

# 年報 Annual Report 2017

---

近畿大学医学部消化器内科学教室





## 目 次

1. 2017 年 Annual Report の発刊にあたって .....	1
2. 消化器内科学業績抜粋 .....	21
3. 消化器内科診療実績 .....	22
4. 近畿大学消化器内科学教室医局員 .....	28
5. 消化器内科学教室業績一覧（2017 年） .....	31
英文論文 .....	32
和文論文 .....	41
招待講演・特別講演（海外） .....	42
招待講演・特別講演（国内） .....	43
学会発表（海外シンポジウム） .....	44
学会発表・抄録（米国及び国際学会） .....	47
学会発表（国内シンポジウム・パネルディスカッション・ワークショップ） .....	51
学会発表（国内一般演題） .....	56
6. 別刷 .....	70



# 2017 年 Annual Report の発刊にあたって

近畿大学消化器内科学教室主任教授 工藤正俊

## 1. 診療活動

診療活動においては平成 28 年度の実績として総稼働額 38 億 4300 万円（附属病院第 2 位）、在院日数は 7.6 日（附属病院第 1 位）、限界利益は外科に肉薄する 20 億円で附属病院第 2 位（1 位は外科全体で 24 億円）、DPC II 以内の退院率は 80% で附属病院第 1 位の成績をあげ大変な診療実績を収めている。一日当たり入院患者は 84.7 人（附属病院第 1 位）、入院延患者数 30,919 人（附属病院第 1 位）、外来延患者数 49,143 人（附属病院第 1 位）、紹介患者数 3,259 件（附属病院第 2 位）、診療所以外の病院からの紹介患者数 1,363 件（附属病院第 1 位）。また 2016 年 10 月からは病床数も 80 床から 95 床へと 15 床増床、2017 年 5 月から 5 床増床され 100 床になった。それにも関わらず稼働率 90-95%、在院日数 6-7 日と以前と同様の数字をキープしている。このようなことから消化器内科の病院収入への貢献は大変に大きいものがある。引き続きこのような高度で active な診療活動を継続していただきたいと考えている。

## 2. 教育活動

教育は当然のことながら大学医学部の役割の極めて根幹を占める重要な部分であります。消化器内科学は消化器コースの内の肝臓の責任科であり、肝臓のユニットを 1 週間担当している他、上部消化管、下部消化管、胆膵のユニットや臨床腫瘍コースならびに画像診断のコースでも講義を担当しております。更には病因・病態のコースの 3 週間のうち 1 週間の責任科として大変多忙な教育活動を行っております。5 年生 6 年生のクリニカルクラークシップも例年 6 年生を常時 6 人程度受け入れており、講義や総括など充実した bed side 教育となるよう全力を尽くしております。国家試験の成績も是非とも向上させなければなりません。

平成 20 年 10 月から病院長に任ぜられ、3 期目となりましたが無事平成 26 年 9 月には任期満了により退任いたしました。その間は公務のために教育活動の多くの部分を渡邊准教授、松井講師はじめ多くの先生方にご負担をおかけすることになってしまい、申し訳なく思っております。消化器コース及び病因・病態コースあるいは日々のクリニカルクラークシップ等の教育活動では決して手を抜かず積極的に行っていくつもりですので何卒ご容赦下さい。この紙面をお借りして感謝とお詫びを申し上げます。

### 3. 研究活動

#### (1) 論文業績

英文論文の発表は1999年消化器内科の設立当初は一桁台でありましたが、年と共に確実に増加し、3年目からは平均20編以上の英文論文がコンスタントに出るようになりました。2010年の英文論文数は51編に達しました。残念ながら2011年は48編、2012年は44編にとどまりました。しかし、2014年からは再び57編と50編の大台に回復しました。また18年間の総インパクトファクターは3901.262点であり英文総論文数は741編ですので、近畿大学消化器内科のような小さな所帯の教室としてはまずまずの結果を残せているのではないかと考えております。来年以降は最低、英文原著論文は60編以上を目標に頑張っていきたいと考えておりますので教室員の皆様の自覚と更なる奮闘を期待致しております。

#### (2) 厚生労働省科学研究費補助金事業研究班の活動

平成22年度に採択された厚労科研（がん臨床部門）「**進行・再発肝細胞癌に対する動注化学療法と分子標的薬併用による新規治療法の確立を目指した臨床試験（Phase III）ならびに効果を予測するbiomarkerの探索研究**」（工藤班）の主任研究者として日本発のエビデンスを創出すべく、努力してまいりました（平成22－24年）。また平成23年度には厚労科研（難病・がん等の疾患分野の医療の実用化部門）「**慢性ウイルス性肝疾患の非侵襲的線化評価法の開発と臨床的有用性の確立**」（工藤班）の主任研究者としても採択され、多くの大学との協同研究を行いました（平成23－25年）。平成26年度には厚生労働科学研究委託費（肝炎等克服実用化研究事業（肝炎等克服緊急対策研究事業））「慢性ウイルス性肝炎の病態把握（重症度・治療介入時期・治療効果判定・予後予測）のための非侵襲的病態診断アルゴリズムの確立」という課題が採択され、平成26年度には平成27年度日本医療研究開発機構（AMED）の委託費となりました。平成30年度、令和元年度からは（臨床研究等ICT基盤構築・人工知能実装研究事業）「人工知能の利活用を見据えた超音波デジタル画像のナショナルデータベース構築基盤整備に関する研究」（平成30年度）と平成31年度からは「超音波デジタル画像のナショナルデータベース構築と人工知能支援型超音波診断システム開発に関する研究」が採択され、日本超音波医学会理事長としてAI開発の研究が進行中です。

またその他にも下記の厚労科研の分担研究者として教室の先生方に実務を担当して頂いております。この場をお借りして感謝申し上げます。

## (3) Research Conference

English Research Conference 出席状況

	2012		2013		2014		2015		2016		2017	
	出席数	出席率	出席数	出席率	出席数	出席率	出席数	出席率	出席数	出席率	出席数	出席率
工藤	32/32	100%	25/25	100%	22/22	100%	21/21	100%	28/28	100%	26/26	100%
檜田	27/32	84%	19/25	76%	20/22	91%	16/21	76%	20/28	71%	22/26	84%
辻	－	－	－	－	－	－	－	－	－	－	－	－
西田	24/32	75%	10/25	40%	4/22	18%	13/21	62%	9/28	32%	7/26	26%
渡邊	－	－	－	－	－	－	－	－	－	－	12/26	46%
北野	25/32	78%	21/25	84%	12/22	55%	9/21	43%	2/28	7%	－	－
松井	30/32	94%	23/25	92%	20/22	91%	21/21	100%	25/28	89%	26/26	100%
上嶋	9/32	28%	6/25	24%	5/22	23%	9/21	43%	15/28	43%	5/26	19%
櫻井	25/32	78%	15/25	60%	15/22	68%	14/21	67%	20/28	71%	22/26	84%
依田	－	－	－	－	－	－	－	－	－	－	26/26	100%
南(康)	31/32	97%	22/25	88%	19/22	86%	20/21	95%	15/28	54%	22/26	84%
萩原	10/32	31%	9/25	36%	4/22	18%	12/21	57%	8/28	29%	6/26	23%
竹中	－	－	－	－	－	－	－	－	20/28	71%	14/26	53%
米田	－	－	－	－	22/22	100%	17/21	81%	23/28	82%	21/26	80%
田北	9/23	39%	12/25	48%	4/22	18%	8/21	38%	13/28	46%	8/26	30%
永井	23/32	72%	14/25	56%	－	－	14/21	67%	16/28	57%	17/26	65%
今井	13/32	41%	7/25	28%	8/22	36%	16/21	76%	－	－	17/26	65%
山雄	－	－	14/25	56%	19/22	86%	16/21	76%	22/28	79%	22/26	84%
山田	23/25	92%	15/25	60%	6/22	27%	8/21	38%	－	－	11/26	42%
鎌田	16/32	50%	9/25	36%	6/22	27%	15/21	71%	27/27	96%	7/26	26%
高山	16/32	50%	16/25	64%	4/22	18%	－	－	－	－	－	－
宮田	22/32	69%	15/25	60%	17/22	77%	11/21	52%	18/28	64%	13/26	50%
松田	－	－	－	－	－	－	9/21	43%	－	－	－	－
三長	－	－	－	－	－	－	11/21	52%	19/28	68%	12/26	46%
河野(匡)	－	－	－	－	20/22	91%	8/21	38%	12/28	43%	16/26	61%
中井	－	－	－	－	－	－	－	－	－	－	12/26	46%
山崎	－	－	－	－	－	－	－	－	－	－	－	－
大本	29/32	91%	19/25	76%	18/22	82%	15/21	71%	13/28	46%	14/26	53%

千品	29/32	91%	22/25	88%	17/22	77%	10/21	48%	10/28	48%	13/26	50%
南(知)	-	-	21/25	84%	19/22	86%	16/21	76%	18/28	64%	13/26	50%
正木	-	-	-	-	-	-	-	-	-	-	-	-
岡本	-	-	-	-	-	-	-	-	15/28	54%	24/26	92%
岡元	-	-	12/25	48%	18/22	82%	14/21	67%	19/28	68%	22/26	84%
石川	-	-	-	-	-	-	-	-	-	-	19/26	73%
橋本	-	-	-	-	-	-	-	-	-	-	-	-
木下	-	-	-	-	-	-	-	-	-	-	21/26	80%
高田	-	-	-	-	-	-	-	-	-	-	13/26	50%
吉川	-	-	-	-	-	-	-	-	-	-	-	-
河野(辰)	-	-	-	-	-	-	-	-	-	-	16/26	61%
高島	-	-	-	-	-	-	-	-	-	-	19/26	73%
田中	-	-	-	-	-	-	-	-	-	-	19/26	73%
半田	-	-	-	-	-	-	-	-	-	-	21/26	80%
福永	-	-	-	-	-	-	-	-	-	-	17/26	65%
吉田	-	-	-	-	-	-	-	-	-	-	16/26	61%
大塚	-	-	-	-	-	-	-	-	-	-	-	-
益田	-	-	-	-	-	-	-	-	-	-	-	-
松村	-	-	-	-	-	-	-	-	-	-	-	-

#### 4. 学会活動および海外における活動

2017 年における国内の学会発表については 26 演題、国際学会（米国及び国際学会＋シンポ・パネル）の発表については 46 演題、海外特別講演は 6、国内特別講演は 44 でありました。私自身の海外出張（特別講演・招待講演のみ）は 2017 年は 26 回となりました。

##### 1. 1月12日－13日

China Lenvima Launch Meeting Eisai China Advisory Boardに参加 (Shanghai, China)

##### 2. 1月17日－19日

消化器癌シンポジウムに参加 (ASCO-GI 2017) (San Francisco, USA)

##### 3. 2月14日

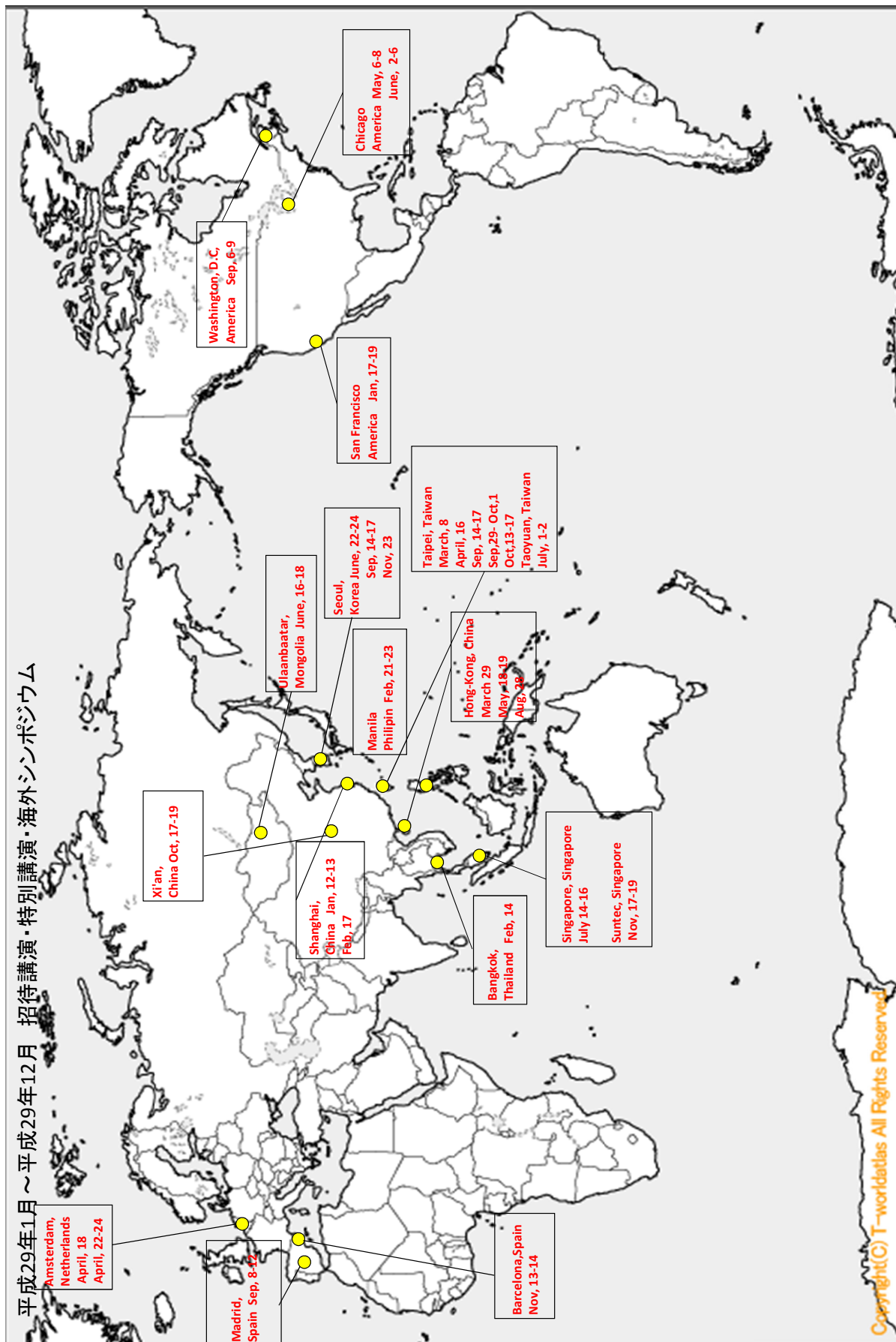
EMERALD-1 (D933GC00001) 試験 Investigator meetingに参加 (Bangkok, Thailand)

##### 4. 2月17日

第26回アジア太平洋肝臓病学会議年次総会にて招待講演 (APASL 2017) (Shanghai, China)

5. 2月21日－23日  
APASL2017Manilaにて発表 (Manila, Philipin)
6. 3月8日  
INTR@PID BTC047 Investigator Meetingに参加 (Taipei, Taiwan)
7. 3月29日  
Hepatocellular Carcinoma Symposiumに参加 (Hong Kong, China)
8. 4月17日－4月23日  
欧州肝臓病学会 (EASL)2017にて Roche 、バイエル Advisory Boardに参加 (Amsterdam, Netherland)
9. 4月15日－4月16日  
バイエル Advisory Boardにて講演 (Taipei, Taiwan)
10. 5月6日－5月9日  
米国消化器病週間に参加 (DDW2017) (Chicago, USA)
11. 5月19日－5月20日  
香港国際腫瘍学会にて講演 (The Hong Kong International Oncology Forum 2017) (Hong Kong, China)
12. 6月2日－6月6日  
第53回癌治療学会議に参加 (ASCO 2017) (Chicago, USA)
13. 6月16日－6月17日  
アジア太平洋肝臓学病学会シングルトピックカンファレンスにて講演 (APASL-STC2017) (Ulaanbaatar, Mongolia)
14. 6月17日－6月18日  
APECHO2017 Advisory Boardに参加 (APASL-STC2017) (Shanghai, China)
15. 6月22日－6月23日  
第24回アジア太平洋癌学会にて講演 (APCC) (Seoul, Korea)
16. 7月1日－7月2日  
台湾におけるネクサバール錠発売10周年記念講演会にて特別講演 (Taoyuan, Taiwan)
17. 7月14日－7月16日  
第8回アジア太平洋肝癌専門家会議にて講演 (APPLE 2017) (Singapore, Singapore)
18. 8月28日  
アストラゼネカ Advisory Boardにて特別講演 (Hong Kong, China)
19. 9月8日－9月12日  
欧州臨床腫瘍学会に参加 (ESMO2017) (Madrid, Spain)
20. 9月14日－9月17日  
国際肝癌学会に参加 (International Liver Cancer Association 2017) (Taipei, Taiwan)
21. 9月29日－10月1日  
Taiwan Digestive Disease Week 2017にて特別講演 (TDDW) (Taipei, Taiwan)
22. 10月13日－17日  
The 9th Asian Conference on Ultrasound Contrast Imagingにて特別講演 (ACUCI) (Taipei,

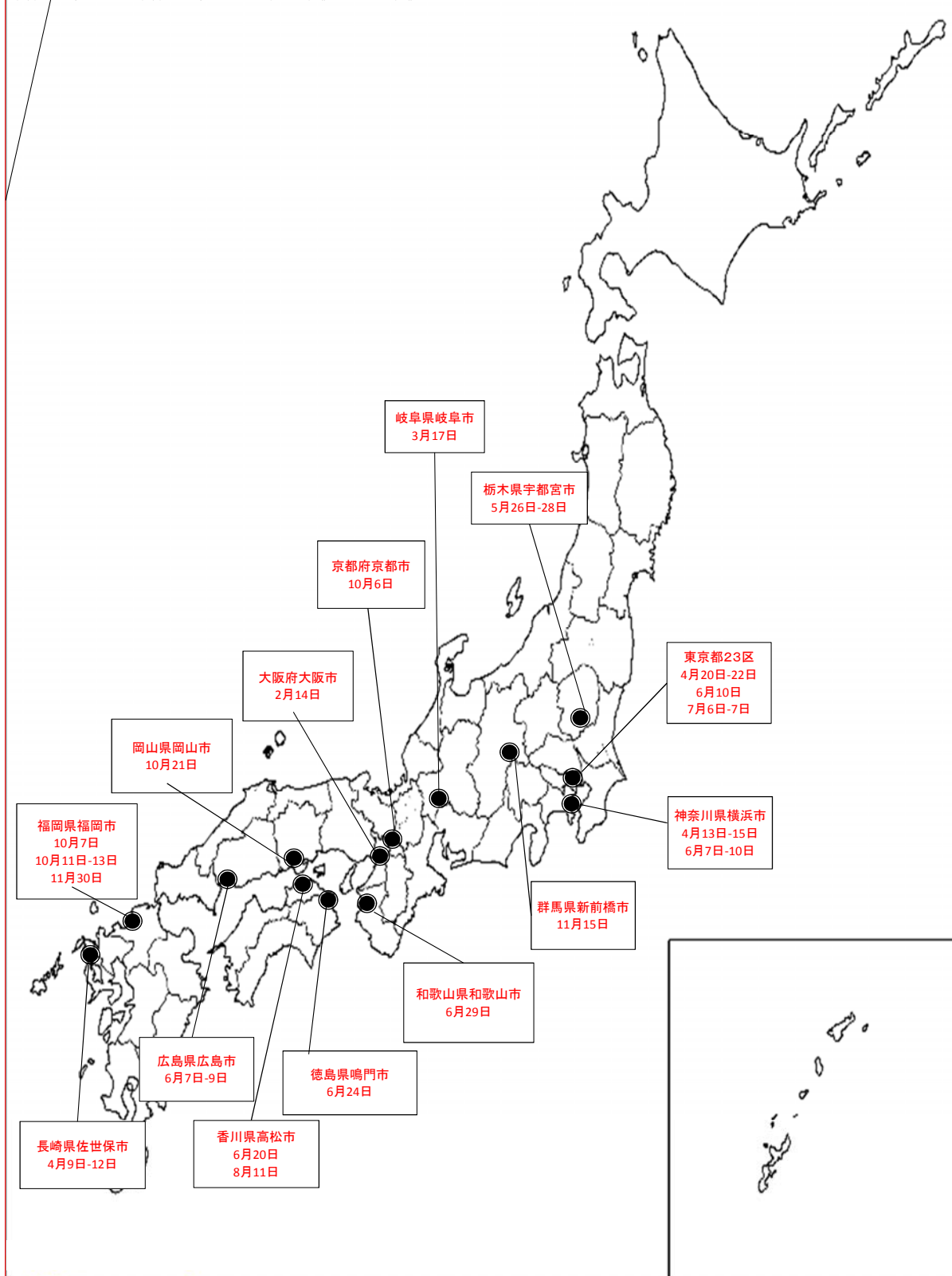
平成29年1月～平成29年12月 招待講演・特別講演・海外シンポジウム



Copyright(C) T-world All Rights Reserved



平成29年1月～平成29年12月 招待講演・特別講演



- Taiwan)
23. 10月17日－19日  
2017年日中笹川医学協力プロジェクト超音波実用技術研修に参加（西安，中国）
24. 11月13日－14日  
バルセロナ Education Meeting にて講演（Barcelona, Spain）
25. 11月17日－19日  
欧州臨床腫瘍学会アジアにて発表（ESM02017）（Suntec, Singapore）
26. 11月23日  
第1回韓国消化器病学会週間にて講演（KDDW）（Seoul, Korea）

## 5. 留学生受け入れ

Bangladesh からの留学生（日本超音波医学会の Fellowship 留学制度による）の Dr. Shahinur Haque も 2017 年 5 月 16 日から 11 月 16 日の 6 か月間消化器内科に在籍し、超音波診断、造影エコー、RFA、EUS さらには核医学診断なども研修された。教室員にもよく溶け込んで頂いて教室員とも「飲みケーション」も積極的に図っていたようである。

一方、日本消化器病学会からの Fellowship 留学制度により台湾から Dr. Sz-Iuan Shiu も消化器内視鏡を中心に当教室において 2017 年 8 月 1 日から 11 月 30 日まで留学生として滞在した。

## 6. 人事について

その他、昨年の一年間のスタッフの動向を以下に述べる。

2017 年 3 月には朝隈 豊先生がお父様の医院の継承するために、また足立哲平先生があだち医院の継承のため退職し開業された。また 2017 年 7 月末 矢田典久先生が京都で「矢田消化器内視鏡クリニック」開業のため退職、2017 年 9 月末、有住忠晃先生も 10 月からの串本赴任に合わせて退職された。結果的に 2017 年には 4 名が退職された。

それに代わる新入局者であるが 2017 年 4 月には新進気鋭の 7 名の近畿大学卒業の後期レジデント（福永朋洋先生、河野辰哉先生、半田康平先生、高島耕太先生、吉田晃浩先生、田中秀和先生）に入局して頂き消化器内科も一気に活気づいた。また県立尼崎病院からは中井敦史先生（平成 22 年徳島大学卒業）、和歌山県立医科大学から木下 淳先生（平成 25 年和歌山医大卒業）、名古屋セントラル病院から石川 嶺先生（平成 24 年近畿大学医学部卒業）、済生会泉尾病院からは高田隆太郎先生（平成 26 年近畿大学医学部卒業）が入局され、計 10 名もの若者が新しく消化器内科に加わって頂いた。

来年度も新しい大学院生・後期レジデントとして数名の新人を迎える予定である。これら若く活気あるニューフェースと一緒に、消化器内科を益々、充実・発展させたいと考えている。

また、短期の研修生として岸和田徳洲会病院から古田朗人先生を 10 月から 12 月 31 日までの

約3か月間受け入れた。

## 7. 学会主催

教室主催の学会としては2017年9月1-2日上嶋一臣講師が高野山においてリザーバー研究会を主催した。当初、高野山で開催するなどという奇抜なアイデアでは参加者が激減するのではと心配していたが200名弱の参加者を得て大変好評であった。また、秘書の朝隈さんの実家である安養院はとても好評で、また弟さんが住職を務められているとのことで、家族の方の温かいおもてなしのみならず高野山の他のお寺の方にもおもてなし頂いた会長招宴は大変に好評であった。また、奥の院への散歩をする時間もあり十分に「気」と「パワー」を頂いた研究会であった。山下弘子さんによる特別講演も素晴らしく、多くの参加者の感動を呼んだ。

## 8. 新専門医制度

ここ数年、議論が活発に行われてきた新内科専門医制度はいよいよ2018年4月から開始される見込みとなった。また、この内科専門医研修では内科専門医研修と subspeciality の研修を平行して行う、いわゆる平行研修が認められ、肝臓専門医および消化器病専門医の研修が内科専門医と共に同時に開始できる従来同様の制度となった。これは subspeciality の専門医取得までの時間のロスが少なく従来と同じくらいの期間で消化器病専門医や肝臓専門医の取得が可能となり結果として良かったと思っている。また、超音波専門医の研修制度も今後見直しがなされる予定である。消化器内視鏡専門医についてはまだ若干、不透明な状況である。

## 9. おわりに

この半世紀、各医学分野における専門の細分化は例外なく進められてきている。内科学から消化器内科学が分離・独立し、さらに上部消化管、下部消化管、肝臓、胆膵と細分化の傾向が顕著である。しかし内科学を包括的学問分野と捉えた場合、知識の連携・統合が本質であり、極く狭い領域しか知らない医師は真の消化器内科医とは言えない。信頼される医師とは広い知識を持ちつつ、ある領域については特に深い見識と技術を持つ organ specialist であり、かつ総合消化器内科医でもあるべきである。内科学全体の広い知識 (generalist) に裏打ちされた organ specialist としての消化器内科医という医師像を目指して医局員の皆様には日夜努力して頂きたいと考えている。今後とも教室員が一丸となって日本だけでなく世界に発信できる現在の教室の高いアクティビティを維持し続け更に発展させて頂けるよう医局員一同には引き続き粉骨砕身、刻苦勉励を切にお願いする次第である。

2017年3月 大阪狭山にて

## 工藤正俊（くどうまさとし）

（令和2年9月更新）



昭和29年	愛媛県西条市生まれ
昭和53年	京都大学医学部 卒業
同	京都大学医学部附属病院 勤務（研修医）
昭和54年	神戸市立中央市民病院内科 勤務（研修医）
昭和55年	同 消化器内科 医員
昭和60年	同 消化器内科 副医長
昭和62年	カリフォルニア大学留学（デービスメディカルセンター）
平成元年	神戸市立中央市民病院消化器内科 副医長 復職
平成4年	同 消化器内科 医長
平成9年	近畿大学医学部第2内科学 助教授
平成11年	近畿大学医学部消化器内科学 主任教授 現在に至る

### （その他大学内役職）

平成19年-20年	近畿大学医学部附属病院副病院長
平成20年-26年	近畿大学医学部附属病院病院長
平成27年-現在	学校法人近畿大学理事（医学部・附属病院担当理事）

### （現在の併任）

近畿大学医学部奈良病院消化器内科 教授（兼務）
神戸市立中央市民病院消化器内科 顧問（兼務）

## 主な所属学会等

日本消化器関連学会機構(JDDW)(理事・国際委員会委員)、日本消化器病学会(執行評議員・指導医・専門医)、日本肝臓学会(理事・国際委員会委員長・指導医・専門医)、日本消化器内視鏡学会(社団評議員・指導医・専門医)、日本超音波医学会(理事長・国際交流委員会委員長・指導医・専門医)、日本内科学会(評議員・認定内科医)、日本高齢消化器病学会(理事)、日本癌学会(評議員)、日本臨床腫瘍学会(協議員)、日本核医学会(評議員・専門医)、日本肝癌研究会(常任幹事・事務局代表・追跡調査委員長)、日本肝がん分子標的治療研究会(代表世話人・事務局代表)、日本肝移植研究会(世話人)、肝血流動態イメージ研究会(世話人)、日本腹部造影エコー・ドプラ診断研究会(代表世話人・事務局)、肝癌治療シミュレーション研究会(副代表幹事)、超音波治療研究会(常任世話人)、日本消化器内視鏡財団(評議員)、米国肝臓学会(AASLD)(肝癌部門企画運営委員: Steering Committee of hepatobiliary malignancy)、米国消化器病学会(AGA)、米国消化器内視鏡学会(ASGE)、世界肝臓学会(IASL)、欧州肝臓学会(EASL)、など

## 委員・資格など

- ・ 世界超音波医学会(WFUMB) Immediate Past President(前理事長)
- ・ アジア超音波医学会(AFSUMB) Immediate Past President(前理事長)
- ・ アジア太平洋肝癌学会(APPLE) President(理事長)
- ・ 国際肝癌学会(ILCA) 理事(Founding Board Member, Governing Board Council Member)
- ・ 米国肝臓学会(AASLD) 肝癌部門運営委員会委員(Steering Committee Member)
- ・ 日本肝がん臨床研究機構(JLOG) (理事長)
- ・ 世界保健機構(WHO) Blue Book「Classification of the Tumor」改訂委員(平成21年5月1日)
- ・ ウイルス肝炎研究財団 日米医学協力研究会肝炎専門部会研究員
- ・ International Liver Thought Leadership Study (ILCS), Council member
- ・ 全国医学部長病院長会議 理事(平成26年5月17日 - 平成28年)
- ・ IASGO 癌分子標的治療国際委員長 (Executive Board President of International IASGO Molecular Targeting Therapy Section)(平成26年12月6日 - 現在)
- ・ ILCA School of Liver Cancer Committee Member(平成27年4月30日 - 現在)
- ・ Editor-in-Chief「Liver Cancer」(Karger, Basel)(2012年 - 現在)

## 受賞

- ・ 米国核医学会 Berson-Yalow Award 受賞(平成元年6月)
- ・ 日本対がん協会がん研究助成奨励賞 受賞(平成4年3月)
- ・ 日本消化器病学会奨励賞 受賞(平成4年4月)
- ・ 日本超音波医学会優秀論文賞「菊池賞」受賞(平成4年5月21日)
- ・ 日本核医学会賞 受賞(平成5年10月)
- ・ 米国超音波医学会(AIUM) 学会賞受賞(平成15年6月4日)
- ・ ボローニャ大学医学部医学会名誉会員賞(平成18年9月15日)

- ・ フィリピン超音波医学会名誉会員(Honorary Member of PSUCMI)(平成20年3月19日)
- ・ アジア太平洋消化器病学会(APDW) OKUDA Award受賞(平成20年9月13日)
- ・ 北米放射線学会 Certificate of Merit受賞(平成20年)
- ・ インド肝臓学会Madangopalan Award受賞(平成21年3月28日)
- ・ 北米放射線学会 Cum Laude 賞受賞(平成21年12月)(7000編の論文中上位10編に採択)
- ・ 日本肝臓学会「日本肝臓学会機関誌 Highest Citation 賞」受賞(平成22年6月)
- ・ JISAN Lecture Award Presented by Korean Society of Ultrasound in Medicine(平成22年5月)
- ・ 米国超音波医学会名誉会員賞(AIUM Honorary Member Award)受賞(平成23年4月)
- ・ 日本肝臓学会「日本肝臓学会機関誌 Highest Citation 賞」受賞(平成23年6月)(2回目)
- ・ Romanian Society of Ultrasound in Medicine and Biology (SRUMB) Honorary Award受賞(平成23年6月)
- ・ 北米放射線学会 Certificate of Merit受賞(平成23年11月)(2回目)
- ・ USE 論文賞(応用物理学会論文賞)受賞(平成24年11月)
- ・ Lorenzo Capussotti Award受賞(from IASGO)(平成26年12月)
- ・ 韓国超音波医学会名誉会員賞(KSUM honorary Award)受賞(平成30年5月25日)
- ・ 日本肝臓学会 織田賞受賞(平成30年6月13日)
- ・ 台湾超音波医学会名誉会員賞(TSUM Honorary Member Award)受賞(平成30年10月13日)
- ・ SGHがん特別賞受賞(平成30年12月1日)
- ・ Desai Memorial Lecture Award from Education Universe and Care Foundation(平成30年12月16日)
- ・ Highly Cited Researcher 2019 受賞(Clarivate Analytics)(令和元年11月19日)(日本人唯一の選出)

## 著書(単著)

- ・ Contrast Harmonic Imaging in the Diagnosis and Treatment of Liver Tumors(Springer-Verlag 2003)
- ・ 肝腫瘍における造影ハーモニックイメージング(医学書院 2001)

## 編集

- ・ 松井 修, 工藤正俊, 編集: 消化器疾患の造影エコーUp Date. 南江堂, 東京, 2003.
- ・ 工藤正俊, 編集: 肝細胞癌治療の最近の進歩, 消化器病セミナー97, へるす出版, 東京, 2004.
- ・ 河田純男, 白鳥康史, 工藤正俊, 榎本信幸, 編集, 小俣政男, 監修: 肝疾患Review 2004, 日本メディカルセンター, 東京, 2004.
- ・ 河田純男, 白鳥康史, 工藤正俊, 榎本信幸, 編集, 小俣政男, 監修: 肝疾患Review 2006-2007, 日本メディカルセンター, 東京, 2006.



- ・ 河田純男, 横須賀收, 工藤正俊, 榎本信幸, 編集, 小俣政男, 監修: 肝疾患Review 2008-2009, 日本メディカルセンター, 東京, 2008.
- ・ 河田純男, 横須賀收, 工藤正俊, 榎本信幸, 編集, 小俣政男, 監修: 肝疾患Review 2010-2011, 日本メディカルセンター, 東京, 2010.
- ・ 幕内雅敏, 菅野健太郎, 工藤正俊, 編集: 今日の消化器疾患治療指針 第3版, 医学書院, 東京, 2010.
- ・ 工藤正俊, 泉 並木, 編集: 症例から学ぶ ウイルス肝炎の治療戦略. (株)診断と治療社, 東京, 2010.
- ・ 工藤正俊, 編集: 肝細胞癌の分子標的治療, アークメディア, 東京, 2010.
- ・ 山雄健次, 工藤正俊, 編集: 見逃し、誤りを防ぐ! 肝・胆・膵癌画像診断アトラス, 羊土社, 東京, 2010.
- ・ 工藤正俊, 編集: 医学のあゆみ「肝癌の分子標的治療」, 医歯薬出版株式会社, 東京, 2011.
- ・ 工藤正俊, 編集: 「肝細胞がん診療の進歩: Up-To-Data」, 最新医学社, 大阪, 2011.
- ・ 工藤正俊, 編集: 朝倉内科学, 矢崎義雄, 「総編集」, 朝倉書店, 東京, 2013.
- ・ 工藤正俊, 國分茂博, 編集: EOB-MRI/ ソナゾイド造影超音波による肝癌の診断と治療, 医学書院, 東京, 2013.
- ・ 工藤正俊, 編集: 日本臨床増刊号 最新肝癌学, 日本臨床社, 大阪, 2015.
- ・ 工藤正俊, 編集: 最新医学 別冊「診断と治療のABC103 肝がん」, 最新医学社, 大阪, 2015.
- ・ 千葉 勉, 日比紀文, 東 健, 榎本信幸, 金子周一, 工藤正俊, 坂井田 功, 下瀬川 徹, 茶山一彰, 三輪洋人, 本郷道夫, 渡辺 守, 編集: An International Journal of Gastroenterology and Hepatology「GUT」日本語版 Vol. 7, No. 4, 2015.
- ・ 工藤正俊, 企画: 肝胆膵 75巻2号 特集企画. 特集「肝細胞癌の化学療法が変わる」, 肝胆膵, 2017.
- ・ 工藤正俊, 監修: 肝細胞癌に対するレゴラフェニブ治療. アークメディア, 東京, 2017.
- ・ 工藤正俊, 編集: 消化器内科診療レジデントマニュアル. 医学書院, 東京, 2018.
- ・ 工藤正俊, 総監修: レンバチニブによる肝細胞癌治療. アークメディア, 東京, 2019.
- ・ 工藤正俊, 総監修: ラムシルマブによる肝細胞癌治療. アークメディア, 東京, 2020.
- ・ 工藤正俊, 企画: 医学のあゆみ 273巻13号「肝細胞癌治療のパラダイムシフト～分子標的薬、免疫チェックポイント阻害薬の登場を受けて～」. 医学のあゆみ, 2020.

#### Editor-in-Chief:

- ・ Liver Cancer (Basel) (5.944)

#### Associate Editor:

- ・ Journal of Oncology (Germany), 肝胆膵(アークメディア))

## EDITORIAL BOARD:

国際学術雑誌: International Journal of Clinical Oncology (Tokyo) Ultrasound in Medicine and Biology (ELSEVIER, New York) Hepatology International (Springer, New York) Liver International (Blackwell, UK) World Journal of Gastroenterology Liver Cancer Review Letters

国内学術雑誌: 肝胆膵、その他の学会誌 (3)

## 論文査読委員

J Clin Oncol(28.245) , Lancet Oncol(35.386), Gastroenterology(19.233), Hepatology(14.971) , J Hepatol(18.946), Oncologist(5.252), Am J Gastroenterol(10.241), Endoscopy(6.381), Clin Exp Metastas(2.513), Cancer Sci(4.751) , Expert Rev Mol Diagn(2.347) , Eur Radiol(3.962) , Liver Int(5.542), J Gastroenterol(5.130) , Eur J Clin Invest(2.784), J Nucl Med(7.354), J Gastroen Hepatol(3.632), Oncology-Basel (International Journal of Cancer Research and Treatment)(2.278), Ultrasound Med Biol(2.205) , Acta Paediatr(2.265), Hepatol Int(5.490) , Eur J Gastroen Hepat(2.198), J Hepato-Bil-Pan Scu (2.353), Hepatol Res(3.440), Int J Clin Oncol(2.503), Jpn J Clin Oncol(2.183), Internal Med(0.956), J Clin Ultrasound(0.820), Biomark Med(2.268), Hepato-Gastroenterol(0.792), Ann Nucl Med(1.648), Expert Review of Anticancer Treatment(2.347), J Cancer Res Ther (1.392), CSR National Registry(0), J Gastrointest Liver (2.063), Cancer Informatics(0), Expert Review of Proteomics and Future Oncology(0)

## SCIENTIFIC PAPER PUBLICATION:

### 学術論文等:

英文論文: 959(IF: 5430.285, H-Index 83)

和文論文: 948

教科書(単著) 英文: 2 和文: 6

分担執筆 英文: 21 和文: 270

### 特別講演・招待講演・教育講演:

国際学会: 415

国内学会: 768

## 文部科学省科学研究費補助金

「肝細胞癌の発生・進展における腫瘍血管構築の分子機構と血流画像-基盤研究(B)」

(主任研究者: 工藤正俊)

平成10年度(1998年度) 研究費総額: 3,700,000円

平成11年度(1999年度) 研究費総額: 2,300,000円

平成12年度(2000年度) 研究費総額: 2,000,000円



「肝細胞癌の発癌・進展における腫瘍血管構築の精密血流画像解析とその分子機構の解明－基盤研究(C)」(主任研究者：工藤正俊)

平成14年度(2002年度) 研究費総額：1,800,000円

平成15年度(2003年度) 研究費総額：1,200,000円

「肝発癌の進展と血流動態および肝類洞細胞機能変化：造影ハーモニック法による病態解明－基盤研究(C)」(主任研究者：工藤正俊)

平成16年度(2004年度) 研究費総額：2,300,000円

平成17年度(2005年度) 研究費総額：1,400,000円

「精密血流画像解析法の新規開発による動・門脈血流の分離定量評価と肝発癌研究への応用－基盤研究(B)」(主任研究者：工藤正俊)

平成18年度(2006年度) 研究費総額：10,300,000円

平成19年度(2007年度) 研究費総額：2,860,000円

平成20年度(2008年度) 研究費総額：1,950,000円

「高分解能超音波内視鏡造影による膵微小循環動態の検討—診断および治療への応用－基盤研究(C)」(主任研究者：北野雅之)

分担研究者 工藤正俊

平成15年度(2003年度) 研究費総額：1,900,000円

平成16年度(2004年度) 研究費総額：1,100,000円

平成17年度(2005年度) 研究費総額：600,000円

「超音波内視鏡下バイオセンサー穿刺法の開発—膵疾患局所情報入手と評価－基盤研究(C)」  
(主任研究者：北野雅之)

分担研究者 工藤正俊

平成18年度(2006年度) 研究費総額：1,600,000円

平成19年度(2007年度) 研究費総額：1,560,000円

平成20年度(2008年度) 研究費総額：910,000円

「肝細胞癌の発癌・進展の分子機序：造影超音波クーパー相と遺伝子発現を用いた融合解析－挑戦的萌芽研究」(主任研究者：工藤正俊)

平成23年度(2011年度) 研究費総額：2,340,000円

平成24年度(2012年度) 研究費総額：1,430,000円

「肝細胞癌のソラフェニブ著効例における感受性規定遺伝子変異の探索－挑戦的萌芽研究」  
(主任研究者：西尾和人)

分担研究者 工藤正俊

平成23年度(2011年度) 研究費総額: 4,030,000円 / 配分額: 500,000円

「超音波内視鏡を用いた胆膵疾患診断・治療システムの開発-基盤研究(C)」

(主任研究者: 北野雅之)

分担研究者 工藤正俊

平成22年度(2010年度) 研究費総額: 1,950,000円 / 配分額: 100,000円

平成23年度(2011年度) 研究費総額: 1,430,000円 / 配分額: 100,000円

平成24年度(2012年度) 研究費総額: 1,040,000円 / 配分額: 100,000円

「ガンキリンのプロテアソーム制御機構を利用した展開医療研究-基盤研究(C)」

(主任研究者: 櫻井俊治)

分担研究者 工藤正俊

平成23年度(2011年度) 研究費総額: 2,080,000円 / 配分額: 200,000円

平成24年度(2012年度) 研究費総額: 1,950,000円 / 配分額: 200,000円

平成25年度(2013年度) 研究費総額: 2,080,000円 / 配分額: 200,000円

「FGF3遺伝子増幅による肝細胞癌ソラフェニブ治療の効果予測-基盤研究(A)」

(主任研究者: 西尾和人)

分担研究者 工藤正俊

平成24年度(2012年度) 研究費総額: 17,420,000円 / 配分額: 1,000,000円

平成25年度(2013年度) 研究費総額: 17,490,000円 / 配分額: 1,000,000円

平成26年度(2014年度) 研究費総額: 9,100,000円 / 配分額: 600,000円

「超音波ビスコエラストグラフィ: 複合励振による組織粘弾性の定量的可視化技術の開発-基盤研究(A)」(主任研究者: 椎名毅)

分担研究者 工藤正俊

平成25年度(2013年度) 研究費総額: 26,780,000円 / 配分額: 1,040,000円

平成26年度(2014年度) 研究費総額: 11,960,000円 / 配分額: 650,000円

平成27年度(2015年度) 研究費総額: 7,800,000円 / 配分額: 400,000円

「大腸癌、炎症性腸疾患における新規治療標的分子およびバイオマーカーの探索-基盤研究(C)」

(主任研究者: 櫻井俊治)

分担研究者 工藤正俊

平成26年度(2014年度) 研究費総額: 1,170,000円 / 配分額: 200,000円

平成27年度(2015年度) 研究費総額: 1,820,000円 / 配分額: 100,000円

平成28年度(2016年度) 研究費総額: 1,820,000円 / 配分額: 100,000円

「膵疾患の診断能・予後の向上を目指した超音波内視鏡技術の開発－基盤研究(C)」

(主任研究者：北野雅之)

分担研究者 工藤正俊

平成25年度(2013年度) 研究費総額：2,080,000円 / 配分額：150,000円

平成26年度(2014年度) 研究費総額：1,820,000円 / 配分額：150,000円

平成27年度(2015年度) 研究費総額：1,700,000円 / 配分額：100,000円

「血清分泌型マイクロRNAを用いたソラフェニブ治療効果予測マーカーの開発－基盤研究(C)」

(主任研究者：工藤正俊)

平成27年度(2015年度) 研究費総額：1,950,000円

平成28年度(2016年度) 研究費総額：1,950,000円

平成29年度(2017年度) 研究費総額：780,000円

「剪断波伝搬モデルに基づく定量的組織粘・弾性影像法の開発と肝線維化早期診断法の研究－新学術領域研究(研究領域提案型)」(主任研究者：椎名毅)

分担研究者 工藤正俊

平成27年度(2015年度) 研究費総額：2,210,000円 / 配分額：0円

平成28年度(2016年度) 研究費総額：2,600,000円 / 配分額：400,000円

「超音波・光伝播モデルに基づく組織脂肪化・線維化の定量的評価と肝疾患診断への応用－新学術領域研究(研究領域提案型)」(主任研究者：椎名毅)

分担研究者 工藤正俊

平成29年度(2017年度) 研究費総額：2,210,000円 / 配分額：100,000円

平成30年度(2018年度) 研究費総額：2,210,000円 / 配分額：100,000円

「革新的超音波内視鏡技術の開発：膵癌の早期診断・予後改善を目指して－基盤研究(C)」

(主任研究者：北野雅之)

分担研究者 工藤正俊

平成28年度(2016年度) 研究費総額：1,820,000円 / 配分額：100,000円

平成29年度(2017年度) 研究費総額：1,560,000円 / 配分額：100,000円

平成30年度(2018年度) 研究費総額：1,300,000円 / 配分額：100,000円

「発癌とストレス応答の分子基盤解明とその臨床応用」(主任研究者：櫻井俊治)

分担研究者 工藤正俊

平成29年度(2017年度) 研究費総額：1,690,000円 / 配分額：200,000円

平成30年度(2018年度) 研究費総額：1,170,000円 / 配分額：200,000円

平成31年度（2019年度） 研究費総額：1,430,000円 / 配分額：100,000円

「肝癌惹起性HBx変異の存在下で形成される腫瘍微小免疫環境の解析-基盤研究(C)」

(主任研究者：萩原智)

分担研究者 工藤正俊

平成30年度（2018年度） 研究費総額：1,430,000円 / 配分額：100,000円

平成31年度（2019年度） 研究費総額：1,170,000円 / 配分額：100,000円

令和2年度（2020年度） 研究費総額：1,690,000円 / 配分額：100,000円

「肝細胞癌におけるチロシンキナーゼ阻害剤の免疫微小環境への影響に関する研究-基盤研究(C)」

(主任研究者：工藤正俊)

平成30年度（2018年度） 研究費総額：1,690,000円

平成31年度（2019年度） 研究費総額：2,210,000円

令和2年度（2020年度） 研究費総額：520,000円

「自然免疫担当分子RIP2を標的とする炎症性腸疾患の新規治療法の開発-基盤研究(C)」

(主任研究者：渡邊 智裕)

分担研究者 工藤正俊

平成31年度（2019年度） 研究費総額：1,430,000円 / 配分額：100,000円

令和2年度（2020年度） 研究費総額：1,430,000円 / 配分額：100,000円

令和3年度（2021年度） 研究費総額：1,430,000円 / 配分額：100,000円（予定）

「免疫制御機構に注目した難病新規治療戦略の開発-基盤研究(C)」

(主任研究者：櫻井 俊治)

分担研究者 工藤正俊

令和2年度（2020年度） 研究費総額：1,950,000円 / 配分額：50,000円

令和3年度（2021年度） 研究費総額：1,430,000円 / 配分額：50,000円（予定）

令和4年度（2022年度） 研究費総額：1,040,000円 / 配分額：50,000円（予定）

「消化器疾患領域の透視化医療処置における被ばく線量測定(全国多施設前向き観察研究)-基盤研究(C)」(主任研究者：竹中 完)

分担研究者 工藤正俊

令和2年度（2020年度） 研究費総額：2,470,000円 / 配分額：100,000円

令和3年度（2021年度） 研究費総額：780,000円 / 配分額：100,000円（予定）

令和4年度（2022年度） 研究費総額：390,000円 / 配分額：100,000円（予定）

## 厚生科学研究費補助金

厚生科学研究費補助金(肝炎等克服緊急対策研究事業)

「肝がん患者のQOL向上に関する研究」(班長：藤原研司)

分担研究者 工藤正俊

平成14年度(2002年度) 研究費総額：18,700,000円 / 配分額：1,500,000円

平成15年度(2003年度) 研究費総額：14,000,000円 / 配分額：1,000,000円

平成16年度(2004年度) 研究費総額：13,700,000円 / 配分額：2,500,000円

厚生科学研究費補助金(肝炎等克服緊急対策研究事業)

「肝がん患者のQOL向上に関する研究」(班長：藤原研司)

分担研究者 工藤正俊

平成18年度(2006年度) 研究費総額：22,000,000円 / 配分額：2,000,000円

平成19年度(2007年度) 研究費総額：14,000,000円 / 配分額：1,300,000円

平成20年度(2008年度) 研究費総額：13,230,000円 / 配分額：1,250,000円

厚生科学研究費補助金(肝炎等克服緊急対策研究事業)

「血小板低値例へのインターフェロン治療法の確立を目指した基礎および臨床的研究」(班長：西口修平)

分担研究者 工藤正俊

平成21年度(2009年度) 研究費総額：20,000,000円 / 配分額：700,000円

平成22年度(2010年度) 研究費総額：20,000,000円 / 配分額：800,000円

平成23年度(2011年度) 研究費総額：17,000,000円 / 配分額：800,000円

厚生科学研究費補助金(がん臨床研究事業)

「初発肝細胞癌に対する肝切除とラジオ波焼灼両方の有効性に関する多施設共同研究」(班長：國土典宏)

分担研究者 工藤正俊

平成21年度(2009年度) 研究費総額：25,500,000円 / 配分額：200,000円

平成22年度(2010年度) 研究費総額：25,895,000円 / 配分額：200,000円

平成23年度(2011年度) 研究費総額：20,082,000円 / 配分額：150,000円

厚生科学研究費補助金(肝炎等克服緊急対策研究事業)

「肝がんの新規治療法に関する研究」(班長：本多政夫)

分担研究者 工藤正俊

平成21年度(2009年度) 研究費総額：52,800,000円 / 配分額：2,000,000円

平成22年度(2010年度) 研究費総額：52,800,000円 / 配分額：2,000,000円

平成23年度(2011年度) 研究費総額：55,277,000円 / 配分額：2,000,000円

厚生科学研究費補助金(がん臨床研究事業)

「進行・再発肝細胞癌に対する動注化学療法と分子標的薬併用による新規治療法の確立を目指した臨床試験(Phase III)ならびに効果を予測するbiomarkerの探索研究」

(班長：工藤正俊)

平成22年度(2010年度) 研究費総額：45,750,000円

平成23年度(2011年度) 研究費総額：32,500,000円

平成24年度(2012年度) 研究費総額：30,000,000円

厚生科学研究費補助金(難治性疾患克服研究事業)

「多発肝のう胞症に対する治療ガイドライン作成と試料バンクの構築」

(班長：大河内信弘)

分担研究者 工藤正俊

平成22年度(2010年度) 研究費総額：12,285,000円 / 配分額：700,000円

平成23年度(2011年度) 研究費総額：10,000,000円 / 配分額：700,000円

平成24年度(2012年度) 研究費総額：11,700,000円 / 配分額：0円

厚生科学研究費補助金(難病・がん等の疾患分野の医療の実用化研究事業)

「慢性ウイルス性肝疾患の非侵襲的線維化評価法の開発と臨床的有用性の確立」

(班長：工藤正俊)

平成23年度(2011年度) 研究費総額：58,500,000円

平成24年度(2012年度) 研究費総額：57,000,000円

平成25年度(2013年度) 研究費総額：50,000,000円

厚生科学研究費補助金(難病・がん等の疾患分野の医療の実用化研究事業)

「慢性ウイルス性肝疾患患者の情報収集の在り方等に関する研究」(班長：相崎英樹)

分担研究者 工藤正俊

平成23年度(2011年度) 研究費総額：40,000,000円 / 配分額：1,500,000円

平成24年度(2012年度) 研究費総額：35,500,000円 / 配分額：1,500,000円

平成25年度(2013年度) 研究費総額：35,500,000円 / 配分額：1,500,000円

厚生科学研究費補助金(肝炎等克服実用化研究事業)

「肝がん研究の推進及び肝がん患者等への支援のための最適な仕組みの構築を目指した研究」

(班長：小池和彦)

分担研究者 工藤正俊

平成29年度(2017年度) 研究費総額：2,000,000円 / 配分額：0円

「肝がん・重度肝硬変の治療に係るガイドラインの作成等に資する研究」

(班長：小池和彦)

分担研究者 工藤正俊

平成30年度（2018年度） 研究費総額：70,000,000円 / 配分額：2,000,000円

令和 1年度（2019年度） 研究費総額：70,000,000円 / 配分額：2,000,000円

令和 2年度（2020年度） 研究費総額：70,000,000円 / 配分額：2,000,000円

令和 3年度（2021年度） 研究費総額：－ 円 / 配分額：－ 円

令和 4年度（2022年度） 研究費総額：－ 円 / 配分額：－ 円

厚生科学研究委託事業(肝炎等克服実用化研究事業(肝炎等克服緊急対策研究事業))

「慢性ウイルス性肝炎の病態把握(重症度・治療介入時期・治療効果判定・予後予測)のための非侵襲的病態診断アルゴリズムの確立」(班長：工藤正俊)

平成26年度（2014年度） 研究費総額：40,300,000円

#### 国立研究開発法人日本医療研究開発機構（AMED）

(肝炎等克服実用化研究事業(肝炎等克服緊急対策研究事業))

「慢性ウイルス性肝炎の病態把握(重症度・治療介入時期・治療効果判定・予後予測)のための非侵襲的病態診断アルゴリズムの確立」

主任研究者 工藤正俊

平成27年度（2015年度） 研究費総額：44,220,000円

平成28年度（2016年度） 研究費総額：33,800,000円

(臨床研究等 ICT 基盤構築・人工知能実装研究事業)

「人工知能の利活用を見据えた超音波デジタル画像のナショナルデータベース構築基盤整備に関する研究」

主任研究者 工藤正俊

平成30年度（2018年度） 研究費総額：190,000,000円

「超音波デジタル画像のナショナルデータベース構築と人工知能支援型超音波診断システム開発に関する研究」

主任研究者 工藤正俊

平成31年度（2019年度） 研究費総額：61,990,900円

令和 2年度（2020年度） 研究費総額：50,030,759円

「医療ビッグデータ利活用を促進するクラウド基盤・AI画像解析に関する研究」(主任研究者：合田憲人)(分担課題名:人工知能の開発に資する超音波画像データとアノテーションに関する研究)

分担研究者 工藤正俊



平成31年度（2019年度） 研究費総額：82,999,982円 / 配分額：0円

令和 2年度（2020年度） 研究費総額：124,879,298円 / 配分額：0円

### ガイドライン策定委員会委員

- ・ 「科学的根拠に基づく肝臓診療ガイドライン」(日本肝臓学会編)，金原出版
- ・ 「慢性肝炎の治療ガイドライン」(日本肝臓学会編)，文光堂
- ・ 「肝臓診療マニュアル」(日本肝臓学会編)，医学書院
- ・ 「肝臓治療効果判定基準」(日本肝臓学会取扱い規約委員会編)，肝臓
- ・ 臨床病理「肝臓取り扱い規約」(日本肝臓学会編)
- ・ Clinical Practice Guidelines for Hepatocellular Carcinoma, Japan Society of Hepatology, Hepatology Research
- ・ General Rules for the Clinical and Pathological Study of Primary Liver Cancer, 3<sup>rd</sup> English Version, Liver Cancer Study Group of Japan, Kanehara, Tokyo, 2010
- ・ Response Evaluation criteria in the Cancer of the Liver (RECICL), Liver Cancer Study Group of Japan, Hepatology Research
- ・ 「多発肝のう胞症に対する治療ガイドライン」
- ・ RECICL 2014 update版, Hepatology Research

### ガイドライン策定

- ・ 日本肝臓学会 肝臓診療ガイドライン作成委員(2009年, 2013年, 2017年, 2021年)
- ・ 日本肝臓学会 肝臓診療マニュアル作成委員会委員(2010年, 2015年, 2020年)
- ・ 日本肝臓学会 慢性肝炎治療ガイドライン作成委員会委員
- ・ 日本肝臓学会 多発性肝嚢胞治療ガイドライン作成委員会委員
- ・ 日本超音波医学会 肝臓のエラストグラフィ作成委員会委員長
- ・ 世界超音波医学会 エラストグラフィガイドライン作成委員会委員長

### 特許取得

発明の名称： ソラフェニブの効果予測方法

出願番号： 特願2011-104275

出願日： 2011年5月9日

発明者： 荒尾徳三、松本和子、西尾和人、工藤正俊

出願人： 学校法人近畿大学

発明の名称： N型糖鎖を利用した膵臓癌の診断方法

公開番号： 特許公開2009-270996

公開日： 2009年11月19日

発明者： 荒尾徳三、松本和子、西尾和人、坂本洋城、北野雅之、工藤正俊

出願人： 住友ベークライト株式会社



## 全国規模の学会・研究会事務局

- ・ 日本肝臓研究会(事務局・追跡調査委員長・常任幹事)
- ・ 日本腹部造影エコー・ドプラ診断研究会(代表世話人・事務局)
- ・ NPO法人日本肝がん臨床研究機構(理事長・事務局)
- ・ 日本肝がん分子標的治療研究会(代表世話人・事務局)

## 全国規模の研究会世話人・役員

平成 6年 4月－ 8年 3月	日本超音波医学会腹部造影エコー研究部会幹事
平成 7年11月－現在	肝血流動態イメージ研究会世話人
平成 8年 4月－現在	日本腹部造影エコー・ドプラ造影研究会世話人（事務局兼務） (平成25年より代表世話人)
平成 9年 7月－現在	肝動脈塞栓療法研究会世話人
平成10年－現在	国際造影超音波研究会 (現、Asia Contrast Ultrasound Imaging Society)世話人
平成11年10月－現在	臨床消化器病研究会世話人
平成11年 7月－現在	西日本肝臓研究会世話人
平成13年 5月－現在	肝疾患フォーラム世話人
平成14年 4月－現在	犬山シンポジウム会員
平成14年 9月－現在	日本消化器画像診断研究会世話人
平成16年－現在	Liver Forum in Kyoto世話人
平成18年－現在	肝臓治療シミュレーション研究会副代表幹事
平成19年11月－現在	日本超音波治療研究会常任世話人
平成20年－現在	日本肝がん分子標的治療研究会(代表世話人)

## 関西地区研究会代表世話人

- ・ 平成11年－平成19年 関西造影超音波研究会(代表世話人)
- ・ 平成13年－現在 関西B型肝炎研究会(代表世話人)
- ・ 平成14年－現在 肝臓局所治療研究会(代表世話人)
- ・ 平成14年－現在 大阪消化器化学療法懇話会(代表世話人)
- ・ 平成15年－現在 臨床消化器病フォーラム(代表世話人)
- ・ 平成18年－平成22年 Bay Area Gut Club(代表世話人)
- ・ 平成18年－平成22年 South Osaka Liver Club(代表世話人)
- ・ 平成19年－現在 関西肝血流動態イメージ研究会(代表世話人)
- ・ 平成20年－現在 Kinki Liver Club(代表世話人)
- ・ 平成21年－現在 南大阪肝疾患研究会(代表世話人)
- ・ 平成21年－現在 南大阪肝胆膵疾患研究会(代表世話人)

## 関西地区研究会世話人

- ・ 平成 2年-現在 大阪肝穿刺生検治療研究会世話人
- ・ 平成 6年-現在 兵庫インターベンショナルラディオロジー研究会世話人
- ・ 平成 8年-現在 肝胆膵治療フォーラム・神戸世話人
- ・ 平成 9年-現在 京都肝疾患懇話会世話人
- ・ 平成 9年-現在 肝臓分子生物学研究会
- ・ 平成11年-平成18年 肝代謝コロキウム世話人
- ・ 平成11年-現在 大阪肝胆膵懇話会世話人
- ・ 平成11年-現在 南大阪肝胆膵疾患研究会世話人
- ・ 平成11年-現在 南大阪消化器病懇話会世話人
- ・ 平成11年-現在 南大阪肝疾患研究会世話人
- ・ 平成11年-平成24年 消化器ラウンドテーブルディスカッション世話人
- ・ 平成11年-平成18年 泉州肝臓病研究会世話人
- ・ 平成11年-平成18年 大阪肝炎ミーティング世話人
- ・ 平成12年-現在 大阪肝臓病談話会世話人
- ・ 平成12年-現在 関西経皮内視鏡的胃瘻造設術研究会世話人
- ・ 平成12年-現在 肝疾患座談会 in Kyoto世話人
- ・ 平成12年-現在 近畿肝癌談話会常任幹事
- ・ 平成13年-現在 関西肝血流動態イメージ研究会世話人
- ・ 平成16年-平成23年 あおい肝臓研究会世話人
- ・ 平成18年-現在 大阪肝臓ミーティング世話人
- ・ 平成19年-現在 近畿・超音波内視鏡研究会顧問

## 全国規模の国内研究会主催（会長）

- ・ 1997年 2月 第3回肝血流動態イメージ研究会(神戸)
- ・ 1996年10月 第1回日本造影エコー・ドプラ診断研究会(神戸)
- ・ 2005年 2月 第11回肝血流動態イメージ研究会(横浜)
- ・ 2007年 9月 第2回肝癌治療シミュレーション研究会(大阪)
- ・ 2008年 9月 第49回日本消化器画像診断研究会(大阪)
- ・ 2010年 1月 第1回日本肝癌分子標的治療研究会(神戸)
- ・ 2014年 2月 第20回肝血流動態・機能イメージ研究会(大阪)

## 国内学会主催（会長）

- ・ 第45回日本肝臓学会総会(2009年6月), 神戸
- ・ 第83回日本超音波医学会学術集会(2010年5月), 京都
- ・ 第50回日本肝癌研究会(2014年6月), 京都
- ・ 第89回日本超音波医学会学術集会(2016年5月), 京都

### 近畿地区学会主催（会長）

- ・ 第82回日本消化器内視鏡学会近畿支部例会(2009年8月)
- ・ 第95回日本消化器病学会近畿支部例会(2011年8月)

### 近畿地区学会主催（会長）

- ・ 第82回日本消化器内視鏡学会近畿支部例会(2009年8月)
- ・ 第95回日本消化器病学会近畿支部例会(2011年8月)
- ・ 第214回日本内科学会近畿地方会(2016年12月)

### 国際学会主催（会長）

- ・ JSH Single Topic Conference on HCC (2005年), Awaji-shima
- ・ The 3<sup>rd</sup> International Kobe Liver Cancer Symposium on HCC(IKLS) (2009年6月), Kobe
- ・ The 2<sup>nd</sup> Asia Pacific Primary Liver Cancer Expert Meeting (APPLE) (2011年7月), Osaka
- ・ The 14<sup>th</sup> WFUMB 2013 (世界超音波医学会) (2013年5月), Sao Paulo (Co-President with Leandro Fernandez and Giovanni Guido Cerri)
- ・ The 4<sup>th</sup> International Kyoto Liver Cancer Symposium(IKLS) (2014年6月6-7日), Kyoto
- ・ the 8<sup>th</sup> International Liver Cancer Association(ILCA) (国際肝癌学会) (2014年9月5日-7日), Kyoto (Co-President with Peter Galle)
- ・ The 6<sup>th</sup> Asia Pacific Primary Liver Cancer Expert Meeting (APPLE) (2015年7月), Osaka
- ・ AFSUMB 2016 (アジア超音波医学会) (2016年5月), Kyoto
- ・ ACUCI (アジア造影超音波医学会) (2016年5月), Kyoto

## 2017年度表彰式一覧

### ➤ Highest Impact Factor Award 2017（最高インパクトファクター賞）

1 位 米田頼晃 9.566 (Am J Gastroenterol)  
2 位 西田直生志 7.854 (Liver Cancer)  
2 位 有住忠晃 7.854 (Liver Cancer)

※ 4 位 渡邊智裕 7.478 (Mucosal Immunol)  
※ 工藤正俊 7.854 (Liver Cancer)

### ➤ Most Numbers of Paper Award 2017（最多英文論文発表賞）

1 位 鎌田 研 7 本 (World J Gastroenterol × 1, Oncology-Basel × 2, Arab J Gastroenterol × 1, Dig Liver Dis × 1, J Gastroen Hepatol × 1, Gastrointest Endosc × 1)  
1 位 三長孝輔 7 本 (Gastrointest Endosc × 1, Dig Endosc × 1, Endoscopy × 1, Surg Endosc × 1, Oncology-Basel × 1, J Med Ultrason × 1, Endosc Ultrasound × 1)

※ 3 位 西田直生志 5 本 (Liver Cancer × 1, Oncology-Basel × 2, Clin Ther × 1, Digest Dis × 1)  
※ 工藤正俊 14 本

### ➤ Total Highest Impact Factor Award 2017（累積最高インパクトファクター賞）

1 位 三長孝輔 24.375 (7 本)  
2 位 鎌田 研 21.575 (7 本)  
  
※ 3 位 西田 直生志 (5 本)  
※ 工藤正俊 59.538 (14 本)

### ➤ 最多入院受持患者賞

1 位 竹中 完 3,109 人  
2 位 山雄健太郎 1,376 人  
  
※ 3 位 米田頼晃 1,259 人

### ➤ 最多緊急内視鏡賞

1 位 高島耕太 41 件  
2 位 田中秀和 34 件  
  
※ 3 位 半田康平 33 件

### ➤ 最多外来患者診療賞

1 位 萩原 智 3,198 人  
2 位 上嶋一臣 2,964 人  
  
※ 3 位 松井繁長 2,861 人  
※ 工藤正俊 1,239 人

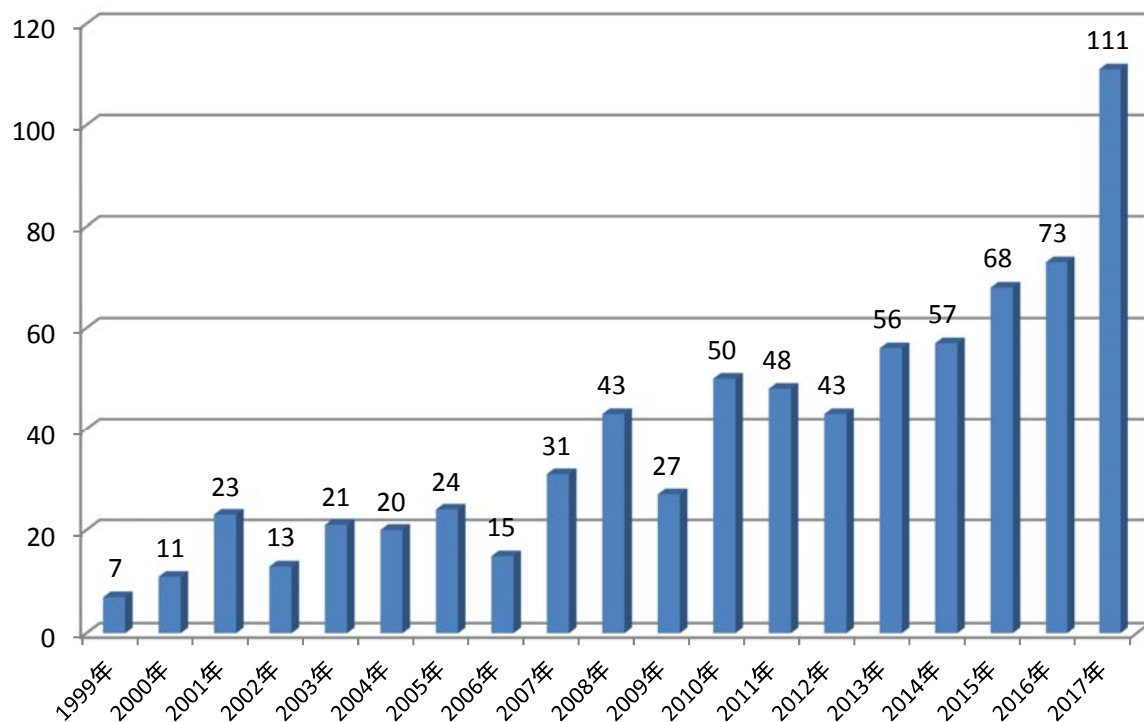
## 消化器内科学教室業績抜粋

	1999	2000	2001	2002	2003	2004	2005	2006	2007
英文論文 (Impact Factor)	7 57.1	11 61.526	23 80.163	13 29.11	21 75.988	20 99.181	24 92.954	15 59.849	31 127.014
和文論文 (著書・分担執筆を含む)	37	41	43	34	31	54	45	39	45
海外学会発表	2	9	4	6	24	23	14	14	17
国内学会発表	46	56	71	113	105	79	69	52	79
海外特別講演	0	11	4	11	8	18	16	25	18
国内特別講演	37	40	40	52	37	38	39	27	36
単著教科書			1		1 (英文)				

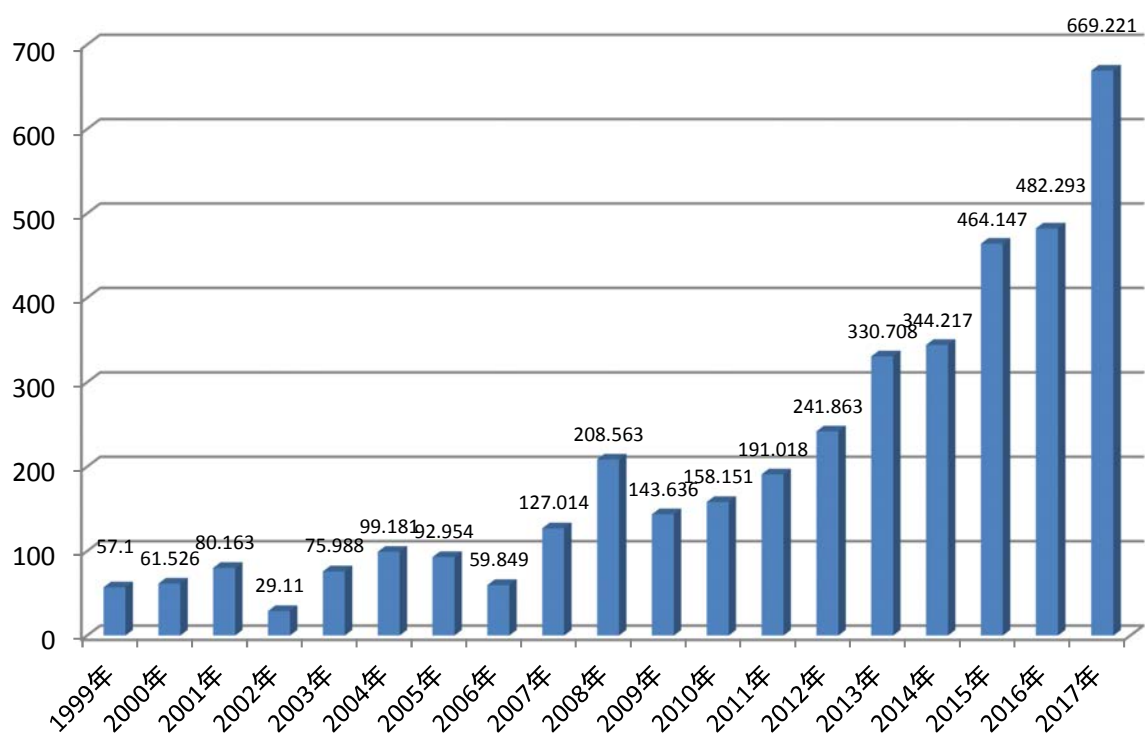
令和2年10月現在

2008	2009	2010	2011	2012	2013	2014	2015	2016	2017	計
43 208.563	27 143.636	50 158.151	48 191.018	43 241.863	56 330.708	57 344.217	68 464.147	73 482.293	111 669.221	741 3916.702
74	81	126	59	54	17	21	55	15	43	914
26	20	34	64	52	35	37	32	47	37	497
87	65	96	100	118	117	105	98	69	93	1618
36	34	42	28	34	33	16	19	16	7	376
39	62	94	75	59	43	28	40	34	35	818
										2

### 近畿大学医学部消化器内科 英文論文総数(741編)



### 近畿大学医学部消化器内科 英文論文 Impact Factor総数 (IF=3916.702)

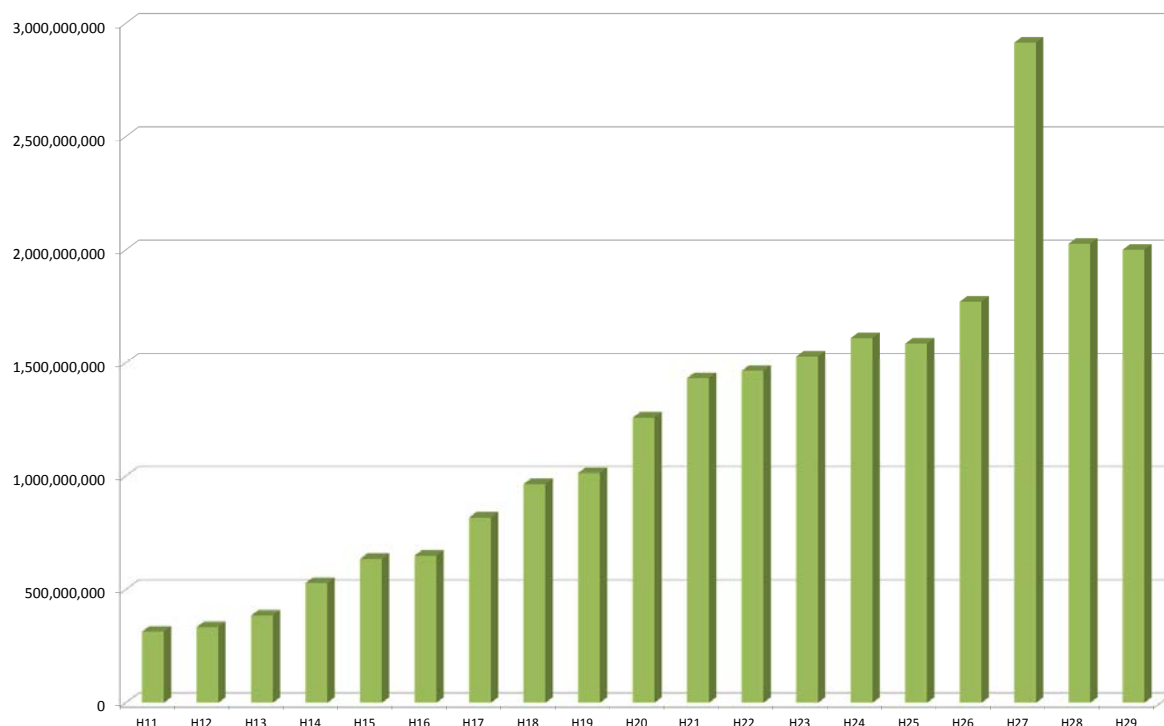


## 消化器内科年度別診療実績

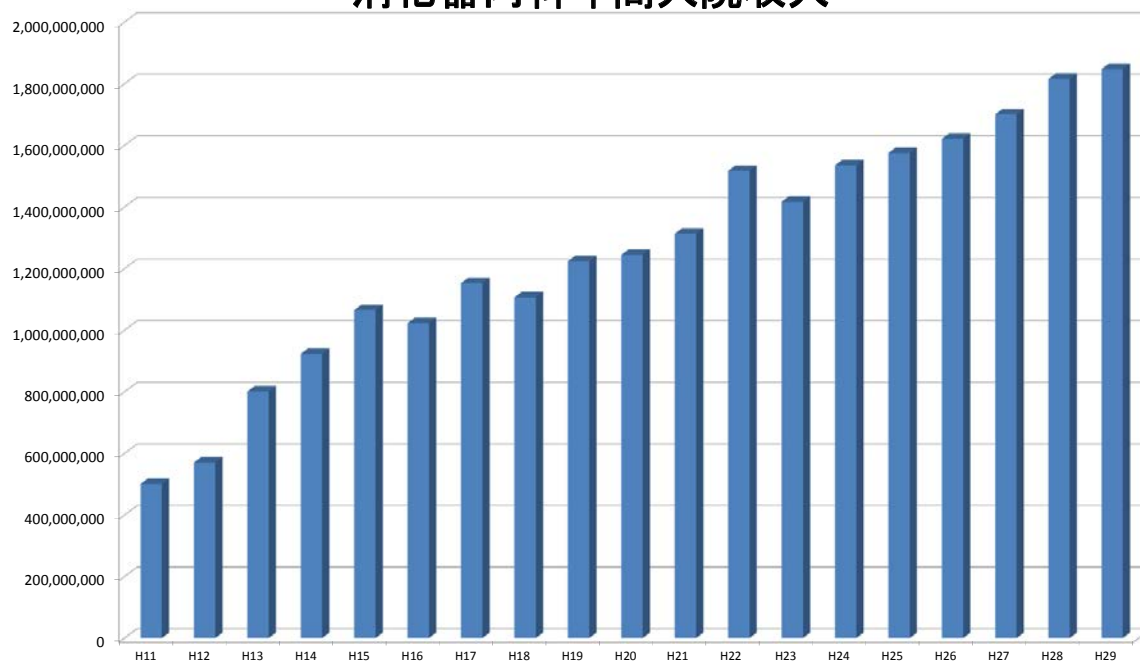
	H11	H12	H13	H14	H15	H16	H17	H18	H19	H20
稼働床	40	44	44	44	60	78	78	77	76	73
稼働率	107.2%	98.5%	126.7%	148.2%	121.0%	89.5%	95.3%	89.2%	94.7%	96.3%
日平均入院患者数	40.0	43.3	55.8	65.2	72.6	69.8	74.4	68.7	72.0	70.3
平均在院日数	31.1	25.6	21.4	18.6	15.4	14.7	12.8	10.7	10.5	9.6
年間入院収入	501,570,188	570,616,464	801,199,124	923,171,333	1,065,481,449	1,023,271,279	1,152,778,111	1,106,484,453	1,224,122,968	1,244,806,271
年間外来収入	314,641,639	334,517,979	386,084,329	530,035,297	635,562,806	649,876,475	818,049,485	966,247,389	1,013,910,559	1,257,804,553
消化器内科年間収入	816,211,827	905,134,443	1,187,283,453	1,453,206,630	1,701,044,255	1,673,147,754	1,970,827,596	2,072,731,842	2,238,033,527	2,502,610,824

	H21	H22	H23	H24	H25	H26	H27	H28	H29
稼働床	85	84	84	84	80	80	80	95	101
稼働率	91.8%	89.9%	85.8%	89.0%	91.0%	93.9%	98.7%	96.8%	89.3%
日平均入院患者数	70.3	76.1	72.0	74.7	77.0	75.1	78.9	84.7	88.7
平均在院日数	9	8.6	7.9	7.2	7.2	6.7	7.0	7.6	6.9
年間入院収入	1,312,812,506	1,516,925,835	1,417,104,402	1,535,069,456	1,575,321,748	1,621,531,082	1,700,694,167	1,816,140,190	1,847,155,829
年間外来収入	1,432,350,698	1,464,645,183	1,529,385,181	1,610,826,432	1,586,645,573	1,771,578,798	2,914,910,768	2,027,534,890	2,001,226,787
消化器内科年間収入	2,745,163,204	2,981,571,018	2,946,489,583	3,145,895,888	3,161,967,321	3,393,109,880	4,615,604,935	3,843,675,080	3,848,382,616

# 消化器内科年間外来収入

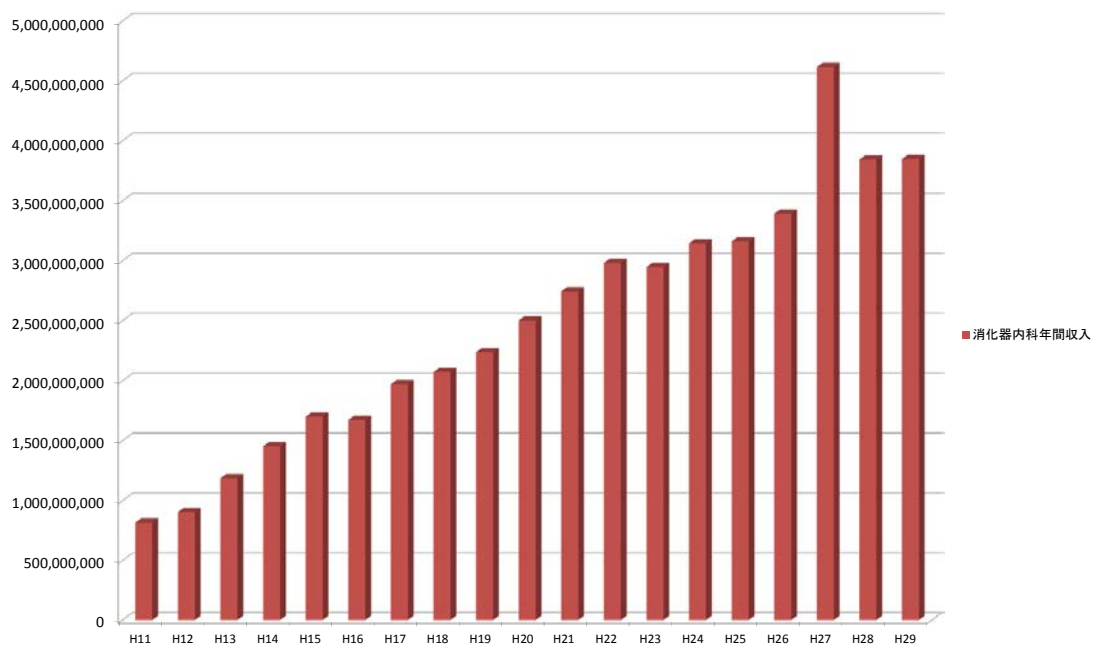


# 消化器内科年間入院収入

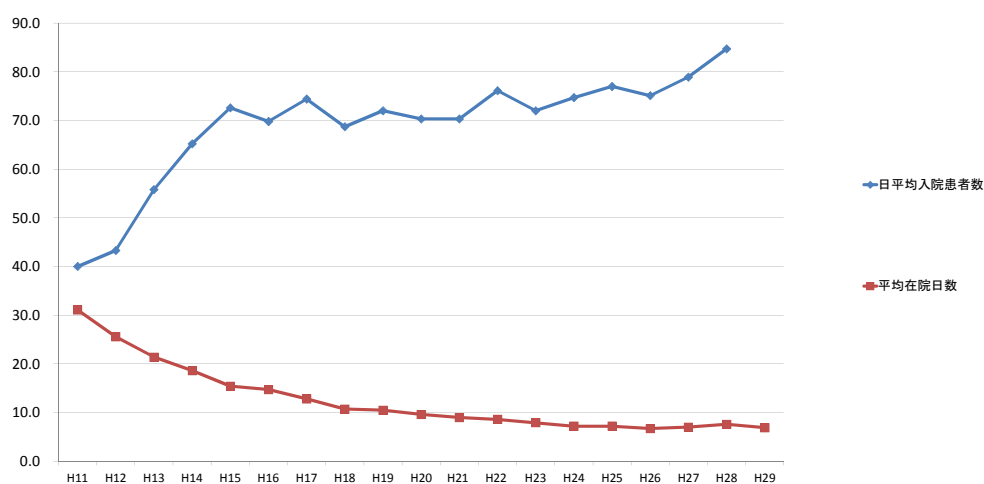




## 消化器内科年間総収入



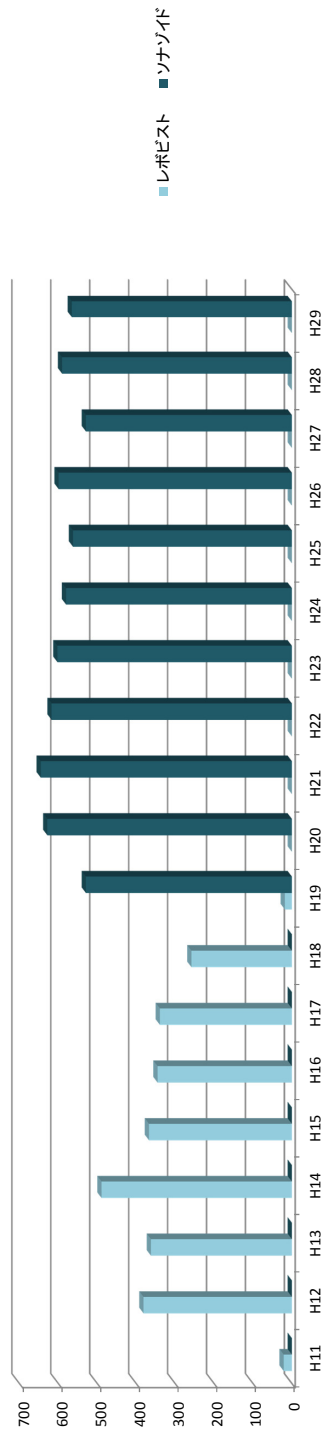
## 消化器内科入院診療実績



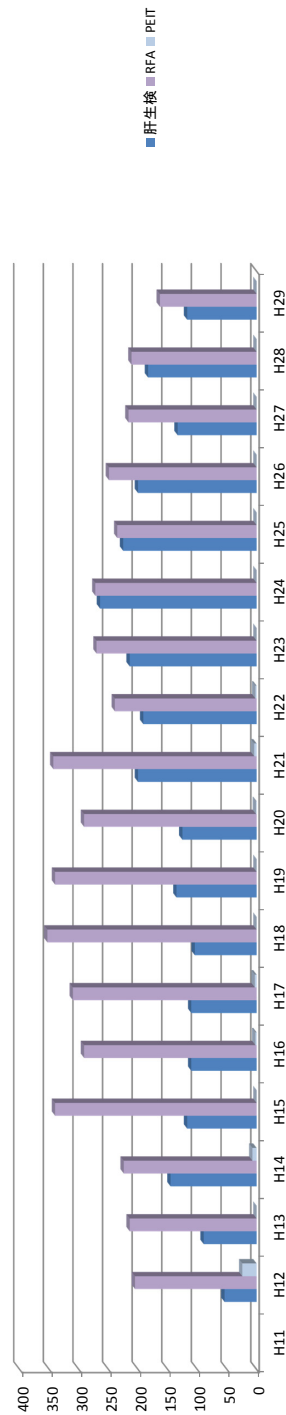
## エコー室件数

1月-12月	H11	H12	H13	H14	H15	H16	H17	H18	H19	H20	H21	H22	H23	H24	H25	H26	H27	H28	H29
肝生検		54	89	145	117	110	110	104	135	125	200	191	214	264	225	200	133	183	117
RFA		205	214	224	340	291	310	353	340	291	343	239	270	272	235	249	216	211	163
PEIT		24	0	7	0	2	3	0	0	1	4	2	0	0	0	0	0	0	0
レボビスト	21	381	362	489	367	345	339	258	18	0	0	0	0	0	0	0	0	0	0
ソナゾイド	0	0	0	0	0	0	0	0	529	628	645	617	602	580	562	599	529	590	565

### 腹部造影エコー検査



### 経皮的局所治療・肝生検総件数



平成29年11月現在

## 内視鏡部年報

検 査	H26	H27	H28	H29
胃・十二指腸 球部(EUS含む)	9003	8993	8487	8422
超音波内視鏡 (胃)	42	53	72	82
超音波内視鏡 (胆膵)	1603	1817	1609	1599
胃・十二指腸 ポリペク	4	40	3	6
胃・十二指腸 EMR	206	236	224	227
止血・上部	125	158	165	160
食道静脈瘤結紮術 (EVL)	51	63	56	62
硬化療法 (EIS)	0	7	9	10
EISL	29	25	28	37
食道ブジー	163	153	69	83
経皮内視鏡的胃瘻造設術 (PEG)	73	68	59	65
ステント留置 (食道)	10	11	16	14
ステント留置 (胃・十二指腸)	33	38	24	40
イレウス管 (経口)	45	54	64	69
トロビン撒布	30	25	24	33
異物除去	371	405	415	203
大腸ファイバースコピー(EUS含む)	3903	3928	3813	3938
超音波内視鏡 (大腸)	12	10	14	21
大腸ポリペク・EMR (大腸ESD含む)	769	729	760	846
止血 大腸	50	42	40	37
異物除去	30	25	24	0
大腸ブジー	6	8	7	7
(経肛門) イレウス管	45	54	64	2
小腸ファイバースコピーのみ	97	125	95	104
小腸 ポリペク	0	0	1	0
小腸EMR	4	1	4	4
止血 小腸	5	5	3	6
小腸ブジー	0	0	7	0
小腸カプセル内視鏡	34	17	34	47
胆道ドレナージ	278	349	382	304
乳頭切開	120	127	127	130
乳頭バルーン拡張術	2	1	1	1
結石除去	125	106	129	127
気管支ファイバースコピー	495	542	544	521
胸腔鏡	—	—	17	20
予約外内視鏡検査	1117	1101	846	677

## 近畿大学 消化器内科学教室医局員

(令和元年9月現在)

主任教授	工藤正俊	S53	肝臓・消化器・肝癌の診断と治療
教授（内視鏡部）	樫田博史	S58	下部消化管
	辻 直子	S60	上部消化管
准教授	汐見幹夫	S55	上部・胆膵内視鏡（関空クリニック所長・教授兼務）
	西田直生志	S60	肝臓病学・肝癌の分子生物学
	渡邊智裕	H5	消化管全般
講師	松井繁長 (医局長)	H3	食道静脈瘤止血・上部消化管
医学部講師	上嶋一臣	H7	慢性肝炎・肝癌の治療
	櫻井俊治 (病棟医長)	H7	上部消化管・分子生物学
	依田 広 (外来医長)	H8	肝疾患・消化器一般
	南 康範	H9	肝疾患・消化器一般
	萩原 智	H10	肝疾患・消化器一般
	竹中 完	H13	胆膵疾患・消化器一般
	米田頼晃	H13	消化器一般
	田北雅弘	H15	肝疾患・消化器一般
	永井知行	H16	消化器一般
	山雄健太郎	H18	胆膵疾患・消化器一般
医学部助教	本庶 元	H5	胆膵疾患・消化器一般
	鎌田 研	H19	胆膵疾患・消化器一般
	三長孝輔	H19	胆膵疾患・消化器一般
	山田光成	H19	消化器一般
	青木智子	H20	肝疾患・消化器一般
	大本俊介	H20	消化器一般
	千品寛和 (富田林病院出向中)	H22	消化器一般
	河野匡志	H22	消化器一般
	中井敦史	H22	胆膵疾患・消化器一般
	山崎友裕	H22	胆膵疾患・消化器一般
	南 知宏	H23	消化器一般
	正木 翔	H23	消化器一般
	岡元寿樹 (串本病院出向中)	H23	消化器一般
	岡本彩那	H24	胆膵疾患・消化器一般
	高田隆太郎 (奈良病院出向中)	H24	肝疾患・消化器一般
	福永明洋 (奈良病院出向中)	H24	胆膵疾患・消化器一般

	河野辰哉	H24	消化器一般
	半田康平 (府中病院出向中)	H24	消化器一般
	高島耕太	H24	消化器一般
	吉田晃浩	H24	消化器一般
	田中秀和	H24	消化器一般
	吉川智恵	H24	胆膵疾患・消化器一般
	橋本有人 (奈良病院出向中)	H25	胆膵疾患・消化器一般
	松村まり子	H25	消化器一般
	大塚康生 (富田林病院出向中)	H25	消化器一般
	益田康弘	H25	消化器一般
大学院生	石川 嶺 (3年)	H24	胆膵疾患・消化器一般
	山崎友裕 (2年)	H22	胆膵疾患・消化器一般
	本庶 元 (1年)	H 5	消化器一般
	高島耕太 (1年)	H24	消化器一般
	高田隆太郎 (1年)	H24	消化器一般
専攻医	吉川馨介	H29	消化器一般
	野村健司	H29	消化器一般
	友岡瑞貴	H29	消化器一般
	吉田早希	H29	消化器一般
実験助手	升本知子		
	小崎秀人		
臨床研究補助	児玉美由紀		
教授秘書	田中真紀		
	本廣佳香		
	上野由紀子		
日本肝癌研究会	田村利恵		
	上妻智子		
医局秘書	胡桃由佳		
	朝隈 智		
	市井由紀		
近大奈良病院	川崎俊彦、水野成人、川崎正憲、高山政樹、茂山朋広、奥田英之		

## 部門別医師構成

### ○消化管グループ

檜田博史、辻 直子、渡邊智裕、松井繁長、櫻井俊治、米田頼晃、  
永井知行、山田光成、本庶 元、河野匡志、正木 翔、岡元寿樹  
橋本有人

### ○胆膵グループ

汐見幹夫、竹中 完、山雄健太郎、鎌田 研、三長孝輔、大本俊介、  
中井敦史、石川 嶺、山崎友裕、岡本彩那、田中隆光

### ○肝グループ

工藤正俊、西田直生志、上嶋一臣、依田 広、南 康範、萩原 智、  
田北雅弘、南 知宏、青木智子、千品寛和、盛田真弘

# 消化器内科学教室業績一覧

## (2017 年)

## I. 英文論文

1. 2017 Watanabe T, Asano N, Kudo M, Strober W: Nucleotide-binding oligomerization domain 1 and gastrointestinal disorders. *Proc Jpn Acad Ser B Phys Biol Sci* 93:578-599, 2017. (IF=3.000)
2. 2017 Otsuka Y, Kamata K, Takenaka M, Minaga K, Tanaka H, Kudo M: Electronic hydraulic lithotripsy by antegrade digital cholangioscopy through endoscopic ultrasound-guided hepaticojunostomy. *Endoscopy* 49:E316-E318, 2017. (IF=7.341)
3. 2017 Minaga K, Takenaka M, MD, Miyata T, Yamao K, Kitano M, Kudo M: Achievement of long-term stent patency in endoscopic ultrasonography-guided right bile duct drainage after left hepatic lobectomy (with video). *Endosc Ultrasound* 6:412-413, 2017. (IF=4.489)
4. 2017 Kawakami H, Tanizaki J, Tanaka K, Haratani K, Hayashi H, Takeda M, Kamata K, Takenaka M, Kimura M, Chikugo T, Sato T, Kudo M, Ito A, Nakagawa K: Imaging and clinicopathological features of nivolumab-related cholangitis in patients with non-small cell lung cancer. *Invest New Drugs* 35:529-536, 2017. (IF=3.525)
5. 2017 Kamata K, Takenaka M, Minaga K, Omoto S, Miyata T, Yamao K, Imai H, Kudo M: Stent migration during EUS-guided hepaticogastrostomy in a patient with massive ascites: troubleshooting using additional EUS-guided antegrade stenting. *Arab J Gastroenterol* 18:120-121, 2017. (IF=1.013)
6. 2017 Imoto M, Yoshida K, Maeda Y, Nakae KI, Kudo M, Sakurabayashi I, Yamada T, Kamisako T: A case of waldenstrom macroglobulinemia with temporary appearance of 7S IgM half molecule. *Clin Lab* 63:983-989, 2017. (IF=0.940)
7. 2017 Arizumi T, Ueshima K, Iwanishi M, Minami T, Chishina H, Kono M, Takita M, Yada N, Hagiwara S, Minami Y, Ida H, Komeda Y, Takenaka M, Sakurai T, Watanabe T, Nishida N, Kudo M: The overall survival of patients with hepatocellular carcinoma correlates with the newly defined time to progression after transarterial chemoembolization. *Liver Cancer* 6:227-235, 2017. (IF=9.720)
8. 2017 Banno E, Togashi Y, de Velasco MA, Mizukami T, Nakamura Y, Terashima M, Sakai K, Fujita Y, Kamata K, Kitano M, Kudo M, Nishio K: Clinical significance of Akt2 in advanced pancreatic cancer treated with erlotinib. *Int J Oncol* 50:2049-2058, 2017. (IF=3.899)
9. 2017 Watanabe T, Yamashita K, Arai Y, Minaga K, Kamata K, Nagai T, Komeda Y, Takenaka M, Hagiwara S, Ida H, Sakurai T, Nishida N, Strober W, Kudo M: Chronic fibro-inflammatory responses in autoimmune pancreatitis depend on IFN- $\alpha$  and IL-33 produced by plasmacytoid dendritic cells. *J Immunol* 198:3886-3896, 2017. (IF=4.886)
10. 2017 Hiraoka A, Kumada T, Kudo M, Hirooka M, Tsuji K, Itobayashi E, Kariyama K, Ishikawa T, Tajiri K, Ochi H, Tada T, Toyoda H, Nouse K, Kawasaki H, Hiasa Y, Michitaka K on behalf of the Real-Life Practice Experts for HCC (RELPEC) Study Group and HCC 48 Group: Albumin-bilirubin (ALBI) grade as part of the evidence-based clinical practice guideline for HCC of the Japan Society of Hepatology: a comparison with the liver damage and Child-Pugh classifications. *Liver Cancer* 6:204-215, 2017. (IF=9.720)
11. 2017 Lencioni R, Montal R, Torres F, Park JW, Decaens T, Boucher E, Raoul JL, Kudo M, Chang C, Rios J, Boige V, Assenat E, Kang YK, Lim HY, Walters I, Llovet JM: Objective response by mRECIST as a predictor and potential surrogate end point of overall survival in advanced hepatocellular carcinoma. *J Hepatol* 66:1166-1172, 2017. (IF=20.582)
12. 2017 Ikeda M, Shimizu S, Sato T, Morimoto M, Kojima Y, Inaba Y, Hagihara A, Kudo M,



- Nakamori S, Kaneko S, Sugimoto R, Tahara T, Ohmura T, Yasui K, Sato K, Ishii H, Furuse J, Okusaka T: Reply to the Letter to the editor 'Sorafenib plus hepatic arterial infusion chemotherapy with cisplatin versus Sorafenib for advanced hepatocellular carcinoma: randomized phase II trial' by Fornaro et al. **Ann Oncol** 28:903-904, 2017. (IF=18.274)
13. 2017 Toguchi M, Tsurusaki M, Yada N, Sofue K, Hyodo T, Onoda M, Numoto I, Matsuki M, Imaoka I, Kudo M, Murakami T: Magnetic resonance elastography in the assessment of hepatic fibrosis: a study comparing transient elastography and histological data in the same patients. **Abdom Radiol** 42:1659-1666, 2017. (IF=2.429)
  14. 2017 Hyodo T, Yada N, Hori M, Maenishi O, Lamb P, Sasaki K, Onoda M, Kudo M, Mochizuki T, Murakami T: Multimaterial decomposition algorithm for the quantification of liver fat content using fast-kilovolt-peak switching dual-energy CT: clinical evaluation. **Radiology** 283:108-118, 2017. (IF=7.931)
  15. 2017 Howell J, Pinato D, Ramaswami R, Bettinger D, Arizumi T, Ferrari C, Yen C, Gibbin A, Burlone M, Guaschino G, Sellers L, Black J, Pirisi M, Kudo M, Thimme R, Park JW, Sharma R: On-target sorafenib toxicity predicts improved survival in hepatocellular carcinoma: a multi-centre, prospective study. **Aliment Pharm Ther** 45:1146-1155, 2017. (IF=7.515)
  16. 2017 Ikeda K, Kudo M, Kawazoe S, Osaki Y, Ikeda M, Okusaka T, Tamai T, Suzuki T, Hisai T, Hayato S, Okita K, Kumada H: Phase 2 Study of Lenvatinib in patients with advanced hepatocellular carcinoma. **J Gastroenterol** 52:512-519, 2017. (IF=6.132)
  17. 2017 Kudo M, Hatano E, Ohkawa S, Fujii H, Masumoto A, Furuse J, Wada Y, Ishii H, Obi S, Kaneko S, Kawazoe S, Yokosuka O, Ikeda M, Ukai K, Morita S, Tsuji A, Kudo T, Shimada M, Osaki Y, Tateishi R, Sugiyama G, Abada PB, Yang L, Okusaka T, Zhu AX: Ramucirumab as second-line treatment in patients with advanced hepatocellular carcinoma: Japanese subgroup analysis of the REACH trial. **J Gastroenterol** 52:494-503, 2017. (IF=6.132)
  18. 2017 Minami Y, Takita M, Tsurusaki M, Yagyu Y, Ueshima K, Murakami T, Kudo M: Semiquantitative prediction of early response of conventional transcatheter arterial chemoembolization for hepatocellular carcinoma using postprocedural plain cone-beam computed tomography. **Hepatol Res** 47:E113-E119, 2017. (IF=3.165)
  19. 2017 Watanabe T, Yamashita K, Kudo M: IgG4-related disease and innate immunity. **Curr Top Microbiol Immunol** 401:115-128, 2017. (IF=3.095)
  20. 2017 Minaga K, Kitano M, Gon C, Yamao K, Imai H, Miyata T, Kamata K, Omoto S, Takenaka M, Kudo M: Endoscopic ultrasonography-guided choledochoduodenostomy using a newly designed laser-cut metal stent: feasibility study in a porcine model. **Dig Endosc** 29:211-217, 2017. (IF=4.774)
  21. 2017 Watanabe T, Kudo M, Strober W: Immunopathogenesis of pancreatitis. **Mucosal Immunol** 10:283-298, 2017. (IF=6.726)
  22. 2017 Komeda Y, Kashida H, Sakurai T, Kono M, Nagai T, Asakuma Y, Hagiwara S, Matsui S, Watanabe T, Chikugo T, Kudo M: A case of type II enteropathy-associated T-cell lymphoma (EATL) in a patient with ulcerative colitis. **Am J Gastroenterol** 112:833, 2017. (IF=10.171)
  23. 2017 Pinato DJ, Ramaswami R, Arizumi T, Ferrari C, Gibbin A, Burlone M, Guaschino G, Tonitto P, Black J, Sellers L, Kudo M, Pirisi M, Sharma R: Integration of the cancer-related inflammatory response as a stratifying biomarker of survival in hepatocellular carcinoma treated with sorafenib. **Oncotarget** 8:36161-36170, 2017. (IF=5.168)

24. 2017 Sakurai T, Higashitsuji H, Kashida H, Watanabe T, Komeda Y, Nagai T, Hagiwara S, Kitano M, Nishida N, Abe T, Kiyonari H, Ithoh K, Fujita J, **Kudo M**: The oncoprotein gankyrin promotes the development of colitis-associated cancer through activation of STAT3. **Oncotarget** 8:24762-24776, 2017. (IF=5.168)
25. 2017 **Kudo M**, Moriguchi M, Numata K, Hidaka H, Tanaka H, Ikeda M, Kawazoe S, Ohkawa S, Sato Y, Kaneko S, Furuse J, Takeuchi M, Fang X, Date Y, Takeuchi M, Okusaka T: S-1 versus placebo in patients with sorafenib-refractory advanced hepatocellular carcinoma (S-CUBE): a randomised, double-blind, multicentre, phase 3 trial. **Lancet Gastroenterol Hepatol** 2:407-417, 2017. (IF=14.789)
26. 2017 El-Khoueiry AB, Sangro B, Yau T, Crocenzi TS, **Kudo M**, Hsu C, Kim TY, Choo SP, Trojan J, Welling TH, Meyer T, Kang YK, Yeo W, Chopra A, Anderson J, dela Cruz C, Lang L, Neely J, Tang H, Dastani HB, Melero I: Nivolumab in patients with advanced hepatocellular carcinoma (CheckMate040): results of phase 1/2 dose escalation and expansion. **Lancet** 389:2492-2502, 2017. (IF=60.392)
27. 2017 Nishie A, Goshima S, Haradome H, Hatano E, Imai Y, **Kudo M**, Matsuda M, Motosugi U, Saito S, Yoshimitsu K, Crawford B, Kruger E, Ball G, Honda H: Cost-effectiveness of EOB- MRI for hepatocellular carcinoma in Japan. **Clin Ther** 39:738-750, 2017. (IF=3.119)
28. 2017 Kamata K, Kitano M, Omoto S, Miyata T, Minaga K, Yamao K, Imai H, Takenaka M, **Kudo M**: Endoscopic ultrasound-guided gallbladder drainage for acute cholecystitis: long-term outcomes after removal of a self-expandable metal stent. **World J Gastroenterol** 23:661-667, 2017. (IF=3.665)
29. 2017 Pinato DJ, Sharma R, Allara E, Yen C, Arizumi T, Kubota K, Bettinger D, Jang JW, Smirne C, Kim YW, **Kudo M**, Howell J, Ramaswami R, Burlone ME, Guerra V, Thimme R, Ishizuka M, Stebbing J, Pirisi M, Carr BI: The ALBI grade provides objective hepatic reserve estimation across each BCLC stage of hepatocellular carcinoma. **J Hepatol** 66:338-346, 2017. (IF=20.582)
30. 2017 Pinato DJ, Yen C, Bettinger D, Ramaswami R, Arizumi T, Ward C, Pirisi M, Burlone ME, Thimme R, **Kudo M**, Sharma R: The albumin-bilirubin grade improves hepatic reserve estimation post-sorafenib failure: implications for drug development. **Aliment Pharm Ther** 45:714-722, 2017. (IF=7.515)
31. 2017 Sakurai T, Kashida H, Komeda Y, Nagai T, Hagiwara S, Watanabe T, Kitano M, Nishida N, Fujita J, **Kudo M**: Stress response protein RBM3 promotes the development of colitis-associated cancer. **Inflamm Bowel Dis** 23:57-65, 2017. (IF=4.261)
32. 2017 Minaga K, Kitano M, Yamashita Y, Nakatani Y, **Kudo M**: Stent migration into the abdominal cavity after EUS-guided hepaticogastrostomy. **Gastrointest Endosc** 85:263-264, 2017. (IF=6.890)
33. 2017 **Kudo M**: Immune checkpoint blockade in hepatocellular carcinoma: 2017 update. **Liver Cancer** 6:1-12, 2017. (IF=9.720)
34. 2017 **Kudo M**: Molecular targeted agents for hepatocellular carcinoma: current status and future perspectives. **Liver Cancer** 6:101-112, 2017. (IF=9.720)
35. 2017 Komeda Y, Kashida H, Sakurai T, Tribonias G, Okamoto K, Kono M, Yamada M, Adachi T, Mine H, Nagai T, Asakuma Y, Hagiwara S, Matsui S, Watanabe T, Kitano M, Chikugo T, Chiba Y, **Kudo M**: Removal of diminutive colorectal polyps: a prospective randomized clinical trial between cold snare polypectomy and hot forceps biopsy. **World J Gastroenterol** 23:328-335, 2017. (IF=3.665)
36. 2017 Bruix J, Qin S, Merle P, Granito A, Huang YH, Bodoky G, Pracht M, Yokosuka O, Rosmorduc O, Breder V, Gerolami, Masi G, Ross P, Song T, Bronowicki JP,

- Ollivier-Hourmand I, Kudo M, Cheng AL, Llovet JM, Finn RS, LeBerre MA, Baumhauer A, Meinhardt G, Han G, on behalf of the RESORCE Investigators: Regorafenib for patients with hepatocellular carcinoma who progressed on sorafenib treatment (RESORCE): a randomised, double-blind, placebo-controlled, phase 3 trial. **Lancet** 389:56–66, 2017. (IF=60.392)
37. 2017 Hyodo T, Yada N, Hori M, Maenishi O, Lamb P, Sasaki K, Onoda M, Kudo M, Mochizuki T, Murakami T: Multimaterial decomposition algorithm for the quantification of liver fat content using fast-kilovolt-peak switching dual-energy CT: experimental validation. **Radiology** 282:381–389, 2017. (IF=7.931)
  38. 2017 Piscaglia F, Kudo M, Han KH, Sirlin C: Diagnosis of hepatocellular carcinoma with non-invasive imaging: a plea for worldwide adoption of standard and precise terminology for describing enhancement criteria. **Ultraschall Med** 38:9–11, 2017. (IF=4.966)
  39. 2017 Kudo M: Immune checkpoint inhibitors in hepatocellular carcinoma: basics and ongoing clinical trials. **Oncology** 92:50–62, 2017. (IF=2.262)
  40. 2017 Kono M, Minami Y, Iwanishi M, Minami T, Chishina H, Arizumi T, Komeda Y, Sakurai T, Takita M, Yada N, Ida H, Hagiwara S, Ueshima K, Nishida N, Kudo M: Contrast-enhanced tissue harmonic imaging versus phase inversion harmonic sonographic imaging for the delineation of hepatocellular carcinomas. **Oncology** 92:29–34, 2017. (IF=2.642)
  41. 2017 Kwok WY, Hagiwara S, Nishida N, Watanabe T, Sakurai T, Ida H, Minami Y, Takita M, Minami T, Iwanishi M, Chishina H, Kono M, Ueshima K, Komeda Y, Arizumi T, Enoki E, Nakai T, Kumabe T, Nakashima O, Kondo F, Kudo M: Malignant transformation of hepatocellular adenoma. **Oncology** 92:16–28, 2017. (IF=2.642)
  42. 2017 Hagiwara S, Nishida N, Watanabe T, Sakurai T, Ida H, Minami Y, Takita M, Minami T, Iwanishi M, Chishina H, Ueshima K, Komeda Y, Arizumi T, Kudo M: Outcome of combination therapy with sofosbuvir and ledipasvir for chronic type C liver disease. **Oncology** 92:3–9, 2017. (IF=2.642)
  43. 2017 Kudo M: A new horizon in liver disease. **Oncology** 92:1–2, 2017. (IF=2.642)
  44. 2017 Yada N, Sakurai T, Minami T, Arizumi T, Takita M, Hagiwara S, Ida H, Ueshima K, Nishida N, Kudo M: Influence of liver inflammation on liver stiffness measurement in patients with autoimmune hepatitis evaluation by combinational elastography. **Oncology** 92:10–15, 2017. (IF=2.642)
  45. 2017 Nishida N, Kudo M: Immunological microenvironment of hepatocellular carcinoma and its clinical implication. **Oncology** 92:40–49, 2017. (IF=2.642)
  46. 2017 Tochio H, Tamaki E, Imai Y, Iwasaki N, Minowa K, Chung H, Sugimoto Y, Inokuma T, Kudo M: CD68-positive cells in hepatic angiosarcoma. **Oncology** 92:35–39, 2017. (IF=2.642)
  47. 2017 Kudo M: A new era of systemic therapy for hepatocellular carcinoma with regorafenib and lenvatinib. **Liver Cancer** 6:177–184, 2017. (IF=9.720)
  48. 2017 Kudo M: Albumin-Bilirubin grade and hepatocellular carcinoma treatment algorithm. **Liver Cancer** 6:185–188, 2017. (IF=7.854)
  49. 2017 Nishida N, Nishida N, Arizumi T, Hagiwara S, Ida H, Sakurai T, Kudo M: Serum microRNA profile that predict initial effect of sorafenib in patients with advanced hepatocellular carcinoma. **Liver Cancer** 6:113–125, 2017. (IF=9.720)
  50. 2017 Chau I, Peck-Radosavljevic M, Borg C, Malfertheiner P, Seitz JF, Park JO, Ryoo BY, Yen CJ, Kudo M, Poon R, Pastorelli D, Blanc JF, Chung HC, Baron AD, Okusaka T, Bowman L, Cui ZL, Girvan AC, Abada PB, Yang L, Zhu AX: Ramucirumab as second-line treatment in patients with advanced hepatocellular carcinoma following

- first-line therapy with sorafenib: patient-focused outcome results from the randomised phase III REACH study. **Eur J Cancer** 81:17-25, 2017. (IF=7.275)
51. 2017 Omata M, Cheng AL, Kokudo N, Kudo M, Lee JM, Jia J, Tateishi R, Han KH, Chawla YK, Shiina S, Jafri W, Payawal DA, Ohki T, Ogasawara S, Chen PJ, Lesmana CRA, Lesmana LA, Gani RA, Obi S, Dokmeci AK, Sarin SK: Asia-Pacific clinical practice guidelines on the management of hepatocellular carcinoma: a 2017 update. **Hepatol Int** 11:317-370, 2017. (IF=5.102)
  52. 2017 Kokudo T, Hasegawa K, Matsuyama Y, Takayama T, Izumi N, Kadoya M, Kudo M, Kubo S, Sakamoto M, Nakashima O, Kumada T, Kokudo N, Liver Cancer Study Group of Japan: Liver resection for hepatocellular carcinoma associated with hepatic vein invasion: a Japanese nationwide survey. **Hepatology** 66:510-517, 2017. (IF=14.679)
  53. 2017 Kamata K, Takenaka M, Tsurusaki M, Kudo M: Portal vein stenting for portal vein stenosis caused by bile duct cancer. **Dig Liver Dis** 49:1282, 2017. (IF=3.570)
  54. 2017 Matsui S, Kashida H, Asakuma Y, Kudo M: Endoscopic Treatment of Tracheoesophageal Fistula using the Over-The-Scope-Clip System. **Ann Gastrol** 30:578, 2017. (IF=0.000)
  55. 2017 Hagiwara S, Nishida N, Park AM, Komeda Y, Sakurai T, Watanabe T, Kudo M: Contribution of C1485T mutation in the HBx gene to human and murine hepatocarcinogenesis. **Sci Rep** 7:10440, 2017. (IF=3.998)
  56. 2017 Kudo M: Lenvatinib in advanced hepatocellular carcinoma. **Liver Cancer** 6:253-263, 2017. (IF=9.720)
  57. 2017 Hiraoka A, Michitaka K, Kumada T, Izumi N, Kadoya M, Kokudo N, Kubo S, Matsuyama Y, Nakashima O, Sakamoto M, Takayama T, Kokudo T, Kashiwabara K, Kudo M, The Liver Cancer Study Group of Japan: Validation and potential of albumin-bilirubin grade and prognostication in a nationwide survey of 46,681 hepatocellular carcinoma patients in japan: the need for a more detailed evaluation of hepatic function. **Liver Cancer** 6:325-336, 2017. (IF=9.720)
  58. 2017 Hiraoka A, Michitaka K, Kumada, Kudo M: ALBI score as a novel tool in staging and treatment planning for hepatocellular carcinoma: advantage of ALBI grade for universal assessment of hepatic function. **Liver Cancer** 6:377-379, 2017. (IF=9.720)
  59. 2017 Kudo M: New Era in the Treatment of Chronic Liver Diseases and Liver Cancer: State-of-the Art Progress in 2017. **Digest Dis** 35:493-497, 2017. (IF=2.493)
  60. 2017 Kitahata S, Hiraoka A, Kudo M, Murakami T, Ochi M, Izumoto H, Ueki H, Kaneto M, Aibiki T, Okudaira T, Yamago H, Miyamoto Y, Iwasaki R, Tomida H, Mori K, Kishida M, Miyata H, Tsubouchi E, Hirooka M, Koizumi Y, Ninomiya T, Hiasa Y, Michitaka K: Abdominal ultrasound findings of tumor-forming hepatic malignant lymphoma. **Digest Dis** 35:498-505, 2017. (IF=2.493)
  61. 2017 Tsutsui A, Harada K, Tsuneyama K, Senoh T, Nagano T, Takaguchi K, Ando M, Nakamura S, Mizobuchi K, Kudo M: Clinicopathological study of autoimmune hepatitis cases that were difficult to differentiate from drug-induced liver injury. **Digest Dis** 35:506-514, 2017. (IF=2.493)
  62. 2017 Yada N, Tamaki N, Koizumi Y, Hirooka M, Nakashima O, Hiasa Y, Izumi N, Kudo M: Diagnosis of fibrosis and activity by a combined use of strain and shear wave imaging in patients with liver disease. **Digest Dis** 35:515-520, 2017. (IF=2.493)
  63. 2017 Kobayashi N, Kumada T, Toyoda H, Tada T, Ito T, Kage M, Okanoue T, Kudo M: Ability of cytokeratin-18 fragments and FIB-4 index to diagnose overall and mild fibrosis nonalcoholic steatohepatitis in Japanese nonalcoholic fatty liver disease patients. **Digest Dis** 35:521-530, 2017. (IF=2.493)
  64. 2017 Imoto S, Kim SR, Amano K, Iio E, Yoon S, Hirohata S, Yano Y, Ishikawa T,

- Katsushima S, Komeda T, Fukunaga T, Chung H, Kokuryu H, Horie Y, Hatae T, Fujinami A, Kim SK, Kudo M, Tanaka Y: Serum IFN- $\lambda$ 3 levels correlate with serum HCV RNA levels in symptomatic patients with acute hepatitis C. **Digest Dis** 35:531-540, 2017. (IF=2.493)
65. 2017 Seo K, Kim SK, Kim SR, Ohtani A, Kobayashi M, Kato A, Morimoto E, Saijo Y, Kim KI, Imoto S, Kim CW, Yano Y, Kudo M, Hayashi Y: Comparison of Sofosbuvir plus Ribavirin treatment with pegylated interferon plus Ribavirin treatment for chronic hepatitis C genotype 2. **Digest Dis** 35:541-547, 2017. (IF=2.493)
66. 2017 Umehara Y, Hagiwara S, Nishida N, Sakurai T, Ida H, Minami Y, Takita M, Minami T, Chishina H, Ueshima K, Komeda Y, Arizumi T, Watanabe T, Kudo M: Hepatocarcinogenesis is associated with serum albumin levels after sustained virological responses with interferon based therapy in patients with hepatitis C. **Digest Dis** 35:548-555, 2017. (IF=2.493)
67. 2017 Kono M, Nishida N, Hagiwara S, Minami T, Chishina H, Arizumi T, Minaga K, Kamata K, Komeda Y, Sakurai T, Takenaka M, Takita M, Yada N, Ida H, Minami Y, Ueshima K, Watanabe T, Kudo M: Unique characteristics associated with sustained liver damage in chronic hepatitis C patients treated with direct acting antivirals. **Digest Dis** 35: 556-564, 2017. (IF=2.493)
68. 2017 Ida H, Hagiwara S, Kono M, Minami T, Chishina H, Arizumi T, Takita M, Yada N, Minami Y, Ueshima K, Nishida N, Kudo M: Hepatocellular carcinoma after achievement of sustained viral response with daclatasvir and asunaprevir in patients with chronic hepatitis C virus infection. **Digest Dis** 35: 565-573, 2017. (IF=2.493)
69. 2017 Iwamoto T, Imai Y, Igura T, Kogita S, Sawai Y, Fukuda K, Yamaguchi Y, Matsumoto Y, Nakahara M, Morimoto O, Ohashi H, Fujita N, Kudo M, Takehara T: Non-hypervascular hypointense hepatic nodules during the hepatobiliary phase of Gd-EOB-DTPA-enhanced MRI as a risk factor of intrahepatic distant recurrence after radiofrequency ablation of hepatocellular carcinoma. **Digest Dis** 35:574-582, 2017. (IF=2.493)
70. 2017 Arizumi T, Minami T, Chishina H, Kono M, Takita M, Yada N, Hagiwara S, Minami Y, Ida H, Ueshima K, Kamata K, Minaga K, Komeda Y, Takenaka M, Sakurai T, Watanabe T, Nishida N, Kudo M: Impact of Tumor Factors on survival in Patients with Hepatocellular Carcinoma classified based on Kinki Criteria Stage B2. **Digest Dis** 35:583-588, 2017. (IF=2.493)
71. 2017 Arizumi T, Minami T, Chishina H, Kono M, Takita M, Yada N, Hagiwara S, Minami Y, Ida H, Ueshima K, Kamata K, Minaga K, Komeda Y, Takenaka M, Sakurai T, Watanabe T, Nishida N, Kudo M: Time to transcatheter arterial chemoembolization refractoriness in patients with hepatocellular carcinoma in Kinki criteria stages B1 and B2. **Digest Dis** 35:589-597, 2017. (IF=2.493)
72. 2017 Ishikawa T, Imai M, Owaki T, Sato H, Nozawa Y, Sano T, Iwanaga A, Seki K, Honma T, Yoshida T, Kudo M: Hemodynamic Changes on Cone-Beam Computed Tomography during Balloon-Occluded Transcatheter Arterial Chemoembolization Using Miriplatin for Hepatocellular Carcinoma: A Preliminary Study. **Digest Dis** 35:598-601, 2017. (IF=2.493)
73. 2017 Hiraoka A, Kumada T, Kudo M, Hirooka M, Koizumi Y, Hiasa Y, Tajiri K, Toyoda H, Tada T, Ochi H, Joko K, Shimada N, Deguchi A, Ishikawa T, Imai M, Tsuji K, Michitaka K: Hepatic function during repeated TACE procedures and prognosis after introducing sorafenib in patients with unresectable hepatocellular carcinoma: multicenter analysis. **Digest Dis** 35:602-610, 2017. (IF=2.493)



74. 2017 Ueshima K, Nishida N, Kudo M: Sorafenib-regorafenib sequential therapy in advanced hepatocellular carcinoma: a single-institute experience. **Digest Dis** 35:611-617, 2017. (IF=2.493)
75. 2017 Nishida N, Kudo M: Role of immune checkpoint blockade in the treatment for human hepatocellular carcinoma. **Digest Dis** 35:618-622, 2017. (IF=2.493)
76. 2017 Sakurai T, Yada N, Hagiwara S, Arizumi T, Minaga K, Kamata K, Takenaka M, Minami Y, Watanabe T, Nishida N, Kudo M: Gankyrin induces STAT3 activation in tumor microenvironment and sorafenib resistance in hepatocellular carcinoma. **Cancer Sci** 108:1996-2003, 2017. (IF=4.966)
77. 2017 Kamata K, Takenaka M, Minaga, Kudo M: Utility of contrast-enhanced harmonic EUS for evaluating the effects of steroid therapy in a case of IgG4-negative focal autoimmune pancreatitis. **Gastrointest Endosc** 86:1177-1179, 2017. (IF=6.890)
78. 2017 Toyoda H, Tada T, Johnson PJ, Izumi N, Kadoya M, Kaneko S, Kokudo N, Ku Y, Kubo S, Kumada T, Matsuyama Y, Nakashima O, Sakamoto M, Takayama T, Kudo M; Liver Cancer Study Group of Japan: Validation of serological models for staging and prognostication of HCC in patients from a Japanese nationwide survey. **J Gastroenterol** 52:1112-1121, 2017. (IF=6.132)
79. 2017 Minaga K, Takenaka M, Kamata K, Miyata T, Yamao K, Imai H, Kudo M: Endoscopic ultrasound-guided choledochoduodenostomy with novel use of contrast-enhanced harmonic imaging. **Endoscopy** 49:E281-E282, 2017. (IF=7.341)
80. 2017 Komeda Y, Watanabe R, Matsui S, Kashida H, Sakurai T, Kono M, Minaga K, Nagai T, Hagiwara S, Enoki E, Kudo M: A case of small invasive gastric cancer arising from Helicobacter pylori-negative gastric mucosa: Fundic gland-type adenocarcinoma. **J Gastroen Hepatol** 1:74-75, 2017. (IF=3.437)
81. 2017 Minaga K, Takenaka M, Kitano M, Chiba Y, Imai H, Yamao K, Kamata K, Miyata T, Omoto S, Sakurai T, Watanabe T, Nishida N, Kudo M: Rescue EUS-guided intrahepatic biliary drainage for malignant hilar biliary stricture after failed transpapillary re-intervention. **Surg Endosc** 31:4764-4772, 2017. (IF=3.149)
82. 2017 Kamata K, Takenaka M, Kitano M, Omoto S, Miyata T, Minaga K, Yamao K, Imai H, Sakurai T, Watanabe T, Nishida N, Chikugo T, Chiba Y, Imamoto H, Yasuda T, Lisotti A, Fusaroli P, Kudo M: Contrast-enhanced harmonic endoscopic ultrasonography for differential diagnosis of submucosal tumors of the upper gastrointestinal tract. **J Gastroen Hepatol** 32:1686-1692, 2017. (IF=3.437)
83. 2017 Yen C, Sharma R, Rimassa L, Arizumi T, Bettinger D, Choo HY, Pressiani T, Burlone ME, Pirisi M, Giordano L, Abdulrahman A, Kudo M, Thimme R, Park JW, Pinato DJ: Treatment stage migration maximizes survival outcomes in patients with hepatocellular carcinoma treated with sorafenib: an observational study. **Liver Cancer** 6:313-324, 2017. (IF=9.720)
84. 2017 Kudo M: New Paradigm in Gastrointestinal Cancer Treatment. **Oncology** 93:1-8, 2017. (IF=2.642)
85. 2017 Okamoto K, Matsui S, Watanabe T, Asakuma Y, Komeda Y, Okamoto A, Ishikawa R, Kono M, Yamada M, Nagai T, Arizumi T, Minaga, K, Kamata K, Yamao K, Takenaka M, Sakurai T, Nishida N, Kashida H, Chikugo T, Kudo M: Clinical analysis of esophageal stricture in patients treated with intralesional triamcinolone injection after endoscopic submucosal dissection for superficial esophageal cancer. **Oncology** 93:9-14, 2017. (IF=2.642)
86. 2017 Adachi T, Matsui S, Watanabe T, Okamoto K, Okamoto A, Kono M, Yamada M, Nagai T, Komeda Y, Minaga K, Kamata K, Yamao K, Takenaka M, Asakuma Y, Sakurai T, Nishida N, Kashida H, Kudo M: Comparative study of clarithromycin vs. metronidazole-based

- triple therapy as first-line eradication for *Helicobacter pylori*. **Oncology** 93:15-19, 2017. (IF=2.642)
87. 2017 Yamada M, Sakurai T, Komeda Y, Nagai T, Kamata K, Minaga K, Watanabe T, Nishida N, Kashida H, **Kudo M**: Clinical significance of Bmi1 expression in inflammatory bowel disease. **Oncology** 93:20-26, 2017. (IF=2.642)
  88. 2017 Sakurai T, Adachi T, Kono M, Arizumi T, Kamata K, Minaga K, Yamao K, Komeda Y, Takenaka M, Hagiwara S, Watanabe T, Nishida N, Kashida H, **Kudo M**: Prophylactic Suturing Closure is Recommended after Endoscopic Treatment of Colorectal Tumors in Patients with Antiplatelet/Anticoagulant Therapy. **Oncology** 93:27-29, 2017. (IF=2.642)
  89. 2017 Komeda Y, Handa H, Watanabe T, Nomura T, Kitahashi M, Sakurai T, Okamoto A, Minami T, Kono M, Arizumi T, Takenaka M, Hagiwara S, Matsui S, Nishida N, Kashida H, **Kudo M**: Computer-aided diagnosis based on convolutional neural network system for colorectal polyp classification: preliminary experience. **Oncology** 93: 30-34, 2017. (IF=2.642)
  90. 2017 Okamoto K, Watanabe T, Komeda Y, Kono T, Takashima K, Okamoto A, Kono M, Yamada M, Arizumi T, Kamata K, Minaga K, Yamao K, Nagai T, Asakuma Y, Takenaka M, Sakurai T, Matsui S, Nishida N, Chikugo T, Kashida H, **Kudo M**: Risk factors for postoperative bleeding in endoscopic submucosal dissection of colorectal tumors. **Oncology** 93:35-42, 2017. (IF=2.642)
  91. 2017 Ogawa S, Ishii T, Minaga K, Nakatani Y, Hatamaru K, Akamatsu T, Seta T, Urai S, Uenoyama Y, Yamashita Y, **Kudo M**: The feasibility of 18-mm diameter colonic stents for obstructive colorectal cancers. **Oncology** 93: 43-48, 2017. (IF=2.642)
  92. 2017 Komeda Y, Kashida H, Sakurai T, Asakuma Y, Tribonias G, Nagai T, Kono M, Minaga K, Takenaka M, Arizumi T, Hagiwara S, Matsui S, Watanabe T, Nishida N, Chikugo T, Chiba Y, **Kudo M**: Magnifying narrow band imaging (NBI) for the diagnosis of localized colorectal lesions using the Japan NBI Expert Team (JNET) classification. **Oncology** 93:49-54, 2017. (IF=2.642)
  93. 2017 Omoto S, Takenaka M, Kitano M, Miyata T, Kamata K, Minaga K, Arizumi T, Yamao K, Imai H, Sakamoto H, Harwani Y, Sakurai T, Watanabe T, Nishida N, Takeyama Y, Chiba Y, **Kudo M**: Characterization of pancreatic tumors with quantitative perfusion analysis in contrast-enhanced harmonic endoscopic ultrasonography. **Oncology** 93:55-60, 2017. (IF=2.642)
  94. 2017 Takenaka M, Masuda A, Shiomi H, Yagi Y, Zen Y, Sakai A, Kobayashi T, Arisaka Y, Okabe Y, Kutsumi H, Toyama H, Fukumoto T, Ku Y, **Kudo M**, Azuma T: Chronic pancreatitis finding by endoscopic ultrasonography in the pancreatic parenchyma of intraductal papillary mucinous neoplasms Is associated with invasive intraductal papillary mucinous carcinoma. **Oncology** 93: 61-68, 2017. (IF=2.642)
  95. 2017 Imai H, Takenaka M, Omoto S, Kamata K, Miyata T, Minaga K, Yamao K, Sakurai T, Nishida N, Watanabe T, Kitano M, **Kudo M**: Utility of endoscopic ultrasound-guided hepaticogastrostomy with antegrade stenting for malignant biliary obstruction after failed endoscopic retrograde cholangiopancreatography. **Oncology** 93:69-75, 2017. (IF=2.642)
  96. 2017 Kamata K, Takenaka M, Nakai A, Omoto S, Miyata T, Minaga K, Matsuda T, Yamao K, Imai H, Chiba Y, Sakurai T, Watanabe T, Nishida N, Chikugo T, Matsumoto I, Takeyama Y, **Kudo M**: Association between the risk factors for pancreatic ductal adenocarcinoma and those for malignant intraductal papillary mucinous neoplasm. **Oncology** 93:102-106, 2017. (IF=2.642)
  97. 2017 Minaga K, Takenaka M, Katanuma A, Kitano M, Yamashita Y, Kamata K, Yamao

- K, Watanabe T, Maguchi H, **Kudo M**: Needle tract seeding: an overlooked rare complication of endoscopic ultrasound-guided fine-needle aspiration. **Oncology** 93:107-112, 2017. (IF=2.642)
98. 2017 Yamao K, Takenaka M, Imai H, Nakai A, Omoto S, Kamata K, Minaga K, Miyata T, Sakurai T, Watanabe T, Nishida N, Matsumoto I, Takeyama Y, Chikugo T, **Kudo M**: Primary hepatic adenosquamous carcinoma associated with primary sclerosing cholangitis. **Oncology** 93:67-80, 2017. (IF=2.642)
  99. 2017 Yamao K, Takenaka M, Nakai A, Omoto S, Kamata K, Minaga K, Miyata T, Imai H, Sakurai T, Watanabe T, Nishida N, Matsumoto I, Takeyama Y, Chikugo T, **Kudo M**: Detection of High-grade pancreatic intraepithelial neoplasia without morphological changes of the main pancreatic duct over long period: Importance for close follow-up for confirmation. **Oncology** 93:81-86, 2017. (IF=2.642)
  100. 2017 Kamata K, Takenaka M, Minaga K, Sakurai T, Watanabe T, Nishida N, **Kudo M**: EUS-guided pancreatic duct drainage for repeat pancreatitis in a patient with pancreatic cancer. **Oncology** 93:87-88, 2017. (IF=2.642)
  101. 2017 Sakamoto H, Harada S, Nishioka N, Maeda K, Kurihara T, Sakamoto T, Higuchi K, Kitano M, Takeyama Y, Kogire M, **Kudo M**: A social program for the early detection of pancreatic cancer: the kishiwada katsuragi project. **Oncology** 93:89-97, 2017. (IF=2.642)
  102. 2017 Miyata T, Takenaka M, Omoto S, Kamata K, Minaga K, Yamoo K, Imai H, **Kudo M**: A case of pancreatic carcinoma in situ diagnosed by repeated pancreatic juice cytology. **Oncology** 93:98-101, 2017. (IF=2.642)
  103. 2017 Ogawa C, Morita M, Omura A, Noda T, Kubo A, Matsunaka T, Tamaki H, Shibatoe M, Tsutsui A, Senoh T, Nagano T, Takaguchi K, Tani J, Morishita A, Yoneyama H, Masaki T, Moriya A, Ando M, Deguchi A, Kokudo Y, Minami Y, Ueshima K, Sakurai T, Nishida N, **Kudo M**: Hand-foot syndrome and post-progression treatment are the good predictors of better survival in advanced hepatocellular carcinoma treated with sorafenib: a multicenter study. **Oncology** 93:113-119, 2017. (IF=2.642)
  104. 2017 Izumoto H, Hiraoka A, Ishimaru Y, Murakami T, Kitahata S, Ueki H, Aibiki T, Okudaira T, Miyamoto Y, Yamago H, Iwasaki R, Tomida H, Mori K, Kishida M, Tsubouchi E, Miyata H, Ninomiya T, Kawasaki H, Hirooka M, Matsuura B, Abe M, Hiasa Y, Kojiro M, **Kudo M**: Validation of newly proposed time to transarterial chemoembolization progression in intermediate-stage hepatocellular carcinoma cases. **Oncology** 93:120-126, 2017. (IF=2.642)
  105. 2017 **Kudo M**, Arizumi T: Transarterial Chemoembolization in Combination with Molecular Targeted Agent: Lessons from Negative Trials (Post-TACE, BRISK-TA, SPACE, ORIENTAL, and TACE-2). **Oncology** 93:127-134, 2017. (IF=2.642)
  106. 2017 **Kudo M**: Systemic Therapy for Hepatocellular Carcinoma: 2017 Update. **Oncology** 93:135-146, 2017. (IF=2.642)
  107. 2017 **Kudo M**: Immuno-Oncology in Hepatocellular Carcinoma: 2017 Update. **Oncology** 93:147-159, 2017. (IF=2.642)
  108. 2017 Nishida N, **Kudo M**: Oncogenic signal and tumor microenvironment in hepatocellular carcinoma. **Oncology** 93:160-164, 2017. (IF=2.642)
  109. 2017 Ogura T, Onda S, Takagi W, Sano T, Okuda A, Masuda D, Yamamoto K, Miyano A, Kitano M, Takeuchi T, Fukunishi S, Higuchi K: Clinical utility of Endoscopic ultrasound-guided biliary drainage as a rescue of re-intervention procedure for high-grade hilar stricture. **J Gastroenterol Hepatol** 32:163-168, 2017. (IF=6.132)
  110. 2017 Kimura M, Kashida H, Enoki E, Hasegawa H: Early histologic detection of Lanthanum deposition in gastric mucosa after Lanthanum carbonate therapy.



Rinsho-byori 65: 413-418, 2017. (IF=0.000)

111. 2017 Ishii T, Minaga K, Ogawa S, Ikenouchi M, Yoshikawa T, Akamatsu T, Seta T, Urai S, Uenoyama Y, Yamashita Y: Effectiveness and safety of metallic stent for ileocecal obstructive colon cancer: a report of 4 cases. *Endosc Int Open* 5: E834-E838, 2017. (IF=0.000)

## Ⅱ. 和文論文

1. 2017 鎌田 研, 竹中 完, 北野雅之, 工藤正俊: IPMN経過観察におけるEUSの有用性. 特集「今IPMNをどう診るか」, 肝胆膵 74:583-586, 2017.
2. 2017 鎌田 研, 竹中 完, 北野雅之, 大本俊介, 三長孝輔, 宮田 剛, 山雄健太郎, 今井元, 工藤正俊: 膵癌早期診断におけるEUSの役割. 膵臓 32:38-44, 2017.
3. 2017 工藤正俊: 肝細胞癌の治療-内科的治療. 臨床と研究 94:583-591, 2017.
4. 2017 松井繁長, 樫田博史, 河野匡史, 岡元寿樹, 米田頼晃, 永井知行, 朝隈 豊, 櫻井俊治, 渡邊智裕, 工藤正俊: アミロイドーシスを疑う胃病変. 消化器内視鏡 29:756-758, 2017.
5. 2017 工藤正俊: 各論: 免疫チェックポイント阻害薬の役割, 肝がん. 特集「なぜ免疫チェックポイント阻害薬はがんに効くのか」. 消化器病学サイエンス 1:35-41, 2017.
6. 2017 松井繁長, 樫田博史, 田中梨絵, 高山政樹, 峯 宏昌, 足立哲平, 米田頼晃, 永井知行, 朝隈 豊, 櫻井俊治, 工藤正俊, 筑後孝章, 月山雅之: 粘膜下腫瘍様形態を呈した胃神経周膜腫(perineurioma)の1例. 早期胃がん研究会症例. 胃と腸 52:1098-1106, 2017.
7. 2017 有住忠明, 工藤正俊: 肝動脈化学塞栓療法(TACE)の適応の再考①BCLC-Bの亜分類とTACEの適応. *The Liver Cancer Journal* 6:26-29, 2017.
8. 2017 上嶋一臣, 工藤正俊: 肝細胞癌に対する薬物療法のエビデンスとトピックス. 日本消化器病学会雑誌, 114:1621-1628, 2017.
9. 2017 工藤正俊: 肝細胞癌に対する分子標的治療. 特集「肝癌診療A to Z」. 肝臓クリニカルアップデート 3:155-163, 2017.
10. 2017 工藤正俊, 池田公史, 古瀬純司, 小笠原定久: 特別座談会「急激に変貌する肝細胞癌の薬物療法を語る」, 特集 肝細胞癌の化学療法が変わる. 肝胆膵 75:187-208, 2017.
11. 2017 有住忠晃, 工藤正俊: 分子標的治療時代におけるIntermediate stage肝癌の亜分類の重要性を考える. 肝胆膵 75:253-256, 2017.
12. 2017 上嶋一臣, 工藤正俊: 動注化学療法は生き残れるか—エビデンスからみた動注化学療法の今後—. 特集「肝細胞癌の化学療法が変わる」. 肝胆膵 75:363-367, 2017.
13. 2017 有住忠晃, 工藤正俊: TACE併用 (Post TACE, BRISK-TA, SPACE, ORIENTAL, TACE-2) —標的分子と結果の概要・失敗原因の考察—. 特集「肝細胞癌の化学療法が変わる」. 肝胆膵 75:398-406, 2017.
14. 2017 上嶋一臣, 工藤正俊: ソラフェニブ・レゴラフェニブ sequential療法の効果を考察する. 特集「肝細胞癌の化学療法が変わる」. 肝胆膵 75:437-439, 2017.
15. 2017 工藤正俊: レンバチニブ第III相試験 (REFLECT試験)からみえてきたもの—いかに効果を引き出すか—. 特集「肝細胞癌の化学療法が変わる」. 肝胆膵 75:466-471, 2017.
16. 2017 工藤正俊: 肝癌における免疫チェックポイント阻害剤と既存治療との組み合わせ治療 (根治後アジュバント・TACE併用・ほかの免疫療法) 開発の現状と今後の展望. 特集「肝細胞癌の化学療法が変わる」. 肝胆膵 75: 522-528, 2017.
17. 2017 渡邊智裕, 三長孝輔, 鎌田研, 山雄健太郎, 竹中完, 工藤正俊: 膵炎における腸管免疫機構破綻と重症化機序. 肝胆膵 75:991-996, 2017.
18. 2017 上嶋一臣, 工藤正俊: 肝細胞癌に対する薬物療法のエビデンスとトピックス 肝細胞癌診断治療におけるエビデンスとトピックス. 日本消化器病学会誌 114: 1621-1628, 2017.
19. 2017 上嶋一臣, 工藤正俊: 日本における新薬開発と今後の展望. 消化器・肝臓内科2(1):1-7, 2017.
20. 2017 工藤正俊: 私の座右の銘“全ての出来事には理由がある”. 特集: ターニングポイントを迎えた肝癌診療. クリニシャン 659: 712-715, 2017.

21. 2017 工藤正俊：肝癌診療のブレイクスルー—世界に誇る肝癌診療の構築. 特集：ターニングポイントを迎えた肝癌診療. クリニシアン 659: 716-737, 2017.
22. 2017 小川 力, 工藤正俊：肝生検での診断が可能であった、AFP-L3陽性の細胆管細胞癌 (CoCC) の一例. 第17回肝血流動態イメージ研究会記録集 93-96, 2017.
23. 2017 工藤正俊：公益社団法人日本超音波医学会第89回学術集会 アジア超音波医学生物学会第12回学術集会およびアジア造影超音波医学会第8回学術集会を終えて. Jpn J Med Ultrasonics 44:193-199, 2017.
24. 2017 工藤正俊, 黒崎雅之, 池田公史, 小笠原定久：座談会；切除不能な肝細胞癌に対するスチバーガ治療～2nd line治療における世界初のエビデンス創出およびネクサバルとの sequential therapyへの期待～. Medical Tribune Web, 2017.
25. 2017 渡邊智裕, 工藤正俊：パターン認識受容体. 消化器病学サイエンス 1:150-152, 2017.
26. 2017 高山政樹, 大原裕士郎, 秦 康倫, 木下大輔, 奥田英之, 川崎俊彦, 水野成人, 若狭朋子, 太田善夫, 工藤正俊：悪性黒色腫に対しニボルマブ投与中に潰瘍性大腸炎類似の大腸炎を認めた1例. 日本消化器内視鏡学会雑誌 59:450-455, 2017.
27. 2017 工藤正俊：序文. 肝細胞癌に対するレゴラフェニブ治療, アークメディア, 東京, pp3-9, 2017.
28. 2017 工藤正俊, 吉野孝之, 黒崎雅之, 山下竜也, 森口理久：特別座談会「レゴラフェニブの登場により肝細胞癌治療のパラダイムはどう変わるのか」. 肝細胞癌に対するレゴラフェニブ治療, アークメディア, 東京, pp15-40, 2017.
29. 2017 上嶋一臣, 工藤正俊：レゴラフェニブの第III相試験の経験症例からわかること-市販後経験例も含めて-. 肝細胞癌に対するレゴラフェニブ治療, アークメディア, 東京, pp77-85, 2017.
30. 2017 工藤正俊：ソラフェニブ・レゴラフェニブsequential療法の可能性. 肝細胞癌に対するレゴラフェニブ治療, アークメディア, 東京, pp100-107, 2017.
31. 2017 鎌田 研, 竹中 完：内視鏡的逆行性膵管造影. 新世代の膵癌診療・治療バイブル—研修医・レジデント必携. メディア出版, pp79-83, 2017.
32. 2017 西潟まり, 置田和代, 小口那代, 榎田博史：消化管出血に対する緊急内視鏡的止血術の看護・解除. 消化器看護がん・化学療法・内視鏡 22: 74-79, 2017.
33. 2017 河野匡志, 松井繁長, 榎田博史：家族性大腸腺腫症 (FAP) を疑う胃病変. 消化器内視鏡 29: 768-770, 2017.
34. 2017 榎田博史：大腸内視鏡の偶発症予防と対応. 消化器内視鏡 29: 2018-2033, 2017.
35. 2017 榎田博史, 島田光生 編集担当：消化器のひろば No. 11, 日本消化器病学会, 2017.
36. 2017 榎田博史：大腸鋸歯状病変. 消化器内視鏡 29: 1491-1496, 2017.
37. 2017 榎田博史, 山野泰穂, 田村 智：ポリペクトミー, コールドポリペクトミー, EMR, 分割EMR. 日本消化器内視鏡学会監修, 日本消化器内視鏡学会卒後教育委員会責任編集, 消化器内視鏡ハンドブック改訂第2版 pp394-405, 日本メディカルセンター, 2017.
38. 2017 榎田博史：内視鏡所見から全身を診る—診断のストラテジー—. 消化器内視鏡 29: 646-649, 2017
39. 2017 榎田博史：大腸内視鏡挿入. 消化器内視鏡 29: 509-513, 2017.
40. 2017 榎田博史：大腸ポリペクトミー・コールドポリペクトミー・EMRのコツ. Gastroenterol Endosc 59: 311-325, 2017
41. 2017 榎田博史, 米田頼晃, 岡元寿樹, 足立哲平, 永井知行, 朝隈 豊, 櫻井俊治, 渡邊智裕：内視鏡所見からみた腸炎の鑑別診断. 消化器内視鏡 29: 20-30, 2017
42. 2017 榎田博史：腸管虚血 (急性腸間膜虚血, 虚血性大腸炎). 福井次矢, 高木 誠, 小室一成 総編集：今日の治療指針2017年版, pp 472-473, 医学書院, 2017.
43. 2017 宇谷 厚志, 岩永 聡, 小池 雄太, 大久保 佑美, 鋤塚 大, 遠藤 雄一郎, 谷崎 英昭, 金田 眞理, 簗持 淳, 三長 孝輔, 荻 朋男, 山本 洋介, 池田 聡司, 築城 英子, 田村 寛, 前村 浩二, 北岡 隆：「弾性線維性仮性黄色腫診療ガイドライン」策定委員会. 日本皮膚科学会ガイドライン, 弾性線維性仮性黄色腫診療ガイドライン(2017年版), 日本皮膚科学

### Ⅲ. 招待講演・特別講演（海外）

1. **Kudo M**: Invited Lecture “TACE”, the 26th Conference of Asian Pacific Association for the Study of the Liver (APASL 2017), Shanghai, China, February 17, 2017.
2. **Kudo M**: Invited Lecture “Molecular targeted therapy for HCC: current status and future perspective.” Luncheon Seminar 18 “Diagnosis and treatment of liver cancer”, The 6th Biennial Congress of the Asian-Pacific Hepato-Pancreato-Biliary Association (6th A-PHPBA), The 29th Meeting of Japanese Society of Hepato-Biliary-Pancreatic Surgery (29th JSHBPS), Pacifico Yokohama, Kanagawa, June 7-10, 2017.
3. **Kudo M**: Special Lecture (V) “Impact of surveillance and diagnosis on survival in HCC patients”, Taiwan Digestive Disease Week 2017 (TDDW), Taipei, Taiwan, September 29-October 1, 2017.
4. **Kudo M**: Special Lecture “US-US overlay fusion imaging in the evaluation of treatment response after RFA.” The 9th Asian Conference on Ultrasound Contrast Imaging (ACUCI) 2017, Taipei, Taiwan, October 13-17, 2017.
5. **Kudo M**: Special Lecture “CEUS for pancreatobiliary diseases.” The 9th Asian Conference on Ultrasound Contrast Imaging (ACUCI) 2017, Taipei, Taiwan, October 13-17, 2017.
6. **Kudo M**: Sonazoid-enhanced US in the management of HCC. 2017年日中笹川医学協力プロジェクト超音波実用技術研修, 西安, 中国, October 17-19, 2017.
7. **Kudo M**: Locally advanced, non-resectable disease. ESMO ASIA 2017, Singapore, November 17-19, 2017.

### Ⅳ. 招待講演・特別講演（国内）

1. 工藤正俊: 特別講演「肝がんの薬剤治療の現況と薬剤の開発状況」, 社内サテライト研修, 平成29年2月14日, ユーザイ大阪コミュニケーションオフィス, 大阪.
2. 工藤正俊: 特別講演「内科医からみた肝画像診断の役割」, Radiology Update in Gifu, 平成29年3月17日, 岐阜グランドホテル, 岐阜.
3. 工藤正俊: シンポジスト; 総合討論・症例提示, Radiology Update in Gifu, 平成29年3月17日, 岐阜グランドホテル, 岐阜.
4. 工藤正俊, 長谷川雄一, 小川眞広: ディスカッサー; 男女共同参画委員会企画「日本超音波医学会が取り組むキャリア支援」, 日本超音波医学会第90回学術, 平成29年5月26-28日, 栃木県総合文化センター, 宇都宮東武ホテルグランデ, ホテルニューイタヤ, 栃木.
5. 工藤正俊: 特別講演「肝細胞癌に対する分子標的治療: 現況と今後の展望」, Specific Molecule Antiviral Treatment Tokyo Hepatitis C (SMART C), 平成29年6月10日, ザ・キャピトルホテル東急, 東京.
6. 工藤正俊: 特別講演2「肝細胞癌の分子標的治療: 最新の話」, 第6回香川肝がん分子標的治療研究会, 平成29年6月20日, リーガホテルゼスト高松, 香川.
7. 工藤正俊: 特別講演「肝細胞癌の分子標的治療: 現状と今後の展望」, 第16回日本肝癌分子標的治療研究会, 平成29年6月24日, ルネッサンスリゾートナルト, 徳島.
8. 工藤正俊: 特別講演I「肝細胞癌に対する薬物治療の新たな展開〜ASCO2017の最新発表を踏まえて〜」, 肝疾患学術講演会, 平成29年6月29日, ホテルグランヴィア和歌山, 和歌山.
9. 工藤正俊: 特別講演「肝癌の薬物療法が変わる」, 近畿・中国四国肝疾患研究会, 平成29年8月11日, JRホテルクレメント高松, 香川.
10. 工藤正俊: 特別講演「レンバチニブ」, レンバチニブ(Lenvatinib), 第53回日本肝癌研究会, 平成29年7月6-7日, 京王プラザホテル, 東京.
11. 工藤正俊: 特別講演「肝細胞癌診療のブレークスルー〜薬物療法が変わる〜」, スチバーガ錠HCC

承認記念講演会in京都，平成29年10月6日，ウェスティン都ホテル京都，京都。

12. 工藤正俊：特別講演「急激に変貌する肝細胞癌の薬物治療」，第17回肝癌治療研究会，平成29年10月7日，ホテルセントラザ博多，福岡。
13. 工藤正俊：特別講演II「肝細胞癌診療のブレイクスルー薬物療法が変わる」，第18回岡山肝癌研究会，平成29年10月21日，ホテルグランヴィア岡山，岡山。
14. 工藤正俊：特別講演「肝細胞癌薬物治療のブレイクスルー」，第168回群馬肝癌検討会特別講演会，平成29年11月15日，ホテルラシーネ新前橋，群馬。
15. 工藤正俊：基調講演「進行肝細胞癌治療における最新治療：基礎と臨床の立場から」，シンポジウム7，第42回日本肝臓学会西部会，平成29年11月30日，ヒルトン福岡シーホーク，福岡。
16. 榎田博史：特別講演「適切な診断と適応に基づいた 大腸 ESD/EMR」．第8回福岡宮崎消化管セミナー，平成29年1月11日，宮崎。
17. 榎田博史：特別講演「早期大腸癌の見つけ方．その腫瘍見逃していませんか？」，第4回京都広小路ライブセミナー，平成29年1月21日，京都。
18. 萩原 智：特別講演「肝臓病と採血データの見方」，日本肝臓学会主催平成28年度「肝がん撲滅運動」，平成29年1月29日，ビッグ・アイ，大阪。
19. 南 康範：特別講演「B型肝炎：治療の現在」，日本肝臓学会主催平成28年度「肝がん撲滅運動」，平成29年1月29日，ビッグ・アイ，大阪。
20. 依田 広：特別講演「C型肝炎の最新治療」，日本肝臓学会主催平成28年度「肝がん撲滅運動」，平成29年1月29日，ビッグ・アイ，大阪。
21. 千品寛和：特別講演「肝硬変とは？～診断と治療～」，日本肝臓学会主催平成28年度「肝がん撲滅運動」，平成29年1月29日，ビッグ・アイ，大阪。
22. 南 知宏：特別講演「肝臓病の薬と肝がんの予防」，日本肝臓学会主催平成28年度「肝がん撲滅運動」，平成29年1月29日，ビッグ・アイ，大阪。
23. 田北雅弘：特別講演「内科での治療～ラジオ波焼灼術と肝動脈塞栓術～」，日本肝臓学会主催平成28年度「肝がん撲滅運動」，平成29年1月29日，ビッグ・アイ，大阪。
24. 有住忠晃：特別講演「肝がん治療薬の最新動向」，日本肝臓学会主催平成28年度「肝がん撲滅運動」，平成29年1月29日，ビッグ・アイ，大阪。
25. 榎田博史：特別講演 炎症性腸疾患のトレンド：一般消化器医が知っておくべき事．炎症性腸疾患勉強会，平成29年2月8日，大阪。
26. 上嶋一臣：特別講演「ここまできた肝細胞癌の化学療法～分子標的薬と免疫チェックポイント阻害薬の進歩～」．第36回南大阪肝疾患研究会，平成29年2月17日，ホテル・アゴーラリージェンシー堺，大阪。
27. 松井繁長：特別講演「GERDの現状と今後の展望」．中河内消化器フォーラム，平成29年3月9日，ザ・リッツ・カールトン大阪，大阪。
28. 萩原 智：特別講演「当院におけるウイルス性肝炎治療」，阪南肝炎セミナー，平成29年3月23日，ホテル・アゴーラリージェンシー堺，大阪。
29. 萩原 智：特別講演「当院におけるウイルス性肝炎診療」，泉州消化器病談話会，平成29年3月25日，市立岸和田市民病院，大阪。
30. 榎田博史：特別講演「大腸腫瘍：適格な診断に基づいた ESD/EMR/cold polypectomy」，Takeda GI Forum，平成29年4月1日，岩手。
31. 上嶋一臣：肝・消化器進行癌治療の未来．特別講演①．第14回日本消化器癌研究会，平成29年5月16日，甲府富士屋ホテル2階「桃源」，山梨。
32. 上嶋一臣：特別講演1「Intermediate stageの亜分類からみたTACE対象の絞り込みとTACE不応の適切な判断」，第6回香川肝がん分子標的治療研究会，平成29年6月20日，リーガホテルゼスト高松，香川。
33. 榎田博史：特別講演「大腸腫瘍の内視鏡診断と治療」，第1回 和歌山消化器内視鏡ライブデモンストラションコースきのくにライブ，平成29年7月27日，和歌山。
34. 萩原 智：特別講演「C型肝炎治療のピットフォール．倉敷肝炎ネットワークセミナー」．倉敷中央病院総合保険管理センター古久賀ホール，平成29年7月28日，岡山。



35. 南 康範: 特別講演「Ablative marginの可視化: Hepatic GuideとUS-US overlay fusionの有用性」. 日本超音波医学会第38回中部地方会, 平成29年9月10日, 金沢大学附属病院外来診療棟4階玉ホール, CPDセンター, 石川.

## V. 学会発表 (海外シンポジウム)

1. **Kudo M**: New HCC Diagnosis. Session5 “HCC-2”, The Asian Pacific Association for the Study of the Liver (APASL STC 2017), April 10-12, 2017, ホテルオークラ・ハウステンボス, 長崎.
2. **Kudo M**: Latest Advances in Using Molecular Targeted Therapy in Advanced HCC Patients. Concurrent Session 3 “Hepatocellular Cancer”, Hong Kong International Oncology Forum 2017, May 19, 2017, Hong Kong.
3. **Kudo M**: Treatment Strategy of Intermediate Stage HCC. Symposium 43 (Keynote) ” Strategy for Intermediate Stage of HCC”, 第6回アジア太平洋肝胆膵学会(6th A-PHPBA), 第29回日本肝胆膵外科学会学術集会(29th JSHBPS), June 7-10, 2017, パシフィコ横浜, 神奈川.
4. **Kudo M**: Systemic Therapy for Hepatocellular Carcinoma: current Status and Future Perspective. KEYNOTE LECTURE II (KL-2-1), APASL Single Topic Conference 2017 Mongolia, 6th HCV Conference on HCV and CO-INFECTIONS, June 16-18, 2017, Ulaanbaatar, Mongolia.
5. **Kudo M**: Response Assessment and Interpretation: Comparing Systemic And Loco-regional Therapies. Master Class: Workshop: Master Class for Hepatocellular Carcinoma, 24th Asia Pacific Cancer Conference (APCC), June 22-24, 2017, COEX Seoul, Korea.
6. **Kudo M**: HCC treatment landscape-the Asian perspective- HCC treatment guidelines, Asian perspective- Experience sharing from Japan. Necavar 10-years Anniversary, Jul 1-2, 2017, Taiwan.
7. Ueshima K, **Kudo M**, Izumi N, Kadoya M, Kubo M, Kumada T, Kokudo N, Takayama T, Sakamoto M, Nakashima O, Matsuyama Y: Validation of three staging systems for hepatocellular carcinoma (JIS score, biomarker-combined JIS score and BCLC system) in 4,649 cases from a Japanese nationwide survey. 国際シンポジウム2「肝細胞癌のStaging」, The 53rd Annual Meeting of Liver Cancer Study Group of Japan, July 6-7, 2017, Keio Plaza Hotel, Tokyo.
8. Hasegawa K, **Kudo M**, Izumi N, Kadoya M, Kubo S, Kumada T, Sakamoto M, Takayama T, Nakajima O, Matsuyama Y, Kokudo N: The Current Situations and Future Perspectives of the Japanese Nationwide Survey of Patients with Primary Liver Cancer. 国際シンポジウム3「肝悪性腫瘍のRegistry」, The 53rd Annual Meeting of Liver Cancer Study Group of Japan, July 6-7, 2017, Keio Plaza Hotel, Tokyo.
9. **Kudo M**: Treatment of advanced hepatocellular carcinoma: Future perspective. シンポジウム26「これからの進行肝細胞がん治療」, 2017 the Japanese Society of Medical Oncology Annual Meeting, July 27-29, 2017, Kobe Convention Center/ Junko Fukutake Hall, Hyogo/ Okayama.
10. Shiori Fujii, Makoto Yamakawa, Kengo Kondo, Takeshi Namita, Masatoshi Kudo, Tsuyoshi Shiina: Evaluation of shear wave dispersion caused by fibrous structure and tissue viscosity using hepatic fibrosis progression and histological models. 2017 IEEE International Ultrasonics Symposium (IUS), September 6-9, 2017, Washington, D.C, USA.
11. **Kudo M**: How to Improve Survival Outcome and Use Molecular Targeted Agent in HCC Patients? Symposium (XI) ” Innovation and New Approaches in Hepatocellular Carcinoma.”, Taiwan Digestive Disease Week 2017 (TDDW), Taipei, Taiwan, September 29-October 1, 2017.
12. Sakurai T, Kashida H, **Kudo M**: A new strategy to personalize surveillance program for colitis-associated cancer. International Session (Symposium)9 (JGES・JSGE・JSGS) “Surveillance colonoscopy for ulcerative colitis; Up-to-date procedure and therapeutic strategy” Japan Digestive Disease Week (JDDW) 2017 Fukuoka, October 12-15, 2017,

Fukuoka.

13. Minami Y: Contrast US for HCC. Taiwan Liver Cancer Association 2017 (Innovation and advances in Hepatocellular Carcinoma), May 20-21, 2017, Taiwan.
14. Kashida H: Instructor of hands-on seminar. 5th International teaching course on gastrointestinal endoscopy, Athens, February 3-4, 2017.
15. Kashida H: Lecture: Endoscopic submucosal dissection (ESD). 5th International teaching course on gastrointestinal endoscopy, Athens, February 3-4, 2017.
16. Minami Y: Fusion Image and Contrast Enhanced Ultrasonography in Assessing Ablation Effect. TATA 2017 Annual Meeting, Kaoshiung Chang Gung Memorial Hospital, Taiwan, February 12, 2017.
17. Nemoto D, Kashida H, Hewett DG, Hayashi Y, Yamamoto H, Togashi K: Blue Laser Imaging for the identification of deep submucosal invasion in colorectal cancers: a reading test in Western & Japanese endoscopists. Digestive Disease Week (DDW) 2017, Chicago, USA, May 6-9, 2017.
18. Asai S, Kawamura T, Takeuchi Y, Yokota I, Akamine E, Kato M, Akamatsu T, Tada K, Komeda Y, Iwatate M, Kawakami K, Nishikawa M, Watanabe D, Yamauchi A, Fukata N, Shimatani M, Ooi M, Fujita K, Sano Y, Kashida H, Hirose S, Iwagami H, Uedo N, Teramukai S, Tanaka K: A comparison between cold snare polypectomy and hot snare polypectomy for resection rate of subcentimeter colorectal polyps: a multicenter randomized controlled trial (CRESCENT study). Digestive Disease Week (DDW) 2017, Chicago, USA, May 6-9, 2017.
19. 米田頼晃: Therapeutic Strategies for Four Subtypes of Laterally Spreading Tumors of Colorectum. 11th Global Gastroenterologists Meeting, Gastro 2017, Italy Rome, June 13, 2017.
20. 2017 Kashida H: Instructor of hands-on seminar. 3rd APSDE MGA Local workshop on OGD and Colonoscopy, Yangon, June 14-16, 2017.
21. 2017 Kashida H: Lecture, Capsule endoscopy. 3rd APSDE MGA Local workshop on OGD and Colonoscopy, Yangon, June 14-16, 2017.
22. Kashida H: Lecture, Contrast endoscopy. 3rd APSDE MGA Local workshop on OGD and Colonoscopy, Yangon, June 14-16, 2017.
23. 2017 Kashida H: Live Demonstration, Conference with international participation "Endoscopic Diagnosis and Treatment of Diseases of Gastrointestinal Tract", Moscow, June 21-22, 2017.
24. 2017 Kashida H: Lecture, Endoscopic treatment of colon lesions. Conference with international participation "Endoscopic Diagnosis and Treatment of Diseases of Gastrointestinal Tract", Moscow, June 21-22, 2017.
25. 2017 Kashida H: Lecture, Endoscopic diagnosis of colorectal non-polypoid lesions. Conference with international participation "Endoscopic Diagnosis and Treatment of Diseases of Gastrointestinal Tract", Moscow, June 21-22, 2017.
26. Kashida H: Lecture, How to prevent recurrence and follow up the patient after endoscopic treatment for large colorectal tumors. The 24th EUS and the 21st Early GI cancer Conference of Taiwan, Taipei, June 25, 2017.
27. Kashida H: Instructor of hands-on training. Masterclass in colonoscopy, Bologna, June 29-30, 2017.
28. Kashida H: Live Demonstration. Masterclass in colonoscopy, Bologna, June 29-30, 2017.
29. Kashida H: Lecture, The Japan Narrow band imaging Expert Team (JNET) classification. Masterclass in colonoscopy, Bologna, June 29-30, 2017.
30. Kashida H: Lecture, Two-hand technique of colonoscopic intubation. Masterclass in colonoscopy, Bologna, June 29-30, 2017.
31. Kashida H: Lecture, Characterization of colorectal superficial neoplastic lesions.

Masterclass in colonoscopy, Bologna, June 29-30, 2017.

32. 2017 Ueshima K: ISY2-1 Validation of three staging systems for hepatocellular carcinoma (JIS score, biomarker combined JIS score and BCLC system) in 4,649 cases from a Japanese nationwide survey. International symposium 2. The Staging Systems of Hepatocellular Carcinoma 53rd. Liver Cancer Study Group of Japan Annual Meeting, July 6, 2017, Tokyo.
33. Kashida H: New techniques and new instruments for EMR/ESD. Symposium VI: The Korean Society of Coloproctology (KSCP) – The Japan Society of Coloproctology (JSCP) Joint Symposium. Session II How to manage lateral spreading tumor International Colorectal Research Summit 2017, Seoul, September 2-3, 2017.
34. Kawamura T, Takeuchi Y, Asai S, Yokota I, Akamine E, Kato M, Akamatsu T, Tada K, Komeda Y, Iwatate M, Kawakami K, Nishikawa M, Watanabe D, Yamauchi A, Fukata N, Shimatani M, Ooi M, Fujita K, Sano Y, Kashida H, Hirose S, Iwagami H, Uedo N, Teramukai S, Tanaka K: A comparison of the resection rate for cold and hot snare polypectomy for 4-9 mm colorectal polyps: a multicenter randomized controlled trial (CRESCENT study). Gut on line first, September 28, 2017.
35. Kawamura T, Takeuchi Y, Asai S, Yokota I, Akamine E, Kato M, Akamatsu T, Tada K, Komeda Y, Iwatate M, Kawakami K, Nishikawa M, Watanabe D, Yamauchi A, Fukata N, Shimatani M, Ooi M, Fujita K, Sano Y, Kashida H, Hirose S, Iwagami H, Uedo N, Teramukai S, Tanaka K: The efficacy of cold snare polypectomy in achieving complete resection of subcentimetre colorectal polyps: a multicenter randomized controlled trial (CRESCENT study). 25th UEGW, Barcelona, October 28-November 1, 2017.
36. Kashida H, Shiu SI: Newly developed EMR/ESD instruments. Asian Session “How to manage lateral spreading tumor” 第72回日本大腸肛門病学会学術集会, 平成29年11月10-11日, 福岡.
37. Minami Y: Real-time Evaluation of Ablative Margin in Radiofrequency Ablation for Hepatocellular Carcinoma: Usefulness of US-US Overlay Image Fusion. “Branch Venue of Image Changes on Ablation and Response Evaluation” Asian Conference on Tumor Ablation (ACTA) 2017, Guangzhou, China, November 16-18, 2017.
38. Kashida H: Lecture How to perform IEE - focus on NBI and magnification. Image-enhanced endoscopy (IEE) Course, Taichung, December 3, 2017.
39. Kashida H: Instructor in hands-on training Image-enhanced endoscopy (IEE) Course, Taichung, December 3, 2017
40. 2017 Ueshima K: Treatment Strategy for Intermediate Stage HCC. PRECEPTORSHIP PROGRAM Standardization of treatment HCC Intermediate stage. National Cancer Hospital, Hanoi, Vietnam, December 7, 2017.
41. 2017 Ueshima K: How to decide the treatment strategy for intermediate stage HCC & Advices for National Cancer Hospital HCC. PRECEPTORSHIP PROGRAM Standardization of treatment HCC Intermediate stage. National Cancer Hospital, Hanoi, Vietnam, December 7, 2017.
42. Kashida H: Lecture, Endoscopic treatment for colorectal cancer. Endoscopic session, Post Graduate Course: Gastrointestinal Oncology in Practice, International Association of Surgeons Gastro- enterologists & Oncologists Thailand Chapter (IASGO-TH), Bangkok, December 9-10, 2017.
43. 2017 Kashida H: Presenter, Case discussion, Post Graduate Course: Gastrointestinal Oncology in Practice, International Association of Surgeons Gastro- enterologists & Oncologists Thailand Chapter (IASGO-TH), Bangkok, December 9-10, 2017.
44. 2017 Kashida H: Lecture, Colorectal ESD. Master VDO session, Post Graduate Course: Gastrointestinal Oncology in Practice, International Association of Surgeons Gastro- enterologists & Oncologists Thailand Chapter (IASGO-TH), Bangkok,

VI. 学会発表・抄録 (米国及び国際学会)

1. Kudo M, Bruix J, Merle P, Granito A, Huang YH, Bodoky G, Yokosuka O, Rosmorduc O, Breder V, Gerolami R, Masi G, Ross PJ, Qin S, Song T, Bronowicki JP, Ollivier-Hourmand I, LeBerre MA, Baumhauer A, Meinhardt G, Han G, on behalf of the RESORCE Investigators: Efficacy and safety of regorafenib versus placebo in patients with hepatocellular carcinoma (HCC) progressing on sorafenib: results of the international, randomized phase 3 RESORCE trial. 15th Japan Association of Molecular Targeted Therapy for HCC, Iino hall & Conference Center, Tokyo, January 14, 2017.
2. Kudo M: Resminostat and sorafenib combination therapy for advanced hepatocellular carcinoma in patients previously untreated with systemic chemotherapy. American Society of Clinical Oncology, 2017 Gastrointestinal Cancers Symposium (ASCO-GI 2017), San Francisco, USA, January 19-21, 2017.
3. Finn RS, Chan SL, Zhu AX, Knox J, Cheng AL, Siegel AB, Bautista O, Kudo M: Randomized phase 3 study of pembrolizumab versus best supportive care for second-line advanced hepatocellular carcinoma. American Society of Clinical Oncology, 2017 Gastrointestinal Cancers Symposium (ASCO-GI 2017), San Francisco, USA, January 19-21, 2017.
4. Zhu AX, Knox J, Kudo M, Chan S, Finn R, Siegel A, Ma J, Cheng AL: Phase 2 study of pembrolizumab in patients with previously treated advanced hepatocellular carcinoma. American Society of Clinical Oncology, 2017 Gastrointestinal Cancers Symposium (ASCO-GI 2017), San Francisco, USA, January 19-21, 2017.
5. Melero I, Sangro B, Yau T, Hsu C, Kudo M, Crocenzi TS, Kim TY, Choo SP, Trojan J, Meyer T, Welling TH, Yeo W, Chopra A, Anderson J, dela Cruz C, Lang L, Neely J, Tang H, El-Khoueiry AB: Nivolumab dose escalation and expansion in patients with advanced hepatocellular carcinoma (HCC): the CheckMate 040 study. American Society of Clinical Oncology, 2017 Gastrointestinal Cancers Symposium (ASCO-GI 2017), San Francisco, USA, January 19-21, 2017.
6. Bruix J, Merle P, Granito A, Huang YH, Bodoky G, Pracht M, Yokosuka O, Gerolami R, Masi G, Ross PF, Qin S, Song T, Bronowicki JP, Ollivier-Hourmand I, Kudo M, Le Berre MA, Beinhardt G, Han G, on behalf of RESORCE investigators: Survival by pattern of tumor progression during prior sorafenib (SOR) treatment in patients with hepatocellular carcinoma (HCC) in the phase 3 RESORCE trial comparing second-line treatment with regorafenib (REG) or placebo. American Society of Clinical Oncology, 2017 Gastrointestinal Cancers Symposium (ASCO-GI 2017), San Francisco, USA, January 19-21, 2017.
7. Ikeda M, Ikeda K, Kudo M, Osaki Y, Okusaka T, Tamai T, Suzuki T, Hisai T, Miyagishi H, Okita K, Kumada H: Subgroup analyses of a phase 2 study of lenvatinib (E7080), a multitargeted tyrosine kinase inhibitor, in patients with advanced hepatocellular carcinoma (HCC). American Society of Clinical Oncology, 2017 Gastrointestinal Cancers Symposium (ASCO-GI 2017), San Francisco, USA, January 19-21, 2017.
8. Merle P, Granito A, Huang YH, Bodoky G, Pracht M, Yokosuka O, Rosmorduc O, Breder V, Gerolami R, Masi G, Ross P, Qin S, Song T, Bronowicki JP, Ollivier-Hourmand I, Kudo M, Schliep S, Fiala-Buskes S, Meinhardt G, Bruix J on behalf of the RESORCE Investigators: Time course of treatment-emergent adverse events (TEAEs) in the randomized, controlled phase 3 RESORCE trial of regorafenib for patients with hepatocellular carcinoma progressing on sorafenib treatment. EASL HCC Summit 2017, Geneva, Switzerland, February 2-5, 2017.
9. Hong S, Cheng AL, Raoul JL, Lee HC, Kudo M, Nakajima K, Peck-Radosavljevic M, on



- behalf of the OPTIMIS Investigators: Regional use of sorafenib after transarterial chemoembolization (TACE) in Chinese patients with hepatocellular carcinoma (HCC): results from the second interim analysis of OPTIMIS. The 26th Conference of the Asian Pacific Association for the Study of the Liver (APASL), Shanghai, China, February 15-19, 2017.
10. Bruix J, Merle P, Granito A, Huang YH, Bodoky G, Pracht M, Yokosuka O, Gerolami R, Masi G, Ross PJ, Qin S, Song T, Bronowicki JP, Ollivier-Hourmand I, Kudo M, LeBerre MA, Meinhardt G, Han G, on behalf of the RESORCE Investigators: Analysis of overall survival (OS) by pattern of progression of hepatocellular carcinoma (HCC) during prior sorafenib treatment in the randomized phase 3 RESORCE trial comparing regorafenib with placebo. The 26th Conference of the Asian Pacific Association for the Study of the Liver (APASL), Shanghai, China, February 15-19, 2017.
  11. Yamao K, Kitano M, Takenaka M, Kayahara T, Ishida E, Yamamoto H, Yoshiawa T, Minaga K, Yamashita Y, Asada M, Okabe Y, Osaki Y, Ikemoto J, Hanada K, Kudo M: Outcomes of biliary drainage in pancreatic cancer patients with an indwelling gastroduodenal stent: a multicenter retrospective study in west japan. (Postor). Digestive Disease Week (DDW 2017), Chicago, USA, May 6-9, 2017.
  12. Yada N, Sakurai T, Kudo M: Prospective risk analysis of hepatocellular carcinoma in patients with chronic hepatitis C by ultrasound strain imaging. American Institute of Ultrasound in Medicine (AIUM), Florida, USA, March 25-29, 2017.
  13. Yen C, Sharma R, Rimassa L, Arizumi T, Bettinger D, Evans J, Pressiani T, Burlone ME, Pirisi M, Giordano L, Howell J, Kudo M, Thimme R, Park JW, Pinato DJ: Treatment-stage migration maximizes survival outcomes in patients with hepatocellular carcinoma treated with sorafenib: an observational study. The International Liver Congress 2017 (EASL 2017), Amsterdam, the Netherlands, February 2-5, 2017.
  14. Sangro B, Yau T, Hsu C, Kudo M, Crocenzi TS, Choo SP, Meyer T, Welling TH, Yeo W, Chopra A, Baakili A, dela Cruz C, Lang L, Neely J, Melero I, El-Khoueiry AB, Trojan J: Nivolumab in sorafenib-experienced patients with advanced hepatocellular carcinoma (HCC) with or without chronic viral hepatitis: CheckMate 040 study. The International Liver Congress 2017 (EASL 2017), Amsterdam, the Netherlands, April 19-23, 2017.
  15. Komeda Y, Kashida H, Sakurai T, Asakuma Y, Nagai T, Matsui S, Watanabe T, Kudo M: Diagnosis of localized colorectal lesions with magnifying narrow band imaging (NBI) using Japan NBI Expert Team (JNET) classification: a cross sectional study. Digestive Disease Week (DDW 2017), Chicago, USA, May 6-9, 2017.
  16. Komeda Y, Kashida H, Sakurai T, Asakuma Y, Nagai T, Matsui S, Watanabe T, Kudo M: Follow-up examination of the recurrence after endoscopic treatment of colorectal tumors. Digestive Disease Week (DDW 2017), Chicago, USA, May 6-9, 2017.
  17. Hiroshi Ida, Naoshi Nishida, Satoru Hagiwara, Masatoshi Kudo : Analysis of hepatocellular carcinoma after achievement of sustained viral response with daclatasvir and asunaprevir for hepatitis C virus infection. The Asian Pacific Association for the Study of the Liver (APASL), Single Topic Conference 2017 Nagasaki, JRハウステンボス, Nagasaki, April 10-11. 2017.
  18. Crocenzi TS, El-Khoueiry AB, Yau TC, Melero I, Sangro B, Kudo M, Hsu C, Trojan J, Kim TY, Choo SP, Meyer T, Kang YK, Yeo W, Chopra A, Baakili A, Dela Cruz CM, Lang L, Neely J, Welling T: Nivolumab (nivo) in sorafenib (sor)-naive and -experienced pts with advanced hepatocellular carcinoma (HCC): CheckMate 040 study. Annual Meeting of American Society of Clinical Oncology (ASCO 2017), Chicago, USA, June 2-6, 2017.
  19. Finn RS, Chan SL, Zhu AX, Knox J, Cheng AL, Siegel AB, Bautista O, Kudo M: Phase 3 randomized study of pembrolizumab vs best supportive care for second-line advanced

- hepatocellular carcinoma: KEYNOTR-240. Annual Meeting of American Society of Clinical Oncology (ASCO 2017), Chicago, USA, June 2-6, 2017.
20. Cheng AL, Finn RS, Qin F, Han KH, Ikeda K, Piscaglia F, Baron AD, Park JW, Han G, Jassem J, Blanc JF, Vogel A, Komov D, Evans TRJ, Lopez-Lopez C, Dutcus CE, Ren M, Kraljevic S, Tamai T, Kudo M: Phase 3 trial of lenvatinib (LEN) vs sorafenib (SOR) in first-line treatment of patien (pts) with unresectable hepatocellular carcinoma (uHCC). Annual Meeting of American Society of Clinical Oncology (ASCO 2017), Chicago, USA, June 2-6, 2017.
  21. Merle P, Granito A, Huang Y-H, Bodoky G, Yokosuka O, Rosmorduc O, Breder V, Gerolami R, Masi G, Ross P J, Qin S, Song T, Bronowicki J-P, Ollivier-Hourmand I, Kudo M, LeBerre M-A, Baumhauer A, Meinhardt G, Han G, Bruix J on behalf of the RESORCE Investigators: Updated overall survival analysis and further exploratory analyses from the international, phase 3, randomized, placebo-controlled RESORCE trial of regorafenib for patients with hepatocellular carcinoma who progressed on sorafenib treatment. International Liver Cancer Association (ILCA) 11th Annual Conference, Seoul, South Korea, September 15-17, 2017.
  22. Sakurai T, Kudo M, Nagai T, Kashida H: Gankyrin induces STAT3 activation in tumour microenvironment and sorafenib resistance in hepatocellular carcinoma. The 76th Annual meeting of the Japanese Cancer Association, Yokohama, September 28-30, 2017.
  23. Kudo M: CEUS in the Diagnosis and Treatment for Malignant Liver Tumors. The 16th World Congress of the world federation for ultrasound in medicine and biology (WFUMB) 2017, Taipei, Taiwan, October 13-17, 2017.
  24. Merle P, Granito A, Huang YH, Bodoky G, Pracht M, Yokosuka O, Rosmorduc O, Breder V, Gerolami R, Masi G, Ross P, Qin S, Song T, Bronowicki JP, Ollivier-Hourmand I, Kudo M, Schlief S, Fiala-Buskes S, Meinhardt G, Bruix J on behalf of the RESORCE Investigators: Time course of treatment-emergent adverse events (TEAEs) in the randomized, controlled phase 3 RESORCE trial of regorafenib for patients with hepatocellular carcinoma progressing on sorafenib treatment. American Association for the study of liver diseases (AASLD 2017), Washington DC, USA, October 20-24, 2017.
  25. Komeda Y, Kashida H, Sakurai T, Nagai T, Matsui S, Kudo M: Appropriate intervals to look for local recurrence after endoscopic treatment of colorectal neoplasms. 25th UEGW, Barcelona, October 28-November 1, 2017.
  26. Nagai T, Matsui S, Kashida H, Komeda Y, Sakurai T, Kudo M: Bleeding after endoscopic resection for early gastric lesions in patients on antithrombotic therapy. 25th UEGW, Barcelona, October 28-November 1, 2017.
  27. Cheng AL, Raoul JL, Lee HC, Kudo M, Nakajima K, Peck-Radosavljevic M on behalf of the OPTIMIS Investigators: An international observational study to assess the use of sorafenib after transarterial chemoembolization (TACE) in patients with hepatocellular carcinoma (HCC): OPTIMIS interim analysis. World Conference on Interventional Oncology (WCIO 2017), Boston, USA, June 8-11, 2017.
  28. Melero I, El-Khoueiry AB, Yau T, Hsu C, Kudo M, Crocenzi T, Kim TY, Choo SP, Trojan J, Willing TH, Kang YK, Yeo W, Chopra A, Baakili A, dela Cruz C, Lang L, Sangro B, Meyer T: Efficacy and safety of nivolumab in patients with advanced hepatocellular carcinoma analyzed by patient age: a sub-analysis of the CheckMate 040 study. 19th ESMO World Congress on Gastrointestinal Cancer 2017 (ESMO-GI 2017), Barcelona, Spain, June 28-July 1, 2017.
  29. Bruix J, Merle P, Granito A, Huang YH, Bodoky G, Yokosuka O, Rosmorduc O, Breder V, Gerolami R, Masi G, Ross PJ, Qin S, Song T, Bronowicki JP, Ollivier-Hourmand I, Kudo M, LeBerre MA, Baumhauer A, Meinhardt G, Han G, on behalf of the RESORCE Investigators:

- Updated overall survival (OS) analysis from the international, phase 3, randomized, placebo-controlled RESORCE trial of regorafenib for patients with hepatocellular carcinoma (HCC) who progressed on sorafenib treatment. 19th ESMO World Congress on Gastrointestinal Cancer 2017 (ESMO-GI 2017), Barcelona, Spain, June 28-July 1, 2017.
30. Itonaga M, Kitano M, Kawaji Y, Abe H, Takashi T, Nuta J, Hatamaru K, Omoto S, Minaga K, Kamata K, Miyata T, Yamao K, Imai H, Takenaka M, Kudo M: Endoscopic ultrasonography-guided biliary drainage without dilation device using a thin delivery-system stent: A preclinical study. 25th UEG Week 2017, Barcelona, Spain, October 28- November 1, 2017.
  31. Chan SL, Finn RS, Zhu AX, Knox J, Cheng AL, Siegel AB, Bautista O, Kudo M: Phase 3, randomized KEYNOTE-240 study of pembrolizumab (Pembro) versus best supportive care (BSC) for second-line advanced hepatocellular carcinoma (HCC). European Society for Medical Oncology (ESMO)-ASIA 2017, Singapore, November 18, 2017.
  32. Vogel A, Qin S, Kudo M, Hudgens S, Yamashita T, Yoon JH, Fartoux L, Simon K, Lopez C, Sung M, Dutcus C, Kraljevic S, Tamai T, Grunow N, Meier G, Breder V: Health-related quality of life (HRQOL) and disease symptoms in patients with unresectable hepatocellular carcinoma (HCC) treated with lenvatinib (LEN) or sorafenib (SOR). AASLD 2017.
  33. Aoki T, Kubota K, Matsumoto T, Izumi N, Kadoya M, Kubo S, Kumada T, Kokudo N, Sakamoto M, Takayama T, Nakashima O, Matsuyama Y, Kudo M, for the Liver Cancer Study Group of Japan: Significance of surgical margin in patients with single hepatocellular carcinoma undergoing curative hepatic resection: an analysis using nationwide survey data in Japan. AASLD 2017.
  34. Lee HC, Cheng AL, Raoul JL, Kudo M, Nakajima K, Peck-Radosavljevic M: Deterioration of Liver Function after Transarterial Chemoembolization (TACE) in Hepatocellular Carcinoma (HCC): An Exploratory Analysis of OPTIMIS, an International Observational Study Assessing the Use of Sorafenib after TACE. AASLD 2017.
  35. Kashida H: Instructor of hands-on seminar. 5th International teaching course on gastrointestinal endoscopy, Athens, Febraury 3-4, 2017.
  36. Kashida H: Lecture: Endoscopic submucosal dissection (ESD). 5th International teaching course on gastrointestinal endoscopy, Athens, Febraury 3-4, 2017.
  37. Minami Y: Fusion Image and Contrast Enhanced Ultrasonography in Assessing Ablation Effect. TATA 2017 Annual Meeting, Kaoshiung Chang Gung Memorial Hospital, Taiwan, Febraury 12, 2017.

## Ⅶ. 学会発表（国内シンポジウム・パネルディスカッション・ワークショップ）

1. 米田頼晃, 檜田博史, 橋本有人, 岡元寿樹, 河野匡志, 山田光成, 足立哲平, 峯宏昌, 永井知行, 朝隈 豊, 櫻井俊治, 松井繁長, 渡邊智裕, 工藤正俊: 大腸腫瘍内視鏡治療後の局所再発に対するサーベイランスについて. ワークショップ7「大腸腫瘍の診断とサーベイランス法の最前線」, 第13回日本消化管学会総会学術集会, 平成29年2月10日, 名古屋国際会議場, 名古屋.
2. 宮田 剛, 竹中 完, 工藤正俊: ERCP後膵炎早期発見におけるERCP直後CT撮影の有用性. ワークショップ2「胆膵領域における診断と治療の新たな展開」, 第106回日本消化器病学会近畿支部例会, 平成29年2月25日, 大阪国際交流センター, 大阪.
3. 岩西美奈, 辻 直子, 川崎正憲, 松本 望, 尾崎信人, 米田 円, 谷池聡子, 井上達夫, 梅原康湖, 富田崇文, 前倉俊治, 落合 健, 工藤正俊: PPIによる胃低腺ポリープの変化についての検討. Young Investigator Session1「直動・胃・十二指腸」, 第106回日本消化器病学会近畿支部例会, 平成29年2月25日, 大阪国際交流センター, 大阪.
4. 森本真衣, 奥田英之, 秦 康倫, 木下大輔, 高山政樹, 岡崎典久, 川崎俊彦, 水野成人, 若狭朋子, 太田善夫, 工藤正俊: 多発する多血性肝腫瘍を認めた若年女性の1例. Freshman Session 8「肝臓(4)」, 第106回日本消化器病学会近畿支部例会, 平成29年2月25日, 大阪国際交流セン

ター, 大阪.

5. 和田祐太郎, 三長孝輔, 竹中 完, 大本俊介, 鎌田研, 宮田 剛, 山雄健太郎, 樫田博史, 工藤正俊: 緊急EUS-guided choledochoduodenostomyが有効であった総胆管結石性胆管炎の一例. Freshman Session 9「胆道」, 第106回日本消化器病学会近畿支部例会, 平成29年2月25日, 大阪国際交流センター, 大阪.
6. 神山真紀子, 山雄健太郎, 大本俊介, 鎌田 研, 三長孝輔, 宮田 剛, 今井 元, 竹中 完, 工藤正俊, 松本逸平, 竹山宜典, 筑後孝章: 主膵管狭窄を嚴重に経過観察することで診断し得た膵上皮内癌の1例. Freshman Session 10「膵臓」, 第106回日本消化器病学会近畿支部例会, 平成29年2月25日, 大阪国際交流センター, 大阪.
7. 中野省吾, 鎌田 研, 竹中 完, 大本俊介, 宮田 剛, 三長孝輔, 山雄健太郎, 工藤正俊: 膵炎を繰り返す膵頭部癌に対して超音波内視鏡下膵管ドレナージ術を施行した一例. Freshman Session 11「膵臓・その他」, 第106回日本消化器病学会近畿支部例会, 平成29年2月25日, 大阪国際交流センター, 大阪.
8. 工藤正俊: Molecular Targeted Therapy for Hepatocellular Carcinoma: Current Status and Future Perspective. シンポジウム4「肝細胞癌の治療戦略」, 第76回日本医学放射線学会総会, 平成29年4月13-16日, パシフィコ横浜, 神奈川.
9. 鎌田 研, 竹中 完, 工藤正俊: EUSによるIPMN併存膵癌の早期発見と問題点. パネルディスカッション「IPMNの診断と治療の進歩」, 第103回日本消化器病学会総会, 平成29年4月20-22日, 京王プラザホテル, 東京.
10. 鎌田 研, 竹中 完, 工藤正俊: 胃粘膜下腫瘍における造影ハーモニックEUSによる悪性抽出能の検討. パネルディスカッション07「上部消化管粘膜下腫瘍のマネージメントー経験とエビデンスに基づく食道・胃粘膜下腫瘍の診断と治療指針ー」, 第93回日本消化器内視鏡学会総会, 平成29年5月11-13日, 大阪国際会議場・リーガロイヤルホテル, 大阪.
11. 西田直生志, 工藤正俊: PD-L1陽性肝癌の臨床病理学的特徴と遺伝子変異プロファイル. シンポジウム8「肝発癌メカニズムのパラダイムシフトとこれからの展望」, 第103回日本消化器病学会総会, 平成29年4月20-22日, 京王プラザホテル, 東京.
12. 櫻井俊治, 樫田博史, 工藤正俊: STAT3 に注目した分子標的薬の治療効果予測. ワークショップ7「進行大腸がん治療のup to date」, 第103回日本消化器病学会総会, 平成29年4月20-22日, 京王プラザホテル, 東京.
13. 矢田典久, 櫻井俊治, 工藤正俊: Strain imaging によるC 型慢性肝疾患の肝発癌リスク予測. ワークショップ12「肝画像診断の進歩」, 第103回日本消化器病学会総会, 平成29年4月20-22日, 京王プラザホテル, 東京.
14. 南 康範, 西田直生志, 工藤正俊: US-US image fusionを用いた肝細胞癌へのラジオ派焼灼術の有用性. ワークショップ12「肝画像診断の進歩」, 第103回日本消化器病学会総会, 平成29年4月20-22日, 京王プラザホテル, 東京.
15. 小川 力, 柴峠光成, 工藤正俊: 汎用型ワークステーションを用いた新しいTACE治療の試み. ワークショップ12「肝画像診断の進歩」, 第103回日本消化器病学会総会, 平成29年4月20-22日, 京王プラザホテル, 東京.
16. 竹中 完, 山雄健太郎, 工藤正俊: 早期慢性肝炎EUS所見の臨床的意義について. ワークショップ13「早期慢性肝炎をめぐる諸問題」, 第103回日本消化器病学会総会, 平成29年4月20-22日, 京王プラザホテル, 東京.
17. 松井繁長, 樫田博史, 工藤正俊: 噴門部静脈瘤合併巨木型食道静脈瘤にはEISL. シンポジウム4「決定版! これが今の食道胃静脈瘤治療だ!」, 第93回日本消化器内視鏡学会総会, 平成29年5月11-13日, 大阪国際会議場・リーガロイヤルホテル, 大阪.
18. 山雄健太郎, 竹中 完, 工藤正俊: 切除不能悪性胃十二指腸狭窄症例に対する胃十二指腸ステント留置の予後予測因子の検討. ワークショップ01「緩和医療における内視鏡の役割」, 第93回日本消化器内視鏡学会総会, 平成29年5月11-13日, 大阪国際会議場・リーガロイヤルホテル, 大阪.
19. 宮田 剛, 竹中 完, 工藤正俊: 経乳頭処置困難総胆管結石症例に対するEUS ガイド下治療の意義. ワークショップ04「治療に難渋する胆管結石の治療ストラテジー」, 第93回日本消化器内視



- 鏡学会総会，平成29年5月11-13日，大阪国際会議場・リーガロイヤルホテル，大阪。
20. 米田頼晃，樫田博史，工藤正俊：The Japan NBI Expert Team(JNET)分類Type 2B 病変の取り扱い. パネルディスカッション05「大腸拡大JNET 分類の有用性と今後の課題」，第93回日本消化器内視鏡学会総会，平成29年5月11-13日，大阪国際会議場・リーガロイヤルホテル，大阪。
  21. 永井知行，樫田博史，工藤正俊：当院主催のESD/EMR・大腸内視鏡挿入法のハンズオンセミナーの検証. パネルディスカッション10「ハンズオンセミナーを検証する」，第93回日本消化器内視鏡学会総会，平成29年5月11-13日，大阪国際会議場・リーガロイヤルホテル，大阪。
  22. 三長孝輔，竹中 完，工藤正俊：経乳頭のre-intervention 困難例の悪性肝門部胆道閉塞に対するEUS 下胆道ドレナージの有用性. パネルディスカッション11「EUS 下胆道ドレナージ（戦略と安全な手技）」，第93回日本消化器内視鏡学会総会，平成29年5月11-13日，大阪国際会議場・リーガロイヤルホテル，大阪。
  23. 竹中 完，東 健，工藤正俊：当院におけるERCP 教育の工夫(drawing pictures method/CD method). パネルディスカッション14「胆膵内視鏡における安全かつ効果的な教育法」，第93回日本消化器内視鏡学会総会，平成29年5月11-13日，大阪国際会議場・リーガロイヤルホテル，大阪。
  24. 矢田典久，依田 広，工藤正俊：各種超音波エラストグラフィデバイスの進歩とその有用性. シンポジウム 消化器2 消化器横断領域「消化器領域における超音波最新技術」，日本超音波医学会第90回学術集会，平成29年5月26-28日，栃木県総合文化センター，宇都宮東武ホテルグランデ，ホテルニューイタヤ，栃木。
  25. 竹中 完，大本俊介，三長孝輔，宮田 剛，鎌田 研，山雄健太郎，今井 元，樫田博史，工藤正俊：早期慢性膵炎EUS所見の臨床的意義について. パネルディスカッション 消化器1 膵臓「慢性膵炎診断における超音波の役割」，日本超音波医学会第90回学術集会，平成29年5月26-28日，栃木県総合文化センター，宇都宮東武ホテルグランデ，ホテルニューイタヤ，栃木。
  26. 南 康範，工藤正俊：ラジオ波焼灼術後のバブルによる高エコー域を壊死部とみなして良いか？ワークショップ 消化器1 肝臓「肝腫瘍に対する穿刺・治療の進歩」，日本超音波医学会第90回学術集会，平成29年5月26-28日，栃木県総合文化センター，宇都宮東武ホテルグランデ，ホテルニューイタヤ，栃木。
  27. 工藤正俊：肝臓診療ガイドライン. 特別企画2「日本肝臓学会ガイドラインup to date」，第53回日本肝臓学会総会，平成29年6月9日，広島国際会議場，広島。
  28. 工藤正俊：肝細胞癌の治療アルゴリズムー穿刺局所療法・TACE・化学療法ー. 特別企画2「日本肝臓学会ガイドラインup to date」B型肝炎治療ガイドライン，第53回日本肝臓学会総会，平成29年6月9日，広島国際会議場，広島。
  29. 永井知行，松井繁長，樫田博史，工藤正俊：抗血栓薬服用者の胃病変に対する内視鏡的治療の安全の評価検討. シンポジウム1「上部消化管内視鏡治療の現状と課題」，第98日本消化器内視鏡学会近畿支部例会，平成29年6月17日，神戸ポートピアホテル，兵庫。
  30. 岡元寿樹，米田頼晃，朝隈 豊，樫田博史，工藤正俊：大腸ESDにおける抗血栓薬の影響に関する検討. シンポジウム2「下部消化器内視鏡治療の現状と課題」，第98日本消化器内視鏡学会近畿支部例会，平成29年6月17日，神戸ポートピアホテル，兵庫。
  31. 三長孝輔，竹中 完，宮田 剛，樫田博史，工藤正俊：経乳頭処置困難総胆管結石症例に対するEUSガイド下治療の成績. ワークショップ1「Interventional EUSによる胆膵診療の現状と新たな展開」，第98日本消化器内視鏡学会近畿支部例会，平成29年6月17日，神戸ポートピアホテル，兵庫。
  32. 山雄健太郎，竹中 完，樫田博史，工藤正俊：当院におけるself-expandable metallic stent留置の工夫～BONASTENTの使用経験を添えて～. ビデオワークショップ「安全で確実なERCP関連処置を目指して一手技のコツからトラブルシューティングまで」，第98日本消化器内視鏡学会近畿支部例会，平成29年6月17日，神戸ポートピアホテル，兵庫。
  33. 今村修三，秦 康倫，岡崎典久，木下大輔，高山政樹，奥田英之，川崎俊彦，水野成人，工藤正俊，若狭朋子，太田善夫，盛田圭紀，石黒信吾，橋本恵介：内視鏡的粘膜下層剥離術にて切除した胃底腺胃癌の1例. Fresh Endoscopist Session 1 消化管1，第98日本消化器内視鏡学会近畿支部例会，平成29年6月17日，神戸ポートピアホテル，兵庫。

34. 河野辰哉, 松井繁長, 岡本彩那, 岡元寿樹, 河野匡志, 足立哲平, 米田頼晃, 永井知行, 朝隈 豊, 櫻井俊治, 渡邊智裕, 樫田博史, 工藤正俊: ESDを施行した胃低腺型胃癌の検討. Young Endoscopist Session 3 「胃」, 第98日本消化器内視鏡学会近畿支部例会, 平成29年6月17日, 神戸ポートピアホテル, 兵庫.
35. 高島耕大, 樫田博史, 朝隈 豊, 岡本彩那, 岡元寿樹, 河野匡志, 山田光成, 足立哲平, 米田頼晃, 櫻井俊治, 松井繁長, 渡邊智裕, 工藤正俊: 大腸早期印環細胞癌の一例. Young Endoscopist Session 7 「小腸・大腸」, 第98日本消化器内視鏡学会近畿支部例会, 平成29年6月17日, 神戸ポートピアホテル, 兵庫.
36. 中井敦史, 宮田 剛, 竹中 完, 大本俊介, 鎌田 研, 三長孝輔, 山雄健太郎, 樫田博史, 工藤正俊: SpyGlassTM DSを用いた電気水圧衝撃波結石破碎術 (EHL) が有用であった巨大総胆管結石の一例. Young Endoscopist Session 8 「胆道」, 第98日本消化器内視鏡学会近畿支部例会, 平成29年6月17日, 神戸ポートピアホテル, 兵庫.
37. 鎌田 研, 竹中 完, 山雄健太郎, 三長孝輔, 宮田 剛, 大本俊介, 今井 元, 工藤正俊: 胃全摘後の総胆管結石性胆管炎に対して超音波内視鏡下管内胆管空腸吻合術が有用であった一例. Fresh Endoscopist Session 4 「胆膵」, 第98日本消化器内視鏡学会近畿支部例会, 平成29年6月17日, 神戸ポートピアホテル, 兵庫.
38. 大塚康生, 鎌田 研, 竹中 完, 山雄健太郎, 三長孝輔, 宮田 剛, 大本俊介, 今井 元, 工藤正俊: 急性膵炎の経過中に来たした肝障害の原因精査に超音波内視鏡が有用であった一例. Fresh Endoscopist Session 4 「胆膵」, 第98日本消化器内視鏡学会近畿支部例会, 平成29年6月17日, 神戸ポートピアホテル, 兵庫.
39. 櫻井俊治, 工藤正俊, 有住忠明, 田北雅弘, 矢田典久, 萩原 智, 南 康範, 依田 広, 上嶋一臣, 西田直生志: STAT3制御分子に注目した肝細胞癌のソラフェニブ治療効果予測の可能性. プレナリーセッション1. 第16回日本肝がん分子標的治療研究会, 平成29年6月24日, ルネッサンスリゾートナルト, 徳島.
40. 南 康範, 工藤正俊: US-US overlay image fusionを用いたラジオ波焼灼術の有用性: 従来治療との比較. ワークショップ4 「肝癌治療におけるナビゲーションの有用性と将来性」, 第53回日本肝癌研究会, 平成29年7月6-7日, 京王プラザホテル, 東京.
41. 小川 力, 盛田真弘, 大村亜紀奈, 野田晃世, 出田雅子, 久保敦司, 石川哲朗, 松中寿浩, 玉置敬之, 柴峠光成, 工藤正俊: 鎮静下RFAにおける3D-GPS markerの使用経験と課題. ワークショップ4 「肝癌治療におけるナビゲーションの有用性と将来性」, 第53回日本肝癌研究会, 平成29年7月6-7日, 京王プラザホテル, 東京.
42. 上嶋一臣, 工藤正俊, 泉 並木, 角谷眞澄, 久保正二, 熊田 卓, 國土典宏, 高山忠利, 坂元亨宇, 中島 収, 松山 裕: Intermediate stage HCCの新しい亜分類と治療方針ー全国原発性肝癌追跡調査46997例の解析からー. パネルディスカッション1 「Intermediate stage肝癌の標準治療はなにか?: エビデンスとコンセンサス」, 第53回日本肝癌研究会, 平成29年7月6-7日, 京王プラザホテル, 東京.
43. 國土典宏, 工藤正俊, 長谷川潔: 第4版改訂のコンセプト. シンポジウム4 「肝癌診療ガイドライン第4版公聴会: エビデンスとコンセンサス」, 第53回日本肝癌研究会, 平成29年7月6-7日, 京王プラザホテル, 東京.
44. 海堀昌樹, 吉井健悟, 横田 勲, 長谷川潔, 高山忠利, 久保正二, 權 雅憲, 長島文夫, 泉 並木, 角谷眞澄, 工藤正俊, 熊田 卓, 坂元亨宇, 中島 収, 松山 裕, 國土典宏: 肝癌研究会追跡調査よりみた高齢肝細胞癌に対する外科的切除の意義. パネルディスカッション7 「超高齢者肝癌の治療 (切除か非切除か)」, 第53回日本肝癌研究会, 平成29年7月6-7日, 京王プラザホテル, 東京.
45. 國土貴嗣, 長谷川潔, 高山忠利, 泉 並木, 角谷眞澄, 工藤正俊, 久保正二, 坂元亨宇, 中島 収, 熊田 卓, 國土典宏: 肝静脈腫瘍栓合併肝細胞癌に対する外科的切除の意義の検討ー肝癌研究会追跡調査より. パネルディスカッション4 「高度進行肝細胞癌 (Vp3以上、Vv2以上) に対する集学的治療: エビデンスとコンセンサス」, 第53回日本肝癌研究会, 平成29年7月6-7日, 京王プラザホテル, 東京.

46. 三長孝輔, 竹中 完, 宮田 剛, 中井敦史, 大本俊介, 鎌田 研, 山雄健太郎, 今井 元, 渡邊智裕, 工藤正俊: EUSガイド下神経ブロックの成績と治療効果予測因子の検討. ビデオシンポジウム12「超音波内視鏡を用いた膵疾患診療ー基本から応用までー」, 第48回日本膵臓学会大会, 平成29年7月14-15日, 京都市勧業館みやこめっせ, 京都.
47. 竹中 完, 大本俊介, 三長孝輔, 鎌田 研, 宮田 剛, 山雄健太郎, 今井 元, 工藤正俊: 早期慢性膵炎のEUS所見の妥当性, 早期治療介入の意義について. パネルディスカッション1「慢性膵炎の進展予防を目的とした治療ーその適応と限界ー」, 第48回日本膵臓学会大会, 平成29年7月14-15日, 京都市勧業館みやこめっせ, 京都.
48. 竹中 完, 大本俊介, 三長孝輔, 鎌田 研, 宮田 剛, 山雄健太郎, 今井 元, 工藤正俊: 当院におけるWONに対するstep-up approachの検討. パネルディスカッション3「急性膵炎の後期合併症に対する手術・インターベンション治療の現状と課題」, 第48回日本膵臓学会大会, 平成29年7月14-15日, 京都市勧業館みやこめっせ, 京都.
49. 竹中 完, 大本俊介, 三長孝輔, 鎌田 研, 宮田 剛, 山雄健太郎, 今井 元, 工藤正俊: 慢性膵炎に対する経乳頭的金属ステント留置, 短期間抜去の有用性. ミニワークショップ3-1「肝疾患診療におけるERCPの役割を見直す」, 第48回日本膵臓学会大会, 平成29年7月14-15日, 京都市勧業館みやこめっせ, 京都.
50. 三長孝輔, 竹中 完, 宮田 剛, 中井敦史, 大本俊介, 鎌田 研, 山雄健太郎, 今井 元, 渡邊智裕, 工藤正俊: EUSガイド下神経ブロックの成績と治療効果予測因子の検討. ビデオシンポジウム12「超音波内視鏡を用いた膵疾患診療ー基本から応用までー」, 第48回日本膵臓学会大会, 平成29年7月14-15日, 京都市勧業館みやこめっせ, 京都.
51. 竹中 完, 大本俊介, 三長孝輔, 鎌田 研, 宮田 剛, 山雄健太郎, 今井 元, 工藤正俊: 早期慢性膵炎のEUS所見の妥当性, 早期治療介入の意義について. パネルディスカッション1「慢性膵炎の進展予防を目的とした治療ーその適応と限界ー」, 第48回日本膵臓学会大会, 平成29年7月14-15日, 京都市勧業館みやこめっせ, 京都.
52. 竹中 完, 大本俊介, 三長孝輔, 鎌田 研, 宮田 剛, 山雄健太郎, 今井 元, 工藤正俊: 当院におけるWONに対するstep-up approachの検討. パネルディスカッション3「急性膵炎の後期合併症に対する手術・インターベンション治療の現状と課題」, 第48回日本膵臓学会大会, 平成29年7月14-15日, 京都市勧業館みやこめっせ, 京都.
53. 竹中 完, 大本俊介, 三長孝輔, 鎌田 研, 宮田 剛, 山雄健太郎, 今井 元, 工藤正俊: 慢性膵炎に対する経乳頭的金属ステント留置, 短期間抜去の有用性. ミニワークショップ3-1「肝疾患診療におけるERCPの役割を見直す」, 第48回日本膵臓学会大会, 平成29年7月14-15日, 京都市勧業館みやこめっせ, 京都.
54. 松井繁長, 檜田博史, 工藤正俊: 巨木型食道静脈瘤に対するmodified EISL. ビデオワークショップ4「EISー私はこうしているー」, 第24回日本門脈圧亢進症学会総会, 平成29年9月14-15日, 東京コンベンションホール, 東京.
55. 中井敦史, 竹中 完, 宮田 剛, 工藤正俊: 膵胆道腫瘍のリンパ節転移診断における造影ハーモニックEUSの有用性. パネルディスカッション「胆膵疾患診療の最前線」, 日本消化器病学会近畿支部第107回例会, 平成29年9月23日, 大阪国際交流センター, 大阪.
56. 吉田晃浩, 山雄健太郎, 中井敦史, 大本俊介, 鎌田 研, 三長孝輔, 宮田 剛, 今井 元, 竹中 完, 檜田博史, 工藤正俊, 里井俊平, 松本逸平, 竹中宜典, 前西 修: 肝原発MCNと鑑別が困難であった腸間膜神経鞘腫の一例. Young Investigator Session 3 肝2, 日本消化器病学会近畿支部第107回例会, 平成29年9月23日, 大阪国際交流センター, 大阪.
57. 大賀智行, 宮田 剛, 竹中 完, 中井敦史, 三長孝輔, 鎌田 研, 山雄健太郎, 今井 元, 工藤正俊: 食道癌、肺癌、膵臓癌の異時性3重複癌の1例. Freshman Session 3 膵, 日本消化器病学会近畿支部第107回例会, 平成29年9月23日, 大阪国際交流センター, 大阪.
58. 久家沙希那, 永井知行, 松井繁長, 河野辰哉, 高島耕大, 木下 淳, 岡本彩那, 岡元寿樹, 石川 嶺, 山田光成, 河野匡志, 米田頼晃, 櫻井俊治, 渡邊智裕, 檜田博史, 工藤正俊: カテーテルアブレーション後に急性胃拡張を来した2例. Freshman Session 6 胃・十二指腸1, 日本消化器病学会近畿支部第107回例会, 平成29年9月23日, 大阪国際交流センター, 大阪.



59. 田中秀和, 鎌田 研, 三長孝輔, 竹中 完, 中井敦史, 大本俊介, 宮田 剛, 山尾健太郎, 今井元, 櫻井俊治, 西田直生志, 渡邊智裕, 樫田博史, 工藤正俊: Roux-en-Y 再建後の輸入脚狭窄に対してショートタイプシングルバルーン内視鏡を用いて消化管ステント留置術を行った1例. Yung Investigator Session10 胃・十二指腸3, 日本消化器病学会近畿支部第107回例会, 平成29年9月23日, 大阪国際交流センター, 大阪.
60. 米田頼晃, 樫田博史, 工藤正俊: 早期直腸癌に対する内視鏡治療について. パネルディスカッション「早期直腸がんに対する治療戦略」, 第72回日本大腸肛門病学会学術集会, 平成29年11月10-11日, 福岡.
61. 山雄健太郎, 竹中 完, 樫田博史, 工藤正俊: Stage 0, I 膵癌の発見におけるEUSの役割. ワークショップ2「胆膵癌の早期発見における内視鏡の役割」, 第99回日本消化器内視鏡学会近畿支部例会, 平成29年11月18日, 京都テルサ, 京都.
62. 山田信広, 米田頼晃, 三長孝輔, 河野辰哉, 高島耕太, 木下 淳, 石川 嶺, 岡本彩那, 岡元寿樹, 山田光成, 河野匡志, 永井知行, 櫻井俊治, 松井繁長, 渡邊智裕, 樫田博史, 工藤正俊: 超音波内視鏡下吸引細胞診 (EUS-FNA) にて診断に至ったスキルス胃癌の1例. Fresh Endoscopist Session 2「胃」, 第99回日本消化器内視鏡学会近畿支部例会, 平成29年11月18日, 京都テルサ, 京都.
63. 永井知行, 櫻井俊治, 樫田博史, 工藤正俊: 糞便移植を実施した潰瘍性大腸炎患者の2症例. パネルディスカッション2「下部消化管炎症性疾患の診断と治療」, 第99回日本消化器内視鏡学会近畿支部例会, 平成29年11月18日, 京都テルサ, 京都.
64. 田中秀和, 三長孝輔, 竹中 完, 鎌田 研, 中井敦史, 大本俊介, 宮田 剛, 山雄健太郎, 今井元, 渡邊智裕, 樫田博史, 工藤正俊, 榎木英介, 木村雅友: 術前診断が困難であり経口膵管鏡による直接生検で診断しえた膵神経内分泌癌の1例. Young Endoscopist Session 6「膵臓」, 第99回日本消化器内視鏡学会近畿支部例会, 平成29年11月18日, 京都テルサ, 京都.
65. 中野省吾, 松井繁長, 高島耕太, 河野辰哉, 石川 嶺, 岡元寿樹, 山田光成, 河野匡志, 木下淳, 米田頼晃, 永井知行, 朝隈 豊, 櫻井俊治, 渡邊智裕, 樫田博史, 工藤正俊: 止血に難渋した十二指腸静脈瘤出欠の1例. Fresh Endoscopist Session 5「十二指腸・小腸」, 第99回日本消化器内視鏡学会近畿支部例会, 平成29年11月18日, 京都テルサ, 京都.
66. 吉川馨介, 木下 淳, 櫻井俊治, 高島耕太, 河野辰哉, 石川 嶺, 岡本彩那, 河野匡志, 岡元寿樹, 山田光成, 永井知行, 米田頼晃, 松井繁長, 渡邊智裕, 樫田博史, 工藤正俊: 大網裂孔ヘルニアによるレイウスの1例. Fresh Endoscopist Session 5「十二指腸・小腸」, 第99回日本消化器内視鏡学会近畿支部例会, 平成29年11月18日, 京都テルサ, 京都.
67. 福永朋洋, 永井知行, 櫻井俊治, 岡元寿樹, 岡本彩那, 河野匡志, 山田光成, 米田頼晃, 松井繁長, 渡邊智裕, 樫田博史, 工藤正俊: 空腸穿通魚骨を小腸内視鏡にて除去し得た一例. Young Endoscopist Session 9「小腸・その他」, 第99回日本消化器内視鏡学会近畿支部例会, 平成29年11月18日, 京都テルサ, 京都.
68. 萩原 智: Naiveに対する各DAA治療不成功例の特徴. パネリスト. XIMENCY発売記念講演会 1st Announcement, 平成29年7月22日, 東京プリンスホテル, 東京.

## VIII. 学会発表 (国内一般演題)

1. 岡本彩那, 樫田博史, 米田頼晃, 岡元寿樹, 河野匡志, 足立哲平, 永井知行, 朝隈 豊, 櫻井俊治, 松井繁長, 渡邊智裕, 工藤正俊: 腸管症型T細胞リンパ腫の一例. 一般演題 小腸, 第106回日本消化器病学会近畿支部例会, 平成29年2月25日, 大阪国際交流センター, 大阪.
2. 國土貴嗣, 長谷川 潔, 松山 裕, 高山忠利, 泉 並木, 角谷真澄, 工藤正俊, 坂元亨宇, 中島収, 國土典宏: 血管腫瘍栓合併肝細胞癌に対する外科的切除の意義の検討-肝癌研究会追跡調査より. 第72回日本消化器外科学会総会, 平成29年7月20-22日, 金沢, 石川.
3. 西田直生志, 岩西美奈, 南 知宏, 千品寛和, 河野匡志, 有住忠晃, 田北雅弘, 矢田典久, 依田 広, 萩原 智, 南 康範, 上嶋一臣, 工藤正俊: Locked Nucleic Acidsを用いた血清中マイクロRNA定量とソラフェニブ治療に対する反応予測. 第15回日本肝がん分子標的治療研究会, 平成29年1月14日, イイノホール&カンファレンスセンター, 東京.



4. 盛田真弘, 小川 力, 川井伸彦, 三野 智, 野田晃世, 出田雅子, 久保敦司, 松中寿浩, 玉置敬之, 紫峠光成, 村川佳子, 日野賢志, 西田知紗, 横井靖世, 河合直之, 丸山哲夫, 木太秀行, 大西宏明, 工藤正俊: 造影USにて破裂性肝膿瘍が予測できた一例. 第30回日本腹部造影エコー・ドプラ診断研究会, 平成29年4月8日, 米子コンベンションセンター, 鳥取.
5. 川井伸彦, 小川 力, 三野 智, 盛田真弘, 野田晃世, 出田雅子, 久保敦司, 松中寿浩, 玉置敬之, 紫峠光成, 村川佳子, 日野賢志, 西田知紗, 横井靖世, 河合直之, 丸山哲夫, 木太秀行, 大西宏明, 工藤正俊: 造影USにて診断した虚血性鼠径ヘルニアの一例. 第30回日本腹部造影エコー・ドプラ診断研究会, 平成29年4月8日, 米子コンベンションセンター, 鳥取.
6. 小川 力, 川井伸彦, 三野 智, 盛田真弘, 野田晃世, 出田雅子, 久保敦司, 松中寿浩, 玉置敬之, 紫峠光成, 村川佳子, 日野賢志, 西田知紗, 横井靖世, 河合直之, 丸山哲夫, 木太秀行, 大西宏明, 工藤正俊: コンパニオン診断時代における造影USの役割とその啓蒙. 第30回日本腹部造影エコー・ドプラ診断研究会, 平成29年4月8日, 米子コンベンションセンター, 鳥取.
7. 岡元寿樹, 工藤正俊: 広範囲食道表在癌ESD 後の狭窄に対する治療成績の検討. 一般演題口演36 食道-狭窄2, 第93回日本消化器内視鏡学会総会, 平成29年5月11-13日, 大阪国際会議場・リーガロイヤルホテル, 大阪.
8. 辻直子, 川崎正憲, 梅原康湖, 松本望, 工藤正俊: 胃前庭部たこいぼびらんとH. pyloriの関連. 一般演題口演74 胃-HP関連, 第93回日本消化器内視鏡学会総会, 平成29年5月11-13日, 大阪国際会議場・リーガロイヤルホテル, 大阪.
9. 中井敦史, 山雄健太郎, 大本俊介, 鎌田研, 三長孝輔, 宮田剛, 今井元, 竹中 完, 松本逸平, 竹山宜典, 筑後孝章, 工藤正俊: 硬化性胆管炎と診断された膵癌、閉塞性黄疸の1例. 一般演題ポスター12 膵-症例, 第93回日本消化器内視鏡学会総会, 平成29年5月11-13日, 大阪国際会議場・リーガロイヤルホテル, 大阪.
10. 奥田英之, 高山政樹, 木下大輔, 秦 康倫, 岡崎能久, 川崎俊彦, 水野成人, 若狭朋子, 太田善夫, 工藤正俊: 当院における小児上部消化管内視鏡検査の現状. 一般演題講演92 胃-その他2, 第93回日本消化器内視鏡学会総会, 平成29年5月11-13日, 大阪国際会議場・リーガロイヤルホテル, 大阪.
11. 井本 勉, 天野恵介, 飯尾悦子, 勝島慎二, 米田俊貴, 福永豊和, 堀江 裕, 鄭 浩柄, 國立裕之, 金 秀基, 金 守良, 工藤正俊, 田中靖人: 散発性急性C型肝炎例に於ける血清type-1 IFN s 及びtype-3 IFN s 値の動態とその臨床的意義. セッション (一般公演), 第53回日本肝臓学会総会, 平成29年6月8-9日, 広島国際会議場, 広島.
12. 河野匡志, 西田直生志, 南 知宏, 千品寛和, 有住忠晃, 田北雅弘, 依田 広, 矢田典久, 南康範, 萩原 智, 上嶋一臣, 工藤正俊: DAA投与におけるSVR後のAFP及びALT異常値と関連する臨床背景の検討. セッション (一般公演), 第53回日本肝臓学会総会, 平成29年6月8-9日, 広島国際会議場, 広島.
13. 南 康範, 西田直生志, 工藤正俊: US-US overlay image fusionを用いたラジオ波焼灼術の有効性: 従来法と野比較. セッション (一般公演), 第53回日本肝臓学会総会, 平成29年6月8-9日, 広島国際会議場, 広島.
14. 鎌田 研, 竹中 完, 大本俊介, 宮田 剛, 三長孝輔, 山雄健太郎, 今井 元, 筑後孝章, 安田卓司, 工藤正俊: 造影ハーモニックEUSによる上部消化管粘膜下腫瘍の鑑別診断~EUS-FNA診断との併用~. 奨励賞演題「消化器 奨励賞」, 日本超音波医学会第90回学術集会, 平成29年5月26-28日, 栃木県総合文化センター, 宇都宮東武ホテルグランデ, ホテルニューイタヤ. 栃木.
15. 青木 琢, 窪田敬一, 松本尊嗣, 泉 並木, 角谷眞澄, 久保正二, 熊田 卓, 國土典宏, 坂元亨宇, 高山忠利, 中島 収, 松山裕, 工藤正俊: 肝細胞癌に対する肝切除における、surgical marginの意義の検討: 追跡調査データを用いた解析. 一般演題「肝切除(1)」, 第53回日本肝臓学会総会, 平成29年7月6-7日, 京王プラザホテル, 東京.
16. 竹中 完, 山雄健太郎, 鎌田 研, 三長 孝輔, 宮田 剛, 今井 元, 松本逸平, 竹山宜典, 前西 修, 工藤正俊: 術前に肝原発嚢胞性病変が疑われた腸間膜由来神経鞘腫の1例. 口演20 肝・その他, 第67回日本消化器画像診断研究会, 平成29年9月15-16日, 札幌プリンスホテル国際館パミール, 北海道.

17. 横川美香, 前野知子, 市島真由美, 塩見香織, 前川 清, 依田 広, 南 康範, 工藤正俊: FNHのLMI-THI造影の検討. 一般演題9「消化器3(造影)」, 日本超音波医学会第44回関西地方会学術集会, 第21回関西地方講習会, 平成29年9月23日, 大阪国際会議場(グランキューブ大阪), 大阪.
18. 永井知行, 松井繁長, 岡本彩那, 岡元寿樹, 河野匡志, 山田光成, 米田頼晃, 櫻井俊治, 渡邊智裕, 樫田博史, 工藤正俊: 抗血栓薬服用者に対する胃病変のESD/EMRの安全性評価検討. 第94回日本消化器内視鏡学会総会 Japanese Digestive Disease Week (JDDW) 2017 Fukuoka, 平成29年10月12-15日, 福岡.
19. 岡元寿樹, 米田頼晃, 樫田博史, 岡本彩那, 河野匡志, 永井知行, 櫻井俊治, 松井繁長, 渡邊智裕, 工藤正俊: 抗血栓薬内服での大腸ESDにおける検討. 第59回日本消化器病学会大会 Japanese Digestive Disease Week (JDDW) 2017 Fukuoka, 平成29年10月12-15日, 福岡.
20. 木下大輔, 秦 康倫, 岡崎能久, 高山政樹, 奥田英之, 川崎正憲, 水野成人, 川崎俊彦, 若狭朋子, 太田善夫, 工藤正俊, 森田圭紀: ESDにより切除しえた、巨大直腸腫瘍の1例. 一般演題「大腸2」, 第99回日本消化器内視鏡学会近畿支部例会, 平成29年11月18日, 京都テルサ, 京都.
21. 岡本彩那, 田北雅弘, 半田康平, 高田隆太郎, 福永朋洋, 南 知宏, 河野匡志, 千品寛和, 有住忠晃, 南 康範, 依田 広, 櫻井俊治, 上嶋一臣, 西田直生志, 工藤正俊: リザーバー留置後に十二指腸よりカテーテルの逸脱を認めた一例. 一般演題「十二指腸・小腸」, 第99回日本消化器内視鏡学会近畿支部例会, 平成29年11月18日, 京都テルサ, 京都.
22. 河野匡志, 西田直生志, 千品寛和, 南 知宏, 有住忠晃, 田北雅弘, 矢田典久, 萩原 智, 南 康範, 上嶋一臣, 工藤正俊: DAA投与におけるSVR後のAFP異常値と関連する臨床背景の検討. 一般演題, 第42回日本肝臓学会西部会, 平成29年11月30日, ヒルトン福岡シーホーク, 福岡.
23. 福永朋洋, 萩原 智, 半田康平, 高田隆太郎, 岡本彩那, 南 知宏, 河野匡志, 千品寛和, 有住忠晃, 田北雅弘, 南 康範, 依田 広, 上嶋一臣, 西田直生志, 工藤正俊: 胃への遠隔転移を認めた肝細胞癌の一例. 若手医師症例報告奨励賞, 第42回日本肝臓学会西部会, 平成29年11月30日, ヒルトン福岡シーホーク, 福岡.
24. 高田隆太郎, 萩原 智, 福永朋洋, 半田康平, 岡本彩那, 南 知宏, 河野匡志, 千品寛和, 有住忠晃, 田北雅弘, 南 康範, 依田 広, 上嶋一臣, 西田直生志, 工藤正俊: 真性多血症にBudd-Chiari症候群を伴った1例. 若手医師症例報告奨励賞, 第42回日本肝臓学会西部会, 平成29年11月30日, ヒルトン福岡シーホーク, 福岡.
25. 半田康平, 萩原 智, 福永朋洋, 高田隆太郎, 岡本彩那, 南 知宏, 河野匡志, 千品寛和, 有住忠晃, 田北雅弘, 南 康範, 依田 広, 上嶋一臣, 西田直生志, 工藤正俊: 腹壁静脈瘤破裂に対し直接穿刺にて硬化療法を施行した2例. 若手医師症例報告奨励賞, 第42回日本肝臓学会西部会, 平成29年11月30日, ヒルトン福岡シーホーク, 福岡.
26. 工藤正俊: 急激に変貌する肝癌の薬物療法: 免疫療法を含めて. 講演II. 中・四国肝疾患研究会, 平成29年12月28日, JRホテルクレメント高松, 香川.
27. 樫田博史: ～知っておきたい～ちょっと珍しい上部消化管病変. 堺市医師会消化器談話会, 平成29年1月14日, 大阪.
28. 萩原 智: 当院におけるDAAs治療成績. エレルサ®・グラジナ®発売記念講演会in南大阪, 平成29年2月18日, シェラトン都ホテル大阪, 大阪.
29. 上嶋一臣: 肝細胞癌の集学的治療～肝硬変のマネジメントの重要性を含めて～. 肝疾患治療セミナー, 肝疾患とかゆみ, 平成29年2月18日, 大阪.
30. 上嶋一臣: 肝細胞癌の集学的治療～肝硬変のマネジメントから肝細胞癌の最新治療まで～, レミッチェリアフォーラムin南大阪, 平成29年2月23日, 大阪.
31. 樫田博史: 大腸がんに関する地域連携の在り方. 平成28年度近畿大学医学部附属病院「がん診療連携医の会」, 平成29年3月11日.
32. 松井繁長: GERDの現状と今後の展望. 東牟婁郡医師会学術講演会. 平成29年3月30日, くしもと町立病院, 和歌山.
33. 萩原 智: 当院におけるDAAs治療成績. 第13回Kinki Liver Club, 平成29年3月31日, スイスホテル南海大阪, 大阪.
34. 上嶋一臣: ここまできた肝細胞癌の化学療法～分子標的薬の現状と免疫チェックポイント阻害剤

- に対する期待～. 第13回Kinki Liver Club, 平成29年3月31日, スイスホテル南海大阪, 大阪.
35. 岡元寿樹, 松井繁長, 樫田博史, 河野匡志, 山田光成, 足立哲平, 永井知行, 朝隈 豊, 米田頼晃, 櫻井俊治: 広範囲食堂表在癌ESD後の狭窄に対する治療成績の検討. 一般演題 口演36「食道-狭窄2」. 第93回日本消化器内視鏡学会総会, 平成29年5月11-13日, 大阪国際会議場, リーガロイヤルホテル, 大阪.
  36. 根本大樹, 樫田博史, 富樫一智: BLI拡大大腸内視鏡におけるJNET分類とNICE分類: 大腸T1b癌の読影試験からの考察. 一般演題 ポスター55「大腸-診断」. 第93回日本消化器内視鏡学会総会, 平成29年5月11-13日, 大阪国際会議場, リーガロイヤルホテル, 大阪.
  37. 岡部義信, 竹中 完: ザ・プラスチックテント -Future&Past-. スポンサーイベント「モーニングセミナー4」. 第93回日本消化器内視鏡学会総会, 平成29年5月11-13日, 大阪国際会議場, リーガロイヤルホテル, 大阪.
  38. 中井陽介, 竹中 完: ザ胆膵手術を極める... 結石除去&ドレナージデバイス進化と特性. スポンサーイベント「ランチョンセミナー13」. 第93回日本消化器内視鏡学会総会, 平成29年5月11-13日, 大阪国際会議場, リーガロイヤルホテル, 大阪.
  39. 土田幸平, 岩下拓司, 渋谷悟朗, 井上宏之, 鎌田 研: 膵腫瘍性病変に対する新規のcore biopsy needleを用いたEUS-FNAにおける組織診断能の検討. 一般演題 ポスター48「膵-EUS-FNA」. 第93回日本消化器内視鏡学会総会, 平成29年5月11-13日, 大阪国際会議場, リーガロイヤルホテル, 大阪.
  40. 樫田博史: 中継先及び術者;ライブ中継「消化管セッション」. 第93回日本消化器内視鏡学会総会, 平成29年5月11-13日, 大阪国際会議場, リーガロイヤルホテル, 大阪.
  41. 岡元寿樹, 松井繁長, 樫田博史, 河野匡志, 山田光成, 足立哲平, 永井知行, 朝隈豊, 米田頼晃, 櫻井俊治: 広範囲食道表在癌 ESD後の狭窄に対する治療成績の検討. 第93回日本消化器内視鏡学会総会, 平成29年5月11-13日, 大阪国際会議場, リーガロイヤルホテル, 大阪.
  42. 斎藤 豊, 松田尚久, 中島 健, 坂本 琢, 山田真善, 高丸博之, The Japan NBI Expert Team (JNET: 斎藤 豊 松田尚久 中島 健 坂本 琢 斎藤彰一 池松弘朗 和田祥城 岡 志郎 河野弘志 佐野 寧 田中信治 藤井隆広 工藤進英 浦岡俊夫 小林 望 中村尚志 堀田欣一 堀松高博 坂本直人 傳 光義 鶴田 修 樫田博史 竹内洋司 町田浩久 日下利広 吉田直久 平田一郎 寺井 毅 山野泰穂 金子和弘 山口裕一郎 玉井尚人 中野(丸山)尚子 林 奈那 岩館峰雄 石川秀樹 吉田茂昭): 基調講演 The Japan NBI Expert Team(JNET)大腸拡大 Narrow Band Imaging(NBI)分類の紹介. パネルディスカッション「大腸拡大 JNET 分類の有用性と今後の課題」, 第93回日本消化器内視鏡学会総会, 平成29年5月11-13日, 大阪国際会議場・リーガロイヤルホテル, 大阪.
  43. 根本大樹, 樫田博史, 富樫一智: BLI 拡大大腸内視鏡における JNET 分類と NICE 分類: 大腸 T1b 癌の読影試験からの考察. 第93回日本消化器内視鏡学会総会, 平成29年5月11-13日, 大阪国際会議場・リーガロイヤルホテル, 大阪.
  44. 樫田博史: ライブデモンストレーション演者. 第93回日本消化器内視鏡学会総会, 平成29年5月11-13日, 大阪国際会議場・リーガロイヤルホテル, 大阪.
  45. 依田 広: C型肝炎に対するダクラタスビル・アスナプレビル併用療法後のSVR後肝発癌についての検討. 第2回関西肝疾患フォーラム, 2017年5月20日, 帝国ホテル大阪, 大阪.
  46. 松井繁長: GERD診療における現状と今後の展望. 2017年近畿大学医学部同窓会大阪市支部学術講演会, 平成29年5月20日, スイスホテル南海大阪, 大阪.
  47. 萩原 智: 高岡美樹のべっぴんラジオ「C型肝炎について病気や新しい治療をテーマにお届けします。」. ラジオ大阪, 平成29年6月6日.
  48. 南 康範: Precision RFAを目指して～可変型電極ができること～. ランチョンセミナー11「これからのRFA治療～可変型電極がもたらすinnovation～」. 第53回日本肝臓学会総会, 平成29年6月8日, リーガロイヤルホテル広島, 広島.
  49. 櫻井俊治: 潰瘍性大腸炎・クローン病ってどんな病気? 市民公開講座, 平成29年6月3日, プリメールアートホール, 大阪.
  50. 松井繁長: 吐下血について. 平成29年度救急講演会, 平成29年6月20-21日, 近畿大学医学部付属



病院円形棟小講堂，大阪。

51. 松井繁長：十二指腸静脈瘤に対するアプローチ．第26回近畿食道・胃静脈瘤研究会，平成29年6月24日，AP大阪梅田，大阪。
52. 上嶋一臣：TACE不応の見極めの重要性～分子標的療法・肝動注化学療法移行へのベストタイミング～．HCC 分子標的治療 Forum in 大分，平成29年6月30日，大分。
53. 松井繁長：抗血栓薬による消化管粘膜傷害について．第I部消化管領域，Stroke Prevention in Atrial Fibrillation Forum in OSAKA，平成29年7月1日，セントレジスホテル大阪，大阪。
54. 松井繁長：基調講演「GERD診療の最新話題」．第19回近畿超音波内視鏡研究会クリニカルカンファレンス，平成29年7月1日，AP大阪梅田茶屋町，大阪。
55. 萩原 智：C型肝炎治療のピットフォール．Smart Life Symposium in 多治見．平成29年7月5日，オースタット国際ホテル多治見，滋賀。
56. 上嶋一臣：PD1-5 Intermediate stage HCCの新しい亜分類と治療方針ー全国原発性肝癌追跡調査46997例の解析からー．パネルディスカッション1 「Intermediate stage肝癌の標準治療はなにか？：エビデンスとコンセンサス」，第53回日本肝癌研究会，平成29年7月6日，東京。
57. 樫田博史：大腸疾患最近の話題～便通異常から大腸癌まで～．八尾市医師会学術講演会，平成29年7月8日。
58. 上嶋一臣：高度脈管侵襲（Vp3, 4）を伴う肝細胞癌に対する治療選択～内科の立場から～第17回関西肝血流動態・機能イメージ研究会III. [Debate session] 平成29年7月8日，大阪。
59. 依田 広：C型肝炎に対するDAA投与後SVR後初発肝発癌についての検討．第17回関西肝血流動態・機能イメージ研究会，平成29年7月8日，梅田スカイビル，大阪。
60. 萩原 智：C型肝炎治療のピットフォール～より安全に確実にSVRを目指すために～．G-STATION-Lecture-，WEB講演会，平成29年7月13日。
61. 上嶋一臣：Sorafenib - Regorafenib sequential therapyを見据えたTACE不応の見極め．鹿児島肝癌分子標的治療研究会，平成29年7月14日，鹿児島。
62. 上嶋一臣：TACE不応の見極めの重要性～分子標的療法・肝動注化学療法移行へのベストタイミング～．島根HCC治療セミナー，平成29年7月19日，島根。
63. 上嶋一臣：Sorafenib-Regorafenib sequential therapyを見据えたTACE不応の見極め治療戦略．大阪市立大学関連Nexavar HCC 講演会，平成29年7月20日，大阪。
64. 樫田博史：ライブデモンストレーション演者．第1回 和歌山消化器内視鏡ライブデモンストレーションコースきのくにライブ，平成29年7月27日，和歌山。
65. 萩原 智：室臨床におけるエレルサ®/グラジナ®の使用成績．肝炎インターネット講演会．平成29年8月9日。
66. 樫田博史：Kindai Univ. ESD/EMR Hands-on Seminar，平成29年8月20日，大阪。
67. 松井繁長：治療に難渋した食道気管支瘻の1例．症例から学ぶ．第9回南大阪消化器疾患“なんでも相談”会，平成29年8月31日，スイスホテル南海大阪，大阪。
68. 上嶋一臣：リザーバー研究会主導臨床研究の提案．特別企画「リザーバー動注化学療法のいままでそしてこれから」．第42回リザーバー研究会，平成29年9月1-2日，高野山大学松下講堂・黎明館，和歌山。
69. 上嶋一臣：肝細胞癌に対する分子標的薬・免疫チェックポイント阻害剤治療の進歩～肝動注化学療法はどうなるの？～．イブニングセミナー．第42回リザーバー研究会，平成29年9月1-2日，高野山大学松下講堂・黎明館，和歌山。
70. 南 康範：Ablative margin の可視化：Hepatic GuideとUS-US overlay fusionの有用性．ランチョンセミナー1．日本超音波医学会 第53回中国地方会学術集会，第16回中国地方会講習会，平成29年9月2日，倉敷市芸文館，岡山。
71. 上嶋一臣：肝炎・肝硬変・肝細胞癌の薬物療法～DAAから分子標的薬、免疫チェックポイント阻害薬まで～．福井肝臓懇話会，平成29年9月6日，福井。
72. 上嶋一臣：肝細胞癌の集学的治療～肝硬変のマネジメントから肝細胞癌の最新治療まで～肝疾患と痒みエリアフォーラムin上本町「慢性肝疾患患者のQOL向上を目指して」平成29年9月8日，大阪。

73. 上嶋一臣：肝細胞癌に対する分子標的薬の現状～Sequential therapyの意義～. 第17回肝疾患フォーラム学術集会, 平成29年9月9日, 大阪.
74. 萩原 智：ハーボニー配合錠の心・腎・肝機能への影響. G-STATION-Lecture-, WEB講演会, 平成29年9月13日.
75. 上嶋一臣：ソラフェニブ・レゴラフェニブSequential Therapyが臨床に与えるインパクト. NEXT Symposium, 平成29年9月16日.
76. 萩原 智：講演I「TAF（テノホビルアラフェナミド）の初期使用経験について」. 第2回南大阪肝疾患診療連携セミナー, 平成29年9月21日, スイスホテル南海大阪, 大阪
77. 上嶋一臣：講演II「肝細胞癌薬物療法のパラダイムシフト～分子標的薬・免疫チェックポイント阻害剤の登場により治療体系がどう変わるか～」. 第2回南大阪肝疾患診療連携セミナー, 平成29年9月21日, スイスホテル南海大阪, 大阪.
78. 上嶋一臣：症例提示 レゴラフェニブの導入時期 Expert Summit Meeting 2017 Regorafenib HCC 2nd line, 平成29年9月23日, 東京.
79. 上嶋一臣：進行肝細胞癌に対する治療戦略～全身化学療法時代における局所療法の位置づけ～. 第3回山口県肝臓癌研究会, 平成29年9月29日, 山口.
80. 榎田博史：教育講演「炎症性腸疾患における内視鏡診断」, 第31回日本臨床内科医学会, 平成29年10月8-9日, 大阪.
81. 榎田博史：基調講演. 前回のJGES Core Session の報告. ワークショップ「Innovative therapeutic endoscopy大腸 ESD/EMRの課題と将来展望」, 第94回日本消化器内視鏡学会総会（第59回日本消化器病学会大会、第15回日本消化器外科学会大会）Japanese Digestive Disease Week (JDDW) 2017 Fukuoka, 平成29年10月12-15日, 福岡.
82. 上嶋一臣：Intermediate～Advanced stage HCCの治療戦略-分子標的療法・肝動注化学療法移行へのベストタイミング-. 阪神HCC治療研究会, 平成29年10月27日, 兵庫
83. 松井繁長：GERD診療における現状と今後の展望. 大阪狭山市地域連携講演会, 平成29年10月28日, 大阪.
84. 萩原 智：講演I 肝臓領域. 大阪和歌山消化器疾患カンファレンス, 平成29年11月3日, 和歌山.
85. 上嶋一臣：講演I 肝臓領域. 大阪和歌山消化器疾患カンファレンス, 平成29年11月3日, 和歌山.
86. 鎌田 研：講演II 胆膵領域. 大阪和歌山消化器疾患カンファレンス, 平成29年11月3日, 和歌山.
87. 上嶋一臣：Intermediate～Advanced stage HCCの治療戦略-Sorafenib-Regorafenib sequential therapyを見据えた治療の組み立て-. 肝臓NEXT Symposium in 浜松, 平成29年11月15日, 静岡.
88. 上嶋一臣：Intermediate～Advanced stage HCCの治療戦略 -Sorafenib-Regorafenib sequential therapyを見据えた治療の組み立て- 北摂肝臓治療研究会, 平成29年11月17日. 大阪.
89. 上嶋一臣：肝細胞癌の集学的治療～肝硬変のマネジメントから肝細胞癌の最新治療まで～. 第105回さがみりばーカンファレンス, 平成29年11月20日, 神奈川
90. 上嶋一臣：肝細胞癌に対する化学療法の進歩と支持療法の重要性. ランチョンセミナー6「病態に応じた肝疾患のトータルケア」, 第42回日本肝臓学会西部会, 平成29年11月30日, 福岡.
91. 萩原 智：ウイルス性肝炎の最新情報. 大阪狭山市医師会学術講演会. 平成29年12月6日, 旧狭山美原医療保険センター, 大阪.
92. 米田頼晃：当院におけるUCとCDの治療連携, 大阪IBDネットワーク, 平成29年12月9日, ホテル・アゴーラ リージェンシー堺, 大阪
93. 上嶋一臣、千品 寛： 進行肝細胞癌患者に対するニボルマブの第I/II相試験（CheckMate040試験）監訳 GI cancer-net 消化器癌治療の広場<<http://www.gi-cancer.net/gi/>>.



別刷

# Stress Response Protein RBM3 Promotes the Development of Colitis-associated Cancer

Toshiharu Sakurai, MD,\* Hiroshi Kashida, MD,\* Yoriaki Komeda, MD,\* Tomoyuki Nagai, MD,\* Satoru Hagiwara, MD,\* Tomohiro Watanabe, MD,\* Masayuki Kitano, MD,\* Naoshi Nishida, MD,\* Jun Fujita, MD,<sup>†,‡</sup> and Masatoshi Kudo, MD\*

**Background:** Colitis-associated cancer (CAC) is caused by chronic intestinal inflammation and often results from refractory inflammatory bowel disease (IBD). Stress response proteins Cirp and HSPA4 are involved in the refractory clinical course and development of CAC. RNA-binding motif protein 3 (RBM3) is induced in response to various stresses and is upregulated in several cancers. However, the role of RBM3 in CAC is unclear.

**Methods:** We assessed RBM3 expression and function in 263 human intestinal mucosa samples from patients with IBD and in *Rbm3*-deficient (*Rbm3*<sup>-/-</sup>) mice.

**Results:** Expression of RBM3 was correlated with the expression of stress response proteins Cirp, HSPA4, and HSP27 in the colonic mucosa of patients with IBD. Significant correlation was observed between the expression of RBM3 and that of Bcl-xL or stem cell markers. RBM3 expression increased and significantly correlated with R-spondin expression in the colonic mucosa of patients with refractory IBD, a condition associated with increased cancer risk, and RBM3 was overexpressed in human CACs. In the murine CAC model, *Rbm3* deficiency decreased R-spondin and Bcl-xL expression and increased apoptotic cell number in the colonic mucosa, leading to reduced tumor multiplicity. Transplantation of wild-type and *Rbm3*<sup>-/-</sup> bone marrow did not alter tumor burden, indicating the importance of RBM3 in epithelial cells.

**Conclusions:** Our findings indicated that RBM3 was required for efficient inflammatory carcinogenesis in the murine CAC model and suggested that RBM3 could be a predictive biomarker of CAC risk and a new therapeutic target for cancer prevention in patients with IBD.

(*Inflamm Bowel Dis* 2017;23:57–65)

**Key Words:** Bcl-xL, inflammatory bowel disease, R-spondin, CD133

Chronic intestinal inflammation, as that observed in patients with inflammatory bowel disease (IBD), is a risk factor of colitis-associated cancer (CAC).<sup>1,2</sup> IBD comprises Crohn's disease (CD) and ulcerative colitis (UC) and is characterized by marked infiltration of inflammatory cells into the affected mucosa. However, mechanisms underlying the pathogenesis of CAC are poorly understood. Previously, we found that induction of stress response proteins Cirp and heat shock protein A4

(HSPA4) in patients with long-standing inflammation of the mucosa promoted the development of refractory colitis and CAC.<sup>3,4</sup> A recent study showed that Cirp is released into the circulation.<sup>5</sup> Analysis of serum Cirp levels may increase the identification rate of patients who are at a high risk of developing CAC and hepatocellular carcinoma.<sup>3,6</sup> Moreover, HSPA4 expression could predict poor therapeutic response of patients with IBD to steroids.<sup>4</sup> These data suggest that long-term inflammation induces treatment resistance, refractory clinical course, and eventually cancer through the stress response of host.

Crypt stem cells represent the cells of origin of intestinal neoplasias. Both mouse and human intestinal stem cells can be cultured in a medium containing stem cell-specific factors, such as R-spondin and Noggin, over long periods to produce epithelial organoids that remain genetically and phenotypically stable.<sup>7</sup> Colorectal cancers arise from the loss of homeostasis of the intestinal epithelium and hyperproliferation of the crypt epithelium. Kim et al<sup>8</sup> showed that R-spondin induced hyperproliferation of the crypt epithelium in mice. Consistently, R-spondin has been reported to promote the development of colorectal cancer.<sup>9</sup> Endogenous R-spondin is mainly localized in intestinal epithelial cells.<sup>10</sup>

Similar to Cirp and HSPA4, RNA-binding motif protein 3 (RBM3) is induced under various conditions, including hypoxia

Supplemental digital content is available for this article. Direct URL citations appear in the printed text and are provided in the HTML and PDF versions of this article on the journal's Web site (<http://www.ibdjournal.org>).

Received for publication May 19, 2016; Accepted September 28, 2016.

From the \*Department of Gastroenterology and Hepatology, Faculty of Medicine, Kindai University, Osaka-Sayama, Japan; †Department of Clinical Molecular Biology, Graduate School of Medicine, Kyoto University, Kyoto, Japan; and ‡Kaifukuki Rehabilitation Ward, Biwako-Chuo Hospital, Otsu, Japan.

Supported by grants from the Japan Foundation for Research and Promotion of Endoscopy, the Japan Society of Gastroenterology, a Grant-in-Aid for Scientific Research (26460979), and Health Labour Sciences Research Grant.

The authors have no conflict of interest to disclose.

Reprints: Toshiharu Sakurai, MD, Department of Gastroenterology and Hepatology, Kindai University, 377-2 Ohno-Higashi, Osaka-Sayama, Osaka 589-8511, Japan (e-mail: sakurai@med.kindai.ac.jp).

Copyright © 2016 Crohn's & Colitis Foundation of America, Inc.

DOI 10.1097/MIB.0000000000000968

Published online 7 December 2016.



and cold stress<sup>11,12</sup> and is upregulated in several cancers.<sup>13–15</sup> In the present study, we examined whether RBM3 was involved in the tumorigenesis of CAC by using human colonic tissue samples and *Rbm3*-deficient (*Rbm3*<sup>−/−</sup>) mice and found that RBM3 promoted colorectal tumorigenesis by inhibiting apoptosis and by increasing R-spondin expression in the gut. In patients with IBD, refractory inflammation was associated with increased RBM3 expression in the colonic mucosa, which enhanced the risk of CAC. To the best of our knowledge, this is the first study on RBM3 as a possible regulator of tumorigenesis in patients with IBD.

## MATERIALS AND METHODS

### Human Tissue Samples

In all, 263 intestinal mucosa samples from patients with IBD (36 patients with CD and 209 patients with UC) and 18 normal colonic mucosa samples from patients without IBD were obtained endoscopically at Kindai University Hospital between January 2011 and March 2014. The study participants comprised 38 patients in remission and 207 patients with active IBD, including 100 patients with refractory IBD. The tissue samples were collected from involved areas of the intestine. Active inflammation was defined as a Mayo endoscopic score of  $\geq 2$  in patients with UC and presence of ulcers in patients with CD or presence of symptoms. Patients with refractory IBD were defined as those with active IBD for  $>6$  months at the time of biopsy. Colonic mucosae surrounding colonic tumors that were endoscopically resected were used as control mucosae in Figure 4A. CAC specimens were obtained from 10 patients who had undergone surgery. Informed consent for utilization of the tissue samples for analysis was obtained from all the patients. All study protocols conformed to the ethical guidelines of the Declaration of Helsinki (1975) and were approved by the appropriate institutional review boards.

### Mice and Treatment

*Rbm3*<sup>−/−</sup> mice were obtained from Prof. Tadatsugu Taniguchi of the University of Tokyo. Sex- and age-matched C57BL/6:129P *Rbm3*<sup>−/−</sup> mice and their wild-type (WT) littermates (age, 8–12 weeks) received 2.5% (wt/vol) dextran sodium sulfate (DSS; molecular weight, 36–50 kDa; MP Biomedicals, Solon, OH) in drinking water for 7 days. For developing the murine model of CAC, the mice were intraperitoneally injected with 12.5 mg/kg azoxymethane (AOM; Sigma-Aldrich, Tokyo, Japan). After 5 days, the mice were given drinking water containing 2.0% DSS for 5 days, followed by regular water for 16 days. This cycle was repeated 3 times. Next, the mice were given drinking water containing 1.5% DSS for 4 days, followed by regular water for 7 days. After euthanization, the colon was excised from the ileocecal junction to the anus, cut longitudinally, and prepared for histological evaluation. Inflammatory cell infiltration score and epithelial injury score were assessed as described previously.<sup>3</sup> Bone marrow transplantation experiments were

performed as described previously,<sup>3</sup> with slight modifications. Bone marrow (BM) from the tibia and femur was washed twice in Hanks balanced salt solution, and  $10^7$  BM cells were injected into the tail vein of lethally irradiated (11 Gy) recipient mice. All animal procedures were performed in accordance with approved protocols and with the recommendations for the proper care and use of laboratory animals. This study was approved by the Medical Ethics Committee of the Faculty of Medicine, Kindai University.

### Biochemical and Immunohistochemical Analyses

Quantitative polymerase chain reaction, immunoblotting, and immunohistochemical analysis were performed as described previously.<sup>3,4,16</sup> Primer sequences for quantitative polymerase chain reaction are given in Table 1 (Supplemental Digital Content 1, <http://links.lww.com/IBD/B381>). The following antibodies were used for performing immunoblotting: anti- $\beta$ -actin antibody (Sigma-Aldrich) and anti-Bcl-xL antibody (Cell Signaling, Danvers, MA). Anti-RBM3 polyclonal antibody was developed as described previously.<sup>11</sup> Immunohistochemical analysis was performed using ImmPRESS reagents (Vector Laboratory, Burlingame, CA), according to the manufacturer's recommendations. Apoptosis in paraffin-embedded tissue sections was determined by performing immunofluorescent TdT-mediated dUTP nick-end labeling (TUNEL) assay with In Situ Apoptosis Detection Kit (Takara, Tokyo, Japan) and a confocal laser microscope (FluoView FV10i; Olympus, Tokyo, Japan), according to the manufacturer's instructions. Nuclei were stained with 4,6'-diamidino-2-phenylindole to count the total number of cells per crypt. A minimum of 10 crypts with a normal morphology were counted per section. TUNEL-positive crypts were counted from 100 randomly selected crypts.

### Statistical Analysis

Differences were analyzed using Student's *t* test, and relationship between the expression of several genes was analyzed using Spearman's rank correlation test. Variables of more than 2 conditions were compared using analysis of variance and post hoc Tukey–Kramer honestly significant difference multiple comparison test.  $P < 0.05$  was considered statistically significant.

## RESULTS

### RBM3 Expression Is Significantly Correlated with Bcl-xL and Stem Cell Marker Expression in the Colonic Mucosa of Patients with IBD

Long-standing intestinal inflammation increases the expression of cold-inducible proteins, such as Cirp and HSPA4, in the colonic mucosa of patients with IBD.<sup>3,4</sup> Because RBM3 is also induced by cold shock, we examined the association between the expression of RBM3 and that of other stress response proteins. RBM3 expression was significantly correlated with HSPA4, Cirp, and HSP27 expression (linear coefficients of

0.67, 0.58, and 0.52, respectively) in the colonic mucosa of patients with UC (Fig. 1A–C). Like Cirp and HSPA4, RBM3 expression was also correlated with Bcl-2 and Bcl-xL expression (Fig. 1D, E).

Cirp and HSPA4 increase the number of Sox2-positive cells in the chronically inflamed colon.<sup>3,4</sup> Moreover, expression of Cirp and HSPA4 is correlated with that of several stem cell markers such as Sox2 and Lgr5 in patients with IBD.<sup>3,4</sup> RBM3 increases stem cell characteristics of colorectal cancer cells.<sup>15</sup> Expectedly, we observed that RBM3 expression was significantly correlated with Sox2 and Lgr5 expression in the colonic mucosa of patients with UC and CD (Fig. 2). These data suggested that RBM3 functioned as a tumor promoter similar to stress response proteins Cirp and HSPA4.

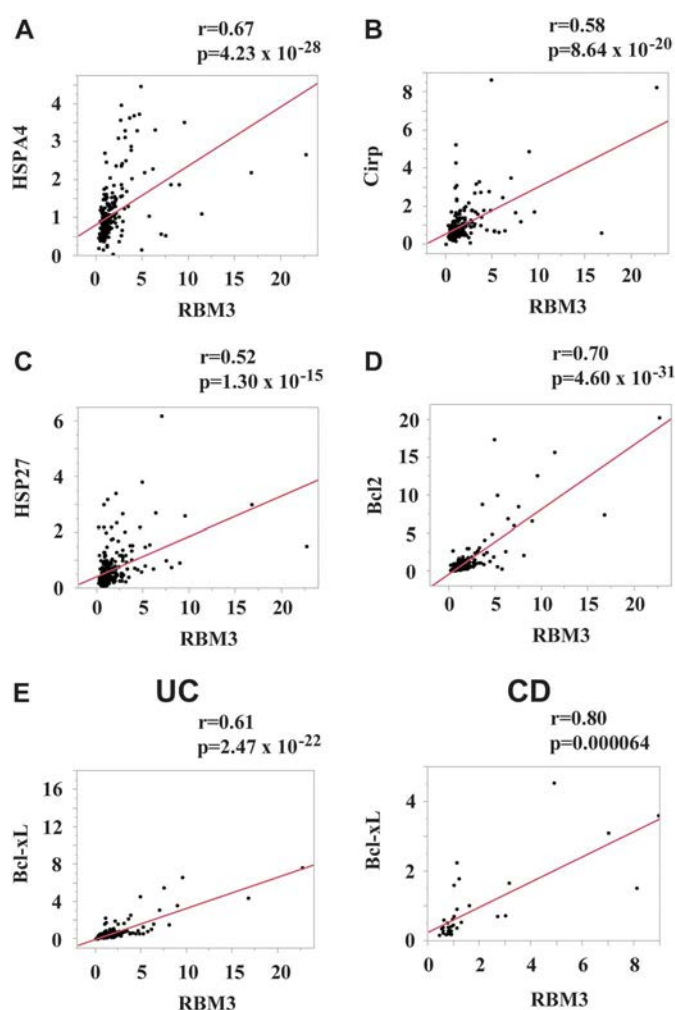


FIGURE 1. A–D, Association between RBM3 and other stress response proteins in the colonic mucosa of patients with UC. E, Association between RBM3 and Bcl-xL in the colonic mucosa of patients with UC and CD. Scatter plot of relative messenger RNA levels of *RBM3* and the indicated genes in the human colonic mucosa. The messenger RNA level of each gene in the normal colon of an individual without IBD was given an arbitrary value of 1.0.

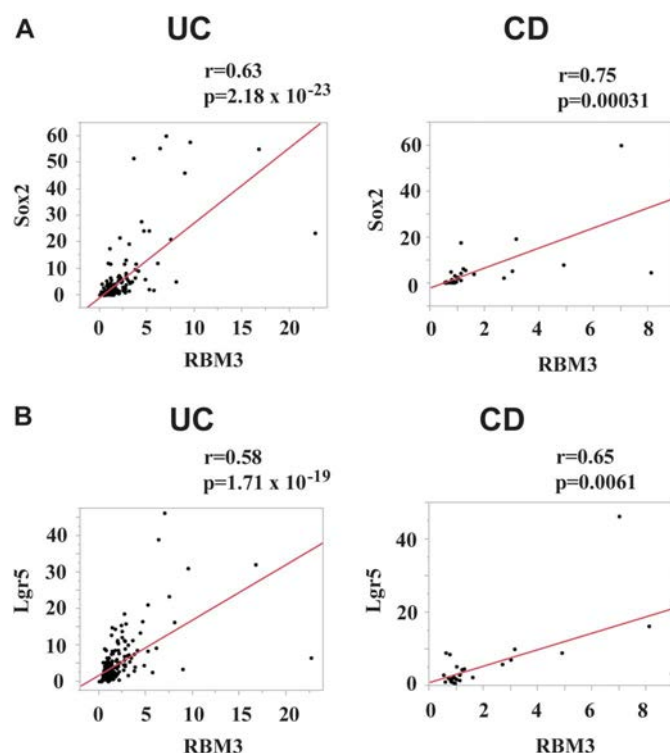


FIGURE 2. A and B, Association between RBM3 and stem cell markers in the colonic mucosa of patients with UC and CD. Scatter plot of relative messenger RNA levels of *RBM3* and the indicated genes in the human colonic mucosa. The messenger RNA level of each gene in the normal colon of an individual without IBD was given an arbitrary value of 1.0.

In this study, patients with refractory IBD are defined as those with long-term colonic inflammation lasting for more than 6 months. In the colonic mucosa of refractory UC, a stronger correlation between RBM3 and Bcl-xL expression was found compared with that in nonrefractory active UC (Fig. 3A). Similarly, we found a significant correlation between RBM3 and R-spondin expression in refractory UC but not in nonrefractory active UC (Fig. 3B). These data suggest that RBM3 would regulate the expression of Bcl-xL and R-spondin in the setting of chronic inflammation.

### RBM3 Expression Is Increased in Patients with Refractory IBD and CAC

In patients with refractory IBD, Cirp expression is higher in inflammatory cells than in epithelial cells, whereas HSPA4 expression is similar in both inflammatory and epithelial cells.<sup>3,4</sup> Immunohistochemical analysis was performed to identify RBM3-expressing cells in the human intestine. In the chronically inflamed mucosa, RBM3 was expressed in both epithelial and inflammatory cells (Fig. 4A), which was similar to that observed with HSPA4.

Cirp and HSPA4 expression increases in the colonic mucosa of patients with refractory IBD.<sup>3,4</sup> We determined

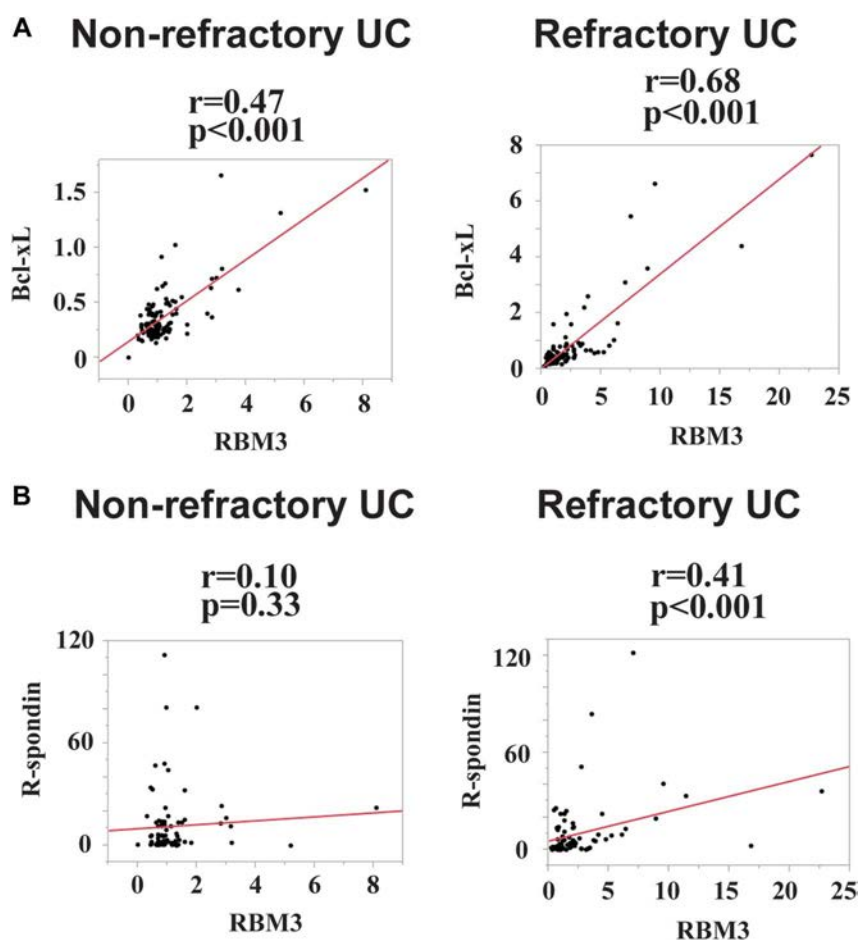


FIGURE 3. A and B, Association between RBM3 and Bcl-xL or R-spondin expression in the intestinal mucosa of patients with nonrefractory active UC and refractory UC. Scatter plot of relative messenger RNA levels of *RBM3* and the indicated genes in the human colonic mucosa. The messenger RNA level of each gene in the normal colon of an individual without IBD was given an arbitrary value of 1.0.

whether RBM3 expression was associated with the clinical status of patients with IBD. RBM3 expression levels increased in patients with refractory IBD who had long-term inflammation compared with those in controls, patients with IBD in remission, and patients with nonrefractory active IBD (Fig. 4B). Chronic inflammation often precedes or accompanies many cancers. In this study, we observed that RBM3 was overexpressed in all the examined patients with CAC. Moreover, we observed that tumor cells preferentially but not exclusively expressed RBM3 (Fig. 4C).

### RBM3 Deficiency Attenuated Tumorigenesis in the Murine CAC Model

Chronic inflammation increases the risk of intestinal cancer in patients with IBD.<sup>1,2</sup> To investigate the precise pathogenic mechanisms underlying IBD-associated colorectal carcinogenesis, we used an AOM-treated plus DSS-treated mouse model and examined the role of RBM3 in CAC. Treatment with AOM plus DSS significantly decreased the number but not the size of tumors

in *Rbm3*<sup>-/-</sup> mice compared with those in WT mice (Fig. 5A, B). Histological examination of hematoxylin and eosin–stained tissue sections of rolled-up colons did not show any differences between tumors in WT and *Rbm3*<sup>-/-</sup> mice (data not shown). However, RBM3 was expressed in both epithelial and inflammatory cells in the surrounding nontumor tissues and was preferentially expressed in tumor cells (Fig. 5C), which is consistent with the findings in humans (Fig. 4).

A decrease in tumor multiplicity in *Rbm3*<sup>-/-</sup> mice suggested that RBM3 may be playing a role in initiated or early tumor progenitor cell survival, as opposed to influencing tumor promotion, in which case similar number of tumors, but smaller tumors, would be expected. Given the involvement of RBM3 in the initiation of colorectal cancer, RBM3 might act in nontransformed colonic tissues rather than in established tumors. Therefore, we focused on nontumor tissues but not on tumor tissues. A stem cell–specific factor R-spondin is required for maintaining intestinal stem cells<sup>7</sup> and for inducing hyperproliferation of the crypt epithelium,<sup>8</sup> which would promote colorectal



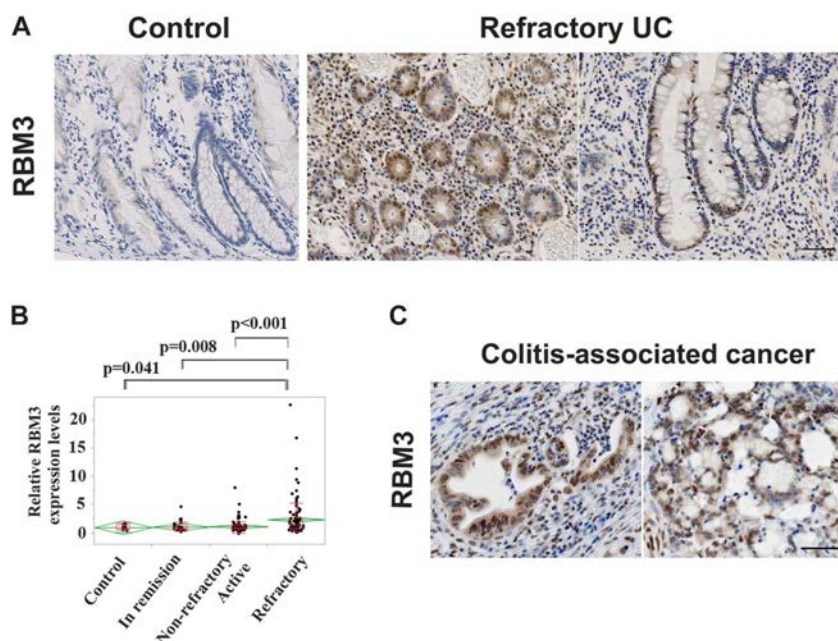


FIGURE 4. Increased expression of RBM3 in the intestinal mucosa of patients with refractory IBD and CAC. A, Representative images of immunohistochemical staining of RBM3 in the colonic tissues of patients with treatment-refractory UC and of controls; scale bar, 50  $\mu$ m. B, *RBM3* messenger RNA expression in the human colonic mucosa of patients without IBD (Control;  $n = 18$ ), patients with IBD in remission (In remission;  $n = 38$ ), patients with nonrefractory active UC (Nonrefractory active;  $n = 107$ ), and patients with refractory UC (Refractory;  $n = 100$ ) was analyzed by performing quantitative polymerase chain reaction.  $P$  values were calculated using post hoc Tukey–Kramer honestly significant difference multiple comparison test.  $F$  and  $P$  values obtained using analysis of variance are as follows:  $F = 7.3$  and  $P = 0.0001$ . C, Representative images of immunostaining of CAC tissues by using anti-RBM3 antibody; scale bar, 50  $\mu$ m.

carcinogenesis.<sup>9</sup> Expression of R-spondin and cancer stem cell marker CD133 was decreased in the colons of *Rbm3*<sup>-/-</sup> mice compared with that in the colons of WT mice (Fig. 5D). Expression of Noggin, another stem cell-specific factor, and Sox2 was slightly decreased in the colons of *Rbm3*<sup>-/-</sup> mice (Fig. 5D). Tumor-derived R-spondin augments  $\beta$ -catenin signaling.<sup>9</sup> However, expression of *Lgr5*, a downstream target gene of WNT/ $\beta$ -catenin signaling pathway, was not affected by *Rbm3* deletion in the tumors of *Rbm3*<sup>-/-</sup> mice (data not shown).

Because RBM3 expression was significantly correlated with Bcl-xL expression in humans (Figs. 2 and 3), we speculated that RBM3 regulated Bcl-xL expression. Expectedly, RBM3 deficiency decreased Bcl-xL expression in the colons of AOM-treated plus DSS-treated WT mice (Fig. 5D). In contrast, Bcl-xL expression did not decrease in the tumors of AOM-treated plus DSS-treated *Rbm3*<sup>-/-</sup> mice (Fig. 5D). Tumor and nontumor cells use different mechanisms to regulate gene expression. In tumor cells, Bcl-xL expression might be upregulated in an RBM3-independent manner. To confirm the role of RBM3 in apoptosis, we compared apoptosis induction in AOM-treated plus DSS-treated WT and *Rbm3*<sup>-/-</sup> mice. Gut apoptosis was >2-fold higher in AOM-treated plus DSS-treated *Rbm3*<sup>-/-</sup> mice than in AOM-treated plus DSS-treated WT mice (Fig. 6A). Bcl-xL was expressed in both epithelial cells and inflammatory cells (Fig. 6B), which was consistent with the cellular distribution

of RBM3 (Fig. 5C). In tumors, RBM3 did not affect apoptosis induction (Fig. 6A). Collectively, these results suggested that RBM3 protects intestinal cells from clearance due to inflammation in the murine CAC model.

To assess the effect of RBM3 on acute inflammation, experimental colitis was induced by treating mice with 2.5% DSS for 7 days. Inflammatory cell infiltration into the colon and epithelial injury were not affected by RBM3 disruption (see Fig. S1A, B, Supplemental Digital Content 2, <http://links.lww.com/IBD/B382>). No significant difference in messenger RNA levels of Bcl-xL, R-spondin, and CD133 was found between control mice and RBM3-deficient mice (see Fig. S2, Supplemental Digital Content 3, <http://links.lww.com/IBD/B383>). In Caco2 cells, an immortalized line of human colorectal cancer cell, knockdown of RBM3, did not reduce the expression of Bcl-xL, R-spondin, and CD133 (see Fig. S3, Supplemental Digital Content 4, <http://links.lww.com/IBD/B384>). These data suggest that RBM3 might contribute to the enhanced colonic expression of these genes in a non-cell-autonomous manner.

### RBM3 Upregulates R-Spondin Expression and Promotes Tumorigenesis Through Epithelial Cells

To functionally characterize the contribution of different cell populations to colorectal tumorigenesis, we developed

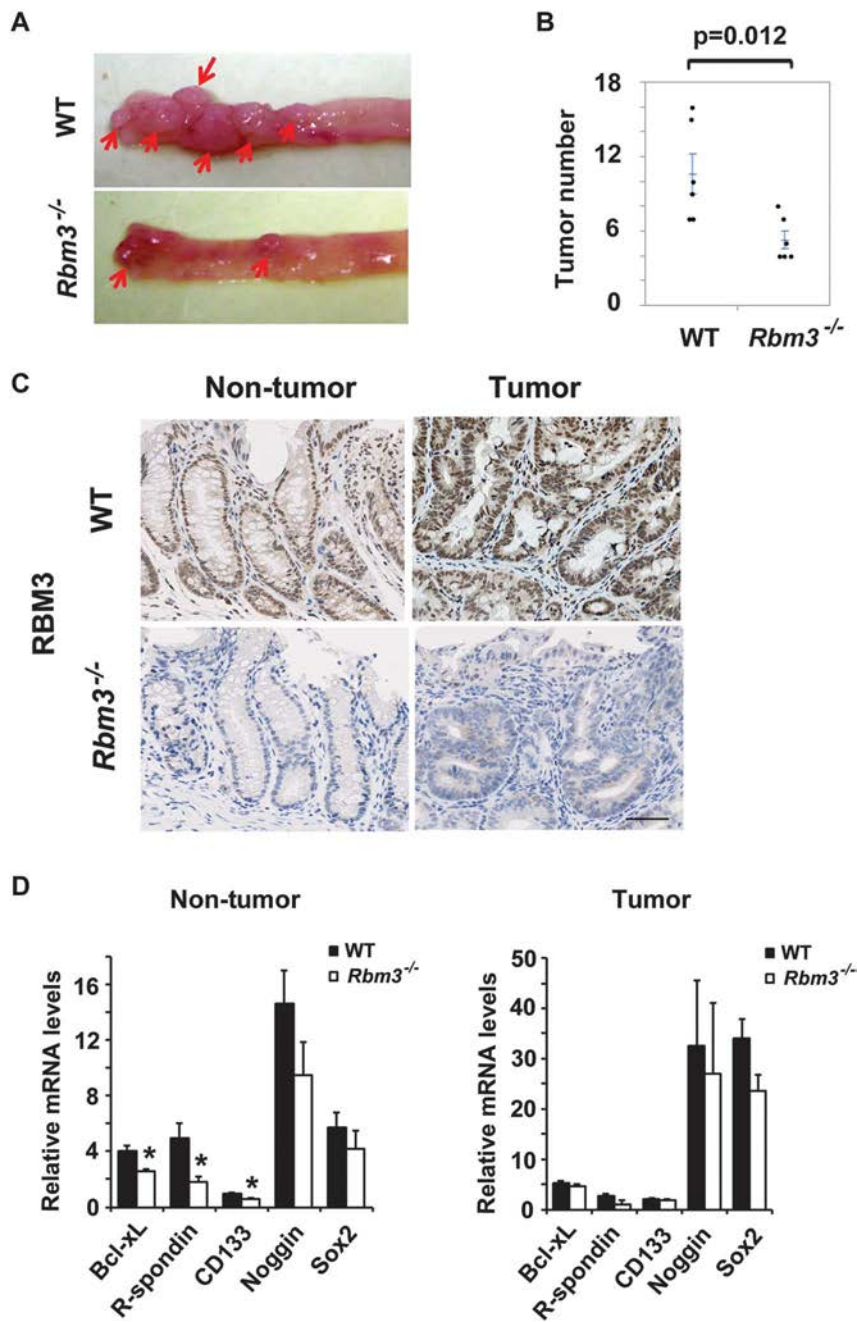


FIGURE 5. Deficiency of RBM3 affects colonic tumorigenesis in the murine model of CAC. A, Typical examples of macroscopic tumorigenesis in the murine CAC model. Colons were cut longitudinally. B, Tumor number (WT mice, n = 6; *Rbm3*<sup>-/-</sup> mice, n = 6). C, Results of immunohistochemical staining of the colonic sections of AOM-treated plus DSS-treated WT and *Rbm3*<sup>-/-</sup> mice. Nontumor and tumor tissues obtained from the murine CAC model were stained with anti-RBM3 antibody; scale bar, 50  $\mu$ m. D, RNA was extracted from nontumorous and tumorous colonic tissues. Relative levels of messenger RNA, as determined by performing quantitative polymerase chain reaction were normalized to those of actin messenger RNA. Level of each messenger RNA in untreated colonic tissues was given an arbitrary value of 1.0.

RBM3-chimeric mice by using a combination of gamma irradiation and bone marrow transplantation. Nontransplanted control mice survived for <2 weeks after the irradiation, indicating the ablation of endogenous BM. Transplanted mice were allowed to

recover for 2 months before treating them with AOM plus DSS. *Rbm3*<sup>-/-</sup> mice transplanted with WT or *Rbm3*<sup>-/-</sup> BM had significantly smaller tumor burden than WT mice transplanted with WT BM (Fig. 6C). WT mice transplanted with WT and *Rbm3*<sup>-/-</sup>

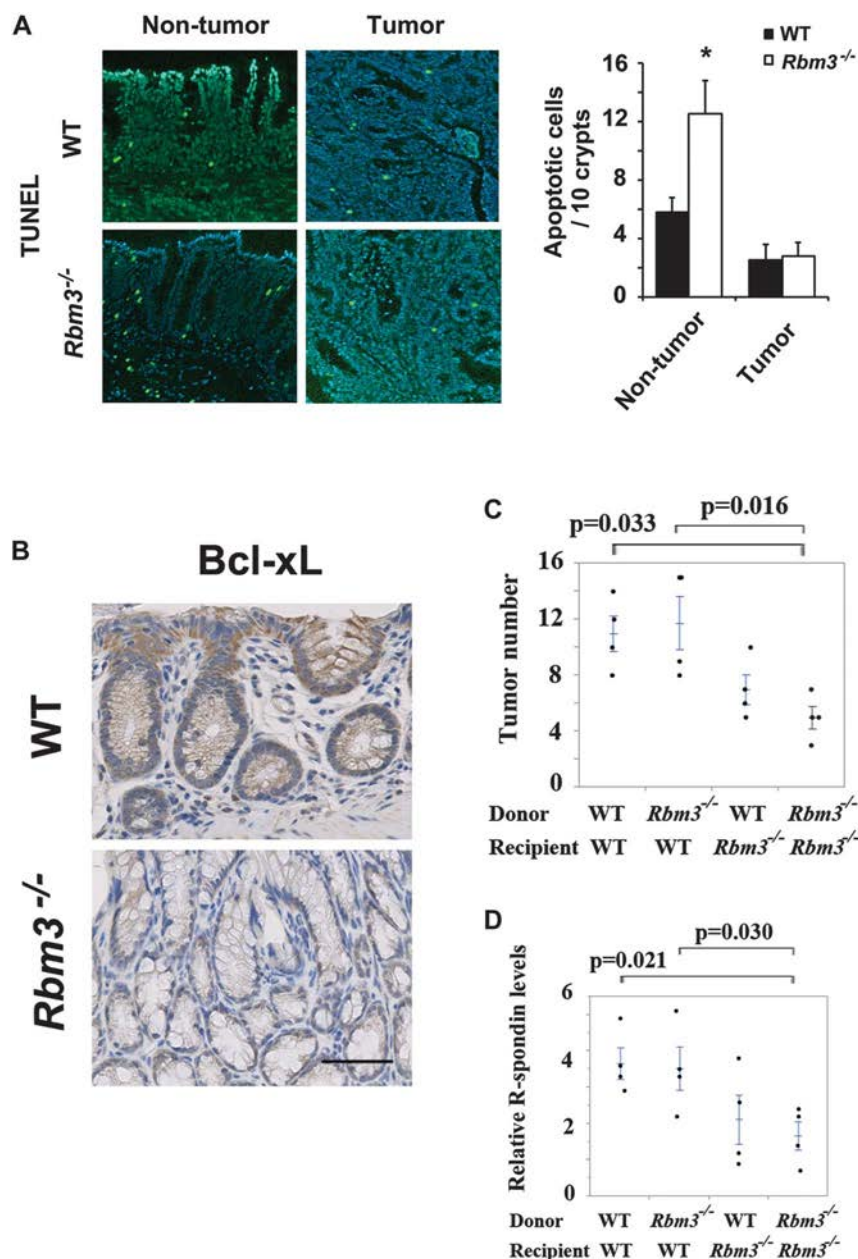


FIGURE 6. RBM3 upregulates R-spondin expression and promotes tumorigenesis through epithelial cell populations. A, TUNEL staining of colonic tissues and tumors of WT and *Rbm3*<sup>-/-</sup> mice treated with AOM plus DSS. Apoptotic index was calculated by counting TUNEL signals in 100 crypts. B, Representative images of immunohistochemical staining of Bcl-xL in the colonic tissues of WT mice and *Rbm3*<sup>-/-</sup> mice treated with AOM and DSS; scale bar, 50  $\mu$ m. C, WT mice transplanted with WT or *Rbm3*<sup>-/-</sup> BM and *Rbm3*<sup>-/-</sup> mice transplanted with WT or *Rbm3*<sup>-/-</sup> BM. Number of tumors in each group of mice is as follows: WT BM/WT mice, n = 4; *Rbm3*<sup>-/-</sup> BM/WT mice, n = 4; WT BM/*Rbm3*<sup>-/-</sup> mice, n = 4; *Rbm3*<sup>-/-</sup> BM/*Rbm3*<sup>-/-</sup> mice, n = 4. P values were calculated using post hoc Tukey–Kramer honestly significant difference multiple comparison test. D, RNA was extracted from nontumorous colonic tissues. Relative levels of R-spondin messenger RNA, as determined by performing quantitative polymerase chain reaction, were normalized to those of actin messenger RNA. R-spondin messenger RNA levels in untreated colonic tissues were given an arbitrary value of 1.0; n = 4 per group.

BM showed equivalent tumor numbers (Fig. 6C). *Rbm3*<sup>-/-</sup> mice transplanted with *Rbm3*<sup>-/-</sup> or WT BM showed decreased R-spondin expression compared with WT mice transplanted with WT BM (Fig. 6D). WT mice transplanted with WT and *Rbm3*<sup>-/-</sup>

BM showed equivalent R-spondin expression levels (Fig. 6D). These data indicated that RBM3 acted in the epithelial compartment to upregulate R-spondin expression and to enhance colorectal tumorigenesis.



## DISCUSSION

Stress response pathways play important roles in cancers arising from the loss of intestinal epithelial homeostasis. Stress triggers important adaptive responses to maintain homeostasis. One adaptive response is the induction of stress response proteins that act as chaperones and protect host from different stresses. However, increased and decreased stress response induces pathogenic conditions, such as inflammation and carcinogenesis.<sup>17</sup> Increased expression of stress response proteins Cirp and HSPA4 promotes the development of refractory colitis and colorectal cancers.<sup>3,4</sup> Here, we showed that the stress response protein RBM3, which is upregulated in patients with refractory IBD, promoted colorectal tumorigenesis. The association between IBD and CAC is well established. The cumulative risk of developing colorectal cancer after 20 years is 7% in patients with UC and 8% in patients with CD.<sup>2</sup> In addition, it is clear that chronic inflammation plays a causative role in the transition to adenocarcinoma in IBD.<sup>1,2</sup> Periodic colonoscopic surveillance with multiple biopsies is the conventional method for the early detection of colitis-associated dysplasia or cancer. However, such surveillance programs have several limitations,<sup>18</sup> and surveillance strategies need to be appropriately personalized. One of the challenges in colonoscopy for cancer surveillance is the lack of risk stratification. Therefore, analyzing the expression levels of stress response proteins may be effective for improving the identification of patients with IBD who are at a high risk of CAC. A future large-scale study involving patients with different stages of IBD will be crucial for determining whether Cirp, HSPA4, and RBM3 can be used as biomarkers for predicting the risk of colorectal carcinogenesis.

Although *RBM3* messenger RNA and protein expression is upregulated in human tumors, the clinical implications of RBM3 in tumors are controversial.<sup>13–15,19–21</sup> In contrast, RBM3 induces the growth of nontransformed cells in an anchorage-independent manner,<sup>13</sup> suggesting that RBM3 would expand transformed cells and act as a tumor promoter in nontransformed colonic mucosa. Because crypt stem cells represent the cells of origin of intestinal neoplasias, stem cell-specific factors, such as WNT, R-spondin, noggin, and epidermal growth factor, would promote the growth of cancer stem cells and intestinal stem cells in a paracrine manner.<sup>7–9</sup> Bone marrow transplantation experiments indicated that RBM3 upregulated R-spondin expression and promoted tumorigenesis through epithelial cell populations. We showed that RBM3 deficiency decreased Bcl-xL expression and increased apoptosis in nontumor tissues but not in tumor tissues of AOM-treated plus DSS-treated mice. RBM3 may protect early progenitor cells from clearance due to chronic inflammation. Because endogenous R-spondin is mainly localized in intestinal epithelial cells,<sup>10</sup> RBM3 might increase R-spondin expression through inhibiting apoptosis of epithelial cells. Furthermore, RBM3 can bind the transcripts to regulate the expression of several genes.<sup>12</sup> RBM3 might regulate expression of R-spondin and Bcl-xL genes posttranscriptionally as well.

Chronic inflammation enhances stress-induced Cirp and HSPA4 expression in patients with IBD.<sup>3,4</sup> Here, we found that

RBM3 expression increased because of refractory and long-term inflammation in the human colonic mucosa. Because Cirp and RBM3 are 2 evolutionarily conserved RNA-binding proteins that are transcriptionally upregulated in response to low temperature,<sup>22</sup> hypothermia might occur in the chronically inflamed colonic mucosa. Hypoxia, which increases in chronic inflammatory diseases, including IBD, upregulates Cirp and RBM3 expression,<sup>12</sup> which may be one of the reasons for the induction of RBM3 expression by chronic inflammation. However, the exact mechanisms underlying the regulation of RBM3 expression by long-term inflammation are unknown.

In summary, our results suggested that chronic inflammation-induced RBM3 inhibited apoptosis and augmented cancer stem cell expansion by upregulating Bcl-xL and R-spondin expression, thus increasing tumorigenesis. Thus, RBM3 would be a promising biomarker for predicting the risk of cancer and a new therapeutic target for cancer prevention in patients with IBD.

## REFERENCES

1. Itzkowitz SH, Yio X. Inflammation and cancer IV. Colorectal cancer in inflammatory bowel disease: the role of inflammation. *Am J Physiol Gastrointest Liver Physiol*. 2004;287:G7–G17.
2. Gillen CD, Walmsley RS, Prior P, et al. Ulcerative colitis and Crohn's disease: a comparison of the colorectal cancer risk in extensive colitis. *Gut*. 1994;35:1590–1592.
3. Sakurai T, Kashida H, Watanabe T, et al. Stress response protein cirp links inflammation and tumorigenesis in colitis-associated cancer. *Cancer Res*. 2014;74:6119–6128.
4. Adachi T, Sakurai T, Kashida H, et al. Involvement of heat shock protein a4/apg-2 in refractory inflammatory bowel disease. *Inflamm Bowel Dis*. 2015;21:31–39.
5. Qiang X, Yang WL, Wu R, et al. Cold-inducible RNA-binding protein (CIRP) triggers inflammatory responses in hemorrhagic shock and sepsis. *Nat Med*. 2013;19:1489–1495.
6. Sakurai T, Yada N, Watanabe T, et al. Cold-inducible RNA-binding protein promotes the development of liver cancer. *Cancer Sci*. 2015;106:352–358.
7. Drost J, van Jaarsveld RH, Ponsioen B, et al. Sequential cancer mutations in cultured human intestinal stem cells. *Nature*. 2015;521:43–47.
8. Kim KA, Kakitani M, Zhao J, et al. Mitogenic influence of human R-spondin1 on the intestinal epithelium. *Science*. 2005;309:1256–1259.
9. Chartier C, Raval J, Axelrod F, et al. Therapeutic targeting of tumor-derived R-spondin attenuates  $\beta$ -catenin signaling and tumorigenesis in multiple cancer types. *Cancer Res*. 2016;76:713–723.
10. Zhao J, de Vera J, Narushima S, et al. R-spondin1, a novel intestinotrophic mitogen, ameliorates experimental colitis in mice. *Gastroenterology*. 2007;132:1331–1343.
11. Danno S, Nishiyama H, Higashitsuji H, et al. Increased transcript level of RBM3, a member of the glycine-rich RNA-binding protein family, in human cells in response to cold stress. *Biochem Biophys Res Commun*. 1997;236:804–807.
12. Wellmann S, Bühner C, Moderegger E, et al. Oxygen-regulated expression of the RNA-binding proteins RBM3 and CIRP by a HIF-1-independent mechanism. *J Cell Sci*. 2004;117:1785–1794.
13. Sureban SM, Ramalingam S, Natarajan G, et al. Translation regulatory factor RBM3 is a proto-oncogene that prevents mitotic catastrophe. *Oncogene*. 2008;27:4544–4556.
14. Melling N, Simon R, Mirlacher M, et al. Loss of RNA-binding motif protein 3 expression is associated with right-sided. *Histopathology*. 2016;68:191–198.
15. Venugopal A, Subramaniam D, Balmaceda J, et al. RNA binding protein RBM3 increases  $\beta$ -catenin signaling to increase stem cell characteristics in colorectal cancer cells. *Mol Carcinog*. 2015;55:1503–1516.
16. Sakurai T, Kashida H, Hagiwara S, et al. Heat shock protein A4 controls cell migration and gastric ulcer healing. *Dig Dis Sci*. 2015;60:850–857.

17. Park SH, Moon Y. Integrated stress response-altered pro-inflammatory signals in mucosal immune-related cells. *Immunopharmacol Immunotoxicol*. 2013; 35:205–214.
18. Gupta RB, Harpaz N, Itzkowitz S, et al. Histologic inflammation is a risk factor for progression to colorectal neoplasia in ulcerative colitis: a cohort study. *Gastroenterology*. 2007;133:1099–1105.
19. Olofsson SE, Nodin B, Gaber A, et al. Low RBM3 protein expression correlates with clinical stage, prognostic classification and increased risk of treatment failure in testicular non-seminomatous germ cell cancer. *PLoS One*. 2015;10:e0121300.
20. Zeng Y, Wodzinski D, Gao D, et al. Stress-response protein RBM3 attenuates the stem-like properties of prostate cancer cells by interfering with CD44 variant splicing. *Cancer Res*. 2013;73: 4123–4133.
21. Hjelm B, Brennan DJ, Zendeckroth N, et al. High nuclear RBM3 expression is associated with an improved prognosis in colorectal cancer. *Proteomics Clin Appl*. 2011;5:624–635.
22. Zhu X, Bühner C, Wellmann S. Cold-inducible proteins CIRP and RBM3, a unique couple with activities far beyond the cold. *Cell Mol Life Sci*. 2016;73:3839–3859.

Original Paper

# MicroRNAs for the Prediction of Early Response to Sorafenib Treatment in Human Hepatocellular Carcinoma

Naoshi Nishida Tadaaki Arizumi Satoru Hagiwara Hiroshi Ida  
Toshiharu Sakurai Masatoshi Kudo

Department of Gastroenterology and Hepatology, Kindai University Faculty of Medicine,  
Osaka, Japan

## Key Words

Hepatocellular carcinoma · microRNA · Molecular targeted therapy · Biomarkers · Treatment

## Abstract

**Background:** Several studies suggest the role of circulating microRNAs (miRNAs) as biomarkers of hepatocellular carcinoma (HCC). However, the serum miRNA profile associated with the response to sorafenib remains to be elucidated. The aim of this study was to clarify the specific miRNAs in serum that could predict the early response of HCC to sorafenib treatment.

**Summary:** Analyzing the sera from 16 HCC patients, we selected five miRNAs that showed differences in serum levels between patients with and without tumor responses among 179 known secretory miRNAs by using locked nucleic acid probe-based quantitative PCR. Through further analysis using a validation cohort that included 53 HCC patients who underwent sorafenib treatment and 8 healthy control subjects, we found that miR-181a-5p and miR-339-5p showed significant differences in serum levels among patients with partial response (PR), stable disease (SD), and progressive disease (PD), where PR patients showed the highest and PD the lowest levels. We also analyzed the factors associated with disease control (DC; PR or SD) 3 months after the initiation of sorafenib treatment; patients with DC showed a significantly higher level of serum miR-181a-5p than non-DC patients or healthy control subjects ( $p = 0.0349$  and  $0.0180$  for DC vs. non-DC and control vs. non-DC by Tukey-Kramer test, respectively). We further conducted multivariate analysis among HCC patients with Barcelona Clinic Liver Cancer stage C using extrahepatic metastasis, serum decarboxyprothrombin, and miR-181a-5p levels as covariables; serum miR-181a-5p was the only independent factor for achieving DC ( $p = 0.0092$ , odds ratio 0.139, and 95% confidence interval 0.011–0.658). In addition, miR-181a-5p level was also the only independent factor affecting overall survival ( $p = 0.0194$ , hazard ratio 0.267, and 95% confidence interval 0.070–0.818). **Key Messages:** A high serum level of miR-181a-5p before treatment is associated with DC after the initiation of sorafenib.

© 2016 S. Karger AG, Basel

Naoshi Nishida, MD  
Department of Gastroenterology and Hepatology  
Kindai University Faculty of Medicine  
337-2 Ohno-higashi, Osaka-sayama, Osaka 589-8511 (Japan)  
E-Mail naoshi@med.kindai.ac.jp

## Introduction

Hepatocellular carcinoma (HCC) is one of the leading causes of cancer death worldwide [1]. Despite recent advancements in the diagnosis and treatment of HCC, the prognosis of the patients at an advanced stage, where curative treatments are not applicable, is still unsatisfactory.

Noncurative treatment of HCC mainly consists of transcatheter-based treatment and molecular targeting treatment [2]; to date, sorafenib is the only agent that has improved the time-to-progression and overall survival (OS) in advanced stages of HCC with vascular invasion and extrahepatic spread [3]. According to the Barcelona Clinic Liver Cancer (BCLC) algorithm that refers to disease staging and treatment allocation, sorafenib is proposed as a first-line treatment for cases with BCLC stage C, where cancer has spread into blood vessels or extrahepatic tissues [4]. However, a considerable number of HCC patients with BCLC stage C are refractory to sorafenib; some of these patients may have a survival benefit from transcatheter-based treatment if intrahepatic tumor could be considered as a main prognostic factor for survival [5]. On the other hand, a subset of HCC patients with BCLC stage B, where transcatheter chemoembolization (TACE) is recommended, might be refractory to TACE but respond to sorafenib [6]. From this point of view, it is important to develop a biomarker to narrow down the subgroup of the patients who have a survival benefit from sorafenib treatment.

Recently, a number of studies have reported that microRNAs (miRNAs) could be key players in the pathogenesis of liver cancer [7]. Given that a single miRNA targets multiple mRNAs, the alteration of multiple pathways attributed to the miRNA profile may act in concert and affect the sensitivity of HCC cells to sorafenib [8–10]. To date, several reports have suggested that miRNAs could influence the cellular response to drugs, and a profile of the miRNAs in peripheral blood could be biomarkers for the drug response of HCC [11–13]. However, the performance of miRNAs as biomarkers for the response to sorafenib treatment remains to be elucidated.

Moreover, several issues need to be addressed for the quantification of serum miRNAs [14]. For example, the low concentration of miRNAs in peripheral blood could give rise to unreliable quantification, and nonspecific miRNAs derived from apoptotic bodies due to the injury of liver tissue and blood cells could act as noise in the measurement of target miRNAs. In addition, a reference for the quantification of miRNAs in peripheral blood has not yet been established. In this study, we attempted to address these important issues using locked nucleic acid (LNA) probes for quantitative PCRs (qPCRs). LNA is a modified RNA nucleotide, and qPCR using LNA probes provides enhanced sensitivity and specificity for quantification [15]. In this study, we specifically focused on the 179 known secretory miRNAs present in peripheral blood, and performed quantification using several reference miRNAs that are abundant in serum as a control of quantification. These procedures allowed us to perform stable quantification and eliminate the background noise of miRNAs in serum. Using screening and validation cohorts, we examined the secretory miRNAs in peripheral blood that could help identify the subclass of HCC patients who would likely respond to sorafenib treatment.

## Materials and Methods

### *Patients and Screening of Serum miRNAs Associated with Tumor Response to Sorafenib Therapy*

For the screening of miRNAs that could predict the initial response to sorafenib, we selected 8 HCC patients who showed partial response (PR) to sorafenib treatment at 3 months after the initiation of the treatment as well as 8 patients with progressive disease (PD) at 1 month after treatment initiation (screening cohort). The sera were collected before the initiation of sorafenib. The tumor response was evaluated

according to the criteria outlined in the modified Response Evaluation Criteria in Solid Tumors (mRECIST) [16]. The characteristics of the screening cohort that consisted of the PR and PD patients are shown in online supplementary table 1 (for all online suppl. material, see [www.karger.com/doi/10.1159/000449475](http://www.karger.com/doi/10.1159/000449475)). Using the serum from the screening cohort that was collected before the initiation of sorafenib, we selected the miRNAs that showed differences in serum levels between the PR and PD cases.

In the next step, we selected 53 consecutive patients who underwent sorafenib treatment for more than 1 month between July 2009 and May 2013 as a validation cohort. Among the 53 patients, 12 received sorafenib treatment as an initial therapy for HCC. On the other hand, 41 patients underwent several treatments before sorafenib, and the last treatment before sorafenib was as follows: 26 patients received TACE, 7 underwent hepatic arterial infusion chemotherapy, 5 received radiofrequency ablation, one underwent surgical resection and 2 received other molecular targeting agent.

The collection of serum was performed within 1 week prior to the initiation of treatment, and serum was stored at  $-80^{\circ}\text{C}$  until the measurement of miRNA. The characteristics of the validation cohort are listed in table 1. Briefly, the median age of the patients was 74 years of age (67.5–79.5), with 45 males and 8 females. Thirteen were positive for hepatitis surface antigen (HBsAg), 22 were positive for hepatitis C virus antibody, and 18 were negative for both. Eight patients were classified as Barcelona Clinic or Liver Cancer (BCLC) stage A, 15 were stage B, and 30 were stage C. Twenty-three patients showed extrahepatic metastasis and 11 had vascular invasion. The median duration of sorafenib treatment was 99 days (24–567 days). Fifteen patients discontinued sorafenib administration before the 3rd month of treatment due to the diagnosis of PD or noncompliance with treatment. We also measured the serum miRNA levels from 8 healthy volunteers ranging in age from 23 to 77 years old. Informed consent was obtained from each patient, and the study protocol conforms to the ethical guidelines of the 1975 Declaration of Helsinki. This study was approved by the institution's research committee.

#### *Follow-Up and Assessment of Response*

After the initiation of sorafenib, the response to the therapy was assessed at 1 and 3 months; complete response (CR), PR, stable disease (SD), and PD were determined based on the radiological findings obtained from contrast-enhanced computed tomography that were reviewed by 2 independent radiologists in a nonblinded fashion. Extrahepatic metastasis was also evaluated as required using chest X-ray, bone scintigraphy, or fluorodeoxyglucose positron emission tomography [6]. We also defined the disease control rate (DCR) as the total number of the patients with CR, PR, and SD divided by the number of all patients, and the patients were classified under disease control (DC) or not based on the contrast-enhanced computed tomography findings 3 months after the initiation of sorafenib [3]. Blood chemical tests, and serum  $\alpha$ -fetoprotein and decarboxyprothrombin (DCP) levels were also measured monthly.

#### *Extraction of Total RNA from Serum and cDNA Synthesis*

Total RNA including miRNA was isolated from 250  $\mu\text{l}$  of serum using the miRNeasy mini-kit according to the manufacturer's protocol (Qiagen, Hilden, Germany); 1  $\mu\text{g}$  of carrier MS2 RNA was added to each serum sample (F. Hoffmann-La Roche, Ltd, Basel, Switzerland). We also used a set of synthetic RNA spike-ins (RNA spike-in kit; UniRT) for quality control, such as monitoring RNA isolation efficiency, interplate calibration, cDNA synthesis, and qPCR (Exiqon, Vedbaek, Denmark). RNA was eluted into 50  $\mu\text{l}$  of DNase/RNase-free water. For the reverse transcription, 2  $\mu\text{l}$  of template total RNA solution was added to 2  $\mu\text{l}$  of 5 $\times$  reaction buffer, 4.5  $\mu\text{l}$  of nuclease-free water, 1  $\mu\text{l}$  of enzyme mix, and 0.5  $\mu\text{l}$  of enzyme mix synthetic RNA spike-ins, according to the manufacture's protocol (Universal cDNA Synthesis Kit II; Exiqon).

#### *Quantification of Serum miRNA Levels*

For the screening of miRNAs that predict an early response to sorafenib treatment and reliable detection of low amounts of serum miRNA, we used a serum/plasma focus miRNA PCR panel containing 179 miRNA primer sets focused on secreted serum/plasma relevant human miRNAs, and ExiLent SYBR Green master mix (Exiqon, Vedbaek, Denmark). For the stability measurements of low level of miRNAs, an LNA probe, a novel type of nucleic acid analog that could distinguish a 1-bp mismatch, was used to obtain enhanced sensitivity and specificity of qPCR. The qPCR was performed using the StepOne real-time detection system (Applied Biosystems, Foster City, Calif., USA). The expression level of five reference miRNAs abundantly detected in serum (miR-95-5p, miR-103a-3p, miR-191-5p, miR-423-3p, and miR-425-5p) was measured, and their mean value was applied as an internal control for quantification [17, 18]. We applied the comparative cycle threshold method for relative quantification of miRNAs within the input according to the manufac-



**Table 1.** Clinical characteristics of the validation cohort

Clinical factors	Characteristics of the patients <sup>1</sup>
Age, years	74 (67.5 to 79.5)
Sex	
Male	45
Female	8
Etiology	
HBV	13
HCV	22
NBNC	18
Maximum tumor size, cm	3.7 (2.1 to 7.25)
Number of tumors	
≤5	25
≥6	28
BCLC stage	
A	8
B	15
C	30
Extrahepatic metastasis	
Without	30
With	23
Portal vein thrombosis	
Without	42
With	11
Serum AFP level before treatment, ng/ml	70 (10 to 4,846)
Serum DCP level before treatment, mAU/ml	1,185 (68.5 to 7,865)
Initial dose of sorafenib	
200 mg	1
400 mg	16
800 mg	36
Duration of sorafenib treatment, days	99 (56 to 233.5)
Response to sorafenib	
ΔAFP at 1 month after the initiation <sup>2</sup>	0.03 (–0.27 to 0.57)
ΔDCP at 1 month after the initiation <sup>3</sup>	1.80 (0.34 to 3.31)
At 1 month after the initiation	
PR	11
SD	22
PD <sup>4</sup>	20
At 3 months after the initiation	
PR	7
SD	9
PD <sup>5</sup>	22
DCR at 3 months after the initiation <sup>6</sup>	16/53 (30.2%)

AFP =  $\alpha$ -Fetoprotein. <sup>1</sup> Median value (25th to 75th percentiles) for contentious variables, and number of cases for categorical variables are shown as characteristics of the patients. <sup>2</sup> Differences of serum AFP level between before and at 1 month after the initiation of sorafenib; the  $\Delta$ AFP is calculated as (AFP level after the treatment – baseline AFP level) divided by baseline AFP level. A minus score indicates a decrease in APF compared with a baseline value. <sup>3</sup> Differences of serum DCP level between before and at 1 month after the initiation of sorafenib; the  $\Delta$ DCP is calculated as (DCP level after the treatment – baseline DCP level) divided by baseline DCP level. A minus score indicates a decrease in DCP compared with a baseline value. <sup>4</sup> Response at 1 month after the initiation of sorafenib was not determined in one patients. <sup>5</sup> Sorafenib treatment was stopped before the 3rd month in 15 patients because of the disease progression. These patients were not evaluated for response at 3 months after the initiation. <sup>6</sup> DCR was calculated as total number of the patients with PR and SD divided by total number of all patients.



**Table 2.** Candidates of serum miRNAs for the prediction of early response to sorafenib

Candidate miRNA <sup>1</sup>	Mean ΔCq	PR group, median ΔCq (distribution)	PD group, median ΔCq (distribution)	p value by Student's t test	p value by Mann-Whitney U test	miRNA levels in PR group vs. PD group
hsa-miR-136-5p	6.707	5.572 (4.954–7.162)	7.957 (7.146–7.996)	0.0046	0.0275	increased
<b>hsa-miR-17-5p</b>	5.361	5.630 (5.016–8.622)	4.919 (3.842–5.048)	0.0144	0.0023	decreased
<b>hsa-miR-181a-5p</b>	2.555	2.098 (1.720–3.388)	2.972 (2.112–3.554)	0.0238	0.0357	increased
hsa-miR-182-5p	7.455	7.648 (7.272–9.466)	6.918 (6.046–8.044)	0.0275	0.0618	decreased
<b>hsa-miR-33a-5p</b>	5.520	4.987 (4.066–5.744)	5.976 (4.818–8.374)	0.0342	0.0357	increased
hsa-miR-335-5p	6.684	6.279 (4.578–7.31)	6.903 (5.784–8.916)	0.0423	0.0587	increased
<b>hsa-miR-339-5p</b>	5.958	5.804 (4.568–6.414)	6.254 (5.348–7.368)	0.0428	0.0587	increased
<b>hsa-miR-148b-3p</b>	2.068	1.950 (0.628–2.270)	2.474 (1.574–3.118)	0.0443	0.0587	increased

<sup>1</sup> miRNAs that showed a difference of serum levels between PR and PD groups with  $p < 0.05$  by Student's t test. miRNAs with  $p < 0.05$  by Mann-Whitney U test, and mean  $\Delta Cq < 6$  are shown in bold.

turer's instruction. We performed duplicate measurements per experiment, and the mean number of cycles required for the fluorescent signal to reach the threshold (quantification cycle; Cq) was determined for each sample. The Cq was determined automatically by the StepOne real-time detection system (Applied Biosystems). The difference of Cq between the target miRNA and a mean of the five reference miRNAs ( $\Delta Cq$ ) was considered as a relative value of serum miRNA level for each sample [18]. Specificity of amplification was confirmed using melting curve analysis for each amplification (online suppl. fig. 1). Since serum miRNAs derived from blood cells should affect the measurement of miRNA from HCC cells, the serum level of three miRNAs abundantly present in blood cells (miR-16, miR-451, and miR-23a) was also examined to monitor hemolysis [18]. For the validation of miRNAs that are associated with early response to sorafenib, we also applied LNA miRNA primer-based qPCR.

### Statistics

For comparing contentious variables, the Wilcoxon rank-sum test, Kruskal-Wallis test and Student's t test, or one-way factorial analysis of variance (ANOVA) was applied. For multiple comparisons, the Tukey-Kramer test or Wilcoxon rank-sum test with Bonferroni correction was applied. For categorical comparisons of clinical data, the  $\chi^2$  test or Fisher's exact test was used. For the interassay variation, Pearson's correlation test was applied; the percentage coefficient of variation (%CV) was calculated. For the survival analysis, we applied Kaplan-Meier analysis and calculated a p value using the log-rank test. Variables with a p value of  $< 0.05$  on univariate analysis were further analyzed by the Cox proportional-hazards regression model to determine the independent determinants of outcome variables. All p values were two-sided, and  $p < 0.05$  was considered statistically significant. All statistical analyses were calculated using the JMP version 4.05J software (SAS Institute Inc., Cary, N.C., USA).

## Results

### Screening of Serum miRNAs Associated with Early Response to Sorafenib

Initially, we conducted a screening of miRNAs associated with early response to sorafenib among 179 secreted miRNAs in serum. For this purpose, we compared serum miRNA levels between 8 HCC patients who showed PR for 3 months (PR group) and 8 HCC patients who were diagnosed as PD 1 month after initiation of treatment (PD group) (online suppl. fig. 2). Eight miRNAs showed significant differences in serum levels between the PR and PD groups with p values of  $< 0.05$  by Student's t test (table 2). Among them, we further selected 5 miRNAs, miR-17-5p, miR-181a-5p, miR-33a-5p, miR-339-5p, and miR-148b-3p, as candidates for validation as these miRNAs showed differences in serum levels even with the nonparametric method ( $p < 0.0587$  by Wilcoxon rank-sum test) and were present at a high enough concentration in serum to allow for quantification ( $\Delta Cq < 6$ ) (table 2). Of them, 4 showed a decrease

in  $\Delta Cq$  in the PR group compared with that of the PD group, and 1 miRNA showed an increased  $\Delta Cq$  in the PR group.

#### *Initial Response to Sorafenib among HCC Patients in the Validation Cohort*

Among the 53 patients in the validation cohort, no patients were diagnosed as CR at either 1 or 3 months after the initiation of treatment. Eleven (11/53, 20.8%), 22 (22/53, 41.5%), and 20 (20/53, 37.7%) patients comprised the PR, SD, and PD groups at 1 month, respectively. Of them, 5 and 10 patients who were classified as SD and PD, respectively, 1 month after the initiation of sorafenib, discontinued treatment due to tumor progression. The response at 3 months was evaluated in 38 patients; 7 (7/38, 18.4%), 9 (9/38, 23.7%), and 22 (22/38, 57.9%) patients were diagnosed as PR, SD, and PD, respectively. No patients in the PR group at the first month of the treatment were diagnosed as CR afterwards. Thus, the DCR at 3 months, calculated as the number of patients with PR and SD for 3 months divided by the total number of patients who received sorafenib, was 30.2% (16/53).

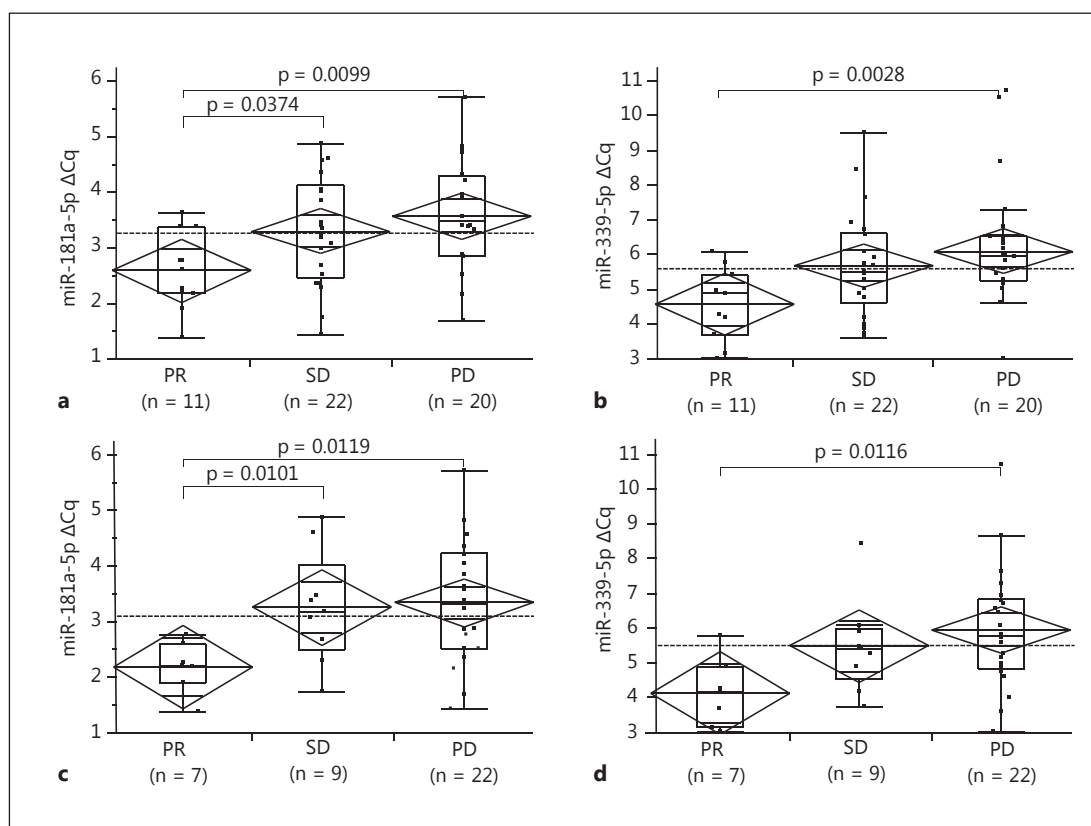
#### *Validation of Serum miRNAs That Predict Early Response to Sorafenib*

We confirmed the association of serum miRNA levels with tumor response 1 and 3 months after the initiation of sorafenib for five different miRNAs selected from the validation cohort. Of them, miR-181a-5p and miR-339-5p showed significant differences in serum levels 1 month after the initiation of sorafenib among the PR, SD, and PD groups by both ANOVA and nonparametric Kruskal-Wallis tests ( $p = 0.0223$  and  $0.0256$  by ANOVA and Kruskal-Wallis tests for miR-181a-5p, respectively;  $p = 0.0244$  and  $0.0133$  by ANOVA and Kruskal-Wallis tests for miR-339a-5p, respectively, fig. 1a, b). These miRNA levels also showed significant differences 3 months after treatment initiation among the sera from the three groups ( $p = 0.0333$  and  $0.0271$  by ANOVA and Kruskal-Wallis tests for miR-181a-5p, respectively;  $p = 0.0323$  and  $0.0290$  by ANOVA and Kruskal-Wallis tests for miR-339a-5p, respectively, fig. 1c, d). Interestingly, there was a clear trend between tumor response and the  $\Delta Cq$  of miRNAs; in patients with PR it is the smallest, and in those with PD it is the largest (fig. 1).

Using healthy subjects as a control, we compared the serum miRNA levels between patients with and without DC 3 months after treatment. Although the  $\Delta Cq$  of miR-339-5p is larger in patients without DC (non-DC) than those with DC by nonparametric analyses ( $p = 0.0341$  among 3 groups by the Kruskal-Wallis tests, and  $p = 0.0143$  between DC and non-DC by Wilcoxon rank-sum test with Bonferroni correction; fig. 2a), a significant difference was not detected using ANOVA ( $p = 0.0742$ ). On the other hand, non-DC patients showed significantly larger  $\Delta Cq$  of miR-181a-5p than DC patients as well as control subjects in both parametric and nonparametric analyses ( $p = 0.0048$  by ANOVA,  $p = 0.0349$  and  $0.0180$  for DC vs. non-DC and control vs. non-DC by Tukey-Kramer test, respectively;  $p = 0.0032$  by Kruskal-Wallis tests,  $p = 0.0150$  and  $p = 0.0038$  for DC vs. non-DC and control vs. non-DC by Wilcoxon rank-sum test with Bonferroni correction, respectively; fig. 2b).

#### *Interassay Variation for Quantification of Serum miRNAs*

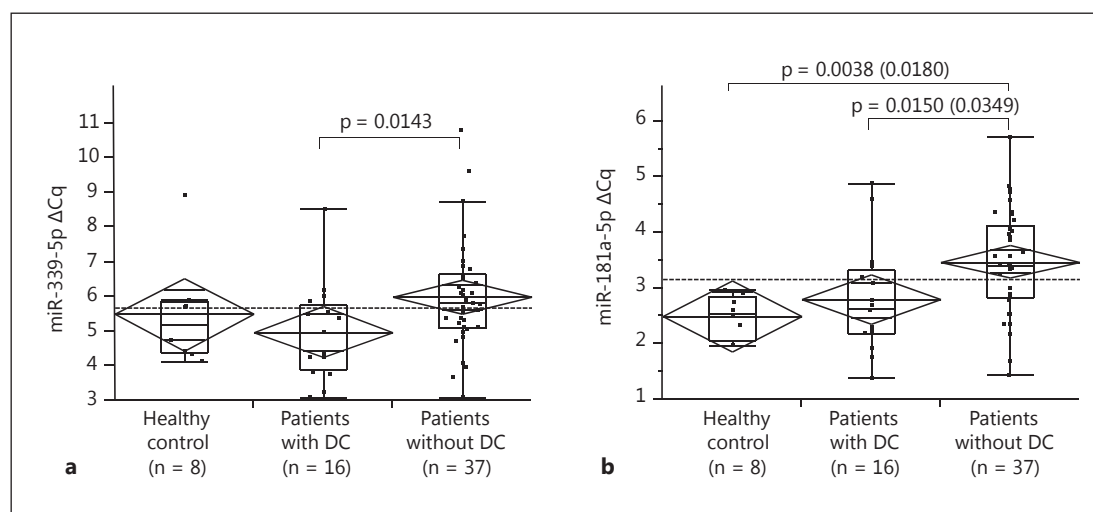
Using sera from 19 HCC patients, we evaluated interassay variation for miR-181a-5p and miR-338-5p. For this propose, we compared the  $\Delta Cq$  based on the mean value of five reference miRNAs (shown in Materials and Methods) with those based on the mean of two reference miRNAs (miR-95-5p, miR-423-3p). The  $\Delta Cq$  from two assays was more correlated in miR-181a-5p than in miR-338-5p ( $R^2 = 0.7804$ ,  $p < 0.0001$  for miR-181a-5p, and  $R^2 = 0.418$ ,  $p = 0.0068$  for miR-339-5p by Pearson's correlation coefficient; fig. 3). In addition, the interassay %CV is smaller in miR-181a-5p than in miR-338-5p (%CV = 16.6 and 28.6% for miR-181a-5p and miR-338-5p, respectively), suggesting that miR-181a-5p is more suitable for the evaluation of serum levels than miR-338-5p in a clinical setting.



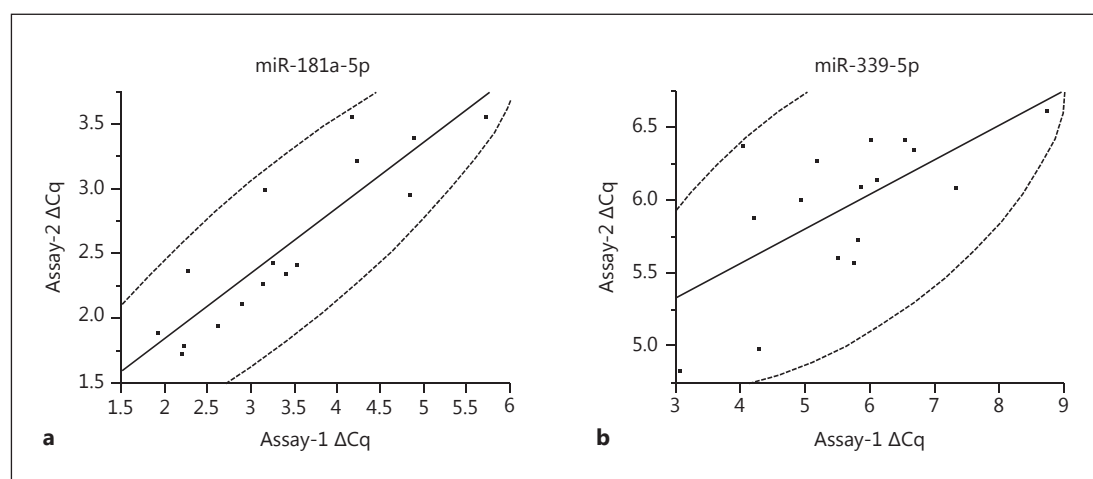
**Fig. 1.** Association between  $\Delta Cq$  of serum miRNAs and tumor response after the initiation of sorafenib. Diamond and lines in the diamond indicate the means and 95% CIs of each subgroup; boxes and whiskers denote 75 and 95% distributions, and the lines in the boxes show median values, respectively. Dashed lines in the each panel represent the mean value of all patients. p values between each group shown in the panels were calculated using Wilcoxon rank-sum test with Bonferroni correction. **a**  $\Delta Cq$  of serum miR-181a-5p among the patients who showed PR, SD, and PD at 1 month after the initiation of sorafenib. The difference was significant between 3 groups by both ANOVA and Kruskal-Wallis tests [ $p = 0.0223$ ,  $F(2, 52) = 4.12$  by ANOVA and  $p = 0.0256$  by Kruskal-Wallis tests, respectively]. **b**  $\Delta Cq$  of serum miR-339-5p among the patients who showed PR, SD, and PD at 1 month after the initiation of sorafenib. The difference was significant between 3 groups by both ANOVA and Kruskal-Wallis tests [ $p = 0.0244$ ,  $F(2, 52) = 4.00$  by ANOVA and  $p = 0.0133$  by Kruskal-Wallis tests]. **c**  $\Delta Cq$  of serum miR-181a-5p among the patients who showed PR, SD, and PD at 3 months after the initiation of sorafenib. The difference was significant between 3 groups by both ANOVA and Kruskal-Wallis tests [ $p = 0.0333$ ,  $F(2, 37) = 3.76$  by ANOVA and  $p = 0.0271$  by Kruskal-Wallis tests]. **d**  $\Delta Cq$  of serum miR-339-5p among the patients who showed PR, SD, and PD at 3 months after the initiation of sorafenib. The difference was significant between 3 groups by both ANOVA and Kruskal-Wallis tests [ $p = 0.0323$ ,  $F(2, 37) = 3.79$  by ANOVA and  $p = 0.0290$  by Kruskal-Wallis tests].

#### Clinical Factors That Predict DC for Sorafenib Treatment

Before treatment, we studied clinical factors that were associated with DC. For this purpose, we categorized contentious variables of age, maximum tumor size, and number of tumor into two groups using their median values shown in table 1. Among the variables examined, BCLC stage, extrahepatic metastasis, DCP level before treatment, and the  $\Delta Cq$  of miR-181a-5p and miR-338-5p were significantly associated with DC at 3 months after sorafenib treatment ( $p = 0.0093$  and  $0.0173$  for BCLC stage and extrahepatic metastasis by Pearson's  $\chi^2$  test, respectively;  $p = 0.0135$ ,  $0.0146$ , and  $0.0139$  for DCP level, and  $\Delta Cq$  of miR-



**Fig. 2.** Association between  $\Delta Cq$  of serum miRNAs and DC at 3 months after the initiation of sorafenib. Patients with DC were defined as patients with PR or SD for 3 months. Diamond and lines in the diamond indicate the means and 95% CIs of each subgroup; boxes and whiskers denote 75 and 95% distributions, and the lines in the boxes show median values, respectively. Dashed lines in each panel represent the mean value of all patients. p values between each group shown in the panels were calculated using Wilcoxon rank-sum test with Bonferroni correction. **a**  $\Delta Cq$  of serum miR-339-5p among the healthy control, patients with and without DC at 3 months after the initiation of sorafenib.  $p = 0.0742$ ,  $F(2, 60) = 2.72$  by ANOVA and  $p = 0.0341$  by Kruskal-Wallis tests, respectively. **b**  $\Delta Cq$  of serum miR-181a-5p among the healthy control and patients with and without DC at 3 months after the initiation of sorafenib.  $p = 0.0048$ ,  $F(2, 60) = 5.87$  by ANOVA and  $p = 0.0032$  by Kruskal-Wallis tests. In addition to the p values calculated using Wilcoxon rank-sum test with Bonferroni correction ( $p = 0.0150$  and  $0.0038$  for DC vs. non-DC and control vs. non-DC, respectively), the p values by post hoc Tukey-Kramer test are also shown in parentheses ( $p = 0.0349$  and  $0.0180$  for DC vs. non-DC and control vs. non-DC, respectively).



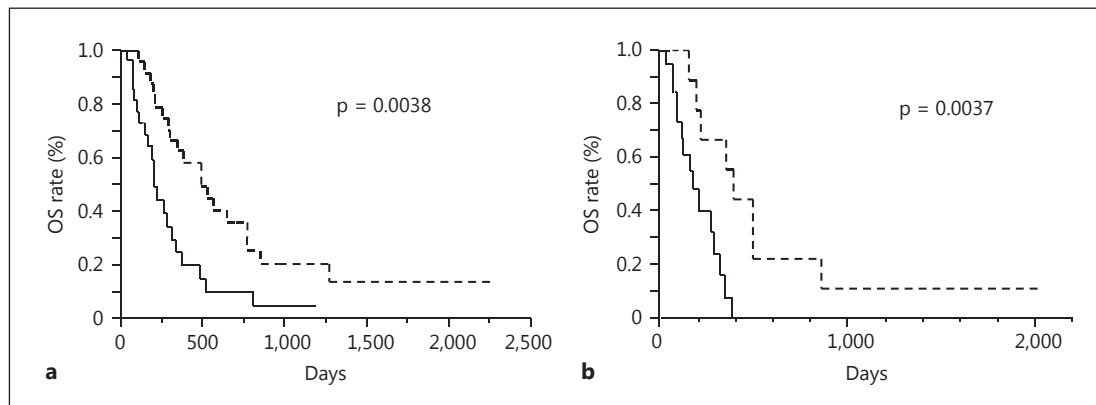
**Fig. 3.** Interassay variation for quantification of serum miRNAs. The  $\Delta Cq$  values based on the mean value of 5 kinds of reference miRNAs (assay-1) and those based on the mean of 2 kinds of reference miRNAs (assay-2) were compared. The dashed curves represent 95% confidence ellipse area. **a** Interassay variation for  $\Delta Cq$  of serum miR-181a-5p.  $R^2 = 0.418$ ,  $p = 0.0068$  by Pearson's correlation coefficient. **b** Interassay variation for  $\Delta Cq$  of serum miR-339-5p.  $R^2 = 0.7804$ ,  $p < 0.0001$  by Pearson's correlation coefficient.

**Table 3.** Associations between characteristics before treatment and disease control after the initiation of sorafenib

Characteristics before treatment	Patients with DC <sup>2</sup>	Patients without DC <sup>2</sup>	Univariate p value <sup>3</sup>	Multivariate <sup>4</sup>	
				p value	OR (95% CI)
Age <sup>1</sup>					
≤73 years	9	16	0.3839	–	–
≥74 years	7	21			
Sex					
Male	13	32	0.6249	–	–
Female	3	5			
Virus					
HBV	5	8	0.3039	–	–
HCV	8	14			
NBNC	3	15			
Size <sup>1</sup>					
<3.6 cm	7	19	0.6133	–	–
>3.7 cm	9	18			
Number of tumors <sup>1</sup>					
<5	10	15	0.1415	–	–
>6	6	22			
BCLC stage			<b>0.0093</b>	<b>0.0475</b>	
A	4	4			
B	8	7			
C	4	26			
BCLC-B/A				0.7230	0.71 (0.10–4.68) <sup>5</sup>
BCLC-C/A				<b>0.0430</b>	<b>0.14 (0.02–0.94)</b>
BCLC-C/B				<b>0.0387</b>	<b>0.20 (0.04–0.93)</b>
Extrahepatic metastasis					
Without	13	17	<b>0.0173</b>	–	–
With	3	20			
Portal vein thrombosis					
Without	14	28	0.3298	–	–
With	2	9			
AFP level before treatment, ng/ml	158 (16–1,527.25)	65 (7–5,367.5)	0.8691	–	
DCP level before treatment, mAU/ml	142.5 (27.25–1,785.25)	3,431 (178.5–17,700)	<b>0.0135</b>	0.9092	1 (1–1)
ΔCq of serum miR-181a-5p	2.65 (2.20–3.35)	3.42 (2.82–4.14)	<b>0.0146</b>	0.2864	0.63 (0.26–1.47)
ΔCq of serum miR-339-5p	4.92 (3.86–5.73)	5.74 (5.04–6.58)	<b>0.0139</b>	0.2378	0.70 (0.36–1.26)

AFP = α-Fetoprotein. <sup>1</sup> Contentious variables of these factors are categorized using the median value shown in table 1. <sup>2</sup> Number of the patients of each group for categorical variables or median value (25th–75th percentiles) for contentious variables are shown. <sup>3</sup> p values by the  $\chi^2$  test or Fisher's exact test for categorical variables or the Wilcoxon rank-sum test for contentious variables are shown. <sup>4</sup> We applied multiple logistic regression analysis and calculated the p value and OR. Bold denotes p < 0.05. <sup>5</sup> p values and OR between two categories of BCLC stage.

181a-5p and miR-338-5p by Wilcoxon rank-sum test, respectively; table 3). Since extrahepatic metastasis is a component of the BCLC staging system, we eliminated the extrahepatic metastasis variable and conducted multivariate analysis using BCLC stage, DCP level, and the ΔCq of miR-181a-5p and miR-338-5p as covariables; only BCLC stage was revealed as an independent factor with borderline significance [p = 0.0475, odds ratio (OR) of BCLC-C/BCLC-A for DC 0.14, 95% confidence interval (CI) 0.02–0.94, and OR for BCLC-C/BCLC-B for DC 0.20, 95% CI 0.04–0.93; table 3]. As sorafenib is usually recommended in BCLC-C cases, and miR-181a-5p should be more suitable for quantification than miR-338-5p in a real clinical setting because of the lower interassay variation, we further conducted multivariate analysis using extrahepatic metastasis, serum DCP and miR-181a-5p levels before the treatment among



**Fig. 4.** Kaplan-Meier curve for OS after initiation of sorafenib treatment in serum miR-181a-5p high and low groups. The patients were categorized as the high serum miR-181a-5p and the low serum miR-181a-5p groups based on the  $\Delta Cq$  cutoff value of 3.25. The solid line shows the survival curve for the low serum miR-181a-5p group and the dashed line for the high serum miR-181a-5p group. p values by log-rank test are shown. **a** Kaplan-Meier curve for all HCC patients. Among the 53 patients examined, 25 were classified as the high serum miR-181a-5p group (6 were censored cases) and 28 were members of the low serum miR-181a-5p group (7 were censored). Median periods of OS (25th–75th percentile) were 489 days (272–849) for the high serum miR-181a-5p group and 198 days (111–336) for the low serum miR-181a-5p group. **b** Kaplan-Meier curve among patients with BCLC-C HCC. Among the 30 HCC patients with BCLC-C tumor, 10 were classified as the high serum miR-181a-5p group (2 were censored cases) and 20 were members of the low serum miR-181a-5p group (5 were censored). Median periods of OS (25th–75th percentile) were 382 days (204–489) for the high serum miR-181a-5p group and 164 days (80–279) for the low serum miR-181a-5p group.

BCLC-C cases. The analysis revealed that the  $\Delta Cq$  of miR-181a-5p, representing the serum miRNA levels, was the only independent factor for predicting DC ( $p = 0.0092$ , OR for DC = 0.139, 95% CI 0.011–0.658).

#### *Serum miR-181a-5p Level Predicts Survival after Sorafenib Treatment*

Finally, we determined the serum  $\Delta Cq$  of miR-181a-5p before treatment that best reflected the DC at 3 months after initiation of sorafenib using receiver operating characteristic analysis. A  $\Delta Cq$  cutoff value of 3.25 provides the best discrimination of DC cases from non-DC cases with a sensitivity of 0.7500 and 1 – specificity of 0.3243 (online suppl. fig. 2).

Using the  $\Delta Cq$  cutoff value of 3.25, we classified the HCC patients into the high serum miR-181a-5p and the low serum miR-181a-5p groups, and analyzed the survival after the initiation of sorafenib treatment using patient's death as an endpoint. The univariate analysis revealed that OS was significantly longer in patients with a high serum miR-181a-5p level than in those with a low level among all 53 HCC cases as well as the 30 BCLC-C cases ( $p = 0.0038$  and  $0.0037$  for all the cases and the BCLC-C cases, respectively, fig. 4a, b). Among other clinical characteristics, such as age, sex, maximum tumor size, number of tumors, presence of extrahepatic metastasis and portal vein thrombosis, number of tumors was also significantly associated with the duration of OS among the BCLC-C cases ( $p = 0.0194$  by log-rank test, online suppl. table 2). We further conducted multivariate analysis using number of tumor (categorized as  $\leq 5$  and  $\geq 6$ ) and serum miR-181a-5p level as covariables and found that miR-181a-5p level was the independent factor for OS ( $p = 0.0194$ , hazard ratio 0.267, and 95% CI 0.070–0.818, online suppl. table 2).



## Discussion

Despite recent progress in the diagnosis and treatment of HCC, the prognosis of patients with advanced HCC is still unsatisfactory. Currently, sorafenib is the only systemic agent that shows improvement of progression-free and overall survival for advanced HCC patients with vascular invasion and extrahepatic spread, or in those who failed to respond to TACE [2, 3]. Previously, we reported that DC after initiation of sorafenib is associated with improved OS in patients with advanced HCC [6]. Therefore, prediction of the initial response to this molecular-targeting agent is critical for the management of HCC, the needs of which are still unmet. In this study, we addressed this important issue and showed serum miRNA profiles that are associated with DC after the initiation of sorafenib treatment.

It is well described that miRNAs target several molecules that are critical for the development and biological behavior of cancer including HCC. So far, a number of studies have shown the role of miRNAs in the pathogenesis of liver disease including HCC [19]. Moreover, miRNAs detected in circulating blood are usually present within microvesicles such as exosomes [20, 21]; the circulating miRNAs could be markers of HCC progression [22]. However, it is difficult to evaluate the serum miRNA profiles from cancer cells for several reasons. For example, serum miRNA levels may be affected by the degradation of noncancerous cells, especially those derived from hematopoietic cells [14]. In addition, as serum miRNAs should be in exosomes as well as apoptotic bodies, a certain type of miRNA could be overestimated in HCC cases with degradation and vascular invasion [19]. Furthermore, serum miRNA levels are generally low, and the application of a universal internal control of miRNAs for quantification is controversial [14]. To address these issues, we used a qPCR panel specially focused on detecting serum miRNAs that have been previously reported in the literature. [18] For this PCR panel, we used LNA probes to provide enhanced sensitivity and specificity of qPCR with five reference miRNAs serving as an internal control. We also used ideal monitors for several steps of the quantification procedure. Through the analysis of screening and validation, we found miR-181a-5p is the best candidate as a serum biomarker for predicting early response of sorafenib in HCC treatment.

In this study, we applied the comparative cycle threshold methods for relative quantification for evaluating serum miRNAs [23], and found that an increase in  $\Delta Cq$  was detected in HCC patients with non-DC compared to DC patients for miR-181a-5p and miR-338-5p. As  $\Delta Cq$  was calculated as a difference of  $Cq$  between target and control miRNAs ( $Cq$  of target subtracted by that of control), a larger  $\Delta Cq$  implies a lower level of serum miRNAs. Interestingly, there is no statistical difference in the serum level of these miRNAs between HCC patients with DC and normal healthy controls; a significant decrease in serum levels was detected in HCC patients with non-DC for serum miR-181a-5p and miR-338-5p. In addition, a dose-dependent relationship was observed between serum miRNA levels and tumor responses, where the serum level was the highest in the PR and the lowest in the PD group, suggesting a biological role of serum miRNAs in tumor behavior; miR-181a-5p and miR-338-5p in serum might provide a tumor-suppressive effect during sorafenib therapy. Currently, the role of miR-181a-5p and miR-338-5p in the pathogenesis of cancer is controversial. Previous reports suggest that the plasma level of miR-338-5p is higher in HCC patients than in healthy controls [24]. On the other hand, the expression of pre-miR-338-5p induced a decrease in cell proliferation and cell cycle arrest in glioblastoma cells; miR-338-5p sensitizes tumors to radiation through regulation of genes involved in DNA damage response [25]. Our result suggested that miR-338-5p might have a role in the induction of tumor response to sorafenib treatment, although the quantification of serum miR-338-5p is unstable compared to that of miR-181a-5p because of a lower level of the initial copy number. Regarding miR-181a-5p, the overexpression in tumorous tissue was reportedly associated with shorter

survival in patients with ovarian cancer who underwent neoadjuvant chemotherapy [26]. However, another report suggested that a reduction of serum miR-181a-5p was observed in breast cancer patients [27]. Recently, it was reported that miR-181a-5p inhibits cancer cell migration and angiogenesis through downregulation of matrix metalloproteinase-14 in aggressive human breast and colon cancers [28]. More importantly, it has also been reported that miR-181a-5p, which directly targets c-Met, is downregulated in HCC and suppresses motility, invasion, and branching-morphogenesis; the loss of miR-181a-5p expression led to the activation of c-Met-mediated oncogenic signaling in hepatocarcinogenesis [29]. A recent study suggested that c-Met could activate p38 $\alpha$  mitogen-activated protein kinase, which could be a molecule involved in the escape pathway of sorafenib-resistance [30]. Taken together, it is conceivable that miR-181a-5p acts as a tumor suppressor in HCC, and its expression might have a synergic antitumor effect with the multikinase inhibitor. Further study is required to understand the role of miR-181a-5p in HCC pathogenesis and chemoresistance.

As mentioned before, we have reported that DC after the initiation of sorafenib is associated with improved OS in patients with advanced HCC [6]; the presented data also show that high serum miR-181a-5p levels are associated with both high DCR and long OS in patients with BCLC-C HCC, although the data might be biased because of the nature of retrospective analyses. Therefore, analyzing a miR-181a-5p level should be informative for initiating sorafenib treatment in HCC with advanced stage.

Although we screened candidate miRNAs for predicting DC in sorafenib treatment using a serum secreted miRNA panel and confirmed the relationships with validation cohort, the limitation of this study is mainly attributed to the relatively small size of the sample. Therefore, the results of this study should be reevaluated using a larger cohort. Further study will allow us to understand the predictive value of serum miRNAs in the tumor behavior during sorafenib therapy.

## Acknowledgements

The authors thank Ms. Ikuko Kagami for technical assistance. This work was supported in part by a grant-in-aid for scientific research (KAKENHI: 15K09028) from the Japanese Society for the Promotion of Science.

## Disclosure Statement

The authors declare that they have no conflict of interest.

## References

- 1 Torre LA, Bray F, Siegel RL, Ferlay J, Lortet-Tieulent J, Jemal A: Global cancer statistics, 2012. *CA Cancer J Clin* 2015;65:87–108.
- 2 Kudo M: Treatment of advanced hepatocellular carcinoma with emphasis on hepatic arterial infusion chemotherapy and molecular targeted therapy. *Liver Cancer* 2012;1:62–70.
- 3 Llovet JM, Ricci S, Mazzaferro V, Hilgard P, Gane E, Blanc JF, de Oliveira AC, Santoro A, Raoul JL, Forner A, Schwartz M, Porta C, Zeuzem S, Bolondi L, Greten TF, Galle PR, Seitz JF, Borbath I, Haussinger D, Giannaris T, Shan M, Moscovici M, Voliotis D, Bruix J; SHARP Investigators Study Group: Sorafenib in advanced hepatocellular carcinoma. *N Engl J Med* 2008;359:378–390.
- 4 Bruix J, Sherman M, American Association for the Study of Liver Diseases: Management of hepatocellular carcinoma: an update. *Hepatology* 2011;53:1020–1022.

- 5 Yamasaki T, Kimura T, Kurokawa F, Aoyama K, Ishikawa T, Tajima K, Yokoyama Y, Takami T, Omori K, Kawaguchi K, Tsuchiya M, Terai S, Sakaida I, Okita K: Prognostic factors in patients with advanced hepatocellular carcinoma receiving hepatic arterial infusion chemotherapy. *J Gastroenterol* 2005;40:70–78.
- 6 Arizumi T, Ueshima K, Chishina H, Kono M, Takita M, Kitai S, Inoue T, Yada N, Hagiwara S, Minami Y, Sakurai T, Nishida N, Kudo M: Duration of stable disease is associated with overall survival in patients with advanced hepatocellular carcinoma treated with sorafenib. *Dig Dis* 2014;32:705–710.
- 7 Borel F, Konstantinova P, Jansen PL: Diagnostic and therapeutic potential of miRNA signatures in patients with hepatocellular carcinoma. *J Hepatol* 2012;56:1371–1383.
- 8 Bai S, Nasser MW, Wang B, Hsu SH, Datta J, Kutay H, Yadav A, Nuovo G, Kumar P, Ghoshal K: MicroRNA-122 inhibits tumorigenic properties of hepatocellular carcinoma cells and sensitizes these cells to sorafenib. *J Biol Chem* 2009;284:32015–32027.
- 9 Shimizu S, Takehara T, Hikita H, Kodama T, Miyagi T, Hosui A, Tatsumi T, Ishida H, Noda T, Nagano H, Doki Y, Mori M, Hayashi N: The let-7 family of microRNA inhibits Bcl-xL expression and potentiates sorafenib-induced apoptosis in human hepatocellular carcinoma. *J Hepatol* 2010;52:698–704.
- 10 Mao K, Zhang J, He C, Xu K, Liu J, Sun J, Wu G, Tan C, Zeng Y, Wang J, Xiao Z: Restoration of miR-193b sensitizes hepatitis B virus-associated hepatocellular carcinoma to sorafenib. *Cancer Lett* 2014;352:245–252.
- 11 Gyongyosi B, Vegh E, Jaray B, Szekely E, Fassan M, Bodoky G, Schaff Z, Kiss A: Pretreatment microRNA level and outcome in sorafenib-treated hepatocellular carcinoma. *J Histochem Cytochem* 2014;62:547–555.
- 12 Vaira V, Roncalli M, Carnaghi C, Favarsani A, Maggioni M, Augello C, Rimassa L, Pressiani T, Spagnuolo G, Di Tommaso L, Fagioli S, Rota Caremoli E, Barberis M, Labianca R, Santoro A, Bosari S: MicroRNA-425-3p predicts response to sorafenib therapy in patients with hepatocellular carcinoma. *Liver Int* 2015;35:1077–1086.
- 13 Nishida N, Kitano M, Sakurai T, Kudo M: Molecular mechanism and prediction of sorafenib chemoresistance in human hepatocellular carcinoma. *Dig Dis* 2015;33:771–779.
- 14 Ono S, Lam S, Nagahara M, Hoon DS: Circulating microRNA biomarkers as liquid biopsy for cancer patients: pros and cons of current assays. *J Clin Med* 2015;4:1890–1907.
- 15 Lind K, Stahlberg A, Zoric N, Kubista M: Combining sequence-specific probes and DNA binding dyes in real-time PCR for specific nucleic acid quantification and melting curve analysis. *BioTechniques* 2006;40:315–319.
- 16 Lencioni R, Llovet JM: Modified RECIST (mRECIST) assessment for hepatocellular carcinoma. *Semin Liver Dis* 2010;30:52–60.
- 17 Gadkar V, Filion M: New developments in quantitative real-time polymerase chain reaction technology. *Curr Issues Mol Biol* 2014;16:1–6.
- 18 Ameling S, Kacprowski T, Chilukoti RK, Malsch C, Liebscher V, Suhre K, Pietzner M, Friedrich N, Homuth G, Hammer E, Volker U: Associations of circulating plasma microRNAs with age, body mass index and sex in a population-based study. *BMC Med Genomics* 2015;8:61.
- 19 Szabo G, Bala S: MicroRNAs in liver disease. *Nat Rev Gastroenterol Hepatol* 2013;10:542–552.
- 20 Reid G, Kirschner MB, van Zandwijk N: Circulating microRNAs: association with disease and potential use as biomarkers. *Crit Rev Oncol Hematol* 2011;80:193–208.
- 21 Lemoine S, Thabut D, Housset C, Moreau R, Valla D, Boulanger CM, Rautou PE: The emerging roles of microvesicles in liver diseases. *Nat Rev Gastroenterol Hepatol* 2014;11:350–361.
- 22 Murakami Y, Toyoda H, Tanahashi T, Tanaka J, Kumada T, Yoshioka Y, Kosaka N, Ochiya T, Taguchi YH: Comprehensive miRNA expression analysis in peripheral blood can diagnose liver disease. *PLoS One* 2012;7:e48366.
- 23 Goll R, Olsen T, Cui G, Florholmen J: Evaluation of absolute quantitation by nonlinear regression in probe-based real-time PCR. *BMC Bioinformatics* 2006;7:107.
- 24 Chen Y, Chen J, Liu Y, Li S, Huang P: Plasma miR-15b-5p, miR-338-5p, and miR-764 as biomarkers for hepatocellular carcinoma. *Med Sci Monit* 2015;21:1864–1871.
- 25 Besse A, Sana J, Lakomy R, Kren L, Fadrus P, Smrcka M, Hermanova M, Jancalek R, Reguli S, Lipina R, Svoboda M, Slampa P, Slaby O: MiR-338-5p sensitizes glioblastoma cells to radiation through regulation of genes involved in DNA damage response. *Tumour Biol* 2016;37:7719–7727.
- 26 Petrillo M, Zannoni GF, Beltrame L, Martinelli E, DiFeo A, Paracchini L, Craparotta I, Mannarino L, Vizzielli G, Scambia G, D'Incalci M, Romualdi C, Marchini S: Identification of high-grade serous ovarian cancer miRNA species associated with survival and drug response in patients receiving neoadjuvant chemotherapy: a retrospective longitudinal analysis using matched tumor biopsies. *Ann Oncol* 2016;27:625–634.
- 27 Ferracin M, Lupini L, Salamon I, Saccenti E, Zanzi MV, Rocchi A, Da Ros L, Zagatti B, Musa G, Bassi C, Mangolini A, Cavallero G, Frassoldati A, Volpato S, Carcoforo P, Hollingsworth AB, Negrini M: Absolute quantification of cell-free microRNAs in cancer patients. *Oncotarget* 2015;6:14545–14555.
- 28 Li Y, Kuscus C, Banach A, Zhang Q, Pulkoski-Gross A, Kim D, Liu J, Roth E, Li E, Shroyer KR, Denoya PI, Zhu X, Chen L, Cao J: MiR-181a-5p inhibits cancer cell migration and angiogenesis via downregulation of matrix metalloproteinase-14. *Cancer Res* 2015;75:2674–2685.
- 29 Korhan P, Erdal E, Atabey N: Mir-181a-5p is downregulated in hepatocellular carcinoma and suppresses motility, invasion and branching-morphogenesis by directly targeting c-Met. *Biochem Biophys Res Commun* 2014;450:1304–1312.
- 30 Rudalska R, Dauch D, Longerich T, McJunkin K, Wuestefeld T, Kang TW, Hohmeyer A, Pesic M, Leibold J, von Thun A, Schirmacher P, Zuber J, Weiss KH, Powers S, Malek NP, Eilers M, Sipos B, Lowe SW, Geffers R, Laufer S, Zender L: In vivo RNAi screening identifies a mechanism of sorafenib resistance in liver cancer. *Nat Med* 2014;20:1138–1146.

## Commentary

In 1896, Lambert reported the first case of a hepatic abscess secondary to foreign body perforation. Since then, several cases of foreign bodies causing adverse events have been described. Fish bones are the leading ingested foreign bodies in areas where fish consumption is highly prevalent. Most of them pass uneventfully within 1 week, with only 10% to 20% causing intraluminal injury. As with this particular person, many patients have no memory of foreign body ingestion, nor do they remember once the diagnosis is made, so the bones may remain undetected. Although most accidentally ingested fish bones migrate distally inside the lumen, they may also remain embedded inside the thick gastric wall without full perforation and may result in abscess or granuloma formation. When the location and nature of a fish bone is being determined, plain radiography has a sensitivity of 32% because of the radiolucent character of the bones. EUS is a valuable tool; previous studies have shown that it leads to the diagnosis in 74% of cases and changes management in 57% of cases. The available endoscopic tools for removal of foreign bodies include forceps, balloon extraction, bougienage, and magnetic extraction. In 2011, Seo et al reported the first case of ESD for endoscopic removal of impacted magnets. That procedure had also been previously used once for definitive diagnosis and management of toothpick ingestion. This case encourages endoscopists to consider emerging procedures, such as ESD, as an alternative for difficult cases such as embedded foreign bodies. A fish-bone granuloma should be kept in mind when a submucosal mass is found in the GI tract.

**Katherine Mejía, MD**

**Universidad de los Andes, Bogotá, Columbia**

**Massimo Raimondo, MD**

**Associate Editor for Focal Points**

## Stent migration into the abdominal cavity after EUS-guided hepaticogastrostomy



A 73-year-old man had advanced multifocal hepatocellular carcinoma and had undergone endoscopic transpapillary bilateral metal stenting for hilar biliary obstruction. He was readmitted because of the recurrence of obstructive jaundice. Repeated ERCP was attempted; however, drainage of the left side was unsuccessful. Hence, we performed EUS-guided hepaticogastrostomy. A 4-mm left intrahepatic bile duct was punctured with a 19-gauge needle, and a 0.025-inch guidewire was inserted. The fistula was dilated with a tapered-tip ERCP catheter; subsequently, a covered metal stent (Niti-S Biliary Cover Stent, 6 × 80 mm; Taewoong Medical, Seoul, Korea) was deployed (**A**). On the day after the procedure, the patient had 2 episodes of vomiting. CT revealed that the proximal end of the stent was buried in the gastric wall (**B**). Emergent gastroscopy confirmed stent migration from the gastric lumen (**C**). A laparotomy was immediately performed. The migrated stent could be seen in the abdominal cavity (**D**). The stent was reinserted through the fistula into the gastric lumen and was sutured to prevent migration. After surgery, the jaundice resolved. The patient died 142 days after the procedure as a result of progression

of his underlying liver disease. However, he was free of obstructive jaundice until death.

### DISCLOSURE

*All authors disclosed no financial relationships relevant to this publication.*

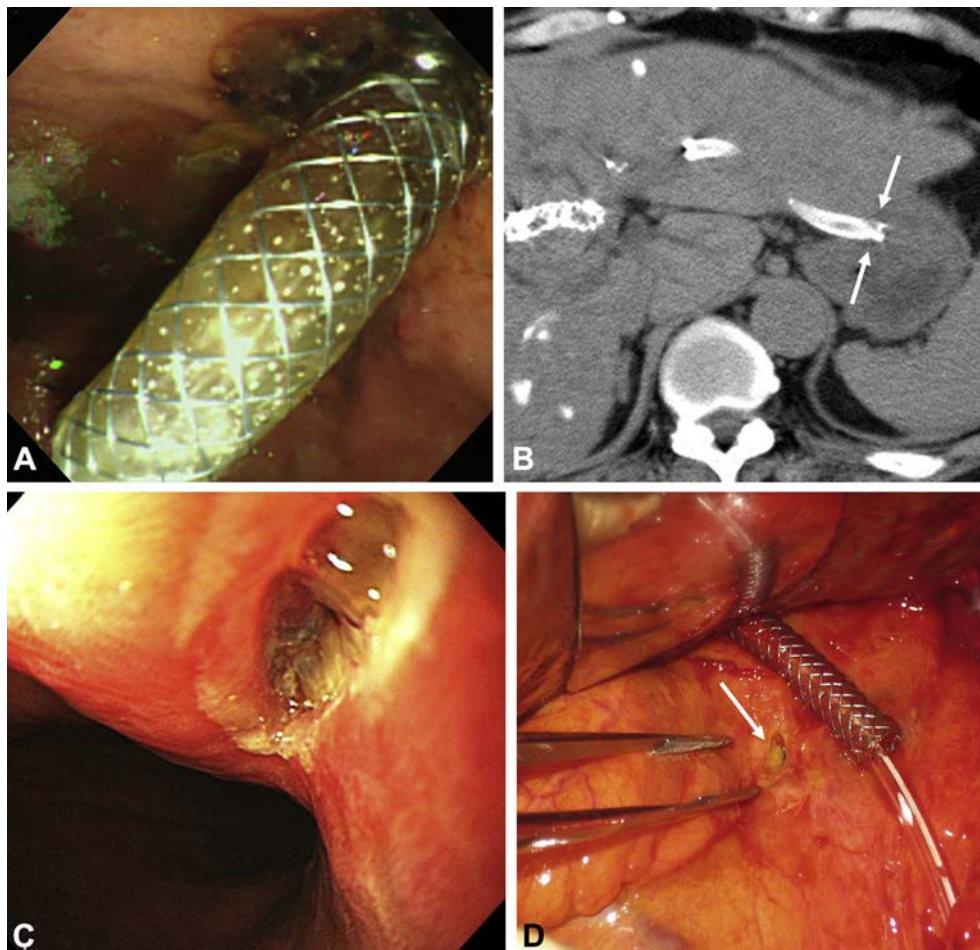
**Kosuke Minaga, MD**, Department of Gastroenterology and Hepatology, Kinki University Hospital, Faculty of Medicine, Osaka-Sayama, Japan, Department of Gastroenterology and Hepatology, Japanese Red Cross Society Wakayama Medical Center, Wakayama, Japan, **Masayuki Kitano, MD, PhD**, Department of Gastroenterology and Hepatology, Kinki University Hospital, Faculty of Medicine, Osaka-Sayama, Japan, **Yukitaka Yamashita, MD, PhD**, Yasuki Nakatani, MD, Department of Gastroenterology and Hepatology, Japanese Red Cross Society Wakayama Medical Center, Wakayama, Japan, **Masatoshi Kudo, MD, PhD**, Department of Gastroenterology and Hepatology, Kinki University Hospital, Faculty of Medicine, Osaka-Sayama, Japan

<http://dx.doi.org/10.1016/j.gie.2016.03.016>

## Commentary

ERCP is the standard drainage technique for biliary obstruction. Although it has a success rate of >90%, it can fail as a result of anatomic difficulties such as surgically altered anatomy, gastric and duodenal obstruction, periampullary diverticula, and





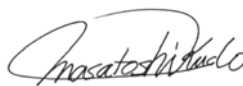
tumor infiltration. This case clearly portrays the latter condition. When failure occurs, percutaneous transhepatic biliary drainage (PTBD) and surgery are considered as alternative interventions. However, these are associated with major adverse events in 4% to 25% of cases, negatively affecting the patient's quality of life. In 2001, the first case of EUS-guided biliary drainage was reported. Since then, major advances have been made, and 3 different approaches have been developed: (1) EUS-guided transluminal biliary drainage, (2) the EUS rendezvous technique, and (3) the EUS antegrade approach. This is a nice case describing the first method. According to a meta-analysis conducted by Khan et al, EUS-guided biliary drainage has a success rate of 90% and an adverse events rate of 17%. The reported adverse events of this technique include stent migration, bleeding, pneumoperitoneum, bile peritonitis, and acute cholangitis. Stent migration is a serious event, especially early after the procedure. To address it, Ogura et al recently evaluated the factors related to stent dysfunction. The study revealed that a stent length  $\geq 3$  cm in the luminal portion can prevent stent migration after its deployment. Furthermore, longer luminal length is related to decreased stent impaction and gastrobiliary reflux, leading to long-term stent patency. This adverse event would probably have been prevented if a longer stent had been used. Observational studies comparing traditional approaches, including PTBD and surgery, versus EUS-guided biliary drainage have shown that both techniques have equal technical success and adverse events profile. However, the development of specially designed stents and assessment of the technique are mandatory for generalization of this endoscopic approach. In this particular situation, it was the appropriate tool for successful resolution of obstructive jaundice, especially in a patient with an infiltrating tumor. This case shows how important it is to consider emerging endoscopic techniques to accomplish never-imagined solutions.

**Katherine Mejía, MD**  
**Universidad de los Andes, Bogotá, Columbia**

**Massimo Raimondo, MD**  
**Associate Editor for Focal Points**

# Immune Checkpoint Blockade in Hepatocellular Carcinoma: 2017 Update

*Prof. M. Kudo*



Editor *Liver Cancer*



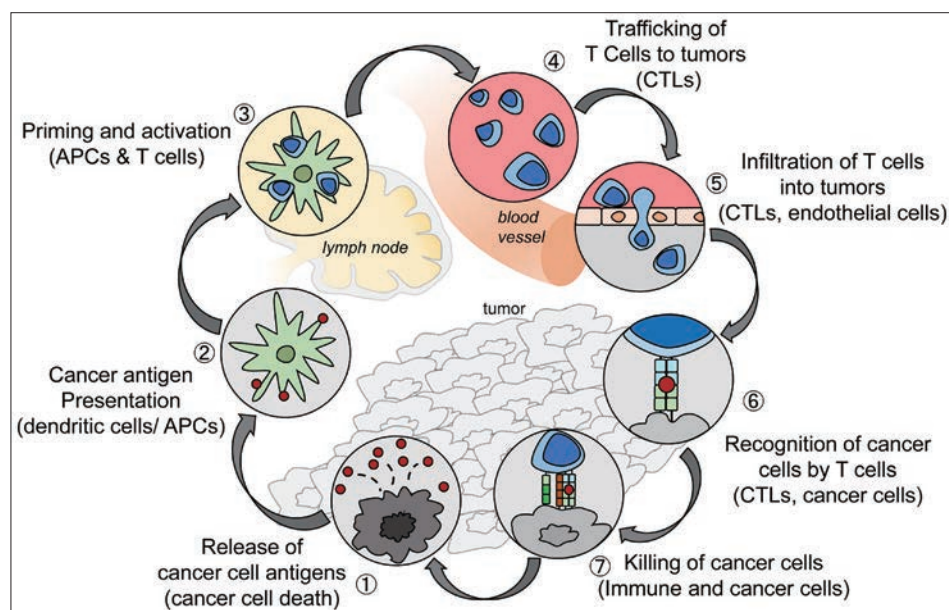
## Introduction

The immune checkpoint molecule programmed cell death 1 (PD-1) was discovered in 1992 by Professor Tasuku Honjo and his research team at Kyoto University [1]. They later discovered that PD-1 is involved in immunosuppression and is a receptor that acts as a “brake” for the immune response in knockout mice. In 2000, a joint research project between the Honjo group at Kyoto University and the Genetics Institute together with Harvard University discovered the ligands of PD-1 (PD-L1 and PD-L2) [2–5]. In 2002, Iwai et al. [6] found that enhancing immune activation by inhibiting the binding of PD-1 to its ligands in mouse models markedly enhanced antitumor activity. In 2005, Ono Pharmaceutical and the American company Medarex took note of these findings and developed nivolumab, a human anti-PD-1 antibody. That same year, the U.S. Food and Drug Administration (FDA) recognized nivolumab as an investigational new drug, thereby enabling clinical trials to be started in the United States. In 2009, Bristol-Myers Squibb and Ono Pharmaceutical (BMS/ONO) began joint clinical trials of nivolumab. The results of clinical trials in patients with melanoma led to the approval of an anti-PD-1 antibody for the treatment of melanoma in Japan in July 2014, before any other country in the world. Nivolumab has also been evaluated in a series of clinical trials for non-small cell lung cancer and renal cell carcinoma and has yielded favorable outcomes.

In 1995, Dr. James Allison of the University of Texas discovered that another molecule, called cytotoxic T-lymphocyte-associated antigen (CTLA-4) [7], serves as an indicator of immune cell suppression [7]. In 1996, his team showed that tumors disappeared in mice treated with an antibody that inhibits the function of CTLA-4 [8]. CTLA-4 is also an immune checkpoint molecule. Bristol-Myers developed an anti-CTLA-4 antibody called ipilimumab, which was approved for the treatment of melanoma in the United States in March 2011 and in Europe in July 2011 [9]. It was later approved in Japan in July 2015.

When cancer cells develop, antigen-presenting cells (APCs) recognize tumor-associated antigens (TAAs), triggering in the lymph nodes the activation of immature T cells that will become CD8-positive T cells (the priming phase). Once activated, the T cells travel throughout the bloodstream and reach the tumor site. There, they attempt to attack tumor cells by



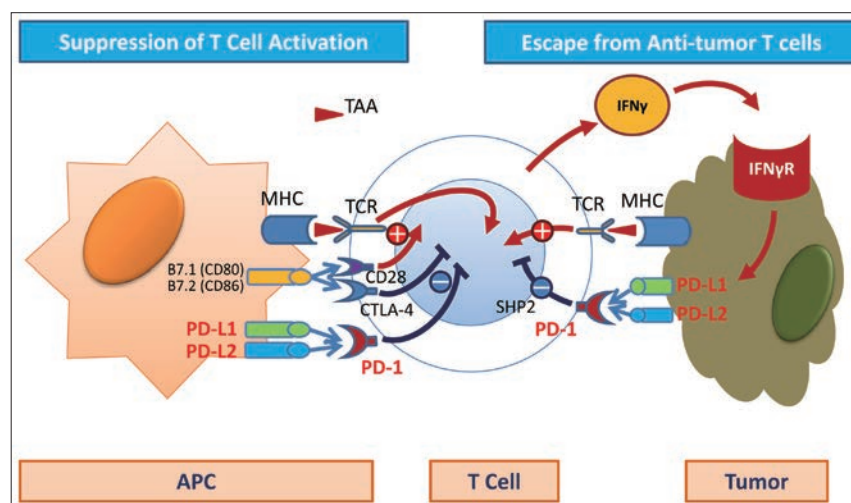


**Fig. 1.** The cancer–immunity cycle. The generation of immunity to cancer is a cyclic process that leads to an accumulation of immune-stimulatory factors. This cycle can be divided into seven major steps, starting with the release of antigens from cancer cells and ending with the killing of cancer cells. CTLs=cytotoxic T lymphocytes. Reproduced with permission from Chen DS, et al. [10]

releasing molecules such as perforin and granzymes (the effector phase) (fig 1) [10]. Moreover, recognition of TAAs by T cell receptors (TCR) triggers the release of interferon gamma (IFN- $\gamma$ ) and other cytokines by CD8-positive T cells in an attempt to attack the cancer. However, tumor cells protect themselves by expressing IFN- $\gamma$  induced PD-L1 or PD-L2, which binds to PD-1. When this happens, PD-1/PD-L1 binding attenuate the antitumor immune response, thereby weakening the attacking power of the T cells. This is called immune escape or immune tolerance (fig. 2). The anti-PD-1 antibody blocks PD-1 on activated T cells from binding to PD-L1 or PD-L2 on APCs or tumor cells. This removes the “brake” on the immune system and restores the ability of T cells to attack tumor cells (fig. 3). Unlike conventional chemotherapy or molecular targeted therapy, anti-PD-1 antibody achieves its antitumor effect by restoring the original potential of the natural human immune system as a powerful and precise weapon against cancer cells [11–22]. Antibodies against PD-L1 expression in the cancer tissue are believed to have a similar effect [23]. The recognition of “immuno-oncology” using immune checkpoint inhibitors was considered the “Breakthrough of the Year” by the American journal *Science* in 2013, and immuno-oncology has been widely publicized. PD-L1 also serves as a biomarker that predicts the response to anti-PD-1 antibody [24]. In addition, Kupffer-phase Sonazoid contrast-enhanced ultrasonography is an effective imaging method for predicting the response to treatment with anti-PD-1 antibody [25].

### Development of Immune Checkpoint Inhibitors for Hepatocellular Carcinoma (HCC)

Promising results from an interim analysis of a phase I/II trial of the anti-PD-1 antibody nivolumab (CheckMate-040 trial dose-escalation cohort) were presented at the 2015 American Society of Clinical Oncology (ASCO) Annual Meeting held in Chicago [26, 27]. This

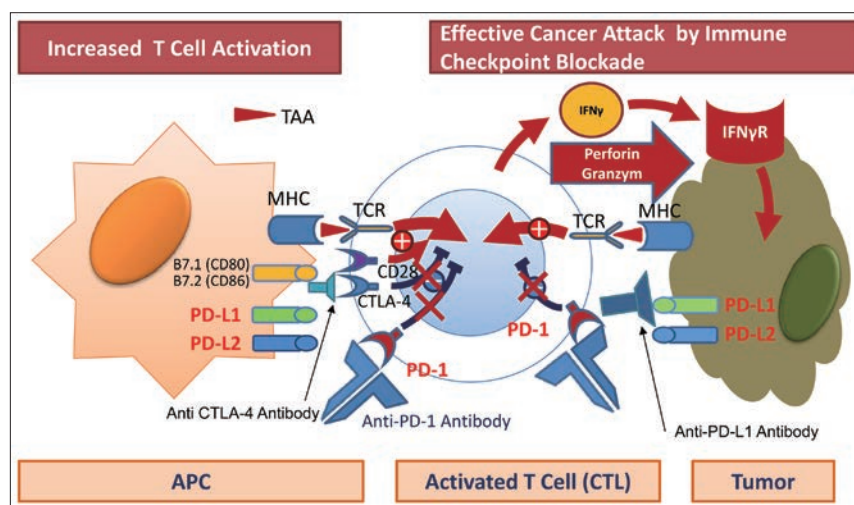


**Fig. 2.** Immune checkpoint molecule: PD-1, PD-L1, CTLA-4. Immune checkpoint molecules such as PD-1, PD-L1, and CTLA-4 play an important role in the immune escape of cancer cells from activated CD8-positive T cells. MHC=major histocompatibility complex; IFNγR=interferon gamma receptor.

dose-escalation study demonstrated the safety of nivolumab at doses of 3 mg/kg and 10 mg/kg in HCC patients with hepatitis C virus (HCV) infection, patients with hepatitis B virus (HBV) infection, and uninfected patients. The interim results of the dose-escalation study also demonstrated the efficacy of nivolumab at doses ranging from 0.1 to 10 mg/kg. Of the 47 patients included in the study, 33 (70%) had extrahepatic metastasis, 6 (13%) had vascular invasion, and 32 (68%) had previously been treated with sorafenib, i.e., the study population had relatively advanced cancer. Patients were treated with anti-PD-1 antibody, and an interim analysis was performed on March 12, 2015. At that point, 17 patients were still receiving treatment and 30 had completed or discontinued treatment. The reasons for discontinuation were disease progression in 26 patients, complete response (CR) in two patients, and adverse events in two patients. The adverse events leading to discontinuation were increased bilirubin (n=1) and an event unrelated to the study drug (n=1). The only grade 4 event (graded using the Common Terminology Criteria for Adverse Events) was increased lipase, and the only grade 3 events were elevated aspartate aminotransferase (AST) levels in five patients (11%) and elevated alanine aminotransferase (ALT) levels in four patients (9%). No serious liver dysfunction or autoimmune disease was reported.

The response rate was 19% (n=8), including the two CRs (5%). The disease control rate (DCR) was also very favorable: 67% of patients (n=28) maintained stable disease (SD) or better, whereas only 33% (n=14) developed progressive disease (PD).

Waterfall plots showed that the tumor size decreased to some extent in all cohorts (i.e., uninfected, HBV-infected, and HCV-infected HCC patients). The durability of treatment responses is particularly noteworthy. The two patients who had a CR achieved it within 3 months and maintained it for 18 months. Another patient who showed a partial response (PR) (almost a CR in fact) showed SD at approximately 11 months while the PR occurred at approximately 13 months. A durable response was achieved in all patients with a PR or SD, and no patient developed PD because of resistance. In summary, treatment of liver cancer with anti-PD-1 antibody yielded a durable response comparable to that achieved in other types of cancer. This property is highly characteristic of immune checkpoint inhibitors and merits attention. The two patients who had a CR achieved it within 3 months and maintained the response for 18 months or longer, even after discontinuing the anti-PD-1 antibody a few months after the



**Fig. 3.** Immune checkpoint blockade: anti-PD-1, anti-PD-L1, and anti CTLA-4 antibody. Anti-PD-1, anti-PD-L1, and anti-CTLA-4 antibodies restore cytotoxic T cell activity, resulting in tumor attack by perforin and granzyme.

CR. Almost all patients who showed a PR achieved it within 3 months of treatment. One of the cases presented at ASCO 2015 was a patient with countless bilobar HCCs, all of which resolved completely after 6 weeks; this was accompanied by a decrease in alpha-fetoprotein from 21,000 to 283 ng/ml. Another patient showed a decrease in tumor size from 10 cm to about 2 cm after 48 weeks, which demonstrates the durability of the response. The overall 12-month survival rate was a favorable 62%, which is a very promising outcome considering the unfavorable tumor characteristics of the study population.

The interim results of this trial can be summarized in three points: First, monotherapy with the anti-PD-1 antibody nivolumab has a favorable safety profile for HCC that is comparable with its safety profile for the treatment of other types of cancer. Second, nivolumab can be used safely in patients infected with HBV or HCV. Third, immunotherapy yields both a very high response rate and a durable response. This long-lasting effect was observed at all dose levels and in all cohorts (uninfected, HBV-infected, and HCV-infected).

The team conducting this phase I/II trial designed an expansion study using a fixed dose of 3 mg/kg of nivolumab in three cohorts as follows: patients with no HBV or HCV infection who were sorafenib-naïve ( $n=50$ ) or who had developed PD after treatment with sorafenib ( $n=50$ ); HCV-infected patients ( $n=50$ ); and HBV-infected patients ( $n=50$ ). The results of the expansion study and the final results from the dose-escalation study were presented at ASCO 2016.

### Clinical Trials in Progress

According to the results presented at ASCO 2016, 35 of the 214 patients (16%) in the expansion cohort (CheckMate-040 cohort 2) had a tumor response [28] (table 1). The response rate was 20% for uninfected sorafenib-naïve or sorafenib-intolerant HCC patients, 19% for uninfected sorafenib-treated patients with PD, 14% for HCV-infected patients, and 12% for HBV-infected patients. The 9-month survival rate was a favorable 70.8%. Grade 3-4 adverse events of elevated AST and ALT levels were observed in this expansion cohort at low

**Table 1.** CheckMate 040 dose-expansion cohort (n=214) investigator-assessed best overall response (RECIST v1.1)

	Uninfected: sorafenib naïve/ intolerant (n=54)	Uninfected: sorafenib progressors (n=58)	HCV (n=51)	HBV (n=51)	Total (n=214)
Objective response, n (%)	11 (20)	11 (19)	7 (14)	6 (12)	35 (16)
CR	0	2 (3)	0	0	2 (1)
PR	11 (20)	9 (16)	7 (14)	6 (12)	33 (15)
SD	32 (59)	27 (47)	29 (57)	23 (45)	111 (52)
PD	11 (20)	18 (31)	12 (24)	22 (43)	63 (29)
Not evaluable	0	2 (3)	3 (6)	0	5 (2)

RECIST=response evaluation criteria in solid tumors. Reproduced with permission from Sangro B, et al. [28]

**Table 2.** CheckMate 040 dose-expansion cohort (n=214) treatment-related adverse events (TRAEs)

	Uninfected (n=112)		HCV (n=51)		HBV (n=51)		Total (n=214)	
	Any grade	Grade 3-4	Any grade	Grade 3-4	Any grade	Grade 3-4	Any grade	Grade 3-4
Patients with any TRAE, n (%)	72 (64)	21 (19)	37 (73)	15 (29)	30 (59)	3 (6)	139 (65)	39 (18)
Symptomatic TRAEs reported in >4% of all patients								
Fatigue	31 (28)	2 (2)	7 (14)	0	7 (14)	0	45 (21)	2 (1)
Pruritus	11 (10)	0	11 (22)	0	11 (22)	0	33 (15)	0
Rash	12 (11)	1 (1)	8 (16)	0	6 (12)	0	26 (12)	1 (0.5)
Diarrhea	16 (14)	2 (2)	3 (6)	0	1 (2)	1 (2)	20 (9)	3 (1)
Nausea	8 (7)	0	6 (12)	0	0	0	14 (7)	0
Decreased appetite	5 (5)	0	2 (4)	0	3 (6)	0	10 (5)	0
Dry mouth	5 (4)	0	1 (2)	0	2 (4)	0	8 (4)	0
Laboratory-value TRAEs reported in >4% of all patients								
ALT increased	6 (5)	2 (2)	7 (14)	4 (8)	2 (4)	0	15 (7)	6 (3)
AST increased	7 (6)	3 (3)	6 (12)	6 (12)	0	0	13 (6)	9 (4)
Platelet count decreased	4 (4)	1 (1)	3 (6)	2 (4)	5 (10)	1 (2)	8 (4)	3 (1)
Anemia	2 (2)	0	3 (6)	1 (2)	3 (6)	0	8 (4)	1 (0.5)

Reproduced with permission from Sangro B, et al. [28]

rates of 6% (13/139) and 7% (15/139), respectively (table 2). Considering that 66% of the 214 patients had been previously treated with sorafenib, and a high percentage of patients had advanced cancer, a 9-month survival rate of 70.8% is an excellent result (tables 3, 4).

The results of additional analysis of the dose-escalation cohort of 48 patients (CheckMate-040 cohort 1) showed a tumor response in seven patients (15%); the response rate was 13% in the uninfected group, 30% in the HCV-infected group, and 7% in the HBV-infected group [29] (tables 5–7).

The team conducting this phase I/II trial in addition to cohort 1 and 2, a randomized controlled study comparing nivolumab with sorafenib (cohort 3), a study of combination therapy

**Table 3.** CheckMate 040 dose-expansion cohort (n=214) baseline patient characteristics and prior treatment history

	Uninfected: sorafenib naïve/ intolerant (n=54)	Uninfected: sorafenib progressors (n=58)	HCV (n=51)	HBV (n=51)	Total (n=214)
Median age (range), years	66 (20–83)	65 (19–80)	65 (53–81)	55 (22–81)	64 (19–83)
Male, n (%)	46 (85)	43 (74)	43 (84)	39 (77)	171 (80)
Ethnicity, n (%)					
White	36 (67)	35 (60)	30 (59)	4 (8)	105 (49)
Black/African American	1 (2)	1 (2)	2 (4)	2 (4)	6 (3)
Asian	16 (30)	22 (38)	18 (35)	45 (88)	101 (47)
Other	1 (2)	0	1 (2)	0	2 (1)
Extrahepatic metastases, n (%)	42 (78)	43 (74)	30 (59)	46 (90)	161 (75)
Vascular invasion, n (%)	1 (2)	3 (5)	5 (10)	6 (12)	15 (7)
Child–Pugh score, n (%)					
5	41 (76)	38 (66)	27 (53)	44 (86)	150 (70)
6	12 (22)	20 (34)	21 (41)	7 (14)	60 (28)
7	1 (2)	0	2 (4)	0	3 (1)
9	0	0	1 (2)	0	1 (0.5)
α-Fetoprotein >200 µg/L, n (%)	15 (28)	26 (45)	18 (35)	27 (53)	86 (40)
Prior treatment type, n (%)					
Surgical resection	29 (54)	37 (64)	19 (37)	40 (78)	125 (58)
Radiotherapy	7 (13)	17 (29)	5 (10)	12 (24)	41 (19)
Local treatment for HCC	25 (46)	33 (57)	29 (57)	40 (78)	127 (59)
Systemic therapy	22 (41)	57 (98)	32 (63)	46 (90)	157 (73)
Sorafenib	15 (28)	56 (97)	30 (59)	40 (78)	141 (66)

Reproduced with permission from Sangro B, et al. [28]

**Table 4.** CheckMate 040 dose-expansion cohort (n=214) overall survival rates

Survival rate, %(95% CI) <sup>a</sup>	Uninfected: sorafenib naïve/ intolerant (n=54)	Uninfected: sorafenib progressors (n=58)	HCV (n=51)	HBV (n=51)	Total (n=214)
6-Month	89.8 (77.1, 95.6)	75.6 (61.5, 85.2)	82.1 (61.3, 92.4)	83.3 (67.6, 91.8)	82.5 (75.8, 87.5)
9-Month	79.8 (50.6, 92.8)	NC	NC	NC	70.8 (56.6, 81.1)

<sup>a</sup>Estimated using the Kaplan–Meier method. CI=confidence interval; NC=not calculated. Reproduced with permission from Sangro B, et al. [28]

with the anti-CTLA-4 antibody ipilimumab (cohort 4), and a study of nivolumab in Child–Pugh B patients (cohort 5).

Other ongoing trials include the dose-expansion study (cohort 2), a phase III trial comparing first-line nivolumab (anti-PD-L1 antibody) with sorafenib, a phase III trial of pembrolizumab as second-line therapy after sorafenib failure, and a phase II trial of combination therapy with the anti-PD-L1 antibody durvalumab and the anti-CTLA-4 antibody tremelimumab (table 8). The results of a clinical trial of an anti-CTLA-4 antibody for the treatment of HCC were published in the *Journal of Hepatology* in 2013. However, the anti-CTLA-4 antibody



**Table 5.** CheckMate 040 dose-escalation cohort (n=48) baseline patient characteristics and prior treatment history

	Uninfected (n=23)	HCV (n=10)	HBV (n=15)	Total (n=48)
Median age (range), years	61 (22–79)	67 (55–83)	62 (41–75)	62 (22–83)
≥65 years, n (%)	8 (35)	6 (60)	6 (40)	20 (42)
Male, n (%)	17 (74)	6 (60)	13 (87)	36 (75)
Ethnicity, n (%)				
White	19 (83)	8 (80)	1 (7)	28 (58)
Asian	2 (9)	2 (17)	14 (88)	18 (38)
Black	2 (9)	0	0	2 (4)
Extrahepatic metastases, n (%)	18 (78)	6 (60)	13 (87)	37 (77)
Vascular invasion, n (%)	3 (13)	1 (10)	2 (13)	6 (13)
Child–Pugh score, n (%)				
5	19 (83)	8 (80)	14 (93)	41 (85)
6	4 (17)	2 (20)	1 (7)	7 (15)
α-Fetoprotein >200 µg/L, n (%) <sup>a</sup>	8 (35)	3 (30)	8 (53)	19 (40)
Prior treatment type, n (%)				
Surgical resection	15 (65)	8 (80)	13 (87)	36 (75)
Radiotherapy <sup>b</sup> (external or internal)	6 (26)	2 (20)	2 (13)	10 (21)
Local treatment for HCC <sup>c</sup>	11 (48)	8 (80)	12 (80)	31 (65)
Systemic therapy	18 (78)	6 (60)	15 (100)	39 (81)
Sorafenib	16 (70)	5 (50)	14 (93)	35 (73)

<sup>a</sup>Baseline α-fetoprotein values were missing for one uninfected patient; <sup>b</sup>Could include radioembolization; <sup>c</sup>TACE, RFA, or percutaneous ethanol injection. Reproduced with permission from El-Khoueiry AB, et al. [29]

**Table 6.** CheckMate 040 dose-escalation cohort (n=48) TRAE

	Total (n=48)	
	Any grade	Grade 3-4
Patients with any TRAE, n (%)	38 (79)	12 (25)
Symptomatic TRAEs reported in >5% of all patients, n (%)		
Rash	11 (23)	0
Pruritus	7 (15)	0
Diarrhea	4 (8)	0
Asthenia	3 (6)	0
Decreased appetite	3 (6)	0
Dry mouth	3 (6)	0
Fatigue	3 (6)	1 (2)
Laboratory-value TRAEs reported in >5% of all patients, n (%)		
AST increased	10 (21)	5 (10)
Lipase increased	10 (21)	6 (13)
Amylase increased	9 (19)	1 (2)
ALT increased	7 (15)	3 (6)
Anemia	3 (6)	1 (2)
Hypoalbuminemia	3 (6)	0
Hyponatremia	3 (6)	0

Reproduced with permission from El-Khoueiry AB, et al. [29]



**Table 7.** CheckMate 040 dose-escalation cohort (n=48) investigator-assessed best overall response (RECIST v1.1)

	Uninfected (n=23)	HCV (n=10)	HBV (n=15)	Total (n=48)
Objective response, n (%)	3 (13)	3 (30)	1 (7)	7 (15)
CR	2 (9)	1 (10)	0	3 (6)
PR	1 (4)	2 (20)	1 (7)	4 (8)
SD	13 (57)	5 (50)	6 (40)	24 (50)
PD	6 (26)	2 (20)	7 (47)	15 (31)
Not evaluable	1 (4)	0	1 (7)	2 (4)
Ongoing response, n (%)	1 (33)	0	0	1 (14)

Reproduced with permission from El-Khoueiry AB, et al. [29]

was associated with a slightly higher rate of adverse events than the anti-PD-1 antibody [30] (table 9).

### Future Perspectives

The previously described interim analysis results from the phase I/II trial for HCC (dose-expansion cohort) that were presented at ASCO 2016 involved monotherapy with anti-PD-1 antibody. The anti-PD-1 antibody nivolumab has been approved for certain malignancies, including melanoma, non-small-cell lung cancer, and kidney cancer, and is expected to yield favorable outcomes in ongoing trials for many other types of cancer [31–36]. HCC requires different treatment strategies compared with other solid tumors or hematologic malignancies because it is extremely heterogeneous, does not have any major driver mutations, and cannot be treated with drugs that reduce hepatic functional reserve. The outcomes of this phase I/II dose-expansion trial indicate that the anti-PD-1 antibody is a promising treatment for HCC.

Additionally, as mentioned in the previous section, many pharmaceutical companies have started phase III trials and other early phase clinical trials of anti-PD-1/PD-L1 antibody for the treatment of HCC, the results of which are eagerly awaited.

There are unmet needs in HCC management in various settings, including neoadjuvant or adjuvant therapy with resection or ablation, combination of anti-PD-1 antibody with transcatheter arterial chemoembolization (TACE) [37, 38], and first- and second-line treatment. The immune checkpoint-inhibiting anti-PD-1, anti-PD-L1, and anti-CTLA-4 antibodies may prove useful for adjuvant therapy or combination therapy in all these settings. Immune checkpoint inhibitors could be particularly effective for the treatment of inflammation induced by TACE or radiofrequency ablation (RFA) [39, 40], which releases highly antigenic neoantigens into the bloodstream. A clinical trial of adjuvant therapy with anti-CTLA-4 antibody after TACE and RFA is currently underway (table 9). The results of the interim analysis for that trial were presented at ASCO 2016. Adjuvant therapy with anti-CTLA-4 antibody after non-curative RFA or TACE caused an increase in CD3-positive and CD8-positive cells, even for untreated nodules [41].

A most promising topic in this area is the combination of these antibodies (anti-PD-1/PD-L1 antibodies) with other drugs. Potential drug combinations include anti-CTLA4 antibodies (ipilimumab and tremelimumab) and molecular targeted drugs (sorafenib and oth-

**Table 8.** Current trials of immune checkpoint inhibitors

Drug	Trial name	Clinicaltrials.gov	Company	Phase	n	Line of therapy	Design	Endpoint	Status
<b>Nivolumab</b>									
Nivolumab (PD-1 Ab)	CheckMate 040	NCT01658878	BMS/ONO	I/II	42	1/2I	Cohort 1: Dose escalation	DLT/MTD	Completed
/ipilimumab (PD-L1 Ab)	CheckMate 040	NCT01658878	BMS/ONO	I/II	214	1/2I	Cohort 2: Dose expansion	ORR	Completed
	CheckMate 040	NCT01658878	BMS/ONO	I/II	200	1I	Cohort 3: Nivolumab vs sorafenib	ORR	Completed
	CheckMate 040	NCT01658878	BMS/ONO	I/II	120	2I	Cohort 4: Nivolumab + ipilimumab	Safety/tolerability	Completed
Nivolumab (PD-1 Ab)	CheckMate 459	NCT02576509	ONO	III	726	1I	Nivolumab vs sorafenib	TTP/OS	Recruiting
<b>Pembrolizumab</b>									
Pembrolizumab (PD-1 Ab)	KEYNOTE-224	NCT02702414	MSD	II	100	2I	Pembrolizumab (1 arm)	ORR	Completed
Pembrolizumab (PD-1 Ab)	KEYNOTE-240	NCT02702401	MSD	III	408	2I	Pembrolizumab vs placebo	PFS/OS	Recruiting
<b>Durvalumab</b>									
Durvalumab (PD-L1 Ab)	-	NCT02519348	AstraZeneca	II	144	1/2I	Durvalumab (Arm A) Tremelimumab (Arm B) Durvalumab + tremelimumab (Arm C)	Safety/tolerability	Recruiting

DLT/MTD=dose-limiting toxicity/maximum tolerated dose; ORR=overall response rate; TTP/OS=time to progression/overall survival; PFS=progression-free survival.

**Table 9.** Clinical trials of CTLA-4 antibody for the treatment of HCC

NCT no.	Agent	Design	Status	n	Stage	Results
01008358	Tremelimumab	II	Complete	20	III/IV	PR=17.6%, DCR=76% TTP=6.5 months HCV virologic response Grade 3 AST/ALT=45%
01853618	Tremelimumab + TACE/RFA/ cryoablation	I	Ongoing	29 14 TACE 10 RFA 5 Cryoablation	III/IV	Safe, feasible Immune cell infiltration (+) TTP=5.7 month Reduction in HCV viral load

ers). The combination of nivolumab and ipilimumab has yielded treatment outcomes superior to those of monotherapy with either drug in melanoma [31, 42].

Rapid advances in the field of immunotherapy have been made in other types of cancer. The FDA designated nivolumab as a breakthrough therapy in September 2014, and later did the same for pembrolizumab. This raised hopes that anti-PD-1 and anti-PD-L1 antibodies will be approved for the treatment of HCC in the near future. The outcomes of liver cancer treatment strategies are widely expected to improve through the application of multidrug and locoregional therapies centered on immune checkpoint inhibitors. The field is in the middle of a paradigm shift in not only systemic therapy, but also comprehensive treatment strategies, including locoregional therapy for liver cancer.

## Conclusion

Having advanced through the first stage of chemotherapy centered on cytotoxic agents and the second stage of chemotherapy centered on molecular targeted therapies, we are now poised to enter a third stage of cancer treatment strategies centered on immune checkpoint inhibitors. These strategies promise to become an essential element in cancer treatment, and advances in this area will bring the paradigm shift in cancer treatment.

## References

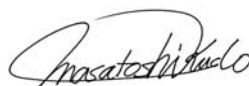
- 1 Ishida Y, Agata Y, Shibahara K, Honjo T: Induced expression of PD-1, a novel member of the immunoglobulin gene superfamily, upon programmed cell death. *EMBO J* 1992;11:3887–3895.
- 2 Freeman GJ, Long AJ, Iwai Y, Bourque K, Chernova T, Nishimura H, Fitz LJ, Malenkovich N, Okazaki T, Byrne MC, Horton HF, Fouser L, Carter L, Ling V, Bowman MR, Carreno BM, Collins M, Wood CR, Honjo T: Engagement of the PD-1 immunoinhibitory receptor by a novel B7 family member leads to negative regulation of lymphocyte activation. *J Exp Med* 2000;192:1027–1034.
- 3 Carter L, Fouser LA, Jussif J, Fitz L, Deng B, Wood CR, Collins M, Honjo T, Freeman GJ, Carreno BM: PD-1:PD-L inhibitory pathway affects both CD4(+) and CD8(+) T cells and is overcome by IL-2. *Eur J Immunol* 2002;32:634–643.
- 4 Latchman Y, Wood CR, Chernova T, Chaudhary D, Borde M, Chernova I, Iwai Y, Long AJ, Brown JA, Nunes R, Greenfield EA, Bourque K, Boussiotis VA, Carter LL, Carreno BM, Malenkovich N, Nishimura H, Okazaki T, Honjo T, Sharpe AH, Freeman GJ: PD-L2 is a second ligand for PD-1 and inhibits T cell activation. *Nat Immunol* 2001;2:261–268.
- 5 Okazaki T, Honjo T: PD-1 and PD-1 ligands: from discovery to clinical application. *Int Immunol* 2007;19:813–824.
- 6 Iwai Y, Ishida M, Tanaka Y, Okazaki T, Honjo T, Minato N: Involvement of PD-L1 on tumor cells in the escape from host immune system and tumor immunotherapy by PD-L1 blockade. *Proc Natl Acad Sci USA* 2002;99:12293–12297.
- 7 Krummel MF, Allison JP: CD28 and CTLA-4 have opposing effects on the response of T cells to stimulation. *J Exp Med* 1995;182:459–465.

- 8 Leach DR, Krummel MF, Allison JP: Enhancement of antitumor immunity by CTLA-4 blockade. *Science* 1996;271:1734–1736.
- 9 Sharma P, Allison JP: The future of immune checkpoint therapy. *Science* 2015;348:56–61.
- 10 Chen DS, Mellman I: Oncology meets immunology: the cancer-immunity cycle. *Immunity* 2013;39:1–10.
- 11 Sznol M, Chen L: Antagonist antibodies to PD-1 and B7-H1 (PD-L1) in the treatment of advanced human cancer. *Clin Cancer Res* 2013;19:1021–1034.
- 12 Herbst RS, Soria JC, Kowanetz M, Fine GD, Hamid O, Gordon MS, Sosman JA, McDermott DF, Powderly JD, Gettinger SN, Kohrt HE, Horn L, Lawrence DP, Rost S, Leabman M, Xiao Y, Mokatrin A, Koeppen H, Hegde PS, Mellman I, Chen DS, Hodi FS: Predictive correlates of response to the anti-PD-L1 antibody MPDL3280A in cancer patients. *Nature* 2014;515:563–567.
- 13 Shih K, Arkenau HT, Infante JR: Clinical impact of checkpoint inhibitors as novel cancer therapies. *Drugs* 2014;74:1993–2013.
- 14 Philips GK, Atkins M: Therapeutic uses of anti-PD-1 and anti-PD-L1 antibodies. *Int Immunol* 2015;27:39–46.
- 15 Mahoney KM, Freeman GJ, McDermott DF: The next immune-checkpoint Inhibitors: PD-1/PD-L1 blockade in melanoma. *Clin Ther* 2015;37:764–782.
- 16 Harshman LC, Drake CG, Wargo JA, Sharma P, Bhardwaj N: Cancer immunotherapy highlights from the 2014 ASCO Meeting. *Cancer Immunol Res* 2014;2:714–719.
- 17 Topalian SL, Drake CG, Pardoll DM: Targeting the PD-1/B7-H1(PD-L1) pathway to activate anti-tumor immunity. *Curr Opin Immunol* 2012;24:207–212.
- 18 Merelli B, Massi D, Cattaneo L, Mandalà M: Targeting the PD1/PD-L1 axis in melanoma: biological rationale, clinical challenges and opportunities. *Crit Rev Oncol Hematol* 2014;89:140–165.
- 19 Le DT, Uram JN, Wang H, Bartlett BR, Kemberling H, Eyring AD, Skora AD, Luber BS, Azad NS, Laheru D, Biedrzycki B, Donehower RC, Zaheer A, Fisher GA, Crocenzi TS, Lee JJ, Duffy SM, Goldberg RM, de la Chapelle A, Koshiji M, Bhajee F, Huebner T, Hruban RH, Wood LD, Cuka N, Pardoll DM, Papadopoulos N, Kinzler KW, Zhou S, Cornish TC, Taube JM, Anders RA, Eshleman JR, Vogelstein B, Diaz LA Jr: PD-1 blockade in tumors with mismatch-repair deficiency. *N Engl J Med* 2015;372:2509–2520.
- 20 Droezer RA, Hirt C, Viehl CT, Frey DM, Nebiker C, Huber X, Zlobec I, Eppenberger-Castori S, Tzankov A, Rosso R, Zuber M, Muraro MG, Amicarella F, Cremonesi E, Heberer M, Iezzi G, Lugli A, Terracciano L, Sconocchia G, Oertli D, Spagnoli GC, Tornillo L: Clinical impact of programmed cell death ligand 1 expression in colorectal cancer. *Eur J Cancer* 2013;49:2233–2242.
- 21 Ribas A: Tumor immunotherapy directed at PD-1. *N Engl J Med* 2012;366:2517–2519.
- 22 Hamid O, Robert C, Daud A, Hodi FS, Hwu WJ, Kefford R, Wolchok JD, Hersey P, Joseph RW, Weber JS, Dronca R, Gangadhar TC, Patnaik A, Zarour H, Joshua AM, Gergich K, Ellassaiss-Schaap J, Algazi A, Mateus C, Boasberg P, Tumeh PC, Chmielowski B, Ebbinghaus SW, Li XN, Kang SP, Ribas A: Safety and tumor responses with lambrolizumab (anti-PD-1) in melanoma. *N Engl J Med* 2013;369:134–144.
- 23 Brahmer JR, Tykodi SS, Chow LQ, Hwu WJ, Topalian SL, Hwu P, Drake CG, Camacho LH, Kauh J, Odunsi K, Pitot HC, Hamid O, Bhatia S, Martins R, Eaton K, Chen S, Salay TM, Alaparthi S, Grosso JF, Korman AJ, Parker SM, Agrawal S, Goldberg SM, Pardoll DM, Gupta A, Wigginton JM: Safety and activity of anti-PD-L1 antibody in patients with advanced cancer. *N Engl J Med* 2012;366:2455–2465.
- 24 Gao Q, Wang XY, Qiu SJ, Yamato I, Sho M, Nakajima Y, Zhou J, Li BZ, Shi YH, Xiao YS, Xu Y, Fan J: Overexpression of PD-L1 significantly associates with tumor aggressiveness and postoperative recurrence in human hepatocellular carcinoma. *Clin Cancer Res* 2009;15:971–979.
- 25 Tochio H, Sugahara M, Imai Y, Tei H, Suginosita Y, Imawaki N, Sasaki I, Hamada M, Minowa K, Inokuma T, Kudo M: Hyperenhanced rim surrounding liver metastatic tumors in the postvascular phase of sonazoid-enhanced ultrasonography: a histological indication of the presence of Kupffer cells. *Oncology* 2015;89(suppl 2):33–41.
- 26 Anthony B, El-Khoueiry IM, Todd S, Crocenzi, et al: Phase I/II safety and antitumor activity of nivolumab in patients with advanced hepatocellular carcinoma (HCC): CA209-040. *J Clin Oncol* 2015;33(suppl; abstr LBA101)
- 27 Kudo M: Immune checkpoint blockade in hepatocellular carcinoma. *Liver Cancer* 2015;4:201–207.
- 28 Sangro B, et al: Safety and antitumor activity of nivolumab (nivo) in patients (pts) with advanced hepatocellular carcinoma (HCC): Interim analysis of dose-expansion cohorts from the phase 1/2 CheckMate-040 study. *J Clin Oncol* 2016;34 (suppl; abstr 4078)
- 29 El-Khoueiry AB, et al: Phase I/II safety and antitumor activity of nivolumab (nivo) in patients (pts) with advanced hepatocellular carcinoma (HCC): Interim analysis of the CheckMate-040 dose escalation study. *J Clin Oncol* 2016;34 (suppl; abstr 4012)
- 30 Sangro B, Gomez-Martin C, de la Mata M, Iñarrairaegui M, Garralda E, Barrera P, Riezu-Boj JI, Larrea E, Alfaro C, Sarobe P, Lasarte JJ, Pérez-Gracia JL, Melero I, Prieto J: A clinical trial of CTLA-4 blockade with tremelimumab in patients with hepatocellular carcinoma and chronic hepatitis C. *J Hepatol* 2013;59:81–88.
- 31 Wolchok JD, Kluger H, Callahan MK, Postow MA, Rizvi NA, Lesokhin AM, Segal NH, Ariyan CE, Gordon RA, Reed K, Burke MM, Caldwell A, Kronenberg SA, Agunwamba BU, Zhang X, Lowy I, Inzunza HD, Feely W, Horak CE, Hong Q, Korman AJ, Wigginton JM, Gupta A, Sznol M: Nivolumab plus ipilimumab in advanced melanoma. *N Engl J Med* 2013;369:122–133.

- 32 Ansell SM, Lesokhin AM, Borrello I, Halwani A, Scott EC, Gutierrez M, Schuster SJ, Millenson MM, Cattry D, Freeman GJ, Rodig SJ, Chapuy B, Ligon AH, Zhu L, Grosso JF, Kim SY, Timmerman JM, Shipp MA, Armand P: PD-1 blockade with nivolumab in relapsed or refractory Hodgkin's lymphoma. *N Engl J Med* 2015;372:311–319.
- 33 Robert C, Schachter J, Long GV, Arance A, Grob JJ, Mortier L, Daud A, Carlino MS, McNeil C, Lotem M, Larkin J, Lorigan P, Neyns B, Blank CU, Hamid O, Mateus C, Shapira-Frommer R, Kosh M, Zhou H, Ibrahim N, Ebbinghaus S, Ribas A, KEYNOTE-006 investigators: Pembrolizumab versus ipilimumab in advanced melanoma. *N Engl J Med* 2015;372:2521–2532.
- 34 Garon EB, Rizvi NA, Hui R, Leighl N, Balmanoukian AS, Eder JP, Patnaik A, Aggarwal C, Gubens M, Horn L, Carcereny E, Ahn MJ, Felip E, Lee JS, Hellmann MD, Hamid O, Goldman JW, Soria JC, Dolled-Filhart M, Rutledge RZ, Zhang J, Luncford JK, Rangwala R, Lubiniecki GM, Roach C, Emancipator K, Gandhi L, KEYNOTE-001 Investigators: Pembrolizumab for the treatment of non-small-cell lung cancer. *N Engl J Med* 2015;372:2018–2028.
- 35 Brahmer J, Reckamp KL, Baas P, Crinò L, Eberhardt WE, Poddubskaya E, Antonia S, Pluzanski A, Vokes EE, Holgado E, Waterhouse D, Ready N, Gainor J, Arén Frontera O, Havel L, Steins M, Garassino MC, Aerts JG, Domine M, Paz-Ares L, Reck M, Baudelet C, Harbison CT, Lestini B, Spigel DR: Nivolumab versus docetaxel in advanced squamous-cell non-small-cell lung cancer. *N Engl J Med* 2015;373:123–135.
- 36 Larkin J, Chiarion-Sileni V, Gonzalez R, Grob JJ, Cowey CL, Lao CD, Schadendorf D, Dummer R, Smylie M, Rutkowski P, Ferrucci PF, Hill A, Wagstaff J, Carlino MS, Haanen JB, Maio M, Marquez-Rodas I, McArthur GA, Ascierto PA, Long GV, Callahan MK, Postow MA, Grossmann K, Sznol M, Dreno B, Bastholt L, Yang A, Rollin LM, Horak C, Hodi FS, Wolchok JD: Combined nivolumab and ipilimumab or monotherapy in untreated melanoma. *N Engl J Med* 2015;373:23–34.
- 37 Kudo M: Locoregional therapy for hepatocellular carcinoma. *Liver Cancer* 2015;4:163–164.
- 38 Tsurusaki M, Murakami T: Surgical and locoregional therapy of HCC: TACE. *Liver Cancer* 2015;4:165–175.
- 39 Kang TW, Rhim H: Recent advances in tumor ablation for hepatocellular carcinoma. *Liver Cancer* 2015;4:176–187.
- 40 Lencioni R, de Baere T, Martin RC, Nutting CW, Narayanan G: Image-guided ablation of malignant liver tumors: recommendations for clinical validation of novel thermal and non-thermal technologies – a Western perspective. *Liver Cancer* 2015;4:208–214.
- 41 Duffy A, Makarova-Rusher OV, Pratt D, Kleiner DE, Ulahannan S, Mabry D, et al: Tremelimumab, a monoclonal antibody against CTLA-4, in combination with subtotal ablation (trans-catheter arterial chemoembolization (TACE), radiofrequency ablation (RFA) or cryoablation) in patients with hepatocellular carcinoma (HCC) and biliary tract carcinoma (BTC). *J Clin Oncol* 2016;34 (suppl; abstr 4073).
- 42 Postow MA, Chesney J, Pavlick AC, Robert C, Grossmann K, McDermott D, Linette GP, Meyer N, Giguere JK, Agarwala SS, Shaheen M, Ernstoff MS, Minor D, Salama AK, Taylor M, Ott PA, Rollin LM, Horak C, Gagnier P, Wolchok JD, Hodi FS: Nivolumab and ipilimumab versus ipilimumab in untreated melanoma. *N Engl J Med* 2015;372:2006–2017.

**Editorial**

# Molecular Targeted Agents for Hepatocellular Carcinoma: Current Status and Future Perspectives

*Prof. M. Kudo**Editor Liver Cancer***Introduction**

Locoregional therapy is the primary treatment for hepatocellular carcinoma (HCC). Sorafenib was approved as a first-line systemic therapy for advanced HCC with associated extrahepatic spread and/or vascular invasion in 2007. However, there are several limitations associated with sorafenib therapy. To overcome these problems, various clinical trials have been conducted to develop additional molecular targeted agents for HCC. However, all of the clinical trials conducted thus far, except for a recent trial using regorafenib, have been unsuccessful, emphasizing the difficulties associated with drug development for HCC. In this editorial, we review the current status and future prospects of molecular targeted agents that are being developed for HCC.

**Sorafenib**

The multikinase inhibitor sorafenib was the first oral molecular targeted agent to show a survival benefit in patients with HCC [1, 2]. In Japan, sorafenib was approved for national health insurance coverage in May 2009, and it has since been administered to more than 26,000 patients.



**Table 1.** Phase III clinical trials for HCC

Target population		Design	Trial name	Presentation	Publication
Early	Adjuvant (prevention of recurrence)	1. Peretinoin vs. placebo <sup>a</sup>	NIK-333	ASCO 2010	JG 2014
		2. Sorafenib vs. placebo <sup>a</sup>	STORM	ASCO 2014	Lancet-O 2015
		3. Peretinoin vs. placebo	NIK-333/K-333	Ongoing	
Intermediate	Improvement of TACE	1. TACE +/- sorafenib <sup>a</sup>	Post-TACE	ASCO-GI 2010	EJC 2011
		2. TACE +/- brivanib <sup>a</sup>	BRISK-TA	ILCA 2013	Hepatol 2014
		3. TACE +/- orantinib <sup>a</sup>	ORIENTAL	EASL 2015	
Advanced	First line	1. Sorafenib vs. sunitinib <sup>a</sup>	SUN1170	ASCO 2011	JCO 2013
		2. Sorafenib vs. brivanib <sup>a</sup>	BRISK-FL	AASLD 2012	JCO 2013
		3. Sorafenib vs. linifanib <sup>a</sup>	LiGHT	ASCO-GI 2013	JCO 2015
		4. Sorafenib +/- HAIC <sup>a</sup>	SILIUS	EASL 2016	
		5. Sorafenib vs. lenvatinib	REFLECT	Ongoing	
		6. Sorafenib vs. nivolumab	CheckMate 459	Ongoing	
	Second line	1. Brivanib vs. placebo <sup>a</sup>	BRISK-PS	EASL 2012	JCO 2013
		2. Everolimus vs. placebo <sup>a</sup>	EVOLVE-1	ASCO-GI 2014	JAMA 2014
		3. Ramucirumab vs. placebo <sup>a</sup>	REACH	ESMO 2014	Lancet-O 2015
		4. S-1 vs. placebo <sup>a</sup>	S-CUBE	ASCO 2015	
		5. Regorafenib vs. placebo <sup>b</sup>	RESORCE	WCGI 2016	
		6. Tivantinib vs. placebo	JET-HCC	Ongoing	
		7. Ramucirumab vs. placebo	REACH-2	Ongoing	
		8. Pembrolizumab vs. placebo	KEYNOTE-240	Ongoing	

HAIC, hepatic arterial infusion chemotherapy. <sup>a</sup> RCT halted or with negative results. <sup>b</sup> RCT with positive results.

## Current Status of the Development of Molecular Targeted Agents

Clinical trials are being conducted to develop molecular targeted agents for various stages of liver cancer, including the following: early-stage HCC, in which surgical resection or radiofrequency ablation is indicated; intermediate-stage HCC, in which transcatheter arterial chemoembolization (TACE) is indicated; and advanced-stage HCC, in which sorafenib is indicated.

### Early-Stage HCC

The Sorafenib as Adjuvant Treatment in the Prevention of Recurrence of Hepatocellular Carcinoma (STORM) study, in which sorafenib was used to suppress HCC recurrence after curative therapy, revealed no difference in recurrence-free survival between the sorafenib and placebo groups, demonstrating that sorafenib was not efficacious at suppressing recurrence [3].

Peretinoin, an orally administered acyclic retinoid agent, is structurally similar to vitamin A and functions as a transcription activator and an inducer of differentiation. It is thought to remove precancerous HCC cells by inducing apoptosis and to inhibit carcinogenesis by promoting differentiation. A phase II/III study was launched to investigate the ability of peretinoin to suppress HCC recurrence, but the efficacy of peretinoin could not be evaluated due to problems with dosing [4]. A follow-up phase III trial has been initiated now that the dosing problems have been addressed (Table 1).

### *Intermediate-Stage HCC*

Residual tumor and tumor recurrence are inevitable after TACE, because it is not a curative therapy. Since TACE can itself induce angiogenesis, the use of antiangiogenic agents after TACE greatly suppresses tumor recurrence and regrowth, and may even extend the duration of tumor suppression by TACE. This allows TACE to be performed less frequently, enabling preservation of liver function. Globally, many clinical trials have investigated the efficacy of sorafenib as a post-TACE adjuvant therapy. A study in Japan and Korea investigated time to progression (TTP) in patients treated with sorafenib after TACE but found that sorafenib did not prolong TTP in these patients [5].

In the SPACE study, a phase II study of sorafenib or placebo in combination with TACE with doxorubicin drug-eluting beads [6], the primary endpoint of TTP was achieved; however, the study outcome was considered negative because of the clinically insignificant difference between the sorafenib and placebo arms. Other large-scale studies, such as the Eastern Cooperative Oncology Group (ECOG) 1208 study and the TACE2 study, had to be discontinued due to insufficient enrollment. The outcome of the TACE2 study was reported in detail at the 2016 American Society of Clinical Oncology (ASCO) Annual Meeting [7]. The Transcatheter Arterial Chemoembolization Therapy in Combination with Sorafenib (TACTICS) study conducted in Japan is the only large-scale clinical trial that is currently underway. As shown in Table 1, negative outcomes have also been reported in studies with other agents, including the Brivanib versus Placebo as Adjuvant Therapy to Transarterial Chemoembolization in Patients with Unresectable Hepatocellular Carcinoma (BRISK-TA) study [8], a phase III study on brivanib (an inhibitor of vascular endothelial growth factor receptor [VEGFR] and fibroblast growth factor receptor [FGFR]), and the Orantinib in Combination with Transcatheter Arterial Chemoembolization in Patients with Unresectable Hepatocellular Carcinoma (ORIENTAL) study, a phase III study on orantinib (an inhibitor of VEGFR, platelet-derived growth factor receptor [PDGFR], and FGFR [9]).

### *Advanced-Stage HCC*

Many trials have been conducted to develop molecular targeted agents that can replace sorafenib as a more potent and safe first-line therapy. However, the superiority or noninferiority of sunitinib, brivanib, and linifanib to sorafenib could not be proven [10–12]. A phase III study comparing lenvatinib and sorafenib has recently been concluded, and the results are eagerly awaited. The target molecules of lenvatinib are VEGFR1–3, FGFR1–4, RET, and c-Kit.

Clinical trials of brivanib, everolimus (an inhibitor of mTOR [mechanistic target of rapamycin]), and ramucirumab (a human monoclonal antibody against VEGFR2) were conducted with the aim of developing second-line agents for patients unresponsive to or intolerant of sorafenib, but they failed to show superiority to the placebo (Table 1) [13–15]. However, because ramucirumab was highly effective in a group of patients with elevated serum  $\alpha$ -fetoprotein (AFP), a phase III study of ramucirumab is currently underway on patients with serum AFP levels  $\geq 400$  ng/ml. Recently, on June 30, 2016, positive data from the RESORCE study of regorafenib, an inhibitor of a broad range of kinases including VEGFR, PDGFR, FGFR, TIE2, Kit, RET, and RAF, were presented at the World Congress on Gastrointestinal Cancer (WCGC). As a groundbreaking result, overall survival (OS), the primary endpoint of the study, was significantly improved in patients that received regorafenib as a second-line therapy (median survival time: 10.6 months, vs. 7.8 months in the placebo group; hazard ratio: 0.62; 95% confidence interval: 0.50–0.78;  $p < 0.001$ ) (Table 2). Importantly, the study design might have contributed to the positive outcome. First, the study included a group of patients who progressed while on sorafenib, but these patients were required to have received  $\geq 400$  mg of sorafenib for at least 20 of 28 days prior to enrollment in the RESORCE trial; patients who discontinued sorafenib due to poor tolerability were excluded. Second, vascular invasion and extrahepatic spread were treated as independent stratification factors because

**Table 2.** Results of the RESORCE trial

	Regorafenib	Placebo	HR (95% CI); <i>p</i> value
Subjects, <i>n</i>	379	194	
BCLC stage C, %	88	87	
Treatment duration, months	3.6 (0.03–29.4)	1.9 (0.2–27.4)	
OS, months	10.6	7.8	0.62 (0.50–0.78); <i>p</i> < 0.001
PFS, months	3.1	1.5	0.46 (0.37–0.56); <i>p</i> < 0.001
TTP, months	3.2	1.5	0.44 (0.36–0.55)
DCR, %	65.2	36.1	<i>p</i> < 0.001
ORR, %	10.6	4.1	<i>p</i> < 0.005
Adverse events grade ≥3, %	79.7	58.5	

BCLC, Barcelona Clinic Liver Cancer; OS, overall survival; PFS, progression-free survival; TTP, time to progression; DCR, disease control rate; ORR, overall response rate; HR, hazard ratio; CI, confidence interval.

**Table 3.** Imbalance between the brivanib and placebo arms

Demographic or characteristic	Brivanib ( <i>n</i> = 263)		Placebo ( <i>n</i> = 132)	
	<i>n</i>	%	<i>n</i>	%
Reason for sorafenib discontinuation				
Progression	227	86	116	88
Intolerance	35	13	16	12
Distant metastasis	171	65	84	64
Vascular invasion	81	31	24	18
Portal vein invasion and/or thrombosis	65	25	16	12
Cited and modified from Llovet et al. [13].				

of the lessons learned from the failed brivanib trial (Table 3). As for other agents, a clinical trial of the c-MET inhibitor tivantinib is currently underway (Table 1).

### Problems Associated with Clinical Trials of Molecular Targeted Agents for HCC

As stated above, numerous drug development trials ended with negative outcomes, and a number of potential reasons for these results have been proposed.

#### *Problems Associated with the Heterogeneity of HCC*

Compared with other types of cancer, HCC is very heterogeneous. In particular, HCC is a multicentric tumor, and its characteristics can vary from nodule to nodule, even within an individual patient. Consequently, the efficacy of molecular targeted agents is highly variable. Clinical trials use the Child-Pugh liver function score and the TNM tumor stage as inclusion criteria. Thus, a seemingly clinically homogeneous group of patients included in a study may actually be biologically heterogeneous. Therefore, to restrict the patient population to a biologically homogeneous group, drug development trials have started to rely on biomarkers [16]. A representative example is a trial of tivantinib, which inhibits the hepatocyte growth factor receptor c-MET [17]. This phase II study has shown the efficacy of tivantinib in patients with HCC expressing high levels of c-MET, even though in this group of patients, the prognosis is generally poor. Currently, a placebo-controlled phase III study is being conducted only on

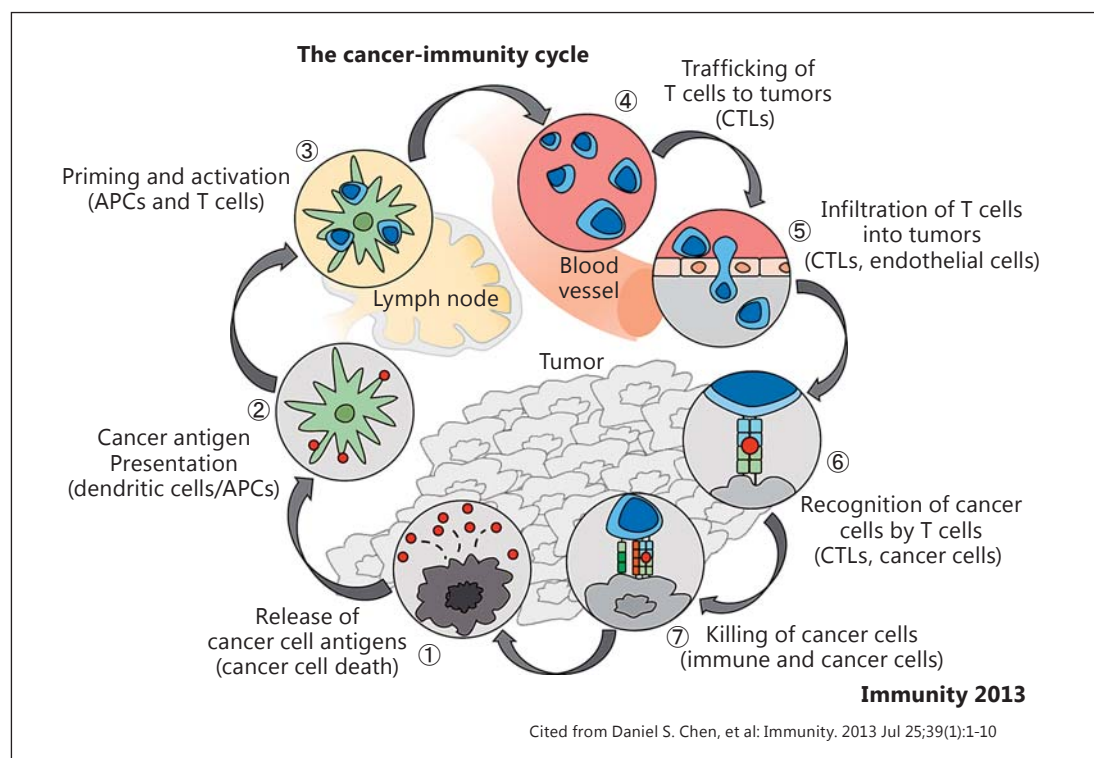
patients with tumors expressing high levels of c-MET. However, selecting patients based on biomarkers does not address the problem of tumor characteristics varying from nodule to nodule within the same patient. In other words, the possibility of sampling variability cannot be eliminated. Indeed, the outcome of a study using a mutation of RAS as a biomarker to investigate the efficacy of the MEK inhibitor refametinib was also unfavorable. These problems may be resolved once more effective serum biomarkers are identified. A phase II clinical trial of the TGF (transforming growth factor)- $\beta$  receptor inhibitor galunisertib is currently underway, and improved OS and reduced TGF- $\beta_1$  levels in patients with normal AFP values were reported at the 2016 ASCO Annual Meeting [18].

#### *Problems Associated with Stratification Factors*

In general, stratification factors are stipulated to prevent bias during randomization. The proper handling of vascular invasion and extrahepatic spread is considered important in patients with HCC. The design of many ongoing clinical trials involves an allocation factor specifying “either vascular invasion or extrahepatic spread” or “neither vascular invasion nor extrahepatic spread.” However, because vascular invasion is an extremely poor prognostic factor for HCC, assigning vascular invasion to the same category as extrahepatic spread may have influenced the outcome of clinical trials. In other words, if the active drug group contains more patients with vascular invasion while the placebo group includes more patients with extrahepatic spread, such a sampling bias will put the active drug groups at a disadvantage. In fact, this actually happened in a clinical trial of brivanib as second-line therapy (Table 3) [13]. In the RESORCE trial, which reported a positive outcome, patients were stratified separately by vascular invasion and by extrahepatic spread [19].

#### *Influence of Post-Trial Treatment*

Post-progression survival (PPS) is defined as the interval between a diagnosis of progressive disease and the patient’s death; OS is expressed by the equation  $OS = PFS + PPS$ , where PFS is progression-free survival. Even when a statistical difference in PFS is observed, this might not be reflected in OS if PPS is sufficiently long. Indeed, OS correlated with PPS more strongly than with PFS in a clinical trial of sorafenib [20]. Locoregional therapy is the mainstay of treatment for HCC, but molecular targeted agents are indicated for cases where locoregional therapy is no longer practical. However, even after following the recommended therapeutic guidelines, locoregional therapy is often applied as a post-trial treatment, if the patient’s general condition is stable. This rarely happens with other types of cancer and is an issue unique to HCC due to the availability of effective locoregional therapies such as intra-arterial infusion chemotherapy or TACE. It is therefore possible that if PPS is prolonged by effective post-trial treatments, there may be no significant difference in OS, the primary endpoint of the trial [21]. In addition, clinical trials of agents other than regorafenib use intolerance to sorafenib as an inclusion criterion; however, this is thought to augment the influence of post-trial treatments. Patients who progressed after administration of sorafenib are defined as unresponsive to sorafenib; they have a relatively advanced tumor burden and are in poor condition overall. By contrast, patients defined as intolerant to sorafenib, who discontinued the treatment due to adverse events, remain in a relatively stable condition. Clinically stable patients are more likely to be subjected to various post-trial treatments, particularly to locoregional therapy, regardless of whether they have received a second-line agent or a placebo during the trial. The outcome of a subanalysis of a phase II study of axitinib supports this contention. This analysis revealed that OS in the axitinib arm was much better than in the placebo arm when patients who discontinued therapy due to adverse events were excluded [22]. Taking this into consideration, clinical trials of second-line agents should enroll only those patients unresponsive to sorafenib, as was done in the RESORCE study [19].



**Fig. 1.** The cancer-immunity cycle. Naïve T cells are activated by signals from antigen-presenting cells (APCs), which recognize the cancer cell antigens in the lymph node. At the tumor, activated T cells attack the cancer cells. CTLs, cytotoxic T lymphocytes.

As stated earlier, the clinical trial of regorafenib excluded patients intolerant to sorafenib. This decision was made primarily because regorafenib and sorafenib have similar toxicological profiles due to their structural similarity [19]. However, because patients intolerant to sorafenib were excluded, post-trial treatments were limited, resulting in a favorable outcome. This superior trial design resulted in a shorter PPS and therefore a greater difference in OS, clarifying the benefits of regorafenib therapy.

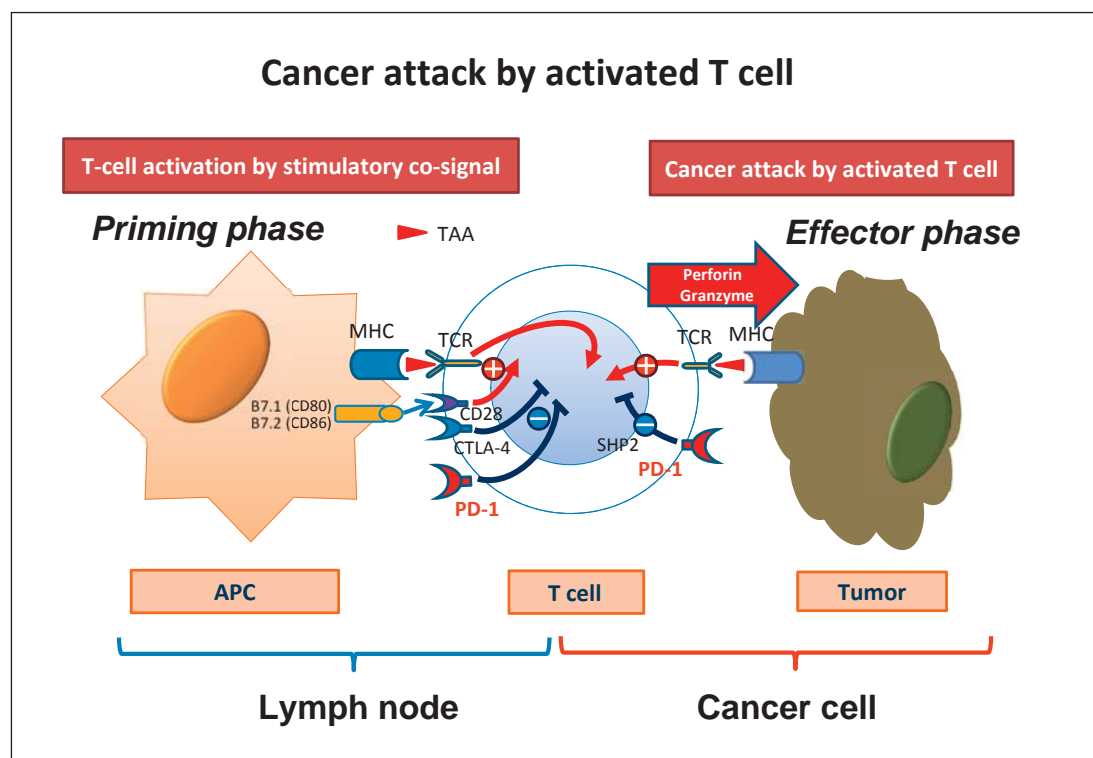
#### *Hepatic Functional Reserve*

Since many patients with HCC have an underlying chronic liver disease, such as cirrhosis, it is important to consider the effect of therapy on liver function. Most clinical trials enroll patients with Child-Pugh class A liver function (Child-Pugh score of 5–6 points). However, prognoses differ substantially between patients with a score of 5 and those with 6 points. Therefore, in the case of HCC, it may be necessary to include Child-Pugh scores of 5 and 6 as separate stratification factors.

#### **Immune Checkpoint Inhibitors**

An antibody against programmed cell death protein 1 (PD-1) has been gaining attention as an immune checkpoint inhibitor in recent years (Fig. 1–3). At the 2015 ASCO Annual Meeting, a phase I study of anti-PD-1 (nivolumab) in patients with HCC reported a favorable outcome, with 2 complete and 7 partial responses and an overall response rate of 19% [23].





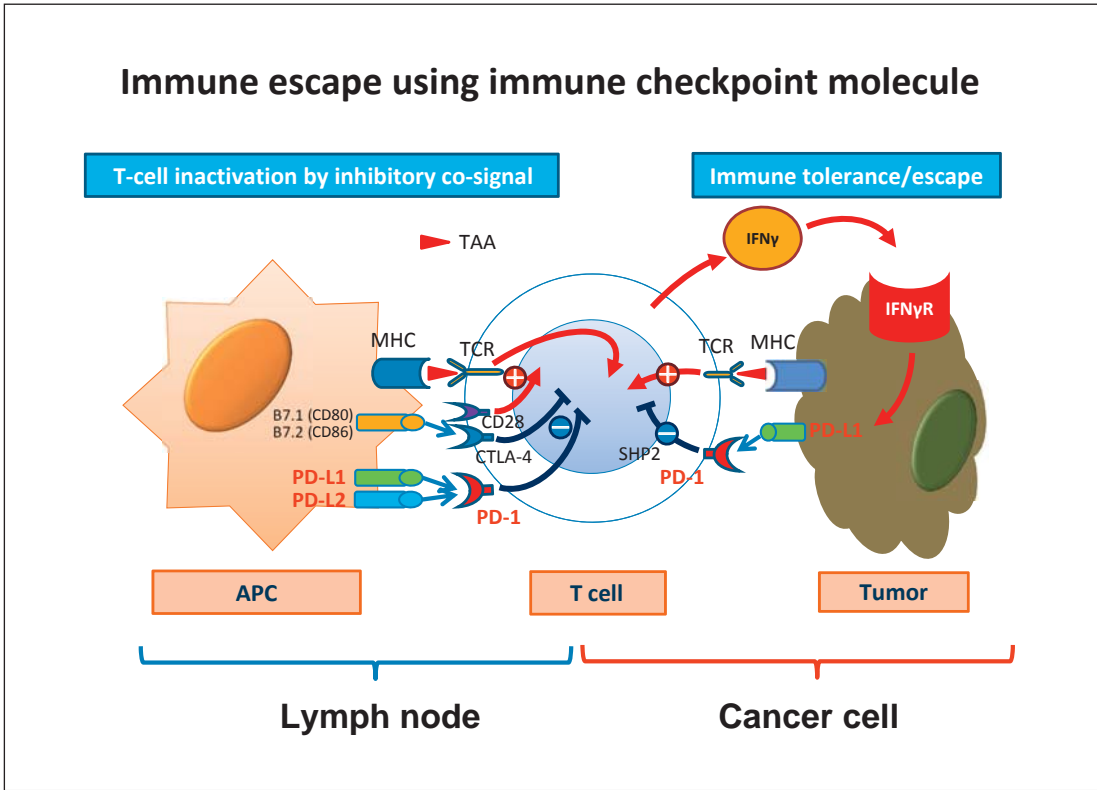
**Fig. 2.** After the recognition of tumor-associated antigen (TAA) by the T-cell receptor (TCR), a co-stimulatory signal by binding B7 and CD28, naïve T cells are activated. Consequently, the activated T cells attack the cancer cells by recognizing the TAA. Cancer cells are killed by activated T cells by producing perforin and granzyme. APC, antigen-presenting cell.

In Japan, a phase I/II study of nivolumab with dose expansion cohorts began in the summer of 2015. The outcomes of the dose escalation and dose expansion trials were reported at the 2016 ASCO Annual Meeting [24, 25] (Table 4). Furthermore, other reports included the design of a phase III clinical trial [26] and a study of combination therapy with anti-PD-1 and cytotoxic T-lymphocyte-associated protein 4 (CTLA-4) (Tables 5, 6) [27]. However, due to extremely expensive drug prices, it is very likely that the medical costs of these agents will strain nations' finances when approved for clinical use. Therefore, an urgent challenge today is to discover biomarkers that predict treatment response and thus offer a clear indication for their use.

### Master Protocols

Drug development trials have high research and development costs and also require a huge effort to recruit participants. In the USA, the Lung Cancer Master Protocol (Lung-MAP) for patients with squamous cell lung cancer was launched in 2014 (Fig. 4) [28]. Patients were screened for alterations in cancer-related genes and were assigned to a trial arm best suited to each subject's genomic profile. This streamlined patient registration made the process more efficient, helping to reduce drug development costs. From the perspective of medical cost reduction, it may become possible to assign an appropriate agent to each patient. Clearly, this will be also extremely beneficial for patients with HCC and we await its early incorpo-





**Fig. 3.** The immune checkpoint molecules PD-1, PD-L1, and CTLA-4 play an impact role in the cancer's escape from activated T cells (cancer immunotolerance/escape). APC, antigen-presenting cell; TAA, tumor-associated antigen; TCR, T-cell receptor.

**Table 4.** Objective response to nivolumab

	Uninfected: sorafenib naïve/ intolerant (n = 54)	Uninfected: sorafenib progressors (n = 58)	HCV (n = 51)	HBV (n = 51)	Total (n = 214)
Objective response	11 (20)	11 (19)	7 (14)	6 (12)	35 (16)
Partial response	0 (0)	2 (3)	0 (0)	0 (0)	2 (1)
Stable disease	32 (59)	27 (47)	29 (57)	23 (45)	111 (52)
Progressive disease	11 (20)	18 (31)	12 (24)	22 (43)	63 (29)
Not evaluable	0 (0)	2 (3)	3 (6)	0 (0)	5 (2)

Data are presented as n (%). Cited from El-Khoueiry et al. [25]. HCV, hepatitis C virus; HBV, hepatitis B virus.

ration. Such results could contribute substantially to the health care economy. Of course, this cannot be achieved by a single pharmaceutical manufacturer but requires the cooperation of multiple manufacturers. Public organizations should also be involved, so that this effort can be made within a public-private integrated project. In Japan, a similar project, SCRUM-Japan, was launched for patients with lung and gastrointestinal cancer including hepatobiliary and pancreatic cancer. Headed by the National Cancer Center, it is currently being tested at various institutions.

**Table 5.** Current trials of immune checkpoint inhibitors

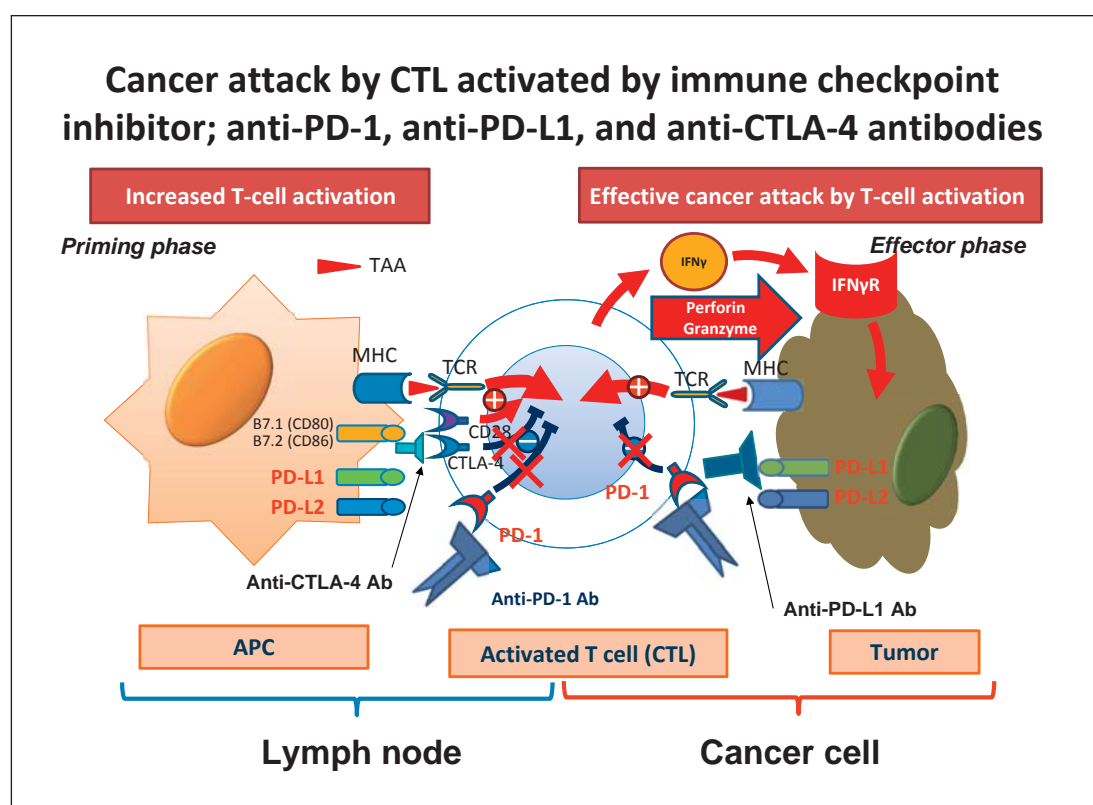
Drug	Trial name	Clinicaltrials.gov No.	Company	Phase	Subjects, n	Line of therapy	Design	Endpoint	Status
<i>Nivolumab</i> Nivolumab (PD-1 Ab)/ ipilimumab (PD-L1 Ab)	CheckMate 040	NCT01658878	BMS/ONO	I/II	42	1L/2L	Cohort 1: dose escalation	DLT/MTD	Completed
	CheckMate 040	NCT01658878	BMS/ONO	I/II	214	1L/2L	Cohort 2: dose expansion	ORR	Completed
	CheckMate 040	NCT01658878	BMS/ONO	I/II	200	1L	Cohort 3: nivolumab vs. sorafenib	ORR	Completed
	CheckMate 040	NCT01658878	BMS/ONO	I/II	120	2L	Cohort 4: nivolumab + ipilimumab	Safety/ tolerability	Completed
Nivolumab (PD-1 Ab)	CheckMate 459	NCT02576509	ONO	III	726	1L	Nivolumab vs. sorafenib	TTP/OS	Recruiting
<i>Pembrolizumab</i> Pembrolizumab (PD-1 Ab) Pembrolizumab (PD-1 Ab)	KEYNOTE-224	NCT02702414	MSD	II	100	2L	Pembrolizumab (1 arm)	ORR	Completed
	KEYNOTE-240	NCT02702401	MSD	III	408	2L	Pembrolizumab vs. placebo	PFS/OS	Recruiting
<i>Durvalumab</i> Durvalumab (PD-L1 Ab)/ tremelimumab (CTLA-4 Ab)	-	NCT02519348	AstraZeneca	II	144	1L/2L	Durvalumab (arm A) Tremelimumab (arm B) Durvalumab + tremelimumab (arm C)	safety/ tolerability	Recruiting

Ab, antibody; BMS, Bristol-Myers Squibb; ONO, Ono Pharmaceutical Co., Ltd.; MSD, MSD K.K.; 1L, first line; 2L, second line; DLT, dose-limiting toxicity; MTD, maximum tolerated dose; ORR, overall response rate; TTP, time to progression; OS, overall survival; PFS, progression-free survival.

**Table 6.** Clinical trials of CTLA-4 antibody in hepatocellular carcinoma

NCT No.	Agent	Design	Status	Subjects, <i>n</i>	Stage	Results
01008358	Tremelimumab	II	Complete	20	III/IV	PR = 17.6%, DCR = 76% TTP = 6.5 months HCV virologic response Grade 3 AST/ALT = 45%
01853618	Tremelimumab + TACE/RFA/cryoablation	I	Ongoing	29 (14 TACE; 10 RFA; 5 cryoablation)	III/IV	Safe, feasible Immune cell infiltration (+) TTP = 5.7 months Reduction in HCV viral load

RFA, radiofrequency ablation; PR, partial response; DCR, disease control rate; TTP, time to progression; HCV, hepatitis C virus.



**Fig. 4.** Anti-PD-1, anti-PD-L1, and anti-CTLA-4 antibodies restore T-cell activation, leading to an effective cancer attack by the immune system. APC, antigen-presenting cell; TAA, tumor-associated antigen; TCR, T-cell receptor; CTL, cytotoxic T lymphocyte.

## Conclusion

Here, we reviewed the current development status of molecular targeted agents and future trends in drug development for HCC. Because of the difficulties involved in developing novel agents, the positive outcome obtained with regorafenib is exciting news and may change

the treatment paradigm for HCC. While expectations are rising for immunotherapy, new patient selection criteria are also emerging based on biological homogeneity as determined by biomarkers. This differs from the conventional selection criteria based on liver function and TNM stage. Furthermore, to reduce medical costs, it is necessary to put drug development into a broader perspective by, for example, incorporating new concepts such as the master protocol system into clinical trials.

## References

- 1 Llovet JM, Ricci S, Mazzaferro V, Hilgard P, Gane E, Blanc JF, de Oliveira AC, Santoro A, Raoul JL, Forner A, Schwartz M, Porta C, Zeuzem S, Bolondi L, Greten TF, Galle PR, Seitz JF, Borbath I, Häussinger D, Giannaris T, Shan M, Moscovici M, Voliotis D, Bruix J; SHARP Investigators Study Group: Sorafenib in advanced hepatocellular carcinoma. *N Engl J Med* 2008;359:378–390.
- 2 Cheng AL, Kang YK, Chen Z, Tsao CJ, Qin S, Kim JS, Luo R, Feng J, Ye S, Yang TS, Xu J, Sun Y, Liang H, Liu J, Wang J, Tak WY, Pan H, Burock K, Zou J, Voliotis D, Guan Z: Efficacy and safety of sorafenib in patients in the Asia-Pacific region with advanced hepatocellular carcinoma: a phase III randomised, double-blind, placebo-controlled trial. *Lancet Oncol* 2009;10:25–34.
- 3 Bruix J, Takayama T, Mazzaferro V, Chau GY, Yang J, Kudo M, Cai J, Poon RT, Han KH, Tak WY, Lee HC, Song T, Roayaie S, Bolondi L, Lee KS, Makuuchi M, Souza F, Berre MA, Meinhardt G, Llovet JM; STORM Investigators: Adjuvant sorafenib for hepatocellular carcinoma after resection or ablation (STORM): a phase 3, randomised, double-blind, placebo-controlled trial. *Lancet Oncol* 2015;16:1344–1354.
- 4 Okita K, Izumi N, Matsui O, Tanaka K, Kaneko S, Moriwaki H, Ikeda K, Osaki Y, Numata K, Nakachi K, Kokudo N, Imanaka K, Nishiguchi S, Okusaka T, Nishigaki Y, Shiomi S, Kudo M, Ido K, Karino Y, Hayashi N, Ohashi Y, Makuuchi M, Kumada H; Peretinoin Study Group: Peretinoin after curative therapy of hepatitis C-related hepatocellular carcinoma: a randomized double-blind placebo-controlled study. *J Gastroenterol* 2015;50:191–202.
- 5 Kudo M, Imanaka K, Chida N, Nakachi K, Tak WY, Takayama T, Yoon JH, Hori T, Kumada H, Hayashi N, Kaneko S, Tsubouchi H, Suh DJ, Furuse J, Okusaka T, Tanaka K, Matsui O, Wada M, Yamaguchi I, Ohya T, Meinhardt G, Okita K: Phase III study of sorafenib after transarterial chemoembolisation in Japanese and Korean patients with unresectable hepatocellular carcinoma. *Eur J Cancer* 2011;47:2117–2127.
- 6 Lencioni R, Llovet JM, Han G: Sorafenib or placebo in combination with transarterial chemoembolization (TACE) with doxorubicin-eluting beads (debdox) for intermediate-stage hepatocellular carcinoma (HCC): phase II, randomized, double-blind space trial (abstract). *J Clin Oncol* 2012;30(suppl 4):LBA154.
- 7 Meyer T, Fox R, Ma YT, Ross PJ, James M, Struggess R, Stubbs C, Wall L, Watkinson A, Hacking N, Evans T, Collins P, Hubner R, Cunningham D, Primrose JN, Johnson PJ, Palmer DH: TACE 2: a randomized placebo-controlled, double-blinded, phase III trial evaluating sorafenib in combination with transarterial chemoembolisation (TACE) in patients with unresectable hepatocellular carcinoma (HCC) – background (abstract). *J Clin Oncol* 2016;34(suppl 2016 ASCO Annu Meet):4018.
- 8 Kudo M, Han G, Finn RS, Poon RT, Blanc JF, Yan L, Yang J, Lu L, Tak WY, Yu X, Lee JH, Lin SM, Wu C, Tanwandee T, Shao G, Walters IB, Dela Cruz C, Poulart V, Wang JH: Brivanib as adjuvant therapy to transarterial chemoembolization in patients with hepatocellular carcinoma: a randomized phase III trial. *Hepatology* 2014;60:1697–1707.
- 9 Park JW, Cheng AL, Kudo M, Park JH, Liang PC, Hidaka H, Izumi N, Heo J, Lee YJ, Sheen IS, Chiu CF, Arioka H, Morita S, Arai Y: A randomized, double-blind, placebo-controlled phase III trial of TSU-68 (Orantinib) combined with transcatheter arterial chemoembolization in patients with unresectable hepatocellular carcinoma. *J Hepatol* 2015;62:S189–S190.
- 10 Cheng AL, Kang YK, Lin DY, Park JW, Kudo M, Qin S, Chung HC, Song X, Xu J, Poggi G, Omata M, Pitman Lowenthal S, Lanzalone S, Yang L, Lechuga MJ, Raymond E: Sunitinib versus sorafenib in advanced hepatocellular cancer: results of a randomized phase III trial. *J Clin Oncol* 2013;31:4067–4075.
- 11 Johnson PJ, Qin S, Park JW, Poon RT, Raoul JL, Philip PA, Hsu CH, Hu TH, Heo J, Xu J, Lu L, Chao Y, Boucher E, Han KH, Paik SW, Robles-Aviña J, Kudo M, Yan L, Sobhonslidsuk A, Komov D, Decaens T, Tak WY, Jeng LB, Liu D, Ezzeddine R, Walters I, Cheng AL: Brivanib versus sorafenib as first-line therapy in patients with unresectable, advanced hepatocellular carcinoma: results from the randomized phase III BRISK-FL study. *J Clin Oncol* 2013;31:3517–3524.
- 12 Cainap C, Qin S, Huang WT, Chung JJ, Pan H, Cheng Y, Kudo M, Kang YK, Chen PJ, Toh HC, Gorbunova V, Eskens FA, Qian J, McKee MD, Ricker JL, Carlson DM, El-Nowiem S: Linifanib versus sorafenib in patients with advanced hepatocellular carcinoma: results of a randomized phase III trial. *J Clin Oncol* 2015;33:172–179.
- 13 Llovet JM, Decaens T, Raoul JL, Boucher E, Kudo M, Chang C, Kang YK, Assenat E, Lim HY, Boige V, Mathurin P, Fartoux L, Lin DY, Bruix J, Poon RT, Sherman M, Blanc JF, Finn RS, Tak WY, Chao Y, Ezzeddine R, Liu D, Walters I, Park JW: Brivanib in patients with advanced hepatocellular carcinoma who were intolerant to sorafenib or for whom sorafenib failed: results from the randomized phase III BRISK-PS study. *J Clin Oncol* 2013;31:3509–3516.

- 14 Zhu AX, Kudo M, Assenat E, Cattani S, Kang YK, Lim HY, Poon RT, Blanc JF, Vogel A, Chen CL, Dorval E, Peck-Radosavljevic M, Santoro A, Daniele B, Furuse J, Jappe A, Perraud K, Anak O, Sellami DB, Chen LT: Effect of everolimus on survival in advanced hepatocellular carcinoma after failure of sorafenib: the EVOLVE-1 randomized clinical trial. *JAMA* 2014;312:57–67.
- 15 Zhu AX, Park JO, Ryoo BY, Yen CJ, Poon R, Pastorelli D, Blanc JF, Chung HC, Baron AD, Pfiffer TE, Okusaka T, Kubackova K, Trojan J, Sastre J, Chau I, Chang SC, Abada PB, Yang L, Schwartz JD, Kudo M; REACH Trial Investigators: Ramucirumab versus placebo as second-line treatment in patients with advanced hepatocellular carcinoma following first-line therapy with sorafenib (REACH): a randomised, double-blind, multicentre, phase 3 trial. *Lancet Oncol* 2015;16:859–870.
- 16 Villanueva A: Rethinking future development of molecular therapies in hepatocellular carcinoma: a bottom-up approach. *J Hepatol* 2013;59:392–395.
- 17 Santoro A, Rimassa L, Borbath I, Daniele B, Salvagni S, Van Laethem JL, Van Vlierberghe H, Trojan J, Kolligs FT, Weiss A, Miles S, Gasbarrini A, Lencioni M, Cicalese L, Sherman M, Gridelli C, Buggisch P, Gerken G, Schmid RM, Boni C, Personeni N, Hassoun Z, Abbadessa G, Schwartz B, Von Roemeling R, Lamar ME, Chen Y, Porta C: Tivantinib for second-line treatment of advanced hepatocellular carcinoma: a randomised, placebo-controlled phase 2 study. *Lancet Oncol* 2013;14:55–63.
- 18 Faivre SJ, Santoro A, Gane E, Kelley RK, Hourmand IO, Assenat E, Gueorguieva I, Cleverly A, Desai D, Lahn M, Raymond E, Benhadji KA, Giannelli G: A phase 2 study of galunisertib, a novel transforming growth factor-beta (TGF- $\beta$ ) receptor I kinase inhibitor, in patients with advanced hepatocellular carcinoma (HCC) and low serum alpha fetoprotein (AFP) (abstract). *J Clin Oncol* 2016;34(suppl 2016 ASCO Annu Meet):4070.
- 19 Kudo M: Regorafenib as second-line systemic therapy may change the treatment strategy and management paradigm for hepatocellular carcinoma. *Liver Cancer* 2016;5:235–244.
- 20 Terashima T, Yamashita T, Takata N, Nakagawa H, Toyama T, Arai K, Kitamura K, Yamashita T, Sakai Y, Mizukoshi E, Honda M, Kaneko S: Post-progression survival and progression-free survival in patients with advanced hepatocellular carcinoma treated by sorafenib. *Hepatol Res* 2016;46:650–656.
- 21 Reig M, Rimola J, Torres F, Darnell A, Rodriguez-Lope C, Forner A, Llarch N, Ríos J, Ayuso C, Bruix J: Postprogression survival of patients with advanced hepatocellular carcinoma: rationale for second-line trial design. *Hepatology* 2013;58:2023–2031.
- 22 Kudo M, Park JW, Obi S, Qin S, Assenat E, Umeyama Y, Chakrabarti D, Valota O, Fujii Y, Martini JF, Williams JA, Kang YK: Regional differences in efficacy/safety/biomarkers in a randomised study of axitinib in 2nd line patients (pts) with advanced hepatocellular carcinoma (HCC) (abstract). *J Clin Oncol* 2016;34(suppl 4S 2016 Gastrointest Cancers Symp):329.
- 23 Anthony B, El-Khoueiry IM, Todd S, Crocenzi, et al: Phase I/II safety and antitumor activity of nivolumab in patients with advanced hepatocellular carcinoma (HCC): CA209-040 (abstract). *J Clin Oncol* 2015;33(suppl):LBA101.
- 24 Sangro B, Melero I, Yau TC, Hsu C, Kudo M, Crocenzi TS, Kim TY, Choo SP, Trojan J, Meyer T, Kang YK, Anderson J, Dela Cruz C, Lang L, Neely J, El-Khoueiry AB: Safety and antitumor activity of nivolumab (nivo) in patients (pts) with advanced hepatocellular carcinoma (HCC): interim analysis of dose-expansion cohorts from the phase 1/2 CheckMate-040 study (abstract). *J Clin Oncol* 2016;34(suppl 2016 ASCO Annu Meet):4078.
- 25 El-Khoueiry AB, Sangro B, Yau TC, Crocenzi TS, Welling TH, Yeo W, Chopra A, Anderson J, Dela Cruz C, Lang L, Neely J, Melero I: Phase I/II safety and antitumor activity of nivolumab (nivo) in patients (pts) with advanced hepatocellular carcinoma (HCC): interim analysis of the checkmate-040 dose escalation study (abstract). *J Clin Oncol* 2016;34(suppl 2016 ASCO Annu Meet):4012.
- 26 Sangro B, Park JW, Dela Cruz C, Anderson J, Lang L, Neely J, Shaw JW, Cheng AL: A randomized, multicenter, phase 3 study of nivolumab versus sorafenib as first-line treatment in patients (pts) with advanced hepatocellular carcinoma (HCC): CheckMate-459 (abstract). *J Clin Oncol* 2016;34(suppl 2016 ASCO Annu Meet):TPS4147.
- 27 Abou-Alfa G, Sangro B, Morse M, Zhu AX, Kim RD, Cheng AL, Kudo M, Kang YK, Chan SL, Antal J, Boice J, Xiao F, Morris SR, Bendell J; 022 Study Group: Phase 1/2 study of durvalumab and tremelimumab as monotherapy and in combination in patients with unresectable hepatocellular carcinoma (HCC) (abstract). *J Clin Oncol* 2016;34(suppl 2016 ASCO Annu Meet):TPS3103.
- 28 Lung-MAP. <http://www.lung-map.org/>.

## Randomized Clinical Trial

# Removal of diminutive colorectal polyps: A prospective randomized clinical trial between cold snare polypectomy and hot forceps biopsy

Yoriaki Komeda, Hiroshi Kashida, Toshiharu Sakurai, George Tribonias, Kazuki Okamoto, Masashi Kono, Mitsunari Yamada, Teppei Adachi, Hiromasa Mine, Tomoyuki Nagai, Yutaka Asakuma, Satoru Hagiwara, Shigenaga Matsui, Tomohiro Watanabe, Masayuki Kitano, Takaaki Chikugo, Yasutaka Chiba, Masatoshi Kudo

Yoriaki Komeda, Hiroshi Kashida, Toshiharu Sakurai, George Tribonias, Kazuki Okamoto, Masashi Kono, Mitsunari Yamada, Teppei Adachi, Hiromasa Mine, Tomoyuki Nagai, Yutaka Asakuma, Satoru Hagiwara, Shigenaga Matsui, Tomohiro Watanabe, Masayuki Kitano, Takaaki Chikugo, Yasutaka Chiba, Masatoshi Kudo, Department of Gastroenterology and Hepatology, Kindai University Faculty of Medicine, Osaka-Sayama, Osaka 589-8511, Japan

Takaaki Chikugo, Department of Pathology, Kindai University Faculty of Medicine, Osaka-Sayama, Osaka 589-8511, Japan

Yasutaka Chiba, Clinical Research Center, Kindai University Hospital, Osaka-Sayama, Osaka 589-8511, Japan

**Author contributions:** Komeda Y and Kitano M were involved in the study conception and design; Komeda Y drafted the article and analyzed and interpreted the data; Kashida H and Kudo M performed critical revision of the article for important intellectual content; Tribonias G, Okamoto K, Kono M, Yamada M, Adachi T, Hagiwara S, Matsui S, and Watanabe T collected data; Kashida H, Komeda Y, Sakurai T, Mine H, Nagai T, and Asakuma Y performed endoscopic procedure; Chiba Y performed statistical analysis; Chikugo T conducted pathologic evaluation; all authors performed the final approval of the article.

**Institutional review board statement:** The study was reviewed and approved by the Ethics Committee of the Kindai University Faculty of Medicine.

**Clinical trial registration statement:** This study is registered at <http://www.umin.ac.jp/ctr/index.htm>. The registration identification number is UMIN000015016.

**Informed consent statement:** All study participants provided informed written consent prior to study enrollment.

**Conflict-of-interest statement:** None to declare.

**Data sharing statement:** The technical appendix, statistical code, and data set are available from the corresponding author.

**Open-Access:** This article is an open-access article which was selected by an in-house editor and fully peer-reviewed by external reviewers. It is distributed in accordance with the Creative Commons Attribution Non Commercial (CC BY-NC 4.0) license, which permits others to distribute, remix, adapt, build upon this work non-commercially, and license their derivative works on different terms, provided the original work is properly cited and the use is non-commercial. See: <http://creativecommons.org/licenses/by-nc/4.0/>

**Manuscript source:** Unsolicited manuscript

**Correspondence to:** Yoriaki Komeda, MD, Department of Gastroenterology and Hepatology, Kindai University Faculty of Medicine, 377-2 Ohno-Higashi, Osaka-Sayama, Osaka 589-8511, Japan. [y-komme@mvb.biglobe.ne.jp](mailto:y-komme@mvb.biglobe.ne.jp)  
Telephone: +81-72-3660221-3525  
Fax: +81-72-3672880

Received: August 8, 2016  
Peer-review started: August 9, 2016  
First decision: September 20, 2016  
Revised: October 19, 2016  
Accepted: November 13, 2016  
Article in press: November 13, 2016  
Published online: January 14, 2017

## Abstract

### AIM

To compare the efficacy and safety of cold snare polypectomy (CSP) and hot forceps biopsy (HFB) for diminutive colorectal polyps.



## METHODS

This prospective, randomized single-center clinical trial included consecutive patients  $\geq 20$  years of age with diminutive colorectal polyps 3-5 mm from December 2014 to October 2015. The primary outcome measures were *en-bloc* resection (endoscopic evaluation) and complete resection rates (pathological evaluation). The secondary outcome measures were the immediate bleeding or immediate perforation rate after polypectomy, delayed bleeding or delayed perforation rate after polypectomy, use of clipping for bleeding or perforation, and polyp retrieval rate. Prophylactic clipping after polyp removal wasn't routinely performed.

## RESULTS

Two hundred eight patients were randomized into the CSP (102), HFB (106) and 283 polyps were evaluated (CSP: 148, HFB: 135). The *en-bloc* resection rate was significantly higher with CSP than with HFB [99.3% (147/148) *vs* 80.0% (108/135),  $P < 0.0001$ ]. The complete resection rate was significantly higher with CSP than with HFB [80.4% (119/148) *vs* 47.4% (64/135),  $P < 0.0001$ ]. The immediate bleeding rate was similar between the groups [8.6% (13/148) *vs* 8.1% (11/135),  $P = 1.000$ ], and endoscopic hemostasis with hemoclips was successful in all cases. No cases of perforation or delayed bleeding occurred. The rate of severe tissue injury to the pathological specimen was higher HFB than CSP [52.6% (71/135) *vs* 1.3% (2/148),  $P < 0.0001$ ]. Polyp retrieval failure was encountered CSP (7), HFB (2).

## CONCLUSION

CSP is more effective than HFB for resecting diminutive polyps. Further long-term follow-up study is required.

**Key words:** Cold snare polypectomy; Colonoscopy; Polypectomy; Colorectal diminutive polyps; Hot forceps biopsy

© The Author(s) 2017. Published by Baishideng Publishing Group Inc. All rights reserved.

**Core tip:** Cold snare polypectomy (CSP) is more effective in terms of both endoscopic *en-bloc* resection rate and pathological complete resection rate than hot forceps biopsy (HFB) for resecting diminutive polyps. Moreover, CSP and HFB did not result in any serious adverse events such as delayed bleeding and perforation.

Komeda Y, Kashida H, Sakurai T, Tribonias G, Okamoto K, Kono M, Yamada M, Adachi T, Mine H, Nagai T, Asakuma Y, Hagiwara S, Matsui S, Watanabe T, Kitano M, Chikugo T, Chiba Y, Kudo M. Removal of diminutive colorectal polyps: A prospective randomized clinical trial between cold snare polypectomy and hot forceps biopsy. *World J Gastroenterol* 2017; 23(2): 328-335 Available from: URL: <http://www.wjgnet.com/1007-9327/full/v23/i2/328.htm> DOI: <http://dx.doi.org/10.3748/wjg.v23.i2.328>

## INTRODUCTION

The United States National Polyp Study demonstrated that a clean colon (*i.e.*, a colon in which all adenomatous polyps have been eliminated) significantly decreases the mortality rate for colorectal cancer<sup>[1]</sup>. Accordingly, there is a need to consider the resection of neoplastic polyps, including diminutive polyps, when performing colonoscopy. Cold snare polypectomy (CSP) is becoming a common method for resecting small or diminutive polyps without using submucosal injections or electrocautery, and it is regarded as a safe treatment in Western countries<sup>[2]</sup>. Recently, it has also gradually gained popularity in Japan<sup>[3-5]</sup>. The advantages of CSP are that electrocautery-related damages to the submucosal vascular tissue are prevented and there are fewer restrictions on patients' postoperative activity or diet. Low rates of postoperative bleeding and perforation can also be expected, because electrocautery is not used during CSP.

Hot forceps biopsy (HFB) is another method used to remove diminutive polyps; it has been widely used in Japan, because it is comparatively easy to use. Although the HFB approach is advantageous in that possible adenomatous remnants are fulgurated and the blood vessels are coagulated, it also has disadvantages associated with electrocautery, such as perforation and delayed bleeding<sup>[6,7]</sup>. To our knowledge, CSP and HFB have not been directly compared. We hypothesized that CSP would be more effective than HFB for resecting diminutive polyps 3-5 mm. Therefore, the present study aimed to compare the efficacy and safety of CSP and HFB for removing colorectal polyps measuring 3-5 mm.

## MATERIALS AND METHODS

### Study design, subjects, and methods

This prospective, randomized, single-center comparison study was conducted from December 2014 to October 2015. The inclusion criteria were consecutive patients over 20 years old and those who were scheduled to undergo the removal of colorectal polyps measuring 3-5 mm. The preoperative exclusion criteria were patients with inflammatory bowel disease, polyposis, polyps suggestive of cancer, and hyperplastic polyps measuring less than 5 mm in the distal colon. Similar to hyperplastic polyps less than 5 mm, typical hyperplastic polyps featuring white, flat protrusions with a diameter of 5 mm or less, which are frequently observed in the distal colon (rectum and sigmoid colon), reportedly exhibit no relationship with adenoma onset in the future, and guidelines state that no proactive action is required. The intra-operative exclusion criteria were patients converted to endoscopic mucosal resection (EMR), those with polyp retrieval failure, and patients with non-neoplastic polyps. Patients presenting with diminutive polyps were assigned to either the CSP or HFB group using computer-generated random sequencing. The polyp size was estimated on the basis

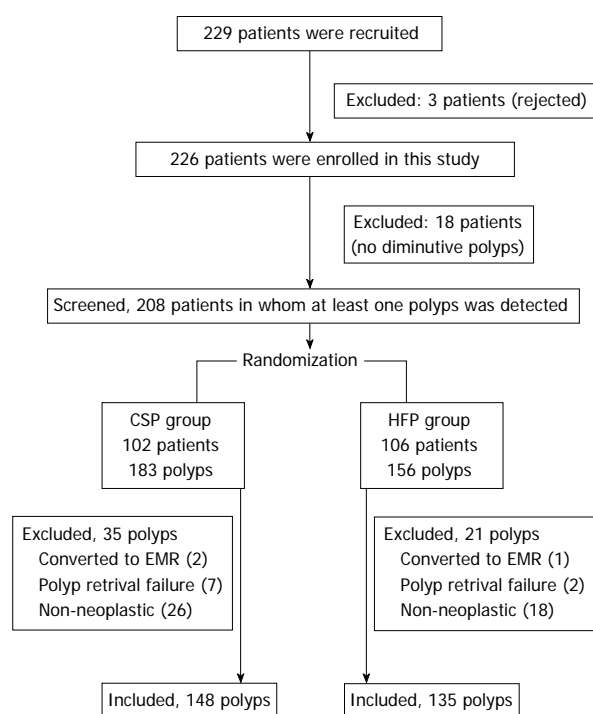


Figure 1 Enrollment flowchart. CSP: Cold snare polypectomy; HFB: Hot forceps biopsy; EMR: Endoscopic mucosal resection.

of the maximum width of the opened snare or HFB. Endoscopic and pathological images obtained during the tests were de-identified, and they were used to make diagnoses on the basis of the findings. No limit was set for the number of polyps removed per patient. Each polypectomy was considered independent of the others.

The study was approved by the institutional ethics committee (registration number 26-180; date: Dec 2 2014), and it was registered with the University Hospital Medical Information Network (UMIN ID: 000015016; date of registration: Sep 1, 2014). Written informed consent was obtained from all patients.

### Outcome measures

The primary outcome measures were as follows: the *en-bloc* resection rate (endoscopic evaluation was used to confirm the tumor-free cut margin with magnified endoscopic view) and complete resection rate (pathological evaluation was used to confirm the tumor-free cut margin in microscopic view). The secondary outcome measures were as follows: the immediate bleeding or immediate perforation rate after polypectomy, delayed bleeding or delayed perforation rate after polypectomy, use of clipping for bleeding or perforation, and polyp retrieval rate.

Immediate bleeding was defined as spurting or oozing blood that continued for more than 1 min following resection that was stopped with hemoclips. Delayed bleeding was clinically defined as evident

hematochezia after the patient was removed from the endoscopic room; this was confirmed by a questionnaire at the time of the patient's next hospital visit (7-10 d after treatment). Prophylactic clipping after polyp removal was not routinely performed, except in patients with immediate bleeding or in those with a high risk for perforation, patients with a bleeding tendency, those taking antithrombotic agents, *etc.*

### Endoscopic procedures

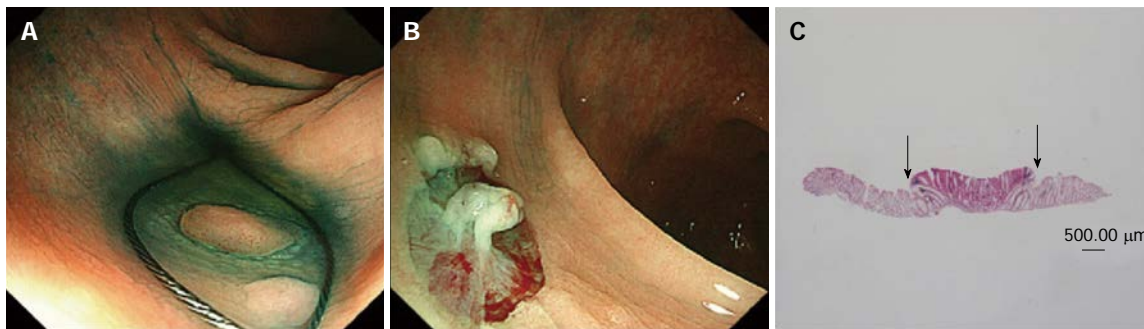
All colonoscopic procedures were performed by six experienced endoscopists (H.K., T.S., Y.A., Y.K., T.N., and H.M.) who had each performed more than 1000 polypectomies before. No colonoscopist had performed CSP before this trial. High-definition endoscopes (PCF-Q260AZI, CF-H260AZI, CF-HQ290I; Olympus Medical Systems, Tokyo, Japan) were used in this study. Patients drank a polyethylene glycol-electrolyte solution (Ajinomoto Pharmaceutical Co., Tokyo, Japan) for bowel preparation. Two types of snares were used for CSP: the Profile snare and Captivator-II Snare (Boston Scientific, Natick, MA, United States), both of which are approved for cold polypectomy in Japan. Each endoscopist chose which snare they preferred. In addition, the FD-1U-1 forceps (Olympus) was used to perform HFB. The respective maximum widths of the FD-1U-1 forceps, Profile snare, and Captivator-II Snare were 7, 10, and 11 mm.

During CSP, the polyps were resected without injection or electrocautery, and some of the surrounding normal mucosa was removed (Figure 1). The transected polyps in the CSP group were vacuumed into a trap and were collected (Figure 2). During HFB, an electrocautery with coagulating current at 25-30 W in the setting of the electrosurgical unit VIO300D (Erbe Elektromedizin, Tuebingen, Germany) was applied to the polyp until the white coagulum was seen at the polyp base (Figure 3)<sup>[8]</sup>, and then the polyp was removed by gently pulling it from the mucosa. The resected polyps in the HFB group were collected in the cup of the forceps.

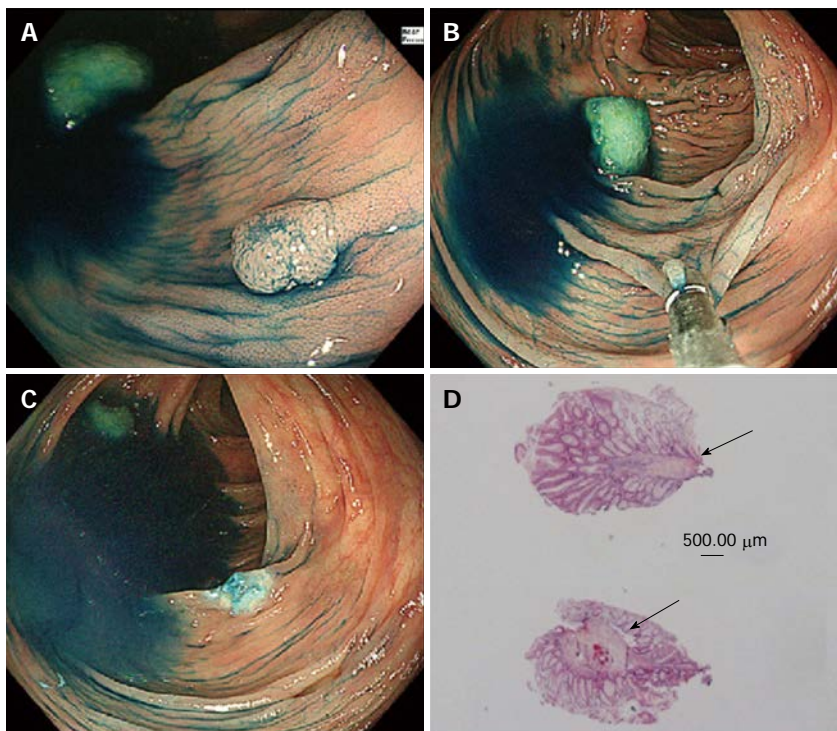
All tissue specimens were examined by an experienced pathologist (T.T.) who was blinded to the clinical information concerning the patient and polyp, and to how the polyp was resected. The vertical and lateral cut margins and tissue damage were evaluated with a hematoxylin and eosin stain.

### Sample size calculation and statistical analysis

The sample size was calculated on the basis of the overall estimated complete resection rate. We assumed that it would be 95% in the CSP group and 80% in the HFB group according to the results of previous reports (93% and 83%, respectively)<sup>[9,10]</sup>. Thus, the needed sample size was 150 polyps per group with a significance level of 5% (two-tailed) and power of 80% when the Fisher exact test was used to confirm superiority of CSP to HFB. We assumed a dropout rate



**Figure 2** Technique for cold snare polypectomy. A: Chromoendoscopy was used to detect the polyp and surrounding normal mucosa, which were captured with a snare, and resection was performed without electrocautery; B: The mucosal defect was assessed to ensure complete resection and no persistent bleeding; C: The free cut-margin was negative for neoplastic tissue (area between the arrows).



**Figure 3** Technique for hot forceps biopsy. A: A slightly protruded polyp was detected with magnified chromoendoscopy; B: The polyp was captured in the cup of the forceps and gently pulled from the mucosa; C: The electrocautery current was applied to the polyp until the color changed to white at the polyp base. Then the polyp was completely removed from the mucosa; D: Pathologic evaluation of the free cut-margin was difficult to perform because of a thermal tissue injury (arrow).

of 10%; thus, we determined that the sample size should be 165 polyps per group.

Categorical variables were compared with the Fisher exact test, and continuous variables were compared with the *t*-test. To determine predictive factors of complete resection, we conducted multivariable logistic regression analysis with the resection method (CSP or HFB) and polyp characteristics (location, shape, and histology) as explanatory variables.

We performed a modified intention-to-treat (ITT) analysis. In our modified ITT analysis, we considered polyps converted to EMR and polyp retrieval failure as incomplete *en-bloc* resection and pathological resection. We excluded the non-neoplastic polyps

from ITT analysis because endoscopic/pathological evaluation of these polyps could not originally be performed. The target of modified ITT analysis was 157 polyps in CSP and 138 polyps in HFB.

All statistical analyses were performed using SAS software, version 9.4 (SAS Institute, Cary, NC, United States). Statistical review of the study was performed by a biomedical statistician.

## RESULTS

### *Patients' and polyps' characteristics*

Two hundred eight patients were enrolled in the study [mean  $\pm$  SD: age 69.0  $\pm$  8.0 years (range 35-87



**Table 1 Patients' baseline characteristics *n* (%)**

	CSP group ( <i>n</i> = 102)	HFB group ( <i>n</i> = 106)	<i>P</i> value
Age (yr), mean (SD)	69.4 (8.0)	68.9 (7.9)	0.60
Female sex	32 (31.3)	31 (29.2)	0.76
Use of antithrombotic agents	4 (3.9)	3 (2.8)	0.72

CSP: Cold snare polypectomy; HFB: Hot forceps biopsy.

**Table 2 Polyps' characteristics**

	CSP group	HFB group	<i>P</i> value
Total No. of polyps	148	135	
Polyp size (mm) mean ± SD	4.2 (1.0)	3.8 (1.0)	
No. of polyps per patient, mean	1.5	1.3	
Location			0.10
Right <sup>1</sup> /Left <sup>2</sup>	44/104	53/82	
Shape			0.09
Protruded	107	110	
Flat	41	25	
Histology			0.16
High-grade adenoma	12	3	
Low-grade adenoma	124	126	
SSA/P	6	4	
Hyperplastic polyp	3	2	
Other	3	0	

<sup>1</sup>Located from the cecum to the splenic flexure; <sup>2</sup>Located from the splenic flexure to the rectum. SSA/P: Sessile serrated adenoma/polyp; CSP: Cold snare polypectomy; HFB: Hot forceps biopsy.

years), 31% women], and we excluded 3 patients who were rejected (the rejection rate for inclusion in the trial was 1.3%: 3/229) and 18 patients who had no diminutive polyps (7.9%: 18/229). After randomization was performed, 102 patients were allocated to the CSP group, and 106 were allocated to the HFB group. A flowchart of the study enrollment is shown in Figure 1. The mean ages were 69.4 ± 9.4 in the CSP group and 68.9 ± 7.9 in the HFB group. The mean number of resected polyps per patient was 1.5 in the CSP group and 1.3 in the HFB group. Finally, 283 polyps (CSP group: 148 polyps, HFB group: 135 polyps) were evaluated after excluding some polyps (polyps removed with EMR, polyps that could not be retrieved, and non-neoplastic polyps). There was no significant difference between the two groups with regard to the characteristics of the patients and polyps (Tables 1 and 2). According to the pathological diagnosis, tubular adenoma with low-grade dysplasia accounted for 83.4% of polyps in the CSP group and 93.3% in the HFB group.

### Primary and secondary outcomes

The *en-bloc* resection rate was significantly higher with CSP than with HFB [99.3% (147/148) vs 80.0% (108/135), *P* < 0.0001]. The complete resection rate

was significantly higher with CSP than with HFB [80.4% (119/148) vs 47.4% (64/135), *P* < 0.0001]; however, there were 6 polyps in the CSP group that broke into pieces during retrieval by aspiration (Table 3). The immediate bleeding rate was similar between the two groups [CSP group: 8.8% (13/148) vs HFB group: 8.1% (11/135), *P* = 1.000]. Endoscopic hemostasis with hemoclips was successful in cases of immediate bleeding. Serious adverse events such as perforation or delayed bleeding did not occur in any case, although prophylactic clipping after polyp removal was not routinely performed, except in cases of immediate bleeding or in those with a high risk of bleeding.

The rate of tissue injury according to the pathologic specimen was higher in the HFB group than in the CSP group [52.6% (71/135) vs 1.3% (2/148), *P* < 0.0001]. The frequency of polyp retrieval failure was higher in the CSP group than in the HFB group (7/148 vs 2/135). There was no significant difference between the Profile snare and Captivator II Snare for CSP in terms of all the factors (Table 4).

The results of this modified ITT analysis were that the *en-bloc* resection rate was significantly higher with CSP than with HFB [87.9% (138/157) vs 76.0% (105/138), *P* < 0.0001]. The complete resection rate was significantly higher with CSP than with HFB [70.1% (110/157) vs 44.2% (61/138), *P* < 0.0001]. There was no significant difference between the original data and modified ITT analysis.

Multivariable logistic regression analysis showed that the resection method (CSP vs HFB) was the strongest predictive factor for complete resection (Table 5).

## DISCUSSION

We demonstrated that CSP is more effective than HFB for resecting diminutive polyps 3–5 mm. Recently, in a randomized controlled trial at a single center, Lee *et al*<sup>[9]</sup> reported that CSP was superior to CFP for removing small polyps ≤ 5 mm (93% vs 76%, *P* = 0.009). Kim *et al*<sup>[11]</sup> also demonstrated that the overall complete resection rate was significantly higher in the CSP group than in the CFP (96.6% vs 82.6%, *P* = 0.01) for polyps ≤ 7 mm. Authors of a pilot study conducted in Japan reported that the rate of complete resection after CSP for polyps < 10 mm was 60%<sup>[3]</sup>. The present study's findings showed that the overall complete resection rate for polyps 3–5 mm was significantly higher with CSP than with HFB, although six polyps in the CSP group could not be evaluated because they broke into pieces in the working channel of the scope during aspiration. In 19.6% of patients in the CSP group, the resected free cut-margin was very close to the lesion, thus it was considered unclear (*i.e.*, tumor involvement of the horizontal margin could not be determined).

In the present study, the HFB group had a low

**Table 3 Outcomes and adverse events among the patients**

	CSP group (95%CI)	HFB group (95%CI)	P value
Endoscopic evaluation	147/148 = 99.3%	108/135 = 80.0%	< 0.0001
<i>En-bloc</i> resection rate with free cut-margin	(92.3%-100.0%)	(72.3%-86.4%)	
Pathologic evaluation	119/148 = 80.4%	64/135 = 47.4%	< 0.0001
Complete resection rate with free cut-margin	(73.1%-86.5%)	(38.8%-56.2%)	
Histological tissue injury	2/148 = 1.3%	71/135 = 52.6%	< 0.0001
(0.2%-4.8%)		(43.8%-61.2%)	
Adverse event			
Immediate bleeding	13/148 = 8.8%	11/135 = 8.1%	1.00
(4.8%-14.6%)		(4.1%-14.1%)	
Delayed bleeding	0	0	
Perforation	0	0	

CSP: Cold snare polypectomy; HFB: Hot forceps biopsy.

**Table 4 Outcomes and adverse events in terms of the snares used for cold snare polypectomy**

	Profile snare (95%CI)	Captivator-II snare (95%CI)	P value
Endoscopic evaluation	88/88 = 100%	59/60 = 98.3%	0.41
<i>En-bloc</i> resection rate with free cut-margin	(95.9%-100.0%)	(91.2%-100.0%)	
Pathologic evaluation	75/88 = 85.2%	44/60 = 73.3%	0.09
Complete resection rate with free cut-margin	(76.1%-91.9%)	(60.3%-83.9%)	
Histological tissue injury	0/88 = 0%	2/60 = 3.3%	0.16
(0.0%-4.1%)		(0.4%-11.5%)	
Adverse event			
Immediate bleeding	9/88 = 10.2%	4/60 = 6.7%	0.56
(4.8%-18.5%)		(1.8%-16.2%)	
Delayed bleeding	0	0	
Perforation	0	0	

There were no differences in the type or number of polyps in these groups. CSP: Cold snare polypectomy.

**Table 5 Results of multivariable logistic regression analysis of the complete resection rate**

Variable	Odds ratio (95%CI)	P value
Resection method		
CSP/HFB	4.70 (2.68-8.24)	< 0.0001
Location		
Left <sup>1</sup> /Right <sup>2</sup>	1.24 (0.71-2.17)	0.45
Shape		
Flat/protruded	0.94 (0.50-1.78)	0.85
Histology		
Non-TA/TA	1.34 (0.44-4.08)	0.61

<sup>1</sup>Located from the cecum to the splenic flexure; <sup>2</sup>Located from the splenic flexure to the rectum. CSP: Cold snare polypectomy; HFB: Hot forceps biopsy; TA: Tubular adenoma.

complete resection rate of 47.4%, significantly low rate 80.0% with *en-bloc* resection, and substantial tissue damage due to electric resection. It is concerning that HFB caused so much thermal damage to the specimen that it made the pathological diagnosis difficult.

The current study also demonstrated similar immediate bleeding rates in both groups, and endoscopic hemostasis with hemoclips was successful in these cases. Horiuchi *et al*<sup>[12]</sup> reported that CSP was used safely even in patients taking antiplatelet agents and in those in which therapeutic levels of anticoagulation

were achieved, although the sample size was small.

In our study, no perforation or delayed bleeding occurred in any case. The first author previously reported on an animal experiment conducted in pigs at another institution, and no perforation occurred with CSP for large polyps exceeding 1 cm<sup>[13]</sup>. In the present study, two polyps could not be resected with CSP because there was too much resistance during snaring; therefore, they were converted with conventional EMR using an injection and electrical current was used. These cases were excluded from further evaluation. Accordingly, a very low incidence of perforation can be expected in CSP. The change in the resection method may have contributed to the low rate perforation.

A previous study reported a perforation rate of 0.05% after HFB, including one case of death<sup>[14]</sup>. In the present study, no serious adverse events (delayed bleeding, perforation, or post-coagulation syndrome) were observed in HFB group. Although Williams reported a rate of 95% for specimens with interpretable histological features<sup>[8]</sup>, our study demonstrated that the rate of severe histological tissue injury was higher in the HFB group than in the CSP group.

Polyp retrieval failure occurred in seven patients in the CSP group and two patients in the HFB group. This corresponds with a previously reported result that specimen retrieval is more difficult when the polyp size

is  $\leq 5$  mm<sup>[15]</sup>.

There were some limitations to this study. It was performed at a single university hospital. We only used the two types of snares that are approved for cold resection in Japan; thus, our results may not be applicable to other snares. In this study, we did not assess the amount of time required using each of the two techniques for complete polyp resection in each colonoscopy because the time for polypectomy did not differ between cold forceps polypectomy as almost same technique of HFB and CSP in a previous study<sup>[16]</sup>. We did not compare the two procedures. Lastly, the study did not include long-term follow-up after resection.

In conclusion, our results showed that CSP is more effective than HFB for resecting diminutive polyps. The endoscopic *en-bloc* resection rate and pathologic complete resection rate were lower with HFB, as histological evaluation in the HFB group was difficult due to tissue injury. Serious adverse events such as delayed bleeding and perforation did not occur in either group. Further study with long-term follow-up is required.

## COMMENTS

### Background

The advantages of cold snare polypectomy (CSP) are that electrocautery-related damage to the submucosal vascular tissue is prevented, and there are fewer restrictions on patients' postoperative activity and diet. Low rates of postoperative bleeding and perforation can also be expected, because electrocautery is not used during CSP. Hot forceps biopsy (HFB) is another method used to remove diminutive polyps because it is comparatively easy to use. CSP and HFB have not previously been directly compared.

### Research frontiers

A few human studies in the West have suggested that CSP is a safe treatment without electrocautery-related damages and HFB has disadvantages associated with electrocautery, such as perforation and delayed bleeding.

### Innovations and breakthroughs

This is the first randomized controlled prospective study to compare the efficacy of CSP and HFB. CSP is more effective in terms of both endoscopic *en-bloc* resection rate and pathological complete resection rate than HFB for resecting diminutive polyps, as histological evaluation with HFB was difficult due to tissue injury.

### Applications

CSP is preferable under the removal of colorectal diminutive polyps without polyps suggestive of cancer, and hyperplastic polyps measuring less than 5 mm in the distal colon.

### Terminology

CSP is a method for resecting diminutive polyps without using submucosal injections or electrocautery. HFB captures the polyp in the cup of the forceps and gently pulls it from the mucosa with electrocautery.

### Peer-review

This study showed a topic of interest in clinical practice.

## REFERENCES

1 Winawer SJ, Zauber AG, Ho MN, O'Brien MJ, Gottlieb LS,

Sternberg SS, Wayne JD, Schapiro M, Bond JH, Panish JF. Prevention of colorectal cancer by colonoscopic polypectomy. The National Polyp Study Workgroup. *N Engl J Med* 1993; **329**: 1977-1981 [PMID: 8247072 DOI: 10.1056/NEJM199312303292701]

- 2 Repici A, Hassan C, Vitetta E, Ferrara E, Manes G, Gullotti G, Princiotta A, Dulbecco P, Gaffuri N, Bettoni E, Pagano N, Rando G, Strangio G, Carlino A, Romeo F, de Paula Pessoa Ferreira D, Zullo A, Ridola L, Malesci A. Safety of cold polypectomy for  $\leq 10$  mm polyps at colonoscopy: a prospective multicenter study. *Endoscopy* 2012; **44**: 27-31 [PMID: 22125197 DOI: 10.1055/s-0031-1291387]
- 3 Takeuchi Y, Yamashina T, Matsuura N, Ito T, Fujii M, Nagai K, Matsui F, Akasaka T, Hanaoka N, Higashino K, Iishi H, Ishihara R, Thorlacius H, Uedo N. Feasibility of cold snare polypectomy in Japan: A pilot study. *World J Gastrointest Endosc* 2015; **7**: 1250-1256 [PMID: 26634041 DOI: 10.4253/wjge.v7.i17.1250]
- 4 Hewett DG, Rex DK. Colonoscopy and diminutive polyps: hot or cold biopsy or snare? Do I send to pathology? *Clin Gastroenterol Hepatol* 2011; **9**: 102-105 [PMID: 20951831 DOI: 10.1016/j.cgh.2010.09.024]
- 5 Uraoka T, Rambaran H, Matsuda T, Fujii T, Yahagi N. Cold polypectomy techniques for diminutive polyps in the colorectum. *Dig Endosc* 2014; **26** Suppl 2: 98-103 [PMID: 24750157 DOI: 10.1111/den.12252]
- 6 Gilbert DA, DiMarino AJ, Jensen DM, Katon RM, Kimmey MB, Laine LA, MacFaydyen BV, Michaelitz-Onody PA, Zuckerman G. Status evaluation: biliary stents. American Society for Gastrointestinal Endoscopy. Technology Assessment Committee. *Gastrointest Endosc* 1992; **38**: 750-752 [PMID: 1473699]
- 7 Metz AJ, Moss A, McLeod D, Tran K, Godfrey C, Chandra A, Bourke MJ. A blinded comparison of the safety and efficacy of hot biopsy forceps electrocauterization and conventional snare polypectomy for diminutive colonic polypectomy in a porcine model. *Gastrointest Endosc* 2013; **77**: 484-490 [PMID: 23199650 DOI: 10.1016/j.gie.2012.09.014]
- 8 Wayne JD. Techniques of polypectomy: hot biopsy forceps and snare polypectomy. *Am J Gastroenterol* 1987; **82**: 615-618 [PMID: 3605021]
- 9 Lee CK, Shim JJ, Jang JY. Cold snare polypectomy vs. Cold forceps polypectomy using double-biopsy technique for removal of diminutive colorectal polyps: a prospective randomized study. *Am J Gastroenterol* 2013; **108**: 1593-1600 [PMID: 24042189 DOI: 10.1038/ajg.2013.302]
- 10 Vanagunas A, Jacob P, Vakil N. Adequacy of "hot biopsy" for the treatment of diminutive polyps: a prospective randomized trial. *Am J Gastroenterol* 1989; **84**: 383-385 [PMID: 2648816]
- 11 Kim JS, Lee BI, Choi H, Jun SY, Park ES, Park JM, Lee IS, Kim BW, Kim SW, Choi MG. Cold snare polypectomy versus cold forceps polypectomy for diminutive and small colorectal polyps: a randomized controlled trial. *Gastrointest Endosc* 2015; **81**: 741-747 [PMID: 25708763 DOI: 10.1016/j.gie.2014.11.048]
- 12 Horiuchi A, Nakayama Y, Kajiyama M, Tanaka N, Sano K, Graham DY. Removal of small colorectal polyps in anticoagulated patients: a prospective randomized comparison of cold snare and conventional polypectomy. *Gastrointest Endosc* 2014; **79**: 417-423 [PMID: 24125514 DOI: 10.1016/j.gie.2013.08.040]
- 13 Tribonias G, Komeda Y, Voudoukis E, Bassioulas S, Viazis N, Manola ME, Giannikaki E, Papalois A, Paraskeva K, Karamanolis D, Paspatis GA. Cold snare polypectomy with pull technique of flat colonic polyps up to 12 mm: a porcine model. *Ann Gastroenterol* 2015; **28**: 141-143 [PMID: 25609218]
- 14 Wadas DD, Sanowski RA. Complications of the hot biopsy forceps technique. *Gastrointest Endosc* 1988; **34**: 32-37 [PMID: 3258260]
- 15 Komeda Y, Suzuki N, Sarah M, Thomas-Gibson S, Vance M, Fraser C, Patel K, Saunders BP. Factors associated with failed polyp retrieval at screening colonoscopy. *Gastrointest Endosc* 2013; **77**: 395-400 [PMID: 23211749 DOI: 10.1016/j.gie.2012.10.007]



- 16 **Park SK**, Ko BM, Han JP, Hong SJ, Lee MS. A prospective randomized comparative study of cold forceps polypectomy by using narrow-band imaging endoscopy versus cold snare

polypectomy in patients with diminutive colorectal polyps. *Gastrointest Endosc* 2016; **83**: 527-532.e1 [PMID: 26358331 DOI: 10.1016/j.gie.2015.08.053]

**P- Reviewer:** Koker IH, Mori Y, Saligram S **S- Editor:** Yu J  
**L- Editor:** A **E- Editor:** Zhang FF





Published by **Baishideng Publishing Group Inc**  
8226 Regency Drive, Pleasanton, CA 94588, USA  
Telephone: +1-925-223-8242  
Fax: +1-925-223-8243  
E-mail: [bpgoffice@wjgnet.com](mailto:bpgoffice@wjgnet.com)  
Help Desk: <http://www.wjgnet.com/esps/helpdesk.aspx>  
<http://www.wjgnet.com>



ISSN 1007-9327



© 2017 Baishideng Publishing Group Inc. All rights reserved.



# Regorafenib for patients with hepatocellular carcinoma who progressed on sorafenib treatment (RESORCE): a randomised, double-blind, placebo-controlled, phase 3 trial

Jordi Bruix, Shukui Qin, Philippe Merle, Alessandro Granito, Yi-Hsiang Huang, György Bodoky, Marc Pracht, Osamu Yokosuka, Olivier Rosmorduc, Valeriy Breder, René Gerolami, Gianluca Masi, Paul J Ross, Tianqiang Song, Jean-Pierre Bronowicki, Isabelle Ollivier-Hourmand, Masatoshi Kudo, Ann-Lii Cheng, Josep M Llovet, Richard S Finn, Marie-Aude LeBerre, Annette Baumhauer, Gerold Meinhardt, Guohong Han, on behalf of the RESORCE Investigators\*

## Summary

**Background** There are no systemic treatments for patients with hepatocellular carcinoma (HCC) whose disease progresses during sorafenib treatment. We aimed to assess the efficacy and safety of regorafenib in patients with HCC who have progressed during sorafenib treatment.

**Methods** In this randomised, double-blind, parallel-group, phase 3 trial done at 152 sites in 21 countries, adults with HCC who tolerated sorafenib ( $\geq 400$  mg/day for  $\geq 20$  of last 28 days of treatment), progressed on sorafenib, and had Child-Pugh A liver function were enrolled. Participants were randomly assigned (2:1) by a computer-generated randomisation list and interactive voice response system and stratified by geographical region, Eastern Cooperative Oncology Group performance status, macrovascular invasion, extrahepatic disease, and  $\alpha$ -fetoprotein level to best supportive care plus oral regorafenib 160 mg or placebo once daily during weeks 1–3 of each 4-week cycle. Investigators, patients, and the funder were masked to treatment assignment. The primary endpoint was overall survival (defined as time from randomisation to death due to any cause) and analysed by intention to treat. This trial is registered with ClinicalTrials.gov, number NCT01774344.

**Findings** Between May 14, 2013, and Dec 31, 2015, 843 patients were screened, of whom 573 were enrolled and randomised (379 to regorafenib and 194 to placebo; population for efficacy analyses), and 567 initiated treatment (374 received regorafenib and 193 received placebo; population for safety analyses). Regorafenib improved overall survival with a hazard ratio of 0.63 (95% CI 0.50–0.79; one-sided  $p < 0.0001$ ); median survival was 10.6 months (95% CI 9.1–12.1) for regorafenib versus 7.8 months (6.3–8.8) for placebo. Adverse events were reported in all regorafenib recipients (374 [100%] of 374) and 179 (93%) of 193 placebo recipients. The most common clinically relevant grade 3 or 4 treatment-emergent events were hypertension (57 patients [15%] in the regorafenib group vs nine patients [5%] in the placebo group), hand-foot skin reaction (47 patients [13%] vs one [1%]), fatigue (34 patients [9%] vs nine patients [5%]), and diarrhoea (12 patients [3%] vs no patients). Of the 88 deaths (grade 5 adverse events) reported during the study (50 patients [13%] assigned to regorafenib and 38 [20%] assigned to placebo), seven (2%) were considered by the investigator to be related to study drug in the regorafenib group and two (1%) in the placebo group, including two patients (1%) with hepatic failure in the placebo group.

**Interpretation** Regorafenib is the only systemic treatment shown to provide survival benefit in HCC patients progressing on sorafenib treatment. Future trials should explore combinations of regorafenib with other systemic agents and third-line treatments for patients who fail or who do not tolerate the sequence of sorafenib and regorafenib.

**Funding** Bayer.

## Introduction

The treatment of hepatocellular carcinoma (HCC) follows well established guidelines.<sup>1–3</sup> Surgical resection, transplantation, and ablation are potential curative options for early-stage disease, whereas chemo-embolisation is recommended for patients with preserved liver function and disease confined to the liver generally without vascular invasion. For patients who are not or who are no longer candidates for locoregional therapy, the oral multikinase inhibitor sorafenib is the only systemic treatment shown to

provide a clinically significant improvement in overall survival.<sup>4,5</sup> Since the results with sorafenib were published almost 10 years ago, all phase 3 trials assessing novel systemic drugs have failed to improve outcomes over sorafenib in the first-line setting<sup>6–10</sup> or in the second-line setting following sorafenib.<sup>11–14</sup> In second-line trials in patients who have failed sorafenib, overall survival in the placebo group is about 8 months.<sup>11–14</sup> Therefore, there is an unmet need for effective systemic therapies for HCC, particularly after treatment with sorafenib.

Lancet 2017; 389: 56–66

Published Online  
December 5, 2016

[http://dx.doi.org/10.1016/S0140-6736\(16\)32453-9](http://dx.doi.org/10.1016/S0140-6736(16)32453-9)

This online publication has been corrected. The corrected version first appeared at thelancet.com on January 5, 2017

See [Comment](#) page 4

\*Full list of investigators can be found in the appendix

Barcelona Clinic Liver Cancer (BCLC) Group, Liver Unit, IDIBAPS-Hospital Clínic de

Barcelona, CIBERehd, Universitat de Barcelona, Catalonia, Spain (J Bruix MD, Prof J M Llovet MD); Chinese

People's Liberation Army Cancer Center of Nanjing Bai Hospital, Nanjing, China (Prof S Qin MD); Groupement

Hospitalier Lyon Nord, Hepatology Unit, Lyon, France (Prof P Merle MD); Department

of Medical and Surgical Sciences, University of Bologna, S Orsola-Malpighi Hospital, Bologna, Italy

(A Granito MD); Division of Gastroenterology and

Hepatology, Taipei Veterans General Hospital, Institute of Clinical Medicine, National

Yang-Ming University, Taipei, Taiwan (Prof Y-H Huang MD); St Laszlo Teaching Hospital,

Budapest, Hungary (G Bodoky MD); Service

d'Oncologie Médicale, Centre Eugène Marquis, Rennes,

France (M Pracht MD); Department of

Gastroenterology and Nephrology, Chiba University,

Chiba, Japan (Prof O Yokosuka MD);

Department of Hepatology, Hôpital de la Pitié-Salpêtrière,

Assistance Publique-Hôpitaux de Paris and Université Pierre

et Marie Curie, Sorbonne Universités, Paris, France

## Research in context

## Evidence before this study

We searched PubMed for articles published between Jan 1, 2008, and Oct 26, 2016, with no language restrictions, reporting on the treatment of patients with advanced hepatocellular carcinoma (HCC) who failed sorafenib treatment using the search terms ("advanced hepatocellular carcinoma" OR "advanced hepatocellular cancer") AND "sorafenib", filtering for articles describing phase 3 clinical trials. We also searched abstracts of the annual meeting of the American Society of Clinical Oncology, using the search term "advanced hepatocellular carcinoma", limiting the results to phase 3 trials published or presented during the past 2 years. The search resulted in 15 articles or abstracts, of which three were excluded (two subanalyses and one report of maintenance sorafenib therapy following the combination of transcatheter arterial chemoembolisation and radiotherapy). Of the remaining 12 publications, two were reports of the pivotal trials of sorafenib for advanced HCC; five reported the first-line use of a novel drug or the novel combination of a drug with sorafenib compared with a sorafenib control; and five reported the second-line use of a novel agent in patients who had failed sorafenib. None of the trials assessing novel agents or novel combinations of agents in the first-line setting met the primary endpoint to show improved overall survival over sorafenib.

Similarly, none of the drugs assessed in the second-line setting in patients previously treated with sorafenib who stopped because of disease progression or intolerance showed improvement over placebo. Therefore, new effective systemic therapies for patients with advanced HCC who fail sorafenib treatment are needed.

## Added value of this study

Until now, no systemic agent has been shown to improve survival over placebo in patients with advanced HCC who fail sorafenib treatment. The results of RESORCE show that treatment with regorafenib resulted in a significant improvement in overall survival compared with placebo in patients with disease progression on sorafenib. Significant improvement over placebo was also shown for the secondary endpoints of progression-free survival, time to progression, disease control, and overall tumour response.

## Implications of all the available evidence

This phase 3 trial of regorafenib is the first to show an overall survival benefit compared with placebo in patients who failed sorafenib treatment. Future trials should explore combinations of regorafenib with other systemic agents and third-line treatments for patients who fail or who do not tolerate the sequence of sorafenib and regorafenib.

Regorafenib is an oral multikinase inhibitor that blocks the activity of protein kinases involved in angiogenesis, oncogenesis, metastasis, and tumour immunity.<sup>15,16</sup> It has a distinct molecular target profile and had more potent pharmacological activity than sorafenib in preclinical studies.<sup>15,17</sup> Regorafenib is approved as monotherapy for the treatment of treatment-refractory metastatic colorectal cancer and gastrointestinal stromal tumours at a dose of 160 mg once daily for the first 3 weeks of each 4-week cycle.<sup>18–20</sup> Based on results of a single-arm phase 2 study showing antitumour activity and acceptable tolerability,<sup>21</sup> we aimed to assess the efficacy and safety of regorafenib in patients with HCC who progressed during sorafenib treatment.

## Methods

## Study design and participants

This randomised, double-blind, placebo-controlled international phase 3 trial was done at 152 centres in 21 countries in North America, South America, Europe, Asia, and Australia.

Eligible patients were adults with HCC confirmed by pathological assessment or non-invasive assessment according to the American Association for the Study of Liver Diseases criteria for patients with confirmed cirrhosis,<sup>1</sup> and had to have at least one measurable lesion by modified Response Evaluation Criteria in Solid Tumors for HCC (mRECIST)<sup>22</sup> and RECIST version 1.1. Patients were Barcelona Clinic Liver Cancer (BCLC)

stage B or C,<sup>23</sup> could not benefit from resection, local ablation, or chemoembolisation, and must have had documented radiological progression during sorafenib treatment as defined in a study-specific radiology charter. They must have tolerated sorafenib ( $\geq 400$  mg daily for at least 20 of the 28 days before discontinuation) and received their last sorafenib dose within 10 weeks of randomisation. They were required to have Child-Pugh A liver function. Patients were excluded if they had received any other previous systemic treatment for HCC or if they discontinued sorafenib for toxicity (see appendix pp 5–7 for full inclusion and exclusion criteria).

All patients provided written informed consent. The trial was approved by each centre's ethics committee or institutional review board and complied with Good Clinical Practice guidelines, the Declaration of Helsinki, and applicable local laws.

## Randomisation and masking

Patients were randomly assigned (2:1) to regorafenib or placebo using a computer-generated randomisation list prepared by the funder. Randomisation was stratified by geographical region (Asia vs rest of world), macrovascular invasion (yes vs no), extrahepatic disease (yes vs no),  $\alpha$ -fetoprotein concentration ( $<400$  ng/mL vs  $\geq 400$  ng/mL), and Eastern Cooperative Oncology Group (ECOG) performance status (0 vs 1). The proportion of patients recruited from Asia was limited to 40%. Investigators, patients, and the funder were masked to treatment

(Prof O Rosmorduc MD); Russian Cancer Research Center n.a.N.Blokhin, Moscow, Russia (V Breder MD); CHU Timone, Université de la Méditerranée, Marseille, France (Prof R Gerolami MD); Azienda Ospedaliero-Universitaria Pisana, Pisa, Italy (G Masi MD); King's College Hospital NHS Foundation Trust, London, UK (P J Ross FRCP); Tianjin Medical University Cancer Hospital, Tianjin, China (T Song PhD); INSERM 954, CHU de Nancy, Université de Lorraine, Nancy, France (Prof J-P Bronowicki MD); Service d'Hépatogastroentérologie, CHU, Caen, France (I Ollivier-Hourmand MD); Kindai University Faculty of Medicine, Osaka, Japan (Prof M Kudo MD); Department of Medical Oncology, National Taiwan University Hospital, Taipei, Taiwan (Prof A-L Cheng MD); Liver Cancer Program, Division of Liver Diseases, Tisch Cancer Institute, Department of Medicine, Icahn School of Medicine at Mount Sinai, New York, NY, USA (Prof J M Llovet MD); Institutació Catalana de Recerca i Estudis Avançats (ICREA), Barcelona, Spain (Prof J M Llovet); Department of Medicine, Division of Hematology/Oncology, David Geffen School of Medicine at UCLA, Los Angeles, CA, USA (R S Finn MD); Bayer HealthCare SAS, Loos, France (M-A LeBerge MSc); Bayer Pharmaceuticals, Bayer Vital GmbH, Leverkusen, Germany (A Baumhauer MD); Bayer HealthCare Pharmaceuticals, Whippany, NJ, USA (G Meinhardt MD); and The First Affiliated Hospital (Xijing Hospital) of the Fourth Military Medical University, Xi'an, China (Prof G Han MD)

Correspondence to: Dr Jordi Bruix, BCLC Group, Liver Unit, Hospital Clinic, University of Barcelona, IDIBAPS, CIBEREHD, Villarroel 170, Barcelona 08036, Spain  
jbruix@clinic.ub.es

See Online for appendix

assignment. The randomisation number for each patient was assigned based on information obtained from the interactive voice-response system. Tablets with identical appearance were used for regorafenib and placebo.

### Procedures

Patients received 160 mg regorafenib (four 40 mg tablets) orally or matching placebo once daily for the first 3 weeks of each 4-week cycle. All patients received best supportive care. Other investigational antitumour drugs, antineoplastic chemotherapy, hormonal therapy, or immunotherapy were not allowed. Treatment continued until disease progression as defined by mRECIST, clinical progression (defined as an ECOG performance score  $\geq 3$  or symptomatic deterioration, including increased liver function tests), death, unacceptable toxicity, withdrawal of consent by the patient, or decision by the treating physician that discontinuation would be in the patient's best interest. Patients were followed up for tumour assessments every 6 weeks for the first eight

cycles and every 12 weeks thereafter during treatment. Treatment could be continued beyond progression if the investigator judged that the patient would benefit from continued treatment. Patients assigned to placebo could receive regorafenib after the primary analysis.

Treatment interruptions and dose reductions (to 120 mg, then 80 mg) were allowed to manage toxicity (appendix pp 12–15). The regorafenib dose could be re-escalated to a maximum of 160 mg at the investigator's discretion once toxicities were resolved. If further dose reduction was required, treatment was discontinued.

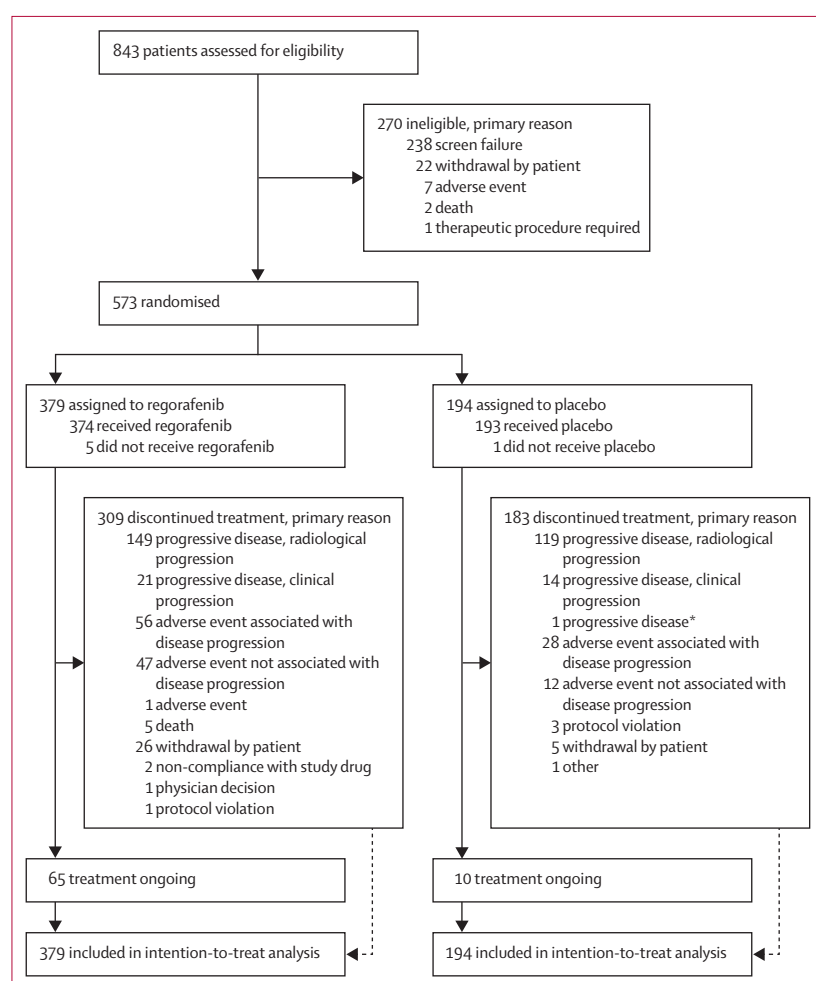
### Outcomes

The primary endpoint was overall survival (time from randomisation to death due to any cause), analysed by intention to treat (ITT). Secondary efficacy endpoints were progression-free survival (randomisation to radiological or clinical disease progression or death; by ITT), time to progression (randomisation to radiological or clinical disease progression; by ITT), objective response rate (patients with complete or partial response), and disease control rate (patients with complete response, partial response, or stable disease maintained for  $\geq 6$  weeks), assessed by investigators using mRECIST<sup>22</sup> and RECIST 1.1 (appendix p 7).

Health-related quality of life (HRQoL) was a tertiary outcome assessed using the Functional Assessment of Cancer Therapy (FACT)–General (FACT-G), FACT–Hepatobiliary (FACT-Hep), EQ-5D, and EQ-VAS questionnaires.<sup>24,25</sup> The following tertiary endpoints are not reported here: pharmacokinetics of regorafenib, and biomarker evaluation. Safety was assessed by adverse events, laboratory abnormalities, vital signs, and electrocardiography. Safety was monitored continuously throughout the study, and patients underwent safety evaluations at every cycle. Concentrations of alanine aminotransferase (ALT), aspartate aminotransferase (AST), and bilirubin were assessed weekly during the first two cycles. Adverse events were graded using National Cancer Institute Common Terminology Criteria for Adverse Events (NCI-CTCAE) version 4.03 (appendix p 7 for further assessments) and seriousness of adverse events was recorded. Investigators were blinded to study treatment for assessment of whether a death was considered related to study drug.

### Statistical analysis

Using a per-protocol one-sided  $\alpha$  of 0.025, a 2:1 randomisation between regorafenib and placebo, and assuming a median overall survival of 8 months in the placebo group, the study would have 90% power to detect a 43% increase in overall survival with regorafenib (assumed median survival 11.4 months) compared with placebo at 370 deaths and requiring 560 patients. For the primary efficacy endpoint of overall survival, the groups were compared using a log-rank test, stratified by the



**Figure 1: Trial profile**

\*Patient had radiological progression but continued treatment, and terminated treatment when the investigator judged that the patient was no longer experiencing clinical benefit.

	Regorafenib (n=379)	Placebo (n=194)
Sex		
Male	333 (88%)	171 (88%)
Female	46 (12%)	23 (12%)
Age, years	64 (54–71)	62 (55–68)
Race		
White	138 (36%)	68 (35%)
Asian	156 (41%)	78 (40%)
Black	6 (2%)	2 (1%)
Other/not reported	79 (21%)	46 (24%)
Geographical region		
Rest of world	236 (62%)	121 (62%)
Asia*	143 (38%)	73 (38%)
ECOG performance status		
0	247 (65%)	130 (67%)
1	132 (35%)	64 (33%)
Macrovascular invasion	110 (29%)	54 (28%)
Extrahepatic disease	265 (70%)	147 (76%)
Macrovascular invasion and/or extrahepatic disease	304 (80%)	162 (84%)
Lung, target lesion†	98 (26%)	48 (25%)
Lymph node, target lesion†	58 (15%)	36 (19%)
Lung, non-target lesion†	121 (32%)	57 (29%)
Lymph node, non-target lesion†	61 (16%)	29 (15%)
Pattern of progression on previous sorafenib treatment		
New extrahepatic lesion	153 (40%)	80 (41%)
New intrahepatic lesion	168 (44%)	88 (45%)
Growth of intrahepatic or extrahepatic lesions, or both	307 (81%)	156 (80%)
α-fetoprotein ≥400 ng/mL	162 (43%)	87 (45%)
Child–Pugh class‡		
A	373 (98%)	188 (97%)
B	5 (1%)	6 (3%)
BCLC stage		
A (early)	1 (<1%)	0
B (intermediate)	53 (14%)	22 (11%)
C (advanced)	325 (86%)	172 (89%)

(Table 1 continues in next column)

aforementioned randomisation factors. The hazard ratio (HR) for overall survival and its 95% CI were calculated using the stratified Cox model. An interim futility analysis was done after 30% of the events had occurred; futility boundaries were not crossed. For analyses of time to progression and progression-free survival, groups were compared using a log-rank test stratified by the factors used in the analyses of the primary endpoint. The response rates and disease control rates in the two groups were compared using the Cochran–Mantel–Haenszel test, with adjustment for the stratification factors.

	Regorafenib (n=379)	Placebo (n=194)
(Continued from previous column)		
Liver cirrhosis (investigator assessed)	285 (75%)	144 (74%)
Aetiology of HCC§		
Hepatitis B	143 (38%)	73 (38%)
Alcohol use	90 (24%)	55 (28%)
Hepatitis C	78 (21%)	41 (21%)
Unknown	66 (17%)	32 (16%)
Non-alcoholic steatohepatitis	25 (7%)	13 (7%)
Other	28 (7%)	10 (5%)
Number of target lesions (mRECIST)¶		
1	67 (18%)	31 (16%)
2	175 (46%)	88 (45%)
3	68 (18%)	37 (19%)
4	43 (11%)	26 (13%)
5	19 (5%)	12 (6%)
Time from initial HCC diagnosis to start of study treatment, months		
Median (IQR)	21 (11–38)	20 (12–32)
Mean (SD)	29 (28)	27 (22)
Duration of sorafenib treatment, months	7·8 (4·2–14·5)	7·8 (4·4–14·7)
Time from progression on sorafenib to start of study treatment, months	1·4 (0·9–2·3)	1·4 (0·9–2·2)
Time from discontinuation of sorafenib to start of study treatment, months	0·9 (0·7–1·3)	0·9 (0·7–1·3)

Data are n (%) or median (IQR), unless otherwise specified. BCLC=Barcelona Clinic Liver Cancer. ECOG=Eastern Cooperative Oncology Group. HCC=hepatocellular carcinoma. mRECIST=modified RECIST for HCC. \*Includes patients from China, Japan, South Korea, Singapore, and Taiwan. †RECIST version 1.1. ‡The Child–Pugh system describes liver disease severity: patients are divided into classes from A to C, with class C representing the worst prognosis. Child–Pugh class was missing in one patient in the regorafenib group. Those patients who progressed to Child–Pugh B after screening and before randomisation were included. §Patients could have more than one aetiology of HCC. ¶n=372 in the regorafenib group.

**Table 1: Baseline characteristics (efficacy population)**

For HRQoL assessments, an analysis-of-covariance model was used to compare the time-adjusted area under the curve (AUC) between groups with covariates for baseline scores and stratification factors. The least-squares mean (LSM) with 95% CI was estimated for each treatment group and for the difference between groups.

Data were analysed with SAS, version 9.2 (SAS Institute Inc, Cary, NC, USA). The primary analysis was by intention to treat; safety analyses included all patients who received at least one dose of study drug. The study was overseen by a data safety monitoring committee.

This trial is registered with ClinicalTrials.gov, number NCT01774344.



### Role of the funding source

The funder (Bayer) provided the study drug and worked with the principal investigator (JB) and the study steering committee to design the study. Data collection and interpretation, and preparation of this report, were done by the investigators and the funder. Statistical analyses were performed by the funder. All authors reviewed this

report and approved the submission for publication, had full access to the data, and vouch for the completeness and accuracy of the data and adherence of the study to the protocol. The funder funded writing assistance.

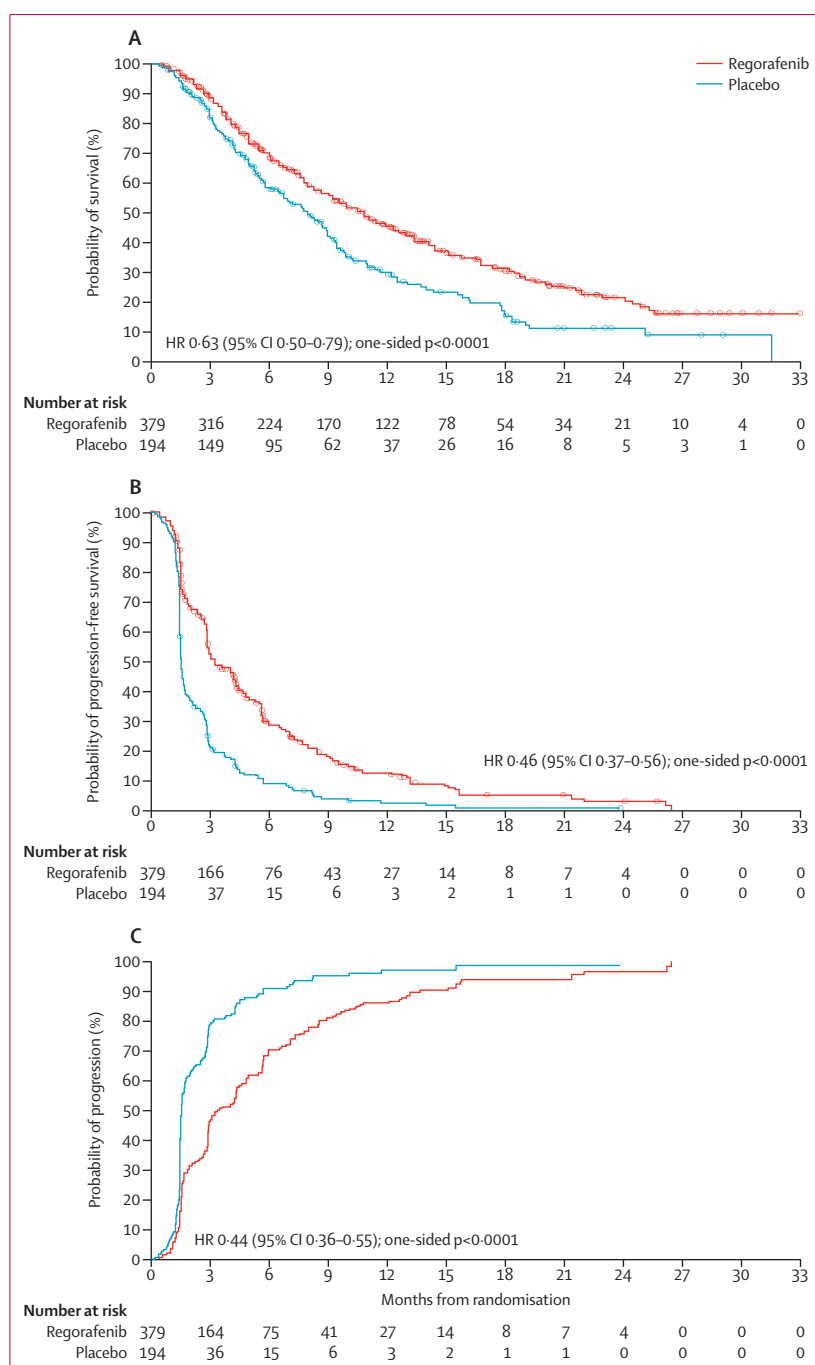
### Results

Between May 14, 2013, and Dec 31, 2015, 843 patients were screened, of whom 573 were enrolled and randomised (379 to regorafenib and 194 to placebo; population for efficacy analyses; figure 1). 216 patients (38%) were from Asia. Overall, 567 patients (99%) started treatment (374 in the regorafenib group and 193 in the placebo group) and comprise the safety analysis population. Treatment groups were similar with respect to baseline demographics, tumour burden, ECOG performance status, aetiology, and severity of liver disease (table 1). We also assessed the pattern of progression during sorafenib treatment because this parameter has been shown to influence outcomes and could distort the results of second-line studies.<sup>26</sup> A potential imbalance in the pattern of progression on previous sorafenib was ruled out because the distribution of the different categories was similar across the treatment groups. Specifically, the development of new extrahepatic sites during previous sorafenib, which was recently shown to be associated with a worse prognosis,<sup>26</sup> was present in 153 (40%) patients in the regorafenib group and 80 (41%) in the placebo group. Similarly, growth of existing lesions (intrahepatic or extrahepatic; 307 [81%] patients in the regorafenib group and 156 [80%] patients in the placebo group) or new intrahepatic sites (168 [44%] patients in the regorafenib group and 88 [45%] patients in the placebo group) were balanced between treatment groups.

Median time on sorafenib was 7·8 months (IQR 4·2–14·5) in the regorafenib group and 7·8 months (4·4–14·7) in the placebo group. Median time from progression on sorafenib was similar in both groups (1·4 months [IQR 0·9–2·3] in the regorafenib group vs 1·4 months [0·9–2·2] in the placebo group), as was the median time from discontinuation of sorafenib to the start of study treatment (0·9 months [IQR 0·7–1·3] in both groups).

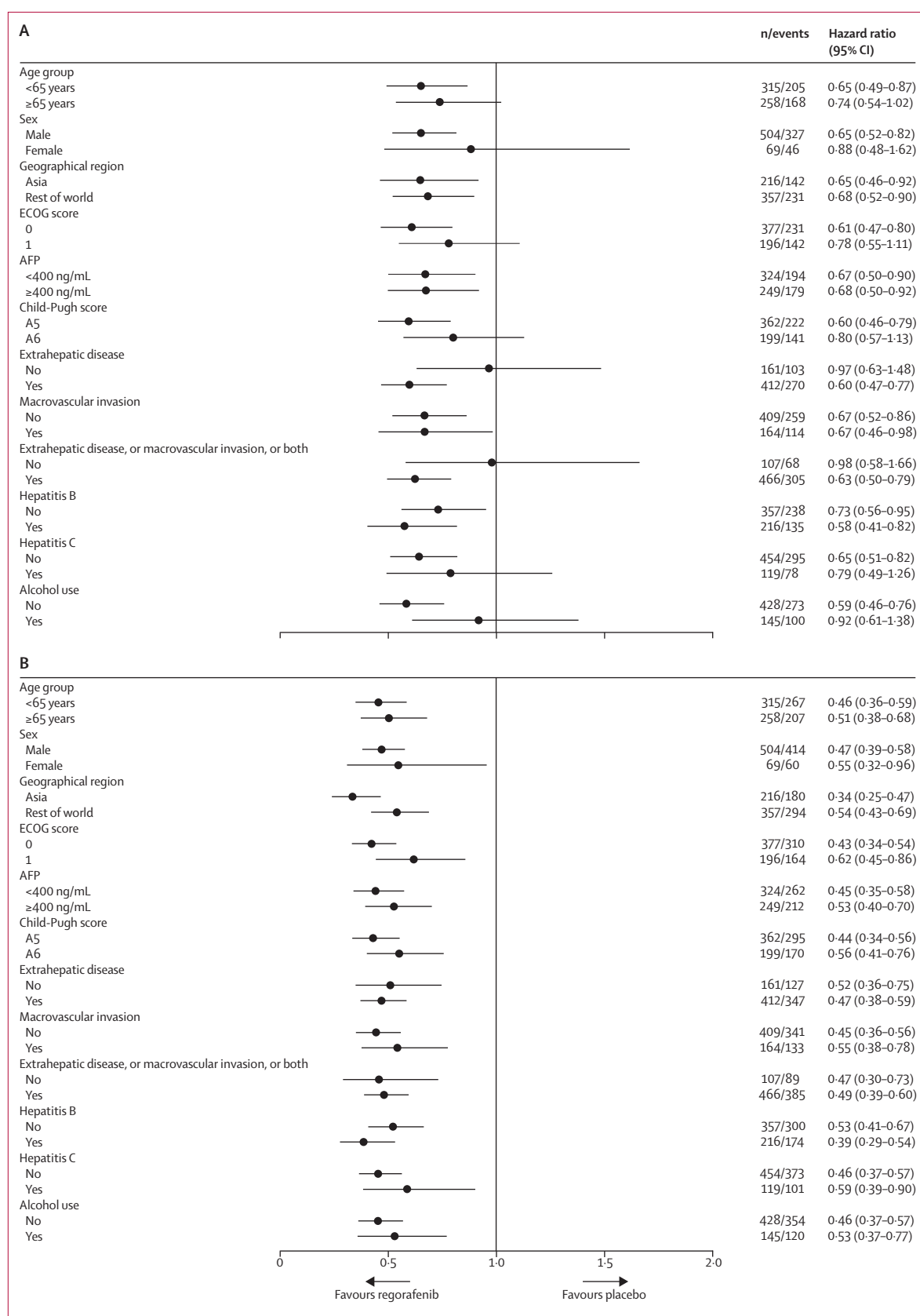
Of patients who started treatment, 309 (83%) receiving regorafenib and 183 (95%) receiving placebo discontinued study treatment (figure 1). The most common reason for discontinuation was disease progression (226 [60%] in the regorafenib group and 162 [84%] in the placebo group). Median treatment duration was 3·6 months (IQR 1·6–7·6) with regorafenib and 1·9 months (1·4–3·9) with placebo; mean durations were 5·9 months (SD 6·0) and 3·3 months (3·9), respectively. Mean daily dose of regorafenib was 144·1 mg (SD 21·3) and of placebo was 157·4 mg (10·3). Excluding treatment delays or interruptions, almost half of the regorafenib group (184 [49%] of 374) received the full protocol dose (160 mg/day) with no reductions.

At the cutoff date for the final analysis (Feb 29, 2016) and a median follow-up of 7·0 months (IQR 3·7–12·6),



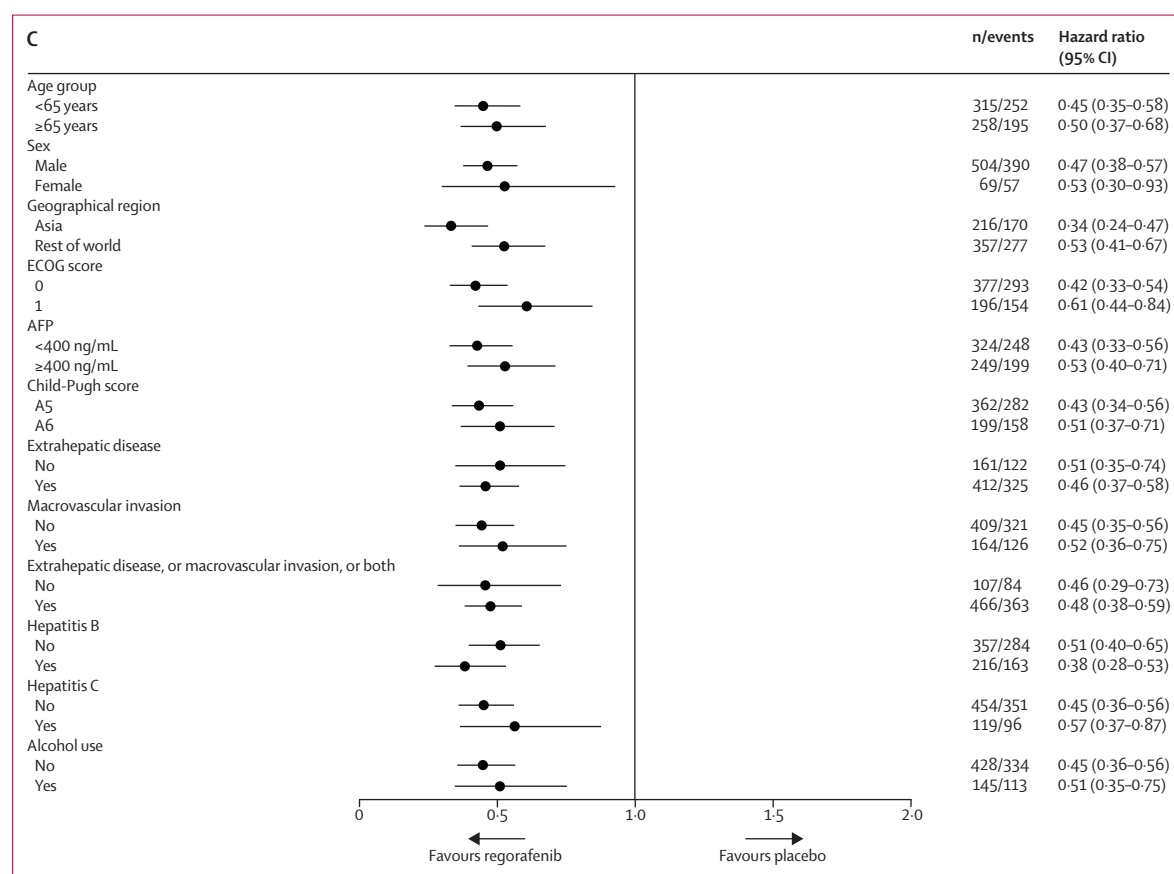
**Figure 2:** Kaplan-Meier analysis of overall survival (A), progression-free survival (mRECIST; B), and time to progression (mRECIST; C)

mRECIST=modified RECIST for hepatocellular carcinoma.



(Figure 3 continues on next page)

(Figure continued from previous page)



**Figure 3:** Overall survival (A), progression-free survival (mRECIST; B), and time to progression (mRECIST; C) in selected subgroups  
AFP=α-fetoprotein. ECOG=Eastern Cooperative Oncology Group. mRECIST=modified RECIST.

373 (65%) of the 573 randomised patients had died (233 [61%] of 379 in the regorafenib group and 140 [72%] of 194 in the placebo group). Median overall survival was 10.6 months (95% CI 9.1–12.1) with regorafenib and 7.8 months (6.3–8.8) with placebo (HR 0.63 [95% CI 0.50–0.79]; one-sided  $p < 0.0001$ ; figure 2A). The improvement in overall survival with regorafenib was maintained in all preplanned subgroup analyses (figure 3A; appendix p 16).

Median progression-free survival by mRECIST was 3.1 months (95% CI 2.8–4.2) with regorafenib and 1.5 months (1.4–1.6) with placebo (figure 2B). Median time to progression by mRECIST was 3.2 months (95% CI 2.9–4.2) with regorafenib and 1.5 months (1.4–1.6) with placebo (figure 2C). Predefined subgroup analysis for progression-free survival and time to progression also showed a consistent benefit (figures 3B,C). The HRs for progression-free survival and time to progression assessed by RECIST 1.1 were comparable (appendix pp 8–11).

Two patients (1% [95% CI <1–2]) in the regorafenib group versus no patients in the placebo group had a complete response and 38 patients (10% [7–14]) in the

regorafenib group versus eight patients (4% [2–8]) in the placebo group had a partial response by mRECIST as assessed by investigators (table 2). 40 (11%) of 379 patients in the regorafenib group versus eight (4%) of 194 patients in the placebo group achieved an objective response ( $p = 0.0047$ ). 247 (65%) of 379 patients in the regorafenib group versus 70 (36%) of 194 patients in the placebo group achieved disease control ( $p < 0.0001$ ). A significant improvement in tumour response and disease control was also shown using RECIST 1.1 (appendix p 16). Tumour shrinkage (any decrease in the sum of diameters of target lesions) was reported in 49% (184/379) of patients in the regorafenib group and 23% (44/194) of patients in the placebo group (appendix p 17). Duration of response and duration of stable disease are reported in the appendix (p 17).

All (374/374) patients who received regorafenib and 179 (93%) of 193 patients who received placebo had at least one treatment-emergent adverse event; these were deemed possibly study-drug related in 346 (93%) patients who received regorafenib and 100 (52%) patients who received placebo (table 3). The most common clinically relevant grade 3 or 4 events were hypertension (57 patients [15%] in

	Regorafenib (n=379)	Placebo (n=194)
Best overall response*		
Complete response	2 (1%; <1–2)	0
Partial response	38 (10%; 7–14)	8 (4%; 2–8)
Stable disease	206 (54%; 49–59)	62 (32%; 26–39)
Non-complete response/ non-progressive disease	1 (<1%; 0–2)	0
Progressive disease	86 (23%; 19–27)	108 (56%; 48–63)
Not evaluable	19 (5%; 3–8)	8 (4%; 2–8)
Not assessed	27 (7%; 5–10)	8 (4%; 2–8)
Clinical progression†	86 (23%; 19–27)	40 (21%; 15–27)
Objective response (complete response + partial response)*	40 (11%)‡	8 (4%)‡
Disease control*	247 (65%)§	70 (36%)§

Data are n (%; 95% CI). \*Based on radiological review using modified Response Evaluation Criteria in Solid Tumors for HCC (mRECIST).<sup>22</sup> †Defined as worsening of ECOG performance status or symptomatic deterioration including increase in liver function tests. ‡One-sided p=0.0047. §One-sided p<0.0001.

**Table 2: Tumour response (efficacy population)**

the regorafenib group vs nine patients [5%] in the placebo group), hand-foot skin reaction (47 patients [13%] vs one [1%]), fatigue (34 patients [9%] vs nine patients [5%]), and diarrhoea (12 patients [3%] vs no patients). The frequency of hepatobiliary disorders was higher with placebo (18% [34/193]) than with regorafenib (11% [40/374]). Serious adverse events occurred in 166 (44%) patients assigned to regorafenib and 90 (47%) patients assigned to placebo and were attributed to study drug in 39 (10%) patients assigned to regorafenib and five (3%) patients assigned to placebo. Of the 88 deaths (grade 5 adverse events) reported during the study (50 patients [13%] assigned to regorafenib and 38 [20%] assigned to placebo), seven (2%) were considered by the investigator to be related to study drug in the regorafenib arm and two (1%) in the placebo arm, including two patients (1%) with hepatic failure in the placebo group (appendix p 18). 21 (6%) of 374 patients in the regorafenib group had grade 3 or higher treatment-emergent bleeding events versus 15 (8%) of 193 patients in the placebo group (appendix p 18). 255 (68%) of 374 patients in the regorafenib group had interruptions or dose reductions due to adverse events versus 60 (31%) of 193 patients in the placebo group. Similarly, 93 (25%) of 374 patients in the regorafenib group discontinued due to adverse events versus 37 (19%) of 193 patients in the placebo group. Drug-related adverse events led to interruptions or dose reductions in 202 (54%) patients in the regorafenib group and 20 (10%) patients in the placebo group, and to discontinuations in 39 (10%) patients in the regorafenib group and seven (4%) patients in the placebo group. The most common adverse events leading to discontinuation more frequently with regorafenib were increase in AST concentration (eight [2%] of 374 patients in the regorafenib group vs three [2%] of

193 patients in the placebo group), hand-foot skin reaction (seven [2%] vs none), and ALT increase (four [1%] vs none).

No clinically meaningful differences were noted between the regorafenib and placebo groups in HRQoL. Overall changes from baseline in EQ-5D and FACT-Hep were similar in the two groups. In the LSM time-adjusted AUC analysis of the EQ-5D and FACT-Hep, the scores were lower in the regorafenib group than in the placebo group, and specifically the scores of the FACT-Hep Total and Trial Outcome Index (a subscale of the FACT-Hep) were statistically lower in the regorafenib group than in the placebo group ( $p=0.0006$  and  $p<0.0001$ , respectively); however, minimally important thresholds for the differences as established in the literature were not met (appendix p 19).<sup>24,25</sup>

## Discussion

Our study shows that regorafenib provides a significant and clinically meaningful improvement in overall survival in patients with HCC progressing during sorafenib treatment. This finding was associated with an increase in median survival from 7.8 months to 10.6 months. This survival benefit was maintained in the prespecified subgroup analyses, including geographical region and aetiology, and was accompanied by significant improvements in progression-free survival, time to progression, and objective response, and disease control rate. Two patients treated with regorafenib had a complete tumour response by mRECIST, which excludes necrosis of the target lesion from the tumour measurement. These responses would also have been classified as complete using conventional European Association for the Study of the Liver criteria.<sup>27</sup> Interestingly, we noted similar outcomes using mRECIST and RECIST 1.1 for progression-free survival and time to progression.

The survival of the placebo group in our study is consistent with previous second-line studies in HCC at about 8 months.<sup>11–14</sup> Use of five stratification factors ensured that the trial groups were fully balanced for commonly assessed patient and disease characteristics; however, we also analysed the distribution of patients across treatment groups according to the pattern of progression under sorafenib. Pattern of progression has recently been found to be a major factor affecting outcome and potentially confounding study results if not balanced across study groups.<sup>26</sup> Although new intrahepatic sites or growth of known tumour lesions have been shown to have a moderate effect on post-progression survival, the development of new vascular invasion or extrahepatic spread is a significant predictor of a worse survival.<sup>26</sup> Pattern of progression under previous sorafenib was balanced in this study.

All primary and secondary efficacy outcomes in this sorafenib pretreated population seem numerically better than those with sorafenib in the first-line setting.<sup>4,5</sup> This might be because regorafenib is more pharmacologically

	Treatment-emergent						Treatment-emergent drug-related					
	Regorafenib (n=374)			Placebo (n=193)			Regorafenib (n=374)			Placebo (n=193)		
	Any grade	Grade 3	Grade 4	Any grade	Grade 3	Grade 4	Any grade	Grade 3	Grade 4	Any grade	Grade 3	Grade 4
Any adverse event	374 (100%)	208 (56%)	40 (11%)	179 (93%)	61 (32%)	14 (7%)	346 (93%)	173 (46%)	14 (4%)	100 (52%)	31 (16%)	1 (1%)
Hand-foot skin reaction	198 (53%)	47 (13%)	NA	15 (8%)	1 (1%)	NA	196 (52%)	47 (13%)	NA	13 (7%)	1 (1%)	NA
Diarrhoea	155 (41%)	12 (3%)	0	29 (15%)	0	0	125 (33%)	9 (2%)	0	18 (9%)	0	0
Fatigue	151 (40%)	34 (9%)	NA	61 (32%)	9 (5%)	NA	110 (29%)	24 (6%)	NA	37 (19%)	3 (2%)	NA
Hypertension	116 (31%)	56 (15%)	1 (<1%)	12 (6%)	9 (5%)	0	87 (23%)	48 (13%)	1 (<1%)	9 (5%)	6 (3%)	0
Anorexia	116 (31%)	10 (3%)	0	28 (15%)	4 (2%)	0	88 (24%)	10 (3%)	0	12 (6%)	0	0
Increased blood bilirubin	108 (29%)	37 (10%)	2 (1%)	34 (18%)	15 (8%)	6 (3%)	70 (19%)	24 (6%)	1 (<1%)	7 (4%)	4 (2%)	0
Abdominal pain	105 (28%)	13 (3%)	NA	43 (22%)	8 (4%)	NA	34 (9%)	5 (1%)	NA	5 (3%)	0	NA
Increased AST	92 (25%)	37 (10%)	4 (1%)	38 (20%)	19 (10%)	3 (2%)	48 (13%)	16 (4%)	3 (1%)	15 (8%)	9 (5%)	1 (1%)
Fever	72 (19%)	0	0	14 (7%)	0	0	14 (4%)	0	0	4 (2%)	0	0
Nausea	64 (17%)	2 (1%)	NA	26 (13%)	0	NA	40 (11%)	1 (<1%)	NA	13 (7%)	0	NA
Constipation	65 (17%)	1 (<1%)	0	22 (11%)	1 (1%)	0	24 (6%)	0	0	3 (2%)	0	0
Ascites	58 (16%)	16 (4%)	0	31 (16%)	11 (6%)	0	8 (2%)	3 (1%)	0	1 (1%)	1 (1%)	0
Anaemia	58 (16%)	16 (4%)	2 (1%)	22 (11%)	10 (5%)	1 (1%)	23 (6%)	5 (1%)	1 (<1%)	2 (1%)	1 (1%)	0
Limb oedema	60 (16%)	2 (1%)	NA	24 (12%)	0	NA	12 (3%)	1 (<1%)	NA	1 (1%)	0	NA
Increased ALT	55 (15%)	10 (3%)	2 (1%)	22 (11%)	5 (3%)	0	29 (8%)	6 (2%)	2 (1%)	8 (4%)	2 (1%)	0
Hypoalbuminaemia	57 (15%)	6 (2%)	0	16 (8%)	1 (1%)	0	9 (2%)	2 (1%)	0	0	0	0
General disorders and administration site conditions, other	53 (14%)	16 (4%)	2 (1%)	29 (15%)	6 (3%)	3 (2%)	8 (2%)	5 (1%)	0	2 (1%)	1 (1%)	0
Weight loss	51 (14%)	7 (2%)	NA	9 (5%)	0	NA	27 (7%)	4 (1%)	NA	3 (2%)	0	NA
Oral mucositis	47 (13%)	4 (1%)	0	6 (3%)	1 (1%)	0	42 (11%)	4 (1%)	0	5 (3%)	1 (1%)	0
Vomiting	47 (13%)	3 (1%)	0	13 (7%)	1 (1%)	0	27 (7%)	1 (<1%)	0	5 (3%)	0	0
Investigations, other	40 (11%)	4 (1%)	0	11 (6%)	1 (1%)	0	18 (5%)	1 (<1%)	0	0	0	0
Back pain	42 (11%)	6 (2%)	1 (<1%)	17 (9%)	2 (1%)	0	2 (1%)	1 (<1%)	0	2 (1%)	0	0
Thrombocytopenia	39 (10%)	13 (3%)	1 (<1%)	5 (3%)	0	0	19 (5%)	7 (2%)	1 (<1%)	2 (1%)	0	0
Cough	40 (11%)	1 (<1%)	NA	14 (7%)	0	NA	4 (1%)	0	NA	2 (1%)	0	NA
Hypophosphataemia	37 (10%)	30 (8%)	2 (1%)	4 (2%)	3 (2%)	0	22 (6%)	16 (4%)	2 (1%)	2 (1%)	1 (1%)	0
Hoarseness	39 (10%)	0	NA	1 (1%)	0	NA	34 (9%)	0	NA	0	0	NA

Data are n (%). Adverse events were graded using NCI-CTCAE version 4.03. ALT=alanine aminotransferase. AST=aspartate aminotransferase. NA=not applicable. NCI-CTCAE=National Cancer Institute Common Terminology Criteria for Adverse Events. \*Events listed are treatment-emergent adverse events occurring in at least 10% of patients in either treatment group.

**Table 3: Treatment-emergent adverse events and treatment-emergent drug-related adverse events\* (safety population)**

active than is sorafenib,<sup>15</sup> and could also be because tolerability to regorafenib was improved for patients tolerant to sorafenib due to the somewhat overlapping adverse-event profiles of the two drugs. As multikinase inhibitors, the antitumour activity of regorafenib and sorafenib could extend beyond their antiangiogenic properties to a direct effect on tumour and stromal cells that modulate inflammatory and immune processes.<sup>28</sup> Recent phase 3 trials in HCC assessing multikinase inhibitors having profiles that partly overlap with regorafenib have failed to improve outcomes over sorafenib or versus placebo after sorafenib.<sup>6–8,11</sup> The results of this study suggest that the sequential use of two multikinase inhibitors with partly overlapping target profiles provides a survival benefit in HCC. Regorafenib has been shown to improve survival in patients with gastrointestinal stromal tumours after failure of two multikinase inhibitors (imatinib and sunitinib).<sup>19</sup>

This study was designed to assess a new systemic treatment for patients with HCC progressing on first-line therapy and incorporated lessons from previous phase 3 trials that failed to meet their primary endpoint.<sup>6–14</sup> Only patients with Child-Pugh A liver function were included to avoid the potential confounding effect of impaired liver function on survival. To ensure that treatment groups were balanced with respect to relevant prognostic factors, randomisation was stratified by  $\alpha$ -fetoprotein concentrations and ECOG performance status. However, unlike in previous studies,<sup>4,11</sup> macrovascular invasion and extrahepatic disease were separate stratification factors. We also stratified for geographical region because of differences in access to cancer care and the use of locoregional therapies. Although the trial was not stratified for aetiology, geographical region accounts partly for the aetiology of HCC because hepatitis B virus infection is the

predominant underlying cause of HCC in most Asian countries.

The safety of regorafenib in HCC in this study is consistent with the safety profile of regorafenib in other gastrointestinal malignancies, and with no new safety concerns.<sup>18,19</sup> The most common grade 3 or 4 adverse events included hypertension, hand–foot skin reaction, fatigue, and diarrhoea. Exclusion of patients who were unable to tolerate sorafenib could have reduced the occurrence of severe adverse events; 10% of patients discontinued treatment due to a regorafenib-related adverse event. Although underlying liver dysfunction is expected to be more common in patients with HCC, the rates of liver-related adverse events and liver failure in the regorafenib group were not higher in this study compared with in other regorafenib trials.<sup>18,19</sup> In this study, the only two cases of drug-related death due to liver failure occurred in the placebo group. Although adverse events in the regorafenib group led to higher rates of treatment interruptions and dose reductions than did those in the placebo group, the median treatment duration was longer with regorafenib than with placebo. Assessments using standard, validated measures of quality of life in patients with hepatobiliary cancer showed no clinically meaningful differences between the groups.

Although biomarker-based treatment decisions have become standard of care in certain tumour types, no baseline markers predictive of treatment benefit have been identified for patients with HCC.<sup>29,30</sup> Exploratory studies have suggested that there is an association between certain adverse events, most notably hand–foot skin reaction, and overall survival and time to progression.<sup>31</sup> However, because this approach is based on post-randomisation events, it does not inform the selection of patients who could derive a greater treatment benefit.

A potential limitation of the study is that it was undertaken in patients who progressed during previous sorafenib treatment, and therefore firm conclusions about the efficacy of regorafenib in patients who do not tolerate sorafenib cannot be drawn. In addition, special populations, such as patients co-infected with HIV, are not included here.

The results of this study represent a significant advance in addressing an unmet need in the treatment of HCC. All previous second-line trials of novel agents have failed,<sup>11–14</sup> thus no effective systemic therapies after progression on sorafenib are currently available. These data underscore that prolonging exposure to multikinase inhibitors such as the sequence of sorafenib and regorafenib in conjunction with proper management of adverse events can lead to an extension in survival. In conclusion, this study met its primary endpoint showing that regorafenib improves overall survival in patients with HCC who had disease progression during first-line treatment with sorafenib.

#### Contributors

JB, M-AL, RSF, and GMe conceived and designed the study. JB, SQ, PM, AG, Y-HH, GB, MP, OY, OR, VB, RG, GMa, PJR, TS, J-PB, IO-H, MK,

A-LC, JML, RSF, M-AL, AB, GMe, and GH collected the data. JB, M-AL, AB, and GMe analysed and interpreted the data. All authors participated in the drafting, review, and approval of the report and in the decision to submit for publication.

#### Declaration of interests

JB has received grants and personal fees from Bayer; consultancy and advisory fees from Bayer and Novartis; and consultancy fees from Gilead, AbbVie, Kowa, BTG, ArQule, Terumo, Bristol-Myers Squibb, Boehringer Ingelheim, OSI, Roche, Eisai, Sirtex, and Onxeo. PM has received consultancy fees from Bayer. OY has received grants from Gilead Sciences, MSD, Bayer, Mitsubishi Tanabe Pharma, and Bristol-Myers Squibb. OR has received personal fees from Transgene and Bristol-Myers Squibb. VB has received personal fees from Bayer, Boehringer Ingelheim, Pfizer, MSD, and Roche; and non-financial support from Boehringer Ingelheim, Pfizer, and MSD. RG has received advisory fees from Bayer France. PJR has received personal fees from Bayer, Celgene, Roche, Merck, and Sirtex; advisory fees from Bayer, Baxalta, Amgen, and Sanofi; speaker fees from Celgene; and support for attending meetings from Bayer, Celgene, and Merck. J-PB has received grants from Bayer during the conduct of the study and lecturing and consultancy fees from Bayer. IO-H has received grants and personal fees from Bayer; personal fees from Gilead, Intercept, Daiichi Sankyo, AbbVie, and Boehringer Ingelheim; grants from Lilly; and non-financial support from Gilead, MSD, and AbbVie. MK has received grants from Chugai, Otsuka, Takeda, Taiho, Sumitomo Dainippon, Daiichi Sankyo, MSD, Eisai, Bayer, and AbbVie; lecturing fees from Bayer, Eisai, MSD, and Ajinomoto; and advisory and consultancy fees from Bayer, Eisai, Kowa, MSD, Bristol-Myers Squibb, Chugai, and Taiho. A-LC has received consultancy fees from Novartis, Eisai, MSD, Bayer, Ono Pharmaceuticals, Bristol-Myers Squibb, and Merck Serono. JML has received grants from Bayer, Bristol-Myers Squibb, Blueprint Medicines, and Boehringer Ingelheim; and consultancy fees from Bayer, Bristol-Myers Squibb, Blueprint Medicines, Boehringer Ingelheim, Lilly Pharmaceuticals, Celsion, Biocompatibles, and Novartis. RSF has received grants, consultancy fees, and travel support from Bayer, Pfizer, Novartis, and Bristol-Myers Squibb. M-AL is an employee of Bayer. AB is an employee of Bayer. GMe is an employee of Bayer and owns stock in Bayer. GH has received a grant and advisory board and speaker fees from Bayer. SQ, AG, Y-HH, GB, MP, GMa, and TS declare no competing interests.

#### Acknowledgments

This study was funded by Bayer. Editorial assistance in the preparation of this manuscript was provided by Ann Contijoch (Bayer) and Jennifer Tobin (Choice Healthcare Solutions, with financial support from Bayer). We thank the patients who participated in the RESORCE trial, their families, the RESORCE investigators, and the members of the Data Safety Monitoring Committee: Morris Sherman, Bruno Daniele, Gregory J Gores, and KyungMann Kim.

#### References

- 1 Bruix J, Sherman M. Management of hepatocellular carcinoma: an update. *Hepatology* 2011; **53**: 1020–22.
- 2 Llovet JM, Ducreux M, Lencioni R, et al. EASL-EORTC clinical practice guidelines: management of hepatocellular carcinoma. *J Hepatol* 2012; **56**: 908–43.
- 3 Kudo M, Matsui O, Izumi N, et al. JSH Consensus-based clinical practice guidelines for the management of hepatocellular carcinoma: 2014 update by the Liver Cancer Study Group of Japan. *Liver Cancer* 2014; **3**: 458–68.
- 4 Llovet JM, Ricci S, Mazzaferro V, et al. Sorafenib in advanced hepatocellular carcinoma. *N Engl J Med* 2008; **359**: 378–90.
- 5 Cheng AL, Kang YK, Chen Z, et al. Efficacy and safety of sorafenib in patients in the Asia-Pacific region with advanced hepatocellular carcinoma: a phase III randomised, double-blind, placebo-controlled trial. *Lancet Oncol* 2009; **10**: 25–34.
- 6 Cheng AL, Kang YK, Lin DY, et al. Sunitinib versus sorafenib in advanced hepatocellular cancer: results of a randomized phase III trial. *J Clin Oncol* 2013; **31**: 4067–75.
- 7 Johnson PJ, Qin S, Park JW, et al. Brivanib versus sorafenib as first-line therapy in patients with unresectable, advanced hepatocellular carcinoma: results from the randomized phase III BRISK-FL study. *J Clin Oncol* 2013; **31**: 3517–24.



- 8 Cainap C, Qin S, Huang WT, et al. Linifanib versus sorafenib in patients with advanced hepatocellular carcinoma: results of a randomized phase III trial. *J Clin Oncol* 2015; **33**: 172–79.
- 9 Zhu AX, Rosmorduc O, Evans TR, et al. SEARCH: a phase III, randomized, double-blind, placebo-controlled trial of sorafenib plus erlotinib in patients with advanced hepatocellular carcinoma. *J Clin Oncol* 2015; **33**: 559–66.
- 10 Abou-Alfa GK, Niedzwieski D, Knox JJ, et al. Phase III randomized study of sorafenib plus doxorubicin versus sorafenib in patients with advanced hepatocellular carcinoma (HCC): CALGB 80802 (Alliance). *Proc Am Soc Clin Oncol* 2016; **34**: abstr 4003.
- 11 Llovet JM, Decaens T, Raoul JL, et al. Brivanib in patients with advanced hepatocellular carcinoma who were intolerant to sorafenib or for whom sorafenib failed: results from the randomized phase III BRISK-PS study. *J Clin Oncol* 2013; **31**: 3509–16.
- 12 Zhu AX, Kudo M, Assenat E, et al. Effect of everolimus on survival in advanced hepatocellular carcinoma after failure of sorafenib: the EVOLVE-1 randomized clinical trial. *JAMA* 2014; **312**: 57–67.
- 13 Zhu AX, Park JO, Ryoo BY, et al. Ramucirumab versus placebo as second-line treatment in patients with advanced hepatocellular carcinoma following first-line therapy with sorafenib (REACH): a randomised, double-blind, multicentre, phase 3 trial. *Lancet Oncol* 2015; **16**: 859–70.
- 14 Abou-Alfa GK, Qin S, Ryoo BY, et al. Phase III randomized study of second-line ADI-peg 20 (A) plus best supportive care versus placebo (P) plus best supportive care in patients (pts) with advanced hepatocellular carcinoma (HCC). *Proc Am Soc Clin Oncol* 2016; **34**: abstr 4017.
- 15 Wilhelm SM, Dumas J, Adnane L, et al. Regorafenib (BAY 73-4506): a new oral multikinase inhibitor of angiogenic, stromal and oncogenic receptor tyrosine kinases with potent preclinical antitumor activity. *Int J Cancer* 2011; **129**: 245–55.
- 16 Abou-Elkacem L, Arns S, Brix G, et al. Regorafenib inhibits growth, angiogenesis, and metastasis in a highly aggressive, orthotopic colon cancer model. *Mol Cancer Ther* 2013; **12**: 1322–31.
- 17 Wilhelm SM, Carter C, Tang L, et al. BAY 43-9006 exhibits broad spectrum oral antitumor activity and targets the RAF/MEK/ERK pathway and receptor tyrosine kinases involved in tumor progression and angiogenesis. *Cancer Res* 2004; **64**: 7099–109.
- 18 Grothey A, Van Cutsem E, Sobrero A, et al. Regorafenib monotherapy for previously treated metastatic colorectal cancer (CORRECT): an international, multicentre, randomised, placebo-controlled, phase 3 trial. *Lancet* 2013; **381**: 303–12.
- 19 Demetri GD, Reichardt P, Kang YK, et al. Efficacy and safety of regorafenib for advanced gastrointestinal stromal tumours after failure of imatinib and sunitinib (GRID): an international, multicentre, randomised, placebo-controlled, phase 3 trial. *Lancet* 2013; **381**: 295–302.
- 20 Stivarga Prescribing Information. Whippany, NJ: Bayer HealthCare Pharmaceuticals; 2016.
- 21 Bruix J, Tak WY, Gasbarrini A, et al. Regorafenib as second-line therapy for intermediate or advanced hepatocellular carcinoma: multicentre, open-label, phase II safety study. *Eur J Cancer* 2013; **49**: 3412–19.
- 22 Lencioni R, Llovet JM. Modified RECIST (mRECIST) assessment for hepatocellular carcinoma. *Semin Liver Dis* 2010; **30**: 52–60.
- 23 Bruix J, Reig M, Sherman M. Evidence-based diagnosis, staging, and treatment of patients with hepatocellular carcinoma. *Gastroenterology* 2016; **150**: 835–53.
- 24 Steel JL, Eton DT, Cella D, Olek MC, Carr BI. Clinically meaningful changes in health-related quality of life in patients diagnosed with hepatobiliary carcinoma. *Ann Oncol* 2006; **17**: 304–12.
- 25 Pickard AS, Neary MP, Cella D. Estimation of minimally important differences in EQ-5D utility and VAS scores in cancer. *Health Qual Life Outcomes* 2007; **5**: 70.
- 26 Reig M, Rimola J, Torres F, et al. Postprogression survival of patients with advanced hepatocellular carcinoma: rationale for second-line trial design. *Hepatology* 2013; **58**: 2023–31.
- 27 Bruix J, Sherman M, Llovet JM, et al. Clinical management of hepatocellular carcinoma. Conclusions of the Barcelona-2000 EASL conference. European Association for the Study of the Liver. *J Hepatol* 2001; **35**: 421–30.
- 28 Mazzocchi G, Miele L, Oben J, Grieco A, Vinciguerra M. Biology, epidemiology, clinical aspects of hepatocellular carcinoma and the role of sorafenib. *Curr Drug Targets* 2016; **17**: 783–99.
- 29 Llovet JM, Peña CE, Lathia CD, et al. Plasma biomarkers as predictors of outcome in patients with advanced hepatocellular carcinoma. *Clin Cancer Res* 2012; **8**: 2290–300.
- 30 Zhu AX, Kang YK, Rosmorduc O, et al. Biomarker analyses of clinical outcomes in patients with advanced hepatocellular carcinoma treated with sorafenib with or without erlotinib in the SEARCH trial. *Clin Cancer Res* 2016; **22**: 4870–79.
- 31 Reig M, Torres F, Rodriguez-Lope C, et al. Early dermatologic adverse events predict better outcome in HCC patients treated with sorafenib. *J Hepatol* 2014; **61**: 318–24.

# Multimaterial Decomposition Algorithm for the Quantification of Liver Fat Content by Using Fast-Kilovolt-Peak Switching Dual-Energy CT: Experimental Validation<sup>1</sup>

Tomoko Hyodo, MD  
Masatoshi Hori, MD, PhD  
Peter Lamb, MS  
Kosuke Sasaki, MS  
Tetsuya Wakayama, PhD  
Yasutaka Chiba, PhD  
Teruhito Mochizuki, MD  
Takamichi Murakami, MD, PhD

## Purpose:

To assess the ability of fast-kilovolt-peak switching dual-energy computed tomography (CT) by using the multimaterial decomposition (MMD) algorithm to quantify liver fat.

## Materials and Methods:

Fifteen syringes that contained various proportions of swine liver obtained from an abattoir, lard in food products, and iron (saccharated ferric oxide) were prepared. Approval of this study by the animal care and use committee was not required. Solid cylindrical phantoms that consisted of a polyurethane epoxy resin 20 and 30 cm in diameter that held the syringes were scanned with dual- and single-energy 64-section multidetector CT. CT attenuation on single-energy CT images (in Hounsfield units) and MMD-derived fat volume fraction (FVF; dual-energy CT FVF) were obtained for each syringe, as were magnetic resonance (MR) spectroscopy measurements by using a 1.5-T imager (fat fraction [FF] of MR spectroscopy). Reference values of FVF ( $FVF_{ref}$ ) were determined by using the Soxhlet method. Iron concentrations were determined by inductively coupled plasma optical emission spectroscopy and divided into three ranges (0 mg per 100 g, 48.1–55.9 mg per 100 g, and 92.6–103.0 mg per 100 g). Statistical analysis included Spearman rank correlation and analysis of covariance.

## Results:

Both dual-energy CT FVF ( $\rho = 0.97$ ;  $P < .001$ ) and CT attenuation on single-energy CT images ( $\rho = -0.97$ ;  $P < .001$ ) correlated significantly with  $FVF_{ref}$  for phantoms without iron. Phantom size had a significant effect on dual-energy CT FVF after controlling for  $FVF_{ref}$  ( $P < .001$ ). The regression slopes for CT attenuation on single-energy CT images in 20- and 30-cm-diameter phantoms differed significantly ( $P = .015$ ). In sections with higher iron concentrations, the linear coefficients of dual-energy CT FVF decreased and those of MR spectroscopy FF increased ( $P < .001$ ).

## Conclusion:

Dual-energy CT FVF allows for direct quantification of fat content in units of volume percent. Dual-energy CT FVF was larger in 30-cm than in 20-cm phantoms, though the effect of object size on fat estimation was less than that of CT attenuation on single-energy CT images. In the presence of iron, dual-energy CT FVF led to underestimation of  $FVF_{ref}$  to a lesser degree than FF of MR spectroscopy led to overestimation of  $FVF_{ref}$ .

© RSNA, 2016

Online supplemental material is available for this article.

<sup>1</sup> From the Department of Radiology, Kindai University Faculty of Medicine, 377-2 Ohno-Higashi, Osaka-Sayama, Osaka 589-8511, Japan (T.H., T. Murakami); Department of Radiology, Osaka University Graduate School of Medicine, Suita, Japan (M.H.); CT Research Group (K.S.) and MR Applications and Workflow Group (T.W.), GE Healthcare Japan, Hino, Japan; Biomedical Image Analysis Laboratory, GE Global Research, Niskayuna, NY (P.L.); Clinical Research Center, Kindai University Hospital, Osaka-Sayama, Japan (Y.C.); and Department of Diagnostic and Therapeutic Radiology, Ehime University Graduate School of Medicine, Toon, Japan (T. Mochizuki). Received January 18, 2016; revision requested March 14; revision received May 29; accepted June 8; final version accepted June 13. Address correspondence to T.H. (e-mail: [neneth@m.ehime-u.ac.jp](mailto:neneth@m.ehime-u.ac.jp)).

© RSNA, 2016

**Q**uantification of fat content in the liver is important when assessing fatty liver disease and when selecting donors for living donor

### Advances in Knowledge

- The multimaternal decomposition (MMD) algorithm allows for direct quantification of fat content in units of volume percent by using dual-energy (DE) CT data, with linear coefficients against a reference standard for 20- and 30-cm-diameter phantoms in the absence of iron of 0.93 and 0.92 ( $P < .001$  each).
- Cylindrical phantom size had a significant effect on MMD-derived fat volume fraction (FVF) after controlling for reference values of FVF ( $FVF_{ref}$ ) ( $P < .001$ ), and DE CT FVF for the 30-cm phantom was similar to  $FVF_{ref}$  and was about 5% larger than was the 20-cm phantom at any level of  $FVF_{ref}$ .
- The linear regression slopes for CT attenuation on single-energy CT images in the 20- and 30-cm-diameter phantoms differed significantly ( $P = .015$ ), and the y-intercept was larger for the 20-cm than for the 30-cm phantom (78 HU and 71 HU); the difference of CT attenuation on single-energy CT images was smaller at higher  $FVF_{ref}$ .
- The presence of iron reduced DE CT FVF (linear correlation coefficients [LCC] for iron concentrations of 0 mg per 100 g, 48.1–55.9 mg per 100 g, and 92.6–103.0 mg per 100 g for a 30-cm phantom were 0.92, 0.88, and 0.87;  $P < .001$ ) while it increased fat fraction (FF) estimated by MR spectroscopy (LCC for iron concentrations of 0 mg per 100 g, 48.1–55.9 mg per 100 g, and 92.6–103.0 mg per 100 g were 1.09 [ $P = .012$ ], 1.19 [ $P = .001$ ], and 1.66 [ $P < .001$ ]), with a smaller effect for DE CT FVF than for FF of MR spectroscopy.

liver transplantation (1). Although liver biopsy remains the reference standard for liver fat quantification, this method is associated with sampling error, as a typical adult biopsy sample corresponds to just 0.002% of the entire liver (2). Moreover, liver biopsy is an invasive procedure (3), with complication rates ranging from 0.6% to 18% (4–6).

Noninvasive imaging and assessment of liver-fat concentration, therefore, is of increasing clinical interest (2,3). Current imaging-based fat-quantification techniques include those associated with magnetic resonance (MR) imaging, ultrasonography (US), and computed tomography (CT), with MR methods considered optimal for liver-fat quantification (7). However, MR methods are acquisition time consuming (8,9); the imaging range per examination is narrower, and specific analyses, such as MR elastography, require additional data acquisition. Furthermore, intrahepatic iron has been shown to reduce the accuracy of fat measurement (10,11).

Although US is widely used to assess hepatic steatosis, conventional B-mode US is less quantitative, with relatively poor interobserver and interequipment reproducibility (3,12). At conventional single-energy CT, liver fat is quantified with attenuation in Hounsfield units, a method based on an inverse relationship between liver fat content and liver attenuation (3). However, CT attenuation measurements are only semiquantitative (13), with liver fat concentration heuristically inferred. Moreover, CT attenuation may be altered by the presence of iron and glycogen in the liver, the patient's hematocrit, and drugs such as amiodarone (14). Because of beam hardening, which results from the polychromatic nature of the x-ray beam, CT attenuation of the liver can

decrease in patients who are larger in size, which would require normalization by attenuation of the spleen (15,16).

Multimaterial decomposition (MMD), developed for fast kilovolt-peak-switching dual-energy CT (17), is a technique that can discriminate among two or more different materials simultaneously. This method displays fat volume fraction (FVF) images, which enables quantitative and visual assessment of the fat content in the liver. Additionally, projection-based methods at dual-energy CT are in principle more effective for beam-hardening correction (18), which suggests that the MMD technique may be less affected by body size than single-energy CT, as in virtual monochromatic images.

The purpose of this phantom study was to assess the ability of fast-kilovolt-peak switching dual-energy CT by using the MMD algorithm to quantify liver fat. The susceptibility to object size and iron was investigated and compared with the results of single-energy CT and MR spectroscopy, respectively.

### Materials and Methods

Three authors (P.L., K.S., and T.W.) are employees of GE, the manufacturer of the CT and MR imaging systems and the MMD software used in this study. The other authors, who are not

#### Published online before print

10.1148/radiol.2016160129 Content code: CT

Radiology 2017; 282:381–389

#### Abbreviations:

FF = fat fraction  
FVF = fat volume fraction  
 $FVF_{ref}$  = reference value of FVF  
MMD = multimaterial decomposition

#### Author contributions:

Guarantor of integrity of entire study, T. Murakami; study concepts/study design or data acquisition or data analysis/interpretation, all authors; manuscript drafting or manuscript revision for important intellectual content, all authors; approval of final version of submitted manuscript, all authors; agrees to ensure any questions related to the work are appropriately resolved, all authors; literature research, T.H., T. Mochizuki, T. Murakami; experimental studies, T.H., K.S., T.W.; statistical analysis, T.H., M.H., Y.C.; and manuscript editing, T.H., M.H., P.L., T.W., T. Murakami

Conflicts of interest are listed at the end of this article.

### Implication for Patient Care

- The results of this study may have clinical utility for noninvasive diagnosis, treatment, and monitoring of patients with fatty livers by using DE CT.

Table 1

## Material Composition of the Syringes

Syringe No.	Preparation			Measured Reference Value	
	Pig Liver (mL)	Lard (mL)	Iron* (mg)	FVF (%)	Iron (mg per 100 g)
1	90	0	0	3	0
2	80	10	...	12	0
3	70	20	...	23	0
4	60	30	...	33	0
5	40	50	...	58	0
6	90	0	40	3	48.1
7	80	10	...	12	51.5
8	70	20	...	23	51.0
9	60	30	...	33	51.9
10	40	50	...	58	55.9
11	90	0	80	3	92.6
12	80	10	...	13	95.1
13	70	20	...	23	98.2
14	60	30	...	32	101.0
15	40	50	...	62	103.0

Note.—Measured reference values of fat are reported as the reference values of FVF (FVF<sub>ref</sub>) in our study.

\* Saccharated iron oxide (20 mg of iron per milliliter) diluted with distilled water (total volume, 10 mL).

GE employees, had control of the data and information that might present a conflict of interest for the employee authors.

### Swine Liver Phantom

The animal care and use committee of Kindai University Faculty of Medicine, Osaka, Japan, did not require their approval for the study. Liver from a freshly slaughtered swine obtained from an abattoir was homogenized and deaerated with a vacuum deaerator for 20 minutes at room temperature. Fifteen mixtures that contained varying proportions of the swine liver, lard (Pure Lard, Megmilk Snow Brand, Sapporo, Japan; specific gravity, 0.8), and iron (saccharated ferric oxide, Fesin, Nichi-Iko, Toyama, Japan; 20 mg of iron per milliliter; 40 mg of iron per 2 mL ampule) were prepared and again deaerated until air bubbles were undetectable for 5–20 minutes (longer times were needed for the mixtures that contained more fat) (Table 1). Iron content for mixtures was intended to be at roughly three levels (see Statistical Analysis) to a maximum of about 100 mg per 100 g because iron content measured by biomagnetometry with a superconducting

quantum interference device (19) was reported to be less than 40 mg per 100 g of liver (wet weight) in healthy individuals and 60.6 mg per 100 g of liver (wet weight)  $\pm$  46.4 (standard deviation) in patients with nonalcoholic fatty liver disease (20). After measuring the weight of 100 mL of each mixture to determine its specific gravity, 15 plastic syringes were filled with the mixtures and inserted into holes in a cylindrical phantom (Kyoto Kagaku, Kyoto, Japan) at CT scanning. The cylindrical phantom, made from water-equivalent material (ToughWater, Kyoto Kagaku; consisting of a polyurethane epoxy resin), was 30 cm in diameter and 8 cm in length; however, it contained a removable outer ring, which effectively created a smaller phantom with a diameter of 20 cm. Each phantom had five holes, or inserts, 20 mm in diameter (Fig 1a and 1b). Immediately after CT scanning, the same 15 syringes were used in MR data acquisition. Reference values for the amounts of fat and iron in each syringe were determined by Japan Food Research Laboratory. FVF<sub>ref</sub> was calculated from the results of the Soxhlet extraction method (21,22) (measuring precision, 0.1 g per 100 g)

and the specific gravity of the contents of each syringe. Iron concentrations were measured by using inductively coupled plasma optical emission spectroscopy (Vista-Pro, Agilent Technologies, Tokyo, Japan; measuring precision, 0.1 mg per 100 g). Syringes numbered 5, 10, and 15 were excluded from the study because they appeared to be heterogeneous at CT imaging (Fig 1c and 1d) and at three-dimensional fast spoiled gradient-recalled-echo MR imaging (Fig 2a).

### CT Acquisition and Image Analysis

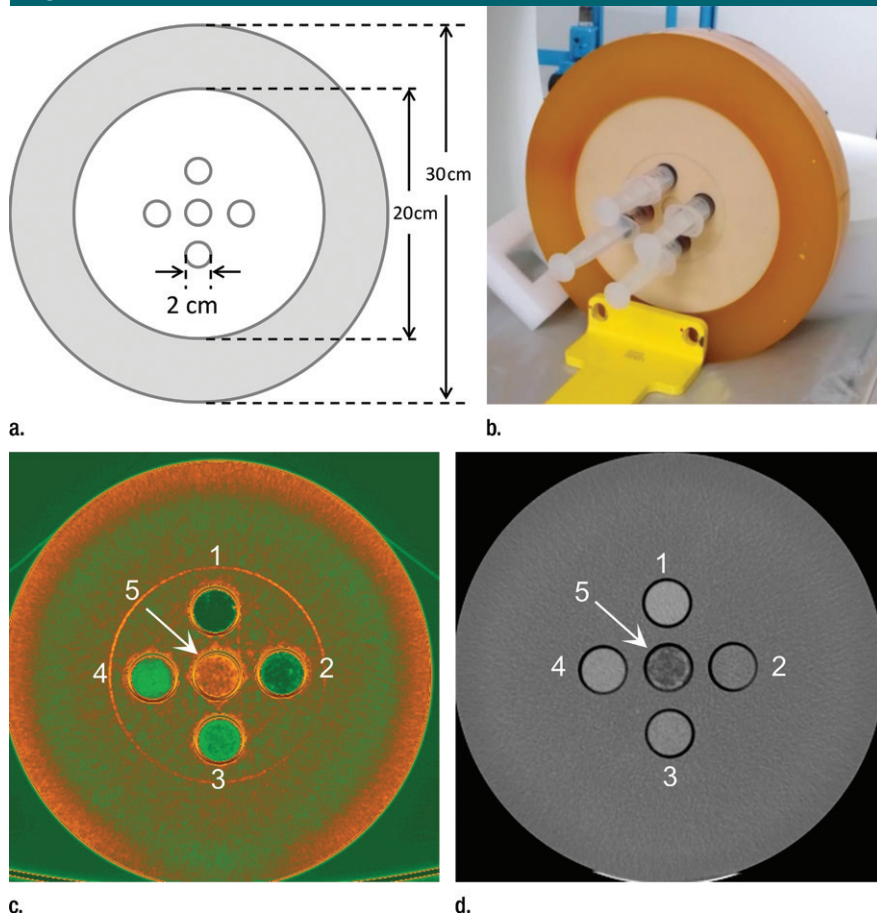
Cylindrical phantoms (diameter, 20 cm and 30 cm) that contained the syringes were scanned by using fast-kilovolt-peak switching dual-energy CT (80 and 140 kVp) and conventional single-energy CT (120 kVp) with a 64-section multi-detector CT scanner (Discovery CT750 HD; GE Healthcare, Milwaukee, Wis). In both scanning modes, data sets were acquired with helical scanning (gantry rotation speed, 0.5; detector configuration, 0.625  $\times$  64 mm; helical pitch, 1.375). Tube current and CT dose index volume were 640 mA and 15.64 mGy, respectively, for the dual-energy mode, and 500 mA and 13.82 mGy, respectively, for the single-energy mode.

FVF images of 5-mm thickness were generated from dual-energy CT data at a local workstation (AW VolumeShare 5; GE Healthcare) by using MMD software currently not commercially available (GE Healthcare), shown in Figure 1c (17). The MMD algorithm quantifies liver fat by two-material decomposition by using fat and healthy liver tissue as the material pair. The output of the MMD algorithm consists of FVF images in units of volume percent, and each voxel in the FVF image represents that voxel's volume percentage of fat.

MMD-based FVF (dual-energy CT FVF, in percent) measurements were made by placing a region of interest (cross-sectional area, 236.6 mm<sup>2</sup>; 689 voxels) on three contiguous FVF sections within the area that corresponded to the syringe at a workstation (AW VolumeShare 5; GE Healthcare). The size of the regions of interest was kept constant among all sections and



Figure 1



**Figure 1:** Phantoms for CT. **(a)** Schematic of the phantom holder. The whole thing is composed of water-equivalent material. The outer ring (shaded area) is removable. **(b)** Photograph of the phantom. **(c)** FVF image from dual-energy CT data and **(d)** standard single-energy CT (120-kVp) images. Numbers in **c** and **d** represent the syringe numbers shown in Table 1. Syringe number 5 demonstrated an attenuation that appeared to be heterogeneous.

syringes by applying the copy-and-paste function. The individual data points were used in analyses. CT attenuation (single-energy CT in Hounsfield units) was similarly obtained on single-energy CT images, which also had a section thickness of 5 mm (Fig 1d).

### MR Spectroscopy

MR imaging and proton spectroscopy were performed on the 15 syringes by using a 1.5-T clinical imager (Signa HDxt; GE Healthcare) with a 12-channel head coil (Fig 2a). Single-voxel MR spectroscopy data were collected by single shot-point-resolved spectroscopy without water saturation (23). A voxel

on each phantom syringe measured  $15 \times 15 \times 15 \text{ mm}^3$ . The acquisition parameters were as follows: echo time, 28 msec; one signal average; and spectral width, 2500 Hz with 2048 sampling points. No dummy radiofrequency excitation was applied. The areas of the fat and water peaks were measured on each acquired spectrum. Fat fraction (FF) was calculated from the results of MR spectroscopy (FF of MR spectroscopy, in percent) by using the following equation:  $\text{FF of MR spectroscopy} = \text{fat peak area} / (\alpha \times \text{water area} + \text{fat peak area})$  (Fig 2b), where  $\alpha = 0.83$  and is the calibration factor obtained from standard curves (Appendix E1 [online]).

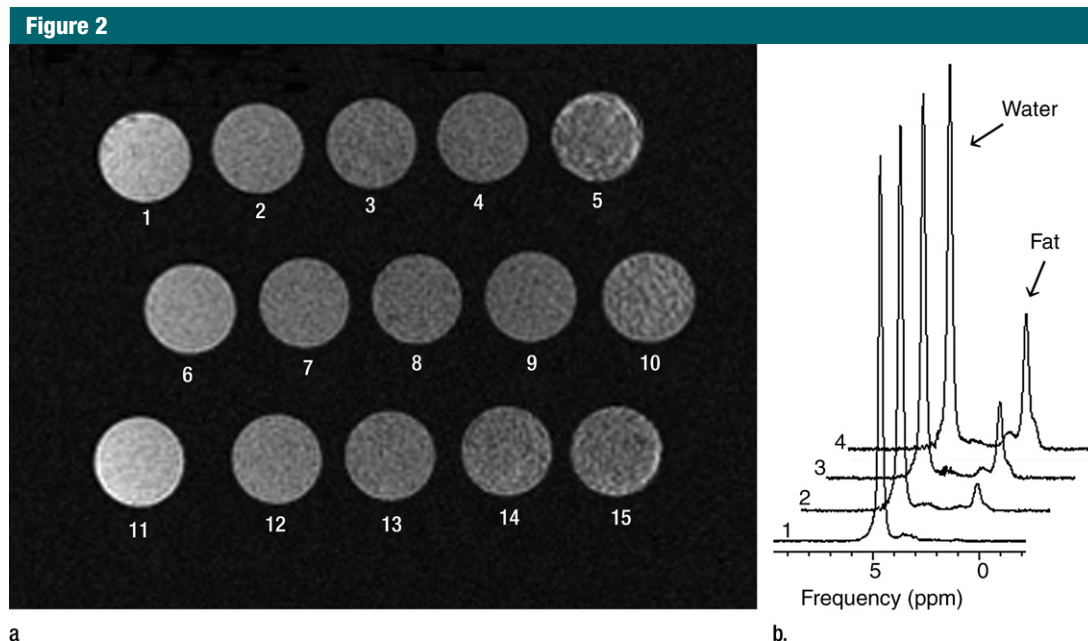
### Statistical Analysis

Statistical software (R Package version 2.12.0; R Foundation for Statistical Computing, Vienna, Austria) was used for statistical analysis (24). A *P* value less than .05 was considered to indicate statistical significance. To compare the effects of phantom size on the results of dual-energy CT and single-energy CT, the relationships between CT measurements (dual-energy CT FVF and Hounsfield unit single-energy CT in each of the two phantom sizes) and  $\text{FVF}_{\text{ref}}$  for the syringes without iron (numbered 1–4 in Table 1) were assessed by using Spearman rank correlation coefficient ( $\rho$ ) and linear regression analyses. The regression lines for both phantom sizes were assessed by analysis of covariance to determine if beam hardening had statistically significant effects on measurements at single-energy CT and dual-energy CT.

To assess the influence of iron on fat measurements made by using dual-energy CT and MR spectroscopy, the linear regression lines for dual-energy CT FVF and FF of MR spectroscopy were compared by using analysis of covariance at three levels of iron, and syringes 1–4, 6–9, and 11–14 (Table 1) contained iron concentrations of 0 mg per 100 g, 48.1–55.9 mg per 100 g, and 92.6–103.0 mg per 100 g, respectively.

### Results

Table 1 shows reference values for the amounts of fat and iron in the syringes. Syringes without lard (syringe number 1, 6, and 11) contained FF of 3%. Figure 3 shows the influence of the size of the cylindrical phantom on the relationship between  $\text{FVF}_{\text{ref}}$  of syringes numbered 1–4 and the corresponding CT measurements (dual-energy CT FVF and CT attenuation on single-energy CT images). For both phantom sizes,  $\text{FVF}_{\text{ref}}$  positively correlated with dual-energy CT FVF ( $\rho = 0.97$ ;  $P < .001$ ) (Fig 3a), whereas it negatively correlated with CT attenuation on single-energy CT images ( $\rho = -0.97$ ;  $P < .001$ ) (Fig 3b). Analysis of covariance showed that phantom size had a significant effect on dual-energy CT FVF after controlling for  $\text{FVF}_{\text{ref}}$ .



**Figure 2:** (a) MR image of liver fat phantom by three-dimensional fast spoiled gradient-recalled-echo sequence (repetition time [msec]/echo time [msec], 50.8/3.5; flip angle, 10°; echo time interval, 6 msec; eight echoes; bandwidth, 31.3k Hz; 256 × 256 matrix). (b) Graph shows examples of MR spectroscopy (syringes 1–4). Ppm = parts per million.

( $P < .001$ ). The adjusted mean was significantly higher for the 30-cm than for the 20-cm-diameter phantom (18.3 vs 15.5, respectively;  $P < .001$ ). The scatterplot with regression lines showed that dual-energy CT FVF for the 30-cm phantom was similar to  $FVF_{ref}$  and was about 5% larger than for the 20-cm phantom at any level of  $FVF_{ref}$  (Fig 3a). Analysis of covariance for CT attenuation on single-energy CT images yielded a significant difference between the slopes of 20- and 30-cm (diameter) phantoms ( $P = .015$ ); y-intercept was larger for the 20-cm than for the 30-cm phantom (78 HU and 71 HU, respectively), and the difference in CT attenuation on single-energy CT images was smaller at higher  $FVF_{ref}$  (eg, 28 HU and 23 HU, respectively, at  $FVF_{ref}$  of 30%) (Fig 3b).

Dual-energy CT FVF for both phantom sizes and FF of MR spectroscopy as a function of  $FVF_{ref}$  were plotted for three ranges of iron concentration (0 mg per 100 g, 48.1–55.9 mg per 100 g, and 92.6–103.0 mg per 100 g; Fig 4) and fit by using linear regression (Table 2). Analysis of covariance showed significant differences in slopes among dual-energy

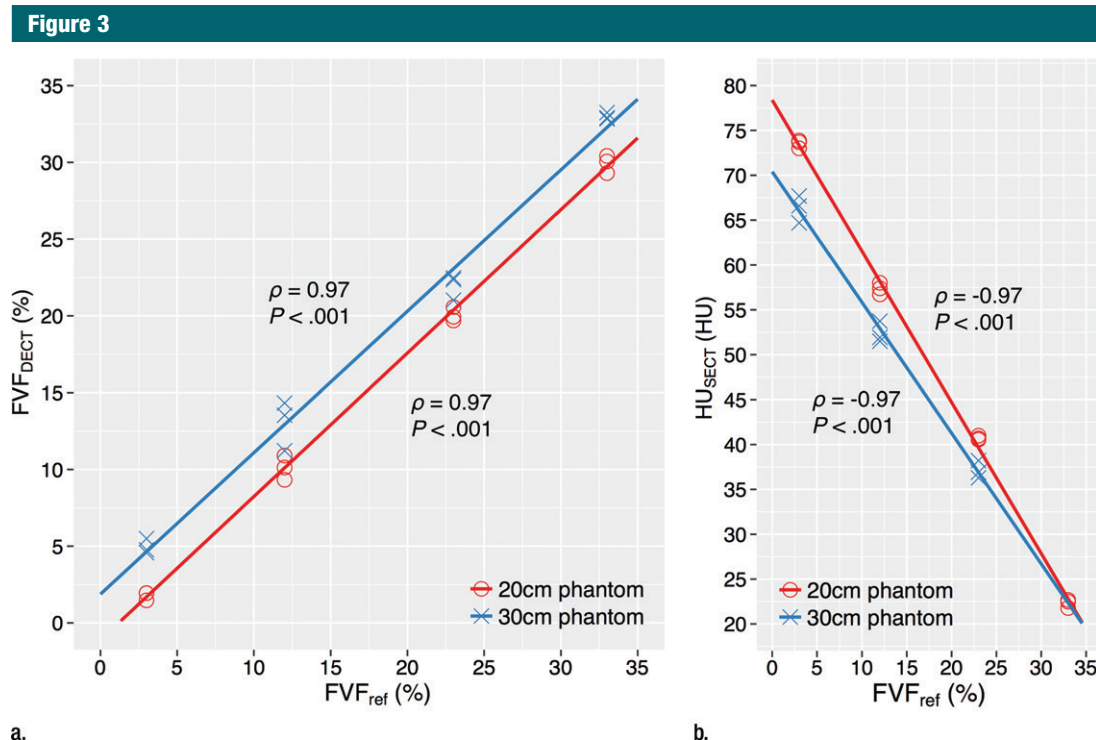
CT FVF for 20- and 30-cm (diameter) phantoms and FF of MR spectroscopy for all three ranges ( $P < .001$ ; Table 2). At an iron concentration of 0 mg per 100 g, the linear coefficients of dual-energy CT FVF for 20- and 30-cm (diameter) phantoms and FF of MR spectroscopy were approximately 1.00 (0.93, 0.92, and 1.09, respectively; respective  $P$  values were  $< .001$ ,  $< .001$ , and .012) and the regression lines were close to one another (Fig 4a). At higher concentrations of iron, the linear coefficients for dual-energy CT FVF decreased and the linear coefficients for FF of MR spectroscopy increased, which resulted in the further separation of the regression lines for dual-energy CT FVF and FF of MR spectroscopy. Within each range, dual-energy CT FVF led to underestimation of  $FVF_{ref}$  to a lesser degree than FF of MR spectroscopy led to overestimation of  $FVF_{ref}$  at higher  $FVF_{ref}$  (Fig 4b and 4c).

### Discussion

Although dual-energy CT FVF ( $\rho = 0.96$ ) and CT attenuation on single-energy CT images ( $\rho = -0.96$ ) showed

similarly strong correlations with  $FVF_{ref}$ , one advantage of the MMD method over CT attenuation in single-energy CT is the ability of the former to directly measure fat content in units of volume percent. In addition, dual-energy CT FVF was expected to be more susceptible to cylindrical phantom size (a surrogate for patient body size) than CT attenuation on single-energy CT images. We found, however, that dual-energy CT FVF was larger and CT attenuation on single-energy CT images was smaller in 30-cm than in 20-cm phantoms, which indicated that both the MMD method and single-energy CT were affected by beam hardening. One reason is that material decomposition images are based on two different polychromatic x-ray beams, each of which has a different degree of beam hardening. However, CT attenuation on single-energy CT images might be more affected by beam hardening than dual-energy CT FVF because CT attenuation on single-energy CT images for the 30-cm phantom was closer to CT attenuation on single-energy CT images for the 20-cm phantom at higher  $FVF_{ref}$ . It





**Figure 3:** Scatterplots of  $FVF_{ref}$  versus CT measurements for the fatty liver phantoms without iron. The red and blue lines represent the regression lines for the 20- and 30-cm-diameter cylindrical phantoms, respectively. Spearman correlation coefficients and associated  $P$  values are shown. **(a)** Scatterplot of the data and regression lines for the FVF measured by using dual-energy CT ( $FVF_{DECT}$ ). **(b)** Scatterplot of the data and regression lines for the CT attenuation at single-energy CT ( $HU_{SECT}$ ).

should be considered that the essential difference between dual-energy CT and single-energy CT is difficult to determine by using clinical equipment because beam-hardening correction is optimized in each system. An analysis of covariance showed that regardless of  $FVF_{ref}$ , dual-energy CT FVF in 30-cm (diameter) phantom was higher than in 20-cm phantom. Because patients who undergo liver fat quantification usually have larger body size, it would be acceptable that dual-energy CT FVF in 30-cm phantom was closer to  $FVF_{ref}$  than in 20-cm phantom.

The use of inductively coupled plasma optical emission spectroscopy ensured that the amount of iron (0–103.0 mg per 100 g) in the phantoms varied from that observed in healthy patients to that observed in pathologic states, including in patients with non-alcoholic fatty liver disease, although liver iron concentration may be higher in other diseases. For example, greater

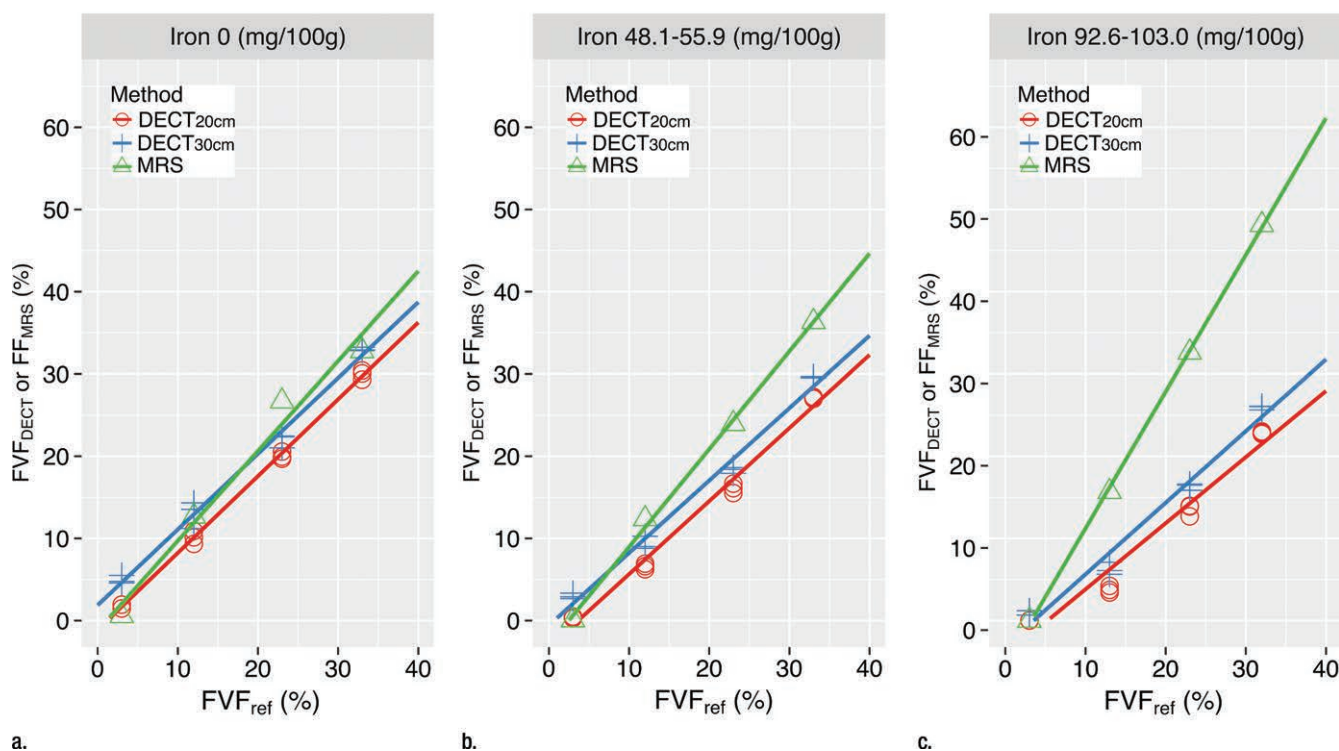
than 100 mg per 100 g of liver (wet weight) was defined as the criterion for hereditary hemochromatosis, and severe iron overload (>350 mg per 100 g liver wet weight) resulted in clinically relevant liver damage (25). Syringes that contained more lard also contained more iron per unit volume, which accentuated the effects of iron when iron concentrations were 48.1–55.9 mg per 100 g and 92.6–103.0 mg per 100 g. However, our phantom study indicated that the presence of iron decreased measured fat content measured by the MMD method while it increased fat content measured by MR spectroscopy, and the latter validated the results of previous studies (26).

Linear regression analysis and analysis of covariance suggested that MR spectroscopy and MMD leads to overestimation and underestimation, respectively, of liver fat volume, and that MR spectroscopy may yield more errors than the MMD method

for assessment of patients with more liver fat and who had iron deposition in their livers, including patients with chronic hepatic diseases and hemochromatosis. Meanwhile, MMD software could be affected by iron deposition and patient body size. Specifically, liver fat content may be underestimated in a small patient with high iron content in the liver, as also shown by the CT attenuation value at single-energy CT (27).

The overall accuracy of MMD can be improved by augmenting the algorithm to account for the presence of iron (and any other confounding materials) in the liver parenchyma (17). However, accounting for iron in the context of fat quantification is challenging. First, initial experiments during MMD software development indicated that fat, healthy liver tissue, and iron all lie along the same line or direction in linear attenuation space (Fig E1 [online]). Three

Figure 4



**Figure 4:** (a–c) Linear regression relationships between  $FVF_{ref}$  and FVF measured with dual-energy CT FVF ( $FVF_{DECT}$ ; DECT) and FF of MR spectroscopy ( $FF_{MRS}$ ; MRS) for each range of iron concentration (a, 0 mg per 100 g; b, 48.1–55.9 mg per 100 g; c, 92.6–103.0 mg per 100 g). The red and blue lines represent the regression lines for dual-energy CT FVF in the 20- and 30-cm-diameter cylindrical phantoms, respectively. The green line represents the regression line for FF of MR spectroscopy.

Table 2

## Comparison of the Slopes of Regression Lines of FVF

Iron Level	Slope of Regression Lines of FVF		PValue*
	Linear Coefficient	PValue	
0 mg per 100 g			<.001
Dual-energy CT 20 cm	0.93	<.001	
Dual-energy CT 30 cm	0.92	<.001	
MR spectroscopy	1.09	.012	
48.1–55.9 mg per 100 g			<.001
Dual-energy CT 20 cm	0.89	<.001	
Dual-energy CT 30 cm	0.88	<.001	
MR spectroscopy	1.19	.001	
92.6–103.0 mg per 100 g			<.001
Dual-energy CT 20 cm	0.80	<.001	
Dual-energy CT 30 cm	0.87	<.001	
MR spectroscopy	1.66	<.001	

Note.—MMD in dual-energy CT was measured in phantoms with diameters of 20 cm and 30 cm.

\* P values reflect the homogeneity of regression slopes at within-iron levels.

materials lying along the same line is problematic because it is difficult to get a unique linear combination of the three materials. Second, iron is not the only heavy metal that can be found in the liver. For example, copper, which accumulates in the liver in Wilson disease, has a similar atomic number to that of iron (respective atomic numbers, 29 and 26). Thus, it would be difficult to differentially quantify these two metals because the attenuation of x-ray beams would be similar. Whereas some publications indicated that iron can be quantified from fat and iodinated contrast agents in phantoms or animal models (28–30), this work has not been extended to patients.

Other than the fast-kilovolt-peak switching approach, several techniques were proposed for dual-energy imaging (31). Because MMD is model based and

uses National Institute of Standards and Technology–measured values (32) to obtain material triangle vertices in the linear attenuation space (17), the MMD technique itself is generalizable. To our knowledge, the ability of dual-energy CT systems to reproduce the same or similar attenuation values for the same object that is imaged has not been determined. Thus, adjustments may be needed among different dual-energy CT systems, manufacturers, or vendors.

This study had several limitations. First, because the MR spectroscopy protocol used a single echo time, T2 correction could not be applied. Iron may have resulted in an overestimate of FF at MR spectroscopy had the T2 correction been applied (11). In addition, the lower specific gravity (ie, fewer electrons per unit volume) of the lard we used may have improved the performance of MMD because of differences in attenuation coefficients between liver and fat tissue. The accuracy of MMD software should be further investigated in vivo.

In conclusion, dual-energy CT-based MMD method is promising for noninvasive quantification of hepatic steatosis, with lower susceptibility to object size than attenuation values at single-energy CT and lower susceptibility to iron compared with MR spectroscopy. Iron concentration, however, is a confounding factor for both MMD and MR spectroscopy, resulting in underestimation and overestimation, respectively, of fat content.

**Acknowledgments:** We thank Masayuki Kudo, PhD, RT, and Atsuo Kimura, PhD, for their advice and constructive comments on our work.

**Disclosures of Conflicts of Interest:** T.H. disclosed no relevant relationships. M.H. disclosed no relevant relationships. P.L. Activities related to the present article: disclosed no relevant relationships. Activities not related to the present article: author disclosed employment with GE; author was issued a patent for liver fat quantification that encompasses the algorithm reported herein. Other relationships: disclosed no relevant relationships. K.S. Activities related to the present article: disclosed no relevant relationships. Activities not related to the present article: author dis-

closed personal fees from employment with GE Healthcare. Other relationships: disclosed no relevant relationships. T.W. Activities related to the present article: disclosed no relevant relationships. Activities not related to the present article: author disclosed personal fees from employment with GE Healthcare. Other relationships: disclosed no relevant relationships. Y.C. disclosed no relevant relationships. T. Mochizuki disclosed no relevant relationships. T. Murakami disclosed no relevant relationships.

## References

1. Brandhagen D, Fidler J, Rosen C. Evaluation of the donor liver for living donor liver transplantation. *Liver Transpl* 2003;9(10 Suppl 2):S16–S28.
2. Sanai FM, Keefe EB. Liver biopsy for histological assessment: The case against. *Saudi J Gastroenterol* 2010;16(2):124–132.
3. Schwenzer NF, Springer F, Schraml C, Stefan N, Machann J, Schick F. Non-invasive assessment and quantification of liver steatosis by ultrasound, computed tomography and magnetic resonance. *J Hepatol* 2009;51(3):433–445.
4. Gunneson TJ, Menon KV, Wiesner RH, et al. Ultrasound-assisted percutaneous liver biopsy performed by a physician assistant. *Am J Gastroenterol* 2002;97(6):1472–1475.
5. Weigand K, Weigand K. Percutaneous liver biopsy: retrospective study over 15 years comparing 287 inpatients with 428 outpatients. *J Gastroenterol Hepatol* 2009;24(5):792–799.
6. Szymczak A, Simon K, Inglot M, Gladysz A. Safety and effectiveness of blind percutaneous liver biopsy: analysis of 1412 procedures. *Hepat Mon* 2012;12(1):32–37.
7. Patel KD, Abeysekera KW, Marlais M, et al. Recent advances in imaging hepatic fibrosis and steatosis. *Expert Rev Gastroenterol Hepatol* 2011;5(1):91–104.
8. Joy D, Thava VR, Scott BB. Diagnosis of fatty liver disease: is biopsy necessary? *Eur J Gastroenterol Hepatol* 2003;15(5):539–543.
9. Taouli B, Ehman RL, Reeder SB. Advanced MRI methods for assessment of chronic liver disease. *AJR Am J Roentgenol* 2009;193(1):14–27.
10. Horng DE, Hernando D, Hines CD, Reeder SB. Comparison of R2\* correction methods for accurate fat quantification in fatty liver. *J Magn Reson Imaging* 2013;37(2):414–422.
11. Lee SS, Lee Y, Kim N, et al. Hepatic fat quantification using chemical shift MR imaging and MR spectroscopy in the presence of hepatic iron deposition: validation in phantoms and in patients with chronic liver disease. *J Magn Reson Imaging* 2011;33(6):1390–1398.
12. Duman DG, Celikel C, Tüney D, Imeryüz N, Aysar E, Tözün N. Computed tomography in nonalcoholic fatty liver disease: a useful tool for hepatosteatosis assessment? *Dig Dis Sci* 2006;51(2):346–351.
13. Sanyal AJ; American Gastroenterological Association. AGA technical review on nonalcoholic fatty liver disease. *Gastroenterology* 2002;123(5):1705–1725.
14. Qayyum A. MR spectroscopy of the liver: principles and clinical applications. *RadioGraphics* 2009;29(6):1653–1664.
15. Kodama Y, Ng CS, Wu TT, et al. Comparison of CT methods for determining the fat content of the liver. *AJR Am J Roentgenol* 2007;188(5):1307–1312.
16. Brancatelli G. Science to practice: Should biopsy be performed in potential liver donors when unenhanced CT shows an unacceptable degree of steatosis for transplantation? *Radiology* 2006;239(1):1–2.
17. Mendonca PR, Lamb P, Sahani DV. A flexible method for multi-material decomposition of dual-energy CT images. *IEEE Trans Med Imaging* 2014;33(1):99–116.
18. Yu L, Leng S, McCollough CH. Dual-energy CT-based monochromatic imaging. *AJR Am J Roentgenol* 2012;199(5 Suppl):S9–S15.
19. Brittenham GM, Farrell DE, Harris JW, et al. Magnetic-susceptibility measurement of human iron stores. *N Engl J Med* 1982;307(27):1671–1675.
20. Bugianesi E, Manzini P, D'Antico S, et al. Relative contribution of iron burden, HFE mutations, and insulin resistance to fibrosis in nonalcoholic fatty liver. *Hepatology* 2004;39(1):179–187.
21. Carpenter C. Determination of fat content. In: Nielsen SS, ed. *Protein analysis laboratory manual*. 2nd ed. New York: Springer, 2010; 31–32.
22. Palmisciano Bedê T, Pascoal AC, Hauaji Facó L, et al. Effect of the intake of liquids rich in polyphenols on blood pressure and fat liver deposition in rats submitted to high-fat diet. *Nutr Hosp* 2015;31(6):2539–2545.
23. Bottomley PA. Spatial localization in NMR spectroscopy in vivo. *Ann N Y Acad Sci* 1987;508:333–348.
24. R Development Core Team. *R: A language and environment for statistical computing*. Vienna, Austria: R Foundation for Statistical Computing, 2010.

25. Nielsen P, Engelhardt R, Düllmann J, Fischer R. Non-invasive liver iron quantification by SQUID-biosusceptometry and serum ferritin iron as new diagnostic parameters in hereditary hemochromatosis. *Blood Cells Mol Dis* 2002;29(3):451–458.
26. Hayashi N, Miyati T, Minami T, et al. Quantitative analysis of hepatic fat fraction by single-breath-holding MR spectroscopy with  $T_2$  correction: phantom and clinical study with histologic assessment. *Radiol Phys Technol* 2013;6(1):219–225.
27. Pickhardt PJ, Park SH, Hahn L, Lee SG, Bae KT, Yu ES. Specificity of unenhanced CT for non-invasive diagnosis of hepatic steatosis: implications for the investigation of the natural history of incidental steatosis. *Eur Radiol* 2012;22(5):1075–1082.
28. Ma J, Song ZQ, Yan FH. Separation of hepatic iron and fat by dual-source dual-energy computed tomography based on material decomposition: an animal study. *PLoS One* 2014;9(10):e110964.
29. Fischer MA, Reiner CS, Raptis D, et al. Quantification of liver iron content with CT-added value of dual-energy. *Eur Radiol* 2011;21(8):1727–1732.
30. Fischer MA, Gnannt R, Raptis D, et al. Quantification of liver fat in the presence of iron and iodine: an ex-vivo dual-energy CT study. *Invest Radiol* 2011;46(6):351–358.
31. Marin D, Boll DT, Mileto A, Nelson RC. State of the art: dual-energy CT of the abdomen. *Radiology* 2014;271(2):327–342.
32. Hubbell JH, Seltzer SM. Tables of X-Ray Mass Attenuation Coefficients and Mass Energy-Absorption Coefficients from 1 keV to 20 MeV for Elements Z = 1 to 92 and 48 Additional Substances of Dosimetric Interest: National Institute of Standards and Technology Web site. <http://www.nist.gov/pml/data/xraycoef/>. Published May 1996. Updated July 2004. Accessed May 9, 2016.

## Diagnosis of Hepatocellular Carcinoma with Non-Invasive Imaging: a Plea for Worldwide Adoption of Standard and Precise Terminology for Describing Enhancement Criteria

Diagnose des hepatozellulären Karzinoms mittels nicht-invasiver Bildgebung: Ein Plädoyer für die weltweite Umsetzung einer standardisierten und präzisen Fachterminologie zur Beschreibung des Enhancements



Fabio Piscaglia



Masatoshi Kudo



Kwang-Hyub Han



Claude Sirlin

### Correspondence

Prof. Fabio Piscaglia

Dpt of Medical and Surgical Sciences DIMEC Unit of Internal Medicine  
via Albertoni 15

40138 Bologna

Italy

fabio.piscaglia@unibo.it

### Bibliography

DOI <http://dx.doi.org/10.1055/s-0042-124204>

Published online: 2017 | *Ultraschall in Med* 2017; 38: 9–11

© Georg Thieme Verlag KG Stuttgart · New York

ISSN 0172-4614

Hepatocellular carcinoma in cirrhosis is unique in oncology since a definitive diagnosis based on non-invasive imaging can be used without biopsy confirmation to determine even the most radical therapies such as liver transplantation. Given the enormous responsibility assigned to non-invasive imaging in guiding HCC management one would expect that there would be standardized terminology in use throughout the world for describing the diagnostic imaging criteria. Surprisingly, this is not the case. Different guidelines have adopted different terminology for assessing the temporal enhancement characteristics of HCC. The adoption of different terminology by different guidelines, even if intended to have similar meaning, contributes to inconsistency in clinical care, causes confusion in research, and is a barrier to progress in the field.

It is time to standardize the terminology for describing temporal enhancement criteria, which will be suggested at the end of the present editorial in line with recently published relevant documents in this field.

A summary of the current guidelines and of the variance of the terminology is useful to understand the potential causes of variability and misunderstandings. Guidelines released by the AASLD in 2005 [1] recognized the need to incorporate imaging features from both the arterial phase and the subsequent venous/delayed phase. This was done to help avoid false-positive diagnosis of perfusion disturbances caused by arterioportal shunting which also can manifest with hyperenhancement in the arterial phase. The criteria for the diagnosis of HCC was a lesion

showing “arterial hypervascularity that washes out in the early or delayed venous phase” [1]. The update of these guidelines in 2011 adopted the wording of “intense arterial uptake followed by wash out in the venous-delayed phases” [2]. Although the AASLD guidelines should be lauded for recognizing the importance of “washout”, the terminology advocated by the AASLD is suboptimal. The term “hypervascularity” is ambiguous as it encompasses multiple different pathophysiological alterations – including number and size of vessels, type of vessels, quality of their walls (fenestrated or not fenestrated sinusoids, capillarization), degree of vascular tone, etc. – most of which cannot be assessed reliably by imaging. A descriptive term would be more appropriate. In this sense, the usage of “intense arterial uptake” in the 2011 update is an improvement [2], but remains suboptimal for several reasons. In a liver with only arterial inflow and no portal perfusion (e. g. a patient with reversal of portal flow due to portal hypertension or TIPS), any part of the liver, including benign parenchyma, has intense arterial “uptake”. Moreover, no cancer and no part of the liver, literally takes up contrast agents in the arterial phase. Even contrast agents that eventually are transported into liver cells via membrane transporters do not enter cells in any meaningful concentration during the arterial phase. Thus the wording, “intense arterial uptake”, is pathophysiologically incorrect and cannot be considered appropriate.

The EASL 2012 guidelines [3] as well as the Spanish guidelines [4] utilized similar imperfect terminology as the AASLD guidelines

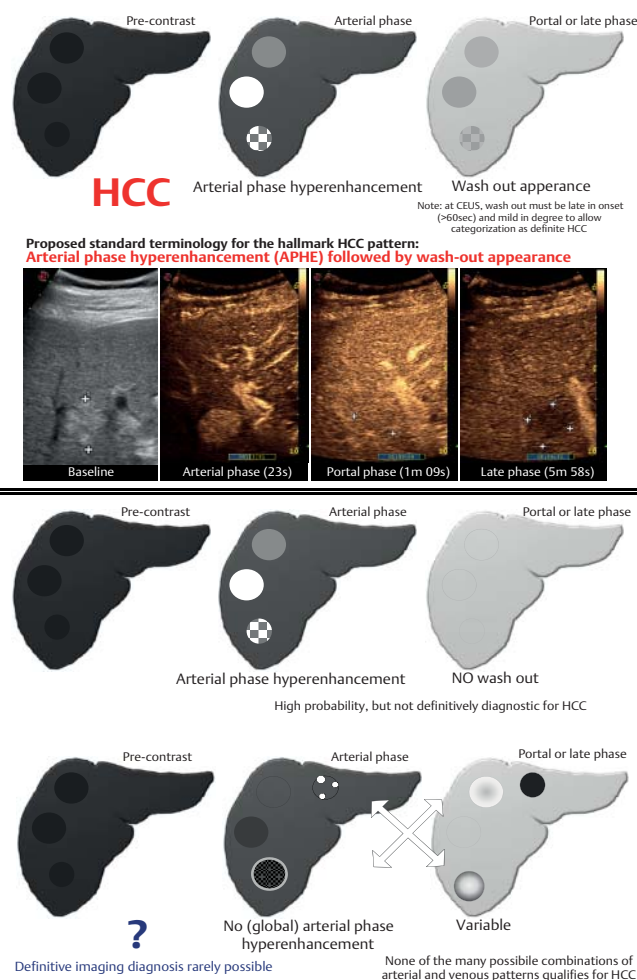


(“hypervascular in the arterial phase with washout in the portal venous or delayed phases” and “radiological hallmark, i. e. contrast uptake in the arterial phase and washout in the venous/late phase” or respectively “una captación de contraste en fase arterial seguido de lavado en fases venosas”). Also the Korean guidelines [5] (“hypervascularity in the arterial phase”) and Japanese guidelines [6] (“intense arterial enhancement”) adopt similar suboptimal definitions. The Italian position paper in 2013 [7] defined more clearly the diagnostic pattern in connection to both the arterial and portal patterns (homogeneous hyper-enhancement of the lesion in the arterial phase, followed by hypo-enhancement in the venous or delayed phase), but created confusion in its accompanying figure where it reported, “typical feature: wash-in and wash-out”. More properly, the term “wash-in” should be used to refer to the phase of arrival of the contrast during the arterial phase, up to reaching the peak signal intensity [8], but not to describe the degree of contrast enhancement. Using the term “wash-in” to describe the degree of arterial-phase enhancement is inappropriate and should not be considered synonymous of hyperenhancement.

The term wash-out may cause similar confusion. For example, the term “wash-out phase” refers to the time period between peak contrast enhancement intensity and disappearance of contrast [8] – i. e., the phase during which de-enhancement occurs, not the degree of de-enhancement. Moreover, some investigators have used “washout” to refer to a lesion that hyperenhances in the arterial phase relative to the surrounding parenchyma and that becomes isoenhancing in the venous phase. The use of “washout” in this context is justifiable in the sense that the lesion did de-enhance relative to the surrounding parenchyma. However, this temporal enhancement pattern – arterial phase hyperenhancement followed by venous phase isoenhancement – is not specific for HCC. For this reason, the term “wash-out pattern” should be reserved for lesions that, after showing iso or hyperenhancement in the arterial phase, become hypoenhancing in the venous/delayed phase in comparison to the surrounding parenchyma. Accordingly the Canadian guidelines [9] define the “classical radiographic appearance of HCC as: a lesion that exhibits higher signal intensity than the surrounding liver in the arterial phase of a contrast-enhanced study and lower signal intensity than the surrounding liver in the venous or the delayed phase of the contrast examination (so-called portal venous ‘washout’)”.

To summarize very few guidelines have provided optimal terminology for the hallmark imaging criteria of HCC.

In recent years, the American College of Radiology has supported the development of the Liver Imaging Reporting And Data System (LI-RADS®) with the aim, among others, to establish consistent, rigorous, and precisely defined terminology for clinical care and research. The LI-RADS® definition of the hallmark enhancement pattern at CT, MRI and CEUS is “arterial phase hyperenhancement (in whole or in part, not rim or peripheral discontinuous globular enhancement) in conjunction with wash-out appearance” (<https://www.acr.org/quality-safety/resources/lirads>), which is in keeping with the clear definitions expressed by the Canadian [9] and Italian [7] documents. Importantly, LI-RADS specifies that at CEUS (see scheme at <https://www.acr.org/quality-safety/resources/lirads>), the washout has to be of mild degree and late, namely starting after 60 seconds, in keeping with recent



► **Fig. 1** Schematic depictions of the patterns of appearance of focal lesions in cirrhosis in the arterial and venous contrast enhancement phases. The diagnostic pattern of HCC is shown, including an example at contrast enhanced ultrasound, in the upper half of the figure: this pattern is herewith proposed to be unequivocally and definitively defined as “arterial phase hyperenhancement (APHE) followed by wash-out appearance”, according to the LI RADS definition of LR5.

publications [10–12] to prevent the misdiagnosis of cholangiocellular carcinoma as HCC [13–17].

Hence, we hereby propose the following as standardized terminology to describe the hallmark temporal enhancement pattern of HCC: “arterial phase hyperenhancement (APHE) followed by washout appearance”. We also propose that the terms arterial phase hyperenhancement and washout appearance be defined as: arterial phase hyperenhancement = enhancement (of the lesion) in the arterial phase that is unequivocally greater than that of the liver; washout appearance = visually assessed temporal reduction in enhancement of the lesion relative to the liver from an earlier to a later phase resulting in portal venous phase hypoenhancement or delayed phase hypoenhancement.

This pattern is typical and diagnostic of HCC (with the additional requirement of mild and late occurrence of hypoenhancement = wash-out for CEUS) (► **Fig. 1**). According to LI-RADS, other imaging feature combinations such as APHE plus capsule appear-



ance also can establish the diagnosis of HCC at CT or MRI, especially since capsule appearance can create the visual perception of “washout” in HCCs without true “washout”, but this, as well as the pattern in the postvascular phase of Sonazoid®, are beyond the scope of the present editorial, which focuses on vascular phases enhancement characteristics.

## Conflict of interest

The authors declare the following conflict of interest: Fabio Piscaglia: Speaker fees: Bayer, Bracco; Advisory board: Bayer; Research contract: Esaote. Member of the board of directors of the International Contrast Ultrasound Society ICUS. Claude Sirlin: Industry grant support: Siemens, GE, Gerber; Consulting and service agreements: Bracco. Kwang-Hyub Han: nothing to disclose. Masatoshi Kudo: Speaker fees: Bayer, Eisai, MSD, Ajinomoto, Grants: Chugai, Otsuka, Takeda, Taiho, Sumitomo Dainippon, Daiichi Sankyo, MSD, Eisai, Bayer, Abbvie Advisory Consulting: Kowa, MSD, BMS, Bayer, Chugai, Taiho.

## References

- [1] Bruix J, Sherman M. Management of hepatocellular carcinoma. *Hepatology* 2005; 42: 1208–1236
- [2] Bruix J, Sherman M. Management of hepatocellular carcinoma: an update. *Hepatology* 2011; 53: 1020–1022
- [3] European Association For The Study Of The Liver, European Organisation For Research and Treatment Of Cancer. EASL-EORTC clinical practice guidelines: management of hepatocellular carcinoma. *J Hepatol* 2012; 56: 908–943
- [4] Forner A, Reig M, Varela M et al. Diagnóstico y tratamiento del carcinoma hepatocelular. Actualización del documento de consenso de la AEEH, SEOM, SERAM, SERVEI y SETH. *Med Clin (Barc)* 2016; 146: 511.e1–511.e22
- [5] Korean Liver Cancer Study Group-National Cancer Center Korea. 2014 Korean Liver Cancer Study Group-National Cancer Center Korea practice guideline for the management of hepatocellular carcinoma. *Korean J Radiol* 2015; 16: 465–522
- [6] Kokudo N, Hasegawa K, Akahane M et al. Evidence-based Clinical Practice Guidelines for Hepatocellular Carcinoma: The Japan Society of Hepatology 2013 update (3rd JSH-HCC Guidelines). *Hepatol Res* 2015; 45: DOI: 10.1111/hept.12464
- [7] Panel AE, Italian Association for the Study of the Liver, Committee AC et al. Position paper of the Italian Association for the Study of the Liver (AISF): the multidisciplinary clinical approach to hepatocellular carcinoma. *Dig Liver Dis* 2013; 45: 712–723
- [8] Dietrich CF, Averkiou MA, Correias JM et al. An EFSUMB introduction into Dynamic Contrast-Enhanced Ultrasound (DCE-US) for quantification of tumour perfusion. *Ultraschall in Med* 2012; 33: 344–351
- [9] Burak KW, Sherman M. Hepatocellular carcinoma: Consensus, controversies and future directions. A report from the Canadian Association for the Study of the Liver Hepatocellular Carcinoma Meeting. *Can J Gastroenterol Hepatol* 2015; 29: 178–184
- [10] Yuan MX, Li R, Zhang XH et al. Factors Affecting the Enhancement Patterns of Intrahepatic Cholangiocarcinoma (ICC) on Contrast-Enhanced Ultrasound (CEUS) and their Pathological Correlations in Patients with a Single Lesion. *Ultraschall in Med* 2016; 37: 609–617
- [11] Schellhaas B, Wildner D, Pfeifer L et al. LI-RADS-CEUS – Proposal for a Contrast-Enhanced Ultrasound Algorithm for the Diagnosis of Hepatocellular Carcinoma in High-Risk Populations. *Ultraschall in Med* 2016; 37: 627–634
- [12] Liu GJ, Wang W, Lu MD et al. Contrast-Enhanced Ultrasound for the Characterization of Hepatocellular Carcinoma and Intrahepatic Cholangiocarcinoma. *Liver Cancer* 2015; 4: 241–252
- [13] Galassi M, Iavarone M, Rossi S et al. Patterns of appearance and risk of misdiagnosis of intrahepatic cholangiocarcinoma in cirrhosis at contrast enhanced ultrasound. *Liver Int* 2013; 33: 771–779
- [14] Vilana R, Forner A, Bianchi L et al. Intrahepatic peripheral cholangiocarcinoma in cirrhosis patients may display a vascular pattern similar to hepatocellular carcinoma on contrast-enhanced ultrasound. *Hepatology* 2010; 51: 2020–2029
- [15] Salvatore V, Gianstefani A, Negrini G et al. Imaging diagnosis of hepatocellular carcinoma: recent advances of contrast-enhanced ultrasonography with SonoVue®. *Liver Cancer* 2016; 5: 55–66
- [16] Wildner D, Bernatik T, Greis C et al. CEUS in hepatocellular carcinoma and intrahepatic cholangiocarcinoma in 320 patients – early or late washout matters: a subanalysis of the DEGUM multicenter trial. *Ultraschall in Med* 2015; 36: 132–139
- [17] Wildner D, Pfeifer L, Goertz RS et al. Dynamic contrast-enhanced ultrasound (DCE-US) for the characterization of hepatocellular carcinoma. *Ultraschall in Med* 2014; 35: 522–527

# Immune Checkpoint Inhibition in Hepatocellular Carcinoma: Basics and Ongoing Clinical Trials

Masatoshi Kudo

Department of Gastroenterology and Hepatology, Kindai University Faculty of Medicine, Osaka-Sayama, Japan

## Key Words

Hepatocellular carcinoma · Immune checkpoint inhibitors · PD-1 antibody · PD-L1 antibody · CTLA-4 antibody · Nivolumab · Pembrolizumab

## Abstract

Clinical trials of antibodies targeting the immune checkpoint inhibitors programmed cell death 1 (PD-1), programmed cell death ligand 1 (PD-L1), or cytotoxic T-lymphocyte-associated protein 4 (CTLA-4) for the treatment of advanced hepatocellular carcinoma (HCC) are ongoing. Expansion cohorts of a phase I/II trial of the anti-PD-1 antibody nivolumab in advanced HCC showed favorable results. Two phase III studies are currently ongoing: a comparison of nivolumab and sorafenib in the first-line setting for advanced HCC, and a comparison of the anti-PD-1 antibody pembrolizumab and a placebo in the second-line setting for patients with advanced HCC who progressed on sorafenib therapy. The combination of anti-PD-1/PD-L1 and anti-CTLA-4 antibodies is being evaluated in other phase I/II trials, and the results suggest that an anti-PD-1 antibody combined with locoregional therapy or other molecular targeted agents is an effective treatment strategy for HCC. Immune checkpoint inhibitors may therefore open new doors to the treatment of HCC.

© 2017 S. Karger AG, Basel

## Introduction

Since immune checkpoint inhibitors were first reported in 2010 [1] and 2012 [2], they have exceeded expectations in clinical studies, the results of which indicate that these agents are highly effective (even in patients with advanced or metastatic liver cancer). The goal of previous cancer immunotherapy has so far been to enhance immune cell activity to kill the cancer cells; however, this does not result in actual activation of the immune system because of the inhibition signal by checkpoint molecules. Consequently, its clinical application remains controversial among clinical researchers in this field. Recently, many clinicians have become involved in the development of immune checkpoint inhibitors, which release the ‘brakes’ on the immune system, restoring its activity to normal levels. Their use in cancer immunotherapy is now actively promoted by both companies and academics worldwide. The journal *Science* selected cancer immunotherapy as its Breakthrough of the Year in 2013, and *Nature* featured the use of immune checkpoint blockade in cancer as a sensational paradigm shift in cancer therapy. Various industry/academia collaborations are ongoing, with the field developing at an amazing speed. Cancer immunotherapy has been described as the ‘beginning of new cancer therapy’ [3]; it has also been said that ‘cancer immunotherapy comes of age’ [4].

KARGER

© 2017 S. Karger AG, Basel

E-Mail karger@karger.com  
www.karger.com/ocl

Prof. Masatoshi Kudo  
Department of Gastroenterology and Hepatology  
Kindai University Faculty of Medicine  
377-2 Ohno-Higashi, Osaka-Sayama, Osaka 589-8511 (Japan)  
E-Mail m-kudo@med.kindai.ac.jp

The first protein identified as an immune checkpoint molecule was programmed cell death 1 (PD-1), which was discovered by Prof. Tasuku Honjo (Kyoto University) in 1992 [5]. Subsequent reports described its involvement in immune regulation and its function as a receptor that ‘puts the brakes’ on immune responses. In 2000, the PD-1 ligands PD-L1 and PD-L2 were identified by a collaborative project between Prof. Honjo’s group at Kyoto University and a group at Harvard University [6, 7]. In 2002, Iwai et al. [8] blocked the interaction between PD-1 and its ligands in a mouse model and found that the resulting increase in the strength of the immune response led to a marked increase in anticancer activity. Based on these findings, Ono Pharmaceutical Co., Ltd. (Japan) and Medarex (later acquired by Bristol-Myers Squibb; both based in the USA) successfully created the humanized anti-PD-1 antibody, nivolumab, in 2005, and clinical trials in humans were initiated in the USA in 2006. Bristol-Myers Squibb and Ono Pharmaceutical Co., Ltd. collaborated and jointly conducted a clinical study in 2009. Nivolumab was first approved for use as a treatment for melanoma in Japan in 2014. Nivolumab is currently approved for the treatment of melanomas, non-small-cell lung cancer, and kidney cancer in the USA. In Japan, it was approved for the treatment of non-small-cell lung cancer in 2015 and for kidney cancer in 2016. In addition to nivolumab, pembrolizumab (an anti-PD-1 antibody developed by Merck) is now an approved agent for the treatment of melanoma and non-small-cell lung cancer in the USA.

A series of clinical trials are currently examining these two anti-PD-1 antibodies for the treatment of head and neck cancer, breast cancer, Hodgkin’s lymphoma, hepatocellular carcinoma (HCC), and bladder cancer, and favorable outcomes were reported at the annual meetings of the American Society of Clinical Oncology (ASCO) and the European Society of Medical Oncology in 2016. These results suggest that antibodies against PD-1 and its ligand PD-L1 will soon be approved for the treatment of many types of cancer.

In 1995, James Allison at the University of Texas MD Anderson Cancer Center found that a different immune checkpoint molecule, cytotoxic T-lymphocyte-associated protein 4 (CTLA-4), acts as a regulator of immune cells [9]. In 1996, he demonstrated tumor regression in mice treated with antibodies that inhibit CTLA-4 function [10]. An antibody against this molecule, ipilimumab, was subsequently developed by Bristol-Myers Squibb and was approved as an anti-melanoma agent in the USA in March 2011, in Europe in July 2011 [11], and in Japan in 2015.

Clinical trials of monotherapy or combination therapy using one or multiple antibodies against PD-1, PD-L1, or CTLA-4 for the treatment of HCC are currently ongoing, reflecting the rapid progress in this field. This review outlines the basics of immune checkpoint inhibitors and the current status of clinical trials.

### Theoretical Mechanism of Antitumor Immunity

When cells become cancerous, major histocompatibility complex (MHC) molecules on antigen-presenting cells (APCs) recognize tumor-associated antigens. The APCs then migrate to lymph nodes where they present antigens to T cell receptors expressed on immature T cells. However, antigen stimulation alone is insufficient for activation of immature T cells; an additional co-stimulatory signal is required. Upon this second signal, namely, binding of CD28 on T cells to CD80/B7-1 or CD86/B7-2 on APCs, CD8 T cells become activated (priming phase) (fig. 1, 2). These activated T cells then migrate to the tumor site via the bloodstream and recognize tumor antigens presented by MHC molecules on tumor cells, triggering an attack on the tumor cells via perforin and granzymes (effector phase) (fig. 1, 2). This process is known as the cancer-immunity cycle (fig. 1) [12].

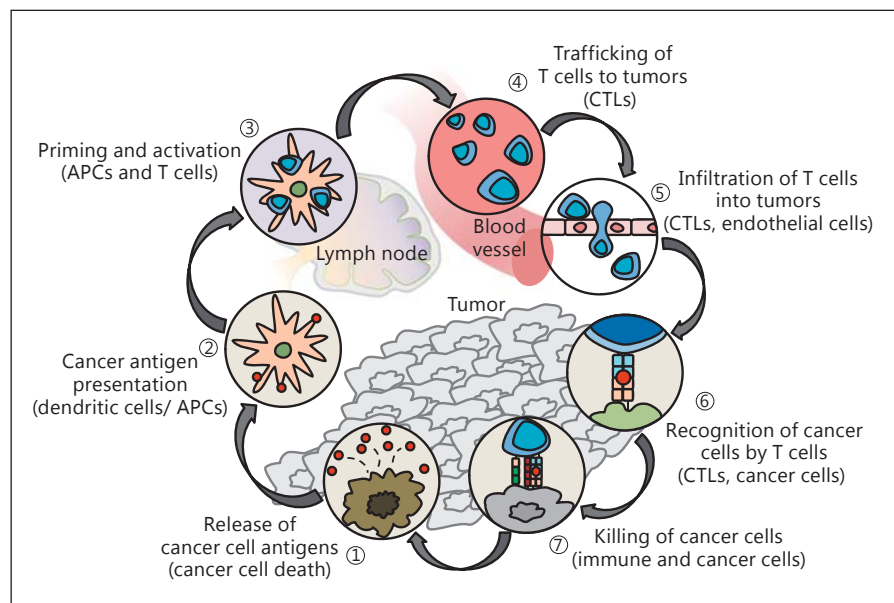
The effect of a T cell attack does not last long. To increase antitumor immunity, several conventional approaches for boosting immune responses, such as therapy with peptides, dendritic cells, cytokines, and lymphokine-activated killer cells, have been investigated. However, at the time these strategies were developed, the brake function in immunity (i.e., immune tolerance or escape) was not fully understood. Therefore, the therapeutic effect of these immune-stimulating agents remained insufficient, which led researchers to question whether these approaches were clinically applicable. In fact, since the brake and the accelerator can be stimulated simultaneously in the immune system, the effects of immune activation are limited. There are two main mechanisms for cancer immune escape: one that occurs in the lymph nodes and another at the tumor site.

### Cancer Immune Escape

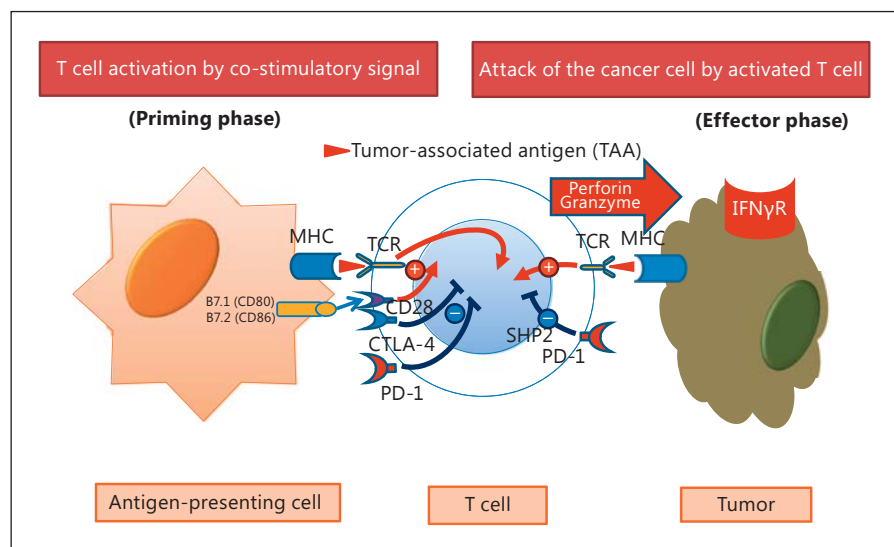
#### *The CTLA-4 Pathway*

The CTLA-4 pathway functions solely within the lymph nodes and regulates the proliferation of activated lymphocytes. CTLA-4 is expressed constitutively on reg-

**Fig. 1.** The cancer-immunity cycle. Cited from Chen and Mellman [12].



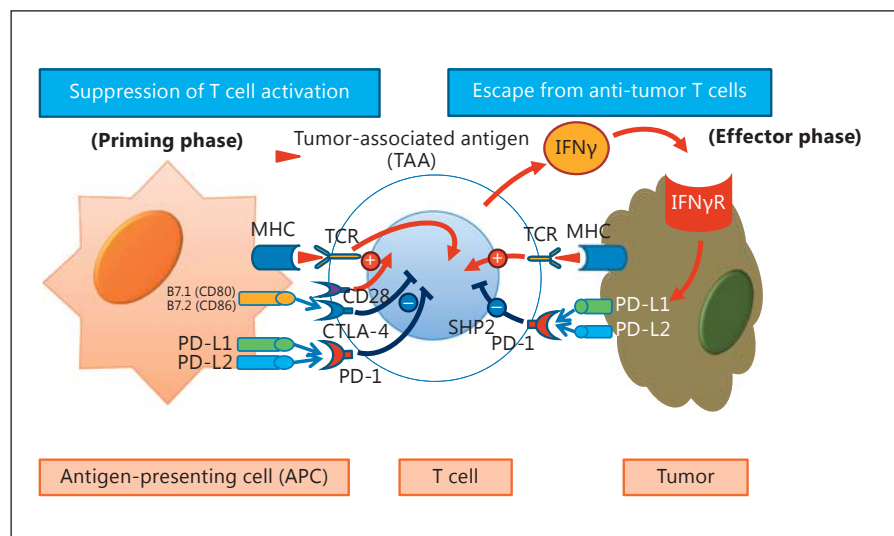
**Fig. 2.** Cancer attack by activated T cells. Presentation of tumor-associated antigen by the major histocompatibility complex (MHC) expressed by the antigen-presenting cell leads to the release of an activating signal in combination with a co-stimulatory signal via the B7-CD28 pathway, resulting in activation of T cells in the lymph node. Subsequently, in the cancer microenvironment, activated T cells attack the tumor by releasing perforin or granzymes.



ulatory T cells (Tregs) and transiently on a broad range of T cells at the early activation stage (24–48 h). B7-1 and B7-2 (the molecules mediating the second stimulatory signal mentioned above) also bind to CTLA-4, and their affinity for CTLA-4 is 10 times as strong as it is for CD28. Therefore, these ligands favor binding to CTLA-4 over binding to CD28, and activation of T cell does not occur. CTLA-4 prevents excessive T cell immune responses by halting physiologically unnecessary T cell activity. However, in anticancer immunity, this acts as a brake on the activation and proliferation of valuable activated T cells that recognize cancer antigens (fig. 3).

Therapy with an anti-CTLA-4 antibody aims to release this brake on T cell activation in the lymph nodes. The use of a CTLA-4 antibody for cancer treatment was first suggested in 1996 by Allison [10], who worked on a mouse model wherein an inhibitory antibody against CTLA-4 eliminated tumors. Given that CTLA-4 is most strongly expressed on Tregs, the mechanism of action of anti-CTLA-4 antibodies may involve inhibition of Treg activity. Two antibodies against CTLA-4, ipilimumab and tremelimumab, are currently being actively investigated in clinical trials (table 1).

**Fig. 3.** Cancer immune escape by the immune checkpoint molecules PD-1, PD-L1, and CTLA-4. Immune escape is induced in cancer via the PD-1/PD-L1 axis. T cell activation is also suppressed by the B-7/CTLA-4 axis.



**Table 1.** Immune checkpoint inhibitors

Target cell	Target molecule	Development code	Drug name	Commercial name	Antibody	Company
T lymphocyte	PD-1	BMS-36558 ONO-4538	nivolumab	Optivo	fully human IgG4 antibody	Ono/BMS
	PD-1	MK-4375	pembrolizumab	Keytruda	humanized IgG4 antibody	Merck
Tumor cell	PD-L1	MPDL3280A	atezolizumab	not approved	fully humanized IgG1 antibody	Roche
	PD-L1	MEDI4736	durvalumab	not approved	humanized IgG1 antibody	AstraZeneca
	PD-L1	MSB-0010718C	avelumab	not approved	humanized IgG1 antibody	Merck Serono
T lymphocyte	CTLA-4	BMS-734016	ipilimumab	Yervoy	fully humanized IgG1 antibody	BMS Medarex
	CTLA-4	MEDI1123	tremelimumab	not approved	fully humanized IgG2 antibody	AstraZeneca MedImmune

Ono = Ono Pharmaceutical Co., Ltd.; BMS = Bristol-Myers Squibb.

### The PD-1/PD-L1 Pathway

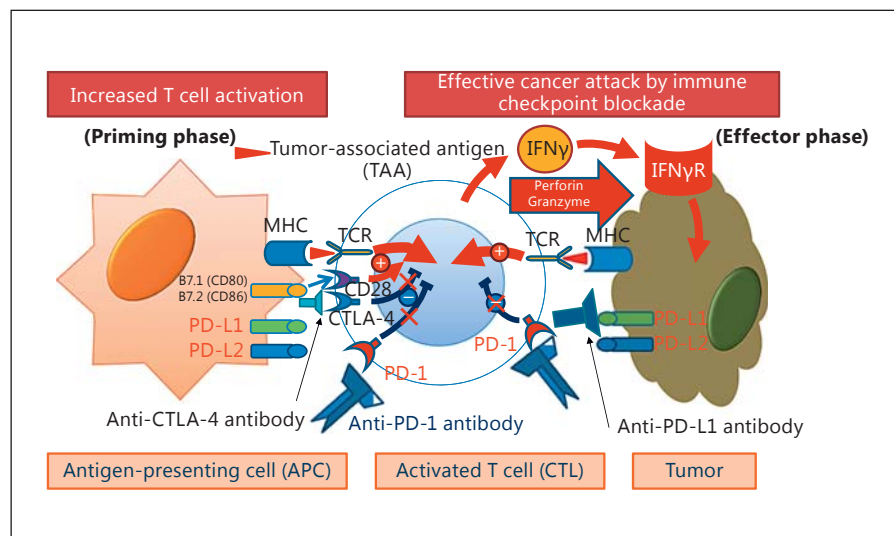
PD-1 is an immune co-inhibitory receptor expressed on T cells, B cells, NK cells, and myeloid cells. On T cells, PD-1 suppresses antigen-specific T cell activation through interactions with its ligands PD-L1 and PD-L2. PD-L1 is expressed on dendritic cells and in a broad range of tissues, including blood vessels, the myocardium, lung, and placenta, while PD-L2 expression is restricted to dendrit-

ic cells. PD-1 is rarely expressed on peripheral blood lymphocytes in normal mice and healthy humans; it is expressed selectively on T cells at the late activation stage in association with infection or an immune response (e.g., inflammation). Expression of PD-1 is particularly strong in effector T cells in peripheral tissues.

In contrast to PD-1, PD-L1 is constitutively expressed in normal peripheral tissues and on most immune cells



**Fig. 4.** Cancer attack by immune checkpoint blockade with anti-PD-1, anti-PD-L1, or anti-CTLA-4 antibody. T cell activation and effective cancer attack are restored by anti-CTLA-4, anti-PD-1, and anti-PD-L1 antibodies.



during the initiation of the immune response. The majority of cancer cells also express this molecule through the mechanism described below. Conversely, PD-L2 expression is selective and limited to APCs, suggesting its involvement in T cell activation in the lymph node. Taken together, these observations explain why antibodies against PD-1 and PD-L1 are equally effective while PD-L2 plays a limited role in anticancer immunity.

When T cell receptors on activated T cells recognize cancer antigens presented by MHC molecules on cancer cells, perforin and granzymes are released to attack the cancer cells. At the same time, interferon- $\gamma$  and other cytokines are released by the activated T cells. In response to these cytokines, cancer cells upregulate PD-L1, which binds to PD-1 on the T cells, thereby weakening the T cell attack (i.e., resulting in immune escape or immune tolerance) (fig. 3).

Administration of anti-PD-1 antibodies releases this brake mechanism and allows T cells to remain active despite the inhibitory molecules expressed by the tumor (fig. 4). In other words, unlike conventional chemotherapy and molecular targeted therapy, this approach takes advantage of the immune system's natural antitumor response and aims to amplify and prolong it [13–24]. Antibodies to PD-L1 have an effect similar to that of PD-1 antibodies. PD-L1 overexpression is a marker of tumor aggressiveness [25]. PD-L1 is also being explored as a potential biomarker to predict the efficacy of anti-PD-1 therapy. Patients with high PD-L1 expression may be more likely to respond well to anti-PD-1 therapy.

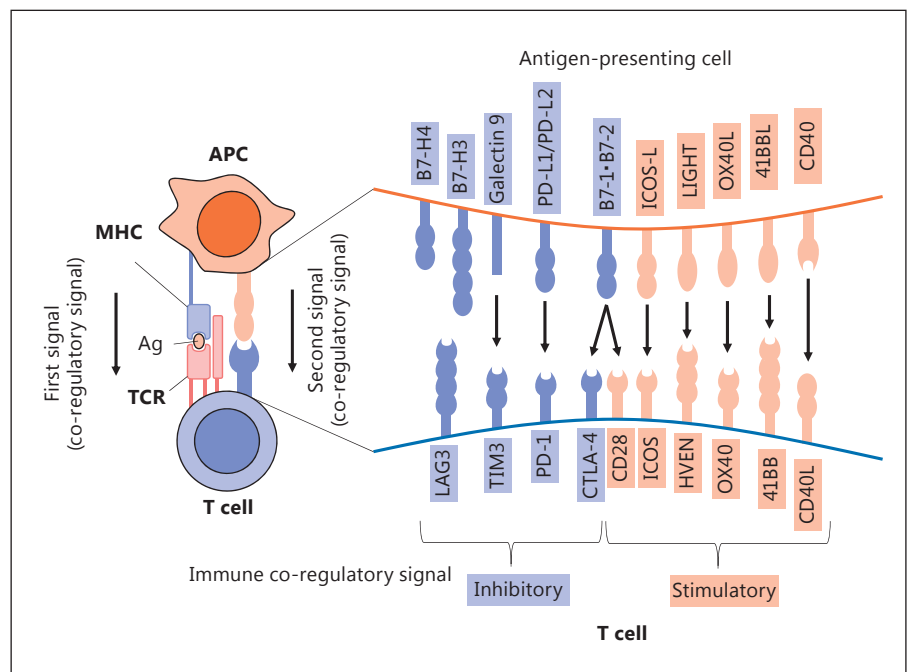
### Results from Previous Studies with Anti-PD-1 Antibodies

Approved immune checkpoint inhibitors include nivolumab and pembrolizumab (anti-PD-1 antibodies) as well as ipilimumab (an anti-CTLA-4 antibody). Other agents under development include tremelimumab (an anti-CTLA-4 antibody) and durvalumab, avelumab, and atezolizumab (anti-PD-L1 antibodies) (table 1).

A study of pembrolizumab demonstrated the marked effect of an anti-PD-1 antibody when used to treat DNA mismatch repair (MMR)-deficient colorectal cancer and other types of solid tumor [21].

Clinical trials are currently underway to evaluate immune checkpoint inhibitors for the treatment of various types of cancer, including esophageal cancer, gastric cancer, MMR-deficient colorectal cancer, head and neck cancer, breast cancer, small-cell lung cancer, Hodgkin's lymphoma, ovarian cancer, and bladder cancer.

The response rates to anti-PD-1 monotherapy are 10–30% overall, but response rates are much higher in extremely immunogenic tumors such as malignant melanoma and Hodgkin's disease. Disease control rates, which include patients with stable disease (SD), are around 70% overall, suggesting that approximately 30% of patients do not respond to anti-PD-1 antibody monotherapy. Although the causes of nonresponsiveness remain unclear, one possibility is that there may be additional molecules involved in immune escape other than PD-1, PD-L1/2, and CTLA-4. This question might be answered by the development of antibodies that block oth-



**Fig. 5.** Immune co-regulatory signals related to the immune checkpoint. There are two types of co-regulatory signals: inhibitory signals and stimulatory signals.

**Table 2.** Investigator-assessed best overall response (RECIST v1.1)

	Uninfected: sorafenib-naïve or -intolerant (n = 54)	Uninfected: sorafenib progressors (n = 58)	HCV (n = 51)	HBV (n = 51)	Total (n = 214)
Objective response	11 (20%)	11 (19%)	7 (14%)	6 (12%)	35 (16%)
Complete response	0	2 (3%)	0	0	2 (1%)
Partial response	11 (20%)	9 (16%)	7 (14%)	6 (12%)	33 (15%)
Stable disease	32 (59%)	27 (47%)	29 (57%)	23 (45%)	111 (52%)
Progressive disease	11 (20%)	18 (31%)	12 (24%)	22 (43%)	63 (29%)
Not evaluable	0	2 (3%)	3 (6%)	0	5 (2%)

CheckMate 040 Dose Expansion Cohort (n = 214). Cited from Sangro et al. [42].

er inhibitory immune checkpoint molecules such as TIM3 or LAG3, or by the development of agonists of activation signals (fig. 5).

### Combination Immunotherapy

A different approach to anticancer immunotherapy is combination therapy to simultaneously block the suppressive signals of both PD-1 and a CTLA-4. The objective of this strategy is to achieve a stronger therapeutic effect than what can be achieved with single-agent therapy. The advantages of such an approach have been

shown for the treatment of malignant melanoma [26]. The rationale of this strategy is based on the idea that if CD8-positive T cells do not exist in cancer tissues, blockade of the PD-1/PD-L1 pathway cannot be expected to be efficacious. Therefore, blocking CTLA-4 may be an effective strategy to increase the number of activated CD8-positive T cells that infiltrate the tumor tissue. Indeed, a combination trial of an anti-CTLA-4 antibody and a PD-1/PD-L1 antibody for the treatment of HCC is in the early stages (table 2). A three-arm phase I/II trial is currently investigating the combination of nivolumab (anti-PD-1) and ipilimumab (anti-CTLA-4) at varying doses and intervals. Another three-arm trial

is currently comparing the efficacy and safety of combination therapy with durvalumab (anti-PD-L1) and tremelimumab (anti-CTLA-4) with the corresponding monotherapies. The results of these trials are eagerly awaited.

A different approach is pretreatment of HCC with transcatheter arterial chemoembolization, radiofrequency ablation, or radiation to induce inflammation or thermocoagulation, thereby creating conditions that favor tumor neoantigen generation prior to the initiation of immunotherapy. This type of pretreatment is expected to be beneficial when cancer antigen recognition has not been established due to a lack of neoantigen release. An investigator-initiated clinical trial of this approach was recently initiated in stage III and IV HCC patients [27].

### **Biomarkers in Immune Checkpoint Blockade**

In 2010, Brahmer et al. [28] showed that PD-1 pathway inhibitors have a stronger therapeutic effect in patients with high levels of PD-L1 expression. The level of PD-L1 expression in tumors can vary greatly throughout the course of treatment [14, 29]. Furthermore, differences in the timing and method of specimen collection (biopsy or surgical specimens), the preparation of the specimen (paraffin-embedded or frozen), the evaluation method (immunohistochemistry, quantitative PCR, or Western blotting), and the cutoff values used also greatly influence the apparent PD-L1 expression.

Only 10–30% of patients respond to anti-PD-1/PD-L1 therapy, and even when patients with SD are included, the drug is effective in only 70% of them; the remaining 30% do not respond at all to immune checkpoint inhibitors. In practice, although disease progression is sometimes observed immediately after initiation of therapy, treatment must be continued in nonresponders because of the possibility of pseudoprogression. Some responders also require long-term administration of the therapy. Therefore, the identification of biomarkers to predict response is urgently needed, both from the perspective of the effective use of medical resources and to prevent adverse effects caused by unnecessary treatment. There are several highly promising candidate predictors of a therapeutic effect: PD-L1 expression in tumor tissue, the number of tumor-infiltrating lymphocytes, and the presence of CD8-positive T cells in the cancer microenvironment. Kupffer phase findings in Sonazoid contrast-enhanced ultrasound are another possible imaging biomarker that may predict the effect of anti-PD-1 therapy [30].

The possibility of MMR deficiency serving as a biomarker for the therapeutic effect of pembrolizumab, an anti-PD-1 antibody, was demonstrated in a clinical study examining three cohorts: 25 patients with MMR-deficient colorectal cancer, 25 patients with MMR-normal colorectal cancer, and 21 patients with MMR-deficient cancers other than colorectal cancer [21]. The response rate and disease control rate were 62 and 92%, respectively, in MMR-deficient colorectal cancer patients, and 60 and 70%, respectively, in patients with MMR-deficient noncolorectal cancer, while both rates were extremely low (0 and 16%, respectively) in MMR-normal colorectal patients.

Rapid advances in high-throughput analysis techniques should enable the identification and verification of more effective biomarkers in cancer immunotherapy. An example of such high-throughput analysis is mutanome analysis, where next-generation sequencing is globally performed in cancer genomes to search for biomarkers. Another example is immunome analysis, which employs T cell repertoire analysis, microarray analysis, and protein analysis. The results of these studies are leading to the identification of biomarkers for various cancers.

### **Adverse Events**

The toxicities associated with immune checkpoint inhibitors are milder than those of cytotoxic anticancer agents and molecular targeted agents. However, immune checkpoint inhibition can induce adverse events related to autoimmunity such as hyperthyroidism, hypothyroidism, type 1 diabetes mellitus, myasthenia gravis, rheumatoid arthritis, or Addison's disease. Many of these adverse events can be controlled by withdrawal of immune checkpoint inhibitors and initiation of steroid therapy. Immune-related adverse events are least frequent in patients treated with anti-PD-L1 antibodies and most frequent in patients treated with anti-CTLA-4 antibodies (fig. 4) [31]. Other adverse events include dry mouth, hepatitis, dermatopathy, pancreatitis, pneumonitis, adrenal insufficiency, enteritis, arthritis, and uveitis.

### **Results of Clinical Trials in HCC**

Long-awaited results from an interim analysis of a phase I/II trial of nivolumab (anti-PD-1) in patients with advanced HCC (CA209-040 trial) were presented at the 2015 ASCO meeting held in Chicago [32]. A dose escalation study showed that nivolumab was safely adminis-

**Table 3.** Overall survival rates (percentage with 95% confidence interval in parentheses<sup>1</sup>)

	Uninfected: sorafenib-naïve or -intolerant (n = 54)	Uninfected: sorafenib progressors (n = 58)	HCV (n = 51)	HBV (n = 51)	Total (n = 214)
6 months	89.8 (77.1–95.6)	75.6 (61.5–85.2)	82.1 (61.3–92.4)	83.3 (67.6–91.8)	82.5 (75.8–87.5)
9 months	79.8 (50.6–92.8)	not calculated	not calculated	not calculated	70.8 (56.6–81.1)

<sup>1</sup> Estimated using the Kaplan-Meier method. CheckMate 040 Dose Expansion Cohort (n = 214). Cited from Sangro et al. [42].

tered up to a dose of 3 ml/kg in hepatitis C virus (HCV)-infected, hepatitis B virus (HBV)-infected, and uninfected individuals, and confirmed the safety of nivolumab at 10 ml/kg in the uninfected group. At the same time, the efficacy of nivolumab in a range from 0.1 to 3 ml/kg was also reported. Among a total of 47 subjects, 33 (70%) had extrahepatic metastasis, 6 (13%) had vascular invasion, and 32 (68%) had a history of sorafenib therapy, suggesting that these patients had relatively advanced liver cancers. The report (interim analysis date: March 12, 2015) indicated that 17 patients remained on nivolumab therapy, while therapy was completed or discontinued in 30 patients because of disease progression in 26 patients, an adverse event in 2 patients (elevated bilirubin in one and an unrelated event in the other), and a complete response (CR) in 2 patients. The only CTCAE grade IV adverse event was elevation of lipase levels. Grade III increases in aspartate amino transferase levels were seen in 5 (11%) patients, and increases in alanine amino transferase levels were seen in 4 (9%) patients. Autoimmune disease and hepatic dysfunction, which were the adverse events of initial concern, were not observed.

The response rate was 19% (8 patients) and the CR rate was 5% (2 patients). The disease control rate (including SD cases) was 67% (28 patients), while progressive disease (PD) occurred in 33% of patients (14 cases). Waterfall plots revealed a tumor size reduction in all cohorts (HBV patients, HCV patients, and uninfected patients). The responders showed a notable, durable response. Two patients achieved CR at ≤3 months and remained in remission for 18 months. A sustained response was seen in all partial response (PR) and SD cases, and reversion to PD due to acquisition of resistance was not observed in any case. Taken together, these results confirmed that treatment with the anti-PD-1 antibody nivolumab produced a durable response in patients with HCC, as reported in patients with other types of cancer. This is the most unique and notable characteristic of immune checkpoint inhibitors, especially considering that 2 patients achieved

CR within 3 months and maintained this response for longer than 18 months despite the termination of nivolumab therapy several months after CR was achieved.

In most patients who achieved CR/PR, the response was evident within 3 months. In clinical cases presented at ASCO 2015, a large number of multiple HCCs disappeared after 6 weeks of therapy, and the alpha-fetoprotein level in 1 case dropped from 21,000 to 283 ng/ml. The overall survival rate at 12 months was 62%. Furthermore, a continuous reduction in tumor size (from approximately 10 to 2 cm) was observed in a patient after 48 weeks. Taken together, these outcomes are very promising, especially considering the poor tumor-related patient characteristics in this patient cohort.

In summary, monotherapy with nivolumab, an anti-PD-1 antibody, had a favorable safety profile in patients with HCC (comparable to that seen in patients with other types of cancer); it can be used safely in patients with HBV and HCV infection, and its high response rate was groundbreaking compared to the rates achievable with other types of immunotherapy. Durable responses were seen at all dose levels regardless of etiology (HBV, HCV, and uninfected cohorts).

Since then, a fixed dose of 3 mg/kg of nivolumab was planned in expansion cohorts of 50 uninfected patients with PD after sorafenib treatment failure, 50 uninfected patients who were sorafenib-naïve or -intolerant, 50 HCV-infected patients, and 50 HBV-infected patients. Outcomes of the fixed dose trial and the final results of the dose escalation study were reported at the 2016 ASCO meeting.

### Ongoing Clinical Trials

According to the outcomes reported at the 2016 ASCO meeting, 35 (16%) of the 214 patients in the dose expansion cohort achieved a response, including 2 (1%) who achieved CR and 33 (15%) who achieved PR (table 2).

**Table 4.** Baseline patient characteristics and prior treatment history

	Uninfected: sorafenib-naïve or -intolerant (n = 54)	Uninfected: sorafenib progressors (n = 58)	HCV (n = 51)	HBV (n = 51)	Total (n = 214)
Age, years	66 (20–83)	65 (19–80)	65 (53–81)	55 (22–81)	64 (19–83)
Male	46 (85%)	43 (74%)	43 (84%)	39 (77%)	171 (80%)
Race					
White	36 (67%)	35 (60%)	30 (59%)	4 (8%)	105 (49%)
Black/African American	1 (2%)	1 (2%)	2 (4%)	2 (4%)	6 (3%)
Asian	16 (30%)	22 (38%)	18 (35%)	45 (88%)	101 (47%)
Other	1 (2%)	0	1 (2%)	0	2 (1%)
Extrahepatic metastases	42 (78%)	43 (74%)	30 (59%)	46 (90%)	161 (75%)
Vascular invasion	1 (2%)	3 (5%)	5 (10%)	6 (12%)	15 (7%)
Child-Pugh score					
5	41 (76%)	38 (66%)	27 (53%)	44 (86%)	150 (70%)
6	12 (22%)	20 (34%)	21 (41%)	7 (14%)	60 (28%)
7	1 (2%)	0	2 (4%)	0	3 (1%)
9	0	0	1 (2%)	0	1 (0.5%)
Alpha-fetoprotein >200 µg/l	15 (28%)	26 (45%)	18 (35%)	27 (53%)	86 (40%)
Prior treatment type					
Surgical resection	29 (54%)	37 (64%)	19 (37%)	40 (78%)	125 (58%)
Radiotherapy	7 (13%)	17 (29%)	5 (10%)	12 (24%)	41 (19%)
Local treatment for HCC	25 (46%)	33 (57%)	29 (57%)	40 (78%)	127 (59%)
Systemic therapy	22 (41%)	57 (98%)	32 (63%)	46 (90%)	157 (73%)
Sorafenib	15 (28%)	56 (97%)	30 (59%)	40 (78%)	141 (66%)

Figures are given as mean (range) or n (%). CheckMate 040 Dose Expansion Cohort (n = 214). Cited from Sangro et al. [42].

Furthermore, 111 patients (52%) had SD and 63 (29%) had PD (table 3).

The response rates in the cohorts of uninfected patients who were sorafenib-naïve or -intolerant, uninfected patients with PD after sorafenib treatment failure, HCV-infected patients, and HBV-infected patients were 20, 19, 14, and 12%, respectively (table 3). Nine-month survival was favorable (70%) (table 4). Considering that a high proportion (66%) progressed on sorafenib treatment (table 5), these outcomes appear to be extremely good. The frequency of adverse events was also extremely low. The most concerning treatment-related adverse event was hepatic dysfunction; however, only 9 (4%) and 6 (3%) patients showed grade 3–4 increases in aspartate amino transferase and alanine amino transferase levels, respectively (table 6). These figures were comparable to those reported in nivolumab-treated patients with other types of cancer. Severe hepatic dysfunction related to nivolumab therapy in patients with viral hepatitis, which was an original concern, was not observed in any patient.

Additional analysis of the dose escalation cohort (48 patients) showed that 3 (6%) and 4 (8%) patients achieved CR and PR, respectively, while 24 (50%) and 15 (13%) had SD

and PD, respectively. The response rate was 13% in the noninfected group and 30% and 7% in the HCV- and HBV-infected groups, respectively (table 5). In this CA209-040 phase I/II trial, a dose escalation cohort (cohort 2), a cohort for randomized comparison against sorafenib (cohort 3), and a combination therapy cohort (with an anti-CTLA-4 antibody, ipilimumab) (cohort 4), in addition to the dose escalation cohort (cohort 1), were tested and registered. Furthermore, based on the tolerability and low frequency of hepatic dysfunction observed in patients with liver cirrhosis, a trial of nivolumab in patients with Child-Pugh B HCC (cohort 5) was initiated (table 2).

Following these trials, a phase III trial directly comparing nivolumab with sorafenib was initiated, as was a clinical trial investigating the efficacy of second-line pembrolizumab in patients who did not respond to sorafenib. Monotherapy with an anti-PD-1 antibody (nivolumab or pembrolizumab) or combination therapy is expected to be successful. A clinical trial examining the use of an anti-CTLA-4 antibody in HCC has also been conducted, but the results, reported in the *Journal of Hepatology* in 2013, indicated more adverse events than those caused by anti-PD-1 antibodies [33].



**Table 5.** Treatment-related adverse events (TRAEs)

	Uninfected (n = 112)		HCV (n = 51)		HBV (n = 51)		Total (n = 214)	
	any grade	grade 3–4	any grade	grade 3–4	any grade	grade 3–4	any grade	grade 3–4
Patients with any TRAE	72 (64%)	21 (19%)	37 (73%)	15 (29%)	30 (59%)	3 (6%)	139 (65%)	39 (18%)
<i>Symptomatic TRAEs reported in &gt;4% of all patients</i>								
Fatigue	31 (28%)	2 (2%)	7 (14%)	0	7 (14%)	0	45 (21%)	2 (1%)
Pruritus	11 (10%)	0	11 (22%)	0	11 (22%)	0	33 (15%)	0
Rash	12 (11%)	1 (1%)	8 (16%)	0	6 (12%)	0	26 (12%)	1 (0.5%)
Diarrhea	16 (14%)	2 (2%)	3 (6%)	0	1 (2%)	1 (2%)	20 (9%)	3 (1%)
Nausea	8 (7%)	0	6 (12%)	0	0	0	14 (7%)	0
Decreased appetite	5 (5%)	0	2 (4%)	0	3 (6%)	0	10 (5%)	0
Dry mouth	5 (4%)	0	1 (2%)	0	2 (4%)	0	8 (4%)	0
<i>Laboratory-value TRAEs reported in &gt;4% of all patients</i>								
ALT increased	6 (5%)	2 (2%)	7 (14%)	4 (8%)	2 (4%)	0	15 (7%)	6 (3%)
AST increased	7 (6%)	3 (3%)	6 (12%)	6 (12%)	0	0	13 (6%)	9 (4%)
Platelet count decreased	4 (4%)	1 (1%)	3 (6%)	2 (4%)	5 (10%)	1 (2%)	8 (4%)	3 (1%)
Anemia	2 (2%)	0	3 (6%)	1 (2%)	3 (6%)	0	8 (4%)	1 (0.5%)

CheckMate 040 dose expansion cohort (n = 214). Cited from Sangro et al. [42]. ALT = Alanine amino transferase; AST = aspartate amino transferase.

**Table 6.** Current clinical trials of immune checkpoint inhibitors for HCC

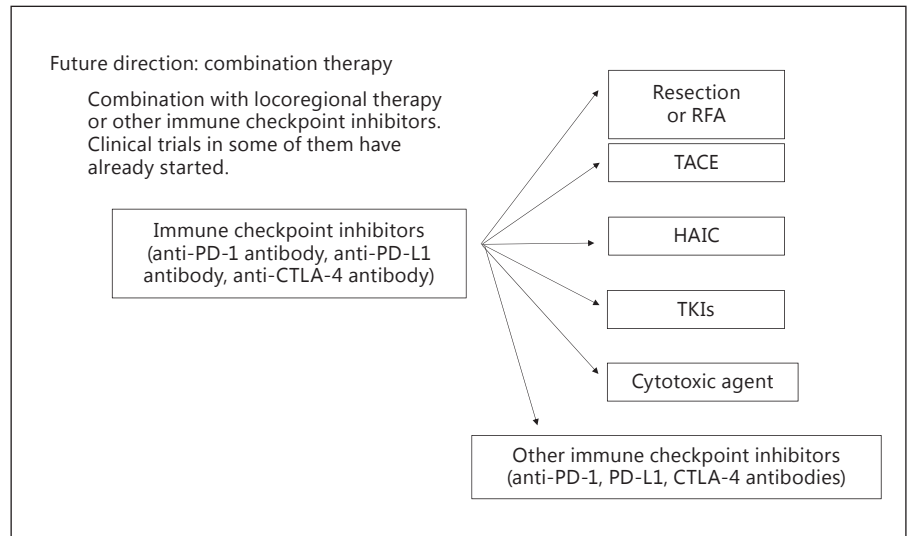
Drug	Trial name	ClinicalTrials.gov	Company	Phase	n	Line of therapy	Design	Endpoint	Status
<b>Nivolumab</b>									
Nivolumab (PD-1 Ab)	CheckMate 040	NCT01658878	BMS/ONO	I/II	42	1L/2L	cohort 1: dose escalation	DLT/MTD	completed
Nivolumab (PD-1 Ab)	CheckMate 040	NCT01658878	BMS/ONO	I/II	214	1L/2L	cohort 2: dose expansion	ORR	completed
Nivolumab (PD-1 Ab)	CheckMate 040	NCT01658878	BMS/ONO	I/II	200	1L	cohort 3: nivolumab vs. sorafenib	ORR	completed
Nivolumab (PD-1 Ab)/ ipilimumab (CTLA-4 Ab)	CheckMate 040	NCT01658878	BMS/ONO	I/II	120	2L	cohort 4: nivolumab + ipilimumab	safety/ tolerability	completed
Nivolumab (PD-1 Ab)	CheckMate 040	NCT01658878	BMS/ONO	I/II	–	1L/2L	cohort 5: nivolumab (Child B patients)	safety/ tolerability	recruiting
Nivolumab (PD-1 Ab)	CheckMate 459	NCT02576509	ONO	III	726	1L	nivolumab vs. sorafenib	TTP/OS	recruiting
<b>Pembrolizumab</b>									
Pembrolizumab (PD-1 Ab)	KEYNOTE-224	NCT02702414	MSD	II	100	2L	pembrolizumab (1 arm)	ORR	completed
Pembrolizumab (PD-1 Ab)	KEYNOTE-240	NCT02702401	MSD	III	408	2L	pembrolizumab vs. placebo	PFS/OS	recruiting
<b>Durvalumab</b>									
Durvalumab (PD-L1 Ab)/ tremelimumab (CTLA-4 Ab)	–	NCT02519348	AstraZeneca	II	144	1L/2L	durvalumab (arm A); tremelimumab (arm B); durvalumab + tremelimumab (arm C)	safety/ tolerability	recruiting

BMS = Bristol-Myers Squibb; DLT = dose-limiting toxicity; MTD = maximum tolerated dose; Ono = Ono Pharmaceutical Co., Ltd.; ORR = overall response rate; OS = overall survival; PFS = progression-free survival; TTP = time to progression.

## Future Prospects

The outcomes described above, which were reported at the 2015 and 2016 ASCO meetings, were interim analysis results of phase I/II trials of monotherapy with an anti-PD-1 antibody (nivolumab) in HCC patients. Ni-

volumab is approved for the treatment of melanoma, non-small-cell lung cancer, and kidney cancer (in the USA), and similar effects in other types of cancer are expected. HCC is an extremely heterogeneous cancer, does not have a clear driver mutation, and cannot be treated with agents that reduce hepatic functional reserve; there-



**Fig. 6.** Treatment strategy using immune checkpoint inhibitors. RFA = Radiofrequency ablation; TACE = transcatheter arterial chemoembolization.

fore, different therapeutic strategies from those used for other types of solid tumors and hematologic malignancies are needed. Based solely on the outcomes of the phase I/II trials, anti-PD-1 antibody therapy seems highly promising, and several pharmaceutical companies have started clinical trials in HCC patients. The outcomes of these studies are eagerly awaited.

There are unmet needs at various stages of HCC treatment, such as neoadjuvants and adjuvants after resection [34, 35] and ablation [36–38], combination therapy with transcatheter arterial chemoembolization [39–41], and first- and second-line treatments. Novel antibodies against PD-1 and PD-L1 may be beneficial at these stages. Their combination with other anti-angiogenic agents, locoregional therapy, another checkpoint inhibitor such as an anti-CTLA-4 antibody (ipilimumab or tremelimumab), or with a molecular targeted agent (e.g., sorafenib or lenvatinib) appears promising. Indeed, combination therapy with nivolumab and ipilimumab produces better therapeutic outcomes than the corresponding monotherapies [12].

The development of combination immunotherapy for the treatment of other types of cancer is rapidly advancing. Nivolumab became an FDA-designated breakthrough therapy in September 2014, followed by pembrolizumab. Antibodies against PD-1/PD-L1 and CTLA-4 are expected to be approved for the treatment of additional types of cancer, particularly in the setting of liver cancer, where they are expected to be implemented in the very near future.

Immune checkpoint inhibitors will play a major role in combination with other chemotherapies and locore-

gional therapies as treatment strategies against liver cancer, with high hopes for improved therapeutic outcomes (fig. 6). We are in the middle of a paradigm shift, not only for systemic therapy, but also for multimodal therapeutic strategies against liver cancer. There is no doubt that immune checkpoint inhibitors will play a key role.

## Conclusion

Anticancer therapy has progressed through the first and second stages of treatment strategies with cytotoxic agents and molecular targeted agents, respectively. We are now about to enter the third stage with immune checkpoint blockade. Immune checkpoint inhibitor-based strategies will soon become the mainstay of anticancer treatment for liver cancer, and we will continue to watch the rapid advances in the therapeutic use of immune checkpoint inhibitors with great interest.

## Disclosure Statement

The author declares no conflicts of interest regarding the publication of this paper.

## References

- Hodi FS, O'Day SJ, McDermott DF, Weber RW, Sosman JA, Haanen JB, Gonzalez R, Robert C, Schadendorf D, Hassel JC, Akerley W, van den Eertwegh AJ, Lutzky J, Lorigan P, Vaubel JM, Linette GP, Hogg D, Ottensmeier CH, Lebbe C, Peschel C, Quirt I, Clark JI, Wolchok JD, Weber JS, Tian J, Yellin MJ, Nichol GM, Hoos A, Ura WJ: Improved survival with ipilimumab in patients with metastatic melanoma. *N Engl J Med* 2010;363:711–723.
- Brahmer JR, Tykodi SS, Chow LQ, Hwu WJ, Topalian SL, Hwu P, Drake CG, Camacho LH, Kauh J, Odunsi K, Pitot HC, Hamid O, Bhatia S, Martins R, Eaton K, Chen S, Salay TM, Alaparthi S, Grosso JF, Korman AJ, Parker SM, Agrawal S, Goldberg SM, Pardoll DM, Gupta A, Wigginton JM: Safety and activity of anti-PD-L1 antibody in patients with advanced cancer. *N Engl J Med* 2012;366:2455–2465.
- Mellman I, Coukos G, Dranoff G: Cancer immunotherapy comes of age. *Nature* 2011;480:480–489.
- Kirkwood JM, Butterfield LH, Tarhini AA, Zarour H, Kalinski P, Ferrone S: Immunotherapy of cancer in 2012. *CA Cancer J Clin* 2012;62:309–335.
- Ishida Y, Agata Y, Shibahara K, Honjo T: Induced expression of PD-1, a novel member of the immunoglobulin gene superfamily, upon programmed cell death. *EMBO J* 1992;11:3887–3895.
- Freeman GJ, Long AJ, Iwai Y, Bourque K, Chernova T, Nishimura H, Fitz LJ, Malenkovich N, Okazaki T, Byrne MC, Horton HF, Fouser L, Carter L, Ling V, Bowman MR, Carreno BM, Collins M, Wood CR, Honjo T: Engagement of the PD-1 immunoinhibitory receptor by a novel B7 family member leads to negative regulation of lymphocyte activation. *J Exp Med* 2000;192:1027–1034.
- Latchman Y, Wood CR, Chernova T, Chaudhary D, Borde M, Chernova I, Iwai Y, Long AJ, Brown JA, Nunes R, Greenfield EA, Bourque K, Boussiotis VA, Carter LL, Carreno BM, Malenkovich N, Nishimura H, Okazaki T, Honjo T, Sharpe AH, Freeman GJ: PD-L2 is a second ligand for PD-1 and inhibits T cell activation. *Nat Immunol* 2001;2:261–268.
- Iwai Y, Ishida M, Tanaka Y, Okazaki T, Honjo T, Minato N: Involvement of PD-L1 on tumor cells in the escape from host immune system and tumor immunotherapy by PD-L1 blockade. *Proc Natl Acad Sci USA* 2002;99:12293–12297.
- Krummel MF, Allison JP: CD28 and CTLA-4 have opposing effects on the response of T cells to stimulation. *J Exp Med* 1995;182:459–465.
- Leach DR, Krummel MF, Allison JP: Enhancement of antitumor immunity by CTLA-4 blockade. *Science* 1996;271:1734–1736.
- Sharma P, Allison JP: The future of immune checkpoint therapy. *Science* 2015;348:56–61.
- Chen DS, Mellman I: Oncology meets immunology: the cancer-immunity cycle. *Immunity* 2013;39:1–10.
- Sznol M, Chen L: Antagonist antibodies to PD-1 and B7-H1 (PD-L1) in the treatment of advanced human cancer. *Clin Cancer Res* 2013;19:1021–1034.
- Herbst RS, Soria JC, Kowanetz M, Fine GD, Hamid O, Gordon MS, Sosman JA, McDermott DF, Powderly JD, Gettinger SN, Kohrt HE, Horn L, Lawrence DP, Rost S, Leabman M, Xiao Y, Mokatrini A, Koeppe H, Hegde PS, Mellman I, Chen DS, Hodi FS: Predictive correlates of response to the anti-PD-L1 antibody MPDL3280A in cancer patients. *Nature* 2014;515:563–567.
- Shih K, Arkenau HT, Infante JR: Clinical impact of checkpoint inhibitors as novel cancer therapies. *Drugs* 2014;74:1993–2013.
- Philips GK, Atkins M: Therapeutic uses of anti-PD-1 and anti-PD-L1 antibodies. *Int Immunol* 2015;27:39–46.
- Mahoney KM, Freeman GJ, McDermott DF: The next immune-checkpoint inhibitors: PD-1/PD-L1 blockade in melanoma. *Clin Ther* 2015;37:764–782.
- Harshman LC, Drake CG, Wargo JA, Sharma P, Bhardwaj N: Cancer immunotherapy highlights from the 2014 ASCO meeting. *Cancer Immunol Res* 2014;2:714–719.
- Topalian SL, Drake CG, Pardoll DM: Targeting the PD-1/B7-H1 (PD-L1) pathway to activate anti-tumor immunity. *Curr Opin Immunol* 2012;24:207–212.
- Merelli B, Massi D, Cattaneo L, Mandala M: Targeting the PD1/PD-L1 axis in melanoma: biological rationale, clinical challenges and opportunities. *Crit Rev Oncol Hematol* 2014;89:140–165.
- Le DT, Uram JN, Wang H, Bartlett BR, Kemberling H, Eyring AD, Skora AD, Luber BS, Azad NS, Laheru D, Biedrzycki B, Donehower RC, Zaheer A, Fisher GA, Crocenzi TS, Lee JJ, Duffy SM, Goldberg RM, de la Chapelle A, Koshiji M, Bhajee F, Huebner T, Hruban RH, Wood LD, Cuka N, Pardoll DM, Papadopoulos N, Kinzler KW, Zhou S, Cornish TC, Taube JM, Anders RA, Eshleman JR, Vogelstein B, Diaz LA Jr: PD-1 blockade in tumors with mismatch-repair deficiency. *N Engl J Med* 2015;372:2509–2520.
- Droeser RA, Hirt C, Viehl CT, Frey DM, Nebiker C, Huber X, Zlobec I, Eppenberger-Castori S, Tzankov A, Rosso R, Zuber M, Muraro MG, Amicarella F, Cremonesi E, Heberer M, Iezzi G, Lugli A, Terracciano L, Scocchia G, Oertli D, Spagnoli GC, Tornillo L: Clinical impact of programmed cell death ligand 1 expression in colorectal cancer. *Eur J Cancer* 2013;49:2233–2242.
- Ribas A: Tumor immunotherapy directed at PD-1. *N Engl J Med* 2012;366:2517–2519.
- Hamid O, Robert C, Daud A, Hodi FS, Hwu WJ, Kefford R, Wolchok JD, Hersey P, Joseph RW, Weber JS, Dronca R, Gangadhar TC, Patnaik A, Zarour H, Joshua AM, Gergich K, Ellassa-Schaap J, Algazi A, Mateus C, Boasberg P, Tume PC, Chmielowski B, Ebbinghaus SW, Li XN, Kang SP, Ribas A: Safety and tumor responses with lambrolizumab (anti-PD-1) in melanoma. *N Engl J Med* 2013;369:134–144.
- Gao Q, Wang XY, Qiu SJ, Yamato I, Sho M, Nakajima Y, Zhou J, Li BZ, Shi YH, Xiao YS, Xu Y, Fan J: Overexpression of PD-L1 significantly associates with tumor aggressiveness and postoperative recurrence in human hepatocellular carcinoma. *Clin Cancer Res* 2009;15:971–979.
- Larkin J, Chiarion-Sileni V, Gonzalez R, Grob JJ, Cowey CL, Lao CD, Schadendorf D, Dummer R, Smylie M, Rutkowski P, Ferrucci PF, Hill A, Wagstaff J, Carlino MS, Haanen JB, Maio M, Marquez-Rodas I, McArthur GA, Ascierto PA, Long GV, Callahan MK, Postow MA, Grossmann K, Sznol M, Dreno B, Bastholt L, Yang A, Rollin LM, Horak C, Hodi FS, Wolchok JD: Combined nivolumab and ipilimumab or monotherapy in untreated melanoma. *N Engl J Med* 2015;373:23–34.
- Duffy A, Makarova-Rusher OV, Pratt D, Kleiner DE, Ulahannan S, Mabry D, Fioravanti S, Walker M, Carey S, Figg WD, Steinberg SM, Anderson V, Levy E, Krishnasamy V, Wood BJ, Gretten TF: Tremelimumab: a monoclonal antibody against CTLA-4 – in combination with subtotal ablation (trans catheter arterial chemoembolization (TACE), radiofrequency ablation (RFA) or cryoablation) in patients with hepatocellular carcinoma (HCC) and biliary tract carcinoma (BTC). *J Clin Oncol* 2016;34(suppl):abstr 4073.
- Brahmer JR, Drake CG, Wollner I, Powderly JD, Picus J, Sharfman WH, Stankevich E, Pons A, Salay TM, McMiller TL, Gilson MM, Wang C, Selby M, Taube JM, Anders R, Chen L, Korman AJ, Pardoll DM, Lowy I, Topalian SL: Phase I study of single-agent anti-programmed death-1 (MDX-1106) in refractory solid tumors: safety, clinical activity, pharmacodynamics, and immunologic correlates. *J Clin Oncol* 2010;28:3167–3175.
- Taube JM, Anders RA, Young GD, Xu H, Sharma R, McMiller TL, Chen S, Klein AP, Pardoll DM, Topalian SL, Chen L: Colocalization of inflammatory response with B7-H1 expression in human melanocytic lesions supports an adaptive resistance mechanism of immune escape. *Sci Transl Med* 2012;4:127ra37.
- Tochio H, Sugahara M, Imai Y, Tei H, Suginoshita Y, Imawaki N, Sasaki I, Hamada M, Minowa K, Inokuma T, Kudo M: Hyperenhanced rim surrounding liver metastatic tumors in the postvascular phase of Sonazoid-enhanced ultrasonography: a histological indication of the presence of Kupffer cells. *Oncology* 2015;89(suppl 2):33–41.

- 31 Michot JM, Bigenwald C, Champiat S, Collins M, Carbone F, Postel-Vinay S, Berdelou A, Varga A, Bahleda R, Hollebecque A, Massard C, Fuerea A, Ribrag V, Gazzah A, Armand JP, Amellal N, Angevin E, Noel N, Boutros C, Mateus C, Robert C, Soria JC, Marabelle A, Lambotte O: Immune-related adverse events with immune checkpoint blockade: a comprehensive review. *Eur J Cancer* 2016;54:139–148.
- 32 El-Khoueiry A, Melero I, Crocenzi TS: Phase I/II safety and antitumor activity of nivolumab in patients with advanced hepatocellular carcinoma (HCC): CA209-040. *J Clin Oncol* 2015;33(suppl):abstr LBA101.
- 33 Sangro B, Gomez-Martin C, de la Mata M, Inarrairaegui M, Garralda E, Barrera P, Riezu-Boj JI, Larrea E, Alfaro C, Sarobe P, Lasarte JJ, Perez-Gracia JL, Melero I, Prieto J: A clinical trial of CTLA-4 blockade with tremelimumab in patients with hepatocellular carcinoma and chronic hepatitis C. *J Hepatol* 2013; 59:81–88.
- 34 Kudo M: Surveillance, diagnosis, treatment, and outcome of liver cancer in Japan. *Liver Cancer* 2015;4:39–50.
- 35 Poon RT, Cheung TT, Kwok PC, Lee AS, Li TW, Loke KL, Chan SL, Cheung MT, Lai TW, Cheung CC, Cheung FY, Loo CK, But YK, Hsu SJ, Yu SC, Yau T: Hong Kong consensus recommendations on the management of hepatocellular carcinoma. *Liver Cancer* 2015;4: 51–69.
- 36 Kudo M: Locoregional therapy for hepatocellular carcinoma. *Liver Cancer* 2015;4:163–164.
- 37 Kang TW: Recent advances in tumor ablation for hepatocellular carcinoma. *Liver Cancer* 2015;4:176–187.
- 38 Lencioni R, de Baere T, Martin RC, Nutting CW, Narayanan G: Image-guided ablation of malignant liver tumors: recommendations for clinical validation of novel thermal and non-thermal technologies – a Western perspective. *Liver Cancer* 2015;4:208–214.
- 39 Raoul JL, Gilibert M, Piana G: How to define transarterial chemoembolization failure or refractoriness: a European perspective. *Liver Cancer* 2014;3:119–124.
- 40 Tsurusaki M, Murakami T: Surgical and locoregional therapy of HCC: TACE. *Liver Cancer* 2015;4:165–175.
- 41 Arizumi T, Ueshima K, Minami T, Kono M, Chishina H, Takita M, Kitai S, Inoue T, Yada N, Hagiwara S, Minami Y, Sakurai T, Nishida N, Kudo M: Effectiveness of sorafenib in patients with transcatheter arterial chemoembolization (TACE) refractory and intermediate-stage hepatocellular carcinoma. *Liver Cancer* 2015;4:253–262.
- 42 Sangro B, Melero I, Yau TC, Hsu C, Kudo M, Crocenzi TS, Kim TY, Choo SP, Trojan J, Meyer T, Kang YK, Anderson J, Dela Cruz C, Lang L, Neely J, El-Khoueiry AB: Safety and antitumor activity of nivolumab (nivo) in patients (pts) with advanced hepatocellular carcinoma (HCC): interim analysis of dose-expansion cohorts from the phase 1/2 CheckMate-040 study. *J Clin Oncol* 2016; 34(suppl):abstr 4078.

# Contrast-Enhanced Tissue Harmonic Imaging versus Phase Inversion Harmonic Sonographic Imaging for the Delineation of Hepatocellular Carcinomas

Masashi Kono Yasunori Minami Mina Iwanishi Tomohiro Minami  
Hirokazu Chishina Tadaaki Arizumi Yoriaki Komeda Toshiharu Sakurai  
Masahiro Takita Norihisa Yada Hiroshi Ida Satoru Hagiwara  
Kazuomi Ueshima Naoshi Nishida Masatoshi Kudo

Department of Gastroenterology and Hepatology, Kindai University Faculty of Medicine, Osaka-Sayama, Japan

## Key Words

Contrast harmonic imaging · Contrast tissue harmonic imaging with low mechanical index · Hepatocellular carcinoma · Sonazoid

## Abstract

**Objective:** To compare contrast tissue harmonic imaging (THI) with low mechanical index (MI) and conventional contrast harmonic imaging (CHI) with respect to lesion visibility of hepatocellular carcinoma (HCC). **Methods:** One hundred and twenty-five patients (84 men and 41 women, age range 39–94 years, mean age 74 years) with 100 naïve HCCs and 30 lesions after radiofrequency ablation (RFA) for HCC were evaluated. One hundred and four patients had liver cirrhosis of Child-Pugh class A, and the remaining 21 had Child-Pugh class B cirrhosis. The lesion conspicuity and intratumoral echogenicity during the postvascular phase were compared using conventional CHI and contrast THI with low MI. **Results:** The MI values ranged from 0.20 to 0.30 on convention-

al CHI and from 0.30 to 0.35 on contrast THI. Regarding HCC lesion conspicuity, contrast THI with low MI was clearer in 79 lesions (60.8%), equal in 34 lesions (26.2%), and less clear in 17 lesions (13.1%) when compared with conventional CHI. The lesion conspicuity with contrast THI was significantly better than that with conventional CHI ( $p < 0.01$ ). All of the postablative lesions were well delineated in patients who received RFA. **Conclusion:** Low-MI contrast THI was superior to conventional CHI with respect to lesion visibility of HCCs and might offer good imaging for the guiding of RFA.

© 2016 S. Karger AG, Basel

## Introduction

Contrast harmonic sonographic imaging can depict tumor vascularity sensitively and accurately and is able to characterize liver tumors, recognize hepatocellular carcinoma (HCC) dedifferentiation, evaluate treatment efficacy, and guide ablation therapy for unresectable HCC



[1–13]. Several contrast harmonic software applications have been developed for contrast-enhanced ultrasound (CEUS) examination, although the most promising techniques are phase inversion and amplitude modulation [14, 15]. Harmonic imaging techniques, which utilize the nonlinear properties of tissue and contrast agent, can partially reduce some artifacts. Contrast harmonic imaging (CHI) exploits the nonlinear oscillations of microbubbles in contrast agents that produce harmonic overtones of the original sound wave [16, 17]. However, in patients with liver cirrhosis, it is often difficult to identify hepatic lesions on CEUS [18]. This could be due to a decrease in Kupffer cells and/or their function in patients with cirrhosis and tissue background suppression.

Tissue harmonic imaging (THI) is a form of native harmonic imaging that provides a better signal-to-noise ratio and reduced side lobe artifacts, resulting in better performance in scanning obese patients and patients with poor acoustic windows [19–22]. The contrast-to-tissue ratio in harmonic imaging is generally limited by the tissue background signal comprising both the leakage harmonic signal and the tissue harmonic signal. The technique of low-mechanical index (MI) THI using contrast media can offer a better contrast-to-tissue ratio at the cost of blood flow signals from ultrasound contrast agents. Therefore, contrast THI with low MI could offer an overlay view of conventional THI and contrast imaging. Contrast THI with low MI might be good for detail resolution, image quality, focal abnormality margin sharpness, and penetration for hepatic imaging.

The purpose of this study was to conduct a retrospective evaluation of contrast THI with low MI for imaging of cirrhotic liver tissue and HCCs compared with conventional CHI with respect to lesion visibility.

## Subjects and Methods

Approval for this retrospective study was obtained from the local ethical review board.

### Subjects

Between April 2013 and October 2014, 125 patients with 130 HCCs were enrolled in our study (table 1). A specific tumor diagnosis was made after CEUS and compared with the correct, final diagnosis based on additional imaging techniques or histology. The patient population included 84 men and 41 women (age range 39–94 years, mean  $\pm$  SD 74  $\pm$  9.1 years). One hundred and four patients had liver cirrhosis of Child-Pugh class A, and the remaining 21 had Child-Pugh class B cirrhosis. One hundred HCCs were treatment-naïve nodules, and the remaining 30 lesions had received prior therapies 1 day after radiofrequency ablation (RFA) for HCCs.

**Table 1.** Baseline clinical characteristics of the patients

Number of patients	125
Number of tumors evaluated	130
Sex	
Male	84
Female	41
Age, years	
Mean $\pm$ SD	74 $\pm$ 9.1
Range	39–94
Etiology	
HBV	10
HCV	104
NonBNonC	11
Child-Pugh class	
A	104
B	21
C	0
Tumor location	
Left lateral	28
Left medial	17
Right medial	37
Right lateral	45
Segment 1	3
Tumor size, cm	
Mean $\pm$ SD	1.6 $\pm$ 1.1
Range	0.5–6.0
Tumor depth, cm	
Mean $\pm$ SD	7.3 $\pm$ 2.6
Range	3–14

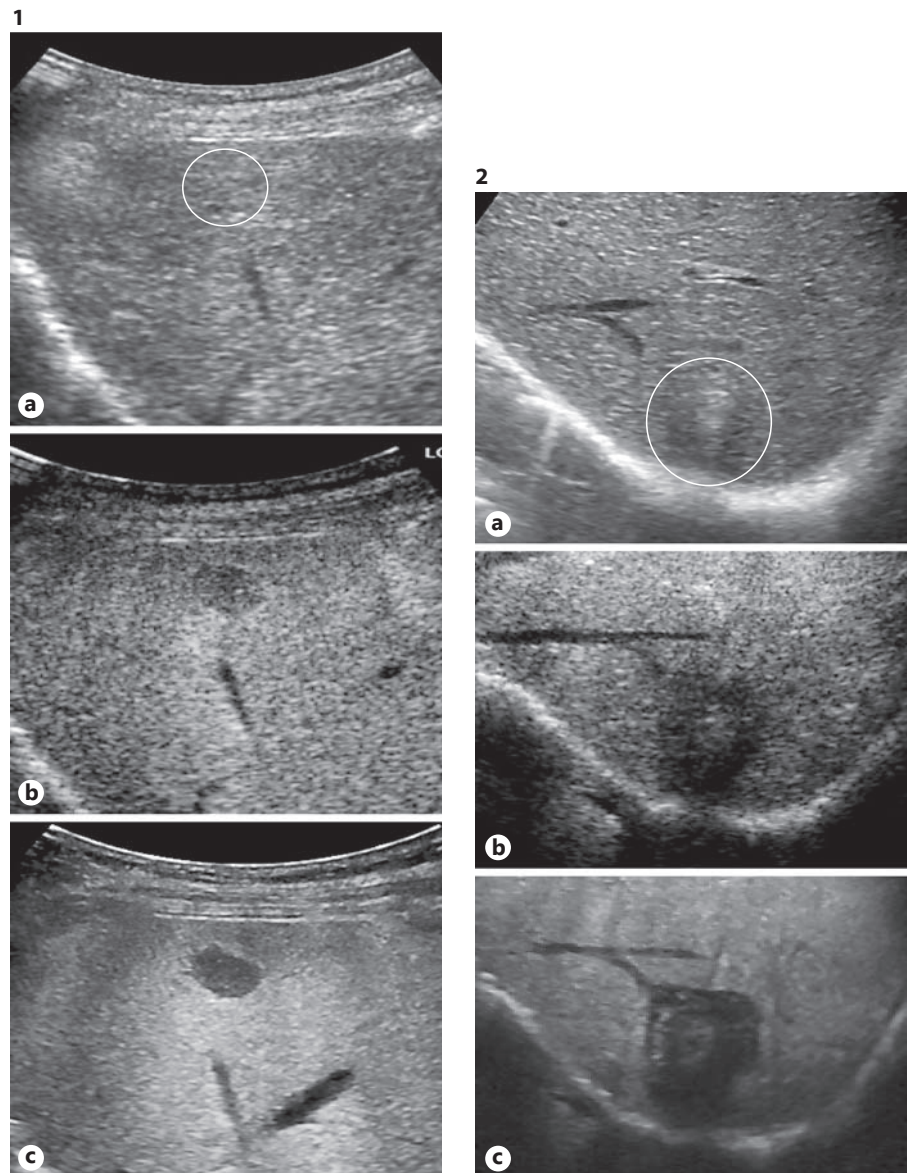
HBV = Hepatitis B virus; HCV = hepatitis C virus.

### Ultrasound Equipment and Examination

All examinations were performed using the same ultrasound unit (LOGIQ E9, GE Healthcare, Chalfont St. Giles, UK) with a 4.0-MHz convex ultrasound probe (C1–6) or a 2- to 8-MHz linear probe (9L). The convex probe was usually used to obtain images, while the linear probe was used to assess nodules on the liver surface. To provide a baseline reference for the examination, a conventional gray-scale sonography was performed first to assess the localization, size, and echogenicity of the lesion in comparison with the surrounding liver tissue.

CHI was performed with the phase inversion method using a convex probe or with the amplitude modulation method using a linear probe at a low MI, automatically defined by the software, and the focus was placed deeper than the nodule plane to avoid rapid destruction of the microbubbles. After the administration of Sonazoid (Daiichi-Sankyo, Tokyo, Japan), the hepatic arteries, the portal veins, and background liver parenchyma were gradually enhanced (vascular phase image). Approximately 10 min after the injection, the liver was scanned again to observe the postvascular image (Kupffer image). After the examination of CHI during the postvascular phase, the contrast-imaging mode was manually changed to conventional THI at a low MI ( $<0.35$ ).

The lesion conspicuity and intratumoral echogenicity during the postvascular phase were compared with conventional CHI and con-



**Fig. 1.** Small HCC in segment 8 of the liver in a 91-year-old man. **a** B-mode ultrasound showed a small isoechoic nodule with an indistinct border (circle). **b** Conventional CHI depicted a defect image of the lesion during the postvascular phase. **c** On contrast THI with low MI, the border of the defect image was more sharply demonstrated.

**Fig. 2.** Post-RFA HCC lesion in segment 2 of the liver in an 86-year-old woman. **a** B-mode ultrasound showed a hypoechoic lesion with an indistinct border (circle). **b** Conventional CHI displayed a defect image of the lesion during the postvascular phase. **c** On contrast THI, the border of the defect image was more sharply demonstrated.

trast THI with low MI. However, the detection of intratumoral vascularity on contrast THI was not assessed in this study. The lesion conspicuities using CHI and contrast THI were evaluated by subjective visual review in terms of lesion border definition, lesion contrast, etc. The lesion echogenicity was divided into hypoechoic, isoechoic, or hyperechoic regions with respect to the background liver.

#### Contrast Agent

Sonazoid consists of perfluorocarbon-containing microbubbles stabilized by a phospholipid monolayer. The bubble diameter range is approximately 2–3  $\mu\text{m}$ , and the concentration is  $10^6$  microbubbles per milliliter. This contrast agent was reconstituted with 2 ml sterile water for injection. The anticipated clinical dose for imaging of liver lesions is 0.010 ml encapsulated gas per kilogram of body weight. Each injection of contrast agent was followed immediately by a saline flush (10 ml). In patients with multiple

liver lesions, each lesion was analyzed separately with one bolus injection of contrast medium per lesion.

#### Statistical Analysis

Data were expressed as means  $\pm$  standard deviations. Differences were compared with the  $\chi^2$  test and unpaired Student's *t* test. A *p* value  $<0.05$  was considered to be significant.

#### Results

On baseline ultrasound, 45 (34.6%) of the 130 observed nodules were located in the left lobes of the livers, 82 (63.1%) were in the right lobes, and 3 (2.3%) were in

**Table 2.** Echo signals in lesions compared with B-mode, CHI, and contrast THI (n = 130)

B-mode		CHI		Contrast THI	
High	49	high	2	high	2
		iso	3	iso	4
		low	44	low	43
Iso	5	high	0	high	0
		iso	0	iso	1
		low	5	low	4
Low	76	high	0	high	0
		iso	3	iso	5
		low	73	low	71

**Table 3.** Characteristics of ultrasound technologies: CHI vs. contrast THI

	CHI	Contrast THI
MI	0.20–0.30	0.30–0.35
Spatial resolution	○	◎
Frame rate	12–16	15–25
Deep penetration	△	◎
Spatial compound	×	◎
Suppression of tissue background signal	◎	○

◎ = Excellent; ○ = good; △ = fair; × = poor.

segment 1 (table 1). The maximal diameter of the tumors ranged from 0.5 to 6.0 cm ( $1.6 \pm 1.1$  cm) on ultrasound. The distance from the skin to the deepest edge of the tumor lesions ranged from 2.0 to 14 cm ( $6.6 \pm 3.1$  cm). The MI values ranged from 0.20 to 0.30 on conventional CHI and from 0.30 to 0.35 on contrast THI.

Regarding HCC lesion conspicuity in patients with liver cirrhosis, contrast THI with low MI was clearer in 79 lesions (60.8%), equal in 34 lesions (26.2%), and less clear in 17 lesions (13.1%) when compared with conventional CHI (fig. 1). The lesion conspicuity with contrast THI was significantly better than that with conventional CHI ( $p < 0.01$ ). In patients who had received RFA, all of the postablative lesions were well delineated (fig. 2). The depths of the lesions (the distance from the surface of the skin to the far edge of the lesion) ranged from 4 to 14 cm ( $7.6 \pm 3.1$  cm) in the clear conspicuity with contrast THI

group and from 4 to 10 cm ( $5.4 \pm 2.9$  cm) in the clear conspicuity with conventional CHI group. There was a significant difference in the depths of lesions between these two groups ( $p = 0.03$ ).

The numbers of lesions that showed hyperechogenicity, isoechogenicity, and hypoechogenicity on B-mode ultrasound were 49 (37.7%), 5 (3.8%), and 76 (58.5%), respectively. On the whole, contrast THI and conventional CHI depicted hypoechogenicity better during the post-vascular phase [90.8% (118/130) vs. 93.8% (122/130),  $p = 0.49$ ] (table 2).

## Discussion

Our study investigated whether low-MI contrast THI can obtain clear images of HCC in patients with liver cirrhosis. To the best of our knowledge, this is the first report using contrast THI with low MI for HCC. By controlling the ultrasound power, the destruction of the bubbles could be easily controlled. Our results showed that low-MI contrast THI was superior to conventional CHI in delineating the lesion borders.

Some key factors could be considered in this improvement of lesion conspicuity on low-MI contrast THI (table 3). The first is the limitation of canceling the background signals. Contrast THI demonstrated not only harmonic signals from microbubbles, but also from the fibrous capsule of HCC. The second factor is deeper penetration. Contrast THI could offer deeper ultrasound penetration than conventional CHI, and thus a wide viewing image could be obtained [19, 23–25]. The third is the higher frame rate of THI needed to create a smooth moving image compared with CHI. The fourth factor is the special compound imaging. THI has a special compound imaging mode that uses electronic beam steering of a transducer array to rapidly acquire several overlapping scans of an object from different view angles. Real-time spatial compound imaging can provide improved contrast resolution and tissue differentiation by reducing speckle, clutter, and other acoustic artifacts [26, 27].

Now that we understand the differences between conventional CHI and contrast THI, we can select the most appropriate imaging application for different purposes. Low-MI contrast THI was able to clearly depict the lesion borders in some HCC patients. Thus, contrast THI has the potential to provide better sonographic images for the guidance of RFA because of easy targeting of HCC nodules. When the signals of vascularity should be focused upon for the differential diagnosis of liver tumors, con-



ventional CHI may be more useful. Even though vascular images were not evaluated with contrast THI in this study, the blood flow images could be created by enhancing the signals of microbubble resonance while canceling background echo signals effectively. In THI with contrast agents, intratumoral intensity might be influenced by background intratumoral echo signals.

The principal limitation of this study was its retrospective design. The second was that this study could suffer from selection bias and/or information bias because the HCC patients enrolled received CEUS examinations according to tumor size and/or number. Another limitation is the preliminary nature of this study with a relatively

small number of patients. Further prospective studies of this technique with larger numbers of patients are warranted.

In conclusion, low-MI contrast THI was superior to conventional CHI in the delineation of liver lesions and might have the potential to provide better sonographic images for RFA guidance and early response assessment of RFA.

## Disclosure Statement

The authors have no conflict of interest to declare.

## References

- Ding H, Kudo M, Onda H, Suetomi Y, Minami Y, Maekawa K: Hepatocellular carcinoma: depiction of tumor parenchymal flow with intermittent harmonic power Doppler US during the early arterial phase in dual-display mode. *Radiology* 2001;220:349–356.
- Hatanaka K, Kudo M, Minami Y, Maekawa K: Sonazoid-enhanced ultrasonography for diagnosis of hepatic malignancies: comparison with contrast-enhanced CT. *Oncology* 2008;75(suppl 1):42–47.
- Minami Y, Kudo M, Kawasaki T, Chung H, Ogawa C, Shiozaki H: Treatment of hepatocellular carcinoma with percutaneous radiofrequency ablation: usefulness of contrast harmonic sonography for lesions poorly defined with B-mode sonography. *AJR Am J Roentgenol* 2004;183:153–156.
- Kudo M, Hatanaka K, Maekawa K: Newly developed novel ultrasound technique, defect reperfusion ultrasound imaging, using Sonazoid in the management of hepatocellular carcinoma. *Oncology* 2010;78(suppl 1):40–45.
- Xia Y, Kudo M, Minami Y, Hatanaka K, Ueshima K, Chung H, Hagiwara S, Inoue T, Ishikawa E, Kitai S, Takahashi S, Tatsumi C, Ueda T, Hayaishi S, Maekawa K: Response evaluation of transcatheter arterial chemoembolization in hepatocellular carcinomas: the usefulness of Sonazoid-enhanced harmonic sonography. *Oncology* 2008;75(suppl 1):99–105.
- Minami Y, Kudo M, Chung H, Kawasaki T, Yagyu Y, Shimono T, Shiozaki H: Contrast harmonic sonography-guided radiofrequency ablation therapy versus B-mode sonography in hepatocellular carcinoma: prospective randomized controlled trial. *AJR Am J Roentgenol* 2007;188:489–494.
- Minami Y, Kudo M, Hatanaka K, Kitai S, Inoue T, Hagiwara S, Chung H, Ueshima K: Radiofrequency ablation guided by contrast harmonic sonography using perfluorocarbon microbubbles (Sonazoid) for hepatic malignancies: an initial experience. *Liver Int* 2010;30:759–764.
- Kudo M, Matsui O, Izumi N, Iijima H, Kadoya M, Imai Y, Okusaka T, Miyayama S, Tsuchiya K, Ueshima K, Hiraoka A, Ikeda M, Ogawara S, Yamashita T, Minami T, Yamakado K; Liver Cancer Study Group of Japan: JSH Consensus-Based Clinical Practice Guidelines for the Management of Hepatocellular Carcinoma: 2014 Update by the Liver Cancer Study Group of Japan. *Liver Cancer* 2014;3:458–468.
- Kudo M: Surveillance, diagnosis, treatment, and outcome of liver cancer in Japan. *Liver Cancer* 2015;4:39–50.
- Kudo M: Clinical practice guidelines for hepatocellular carcinoma differ between Japan, United States, and Europe. *Liver Cancer* 2015;4:85–95.
- Minami Y, Kudo M: Imaging modalities for assessment of treatment response to nonsurgical hepatocellular carcinoma therapy: contrast-enhanced US, CT, and MRI. *Liver Cancer* 2015;4:106–114.
- Chen BB, Murakami T, Shih TT, Sakamoto M, Matsui O, Choi BI, Kim MJ, Lee JM, Yang RJ, Zeng MS, Chen RC, Liang JD: Novel imaging diagnosis for hepatocellular carcinoma: consensus from the 5th Asia-Pacific Primary Liver Cancer Expert Meeting (APPLE 2014). *Liver Cancer* 2015;4:215–227.
- Liu GJ, Wang W, Lu MD, Xie XY, Xu HX, Xu ZF, Chen LD, Wang Z, Liang JY, Huang Y, Li W, Liu JY: Contrast-enhanced ultrasound for the characterization of hepatocellular carcinoma and intrahepatic cholangiocarcinoma. *Liver Cancer* 2015;4:241–252.
- Eckersley RJ, Chin CT, Burns PN: Optimising phase and amplitude modulation schemes for imaging microbubble contrast agents at low acoustic power. *Ultrasound Med Biol* 2005;31:213–219.
- Harvey CJ, Blomley MJ, Eckersley RJ, Heckemann RA, Butler-Barnes J, Cosgrove DO: Pulse-inversion mode imaging of liver specific microbubbles: improved detection of sub-centimetre metastases. *Lancet* 2000;355:807–808.
- Burns PN, Wilson SR, Simpson DH: Pulse inversion imaging of liver blood flow: improved method for characterizing focal masses with microbubble contrast. *Invest Radiol* 2000;35:58–71.
- Strobel D, Raeker S, Martus P, Hahn EG, Becker D: Phase inversion harmonic imaging versus contrast-enhanced power Doppler sonography for the characterization of focal liver lesions. *Int J Colorectal Dis* 2003;18:63–72.
- Bolondi L, Gaiani S, Celli N, Golfieri R, Grigioni WF, Leoni S, Venturi AM, Piscaglia F: Characterization of small nodules in cirrhosis by assessment of vascularity: the problem of hypovascular hepatocellular carcinoma. *Hepatology* 2005;42:27–34.
- Chiou SY, Forsberg F, Fox TB, Needleman L: Comparing differential tissue harmonic imaging with tissue harmonic and fundamental gray scale imaging of the liver. *J Ultrasound Med* 2007;26:1557–1563.
- Shapiro RS, Wagreich J, Parsons RB, Stanca-to-Pasik A, Yeh HC, Lao R: Tissue harmonic imaging sonography: evaluation of image quality compared with conventional sonography. *AJR Am J Roentgenol* 1998;171:1203–1206.

- 21 Rosenthal SJ, Jones PH, Wetzel LH: Phase inversion tissue harmonic sonographic imaging: a clinical utility study. *AJR Am J Roentgenol* 2001;176:1393–1398.
- 22 Sodhi KS, Sidhu R, Gulati M, Saxena A, Suri S, Chawla Y: Role of tissue harmonic imaging in focal hepatic lesions: comparison with conventional sonography. *J Gastroenterol Hepatol* 2005;20:1488–1493.
- 23 Lencioni R, Cioni D, Bartolozzi C: Tissue harmonic and contrast-specific imaging: back to gray scale in ultrasound. *Eur Radiol* 2002;12: 151–165.
- 24 Anvari A, Forsberg F, Samir AE: A primer on the physical principles of tissue harmonic imaging. *Radiographics* 2015;35:1955–1964.
- 25 Choudhry S, Gorman B, Charboneau JW, Tradup DJ, Beck RJ, Kofler JM, Groth DS: Comparison of tissue harmonic imaging with conventional US in abdominal disease. *Radiographics* 2000;20:1127–1135.
- 26 Oktar SO, Yucel C, Ozdemir H, Uluturk A, Isik S: Comparison of conventional sonography, real-time compound sonography, tissue harmonic sonography, and tissue harmonic compound sonography of abdominal and pelvic lesions. *AJR Am J Roentgenol* 2003; 181:1341–1347.
- 27 Cha JH, Moon WK, Cho N, Chung SY, Park SH, Park JM, Han BK, Choe YH, Cho G, Im JG: Differentiation of benign from malignant solid breast masses: conventional US versus spatial compound imaging. *Radiology* 2005; 237:841–846.



# Malignant Transformation of Hepatocellular Adenoma

Wing Yee Kwok<sup>a</sup> Satoru Hagiwara<sup>a</sup> Naoshi Nishida<sup>a</sup> Tomohiro Watanabe<sup>a</sup>  
Toshiharu Sakurai<sup>a</sup> Hiroshi Ida<sup>a</sup> Yasunori Minami<sup>a</sup> Masahiro Takita<sup>a</sup> Tomohiro Minami<sup>a</sup>  
Mina Iwanishi<sup>a</sup> Hirokazu Chishina<sup>a</sup> Masashi Kono<sup>a</sup> Kazuomi Ueshima<sup>a</sup> Yoriaki Komeda<sup>a</sup>  
Tadaaki Arizumi<sup>a</sup> Eisuke Enoki<sup>b</sup> Takuya Nakai<sup>c</sup> Tsutomu Kumabe<sup>d</sup> Osamu Nakashima<sup>e</sup>  
Fukuo Kondo<sup>f</sup> Masatoshi Kudo<sup>a</sup>

Departments of <sup>a</sup>Gastroenterology and Hepatology, <sup>b</sup>Pathology, and <sup>c</sup>Surgery, Kindai University Faculty of Medicine, Osaka-Sayama, <sup>d</sup>Kumabe Clinic, Kikuchi, <sup>e</sup>Department of Clinical Laboratory Medicine, Kurume University Hospital, Kurume, and <sup>f</sup>Department of Pathology, Teikyo University Hospital, Tokyo, Japan

## Key Words

Hepatocellular adenoma · Malignant transformation · Gadoteric acid-enhanced magnetic resonance imaging

## Abstract

The patient was a 20-year-old male in whom a hepatic hypervascular mass accompanied by intratumoral hemorrhage was detected on examination for epigastric pain. Based on the enlargement of the mass and diagnostic imaging, hepatocellular adenoma (HCA) was suspected and hepatectomy was performed. The lesion was diagnosed as malignant transformation of  $\beta$ -catenin-activated HCA. There are only few reports of cases with malignant transformation of HCA in Japan; it is necessary to accumulate cases to investigate it.

© 2016 S. Karger AG, Basel

## Introduction

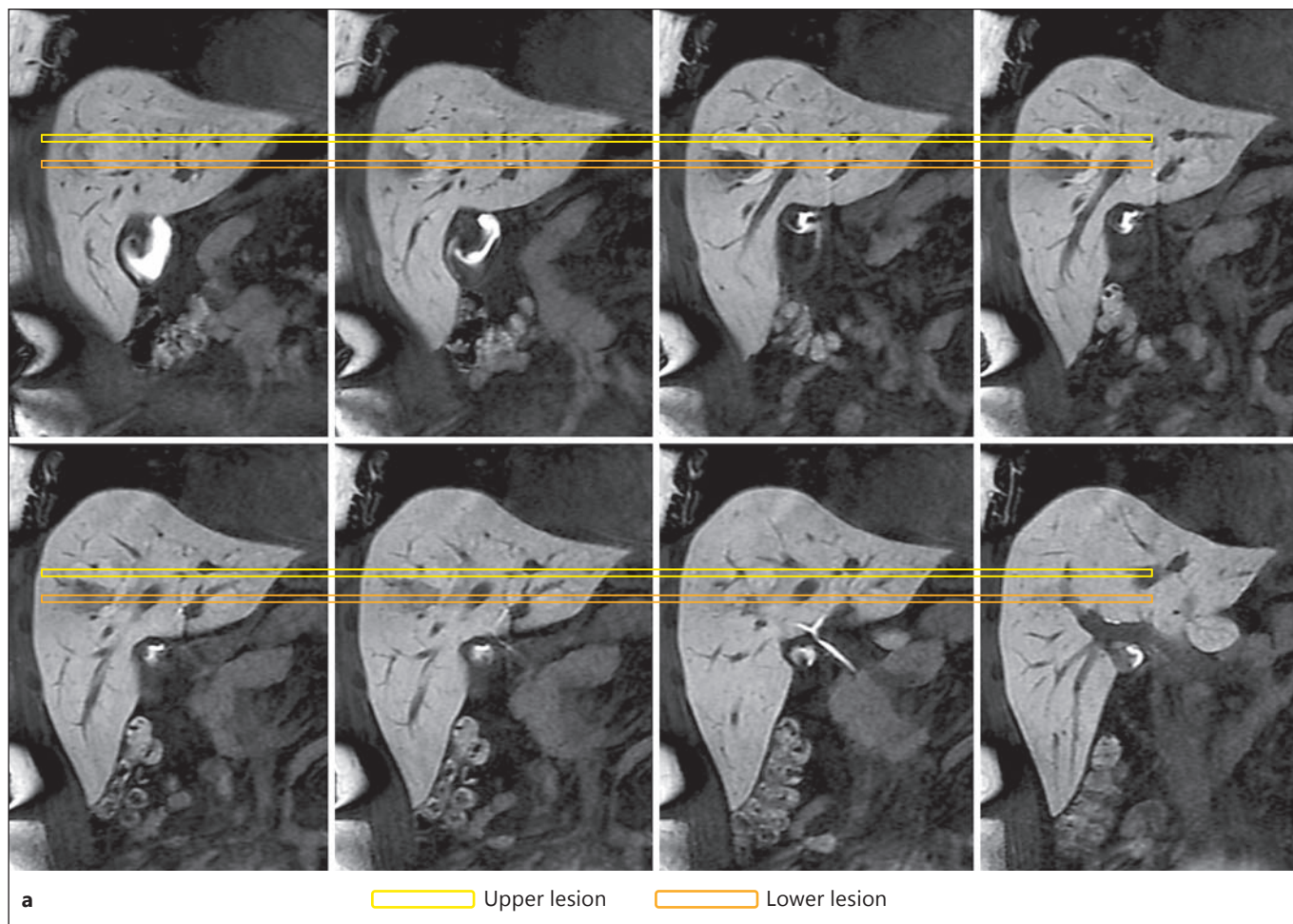
Reportedly, the incidence of hepatocellular adenoma (HCA) in Western countries is 3–4 in 100,000 people, and there are many reports in the literature regarding HCA [1–3]. In contrast, HCA is a very rare disease in Asia, par-

ticularly in Japan. The risks of hemorrhage and malignant transformation have been well reported from Western countries, but cases of malignant transformation of HCA have not been reported in Japan so far [4, 5]. HCA presents as a hypervascular nodule and is thus sometimes difficult to differentiate from hepatocellular carcinoma (HCC) [6]. Herein we report the case of HCA with malignant transformation in a young male whose pathological study gives us a deep insight into this disease.

## Case Presentation

The 20-year-old male patient was referred to our hospital for the purpose of examination and treatment of a hepatic mass. The patient and family members did not show any medical history of disease. He did not report habitual alcohol drinking or cigarette smoking.

Epigastric pain suddenly developed on May 26, 2012. The patient visited a clinic where a hepatic tumor was detected in segment 8 (S8). Percutaneous biopsy of the mass was performed and revealed no malignant finding. However, an increased level of serum des-gamma-carboxy prothrombin (DCP) (103 mAU/ml) was observed; the patient visited the Gastroenterological Surgery Department of our hospital on August 9, 2012. A benign mass was suspected based on gadoteric acid-enhanced magnetic resonance im-



**Fig. 1. a** A mass containing various components was present in S8. **b** The upper lesion of the mass was intensely stained in the early phase on Gd-EOB-MRI and slightly washed out in the delayed phase, and regions with reduced and increased EOB uptakes were

mixed in the hepatobiliary phase. **c** An avascular area assumed to be a hematoma was present in the center of the mass in the lower lesion.

(For Figure 1b and c see next page.)

aging (Gd-EOB-MRI), and regular follow-up of its course was started. Since the mass enlarged, the patient was referred to the Department of Gastroenterology on August 28, 2014. His height was 180 cm, body weight 113.7 kg, and BMI 35.1, with no abdominal finding or hepatosplenomegaly.

#### Blood Chemical Tests

The results of initial blood chemical tests on arrival to the Department of Surgery are shown in table 1; slight increases in WBC and CRP were noted. All HBV and HCV virus markers were negative. Elevation of the serum DCP level to 123 mAU/ml was observed.

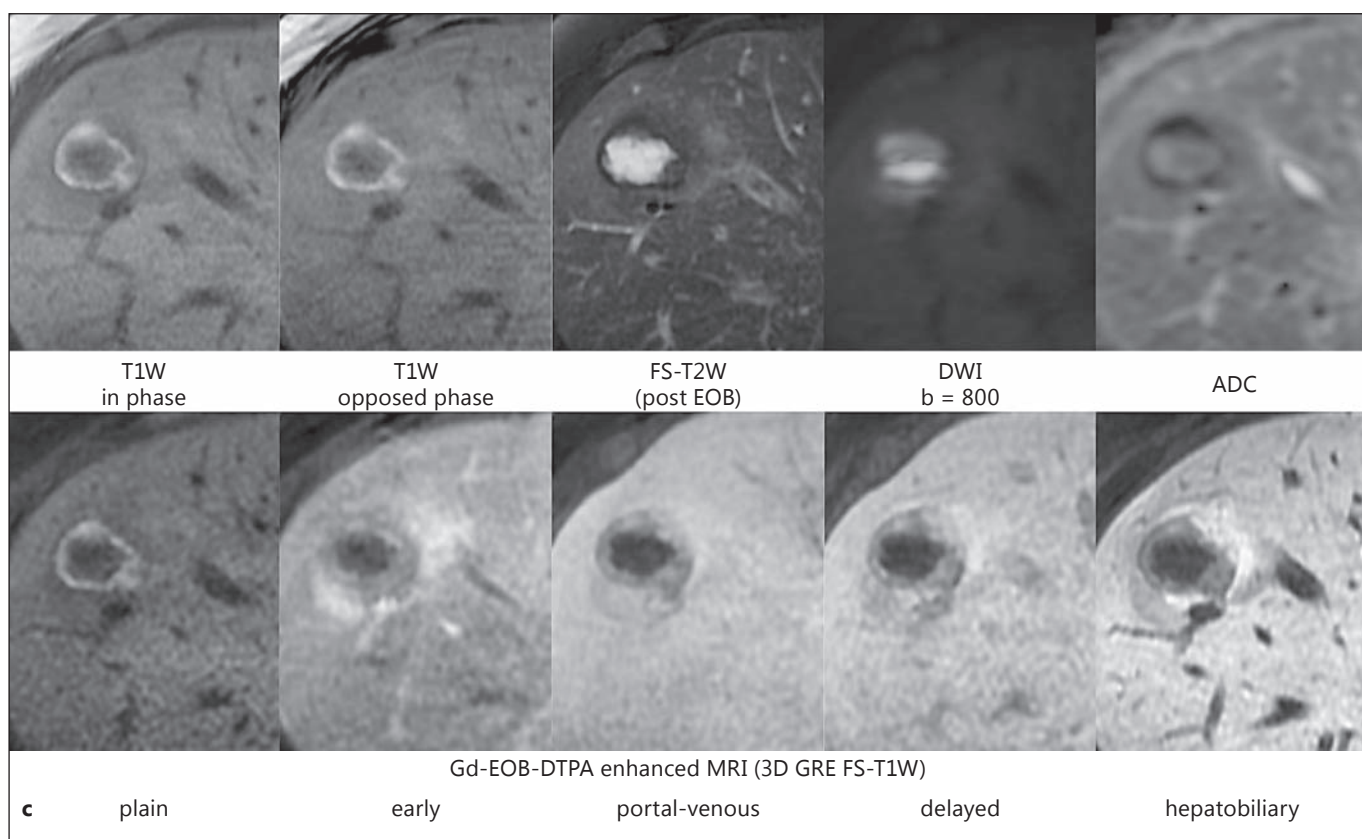
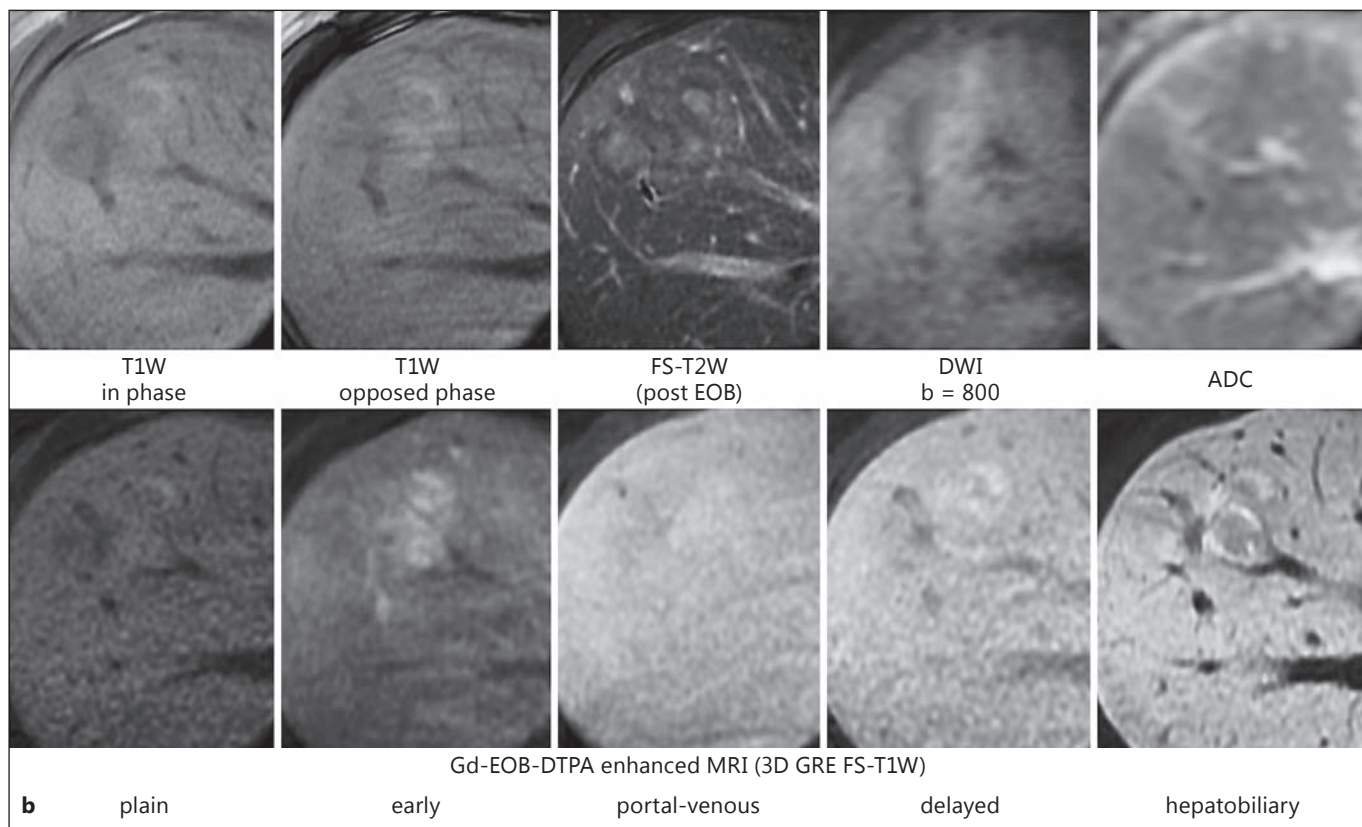
#### Gd-EOB-MRI Findings

On arrival to the Department of Surgery in August 2012, a mass containing various components was present in S8 (fig. 1a). The upper lesion of the mass was intensely stained in the early phase on

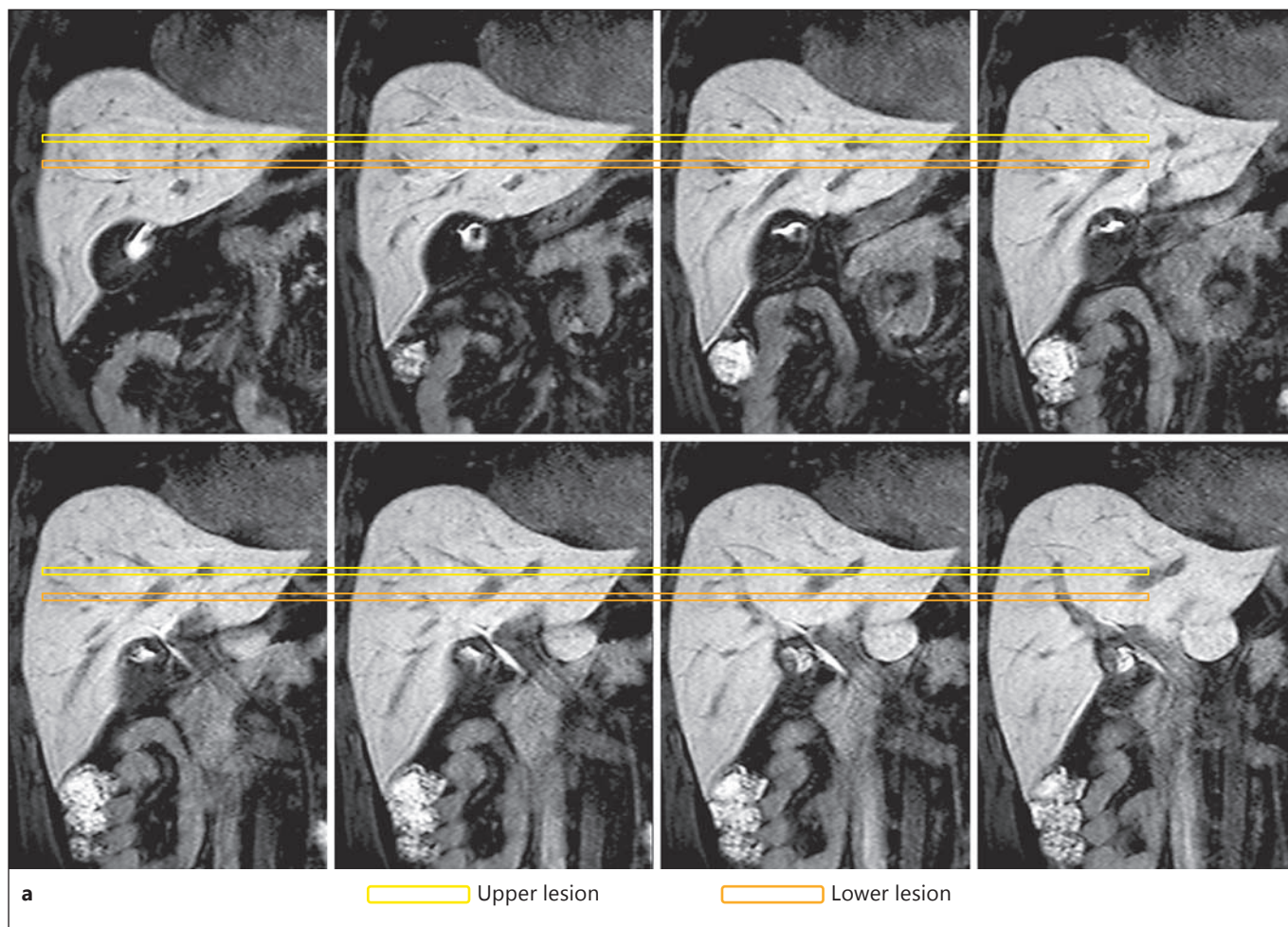
**Table 1.** Blood test findings on arrival to the Department of Surgery

<b>Hematology</b>		<b>Biochemistry</b>	
WBC	10,400 $\mu$ l	CRP	0.315 mg/dl
RBC	$5.42 \times 10^4/\mu$ l	BUN	10 ng/dl
Hb	15.8 g/dl	Cr	0.74 mg/dl
Ht	46.6%	FBS	81 mg/dl
PLT	$41.5 \times 10^4/\mu$ l	HbA1c	5.8%
<b>Coagulation</b>		ALB	4.4 g/dl
PT	108.1%	T-bil	0.4 mg/dl
INR	0.97 index	ALT	31 IU/l
APTT	25.2 s	ALP	247 IU/l
<b>Virus marker</b>		TC	176 mg/dl
HBsAg	(-)	Trig	491 mg/dl
HBcAb	(-)	<b>Tumor marker</b>	
HBsAb	(-)	AFP	2 ng/ml
HCVAb	(-)	DCP	123 mAU/ml

AFP = Alpha-fetoprotein; PLT = platelets; PT = prothrombin time; RBC = red blood cells; WBC = white blood cells.







**Fig. 2. a** Compared with the EOB-MRI findings from August 2012, the mass had apparently enlarged. **b** The upper lesion of the mass was intensely stained in the early phase on Gd-EOB-MRI and slightly washed out in the delayed phase, and regions with reduced and increased EOB uptakes were mixed in the hepatobiliary phase.

**c** On the other hand, in the lower lesion, the margin of the mass was intensely stained in the early phase and slightly washed out in the delayed phase. The hematoma in the center of the mass pointed out on the previous MRI had been absorbed and replaced by a mass with an increased EOB uptake in the hepatobiliary phase.

(For Figure 2b and c see next page.)

Gd-EOB-MRI and slightly washed out in the delayed phase. The image in the hepatobiliary phase revealed mixed regions in terms of reduced and increased EOB uptakes (fig. 1b). In contrast, in the lower lesion, an avascular area assumed to be a hematoma was present in the center of the mass (fig. 1c).

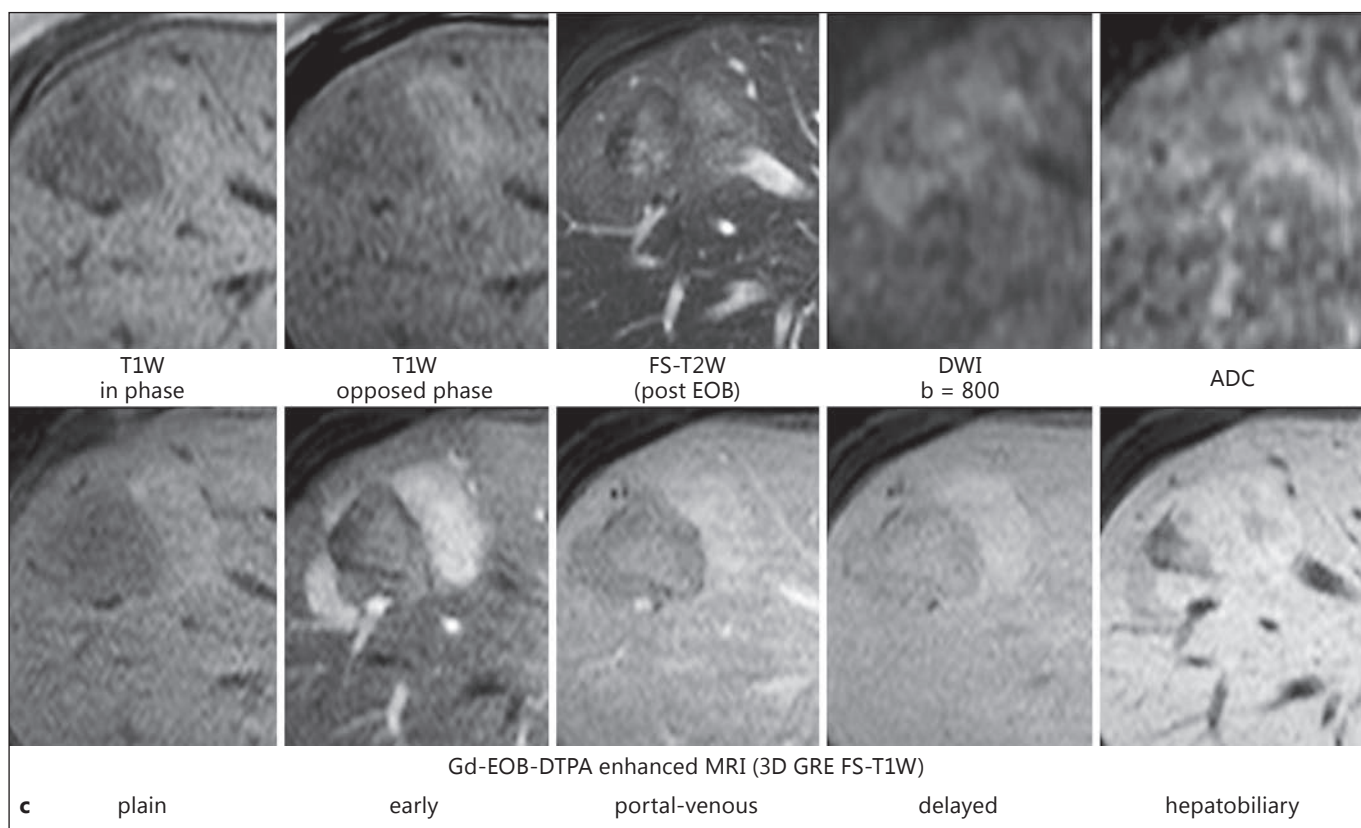
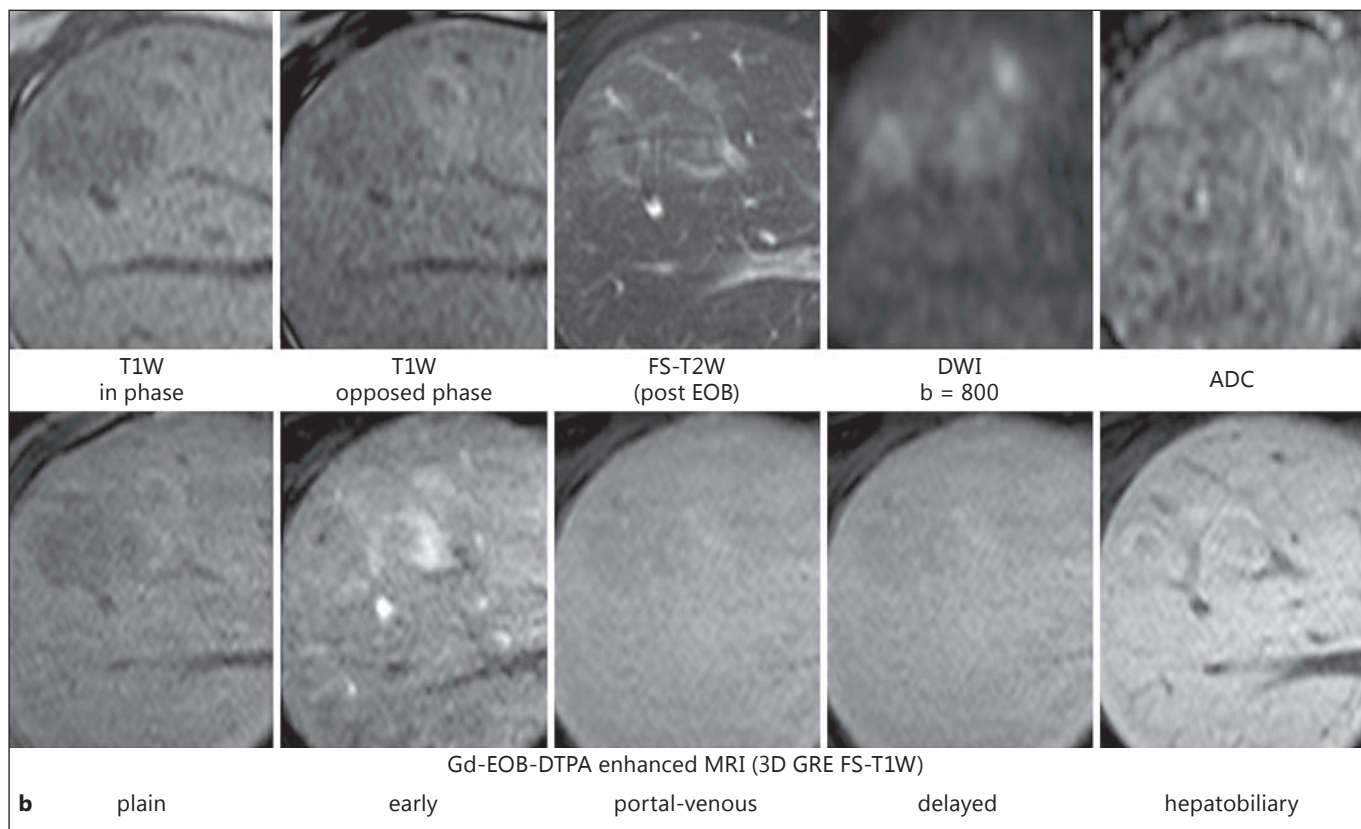
In August 2013, about 1 year after the previous Gd-EOB-MRI, the mass had apparently enlarged (fig. 2a) compared with August 2012. The upper lesion of the mass was intensely stained in the early phase on Gd-EOB-MRI and slightly washed out in the delayed phase. Heterogeneous regions for uptake of EOB were confirmed in the hepatobiliary phase (fig. 2b). In the lower lesion, the margin of the mass was intensely stained in the early phase and slightly washed out in the delayed phase. The hematoma previously observed in the center of the mass had been absorbed and replaced by a mass with an increased EOB uptake in the hepatobiliary phase (fig. 2c).

#### Abdominal Contrast Computed Tomography

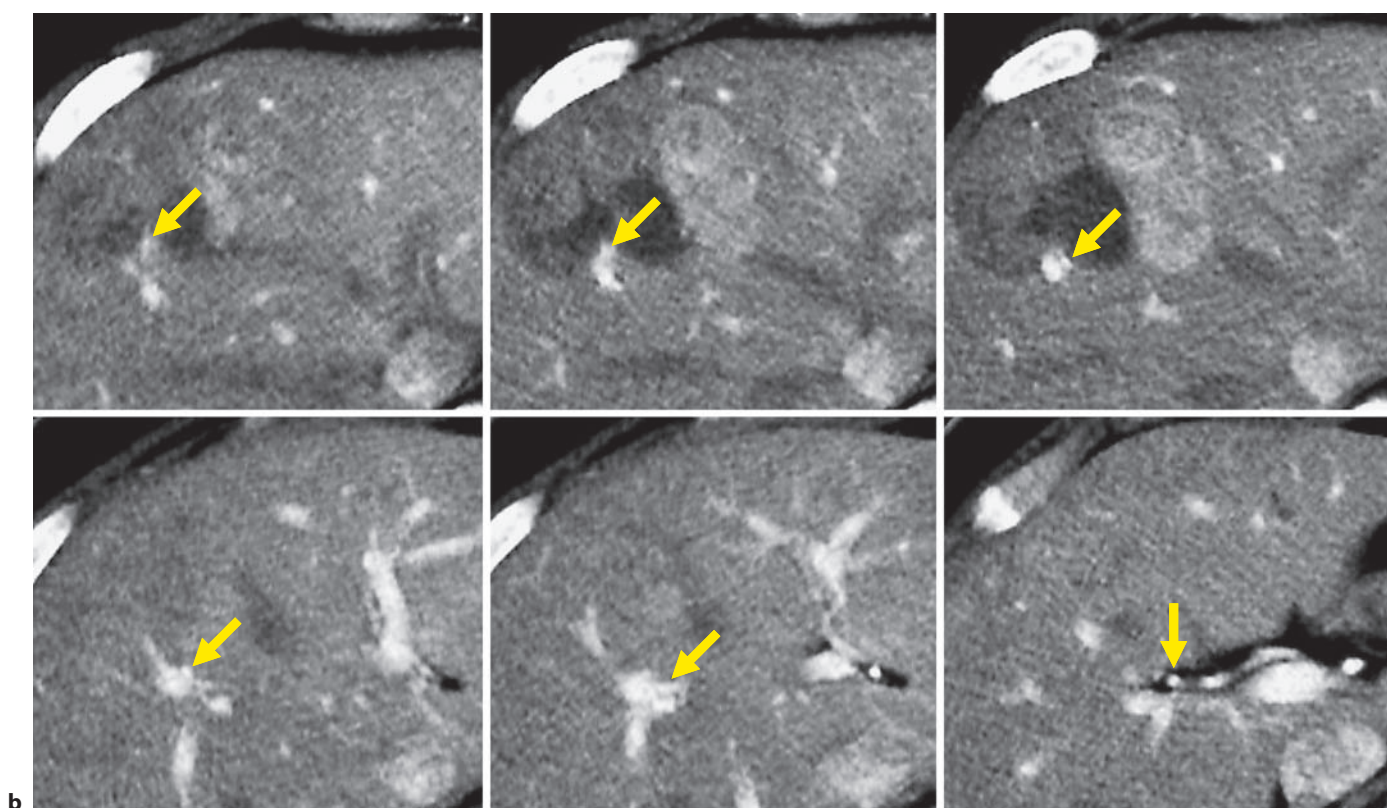
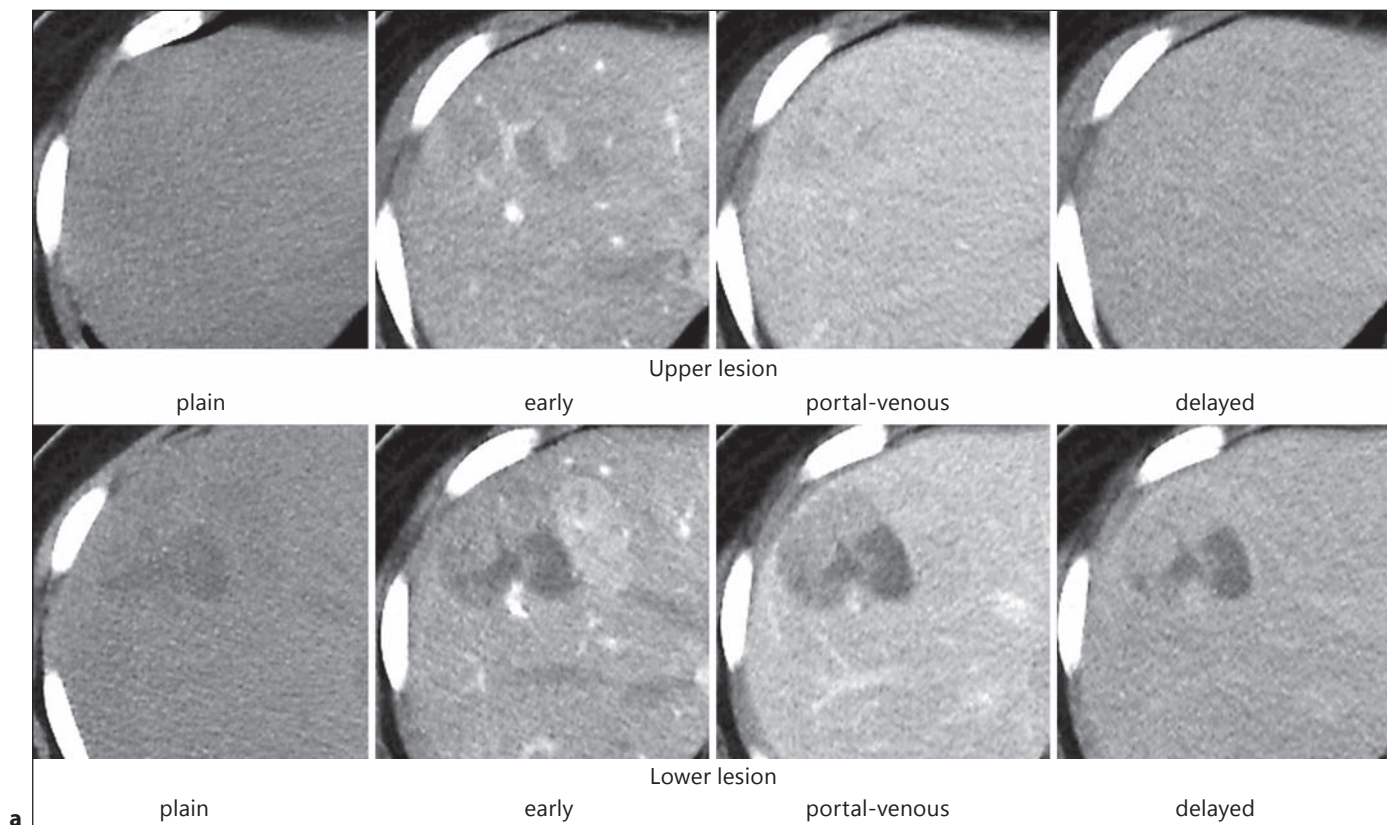
When the patient was referred to the Department of Gastroenterology in August 2014, heterogeneous regions for vascularity, showing abundant and scarce blood flows, was observed in both the upper and lower lesions of the mass (fig. 3a). The portal vein was also observed to penetrate the mass (fig. 3b).

#### Abdominal Contrast-Enhanced Ultrasound

When the patient was referred to the Department of Gastroenterology in August 2014, the mass was entirely stained in the early vascular phase, and a heterogeneously attenuated image of the entire mass was observed in the postvascular phase. In addition, the hepatic vein was the route of blood discharge from the mass (figure not shown).







(For legend see next page.)

### Treatment Course

Since the tumor was enlarged, the serum DCP level was high, and primary HCC or malignant transformation of HCA was strongly suspected on diagnostic imaging, two segments in the central liver were resected at the Department of Surgery.

### Resected Specimen and Schematic Diagram

On macroscopic observation and H&E staining of the resected specimen, HCC regions were scattered in the HCA tissue. In addition, hemorrhage and necrosis were noted within the tumor (fig. 4a). These are presented in the schematic diagram (fig. 4b). This nodular lesion consisted of three kinds of neoplastic lesions as follows: (1) HCA region (GS-positive, SAA-negative), blue region; (2) HCA region (GS-positive, SAA-positive), orange-colored region; and (3) HCC (GS-positive, SAA-positive), red regions.

### Histological and Immunohistochemical Findings of the Boundary between the HCA Region and the Normal Liver

In the boundary between the HCA region and the normal liver (fig. 5a), the artery in the portal tract was abnormally thick compared with the portal vein and bile duct (fig. 5b) (the d region of normal liver is shown in yellow in fig. 4b). In the HCA region, which corresponds to the e region in figure 4b (shown in blue), similar to those shown in figure 5b, the artery in the portal tract was abnormally thick compared with the portal vein and the bile duct (fig. 5c). In the HCA region, which corresponded to the f region in figure 4b (shown in blue), the artery was not abnormally thick, but the portal vein and the bile duct were retained (fig. 5d). These pathological findings were different from those of conventional HCA.

In the HCA region, which corresponded to the c region in figure 4b (shown in blue), mild cellular and structural atypia was observed; no invasive growth was noted in the portal region (fig. 6a, b). GS immunostaining was diffusely positive (fig. 6c) without any nuclear accumulation of  $\beta$ -catenin (fig. 6d), and SAA immunostaining was also negative (fig. 6e). In the b region of HCA, shown in orange in figure 4b, mild cellular and structural atypia was observed, and no invasive growth was noted in the portal tract (fig. 7a, b). GS immunostaining was diffusely positive (fig. 7c), nuclear accumulation of  $\beta$ -catenin was noted on immunostaining (fig. 7d), and SAA immunostaining was positive (fig. 7e). Because of definite nuclear accumulation of  $\beta$ -catenin, this tumor was diagnosed as  $\beta$ -catenin-activated HCA.

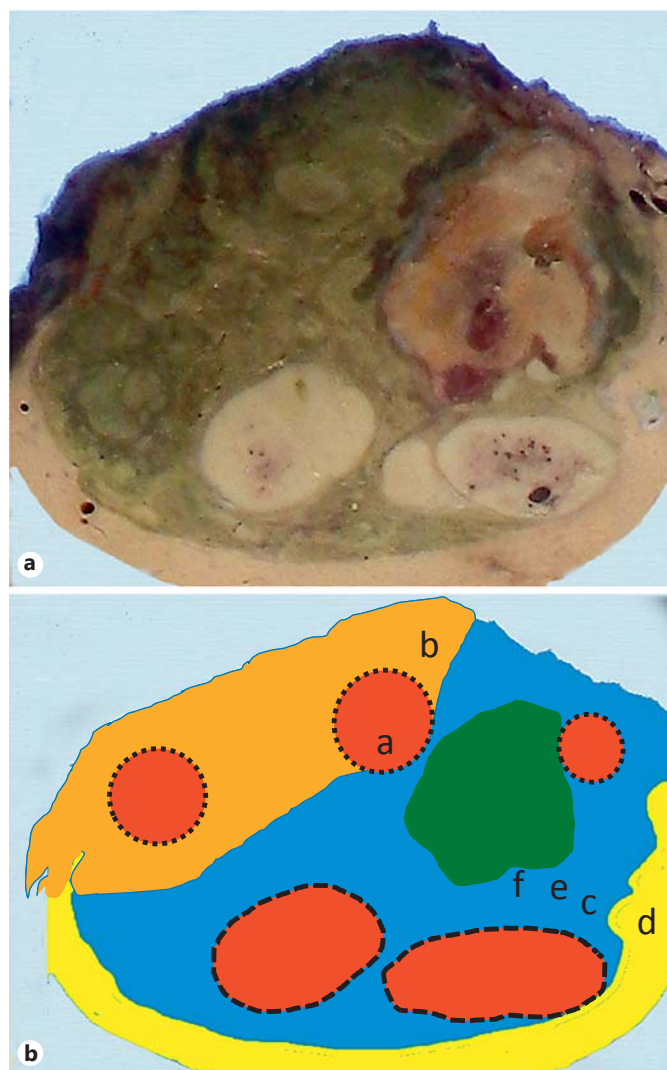
In the HCC region that corresponded to the regions shown in red in figure 4b, well-differentiated HCC with a slightly disturbed trabecular structure was detected on H&E staining (fig. 8a). On Masson trichrome staining, the tumor tissue invaded the vascular wall and reached right below the vascular endothelium or was exposed to the vascular lumen (fig. 8b). The tumor tissue was diffusely positive on GS immunostaining (fig. 8c), and nuclear accumulation was not found on immunostaining (fig. 8d). SAA immunostaining was also positive (fig. 8e).

Based on the above findings, the final pathological diagnosis was HCA ( $\beta$ -catenin-activated type) with a component of malignant transformation.

**Fig. 3.** Images from referral to the Department of Gastroenterology in August 2014. **a** Regions with abundant and scarce blood flow were mixed in both the upper and lower lesions of the mass. **b** The portal vein was observed to penetrate the mass.

### Discussion

Generally, HCA is a benign tumor developing in the liver without chronic hepatitis or hepatic cirrhosis. It has recently been clarified that HCA develops due to gene aberration [7, 8]. According to the WHO classification, HCA is roughly classified into four types through the genotype- and phenotype-based subtype classification. Previous reports from Western countries have shown that the inactive hepatocyte nuclear factor (HNF) 1 $\alpha$  type of



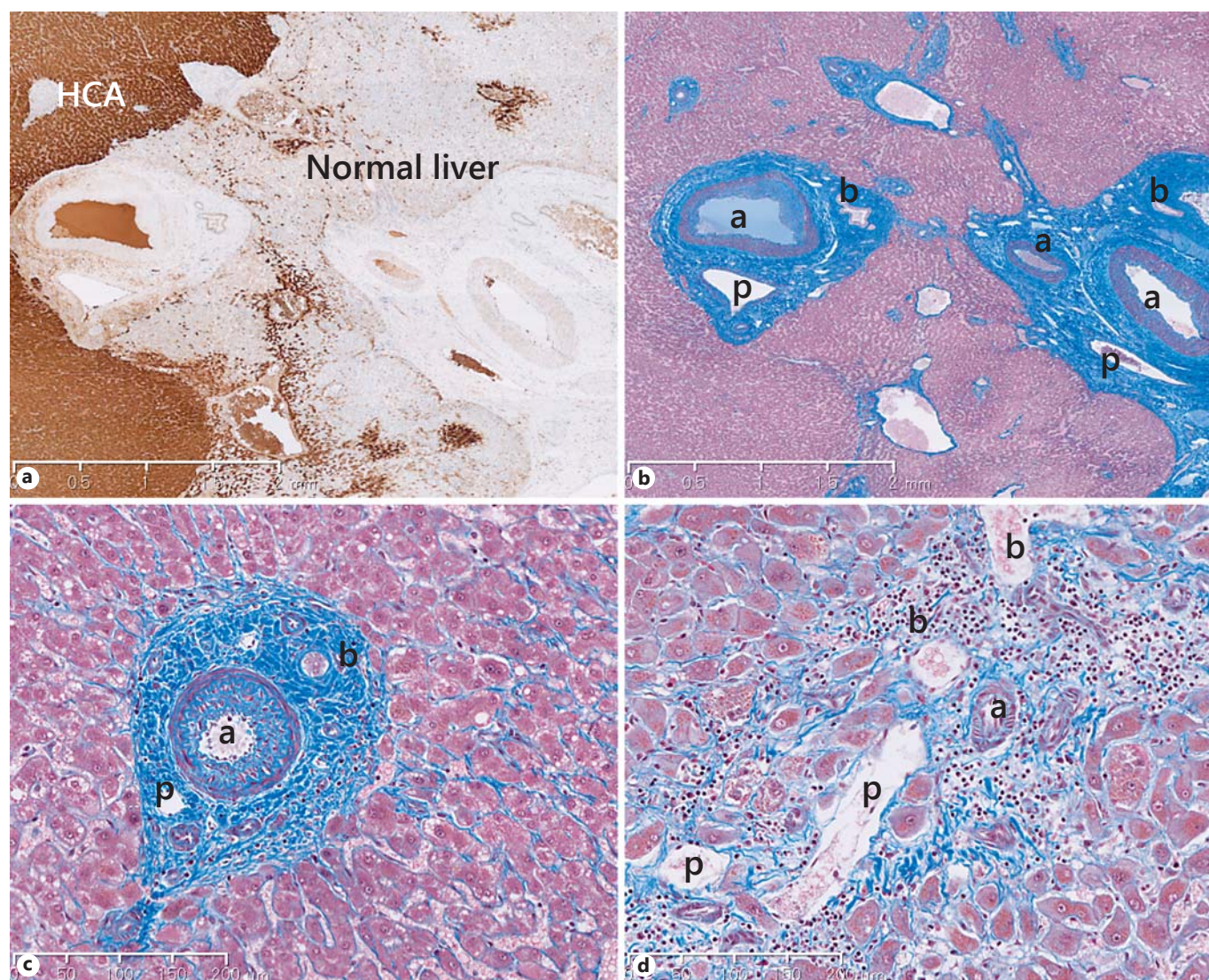
**Fig. 4.** **a** Macroscopic findings of the resected specimen. The tumor consisted of various components. **b** Schematic diagram of the resected specimen. Red: HCC regions (GS-positive, SAA-positive). Blue: HCA region (GS-positive, SAA-negative). Orange: HCA region (GS-positive, SAA-positive). Green: Necrosis and hemorrhage. Yellow: Normal liver.



HCA develops based on the *HNF1A* gene mutation, and that its phenotype is negative for the expression of liver fatty acid-binding protein. It reportedly develops mainly in women and is associated with oral contraceptives. HCC scarcely takes place in this subtype [7–9]. On the other hand, inflammatory HCA is caused by mutations of the *gp130* and *STAT3* genes, and SAA and CRP are positive as its phenotype [10–13]. It occurs in both genders, and obesity and alcohol drinking are reported as risk fac-

tors. Reportedly, the frequency of HCC emergence from  $\beta$ -catenin-activated HCA is considerably high [7, 8]. Gene mutation and histological characteristics are unclear in the unclassifiable types.

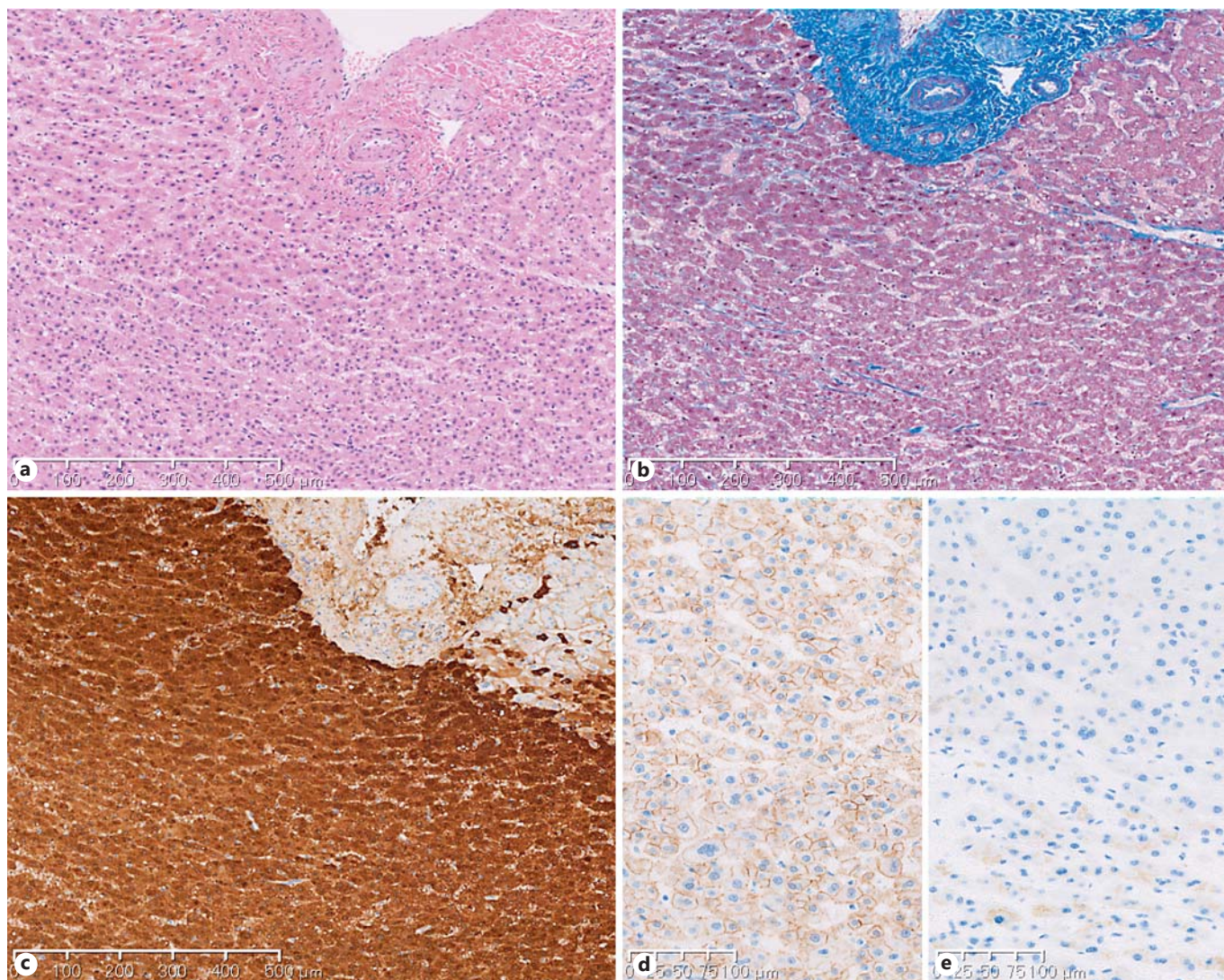
Beta-catenin-activated HCA should be attributed to the *CTNNB1* mutation; immunohistochemical analyses revealed positivity for GS and nuclear  $\beta$ -catenin [7, 8, 14]. The frequency of its malignant transformation is higher than those of the other subtypes in Western countries, but



**Fig. 5.** Boundary between the HCA region and normal liver. **a** GS immunostaining. Boundary between the HCA region and normal liver (d region shown in yellow in fig. 4b). Bar: 2 mm. **b** Masson trichrome staining of the same region. The artery (a) in the portal tract was abnormally thick compared with the portal vein (p) and the bile duct (b). Bar: 200  $\mu$ m. **c** The e region in the HCA nodule re-

gion shown in figure 4b. Similar to **b**, the artery (a) in the portal tract was abnormally thick compared with the portal vein (p) and the bile duct (b). Bar: 200  $\mu$ m. **d** The f region in the deep region of the HCA nodule shown in figure 4b. The artery was not abnormally thick, but the portal vein (p) and bile duct (b) were retained. Bar: 200  $\mu$ m.





**Fig. 6.** HCA region (c region shown in blue in fig. 4b). **a** Mild cellular and structural atypia was observed, and no infiltration was noted in the portal region. Bar: 500 µm. **b** Masson trichrome staining. No invasive growth was noted in the portal tract. Bar: 500 µm.

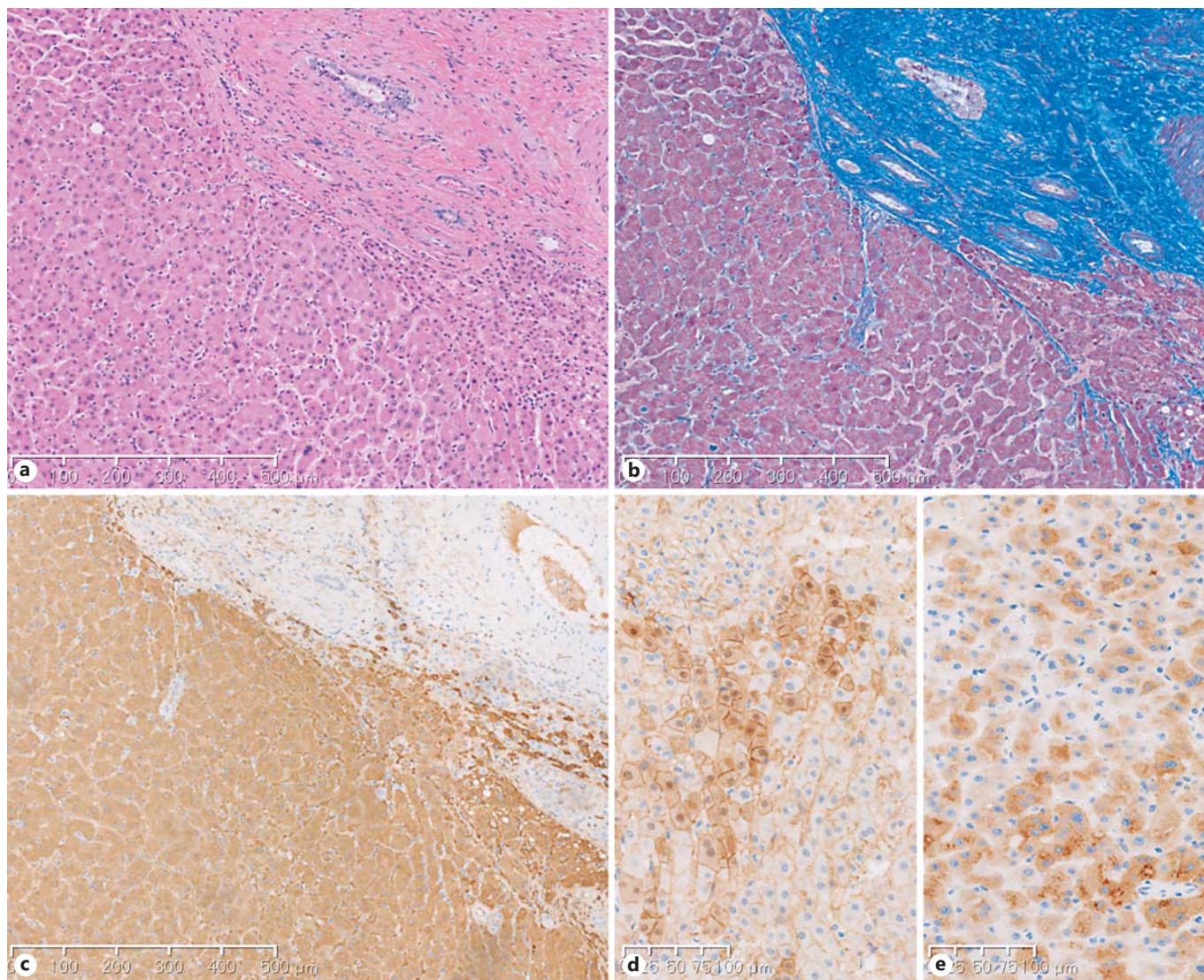
**c** GS immunostaining was diffusely positive. Bar: 500 µm. **d** Beta-catenin immunostaining. No nuclear accumulation was noted. Bar: 100 µm. **e** SAA immunostaining was negative. Bar: 100 µm.

there have been only few reports in the literature regarding malignant transformation of HCA in Japan [4]. Thus the present case, in which the surgical specimen was pathologically examined, is valuable for understanding the difference of HCC pathogenesis based the HCA sub-type.

The characteristic imaging findings of this case were: (1) the main part of the tumor exhibited hypervascularity; (2) there were also mixed lesions with hyper- and hypovascular pattern; (3) presence of intratumoral hemorrhage; (4) penetration of the portal vein into the tumor;

(5) there were slightly high-intensity regions on diffusion-weighted imaging, which were regarded as nontumorous liver based on apparent diffusion coefficient map; (6) heterogeneous high-intensity regions were observed in the hepatocellular phase on Gd-EOB-DTPA contrast-enhanced MRI; (7) the entire tumor represented a heterogeneously attenuated image on the Kupffer phase of contrast-enhanced ultrasound. Based on the unique feature of imaging, it could be speculated for differential diagnosis that there was intratumoral hemorrhage that was detected as heterogeneously high-intensity regions in





**Fig. 7.** HCA region (b region shown in orange in fig. 4b). **a** Mild cellular and structural atypia was observed and no infiltration was noted in the portal region Bar: 500  $\mu$ m. **b** Masson trichrome staining. No invasive growth was noted. Bar: 500  $\mu$ m. **c** GS immuno-

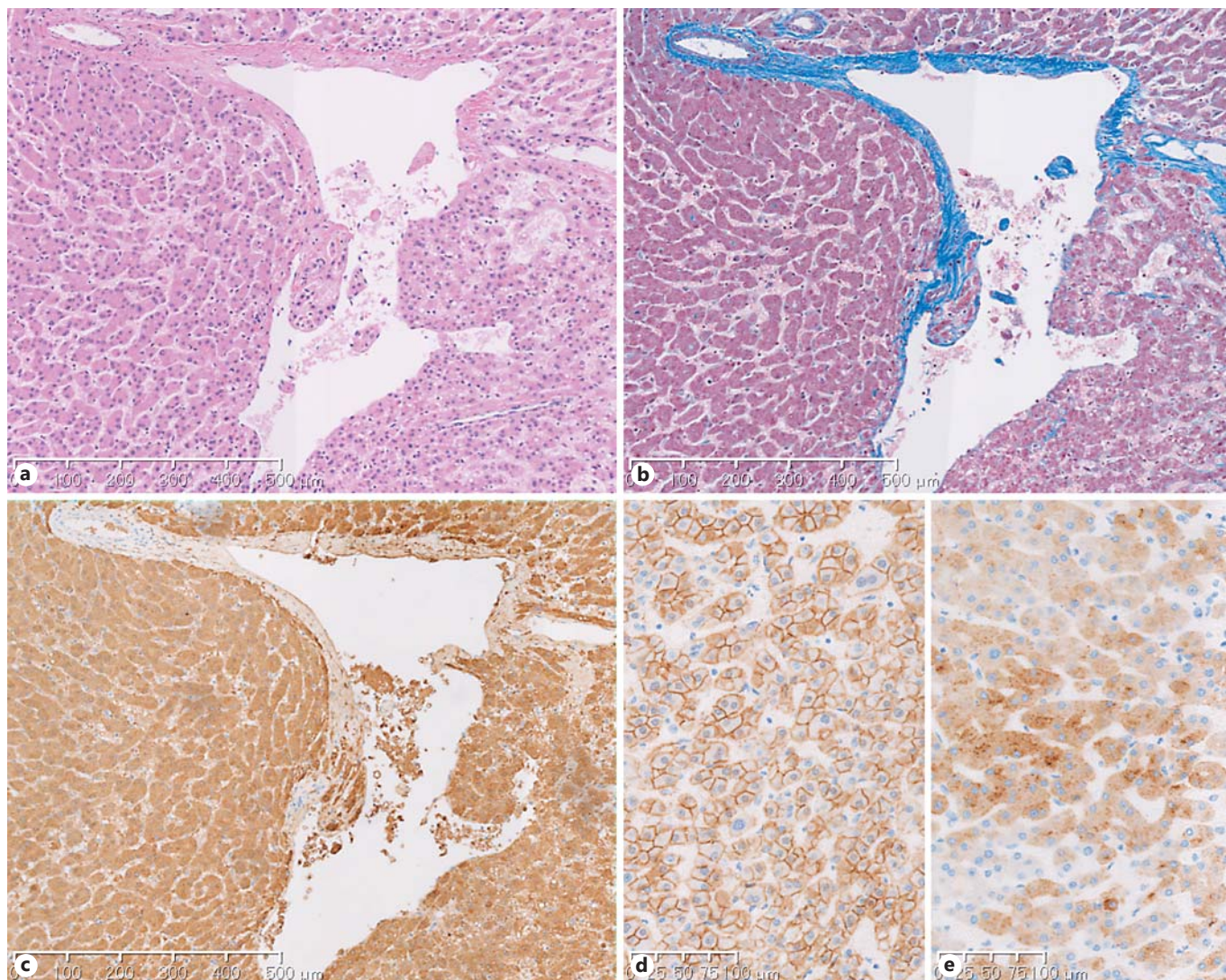
staining was diffusely positive. Bar: 500  $\mu$ m. **d** Nuclear accumulation was observed on  $\beta$ -catenin immunostaining. Bar: 100  $\mu$ m. **e** SAA immunostaining was positive. Bar: 100  $\mu$ m.

the hepatocellular phase of Gd-EOB-DTPA contrast-enhanced MRI. Several types of tumors are known to show hemorrhage in the mass, such as HCC [15], HCA [16], metastatic tumors of lung and renal cancers [17], and angiomyolipoma (AML) [18]. In the present patient, imaging studies revealed no findings of metastatic liver tumor or AML; neither metastatic liver tumor nor AML show any enhancement on Gd-EOB-DTPA in the hepatocellular phase on contrast-enhanced MRI. On the other hand, focal nodular hyperplasia is known as a hypervas-

cular tumor, but intratumoral hemorrhage should be rare, indicating the low priority for diagnosis.

HCC and HCA may present as heterogeneous high-intensity masses in the hepatocellular phase on Gd-EOB-DTPA contrast-enhanced MRI [19–21]. Generally, high intensity in the hepatocellular phase suggests a benign or less malignant tumor. However, since OATP8 is under the control of Wnt/ $\beta$ -catenin signaling,  $\beta$ -catenin-activated HCA may well show increased intensity in the hepatocellular phase on EOB-MRI. Indeed, OATP8 is





**Fig. 8.** HCC region (a region shown in red in fig. 4b). **a** H&E staining. Well-differentiated HCC with a slightly disturbed trabecular structure. Bar: 500  $\mu$ m. **b** Masson trichrome staining. Tumor tissue invaded into the vascular wall and reached right below the vascular endothelium or was exposed to the vascular lumen. Bar: 500  $\mu$ m.

**c** GS immunostaining. Tumor tissue was diffusely positive. Bar: 500  $\mu$ m. **d** Beta-catenin immunostaining. Nuclear accumulation was not found. Bar: 100  $\mu$ m. **e** SAA immunostaining was positive. Bar: 100  $\mu$ m.

pathologically well preserved in  $\beta$ -catenin-activated HCA [22]. As malignant transformation is most likely in the  $\beta$ -catenin-activated HCA than any other types of HCA, HCA showing the high intensity in the hepatocellular phase of EOB-MRI should be observed carefully in clinical practice.

Regarding the characteristics of the pathological findings, a thickened artery wall was detected in the portal tract located at the boundary between the HCA and normal liver, suggesting the presence of abnormal blood flow

in the background liver and HCA. However, inside the HCA nodule, the components of portal tract were retained, which was different from typical HCA. Generally, no abnormal blood flow is present in the surrounding normal liver of HCA cases. Therefore, a benign nonneoplastic hepatocellular nodule may have emerged from the liver, carrying abnormal blood flow in advance of HCA formation. The reports regarding HCA development from a benign nonneoplastic hepatocellular nodule also support this hypothesis [23–25].

Based on the immunopathological findings, the mass should subsequently acquire the nuclear  $\beta$ -catenin accumulation-positive and GS-positive characters (c region, blue in fig. 4b) as well as SAA-positive character (b region, orange in fig. 4b), which led to the diagnosis of  $\beta$ -catenin-activated HCA. In this case, the nuclear  $\beta$ -catenin accumulation is limited to a small region. In general, not all regions of  $\beta$ -catenin-activated HCA exhibit diffuse nuclear accumulation. Therefore, nuclear accumulation in the b region (orange in fig. 4b) provides evidence for  $\beta$ -catenin-activated HCA. In the WHO classification, HCA is diagnosed mainly based on gene mutation and immunopathological findings. However, in patients showing abnormal blood flow in the background liver, it seems to be difficult to understand the development of HCA based on only immunopathological findings.

Although as described above the factors of HCA development are controversial, the diagnosis of  $\beta$ -catenin-activated HCA is solid in this case, where HCC with a similar immunopathological feature and structural atypia might develop from the  $\beta$ -catenin-activated HCA. Many cases of malignant transformation from HCA have

been reported in Western countries. However, to our best knowledge, this is the first Japanese case reported, the reason for the discrepancy of the frequency between Western countries and Japan remaining to be elucidated.

## Conclusion

We encountered a young patient with malignant transformation of  $\beta$ -catenin-activated HCA. Beta-catenin-activated HCA may show characteristic findings, such as high intensity in the hepatocellular phase on EOB-MRI. HCA might develop based on the intrahepatic abnormal blood flow, which finally reaches malignant transformation. In Japan, malignant transformation of HCA is very rare, but further accumulation of cases and investigation are necessary.

## Disclosure Statement

The authors have no conflicts of interest to declare.

## References

- 1 Bioulac-Sage P, Laumonier H, Couchy G, Le Bail B, Sa Cunha A, Rullier A, et al: Hepatocellular adenoma management and phenotypic classification: the Bordeaux experience. *Hepatology* 2009;50:481–489.
- 2 Bioulac-Sage P, Balabaud C, Zucman-Rossi J: Subtype classification of hepatocellular adenoma. *Dig Surg* 2010;27:39–45.
- 3 Deneve JL, Pawlik TM, Cunningham S, Clary B, Reddy S, Scoggins CR, et al: Liver cell adenoma: a multicenter analysis of risk factors for rupture and malignancy. *Ann Surg Oncol* 2009;16:640–648.
- 4 Tokoro T, Kato Y, Sugioaka A, Mizoguchi Y: Malignant transformation of hepatocellular adenoma over a decade. *BMJ Case Rep* 2014; 2014:bcr2014205261.
- 5 Kudo M: Malignant transformation of hepatocellular adenoma: how frequently does it happen? *Liver Cancer* 2015;4:1–5.
- 6 Murakami T, Tsurusaki M: Hypervascular benign and malignant liver tumors that require differentiation from hepatocellular carcinoma: key points of imaging diagnosis. *Liver Cancer* 2014;3:85–96.
- 7 Bioulac-Sage P, Rebouissou S, Thomas C, Blanc JF, Saric J, Sa Cunha A, et al: Hepatocellular adenoma subtype classification using molecular markers and immunohistochemistry. *Hepatology* 2007;46:740–748.
- 8 Nault JC, Bioulac-Sage P, Zucman-Rossi J: Hepatocellular benign tumors – from molecular classification to personalized clinical care. *Gastroenterology* 2013;144:888–902.
- 9 Bluteau O, Jeannot E, Bioulac-Sage P, Marques JM, Blanc JF, Bui H, et al: Bi-allelic inactivation of TCF1 in hepatic adenomas. *Nat Genet* 2002;32:312–315.
- 10 Rebouissou S, Amessou M, Couchy G, Pousin K, Imbeaud S, Pilati C, et al: Frequent in-frame somatic deletions activate gp130 in inflammatory hepatocellular tumours. *Nature* 2009;457:200–204.
- 11 Pilati C, Amessou M, Bihl MP, Balabaud C, Nhieu JT, Paradis V, et al: Somatic mutations activating STAT3 in human inflammatory hepatocellular adenomas. *J Exp Med* 2011; 208:1359–1366.
- 12 Nault JC, Fabre M, Couchy G, Pilati C, Jeannot E, Tran Van Nhieu J, et al: GNAS-activating mutations define a rare subgroup of inflammatory liver tumors characterized by STAT3 activation. *J Hepatol* 2012;56:184–191.
- 13 Pilati C, Letouze E, Nault JC, Imbeaud S, Boulai A, Calderaro J, et al: Genomic profiling of hepatocellular adenomas reveals recurrent FRK-activating mutations and the mechanisms of malignant transformation. *Cancer Cell* 2014;25:428–441.
- 14 Chen YW, Jeng YM, Yeh SH, Chen PJ: p53 gene and Wnt signaling in benign neoplasms: beta-catenin mutations in hepatic adenoma but not in focal nodular hyperplasia. *Hepatology* 2002;36:927–935.
- 15 Srinivasa S, Lee WG, Aldameh A, Koea JB: Spontaneous hepatic haemorrhage: a review of pathogenesis, aetiology and treatment. *HPB (Oxford)* 2015;17:872–880.
- 16 Addeo P, Cesaretti M, Fuchshuber P, Langel-la S, Simone G, Oussoultzoglou E, et al: Outcomes of liver resection for haemorrhagic hepatocellular adenoma. *Int J Surg* 2016;27:34–38.
- 17 Kadowaki T, Hamada H, Yokoyama A, Ito R, Ishimaru S, Ohnishi H, et al: Hemoperitoneum secondary to spontaneous rupture of hepatic metastasis from lung cancer. *Intern Med* 2005;44:290–293.
- 18 Occhionorelli S, Dellachiesa L, Stano R, Cappellari L, Tartarini D, Severi S, et al: Spontaneous rupture of a hepatic epithelioid angiolipoma: damage control surgery. A case report. *G Chir* 2013;34:320–322.
- 19 Lee S, Kim SH, Park CK, Kim YS, Lee WJ, Lim HK: Comparison between areas with Gd-EOB-DTPA uptake and without in hepatocellular carcinomas on Gd-EOB-DTPA-enhanced hepatobiliary-phase MR imaging: pathological correlation. *J Magn Reson Imaging* 2010;32:719–725.

- 20 Yoneda N, Matsui O, Kitao A, Kozaka K, Gabata T, Sasaki M, et al: Beta-catenin-activated hepatocellular adenoma showing hyperintensity on hepatobiliary-phase gadoxetic-enhanced magnetic resonance imaging and overexpression of OATP8. *Jpn J Radiol* 2012; 30:777–782.
- 21 Suh CH, Kim KW, Kim GY, Shin YM, Kim PN, Park SH: The diagnostic value of Gd-EOB-DTPA-MRI for the diagnosis of focal nodular hyperplasia: a systematic review and meta-analysis. *Eur Radiol* 2015;25:950–960.
- 22 Fukusato T, Soejima Y, Kondo F, Inoue M, Watanabe M, Takahashi Y, et al: Preserved or enhanced OATP1B3 expression in hepatocellular adenoma subtypes with nuclear accumulation of  $\beta$ -catenin. *Hepatol Res* 2015;45: E32–E42.
- 23 Sanada Y, Mizuta K, Niki T, Tashiro M, Hirata Y, Okada N, et al: Hepatocellular nodules resulting from congenital extrahepatic portosystemic shunts can differentiate into potentially malignant hepatocellular adenomas. *J Hepatobiliary Pancreat Sci* 2015;22: 746–756.
- 24 Handra-Luca A, Paradis V, Vilgrain V, Dubois S, Durand F, Belghiti J, et al: Multiple mixed adenoma-focal nodular hyperplasia of the liver associated with spontaneous intrahepatic porto-systemic shunt: a new type of vascular malformation associated with the multiple focal nodular hyperplasia syndrome? *Histopathology* 2006;48:309–311.
- 25 Kondo F, Fukusato T, Kudo M: Pathological diagnosis of benign hepatocellular nodular lesions based on the new World Health Organization classification. *Oncology* 2014;87(suppl 1):37–49.



# Outcome of Combination Therapy with Sofosbuvir and Ledipasvir for Chronic Type C Liver Disease

Satoru Hagiwara Naoshi Nishida Tomohiro Watanabe Toshiharu Sakurai  
Hiroshi Ida Yasunori Minami Masahiro Takita Tomohiro Minami  
Mina Iwanishi Hirokazu Chishina Kazuomi Ueshima Yoriaki Komeda  
Tadaaki Arizumi Masatoshi Kudo

Department of Gastroenterology and Hepatology, Kindai University Faculty of Medicine, Osaka-Sayama, Japan

## Key Words

Sofosbuvir · Ledipasvir · Chronic type C liver disease

## Abstract

**Introduction:** Recently, the treatment of chronic hepatitis C has markedly advanced. A phase III clinical study of combination therapy with sofosbuvir (SOF) and ledipasvir (LDV) was conducted in Japan, and the additive therapeutic effects were reported. In this study, we report the results of treatment in our hospital. **Methods:** Of 147 patients with chronic type C liver disease who had consulted our hospital since September 2015 and received SOF/LDV therapy, in 91 subjects a sustained virological response of 12 weeks (SVR12) could be evaluated. **Results:** In all 91 patients, end treatment response was achieved. Subsequently, recrudescence was noted in 1 before the completion of treatment (week 12); an SVR12 was achieved in 90 patients (99%). The following adverse reactions were observed in 3 patients (3.3%): bradycardia, paroxysmal atrial fibrillation, and heart failure with QT prolongation, which were associ-

ated with heart disease. **Conclusion:** A favorable SVR was achieved by SOF/LDV therapy even in elderly patients, those with liver cirrhosis, or those having undergone radical treatment of liver cancer. Furthermore, a high tolerance was demonstrated, but adverse reactions associated with the heart may appear in patients with heart disease as an underlying disease; strict management during treatment is necessary.

© 2016 S. Karger AG, Basel

## Introduction

Chronic hepatitis C is one of the major etiologies of hepatocellular carcinoma [1–3], which is the third leading cause of cancer death. Therefore, treatment of hepatitis C is an important issue to prevent hepatocarcinogenesis [4]. Recently, the treatment of chronic hepatitis C has markedly advanced. In 2011, telaprevir [5–7] was approved as a directly acting antiviral agent. In 2013, simeprevir was approved [8–12]; the efficacy has

**Table 1.** Patient background (n = 91)

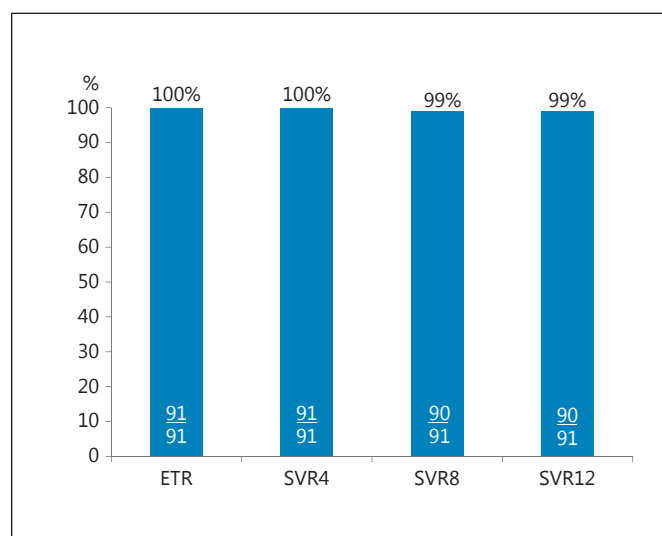
Age, years	
Median (range)	71 (36–88)
≥65 years, n (%)	65 (71)
≥75 years, n (%)	41 (45)
Male sex, n (%)	38 (42)
Cirrhosis, n (%)	34 (37)
History of hepatocellular carcinoma, n (%)	23 (25)
Prior therapy	
Naïve, n (%)	31 (34)
No response, n (%)	12 (13)
Relapse, n (%)	4 (4)
Intolerant, n (%)	8 (9)
Ineligible, n (%)	36 (40)

**Table 2.** NS5A resistance mutations at baseline (n = 91)

Negative, n (%)	8 (9)
Y93H, n (%)	11 (12)
Y93H+L31M, n (%)	2 (2)
No measurement, n (%)	70 (77)

improved. However, it is necessary to combine these agents with peginterferon and ribavirin (RBV), raising the issue of tolerance. In other words, hepatitis C virus eradication has been successfully achieved in young patients and, as a result, the proportions of elderly patients in whom treatment was unsuccessful or discontinued and of those with deterioration of fibrosis have increased.

On this background, the necessity of developing a more tolerable, effective treatment method has been emphasized. In Japan, the first interferon (IFN)-free regimen, a combination therapy with asunaprevir and daclatasvir, became commercially available in September 2014 [13–16]. This therapy has been increasingly indicated for elderly patients and those with underlying diseases in comparison with treatments with IFN, decreasing the incidence of adverse reactions. On the other hand, the therapeutic effects were markedly reduced in patients with resistance mutations at baseline, and adverse reactions, such as liver dysfunction, made it difficult to continue treatment in some patients, raising issues. Based on such a background, a phase III clinical study of combination therapy with sofosbuvir (SOF) and ledipasvir (LDV) was conducted in Japan, and the additive therapeutic effects were reported [17]. In this study, we report the results of treatment in our hospital.

**Fig. 1.** Virological reactivity. In all 91 patients, end treatment response (ETR) was achieved. Subsequently, recrudescence was noted in 1 before the completion of treatment (week 12); an SVR12 was achieved in 90 patients (99%).

## Methods

### Patients and Treatment Schedule

Of 147 patients with chronic type C liver disease who had consulted our hospital since September 2015 and received SOF/LDV therapy, in 91 subjects a sustained virological response of 12 weeks (SVR12) could be evaluated. The administration period was 12 weeks, and follow-up was performed until 12 weeks after the completion of treatment. SOF at 400 mg and LDV at 90 mg were orally administered once a day.

### Resistance Test

Hepatitis C virus NS5A and NS3/4A resistance was measured using the PCR-invader method. Strains with a mutant virus rate of <1% were regarded as negative, those with a mutant virus rate of 1–19% as weakly positive, and those with a mutant virus rate of ≥20% as positive.

### Statistical Analysis

Changes in hepatic reserve, estimated glomerular filtration rate (eGFR), and corrected QT (QTc) were analyzed using Student's t test. A p value of 0.05 was regarded as significant.

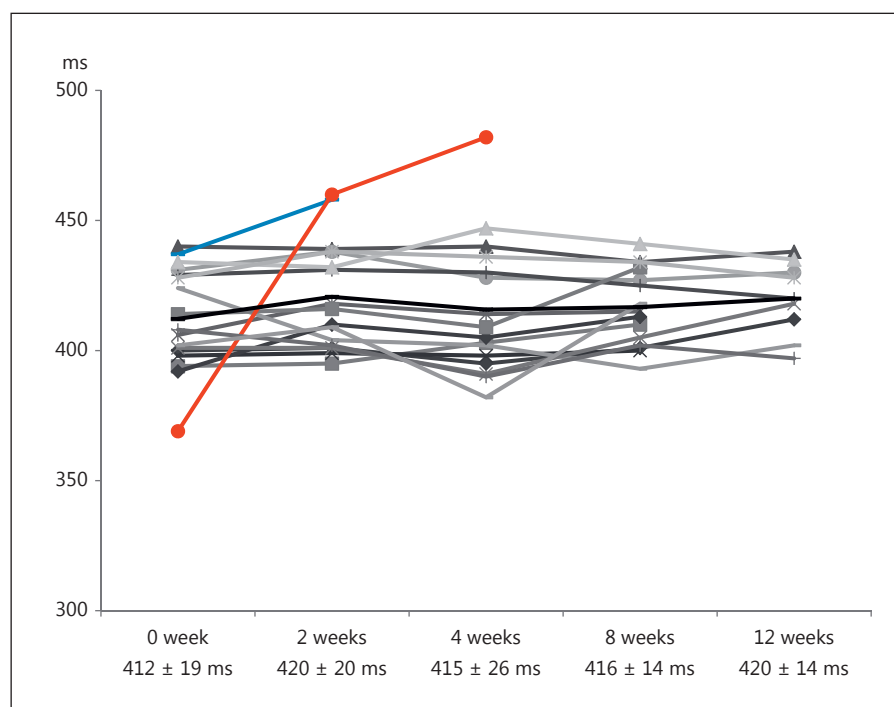
## Results

### Patients

Of 147 patients with chronic type C liver disease who had consulted our hospital since September 2015 and received SOF/LDV therapy, in 91 subjects an SVR12 could



**Fig. 2.** Changes in QTc before and during treatment. In 17 patients who underwent electrocardiography before treatment and every 2 weeks during treatment, the QTc interval was measured. In 2 (11.7%) of the 17 patients, the QTc interval was markedly prolonged (from 369 to 482 ms and from 437 to 458 ms, respectively).



**Table 3.** Adverse reactions leading to the discontinuation of oral administration

Adverse reaction	Onset time	Outcome	SVR	Age	Sex	Cirrhosis	eGFR	Underlying disease
Bradycardia, QT prolongation	day 14	recovery through drug withdrawal alone	SVR12	75	F	absent	77	absent
Paroxysmal atrial fibrillation	day 34	recovery through administration and discontinuation	SVR12	79	F	absent	52	paroxysmal atrial fibrillation
QT prolongation, heart failure	day 77	recovery through administration and discontinuation	SVR12	78	F	present	84	heart failure

be evaluated. The median age was 71 years. Patients aged 65 years or older accounted for 71% (n = 65), and those aged 75 years or older accounted for 45% (n = 41). The subjects' age was more advanced than in the phase III clinical trial in Japan. Furthermore, they included 34 patients with liver cirrhosis (37%) and 23 patients having undergone radical treatment of liver cancer (25%). Concerning previous treatment, 31 patients (34%) had not received any biological preparation. There were 12 (13%) nonresponders to IFN, and recrudescence was noted in 4 (4%). IFN was inappropriate/intolerable in 44 (49%), showing the highest percentage (table 1).

#### NS5A Resistance Mutations at Baseline

Eight patients (9%) were negative for NS5A resistance mutations. Y93H was detected in 11 patients (12%), and Y93H+L31M in 2 (2%). Measurement was not performed in 70 (77%) (table 2).

#### Virological Reactiveness

In all 91 patients, end treatment response was achieved. Subsequently, recrudescence was noted in 1 before the completion of treatment (week 12); an SVR12 was achieved in 90 patients (99%) (fig. 1).

### Virological Ineffectiveness

After completion of the 12-week treatment, recrudescence was noted in 1 patient. This patient had multiple resistant strains, Y93H and L31M, at baseline.

### Adverse Reactions Leading to the Discontinuation of Oral Administration

Such adverse reactions were observed in 3 patients (3.3%): bradycardia, paroxysmal atrial fibrillation, and heart failure with QT prolongation, which were associated with heart disease. Furthermore, many patients had heart disease as an underlying disease (table 3).

### Changes in QTc before/during Treatment

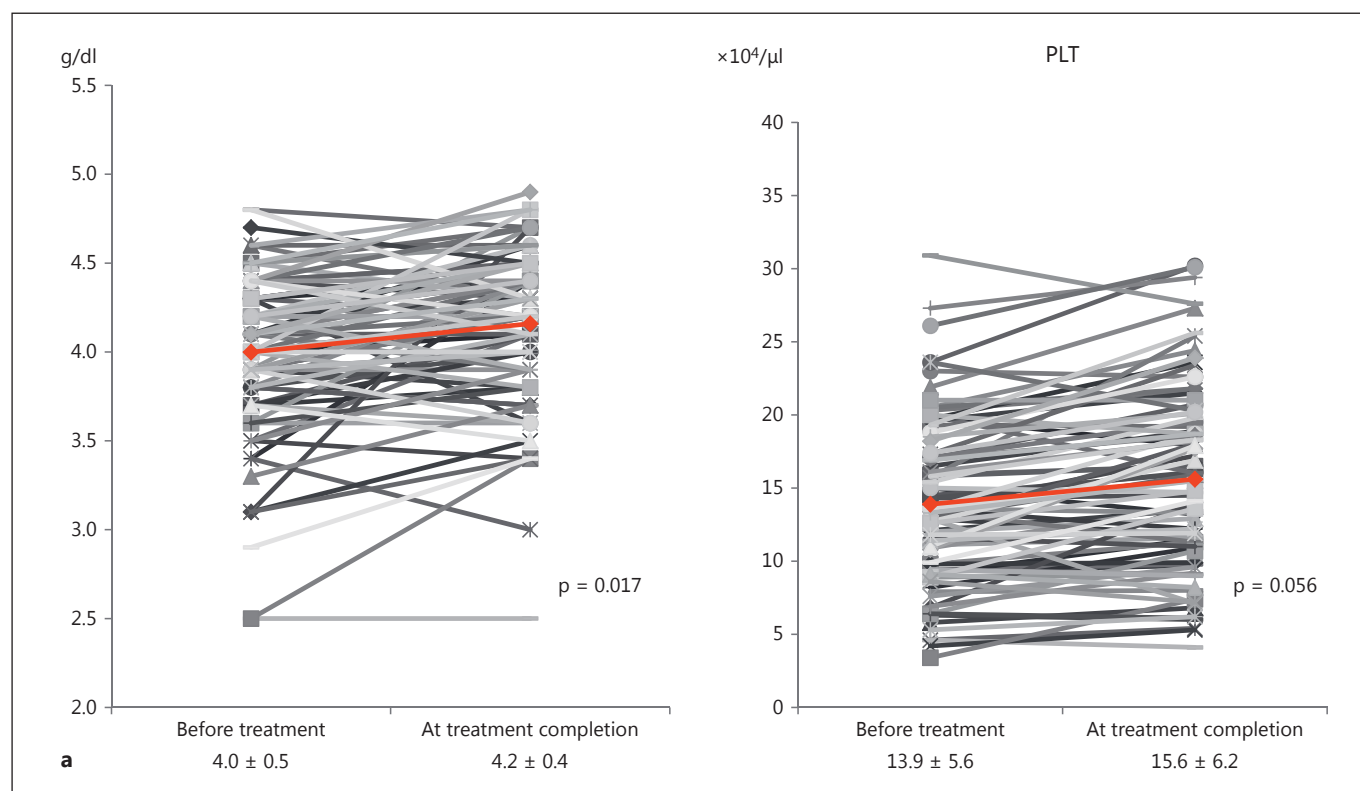
In 17 patients who underwent electrocardiography before treatment and every 2 weeks during treatment, the QTc interval was measured. In 2 (11.7%) of the 17 patients, the QTc interval was markedly prolonged (from 369 to 482 ms and from 437 to 458 ms, respectively) (fig. 2).

### Changes in Hepatic Reserve before and after Treatment

The serum albumin levels at the time of treatment introduction and its completion were  $4.0 \pm 0.5$  and  $4.2 \pm 0.4$  (mean  $\pm$  SD), respectively, showing a significant increase ( $p = 0.017$ ) (fig. 3a). When reviewing the results with respect to diseases (chronic hepatitis and liver cirrhosis), there was no difference in patients with chronic hepatitis (fig. 3b), whereas there was a significant improvement (from  $3.7 \pm 0.5$  to  $4.0 \pm 0.5$ ) in those with liver cirrhosis (fig. 3c,  $p = 0.013$ ). In the latter, there was a significant improvement in the platelet count (from  $8.8 \pm 2.7$  to  $10.3 \pm 3.5$ ) ( $p = 0.049$ ).

### Changes in the Kidney Function (eGFR) before and after Treatment

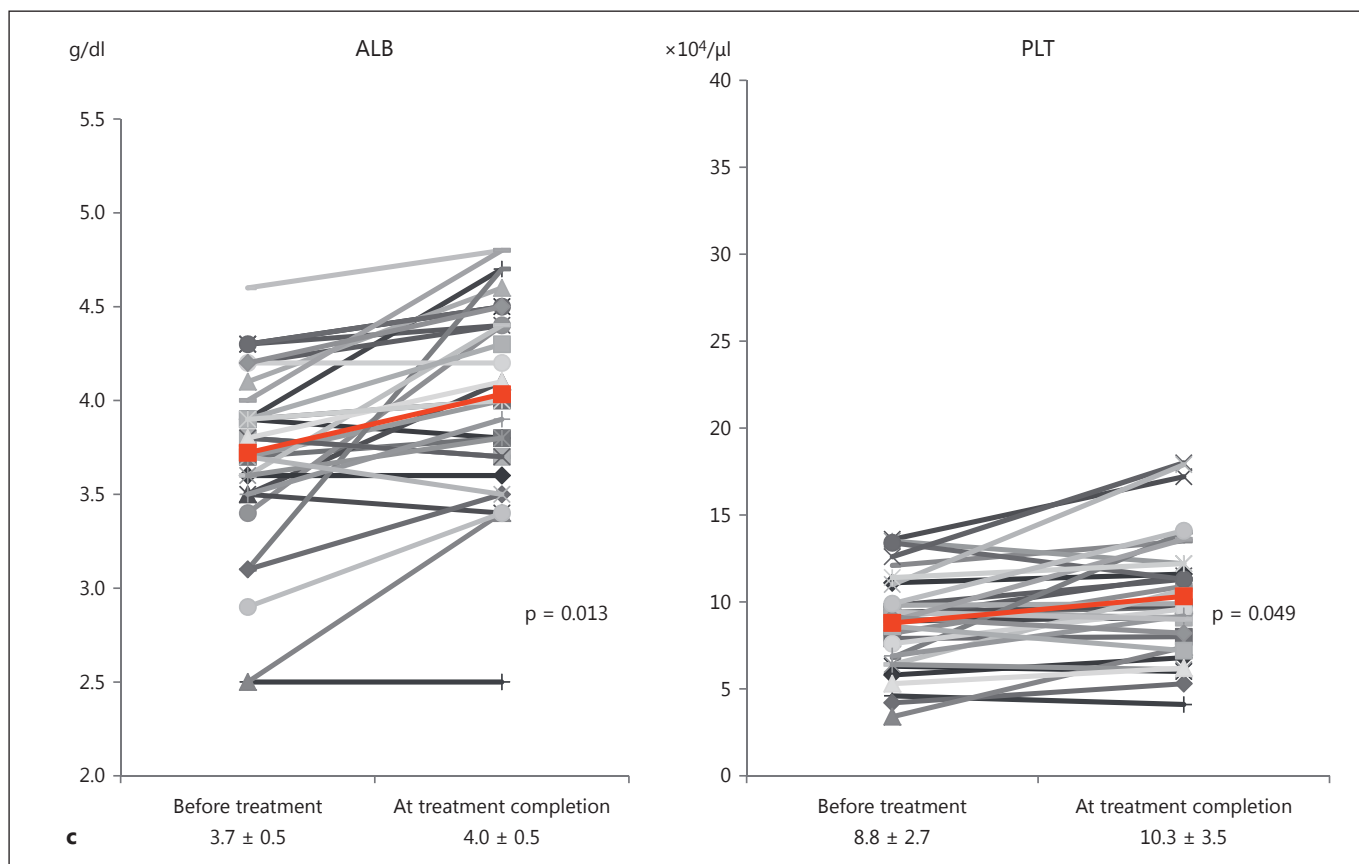
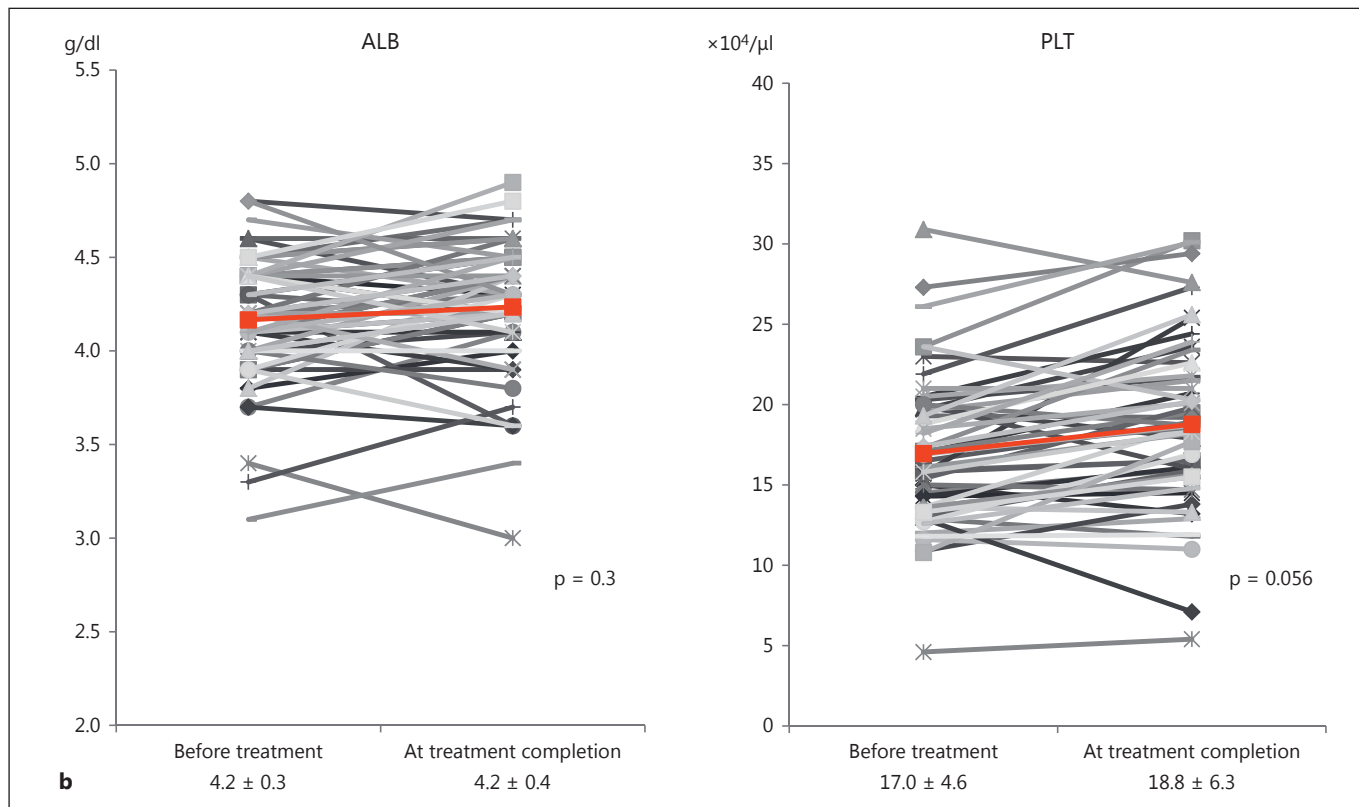
Overall, the eGFRs at the time of treatment introduction and its completion were  $73.0 \pm 16.0$  and  $71.3 \pm 15.0$  (mean  $\pm$  SD), respectively; there was no exacerbation. In patients with an eGFR of  $<60$  at the time of treatment introduction, there was no further exacerbation either (fig. 4).

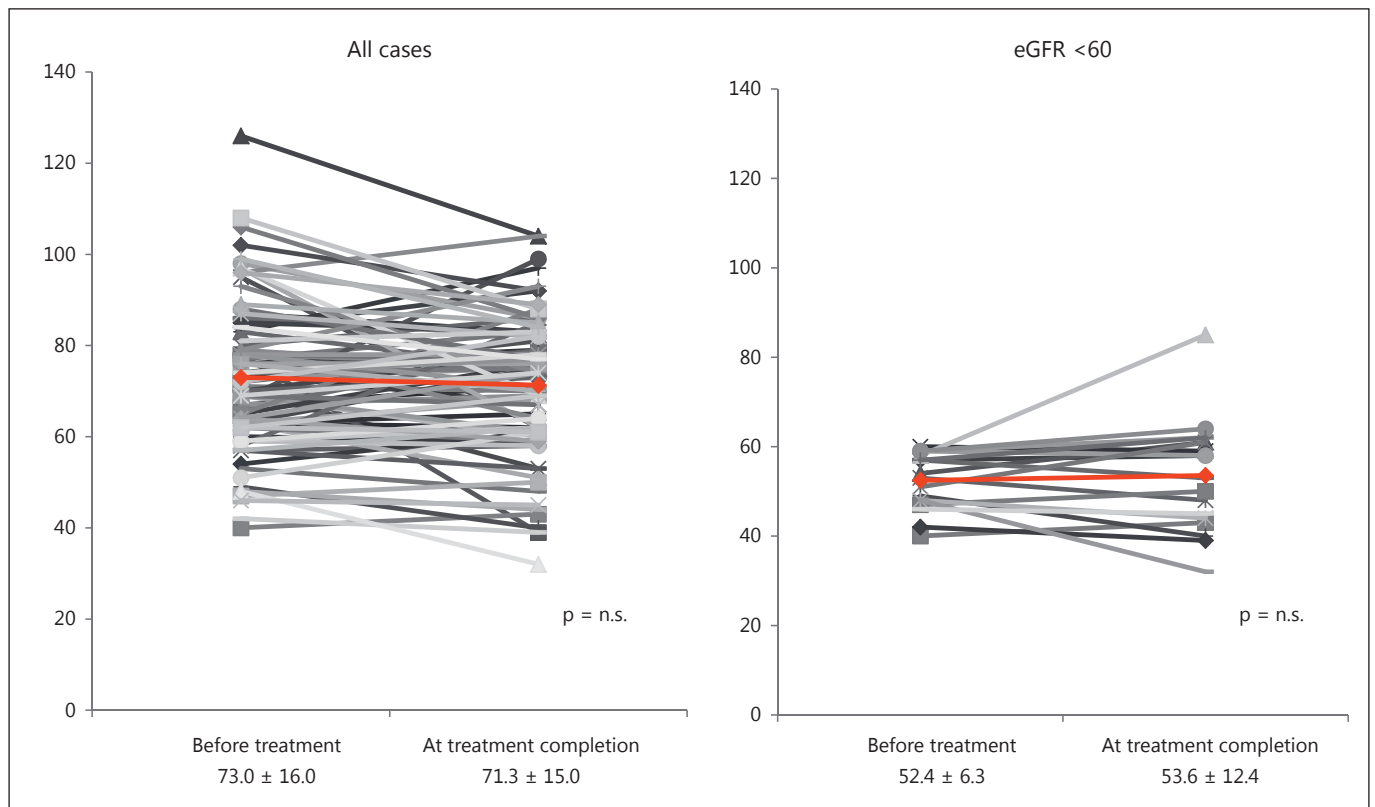


**Fig. 3. a** Changes in hepatic reserve before and after treatment. The serum albumin (ALB) levels at the time of treatment introduction and its completion were  $4.0 \pm 0.5$  and  $4.2 \pm 0.4$  (mean  $\pm$  SD), respectively, showing a significant increase ( $p = 0.017$ ). **b, c** When reviewing the results with respect to chronic hepatitis and liver cir-

rhosis, there was no difference in patients with chronic hepatitis (**b**), whereas there was a significant improvement (from  $3.7 \pm 0.5$  to  $4.0 \pm 0.4$ ) in those with liver cirrhosis (**c**,  $p = 0.013$ ). In the latter, there was a significant improvement in the platelet count (PLT) (from  $8.8 \pm 2.7$  to  $10.3 \pm 3.5$ ) ( $p = 0.049$ ).

(For rest of figure see next page.)





**Fig. 4.** Changes in kidney function (eGFR) before and after treatment. Overall, the eGFRs at the time of treatment introduction and its completion were  $73.0 \pm 16.0$  and  $71.3 \pm 15.0$  (mean  $\pm$  SD), respectively; there was no exacerbation. In patients with an eGFR of  $<60$  at the time of treatment introduction, there was no further exacerbation either. n.s. = Not significant.

## Discussion

The phase III clinical study of SOF/LDV in Japan showed an SVR12 of 100%. On the other hand, an SVR was not achieved in 3 of 170 patients receiving combination therapy with SOF/LDV and RBV: administration was discontinued due to exanthema and cardiac arrest in 2, respectively, and recrudescence was noted after the completion of administration in 1 [17]. In our hospital, an SVR12 was achieved in 90 (99%) of the 91 patients. The remaining patient, in whom an SVR was not achieved, had multiple Y93H and L31M resistance at baseline, and recrudescence was noted 5 weeks after the completion of treatment. In the phase III clinical study, there was no difference in the therapeutic effects related to the presence or absence of resistance in the NS5A region at baseline. Furthermore, an SVR12 was achieved even in patients with multiple Y93H and L31M resistance [17]. No study has reported the effects of SOF/LDV on multiple resis-

tance in the NS5A region in a large number of patients. In the ELECTRON study, effects of SOF/RBV on G1 were obtained in 10–84% of the patients [18, 19], suggesting that the effects of SOF/LDV in patients with multiple NS5A resistance are limited.

Adverse reactions leading to the discontinuation of oral administration were observed in 3 patients (3.3%): bradycardia, paroxysmal atrial fibrillation, and heart failure with QT prolongation, which were associated with heart disease. Furthermore, many patients had heart disease as an underlying disease. In 2 of 17 patients in whom electrocardiograms could be serially measured, the QTc interval was markedly prolonged (from 369 to 482 ms and from 437 to 458 ms, respectively). There are patients with latent QTc prolongation in the absence of symptoms, although we cannot conclude this due to the small number of patients; therefore, strict electrocardiographic monitoring may be necessary during this therapy.

The hepatic reserve had improved at the completion of treatment. Concerning kidney function, we considered the influence of SOF, which is excreted in the kidneys, but there was no influence on kidney function in this study.

In conclusion, a favorable SVR was achieved by SOF/LDV therapy even in elderly patients, those with liver cirrhosis, or those after the radical treatment of hepatocellular carcinoma. Furthermore, a high tolerance was dem-

onstrated, but adverse reactions associated with the heart may appear in patients with heart disease as an underlying disease; strict management during treatment is necessary.

## Disclosure Statement

The authors have no conflicts of interest to declare.

## References

- 1 Kudo M, Matsui O, Izumi N, Iijima H, Kadoya M, Imai Y, Okusaka T, Miyayama S, Tsuchiya K, Ueshima K, Hiraoka A, Ikeda M, Ogawara S, Yamashita T, Minami T, Yamakado K: JSH Consensus-Based Clinical Practice Guidelines for the Management of Hepatocellular Carcinoma: 2014 Update by the Liver Cancer Study Group of Japan. *Liver Cancer* 2014;3:458–468.
- 2 Kudo M: Surveillance, diagnosis, treatment, and outcome of liver cancer in Japan. *Liver Cancer* 2015;4:39–50.
- 3 Kudo M: Clinical practice guidelines for hepatocellular carcinoma differ between Japan, United States, and Europe. *Liver Cancer* 2015; 4:85–95.
- 4 Kudo M: Prediction of hepatocellular carcinoma incidence risk by ultrasound elastography. *Liver Cancer* 2014;3:1–5.
- 5 Kumada H, Toyota J, Okanoue T, Chayama K, Tsubouchi H, Hayashi N: Telaprevir with peginterferon and ribavirin for treatment-naïve patients chronically infected with HCV of genotype 1 in Japan. *J Hepatol* 2012;56:78–84.
- 6 Jacobson IM, McHutchison JG, Dusheiko G, Di Bisceglie AM, Reddy KR, Bzowej NH, Marcellin P, Muir AJ, Ferenci P, Flisiak R, George J, Rizzetto M, Shouval D, Sola R, Terg RA, Yoshida EM, Adda N, Bengtsson L, Sankoh AJ, Kieffer TL, George S, Kauffman RS, Zeuzem S: Telaprevir for previously untreated chronic hepatitis C virus infection. *N Engl J Med* 2011;364:2405–2416.
- 7 Zeuzem S, Andreone P, Pol S, Lawitz E, Diago M, Roberts S, Focaccia R, Younossi Z, Foster GR, Horban A, Ferenci P, Nevens F, Mullhaupt B, Pockros P, Terg R, Shouval D, van Hoek B, Weiland O, Van Heeswijk R, De Meyer S, Luo D, Boogaerts G, Polo R, Picchio G, Beumont M: Telaprevir for retreatment of HCV infection. *N Engl J Med* 2011;364:2417–2428.
- 8 Hayashi N, Izumi N, Kumada H, Okanoue T, Tsubouchi H, Yatsuhashi H, Kato M, Ki R, Komada Y, Seto C, Goto S: Simeprevir with peginterferon/ribavirin for treatment-naïve hepatitis C genotype 1 patients in Japan: CONCERTO-1, a phase III trial. *J Hepatol* 2014;61:219–227.
- 9 Izumi N, Hayashi N, Kumada H, Okanoue T, Tsubouchi H, Yatsuhashi H, Kato M, Ki R, Komada Y, Seto C, Goto S: Once-daily simeprevir with peginterferon and ribavirin for treatment-experienced HCV genotype 1-infected patients in Japan: the CONCERTO-2 and CONCERTO-3 studies. *J Gastroenterol* 2014;49:941–953.
- 10 Kumada H, Hayashi N, Izumi N, Okanoue T, Tsubouchi H, Yatsuhashi H, Kato M, Rito K, Komada Y, Seto C, Goto S: Simeprevir (TMC435) once daily with peginterferon-alpha-2b and ribavirin in patients with genotype 1 hepatitis C virus infection: the CONCERTO-4 study. *Hepatol Res* 2015;45:501–513.
- 11 Jacobson IM, Dore GJ, Foster GR, Fried MW, Radu M, Rafalsky VV, Moroz L, Craxi A, Peeters M, Lenz O, Ouwkerk-Mahadevan S, De La Rosa G, Kalmeijer R, Scott J, Sinha R, Beumont-Mauviel M: Simeprevir with pegylated interferon alfa 2a plus ribavirin in treatment-naïve patients with chronic hepatitis C virus genotype 1 infection (QUEST-1): a phase 3, randomised, double-blind, placebo-controlled trial. *Lancet* 2014;384:403–413.
- 12 Manns M, Marcellin P, Poordad F, de Araujo ES, Buti M, Horsmans Y, Janczewska E, Vilamil F, Scott J, Peeters M, Lenz O, Ouwkerk-Mahadevan S, De La Rosa G, Kalmeijer R, Sinha R, Beumont-Mauviel M: Simeprevir with pegylated interferon alfa 2a or 2b plus ribavirin in treatment-naïve patients with chronic hepatitis C virus genotype 1 infection (QUEST-2): a randomised, double-blind, placebo-controlled phase 3 trial. *Lancet* 2014;384:414–426.
- 13 Chayama K, Takahashi S, Toyota J, Karino Y, Ikeda K, Ishikawa H, Watanabe H, McPhee F, Hughes E, Kumada H: Dual therapy with the nonstructural protein 5A inhibitor, daclatasvir, and the nonstructural protein 3 protease inhibitor, asunaprevir, in hepatitis C virus genotype 1b-infected null responders. *Hepatology* 2012;55:742–748.
- 14 Karino Y, Toyota J, Ikeda K, Suzuki F, Chayama K, Kawakami Y, Ishikawa H, Watanabe H, Hernandez D, Yu F, McPhee F, Kumada H: Characterization of virologic escape in hepatitis C virus genotype 1b patients treated with the direct-acting antivirals daclatasvir and asunaprevir. *J Hepatol* 2013;58:646–654.
- 15 Suzuki Y, Ikeda K, Suzuki F, Toyota J, Karino Y, Chayama K, Kawakami Y, Ishikawa H, Watanabe H, Hu W, Eley T, McPhee F, Hughes E, Kumada H: Dual oral therapy with daclatasvir and asunaprevir for patients with HCV genotype 1b infection and limited treatment options. *J Hepatol* 2013;58:655–662.
- 16 Kumada H, Suzuki Y, Ikeda K, Toyota J, Karino Y, Chayama K, Kawakami Y, Ido A, Yamamoto K, Takaguchi K, Izumi N, Koike K, Takehara T, Kawada N, Sata M, Miyagoshi H, Eley T, McPhee F, Damokosh A, Ishikawa H, Hughes E: Daclatasvir plus asunaprevir for chronic HCV genotype 1b infection. *Hepatology* 2014;59:2083–2091.
- 17 Mizokami M, Yokosuka O, Takehara T, Sakamoto N, Korenaga M, Mochizuki H, Nakane K, Enomoto H, Ikeda F, Yanase M, Toyoda H, Genda T, Umemura T, Yatsuhashi H, Ide T, Toda N, Nirei K, Ueno Y, Nishigaki Y, Betular J, Gao B, Ishizaki A, Omote M, Mo H, Garrison K, Pang PS, Knox SJ, Symonds WT, McHutchison JG, Izumi N, Omata M: Ledipasvir and sofosbuvir fixed-dose combination with and without ribavirin for 12 weeks in treatment-naïve and previously treated Japanese patients with genotype 1 hepatitis C: an open-label, randomised, phase 3 trial. *Lancet Infect Dis* 2015;15:645–653.
- 18 Gane EJ, Stedman CA, Hyland RH, Ding X, Svarovskaia E, Symonds WT, Hinds RG, Berrey MM: Nucleotide polymerase inhibitor sofosbuvir plus ribavirin for hepatitis C. *N Engl J Med* 2013;368:34–44.
- 19 Gane EJ, Stedman CA, Hyland RH, Ding X, Svarovskaia E, Subramanian GM, Symonds WT, McHutchison JG, Pang PS: Efficacy of nucleotide polymerase inhibitor sofosbuvir plus the NS5A inhibitor ledipasvir or the NS5B non-nucleoside inhibitor GS-9669 against HCV genotype 1 infection. *Gastroenterology* 2014;146:736–743.e1.



# A New Horizon in Liver Disease

Masatoshi Kudo

Department of Gastroenterology and Hepatology, Kindai University Faculty of Medicine, Osaka-Sayama, Japan

On May 26–27, 2016, the 6th International Kyoto Liver Cancer Symposium (IKLS) was held in Kyoto in conjunction with the 89th annual meeting of the Japan Society of Ultrasonics in Medicine (JSUM), the 8th Asian Conference on Ultrasound Contrast Imaging (ACUCI), the 12th congress of the Asian Federation of Societies for Ultrasound in Medicine and Biology (AFSUMB), and the 36th annual meeting of the Japan Association of Breast and Thyroid Sonology (JABTS). The theme of this symposium was ‘A New Horizon in Liver Disease’.

The 1st IKLS was held on Awaji Island, Hyogo, in 2005, in conjunction with a single-topic conference on hepatocellular carcinoma (HCC) organized by the Japan Society of Hepatology (JSH) (Congress President: Prof. M. Kudo). The 2nd IKLS was held in Kobe in 2009, in conjunction with the 45th annual congress of the JSH (Congress President: Prof. M. Kudo). The 3rd IKLS was held in Osaka in 2011, in conjunction with the 2nd Asian Pacific Primary Liver Cancer Expert (APPLE) Meeting (Congress President: Prof. M. Kudo). The 4th IKLS was held in 2014 in Kyoto, in conjunction with the 50th annual congress of the Liver Cancer Study Group of Japan (Congress President: Prof. M. Kudo). The 5th IKLS was held in 2015 in Kyoto, in conjunction with the 6th APPLE Meeting (Congress President: Prof. M. Kudo).

All of these symposia were successful. This issue of *Oncology* includes selected articles from the 6th IKLS.

Hagiwara et al. [1] describe the outcome of combination therapy with sofosbuvir and ledipasvir for those with

chronic viral type C liver disease. They conclude that a favorable sustained viral response was achieved by sofosbuvir/ledipasvir therapy, even in elderly patients, those with liver cirrhosis, and those who underwent curative treatment for liver cancer.

Yada et al. [2] describe the influence of liver inflammation on measurements of liver stiffness in patients with autoimmune hepatitis. They conclude that the simultaneous use of shear wave and strain imaging [3], i.e., combination elastography, was useful for evaluating not only the degree of liver fibrosis, but also the degree of liver inflammation.

Kwok et al. [4] report a case of malignant transformation of hepatocellular adenoma (HCA) in a 20-year-old male; this disease is very rare in Japan. Although the factors underlying HCA development are unclear, the diagnosis of  $\beta$ -catenin-activated HCA was correct in this case, in which HCC with similar immunopathological features and structural atypia might have developed from  $\beta$ -catenin-activated HCA. To the best of their knowledge, this is the first case to be reported in Japan [5, 6], although many such cases have been reported in Western countries.

Kono et al. [7] state that low mechanical index contrast tissue harmonic imaging was superior to conventional contrast harmonic imaging [8, 9] for the delineation of hepatic nodular lesions, and might provide better sonographic images to guide radiofrequency ablation and early responses to this type of treatment.

Tochio et al. [10] report 4 cases of hepatic angiomylipoma showing an abundance of CD68-positive cells. This was initially suggested by imaging [11], i.e., positive uptake of a contrast agent within the tumor during the postvascular (Kupffer) phase of Sonazoid-enhanced ultrasonography, and was finally confirmed pathologically by immunohistochemical staining for CD68. This is the first report that CD68-positive cells are abundant in hepatic angiomylipoma [12].

Nishida and Kudo [13] describe the immunological microenvironment of HCC and its clinical implications. They state that the immune response to HCC is determined by the balance between tumor antigenicity and the immunological microenvironment within cancer tissues. The former is also attributed to the accumulation of mutations and aberrations in cellular signaling pathways [14]. They conclude that an immunosuppressive microenvironment within an HCC tumor may result in resistance to immunotherapies such as immune checkpoint blockade [15]; therefore, modification of the tumor microenvironment may restore normal anticancer immune responses.

Kudo [16] describes both basic research and ongoing clinical trials of immune checkpoint inhibitors with respect to HCC. The author states that the results of a phase I/II nivolumab trial are promising, with patients tolerating the treatment well. Currently, two phase III trials are ongoing: one is a first-line trial of nivolumab and the other is a second-line trial of pembrolizumab. Furthermore, combination trials of PD-1/PD-L1 and CTLA-4 in advanced HCC patients are ongoing, as are combination trials of locoregional therapy with immune checkpoint inhibitors [17]. The author notes that immune checkpoint inhibitors will open new avenues for the treatment of HCC.

Finally, I firmly believe that the articles presented herein will provide new insight into recent advances in the field of liver disease; thus, this issue will be a most valuable resource for all the readers of *Oncology*.

## Disclosure Statement

The author declares no conflict of interest regarding this study.

## References

- Hagiwara S, Nishida N, Watanabe T, Sakurai T, Ida H, Minami Y, Takita M, Minami T, Iwanishi M, Chishina H, Ueshima K, Komeda Y, Arizumi T, Kudo M: Outcome of combination therapy with sofosbuvir and ledipasvir for chronic type C liver disease. *Oncology* DOI: 10.1159/000451010.
- Yada N, Sakurai T, Minami T, Arizumi T, Takita M, Hagiwara S, Ida H, Ueshima K, Nishida N, Kudo M: Influence of liver inflammation on liver stiffness measurement in patients with autoimmune hepatitis evaluation by combinational elastography. *Oncology* DOI: 10.1159/000451011.
- Kudo M: Prediction of hepatocellular carcinoma incidence risk by ultrasound elastography. *Liver Cancer* 2014;3:1–5.
- Kwok WY, Hagiwara S, Nishida N, Watanabe T, Sakurai T, Ida H, Minami Y, Takita M, Minami T, Iwanishi M, Chishina H, Kono M, Ueshima K, Komeda Y, Arizumi T, Enoki E, Nakai T, Kumabe T, Nakashima O, Kondo F, Kudo M: Malignant transformation of hepatocellular adenoma. *Oncology* DOI: 10.1159/000451012.
- Kudo M: Malignant transformation of hepatocellular adenoma: how frequently does it happen? *Liver Cancer* 2015;4:1–5.
- Kudo M: Surveillance, diagnosis, treatment, and outcome of liver cancer in Japan. *Liver Cancer* 2015;4:39–50.
- Kono M, Minami Y, Iwanishi M, Minami T, Chishina H, Arizumi T, Komeda Y, Sakurai T, Takita M, Yada N, Ida H, Hagiwara S, Ueshima K, Nishida N, Kudo M: Contrast-enhanced tissue harmonic imaging versus phase inversion harmonic sonographic imaging for the delineation of hepatocellular carcinomas. *Oncology* DOI: 10.1159/000451014.
- Minami Y, Kudo M: Imaging modalities for assessment of treatment response to nonsurgical hepatocellular carcinoma therapy: contrast-enhanced US, CT, and MRI. *Liver Cancer* 2015;4:106–114.
- Liu GJ, Wang W, Lu MD, Xie XY, Xu HX, Xu ZF, Chen LD, Wang Z, Liang JY, Huang Y, Li W, Liu JY: Contrast-enhanced ultrasound for the characterization of hepatocellular carcinoma and intrahepatic cholangiocarcinoma. *Liver Cancer* 2015;4:241–252.
- Tochio H, Tamaki E, Imai Y, Iwasaki N, Minowa K, Chung H, Sugino Y, Inokuma T, Kudo M: CD68-positive cells in hepatic angiomylipoma. *Oncology* DOI: 10.1159/000451013.
- Murakami T, Tsurusaki M: Hypervascular benign and malignant liver tumors that require differentiation from hepatocellular carcinoma: key points of imaging diagnosis. *Liver Cancer* 2014;3:85–96.
- Kudo M: Clinical practice guidelines for hepatocellular carcinoma differ between Japan, United States, and Europe. *Liver Cancer* 2015;4:85–95.
- Nishida N, Kudo M: Immunological microenvironment of hepatocellular carcinoma and its clinical implication. *Oncology* DOI: 10.1159/000451015.
- Kudo M: Recent advances in bioinformatics reveal the molecular heterogeneity of hepatocellular carcinoma. *Liver Cancer* 2014;3:68–70.
- Kudo M: Immune checkpoint blockade in hepatocellular carcinoma. *Liver Cancer* 2015;4:201–207.
- Kudo M: Immune checkpoint inhibition in hepatocellular carcinoma: basics and ongoing clinical trials. *Oncology* DOI: 10.1159/000451016.
- Kim HY, Park JW: Clinical trials of combined molecular targeted therapy and locoregional therapy in hepatocellular carcinoma: past, present, and future. *Liver Cancer* 2014;3:9–17.

# Influence of Liver Inflammation on Liver Stiffness Measurement in Patients with Autoimmune Hepatitis Evaluation by Combinational Elastography

Norihisa Yada Toshiharu Sakurai Tomohiro Minami Tadaaki Arizumi  
Masahiro Takita Satoru Hagiwara Hiroshi Ida Kazuomi Ueshima  
Naoshi Nishida Masatoshi Kudo

Department of Gastroenterology and Hepatology, Kindai University Faculty of Medicine, Osaka-Sayama, Japan

## Key Words

Combinational elastography · Shear wave imaging · Transient elastography · Strain imaging · Real-time tissue elastography · Autoimmune hepatitis

## Abstract

**Objective:** In order to evaluate the influence of liver inflammation on liver stiffness measurement (LSM) by the simultaneous use of shear wave and strain imaging (combinational elastography), shear wave and strain imaging were compared before and after initial therapy for autoimmune hepatitis (AIH). **Methods:** Nine AIH patients initially treated with steroid were enrolled. Transient elastography and real-time tissue elastography were performed just before and 1 month after the start of initial steroid treatment. Blood samples, LSM, and the liver fibrosis index (LFI) were compared. **Results:** Aspartate aminotransferase ( $p = 0.002$ ) and alanine aminotransferase (ALT) ( $p = 0.015$ ) were significantly decreased after initial treatment. The LSM was  $15.5 \pm 9.6$  kPa at baseline, decreasing to  $7.2 \pm 2.3$  kPa after initial treatment ( $p = 0.034$ ). The LFI was  $1.67 \pm 0.67$  at baseline and  $1.61 \pm 0.66$

after initial treatment; no significant change in LFI was recognized ( $p = 0.842$ ). Between  $\Delta$ ALT and  $\Delta$ LSM, a significant regression equation could be calculated as follows:  $\Delta$ ALT =  $-0.55 + 0.654 \times \Delta$ LSM. **Conclusions:** Combinational elastography was useful in evaluating not only the degree of liver fibrosis, but also the degree of liver inflammation in AIH.

© 2017 S. Karger AG, Basel

## Introduction

In recent years, ultrasound elastography has been attracting attention as a noninvasive diagnostic tool for liver fibrosis [1–7]. Evaluation of liver fibrosis is important in the prediction of hepatocellular carcinoma incidence risk and prognosis [8–10]. Ultrasound elastography can be classified into two groups depending on the measurement of physical quantities. Shear wave imaging measures the propagation speed of a shear wave, and strain imaging displays the relative strain of the tissue [11–14].

Autoimmune hepatitis (AIH) is one of the autoimmune diseases where steroids and immunosuppressants

are remarkably effective [15]. While shear wave imaging has been reported to be useful in the detection of fibrosis in the diagnosis of AIH, it has also been reported that liver stiffness varies greatly depending on the level of hepatic inflammation activity [16, 17]. In several liver diseases both of these elastography methods are useful to diagnose the degree of liver fibrosis, but it is said that only shear wave imaging is influenced by liver inflammation, jaundice, liver congestion, etc. [5, 15, 18–21]. However, the degree of influence on liver stiffness by liver inflammation has not been examined so far.

The objective of this study was to examine the influence of liver inflammation on the degree of liver stiffness measurement (LSM) with the simultaneous use of shear wave and strain imaging (combinational elastography).

## Patients and Methods

### Patients

This prospective study was performed at Kindai University Hospital (Osaka-Sayama, Japan). From July 2010 to May 2012, consecutive patients with AIH, who were initially treated with steroid, were enrolled. AIH was diagnosed using the Japanese diagnostic criteria for AIH published in 1996 [22]. Patients were excluded if they consumed >20 g alcohol per day. Patients with histories of viral hepatitis, drug-induced hepatitis, primary biliary hepatitis, primary sclerosing cholangitis, IgG4-related disease, hemochromatosis,  $\alpha$ 1-antitrypsin deficiency, or Wilson's disease were also excluded. The study protocol conformed to the Declaration of Helsinki and was approved by the ethics committee at the Kindai University Faculty of Medicine. Each patient provided informed consent to participate in the study.

### Clinical and Laboratory Assessments

Clinical data were collected at the start of initial therapy with steroid. The relevant clinical data recorded were age, sex, height, and weight. The body mass index was calculated as weight (in kg) divided by height (in m) squared. The presence or absence of jaundice, congestive liver, pleural effusion, and ascites and encephalopathy was confirmed by physical findings and inspection of various images. Blood samples were taken after overnight fasting on the same day as elastography was performed. Laboratory tests, including the measurement of aspartate aminotransferase (AST), alanine aminotransferase (ALT), total bilirubin levels, and platelet counts, were conducted using automated methods.

### Histological Liver Assessment

Percutaneous ultrasound-guided liver biopsy was performed on the right lobe of the liver using a Tru-Cut semiautomatic 18-gauge needle apparatus (Monopty; CR Bard, Tempe, Ariz., USA) within 2 weeks before the start of the initial treatment. The liver biopsy specimens were fixed in formalin, embedded in paraffin, and stained with hematoxylin and eosin, and Masson's trichrome stain. All biopsy specimens were examined by pathologists who were blinded to the patient characteristics. Liver fibrosis was

**Table 1.** Patients' baseline characteristics

Age, years	66.6±2.2
Males	1 (11.1%)
Females	8 (88.9%)
Height, cm	154.6±8.5
Weight, kg	54.3±11.5
BMI	22.8±5.4
F stage	
0	0
1	1
2	4
3	4
4	0
Jaundice	0
Liver congestion	0
Pleural effusion	0
Ascites	0
Encephalopathy	0

**Table 2.** Elastographic and hematological data before and after initial treatment

	Before initial treatment	After initial treatment	p value
LSM, kPa	15.5±9.6	7.2±2.3	0.034
LFI	1.67±0.67	1.61±0.66	0.842
AST, IU/l	274.7±168.3	22.9±7.5	0.002
ALT, IU/l	360.6±319.5	29.8±13.5	0.015
Serum bilirubin, g/dl	1.1±0.4	0.9±0.3	0.418
Platelet count, ×10 <sup>9</sup> /l	18.8±7.6	20.0±6.5	0.733

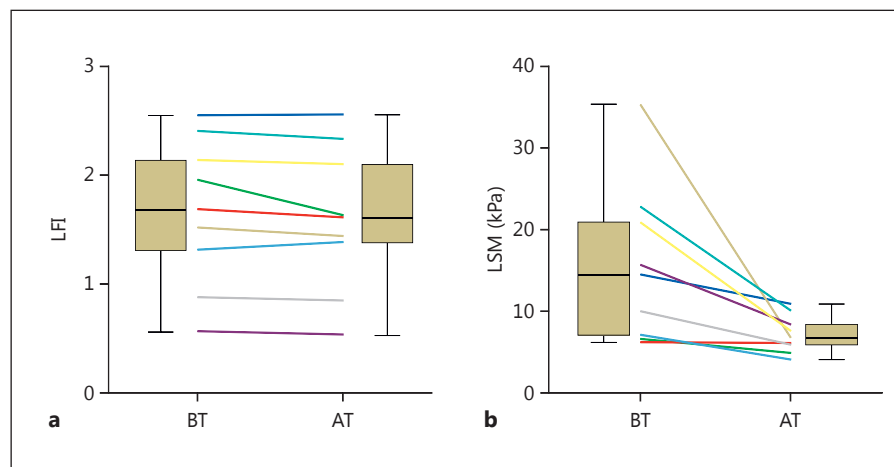
The mean values of LSM, LFI, AST, ALT, serum bilirubin, and platelet count before and after initial treatment are given. There were significant decreases in LSM ( $p = 0.034$ ), AST ( $p = 0.002$ ), and ALT ( $p = 0.015$ ). ALT = Alanine aminotransferase; AST = aspartate aminotransferase; LFI = liver fibrosis index; LSM = liver stiffness measurement.

scored using the New Inuyama classification. The stage of fibrosis was classified from F0 to F4 as follows: F0 = no fibrosis; F1 = fibrosis portal expansion; F2 = bridging fibrosis (portal-portal or portal-central linkage); F3 = bridging fibrosis with lobular distortion (disorganization); and F4 = cirrhosis [23].

### Transient Elastography

Transient elastography (TE) was performed using a dedicated LSM device, namely a FibroScan 502 with the M-probe (Echosens, Paris, France). TE was carried out just before and 1 month after the start of the initial treatment. The procedure was performed on the right lobe of the liver through the intercostal space, with patients in the supine position. Examinations that achieved no successful measurements after ≥10 attempts were deemed failures. The median LSM value (in kPa) was considered as being representative of

**Fig. 1.** Line graph and box-and-whisker plot of LFI and LSM changes. The color of the line graph is the same in LFI (a) and LSM (b) in each case. The LSM was  $15.5 \pm 9.6$  kPa at baseline and decreased to  $7.2 \pm 2.3$  kPa after initial treatment ( $p = 0.034$ ). The LFI was  $1.67 \pm 0.67$  at baseline and  $1.61 \pm 0.66$  after the initial treatment; there was no significant change in LFI ( $p = 0.842$ ). LFI = Liver fibrosis index; LSM = liver stiffness measurement; BT = before treatment; AT = after treatment.



the elastic modulus of the liver. As an indicator of variability, the ratio of the interquartile range (IQR) of the LSM to the median value (IQR/M) was calculated. Examinations with <10 valid measurements or an IQR/M >30% or a success rate <60% were considered potentially unreliable [19].

#### Real-Time Tissue Elastography

Real-time tissue elastography (RTE) and TE were performed on the same day, just before and 1 month after the start of the initial treatment, and continued until the next TE. The procedure was performed after overnight fasting using ultrasound (EUB-8500 or HI VISION Ascendus; Hitachi, Tokyo, Japan) and an EUP-L52 linear type probe (3–7 MHz; Hitachi), by means of a previously reported method [4, 6]. The liver fibrosis index (LFI) was calculated using a multiple regression equation with feature values obtained from RTE images, for the diagnosis of liver fibrosis in patients with chronic hepatitis C [1]. An examiner who was unaware of the patient's background selected 10 high-quality images for the estimation of the median LFI. In the current study, the median LFI was used as an objective evaluation of RTE values.

#### Statistical Analysis

Descriptive statistics are shown as mean  $\pm$  SD, median (range), or percentage, as appropriate. Correlation between the data was tested using nonparametric Spearman rank correlation analysis. Differences were considered statistically significant at  $p$  values <0.05. Analysis was performed using the SPSS Statistics 20 software (IBM, Armonk, N.Y., USA).

## Results

#### Demographics and Baseline Features

A total of 9 cases were enrolled. The clinical characteristics and laboratory data are shown in table 1. Eight patients (88.9%) were women. The patients' mean age was  $66.6 \pm 2.2$  years. In the pathological diagnosis, 1 case was

in F1, 4 cases were in F2, and 4 cases were in F3 (table 1). Jaundice, congestive liver, pleural effusion, ascites, and encephalopathy were not observed (table 1). The LSM and LFI were measurable in all cases. There was no significant correlation between elastographic and hematological data at baseline.

#### Comparison of Hematological Laboratory Findings, Liver Stiffness, and LFI at Baseline and after Initial Treatment

AST ( $p = 0.002$ ) and ALT ( $p = 0.015$ ) levels were significantly decreased after the initial treatment with steroid. However, there was no significant change in serum bilirubin level ( $p = 0.418$ ) or platelet count ( $p = 0.733$ ) (table 2). The LSM was  $15.5 \pm 9.6$  kPa at baseline and decreased to  $7.2 \pm 2.3$  kPa after initial treatment ( $p = 0.034$ ). The LFI was  $1.67 \pm 0.67$  at baseline and  $1.61 \pm 0.66$  after the initial treatment; there was no significant change in LFI ( $p = 0.842$ ) (fig. 1; table 2).

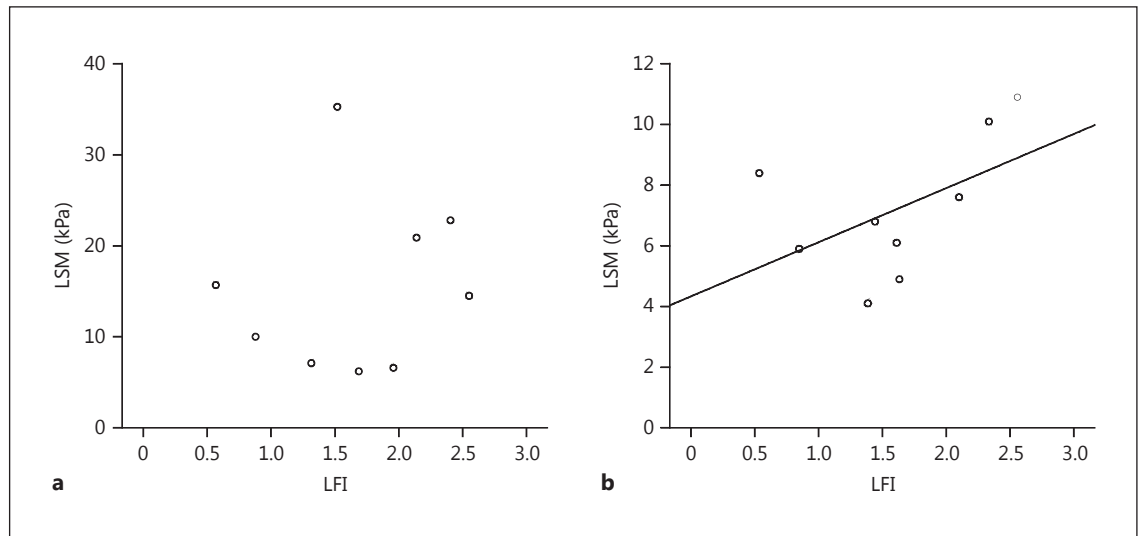
#### Relationship between LFI and LSM

At baseline, LFI and LSM were not significantly correlated, but a strong correlation was observed between LFI and LSM after initial therapy (fig. 2).

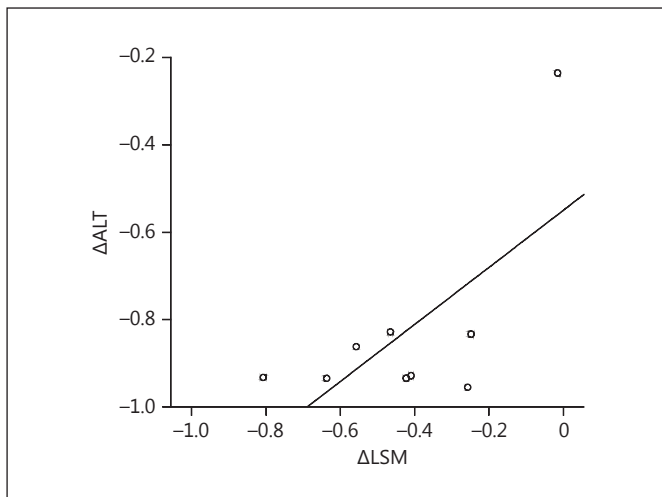
#### Relationship between $\Delta$ LFI and $\Delta$ LSM

$\Delta$ AST,  $\Delta$ ALT, and  $\Delta$ LSM represent the amount of change in AST, ALT, and LSM, calculated as follows: (date after treatment – date at baseline)/date at baseline. The trend in  $\Delta$ LSM correlated with the trend in  $\Delta$ AST and  $\Delta$ ALT. Between  $\Delta$ ALT and  $\Delta$ LSM, a significant regression equation could be calculated as follows:  $\Delta$ ALT =  $-0.55 + 0.654 \times \Delta$ LSM (fig. 3).





**Fig. 2.** Scatter diagram of the relationship between LFI and LSM before (a) and after initial treatment (b). A strong correlation was observed between LFI and LSM after initial therapy. LFI = Liver fibrosis index; LSM = liver stiffness measurement.



**Fig. 3.** Relationship between  $\Delta$ ALT and  $\Delta$ LSM.  $\Delta$ ALT and  $\Delta$ LSM represent the amount of change in ALT and LSM, calculated as follows: (date after treatment – date at baseline)/date at baseline. Between  $\Delta$ ALT and  $\Delta$ LSM, a significant regression equation could be calculated as follows:  $\Delta$ ALT =  $-0.55 + 0.654 \times \Delta$ LSM. ALT = Alanine aminotransferase; LSM = liver stiffness measurement.

#### *LFI and LSM in the Various Fibrosis Stages*

The LFI gradually increased in accordance with the progress of liver fibrosis. Baseline LSM also significantly increased in accordance with the progress of liver fibrosis (fig. 4).

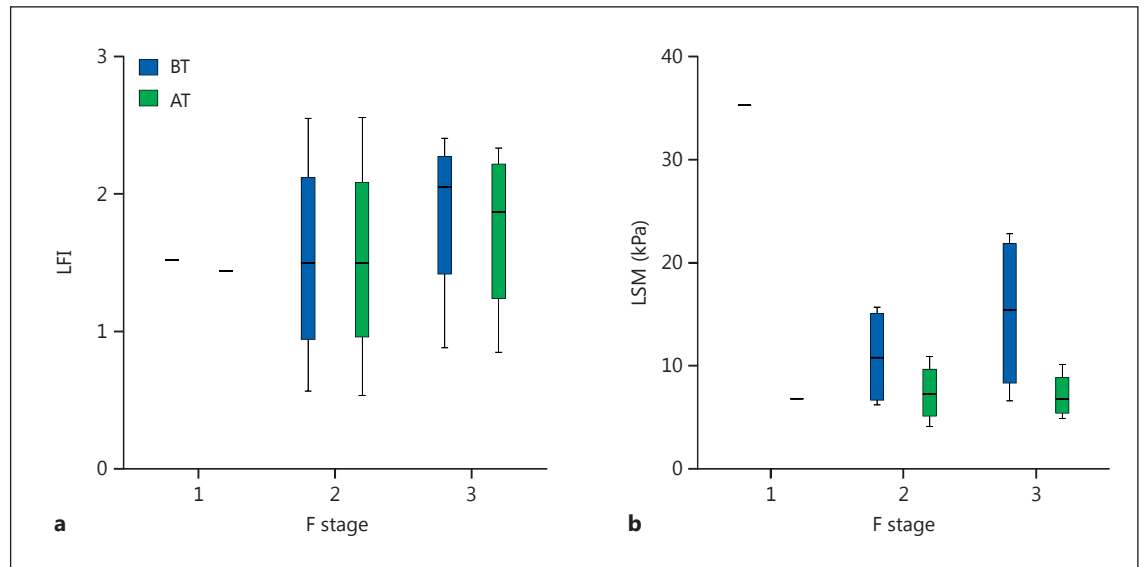
#### **Discussion**

Since the mean LSM at baseline was very high ( $15.5 \pm 9.6$  kPa), in some cases it might be misdiagnosed as cirrhosis. After initial treatment the LSM was significantly reduced to  $7.2 \pm 2.3$  kPa. The observation interval was only 1 month; liver fibrosis seemed not to have changed.

There were no jaundice or liver congestion cases in this study. Moreover, such a relationship between  $\Delta$ ALT and  $\Delta$ LSM could be established ( $\Delta$ ALT =  $-0.55 + 0.654 \times \Delta$ LSM), so the main cause of the reduction in LSM was considered to be an improvement in inflammation. Thus, at baseline the mean LSM seems to have been mainly influenced by inflammation and liver fibrosis. After treatment, the inflammation was assumed to be substantially healed, and liver stiffness after treatment could be assumed to reflect only the effect of hepatic fibrosis.

In the current study, we used TE for shear wave imaging; however, TE can be substituted by other shear wave imaging devices, because there is a strong correlation between LSM and the liver stiffness calculated by other shear wave imaging devices [7].

On the other hand, the LFI was not changed after initial treatment; it seems to be mainly influenced by liver fibrosis, not by inflammation. In my opinion, since the liver fibrosis level can be evaluated by the LFI, it is possible to predict the LSM corresponding to the liver fibro-



**Fig. 4.** LFI and LSM in the various liver fibrosis stages before and after initial treatment. The LFI (a) and the LSM (b) of each fibrosis stage were divided into before and after treatment. The LFI gradually increased in accordance with the progress of liver fibrosis. The baseline LSM also significant increased in accordance with the progress of liver fibrosis. LFI = Liver fibrosis index; LSM = liver stiffness measurement; BT = before treatment; AT = after treatment.

sis. If the LSM at pretreatment is much greater than the predictive value using the LFI, it can be determined that the degree of inflammation is high. In this way, if there is a discrepancy of LSM and LFI with the simultaneous use of shear wave and strain imaging (combinational elastography), the other influence to accelerate the propagation speed of shear wave, such as inflammation, jaundice, or liver congestion, could be grasped.

Unfortunately the sample size of this study was too small, so the degree of predictive evaluation of inflammation could not be determined accurately. It is necessary to verify this by studying further cases, with other liver diseases or conditions. At least, combinational elastography was useful in evaluating not only the degree of liver fibrosis, but also the degree of liver inflammation in AIH.

## Conclusions

Changes in LSM, LFI, and hematological features were examined before and after the initial treatment of patients with AIH. After successful treatment with steroid, AST and ALT levels promptly improved and the LSM also greatly decreased. However, there was no significant change in LFI. Using shear wave imaging and

strain imaging simultaneously (combinational elastography), it may be possible to determine not only the degree of liver fibrosis, but also the degree of severity of conditions such as liver inflammation in AIH.

## Acknowledgment

This research was supported by the Research Program on Hepatitis of the Japan Agency for Medical Research and Development (AMED).

## Disclosure Statement

The authors declare that they have no conflicts of interest.

## References

- 1 Fujimoto K, Kato M, Tonomura A, Yada N, Tatsumi C, Oshita M: Non-invasive evaluation method of the liver fibrosis using real-time tissue elastography – usefulness of judgment liver fibrosis stage by liver fibrosis index (LF Index). *Kanzo* 2010;51:539–541.
- 2 Tatsumi C, Kudo M, Ueshima K, Kitai S, Ishikawa E, Yada N, Hagiwara S, Inoue T, Minami Y, Chung H, Maekawa K, Fujimoto K, Kato M, Tonomura A, Mitake T, Shiina T: Non-invasive evaluation of hepatic fibrosis for type C chronic hepatitis. *Intervirol* 2010;53:76–81.

- 3 Fujimoto K, Kato M, Kudo M, Yada N, Shiina T, Ueshima K, Yamada Y, Ishida T, Azuma M, Yamasaki M, Yamamoto K, Hayashi N, Takehara T: Novel image analysis method using ultrasound elastography for noninvasive evaluation of hepatic fibrosis in patients with chronic hepatitis C. *Oncology* 2013;84(suppl 1):3–12.
- 4 Yada N, Kudo M, Morikawa H, Fujimoto K, Kato M, Kawada N: Assessment of liver fibrosis with real-time tissue elastography in chronic viral hepatitis. *Oncology* 2013;84(suppl 1):13–20.
- 5 Yada N, Kudo M, Kawada N, Sato S, Osaki Y, Ishikawa A, Miyoshi H, Sakamoto M, Kage M, Nakashima O, Tonomura A: Noninvasive diagnosis of liver fibrosis: utility of data mining of both ultrasound elastography and serological findings to construct a decision tree. *Oncology* 2014;87(suppl 1):63–72.
- 6 Yada N, Sakurai T, Minami T, Arizumi T, Takita M, Inoue T, Hagiwara S, Ueshima K, Nishida N, Kudo M: Ultrasound elastography correlates treatment response by antiviral therapy in patients with chronic hepatitis C. *Oncology* 2014;87(suppl 1):118–123.
- 7 Yada N, Sakurai T, Minami T, Arizumi T, Takita M, Hagiwara S, Ueshima K, Ida H, Nishida N, Kudo M: A newly developed shear wave elastography modality: with a unique reliability index. *Oncology* 2015;89(suppl 2): 53–59.
- 8 Kudo M: Prediction of hepatocellular carcinoma incidence risk by ultrasound elastography. *Liver Cancer* 2014;3:1–5.
- 9 Kudo M: Surveillance, diagnosis, treatment, and outcome of liver cancer in Japan. *Liver Cancer* 2015;4:39–50.
- 10 Kudo M: Clinical practice guidelines for hepatocellular carcinoma differ between Japan, United States, and Europe. *Liver Cancer* 2015; 4:85–95.
- 11 Kudo M, Shiina T, Moriyasu F, Iijima H, Tateishi R, Yada N, Fujimoto K, Morikawa H, Hirooka M, Sumino Y, Kumada T: JSUM ultrasound elastography practice guidelines: liver. *J Med Ultrason* (2001) 2013;40:325–357.
- 12 Shiina T: JSUM ultrasound elastography practice guidelines: basics and terminology. *J Med Ultrason* (2001) 2013;40:309–323.
- 13 Ferraioli G, Filice C, Castera L, Choi BI, Sporea I, Wilson SR, Cosgrove D, Dietrich CF, Amy D, Bamber JC, Barr R, Chou YH, Ding H, Farrokh A, Friedrich-Rust M, Hall TJ, Nakashima K, Nightingale KR, Palmeri ML, Schafer F, Shiina T, Suzuki S, Kudo M: WFUMB guidelines and recommendations for clinical use of ultrasound elastography: Part 3: liver. *Ultrasound Med Biol* 2015;41: 1161–1179.
- 14 Shiina T, Nightingale KR, Palmeri ML, Hall TJ, Bamber JC, Barr RG, Castera L, Choi BI, Chou YH, Cosgrove D, Dietrich CF, Ding H, Amy D, Farrokh A, Ferraioli G, Filice C, Friedrich-Rust M, Nakashima K, Schafer F, Sporea I, Suzuki S, Wilson S, Kudo M: WFUMB guidelines and recommendations for clinical use of ultrasound elastography: Part 1: basic principles and terminology. *Ultrasound Med Biol* 2015;41:1126–1147.
- 15 Yada N, Kudo M, Chung H, Watanabe T: Autoimmune hepatitis and immunoglobulin G4-associated autoimmune hepatitis. *Dig Dis* 2013;31:415–420.
- 16 Xu Q, Sheng L, Bao H, Chen X, Guo C, Li H, Ma X, Qiu D, Hua J: Evaluate of transient elastography in assessing liver fibrosis in patients with autoimmune hepatitis. *J Gastroenterol Hepatol* 2016, Epub ahead of print.
- 17 Hartl J, Denzer U, Ehlken H, Zenouzi R, Peiseler M, Sebode M, Hübener S, Pannicke N, Weiler-Normann C, Quaas A, Lohse AW, Schramm C: Transient elastography in autoimmune hepatitis: timing determines the impact of inflammation and fibrosis. *J Hepatol* 2016;65:769–775.
- 18 Arena U, Vizzutti F, Corti G, Ambu S, Stasi C, Bresci S, Moscarella S, Boddi V, Petrarca A, Laffi G, Marra F, Pinzani M: Acute viral hepatitis increases liver stiffness values measured by transient elastography. *Hepatology* 2008; 47:380–384.
- 19 Cebbold JF, Taylor-Robinson SD: Transient elastography in acute hepatitis: all that's stiff is not fibrosis. *Hepatology* 2008;47:370–372.
- 20 Millonig G, Reimann FM, Friedrich S, Fonouni H, Mehrabi A, Büchler MW, Seitz HK, Mueller S: Extrahepatic cholestasis increases liver stiffness (FibroScan) irrespective of fibrosis. *Hepatology* 2008;48:1718–1723.
- 21 Colli A, Pozzoni P, Berzuini A, Gerosa A, Canovi C, Molteni EE, Barbarini M, Bonino F, Prati D: Decompensated chronic heart failure: increased liver stiffness measured by means of transient elastography. *Radiology* 2010;257:872–878.
- 22 Research Program of Intractable Disease provided by the Ministry of Health, Labor, and Welfare of Japan: Guidelines for the diagnosis of autoimmune hepatitis. *Kanzo* 1996;37: 298–300.
- 23 Ichida F, Tsuji T, Omata M, Ichida T, Inoue K, Kamimura T, Yamada G, Hino K, Yokosuka O, Suzuki H: New Inuyama classification; new criteria for histological assessment of chronic hepatitis. *Int Hepatol Commun* 1996;6:112–119.

# Immunological Microenvironment of Hepatocellular Carcinoma and Its Clinical Implication

Naoshi Nishida Masatoshi Kudo

Department of Gastroenterology and Hepatology, Kindai University Faculty of Medicine, Osaka-Sayama, Japan

## Key Words

Hepatocellular carcinoma · Neoantigen · Mutation · Immune exhaustion · Immune checkpoint

## Abstract

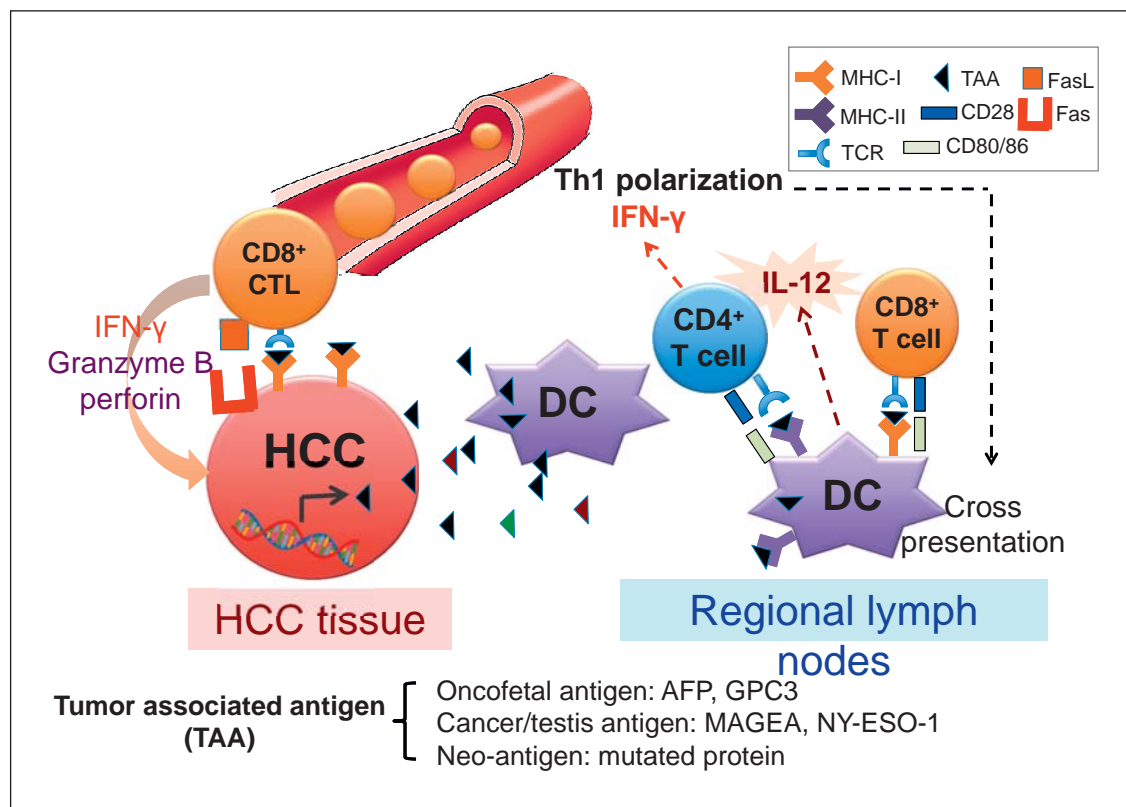
Despite recent advances in the treatment of hepatocellular carcinoma (HCC), the prognosis of patients with advanced stage of disease remains unfavorable. Several immune therapies have been applied to HCC, and their responses have not been satisfactory. The immune response to cancer is determined by the balance between the antigenicity of the tumor and the microenvironment of cancer tissues. Generally, accumulated genetic mutations are observed in HCC, which may lead to increased neoantigens on cancer cells with high antigenicity. However, cancer cells may evade the immune system because of alterations in molecules and cellular pathways involved in antigen processing and presentation. In addition, hypoxia in tissue induces several cytokines, chemokines, and immunosuppressive molecules from HCC cells and stromal cells. These cells also produce cytokines that attract regulatory T cells infiltrating tumor tissues and contribute to establishing an immunosuppressive microenvironment. Some cancers show a good response to immune checkpoint therapy. However, prolonged stabilization of dis-

ease for this treatment is reportedly 12–41% in patients with advanced cancer. Therefore, immunosuppressive forces in the microenvironment of HCC may cause resistance to immune therapy, and modification of the tumor microenvironment may restore normal anticancer immunity. In this review, we focus on the immunological microenvironment of HCC tissues and discuss how the immunosuppressive environment of HCC should be modulated to achieve a favorable response to immune therapy, such as immune checkpoint therapy, in HCC.

© 2016 S. Karger AG, Basel

## Introduction

Hepatocellular carcinoma (HCC) is one of the leading causes of cancer death, and the prognosis of patients with advanced tumors that are not suitable for locoregional treatment remains unfavorable [1–5]. Several types of immune therapies have been applied for the treatment for advanced cancer, including HCC, yet the response of HCC to immune therapy has not been satisfactory. However, since the degree of lymphocyte infiltration in HCC tissues is closely associated with recurrence after liver resection and transplantation [6, 7], the immune response



**Fig. 1.** Recognition and immune rejection of HCC cell by CTLs. DCs become active through the uptake and recognition of TAAs by the pattern recognition receptors. Activated DCs express co-stimulatory factors (CD80 and CD86) and IL-12, migrate to the regional lymph nodes, and present the processed antigen on MHC class II molecules for recognition by naïve CD4+ T cells. The activated CD4+ T cells differentiate to IFN-γ-producing type 1 Th cells (Th1 polarization). Th1 cells also help DCs to present exog-

enous antigens on MHC class I molecules to CD8+ T cells (cross-presentation), which induces the development of CD8+ CTLs. CTLs exert anticancer effects by producing IFN-γ and releasing granzyme B and perforin. Fas-dependent mechanisms also contribute to the cytotoxic effect of T cells. AFP = Alpha-fetoprotein; MAGEA = melanoma-associated antigen; NY-ESO-1 = New York esophageal squamous cell carcinoma-1.

should be critical for eliminating HCC cells [8, 9]. It was recently reported that some types of cancers, such as melanoma, non-small-cell lung cancer, and renal cell carcinoma, showed a good response to immune checkpoint therapy using antibodies against programmed cell death protein 1 (PD-1), programmed cell death 1 ligand 1 (PD-L1), and cytotoxic T-lymphocyte-associated protein 4 (CTLA-4) [9–11]. However, tumor antigenicity and background immune conditions differ among individuals, affecting the response to immune therapies, including immune checkpoint blockade [8]. In this review, we focus on the immunological microenvironment of HCC tissues in the context of the disturbance of immunity in cancer and discuss how the immunosuppressive microenvironment of HCC should be modulated to achieve a favorable response in the immune therapy of HCC.

## Immune Response and Rejection of Cancer Cells

Antigen uptake by dendritic cells (DCs) triggers the immune response and rejection of cancer cells. DCs become active through the recognition of specific molecular structures, such as pathogen-associated molecular patterns (PAMPs) in pathogens and damage-associated molecular patterns (DAMPs) in damaged cells, by the pattern recognition receptors. Activated DCs express co-stimulatory factors (CD80 and CD86), and inflammatory cytokines (such as interleukin-12, IL-12) migrate to the regional lymph nodes and present the processed antigen on major histocompatibility complex (MHC) class II molecules for recognition by naïve CD4+ T cells (fig. 1). Subsequently, the activation and proliferation of CD4+ T cells are triggered by binding of the antigen on MHC class



II to T cell receptor (TCR) and CD80/CD86 to CD28 on the lymphocyte. The activated CD4<sup>+</sup> T cells express the CD40 ligand that binds to CD40 on antigen-presenting cells (APCs), leading to the production of IL-12 from APCs, and enhances the differentiation of CD4<sup>+</sup> T cells to interferon gamma (IFN- $\gamma$ )-producing type 1 T helper (Th1) cells (Th1 polarization). Accordingly, Th1 cells help DCs to present exogenous antigens on MHC class I molecules to CD8<sup>+</sup> T cells (cross-presentation), which induces the development of CD8<sup>+</sup> cytotoxic T lymphocytes (CTLs). CTLs exert anticancer effects by producing IFN- $\gamma$  and releasing granzyme B and perforin (fig. 1). They also have cytotoxic effects in cancer cells by interacting with TNF receptor superfamily member 6 (Fas) and TNF ligand superfamily member 10 on cancer cells. These processes may act in concert; sufficient induction of the Th1 response and proliferation of anticancer CTLs may be critical for the immune reaction to cancer.

### Cells and Cytokines Related to Immune Response and Suppression in HCC

#### *Helper T Cells and Related Cytokines*

As described above, naïve CD4<sup>+</sup> T cells are activated through the recognition of antigens on MHC class II molecules and co-stimulatory factors on DCs; the differentiation of CD4<sup>+</sup> T cells depends on the profile of cytokines from APCs and CD4<sup>+</sup> T cells. In the presence of IL-12 and IFN- $\gamma$ , CD4<sup>+</sup> T cells express Th1-specific T-box 1 transcription factor and differentiate into Th1 cells, leading to the activation of CD8<sup>+</sup> T cells (or CTLs) and macrophages. In the presence of IL-4, CD4<sup>+</sup> T cells express the transcription factor GATA binding protein 3, which induces the differentiation of CD4<sup>+</sup> T cells to Th2 cells. Th2 cells produce Th2 cytokines, such as IL-4, IL-5, and IL-13, and enhance the humoral immune response. It has been reported that increased expression of Th1 cytokines in HCC tissues is associated with longer patient survival, whereas expression of Th2 cytokines is associated with vascular invasion and the metastatic recurrence of cancer [12].

The presence of transforming growth factor beta (TGF- $\beta$ ) and IL-2 induces the expression of the master transcription factor forkhead box P3 (FOXP3), which induces the differentiation of naïve CD4<sup>+</sup> T cells to regulatory T cells (Tregs). These cells may play an important role in the immunosuppressive environment of cancer cells [13]. Naïve CD4<sup>+</sup> T cells also differentiate into Th17 cells in the presence of IL-6 and TGF- $\beta$ . Th17 cells play a

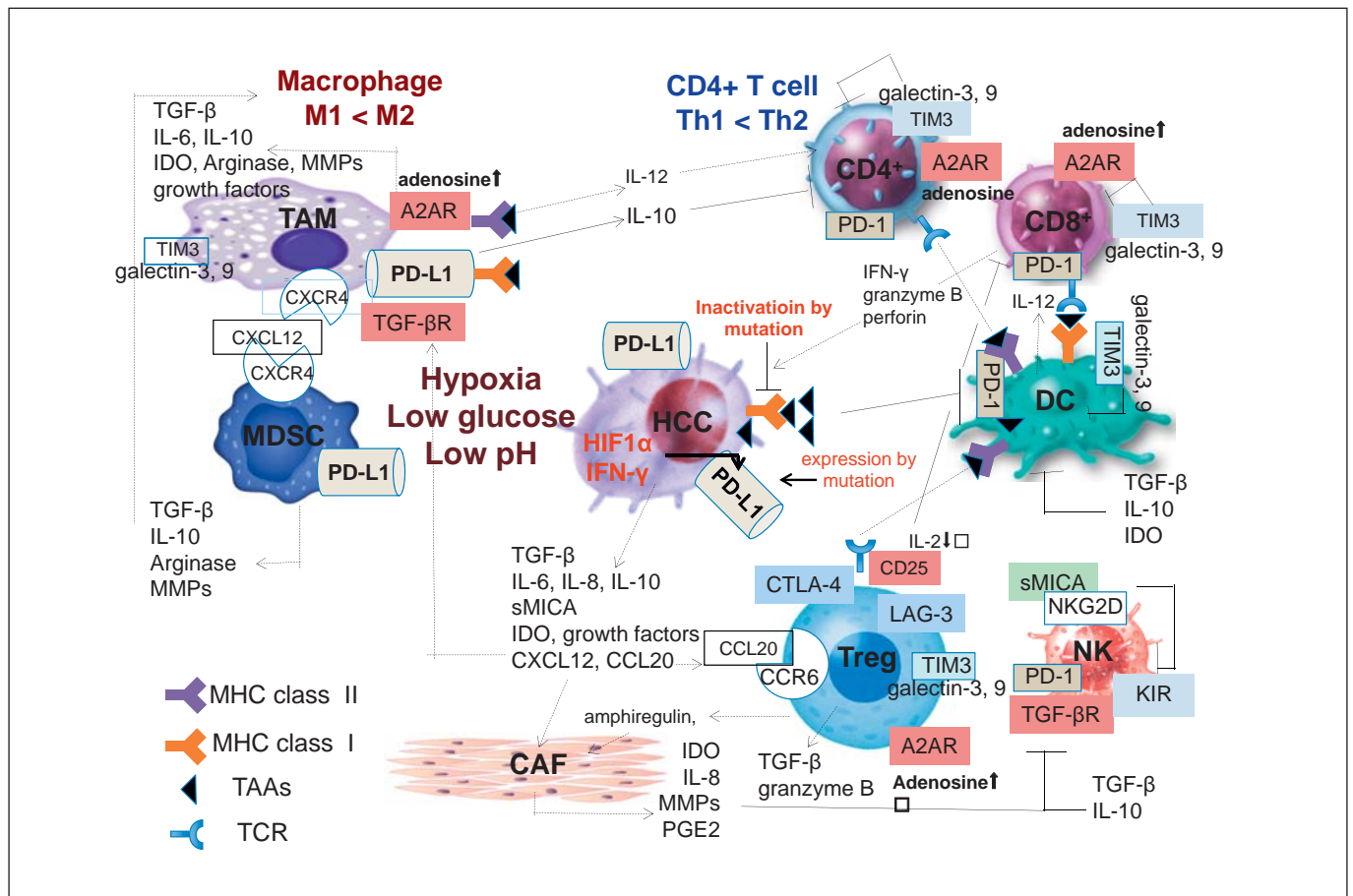
role in the activation of neutrophils and the progression of inflammation.

The recognition of antigen and CD80/86 induces activation of the PI3K-Akt-mTOR pathway in CD8<sup>+</sup> T cells through signaling from TCR and CD28. One of the downstream targets of mTOR, interferon regulatory factor 4, induces Th1-specific T-box 1 transcription factor as well as hypoxia-inducible factor 1- $\alpha$  (HIF-1 $\alpha$ ). The latter induces glucose transporter 1 on the T cell membrane, enhances glycolysis, and plays a role in its effector function. It is also known that immune checkpoint molecules, such as CTLA-4 and PD-1, suppress activation of the PI3K-Akt-mTOR pathway in T cells [14, 15].

Adenosine triphosphate (ATP) is also considered critical for the effector function of T cells. Extracellular ATP stimulates the production of IL-2 in CD8<sup>+</sup> T cells by increasing the intracellular concentration of calcium [16]. In contrast, adenosine binds to the adenosine A2A receptor on T cells and decreases intracellular calcium concentration. This process suppresses the proliferation and cytotoxic effects of CD8<sup>+</sup> cells and reduces Th1 cytokines (fig. 2) [16].

#### *Regulatory T Cells*

Tregs play a central role in peripheral immune tolerance that acts as a regulator of self-reactive T cells. Tregs constitutively express CTLA-4 and glucocorticoid-induced TNF receptor; their expression is regulated by FOXP3 [13]. In contrast to the stimulatory receptor CD28 on T cells, CTLA-4 acts as a repressive receptor to CD80/CD86 and inhibits T cell activation. Tregs also possess IL-2 receptor subunit  $\alpha$  (CD25) and reduce IL-2 in the microenvironment by associating with CD25. As IL-2 is essential for the differentiation and proliferation of CTLs, a decrease in IL-2 is expected to induce immune suppression (fig. 2). In addition, Tregs convert extracellular ATP into adenosine through the function of CD38 and CD78; adenosine binds to the adenosine A2A receptor on effector T cells and suppresses its function [17]. Tregs also produce several regulatory cytokines for immune reactions [18]. For example, TGF- $\beta$  and IL-35, which are produced by Tregs, exert suppressive effects on T cell proliferation. Granzyme B from Tregs induces the apoptosis of effector T cells [19]; Tregs express an epidermal growth factor ligand, amphiregulin, which promotes the proliferation of epithelial cells and induces the extracellular matrix [20, 21]. These effects act in concert and contribute to establishing the immunosuppressive microenvironment of HCC tissue (fig. 2). Recently, several studies have shown that cancer cells can induce chemokines that



**Fig. 2.** Immune cells, cytokines, and molecules that contribute to the immunosuppressive microenvironment in HCC. A2AR = Human adenosine receptor A2A; CAF = cancer-associated fibroblast; CXCL12 = stromal cell-derived factor α; LAG-3 = lymphocyte activation gene 3; MMP = matrix metalloprotease; PGE2 = prostaglandin E2.

may help Tregs to migrate into cancerous tissues [22]. Recruitment of Tregs reportedly fosters tumor progression and is associated with the poor prognosis of HCC; the chemokine C-C motif ligand 20 cooperates with its receptor chemokine receptor 6 and induces Tregs to HCC [23].

#### Dendritic Cells

DCs link the innate immune systems to adaptive systems; the main function of DCs is to process antigens and present them on MHC molecules to T cells. As described above, activation of DCs takes place through the recognition of molecules with specific structures such as PAMPs and DAMPs with the pattern recognition receptors [24]. They produce cytokines responsible for the adaptive immune response, such as IL-12 and type 1 interferon,

which initiate the adaptive immune response. Once activated, they induce expression of MHC class II and co-stimulatory factor CD80/86, migrate to the regional lymph nodes, and interact with and activate T cells (fig. 1). In addition, cross-presentation of processed antigens by DCs induces the activation of CD8+ T cells that act as CTLs. As several DAMPs can be released from cancer cells during inflammation and cell death, cross-presentation by DCs is critical for initiating an immune response to cancer (fig. 1). It has also been reported that CD14+ DCs express high levels of CTLA-4 and suppress T cell effects by inducing IL-10 and indoleamine 2,3-dioxygenase (IDO) [25]. The enzymatic action of IDO depletes tryptophan in the microenvironment, leading to the inhibition of antigen-specific T cell proliferation.

### Macrophages

Macrophages are found in all types of tissues and exert a phagocyte function. In addition, they play a critical role in innate and adaptive immunity by recruiting other types of immune cells and presenting antigens to T cells. Macrophages in cancerous tissues (tumor-associated macrophages, TAMs) are mainly derived from monocytes from the bone marrow and spleen. They represent different functions and features based on the tissue microenvironments. Generally, in the presence of Th1 cytokines, such as IFN- $\gamma$  and Toll-like receptor ligands, macrophages express Th1 cytokines, inflammatory cytokines (such as IL-1 $\beta$ , IL-6, IL-12, and TNF- $\alpha$ ), reactive oxygen species (ROS), and nitric oxide (NO); macrophages play a critical role in pro-inflammatory response and pathogen clearance. They also induce the cytotoxicity of target cells, which is critical for anticancer immunity, and they are known as M1 macrophages. In contrast, Th2 cytokines (such as IL-4 and IL-13) and TGF- $\beta$  induce M2 macrophages that are important for the anti-inflammatory response, wound healing, angiogenesis, and tissue remodeling. M2 macrophages produce tumor-promoting and immunosuppressive cytokines and growth factors related to tissue regeneration and angiogenesis, such as IL-10, TGF- $\beta$ , arginase, prostaglandin E2, matrix metalloproteinase 7/9, epidermal growth factor, insulin-like growth factor, vascular endothelial growth factor (VEGF), and platelet-derived growth factor (PDGF) [26]. Therefore, the balance between M1 and M2 in TAMs is important for cancer immune therapy (fig. 2).

Several bone marrow-derived cells resembling macrophages have also been detected in cancer tissues. These are considered precursors of granulocytes, monocytes, and macrophages and are known as myeloid-derived suppressor cells (MDSCs) [27]. These cells are recruited upon stimulation of cytokines from cancer cells and exert immunosuppressive and tumor-promoting effects. From an immunological perspective, they disturb both CD4+ and CD8+ responses through the enzymatic activity of arginase and arginine depletion [28] and induce ROS and NO, which leads to disruption of TCR signaling (fig. 2) [29]. TGF- $\beta$  and IL-10 from MDSCs suppress natural killer (NK) cell activity and induce the expansion of Tregs, respectively [30]. The number of MDSCs is reportedly associated with the aggressiveness of HCC [28, 31].

The Th1/Th2 and M1/M2 balance in cancer tissues may also be affected by the interaction between MDSCs and TAMs. IL-10 derived from MDSCs downregulates IL-12 in TAMs, leading to Th2 polarization. IL-4 from Th2 induces the development of M2 macrophages (fig. 2).

### NK Cells

NK cells also show a cytotoxic effect among the cells involved in the innate immune system. The role of NK cells is similar to that of CTLs in the adaptive immune system. Compared to T cells, NK cells react more quickly during immune reactions. Typically, CTLs recognize antigens on MHC and subsequently release cytokines, leading to cell lysis and apoptosis. NK cells can also recognize target cells in the absence of MHC. This ability is particularly important because cancer cells that are missing MHC I molecules can be detected and killed only by NK cells.

The mechanism of how NK cells target cancer cells missing MHC I molecules is mainly attributed to the balance in the signals from killer activation receptors (KARs) and inhibitory receptors in this cell. There are different types of KARs; one of the KARs is known as natural killer group 2D (NKG2D), which is a group of inhibitory receptors including inhibitory killer-cell immunoglobulin-like receptors (KIRs) and receptors known as immune checkpoint molecules, such as PD-1 and T-cell immunoglobulin and mucin-domain containing-3 (TIM3). For target detection, NK cells examine the target cell surface using KIRs and determine the expression level of MHC class I molecules. If engagement of KIRs to MHC class I molecules is insufficient, killing of the target cell proceeds. However, sufficient binding of MHC class I molecules to KIRs prevents killing of the target cell because the killing signal is overridden by the suppression signal.

The NKG2D ligand is known to be unregulated by DNA damage and cell stress in target cells [32]. In contrast, chronic exposure of the NKG2D ligand to NK cells can lead to downregulation of NKG2D and induce anergy of this cell [33]. Stress-induced molecules, such as MHC class I polypeptide-related sequence A and B (MICA and MICB), are ligands of NKG2D and contribute to cancer elimination by NK cells. Although MICA and MICB are induced by DNA damage in many cancers [34], the soluble forms of MICs (sMICs), which are reportedly expressed in HCC, downregulate NKG2D and inhibit NK cells from killing the target (fig. 2) [35–37]. Another stress-induced ligand, the unique long 16 binding protein family, also binds to NKG2D and downregulates its expression in poorly differentiated HCCs. In addition, the recurrence of HCC in patients was significantly associated with downregulation of ULBP1 after resection [38]. A recent report showed that the soluble form of another NKG2D ligand, soluble murine UL16-binding protein-like transcript 1, could maintain NK function by preventing NKG2D downregulation in mice [39]. Taken together,

er, inhibition of NK cell anergy in cancer immunity should be a strategy for cancer immune therapy. A recent report suggested that a subset of NK T cells with FOXP3+ had an immunosuppressive function in human HCC [40].

#### *Hepatic Stellate Cells, Endothelial Cells, and Cancer-Associated Fibroblasts*

Hepatic stellate cells and endothelial cells produce the C-X-C motif chemokine 12 (CXCL12)/stromal cell-derived factor 1. CXCL12 induces tumor growth, migration, and invasiveness through C-X-C chemokine receptor type 4 (CXCR4) on cancer cells and also recruits endothelial progenitors for tumor angiogenesis. Moreover, MDSCs, which play a crucial role in the immunosuppressive tumor environment, are recruited to tumors in a CXCL12/CXCR4-dependent manner (fig. 2) [41]. These tumor microenvironments of HCC, where the recruitment and retention of immunosuppressive cells take place [42], should disturb effective immune therapies. Endothelial cells also induce Treg induction in a TGF- $\beta$ -dependent manner [43]. These cells also express FasL, which plays a role in tumor invasion into the parenchyma and elimination of infiltrating CTLs [44]. Cancer-associated fibroblasts also reportedly produce prostaglandin E2 and IDO to suppress NK function (fig. 2) [45].

#### **Antigenicity of HCC Cells and Tumor-Associated Antigens/Neoantigens**

CTLs can recognize specific antigens processed and presented on MHC class I molecules. Several types of molecules in cancer cells can act as tumor-associated antigens (TAAs), such as cancer/testis (CT) antigens and differentiation antigens.

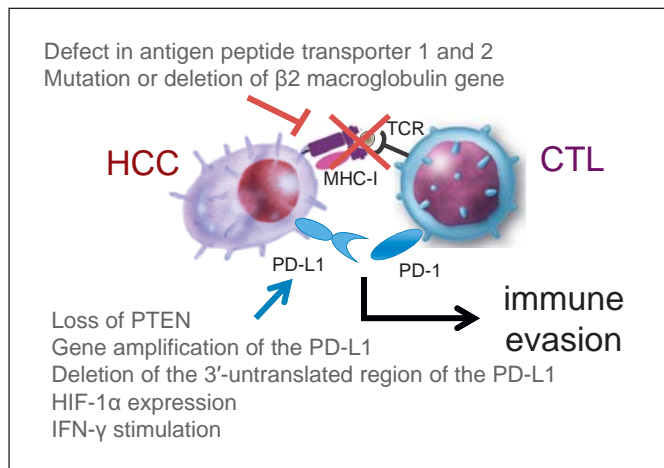
Peptides specifically observed in the testis, ovary, and placenta may be detected in cancerous tissues, which are known as CT antigens. As germ cells do not express MHC molecules, CTLs that recognize CT antigens are typically not harmful to normal tissues and selectively attack cancer cells. Melanoma antigen and CT antigen 1 are isolated from melanoma and esophageal cancer; they are also detected in other types of cancers, including HCC [46]. TAAs such as oncofetal protein present in cancer cells are sometimes observed in corresponding normal tissues;  $\alpha$ -fetoprotein and glypican-3 (GPC3) may also be a TAA in HCC. It has been reported that T cells expressing GPC3-targeted chimeric antigen receptor eliminated GPC3-positive HCC cells [47].

HCC generally accumulates a variety of genetic and epigenetic alterations [48–54], and the products of mutated genes may be cancer-specific neoantigens. In contrast to TAAs, neoantigens are not exposed to the immune system before the emergence of cancer cells, potentially making them ideal targets for the immune reaction. Abnormal products generated by point mutations, gene amplifications, abnormal splicing, and fusion genes may be targets of CTLs. In this case, common mutations specific for certain types of cancers may be good candidates for targeting. For example, overexpression of telomerase reverse transcriptase, which activates promoter mutation and integration of hepatitis B virus in the promoter as well as gene amplification, is common in HCC; vaccination using telomerase peptide has been reported in HCC [55]. However, as cancer cells with high antigenicity should be eliminated during clonal expansion by anticancer immune reactions, the established tumor may become resistant to immune rejection. In addition, cancers caused by few common driver mutations show fewer antigenic characteristics compared to those with many passenger mutations because of the lower levels of neoantigens. For example, cancers with mismatch-repair deficiency carry numerous passenger mutations and show a good response to immune checkpoint blockade [11]. However, cancer is heterogeneous in terms of profile of mutations, and complete elimination of cancerous tissues may be difficult.

#### **Immunological Microenvironment and Treatment of HCC**

As described above, immune cell functions are affected by the background condition of the immune system and the antigenicity of the tumor (fig. 2). During tumor development, cells with strong antigenicity should be removed by the host immune system. For example, the response of anti-TAA CD8+ T cell is higher in cases with early-stage HCC than those with advanced-stage HCC [46]; the immunosuppressive microenvironment with defects of effector T cells is more prevalent in advanced HCC tissues [56]. Chronic stimulation of TAAs can induce the expression of immune regulatory receptors and ligands and cytokines that lead to the anergy of immune cells. In HCC patients, it was reported that anti-TAA CD8+ T cells in the peripheral blood induced IFN- $\gamma$  upon stimulation; tumors infiltrating CD8+ T cells failed to do so [46]. In addition, cancer cells may have defects in the processing and presentation of TAAs, which may be a





**Fig. 3.** T cell exhaustion in the cancer microenvironment. Mutation or deletion of antigen peptide transporter and  $\beta 2$  microglobulin causes defects in MHC class I molecules. On the other hand, constitutive activation of the gene coding for PD-L1 should impair the response to cancer cells. The expression of PD-L1 is induced by the loss of phosphatase and tensin homolog deleted from chromosome 10 (PTEN) in glioma. Amplification of the PD-L1 coding gene and stabilization of PD-L1 mRNA caused by deletion of the 3'-untranslated region of this gene also induce increased expression of PD-L1 in leukemia, B cell lymphoma, and gastric cancer. HIF-1 $\alpha$  and stimulation by IFN- $\gamma$  also increase PD-L1 expression in the tumor.

target of the immune system [57]; mutation or deletion of  $\beta 2$  microglobulin causes defects in MHC class I molecules (fig. 3) [58]. Immune checkpoint molecules, such as CTLA-4, PD-1, TIM3, lymphocyte-activating gene 3 protein, and B and T lymphocyte attenuator, are also involved in establishing an immunosuppressive environment of cancer. Constitutive activation of the gene coding for PD-L1 should impair the response to cancer cells. For example, the expression of PD-L1 is induced by the loss of phosphatase and tensin homolog deleted from chromosome 10 in glioma. Amplification of the PD-L1 coding gene and stabilization of PD-L1 mRNA caused by deletion of the 3'-untranslated region of this gene also induce increased expression of PD-L1 in adult T-cell leukemia, B-cell lymphoma, and gastric cancer [59, 60]. In addition, PD-L1 is a direct target of HIF-1 $\alpha$ . As hypoxia is a common feature of HCC tissue, HIF-1 $\alpha$  may increase PD-L1 expression in the tumor as well as MDSCs and macrophages in HCC (fig. 3) [61]. The binding of PD-1 to PD-L1 on macrophages induces IL-10 release and CD4 $^{+}$  T-cell repression. High expression of PD-L1 and PD-1 in HCC, CD8 $^{+}$  T cells, and DCs is associated with tumor

aggressiveness and recurrence after HCC resection [62–64]. TIM3 and its ligand, galectin-3, also suppress the T-cell response. Infiltrating CD4 $^{+}$  and CD8 $^{+}$  T cells in HCC also show increased expression of TIM3 [65].

Activation of cellular signaling pathways in cancer also induces the expression of several cytokines and growth factors; these also contribute to the establishment of the immunosuppressive environment in HCC tissues. For example, TGF- $\beta$ , IL-6, IL-8, IL-10, IDO, arginase, adenosine, lactic acid, VEGF, PDGF, EGFR ligands, sIL-2, sMICA, Tregs inducing chemokines, and immune checkpoint-related molecules may be derived from HCC and stromal cells around the tumor; these molecules may act in concert and induce Treg accumulation and Th2 and M2 polarization along with HCC progression (fig. 2) [23, 28, 59, 60, 66–73].

In HCC, it has been reported that Tregs suppress DC function through CTLA-4 on their surface. This prevents CD28 binding to CD80/86 and downregulates the stimulation of CD4 $^{+}$  and CD8 $^{+}$  T cells. In addition, CTLA-4 induces immunosuppressive molecules such as IL-10, arginase, and IDO. IDO is an enzyme involved in the kynurenine pathway and depletes tryptophan. Through this enzymatic effect, T-cell activation is inhibited, Treg function is enhanced, and naïve CD4 $^{+}$  T cells are prone to differentiate into Tregs.

IDO is expressed in HCC as well as cancer-associated fibroblasts [45, 67]. It has also been reported that IFN- $\gamma$  from activated T cells upregulates IDO in macrophages and suppresses T-cell proliferation in HCC; IDO inhibitors can reverse this process [74]. The enzymatic action of arginase also depletes L-arginine and induces immune suppression. The hypoxic environment of HCC can induce arginase in TAMs and MDSCs.

IFN- $\gamma$  from CD4 $^{+}$  and CD8 $^{+}$  T cells, which is critical for the induction of CTLs, induces PD-L1 on APCs and cancer cells and causes T-cell exhaustion. It also stimulates TAMs to induce galectin-9 and IL-6, which in turn induces IL-10 production from MDSCs. Galectins, such as galectin-1, -3, and -9, are also associated with the immune escape of HCC cells (fig. 2), and galectin-3 is associated with the poor prognosis of HCC [75]. Galectin-1 is also known as a driver of Th2 polarization and as an inducer of Tregs [76]. As described above, both galectin-3 and galectin-9 are ligands of TIM3.

Cancer cells can release stromal cell-derived factor 1/CXCL12 to induce MDSCs. MDSCs promote tumor progression and angiogenesis through VEGF production [31]. They also mediate immunosuppression by disturbing NK and T-cell functions through TGF- $\beta$ , IL-10, ROS,



and prostaglandin E2 production as well as the enzymatic action of IDO (fig. 2). It has been reported that HCC and Tregs produce and respond to the EGFR ligand amphiregulin, which induces HCC growth and stimulates Tregs [21, 68]. Hypoxia can induce PD-L1 in HCC and MDSCs; the latter produces IL-10, TGF- $\beta$ , and arginase. Adenosine blocks the effector function of CD4+ and CD8+ T cells and inhibits macrophages. In addition, it also induces pro-antigenic molecules such as PDGF, VEGF, and lactic acid and contributes to HCC progression.

## Conclusion

The immune response to HCC is determined by the balance between the antigenicity of the tumor and immunological microenvironment of cancer tissues. The former is also attributed to the accumulation of mutations and alterations in cellular signaling in cancer cells. Genetic and environmental factors of individuals related to

immunity also affect the immune response to cancer. Immunosuppressive forces in the microenvironment of HCC may cause the resistance to immune therapy including immune checkpoint blockade, and modification of the tumor microenvironment may restore normal anti-cancer immunity. Therefore, comprehensive analyses of cancer tissues in terms of mutation, gene expression, cytokines/chemokines, and infiltrated cell profiles are necessary for the development of personalized immune therapy in HCC.

## Author Contributions

N. Nishida drafted the manuscript and wrote the final version. M. Kudo approved the final version of the manuscript.

## Disclosure Statement

The authors have no conflict of interest to declare.

## References

- Kang TW, Rhim H: Recent advances in tumor ablation for hepatocellular carcinoma. *Liver Cancer* 2015;4:176–187.
- Kudo M: Locoregional therapy for hepatocellular carcinoma. *Liver Cancer* 2015;4:163–164.
- Kudo M: Surveillance, diagnosis, treatment, and outcome of liver cancer in Japan. *Liver Cancer* 2015;4:39–50.
- Tsurusaki M, Murakami T: Surgical and locoregional therapy of HCC: TACE. *Liver Cancer* 2015;4:165–175.
- Lencioni R, de Baere T, Martin RC, Nutting CW, Narayanan G: Image-guided ablation of malignant liver tumors: recommendations for clinical validation of novel thermal and non-thermal technologies – a Western perspective. *Liver Cancer* 2015;4:208–214.
- Wada Y, Nakashima O, Kutami R, Yamamoto O, Kojiro M: Clinicopathological study on hepatocellular carcinoma with lymphocytic infiltration. *Hepatology* 1998;27:407–414.
- Unitt E, Marshall A, Gelson W, Rushbrook SM, Davies S, Vowler SL, Morris LS, Coleman N, Alexander GJ: Tumour lymphocytic infiltrate and recurrence of hepatocellular carcinoma following liver transplantation. *J Hepatol* 2006;45:246–253.
- Prieto J, Melero I, Sangro B: Immunological landscape and immunotherapy of hepatocellular carcinoma. *Nat Rev Gastroenterol Hepatol* 2015;12:681–700.
- Kudo M: Immune checkpoint blockade in hepatocellular carcinoma. *Liver Cancer* 2015;4:201–207.
- Brahmer JR, Tykodi SS, Chow LQ, Hwu WJ, Topalian SL, Hwu P, Drake CG, Camacho LH, Kauh J, Odunsi K, Pitot HC, Hamid O, Bhatia S, Martins R, Eaton K, Chen S, Salay TM, Alaparthi S, Grosso JF, Korman AJ, Parker SM, Agrawal S, Goldberg SM, Pardoll DM, Gupta A, Wigginton JM: Safety and activity of anti-PD-L1 antibody in patients with advanced cancer. *N Engl J Med* 2012;366:2455–2465.
- Le DT, Uram JN, Wang H, Bartlett BR, Kemberling H, Eyring AD, Skora AD, Luber BS, Azad NS, Laheru D, Biedrzycki B, Donehower RC, Zaheer A, Fisher GA, Crocenzi TS, Lee JJ, Duffy SM, Goldberg RM, de la Chapelle A, Koshiji M, Bhajee F, Huebner T, Hruban RH, Wood LD, Cuka N, Pardoll DM, Papadopoulos N, Kinzler KW, Zhou S, Cornish TC, Taube JM, Anders RA, Eshleman JR, Vogelstein B, Diaz LA Jr: PD-1 blockade in tumors with mismatch-repair deficiency. *N Engl J Med* 2015;372:2509–2520.
- Budhu A, Forgues M, Ye QH, Jia HL, He P, Zanetti KA, Kammula US, Chen Y, Qin LX, Tang ZY, Wang XW: Prediction of venous metastases, recurrence, and prognosis in hepatocellular carcinoma based on a unique immune response signature of the liver microenvironment. *Cancer Cell* 2006;10:99–111.
- Hori S, Nomura T, Sakaguchi S: Control of regulatory T cell development by the transcription factor Foxp3. *Science* 2003;299:1057–1061.
- Parry RV, Chemnitz JM, Frauwirth KA, Lanfranco AR, Braunstein I, Kobayashi SV, Linsley PS, Thompson CB, Riley JL: CTLA-4 and PD-1 receptors inhibit T-cell activation by distinct mechanisms. *Mol Cell Biol* 2005;25:9543–9553.
- Patsoukis N, Bardhan K, Chatterjee P, Sari D, Liu B, Bell LN, Karoly ED, Freeman GJ, Petkova V, Seth P, Li L, Boussiotis VA: PD-1 alters T-cell metabolic reprogramming by inhibiting glycolysis and promoting lipolysis and fatty acid oxidation. *Nat Commun* 2015;6:6692.
- Cekic C, Linden J: Purinergic regulation of the immune system. *Nat Rev Immunol* 2016;16:177–192.
- Josefowicz SZ, Lu LF, Rudensky AY: Regulatory T cells: mechanisms of differentiation and function. *Ann Rev Immunol* 2012;30:531–564.
- Chen X, Du Y, Lin X, Qian Y, Zhou T, Huang Z: CD4+CD25+ regulatory T cells in tumor immunity. *Int Immunopharmacol* 2016;34:244–249.
- Vignali DA, Collison LW, Workman CJ: How regulatory T cells work. *Nat Rev Immunol* 2008;8:523–532.

- 20 Berasain C, Castillo J, Perugorria MJ, Prieto J, Avila MA: Amphiregulin: a new growth factor in hepatocarcinogenesis. *Cancer Lett* 2007;254:30–41.
- 21 Zaiss DM, van Loosdregt J, Gorlani A, Bekker CP, Grone A, Sibilia M, van Bergen en Henegouwen PM, Roovers RC, Coffe PJ, Sijts AJ: Amphiregulin enhances regulatory T cell-suppressive function via the epidermal growth factor receptor. *Immunity* 2013;38:275–284.
- 22 Serrels A, Lund T, Serrels B, Byron A, McPherson RC, von Kriegsheim A, Gomez-Cuadrado L, Canel M, Muir M, Ring JE, Maniati E, Sims AH, Pachter JA, Brunton VG, Gilbert N, Anderton SM, Nibbs RJ, Frame MC: Nuclear FAK controls chemokine transcription, Tregs, and evasion of anti-tumor immunity. *Cell* 2015;163:160–173.
- 23 Chen KJ, Lin SZ, Zhou L, Xie HY, Zhou WH, Taki-Eldin A, Zheng SS: Selective recruitment of regulatory T cell through CCR6-CCL20 in hepatocellular carcinoma fosters tumor progression and predicts poor prognosis. *PLoS One* 2011;6:e24671.
- 24 Kono H, Rock KL: How dying cells alert the immune system to danger. *Nat Rev Immunol* 2008;8:279–289.
- 25 Han Y, Chen Z, Yang Y, Jiang Z, Gu Y, Liu Y, Lin C, Pan Z, Yu Y, Jiang M, Zhou W, Cao X: Human CD14<sup>+</sup> CTLA-4<sup>+</sup> regulatory dendritic cells suppress T-cell response by cytotoxic T-lymphocyte antigen-4-dependent IL-10 and indoleamine-2,3-dioxygenase production in hepatocellular carcinoma. *Hepatology* 2014;59:567–579.
- 26 Quezada SA, Peggs KS, Simpson TR, Allison JP: Shifting the equilibrium in cancer immunoeediting: from tumor tolerance to eradication. *Immunol Rev* 2011;241:104–118.
- 27 Llovet JM, Bruix J: Systematic review of randomized trials for unresectable hepatocellular carcinoma: chemoembolization improves survival. *Hepatology* 2003;37:429–442.
- 28 Hoechst B, Ormandy LA, Ballmaier M, Lehner F, Kruger C, Manns MP, Greten TF, Korangy F: A new population of myeloid-derived suppressor cells in hepatocellular carcinoma patients induces CD4<sup>+</sup>CD25<sup>+</sup>Foxp3<sup>+</sup> T cells. *Gastroenterology* 2008;135:234–243.
- 29 Nagaraj S, Gupta K, Pisarev V, Kinarsky L, Sherman S, Kang L, Herber DL, Schneck J, Gabrilovich DI: Altered recognition of antigen is a mechanism of CD8<sup>+</sup> T cell tolerance in cancer. *Nat Med* 2007;13:828–835.
- 30 Li H, Han Y, Guo Q, Zhang M, Cao X: Cancer-expanded myeloid-derived suppressor cells induce anergy of NK cells through membrane-bound TGF-beta 1. *J Immunol* 2009;182:240–249.
- 31 Arihara F, Mizukoshi E, Kitahara M, Takata Y, Arai K, Yamashita T, Nakamoto Y, Kaneko S: Increase in CD14+HLA-DR<sup>-</sup>/low myeloid-derived suppressor cells in hepatocellular carcinoma patients and its impact on prognosis. *Cancer Immunol Immunother* 2013;62:1421–1430.
- 32 Gasser S, Orsulic S, Brown EJ, Raulet DH: The DNA damage pathway regulates innate immune system ligands of the NKG2D receptor. *Nature* 2005;436:1186–1190.
- 33 Coudert JD, Scarpellino L, Gros F, Vivier E, Held W: Sustained NKG2D engagement induces cross-tolerance of multiple distinct NK cell activation pathways. *Blood* 2008;111:3571–3578.
- 34 Champsaur M, Lanier LL: Effect of NKG2D ligand expression on host immune responses. *Immunol Rev* 2010;235:267–285.
- 35 Groh V, Wu J, Yee C, Spies T: Tumour-derived soluble MIC ligands impair expression of NKG2D and T-cell activation. *Nature* 2002;419:734–738.
- 36 Jinushi M, Takehara T, Tatsumi T, Hiramatsu N, Sakamori R, Yamaguchi S, Hayashi N: Impairment of natural killer cell and dendritic cell functions by the soluble form of MHC class I-related chain A in advanced human hepatocellular carcinomas. *J Hepatol* 2005;43:1013–1020.
- 37 Kohga K, Takehara T, Tatsumi T, Ohkawa K, Miyagi T, Hiramatsu N, Kanto T, Kasugai T, Katayama K, Kato M, Hayashi N: Serum levels of soluble major histocompatibility complex (MHC) class I-related chain A in patients with chronic liver diseases and changes during transcatheter arterial embolization for hepatocellular carcinoma. *Cancer Sci* 2008;99:1643–1649.
- 38 Kamimura H, Yamagiwa S, Tsuchiya A, Takamura M, Matsuda Y, Ohkoshi S, Inoue M, Wakai T, Shirai Y, Nomoto M, Aoyagi Y: Reduced NKG2D ligand expression in hepatocellular carcinoma correlates with early recurrence. *J Hepatol* 2012;56:381–388.
- 39 Deng W, Gowen BG, Zhang L, Wang L, Lau S, Iannello A, Xu J, Rovis TL, Xiong N, Raulet DH: Antitumor immunity. A shed NKG2D ligand that promotes natural killer cell activation and tumor rejection. *Science* 2015;348:136–139.
- 40 Li X, Peng J, Pang Y, Yu S, Yu X, Chen P, Wang W, Han W, Zhang J, Yin Y, Zhang Y: Identification of a FOXP3<sup>+</sup>CD3<sup>+</sup>CD56<sup>+</sup> population with immunosuppressive function in cancer tissues of human hepatocellular carcinoma. *Sci Rep* 2015;5:14757.
- 41 Chen Y, Huang Y, Reiberger T, Duyverman AM, Huang P, Samuel R, Hiddingh L, Roberge S, Koppel C, Lauwers GY, Zhu AX, Jain RK, Duda DG: Differential effects of sorafenib on liver versus tumor fibrosis mediated by stromal-derived factor 1 alpha/C-X-C receptor type 4 axis and myeloid differentiation antigen-positive myeloid cell infiltration in mice. *Hepatology* 2014;59:1435–1447.
- 42 Obermajer N, Muthuswamy R, Odunsi K, Edwards RP, Kalinski P: PGE(2)-induced CXCL12 production and CXCR4 expression controls the accumulation of human MDSCs in ovarian cancer environment. *Cancer Res* 2011;71:7463–7470.
- 43 Carambia A, Freund B, Schwinge D, Heine M, Laschtowitz A, Huber S, Wraith DC, Korn T, Schramm C, Lohse AW, Heeren J, Herkel J: TGF-beta-dependent induction of CD4<sup>+</sup>CD25<sup>+</sup>Foxp3<sup>+</sup> Tregs by liver sinusoidal endothelial cells. *J Hepatol* 2014;61:594–599.
- 44 Motz GT, Santoro SP, Wang LP, Garrabrant T, Lastra RR, Hagemann IS, Lal P, Feldman MD, Benencia F, Coukos G: Tumor endothelium FasL establishes a selective immune barrier promoting tolerance in tumors. *Nat Med* 2014;20:607–615.
- 45 Li T, Yang Y, Hua X, Wang G, Liu W, Jia C, Tai Y, Zhang Q, Chen G: Hepatocellular carcinoma-associated fibroblasts trigger NK cell dysfunction via PGE2 and IDO. *Cancer Lett* 2012;318:154–161.
- 46 Flecken T, Schmidt N, Hild S, Gostick E, Drognitz O, Zeiser R, Schemmer P, Bruns H, Eiermann T, Price DA, Blum HE, Neumann-Haefelin C, Thimme R: Immunodominance and functional alterations of tumor-associated antigen-specific CD8<sup>+</sup> T-cell responses in hepatocellular carcinoma. *Hepatology* 2014;59:1415–1426.
- 47 Gao H, Li K, Tu H, Pan X, Jiang H, Shi B, Kong J, Wang H, Yang S, Gu J, Li Z: Development of T cells redirected to glypican-3 for the treatment of hepatocellular carcinoma. *Clin Cancer Res* 2014;20:6418–6428.
- 48 Nishida N, Nagasaka T, Nishimura T, Ikai I, Boland CR, Goel A: Aberrant methylation of multiple tumor suppressor genes in aging liver, chronic hepatitis, and hepatocellular carcinoma. *Hepatology* 2008;47:908–918.
- 49 Nishida N, Goel A: Genetic and epigenetic signatures in human hepatocellular carcinoma: a systematic review. *Curr Genomics* 2011;12:130–137.
- 50 Nishida N, Kudo M, Nagasaka T, Ikai I, Goel A: Characteristic patterns of altered DNA methylation predict emergence of human hepatocellular carcinoma. *Hepatology* 2012;56:994–1003.
- 51 Nishida N, Arizumi T, Takita M, Kitai S, Yada N, Hagiwara S, Inoue T, Minami Y, Ueshima K, Sakurai T, Kudo M: Reactive oxygen species induce epigenetic instability through the formation of 8-hydroxydeoxyguanosine in human hepatocarcinogenesis. *Dig Dis* 2013;31:459–466.
- 52 Nishida N, Kudo M: Recent advancements in comprehensive genetic analyses for human hepatocellular carcinoma. *Oncology* 2013;84(suppl 1):93–97.
- 53 Nishida N, Kudo M: Alteration of epigenetic profile in human hepatocellular carcinoma and its clinical implications. *Liver Cancer* 2014;3:417–427.
- 54 Nishida N, Nishimura T, Nakai T, Chishina H, Arizumi T, Takita M, Kitai S, Yada N, Hagiwara S, Inoue T, Minami Y, Ueshima K, Sakurai T, Kudo M: Genome-wide profiling of DNA methylation and tumor progression in human hepatocellular carcinoma. *Dig Dis* 2014;32:658–663.

- 55 Greten TF, Forner A, Korangy F, N'Kontchou G, Barget N, Ayuso C, Ormandy LA, Manns MP, Beaugrand M, Bruix J: A phase II open label trial evaluating safety and efficacy of a telomerase peptide vaccination in patients with advanced hepatocellular carcinoma. *BMC Cancer* 2010;10:209.
- 56 Willimsky G, Schmidt K, Loddenkemper C, Gellermann J, Blankenstein T: Virus-induced hepatocellular carcinomas cause antigen-specific local tolerance. *J Clin Invest* 2013;123:1032–1043.
- 57 Mittal D, Gubin MM, Schreiber RD, Smyth MJ: New insights into cancer immunoediting and its three component phases – elimination, equilibrium and escape. *Curr Opin Immunol* 2014;27:16–25.
- 58 Bernal M, Ruiz-Cabello F, Concha A, Paschen A, Garrido F: Implication of the beta2-microglobulin gene in the generation of tumor escape phenotypes. *Cancer Immunol Immunother* 2012;61:1359–1371.
- 59 Blay J, White TD, Hoskin DW: The extracellular fluid of solid carcinomas contains immunosuppressive concentrations of adenosine. *Cancer Res* 1997;57:2602–2605.
- 60 Colegio OR, Chu NQ, Szabo AL, Chu T, Roberg AM, Jairam V, Cyrus N, Brokowski CE, Eisenbarth SC, Phillips GM, Cline GW, Phillips AJ, Medzhitov R: Functional polarization of tumour-associated macrophages by tumour-derived lactic acid. *Nature* 2014;513:559–563.
- 61 Noman MZ, Desantis G, Janji B, Hasmim M, Karray S, Dessen P, Bronte V, Chouaib S: PD-L1 is a novel direct target of HIF-1alpha, and its blockade under hypoxia enhanced MDSC-mediated T cell activation. *J Exp Med* 2014;211:781–790.
- 62 Gao Q, Wang XY, Qiu SJ, Yamato I, Sho M, Nakajima Y, Zhou J, Li BZ, Shi YH, Xiao YS, Xu Y, Fan J: Overexpression of PD-L1 significantly associates with tumor aggressiveness and postoperative recurrence in human hepatocellular carcinoma. *Clin Cancer Res* 2009;15:971–979.
- 63 Krempski J, Karyampudi L, Behrens MD, Erskine CL, Hartmann L, Dong H, Goode EL, Kalli KR, Knutson KL: Tumor-infiltrating programmed death receptor-1+ dendritic cells mediate immune suppression in ovarian cancer. *J Immunol* 2011;186:6905–6913.
- 64 Shi F, Shi M, Zeng Z, Qi RZ, Liu ZW, Zhang JY, Yang YP, Tien P, Wang FS: PD-1 and PD-L1 upregulation promotes CD8(+) T-cell apoptosis and postoperative recurrence in hepatocellular carcinoma patients. *Int J Cancer* 2011;128:887–896.
- 65 Li H, Wu K, Tao K, Chen L, Zheng Q, Lu X, Liu J, Shi L, Liu C, Wang G, Zou W: Tim-3/galectin-9 signaling pathway mediates T-cell dysfunction and predicts poor prognosis in patients with hepatitis B virus-associated hepatocellular carcinoma. *Hepatology* 2012;56:1342–1351.
- 66 Yan W, Liu X, Ma H, Zhang H, Song X, Gao L, Liang X, Ma C: Tim-3 fosters HCC development by enhancing TGF- $\beta$ -mediated alternative activation of macrophages. *Gut* 2015;64:1593–1604.
- 67 Pan K, Wang H, Chen MS, Zhang HK, Weng DS, Zhou J, Huang W, Li JJ, Song HF, Xia JC: Expression and prognosis role of indoleamine 2,3-dioxygenase in hepatocellular carcinoma. *J Cancer Res Clin Oncol* 2008;134:1247–1253.
- 68 Castillo J, Goni S, Latasa MU, Perugorria MJ, Calvo A, Muntane J, Bioulac-Sage P, Balabaud C, Prieto J, Avila MA, Berasain C: Amphiregulin induces the alternative splicing of p73 into its oncogenic isoform DeltaEx2p73 in human hepatocellular tumors. *Gastroenterology* 2009;137:1805–1815.e1–4.
- 69 Gessi S, Merighi S, Sacchetto V, Simioni C, Borea PA: Adenosine receptors and cancer. *Biochim Biophys Acta* 2011;1808:1400–1412.
- 70 Hato T, Goyal L, Greten TF, Duda DG, Zhu AX: Immune checkpoint blockade in hepatocellular carcinoma: current progress and future directions. *Hepatology* 2014;60:1776–1782.
- 71 Yan W, Han P, Zhou Z, Tu W, Liao J, Li P, Liu M, Tian D, Fu Y: Netrin-1 induces epithelial-mesenchymal transition and promotes hepatocellular carcinoma invasiveness. *Dig Dis Sci* 2014;59:1213–1221.
- 72 Zhang Z, Zhang Y, Sun XX, Ma X, Chen ZN: MicroRNA-146a inhibits cancer metastasis by downregulating VEGF through dual pathways in hepatocellular carcinoma. *Mol Cancer* 2015;14:5.
- 73 Lu Y, Lin N, Chen Z, Xu R: Hypoxia-induced secretion of platelet-derived growth factor-BB by hepatocellular carcinoma cells increases activated hepatic stellate cell proliferation, migration and expression of vascular endothelial growth factor-A. *Mol Med Rep* 2015;11:691–697.
- 74 Zhao Q, Kuang DM, Wu Y, Xiao X, Li XF, Li TJ, Zheng L: Activated CD69+ T cells foster immune privilege by regulating IDO expression in tumor-associated macrophages. *J Immunol* 2012;188:1117–1124.
- 75 Cedeno-Laurent F, Dimitroff CJ: Galectins and their ligands: negative regulators of anti-tumor immunity. *Glycoconj J* 2012;29:619–625.
- 76 Cedeno-Laurent F, Opperman M, Barthel SR, Kuchroo VK, Dimitroff CJ: Galectin-1 triggers an immunoregulatory signature in Th cells functionally defined by IL-10 expression. *J Immunol* 2012;188:3127–3137.

# CD68-Positive Cells in Hepatic Angiomyolipoma

Hitoshi Tochio<sup>a</sup> Eriko Tamaki<sup>a</sup> Yukihiro Imai<sup>b</sup> Nobuhiro Iwasaki<sup>a</sup>  
Kazushi Minowa<sup>a</sup> Hobyung Chung<sup>c</sup> Yoshiki Suginoshta<sup>c</sup> Tetsurou Inokuma<sup>c</sup>  
Masatoshi Kudo<sup>d</sup>

Departments of <sup>a</sup>Clinical Laboratory Medicine, <sup>b</sup>Clinical Pathology, and <sup>c</sup>Internal Medicine, Division of Gastroenterology and Hepatology, Kobe City Medical Center General Hospital, Kobe, and <sup>d</sup>Department of Gastroenterology and Hepatology, Kindai University Faculty of Medicine, Osaka-Sayama, Japan

## Key Words

Sonazoid · Contrast-enhanced ultrasonography · Angiomyolipoma · CD68

## Abstract

Four resected specimens of hepatic angiomyolipoma in which uptake of Sonazoid was observed in the postvascular phase of Sonazoid-enhanced ultrasonography were analyzed. Macrophage localization in the tumor was revealed pathologically by immunohistochemical staining for CD68. CD68-positive cells were observed in the tumor in all cases. The density of CD68-positive cells was 100/mm<sup>2</sup>, and the ratio of CD68-positive cell density in the tumor to that in the surrounding parenchyma was 32–171%. These results suggested that the uptake of the contrast agent Sonazoid was related to the density of CD68-positive cells.

© 2016 S. Karger AG, Basel

## Introduction

Hepatic angiomyolipoma (AML) is a relatively rare tumor typically observed as a hypervascular lesion in the arterial phase and a defective lesion in the postvascular phase of contrast-enhanced ultrasonography (CEUS)

with Sonazoid [1–8]. However, accurate assessment is not possible in the postvascular phase of CEUS because of hyperechoic areas on B-mode ultrasonography (US) that reflect the fat component in the tumor. In cases of hepatocellular carcinoma (HCC) observed as a hyperechoic lesion, a combination of conventional observation with a low-mechanical index (MI) mode and examination with a high-MI mode increased the accuracy of lesion assessment [9–12]. This method has been used to observe the postvascular phase, and to date 4 cases of hepatic AML with Sonazoid uptake in the lesion have been identified. Histopathological study of the 4 resected AML lesions revealed the localization of macrophages in the resected specimens. The present study elucidated the mechanism underlying the uptake of Sonazoid in these lesions.

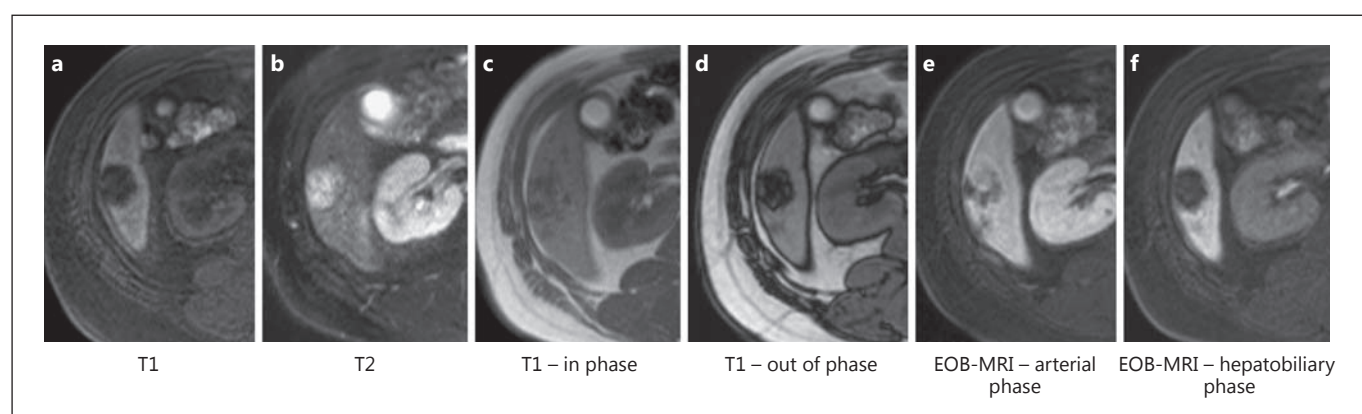
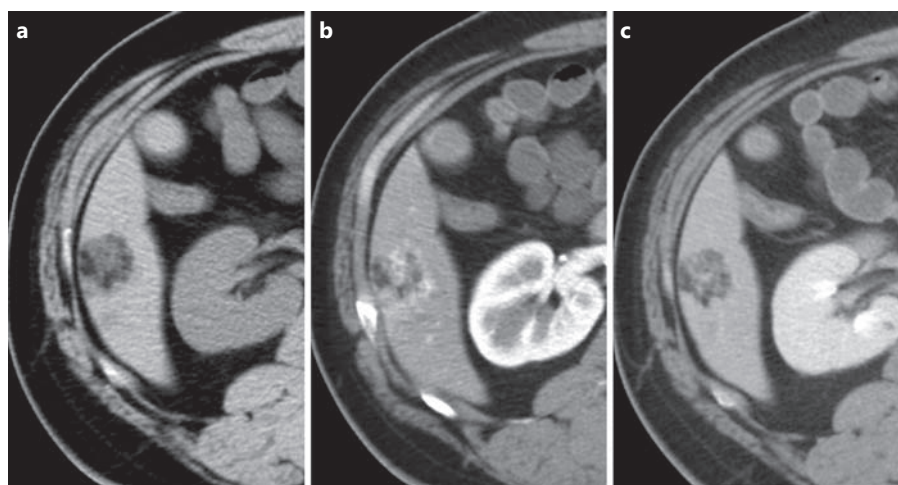
## Subjects and Methods

### Subjects

Four hepatic AML tumors from 4 patients (1 man and 3 women; mean age 45 ± 10 years) resected at our hospital between March 2012 and May 2015 were examined. The tumor diameter in the histological specimens ranged from 3.6 to 11.0 cm. The tumor was observed as a hyperechoic lesion in 2 cases and as a hypoechoic lesion in 2 cases by B-mode US. However, during the postvascular phase, the tumor was observed as a hypoechoic le-



**Fig. 1.** Dynamic CT image in a patient with hepatic angiomyolipoma in his 40s. **a** Plain CT shows a hypodense tumor measuring 3.6 cm in diameter, suggesting a fatty component in the tumor. **b** Arterial-phase CT shows arterial enhancement within the tumor. **c** Portal-venous-phase CT shows a slight washout in the tumor.



**Fig. 2.** Plain and gadolinium ethoxybenzyl diethylenetriamine penta-acetic acid (Gd-EOB-DTPA)-MRI image in a patient with hepatic angiomyolipoma in his 40s. **a** T1-weighted image shows a low-intensity nodule in segment 6. **b** T2-weighted image shows a high-intensity nodule in segment 6. **c** In-phase image shows an

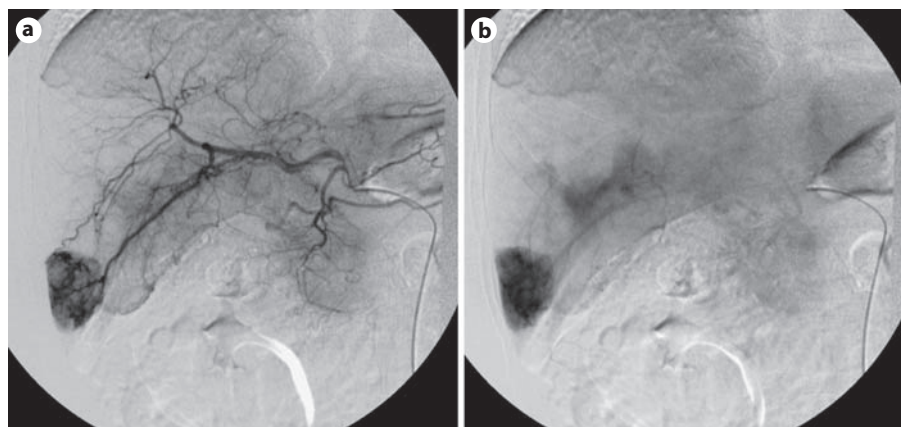
isointense nodule. **d** Out-of-phase image shows a low-intensity nodule, suggesting a fatty component in the nodule. **e** Arterial phase of dynamic EOB-MRI shows arterial enhancement. **f** Hepatobiliary phase of EOB-MRI shows a low-intensity nodule, with no hepatocyte within the tumor.

**Table 1.** Imaging and pathological results of CD68-positive cells in AML

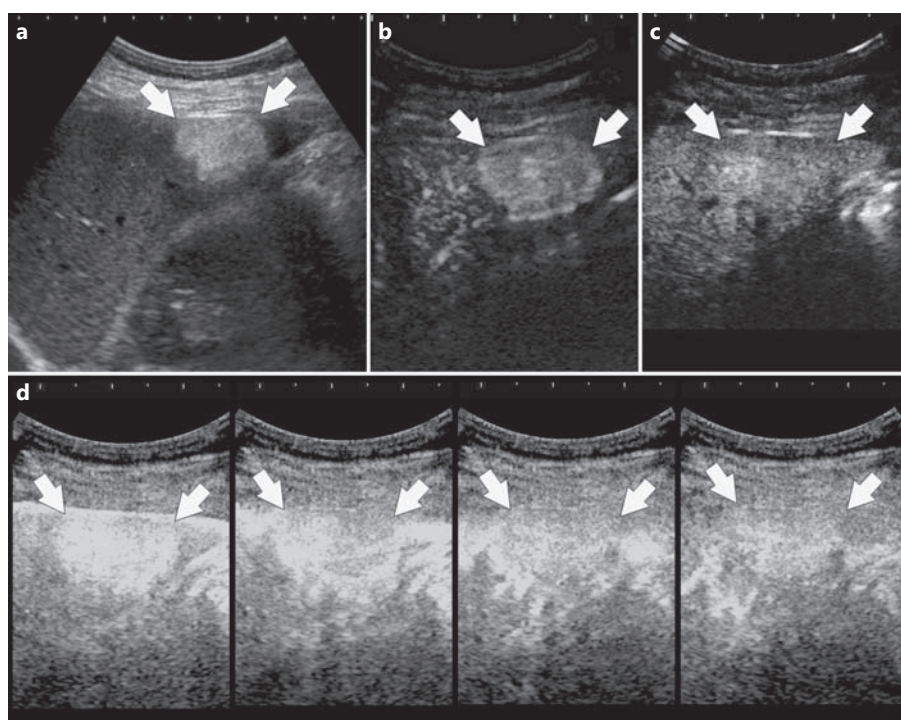
Age, years/ sex	Diameter, cm	B-mode US	Postvascular phase of Sonazoid-enhanced US		CD68-positive cells in AML	
			low MI	high MI	density, per mm <sup>2</sup>	ratio of density compared with surrounding liver, %
40s/M	3.6	hyper	iso	Sonazoid uptake (+)	681	171
60s/F	6.5	hypo	hypo	Sonazoid uptake (+)	124	32
30s/F	8.5	hypo	hypo	Sonazoid uptake (+)	340	121
30s/F	11.0	hyper	iso	Sonazoid uptake (+)	129	68



**Fig. 3.** Digital subtraction angiography (DSA) image in a patient with hepatic angiomyolipoma in his 40s. **a** Arterial phase of DSA shows a hypervascular tumor. **b** Venous phase of DSA shows tumor staining and early venous drainage from the tumor.



**Fig. 4.** Ultrasonography (US) image in a patient with hepatic angiomyolipoma in his 40s. **a** A hyperechoic nodule is demonstrated on B-mode US. **b** Hypervascularity is shown in the arterial phase of contrast-enhanced US (CEUS) with Sonazoid. **c** No perfusion defect is seen in the postvascular phase of CEUS with a low mechanical index (MI = 0.20). **d** The presence of Sonazoid is clearly demonstrated with flash imaging using high acoustic power (MI = 1.3).



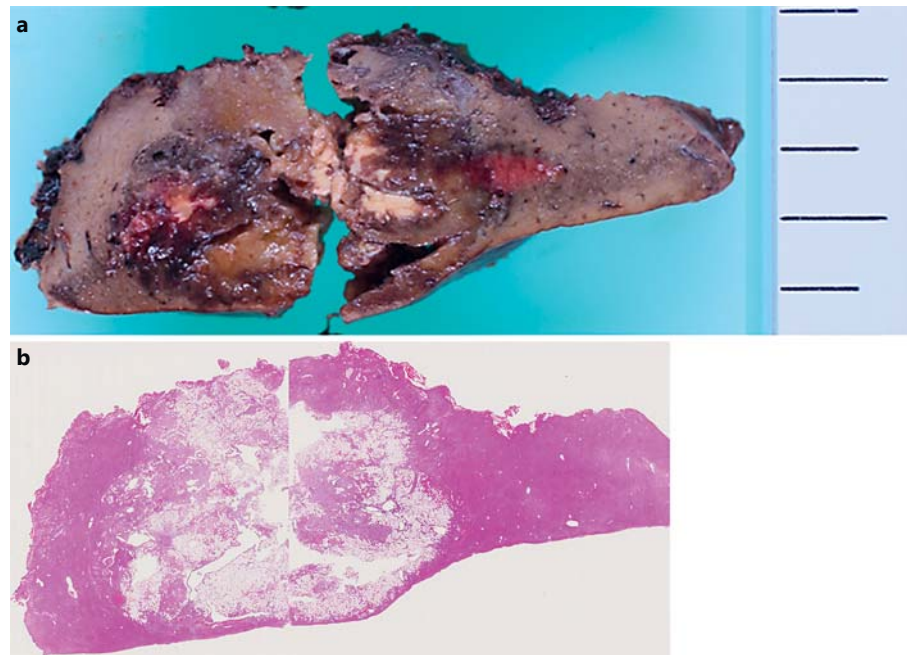
sion in 2 cases and as an isoechoic area in 2 cases (15 min to 12 h after intravenous injection of Sonazoid) by low-MI (0.20–0.24) CEUS imaging. The presence of intratumoral Sonazoid was confirmed in all 4 cases by flash imaging with a high MI (1.0–1.2).

#### Methods

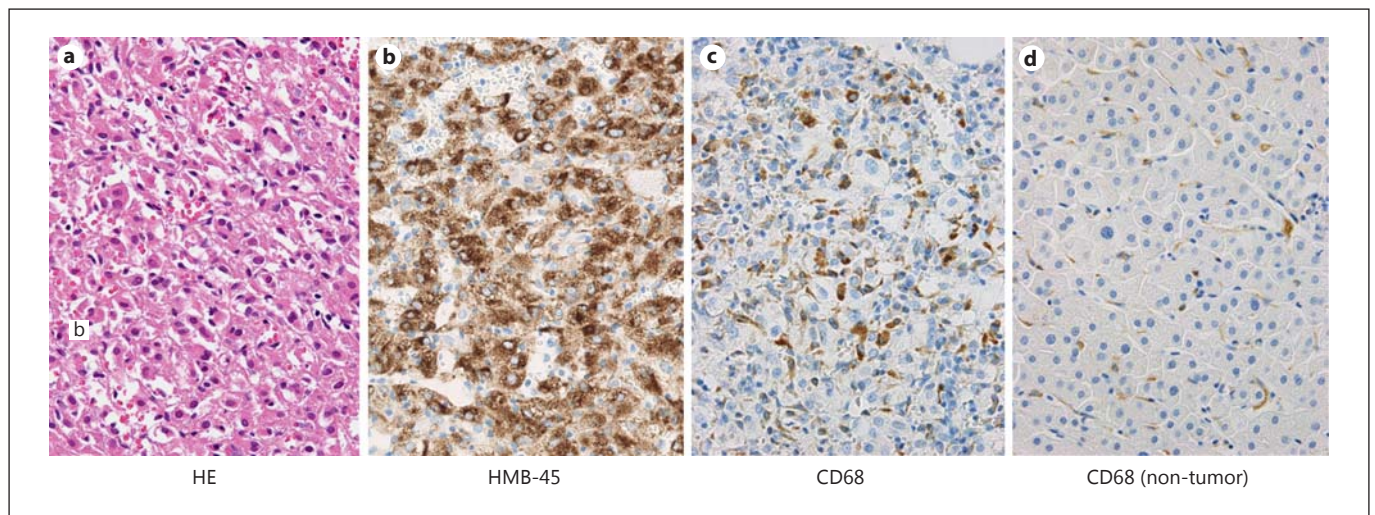
Slices of the resected AML specimens were subjected to immunohistochemical staining using an anti-CD68 antibody (KP1: IS609, Dako). High magnification ( $\times 40$ ) of the tumor area and the non-tumor area (three randomly selected areas each) was performed to obtain the CD68-positive cell count. The densities of CD68-positive cells in tumor areas were calculated. The ratio of CD68-positive cell density in the tumor to that in the surrounding liver parenchyma was also calculated.

#### Results

CD68-positive cells were present in the AML lesion, and the CD68-positive cell density was  $\geq 100$  cells/mm<sup>2</sup> in all 4 cases. The ratio of CD68-positive cell density in the tumor to that in the surrounding parenchyma was  $\geq 32\%$  in all cases (32–171%) (table 1; fig. 1–6). The results of dynamic CT, EOB-MRI, angiography, US, and CEUS are shown in figures 1–4. The results of the pathological study, including immunohistochemical staining, are shown in figures 5 and 6.



**Fig. 5.** Resected specimen of a patient with hepatic angiomyolipoma in his 40s. **a** Macroscopic view of the resected specimen. **b** Magnification view image of the resected specimen suggests the presence of abundant fatty cells in the tumor.



**Fig. 6.** Histopathology in a patient with hepatic angiomyolipoma in his 40s. **a** Histopathological features of the tumor (hematoxylin and eosin [HE] stain,  $\times 40$ ). **b** Immunohistochemical (IHC) staining shows HMB-45-positive cells in the tumor, confirming this

nodule as angiomyolipoma. **c** IHC staining shows CD68-positive cells in the tumor. The ratio of CD68-positive cell density in the tumor to that in the surrounding parenchyma was 171%. **d** IHC staining of CD68 in the surrounding non-tumor parenchyma.

## Discussion

Postvascular phase imaging by Sonazoid-enhanced US utilizes the phagocytic properties of macrophages such as Kupffer cells [13]. Residual Sonazoid may indicate the presence of macrophages in AML lesions, which appear

as low-intensity regions on ferumoxide-enhanced magnetic resonance imaging, as shown by Ketelslegers et al. [14]. However, the current study is the first to report the localization of macrophages in AMLs at a density detectable by CEUS with Sonazoid.



Immunohistochemical staining for CD68 detects histiocytes, including Kupffer cells and macrophages. CD68-positive cells were detected within tumors in all AML cases in this study, and Sonazoid uptake in the tumors was observed by CEUS with Sonazoid. The mean distribution density ratio was 98% (lowest density ratio 32%), which was higher than previously reported levels (approximately 20%) in HCC and metastatic liver cancer [15]. This difference is likely to be associated with the mechanism by which Sonazoid is taken up by hepatic AML.

CD68-positive cells detected in HCC and metastatic liver cancer are considered to be migrating macrophages, which differ from Kupffer cells that are resident macrophages in the sinusoids [15]. The CD68-positive cells within the AML detected in the present study are likely to be histiocytes, such as migrating macrophages. It would be interesting to determine why these cells are densely localized in hepatic AML, but not in HCC or metastatic liver cancer.

Furthermore, given that Sonazoid can be partially phagocytosed by vascular endothelial cells, the abundance of blood vessels may be the determining factor in Sonazoid uptake in AML. This possibility should be investigated in future studies.

## Conclusion

CD68-positive cells were observed within AML lesions in which Sonazoid uptake was detected in the postvascular phase of Sonazoid-enhanced US. The cell density ratio was  $\geq 32\%$  (32–171%). These cells were likely to be migrating macrophages rather than Kupffer cells.

## Disclosure Statement

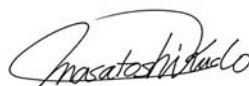
The authors declare no conflict of interest regarding this study.

## References

- 1 Kudo M: Defect reperfusion imaging with Sonazoid®: a breakthrough in hepatocellular carcinoma. *Liver Cancer* 2016;5:1–7.
- 2 Murakami T, Tsurusaki M: Hypervascular benign and malignant liver tumors that require differentiation from hepatocellular carcinoma: key points of imaging diagnosis. *Liver Cancer* 2014;3:85–96.
- 3 Kudo M, Matsui O, Izumi N, Iijima H, Kadoya M, Imai Y, Okusaka T, Miyayama S, Tsuchiya K, Ueshima K, Hiraoka A, Ikeda M, Ogasawara S, Yamashita T, Minami T, Yamakado K: JSH consensus-based clinical practice guidelines for the management of hepatocellular carcinoma: 2014 update by the Liver Cancer Study Group of Japan. *Liver Cancer* 2014;3:458–468.
- 4 Kudo M: Surveillance, diagnosis, treatment, and outcome of liver cancer in Japan. *Liver Cancer* 2015;4:39–50.
- 5 Kudo M: Clinical practice guidelines for hepatocellular carcinoma differ between Japan, United States, and Europe. *Liver Cancer* 2015;4:85–95.
- 6 Kudo M, Hatanaka K, Maekawa K: Sonazoid-enhanced ultrasound in the diagnosis and treatment of hepatic tumors. *J Med Ultrasound* 2008;16:130–139.
- 7 Kudo M, Hatanaka K, Maekawa K: Defect reperfusion imaging, a newly developed novel technology using Sonazoid in the treatment of hepatocellular carcinoma. *J Med Ultrasound* 2008;16:169–176.
- 8 Kudo M, Hatanaka K, Maekawa K: Newly developed novel ultrasound technique, defect reperfusion ultrasound imaging, using Sonazoid in the management of hepatocellular carcinoma. *Oncology* 2010;78(suppl 1):40–45.
- 9 Numata K, Luo W, Morimoto M, Kondo M, Kunishi Y, Sasaki T, Nozaki A, Tanaka K: Contrast enhanced ultrasound of hepatocellular carcinoma. *World J Radiol* 2010;2:68–82.
- 10 Edey AJ, Ryan SM, Beese RC, Gordon P, Sidhu PS: Ultrasound imaging of liver metastases in the delayed parenchymal phase following administration of Sonazoid using a destructive mode technique (agent detection imaging). *Clin Radiol* 2008;63:1112–1120.
- 11 Shiozawa K, Watanabe M, Ikehara T, Kogame M, Shinohara M, Shinohara M, Ishii K, Igarashi Y, Makino H, Sumino Y: Evaluation of hemodynamics in focal steatosis and focal spared lesion of the liver using contrast-enhanced ultrasonography with Sonazoid. *Radiol Res Pract* 2014;2014:604594.
- 12 Luo W, Numata K, Kondo M, Morimoto M, Sugimori K, Hirasawa K, Nozaki A, Zhou X, Tanaka K: Sonazoid-enhanced ultrasonography for evaluation of the enhancement patterns of focal liver tumors in the late phase by intermittent imaging with a high mechanical index. *J Ultrasound Med* 2009;28:439–448.
- 13 Iijima H: Contrast ultrasound imaging (in Japanese). *Kanzo* 2006;47:173–180.
- 14 Ketelslegers E, Van Beers BE, Sempoux C: Angiomyolipoma of the liver: ferumoxides-enhanced MR imaging. *Eur Radiol* 2000;10:1401–1403.
- 15 Goto K: Localization of CD68 positive cells in nodular lesions of the liver (in Japanese). *Kanzo* 1997;38:19–26.

**Editorial**

# A New Era of Systemic Therapy for Hepatocellular Carcinoma with Regorafenib and Lenvatinib

*Prof. M. Kudo**Editor Liver Cancer***Introduction**

The SHARP study in 2007 [1] and the Asia Pacific study in 2008 [2] led to the worldwide approval of sorafenib as the standard therapy for unresectable hepatocellular carcinoma (HCC). However, clinical trials investigating sunitinib [3], brivanib [4], and linifanib [5] as first-line treatments, with sorafenib as a control arm, failed to meet their primary endpoint of improving overall survival (OS). In addition, global phase III studies investigating second-line therapy with brivanib [6], everolimus [7], and ramucirumab [8], and a regional trial investigating S-1 (tegafur/gimeracil/oteracil) in Japan, were unsuccessful (Table 1). Thus, sorafenib was the only systemic therapeutic agent available for HCC, and for some time no options were available for patients with progressive disease or those intolerant to sorafenib. However, between June 2016 and January 2017, promising results of global phase III studies were reported. The results of a trial of regorafenib were reported at a conference [9] and in a journal [10], and results with lenvatinib were reported in a press release [11], indicating the arrival of a new era of liver cancer therapy.

**Sorafenib-Regorafenib Sequential Therapy**

Sorafenib is the standard treatment for advanced-stage HCC (Barcelona Clinic Liver Cancer [BCLC] stage C) and the only therapeutic agent for advanced-stage HCC with vascular invasion and/or extrahepatic spread. However, in addition to patients with advanced-stage

**Table 1.** Phase III clinical trials for HCC

Target population	Design	Trial name	Presentation	Publication
<i>Early</i>				
Adjuvant (prevention of recurrence)	1 Peretinoin vs. placebo <sup>a</sup>	NIK-333	ASCO 2010	JG 2014
	2 Sorafenib vs. placebo <sup>a</sup>	STORM	ASCO 2014	Lancet-O 2015
	3 Peretinoin vs. placebo	NIK-333/K-333	Ongoing	
<i>Intermediate</i>				
Improvement of TACE	1 TACE +/- sorafenib <sup>a</sup>	Post-TACE	ASCO-GI 2010	EJC 2011
	2 TACE +/- brivanib <sup>a</sup>	BRISK-TA	ILCA 2013	Hepatol 2014
	3 TACE +/- orantinib <sup>a</sup>	ORIENTAL	EASL 2015	
<i>Advanced</i>				
First line	1 Sorafenib vs. sunitinib <sup>a</sup>	SUN1170	ASCO 2011	JCO 2013
	2 Sorafenib vs. brivanib <sup>a</sup>	BRISK-FL	AASLD 2012	JCO 2013
	3 Sorafenib vs. linifanib <sup>a</sup>	LiGHT	ASCO-GI 2013	JCO 2015
	4 Sorafenib +/- HAIC <sup>a</sup>	SILIUS	EASL 2016	
	5 Sorafenib vs. lenvatinib	REFLECT	TBD	
	6 Sorafenib vs. nivolumab	CheckMate 459	Ongoing	
Second line	1 Brivanib vs. placebo <sup>a</sup>	BRISK-PS	EASL 2012	JCO 2013
	2 Everolimus vs. placebo <sup>a</sup>	EVOLVE-1	ASCO-GI 2014	JAMA 2014
	3 Ramucirumab vs. placebo <sup>a</sup>	REACH	ESMO 2014	Lancet-O 2015
	4 S-1 vs. placebo <sup>a</sup>	S-CUBE	ASCO-GI 2015	
	5 Regorafenib vs. placebo <sup>b</sup>	RESORCE	WCGI 2016	Lancet 2017
	6 Tivantinib vs. placebo	JET-HCC	Ongoing	
	7 Ramucirumab vs. placebo	REACH-2	Ongoing	
	8 Pembrolizumab vs. placebo	KEYNOTE-240	Ongoing	

HCC, hepatocellular carcinoma; TACE, transarterial chemoembolization; HAIC, hepatic arterial infusion chemotherapy. <sup>a</sup> Trial halted or with negative results. <sup>b</sup> Trial with positive results.

HCC (BCLC-C), patients with intermediate-stage HCC (BCLC-B) were included in the SHARP study and the Asia Pacific study; therefore, sorafenib is a widely approved agent for systemic therapy not only for advanced-stage HCC but also for unresectable HCC (including intermediate-stage HCC). In fact, sorafenib is often administered to patients with intermediate-stage HCC (BCLC-B) in clinical practice and to 16.4–19.6% of patients in clinical trials worldwide [3–5].

The population of patients with intermediate-stage HCC is extremely heterogeneous, comprising 3 main subpopulations: (1) patients with a good prognosis who can be treated with curative therapy, (2) those for whom transarterial chemoembolization (TACE) is indicated, and (3) those for whom TACE is not recommended. This subclassification of intermediate-stage HCC recently became a well-discussed issue, and the Kinki criteria are used to subclassify patients with intermediate-stage HCC [12, 13]. The OS of patients with B1, B2, and B3 HCC according to the Kinki criteria corresponds to that of patients with HCC of BCLC stages A, B, and C. In addition, patients with BCLC substage B2 HCC, especially those with multiple HCC tumors in both lobes, are not good candidates for TACE. For patients with intermediate-stage HCC (BCLC-B) who do not respond to TACE, an early switch to sorafenib therapy (rather than repeat ineffective TACE) results in a better survival benefit; therefore, early identification of patients that are refractory to TACE is crucial [14–17]. These data underscore the importance of establishing globally recognized, common criteria for identifying TACE failure/refractory patients in order to improve the survival of HCC patients [18].



**Table 2.** Results of the RESORCE trial

	Regorafenib	Placebo	HR (95% CI); <i>p</i> value
Subjects, <i>n</i>	379	194	
BCLC stage C, %	86	89	
Treatment duration, months	3.6 (1.6–7.6)	1.9 (1.4–3.9)	
OS, months	10.6 (9.1–12.1)	7.8 (6.3–8.8)	0.63 (0.50–0.79); <i>p</i> < 0.0001
PFS (mRECIST), months	3.1 (2.8–4.2)	1.5 (1.4–1.6)	0.46 (0.37–0.56); <i>p</i> < 0.0001
TTP (mRECIST), months	3.2 (2.9–4.2)	1.5 (1.4–1.6)	0.44 (0.36–0.55); <i>p</i> < 0.0001
DCR, %	65	36	<i>p</i> < 0.0001
ORR, %	11	4	<i>p</i> = 0.0047
Adverse events (grade ≥3), %	79.7	58.5	

Values are presented as median (range) unless specified otherwise. BCLC, Barcelona Clinic Liver Cancer; OS, overall survival; PFS, progression-free survival; TTP, time to progression; DCR, disease control rate; ORR, objective response rate.

The results of the RESORCE study were published recently [10]. The success of the study is attributed to the following 3 points: (1) patients for whom sorafenib therapy was terminated because of adverse events were excluded from the trial, and second-line therapy with regorafenib was provided to HCC patients who had significant disease progression during sorafenib therapy; (2) vascular invasion and extrahepatic spread were considered as separate stratification factors to avoid imbalance in the 2 arms (test agent vs. placebo); and (3) patients showing tolerance to sorafenib (patients who tolerated 400 mg sorafenib daily for a minimum of 20 days within the last 28 days before radiological progression) were enrolled. This trial design prevented the risk of dropouts due to adverse events associated with regorafenib (since the toxicity of regorafenib is similar to that of sorafenib) and minimized the effect of post-trial treatment after disease progression [18]. According to the results of the RESORCE trial, the median OS (mOS) of patients treated with regorafenib was 10.6 months (7.8 for placebo; HR 0.63; *p* < 0.0001) (Table 2). Subgroup analysis revealed that the HR of OS in patients with a Child-Pugh score of 5 was significantly better than that in patients with a Child-Pugh score of 6 (0.60 [0.40–0.79] vs. 0.80 [0.57–1.13]). This also supports the following approach to improving prognosis in the future: an early switch to sorafenib when patients become refractory to TACE and still have good liver function, such as with a Child-Pugh score of 5, with a subsequent switch to regorafenib as soon as possible after patients have shown progressive disease on sorafenib.

An exploratory analysis of the RESORCE trial showed a favorable OS of 26 months from the start of sorafenib therapy among patients who received sorafenib-regorafenib sequential therapy (19.2 months in the placebo group) [19]. These are extremely important data, because the 26-month prognosis is comparable with the conventional figure after TACE for patients with intermediate-stage HCC [20]. To date, 3 prospective phase III trials evaluating combination therapy with sorafenib and TACE have been performed (Table 1). The results of 2 of these trials have been published: the Japan-Korea TACE study (*n* = 450) [21] and the brivanib-TACE (BRISK-TA) study, which evaluated adjuvant brivanib therapy in combination with TACE (*n* = 502) [20]. Because the mOS was not reached in the placebo arm in the post-TACE study, the BRISK-TA study is currently the only prospective phase III study that investigated the OS with TACE and provided a valid mOS for the placebo arm. Since this was a randomized controlled trial (RCT) of TACE (with the largest number of patients included in any trial worldwide) and the placebo arm was free from selection bias, it provides standard outcomes for TACE worldwide. Additionally, most (82%) of the patients in the BRISK-TA study had

**Table 3.** Comparison of mOS between TACE and sorafenib-regorafenib sequential therapy

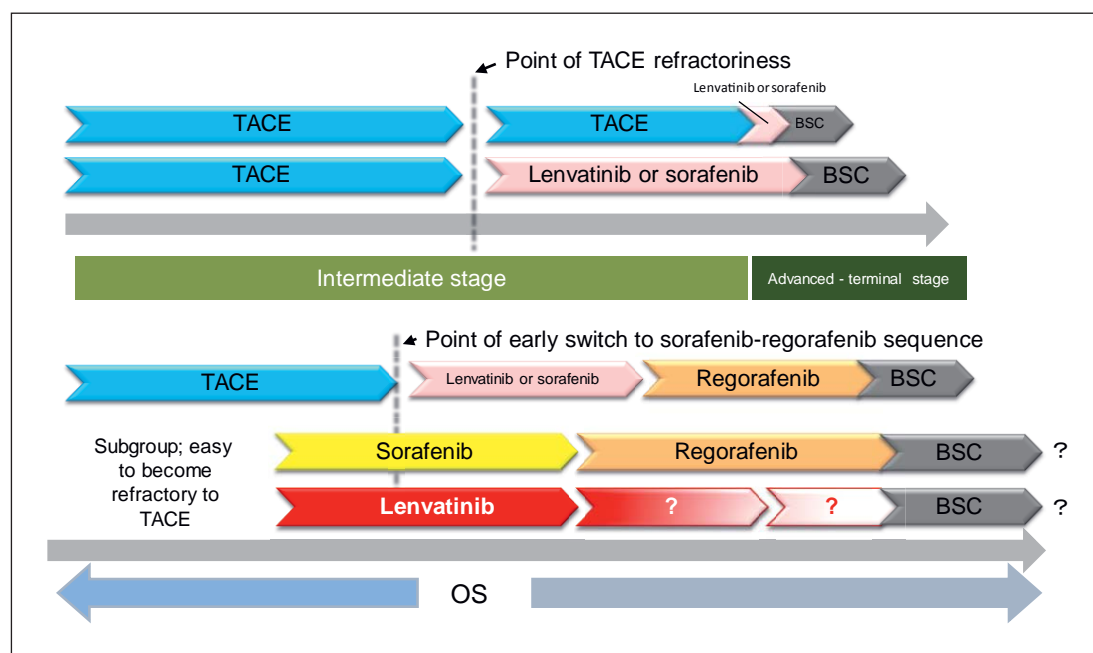
	TACE (placebo arm of brivanib-TACE trial) [20]	Sorafenib-regorafenib sequential therapy (RESORCE trial) [10, 19]
Subjects, <i>n</i>	253	379
Child-Pugh class, <i>n</i> (%)		
A	231 (91)	373 (98)
B	20 (8)	5 (1)
C	2 (1)	0 (0)
BCLC stage, <i>n</i> (%)		
A	57 (23)	1 (0 < 1)
B	150 (59)	53 (14)
C	44 (17)	325 (86)
D	2 (1)	0 (0)
mOS, months	26.1	26

mOS, median overall survival; TACE, transarterial chemoembolization; BCLC, Barcelona Clinic Liver Cancer.

early- or intermediate-stage HCC (BCLC-B, 59%; BCLC-A, 23%) and only 17% had advanced-stage HCC. Conversely, 86% of the patients in the RESORCE trial had advanced-stage HCC (BCLC-C), even though the detailed status of BCLC stage at the start of sorafenib therapy is not disclosed. A simple comparison of OS between the 2 cohorts in different RCTs shows similar outcomes: 26.1 months for the control arm of BRISK-TA versus 26 months for sorafenib-regorafenib sequential therapy (Table 3). Although comparing one arm from an RCT with an arm from exploratory analysis of a different RCT may not be appropriate, both were well-designed prospective randomized clinical trials that minimized the effect of selection bias. Considering that the patients in the sorafenib-regorafenib sequential therapy trial overwhelmingly had advanced-stage HCC, the OS in the study, which is comparable to that in BRISK-TA, is extremely impressive. There is no doubt that the group of subjects with advanced-stage HCC were superselected; nevertheless, the effect of sorafenib-regorafenib sequential therapy in patients with advanced-stage HCC is comparable to that of TACE in those for whom TACE is indicated.

Since the prognosis after sorafenib-regorafenib sequential therapy is promising, the appropriate time to start sorafenib therapy may need to be reconsidered. Conventionally, patients are switched from TACE to systemic therapy when they become refractory to TACE; however, a more proactive approach, such as the earlier introduction of systemic therapy to subgroups of patients who are likely to become refractory to TACE when their liver function is still preserved (Child-Pugh A), may be beneficial (Fig. 1).

Another unaddressed question is the proportion of patients who can be treated by sorafenib-regorafenib sequential therapy. In other words, even after the approval of regorafenib, further studies are needed to obtain real-world data on the percentage of patients undergoing sorafenib therapy who can complete the therapy and also complete regorafenib therapy after failure of sorafenib treatment and disease progression. However, the optimal time point to determine TACE refractoriness should not be missed, since the prognosis after sorafenib-regorafenib sequential therapy is good (26 months from the initiation of sorafenib therapy). Early identification of subgroups likely to become refractory to TACE is also important (Fig. 2). The selection of patients who are likely to respond to systemic therapy is a valid and important line of inquiry regarding therapy with other agents, including lenvatinib (discussed below) and sorafenib.



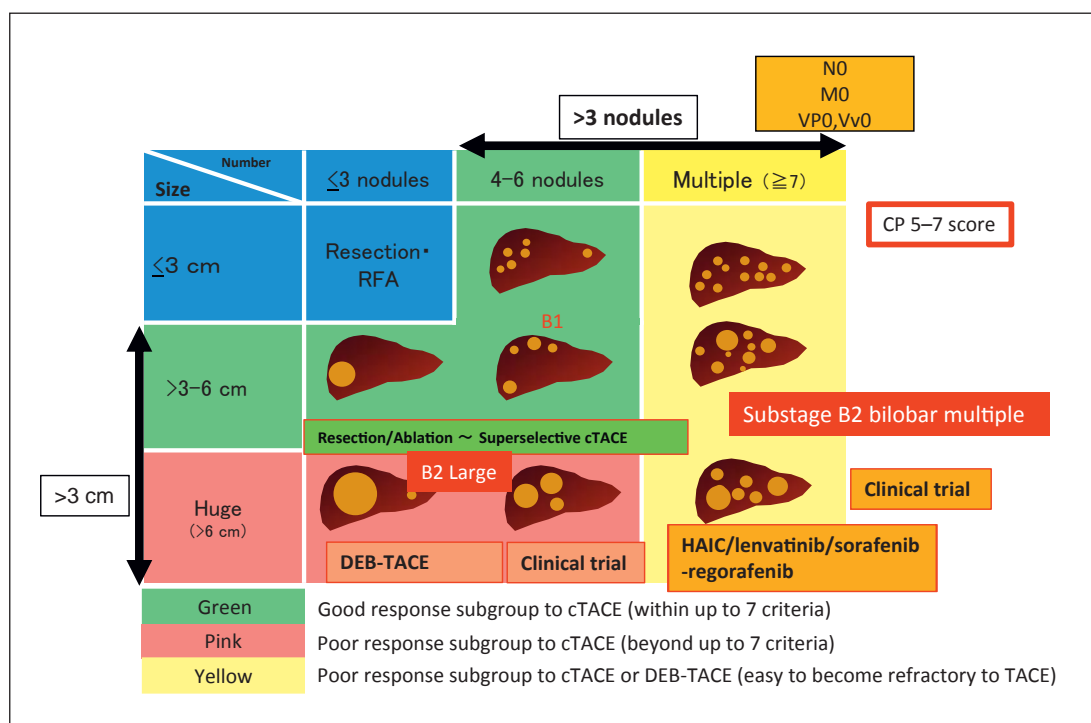
**Fig. 1.** Treatment strategy for systemic therapy for hepatocellular carcinoma. Identification of the subgroup that easily develops to transarterial chemoembolization (TACE) failure/refractoriness may be important. For that subgroup, systemic therapy with a lenvatinib/sorafenib-regorafenib sequence may be a more adequate treatment strategy than repeating ineffective TACE for improving patient survival/benefit. BSC, best supportive care; OS, overall survival.

### A New First-Line Therapy Option: Lenvatinib

Lenvatinib is an oral multi-tyrosine kinase receptor inhibitor that targets VEGF receptors 1–3, FGFR 1–4, PDGFR $\alpha$ , and the KIT and RET proto-oncogenes. It is approved worldwide for the treatment of radioactive iodine-refractory differentiated thyroid cancer. A phase II study evaluating lenvatinib for HCC treatment showed good outcomes, with an mOS of 18.7 months, a time to progression (TTP) of 7.4 months, an objective response rate (ORR) of 37%, and a disease control rate of 78% (according to the modified Response Evaluation Criteria in Solid Tumors [RECIST]) [22]. Considering that the ORR in the control arm of the BRISK-TA study was 42%, the ORR of 37% among those treated with lenvatinib may indicate that the levels of tumor necrosis induced by lenvatinib are similar to those induced by TACE (Table 4).

A worldwide press release by Eisai Co., Ltd. (January 25, 2017) revealed the results of the phase III REFLECT trial involving 954 patients with unresectable HCC [11]. Achievement of the primary endpoint (OS) in the lenvatinib trial was not inferior to that with sorafenib. The secondary endpoints (progression-free survival, TTP, and ORR) also showed that lenvatinib is statistically superior to sorafenib, with clinical significance. Details will be reported at relevant conferences and in journals. The approval of lenvatinib as a novel agent for unresectable HCC in Asia, Japan, Europe, and the USA is anticipated. The improvement of OS with lenvatinib, which is similar to that reported for sorafenib, will likely lead to the approval of lenvatinib as a first-line agent, in addition to sorafenib, for unresectable HCC.

Once lenvatinib will be approved and will become available for treating HCC patients, criteria for the differential use of lenvatinib and sorafenib in the clinical setting will need to be established. The benefits of sorafenib-regorafenib sequential therapy were demonstrated



**Fig. 2.** Heterogeneity and treatment strategy for intermediate-stage hepatocellular carcinoma. Substage B2 (bilobar multiple nodules) may be a candidate for clinical trials of transarterial chemoembolization (TACE) combination therapy with tyrosine kinase inhibitors or immunotherapy. This subgroup may easily become refractory to TACE. CP, Child-Pugh; RFA, radiofrequency ablation; cTACE, conventional subsegmental Lipiodol TACE; DEB, drug-eluting beads; HAIC, hepatic arterial infusion chemotherapy. Modified with permission by Kudo et al. [12].

**Table 4.** Comparison of ORR and DCR between TACE and lenvatinib

	TACE (placebo arm of brivanib-TACE trial) [20]	Lenvatinib (phase II trial) [22]
Subjects, <i>n</i>	253	46
Child-Pugh class, <i>n</i> (%)		
A	231 (91)	45 (97.8)
B	20 (8)	1 (2.2)
C	2 (1)	
BCLC stage, <i>n</i> (%)		
A	57 (23)	0 (0)
B	150 (59)	19 (41.3)
C	44 (17)	27 (58.7)
D	2 (1)	0 (0)
ORR, <i>n</i> (%)	106 (42)	17 (37)
DCR, <i>n</i> (%)	199 (79)	36 (78)

ORR, objective response rate; DCR, disease control rate; TACE, transarterial chemoembolization; BCLC, Barcelona Clinic Liver Cancer

in a solid reliable prospective study [10, 19]. Second-line therapy with regorafenib resulted in significant improvement in patients who had suffered disease progression while on first-line sorafenib, with an mOS of 26 months from the start of sorafenib therapy, even in a group with predominantly advanced-stage HCC (BCLC-C) [19]. However, it is pertinent to note that the subject population was carefully selected.

On the other hand, lenvatinib showed clinically significant antitumor effects (progression-free survival, TTP, and ORR) superior to sorafenib, as disclosed by a press release [11] and phase II trial results [22]. This therapeutic agent is expected to be as effective as TACE in terms of reducing tumor size and inducing tumor necrosis. In some cases, it is expected to permit conversion from systemic therapy to TACE or curative options such as resection or ablation [23–26]. This is a potential advantage of lenvatinib.

For all intents and purposes, the arrival of regorafenib and lenvatinib provides the possibility of systemic therapy as an option for a subgroup of patients with intermediate-stage HCC who easily become or are refractory to TACE, in addition to those with advanced-stage HCC. Patients with intermediate-stage HCC who are likely to become refractory to TACE need to be identified to allow proactive intervention with systemic therapy (Fig. 1).

## Conclusion

The results of phase III studies investigating 2 new therapeutic agents for HCC – namely, regorafenib and lenvatinib – were recently disclosed. The former was presented at a conference in June 2016, and results were published in a journal in January 2017; the latter was announced in a press release in January 2017. Sorafenib-regorafenib sequential therapy is of particular interest. The performance of lenvatinib will remain unclear until relevant congresses or publications; however, based on the contents of the press release, it is very likely to be indicated for the first-line treatment of unresectable HCCs. This suggests that additional therapeutic options will become available for patients with intermediate-stage (BCLC-B) as well as advanced-stage (BCLC-C) HCC.

## References

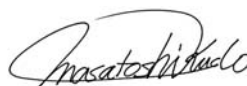
- 1 Llovet JM, Ricci S, Mazzaferro V, et al: Sorafenib in advanced hepatocellular carcinoma. *N Engl J Med* 2008;359:378–390.
- 2 Cheng AL, Kang YK, Chen Z, et al: Efficacy and safety of sorafenib in patients in the Asia-Pacific region with advanced hepatocellular carcinoma: a phase III randomised, double-blind, placebo-controlled trial. *Lancet Oncol* 2009;10:25–34.
- 3 Cheng AL, Kang YK, Lin DY, et al: Sunitinib versus sorafenib in advanced hepatocellular cancer: results of a randomized phase III trial. *J Clin Oncol* 2013;31:4067–4075.
- 4 Johnson PJ, Qin S, Park JW, et al: Brivanib versus sorafenib as first-line therapy in patients with unresectable, advanced hepatocellular carcinoma: results from the randomized phase III BRISK-FL study. *J Clin Oncol* 2013;31:3517–3524.
- 5 Cainap C, Qin S, Huang WT, et al: Linifanib versus sorafenib in patients with advanced hepatocellular carcinoma: results of a randomized phase III trial. *J Clin Oncol* 2015;33:172–179.
- 6 Llovet JM, Decaens T, Raoul JL, et al: Brivanib in patients with advanced hepatocellular carcinoma who were intolerant to sorafenib or for whom sorafenib failed: results from the randomized phase III BRISK-PS study. *J Clin Oncol* 2013;31:3509–3516.
- 7 Zhu AX, Kudo M, Assenat E, et al: Effect of everolimus on survival in advanced hepatocellular carcinoma after failure of sorafenib: the EVOLVE-1 randomized clinical trial. *JAMA* 2014;312:57–67.
- 8 Zhu AX, Park JO, Ryoo BY, et al: Ramucirumab versus placebo as second-line treatment in patients with advanced hepatocellular carcinoma following first-line therapy with sorafenib (REACH): a randomised, double-blind, multicentre, phase 3 trial. *Lancet Oncol* 2015;16:859–870.



- 9 Bruix J, Merle P, Granito A, et al: Efficacy and safety of regorafenib versus placebo in patients with hepatocellular carcinoma (HCC) progressing on sorafenib: results of the international, randomized phase 3 RESORCE trial (abstract LBA-03). *Ann Oncol* 2016;27(suppl 2):ii140–ii141.
- 10 Bruix J, Qin S, Merle P, et al: Regorafenib for patients with hepatocellular carcinoma who progressed on sorafenib treatment (RESORCE): a randomised, double-blind, placebo-controlled, phase 3 trial. *Lancet* 2017; 389:56–66.
- 11 Eisai Co., Ltd.: Phase III trial of anticancer agent Lenvima® as first-line treatment for unresectable hepatocellular carcinoma meets primary endpoint. News Release No. 17-06, January 25, 2017.
- 12 Kudo M, Arizumi T, Ueshima K, et al: Subclassification of BCLC B stage hepatocellular carcinoma and treatment strategies: proposal of modified Bolondi's subclassification (Kinki criteria). *Dig Dis* 2015;33:751–758.
- 13 Arizumi T, Ueshima K, Iwanishi M, et al: Validation of Kinki criteria, a modified substaging system, in patients with intermediate stage hepatocellular carcinoma. *Dig Dis* 2016;34:671–678.
- 14 Ogasawara S, Chiba T, Ooka Y, et al: Efficacy of sorafenib in intermediate-stage hepatocellular carcinoma patients refractory to transarterial chemoembolization. *Oncology* 2014;87:330–341.
- 15 Arizumi T, Ueshima K, Chishina H, et al: Validation of the criteria of transcatheter arterial chemoembolization failure or refractoriness in patients with advanced hepatocellular carcinoma proposed by the LCSGJ. *Oncology* 2014;87(suppl 1):32–36.
- 16 Kudo M, Matsui O, Izumi N, et al: Transarterial chemoembolization failure/refractoriness: JSH-LCSGJ criteria 2014 update. *Oncology* 2014;87(suppl 1):22–31.
- 17 Arizumi T, Ueshima K, Minami T, et al: Effectiveness of sorafenib in patients with transcatheter arterial chemoembolization (TACE) refractory and intermediate-stage hepatocellular carcinoma. *Liver Cancer* 2015;4:253–262.
- 18 Kudo M: Regorafenib as second-line systemic therapy may change the treatment strategy and management paradigm for hepatocellular carcinoma. *Liver Cancer* 2016;5:235–244.
- 19 Finn RS, Merle P, Granito A, et al: Outcomes with sorafenib (SOR) followed by regorafenib (REG) or placebo (PBO) for hepatocellular carcinoma (HCC): results of the international, randomized phase 3 RESORCE trial. *J Clin Oncol* 2017;35(suppl 4S):abstract 344.
- 20 Kudo M, Han G, Finn RS, et al: Brivanib as adjuvant therapy to transarterial chemoembolization in patients with hepatocellular carcinoma: a randomized phase III trial. *Hepatology* 2014;60:1697–1707.
- 21 Kudo M, Imanaka K, Chida N, et al: Phase III study of sorafenib after transarterial chemoembolisation in Japanese and Korean patients with unresectable hepatocellular carcinoma. *Eur J Cancer* 2011;47:2117–2127.
- 22 Ikeda K, Kudo M, Kawazoe S, et al: Phase 2 study of lenvatinib in patients with advanced hepatocellular carcinoma. *J Gastroenterol* 2016, Epub ahead of print.
- 23 Kudo M, Izumi N, Sakamoto M, et al: Survival analysis over 28 years of 173,378 patients with hepatocellular carcinoma in Japan. *Liver Cancer* 2016;5:190–197.
- 24 Kudo M: Surveillance, diagnosis, treatment, and outcome of liver cancer in Japan. *Liver Cancer* 2015;4:39–50.
- 25 Kudo M: Locoregional therapy for hepatocellular carcinoma. *Liver Cancer* 2015;4:163–164.
- 26 Tsurusaki M, Murakami T: Surgical and locoregional therapy of HCC: TACE. *Liver Cancer* 2015;4:165–175.

**Editorial**

# Albumin-Bilirubin Grade and Hepatocellular Carcinoma Treatment Algorithm

*Prof. M. Kudo**Editor Liver Cancer*

The selection of treatment options for hepatocellular carcinoma (HCC) requires critical consideration of hepatic functional reserve in addition to tumor burden (e.g., size and number of HCC nodules [tumor node metastasis stage]). Presently, the Child-Pugh classification is the most common worldwide measure used to assess hepatic functional reserve for the selection of treatment options for HCC [1]. The Child-Pugh classification is used in the American (AASLD [2]), European (EASL-EORTC [3]), Asian (APASL [4]), and Japanese (consensus-based [5, 6] and evidence-based [7–9]) guidelines.

However, there are several issues associated with the Child-Pugh scoring system. First, it includes the subjective criteria of hepatic encephalopathy and ascites in addition to albumin and bilirubin levels. Second, the classification of albumin levels and ascites together is not adequate because they are interrelated factors. Furthermore, converting prothrombin time into the international normalized ratio produces a score of 1 in many patients. Nonetheless, the Child-Pugh score remains the standard measure for selecting treatment options for HCC in clinical practice and clinical trials.

In Japan, a classification called the liver damage grade, which was developed by the Liver Cancer Study Group of Japan (LCSGJ), has been used historically instead of the Child-Pugh score [10]. This classification resembles the Child-Pugh classification but replaces 1 of the 5 factors (hepatic encephalopathy) by the results from the indocyanine green retention test at

See related article by Hiraoka et al.: Albumin-Bilirubin (ALBI) Grade as Part of the Evidence-Based Clinical Practice Guideline for HCC of the Japan Society of Hepatology: A Comparison with the Liver Damage and Child-Pugh Classifications. Liver Cancer DOI: 10.1159/000452846, published on pp. 204–215.

15 min (ICG R15). It is considered a more accurate assessment of hepatic functional reserve than the Child-Pugh classification. The difference between the 2 systems is particularly marked when comparing candidates for hepatectomy; namely, patients with Child-Pugh class A and liver damage grade A. Studies show that Child-Pugh class A is broader and encompasses a larger patient population than liver damage grade A [11, 12]. Liver damage grade is also superior to the Child-Pugh classification for determining whether hepatectomy is indicated [12]. The ICG R15, a factor in the liver damage grading system, is also important for determining the resectable area from the perspective of hepatic functional reserve [13–15]. Makuuchi et al. [15] established the Makuuchi criteria for determining the method of hepatectomy (enucleation, partial hepatectomy, subsegmentectomy, segmentectomy, or resection of 2 or more segments) based on the ICG R15 and total bilirubin values. The Makuuchi criteria enable a safe hepatectomy; therefore, this approach has become the gold standard for selecting the method of hepatectomy not only in Japan [15, 16] but also in other countries [17]. However, there are problems associated with the liver damage grade. First, obtaining ICG R15 values requires injection of ICG in addition to blood collection. Second, injection of ICG for the ICG test can induce anaphylactic shock. Third, accurate values cannot be calculated for patients with marked constitutional jaundice or a portosystemic shunt. Therefore, the ICG R15 test is rarely performed prior to nonsurgical treatments, such as radiofrequency ablation or transcatheter arterial chemoembolization, in patients with relatively good liver function, even in Japan. This is also why the Japanese Evidence-Based Clinical Practice Guidelines list both the Child-Pugh classification and liver damage grade as methods for assessing hepatic functional reserve. The liver damage grade is useful for determining whether hepatectomy is indicated and for determining the size of the liver allowing resection, but it is not useful for the application of nonsurgical treatment.

The albumin-bilirubin (ALBI) grade was proposed as a means of overcoming the previously described issues with the Child-Pugh classification and liver damage grade by calculating a score based on recent albumin and bilirubin levels [18]. This has since then been the subject of many studies [19–25], with the conclusion that the ALBI grade is more accurate than the Child-Pugh classification for assessing hepatic functional reserve.

Hiraoka et al. [26] performed the first study comparing the ALBI grade with the LCSGJ liver damage grade, and the results were reported in this issue of *Liver Cancer*. Consistent with previous studies, Hiraoka et al. [26] showed that the ALBI grade was superior to the Child-Pugh classification. They also found that the ALBI grade can assess hepatic functional reserve with comparable efficacy to the liver damage grade. In addition, patients with ALBI scores of 1 and 2 showed a distribution of ICG R15 levels similar to that of patients with liver damage grades A and B. The ALBI score was well correlated with the ICG R15 ( $r = 0.616$ ,  $p < 0.001$ ), making it possible to roughly estimate the ICG R15 from the ALBI score. Based on the Makuuchi criteria, patient cohorts with an ICG R15 <10, 10–19, and 20–30% are considered candidates for two-segmentectomy, segmentectomy, and subsegmentectomy, respectively. Although the ICG R15 is an important factor for determining the resectable area, Hiraoka et al. [26] found that the ALBI score can also be used to identify groups corresponding to such ranges of ICG R15 values. Specifically, they found that the ALBI score for predicting an ICG R15 of <10% was  $-2.623$  (AUC, 0.798), the ALBI score for predicting an ICG R15 of 10–20% was  $-2.470$  (AUC, 0.791), and the ALBI score for predicting an ICG R15 of 20–30% was  $-2.222$  (AUC, 0.843). Although they noted that performing an ICG R15 test may be an additional option, particularly for patients who require resection, they showed that the ALBI score can fundamentally replace the liver damage grade, since the ICG R15 can be correctly predicted by the ALBI score.

In the Japanese evidence-based treatment algorithm [7], liver damage grade is used only when hepatectomy will be performed, whereas the Child-Pugh classification is used for

patients receiving nonsurgical treatment [9, 27–29]. However, this is essentially a double standard, which is undesirable for clinical practice guidelines. Hiraoka et al. [26] proposed that the ALBI grade is a better measure to address this issue because the score is highly accurate for both nonsurgical and surgical treatments. This is a reasonable and clear-cut message.

In conclusion, the use of the ALBI grade instead of the Child-Pugh classification or liver damage grade to assess hepatic functional reserve for determining treatment options for HCC is a rational proposal not only in clinical practice but also as part of the guidelines. However, it may take some time for clinicians to widely adopt the ALBI grade in the clinical setting because it was only recently introduced into clinical practice.

*Masatoshi Kudo, MD, PhD, Editor-in-Chief*

## References

- 1 Pugh RN, Murray-Lyon IM, Dawson JL, et al: Transection of the oesophagus for bleeding oesophageal varices. *Br J Surg* 1973;60:646–649.
- 2 Bruix J, Sherman M: Management of hepatocellular carcinoma: an update. *Hepatology* 2011;53:1020–1022.
- 3 Llovet JM, Ducreux M, et al: EASL-EORTC clinical practice guidelines: management of hepatocellular carcinoma. *J Hepatol* 2012;56:908–943.
- 4 Omata M, Lesmana LA, Tateishi R, et al: Asian Pacific Association for the Study of the Liver consensus recommendations on hepatocellular carcinoma. *Hepatol Int* 2010;4:439–474.
- 5 Kudo M, Matsui O, Izumi N, et al: JSH consensus-based clinical practice guidelines for the management of hepatocellular carcinoma: 2014 update by the Liver Cancer Study Group of Japan. *Liver Cancer* 2014;3:458–468.
- 6 Kudo M, Matsui O, Izumi N, et al: Transarterial chemoembolization failure/refractoriness: JSH-LCSGJ criteria 2014 update. *Oncology* 2014;87(suppl 1):22–31.
- 7 Kokudo N, Hasegawa K, Akahane M, et al: Evidence-based clinical practice guidelines for hepatocellular carcinoma: the Japan Society of Hepatology 2013 update (3rd JSH-HCC guidelines). *Hepatol Res* 2015;45.
- 8 The Liver Cancer Study Group of Japan: The criteria for the evaluation of direct treatment effects in hepatocellular carcinoma (in Japanese). *Acta Hepatol Jpn* 2004;45:380–385.
- 9 Kudo M: Clinical practice guidelines for hepatocellular carcinoma differ between Japan, United States, and Europe. *Liver Cancer* 2015;4:85–95.
- 10 Liver Cancer Study Group of Japan: General Rules for the Clinical and Pathological Study of Primary Liver Cancer, 3rd English edition. Tokyo, Kanehara & Co, Ltd, 2010.
- 11 Chung H, Kudo M, Haji S, et al: A proposal of the modified liver damage classification for hepatocellular carcinoma. *Hepatol Res* 2006;34:124–129.
- 12 Omagari K, Ohba K, Kadokawa Y, et al: Comparison of the grade evaluated by “liver damage” of Liver Cancer Study Group of Japan and Child-Pugh classification in patients with hepatocellular carcinoma. *Hepatol Res* 2006;34:266–272.
- 13 Greco E, Nanji S, Bromberg IL, et al: Predictors of peri-operative morbidity and liver dysfunction after hepatic resection in patients with chronic liver disease. *HPB (Oxford)* 2011;13:559–565.
- 14 Lau H, Man K, Fan ST, et al: Evaluation of preoperative hepatic function in patients with hepatocellular carcinoma undergoing hepatectomy. *Br J Surg* 1997;84:1255–1259.
- 15 Makuuchi M, Kosuge T, Takayama T, et al: Surgery for small liver cancers. *Semin Surg Oncol* 1993;9:298–304.
- 16 Imamura H, et al: One thousand fifty-six hepatectomies without mortality in 8 years. *Arch Surg* 2003;138:1198–1206; discussion 1206.
- 17 Torzilli G, Makuuchi M, Inoue K, et al: No-mortality liver resection for hepatocellular carcinoma in cirrhotic and noncirrhotic patients: is there a way? A prospective analysis of our approach. *Arch Surg* 1999;134:984–992.
- 18 Johnson PJ, Berhane S, Kagebayashi C, et al: Assessment of liver function in patients with hepatocellular carcinoma: a new evidence-based approach – the ALBI grade. *J Clin Oncol* 2015;33:550–558.
- 19 Wang YY, Zhong JH, Su ZY, et al: Albumin-bilirubin versus Child-Pugh score as a predictor of outcome after liver resection for hepatocellular carcinoma. *Br J Surg* 2016, Epub ahead of print.
- 20 Toyoda H, Lai PB, O’Beirne J, et al: Long-term impact of liver function on curative therapy for hepatocellular carcinoma: application of the ALBI grade. *Br J Cancer* 2016;114:744–750.
- 21 Hiraoka A, Kumada T, Noso K, et al: Proposed new sub-grouping for intermediate-stage hepatocellular carcinoma using albumin-bilirubin grade. *Oncology* 2016;91:153–161.
- 22 Hiraoka A, Kumada T, Michitaka K, et al: Usefulness of albumin-bilirubin grade for evaluation of prognosis of 2,584 Japanese patients with hepatocellular carcinoma. *J Gastroenterol Hepatol* 2016;31:1031–1036.

- 23 Edeline J, Blanc JF, Johnson P, et al: A multicentre comparison between Child Pugh and albumin-bilirubin scores in patients treated with sorafenib for hepatocellular carcinoma. *Liver Int* 2016;36:1821–1828.
- 24 Chan AW, Kumada T, Toyoda H, et al: Integration of albumin-bilirubin (ALBI) score into Barcelona Clinic Liver Cancer (BCLC) system for hepatocellular carcinoma. *J Gastroenterol Hepatol* 2016;31:1300–1306.
- 25 Chan AW, Chong CC, Mo FK, et al: Incorporating albumin-bilirubin grade into the cancer of the liver Italian program system for hepatocellular carcinoma. *J Gastroenterol Hepatol* 2017;32:221–228.
- 26 Hiraoka A, Kumada T, Kudo M, et al: Albumin-bilirubin (ALBI) grade as part of the Japan Society of Hepatology: a comparison with liver damage and Child-Pugh classifications. *Liver Cancer* 2017;6:204–215.
- 27 Kudo M: Surveillance, diagnosis, treatment, and outcome of liver cancer in Japan. *Liver Cancer* 2015;4:39–50.
- 28 Kudo M: Locoregional therapy for hepatocellular carcinoma. *Liver Cancer* 2015;4:163–164.
- 29 Tsurusaki M, Murakami T: Surgical and locoregional therapy of HCC: TACE. *Liver Cancer* 2015;4:165–175.



# The albumin–bilirubin grade improves hepatic reserve estimation post-sorafenib failure: implications for drug development

D. J. Pinato\*, C. Yen\*, D. Bettinger†, R. Ramaswami\*, T. Arizumi‡, C. Ward\*, M. Pirisi§¶, M. E. Burlone§, R. Thimme†, M. Kudo‡ & R. Sharma\*

\*Department of Surgery & Cancer, Hammersmith Campus of Imperial College London, London, UK.

†Department of Medicine II, University Hospital Freiburg, Freiburg, Germany.

‡Department of Gastroenterology and Hepatology, Kindai University School of Medicine, Osaka, Japan.

§Department of Translational Medicine, Università degli Studi del Piemonte Orientale “A. Avogadro”, Novara, Italy.

¶Interdisciplinary Research Center of Autoimmune Diseases, Università degli Studi del Piemonte Orientale “A. Avogadro”, Novara, Italy.

## Correspondence to:

Dr R. Sharma, Department of Surgery & Cancer, Imperial College London Hammersmith Campus, Du Cane Road, W12 0HS London, UK.  
E-mail: r.sharma@imperial.ac.uk

## Publication data

Submitted 1 October 2016  
First decision 20 October 2016  
Resubmitted 20 October 2016  
Resubmitted 23 November 2016  
Accepted 24 November 2016  
EV Pub Online 24 January 2017

The Handling Editor for this article was Professor Peter Hayes, and it was accepted for publication after full peer-review.

## SUMMARY

### Background

Drug development in hepatocellular carcinoma (HCC) is limited by disease heterogeneity, with hepatic reserve being a major source of variation in survival outcomes. The albumin–bilirubin (ALBI) grade is a validated index of liver function in patients with HCC.

### Aim

To test the accuracy of the ALBI grade in predicting post-sorafenib overall survival (PSOS) in patients who permanently discontinued treatment.

### Methods

From a prospectively maintained international database of 447 consecutive referrals, we derived 386 eligible patients treated with sorafenib within Barcelona Clinic Liver Cancer C stage (62%), 75% of whom were of Child class A at initiation. Clinical variables at sorafenib discontinuation were analysed for their impact on post-sorafenib overall survival using uni- and multivariable analyses.

### Results

Median post-sorafenib overall survival of the 386 eligible patients was 3.4 months and median sorafenib duration was 2.9 months, with commonest causes of cessation being disease progression (68%) and toxicity (24%). At discontinuation, 92 patients (24%) progressed to terminal stage, due to worsening Child class to C in 40 (10%). Median post-sorafenib overall survival in patients eligible for second-line therapies ( $n = 294$ ) was 17.5, 7.5 and 1.9 months according respectively to ALBI grade 1, 2 and 3 ( $P < 0.001$ ).

### Conclusions

The ALBI grade at sorafenib discontinuation identifies a subset of patients with prolonged stability of hepatic reserve and superior survival. This may allow improved patient selection for second-line therapies in advanced HCC.

*Aliment Pharmacol Ther* 2017; **45**: 714–722

## INTRODUCTION

In patients with hepatocellular carcinoma (HCC), liver cirrhosis carries an independent clinical course from that of neoplastic disease progression<sup>1</sup> and often represents a barrier to the provision of active anti-cancer treatment.<sup>2</sup> This is particularly true in the more advanced stages of the disease, where liver dysfunction together with deteriorating performance status (PS)<sup>3</sup> remain the strongest adverse prognostic factors.<sup>4, 5</sup>

Sorafenib remains the only first-line treatment option of proven survival benefit in advanced HCC.<sup>6, 7</sup> However, depth and length of response to sorafenib are modest, with <2% objective response rates. Even in patients who achieve initial disease control, progression inexorably occurs within a median interval of 3 months.<sup>8</sup>

Pre-registrative clinical trials of sorafenib in HCC were originally conducted in highly selected populations, as evidenced by high screening failure rates approaching 30%.<sup>6</sup> Whilst clinically developed in patients with optimal liver function, subsequent implementation of sorafenib in routine practice to include subjects with a wider variation in hepatic reserve and PS has highlighted numerous challenges in the clinical management of these patients.<sup>9</sup> In the clinic, neoplastic disease progression, deteriorating PS, hepatic decompensation or unacceptable treatment-related toxicity are the leading causes of permanent sorafenib discontinuation.<sup>10, 11</sup> At treatment cessation, the majority of patients will only qualify for best supportive care, whereas a smaller proportion might be suitable for second-line therapies, an area that is currently at the focus of intense clinical research efforts.<sup>12</sup>

Adequate hepatic function is a universal pre-requisite to access experimental therapies. However, it has been recently suggested that the prognostic ability of the Child class, the scoring system traditionally employed to evaluate liver function based on five parameters, might be outclassed by a novel, more objective biochemical nomogram solely composed of serum albumin and bilirubin, the ALBI grade.<sup>13</sup> The improved clinical utility of this score stems from its ability to further dissect patient groups with different survival outcomes within each Child functional class<sup>14</sup> as well as Barcelona Clinic Liver Cancer (BCLC) stage of HCC.<sup>15</sup>

More accurate prognostic predictors of liver functional reserve are highly required in patients who fail sorafenib treatment, given that a proportion of patients might be eligible for further lines of anti-cancer treatment in an experimental setting. Whilst previous studies have focused on the radiological pattern of progression on

sorafenib as a predictor of survival, this trait, while biologically important and potentially useful as a stratification factor in second-line studies, does not influence patients' eligibility to further lines of therapy, for which the main barriers are represented by progression to terminal-stage disease either due to worsening PS or liver decompensation.<sup>16</sup>

Furthermore, as an improved marker of functional reserve, the ALBI grade might be useful to facilitate patient stratification according to their risk of toxicity from systemic anti-cancer treatment, a non-negligible concern in patients with underlying impairment of hepatic drug clearance.<sup>17</sup>

We therefore conducted a study to ascertain the prognostic value of the ALBI grade in patients who permanently discontinued sorafenib treatment in a large collaborative study including patients from Europe, and Asia.

## PATIENTS AND METHODS

The study population derives from a prospectively maintained, multi-centre patient dataset including 447 consecutive patients treated with sorafenib between 2008 and 2015 within an international research consortium. We excluded 30 patients who were on sorafenib and further 39 due to incomplete data (Figure 1). The final dataset ( $n = 386$ ) comprised 191 patients from three European institutions including 76 (20%) treated at Imperial College London (UK), 44 (11%) from the Academic Liver Unit in Novara (Italy) and 71 patients (18%) treated at the University Hospital in Freiburg (Germany). These patients were incorporated into a larger dataset of 195 subjects (51%) with similar features treated at the Kindai University Faculty of Medicine in Osaka (Japan).

The primary aim was to evaluate the ALBI grade as a predictor of post-sorafenib overall survival (PSOS) and verify its accuracy in comparison with Child class. PSOS was calculated from the time of sorafenib discontinuation to the time of death/last-documented follow-up. Post-sorafenib treatment status was documented for all patients.

The ALBI was calculated using the formula: linear predictor =  $(\log_{10} \text{bilirubin} \times 0.66) + (\text{albumin} \times -0.085)$ , where bilirubin is expressed in  $\mu\text{mol/L}$  and albumin in g/L. Patients were categorised as ALBI grade 1 if the linear predictor  $\leq -2.60$ ; ALBI grade 2 if more than  $-2.60$  to  $\leq -1.39$  and ALBI grade 3 if  $> -1.39$ .<sup>13</sup>

All patients were diagnosed with HCC in accordance to international guidelines.<sup>18</sup> Sorafenib was administered

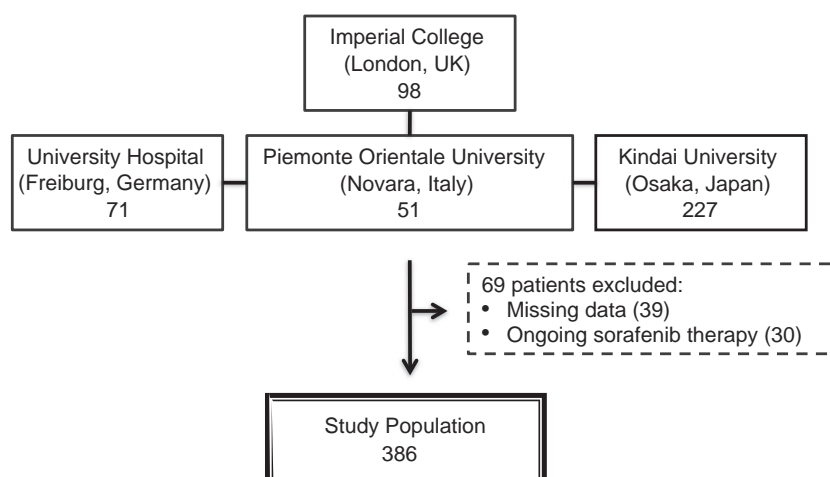


Figure 1 | Study flow chart.

in accordance to the BCLC treatment algorithm to stage C patients or earlier if, on the basis of a multi-disciplinary discussion, they were deemed unfit for or had failed prior loco-regional therapies. Routine clinical reviews during sorafenib therapy were performed at each cycle of treatment and included physical examination, blood test review and adverse events evaluation. Reporting of sorafenib-related AEs followed NCI Common Terminology Criteria for Adverse Events (CTCAE) version 3.<sup>19</sup>

Clinical data at sorafenib commencement and discontinuation included complete blood count, liver function tests, alpha-fetoprotein (AFP) levels and the international normalised ratio value for prothrombin time. Radiological staging of the disease was performed using computerised tomography (CT) and/or magnetic resonance imaging as clinically required. Computation of the ALBI grade,<sup>13</sup> Child functional class and BCLC stage followed standard pre-published methodology.<sup>20</sup> Periodic restaging using triple-phase CT during sorafenib treatment was performed at 8–12 weekly intervals.<sup>21</sup> Reasons for permanent sorafenib cessation included disease progression, unacceptable toxicity defined by grade 2–4 AEs not responding to dose reductions and/or temporary sorafenib discontinuation. In patients with multiple causes for treatment discontinuation (i.e. liver decompensation or unacceptable toxicity), tumour progression was considered the primary cause if confirmed radiologically.<sup>10</sup> The study was conducted in accordance to Good Clinical Practice standards following the ethical guidelines published in the Declaration of Helsinki.

### Statistical analysis

Univariable analysis survival followed Kaplan–Meier methodology and log-rank statistics. Cox proportional hazards regression models were for multivariable

analyses of survival, following formal assessment of the proportional-hazard assumption for each variable using log-likelihood ratio tests over time.<sup>22</sup> Receiver operating characteristic (ROC) methodology was used to test the accuracy of the candidate biomarkers in predicting 90-days mortality.<sup>23</sup> Harrell's concordance index method (*c*-index) was used to rank the different staging systems according to their capacity of discriminating patients according to outcome. Where we assessed the predictive ability of a Cox proportional hazards model, we compared the actual survival outcomes of usable pairs of patients with the values of their estimated prognostic indices from the Cox model. Where the assessment of prediction of multiple biomarkers was performed, the *c*-index was adjusted within the R package for the over-optimism produced by modelling, and assessment being done on the same data via comparison with 150 bootstrap samples. For all analyses, a  $P \leq 0.05$  was considered statistically significant. Statistical analyses were performed using SPSS package version 20.0 (IBM Inc., Chicago, IL, USA) and R Statistical Computing Environment (R Foundation, Vienna, Austria).

## RESULTS

### Patient characteristics

Patient features are presented in Table 1. The majority of patients were of BCLC-C stage ( $n = 248$ , 62%). The predominant aetiological factors of chronic liver disease were HCV infection ( $n = 150$ , 39%), HBV infection ( $n = 62$ , 16%) and alcohol excess ( $n = 72$ , 19%). In total, 290 patients (75%) Child class A at sorafenib initiation, whereas 96 (25%) were of Child B class. All patients had a PS  $\leq 1$  at sorafenib initiation. Sorafenib discontinuation followed primarily progression of disease in 263 patients

**Table 1 | Clinical characteristics of the studied patients**

Characteristic	N = 386 (%)
Age in years, median (range)	71 (33–92)
Gender	
Male	309 (80)
Female	77 (20)
Aetiology of liver disease	
Viral	209 (54)
Non viral	177 (46)
AFP (ng/mL)	
<400	244 (63)
>400	142 (37)
Albumin (g/L), median (range)	30 (16–48)
Bilirubin (μmol/L), median (range)	21 (3–439)
AST (IU/L), median (range)	75 (11–2462)
ALT (IU/L), median (range)	48 (10–1350)
INR, median (range)	1.1 (0.6–3.5)
Platelet count, median (range)	141 (14–673)
Child–Turcotte Pugh Score	
A5	77 (20)
A6	78 (21)
B7	77 (21)
B8	67 (18)
B9	38 (10)
C10	31 (8)
C11	4 (1)
C12	5 (1)
ALBI grade	
Grade 1	27 (7)
Grade 2	171 (45)
Grade 3	188 (48)
Tumour morphology	
Unifocal	36 (10)
Multifocal (<50% of liver replacement)	221 (57)
Massive (>50% of liver replacement)	129 (32)
Maximum diameter of largest lesion (cm), median (range)	4.2 (1–20)
Extrahepatic spread	
Absent	239 (63)
Present	147 (37)
Portal vein involvement	
Absent	287 (74)
Present	99 (26)
BCLC stage at sorafenib initiation	
A–B	154 (38)
C	248 (62)
BCLC stage at sorafenib cessation	
B	105 (27)
C	189 (49)
D	92 (24)
Prior treatment for HCC	
Orthotopic liver transplantation	2 (1)
Surgical resection	62 (16)
Radiofrequency ablation	114 (30)
Transarterial chemoembolisation	231 (60)
Other	53 (14)
Number of prior treatments lines	

**Table 1 | (Continued)**

Characteristic	N = 386 (%)
0	77 (20)
1	156 (40)
2	93 (24)
≥ 3	60 (16)
Subsequent treatment for HCC	
Best supportive care	300 (78)
Further anti-cancer treatment	86 (22)
Sorafenib discontinuation	
Progressive disease	263 (64)
Toxicity	91 (24)
Liver failure	24 (6)
Others	8 (2)

All clinicopathological variables refer to the moment of sorafenib discontinuation unless otherwise stated.

(64%), followed by unacceptable toxicity in 91 (24%). The most common sorafenib-related AEs occurring at any grade during treatment were diarrhoea ( $n = 143$ , 37%), palmo-plantar erythrodysesthesia (PPE) ( $n = 139$ , 36%) and fatigue ( $n = 88$ , 22%). Similarly, when considering AEs ≥Grade 2, PPE was the most prevalent ( $n = 33$ , 9%) followed by diarrhoea ( $n = 24$ , 6%) and fatigue ( $n = 21$ , 5%). In total 196 patients (51%) had experienced at least 1 Grade 2 AE during sorafenib treatment, whereas 104 (27%) had experienced at least 1 Grade 3 AE. Toxicity prompted permanent sorafenib dose reductions in 59 patients (15%).

At the time of sorafenib discontinuation, the stage-distribution according to BCLC had significantly changed compared to baseline, with the majority of patients clustering within BCLC-C criteria ( $n = 189$ , 49%) followed by BCLC-B ( $n = 105$ , 27%) and D ( $n = 92$ , 24%). Stage migration to BCLC-D derived from progression to Child class to C in 39 patients (10%) and worsening PS to >2 in 53 patients (14%). Following sorafenib discontinuation, the majority of patients received best supportive care ( $n = 294$ , 76%). Of the 92 patients (24%) who received further active treatment, 24 (6%) received >1 line of therapy.

#### Post-sorafenib overall survival

At the time of analysis (April 2016), there were 298 deaths (77%). Patients were followed up for a median of 13 months (range 1–70 months). Median duration of treatment was 2.9 months (range 1–53 months). Median OS from the time of sorafenib initiation was 9.4 months (95% CI 7.6–11.0), whereas median PSOS was

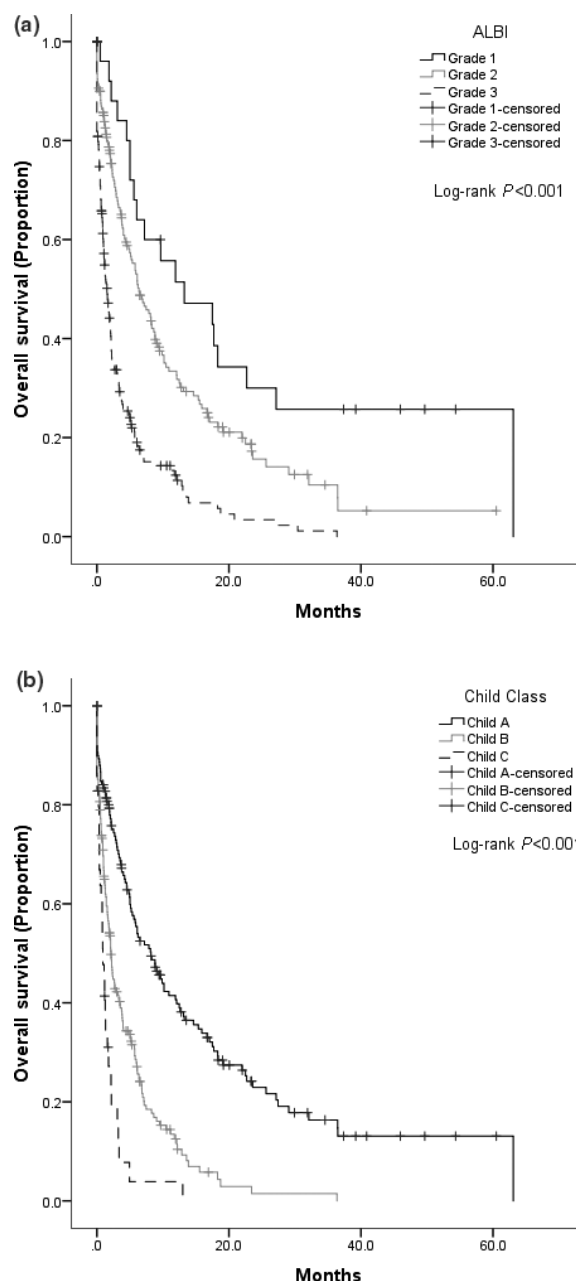
3.4 months (95% CI 2.5–4.3). The median PSOS considering BCLC stage at sorafenib discontinuation was 9 months (95% CI 5.7–12.3) for stage B, 3.6 months for stage C (95% CI 2.4–4.7) and 1.1 months for stage D (95% CI 0.5–1.6). The hazard ratio (HR) between C and B was 2.0 (95% CI 1.4–2.7) and between D and B was 3.5 (95% CI 2.5–5.1) (log-rank  $P < 0.001$ ). Patients withdrawing sorafenib due to AEs had an improved median survival of 5.8 months (95% CI 3.4–8.1) compared to 2.6 (95% CI 1.9–3.4) in patients who progressed on treatment (HR 0.65 95% CI 0.52–0.84, log-rank  $P < 0.001$ ). We verified the relationship between a number of clinicopathological traits at sorafenib discontinuation and PSOS including the presence of extrahepatic spread [median PSOS 4.9 vs. 3.4 months, HR 1.4 (95% CI 1.1–1.9), log-rank  $P = 0.01$ ] and AFP >400 (median PSOS 5.0 vs. 2.9 months, HR 1.3 [95% CI 1.1–1.7], log-rank  $P = 0.02$ ).

#### Prognostic comparison of Child class and ALBI grade at sorafenib discontinuation

For this study, we focused on a comparative analysis of biomarkers of liver functional reserve. The ALBI grade was calculated in all patients. When categorised according to ALBI, patients with grade 1 ( $n = 27$ ) had a median OS of 13 months (95% CI 1.0–25) compared to 6.3 of grade 2 ( $n = 171$ , range 4.3–8.3) and 1.6 of grade 3 ( $n = 188$ , 1.0–2.0; log-rank  $P < 0.001$ ). The HR between ALBI 2 and 1 was 1.7 (95% CI 1.1–2.9) and between ALBI 3 and ALBI 1 was 4.1 (95% CI 2.5–6.8) (Figure 2a).

Child classification was derived in 377 patients (98%). Child class was associated with post-sorafenib survival with median OS of 8.2 months (95% CI 5.2–11) for Child A ( $n = 160$ ), 2.1 months (95% CI 1.6–2.6) for Child B ( $n = 178$ ) and 1 month for Child C patients ( $n = 39$ , 95% CI 0.5–1.3, log-rank  $P < 0.001$ ; Figure 2b). The HR between Child class B and A was 2.4 (95% CI 1.8–3.1) and between Child C and A was 4.7 (95% CI 3.0–7.2). A comparison of ALBI grade and Child class for the 377 patients with both scores available is reported in Table S1.

We further investigated the prognostic relationship between ALBI and Child class by evaluating the stratifying potential of the ALBI across each Child class. The analysis was limited to Child A and B classes because the entire patients with Child C were co-classified as ALBI Grade 3. As shown in Table S2, the ALBI could sub-classify patients within Child A according to significantly different survival times ranging from a median OS of 17.5–1.0 months across the three ALBI grades. This was not replicated in Child B patients where the ALBI was not prognostic.



**Figure 2** | Kaplan–Meier curves describing the overall survival of patients with HCC ( $n = 386$ ) at sorafenib discontinuation categorised according to albumin–bilirubin (ALBI) grade (a) and Child class (b).

We performed further subgroup analyses by excluding patients who, according to current guidelines, displayed untreatable disease progression at sorafenib discontinuation (i.e. patients migrating to BCLC-D stage,  $n = 92$ , 24%). In a subset of 294 potential candidates for second-line therapies, the ALBI grade was predictive of survival with median OS of 17.5 months (95% HR 9.0–26) for ALBI 1 ( $n = 24$ ), 7.5 months for ALBI 2 (95% CI 5.4–9.5)



and 1.9 months for ALBI 3 (95% CI 1.4–2.4; log-rank  $P < 0.001$ ; Figure 3a). Similarly, patients with Child class A ( $n = 135$ ) had better median OS at 10 months (95% CI 7–13) compared to Child B ( $n = 153$ ) whose median OS was 2.2 (95% CI 1.6–2.8) (Figure 3b).

In the same subset of 294 patients, we comparatively tested ALBI grade and Child class for their independent predictive role in estimating PSOS. We tested ALBI and

Child class in concurrent, multivariable Cox regression models adjusted for the confounding effect of BCLC stage at discontinuation and subsequent treatment. Multivariable analysis of survival confirmed both ALBI and Child class as independent predictors of PSOS (Table 2).

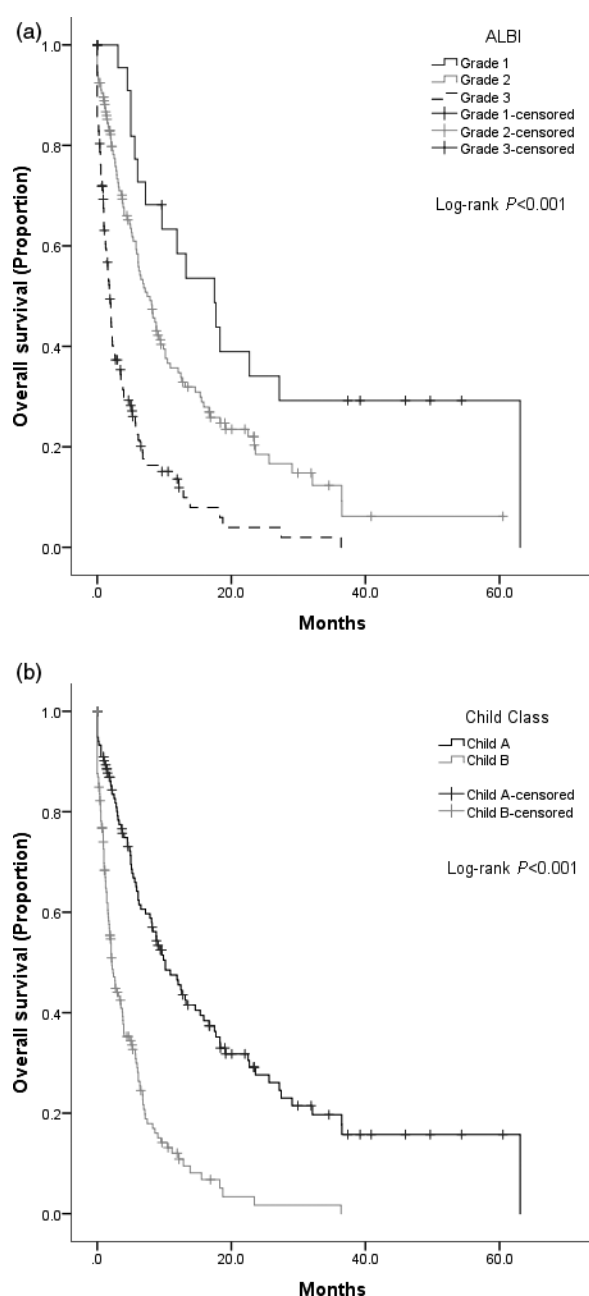
As shown in Figure 4 ROC curve analysis confirmed optimal prognostic accuracy of both ALBI and Child class in predicting 90-days mortality rates, where the ALBI grade displayed better accuracy with an area under the ROC curve (AUROC) of 0.69 (95% CI 0.63–0.75) over Child class 0.66 (0.59–0.72;  $P < 0.001$ ).

We compared the predictive ability of ALBI and Child class in estimating PSOS using Harrel's c-index. In the whole study population ( $n = 386$ ), ALBI was superior to Child class (c-index 0.64 vs. 0.62). ALBI displayed highest accuracy in patients considered eligible to second-line therapies ( $n = 294$ ) (c-index 0.65 vs. 0.63 for Child class), whereas both scores had significantly lower accuracy in patients experiencing untreatable disease progression ( $n = 92$ ) (c-index 0.54 for ALBI and 0.53 for Child class).

## DISCUSSION

The provision of safe and effective systemic anti-cancer treatment in patients with HCC has been traditionally hindered by the concurrent presence of liver dysfunction, which imposes a significant toll on patients' survival and ability to tolerate systemic therapies.<sup>24</sup> In the drug development process, cirrhosis limits enrolment of patients with HCC to early phase clinical trials due to safety concerns stemming from liver dysfunction, reducing the detection of early efficacy signals from novel investigational medicinal products. In later stage trials where treatment efficacy testing is powered on survival benefit, liver dysfunction is a major confounder in influencing the mortality of patients with advanced HCC independently from the progression of malignancy.<sup>25</sup> Such confounding role has affected the clinical development of sorafenib, where unsurprisingly, despite homogeneity in screening criteria and treatment schedules, patients enrolled into the SHARP and Asian Pacific trials had different survival, suggesting that subtle variations in liver function might have at least in part accounted for the observed heterogeneity in trial outcomes.<sup>6, 7</sup>

Accumulating evidence suggests the ALBI grade as a more accurate predictor of liver functional reserve across the various stages of HCC compared to standard Child classification,<sup>13, 14</sup> including patients with advanced HCC.<sup>26, 27</sup> In our multi-institutional study including a large cohort of patients treated with sorafenib, we demonstrated for the first time the independent

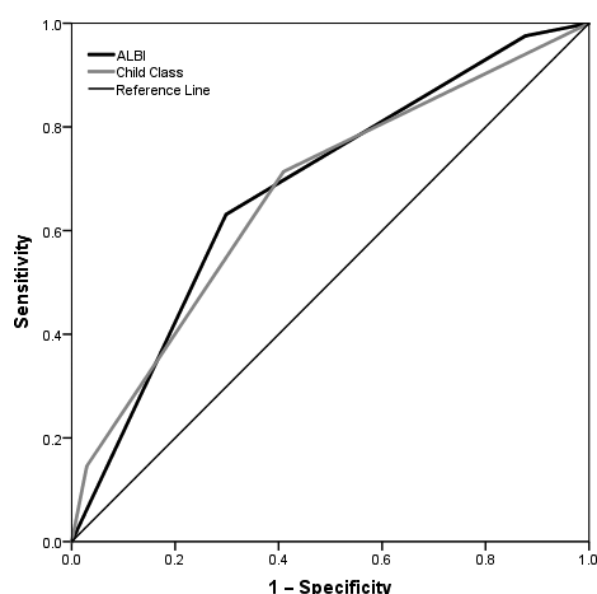


**Figure 3** | Kaplan–Meier curves describing the overall survival of candidates for second-line treatment ( $n = 294$ ) stratified by albumin–bilirubin (ALBI) grade (a) and Child class (b).

**Table 2** | Multivariable cox regression analyses evaluating the prognostic role of Child class and ALBI grade in candidates for second-line systemic therapies (*n* = 294)

	ALBI, Unadjusted		ALBI, Adjusted*		CTP, Unadjusted		CTP, Adjusted*	
	HR (95% CI)	P-value	HR (95% CI)	P-value	HR (95% CI)	P-value	HR (95% CI)	P-value
<b>ALBI</b>								
2 vs. 1	1.9 (1.1–3.3)	0.02	1.8 (1.0–3.2)	0.03				
3 vs. 1	4.7 (2.7–8.4)	<0.001	4.0 (2.2–7.1)	<0.001				
<b>BCLC</b>								
C vs. B			1.8 (1.3–2.4)	<0.001			1.9 (1.3–2.5)	<0.001
<b>Subsequent therapy</b>								
Yes vs. No			0.4 (0.3–0.5)	<0.001			0.4 (0.3–0.6)	<0.001
<b>Child class</b>								
B vs. A					3.0 (2.2–4.0)	<0.001	2.4 (1.8–3.4)	<0.001

\* Coefficients adjusted for post-sorafenib BCLC stage and subsequent therapy status.

**Figure 4** | The comparison of the albumin–bilirubin (ALBI) grade and Child class in predicting 90-days mortality rate using ROC curve analysis (*n* = 386).

prognostic ability of the ALBI in predicting PSOS. In unselected patients who failed sorafenib therapy, the ALBI grade calculated at the moment of permanent sorafenib discontinuation was capable of differentiating patient subgroups with up to a 3-fold difference in median survival times across the diverse strata.

Interestingly, the prognostic accuracy of the ALBI was preserved following exclusion of patients who, based on BCLC stage at sorafenib withdrawal, were unfit for second-line therapies. An even stronger and clinically important stratifying potential of the ALBI grade transpired by restricting our analysis of survival to patients

in Child A functional class, in whom preservation of an ALBI grade 1 at treatment discontinuation predicted for median survival times in excess of 17 months, reducing to 8 months for ALBI grade 2.

It has been suggested that the improved accuracy of ALBI, especially within Child A criteria, is secondary to the modification of pre-defined cut-off points for albumin and bilirubin, which might allow clinicians to capture more subtle differences in the biosynthetic function of the cirrhotic liver.<sup>27–29</sup> Certainly, abandoning scoring of encephalopathy, ascites or coagulopathy, two of which require subjective assessments, does not reduce the accuracy of the ALBI in predicting survival nor 90-days mortality rates, a landmark survival endpoint that investigators often use to assess the suitability of patients to clinical trials. Interestingly, whilst 92% of ALBI grade 1 patients satisfied Child A criteria, such proportion reduced to 73% in ALBI grade 2 patients and 3% in ALBI grade 3, suggesting a potentially higher prognostic heterogeneity in grade 2 patients due to the contribution of diverse functional subclasses.<sup>30</sup>

This is not the first study to highlight, amongst other factors, the key role of deteriorating liver function as a predictor of survival in patients with advanced HCC who might be otherwise fit for second-line therapies. The role of Child class deterioration was reported by Reig *et al.*, although survival analysis was limited to only 85 patients, who had all discontinued sorafenib due to disease progression.<sup>16</sup> Likewise, despite not having directly tested Child class, Iavarone and colleagues provide convincing confirmation of the adverse prognostic role of a composite panel of individual biomarkers of impaired liver function including albumin, bilirubin, prothrombin time as well as clinically overt hepatic

decompensation as predictors of mortality.<sup>10</sup> Based on our data, the maximal improvement in prognostication conferred by the ALBI grade is evident in patients who fulfil Child A criteria, a point which may limit the applicability of this score in patients with intermediate to advanced liver dysfunction.

In contrast to the previous studies, we prospectively followed up a larger, multi-institutional cohort of patients from Europe and Asia, to control for the heterogeneity in survival generated by varying aetiological factors and tumour burden. In addition, our analysis of survival is also controlled for post-progression treatment status, an established confounder in estimating OS not taken into account in previous studies. These methodological strengths allow our observation to be controlled for a number of important sources of systematic bias, suggesting that the independent prognostic value of the ALBI is a true finding and generalisable to patients of diverse geographical origin, ethnicity and aetiology.<sup>31</sup>

In conclusion, this study validates the ALBI grade as a prognostic index in HCC patients who permanently discontinued sorafenib. The increased accuracy of the ALBI comes at no additional costs, as it relies on routinely available, objective biochemical indices. Due to limited evidence-based treatment options in patients who fail sorafenib,<sup>32</sup> the enhanced discriminative power of the ALBI in advanced HCC is particularly important for optimal patient stratification, especially in suitable candidates for clinical trials.<sup>33</sup> The accurate definition of patient subpopulations with prolonged stability in liver functional reserve might enhance efficacy testing in phase II–III trials by reducing the heterogeneity stemming from concomitant liver failure.<sup>12</sup> This is particularly important in trial design, where inaccurate assumptions over predicted survival times in placebo group as well as the choice of pre-planned stratification factors has been a problematic issue in the development of molecularly targeted therapies in the second-line setting.<sup>34</sup>

Secondly, improved hepatic reserve phenotyping might help mitigating the risks stemming from systemic toxicity, a nontrivial issue in patients with HCC where treatment discontinuation due to AEs is higher than other malignancies,<sup>35</sup> and has in the past led to the premature termination of development of sunitinib due to concerns over excessive mortality in the treatment arm. Although exploring the relationship between ALBI grade and toxicity from systemic treatment was beyond the aims of our

study, this should be formally evaluated in future prospective trials.

Although the relatively limited sample size is a potential limitation to our study, the survival times and clinicopathological features describing our cohort are similar to previous studies to suggest our results are generalisable to the broader population of patients with HCC who fail sorafenib therapy.<sup>10, 16, 36</sup> Moreover, the choice of evaluating this score in a large, multi-institutional patient dataset limits the chances of selection bias.

In the absence of convincingly robust molecular biomarkers to dissect the biological heterogeneity of advanced HCC, our study is the first to support the use of the ALBI as an accurate, objective and reproducible marker of liver function in HCC. The prognostic relationship between ALBI and survival in patients should be further defined in independent studies in a view to facilitate the full clinical implementation of this promising biomarker.

## SUPPORTING INFORMATION

Additional Supporting Information may be found in the online version of this article:

**Table S1.** Concordance between Child–Turcotte Pugh and ALBI-based liver functional classification ( $n = 377$ ).

**Table S2.** The prognostic relationship between Child–Turcotte Pugh and ALBI ( $n = 342$ ).

## AUTHORSHIP

*Guarantor of the Article:* Dr Rohini Sharma.

*Authors contributions:* DJP, RS: Study concept and design, DJP, TA, CY, CW, CS, DB, RT, MK, MP: Acquisition of data, DJP, RS: Analysis and interpretation of data, DJP, RS: Drafting of the manuscript, DJP, DB, TA, CY, CW, MP, MB, RT, RR, MK, RS: Critical revision of the manuscript for important intellectual content, DJP, RR: Statistical analysis, DJP, RS: Obtained funding, MP, MK, RT: Administrative, technical or material support, DJP, RT, MK, MP, RS: Study supervision. All authors approved the final version of the manuscript prior to submission.

## ACKNOWLEDGEMENTS:

*Declaration of personal interests:* None.

*Declaration of funding interests:* DJP is supported by the National Institute for Health Research (NIHR) as well as grant funding from the Academy of Medical Sciences and the Imperial NIHR Biomedical Research Centre (BRC). DB is supported by the Berta-Ottenstein Programme, Faculty of Medicine, University of Freiburg, Germany. This project was funded in part by the Academy of Medical Sciences (AMS, Grant ID SGL013/1021 awarded to DJP). The AMS starter grant scheme is supported by the Academy of Medical Sciences, The Wellcome Trust, Medical Research Council, British Heart Foundation, Arthritis Research UK, the Royal College of Physicians and Diabetes UK.

## REFERENCES

- Durand F, Valla D. Assessment of prognosis of cirrhosis. *Semin Liver Dis* 2008; **28**: 110–22.
- Worns MA, Weinmann A, Pflingst K, *et al.* Safety and efficacy of sorafenib in patients with advanced hepatocellular carcinoma in consideration of concomitant stage of liver cirrhosis. *J Clin Gastroenterol* 2009; **43**: 489–95.
- Doyle A, Marsh P, Gill R, *et al.* Sorafenib in the treatment of hepatocellular carcinoma: a multi-centre real-world study. *Scand J Gastroenterol* 2016; **51**: 979–85.
- Al-Rajabi R, Patel S, Ketchum NS, *et al.* Comparative dosing and efficacy of sorafenib in hepatocellular cancer patients with varying liver dysfunction. *J Gastrointest Oncol* 2015; **6**: 259–67.
- Federico A, Orditura M, Cotticelli G, *et al.* Safety and efficacy of sorafenib in patients with advanced hepatocellular carcinoma and Child-Pugh A or B cirrhosis. *Oncol Lett* 2015; **9**: 1628–32.
- Llovet JM, Ricci S, Mazzaferro V, *et al.* Sorafenib in advanced hepatocellular carcinoma. *N Engl J Med* 2008; **359**: 378–90.
- Cheng AL, Kang YK, Chen Z, *et al.* Efficacy and safety of sorafenib in patients in the Asia-Pacific region with advanced hepatocellular carcinoma: a phase III randomised, double-blind, placebo-controlled trial. *Lancet Oncol* 2009; **10**: 25–34.
- Llovet JM, Bruix J. Molecular targeted therapies in hepatocellular carcinoma. *Hepatology* 2008; **48**: 1312–27.
- Lencioni R, Kudo M, Ye SL, *et al.* GIDEON (Global Investigation of therapeutic DEcisions in hepatocellular carcinoma and Of its treatment with sorafenib): second interim analysis. *Int J Clin Pract* 2014; **68**: 609–17.
- Iavarone M, Cabibbo G, Biolato M, *et al.* Predictors of survival in patients with advanced hepatocellular carcinoma who permanently discontinued sorafenib. *Hepatology* 2015; **62**(3): 784–91.
- Pinter M, Sieghart W, Hucke F, *et al.* Prognostic factors in patients with advanced hepatocellular carcinoma treated with sorafenib. *Aliment Pharmacol Ther* 2011; **34**: 949–59.
- Maida M, Iavarone M, Raineri M, Camma C, Cabibbo G. Second line systemic therapies for hepatocellular carcinoma: reasons for the failure. *World J Hepatol* 2015; **7**: 2053–7.
- Johnson PJ, Berhane S, Kagebayashi C, *et al.* Assessment of liver function in patients with hepatocellular carcinoma: a new evidence-based approach-the ALBI grade. *J Clin Oncol* 2015; **33**: 550–8.
- Hiraoka A, Kumada T, Michitaka K, *et al.* Usefulness of albumin-bilirubin grade for evaluation of prognosis of 2584 Japanese patients with hepatocellular carcinoma. *J Gastroenterol Hepatol* 2016; **31**: 1031–6.
- Chan AW, Kumada T, Toyoda H, *et al.* Integration of albumin-bilirubin (ALBI) score into Barcelona clinic liver cancer (BCLC) system for hepatocellular carcinoma. *J Gastroenterol Hepatol* 2016; **31**: 1300–6.
- Reig M, Rimola J, Torres F, *et al.* Postprogression survival of patients with advanced hepatocellular carcinoma: rationale for second-line trial design. *Hepatology* 2013; **58**: 2023–31.
- Palmer DH, Johnson PJ. Evaluating the role of treatment-related toxicities in the challenges facing targeted therapies for advanced hepatocellular carcinoma. *Cancer Metastasis Rev* 2015; **34**: 497–509.
- European Association for the Study of the Liver, European Organisation for Research and Treatment of Cancer. EASL-EORTC clinical practice guidelines: management of hepatocellular carcinoma. *J Hepatol* 2012; **56**: 908–43.
- NCI Common Terminology Criteria for Adverse Events (CTCAE) v.4. 4.03 ed. Bethesda; 2010.
- Llovet JM, Bru C, Bruix J. Prognosis of hepatocellular carcinoma: the BCLC staging classification. *Semin Liver Dis* 1999; **19**: 329–38.
- Lencioni R, Llovet JM. Modified RECIST (mRECIST) assessment for hepatocellular carcinoma. *Semin Liver Dis* 2010; **30**: 52–60.
- Pinato DJ, Stebbing J, Ishizuka M, *et al.* A novel and validated prognostic index in hepatocellular carcinoma: the inflammation based index (IBI). *J Hepatol* 2012; **57**: 1013–20.
- Hanley JA. Receiver operating characteristic (ROC) methodology: the state of the art. *Crit Rev Diagn Imaging* 1989; **29**: 307–35.
- Pinter M, Sieghart W, Graziadei I, *et al.* Sorafenib in unresectable hepatocellular carcinoma from mild to advanced stage liver cirrhosis. *Oncologist* 2009; **14**: 70–6.
- Villanueva A, Hernandez-Gea V, Llovet JM. Medical therapies for hepatocellular carcinoma: a critical view of the evidence. *Nat Rev Gastroenterol Hepatol* 2013; **10**: 34–42.
- Hollebecque A, Cattani S, Romano O, *et al.* Safety and efficacy of sorafenib in hepatocellular carcinoma: the impact of the Child-Pugh score. *Aliment Pharmacol Ther* 2011; **34**: 1193–201.
- Edeline J, Blanc JF, Johnson P, *et al.* A multicenter comparison between Child Pugh and ALBI scores in patients treated with sorafenib for hepatocellular carcinoma. *Liver Int* 2016; **36**: 1821–28.
- Toyoda H, Lai PB, O’Beirne J, *et al.* Long-term impact of liver function on curative therapy for hepatocellular carcinoma: application of the ALBI grade. *Br J Cancer* 2016; **114**: 744–50.
- Chan AW, Chong CC, Mo FK, *et al.* Incorporating albumin-bilirubin grade into the cancer of the liver Italian program system for hepatocellular carcinoma. *J Gastroenterol Hepatol* 2016; doi: 10.1111/jgh.13457.
- D’Amico G, Garcia-Tsao G, Pagliaro L. Natural history and prognostic indicators of survival in cirrhosis: a systematic review of 118 studies. *J Hepatol* 2006; **44**: 217–31.
- Kudo M, Lencioni R, Marrero JA, *et al.* Regional differences in sorafenib-treated patients with hepatocellular carcinoma: GIDEON observational study. *Liver Int* 2016; **36**: 1196–205.
- Bruix J, Qin S, Merle P, *et al.* Regorafenib for patients with hepatocellular carcinoma who progressed on sorafenib treatment (RESORCE): a randomised, double-blind, placebo-controlled, phase 3 trial. *Lancet* 2016; doi: 10.1016/S0140-6736(16)32453-9 [Epub ahead of print].
- He AR, Goldenberg AS. Treating hepatocellular carcinoma progression following first-line sorafenib: therapeutic options and clinical observations. *Therap Adv Gastroenterol* 2013; **6**: 447–58.
- Llovet JM, Decaens T, Raoul JL, *et al.* Brivanib in patients with advanced hepatocellular carcinoma who were intolerant to sorafenib or for whom sorafenib failed: results from the randomized phase III BRISK-PS study. *J Clin Oncol* 2013; **31**: 3509–16.
- Bolos D, Finn RS. Systemic therapy in HCC: lessons from brivanib. *J Hepatol* 2014; **61**: 947–50.
- Terashima T, Yamashita T, Takata N, *et al.* Post-progression survival and progression-free survival in patients with advanced hepatocellular carcinoma treated by sorafenib. *Hepatol Res* 2016; **46**: 650–6.



# The ALBI grade provides objective hepatic reserve estimation across each BCLC stage of hepatocellular carcinoma

David J. Pinato<sup>1,\*†</sup>, Rohini Sharma<sup>1,†</sup>, Elias Allara<sup>2</sup>, Clarence Yen<sup>1</sup>, Tadaaki Arizumi<sup>3</sup>, Keiichi Kubota<sup>4</sup>, Dominik Bettinger<sup>5</sup>, Jeong Won Jang<sup>6</sup>, Carlo Smirne<sup>7</sup>, Young Woon Kim<sup>6</sup>, Masatoshi Kudo<sup>3</sup>, Jessica Howell<sup>1</sup>, Ramya Ramaswami<sup>1</sup>, Michela E. Burlone<sup>7</sup>, Vito Guerra<sup>8</sup>, Robert Thimme<sup>5</sup>, Mitsuru Ishizuka<sup>4</sup>, Justin Stebbing<sup>1</sup>, Mario Pirisi<sup>7</sup>, Brian I. Carr<sup>9</sup>

<sup>1</sup>Department of Surgery & Cancer, Imperial College London, Hammersmith Hospital, Du Cane Road, W120HS London, UK;

<sup>2</sup>NIHR Blood and Transplant Research Unit, Department of Public Health and Primary Care, University of Cambridge, Cambridge CB1 8RN, UK; <sup>3</sup>Department of Gastroenterology and Hepatology, Kinki University School of Medicine, Osaka-Sayama, Osaka, Japan; <sup>4</sup>Department of Gastroenterological Surgery, Dokkyo Medical University, Mibu, Tochigi 321-0293, Japan;

<sup>5</sup>Department of Medicine II, University Hospital Freiburg, Freiburg, Germany; <sup>6</sup>Department of Internal Medicine, The Catholic University of Korea Incheon St. Mary's Hospital, Seoul, Republic of Korea; <sup>7</sup>Department of Translational Medicine, Università degli Studi del Piemonte Orientale "A. Avogadro", Via Solaroli 17, Novara, Italy; <sup>8</sup>IRCCS De Bellis, National Institute for Digestive Diseases, Castellana Grotte, Italy; <sup>9</sup>Izmir Biomedicine and Genome Centre, Dokuz Eylul University, Izmir, Turkey

**Background & Aims:** Overall survival (OS) is a composite clinical endpoint in hepatocellular carcinoma (HCC) due to the mutual influence of cirrhosis and active malignancy in dictating patient's mortality. The ALBI grade is a recently described index of liver dysfunction in hepatocellular carcinoma, based solely on albumin and bilirubin levels. Whilst accurate, this score lacks cross-validation, especially in intermediate stage HCC, where OS is highly heterogeneous.

**Methods:** We evaluated the prognostic accuracy of the ALBI grade in estimating OS in a large, multi-centre study of 2426 patients, including a large proportion of intermediate stage patients treated with chemoembolization (n = 1461) accrued from Europe, the United States and Asia.

**Results:** Analysis of survival by primary treatment modality confirmed the ALBI grade as a significant predictor of patient OS after surgical resection ( $p < 0.001$ ), transarterial chemoembolization ( $p < 0.001$ ) and sorafenib ( $p < 0.001$ ). Stratification by Barcelona Clinic Liver Cancer stage confirmed the independent prognostic value of the ALBI across the diverse stages of the disease, geographical regions of origin and time of recruitment to the study ( $p < 0.001$ ).

**Conclusions:** In this large, multi-centre retrospective study, the ALBI grade satisfied the criteria for accuracy and reproducibility following statistical validation in Eastern and Western HCC

patients, including those treated with chemoembolization. Consideration should be given to the ALBI grade as a stratifying biomarker of liver reserve in routine clinical practice.

**Lay summary:** Liver failure is a key determinant influencing the natural history of hepatocellular carcinoma (HCC). In this large multi-centre study we externally validate a novel biomarker of liver functional reserve, the ALBI grade, across all the stages of HCC.

© 2016 European Association for the Study of the Liver. Published by Elsevier B.V. All rights reserved.

## Introduction

The mortality from hepatocellular carcinoma (HCC), the third most lethal malignancy on a global scale, is increasing despite best diagnostic and therapeutic efforts [1].

In contrast with most solid tumours, the prognosis of patients with HCC is not solely influenced by the extent of anatomic spread of the cancer but equally, if not more importantly, by the degree of functional impairment that accompanies liver cirrhosis [2].

A wide variety of prognostic algorithms have been proposed over the years, aimed at overcoming the limitations of Tumour-Node-Metastasis classification. These have variably integrated clinical domains shown to be harbingers of worse clinical outcome [3], including tumour mass and extent, liver dysfunction, poor performance status and blood alpha-fetoprotein (AFP) levels, however they have variable reported accuracy for survival prediction across early to advanced-stage HCC. Most models quantify liver functional status using the Child-Turcotte-Pugh (CTP) score, a classification originally devised in 1964 and later modified to estimate the risk of perioperative mortality in patients considered for surgical porto-systemic shunting.

**Keywords:** Prognosis; Carcinoma; Hepatocellular; Liver failure; ALBI; Albumins; Bilirubin; Retrospective studies; Biomarkers.

Received 22 December 2015; received in revised form 22 August 2016; accepted 8 September 2016; available online 24 September 2016

\* Corresponding author. Address: NIHR Academic Clinical Lecturer in Medical Oncology, Imperial College London Hammersmith Campus, Du Cane Road, W12 0HS London, UK. Tel.: +44 (0)7564016996.

E-mail address: david.pinato@imperial.ac.uk (D.J. Pinato).

<sup>†</sup> These authors contributed equally as joint-first authors.





Whilst having been widely adopted as a convenient, non-invasive indicator of liver function, the CTP score is limited by several constraints. Firstly, not all the constituents of the score have equal accessibility and reproducibility. The presence of ascites often requires ultrasound confirmation, whilst the assessment of minimal encephalopathy can be clinically challenging and subjective [4]. Secondly, the cut-off points pre-fixed for objective laboratory variables including albumin, bilirubin and prothrombin time are arbitrary, so that patients at the extremes of the distribution are classified equally as patients with marginally deranged laboratory parameters, producing so called “floor” and “ceiling effects”, which ultimately limit accurate prognostication [5]. Thirdly, apart from ascites grade, the CTP score does not include platelet counts or other biomarkers to indicate portal hypertension, a highly lethal complication of cirrhosis that can coexist within each CTP functional class [6]. The importance of diagnosing portal hypertension in HCC strongly emerges from the Barcelona Clinic Liver Cancer (BCLC) prognostic algorithm; the most widely adopted staging system of HCC in Western countries, where invasive measurement of hepatic venous pressure gradients is reserved for patients who are considered for radical treatments [7].

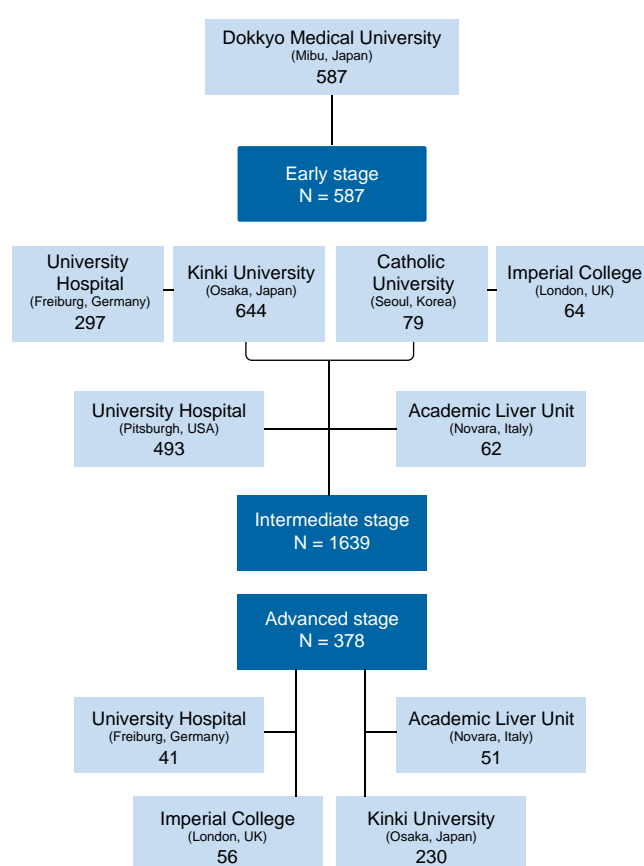
A number of alternative non-invasive biomarkers of liver function have been proposed, including the model for end-stage liver disease (MELD) that takes into account serum creatinine, bilirubin and the international normalized prothrombin time ratio (INR) to derive a continuous score. Whilst useful in prioritizing candidates for liver transplantation [8], the MELD score has demonstrated prognostic limitations [9] and is not routinely used outside this setting, having failed to demonstrate an increased clinical utility over CTP in patients who are not amenable to liver transplantation [5]. Other markers have been evaluated as non-invasive indicators of fibrosis, initially to replace the need for histology in the assessment of severity of chronic liver disease [10]. However, these only partially reproduce the synthetic and metabolic functions of the liver and the advent of transient elastography has re-defined their clinical role [11].

Recently, an alternative measure of liver function based solely on albumin and bilirubin, the ALBI grade, has been proposed in patients with HCC [12]. The ALBI grade is a prognostic nomogram emerging from the multivariate screen of routine clinicopathologic variables in a large, international cohort of patients with HCC, further validated in a separate group of cirrhotic patients without cancer. Whilst appealing due to its potential to objectively dissect prognostically diverse subgroups within CTP classes, the ALBI grade was generated retrospectively and lacks external validation in independent studies: a necessary step before routine clinical use due to the risk of statistical over-fitting in determining true prognostic accuracy. Secondly, the ALBI score has not been characterized in intermediate stage HCC, the most critical subset of patients in terms of prognostic assessment where survival is highly heterogeneous, ranging from 11 to 45 months [13].

The aim of this study was therefore to independently validate the prognostic value of the ALBI grade across all BCLC stages in a large collaborative study including patients from Europe, United States and Asia.

## Patients and methods

The study population consisted of multiple, independently collected retrospective cohorts of consecutively recruited patients diagnosed with HCC either on imaging or by histologic criteria according to international guidelines [14] (Fig. 1). Patients



**Fig. 1. Study flow diagram illustrating patient disposition across the studied cohorts.**

were recruited from tertiary referral centres with specialist multidisciplinary services for HCC management as part of an international research consortium to ensure adequate representation of all disease stages and aetiology of chronic liver disease. Patients who underwent liver transplantation as primary therapy for HCC were excluded. The patient population considered for this study was accrued as part of routine clinical care and was not selected amongst clinical trial participants.

Demographic data, complete blood count including liver function tests, AFP and the INR value for prothrombin time were reconstructed from electronic medical records. Patients were staged using computerized tomography (CT) and/or magnetic resonance imaging as clinically required to derive the number of focal hepatic lesions and maximum tumour diameter detected during contrast enhancement. Computation of CTP functional class and BCLC stage followed standard pre-published methodology [15]. The ALBI grade was calculated using the following equation: linear predictor =  $(\log_{10} \text{bilirubin } \mu\text{mol/L} \times 0.66) + (\text{albumin g/L} \times -0.085)$ . The continuous linear predictor was further categorised into three different grades for prognostic stratification purposes: grade 1 (less than  $-2.60$ ), grade 2 (between  $-2.60$  and  $-1.39$ ) and grade 3 (above  $-1.39$ ) as previously described [12].

The primary clinical endpoint of the study was overall survival (OS), calculated from the date of initiation of treatment (surgery, first chemoembolization or initiation of sorafenib) to the date of death and/or last follow-up. Due to the significant heterogeneity in the study population, survival analysis was stratified by treatment modality to include patients treated with curative resection and palliative patients amenable to locoregional therapies and systemic treatment with sorafenib.

### Surgical resection cohort (n = 587)

To validate the score in early stage HCC, we utilised a cohort of 587 previously reported patients who underwent hepatic resection between April 2000 and 2012 as primary radical treatment for HCC at the Department of Gastroenterological Surgery, Dokkyo Medical University Hospital (Japan) as previously described [16].

## Research Article

### Locoregional therapy (LRT) cohort (n = 1461)

Due to the documented survival heterogeneity in intermediate stage HCC and the diverse treatment protocols and re-treatment criteria for transarterial chemo-embolization (TACE) adopted in Europe, USA and Asia we opted to cross-validate the ALBI grade in different patient cohorts according to geographical region to fully ascertain its reproducibility: LRT-USA, LRT-Europe and LRT-Asia.

From a large, prospectively maintained database of 1202 patients treated at the University of Pittsburgh (USA) we derived a first dataset of 315 individuals with biopsy-proven HCC who were not candidates for surgical resection, RFA or hepatic transplantation and who received conventional selective cisplatin-TACE from 1989 to 2005 [17].

The European dataset of 423 patients included 297 subjects (70%) who underwent conventional frontline selective/superselective TACE at the University Hospital Freiburg (Germany) between 2003 and 2015; a second group of 64 treated at Imperial College London (UK) between 2001 and 2012 and a third subgroup of 62 patients from the Academic Liver Unit in Novara (Italy), treated between 2004 and 2013.

A larger Asian dataset of 723 patients combined 79 (11%) from St. Mary's Hospital Catholic University of Korea at Incheon (Republic of South Korea), prospectively recruited between June 2011 and July 2012, and a further 644 (89%) consecutive patients with unresectable HCC treated with TACE at the Kinki University Faculty of Medicine (Japan) between January 2004 and August 2013. Conventional selective or superselective TACE was administered following multidisciplinary discussion as reported by Pinato *et al.* [18]. In both European and Asian datasets radiologic response to TACE based followed the modified response evaluation criteria in solid tumours (mRECIST) [19] on contrast-enhanced CT scan, 6–8 weeks post-TACE. None of the patients included in the Asian dataset were part of the original ALBI qualification study.

### Sorafenib cohort (n = 378)

A multi-centre dataset of 378 patients with advanced HCC receiving sorafenib between 2008 and 2015 was constructed including 147 from three European institutions including 56 (15%) from Imperial College London (UK), 51 (13%) from the Academic Liver Unit in Novara (Italy) and 41 (11%) from the University Hospital in Freiburg (Germany). These patients were merged with a larger dataset of 230 subjects (61%) with similar characteristics recruited from the Kinki University Faculty of Medicine (Japan).

### Statistical analysis

Univariate analysis of the different clinical factors associated with survival was performed using Kaplan-Meier curves, with differences in OS between each stratum being tested using log-rank statistics. The independent prognostic value of each factor was further tested using by Cox proportional hazards regression models [16]. Formal assessment of the proportional-hazard assumption by means of log-likelihood ratio tests over time-bands yielded no evidence that the effects of the ALBI and CTP scores varied over time (ALBI,  $p = 0.078$ ; CTP,  $p = 0.1325$ ). Analyses of survival were performed using SPSS package version 20.0 (IBM Inc., USA).

Harrell's concordance index method (c-index) was used to rank the different staging systems according to their capacity of discriminating patients according to outcome. For this purpose, we assessed the effect of the candidate risk factors using the Cox model using R [20] and the Statistical Analysis System (SAS, Cary, NC, USA). We used the rms packages of Dr. Frank Harrell [21] to identify a subset of predictors by backward elimination as previously described [16]. Where we assessed the predictive ability of a Cox proportional hazards model, we compared the actual survival outcomes of usable pairs of patients with the values of their estimated prognostic indices from the Cox model to generate a c-index statistic. To correct for the overoptimism generated during model selection, the c-index statistic was internally validated using established bootstrapping techniques with 150 iterations.

## Results

Characteristics of the studied populations are presented in Table 1. Median OS was 54 months for the surgical cohort, whilst in the LRT cohorts survival ranged between 10 and 36 months,

being worse in the LRT-USA cohort. Patient in the sorafenib cohort had a median OS of 9 months (Table 1).

### Surgical resection cohort

Of the 587 patients treated with liver resection, 381 (65%) satisfied BCLC-A criteria, whilst 44 patients (7%) were of BCLC-C stage due to presence of nodal spread in seven patients (1%) and performance status of 1 in 38 (6%). The most prevalent aetiology was hepatitis C virus (HCV) infection ( $n = 395$ , 67%) followed by hepatitis B virus (HBV) ( $n = 146$ , 25%). Median follow-up time was 41 months (range 6–143 months) and the overall event rate was 54%. The majority of patients were of CTP class A ( $n = 477$ , 81%).

When considering OS classified according to the ALBI grade median OS was 82 months (range 58–105) in patients with ALBI grade 1 ( $n = 127$ , 22%), 50 months (44–55) for ALBI 2 ( $n = 435$ , 77%) and 42 months for ALBI 3 ( $n = 25$ , 4%), (HR 1.7, 95%CI 1.3–2.2,  $p < 0.001$ ) (Fig. 2A). We then considered solely patients with CTP A ( $n = 477$ ), who are optimal candidates for resection, and confirmed ALBI grade as a strong predictor of OS in this patient group with a median OS of 82 months (range 58–105) for ALBI 1 ( $n = 127$ , 26%) and 51 months (range 45–56) for ALBI 2 ( $n = 350$ , 74%) (HR 1.7, 95%CI 1.3–2.2,  $p < 0.001$ ) (Fig. 2B).

Multivariable analysis of survival confirmed advanced ALBI as a significant predictor of worse OS in a Cox regression model adjusted for BCLC stage. Individual hazard ratios are presented in Table 2.

The predictive ability of the ALBI grade was tested in comparison with CTP by means of Harrell's concordance index. ALBI displayed an overall better discriminatory ability in predicting OS with a c-score of 0.57 (95%CI 0.54–0.59) when considered alone and 0.67 (95%CI 0.63–0.70) following adjustment by BCLC stage, compared to CTP class (c-score 0.54, 95% CI 0.54–0.59).

### Locoregional therapy cohort

The 315 patients from the United States were treated with conventional TACE as described before [17], the majority were BCLC-B ( $n = 272$ , 86%) and within CTP class A ( $n = 220$ , 70%). Median follow-up was 10 months (range 1–151 months). Most patients were cirrhotic ( $n = 238$ , 76%) with alcohol excess ( $n = 221$ , 70%), HCV ( $n = 113$ , 40%) and HBV infection ( $n = 81$ , 28%) being the most prevalent risk factors. Stratification of OS by ALBI showed a deterioration in median OS from 15.4 months (range 11–20 months) in grade 1 ( $n = 41$ , 13%), to 11 months (range 8.3–14 months) in grade 2 ( $n = 209$ , 66%) and 4.5 months (range 3–6 months) in grade 3 ( $n = 65$ , 21%) (HR 1.4, 95% CI 1.1–1.7,  $p = 0.002$ ) (Fig. 2C). As shown in Fig. 2C and in Table 2, we found no statistically significant difference in OS between patients of ALBI grade 1 and 2 in this patient cohort.

The majority of LRT-Europe cohort ( $n = 423$ ) received TACE within BCLC-B staging criteria ( $n = 310$ , 73%) and CTP A ( $n = 307$ , 72%) with the remaining 113 exceeding these criteria due to segmental portal vein thrombosis not contra-indicating TACE ( $n = 40$ , 9%), extra-hepatic spread ( $n = 1$ , 0.2%) or PS = 1 ( $n = 71$ , 17%). Alcohol excess was the most prevalent etiologic factor ( $n = 160$ , 38%) followed by HCV infection ( $n = 115$ , 27%). Median follow-up time was 27 months (range 1–162 months), with a mortality rate of 72%. Patient stratification according to ALBI revealed grade 1 ( $n = 139$ , 33%) predicted for median survival of 39 months (range 33–44 months) compared to 18 months (range

Table 1. Clinico-pathologic features of the individual patient cohorts included in the study.

Characteristic	Surgical resection cohort (n = 587)	Locoregional therapy cohort (n = 1461)			Sorafenib cohort (n = 378)
Center	Japan	USA	Europe	Asia	Europe and Japan
Patient number	587	315	423	723	378
Accrual period	2000–2012	1989–2005	2001–2013	2004–2013	2008–2015
Age in years					
Median	68	64	69	72	63
Range	28–85	22–93	33–88	32–89	(32–95)
Gender					
Male	469 (80)	239 (76)	350 (83)	512 (71)	296 (78)
Female	118 (20)	76 (24)	73 (17)	210 (29)	82 (22)
Aetiology of liver disease					
Viral	541 (93)	162 (52)	162 (39)	581 (80)	165 (44)
Non-viral	46 (7)	123 (38)	222 (52)	142 (20)	213 (56)
Non-characterized	–	30 (10)	39 (9)		
Child-Turcotte-Pugh class					
A5	224 (38)	220 (70)	211 (50)	355 (50)	171 (45)
A6	253 (43)	–	96 (22)	187 (26)	109 (29)
B7	93 (16)	95 (30)	55 (13)	102 (14)	60 (16)
B8	17 (3)	–	36 (9)	49 (6)	30 (8)
B9	0 (0)	–*	25 (6)	30 (3)	8 (2)
Bilirubin, $\mu\text{mol/L}$					
Median	10	17	17	14	14
IQR	5	17	14	9	12
Albumin, g/L					
Median	34	32	37	37	36
IQR	7	8	8	8	8
AST, IU/L					
Median	36	81	59	49	57
IQR	22	95	59	36	51
ALT, IU/L					
Median	32	59	45	37	38
IQR	26	53	49	32	38
Platelet count					
Median	131	125	140	115	146
IQR	87	140	98	77	119
Alpha-fetoprotein, ng/ml					
Median	29.5	73	23.6	28	184
IQR	227	2078	234	200	3413
INR**					
Median	1.1	12.9**	1.1	1.0	1.1
Range	1.0–3.0	10.5–21.6	0.9–3.4	1.0–2.0	(1.0–2.2)
Maximum tumour diameter					
Median	3	6	5	2	4.0
Range	1–15	1–23	0.9–20	2–17	(1–20)
Tumour morphology					
Oligofocal (1–2 nodules)	–	151 (40)	177 (42)	250 (40)	63 (17)
Multifocal (>3 nodules)		164 (60)	246 (58)	473 (60)	314 (83)
Portal vein thrombosis					
Absent	587 (587)	315 (100)	383 (91)	664 (92)	277 (73)
Present	0 (0)	0 (0)	40 (9)	59 (8)	101 (27)
Extra-hepatic spread					
Absent	580 (99)	315 (100)	423 (100)	693 (96)	255 (68)
Present	7 (1)	0 (0)	0 (0)	29 (4)	123 (32)
BCLC stage					
A	381 (65)	43 (14)	75 (18)	270 (37)	40 (10)
B	162 (28)	272 (86)	236 (56)	390 (54)	109 (29)
C	44 (7)	0 (0)	112 (26)	63 (9)	229 (61)
D	0 (0)	0 (0)	0 (0)	0 (0)	0 (0)
ALBI grade					
Grade 1	127 (22)	41 (13)	140 (33)	156 (22)	105 (27)
Grade 2	435 (77)	209 (66)	253 (60)	482 (67)	238 (63)
Grade 3	25 (4)	65 (21)	30 (7)	85 (12)	35 (9)

(Continued on next page)

## Research Article

**Table 1** (continued)

Characteristic	Surgical resection cohort (n = 587)	Locoregional therapy cohort (n = 1461)	Sorafenib cohort (n = 378)
Overall survival, months			
Median	54.0	10	25.0
95% CI	48.5–59.4	7.8–11.7	21.4–28.6
			32.3–40.0
			1.0–74.0

IQR, interquartile range; CI, confidence interval.

\* Data clustered in Child Turcotte Pugh class (A, n = 220; B = 95).

\*\* Expressed in seconds as prothrombin time (PT) in the USA cohort. Normal range <13 s.

14.3–21.6) for ALBI 2 (n = 251, 60%) and 18 months for ALBI 3 (n = 30, 7%) (range 14.8–21.1, HR 1.4, 95%CI 1.2–1.8,  $p < 0.001$ ) with no significant difference between grades 2 and 3 (Fig. 2D).

Staging characteristics were similar in the LRT-Asia cohort of 723 patients, 660 (91%) being within BCLC-B stage and 79% CTP A (n = 575) with the exception 63 subjects who exceeded intermediate stage due to visceral metastatic spread (n = 29, 4%) and/or segmental portal vein involvement (n = 59, 8%). HCC was mostly HCV (n = 454, 70%) or HBV-related (127, 18%). Patients with ALBI grade 1 (n = 156, 22%) had a median OS of 51.8 months (range 45–57 months) compared to 34 months (range 30–39 months) of ALBI 2 (n = 482, 67%) and 21 (range 14–28 months) of ALBI 3 (n = 85, 12%) (HR 1.7, 1.4–2.0,  $p < 0.001$ ) (Fig. 2E).

To verify its independent prognostic value, the ALBI grade was jointly tested with other prognostic factors including CTP and BCLC stage in alternative multivariate Cox regression model. The effect of ALBI in predicting patients' OS across each of the LRT cohorts is reported in Table 2.

The discriminatory capacity of the ALBI grade as calculated by the corresponding c-index score was substantially homogeneous across each LRT cohort, ranging from 0.57 to 0.58 when ALBI was considered alone, and 0.58–0.65 when adjusted for BCLC stage. Individual c-index scores for ALBI and CTP are presented in Table 2.

### Sorafenib cohort

Sorafenib was prescribed to 229 patients (61%) in BCLC-C stage, 280 (74%) within CTP class A. Aetiology of chronic liver disease included HCV (n = 161, 43%), HBV infection (n = 62, 16%) and alcohol excess (n = 56, 15%). Patients were followed up for a median of 13 months (range 1–74 months). There were 264 deaths (70%) in total. Median duration of treatment was 2.8 months (range 1–70 months). At time of analysis, 16 patients were actively receiving sorafenib (4%), whilst the remaining had discontinued due to radiologic progression (n = 181, 48%), unacceptable toxicity (n = 105, 28%), death (n = 28, 4%) or other causes (n = 48, 13%). The most common adverse events, occurring at any grade, were diarrhoea (n = 134, 35%) and palmar-plantar erythrodysesthesia (n = 131, 35%) requiring permanent dose modifications in 87 patients (23%). Periodic restaging during sorafenib therapy according to mRECIST criteria was available in 222 patients. Best radiologic response included disease progression (n = 119, 31%), stable disease (n = 65, 17%), partial (n = 31, 8%) and complete response (n = 7, 1%). When categorised according to ALBI patients with grade 1 had a median OS of 16 months (range 12–20) compared to 7.6 of grade 2 (range 5.9–9.3) and 4.8 of grade 3 (range 3–6.6) (HR 1.6, 95%CI 1.3–2.0,  $p < 0.001$ ) (Fig. 2F).

Multivariable analysis of survival confirmed ALBI as an independent predictor of patients' OS in advanced disease (Table 2).

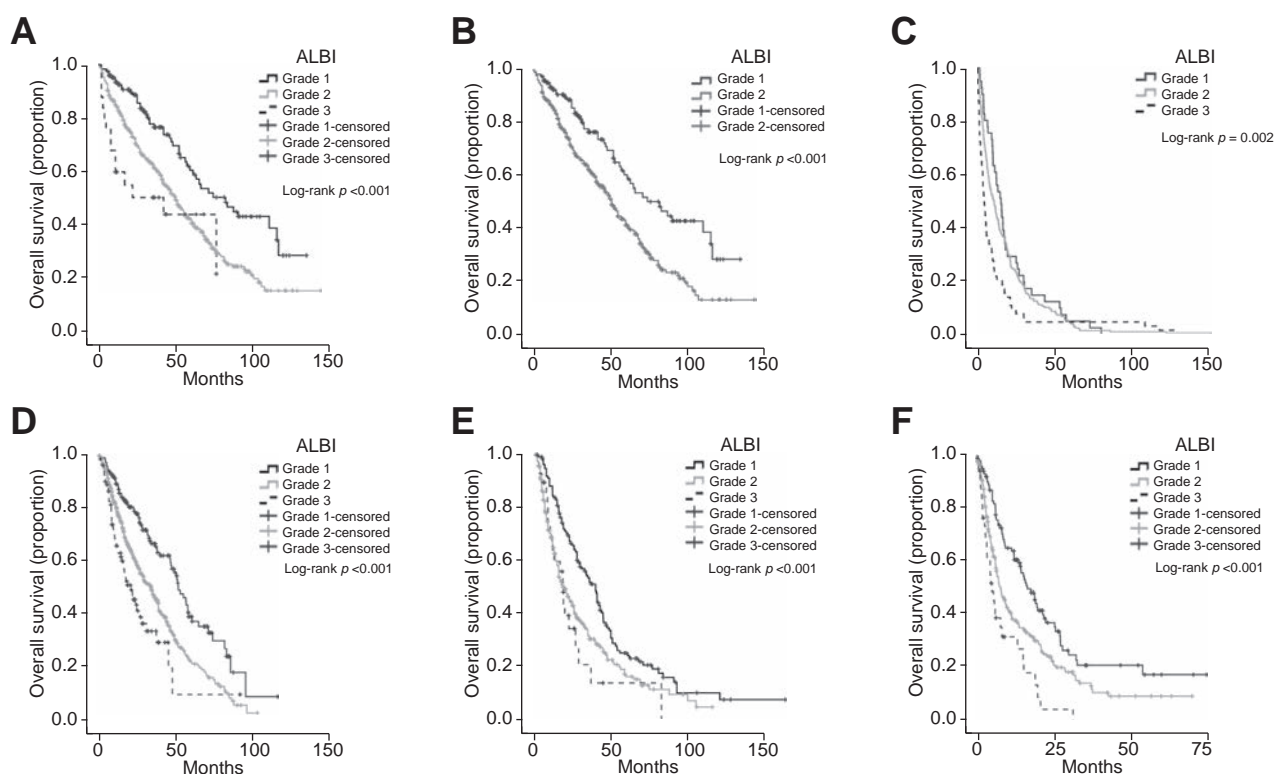
### The prognostic relationship between ALBI and BCLC: interaction with time

We further confirmed the prognostic validity of the ALBI grade in a pooled analysis of patients belonging to the entire study population (n = 2426). As shown in Table 3, the ALBI grade was confirmed as a predictor of OS following adjustment for BCLC stage. Given the wide accrual times (1989–2015) we performed further analyses of survival by including an interaction term between the scores of interest (either ALBI or CTP) and start time of therapy, dichotomized as prior to or after year 2000, to reflect subsequent adoption of the BCLC treatment allocation algorithm. Whilst there was no evidence of a change in the effect of the CTP score on OS before and after year 2000 ( $p = 0.5982$ ), there was some evidence of a variation in the effect of the ALBI score alone ( $p = 0.0031$ ) and in combination with BCLC ( $p = 0.0637$ ). The estimates of these two models stratified by time are presented in Table 4. Stratified analyses provide evidence of a predictive effect of the ALBI score on survival both in the pre- and post-year 2000 datasets, both in unadjusted and adjusted analyses, although the effects of the score were greater in the post year 2000 dataset.

### Discussion

HCC arises as a complication of chronic liver disease and cirrhosis in the vast majority of cases. The prognostic interaction between progressive malignancy and underlying liver functional impairment poses a unique challenge in the provision of optimal treatment strategies in the individual patient [22]. The geographical distribution of different etiologic factors and the diverse accessibility to various treatment modalities are amongst the factors that make the clinical course of HCC particularly variable across countries and institutions [23]. This is particularly true for intermediate stage HCC, where the variation in tumour burden, hepatic reserve combined with the recognized heterogeneity in locoregional treatment schedules exert a crucial impact on patients' survival, which recognizes a >20 months variation in this patient subpopulation [24]. The acknowledged clinical heterogeneity of HCC suggests the need for objective, reproducible and accurate prognostic biomarkers to improve patient outcomes [25].

In our large, collaborative, multi-institutional study we sought to independently validate the prognostic ability of the ALBI grade, a recently qualified nomogram suggested to more accurately predict patients' mortality by solely combining albumin and



**Fig. 2.** Kaplan-Meier curve analysis showing the effect of the ALBI grade as predictor of overall survival across each primary treatment modality in HCC. (A) Surgically resected patients. (B) Surgically resected patients within Child-Turcotte-Pugh Class A criteria. (C) Patients treated with locoregional therapy from USA, (D) Europe and (E) Asia. (F) Patients treated with sorafenib.

bilirubin levels without the need for subjective determinants of liver failure including ascites and encephalopathy.

Using a stage-stratified approach, we investigated the prognostic ability of the ALBI in both curative and palliative settings, demonstrating adequate and clinically meaningful stratifying potential for the score across all the BCLC stages of the disease.

In early stage HCC, we demonstrated that the ALBI grade could predict worse prognosis within CTP A class patients, who are universally recognized as optimal candidates for surgical resection [26]. Whilst our findings in early stage disease are retrospective and based on a single-centre experience, they corroborate previous evidence showing that the ALBI may overcome the prognostic limitations of the CTP classification, allowing for a more subtle quantification of hepatic reserve in patients with grossly preserved synthetic function, perhaps by abolishing “floor” and “ceiling” effects applying to CTP class computation. Clinically, in fact, these patients rarely display evidence of significant coagulopathy, refractory ascites or encephalopathy, a point that strengthens the relevance of pre-operative albumin and bilirubin in the prognostic assessment of surgical candidates [27].

An increasing number of studies have tested the prognostic accuracy of the ALBI grade in multi-institutional cohorts and recently proposed its integration with routinely used prognostic models including TNM [28] and BCLC [29]. However, in a recent study by Hiraoka, which only included Japanese patients, representation of BCLC-B patients accounted for only 12% of the total of patients studied [28], and similar figures apply to the Chan study where a high proportion of patients (up to 33%) received

best supportive care only, a factor that has influenced survival outcomes [29].

To our knowledge, this is the first study to provide evidence of the clinical utility of the ALBI grade in a large, multi-institutional cohort of patients who received TACE for unresectable HCC, largely within BCLC-B criteria. We confirmed the ALBI as an accurate predictor of patients' survival in this patient group. Due to the expected heterogeneity in patients' survival stemming from both patient features and treatment schedules across continents, we opted to validate the prognostic ability of the ALBI separately by constructing three geographically distinct patient cohorts characterized by diverse ethnicity and underlying aetiology. Unsurprisingly, despite relatively balanced tumour staging features and CTP class, survival was significantly different across the three studied cohorts, being worse in US patients compared to the European and Asian cohorts.

Whilst median survival for the European and Asian cohorts is in line with the life expectancy of patients currently presenting with BCLC-B HCC [24], American patients were mostly treated prior to the dissemination of the BCLC algorithm in the early 2000s: although reconstructed retrospectively by medical records review, the algorithm did not guide treatment allocation in these patients, with inherent implications in terms of survival [15]. It is also likely that an equally important influence on survival might have derived from the evolving technical improvements in the delivery of TACE within the accrual period (1989–2005). Stratified analyses according to time provide evidence that the prognostic role of the ALBI grade was preserved in patients assessed prior to and following the dissemination of the BCLC



## Research Article

**Table 2. Survival analyses for the ALBI score across the studied patient cohorts.**

	ALBI, unadjusted		ALBI, adjusted for BCLC		CTP, unadjusted	
Surgical resection cohort (n = 587)						
ALBI, HR (95% CI)						
2 vs. 1	1.86 (1.36–2.54)	p <0.001	1.62 (1.18–2.22)	p = 0.02		
3 vs. 1	2.57 (1.47–4.69)	p <0.001	1.84 (1.0–3.39)	p = 0.04		
BCLC, HR (95% CI)						
B vs. A			1.79 (1.40–2.29)	p <0.001		
C vs. A			4.03 (2.81–5.78)	p <0.001		
CTP, HR (95% CI)						
B vs. A					1.37 (1.04–1.82)	p = 0.02
C-index (95% CI)*	0.57 (0.54–0.59)		0.67 (0.63–0.7)		0.54 (0.51–0.57)	
Locoregional therapy cohort USA (n = 315)						
ALBI, HR (95% CI)						
2 vs. 1	1.16 (0.83–1.63)	p = 0.12	1.23 (0.88–1.73)	p = 0.23		
3 vs. 1	1.89 (1.22–2.70)	p = 0.003	1.92 (1.29–2.86)	p = 0.001		
BCLC, HR (95% CI)						
B vs. A			1.40 (1.05–1.97)	p = 0.04		
CTP, HR (95% CI)						
B vs. A					1.56 (1.22–1.99)	p <0.001
C-index (95% CI)*	0.57 (0.54–0.61)		0.58 (0.54–0.62)		0.57 (0.53–0.60)	
Locoregional therapy cohort Europe (n = 423)						
ALBI, HR (95% CI)						
2 vs. 1	1.59 (1.24–2.03)	p <0.001	1.66 (1.29–2.12)	p <0.001		
3 vs. 1	1.95 (1.21–3.13)	p = 0.006	1.96 (1.22–3.15)	p = 0.005		
BCLC, HR (95% CI)						
B vs. A			2.24 (1.54–3.26)	p <0.001		
C vs. A			3.50 (2.35–5.22)	p <0.001		
CTP, HR (95% CI)						
B vs. A					1.62 (1.24–2.11)	p <0.001
C-index (95% CI)*	0.58 (0.55–0.61)		0.65 (0.62–0.68)		0.56 (0.53–0.59)	
Locoregional therapy cohort Asia (n = 723)						
ALBI, HR (95% CI)						
2 vs. 1	1.78 (1.37–2.32)	p <0.001	1.89 (1.45–2.46)	p <0.001		
3 vs. 1	2.73 (1.88–3.97)	p <0.001	2.86 (1.96–4.17)	p <0.001		
BCLC, HR (95% CI)						
B vs. A	1.75 (1.40–2.19)	p <0.001				
C vs. A	3.59 (2.53–5.11)	p <0.001				
CTP, HR (95% CI)						
B vs. A					4.37 (1.39–13.75)	p <0.001
C-index (95% CI)*	0.58 (0.55–0.6)		0.65 (0.63–0.68)		0.55 (0.51–0.58)	
Sorafenib cohort (n = 378)						
ALBI, HR (95% CI)						
2 vs. 1	1.61 (1.21–2.14)	p <0.001	1.68 (1.26–2.25)	p <0.001		
3 vs. 1	2.78 (1.79–4.33)	p <0.001	2.69 (1.72–4.19)	p <0.001		
BCLC, HR (95% CI)						
B vs. A			2.15 (1.29–3.57)	p <0.001		
C vs. A			2.77 (1.71–4.48)	p <0.001		
CTP, HR (95% CI)						
B vs. A					1.57 (1.19–2.07)	p <0.001
C-index (95% CI)*	0.58 (0.55–0.61)		0.63 (0.59–0.66)		0.55 (0.52–0.58)	

HR, hazard ratio. CI, confidence interval.

\* Bootstrap 95% CI, 150 replications.

treatment guidelines. Interestingly, the effect of the score in influencing patients' survival was greater in the post year 2000 dataset, a finding that might correlate with an improved patient selection and more homogeneous management over time (Table 4).

Whilst these considerations over patients' homogeneity should be acknowledged when interpreting our results, the preserved accuracy of the ALBI in each of the studied cohorts further strengthens its independence as a prognostic predictor in HCC

despite heterogeneity in ethnicity, accrual period, disease etiology, patient selection and management strategies. Crucially, in our study, the ALBI grade displayed comparable accuracy to CTP in estimating mortality prior to TACE suggesting that combination of pre-treatment albumin and bilirubin are indeed the strongest predictors of the CTP classification. This is not a novel finding in intermediate stage HCC, where a number of scores relying on pre-treatment albumin and bilirubin levels have been proposed to guide TACE administration in HCC, with the intent of

**Table 3. Analyses of survival for ALBI, BCLC and CTP in the entire study population (n = 2426).**

	ALBI, unadjusted		ALBI, adjusted for BCLC		CTP, unadjusted	
ALBI, HR (95% CI)						
2 vs. 1	1.49 (1.32–1.69)	<i>p</i> <0.001	1.63 (1.44–1.84)	<i>p</i> <0.001		
3 vs. 1	2.55 (2.12–3.06)	<i>p</i> <0.001	2.57 (2.14–3.09)	<i>p</i> <0.001		
BCLC, HR (95% CI)						
B vs. A			2.41 (2.13–2.72)	<i>p</i> <0.001		
C vs. A			4.19 (3.61–4.86)	<i>p</i> <0.001		
CTP, HR (95% CI)						
B vs. A					1.60 (1.43–1.80)	<i>p</i> <0.001
C-index (95% CI)*	0.57 (0.56–0.59)		0.68 (0.67–0.69)		0.56 (0.54–0.57)	

HR, hazard ratio; CI, confidence interval.

\* Bootstrap 95% CI, 150 replications.

**Table 4. Analyses of survival for ALBI grade stratified by time.**

	ALBI, unadjusted	ALBI, adjusted for BCLC
<b>Pre year 2000</b>		
N deaths/patients	423/423	423/423
ALBI, HR (95% CI)		
2 vs. 1	1.26 (0.95–1.68)	1.27 (0.95–1.7)
3 vs. 1	1.85 (1.25–2.74)	2.11 (1.42–3.13)
BCLC, HR (95% CI)		
B vs. A		1.63 (1.13–2.35)
C vs. A		2.41 (1.68–3.46)
<b>Post year 2000</b>		
N deaths/patients	651/993	651/993
ALBI, HR (95% CI)		
2 vs. 1	1.91 (1.57–2.31)	1.82 (1.5–2.21)
3 vs. 1	4.47 (3.31–6.03)	4.43 (3.27–6.01)
BCLC, HR (95% CI)		
B vs. A		2.16 (1.75–2.69)
C vs. A		6.52 (5.13–8.28)

HR, hazard ratio; CI, confidence interval.

sparing patients with poor prognostic features from potentially futile locoregional therapies and migrate them to systemic treatment or best supportive care [30–32]. Despite having potential clinical utility, our experience suggests that patient heterogeneity and differences in cut-off values for variables including bilirubin [18], may influence the prognostic performance of these algorithms, a limitation that is not shared by the ALBI grade where albumin and bilirubin are considered as continuous variables, preserving their prognostic accuracy in full.

Our study also demonstrates that the ALBI grade is a prognostic maker in advanced HCC, a patient population with limited life expectancy and restricted treatment options. Based on our results, the ALBI grade was superior to CTP in identifying patients at risk of early mortality prior to sorafenib initiation as well as an independent predictor of OS. These features are of greater consequence in advanced HCC, a patient population at the focus of intense research efforts. The post-registrative extension of sorafenib therapy to early stage CTP B patients has in fact demonstrated that patients with intermediate derangement in their liver biochemistry can still benefit from treatment [33] in absence of excessive toxicities [34]. In this context, a more accurate index of liver function such as the ALBI grade might optimize safe administration of experimental therapies in advanced HCC, therefore facilitating efficacy testing of investigational medicinal compounds.

In conclusion, this study provides compelling evidence that the ALBI grade is a validated prognostic index across all BCLC stages of disease. Because it relies on two single inexpensive

and widely available laboratory parameters, the ALBI grade is more objective and can be rapidly computed at the bedside, without the need for special tests.

With c-index values showing moderate discriminative ability in predicting mortality from deteriorating liver function across each stage of HCC, the ALBI grade emerges as an equal and, in some instances, superior biomarker to routinely available liver functional staging systems such as the CTP class. The prognostic performance of the ALBI grade is particularly appealing in intermediate stage disease, where we have shown it to be a widely generalizable biomarker able to overcome the heterogeneity of survival of BCLC-B stage.

The retrospective nature of our study and the relatively wide accrual times characterizing some of the recruited cohorts should be acknowledged as limitations. However, our survival analysis is robustly built on a process of independent cross-validation in large multi-institutional cohorts, which limits the potential for selection bias.

In summary, this study has validated the ALBI grade as an objective, inexpensive, readily available stratifying biomarker of poor liver reserve in HCC. Consideration should be given to its prospective validation in future clinical studies to facilitate its use in routine clinical practice.

### Financial support

DJP is supported by the National Institute for Health Research (NIHR) and has received grant funding from Action Against Cancer and the Imperial NIHR Biomedical Research Centre (BRC). This work was funded in part by the Academy of Medical Sciences (Grant nr. SGL013/1021) awarded to DJP. DB is supported the Berta-Ottenshein-Programme, Faculty of Medicine, University of Freiburg.

### Conflict of interest

The authors who have taken part in this study declared that they do not have anything to disclose regarding funding or conflict of interest with respect to this manuscript.

### Authors' contributions

Study concept and design: DJP, RS, BIC. Acquisition of data: DJP, TA, JWJ, CS, YWK, MK, MP, DB, RT, CY, DB. Analysis and interpretation of data: DJP, EA RR, MP, RS, JS, JH. Drafting of the

## Research Article

manuscript: DJP, RS, EA, BIC, JH. Critical revision of the manuscript for important intellectual content: All the authors. Statistical analysis: DJP, RR, EA, JH.

Obtained funding: DJP, JWJ, RS, MP. Administrative, technical, or material support: MP, MK, JWJ, RT, JS. Study supervision: DJP, JWJ, MK, MP, RS, JS.

### Acknowledgements

The authors would like to acknowledge Dr. Les Huson for his statistical support. This work was presented orally by DJP at the European Association for the Study of the Liver (EASL) 2016 International Liver Meeting, Barcelona.

### Supplementary data

Supplementary data associated with this article can be found, in the online version, at <http://dx.doi.org/10.1016/j.jhep.2016.09.008>.

### References

- [1] Jemal A, Siegel R, Xu J, Ward E. Cancer statistics, 2010. *CA Cancer J Clin* 2010;60:277–300.
- [2] Schutte K, Bornschein J, Malfertheiner P. Hepatocellular carcinoma—epidemiological trends and risk factors. *Dig Dis* 2009;27:80–92.
- [3] Llovet JM, Bruix J. Novel advancements in the management of hepatocellular carcinoma in 2008. *J Hepatol* 2008;48:S20–S37.
- [4] Durand F, Valla D. Assessment of prognosis of cirrhosis. *Semin Liver Dis* 2008;28:110–122.
- [5] Cholongitas E, Papatheodoridis GV, Vangeli M, Terreni N, Patch D, Burroughs AK. Systematic review: The model for end-stage liver disease—should it replace Child-Pugh's classification for assessing prognosis in cirrhosis? *Aliment Pharmacol Ther* 2005;22:1079–1089.
- [6] Procopet B, Tantau M, Bureau C. Are there any alternative methods to hepatic venous pressure gradient in portal hypertension assessment? *J Gastrointest Liver Dis* 2013;22:73–78.
- [7] Cucchetti A, Cescon M, Golfieri R, Piscaglia F, Renzulli M, Neri F, et al. Hepatic venous pressure gradient in the preoperative assessment of patients with resectable hepatocellular carcinoma. *J Hepatol* 2016;64:79–86.
- [8] Wiesner R, Edwards E, Freeman R, Harper A, Kim R, Kamath P, et al. Model for end-stage liver disease (MELD) and allocation of donor livers. *Gastroenterology* 2003;124:91–96.
- [9] Cholongitas E, Marelli L, Shusang V, Senzolo M, Rolles K, Patch D, et al. A systematic review of the performance of the model for end-stage liver disease (MELD) in the setting of liver transplantation. *Liver Transpl* 2006;12:1049–1061.
- [10] Lurie Y, Webb M, Cytter-Kuint R, Shteingart S, Lederkremer GZ. Non-invasive diagnosis of liver fibrosis and cirrhosis. *World J Gastroenterol* 2015;21:11567–11583.
- [11] Singh S, Fujii LL, Murad MH, Wang Z, Asrani SK, Ehman RL, et al. Liver stiffness is associated with risk of decompensation, liver cancer, and death in patients with chronic liver diseases: a systematic review and meta-analysis. *Clin Gastroenterol Hepatol* 2013;11:1573–1584, e1571–e1572; quiz e1588–e1579.
- [12] Johnson PJ, Berhane S, Kagebayashi C, Satomura S, Teng M, Reeves HL, et al. Assessment of liver function in patients with hepatocellular carcinoma: a new evidence-based approach—the ALBI grade. *J Clin Oncol* 2015;33:550–558.
- [13] Dufour JF, Bargellini I, De Maria N, De Simone P, Goulis I, Marinho RT. Intermediate hepatocellular carcinoma: current treatments and future perspectives. *Ann Oncol* 2013;24:ii24–ii29.
- [14] European Association for the Study of the Liver/European Organisation for Research and Treatment of Cancer. EASL-EORTC clinical practice guidelines: management of hepatocellular carcinoma. *J Hepatol* 2012;56:908–943.
- [15] Llovet JM, Bru C, Bruix J. Prognosis of hepatocellular carcinoma: the BCLC staging classification. *Semin Liver Dis* 1999;19:329–338.
- [16] Pinato DJ, Stebbing J, Ishizuka M, Khan SA, Wasan HS, North BV, et al. A novel and validated prognostic index in hepatocellular carcinoma: the inflammation based index (IBI). *J Hepatol* 2012;57:1013–1020.
- [17] Carr BI, Kondragunta V, Buch SC, Branch RA. Therapeutic equivalence in survival for hepatic arterial chemoembolization and yttrium 90 microsphere treatments in unresectable hepatocellular carcinoma: a two-cohort study. *Cancer* 2010;116:1305–1314.
- [18] Pinato DJ, Arizumi T, Allara E, Jang JW, Smirne C, Kim YW, et al. Validation of the hepatoma arterial embolization prognostic score in European and Asian populations and proposed modification. *Clin Gastroenterol Hepatol* 2015;13:e1202.
- [19] Lencioni R, Llovet JM. Modified RECIST (mRECIST) assessment for hepatocellular carcinoma. *Semin Liver Dis* 2010;30:52–60.
- [20] Team RC. R: A language and environment for statistical computing. Vienna: R Foundation for Statistical Computing; 2014.
- [21] Harrell FE. *Regression Modeling Strategies*. 3.0 ed; 2010.
- [22] Liu PH, Hsu CY, Hsia CY, Lee YH, Su CW, Huang YH, et al. Prognosis of hepatocellular carcinoma: assessment of eleven staging systems. *J Hepatol* 2016;64:601–608.
- [23] de Lope CR, Tremosini S, Forner A, Reig M, Bruix J. Management of HCC. *J Hepatol* 2012;56:S75–S87.
- [24] Sangro B, Salem R. Transarterial chemoembolization and radioembolization. *Semin Liver Dis* 2014;34:435–443.
- [25] Bolondi L, Burroughs A, Dufour JF, Galle PR, Mazzaferro V, Piscaglia F, et al. Heterogeneity of patients with intermediate (BCLC B) Hepatocellular Carcinoma: proposal for a subclassification to facilitate treatment decisions. *Semin Liver Dis* 2012;32:348–359.
- [26] Llovet JM, Schwartz M, Mazzaferro V. Resection and liver transplantation for hepatocellular carcinoma. *Semin Liver Dis* 2005;25:181–200.
- [27] Sacco R, Antonucci M, Bresci G, Corti A, Giacomelli L, Mismas V, et al. Curative therapies for hepatocellular carcinoma: an update and perspectives. *Expert Rev Anticancer Ther* 2016;16:169–175.
- [28] Hiraoka A, Kumada T, Michitaka K, Toyoda H, Tada T, Ueki H, et al. Usefulness of albumin-bilirubin (ALBI) grade for evaluation of prognosis of 2584 Japanese patients with hepatocellular carcinoma. *J Gastroenterol Hepatol* 2016;31:1031–1036.
- [29] Chan AW, Kumada T, Toyoda H, Tada T, Chong CC, Mo FK, et al. Integration of albumin-bilirubin (ALBI) score into Barcelona clinic liver cancer (BCLC) system for hepatocellular carcinoma. *J Gastroenterol Hepatol* 2016;31:1300–1306.
- [30] Kadalayil L, Benini R, Pallan L, O'Beirne J, Marelli L, Yu D, et al. A simple prognostic scoring system for patients receiving transarterial embolisation for hepatocellular cancer. *Ann Oncol* 2013;24:2565–2570.
- [31] Pinato DJ, Karamanakis G, Arizumi T, Adjogatse D, Kim YW, Stebbing J, et al. Dynamic changes of the inflammation-based index predict mortality following chemoembolisation for hepatocellular carcinoma: a prospective study. *Aliment Pharmacol Ther* 2014;40:1270–1281.
- [32] Huckle F, Pinter M, Graziadei I, Bota S, Vogel W, Muller C, et al. How to STATE suitability and START transarterial chemoembolization in patients with intermediate stage hepatocellular carcinoma. *J Hepatol* 2014;61:1287–1296.
- [33] Pressiani T, Boni C, Rimassa L, Labianca R, Fagioli S, Salvagni S, et al. Sorafenib in patients with Child-Pugh class A and B advanced hepatocellular carcinoma: a prospective feasibility analysis. *Ann Oncol* 2013;24:406–411.
- [34] Lg DAF, Barroso-Sousa R, Bento AD, Blanco BP, Valente GL, Pfiffer TE, et al. Safety and efficacy of sorafenib in patients with Child-Pugh B advanced hepatocellular carcinoma. *Mol Clin Oncol* 2015;3:793–796.

## Retrospective Study

# Endoscopic ultrasound-guided gallbladder drainage for acute cholecystitis: Long-term outcomes after removal of a self-expandable metal stent

Ken Kamata, Mamoru Takenaka, Masayuki Kitano, Shunsuke Omoto, Takeshi Miyata, Kosuke Minaga, Kentaro Yamao, Hajime Imai, Toshiharu Sakurai, Tomohiro Watanabe, Naoshi Nishida, Masatoshi Kudo

Ken Kamata, Mamoru Takenaka, Masayuki Kitano, Shunsuke Omoto, Takeshi Miyata, Kosuke Minaga, Kentaro Yamao, Hajime Imai, Toshiharu Sakurai, Tomohiro Watanabe, Naoshi Nishida, Masatoshi Kudo, Department of Gastroenterology and Hepatology, Kindai University Faculty of Medicine, Osaka-Sayama 589-8511, Japan

**Author contributions:** All authors helped to perform the research; Kamata K and Takenaka M wrote the manuscript and analyzed the data; Kamata K performed the procedures; Takenaka M drafted the conception and design; Kitano M, Omoto S, Miyata T, Minaga K, Yamao K, Imai H, Sakurai T, Watanabe T, Nishida N and Kudo M contributed to writing the manuscript; Kitano M and Kudo M also contributed to drafting conception and design.

Supported by the Japan Society for the Promotion of Science and the Japanese Foundation for the Research and Promotion of Endoscopy No. 22590764 and No. 25461035.

**Institutional review board statement:** This study was reviewed and approved by the Ethics Committee of the Kindai University Hospital.

**Informed consent statement:** Patients were not required to give informed consent to the study because the analysis used anonymous clinical data that were obtained after each patient agreed to treatment by written consent.

**Conflict-of-interest statement:** All authors declare no conflicts-of-interest related to this article.

**Data sharing statement:** No additional data are available.

**Open-Access:** This article is an open-access article which was selected by an in-house editor and fully peer-reviewed by external reviewers. It is distributed in accordance with the Creative Commons Attribution Non Commercial (CC BY-NC 4.0) license, which permits others to distribute, remix, adapt, build upon this work non-commercially, and license their derivative works on different terms, provided the original work is properly cited and

the use is non-commercial. See: <http://creativecommons.org/licenses/by-nc/4.0/>

**Manuscript source:** Unsolicited manuscript

**Correspondence to:** Mamoru Takenaka, MD, PhD, Department of Gastroenterology and Hepatology, Kindai University Faculty of Medicine, 377-2 Ohno-Higashi, Osaka-Sayama 589-8511, Japan. [mamoxyo45@gmail.com](mailto:mamoxyo45@gmail.com)  
Telephone: +81-72-3660221  
Fax: +81-72-3672880

Received: October 5, 2016  
Peer-review started: October 7, 2016  
First decision: November 9, 2016  
Revised: November 15, 2016  
Accepted: December 2, 2016  
Article in press: December 2, 2016  
Published online: January 28, 2017

## Abstract

### AIM

To assess the long-term outcomes of this procedure after removal of self-expandable metal stent (SEMS). The efficacy and safety of endoscopic ultrasound-guided gallbladder drainage (EUS-GBD) with SEMS were also assessed.

### METHODS

Between January 2010 and April 2015, 12 patients with acute calculous cholecystitis, who were deemed unsuitable for cholecystectomy, underwent EUS-GBD with a SEMS. EUS-GBD was performed under the guidance of EUS and fluoroscopy, by puncturing the gallbladder with a needle, inserting a guidewire, dilating the puncture hole, and placing a SEMS. The

SEMS was removed and/or replaced with a 7-Fr plastic pigtail stent after cholecystitis improved. The technical and clinical success rates, adverse event rate, and recurrence rate were all measured.

## RESULTS

The rates of technical success, clinical success, and adverse events were 100%, 100%, and 0%, respectively. After cholecystitis improved, the SEMS was removed without replacement in eight patients, whereas it was replaced with a 7-Fr pigtail stent in four patients. Recurrence was seen in one patient (8.3%) who did not receive a replacement pigtail stent. The median follow-up period after EUS-GBD was 304 d (78-1492).

## CONCLUSION

EUS-GBD with a SEMS is a possible alternative treatment for acute cholecystitis. Long-term outcomes after removal of the SEMS were excellent. Removal of the SEMS at 4-wk after SEMS placement and improvement of symptoms might avoid migration of the stent and recurrence of cholecystitis due to food impaction.

**Key words:** Endoscopic ultrasound-guided gallbladder drainage; Cholecystitis; Endoscopic ultrasound-guided biliary drainage

© The Author(s) 2017. Published by Baishideng Publishing Group Inc. All rights reserved.

**Core tip:** Endoscopic ultrasound-guided gallbladder drainage (EUS-GBD) was recently used to treat acute cholecystitis. The aim of this study was to assess the utility of removal of self-expandable metal stent (SEMS) at 4-wk after EUS-GBD. Twelve patients with acute calculous cholecystitis underwent EUS-GBD with a SEMS. The rates of technical success, clinical success, and adverse events were 100%, 100%, and 0%, respectively. Recurrence was seen in one patient (8.3%). The median follow-up period after EUS-GBD was 304 d. Removal of the SEMS at 4-wk after SEMS placement might avoid migration of the stent and recurrence of cholecystitis due to food impaction.

Kamata K, Takenaka M, Kitano M, Omoto S, Miyata T, Minaga K, Yamao K, Imai H, Sakurai T, Watanabe T, Nishida N, Kudo M. Endoscopic ultrasound-guided gallbladder drainage for acute cholecystitis: Long-term outcomes after removal of a self-expandable metal stent. *World J Gastroenterol* 2017; 23(4): 661-667 Available from: URL: <http://www.wjgnet.com/1007-9327/full/v23/i4/661.htm> DOI: <http://dx.doi.org/10.3748/wjg.v23.i4.661>

## INTRODUCTION

Laparoscopic cholecystectomy is the standard

treatment for acute cholecystitis caused by cholecystolithiasis<sup>[1,2]</sup>. For patients at high surgical risk, percutaneous transhepatic gallbladder aspiration (PTGBA) or percutaneous transhepatic gallbladder drainage (PTGBD) can be selected for treatment of cholecystitis. However, the efficacy rate of PTGBA is insufficient (61%-77%), and PTGBD involves an external drainage tube, which decreases the ability of the patient to carry out their normal daily activities<sup>[3,4]</sup>. Recently, endoscopic ultrasound-guided gallbladder drainage (EUS-GBD) was developed for acute cholecystitis<sup>[5-17]</sup>. Jang *et al*<sup>[14]</sup> showed that EUS-GBD was comparable with PTGBD in terms of its technical feasibility, efficacy, and procedural safety.

The aim of this study was to evaluate the outcomes of EUS-GBD in patients with acute calculous cholecystitis deemed unsuitable for cholecystectomy. The examined procedure used a self-expandable metal stent (SEMS), and we also assessed the long-term outcomes of the procedure following removal of the SEMS.

## MATERIALS AND METHODS

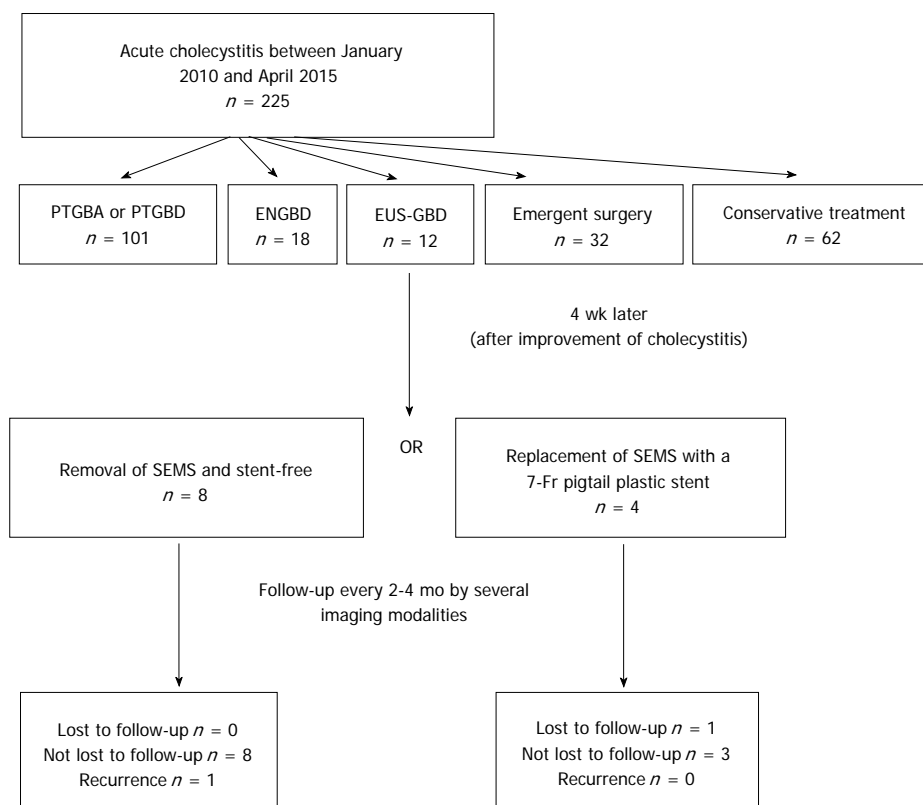
### Patients

Between January 2006 and October 2014, 225 patients with acute cholecystitis due to gallstones visited our hospital. Among these, 101, 18, 32, and 62 patients underwent PTGBA and/or PTGBD, endoscopic naso-gallbladder drainage, emergent surgery and conservative treatment, respectively. The remaining 12 patients with acute calculous cholecystitis, who were deemed unsuitable for cholecystectomy because of poor surgical performance indications and had a risk of self-removal of drainage tube, underwent EUS-GBD. Cases of cholecystitis due to deployment of the metal stent and the cases that cystic duct was obstructed due to advanced cancer were excluded from this study. The surgical performance indications for all patients were poor (class III or IV on the American Society of Anesthesiologists (ASA) Physical Status classification system). These patients were identified by retrospective review of the medical database of our hospital. Acute calculous cholecystitis was diagnosed in all patients on the basis of the characteristic clinical features (abdominal pain and fever), laboratory data (high level of serum C-reactive protein; CRP), and imaging studies. The study was approved by the institutional review board of the Kinki University Faculty of Medicine, and informed consent was obtained from the patients after explaining to them that we could perform PTGBA, PTGBD, or EUS-GBD.

### EUS-GBD technique

An echoendoscope (GF-UCT240-AL5, Olympus, Tokyo, Japan) was introduced into the stomach or duodenum. The echoendoscope images were used to ensure that gallstones were present in the swollen





**Figure 1** Strategy of endoscopic ultrasound-guided gallbladder drainage procedure. ENGBD: Endoscopic naso-gallbladder drainage; EUS-GBD: Endoscopic ultrasound-guided gallbladder drainage; PTGBA: Percutaneous transhepatic gallbladder aspiration; PTGBD: Percutaneous transhepatic gallbladder drainage; SEMS: Self-expandable metal stent.

gallbladder before EUS-GBD was performed. After visualization of the swollen gallbladder adjacent to the antrum or duodenal bulb, the echoendoscope was manipulated until an appropriate puncture route, free from interposing vessels, was identified. The puncture site was selected as the region where the distance between the gastrointestinal tract and the gallbladder was smallest (1 cm or less). When both the stomach and duodenum provided equally good access, the duodenum was selected as the puncture site because it was easier to maintain the scope position at the duodenum than at the stomach.

The neck or body of the gallbladder was generally chosen as the ideal target, and was then punctured with a 19G needle (EchoTip Ultra, Cook Medical, Limerick, Ireland) under endosonographic guidance. The gallbladder was then irrigated with a saline solution through the 19G needle, using a 20 mL syringe. Irrigation was performed at least ten times, and was continued until the color of the bile became weak. This was performed to prevent peritonitis due to bile leakage immediately after the gallbladder was punctured. Thereafter, a sufficient length of 0.035 inch guidewire (Revowave, Piolax, Kanagawa, Japan) was inserted into the gallbladder lumen until there were more than two coils present. The puncture tract was then serially dilated using either biliary

dilation catheters (6F-7F-9F, Soehendra Biliary Dilation Catheter, Cook, Bloomington, IN, United States) or a balloon dilator (Max Pass 4 mm, Olympus, Tokyo, Japan) over the guidewire. If passing dilators or balloons proved difficult, electrocautery was planned to be used. A SEMS (10 mm in diameter, 6 cm in length, Wallflex partially covered stent, Boston Scientific, Natick, MA, United States) was deployed between the gallbladder and the stomach or duodenum. If functional success was obtained, the SEMS was removed and/or replaced with a 7-Fr plastic pigtail stent (4 or 6 cm in length) 4 wk after the original EUS-GBD (Figure 1). Where possible, the stent was replaced after removal of the SEMS in order to keep the fistula considering the possibility of the recurrence. This technique was approved by the institutional review board of the Kinki University Faculty of Medicine.

#### Follow-up after EUS-GBD

Several imaging modalities including ultrasonography, computed tomography (CT), fistulography, and/or EUS were performed to determine if gallstones remained in the gallbladder before removal of the SEMS. CT (looking for air images in the gallbladder) and/or fistulography were performed to determine if the fistula remained open 1 wk after removal of the SEMS. After removal of the SEMS, patients were continually followed up by

**Table 1 Patient characteristics**

Characteristics	
Age, mean $\pm$ SD, yr	76.3 $\pm$ 12.1
Sex, male/female	9/3
Underlying condition	
III	66.7% (8/12)
IV	33.3% (4/12)
Advanced malignancy	8.3% (1/12)
White blood cell count (mean, range)	14525 (9100-21300) per $\mu$ L
C-reactive protein (mean, range)	15.7 (2.0-32.7) mg/dL

**Table 2 Outcomes of endoscopic ultrasound-guided gallbladder drainage**

Technical success rate	100% (12/12)
Functional success rate	100% (12/12)
Rate of removal	67% (8/12)
Rate of replacement	33% (4/12)
Adverse events	0% (0/12)
Recurrence of cholecystitis	8.3% (1/12)
Follow-up period, days [median, range]	304 (78-1492)
Patient status on follow-up	
Alive	91.7% (11/12)
Dead	8.3% (1/12)

SEMS: Self-expandable metal stent.

blood tests and imaging modalities every 2-4 mo. It was determined whether the cystic duct was patent before and after removal of the SEMS by performing fistulography and/or EUS.

### Assessment of outcomes

The long-term outcomes of EUS-GBD after removal of SEMS was the primary outcomes in this study. The outcomes assessed were technical and clinical success rates, adverse events rate, and recurrence rate. Technical success was defined as successful stent deployment between the gallbladder lumen and the stomach or duodenum. Clinical success was defined as improvement of typical clinical symptoms within 3 d, with confirmatory laboratory tests, with or without improved radiologic findings<sup>[14]</sup>. The incidence of the following adverse events was assessed: peritonitis, bile leakage, bleeding, stent migration, and stent occlusion. Recurrence of acute cholecystitis after EUS-GBD was defined on the basis of the characteristic clinical features, laboratory data, and imaging studies.

### Statistical analysis

Continuous variables are expressed as median or mean values with standard deviation or range. All statistical analyses were performed using SAS software version 9.1 (SAS Institute, Cary, NC, United States).

## RESULTS

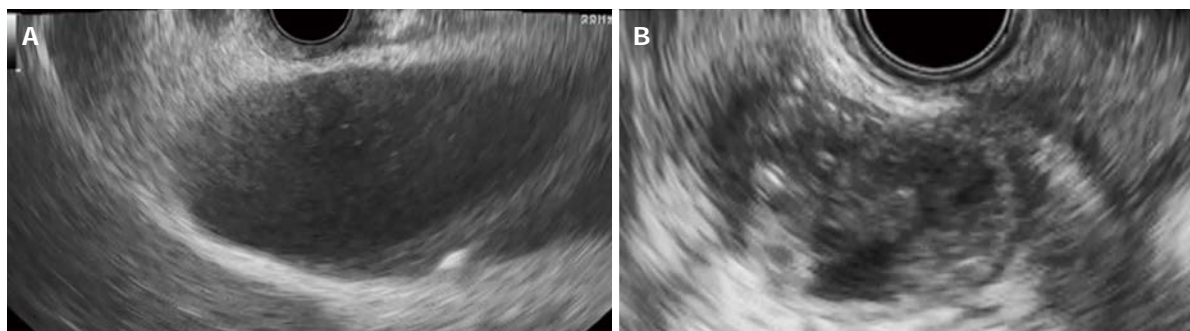
Table 1 shows the patients' characteristics. In total, 12 patients (mean age 76 years, 9 men and 3 women)

underwent EUS-GBD. Eight patients were ASA class III, and the others were ASA class IV. One patient had advanced ovarian cancer which expected long-term survival and there was no influence of the tumor on the cystic duct. Blood examination revealed a mean white blood cell (WBC) count of 14525 cells per  $\mu$ L and a mean CRP level of 15.7 mg/dL. All cases were moderate cholecystitis. The diameter of gallstones was less than 10 mm in all patients. The EUS-GBD procedure was performed *via* the stomach or duodenum in three and nine cases, respectively. The distance between the gastrointestinal tract and the gallbladder was 1 cm or less in all cases. Dilation of the puncture site was performed by biliary dilation and/or balloon catheters without using electrocautery. Table 2 shows the outcomes of EUS-GBD. The technical success and clinical success rates were both 100% (12/12), with no adverse events recorded. At day 3 post-EUS-GBD, the mean WBC count and mean CRP were 7075 cells per  $\mu$ L and 2.37 mg/dL, respectively. The SEMS was removed from eight patients 4 wk after the EUS-GBD. In these eight patients, the plastic pigtail stent was not deployed after removal of the SEMS because the guidewire could not be sufficiently inserted due to shrinkage of the gallbladder by the EUS-GBD treatment. In the remaining four patients, the SEMS was replaced with a 7-Fr plastic double pigtail stent 4 wk after EUS-GBD. The median post-EUS-GBD follow-up period for these 12 patients was 304 d. During the follow-up period, one of the patients (8.3%) died due to advanced cancer. At the time the records were subjected to retrospective evaluation (April 1, 2016), recurrence was present in one of the patients (8.3%) who did not receive a replacement pigtail stent (Figure 2). In four patients received replacement of SEMS with a 7-Fr plastic double pigtail stent, the stent was kept permanently in all of those patients.

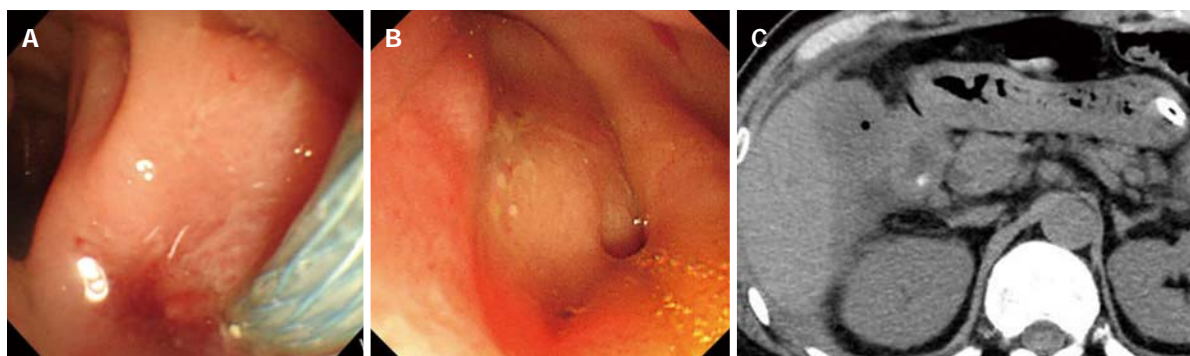
Before removal of the SEMS, gallstones did not remain in the gallbladder in all cases. One week after removal of the SEMS, air in the gallbladder was imaged by CT in nine cases (Figure 3). The other three cases that did not show air images in the gallbladder were cases in which the double pigtail plastic stents were not deployed. Fistulography was performed in eight cases that did not undergo replacement of the stent. Among these, fistulography images of the gallbladder were obtained in three cases. In total, the fistula was confirmed by CT and/or fistulography in 9 of 12 cases. Cystic duct patency was confirmed by fistulography and/or EUS before as well as 1 week after removal of the SEMS in all cases.

## DISCUSSION

The aim of the current study was to evaluate the feasibility of EUS-GBD for patients with acute calculous cholecystitis, who were deemed unsuitable for cholecystectomy. In this study, both technical and



**Figure 2** Endosonographic image. A: Endosonographic image before gallbladder drainage. Contents in the gallbladder were mainly sludge without apparent gallstones; B: Endosonographic image at the time of recurrence of cholecystitis. Sludge volume in the gallbladder was more increased than when gallbladder drainage was performed.



**Figure 3** Esophagogastroduodenoscopy and computed tomography. A: Esophagogastroduodenoscopy image of deployment of the metal stent in the duodenum; B: Esophagogastroduodenoscopy image of the fistula 1 wk after removal of the metal stent; C: Computed tomography after removal of the metal stent showing air image in the gallbladder.

clinical success was achieved in the treatment of acute cholecystitis in all 12 patients. One of the risks of EUS-GBD is bile leakage into the peritoneal space, which can cause bile peritonitis. The bile leakage is caused by migration of the stent exposing the gap between the puncture tract and the stent<sup>[5,6,8]</sup>. In the present study, several techniques were used to avoid such bile leakage. Firstly, the guidewire was inserted until at least two full coils were in the lumen. The gallbladder lumen has more space for coiling than the bile duct, and yields better stability. Secondly, we irrigated the gallbladder lumen with saline solution after puncturing the gallbladder and before proceeding to the next step. This irrigation procedure may reduce the chance of peritonitis due to bile leakage during dilation. We also used SEMs in our study, and, compared with plastic stents, SEMs are better at sealing the gap between the stent and the needle tracts in the gallbladder wall, thus preventing bile leakage<sup>[8]</sup>. As a result, no adverse events occurred in this study. In a systematic review of EUS-guided biliary drainage by Wang *et al*<sup>[18]</sup> in 2016, the rate of adverse events was 38.46% in the group in which cystotomes were used during dilation of the puncture site, which was higher than that in the group in which dilators or balloons were used. Dilation of the puncture site was performed by biliary dilation and/

or balloon catheters without using electrocautery in this study. This might be another reason why there were no adverse events in this study.

During a long-term follow-up with a median period of 275 d, Choi *et al*<sup>[19]</sup> reported that stent distal migration was noted in two patients (3.6%), one at 170 d and the other at 303 d post-EUS-GBD. They also reported recurrence of acute cholecystitis due to food impaction. To avoid stent migration and food impaction into the gallbladder, we either removed the SEMS, or replaced it with a pigtail plastic stent, 4 wk after EUS-GBD. In our study, there was neither stent migration nor food impaction. Performance of these additional procedures after EUS-GBD may prevent such complications.

Recently, the use of lumen-apposing metal stents (LAMS) with anchor flanges and flares for EUS-GBD resulted in excellent outcomes<sup>[13,15,20]</sup>. With a LAMS, the distance between the gastrointestinal tract and the gallbladder needs to be 1 cm or less<sup>[19]</sup>. In terms of this, a conventional biliary SEMS may have allowed us more freedom in selecting the puncture site, although this is not certain because the distance was 1 cm or less in all cases in this study.

In a study examining the use of LAMS for high-risk surgical patients with acute cholecystitis<sup>[20]</sup>, Walter

*et al.*<sup>[20]</sup> reported that technical success was 90%, and clinical success was 96%, and that no migration was seen in any patients. In 15 of the 27 patients with technical success, LAMS were removed approximately 3 mo after EUS-GBD, whereas they were left in place in the other 12 patients. Removal of the LAMS was not achieved due to tissue overgrowth in two patients. Two patients also developed a LAMS obstruction. Thus, long-term deployment of metal stents in EUS-GBD could cause adverse events, including food impaction. Therefore, early removal of the metal stent after EUS-GBD, at a time of around 4 wk (as in the present study), may be considered desirable. However, we did observe a recurrence of acute cholecystitis in one patient (8.3%), where the SEMS was not replaced with a pigtail stent. There is a possibility that this patient recurred cholecystitis due to uncertain small gallstones or sludge remaining after EUS-GBD. Therefore, replacement with a pigtail plastic stent may be helpful for avoiding recurrence. Another reason for the low recurrence rate in this study might be that no gallstones remained in the gallbladder before removal of the SEMS in all cases.

Moon *et al.*<sup>[21]</sup> reported that gross pathology showed adherence of the gallbladder to the stomach wall around the site of cholecystogastrostomy 4 wk after LAMS removal in an animal study. We also performed a preliminary examination of EUS-guided biliary drainage using a conventional biliary SEMS in an animal study using five pigs. We found that at autopsy 1 wk after the procedure, fistulas were created between the bile duct and duodenum in all pigs<sup>[22]</sup>. Thus, a strong fistula might develop between the gallbladder and the gastrointestinal tract within 4 wk using a conventional biliary SEMS as well as a LAMS. This study has a few limitations. Firstly, the number of EUS-GBD cases was low, and all cases were from a single institute. Secondly, the indications for EUS-GBD were limited to those patients deemed unsuitable for cholecystectomy. A larger study comparing the efficacy and safety of EUS-GBD with and without early SEMS removal is warranted. However, a large number of institutions are needed to obtain the required number of patients, otherwise the criteria used for patient selection should be less strict.

In a systematic review of EUS-GBD, LAMS seemed to have a high potential in terms of efficacy and safety; however, the technical success of LAMS (91.5%) was lower than that of conventional biliary SEMS (98.6%)<sup>[23]</sup>. Further studies including long-term results are required to investigate whether SEMS or LAMS are better for EUS-GBD. EUS-GBD with SEMS is a possible alternative treatment for acute cholecystitis. Long-term outcomes after removal of SEMS were promising. Removal of the SEMS after SEMS placement and improvement of symptoms might avoid migration of the stent and recurrence of cholecystitis due to food impaction.

## COMMENTS

### Background

Laparoscopic cholecystectomy is the standard treatment for acute cholecystitis caused by cholelithiasis. For patients at high surgical risk, percutaneous transhepatic gallbladder aspiration (PTGBA) or percutaneous transhepatic gallbladder drainage (PTGBD) can be selected for treatment of cholecystitis. However, the efficacy rate of PTGBA is insufficient (61%-77%), and PTGBD involves an external drainage tube, which decreases the ability of the patient to carry out their normal daily activities. Recently, endoscopic ultrasound-guided gallbladder drainage (EUS-GBD) was developed for acute cholecystitis.

### Research frontiers

There were few reports on long term outcomes of EUS-GBD. This study, the Long-term outcomes after removal of self-expandable metal stent (SEMS), was first report and the results of this study contribute to clarifying the potential of this procedure for acute cholecystitis.

### Innovations and breakthroughs

In this study, EUS-GBD using SEMS was a useful for removal of gallstones in the gallbladder. Gallstones disappeared after EUS-GBD in all cases. During long-term follow-up period after the removal of the SEMS, the recurrence of the cholecystitis was seen in only one patient (8.3%) and there were no complications.

### Applications

This study suggests that EUS-GBD using SEMS and removal of the SEMS 4 wk after the procedure are useful for patients with cholecystitis who were deemed unsuitable for cholecystectomy.

### Peer-review

This study described the use of EUS-GBD for the treatment of acute cholecystitis in patients deemed unsuitable for surgical procedures. Long-term outcomes after removal of SEMS were promising. Removal of the SEMS after SEMS placement and improvement of symptoms might avoid migration of the stent and recurrence of cholecystitis due to food impaction. A larger study comparing the efficacy and safety of EUS-GBD with and without early SEMS removal is warranted.

## REFERENCES

- 1 Reddick EJ, Olsen DO. Laparoscopic laser cholecystectomy. A comparison with mini-lap cholecystectomy. *Surg Endosc* 1989; **3**: 131-133 [PMID: 2530643 DOI: 10.1007/BF00591357]
- 2 Dubois F, Icard P, Berthelot G, Levard H. Coelioscopic cholecystectomy. Preliminary report of 36 cases. *Ann Surg* 1990; **211**: 60-62 [PMID: 2294845]
- 3 Chopra S, Dodd GD, Mumbower AL, Chintapalli KN, Schwesinger WH, Sirinek KR, Dorman JP, Rhim H. Treatment of acute cholecystitis in non-critically ill patients at high surgical risk: comparison of clinical outcomes after gallbladder aspiration and after percutaneous cholecystostomy. *AJR Am J Roentgenol* 2001; **176**: 1025-1031 [PMID: 11264103 DOI: 10.2214/ajr.176.4.1761025]
- 4 Ito K, Fujita N, Noda Y, Kobayashi G, Kimura K, Sugawara T, Horaguchi J. Percutaneous cholecystostomy versus gallbladder aspiration for acute cholecystitis: a prospective randomized controlled trial. *AJR Am J Roentgenol* 2004; **183**: 193-196 [PMID: 15208137 DOI: 10.2214/ajr.183.1.1830193]
- 5 Baron TH, Topazian MD. Endoscopic transduodenal drainage of the gallbladder: implications for endoluminal treatment of gallbladder disease. *Gastrointest Endosc* 2007; **65**: 735-737 [PMID: 17141230 DOI: 10.1016/j.gie.2006.07.041]
- 6 Súttil JC, Betes M, Muñoz-Navas M. Gallbladder drainage guided by endoscopic ultrasound. *World J Gastrointest Endosc* 2010; **2**:



- 203-209 [PMID: 21160934 DOI: 10.4253/wjge.v2.i6.203]
- 7 **Lee SS**, Park DH, Hwang CY, Ahn CS, Lee TY, Seo DW, Lee SK, Kim MW. EUS-guided transmural cholecystostomy as rescue management for acute cholecystitis in elderly or high-risk patients: a prospective feasibility study. *Gastrointest Endosc* 2007; **66**: 1008-1012 [PMID: 17767933 DOI: 10.1016/j.gie.2007.03.1080]
  - 8 **Takasawa O**, Fujita N, Noda Y, Kobayashi G, Ito K, Horaguchi J, Obana T. Endosonography-guided gallbladder drainage for acute cholecystitis following covered metal stent deployment. *Dig Endosc* 2009; **21**: 43-47 [PMID: 19691802 DOI: 10.1111/j.1443-1661.2008.00822.x]
  - 9 **Itoi T**, Itokawa F, Kurihara T. Endoscopic ultrasonography-guided gallbladder drainage: actual technical presentations and review of the literature (with videos). *J Hepatobiliary Pancreat Sci* 2011; **18**: 282-286 [PMID: 20652716 DOI: 10.1007/s00534-010-0310-4]
  - 10 **Song TJ**, Park DH, Eum JB, Moon SH, Lee SS, Seo DW, Lee SK, Kim MH. EUS-guided cholecystoenterostomy with single-step placement of a 7F double-pigtail plastic stent in patients who are unsuitable for cholecystectomy: a pilot study (with video). *Gastrointest Endosc* 2010; **71**: 634-640 [PMID: 20189528 DOI: 10.1016/j.gie.2009.11.024]
  - 11 **Jang JW**, Lee SS, Park DH, Seo DW, Lee SK, Kim MH. Feasibility and safety of EUS-guided transgastric/transduodenal gallbladder drainage with single-step placement of a modified covered self-expandable metal stent in patients unsuitable for cholecystectomy. *Gastrointest Endosc* 2011; **74**: 176-181 [PMID: 21704816 DOI: 10.1016/j.gie.2011.03.1120]
  - 12 **Kamata K**, Kitano M, Komaki T, Sakamoto H, Kudo M. Transgastric endoscopic ultrasound (EUS)-guided gallbladder drainage for acute cholecystitis. *Endoscopy* 2009; **41** Suppl 2: E315-E316 [PMID: 19921608 DOI: 10.1055/s-0029-1215258]
  - 13 **Itoi T**, Binmoeller KF, Shah J, Sofuni A, Itokawa F, Kurihara T, Tsuchiya T, Ishii K, Tsuji S, Ikeuchi N, Moriyasu F. Clinical evaluation of a novel lumen-apposing metal stent for endosonography-guided pancreatic pseudocyst and gallbladder drainage (with videos). *Gastrointest Endosc* 2012; **75**: 870-876 [PMID: 22301347 DOI: 10.1016/j.gie.2011.10.020]
  - 14 **Jang JW**, Lee SS, Song TJ, Hyun YS, Park DY, Seo DW, Lee SK, Kim MH, Yun SC. Endoscopic ultrasound-guided transmural and percutaneous transhepatic gallbladder drainage are comparable for acute cholecystitis. *Gastroenterology* 2012; **142**: 805-811 [PMID: 22245666 DOI: 10.1053/j.gastro.2011.12.051]
  - 15 **de la Serna-Higuera C**, Pérez-Miranda M, Gil-Simón P, Ruiz-Zorrilla R, Díez-Redondo P, Alcaide N, Sancho-del Val L, Nuñez-Rodríguez H. EUS-guided transenteric gallbladder drainage with a new fistula-forming, lumen-apposing metal stent. *Gastrointest Endosc* 2013; **77**: 303-308 [PMID: 23206813 DOI: 10.1016/j.gie.2012.09.021]
  - 16 **Ogura T**, Masuda D, Imoto A, Umegaki E, Higuchi K. EUS-guided gallbladder drainage and hepaticogastrostomy for acute cholecystitis and obstructive jaundice (with video). *Endoscopy* 2014; **46** Suppl 1 UCTN: E75-E76 [PMID: 24639366]
  - 17 **Teoh AY**, Binmoeller KF, Lau JY. Single-step EUS-guided puncture and delivery of a lumen-apposing stent for gallbladder drainage using a novel cautery-tipped stent delivery system. *Gastrointest Endosc* 2014; **80**: 1171 [PMID: 24830582 DOI: 10.1016/j.gie.2014.03.038]
  - 18 **Wang K**, Zhu J, Xing L, Wang Y, Jin Z, Li Z. Assessment of efficacy and safety of EUS-guided biliary drainage: a systematic review. *Gastrointest Endosc* 2016; **83**: 1218-1227 [PMID: 26542374 DOI: 10.1016/j.gie.2015.10.033]
  - 19 **Choi JH**, Lee SS, Choi JH, Park DH, Seo DW, Lee SK, Kim MH. Long-term outcomes after endoscopic ultrasonography-guided gallbladder drainage for acute cholecystitis. *Endoscopy* 2014; **46**: 656-661 [PMID: 24977397 DOI: 10.1055/s-0034-1365720]
  - 20 **Walter D**, Teoh AY, Itoi T, Pérez-Miranda M, Larghi A, Sanchez-Yague A, Siersema PD, Vleggaar FP. EUS-guided gall bladder drainage with a lumen-apposing metal stent: a prospective long-term evaluation. *Gut* 2016; **65**: 6-8 [PMID: 26041748 DOI: 10.1136/gutjnl-2015-309925]
  - 21 **Moon JH**, Choi HJ, Kim DC, Lee YN, Kim HK, Jeong SA, Lee TH, Cha SW, Cho YD, Park SH, Jeong S, Lee DH, Isayama H, Itoi T. A newly designed fully covered metal stent for lumen apposition in EUS-guided drainage and access: a feasibility study (with videos). *Gastrointest Endosc* 2014; **79**: 990-995 [PMID: 24721518 DOI: 10.1016/j.gie.2014.02.015]
  - 22 **Minaga K**, Kitano M, Gon C, Yamao K, Imai H, Miyata T, Kamata K, Omoto S, Takenaka M, Kudo M. Endoscopic ultrasonography-guided choledochoduodenostomy using a newly designed laser-cut metal stent: Feasibility study in a porcine model. *Dig Endosc* 2016; Epub ahead of print [PMID: 27681160]
  - 23 **Andrioni A**, Buda A, Vieceli F, Khashab MA, Hassan C, Repici A. Endoscopic ultrasound-guided transmural stenting for gallbladder drainage in high-risk patients with acute cholecystitis: a systematic review and pooled analysis. *Surg Endosc* 2016; **30**: 5200-5208 [PMID: 27059975]

**P- Reviewer:** Cariati A, Tsuyuguchi T, Tuncyurek O **S- Editor:** Qi Y

**L- Editor:** A **E- Editor:** Wang CH







Published by **Baishideng Publishing Group Inc**  
8226 Regency Drive, Pleasanton, CA 94588, USA  
Telephone: +1-925-223-8242  
Fax: +1-925-223-8243  
E-mail: [bpgoffice@wjgnet.com](mailto:bpgoffice@wjgnet.com)  
Help Desk: <http://www.wjgnet.com/esps/helpdesk.aspx>  
<http://www.wjgnet.com>



ISSN 1007-9327



© 2017 Baishideng Publishing Group Inc. All rights reserved.

**Original Paper**

# Albumin-Bilirubin (ALBI) Grade as Part of the Evidence-Based Clinical Practice Guideline for HCC of the Japan Society of Hepatology: A Comparison with the Liver Damage and Child-Pugh Classifications

Atsushi Hiraoka<sup>a</sup> Takashi Kumada<sup>b</sup> Masatoshi Kudo<sup>c</sup> Masashi Hirooka<sup>d</sup>  
Kunihiko Tsuji<sup>e</sup> Ei Itobayashi<sup>f</sup> Kazuya Kariyama<sup>g</sup> Toru Ishikawa<sup>h</sup>  
Kazuto Tajiri<sup>i</sup> Hironori Ochi<sup>j</sup> Toshifumi Tada<sup>b</sup> Hidenori Toyoda<sup>b</sup>  
Kazuhiro Nouse<sup>g</sup> Kouji Joko<sup>j</sup> Hideki Kawasaki<sup>a</sup> Yoichi Hiasa<sup>d</sup>  
Kojiro Michitaka<sup>a</sup> on behalf of the Real-Life Practice Experts for HCC (RELPEC)  
Study Group and HCC 48 Group (hepatocellular carcinoma experts from 48 clinics)

<sup>a</sup>Gastroenterology Center, Ehime Prefectural Central Hospital, Ehime, <sup>b</sup>Department of Gastroenterology and Hepatology, Ogaki Municipal Hospital, Gifu, <sup>c</sup>Department of Gastroenterology and Hepatology, Kinki University Faculty of Medicine, Osaka-Sayama, <sup>d</sup>Department of Gastroenterology and Metabolism, Ehime University Graduate School of Medicine, Ehime, <sup>e</sup>Center of Gastroenterology, Teine Keijinkai Hospital, Sapporo, <sup>f</sup>Department of Gastroenterology, Asahi General Hospital, Asahi, <sup>g</sup>Department of Gastroenterology, Okayama City Hospital, Okayama, <sup>h</sup>Department of Gastroenterology, Saiseikai Niigata Daini Hospital, Niigata, <sup>i</sup>Department of Gastroenterology, Toyama University Hospital, Toyama, and <sup>j</sup>Hepato-Biliary Center, Matsuyama Red Cross Hospital, Matsuyama, Japan

**Keywords**

ALBI grade · Indocyanine green · Liver damage · Child-Pugh · Hepatocellular carcinoma

**Abstract**

**Aim/Background:** The purpose of this study was to evaluate the validity of 3 classifications for assessing liver function, the liver damage and Child-Pugh classifications and the newly proposed albumin-bilirubin (ALBI) grade, in order to examine the feasibility of evaluating hepatic function using ALBI grade with the hepatocellular carcinoma (HCC) treatment algorithm used in Japan. **Methods:** We analyzed the medical records of 3,495 Japanese HCC patients

See related article by Kudo: Albumin-Bilirubin Grade and Hepatocellular Carcinoma Treatment Algorithm. DOI 10.1159/000462199, published on pp. 185–188.

Atsushi Hiraoka, MD, PhD  
Gastroenterology Center, Ehime Prefectural Central Hospital  
Kasuga-Cho 83  
Matsuyama, Ehime 790-0024 (Japan)  
E-Mail hirage@m.ehime-u.ac.jp

admitted from 2000 to 2015, which were comprised of 1,580 patients hospitalized in the Ehime Prefecture area and used as a training cohort (Ehime group), and 1,915 others who were used for validation (validation group). ALBI score used for grading ( $\leq -2.60$  = grade 1, greater than  $-2.60$  to  $\leq -1.39$  = grade 2, greater than  $-1.39$  = grade 3) as well as clinical features and prognosis (Japan Integrated Staging [JIS], modified JIS, ALBI-TNM [ALBI-T] score) were retrospectively investigated. **Results:** For prediction of liver damage A, the values for sensitivity and specificity, positive predictive and negative predictive values, and positive and negative likelihood ratios of ALBI-1 and Child-Pugh A were similar among the 2 groups. Akaike information criterion results showed that prognosis based on ALBI grade/ALBI-T score was better than that based on liver damage/modified JIS score and Child-Pugh/JIS score (22,291.8/21,989.4, 22,379.6/22,076.0, 22,392.1/22,075.1, respectively). The cutoff values for ALBI score for indocyanine green retention rate at 15 min (ICG-R15)  $<10$ ,  $<20$ , and  $<30\%$  were  $-2.623$  (area under the curve [AUC]: 0.798),  $-2.470$  (AUC: 0.791), and  $-2.222$  (AUC: 0.843), respectively. The distribution of ICG-R15 ( $<10\%$ , 10 to  $<20\%$ , 20 to  $<30\%$ , and  $\geq 30\%$ ) for ALBI grade 1 was similar to that for liver damage A. There were only small differences with regard to therapeutic selection with the Japanese HCC treatment algorithm between liver damage and ALBI grade. **Conclusion:** ALBI grade is a useful and easy classification system for assessment of hepatic function for therapeutic decision making.

© 2017 S. Karger AG, Basel

## Introduction

In Japan, the degree of liver damage as a guide to liver function (liver damage classification) [1] has been defined based on ascites, serum bilirubin, serum albumin, indocyanine green retention rate at 15 min (ICG-R15) (%), and prothrombin time activity (%) by the Liver Cancer Study Group of Japan (LCSGJ) (Table 1). The liver damage classification is utilized for evaluation of hepatic function with the hepatocellular carcinoma (HCC) treatment algorithm of the evidence-based Japan Society of Hepatology (JSH) guideline [2, 3]. Moreover, ICG-R15 has been reported to be a useful marker for predicting the hepatic function of a safely resectable segment in patients with HCC [4–6]. However, ICG-R15 data are not easily obtained in all patients, because ICG injection is needed. On the other hand, the Child-Pugh classification [7] is used worldwide for evaluation of hepatic function in patients with liver cirrhosis. As for the weak points of the Child-Pugh classification, some factors are subjective (ascites, encephalopathy), while interrelated factors (serum albumin, ascites) also exist. Omagari et al. [8] reported that the liver damage classification is a more effective evaluation method for patients with early stage HCC as compared to the Child-Pugh classification. Recently, a simple evaluation method for hepatic function, termed albumin-bilirubin (ALBI) grade, which is calculated using only serum albumin and total bilirubin, has been proposed [9], and some have reported its usefulness for HCC treatment planning [9–16].

ALBI grade [13] and liver damage [8] have been reported to have better capability for evaluation of hepatic function in Japanese HCC patients as compared to the Child-Pugh classification, though few studies have assessed the correlation between them. In the present study, we investigated the clinical usefulness of the ALBI grade by comparing it with both the liver damage and Child-Pugh classifications to analyze whether the ALBI grade can be substituted for the liver damage classification in the evidence-based JSH guideline.

**Table 1.** Degree of liver damage used by LCSGJ

	LD A	LD B	LD C
Ascites	none	controllable	uncontrollable
Serum bilirubin, mg/dL	<2.0	2.0–3.0	>3.0
Serum albumin, g/dL	>3.5	3.0–3.5	<3.0
ICG-R15, %	<15	15–40	>40
Prothrombin activity, %	>80	50–80	<50

The degree of liver damage is decided based on the highest grade that contains at least 2 findings. When there are factors B and C, the degree is recommended as class B. LD, liver damage; ICG-R15, indocyanine green retention rate after 15 min.

## Materials and Methods

### Patients

From 2000 to 2015, 3,495 patients with naive HCC were examined using ICG-R15 at 9 different institutions (Ehime Prefectural Hospital [ $n = 940$ ], Ehime University Hospital [ $n = 268$ ], Matsuyama Red Cross Hospital [ $n = 372$ ], Ogaki Municipal Hospital [ $n = 844$ ], Okayama City Hospital [ $n = 135$ ], Teine Keijinkai Hospital [ $n = 546$ ], Asahi General Hospital [ $n = 124$ ], Saiseikai Niigata Hospital [ $n = 111$ ], Toyama University Hospital [ $n = 155$ ]). After receiving informed consent, ICG-R15 was determined following a bolus injection of ICG (0.5 mg/kg) prior to therapy for HCC. ALBI score was calculated based on serum albumin and total bilirubin using the following formula, ALBI-score:  $(\log_{10} \text{bilirubin } [\mu\text{mol/L}] \times 0.66) + (\text{albumin } [\text{g/L}] \times -0.085)$ , while ALBI grade was defined by the resulting score ( $\leq -2.60$  = grade 1, greater than  $-2.60$  to  $\leq -1.39$  = grade 2, greater than  $-1.39$  = grade 3) [9].

Patients positive for anti-hepatitis C virus (HCV) were judged to have HCC due to HCV, and those positive for hepatitis B virus surface antigen (HBsAg) were judged to have HCC due to hepatitis B virus (HBV). Those without anti-HCV and HBsAg were defined as negative for both HBV and HCV (nonBnonC).

### Comparison between Three Methods for Evaluation of Hepatic Function

We examined the relationship between the liver damage (Table 1) and Child-Pugh classifications and the ALBI grade using a validation cohort. Patients treated at institutions located in Ehime Prefecture (Ehime Prefectural Hospital, Ehime University Hospital, Matsuyama Red Cross Hospital) were defined as the training cohort ( $n = 1,580$ , Ehime group), while the others were used as the validation cohort ( $n = 1,915$ , validation group). For predicting liver damage class A, which often has good values of ICG-R15, the sensitivity, specificity, positive predictive value (PPV), negative predictive value (NPV), positive likelihood ratio, and negative likelihood ratio of ALBI grade 1 and Child-Pugh class A were estimated in both groups.

The number of patients was investigated in each arm of the therapeutic option of the evidence-based JSH guideline [2, 3], with each grade used for assessment of hepatic function. In addition, we retrospectively evaluated the prognosis shown by each classification for hepatic function, and the prognosis shown by 3 different prognostic staging systems [Japan Integrated Staging (JIS) score, modified JIS score, ALBI-TNM (ALBI-T) score]. The distribution of ICG-R15 in each classification of hepatic function was investigated. JIS score was calculated using TNM stage of LCSGJ and Child-Pugh class [17, 18], modified JIS score using TNM stage of LCSGJ and liver damage [19], and ALBI-T using TNM stage of LCSGJ and ALBI grade [13].

### Diagnosis and Surveillance of HCC Patients

HCC was diagnosed based on an increasing course of  $\alpha$ -fetoprotein, as well as dynamic CT [20], magnetic resonance imaging, contrast-enhanced US with perflubutane (Sonazoid®, Daiichi Sankyo Co., Ltd., Tokyo, Japan) [21], and/or pathological findings. TNM stage was determined as reported in studies for staging of HCC conducted by the LCSGJ, ed 6 [1].

### Treatment Criteria

After 2005, all treatments were performed following the Japanese practical guidelines for HCC [2, 3], whenever possible. All treatments were performed after obtaining written informed consent from the

patient. The study protocol was approved by the Institutional Ethics Committee of Ehime Prefectural Central Hospital (No. 28-30).

#### Statistical Analysis

Data are expressed as median values or interquartile range (IQR). Statistical analyses were performed using the Student *t* test, Mann-Whitney U test,  $\chi^2$  test, Pearson test, log-rank test, and Kaplan-Meier methods. A *p* value <0.05 was considered to indicate statistical significance. Akaike information criterion (AIC) for prognosis with each method, receiver operating characteristic (ROC), and the area under the curve (AUC) were calculated for comparisons between the ALBI score and ICG-R15. All statistical analyses were performed using Easy R (EZR) (Saitama Medical Center, Jichi Medical University, Saitama, Japan) [22], a graphical user interface for R (The R Foundation for Statistical Computing, Vienna, Austria) [23].

## Results

### Clinical Backgrounds of Enrolled Patients

The total number of patients diagnosed with and/or treated for HCC from 2000 to 2015 at our institutions was 7,565, of whom 3,495 (46.2%; 2,488 males, 1,007 females; median age 70 years old, IQR 62–75 years) were enrolled in the present study. Their clinical backgrounds are shown in Table 2. HCV was the diagnosis in 2,257, HBV in 506, HBV and HCV in 18, and nonBnonC in 714 patients. In the comparisons between the Ehime and validation groups, there were significant differences with regard to gender, AST, ALT, platelets, total bilirubin, ascites, encephalopathy, ICG-R15, liver damage classification, Child-Pugh classification, ALBI grade, tumor number (single and multiple),  $\alpha$ -fetoprotein ( $\geq 100$  ng/mL), des- $\gamma$ -carboxy prothrombin, and therapies (Table 2).

Surgical resection was performed in 1,274 (36.5%) patients, radiofrequency ablation (RFA) [24, 25] in 1,652 (47.3%), percutaneous ethanol injection in 51 (1.5%), and transcatheter arterial chemoembolization in 462 (13.2%), while other treatments including supportive care were performed in 56 (1.6%).

Grade distribution for each of the 3 hepatic function assessment methods is shown in Table 3. In the Ehime group, the values for sensitivity, specificity, PPV, NPV, positive likelihood ratio, and negative likelihood ratio for predicting liver damage class A based on ALBI grade 1 were 0.677, 0.851, 0.831, 0.708, 4.534 (95% CI: 3.800–5.409), and 0.380 (95% CI: 0.343–0.421), respectively, while those based on Child-Pugh class A were 0.999, 0.413, 0.649, 0.997, 1.703 (95% CI: 1.604–1.808), and 0.003 (95% CI: 0.000–0.021), respectively. In the validation group, those values for predicting liver damage class A based on ALBI grade 1 were 0.632, 0.906, 0.908, 0.628, 6.739 (95% CI: 5.393–8.422), and 0.406 (95% CI: 0.375–0.439), respectively, and those based on Child-Pugh class A were 0.995, 0.438, 0.721, 0.983, 0.769, 1.771 (95% CI: 1.664–1.885), and 0.012 (95% CI: 0.005–0.027), respectively. Similar tendencies for these values were seen in both groups. For all 3,495 enrolled patients, the values for sensitivity, specificity, PPV, NPV, positive likelihood ratio, and negative likelihood ratio for predicting liver damage class A based on ALBI grade 1 were 0.651, 0.879, 0.873, 0.664, 0.751, 5.373 (95% CI: 4.677–6.171), and 0.397 (95% CI: 0.373–0.423), respectively, and those based on Child-Pugh class A were 0.996, 0.426, 0.689, 0.989, 0.746, 1.736 (95% CI: 1.663–1.813), and 0.008 (95% CI: 0.004–0.018), respectively.

When each grade was used for assessment of hepatic function with the evidence-based JSH guideline, after exclusion of patients with major vein invasion, extrahepatic metastasis, and/or rupture (*n* = 209), the numbers of patients in arms 1, 2, 3, 4, and 5 of the algorithm with the use of the liver damage classification were 2,138, 554, 257, 203, and 134, respectively, while the numbers of patients in those arms using the Child-Pugh classification were



**Table 2.** Clinical backgrounds of patients and comparisons between the Ehime and validation groups

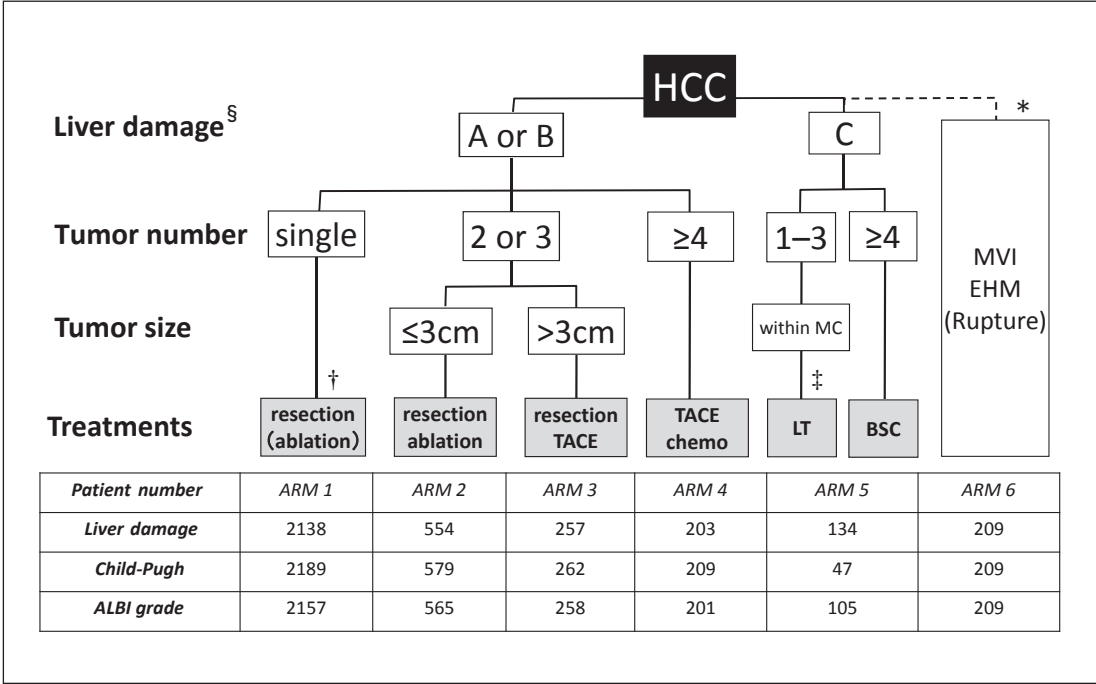
	Ehime group (n = 1,580)	Validation group (n = 1,915)	Total (n = 3,495)
Age, years <sup>a</sup>	69 (62–76)	70 (63–75)	70 (62–75)
Gender, male:female	1,111:469	1,377:538**	2,488:1,007
Etiology, HCV:HBV:HBV&HCV:nonBnon C	1,107:166:12:295	1,150:340:6:419	2,257:506:18:714
AST, IU/L <sup>a</sup>	52 (36–76)	47 (33–67)**	50 (35–72)
ALT, IU/L <sup>a</sup>	42 (27–66)	40 (26–63)*	41 (27–64)
Platelets, ×10 <sup>4</sup> cells/μL <sup>a</sup>	11.0 (7.8–15.4)	11.9 (8.4–16.4)**	11.4 (8.1–15.8)
Total bilirubin, mg/dL <sup>a</sup>	0.8 (0.6–1.1)	0.7 (0.6–1.0)**	0.8 (0.6–1.0)
Albumin, g/dL <sup>a</sup>	3.8 (3.4–4.2)	3.8 (3.5–4.1)	3.8 (3.4–4.1)
Prothrombin time, % <sup>a</sup>	84.1 (73.2–95.5)	87.6 (75.0–96.7)	86.0 (74.0–96.0)
Ascites, none:mild:moderate to severe	1,442:104:34	1,822:86:7**	3,264:190:41
Encephalopathy, none:grade I–II:grade III–IV	1,578:2:0	1,857:53:5**	3,435:55:5
ICG-R15, % <sup>a</sup>	21.0 (13.0–33.6)	16.0 (10.6–23.0)**	17.4 (11.3–28.1)
Liver damage, A:B:C	823:658:99	1,137:735:43**	1,960:1,393:142
Child-Pugh, A:B:C	1,266:282:32	1,568:329:18*	2,834:611:50
ALBI grade, 1:2:3	670:834:76	792:1,086:37**	1,462:1,920:113
Tumor size, cm <sup>a</sup>	2.3 (1.6–3.6)	2.4 (1.6–3.5)	2.3 (1.6–3.5)
Tumor number, single:multiple	956:624	1,328:587**	2,284:1211
TNM stage of LCSGJ, I:II:III:IV	408:728:345:99	574:914:371:56**	982:1,642:716:155
AFP, ng/mL, <100:≥100:ND	1,181:393:6	1,055:277:583**	2,236:670:589
AFP-L3, %, <10:≥10:ND	1,057:378:145	859:271:785	1,916:649:930
DCP, mAU/mL, <100:≥100:ND	917:638:25	856:436:623**	1,773:1,074:648
Treatment, resection:RFA:PEI:TACE:other	400:833:40:265:42	874:819:11:197:14**	1,274:1,652:51:462:56

\*  $p < 0.05$ , \*\*  $p < 0.01$ , comparison between Ehime and validation groups. IQR, interquartile range; HCV, hepatitis C virus; HBV, hepatitis B virus; nonBnonC, negative for both HBV and HCV; AST, aspartate amino transferase; ALT, alanine transferase; ICG-R15, indocyanine green retention rate after 15 min; ALBI grade, albumin-bilirubin grade; TNM stage, tumor node metastasis stage; LCSGJ, Liver Cancer Study Group of Japan; ND, no data; AFP, α-fetoprotein; AFP-L3, lens culinaris agglutinin A-reactive fraction of AFP; DCP, des-γ-carboxy prothrombin; RFA, radiofrequency ablation; PEI, percutaneous ethanol injection; TACE, transcatheter arterial chemoembolization. <sup>a</sup> Median (IQR).

**Table 3.** Comparison of patient distribution between liver damage, Child-Pugh, and ALBI grade

	Ehime group (n = 1,580)			Validation group (n = 1,915)		
	LD A	LD B	LD C	LD A	LD B	LD C
ALBI-1	557	113	0	719	73	0
ALBI-2	266	527	41	417	645	24
ALBI-3	0	18	58	1	17	19
	LD A	LD B	LD C	LD A	LD B	LD C
CP A	822	440	4	1,131	435	2
CP B	1	206	75	6	293	30
CP C	0	12	20	0	7	11
	CP A	CP B	CP C	CP A	CP B	CP C
ALBI-1	664	6	0	785	7	0
ALBI-2	602	223	9	783	297	6
ALBI-3	0	53	23	0	25	12

LD, liver damage; CP, Child-Pugh; ALBI, albumin-bilirubin grade.

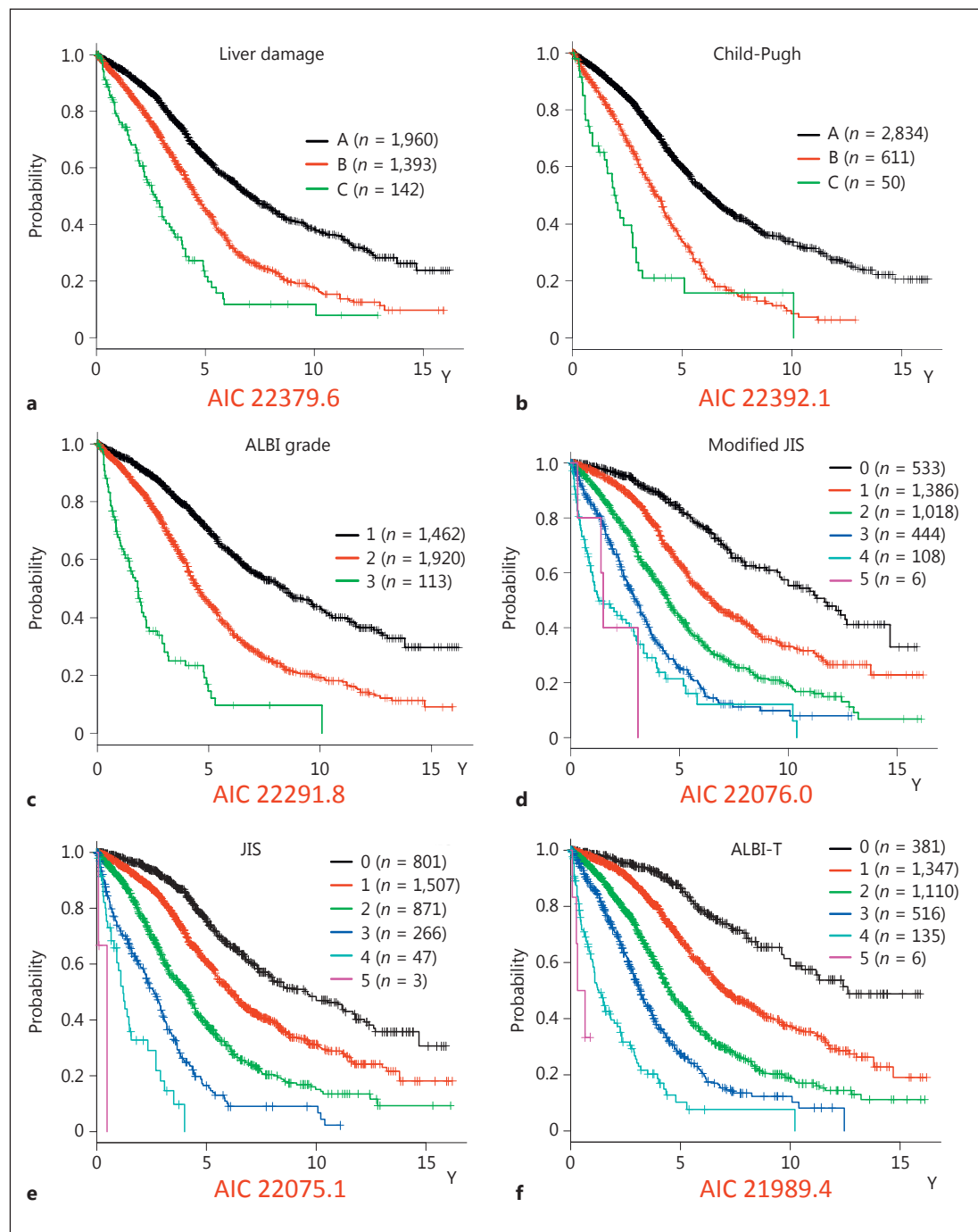


**Fig. 1.** HCC treatment algorithm of the evidence-based Japan Society of Hepatology (JSH) guideline and distribution of patients with 3 hepatic function assessment tools. <sup>§</sup> Child-Pugh classification may also be used when nonsurgical treatment is considered. <sup>†</sup> Can be selected for tumors with a diameter  $\leq 3$  cm. <sup>‡</sup> Patients aged  $\leq 65$  years. \* In some cases, liver resection, chemotherapy, and embolization therapy may be selected for patients with Child-Pugh class A along with vascular invasion, while chemotherapy is recommended for patients with Child-Pugh class A disease with extrahepatic metastasis. TACE, transcatheter arterial chemo-embolization; MC, Milan criteria (single lesion  $\leq 5$  cm or 2–3 lesions each  $\leq 3$  cm); LT, liver transplantation; BSC, best supportive care; MVI, major vessels invasion; EHM, extrahepatic metastasis; ALBI grade, albumin-bilirubin grade.

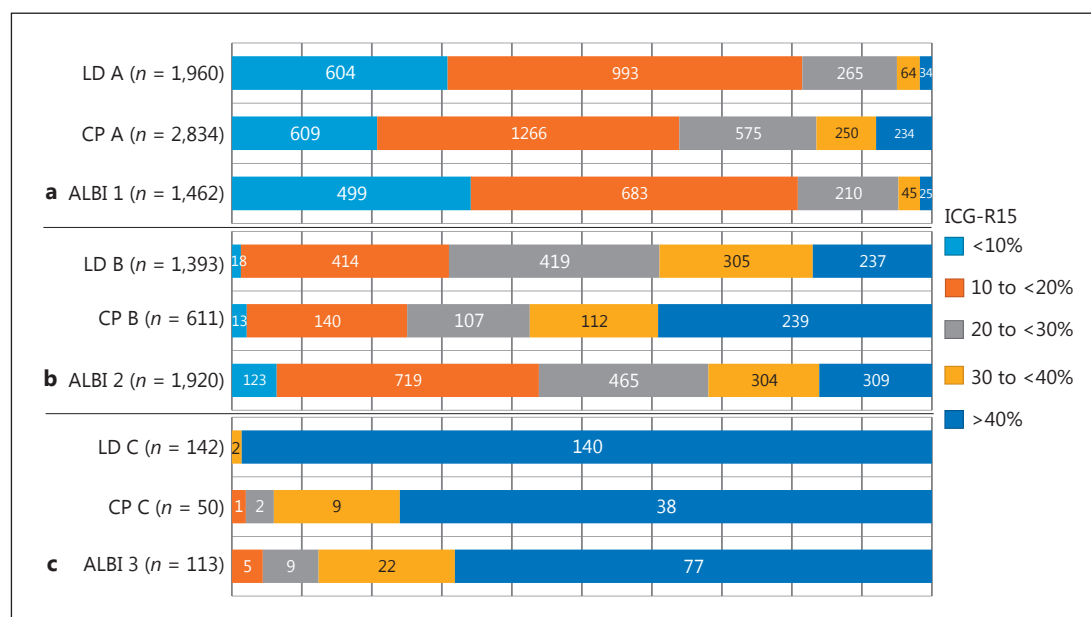
2,189, 579, 262, 209, and 47, respectively, and using ALBI grade were 2,157, 565, 258, 201, and 105, respectively (Fig. 1).

Prognosis for each grade according to each hepatic function assessment method was also examined (Fig. 2a–c). The value obtained with the AIC for prognosis by ALBI grade was lower as compared to the liver damage and Child-Pugh values (22,291.8, 22,379.6, and 22,392.1, respectively). Similarly, that for prognosis according to ALBI-T score was lower than those according to modified JIS and JIS scores (21,989.4, 22,076.0, and 22,075.1, respectively) (Fig. 2d–f).

The distribution of levels of ICG-R15 in each assessment is shown in Figure 3. Those of ICG-R15  $<10\%$ , 10 to  $<20\%$ , 20 to  $<30\%$ , and  $\geq 30\%$  for liver damage class A and B were similar to those for ALBI grade 1 and 2 (Fig. 3). ALBI score showed a good relationship with ICG-R15 ( $r = 0.616$ ,  $p < 0.001$ ) (Fig. 4a). The cutoff values for ALBI score obtained by calculating ROC and AUC values for prediction of ICG-R15 ( $<10\%$ ) were  $-2.623$  and  $0.798$ , respectively, while those for ICG-R15 ( $<20\%$ ) were  $-2.470$  and  $0.791$ , respectively, and for ICG-R15 ( $<30\%$ ) were  $-2.222$  and  $0.843$ , respectively (Fig. 4b–d).



**Fig. 2.** **a** Overall survival rates of patients according to liver damage classification (Akaike information criterion, AIC: 22,379.6). **b** Overall survival rates of patients according to the Child-Pugh classification (AIC: 22,392.1). **c** Overall survival rates of patients according to albumin-bilirubin (ALBI) grade (AIC: 22,291.8). **d** Overall survival rates of patients according to modified Japan Integrated scoring system (JIS) score (AIC: 22,076.0). **e** Overall survival rates of patients according to JIS score (AIC: 22,075.1). **f** Overall survival rates of patients according to ALBI-tumor node metastasis (ALBI-T) score (AIC: 21,989.4).

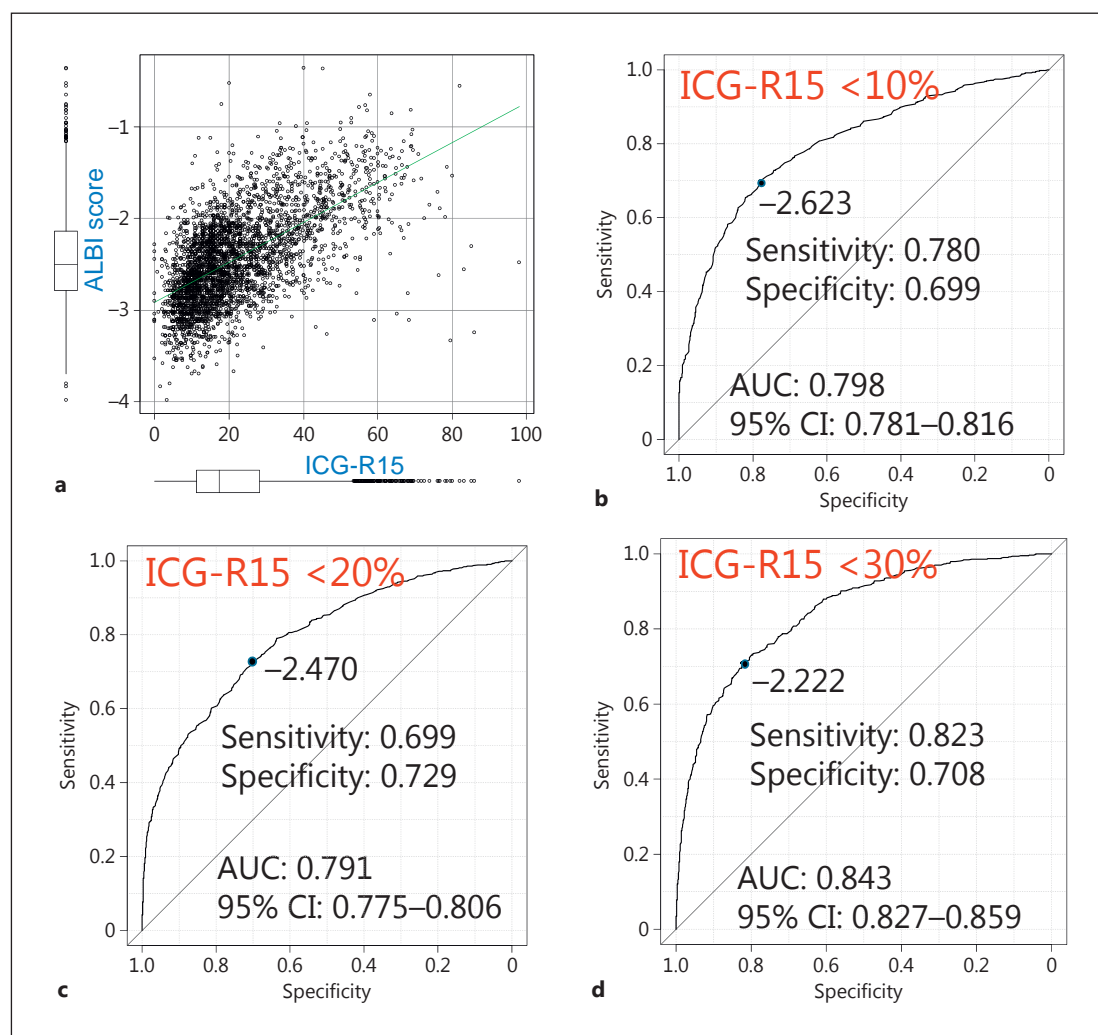


**Fig. 3.** Distribution of level of indocyanine green retention rate at 15 min (ICG-R15). **a** Comparison between liver damage (LD) class A, Child-Pugh (CP) class A, and albumin-bilirubin (ALBI) grade 1. **b** Comparison between LD class B, CP class B, and ALBI grade 2. **c** Comparison between LD class C, CP class C, and ALBI grade 3.

## Discussion

Therapy for HCC in Japanese patients is generally performed according to the HCC treatment algorithm described in the “guidelines for liver cancer treatment based on scientific evidence” using the liver damage classification in the evidence-based JSH guideline [2, 3]. The liver damage classification, which requires ICG test results, has been reported to be more effective for evaluation of hepatic function than the Child-Pugh classification [26, 27]. On the other hand, the Child-Pugh classification may also be used in the evidence-based JSH guideline for consideration of nonsurgical treatment [3]. In fact, the ICG test was performed only in 46.2% of the present patients with HCC in all institutions. In addition, there are issues related to bolus injection of ICG, needed for an ICG test, and allergy to ICG, and constitutional ICG excretory defect [28] and the possibility of underestimation of hepatic function for patients who have a progressed portal-venous shunt [29] have been reported. Moreover, there might also be problems when liver damage and Child-Pugh, which has been reported to be inferior to liver damage [8], are used together in the evidence-based JSH guideline. The newly proposed ALBI grade [9] was shown to provide a better estimation of hepatic function than the Child-Pugh classification [13], and can be calculated with only albumin and total bilirubin data. Indeed, no need for imaging assessment of ascites, encephalopathy, subjective evaluation, or ICG-R15 is thought to be an advantage of ALBI grade as compared with the other classifications. In the present analysis, when ALBI grade was used for assessment of hepatic function in the Japanese HCC treatment algorithm, the distribution of patients in each therapeutic option arm was similar as compared to the liver damage classification.

No comparisons between the liver damage classification and ALBI grade have previously been made. In the present study, the Ehime and validation groups showed a similar tendency for predicting liver damage class A between ALBI grade and the Child-Pugh classification, and



**Fig. 4.** **a** Relationship between albumin-bilirubin (ALBI) score and indocyanine green retention rate at 15 min (ICG-R15) ( $r = 0.616$ ,  $p < 0.001$ ). **b** The cutoff value of ALBI score for predicting ICG-R15 (<10%) by calculating receiver operating characteristic (ROC) was  $-2.623$  (sensitivity: 0.780, specificity 0.699, AUC: 0.798). **c** The cutoff value of ALBI score for predicting ICG-R15 (<20%) by ROC was  $-2.470$  (sensitivity: 0.699, specificity 0.729, AUC: 0.791). **d** The cutoff value of ALBI score for predicting ICG-R15 (<30%) by ROC was  $-2.222$  (sensitivity: 0.823, specificity 0.708, AUC: 0.843).

the positive likelihood ratio of ALBI grade 1 for liver damage class A was good. However, as compared to the Child-Pugh classification, the frequency of patients categorized as requiring transplantation or supportive care due to decompensated classification (arm 5) was increased in the order of ALBI grade and liver damage. Child-Pugh classification had a tendency to overestimate, while liver damage had a tendency to underestimate hepatic function. In a comparison of AIC for prognosis assessment, ALBI grade and ALBI-T score were better than the others. These results suggest that ALBI grade has a superior ability for assessment of hepatic function in patients with HCC.

Surgical resection plays a very important role for improving the prognosis of HCC patients, especially in those with a low number of small-sized tumors (e.g., Milan criteria [30]). Bennett and Blumgart [31] reported that ICG-R15 was unnecessary for deciding on the indication for resection or selection of surgery. However, the ICG test has been described in many reports



as an important examination in patients treated with surgical resection. Makuuchi and colleagues noted the efficacy of ICG test results for decision making in regard to resectable area and proposed the Makuuchi criteria [6, 32], while Torzilli et al. [33] reported satisfactory results following hepatic resection, with a 30-day postoperative mortality of 0% when the criteria were considered for selecting patients to undergo surgery. Ariizumi et al. [34] also reported that the rates of postoperative liver failure and mortality were higher in patients with ICG-R15 (10% or higher) compared to others who underwent a right hepatectomy or trisectionectomy for HCC (23 vs. 2%,  $p = 0.002$ , and 11 vs. 0%,  $p = 0.016$ , respectively).

In addition to the ICG test, development of intraoperative ultrasonically guided subsegmentectomy techniques [35, 36] has made surgical resection safer [37]. In a follow-up survey conducted in Japan ( $n = 54,145$ ), hospital mortality after a resection procedure was reported to be 2.6% [38]. When evaluation for hepatic function was done using ALBI grade, most patients with ALBI grade 1 showed an ICG-R15 value lower than 30%. The Makuuchi criteria define resectable segments according to ICG-R15 level ( $<10\% = >2$  segments,  $10$  to  $<20\% = 1$  segment,  $20$  to  $<30\% =$  subsegment,  $30$  to  $<40\% =$  partial,  $\geq 40\% =$  enucleation) [6, 32]. In the present study, the distribution of ICG-R15 levels in ALBI grade 1 was similar to that in liver damage class A. Based on this result, we consider that the ICG test can be used if necessary, depending on the area scheduled for hepatectomy (e.g., subsegmental, segmental, lobectomy) in patients graded as ALBI-1, and when hepatectomy is considered for patients graded as ALBI-2. Thus, ALBI grade might help to solve difficulties associated with performing the ICG test in HCC patients and the inferiority of assessment with the Child-Pugh classification for hepatic function.

The present study has some limitations, including its retrospective nature. Further investigations with greater numbers of cases are needed to confirm our findings. The majority of the present cohort was considered for resection or RFA, and additional patients with liver damage class C should be analyzed. Of course, each parameter is only one of many indicators available for estimation of hepatic function, and a group of patients cannot be clearly divided into different therapeutic strategies using only a single parameter. Nevertheless, our findings indicate that ALBI grade is a simple but informative clinical indicator for planning treatment against HCC and is considered as adequate for use in the HCC algorithm.

## Disclosure Statement

None of the authors has financial conflicts of interest to disclose concerning this study.

## References

- 1 Liver Cancer Study Group of Japan: The General Rules for the Clinical and Pathological Study of Primary Liver Cancer, ed 6. Tokyo, Kanehara & Co, 2015, pp 26–30.
- 2 Kokudo N, Hasegawa K, Akahane M, Igaki H, Izumi N, Ichida T, Uemoto S, Kaneko S, Kawasaki S, Ku Y, Kudo M, Kubo S, Takayama T, Tateishi R, Fukuda T, Matsui O, Matsuyama Y, Murakami T, Arii S, Okazaki M, Makuuchi M: Evidence-based Clinical Practice Guidelines for Hepatocellular Carcinoma: The Japan Society of Hepatology 2013 update (3rd JSH-HCC Guidelines). *Hepatol Res* 2015;45:123–127.
- 3 The Japan Society of Hepatology: Clinical Practice Guidelines for Hepatocellular Carcinoma 2013. [http://www.jsh.or.jp/English/examination\\_en](http://www.jsh.or.jp/English/examination_en).
- 4 Greco E, Nanji S, Bromberg IL, Shah S, Wei AC, Moulton CA, Greig PD, Gallinger S, Cleary SP: Predictors of perioperative morbidity and liver dysfunction after hepatic resection in patients with chronic liver disease. *HPB (Oxford)* 2011;13:559–565.
- 5 Lau H, Man K, Fan ST, Yu WC, Lo CM, Wong J: Evaluation of preoperative hepatic function in patients with hepatocellular carcinoma undergoing hepatectomy. *Br J Surg* 1997;84:1255–1259.
- 6 Makuuchi M, Kosuge T, Takayama T, Yamazaki S, Kakazu T, Miyagawa S, Kawasaki S: Surgery for small liver cancers. *Semin Surg Oncol* 1993;9:298–304.

- 7 Pugh RN, Murray-Lyon IM, Dawson JL, Pietroni MC, Williams R: Transection of the oesophagus for bleeding oesophageal varices. *Br J Surg* 1973;60:646–649.
- 8 Omagari K, Ohba K, Kadokawa Y, Hazama H, Masuda J, Kinoshita H, Matsuo I, Ohnita K, Mizuta Y, Hayashida K, Kohno S: Comparison of the grade evaluated by “Liver damage” of Liver Cancer Study Group of Japan and Child-Pugh classification in patients with hepatocellular carcinoma. *Hepatol Res* 2006;34:266–272.
- 9 Johnson PJ, Berhane S, Kagebayashi C, Satomura S, Teng M, Reeves HL, O’Beirne J, Fox R, Skowronska A, Palmer D, Yeo W, Mo F, Lai P, Iñarrairaegui M, Chan SL, Sangro B, Miksad R, Tada T, Kumada T, Toyoda H: Assessment of liver function in patients with hepatocellular carcinoma: a new evidence-based approach-the ALBI grade. *J Clin Oncol* 2015;33:550–558.
- 10 Wang YY, Zhong JH, Su ZY, Huang JF, Lu SD, Xiang BD, Ma L, Qi LN, Ou BN, Li LQ: Albumin-bilirubin versus Child-Pugh score as a predictor of outcome after liver resection for hepatocellular carcinoma. *Br J Surg* 2016; 103:725–734.
- 11 Toyoda H, Lai PB, O’Beirne J, Chong CC, Berhane S, Reeves H, Manas D, Fox RP, Yeo W, Mo F, Chan AW, Tada T, Iñarrairaegui M, Vogel A, Schweitzer N, Chan SL, Sangro B, Kumada T, Johnson PJ: Long-term impact of liver function on curative therapy for hepatocellular carcinoma: application of the ALBI grade. *Br J Cancer* 2016; 114:744–750.
- 12 Hiraoka A, Kumada T, Nouse K, Tsuji K, Itobayashi E, Hirooka M, Kariyama K, Ishikawa T, Tada T, Toyoda H, Kawasaki H, Hiasa Y, Michitaka K: Proposed new sub-grouping for intermediate-stage hepatocellular carcinoma using albumin-bilirubin grade. *Oncology* 2016;91:153–161.
- 13 Hiraoka A, Kumada T, Michitaka K, Toyoda H, Tada T, Ueki H, Kaneto M, Aibiki T, Okudaira T, Kawakami T, Kawamura T, Yamago H, Suga Y, Miyamoto Y, Tomida H, Azemoto N, Mori K, Miyata H, Ninomiya T, Kawasaki H: Usefulness of albumin-bilirubin grade for evaluation of prognosis of 2584 Japanese patients with hepatocellular carcinoma. *J Gastroenterol Hepatol* 2016;31:1031–1036.
- 14 Edeline J, Blanc JF, Johnson P, Campillo-Gimenez B, Ross P, Ma YT, King J, Hubner RA, Sumpter K, Darby S, Evans J, Iwuij C, Swinson D, Collins P, Patel K, Muazzam I, Palmer DH, Meyer T: A multicenter comparison between Child Pugh and ALBI scores in patients treated with sorafenib for hepatocellular carcinoma. *Liver Int* 2016;36:1821–1828.
- 15 Chan AW, Kumada T, Toyoda H, Tada T, Chong CC, Mo FK, Yeo W, Johnson PJ, Lai PB, Chan AT, To KF, Chan SL: Integration of albumin-bilirubin (ALBI) score into Barcelona Clinic Liver Cancer (BCLC) system for hepatocellular carcinoma. *J Gastroenterol Hepatol* 2016;31:1300–1306.
- 16 Chan AW, Chong CC, Mo FK, Wong J, Yeo W, Johnson PJ, Yu S, Lai PB, Chan AT, To KF, Chan SL: Incorporating Albumin-Bilirubin grade into the Cancer of the Liver Italian Program system for hepatocellular carcinoma. *J Gastroenterol Hepatol*, Epub ahead of print.
- 17 Kudo M, Chung H, Haji S, Osaki Y, Oka H, Seki T, Kasugai H, Sasaki Y, Matsunaga T: Validation of a new prognostic staging system for hepatocellular carcinoma: the JIS score compared with the CLIP score. *Hepatology* 2004;40:1396–1405.
- 18 Kudo M, Chung H, Osaki Y: Prognostic staging system for hepatocellular carcinoma (CLIP score): its value and limitations, and a proposal for a new staging system, the Japan Integrated Staging Score (JIS score). *J Gastroenterol* 2003;38:207–215.
- 19 Ikai I, Takayasu K, Omata M, Okita K, Nakanuma Y, Matsuyama Y, Makuuchi M, Kojiro M, Ichida T, Arii S, Yamaoka Y: Liver Cancer Study Group of Japan: A modified Japan Integrated Stage score for prognostic assessment in patients with hepatocellular carcinoma. *J Gastroenterol* 2006;41:884–892.
- 20 Bruix J, Sherman M: Management of hepatocellular carcinoma. *Hepatology* 2005;42:1208–1236.
- 21 Hiraoka A, Hiasa Y, Onji M, Michitaka K: New contrast enhanced ultrasonography agent: impact of Sonazoid on radiofrequency ablation. *J Gastroenterol Hepatol* 2011;26:616–618.
- 22 Kanda Y: Investigation of the freely available easy-to-use software “EZ” for medical statistics. *Bone Marrow Transplant* 2013;48:452–458.
- 23 R Development Core Team Rfsc: R: A Language and Environment for Statistical Computing. Vienna, The R Foundation for Statistical Computing, 2005.
- 24 Hiraoka A, Michitaka K, Horiike N, Hidaka S, Uehara T, Ichikawa S, Hasebe A, Miyamoto Y, Ninomiya T, Sogabe I, Ishimaru Y, Kawasaki H, Koizumi Y, Hirooka M, Yamashita Y, Abe M, Hiasa Y, Matsuura B, Onji M: Radiofrequency ablation therapy for hepatocellular carcinoma in elderly patients. *J Gastroenterol Hepatol* 2010;25: 403–407.
- 25 Hiraoka A, Horiike N, Yamashita Y, Koizumi Y, Doi K, Yamamoto Y, Hasebe A, Ichikawa S, Yano M, Miyamoto Y, Ninomiya T, Otomi Y, Kokame M, Iwamura T, Ishimaru Y, Sogabe I, Kashiwara K, Nishiura S, Ootani H, Takamura K, Kawasaki H: Efficacy of radiofrequency ablation therapy compared to surgical resection in 164 patients in Japan with single hepatocellular carcinoma smaller than 3 cm, along with report of complications. *Hepatogastroenterology* 2008;55:2171–2174.
- 26 Watanabe Y, Kumon K: Assessment by pulse dye-densitometry indocyanine green (ICG) clearance test of hepatic function of patients before cardiac surgery: its value as a predictor of serious postoperative liver dysfunction. *J Cardiothorac Vasc Anesth* 1999;13:299–303.
- 27 Erdogan D, Heijnen BH, Bennink RJ, Kok M, Dinant S, Straatsburg IH, Gouma DJ, van Gulik TM: Preoperative assessment of liver function: a comparison of 99mTc-Mebrofenin scintigraphy with indocyanine green clearance test. *Liver Int* 2004;24:117–123.

- 28 Taketazu F, Sanada I, Ngamatsu N, Mukai R, Suetomo Y, Toyoda N, Takada M, Hida K, Kubota K, Maezawa M, Takaku F: A case of hereditary elliptocytosis associated with constitutional indocyanine green excretory defect. *Jpn J Med* 1984;23:139–143.
- 29 Hiraoka A, Kurose K, Hamada M, Azemoto N, Tokumoto Y, Hirooka M, Hasebe A, Kumagi T, Hirata M, Michitaka K, Minami H, Murakami M, Isobe Y, Horiike N, Onji M: Hepatic encephalopathy due to intrahepatic portosystemic venous shunt successfully treated by interventional radiology. *Intern Med* 2005;44:212–216.
- 30 Mazzaferro V, Regalia E, Doci R, Andreola S, Pulvirenti A, Bozzetti F, Montalto F, Ammatuna M, Morabito A, Gennari L: Liver transplantation for the treatment of small hepatocellular carcinomas in patients with cirrhosis. *N Engl J Med* 1996;334:693–699.
- 31 Bennett JJ, Blumgart LH: Assessment of hepatic reserve prior to hepatic resection. *J Hepatobiliary Pancreat Surg* 2005;12:10–15.
- 32 Imamura H, Seyama Y, Kokudo N, Maema A, Sugawara Y, Sano K, Takayama T, Makuuchi M: One thousand fifty-six hepatectomies without mortality in 8 years. *Arch Surg* 2003;138:1198–1206; discussion 1206.
- 33 Torzilli G, Makuuchi M, Inoue K, Takayama T, Sakamoto Y, Sugawara Y, Kubota K, Zucchi A: No-mortality liver resection for hepatocellular carcinoma in cirrhotic and noncirrhotic patients: is there a way? A prospective analysis of our approach. *Arch Surg* 1999;134:984–992.
- 34 Ariizumi S, Yamamoto M, Takasaki K: Right hepatectomy for hepatocellular carcinoma in patients with an indocyanine green retention rate at 15 minutes of 10% or higher. *Dig Surg* 2009;26:135–142.
- 35 Makuuchi M, Hasegawa H, Yamazaki S: Ultrasonically guided subsegmentectomy. *Surg Gynecol Obstet* 1985;161:346–350.
- 36 Makuuchi M, Hasegawa H, Yamazaki S: Intraoperative ultrasonic examination for hepatectomy. *Ultrasound Med Biol* 1983;suppl 2:493–497.
- 37 Kudo M, Izumi N, Ichida T, Ku Y, Kokudo N, Sakamoto M, Takayama T, Nakashima O, Matsui O, Matsuyama Y: Report of the 19th follow-up survey of primary liver cancer in Japan. *Hepatol Res* 2016;46:372–390.
- 38 Ikai I, Arii S, Okazaki M, Okita K, Omata M, Kojiro M, Takayasu K, Nakanuma Y, Makuuchi M, Matsuyama Y, Monden M, Kudo M: Report of the 17th Nationwide Follow-up Survey of Primary Liver Cancer in Japan. *Hepatol Res* 2007;37:676–691.



# S-1 versus placebo in patients with sorafenib-refractory advanced hepatocellular carcinoma (S-CUBE): a randomised, double-blind, multicentre, phase 3 trial

Masatoshi Kudo, Michihisa Moriguchi, Kazushi Numata, Hisashi Hidaka, Hironori Tanaka, Masafumi Ikeda, Seiji Kawazoe, Shinichi Ohkawa, Yozo Sato, Shuichi Kaneko, Junji Furuse, Madoka Takeuchi, Xuemin Fang, Yoshito Date, Masahiro Takeuchi, Takuji Okusaka

## Summary

**Background** Unresectable advanced hepatocellular carcinoma is a heterogeneous disease, for which sorafenib is the first targeted agent approved for first-line therapy, and treatment options for patients with sorafenib-refractory advanced hepatocellular carcinoma are limited. We assessed the efficacy and safety of S-1, a chemotherapeutic agent based on fluorouracil, in patients with sorafenib-refractory advanced hepatocellular carcinoma.

**Methods** We did a randomised, double-blind, placebo-controlled, phase 3 study done at 57 sites in Japan. Patients with advanced hepatocellular carcinoma who were ineligible for surgical or local-regional therapy and judged refractory to sorafenib (ie, had progressed on sorafenib or had discontinued sorafenib because of adverse events) were randomly assigned (2:1) to receive oral S-1 (weight-banded 80 mg/m<sup>2</sup> [80–120 mg per day]), or placebo, twice per day for 28 days consecutively, followed by a minimum 14 day drug-free period. This cycle was repeated until disease progression or the patient became intolerant to the study treatment. Patients were stratified by site and presence or absence of extrahepatic metastasis or vascular invasion. The primary endpoint was overall survival, assessed in the full analysis set (ie, all patients who were treated with study drug except any individuals who were found not to have hepatocellular carcinoma or who were found to have active double cancer). Patients, medical staff, investigators, and the sponsor were masked to treatment assignment. Blinding was maintained even after study treatment concluded. This study is registered with JapicCTI, number JapicCTI-090920, and has been completed.

**Findings** Between Oct 26, 2009, and Aug 22, 2012, we screened 399 patients. 65 patients were excluded due to not meeting criteria (n=61), declining to participate (n=3), or other reasons (n=1). 334 patients were randomly assigned to receive either S-1 (n=223) or placebo (n=111). One patient in the S-1 group did not receive treatment, and was thus excluded from analyses. At data cutoff, median follow-up was 32·4 months (IQR 24·0–34·7) in the S-1 group and 32·9 months (23·7–39·5) in the placebo group. Median overall survival was 11·1 months (95% CI 9·7–13·1) in the S-1 group and 11·2 months (9·2–12·8) in the placebo group (hazard ratio 0·86, 95% CI 0·67–1·10; p=0·220). The most frequently reported adverse events were skin hyperpigmentation (123 [55%] of 222 patients in the S-1 group vs nine [8%] of 111 patients in the placebo group), decreased appetite (104 [47%] vs 21 [19%]), fatigue (102 [46%] vs 20 [18%]), diarrhoea (77 [35%] vs 14 [13%]), and increased blood bilirubin (77 [35%] vs 14 [13%]). Serious adverse events were reported in 90 (41%) of 222 patients in the S-1 group and 24 (22%) of 111 patients in the placebo group. Five treatment-related deaths were reported in the S-1 group.

**Interpretation** S-1 did not prolong overall survival in patients with sorafenib-refractory advanced hepatocellular carcinoma. Further research is needed to identify subgroups of patients who might benefit from S-1.

**Funding** Taiho Pharmaceuticals.

## Introduction

Hepatocellular carcinoma, the most common type of liver cancer, is a major public health concern. According to GLOBOCAN 2012 data, liver cancer is the sixth most common cancer worldwide, and the second most common cause of cancer-related deaths.<sup>1</sup> Sorafenib is the first targeted agent approved as first-line therapy for patients with advanced hepatocellular carcinoma.<sup>2,3</sup> Although no treatment regimen has been established for the second-line setting of advanced hepatocellular carcinoma,<sup>4–6</sup> regorafenib showed a significant improvement in overall survival in a phase 3 study (RESORCE)<sup>7</sup> for patients whose disease had progressed after treatment with sorafenib.

S-1 is an oral fluoropyrimidine that inhibits dihydropyrimidine dehydrogenase, comprised of tegafur (a prodrug of fluorouracil and the main cytotoxic effector), gimeracil (a potent dihydropyrimidine dehydrogenase inhibitor), and oteracil (an inhibitor of phosphorylation of fluorouracil in the gastrointestinal tract) in a molar ratio of 1:0·4:1. Use of S-1 resulted in a prolonged effective concentration of fluorouracil in the liver.<sup>8,9</sup> S-1 is approved in Japan for various solid tumours (gastric cancer, head and neck cancer, colorectal cancer, non-small-cell lung cancer, inoperable or recurrent breast cancer, pancreatic cancer, and biliary tract cancer) as a single agent or in combination with other

*Lancet Gastroenterol Hepatol* 2017

Published Online  
April 6, 2017  
[http://dx.doi.org/10.1016/S2468-1253\(17\)30072-9](http://dx.doi.org/10.1016/S2468-1253(17)30072-9)

See Online/Comment  
[http://dx.doi.org/10.1016/S2468-1253\(17\)30104-8](http://dx.doi.org/10.1016/S2468-1253(17)30104-8)  
Department of Gastroenterology and Hepatology, Kindai University Faculty of Medicine, Osaka, Japan (M Kudo MD); Department of Gastroenterology, Kyoto Prefectural University of Medicine, Kyoto, Japan (M Moriguchi MD); Department of Diagnostic Radiology, Shizuoka Cancer Center Hospital, Shizuoka, Japan (M Moriguchi); Gastroenterological Center, Yokohama City University Medical Center, Yokohama, Japan (K Numata MD); Department of Gastroenterology, Kitasato University Hospital, Kanagawa, Japan (H Hidaka MD); Division of Hepatobiliary and Pancreatic Disease, Department of Internal Medicine, Hyogo College of Medicine, Hyogo, Japan (H Tanaka MD); Department of Gastroenterology and Hepatology, Takarazuka Municipal Hospital, Hyogo, Japan (H Tanaka); Department of Hepatobiliary and Pancreatic Oncology, National Cancer Center Hospital East, Kashiwa, Japan (M Ikeda MD); Department of Internal Medicine, Saga-ken Medical Centre KOSEIKAN, Saga, Japan (S Kawazoe MD); Division of Hepatobiliary and Pancreatic Medical Oncology, Kanagawa Cancer Center, Yokohama, Japan (S Ohkawa MD); Department of Diagnostic and Interventional Radiology, Aichi Cancer Center Hospital, Nagoya, Japan (Y Sato MD);

Department of  
Gastroenterology, Kanazawa  
University Hospital, Ishikawa,  
Japan (S Kaneko MD);  
Department of Medical  
Oncology, Kyorin University  
School of Medicine, Tokyo,  
Japan (J Furuse MD); Keio  
University, Tokyo, Japan  
(Mad Takeuchi MS, Y Date MS);  
Department of Clinical  
Medicine, Kitasato University  
School of Pharmacy, Tokyo,  
Japan  
(Mas Takeuchi ScD, X Fang PhD);  
and Department of  
Hepatobiliary and Pancreatic  
Oncology, National Cancer  
Center Hospital, Tokyo, Japan  
(T Okusaka MD)

Correspondence to:  
Dr Masatoshi Kudo, Department  
of Gastroenterology and  
Hepatology, Kindai University  
Faculty of Medicine,  
Osaka-Sayama, Osaka  
589-8511, Japan  
m-kudo@med.kindai.ac.jp

## Research in context

### Evidence before this study

We searched PubMed and abstracts of major oncology congresses with keywords including "hepatocellular carcinoma", "HCC", "sorafenib", "molecular targeted therapies", and "prognostic factors" for papers published between May 1, 2008, and Dec 31, 2015. The search was restricted to articles published in English. Sorafenib is the only targeted agent approved for patients with advanced hepatocellular carcinoma. No available treatments have shown clinical benefit as second-line treatment after sorafenib.

### Added value of this study

In patients with sorafenib-refractory advanced hepatocellular carcinoma, S-1 was not superior to placebo in terms of overall

survival. Based on patient characteristics, we identified a potential high-response population that might benefit from S-1.

### Implications of all the available evidence

Unresectable advanced hepatocellular carcinoma is a complex carcinoma with high heterogeneity that has few chemotherapeutic options. Sorafenib remains the only effective first-line treatment for patients with advanced hepatocellular carcinoma who are not amenable to surgery and local-regional therapy, and treatment options are extremely limited for patients who become refractory to sorafenib. Further assessment of the efficacy of S-1 in a high-response population as suggested by our exploratory predictive enrichment approach might be worthwhile.

chemotherapy drugs such as cisplatin. S-1 is also approved in other Asian countries (Korea, China, Singapore, Taiwan, Thailand, Hong Kong, Malaysia, Israel, and Vietnam, as of July, 2015) for one or more of the previously described indications, and in Europe for treatment of advanced gastric cancer when given in combination with cisplatin.

Results of a multicentre phase 1/2 study<sup>9</sup> of S-1 in patients with advanced hepatocellular carcinoma were encouraging, with a response rate of 21.7% (five of 23 patients), median progression-free survival of 3.7 months, and overall survival of 16.6 months. Although no data are available on the efficacy of systemic chemotherapy using fluorouracil for patients with advanced hepatocellular carcinoma, the phase 1/2 study of S-1 suggested favourable efficacy and tolerability for these patients. Furthermore, the studies of combination chemotherapy of S-1 with interferon alpha also suggested favourable efficacy for patients with advanced hepatocellular carcinoma.<sup>10,11</sup>

When our study was planned, sorafenib was the only effective treatment for patients with advanced hepatocellular carcinoma, and new treatment options were desired for sorafenib-refractory advanced hepatocellular carcinoma. We planned to do a randomised, double-blind, placebo-controlled, comparative phase 3 study of S-1 to investigate a therapy for patients with advanced hepatocellular carcinoma who discontinued sorafenib treatment due to disease progression or adverse drug reaction.

A common challenge when investigating new agents for advanced hepatocellular carcinoma is the high degree of patient heterogeneity associated with the disease (eg, tumour stage, liver function, performance status, and general health of patients).<sup>12</sup> Although precision medicines are becoming more widespread, identification of appropriate treatment strategies that take individual variability into account can have a substantial effect on outcomes for patients with hepatocellular carcinoma.<sup>13</sup>

Predictive enrichment strategy, a new concept proposed by the US Food and Drug Administration (FDA),<sup>14</sup> calls for a systematic, prespecified procedure to identify a patient population that will benefit most from a particular treatment,<sup>15</sup> which can be accomplished by analysing the results of a single study or a series of studies done under similar settings. Therefore, we did a post-hoc exploratory predictive enrichment strategy analysis in this study.

## Methods

### Study design

This randomised, double-blind, placebo-controlled, comparative phase 3 study (S-CUBE) was done at 57 sites (academic medical centres and community practices) in Japan. The study was approved by each site's institutional review board and was done in accordance with the Declaration of Helsinki and Good Clinical Practice Guidelines.

### Patients

We screened patients for eligibility within 15 days of registration. Eligible patients were aged 20 years or older with histologically, cytologically, or clinically confirmed hepatocellular carcinoma (a typical profile of malignancy in imaging and alpha-fetoprotein [AFP] or protein-induced vitamin K absence or antagonist-II [PIVKA-II] levels exceeding the laboratory reference range); ineligible for surgical or local-regional therapy (eg, percutaneous local therapy and transcatheter arterial (chemo)embolisation [TA(C)E]); and previously treated with but adjudged refractory to sorafenib (ie, disease progression while taking sorafenib or discontinued due to an adverse event). Eligible patients had discontinued sorafenib at least 15 days before registration and had at least one target lesion as assessed by Response Evaluation Criteria In Solid Tumors (RECIST) version 1.1 criteria; Child-Pugh score of 5–7; Eastern Cooperative Oncology Group (ECOG) performance status of 0–1; and adequate haematological, renal, and liver function.



Patients were excluded if they had undergone hepatectomy, percutaneous local therapy, TA(C)E or hepatic arterial infusion chemotherapy within 30 days of registration or had a history of liver transplantation. Patients were also excluded if they had brain metastasis; history of hepatic artery infusion chemotherapy with fluorouracil or S-1; received any systemic chemotherapy after sorafenib for hepatocellular carcinoma; tumour vascular invasion in Vp4 (portal trunk and contralateral portal branch), Vv3 (inferior vena cava), B3 (primary bile duct branch), and B4 (common bile duct); serious complications; clinical hepatic encephalopathy; intractable or refractory ascites; pleural effusion or pericardial effusion; or active double cancer (appendix pp 2–3). All patients provided written informed consent.

### Randomisation and masking

Eligible patients were randomly assigned (2:1) via an interactive web response system to receive S-1 or placebo. Randomisation was stratified by minimisation, based on study site and presence or absence of extrahepatic metastasis or vascular invasion (portal vein, hepatic vein, bile duct, or of branch). The study investigators enrolled patients and the randomisation sequence, generated by Bell Medical Solutions (Tokyo, Japan), was independent of the study sponsor. S-1 and placebo were identical except for the active ingredients. Patients, medical staff, investigators, and the sponsor were masked to treatment assignment. Blinding was maintained even after study treatment.

### Procedures

The dose of S-1 (80 mg/m<sup>2</sup>) was selected on the basis of the results of a phase 1/2 study of S-1 for patients with advanced hepatocellular carcinoma,<sup>9</sup> and the daily dose for each patient was determined in bands, based on the body surface area of each patient at the time of registration (80 mg for <1.25 m<sup>2</sup>, 100 mg for 1.25 to <1.50 m<sup>2</sup>; and 120 mg for ≥1.50 m<sup>2</sup>).

In the first cycle of treatment, oral S-1 was given twice daily, within 1 h of breakfast and the evening meal, for 28 days consecutively (total 56 doses). Patients in the placebo group received identical placebo capsules of S-1 at the same schedule as the S-1 group. Then, patients underwent a minimum 14-day, drug-free period followed by a second cycle. Cycles continued until one of the criteria for discontinuation of study drug was met—ie, disease progression or intolerable adverse event. Details of permitted dose reductions or interruptions can be found in the appendix (pp 4–5).

Vital signs and laboratory values were assessed every 2 weeks until cycle 4, and every 3 weeks thereafter during the treatment period. Local radiological imaging was performed at baseline, every 6 weeks during the first 24 weeks of treatment, and every 12 weeks thereafter until one of the criteria for imaging was met—ie, initiation of a new therapy for hepatocellular carcinoma, consent

withdrawal for imaging follow-up, investigators' decision from the safety point of view, or patient's death. Survival follow-up was done every 12 weeks after the discontinuation of imaging follow-up. Study drug administration after the treatment period and crossover of treatment were not allowed.

### Outcomes

The primary endpoint was overall survival (defined as the time from date of random assignment to date of death). Patients who had not died or who were lost to follow-up were censored on the last date on which they were known to have been alive. Secondary endpoints included progression-free survival (defined as the time from date of randomisation to date of first observation of disease progression or death due to any cause), time to progression (defined by the time from date of randomisation to date of first observation of disease progression), time to treatment failure (defined by the time from date of randomisation to date of completion of the study treatment), the proportion of patients with an objective tumour response (defined as the proportion of patients having partial response or complete response as their best overall response assessment), and incidence of adverse events. Exploratory objectives were to identify a potential high-response population that is more likely to respond to S-1 using a predictive enrichment strategy and patient mapping, and assess the efficacy (ie, overall survival) of S-1 versus placebo in the high-response population. Treatment response was assessed on the basis of the RECIST version 1.1 criteria by centralised review, and safety was assessed according to the Common Terminology Criteria for Adverse Events (CTCAE) version 3.0, until 30 days after last dose of the study drug.

### Statistical analysis

The full analysis set (ie, all patients who were treated with study drug except any individuals who were found not to have hepatocellular carcinoma or who were found to have active double cancer) was used for efficacy analyses and the safety analysis set (ie, all patients except those who did not receive study drug) was used for safety analyses. Efficacy and safety analyses were planned when 250 deaths had occurred, and at least 1.5 years had passed after assignment of the final patient. At the time of trial planning, survival after sorafenib was unclear, due to the lack of information on sorafenib treatment in Japan. The expected median overall survival in the placebo group was estimated on the basis of the results of a phase 3 study of sorafenib,<sup>3</sup> and experiences in Japan (personal communication). In the reference study,<sup>3</sup> the difference between overall survival and progression-free survival in the sorafenib group was around 5 months. Japanese investigators had considered that survival of Japanese patients with advanced hepatocellular carcinoma might be longer than the results of the study. The expected median overall survival in the S-1 group

See Online for appendix

was estimated to be 3.5 months longer than the placebo group, based on the results of phase 1/2 study of S-1 for hepatocellular carcinoma.<sup>9</sup> Therefore, the expected median survival was estimated to be 10 months in the S-1 group and 6.5 months in the placebo group. The power under the alternative hypothesis was deemed to be approximately 90% to detect the superiority of S-1 over placebo to prolong overall survival with two-sided 5% significance. Assuming survival would be distributed in accordance with exponential distribution, a total of 250 deaths were expected, and assuming that 5% of the patients would be excluded from the full analysis set, we planned to enrol 330 patients (220 patients in the S-1 group and 110 patients in the placebo group, 2:1 ratio selected for ethical reasons). Survival for each group was summarised using Kaplan-Meier curves and was further characterised in terms of median value, survival probability at 12 months, and 95% CIs. The difference in overall survival between the two groups was assessed using an unstratified log-rank test with two-sided 5% significance level. Hazard ratios (HRs) were calculated using the Cox proportional hazard model. We did a sensitivity analysis of overall survival for the full analysis set using a stratified log-rank test adapted for the stratifying factors for randomisation. We analysed secondary time-to-event endpoints in a similar way to the primary endpoint. We summarised objective tumour responses by treatment group and analysed the difference between groups using the Fisher's exact test with a one-sided alternative hypothesis. The proportion of adverse events was listed by group. We planned one interim analysis to test for early evidence of potential

inferiority of S-1 versus placebo to judge whether premature discontinuation was necessary in terms of safety. Data were to be locked when a total of 100 patients from both groups had completed two cycles of treatment. The independent data monitoring committee (IDMC) was to assess the incidence of serious adverse events, reasons for discontinuation, and treatment period under non-blinded conditions.

A post-hoc exploratory predictive enrichment analysis was performed by the method proposed by Li and colleagues,<sup>15</sup> in which data are divided into two sets—a training sample and a validation sample. The training sample is used for patient scoring, obtaining prediction Z score, and iterative random-cross-validation within the sample. The results from the training sample are then validated in the validation sample. However, in this study, all patients administered study drug were used for the training and validation samples due to the small sample size. For further characterisation of the statistically enriched subgroup, patient mapping was applied to identify a high-response population, for which patients were plotted on two-dimensional, multivariable plots using the predictive enrichment score and patient covariate values. A high-response population was identified by patient mapping and clinical considerations. This post-hoc exploratory predictive enrichment analysis was planned between completion of enrolment and data lock for the primary analysis.

Data were analysed using SAS version 9.2 (primary analysis) and R version 3.2.0 (exploratory analysis) software. This trial is registered with Japan Pharmaceutical Information Center Clinical Trial, number JapicCTI-090920.

### Role of the funding source

The funder of the study was involved in the study design, data collection, data analysis, data interpretation, writing of the report, and decision to submit the report for publication. The corresponding author had full access to all the data in the study and had final responsibility for the decision to submit.

### Results

Between Oct 26, 2009, and Aug 22, 2012, we screened 399 patients. 65 patients were excluded (figure 1). 334 patients were randomly assigned to receive either S-1 (n=223) or placebo (n=111). Of these patients, 333 received the study drug (222 in the S-1 group; 111 in the placebo group) from 53 sites in Japan (figure 1). The planned interim analysis was done in July, 2011, and the IDMC recommended continuing the trial. Baseline patient characteristics were similar between treatment groups (table 1). All patients had previously received sorafenib and 224 (67%) of the patients had discontinued sorafenib due to progressive disease. 208 (62%) of 333 patients had advanced disease (stage IV per tumour-node-metastasis [TNM] staging system of Liver

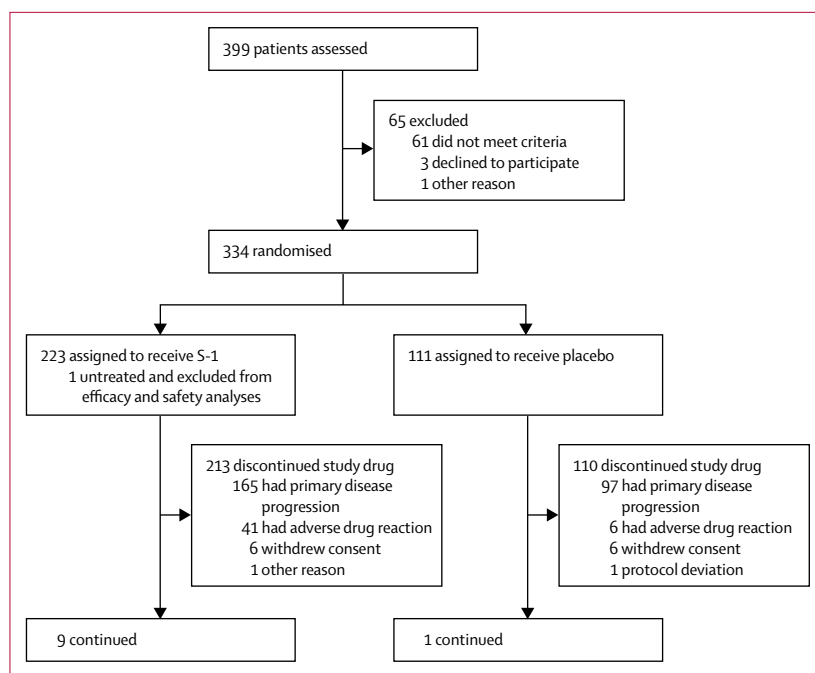


Figure 1: Trial profile

	S-1 group (n=222)	Placebo group (n=111)
Sex		
Male	183 (82%)	85 (77%)
Female	39 (18%)	26 (23%)
Age (years)	70 (64–75)	70 (64–75)
ECOG performance status		
1	34 (15%)	21 (19%)
0	188 (85%)	90 (81%)
Cirrhosis		
No	71 (32%)	35 (32%)
Yes	151 (68%)	76 (68%)
Cause		
HBsAg positive	44 (20%)	26 (23%)
HCV Ab positive	121 (55%)	59 (53%)
Reason for discontinuation of sorafenib		
Disease progression	147 (66%)	77 (69%)
Adverse event	75 (34%)	34 (31%)
Treatment duration of sorafenib (days)	113 (53–196)	90 (45–150)
Child-Pugh score		
5	104 (47%)	45 (41%)
6	76 (34%)	45 (41%)
7	42 (19%)	21 (19%)
TNM stage <sup>16</sup>		
I	0 (0%)	1 (<1%)
II	18 (8%)	8 (7%)
III	65 (29%)	33 (30%)
IVA	38 (17%)	25 (23%)
IVB	101 (45%)	44 (40%)
BCLC staging system		
Early	7 (3%)	1 (<1%)
Intermediate	69 (31%)	36 (32%)
Advanced	146 (66%)	74 (67%)

(Table 1 continues in next column)

	S-1 group (n=222)	Placebo group (n=111)
(Continued from previous column)		
Vascular invasion or extrahepatic metastasis		
No	83 (37%)	41 (37%)
Yes	139 (63%)	70 (63%)
Extrahepatic metastasis		
No	101 (45%)	53 (48%)
Yes	121 (55%)	58 (52%)
Site of measurable lesions		
Liver	178 (80%)	94 (85%)
Lung	58 (26%)	22 (20%)
Adrenal gland	14 (6%)	4 (4%)
Lymph node	41 (18%)	18 (16%)
Peritoneum	9 (4%)	5 (5%)
Other	12 (5%)	6 (5%)
Vascular invasion		
No	186 (84%)	88 (79%)
Yes	36 (16%)	23 (21%)
Portal venous invasion at the first portal branch (Vp3)		
No	208 (94%)	108 (93%)
Yes	14 (6%)	8 (7%)
AFP (ng/mL)		
<400	131 (59%)	62 (56%)
≥400	91 (41%)	49 (44%)
PIVKA-II (mAU/mL)		
<400	84 (38%)	44 (40%)
400–10 000	99 (45%)	51 (46%)
≥10 000	39 (18%)	16 (14%)

Data are n (%) or median (IQR). ECOG=Eastern Cooperative Oncology Group. HBsAg=hepatitis B surface antigen. HCV Ab=hepatitis C virus antibodies. TNM=tumour node metastasis. BCLC=Barcelona clinic liver cancer. AFP=alpha fetoprotein. PIVKA-II=protein-induced vitamin K absence or antagonist-II.

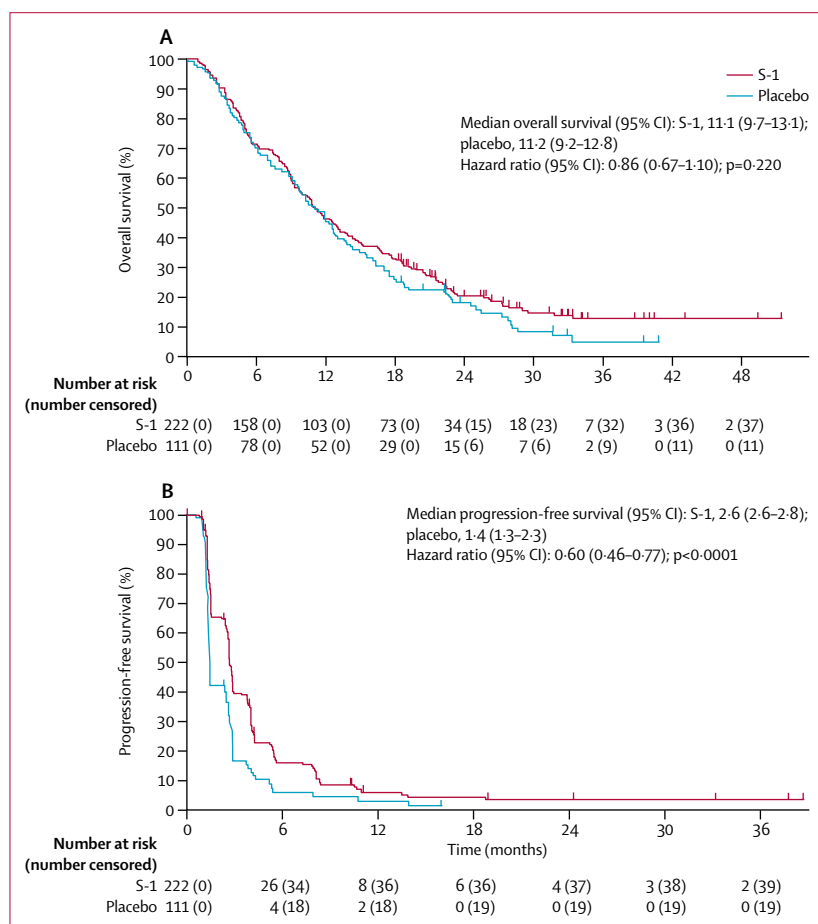
**Table 1: Baseline patient and tumour characteristics**

Cancer Study Group of Japan [LCSGJ]<sup>16</sup>), and 27 (8%) had early disease (stage I–II<sup>16</sup>). 270 (81%) patients had good hepatic function (Child-Pugh A; score 5–6) and 278 (83%) patients were in good general condition (ECOG performance status 0).

Median treatment duration was 3.5 months (IQR 1.4–7.9) in the S-1 group and 2.0 months (1.0–3.8) in the placebo group. The median relative dose intensity in the S-1 group was 85.26% (IQR 69.12–98.81). At data cutoff (Feb 22, 2014), 323 (97%) of 333 patients had discontinued treatment (213 [96%] of 222 patients in the S-1 group and 110 [99%] of 111 patients in the placebo group) due to disease progression (165 [77%] of 213 patients in the S-1 group, 97 [88%] of 110 in the placebo group) or adverse events (41 [19%] in the S-1 group, six [5%] in the placebo group). Post-study treatments, such as systemic chemotherapy, TA(C)E, and hepatic artery infusion chemotherapy, were given to 111 (50%) of 222 patients in the S-1 group and 85 (77%) of 111 patients in the placebo group; six (7%) of 85 patients

in the placebo group were treated with S-1 after the study (appendix p 9).

At data cutoff on Feb 22, 2014, 183 deaths had occurred in the S-1 group, and 100 deaths had occurred in the placebo group. Median follow-up was 32.4 months (IQR 24.0–34.7) in the S-1 group and 32.9 months (23.7–39.5) in the placebo group. Median overall survival was 11.1 months (95% CI 9.7–13.1) in the S-1 group and 11.2 months (9.2–12.8) in the placebo group. There was no significant difference between groups for overall survival (HR 0.86, 95% CI 0.67–1.10;  $p=0.22$ , figure 2A). 12-month overall survival was 46.4% (95% CI 39.8–53.0) in the S-1 group and 46.8% (37.6–56.1) in the placebo group; 24-month overall survival was 20.5% (14.9–26.0) in the S-1 group and 18.2% (10.9–25.6) in the placebo group. There was no significant difference in the proportion of patients with an objective response: 12 (5%, 95% CI 3–9) patients in the S-1 group had an objective response, as did one (1%, 95% CI 0–5) in the placebo group ( $p=0.068$ ; table 2).



**Figure 2: Kaplan-Meier curves**

(A) Overall survival of the full analysis set. (B) Progression-free survival of the full analysis set.

	S-1 group (n=222)	Placebo group (n=111)
Complete response	0	0
Partial response	12 (5%)	1 (<1%)
Stable disease	84 (38%)	26 (23%)
Progressive disease	107 (48%)	74 (67%)
Not assessable	19 (9%)	10 (9%)

Data are n (%).

**Table 2: Best tumour response**

By contrast, median progression-free survival was 2.6 months (95% CI 2.6–2.8) in the S-1 group and 1.4 months (1.3–2.3) in the placebo group. Progression-free survival was significantly improved in the S-1 group compared with placebo group (HR 0.60, 95% CI 0.46–0.77;  $p<0.0001$ , figure 2B). More patients in the S-1 group achieved disease control (ie, a complete or partial response, or stable disease) than did those in the placebo group: 96 (43%, 95% CI 37–50) patients achieved disease control in the S-1 group, as did 27 (24%, 17–33) in the placebo group ( $p=0.001$ ; table 2). Median time to

progression was 2.6 months (95% CI 2.6–2.8) in the S-1 group and 1.4 months (1.3–2.3) in the placebo group (HR 0.59, 95% CI 0.46–0.76;  $p<0.0001$ ). Median time to treatment failure was 3.5 months (95% CI 2.4–3.9) in the S-1 group and 2.0 months (1.0–2.3) in the placebo group (HR 0.63, 95% CI 0.50–0.80;  $p=0.0001$ ). The sensitivity analysis for overall survival also showed no significant difference between groups (stratified log-rank  $p=0.25$ ). Subgroup analysis suggested that efficacy of S-1 on overall survival depends on patient characteristics. Although not significant, risk of death seemed to be lower for Child-Pugh A versus B (score 7), TNM stage III–IV versus stage I–II, and ECOG performance status 0 versus 1 in both treatment groups (appendix p 6).

A post-hoc exploratory predictive enrichment analysis was applied to the data from all 333 patients who received study drug. An enriched group was identified based on selected clinically relevant baseline covariates (TNM stage, ECOG performance status, Child-Pugh score, AFP, and PIVKA-II; individual enrichment scores were not provided). Each individual score reflected an anticipated average treatment difference for future patients who share similar baseline profiles. All patients were ranked based on their enrichment scores, and the population with a better response was identified using 500 random cross-validations. In this case, patients in the top 70% by mean predicted Z score (234 of 333 patients [155 in the S-1 group and 79 in the placebo group]) were selected as the enriched subgroup. In the enriched subgroup, risk of death was significantly lower in the S-1 group than in the placebo group (HR 0.72, 95% CI 0.54–0.97; log-rank  $p=0.027$ , appendix p 7). A high-response population of 219 patients was identified using patient mapping based on the enrichment score. High-response patient characteristics were Child-Pugh A and TNM stage III–IV, and low levels of tumour markers (AFP <400 ng/mL or PIVKA-II <10000 mAU/mL; appendix p 8). In this population, median overall survival was 14.0 months (95% CI 11.7–17.7) in the S-1 group and 12.3 months (10.3–14.2) in the placebo group (HR 0.69, 95% CI 0.51–0.93;  $p=0.016$ , figure 3).

Overall, 221 (>99%) of 222 patients in the S-1 group had at least one adverse event, and 205 (92%) had at least one adverse drug reaction. In the placebo group, 90 (81%) of 111 patients had at least one adverse event and 56 (50%) patients had at least one adverse drug reaction. Adverse events that occurred in 30% or more of 222 patients in the S-1 group were skin hyperpigmentation (123 [55%]), decreased appetite (104 [47%]), fatigue (102 [46%]), diarrhoea (77 [35%]), and increased blood bilirubin (77 [35%]); these events were more common in the S-1 group than in the placebo group (skin hyperpigmentation: nine [8%] of 111 patients in the placebo group; decreased appetite: 21 [19%]; fatigue: 20 [18%]; diarrhoea: 14 [13%]; and increased blood bilirubin 14 [13%]). Grade 3 or higher adverse events that

occurred in 10% or more of patients in the S-1 group were decreased neutrophil count, decreased lymphocyte count, decreased white blood cell count, increased blood bilirubin, and decreased platelet count (table 3).

114 of 333 patients had 186 serious adverse events. Of these, 90 (41%) of 222 patients receiving S-1 had a total of 154 events, and 24 (22%) of 111 patients receiving placebo had a total of 32 events. Of the serious adverse events in the S-1 group, 60 events that occurred in 43 patients were considered adverse drug reactions by the investigator. The most common serious adverse events in the S-1 group were ascites (n=15), hepatic failure (n=8), bone fracture (n=8), oesophageal varices haemorrhage (n=7), and pleural effusion (n=7). Dose reductions and interruptions were higher in the S-1 group than in the placebo group. Adverse events leading to dose interruption during administration within any cycle occurred in 108 (49%) of 222 patients and adverse events leading to rest period extension occurred in 80 (36%) of 222 patients in the S-1 group. Adverse events that led to dose reduction during administration within any cycle occurred in 22 (10%) of 222 patients, and adverse events that led to dose reduction from the subsequent cycle occurred in 53 (24%) of 222 patients in the S-1 group (appendix p 10). Study drug was discontinued due to adverse events in 41 (19%) of the 213 patients who had discontinued the study treatment by the time of data cutoff in the S-1 group. Overall, five treatment-related deaths were reported in the S-1 group; two were early deaths (deaths that occurred within 60 days of starting the treatment); causes of treatment-related early death were decreased white blood cell count, pneumonia, and disseminated intravascular coagulation in one patient; and hepatic failure in a second patient. Other causes of treatment-related death were pneumonitis, ascites or increased blood bilirubin, and acute respiratory distress syndrome. Of the adverse events considered by the investigators to cause death, hepatic failure and ascites or increased blood bilirubin were considered by the sponsor to be caused by aggravation of primary disease or hepatic cirrhosis, and unrelated to S-1.

## Discussion

S-1 was not superior to placebo in prolonging overall survival in patients with sorafenib-refractory advanced hepatocellular carcinoma. However, patients treated with S-1 showed significantly longer progression-free survival than those treated with placebo.

There are a number of potential explanations for there being no difference in overall survival between groups. Median overall survival in the placebo group in this study (11.2 months) was longer than that in other phase 3 trials of targeted second-line treatment after sorafenib (7.8 months for regorafenib,<sup>7</sup> 8.2 months for brivanib,<sup>4</sup> 7.3 months for everolimus,<sup>5</sup> and 7.6 months for ramucirumab<sup>6</sup>). In this study, a third of the patients had poor tolerance to sorafenib, reflecting patient background. Moreover, the proportion of patients in

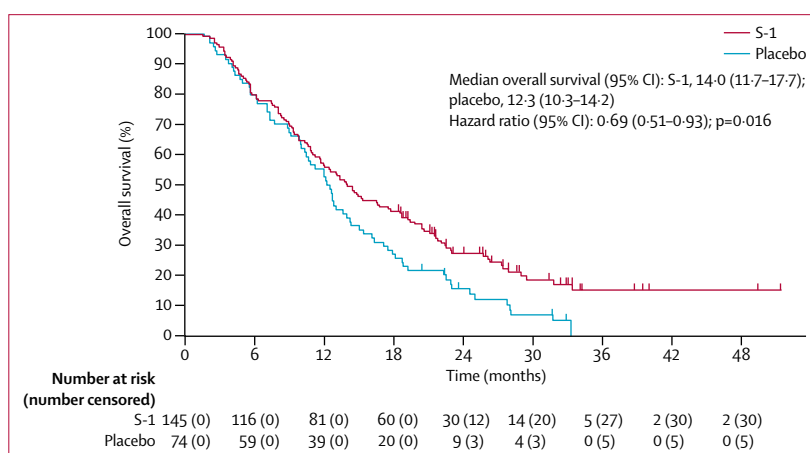


Figure 3: Kaplan-Meier curve for overall survival in the exploratory high-response population

this study who had good performance status (ECOG performance status 0) or early to intermediate tumour stage (BCLC stage A or B) was also higher than those of other studies. As a result, our group of patients might be considered to have had fairly favourable prognoses; their ability to receive local-regional therapy such as TA(C)E as a post-study treatment could have contributed to the outcome. Furthermore, the high quality of supportive care for patients with advanced hepatocellular carcinoma in Japan might also have been a contributor to favourable outcome. Local-regional therapy is often used, especially in Japan, as a post-trial treatment when patients maintain general condition and hepatic function, as control of intrahepatic lesions is an important prognostic factor even in patients with advanced hepatocellular carcinoma who have extrahepatic metastasis.<sup>17</sup> In general, overall survival is the sum of progression-free survival and post-progression survival, thus even significant differences in progression-free survival can be cancelled out if post-progression survival is prolonged.<sup>18</sup> Indeed, overall survival has been shown to have a stronger association with post-progression survival than progression-free survival in a clinical study for advanced hepatocellular carcinoma.<sup>19</sup> Similarly, prolonged post-progression survival might have made it difficult for a difference in progression-free survival to translate into a difference in overall survival in this study.

Half of the patients in the S-1 group received post-study treatment, compared with more than three-quarters of those in the placebo group. This difference might also have affected the outcome of this study. Disease heterogeneity, which makes enrolling a uniform patient population difficult despite stringent inclusion and exclusion criteria, might also be a confounding factor in this study. General health, tumour stage, and liver function are prognostic factors for patients with advanced hepatocellular carcinoma, making the assessment of drug efficacy complex for this type of cancer. Moreover, patients who discontinued sorafenib treatment due to



	S-1 group (n=222)					Placebo group (n=111)				
	Grade 1	Grade 2	Grade 3	Grade 4	Grade 5	Grade 1	Grade 2	Grade 3	Grade 4	Grade 5
<b>Haematological adverse events</b>										
Platelet count decreased	9 (4%)	15 (7%)	23 (10%)	1 (<1%)	0	2 (2%)	1 (<1%)	1 (<1%)	0	0
Haemoglobin decreased	7 (3%)	16 (7%)	17 (8%)	5 (2%)	0	2 (2%)	5 (5%)	0	0	0
White blood cell count decreased	2 (<1%)	16 (7%)	26 (12%)	0	1 (<1%)	0	4 (4%)	1 (<1%)	0	0
Neutrophil count decreased	1 (<1%)	13 (6%)	28 (13%)	2 (<1%)	0	0	2 (2%)	3 (3%)	0	0
Lymphocyte count decreased	0	5 (2%)	25 (11%)	4 (2%)	0	0	3 (3%)	5 (5%)	1 (<1%)	0
<b>Non-haematological adverse events</b>										
Skin hyperpigmentation	105 (47%)	18 (8%)	0	0	0	9 (8%)	0	0	0	0
Decreased appetite	53 (24%)	36 (16%)	15 (7%)	0	0	11 (10%)	8 (7%)	2 (2%)	0	0
Fatigue	53 (24%)	34 (15%)	15 (7%)	0	0	12 (11%)	6 (5%)	2 (2%)	0	0
Blood bilirubin increased	10 (5%)	41 (18%)	23 (10%)	2 (<1%)	1 (<1%)	0	6 (5%)	6 (5%)	2 (2%)	0
Diarrhoea	52 (23%)	17 (8%)	8 (4%)	0	0	10 (9%)	3 (3%)	1 (<1%)	0	0
Peripheral oedema	40 (18%)	25 (11%)	1 (<1%)	0	0	8 (7%)	4 (4%)	1 (<1%)	0	0
Ascites	9 (4%)	42 (19%)	12 (5%)	0	1 (<1%)	1 (<1%)	4 (4%)	7 (6%)	0	0
Nausea	48 (22%)	12 (5%)	1 (<1%)	0	0	10 (9%)	3 (3%)	0	0	0
Stomatitis	29 (13%)	18 (8%)	1 (<1%)	0	0	9 (8%)	0	0	0	0
Exfoliative rash	28 (13%)	16 (7%)	3 (1%)	0	0	8 (7%)	5 (5%)	0	0	0
Vomiting	28 (13%)	11 (5%)	2 (<1%)	0	0	6 (5%)	1 (<1%)	0	0	0
Pruritus	31 (14%)	5 (2%)	1 (<1%)	0	0	4 (4%)	0	0	0	0
Blood albumin decreased	3 (1%)	27 (12%)	6 (3%)	0	0	2 (2%)	8 (7%)	1 (<1%)	0	0
Epistaxis	34 (15%)	1 (<1%)	1 (<1%)	0	0	3 (3%)	0	0	0	0
Upper respiratory tract infection	21 (9%)	14 (6%)	1 (<1%)	0	0	13 (12%)	4 (4%)	0	0	0
Constipation	26 (12%)	7 (3%)	2 (<1%)	0	0	8 (7%)	2 (2%)	0	0	0
Pyrexia	26 (12%)	5 (2%)	0	0	0	9 (8%)	1 (<1%)	0	0	0
Dysgeusia	22 (10%)	8 (4%)	0	0	0	4 (4%)	1 (<1%)	0	0	0
Lacrimation increased	16 (7%)	8 (4%)	2 (<1%)	0	0	1 (<1%)	0	0	0	0
Abdominal pain	16 (7%)	8 (4%)	2 (<1%)	0	0	5 (5%)	7 (6%)	1 (<1%)	0	0
Aspartate aminotransferase increased	2 (<1%)	5 (2%)	19 (9%)	0	0	1 (<1%)	3 (3%)	11 (10%)	0	0
Pleural effusion	6 (3%)	11 (5%)	6 (3%)	0	0	2 (2%)	0	1 (<1%)	0	0

Data are from the safety analysis set. Data are n (%).

**Table 3: Safety summary of events occurring in 10% or more of patients by grade**

adverse drug reactions, and not just those who were refractory to sorafenib, as in the RESORCE trial,<sup>7</sup> were eligible for our study. Furthermore, subgroup analyses suggested that the efficacy of S-1 may vary depending on different patient characteristics, which might be a major factor that contributed to the outcome of this study.

To address potential variation in drug efficacy based on patient characteristics, a predictive enrichment strategy was used to identify a population that might benefit from S-1 (potential high-response population). Such enrichment strategies have recently been put forward by the FDA.<sup>14</sup> In the enriched and high-response populations, S-1 significantly improved overall survival compared with placebo. Results also suggested that Child-Pugh class, TNM stage, and tumour marker levels were important efficacy predictors of S-1 treatment. Showing the efficacy of chemotherapeutic agents is difficult in some patients with advanced hepatocellular

carcinoma, including those with TNM stage I–II, who are mainly surgically treated and have long survival durations;<sup>16,20</sup> those with Child-Pugh B or C, who have liver dysfunction and for whom death from cirrhosis could potentially mask treatment-related antitumour efficacy;<sup>21</sup> and those with highly malignant hepatocellular carcinoma, who typically have extremely high tumour marker (AFP and PIVKA-II) levels.<sup>22</sup>

Results of this study indicate that patients with TNM stage III–IV, Child-Pugh A, and low levels of tumour marker (AFP <400 ng/mL or PIVKA-II <10000 mAU/mL) respond well to treatment with S-1. Given that these indicators are easily identifiable, determining the appropriateness of S-1 therapy for patients with sorafenib-refractory advanced hepatocellular carcinoma is potentially feasible. However, further studies should be done to assess the benefit of S-1 treatment in the potential high-response population before this approach is adopted.

The RESORCE study<sup>7</sup> differs from other second-line setting studies, including this study, that have negative outcomes, in that only RESORCE has excluded patients intolerant of sorafenib.<sup>4-7</sup> This exclusion might have minimised the effect of post-study treatment and reduced the heterogeneity of the enrolled patients. As a result, regorafenib showed significant improvement in terms of overall survival compared with placebo. Together with our exploratory analysis, it seems that focused patient selection is likely to be an important factor for clinical development of treatments for advanced hepatocellular carcinoma.

The safety profile of S-1 differs from targeted therapies such as sorafenib and regorafenib. These targeted therapies are associated with skin toxicity and hypertension,<sup>7,23</sup> whereas treatment with S-1 was associated with bone marrow and gastrointestinal toxicity. The skin toxicity of S-1—such as hyperpigmentation—was mild, and different from hand-foot skin reaction, which is known as a major adverse event related to sorafenib. In this study, most S-1-related adverse events were controlled by dose reduction, interruption, or discontinuation. Fewer patients discontinued treatment because of adverse drug reaction in our study than in studies assessing other treatments.<sup>4</sup> In fact, median treatment duration was longer than median progression-free survival or time to progression in this study, suggesting that toxicity of S-1 was not a major issue. The timing of discontinuation of study treatment depended on investigators, whereas progression-free survival was based on centralised tumour assessment, which can be considered the reason for the median duration of treatment being longer than median progression-free survival in this study.

Since patients with advanced hepatocellular carcinoma have decreased liver function because of the presence of hepatic complications such as hepatitis and liver cirrhosis,<sup>24</sup> and since S-1 is metabolised in the liver,<sup>25</sup> S-1 treatment was predicted to be associated with high rates of adverse events.<sup>26</sup> In this study, although rates of all grade adverse events and grade 3 or greater adverse events (ie, bone marrow and gastrointestinal toxicity, and toxicity related to liver function) were slightly higher, the safety profile of S-1 in this study is similar to that reported in previous studies for other cancers in Asia.<sup>27-30</sup> Continuous administration of S-1 treatment is feasible by appropriate intervention including dose reduction and interruption in patients with sorafenib-refractory advanced hepatocellular carcinoma. However, attention should be paid to patients with advanced liver dysfunction and vascular invasion, since grade 3 or higher bone marrow toxicity and toxicity associated with liver function occur more often in patients with Child-Pugh B and portal venous invasion at the first portal branch (Vp3). One death related to bone marrow suppression and one due to pneumonitis were observed in this study. Although these adverse reactions were known to be associated with S-1, caution should be taken in administration of S-1 to patients with advanced hepatocellular carcinoma.

Given that the RESORCE study excluded patients intolerant to sorafenib, such patients represent an unmet medical need. Although we did not demonstrate superiority of S-1 over placebo in terms of overall survival in patients with advanced hepatocellular carcinoma that was refractory to sorafenib (ie, patients who had progressed while on sorafenib, or who discontinued sorafenib because of adverse events), there was significantly longer progression-free survival with S-1 than with placebo, and we identified a potential high-response population by use of a predictive enrichment approach.

Our study suggests that S-1 might be a treatment option for selected sorafenib-intolerant patients, although further investigation and validation are needed.

#### Contributors

MK, SKan, JF, MasT, and TO conceived and designed the study. MK, MM, KN, HH, HT, MI, SKaw, SO, YS, SKan, and JF collected the data. MK, SKan, JF, MadT, XF, YD, MasT, and TO analysed and interpreted the data. All authors were involved in the drafting, review, and approval of the report and the decision to submit for publication.

#### Declaration of interests

During this work, MK, SKan, JF, and TO report grants, personal fees, and non-financial support from Taiho. MM, KN, HH, HT, MI, SKaw, SO, and YS report grants and non-financial support from Taiho. MasT reports personal fees from Taiho. Outside the submitted work, MK reports grants, personal fees, and non-financial support from Taiho, Bayer, Bristol-Myers Squibb, Chugai, Kowa, Otsuka, and Eisai, grants and non-financial support from Eli Lilly, Pfizer, Novartis, Takeda, Sumitomo Dainippon, and Daiichi Sankyo, personal fees from Ajinomoto and Kaken; MM reports grants and non-financial support from Taiho, Pfizer, Bayer, Kowa, Kyowa Hakko Kirin, and Yakult; KN reports grants, personal fees, and non-financial support from Bayer, grants and non-financial support from Kowa, Eisai, Kyowa Hakko Kirin, and Novartis, personal fees from Daiichi Sankyo; HH reports grants, personal fees, and non-financial support from Taiho, Otsuka, Takeda, Daiichi Sankyo, Eisai, Shionogi, Sumitomo Dainippon, and Gilead Sciences, grants and non-financial support from Ajinomoto and Nihon pharmaceutical, personal fees from Bristol-Myers Squibb, AbbVie, EA Pharma, and Ono; HT reports grants, personal fees, and non-financial support from Bayer, grants and non-financial support from Shionogi, personal fees from Daiichi Sankyo, Century Medical, Philips, AbbVie, GE Healthcare Japan, Gilead Sciences, Bristol-Myers Squibb, AstraZeneca, Daiichi Sankyo, Mitsubishi Tanabe, Nipro, and Sumitomo Dainippon; MI reports grants, personal fees, and non-financial support from Bayer, Novartis, Merck Serono, Kyowa Hakko Kirin, Yakult, Sumitomo Dainippon, Taiho, Eli Lilly, Chugai, and Eisai, grants and non-financial support from Otsuka, OncoTherapy Science, Boehringer Ingelheim, Kowa, Ono, AstraZeneca, Pfizer, GlaxoSmithKline, Zeria, and Baxter, personal fees from Taiwan Digestive Disease Week, Ako City Hospital, Bristol-Myers Squibb, Abbott, Takeda Bio Development Center, Guerbet Japan, Nano Carrier, Nippon Kayaku, and Daiichi Sankyo; SKaw reports grants and non-financial support from Taiho, Bristol-Myers Squibb, Chugai, MSD, Yakult, and Kowa, personal fees from Otsuka; SO reports grants, personal fees, and non-financial support from Taiho, Eli Lilly, and Yakult, grants and non-financial support from AstraZeneca, Chugai, OncoTherapy Science and Sumitomo Dainippon, personal fees from Eisai, Daiichi Sankyo, Pfizer, MSD, and Boehringer Ingelheim; YS reports grants and non-financial support from Taiho, Kyowa Hakko Kirin, Boehringer Ingelheim, Eisai, and Astellas, personal fees from Bayer, Novartis, Daiichi Sankyo, Boston Scientific, OncoTherapy Science and Micron; SKan reports grants, personal fees, and non-financial support from Taiho and Bayer, grants and personal fees from Toray, Zeria, MSD, Sumitomo Dainippon, Mitsubishi Tanabe, Bristol-Myers Squibb, Daiichi Sankyo, Chugai, Eisai, and Taisho Toyama, grants and non-financial support from Roho, Kubix, Yakult, JIMRO, Aska, AbbVie, Abbott, Kyorin, and Janssen, grants from Mochida, Shionogi, Kyowa Hakko Kirin, Eli Lilly, Boehringer Ingelheim, AstraZeneca, Astellas, Novo Nordisk, Novartis, Teijin Pharma,

Takeda, and Ono, personal fees from Ajinomoto, Otsuka, GlaxoSmithKline, Kowa, and MOS; JF reports grants and personal fees and non-financial support from Taiho, Ono, Merck Serono, Zeria, Eli Lilly, Takeda, Chugai, Bayer, Yakult, Sumitomo Dainippon, Daiichi Sankyo, Shionogi, Novartis, J-Pharma, Nippon Kayaku, Bristol-Myers Squibb, Kyowa Hakko Kirin, Mochida, and Astellas, grants and non-financial support from OncoTherapy Science, GlaxoSmithKline, Torii, Janssen, Sanofi, Hisamitsu and Pfizer, personal fees from Eisai, Fujifilm, Merck Serono, Otsuka, Boehringer Ingelheim, AstraZeneca, Mitsubishi Tanabe, MSD, Meiji Seika, Ajinomoto, Sawai, and Sandoz; YD reports personal fees from Hitachi Consulting; MasT reports personal fees from AstraZeneca, Hisamitsu, AbbVie, Kyorin, Sanofi, Takeda, Mitsubishi Tanabe, and Kowa; TO reports grants, personal fees, and non-financial support from Chugai Eli Lilly, Eisai, Novartis, Yakult, Onco Therapy Science, Taiho, Boehringer Ingelheim, Merck Serono, Ono, Bayer, Pfizer, AstraZeneca, Sumitomo Dainippon, Zeria, Nobelpharma, and Nano Carrier, grants and non-financial support from Shizuoka Industry, Takeda Bio Development Center, Otsuka, Scti Medical Labo K.K., Kowa, Kyowa Hakko Kirin, and Baxter, personal fees from Celgene, MSD, Fujifilm RI Pharma, Bristol-Myers Squibb, Nippon Chemiphar, Amgen, and Daiichi Sankyo. MadT, XF, and YD have nothing to disclose.

#### Acknowledgments

We thank all the patients, their families, and the investigators who participated in the study; all the independent data monitoring committee members (Yuh Sakata, Keisuke Aiba, Yasuaki Arai, and Tetsutaro Hamano); medical adviser Shigeki Arai; and Yasuyoshi Watanabe, Taiho Pharmaceutical for his support in compiling this report. We also thank Disha Dayal and Maribeth Bogush of Cactus Communications for medical writing assistance for the manuscript, funded by Taiho Pharmaceutical. The authors retained full control of the manuscript content. This study was sponsored by Taiho Pharmaceutical.

#### References

- 1 Ferlay J, Soerjomataram I, Dikshit R, et al. Cancer incidence and mortality worldwide: sources, methods and major patterns in GLOBOCAN 2012. *Int J Cancer* 2015; **136**: E359–86.
- 2 Cheng AL, Kang YK, Chen Z, et al. Efficacy and safety of sorafenib in patients in the Asia-Pacific region with advanced hepatocellular carcinoma: a phase III randomised, double-blind, placebo-controlled trial. *Lancet Oncol* 2009; **10**: 25–34.
- 3 Llovet JM, Ricci S, Mazzaferro V, et al. Sorafenib in advanced hepatocellular carcinoma. *N Engl J Med* 2008; **359**: 378–90.
- 4 Llovet JM, Decaens T, Raoul JL, et al. Brivanib in patients with advanced hepatocellular carcinoma who were intolerant to sorafenib or for whom sorafenib failed: results from the randomized phase III BRISK-PS study. *J Clin Oncol* 2013; **31**: 3509–16.
- 5 Zhu AX, Kudo M, Assenat E, et al. Effect of everolimus on survival in advanced hepatocellular carcinoma after failure of sorafenib: the EVOLVE-1 randomized clinical trial. *JAMA* 2014; **312**: 57–67.
- 6 Zhu AX, Park JO, Ryoo BY, et al. Ramucirumab versus placebo as second-line treatment in patients with advanced hepatocellular carcinoma following first-line therapy with sorafenib (REACH): a randomised, double-blind, multicentre, phase 3 trial. *Lancet Oncol* 2015; **16**: 859–70.
- 7 Bruix J, Qin S, Merle P, et al. Regorafenib for patients with hepatocellular carcinoma who progressed on sorafenib treatment (RESORCE): a randomised, double-blind, placebo-controlled, phase 3 trial. *Lancet* 2017; **389**: 56–66.
- 8 Shirasaka T, Nakano K, Takechi T, et al. Antitumor activity of 1 M tegafur-0.4 M 5-chloro-2,4-dihydroxypyridine-1 M potassium oxonate (S-1) against human colon carcinoma orthotopically implanted into nude rats. *Cancer Res* 1996; **56**: 2602–06.
- 9 Furuse J, Okusaka T, Kaneko S, et al. Phase I/II study of the pharmacokinetics, safety and efficacy of S-1 in patients with advanced hepatocellular carcinoma. *Cancer Sci* 2010; **101**: 2606–11.
- 10 Nakamura M, Nagano H, Marubashi S, et al. Pilot study of combination chemotherapy of S-1, a novel oral DPD inhibitor, and interferon-alpha for advanced hepatocellular carcinoma with extrahepatic metastasis. *Cancer* 2008; **112**: 1765–71.
- 11 Ueshima K, Kudo M, Nagai T, et al. Combination therapy with S-1 and pegylated interferon alpha for advanced hepatocellular carcinoma. *Oncology* 2008; **75** (suppl 1): 106–13.
- 12 Llovet JM, Hernandez-Gea V. Hepatocellular carcinoma: reasons for phase III failure and novel perspectives on trial design. *Clin Cancer Res* 2014; **20**: 2072–79.
- 13 Collins FS, Varmus H. A new initiative on precision medicine. *N Engl J Med* 2015; **372**: 793–95.
- 14 US Food and Drug Administration. Guidance for industry enrichment strategies for clinical trials to support approval of human drugs and biological products, draft guidance. 2012. <http://www.fda.gov/downloads/drugs/guidancecomplianceregulatoryinformation/guidances/ucm332181.pdf> (accessed Nov 2, 2016).
- 15 Li J, Zhao L, Tian L, et al. A predictive enrichment procedure to identify potential responders to a new therapy for randomized, comparative controlled clinical studies. *Biometrics* 2016; **72**: 877–87.
- 16 Kudo M, Izumi N, Kokudo N, et al. Management of hepatocellular carcinoma in Japan: consensus-based clinical practice guidelines proposed by the Japan Society of Hepatology (JSH) 2010 updated version. *Dig Dis* 2011; **29**: 339–64.
- 17 Uchino K, Tateishi R, Shiina S, et al. Hepatocellular carcinoma with extrahepatic metastasis: clinical features and prognostic factors. *Cancer* 2011; **117**: 4475–83.
- 18 Broglio KR, Berry DA. Detecting an overall survival benefit that is derived from progression-free survival. *J Natl Cancer Inst* 2009; **101**: 1642–49.
- 19 Terashima T, Yamashita T, Takata N, et al. Post-progression survival and progression-free survival in patients with advanced hepatocellular carcinoma treated by sorafenib. *Hepatol Res* 2016; **46**: 650–56.
- 20 Kudo M, Izumi N, Ichida T, et al. Report of the 19th follow-up survey of primary liver cancer in Japan. *Hepatol Res* 2016; **46**: 372–90.
- 21 Llovet JM, Di Bisceglie AM, Bruix J, et al. Design and endpoints of clinical trials in hepatocellular carcinoma. *J Natl Cancer Inst* 2008; **100**: 698–711.
- 22 Kamiyama T, Yokoo H, Kakisaka T, et al. Multiplication of alpha-fetoprotein and protein induced by vitamin K absence-II is a powerful predictor of prognosis and recurrence in hepatocellular carcinoma patients after a hepatectomy. *Hepatol Res* 2015; **45**: E21–31.
- 23 Lencioni R, Kudo M, Ye SL, et al. GIDEON (Global Investigation of therapeutic DEcisions in hepatocellular carcinoma and Of its treatment with sorafenib): second interim analysis. *Int J Clin Pract* 2014; **68**: 609–17.
- 24 Llovet JM, Burroughs A, Bruix J. Hepatocellular carcinoma. *Lancet* 2003; **362**: 1907–17.
- 25 Ikeda K, Yoshisue K, Matsushima E, et al. Bioactivation of tegafur to 5-fluorouracil is catalyzed by cytochrome P-450 2A6 in human liver microsomes in vitro. *Clin Cancer Res* 2000; **6**: 4409–15.
- 26 Ueno H, Okada S, Okusaka T, Ikeda M, Kuriyama H. Phase I and pharmacokinetic study of 5-fluorouracil administered by 5-day continuous infusion in patients with hepatocellular carcinoma. *Cancer Chemother Pharmacol* 2002; **49**: 155–60.
- 27 Koizumi W, Narahara H, Hara T, et al. S-1 plus cisplatin versus S-1 alone for first-line treatment of advanced gastric cancer (SPIRITS trial): a phase III trial. *Lancet Oncol* 2008; **9**: 215–21.
- 28 Nagashima F, Ohtsu A, Yoshida S, Ito K. Japanese nationwide post-marketing survey of S-1 in patients with advanced gastric cancer. *Gastric Cancer* 2005; **8**: 6–11.
- 29 Ueno H, Ioka T, Ikeda M, et al. Randomized phase III study of gemcitabine plus S-1, S-1 alone, or gemcitabine alone in patients with locally advanced and metastatic pancreatic cancer in Japan and Taiwan: GEST study. *J Clin Oncol* 2013; **31**: 1640–48.
- 30 Takashima T, Mukai H, Hara F, et al. Taxanes versus S-1 as the first-line chemotherapy for metastatic breast cancer (SELECT BC): an open-label, non-inferiority, randomised phase 3 trial. *Lancet Oncol* 2016; **17**: 90–98.

SCIENCE IS DEMANDING.  
THAT'S WHY SCIENTISTS WORK SMART.



This information is current as  
of November 19, 2018.

## Chronic Fibro-Inflammatory Responses in Autoimmune Pancreatitis Depend on IFN- $\alpha$ and IL-33 Produced by Plasmacytoid Dendritic Cells

Tomohiro Watanabe, Kouhei Yamashita, Yasuyuki Arai,  
Kosuke Minaga, Ken Kamata, Tomoyuki Nagai, Yoriaki  
Komeda, Mamoru Takenaka, Satoru Hagiwara, Hiroshi Ida,  
Toshiharu Sakurai, Naoshi Nishida, Warren Strober and  
Masatoshi Kudo

*J Immunol* 2017; 198:3886-3896; Prepublished online 3  
April 2017;  
doi: 10.4049/jimmunol.1700060  
<http://www.jimmunol.org/content/198/10/3886>

**Supplementary  
Material** <http://www.jimmunol.org/content/suppl/2017/04/01/jimmunol.1700060.DCSupplemental>

**References** This article **cites 47 articles**, 13 of which you can access for free at:  
<http://www.jimmunol.org/content/198/10/3886.full#ref-list-1>

**Why *The JI*? Submit online.**

- **Rapid Reviews! 30 days\*** from submission to initial decision
- **No Triage!** Every submission reviewed by practicing scientists
- **Fast Publication!** 4 weeks from acceptance to publication

*\*average*

**Subscription** Information about subscribing to *The Journal of Immunology* is online at:  
<http://jimmunol.org/subscription>

**Permissions** Submit copyright permission requests at:  
<http://www.aai.org/About/Publications/JI/copyright.html>

**Email Alerts** Receive free email-alerts when new articles cite this article. Sign up at:  
<http://jimmunol.org/alerts>

*The Journal of Immunology* is published twice each month by  
The American Association of Immunologists, Inc.,  
1451 Rockville Pike, Suite 650, Rockville, MD 20852  
Copyright © 2017 by The American Association of  
Immunologists, Inc. All rights reserved.  
Print ISSN: 0022-1767 Online ISSN: 1550-6606.





# Chronic Fibro-Inflammatory Responses in Autoimmune Pancreatitis Depend on IFN- $\alpha$ and IL-33 Produced by Plasmacytoid Dendritic Cells

Tomohiro Watanabe,\*<sup>†</sup> Kouhei Yamashita,<sup>‡</sup> Yasuyuki Arai,<sup>‡</sup> Kosuke Minaga,\*  
Ken Kamata,\* Tomoyuki Nagai,\* Yoriaki Komeda,\* Mamoru Takenaka,\*  
Satoru Hagiwara,\* Hiroshi Ida,\* Toshiharu Sakurai,\* Naoshi Nishida,\* Warren Strober,<sup>†</sup>  
and Masatoshi Kudo\*

In previous studies, we found that human IgG4-related autoimmune pancreatitis (AIP) and murine AIP are driven by activation of plasmacytoid dendritic cells (pDCs) producing IFN- $\alpha$ . In the present studies we examined additional roles of pDC-related mechanisms in AIP pathogenesis, particularly those responsible for induction of fibrosis. We found that in murine AIP (MRL/Mp mice treated with polyinosinic-polycytidylic acid) not only the pancreatic infiltration of immune cells but also the development of fibrosis were markedly reduced by the depletion of pDCs or blockade of type I IFN signaling; moreover, such treatment was accompanied by a marked reduction of pancreatic expression of IL-33. Conversely, polyinosinic-polycytidylic acid-induced inflamed pancreatic tissue in murine AIP exhibited increased expression of type I IFNs and IL-33 (and downstream IL-33 cytokines such as IL-13 and TGF- $\beta$ 1). pDCs stimulated by type I IFN were the source of the IL-33 because purified populations of these cells isolated from the inflamed pancreas produced a large amount of IL-33 upon activation by TLR9 ligands, and such production was abrogated by the neutralization of type I IFN. The role of IL-33 in murine AIP pathogenesis was surprisingly important because blockade of IL-33 signaling by anti-ST2 Ab attenuated both pancreatic inflammation and accompanying fibrosis. Finally, whereas patients with both conventional pancreatitis and IgG4-related AIP exhibited increased numbers of acinar cells expressing IL-33, only the latter also exhibited pDCs producing this cytokine. These data thus suggest that pDCs producing IFN- $\alpha$  and IL-33 play a pivotal role in the chronic fibro-inflammatory responses underlying murine AIP and human IgG4-related AIP. *The Journal of Immunology*, 2017, 198: 3886–3896.

**C**linicopathological analysis of autoimmune pancreatitis (AIP) as well as other inflammations often accompanying AIP such as sialadenitis or autoimmune cholangitis has established that these diseases are organ-specific manifestations of a systemic autoimmune fibroinflammatory disorder that can affect

many organs, sometimes simultaneously. These inflammations are now called IgG4-related diseases (IgG4-RD) because the inflammation is in each case marked by the presence of elevated serum levels of IgG4 as well as a massive infiltration of affected organs with IgG4-expressing plasmacytes (1–4). Additionally, these inflammations are characterized by the presence of storiform fibrosis and, in some cases, obliterative phlebitis (1–4).

Despite the fact that elevated levels of serum IgG4 and infiltration of IgG4-expressing plasmacytes in affected organs are diagnostic of IgG4-RD, the pathophysiological role of this IgG4 subtype is poorly understood. One possibility is that the presence of IgG4 in IgG4-RD inflammations is an epiphenomenon of the unique fibro-inflammatory response characterizing this disease rather than its cause because this IgG4 subtype has only a limited ability to bind to complement and Fc $\gamma$  receptors (5). This idea is favored by studies showing that IgG1, but not IgG4, purified from serum of patients with IgG4-RD causes pancreatic injury upon injection into neonatal mice (6). Contrary evidence, however, comes from studies showing that autoantigen-specific IgG4 Abs have been identified as a cause of small vessel vasculitis and membranous nephropathy (7, 8); it thus remains possible that IgG4 is playing a pathologic role in at least some of the manifestations of IgG4-RD.

One major line of investigation of IgG4-RD pathogenesis has been studies of T cell cytokine responses focusing quite logically on Th2 cytokines that might enhance B cell production of IgG4, such as IL-4, IL-10, and IL-13 (9–12). These studies disclosed an increased accumulation of Th2 cells or regulatory T cells producing IL-4, IL-10, and IL-13 in the peripheral blood and

\*Department of Gastroenterology and Hepatology, Kindai University Faculty of Medicine, Osaka-Sayama, Osaka 589-8511, Japan; <sup>†</sup>Mucosal Immunity Section, Laboratory of Host Defenses, National Institute of Allergy and Infectious Diseases, National Institutes of Health, Bethesda, MD 20892; and <sup>‡</sup>Department of Hematology and Oncology, Kyoto University Graduate School of Medicine, Kyoto 606-8507, Japan

Received for publication January 11, 2017. Accepted for publication March 8, 2017.

This work was supported by a Grant-in-Aid for Scientific Research (15K15370) from the Japan Society for the Promotion of Science, the Kato Memorial Trust for Nambyo Research, the Naito Foundation, the Yakult Bioscience Foundation, the SENSHIN Medical Research Foundation, Special Coordination Funds from the Ministry of Education, Culture, Sports, Science and Technology of Japan and Astellas Pharma Inc. in the Creation of Innovation Centers for Advanced Interdisciplinary Research Areas Program, and by Health and Labor Sciences Research Grants for Research on Intractable Diseases from the Ministry of Health, Labor and Welfare, Japan.

Address correspondence and reprint requests to Dr. Tomohiro Watanabe, Department of Gastroenterology and Hepatology, Kindai University Faculty of Medicine, 377-2 Ohno-Higashi, Osaka-Sayama, Osaka 589-8511, Japan. E-mail addresses: tomohiro@med.kindai.ac.jp and tmhrwtb@kuhp.kyoto-u.ac.jp

The online version of this article contains supplemental material.

Abbreviations used in this article: AIP, autoimmune pancreatitis; BDCA, blood DC Ag; CCKR, cholecystokinin receptor; DC, dendritic cell; HPF, high-power field; IFNAR, type I IFN receptor; IgG4-RD, IgG4-related disease; NET, neutrophil extracellular trap; NOD, nucleotide-binding oligomerization; pDC, plasmacytoid dendritic cell; PDCA, pDC Ag; PMNC, pancreatic mononuclear cell; poly(I:C), polyinosinic-polycytidylic acid; PSC, pancreatic satellite cell; SMA, smooth muscle actin.

Copyright © 2017 by The American Association of Immunologists, Inc. 0022-1767/17/\$30.00

www.jimmunol.org/cgi/doi/10.4049/jimmunol.1700060



affected organs of patients with IgG4-RD (13, 14). Perhaps more importantly, they showed that there was a positive correlation between circulating numbers of T follicular helper 2 cells and serum levels of IgG4 in these patients (15). These findings thus suggested that various T cells generated during an abnormal adaptive immune response contribute to the pathogenesis of IgG4-RD; however, it remained possible that the development of these T cells is secondary to a more fundamental innate immune defect.

Initial evidence for the latter came from studies in which we showed that B cells can be induced to produce IgG4 by APCs activated by TLRs or nucleotide-binding oligomerization domain (NOD)-like receptor ligands (16, 17). Additionally, we showed that monocytes, basophils, and plasmacytoid dendritic cells (pDCs) isolated from patients with IgG4-RD enhance IgG4 production by B cells from healthy controls in a T cell-independent manner (16–18). These studies therefore showed that innate cell abnormalities could account for increased IgG4 production in IgG4-RD.

Further and more convincing evidence that innate cells participate in the pathogenesis of IgG4-RD came from studies of a murine model of AIP, that is, MRL/Mp mice treated with repeated injections of polyinosinic-polycytidylic acid [poly(I:C)] (19, 20). Such mice exhibit similar pathological findings to human IgG4-related AIP such as massive infiltration of immune cells, destruction of pancreas acinar architecture, and fibrosis. Utilizing this murine model of AIP, we found that the development of AIP is accompanied by pancreatic accumulation of pDCs producing IFN- $\alpha$  and that the development of AIP is markedly attenuated by the depletion of pDCs or the blockade of IFN- $\alpha$  signaling (18). In accordance with these murine studies, we also showed that pDCs isolated from patients with IgG4-RD enhance IgG4 production by B cells from healthy controls in an IFN- $\alpha$ -dependent manner. Thus, these studies provide strong evidence that both murine AIP and human IgG4-related AIP are characterized by activation of pDCs producing IFN- $\alpha$ .

Although pancreatic fibrosis, especially storiform fibrosis, is one of the typical pathological findings of human IgG4-related AIP (1–4), the molecular mechanisms leading to the development of such fibrosis have not been fully understood. One possibility is that it involves the secretion of IL-33, a cytokine produced by nonhematopoietic cells that has been shown to induce hepatic and intestinal fibrosis through its ability to promote the production of profibrogenic mediators such as IL-13 and TGF- $\beta$ 1 (21–23). In line with these findings, we recently reported that IL-33 secretion by pancreatic acinar cells under the influence of type I IFN plays an important role in the development of pancreatic fibrosis occurring in a model of conventional pancreatitis (24, 25). These findings led us in the present studies to explore the possibility that IL-33 production plays a key role in the pathogenesis of IgG4-related AIP, particularly that relating to fibrosis. In this study, we provide the evidence that chronic fibro-inflammatory responses in human IgG4-related AIP and murine AIP are mediated by pDCs producing both IFN- $\alpha$  and IL-33.

## Materials and Methods

### Induction of AIP in MRL/Mp mice

Female MRL/Mp mice were purchased from Japan SLC (Shizuoka, Japan) and reared at the Kyoto University animal facility under specific pathogen-free conditions. The ethical permission of this study was obtained by the Review Boards of Kyoto University Graduate School of Medicine and Kindai University Faculty of Medicine. Female MRL/Mp mice at 6 wk old were treated with an i.p. injection of poly(I:C) (100  $\mu$ g; InvivoGen, San

Diego, CA) twice a week for a total of 14 or 16 times to induce experimental AIP as previously described (18). To deplete pDCs and to neutralize type I IFN-mediated signaling pathways, mice were treated with Ab against bone marrow stromal cell Ag 2 (100  $\mu$ g; 120G8; Dendritics, Lyon, France) and Ab against type I IFN receptor (IFNAR; 100  $\mu$ g; BD Biosciences, San Jose, CA) prior to each poly(I:C) injection (18). Additionally, mice were treated with Ab against IL-33 receptor, ST2 (100  $\mu$ g; R&D Systems, Minneapolis, MN), to neutralize IL-33-mediated signaling pathways prior to each poly(I:C) injection (24). Mice treated with rat IgG (100  $\mu$ g; Sigma-Aldrich, St. Louis, MO) or mouse IgG (100  $\mu$ g; Sigma-Aldrich) were used as control mice. Pancreatic levels of hydroxyproline were determined by the hydroxyproline assay kit (QuickZyme Biosciences, Leiden, the Netherlands) (24).

### Histology, immunohistochemical, and immunofluorescence analysis

Pancreatic samples obtained from MRL/Mp mice treated with poly(I:C) were subjected to fixation with 10% formalin followed by H&E staining. Pathological assessment was performed by using a scoring system for AIP as previously described (18–20). Pancreas inflammation was scored as follows: 0, pancreas without mononuclear cell infiltration; 1, mononuclear cell aggregation and/or infiltration within the interstitium with no parenchymal destruction; 2, focal parenchymal destruction with mononuclear cell infiltration; 3, diffuse parenchymal destruction but some intact parenchymal areas retained; 4, almost all pancreatic tissue, except the pancreatic islets, destroyed or replaced with fibrosis or adipose tissue (18–20). Immunofluorescence staining was performed using anti-pDC Ag (PDCA)-1 Ab (eBioscience, San Diego, CA) and anti-IL-33 Ab (Abcam, Cambridge, MA) followed by incubation with Alexa Fluor 488- or 546-conjugated anti-rat or anti-mouse IgG (Life Technologies, Carlsbad, CA). For visualization of pancreatic fibrosis, anti-IL-33 Ab (Abcam), anti-fibronectin Ab (Abcam), and anti-smooth muscle actin (SMA) Ab (Abcam) were used as primary Abs as previously described (24). Sirius red staining was performed using a picrosirius red stain kit (Polysciences, Warrington, PA). At least two immunofluorescence and immunohistochemical images were taken by microscopy (Biozero, BZ-8100; Keyence, Osaka, Japan) from each slide. Positive areas were calculated by using hybrid cell count software (Keyence) according to the manufacturer's protocol.

### ELISA

Protein concentrations of cytokines were determined by ELISA. Concentrations of IFN- $\alpha$  and IFN- $\beta$  were determined by ELISA kits from R&D Systems. Concentrations of IL-13 and IL-33 were determined by ELISA kits from eBioscience. Concentration of TGF- $\beta$ 1 was determined by an ELISA kit from Promega (Madison, WI).

### Isolation of pancreatic mononuclear cells and flow cytometric analysis

Pancreatic mononuclear cells (PMNCs) were isolated from the pancreas of MRL/Mp mice treated with poly(I:C) as previously described (18). PMNCs were stained with FITC, PE, or allophycocyanin-conjugated B220 Ab (eBioscience), PDCA-1 Ab (eBioscience), Gr-1 Ab (eBioscience), CD3 Ab (eBioscience), and CD11b Ab (BD Biosciences) and then subjected to flow cytometric analysis by using an Accuri C6 flow cytometer (BD Biosciences) and CFlow Plus software (BD Biosciences). In some experiments, pDCs were isolated from PMNCs using a mouse pDC isolation kit (Miltenyi Biotec, Auburn, CA). The purity of this method was >90% when pDCs were defined as B220<sup>low</sup>PDCA-1<sup>+</sup> cells (18). Whole PMNCs, pancreatic pDCs, and pDC-depleted cell fractions ( $1 \times 10^6$ /ml) were stimulated with poly(I:C) (25  $\mu$ g/ml) and/or CpG (1  $\mu$ M; InvivoGen) for 48 h for measurement of the production of IFN- $\alpha$ , IFN- $\beta$ , and IL-33.

### Immunofluorescence staining of human pancreas tissue

Paraffin-embedded pancreatic tissue samples resected from patients with IgG4-related AIP ( $n = 5$ ), patients with chronic alcoholic pancreatitis ( $n = 5$ ), and patients with pancreatic cancer ( $n = 5$ ) were prepared as previously described (18). Noncancerous portions of pancreas tissue from patients with pancreatic cancer were used as controls. Ethical permission for this study was obtained by the Review Boards of Kyoto University Graduate School of Medicine and Kindai University Faculty of Medicine. Immunofluorescence staining was performed by using anti-IL-33 Ab (Abcam), anti-amylase Ab (Abcam), and anti-blood DC Ag (BDCA)2 Ab (Miltenyi Biotec) followed by incubation with Alexa Fluor 488- or 546-conjugated anti-rabbit or anti-mouse IgG (Life Technologies).

### Statistical analysis

A Student *t* test was used to evaluate the significance of the differences. Statistical analysis was performed with Prism (GraphPad Software, La Jolla, CA). A *p* value <0.05 was regarded as statistically significant.

## Results

### *MRL/Mp mice subjected to repeated administration of poly(I:C) develop AIP accompanied by fibrosis*

To elucidate the molecular mechanisms accounting for the development of pancreatic inflammation and accompanying fibrosis in AIP, we used a well-established animal model of human IgG4-related AIP consisting of MRL/Mp mice treated with i.p. injections of poly(I:C) (see *Materials and Methods*). As shown in previous studies and mentioned in the *Introduction*, such mice develop a pancreatitis similar to that in human IgG4-related AIP (18, 26).

In initial studies we focused on the development of pancreatic fibrosis in MRL/Mp mice with AIP on the assumption that elucidation of this feature of AIP would disclose new innate mechanisms relating to AIP pathogenesis. Accordingly, we treated mice with i.p. injection of poly(I:C) and after the 16th injection harvested pancreatic tissue to measure collagen deposition and activation of pancreatic satellite cells (PSCs) by sirius red and  $\alpha$ -SMA staining, respectively (24, 27). Upon pathological inspection as well as semiquantitative assessment of the extent of stained areas, the pancreatic tissues of poly(I:C)-treated MRL/Mp mice were quite positive for sirius red or  $\alpha$ -SMA staining, whereas tissues of untreated MRL/Mp mice were more or less negative (Fig. 1A, 1B). Additionally, repeated injection of poly(I:C) led to a marked increase in pancreatic tissue expression of collagen as assessed by the measurement of hydroxyproline as well as areas positive for fibronectin, a prototypical extracellular matrix protein associated with fibrosis (24) (Fig. 1A, 1B). These immunohistochemical and biochemical analyses show that the pancreatitis in MRL/Mp mice treated with repeated injections of poly(I:C) is accompanied by severe fibrosis.

### *Pancreatic fibrosis in MRL/Mp mice depends on the activation of pDCs*

In further studies we sought evidence that fibrosis in AIP of poly(I:C)-treated MRL/Mp mice noted above is an integral part of the inflammatory program associated with AIP in this model and is therefore likely to be caused by the activation of pDCs and their production of type I IFNs shown previously to drive this experimental AIP (18). In this study, we took advantage of the fact that in previous studies we showed that administration of a pDC-depleting Ab (120G8 Ab) or neutralization of type I IFN signaling pathways by an IFNAR Ab to poly(I:C)-treated MRL/Mp mice efficiently prevented the development of the AIP-associated inflammatory changes in the pancreas of these mice (18). Thus, these previous findings allowed us to determine in the current study whether prevention of AIP-related inflammatory changes caused by accumulation of pDCs also affects the development of pancreatic fibrosis.

In initial studies along these lines we administered 120G8 Ab to poly(I:C)-treated MRL/Mp mice to prevent pDC accumulation into the pancreas. The specificity of this Ab for pDCs has been established in previous studies (28) as well as in current studies evaluating the effect of such administration on various cell types. As shown in Supplemental Fig. 1, flow cytometric studies of pancreatic cells from poly(I:C)-treated mice confirmed that administration of 120G8 Ab results in a greatly decreased percentage of B220<sup>low</sup>PDCA-1<sup>+</sup> cells (pDCs), but no significant change in the percentage of CD3<sup>+</sup> T cells, B220<sup>+</sup> B cells, Gr-1<sup>+</sup> gran-

ulocytes, or CD11b<sup>+</sup> myeloid cells as compared with administration of control Ab. The distant possibility that such treatment can also target conventional CD11c<sup>hi</sup> DCs producing type I IFN does not detract from the fact that its main target is pDCs producing this cytokine. We found that administration of 120G8 Ab prevented the development of AIP-associated pancreatic inflammation as well as the development of pancreatic fibrosis in poly(I:C)-treated MRL/Mp mice, with the latter assessed by tissue staining with sirius red,  $\alpha$ -SMA, and fibronectin (Fig. 2A). In parallel studies we found that the administration of an IFNAR-blocking Ab also prevented the development of pancreatic fibrosis (Fig. 2B). Taken together, these data strongly suggest that the development of pancreatic fibrosis in this experimental model of AIP and accompanying fibrosis is part of the inflammatory program underlying pancreatitis in this model and, as such, depends on type I IFN signaling pathways initiated by pDC activation.

### *Pancreatitis in MRL/Mp mice with AIP is associated with increased levels of type I IFNs and IL-33*

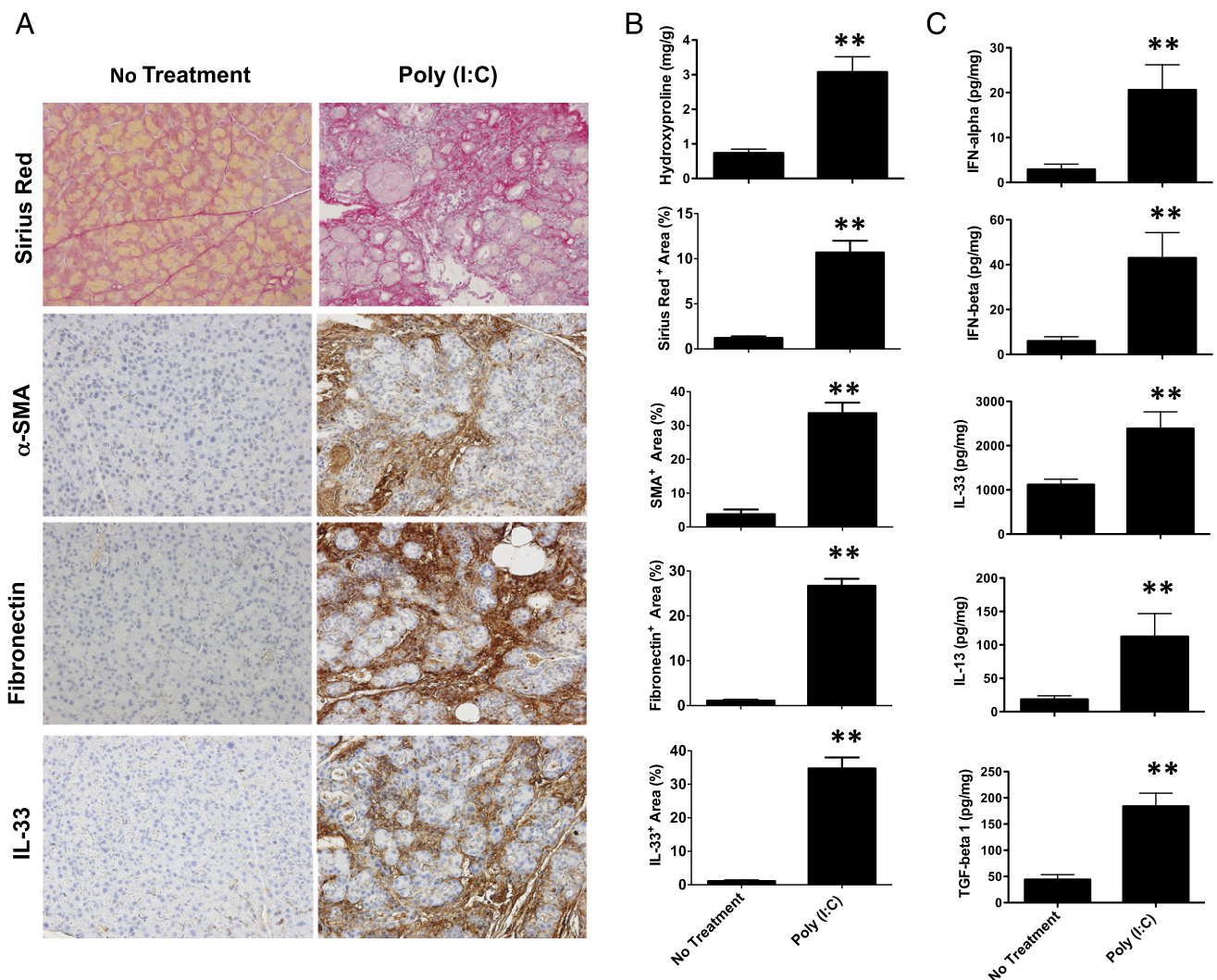
In previous studies we established a model of pancreatitis reflecting patients with non-autoimmune chronic pancreatitis (i.e., conventional pancreatitis) in which mice are subjected to repeated administration of cerulein (cholecystokinin receptor [CCKR] agonist) and NOD1 ligand, FK156, or FK565 (24, 25, 29). Using this model we showed that type I IFN signaling pathways mediate both pancreatic inflammation and fibrosis through induction of IL-33, IL-13, and TGF- $\beta$ 1. We therefore hypothesized that type I IFNs derived from pDCs in MRL/Mp mice with AIP also cause inflammation and fibrosis in this model via a related cytokine mechanism.

To investigate this possibility we first determined whether AIP (and fibrosis) in MRL/Mp mice is accompanied by increased levels of type I IFNs as predicted in the pDC depletion studies or IFNAR blockade studies noted above and in a previous study (18), and this, in turn, is accompanied by increased expression of IL-33, IL-13, and TGF- $\beta$ 1. Indeed, pancreatic expression of both IFN- $\alpha$  and IFN- $\beta$  as assessed by ELISA was markedly increased upon repeated injection of poly(I:C), and this increase was parallel to an increase in the expression of IL-33, IL-13, and TGF- $\beta$ 1 (Fig. 1A, 1C). Moreover, depletion of pDCs as well as blockade of IFNAR in MRL/Mp mice were accompanied by a marked reduction in IL-33 expression that occurred along with a reduction in pancreatic fibrosis (Fig. 2). These data therefore show that pancreatic inflammation and fibrosis in MRL/Mp mice with AIP are in fact accompanied by enhanced expression of cytokines previously associated with pancreatic inflammation in a model of conventional chronic pancreatitis.

### *Type I IFN-stimulated pDCs in MRL/Mp mice with AIP produce IL-33*

In our previous report noted above, in which conventional pancreatitis induced by repeated administration of CCKR agonist and NOD1 ligand was studied, we showed that IL-33 in this model is produced by pancreatic acinar cells (24, 25). To determine whether acinar cells expressing amylase were also the source of IL-33 in MRL/Mp mice with AIP, we stained the inflamed pancreatic tissue with Abs to detect IL-33 in cells expressing either amylase or  $\alpha$ -SMA (the latter PSCs) and found no dual staining cells (data not shown). We thus concluded that neither acinar cells nor PSCs were cellular sources of IL-33 in MRL/Mp mice with AIP.

Based on these data, we hypothesized that a pancreatic hematopoietic cell was the source of IL-33 production. To investigate



**FIGURE 1.** Repeated injection of poly(I:C) induces pancreatic fibrosis in MRL/Mp mice. MRL/Mp mice ( $n = 5$ ) were treated with poly(I:C) (100  $\mu$ g) twice a week for a total of 16 times. Mice were sacrificed 3 h after the last injection and pancreatic samples were prepared. Nontreated mice ( $n = 7$ ) were used as controls. **(A and B)** Pancreas tissues were stained with sirius red, anti- $\alpha$ -SMA Ab, anti-fibronectin Ab, and anti-IL-33 Ab. Representative images of sirius red,  $\alpha$ -SMA, fibronectin, and IL-33 staining are shown. Original magnification  $\times 400$ . **(A)** The areas positive for sirius red,  $\alpha$ -SMA, fibronectin, and IL-33 staining and pancreatic levels of hydroxyproline are shown **(B)**. **(C)** Concentrations of IFN- $\alpha$ , IFN- $\beta$ , IL-33, IL-13, and TGF- $\beta$ 1 in the pancreas lysates were determined by ELISA. Results are shown as mean  $\pm$  SE. \*\* $p < 0.01$ , as compared with nontreated mice.

this idea, PMNCs were isolated from poly(I:C)-treated or untreated MRL/Mp mice and then stimulated with poly(I:C) and/or CpG in vitro. PMNCs from MRL/Mp mice treated with poly(I:C) in vivo produced greatly increased amounts of type I IFNs upon in vitro stimulation with poly(I:C) and/or CpG as compared with mice without in vivo treatment (Fig. 3A). In contrast, whereas these PMNCs produced increased amounts of IL-33 upon stimulation with CpG, they did not produce increased amounts of IL-33 upon stimulation with poly(I:C) (Fig. 3A); this is presumably because pDCs do not express the receptor for poly(I:C), TLR3 (30, 31). In related studies we found that IL-33 production by PMNCs from treated mice was greatly diminished by the addition of anti-IFNAR Ab to the culture (Fig. 3B).

In further studies addressing the source of the IL-33, we obtained pDC-enriched and pDC-depleted cell populations from the PMNCs by MACS sorting (enriched cells containing  $>90\%$  pure pDCs by flow cytometry, data not shown) and then stimulated these cell populations with poly(I:C) and/or CpG. As expected from the studies described above, the purified pDC populations exhibited both robust IFN- $\alpha$  and IL-33 production upon stimulation with

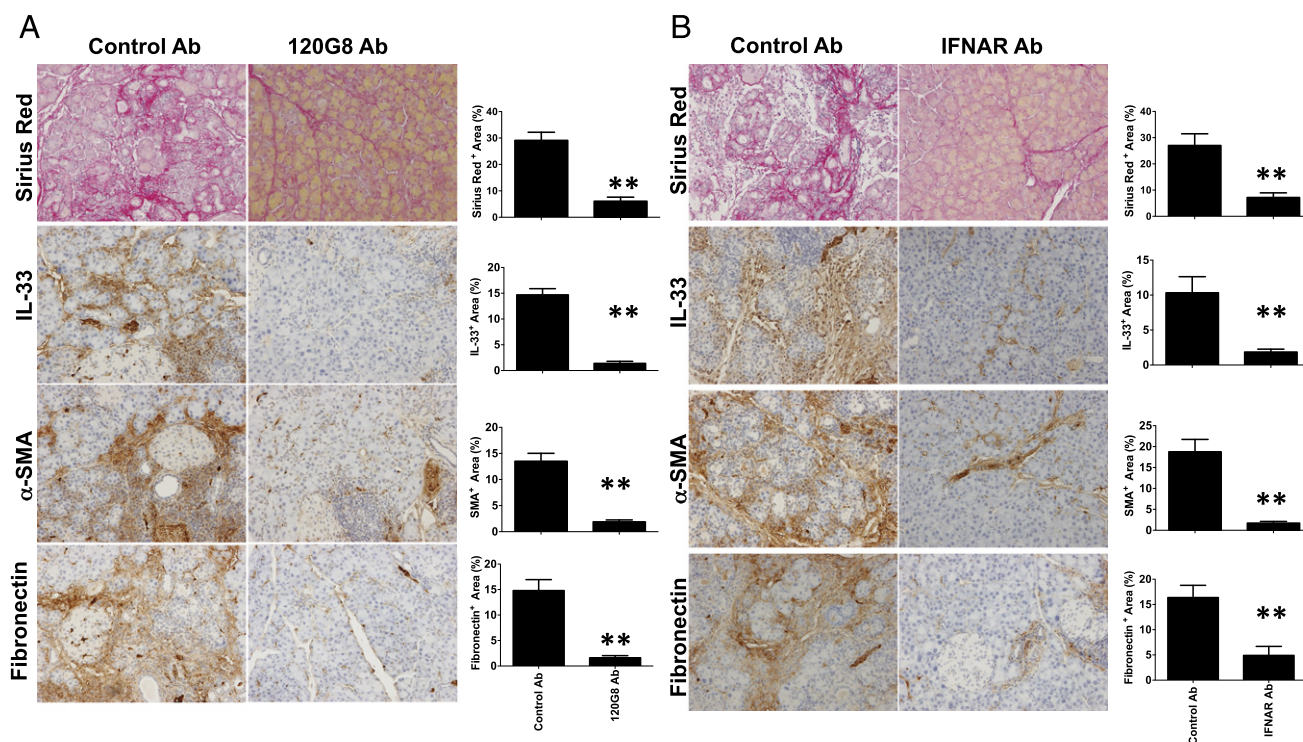
CpG but not poly(I:C), whereas the PMNCs depleted of pDCs exhibited markedly diminished IFN- $\alpha$  and IL-33 production upon stimulation with both stimulants (Fig. 3C).

In a final series of studies on the cellular origin of IL-33 in AIP, we performed dual immunofluorescence analysis of inflamed pancreatic tissue and found that most pancreatic pDCs expressing PDCA-1, a specific pDC marker, were positive for IL-33 staining (Fig. 3D). Taken together, these data provided evidence that pDC cell populations in the inflamed pancreas of poly(I:C)-treated MRL/Mp mice are not only the source of the IL-33, but also that such IL-33 production is dependent on type I IFN production by the pDCs.

#### *Pancreatic inflammation and fibrosis in murine AIP depends on secretion of IL-33*

Having shown that IL-33 secretion and other profibrotic cytokines occur in MRL/Mp mice with AIP in a type I IFN-dependent manner, we next wanted to determine the role of IL-33 in the development of both inflammation and fibrosis in the AIP. To this end, MRL/Mp mice were administered Ab against the receptor for IL-33, ST2, to neutralize IL-33 function by blockade of its





**FIGURE 2.** The development of pancreatic fibrosis depends on signaling pathways mediated by pDC-derived type I IFN. **(A)** MRL/Mp mice ( $n = 5$ ) were treated with the pDC-depleting Ab (120G8 Ab, 100  $\mu$ g,  $n = 5$ ) or control Ab (100  $\mu$ g,  $n = 5$ ) prior to each poly(I:C) (100  $\mu$ g) injection. Mice in each group received poly(I:C) injection twice a week for a total of 14 times. Pancreas tissues were stained with sirius red, anti-IL-33 Ab, anti- $\alpha$ -SMA Ab, and anti-fibronectin Ab. Representative images of sirius red,  $\alpha$ -SMA, fibronectin, and IL-33 staining are shown. Original magnification (left)  $\times 400$ . The areas positive for sirius red,  $\alpha$ -SMA, fibronectin, and IL-33 staining are shown (right). **(B)** MRL/Mp mice ( $n = 5$ ) were treated with the Ab against IFNAR (100  $\mu$ g,  $n = 5$ ) or control Ab (100  $\mu$ g,  $n = 4$ ) prior to each poly(I:C) (100  $\mu$ g) injection. Mice in each group received poly(I:C) injection twice a week for a total of 14 times. Pancreas tissues were stained with sirius red, anti-IL-33 Ab, anti- $\alpha$ -SMA Ab, and anti-fibronectin Ab. Representative images of sirius red,  $\alpha$ -SMA, fibronectin, and IL-33 staining are shown. Original magnification (left)  $\times 400$ . The areas positive for sirius red,  $\alpha$ -SMA, fibronectin, and IL-33 staining are shown (right). Results are shown as mean  $\pm$  SE. \*\* $p < 0.01$ , as compared with control Ab-treated mice.

signaling pathway, as previously described (24). We found that administration of anti-ST2 Ab (as compared with control Ab) significantly reduced the level of inflammation in MRL/Mp mice with AIP as assessed by H&E staining and pathology scores (Fig. 4A). Additionally, administration of anti-ST2 Ab (as compared with control Ab) markedly reduced the level of pancreatic fibrosis in MRL/Mp mice with AIP as assessed by quantitative hydroxyproline assay and tissue staining with  $\alpha$ -SMA or fibronectin (Fig. 4B–D). This reduction in pancreatic fibrosis by administration of anti-ST2 Ab was accompanied by, and was thus at least partially due to, reduction in the secretion of IL-13 and TGF- $\beta$ 1, that is, factors previously shown to be induced by IL-33, either directly or indirectly (24). Finally, as shown in Fig. 4E, the cause of the reduced inflammation in MRL/Mp mice with AIP due to the blockade of IL-33-mediated signaling pathways was revealed in studies that showed that such blockade led to decreased pancreatic accumulation of pDCs defined as PDCA-1<sup>+</sup> B220<sup>low</sup> cells (18). Such a reduction in pDC accumulation induced by the blockade of IL-33-mediated signaling pathways might be explained by an effect on the attenuation of pancreatic inflammation rather than a specific effect on the function of pDCs because administration of ST2 Ab in the model of chronic pancreatitis results in greatly reduced amounts of proinflammatory cytokine production, including reduction in IL-6, TNF- $\alpha$ , and MCP-1 as shown in previous studies (24).

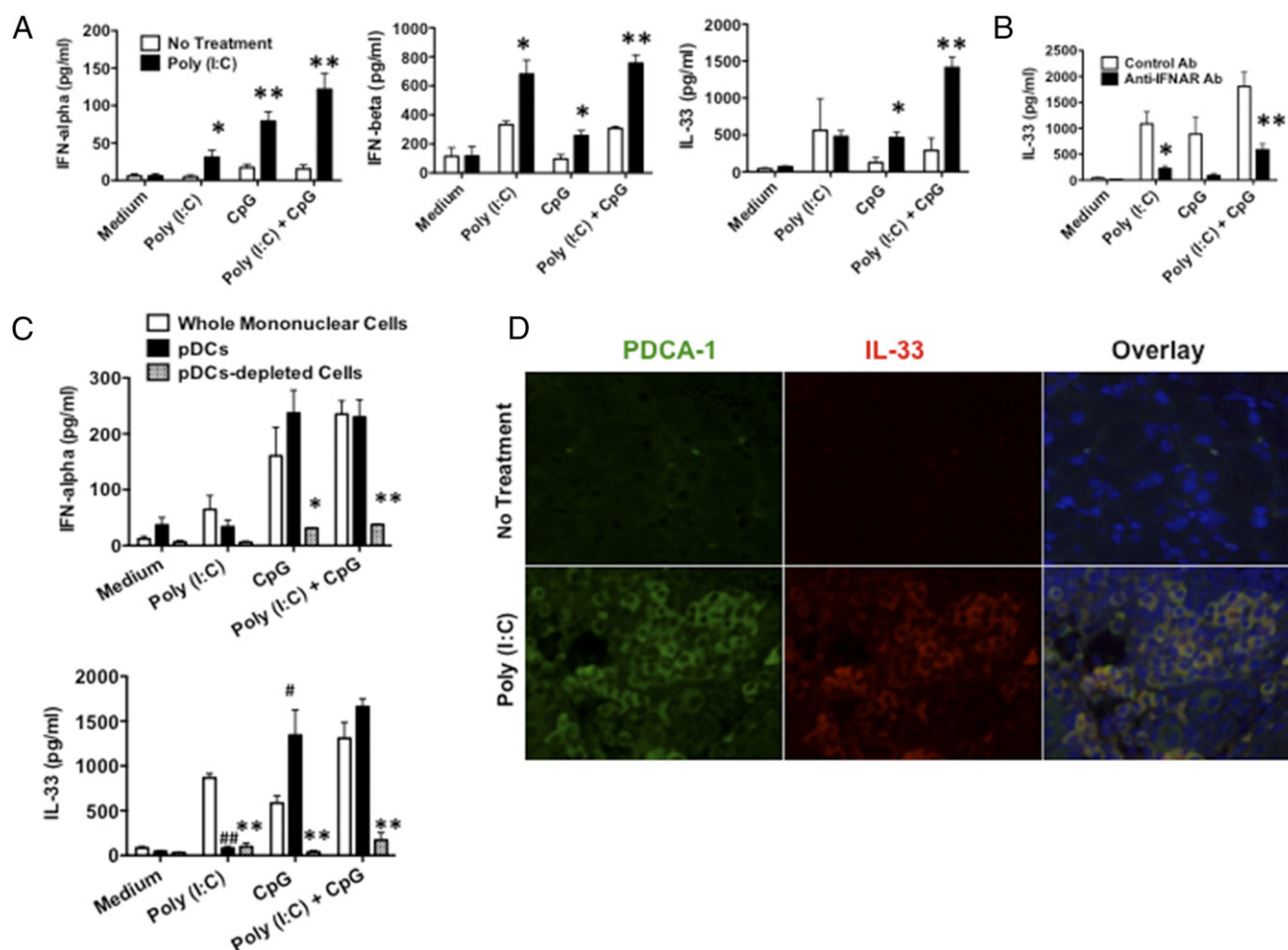
Taken together, these data suggest that murine experimental AIP is characterized by pDC-mediated type I IFN production followed by the secretion of proinflammatory and/or profibrotic cytokines such as IL-33, IL-13, and TGF- $\beta$ 1 and that IL-33 is a potent in-

ducer of both pancreatic inflammation and pancreatic fibrosis as in the case of experimental chronic pancreatitis induced by CCKR and NOD1 agonists (24).

#### *Pancreatic acinar cells expressing IL-33 are increased in human chronic pancreatitis and IgG4-related AIP*

Having identified the profibrogenic and proinflammatory properties of IL-33 in murine AIP, we assessed the expression of this cytokine in human pancreatic diseases. These studies were facilitated by access to surgical pancreatic specimens obtained from patients with chronic alcoholic pancreatitis ( $n = 3$ ) and human IgG4-related AIP ( $n = 3$ ) as well as from one control patient as previously described (18). In baseline studies of levels of fibrosis we found that tissue specimens from patients with both forms of pancreatitis exhibited considerable but equivalent levels of fibrosis as assessed by  $\alpha$ -SMA staining (Fig. 5A). In contrast, expression of  $\alpha$ -SMA was barely seen in tissue specimens from the noncancerous portions of the pancreas with pancreatic cancer (Supplemental Fig. 2A). Thus, human chronic pancreatitis and IgG4-related AIP generate comparable levels of fibrosis.

We next evaluated the expression of IL-33 in acinar cells in tissue specimens from chronic alcoholic pancreatitis ( $n = 4$ ) and IgG4-related AIP patients ( $n = 4$ ) (as well as in control tissues). We found that most amylase<sup>+</sup> acinar cells in specimens from both patients with chronic pancreatitis and IgG4-related AIP were positive for IL-33 staining (Fig. 5B), whereas pancreatic acinar cells in tissue samples from one control patient (noncancerous portions of the pancreatic tissue with pancreatic cancer) were negative for IL-33 staining (Supplemental Fig. 2B). Additionally,



**FIGURE 3.** Pancreatic pDCs produce IL-33 in a type I IFN-dependent manner. MRL/Mp mice ( $n = 4$ ) were treated with poly(I:C) (100  $\mu$ g) twice a week for a total of 16 times. Mice were sacrificed 3 h after the last injection and pancreatic samples were prepared. Nontreated mice ( $n = 4$ ) were used as controls. **(A)** PMNCs ( $1 \times 10^6$ /ml) were stimulated with poly(I:C) (25  $\mu$ g/ml) and/or CpG (1  $\mu$ M) for 48 h to measure the production of IFN- $\alpha$ , IFN- $\beta$ , and IL-33. Results are shown as mean  $\pm$  SE. \* $p < 0.05$ , \*\* $p < 0.01$ , as compared with PMNCs from nontreated mice. **(B)** PMNCs ( $1 \times 10^6$ /ml) isolated from poly(I:C)-treated mice were stimulated with poly(I:C) (25  $\mu$ g/ml) and/or CpG (1  $\mu$ M) for 48 h to measure the production of IL-33 in the presence of anti-IFNAR Ab (50  $\mu$ g/ml) or control Ab (50  $\mu$ g/ml). Results are shown as mean  $\pm$  SE. \* $p < 0.05$ , \*\* $p < 0.01$ , as compared with control Ab-treated cells. **(C)** PMNCs isolated from poly(I:C)-treated mice were separated into pDCs and a pDC-depleted fraction. Whole PMNCs ( $1 \times 10^6$ /ml), pDCs ( $1 \times 10^6$ /ml), and pDC-depleted cells ( $1 \times 10^6$ /ml) were stimulated with poly(I:C) (25  $\mu$ g/ml) and/or CpG (1  $\mu$ M) for 48 h to measure the production of IFN- $\alpha$  and IL-33. Results are shown as mean  $\pm$  SE. \* $p < 0.05$ , \*\* $p < 0.01$ , as compared with whole PMNCs; # $p < 0.05$ , ## $p < 0.01$ , as compared with whole PMNCs. **(D)** Representative images of pancreatic tissues stained with PDCA-1 and IL-33. Original magnification  $\times 1200$ . Pancreas tissues were stained with PDCA-1 (green) and IL-33 (red). Nuclei were counterstained with DAPI.

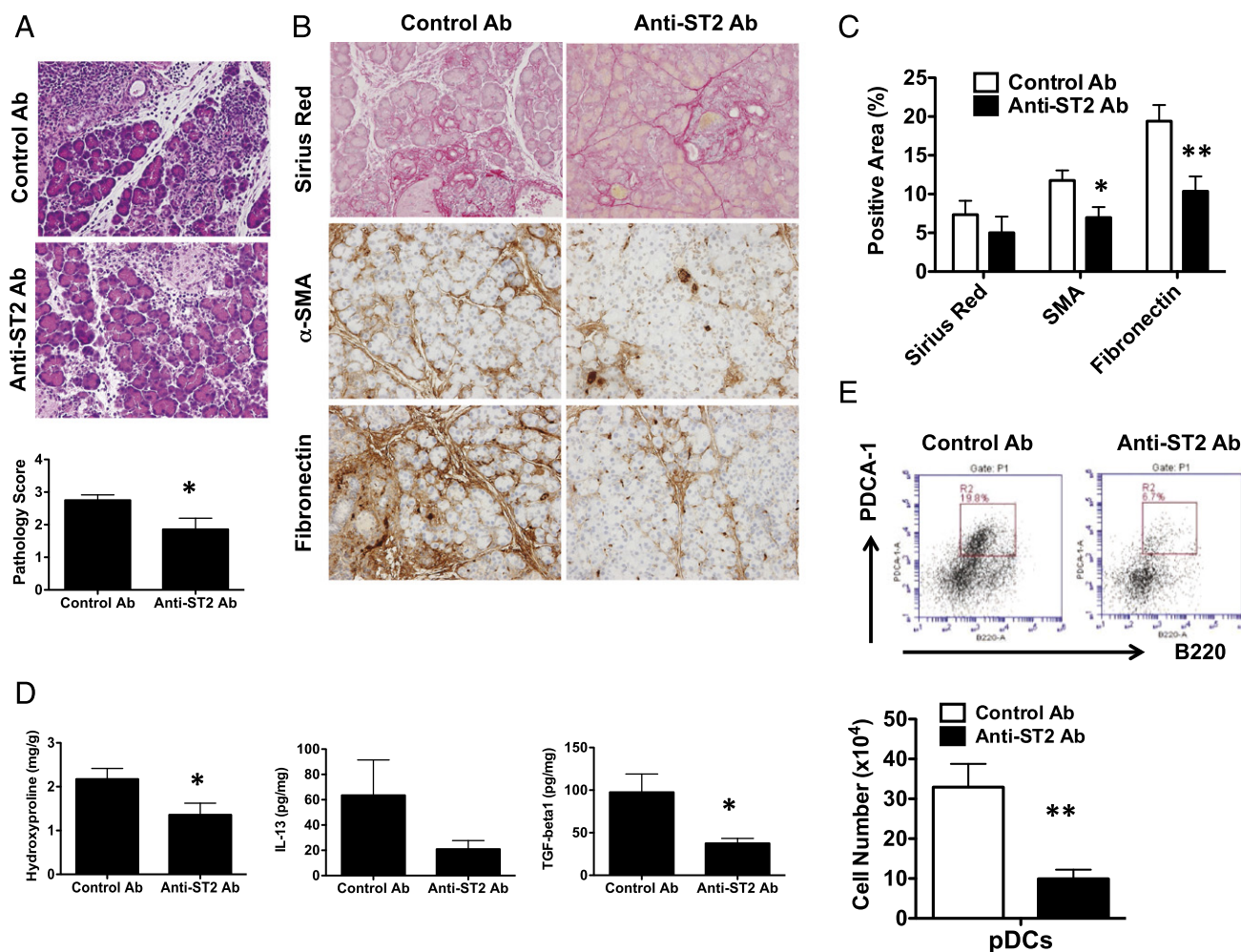
semiquantitative enumeration of acinar cells expressing IL-33 in these pancreatic specimens performed by counting the numbers of amylase<sup>+</sup>IL-33<sup>+</sup> cells, amylase<sup>+</sup>IL-33<sup>-</sup> cells, and amylase<sup>-</sup>IL-33<sup>+</sup> cells in high-power fields (HPFs) revealed no significant difference in IL-33<sup>+</sup> acinar cell numbers in tissues from patients with human chronic pancreatitis and IgG4-related AIP (Fig. 5B). These studies thus revealed that human chronic pancreatitis and IgG4-related AIP are similar to murine chronic pancreatitis induced by administration of CCKR agonist and NOD1 ligand mentioned above in which pancreatic acinar cells were also found to express IL-33; however, such acinar cells expressing IL-33 were not found in the murine model of AIP.

#### *pDCs expressing IL-33 accumulate in the pancreas of human IgG4-related AIP*

Finally, we focused on the expression of IL-33 in pDCs in chronic fibro-inflammatory disorders of the pancreas, again utilizing surgical pancreatic tissue specimens obtained from patients with chronic alcoholic pancreatitis ( $n = 5$ ), human IgG4-related AIP

( $n = 5$ ), and control patients (noncancerous portions of the pancreatic tissue from patients with pancreatic cancer,  $n = 5$ ). In this case we found accumulations of BDCA2<sup>+</sup> pDCs in tissues from patients with IgG4-related AIP, but not in tissues from patients with chronic pancreatitis or controls (Fig. 6A). To verify these tissue staining results we then performed semiquantitative enumeration of pDCs expressing IL-33 in these pancreatic disorders by counting the numbers of BDCA2<sup>+</sup>IL-33<sup>+</sup> cells, BDCA2<sup>+</sup>IL-33<sup>-</sup> cells, and BDCA2<sup>-</sup>IL-33<sup>+</sup> cells in HPFs. We found that the numbers of pDCs expressing IL-33, which were defined as IL-33<sup>+</sup>BDCA2<sup>+</sup> cells, were significantly higher in the pancreas of patients with IgG4-related AIP, as compared with those with chronic pancreatitis or controls (Fig. 6B). Because pancreatic accumulation of BDCA2<sup>+</sup> pDCs expressing IFN- $\alpha$  was seen in patients with IgG4-related AIP but not in patients with chronic pancreatitis in our previous report (18), these data support the idea that human IgG4-related AIP is uniquely characterized by the pancreatic infiltration of pDCs producing both IFN- $\alpha$  and IL-33 and, as such, is similar to AIP in MRL/Mp mice.





**FIGURE 4.** IL-33-mediated signaling pathways are involved in the development of chronic fibro-inflammatory responses of the pancreas. MRL/Mp mice ( $n = 7$ ) were treated with anti-ST2 Ab (100  $\mu$ g,  $n = 7$ ) or control Ab (100  $\mu$ g,  $n = 8$ ) prior to each poly(I:C) (100  $\mu$ g) injection. Mice in each group received poly(I:C) injection twice a week for a total of 14 times. **(A)** Pancreas tissues were stained with H&E. Representative image of the pancreas (original magnification  $\times 400$ ) and pathological scores of AIP are shown. **(B and C)** Pancreas tissues were stained with sirius red, anti- $\alpha$ -SMA Ab, and anti-fibronectin Ab. Representative images of sirius red,  $\alpha$ -SMA, and fibronectin staining are shown. Original magnification in (B)  $\times 400$ . The areas positive for sirius red,  $\alpha$ -SMA, and fibronectin are shown (C). **(D)** Concentrations of hydroxyproline, IL-13, and TGF- $\beta$ 1 in the pancreas lysates are shown. **(E)** Pancreatic accumulation of pDCs in mice treated with anti-ST2 Ab or control Ab. Representative dot plots of flow cytometric analysis. PMNCs were stained with B220 and PDCA-1. pDCs were defined as B220<sup>low</sup>PDCA-1<sup>+</sup> cells and the total numbers of pDCs in each mice were determined. Results are shown as mean  $\pm$  SE. \* $p < 0.05$ , \*\* $p < 0.01$ , as compared with control Ab-treated mice.

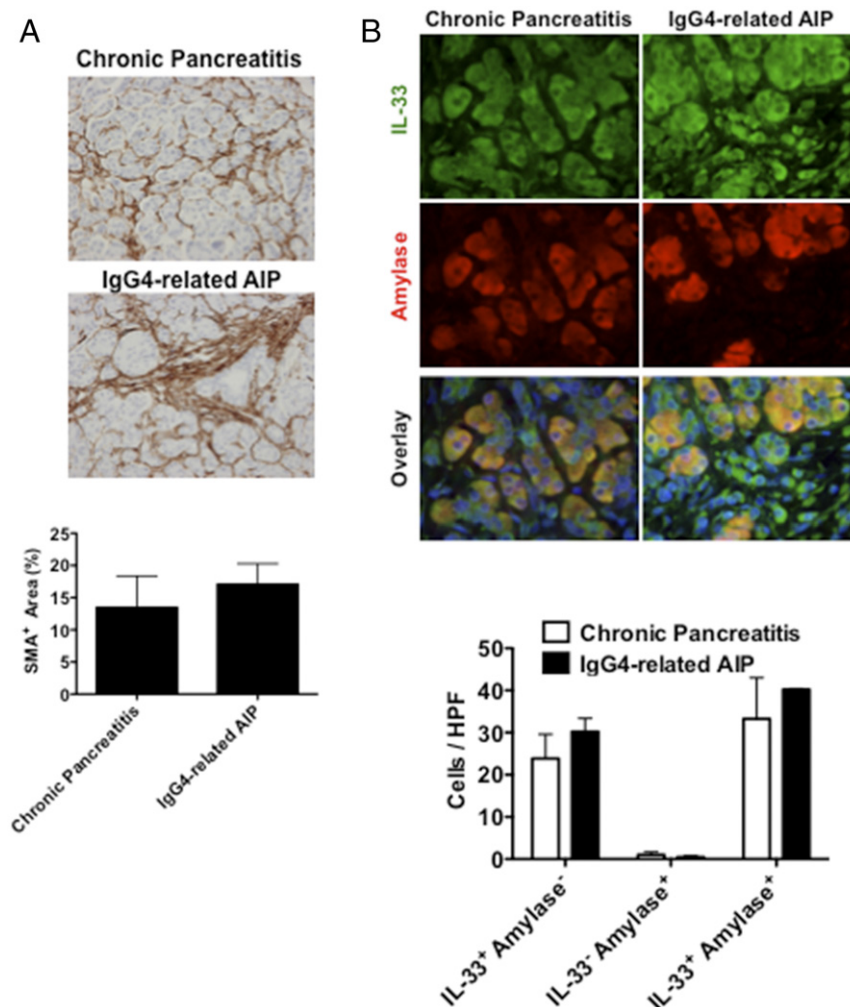
## Discussion

Although massive infiltration of lymphocytes and plasmacytes accompanied by fibrosis is a well-established histological feature of human AIP, the molecular mechanisms accounting for the development of these chronic fibro-inflammatory effects are still poorly understood (1, 32). In this study, we established, to our knowledge for the first time, that IL-33 is a major proinflammatory factor in mice with experimental AIP [MRL/Mp mice administered poly(I:C)], particularly with respect to fibrosis formation. The various studies leading to this conclusion consisted of the following: first, the development of murine AIP was shown to be associated with pancreatic infiltration of pDCs and with enhanced expression of both type I IFNs and IL-33 (as well as profibrotic factors downstream of IL-33, IL-13, and TGF- $\beta$ 1). Second, the depletion of pDCs in these mice by a pDC-depleting Ab (120G8 Ab) or the blockade of type I IFN signaling by anti-IFNAR Ab led to marked reduction in the expression of IL-33. Third, PMNCs isolated from mice treated with poly(I:C) produced a large amount of type I IFN and IL-33 upon stimulation with poly(I:C) and/or CpG in vitro,

and pDCs were identified as producers of these cytokines. Fourth, such IL-33 production was dependent on type I IFN signaling because it was blocked by the presence of anti-IFNAR Ab. Fifth, and finally, the blockade of IL-33-mediated signaling pathways by a neutralizing Ab against its receptor, ST2, led to a significant reduction in pancreatic inflammation and its associated fibrosis. These studies provide further evidence of the importance of pDCs in the pathogenesis of murine AIP in that they show that this cell is the origin of two major cytokines causing the fibro-inflammatory responses, type I IFN and IL-33. Note that in parallel with these findings, we found that pancreatitis in human IgG4-related AIP is also marked by infiltration of pancreatic tissue with pDCs producing IL-33 and IFN- $\alpha$  (but not tissue from patients with chronic alcoholic pancreatitis). This implies that pDC production of type I IFN and IL-33 is involved in the immunopathogenesis of human IgG4-related AIP.

IL-33, the cytokine shown in this study to be produced by pathogenic pDCs in AIP, is a member of the IL-1 family of cytokines that usually resides in the nucleus of a cell bound to chromatin and that is released into the extracellular milieu upon cell

**FIGURE 5.** Pancreatic acinar cells express IL-33 in chronic alcoholic pancreatitis and IgG4-related AIP. **(A)** Surgical pancreas specimens obtained from patients with chronic alcoholic pancreatitis ( $n = 3$ ) and IgG4-related AIP ( $n = 3$ ) were stained with anti- $\alpha$ -SMA Ab. Representative images of  $\alpha$ -SMA staining (top, original magnification  $\times 400$ ) and the areas positive for  $\alpha$ -SMA staining (bottom) are shown. **(B)** Surgical pancreas specimens were obtained from patients with chronic alcoholic pancreatitis ( $n = 4$ ) and IgG4-related AIP ( $n = 4$ ). Immunofluorescence stainings show the presence of IL-33-expressing acinar cells (top, original magnification  $\times 1200$ ). Pancreas tissues were stained with anti-IL-33 Ab (green) and anti-amylase Ab (red). Nuclei were counterstained with DAPI. The numbers of cells positive for IL-33 and/or amylase were counted in HPFs. Results are shown as mean  $\pm$  SE.



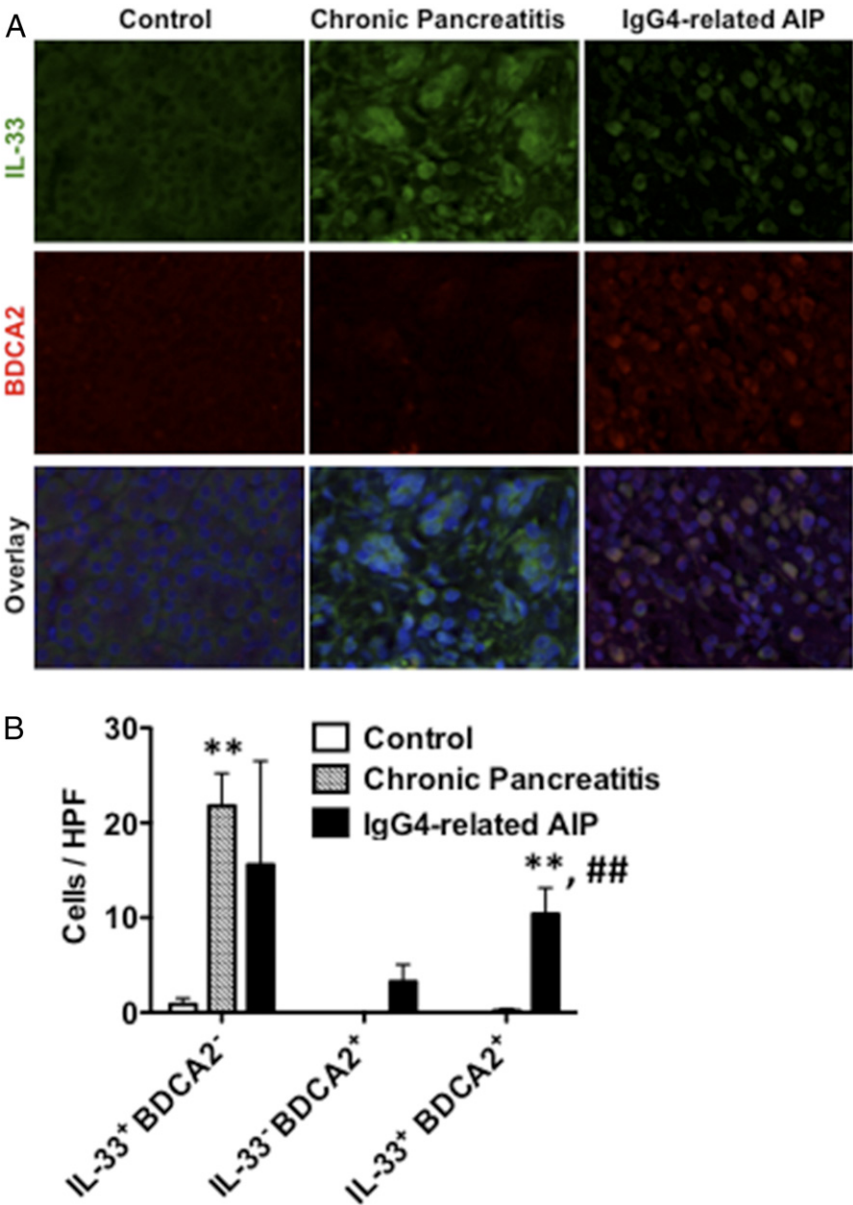
death or, alternatively, by “unconventional” release mechanisms (33). Acting via the ST2 receptor on a variety of cells, including Th2 and group 2 innate lymphoid cells, it induces Th2 cytokine responses and other proinflammatory responses (23). Indeed, recent studies by Furukawa et al. (34) implicate the role of IL-33 as an inducer of Th2 responses in IgG4-RD. However, it also activates Th1 responses in cytotoxic antiviral T cells (35). IL-33 has an ambiguous relationship to gut inflammation: on the one hand, polymorphisms in the IL-33 and ST2 genes appear to be risk factors in both Crohn disease and ulcerative colitis (36), and there is increased IL-33 expression in ulcerative colitis tissues (37); on the other hand, IL-33-deficient mice are more susceptible to experimental gut inflammation possibly because IL-33 is necessary for optimal IgA responses that regulate the gut microbiome (38). The important role of IL-33 in the pathogenesis of experimental AIP shown in the present study, as well as in experimental mouse conventional pancreatitis (24, 39), is not yet completely understood. With respect to IL-33 involvement in the underlying AIP-associated inflammation, IL-33 secretion could be contributing to the production of Th2 cytokines in AIP mentioned in the *Introduction* and in this way to the generation of autoantibodies that are produced in this disease. As shown in our previous studies, such autoantibodies could form immune complexes that stimulate the formation of neutrophil extracellular traps (NETs) by neutrophils followed by NET induction of IFN- $\alpha$  by pDCs (18). IL-33 can also be more directly involved in development of the pancreatic inflammation by its induction of Th1 cytokines that, as mentioned

above, stimulate the function of cytotoxic T cells. To these hypothetical functions of IL-33 in AIP, one can add a more definite function, the ability of IL-33 to induce various downstream cytokines previously demonstrated to have profibrotic functions, IL-13 and TGF- $\beta$ 1 (40, 41). This was shown by the dramatic decrease in fibrosis in murine AIP caused by the blockade of IL-33 signaling and the accompanying downregulation of pancreatic expression of IL-13 and TGF- $\beta$ 1. Thus, one of the most interesting findings in this study is the identification of IL-33 as the major mediator of fibrosis in experimental AIP and, by extension, to human IgG4-related AIP.

The blockade of IL-33-mediated signaling pathways by ST2 Ab led to decreased pancreatic accumulation of pDCs defined as PDCA-1<sup>+</sup>B220<sup>low</sup> cells (Fig. 4E). Whereas in this study the mechanism accounting for such reduction in pDC accumulation is not addressed, in our previous study (24), we showed that blockade of IL-33 signaling in the model of chronic pancreatitis results in greatly reduced amounts of proinflammatory cytokine production, including reduction in IL-6, TNF- $\alpha$ , and MCP-1. Thus, the reason why pDCs are reduced with anti-ST2 Ab treatment appears not to be due to a specific effect on pDCs but rather to a global effect on the attenuation of pancreatic inflammation.

One question arising from the present study is whether IL-33 produced by pDCs enhances IgG4 production by B cells. In this regard, Akiyama et al. (15) reported that there is no correlation between serum levels of IL-33 and IgG4 in patients with IgG4-RD. This study thus suggested that it is unlikely that IL-33

**FIGURE 6.** Pancreatic pDCs express IL-33 in IgG4-related AIP, but not in chronic alcoholic pancreatitis. Surgical pancreas specimens were obtained from patients with chronic alcoholic pancreatitis ( $n = 5$ ), IgG4-related AIP ( $n = 5$ ), and pancreatic cancer ( $n = 5$ ). Noncancerous portions of the tissues from pancreas cancer patients were used as controls ( $n = 5$ ). Pancreatic tissues were stained with anti-IL-33 Ab (green) and anti-BDCA2 Ab (red). Pancreas tissues were counterstained with DAPI. **(A)** Representative images of immunofluorescence staining. Original magnification  $\times 1200$ . **(B)** The numbers of cells positive for IL-33 and/or BDCA2 were counted in HPFs. Results are shown as mean  $\pm$  SE.  $^{###}p < 0.01$ , as compared with chronic alcoholic pancreatitis;  $^{**}p < 0.01$ , as compared with controls.



enhances IgG4 production by B cells; however, additional studies of IL-33 effects on B cells in the presence of type I IFN are necessary to be sure of this conclusion.

In our previous studies of an experimental model of chronic pancreatitis induced by repeated injection of CCKR agonist, cerulein, in combination with NOD1 ligand, FK156, or FK565 (24, 29), we elucidated important aspects of the molecular mechanisms leading to the chronic fibro-inflammatory responses likely causing non-autoimmune conventional acute and chronic pancreatitis in humans. A key feature of this model is that initial acinar cell injury caused by CCKR-induced intra-acinar cell activation of pancreatic enzymes leads to the translocation of commensal organisms bearing NOD1 ligand into the circulation and thereby NOD1-induced acinar cell production of type I IFN. The latter then played a critical role in the pathogenic process by promoting the influx of inflammatory macrophages into the pancreas and the induction of cytotoxic cytokines that cause further acinar cell injury and release of IL-33. As shown by the fact that the chronic pancreatitis and associated fibrosis induced in this model are markedly attenuated by administration of an Ab that blocks IL-33 signaling (anti-ST2 Ab), the IL-33 thus generated makes a major

contribution to the underlying pathologic responses driving the pancreatitis. These characteristics of the murine model of conventional pancreatitis are similar to those of the murine model of AIP in poly(I:C)-treated MRL/Mp mice in that in both models a type I IFN/IL-33 axis plays a critical role in the development of the pancreatic inflammation; this conclusion is highlighted by the fact that AIP is also markedly attenuated by the blockade of type I IFN and IL-33 by anti-IFNAR and anti-ST2 Abs, respectively. Note, however, that as discussed below, the cellular source of the IL-33 in the two models and in the human diseases they represent is somewhat different.

Whereas the present study identified pancreatic pDCs as the key cellular element mediating murine experimental AIP, it did not address the nature of the activators of pDCs in either murine or human AIP. One possible activator already alluded to above is NETs, which we have previously identified in the pancreas of both murine and human AIP (18). These are web-like structures composed of extracellular DNA, chromatin, and molecules derived from neutrophil granules (42, 43) that can be induced to form in the pancreas by neutrophil exposure to Ab-Ag complexes, possibly those composed of Ags released by the neutrophils and Abs



generated by the pathologic process (18). In support of this possibility, we have shown with in vitro studies that NETs induce pDCs obtained from patients with human IgG4-related AIP to produce IFN- $\alpha$  and stimulate pDC induction of IgG4 by cocultured B cells (18). In addition to NETs, microbe-associated molecular patterns derived from intestinal microflora may also serve as activators of pDCs in IgG4-related AIP. In support of this notion, pDCs isolated from poly(I:C)-treated MRL/Mp mice produced a large amount of IFN- $\alpha$  and IL-33 upon stimulation with CpG, a substance mimicking bacterial dsDNA. The possibility that microbe-associated molecular patterns act as pDC activators in AIP is attractive because it suggests that this form of pancreatic inflammation is initiated and/or driven by gut bacterial components. Evidence that this is in fact the case comes from preliminary studies in which we have observed that bowel sterilization by a broad range of antibiotics prevented the development of experimental AIP in MRL/Mp mice (data not shown). However, further studies defining the gut microbiome in AIP as well as the demonstration that gut bacteria are translocated into the circulation and can thus contact pancreatic cells will be required to fully establish this concept.

Our purification and depletion studies utilizing PMNCs obtained from tissues of MRL/Mp mice with experimental AIP as well as immunofluorescence studies of these tissues revealed that pDCs are the main cellular sources of IL-33 in this model. Such production depended on type I IFN signaling because pancreatic expression of IL-33 was markedly reduced either by the depletion of pDCs or by the neutralization of type I IFN signaling. This fits well with the finding that transcription of IL-33 requires transactivation of IFN regulatory factor 7, a critical transcription factor highly expressed in pDCs (44). Interestingly, pancreatic pDCs from MRL/Mp mice with AIP do not respond to poly(I:C) likely due to the fact that pDCs do not express a receptor that recognizes dsRNA, TLR3 (30, 31). This, at first sight, appears to be at odds with the fact that stimulation of MRL/Mp mice with poly(I:C) is shown in these and previous studies to be the inducer of pancreatic pDCs that are responsible for the AIP developing in these mice. The resolution of this apparent contradiction lies in the fact that poly(I:C) is a type I IFN inducer via its stimulation of TLR3 on conventional DCs (45). Such type I IFN production by conventional DCs can lead to the induction of Flt3 ligand, a factor necessary for differentiation and expansion of pDCs (46); moreover, type I IFN enhances the inductive effect of Flt3 ligand on pDCs (47). Thus, poly(I:C) administration via its effect on type I IFN production can induce differentiation and expansion of pDCs when administered to MRL/Mp mice, even though it cannot directly stimulate pDCs because the latter lack TLR3 expression.

IL-33 is not expressed in pancreatic acinar cells in this model although it is expressed in acinar cells of humans with IgG4-related AIP. The latter finding indicates that in the human disease acinar cells also contribute to IL-33 production, although in this situation such production may be redundant. A somewhat different situation regarding IL-33 secretion exists in relationship to pancreatitis in both patients with chronic alcoholic pancreatitis and in the murine model of chronic pancreatitis described extensively above in which pancreatitis is induced by administration of CCKR agonist and NOD1 ligand (24, 25). In this form of pancreatitis acinar cells are the main, if not sole, source of IL-33 secretion, and pDCs producing this cytokine are not observed. Because in the murine model of chronic pancreatitis, administration of anti-ST2 Ab and consequent blockade of IL-33 signaling resulted in reduced inflammation and prevented fibrosis, it is reasonable to conclude that IL-33 from this cellular source is functionally capable of medi-

ating fibrosis and perhaps other proinflammatory functions in human chronic pancreatitis (24, 25).

In conclusion, our findings show that both human IgG4-related AIP and murine AIP are characterized by pancreatic accumulation of pDCs producing IFN- $\alpha$  and IL-33. In the case of murine AIP, we provide evidence that chronic fibro-inflammatory responses in AIP can be prevented by the depletion of pDCs, by the neutralization of type I IFN signaling pathways, and by the neutralization of IL-33 signaling pathways. Thus, patients with IgG4-related AIP can be treated with the blockade of type I IFN or IL-33-mediated signaling pathways. Confirmation of this idea awaits human clinical studies addressing the efficacy of anti-ST2 Ab or anti-IFNAR Ab in human IgG4-related AIP.

## Disclosures

The authors have no financial conflicts of interest.

## References

- Stone, J. H., Y. Zen, and V. Deshpande. 2012. IgG4-related disease. *N. Engl. J. Med.* 366: 539–551.
- Kamisawa, T., and A. Okamoto. 2006. Autoimmune pancreatitis: proposal of IgG4-related sclerosing disease. *J. Gastroenterol.* 41: 613–625.
- Okazaki, K., K. Uchida, and T. Fukui. 2008. Recent advances in autoimmune pancreatitis: concept, diagnosis, and pathogenesis. *J. Gastroenterol.* 43: 409–418.
- Yamamoto, M., H. Takahashi, and Y. Shinomura. 2014. Mechanisms and assessment of IgG4-related disease: lessons for the rheumatologist. *Nat. Rev. Rheumatol.* 10: 148–159.
- Aalberse, R. C., S. O. Stapel, J. Schuurman, and T. Rispens. 2009. Immunoglobulin G4: an odd antibody. *Clin. Exp. Allergy* 39: 469–477.
- Shiokawa, M., Y. Kodama, K. Kuriyama, K. Yoshimura, T. Tomono, T. Morita, N. Kakiuchi, T. Matsumori, A. Mima, Y. Nishikawa, et al. 2016. Pathogenicity of IgG in patients with IgG4-related disease. *Gut* 65: 1322–1332.
- Tomas, N. M., L. H. Beck, Jr., C. Meyer-Schwesinger, B. Seitz-Polski, H. Ma, G. Zahner, G. Dolla, E. Hoxha, U. Helmchen, A. S. Dabert-Gay, et al. 2014. Thrombospondin type-1 domain-containing 7A in idiopathic membranous nephropathy. *N. Engl. J. Med.* 371: 2277–2287.
- Hussain, A., T. Pankhurst, M. Goodall, R. Colman, R. Jefferis, C. O. Savage, and J. M. Williams. 2009. Chimeric IgG4 PR3-ANCA induces selective inflammatory responses from neutrophils through engagement of Fc $\gamma$  receptors. *Immunology* 128: 236–244.
- Jeannin, P., S. Lecoanet, Y. Delneste, J. F. Gauchat, and J. Y. Bonnefoy. 1998. IgE versus IgG4 production can be differentially regulated by IL-10. *J. Immunol.* 160: 3555–3561.
- Punnonen, J., G. Aversa, B. G. Cocks, A. N. McKenzie, S. Menon, G. Zurawski, R. de Waal Malefyt, and J. E. de Vries. 1993. Interleukin 13 induces interleukin 4-independent IgG4 and IgE synthesis and CD23 expression by human B cells. *Proc. Natl. Acad. Sci. USA* 90: 3730–3734.
- Satoguina, J. S., T. Adjibimey, K. Arndts, J. Hoch, J. Oldenburg, L. E. Layland, and A. Hoerauf. 2008. Tr1 and naturally occurring regulatory T cells induce IgG4 in B cells through GITR/GITR-L interaction, IL-10 and TGF- $\beta$ . *Eur. J. Immunol.* 38: 3101–3113.
- Akitake, R., T. Watanabe, C. Zaima, N. Uza, H. Ida, S. Tada, N. Nishida, and T. Chiba. 2010. Possible involvement of T helper type 2 responses to Toll-like receptor ligands in IgG4-related sclerosing disease. *Gut* 59: 542–545.
- Zen, Y., T. Fujii, K. Harada, M. Kawano, K. Yamada, M. Takahira, and Y. Nakanuma. 2007. Th2 and regulatory immune reactions are increased in immunoglobulin G4-related sclerosing pancreatitis and cholangitis. *Hepatology* 45: 1538–1546.
- Miyoshi, H., K. Uchida, T. Taniguchi, S. Yazumi, M. Matsushita, M. Takaoka, and K. Okazaki. 2008. Circulating naive and CD4<sup>+</sup>CD25<sup>high</sup> regulatory T cells in patients with autoimmune pancreatitis. *Pancreas* 36: 133–140.
- Akiyama, M., K. Suzuki, K. Yamaoka, H. Yasuoka, M. Takeshita, Y. Kaneko, H. Kondo, Y. Kassai, T. Miyazaki, R. Morita, et al. 2015. Number of circulating follicular helper 2 T cells correlates with IgG4 and interleukin-4 levels and plasmablast numbers in IgG4-related disease. *Arthritis Rheumatol.* 67: 2476–2481.
- Watanabe, T., K. Yamashita, S. Fujikawa, T. Sakurai, M. Kudo, M. Shiokawa, Y. Kodama, K. Uchida, K. Okazaki, and T. Chiba. 2012. Activation of Toll-like receptors and NOD-like receptors is involved in enhanced IgG4 responses in autoimmune pancreatitis. *Arthritis Rheum.* 64: 914–924.
- Watanabe, T., K. Yamashita, T. Sakurai, M. Kudo, M. Shiokawa, N. Uza, Y. Kodama, K. Uchida, K. Okazaki, and T. Chiba. 2013. Toll-like receptor activation in basophils contributes to the development of IgG4-related disease. *J. Gastroenterol.* 48: 247–253.
- Arai, Y., K. Yamashita, K. Kuriyama, M. Shiokawa, Y. Kodama, T. Sakurai, K. Mizugishi, K. Uchida, N. Kadowaki, A. Takaori-Kondo, et al. 2015. Plasmacytoid dendritic cell activation and IFN- $\alpha$  production are prominent features of murine autoimmune pancreatitis and human IgG4-related autoimmune pancreatitis. *J. Immunol.* 195: 3033–3044.

19. Asada, M., A. Nishio, T. Akamatsu, J. Tanaka, K. Saga, M. Kido, N. Watanabe, K. Uchida, T. Fukui, K. Okazaki, and T. Chiba. 2010. Analysis of humoral immune response in experimental autoimmune pancreatitis in mice. *Pancreas* 39: 224–231.
20. Kanno, H., M. Nose, J. Itoh, Y. Taniguchi, and M. Kyogoku. 1992. Spontaneous development of pancreatitis in the MRL/Mp strain of mice in autoimmune mechanism. *Clin. Exp. Immunol.* 89: 68–73.
21. Fichtner-Feigl, S., W. Strober, E. K. Geissler, and H. J. Schlitt. 2008. Cytokines mediating the induction of chronic colitis and colitis-associated fibrosis. *Mucosal Immunol.* 1(Suppl. 1): S24–S27.
22. McHedlidze, T., M. Waldner, S. Zopf, J. Walker, A. L. Rankin, M. Schuchmann, D. Voehringer, A. N. McKenzie, M. F. Neurath, S. Pflanz, and S. Wirtz. 2013. Interleukin-33-dependent innate lymphoid cells mediate hepatic fibrosis. *Immunity* 39: 357–371.
23. Cayrol, C., and J. P. Girard. 2014. IL-33: an alarmin cytokine with crucial roles in innate immunity, inflammation and allergy. *Curr. Opin. Immunol.* 31: 31–37.
24. Watanabe, T., Y. Sadakane, N. Yagama, T. Sakurai, H. Ezoe, M. Kudo, T. Chiba, and W. Strober. 2016. Nucleotide-binding oligomerization domain 1 acts in concert with the cholecystokinin receptor agonist, cerulein, to induce IL-33-dependent chronic pancreatitis. *Mucosal Immunol.* 9: 1234–1249.
25. Watanabe, T., M. Kudo, and W. Strober. 2017. Immunopathogenesis of pancreatitis. *Mucosal Immunol.* 10: 283–298.
26. Schwaiger, T., C. van den Brandt, B. Fitzner, S. Zaatreh, F. Kraatz, A. Dummer, H. Nizze, M. Evert, B. M. Bröker, M. C. Brunner-Weinzierl, et al. 2014. Autoimmune pancreatitis in MRL/Mp mice is a T cell-mediated disease responsive to cyclosporine A and rapamycin treatment. *Gut* 63: 494–505.
27. Masamune, A., and T. Shimosegawa. 2013. Pancreatic stellate cells—multifunctional cells in the pancreas. *Pancreatology* 13: 102–105.
28. Asselin-Paturel, C., G. Brizard, J. J. Pin, F. Brière, and G. Trinchieri. 2003. Mouse strain differences in plasmacytoid dendritic cell frequency and function revealed by a novel monoclonal antibody. *J. Immunol.* 171: 6466–6477.
29. Tsuji, Y., T. Watanabe, M. Kudo, H. Arai, W. Strober, and T. Chiba. 2012. Sensing of commensal organisms by the intracellular sensor NOD1 mediates experimental pancreatitis. *Immunity* 37: 326–338.
30. Edwards, A. D., S. S. Diebold, E. M. Slack, H. Tomizawa, H. Hemmi, T. Kaisho, S. Akira, and C. Reis e Sousa. 2003. Toll-like receptor expression in murine DC subsets: lack of TLR7 expression by CD8 $\alpha^+$  DC correlates with unresponsiveness to imidazoquinolines. *Eur. J. Immunol.* 33: 827–833.
31. Kadowaki, N., S. Ho, S. Antonenko, R. W. Malefyt, R. A. Kastelein, F. Bazan, and Y. J. Liu. 2001. Subsets of human dendritic cell precursors express different Toll-like receptors and respond to different microbial antigens. *J. Exp. Med.* 194: 863–869.
32. Hart, P. A., Y. Zen, and S. T. Chari. 2015. Recent advances in autoimmune pancreatitis. *Gastroenterology* 149: 39–51.
33. Lefrançois, E., and C. Cayrol. 2012. Mechanisms of IL-33 processing and secretion: differences and similarities between IL-1 family members. *Eur. Cytokine Netw.* 23: 120–127.
34. Furukawa, S., M. Moriyama, K. Miyake, H. Nakashima, A. Tanaka, T. Maehara, M. Iizuka-Koga, H. Tsuboi, J. N. Hayashida, N. Ishiguro, et al. 2017. Interleukin-33 produced by M2 macrophages and other immune cells contributes to Th2 immune reaction of IgG4-related disease. *Sci. Rep.* 7: 42413.
35. Baumann, C., W. V. Bonilla, A. Fröhlich, C. Helmstetter, M. Peine, A. N. Hegazy, D. D. Pinschewer, and M. Löhnig. 2015. T-bet- and STAT4-dependent IL-33 receptor expression directly promotes antiviral Th1 cell responses. *Proc. Natl. Acad. Sci. USA* 112: 4056–4061.
36. Latiano, A., O. Palmieri, L. Pastorelli, M. Vecchi, T. T. Pizarro, F. Bossa, G. Merla, B. Augello, T. Latiano, G. Corritore, et al. 2013. Associations between genetic polymorphisms in IL-33, IL1R1 and risk for inflammatory bowel disease. *PLoS One* 8: e62144.
37. Kobori, A., Y. Yagi, H. Imaeda, H. Ban, S. Bamba, T. Tsujikawa, Y. Saito, Y. Fujiyama, and A. Andoh. 2010. Interleukin-33 expression is specifically enhanced in inflamed mucosa of ulcerative colitis. *J. Gastroenterol.* 45: 999–1007.
38. Malik, A., D. Sharma, Q. Zhu, R. Karki, C. S. Guy, P. Vogel, and T. D. Kanneganti. 2016. IL-33 regulates the IgA-microbiota axis to restrain IL-1 $\alpha$ -dependent colitis and tumorigenesis. *J. Clin. Invest.* 126: 4469–4481.
39. Masamune, A., T. Watanabe, K. Kikuta, K. Satoh, A. Kanno, and T. Shimosegawa. 2010. Nuclear expression of interleukin-33 in pancreatic stellate cells. *Am. J. Physiol. Gastrointest. Liver Physiol.* 299: G821–G832.
40. Shinozaki, S., H. Mashima, H. Ohnishi, and K. Sugano. 2010. IL-13 promotes the proliferation of rat pancreatic stellate cells through the suppression of NF- $\kappa$ B/TGF- $\beta$ 1 pathway. *Biochem. Biophys. Res. Commun.* 393: 61–65.
41. Xue, J., V. Sharma, M. H. Hsieh, A. Chawla, R. Murali, S. J. Pandol, and A. Habtezion. 2015. Alternatively activated macrophages promote pancreatic fibrosis in chronic pancreatitis. *Nat. Commun.* 6: 7158.
42. Garcia-Romo, G. S., S. Caielli, B. Vega, J. Connolly, F. Allantaz, Z. Xu, M. Punaro, J. Baisch, C. Guiducci, R. L. Coffman, et al. 2011. Netting neutrophils are major inducers of type I IFN production in pediatric systemic lupus erythematosus. *Sci. Transl. Med.* 3: 73ra20.
43. Lande, R., D. Ganguly, V. Facchinetti, L. Frasca, C. Conrad, J. Gregorio, S. Meller, G. Chamilos, R. Sebasigari, V. Riccieri, et al. 2011. Neutrophils activate plasmacytoid dendritic cells by releasing self-DNA-peptide complexes in systemic lupus erythematosus. *Sci. Transl. Med.* 3: 73ra19.
44. Sun, L., Z. Zhu, N. Cheng, Q. Yan, and R. D. Ye. 2014. Serum amyloid A induces interleukin-33 expression through an IRF7-dependent pathway. *Eur. J. Immunol.* 44: 2153–2164.
45. Akira, S., and K. Takeda. 2004. Toll-like receptor signalling. *Nat. Rev. Immunol.* 4: 499–511.
46. Franchini, M., H. Hefti, S. Vollstedt, B. Glanzmann, M. Riesen, M. Ackermann, P. Chaplin, K. Shortman, and M. Suter. 2004. Dendritic cells from mice neonatally vaccinated with modified vaccinia virus Ankara transfer resistance against herpes simplex virus type 1 to naive one-week-old mice. *J. Immunol.* 172: 6304–6312.
47. Chen, Y. L., T. T. Chen, L. M. Pai, J. Wesoly, H. A. Bluyssen, and C. K. Lee. 2013. A type I IFN-Flt3 ligand axis augments plasmacytoid dendritic cell development from common lymphoid progenitors. *J. Exp. Med.* 210: 2515–2522.





# Cost-effectiveness of EOB-MRI for Hepatocellular Carcinoma in Japan

Akihiro Nishie, MD, PhD<sup>1</sup>; Satoshi Goshima, MD, PhD<sup>2</sup>; Hiroki Haradome, MD, PhD<sup>3</sup>; Etsuro Hatano, MD, PhD<sup>4</sup>; Yasuharu Imai, MD, PhD<sup>5</sup>; Masatoshi Kudo, MD, PhD<sup>6</sup>; Masanori Matsuda, MD, PhD<sup>7</sup>; Utaroh Motosugi, MD, PhD<sup>7</sup>; Satoshi Saitoh, MD<sup>8</sup>; Kengo Yoshimitsu, MD, PhD<sup>9</sup>; Bruce Crawford, MA, MPH<sup>10</sup>; Eliza Kruger, MHEcon<sup>10</sup>; Graeme Ball, MA<sup>10</sup>; and Hiroshi Honda, MD, PhD<sup>1</sup>

<sup>1</sup>Kyushu University, Fukuoka, Japan; <sup>2</sup>Gifu University Hospital, Gifu, Japan; <sup>3</sup>Nihon University Hospital, Tokyo, Japan; <sup>4</sup>Hyogo University Hospital, Hyogo, Japan; <sup>5</sup>Ikeda Municipal Hospital, Osaka, Japan; <sup>6</sup>Kindai University Hospital, Osaka, Japan; <sup>7</sup>Yamanashi University, Yamanashi, Japan; <sup>8</sup>Toranomon Hospital, Tokyo, Japan; <sup>9</sup>Fukuoka University Hospital, Fukuoka, Japan; and <sup>10</sup>QuintilesIMS, Tokyo, Japan

## ABSTRACT

**Purpose:** The objective of the study was to evaluate the cost-effectiveness of gadoxetic acid-enhanced magnetic resonance imaging (EOB-MRI) in the diagnosis and treatment of hepatocellular carcinoma (HCC) in Japan compared with extracellular contrast media-enhanced MRI (ECCM-MRI) and contrast media-enhanced computed tomography (CE-CT) scanning.

**Methods:** A 6-stage Markov model was developed to estimate lifetime direct costs and clinical outcomes associated with EOB-MRI. Diagnostic sensitivity and specificity, along with clinical data on HCC survival, recurrence, treatment patterns, costs, and health state utility values, were derived from predominantly Japanese publications. Parameters unavailable from publications were estimated in a Delphi panel of Japanese clinical experts who also confirmed the structure and overall approach of the model. Sensitivity analyses, including one-way, probabilistic, and scenario analyses, were conducted to account for uncertainty in the results.

**Findings:** Over a lifetime horizon, EOB-MRI was associated with lower direct costs (¥2,174,869) and generated a greater number of quality-adjusted life years (QALYs) (9.502) than either ECCM-MRI (¥2,365,421, 9.303 QALYs) or CE-CT (¥2,482,608, 9.215 QALYs). EOB-MRI was superior to the other diagnostic strategies considered, and this finding was robust over sensitivity and scenario analyses. A majority of the direct costs associated with HCC in Japan were found to be costs of treatment. The model results revealed the superior cost-effectiveness of the

EOB-MRI diagnostic strategy compared with ECCM-MRI and CE-CT.

**Implications:** EOB-MRI could be the first-choice imaging modality for medical care of HCC among patients with hepatitis or liver cirrhosis in Japan. Widespread implementation of EOB-MRI could reduce health care expenditures, particularly downstream treatment costs, associated with HCC. (*Clin Ther.* 2017;39:738–750) © 2017 Elsevier HS Journals, Inc. All rights reserved.

**Key words:** CT, cost, economic evaluation, gadoxetic acid, hepatocellular carcinoma, liver imaging, MRI.

## INTRODUCTION

Hepatocellular carcinoma (HCC) is the third most frequent cause of cancer-related mortality worldwide.<sup>1</sup> It is the fifth most common cancer among men and the eighth most common cancer among women.<sup>1</sup> Infection with the hepatitis B virus (HBV) or hepatitis C virus (HCV) are jointly responsible for ~80% of HCC cases.<sup>2</sup> Japan has the second largest number of patients with HCC in the world; HCC reportedly accounts for 94% of all primary liver cancers, and an estimated 32,000 people die of primary liver cancer in Japan each year.<sup>3</sup>

Accepted for publication March 3, 2017.

<http://dx.doi.org/10.1016/j.clinthera.2017.03.006>

0149-2918/\$ - see front matter

© 2017 Elsevier HS Journals, Inc. All rights reserved.

For patients with HCC, number of tumors, tumor size, hepatic function, and the presence of metastases jointly determine disease management. Approved therapies for HCC in Japan include liver resection (LR), liver transplantation (LT), radiofrequency ablation (RFA), transarterial chemoembolization (TACE), and both intra-arterial and systemic chemotherapy.<sup>4</sup> Although LR and LT have the potential to cure the disease, they are typically offered to only 30% to 40% of patients with HCC at early stages of the disease.<sup>5</sup> As a potentially curative treatment for both HCC and cirrhosis, LT in particular may be preferred over other treatment alternatives. However, in Japan, deceased donor LT is not available in most cases of cirrhosis, leaving only living donor LT as an option. Given the small number of living donors available, patients often have no choice but to use their own liver as long as possible. HCC should therefore be treated at an early stage to avoid reducing liver function in these patients. In addition, early detection of HCC may prevent the progression to metastatic disease. Diagnostic precision in the detection, localization, and characterization of liver tumors also reduces the need for additional diagnostic procedures.

Advances in diagnostic imaging techniques, such as the introduction of contrast media-enhanced magnetic resonance imaging (MRI), have enabled imaging-based diagnosis of HCC in many patients. Gadolinium ethoxybenzyl diethylenetriamine pentaacetic acid (gadoteric acid) is a contrast agent used for the detection and characterization of liver tumors in patients with known or suspected liver disease.<sup>6</sup> Gadoteric acid is an extracellular interstitial compound with a partial hepatobiliary secretion, and it can be administered by bolus injection for evaluation of vascularization. Gadoteric acid-enhanced MRI (EOB-MRI) has demonstrated improved sensitivity in the characterization of most tumor types compared with nonenhanced MRI, computed tomography (CT) scanning, and alternative contrast agents.<sup>7</sup> The most significant advantage of this improvement in diagnostic sensitivity over other imaging techniques is the high detectability of small lesions as well as nonhypervascular HCC. This approach allows early detection of HCC by EOB-MRI.

Very few studies have investigated the cost-effectiveness of EOB-MRI, and existing studies have not assessed downstream costs or effects after diagnosis.<sup>8</sup> The cost-effectiveness of EOB-MRI as a

diagnostic strategy for patients at high risk of HCC in Japan is currently unknown.<sup>9–14</sup> The present study was therefore conducted to evaluate the cost-effectiveness of EOB-MRI in the diagnosis and treatment of HCC in Japan after preliminary screening with ultrasound in which HCC was suspected.

## PATIENTS AND METHODS

### Model Overview

This economic evaluation considered the Japanese population of people experiencing chronic infection with HBV, HCV, or liver cirrhosis. Japanese guidelines define these individuals as patients at high risk for HCC.<sup>2</sup> This analysis compares the diagnostic strategy of EOB-MRI against extracellular contrast media-enhanced MRI (ECCM-MRI) and contrast media-enhanced CT (CE-CT), 3 diagnostic methods commonly used for confirming HCC in Japan after preliminary ultrasound screening in which HCC is suspected.<sup>2</sup> The perspective taken in these analyses was that of the Ministry of Health, Labour and Welfare (MHLW); as such, only direct costs were considered.

### Model Structure

Because HBV, HCV, liver cirrhosis, and HCC are chronic diseases that affect patients over a lifetime, a Markov model was developed to evaluate the cost-effectiveness of EOB-MRI compared with either ECCM-MRI or CE-CT in the treatment and diagnosis of HCC among high-risk Japanese patients. The model was developed as a 6-state cohort Markov model, in line with model structures presented in previously published cost-effectiveness studies (Figure 1).<sup>15–18</sup> The cycle length was chosen as 6 months to reflect the period over which the Japanese Evidence-Based Clinical Practice Guidelines for Hepatocellular Carcinoma recommend tumor marker measurements and ultrasound diagnostic testing be performed for patients with chronic HBV, chronic HCV, or liver cirrhosis.<sup>2</sup> Health states in the model included the entry state of no HCC (patients stratified according to Child-Pugh [CP] liver function of A [CPA], B [CPB], or C [CPC]), HCC, HCC remission, LT, end-stage care, and death. Mortality risk was calculated as a function of patient age, disease status, and CP liver function. Background mortality was derived from Japanese life tables.<sup>19</sup> All transitions between health states were assumed to

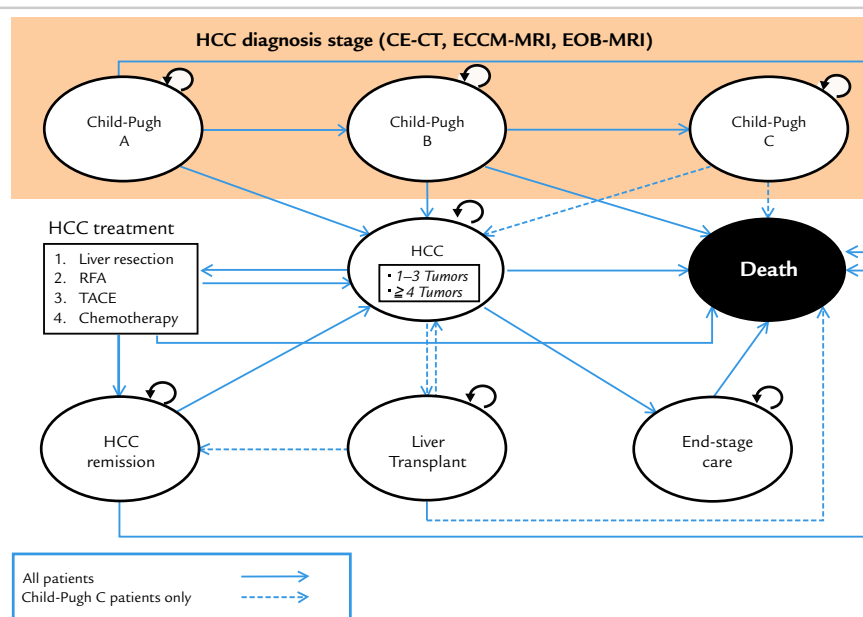


Figure 1. Markov model flow diagram. CE-CT = contrast media-enhanced computed tomography scan; ECCM = extracellular contrast media-enhanced; EOB = gadoxetic acid-enhanced; HCC = hepatocellular carcinoma; ICER = incremental cost-effectiveness ratio; LY = life year; MRI = magnetic resonance imaging; RFA = radiofrequency ablation; TACE = transarterial chemoembolization; QALY = quality-adjusted life year.

occur half way through each 6-month cycle. The impact of varying base case transition probability values was explored in sensitivity analyses.

The base case time horizon was lifetime, as recommended by international pharmacoeconomic modeling guidelines for the evaluation of chronic diseases.<sup>20,21</sup> However, results are also presented for several alternative time horizons to more fully inform readers and decision-makers regarding costs and outcomes. In accordance with the guideline for economic evaluation of health care technologies in Japan, both costs and outcomes were discounted at an annual rate of 2%.<sup>20</sup>

From the initial entry health state, and at each subsequent cycle, patients could either remain in their current health state, transition to a state of worsening CP liver function, progress to HCC, or transition to the absorbing health state of death. For patients who developed HCC, it was assumed that a 2-step diagnostic process was undertaken in which ultrasound was used to identify suspected HCC followed by confirmation through a secondary diagnostic process as recommended by the Japanese Evidence-Based Clinical Practice Guidelines for Hepatocellular Carcinoma.<sup>2</sup> Secondary diagnostic options included

EOB-MRI, ECCM-MRI, and CE-CT. The proportion of patients correctly identified through these secondary diagnostic processes was a function of the sensitivity and specificity of the respective diagnostic instrument. Patients who were identified as having HCC were stratified into 1 of 2 groups according to the number of identified tumors (either 1–3 or  $\geq 4$  tumors). Treatment for these patients with HCC was then determined based on CP status and number of tumors. Patients whose disease status remained undiagnosed after the diagnostic process could either experience disease progression categorized according to the number of tumors, transition to end-stage care, or die.

For patients with 1 to 3 tumors, it was also assumed that 50% of patients received LR as first-line therapy and 50% received RFA as first-line therapy. All patients with  $\geq 4$  tumors were assumed to receive TACE as first-line therapy, following recommendations in the Japanese Evidence-Based Clinical Practice Guidelines for Hepatocellular Carcinoma.<sup>2</sup> These assumptions were validated by the Delphi panel participants.

After the first-line treatment, patients with HCC with 1 to 3 tumors could transition to the HCC

remission health state, experience treatment failure (remain in the HCC health state), or die. Patients who failed the first treatment during any given 6-month cycle could progress to a second line of treatment in the following cycle. For second-line treatment among patients with 1 to 3 tumors, it was assumed that 50% of patients received LR and 50% received RFA. For those who failed the second treatment, a third line of treatment using TACE was made available. Treatment failure rates for each treatment modality were calculated as the number of patients who experienced disease recurrence in a given cycle. Patients with HCC who had received 3 lines of therapy transitioned to end-stage care, which could include either chemotherapy with the biologic agent sorafenib or palliative care, as indicated in the Japanese Evidence-Based Clinical Practice Guidelines for Hepatocellular Carcinoma.<sup>2</sup> It was assumed that for all CPA and CPB patients who failed 3 lines of therapy, 50% would receive chemotherapy and 50% would receive palliative care. For CPC patients, all patients were assumed to receive palliative care after treatment failure. These assumptions were validated during the Delphi panel process.

The reference strategy was EOB-MRI, and the incremental comparisons of interest were therefore EOB-MRI versus ECCM-MRI and EOB-MRI versus CE-CT, respectively. Primary outcomes are expressed in terms of incremental cost per quality-adjusted life year (QALY), calculated by using incremental cost-effectiveness ratios (ICERs). In accordance with economic modeling guidelines, ICERs were not calculated for strategies that were dominated.<sup>22</sup> Additional outcomes include number of new HCC cases, number of HCC deaths, and both discounted and undiscounted life-years.

### Clinical Inputs

A targeted literature review was conducted to identify previous literature on HCC diagnostic and treatment strategies. The scope of each search strategy was defined in terms of patient population, intervention, comparator, and outcome, together with the design of the studies considered. In addition to the targeted literature review, a Delphi panel of 9 Japanese physicians with expertise in gastroenterology, radiology, hepatology, surgery, and biliary-pancreatic surgery was convened to identify input parameter values not identified in the literature

search. The Delphi panel consisted of 2 rounds of anonymous responses. Clinical assumptions and the overall approach of the model were confirmed by the Delphi panel, and the clinical pathway was reviewed and revised according to the panel's suggestions.

All patients at high risk of HCC entered the model with chronic HBV, HCV, or liver cirrhosis, stratified according to CP status A, B, or C. The initial CP distribution among patients and the transition probabilities between CP categories were derived from a recent Japanese study of Japanese patients with chronic HCV, which was then validated by the Delphi panel experts (Figure 1).<sup>23</sup> The proportion of high-risk patients who developed HCC was derived from a Japanese longitudinal study of 2215 patients with chronic viral hepatitis.<sup>24</sup> Due to the paucity of data regarding HCC according to CP status, the risk of developing HCC was assumed to be the same across CP categories. The proportion of patients with HCC identified as having 1 to 3 tumors was obtained from the expert Delphi panel, and the proportion having  $\geq 4$  tumors was assumed to be 1 minus this value. The proportion of untreated patients transitioning from 1 to 3 tumors to either  $\geq 4$  tumors, end-stage disease, or death, according to CP status, was also obtained from the Delphi panel questionnaire. The base case mortality rate was estimated as a function of both age (using Japanese life tables) and the excess mortality due to liver function and underlying disease (eg, HCV, HBV, liver cirrhosis) as reported in the recent Japanese study.<sup>23</sup>

Japanese patients diagnosed with HCC could receive  $\geq 1$  of the following treatments: LR, RFA, TACE or, for those with advanced stages of liver dysfunction, LT was assumed. Overall survival data associated with LR, LT, and treatment with TACE or RFA were derived from studies conducted in Japan.<sup>25,26</sup> The maximum age to receive a LT was assumed to be 65 years, as specified in the Japanese HCC guidelines.<sup>2</sup> Overall survival rates for patients who transitioned to palliative care or received chemotherapy were derived from a Japanese study.<sup>25</sup> Patients with HCC in the model who received chemotherapy or palliative care were assumed to continue these treatments until death. Survival rates reported in the identified studies were transformed to 6-month survival probabilities by using a standard mathematical formula.<sup>27</sup> Alternate overall survival values were explored in

sensitivity analyses in which the base case values were varied by  $\pm 20\%$ .

Recurrence rates for patients treated with either LR, LT, or TACE were derived from 2 recent Japanese studies of patients with HCC.<sup>26,28,29</sup> Because Japanese data on recurrence after RFA treatment were not identified during the literature review, the recurrence rate was derived from a recent Chinese comparative cohort study of 597 patients with HCC.<sup>30</sup> Alternative values ( $\pm 20\%$  of the base case values) for overall survival and recurrence were examined in sensitivity analyses to account for uncertainty.

The Japanese Evidence-Based Clinical Practice Guidelines for Hepatocellular Carcinoma classify patients according to HCC tumor size.<sup>2</sup> However, due to the unavailability of Japanese data on tumor size in determination of diagnostic accuracy, a simplifying assumption was made based on the number of HCC tumors (either 1–3 or  $\geq 4$  tumors). The proportion of patients with 1 to 3 tumors and  $\geq 4$  tumors treated with LR, LT, or RFA, according to CP status, was provided by the expert Delphi panel participants. The Delphi panel also provided the proportion of patients who receive palliative care, stratified according to CP status. All clinical values used in the model are presented in **Supplemental Table I** (as shown in the online version at <http://dx.doi.org/10.1016/j.clinthera.2017.03.006>).

For all analyses, the diagnostic specificity of preliminary ultrasound screening (0.96) was derived from a diagnostic study conducted in the United States of HCC in patients with cirrhosis.<sup>31</sup> Diagnostic sensitivity and specificity values for each of the 3 diagnostic modalities examined in the model were reported in the literature according to tumor size, either  $< 2$  cm, 2 to 4 cm, or  $> 4$  cm in diameter, or for all sizes. Average sensitivity and specificity values across all relevant studies were calculated, weighted by the total number of patients and total number of tumors in each study. In the base case, weighted averages across studies of tumors of all sizes were used. This approach may be conservative because the reported sensitivity of ECCM-MRI and CE-CT is lower for smaller tumor sizes compared with that of EOB-MRI.<sup>10,14,31,32</sup>

Diagnostic sensitivity and specificity values for CE-CT and EOB-MRI were calculated based on the results of a recently published meta-analysis of 9 studies of patients with HCC, which included

3 Japanese studies.<sup>9</sup> Diagnostic sensitivity values for ECCM-MRI were not identified in recent Japanese studies or meta-analyses, and therefore a weighted average across 3 identified studies among patients with HCC from South Korea was used in the model.<sup>10,13,14</sup> Specificity data for ECCM-MRI were calculated as a weighted average derived from 2 published studies of patients with HCC from South Korea and the United States, respectively.<sup>10,11</sup> Due to a paucity of data, diagnostic values for patients with 1 to 3 tumors and  $\geq 4$  tumors were assumed to be the same. All diagnostic parameter values used in the model are presented in **Supplemental Table II** (as shown in the online version at <http://dx.doi.org/10.1016/j.clinthera.2017.03.006>).

### Health Care Resource Utilization and Costs

Because the present analysis was conducted from the public payer perspective of the MHLW, only direct costs were included. The costs of productivity loss, including absenteeism and presenteeism, were not considered. However, because unit costs were derived from MHLW databases, as recommended by Japanese guidelines, patient out-of-pocket expenses were assumed to be included in the estimates.

Unit costs consisted of the direct costs of diagnostic procedures, treatment courses, and other health care resource utilization costs. The respective unit costs for ultrasound, ECCM-MRI, EOB-MRI, and CE-CT were gathered from the MHLW Reimbursement Information Service.<sup>33</sup> The per-procedure unit costs for treatment modalities included LR, LT, RFA, and TACE. Unit costs for the LR, RFA, and TACE treatment modalities were taken from the MHLW's Reimbursement Information Service and included cost of treatment procedures and associated hospitalization. For use in the model, the unit cost of TACE was multiplied by 1.6 to account for the fact that 60% of patients receive a second course of TACE therapy, as per the recommendations of the expert Delphi panel. The unit cost of LT was taken from a cost analysis of adult-adult living donors for LT in Japan.<sup>34</sup>

Other health care resource utilization unit costs included chemotherapy with sorafenib and unit costs associated with palliative or end-stage care. The cost of sorafenib was estimated based on standard dosing in Japan of 800 mg/d (200 mg per pill) multiplied by 182 days. The unit cost was taken from the MHLW's Reimbursement Information Service.<sup>33</sup> The median



duration of sorafenib therapy among patients with HCC in Japan was reported to be 17.4 weeks and 7.6 weeks for CPA and CPB patients, respectively.<sup>35</sup> Therefore, it was assumed in the model that the cost of sorafenib therapy would be limited to one 6-month cycle. Palliative care costs were estimated as the 6-month cost of hospitalization from the MHLW's Reimbursement Information Service. For this calculation, it was assumed that 50% of patients were treated as inpatients and 50% of patients were treated in the outpatient setting. All unit costs were converted to 6-month costs for use in the model.

All patients were assumed to receive diagnostic ultrasound and secondary confirmatory diagnostic tests every 6 months. Patients whose ultrasound results were positive (including both true HCC and false-positive results) underwent confirmatory diagnostic testing with either CE-CT, ECCM-MRI, or EOB-MRI. Costs pertaining to false-positive findings were assumed to be the cost of the additional diagnostic tests needed to confirm the decision to treat. The unit cost of EOB-MRI, ECCM-MRI, and CE-CT was used for estimating the cost of false-positive findings for each diagnostic strategy. Additional diagnostic costs were not considered for true positive findings. Patients receiving palliative care or chemotherapy who died at any point during a given 6-month period (ie, 1 cycle in the model) were assumed to die halfway through the cycle and were therefore assigned 50% of the 6-month costs of chemotherapy or palliative care, respectively. All costs used in the model are presented in [Supplemental Table III](#) (as shown in the online version at <http://dx.doi.org/10.1016/j.clinthera.2017.03.006>).

### Health State Utilities

For use in economic evaluation, health-related quality of life is typically reported in the form of utility values on a scale between 0 and 1 (0 indicating death, and 1 indicating the best possible state of health). The EuroQoL 5 Dimensions questionnaire (EQ-5D) utility index has been shown to be a valid and responsive outcome measure among patients with chronic hepatic diseases, and Japanese studies have provided EQ-5D utility values for patients infected with HCV.<sup>36,37</sup> Results from a Japanese study reported utility estimates for both HBV and HCV patients stratified according to age group, and the present model uses the utility estimates for the patients

aged 40 to 49 years from this publication in the base case.<sup>37</sup>

For patients undergoing an LT procedure, the utility value for the first year after the transplant and for subsequent years was derived from a previously published cost-effectiveness analysis of patients with HCC.<sup>17</sup> Temporary utility decrements associated with HCC treatment modalities were not available in the Japanese literature and thus were taken from international sources. For LR, the temporary utility decrement was derived from a systematic review and economic evaluation from the United Kingdom of ablative therapies for the management of liver metastases.<sup>38</sup> For RFA-treated patients, the temporary utility decrement was taken from the same study. Previous studies have shown that TACE results in lower quality of life relative to RFA and higher quality of life relative to LR.<sup>39</sup> Therefore, on the basis of this information, and because a published estimate was not identified for the temporary decrement associated with TACE, the temporary TACE decrement was assumed to be the mid-point of the decrement for LR and the decrement for RFA. The utility value corresponding to treatment with chemotherapy with sorafenib was derived from a study by the National Institute for Health and Care Excellence in the United Kingdom of sorafenib treatment for advanced HCC.<sup>40</sup> All utility values used in the model are presented in [Supplemental Table IV](#) (as shown in the online version at <http://dx.doi.org/10.1016/j.clinthera.2017.03.006>). To account for uncertainty in utility estimates, base case utility values were varied by  $\pm 20\%$  in sensitivity analyses.

### Sensitivity Analyses

Models are necessarily simplified approximations of actual clinical practice and patient experience. As a result, uncertainty in terms of both model input values and structural assumptions should be characterized through sensitivity analysis. One-way (deterministic) sensitivity analysis involves varying input parameter values one at a time and assessing the impact of these variations on the results. To assess the simultaneous impact of changes in multiple input parameter values, a Monte Carlo simulation was performed. This probabilistic technique involves simulating the model results numerous times by using sampling with replacement to create a probability distribution of the results. These results are typically presented in the

Table I. Base case results (deterministic).

Strategy	New HCC Cases	HCC Deaths	LYs: Undiscounted	LYs: Discounted	QALYs	Costs, ¥	Incremental Costs, ¥	Incremental QALYs	ICER
CE-CT	0.871	0.232	10.394	9.696	9.215	2,482,608	-307,739	0.287	Dominated
ECCM-MRI	0.885	0.212	10.488	9.776	9.303	2,365,421	-190,552	0.199	Dominated
EOB-MRI	0.904	0.172	10.683	9.968	9.502	2,174,869	-	-	-

CE-CT = contrast media-enhanced computed tomography scan; ECCM = extracellular contrast media-enhanced; EOB = gadoteric acid-enhanced; HCC = hepatocellular carcinoma; ICER = incremental cost-effectiveness ratio; LY = life year; MRI = magnetic resonance imaging; QALY = quality-adjusted life year.

form of cost-effectiveness acceptability curves in accordance with accepted good research practices.<sup>22</sup>

For each input parameter, a distribution was assumed in the probabilistic analysis. For transition probabilities, utility data, treatment efficacy, treatment proportions, and diagnostic variables, the data were assumed to follow a beta distribution because they are restricted to values between 0 and 1. For all costs, the data were assumed to follow a gamma distribution because the distribution of the data was assumed to be right-skewed and restricted to values > 0.

## RESULTS

### Base Case

Over a lifetime horizon, the per patient undiscounted and discounted LYs generated for each of the diagnostic strategies, respectively, were as follows: CE-CT, 10.394 and 9.696, ECCM-MRI, 10.488 and 9.776; and EOB-MRI 10.683 and 9.968. The number of new HCC cases was highest for the EOB-MRI strategy (0.904), followed by ECCM-MRI (0.885), and CE-CT (0.871). Deaths due to HCC were lowest for EOB-MRI (0.172), followed by ECCM-MRI (0.212); HCC deaths were highest for CE-CT (0.232).

The EOB-MRI strategy generated the greatest number of QALYs (9.502), followed by ECCM-MRI (9.303); CE-CT generated the lowest number of QALYs (9.215). The diagnostic strategy with the lowest costs was EOB-MRI (¥2,174,869), followed by ECCM-MRI (¥2,365,421), and then CE-CT (¥2,482,608). EOB-MRI had lower costs and generated a higher number of QALYs than either ECCM-MRI or CE-CT and therefore was the dominant diagnostic strategy (Table I). The EOB-MRI

diagnostic strategy was observed to remain dominant over alternative time horizons considered of 5, 10, 25, and 50 years. The results for EOB-MRI only ceased to be dominant over a time horizon of 1 year. Because EOB-MRI dominated both comparator diagnostic strategies in the base case, ICERs were not calculated, in accordance with standard pharmacoeconomic analysis practices.<sup>22</sup>

In a detailed breakdown of the base case costs, treatment for HCC was the most costly component: ¥2,212,818 for CE-CT, ¥2,123,319 for ECCM-MRI, and ¥1,943,238 for EOB-MRI (Table II). For the EOB-MRI strategy, higher costs were observed for treatments given in earlier stages of disease such as LT, LR, and RFA. By contrast, the ECCM-MRI and CE-CT diagnostic strategies were associated with higher costs for later stage treatments such as chemotherapy and palliative care. A breakdown of the base case outcomes (Table III) revealed that CPA patients had the highest QALYs across each of the treatment strategies (7.190 for CE-CT, 7.268 for ECCM-MRI, and 7.436 for EOB-MRI).

### Sensitivity Analyses

The results of one-way sensitivity analyses are typically presented in the form of a tornado diagram.<sup>27</sup> Both CE-CT and ECCM-MRI were dominated by EOB-MRI in the base case, and EOB-MRI dominance was maintained across each of the one-way sensitivity analyses conducted. Therefore, in accordance with pharmacoeconomic modeling best practices, the results of the one-way sensitivity analysis were not presented.<sup>22</sup>

For the probabilistic sensitivity analysis, 1000 Monte Carlo simulations were conducted (Figure 2). The

Table II. Disaggregated costs.

Cost Component	CE-CT, ¥	ECCM-MRI, ¥	EOB-MRI, ¥
Additional screening	97,715	59,546	36,752
False-positive finding	1733	7496	1638
Screening	58,394	61,486	76,201
Ultrasound	111,948	113,574	117,040
Treatment	2,212,818	2,123,319	1,943,238
Chemotherapy	727,719	620,267	410,975
Liver resection	206,650	219,898	250,203
LT	590,066	624,491	712,106
Palliative care	354,078	311,423	221,392
RFA	186,254	198,292	225,717
TACE	148,050	148,949	122,845
Total	2,482,608	2,365,421	2,174,869

CE-CT = contrast media-enhanced computed tomography scan; ECCM = extracellular contrast media-enhanced; EOB = gadoxetic acid-enhanced; LT = liver transplant; MRI = magnetic resonance imaging; RFA = radiofrequency ablation; TACE = transarterial chemoembolization; QALY = quality-adjusted life year.

probabilistic results, presented as mean costs and mean QALYs across all simulations, closely matched the base case (deterministic) results, providing validation of the model results and model structure (Table IV). Because both the CE-CT and ECCM-MRI diagnostic strategies were dominated by EOB-MRI in the base case, in accordance with modeling best practices, the cost-effectiveness acceptability curves were not presented.<sup>22</sup>

To assess uncertainty associated with input parameter value data selections, alternative sets of values were chosen based on previously conducted studies. The base case results used imaging modality-specific sensitivity and specificity values reported for tumors of any size. Because EOB-MRI has been suggested to have superior sensitivity for smaller tumor sizes, a scenario analysis was conducted by using alternative sensitivity and specificity values reported for tumor sizes <2 cm.<sup>10,11,14,31,32</sup> The negative incremental costs and positive incremental QALYs between EOB-MRI and the other diagnostic strategies in the

Table III. Disaggregated quality-adjusted life year (QALYs).

QALY Component	CE-CT	ECCM-MRI	EOB-MRI
CPA	7.190	7.268	7.436
CPB	0.687	0.694	0.709
CPC	1.160	1.182	1.237
Treatment	0.178	0.159	0.120
Total	9.215	9.303	9.502

CE-CT = contrast media-enhanced computed tomography scan; CPA = Child-Pugh class A; CPB = Child-Pugh class B; CPC = Child-Pugh class C; ECCM = extracellular contrast media-enhanced; EOB = gadoxetic acid-enhanced; MRI = magnetic resonance imaging.

base case were found to be even more pronounced in this scenario analysis.

A second scenario analysis was conducted by using alternative utility values reported by Levy et al in 2008 as these values have been used in economic evaluations of HCC.<sup>15,41,42</sup> Using the alternative utility values resulted in a lower number of QALYs generated for each diagnostic strategy compared with the base case. The incremental QALYs between EOB-MRI and both ECCM-MRI and CE-CT were also found to be smaller than in the base case; however, EOB-MRI consistently remained the dominant diagnostic strategy.

## DISCUSSION

The primary objective of the present study was to determine, from an MHLW perspective, the cost-effectiveness of EOB-MRI compared with ECCM-MRI and CE-CT among patients at high risk of developing HCC in Japan.

There are a number of strengths associated with the present analysis. One advantage was that the base case time horizon was lifetime, which accounts for the fact that HCC risk and outcomes are relevant for the duration of a patient's life. Results using alternative time horizons were also presented to more fully describe the expected outcomes associated with the 3 diagnostic strategies under analysis.

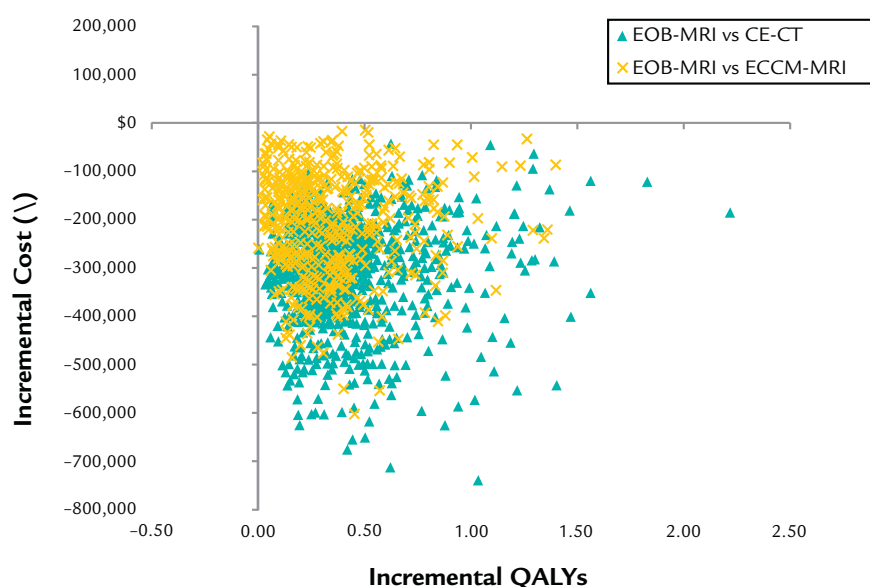


Figure 2. Scatterplot: probabilistic sensitivity analysis. CE-CT = contrast media-enhanced computed tomography scan; ECCM = extracellular contrast media-enhanced; EOB = gadoxetic acid-enhanced; MRI = magnetic resonance imaging; QALY = quality-adjusted life year.

Another advantage is that data from studies conducted in Japan were used almost exclusively, in accordance with the guideline for economic evaluation of health care technologies in Japan.<sup>20</sup> Important differences in demography, epidemiology, characteristics of the health care system, and health care resource availability likely exist, underscoring the importance of using data specific to Japan for localized results. Previous economic evaluations of HCC surveillance and diagnostics by Japanese investigators have relied heavily on data from

foreign sources, which may not be appropriate for evaluating costs and effects among patients in Japan.<sup>8,16</sup>

Previously published pharmacoeconomic studies of HCC in Japan have also tended to focus on either treatment or diagnostics in isolation from one another.<sup>8,16</sup> The present analysis evaluated the costs and outcomes of diagnostic strategies that include the succession of treatments and related outcomes which followed as a result of HCC diagnoses. Fully defined diagnostic strategies, combining both diagnostic

Table IV. Probabilistic results.

Strategy	New HCC Cases	HCC Deaths	LYs: Undiscounted	LYs: Discounted	QALYs	Costs, ¥	Incremental Costs, ¥	Incremental QALYs	ICER
CE-CT	0.923	0.241	10.890	10.103	9.681	2,677,766	-313,765	0.415	Dominated
ECCM-MRI	0.942	0.220	11.034	10.222	9.816	2,554,973	-190,977	0.280	Dominated
EOB-MRI	0.970	0.180	11.319	10.487	10.095	2,363,996	-	-	-

CE-CT = contrast media-enhanced computed tomography scan; ECCM = extracellular contrast media-enhanced; EOB = gadoxetic acid-enhanced; HCC = hepatocellular carcinoma; ICER = incremental cost-effectiveness ratio; LY = life year; MRI = magnetic resonance imaging; QALY = quality-adjusted life year.

procedures and the treatments and outcomes they entail, more accurately capture the true value of diagnostic technologies than considering diagnostics or treatments alone. In this way, the present study provides a basis for improved content validity over previous studies.

In addition, the HCC patient treatment pathway in the present analysis was based on the Japanese Evidence-Based Clinical Practice Guidelines for Hepatocellular Carcinoma, and both unit costs and diagnostic characteristics (sensitivity and specificity) were similar to previously published estimates, which supports the face validity of the model.<sup>8,16</sup> However, EOB-MRI has been shown to have superior diagnostic characteristics over both ECCM-MRI and CE-CT in the detection of tumors  $\leq 2$  cm in diameter. In fact, the availability and use of EOB-MRI for the detection of HCC and its documented capability to differentiate early HCC from dysplastic nodules has been identified as a major breakthrough.<sup>43</sup> Consequently, the base case results of the present analysis may in fact be understating the value of EOB-MRI as a diagnostic strategy for HCC.

The superior diagnostic capability of EOB-MRI in detecting HCC has particular relevance to both patients and the health care system because the need for additional imaging as a result of inadequate initial diagnostic accuracy could result in prolonged patient testing, delayed treatment decisions, and delayed therapeutic interventions.<sup>44</sup> Delayed therapeutic interventions can lead to unnecessary distress and worsening disease for patients as well as generate additional medical costs and excessive burden for the medical system. In the present analysis, diagnosis of HCC using either ECCM-MRI or CE-CT resulted in comparatively later detection of disease for many patients. Although this later detection necessitated fewer up-front treatment costs than EOB-MRI in the short run, it also led to treatment being administered at later stages of disease, resulting in less effective disease management and, ultimately, the need for more intensive and costly treatments such as TACE, chemotherapy, and palliative care. In contrast, EOB-MRI generated higher costs for LR and RFA compared with ECCM-MRI and CE-CT, suggesting that treatment had been provided at earlier stages due to earlier detection of tumors. The results of the present analysis provide some initial confirmatory evidence that the comparatively inferior diagnostic

accuracy associated with ECCM-MRI and CE-CT may lead to suboptimal patient and medical system outcomes.

The present study had a number of limitations. As is unavoidable in pharmacoeconomic modeling, a number of simplifying assumptions were made over the course of model development. These included assumptions regarding input values used in the sensitivity analyses, tumor size and number, stratification of HCC risk, survival, and costing.

A limitation of this study is that uncertainty in input parameter values was arbitrarily modeled at  $\pm 20\%$  of base case values. As such, the sensitivity analyses may not represent the true uncertainty associated with the model input parameter values. However,  $\pm 20\%$  of base case values is likely an overstatement of the true uncertainty.

Published studies reporting the sensitivity and specificity for detecting tumors by sizes categorized in the Japanese treatment guidelines for HCC were not identified in the literature search nor elicited through the Delphi process. Consequently, an assumption was made to stratify patients on the basis of tumor number rather than tumor size. This assumption may have clinical plausibility because patients with a greater number of tumors tend to be at more advanced stages of disease. A study of 557 patients with HCC from the United States identified the presence of multiple tumors as an independent predictor of death, which supports this assumption.<sup>45</sup> Although the assumption could have introduced bias into the model because diagnostic sensitivity and specificity are calculated on the basis of tumor size rather than on tumor number, the potential bias is likely to be in favor of the comparators to EOB-MRI, as EOB-MRI has been shown to have superior diagnostic characteristics for smaller tumor sizes.<sup>10,14,32</sup> As a result, the assumption may be conservative.

Another limitation is that due to lack of published data, the sensitivity and specificity of the diagnostic strategies in the model were assumed to be the same regardless of the number of tumors a patient had. This approach may have biased downward the results for patients with  $\geq 4$  tumors because true sensitivity and specificity of diagnostic tests can be, on average, slightly higher among patients with a greater number of tumors. However, this scenario is likely a conservative assumption in the present analysis, as improved



diagnostic characteristics for patients with  $\geq 4$  tumors would be expected across all 3 diagnostic strategies, and EOB-MRI has a relatively higher baseline sensitivity and specificity. The incrementally higher true sensitivity and specificity values of EOB-MRI for patients with  $\geq 4$  tumors, if used in the analysis, would likely have resulted in greater diagnostic superiority relative to the other strategies. Consequently, the assumption may have had at worst a negligible overall effect or even biased the base case results slightly in favor of the other 2 diagnostic strategies.

In the absence of studies reporting stratification of HCC risk across CP groups, an assumption was made that HCC risk was equal across CP groups. Because HCC risk has been noted to depend on the stage of cirrhosis, this assumption may have biased the results for CPC patients relative to CPA or CPB patients.<sup>46</sup> This bias may have resulted in fewer CPC patients receiving LT and TACE in the model, generating decreased costs relative to the base case. However, these costs would accrue disproportionately between the diagnostic strategies with relatively more costs generated from the ECCM-MRI and CE-CT strategies compared with EOB-MRI. For this reason, this assumption may be considered conservative.

Due to lack of available data, the proportion of untreated patients with 1 to 3 tumors who progress to having  $\geq 4$  tumors was assumed to be the same irrespective of underlying liver function. This outcome may differ from actual clinical practice in which a smaller proportion of patients with CPC liver function may progress to having  $\geq 4$  tumors than patients with either CPA or CPB. However, this assumption concerns a very small proportion of patients and would have a negligible effect on the model results.

In addition, this analysis did not consider the impact of treatment-related adverse events for patients receiving treatment for HCC. However, among patients with HCC receiving treatment with sorafenib, the proportion of patients experiencing treatment-related adverse events has been reported to be relatively low, and would not be expected to materially affect patient overall survival, health-related quality of life, or cost.<sup>35</sup>

## CONCLUSIONS

From the perspective of the MHLW, the cost-effectiveness of EOB-MRI was shown to be superior

to either ECCM-MRI or CE-CT among Japanese patients at high risk of developing HCC. The diagnostic strategy EOB-MRI dominated the other diagnostic strategies, and this finding was robust to both sensitivity and scenario analyses. As a result, in terms of cost-effectiveness, EOB-MRI could be the first-choice imaging modality for medical care of HCC among patients with hepatitis or cirrhosis in Japan. Widespread implementation of EOB-MRI could reduce health care expenditures, particularly downstream treatment costs, associated with HCC.

## ACKNOWLEDGMENTS

This study was funded by Bayer Yakuhin Ltd.

Drs. Honda, Nishie, and Motosugi provided helpful comments in the writing of the manuscript. Drs. Goshima, Haradome, Hatano, Imai, Kudo, Matsuda, Saitoh, and Yoshimitsu participated anonymously in the expert Delphi panel and reviewed the manuscript. Mr. Crawford designed the study, and Mr. Crawford, Mr. Ball, and Ms. Kruger programmed the cost-effectiveness model and wrote the manuscript. All authors approved the final article.

## CONFLICTS OF INTEREST

Bayer Yakuhin Ltd was not involved in the study design, collection, analysis and interpretation of data, writing of the manuscript, or decision to submit the manuscript for publication.

Drs. Nishie, Goshima, Haradome, Hatano, Imai, Kudo, Matsuda, Motosugi, Saitoh, Yoshimitsu, and Honda received an honorarium from Bayer Yakuhin Ltd for participation in this study. Mr. Crawford, Ms. Kruger, and Mr. Ball are employees of QuintilesIMS, a health care consulting firm contracted by Bayer Yakuhin Ltd for this research.

## SUPPLEMENTARY MATERIAL

Supplemental tables accompanying this article can be found in the online version at <http://dx.doi.org/10.1016/j.clinthera.2017.03.006>.

## REFERENCES

1. Yang JD, Roberts LR. Epidemiology and management of hepatocellular carcinoma. *Infect Dis Clin North Am*. 2010;24:899-919.

2. Kokudo N, Hasegawa K, Akahane M, et al. Evidence-based clinical practice guidelines for hepatocellular carcinoma: the Japan Society of Hepatology 2013 update (3rd JSH-HCC Guidelines). *Hepatology Research*. 2015;45:123–127.
3. Ikeda M, Mitsunaga S, Shimizu S, et al. Current status of hepatocellular carcinoma in Japan. *Chinese Clinical Oncology*. 2013;2:40.
4. Huppertz A, Balzer T, Blakeborough A, et al. Improved detection of focal liver lesions at MR imaging: multicenter comparison of gadoxetic acid-enhanced MR images with intraoperative findings. *Radiology*. 2004;230:266–275.
5. Bruix J, Llovet JM. Prognostic prediction and treatment strategy in hepatocellular carcinoma. *Hepatology*. 2002;35:519–524.
6. EOB Primovist label 2015. Accessed 2016/09/20.
7. Chanyaputhipong J, Low SC, Chow PK. Gadoxetate acid-enhanced MR Imaging for HCC: a review for clinicians. *Int J Hepatol*. 2011;489342.
8. Iwata K, Murakami N, Ogasawara K. Cost-effectiveness analysis of the MRI with hepatocyte-specific contrast agent Gd-EOB-DTPA for the detection of metastatic liver tumor. *European Congress of Radiology*. 2012;2012:1–17.
9. Ye F, Liu J, Ouyang H. Gadolinium ethoxybenzyl diethylenetriamine pentaacetic acid (Gd-EOB-DTPA)-enhanced magnetic resonance imaging and multidetector-row computed tomography for the diagnosis of hepatocellular carcinoma: a systematic review and meta-analysis. *Medicine*. 2015;94. e1157–e1157.
10. Kim YK, Kim C, Han Y, Park G. Detection of small hepatocellular carcinoma: can gadoxetic acid-enhanced magnetic resonance imaging replace combining gadopentetate dimeglumine-enhanced and superparamagnetic iron oxide-enhanced magnetic resonance imaging? *Investigative Radiology*. 2010;45:740–746.
11. Park MS, Kim S, Patel J, et al. Hepatocellular carcinoma: detection with diffusion-weighted versus contrast-enhanced magnetic resonance imaging in pretransplant patients. *Hepatology*. 2012;56:140–148.
12. Kasai R, Hasebe T, Takada N, et al. Comparison of diagnostic efficacy of Gd-EOB-DTPA-enhanced MRI and dynamic contrast-enhanced multislice CT in hepatocellular carcinoma. *Journal of the Medical Society of Toho University*. 2012;59:279–289.
13. Youk JH, Lee JM, Kim CS. MRI for detection of hepatocellular carcinoma: comparison of mangafodipir trisodium and gadopentetate dimeglumine contrast agents. *American Journal of Roentgenology*. 2004;183:1049–1054.
14. Park G, Kim Y, Kim C, et al. Diagnostic efficacy of gadoxetic acid-enhanced MRI in the detection of hepatocellular carcinomas: comparison with gadopentetate dimeglumine. *British Journal of Radiology*. 2010;83:1010–1016.
15. Sangmala P, Chaikledkaew U, Tanwandee T, Pongchareonsuk P. Economic evaluation and budget impact analysis of the surveillance program for hepatocellular carcinoma in Thai chronic hepatitis B patients. *Asian Pacific Journal of Cancer Prevention*. 2014;15:8993–9004.
16. Nouse K, Tanaka H, Uematsu S, et al. Cost-effectiveness of the surveillance program of hepatocellular carcinoma depends on the medical circumstances. *Journal of Gastroenterology and Hepatology*. 2008;23:437–444.
17. Arguedas MR, Chen VK, Eloubeidi MA, Fallon MB. Screening for hepatocellular carcinoma in patients with hepatitis C cirrhosis: a cost-utility analysis. *The American Journal of Gastroenterology*. 2003;98:679–690.
18. Lee JM, Kim MJ, Phongkitkarun S, et al. Health economic evaluation of Gd-EOB-DTPA MRI vs ECCM-MRI and multi-detector computed tomography in patients with suspected hepatocellular carcinoma in Thailand and South Korea. *Journal of Medical Economics*. 2016;19:759–768.
19. Ministry of Health Labour and Welfare. Abridged Life Tables For Japan. *Vital, Health and Social Statistics Office*. 2015. Available online: <http://www.mhlw.go.jp/>.
20. Research group on economic evaluation for Japanese public medical benefits. *Guideline for Economic Evaluation of Healthcare Technologies in Japan*. Tokyo; 2013.
21. Siebert U, Alagoz O, Bayoumi AM, et al. State-transition modeling: a report of the ISPOR-SMDM Modeling Good Research Practices Task Force. *Value Health*. 2012;15:812–820.
22. Briggs AH, Weinstein MC, Fenwick EAL, et al. Model parameter estimation and uncertainty: a report of the ISPOR-SMDM modeling good research practices task force. *Value in Health*. 2012;15:835–842.
23. Yatsushashi H. [Study of the prognosis of patients with liver cirrhosis]. [*National Institute of Public Health*]. 2015. [In Japanese].
24. Ikeda K, Saitoh S, Suzuki Y, et al. Disease progression and hepatocellular carcinogenesis in patients with chronic viral hepatitis: a prospective observation of 2215 patients. *Journal of Hepatology*. 1998;28:930–938.
25. Nakano M, Tanaka M, Kuromatsu R, et al. Efficacy, safety, and survival factors for sorafenib treatment in Japanese patients with advanced hepatocellular carcinoma. *Oncology*. 2012;84:108–114.
26. Kaido T, Morita S, Tanaka S, et al. Long-term outcomes of hepatic resection versus living donor liver transplantation for hepatocellular carcinoma: a propensity score-matching study. *Disease Markers*. 2015;2015. [Article ID 425926], <http://dx.doi.org/10.1155/2015/425926>.
27. Briggs A, Sculpher M, Claxton K. *Decision Modeling for Health. Economic Evaluation*. Oxford: Oxford University Press; 2006.
28. Ikeda K. [Comparison of radiofrequency ablation with surgical

- resection]. *[Strides of Medicine]*. 2009;231:215–219. [In Japanese].
29. Matsuda M, Omata F, Fuwa S, et al. Prognosis of patients with hepatocellular carcinoma treated solely with transcatheter arterial chemoembolization: risk factors for one-year recurrence and two-year mortality (preliminary data). *Intern Med*. 2013;52:847–853.
  30. Guo R, Feng X, Xiao S, et al. Short- and long-term outcomes of hepatectomy with or without radiofrequency-assist for the treatment of hepatocellular carcinomas: a retrospective comparative cohort study. *BioScience Trends*. 2015;9: 65–72.
  31. Yu NC, Chaudhari V, Raman SS, et al. CT and MRI improve detection of hepatocellular carcinoma, compared with ultrasound alone, in patients with cirrhosis. *Clinical Gastroenterology and Hepatology*. 2011;9:161–167.
  32. Sano K, Ichikawa T, Motosugi U, et al. Imaging study of early hepatocellular carcinoma: usefulness of gadoxetic acid-enhanced MR imaging. *Radiology*. 2011;261:834–844.
  33. Reimbursement Information Service. Ministry of Health, Labour and Welfare; 2016. [http://www.iryohoken.go.jp/shinryohoshu/search Menu/](http://www.iryohoken.go.jp/shinryohoshu/searchMenu/).
  34. Sakata H, Tamura S, Sugawara Y, Kokudo N. Cost analysis of adult-adult living donor liver transplantation in Tokyo University Hospital. *Journal of Hepato-Biliary-Pancreatic Sciences*. 2011;18:184–189.
  35. Kudo M, Ikeda M, Takayama T, et al. Safety and efficacy of sorafenib in Japanese patients with hepatocellular carcinoma in clinical practice: a subgroup analysis of GIDEON. *Journal of Gastroenterology*. 2016;51:1150–1160.
  36. Scalone L, Ciampichini R, Fagioli S, et al. Comparing the performance of the standard EQ-5D 3L with the new version EQ-5D 5L in patients with chronic hepatic diseases. *Quality of Life Research*. 2013;22:1707–1716.
  37. Hirao T. [Research on health economic evaluation of various measures relating to patients with viral liver disease]. *[National Institute of Public Health]*. 2013. [In Japanese].
  38. Loveman E, Jones J, Clegg AJ, et al. The clinical effectiveness and cost-effectiveness of ablative therapies in the management of liver metastases: systematic review and economic evaluation. *Health Technology Assessment*. 2014;18:1–283.
  39. Toro A, Pulvirenti E, Palermo F, Di Carlo I. Health-related quality of life in patients with hepatocellular carcinoma after hepatic resection, transcatheter arterial chemoembolization, radiofrequency ablation or no treatment. *Surg Oncol*. 2012;21:e23–e30.
  40. Connock M, Bayliss S, Tubeuf S, et al. Sorafenib for the treatment of advanced hepatocellular carcinoma. *Health Technology Assessment*. 2010;14 (Suppl 1):17–21.
  41. Eckman M, Sherman K. The cost-effectiveness of screening for chronic hepatitis B infection in the United States. *Clinical Infectious Diseases*. 2011; 52:1294–1306.
  42. Levy AR, Kowdley KV, Iloeje U, et al. The impact of chronic hepatitis B on quality of life: a multinational study of utilities from infected and uninfected persons. *Value in Health*. 2008;11:527–538.
  43. Ichikawa T. Diagnosis of Pathologically Early HCC with EOB-MRI: experiences and current consensus. *Cancer*. 2014;3898:97–107.
  44. Zech CJ, Korpraphong P, Huppertz A, et al. Randomized multicentre trial of gadoxetic acid-enhanced MRI versus conventional MRI or CT in the staging of colorectal cancer liver metastases. *British Journal of Surgery*. 2014;101:613–621.
  45. Vauthey J, Lauwers G, Esnaola N, et al. Simplified staging for hepatocellular carcinoma. *Journal of Clinical Oncology*. 2002;20:1527–1536.
  46. El-Serag H. Hepatocellular carcinoma. *New England Journal of Medicine*. 2011;365:1118–1127.
- Address correspondence to:** Akihiro Nishie, M.D., Ph.D, 3-1-1 Maidashi, Higashi-ku, Fukuoka 812-8582, Japan. E-mail: anishie@radiol.med.kyushu-u.ac.jp

**SUPPLEMENTARY MATERIAL**See Supplementary [Table SI-IV](#).

Supplementary Table SI. Clinical inputs.

Variable	Base case value	Reference
<b>Transition probabilities</b>		
TP: C-P A → C-P B	0.02	Yatsuhashi 2015
TP: C-P B → C-P C	0.21	Yatsuhashi 2015
TP: C-PA → C-PA + HCC	0.04	Ikeda et al. 1998
TP: C-P B → C-P B + HCC	0.04	Ikeda et al. 1998
TP: C-P C → C-P C + HCC	0.04	Ikeda et al. 1998
Proportion of HCC that is 1-3 nodules (CPA, CPB)	0.848	Delphi panel 2016
Proportion of HCC that is 1-3 nodules (CPC)	0.848	Delphi panel 2016
Excess death C-P A	0.011	Yatsuhashi 2015
Excess death C-P B	0.051	Yatsuhashi 2015
Excess death C-P C	0.117	Yatsuhashi 2015
TP: Untreated 1-3 nodules → 4+ nodules (CPA/CPB)	0.438	Delphi panel 2016
TP: Untreated 1-3 nodules → end-stage disease (CPA/CPB)	0.092	Delphi panel 2016
TP: Untreated 1-3 nodules → Death (CPA/CPB)	0.048	Delphi panel 2016
TP: Untreated 4+ nodules → end-stage disease (CPA/CPB)	0.356	Delphi panel 2016
TP: Untreated 4+ nodules → Death (CPA/CPB)	0.114	Delphi panel 2016
TP: Untreated 1-3 nodules → 4+ nodules/advanced (CPC)	0.438	Delphi panel 2016
TP: Untreated 1-3 nodules → Death (CPC)	0.09	Delphi panel 2016
<b>Proportion of patients receiving HCC treatments</b>		
Proportion of 1-3 HCC treated with LR CPA/CPB	0.5	Delphi panel 2016
Proportion of 1-3 HCC treated with LT CPA/CPB	0	Delphi panel 2016
Proportion of 1-3 HCC treated with RFA CPA/CPB	0.5	Delphi panel 2016
Proportion of 1-3 HCC treated with LR CPC	0	Delphi panel 2016
Proportion of 1-3 HCC treated with LT CPC	1	Delphi panel 2016
Proportion of end-stage CPA/CPB receiving PC	0.2	Delphi panel 2016
Proportion of end-stage CPC receiving PC	0.9	Delphi panel 2016
<b>Treatment efficacy and recurrence</b>		
HCC recurrence following LR	0.05	Ikeda 2009
HCC recurrence following LT	0.012	Kaido et al. 2015
HCC recurrence following RFA	0.098	Guo et al. 2015
HCC recurrence following TACE	0.37	Matsuda et al. 2013
Treatment survival Chemotherapy CPA	0.730	Nakano et al. 2012
Treatment survival Liver resection CPA	0.946	Kudo et al. 2010
Treatment survival Liver transplant CPA	0.906	Kaido et al. 2015
Treatment survival PC CPA	0.818	Sakaguchi et al. 2016
Treatment survival RFA CPA	0.907	Guo et al. 2015
Treatment survival TACE CPA	0.887	Kudo et al. 2010
Treatment survival Chemotherapy CPB	0.730	Nakano et al. 2012
Treatment survival LR CPB	0.926	Kudo et al. 2010

(continued)

Supplementary Table SI. (continued).

Variable	Base case value	Reference
Treatment survival LT CPB	0.906	Kaido et al. 2015
Treatment survival PC CPB	0.624	Sakaguchi et al. 2016
Treatment survival RFA CPB	0.91	Guo et al. 2015
Treatment survival TACE CPB	0.851	Kudo et al. 2010
Treatment survival Chemotherapy CPC	0.730	Nakano et al. 2012
Treatment survival LR CPC	0.926	Kudo et al. 2010
Treatment survival LT CPC	0.906	Kaido et al. 2015
Treatment survival PC CPC	0.624	Sakaguchi et al. 2016
Treatment survival RFA CPC	0.91	Guo et al. 2015
Treatment survival TACE CPC	0.848	Kudo et al. 2010

Abbreviations: CPA, Child-Pugh A; CPB, Child-Pugh B; CPC, Child-Pugh C; HCC, hepatocellular carcinoma; LR, liver resection; LT, liver transplant; PC, palliative care; RFA, radiofrequency ablation; TP, transition probability

Supplementary Table SII. Diagnostic sensitivity and specificity.

Variable (grouped by number of tumors: either 1-3 or 4+)	Base case value	Reference
<b>EOB-MRI</b>		
EOB-MRI Sensitivity 1-3	0.95	Ye et al. 2015
EOB-MRI Specificity 1-3	0.96	Ye et al. 2015
EOB-MRI % HCC 1-3 requiring additional tests	50.3%	Delphi panel 2016
EOB-MRI % CE-CT scan for 2nd test 1-3	69.4%	Delphi panel 2016
EOB-MRI % ECCM-MRI for 2nd test 1-3	0.3%	Delphi panel 2016
EOB-MRI % other for 2nd test 1-3	30.2%	Delphi panel 2016
EOB-MRI Sensitivity 4+	0.95	Ye et al. 2015
EOB-MRI Specificity 4+	0.96	Ye et al. 2015
EOB-MRI % HCC 4+ requiring additional tests	50.3%	Delphi panel 2016
EOB-MRI % CE-CT scan for 2nd test 4+	69.4%	Delphi panel 2016
EOB-MRI % ECCM-MRI for 2nd test 4+	0.3%	Delphi panel 2016
EOB-MRI % other for 2nd test 4+	30.2%	Delphi panel 2016
<b>ECCM-MRI</b>		
ECCM-MRI Sensitivity 1-3	0.79	Weighted average (Youk et al. 2004, Kim et al. 2010, Park et al. 2010)
ECCM-MRI Specificity 1-3	0.89	Weighted average (Kim et al. 2010; Park et al. 2012)
ECCM-MRI % HCC 1-3 requiring additional tests	81.6%	Delphi panel 2016
ECCM-MRI % CE-CT scan for 2nd test 1-3	10.0%	Delphi panel 2016
ECCM-MRI % EOB-MRI for 2nd test 1-3	88.0%	Delphi panel 2016

(continued)



Supplementary Table SII. (continued).

Variable (grouped by number of tumors: either 1-3 or 4+)	Base case value	Reference
ECCM-MRI % other for 2nd test 1-3	2.0%	Delphi panel 2016
ECCM-MRI Sensitivity 4+	0.86	Weighted average (Youk et al. 2004, Kim et al. 2010, Park et al. 2010)
ECCM-MRI Specificity 4+	0.84	Weighted average (Kim et al. 2010; Park et al. 2012)
ECCM-MRI % HCC 4+ requiring additional tests	81.6%	Delphi panel 2016
ECCM-MRI % CE-CT scan for 2nd test 4+	10.0%	Delphi panel 2016
ECCM-MRI % EOB-MRI for 2nd test 4+	88.0%	Delphi panel 2016
ECCM-MRI % other for 2nd test 4+	2.0%	Delphi panel 2016
<b>CE-CT</b>		
CE-CT Sensitivity 1-3	0.74	Ye et al. 2015
CE-CT Specificity 1-3	0.93	Ye et al. 2015
CE-CT % HCC 1-3 requiring additional tests	89.8%	Delphi panel 2016
CE-CT % ECCM-MRI scan for 2nd test 1-3	0.3%	Delphi panel 2016
CE-CT % EOB-MRI for 2nd test 1-3	97.2%	Delphi panel 2016
CE-CT % other for 2nd test 1-3	24.0%	Delphi panel 2016
CE-CT Sensitivity 4+	0.74	Ye et al. 2015
CE-CT Specificity 4+	0.93	Ye et al. 2015
CE-CT % HCC 4+ requiring additional tests	89.8%	Delphi panel 2016
CE-CT % ECCM-MRI scan for 2nd test 4+	0.3%	Delphi panel 2016
CE-CT % EOB-MRI for 2nd test 4+	97.2%	Delphi panel 2016
CE-CT % other for 2nd test 4+	24.0%	Delphi panel 2016
<b>Ultrasound</b>		
Ultrasound sensitivity	0.96	Yu et al. 2011

Abbreviations: CE-CT, contrast-media-enhanced computed tomography; CPA, Child-Pugh A; CPB, Child-Pugh B; CPC, Child-Pugh C; ECCM, extracellular contrast-media-enhanced; EOB, ethoxybenzyl; HCC, hepatocellular carcinoma; MRI, magnetic resonance imaging; PC, palliative care; RFA, radiofrequency ablation

Supplementary Table SIII. Unit costs.

Variable	Base case value	Source
Cost ECCM-MRI	¥32,678	2016 Reimbursement Information Service (Ministry of Health, Labor and Welfare)
Cost EOB-MRI	¥42,417	2016 Reimbursement Information Service (Ministry of Health, Labor and Welfare)
Cost CE-CT	¥30,465	2016 Reimbursement Information Service (Ministry of Health, Labor and Welfare)
Cost CHE	¥3,414,287	2016 Reimbursement Information Service (Ministry of Health, Labor and Welfare)
Cost LR	¥696,200	2016 Reimbursement Information Service (Ministry of Health, Labor and Welfare)
Cost LT	¥8,800,978	Sakata et al. 2011
Cost RFA	¥600,268	2016 Reimbursement Information Service (Ministry of Health, Labor and Welfare)
Cost TACE	¥682,672	2016 Reimbursement Information Service (Ministry of Health, Labor and Welfare)
Cost PC	¥1,106,169	2016 Reimbursement Information Service (Ministry of Health, Labor and Welfare)
Ultrasound	¥5,300	2016 Reimbursement Information Service (Ministry of Health, Labor and Welfare)

Abbreviations: CHE, chemotherapy (Sorafenib); ECCM, extracellular contrast-media-enhanced; EOB, gadoxetic acid-enhanced; LR, liver resection; CE-CT, contrast-media-enhanced computed tomography; MHLW, Ministry of Health, Labor and Welfare; MRI, magnetic resonance imaging; PC, palliative care; RFA, radiofrequency ablation; TACE, transarterial chemoembolization

Supplementary Table SIV. Utility values.

Variable	Base case value	Source
QoL: CHE	0.68	NICE technology appraisal guidance 189 (2010)
QoL: CPA No HCC	0.93	Hirao 2013
QoL: CPB No HCC	0.86	Hirao 2013
QoL: CPC No HCC	0.78	Hirao 2013
QoL: HCC	0.7	Hirao 2013
QoL: LR decrement (4 weeks)	0.17	Loveman et al. 2014
QoL: Liver transplant first 6 months	0.6	Arguedas et al. 2003 (Liver transplant, year 1)
QoL: Liver transplant long term	0.85	Arguedas et al. 2003 (Liver transplant year 2+)
QoL: PC (Palliative care)	0.68	NICE technology appraisal guidance 189 (2010)
QoL: RFA decrement	0.09	Loveman et al. 2014
QoL: TACE decrement	0.13	Assumption: midpoint of LR and RFA decrement

Abbreviations: CHE, chemotherapy (Sorafenib); HCC, hepatocellular carcinoma; LR, liver resection; PC, palliative care; RFA, radiofrequency ablation; TACE, transarterial chemoembolization

# Multimaterial Decomposition Algorithm for the Quantification of Liver Fat Content by Using Fast-Kilovolt-Peak Switching Dual-Energy CT: Clinical Evaluation<sup>1</sup>

Tomoko Hyodo, MD  
 Norihisa Yada, MD  
 Masatoshi Hori, MD, PhD  
 Osamu Maenishi, MD  
 Peter Lamb, MS  
 Kosuke Sasaki, MS  
 Minori Onoda, PhD  
 Masatoshi Kudo, MD, PhD  
 Teruhito Mochizuki, MD  
 Takamichi Murakami, MD, PhD

<sup>1</sup> From the Departments of Radiology (T.H., T. Murakami), Gastroenterology and Hepatology (N.Y., M.K.), and Pathology (O.M.), Kindai University Faculty of Medicine, 377-2 Ohno-Higashi, Osaka-Sayama, Osaka 589-8511, Japan; Department of Radiology, Osaka University Graduate School of Medicine, Suita, Japan (M.H.); GE Healthcare Japan CT Research Group, Hino, Japan (K.S.); GE Global Research, Niskayuna, NY (P.L.); Department of Radiological Technology, Kanazawa University Hospital, Kanazawa, Japan (M.O.); and Department of Diagnostic and Therapeutic Radiology, Ehime University Graduate School of Medicine, Toon, Japan (T.H., T. Mochizuki). Received January 18, 2016; revision requested March 22; revision received August 21; accepted September 22; final version accepted December 20. **Address correspondence** to T.H. (e-mail: [neneth@m.ehime-u.ac.jp](mailto:neneth@m.ehime-u.ac.jp)).

© RSNA, 2017

## Purpose:

To assess the clinical accuracy and reproducibility of liver fat quantification with the multimaterial decomposition (MMD) algorithm, comparing the performance of MMD with that of magnetic resonance (MR) spectroscopy by using liver biopsy as the reference standard.

## Materials and Methods:

This prospective study was approved by the institutional ethics committee, and patients provided written informed consent. Thirty-three patients suspected of having hepatic steatosis underwent non—contrast material—enhanced and triple-phase dynamic contrast-enhanced dual-energy computed tomography (CT) (80 and 140 kVp) and single-voxel proton MR spectroscopy within 30 days before liver biopsy. Percentage fat volume fraction (FVF) images were generated by using the MMD algorithm on dual-energy CT data to measure hepatic fat content. FVFs determined by using dual-energy CT and percentage fat fractions (FFs) determined by using MR spectroscopy were compared with histologic steatosis grade (0–3, as defined by the nonalcoholic fatty liver disease activity score system) by using Jonckheere-Terpstra trend tests and were compared with each other by using Bland-Altman analysis. Real non-contrast-enhanced FVFs were compared with triple-phase contrast-enhanced FVFs to determine the reproducibility of MMD by using Bland-Altman analyses.

## Results:

Both dual-energy CT FVF and MR spectroscopy FF increased with increasing histologic steatosis grade (trend test,  $P < .001$  for each). The Bland-Altman plot of dual-energy CT FVF and MR spectroscopy FF revealed a proportional bias, as indicated by the significant positive slope of the line regressing the difference on the average ( $P < .001$ ). The 95% limits of agreement for the differences between real non-contrast-enhanced and contrast-enhanced FVFs were not greater than about 2%.

## Conclusion:

The MMD algorithm quantifying hepatic fat in dual-energy CT images is accurate and reproducible across imaging phases.

© RSNA, 2017

Online supplemental material is available for this article.

The ability to quantify liver fat is becoming increasingly important for patient care. For example, early diagnosis of nonalcoholic fatty liver disease (NAFLD) is important, as NAFLD can progress from simple steatosis to nonalcoholic steatohepatitis, fibrosis, and cirrhosis. About 20% of patients with a diagnosis of NASH progress to cirrhosis over a 10-year period (1). The earliest indication of NAFLD is hepatic steatosis, defined as accumulation of more than 5% fat across the total hepatocyte area in histologic slices (2,3). In addition to fat quantity, other biopsy-related indicators, such as lobular inflammation, hepatocyte ballooning, and fibrosis, are necessary for proper patient diagnosis along the NAFLD spectrum (2,4,5). Biopsies,

however, have limitations, including sampling errors, observer dependence (6–8), and invasiveness (9). Thus, indicators of hepatic steatosis obtained with imaging methods, including ultrasonography (US), magnetic resonance (MR) imaging, and computed tomography (CT), have been increasingly investigated as possible noninvasive alternatives to biopsy (10–14).

Measurements of CT attenuation can detect fatty liver according to the inverse relationship between liver fat content and liver attenuation (11,15). Although simple and convenient, this technique is semiquantitative (16) and may be unreliable in patients with less than 30% macrovesicular steatosis (17). Furthermore, it is impractical for contrast material-enhanced CT, as the presence of contrast material can skew attenuation measurements (11,18).

Liver fat was first quantified by using dual-energy CT in 1991 (19). Recent advances in dual-energy CT technology, including simultaneous acquisition and differentiation of high- and low-energy data sets, provide more accurate measurements of fat (20). A new multimaterial decomposition (MMD) algorithm, available as a research tool since June 2013, has been developed to quantify liver fat for fast-kilovolt-peak switching dual-energy CT (21,22). Evaluation with MMD has two advantages over evaluation with conventional single-energy CT. First, hepatic fat is directly measured in percentage volume. The fat quantification is performed through

dual-material decomposition using fat and healthy liver tissue as the material pair, and actual fat quantification is performed with a convex constrained least-squares problem (21). Second, the MMD algorithm can quantify liver fat content in both contrast- and non-contrast-enhanced data sets, as shown in rabbits (22). In the contrast-enhanced case, virtual unenhancement (VUE) is applied by using a material triplet triangle consisting of fat, blood, and contrast agent before the above-mentioned fat quantification. If the MMD algorithm shows clinical validity, patient radiation exposure may be reduced by omitting non-contrast-enhanced scans. This is important, as most clinical CT liver imaging protocols include multiphase contrast-enhanced scanning (23,24).

Assessment of the accuracy of the MMD algorithm in our phantom experiments indicated its feasibility for evaluation of hepatic steatosis. This study therefore assessed the accuracy and reproducibility of liver fat quantification with the MMD algorithm in a clinical setting, comparing the

#### Advances in Knowledge

- The multimaterial decomposition (MMD) algorithm generates fat volume fraction (FVF) images from dual-energy CT data, enabling quantification of liver fat content in a clinical setting.
- Bland-Altman analyses of inter- and intraobserver agreement in liver fat measurements showed mean differences of  $-0.3\%$  to  $0.01\%$ .
- Bland-Altman analysis demonstrated a significant proportional bias between MMD-derived FVF and fat fraction estimated at MR spectroscopy (regression coefficient,  $0.42$ ;  $P < .001$ ).
- Bland-Altman comparison of FVF measurements with MMD between real non-contrast-enhanced CT and each phase of contrast-enhanced CT showed agreement for the equilibrium phase (mean difference:  $0.7\%$  [limits of agreement,  $-0.8\%$  to  $2.1\%$ ]), whereas it showed systematic bias according to the quadratic model for the arterial and portal venous phases (coefficient of quadratic term:  $-0.01$  for both;  $P$  values:  $.030$  and  $.026$ , respectively).

#### Implications for Patient Care

- The MMD algorithm adds clinical utility in the quantitative (in units of percentage volume) and visual assessment of liver fat content to dual-energy CT imaging.
- The MMD algorithm is a promising technique for less-invasive assessment of hepatic fat content, as FVF data can be derived from the contrast-enhanced scan, eliminating the need for a separate non-contrast CT scan to derive FVF.

Published online before print

10.1148/radiol.2017160130 Content codes: CT GI

Radiology 2017; 283:108–118

#### Abbreviations:

CI = confidence interval  
 CTDI<sub>vol</sub> = volumetric CT dose index  
 FF = fat fraction  
 FVF = fat volume fraction  
 MMD = multimaterial decomposition  
 NAFLD = nonalcoholic fatty liver disease  
 NPV = negative predictive value  
 PPV = positive predictive value  
 ROC = receiver operating characteristic  
 VUE = virtual unenhancement

#### Author contributions:

Guarantor of integrity of entire study, T. Murakami; study concepts/study design or data acquisition or data analysis/interpretation, all authors; manuscript drafting or manuscript revision for important intellectual content, all authors; manuscript final version approval, all authors; agrees to ensure any questions related to the work are appropriately resolved, all authors; literature research, T.H., N.Y., M.K., T. Mochizuki, T. Murakami; clinical studies, T.H., N.Y., O.M., M.O.; statistical analysis, T.H., M.H.; and manuscript editing, T.H., M.H., P.L., K.S., T. Murakami

Conflicts of interest are listed at the end of this article.

performance of MMD with that of MR spectroscopy, with liver biopsy results used as the reference standard.

### Materials and Methods

Two authors (P.L. and K.S.) are employees of GE, the manufacturer of the CT and MR imaging systems and the MMD software used in this study. The other authors (who are not GE employees) had control of the data and information that might present a conflict of interest for the employee authors.

### Patients

This prospective study was approved by the institutional review board of the Kindai University Faculty of Medicine, and written informed consent was obtained from all patients. Of the 68 patients suspected of having NAFLD (as determined by liver-kidney contrast at US (25) and/or elevated liver enzymes and no evidence of alcohol abuse) who underwent planned liver biopsy between February and October 2012, 40 agreed to participate in this study. Sample size calculation was not performed for the convenience sample (26). All 40 patients underwent MR spectroscopy and triple-phase dynamic contrast-enhanced dual-energy CT fewer than 30 days prior to liver biopsy. Seven patients were excluded, two because of failure to acquire MR spectroscopy data and five because of insufficient scanning time for dynamic CT. This study therefore included 33 patients: 21 women (mean age, 60 years  $\pm$  11 [standard deviation]; range, 30–75 years) and 12 men (mean age, 51 years  $\pm$  7; range, 40–65 years) (Fig 1). The mean body mass index of the 33 patients was 26.7 kg/m<sup>2</sup>  $\pm$  3.6 (range, 18.6–33.3 kg/m<sup>2</sup>). The median interval between CT and biopsy was 10 days (range, 3–30 days) and that between CT and MR spectroscopy was 0 days (range, 0–14 days).

All percutaneous US-guided liver biopsy specimens (each 2 cm in length) were obtained by a single hepatologist (N.Y., with 14 years of experience) using two passes from the right lobe with a Tru-Cut semiautomatic 18-gauge needle

apparatus. Formalin-fixed, paraffin-embedded tissue slices were stained with hematoxylin-eosin or Masson trichrome stain, and liver steatosis in all patients was graded by a single pathologist (O.M., with 21 years of experience, who was blinded to the results of fat measurements at CT and MR imaging) using the NAFLD activity score (NAS) system, where NAS steatosis grades of 0, 1, 2, and 3 indicated less than 5%, 5%–33%, more than 33% to 66%, and more than 66% steatosis, respectively (2). Iron deposition was assessed by means of Berlin blue staining. The pathologist also reviewed all biopsy specimens and categorized them according to the classification system of Matteoni et al (5): type 1, simple steatosis; type 2, steatosis with inflammation; type 3, steatosis with ballooned hepatocytes; and type 4, presence of either Mallory hyaline bodies or fibrosis. Patients with type 3 or 4 steatosis were considered to have nonalcoholic steatohepatitis.

### Data Acquisition

**Dual-energy CT.**—A 64-channel multi-detector CT scanner (Discovery CT750 HD; GE Healthcare, Milwaukee, Wis) was used. Scanning parameters were as follows: dual-energy helical scanning with 80/140-kVp fast switching, 640 mA; rotation time, 0.6 second; helical pitch, 1.375:1; image thickness and image interval, 5.0 mm; and beam width, 40 mm. After the non-contrast-enhanced (hereafter, real non-contrast-enhanced) data acquisition, patients were given (through a 20- or 22-gauge plastic cannula in an antecubital vein) 600 mg iodine per kilogram of body weight of nonionic contrast material containing 300–370 mg/mL iodine over a fixed duration of 30 seconds (27). Specifically, when administered through a 20-gauge cannula, the contrast medium used for patients of less than 60 kg in body weight was iohexol 300 mg I/mL (Omnipaque 300 100 mL or 150 mL, Daiichi-Sankyo, Tokyo, Japan)—that is, the volume of contrast medium was 100 mL (injection rate, 3.3 mL/sec) and 120 mL (injection rate, 4.0 mL/sec) for patients weighing 50 kg and those weighing 60 kg, respectively. Iopamidol

Figure 1

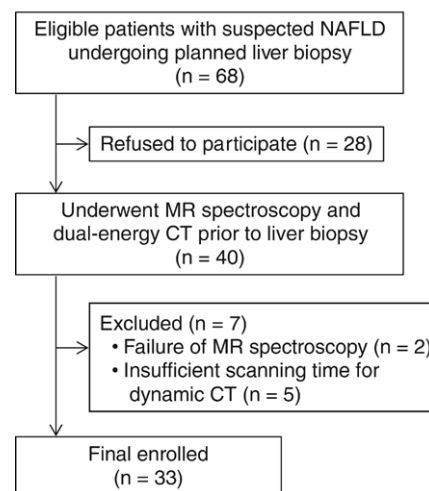


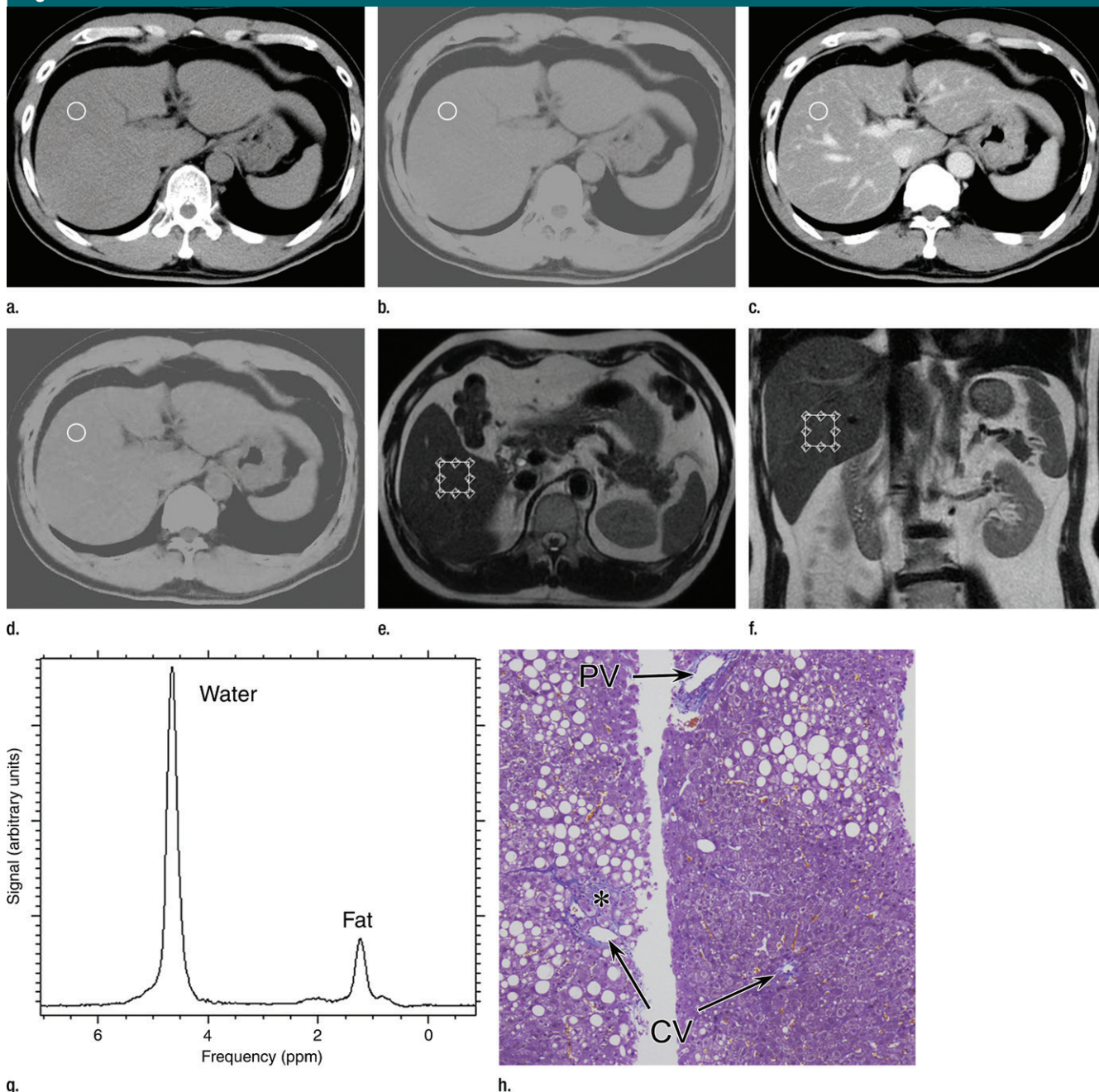
Figure 1: Flow diagram of patient enrollment.

370 mg I/mL (Iopamiron 370 100 mL; Bayer Yakuhin, Osaka, Japan) was used to limit the injection rates to 4.0 and 3.0 mL/sec when contrast medium was administered through 20- and 22-gauge cannulae, respectively. Arterial phase scanning commenced manually 6 seconds after the attenuation value in the region of interest in the abdominal aorta reached a plateau. The intervals between the arterial and portal venous phases and between the portal venous and equilibrium contrast-enhanced phases were 30 and 80 seconds, respectively. Scan duration for the entire liver was 5 seconds per imaging phase. Hepatic fat volume fraction (FVF) images and monochromatic images were reconstructed from real non-contrast-enhanced and all triple-phase contrast-enhanced dual-energy CT data sets, as described in the CT Data Analysis subsection.

**MR spectroscopy.**—Patients were examined by using a 1.5-T clinical MR imaging unit (Signa HDxt; GE Healthcare) with a 12-channel body coil. For single-voxel MR spectroscopy, the volume of interest of size 25  $\times$  25  $\times$  25 mm<sup>3</sup> was set in the planned biopsy site in reference to axial, coronal, and sagittal plane single-shot fast spin-echo localizing images, taking care to avoid large vessels (Fig 2e and 2f). MR spectroscopic data were acquired by using single-shot



Figure 2



**Figure 2:** An example of liver fat measurements by using (a–d) dual-energy CT and (e, f) MR spectroscopy in a 61-year-old man with NAFLD. The biopsy site was planned to be the superficial part of the anterior segment of the liver. However, the fields of measurement for MR spectroscopy and CT differed, as a result of avoiding large vessels with each modality. (a, b) Axial unenhanced CT images reconstructed as (a) a virtual monochromatic 70-keV image and (b) an FVF map. (c, d) Axial portal venous phase CT images reconstructed as (c) a virtual monochromatic 70-keV image and (d) an FVF map. Circles in a–d = locations of measurements. Fat content is measured as CT attenuation value (in Hounsfield units) on (a, c) virtual monochromatic images and as FVF (as a percentage) on (b, d) FVF maps. (e) Axial and (f) coronal T2-weighted MR images show a single voxel of interest for MR spectroscopy (box) placed within the liver parenchyma. (g) The MR spectrum yielded a fat fraction (FF) of 12%. (h) Liver biopsy specimen shows 30% macrovesicular steatosis, classified as grade 1. Slight perisinusoidal fibrosis (\*) was observed. CV = central venous, PV = portal venous. (Masson trichrome stain; original magnification,  $\times 40$ .)

point-resolved spectroscopy with the following parameters: echo time, 28.0 msec; number of signals averaged, one; spectral width, 1.5 kHz; number of sampling points, 2048; and no dummy radiofrequency excitation). A radiologic technologist (M.O., with 7 years of experience in MR spectroscopy of the liver) analyzed and quantified the MR spectroscopic data. Proton density percentage FF obtained from MR spectroscopy was expressed as the ratio of fat peak area to cumulative water and fat peak areas.

### CT Data Analysis

The MMD-based fat quantification algorithm displays FVF images, enabling quantitative and visual assessment of fat content in the liver. Percentage hepatic FVF images that were 5 mm thick were generated from each dual-energy CT scan phase. By using an advanced workstation (AW VolumeShare 5; GE Healthcare), three regions of interest (ROIs) (size, 200 mm<sup>2</sup>) across three contiguous sections were placed in the planned biopsy site, with care to avoid large vessels. The mean value of the three ROIs was calculated. The copy function was used to determine dual-energy CT FVF at the same ROI location for all phases in each patient. Monochromatic images were generated at 70 keV by using 50% adaptive statistical iterative reconstruction (ASiR; GE Healthcare), and filtered back-projection blending and CT attenuation values were measured at the same site in the same manner.

To determine inter- and intraobserver agreement, dual-energy CT FVF was measured independently by two radiologists (T.H. and M.H., with 13 and 17 years of experience in abdominal imaging, respectively; both were blinded to the results of liver biopsy), each of whom repeated the measurements after an interval of 2 weeks. During the second measurements, the readers were blinded to their prior measurements. Images within each measurement session were evaluated in randomized patient order.

The volumetric CT dose index (CTDI<sub>vol</sub>) and dose-length product reported by the CT scanner were recorded.

Size-specific dose estimate was also assessed, as described (28), but was used only as a reference, as the correction factors had been generated for 120 kVp.

### Statistical Analysis

All statistical analyses except the power analysis were performed by using R software (Version 3.0.0; R Foundation for Statistical Computing, Vienna, Austria) (29). Averaged continuous data are reported as means with standard deviations.  $P < .05$  was considered to indicate a statistically significant difference.

Inter- and intraobserver agreement were evaluated by using Bland-Altman analyses and interclass correlation coefficients (ICCs). Interobserver variability was assessed by using mean results from each observer. In Bland-Altman analysis, the 95% confidence interval (CI) for the limits of agreement was determined by using the Student  $t$  distribution (30). ICC was calculated by using two-way random single measures with an absolute agreement condition (ICC [2,1]) for interobserver agreement and one-way random single measures (ICC [1,1]) for intraobserver agreement. Because inter- and intraobserver agreement were both high (see Results), mean values were used for further analysis.

Trends in dual-energy CT FVF (determined only from real non-contrast-enhanced data) and MR spectroscopy FF across histologic steatosis grades were each assessed by using the Jonckheere-Terpstra test (31). To ensure adequate statistical power of the trend test, we performed a retrospective power analysis based on Monte Carlo simulation (number of trials, 1000) with the StudySize software package (Version 3.0; <http://studysize.com/>).

Receiver operating characteristic (ROC) analysis (32) was performed to determine areas under the curve and the optimal Youden index-based cutoff point (33) for each dual-energy CT FVF and MR spectroscopy FF to distinguish histologic grade 0 from grades 1–3. In addition, agreements between FVF and FF were assessed

by using Bland-Altman analysis (30). Proportional bias was assessed with simple linear regression between the averages and the differences between FVF and FF (34).

To verify the accuracy of the VUE algorithm in MMD, the association between dual-energy CT FVF and scan phase, stratified by histologic grade of hepatic steatosis, was analyzed using a generalized estimating equation model with a Gaussian distribution of the dependent variable, an identity link function, and an independent working matrix (35). The same analyses were performed for CT attenuation values. Multiple comparisons of FVF among scan phases were assessed by using the Holm sequentially rejective Bonferroni procedure and Bland-Altman analyses. After we checked them for possible fixed bias, the Bland-Altman plots for agreement between data from each of the three (arterial, portal venous, and equilibrium) scan phases and those from the real non-contrast-enhanced scan seemed to show a quadratic relationship between the means (x-axis) and the differences (y-axis); thus, we fitted the data to a second-order polynomial ( $y = b_0 + b_1x + b_2x^2$ ) to compare the significance of coefficients and the Akaike information criterion (36) of the simple linear regression model ( $y = a_0 + a_1x$ ).

### Results

Figure 2 shows sample images in a patient. Of the 33 patients, four (12%) had a histopathologic diagnosis with no marked fat deposition, whereas six (18%), 17 (52%), and six (18%) patients had Matteoni classification types 1, 2, and 3, respectively. The histologic steatosis grades were grade 0 in five patients (15%), grade 1 in 14 patients (42%), grade 2 in 11 patients (33%), and grade 3 in three patients (9%). None of these patients showed evidence of increased iron at histologic examination.

### Patient Radiation Dose

In all CT examinations, CTDI<sub>vol</sub> per scanning phase was 15.64 mGy. The

mean dose-length product of each phase was  $533 \text{ mGy-cm} \pm 48$  (range, 444–624 mGy-cm). The mean effective diameter was  $27 \text{ cm} \pm 2$  (range, 22–31 cm), and the mean patient size-specific dose estimate was  $22 \text{ mGy} \pm 2$  (range, 19–26.7 mGy).

### Inter- and Intraobserver Agreement of Dual-Energy CT FVF Measurements

Intra- and interobserver agreement of dual-energy CT FVF for each scan phase was very good. The corresponding Bland-Altman plots indicated no bias (Figure E1 [online]). Mean differences for inter- and intraobserver agreement ranged from  $-0.1\%$  to  $0.004\%$  and from  $-0.3\%$  to  $0.01\%$ , respectively (Table 1). Intraclass correlation coefficients for inter- and intraobserver agreement ranged from 0.994 to 0.997 and from 0.992 to 0.999, respectively.

### Comparison of Dual-Energy CT FVF and MR Spectroscopy FF

In this subsection, we deal with dual-energy CT FVF, which was determined only from real non-contrast-enhanced data. The mean values for histologic steatosis grades 0, 1, 2, and 3 were 2.2%, 6.3%, 13.8%, and 20.1% in dual-energy CT FVF and 3.7%, 9.5%, 20.8%, and 34.5% in MR spectroscopy FF, respectively. Both FVF and FF increased with increasing histologic steatosis grade ( $P = .001$  for each trend test) (Fig 3). The statistical power of the trend test for FVF was 0.79. ROC analyses for discrimination between histologic grade 0 and grades 1–3 yielded areas under the curve of 0.88 (95% CI: 0.74, 0.98) for FVF and 0.89 (95% CI: 0.72, 1.00) for FF. A cutoff of 4.6% for FVF had a sensitivity of 82% (23 of 28), a specificity of 100% (five of five), a positive predictive value (PPV) of 100% (23 of 23), and a negative predictive value (NPV) of 50% (five of 10), whereas a cutoff of 9.5% for FF had a sensitivity of 71% (20 of 28), a specificity of 100% (five of five), a PPV of 100% (20 of 20), and an NPV of 38% (five of 13). The Bland-Altman plot showed a proportional bias, as a positive slope was

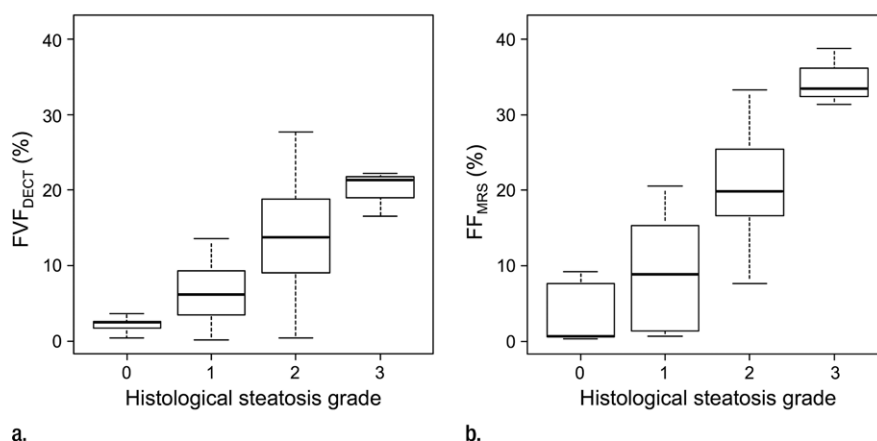
**Table 1**

#### Intra- and Interobserver Agreement of Fat Quantification with Dual-Energy CT

MMD Measurement and Type of Agreement	Mean Difference (%)	Intraclass Correlation Coefficient
<b>Non-contrast enhanced</b>		
Interobserver	−0.1 (−0.8, 0.6)	0.997 (0.995, 0.999)
Intraobserver 1	−0.1 (−0.6, 0.4)	0.998 (0.997, 0.999)
Intraobserver 2	−0.02 (−0.5, 0.4)	0.999 (0.998, 1.000)
<b>Arterial phase</b>		
Interobserver	−0.06 (−0.9, 0.8)	0.997 (0.994, 0.998)
Intraobserver 1	−0.2 (−1.5, 1.1)	0.992 (0.984, 0.996)
Intraobserver 2	0.01 (−0.9, 0.9)	0.996 (0.993, 0.998)
<b>Portal venous phase</b>		
Interobserver	0.004 (−1.0, 1.0)	0.996 (0.991, 0.998)
Intraobserver 1	−0.3 (−1.0, 0.5)	0.996 (0.993, 0.998)
Intraobserver 2	−0.07 (−0.6, 0.4)	0.999 (0.998, 0.999)
<b>Equilibrium phase</b>		
Interobserver	−0.1 (−1.2, 1.0)	0.994 (0.988, 0.997)
Intraobserver 1	−0.3 (−1.5, 0.9)	0.992 (0.984, 0.996)
Intraobserver 2	−0.01 (−0.6, 0.6)	0.998 (0.996, 0.999)

Note.—The data were evaluated by using Bland-Altman analysis, which yielded the mean difference and the limits of agreement (in parentheses) and intraclass correlation coefficients with 95% CIs (in parentheses) for reproducibility between two observers.

**Figure 3**



**Figure 3:** Box plots of FFs measured with both (a) dual-energy CT ( $FVF_{DECT}$ ) and (b) MR spectroscopy ( $FF_{MRS}$ ) in patients with different histologic grades of steatosis. At Jonckheere-Terpstra trend testing, increases in FVF and FF were significantly related to increase in histologic grade ( $P = .001$  for both).

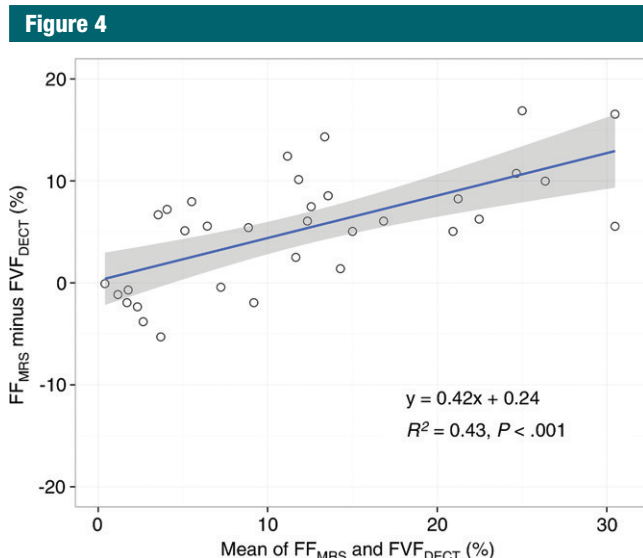
observed (regression coefficient, 0.42;  $P < .001$ , Fig 4).

### Accuracy of VUE Algorithm in MMD

Changes in FVF and CT attenuation value over all scan phases and at each histologic steatosis grade are shown in Figure 5a and 5b, respectively. Generalized estimating equation models revealed that scan phase was significantly

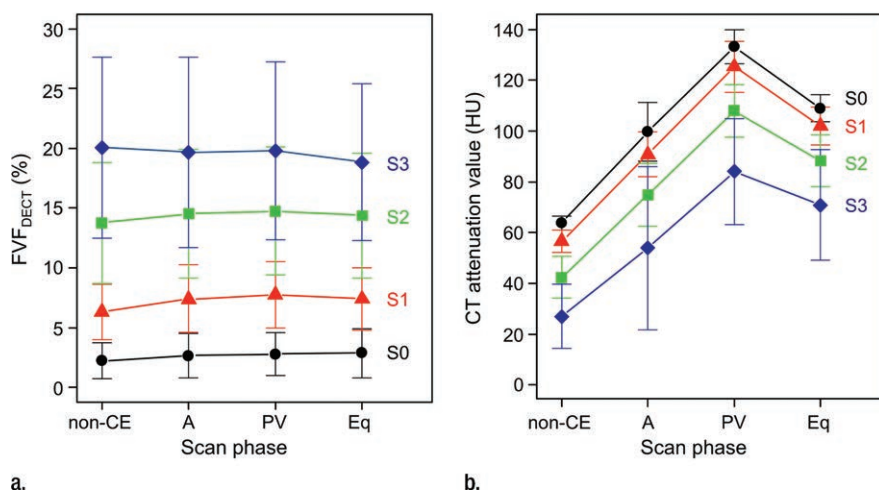
associated with both FVF ( $\beta = 0.2$ ; 95% CI: 0.1, 0.3;  $P < .001$ ) and CT attenuation values ( $\beta = 17.0$ ; 95% CI: 16.0, 17.9;  $P < .001$ ) (Table 2). However, for FVF, the coefficient for scan phase was smaller than that for histologic grading of hepatic steatosis ( $\beta = 6.0$ ; 95% CI: 4.5, 7.6;  $P < .001$ ). The Holm sequentially rejective Bonferroni procedure showed that FVF did





**Figure 4:** Bland-Altman plots show absolute differences in FFs determined by dual-energy CT ( $FVF_{DECT}$ ) and MR spectroscopy ( $FF_{MRS}$ ). Note the slightly skewed distribution of the data, as shown by the sloping regression line (blue line) with 95% CIs for limits of agreement (gray area). The linear regression equation with coefficient of determination,  $R^2$ , and  $P$  value are shown.

**Figure 5**



**Figure 5:** Line charts show changes in (a) FVF obtained with MMD ( $FVF_{DECT}$ ) and (b) CT attenuation values at 70 keV over scan phases. Both charts are colored to show the histologic steatosis grade with the NAFLD activity score system (S 0–3). Means with error bars (95% CIs) are shown. FVF showed an overlap of 95% CIs through the scan phases in each histologic grade, whereas CT attenuation values increased after contrast enhancement, peaking during the portal venous (PV) phase. A = arterial, Eq = equilibrium, non-CE = non-contrast enhanced.

not differ significantly in all comparisons of scan phases ( $P > .05$ ) for each histologic steatosis grade. These results indicate that there was no significant difference in FVF after contrast

enhancement. Bland-Altman analyses of FVF between real non-contrast-enhanced CT data and each phase of contrast-enhanced CT data (Fig 6) evaluated proportional bias as follows:

The coefficients of the simple linear models were not significant in the arterial, portal venous, or equilibrium phases ( $a_1$ : 0.03, 0.03, and  $-0.01$ , respectively; respective  $P$  values: .210, .303, and .811). The coefficients for the quadratic term in the second-order polynomial regression models were statistically significant for the arterial and portal venous phases ( $b_2$ :  $-0.01$  for both; respective  $P$  values: .030 and .026) and were not significant for the equilibrium phase ( $b_2 = -0.01$ ;  $P = .062$ ). The second-order regression model showed a smaller Akaike information criterion (implying a better model) than the first-order regression across the arterial, portal venous, and equilibrium phases (102.1 vs 105.4, 110.1 vs 113.6, and 102.1 vs 104.0, respectively). The plots showed that FVF from the arterial and portal venous phases tended to be larger than that from real non-contrast-enhanced data at mean FVF 10%–20% (Fig 6a and 6b). The mean difference was 0.7%, and the limits of agreement were  $-0.8\%$  to  $2.1\%$  for the equilibrium phase (Fig 6c).

## Discussion

US, CT, and MR imaging are all useful imaging modalities for assessing patients with hepatic disease. MR imaging techniques are generally considered more precise for quantifying liver fat. This is shown by the ability of each modality to help distinguish histologic grade 0 from grades 1–3 (ie, detection of  $> 5\%$  liver fat). For example, the area under the ROC curve, the optimal cutoff value, and its corresponding PPV and NPV were reported as 0.88, 233 dB/m, 75%, and 87%, respectively, for the controlled attenuation parameter (37) at US (10); 0.93, 1.5%, 90%, and 91% at dual-echo chemical shift MR imaging (12); 0.99, 6.4%, 100%, and 71%, respectively, on the six-point Dixon MR imaging method (13); 0.97, 1.8%, 88%, and 91%, respectively, at MR spectroscopy (12); and 0.76, 54 HU, 74%, and 70%, respectively, for CT attenuation at non-contrast-enhanced single-energy CT (120 kVp)

Table 2

**GEE Models of CT Attenuation Value and FF Obtained from Dual-Energy CT Data by Using MMD Algorithm as a Function of Scan Phase and Histologic Steatosis Grade**

Variable	Coefficient	Robust Standard Error for Estimated Coefficient	P Value
FVF according to MMD			
Scan phase	0.2 (0.1, 0.3)	0.06	<.001
NAS steatosis grade	6.0 (4.5, 7.6)	0.8	<.001
CT attenuation value			
Scan phase	17.0 (16.0, 17.9)	0.5	<.001
NAS steatosis grade	−14.0 (−17.5, −10.5)	1.9	<.001

Note.—GEE = generalized estimating equation, NAS = NAFLD activity score. Data in parentheses are 95% CIs.

(12). In our study, the areas under the ROC curves were comparable for dual-energy CT FVF and FF, and dual-energy CT had a practical cutoff of approximately 5% and a PPV of 100%. However, the derivation of thresholds from the test set without independent testing by using the validation set tends to overestimate accuracy, indicating the need for further validation.

The MMD algorithm allowed direct measurement of fat content in units of percentage volume, enabling a direct comparison between dual-energy CT FVF and MR spectroscopy FF in Bland-Altman analysis. It should be noted that fat content at MR spectroscopy is estimated according to the ratio of proton density between fat and water in underlying tissues rather than relative to volume. Strictly speaking, therefore, it would not be appropriate to consider the MR spectroscopy results as indicating FVF, unless the relationship between signal intensity and fat volume is defined by using standard curves. This definition was utilized in our phantom study (38), for example. Although this was a limitation, this comparison revealed systematic proportional bias, indicating that either FVF led to underestimation or that FF led to overestimation of fat content in patients with more fat in the liver. Our phantom study (38) showed a similar trend, but the difference in measured fat content between FVF and FF was larger in the clinical study than in the phantom study. Other causes may include a steatosis-associated

increase in material such as iron (39). Iron uptake was not observed in any biopsy specimens in our study, but that does not rule out the possibility that the measurement site for CT and MR spectroscopy included iron because of differences in the size and location of the object among the methods, as discussed below. This consideration is partially supported by previous studies (20,40) and our phantom experiments (38). Additionally, our MR spectroscopy protocol used a single echo time, preventing application of T2 correction. Thus, the possible presence of pre-existing iron may have resulted in FF overestimating liver fat more than if T2 correction had been applied (40). The discrepancies between dual-energy CT and MR spectroscopy measurements were large enough to prevent consistent assessment of hepatic steatosis, which suggests the need for follow-up studies using the same method.

In addition to fat content, the degrees of fibrosis and inflammation are also important in assessing hepatic steatosis (2). These parameters should be evaluated separately, using methods such as blood tests and elastography techniques based on US or MR imaging.

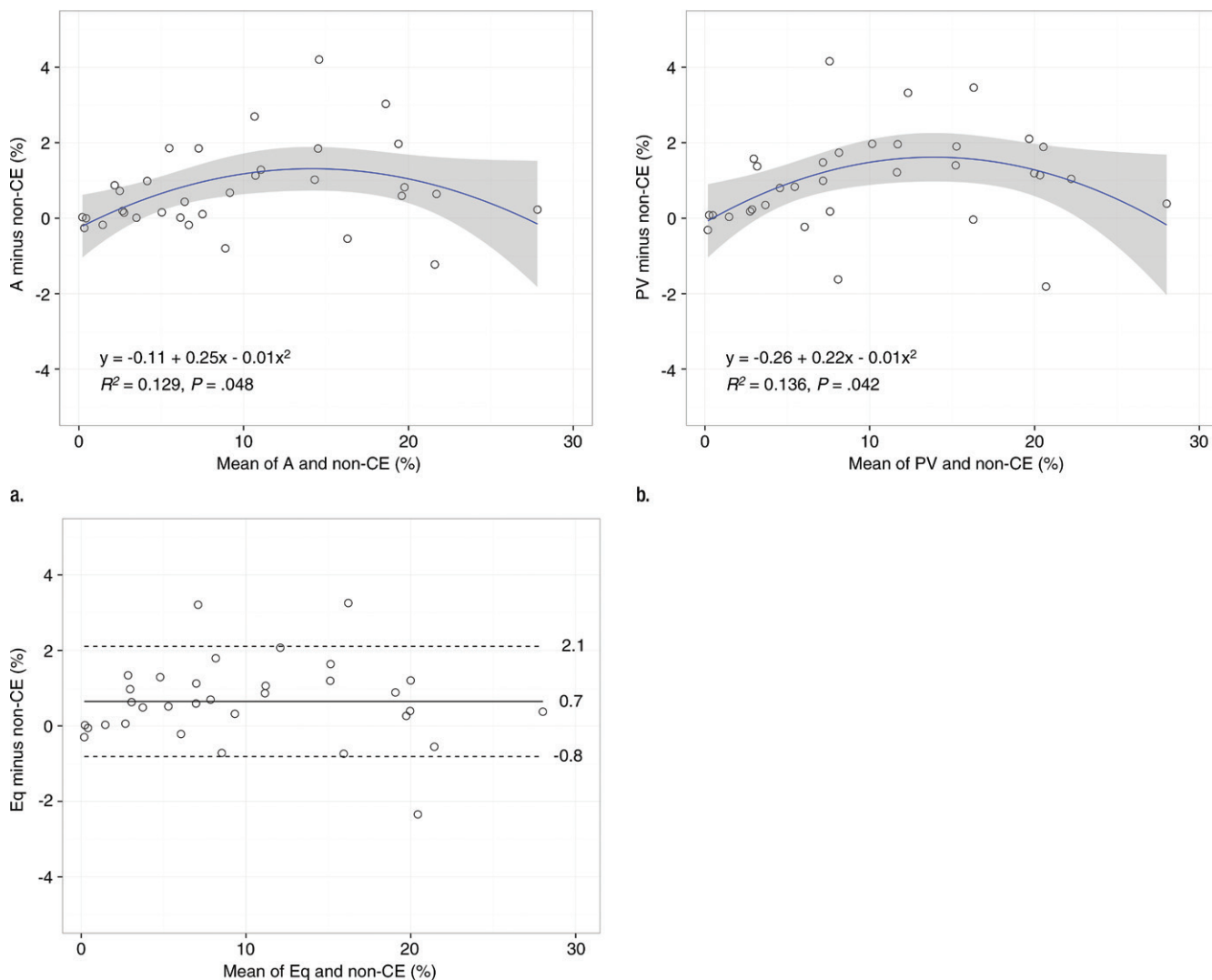
Bland-Altman analyses suggested that FVF from the arterial and portal venous phases is larger than that from real non-contrast-enhanced data at FVF values of about 10%–20%. The quadratic relationship, though possibly caused by outlier(s), was considered to be caused by the VUE step rather

than by the fat quantification step of the MMD algorithm, because our phantom study showed a linear relationship between FVF and the measured reference values of fat in the absence of iodine (38). Thus, hepatic or systemic hemodynamics, which are related to the iodine content of the liver according to arterial and portal venous phase images, may vary among patients with amounts of hepatic fat corresponding to an FVF of about 10%–20%. Additionally, FVF tended to be larger during the equilibrium phase, though the difference was not statistically significant from real non-contrast-enhanced data. Contrast material removal by means of the VUE step is a key component to liver-fat quantification with MMD, and errors in this step can manifest as incorrect FVF measurements. Therefore, this may indicate that the VUE step needs to be modified to account for the different contrast enhancement that can be seen on arterial and portal venous phase images. Our data showed that the differences that fall within limits of agreements were not greater than about 2% in Bland-Altman plots of all three phases of dynamic contrast-enhanced CT data. This was considered clinically acceptable, as the degree of hepatic steatosis is histologically assessed on the basis of more than 5% (2). The equilibrium phase data are the best alternative to real non-contrast-enhanced data for liver-fat volume quantification among the three phases of dynamic contrast-enhanced data, considering that no proportional bias could be detected in the equilibrium phase. An attempt should be made to see if the same applies to larger patient cohorts and cohorts in which the patient habitus is larger.

In this study, dual-energy CT examinations were performed by using the first generation of CT750HD (2009) with a fixed current (640 mA), resulting in a  $\text{CTDI}_{\text{vol}}$  of 15.64 mGy per scan. This value was comparable to the dose for conventional single-energy CT with fixed current but is now considered high. Introduction of the second generation (2011) has made more scan preset variations (combinations of tube



Figure 6



**Figure 6:** Bland-Altman plots show limits of agreement between percentage FVFs assessed by using non-contrast-enhanced CT (*non-CE*) and those assessed by using the (a) arterial (*A*), (b) portal venous (*PV*), and (c) equilibrium (*Eq*) phases at contrast-enhanced CT. The quadratic fit reached significance in a and b; thus, fitting curves (blue) with 95% CIs (gray area) and the regression equation with adjusted  $R^2$  and the  $P$  value are shown. Proportional bias was not evident according to linear ( $y = a_0 + a_1x$ ) or quadratic ( $y = b_0 + b_1x + b_2x^2$ ) functions in c, so the mean of the differences (solid line) and the upper and lower limits of agreement (dotted lines) are shown.

current and rotation speed) available (41). The scan presets can be tailored to a targeted  $\text{CTDI}_{\text{vol}}$  for a comparable single-energy scan using automatic tube-current modulation.

This study had several limitations, including regarding object correspondence. We compared data from CT, MR spectroscopy, and needle biopsy, which differ in sample size (1500, 15625, and

5–10 mm<sup>3</sup>, respectively). Each is sized appropriately for the given method, and we attempted to evaluate the same hepatic site. However, it is possible that we correlated different objects with fat content between the methods. Hepatic fat may be homogeneous or heterogeneous, complicating this problem, as often seen in clinical practice. From the other perspective, a fat map of

the entire liver reconstructed with the MMD algorithm can help gauge the spatial distribution of fat in the liver more quickly and easily.

In addition, MR spectroscopy and CT lump triglycerides and the other lipid fractions (eg, cell membrane lipids) together as fat contents whereas biopsy specimens are specifically assessed for the amount of triglycerides. This may

be a limitation when comparing fat content between different patients or evaluating a time series containing both MR spectroscopy and CT.

In conclusion, the dual-energy CT-based MMD algorithm for liver fat quantification is accurate and reproducible and can be performed on both contrast-enhanced and non-contrast-enhanced data sets, making it a clinically relevant technique. The measurement difference between dual-energy CT and MR spectroscopy increases with the fraction of fat.

**Acknowledgment:** The authors thank Masayuki Kudo, PhD, RT, for his technical expertise and advice regarding the CT system used; and Yasutaka Chiba, PhD, Clinical Research Center, Kindai University Hospital, Osaka-Sayama, Japan, for his helpful suggestions about statistical analysis.

**Disclosures of Conflicts of Interest:** T.H. disclosed no relevant relationships. N.Y. disclosed no relevant relationships. M.H. disclosed no relevant relationships. O.M. disclosed no relevant relationships. P.L. Activities related to the present article: is an employee of General Electric, which is the manufacturer of the CT and MR imaging systems and the MMD software used in this study. Activities not related to the present article: has been issued patent US 8855385 B2. Other relationships: disclosed no relevant relationships. K.S. Activities related to the present article: is an employee of GE Healthcare. Activities not related to the present article: disclosed no relevant relationships. Other relationships: disclosed no relevant relationships. M.O. disclosed no relevant relationships. M.K. disclosed no relevant relationships. T. Mochizuki disclosed no relevant relationships. T. Murakami disclosed no relevant relationships.

## References

- Review Team, LaBrecque DR, Abbas Z, et al. World Gastroenterology Organisation global guidelines: nonalcoholic fatty liver disease and nonalcoholic steatohepatitis. *J Clin Gastroenterol* 2014;48(6):467–473.
- Kleiner DE, Brunt EM, Van Natta M, et al. Design and validation of a histological scoring system for nonalcoholic fatty liver disease. *Hepatology* 2005;41(6):1313–1321.
- Liang W, Menke AL, Driessen A, et al. Establishment of a general NAFLD scoring system for rodent models and comparison to human liver pathology. *PLoS One* 2014;9(12):e115922.
- Brunt EM, Kleiner DE, Wilson LA, Belt P, Neuschwander-Tetri BA; NASH Clinical Research Network (CRN). Nonalcoholic fatty liver disease (NAFLD) activity score and the histopathologic diagnosis in NAFLD: distinct clinicopathologic meanings. *Hepatology* 2011;53(3):810–820.
- Matteoni CA, Younossi ZM, Gramlich T, Boparai N, Liu YC, McCullough AJ. Non-alcoholic fatty liver disease: a spectrum of clinical and pathological severity. *Gastroenterology* 1999;116(6):1413–1419.
- Fassio E, Alvarez E, Domínguez N, Landeira G, Longo C. Natural history of non-alcoholic steatohepatitis: a longitudinal study of repeat liver biopsies. *Hepatology* 2004;40(4):820–826.
- Juluri R, Vuppalanchi R, Olson J, et al. Generalizability of the nonalcoholic steatohepatitis Clinical Research Network histologic scoring system for nonalcoholic fatty liver disease. *J Clin Gastroenterol* 2011;45(1):55–58.
- Vuppalanchi R, Unalp A, Van Natta ML, et al. Effects of liver biopsy sample length and number of readings on sampling variability in nonalcoholic fatty liver disease. *Clin Gastroenterol Hepatol* 2009;7(4):481–486.
- Bravo AA, Sheth SG, Chopra S. Liver biopsy. *N Engl J Med* 2001;344(7):495–500.
- Masaki K, Takaki S, Hyogo H, et al. Utility of controlled attenuation parameter measurement for assessing liver steatosis in Japanese patients with chronic liver diseases. *Hepatol Res* 2013;43(11):1182–1189.
- Kodama Y, Ng CS, Wu TT, et al. Comparison of CT methods for determining the fat content of the liver. *AJR Am J Roentgenol* 2007;188(5):1307–1312.
- van Werven JR, Marsman HA, Nederveen AJ, et al. Assessment of hepatic steatosis in patients undergoing liver resection: comparison of US, CT, T1-weighted dual-echo MR imaging, and point-resolved 1H MR spectroscopy. *Radiology* 2010;256(1):159–168.
- Tang A, Tan J, Sun M, et al. Nonalcoholic fatty liver disease: MR imaging of liver proton density fat fraction to assess hepatic steatosis. *Radiology* 2013;267(2):422–431.
- Reeder SB, Cruite I, Hamilton G, Sirlin CB. Quantitative assessment of liver fat with magnetic resonance imaging and spectroscopy. *J Magn Reson Imaging* 2011;34(4):729–749.
- Ducommun JC, Goldberg HI, Korobkin M, Moss AA, Kressel HY. The relation of liver fat to computed tomography numbers: a preliminary experimental study in rabbits. *Radiology* 1979;130(2):511–513.
- Sanyal AJ; American Gastroenterological Association. AGA technical review on nonalcoholic fatty liver disease. *Gastroenterology* 2002;123(5):1705–1725.
- Limanond P, Raman SS, Lassman C, et al. Macrovesicular hepatic steatosis in living related liver donors: correlation between CT and histologic findings. *Radiology* 2004;230(1):276–280.
- Schwenzer NE, Springer F, Schraml C, Stefan N, Machann J, Schick F. Non-invasive assessment and quantification of liver steatosis by ultrasound, computed tomography and magnetic resonance. *J Hepatol* 2009;51(3):433–445.
- Raptopoulos V, Karellas A, Bernstein J, Reale FR, Constantinou C, Zawacki JK. Value of dual-energy CT in differentiating focal fatty infiltration of the liver from low-density masses. *AJR Am J Roentgenol* 1991;157(4):721–725.
- Fischer MA, Gnannt R, Raptis D, et al. Quantification of liver fat in the presence of iron and iodine: an ex-vivo dual-energy CT study. *Invest Radiol* 2011;46(6):351–358.
- Mendonca PR, Lamb P, Sahani DV. A flexible method for multi-material decomposition of dual-energy CT images. *IEEE Trans Med Imaging* 2014;33(1):99–116.
- Hur BY, Lee JM, Hyunsik W, et al. Quantification of the fat fraction in the liver using dual-energy computed tomography and multiterminal decomposition. *J Comput Assist Tomogr* 2014;38(6):845–852.
- Jacobs JE, Birnbaum BA, Shapiro MA, et al. Diagnostic criteria for fatty infiltration of the liver on contrast-enhanced helical CT. *AJR Am J Roentgenol* 1998;171(3):659–664.
- Cabrera R, Nelson DR. Review article: the management of hepatocellular carcinoma. *Aliment Pharmacol Ther* 2010;31(4):461–476.
- Savarymattu SH, Joseph AE, Maxwell JD. Ultrasound scanning in the detection of hepatic fibrosis and steatosis. *Br Med J (Clin Res Ed)* 1986;292(6512):13–15.
- Obuchowski NA. Special Topics III: bias. *Radiology* 2003;229(3):617–621.
- Awai K, Hiraishi K, Hori S. Effect of contrast material injection duration and rate on aortic peak time and peak enhancement at dynamic CT involving injection protocol with dose tailored to patient weight. *Radiology* 2004;230(1):142–150.
- Boone J, Strauss K, Cody D. Size-specific dose estimates (SSDE) in pediatric and adult body CT examinations. Report of AAPM Task Group 204. College Park, Md: American Association of Physicists in Medicine, 2011.
- R Development Core Team. R: A language and environment for statistical computing. Vienna, Austria: R Foundation for Statistical Computing, 2010.

30. Bland JM, Altman DG. Statistical methods for assessing agreement between two methods of clinical measurement. *Lancet* 1986;1 (8476):307–310.
31. Hollander M, Wolfe D. Nonparametric statistical methods. New York, NY: Wiley, 1999.
32. Fawcett T. An introduction to ROC analysis. *Pattern Recognit Lett* 2006;27(8):861–874.
33. Akobeng AK. Understanding diagnostic tests 3: receiver operating characteristic curves. *Acta Paediatr* 2007;96(5):644–647.
34. Ludbrook J. Confidence in Altman-Bland plots: a critical review of the method of differences. *Clin Exp Pharmacol Physiol* 2010; 37(2):143–149.
35. Zeger SL, Liang KY, Albert PS. Models for longitudinal data: a generalized estimating equation approach. *Biometrics* 1988;44(4):1049–1060.
36. Akaike H. A new look at the statistical model identification. *IEEE Trans Automat Contr* 1974;19(6):716–723.
37. Sasso M, Beaugrand M, de Ledinghen V, et al. Controlled attenuation parameter (CAP): a novel VCTE™ guided ultrasonic attenuation measurement for the evaluation of hepatic steatosis: preliminary study and validation in a cohort of patients with chronic liver disease from various causes. *Ultrasound Med Biol* 2010;36(11):1825–1835.
38. Hyodo T, Hori M, Lamb P, et al. Multi-material decomposition algorithm for the quantification of liver fat content by using fast-kilovolt-peak switching dual-energy CT: experimental validation. *Radiology* 2017;282(2):381–389.
39. Kohgo Y, Ikuta K, Ohtake T, Torimoto Y, Kato J. Iron overload and cofactors with special reference to alcohol, hepatitis C virus infection and steatosis/insulin resistance. *World J Gastroenterol* 2007;13(35):4699–4706.
40. Lee SS, Lee Y, Kim N, et al. Hepatic fat quantification using chemical shift MR imaging and MR spectroscopy in the presence of hepatic iron deposition: validation in phantoms and in patients with chronic liver disease. *J Magn Reson Imaging* 2011;33(6):1390–1398.
41. Machida H, Fukui R, Tanaka I, et al. A method for selecting a protocol for routine body CT scan using Gemstone Spectral Imaging with or without adaptive statistical iterative reconstruction: phantom experiments. *Jpn J Radiol* 2014;32(4):217–223.

## The oncoprotein gankyrin promotes the development of colitis-associated cancer through activation of STAT3

Toshiharu Sakurai<sup>1</sup>, Hiroaki Higashitsuji<sup>2</sup>, Hiroshi Kashida<sup>1</sup>, Tomohiro Watanabe<sup>1</sup>, Yoriaki Komeda<sup>1</sup>, Tomoyuki Nagai<sup>1</sup>, Satoru Hagiwara<sup>1</sup>, Masayuki Kitano<sup>1</sup>, Naoshi Nishida<sup>1</sup>, Takaya Abe<sup>3</sup>, Hiroshi Kiyonari<sup>3,4</sup>, Katsuhiko Itoh<sup>2</sup>, Jun Fujita<sup>2</sup>, Masatoshi Kudo<sup>1</sup>

<sup>1</sup>Department of Gastroenterology and Hepatology, Kindai University Faculty of Medicine, Osaka-Sayama, Osaka, Japan

<sup>2</sup>Department of Clinical Molecular Biology, Kyoto University, Kyoto, Japan

<sup>3</sup>Genetic Engineering Team, RIKEN Center for Life Science Technologies, Kobe, Japan

<sup>4</sup>Animal Resource Development Unit, RIKEN Center for Life Science Technologies, Kobe, Japan

Correspondence to: Toshiharu Sakurai, email: sakurai@med.kindai.ac.jp

Keywords: IBD, TNF, Bmi1, IL-17, treatment resistance

Received: April 20, 2016

Accepted: December 31, 2016

Published: February 01, 2017

Copyright: Sakurai et al. This is an open-access article distributed under the terms of the Creative Commons Attribution License (CC-BY), which permits unrestricted use, distribution, and reproduction in any medium, provided the original author and source are credited.

### ABSTRACT

**Although long-standing colonic inflammation due to refractory inflammatory bowel disease (IBD) promotes the development of colitis-associated cancer (CAC), the molecular mechanisms accounting for the development of CAC remains largely unknown. In this study, we investigated the role of gankyrin in the development of CAC since gankyrin is overexpressed in sporadic colorectal cancers. We analyzed gene expression of colon tissues obtained from 344 patients with IBD and CAC and found that expression of gankyrin was much higher in colonic mucosa of patients with refractory IBD than in those with IBD in remission. Expression of gankyrin was upregulated in inflammatory cells as well as tumor cells in colonic mucosa of patients with CAC. Over-expressing studies utilizing tagged gankyrin-cDNA identified physical interaction between gankyrin and Src homology 2-containing protein tyrosine phosphatase-1 (SHP-1). Importantly, the interaction between gankyrin and SHP-1 leads to inhibition of STAT3 activation and to enhancement of TNF- $\alpha$  and IL-17 in inflammatory cells. To further address the role of gankyrin in the development of CAC, we created mice with intestinal epithelial cell-specific gankyrin ablation (*Vil-Cre;Gankyrin*<sup>fl/fl</sup>) and deletion of gankyrin in myeloid and epithelial cells (*Mx1-Cre;Gankyrin*<sup>fl/fl</sup>). Gankyrin deficiency in myeloid cells, but not in epithelial cells, reduced the activity of mitogen activated protein kinase and the expression of stem cell markers, leading to attenuated tumorigenic potential. These findings provide important insights into the pathogenesis of CAC and suggest that gankyrin is a promising target for developing therapeutic and preventive strategies against CAC.**

### INTRODUCTION

Colorectal cancer is one of the most leading causes of cancer-related death worldwide [1, 2]. Inflammatory bowel diseases (IBD); ulcerative colitis (UC) and Crohn's disease (CD) are thought to result from aberrant activation of the intestinal immune system [3] and are major risk factors for colorectal cancer, so-called colitis-

associated cancer (CAC) [4]. Indeed, patients with IBD with refractory and longstanding colitis bear higher risk of colorectal cancer than individuals in the general population [5]. However, the exact molecular mechanisms underlying CAC remain unclear. In our previous reports, we found that stress response proteins induced in longstanding inflamed mucosa promote the development of CAC [6, 7]. In addition, we found that heat shock protein A4 (HSPA4)

expression could predict poor therapeutic response to steroid in IBD patients. These data suggest that persistent inflammation can result in treatment resistance and refractory clinical course, then thereby increase the risk of CAC in IBD due to enhanced stress protein responses.

Gankyrin (also known as PSMD10, p28 and Nas6p) is an oncoprotein overexpressed in many malignancies including hepatocellular carcinoma, cholangiocellular carcinoma, colorectal cancer and lung cancer [8–12]. Given the fact that gankyrin enhances proliferation and death evasion in cancer cell lines [13–15], uncontrolled cell-autonomous events underlie the pathogenesis of cancer development through over-expression of gankyrin. It should be noted, however, that the tumor microenvironment makes a major contribution and influences the physiology of malignant cells [16] in addition to cell-autonomous events such as proliferation and death evasion. At present, little has been understood regarding the involvement of gankyrin in inflammation-associated cancer.

Here we examined whether gankyrin plays a role in inflammation-associated tumorigenesis in the colon using a murine CAC model in which two kinds of tissue-specific gankyrin-deficient mice, intestinal epithelial cell-specific gankyrin ablation (*Vil-Cre;Gankyrin<sup>fl/fl</sup>*) mice and deletion of gankyrin in both myeloid and epithelial cells (*Mx1-Cre;Gankyrin<sup>fl/fl</sup>*) mice, were employed. We found that expression of gankyrin in myeloid cells rather than in epithelial cells is required for efficient tumorigenesis. Mechanistically, binding of gankyrin to SH2-containing protein tyrosine phosphatase-1 (SHP-1, also known as PTPN6) enhances the pro-inflammatory cytokine responses in myeloid cells through activation of signal transducer and activator of transcription-3 (STAT3) [17, 18] and then promotes colorectal tumorigenesis. Consistent with these results, refractory inflammation is associated with increased gankyrin expression in the colonic mucosa of patients with refractory IBD, which would increase the risk for CAC. Taken together, this study provides the evidence that gankyrin expression underlie the pathogenesis of inflammation-associated tumorigenesis.

## RESULTS

### Gankyrin expression is increased in the colonic mucosa of patients with refractory IBD

In our previous study, we showed that longstanding intestinal inflammation increases the expression of stress response proteins including HSPA4 in the colonic mucosa of IBD patients. Interestingly, such increased expression of HSPA4 was accompanied by that of gankyrin, which suggests possible involvement of gankyrin in the development of long-standing colonic inflammation [7]. Based on these data, in this study we addressed whether an association exists between gankyrin expression and the clinical status of IBD patients. For this purpose, we obtained colonic biopsy specimens from patients with refractory

IBD, non-refractory IBD, and IBD in remission. The disease characteristics were shown in Supplementary Table 1. Gankyrin expression levels were increased in patients with refractory IBD as compared with those in controls or IBD patients in remission (Figure 1A, 1B). By contrast, no significant difference was seen in gankyrin expression levels between non-refractory IBD patients and those in remission (Figure 1B). Serum albumin levels were significantly lower and Mayo endoscopic scores were significantly higher in non-refractory and refractory IBD patients than those in IBD patients in remission (Table S1). Thus, gankyrin expression was associated with the disease activity of IBD.

We then performed immunohistochemical studies to identify the cells expressing gankyrin in the human colon tissues. Gankyrin expression was enhanced in inflammatory cells as well as epithelial cells in chronically inflamed mucosa (Figure 1A). In addition, gankyrin expression was up-regulated in all human CAC cases (total n=10) and was detected in inflammatory cells as well as epithelial cells and tumor cells (Figure 1A). Taken together, these data suggest that expression of gankyrin is up-regulated in inflammatory cells, epithelial cells, and tumor cells in the colonic mucosa of patients with refractory IBD and CAC.

### Gankyrin expression is correlated with expression of pro-inflammatory cytokines and stem cell markers

It is generally accepted that colonic mucosa of patients with IBD is characterized by pro-inflammatory cytokine responses. Th17 pathways induced by myeloid cell production of IL-6 and IL-23 have been implicated in the immuno-pathogenesis of IBD [19]. Therefore, we next assessed the relationship between pro-inflammatory Th17 responses and gankyrin expression in colonic mucosa of IBD. To this end, expression levels of IL-6, IL-23p19, and IL-17A were determined. Gankyrin expression correlated weakly but significantly with IL-6 expression with a linear coefficient of 0.26 in the colonic mucosa of UC patients but not of CD patients (Supplementary Figure 1A-1B). A significant correlation was seen between *Gankyrin* and *IL-17A* or *IL-23p19* mRNA expression in UC patients (Figure 1C–1D). Thus, it is likely that gankyrin could act in concert with pro-inflammatory Th17 responses to cause chronic colonic inflammation.

Having obtained positive correlation between pro-inflammatory cytokine responses and gankyrin, we next turned our attention to a linkage between expression levels of gankyrin and stem cell markers. Leucine-rich repeat-containing G-protein-coupled receptor 5 (*Lgr5*) is a prototypical marker of the self-renewing multipotent adult stem cell populations residing in intestinal crypts that mediate regeneration of the intestinal epithelium [20]. *Lgr5* expressed in intestinal stem cells has also been shown to self-renew and continuously replenish tumor progeny [21]. B cell-specific Moloney murine leukemia virus insertion site 1 (*Bmi1*)

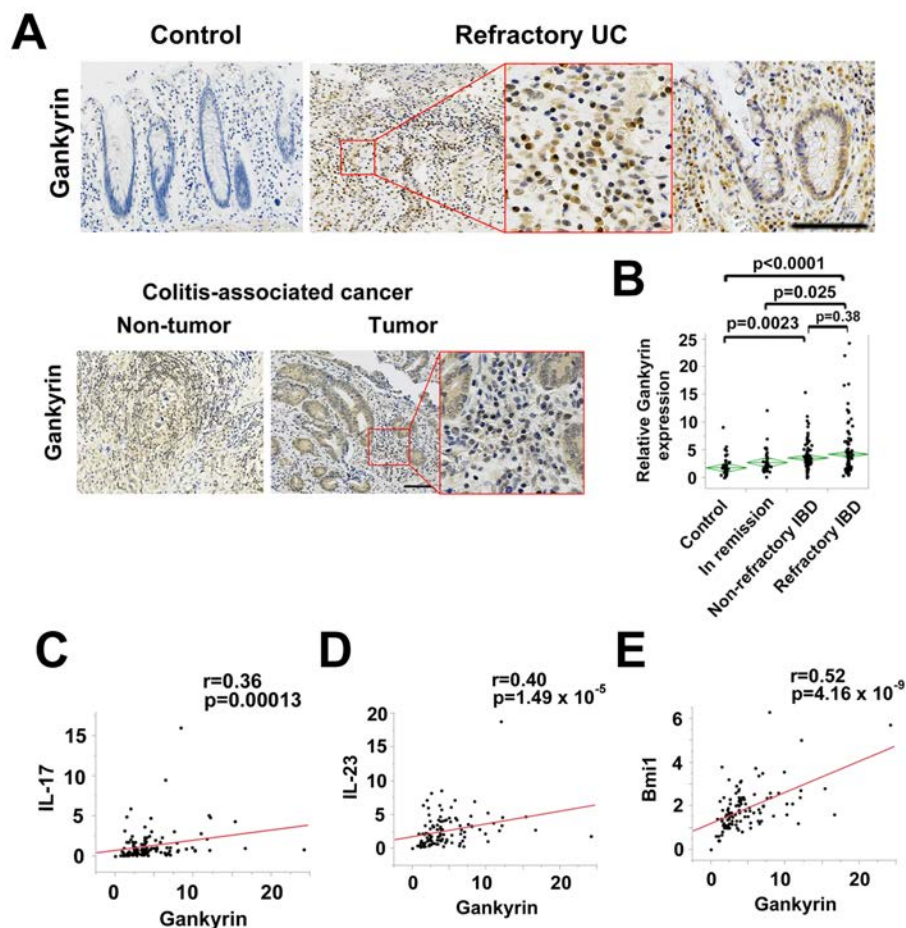


is frequently overexpressed in human sporadic colorectal cancer and the degree of upregulation correlates with disease progression and is predictive of poor patient survival [22]. In mice, *Bmi1* is required for intestinal tumorigenesis [23]. In UC patients, a significant correlation was found between *Lgr5* and *Bmi1* expression (Supplementary Figure 1C). Interestingly, gankyrin expression significantly correlated with *Bmi1* and *Lgr5* expression with linear coefficients of 0.52 and 0.27, respectively in UC and correlated with *Bmi1* expression in CD (Figure 1E and Supplementary Figure 1D–1E). Although gankyrin expression was shown to correlate with stemness factor *Nanog* expression in human sporadic colorectal cancer in previous study [10], no significant correlation was found between the expression of these genes in IBD patients (Supplementary Figure 1F). This positive correlation between gankyrin and *Lgr5* or *Bmi1* suggests that gankyrin might be related with cancer stem cell behavior in IBD patients.

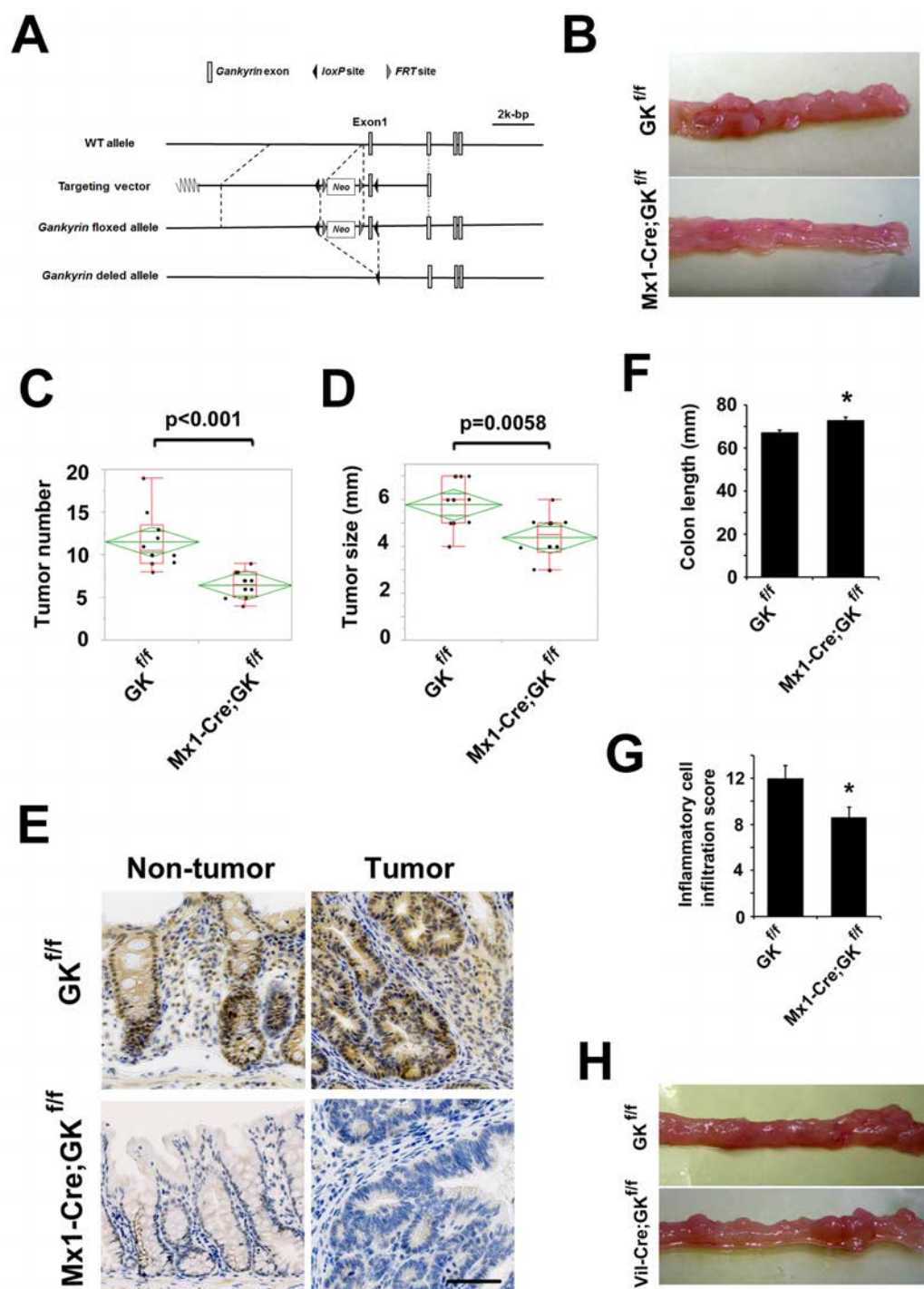
## Gankyrin deficiency attenuates tumorigenesis in the murine CAC model

Chronic inflammation increases intestinal cancer risk in IBD [24]. To investigate the precise pathogenic mechanisms underlying IBD-associated colorectal carcinogenesis, we used the AOM plus DSS mouse model to study the role of gankyrin in CAC. Since gankyrin expression was up-regulated in a wide variety of cells including immune cells, epithelial cells, and tumor cells in human IBD and CAC samples, we initially tried to determine the role of gankyrin in the AOM-DSS mouse model. To this end, we created *Gankyrin*<sup>fl/fl</sup> mice (Figure 2A) and then crossed with *Mx1-Cre* mice to generate *Mx1-Cre*-driven gankyrin deficient mice (termed *Mx1-Cre*;*Gankyrin*<sup>fl/fl</sup> mice).

In the AOM/DSS protocol, a significant decrease was noted in the number and maximum size of tumors in



**Figure 1: Gankyrin expression is increased in the colonic mucosa of patients with refractory IBD.** **A.** Representative images of immunohistochemical findings in human colonic mucosa of patients without IBD and those with refractory UC and human colitis-associated cancer (CAC) using anti-gankyrin antibody. Scale bar, 100  $\mu$ m. **B.** Expression of gankyrin mRNA in normal colonic mucosa (Control,  $n = 54$ ), colonic mucosa of IBD patients in remission (In remission,  $n = 47$ ), those with non-refractory active IBD (Non-refractory,  $n = 115$ ), and those with refractory IBD (Refractory,  $n = 128$ ), as determined by quantitative real-time qPCR. *P* values were calculated by post-hoc Tukey-Kramer HSD multiple comparison. **C-E.** Scatter plot of relative mRNA levels of gankyrin and the respective genes in human colonic mucosa.



**Figure 2: Gankyrin deficiency in myeloid cells attenuates tumorigenesis in the murine CAC model.** **A.** Construction of the wild-type allele, targeting vector, floxed allele and deleted allele of the mouse *Gankyrin* gene. The targeting vector contained the neo<sup>r</sup> cassette for selection, and loxP fragments were located on both sides of exon 1 to delete this exon. **B.** Typical examples of macroscopic tumorigenesis in the CAC model. *Gankyrin*<sup>fl/fl</sup> (GK<sup>fl/fl</sup>) mice and *Mx1-Cre;Gankyrin*<sup>fl/fl</sup> (*Mx1-Cre;GK*<sup>fl/fl</sup>) mice were challenged with AOM and DSS, and colons were cut longitudinally. **C, D.** Tumor number (C) and maximum size (D, GK<sup>fl/fl</sup> mice, n = 10; *Mx1-Cre;GK*<sup>fl/fl</sup> mice, n = 10). **E.** *Mx1-Cre;GK*<sup>fl/fl</sup> mice and GK<sup>fl/fl</sup> mice were challenged with AOM and DSS. Representative images of immunohistochemical detection of gankyrin are shown. Scale bar, 100  $\mu$ m. **F.** Colon length after treatment with AOM and DSS. GK<sup>fl/fl</sup> mice, n = 6; *Mx1-Cre;GK*<sup>fl/fl</sup> mice, n = 6. Data are means  $\pm$  SEM. \**P* < 0.05 compared with GK<sup>fl/fl</sup> mice. **G.** Inflammatory cell infiltration into colonic tissues of GK<sup>fl/fl</sup> mice and *Mx1-Cre;GK*<sup>fl/fl</sup> mice 7 days after the initiation of DSS administration. GK<sup>fl/fl</sup> mice, n = 5; *Mx1-Cre;GK*<sup>fl/fl</sup> mice, n = 5. Data are means  $\pm$  SEM. \**P* < 0.05 compared with GK<sup>fl/fl</sup> mice. **H.** Typical examples of macroscopic tumorigenesis in the CAC model. GK<sup>fl/fl</sup> mice and *Villin-Cre;Gankyrin*<sup>fl/fl</sup> (*Vil-Cre;GK*<sup>fl/fl</sup>) mice were challenged with AOM and DSS, and colons were cut longitudinally.

the *Mx1-Cre;Gankyrin<sup>ff</sup>* mice compared with *Gankyrin<sup>ff</sup>* controls (Figure 2B–2D). These tumors were located in the middle to distal colon, which is similar to human CAC. In *Gankyrin<sup>ff</sup>* mice, gankyrin expression was detected in both epithelial and in lamina propria immune cells of non-tumor colonic tissue by immuno-histochemical analysis. In the colonic tumor lesions, both tumor cells and surrounding stromal cells expressed gankyrin protein (Figure 2E). Gankyrin expression was much lower both in myeloid and epithelial cells of non-tumor colonic tissue of *Mx1-Cre;Gankyrin<sup>ff</sup>* mice as compared with *Gankyrin<sup>ff</sup>* controls. Gankyrin was absent in most of tumors of *Mx1-Cre;Gankyrin<sup>ff</sup>* mice; however, a few tumors expressed gankyrin protein (Figure 2E and Supplementary Figure 2A). Thus, these data utilizing the AOM-DSS model suggest that gankyrin expression in myeloid cells and/or epithelial cells is associated with the development of CAC.

We next assessed the effects of gankyrin deletion on the chronic inflammatory responses in this model. Colon length was measured as one parameter to evaluate the severity of inflammation and was found to be significantly longer in *Mx1-Cre;Gankyrin<sup>ff</sup>* mice than in *Gankyrin<sup>ff</sup>* mice (Figure 2F). Pathological analysis of non-tumor portions showed a marked infiltration of immune cells in *Mx1-Cre;Gankyrin<sup>ff</sup>* mice as compared with *Gankyrin<sup>ff</sup>* mice (Supplementary Figure 2B). No differences in body weight could be detected between *Mx1-Cre;Gankyrin<sup>ff</sup>* mice and *Gankyrin<sup>ff</sup>* mice during the CAC regimen (Supplementary Figure 2C).

To assess the effect of gankyrin on acute inflammation, experimental colitis was induced by treating mice with 2.5% DSS for 7 days. The degree of inflammatory cell infiltration into the colon was lower in *Mx1-Cre;Gankyrin<sup>ff</sup>* mice than in *Gankyrin<sup>ff</sup>* mice (Figure 2G and Supplementary Figure 3A). Apoptosis detected by TUNEL staining was observed primarily in the colonic crypts and was not affected by gankyrin disruption (Supplementary Figure 3B). In addition, no significant difference in body weight was found during the seven-day colitis regimen (Supplementary Figure 3C). These data altogether suggest that loss of gankyrin expression in hematopoietic and non-hematopoietic cells leads to the prevention of CAC development through the attenuation of inflammatory responses.

### Gankyrin in myeloid cells is critical for efficient tumorigenesis in the murine CAC model

To functionally characterize the contribution of different cell populations to colitis development, we created bone marrow-chimeric mice using a combination of gamma irradiation and bone marrow transplantation (BMT). Non-transplanted irradiated mice survived less than 2 weeks after irradiation, indicating successful deletion of BM cells by gamma irradiation. Irradiated animals that received BMT were allowed to recover

for 2 months prior to placing them on the DSS-induced colitis protocol. Inflammatory cell infiltration scores of irradiated gankyrin-intact mice harbouring gankyrin-deficient BM cells was lower than those harbouring gankyrin-intact BM cells (Supplementary Figure 3D), which indicates that gankyrin expressed in hematopoietic cells is involved in the attenuated inflammation observed in *Mx1-Cre;gankyrin<sup>ff</sup>* mice. To address the therapeutic ability of gankyrin inhibition, we injected poly(I:C) into *Mx1-Cre;Gankyrin<sup>ff</sup>* mice and deleted gankyrin after the initiation of DSS treatment. Inflammation was slightly attenuated by gankyrin deletion after the DSS treatment (Supplementary Figure 3E). Consistent with the data shown above, flow-cytometric analysis revealed that CD3<sup>+</sup> T cells, CD11b<sup>+</sup> myeloid cells, and CD20<sup>+</sup> B cells were positive for intracellular gankyrin expression (Supplementary Figure 4A).

In *Mx1-Cre;Gankyrin<sup>ff</sup>* mice, gankyrin was deleted in the liver as well. To confirm the role of gankyrin expression in the colon, we created *Albumin-Cre;gankyrin<sup>ff</sup>* mice where gankyrin is deficient only in the liver (Sakurai et al., unpublished data) and compared *Albumin-Cre;gankyrin<sup>ff</sup>* mice and *gankyrin<sup>ff</sup>* mice in colitis model. No difference in DSS-induced colonic inflammation was seen between *Albumin-Cre;gankyrin<sup>ff</sup>* mice and *gankyrin<sup>ff</sup>* mice (Supplementary Figure 4B), suggesting that gankyrin deficiency in the colon, but not the liver, affects the phenotype observed in DSS-challenged *Mx1-Cre;gankyrin<sup>ff</sup>* mice.

Mice lacking gankyrin only in their intestinal epithelial cells (*Vil-Cre;Gankyrin<sup>ff</sup>* mice) and their littermate controls (*Gankyrin<sup>ff</sup>* mice) were challenged with AOM and DSS to confirm a role of myeloid cells expressing gankyrin. Deletion of gankyrin in enterocytes did not show gross abnormalities. No significant differences were seen in tumor numbers or maximum sizes between *Vil-Cre;Gankyrin<sup>ff</sup>* mice and control *Gankyrin<sup>ff</sup>* mice in the murine CAC model (Figure 2H and Supplementary Figure 5A–5B). Collectively, these data suggest that gankyrin promotes tumorigenesis mainly through its actions in myeloid cells rather than epithelial cells.

### Gankyrin interacts with SHP-1 in myeloid cells

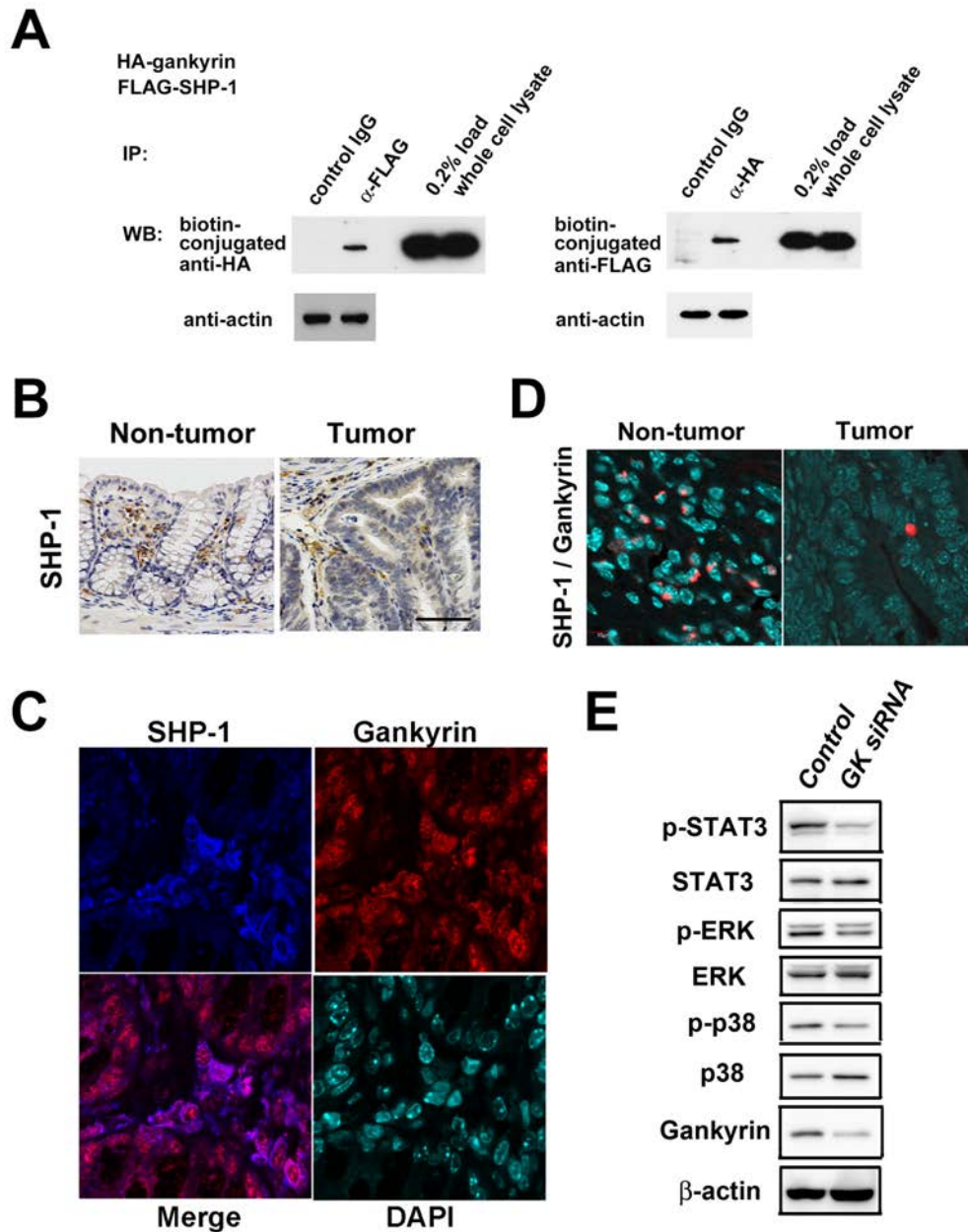
To further characterize the tumorigenic activity of gankyrin, we performed a yeast two-hybrid assay using the full length of gankyrin as bait, and found that gankyrin bound to SHP-1 in the yeast. To confirm that gankyrin interacts with SHP-1 in mammalian cells, U-2 OS cells were co-transfected with plasmids expressing HA-tagged human gankyrin and FLAG-tagged SHP-1. When cell lysates were immunoprecipitated with an anti-FLAG antibody, HA-gankyrin was detected in the precipitates. Reciprocally, SHP-1 was detected in the anti-HA immunoprecipitates from cells co-transfected with plasmid



expressing HA-gankyrin and FLAG-SHP-1 (Figure 3A). Thus, a physical interaction between gankyrin and SHP-1 was confirmed in over-expression studies.

We next addressed a physiological role played by the interaction between gankyrin and SHP-1 in AOM-DSS model. In *Gankyrin<sup>ff</sup>* mice challenged with AOM and DSS, SHP-1 was expressed mainly in inflammatory or stromal cells as well as tumor cells (Figure 3B). Double immunofluorescence staining showed that both gankyrin

and SHP-1 proteins were co-localized in the cytoplasm and the nucleus of these cells (Figure 3C). Finally, we employed the Duolink Assay for the visualization of interaction between gankyrin and SHP-1. The molecular interaction between gankyrin and SHP-1 visualized as red punctate dots were mainly seen in non-epithelial cells, but not epithelial cells (Figure 3D). These data suggest that the molecular interaction between gankyrin and SHP-



**Figure 3: Gankyrin interacts with SHP1 *in vitro* and *in vivo*.** **A.** Coimmunoprecipitation (IP) of exogenous proteins. U-2 OS cells were cotransfected with plasmids expressing HA-gankyrin and FLAG-SHP-1. Immunoprecipitates prepared by IP with indicated antibodies were analyzed by western blotting (WB). **B.** Representative images of immunohistochemical detection of SHP-1 in colonic tissues and tumors of *Gankyrin<sup>ff</sup>* mice treated with AOM and DSS. Scale bar, 100 μm. **C.** Representative images of immunohistochemical detection of SHP-1 and gankyrin in colonic tissues from tumor-harboring *Gankyrin<sup>ff</sup>* mice. **D.** Interaction of gankyrin with SHP-1 was assessed by Duolink Assay in AOM/DSS-treated *Gankyrin<sup>ff</sup>* mice. **E.** Lysates from THP-1 cells transfected with *gankyrin* RNAi (GK siRNA) or control RNAi (Control) were analyzed by WB using indicated antibodies.

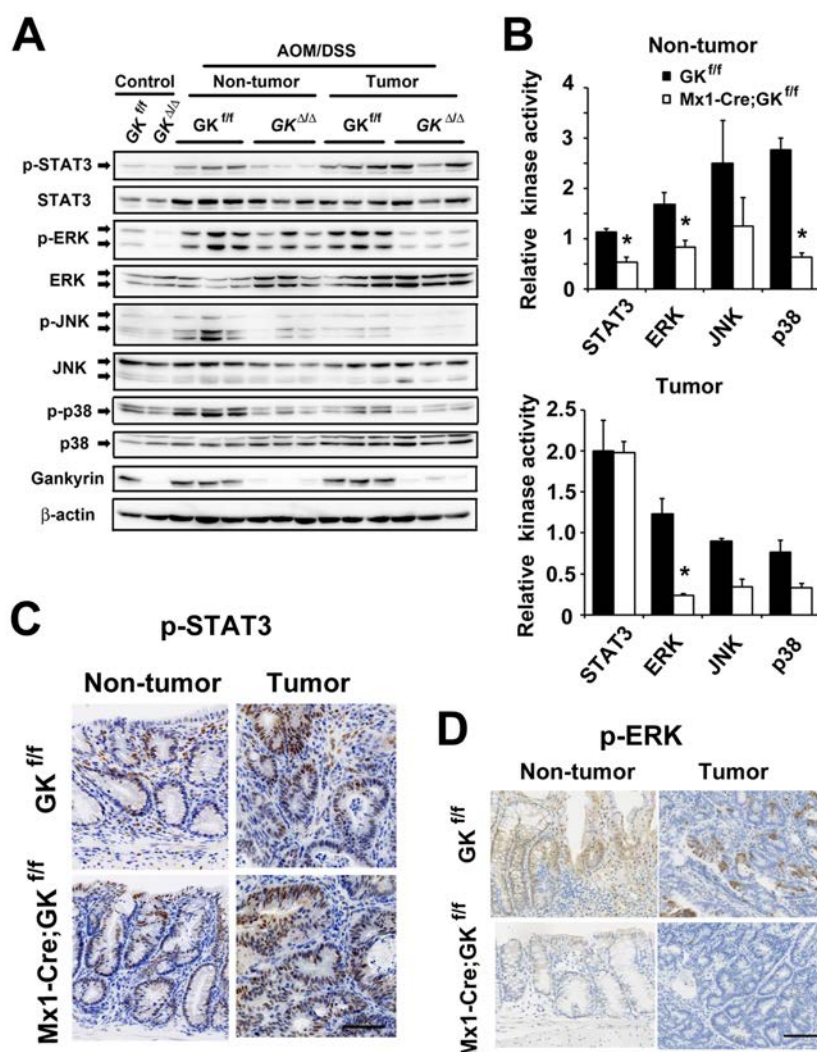
1 is operating in non-epithelial cells i.e., hematopoietic myeloid cells, in AOM-DSS model.

### Interaction of gankyrin with SHP-1 results in activation of STAT3 and MAP kinase

SHP-1 is well-known inhibitor of activation-promoting signaling cascades in hematopoietic cells [25] and negatively regulates signaling by dephosphorylating STAT3, ERK, JNK and p38 [17, 18, 26, 27]. Having obtained the induction of gankyrin-SHP1 interaction in hematopoietic cells, we next assessed the effects of such interaction on these signaling pathways in myeloid cells. To this end, we utilized THP-1 cells, an immortalized line of human monocyte. Knockdown of gankyrin expression

by gankyrin-specific siRNA reduced STAT3 and p38 phosphorylation in immunoblotting analysis (Figure 3E). Thus, gankyrin promotes activation of STAT3 and mitogen-activated protein kinase (MAP kinase). In colon tumor cells, knockdown of gankyrin reduced cell viability while knockdown of SHP-1 increased it (Supplementary Figure 6A). In contrast, overexpression of gankyrin did not affect SHP-1 phosphatase activity probably because of much endogenous gankyrin protein (Supplementary Figure 6B).

Then, we assessed the effects of gankyrin on the signaling pathways *in vivo*. Consistent with the data obtained from human THP-1 cells, *Mx1-Cre;Gankyrin<sup>fl/fl</sup>* mice exhibited reduced activation of STAT3, ERK and p38 compared with *Gankyrin<sup>fl/fl</sup>* controls (Figure 4A and 4B). Immunohistochemical analysis revealed



**Figure 4: Gankyrin activates STAT3 in non-tumor tissues and ERK in tumors.** A. *Mx1-Cre;Gankyrin<sup>fl/fl</sup>* (*Mx1-Cre;GK<sup>fl/fl</sup>*) mice and *Gankyrin<sup>fl/fl</sup>* (*GK<sup>fl/fl</sup>*) mice were challenged with AOM and DSS. Homogenates of non-treated colons (Control), non-tumor colon tissues (Non-tumor) and tumors (Tumor) were gel-separated and immunoblotted with the indicated antibodies. B. Relative kinase activities in non-tumor colon tissues (Non-tumor) and tumors (Tumor) isolated from *Mx1-Cre;Gankyrin<sup>fl/fl</sup>* (*Mx1-Cre;GK<sup>fl/fl</sup>*) mice and *Gankyrin<sup>fl/fl</sup>* (*GK<sup>fl/fl</sup>*) mice challenged with AOM and DSS were assessed by densitometry. Kinase activity in untreated *Gankyrin<sup>fl/fl</sup>* mice was given an arbitrary value of 1. Data are means  $\pm$  SEM. C, D. Representative images of immunohistochemical detection of phosphorylated STAT3 (C) and phosphorylated ERK (D) in non-tumor colon tissues (Non-tumor) and tumors (Tumor). Scale bar, 100  $\mu$ m.



that the activities of STAT3 and ERK were reduced in inflammatory cells but not in intestinal epithelial cells in gankyrin-deficient colons (Figure 4C and 4D). In contrast, tumors isolated from *Mx1-Cre;Gankyrin<sup>ff</sup>* mice showed similar level of phosphorylated STAT3 and lower level of phosphorylated ERK compared with those from control *Gankyrin<sup>ff</sup>* mice (Figure 4A, 4B and 4D). Colorectal tissues isolated from *Vil-Cre;Gankyrin<sup>ff</sup>* mice exhibited similar level of phosphorylated STAT3 and ERK compared with control counterparts (Supplementary Figure 5C). Thus, these data suggest that gankyrin deletion leads to reduced activation of STAT3 and MAP kinase in inflammatory myeloid cells rather than epithelial cells in AOM-DSS model.

We assessed the effect of gankyrin on these signaling pathways in DSS-induced colitis model. Examination of the colonic lysates from DSS-treated *Villin-Cre;Gankyrin<sup>ff</sup>* mice and *Gankyrin<sup>ff</sup>* controls showed that gankyrin deletion resulted in reduced STAT3 phosphorylation but a minor change in ERK phosphorylation (Supplementary Figure 7A), which suggests a possible involvement of gankyrin-SHP1 interaction in the activation of STAT3 and MAP kinase in acute epithelial cell injury.

### Loss of gankyrin in myeloid cells results in reduced expression of cytokines and stem cell markers

The associated immune response was investigated by analyzing colonic cytokine levels. Colonic tissue from *Mx1-Cre;Gankyrin<sup>ff</sup>* mice showed lower levels of pro-inflammatory cytokine TNF- $\alpha$  than that of control mice (Figure 5A) as assessed by qPCR analysis, which would be due to reduced activities of STAT3 and MAP kinase in inflammatory cells. To further characterize the effects of gankyrin on cytokine production, we sought to confirm these findings *in vitro*. In LP cells isolated from DSS-treated colons of *Mx1-Cre;Gankyrin<sup>ff</sup>* mice, expression of TNF- $\alpha$  and IL-17 was decreased compared with those of control mice (Figure 5B), which is consistent with the data in humans (Figure 1C).

It is generally accepted that pro-inflammatory cytokine responses affect the expression of stem cell markers and proliferation of stem cells [28]. Therefore, we addressed the effects of gankyrin deletion on the expression of cancer stem cell markers. Colonic tissue from *Mx1-Cre;Gankyrin<sup>ff</sup>* mice showed lower levels of Bmi1 than that of *Gankyrin<sup>ff</sup>* mice when they were treated with AOM and DSS (Figure 5A). In contrast, no difference was found in the level of Bmi1 between similarly treated *Vil-Cre;Gankyrin<sup>ff</sup>* mice and *Gankyrin<sup>ff</sup>* mice (Supplementary Figure 5D).

In *Mx1-Cre;Gankyrin<sup>ff</sup>* mice, STAT3 activity was decreased in inflammatory cells whilst ERK activity was decreased in tumor cells as well as inflammatory cells. Provirus integration site for Moloney murine leukemia

virus (Pim1) is linked to the development and progression of several cancers including colorectal cancer [29]. Sox9 [sex-determining region Y (SRY)-box 9 protein], an intestinal stem cell marker, plays critical roles during embryogenesis and its activity is required for development, differentiation, and lineage commitment in various tissues including the intestinal epithelium [30]. Since expression of Pim1 and Sox9 requires activation of STAT3 and ERK, respectively, we assessed the expression of Pim1 and Sox9 in AOM-DSS model utilizing conditional gankyrin-deficient mice. Expression of Pim1 was down-regulated in gankyrin-deficient colons compared to control counterparts (Figure 5A). Furthermore, LP cells derived from *Mx1-Cre;Gankyrin<sup>ff</sup>* mice, but not from *Vil-Cre;Gankyrin<sup>ff</sup>* mice, exhibited marked down-regulation of Pim1 mRNA relative to those isolated from *Gankyrin<sup>ff</sup>* mice (Figure 5B and Supplementary Figure 7B). Sox9 mRNA expression was significantly reduced in gankyrin-deficient tumors (Figure 5C). Another stem cell marker achaete-scute complex homolog 2 (Ascl2) is suggested to regulate the development of colorectal cancer via CDX2 [31]. Gankyrin ablation also decreased the expression of Ascl2 (Figure 5C). In addition, expression of cMyc, a prototypical oncogene, was reduced in gankyrin-deficient mice as compared with gankyrin-intact mice (Figure 5C). Taken together, these data support the idea that gankyrin deletion leads to a reduction of pro-inflammatory cytokine responses and expression of cancer stem cell markers through inhibition of STAT3 and/or ERK activation.

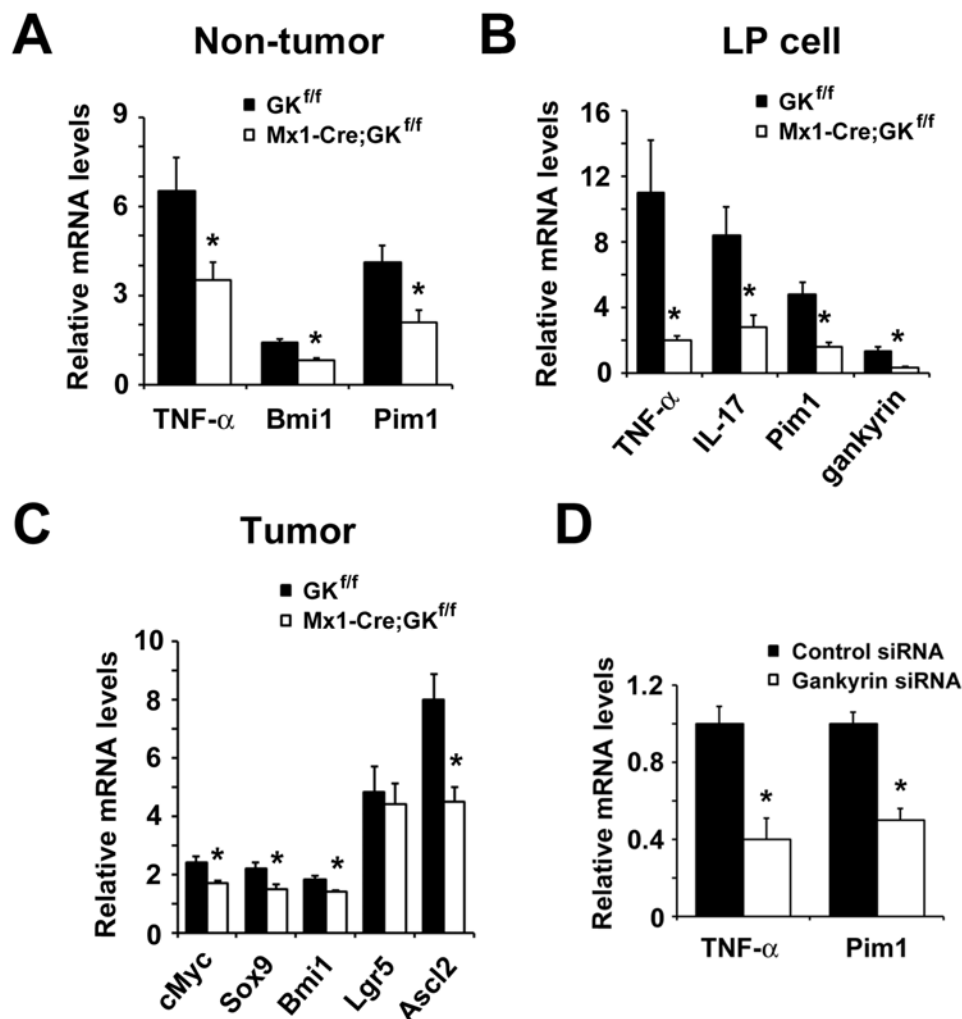
In THP-1 cells, an immortalized line of human monocyte, knockdown of gankyrin reduced the expression of TNF- $\alpha$  and Pim1 (Figure 5D) through the inhibition of p38 and STAT3 activation (Figure 3E). In contrast, the effect of gankyrin on ERK activation was marginal in THP-1 cells (Figure 3E). These data indicate that gankyrin activates STAT3 in a cell-autonomous manner, leading to increased expression of their target genes such as TNF- $\alpha$ , which might at least partially contribute to the enhanced MAP kinase ERK activation in a non-cell-autonomous manner.

## DISCUSSION

In the context of chronic inflammation, cytokines secreted by immune cells contribute to creating the cancer-microenvironment in which activation and proliferation of cancer stem cells are promoted [28]. Indeed, a recent study has suggested that colorectal cancer tissue-derived Foxp3<sup>+</sup> IL-17<sup>+</sup> cells have the capacity to induce cancer-initiating cells *in vitro* [32]. Thus, it is generally accepted that cytokine-mediated inflammatory signaling pathways are important for dedifferentiation and generation of tumor-initiating cells [33]. However, the precise mechanisms accounting for the activation of cancer-initiating cells in response to pro-inflammatory cytokines have been poorly defined. In this study, we provide the evidence

that gankyrin expressed in myeloid cells promote the expansion of cancer-initiating cells through the induction of cancer stem cell markers such as Pim1 and Sox9. As for the mechanisms of gankyrin-induced inflammatory responses by myeloid cells, we show that molecular interaction between gankyrin and SHP1 leads to secretion of pro-inflammatory cytokine. Thus, we have elucidated a part of molecular mechanisms for the development of inflammation-associated colon carcinogenesis by focusing on the function of myeloid cell expression of gankyrin.

Previous studies report that upregulation of gankyrin was detected in many tumor cell lines and primary tumors. Such enhanced expression of gankyrin has been considered to promote the proliferation of cancer cells by inhibiting apoptosis and cell cycle in cell lines [8–14]. However, until now it was not clear whether gankyrin is instrumental for tumor development *in vivo*. In this study, we tried to determine the role of gankyrin in the interface between tumor cells and immune cells. We found that gankyrin upregulates IL-17 expression in



**Figure 5: Loss of gankyrin in myeloid cells results in reduced expression of cytokines and stem cell markers.** **A.** RNA was extracted from non-tumor colon of tumor-harboring *Mx1-Cre;Gankyrin<sup>fl/fl</sup>* (*Mx1-Cre;GK<sup>fl/fl</sup>*) mice and *Gankyrin<sup>fl/fl</sup>* (*GK<sup>fl/fl</sup>*) mice. Relative amounts of mRNA were determined by real-time qPCR and normalized to the amount of actin mRNA. The amount of each mRNA in the untreated colon was given an arbitrary value of 1.0. Data are means  $\pm$  SEM (n = 5). **B.** Effect of gankyrin on gene expression in colonic lamina propria (LP) cells. LP cells were isolated from DSS-treated *Mx1-Cre;Gankyrin<sup>fl/fl</sup>* (*Mx1-Cre;GK<sup>fl/fl</sup>*) mice and *Gankyrin<sup>fl/fl</sup>* (*GK<sup>fl/fl</sup>*) mice and cytokine mRNA expression was analyzed by real-time qPCR. The mRNA expression levels in LP cells from non-treated WT mice were set as 1. **C.** RNA was extracted from tumor tissues of *Mx1-Cre;Gankyrin<sup>fl/fl</sup>* (*Mx1-Cre;GK<sup>fl/fl</sup>*) mice and *Gankyrin<sup>fl/fl</sup>* (*GK<sup>fl/fl</sup>*) mice. Relative amounts of mRNA of ERK target genes cMyc, and stem cell markers Sox9, Bmi1, Lgr5 and Ascl2 were determined by real-time qPCR and normalized to the amount of actin mRNA. The amount of each mRNA in the untreated colon was given an arbitrary value of 1.0. Data are means  $\pm$  SEM (n = 5). **D.** Relative amounts of mRNA of TNF- $\alpha$  and Pim1 from THP-1 cells transfected with *gankyrin* RNAi or control RNAi were determined by real-time qPCR and normalized to the amount of actin mRNA. The amount of each mRNA in the untreated colon was given an arbitrary value of 1.0. Data are means  $\pm$  SEM (n = 3).

lamina propria cells in murine AOM-DSS CAC model. In addition, we showed that expression of gankyrin was positively correlated with that of IL-17A. Recent study by Wang K et al. show that IL-17A exerts its pro-tumorigenic activity through its type A receptor (IL-17RA), which signals directly within transformed colonic epithelial cells to promote early tumor development by activating MAP kinase, especially ERK signaling [34]. Consistent with this report, a significant reduction of IL-17 production was seen in the colonic mucosa of gankyrin-deficient mice upon AOM-DSS treatment, which effect was accompanied by a reduction in MAP kinase activation and in expression of cancer stem cell markers. Thus, IL-17 signaling might mediate the gankyrin-mediated cross-talk between immune cells and tumor cells.

Another pro-inflammatory cytokine associated with the development of CAC through activation of gankyrin is TNF- $\alpha$ . Expression of TNF- $\alpha$  was positively correlated with that of gankyrin in human IBD samples. In addition, TNF- $\alpha$  expression was significantly lower in gankyrin-deficient mice treated with AOM-DSS than in gankyrin-intact mice. Furthermore, gankyrin-knockdown leads to a diminished TNF- $\alpha$  production by human monocytic cells through inhibition of STAT3 and MAP kinase activation, which suggests involvement of gankyrin-mediated signaling pathways for optimal production of TNF- $\alpha$ . Given the fact that TNF- $\alpha$  produced by myeloid cells is a critical player for the longstanding chronic inflammation and CAC [35], the results of the present study provide another important linkage between gankyrin-mediated TNF- $\alpha$  production and colon carcinogenesis.

In this study, we created two kinds of conditional gankyrin-deficient mice; *Mx1-Cre;Gankyrin<sup>fl/fl</sup>* mice and *Vil-Cre;Gankyrin<sup>fl/fl</sup>* mice. Deletion of gankyrin was confirmed in hemopoietic and non-hematopoietic cells in *Mx1-Cre;Gankyrin<sup>fl/fl</sup>* mice whereas deletion was confirmed in epithelial cells in *Vil-Cre;Gankyrin<sup>fl/fl</sup>* mice. The development of CAC induced by AOM-DSS treatment was significantly attenuated in the colon of *Mx1-Cre;Gankyrin<sup>fl/fl</sup>* mice as compared with control *Gankyrin<sup>fl/fl</sup>* mice. In contrast, the development of CAC induced by AOM-DSS treatment was comparable between *Vil-Cre;Gankyrin<sup>fl/fl</sup>* mice and control *Gankyrin<sup>fl/fl</sup>* mice. Similarly, *Mx1-Cre;Gankyrin<sup>fl/fl</sup>* mice exhibited attenuated inflammatory scores upon acute DSS colitis model. In line with this, the development of acute DSS colitis was attenuated in irradiated-gankyrin-intact mice transplanted gankyrin-deficient BM cells as compared with those transplanted with gankyrin-intact BM cells. These studies utilizing two kinds of conditional gankyrin-deficient mice together with BMT experiments strongly suggest a pivotal role played by hematopoietic cells expressing gankyrin in the development of chronic colitis and colitis-associated cancer. Compatible to this idea, gankyrin expression was detected in immune cells of the colon tissue of human CAC and refractory IBD samples. Moreover, pro-

inflammatory cytokine responses such as TNF- $\alpha$  and IL-17 were significantly reduced in the colon tissues of AOM-DSS-treated *Mx1-Cre;Gankyrin<sup>fl/fl</sup>* mice, which effects were again accompanied by a reduction in expression of cancer stem cell markers and in activation of STAT3 and MAP kinase activation. Thus, it is very likely that myeloid cells expressing gankyrin play an indispensable role in the development of chronic colitis and CAC through the enhancement of pro-inflammatory cytokine responses, activation of STAT3 and MAP kinases, and finally expression of cancer stem cell markers. Therefore, present findings show for the first time that as a tumor promoter gankyrin can enhance tumor development through the interaction between tumor cells and immune cells. It should be noted, however, that we cannot exclude a role played by gankyrin-expressing epithelial cells. Gankyrin in epithelial cells would at least partly contribute to tumorigenesis in another type of cancer such as sporadic colorectal cancer rather than CAC.

One question arising from the present study is whether gankyrin expression is up-regulated not only in IBD but also in non-chronic inflammatory diseases such as infectious or ischemic colitis in human samples. In this regards, we do not have enough specimens of non-chronic inflammatory diseases and thus cannot provide the data of gankyrin expression in non-chronic inflammatory diseases. However, our preliminary assay utilizing biopsy samples from Amoebatic dyscentery revealed that the gankyrin expression was found to be lower than that in IBD patients.

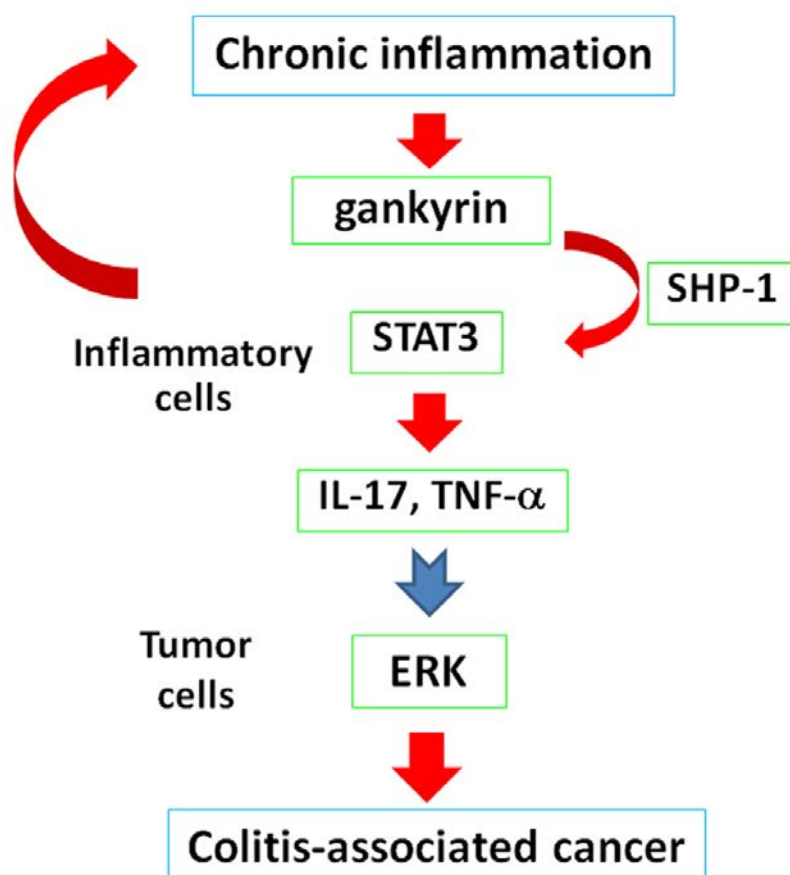
The most feared long-term complication of IBD is CAC as patients with IBD have an increased risk of colorectal cancer [5]. Most cases of CAC arise from dysplasia, and surveillance colonoscopy is therefore recommended to detect dysplasia. Recently, it was suggested that intensified surveillance and endoscopic resection of dysplasia might prevent CAC [36], which is a new strategy to improve quality of life for patients. If we can reliably predict an individual's risk of dysplasia and CAC, surveillance strategies could be appropriately personalized and surveillance programs would become more cost-effective. As shown in the present study, high level of gankyrin expression in the colonic mucosae reflects the presence of refractory inflammation. This suggests that gankyrin can be used as a potential marker for predicting the risk of CAC development. Indeed, expression of gankyrin was increased in human CAC tissues as well. Furthermore, gankyrin expression was reported to be upregulated during the development of another type of cancer [15, 37]. Analyzing the gankyrin level may be utilized to predict the risk of cancer and prognosis of IBD patients.

In this study, we propose that gankyrin expressed in myeloid cells promotes CAC through induction of pro-inflammatory cytokine responses and expression of cancer stem cell markers. The chain of evidence supporting this conclusion consisted first of the fact that gankyrin

expression is correlated with the expression of immune cell-derived pro-inflammatory IL-17-related cytokines and with that of stem cell marker (Lgr5) in the colonic mucosa of IBD patients. Moreover, immuno-histochemical analysis revealed the expression of gankyrin in immune cells migrated into the colonic mucosa of patients with refractory IBD and CAC. These results obtained from human samples were further corroborated in experimental studies utilizing *Mx1-Cre;Gankyrin<sup>ff</sup>* mice and *Vil-Cre;Gankyrin<sup>ff</sup>* mice. As mentioned above, *Mx1-Cre;Gankyrin<sup>ff</sup>* mice lacking gankyrin in hematopoietic cells and epithelial cells, but not *Vil-Cre;Gankyrin<sup>ff</sup>* mice lacking gankyrin in epithelial cells alone, were resistant to the development of acute colitis and inflammation-associated colon tumorigenesis. Importantly, such resistance to inflammation-associated colon tumorigenesis in *Mx1-Cre;Gankyrin<sup>ff</sup>* mice was associated with a significant reduction of pro-inflammatory responses (IL-17 and TNF- $\alpha$ ) and expression of cancer stem cell markers (Bmi1 and Sox9). A final step in the chain of evidence consisted of yeast-two hybrid, over-expression, and gene-silencing studies showing that gankyrin interacts with SHP-1 to induce activation of STAT3 and MAP kinases and then to induce TNF- $\alpha$  production. In accordance with

this, a physical interaction between gankyrin and SHP-1 was detected in immune cells of the colon tissue of gankyrin-intact mice treated with AOM and DSS. Collectively, these data strongly suggest that gankyrin-expressing myeloid cells produce pro-inflammatory cytokines through its interaction with SHP-1 followed by STAT3 activation and then promote CAC through induction of stem cell markers. Thus, we propose gankyrin as a tumor promoter that plays a role in the interface between immune cells and epithelial cells. It should be noted, however, that confirmation of this notion awaits future studies addressing the relationship between gankyrin expression and colon cancer prognosis as well as those addressing the role of gankyrin in immune cells by using myeloid, T cell, or B cell-specific gankyrin deletion mice.

Taken together, gankyrin, whose expression is upregulated by chronic inflammation, increases STAT3 activity and the production of TNF- $\alpha$  and IL-17 by binding to SHP-1 in inflammatory cells, leading to augmented inflammation. Such pro-inflammatory cytokine responses may enhance MAP kinase activity in the tumor and upregulate expression of stem cell markers in the colon. These factors would eventually promote CAC (Figure 6).



**Figure 6: Chronic inflammation increases gankyrin expression in the colonic mucosa of patients with IBD.** In inflammatory cells, gankyrin activates STAT3 by binding to SHP-1, leading to enhanced inflammation. These augmented inflammatory responses would activate ERK in tumors and eventually promote colitis-associated cancer.



Thus, suppression and measurement of gankyrin expression is a promising approach for advanced treatment and personalized management of IBD patients.

## PATIENTS AND METHODS

### Human tissue samples

UC and CD were diagnosed as previously described [38]. In total, 344 intestinal mucosa specimens were obtained by endoscopy from UC patients including 109 cases of refractory UC, 106 cases of non-refractory active UC, 40 cases in remission, as well as 35 CD patients and 54 normal controls without IBD and gankyrin expression was assessed. Among 344 intestinal mucosa specimens, 111 intestinal samples were obtained between April 2011 and March 2013 and analyzed for the expression of several genes. CAC specimens were obtained from 10 patients who had undergone surgery. Refractory IBD was defined according to endoscopic criteria and categorized as being active for more than 6 months. Active inflammation was defined as Mayo endoscopic score  $\geq 2$  in UC cases and a presence of ulcer in CD cases or presence of symptoms. The Mayo score was previously described [39]. The clinical study protocol conformed to the ethical guidelines of the 1975 Declaration of Helsinki and was approved by the relevant institutional review boards.

### Generation of mice with tissue-specific deletion of the gankyrin gene

Targeted ES clones were isolated from HK3i ES cells [40]. Chimeric mice were generated as described [41] and crossed with C57BL/6 mice to obtain heterozygous *Gankyrin*<sup>flox/wt</sup> mice (Accession No. CDB0944K) [42]; *Gankyrin*<sup>flox/wt</sup>, *Mx1-Cre*, and *Villin-Cre* (Jackson laboratory) mice were used to create tissue-specific conditional gankyrin knockout mice, designated here as *Mx1-Cre;Gankyrin*<sup>ff</sup> and *Vil-Cre;Gankyrin*<sup>ff</sup> mice. Induction of *Mx1-Cre* was achieved by 3 intraperitoneal injections of 300  $\mu$ g of poly(I:C) (Sigma-Aldrich, St. Louis, MO) every other day to 4–8-week-old mice.

### Mouse treatment

*Mx1-Cre;Gankyrin*<sup>ff</sup> mice and *Gankyrin*<sup>ff</sup> mice were treated with poly(IC) as described previously [43]. Sex- and age-matched poly(IC)-treated *Mx1-Cre;Gankyrin*<sup>ff</sup> mice (referred to as *Mx1-Cre;Gankyrin*<sup>ff</sup> mice), poly(IC)-treated *Gankyrin*<sup>ff</sup> mice, *Vil-Cre;Gankyrin*<sup>ff</sup> mice and *Gankyrin*<sup>ff</sup> mice (8–16 weeks old) received 2.5% (w/v) dextran sodium sulfate (DSS; molecular weight, 36,000–50,000 kDa; MP Biomedicals, Solon, OH) in drinking water for 7 days. Inflammatory cell infiltration score was assessed as described previously [6]. Isolation of lamina propria (LP) cells was performed as described

previously [6]. As the protocol for the murine CAC model [6], mice were intraperitoneally (i.p.) injected with 12.5 mg/kg azoxymethane (AOM; Sigma-Aldrich). After 5 days, 2.0% DSS was included in the drinking water for 5 days, followed by 16 days of regular water. This cycle was repeated three times. Then, 1.5% DSS was included in the drinking water for 4 days, followed by 7 days of regular water. Upon sacrifice, the colon was excised from the ileocecal junction to the anus, cut open longitudinally, and prepared for histological evaluation. Colons were assessed macroscopically for polyps under a dissecting microscope. All animal procedures were performed according to approved protocols and in accordance with the recommendations for the proper care and use of laboratory animals. The animal study protocol was approved by the Medical Ethics Committee of Kindai University Faculty of Medicine and Institutional Animal Care and Use Committee of RIKEN Kobe.

### Cell culture

THP-1 cells, an immortalized line of human monocyte, were maintained in RPMI-1640 medium (Gibco, Carlsbad, CA) supplemented with 10% fetal bovine serum, containing penicillin (100 U/ml) and streptomycin (100 mg/ml) and transfection of gankyrin siRNA and SHP-1 siRNA (Santa Cruz, Dallas, TX) was carried out using X-treme GENE siRNA Transfection Reagent (Roche, Basel, Switzerland). Caco2 and U-2 OS cells were maintained in DMEM medium (Gibco) supplemented with 10% fetal bovine serum, containing penicillin (100 U/ml) and streptomycin (100 mg/ml) and transfected with plasmid using Fugene (Promega, Madison, WI) and X-treme GENE HP DNA transfection reagent (Roche). Cell viability was assessed using Cell Counting Kit-8 (Dojindo, Tokyo, Japan). Jurkat cells were transfected with a plasmid containing 3HA-gankyrin cDNA.

### Biochemical and immunochemical analyses

Real-time qPCR, immunoblotting, immunoprecipitation and immunohistochemistry were previously described [6, 44]. List of primer sequences and FACS protocols are mentioned in Supplementary Materials and Methods. The following antibodies were used: anti-actin, anti-FLAG, anti-biotin conjugated FLAG (Sigma-Aldrich); anti-Bmi1, anti-phospho-STAT3, anti-STAT3, anti-phospho- extracellular signal-regulated protein kinase (ERK), anti-ERK, anti-phospho-c-Jun N-terminal kinase (JNK), anti-JNK, anti-phospho-p38, anti-p38 (Cell Signaling, Danvers, MA); anti-HA, anti-biotin conjugated HA (Roche), anti-SHP-1 (R&D systems, Minneapolis, MN) and anti-CD3, anti-CD11b, anti-CD20, anti-CD68, anti-CD138 (BD bioscience, San Jose, CA). Generation of anti-gankyrin polyclonal antibody was previously described



[45]. Immunohistochemistry was performed using ImmPRESS™ reagents (Vector Laboratory, Burlingame, CA) according to the manufacturer's recommendations.

Duolink fluorescence method was employed as per manufacturer's recommendations (Sigma Aldrich). Human gankyrin antibody and SHP-1 antibody (R&D systems) were used to assess gankyrin/SHP-1 interactions under confocal laser microscope.

Using the full length of gankyrin as bait, a cDNA library from human fetal intestine was screened by the yeast two-hybrid method, which was done by Invitrogen (Carlsbad, CA). Thirty-seven clones of yeast clones transformed with a human intestinal cDNA library were identified. Each clone proliferated on media containing the histidine inhibitor 3AT and was positive for  $\beta$ -galactosidase staining. DNA sequencing of the rescued plasmids revealed that two clones encoded SHP-1.

Immunofluorescent TUNEL staining was performed to measure apoptosis in paraffin-embedded sections using the *In Situ* Apoptosis Detection Kit as described by the manufacturer (Takara, Tokyo, Japan) and previous report [6]. Nuclei were stained with 4', 6diamidino-2-phenylindole (DAPI) to count the total cells per crypt.

### Statistical analysis

Differences were analyzed using Student's *t*-test. To compare variables of more than 2 conditions, analysis of variance (ANOVA) with post-hoc Tukey-Kramer honestly significant difference (HSD) multiple comparison was applied. The relationship between the expression of several genes was analyzed by Spearman's rank correlation test. *P* values <0.05 were considered significant.

### Abbreviations

Ascl2, achaete-scute complex homolog 2; AOM, azoxymethane; Bmi1, B cell-specific Moloney murine leukemia virus insertion site 1; CAC, colitis-associated cancer; CD, Crohn's disease; DSS, dextran sodium sulfate; ERK, extracellular signal-regulated protein kinase; IBD, inflammatory bowel disease; JNK, c-Jun N-terminal kinase; Lgr5, leucine-rich repeat-containing G-protein-coupled receptor 5; LP, lamina propria; Pim1, provirus integration site for Moloney murine leukemia virus 1; Sox9, sex-determining region Y (SRY)-box 9; STAT3, signal transducer and activator of transcription-3; UC, ulcerative colitis.

### CONFLICTS OF INTEREST

None of the authors have any conflicts to declare.

### GRANT SUPPORT

This research was supported by grants from the the Japan Foundation for Research and Promotion of

Endoscopy and the Japan Society of Gastroenterology, JSPS KAKENHI Grant Number JP26460979 and Health Labour Sciences Research Grant.

### REFERENCES

1. Weir HK, Thun MJ, Hankey BF, Ries LA, Howe HL, Wingo PA, Jemal A, Ward E, Anderson RN, Edwards BK. Annual report to the nation on the status of cancer, 1975-2000, featuring the uses of surveillance data for cancer prevention and control. *J Natl Cancer Inst*. 2003;95:1276-1299.
2. Jemal A, Siegel R, Ward E, Hao Y, Xu J, Thun MJ. Cancer statistics, 2009. *CA Cancer J Clin*. 2009;59:225-249.
3. Xavier RJ, Podolsky DK. Unravelling the pathogenesis of inflammatory bowel disease. *Nature*. 2007;448:427-434.
4. Itzkowitz SH, Yio X. Inflammation and cancer IV. Colorectal cancer in inflammatory bowel disease: the role of inflammation. *Am J Physiol Gastrointest Liver Physiol*. 2004;287:G7-17.
5. Ullman TA, Itzkowitz SH. Intestinal inflammation and cancer. *Gastroenterology*. 2011;140:1807-1816.
6. Sakurai T, Kashida H, Watanabe T, Hagiwara S, Mizushima T, Iijima H, Nishida N, Higashitsuji H, Fujita J, Kudo M. Stress response protein cirp links inflammation and tumorigenesis in colitis-associated cancer. *Cancer Res*. 2014;74:6119-6128.
7. Adachi T, Sakurai T, Kashida H, Mine H, Hagiwara S, Matsui S, Yoshida K, Nishida N, Watanabe T, Itoh K, Fujita J, Kudo M. Involvement of heat shock protein  $\alpha$ 4/apg-2 in refractory inflammatory bowel disease. *Inflamm Bowel Dis*. 2015;21:31-39.
8. Higashitsuji H, Itoh K, Nagao T, Dawson S, Nonoguchi K, Kido T, Mayer RJ, Arai S, Fujita J. Reduced stability of retinoblastoma protein by gankyrin, an oncogenic ankyrin-repeat protein overexpressed in hepatomas. *Nat Med*. 2000;6:96-99.
9. Tang S, Yang G, Meng Y, Du R, Li X, Fan R, Zhao L, Bi Q, Jin J, Gao L, Zhang L, Li H, Fan M, et al. Overexpression of a novel gene gankyrin correlates with the malignant phenotype of colorectal cancer. *Cancer Biol Ther*. 2010;9:88-95.
10. Mine H, Sakurai T, Kashida H, Matsui S, Nishida N, Nagai T, Hagiwara S, Watanabe T, Kudo M. Association of gankyrin and stemness factor expression in human colorectal cancer. *Dig Dis Sci*. 2013;58:2337-2344.
11. Zheng T, Hong X, Wang J, Pei T, Liang Y, Yin D, Song R, Song X, Lu Z, Qi S, Liu J, Sun B, Xie C, et al. Gankyrin promotes tumor growth and metastasis through activation of IL-6/STAT3 signaling in human cholangiocarcinoma. *Hepatology*. 2014;59:935-946.
12. Man JH, Liang B, Gu YX, Zhou T, Li AL, Li T, Jin BF, Bai B, Zhang HY, Zhang WN, Li WH, Gong WL, Li HY, et al. Gankyrin plays an essential role in Ras-induced tumorigenesis through regulation of the RhoA/

- ROCK pathway in mammalian cells. *J Clin Invest*. 2010;120:2829-2841.
13. Higashitsuji H, Higashitsuji H, Itoh K, Sakurai T, Nagao T, Sumitomo Y, Masuda T, Dawson S, Shimada Y, Mayer RJ, Fujita J. The oncoprotein gankyrin binds to MDM2/HDM2, enhancing ubiquitylation and degradation of p53. *Cancer Cell*. 2005;8:75-87.
14. Wang GL, Shi X, Haeffliger S, Jin J, Major A, Iakova P, Finegold M, Timchenko NA. Elimination of C/EBPalpha through the ubiquitin-proteasome system promotes the development of liver cancer in mice. *J Clin Invest*. 2010;120:2549-2562.
15. Fu J, Chen Y, Cao J, Luo T, Qian YW, Yang W, Ren YB, Su B, Cao GW, Yang Y, Yan YQ, Shen F, Wu MC, et al. p28GANK overexpression accelerates hepatocellular carcinoma invasiveness and metastasis via phosphoinositol 3-kinase/AKT/hypoxia-inducible factor-1 $\alpha$  pathways. *Hepatology*. 2011;53:181-192.
16. Radisky DC, Bissell MJ. Cancer. Respect thy neighbor! *Science*. 2004;303:775-7.
17. Yin S, Wu H, Lv J, Wu X, Zhang Y, Du J, Zhang Y. SHP-1 arrests mouse early embryo development through downregulation of Nanog by dephosphorylation of STAT3. *PLoS One*. 2014;9:e86330.
18. Ramachandran IR, Song W, Lapteva N, Seethamagari M, Slawin KM, Spencer DM, Levitt JM. The phosphatase SRC homology region 2 domain-containing phosphatase-1 is an intrinsic central regulator of dendritic cell function. *J Immunol*. 2011;186:3934-3945.
19. McKenzie BS, Kastelein RA, Cua DJ. Understanding the IL-23-IL-17 immune pathway. *Trends Immunol*. 2006;27:17-23.
20. Barker N, van Es JH, Kuipers J, Kujala P, van den Born M, Cozijnsen M, Haegebarth A, Korving J, Begthel H, Peters PJ, Clevers H. Identification of stem cells in small intestine and colon by marker gene Lgr5. *Nature*. 2007;449:1003-1007.
21. Davies EJ, Marsh V, Clarke AR. Origin and maintenance of the intestinal cancer stem cell. *Mol Carcinog*. 2011;50:254-263.
22. Li DW, Tang HM, Fan JW, Yan DW, Zhou CZ, Li SX, Wang XL, Peng ZH. Expression level of Bmi-1 oncoprotein is associated with progression and prognosis in colon cancer. *J Cancer Res Clin Oncol*. 2010;136:997-1006.
23. Maynard MA, Ferretti R, Hilgendorf KI, Perret C, Whyte P, Lees JA. Bmi1 is required for tumorigenesis in a mouse model of intestinal cancer. *Oncogene*. 2014;33:3742-3747.
24. Cannon J. Colorectal Neoplasia and Inflammatory Bowel Disease. *Surg Clin North Am*. 2015;95:1261-1269.
25. Lorenz U. SHP-1 and SHP-2 in T cells: two phosphatases functioning at many levels. *Immunol Rev*. 2009;228:342-359.
26. Xie ZH, Zhang J, Siraganian RP. Positive regulation of c-Jun N-terminal kinase and TNF-alpha production but not histamine release by SHP-1 in RBL-2H3 mast cells. *J Immunol*. 2000;164:1521-1528.
27. Inoue T, Suzuki Y, Mizuno K, Nakata K, Yoshimaru T, Ra C. SHP-1 exhibits a pro-apoptotic function in antigen-stimulated mast cells: positive regulation of mitochondrial death pathways and negative regulation of survival signaling pathways. *Mol Immunol*. 2009;47:222-232.
28. Shigdar S, Li Y, Bhattacharya S, O'Connor M, Pu C, Lin J, Wang T, Xiang D, Kong L, Wei MQ, Zhu Y, Zhou S, Duan W. Inflammation and cancer stem cells. *Cancer Lett*. 2014;345:271-278.
29. Peng YH, Li JJ, Xie FW, Chen JF, Yu YH, Ouyang XN, Liang HJ. Expression of pim-1 in tumors, tumor stroma and tumor-adjacent mucosa co-determines the prognosis of colon cancer patients. *PLoS One*. 2013;8:e76693.
30. Espersen ML, Olsen J, Linnemann D, Høgdall E, Troelsen JT. Clinical implications of intestinal stem cell markers in colorectal cancer. *Clin Colorectal Cancer*. 2015;14:63-71.
31. Shang Y, Pan Q, Chen L, Ye J, Zhong X, Li X, Meng L, Guo J, Tian Y, He Y, Chen W, Peng Z, Wang R. Achaete scute-like 2 suppresses CDX2 expression and inhibits intestinal neoplastic epithelial cell differentiation. *Oncotarget*. 2015;6:30993-31006. doi: 10.18632/oncotarget.5206.
32. Yang S, Wang B, Guan C, Wu B, Cai C, Wang M, Zhang B, Liu T, Yang P. Foxp3+IL-17+ T cells promote development of cancer-initiating cells in colorectal cancer. *J Leukoc Biol*. 2011;89:85-91.
33. Schwitalla S, Fingerle AA, Cammareri P, Nebelsiek T, Göktuna SI, Ziegler PK, Canli O, Heijmans J, Huels DJ, Moreaux G, Rupec RA, Gerhard M, Schmid R, et al. Intestinal tumorigenesis initiated by dedifferentiation and acquisition of stem-cell-like properties. *Cell*. 2013;152:25-38.
34. Wang K, Kim MK, Di Caro G, Wong J, Shalpour S, Wan J, Zhang W, Zhong Z, Sanchez-Lopez E, Wu LW, Taniguchi K, Feng Y, Fearon E, et al. Interleukin-17 receptor a signaling in transformed enterocytes promotes early colorectal tumorigenesis. *Immunity*. 2014;41:1052-1063.
35. Grivennikov SI, Karin M. Inflammatory cytokines in cancer: tumour necrosis factor and interleukin 6 take the stage. *Ann Rheum Dis*. 2011;70:i104-8.
36. Laine L, Kaltenbach T, Barkun A, McQuaid KR, Subramanian V, Soetikno R; SCENIC Guideline Development Panel. SCENIC international consensus statement on surveillance and management of dysplasia in inflammatory bowel disease. *Gastrointest Endosc*. 2015;81:489-501.
37. Su B, Luo T, Zhu J, Fu J, Zhao X, Chen L, Zhang H, Ren Y, Yu L, Yang X, Wu M, Feng G, Li S, et al. Interleukin-1 $\beta$ /Interleukin-1 receptor-associated kinase 1 inflammatory signaling contributes to persistent Gankyrin activation during hepatocarcinogenesis. *Hepatology*. 2015;61:585-597.
38. Bockus gastroenterology, 5<sup>th</sup> edition, Henry L. Bockus, W B Saunders Co. 1995.

39. Sandborn WJ, Sands BE, Wolf DC, Valentine JF, Safdi M, Katz S, Isaacs KL, Wruble LD, Katz J, Present DH, Loftus EV Jr, Graeme-Cook F, Odenheimer DJ, Hanauer SB. Repifermin (keratinocyte growth factor-2) for the treatment of active ulcerative colitis: a randomized, double-blind, placebo-controlled, dose-escalation trial. *Aliment Pharmacol Ther.* 2003;17:1355-1364.
40. Kiyonari H, Kaneko M, Abe S, Aizawa S. Three Inhibitors of FGF Receptor, ERK and GSK3 Establishes Germline-Competent Embryonic Stem Cells of C57BL/6N Mouse Strain with High Efficiency and Stability. *Genesis* 2010;48:317-27.
41. <http://www2.clst.riken.jp/arg/Methods.html>
42. <http://www2.clst.riken.jp/arg/mutant%20mice%20list.html>
43. Sakurai T, He G, Matsuzawa A, Yu GY, Maeda S, Hardiman G, Karin M. Hepatocyte necrosis induced by oxidative stress and IL-1 alpha release mediate carcinogen-induced compensatory proliferation and liver tumorigenesis. *Cancer Cell.* 2008;14:156-165.
44. Sakurai T, Kudo M, Umemura A, He G, Elsharkawy AM, Seki E, Karin M. p38 $\alpha$  Inhibits Liver Fibrogenesis and Consequent Hepatocarcinogenesis by Curtailing Accumulation of Reactive Oxygen Species. *Cancer Res.* 2013;73:215-224.
45. Liu Y, Higashitsuji H, Higashitsuji H, Itoh K, Sakurai T, Koike K, Hirota K, Fukumoto M, Fujita J. Overexpression of gankyrin in mouse hepatocytes induces hemangioma by suppressing factor inhibiting hypoxia-inducible factor-1 (FIH-1) and activating hypoxia-inducible factor-1. *Biochem Biophys Res Commun.* 2013;432:22-27.

## Original Article

## Endoscopic ultrasonography-guided choledochoduodenostomy using a newly designed laser-cut metal stent: Feasibility study in a porcine model

Kosuke Minaga,<sup>1</sup> Masayuki Kitano,<sup>1,2</sup> Chimyon Gon,<sup>3</sup> Kentaro Yamao,<sup>1</sup> Hajime Imai,<sup>1</sup> Takeshi Miyata,<sup>1</sup> Ken Kamata,<sup>1</sup> Shunsuke Omoto,<sup>1</sup> Mamoru Takenaka<sup>1</sup> and Masatoshi Kudo<sup>1</sup>

<sup>1</sup>Department of Gastroenterology and Hepatology, Kindai University Faculty of Medicine, Osaka-Sayama,

<sup>2</sup>Second Department of Internal Medicine, Wakayama Medical University School of Medicine, Wakayama, and

<sup>3</sup>Research and Development Center, Zeon Corporation, Toyama, Japan

**Background and Aim:** Endoscopic ultrasonography (EUS)-guided choledochoduodenostomy (EUS-CDS) is increasingly used in the treatment of malignant distal biliary obstruction. Standardized use of this technique requires improvements in instruments, including more convenient and safer devices. The present study was designed to evaluate the resistance force to migration (RFM) of a newly designed laser-cut metal stent and the feasibility of EUS-CDS using this stent.

**Methods:** This experimental study used a porcine model of biliary dilatation involving five male pigs. The new stent is a fully covered laser-cut stent with anti-migration anchoring hooks. The RFM of the new stents was compared with those of three commercially available covered metal stents using a phantom model. In the animal study, after ligation of Vater's ampulla with endoscopic clips, the dilated common bile duct was punctured under EUS guidance, followed by EUS-CDS using the new stent. One week after the procedure, the stents were removed

endoscopically and the fistulas were assessed after the pigs were killed. Technical feasibility and clinical outcomes were evaluated.

**Results:** Among the four stents, the new stent had the highest RFM. Metal stent placement was successful in all five pigs, with no procedure-related complications occurring during and 1 week after endoscopic intervention. All stents remained in place without migration and were removed easily using a snare. At necropsy, fistulas were created between the bile duct and duodenum in all pigs.

**Conclusion:** EUS-CDS using a newly designed metal stent was feasible and effective in this porcine model of biliary dilatation.

**Key words:** anti-migration, endoscopic ultrasonography (EUS), EUS-guided biliary drainage, EUS-guided choledochoduodenostomy, metal stent

## INTRODUCTION

ENDOSCOPIC PLACEMENT OF biliary stents in patients with biliary malignancy is frequently used to relieve obstructive jaundice.<sup>1–3</sup> Patients with malignant biliary obstruction who fail initial endoscopic retrograde cholangiopancreatography (ERCP) may undergo an alternative procedure, endoscopic ultrasonography (EUS)-guided biliary drainage (EUS-BD).<sup>4–7</sup> Although the transduodenal approach to extrahepatic bile ducts, called EUS-guided choledochoduodenostomy (EUS-CDS), is incre-

easingly used to treat malignant distal biliary obstructions, endoscopic devices dedicated to EUS-BD with transluminal stenting are limited, resulting in device-related shortcomings with this new procedure. This pilot study was designed to evaluate the resistance force to migration (RFM) of a newly designed laser-cut metal stent with anti-migration hooks and the feasibility of carrying out EUS-CDS using this stent in a porcine model of biliary dilatation.

## METHODS

## Stents

THE NEWLY DESIGNED self-expandable metal stent (Hook Stent; Zeon Corporation, Tokyo, Japan; not commercially available), with a diameter of 10 mm and a length of 40 mm, is made of laser-cut nitinol wire fully covered by a polyurethane membrane to prevent bile

**Corresponding:** Masayuki Kitano, Wakayama Medical University School of Medicine, Second Department of Internal Medicine, 811-1 Kimiidera, Wakayama, Wakayama 641-8509, Japan. Email: kitano@wakayama-med.ac.jp

Received 19 July 2016; accepted 23 September 2016.



leakage (Fig. 1a). To prevent inward stent migration, the distal end of the stent has three hooks made from nitinol wire, each with a length of 10 mm and a width of 4 mm (Fig. 1b). Stents are delivered with a 9-Fr pull-back delivery catheter, which is compatible with the working channel of an echoendoscope. The extent of stent shortening is approximately 4%.

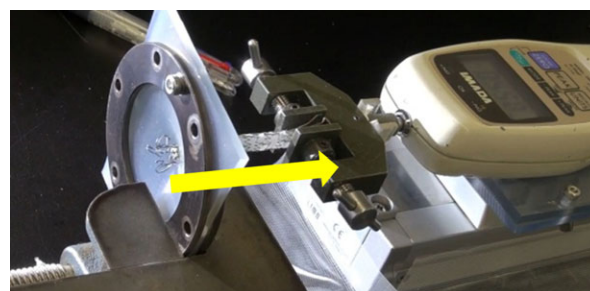
### Phantom experiments used to determine anti-migration

The anti-migration property of the metal stents was assessed as described previously.<sup>8</sup> Briefly, a phantom model of metal stent migration was created using a retraction robot, a 3-mm-thick silicone wall (Shin-etsu Chemical, Tokyo, Japan), and a force gauge (Model DPX-5TR; Imada, Tokyo, Japan) (Fig. 2). The new stent (Hook Stent) and three different commercially available covered metal stents (ZEOSTENT covered; Zeon Corporation, ComVi stent; Taewoong Medical, Gimpo, South Korea, and WallFlex Fully Covered Biliary Metal Stent; Boston Scientific, Natick, MA, USA) were used in this experimental study. The former two are covered stents with a laser-cut structure and the latter two have a braided structure. The metal stents were fixed into a round hole (diameter, 8 mm) in the silicone wall. A force gauge was fixed to the proximal end of the stent. During the experiments, the proximal end of the stent (with the attached force gauge) was retracted at a speed of 1 mm/s using the retraction robot (Fig. 2). Force of the resistance of the stent to retraction in the axial direction, which is denoted as resistance force to migration (RFM), was measured from the time stent retraction started until the time the distal end of the stent was dislocated from the silicone wall.<sup>8</sup> Maximum value of the resistance force generated during retraction was used for analysis. RFM was expressed as the average of five replicate measurements.

## In vivo experiments

### Animals

This study was carried out *in vivo* using a porcine model and was approved by the Institutional Animal Care and Use Committee of Kindai University. All animal experiments were carried out at Research and Development Center, Zeon Corporation (Toyama, Japan). Between August 2015 and January 2016, five male pigs (Camborough hybrids) weighing 35–45 kg underwent endoscopic procedures. No antibiotic agents were given before the procedure. The pigs were fasted for 24 h before the procedure, placed under general anesthesia, and intubated endotracheally. During the procedure, heart rate, respiratory rate, oxygen saturation and body temperature were monitored continuously. The pigs resumed their usual diet (1000 kcal/day) on the day after the procedure.



**Figure 2** Resistance force to migration measurement machine. The machine consists of a retraction robot, a silicone wall, and a force gauge. The Hook Stent (Zeon Corporation, Tokyo, Japan) is fixed into a round hole in the silicone wall and its proximal end is connected to the force gauge device. The stent is retracted from the wall at a speed of 1 mm/s by using the retraction robot.



**Figure 1** Illustration of a newly designed, self-expandable, covered metal stent (Hook Stent; Zeon Corporation, Tokyo, Japan). (a) Each stent, measuring 10 mm in diameter and 40 mm in length, is made of laser-cut nitinol wire and fully covered by a polyurethane membrane. (b) Three hooks made of nitinol wire are attached to the distal end of the stent. Each hook is 10 mm in length and 4 mm in width (arrow).



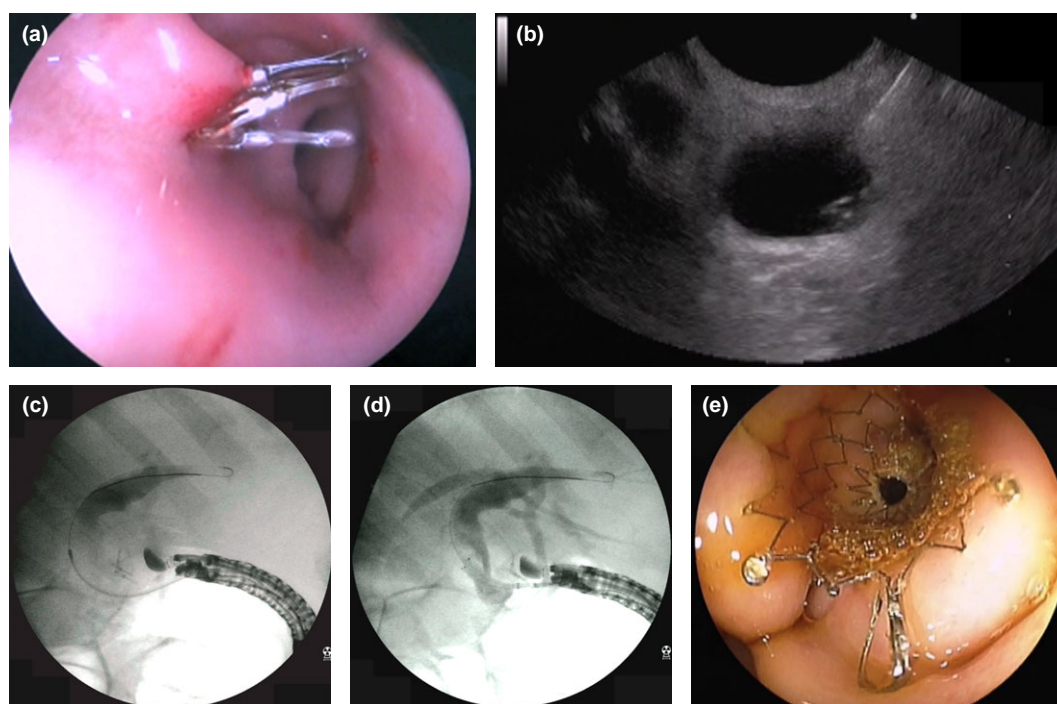
## Endoscopic procedures

First, we created an experimental porcine model of biliary dilatation by modifying the previously established model.<sup>9</sup> The day before EUS-guided drainage, a gastroscope was inserted into the duodenal bulb. Then, Vater's ampulla of each pig was ligated with four endoscopic clips to induce dilatation of the common bile duct (CBD), mimicking obstructive jaundice (Fig. 3a). On the following day, a linear array echoendoscope (EG-530UT2; Fujifilm, Kanagawa, Japan) was introduced into the duodenum. Following visualization of the dilated CBD adjacent to the duodenum (Fig. 3b), the echoendoscope was manipulated until an appropriate puncture route that avoided any intervening vessels was identified. The distal CBD, chosen as the ideal target, was punctured with a 19-gauge aspiration needle (SonoTip ProControl; Medi-Globe, Rosenheim, Germany) under EUS guidance. Bile was aspirated, contrast medium was injected, and a 0.025-inch guidewire (VisiGlide 2; Olympus Medical Systems, Tokyo, Japan) was advanced into the CBD (Fig. 3c). The fistula was dilated using a

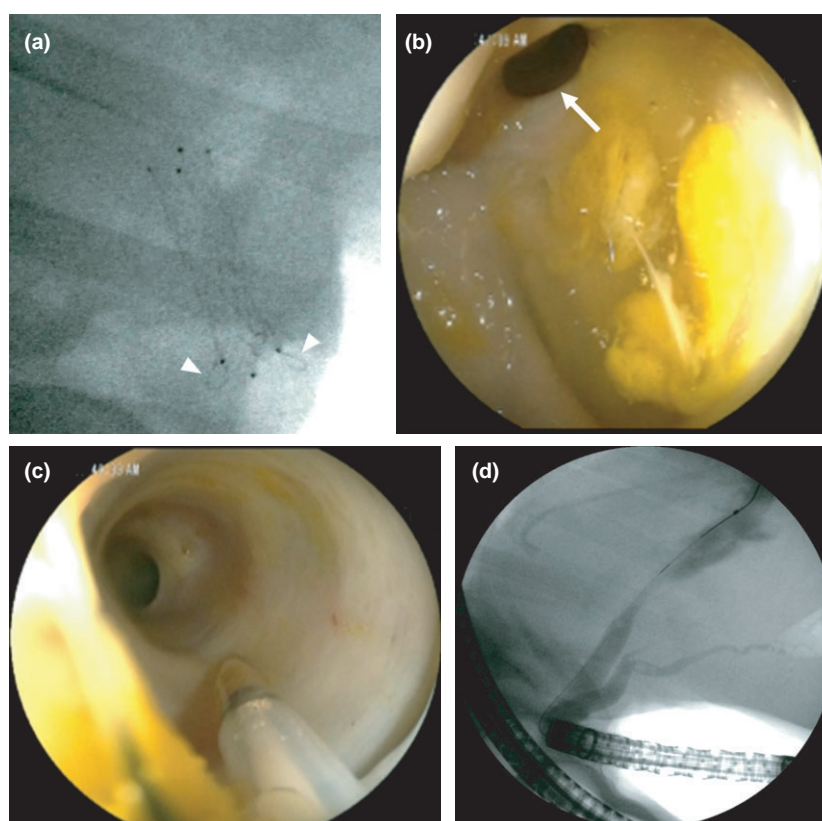
biliary bougie dilator (7-Fr, 9-Fr, Soehendra Biliary Dilation Catheter; Cook Medical, Winston-Salem, NC, USA) or diathermic dilator (6-Fr, Cysto-Gastro-Set; Endo-Flex, Voerde, Germany). Thereafter, a new metal stent (Hook Stent) was deployed between the CBD and the duodenum (Fig. 3d,e). First, the proximal end of the stent was released under fluoroscopic and endosonographic guidance. Once the proximal end of the stent was extended, the delivery system was slightly retracted to adjust the proximal stent position. Afterwards, the stent was further released until a section of 1 cm appeared within the channel of the echoendoscope under fluoroscopic guidance. Then, the delivery catheter of the stent was pushed out and the echoendoscope was pulled out gently while ensuring that the stent had been completely released in the duodenal lumen under endoscopic guidance.

## Post-procedural care and necropsy

A gastroscope was advanced into the duodenum to confirm stent position, and the degree of stent expansion was



**Figure 3** Procedures used in the porcine model of endoscopic ultrasonography (EUS)-guided choledochoduodenostomy with the newly designed laser-cut, covered metal stent. (a) Ligation of Vater's ampulla with multiple endoscopic clips 1 day before EUS-guided drainage. (b) Linear array EUS image showing dilatation of the distal common bile duct (CBD). CBD diameter measured by EUS is 9.5 mm. (c) Fluoroscopic image, showing dilatation of the CBD with ampullary obstruction. After puncturing the CBD, a 0.025-inch guidewire was advanced into the bile duct. (d) After dilating the puncture site, a newly designed covered metallic stent (10-mm wide and 40-mm long) was deployed between the CBD and the duodenum. (e) Endoscopic view of the deployed stent.



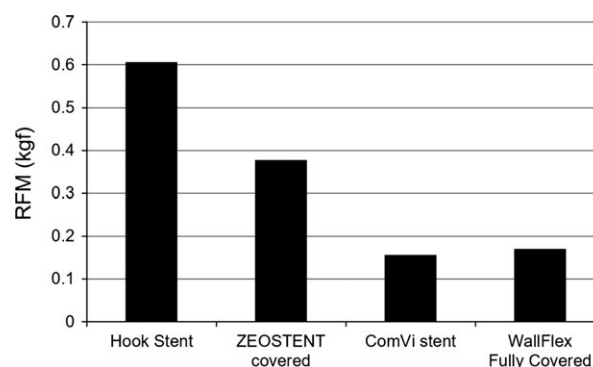
**Figure 4** Post-endoscopic procedural findings in the porcine model. (a) Fluoroscopic image 1 week after the procedure showing that the stent is fully expanded. (b) View showing a mature fistula (arrow) at the site from which the stent had been removed. (c) View showing the common bile duct as seen from the fistula. (d) An endoscopic retrograde cholangiopancreatography catheter was inserted into the fistula and contrast medium was injected. The bile duct was visualized, but there was no leakage of contrast medium into the peritoneal cavity.

assessed under fluoroscopic guidance (Fig. 4a). The stent was removed with a snare, and an ERCP catheter was inserted into the place from which the stent had been removed. Contrast medium was injected to assess whether the medium leaked into the peritoneal cavity (Fig. 4b,c,d). The pigs were killed and dissected, and formation of a fistula between the bile duct and the duodenum was evaluated.

## RESULTS

### Phantom experiments

**FIGURE 5** SHOWS THE results of the RFM measurements. Among the four stents tested, the new stent (Hook Stent) had the highest RFM. Among the three commercially available stents, the laser-cut metal stent (ZEOSTENT covered) had the highest RFM.



**Figure 5** Resistance force to migration of four different covered metal stents.

### In vivo experiments

EUS-CDS was successfully carried out, and newly designed stents were deployed without technical difficulties in all five

pigs. The fistula was dilated using the biliary bougie dilator in four pigs and the diathermic dilator in one pig. Mean  $\pm$  SD CBD diameter, as measured by EUS at the time of puncture, was  $9.8 \pm 1.8$  mm, with all five CBD punctured easily using a 19-gauge aspiration needle. All five pigs survived for 1 week after the procedure without complications. All consumed expected quantities of a standard diet, with none of the animals manifesting signs of peritonitis. Gastroscopy done 1 week after the procedure revealed that all stents had been inserted through the duodenum and that they remained in place without migration. All stents fully expanded and could be removed endoscopically with a snare without difficulty. Subsequent contrast injection into the stent area showed no evidence of leakage into the peritoneal space. At necropsy, one pig showed a small hematoma, but none showed evidence of organ injury or peritonitis. Strong adhesion between the duodenum and the CBD was observed in all five pigs.

## DISCUSSION

SINCE INITIALLY DESCRIBED in 2001,<sup>4</sup> EUS-CDS has been increasingly carried out as an effective alternative in patients with malignant biliary obstruction who fail ERCP.<sup>4–7</sup> A recent systematic analysis of 1192 patients who underwent EUS-BD revealed a cumulative adverse event rate of 23.32%.<sup>10</sup> The most frequent complications were bile leakage, stent migration, bleeding and pneumoperitoneum, which can be serious or even fatal.<sup>10–12</sup> Development of a new comfortable stenting device that prevents complications related to the EUS-BD procedure is therefore needed. To overcome the shortcomings of conventional stents, we developed a newly designed, fully covered, laser-cut metal stent with anti-migration hooks.

Covered metal stents are more prone to migration than uncovered ones.<sup>2,13,14</sup> To reduce stent migration, covered stents have been equipped with various mechanical, anti-migration properties, including different stent frameworks, different membrane materials, high radial force (RF), different flare structures, and inclusion of an anchoring flap.<sup>15–17</sup> Stent flare structure and low RF have been associated directly with stent migration.<sup>8,16,18</sup> RF is the radially outward expanding force that maintains luminal patency at the stricture following stent deployment.<sup>15</sup> Laser-cut stents have a higher RF and much higher resistance to migration than braided stents.<sup>8</sup> Therefore, to prevent migration, we designed a laser-cut covered stent with anti-migration hooks.

Adequate extrahepatic bile duct dilatation is essential for successful EUS-CDS in porcine models. To establish an experimental porcine model of biliary dilatation, we ligated

Vater's ampulla of each pig with four endoscopic clips the day before the EUS-CDS procedure. Lee *et al.*<sup>9</sup> previously created a biliary dilatation porcine model using endoscopic clip closure or endoscopic band ligation of the major papilla followed by argon plasma coagulation in the ampullary orifice. They carried out EUS-guided hepaticogastrostomy puncturing of the intrahepatic bile duct. However, in our study assessing the feasibility of EUS-CDS, the main target of puncturing was the extrahepatic bile duct. Anatomically, the extrahepatic bile duct is thicker than the intrahepatic bile duct; therefore, EUS-CDS can be carried out even when the intrahepatic bile duct is not sufficiently dilated. After simple ligation of the Vater's ampulla with endoscopic clips, mean  $\pm$  SD extrahepatic bile duct diameter was  $9.8 \pm 1.8$  mm on the following day, which was adequate for puncturing with a 19-gauge aspiration needle. Although a suitable porcine model of biliary dilatation is yet to be established, our model is simple and feasible for EUS-CDS.

This pilot study has shown that EUS-CDS using our newly designed metal stent in a porcine model of biliary dilatation was feasible and safe. There was no evidence of stent inward or distal migration, despite these stents being shorter than conventional tubular biliary metal stents. These results suggested that both the stent framework (laser-cut) and the anchoring hooks at the distal end effectively prevented stent migration. One advantage of laser-cut type is that stent shortening is lower than with the braided type, which makes it easy to place a modestly sized stent. Up to now, tubular biliary metal stents longer than 4 cm have been used in the EUS-CDS procedure to prevent stent inward migration; however, this type of stent placement can sometimes make re-intervention difficult and the exposed ends of the stent in the duodenal lumen may cause tissue trauma, resulting in bleeding or perforation.<sup>19</sup> In view of these limitations, shorter exposed stents in the luminal portion equipped with anti-migration properties may be preferable.

Distal stent migration is one of the late adverse events that can occur during follow up.<sup>20</sup> To assess distal stent migration, long-term follow up is needed. In this animal study, the stents were removed endoscopically after 1 week. Therefore, whether or not this new stent can prevent distal stent migration is still unclear. Recently, we reported that the laser-cut stent (ZEOSTENT covered) is more resistant to migration than the braided type in phantom experiments.<sup>8</sup> We surmise that the new laser-cut stent (Hook Stent) may have potential in preventing distal stent migration. Further long-term studies are needed to evaluate the distal anti-migration potential of this new stent.

Recent studies have described the development of a novel, lumen-apposing metal stent (LAMS; AXIOS;

Xlumen, Mountain View, CA, USA).<sup>21–24</sup> These stents allowed the creation of a sealed transluminal conduit between the drainage lumen and the gastrointestinal tract, which may reduce the risk of stent migration and bile leakage. Interventional EUS-guided procedures using LAMS have been reported and shown to have high success rates, especially for the drainage of pancreatic fluids and the gallbladder.<sup>21–24</sup> However, the use of LAMS for EUS-CDS has been described only in case reports and small case series.<sup>25,26</sup> The feasibility and safety of stents specific for EUS-CDS have not been established. Large multicenter studies using stents specific for EUS-CDS, including LAMS and the laser-cut hook stent described in this report, may be useful for biliary drainage.

The present study had several limitations. This study was a small pilot study in animals, with a small sample size and a non-comparative design. The follow-up time was only 1 week, after which the pigs were necropsied. Long-term evaluation of these stents is required. Studies comparing these stents with other conventional stents are needed to evaluate the efficacy and safety of these newly designed, laser-cut, covered metal stents.

In conclusion, EUS-CDS using these newly designed, laser-cut, covered metal stents was shown to be feasible and effective in an experimental porcine model. Clinical trials may be warranted to confirm the feasibility and safety of this promising device.

## ACKNOWLEDGMENTS

THIS STUDY WAS supported by grants from the Japan Society for the Promotion of Science. We thank Zeon Corporation (Tokyo, Japan) for providing stent samples, animals, and for preparing the animal laboratory. We also thank the staff of the Research and Development Center, Zeon Corporation (Toyama, Japan) for their efforts in developing the new stent.

## CONFLICTS OF INTEREST

THE FOLLOWING AUTHORS declare no conflicts of interest: K. Minaga, M. Kitano, K. Yamao, H. Imai, T. Miyata, K. Kamata, S. Omoto, M. Takenaka, M. Kudo. C. Gon works in the Research and Development Center, Zeon Corporation.

## REFERENCES

- Soehendra N, Reynders-Frederix V. Palliative bile duct drainage: a new endoscopic method of introducing a transpapillary drain. *Endoscopy* 1980; **12**: 8–11.
- Isayama H, Komatsu Y, Tsujino T *et al.* A prospective randomised study of “covered” versus “uncovered” diamond stents for the management of distal malignant biliary obstruction. *Gut* 2004; **53**: 729–34.
- Kitano M, Yamashita Y, Tanaka K *et al.* Covered self-expandable metal stents with an anti-migration system improve patency duration without increased complications compared with uncovered stents for distal biliary obstruction caused by pancreatic carcinoma: a randomized multicenter trial. *Am. J. Gastroenterol.* 2013; **108**: 1713–22.
- Giovannini M, Moutardier V, Pesenti, Bories E, Lelong B, Delpero JR. Endoscopic ultrasound-guided bilioduodenal anastomosis: a new technique for biliary drainage. *Endoscopy* 2001; **33**: 898–900.
- Kahaleh M, Hernandez AJ, Tokar J, Adams RB, Shami VM, Yeaton P. Interventional EUS-guided cholangiography: evaluation of a technique in evolution. *Gastrointest. Endosc.* 2006; **64**: 52–9.
- Itoi T, Sofuni A, Itokawa F *et al.* Endoscopic ultrasonography-guided biliary drainage. *J. Hepatobiliary Pancreat. Sci.* 2010; **17**: 611–6.
- Park DH, Jang JW, Lee SS, Seo DW, Lee SK, Kim MH. EUS guided biliary drainage with transluminal stenting after failed ERCP: predictors of adverse events and long-term results. *Gastrointest. Endosc.* 2011; **74**: 1276–84.
- Minaga K, Kitano M, Imai H *et al.* Evaluation of anti-migration properties of biliary covered self-expandable metal stents. *World J. Gastroenterol.* 2016; **22**: 6917–24.
- Lee TH, Choi JH, Lee SS *et al.* A pilot proof-of-concept study of a modified device for one-step endoscopic ultrasound-guided biliary drainage in a new experimental biliary dilatation animal model. *World J. Gastroenterol.* 2014; **21**: 5859–66.
- Wang K, Zhu J, Xing L, Wang Y, Jin Z, Li Z. Assessment of efficacy and safety of EUS-guided biliary drainage: a systematic review. *Gastrointest. Endosc.* 2016; **83**: 1218–27; Epub ahead of print.
- Poincloux L, Rouquette O, Buc E *et al.* Endoscopic ultrasound-guided biliary drainage after failed ERCP: cumulative experience of 101 procedures at a single center. *Endoscopy* 2015; **47**: 794–801.
- Chantarojanasiri T, Aswakul P, Prachayakul V. Uncommon complications of therapeutic endoscopic ultrasonography: what, why, and how to prevent. *World J. Gastrointest. Endosc.* 2015; **7**: 960–8.
- Telford JJ, Carr-Locke DL, Baron TH *et al.* A randomized trial comparing uncovered and partially covered self-expandable metal stents in the palliation of distal malignant biliary obstruction. *Gastrointest. Endosc.* 2010; **72**: 907–14.
- Lee JH, Krishna SG, Singh A *et al.* Comparison of the utility of covered metal stents versus uncovered metal stents in the management of malignant biliary strictures in 749 patients. *Gastrointest. Endosc.* 2013; **78**: 312–24.
- Isayama H, Nakai Y, Toyokawa Y *et al.* Measurement of radial and axial forces of biliary self-expandable metallic stents. *Gastrointest. Endosc.* 2009; **70**: 37–44.



- 16 Park DH, Lee SS, Lee TH *et al.* Anchoring flap versus flared end, fully covered self-expandable metal stents to prevent migration in patients with benign biliary structures: a multicenter, prospective, comparative pilot study (with videos). *Gastrointest. Endosc.* 2011; **73**: 64–70.
- 17 Isayama H, Kawakubo K, Nakai Y *et al.* A novel, fully covered laser-cut nitinol stent with antimigration properties for nonresectable distal malignant biliary obstruction: a multicenter feasibility study. *Gut Liv.* 2013; **7**: 725–30.
- 18 Nakai Y, Isayama H, Kogure H *et al.* Risk factors for covered metallic stent migration in patients with distal malignant biliary obstruction due to pancreatic cancer. *J. Gastroenterol. Hepatol.* 2014; **29**: 1744–9.
- 19 Rimbaş M, Kunda R, Larghi A. Endoscopic ultrasound-guided choledochoduodenostomy as a primary treatment for malignant distal biliary obstruction: is it time for a randomized controlled study? *Endoscopy* 2016; **48**: 686.
- 20 Song TJ, Hyun YS, Lee SS *et al.* Endoscopic ultrasound-guided choledochoduodenostomies with fully covered self-expandable metallic stents. *World J. Gastroenterol.* 2012; **18**: 4435–40.
- 21 Itoi T, Binmoeller KF, Shah J *et al.* Clinical evaluation of a novel lumen-apposing metal stent for endosonography-guided pancreatic pseudocyst and gallbladder drainage (with videos). *Gastrointest. Endosc.* 2012; **75**: 870–6.
- 22 Law R, Grimm IS, Stavas JM, Baron TH. Conversion of percutaneous cholecystostomy to internal transmural gallbladder drainage using an endoscopic ultrasound-guided, lumen-apposing metal stent. *Clin. Gastroenterol. Hepatol.* 2016; **14**: 476–80.
- 23 Siddiqui AA, Adler DG, Nieto J *et al.* EUS-guided drainage of peripancreatic fluid collections and necrosis by using a novel lumen-apposing stent: a large retrospective, multicenter U.S. experience (with videos). *Gastrointest. Endosc.* 2016; **83**: 699–707.
- 24 Walter D, Teoh AY, Itoi T *et al.* EUS-guided gall bladder drainage with a lumen-apposing metal stent: a prospective long-term evaluation. *Gut* 2016; **65**: 6–8.
- 25 Tyberg A, Karia K, Zerbo S, Sharaiha RZ, Kahaleh M. Endoscopic ultrasound-guided choledochojejunostomy with a lumen-apposing metal stent: a shortcut for biliary drainage. *Endoscopy* 2015; **47**(Suppl 1): UCTN: E342–3.
- 26 Brückner S, Arlt A, Hampe J. Endoscopic ultrasound-guided biliary drainage using a lumen-apposing self-expanding metal stent: a case series. *Endoscopy* 2015; **47**: 858–61.



## Phase 2 study of lenvatinib in patients with advanced hepatocellular carcinoma

Kenji Ikeda<sup>1</sup> · Masatoshi Kudo<sup>2</sup> · Seiji Kawazoe<sup>3</sup> · Yukio Osaki<sup>4</sup> · Masafumi Ikeda<sup>5</sup> ·  
Takuji Okusaka<sup>6</sup> · Toshiyuki Tamai<sup>7</sup> · Takuya Suzuki<sup>7</sup> · Takashi Hisai<sup>7</sup> ·  
Seiichi Hayato<sup>7</sup> · Kiwamu Okita<sup>8</sup> · Hiromitsu Kumada<sup>1</sup>

Received: 27 April 2016 / Accepted: 6 September 2016 / Published online: 4 October 2016  
© The Author(s) 2016. This article is published with open access at Springerlink.com

### Abstract

**Background** Lenvatinib is an oral inhibitor of vascular endothelial growth factor receptor 1–3, fibroblast growth factor receptor 1–4, platelet-derived growth factor receptor alpha, RET, and KIT. This phase 2, single-arm, open-label multicenter study evaluated lenvatinib in advanced hepatocellular carcinoma (HCC).

**Methods** Patients with histologically/clinically confirmed advanced HCC who did not qualify for surgical resection or local therapies received lenvatinib at a dosage of 12 mg once daily (QD) in 28-day cycles. The primary efficacy endpoint was time to progression (TTP) per modified Response Evaluation Criteria in Solid Tumors v1.1; secondary efficacy endpoints included objective response rate

(ORR), disease control rate (DCR), and overall survival (OS).

**Results** Between July 2010 and June 2011, 46 patients received lenvatinib at sites across Japan and Korea. The median TTP, as determined by independent radiological review, was 7.4 months [95 % confidence interval (CI): 5.5–9.4]. Seventeen patients (37 %) had partial response and 19 patients (41 %) had stable disease (ORR: 37 %; DCR: 78 %). Median OS was 18.7 months (95 % CI: 12.7–25.1). The most common any-grade adverse events (AEs) were hypertension (76 %), palmar-plantar erythrodysesthesia syndrome (65 %), decreased appetite (61 %), and proteinuria (61 %). Dose reductions and discontinuations due to AEs occurred in 34 (74 %) and 10 patients (22 %), respectively. Median body weight was lower in patients with an early (<30 days) dose withdrawal or reduction than in those without.

**Conclusions** Lenvatinib 12-mg QD showed clinical activity and acceptable toxicity profiles in patients with advanced HCC, but early dose modification was necessary in patients with lower body weight. Further development of lenvatinib in HCC should consider dose modification by body weight.

**Trial registration** ID [www.ClinicalTrials.gov](http://www.ClinicalTrials.gov) NCT00946153.

**Electronic supplementary material** The online version of this article (doi:10.1007/s00535-016-1263-4) contains supplementary material, which is available to authorized users.

✉ Kenji Ikeda  
ikedakenji@tora.email.ne.jp

- <sup>1</sup> Department of Hepatology, Toranomon Hospital, Toranomon 2-2-2, Minato-ku, Tokyo 105-8470, Japan
- <sup>2</sup> Department of Gastroenterology and Hepatology, Kinki University School of Medicine, Osaka, Japan
- <sup>3</sup> Department of Hepatobiliary and Pancreatology, Saga-Ken Medical Centre KOSEIKAN, Saga, Japan
- <sup>4</sup> Department of Gastroenterology and Hepatology, Osaka Red Cross Hospital, Osaka, Japan
- <sup>5</sup> Department of Hepatobiliary and Pancreatic Oncology, National Cancer Center Hospital East, Kashiwa, Japan
- <sup>6</sup> Department of Hepatobiliary and Pancreatic Oncology, National Cancer Center Hospital, Tokyo, Japan
- <sup>7</sup> Eisai Co., Ltd., Tokyo, Japan
- <sup>8</sup> Shunan Memorial Hospital, Yamaguchi, Japan

**Keywords** Hepatocellular carcinoma · Lenvatinib · Tyrosine kinase inhibitor · E7080 · Vascular endothelial growth factor inhibitor

### Introduction

In hepatocellular carcinoma (HCC), which accounts for 85–90 % of primary liver cancers [1], increased expression of vascular endothelial growth factor (VEGF) levels has

been correlated with angiogenic activity, tumor progression, and poor prognosis [2, 3].

Sorafenib is currently the only systemic VEGF-targeted therapy to have demonstrated a survival benefit in patients with advanced HCC [4, 5]. However, the median overall survival (OS) and time to progression (TTP) with sorafenib are only ~1 year and ~4 months, respectively, with frequent dose reductions or discontinuations due to adverse events, including severe skin toxicity [6–8]. Therefore, there is still an unmet need for better therapeutic options for patients with advanced HCC. To date, phase 3 trials of several agents, including sunitinib, brivanib, and linifanib, have failed to demonstrate benefit in advanced HCC [6].

Lenvatinib—an oral, multi-tyrosine kinase receptor inhibitor of VEGF receptors 1–3, fibroblast growth factor (FGF) receptor 1–4, platelet-derived growth factor (PDGF) receptor alpha, and KIT and RET proto-oncogenes [9–11]—was approved for radioiodine-refractory differentiated thyroid cancer at a dose of 24 mg once daily (QD) in 28-day cycles [12]. However, for the clinical development of therapeutics in HCC, re-evaluation of the starting dose of any investigational agent is recommended [13]. In a phase 1 study of lenvatinib in HCC, the maximum tolerable dose in patients with HCC and Child Pugh (CP) class A liver function was 12 mg QD [14]. This dose also showed blood trough concentrations comparable to those with the 25-mg QD dose determined to be the maximum tolerated dose in solid tumors [15] with preliminary evidence of tumor shrinkage. Here we assessed the antitumor activity and safety of lenvatinib in this phase 2 study in patients with advanced HCC.

## Methods

### Patients

Patients ages 20–80 years had clinically confirmed advanced HCC with residual disease not qualifying for surgical resection or local therapies, including transarterial chemoembolization;  $\geq 1$  measurable target lesion by Response Evaluation Criteria in Solid Tumors version 1.1 (RECIST v1.1); [16] 1–3 tumor lesions  $>3$  cm in diameter ( $>5$  cm diameter if only one lesion) or four or more lesions or portal vein invasion, extrahepatic invasion; Eastern Cooperative Oncology Group performance status of 0 or 1; CP score of 5 or 6 (CP class A); platelet count  $\geq 50 \times 10^9/L$ , absolute neutrophil count  $\geq 1.5 \times 10^3/\mu L$ ; aspartate transaminase and alanine transaminase  $\leq 5.0$  times the upper limit of normal; and serum creatinine  $\leq 2.0$  mg/dL or calculated creatinine clearance  $\geq 40$  mL/min. Patients had

to have had a hepatectomy and local therapy for HCC at least 6 and 4 weeks, respectively, prior to study enrollment. Exclusion criteria included clinically symptomatic brain metastasis or meningeal carcinomatosis; receipt of  $\geq 1$  systemic chemotherapy, including targeted therapy or transarterial infusion chemotherapy; QT-corrected interval by the Fredericia method  $>500$  ms at screening; mean blood pressure  $\geq 150/90$  mmHg; presence of a progressive central nervous system disease; or a clinically significant hemorrhagic or thrombotic event within 4 weeks prior to study enrollment.

### Study design and treatment

Patients in this single-arm, open-label multicenter study of lenvatinib monotherapy for advanced HCC (NCT00946153) received daily oral administration of 12 mg lenvatinib (12-mg QD) in 28-day cycles until disease progression, unacceptable toxicity, or withdrawal of consent. Dose interruption and sequential reduction of lenvatinib (to 8- and 4-mg QD) were permitted for drug-related adverse events (AEs; see Online Resource Table S1). Once reduced, the dose could not be re-escalated. The study drug was discontinued if patient recovery time was  $>2$  weeks.

This study was conducted in accordance with local laws, the Declaration of Helsinki, and International Conference on Harmonization Good Clinical Practice guidelines, and with the approval of each institutional review board. All patients provided written informed consent.

### Study assessments

The primary efficacy endpoint was TTP per modified RECIST (mRECIST; modified to evaluate viable lesions) [17] by an independent radiologic review committee (IRRC). mRECIST uses viable target lesions in dynamic computed tomography and is suitable for the assessment of tyrosine kinase inhibitors in HCC [17, 18]. Secondary efficacy endpoints included objective response rate (ORR), disease control rate (DCR), and OS. Tumor response was evaluated every 8 weeks using mRECIST v1.1 by both the IRRC and study investigators. An exploratory analysis to reassess tumors using RECIST v1.1 was also performed by the IRRC. Safety was assessed by physical examinations, clinical and laboratory evaluations, vital signs, and electrocardiograms. AEs were graded according to the National Cancer Institute Common Terminology Criteria for AEs, version 3.0. A pre-dose blood sample was obtained for pharmacokinetic (PK) assessment on days 1, 8, 15, and 22 of cycle 1, and day 1 of cycles 2 and 3, using a validated liquid chromatography–tandem mass spectrometry method [19].

## Statistical considerations

Time-to-event endpoints, including TTP and OS, were summarized using Kaplan–Meier estimates. The sample size of 46 patients was based on an 80 % probability that the lower limit of the two-sided 90 % confidence interval (CI) of median TTP would exceed the threshold of 2.7 months (based on the Sorafenib HCC Assessment Randomized Protocol trial [20]), with an expected median TTP of 4.1 months for lenvatinib. Sample size determination also assumed exponential distribution for TTP, 12 months of enrollment, 6 months of follow-up, and a 10 % patient exclusion/dropout rate. An interim evaluation was conducted when 21–23 patients became evaluable for the 2-month tumor assessment. If the number of patients with progressive disease within 2 months was  $\geq 10$  ( $\geq 80$  % Bayesian posterior probability for proportion of patients with progressive disease at 2 months  $\geq 35$  %), then study discontinuation would be considered due to futility. Follow-up was continued until final analysis was performed when 67 % of patients had died.

## Results

### Patient characteristics

Overall, 46 patients were enrolled and received lenvatinib at 14 sites across Japan and Korea between July 2010 and June 2011. All patients were included in the safety and efficacy analyses. Patient demographics and baseline characteristics are listed in Table 1.

### Efficacy

Median TTP was 7.4 months (95 % CI: 5.5–9.4) as assessed by IRRC per mRECIST (Fig. 1a). Median TTP was 12.8 months (95 % CI: 7.2–14.7) by investigator assessment. Seventeen patients (37 %) achieved a partial response and 19 patients (41 %) had stable disease  $\geq 8$  weeks, with a DCR of 78 % by IRRC (Table 2). Outcomes using RECIST v1.1 criteria are also provided in Table 2. Median OS was 18.7 months (95 % CI: 12.7–25.1; Fig. 1b).

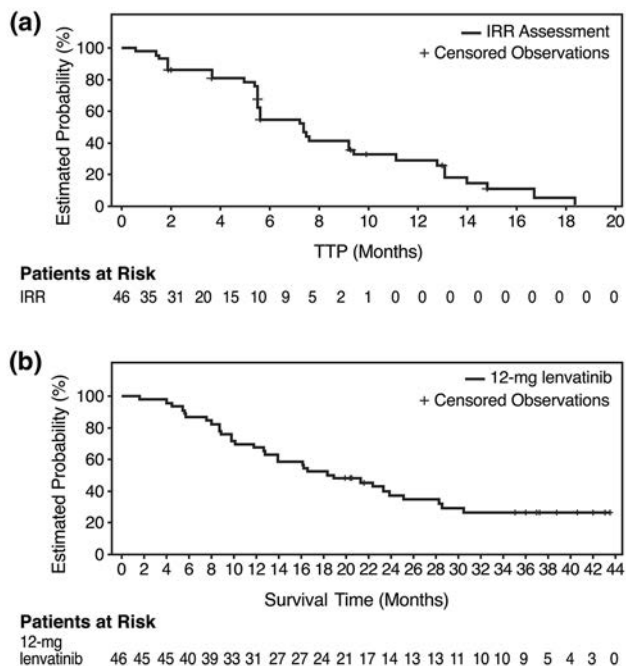
Tumor reduction of target lesions, assessed by IRRC, occurred in 80 % of patients (Fig. 2a–c). Subgroup analyses indicated that lenvatinib clinical activity was maintained regardless of tumor status (with or without extrahepatic spread or portal vein invasion), type of underlying hepatitis [hepatitis B virus (HBV) or hepatitis C virus], receipt of previous chemotherapy, or alpha-fetoprotein levels (AFP;  $<200$  ng/mL or  $\geq 200$  ng/mL; see

**Table 1** Patient demographics and baseline characteristics

Characteristic	Patients ( <i>N</i> = 46)
Median age, years (range)	66.5 (37–80)
Sex, <i>n</i> (%)	
Female	13 (28.3)
Male	33 (71.7)
Region, <i>n</i> (%)	
Japan	43 (93.5)
South Korea	3 (6.5)
Median weight, kg (range)	56.7 (42.8–85.5)
ECOG PS, <i>n</i> (%)	
0	38 (82.6)
1	8 (17.4)
Child Pugh Class, <i>n</i> (%)	
A	45 (97.8)
B	1 (2.2)
BCLC staging, <i>n</i> (%)	
B	19 (41.3)
C	27 (58.7)
Portal vein invasion, <i>n</i> (%)	
Yes	5 (10.8)
No	41 (89.1)
Extrahepatic metastasis, <i>n</i> (%)	
Yes	21 (45.7)
No	25 (54.3)
Cause of HCC, <i>n</i> (%)	
Hepatitis B	15 (32.6)
Hepatitis C	27 (58.7)
Alcohol	2 (4.3)
Non-alcohol-related fatty liver disease	1 (2.2)
Unknown	2 (4.3)
AFP value at baseline <sup>a</sup>	
$<200$ ng/mL	27 (57.7)
$\geq 200$ ng/mL	18 (39.1)
Prior surgery for HCC, <i>n</i> (%)	
No	27 (58.7)
Yes	19 (41.3)
Prior local therapy, <i>n</i> (%)	
No	4 (8.7)
Yes	42 (91.3)
RFA	32 (69.6)
PEI	12 (26.1)
TACE	39 (84.8)
TAE	3 (6.5)
Prior chemotherapy, <i>n</i> (%)	
Sorafenib	6 (13.0)
Other systemic chemotherapy	5 (10.9)
Hepatic intra-arterial chemotherapy	5 (10.9)

*BCLC* Barcelona Clinic Liver Cancer, *ECOG-PS* Eastern Cooperative Oncology Group Performance Status, *HCC* hepatocellular carcinoma, *AFP* alpha-fetoprotein, *PEI* percutaneous ethanol injection, *RFA* radiofrequency ablation, *TACE* transcatheter arterial chemoembolization, *TAE* transarterial embolization

<sup>a</sup> AFP data were unavailable for one patient



**Fig. 1** Kaplan–Meier estimates of **a** TTP and **b** OS. Median TTP was 7.4 months as assessed by an IRRC comprising four independent radiologists. Median OS was 18.7 months. IRRC independent radiologic review committee, TTP time to progression

Online Resource Table S2). On the other hand, AFP levels may affect the prognosis for patients with HCC (Online Resource Figure S1).

## Safety

Median and mean durations of lenvatinib treatment were 7.3 and 9.0 months, respectively. All 46 patients experienced at least one AE. The most common any-grade AEs (Table 3) were hypertension (76 %), palmar-plantar erythrodysesthesia syndrome (PPES; 65 %), decreased appetite (61 %), and proteinuria (61 %). The incidence of serious AEs (SAEs) was 48 %, and the most frequently reported SAE was hepatic encephalopathy (11 %). No

treatment-related deaths were reported. Two patients died within 30 days of receiving their last dose of lenvatinib—one from pneumonia and one from liver tumor rupture.

AEs were generally manageable with dose modifications. Lenvatinib dose reductions due to AEs occurred in 34 patients (74 %). Ten patients (22 %) discontinued study treatment due to toxicity. The most frequently reported AE leading to study drug withdrawal was proteinuria (11 %). Twenty-two patients (48 %) experienced AEs leading to dose withdrawal or dose reduction <30 days after starting lenvatinib. In an exploratory analysis of differences in baseline characteristics between patients who did and did not require an early dose withdrawal or reduction, body weight and minimum concentration of lenvatinib ( $C_{trough}$ ) were identified as potential differentiators (Fig. 3). Median body weight was lower for patients who experienced an early dose withdrawal or reduction (54.1 kg) than for those who did not (67.6 kg) (Fig. 3a). The median  $C_{trough}$  values on cycle 1 day 15 (C1D15) in patients with and without dose modifications were 62.4 and 33.9 ng/mL, respectively (Fig. 3b). The Spearman correlation coefficient between body weight and lenvatinib  $C_{trough}$  at C1D15 was  $-0.64$ .

## Discussion

Multi-tyrosine kinase inhibitors have shown limited success in advanced HCC, with reported TTP ranging from 2.8 to 5.4 months and ORR from 6.9 to 9 % [4, 5, 7, 21, 22]. In this study, lenvatinib 12-mg QD showed promising clinical activity in patients with advanced HCC, with a median TTP of 7.4 months as assessed by IRRC (12.8 months by investigator). Lenvatinib also demonstrated tumor shrinkage in 80 % of patients, with a response rate of 37 % per mRECIST and 24 % per conventional RECIST.

Although progression-free survival is the preferred OS surrogate endpoint in most solid tumor trials, it is a particularly unreliable endpoint in HCC studies, because death from the natural history of cirrhosis may confound results;

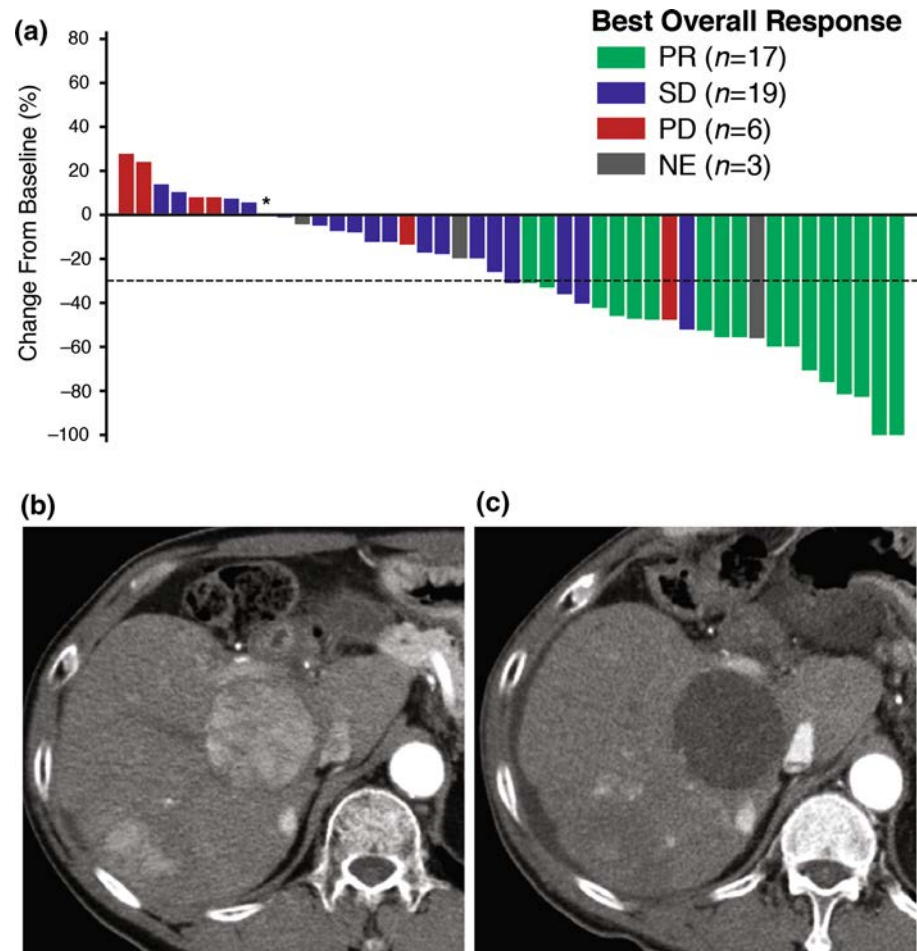
**Table 2** Tumor responses

Response category	Investigator assessment (mRECIST), <i>n</i> = 46	IRRC assessment (mRECIST), <i>n</i> = 46	IRRC assessment (RECIST 1.1), <i>n</i> = 46
Best response, <i>n</i> (%)			
Complete response	0 (0)	0 (0)	0 (0)
Partial response	17 (37)	17 (37)	11 (24)
Stable disease	21 (46)	19 (41)	25 (54)
Progressive disease	5 (11)	6 (13)	6 (13)
Not evaluable	3 (7)	4 (9)	4 (9)
Objective response rate, <i>n</i> (%)	17 (37)	17 (37)	11 (24)
Disease control rate, <i>n</i> (%)	38 (83)	36 (78)	36 (78)

IRRC independent radiologic review committee, mRECIST modified response evaluation criteria in solid tumors



**Fig. 2** **a** Waterfall plot of changes in tumor size by IRRC assessment. One patient was excluded from the plot due to lack of IRRC assessment of target lesion at baseline. The patient marked with an asterisk showed a best overall response of SD. **b** Representative liver lesion of HCC at baseline on arterial phase CT. **c** Representative liver lesion on arterial phase CT after 1 year of lenvatinib treatment. *CT* computed tomography, *HCC* hepatocellular carcinoma, *IRRC* independent radiologic review committee, *PD* progressive disease, *PR* partial response, *SD* stable disease, *NE* not evaluable



TTP is therefore the recommended endpoint for early-stage trials of HCC [13]. In HCC, response rates derived from mRECIST have been shown to better correlate with OS than those from conventional RECIST [18]. Notably, despite a similarity in best overall responses between investigator and independent assessments, the median TTP was substantially different, suggesting a bias by the investigators in determining the timing of disease progression, ostensibly so that their patients could continue therapy.

The median OS in this study was 18.7 months. Although subgroup analyses indicated that median TTP was comparable regardless of baseline AFP levels, OS was longer in the 61 % of patients with lower vs. higher AFP levels (23.5 vs. 13.3 months, respectively). Therefore, it is possible that the long median OS observed in this study may have been driven by those patients with lower baseline AFP levels, because elevated AFP levels are associated with an increased mortality rate in HCC [23]. Other risk factors examined included extrahepatic spread and HBV. In this study, lenvatinib activity was observed even in these patients with poor prognoses; however, this conclusion is limited by the small numbers of patients in each subgroup. Another limitation is the single-arm design of the study,

and the possibility that results may be influenced by patient selection. However, we note that patient characteristics in this study were typical of the population of patients with HCC who required sorafenib therapy in Japan [8, 24].

The most common AEs in this study included hypertension, PPES, decreased appetite, proteinuria, and fatigue, which are well-known class effects of VEGF-targeted therapies and are consistent with the known safety profile of lenvatinib. Although the incidence of grade 3 hypertension was high (54 %), this included patients whose blood pressure was controlled by two or more antihypertensive drugs. No patient required a dose modification or discontinuation due to hypertension; therefore, it was considered to be manageable. Although 65 % of patients experienced PPES, the incidence of grade 3 PPES was only 9 %. The incidence of grade 3 or 4 thrombocytopenia was also high (22 %); however, in all but one patient who discontinued lenvatinib, thrombocytopenia was controllable with dose modifications. There was no report of grade 3 or higher bleeding related to the study drug. Although hepatic encephalopathy was the most common SAE (five patients) in this study, all five patients also had constipation, and three had dehydration—known risk factors for

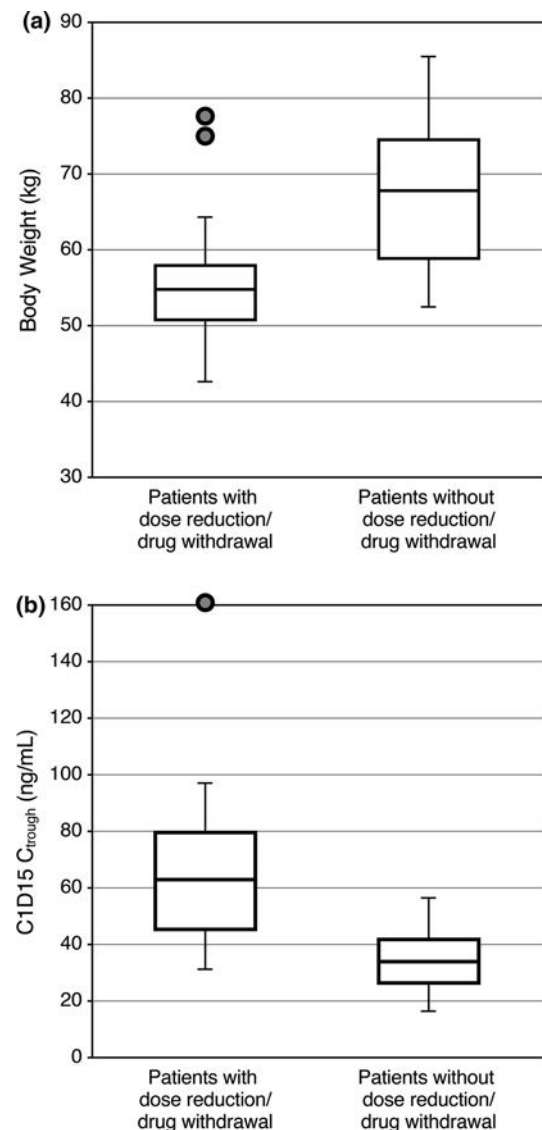


**Table 3** Common adverse events occurring in  $\geq 20$  % of patients

Adverse event	Any grade, n = 46	Grade 3, n = 46	Grade 4, n = 46
Hypertension	35 (76.1)	25 (54.3)	0
Palmar-plantar erythrodysesthesia syndrome	30 (65.2)	4 (8.7)	0
Decreased appetite	28 (60.9)	1 (2.2)	0
Proteinuria	28 (60.9)	9 (19.6)	0
Fatigue	25 (54.3)	0	0
Diarrhea	20 (43.5)	6 (13.0)	0
Constipation	19 (41.3)	0	0
Nausea	17 (37.0)	1 (2.2)	0
Dysphonia	17 (37.0)	0	0
Thrombocytopenia	16 (34.8)	9 (19.6)	1 (2.2)
Peripheral edema	16 (34.8)	0	0
Decreased weight	14 (30.4)	2 (4.3)	0
Neutropenia	13 (28.3)	2 (4.3)	0
Nasopharyngitis	13 (28.3)	0	0
Rash	13 (28.3)	0	0
Increased blood thyroid-stimulating hormone level	12 (26.1)	0	0
Back pain	11 (23.9)	0	0
Stomatitis	11 (23.9)	0	0
Vomiting	11 (23.9)	1 (2.2)	0
Pyrexia	10 (21.7)	0	0
Hypothyroidism	10 (21.7)	0	0
Insomnia	10 (21.7)	0	0

hepatic encephalopathy [25]. These events were managed with dose modifications as well as treatment of constipation and dehydration.

Dose reduction occurred frequently and early in the course of treatment. Because 74 % of patients required a dose reduction due to AEs, we examined possible risk factors for the development of intolerable toxicities. The influence of body weight on the pharmacodynamics of antiangiogenic agents and resultant toxicity patterns is still uncertain [26]. Additionally, increased lenvatinib exposure was found in patients with severe hepatic impairment [27]. It is possible that in patients with HCC, who typically have impaired hepatic function, lenvatinib PK is more affected by body weight than in healthy individuals or patients with other cancers. Furthermore, careful evaluation of the balance between efficacy and toxicity is especially important in studies of patients with HCC, because high toxicity is a common reason for failure of phase 3 clinical trials in this therapeutic area [6]. Therefore, although drug-related AEs were manageable with dose modifications, and there were no drug-related deaths in this study, lenvatinib exposure was observed to be influenced by body weight in patients



**Fig. 3** **a** Boxplot of body weight for patients with vs. without adverse events that led to dose reduction or dose withdrawal within 30 days of lenvatinib treatment initiation. **b** Boxplot of lenvatinib  $C_{trough}$  level 15 days after lenvatinib treatment initiation for patients with vs. without adverse events that led to dose reduction or withdrawal within 30 days.  $C1D15$  cycle 1 day 15,  $C_{trough}$  minimum concentration of lenvatinib

with HCC, and adjustment of the starting dose of lenvatinib by body weight in further clinical development of lenvatinib in HCC is recommended.

In conclusion, the administration of lenvatinib 12-mg QD showed clinical activity and acceptable toxicity profiles in patients with advanced HCC, although early dose modification was necessary for the management of toxicities in patients with lower body weight. Based on these findings, a phase 3 study of lenvatinib in HCC is underway, with planned doses of 8 mg in patients with lower body weight ( $<60$  kg) and 12 mg in those with higher body weight ( $\geq 60$  kg; NCT01761266) [28].

**Acknowledgments** We thank all of the patients who participated in this study and their families, as well as all investigators, physicians, nurses, and clinical research coordinators who helped with the study, including the Independent Radiological Review Committee: Drs. Osamu Matsui (Kanazawa University Hospital), Kazuhiko Ueda (Shinshu University Hospital), Akihiro Tanimoto (Keio University Hospital), and Tatsuya Gomi (Toho University Ohashi Medical Center). We also thank the Efficacy and Safety Evaluation Committee: Drs. Junji Furuse (Kyorin University School of Medicine), Kazuhiko Koike (The University Tokyo), and Shigeki Arai (Hama-matsu Rousai Hospital). Editorial assistance was provided by Oxford PharmaGenesis Inc., and funded by Eisai Inc. The work was supported by Eisai Co., Ltd., Japan.

#### Compliance with ethical standards

**Conflict of interest** Dr. K. Ikeda reports honoraria from Eisai, Dainippon, Sumitomo Pharmaceutical Co., and Olympus, and served in a consulting/advisory role for Eisai during the conduct of study. Dr. Kudo reports honoraria from Bayer, Eisai, MSD, Bristol Myers Squibb, Daiichi, and Sankey, and served in a consulting/advisory role for Eisai, Bristol Myers Squibb, and Eli Lilly. Dr. Kawazoe has nothing to disclose. Dr. Osaki has nothing to disclose. Dr. M. Ikeda reports honoraria from Novartis, Bayer Yakuhin, Bristol Myers Squibb, Abbott Japan, Taiho Pharmaceutical, Eli Lilly Japan, Kowa, OncoTherapy Science, Nippon Kayaku, and Daiichi Sankyo; received research funding from Bayer Yakuhin, Novartis, Merck Serono, Kyowa Hakko Kirin, Yakult, Taiho Pharmaceutical, Eli Lilly Japan, Otsuka Pharmaceutical, OncoTherapy Science, Boehringer Ingelheim, Kowa, Ono Pharmaceutical, Eisai, AstraZeneca, Pfizer Japan, Glaxo Smith Kline, and Zeria Pharmaceutical; and reports travel, accommodation, and other expense reimbursement from Bayer Yakuhin and Eisai. Dr. Okusaka reports honoraria from Chugai Pharmaceutical Co., Ltd, Pfizer Japan Inc., Novartis Pharmaceutical K.K., Taiho Pharmaceutical Co., Ltd., Merck Serono Co., Ltd., Eli Lilly Japan K.K., Dainippon Sumitomo Pharmaceutical Co., Ltd, Eisai Co., Ltd, and Bayer Yakuhin Ltd.; served in a consulting/advisory role for Eli Lilly Japan K.K., Yakult Honsha Co., Ltd., Amgen, Dainippon Sumitomo Pharmaceutical Co., Ltd., Taiho Pharmaceutical Co., Ltd., OncoTherapy Science, Inc., Nobelpharma Co., Ltd., Nippon Boehringer Ingelheim Co., Ltd., Nano Carrier Co., Ltd., Novartis Pharmaceutical K.K., and Zeria Pharmaceutical Co., Ltd.; and received research funding from Chugai Pharmaceutical Co., Ltd., Eli Lilly Japan K.K., Eisai Co., Ltd., Novartis Pharmaceutical K.K., Shizuoka Industry, Takeda Bio Development Center Limited, Yakult Honsha Co., Ltd., OncoTherapy Science, Inc., Otsuka Pharmaceutical Co., Ltd., Taiho Pharmaceutical Co., Ltd., Sceti Medical Laboratory K.K., Nippon Boehringer Ingelheim Co., Ltd., Kowa Company, Ltd., Kyowa Hakko Kirin Co., Ltd, Merck Serono Co., Ltd, Ono Pharmaceutical Co., Ltd, Bayer Yakuhin Ltd., Pfizer Japan Inc., AstraZeneca K.K., and Dainippon Sumitomo Pharmaceutical Co., Ltd. T. Tamai reports employment and stock/other ownership with Eisai Co., Ltd. T. Suzuki reports employment with Eisai Co., Ltd. T. Hisai has nothing to disclose. S. Hayato reports employment with Eisai Co., Ltd. Dr. Okita reports honoraria from Kowa and Eisai Co., Ltd. Dr. Kumada reports honoraria from, and served in a consulting/advisory role for, Eisai Co., Ltd.

**Open Access** This article is distributed under the terms of the Creative Commons Attribution 4.0 International License (<http://creativecommons.org/licenses/by/4.0/>), which permits unrestricted use, distribution, and reproduction in any medium, provided you give appropriate credit to the original author(s) and the source, provide a link to the Creative Commons license, and indicate if changes were made.

#### References

1. El-Serag HB, Rudolph KL. Hepatocellular carcinoma: epidemiology and molecular carcinogenesis. *Gastroenterology*. 2007;132:2557–76.
2. Poon RT, Ho JW, Tong CS, Lau C, Ng IO, Fan ST. Prognostic significance of serum vascular endothelial growth factor and endostatin in patients with hepatocellular carcinoma. *Br J Surg*. 2004;91:1354–60.
3. Bertino G, Demma S, Ardiri A, et al. Hepatocellular carcinoma: novel molecular targets in carcinogenesis for future therapies. *Biomed Res Int*. 2014;2014:203693.
4. Llovet JM, Ricci S, Mazzaferro V, et al. Sorafenib in advanced hepatocellular carcinoma. *N Engl J Med*. 2008;359:378–90.
5. Cheng AL, Kang YK, Chen Z, et al. Efficacy and safety of sorafenib in patients in the Asia-Pacific region with advanced hepatocellular carcinoma: a phase III randomised, double-blind, placebo-controlled trial. *Lancet Oncol*. 2009;10:25–34.
6. Llovet JM, Hernandez-Gea V. Hepatocellular carcinoma: reasons for phase III failure and novel perspectives on trial design. *Clin Cancer Res*. 2014;20:2072–9.
7. Cheng AL, Kang YK, Lin DY, et al. Sunitinib versus sorafenib in advanced hepatocellular cancer: results of a randomized phase III trial. *J Clin Oncol*. 2013;31:4067–75.
8. Ogasawara S, Kanai F, Obi S, et al. Safety and tolerance of sorafenib in Japanese patients with advanced hepatocellular carcinoma. *Hepatol Int*. 2011;5:850–6.
9. Matsui J, Funahashi Y, Uenaka T, Watanabe T, Tsuruoka A, Asada M. Multi-kinase inhibitor E7080 suppresses lymph node and lung metastases of human mammary breast tumor MDA-MB-231 via inhibition of vascular endothelial growth factor-receptor (VEGF-R) 2 and VEGF-R3 kinase. *Clin Cancer Res*. 2008;14:5459–65.
10. Tohyama O, Matsui J, Kodama K, et al. Antitumor activity of lenvatinib (E7080): an angiogenesis inhibitor that targets multiple receptor tyrosine kinases in preclinical human thyroid cancer models. *J Thyroid Res*. 2014;2014:638747.
11. Yamamoto Y, Matsui J, Matsushima T, et al. Lenvatinib, an angiogenesis inhibitor targeting VEGFR/FGFR, shows broad antitumor activity in human tumor xenograft models associated with microvessel density and pericyte coverage. *Vasc Cell*. 2014;6:18.
12. Schlumberger M, Tahara M, Wirth LJ, et al. Lenvatinib versus placebo in radioiodine-refractory thyroid cancer. *N Engl J Med*. 2015;372:621–30.
13. Llovet JM, Di Bisceglie AM, Bruix J, et al. Design and endpoints of clinical trials in hepatocellular carcinoma. *J Natl Cancer Inst*. 2008;100:698–711.
14. Ikeda M, Okusaka T, Mitsunaga S, et al. Safety and pharmacokinetics of lenvatinib in patients with advanced hepatocellular carcinoma. *Clin Cancer Res*. 2016;22:1385–94.
15. Boss DS, Glen H, Beijnen JH, et al. A phase I study of E7080, a multitargeted tyrosine kinase inhibitor, in patients with advanced solid tumours. *Br J Cancer*. 2012;106:1598–604.
16. Eisenhauer EA, Therasse P, Bogaerts J, et al. New response evaluation criteria in solid tumours: revised RECIST guideline (version 1.1). *Eur J Cancer*. 2009;45:228–47.
17. Lencioni R, Llovet JM. Modified RECIST (mRECIST) assessment for hepatocellular carcinoma. *Semin Liver Dis*. 2010;30:52–60.
18. Edeline J, Boucher E, Rolland Y, et al. Comparison of tumor response by Response Evaluation Criteria in Solid Tumors (RECIST) and modified RECIST in patients treated with sorafenib for hepatocellular carcinoma. *Cancer*. 2012;118:147–56.

19. Mano Y, Kusano K. A validated LC-MS/MS method of total and unbound lenvatinib quantification in human serum for protein binding studies by equilibrium dialysis. *J Pharm Biomed Anal.* 2015;114:82–7.
20. Sherman M, Mazzaferro V, Amadori D, et al. Efficacy and safety of sorafenib in patients with advanced hepatocellular carcinoma and vascular invasion or extrahepatic spread: a subanalysis from the SHARP trial [abstract]. *J Clin Oncol.* 26:15S. 2008. (abstr 4584).
21. Johnson PJ, Qin S, Park JW, et al. Brivanib versus sorafenib as first-line therapy in patients with unresectable, advanced hepatocellular carcinoma: results from the randomized phase III BRISK-FL study. *J Clin Oncol.* 2013;31:3517–24.
22. Cainap C, Qin S, Huang WT, et al. Linifanib versus sorafenib in patients with advanced hepatocellular carcinoma: results of a randomized phase III trial. *J Clin Oncol.* 2015;33:172–9.
23. Li P, Wang SS, Liu H, et al. Elevated serum alpha fetoprotein levels promote pathological progression of hepatocellular carcinoma. *World J Gastroenterol.* 2011;17:4563–71.
24. Takeda H, Nishikawa H, Osaki Y, et al. Clinical features associated with radiological response to sorafenib in unresectable hepatocellular carcinoma: a large multicenter study in Japan. *Liver Int.* 2015;35:1581–9.
25. Wright G, Chattree A, Jalan R. Management of hepatic encephalopathy. *Int J Hepatol.* 2011;2011:841407.
26. Verheul HM, Pinedo HM. Possible molecular mechanisms involved in the toxicity of angiogenesis inhibition. *Nat Rev Cancer.* 2007;7:475–85.
27. Shumaker R, Aluri J, Fan J, Martinez G, Pentikis H, Ren M. Influence of hepatic impairment on lenvatinib pharmacokinetics following single-dose oral administration. *J Clin Pharmacol.* 2015;55:317–27.
28. Finn RS, Cheng AL, Ikeda K, et al. A multicenter, open-label, phase 3 trial to compare the efficacy and safety of lenvatinib (E7080) versus sorafenib in first-line treatment of subjects with unresectable hepatocellular carcinoma [abstract]. *J Clin Oncol.* 32:5s. 2014. (abstr TPS4153).

## Ramucirumab as second-line treatment in patients with advanced hepatocellular carcinoma: Japanese subgroup analysis of the REACH trial

Masatoshi Kudo<sup>1</sup> · Etsuro Hatano<sup>2</sup> · Shinichi Ohkawa<sup>3</sup> · Hirofumi Fujii<sup>4</sup> · Akihide Masumoto<sup>5</sup> · Junji Furuse<sup>6</sup> · Yoshiyuki Wada<sup>7</sup> · Hiroshi Ishii<sup>8</sup> · Shuntaro Obi<sup>9</sup> · Shuichi Kaneko<sup>10</sup> · Seiji Kawazoe<sup>11</sup> · Osamu Yokosuka<sup>12</sup> · Masafumi Ikeda<sup>13</sup> · Katsuaki Ukai<sup>14</sup> · Sojiro Morita<sup>15</sup> · Akihito Tsuji<sup>16</sup> · Toshihiro Kudo<sup>17</sup> · Mitsuo Shimada<sup>18</sup> · Yukio Osaki<sup>19</sup> · Ryosuke Tateishi<sup>20</sup> · Gen Sugiyama<sup>21</sup> · Paolo Benjamin Abada<sup>22</sup> · Ling Yang<sup>23</sup> · Takuji Okusaka<sup>24</sup> · Andrew Xiuxuan Zhu<sup>25</sup>

Received: 13 January 2016 / Accepted: 18 July 2016 / Published online: 22 August 2016  
© Japanese Society of Gastroenterology 2016

### Abstract

**Background** REACH evaluated ramucirumab in the second-line treatment of patients with advanced hepatocellular carcinoma. In the intent-to-treat population ( $n = 565$ ), a significant improvement in overall survival (OS) was not observed. In patients with an elevated

baseline  $\alpha$ -fetoprotein (AFP) level (400 ng/mL or greater), an improvement in OS was demonstrated. An analysis of the Japanese patients in REACH was performed.

**Methods** An analysis was performed with the subset of the intent-to-treat population enrolled in Japan ( $n = 93$ ).

**Results** The median OS was 12.9 months for the ramucirumab arm ( $n = 45$ ) and 8.0 months for the placebo arm ( $n = 48$ ) [hazard ratio (HR) 0.621 (95 % confidence interval (CI) 0.391–0.986);  $P = 0.0416$ ]. The median progression-free survival was 4.1 months for the ramucirumab arm and 1.7 months for the placebo arm [HR 0.449 (95 % CI 0.285–0.706);  $P = 0.0004$ ]. The objective

Ling Yang is now at Sanofi.

Takuji Okusaka and Andrew X. Zhu are co-senior authors.

**Electronic supplementary material** The online version of this article (doi:10.1007/s00535-016-1247-4) contains supplementary material, which is available to authorized users.

✉ Masatoshi Kudo  
m-kudo@med.kinki.ac.jp

<sup>1</sup> Kindai University Faculty of Medicine, Osaka-Sayama, Osaka, Japan

<sup>2</sup> Kyoto University Hospital, Kyoto, Japan

<sup>3</sup> Kanagawa Cancer Center, Yokohama, Kanagawa, Japan

<sup>4</sup> Jichi Medical University, Shimotsuke, Tochigi, Japan

<sup>5</sup> Aso Iizuka Hospital, Fukuoka, Japan

<sup>6</sup> Kyorin University School of Medicine Hospital, Tokyo, Japan

<sup>7</sup> National Hospital Organization Kyushu Medical Center, Fukuoka, Japan

<sup>8</sup> The Cancer Institute Hospital of the Japanese Foundation for Cancer Research, Tokyo, Japan

<sup>9</sup> Kyoundo Hospital, Sasaki Institute, Tokyo, Japan

<sup>10</sup> Kanazawa University Hospital, Ishikawa, Japan

<sup>11</sup> Saga-Ken Medical Centre Koseikan, Saga, Japan

<sup>12</sup> Chiba University Hospital, Chiba, Japan

<sup>13</sup> National Cancer Center Hospital East, Chiba, Japan

<sup>14</sup> Sendai Medical Center, Sendai, Miyagi, Japan

<sup>15</sup> Kochi Health Sciences Center, Kochi, Japan

<sup>16</sup> Kagawa University Hospital, Takamatsu, Kagawa, Japan

<sup>17</sup> Osaka University Hospital, Osaka, Japan

<sup>18</sup> Tokushima University Hospital, Tokushima, Japan

<sup>19</sup> Osaka Red Cross Hospital, Osaka, Japan

<sup>20</sup> The University of Tokyo Hospital, Tokyo, Japan

<sup>21</sup> Kurume University Medical Center, Fukuoka, Japan

<sup>22</sup> Eli Lilly and Company, Indianapolis, IN, USA

<sup>23</sup> Eli Lilly and Company, Bridgewater, NJ, USA

<sup>24</sup> National Cancer Center Hospital, Tokyo, Japan

response rates were 11 % for the ramucirumab arm and 2 % for the placebo arm ( $P = 0.0817$ ). The grade 3 or higher treatment-emergent adverse events occurring in more than 5 % of patients with a higher incidence for the ramucirumab arm ( $n = 44$ ) than for the placebo arm ( $n = 47$ ) were ascites (7 % vs 2 %), hypertension (7 % vs 2 %), and cholangitis (7 % vs 0 %). In patients with a baseline AFP level of 400 ng/mL or greater, the median OS was 12.9 months for the ramucirumab arm ( $n = 20$ ) and 4.3 months for the placebo arm ( $n = 22$ ) [HR 0.464 (95 % CI 0.232–0.926);  $P = 0.0263$ ].

**Conclusions** In the Japanese patients in REACH, ramucirumab treatment improved OS, including in patients with a baseline AFP level of 400 ng/mL or greater; improvements in progression-free survival and objective response rate were also demonstrated. The safety profile of ramucirumab was acceptable and well tolerated in Japanese patients.

*ClinicalTrials.gov identifier* NCT01140347.

**Keywords**  $\alpha$ -Fetoprotein · Clinical trial · Japan · Liver neoplasms · Vascular endothelial growth factor receptor 2

## Introduction

Liver cancer is the fifth commonest cancer in men and ninth commonest cancer in women worldwide, and the second commonest cause of cancer death; hepatocellular carcinoma accounts for approximately 70–90 % of primary liver cancers [1, 2]. The incidence rates of liver cancer are highest in East Asia [1], and Japan has one of the highest incidences of liver cancer in the world [1]. The prognosis of patients with liver cancer is considerably better in Japan than in other countries. For example, the observational GIDEON study showed that in hepatocellular carcinoma patients treated with sorafenib, the median survival time was markedly longer in Japan than in Europe, the Asia Pacific region, Latin America, and the USA [3]. The reasons for the longer survival times in Japan remain unclear, but may include differences in cause, population characteristics, screening, and disease management [4–7]. Nonetheless, new and more active treatment options are needed for all patients with hepatocellular carcinoma, including patients in Japan.

Sorafenib is the only systemic therapy shown to improve overall survival (OS) in patients with advanced hepatocellular carcinoma [8, 9]. However, sorafenib is associated with significant toxicity, and approximately 30 % of patients stop taking sorafenib because of intolerance

[10, 11]. Other than sorafenib, no other systemic agent has demonstrated a positive phase III result in the treatment of advanced hepatocellular carcinoma.

Vascular endothelial growth factor (VEGF)-mediated signaling and VEGF receptor 2 mediated signaling have an important role in angiogenesis and tumor growth [12–14]. VEGF is overexpressed in hepatocellular carcinoma and is associated with poorer clinical outcomes, suggesting VEGF-mediated signaling is important in hepatocellular carcinoma pathogenesis and as a therapeutic target [15].

Ramucirumab is a recombinant human IgG1 monoclonal antibody that specifically binds to the extracellular domain of VEGF receptor 2 with high affinity, preventing binding of VEGF ligands and receptor activation [16]. In the phase III REACH trial ( $n = 565$ ), ramucirumab as second-line treatment in patients with advanced hepatocellular carcinoma following first-line therapy with sorafenib did not demonstrate a significant OS improvement over best supportive care (primary end point) [hazard ratio (HR) 0.866 (95 % confidence interval (CI) 0.717–1.046);  $P = 0.1391$ ; median OS 9.2 months for the ramucirumab arm vs 7.6 months for the placebo arm], although improvements were observed in the secondary end points of progression-free survival (PFS) [HR 0.625 (95 % CI 0.522–0.750);  $P < 0.0001$ ] and response rate ( $P < 0.0001$ ) [17]. Ramucirumab was well tolerated, with an acceptable safety profile [17]. A prespecified subgroup analysis of the patient population with a baseline  $\alpha$ -fetoprotein (AFP) level of 400 ng/mL or greater showed an OS improvement in the ramucirumab group [HR 0.674 (95 % CI 0.508–0.895);  $P = 0.0059$ ; median OS 7.8 months for the ramucirumab arm vs 4.2 months for the placebo arm] [17].

To explore the potential differences in efficacy and safety in the Japanese patients receiving ramucirumab, a subgroup analysis of the REACH trial was performed in Japanese patients with advanced hepatocellular carcinoma following first-line therapy with sorafenib.

## Methods

### Study design and patients

Details on the study design and patients for REACH have been published previously [17]. Each center's institutional review board or independent ethics committee approved this study. The study followed the guiding principles of the Declaration of Helsinki and the good clinical practice guidelines of the International Conference on Harmonisation of Technical Requirements for Registration of Pharmaceuticals for Human Use. All patients provided written informed consent before enrollment. This study is registered with ClinicalTrials.gov (NCT01140347).

<sup>25</sup> Massachusetts General Hospital Cancer Center, Harvard Medical School, Boston, MA, USA



## Randomization and procedures

Details on the randomization and procedures have been published previously [17]. Patients were randomly assigned in a 1:1 ratio to receive either ramucirumab at 8 mg/kg or placebo intravenously every 2 weeks until disease progression, unacceptable adverse events, or withdrawal of consent occurred. All patients received best supportive care. Predefined dose modifications were allowed to manage treatment-related adverse events.

## Statistical analysis

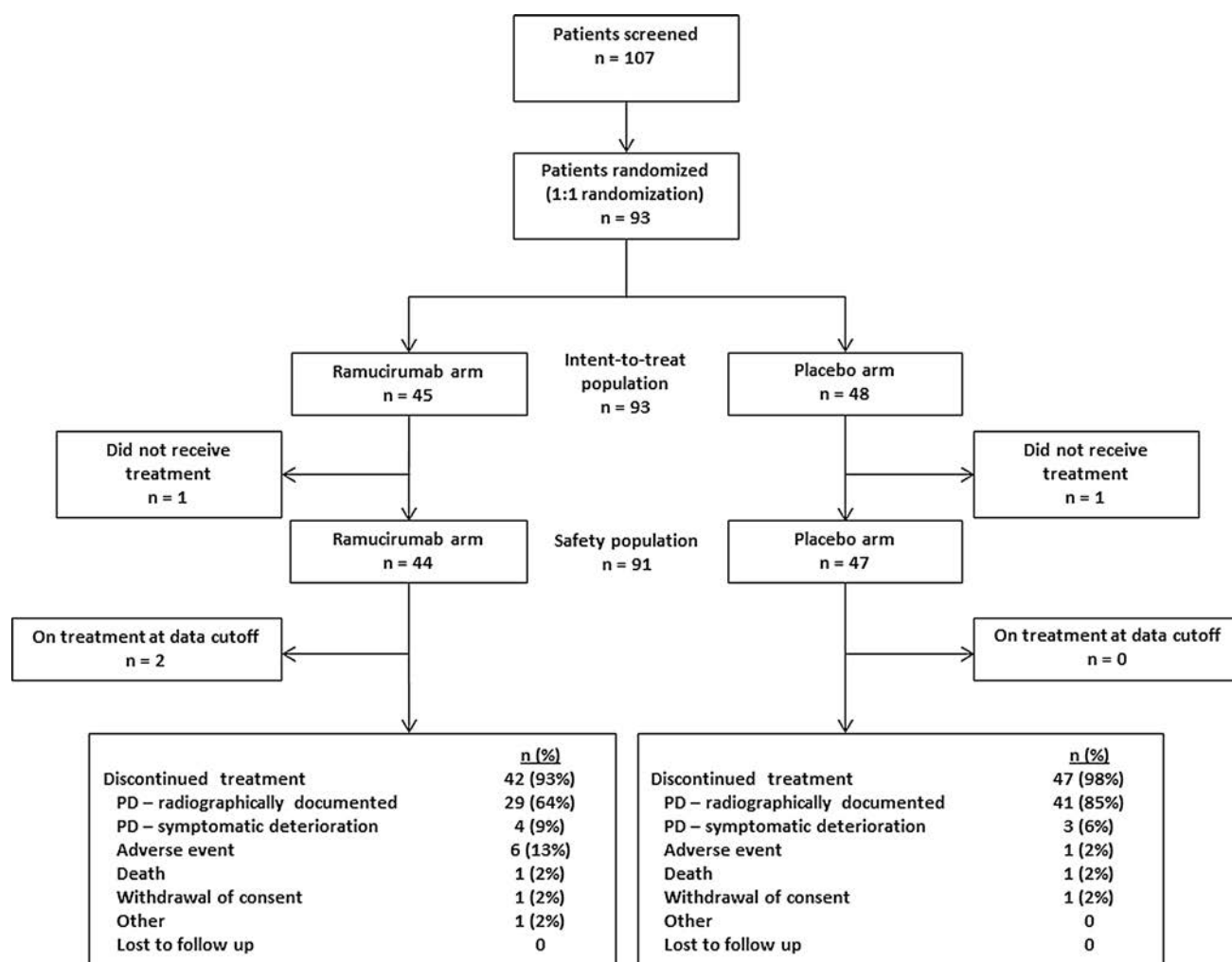
Detailed statistical methods have been published previously [17]. Randomization for the intent-to-treat (ITT) population was stratified by geographic region—region 1 (Brazil, Canada, and the USA) versus region 2 (Europe, Israel, Australia, and New Zealand) versus region 3 (East Asia)—and the cause of liver disease (hepatitis B vs hepatitis C vs other causes). The ITT population

comprised all eligible randomized patients, regardless of study drug administration. The safety population comprised all eligible randomized patients who received any dose of ramucirumab or placebo. The Japanese subgroup was defined as the subset of the ITT population enrolled in Japan; patients of Japanese ethnicity enrolled at sites in countries other than Japan were not included in the Japanese subgroup. Unstratified HRs from a Cox proportional hazards model and *P* values from an unstratified log-rank test are presented for the Japanese subgroup.

## Results

### Patients

Ninety-three Japanese patients were enrolled in the ITT population and randomly assigned to receive either ramucirumab ( $n = 45$ ) or placebo ( $n = 48$ ) (Fig. 1). The



**Fig. 1** REACH trial profile for Japanese patients. *PD* progressive disease

**Table 1** Baseline characteristics of Japanese REACH patients

	Ramucirumab ( <i>n</i> = 45)	Placebo ( <i>n</i> = 48)
Age		
Median (range)	66 (45–85)	67 (25–82)
<65 years	21 (47 %)	22 (46 %)
≥65 years	24 (53 %)	26 (54 %)
Male	35 (78 %)	43 (90 %)
ECOG PS <sup>a</sup>		
0	32 (71 %)	39 (81 %)
1	13 (29 %)	9 (19 %)
Cause of liver disease		
Hepatitis B	14 (31 %)	16 (33 %)
Hepatitis C	21 (47 %)	22 (46 %)
Other	10 (22 %)	12 (25 %)
Baseline Child-Pugh class A	44 (98 %)	47 (98 %)
Macrovascular invasion present	13 (29 %)	12 (25 %)
Extrahepatic spread present	28 (62 %)	33 (69 %)
Baseline BCLC stage		
B	7 (16 %)	11 (23 %)
C	38 (84 %)	37 (77 %)
Prior sorafenib therapy		
Sorafenib only	35 (78 %)	35 (73 %)
Sorafenib and other systemic therapy	10 (22 %)	13 (27 %)
Reason for discontinuation of sorafenib therapy		
Progressive disease	40 (89 %)	40 (83 %)
Toxicity	5 (11 %)	8 (17 %)
Previous locoregional therapy before sorafenib therapy	44 (98 %)	42 (88 %)
α-Fetoprotein		
<400 ng/mL	25 (56 %)	26 (54 %)
≥400 ng/mL	20 (44 %)	22 (46 %)

*BCLC* Barcelona Clinic Liver Cancer staging system, *ECOG PS* Eastern Cooperative Oncology Group, *PS* performance status

<sup>a</sup> PS of 0 indicates asymptomatic, PS of 1 indicates restricted in strenuous activity but ambulatory and able to do light work, and PS of 2 indicates ambulatory and capable of all self-care but unable to work

baseline patient and tumor characteristics were generally well balanced between the treatment arms, with the exception of sex (male, 78 % for the ramucirumab arm vs 90 % for the placebo arm) and Eastern Cooperative Oncology Group performance status 0 (71 % for the ramucirumab arm vs 81 % for the placebo arm) (Table 1). In patients with a baseline AFP level of 400 ng/mL or greater (*n* = 42), the patient and tumor characteristics were similar to those of the overall Japanese subgroup (data not shown). The duration of therapy was longer for the ramucirumab arm (median of 13 weeks) than for the placebo arm (median of 8 weeks), and the median relative dose intensity was similar for both treatment arms (98 % for the ramucirumab arm vs 100 % for the placebo arm) (Table S1).

## Efficacy

In Japanese patients, the median OS was 12.9 months for the ramucirumab arm and 8.0 months for the placebo arm. The improvement in median OS was 4.9 months [HR 0.621 (95 % CI 0.391–0.986); *P* = 0.0416; Fig. 2a]. The median PFS was 4.1 months for the ramucirumab arm and 1.7 months for the placebo arm. The improvement in median PFS was 2.4 months [HR 0.449 (95 % CI 0.285–0.706); *P* = 0.0004; Fig. 2b]. Similar results were demonstrated with stratified analyses (Table S2). Subgroup analyses also favored a ramucirumab survival benefit in Japanese patients with hepatitis B [HR 0.450 (95 % CI 0.183–1.110); *P* = 0.0757] or hepatitis C [HR 0.734 (95 % CI 0.380–1.420); *P* = 0.3590] as the cause of the disease.

The objective response rate (ORR) was higher for the ramucirumab arm [11 % (5 of 45 patients)] than for the placebo arm [2 % (1 of 48 patients);  $P = 0.0817$ ] (Table 2). The disease control rate was higher for the ramucirumab

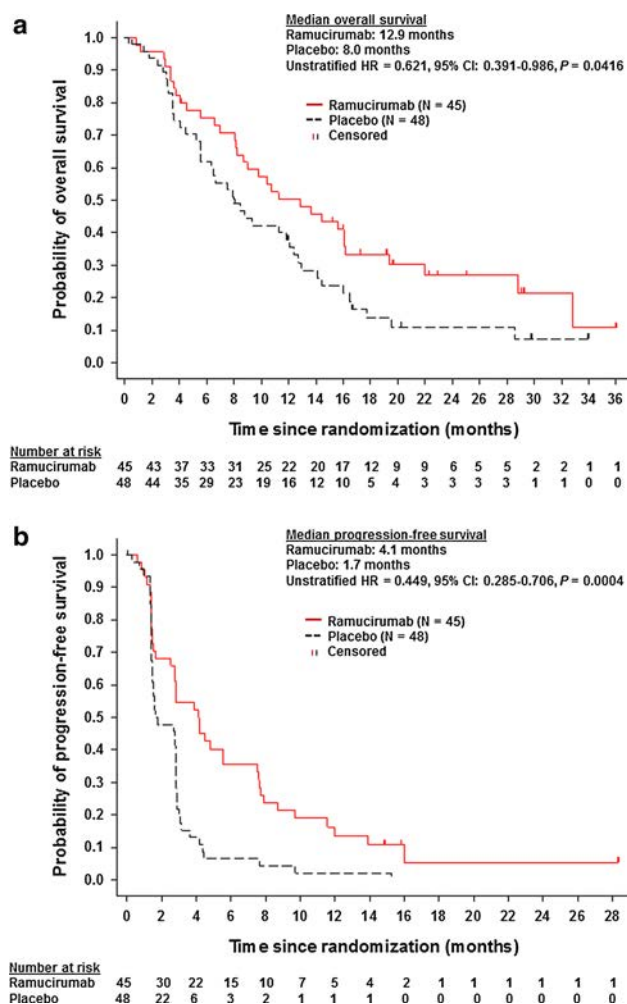
arm [67 % (30 of 45 patients)] than for the placebo arm [46 % (22 of 48 patients);  $P = 0.0462$ ] (Table 2).

Use of posttreatment anticancer systemic therapies in Japanese patients was similar for the ramucirumab arm (38 %) and for the placebo arm (44 %) (Table 3). The types of posttreatment anticancer systemic therapies were similar for both treatment arms (Table 3).

In patients with a baseline AFP level of 400 ng/mL or greater, the median OS was 12.9 months for the ramucirumab arm ( $n = 20$ ) and 4.3 months for the placebo arm ( $n = 22$ ). The improvement in median OS was 8.6 months [HR 0.464 (95 % CI 0.232–0.926);  $P = 0.0263$ ; Fig. 3a]. In patients with a baseline AFP level of less than 400 ng/mL, no OS benefit was observed (Fig. 3b).

### Safety

The Japanese safety population consisted of 44 patients in the ramucirumab arm and 47 patients in the placebo arm. All patients in the ramucirumab arm experienced at least one any-grade treatment-emergent adverse event (TEAE) compared with 87 % of patients in the placebo arm. The TEAEs of grade 3 or higher that occurred in more than 5 % of patients in the ramucirumab arm were ascites [three patients (7 %) vs one patient (2 %)], hypertension [three patients (7 %) vs one patient (2 %)], and cholangitis [three patients (7 %) vs no patients] (Table 4). Most of the other TEAEs that occurred in more than 5 % of patients in the ramucirumab arm were low-grade events (grade 2 or lower). The any-grade TEAEs with an incidence of at least 20 % for at which there was also at least one event of grade 3 or higher in the ramucirumab arm and at least a 10 % difference between the treatment arms were thrombocytopenia [15 patients (34 %) vs 1 patient (2 %)], fatigue [14 patients (32 %) vs 8 patients (17 %)], ascites [13 patients (30 %) vs 2 patients (4 %)], proteinuria [11 patients (25 %) vs 4 patients (9 %)], and hypertension [10 patients (23 %) vs 3 patients (6 %)] (Table 4). Two patients in the ramucirumab arm (hemorrhage of esophageal varices and hepatic failure) and two patients in the



**Fig. 2** Kaplan-Meier estimates of overall survival (a) and progression-free survival (b) for Japanese REACH patients. CI confidence interval, HR hazard ratio

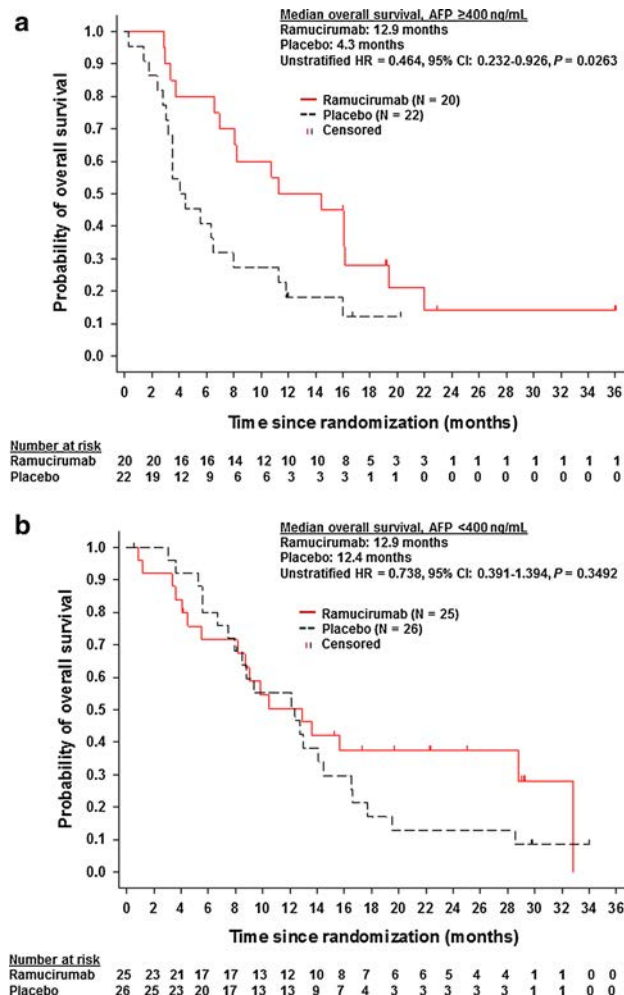
**Table 2** Best overall response in Japanese REACH patients

	Ramucirumab ( $n = 45$ )	Placebo ( $n = 48$ )	$P$
Best overall response			
Complete response	0	0	
Partial response	5 (11 %)	1 (2 %)	
Stable disease	25 (56 %)	21 (44 %)	
Progressive disease	12 (27 %)	22 (46 %)	
Not evaluable or not assessed	3 (7 %)	4 (8 %)	
Objective response rate	11 % (5/45)	2 % (1/48)	0.0817
Disease control rate <sup>a</sup>	67 % (30/45)	46 % (22/48)	0.0462

<sup>a</sup> Best response of complete response, partial response, or stable disease

**Table 3** Posttreatment anticancer systemic therapy in Japanese REACH patients

	Ramucirumab (n = 45)	Placebo (n = 48)
Any treatment	17 (38 %)	21 (44 %)
Chemotherapy	9 (20 %)	11 (23 %)
Anthracycline	2 (4 %)	1 (2 %)
Fluoropyrimidine	6 (13 %)	9 (19 %)
Gemcitabine	0	1 (2 %)
Platinum	1 (2 %)	5 (10 %)
Other	1 (2 %)	1 (2 %)
Immunomodulatory	2 (4 %)	4 (8 %)
Randomized trial	1 (2 %)	0
Targeted antibody (glypican 3)	1 (2 %)	2 (4 %)
Targeted small molecule	6 (13 %)	9 (19 %)
Vascular endothelial growth factor receptor	4 (9 %)	9 (19 %)
Other	2 (4 %)	0

**Fig. 3** Kaplan-Meier estimates of overall survival for Japanese REACH patients with a baseline  $\alpha$ -fetoprotein (AFP) level of 400 ng/mL or greater (a) or less than 400 ng/mL (b). CI confidence interval, HR hazard ratio

placebo arm (septic shock and acute respiratory distress syndrome) experienced a grade 5 event.

The incidence of adverse events of special interest (AESIs) in the ramucirumab arm and the placebo arm are shown in Table 4. The AESIs of grade 3 or higher that occurred in at least 5 % of patients and at a higher rate for the ramucirumab arm than the placebo arm were liver injury/failure [ten patients (23 %) vs five patients (11 %)], hypertension [four patients (9 %) vs one patient (2 %)], bleeding/hemorrhage [three patients (7 %) vs one patient (2 %)], and renal failure [two patients (5 %) vs no patients]. The most commonly noted grade 3 or higher liver injury/failure event was ascites [three patients (7 %) vs one patient (2 %)], and no cases of ascites were of grade 5. The any-grade AESIs that were commoner (at least 10 % difference between the treatment arms) in the ramucirumab arm than in the placebo arm were liver injury/failure [28 patients (64 %) vs 12 patients (26 %)], bleeding/hemorrhage [19 patients (43 %) vs 5 patients (11 %)], proteinuria [12 patients (27 %) vs 4 patients (9 %)], hypertension [11 patients (25 %) vs 3 patients (6 %)], and renal failure [6 patients (14 %) vs 2 patients (4 %)] (Table 4). Most of the any-grade bleeding/hemorrhage events in the ramucirumab arm (12 of 19 bleeding/hemorrhage events) were due to low-grade epistaxis. Most of the any-grade liver injury/failure events in the ramucirumab arm were due to low-grade ascites.

The safety profile of ramucirumab in Japanese patients with a baseline AFP level of 400 ng/mL or greater was similar to the profile observed in the overall Japanese safety population. AESIs for Japanese patients with a baseline AFP level of 400 ng/mL or greater are presented in Table S3.

**Table 4** Adverse events of Japanese REACH patients, irrespective of causality

	Ramucirumab ( <i>n</i> = 44)		Placebo ( <i>n</i> = 47)	
	Any grade	Grade $\geq 3$	Any grade	Grade $\geq 3$
TEAEs in $\geq 5$ % of patients (any grade) with at least one grade $\geq 3$ event in the ramucirumab arm				
Any	44 (100 %)	22 (50 %)	41 (87 %)	12 (26 %)
Thrombocytopenia	15 (34 %)	1 (2 %)	1 (2 %)	0
Fatigue	14 (32 %)	1 (2 %)	8 (17 %)	1 (2 %)
Ascites	13 (30 %)	3 (7 %)	2 (4 %)	1 (2 %)
Proteinuria	11 (25 %)	1 (2 %)	4 (9 %)	0
Decreased appetite	10 (23 %)	2 (5 %)	11 (23 %)	0
Hypertension	10 (23 %)	3 (7 %)	3 (6 %)	1 (2 %)
Increased aspartate aminotransferase level	6 (14 %)	1 (2 %)	7 (15 %)	4 (9 %)
Leukopenia	6 (14 %)	2 (5 %)	2 (4 %)	0
Neutropenia	6 (14 %)	1 (2 %)	0	0
Anemia	5 (11 %)	2 (5 %)	2 (4 %)	0
Hypoalbuminemia	5 (11 %)	1 (2 %)	1 (2 %)	0
Abdominal pain	4 (9 %)	1 (2 %)	4 (9 %)	0
Arthralgia	3 (7 %)	1 (2 %)	0	0
Cholangitis	3 (7 %)	3 (7 %)	0	0
Dehydration	2 (5 %)	1 (2 %)	1 (2 %)	0
Hepatic cirrhosis	2 (5 %)	1 (2 %)	0	0
Hepatic encephalopathy	2 (5 %)	1 (2 %)	0	0
Hepatic failure	2 (5 %)	2 (5 %)	1 (2 %)	1 (2 %)
Hypophosphatemia	2 (5 %)	1 (2 %)	0	0
Esophageal varices	2 (5 %)	1 (2 %)	0	0
Adverse events of special interest				
Any	30 (68 %)	7 (16 %)	13 (28 %)	2 (4 %)
Liver injury/failure <sup>a</sup>	28 (64 %)	10 (23 %)	12 (26 %)	5 (11 %)
Ascites <sup>b</sup>	13 (30 %)	3 (7 %)	2 (4 %)	1 (2 %)
Bleeding/hemorrhage <sup>a</sup>	19 (43 %)	3 (7 %)	5 (11 %)	1 (2 %)
Epistaxis <sup>c</sup>	12 (27 %)	0	3 (6 %)	0
Gastrointestinal hemorrhage <sup>d</sup>	4 (9 %)	2 (5 %)	0	0
Pulmonary hemorrhage <sup>d</sup>	1 (2 %)	0	0	0
Hepatic hemorrhage <sup>d</sup>	0	0	1 (2 %)	1 (2 %)
Proteinuria <sup>a</sup>	12 (27 %)	1 (2 %)	4 (9 %)	0
Hypertension <sup>a</sup>	11 (25 %)	4 (9 %)	3 (6 %)	1 (2 %)
Renal failure <sup>a</sup>	6 (14 %)	2 (5 %)	2 (4 %)	0
Infusion-related reaction <sup>a</sup>	3 (7 %)	0	0	0
Arterial thromboembolism <sup>a</sup>	0	0	0	0
Congestive heart failure <sup>a</sup>	0	0	0	0
Venous thromboembolism <sup>a</sup>	0	0	0	0

TEAE treatment-emergent adverse event

<sup>a</sup> Pooled adverse event term<sup>b</sup> Clinical term<sup>c</sup> Preferred term<sup>d</sup> Pooled adverse event category comprising synonymous MedDRA version 16.1 preferred terms

## Discussion

In the ITT population of the phase III REACH trial, second-line treatment with ramucirumab demonstrated an improvement in OS, and statistically significant improvements in PFS, time to radiographic progression, and ORR, for patients with advanced hepatocellular carcinoma when compared with placebo [17]. Subgroup analyses of the

REACH ITT population suggested that an elevated baseline AFP level of 400 ng/mL or greater could identify patients likely to derive an OS benefit from ramucirumab therapy [17]. In Japanese hepatocellular carcinoma patients treated with ramucirumab, improvements in OS, PFS, and ORR were observed, including an OS benefit for patients with an elevated baseline AFP level of 400 ng/mL or greater.



The results in the Japanese subgroup are notable for the impressive median OS difference (4.9 months) observed for the ramucirumab arm compared with the placebo arm; in the overall REACH ITT population, the median OS difference (1.5 months) was not statistically significant [17]. The OS benefit seen in the overall Japanese subgroup was maintained in the subset of Japanese patients with a baseline AFP level of 400 ng/mL or greater, with an improvement of median OS of 8.6 months and  $P < 0.05$ , despite the small number of patients in this subgroup. The median survival difference between the ramucirumab arm and the placebo arm in the Japanese subgroup is unlikely to be explained by any imbalance in baseline characteristics or posttreatment anticancer systemic therapy. Given the relatively small size of the Japanese subgroup ( $n = 93$ ), it is possible that the OS improvement in the Japanese subgroup is a chance finding. However, the results are consistent with the evidence that ramucirumab has activity in hepatocellular carcinoma, as demonstrated by the results in the ITT population [17].

The reasons for potentially longer survival of ramucirumab-treated Japanese patients compared with the overall REACH ITT population are unclear but may be due to differences in Japanese patient characteristics or disease management that result in greater benefit from an effective therapy [6, 7]. Currently there is no evidence to support a biological mechanism underlying the potential association of improved benefits from ramucirumab treatment in Japanese patients. Differences in disease cause are unlikely to be responsible for the longer survival of ramucirumab-treated Japanese patients compared with the overall REACH ITT population. In the REACH study, hepatitis C was more commonly reported as the cause in the Japanese subgroup (46 % hepatitis C and 32 % hepatitis B) compared with the overall REACH ITT population, in which hepatitis B was more frequent (28 % hepatitis C and 38 % hepatitis B) [17]. In the overall REACH ITT population, hepatitis B or hepatitis C did not significantly alter OS [17]. Hepatitis C is a cause that has traditionally been associated with a better outcome than hepatitis B in patients with advanced hepatocellular carcinoma receiving antiangiogenic therapy. A retrospective analysis of the SHARP study and a phase III study of sunitinib have suggested a greater treatment benefit from antiangiogenic therapy for patients with hepatocellular carcinoma with hepatitis C as the cause [18, 19]. However, analyses of REACH in both the overall ITT population and in Japanese patients in this analysis demonstrate a treatment benefit regardless of the cause, possibly favoring a greater benefit in patients with hepatitis B, and do not support that the cause is a reason to expect a better treatment effect in Japanese patients. Japanese patients in REACH were also likelier to have an Eastern Cooperative Oncology Group performance status

of 0 (76 % of Japanese patients vs 55 % of the overall ITT population), to have had prior locoregional therapy (92 % of Japanese patients vs 73 % of the overall ITT population), and to have posttreatment anticancer systemic therapy (41 % of Japanese patients vs 30 % of the overall ITT population) compared with the overall REACH ITT population [17]. Some of these differences are not only prognostic but might also enhance the probability of deriving a survival benefit in the ramucirumab treatment arm of the Japanese subgroup. Differential ramucirumab activity by ethnicity is unlikely to explain the results in the Japanese subgroup of REACH; ramucirumab studies in advanced gastric cancer did not identify a consistent relationship between ramucirumab activity and geographic region or ethnicity [20, 21].

The observed safety profile for Japanese patients was consistent with that of the overall ITT population among trials of ramucirumab [17, 22, 23]. Ramucirumab was well tolerated, with similar dose intensities for both treatment arms; additionally, most patients discontinued ramucirumab treatment because of progressive disease, and only 14 % of patients in the ramucirumab arm discontinued ramucirumab treatment because of an adverse event. Ascites, hypertension, and cholangitis were the only reported grade 3 or higher adverse events occurring in more than 5 % of Japanese patients with a higher incidence in the ramucirumab arm, and the occurrence of any of these events in the ramucirumab arm was less than 10 %; none of these adverse events were of grade 4 or grade 5. Other adverse events with a higher occurrence in the ramucirumab arm were generally of a low grade. An increase in the incidence of AESIs of liver injury/failure, bleeding/hemorrhage, proteinuria, hypertension, renal failure, and infusion-related reaction was observed in the ramucirumab arm compared with the placebo arm. Similarly to the overall REACH ITT population [17], the increase in the incidence of AESIs of liver injury/failure and bleeding/hemorrhage was primarily due to low-grade ascites and epistaxis respectively.

In the Japanese patients of the REACH trial, ramucirumab treatment improved OS, PFS, and ORR, and demonstrated a manageable safety profile. In Japanese patients treated with ramucirumab with a baseline AFP level of 400 ng/mL or greater, an OS benefit was observed, consistent with observations for patients in the overall REACH ITT population with an elevated baseline AFP level [17]. Further evaluation of ramucirumab in patients with advanced hepatocellular carcinoma is warranted. The REACH-2 trial will evaluate the safety and efficacy of ramucirumab in participants, including Japanese patients, with hepatocellular carcinoma and an elevated baseline AFP level (ClinicalTrials.gov identifier NCT02435433).

**Acknowledgments** We thank the patients, their families, the study sites, and the study personnel who participated in this clinical trial. This study was sponsored by Eli Lilly and Company. Medical writing support was provided by Andrew Sakko, and editorial support was provided by Noelle Gasco, of inVentiv Health Clinical and funded by Eli Lilly and Company.

**Conflict of interest** Junji Furuse has received honoraria from Ajinomoto, Astellas Pharma, Bayer, Bristol-Myers Squibb, Chugai Pharmaceutical, Daiichi Sankyo, Sumitomo Dainippon Pharma, Eisai, Eli Lilly and Company, Hisamitsu Pharmaceutical, Kyowa Hakko Kirin, Nippon Kayaku, Novartis, Meiji Seika Pharma, Merck Serono, Mitsubishi Tanabe Pharma, Ono Pharmaceutical, Sandoz, Sanofi, Shionogi, Sumitomo Group, Taiho Pharmaceutical, Takeda Pharmaceutical, and Yakult, has acted in a consulting or advisory role for Astellas Pharma, AstraZeneca, Bayer, Boehringer Ingelheim, Chugai Pharmaceutical, Eisai, Fujifilm, GlaxoSmithKline, J-Pharma, Janssen Pharmaceutical, Kyowa Hakko Kirin, Merck, Nobelpharma, OncoTherapy Science, Otsuka Pharmaceutical, Taiho Pharmaceutical, Zeria Pharmaceutical, and Yakult, and has received research funding from Bayer, Chugai Pharmaceutical, Daiichi Sankyo, Eli Lilly and Company, GlaxoSmithKline, Merck, Nippon Kayaku, Novartis, OncoTherapy Science, Ono Pharmaceutical, Pfizer, Sanofi, Taiho Pharmaceutical, Takeda Pharmaceutical, Torii Pharmaceutical, and Yakult. Masafumi Ikeda has received honoraria from Abbott, Bayer, Bristol-Myers Squibb, Guerbet, Kyowa Hakko Kirin, Novartis, Takeda Pharmaceutical, and Yakult, has acted in a consulting or advisory role for Bayer, Eisai, Fujifilm, Merck Serono, NanoCarrier, and Sceti Medical, and has received research funding from AstraZeneca, Chugai Pharmaceutical, Sumitomo Dainippon Pharma, Eli Lilly and Company, GlaxoSmithKline, Pfizer, Yakult, and Zeria Pharmaceutical. Hiroshi Ishii has received honoraria from Ajinomoto, Bayer, Daiichi Sankyo, Eli Lilly and Company, Ono Pharmaceutical, Taiho Pharmaceutical, Torii Pharmaceutical, and Yakult. Shinichi Ohkawa has received honoraria from Eli Lilly and Company. Takuji Okusaka has received honoraria from Bayer, Chugai Pharmaceutical, Sumitomo Dainippon Pharma, Eisai, Eli Lilly and Company, Fujifilm, Merck Serono, Novartis, Pfizer, Taiho Pharmaceutical, and Yakult, has acted in a consulting or advisory role for Amgen, Boehringer Ingelheim, Chugai Pharmaceutical, Sumitomo Dainippon Pharma, Eli Lilly and Company, NanoCarrier, Nobelpharma, Novartis, OncoTherapy Science, Ono Pharmaceutical, Taiho Pharmaceutical, Yakult, and Zeria Pharmaceutical, and has received research funding from AstraZeneca, Bayer, Boehringer Ingelheim, Chugai Pharmaceutical, Sumitomo Dainippon Pharma, Eisai, Eli Lilly and Company, Kyowa Hakko Kirin, Merck Serono, Novartis, OncoTherapy Science, Ono Pharmaceutical, Otsuka Pharmaceutical, Pfizer, Sceti Medical, Shizuoka Industry, Taiho Pharmaceutical, Takeda Pharmaceutical, and Yakult. Ryosuke Tateishi has received research funding from Kyowa-Hakko Kirin. Andrew X. Zhu has acted in a consulting or advisory role for Amgen, Exelixis, and Sanofi, has received research funding from Bayer and Onyx Pharmaceutical, and received grants from Eli Lilly and Company during the conduct of the study. Paolo B. Abada and Ling Yang are employees of Eli Lilly and Company. All remaining authors have declared no conflict of interest.

## References

1. Ferlay J, Soerjomataram I, Ervik M, et al. GLOBOCAN 2012 v1.0. Estimated cancer incidence, mortality and prevalence worldwide in 2012: liver cancer. CancerBase no. 11. Lyon: International Agency for Research on Cancer. Available via [http://globocan.iarc.fr/Pages/fact\\_sheets\\_cancer.aspx](http://globocan.iarc.fr/Pages/fact_sheets_cancer.aspx). Accessed 13 Feb 2015.
2. Torre LA, Bray F, Siegel RL, et al. Global cancer statistics, 2012. *CA Cancer J Clin*. 2015;65:87–108.
3. Kudo M, Lencioni R, Marrero JA, et al. Regional differences in sorafenib-treated patients with hepatocellular carcinoma: GIDEON observational study. *Liver Int*. 2016. doi:10.1111/liv.13096.
4. Ikeda M, Mitsunaga S, Shimizu S, et al. Current status of hepatocellular carcinoma in Japan. *Chin Clin Oncol*. 2013;2:40.
5. Bruix J, Gores GJ, Mazzaferro V. Hepatocellular carcinoma: clinical frontiers and perspectives. *Gut*. 2014;63:844–55.
6. Kudo M. Surveillance, diagnosis, treatment, and outcome of liver cancer in Japan. *Liver Cancer*. 2015;4:39–50.
7. Kudo M. Clinical practice guidelines for hepatocellular carcinoma differ between Japan, United States and Europe. *Liver Cancer*. 2015;4:85–95.
8. Llovet JM, Ricci S, Mazzaferro V, et al. Sorafenib in advanced hepatocellular carcinoma. *N Engl J Med*. 2008;359:378–90.
9. Cheng AL, Kang YK, Chen Z, et al. Efficacy and safety of sorafenib in patients in the Asia-Pacific region with advanced hepatocellular carcinoma: a phase III randomised, double-blind, placebo-controlled trial. *Lancet Oncol*. 2009;10:25–34.
10. Lencioni R, Kudo M, Ye SL, et al. GIDEON (Global Investigation of therapeutic DEcisions in hepatocellular carcinoma and Of its treatment with sorafenib): second interim analysis. *Int J Clin Pract*. 2014;68:609–17.
11. Iavarone M, Cabibbo G, Piscaglia F, et al. Field-practice study of sorafenib therapy for hepatocellular carcinoma: a prospective multicenter study in Italy. *Hepatology*. 2011;54:2055–63.
12. Sullivan LA, Brekken RA. The VEGF family in cancer and antibody-based strategies for their inhibition. *MAbs*. 2010;2:165–75.
13. Tugues S, Koch S, Gualandi L, et al. Vascular endothelial growth factors and receptors: anti-angiogenic therapy in the treatment of cancer. *Mol Asp Med*. 2011;32:88–111.
14. Amini A, Masoumi Moghaddam S, Morris DL, et al. The critical role of vascular endothelial growth factor in tumor angiogenesis. *Curr Cancer Drug Targets*. 2012;12:23–43.
15. Zhu AX, Duda DG, Sahani DV, et al. HCC and angiogenesis: possible targets and future directions. *Nat Rev Clin Oncol*. 2011;8:292–301.
16. Sprattlin JL, Cohen RB, Eadens M, et al. Phase I pharmacologic and biologic study of ramucirumab (IMC-1121B), a fully human immunoglobulin G1 monoclonal antibody targeting the vascular endothelial growth factor receptor-2. *J Clin Oncol*. 2010;28:780–7.
17. Zhu AX, Park JO, Ryoo BY, et al. Ramucirumab versus placebo as second-line treatment in patients with advanced hepatocellular carcinoma following first-line therapy with sorafenib (REACH): a randomised, double-blind, multicentre, phase 3 trial. *Lancet Oncol*. 2015;16:859–70.
18. Bruix J, Raoul JL, Sherman M, et al. Efficacy and safety of sorafenib in patients with advanced hepatocellular carcinoma: subanalyses of a phase III trial. *J Hepatol*. 2012;57:821–9.
19. Cheng AL, Kang YK, Lin DY, et al. Sunitinib versus sorafenib in advanced hepatocellular cancer: results of a randomized phase III trial. *J Clin Oncol*. 2013;31:4067–75.
20. Hironaka S, Shimada Y, Sugimoto N, et al. RAINBOW: a global, phase III, randomized, double-blind study of ramucirumab (RAM) plus paclitaxel (PTX) versus placebo (PL) plus PTX in the treatment of metastatic gastroesophageal junction and gastric adenocarcinoma (mGC) following disease progression on first-line platinum- and fluoropyrimidine-containing combination therapy—efficacy analysis in Japanese and Western patients. *J Clin Oncol*. 2014;32(15 Suppl):4005.
21. Muro K, Cheul Oh S, et al. Subgroup analysis of East Asians in RAINBOW: a phase 3 trial of ramucirumab plus paclitaxel for

- advanced gastric cancer. *J Gastroenterol Hepatol*. 2015. doi: [10.1111/jgh.13153](https://doi.org/10.1111/jgh.13153).
22. Fuchs CS, Tomasek J, Yong CJ, et al. Ramucirumab monotherapy for previously treated advanced gastric or gastro-oesophageal junction adenocarcinoma (REGARD): an international, randomised, multicentre, placebo-controlled, phase 3 trial. *Lancet*. 2014;383:31–9.
23. Zhu AX, Finn RS, Mulcahy M, et al. A phase II and biomarker study of ramucirumab, a human monoclonal antibody targeting the VEGF receptor-2, as first-line monotherapy in patients with advanced hepatocellular cancer. *Clin Cancer Res*. 2013;19:6614–23.

# On-target sorafenib toxicity predicts improved survival in hepatocellular carcinoma: a multi-centre, prospective study

J. Howell<sup>\*,†,‡</sup> , D. J. Pinato<sup>\*</sup>, R. Ramaswami<sup>\*</sup>, D. Bettinger<sup>§</sup>, T. Arizumi<sup>¶</sup>, C. Ferrari<sup>\*\*</sup>, C. Yen<sup>\*</sup>, A. Gibbin<sup>\*\*</sup>, M. E. Burlone<sup>\*\*</sup>, G. Guaschino<sup>\*\*</sup>, L. Sellers<sup>\*</sup>, J. Black<sup>\*</sup>, M. Pirisi<sup>¶</sup>, M. Kudo<sup>¶</sup>, R. Thimme<sup>§</sup>, J.-W. Park<sup>††</sup> & R. Sharma<sup>\*</sup>

<sup>\*</sup>Department of Surgery and Cancer, Imperial College London, Hammersmith Hospital, London, UK.

<sup>†</sup>Department of Medicine, University of Melbourne, St Vincent's Hospital, Melbourne, Vic., Australia.

<sup>‡</sup>Centre for Population Health, Macfarlane-Burnet Institute, Melbourne, Vic., Australia.

<sup>§</sup>Department of Medicine II, University Hospital Freiburg, Freiburg, Germany.

<sup>¶</sup>Department of Gastroenterology and Hepatology, Kindai University School of Medicine, Osaka-Sayama, Osaka, Japan.

<sup>\*\*</sup>Department of Translational Medicine, Università degli Studi del Piemonte Orientale "A. Avogadro", Novara, Italy.

<sup>††</sup>Center for Liver Cancer, National Cancer Center, Goyang, Gyeonggi, South Korea.

## Correspondence to:

Dr R. Sharma, Department of Surgery and Cancer, Imperial College London Hammersmith Campus, London, UK. E-mail: r.sharma@imperial.ac.uk

Jessica Howell and David J. Pinato contributed equally to the manuscript.

## Publication data

Submitted 14 December 2016  
First decision 9 January 2017  
Resubmitted 15 January 2017  
Accepted 17 January 2017  
EV Pub Online 2 March 2017

The Handling Editor for this article was Professor Peter Hayes, and it was accepted for publication after full peer-review.

## SUMMARY

### Background

Hepatocellular carcinoma (HCC) is the sixth most common cancer worldwide and has high mortality despite treatment. While sorafenib has a survival benefit for patients with advanced HCC, clinical response is highly variable.

### Aim

To determine whether development of sorafenib toxicity is a prognostic marker of survival in HCC.

### Methods

In this prospective multicentre cohort study, patients with advanced-stage HCC receiving sorafenib were recruited from five international specialist centres. Demographic and clinical data including development and grade of sorafenib toxicity during treatment, radiological response to sorafenib and survival time (months) were recorded prospectively.

### Results

A total of 634 patients with advanced-stage HCC receiving sorafenib were recruited to the study, with a median follow-up of 6692.3 person-months at risk. The majority of patients were male (81%) with Child–Pugh A stage liver disease (74%) and Barcelona Clinic Liver Cancer stage C HCC (64%). Median survival time was 8.1 months (IQR 3.8–18.6 months). 94% experienced at least one sorafenib-related toxicity: 34% diarrhoea, 16% hypertension and 37% hand-foot syndrome (HFS). Twenty-one per cent ceased sorafenib due to toxicity and 59% ceased treatment due to progressive disease or death. On multivariate analysis, sorafenib-related diarrhoea (HR 0.76, 95% CI 0.61–0.95,  $P = 0.017$ ), hypertension (HR 0.531, 95% CI 0.37–0.76,  $P < 0.0001$ ) and HFS (HR 0.65, 95% CI 0.51–0.81,  $P < 0.0001$ ) were all significant independent predictors of overall survival after adjusting for age, severity of liver disease, tumour stage and sorafenib dose.

### Conclusion

Development of sorafenib-related toxicity including diarrhoea, hypertension and hand-foot syndrome is associated with prolonged overall survival in patients with advanced-stage HCC on sorafenib.

*Aliment Pharmacol Ther* 2017; **45**: 1146–1155

## INTRODUCTION

Hepatocellular carcinoma (HCC) is the third most common cause of cancer-related death worldwide, with an escalating global incidence and mortality.<sup>1</sup> Despite extensive research efforts, the oral multi-tyrosine kinase inhibitor (TKI) sorafenib remains the only established treatment with proven efficacy for advanced HCC that is recommended in current HCC management guidelines.<sup>2–4</sup> Clinical response to sorafenib is highly variable<sup>2</sup> and currently there are no validated biomarkers to predict tumour response to therapy. Due to the modest survival benefit of treatment and the potential for sorafenib-related adverse events to worsen patient quality of life, there is an unmet need for better prognostic markers to guide clinicians in initiating and maintaining sorafenib therapy in patients with advanced HCC.

The evolving experience in the clinical use of sorafenib has demonstrated that the development of drug-related toxicity is associated with prolonged survival in advanced HCC.<sup>5–15</sup> Sorafenib-induced diarrhoea,<sup>9, 13, 16</sup> hypertension<sup>9</sup> and hand-foot skin toxicity<sup>6, 9, 16</sup> have been shown to identify a subset of patients with significantly improved survival outcomes. Such trends have been confirmed by further studies showing that treatment cessation due to toxicity predicts longer survival compared to when sorafenib is ceased due to disease progression.<sup>8</sup> Toxicity from TKIs is the result of a complex interplay between the pharmacokinetic profile of the drug and diverse end-organ susceptibility towards the drug or its metabolites. In some instances, drug therapy may produce an exaggerated pharmacodynamic modulation of the target of interest when this is expressed in nontumorous tissues, resulting in so-called ‘on target’ toxicity.<sup>17</sup>

It is hypothesised that ‘on target’ toxicity, while producing undesired effects in noncancerous tissues, might correspond to a clinically desirable, more potent inhibition of the target within the tumour, therefore, acting as a clinical surrogate of efficacy.<sup>18</sup> However, reports on the association between adverse event profiles and survival have been inconsistent and further validation studies to confirm this relationship are needed.<sup>6</sup>

This retrospective analysis of a large, multicentre prospective HCC patient cohort was designed to further investigate whether sorafenib-induced toxicities are independently associated with prolonged survival in advanced HCC.

## PATIENTS AND METHODS

Patients with HCC were consecutively recruited to the study from five tertiary centres with specialist

multidisciplinary services for HCC management: Osaka, Japan (183 patients, 28.9%); Novara, Italy (156, 24.6%); London, UK (103, 16.3%); Freiburg, Germany (71, 11.2%), and Goyang, South Korea (121, 19.1%). Inclusion criteria included all adult patients (>18 years of age) with confirmed HCC who were to commence sorafenib as per standard of care. Exclusion criteria included patients under the age of 18 years. All patients had a diagnosis of HCC based either on imaging or histologic criteria according to international guidelines.<sup>19</sup> Patients were staged using the Barcelona Clinic Liver Cancer (BCLC) staging system, which describes liver functional impairment using the Child–Turcotte–Pugh (CTP) score.<sup>2</sup> Demographic data, imaging and other clinical details including development of sorafenib-mediated adverse events were collected prospectively and were entered directly into a clinical HCC database at the end of the clinic visit by a member of the research team. The primary study endpoint was overall survival (OS) after commencing sorafenib, with the clinical endpoint being either death or end date of study follow-up, censored on the 30 March 2015. The study was approved by local Institutional Ethics Committees and conducted in accordance with the Declaration of Helsinki (update 2004).

## Sorafenib treatment and toxicity development

Patients were commenced on sorafenib therapy in accordance with BCLC guidelines.<sup>19</sup> At each centre, patients were routinely reviewed in the HCC clinic at baseline, 2 weeks, 4–6 weeks and 6–8 weeks post commencement of sorafenib for safety and tolerability review. Patients with decompensated liver disease and performance scores  $\geq 2$  were excluded. Treatment duration, dose modifications and sorafenib tolerability were recorded. Sorafenib was either commenced at full dose or at a lower dose then rapidly titrated up to the recommended dose within 1–2 weeks in order to improve tolerability. Cause for cessation of therapy due to toxicity, patient preference, disease progression or death was also recorded. Tumour response to sorafenib was also recorded, with disease progression defined by mRECIST criteria.<sup>20</sup> The onset of sorafenib-related toxicities including hand-foot syndrome (HFS), diarrhoea, hypertension, nonhand-foot-syndrome, rash and mucositis was recorded, and toxicities were graded according to the Common Toxicity Criteria Adverse Events (version 3.0), using the most severe grade recorded for the purposes of study analysis. To be included in the analysis, toxicities were defined as new diagnoses developing within 6 weeks of commencing maximum intended dose of sorafenib. Diarrhoea was



determined to be sorafenib-related by the treating clinician and members of the research team if temporally associated with commencing sorafenib, in the absence of other causes including infection (excluded by faecal microscopy and culture) or increased lactulose dosing for encephalopathy. Sorafenib-related fatigue was not included in the analysis as fatigue may be multi-factorial and assessment more subjective than other sorafenib-mediated toxicities.

### Statistical methods

Variables were described using mean and standard deviation or median and interquartile range (IQR). Univariate analysis of variables associated with survival was performed using Log-rank testing. Factors shown to be associated with survival on univariate analysis ( $P < 0.10$ ) were included in the multivariable analysis, along with factors well-known to be associated with survival in HCC in the published literature – namely CTP score, BCLC score and age. Multivariable analysis was performed using Cox proportional hazards regression modelling with backward elimination and likelihood ratio testing. Proportional hazards assumption was tested using log-log plots and Schoenfeld residuals. All analyses were performed using STATA version 12.1 (Stata Corporation, College Station, TX, USA).

## RESULTS

Six hundred and thirty-four patients with HCC receiving sorafenib therapy were recruited to the study, with a median follow-up time of 6692.3 person-months at risk. Of these, sorafenib-related toxicity data were available for 620 patients (97.7%). The majority of patients were male (81.1%) with CTP A stage liver cirrhosis (74.1%) and BCLC C stage HCC (64.5%), with a mean age of  $67 \pm 11.3$  years. Thirty-four per cent had hepatitis C, 26% had hepatitis B and 46.2% had alcohol-related liver disease. A total of 489 patients (77.1%) died during follow-up and the median OS time for the cohort was 8.1 months (IQR 3.8–18.6 months). The distribution of clinical factors among the study group is outlined in Table S1.

### Occurrence of sorafenib-related toxicities and their severity within the study group

Almost all patients ceased sorafenib therapy during the study period (96.6%), and the median duration of sorafenib therapy was 3.97 months (IQR 1.6–10.3 months). Indications for treatment withdrawal included unacceptable toxicity in 20.6% (124/602) or progressive HCC or death in 59% (355/602), with 14% due to other reasons.

Overall, 93.8% (595/634) of patients experienced at least one sorafenib-related side effect (grade 1 severity or above) within the first 6 weeks of treatment. In total, 38% of patients developed diarrhoea on sorafenib, 16% developed hypertension, 37% developed HFS, 5% developed nonhand-foot-syndrome skin rash and 2% developed mucositis. Most patients only experienced grade 1 or 2 level sorafenib-related toxicity, with less than 10% of patients experiencing grade 3–4 adverse events. There were no deaths directly attributable to sorafenib treatment. The distribution of sorafenib-related toxicity within the study group, graded by severity, is outlined in Table 1.

### Sorafenib-related toxicities are associated with prolonged OS

The development of any grade toxicity from sorafenib therapy was associated with prolonged survival in patients with a diagnosis of HCC. The median survival time was 8.8 months (IQR 4.3–17.4) in those who developed sorafenib toxicity (irrespective of severity or type),

**Table 1 | Distribution of sorafenib-related toxicities among the study cohort (n = 634)**

Clinical variable (grade of severity)	N (%)
Sorafenib-related diarrhoea (n = 572)	216 (37.8)
1	140 (71.4)
2	44 (22.4)
3	17 (8.7)
4	15 (7.7)
Sorafenib-related hypertension (n = 489)	80 (16.4)
1	44 (55.0)
2	24 (30.0)
3	12 (15.0)
Sorafenib-related hand-foot syndrome (n = 571)	209 (36.6)
1	105 (50.2)
2	57 (27.3)
3	46 (22.0)
4	1 (0.4)
Sorafenib-related nonhand-foot-syndrome rash (n = 571)	30 (5.2)
1	14 (46.7)
2	5 (16.7)
3	6 (20.0)
4	5 (16.7)
Sorafenib-related mucositis (n = 571)	12 (2.1)
1	11 (91.7)
2	1 (8.3)

compared with 5.4 months (IQR 2.7–8.8) in those who did not develop toxicity ( $P = 0.004$ , Figure 1). However, on *post hoc* analysis no difference in OS was observed between patients who ceased therapy due to toxicity compared to patients who ceased therapy for other reasons, such as progressive disease (9.2 months compared with 7.5 months,  $P = 0.354$ ;  $n = 620$ , Figure 2).

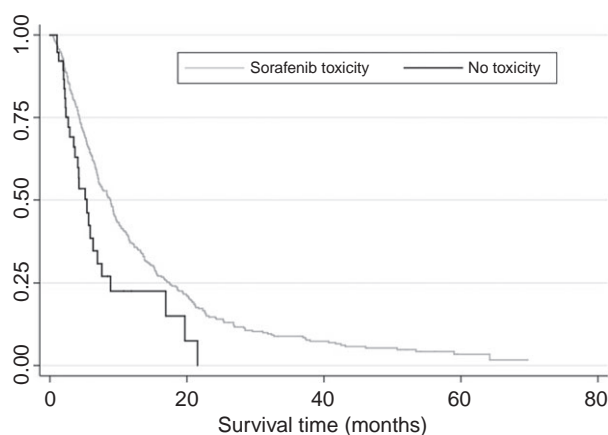
On univariate Log-rank analysis, sorafenib-induced hand-foot-syndrome ( $P < 0.0001$ ), diarrhoea ( $P = 0.004$ ) and hypertension ( $P < 0.0001$ ) were all significantly associated with prolonged survival. In addition, BCLC stage ( $P < 0.0001$ ), CTP class ( $P = 0.034$ ) and age when sorafenib commenced ( $P < 0.0001$ ) were also significantly associated with survival (Table 2).

We further assessed the presence of a linear association between grade of toxicity and survival on univariate analysis. There was no significant linear trend in hazard ratios evident across categories of side effect severity (Table 3). For this reason, we chose to categorise each adverse event as a binary variable (toxicity present or absent) and these were included in a multivariable Cox proportional hazards model. The model was also adjusted for factors associated with HCC survival in our dataset and also known from the published literature, namely CTP class ( $P = 0.034$ ), BCLC stage ( $P < 0.0001$ ) and age when sorafenib was commenced ( $P < 0.0001$ ).<sup>21</sup> A total of 464 patients had complete data for all independent variables of interest and were included in the final multivariable Cox proportional hazards model for

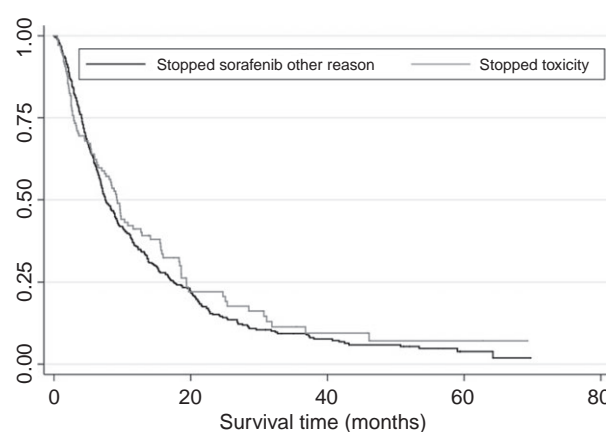
survival. The only significant clinical differences between patients for whom complete data were available and those that did not have complete data available was female preponderance (26.2% compared with 17.5%,  $P = 0.036$ ) and a higher proportion with CTP class B liver disease (36.5% compared with 23.7%,  $P = 0.006$ ) in the group without complete data available (Table S2).

Due to significant heterogeneity in HCV treatment access and eradication rates between international centres during the period of follow-up, hepatitis C diagnosis was not included in our final model presented in Table 4. However, when hepatitis C was included in the multivariable model, sorafenib-related diarrhoea ( $P = 0.019$ ), hypertension ( $P < 0.0001$ ) and HFS ( $P = 0.001$ ) remained significantly associated with OS, with no significant change in hazard ratios (Table S5).

On multivariable analysis, only sorafenib-related diarrhoea (HR 0.78, 95% CI 0.62–0.97,  $P = 0.024$ ), HFS (HR 0.67, 95% CI 0.53–0.84,  $P < 0.0001$ ) and hypertension (HR 0.50, 95% CI 0.35–0.71,  $P < 0.0001$ ) remained significantly associated with prolonged survival when adjusted for BCLC stage, CTP class and age (Table 4). The median survival time was 20.3 months (IQR 8.5–46.1 months) in those who developed hypertension on sorafenib, compared with 7.0 months (IQR 3.3–15.7 months) in those who did not (Figure 3a). Moreover, median survival time was 9.7 months (IQR 8.5–46.1 months) in patients who developed sorafenib-mediated diarrhoea of any severity, compared to



**Figure 1** | Comparison of Kaplan–Meier survival time (months) between HCC patients who developed sorafenib toxicity of any severity grade, compared with HCC patients who did not develop sorafenib toxicity [8.8 months (IQR 4.3–17.4) vs. 5.4 months (IQR 2.7–8.8), Log-rank  $P = 0.004$ ,  $n = 634$ ].



**Figure 2** | Comparison of Kaplan–Meier survival time (months) between HCC patients who ceased sorafenib due to sorafenib-related toxicity and HCC patients who ceased sorafenib for other reasons [9.2 months (IQR 2.87–19.37 months) compared with 7.5 months (IQR 4.07–17.50 months); log-rank  $P = 0.354$ ,  $n = 620$ ].

6.7 months (IQR 3.4–16.3 months) in those who did not (Figure 3b). and median survival was significantly longer in patients with HFS compared to patients without [12.7 months (95% CI 6.6–20.0) compared with 6.4 months (95% CI 2.9–15.1,  $P < 0.0001$ ; Figure 3c].

There were significant differences in age, gender, aetiology of liver disease, CTP class and HCC stage of disease between the patient populations at the participating study centres (Table S3). There was also an association

**Table 2 | Clinical variables associated with survival in patients with advanced HCC on sorafenib on univariate log-rank analysis**

Clinical Variable	Median survival time (IQR; months)	P-value
Sorafenib-related diarrhoea (n = 572)		
Yes	9.7 (5.37–20.0)	0.004
No	6.7 (3.40–16.30)	
Sorafenib-related hypertension (n = 489)		
Yes	20.3 (8.47–46.10)	<0.0001
No	7.0 (3.30–15.68)	
Sorafenib-related hand-foot syndrome (n = 571)		
Yes	12.7 (6.60–23.20)	<0.0001
No	6.4 (2.90–15.10)	
Sorafenib-related rash* (n = 571)		
Yes	9.8 (6.20–20.00)	0.892
No	8.1 (3.80–18.63)	
Sorafenib-related mucositis (n = 571)		
Yes	9.6 (6.30–29.57)	0.861
No	11.6 (4.47–25.07)	
BCLC stage (n = 634)		
A	17.4 (7.40–40.70)	<0.0001
B	9.7 (4.50–20.00)	
C	6.8 (3.10–15.00)	
CTP class (n = 622)		
A	8.9 (4.10–19.50)	0.034
B	6.8 (2.83–16.70)	
Age when commenced sorafenib (years)		
<50	5.4 (2.60–9.00)	<0.0001
50–59	7.5 (3.40–13.40)	
60–69	8.3 (3.70–20.50)	
70–79	9.3 (4.43–20.20)	
≥80	15.5 (5.33–26.93)	
Hepatitis B (n = 486)		
Yes	6.4 (2.87–15.60)	0.100
No	8.9 (4.20–19.37)	
Hepatitis C (n = 615)		
Yes	9.3 (4.70–21.20)	0.010
No	7.5 (3.43–16.67)	
Alcohol (n = 447)		
Yes	6.9 (3.00–12.20)	0.051
No	7.5 (4.11–16.70)	
BCLC, Barcelona Clinic Liver Cancer stage; CTP, Child–Turcotte–Pugh class.		
* Rash excluding hand-foot syndrome.		

between study centre and survival ( $P = 0.001$ ), reflecting the proportion of patients with advanced-stage HCC at each centre. To ensure that study centre was not a confounder for the apparent relationship between sorafenib-mediated toxicity and survival, we adjusted our proportional hazards model for study centre. The addition of study centre did not alter the significant association between sorafenib-mediated hand-foot-syndrome, hypertension or diarrhoea and survival (Table S4), suggesting despite significant clinical differences between the HCC patient cohorts at each study site, centre per se was not a significant confounding factor for survival in our dataset.

#### The association between sorafenib-mediated diarrhoea, HFS, hypertension and survival is independent of dose reductions during treatment

Finally, an important consideration was whether the requirement for dose reductions during treatment was a confounding factor for the apparent association between sorafenib-mediated diarrhoea, hand-foot-syndrome and hypertension and survival. There was no significant difference in survival between those with a sorafenib start dose of 400 mg or less per day (59%) compared with greater than 400 mg per day (41%,  $\chi^2 P = 0.341$ ). There was also no significant difference in sorafenib-mediated toxicity and starting dose ( $\chi^2 P = 0.243$ ). Data describing dose reductions during therapy were only available for 109 patients (25%). However, in a *post hoc* analysis, sorafenib dose reduction was not associated with survival (Log-rank  $P = 0.211$ ) or with development of diarrhoea

**Table 3 | Log-rank univariate association between sorafenib-related toxicity severity and survival in patients with HCC treated with sorafenib**

Clinical variable	HR	95% CI	P-value
Sorafenib-related diarrhoea grade ( <i>n</i> = 572)			
1	0.496	0.390–0.630	<0.0001
2	0.813	0.581–1.139	0.229
3	0.351	0.180–0.686	0.002
4	0.594	0.338–1.045	0.071
Sorafenib-related hypertension grade ( <i>n</i> = 489)			
1	0.299	0.195–0.458	<0.0001
2	0.396	0.238–0.660	<0.0001
3	0.119	0.030–0.481	0.003
Sorafenib-related hand-foot syndrome grade ( <i>n</i> = 571)			
1	0.461	0.353–0.601	<0.0001
2	0.487	0.349–0.678	<0.0001
3	0.335	0.229–0.491	<0.0001
4	1.528	0.214–10.929	0.673

( $\chi^2 P = 0.122$ ) or hypertension ( $\chi^2 P = 0.698$ ). Although limited by incomplete data and small sample size, these data suggest that dose reduction was not a significant confounding factor for the association between diarrhoea, hand-foot-syndrome and hypertension and survival in patients with HCC treated with sorafenib in this study.

## DISCUSSION

Targeted therapies have significantly re-shaped cancer care over the last three decades. The possibility of targeting specific oncogenic molecular traits with orally available, nonmyelosuppressive small molecule inhibitors has significantly broadened the therapeutic armamentarium available for a wide range of solid tumours including HCC.<sup>2</sup> Conventionally, the early-phase clinical development of TKIs has followed that of cytotoxic chemotherapy, in that dose escalation occurs until maximum tolerated dose (MTD) is attained. However, there is increasing evidence that for targeted agents, target modulation does not linearly reflect MTD, making the identification of an optimal biologically active dose in relationship with treatment-induced toxicity a contentious point in early-phase trials.<sup>22</sup>

This study is the largest study to our knowledge to address the prognostic utility of sorafenib toxicity for survival in advanced-stage HCC. In this multi-institutional cohort study, which includes patients of diverse ethnicity and liver disease aetiologies, we demonstrated that the development of sorafenib-related adverse events is associated with a significant survival advantage. Moreover, survival of patients with advanced HCC receiving sorafenib is specifically predicted by development of diarrhoea, HFS and hypertension, but not other sorafenib toxicities. Importantly, when patients were stratified

by well-recognised prognostic factors in HCC,<sup>23, 24</sup> namely CTP class (A vs. B), BCLC class (A, B and C) and age, the significant association between sorafenib-induced diarrhoea, HFS and hypertension and survival remained, with minimal change in hazard ratio, strongly suggesting the absence of confounding or effect modification. These data therefore demonstrate that both sorafenib-mediated diarrhoea, HFS and hypertension are independently associated with survival, across CTP class and HCC BCLC disease stages.

Various groups have previously reported the association between survival and sorafenib toxicity,<sup>5–15</sup> corroborating the evidence from our study that suggests on-target effects of sorafenib may prove useful prognostic biomarkers. Importantly, this association with prolonged survival appears independent of CTP class, age and tumour stage, suggesting broad utility of sorafenib-mediated diarrhoea and hypertension as potential prognostic markers in all patients receiving sorafenib therapy for advanced-stage HCC. This finding was also independent of sorafenib dose reduction during treatment; however, this *post hoc* analysis was only performed in a limited subset of 109 patients.

In this study, the majority of patients experienced at least one grade 1 sorafenib-associated side effect, while cessation due to grade 3 or 4 toxicity was 20%. Our data concur with the original SHARP trial, where over 80% experienced at least one adverse event while on sorafenib therapy compared to 52% in the placebo group and temporary cessation rates due to toxicity were in the order of 38% and permanent cessation rates 11%.<sup>2</sup> In a further Asian study, the cessation rate due to sorafenib toxicity was 19.5%.<sup>4</sup> The mixed Asian and Caucasian sample in this study likely explains why the sorafenib cessation rate due to adverse effects in this study lies between that reported in these two pivotal randomised controlled trials.<sup>25</sup>

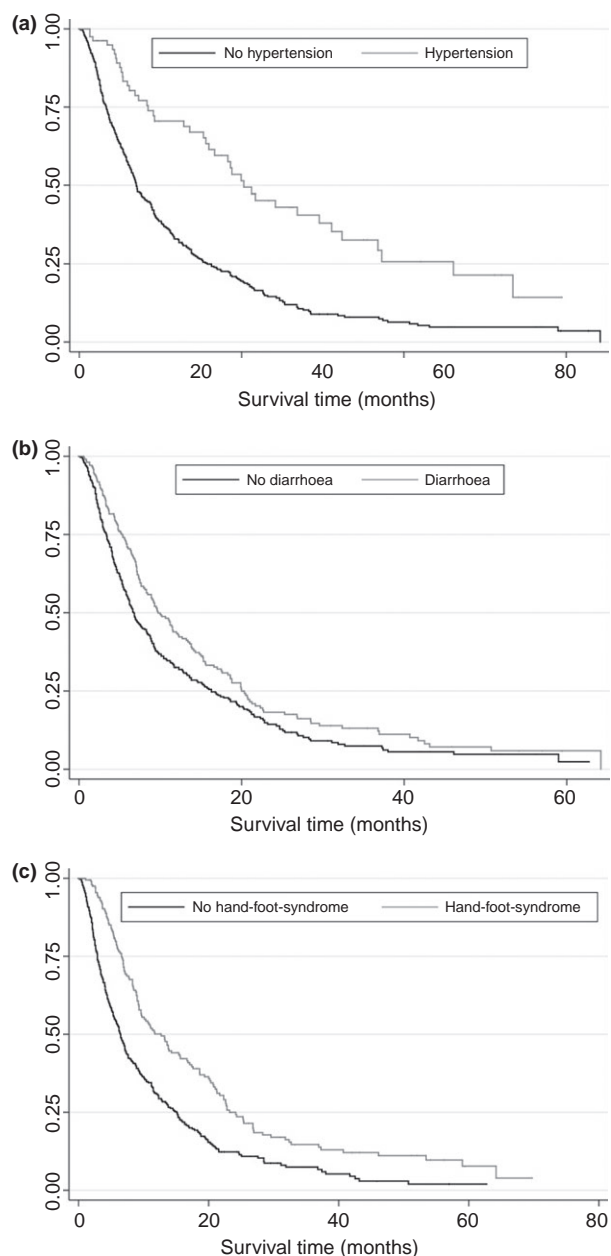
We demonstrated that sorafenib-mediated hypertension was significantly associated with prolonged survival, a finding that has been previously shown by others.<sup>9</sup>

The mechanisms underlying the efficacy of sorafenib, a multi-targeted inhibitor of Raf, Platelet-derived growth factor-receptor (PDGF-R) and Vascular-endothelial growth factor-receptor (VEGF-R), are poorly understood in HCC.<sup>25</sup> Evidence suggests that the anti-tumour-effects at least in part relate to its anti-angiogenic properties.<sup>26</sup>

Arterial hypertension is a well-known class-effect of anti-angiogenics and consolidated evidence from the clinical use of bevacizumab, sunitinib, axitinib and sorafenib suggests that this adverse event might be the surrogate marker of an effective obliteration of tumour

**Table 4 |** Clinical variables associated with survival in patients with advanced HCC on sorafenib: Cox proportional hazards multivariable analysis ( $n = 464$ )

Clinical Variable	HR	95% CI	P-value
Sorafenib-related hypertension	0.500	0.353–0.708	<0.0001
Sorafenib-related diarrhoea	0.776	0.623–0.967	0.024
Sorafenib-related hand-foot-syndrome	0.667	0.531–0.837	<0.0001
BCLC stage	1.266	1.098–1.461	0.001
Age when started sorafenib	0.986	0.977–0.996	0.006
BCLC, Barcelona Clinic Liver Cancer stage.			



**Figure 3** | (a) Comparison of Kaplan–Meier survival time (months) between HCC patients who developed sorafenib-related hypertension compared with HCC patients who did not develop sorafenib-related hypertension [hypertension median survival time 20.3 months (IQR 8.5–46.1), no hypertension 7.0 months (IQR 3.3–15.7), Log-rank  $P < 0.0001$ ,  $n = 489$ ]. (b) Comparison of Kaplan–Meier survival time (months) between HCC patients who developed sorafenib-related diarrhoea compared with HCC patients who did not develop sorafenib-related diarrhoea [diarrhoea median survival time 9.7 months (IQR 5.4–20.0), no diarrhoea 6.7 months (IQR 3.4–16.3), Log-rank  $P = 0.004$ ;  $n = 572$ ]. (c) Comparison of Kaplan–Meier survival time (months) between HCC patients who developed sorafenib-related hand-foot syndrome compared with HCC patients who did not develop sorafenib-related hand-foot-syndrome [hand-foot-syndrome median survival time 12.7 months (IQR 6.6–23.2); no hand-foot-syndrome 6.4 months (IQR 2.9–15.1), Log-rank  $P < 0.0001$ ;  $n = 571$ ].

neovasculation, therefore, substantiating the prognostic value of this adverse event.

Diarrhoea is also a well-described toxicity of sorafenib therapy<sup>27</sup> and several studies including this study have demonstrated an association between diarrhoea and survival.<sup>9, 13, 16</sup> Bettinger *et al.*<sup>13</sup> reported survival was twice as long in patients who developed diarrhoea on sorafenib compared to those who did not (7.1 months vs. 14.1 months). Diarrhoea may therefore represent a marker of on-target drug concentration and efficacy. An alternative potential hypothesis regarding the association between the onset of diarrhoea and sorafenib outcome, may relate to the impact sorafenib has on the gut microbiome. The gut microbiome and the role of bacterial translocation in portal

hypertension and advanced liver disease are well established, contributing to liver decompensation, encephalopathy and spontaneous bacterial peritonitis (SBP) and directly impacting survival.<sup>28–32</sup> Innate immune stimulation via toll-like receptors TLR2 and TLR4 by translocated bacterial products, such as lipopolysaccharide, is well described in liver disease and contributes to inflammatory-mediated liver damage and decompensation.<sup>33</sup> Therapeutic strategies to reduce bacterial translocation include the use of lactulose as both aperient and modulator of nitrogenous bacterial load, as well as antibiotics such as norfloxacin and rifaximin to directly alter the gut microbiome in advanced liver disease.<sup>31, 34, 35</sup> Sorafenib-induced diarrhoea may lead to alterations in gut flora or reduction in the load of nitrogenous commensal bacteria, therefore reducing bacterial translocation and ammonia absorption, akin to the therapeutic effects of lactulose or rifaximin.<sup>33, 36</sup> In turn, this may improve survival by reducing adverse events such as liver decompensation and SBP. However, there is currently no evidence to substantiate this theory and further studies are needed to elucidate the mechanism of the association between sorafenib-mediated diarrhoea and survival.

Several groups have shown hand-foot-syndrome to be associated with survival in sorafenib treatment of advanced HCC.<sup>16</sup> Reig *et al.* demonstrated in a large, well-designed cohort study that skin toxicities requiring dose reduction were associated with prolonged survival in a cohort of 147 HCC patients treated with sorafenib.<sup>5</sup> Cho *et al.* demonstrated skin toxicity was associated with



prolonged survival in a study of 99 predominantly hepatitis B infected patients with BCLC stage C disease.<sup>16</sup> Di Constanzi *et al.*<sup>9</sup> reported that hand-foot-syndrome, hypertension and diarrhoea were all independently associated with prolonged survival in patients receiving sorafenib in a cohort of 226 patients, along with AFP level and radiological response to sorafenib. The authors went on to validate sorafenib toxicities as prognostic markers in a validation cohort of 57 patients. In a further study by Shin *et al.*<sup>15</sup> ( $n = 99$ ), hand-foot-syndrome was found to be associated with survival, but not hypertension. However, several of these studies are limited by their retrospective nature<sup>9, 15, 16</sup> and generally studies have been performed in relatively homogenous cohorts of patients with respect to aetiology of liver disease and ethnicity,<sup>5, 9, 15</sup> with two of the studies performed in Asian cohorts of patients with viral hepatitis. In this study, we also demonstrated a significant association between developing HFS and survival in advanced-stage HCC.

Iavarone *et al.*<sup>8</sup> also demonstrated in a prospective study of 260 patients that cessation of sorafenib due to toxicity compared with ceasing sorafenib for other reasons was associated with prolonged post-sorafenib treatment survival. Though these data support our finding that sorafenib toxicity is associated with survival, unlike Iavarone and colleagues,<sup>8</sup> we did not demonstrate a significantly longer survival time in patients who ceased sorafenib due to toxicity compared with those who ceased sorafenib for other reasons such as disease progression in our large prospective cohort. However, this was not a primary endpoint in our study, which focussed on the association between sorafenib toxicity and survival; therefore, there may have been reduced power to discern a difference in survival between those who ceased sorafenib due to toxicities compared with other reasons in our study. The difference in findings may also be explained by differences in the underlying patient cohort. In the Iavarone study, patients generally had more advanced HCC disease (41% macrovascular invasion compared with 33% in this study), and more advanced liver disease (42% CTP class B compared with 25% in this study). In addition, Iavarone *et al.* classified all patients who ceased sorafenib due to progressive disease and toxicities as ceasing due to progressive disease only, whereas in our study these categories were not mutually exclusive, therefore, some patients who ceased treatment due to side effects may also have had progressive disease in our study.

There are limitations to our study. Data for sorafenib toxicities were incomplete for some participants due to differences in side effect recording practices between the

three centres, particularly for hypertension. While the study cohort was followed prospectively and all data recorded prospectively, data on sorafenib-mediated toxicities were not systematically collected at all centres throughout the study period as this was not a primary objective of the original cohort study design. We did not impute data and did not seek to retrieve missing data retrospectively to reduce observer bias and this limited the number of patients who provided data for the multi-variable analysis, potentially reducing study power to detect associations between sorafenib toxicities and survival. Selection bias may also have been introduced due to systematic differences in patients for whom sorafenib toxicity data were recorded and those who did not have these data recorded. However, we demonstrated that the only significant clinical differences between patients with complete toxicity data and those without was female preponderance and CTP B disease (Table S2). As gender was not associated with survival in our dataset and CTP class was accounted for in the analysis, it is unlikely that these differences resulted in significant bias of the results. Moreover, HCC management was similar in all centres of the study in accordance with international guidelines and recruitment site was not significantly associated with either side effect reporting or with survival (Tables S3 and S4). Finally, adjusting our survival model for treatment centre did not appreciably change the strength of association between sorafenib-related toxicities and survival (Table S4), suggesting centre-related factors were not significant confounding factors in this study.

A further potential confounder for the relationship between sorafenib-mediated toxicity and survival is duration of sorafenib treatment, as longer duration would reasonably be associated with a higher probability of developing toxicity and also surviving longer to remain on sorafenib. In our study, we sought to minimise this effect by only including toxicities that developed within 6 weeks of commencing sorafenib therapy, particularly as adjusting the model for duration of sorafenib is problematic due to strong collinearity between duration of sorafenib and survival. Another limitation was that dose reduction data were only available for 25% of the study cohort and no data were available for temporary dose alterations during treatment. However, *post hoc* analysis of these limited data coupled with the lack of association between sorafenib dose, sorafenib-related toxicities and survival do not support a confounding or effect modifying role of sorafenib dose on the relationship between sorafenib toxicity and survival. Finally, we did not demonstrate a relationship between grade of toxicity and OS. This may reflect the

relatively small numbers of patients per strata available for analysis when OS was stratified by toxicity grade. However, our data are also consistent with published data from the use of TKIs in other malignancies, suggesting that in this drug class it is the presence of toxicity rather than the grade that is prognostic.<sup>37</sup>

In this large, retrospective analysis of prospectively collected sample data, the data demonstrate a clear relationship between the development of diarrhoea, HFS and hypertension and survival in a large cohort of patients receiving sorafenib for advanced HCC, spanning various aetiologies, ethnicities and disease severities. Moreover, hypertension, change in stool frequency and/or consistency and HFS can be reliably determined in the clinic. These data suggest development of these toxicities may have broad applicability as potentially useful prognostic markers across a wide spectrum of HCC patients treated with sorafenib.

## CONCLUSION

The development of sorafenib-related toxicity is associated with prolonged survival in patients with advanced HCC receiving sorafenib therapy. Specifically, development of diarrhoea, hand-foot-syndrome and hypertension are independently associated with prolonged survival, independent of age, underlying liver disease severity or stage of HCC. Development of diarrhoea, hand-foot-syndrome and/or hypertension whilst on sorafenib may therefore prove to be a potentially useful prognostic biomarker in HCC and further validation studies are urgently warranted.

## SUPPORTING INFORMATION

Additional Supporting Information may be found in the online version of this article:

**Table S1.** Distribution of clinical variables within the study cohort ( $n = 634$ ).

**Table S2.** Differences in clinical factors between patients for whom complete sorafenib-related toxicity data were available and those without complete data available (univariate analysis).

**Table S3.** Clinical differences in the HCC patient cohort at each participating centre (univariate analysis).

**Table S4.** Multivariable model for survival in-patients on sorafenib, adjusted for study centre.

**Table S5.** Multivariable Cox proportional hazards model for survival in patients on sorafenib, adjusted for hepatitis C ( $n = 464$ ).

## AUTHORSHIP

*Guarantor of the article:* A/Prof Rohini Sharma.

*Author contributions:* JH lead the study, performed all analyses and wrote the manuscript. DJP also lead the study and wrote the manuscript. RR, DB, TA, CF, CY, AG, MB, GG, LS, JB, MP, MK, RT and JWP all provided data and clinical input into the study and manuscript. RS conceived the study design, supervised the study, provided data and clinical input and provided mentorship for the study. All authors have reviewed and approved a final version of the manuscript.

## ACKNOWLEDGEMENTS

*Declaration of personal interests:* The authors have no disclosures relevant to this study.

*Declaration of funding interests:* JH was supported by a National Medical Research Council of Australia Early Career Fellowship. DJP was supported by the National Institute of Health Research (NIHR). DB was supported by the Berta-Ottenstein-Programme, Faculty of Medicine, University of Freiburg. This project was funded in part by the Academy of Medical Sciences (AMS, Grant ID SGL013/1021 awarded to DJP).

## LINKED CONTENT

This article is linked to Clare et al and Sharma papers. To view these articles visit <https://doi.org/10.1111/apt.14033> and <https://doi.org/10.1111/apt.14067>.

## REFERENCES

1. Ferlay J, Soerjomataram I, Dikshit R, et al. Cancer incidence and mortality worldwide: sources, methods and major patterns in GLOBOCAN 2012. *Int J Cancer* 2015; **136**: E359–86.
2. Llovet JM, Ricci S, Mazzaferro V, et al. Sorafenib in advanced hepatocellular carcinoma. *N Engl J Med* 2008; **359**: 378–90.
3. Abou-Alfa GK, Schwartz L, Ricci S, et al. Phase II study of sorafenib in patients with advanced hepatocellular carcinoma. *J Clin Oncol* 2006; **24**: 4293–300.
4. Cheng AL, Kang YK, Chen Z, et al. Efficacy and safety of sorafenib in patients in the Asia-Pacific region with advanced hepatocellular carcinoma: a phase III randomised, double-blind, placebo-controlled trial. *Lancet Oncol* 2009; **10**: 25–34.
5. Reig M, Torres F, Rodriguez-Lope C, et al. Early dermatologic adverse events predict better outcome in HCC patients treated with sorafenib. *J Hepatol* 2014; **61**: 318–24.
6. Otsuka T, Eguchi Y, Kawazoe S, et al. Skin toxicities and survival in advanced hepatocellular carcinoma patients

- treated with sorafenib. *Hepatol Res* 2012; **42**: 879–86.
7. Kim HY, Park JW, Joo J, *et al.* Worse outcome of sorafenib therapy associated with ascites and Child-Pugh score in advanced hepatocellular carcinoma. *J Gastroenterol Hepatol* 2013; **28**: 1756–61.
8. Iavarone M, Cabibbo G, Biolato M, *et al.* Predictors of survival of patients with advanced hepatocellular carcinoma who permanently discontinued sorafenib. *Hepatology* 2015; **62**: 784–91.
9. Di Costanzo GG, de Stefano G, Tortora R, *et al.* Sorafenib off-target effects predict outcomes in patients treated for hepatocellular carcinoma. *Future Oncol* 2015; **11**: 943–51.
10. Ogasawara S, Chiba T, Ooka Y, *et al.* Sorafenib treatment in Child-Pugh A and B patients with advanced hepatocellular carcinoma: safety, efficacy and prognostic factors. *Invest New Drugs* 2015; **33**: 729–39.
11. Personeni N, Bozzarelli S, Pressiani T, *et al.* Usefulness of alpha-fetoprotein response in patients treated with sorafenib for advanced hepatocellular carcinoma. *J Hepatol* 2012; **57**: 101–7.
12. Vincenzi B, Santini D, Russo A, *et al.* Early skin toxicity as a predictive factor for tumor control in hepatocellular carcinoma patients treated with sorafenib. *Oncologist* 2010; **15**: 85–92.
13. Bettinger D, Schultheiss M, Knuppel E, Thimme R, Blum HE, Spangenberg HC. Diarrhea predicts a positive response to sorafenib in patients with advanced hepatocellular carcinoma. *Hepatology* 2012; **56**: 789–90.
14. Song T, Zhang W, Wu Q, Kong D, Ma W. A single center experience of sorafenib in advanced hepatocellular carcinoma patients: evaluation of prognostic factors. *Eur J Gastroenterol Hepatol* 2011; **23**: 1233–8.
15. Shin SY, Lee YJ. Correlation of skin toxicity and hypertension with clinical benefit in advanced hepatocellular carcinoma patients treated with sorafenib. *Int J Clin Pharmacol Ther* 2013; **51**: 837–46.
16. Cho JY, Paik YH, Lim HY, *et al.* Clinical parameters predictive of outcomes in sorafenib-treated patients with advanced hepatocellular carcinoma. *Liver Int* 2013; **33**: 950–7.
17. Rudmann DG. On-target and off-target-based toxicologic effects. *Toxicol Pathol* 2013; **41**: 310–4.
18. Shah DR, Shah RR, Morganroth J. Tyrosine kinase inhibitors: their on-target toxicities as potential indicators of efficacy. *Drug Saf* 2013; **36**: 413–26.
19. EASL-EORTC Clinical Practice Guidelines management of hepatocellular carcinoma. *J Hepatol* 2012; **56**: 908–43.
20. Lencioni R, Llovet JM. Modified RECIST (mRECIST) assessment for hepatocellular carcinoma. *Semin Liver Dis* 2010; **30**: 52–60.
21. Llovet JM, Burroughs A, Bruix J. Hepatocellular carcinoma. *Lancet* 2003; **362**: 1907–17.
22. Villanueva A, Hernandez-Gea V, Llovet JM. Medical therapies for hepatocellular carcinoma: a critical view of the evidence. *Nat Rev Gastroenterol Hepatol* 2013; **10**: 34–42.
23. Pinter M, Sieghart W, Huckle F, *et al.* Prognostic factors in patients with advanced hepatocellular carcinoma treated with sorafenib. *Aliment Pharmacol Ther* 2011; **34**: 949–59.
24. Hollebecque A, Cattani S, Romano O, *et al.* Safety and efficacy of sorafenib in hepatocellular carcinoma: the impact of the Child-Pugh score. *Aliment Pharmacol Ther* 2011; **34**: 1193–201.
25. Cabrera R, Nelson DR. The management of hepatocellular carcinoma. *Aliment Pharmacol Ther* 2010; **31**: 461–76.
26. Chiang DY, Villanueva A, Hoshida Y, *et al.* Focal gains of VEGFA and molecular classification of hepatocellular carcinoma. *Cancer Res* 2008; **68**: 6779–88.
27. Sohn W, Paik YH, Cho JY, *et al.* Sorafenib therapy for hepatocellular carcinoma with extrahepatic spread: treatment outcome and prognostic factors. *J Hepatol* 2015; **62**: 1112–21.
28. Bajaj JS, Heuman DM, Hylemon PB, *et al.* Altered profile of human gut microbiome is associated with cirrhosis and its complications. *J Hepatol* 2014; **60**: 940–7.
29. Wiest R, Lawson M, Geuking M. Pathological bacterial translocation in liver cirrhosis. *J Hepatol* 2014; **60**: 197–209.
30. Chassaing B, Etienne-Mesmin L, Gewirtz AT. Microbiota-liver axis in hepatic disease. *Hepatology* 2014; **59**: 328–39.
31. Macnaughtan J, Jalan R. Clinical and pathophysiological consequences of alterations in the microbiome in cirrhosis. *Am J Gastroenterol* 2015; **110**: 1399–410; quiz 411.
32. Trivedi PJ, Adams DH. Gut – liver Immunity. *J Hepatol* 2015; **64**: 1187–9.
33. Schwabe RF, Seki E, Brenner DA. Toll-like receptor signaling in the liver. *Gastroenterology* 2006; **130**: 1886–900.
34. European Association for the Study of the L. EASL clinical practice guidelines on the management of ascites, spontaneous bacterial peritonitis, and hepatorenal syndrome in cirrhosis. *J Hepatol* 2010; **53**: 397–417.
35. Vilstrup H, Amodio O, Bajaj J, *et al.* Hepatic encephalopathy in chronic liver disease: 2014 Practice Guidelines by the American Association for the Study of Liver Diseases. *Hepatology* 2014; **60**: 715–35.
36. Pal SK, Li SM, Wu X, *et al.* Stool bacteriomic profiling in patients with metastatic renal cell carcinoma receiving vascular endothelial growth factor-tyrosine kinase inhibitors. *Clin Cancer Res* 2015; **21**: 5286–93.
37. Sharma R, Rivory L, Beale P, Ong S, Horvath L, Clarke SJ. A phase II study of fixed-dose capecitabine and assessment of predictors of toxicity in patients with advanced/metastatic colorectal cancer. *Br J Cancer* 2006; **94**: 964–8.

Company and Five Prime Therapeutics; research funding from Roche-Genentech, Merck, and Eli Lilly and Company; and travel, accommodations, or expenses from Eli Lilly and Company. ZAW reports consulting or advisory role fees from Sirtex; speakers' bureau fees from Genentech; and travel, accommodations, or expenses from Genentech. JCB has declared no conflicts of interest.

## References

1. Roviello G, Pacifico C, Polom K et al. Different efficacy of ramucirumab in patients with metastatic gastric and gastroesophageal junction cancer

according ECOG performance status. *Ann Oncol* 2017; doi: <https://doi.org/10.1093/annonc/mdw657>.

2. Yoon HH, Bendell JC, Braith F et al. Ramucirumab combined with FOLFOX as front-line therapy for advanced esophageal, gastroesophageal junction, or gastric adenocarcinoma: a randomized, double-blind, multi-center Phase II trial. *Ann Oncol* 2016; 27: 2196-2203.

doi:10.1093/annonc/mdw688

Published online 14 February 2017

## Reply to the Letter to the editor 'Sorafenib plus hepatic arterial infusion chemotherapy with cisplatin versus Sorafenib for advanced hepatocellular carcinoma: randomized phase II trial' by Fornaro et al.

We thank Dr Fornaro et al. [1] for their interest in our recent article entitled 'Sorafenib plus hepatic arterial infusion chemotherapy with cisplatin versus sorafenib for advanced hepatocellular carcinoma: randomized phase II trial' [2].

As Fornaro et al. have pointed out, our randomized phase II trial contained some imbalances in regard to the baseline patient characteristics between the two treatment arms. The proportions of patients with hepatitis B virus infection, Barcelona Clinic Liver Cancer Group stage C and portal vein tumor thrombosis (PVTT), which are well-known unfavorable prognostic factors of sorafenib [3], were higher in the SorCDDP arm than in the sorafenib arm, and the survival benefit would have become greater if they had been balanced. Despite PVTT having been a dynamic allocation factor, there was an imbalance between the two arms. In this trial, the randomization was conducted by an independent data center using the minimization method with biased-coin assignment, and the planned random assignment ratio was 2:1. Unlike the use of permutation blocks, the resultant allocation ratio was not exactly 2:1 due to random error of the biased-coin (the actual randomization ratio in this trial was 1.6:1). The randomization method on the program and the allocation log at the data center were re-checked, and no problem was detected. Therefore, we, including our trial statistician (TS), concluded that this was within the range of acceptability of randomization errors and believed that our result was valid, because adjustments were made for the stratification factors, including PVTT, in the primary analysis.

Also, Fornaro et al. mention the potential bias introduced by the high proportion of patients administered subsequent locoregional treatments, including HAIC, transarterial chemoembolization or local ablation in the SorCDDP arm. The proportion of patients receiving subsequent locoregional treatments was slightly higher in the SorCDDP arm than in the Sorafenib arm (29 versus 15 patients; 44.6% versus 36.5%). It was speculated that this difference was a result of the more favorable tumor shrinkage effect of SorCDDP, with the consequent smaller tumor burden and improved hepatic function facilitating the use of further locoregional treatments.

Fornaro et al. show a great interest in the efficacy at the liver sites, not including the extrahepatic sites. The response rate at the

liver sites alone was 25.0% in the SorCDDP arm and 7.3% in the Sorafenib arm, with the overall response rates also being similar. The time to progression at the liver sites were also the same as the overall time to progression. Because most of the enrolled patients in this study had intrahepatic-predominant advanced HCC, the presence of extrahepatic metastases did not significantly affect the tumor response rates or time to progression.

Finally, Fornaro et al. suggest that administration of sorafenib before HAIC could lead to better clinical outcomes considering the sensitized and synergistic effect with cisplatin and the antiangiogenic activity of sorafenib [4, 5]. We thank them as we consider this to be insightful advice for future planning of combined SorCDDP treatment.

M. Ikeda<sup>1\*</sup>, S. Shimizu<sup>1</sup>, T. Sato<sup>2</sup>, M. Morimoto<sup>3</sup>, Y. Kojima<sup>4</sup>, Y. Inaba<sup>5</sup>, A. Hagihara<sup>6</sup>, M. Kudo<sup>7</sup>, S. Nakamori<sup>8</sup>, S. Kaneko<sup>9</sup>, R. Sugimoto<sup>10</sup>, T. Tahara<sup>11</sup>, T. Ohmura<sup>12</sup>, K. Yasui<sup>13</sup>, K. Sato<sup>14</sup>, H. Ishii<sup>15</sup>, J. Furuse<sup>16</sup> & T. Okusaka<sup>17</sup>

<sup>1</sup>Department of Hepatobiliary and Pancreatic Oncology, National Cancer Center Hospital East, Kashiwa; <sup>2</sup>Department of Biostatistics, Kyoto University School of Public Health, Kyoto; <sup>3</sup>Department of Hepatobiliary and Pancreatic Medical Oncology, Kanagawa Cancer Center, Yokohama; <sup>4</sup>Department of Gastroenterology, National Center for Global Health and Medicine Center Hospital, Tokyo; <sup>5</sup>Department of Diagnostic and Interventional Radiology, Aichi Cancer Center Hospital, Nagoya; <sup>6</sup>Department of Hepatology, Osaka City University Hospital, Osaka; <sup>7</sup>Department of Gastroenterology and Hepatology, Kinki University School of Medicine, Osaka; <sup>8</sup>Department of Hepatobiliary and Pancreatic Surgery, Osaka National Hospital, Osaka; <sup>9</sup>Department of Gastroenterology, Kanazawa University Hospital, Kanazawa, Ishikawa; <sup>10</sup>Department of Hepato-Biliary-Pancreatology, National Hospital Organization Kyushu Cancer Center, Fukuoka; <sup>11</sup>Department of Gastroenterology, Saiseikai Utsunomiya Hospital, Tochigi; <sup>12</sup>Department of Gastroenterology, Sapporo Kosei General Hospital, Sapporo; <sup>13</sup>Department of Molecular Gastroenterology and Hepatology, Kyoto Prefectural University of Medicine, Kyoto; <sup>14</sup>Institute for Advancement of Clinical and Translational Science, Kyoto University Hospital, Kyoto; <sup>15</sup>Clinical Research Center, Shikoku Cancer Center, Matsuyama; <sup>16</sup>Department of Medical Oncology, Kyorin University, Tokyo; <sup>17</sup>Department of Hepatobiliary and Pancreatic Oncology, National Cancer Center Hospital, Tokyo, Japan

(\*E-mail: [masiked@east.ncc.go.jp](mailto:masiked@east.ncc.go.jp))

## Funding

The National Cancer Center Research and Development Fund (23-A-22).



## Disclosure

MI has received payment for lectures from Bayer Yakuhin and Nippon Kayaku; consulted for Bayer Yakuhin; received research funding from Bayer Yakuhin. SS has received payment for lectures from Nippon Kayaku. YI has received payment for lectures from Bayer Yakuhin and Nippon Kayaku; received research funding from Bayer Yakuhin and Nippon Kayaku. AH has been on the speakers' bureau for Bayer Yakuhin. T. Ohmura has received payment for lectures from Bayer Yakuhin. JF has received payment for lectures from Bayer Yakuhin and Nippon Kayaku; has been on advisory arrangements for Bayer Yakuhin; received research funding from Bayer Yakuhin and Nippon Kayaku. T. Okusaka has received research funding from Bayer Yakuhin; has received payment for lectures from Nippon Kayaku. Others have none to declare for this study.

## References

1. Fornaro L, Vivaldi C, Lorenzoni G et al. Moving beyond sorafenib alone in advanced hepatocellular carcinoma: is hepatic arterial infusion chemotherapy the best option? *Ann Oncol* 2017. doi: 10.1093/annonc/mdw664.
2. Ikeda M, Shimizu S, Sato T et al. Sorafenib plus hepatic arterial infusion chemotherapy with cisplatin versus sorafenib for advanced hepatocellular carcinoma: randomized phase II trial. *Ann Oncol* 2016; 27: 2090–2096.
3. Bruix J, Raoul JL, Sherman M et al. Efficacy and safety of sorafenib in patients with advanced hepatocellular carcinoma: subanalyses of a phase III trial. *J Hepatol* 2012; 57: 821–829.
4. Heim M, Scharifi M, Zisowsky J et al. The Raf kinase inhibitor BAY 43-9006 reduces cellular uptake of platinum compounds and cytotoxicity in human colorectal carcinoma cell lines. *Anticancer Drugs* 2005; 16: 129–136.
5. Wei Y, Shen N, Wang Z et al. Sorafenib sensitizes hepatocellular carcinoma cell to cisplatin via suppression of Wnt/beta-catenin signaling. *Mol Cell Biochem* 2013; 381: 139–144.

doi:10.1093/annonc/mdx013  
Published online 30 January 2017

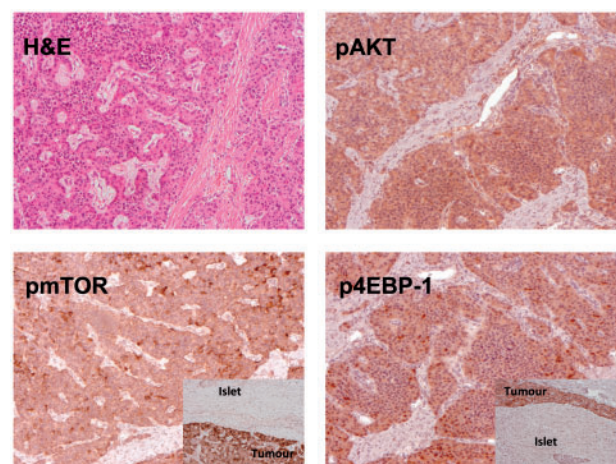
### Successful mTOR inhibitor therapy for a metastatic neuroendocrine tumour in a patient with a germline TSC2 mutation

We here report a 41-year-old patient with tuberous sclerosis and a known germline mutation in the TSC2 gene. During ultrasound tumour screening done for unexplained varicella reactivation a tumour of the left kidney and a lesion in the pancreatic tail were discovered. Pathologic examination of the surgically removed tumours revealed an angiomyolipoma of the left kidney and a well-differentiated neuroendocrine tumour of the pancreas (pT2N0cM0,V0L0) with a proliferative index of 5% (G2). According to guidelines no adjuvant therapy was given and the patient was entered into our 6-monthly follow-up scheme. 12 months after the successful removal of the primary tumour the patient developed four new small lesions in the liver with a MRI-morphology coherent with neuroendocrine tumour metastasis.

The development of pancreatic neuroendocrine tumours in patients with tuberous sclerosis is a rare event with <20 reports in the literature [1]. Therefore, no experience with regard to treatment is available. It is well known, that TSC2 is a negative upstream regulator of the mTOR pathway resulting in an uncontrolled mTOR activation in patients carrying loss of function mutations in TSC1 or TSC2 genes. Indeed, immunohistochemistry of the primary tumour confirmed strong activation of the Akt/mTOR pathway in our patient (Figure 1). Given the positive data on the use of everolimus for benign tumours in patients with tuberous sclerosis we considered starting everolimus as a first line therapy in our patient [2]. On the first treatment control scan done after 3 months we already observed a partial remission of liver metastasis and continued treatment. Six months after the initiation of therapy we achieved a 46% reduction of liver tumour burden with two lesions even no longer visible. Treatment was well tolerated except for grade 2 hypophosphatemia requiring long-term phosphate supplementation.

Apart from using PARP inhibitors for tumour therapy in BRCA mutation carriers to enhance DNA-damage response, this is one of

the rare cases of a successful signalling pathway targeting therapy of a malignant tumour in a patient harbouring a germline mutation in the targeted pathway. Data from a large randomized trial of everolimus in pancreatic neuroendocrine tumours (pNETs) describe halt of tumour growth in the majority of patients, whereas partial tumour regression was only observed in 5% of patients [3]. The strong response towards treatment in our patient was unexpected, but points to a driver function of TSC2 mutations in pNETs directly activating the mTOR pathway. It is open to speculation, whether similar mutations might be found in the subgroup of patients responding well to everolimus treatment. Loss of TSC2 expression is correlated with a poor prognosis in pNET patients, but has not been evaluated as a stratifying factor for therapeutic options [4]. Interestingly, increased activation of the mTOR



**Figure 1.** Immunohistochemistry on a paraffin-embedded tumour specimen of the patient's primary pancreatic tumour showing strong activation of Akt, mTOR and the mTOR downstream target 4-EBP1 in the tumour. Activation of mTOR and 4-EBP1 was higher in tumour cells compared to adjacent normal pancreatic islets (small insert images). Immunohistochemistry was performed using antibodies for phospho-Akt<sup>Thr473</sup>, phospho-mTOR<sup>Thr2448</sup> and phospho-4EBP-1<sup>Thr37/46</sup> (all from Cell Signalling, Danvers, MA).



# Immunopathogenesis of pancreatitis

T Watanabe<sup>1,2</sup>, M Kudo<sup>1</sup> and W Strober<sup>2</sup>

The conventional view of the pathogenesis of acute and chronic pancreatitis is that it is due to a genetic- or environment-based abnormality of intracellular acinar trypsinogen activation and thus to the induction of acinar cell injury that, in turn, sets in motion an intra-pancreatic inflammatory process. More recent studies, reviewed here, present strong evidence that while such trypsinogen activation is likely a necessary first step in the inflammatory cascade underlying pancreatitis, sustained pancreatic inflammation is dependent on damage-associated molecular patterns-mediated cytokine activation causing the translocation of commensal (gut) organisms into the circulation and their induction of innate immune responses in acinar cells. Quite unexpectedly, these recent studies reveal that the innate responses involve activation of responses by an innate factor, nucleotide-binding oligomerization domain 1 (NOD1), and that such NOD1 responses have a critical role in the activation/production of nuclear factor-kappa B and type I interferon. In addition, they reveal that chronic inflammation and its accompanying fibrosis are dependent on the generation of IL-33 by injured acinar cells and its downstream induction of T cells producing IL-13. These recent studies thus establish that pancreatitis is quite a unique form of inflammation and one susceptible to newer, more innovative therapy.

## INTRODUCTION

Pancreatitis is a major inflammatory disease of the gastrointestinal tract and one that has so far been resistant to specific treatment.<sup>1–4</sup> It manifests as an acute or chronic disease, each displaying some overlapping and some unique characteristics: the acute form is a new-onset inflammation occurring in a previously uninflamed pancreas that may resolve before causing permanent damage to the pancreas; in contrast, the chronic form is an ongoing pancreatic inflammation in which the underlying inflammation similar to that driving the acute disease is accompanied by processes leading to pancreatic atrophy and fibrosis.<sup>2,5</sup>

Over the past two decades, a great deal has been learned concerning its pathogenesis, particularly the role of inappropriate trypsinogen activation in the initiation of the inflammatory process. This has been well-discussed in several current reviews and therefore will be only summarized here.<sup>6,7</sup> Until recently, however, the relation of pancreatitis to the gut microbiome and to related factors that drive the pathological immunological response has been shrouded in mystery. In this review, we will focus on this aspect of pancreatitis pathogenesis and try to establish the thesis that innate immune responses are an integral part of the pathogenesis of pancreatitis.

## TRYPSINOGEN ACTIVATION AND PANCREATITIS

The most widely held understanding of the pathogenesis of pancreatitis is that it is an inflammation initiated and/or sustained by a disturbance in pancreatic acinar cell control of pancreatic digestive enzymes.<sup>1–4,6–8</sup> To understand how this may be the case it is important to know that digestive enzymes synthesized in pancreatic acinar cells are normally maintained in an inactive form (i.e., as zymogens such as trypsinogen) while in the acinar cells and in the draining ducts and are converted to an active form (such as trypsin) only upon entry into the gut lumen by enterokinase or trypsin itself.<sup>6–9</sup> Thus, factors that cause premature intra-acinar cell activation of the inactive enzymes have the potential of causing auto-digestion of acinar cells and ensuing events that cause sustained pancreatic inflammation. Several mechanisms of such premature and inappropriate activation of normally inactive zymogens have been put forward and include trypsinogen autoactivation, activation of trypsinogen by lysosomal hydrolase cathepsin B (CatB) caused by shifting of trypsinogen into cellular compartments rich in proteases (lysosomes) and imbalances between degrading and activating acinar cell cathepsins. It should also be noted that activation of pancreatic proteases requires the presence of

<sup>1</sup>Department of Gastroenterology and Hepatology, Kindai University Faculty of Medicine, Osaka-Sayama, Osaka, Japan and <sup>2</sup>Mucosal Immunity Section, Laboratory of Host Defenses, National Institute of Allergy and Infectious Diseases, National Institutes of Health, Bethesda, Maryland, USA. Correspondence: T Watanabe or W Strober (tomohiro@med.kindai.ac.jp or wstrober@niaid.nih.gov)

Received 27 July 2016; accepted 6 October 2016; published online 16 November 2016. doi:10.1038/mi.2016.101

increased intracellular calcium concentrations; thus, disturbances in such concentrations could be a contributing cause of pancreatitis.<sup>6–9</sup>

This “enzyme (trypsin) activation-centered” view of the pathogenesis of pancreatitis derives strong support from studies of genetic defects in humans that pre-dispose individuals to the development of pancreatitis.<sup>10</sup> For example, various mutations in the gene encoding cationic trypsinogen, the main form of trypsinogen subject to activation after secretion (the protease serine 1 (*PRSS1*) gene) cause an autosomal dominant susceptibility to acute and chronic pancreatitis because these mutations render the molecule more susceptible to activation or less able to undergo intracellular autolysis.<sup>10</sup> Similarly, mutations in the gene encoding an inhibitor of activated trypsin that is normally present within the acinar cell (the serine protease inhibitor, Kazal type I (*SPINK1*) gene) that renders the inhibitor incapable of inhibition cause an autosomal recessive susceptibility to pancreatitis.<sup>10</sup>

Additional support for the concept that inappropriate trypsinogen activation initiates pancreatitis comes from studies of experimental models of pancreatitis. The most widely studied of such models is the pancreatitis induced in mice by administration of “supra-maximal” amounts of the pancreatic secretagogue, cholecystokinin (CCK) or, more commonly, by administration of the CCK analog, cerulein. The reason why pancreatitis is caused by high doses of CCK/cerulein (and not physiological doses) is somewhat unclear. However, there is evidence that high-dose CCK/cerulein stimulation causes activation of acinar cells via low-affinity CCK receptors rather than high-affinity receptors and this form of activation has the effect of causing intracellular ultra-structural changes that result in inhibition of acinar cell secretion.<sup>8</sup> This, in turn, results in the rapid accumulation of trypsinogen within acinar cells and exposure of accumulated trypsinogen to factors that result in trypsinogen activation.<sup>8</sup> As indicated by the fact that inhibition or deletion of CatB leads to greatly reduced cerulein-induced pancreatitis, one possible trypsinogen activating factor is the co-localization of zymogen granules with an activating CatB.<sup>8</sup>

A challenge to the concept that trypsinogen activation within acinar cells is a key initiating event in cerulein-induced pancreatitis (i.e., in pancreatitis in general) comes from recent studies showing that mice in whom there is deletion in T7 isoform of trypsinogen (the form of trypsinogen equivalent to “cationic trypsinogen” that has been implicated in acinar cell destruction and pancreatitis in humans) exhibit absence of trypsinogen or chymotrypsin activation and a 50% reduction in acinar cell necrosis following initiation of cerulein-induced pancreatitis. Nevertheless, these mice exhibited similar levels of pancreatitis and lung inflammation as assessed by neutrophil infiltration and pancreatic histology.<sup>11</sup> Moreover, in additional studies in which mice were given repeated doses of cerulein over many weeks to induce chronic pancreatitis, absence of T7 trypsinogen again had no effect on the development of cerulein-induced chronic pancreatitis.<sup>12</sup> In both the studies of acute and chronic pancreatitis, T7-deletion was associated with lack of cerulein-induced chymotrypsin and elastase generation so that

the effect of T7-deletion was apparently not being compensated by increases in the activation of these zymogens. Finally, whereas both acute and chronic cerulein-induced pancreatitis occurred in mice lacking cationic trypsin, these inflammations were accompanied by the early appearance of nuclear factor-kappa B (NF- $\kappa$ B) in acinar cells. This, in turn, implied that induction of a trypsinogen activation-independent inflammatory response was the paramount initiator of pancreatitis.

The overall conclusion drawn from these findings was that whereas early pancreatic injury and inflammation could conceivably occur as a result of trypsinogen activation, both acute and chronic pancreatitis can and does proceed in the absence of such activation. The weakness of this conclusion lies in the fact that deletion of T7 trypsinogen leaves intact the expression of other forms of trypsinogen that can also undergo autoactivation and thus cause pancreatitis in mice if not in humans.<sup>13</sup> Thus, while *in vitro* acinar cell necrosis resulting from exposure to super-maximal CCKR stimulation was shown to be dependent on T7 trypsinogen, *in vivo* acinar cell necrosis induced by cerulein occurred in the absence of T7 trypsinogen, albeit to a reduced extent, presumably due to activation of other trypsinogen isoforms that occurs *in vivo*.<sup>11</sup> On this basis, these studies of T7 trypsinogen deletion do not negate the idea that experimental pancreatitis is initiated if not sustained by dysregulation of trypsinogen activation; on the contrary, this idea still holds as does the concept that experimental pancreatitis mimics human pancreatitis where evidence that abnormalities of trypsinogen activation is a primary cause of pancreatitis is buttressed by genetic studies.

A second set of findings raising a question concerning the trypsin-centered concept of pancreatitis development comes from a recent study showing that genetically engineered mice in whom one can induce activation of trypsinogen in acinar cells in the absence of cerulein stimulation do in fact develop acute pancreatitis associated with acinar cell apoptosis and necrosis.<sup>14</sup> However, in this case trypsinogen activation did not lead to sustained pancreatitis. These findings thus suggest that whereas intracellular trypsinogen activation is dispensable for the development of cerulein-induced pancreatitis as indicated by the T7-deletion studies above, such activation can nevertheless be an initiating cause of pancreatitis. Thus, while they dispute the T7-deletion studies by showing that inappropriate trypsinogen activation can indeed induce acute pancreatitis, they support the T7-deletion studies by showing that other changes in the acinar cells induced by supra-maximal cerulein-mediated CCKR stimulation are necessary to induce a sustained inflammation.<sup>15</sup>

Of particular interest is the relation of trypsinogen activation to the ingestion of alcohol since excess alcohol consumption is one of the leading causes of pancreatitis in humans.<sup>5</sup> However, it is difficult to induce pancreatitis in experimental animals by administration of alcohol alone and it is thus likely that alcohol is not a primary cause of pancreatitis, but rather a secondary cause that potentiates other pancreatitis inducing factors (at least in rodents).<sup>7</sup> One possibility in this context is the known ability of alcohol (i.e., ethanol) to cause increased viscosity of pancreatic secretions and thus to favor obstruction

to pancreatic outflow, a feature of cerulein-induced pancreatitis. The second possibility is that alcohol consumption causes increased gut permeability and the penetration of bacteria and/or bacterial products into the circulation; as discussed more fully below, this results in increased exposure of acinar cells to gut bacterial components and the activation of the NLRP3 (NOD-like receptor family pyrin domain containing-3) inflammasome due to signaling via toll-like receptor 4 (TLR4).<sup>16</sup> This idea is fully supported by the clinical observation that plasma concentrations of endotoxin are elevated in patients with alcoholic-related diseases.<sup>17</sup> The final and perhaps the most important possibility relates to the capacity of ethanol to enhance CCK activation of NF- $\kappa$ B via phosphorylation of protein kinase C (PKC).<sup>18</sup> This last mechanism suggests that ethanol has a direct role in the stimulation of a key signaling pathway necessary to the induction of pancreatic inflammation.

Cigarette smoking is another risk factor for acute and chronic pancreatitis and one that appears to potentiate the effect of alcohol.<sup>19</sup> The mechanisms underlying this association are poorly understood and likely to be multifactorial, reflecting the fact that cigarette smoke contains many factors that might affect a number of aspects of pancreatic inflammation.

#### AUTOPHAGY AND PANCREATITIS

Autophagy is an essential cellular process through which long-lived proteins and cytoplasmic organelles are degraded and used for recycling.<sup>20</sup> In this process, targeted proteins become entrapped in double-membrane autophagic vacuoles and are then subjected to proteolytic digestion when the autophagic vacuoles are fused with lysosomes.<sup>20</sup> Given the fact that pancreatitis is marked by acinar cells in which proteolytic enzymes normally sequestered in protective granules are released into the cytoplasm it was reasonable to assume that defective autophagic function is an important, even primary, cause of pancreatitis (see reviews by Gukovskaya and Gukovsky).<sup>21,22</sup> The most compelling evidence in support of this concept comes from studies of mice with specific deletions of key autophagy genes such as that of Diakopoulos *et al.* who showed that mice with pancreas-specific autophagy-related 5 (ATG5) deficiency, develop chronic pancreatitis accompanied by acinar cells showing evidence of endoplasmic reticulum stress.<sup>23</sup> Likewise, Antonucci *et al.*,<sup>24</sup> showed that mice with pancreatic epithelial cell loss of ATG7, develop chronic pancreatitis and extensive fibrosis, also associated with endoplasmic reticulum stress. Finally, in related studies it was shown by Li *et al.*<sup>25</sup> that mice deficient in I $\kappa$ B kinase  $\alpha$  (IKK $\alpha$ ) develop spontaneous chronic pancreatitis and display elevated levels of acinar cell trypsinogen due to defective degradation of proteins in autophagic vesicles. These pathological changes as well as the presence of enhanced oxidative and endoplasmic reticulum stress were thought to be due to accumulation of protein aggregates dependent on p62, a protein normally cleared by autophagy, since ablation of p62 partially reversed changes due to IKK $\alpha$  deletion. The mechanism of the effect of IKK $\alpha$  deletion on autophagy was somewhat unclear but since

IKK $\alpha$  binds to ATG16L2, defective function of this autophagy protein may be the cause of the defective autophagy.<sup>23,25</sup>

Since deletion of autophagy genes does not occur in human pancreatitis, or even most forms of murine experimental pancreatitis, one must look elsewhere to implicate an autophagy defect in pancreatic inflammation. This could come from autophagic defects arising from abnormalities affecting fusion of lysosomes with autophagosomes or from inhibition of proteolytic degradation of proteins in fused autophagocytic-lysosomal vacuoles.<sup>21</sup> Relating to the first of these possibilities, Fortunato *et al.*, reported that pancreatitis was accompanied by abnormalities in the function of lysosomal associated membrane protein 2 (LAMP2), a protein necessary for the completion of autophagosome-lysosome fusion. These investigators showed that rats subjected to alcohol and lipopolysaccharide (LPS) exposure display impaired autophagic vacuole-lysosome fusion due to the depletion of LAMP2 in pancreatic acinar cells and thus decreased autophagic protein degradation.<sup>26</sup> These findings are supported by those of Mareninova *et al.* who showed more recently that mice deficient in LAMP2 are subject to the spontaneous pancreatitis marked by impaired autophagy.<sup>27</sup> In addition, they are supported by studies in humans that showed reduced expression of LAMP-2 in pancreatic tissue of patients with pancreatitis.

The second of the above possibilities, namely defective degradation of autophagosomal contents, is also reported to be involved in the development of pancreatitis.<sup>28</sup> Thus, Mareninova *et al.* found that autophagosome size and number were greatly increased in pancreatic acinar cells of rats with pancreatitis induced by cerulein or arginine compared with acinar cells of rats subjected to starvation and, furthermore, this was due to greatly decreased protein degradation as compared with starved cells.<sup>28</sup> In addition, Mareninova *et al.* found that cathepsin L (CatL) activity, an enzyme that inhibits trypsin activity by degrading both trypsinogen and trypsin, is impaired in mice with pancreatitis whereas cathepsin B (CatB), an enzyme that converts trypsinogen to trypsin is less impaired. Thus, an imbalance between CatL activity and CatB activity was suggested to be one of the mechanisms by which impaired autophagy contributes to pancreatitis.

Despite these various studies of abnormal autophagy in pancreatitis it remains unclear that this process has a primary role in this form of inflammation. The fact that genetic defects of autophagy components caused by gene deletion can lead to pancreatitis in itself may simply reflect that fact that normal pancreatic cell generation of trypsin requires efficient clearance of non-secreted active enzyme by an autophagic mechanism and pancreatitis ensues in the absence of this mechanism. Alternatively, defects in autophagy may be a secondary effect of the pancreatitis. This could be a consequence of a pancreatitis-induced effect on cathepsin enzymes or other intracellular factors that may impair autophagic function. In support of this possibility, Mareninova *et al.* have shown that CatB causes cleavage of LAMP<sup>27</sup> and it is thus possible that generation of CatB as a result of a pancreatitis inducer (see discussion above)

has an inhibitory effect of autophagic function. It is important to note, however, that even if an autophagy defect is a secondary consequence of pancreatitis it may have a significant ability to aggravate a primary defect since the need to clear increased trypsin generated by the pathological process becomes more critical in the face of a primary defect.

### NECROPTOSIS AND PANCREATITIS

A major feature of pancreatitis, pancreatic acinar cell death, can conceivably occur as a result of apoptosis or necroptosis (programed necrosis). To some extent which of these death processes is operative may be species-dependent since in the rat model of cerulein-induced pancreatitis apoptosis is the dominant cell death process, whereas in the corresponding mouse model, necrosis is the dominant process.<sup>29</sup> These unexpected species differences are likely related to the fact that the molecular processes underlying apoptosis and necrosis are different but related. Under pathological conditions apoptosis is most often mediated by tumor necrosis factor- $\alpha$  (TNF- $\alpha$ ) activation of TNF receptor type 1-associated death domain protein (TRADD)/ Fas-associated protein with death domain (FADD) or receptor-interacting protein kinase 1 (RIP1)/RIP3 followed by activation of caspase-8, the actual “executioner” molecule.<sup>30</sup> In some contrast, necroptosis is mediated by TNF- $\alpha$  activation of RIP1/RIP3 followed by RIP3 binding to and activation of MLKL (mixed lineage kinase domain-like), a newly defined executioner molecule.<sup>31</sup> Various stimuli that cause the generation of TNF- $\alpha$  or, alternatively, TLR3 or TLR4 signaling can result in necroptosis, but the circumstances under which this mechanism of cell death occurs rather than apoptosis remains to be clarified. Since caspase-8 inhibits necroptosis, one possibility is that necroptosis occurs when caspase-8 is not generated or is inactivated; alternatively, it is possible that necroptosis occurs when RIP3 is highly activated, since this kinase is uniquely involved in necroptosis. In line with these possibilities, caspases are activated and RIP is cleaved in rat cerulein pancreatitis whereas an endogenous inhibitor of caspases (XIAP) undergoes degradation in this model.<sup>29</sup> In contrast, caspase induction in the mouse cerulein model leads to increased apoptosis and decreased necrosis. Thus, caspase and RIP levels (or state of activation) seem to determine whether acinar cell death in cerulein pancreatitis is predominantly mediated by apoptosis or necrosis.<sup>29</sup>

In more recent studies of acinar cell death in cerulein pancreatitis in mice, it has been shown that mice with deletions of RIP3 or MLKL are highly resistant to cerulein pancreatitis.<sup>32,33</sup> These findings provide further verification that acinar cell death in murine cerulein pancreatitis is mediated by necroptosis rather than by apoptosis. Whether a similar situation obtains in other forms of murine experimental pancreatitis or in human pancreatitis remains to be seen. This is not a trivial question since the form of cell death occurring in pancreatitis could determine a unique approach to the treatment of the disease. It should be noted, however, that both forms of cell death are initiated by TNF- $\alpha$ , indicating that generation of this cytokine during the inflammation can

mediate either apoptosis or necroptosis and in this sense, pancreatitis in different species and in different models may be similar.

Recently it has been shown that necroptosis is also involved in pancreatic oncogenesis in that expression of RIP1 and RIP3 is elevated in human pancreatic ductal adenocarcinoma and inhibition/deletion of these components lead to decreased tumor progression.<sup>34</sup> This may relate to the fact that RIP1/RIP3-induced necroptosis induces CXCL1 production and SAP130 activation of Mincle, which then leads to the accumulation of myeloid-derived suppressor cells and Mincle-stimulated dendritic cells in the tumor environment that suppress T cells with anti-tumor activity. Whether this complex mechanism influences pancreatitis progression is currently unknown.

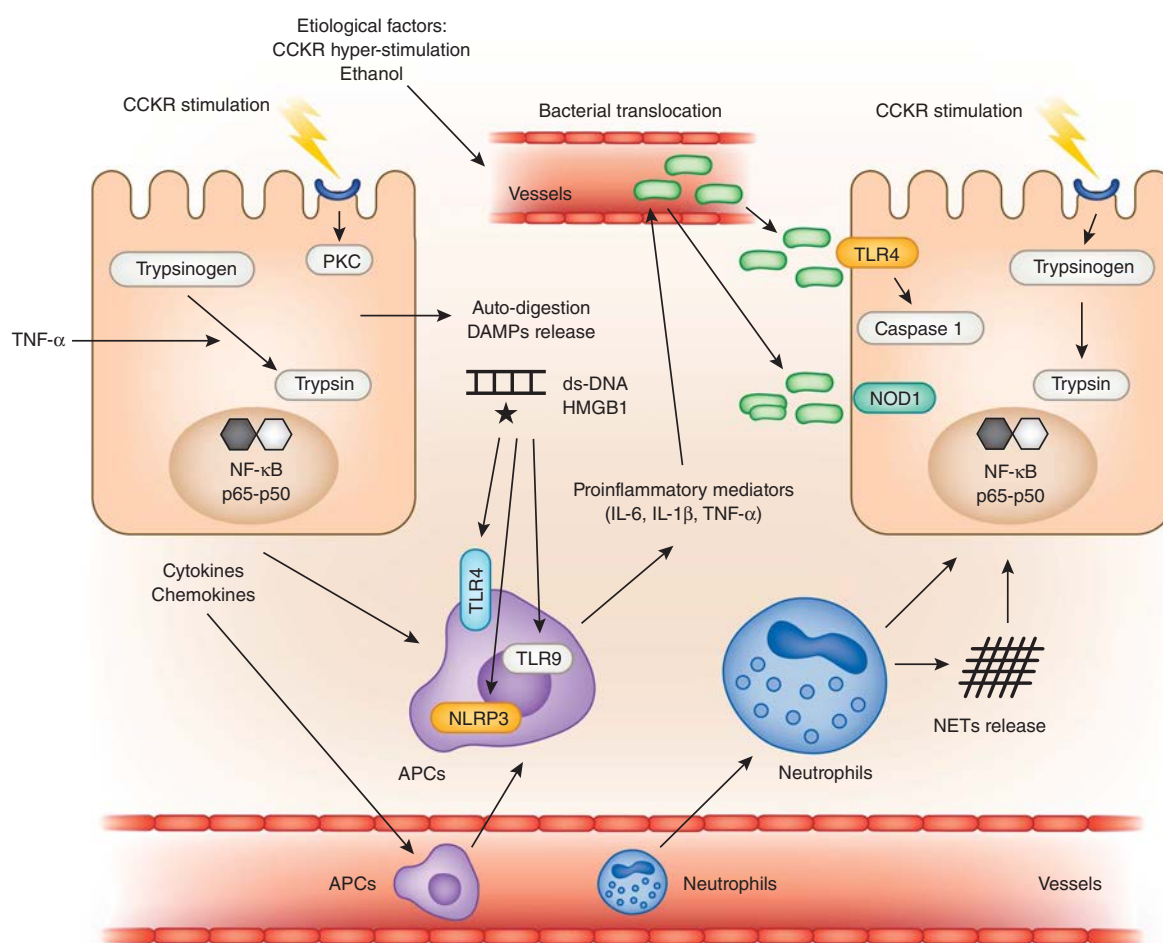
### INITIATION OF INFLAMMATION IN PANCREATITIS BY STIMULATION OF INNATE IMMUNE RESPONSES BY DAMAGE-ASSOCIATED MOLECULAR PATTERNS (DAMPs) AND NEUTROPHIL-EXTRACELLULAR TRAPS (NETs)

Given the fact that the uninflamed pancreas is a sterile organ, the initial cellular injury (as discussed above, most likely triggered by pathological trypsinogen activation) occurs in an aseptic environment (**Figure 1**). Studies of the inflammation nevertheless strongly suggest that it is likely to result from the release of damage-associated molecular patterns (DAMPs) from dying pancreatic acinar cells that then induce inflammation mediated by activation of PRRs (pattern recognition receptors) of the innate immune system.<sup>35</sup> Various kinds of DAMPs, including high-mobility group box protein 1 (HMGB1), self-DNA, nucleosomes (DNA coiled around histone octamers) and adenosine triphosphate have in fact been identified as pancreatitis-associated “danger signals” (i.e., DAMPs) in human and experimental pancreatitis.<sup>36,37</sup> Of these, HMGB1 is of particular interest since Yasuda *et al.*, reported markedly elevated levels of this DAMP in both animals and patients with acute pancreatitis<sup>38,39</sup> and Sawa *et al.*,<sup>40</sup> reported attenuation of experimental pancreatitis is achieved by administration of neutralizing antibodies to HMGB1. It should be noted, however, that intracellular HMGB1 inhibits inflammatory nucleosome release (see discussion below) and may have an inhibitory effect on pancreatitis as an intracellular protein.<sup>37</sup>

Hoque *et al.* have elucidated a possible molecular mechanism mediated by DAMPs-PRR interaction in cerulein-induced pancreatitis. These authors showed that during the early phase of cerulein-induced pancreatitis, self-DNA released from the dying acinar cells activates pancreatic macrophage TLR9, an endosome-linked PRR responsive to bacterial CpG DNA and self-DNA.<sup>35,41,42</sup> In parallel with this event, released adenosine triphosphate induces the activation of P<sub>2</sub>X<sub>7</sub>, a purinergic receptor, which then acts in concert with TLR9 activation to trigger the activation of the NLRP3 inflammasome and the conversion of the pro-IL-1 $\beta$  to mature IL-1 $\beta$ .

Very recently, a DAMP-PRR interaction in pancreatitis involving the AIM2 (absent in melanoma 2) inflammasome has





**Figure 1** Initiating events in the induction of pancreatitis: acinar cell injury and release of DAMPs. This figure depicts the initiating events that result in pancreatitis. A variety of factors, most notably CCKR hyper-stimulation caused in one experimental model by cerulein and perhaps in humans by excessive ethanol ingestion leads via PKC signaling to dysregulation of intracellular acinar proteases and the generation of trypsin from trypsinogen. This causes acinar cell injury and release of DAMPs such as host dsDNA and HMGB1 that then induce APCs in the vicinity of the acinar cells via various TLRs and NLRP3 to produce a mixture of pro-inflammatory cytokines. An important consequence of such release is the induction of changes in intestinal permeability and the translocation of gut commensal microflora into the circulation, where the latter stimulates acinar cells via TLR4 and NOD1. TLR4 signaling leads to the activation of the NLRP3 inflammasome and the production of caspase 1 and IL-1 $\beta$ . NOD1 signaling in cooperation with CCKR signaling results in the activation of NF- $\kappa$ B, TNF- $\alpha$ , and type I IFN factors that sustain the inflammation as shown in **Figure 2**. Another early feature of pancreatitis is the migration of neutrophils into the pancreas, where they enhance trypsinogen activation and cell damage either directly or indirectly via the generation of NETs. APCs, antigen-presenting cells; CCKR, cholecystikinin receptor; DAMPs, damage-associated molecular patterns; dsDNA, double-stranded host DNA; NETs, neutrophil extracellular traps; NF- $\kappa$ B, nuclear factor-kappa B; NLRP3, NOD-like receptor family pyrin domain containing-3; NOD1, nucleotide-binding oligomerization domain 1; PKC, protein kinase C; TLRs, toll-like receptors.

been reported. In this case, the stimulating DAMPs were nucleosomes mentioned above as possible pro-inflammatory DAMPs in pancreatitis. In the relevant studies, Kang *et al.*<sup>43</sup> provided evidence that nucleosome stimulated the AIM2 inflammasome (and IL-1 $\beta$  production) but that such stimulation required dsRNA-activated protein kinase phosphorylation mediated by RAGE (receptor for advanced glycation end products). In addition, they found that both AIM2- and RAGE-deficient mice exhibit reduced L-arginine-induced pancreatitis as well as reduced IL-1 $\beta$  and HMGB1 expression, the latter an inflammasome product, under these circumstances.

Another factor contributing to the initial inflammation of pancreatitis relates to the observation discussed above that stimulation of the innate immune system by DAMPs results in inflammasome activation and the release of IL-1 $\beta$ , the latter a potent neutrophil chemotactic factor via its upregulation of leukocyte adhesion molecules.<sup>44</sup> This observation introduced the possibility that the early neutrophil infiltration characteristic of pancreatitis is both a result and cause of initial pancreatic inflammation.

Initial evidence for the latter possibility came from studies showing that neutrophil infiltration of the pancreas following pancreatitis induction is an early phenomenon and that such



infiltration results in trypsinogen activation.<sup>45,46</sup> Insight into the mechanism of such neutrophil-mediated trypsinogen activation came from subsequent studies showing that taurocholate induction of acute pancreatitis in mice induces formation of extracellular fibrillar and web-like structures, which disappear with treatment with DNase.<sup>47</sup> Such structures were highly reminiscent of neutrophil-extracellular traps (NETs), web-like structures composed of extracellular DNA, chromatin, molecules derived from granules<sup>48,49</sup> and it was thus apparent that neutrophil-derived NETs might be causing trypsinogen activation. Evidence for this possibility has come from the observation that inhibition of NETs formation by the administration of DNase protects mice from pancreatitis induced by taurocholate or L-arginine. Moreover, plasma levels of DNA-histone complexes, i.e., NETs elements, are markedly elevated in patients with acute pancreatitis. Finally, Merza *et al.* have shown that NETs released from neutrophils are potent *in vitro* activators of trypsinogen in acinar cells. Taken together, these results suggest that initial pancreas injury caused by trypsinogen activation induces the migration of neutrophils into the pancreas and this in turn causes further trypsinogen activation via generation of NETs.

The acinar cell death resulting from the release of DAMPs in the early stages of pancreatitis discussed above is a prelude to the translocation of commensal organisms into the circulation and their subsequent stimulation of innate immune responses in acinar cells that sustain the inflammation, as discussed below. An interesting side-light to this phenomenon is the fact that dendritic cells might serve as a break on this phenomenon via their capacity to clear cellular necrotic debris. This is suggested by the fact that depletion of DCs results in intensification of experimental pancreatitis and decreased acinar cell viability.<sup>50</sup>

#### INVOLVEMENT OF MICROBE-ASSOCIATED MOLECULAR PATTERNS (MAMPS) AND PATHOGEN RECOGNITION RECEPTORS (PRRS) IN PANCREATITIS

So far in our discussion of the pathogenesis of pancreatitis we have been concerned mainly with early intra-acinar cell events that are involved in the initiation of inflammation (although these events may be persistent and contribute to ongoing inflammation as well) (**Figure 1**). However, pancreatitis is unique in that the inflammation leads rapidly to changes in the permeability of the bowel wall that allow translocation of intra-luminal bacteria into the circulation and therefore the exposure of acinar cells to pro-inflammatory effects of organisms in the gut microbiome.<sup>51</sup> As we shall see, this may be the major driving force of pancreatic inflammation after its initiation.

The first hint that this is in fact the case came from clinical studies which showed that severe pancreatitis can lead to local and extra-pancreatic complications such as pancreatic necrosis or systemic inflammatory response syndrome or multiple organ dysfunction syndrome,<sup>1,5,51,52</sup> which were shown to be manifestations of pancreatitis largely due to invasion of pancreatic tissue by gut organisms and subsequent dissemination of the latter to distant organs and/or endotoxemia.<sup>51</sup>

Studies of the types of organisms involved were sporadic and incomplete until Li *et al.*<sup>53</sup> conducted a comprehensive study of bacterial invasion in pancreatitis using 16S rRNA-based technology. They found that polymicrobial bacterial DNA can be detected in the circulation of almost 70% of patients with pancreatitis and this percentage increased with increased disease severity. Most of the organisms were similar to those found in the gastrointestinal tract and therefore had probably originated in the bowel lumen; in addition, while in most cases these bacteria consisted of commensal organisms, at least in some instances, organisms considered to be pathogens were also found. It is presumably the latter that account for the more severe complications of bacterial invasion in pancreatitis such as pancreatic necrosis. Although these studies highlight the prevalence of bacterial translocation from the bowel during pancreatitis, they provide no insight into the mechanism of the altered bowel permeability allowing such translocation. Indeed, the mechanism involved is poorly understood although it may involve the release of unique pancreatitis-specific cytokines that affect gut permeability that are not generated in other forms of gut inflammation.

The high rate at which bacteria are found in the circulation of patients with pancreatitis suggest that these bacteria could have a role in disease pathogenesis that transcends their capacity to cause local and systemic infections in a minority of patients. This concept is supported by findings in several animal studies. First, enteric bacteria have been detected in the mesenteric lymph nodes and the translocation of fluorescent beads having the size of bacteria into the pancreas via the peritoneum has been seen upon induction of experimental pancreatitis.<sup>54–56</sup> Second, experimental pancreatitis is in fact accompanied by increased intestinal permeability.<sup>57</sup> Third and finally, bowel sterilization via antibiotic treatment reduces pancreatic inflammation, infection, and mortality in various experimental pancreatitis models.<sup>58–61</sup>

More definitive support for the role of translocated bowel organisms in the pathogenesis of pancreatitis comes from recent studies showing that such translocation is necessary for the development of cerulein-induced pancreatitis. Thus, as shown by Tsuji *et al.*,<sup>58</sup> antibiotic-induced bowel sterilization rendered mice virtually completely resistant to cerulein-induced pancreatitis but such resistance was negated when the bowel sterilization was accompanied by oral administration of a commensal *Escherichia coli* expressing LacZ (ECLACZ) that was resistant to the antibiotics in the bowel sterilization regimen. Thus, colonization of the gut with a commensal organism was both necessary and sufficient for the induction of cerulein pancreatitis.

These studies of the role of the gut microflora in pancreatitis intermesh with studies examining the role of bacteria-associated MAMPs and their capacity to stimulate PRRs such as TLRs and nucleotide-binding domain and leucine-rich repeat-containing receptors (NLRs) in the induction of experimental pancreatic inflammation.<sup>42,62,63</sup> Studies of the role of TLR4, the prototypical PRR that responds to LPS derived from Gram-negative bacteria, was the first PRR to be studied.<sup>42</sup>

It was found that mice deficient in TLR4 are partially protected from acute cerulein-induced pancreatitis<sup>64</sup> and severe lung injury associated with pancreatitis is induced by combined treatment of cerulein and LPS as compared with cerulein alone.<sup>65</sup> As alluded to above, the possible role of TLR4 in causation of pancreatitis has been highlighted in studies of ethanol-induced pancreas injury.<sup>16</sup> The theory is that an ethanol-induced leaky gut syndrome leads to bacterial translocation into the circulation, followed by sensing of LPS by TLR4 expressed in pancreatic acinar cells and activation of the NLRP3 inflammasome. The resulting production of mature IL-1 $\beta$  then aggravates gut permeability changes and contributes to other aspects of pancreatic inflammation. Interestingly, a polymorphism in the *TLR4* gene has been identified as a susceptible factor for acute pancreatitis.<sup>66</sup> This raises the question of whether abnormalities of TLR4 structure or level of expression can enhance TLR4-mediated pro-inflammatory responses leading to pancreatitis in certain individuals.

More impressive studies of the role of a PRR in pancreatitis are those evaluating the role of NOD1 in pancreatitis pathogenesis.<sup>58,67</sup> NOD1 was originally characterized as a cytosolic PRR that detects small peptide components derived from bacterial peptidoglycan associated with gut pathogens.<sup>63</sup> As such, NOD1 was shown to have a protective role in mucosal host defense against various kinds of pathogenic organisms such as *Shigella flexneri*, pathogenic *E. coli*, and *Helicobacter pylori*.<sup>68–71</sup> In later studies, however, it was established that NOD1 is also capable of reacting to peptidoglycan components derived from commensal organisms. This was shown first by the fact that sensing of commensal organisms by NOD1 is required for lymphoid tissue organogenesis.<sup>72</sup> More importantly to the present discussion, it was more recently shown that NOD1 expression on acinar cells and subsequent interactions between NOD1 at this site with commensal organisms is essential to the development of cerulein-induced pancreatitis in that NOD1-deficient mice are almost completely resistant to the induction of this pancreatitis.<sup>58</sup>

The role of bacterial translocation in experimental pancreatitis was further explored in a model of cerulein-induced pancreatitis in which pancreatitis was induced by administration of a low dose of cerulein (that does not itself induce pancreatitis yet is still capable of acinar cell signaling) and FK156, a ligand and activator of NOD1 that also does not itself induce pancreatitis.<sup>58,67</sup> This form of cerulein-induced pancreatitis, termed low-dose cerulein pancreatitis was developed to clearly differentiate the respective roles of NOD1 signaling and CCKR signaling in the pathogenesis of the pancreatitis, as will be discussed in more detail below. Using this model, it could be shown that although IP injection of ECLACZ or low-dose cerulein alone (to mice sterilized by antibiotic treatment) does not cause pancreatitis, administration of both of these factors does cause pancreatitis and that the latter is at least partially dependent on the presence of NOD1. Thus, in this low-dose cerulein model, the NOD1 activation by FK156 is taking the place of translocated bacteria expressing a NOD1

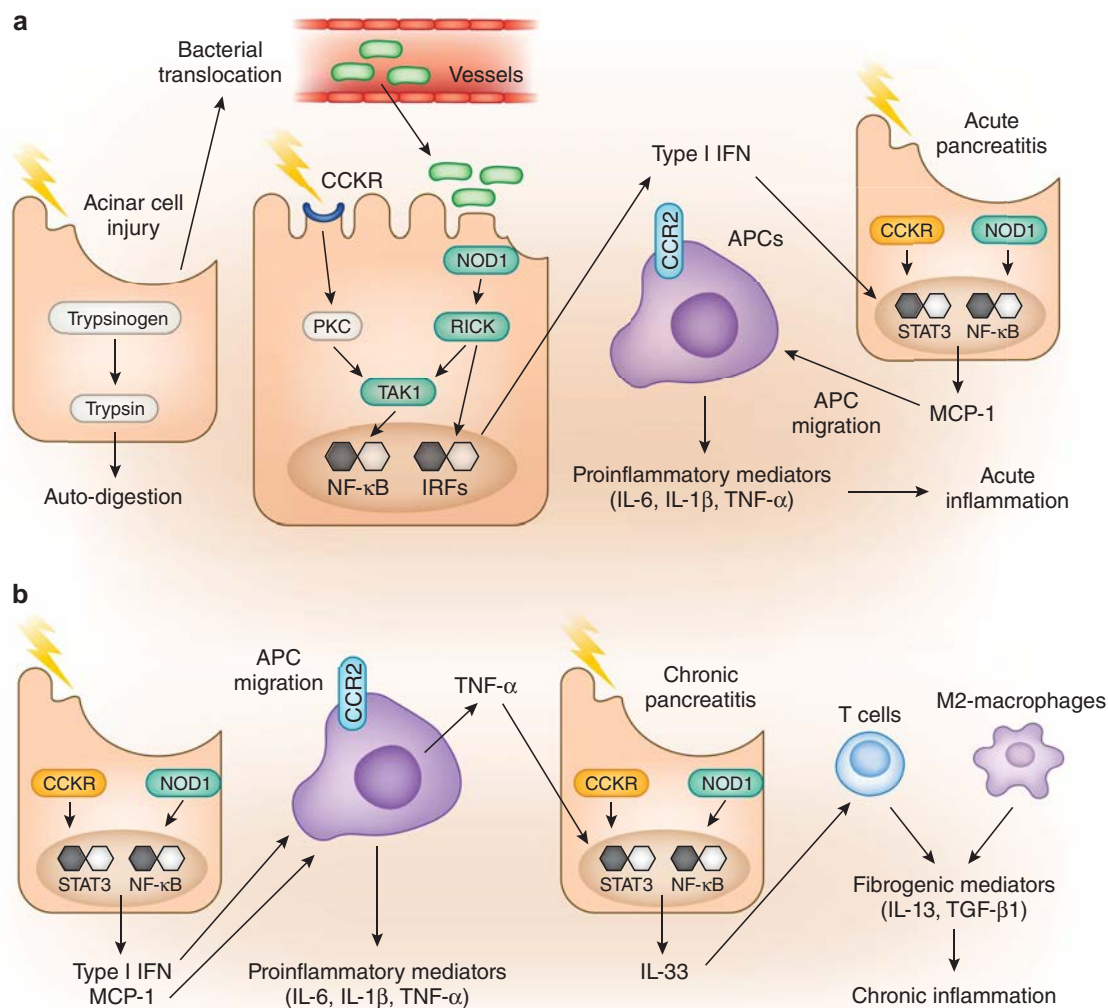
ligand. Finally, in studies addressing bacterial translocation in low-dose cerulein pancreatitis, it could be shown that the level of bacteremia was relatively low in mice treated with low-dose cerulein alone and relatively high in mice treated with both low-dose cerulein and FK156; thus a high level of bacteremia (due to bacterial translocation) requires the initiation of pancreatitis. In further studies addressing the same question, mice with bowel sterilization administered increasing oral doses of ECLACZ and then subjected to low-dose cerulein and FK156 administration exhibited a level of pancreatitis proportional to the ECLACZ dose. This suggested that whereas initiation of low-dose cerulein pancreatitis requires both low-dose cerulein and NOD1 ligand, the pancreatitis is ultimately sustained by the bacterial translocation and *de novo* NOD1 activation caused by the initiated pancreatitis.

Taken together, these results definitively establish that while pancreatic inflammation may be initially triggered by intra-acinar events such as trypsinogen activation, it ultimately depends on subsequent immune responses induced by the activation of components of the innate immune system, notably NOD1.

#### ACTIVATION OF NF- $\kappa$ B IN PANCREATITIS

In the knowledge that innate immune responses at least in part involving NOD1 activation are necessary for induction of cerulein-induced pancreatitis as discussed above and that such activation may lead to NF- $\kappa$ B activation, one might assume that NF- $\kappa$ B activation is a central feature of pancreatic inflammation as it is in the case of other major inflammatory diseases. A host of evidence fully supports this conjecture (**Figure 2**). First, it has been shown that administration of cerulein at doses causing pancreatitis leads to activation of pancreatic NF- $\kappa$ B and that such activation is accompanied by nuclear translocation of p65, p50, and p52 in both gel-shift assays and in immunoblotting studies.<sup>73–76</sup> Second, this activation occurs *pari passu* with the transcription and release of NF- $\kappa$ B pro-inflammatory target genes such as TNF- $\alpha$  and monocyte chemoattractant protein-1 (MCP-1), indicating that NF- $\kappa$ B activation is leading to the synthesis of a host of pro-inflammatory factors that have the potential to drive various aspects of the pancreatic inflammation.<sup>58,77,78</sup> Third, the latter possibility has in fact been established by studies showing that mice deficient in NF- $\kappa$ B/p105, a precursor of p50, are resistant to cerulein-induced pancreatitis as are mice administered low molecular weight-specific inhibitors of NF- $\kappa$ B activation.<sup>79–81</sup> Finally, the development of pancreatitis can be induced in animals treated with intra-pancreatic ductal retrograde infusion of adenovirus-mediated gene delivery of the NF- $\kappa$ B subunit p65.<sup>82</sup>

The relation of NF- $\kappa$ B activation in pancreatitis to aberrant trypsinogen activation has come from studies of an elegant murine model of pancreatitis established by Baumann *et al.*<sup>83</sup> These authors created transgenic mice that regulate the activation of NF- $\kappa$ B by expression of either a dominant negative (DN) or a constitutive active (CA) form of IKK $\beta$  under the control of a tetracycline-responsive elastase promoter. Thus, in this model one of these forms of IKK $\beta$  is overexpressed



**Figure 2** Innate immunological response that sustain pancreatitis and underlie the fibrosis of chronic pancreatitis. This figure depicts the complex series of immunological events that sustain pancreatitis after initial acinar damage and translocation of commensal organisms from the gut into the circulation has occurred, as shown in **Figure 1**. In this figure, five diagrammatic acinar cells are shown, each roughly representing different stages of pancreatitis pathogenesis. **(a)** The first acinar cell (top, on the left) represents the first stage that has been shown in greater detail in **Figure 1**. The top middle and right acinar cells illustrates the fact that signaling via CCKR and NOD1 act in concert to induce activation of NF- $\kappa$ B and IRF and type I IFN expression; these factors then act downstream to induce expression of MCP-1, a chemotactic ligand that draws pro-inflammatory CCR2-bearing macrophages into the pancreas. These macrophages produce a host of pro-inflammatory mediators of the full-blown inflammation; among these are cytokines that support T-cell differentiation into Th1 or Th17 cells. **(b)** The bottom acinar cells represent cells that occur in the pancreas during chronic pancreatitis that have subjected to apoptotic or necrotic cell injury due to secretion of TNF- $\alpha$  by macrophages. This cell injury leads to the generation of IL-33, an alarmin cytokine that acts via the ST2 receptor on T cells to induce fibrogenic mediators, particularly IL-13. The latter may then act on M2-macrophages to induce production of TGF- $\beta$  1 and other downstream fibrogenic factors. This pro-fibrotic program underlies the development of fibrosis that is characteristic of chronic pancreatitis. CCKR, cholecystikinin receptor; CCR2, C-C chemokine receptor type 2; IFN, interferon; IRF, interferon regulatory factor; MCP-1, monocyte chemotactic protein-1; NOD1, nucleotide-binding oligomerization domain 1; NF- $\kappa$ B, nuclear factor-kappa B; TNF, tumor necrosis factor.

exclusively in acinar cells when the mouse is administered tetracycline and this, in turn, leads to either suppressed or activated NF- $\kappa$ B signaling depending on whether DN-IKK $\beta$  and CA-IKK $\beta$  is being overexpressed, respectively.<sup>83</sup> Using these transgenic mice, Baumann *et al.* showed first that expression of CA-IKK $\beta$  in acinar cells leads to spontaneous development of severe pancreatitis, as was the case in the aforementioned studies of intra-ductal adenovirus administration of p65, whereas in contrast, the expression of DN-IKK $\beta$  in acinar cells suppresses cerulein-induced pancreatitis. Furthermore, they showed that overexpression of either

DN-IKK $\beta$  or CA-IKK $\beta$  had no significant effect on cerulein-induced acinar cell trypsinogen activation. Taken together, these studies indicate that NF- $\kappa$ B activation in acinar cells is indispensable for the development of pancreatitis and that CCKR-mediated trypsinogen activation cannot induce pancreatitis in the absence of such activation.

The above studies showing the importance of NF- $\kappa$ B activation in the pathogenesis of pancreatitis do not address the question of whether trypsinogen activation and NF- $\kappa$ B activation are interrelated or independent events. Several reports show that one of the signaling outcomes of CCKR over-

stimulation is the activation of NF- $\kappa$ B via a PKC pathway<sup>84</sup> or a phosphatidylinositol 3-kinase (PI3K) pathway<sup>85</sup> and that pharmacological inhibitors of PKC or PI3K block CCKR induction of NF- $\kappa$ B in pancreatic acinar cells. In addition, blockade of intracellular  $\text{Ca}^{++}$  influx by a chelator also inhibits NF- $\kappa$ B induction owing to the fact that PKC-mediated NF- $\kappa$ B activation in this model requires such influx.<sup>18,73,74,84,86</sup> These findings, however, do not necessarily imply that the other major outcome of CCKR stimulation, trypsinogen activation and trypsin expression, results in NF- $\kappa$ B activation. That it does not was nicely shown by the fact that acinar cell expression of an intracellular mutant trypsinogen subject to conversion to intracellular trypsin by an endogenous protease did not induce NF- $\kappa$ B activation.<sup>87,88</sup> Thus, the conclusion that can be drawn from these various studies is that whereas CCKR over-stimulation does indeed induce both NF- $\kappa$ B activation and trypsinogen activation, these two events are independent.<sup>73</sup> An additional aspect relating to the outcome of CCKR signaling is that the induction of NF- $\kappa$ B activation is accompanied by the induction of TNF- $\alpha$  production. As discussed below, this important attribute of CCKR signaling plays into the mechanism of acinar cell damage mediated by infiltrating macrophages.

If indeed CCKR over-stimulation leads to NF- $\kappa$ B activation and the latter is sufficient for the development of pancreatitis as implied by the Bauman *et al.*, studies discussed above, why is it that high-dose administration of cerulein is not in itself capable of inducing acute pancreatitis in mice subjected to bowel sterilization and are not able to develop either acute or chronic pancreatitis in the absence of NOD1? A possible answer to this important question came from signaling studies obtained from mice subjected to the low-dose cerulein-induced pancreatitis developed by Tsuji *et al.* alluded to above in which the pancreatitis had been induced by administration of a low dose of cerulein together with a NOD1 ligand, neither of which is able to induce pancreatitis when administered alone.<sup>58,67</sup> The acinar cells from the pancreatitis in these mice were attractive targets of signaling studies because they suggested that whereas neither low-dose cerulein nor NOD1 ligand can induce a sufficient amount of NF- $\kappa$ B to support pancreatitis when administered alone these stimuli can do so when administered together.

In the relevant studies, it was found that administration of a low dose of cerulein alone resulted in acinar cell PKC activation followed by the interaction between PKC and TGF- $\beta$ -activated kinase (TAK1).<sup>58</sup> However, such TAK1 activation was not sufficient for induction of NF- $\kappa$ B. On a separate track, administration of NOD1 ligand alone activated acinar cell receptor-interacting serine-threonine kinase (RICK), its immediate downstream signaling partner, but such RICK activation was again not itself sufficient for the activation of NF- $\kappa$ B. In contrast, simultaneous activation of CCKR and NOD1 by a low dose of cerulein and NOD1 ligand led to interaction between RICK and TAK1 as well as substantial activation of NF- $\kappa$ B.<sup>58</sup> These findings thus implied that cerulein signaling via CCKR and NOD1 activation acts in a cooperative fashion to

induce NF- $\kappa$ B during the induction of pancreatitis. With respect to the fact that high-dose cerulein administration cannot induce pancreatitis in the absence of NOD1 signaling, the above results are most consistent with the view that despite *in vitro* studies showing that CCKR over-stimulation can give rise of NF- $\kappa$ B activation, such stimulation is, in reality, an inadequate inducer of pancreatitis in the absence of NOD1 stimulation. On the other hand, it can give rise to a sufficient initial acinar cell DAMPs response and induction of cytokines that cause changes in bowel permeability and entry of NOD1-stimulating microflora. Finally, it is important to point out that, as discussed below, NOD1 signaling is essential to the development of pancreatitis by mechanisms that involve NF- $\kappa$ B and signal transducer and activator of transcription 3 (STAT3) signaling; it is therefore reasonable to postulate that even if CCKR over-stimulation is sufficient to cause NF- $\kappa$ B activation by itself, such activation alone is not sufficient for the development of pancreatitis.

#### NF- $\kappa$ B/STAT3-MEDIATED MCP-1 INDUCTION AND MACROPHAGE INVASION IN PANCREATITIS

Activation of NF- $\kappa$ B in cerulein-induced pancreatitis by the mechanisms discussed above is an essential component of the mechanisms of inflammation driving this disease (Figure 2). One of the most important of these mechanisms (to which we will now turn our attention) is that underlying the induction of CCL2 (MCP-1), a chemokine necessary for the influx of inflammatory macrophages into the pancreas.

In studies of low-dose cerulein pancreatitis addressing this issue, it was found that NOD1 stimulation by its ligand FK156, in combination with low-dose cerulein administration induces MCP-1 as well as IL-6 production and, as before, such NOD1 stimulation mimics the effect of IP administration of commensal bacteria (e.g., ECLACZ).<sup>58</sup> In addition, NOD1/low-dose cerulein administration causes the pancreatic infiltration of large numbers of CD11b<sup>+</sup> myeloid cells bearing C-C chemokine receptor type 2 (CCR2). This was in accord with previous studies that have shown that MCP-1 has a role in the macrophage-dependent inflammatory response characterizing pancreatitis.<sup>89</sup> In further studies of the low-dose cerulein pancreatitis model it was shown that CCR2-deficient mice exhibit decreased evidence of pancreatitis along with decreased infiltration of CD11b<sup>+</sup> macrophages.<sup>58</sup> In addition, studies of bone marrow chimeras allowed one to establish that NOD1-bearing non-hematopoietic cells (i.e., acinar cells) were necessary for the development of pancreatitis as well as the induction of MCP-1 in this model. Finally, studies of isolated pancreatic acinar cells from untreated mice showed that NOD1 stimulation was sufficient to induce substantial amounts of MCP-1 secretion but that the latter was augmented by low-dose cerulein stimulation. Together, these studies established that MCP-1 production is an essential initial step in the induction of cerulein-induced pancreatitis and that such production is dependent on NOD1/cerulein stimulation of acinar cells.

The above findings set the stage for studies defining the signaling pathways underlying MCP-1 induction. In initial



studies along these lines the findings of Deshmane *et al.*<sup>90</sup> showing that STAT3 and NF- $\kappa$ B activation underlies induction of MCP-1 were verified with studies showing that expression of phospho-STAT3 (pSTAT3) and phospho-I $\kappa$ B $\alpha$  (pI $\kappa$ B $\alpha$ ) was present in the pancreas of NOD1-intact mice treated with NOD1 ligand/low-dose cerulein but was not seen in the pancreas of NOD1-deficient mice. In addition, these findings were confirmed by studies of bone marrow chimeras either expressing NOD1 or not expressing NOD1 in acinar cells.<sup>58</sup> Finally, the role of STAT3 and NF- $\kappa$ B in MCP-1 induction was explored with specific inhibitors of these factors. It was found that administration of JSI-124, a specific inhibitor of STAT3 in combination with IMD-0354, a NF- $\kappa$ B inhibitor led to complete prevention of low-dose cerulein pancreatitis and MCP-1 production. It was thus evident that MCP-1 production was dependent on signaling mediated by both STAT3 and NF- $\kappa$ B.

In further exploration of MCP-1 induction in low-dose cerulein-induced pancreatitis the mechanism of STAT3 activation in this model was examined. As mentioned above, one outcome of NOD1/low-dose cerulein administration to mice was pancreatic production of IL-6, a cytokine known to induce STAT3 activation and, therefore, potentially involved in MCP-1 production. That this was in fact the case was established with studies showing that MCP-1 production by NOD1/low-dose cerulein stimulated acinar cells was partially blocked by the neutralization of the IL-6 signaling pathway.<sup>58</sup>

A second potential mechanism of STAT3 activation in this model was suggested by the fact that NOD1 was known to have the unique ability to induce type I IFN, a factor that causes STAT3 (as well as STAT1) activation.<sup>58</sup> Such induction of type I IFN by NOD1 had been shown to be due to its ability to activate a multistep signaling pathway involving first the activation of interferon regulatory factor 7 (IRF7) and second the priming of the IFN-stimulated gene factor 3 pathway (ISGF3) by IRF7-induced type I IFN via the IFN $\alpha\beta$ R (IFNAR).<sup>71</sup> Indeed, it could be shown that pancreatitis in the NOD1/low-dose cerulein model was attenuated in mice lacking IFNAR and this was associated with both reduced STAT3 and MCP-1 expression. It should be noted that low-dose cerulein also induces STAT3 via CCKR-activation of janus activating kinase 2,<sup>91</sup> so that both NOD1 and cerulein signaling again act cooperatively to induce STAT3 activation, albeit by a different mechanism than that governing NF- $\kappa$ B induction.

Taken together, these various studies established that STAT3 activation in low-dose cerulein pancreatitis (and by extension in pancreatitis in general) is a complex process involving both IL-6 induction mainly due to NF- $\kappa$ B activation and type I IFN production mainly due to NOD1 activation. Although the essential outline of the signaling pathways have been defined in the acute model of low-dose cerulein pancreatitis, similar pathways probably apply to the chronic model of cerulein pancreatitis wherein low-dose cerulein and NOD1 ligand is administered for a more prolonged period.<sup>67</sup> This is evident from the fact that mice deficient in IFNAR are resistant to the development of chronic pancreatitis. Finally, it is important to

point out that whereas STAT3 activation has a central role in pancreatitis development in relation to induction of MCP-1 and inflammatory macrophage infiltration it also has a role in the inflammation via its involvement of cytokines that contribute to the inflammation such as type I IFN and IL-6.<sup>67</sup>

As discussed above, there is compelling evidence that activation of NF- $\kappa$ B and STAT3 in acinar cells is a central event for the development of experimental (murine) pancreatitis. However, our knowledge regarding the activation status of these transcription factors in human pancreatitis is very limited and somewhat paradoxical. Analysis of the status of NF- $\kappa$ B and STAT3 in the peripheral blood cells but not the pancreatic tissue of pancreatitis patients, provided unexpected evidence that activation of NF- $\kappa$ B, STAT1, and STAT3 is reduced in acute pancreatitis patients as compared with those from healthy controls.<sup>92–94</sup> The molecular mechanisms accounting for such reduced activation are not fully understood, but could involve tolerogenic responses to MAMPs expressed by translocated intestinal organisms. Thus, tolerance to MAMPs may be one possible mechanism accounting for reduced innate immune responses to the same or other MAMPs in pancreatitis.<sup>95</sup>

#### THE ROLE OF TYPE I IFN IN PANCREATITIS

Mice deficient in IFNAR and thus unable to signal via type I IFN are resistant to both the development of acute low-dose cerulein-induced pancreatitis (as already mentioned) as well as chronic low-dose cerulein-induced pancreatitis<sup>58,67</sup> (Figure 2). Although this is partly explained by its role in the induction of STAT3 and MCP-1 in acinar cells, it also is due to various effects of this cytokine on macrophage effector function. The role of type I IFN in macrophage effector function is immediately evident from studies showing recruitment and maturation of the Ly6<sup>hi</sup> monocytes is uniquely dependent on type I IFN induction of CCR2 expression, which, as noted above, is the receptor for MCP-1.<sup>96</sup> Thus, type I IFN is responsible for both the receptor and ligand aspects of the chemotaxis mediating macrophage infiltration of the pancreas.

Yet another role of type I IFN in relation to macrophage effector function in pancreatitis relates to evidence that it induces macrophage TNF- $\alpha$  production. As noted in the discussion above, myeloid cells in cerulein-induced pancreatitis cause necroptotic acinar cell death via production of TNF- $\alpha$ . Evidence that type I IFN is involved in such production came from studies of pancreatic cells extracted from mice with chronic cerulein-induced pancreatitis wherein it was observed that pancreatic acinar cells co-cultured with pancreatic CD11b<sup>+</sup> macrophages release greatly increased amounts of IL-33, a cytokine associated with acinar cell death (see discussion below) and that such IL-33 release is inhibited by anti-IFNAR Ab (presumably blocking type I IFN stimulation of the macrophages) or anti-TNF- $\alpha$  Ab (presumably blocking TNF- $\alpha$  stimulation of acinar cells).<sup>67</sup> The capacity of type I IFN to induce macrophage TNF- $\alpha$  production is supported by a prior study by Mancuso *et al.*<sup>97</sup> showing that such production induced by live bacteria is mediated by type I IFN signaling.



### PRO-INFLAMMATORY CYTOKINE ACTIVITY IN PANCREATITIS ARISING FROM INNATE IMMUNE RESPONSES

The basic picture of pancreatitis pathogenesis suggested above is that acinar cell damage initiated by various causes of dysregulated trypsinogen activation leads to the release of DAMPs that then react with PRRs on antigen-presenting cells (APCs) to cause the generation of cytokines that induce a change in bowel wall permeability (**Figure 2**). This, in turn, leads to the entry of commensal organism into the circulation and the activation of NOD1 (and possibly TLR4 as well) that, in concert with CCKR signaling causes activation of NF- $\kappa$ B, a type I IFN response and ongoing pro-inflammatory cytokine elaboration by PRR-expressing (but as yet poorly defined) APCs responsive to DAMPs and MAMPs.<sup>35,42,63</sup> Consistent with this scenario, patients with acute pancreatitis exhibit elevated serum levels of various pro-inflammatory cytokines such as IL-6, IL-1 $\beta$ , and TNF- $\alpha$ ,<sup>98–100</sup> and elevated serum levels of various chemokines such as IL-8, MCP-1, and macrophage migration inhibitory factor, which presumably arise from activated cells in the pancreas.<sup>100–102</sup>

These “generic” pro-inflammatory factors drive (or aggravate) the pancreatic inflammation in various specific and/or nonspecific ways. For instance, IL-6, one of the prototypical inflammatory cytokines, may enhance inflammation by its role in the generation of pathological T helper type 17 (Th17) cells or, as discussed above, its contribution to the induction of MCP-1 and the entry of inflammatory macrophages into the pancreas. In any case, it has been shown that administration of anti-IL-6 Ab to mice with pancreatitis induced by cerulein and LPS leads to marked attenuation of the pancreatitis as well as accompanying pulmonary inflammation.<sup>103</sup> It should be noted, however, that IL-6 can have anti-inflammatory effects as well. This is shown by the fact that mice genetically deficient in IL-6 exhibit more severe cerulein-induced pancreatitis as compared with IL-6-intact mice.<sup>104</sup> This contrary finding may be due to the fact that a genetic deletion of IL-6 leads to profound disruption of pro-inflammatory machinery necessary for pancreas homeostasis, than does-acute administration of anti-IL-6 Ab.

IL-1 $\beta$  is a second prototypic pro-inflammatory cytokine associated with the pathogenesis of human acute pancreatitis.<sup>98</sup> This cytokine could be mediating pancreatic inflammation in multiple ways including its ability to induce neutrophil infiltration into sites of inflammation and its more general effect on the induction of other pro-inflammatory cytokines and chemokines.<sup>36</sup> Interestingly, there is evidence that a precursor form of this cytokine is induced by DAMPs acting via TLR9, suggesting that IL-1 $\beta$  may have a role in the induction of enhanced gut permeability to commensal organisms.<sup>41</sup> The precursor form of IL-1 $\beta$  is converted into an active form via the NLRP3 inflammasome and thus mice deficient in NLRP3 inflammasome component are resistant to the induction of cerulein-induced pancreatitis.<sup>41,62</sup> Moreover, attenuation of experimental pancreatitis in the absence of TLR9 is accompanied by the presence of pancreatic APCs with impaired

production of IL-1 $\beta$  as well as pro-IL-1 $\beta$ , suggesting that IL-1 $\beta$  has an autocrine effect on its own synthesis.<sup>41</sup>

TNF- $\alpha$  is a third prototypic pro-inflammatory cytokine involved in pancreatitis pathogenesis and one that appears to have a central role in experimental pancreatitis. As discussed above, this cytokine is induced in pancreatic APCs and is therefore a prime suspect for causing the initial injury to acinar cells occurring in response to excessive CCKR stimulation. This possibility has recently been supported by Sendler *et al.*<sup>105</sup> who showed that stimulation of pancreatic acinar cells by TNF- $\alpha$  causes direct activation of pancreatic enzymes and thus leads to premature protease activation and cell necrosis. Type I IFN may also have an important pathological role by its ability to induce CCR2, the chemokine receptor attracting pro-inflammatory macrophages expressing TNF- $\alpha$  into the pancreas, as already discussed above. These macrophages are cellular source of TNF- $\alpha$  in the inflamed pancreas of cerulein-induced pancreatitis<sup>106,107</sup> and, as also discussed above, may be the important driver of sustained acinar cell necroptosis. These various ways in which TNF- $\alpha$  acts to facilitate pancreatic inflammation provide ample explanation for the fact that the administration of infliximab (monoclonal TNF- $\alpha$  antibody) ameliorates cerulein-induced pancreatic inflammation.<sup>106</sup> Thus, it is clear that TNF- $\alpha$  has a critical role in the development of experimental pancreatitis. However, confirmation that this cytokine has an equally important role in human pancreatitis awaits the studies of human cells obtained from the inflamed pancreas as well as studies addressing the therapeutic effect of infliximab (anti-TNF- $\alpha$  Ab) administration to patients.

Recently it has become evident that yet another pro-inflammatory cytokine, IL-33, is an essential element in the pathogenesis of pancreatitis. IL-33 is an “alarmin” cytokine released from dying cells.<sup>108</sup> Therefore, it is not surprising that serum levels of IL-33 are elevated in patients with severe acute pancreatitis, a condition associated with massive pancreatic acinar cell death.<sup>109</sup> The role of IL-33 in pancreatitis was extensively analyzed in studies of the chronic model of pancreatitis described by Watanabe *et al.*,<sup>67</sup> in which, as discussed above, chronic pancreatitis is induced by repeated administration of NOD1 ligand and a low dose of cerulein. This model was of particular relevance for the study of IL-33 because it is marked by the development of fibrosis, a feature of chronic pancreatitis that is driven by IL-33.

The important finding that emerged from these studies was that blocking of IL-33 activity by administration of antibody neutralizing the IL-33 receptor (ST2) to mice subjected to the chronic pancreatitis regimen led to reduction in pancreatic infiltration of immune cells and fibrosis accompanied by decreased pancreatic expression of both pro-inflammatory mediators such as IL-6, TNF- $\alpha$ , and MCP-1 and pro-fibrogenic mediators such as IL-13 and TGF- $\beta$ 1.<sup>67</sup> It was thus apparent that IL-33 production has a major role in the pathogenesis of chronic pancreatitis.

In further studies of IL-33 using this model, the source of the IL-33 was probed with bone marrow transplantation studies,

wherein it was found that induction of chronic pancreatitis was accompanied by IL-33 expression in irradiated NOD1-intact mice transplanted with NOD1-deficient BM cells, but not in irradiated NOD1-deficient mice transplanted with NOD1-intact BM cells; thus, these studies suggested that NOD1 stimulation of non-hematopoietic cells, most likely pancreatic acinar cells were the probable source of the IL-33.<sup>67</sup> In related studies it was found that such acinar cell IL-33 production required the presence of intact type I IFN signaling since mice deficient in IFNAR exhibited a marked decrease in such production as well as resistance to the development of chronic pancreatitis.<sup>67</sup> This correlates with the fact that, as described above, type I IFN induces TNF- $\alpha$  production by infiltrating macrophages and, in addition co-culture of acinar cells with TNF- $\alpha$ -producing CD11b<sup>+</sup> APCs obtained from inflamed pancreatic tissue is associated with enhanced IL-33 production. Overall, these findings are compatible with the view that pathological macrophages producing TNF- $\alpha$  under the influence of type I IFN induce acinar cell death and release of IL-33. Then, as suggested by studies conducted by Kempuraj *et al.*,<sup>110</sup> such IL-33 release induces production of pro-inflammatory cytokines by intact acinar cells.

Also relevant to the role of IL-33 in pancreatitis is the recent finding by Xue *et al.*<sup>111</sup> that alternatively activated M2 macrophages are numerous in chronic pancreatitis in humans and mice with chronic cerulein-induced pancreatitis. Such M2-macrophages bear surface IL-4R $\alpha$  and are induced by IL-4 and IL-13; they are thus likely to be regulated by IL-33 since the latter induces T cells producing IL-13 via the ST2 receptor (see discussion below). These M2-macrophages also produce IL-10 and TGF- $\beta$ , the latter a cytokine that may act (in concert with other cytokines) on pancreatic stellate cells that contribute to pancreatic fibrosis via production of extracellular matrix proteins.<sup>111,112</sup> The importance of these cells in chronic pancreatitis was shown by the fact that pharmacological inhibition of IL-4 and IL-13 by a blocking peptide led to reduced fibrosis in the cerulein-induced chronic pancreatitis model.

Finally, it should be noted that the above rather definitive studies showing that IL-33 is a major mediator of pancreatitis are opposed by data from several studies showing that under some condition the IL-33-ST2 signaling pathway has a protective role in that mice lacking expression of the ST2 receptor develop enhanced pancreatitis.<sup>113,114</sup> Thus, additional study of IL-33 effects in pancreatitis is warranted.

#### PRO-INFLAMMATORY CYTOKINE ACTIVITY IN PANCREATITIS ARISING FROM ADAPTIVE IMMUNE RESPONSES

Adaptive immune responses comprised mainly of T-cell responses to specific antigens also contribute to the pathogenesis of pancreatitis (**Figure 2**). As in the case of human colitis or murine experimental colitis models these can consist of either excessive effector Th cell function or deficient regulatory T-cell (Treg) function.<sup>115,116</sup>

Several studies of pancreatitis in humans suggest the involvement of Th1 responses in that peripheral blood cells obtained from patients with acute and chronic pancreatitis produce large amounts of prototypical Th1 cytokines, IFN- $\gamma$  and IL-12, and serum levels of IFN- $\gamma$  in such patients are significantly higher than those in healthy controls.<sup>117–119</sup> This evidence that pancreatitis is associated with a Th1 response is verified by the presence of T cells producing IFN- $\gamma$  in necrotic pancreatic tissue from patients with acute pancreatitis. In contrast to the above human studies, IFN- $\gamma$  has a protective rather than a pathogenic role in cerulein-induced acute pancreatitis since in this case IFN- $\gamma$ -deficient mice exhibit increased cerulein-induced pancreatic injury and NF- $\kappa$ B activation is suppressed by IFN- $\gamma$ .<sup>120</sup> Given the fact that a pathological Th17 response is suppressed by IFN- $\gamma$  through downregulation of IL-23 receptor,<sup>121,122</sup> this protective role of the Th1 response in experimental pancreatitis might be due to the suppression of a pathogenic Th17 response. Compatible to this idea, recent reports support the possible involvement of IL-17 in human acute pancreatitis.<sup>123,124</sup> In any case, the reason that human and mouse studies regarding Th1 responses are discrepant is unknown.

Studies of experimental models of chronic pancreatitis suggest that Th2 responses also contribute to the pathogenesis of pancreatitis. The most compelling data in this regard comes from the aforementioned study of chronic pancreatitis induced by repeated administration of NOD1 ligand and low-dose cerulein conducted by Watanabe *et al.*<sup>67</sup> These authors provided evidence that IL-33 produced by acinar cells acting via the ST2 receptor induces the production of IL-13 and the latter then induces fibrosis via induction of fibrogenic factors such as TGF- $\beta$ 1. This is supported by the fact that neutralization of IL-13 by the administration of anti-IL-13 Ab prevented the development of fibrosis but not inflammation in the chronic pancreatitis model, whereas inhibition of IL-33 by administration of anti-ST2 Ab (as noted above) prevented both fibrosis and inflammation. The source of the IL-13 was mainly Th2 cells since pancreatic CD4<sup>+</sup> T cells isolated from mice with chronic pancreatitis produce large amounts of IL-13. However, it is possible that type 2 innate lymphoid cells (ILC2) stimulated by IL-33 also contribute to the IL-13 production, but this seems unlikely in view of the fact that Rag1-deficient mice do not develop IL-13-mediated fibrosis in the chronic pancreatitis model.<sup>67</sup> Xue *et al.*<sup>111</sup> have suggested that pancreatic stellate cells are a source of IL-13, but this is again unlikely, since staining studies indicate that cells with stellate cell markers are not congruent with cells producing IL-13.<sup>67</sup> As noted above, IL-13 induction of M2-macrophages may be an important mechanism of IL-13 induction of fibrosis inasmuch as these cells produce TGF- $\beta$ 1 and other factors that have direct effects on fibrosis induction and indirect effects via stimulation of pancreatic stellate cells. The latter is supported by the fact that neutralization of IL-13 in the chronic pancreatitis model reduces the number of stellate cells.<sup>67,111</sup>

Recent studies by Ochi *et al.*<sup>125</sup> have delineated TLR4 signaling pathways that favor APC induction of chronic

pancreatitis and/or pancreatitis-associated pancreatic cancer. They have provided evidence that dendritic cells responding to pancreatic antigens support Th2 responses in the absence of the myeloid differentiation primary response gene 88 (MyD88) signaling and that these cells support both pancreatitis and pancreatitis-associated cancer development via TIR-domain-containing adapter-inducing interferon- $\beta$  (TRIF) signaling. It remains to be seen how activation of these alternative signaling pathways relate to various type of cytokine secretion such as IL-33 secretion.

The clinical course of chronic pancreatitis in humans is composed of acute exacerbation phases and stable quiescent phases.<sup>2</sup> It is likely that the latter (stable) phases are due to immunosuppressive responses mediated by Tregs with the capacity to suppress pathogenic adaptive immune responses. Indeed it has been shown that Tregs are present in human chronic pancreatic lesions and mediate suppressor effects via their production of IL-10.<sup>126</sup> These findings in humans are supported by studies of murine models of pancreatitis in that the severity of cerulein-induced acute pancreatitis and the production of TNF- $\alpha$  was shown to be increased following neutralization of endogenous IL-10.<sup>127</sup> In addition, Demols *et al.*<sup>128</sup> report that IL-10 deficiency promotes pancreas fibrosis induced by chronic cerulein challenge and that this fibrogenic response is accompanied by elevated expression of intra-pancreatic TGF- $\beta$ 1. It should be noted, however, that in these mouse studies the cellular source of the IL-10 was not identified and is not yet clear that IL-10 production by regulatory T cells is the only mechanism mediating the quiescent state in chronic pancreatitis.

## CONCLUSION

In this review, we have summarized the complex chain of events that are responsible for the development of acute and chronic pancreatitis. It is now evident that whereas dysregulation of intra-acinar regulation of proteolytic enzymes are the initial spark that ignites the pancreatic inflammatory process, activation of innate immune responses stimulated by translocated commensal organisms is an indispensable element in sustaining and widening the inflammation. Of considerable interest, an unexpected and essential component of that innate response is the stimulation of NOD1 responses in acinar cells and through such stimulation the enhancement of essential pro-inflammatory signaling leading to the activation of NF- $\kappa$ B or the *de novo* production of type I IFN. Finally, a somewhat unique feature of pancreatic inflammation, especially chronic inflammation is the release of IL-33 from damaged acinar cells and thereby the initiation of a pro-fibrotic program mediated by T-cell production of IL-13 and other downstream fibrogenic mediators. It is hoped that this new understanding of pancreatitis will lead to innovative new approaches to its treatment.

## ACKNOWLEDGMENTS

This work was supported by Grant-in-Aid for Scientific Research (15K15370) from the Japan Society for the Promotion of Science, the Kato Memorial Trust for Nambyo Research, and the Health and Labor

Sciences Research Grants for Research on Intractable Diseases from the Ministry of Health, Labor and Welfare, Japan.

## DISCLOSURE

The authors declared no conflict of interest.

© 2017 Society for Mucosal Immunology

## REFERENCES

1. Frossard, J.L., Steer, M.L. & Pastor, C.M. Acute pancreatitis. *Lancet* **371**, 143–152 (2008).
2. Braganza, J.M., Lee, S.H., McCloy, R.F. & McMahon, M.J. Chronic pancreatitis. *Lancet* **377**, 1184–1197 (2011).
3. Steer, M.L., Waxman, I. & Freedman, S. Chronic pancreatitis. *N. Engl. J. Med.* **332**, 1482–1490 (1995).
4. Steinberg, W. & Tenner, S. Acute pancreatitis. *N. Engl. J. Med.* **330**, 1198–1210 (1994).
5. Lankisch, P.G., Apte, M. & Banks, P.A. Acute pancreatitis. *Lancet* **386**, 85–96 (2015).
6. Logsdon, C.D. & Ji, B. The role of protein synthesis and digestive enzymes in acinar cell injury. *Nat. Rev. Gastroenterol. Hepatol.* **10**, 362–370 (2013).
7. Cosen-Binker, L.I. & Gaisano, H.Y. Recent insights into the cellular mechanisms of acute pancreatitis. *Can. J. Gastroenterol.* **21**, 19–24 (2007).
8. Saluja, A.K., Lerch, M.M., Phillips, P.A. & Dudeja, V. Why does pancreatic overstimulation cause pancreatitis? *Annu. Rev. Physiol.* **69**, 249–269 (2007).
9. Bhatia, M. *et al.* Pathophysiology of acute pancreatitis. *Pancreatol.* **5**, 132–144 (2005).
10. Whitcomb, D.C. Genetic aspects of pancreatitis. *Annu. Rev. Med.* **61**, 413–424 (2010).
11. Dawra, R. *et al.* Intra-acinar trypsinogen activation mediates early stages of pancreatic injury but not inflammation in mice with acute pancreatitis. *Gastroenterology* **141**, 2210–2217. e2212 (2011).
12. Sah, R.P., Dudeja, V., Dawra, R.K. & Saluja, A.K. Cerulein-induced chronic pancreatitis does not require intra-acinar activation of trypsinogen in mice. *Gastroenterology* **144**, 1076–1085. e1072 (2013).
13. Nemeth, B.C., Wartmann, T., Halangk, W. & Sahin-Toth, M. Autoactivation of mouse trypsinogens is regulated by chymotrypsin C via cleavage of the autolysis loop. *J. Biol. Chem.* **288**, 24049–24062 (2013).
14. Gaiser, S. *et al.* Intracellular activation of trypsinogen in transgenic mice induces acute but not chronic pancreatitis. *Gut* **60**, 1379–1388 (2011).
15. Ji, B. & Logsdon, C.D. Digesting new information about the role of trypsin in pancreatitis. *Gastroenterology* **141**, 1972–1975 (2011).
16. Hoque, R. & Mehal, W.Z. Inflammasomes in pancreatic physiology and disease. *Am. J. Physiol. Gastrointest. Liver Physiol.* **308**, G643–G651 (2015).
17. Fukui, H., Brauner, B., Bode, J.C. & Bode, C. Plasma endotoxin concentrations in patients with alcoholic and non-alcoholic liver disease: reevaluation with an improved chromogenic assay. *J. Hepatol.* **12**, 162–169 (1991).
18. Satoh, A., Gukovskaya, A.S., Reeve, J.R. Jr., Shimosegawa, T. & Pandol, S.J. Ethanol sensitizes NF- $\kappa$ B activation in pancreatic acinar cells through effects on protein kinase C- $\epsilon$ . *Am. J. Physiol. Gastrointest. Liver Physiol.* **291**, G432–G438 (2006).
19. Alexandre, M., Pandol, S.J., Gorelick, F.S. & Thrower, E.C. The emerging role of smoking in the development of pancreatitis. *Pancreatol.* **11**, 469–474 (2011).
20. Mizushima, N., Levine, B., Cuervo, A.M. & Klionsky, D.J. Autophagy fights disease through cellular self-digestion. *Nature* **451**, 1069–1075 (2008).
21. Gukovskaya, A.S. & Gukovsky, I. Autophagy and pancreatitis. *Am. J. Physiol. Gastrointest. Liver Physiol.* **303**, G993–G1003 (2012).
22. Gukovsky, I., Li, N., Todoric, J., Gukovskaya, A. & Karin, M. Inflammation, autophagy, and obesity: common features in the pathogenesis of pancreatitis and pancreatic cancer. *Gastroenterology* **144**, 1199–1209. e1194 (2013).
23. Diakopoulos, K.N. *et al.* Impaired autophagy induces chronic atrophic pancreatitis in mice via sex- and nutrition-dependent processes. *Gastroenterology* **148**, 626–638. e617 (2015).



24. Antonucci, L. *et al.* Basal autophagy maintains pancreatic acinar cell homeostasis and protein synthesis and prevents ER stress. *Proc. Natl Acad. Sci. USA* **112**, E6166–E6174 (2015).
25. Li, N. *et al.* Loss of acinar cell IKK $\alpha$  triggers spontaneous pancreatitis in mice. *J. Clin. Invest.* **123**, 2231–2243 (2013).
26. Fortunato, F. *et al.* Impaired autolysosome formation correlates with Lamp-2 depletion: role of apoptosis, autophagy, and necrosis in pancreatitis. *Gastroenterology* **137**, 350–360. 360 e351–355 (2009).
27. Mareninova, O.A. *et al.* Lysosome associated membrane proteins maintain pancreatic acinar cell homeostasis: LAMP-2 deficient mice develop pancreatitis. *Cell. Mol. Gastroenterol. Hepatol.* **1**, 678–694 (2015).
28. Mareninova, O.A. *et al.* Impaired autophagic flux mediates acinar cell vacuole formation and trypsinogen activation in rodent models of acute pancreatitis. *J. Clin. Invest.* **119**, 3340–3355 (2009).
29. Mareninova, O.A. *et al.* Cell death in pancreatitis: caspases protect from necrotizing pancreatitis. *J. Biol. Chem.* **281**, 3370–3381 (2006).
30. Conrad, M., Angeli, J.P., Vandenabeele, P. & Stockwell, B.R. Regulated necrosis: disease relevance and therapeutic opportunities. *Nat. Rev. Drug Discov.* **15**, 348–366 (2016).
31. Pasparakis, M. & Vandenabeele, P. Necroptosis and its role in inflammation. *Nature* **517**, 311–320 (2015).
32. He, S. *et al.* Receptor interacting protein kinase-3 determines cellular necrotic response to TNF- $\alpha$ . *Cell* **137**, 1100–1111 (2009).
33. Wu, J. *et al.* Mkl1 knockout mice demonstrate the indispensable role of Mkl1 in necroptosis. *Cell Res.* **23**, 994–1006 (2013).
34. Seifert, L. *et al.* The necrosome promotes pancreatic oncogenesis via CXCL1 and Mincle-induced immune suppression. *Nature* **532**, 245–249 (2016).
35. Kono, H. & Rock, K.L. How dying cells alert the immune system to danger. *Nat. Rev. Immunol.* **8**, 279–289 (2008).
36. Hoque, R., Malik, A.F., Gorelick, F. & Mehal, W.Z. Sterile inflammatory response in acute pancreatitis. *Pancreas* **41**, 353–357 (2012).
37. Kang, R. *et al.* Intracellular Hmgb1 inhibits inflammatory nucleosome release and limits acute pancreatitis in mice. *Gastroenterology* **146**, 1097–1107 (2014).
38. Yasuda, T. *et al.* Increase of high-mobility group box chromosomal protein 1 in blood and injured organs in experimental severe acute pancreatitis. *Pancreas* **34**, 487–488 (2007).
39. Yasuda, T. *et al.* Significant increase of serum high-mobility group box chromosomal protein 1 levels in patients with severe acute pancreatitis. *Pancreas* **33**, 359–363 (2006).
40. Sawa, H. *et al.* Blockade of high mobility group box-1 protein attenuates experimental severe acute pancreatitis. *World J. Gastroenterol.* **12**, 7666–7670 (2006).
41. Hoque, R. *et al.* TLR9 and the NLRP3 inflammasome link acinar cell death with inflammation in acute pancreatitis. *Gastroenterology* **141**, 358–369 (2011).
42. Akira, S. & Takeda, K. Toll-like receptor signalling. *Nat. Rev. Immunol.* **4**, 499–511 (2004).
43. Kang, R. *et al.* The receptor for advanced glycation end products activates the AIM2 inflammasome in acute pancreatitis. *J. Immunol.* **196**, 4331–4337 (2016).
44. Kubes, P. & Mehal, W.Z. Sterile inflammation in the liver. *Gastroenterology* **143**, 1158–1172 (2012).
45. Abdulla, A., Awla, D., Thorlacius, H. & Regner, S. Role of neutrophils in the activation of trypsinogen in severe acute pancreatitis. *J. Leukoc. Biol.* **90**, 975–982 (2011).
46. Frossard, J.L. *et al.* The role of intercellular adhesion molecule 1 and neutrophils in acute pancreatitis and pancreatitis-associated lung injury. *Gastroenterology* **116**, 694–701 (1999).
47. Merza, M. *et al.* Neutrophil extracellular traps induce trypsin activation, inflammation, and tissue damage in mice with severe acute pancreatitis. *Gastroenterology* **149**, 1920–1931. e1928 (2015).
48. Lande, R. *et al.* Neutrophils activate plasmacytoid dendritic cells by releasing self-DNA-peptide complexes in systemic lupus erythematosus. *Sci. Transl. Med.* **3**, 73ra19 (2011).
49. Garcia-Romo, G.S. *et al.* Netting neutrophils are major inducers of type I IFN production in pediatric systemic lupus erythematosus. *Sci. Transl. Med.* **3**, 73ra20 (2011).
50. Bedrosian, A.S. *et al.* Dendritic cells promote pancreatic viability in mice with acute pancreatitis. *Gastroenterology* **141**, 1915–1926. e1911–1914 (2011).
51. Foitzik, T. The enteric factor in pancreatic infection. *Pancreatol.* **1**, 217–223 (2001).
52. Flint, R.S. & Windsor, J.A. The role of the intestine in the pathophysiology and management of severe acute pancreatitis. *HPB (Oxford)* **5**, 69–85 (2003).
53. Li, Q., Wang, C., Tang, C., He, Q., Li, N. & Li, J. Bacteremia in patients with acute pancreatitis as revealed by 16S ribosomal RNA gene-based techniques\*. *Crit. Care Med.* **41**, 1938–1950 (2013).
54. Runkel, N.S., Moody, F.G., Smith, G.S., Rodriguez, L.F., LaRocco, M.T. & Miller, T.A. The role of the gut in the development of sepsis in acute pancreatitis. *J. Surg. Res.* **51**, 18–23 (1991).
55. Gianotti, L., Munda, R., Alexander, J.W., Tchervenkov, J.I. & Babcock, G.F. Bacterial translocation: a potential source for infection in acute pancreatitis. *Pancreas* **8**, 551–558 (1993).
56. Medich, D.S., Lee, T.K., Melhem, M.F., Rowe, M.I., Schraut, W.H. & Lee, K.K. Pathogenesis of pancreatic sepsis. *Am. J. Surg.* **165**, 46–50. discussion 51–42 (1993).
57. Rychter, J.W. *et al.* Pretreatment but not treatment with probiotics abolishes mouse intestinal barrier dysfunction in acute pancreatitis. *Surgery* **145**, 157–167 (2009).
58. Tsuji, Y., Watanabe, T., Kudo, M., Arai, H., Strober, W. & Chiba, T. Sensing of commensal organisms by the intracellular sensor NOD1 mediates experimental pancreatitis. *Immunity* **37**, 326–338 (2012).
59. Mithofer, K., Fernandez-del Castillo, C., Ferraro, M.J., Lewandowski, K., Rattner, D.W. & Warshaw, A.L. Antibiotic treatment improves survival in experimental acute necrotizing pancreatitis. *Gastroenterology* **110**, 232–240 (1996).
60. Fritz, S. *et al.* Prophylactic antibiotic treatment is superior to therapy on-demand in experimental necrotizing pancreatitis. *Crit. Care* **12**, R141 (2008).
61. Foitzik, T., Fernandez-del Castillo, C., Ferraro, M.J., Mithofer, K., Rattner, D.W. & Warshaw, A.L. Pathogenesis and prevention of early pancreatic infection in experimental acute necrotizing pancreatitis. *Ann. Surg.* **222**, 179–185 (1995).
62. Chen, G., Shaw, M.H., Kim, Y.G. & Nunez, G. NOD-like receptors: role in innate immunity and inflammatory disease. *Annu. Rev. Pathol.* **4**, 365–398 (2009).
63. Strober, W., Murray, P.J., Kitani, A. & Watanabe, T. Signalling pathways and molecular interactions of NOD1 and NOD2. *Nat. Rev. Immunol.* **6**, 9–20 (2006).
64. Sharif, R. *et al.* Impact of toll-like receptor 4 on the severity of acute pancreatitis and pancreatitis-associated lung injury in mice. *Gut* **58**, 813–819 (2009).
65. Pastor, C.M. *et al.* Role of Toll-like receptor 4 on pancreatic and pulmonary injury in a mice model of acute pancreatitis associated with endotoxemia. *Crit. Care Med.* **32**, 1759–1763 (2004).
66. Gao, H.K., Zhou, Z.G., Li, Y. & Chen, Y.Q. Toll-like receptor 4 Asp299Gly polymorphism is associated with an increased risk of pancreatic necrotic infection in acute pancreatitis: a study in the Chinese population. *Pancreas* **34**, 295–298 (2007).
67. Watanabe, T. *et al.* Nucleotide-binding oligomerization domain 1 acts in concert with the cholecystokinin receptor agonist, cerulein, to induce IL-33-dependent chronic pancreatitis. *Mucosal Immunol.* **9**, 1234–1249 (2016).
68. Girardin, S.E. *et al.* Nod1 detects a unique muropeptide from gram-negative bacterial peptidoglycan. *Science* **300**, 1584–1587 (2003).
69. Kim, J.G., Lee, S.J. & Kagnoff, M.F. Nod1 is an essential signal transducer in intestinal epithelial cells infected with bacteria that avoid recognition by toll-like receptors. *Infect. Immun.* **72**, 1487–1495 (2004).
70. Viala, J. *et al.* Nod1 responds to peptidoglycan delivered by the *Helicobacter pylori* cag pathogenicity island. *Nat. Immunol.* **5**, 1166–1174 (2004).
71. Watanabe, T. *et al.* NOD1 contributes to mouse host defense against *Helicobacter pylori* via induction of type I IFN and activation of the ISGF3 signaling pathway. *J. Clin. Invest.* **120**, 1645–1662 (2010).

72. Bouskra, D. *et al.* Lymphoid tissue genesis induced by commensals through NOD1 regulates intestinal homeostasis. *Nature* **456**, 507–510 (2008).
73. Rakonczay, Z. Jr, Hegyi, P., Takacs, T., McCarroll, J. & Saluja, A.K. The role of NF-kappaB activation in the pathogenesis of acute pancreatitis. *Gut* **57**, 259–267 (2008).
74. Sah, R.P. & Saluja, A. Molecular mechanisms of pancreatic injury. *Curr. Opin. Gastroenterol.* **27**, 444–451 (2011).
75. Steinle, A.U., Weidenbach, H., Wagner, M., Adler, G. & Schmid, R.M. NF-kappaB/Rel activation in cerulein pancreatitis. *Gastroenterology* **116**, 420–430 (1999).
76. Gukovsky, I., Gukovskaya, A.S., Blinman, T.A., Zaninovic, V. & Pandol, S.J. Early NF-kappaB activation is associated with hormone-induced pancreatitis. *Am. J. Physiol.* **275**, G1402–G1414 (1998).
77. Gukovskaya, A.S. *et al.* Pancreatic acinar cells produce, release, and respond to tumor necrosis factor-alpha. Role in regulating cell death and pancreatitis. *J. Clin. Invest.* **100**, 1853–1862 (1997).
78. Grady, T., Liang, P., Ernst, S.A. & Logsdon, C.D. Chemokine gene expression in rat pancreatic acinar cells is an early event associated with acute pancreatitis. *Gastroenterology* **113**, 1966–1975 (1997).
79. Altavilla, D. *et al.* Attenuated cerulein-induced pancreatitis in nuclear factor-kappaB-deficient mice. *Lab. Invest.* **83**, 1723–1732 (2003).
80. Ethridge, R.T., Hashimoto, K., Chung, D.H., Ehlers, R.A., Rajaraman, S. & Evers, B.M. Selective inhibition of NF-kappaB attenuates the severity of cerulein-induced acute pancreatitis. *J. Am. Coll. Surg.* **195**, 497–505 (2002).
81. Letoha, T. *et al.* *In vitro* and *in vivo* nuclear factor-kappaB inhibitory effects of the cell-penetrating penetratin peptide. *Mol. Pharmacol.* **69**, 2027–2036 (2006).
82. Chen, X., Ji, B., Han, B., Ernst, S.A., Simeone, D. & Logsdon, C.D. NF-kappaB activation in pancreas induces pancreatic and systemic inflammatory response. *Gastroenterology* **122**, 448–457 (2002).
83. Baumann, B. *et al.* Constitutive IKK2 activation in acinar cells is sufficient to induce pancreatitis *in vivo*. *J. Clin. Invest.* **117**, 1502–1513 (2007).
84. Satoh, A. *et al.* PKC-delta and -epsilon regulate NF-kappaB activation induced by cholecystokinin and TNF-alpha in pancreatic acinar cells. *Am. J. Physiol. Gastrointest. Liver Physiol.* **287**, G582–G591 (2004).
85. Gukovsky, I. *et al.* Phosphatidylinositol 3-kinase gamma regulates key pathologic responses to cholecystokinin in pancreatic acinar cells. *Gastroenterology* **126**, 554–566 (2004).
86. Tando, Y., Algul, H., Wagner, M., Weidenbach, H., Adler, G. & Schmid, R.M. Cerulein-induced NF-kappaB/Rel activation requires both Ca<sup>2+</sup> and protein kinase C as messengers. *Am. J. Physiol.* **277**, G678–G686 (1999).
87. Ji, B., Gaiser, S., Chen, X., Ernst, S.A. & Logsdon, C.D. Intracellular trypsin induces pancreatic acinar cell death but not NF-kappaB activation. *J. Biol. Chem.* **284**, 17488–17498 (2009).
88. Han, B., Ji, B. & Logsdon, C.D. CCK independently activates intracellular trypsinogen and NF-kappaB in rat pancreatic acinar cells. *Am. J. Physiol. Cell Physiol.* **280**, C465–C472 (2001).
89. Zhao, H.F. *et al.* Anti-monocyte chemoattractant protein 1 gene therapy attenuates experimental chronic pancreatitis induced by dibutyltin dichloride in rats. *Gut* **54**, 1759–1767 (2005).
90. Deshmane, S.L., Kremlev, S., Amini, S. & Sawaya, B.E. Monocyte chemoattractant protein-1 (MCP-1): an overview. *J. Interferon Cytokine Res.* **29**, 313–326 (2009).
91. Yu, J.H., Kim, K.H. & Kim, H. SOCS 3 and PPAR-gamma ligands inhibit the expression of IL-6 and TGF-beta1 by regulating JAK2/STAT3 signaling in pancreas. *Int. J. Biochem. Cell Biol.* **40**, 677–688 (2008).
92. Satoh, A. *et al.* Nuclear factor kappa B expression in peripheral blood mononuclear cells of patients with acute pancreatitis. *Pancreas* **26**, 350–356 (2003).
93. Oiva, J. *et al.* Patients with acute pancreatitis complicated by organ failure show highly aberrant monocyte signaling profiles assessed by phospho-specific flow cytometry. *Crit. Care Med.* **38**, 1702–1708 (2010).
94. Oiva, J. *et al.* Acute pancreatitis with organ dysfunction associates with abnormal blood lymphocyte signaling: controlled laboratory study. *Crit. Care* **14**, R207 (2010).
95. Liew, F.Y., Xu, D., Brint, E.K. & O'Neill, L.A. Negative regulation of toll-like receptor-mediated immune responses. *Nat. Rev. Immunol.* **5**, 446–458 (2005).
96. Lee, P.Y. *et al.* Type I interferon modulates monocyte recruitment and maturation in chronic inflammation. *Am. J. Pathol.* **175**, 2023–2033 (2009).
97. Mancuso, G. *et al.* Type I IFN signaling is crucial for host resistance against different species of pathogenic bacteria. *J. Immunol.* **178**, 3126–3133 (2007).
98. Mayer, J., Rau, B., Gansauge, F. & Beger, H.G. Inflammatory mediators in human acute pancreatitis: clinical and pathophysiological implications. *Gut* **47**, 546–552 (2000).
99. Malmstrom, M.L. *et al.* Cytokines and organ failure in acute pancreatitis: inflammatory response in acute pancreatitis. *Pancreas* **41**, 271–277 (2012).
100. Berney, T. *et al.* Serum profiles of interleukin-6, interleukin-8, and interleukin-10 in patients with severe and mild acute pancreatitis. *Pancreas* **18**, 371–377 (1999).
101. Regner, S., Appelros, S., Hjalmarsson, C., Manjer, J., Sadic, J. & Borgstrom, A. Monocyte chemoattractant protein 1, active carboxypeptidase B and CAPAP at hospital admission are predictive markers for severe acute pancreatitis. *Pancreatology* **8**, 42–49 (2008).
102. Sakai, Y., Masamune, A., Satoh, A., Nishihira, J., Yamagiwa, T. & Shimosegawa, T. Macrophage migration inhibitory factor is a critical mediator of severe acute pancreatitis. *Gastroenterology* **124**, 725–736 (2003).
103. Chao, K.C., Chao, K.F., Chuang, C.C. & Liu, S.H. Blockade of interleukin 6 accelerates acinar cell apoptosis and attenuates experimental acute pancreatitis *in vivo*. *Br. J. Surg.* **93**, 332–338 (2006).
104. Cuzzocrea, S. *et al.* Absence of endogenous interleukin-6 enhances the inflammatory response during acute pancreatitis induced by cerulein in mice. *Cytokine* **18**, 274–285 (2002).
105. Sendler, M. *et al.* Tumour necrosis factor alpha secretion induces protease activation and acinar cell necrosis in acute experimental pancreatitis in mice. *Gut* **62**, 430–439 (2013).
106. Oruc, N. *et al.* Infliximab: a new therapeutic agent in acute pancreatitis?. *Pancreas* **28**, e1–e8 (2004).
107. Saeki, K. *et al.* CCL2-induced migration and SOCS3-mediated activation of macrophages are involved in cerulein-induced pancreatitis in mice. *Gastroenterology* **142**, 1010–1020. e1019 (2012).
108. Cayrol, C. & Girard, J.P. IL-33: an alarmin cytokine with crucial roles in innate immunity, inflammation and allergy. *Curr. Opin. Immunol.* **31C**, 31–37 (2014).
109. Jiang, Y., An, Y., Jiang, D., Wu, B., Yang, Y. & Sun, D. TNF-alpha regulating interleukin-33 induces acute pancreatic inflammation in rats. *Ann. Clin. Lab. Sci.* **46**, 54–59 (2016).
110. Kempuraj, D., Twait, E.C., Williard, D.E., Yuan, Z., Meyerholz, D.K. & Samuel, I. The novel cytokine interleukin-33 activates acinar cell proinflammatory pathways and induces acute pancreatic inflammation in mice. *PLoS One* **8**, e56866 (2013).
111. Xue, J. *et al.* Alternatively activated macrophages promote pancreatic fibrosis in chronic pancreatitis. *Nat. Commun.* **6**, 7158 (2015).
112. Masamune, A. & Shimosegawa, T. Pancreatic stellate cells—multifunctional cells in the pancreas. *Pancreatology* **13**, 102–105 (2013).
113. Ouziel, R. *et al.* The ST2 pathway is involved in acute pancreatitis: a translational study in humans and mice. *Am. J. Pathol.* **180**, 2330–2339 (2012).
114. Sesti-Costa, R. *et al.* The IL-33/ST2 pathway controls coxsackievirus B5-induced experimental pancreatitis. *J. Immunol.* **191**, 283–292 (2013).
115. Bouma, G. & Strober, W. The immunological and genetic basis of inflammatory bowel disease. *Nat. Rev. Immunol.* **3**, 521–533 (2003).
116. Strober, W. & Fuss, I.J. Proinflammatory cytokines in the pathogenesis of inflammatory bowel diseases. *Gastroenterology* **140**, 1756–1767 (2011).
117. Bhatnagar, A., Wig, J.D. & Majumdar, S. Expression of activation, adhesion molecules and intracellular cytokines in acute pancreatitis. *Immunol. Lett.* **77**, 133–141 (2001).
118. Bhatnagar, A., Wig, J.D. & Majumdar, S. Immunological findings in acute and chronic pancreatitis. *ANZ J. Surg.* **73**, 59–64 (2003).



119. Pietruczuk, M., Dabrowska, M.I., Wereszczynska-Siemiatkowska, U. & Dabrowski, A. Alteration of peripheral blood lymphocyte subsets in acute pancreatitis. *World J. Gastroenterol.* **12**, 5344–5351 (2006).
120. Hayashi, T., Ishida, Y., Kimura, A., Iwakura, Y., Mukaida, N. & Kondo, T. IFN-gamma protects cerulein-induced acute pancreatitis by repressing NF-kappa B activation. *J. Immunol.* **178**, 7385–7394 (2007).
121. Park, H. *et al.* A distinct lineage of CD4 T cells regulates tissue inflammation by producing interleukin 17. *Nat. Immunol.* **6**, 1133–1141 (2005).
122. Harrington, L.E. *et al.* Interleukin 17-producing CD4<sup>+</sup> effector T cells develop via a lineage distinct from the T helper type 1 and 2 lineages. *Nat. Immunol.* **6**, 1123–1132 (2005).
123. Dai, S.R., Li, Z. & Zhang, J.B. Serum interleukin 17 as an early prognostic biomarker of severe acute pancreatitis receiving continuous blood purification. *Int. J. Artif. Organs* **38**, 192–198 (2015).
124. Yang, Z.W., Weng, C.Z., Wang, J. & Xu, P. The role of Card9 overexpression in peripheral blood mononuclear cells from patients with aseptic acute pancreatitis. *J. Cell Mol. Med.* **20**, 441–449 (2016).
125. Ochi, A., Nguyen, A.H., Bedrosian, A.S., Mushlin, H.M. & Zerbakhsh, S. Barilla R *et al.* MyD88 inhibition amplifies dendritic cell capacity to promote pancreatic carcinogenesis via Th2 cells. *J. Exp. Med.* **209**, 1671–1687 (2012).
126. Schmitz-Winnenthal, H. *et al.* Chronic pancreatitis is associated with disease-specific regulatory T-cell responses. *Gastroenterology* **138**, 1178–1188 (2010).
127. Van Laethem, J.L., Eskinazi, R., Louis, H., Rickaert, F., Robberecht, P. & Deviere, J. Multisystemic production of interleukin 10 limits the severity of acute pancreatitis in mice. *Gut* **43**, 408–413 (1998).
128. Demols, A. *et al.* Endogenous interleukin-10 modulates fibrosis and regeneration in experimental chronic pancreatitis. *Am. J. Physiol. Gastrointest. Liver Physiol.* **282**, G1105–G1112 (2002).

## Original Article

## Semiquantitative prediction of early response of conventional transcatheter arterial chemoembolization for hepatocellular carcinoma using postprocedural plain cone-beam computed tomography

Yasunori Minami,<sup>1</sup> Masahiro Takita,<sup>1</sup> Masakatsu Tsurusaki,<sup>2</sup> Yukinobu Yagyu,<sup>2</sup> Kazuomi Ueshima,<sup>1</sup> Takamichi Murakami<sup>2</sup> and Masatoshi Kudo<sup>1</sup>Departments of <sup>1</sup>Gastroenterology and Hepatology, <sup>2</sup>Radiology, Kinki University Faculty of Medicine, Osaka, Japan

**Aim:** To investigate whether plain cone-beam computed tomography (CT) immediately after conventional transcatheter arterial chemoembolization (c-TACE) can help to predict tumor response semiquantitatively in patients with hepatocellular carcinoma (HCC).

**Methods:** Analysis was carried out retrospectively on 262 targeted HCCs in 169 patients treated with c-TACE. Dynamic CT was performed at baseline and 1–4 months after c-TACE. Receiver–operating characteristic curve analysis was undertaken to evaluate whether voxel values of cone-beam CT could predict a complete response and to identify the cut-off value. Final tumor response assessment and early prediction using the retention pattern of iodized oil, the cut-off value of the density, and the combination of the cut-off density value and retention pattern of iodized oil in HCCs on postprocedural cone-beam CT were compared.

**Results:** Complete response was obtained in 72.9% of lesions. According to the pattern of iodized oil uptake, the sensitivity,

specificity, and accuracy for predicting complete response were 85.9%, 70.4%, and 81.7%, respectively by excellent uptake on cone-beam CT. The area under the curve was 0.86 with the optimal cut-off at a voxel value of 200.13. According to not only the density but also the homogeneity of iodized oil retention, the sensitivity, specificity, and accuracy values for predicting complete response were 86.4%, 95.8%, and 88.9%, respectively. The predictive accuracy was significantly better than that of the pattern of iodized oil retention only ( $P = 0.019$ ).

**Conclusion:** The combination of density and visual estimate of homogeneity is superior to either alone in predicting tumor response of c-TACE in HCC patients.

**Key words:** conventional transcatheter arterial chemoembolization, hepatocellular carcinoma, iodized oil, postprocedural plain cone-beam CT, voxel gray value

## INTRODUCTION

TRANSCATHETER ARTERIAL CHEMOEMBOLIZATION is the first-line therapy recommended for patients with intermediate HCC.<sup>1–4</sup> Contrast-enhanced CT or magnetic resonance imaging is commonly used to evaluate the efficacy of c-TACE<sup>5</sup>; however, the guidelines state that the evaluation should be delayed by at least 1 month because iodized oil in viable areas is washed out gradually, even if it filled the tumor immediately after c-TACE.<sup>6–10</sup> Consequently, a time lag between treatment and evaluation of

outcome can arise, and retreatment may be delayed in HCC patients with rapid progressive recurrence.

Cone-beam CT angiography is a substantial advancement in interventional radiology. Several studies have shown that cone-beam CT angiography can be helpful during TACE, mostly in cases of complex hepatic arterial anatomy.<sup>11–17</sup> Additionally, postprocedural plain cone-beam CT can also detect the iodized oil uptake in HCCs,<sup>18,19</sup> and the appearance of iodized oil uptake can be used as an endpoint of the c-TACE procedure. The gray-level values of different soft tissues in the same image remain proportional to their HU values,<sup>20</sup> although the grayscale values of cone-beam CT are not strictly calibrated to conform to HU measurements. It is thus possible to obtain pseudo-HUs from cone-beam CTs. Postprocedural plain cone-beam CT is supposed to distinguish induced

Correspondence: Masatoshi Kudo, Department of Gastroenterology and Hepatology, Kinki University Faculty of Medicine, 377-2 Ohno-higashi Osaka-sayama, 589-8511, Japan. Email: [minkun@med.kindai.ac.jp](mailto:minkun@med.kindai.ac.jp)  
Conflict of interest: The authors have no conflict of interest  
Received 25 January 2016; revision 26 April 2016; accepted 28 April 2016.

necrotic lesions from residual or recurring lesions by assessing the degree of iodized oil accumulation in HCCs. Its use might therefore be beneficial in resolving the time lag problems. The purpose of this study was to assess the usefulness of the combination of the grayscale voxel values and morphology of iodized oil uptake in HCCs on postprocedural plain cone-beam CT as an early predictor of c-TACE response in HCC patients.

## MATERIALS AND METHODS

### Study cohort

APPROVAL FOR THIS retrospective study was obtained from the local ethical review board. Written informed consent to perform c-TACE was obtained from all patients before treatment.

This cohort study was carried out as a retrospective analysis in a single institution. The study included HCC patients who underwent the c-TACE procedure and who had undergone immediate postprocedural plain cone-beam CT and contrast-enhanced multiple-phase CT 1–4 months after c-TACE from April 2011 to July 2014. Patients were considered eligible for c-TACE if the diagnosis of HCC was confirmed by typical radiologic findings 1 month before c-TACE. Additional eligibility criteria included a single large or multiple HCC, naïve or recurrent HCC, Child–Pugh class A or B disease, absent or trace ascites, albumin level > 2.0 g/dL, alanine aminotransferase and aspartate aminotransferase levels of less than five times the upper normal limit, total serum bilirubin level <3.0 mg/dL, prothrombin time – international normalized ratio <1.5, serum creatinine level <2.0 mg/dL, platelet count of at least 30 000/mm<sup>3</sup> and at least partial patency of the portal venous system. Patients with metal spine implants or metallic materials after interventions/abdominal surgery had to be excluded because of their metal artifacts.

### Patient demographics

One hundred and sixty-nine patients with 262 unresectable HCCs were included in our study (Table 1). The patient population included 125 men and 44 women (age range, 43–88 years; mean  $\pm$  SD, 73.9  $\pm$  7.4 years). The maximal diameter of the tumors ranged from 0.5 to 8.9 cm (mean  $\pm$  SD, 2.3  $\pm$  1.2 cm) on contrast-enhanced CT. Each injection was carried out in a superselective (160 patients) or selective (9 patients, 3 in the right hepatic artery and 6 in the left hepatic artery) manner in the case of unifocal lesions or those with multiple feeding vessels, respectively.

**Table 1** Baseline clinical characteristics of patients with hepatocellular carcinoma treated with conventional transcatheter arterial chemoembolization

No. of patients	169
No. of tumors evaluated	262
Sex	
Male	125
Female	44
Age, years	
Mean $\pm$ SD	73.9 $\pm$ 7.4
Range	43–88
Etiology	
HBV	13
HCV	111
NonB/nonC	45
HBV + HCV	0
Child–Pugh class	
A	140
B	29
C	0
Tumor location	
Left lateral	65
Left medial	41
Right medial	97
Right lateral	53
Segment 1	6
Tumor size, cm	
Mean $\pm$ SD	2.3 $\pm$ 1.2
Range	0.5–8.9
Tumor area, cm <sup>2</sup>	
Mean $\pm$ SD	3.8 $\pm$ 5.0
Range	0.3–32.7

Data are presented as mean  $\pm$  standard deviation (SD).  
HBV, hepatitis B virus; HCV, hepatitis C virus.

### Conventional TACE technique

All c-TACE procedures were carried out by two experienced interventional hepatologists and one experienced interventional radiologist (M.T, Y.M, and Y.Y, with 12, 18, and 20 years of experience, respectively), using a consistent approach.

The celiac artery was selectively catheterized using a 4-Fr. catheter. A 2.2-Fr. microcatheter (Shirabe; Piolax, Yokohama, Japan) was advanced coaxially through the catheter into the common or proper hepatic artery. Hepatic angiography was used for evaluation of the feeding vessels, and revealed a single large or multiple HCC in the liver. A microcatheter was positioned as close to the tumor bed as possible before infusion of the emulsion. In HCC patients with multiple feeders, the position of the microcatheter was changed within the same session, and both segmental c-TACE and subsegmental c-TACE were

carried out. Chemoembolization was carried out using 10–30 mg epirubicin (Nippon Kayaku, Tokyo, Japan) dissolved in 1–3 mL distilled water and emulsified with 1–5 mL iodized oil (Lipiodol Ultra-Fluid; Guerbet, Paris, France) followed by the injection of gelatin sponge particles (Gelpart; Nipponkayaku, Tokyo, Japan) 1–2 mm in diameter. The dose of the emulsion depended on the tumor size and vascularity (maximal volume of emulsion, 8 mL). Once slowing of the blood flow was observed after administration of the emulsion, only a small amount of embolic was needed to reach the embolization end-point. However, the occlusion by gelatin sponge particles was often temporary and flow recovered within a few minutes, and a stronger embolic effect was required.<sup>21</sup> The end-point for the administration was stasis in tumor feeding arteries with or without the appearance of iodized oil in portal vein branches. The findings of postprocedural plain cone-beam CT were not used to tailor the c-TACE procedure.

### Cone-beam CT

Plain cone-beam CT was undertaken immediately after c-TACE instead of post-embolization digital subtraction angiography. C-arm cone-beam CT images were obtained using an Innova 4100<sup>IQ</sup> pro angiographic unit (GE Healthcare, Chalfont St. Giles, UK). Cone-beam CT images were acquired using the following parameters: total scanning angle, 200°; rotation speed, 20°/s; acquisition time, 10 s; matrix size, 1500 × 1500; isotropic voxel size, 0.2 mm; and effective field-of-view, 18 cm.<sup>2</sup> During rotation, 300 images were obtained at a frame rate of 30 frames/s. The acquired images were then transferred to an external workstation (Advantage Workstation 4.2; GE Healthcare) where a volume dataset was reconstructed from the CT type dataset consisting of many sections with the thickness of one voxel and visualized with a volume rendering technique.

### Imaging data evaluation

Axial maximum intensity projection images were obtained with a 5-mm slice thickness and 2.5-mm interposition. According to the area of iodized oil accumulation in isolation (excellent, 100% deposition of iodized oil in the lesion; good, 50–99%; fair, 1–49%; poor, 0%),<sup>9</sup> the subjective analysis of iodized oil uptake was evaluated based on the largest diameter dimension of the tumor by a hepatologist (Y.M., with 18 years of experience in abdominal CT interpretation) who was unaware of the tumor response assessment. Moreover, on a computer monitor with implementation of a Picture Archiving and Communication System in our hospital, an ROI was drawn on the

target lesion manually as large as possible to contain the whole tumor on plain cone-beam CT. Soon thereafter, the mean voxel gray value and area (cm<sup>2</sup>) were automatically calculated by multiplying the number of voxels by the unit volume of a voxel.

Final treatment response was blindly assessed at 1–4 months of CT follow-up (mean 58 days, median 51 days, range 28–120 days) by two radiologists (M.T and T.M, with 20 and 29 years of experience, respectively) using mRECIST.<sup>22</sup>

### Statistical analysis

Receiver–operating characteristic curve analyses were used to determine the appropriate cut-off points for the prediction of complete response of c-TACE. Finally, mRECIST assessment and early prediction using the retention pattern of iodized oil, the cut-off value of the density, and the combination of the cut-off density value and retention pattern of iodized oil in HCCs on postprocedural cone-beam CT were compared.

Data are expressed as the mean ± SD, and the Pearson  $\chi^2$ -test was used to test for differences in the distribution of categorical variables. The ROC curves and the AUC were calculated to evaluate whether mean voxel gray values in HCCs on postprocedural plain cone-beam CT predict a complete response on follow-up CT. A cut-off mean voxel gray value in HCC was determined for the optimal differentiation between complete response and incomplete response. For predicting c-TACE response, the sensitivity, specificity, positive predictive value, and negative predictive value were each obtained based on the retention pattern of iodized oil, the cut-off value of the density, and the combination of them on postprocedural cone-beam CT.

Data were analyzed using statistical software (SPSS 12.0; SPSS, Chicago, IL, USA). Significance of statistical tests was taken at  $P < 0.05$ .

## RESULTS

### Tumor response at follow-up CT: Assessment with mRECIST

According to target response analysis, contrast-enhanced CT obtained at 1–4 months of follow-up indicated mRECIST complete response in 72.9% (191/262), partial response in 6.1% (16/262), stable disease in 16.8% (44/262), and progressive disease in 4.2% (11/262). This contrast-enhanced CT was carried out, on average, 57.8 days after c-TACE (median, 51 days; range, 28–120 days). During the first half of the follow-up period, complete response was achieved in 71.3% (107/150).

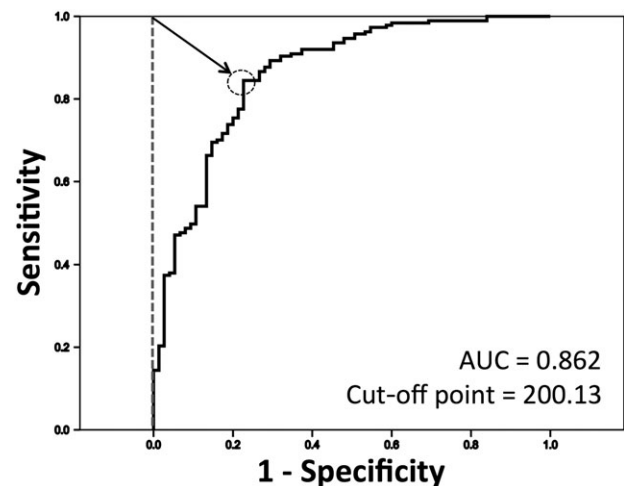
Complete response was achieved in 65.2% (73/112) during the second half of the follow-up period. There was no significant difference in treatment response assessment between the first and second half of the follow-up ( $P = 0.29$ ).

According to the pattern of iodized oil uptake, postprocedural plain cone-beam CT showed uptake to be excellent in 70.6% (185/262), good in 19.5% (51/262), fair in 9.9% (26/262), and poor in 0%. The sensitivity, specificity, positive predictive value, negative predictive value, and accuracy for predicting complete response were 85.9%, 70.4%, 88.6%, 64.9%, and 81.7%, respectively, due to excellent uptake on cone-beam CT (Table 2). If plain cone-beam CT immediately following c-TACE showed good grade iodized oil uptake within HCC, nodular iodized oil uptake was not often observed after a few months.

### Analysis of ROC curve using mean voxel gray value at postprocedural cone-beam CT and prediction of tumor response

All HCCs revealed iodized oil uptake in the lesions on plain cone-beam CT immediately after c-TACE. The mean voxel gray values in HCCs ranged from 20 to 1113 (mean  $\pm$  SD,  $364 \pm 244$ ). Figure 1 shows that the AUC of voxel values was 0.86 (95% confidence interval, 0.81–0.91). Based on the values of sensitivity and specificity, voxel value 200.13 was selected as the cut-off. The sensitivity, specificity, positive predictive value, negative predictive value, and accuracy for predicting complete response were 86.4%, 80.3%, 92.2%, 68.7%, and 84.7%, respectively, with a cut-off voxel value of 200. Actually, some HCCs showed heterogeneous iodized oil accumulation with higher mean voxel values in the ROI than the cut-off level.

With a cut-off voxel value of 200 and excellent iodized oil retention, the sensitivity, specificity, positive predictive



**Figure 1** Receiver–operating characteristic curve as a predictor of complete response to conventional transcatheter arterial chemoembolization on plain cone-beam computed tomography. The cut-off point for complete response was a mean voxel value of 200.13 (dotted circle), with a sensitivity of 85.9% and a specificity of 77.4%. AUC, area under the curve.

value, negative predictive value, and accuracy for predicting complete response were 86.4%, 95.8%, 98.2%, 72.3%, and 88.9%, respectively (Table 3). The predictive accuracy was significantly better than that of the pattern of iodized oil retention alone ( $P = 0.019$ ) (Table 4).

## DISCUSSION

**E**VEN IF THE iodized oil uptake was considered to be good, washout during follow-up sometimes suggested the presence of a viable tumor. For additional diagnostic value of early prediction of c-TACE response, our study investigated whether plain cone-beam CT immediately after c-TACE can help to predict tumor response

**Table 2** Comparison of the pattern of iodized oil uptake only on postprocedural cone-beam computed tomography (CT) and follow-up modified Response Evaluation Criteria in Solid Tumors (mRECIST) assessment

	mmRECIST assessment		
	CR	Not CR	Total
Excellent	164	21	185
Plain cone-beam CT			
Not excellent	27	50	77
Total	191	71	262

CR, complete response.

**Table 3** Comparison of the combination of density and homogeneity of iodized oil uptake on postprocedural plain cone-beam computed tomography (CT) and follow-up modified Response Evaluation Criteria in Solid Tumors (mRECIST) assessment

	mmRECIST assessment		
	CR	Not CR	Total
Voxel value $\geq 200$ and Excellent	165	3	168
Plain cone-beam CT			
Voxel value $< 200$ or Not excellent	26	68	94
Total	191	71	262

CR, complete response.



**Table 4** Sensitivity, specificity, positive and negative predictive values, and accuracy of prediction of transcatheter arterial chemoembolization response with the combination of cut-off and degree of iodized oil uptake, and the pattern of iodized oil uptake only on cone-beam computed tomography

	Sensitivity, %	Specificity, %	PPV, %	NPV, %	Accuracy, %
Combination of cut-off and pattern of iodized oil uptake	86.4	95.8	98.2	72.3	88.9 $P=0.019$
Pattern of iodized oil uptake only	85.9	70.4	88.6	64.9	81.7

NPV, negative predictive value; PPV, positive predictive value.

semiquantitatively in patients with HCC. According to the ROC curve of voxel values as a predictor of complete response, an AUC of 0.86 gave a good correlation, with an optimal cut-off voxel value of 200. The sensitivity, specificity, and accuracy were 85.9%, 77.4%, and 83.6%, respectively. The diagnostic accuracy was shown to be better than that of the pattern of iodized oil retention alone, but was limited because some HCCs showed heterogeneous iodized oil accumulation. Recurrences often occurred at areas of lower voxel value in HCCs. In practical situations, using the only numeric value of the mean voxel value in the ROI has a limited capacity for improving the accuracy of tumor response assessment. Therefore, two indices of lesion density and morphology were applied using plain cone-beam CT on early prediction of c-TACE. Combining the cut-off and excellent iodized oil retention, the sensitivity, specificity, and accuracy for predicting complete response were 86.4%, 95.8%, and 88.9%, respectively. The predictive accuracy was significantly better than that of the iodized oil uptake pattern alone ( $P=0.019$ ). Our results showed that the combination of the cut-off mean voxel gray value and iodized oil retention pattern was positively associated with treatment response assessment per nodule, and could assist in accurate prediction of the response to therapy.

Several researchers have undertaken studies to determine whether cone-beam CT would be appropriate for evaluating the therapeutic efficacy and treatment response after TACE.<sup>23–26</sup> Yu *et al.* reported that well-defined strong arterial enhancement on cone-beam CT was a statistically significant independent predictor of the therapeutic response to c-TACE (OR, 8.08;  $P=0.05$ ).<sup>24</sup> Intraprocedural dual-phase cone-beam CT could be used immediately after TACE with doxorubicin-eluting beads to predict HCC tumor response at 1-month follow-up. Loffroy *et al.* reported that a significant relationship between tumor enhancement at cone-beam CT after TACE and complete and/or partial tumor response at magnetic resonance imaging was found for arterial (OR, 0.95;  $P=0.023$ ) and venous (OR, 0.96;  $P=0.035$ ) phases.<sup>25</sup> The imaging characteristics of different chemoembolic agents differ substantially, thus

requiring different post-treatment cone-beam CT techniques. They administered embolic drug-eluting beads in TACE without using iodized oil, and plain cone-beam CT immediately after drug-eluting bead TACE dose not yield significant imaging findings because of the beads' high permeability to X-rays. It is certain that iodized oil can also easily accumulate in well-enhanced HCCs; however, cone-beam CT hepatic arteriography was not routinely performed in this study. The density enhancement of cone-beam CT hepatic angiography might be easily affected by the volume and/or injection rate of contrast medium, or the location of the catheter tip. Moreover, it is well known that the tumor response is higher in ultraselective TACE and lower in TACE of the proximal hepatic artery.<sup>13,27,28</sup> Therefore, not pre-treatment parameters but post-treatment parameters were focused upon for early prediction of tumor response for c-TACE.

This simple early prediction also eliminates the CT radiation exposure for prediction after c-TACE. Wang *et al.* evaluated the capability of postprocedural cone-beam CT acquired in determining iodized oil retention when compared to 1-day unenhanced CT after TACE.<sup>26</sup> The mean value of tumor volume, iodized oil-deposited regions, calculated average percent iodized oil retention, and HU value of cone-beam CT were not significantly different from those of MDCT. Imai *et al.* compared the mean lesion density of HCCs in HUs on non-enhanced CT imaging immediately after and 1 week after c-TACE.<sup>29</sup> Decreased lesion density was a significant independent predictor associated with a higher local recurrence rate after c-TACE treatment (hazard ratio, 0.46;  $P=0.02$ ). In some clinical studies, CT carried out 1–3 weeks after TACE is often used for early prediction of treatment response.<sup>29–31</sup> Our results indicate that high density iodized oil accumulation within HCCs is difficult to wash out. It is reported that the average effective radiation dose is 8 mSv for a conventional single-phase CT examination of the abdomen and pelvis,<sup>32</sup> which has been associated with an estimated lifetime attributable risk of death from cancer of 0.02%.<sup>33</sup> Martino *et al.* estimated a cumulative effective dose of 30.5–43.1 mSv for a four-phase 64-section multidetector

CT (MDCT) examination of the liver<sup>34</sup>. Unfortunately, no data on the exposure dose from cone-beam CT could be derived from our results. However, Loffroy *et al.* reported that the entrance dose was  $1.42 \text{ mSv} \pm 0.01$  per cone-beam CT for radiation dosimetry experiments.<sup>25</sup> Cone-beam CT can deliver significantly lower doses to patients and achieves similar spatial resolution and low contrast detectability compared to standard diagnostic MDCT from a phantom study.<sup>35</sup> Therefore, it should be emphasized that this early prediction using plain cone-beam CT can replace conventional CT prediction.

Among HCCs with homogeneous accumulation between 150 and 220 grayscale values, the chaotic behavior of c-TACE response was shown in this study. Under this condition, some achieved complete response; however, local treatment failure occurred in the remainder. The advantage of this early prediction is convenience because the images obtained evaluate early response in a series of c-TACE procedures. However, due to the lack of information of intratumoral blood flow, this chaotic behavior could be attributed to the limit of diagnostic accuracy using plain cone-beam CT. Contrast-enhanced ultrasonography can be more sensitive and accurate to detect residual tumor after c-TACE,<sup>36–38</sup> but this examination must be carried out on another day following c-TACE.

On one cone-beam CT section, voxel gray values were measured in this study. Unfortunately, we could not evaluate the capability of postprocedural cone-beam CT in determining iodized oil retention volumetrically. Indeed, patients with marginal recurrence on the periphery of the tumor can be encountered. However, no application can provide tools for quantifying 3-D regions in clinical practice. The further development of computing technology is expected. In this study, voxel values were measured at the level of the maximum diameter of the tumor. As an alternative use, it might be useful to measure voxel values at the level of heterogeneous retention of iodized oil in the tumor. It would seem that most recurrences could happen at the lower voxel value area on plain cone-beam CT.

The principal limitation of this study was its retrospective design, which inherently decreases the statistical strength. Second, this study may have suffered from selection bias. Finally, voxel values in cone-beam CT are not absolute values. Naitoh *et al.* observed a high-level correlation between voxel values of cone-beam CT and bone mineral densities of MDCT ( $r = 0.965$ ).<sup>39</sup> However, it can be supposed that the correlation between voxel values in cone-beam CT and MDCT could become lower at the level of soft tissue. Therefore, the cut-off value of 200 might not have relevance outside of this specific platform.

In conclusion, poor iodized oil accumulation was an unfavorable predictor in HCC patients treated with c-TACE. The pattern of iodized oil uptake on postprocedural cone-beam CT taken alone did not sufficiently correspond to 1–4 months of follow-up mRECIST assessment. The combination of density and visual estimate of homogeneity is superior to either alone in predicting tumor response of c-TACE in HCC patients.

## REFERENCES

- 1 Takayasu K, Arai S, Ikai I *et al.* Prospective cohort study of transarterial chemoembolization for unresectable hepatocellular carcinoma in 8510 patients. *Gastroenterology* 2006; **131**: 461–9.
- 2 Sergio A, Cristofori C, Cardin R *et al.* Transcatheter arterial chemoembolization (TACE) in hepatocellular carcinoma (HCC): the role of angiogenesis and invasiveness. *Am J Gastroenterol* 2008; **103**: 914–21.
- 3 Lencioni R. Chemoembolization for hepatocellular carcinoma. *Semin Oncol* 2012; **39**: 503–9.
- 4 Lencioni R. Chemoembolization in patients with hepatocellular carcinoma. *Liver Cancer* 2012; **1**: 41–50.
- 5 Minami Y, Kudo M. Imaging modalities for assessment of treatment response to nonsurgical hepatocellular carcinoma therapy: contrast-enhanced US, CT, and MRI. *Liver Cancer* 2015; **4**: 106–14.
- 6 Bruix J, Sherman M. Management of hepatocellular carcinoma: an update. *Hepatology* 2010; **53**: 1020–2.
- 7 Omata M, Lesmana LA, Tateishi R *et al.* Asian Pacific Association for the Study of the Liver consensus recommendations on hepatocellular carcinoma. *Hepatol Int* 2010; **4**: 439–74.
- 8 European Association for the Study of the Liver, European Organisation for Research and Treatment of Cancer. EASL-EORTC clinical practice guidelines: management of hepatocellular carcinoma. *J Hepatol* 2012; **56**: 908–43.
- 9 Kudo M, Kubo S, Takayasu K *et al.* Response Evaluation Criteria in Cancer of the Liver (RECICL) proposed by the Liver Cancer Study Group of Japan (2009 Revised Version). *Hepatol Res* 2010; **40**: 686–92.
- 10 Cheng AL, Amarapurkar D, Chao Y *et al.* Re-evaluating transarterial chemoembolization for the treatment of hepatocellular carcinoma: Consensus recommendations and review by an International Expert Panel. *Liver Int* 2014; **34**: 174–83.
- 11 Hirota S, Nakao N, Yamamoto S *et al.* Cone-beam CT with flat-panel-detector digital angiography system: early experience in abdominal interventional procedures. *Cardiovasc Intervent Radiol* 2006; **29**: 1034–8.
- 12 Kakeda S, Korogi Y, Ohnari N *et al.* Usefulness of cone-beam volume CT with flat panel detectors in conjunction with catheter angiography for transcatheter arterial embolization. *J Vasc Interv Radiol* 2007; **18**: 1508–16.
- 13 Miyayama S, Yamashiro M, Okuda M *et al.* Usefulness of cone-beam computed tomography during ultraselective

- transcatheter arterial chemoembolization for small hepatocellular carcinomas that cannot be demonstrated on angiography. *Cardiovasc Intervent Radiol* 2009; 32: 255–64.
- 14 Loffroy R, Lin M, Rao P *et al.* Comparing the detectability of hepatocellular carcinoma by C-arm dual-phase cone-beam computed tomography during hepatic arteriography with conventional contrast-enhanced magnetic resonance imaging. *Cardiovasc Intervent Radiol* 2012; 35: 97–104.
  - 15 Higashihara H, Osuga K, Onishi H *et al.* Diagnostic accuracy of C-arm CT during selective transcatheter angiography for hepatocellular carcinoma: comparison with intravenous contrast-enhanced, biphasic, dynamic MDCT. *Eur Radiol* 2012; 22: 872–9.
  - 16 Miyayama S, Yamashiro M, Hashimoto M *et al.* Blood supply of the main bile duct from the caudate artery and medial subsegmental artery of the hepatic artery: Evaluation using images obtained during transcatheter arterial chemoembolization for hepatocellular carcinoma. *Hepatol Res* 2013; 43: 1175–81.
  - 17 Minami Y, Yagyu Y, Murakami T, Kudo M. Tracking navigation imaging of transcatheter arterial chemoembolization for hepatocellular carcinoma using three-dimensional cone-beam CT angiography. *Liver Cancer* 2014; 3: 53–61.
  - 18 Jeon UB, Lee JW, Choo KS *et al.* Iodized oil uptake assessment with cone-beam CT in chemoembolization of small hepatocellular carcinomas. *World J Gastroenterol* 2009; 15: 5833–7.
  - 19 Chen R, Geschwind JF, Wang Z, Tacher V, Lin M. Quantitative assessment of lipiodol deposition after chemoembolization: comparison between cone-beam CT and multidetector CT. *J Vasc Interv Radiol* 2013; 24: 1837–44.
  - 20 Pauwels R, Nackaerts O, Bellaiche N *et al.* Variability of dental cone beam CT grey values for density estimations. *Br J Radiol* 2013; 86(1021) 20120135. DOI:10.1259/bjr.20120135.
  - 21 de Baere T, Arai Y, Lencioni R *et al.* Treatment of liver tumors with lipiodol TACE: technical recommendations from experts opinion. *Cardiovasc Intervent Radiol* 2016; 39: 334–43.
  - 22 Lencioni R, Llovet JM. Modified RECIST (mRECIST) assessment for hepatocellular carcinoma. *Semin Liver Dis* 2010; 30: 52–60.
  - 23 Tacher V, Radaelli A, Lin M, Geschwind JF. How I do it: Cone-beam CT during transarterial chemoembolization for liver cancer. *Radiology* 2015; 274: 320–34.
  - 24 Yu MH, Kim JH, Yoon JH *et al.* Role of C-arm CT for transcatheter arterial chemoembolization of hepatocellular carcinoma: diagnostic performance and predictive value for therapeutic response compared with gadoxetic acid-enhanced MRI. *AJR Am J Roentgenol* 2013; 201: 675–83.
  - 25 Loffroy R, Lin M, Yenokyan G *et al.* Intraprocedural C-arm dual-phase cone-beam CT: can it be used to predict short-term response to TACE with drug-eluting beads in patients with hepatocellular carcinoma? *Radiology* 2013; 266: 636–48.
  - 26 Wang Z, Lin M, Lesage D *et al.* Three-dimensional evaluation of lipiodol retention in HCC after chemoembolization: a quantitative comparison between CBCT and MDCT. *Acad Radiol* 2014; 21: 393–9.
  - 27 Miyayama S, Matsui O, Yamashiro M *et al.* Ultrasensitive transcatheter arterial chemoembolization with a 2-f tip microcatheter for small hepatocellular carcinomas: relationship between local tumor recurrence and visualization of the portal vein with iodized oil. *J Vasc Interv Radiol* 2007; 18: 365–76.
  - 28 Miyayama S, Mitsui T, Zen Y *et al.* Histopathological findings after ultrasensitive transcatheter arterial chemoembolization for hepatocellular carcinoma. *Hepatol Res* 2009; 39: 374–81.
  - 29 Imai N, Katano Y, Kuzuya T *et al.* An increase in lesion density can predict lower local recurrence after transarterial chemoembolization in patients with hepatocellular carcinoma. *Hepatogastroenterology* 2013; 60: 965–70.
  - 30 Vogl TJ, Trapp M, Schroeder H *et al.* Transarterial chemoembolization for hepatocellular carcinoma: volumetric and morphologic CT criteria for assessment of prognosis and therapeutic success—results from a liver transplantation center. *Radiology* 2000; 214: 349–57.
  - 31 Kwan SW, Fidelman N, Ma E *et al.* Imaging predictors of the response to transarterial chemoembolization in patients with hepatocellular carcinoma: a radiological–pathological correlation. *Liver Transpl* 2012; 18: 727–36.
  - 32 Mettler FA, Huda W, Yoshizumi TT, Mahesh M. Effective doses in radiology and diagnostic nuclear medicine: a catalog. *Radiology* 2008; 248: 254–63.
  - 33 Brenner DJ, Hall EJ. Computed tomography: an increasing source of radiation exposure. *N Engl J Med* 2007; 357: 2277–84.
  - 34 Di Martino M, Marin D, Guerri A, *et al.* Intraindividual comparison of gadoxetate disodium-enhanced MR imaging and 64-section multidetector CT in the Detection of hepatocellular carcinoma in patients with cirrhosis. *Radiology* 2010; 256: 806–16.
  - 35 Bai M, Liu B, Mu H, Liu X, Jiang Y. The comparison of radiation dose between C-arm flat-detector CT (DynaCT) and multi-slice CT (MSCT): a phantom study. *Eur J Radiol* 2012; 81: 3577–80.
  - 36 Liu M, Lin MX, Lu MD *et al.* Comparison of contrast-enhanced ultrasound and contrast-enhanced computed tomography in evaluating the treatment response to transcatheter arterial chemoembolization of hepatocellular carcinoma using modified RECIST. *Eur Radiol* 2015; 25: 2502–11.
  - 37 Rieke J, Seidensticker M, Mohnike K. Noninvasive diagnosis of hepatocellular carcinoma in cirrhotic liver: current guidelines and future prospects for radiological imaging. *Liver Cancer* 2012; 1: 51–8.
  - 38 Minami Y, Kudo M, Kawasaki T *et al.* Transcatheter arterial chemoembolization of hepatocellular carcinoma: usefulness of coded phase-inversion harmonic sonography. *AJR Am J Roentgenol* 2003; 180: 703–8.
  - 39 Naitoh M, Hirukawa A, Katsumata A, Ariji E. Evaluation of voxel values in mandibular cancellous bone: relationship between cone-beam computed tomography and multislice helical computed tomography. *Clin Oral Implants Res* 2009; 20: 503–6.

# IgG4-Related Disease and Innate Immunity

Tomohiro Watanabe, Kouhei Yamashita and Masatoshi Kudo

**Abstract** An increased number of clinicopathological studies on autoimmune pancreatitis, cholangitis, and sialoadenitis have led to the recognition of immunoglobulin G4-related disease (IgG4-RD) as a novel disorder, characterized by elevated levels of serum IgG4 and infiltration of IgG4-expressing plasma cells in the affected organs. Although the immunological background associated with the development of IgG4-RD remains poorly understood, recent studies have suggested involvement of the innate immune response in its pathogenesis. Peripheral blood innate immune cells, such as plasmacytoid dendritic cells and monocytes isolated from patients with IgG4-RD, promote IgG4 production by B cells. Activation of the innate immune response by microbe- and/or damage-associated molecular patterns stimulates production of type I interferon and B cell-activating factor by innate immune cells and results in IgG4 production by B cells. Elucidation of the innate immune response associated with IgG4-RD may help identify a new therapeutic target for this immune disorder.

## Contents

1	Introduction.....	116
2	IgG4-Related Disease (IgG4-RD) and Microbe-Associated Molecular Patterns (MAMPs) and Damage-Associated Molecular Patterns (DAMPs).....	117
2.1	MAMPs and DAMPs.....	117
2.2	IgG4-RD and MAMPs.....	117
2.3	IgG4-RD and DAMPs.....	119
3	IgG4-RD and T Helper Type 2 Cytokines.....	119
4	T Cell-Independent IgG4 Production (Fig. 1).....	121

---

T. Watanabe (✉) · M. Kudo

Department of Gastroenterology and Hepatology, Kindai University Faculty of Medicine,  
377-2 Ohno-Higashi, Osaka-Sayama, Osaka 589-8511, Japan  
e-mail: tmhrwtb@kuhp.kyoto-u.ac.jp

K. Yamashita

Department of Hematology and Oncology, Kyoto University Graduate School of Medicine,  
Kyoto, Kyoto 606-8507, Japan

Current Topics in Microbiology and Immunology (2017) 401: 115–128

DOI 10.1007/82\_2016\_42

© Springer International Publishing Switzerland 2016

Published Online: 22 September 2016

tmhrwtb@kuhp.kyoto-u.ac.jp

5	IgG4-RD and Type I IFN (Fig. 1).....	123
6	Conclusions.....	124
	References.....	125

## 1 Introduction

Immunoglobulin G4-related disease (IgG4-RD) is a chronic multiorgan fibroinflammatory disorder (Stone et al. 2012). It was first described by Japanese physicians and researchers who found elevated levels of serum IgG4 in most patients with autoimmune pancreatitis (AIP) (Hamano et al. 2001; Kamisawa and Okamoto 2006; Masaki et al. 2009; Okazaki et al. 2008). Physicians' awareness and recognition of IgG4-RD have expanded substantially, enabling gastroenterologists and clinical immunologists to establish specific diagnostic criteria. These include the presence of elevated serum IgG4, as well as the massive infiltration of IgG4-expressing plasmacytes in the affected organs (Stone et al. 2012). Various single-organ diseases, such as AIP, sialoadenitis, and retroperitoneal fibrosis, are now considered as organ-specific manifestations of systemic IgG4-RD, because they share an enhanced IgG4 response. Thus, our knowledge of the clinical and epidemiological features of IgG4-RD is expanding rapidly, and IgG4-RD is attracting increasing attention from gastroenterologists and clinical immunologists.

Although the clinical manifestations of IgG4-RD have been established in several organs, our understanding of its immune pathogenesis remains limited. Given the elevated IgG4 serum levels and abundant accumulation of IgG4-expressing plasmacytes in tissues, it is likely that adaptive immunity, rather than innate immunity, plays a pathogenic role in disease development. In fact, the remarkable efficacy of B cell depletion therapy (Carruthers et al. 2015; Khosroshahi et al. 2010) provides strong evidence that adaptive immune cells, such as B and T cells, are involved in the pathogenesis of IgG4-RD. In line with this, recent studies have suggested the involvement of abnormal adaptive immune responses, such as excessive T helper type 2 (TH2), regulatory T cells (Tregs), and plasmablasts (Mattoo et al. 2014b; Miyoshi et al. 2008; Satoguina et al. 2008; Wallace et al. 2015; Zen et al. 2007). However, these studies have not elucidated the abnormal immunological environment that leads to the development of IgG4-RD, and a number of unresolved questions have been raised. These include the identification of antigens recognized by elevated IgG4 levels and the pathogenicity of IgG4 itself. In addition, recent investigations have highlighted the importance of innate immunity in preceding and/or augmenting IgG4 responses driven by adaptive immunity (Akitake et al. 2010; Arai et al. 2015; Fukui et al. 2015; Watanabe et al. 2012, 2013). Thus, the cross talk between adaptive and innate immune responses is associated with the immune pathogenesis of IgG4-RD. In this review, we discuss the innate immune responses associated with IgG4-RD.



## **2 IgG4-Related Disease (IgG4-RD) and Microbe-Associated Molecular Patterns (MAMPs) and Damage-Associated Molecular Patterns (DAMPs)**

### ***2.1 MAMPs and DAMPs***

Danger signals are initially recognized by the innate immune system, which then promotes antigen-specific adaptive immune responses. Innate immunity exerts its host-defense functions immediately upon recognition of microbe-associated molecular patterns (MAMPs) (Akira and Takeda 2004; Chen et al. 2009; Strober et al. 2006) and damage-associated molecular patterns (DAMPs) (Kono and Rock 2008), through germline-encoded pathogen recognition receptors (PRRs). In contrast, adaptive immunity is responsible for delayed effector functions, since it relies on the selection and clonal expansion of antigen-specific B cells and T cells via gene rearrangement. At present, PRRs are categorized into four types: Toll-like receptors (TLRs), nucleotide-binding oligomerization domain (NOD)-like receptors (NLRs), RIG-I-like receptors, and C-type lectin-like receptors (Brubaker et al. 2015). These PRRs are mainly expressed on the cell surface or the cytosolic regions of innate immune cells such as antigen-presenting cells and epithelial cells. Upon microbial infection, MAMPs activate PRRs to eradicate or control microorganisms, in concert with adaptive immune responses against microbe-specific antigens. Under sterile inflammatory conditions, endogenous non-microbial danger molecules released from dying and necrotic cells activate PRRs and have been implicated in the development of autoimmune diseases (Kono and Rock 2008). Recent studies have revealed a possible involvement of MAMPs and DAMPs in the immune pathogenesis of IgG4-RD.

### ***2.2 IgG4-RD and MAMPs***

It is generally accepted that excessive immune reactions toward the intestinal microflora cause inflammatory bowel disease (IBD) (Bouma and Strober 2003). Indeed, significant numbers of patients with Crohn's disease present mutations in caspase recruitment domain 15 (Hugot et al. 2001; Ogura et al. 2001), which encodes NOD2, a sensor for small peptides derived from the bacterial peptidoglycan (Strober et al. 2014). NOD2 polymorphisms associated with Crohn's disease are thought to alter the immune response to gut bacteria and, consequently, the composition of the intestinal microflora (Strober et al. 2014). Thus, studies on the immune pathogenesis of Crohn's disease in the presence of NOD2 mutations have revealed an excessive immune response to MAMPs derived from the intestinal microflora.

Given the lack of definitive genome-wide association or microbiome studies on IgG4-RD, it remains to be seen whether scenario described above applies to this

disorder. Some studies suggest a possible involvement of MAMPs in the development of IgG4-RD. IBD is categorized in two subsets, Crohn's disease and ulcerative colitis. The intestinal mucosa of IBD is characterized by enhanced production of TH1 cytokines, such as interleukin (IL)-12 and interferon (IFN)- $\gamma$ , in Crohn's disease, and TH2 cytokines, such as IL-5 and IL-13, in ulcerative colitis (Bouma and Strober 2003). Extensive immunohistochemical analysis of IgG4-positive plasma cells in the colonic mucosa of IBD patients revealed a significantly higher number of such cells in patients with ulcerative colitis than in those with Crohn's disease (Virk et al. 2014). In addition, in ulcerative colitis, colonic infiltration of IgG4-positive plasma cells was accompanied by severe inflammation (Kuwata et al. 2014). These clinicopathological studies suggest that accumulation and infiltration of IgG4-expressing plasma cells in the colonic mucosa of patients with ulcerative colitis are probably caused by an excessive immune reaction against the intestinal microflora. Supporting this idea, Akitake et al. (2010) reported a case of IgG4-RD presenting abundant infiltration of IgG4-expressing plasmacytes in the ileum and colon without any symptoms of IBD. Furthermore, peripheral blood mononuclear cells isolated from this patient produced large amounts of TH2 cytokines upon stimulation with TLR ligands (Akitake et al. 2010). In line with this case report, the NOD2 ligand, muramyl dipeptide (MDP), has been shown to strongly induce IgG4 production in healthy individuals (Watanabe et al. 2012), which suggests that MAMPs derived from the intestinal microflora may trigger TH2-driven pathogenic responses in IgG4-RD. Repeated administration of heat-killed *Escherichia coli* to C57BL/6 mice induces activation of the innate immune system and the development of chronic fibroinflammatory disorder of the pancreas, akin to human AIP (Haruta et al. 2010; Yanagisawa et al. 2014). Taken together, both human and animal studies provide evidence that MAMPs derived from the intestinal microflora might trigger IgG4-RD through activation of PRRs.

One major question arising from the above hypothesis is whether a significant population of patients with IgG4-RD exhibits clinical symptoms of IBD. To this end, a case-control study revealed that four of 71 patients with AIP had concurrent IBD (Ravi et al. 2009). The simultaneous occurrence of IBD is generally observed in patients with type 2 non-IgG4-associated AIP rather than in patients with type 1 IgG4-associated AIP (Hart et al. 2015). Moreover, Ueki et al. (2015) reported an extremely low incidence of AIP in patients with IBD (Ueki et al. 2015). Thus, previous case-control studies do not support the hypothesis that MAMPs derived from the intestinal microflora are involved in the development of IgG4-RD. Given that intestinal tissue injury is absent even in the presence of massive infiltration of IgG4-expressing plasma cells (Akitake et al. 2010), the underlying immune reactions do not play a pathogenic role in the gut. In this regard, several mechanisms, including Tregs-mediated immune suppression, might protect the intestinal mucosa from tissue injury (Strober et al. 2007). Thus, one possible explanation for the low incidence of IBD in IgG4-RD patients is that pathogenic immune responses leading to colonic injury are suppressed by activation of Tregs. In contrast, these responses might cause tissue injury in sterile organs, such as the pancreas and salivary glands,

due to the absence of regulatory mechanisms. Future studies addressing global immune reactions in the gut mucosa of patients with AIP will confirm this hypothesis.

### 2.3 *IgG4-RD and DAMPs*

DAMPs released from dying or necrotic cells are now recognized as potent activators of the innate immune system (Kono and Rock 2008). The role of DAMPs is highlighted in acute pancreatitis (Hoque et al. 2011, 2012). Double-stranded DNA (dsDNA) released from dying acinar cells upon experimental induction of acute pancreatitis activates TLR9 and NLR family, pyrin domain-containing 3 (NLRP3). These receptors are expressed in antigen-presenting cells and stimulate production of proinflammatory cytokines, such as IL-1 $\beta$  and IL-18 (Hoque et al. 2011, 2012). High-mobility group box chromosomal protein 1 (HMGB1) is a well-studied DAMP capable of inducing sterile inflammation by activating TLR4 (Zong et al. 2013). Yasuda et al. (2006) reported a marked increase in serum levels of HMGB1 in patients with acute pancreatitis. These studies support the idea that DAMPs released from necrotic pancreatic tissues induce the development of acute pancreatitis through activation of the innate immune system. Similarly, several reports suggest the involvement of DAMPs, such as dsDNA, monosodium urate crystals (MSU), and asbestos in the pathogenesis of IgG4-RD. Serum levels of dsDNA are higher in patients with IgG4-RD than in those with chronic pancreatitis or healthy individuals (Arai et al. 2015). Antigen-presenting cells and neutrophils isolated from patients with IgG4-RD induce IgG4 production by B cells upon MSU stimulation (Arai et al. 2015). Furthermore, Toyoshima et al. (2010) reported a case of IgG4-related lung disease in a worker exposed to asbestos, one of the prototypical DAMPs to activate the NLRP3 inflammasome (Toyoshima et al. 2010). It should nevertheless be noted that our knowledge of DAMPs in IgG4-RD is very limited and definitive proof is still lacking at present.

## 3 IgG4-RD and T Helper Type 2 Cytokines

Lesions in patients with IgG4-RD are characterized by enhanced expression of TH2 cytokines, such as IL-4, IL-10, and IL-13, rather than TH1 cytokines, such as IFN- $\gamma$  and IL-12 (Della-Torre et al. 2015; Moriyama et al. 2014; Tanaka et al. 2012). In vitro studies have shown that stimulation of peripheral blood mononuclear cells with IL-4 and/or IL-10 increases IgG4 production in healthy subjects (Jeannin et al. 1998; Punnonen et al. 1993). The involvement of TH2 cytokines partly explains the allergic symptoms and elevated serum IgE levels commonly detected in IgG4-RD patients. It should be noted, however, that such classical TH2 responses might play a pathogenic role only in a defined subpopulation of IgG4-RD. Expansion of cells

expressing IL-4, IL-5, or IL-13 and their lineage transcription factor GATA binding protein 3 (GATA3) (Crotty 2014) has been detected only in IgG4-RD patients with atopic symptoms and not in those without these symptoms (Mattoo et al. 2014a). Co-localization analyses on cells expressing both GATA3 and IL-4, IL-5, or IL-13 have not been performed in the lesions of IgG4-RD patients. Therefore, it is possible that IL-4 and IL-13 may be derived from other types of cells, such as T follicular helper (Tfh) cells (Akiyama et al. 2015; Maehara et al. 2012; Moriyama et al. 2014) and mast cells (Takeuchi et al. 2014, 2015) rather than conventional TH2 cells.

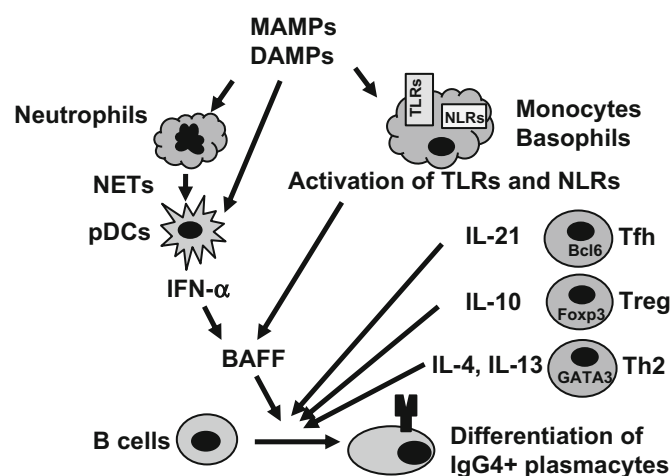
Tfh is a newly defined T helper subset that induces the development of germinal centers and the generation of high-affinity antibodies by B cells (Crotty 2014). Tfh cells express the master transcription factor B cell lymphoma 6 (Bcl6) and the chemokine receptor CXCR5 and produce large amounts of IL-21 (Crotty 2014). Maehara et al. (2012) reported increased IL-21 and BCL6 expression in the ectopic germinal centers of salivary glands from a patient with IgG4-RD (Maehara et al. 2012). Furthermore, flow cytometric analysis by Akiyama et al. (2015) found elevated numbers of CXCR5<sup>+</sup> CD45RA<sup>-</sup> CD4<sup>+</sup> CXCR3<sup>-</sup> CCR6<sup>-</sup> Tfh2 cells in the peripheral blood of IgG4-RD patients. Interestingly, the number of Tfh2 cells correlated with IL-4 and IgG4 serum levels, suggesting that Tfh cells may enhance the production of IgG4 in concert with conventional TH2 cells.

Another important feature of the T cell subset in IgG4-RD is infiltration of Tregs in the lesions (Miyoshi et al. 2008; Zen et al. 2007). Tregs express the master transcription factor, forkhead box protein p3 (Foxp3), and produce immunosuppressive cytokines, such as IL-10 and tumor growth factor (TGF)- $\beta$ 1 (Morikawa and Sakaguchi 2014), as observed in the liver of IgG4-RD patients (Zen et al. 2007). In vitro studies have shown that Tregs induce IgG4 production by B cells through IL-10 and TGF- $\beta$ 1 (Satoguina et al. 2008). Thus, it is likely that Tregs-derived IL-10 and TGF- $\beta$ 1 are associated with enhanced IgG4 production. One major question concerns the mechanism underlying the occurrence of chronic inflammation even in the presence of Tregs in IgG4-RD. In this regard, it should be noted that no studies have addressed the function of Tregs isolated from IgG4-RD patients by using conventional suppression assays. This leaves the possibility that Tregs accumulating in the lesions of IgG4-RD patients cannot fulfill their suppressive activity due to impaired immune regulatory functions, thus leading to chronic fibroinflammatory disorders. Alternatively, activation of Tregs in IgG4-RD may reflect some sort of counter-regulatory response to strong and persistent inflammation.

As suggested above, adaptive immune responses associated with IgG4-RD are mediated by a variety of T cell subsets, including classical TH2 cells, Tfh cells, and Tregs. Even if the elevated cytokine expression observed in IgG4-RD is confirmed to be derived from these T cell subsets, further studies are required to elucidate the cellular and molecular mechanisms accounting for pathological adaptive immune responses.

#### 4 T Cell-Independent IgG4 Production (Fig. 1)

Innate immune responses mediated by MAMPs and DAMPs may be important for the onset and maintenance of abnormal immunological environments leading to IgG4-RD. Watanabe et al. (2012) have addressed the role of TLR- or NLR-mediated signaling pathways in the production of IgG4, and some key findings are summarized herein (Watanabe et al. 2012, 2013). First, MDP was found to be a potent inducer of IgG4 production (Watanabe et al. 2012). Second, MDP activation of NOD2 in monocytes induced the production of B cell-activating factor (BAFF), thereby enhancing IgG4 production through inhibition of B cell apoptosis. These results were obtained from peripheral blood mononuclear cells (PBMCs) of healthy subjects, suggesting the importance of NOD2 activation for IgG4 production in innate immune cells. Third, PBMCs isolated from IgG4-RD patients produced large amounts of IgG4 and BAFF upon stimulation with TLR and NLR ligands. Finally, B cells from healthy controls produced large quantities of IgG4 upon stimulation with TLR and NLR ligands via a T cell-independent manner only when co-cultured with monocytes isolated from patients with IgG4-RD. These results suggest that activation of the innate immune system by TLR and NLR ligands may be a critical step for the increased production of IgG4 and that IgG4 production can be induced without any help by T cells (Watanabe et al. 2012). As for the molecular mechanism accounting for BAFF production, involvement of



**Fig. 1** Innate immune responses associated with IgG4-RD. Damage-associated molecular patterns (DAMPs) and microbe-associated molecular patterns (MAMPs) activate innate immune receptors, such as Toll-like receptors (TLRs) and NOD-like receptors (NLRs) expressed in plasmacytoid dendritic cells (pDCs), monocytes, and basophils. Activation of pDCs by neutrophil extracellular traps (NETs) leads to robust production of IFN- $\alpha$  and BAFF, whereas activation of TLRs and NLRs leads to robust production of BAFF. IgG4 production by B cells is enhanced upon co-culture with pDCs, monocytes, and basophils in a T cell-independent manner. Additionally, regulatory T (Treg), T helper type 2 (Th2), and T follicular helper (Tfh) cells stimulate IgG4 production by B cells through IL-4, IL-10, IL-13, and IL-21



NF- $\kappa$ B activation has been suggested. Inhibition of NF- $\kappa$ B signaling pathways reduces BAFF production by monocytes upon stimulation with MDP (Watanabe et al. 2012). Moreover, the DNA sequence of the BAFF promoter has several functional binding motifs for the NF- $\kappa$ B subunit (He et al. 2003).

Although basophils have been considered effector cells for TH2 and IgE responses, recent studies have highlighted their role in initiating allergic responses (Paul and Zhu 2010; Sokol and Medzhitov 2010). It seems likely that activation of basophils is involved in the immune pathogenesis of IgG4-RD, which is often characterized by elevated serum IgE levels. Indeed, Watanabe et al. (2013) showed that activation of TLRs in basophils stimulated IgG4 production by B cells in a T cell-independent manner (Watanabe et al. 2013). Basophils were found to release large quantities of BAFF upon stimulation with TLR ligands, thereby triggering IgG4 production. More importantly, as with monocytes (Watanabe et al. 2012), it was shown that B cells from healthy controls produced considerable amounts of IgG4 upon stimulation with TLR and NLR ligands only when co-cultured with basophils from IgG4-RD patients. These two studies suggest that activation of TLRs and/or NLRs in monocytes or basophils induces IgG4 production by B cells in a T cell-independent but BAFF-dependent manner. Moreover, monocytes or basophils from IgG4-RD patients produce large quantities of BAFF upon exposure to MAMPs via NF- $\kappa$ B signaling pathways.

Consistent with the above *in vitro* studies (Watanabe et al. 2012, 2013), BAFF serum levels are significantly higher in IgG4-RD patients than in healthy controls or in patients with chronic pancreatitis or pancreatic cancer (Kiyama et al. 2012; Yamanishi et al. 2011). Interestingly, BAFF-mediated signaling pathways seem to be operating in the inflamed pancreas, as confirmed by expression of BAFF and BAFF receptors in cells infiltrating the pancreas of IgG4-related AIP (Yamanishi et al. 2011). In addition, IgD<sup>+</sup> B cells stimulated with BAFF and IL-4 induce Ig class-switch DNA recombination (CSR), giving rise to IgG1, IgG2, IgG3, and IgG4 (Litinskiy et al. 2002). Taken together, these reports have identified BAFF and TH2 cytokines derived from antigen-presenting cells and T cells, respectively, to be responsible for the generation of pathogenic immune responses in IgG4-RD. It should be noted, however, that enhanced IgG4 responses in IgG4-RD cannot be explained by BAFF-mediated pathways alone, since BAFF is a survival and activation factor for B cells rather than a specific inducer for IgG4 CSR (Mackay and Schneider 2009; Mackay et al. 2007).

The above studies on IgG4 and BAFF production in response to MAMPs support the idea that commensal flora-mediated innate immunity is involved in the immunopathogenesis of IgG4-RD. In this scenario, tissue injury initiated by an autoimmune process leads to impaired gut barrier function, followed by entry of intestinal microflora into the splanchnic vascular bed. MAMPs derived from intestinal microflora activate tissue-residing antigen-presenting cells and B cells, thus stimulating production of BAFF and IgG4. This idea is consistent with the observation that IgG4-expressing plasma cells are sometimes seen in the intestinal mucosa of patients with IgG4-RD (Akitake et al. 2010; Deheragoda et al. 2007).

## 5 IgG4-RD and Type I IFN (Fig. 1)

Type I IFNs (IFN- $\alpha$  and IFN- $\beta$ ) are indispensable components of host defenses against viral and bacterial infections (Akira and Takeda 2004). Although rapid induction of type I IFN production is particularly beneficial against viral infections, persistent and excessive release of these pluripotent cytokines causes autoimmune diseases. Detailed and extensive studies using clinical samples from lupus patients have established that excessive production of type I IFN and activation of downstream signaling pathways play a central role in the immune pathogenesis of the disease (Crow 2014a, b; Huang et al. 2015). This was confirmed by enhanced expression of type I IFN-related genes in peripheral blood mononuclear cells from lupus patients (Baechler et al. 2003; Bennett et al. 2003). Since they produce large quantities of IFN- $\alpha$  (Gilliet et al. 2008), plasmacytoid dendritic cells (pDCs) are considered the main promoters of type I IFN signaling pathways in lupus (Crow 2014a, b; Huang et al. 2015). This is particularly true, if they are exposed to immune complexes containing nucleic acids (Crow 2014a, b). Thus, the innate immune response mediated by pDC-derived IFN- $\alpha$  plays a predominant role in the initiation and progression of lupus. This notion is supported by recent genome-wide association studies, which have identified type I IFN-related genes as susceptible loci for lupus (Deng and Tsao 2010).

A recent study by Arai et al. (2015) provides evidence that activation of pDCs and IFN- $\alpha$  production are prominent features of human IgG4-RD and an experimental model of AIP (Arai et al. 2015). MRL/MpJ mice treated with polyinosinic-polycytidylic acid, poly (I:C), exhibit several histological features of chronic autoimmune pancreatitis, such as massive destruction of acinar cell architecture, infiltration of immune cells, and fibrosis (Nishio et al. 2011; Schwaiger et al. 2014). Although human IgG4-related AIP and MRL/MpJ mice treated with poly (I:C) share important clinical findings, common abnormal immune responses have been poorly described. Cytokine and chemokine arrays of pancreatic lysates from MRL/MpJ mice treated with poly (I:C) revealed that type I IFN-related chemokines, such as chemokine (C-X-C motif) ligand (CXCL) 9, 10, and 11, as well as prototypic inflammatory cytokines, such as IL-6 and tumor necrosis factor- $\alpha$ , increased upon induction of experimental AIP (Arai et al. 2015). Indeed, administration of poly (I:C) led to a marked increase of IFN- $\alpha$  and IFN- $\beta$  in the serum of MRL/MpJ mice and accumulation of pDCs in the pancreas. Since both depletion of pDCs and blockade of type I IFN signaling pathways prevent pancreatic inflammation, Arai et al. (2015) propose a pivotal role for pDC-mediated IFN- $\alpha$  signaling pathways in experimental AIP (Arai et al. 2015). In line with the above results, serum levels of IFN- $\alpha$  are significantly higher in patients with IgG4-associated AIP than in healthy controls, or in patients with chronic pancreatitis (Arai et al. 2015). Consistent with a report showing that BAFF expression is directly induced by type I IFN via interferon regulatory factors 1 and 2 (Sjöstrand et al. 2016), elevated IFN- $\alpha$  serum levels are accompanied by BAFF levels. Moreover, infiltration of pDCs producing both IFN- $\alpha$  and BAFF is observed in the pancreas of patients with

IgG4-associated AIP, but not in those with chronic pancreatitis (Arai et al. 2015). Regarding activators of pDCs, two recent studies show that neutrophil extracellular traps (NETs) containing self-DNA and neutrophil-derived proteins are potent inducers of IFN- $\alpha$  production by pDCs in patients with lupus (Garcia-Romo et al. 2011; Lande et al. 2011). In the case of IgG4-RD, NETs may also be involved in increased IFN- $\alpha$  release by pDCs. Arai et al. (2015) report that B cells isolated from healthy individuals produce large quantities of IgG4 when co-cultured with NET-stimulated pDCs isolated from patients with IgG4-RD. Such pDC-mediated IgG4 production by B cells is markedly suppressed by the abrogation of type I IFN signaling pathways, which suggests an important role by pDC-derived IFN- $\alpha$ . Taken together, these results strongly indicate that pDC activation, followed by IFN- $\alpha$  release, is one of the pathogenic immune responses associated with IgG4-RD.

The study described above provides a new insight into the pathogenesis of IgG4-RD, which, like lupus, is characterized by pDC activation and IFN- $\alpha$  production. In addition, autoimmune complexes released by NETs may function as potent activators of pDCs in both immune disorders. Nevertheless, it should be noted that clinicopathological features of IgG4-RD and lupus are completely different, with augmented IgG4 production and storiform fibrosis being observed only in IgG4-RD. Therefore, it is clear that the immunopathogenesis of IgG4-RD cannot be explained solely by pDC activation and ensuing IFN- $\alpha$  production. Future studies aiming to identify immune responses other than the pDC-mediated IFN- $\alpha$  signaling pathways will elucidate the immunopathogenesis of IgG4-RD and help distinguish it from lupus at a cellular and a molecular level.

## 6 Conclusions

IgG4-RD is a newly established disease first proposed by Japanese gastroenterologists and rheumatologists. Although IgG4-RD is characterized by an adaptive response by B cells, recent studies suggest possible involvement of the innate immune system. Expression of IFN- $\alpha$  and BAFF produced by innate immune cells is enhanced in the pancreas of IgG4-RD patients and experimental AIP. Furthermore, pDCs and monocytes isolated from IgG4-RD patients induce a marked increase in IgG4 production by B cells through IFN- $\alpha$  and BAFF, respectively. Although many questions remain to be addressed, these insights into the role of innate immune responses in IgG4-RD pathogenesis support the idea that patients with IgG4-RD can be treated with inhibitors of innate immune cytokines, such as IFN- $\alpha$  and BAFF.

**Acknowledgments** This work was supported by Grant-in-Aid for Scientific Research (25293172, 15K15370) from the Japan Society for the Promotion of Science; the Kato Memorial Trust for Nambyo Research; and the Health and Labor Sciences Research Grants for Research on Intractable Diseases from the Ministry of Health, Labor and Welfare, Japan.

## References

- Akira S, Takeda K (2004) Toll-like receptor signalling. *Nat Rev Immunol* 4:499–511
- Akitake R, Watanabe T, Zaima C, Uza N, Ida H, Tada S, Nishida N, Chiba T (2010) Possible involvement of T helper type 2 responses to Toll-like receptor ligands in IgG4-related sclerosing disease. *Gut* 59:542–545
- Akiyama M, Suzuki K, Yamaoka K, Yasuoka H, Takeshita M, Kaneko Y, Kondo H, Kassai Y, Miyazaki T, Morita R et al (2015) Number of circulating follicular helper 2 T cells correlates with IgG4 and Interleukin-4 levels and plasmablast numbers in IgG4-related disease. *Arthritis Rheumatol* 67:2476–2481
- Arai Y, Yamashita K, Kuriyama K, Shiokawa M, Kodama Y, Sakurai T, Mizugishi K, Uchida K, Kadowaki N, Takaori-Kondo A et al (2015) Plasmacytoid dendritic cell activation and IFN- $\alpha$  production are prominent features of murine autoimmune pancreatitis and human IgG4-related autoimmune pancreatitis. *J Immunol* 195:3033–3044
- Baechler EC, Batliwalla FM, Karypis G, Gaffney PM, Ortmann WA, Espe KJ, Shark KB, Grande WJ, Hughes KM, Kapur V et al (2003) Interferon-inducible gene expression signature in peripheral blood cells of patients with severe lupus. *Proc Natl Acad Sci USA* 100:2610–2615
- Bennett L, Palucka AK, Arce E, Cantrell V, Borvak J, Banchereau J, Pascual V (2003) Interferon and granulopoiesis signatures in systemic lupus erythematosus blood. *J Exp Med* 197:711–723
- Bouma G, Strober W (2003) The immunological and genetic basis of inflammatory bowel disease. *Nat Rev Immunol* 3:521–533
- Brubaker SW, Bonham KS, Zanoni I, Kagan JC (2015) Innate immune pattern recognition: a cell biological perspective. *Annu Rev Immunol* 33:257–290
- Carruthers MN, Topazian MD, Khosroshahi A, Witzig TE, Wallace ZS, Hart PA, Deshpande V, Smyrk TC, Chari S, Stone JH (2015) Rituximab for IgG4-related disease: a prospective, open-label trial. *Ann Rheum Dis* 74:1171–1177
- Chen G, Shaw MH, Kim YG, Nunez G (2009) NOD-like receptors: role in innate immunity and inflammatory disease. *Annu Rev Pathol* 4:365–398
- Crotty S (2014) T follicular helper cell differentiation, function, and roles in disease. *Immunity* 41:529–542
- Crow MK (2014a) Advances in understanding the role of type I interferons in systemic lupus erythematosus. *Curr Opin Rheumatol* 26:467–474
- Crow MK (2014b) Type I interferon in the pathogenesis of lupus. *J Immunol* 192:5459–5468
- Deheragoda MG, Church NI, Rodriguez-Justo M, Munson P, Sandanayake N, Seward EW, Miller K, Novelli M, Hatfield AR, Pereira SP, Webster GJ (2007) The use of immunoglobulin G4 immunostaining in diagnosing pancreatic and extrapancreatic involvement in autoimmune pancreatitis. *Clin Gastroenterol Hepatol* 5:1229–1234
- Della-Torre E, Lanzillotta M, Doglioni C (2015) Immunology of IgG4-related disease. *Clin Exp Immunol* 181:191–206
- Deng Y, Tsao BP (2010) Genetic susceptibility to systemic lupus erythematosus in the genomic era. *Nat Rev Rheumatol* 6:683–692
- Fukui Y, Uchida K, Sakaguchi Y, Fukui T, Nishio A, Shikata N, Sakaida N, Uemura Y, Satoi S, Okazaki K (2015) Possible involvement of Toll-like receptor 7 in the development of type 1 autoimmune pancreatitis. *J Gastroenterol* 50:435–444
- Garcia-Romo GS, Caielli S, Vega B, Connolly J, Allantaz F, Xu Z, Punaro M, Baisch J, Guiducci C, Coffman RL et al (2011) Netting neutrophils are major inducers of type I IFN production in pediatric systemic lupus erythematosus. *Sci Transl Med* 3:73ra20
- Gilliet M, Cao W, Liu YJ (2008) Plasmacytoid dendritic cells: sensing nucleic acids in viral infection and autoimmune diseases. *Nat Rev Immunol* 8:594–606
- Hamano H, Kawa S, Horiuchi A, Unno H, Furuya N, Akamatsu T, Fukushima M, Nikaido T, Nakayama K, Usuda N, Kiyosawa K (2001) High serum IgG4 concentrations in patients with sclerosing pancreatitis. *N Engl J Med* 344:732–738

- Hart PA, Zen Y, Chari ST (2015) Recent advances in autoimmune pancreatitis. *Gastroenterology* 149:39–51
- Haruta I, Yanagisawa N, Kawamura S, Furukawa T, Shimizu K, Kato H, Kobayashi M, Shiratori K, Yagi J (2010) A mouse model of autoimmune pancreatitis with salivary gland involvement triggered by innate immunity via persistent exposure to avirulent bacteria. *Lab Invest* 90:1757–1769
- He B, Raab-Traub N, Casali P, Cerutti A (2003) EBV-encoded latent membrane protein 1 cooperates with BAFF/BLyS and APRIL to induce T cell-independent Ig heavy chain class switching. *J Immunol* 171:5215–5224
- Hoque R, Sohail M, Malik A, Sarwar S, Luo Y, Shah A, Barrat F, Flavell R, Gorelick F, Husain S, Mehal W (2011) TLR9 and the NLRP3 inflammasome link acinar cell death with inflammation in acute pancreatitis. *Gastroenterology* 141:358–369
- Hoque R, Malik AF, Gorelick F, Mehal WZ (2012) Sterile inflammatory response in acute pancreatitis. *Pancreas* 41:353–357
- Huang X, Dorta-Estremera S, Yao Y, Shen N, Cao W (2015) Predominant role of plasmacytoid dendritic cells in stimulating systemic autoimmunity. *Front Immunol* 6:526
- Hugot JP, Chamaillard M, Zouali H, Lesage S, Cezard JP, Belaiche J, Almer S, Tysk C, O'Morain CA, Gassull M et al (2001) Association of NOD2 leucine-rich repeat variants with susceptibility to Crohn's disease. *Nature* 411:599–603
- Jeannin P, Lecoanet S, Delneste Y, Gauchat JF, Bonnefoy JY (1998) IgE versus IgG4 production can be differentially regulated by IL-10. *J Immunol* 160:3555–3561
- Kamisawa T, Okamoto A (2006) Autoimmune pancreatitis: proposal of IgG4-related sclerosing disease. *J Gastroenterol* 41:613–625
- Khosroshahi A, Bloch DB, Deshpande V, Stone JH (2010) Rituximab therapy leads to rapid decline of serum IgG4 levels and prompt clinical improvement in IgG4-related systemic disease. *Arthritis Rheum* 62:1755–1762
- Kiyama K, Kawabata D, Hosono Y, Kitagori K, Yukawa N, Yoshifuji H, Omura K, Fujii T, Mimori T (2012) Serum BAFF and APRIL levels in patients with IgG4-related disease and their clinical significance. *Arthritis Res Ther* 14:R86
- Kono H, Rock KL (2008) How dying cells alert the immune system to danger. *Nat Rev Immunol* 8:279–289
- Kuwata G, Kamisawa T, Koizumi K, Tabata T, Hara S, Kuruma S, Fujiwara T, Chiba K, Egashira H, Fujiwara J et al (2014) Ulcerative colitis and immunoglobulin G4. *Gut Liver* 8:29–34
- Lande R, Ganguly D, Facchinetti V, Frasca L, Conrad C, Gregorio J, Meller S, Chamilos G, Sebasigari R, Riccieri V et al (2011). Neutrophils activate plasmacytoid dendritic cells by releasing self-DNA-peptide complexes in systemic lupus erythematosus. *Sci Transl Med* 3:73ra19
- Litinskiy MB, Nardelli B, Hilbert DM, He B, Schaffer A, Casali P, Cerutti A (2002) DCs induce CD40-independent immunoglobulin class switching through BLyS and APRIL. *Nat Immunol* 3:822–829
- Mackay F, Schneider P (2009) Cracking the BAFF code. *Nat Rev Immunol* 9:491–502
- Mackay F, Silveira PA, Brink R (2007) B cells and the BAFF/APRIL axis: fast-forward on autoimmunity and signaling. *Curr Opin Immunol* 19:327–336
- Maehara T, Moriyama M, Nakashima H, Miyake K, Hayashida JN, Tanaka A, Shinozaki S, Kubo Y, Nakamura S (2012) Interleukin-21 contributes to germinal centre formation and immunoglobulin G4 production in IgG4-related dacryoadenitis and sialoadenitis, so-called Mikulicz's disease. *Ann Rheum Dis* 71:2011–2019
- Masaki Y, Dong L, Kurose N, Kitagawa K, Morikawa Y, Yamamoto M, Takahashi H, Shinomura Y, Imai K, Saeki T et al (2009) Proposal for a new clinical entity, IgG4-positive multiorgan lymphoproliferative syndrome: analysis of 64 cases of IgG4-related disorders. *Ann Rheum Dis* 68:1310–1315



- Mattoo H, Della-Torre E, Mahajan VS, Stone JH, Pillai S (2014a) Circulating Th2 memory cells in IgG4-related disease are restricted to a defined subset of subjects with atopy. *Allergy* 69:399–402
- Mattoo H, Mahajan VS, Della-Torre E, Sekigami Y, Carruthers M, Wallace ZS, Deshpande V, Stone JH, Pillai S (2014b) De novo oligoclonal expansions of circulating plasmablasts in active and relapsing IgG4-related disease. *J Allergy Clin Immunol* 134:679–687
- Miyoshi H, Uchida K, Taniguchi T, Yazumi S, Matsushita M, Takaoka M, Okazaki K (2008) Circulating naïve and CD4+ CD25high regulatory T cells in patients with autoimmune pancreatitis. *Pancreas* 36:133–140
- Morikawa H, Sakaguchi S (2014) Genetic and epigenetic basis of Treg cell development and function: from a FoxP3-centered view to an epigenome-defined view of natural Treg cells. *Immunol Rev* 259:192–205
- Moriyama M, Tanaka A, Maehara T, Furukawa S, Nakashima H, Nakamura S (2014) T helper subsets in Sjögren's syndrome and IgG4-related dacryoadenitis and sialoadenitis: a critical review. *J Autoimmun* 51:81–88
- Nishio A, Asada M, Uchida K, Fukui T, Chiba T, Okazaki K (2011) The role of innate immunity in the pathogenesis of experimental autoimmune pancreatitis in mice. *Pancreas* 40:95–102
- Ogura Y, Bonen DK, Inohara N, Nicolae DL, Chen FF, Ramos R, Britton H, Moran T, Karaliuskas R, Duerr RH et al (2001) A frameshift mutation in *NOD2* associated with susceptibility to Crohn's disease. *Nature* 411:603–606
- Okazaki K, Uchida K, Fukui T (2008) Recent advances in autoimmune pancreatitis: concept, diagnosis, and pathogenesis. *J Gastroenterol* 43:409–418
- Paul WE, Zhu J (2010) How are TH2-type immune responses initiated and amplified? *Nat Rev Immunol* 10:225–235
- Punnonen J, Aversa G, Cocks BG, McKenzie AN, Menon S, Zurawski G, de Waal Malefyt R, de Vries JE (1993) Interleukin 13 induces interleukin 4-independent IgG4 and IgE synthesis and CD23 expression by human B cells. *Proc Natl Acad Sci USA* 90:3730–3734
- Ravi K, Chari ST, Vege SS, Sandborn WJ, Smyrk TC, Loftus EV Jr (2009) Inflammatory bowel disease in the setting of autoimmune pancreatitis. *Inflamm Bowel Dis* 15:1326–1330
- Satoguina JS, Adjobimey T, Arndts K, Hoch J, Oldenburg J, Layland LE, Hoerauf A (2008) Tr1 and naturally occurring regulatory T cells induce IgG4 in B cells through GITR/GITR-L interaction, IL-10 and TGF- $\beta$ . *Eur J Immunol* 38:3101–3113
- Schwaiger T, van den Brandt C, Fitzner B, Zaatreh S, Kraatz F, Dummer A, Nizze H, Evert M, Broker BM, Brunner-Weinzierl MC et al (2014) Autoimmune pancreatitis in MRL/Mp mice is a T cell-mediated disease responsive to cyclosporine A and rapamycin treatment. *Gut* 63:494–505
- Sjöstrand M, Johansson A, Aqrabi L, Olsson T, Wahren-Herlenius M, Espinosa A (2016) The expression of BAFF is controlled by IRF transcription factors. *J Immunol* 196:91–96
- Sokol CL, Medzhitov R (2010) Emerging functions of basophils in protective and allergic immune responses. *Mucosal Immunol* 3:129–137
- Stone JH, Zen Y, Deshpande V (2012) IgG4-related disease. *N Engl J Med* 366:539–551
- Strober W, Murray PJ, Kitani A, Watanabe T (2006) Signalling pathways and molecular interactions of NOD1 and NOD2. *Nat Rev Immunol* 6:9–20
- Strober W, Fuss I, Mannon P (2007) The fundamental basis of inflammatory bowel disease. *J Clin Invest* 117:514–521
- Strober W, Asano N, Fuss I, Kitani A, Watanabe T (2014) Cellular and molecular mechanisms underlying NOD2 risk-associated polymorphisms in Crohn's disease. *Immunol Rev* 260:249–260
- Takeuchi M, Sato Y, Ohno K, Tanaka S, Takata K, Gion Y, Orita Y, Ito T, Tachibana T, Yoshino T (2014) T helper 2 and regulatory T-cell cytokine production by mast cells: a key factor in the pathogenesis of IgG4-related disease. *Mod Pathol* 27:1126–1136
- Takeuchi M, Ohno K, Takata K, Gion Y, Tachibana T, Orita Y, Yoshino T, Sato Y (2015) Interleukin 13-positive mast cells are increased in immunoglobulin G4-related sialadenitis. *Sci Rep* 5:7696

- Tanaka A, Moriyama M, Nakashima H, Miyake K, Hayashida JN, Maehara T, Shinozaki S, Kubo Y, Nakamura S (2012) Th2 and regulatory immune reactions contribute to IgG4 production and the initiation of Mikulicz disease. *Arthritis Rheum* 64:254–263
- Toyoshima M, Chida K, Kono M, Kaida Y, Nakamura Y, Suda T, Sugimura H (2010) IgG4-related lung disease in a worker occupationally exposed to asbestos. *Intern Med* 49:1175–1178
- Ueki T, Kawamoto K, Otsuka Y, Minoda R, Maruo T, Matsumura K, Noma E, Mitsuyasu T, Otani K, Aomi Y et al (2015) Prevalence and clinicopathological features of autoimmune pancreatitis in Japanese patients with inflammatory bowel disease. *Pancreas* 44:434–440
- Virk R, Shinagare S, Lauwers GY, Yajnik V, Stone JH, Deshpande V (2014) Tissue IgG4-positive plasma cells in inflammatory bowel disease: a study of 88 treatment-naïve biopsies of inflammatory bowel disease. *Mod Pathol* 27:454–459
- Wallace ZS, Mattoo H, Carruthers M, Mahajan VS, Della Torre E, Lee H, Kulikova M, Deshpande V, Pillai S, Stone JH (2015) Plasmablasts as a biomarker for IgG4-related disease, independent of serum IgG4 concentrations. *Ann Rheum Dis* 74:190–195
- Watanabe T, Yamashita K, Fujikawa S, Sakurai T, Kudo M, Shiokawa M, Kodama Y, Uchida K, Okazaki K, Chiba T (2012) Activation of toll-like receptors and nucleotide-binding oligomerization domain-like receptors is involved in enhanced IgG4 responses in autoimmune pancreatitis. *Arthritis Rheum* 64:914–924
- Watanabe T, Yamashita K, Sakurai T, Kudo M, Shiokawa M, Uza N, Kodama Y, Uchida K, Okazaki K, Chiba T (2013) Toll-like receptor activation in basophils contributes to the development of IgG4-related disease. *J Gastroenterol* 48:247–253
- Yamanishi H, Kumagi T, Yokota T, Azemoto N, Koizumi M, Kobayashi Y, Abe M, Murakami H, Hiasa Y, Matsuura B et al (2011) Clinical significance of B cell-activating factor in autoimmune pancreatitis. *Pancreas* 40:840–845
- Yanagisawa N, Haruta I, Shimizu K, Furukawa T, Higuchi T, Shibata N, Shiratori K, Yagi J (2014) Identification of commensal flora-associated antigen as a pathogenetic factor of autoimmune pancreatitis. *Pancreatol* 14:100–106
- Yasuda T, Ueda T, Takeyama Y, Shinzeki M, Sawa H, Nakajima T, Ajiki T, Fujino Y, Suzuki Y, Kudoda Y (2006) Significant increase of serum high-mobility group box chromosomal protein 1 levels in patients with severe acute pancreatitis. *Pancreas* 33:359–363
- Zen Y, Fujii T, Harada K, Kawano M, Yamada K, Takahira M, Nakanuma Y (2007) Th2 and regulatory immune reactions are increased in immunoglobulin G4-related sclerosing pancreatitis and cholangitis. *Hepatology* 45:1538–1546
- Zong M, Bruton JD, Grundtman C, Yang H, Li JH, Alexanderson H, Palmblad K, Andersson U, Harris HE, Lundberg IE, Westerblad H (2013) TLR4 as receptor for HMGB1 induced muscle dysfunction in myositis. *Ann Rheum Dis* 72:1390–1399

# Objective response by mRECIST as a predictor and potential surrogate end-point of overall survival in advanced HCC

Riccardo Lencioni<sup>1,†</sup>, Robert Montal<sup>2,†</sup>, Ferran Torres<sup>3,4</sup>, Joong-Won Park<sup>5</sup>, Thomas Decaens<sup>6</sup>, Jean-Luc Raoul<sup>7</sup>, Masatoshi Kudo<sup>8</sup>, Charissa Chang<sup>9</sup>, José Ríos<sup>3,4</sup>, Valerie Boige<sup>10</sup>, Eric Assenat<sup>11</sup>, Yoon-Koo Kang<sup>12</sup>, Ho-Yeong Lim<sup>13</sup>, Ian Walters<sup>14</sup>, Josep M. Llovet<sup>2,9,15,\*</sup>

<sup>1</sup>Department of Interventional Radiology, University of Miami Miller School of Medicine, Sylvester Comprehensive Cancer Center, Miami, FL, USA; <sup>2</sup>Liver Cancer Translational Research Laboratory, BCLC Group, IDIBAPS, Liver Unit, Hospital Clinic, University of Barcelona, Barcelona, Catalonia, Spain; <sup>3</sup>Medical Statistics Core Facility, IDIBAPS, Hospital Clinic, Barcelona, Spain; <sup>4</sup>Biostatistics Unit, Faculty of Medicine, Autonomous University of Barcelona, Barcelona, Spain; <sup>5</sup>Center for Liver Cancer, National Cancer Center, Goyang, Republic of Korea; <sup>6</sup>Service d'Hépatogastro-entérologie, Hôpital Henri Mondor, Faculty of Medicine, University of Paris-Est, and INSERM, Creteil, France; <sup>7</sup>Service d'Oncologie Médicale, Institut Paoli Calmette, Marseille, France; <sup>8</sup>Department of Gastroenterology and Hepatology, Kindai University Faculty of Medicine, Osaka, Japan; <sup>9</sup>Liver Cancer Program, Division of Liver Diseases, Ichan School of Medicine at Mount Sinai, New York, NY, USA; <sup>10</sup>Service de Gastro-entérologie, Institut Gustave Roussy, Villejuif, France; <sup>11</sup>Service d'Hépatogastro-entérologie, Hôpital Saint Eloi, Montpellier Cedex, France; <sup>12</sup>Department of Oncology, Asan Medical Center, Seoul, Republic of Korea; <sup>13</sup>Division of Hematology-Oncology, Samsung Medical Center, Seoul, Republic of Korea; <sup>14</sup>Bristol-Myers Squibb, Wallingford, CT, USA; <sup>15</sup>Institució Catalana de Recerca i Estudis Avançats, Barcelona, Catalonia, Spain

See Editorial, pages 1114–1117

**Background & Aims:** The Modified Response Evaluation Criteria in Solid Tumors (mRECIST) was developed to overcome the limitations of standard RECIST criteria in response assessment of hepatocellular carcinoma (HCC). We aimed to investigate whether objective response by mRECIST accurately predicted overall survival (OS) in patients with advanced HCC treated with systemic targeted therapies and also to preliminarily assess this end-point as a potential surrogate of OS.

**Methods:** Individual patient data from the BRISK-PS randomized phase III trial comparing brivanib vs. placebo (the first to prospectively incorporate mRECIST) were used to analyze objective response as a predictor of OS in a time-dependent covariate analysis. Patients with available imaging scans during follow-up were included ( $n = 334$ ; 85% of those randomized). Moreover, a correlation of the survival probability in deciles vs. the observed objective response was performed to evaluate its suitability as a surrogate end-point.

**Results:** Objective response was observed in 11.5% and 1.9% of patients treated with brivanib and placebo respectively, and was associated with a better survival (median OS 15.0 vs. 9.4 months,  $p < 0.001$ ). In addition, objective response had an independent prognostic value (HR = 0.48; 95% confidence interval

[CI], 0.26–0.91,  $p = 0.025$ ) along with known prognostic factors. Finally, objective response showed promising results as a surrogate of OS in this trial ( $R = -0.92$ ; 95% CI,  $-1$  to  $-0.73$ ,  $p < 0.001$ ). It was an early indicator of the treatment effect (median time to objective response was 1.4 months).

**Conclusions:** Objective response by mRECIST in advanced HCC predicts OS and thus can be considered as a candidate surrogate end-point. Further studies are needed to support this finding.

**Lay summary:** There is a need to identify surrogate end-points for overall survival in advanced hepatocellular carcinoma. We studied patients from the phase III BRISK trial, comparing brivanib treatment with placebo after sorafenib progression. We demonstrate that objective response is an independent predictor of survival and qualifies as a potential surrogate end-point for overall survival in this patient population.

**Clinical trial number:** NCT00825955.

© 2017 European Association for the Study of the Liver. Published by Elsevier B.V. All rights reserved.

## Introduction

In 60% of cases, patients with hepatocellular carcinoma (HCC) are diagnosed when tumors are no longer eligible for potentially curative therapies [1]. In this setting, only two treatments have been included in guidelines after demonstrating survival advantages in randomized controlled trials. Patients at an intermediate stage benefit from chemoembolization and have an estimated median overall survival (OS) of 26 months [2], while at advanced stages, sorafenib extends survival from 8 to almost 11 months [3].

**Keywords:** Liver cancer; Carcinoma, hepatocellular; Advanced BCLC; Brivanib, mRECIST; Objective response; Surrogate end-point; Response evaluation criteria in solid tumours.

Received 5 July 2016; received in revised form 22 December 2016; accepted 3 January 2017; available online 26 January 2017

\* Corresponding author. Address: Laboratori de Recerca Translacional en Oncologia Hepàtica, BCLC-IDIBAPS, Liver Unit, Hospital Clínic, University of Barcelona, Carrer Rosselló 153, Barcelona 08036, Catalonia, Spain. Tel.: +34 93 2279155; fax: +34 93 3129406.

E-mail address: jmllovet@clinic.cat (J.M. Llovet).

<sup>†</sup> These authors contributed equally as joint first authors.



The optimal management of HCC requires an early and accurate assessment of tumor response to therapy, particularly for those patients who experience toxicity [1]. Nevertheless, traditionally established response criteria based on size for tumor burden, as defined by World Health Organization (WHO) criteria or the Response Evaluation Criteria in Solid Tumors (RECIST), have been challenged in HCC due to the nature of effective treatments. Both chemoembolization and sorafenib often induce direct tumor necrosis without critically affecting tumor size [4]. Moreover, valid radiological criteria are crucial for the optimal development of clinical trials testing new therapies for HCC: although the primary goal is to prolong survival, alternative end-points evaluating disease response and progression have been used to assess treatment effectiveness earlier and reduce drug development costs [5].

In addition, controversy remains on what should be an ideal surrogate end-point in HCC research. Objective response was considered an adequate surrogate end-point when assessing benefits of loco-regional therapies [2,6] by European Society for the Study of the Liver (EASL) criteria [7]. These criteria were proposed in 2000 by a panel of experts as an amendment to WHO criteria, considering treatment-induced tumor necrosis and the concept of viable tumor assessment. However, the standardization of RECIST in trials evaluating oncologic therapies led to adopting these criteria for the first time in HCC in the SHARP trial [3]. This landmark trial demonstrated that sorafenib was able to significantly increase OS compared to placebo, despite an objective response rate (ORR) of just 2%. Subsequently, experts convened by the American Association for the Study of Liver Diseases (AASLD) developed a set of guidelines that aimed to provide a common conceptual framework for the design of clinical trials in HCC and endorsed time to progression (TTP) as the optimal secondary end-point in 2008 [5]. At the same time, this provided the basis of the modification of RECIST criteria (mRECIST) [8].

These criteria incorporate the concept of viable tumor assessment, defined as the portions of tumor showing arterial enhancement, and thus providing improved sensitivity for clinical assessment. Moreover, mRECIST also incorporates novel concepts in assessing progression with lymph node involvement, ascites and development of new lesions [5,8] (Fig. 1). Thus, assessment of response by mRECIST was thereafter endorsed by the EASL clinical practice guidelines of management of HCC [1].

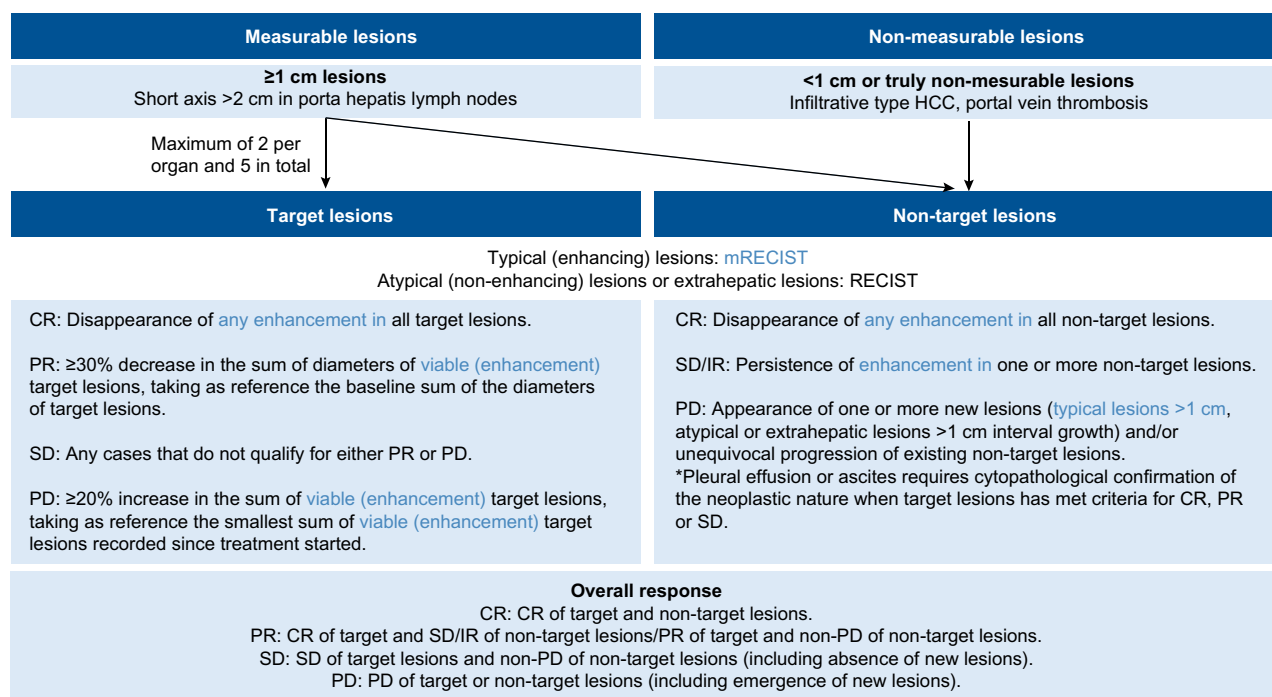
Several studies and one meta-analysis have shown a correlation between objective response by mRECIST and survival in patients treated with loco-regional therapies [9–13]. In advanced HCC cases treated with systemic targeted therapies, few studies suggest a prognostic value of objective response by mRECIST [14–17]. However, their retrospective nature and the absence of a time-dependent multivariate analysis considering immortal time bias, limit the level of evidence in this setting.

We performed an individual patient data analysis of BRISK-PS, a phase III trial comparing brivanib and placebo in the second line setting that was the first to prospectively incorporate mRECIST for the assessment of treatment benefit [18]. The aim was to investigate whether objective response by mRECIST could accurately predict OS in patients with advanced HCC treated by systemic therapies.

## Patients and methods

### BRISK-PS trial design, treatment and assessments

BRISK-PS [18] was a multinational, double-blind, randomized, placebo-controlled, phase III study carried out between February 2009 and June 2011. Three hundred and ninety-five patients were randomly assigned (2:1) to receive brivanib, a dual inhibitor of vascular endothelial growth factor receptor and



**Fig. 1. Response assessment in HCC by mRECIST following the AASLD JNCI guidelines (adapted from ref [8]).** CR, complete response; PR, partial response; SD, stable disease; PD, progressive disease; IR, incomplete responses.

## Research Article

fibroblast growth factor receptor signaling pathways, 800 mg once per day or matching placebo plus best supportive care (BSC). Patients were eligible if they had documented radiographic or symptomatic progression on/after or were intolerant to sorafenib. Patients were required to have one or more measurable target lesions. Other inclusion criteria included liver function of Child-Pugh Class A or B (a total score  $\leq 7$ ) without ascites or encephalopathy an Eastern Cooperative Oncology Group performance status (ECOG PS)  $\leq 2$ , and adequate hematologic, hepatic and renal functions. Stratification was carried out according to reason for sorafenib discontinuation (progression vs. intolerance), ECOG PS score (0 vs. 1–2), distant metastasis and/or macrovascular invasion (yes vs. no) and study site. All patients provided written informed consent before enrollment. The study was approved by the institutional review board or ethics committee at each center and complied with provisions of the Good Clinical Practice guidelines and the Declaration of Helsinki and local laws.

The primary end-point of OS was defined as the time from random assignment until death as a result of any cause. Secondary end-points were TTP and ORR. TTP was defined as the time from random assignment to radiologic disease progression and ORR as the percentage of patients with complete response (CR) or partial response (PR). Tumor measurements were performed every 6 weeks during treatment by contrast-enhanced, computed tomography or magnetic resonance imaging. To define objective response, confirmatory assessments were performed  $\geq 28$  days after the initial demonstration of the response. Assessment was performed by a blinded independent radiologic committee using mRECIST. Results of TTP and ORR were based on central review. Briefly, the study images were subjected to quality control (adherence to image acquisition guidelines and trial protocol) before they were evaluated by two board-certified radiologists with specific expertise in liver imaging. If there was disagreement between the two reviewers in the response assessment at any time point, a third adjudicating radiologist reviewed the case and decided which of the two primary radiologists should be agreed with. In this regard, a previous study showed up to 73% of inter-reader agreement for mRECIST in HCC patients treated with sorafenib and a comparable weighted  $k$  coefficient to RECIST [15].

Overall, 226 of 263 brivanib patients (85.9%) and 108 of 132 placebo patients (81.8%) were evaluable for response because of the presence of baseline and at least one on-study scan. Of the 61 patients not evaluable due to discontinuation of treatment before the first radiological assessment, 27 survived less than 6 weeks.

### Statistical analysis

Analyses were performed using the SPSS v.23 and SAS v.9.4 software packages. A Fisher's exact test was used for comparison of frequency of two categorical variables. Mann-Whitney  $U$  test compared one categorical variable with one continuous variable. The hazard ratio (HR) and their associated confidence interval (CI) for OS were computed by Cox proportional hazard models for the aforementioned stratification factors (reason for sorafenib discontinuation, ECOG PS score, distant metastasis and macrovascular invasion), region, age, sex, race, risk factors, baseline analytical factors (albumin, bilirubin and alpha-fetoprotein [AFP]), nodal metastasis and objective response. Variables associated with OS ( $p$  value  $< 0.10$ ) in univariate analysis were included in multivariate models. Statistics involving evolutionary events were done by means of time-dependent covariate analysis. Survival curves were performed using Landmark Kaplan-Meier method without a fixed time (patients enter the objective response group as soon as they achieved this event); and were compared using the Mantel-Byar test; this method allowed analysis of survival from the point where the variable changed [19,20]. The relationship between probability of survival in deciles and log (odds) (i.e.,  $\log [p/1 - p]$  where  $p$  is the prevalence of the end-point) for ORR was evaluated using Pearson's correlation coefficient and linear regression; the 95% CI for the  $R$  were estimated by bootstrap with 10,000 simulations. The same approach was used to evaluate the association between log HRs for OS and log odds ratios for ORR after dividing the trial into five subgroups at random. All statistical tests were two-tailed and the threshold level of significance was 0.05.

## Results

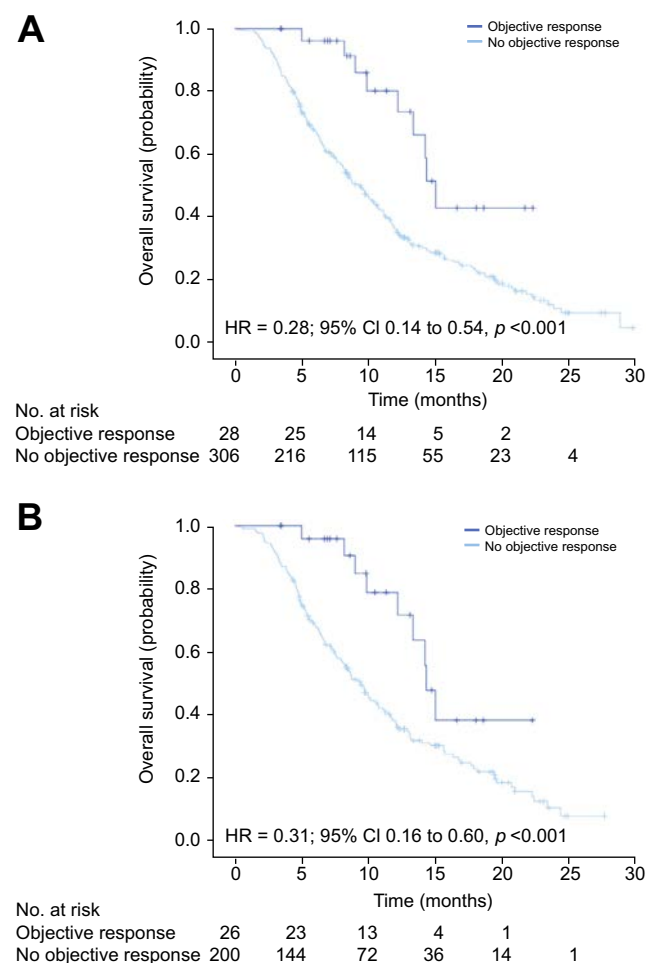
### Objective response by mRECIST as an independent prognostic factor

At the end of follow-up, 233 of the 334 patients with evaluable response had died, with a median OS of 10.1 months (95% CI; 8.6–11.6) and 9.5 (95% CI; 7.4–11.7) for brivanib and placebo groups respectively. There were no statistically significant differ-

ences between treatments (HR = 0.88; 95% CI, 0.67–1.16,  $p = 0.358$ ), as observed in the whole BRISK-PS population (HR = 0.89; 95.8% CI, 0.69–1.15,  $p = 0.331$ ).

There was no CR in either of the two arms among patients evaluated. ORR was 11.5% ( $n = 26/226$ ) with brivanib and 1.9% ( $n = 2/108$ ) with placebo. Overall, considering all patients assessed, those patients achieving objective response ( $n = 28$ ) had a median OS as per landmark analysis of 15.0 months (95% CI; 13.7–16.3), significantly better than the 9.4 (95% CI; 8.2–10.6) months of patients without objective response ( $n = 306$ ) (HR = 0.28; 95%CI 0.14–0.54,  $p < 0.001$ ) (Fig. 2A). Specifically, for patients in the brivanib arm, those with objective response had better survival (14.3 vs. 9.4 months, HR = 0.31; 95%CI 0.16–0.60,  $p < 0.001$ ) (Fig. 2B).

In order to evaluate objective response as a predictor of OS we used a Cox model with objective response as a time-dependent variable, since this variable was measured after entry into the study. Multivariate analysis irrespective of treatment identified objective response by mRECIST as an independent prognostic factor of OS (HR = 0.48; 95% CI, 0.26–0.91,  $p = 0.025$ ) along with nodal metastasis, distant metastasis, macrovascular invasion,



**Fig. 2. Landmark Kaplan-Meier curve of OS between patients with response or not by mRECIST.** (A) Patients in BRISK-PS and (B) in those treated with brivanib.  $p$  value according to Mantel-Byar test.



**Table 1.** Univariate and multivariate time-dependent analysis of OS in BRISK-PS patients who could be assessed for tumor response.

	Univariate analysis		Multivariate analysis	
	HR [95% CI]	p value	HR [95% CI]	p value
Distant metastasis	1.27 [0.96–1.67]	0.094	1.37 [1.05–1.78]	0.019
Macrovascular invasion	1.77 [1.33–2.34]	<0.001	1.54 [1.19–1.99]	0.001
Nodal metastasis	1.52 [1.17–1.99]	0.002	1.36 [1.07–1.73]	0.013
AFP >200 ng/ml	2.02 [1.55–2.62]	<0.001	1.99 [1.56–2.54]	<0.001
Albumin >median <sup>1</sup>	0.58 [0.45–0.75]	<0.001	0.65 [0.51–0.83]	0.001
Bilirubin >median <sup>2</sup>	2.32 [1.78–3.03]	<0.001	2.24 [1.73–2.89]	<0.001
Objective response mRECIST	0.28 [0.14–0.54]	<0.001	0.48 [0.26–0.91]	0.025

Variables not associated with OS in univariate analysis (p value >0.10) were reason for sorafenib discontinuation, ECOG PS score, region, age, sex, race and risk factors.

<sup>1</sup> 3.59 g/dl.

<sup>2</sup> 0.98 mg/dl.

AFP >200 ng/ml, albumin > median and bilirubin > median (Table 1). Objective response maintained independent prognostic value in patients treated with brivanib (HR = 0.50; 95% CI, 0.25–0.99,  $p = 0.047$ ) (Table 2), indicating that objective response by mRECIST captures those patients in which treatment changes the natural history of the disease.

Baseline demographics and disease characteristics that significantly influenced obtaining a higher percentage of objective response by mRECIST after treatment with brivanib were: BCLC A/B stage, absence of distant metastasis and the presence of low and high levels of AFP and albumin, respectively (Table 3).

#### Objective response by mRECIST as a surrogate end-point

To further explore the impact of objective response by mRECIST in the assessment of efficacy of a systemic molecular targeted therapy, we performed a Pearson correlation between the raw survival probability of patients in deciles and the log odds ratios of ORR. This method allowed the determination of the ORR observed in each one of the ten subgroups, sorted by worse to better outcome, and their association. As shown in Fig. 3, treatment effects on ORR and OS were significantly associated ( $R = -0.92$ ; 95% CI,  $-1$  to  $-0.73$ ,  $p < 0.001$ ).

In order to provide additional surrogacy of end-points, a proper correlation between the treatment effect on the surrogate outcome (objective response by mRECIST) and the treatment effect on the clinical outcome (OS) is required. To attempt this, we split the cases in five random subgroups of equal size ( $395/5 = 79$ ). The association between log HRs for OS and log odds ratios for ORR was high ( $R = -0.80$ ; 95% CI,  $-1$  to  $0.23$ ,  $p = 0.091$ ) (Fig. 4).

Of note, median time to objective response was 1.4 months (range: 0.7–8.4) in the 26 patients that reached a PR with brivanib. This means that the first radiological evaluation, conducted at 6 weeks, detects the majority of patients responding to treatment and thus, objective response could be considered an early surrogate end-point.

#### Discussion

OS remains as the main primary end-point in clinical research in oncology and in HCC. However, there is a need to identify a reliable secondary end-point able to recapitulate OS. This will allow ineffective drugs in phase II trials to be discarded, and enable testing new therapies in phase III, where median survivals of patients with intermediate HCC might exceed 30 months, and cross over treatments might dilute the potential benefits during follow-up. Objective response was previously considered a reliable surrogate end-point for loco-regional therapies in HCC [7], but studies assessing response by RECIST criteria failed to capture this benefit. At advanced stages of the disease, performance of objective response by RECIST was disappointing in capturing benefits of sorafenib therapy [3]. As a consequence of these failures, two strategies emerged:

- Assess response according to the 'hallmarks of HCC' for defining viable tumors (mRECIST criteria) [5,8]
- Endorse TTP as a more adequate surrogate end-point, as per the SHARP trial results [5].

The present study defines objective response as an independent prognostic factor for OS, and as a potentially reliable

**Table 2.** Univariate and multivariate time-dependent analysis of OS in patients treated with brivanib and who could be assessed for tumor response in BRISK-PS.

	Univariate analysis		Multivariate analysis	
	HR [95% CI]	p value	HR [95% CI]	p value
Distant metastasis	1.51 [1.06–2.16]	0.022	1.35 [0.97–1.89]	0.076
Macrovascular invasion	1.85 [1.33–2.57]	<0.001	1.64 [1.20–2.24]	0.002
Nodal metastasis	1.60 [1.16–2.22]	0.005	1.30 [0.96–1.77]	0.086
AFP >200 ng/ml	2.16 [1.56–2.99]	<0.001	1.97 [1.44–2.69]	<0.001
Albumin >median <sup>1</sup>	0.56 [0.41–0.77]	<0.001	0.58 [0.43–0.80]	0.001
Bilirubin >median <sup>2</sup>	2.57 [1.85–3.57]	<0.001	2.31 [1.68–3.18]	<0.001
Objective response mRECIST	0.31 [0.16–0.60]	<0.001	0.50 [0.25–0.99]	0.047

Variables not associated with OS in univariate analysis (p value >0.10) were reason for sorafenib discontinuation, ECOG PS score, region, age, sex, race and risk factors.

<sup>1</sup> 3.59 g/dl.

<sup>2</sup> 0.98 mg/dl.

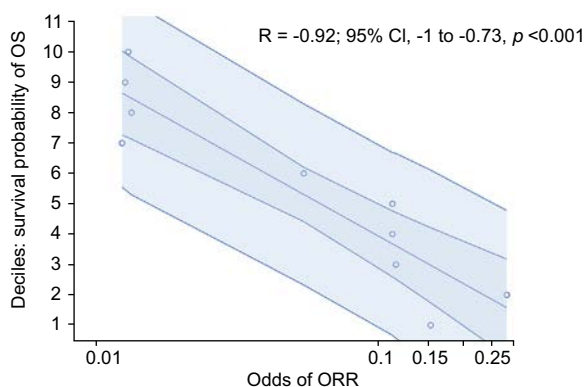
## Research Article

**Table 3. Baseline demographics and disease characteristics in patients with and without objective response by mRECIST after treatment with brivanib.**

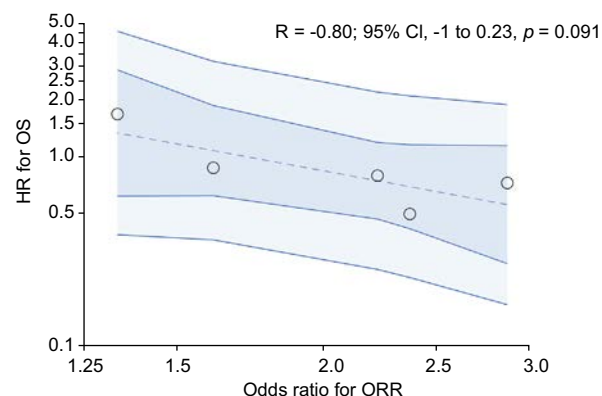
	Objective response (n = 26)	No objective response (n = 200)	p value
Age (median), yr	63 [36–76]	63 [19–85]	0.933
Sex			
Male	23 (88.5)	165 (82.5)	0.583
Female	3 (11.5)	35 (17.5)	
Race			
White	13 (50.0)	84 (42.0)	0.530
Asian	11 (42.3)	103 (51.5)	0.380
Black/African American	0 (0)	10 (5.0)	0.380
Other	2 (7.7)	3 (1.5)	0.100
Region			
America & Europe	16 (61.5)	110 (55.0)	0.675
Asia	10 (38.5)	90 (45.0)	
Risk factors*			
Alcoholic liver disease	6 (23.1)	20 (10.0)	0.093
Hepatitis B	7 (26.9)	80 (40.0)	0.284
Hepatitis C	7 (26.9)	43 (21.5)	0.615
Other	2 (7.7)	7 (3.5)	0.277
Child-Pugh class			
A	26 (100)	189 (94.5)	0.620
B	0 (0)	11 (5.5)	
ECOG PS score			
0	21 (80.8)	125 (62.5)	0.082
1/2	5 (19.2)	75 (37.5)	
Reason for sorafenib discontinuation			
Progression	21 (80.8)	177 (88.5)	0.337
Intolerance	5 (19.2)	23 (11.5)	
BCLC stage			
A/B	9 (34.6)	18 (9.0)	0.001
C	17 (65.4)	182 (91.0)	
Distant metastasis	9 (34.6)	142 (71.0)	0.001
Nodal metastasis	7 (26.9)	76 (38.1)	0.387
Macrovascular invasion	8 (30.8)	61 (30.5)	1.000
AFP (median), ng/ml	24 [2–9101]	353 [1–1.2 × 10 <sup>6</sup> ]	0.001
Albumin (median), g/dl	4.0 [3.0–4.4]	3.5 [2.1–5.0]	0.002
Bilirubin (median), mg/dl	0.9 [0.4–5.7]	0.98 [0.2–15.2]	0.191

(%); [range].

\* 54 patients with more than one risk factor were excluded.



**Fig. 3. Correlation between raw survival probability using deciles and odds of ORR in brivanib patients within BRISK-PS.** Each one of the ten subgroups sorted by worse to better outcome has an observed ORR. The central regression line is their association. Internal and external 95% CI bands identify the uncertainty for expected value of the dependent variable and for the individual predicted value, respectively. Deciles of survival probability =  $-1.293 - 2.261 \cdot \log(\text{Odds (ORR)})$ .



**Fig. 4. Correlation between HR for OS and odds ratio for ORR in five random subsamples of patients within BRISK-PS.** The central regression line is their association. Internal and external 95% CI bands identify the uncertainty for expected value of the dependent variable and for the individual predicted value, respectively.  $\ln(\text{HR for OS}) = 0.621 - 1.139 \cdot \ln(\text{odds ratio for ORR})$ .

surrogate end-point. First, we established an 11.5% ORR by mRECIST in patients treated with brivanib in the setting of BRISK-PS trial. This figure compares well with data from a phase III trial of brivanib in front-line advanced HCC, where an ORR of 12% in those 577 patients randomized to brivanib arm was reported [21]. Furthermore, in this study, ORR for sorafenib was 9%, which is within the range of 9–28% described in several retrospective studies [14–17,22,23]. These figures for sorafenib are far from the 2% ORR described for RECIST [5]. Thus, assessment of mRECIST in patients with advanced HCC treated with anti-angiogenic drugs, might be in line with other alternative criteria developed to measure response in other solid tumors. This is the case for Choi criteria, for the measurement of response in gastrointestinal stromal tumors treated with imatinib [24] or immune-related response criteria for melanomas treated with checkpoint inhibitors [25].

Second, we sought to define if objective response was an independent predictor of OS in advanced HCC. For this purpose, we performed a multivariate time-dependent analysis that defined several variables related to tumoral status (macrovascular invasion, metastases, AFP >200 ng/ml), liver function (bilirubin, albumin) and treatment response measured by mRECIST as independent predictors for survival. This result is critical, since it represents the first requirement to propose ORR as surrogate end-point for OS in advanced HCC. In addition, the level of evidence is high due to the phase III randomized controlled nature of the original study.

Finally, we aimed to explore if ORR could be used as a potential surrogate end-point in HCC. The way to evaluate therapeutic effectiveness in oncology is based upon a statistically significant and clinically meaningful improvement in OS [26]. In clinical research, surrogate end-points are used in order to provide earlier measures of difference in treatment effect than OS [1,27]. In our study, we identified a significant correlation between ORR assessed by mRECIST after brivanib and OS ( $R = -0.92$ ). Notably, most patients with objective response could be identified in the first radiological evaluation conducted at 6 weeks. Moreover, objective response overcomes a limitation of other end-points that include disease stabilization in their definitions (disease control rate, TTP or progression-free survival [PFS]) since these end-points may be influenced by the inherent speed of progression of tumors independently of the effect of the drug [28]. This makes objective response by mRECIST a promising surrogate end-point to evaluate efficacy (if a treatment is effective for a certain condition) after a phase II trial, and thus to decide its further development.

Thus, if ORR is an independent predictor of survival and a potentially good surrogate of OS, we need to explain how the differences in ORR between brivanib and placebo arms (Odds ratio 5.72; 95% CI, 1.41–23.25,  $p = 0.003$ ) were unable to correlate with the lack of survival differences in this trial. The most obvious explanation is that the magnitude of the benefit obtained by a drug certainly depends on the type of ORR benefit (CR vs. PR) and the toxicity. The ORR obtained in the trial according to intention to treat for the brivanib arm was 9.9% (26/263), a figure that is suboptimal to impact on the final OS result. Other effective drugs in cancer such as crizotinib, which achieved a 29% absolute increase in ORR compared to chemotherapy (74% vs. 45%) in non-small cell lung cancer [29], or nivolumab, which achieved 40% ORR in melanoma patients, but with a high rate of complete responses [30], are examples defining a threshold for ORR to directly impact in OS benefit. Therefore, to reliably predict

differences among treatments, a higher magnitude of the difference in terms of quantity (percentage of objective response) and quality (presence of CRs or long-lasting responses) would be necessary. This concept is particularly challenging in the HCC field since, unlike other tumors, the post-progression time is generally longer than TTP and may dilute part of the benefit produced by the drug during treatment [18,31].

The importance of objective response as a surrogate end-point in cancer trials has been acknowledged in some papers by regulatory agencies and used in breakthrough trials [32]. Indeed, 24 of the 25 FDA accelerated marketing approvals for oncologic indications between 2009 and 2014 were based on ORR [33]. This point is of significance since the last randomized studies conducted in HCC have shown inconsistencies between TTP and OS [34]. In this sense, for instance, the two positive trials showed similar OS rates for sorafenib in front-line and regorafenib in second line but with clearly distinct TTP figures [3,35]. Thus, TTP is currently re-visited as a surrogate end-point in trial design for advanced HCC. In order to provide absolutely robust data to enforce recommendations in guidelines, the definitive evidence will be obtained when several randomized trials following mRECIST assessment will be available, allowing this a meta-analysis approach comparing the Pearson correlation coefficient of ORR, TTP or other surrogate end-points with OS [36–40].

In conclusion, these results provide high-level evidence, suggesting that radiological response in advanced HCC by mRECIST captures clinically meaningful outcomes in terms of OS and therefore, if confirmed in other future studies at individual and trial-level [36–40], objective response can be proposed as a complementary surrogate end-point for the efficient development of clinical trials.

### Financial support

Robert Montal is supported by a Rio Hortega grant from Sociedad Española de Oncología Médica – Instituto de Salud Carlos III. Josep M Llovet is supported by grants from the European Commission Horizon 2020 (HEPCAR, proposal number 667273-2), the U.S. Department of Defense (CA150272P1), The Samuel Waxman Cancer Research Foundation, the Spanish National Health Institute (SAF-2013-41027-R) and the Asociación Española contra el Cáncer. The BRISK-PS trial was sponsored by Bristol-Myers Squibb.

### Conflict of interest

The authors who have taken part in this study declared that they do not have any conflict of interest with respect to this manuscript.

### Authors' contributions

Conception and design: RL, RM, FT, IW, JML. Collection of clinical data: RL, JWP, TD, JLR, MK, CC, VB, EA, YKK, HYL, JML. Data analysis and interpretation: RL, RM, FT, JR, IW, JML. Manuscript writing: RL, RM, FT, JR, JML. Critical review of the manuscript: All authors.

# Research Article

## References

Author names in bold designate shared co-first authorship

- [1] EASL-EORTC clinical practice guidelines: management of hepatocellular carcinoma. *J Hepatol* 2012;56:908–943.
- [2] Llovet JM, Real MI, Montaña X, Planas R, Coll S, Aponte J, et al. Arterial embolisation or chemoembolisation vs. symptomatic treatment in patients with unresectable hepatocellular carcinoma: a randomised controlled trial. *Lancet* 2002;359:1734–1739.
- [3] Llovet JM, Ricci S, Mazzaferro V, Hilgard P, Gane E, Blanc J-F, et al. Sorafenib in advanced hepatocellular carcinoma. *N Engl J Med* 2008;359:378–390.
- [4] Jiang T, Zhu AX, Sahani DV, Thomas MB, Zhu AX, Jemal A, et al. Established and novel imaging biomarkers for assessing response to therapy in hepatocellular carcinoma. *J Hepatol* 2013;58:169–177.
- [5] Llovet JM, Di Bisceglie AM, Bruix J, Kramer BS, Lencioni R, Zhu AX, et al. Design and endpoints of clinical trials in hepatocellular carcinoma. *J Natl Cancer Inst* 2008;100:698–711.
- [6] Sala M, Llovet JM, Vilana R, Bianchi L, Solé M, Ayuso C, et al. Initial response to percutaneous ablation predicts survival in patients with hepatocellular carcinoma. *Hepatology* 2004;40:1352–1360.
- [7] Bruix J, Sherman M, Llovet JM, Beaugrand M, Lencioni R, Burroughs AK, et al. Clinical management of hepatocellular carcinoma. Conclusions of the Barcelona-2000 EASL conference. European Association for the Study of the Liver. *J Hepatol* 2001;35:421–430.
- [8] Lencioni R, Llovet J. Modified RECIST (mRECIST) assessment for hepatocellular carcinoma. *Semin Liver Dis* 2010;30:052–60.
- [9] Vincenzi B, Di Maio M, Silletta M, D'Onofrio L, Spoto C, Piccirillo MC, et al. Prognostic relevance of objective response according to EASL criteria and mRECIST criteria in hepatocellular carcinoma patients treated with loco-regional therapies: a literature-based meta-analysis. *PLoS One* 2015;10:e0133488.
- [10] Gillmore R, Stuart S, Kirkwood A, Hameeduddin A, Woodward N, Burroughs AK, et al. EASL and mRECIST responses are independent prognostic factors for survival in hepatocellular cancer patients treated with transarterial embolization. *J Hepatol* 2011;55:1309–1316.
- [11] Prajapati HJ, Spivey JR, Hanish SI, El-rayes BF, Kauh JS, Chen Z, et al. MRECIST and EASL responses at early time point by contrast-enhanced dynamic MRI predict survival in patients with unresectable hepatocellular carcinoma (HCC) treated by doxorubicin drug-eluting beads transarterial chemoembolization (DEB TACE). *Ann Oncol* 2013;24:965–973.
- [12] Jung ES, Kim JHJS, Yoon EL, Lee HJ, Lee SJ, Suh SJ, et al. Comparison of the methods for tumor response assessment in patients with hepatocellular carcinoma undergoing transarterial chemoembolization. *J Hepatol* 2013;58:1181–1187.
- [13] Kim BK, Kim SU, Kim KA, Chung YE, Kim M, Park M, et al. Complete response at first chemoembolization is still the most robust predictor for favorable outcome in hepatocellular carcinoma. *J Hepatol* 2015;62:4–10.
- [14] Edeline J, Boucher E, Rolland Y, Vauléon E, Pracht M, Perrin C, et al. Comparison of tumor response by Response Evaluation Criteria in Solid Tumors (RECIST) and modified RECIST in patients treated with sorafenib for hepatocellular carcinoma. *Cancer* 2012;118:147–156.
- [15] Ronot M, Bouattour M, Wassermann J, Bruno O, Dreyer C, Larroque B, et al. Alternative Response Criteria (Choi, European association for the study of the liver, and modified Response Evaluation Criteria in Solid Tumors [RECIST]) vs. RECIST 1.1 in patients with advanced hepatocellular carcinoma treated with sorafenib. *Oncologist* 2014;19:394–402.
- [16] Takada J, Hidaka H, Nakazawa T, Kondo M, Numata K, Tanaka K, et al. Modified response evaluation criteria in solid tumors is superior to response evaluation criteria in solid tumors for assessment of responses to sorafenib in patients with advanced hepatocellular carcinoma. *BMC Res Notes* 2015;8:609.
- [17] Ogasawara S, Kanai F, Ooka Y, Motoyama T, Suzuki E, Tawada A, et al. Initial response to sorafenib by using enhancement criteria in patients with hepatocellular carcinoma. *Hepatol Int* 2013;7:703–713.
- [18] Llovet JM, Decaens T, Raoul JL, Boucher E, Kudo M, Chang C, et al. Brivanib in patients with advanced hepatocellular carcinoma who were intolerant to sorafenib or for whom sorafenib failed: results from the randomized phase III BRISK-PS study. *J Clin Oncol* 2013;31:3509–3516.
- [19] Anderson JR, Cain KC, Gelber RD. Analysis of survival by tumor response. *J Clin Oncol* 1983;1:710–719.
- [20] Memon K, Kulik L, Lewandowski RJ, Wang E, Riaz A, Ryu RK, et al. Radiographic response to locoregional therapy in hepatocellular carcinoma predicts patient survival times. *Gastroenterology* 2011;141:526–535 e1–e2.
- [21] Johnson PJ, Qin S, Park JW, Poon RT, Raoul JL, Philip PA, et al. Brivanib vs. sorafenib as first-line therapy in patients with unresectable, advanced hepatocellular carcinoma: results from the randomized phase III BRISK-FL study. *J Clin Oncol* 2013;31:3517–3524.
- [22] Kawaoka T, Aikata H, Murakami E, Nakahara T, Naeshiro N, Tanaka M, et al. Evaluation of the mRECIST and  $\alpha$ -fetoprotein ratio for stratification of the prognosis of advanced-hepatocellular-carcinoma patients treated with sorafenib. *Oncology* 2012;83:192–200.
- [23] Spira D, Fenchel M, Lauer UM, Claussen CD, Gregor M, Bitzer M, et al. Comparison of different tumor response criteria in patients with hepatocellular carcinoma after systemic therapy with the multikinase inhibitor sorafenib. *Acad Radiol* 2011;18:89–96.
- [24] Choi H, Chamsangavej C, Faria SC, Macapinlac HA, Burgess MA, Patel SR, et al. Correlation of computed tomography and positron emission tomography in patients with metastatic gastrointestinal stromal tumor treated at a single institution with imatinib mesylate: proposal of new computed tomography response criteria. *J Clin Oncol* 2007;25:1753–1759.
- [25] Hodi FS, Hwu W-J, Kefford R, Weber JS, Daud A, Hamid O, et al. Evaluation of immune-related response criteria and RECIST v1.1 in patients with advanced melanoma treated with pembrolizumab. *J Clin Oncol* 2016;34:1510–1517.
- [26] Booth CM, Tannock I. Reflections on medical oncology: 25 years of clinical trials—where have we come and where are we going? *J Clin Oncol* 2008;26:6–8.
- [27] Wilson MK, Karakasis K, Oza AM. Outcomes and endpoints in trials of cancer treatment: the past, present, and future. *Lancet Oncol* 2015;16:e32–e42.
- [28] Le Tourneau C, Paoletti X, Coquan E, Sablin MP, Zoubir M, Tannock IF. Critical evaluation of disease stabilization as a measure of activity of systemic therapy: Lessons from trials with arms in which patients do not receive active treatment. *J Clin Oncol* 2014;32:260–263.
- [29] Solomon BJ, Mok T, Kim D-W, Wu Y-L, Nakagawa K, Mekhail T, et al. First-line crizotinib vs. chemotherapy in ALK-positive lung cancer. *N Engl J Med* 2014;371:2167–2177.
- [30] Robert C, Long GV, Brady B, Dutriaux C, Maio M, Mortier L, et al. Nivolumab in previously untreated melanoma without BRAF mutation. *N Engl J Med* 2015;372:320–330.
- [31] Zhu AX, Park JO, Ryoo B-Y, Yen C-J, Poon R, Pastorelli D, et al. Ramucirumab vs. placebo as second-line treatment in patients with advanced hepatocellular carcinoma following first-line therapy with sorafenib (REACH): a randomised, double-blind, multicentre, phase 3 trial. *Lancet Oncol* 2015:859–870.
- [32] Johnson JR, Williams G, Pazdur R. End points and United States Food and Drug Administration approval of oncology drugs. *J Clin Oncol* 2003;21:1404–1411.
- [33] Kim C, Prasad V. Strength of validation for surrogate end points used in the US food and drug administration's approval of oncology drugs. *Mayo Clin Proc* 2016;91:713–725.
- [34] Llovet JM, Hernandez-Gea V. Hepatocellular carcinoma: reasons for phase III failure and novel perspectives on trial design. *Clin Cancer Res* 2014;20:2072–2079.
- [35] Bruix J, Qin S, Merle P, Granito A, Huang Y-H, Bodoky G, et al. Regorafenib for patients with hepatocellular carcinoma who progressed on sorafenib treatment (RESORCE): a randomised, double-blind, placebo-controlled, phase 3 trial. *Lancet* 2017;389:56–66.
- [36] Zhao F. Surrogate end points and their validation in oncology clinical trials. *J Clin Oncol* 2016;34:1436–1437.
- [37] Buyse M, Molenberghs G. Criteria for the validation of surrogate endpoints in randomized experiments. *Biometrics* 1998;54:1014–1029.
- [38] Blumenthal GM, Karuri SW, Zhang H, Zhang L, Khozin S, Kazandjian D, et al. Overall response rate, progression-free survival, and overall survival with targeted and standard therapies in advanced non-small-cell lung cancer: US Food and Drug Administration trial-level and patient-level analyses. *J Clin Oncol* 2015;33:1008–1014.
- [39] Tang PA, Bentzen SM, Chen EX, Siu LL. Surrogate end points for median overall survival in metastatic colorectal cancer: literature-based analysis from 39 randomized controlled trials of first-line chemotherapy. *J Clin Oncol* 2007;25:4562–4568.
- [40] Zer A, Prince RM, Amir E, Abdul Razak A. Evolution of randomized trials in advanced/metastatic soft tissue sarcoma: endpoint selection, surrogacy, and quality of reporting. *J Clin Oncol* 2016:1–8.

# Magnetic resonance elastography in the assessment of hepatic fibrosis: a study comparing transient elastography and histological data in the same patients

Masafumi Toguchi<sup>1</sup>,<sup>1b</sup> Masakatsu Tsurusaki,<sup>1</sup> Norihisa Yada,<sup>2</sup> Keitaro Sofue,<sup>3</sup> Tomoko Hyodo,<sup>1</sup> Minori Onoda,<sup>4,5</sup> Isao Numoto,<sup>1</sup> Mitsuru Matsuki,<sup>1</sup> Izumi Imaoka,<sup>1</sup> Masatoshi Kudo,<sup>2</sup> Takamichi Murakami<sup>1</sup>

<sup>1</sup>Department of Radiology, Faculty of Medicine, Kindai University, 377-2 Ohno-Higashi, Osaka-Sayama, Osaka 589-8511, Japan

<sup>2</sup>Department of Gastroenterology and Hepatology, Faculty of Medicine, Kindai University, Osaka-Sayama, Japan

<sup>3</sup>Department of Radiology, Kobe University Graduate School of Medicine, 7-5-2 Kusunoki-cho, Chuo-ku, Kobe 650-0017, Japan

<sup>4</sup>Department of Radiological Technology, Kindai University, 377-2 Ohno-Higashi, Osaka-Sayama, Osaka 589-8511, Japan

<sup>5</sup>Division of Health Sciences, Graduate School of Medical Science, Kanazawa University, 5-11-80 Kodatsuno, Kanazawa, Ishikawa 920-0942, Japan

## Abstract

**Purpose:** To evaluate the quantitative measurement of liver stiffness (LS), compare the diagnostic performance of magnetic resonance elastography (MRE) and ultrasound-based transient elastography (TE), and evaluate two different MRE-based LS measurement methods.

**Methods:** Between October 2013 and January 2015, 116 consecutive patients with chronic liver disease underwent MRE to measure LS (kilopascals; kPa). Of the 116 patients, 51 patients underwent both TE and liver biopsy, and the interval between the liver biopsy and both the MRE and TE was less than 90 days. MRE-derived LS values were measured on the anterior segment of the right lobe (single small round regions of interest per slice; srROIs) and whole right lobe of the liver (free hand region of interest; fhROI), and these values were correlated with pathological fibrosis grades and diagnostic performance.

**Results:** Pathological fibrosis stage was significantly correlated with srROIs ( $r = 0.87$ ,  $p < 0.001$ ), fhROI ( $r = 0.80$ ,  $p < 0.001$ ), and TE ( $r = 0.73$ ,  $p < 0.001$ ). For detection of significant fibrosis ( $\geq F2$ ), advanced fibrosis ( $\geq F3$ ), and cirrhosis, the area under the curve (AUC) associated with the srROIs was largest, and there was a significant difference between srROIs and TE (0.93

vs. 0.82,  $p = 0.006$ ), srROIs and fhROI (0.93 vs. 0.89,  $p = 0.04$ ) for detection of  $\geq F2$ . For advanced fibrosis and cirrhosis detection, AUCs were not significant (0.92–0.96).

**Conclusions:** MRE and TE detected liver fibrosis with comparable accuracy. In particular, the srROIs method was effective for detecting of significant fibrosis.

**Key words:** MR elastography—Transient elastography—Liver fibrosis—Fibrosis assessment—Chronic liver disease

In many chronic liver diseases, liver fibrosis can result in cirrhosis. Patients with cirrhosis are at an increased risk of developing hepatocellular carcinoma, encephalopathy, and varices. In Japan, there are several major causes of liver cirrhosis. Hepatitis C virus accounts for 70% of patients with hepatic cirrhosis, followed by hepatitis B virus (20%), alcoholism (5% to 10%), and other causes including primary biliary cirrhosis, autoimmune hepatitis, and Budd-Chiari syndrome. Recently, non-alcoholic steatohepatitis, which is common in Western countries, has also been increasingly reported as a cause of non-viral chronic hepatitis [1], which is important due to the possibility of the same potential complications associated with viral hepatitis mentioned above. Therefore, the

Correspondence to: Masafumi Toguchi; email: e024163@yahoo.co.jp



evaluation of hepatic fibrosis is necessary for proper management in accordance with the stage, in order to improve the prognosis of patients.

Currently, the most widely used method for the diagnosis of advanced fibrosis is histological assessment from a liver biopsy. However, biopsy of the liver is invasive, and may be complicated by morbidity and even death. With regards to evaluating the effects of treatment for hepatic fibrosis, achieving consistent repeatability has proved to be difficult.

Recently, simple serological markers including the FIB-4 index and the aspartate aminotransferase ratio index have been introduced as non-invasive tests; however, they are not sufficiently accurate for routine clinical use [1]. Some promising studies have demonstrated that liver stiffness (LS) measurements derived via both ultrasound (US)-based elastography and magnetic resonance elastography (MRE) correlate with histological data [2–5]. Modes of US-based elastography such as transient elastography (TE) (Fibroscan; Echo sense, Paris, France), acoustic radiation force imaging (Siemens, Erlangen, Germany), and supersonic shear wave elastography (Aixplorer; Supersonic Imagine, Aix-en-Provence, France) are more commonly used in clinical practice than MRE. The TE technique, which is one of the most common modes of US-based elastography performed worldwide, can quantify localized shear stiffness in the form of a 1-dimensional measurement. Fibroscan measures the velocity of shear waves propagating through the liver tissue [6]. The harder the tissue, the faster the shear wave propagates. In contrast to US-based elastography, MRE is much less operator dependent, and can provide a comprehensive evaluation of the liver, including the presence of a focal disease and complications such as varices.

MRE can provide quantitative maps of tissue stiffness over large regions of the liver. Many researchers have assessed LS by generating regions of interest (ROI) incorporating the whole liver, the right lobe, and a small oval shape in an elastogram [7]. Notably, while specimens obtained via liver biopsy only represent approximately 1/50,000 of the total liver volume [8], it is generally accepted that the process of fibrosis is not homogeneous [9]. Rusak et al. [10] reported that LS exhibited significant variability between the involved segments, and that the most reproducible method was averaging the results derived from cross-sections of whole liver. Thus, with regards to determining the grade of fibrosis based on biopsy specimens, the single small round regions of interest per slice (srROIs) method considering the weighted averages of measured areas is more appropriate than data derived from the whole liver or the right lobe, for evaluating fibrosis. In the past studies, they incorporated the small round ROI in size of 200 mm<sup>2</sup> [3] or 100–150 mm<sup>2</sup> [11], and 1 cm in diameter [12].

Therefore, we evaluated the quantitative measurement of LS by investigating the diagnostic performance of MRE and TE in comparison with histological data, with a particular emphasis on methods of ROI placement in MRE.

## Methods

### Study population

This retrospective study was approved by the relevant institutional review board, and written informed consent was obtained from all patients. From October 2013 to January 2015, 116 consecutive patients with chronic liver disease underwent both MRE and TE to measure LS. Of these patients, liver biopsies were performed, and the interval between the liver biopsy, MRE, and TE was less than 90 days (median, 29 days; range, 1–82 days). One patient with diffuse liver nodules due to sarcoidosis and four patients in whom the LS could not be determined because of technical failure such as T2\* relaxation due to excessive hemosiderin deposit in MRE, obesity, or bowel interference in TE were excluded. Finally, 51 patients (mean age 59.9 years, M:F ratio 21:30) were included. The background of chronic liver diseases in the patients included 6 cases of chronic hepatitis B virus, 17 chronic hepatitis C virus cases, 23 non-alcoholic fatty liver disease cases, three with alcoholic hepatitis, and two with primary biliary cirrhosis. Flow diagram of study population is shown in Fig. 1.

### Histologic assessment

All specimens were obtained via percutaneous US-guided liver biopsy performed on the anterior lobe of the liver with a Tru-Cut semiautomatic 16- or 18-gauge needle apparatus. After standard processing, all specimens were subjected to hematoxylin-and-eosin staining and Masson trichrome staining, to assess the stage of liver fibrosis. Three liver pathologists who were blinded to the patients' characteristics and the results of both TE and MRE as-

### Subjects

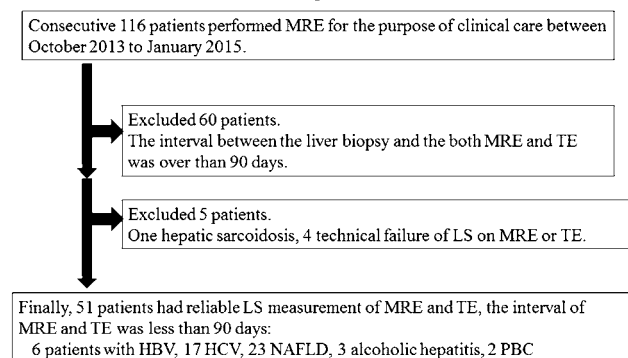
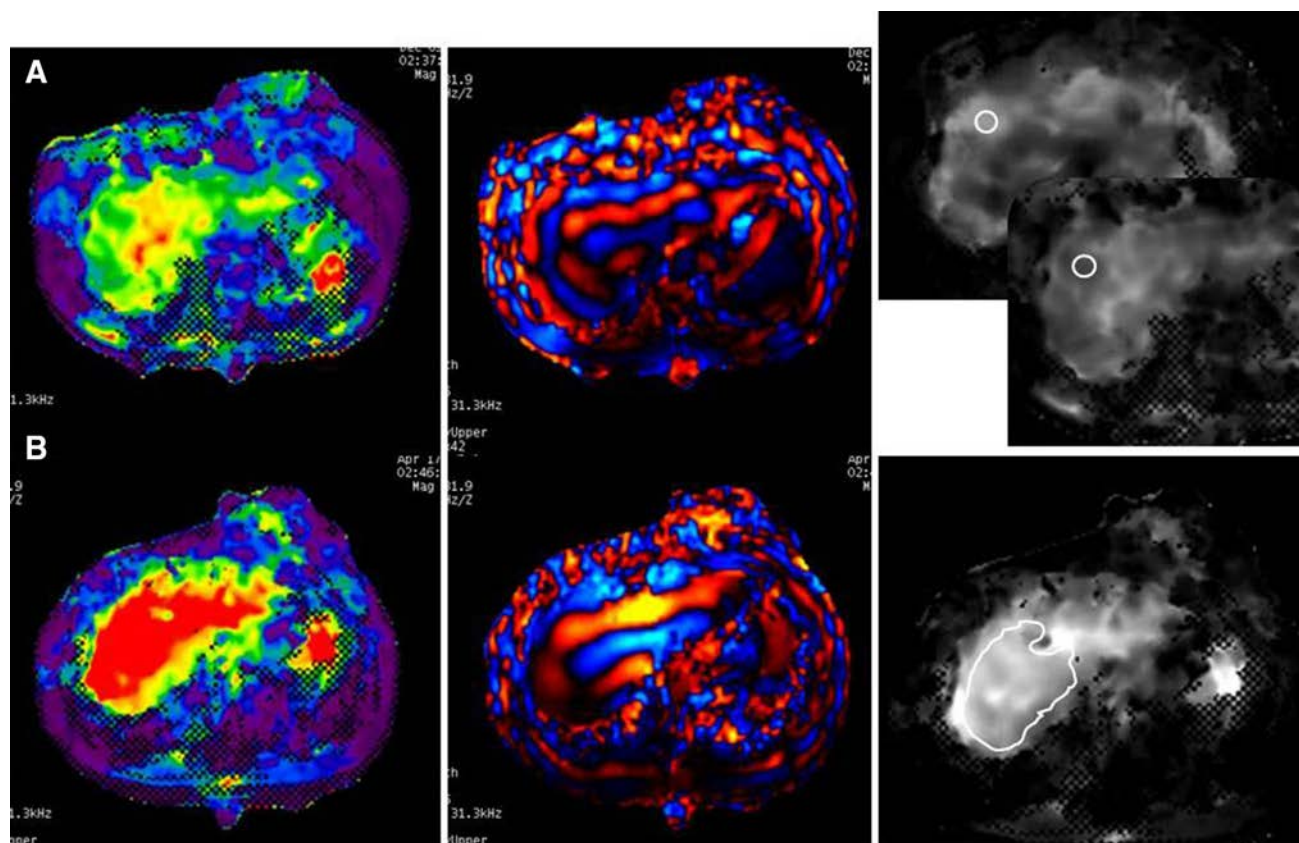


Fig. 1. Flow diagram of study population.



**Fig. 2.** An MRE color map (*left*), wave image (*middle*), and elastogram image (*right*). **A** A case of F1 stage. A small round ROI was placed on the anterior lobe of the liver on the LS map per slice (srROIs method). The averaged LS value was

2.85 kPa. **B** A case of F4 stage. A free hand ROI was placed over the right lobe of the liver on the LS map (fhROI method). The LS value was 9.23 kPa.

essed the stained specimens. We utilized the METAVIR scoring system for the assessment of liver fibrosis. Specifically, fibrosis was divided into five stages: F0, no fibrosis; F1, mild fibrosis (portal fibrosis without septa); F2, moderate fibrosis (portal fibrosis with rare septa); F3, bridging fibrosis (numerous septa connecting portal and/or central areas); and F4, cirrhosis (thick septa with well-formed regenerative nodules) [13].

### MRE technique

All MRE examinations were performed with a 1.5T scanner (1.5T Signa HDxt, GE Healthcare, Milwaukee, Wisconsin) with an 8-channel phased-array coil, and TE was performed with the Fibroscan system (Echosens, Paris, France).

We placed a passive longitudinal driver (MR touch; GE Healthcare) over the patient's right upper quadrant abdominal wall, which generates shear waves with low frequency (60 Hz) in the liver. While the vibrations were transmitted, a two-dimensional phase-contrast gradient echo MRE pulse sequence was performed to capture the propagation of the shear waves [14]. The MRE acquisition parameters utilized were as follows: repetition time

ms/echo time 50/21.6, flip angle 30°, field of view 42 cm, and matrix size 256 × 64. We used the ASSET parallel imaging with an acceleration factor of 2. MRE acquisition of each section required two breath holds, and the duration of each breath hold was 16 s. To achieve a consistent position of the liver for each phase offset, patients held their breath at the end of expiration. After data acquisition was complete, the wave images were automatically processed by the host computer, which then generated elastograms depicting the shear wave stiffness in kPa. Thereby, four noncontiguous axial slices (section thickness 10 mm, intersection gap 3 mm) were obtained in each patient, with the center of the slices located at the portal hilar level corresponding to the biopsy site. In some cases, one of the obtained elastograms was not satisfactory because of an irregular wave reflection, motion artifact, and wave diffraction.

LS values were obtained via two different methods; placing the ROIs on the elastogram image and referring to the wave images where wave propagations were regular and relatively free of reflections and interference patterns. First, in the srROIs method, we placed a single small round ROI on the right anterior lobe of the liver per slice of the elastogram. As a result, the four LS values

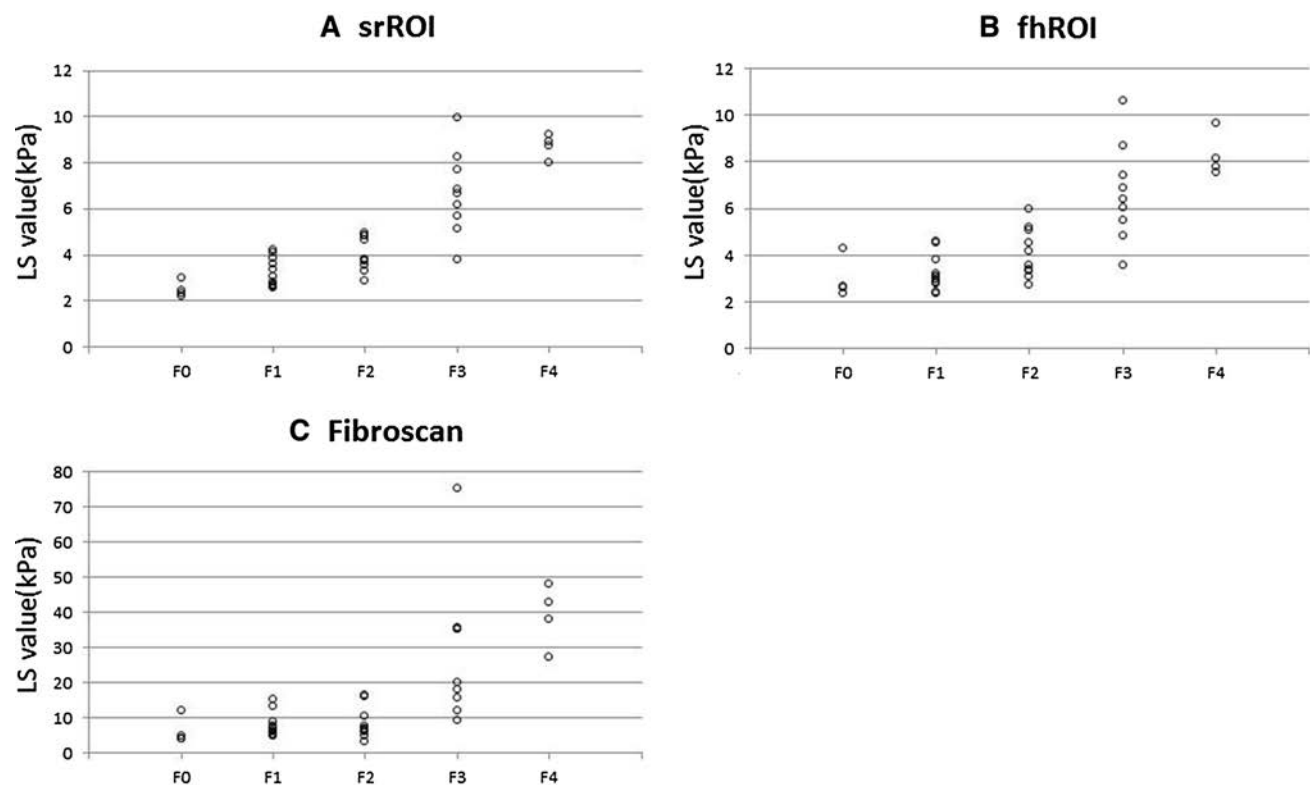


Fig. 3. Scatter plots of the correlations with the three different methods A–C.

	F0 ( <i>n</i> = 6)	F1 ( <i>n</i> = 13)	F2 ( <i>n</i> = 13)	F3 ( <i>n</i> = 15)	F4 ( <i>n</i> = 4)
Small round ROI method	2.44 ± 0.3 (1.96–2.98)	3.24 ± 0.61 (2.60–4.24)	4.14 ± 0.75 (2.88–5.45)	6.74 ± 1.96 (3.78–10.1)	8.73 ± 0.51 (8.03–9.23)
Free hand ROI method	2.72 ± 0.81 (1.93–4.28)	3.39 ± 0.83 (2.35–4.81)	4.18 ± 1.03 (2.68–5.96)	6.56 ± 2.23 (3.56–10.75)	8.27 ± 0.96 (7.54–9.66)
Fibroscan (TE)	5.93 ± 3.18 (3.80–12.1)	7.47 ± 3.35 (3.60–15.3)	8.55 ± 3.96 (3.20–16.3)	22.7 ± 17.8 (6.10–75.0)	39.1 ± 8.77 (27.4–48.0)

The mean LS values based on each of the hisological fibrosis grades for the three different methods assessed

obtained from each elastogram were averaged (Fig. 2A). The average liver area for each slice using the srROIs measurement method was 125 mm<sup>2</sup> (range 101–147 mm<sup>2</sup>). Second, fhROI were placed in the whole right lobe (Fig. 2B). The attending radiologist (M.T), who had 8 years of clinical experience and was blinded to each patient’s clinical history and their US-TE results, carefully avoiding focal lesions, large hepatic vessels, their large branches, liver edges, and motion artifacts by referring to wave images where propagations were regular and relatively free of reflections and interference patterns.

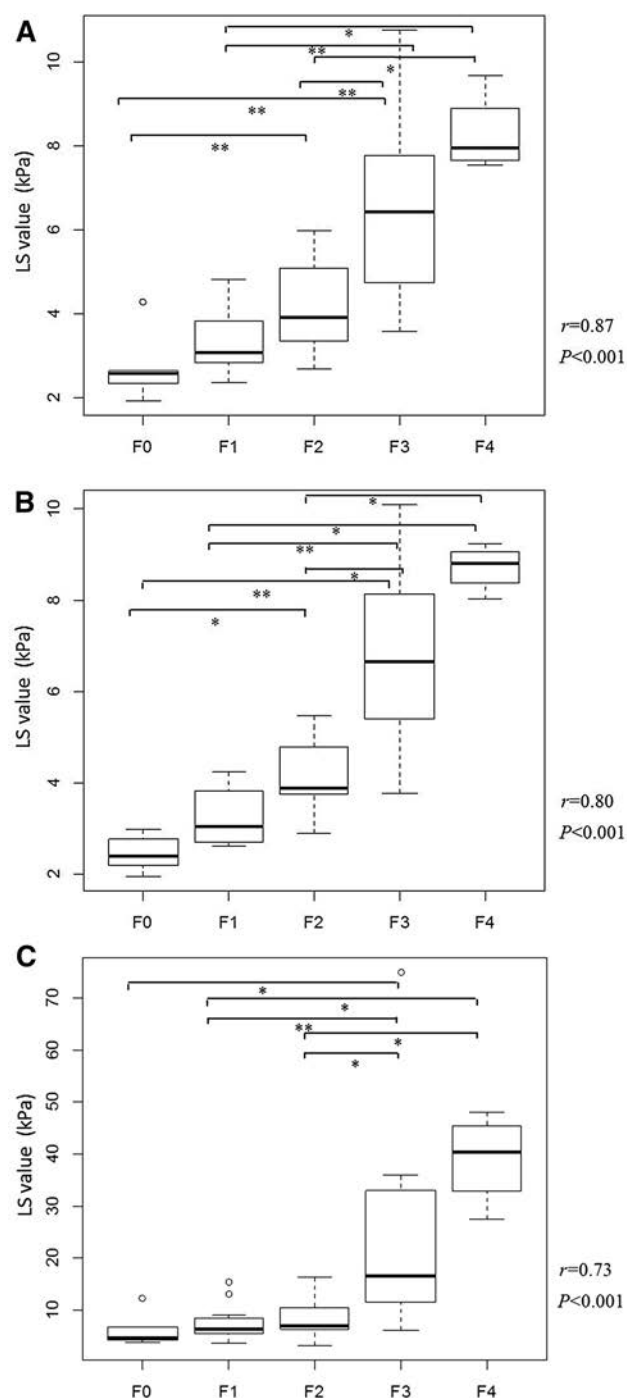
US-TE technique

Fibroscan is one of various modes of TE available, and is categorized as a dynamic form of elastography that can evaluate elasticity by directly measuring the propagating wave velocity associated with an external vibration source. The frequency of the wave was 50 Hz and the LS

values were obtained via the right intercostal approach. This was performed by the same hepatologist with 15 years of clinical experience (NY), who was blinded to each patient’s MRE results, and the results were normalized to the median values of 10 acquisitions with a success rate of >60% and an interquartile range of <30% of the median LS [15]. Particular attention was paid to the stiffness values derived from TE. These values were expressed with reference to Young’s modulus and the stiffness values derived from the MRE shear module [16]; therefore, the Young’s modulus (kPa) values were equivalent to three times those of the values calculated via the MRE shear module.

Statistical analysis

R software (version 2.12.0; R Foundation for Statistical Computing, Vienna, Austria) was used for all statistical analyses [17]. Continuous variables are expressed as the



**Fig. 4.** Box plots representing LS values derived via TE and MRE utilizing the srROIs and fhROI methods. **A** LS values yielded by the srROIs method in the anterior lobes of livers at different fibrosis stages. There was a strong correlation ( $r = 0.87$ ,  $p < 0.001$ ). **B** LS values yielded by the fhROI method in the right lobes of livers at different fibrosis stages. There was a strong correlation ( $r = 0.80$ ,  $p < 0.001$ ). **C** LS values yielded by TE at different fibrosis stages. There was a strong correlation ( $r = 0.73$ ,  $p < 0.001$ ).

mean  $\pm$  SD, and categorical values are expressed as numbers and frequencies. First, a normality test (Shapiro–Wilk test) was performed on the LS values obtained via MRE and US-TE, which determined the choice for the non-parametric test. Correlations between the quantitative values generated via srROIs and fhROI on MRE, US-TE, and histological grades were evaluated via computed Spearman’s rank correlation analysis. Steel–Dwass non-parametric analysis was performed for multiple comparisons between the different histopathological fibrosis stages. To evaluate agreement between the LS values of TE and MRE, a Bland–Altman analysis was performed. The overall predictive ability of MRE and TE for the assessment of fibrosis grades was compared by constructing receiver operating characteristic (ROC) curves which discriminated between significant fibrosis ( $\geq F2$ ), advanced fibrosis ( $\geq F3$ ), and cirrhosis (F4). Respective areas under the curve (AUCs) were then calculated, and the Delong test was performed on the basis of histopathological analysis. A  $p$  value of  $<0.05$  (two-tailed) was considered statistically significant.

## Results

### *Distribution of fibrosis stage and mean LS values*

In patients with biopsy data, the distribution of fibrosis stage was: F0 in 11.8% (6/51), F1 in 25.5% (13/51), F2 in 25.5% (13/51), F3 in 29.4% (15/51), and F4 in 7.8% (4/51). Figure 3 and Table 1 show the scatter plots and mean LS values based on each of the histological fibrosis grades for the three different methods assessed.

### *MRE and TE correlations*

Spearman’s rank correlational analysis yielded a strongly positive statistically significant correlation between the LS values as determined via the srROIs MRE method and histological fibrosis stage ( $r = 0.87$ ,  $p < 0.001$ ), and good correlations between the fhROI method ( $r = 0.80$ ,  $p < 0.001$ ) and the TE method ( $r = 0.73$ ,  $p < 0.001$ ) (Fig. 4A–C).

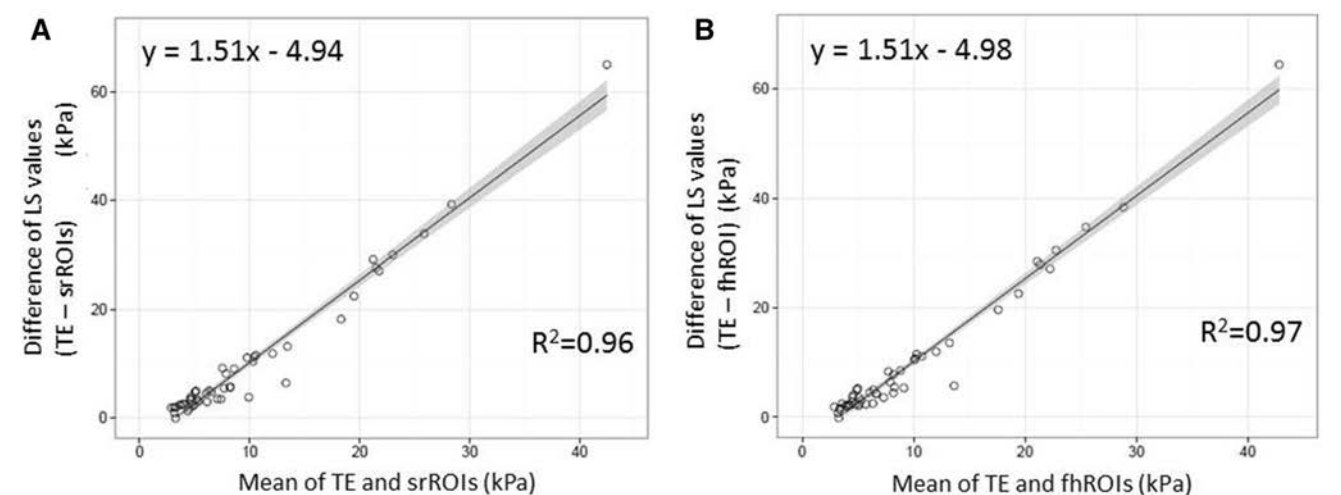
### *Multiple comparisons between different fibrosis stages*

In comparison of the three methods, we were able to distinguish between adjacent histological hepatic fibrosis stages most significantly with the srROIs method (Fig. 4A–C).

### *Agreement between MRE and TE*

Bland–Altman analyses (Fig. 5A for the srROIs method and 5b for the fhROI method) suggested significant





**Fig. 5.** Bland–Altman analyses comparing LS values measured by MRE and TE showed significant proportional bias between TE and each of the two alternative measurement methods investigated. **A** The srROIs method. The existence of proportional bias is suggested by the significant slope of the regression line compared to the average (slope = 1.51,  $p < 0.001$ ). The regression line is shown with 95% individual confidence limit bands. **B** The fhROI method. The existence of proportional bias is suggested by the significant slope of the regression line compared to the average (slope = 1.51,  $p < 0.001$ ). The regression line is shown with 95% individual confidence limit bands.

proportional bias between TE and each of the srROIs and fhROI measurement methods ( $y = 1.51x - 4.94$ ,  $y = 1.51x - 4.98$  respectively,  $p < 0.001$  for both).

Diagnostic performance of MRE and TE

ROC analysis for discriminating significant fibrosis, advanced fibrosis, and cirrhosis provided the respective AUCs, cut-off values, sensitivities, specificities, positive predictive values, negative predictive values, and accuracies (Table 2).

For the detection of significant fibrosis and advanced fibrosis, the AUC associated with MRE using the srROIs method was the highest of all the modes tested. In addition, the Delong test revealed a significant difference between the results yielded by the srROIs method and TE (0.93 vs. 0.82,  $p = 0.006$ ) and between srROIs and fhROI (0.93 vs. 0.89,  $p = 0.04$ ) for detection of significant fibrosis, but not between fhROI and TE (0.89 vs. 0.82,  $p = 0.053$ ). For the detection of advanced fibrosis and cirrhosis, the difference of the AUCs was not significant ( $p = 0.07$ ).

Discussion

In this study, the MRE-derived LS values yielded by the srROIs and fhROI methods were significantly correlated with pathological fibrosis stage ( $r = 0.87$  and  $0.80$  respectively,  $p < 0.001$  for both). The results yielded by TE were also significantly correlated with pathological fibrosis stage, although that correlation was not as strong ( $r = 0.73$ ,  $p < 0.001$ ).

Table 2. ROC analysis

	≥F2 Az value Cut off value Se, Sp, PPV, NPV, accuracy	≥F3 Az value Cut off value Se, Sp, PPV, NPV, accuracy	F4 Az value Cut off value Se, Sp, PPV, NPV, accuracy
MRE small round ROI	0.93 (0.87-1) 3.68kPa 91%, 79%, 88%, 83%, 86%	0.96 (0.91-1) 5.05kPa 89%, 97%, 94%, 94%, 94%	0.94 (0.87-1) 7.86kPa 100%, 89%, 44%, 100%, 90%
MRE free hand ROI	0.89 (0.80-0.98) 3.85kPa 78%, 79%, 86%, 68%, 76%	0.93 (0.85-1) 4.61kPa 84%, 84%, 76%, 90%, 84%	0.94 (0.87-1) 7.86kPa 100%, 91%, 50%, 100%, 92%
Fibroscan (TE)	0.82 (0.70-0.94) 8.85kPa 69%, 84%, 88%, 62%, 76%	0.92 (0.84-1) 11.05kPa 84%, 84%, 76%, 90%, 84%	0.96 (0.90-1) 23.7kPa 100%, 89%, 44%, 100%, 90%

※  $p < 0.05$ , Delong's test

ROC analysis for discriminating ≥F2, ≥F3, and F4 provided the respective AUCs, cut-off values, sensitivities, specificities, positive predictive values, negative predictive values, and accuracies.

The SD tended to increase as fibrosis progressed. Yoon et al. [3] suggested that a wide range in SD values reflected the heterogeneity of fibrosis rather than a measurement error. Moreover, the Bland–Altman analysis demonstrated a proportional bias as fibrosis progressed. The LS values of TE and MRE were expressed as Young’s modulus and shear elasticity modulus, respectively. The Young’s modulus is equal to three times the shear elasticity modulus. Even if the modulus difference was corrected, there was a discrepancy in the corrected LS values. This may have been due to other plural factors involved in the measurement of the LS values: a one-dimensional or two-dimensional measure-



ment, a transient or continuous wave, and a vibration source of 50 or 60 Hz. For example, the MRE using a two-dimensional measurement results in more wave interference from adjacent tissues. The difference between a continuous and transient wave will lead to wave dispersion. The size of vibration source may cause differences in wave diffraction [11, 17–19]. As a result, we postulated that the degree in which fibrosis, congestion, and inflammation influences an LS value may be different between an MRE and TE.

In previous reports on the determination of fibrosis grade via MRE, LS cut-off values have generally corresponded to histological fibrosis grades of F0 (1.5–2.9 kPa) and F4 ( $\geq 5.2$  kPa), and for TE, LS values of F4 were reportedly associated with  $\geq 12$ –14 kPa [8]. The MRE results of the ROC analysis in the current study were very similar to those of previous reports with regards to distinguishing significant fibrosis, advanced fibrosis, and cirrhosis, even for the srROIs method considering weighted average in the right anterior segment of liver. Further, the results of the srROIs method were superior to those of the fhROI method, with respective AUCs of 0.93 vs. 0.89 for significant fibrosis, 0.96 vs. 0.93 for advanced fibrosis, and 0.94 vs. 0.93 for cirrhosis. Notably, with regards to significant fibrosis, the Delong test also revealed a statistically significant difference between AUC of the srROIs and TE (0.93 vs. 0.82,  $p = 0.006$ ), even between AUC of srROIs, and fhROI (0.93 vs. 0.89,  $p = 0.04$ ), but not significant for others.

With regards to MRE, generally methods involving the placement of large ROIs rather than srROIs have been recommended, in order to enable averaging of the parenchymal heterogeneity [12, 20–24]. Lee et al. compared the reliability, reproducibility, and repeatability of three measurement methods: the placement of several small round ROIs in each liver segment, the placement of larger sized ROIs in the whole liver, and the placement of only a small sized ROI in the right anterior segment of liver. They concluded that the former two methods were significantly more reliable than using a single small round ROI alone in an anterior segment of the liver [12]. Rusak et al. concluded that LS varied significantly between segments, but there was less variation between cross-sections of the same segment, even in healthy adults [10]. Therefore, we utilized the srROIs method to calculate the average LS values yielded by a single small round ROI placed on the right lobe of the liver per slice, in order to minimize cross-sectional and inter-segmental variations in LS associated with the biopsy site. Therefore, the consistency within the segments is at least maintained. While the validity of the srROIs method remains to be determined, we suggest that it may yield reasonable consistency with regards to the biopsy site and ROIs placement only within the right anterior lobe of the liver, and may be less affected by inter-segmental variation than more traditional methods, resulting in a

better correlation with the pathological fibrosis stage than methods involving larger ROIs.

In the current study, MRE yielded superior diagnostic results to TE, using the srROIs method. Notably, the method also yielded average stiffness values derived from larger regions of the liver. In this respect, MRE has the potential to replace liver biopsy as a non-invasive imaging procedure as it can assess the whole liver. Moreover, the current study may facilitate more appropriate choices with regards to the two methods of ROI placement investigated. Specifically, while the fhROI method may be more appropriate in cases where evaluation of a larger region of the liver is required (for example, when assessing the effects of hepatitis treatment), the srROIs method may be more appropriate in cases requiring comparisons between biopsy specimens.

The current study had several limitations, in that it was a retrospective study with a relatively small sample size, and included cases of chronic hepatitis with varying etiology. In addition, we did not evaluate reproducibility or reliability. In future studies, the efficacy and clinical adequacy of the srROIs method will be investigated.

Both MRE and US-based TE can be used to assess hepatic fibrosis. In the current study, both methods demonstrated comparable accuracy in patients with chronic liver diseases, with regards to analysis of the liver biopsy specimens. Both methods are non-invasive, and proved useful for evaluating the degree of hepatic fibrosis, particularly with regards to the detection of advanced fibrosis. Additionally, the srROIs and the fhROI methods were both effective, but the srROIs method was superior when comparisons were made based on the biopsy specimens. The results of the current study suggest that the method of ROI placement utilized in cases of hepatic fibrosis should be chosen after careful consideration of the clinical situation.

**Acknowledgement.** We gratefully acknowledge the help of all radiological technologists working in the MRE division of our hospital.

#### Compliance with ethical standards

**Funding** No funding was received for this study.

**Conflict of interest** The authors declare that they have no conflict of interest.

**Ethical approval** All procedures performed in studies involving human participants were in accordance with the ethical standards of the institutional and/or national research committee and with the 1964 Helsinki declaration and its later amendments or comparable ethical standards. For this type of study, formal consent is not required.

**Informed consent** Statement of informed consent was not applicable since the manuscript does not contain any patient data.

#### References

1. Arora A, Sharma P (2012) Non-invasive diagnosis of fibrosis in non-alcoholic fatty liver disease. *J Clin Exp Hepatol* 2:145–155

2. Bensamoun SF, Wang L, Robert L, et al. (2008) Measurement of liver stiffness with two imaging techniques: magnetic resonance elastography and ultrasound elastometry. *J Magn Reson Imaging* 28:1287–1292
3. Yoon JH, Lee JM, Joo I, et al. (2014) Hepatic fibrosis: prospective comparison of MR elastography and US shear-wave elastography for evaluation. *Radiology* 273:772–782
4. Huwart L, Sempoux C, Vicaud E, et al. (2008) Magnetic resonance elastography for the noninvasive staging of liver fibrosis. *Gastroenterology* 135:32–40
5. Bohte AE, de Niet A, Jansen L, et al. (2014) Non-invasive evaluation of liver fibrosis: a comparison of ultrasound-based transient elastography and MR elastography in patients with viral hepatitis B and C. *Eur Radiol* 24:638–648
6. Van Beers BE, Daire JL, Garteiser P (2015) New imaging techniques for liver diseases. *J Hepatol* 62:690–700
7. Venkatesh SK, Yin M, Ehman RL (2013) Magnetic resonance elastography of liver: technique, analysis, and clinical applications. *J Magn Reson Imaging* 37:544–555
8. Hagan M, Asrani SK, Talwalkar J (2015) Non-invasive assessment of liver fibrosis and prognosis. *Expert Rev Gastroenterol Hepatol* 9:1251–1260
9. Pinzani M, Rombouts K, Colagrande S (2005) Fibrosis in chronic liver diseases: diagnosis and management. *J Hepatol* 42(1):S22–S36
10. Rusak G, Zawada E, Lemanowicz A, Serafin Z (2015) Whole-organ and segmental stiffness measured with liver magnetic resonance elastography in healthy adults: significance of the region of interest. *Abdom Imaging* 40:776–782
11. Motosugi U, Ichikawa T, Amemiya F, et al. (2012) Cross-validation of MR elastography and ultrasound transient elastography in liver stiffness measurement: discrepancy in the results of cirrhotic liver. *J Magn Reson Imaging* 35:607–610
12. Lee DH, Lee JM, Han JK, Choi BI (2013) MR elastography of healthy liver parenchyma: normal value and reliability of the liver stiffness value measurement. *J Magn Reson Imaging* 38:1215–1223
13. Bedossa P (1994) Intraobserver and interobserver variations in liver biopsy interpretation in patients with chronic hepatitis C. The French METAVIR cooperative study group. *Hepatology* 20:15–20
14. Rouvière O, Yin M, Dresner MA, et al. (2006) MR elastography of the liver: preliminary results. *Radiology* 240:440–448
15. Yada N, Sakurai T, Minami T, et al. (2014) Ultrasound elastography correlates treatment response by antiviral therapy in patients with chronic hepatitis C. *Oncology* 87(suppl 1):118–123
16. Sandrin L, Fourquet B, Hasquenoph JM, et al. (2003) Transient elastography: a new noninvasive method for assessment of hepatic fibrosis. *Ultrasound Med Biol* 29:1705–1713
17. R Development Core Team. R (2007) A language and environment for statistical computing. Vienna, Austria: The R Foundation for Statistical Computing/2001. ISBN: 3-900051-07-0. <http://www.R-project.org/>
18. Chen J, Talwalkar JA, Yin M, et al. (2001) Early detection of nonalcoholic steatohepatitis in patients with nonalcoholic fatty liver disease by using MR elastography. *Radiology* 259:749–756
19. Wong GL (2013) Update of liver fibrosis and steatosis with transient elastography (Fibroscan). *Gastroenterol Rep* 1:19–26
20. Zhang DY, Friedman SL (2012) Fibrosis-dependent mechanisms of hepatocarcinogenesis. *Hepatology* 56:769–775
21. Yin M, Talwalkar JA, Glaser KJ, et al. (2007) Assessment of hepatic fibrosis with magnetic resonance elastography. *Clin Gastroenterol Hepatol* 5:1207–1213
22. Mitsufuji T, Shinagawa Y, Fujimitsu R, et al. (2013) Measurement consistency of MR elastography at 3.0T: comparison among three different region-of-interest placement methods. *Jpn J Radiol* 31: 336–341
23. Dzyubak B, Glaser K, Yin M, et al. (2013) Automated liver stiffness measurements with magnetic resonance elastography. *J Magn Reson Imaging* 38:371–379
24. Hines CD, Bley TA, Lindstrom MJ, Reeder SB (2010) Repeatability of magnetic resonance elastography for quantification of hepatic stiffness. *J Magn Reson Imaging* 31:725–731

## Integration of the cancer-related inflammatory response as a stratifying biomarker of survival in hepatocellular carcinoma treated with sorafenib

Jessica A. Howell<sup>1,2,3,\*</sup>, David J. Pinato<sup>1,\*</sup>, Ramya Ramaswami<sup>1</sup>, Tadaaki Arizumi<sup>4</sup>, Carlotta Ferrari<sup>5</sup>, Antonello Gibbin<sup>5</sup>, Michela E. Burlone<sup>5</sup>, Giulia Guaschino<sup>5</sup>, Pierluigi Toniutto<sup>6</sup>, James Black<sup>1</sup>, Laura Sellers<sup>1</sup>, Masatoshi Kudo<sup>4</sup>, Mario Pirisi<sup>5</sup> and Rohini Sharma<sup>1</sup>

<sup>1</sup>Department of Surgery and Cancer, Imperial College London, Hammersmith Hospital, London, UK

<sup>2</sup>Centre for Population Health, Burnet Institute, Melbourne, Australia

<sup>3</sup>Department of Medicine, University of Melbourne, Melbourne, Australia

<sup>4</sup>Department of Gastroenterology and Hepatology, Kinki University School of Medicine, Osaka-Sayama, Osaka, Japan

<sup>5</sup>Department of Translational Medicine, Università degli Studi del Piemonte Orientale "A. Avogadro", Novara, Italy

<sup>6</sup>Department of Experimental and Clinical Medicine, University of Udine, Udine, Italy

\* These authors have contributed equally to the work

Correspondence to: Jessica A. Howell, email: jessica.howell@svha.org.au

Keywords: liver cancer, VEGF inhibitor, CLIP score, BCLC, inflammation

Received: March 30, 2016 Accepted: October 13, 2016 Published: February 14, 2017

Copyright: Howell et al. This is an open-access article distributed under the terms of the Creative Commons Attribution License (CC-BY), which permits unrestricted use, distribution, and reproduction in any medium, provided the original author and source are credited.

### ABSTRACT

**Background and Aims:** Response to sorafenib is highly variable in hepatocellular carcinoma (HCC). Baseline inflammatory parameters and treatment toxicities may improve survival prediction in patients on sorafenib therapy.

**Results:** 442 patients with advanced stage HCC on sorafenib were recruited (follow-up 5096 person-months at risk). 88% had BCLC stage B or greater HCC and 72.3% had Child-Pugh A cirrhosis. On Cox multivariate regression, previously-treated HCC (HR 0.579, 95% CI 0.385-0.872,  $p=0.009$ ), Cancer of Liver Italian Program (CLIP) score (HR 1.723, 95% CI 1.462-2.047,  $p<0.0001$ ), baseline red cell distribution width (RDW; HR 1.234, 95% CI 1.115-1.290,  $p<0.0001$ ) and neutrophil to lymphocyte ratio (NLR; HR 1.218, 95% CI 1.108-1.322,  $p<0.0001$ ) were significant independent risks for shorter survival, whilst sorafenib-related diarrhoea was associated with prolonged survival (HR 0.533, 95% CI 0.373-0.763,  $p=0.001$ ). The combination of RD-CLIP score (CLIP score multiplied by RDW)  $\geq 70$  and no treatment-related diarrhoea had good utility for predicting 3-month survival (AUC of 0.808 (95% CI 0.734-0.882), positive predictive value of 86.4% and negative predictive value of 83.3%), compared with CLIP (AUC=0.642) or BCLC score alone (AUC=0.579). RD-CLIP score  $\geq 35$  and no treatment-related diarrhoea had an AUC of 0.787 for predicting 12-month survival.

**Methods:** Patients with HCC were consecutively recruited from three tertiary centres (Japan, Italy and UK) and clinical data were prospectively collected. The primary study endpoint was overall survival (OS) after commencing sorafenib.

**Conclusion:** The novel prognostic index of CLIP score combined with inflammatory marker RDW and treatment-related diarrhoea has good accuracy for predicting overall, 3 month and 12 month survival in patients on sorafenib.

## INTRODUCTION

Hepatocellular carcinoma (HCC) is the sixth most common malignancy worldwide and the third most common cause of cancer-related death [1]. Despite major advances in the diagnosis and therapy of HCC, incidence of HCC is increasing worldwide and mortality remains high despite the global trend of falling cancer death rates over the last decade [1, 2].

Sorafenib, an oral multi-targeted inhibitor of Raf, Platelet-derived (PDGF) and Vascular Endothelial Growth Factor (VEGF) receptors, has proven efficacy for advanced HCC, with a reported median 3-month improvement in patient survival and delayed radiological disease progression by an average of 2 months [3, 4]. However, in the clinical setting overall response rates to sorafenib are highly heterogeneous [3], due to the fact that mortality from HCC is not solely influenced by tumour stage, but also by underlying liver function impairment and patient performance status.

There are currently no validated stratifying biomarkers to predict sorafenib treatment efficacy. Whilst molecular traits including intra-tumour Erk phosphorylation [5] or focal gains in VEGF-A [6] have been postulated as biomarkers of enhanced sorafenib sensitivity, these have not translated into validated, accessible prognostic tests. Given drug-related toxicities and the cost of sorafenib therapy [3, 4, 7], there is an unmet need for inexpensive, accessible clinical biomarkers to help identify patients who are most likely to benefit from sorafenib.

Inflammation is a well-established driver of liver fibrosis and carcinogenesis and inflammatory parameters predict survival in both cirrhosis [8, 9] and HCC [10-14]. Gene expression studies have shown a pro-inflammatory signature in the tumour microenvironment predicts shorter time to recurrence and worse OS in patients receiving radical treatment for HCC [10]. Several groups have previously shown that inflammatory parameters, including the Inflammation-based Index (IBI) and the neutrophil to lymphocyte ratio (NLR), are associated with worse survival in HCC [11-14]. More recently, we demonstrated that stage-dependent deterioration in red cell distribution width (RDW), a marker of anisocytosis, is associated with overall survival in HCC, with the strongest prognostic role of RDW demonstrated in patients with advanced HCC [15]. Moreover, inflammatory parameters such as RDW are inexpensive and accessible biomarkers for survival prediction in HCC.

The aim of this study was to use a multivariable regression model to evaluate the prognostic value of common clinical and biochemical parameters including RDW and systemic inflammatory biomarkers in a large, prospectively recruited mixed-race cohort of HCC patients receiving sorafenib. Based on our survival analysis, we derived a composite Cancer Liver Italian Program

(CLIP) and inflammation-based algorithm to optimise the prediction of survival benefit from sorafenib therapy in HCC.

## RESULTS

Four hundred and forty two patients with HCC were recruited, with a median follow-up time of 7.1 months (IQR 3.4-16.1 months) and overall follow-up time of 5096 person-months at risk. The mean age was 70 +/-10 years and 78% were male. The majority of patients in the cohort had CTP class A (73%) or B (27%) disease, with a median CTP score of 6 (IQR 5-7). With respect to tumour stage, the majority of patients had a BCLC score of B or greater (88%), 29% had portal vein thrombosis (PVT) and 24% had extra-hepatic metastases. Twenty-five percent had received loco-regional treatment prior to sorafenib. A summary of the distribution of clinical variables is outlined in Table 1.

### Clinical variables associated with overall survival after sorafenib therapy

Median duration of sorafenib therapy was 3.97 months (IQR 1.6-10.3 months), with the majority of patients ceasing therapy due to progressive disease (178 of 438 patients in whom follow up data were available, 40.6%) or unacceptable toxicity (111 of 438, 25.3%). Overall, 311 (70.4%) patients died during follow up, with a median survival time of 9.6 months (IQR 4.3-21.3 months) after commencing sorafenib. Three-month survival was 78.5% (346/441) and twelve-month survival was 33% (147/441). Overall response to sorafenib (either complete, partial disease response or stabilisation of disease without radiological progression) occurred in 221 (50.2%) patients, whereas 221 (49.8%) developed progressive HCC on imaging during follow up. The vast majority (363/ 442, 82.1%) of patients experienced at least one side effect of grade 1 or higher severity.

Univariate predictors of OS included age ( $p=0.013$ ), baseline CTP score ( $p<0.0001$ ), NLR ( $p<0.0001$ ), RDW ( $p<0.0001$ ), presence of portal venous thrombosis (PVT,  $p<0.0001$ ), presence of metastases ( $p=0.002$ ), CLIP score ( $p=0.001$ ) and BCLC score ( $p=0.009$ ). Patients who were treatment naïve had longer survival compared to patients who had previously undergone therapy ( $p=0.006$ ). Moreover, development of side effects on sorafenib (of any severity and at any treatment stage), including hypertension  $p<0.0001$ , hand-foot syndrome  $p<0.0001$  and diarrhoea  $p<0.0001$  were univariate predictors of survival (Supplementary Table 1). However, on Cox proportional hazards analysis ( $n=175$  patients who had complete data for all parameters), treatment-naïve compared with previously treated HCC (HR 0.579, 95% CI 0.385-0.872,  $p=0.009$ ), CLIP score (HR 1.723, 95% CI 1.462-2.047,  $p<0.0001$ ), RDW (HR 1.234, 95% CI

**Table 1: Distribution of clinical variables within the cohort (n=442)**

<b>Clinical Variable</b>	
Number of deaths (N, %) (n=442)	311 (70.4%)
Gender N (%) (n=442)	
Male	346 (78.3%)
Female	96 (21.7%)
Mean Age (years) +/- sd (n=442)	69.92 +/- 10.06 years
Median (IQR) ALT ( $\mu\text{mol/L}$ ) (n=438)	41 (26-70)
Median (IQR) total bilirubin ( $\mu\text{mol/L}$ ) (n=442)	16.00 (10.30-23.94)
Median (IQR) albumin (g/L) (n=441)	36 (31-39)
Median (IQR) CTP score (n=441)	6 (5-7)
Median (IQR) neutrophils ( $\times 10^9/\text{L}$ ) (n=438)	3.1 (2.3-4.4)
Median (IQR) lymphocytes ( $\times 10^9/\text{L}$ ) (n=438)	1.30 (0.99-1.73)
Median (IQR) platelets ( $\times 10^9/\text{L}$ ) (n=440)	145.5 (97.0-210.5)
Median (IQR) NLR (n=438)	2.52 (1.68-3.40)
Median (IQR) red cell distribution width (n=425)	14.2 (13.1-16.0)
Viral hepatitis N (%) (n=213)	98 (46.0%)
Alcohol Liver Disease N (%) (n=210)	97 (46.2%)
Tumour morphology N (%) (n=438)	
<50% uninodular	62 (14.2%)
<50% multinodular	257 (58.7%)
>50% multinodular	119 (27.2%)
Median (IQR) AFP (ng/mL) (n=420)	128 (9-1616)
Portal vein thrombosis N (%) (n=442)	128 (29.0%)
Median (IQR) Tumour size (cm) (n=427)	4.2cm (2.1-7.3)
Number of nodules N (%) (n=390)	
1-3 nodules	174 (44.5%)
4-6 nodules	100 (25.6%)
7-10 nodules	102 (26.2%)
Multinodular	8 (2.1%)
Diffuse	6 (1.5%)
Metastases N (%) (n=442)	108 (24.4%)
BCLC score N (%) (n=428)	
A1	12 (2.8%)
A2	2 (0.5%)
A3	3 (0.7%)
A4	34 (7.9%)
B	148 (34.6%)

*(Continued)*



Clinical Variable	
C	225 (52.6%)
D	4 (0.9%)
Median (IQR) CLIP score (n=276)	2 (1-3)
Treatment-naïve versus previously treated HCC (n=204)	
Treatment-naïve HCC	103 (50.5%)
Previously treated HCC	101 (49.5%)
Median (IQR) Sorafenib duration (months) (n=440)	3.97 (1.63-10.30)
Adverse events from sorafenib*:	
Diarrhoea (n=261)	156 (59.78%)
Hypertension (n=168)	77 (45.8%)
Hand-foot syndrome (n=287)	148 (51.7%)
Mucositis (n=118)	12 (10.2%)

\*Adverse events from sorafenib developing during any cycle of treatment

IQR, interquartile range; ALT, alanine aminotransferase; CTP, Child Turcotte Pugh score; NLR, neutrophil to lymphocyte ratio; BCLC, Barcelona Clinic Liver Cancer score; CLIP, Cancer of the Liver Italian Program.

1.115-1.290,  $p<0.0001$ ) and NLR (HR 1.218, 95% CI 1.108-1.322,  $p<0.0001$ ) were all significant independent risks for shorter survival in patients receiving sorafenib. In contrast, sorafenib-related diarrhoea was associated with prolonged survival (HR 0.533, 95% CI 0.373-0.763,  $p=0.001$ ; Table 2).

### RD-CLIP score and diarrhoea predicts three-month survival in patients receiving sorafenib

We further evaluated clinical variables associated with survival endpoints at 3 and 12 months. There was a significant association between 3-month survival and lower CLIP score (OR 0.522, 95% CI 0.382-0.714,  $p<0.0001$ ), lower RDW (OR 0.789, 95% CI 0.688-0.905,  $p=0.001$ ), and sorafenib-mediated diarrhoea (OR 3.682, 95% CI 1.598-9.335,  $p=0.003$ , Table 3), but not NLR.

A combined logistic regression model of these three variables confirmed good predictive accuracy for 3-month survival, with an AUROC of 0.815 (95% CI 0.727-0.896). We then developed a novel prognostic index of baseline RDW multiplied by CLIP score (RD-CLIP), combined with sorafenib-related diarrhoea in a logistic regression model. Using variable cut-offs chosen to maximise sensitivity and specificity, a model using a baseline RD-CLIP score greater than or equal to 70 and the presence of sorafenib-related diarrhoea had an AUROC for predicting three-month survival of 0.808 (95% CI 0.734-0.882), with sensitivity of 97.9%, specificity of 40.5%, positive predictive value of 86.4% and negative predictive value of 83.3%. This was superior to CLIP score alone (AUC=0.642) or BCLC score alone (AUC=0.579).

Median survival time was 2.1 months (IQR 2-2.2 months) in patients with RD-CLIP score greater than or equal to 70 and no sorafenib-mediated diarrhoea, compared with 8.4 months (IQR 4.23-16.8 months) in patients who did not fulfil these criteria (Figure 1A).

Twelve-month survival was also independently associated with lower baseline RDW (OR 0.799, 95% CI 0.665-0.959,  $p=0.016$ ), lower CLIP score (OR 0.663, 95% CI 0.469-0.937,  $p=0.020$ ), and treatment-naïve compared with previously-treated HCC (OR 3.517, 95% CI 1.626-7.610,  $p=0.001$ ) on logistic regression. A non-significant trend was observed between sorafenib-related diarrhoea and twelve-month survival ( $p=0.059$ ). A predictive logistic regression model was optimised for sensitivity and specificity using a modified RD-CLIP cut-off of 35, recurrent HCC and no diarrhoea, with an AUROC of 0.787 (95% CI 0.718-0.857), suggesting moderate utility as a predictive model of twelve-month survival. Sensitivity for twelve-month survival was 44.4%, specificity 85.5%, positive predictive value (PPV) 55.6% and negative predictive value (NPV) was 79.0%. Again, this combination had higher accuracy for 12-month survival than either CLIP score (AUC=0.669) or BCLC score alone (AUC=0.579).

### The association between sorafenib-mediated diarrhoea and RDW and survival is independent of dose reductions during treatment

Finally, an important consideration was whether the requirement for dose reductions during treatment was a confounding factor for the apparent association between

**Table 2: Summary of clinical variables independently associated with survival in patients on sorafenib therapy: results of Cox proportional hazards multivariate analysis (n=175)**

Clinical Variable	HR	95% CI	P-value
Treatment-naïve HCC	0.579	0.385-0.872	0.009
NLR	1.252	1.139-1.377	<0.0001
RDW	1.136	1.056-1.223	0.001
CLIP score	1.383	1.195-1.600	<0.0001
Diarrhoea on sorafenib	0.596	0.417-0.852	0.005

NLR, neutrophil to lymphocyte ratio; RDW, red cell distribution width; AFP, alpha-fetoprotein; CLIP score, Cancer of the Liver Italian Program score. Primary tumour refers to primary diagnosis of tumour, compared with recurrent tumour after previous therapy.

**Table 3: Clinical variables significantly associated with 3 month and 12 month survival in patients on sorafenib therapy (n=232)**

Clinical Variable	OR	95% CI	P-value	AUC	Sensitivity Specificity PPV NPV
3 month survival					
RD-CLIP $\geq$ 70	0.017	0.004-0.075	<0.0001	0.808	Sensitivity 97.9% Specificity 40.5% PPV 86.4% NPV 83.3% Correct identification 86.1%
Diarrhoea on sorafenib	4.990	1.774-14.04	0.002		
12 month survival					
RD-CLIP $\geq$ 35	0.093	0.021-0.415	0.002	0.787	Sensitivity 44.4% Specificity 85.5% PPV 55.6% NPV 79.0% Correct identification 73.6%
Recurrent HCC	3.943	1.652-9.408	0.002		
Diarrhoea on sorafenib	1.777	0.810-3.899	0.152		

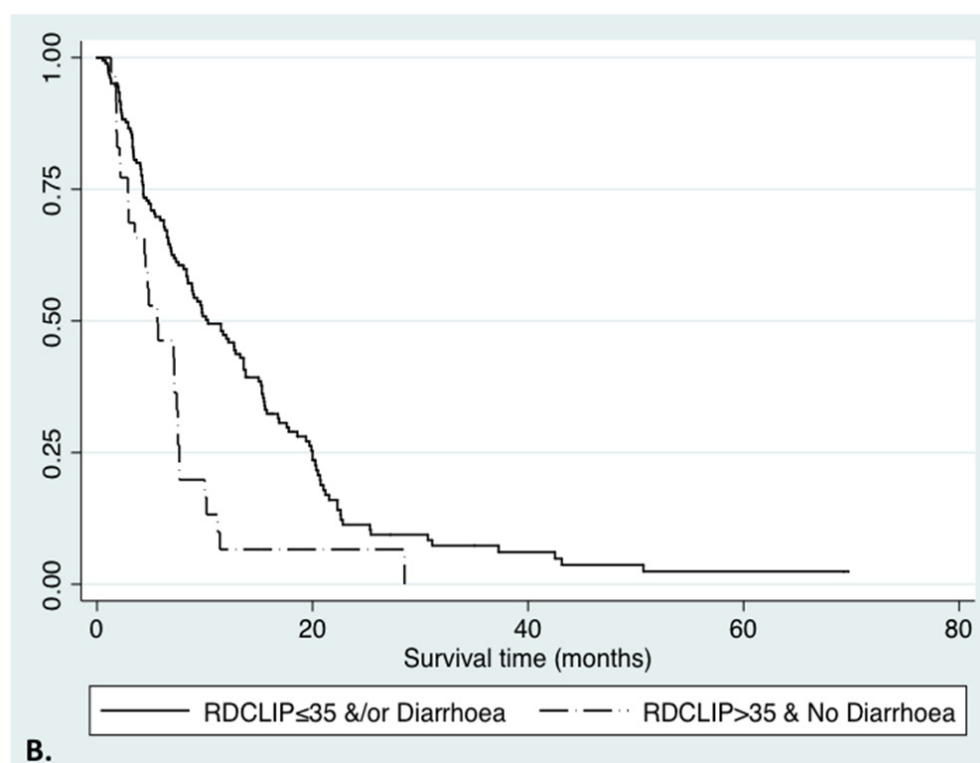
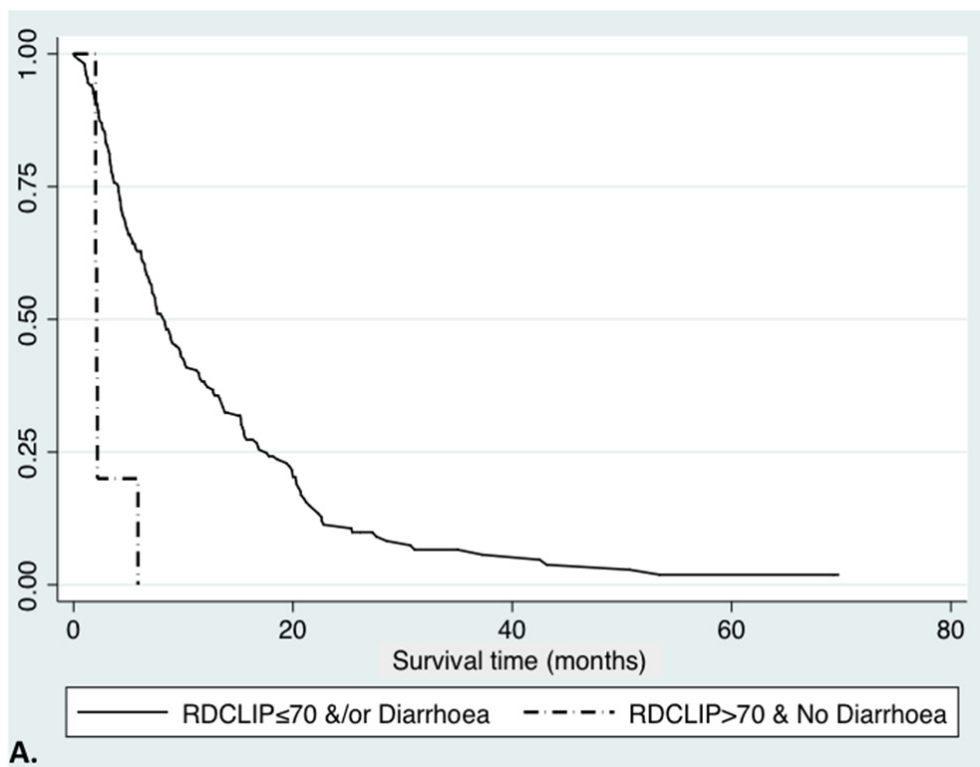
RD, red cell distribution width; CLIP, Cancer of the Liver Italian Program; HCC, hepatocellular carcinoma.

sorafenib-mediated diarrhoea, RDW and survival. Median duration of sorafenib was 3.97 months (IQR 1.63-10.30 months). 261 (59.2%) patients commenced on 400mg sorafenib and 180 (40.8%) were commenced on 800mg daily, with those starting on lower dose rapidly titrated up to target dose. Data describing dose reductions during therapy were only available for 109 patients (25%). However, in a post-hoc analysis, sorafenib dose reduction was not associated with survival (Log-rank  $p=0.211$ ; Wilcoxon rank-sum  $p=0.853$ ) or with development of diarrhoea ( $\chi^2$   $p=0.122$ ) or RDW (Wilcoxon rank-sum  $p=0.842$ ). Though limited by small sample size and available data representing only 25% of the cohort, these data suggest sorafenib dose reduction was not a significant confounding factor for the association between diarrhoea

or RDW and survival in patients with HCC treated with sorafenib in this study.

## DISCUSSION

Survival in advanced HCC is dependent upon the complex interplay between tumour burden and underlying liver disease, which ultimately determines patient outcome. Given the modest survival benefit offered by sorafenib and the frequent need for discontinuation due to poor tolerability, deterioration in liver function or progressive disease, prognostic markers to guide clinical decision-making in patients with advanced HCC are urgently sought. This large, prospective, multicentre study enrolling patients from a wide range of racial backgrounds



**Figure 1: Survival curves in HCC patients receiving sorafenib, defined by RD-CLIP score and treatment-related diarrhoea.** **A.** Kaplan-Meier curve comparing RD-CLIP score greater than 70 and those without treatment-related diarrhoea, to those with RD-CLIP score less than or equal to 70 and/ or treatment-related diarrhoea (2.1 months (IQR 2.0-2.2 months) versus 8.3 months (IQR 4.1-17.6 months); Logrank  $p < 0.0001$ , Wilcoxon  $p < 0.0001$ ). **B.** Kaplan-Meier curve comparing RD-CLIP score greater than 35 and those without treatment-related diarrhoea, to those with RD-CLIP score less than or equal to 35 and/ or treatment-related diarrhoea (5.6 months (IQR 2.8-18.6 months) versus 10.3 months (IQR 4.3-20 months); Logrank  $p < 0.0001$ , Wilcoxon  $p = 0.0003$ ).

and disease aetiologies shows for the first time that the combination of RDW and CLIP score together with treatment-related diarrhoea are superior markers for predicting overall, three-month and twelve-month survival compared with CLIP or BCLC score alone in patients with advanced disease on sorafenib.

RDW reflects inflammation-induced erythroid maturation impairment and has clinical utility as a marker of inflammation in both liver disease [15, 16, 17] and cancer [18]. Inflammation is central to liver damage, fibrogenesis and oncogenesis [10, 19], and inflammatory markers have prognostic value in HCC [20, 21]. Several indices, the Inflammation-based index, IBI; prognostic nutritional index, PNI; and modified Glasgow score, have prognostic utility for survival in HCC. However, no inflammatory scores have been systematically assessed in patients with advanced disease on sorafenib. Importantly, RDW has previously been validated as a marker of overall survival in HCC patients [15], lending credence to the association between RDW and survival in advanced HCC patients receiving sorafenib. This suggests inflammation is a key determinant of survival in advanced HCC, which fits with the known driving role of inflammation in hepatocarcinogenesis [10, 19]. RDW also reflects nutritional status, itself a marker of performance status in cancer and also systemic immune function [15]. Moreover, RDW is an inexpensive and accessible biomarker in patients with HCC receiving sorafenib, as it is already provided in the full blood count.

A key finding of this study is that overall survival, 3 month and 12 month survival were associated with diarrhoea as a side effect of sorafenib use, but not skin toxicities as previously reported. A number of studies have reported off-target effects of sorafenib as prognostic factors, including diarrhoea and skin toxicities [22-31]. Bettinger et al [29] reported survival was twice as long in patients who developed diarrhoea on sorafenib compared to those who did not (7.1 months versus 14.1 months), findings that have been replicated by others [26, 32]. The current study is the largest to date reporting the association between treatment-related diarrhoea and survival, lending strength to these findings.

It is likely that diarrhoea reflects systemic drug levels and drug activity [23, 25, 26, 31, 32]. Evidence suggests that there is survival benefit of sorafenib even in patients who cease drug due to toxicities, compared with those who cease sorafenib due to progressive disease [25], findings that were echoed in our study. Another potential mechanism of improved survival may be through the effects of diarrhoea on the gut microbiome and bacterial translocation, both key determinants of survival in cirrhosis with portal hypertension [33, 34]. Sorafenib-induced diarrhoea may lead to alterations in gut flora or reduction in the load of nitrogenous commensal bacteria, therefore reducing bacterial translocation and ammonia

absorption akin to the therapeutic effects of lactulose or rifaximin on encephalopathy [35].

Though 50% of our patients reported hand-foot skin toxicity, there was no association with survival. However, skin rash other than hand-foot syndrome was uncommon in the cohort (13%) and grade 3-4 HFS was rare, and may explain the lack of association found between skin toxicity and survival in this study. Hypertension has been reported as a prognostic variable for survival [26], however we did not replicate this finding, in line with another previous negative report [23].

CLIP score, but not BCLC score, was prognostic for survival on multivariate analysis. There is good evidence for the prognostic potential of both CLIP and BCLC scores in HCC [1, 36] and they have traditionally been used to stratify those who are most likely to benefit from sorafenib [1, 36]. Key features of both scores, including tumour morphology, size, AFP levels, metastases and PVT have all been shown to predict survival in patients on sorafenib [3, 4, 25, 27, 33, 37-39]. The main differences between BCLC and CLIP scores are greater weight given to CTP class and inclusion of AFP in CLIP [1]. The discrepancy between our finding regarding BCLC score and other reports [39, 40] is not surprising given the relative homogeneity of our patient cohort, with inherent over-representation of patients with well-compensated liver disease and advanced HCC. These data also suggest that AFP is an important prognostic factor for survival in patients on sorafenib, particularly in patients with advanced disease, which is supported by data from the study of the VEGF2 inhibitor, ramucirumab, where patients with higher AFP levels had shorter overall survival [41]. Whilst BCLC remains undoubtedly a useful validated system to prioritize treatment allocation, our study suggests a better stratifying role for CLIP in the prognostic assessment of patients with advanced HCC receiving sorafenib, in line with previous evidence gathered in patients with advanced disease.

Current prognostic scores such as BCLC and CLIP do not include markers of inflammation [1]. However, by combining red cell distribution width with CLIP score and sorafenib-mediated diarrhoea, 3-month survival was predicted with good accuracy (AUC 0.808) and 12 month survival with moderately good accuracy (AUC 0.787), with greater accuracy than CLIP score or BCLC scores alone. Importantly, baseline RD-CLIP and diarrhoea had very high sensitivity for predicting 3-month survival, with a relatively high PPV and NPV in this study population. Our data suggest the addition of inflammatory parameters to prognostic assessments such as CLIP or BCLC significantly improves prediction of patients most likely to benefit from sorafenib, which will inform discussions with patients experiencing side effects and considering treatment cessation or changing to second-line agents.

There are several limitations to our study. This is a pilot cohort study powered to detect clinical variables

associated with overall survival that may prove useful biomarkers of sorafenib survival in future studies. These findings therefore require validation in independent cohorts before they can be incorporated into current HCC management guidelines, however the data are highly suggestive of the merit of further validation studies. We did not evaluate dynamic changes in clinical parameters over time to confirm ongoing prediction of survival and response to treatment, which would be useful to confirm their utility throughout duration of sorafenib therapy. Moreover, diarrhoea is a more subjective measure than RDW or CLIP score for the purposes of survival prediction. However, the current study includes a large cohort of patients and is well-powered to detect significant associations between clinical variables and overall survival, which lends considerable weight to our findings.

## MATERIALS AND METHODS

This is a prospective, observational cohort study of prognostic factors in patients receiving sorafenib for advanced HCC. The primary study endpoint was overall survival (OS) after commencing sorafenib, censored at either death or end date of study follow up (30 March 2015). Clinical factors related to OS and disease progression were determined.

Patients with HCC were consecutively recruited to the study from three tertiary centres with specialist multidisciplinary services for HCC management: Osaka, Japan (183 patients, 41.4%); Novara, Italy (156, 35.4%) and Hammersmith Hospital, Imperial College, London UK (103, 23.3%) from January 1, 2008 until censorship for death or loss to follow up, or the study end date of December 31, 2015. Demographic and clinical data, blood tests and imaging results were collected prospectively. All patients had a diagnosis of HCC based either on imaging or histologic criteria according to international guidelines [1]. Patients were staged using the Barcelona Clinic Liver Cancer (BCLC) and CLIP scores, both of which describe liver functional impairment using the Child Turcotte Pugh score (CTP) [1].

The study was approved by local institutional ethics committees and conducted in accordance with the Declaration of Helsinki (update 2004).

### Sorafenib treatment

Patients were commenced on sorafenib therapy in accordance with BCLC guidelines (BCLC stage C, or BCLC stage B if other factors precluded use of loco-regional therapies). All patients in the study were unsuitable for surgical resection of HCC. Patients with decompensated liver disease and performance scores  $\geq 2$  were excluded. Duration, dose modifications and tolerability to sorafenib were recorded. Cause for cessation of therapy (toxicity, patient preference, disease progression

or death) was also recorded. Disease progression was defined by mRECIST criteria [42].

## Statistical methods

Variables were described using mean and standard deviation or median and interquartile range (IQR), with natural logarithmic transformation of skewed data. NLR was calculated by dividing the neutrophil count by the lymphocyte count. Univariate analysis of variables associated with survival was performed using Log-rank testing. Multivariate analysis was performed using Cox proportional hazards regression modelling using backward elimination and likelihood ratio testing, including variables significantly associated with survival on univariate analysis. Proportional hazards was confirmed using Schoenfeld residuals and visually using log-log plots. Prognostic model building utilised logistic regression modelling with stepwise backward elimination and likelihood ratio testing. Receiver Operator Curve (ROC) analysis determined diagnostic accuracy of regression models for predicting three-month survival and twelve-month survival. All analyses were performed using STATA version 12.1 (Stata Corporation, College Station, Texas, USA).

## CONCLUSION

A novel prognostic index of CLIP score combined with RDW and the presence of treatment-related diarrhoea had good accuracy for determining overall, 3 month and 12 month survival in patients who have commenced sorafenib. Patients with RD-CLIP scores  $\geq 70$  and no treatment-related diarrhoea had median survival of 2.1 months compared with 8.4 months in those who did not fulfil these criteria. The addition of simple, easy-to-measure RDW and sorafenib-related diarrhoea to current prognostic algorithms in advanced HCC management improves accuracy for predicting survival benefit of sorafenib in patients with advanced HCC and warrants further validation in future studies.

## ACKNOWLEDGMENTS

JH is supported by a National Medical Research Council of Australia Early Career Fellowship. DJP is supported by the National Institute of Health Research (NIHR), Academy of Medical Sciences (AMS) and Action Against Cancer.

## CONFLICTS OF INTEREST

The authors have no disclosures relevant to the current study



## FINANCIAL SUPPORT

JH is supported by a National Medical Research Council of Australia Early Career Fellowship. DJP is supported by the National Institute of Health Research (NIHR), Academy of Medical Sciences (AMS) and Action Against Cancer. No specific financial support was provided for this project.

We are grateful to Imperial College for supporting publication costs for the manuscript.

## REFERENCES

1. European Association For The Study Of The Liver, European Organisation For Research And Treatment Of Cancer. EASL-EORTC clinical practice guidelines: management of hepatocellular carcinoma. *J Hepatol*. 2012; 56:908–43.
2. Jemal A, Siegel R, Ward E, Hao Y, Xu J, Murray T, Thun MJ. Cancer statistics, 2008. *CA Cancer J Clin*. 2008; 58:71–96.
3. Llovet JM, Ricci S, Mazzaferro V, Hilgard P, Gane E, Blanc JF, de Oliveira AC, Santoro A, Raoul JL, Forner A, Schwartz M, Porta C, Zeuzem S, et al. Sorafenib in advanced hepatocellular carcinoma. *N Engl J Med*. 2008; 359:378–90.
4. Cheng AL, Kang YK, Chen Z, Tsao CJ, Qin S, Kim JS, Luo R, Feng J, Ye S, Yang TS, Xu J, Sun Y, Liang H, et al. Efficacy and safety of sorafenib in patients in the Asia-Pacific region with advanced hepatocellular carcinoma: a phase III randomised, double-blind, placebo-controlled trial. *Lancet Oncol*. 2009; 10:25–34.
5. Chen D, Zhao P, Li SQ, Xiao WK, Yin XY, Peng BG, Liang LJ. Prognostic impact of pERK in advanced hepatocellular carcinoma patients treated with sorafenib. *Eur J Surg Oncol*. 2013; 39:974–80.
6. Llovet JM. Focal gains of VEGFA: candidate predictors of sorafenib response in hepatocellular carcinoma. *Cancer Cell*. 2014; 25:560–62.
7. Cammà C, Cabibbo G, Petta S, Enea M, Iavarone M, Grieco A, Gasbarrini A, Villa E, Zavaglia C, Bruno R, Colombo M, Craxi A, and WEF study group, and SOFIA study group. Cost-effectiveness of sorafenib treatment in field practice for patients with hepatocellular carcinoma. *Hepatology*. 2013; 57:1046–54.
8. Bernardi M, Moreau R, Angeli P, Schnabl B, Arroyo V. Mechanisms of decompensation and organ failure in cirrhosis: from peripheral arterial vasodilation to systemic inflammation hypothesis. *J Hepatol*. 2015; 63:1272–84.
9. Cazzaniga M, Dionigi E, Gobbo G, Fioretti A, Monti V, Salerno F. The systemic inflammatory response syndrome in cirrhotic patients: relationship with their in-hospital outcome. *J Hepatol*. 2009; 51:475–82.
10. Hernandez-Gea V, Toffanin S, Friedman SL, Llovet JM. Role of the microenvironment in the pathogenesis and treatment of hepatocellular carcinoma. *Gastroenterology*. 2013; 144:512–27.
11. Li X, Chen ZH, Ma XK, Chen J, Wu DH, Lin Q, Dong M, Wei L, Wang TT, Ruan DY, Lin ZX, Xing YF, Deng Y, et al. Neutrophil-to-lymphocyte ratio acts as a prognostic factor for patients with advanced hepatocellular carcinoma. *Tumour Biol*. 2014; 35:11057–63.
12. Zheng YB, Zhao W, Liu B, Lu LG, He X, Huang JW, Li Y, Hu BS. The blood neutrophil-to-lymphocyte ratio predicts survival in patients with advanced hepatocellular carcinoma receiving sorafenib. *Asian Pac J Cancer Prev*. 2013; 14:5527–31.
13. Wei K, Wang M, Zhang W, Mu H, Song TQ. Neutrophil-lymphocyte ratio as a predictor of outcomes for patients with hepatocellular carcinoma undergoing TAE combined with Sorafenib. *Med Oncol*. 2014; 31:969.
14. Morimoto M, Numata K, Moriya S, Kondo M, Nozaki A, Morioka Y, Maeda S, Tanaka K. Inflammation-based prognostic score for hepatocellular carcinoma patients on sorafenib treatment. *Anticancer Res*. 2012; 32:619–23.
15. Smirne C, Grossi G, Pinato DJ, Burlone ME, Mauri FA, Januszewski A, Oldani A, Minisini R, Sharma R, Pirisi M. Evaluation of the red cell distribution width as a biomarker of early mortality in hepatocellular carcinoma. *Dig Liver Dis*. 2015; 47:488–94.
16. Dogan S, Celikbilek M, Zararsiz G, Deniz K, Sivgin S, Guven K, Gursoy S, Ozbakir O, Yucesoy M. Red blood cell distribution width as a non-invasive marker for the assessment of inflammation in non-alcoholic steatohepatitis. *Hepatogastroenterology*. 2015; 62:393–98.
17. Taefi A, Huang CC, Kolli K, Ebrahimi S, Patel M. Red cell distribution width to platelet ratio, a useful indicator of liver fibrosis in chronic hepatitis patients. *Hepatol Int*. 2015; 9:454–60.
18. Riedl J, Posch F, Königsbrügge O, Lötsch F, Reitter EM, Eigenbauer E, Marosi C, Schwarzwinger I, Zielinski C, Pabinger I, Ay C. Red cell distribution width and other red blood cell parameters in patients with cancer: association with risk of venous thromboembolism and mortality. *PLoS One*. 2014; 9:e111440.
19. Greten TF, Duffy AG, Korangy F. Hepatocellular carcinoma from an immunologic perspective. *Clin Cancer Res*. 2013; 19:6678–85.
20. Hashimoto K, Ikeda Y, Korenaga D, Tanoue K, Hamatake M, Kawasaki K, Yamaoka T, Iwatani Y, Akazawa K, Takenaka K. The impact of preoperative serum C-reactive protein on the prognosis of patients with hepatocellular carcinoma. *Cancer*. 2005; 103:1856–64.
21. Sieghart W, Pinter M, Huckle F, Graziadei I, Schöninger-Hekele M, Müller C, Vogel W, Trauner M, Peck-Radosavljevic M. Single determination of C-reactive protein at the time of diagnosis predicts long-term outcome of patients with hepatocellular carcinoma. *Hepatology*. 2013; 57:2224–34.

22. Reig M, Torres F, Rodriguez-Lope C, Forner A, Llach N, Rimola J, Darnell A, Ríos J, Ayuso C, Bruix J. Early dermatologic adverse events predict better outcome in HCC patients treated with sorafenib. *J Hepatol.* 2014; 61:318–24.
23. Otsuka T, Eguchi Y, Kawazoe S, Yanagita K, Ario K, Kitahara K, Kawasoe H, Kato H, Mizuta T, and Saga Liver Cancer Study Group. Skin toxicities and survival in advanced hepatocellular carcinoma patients treated with sorafenib. *Hepatol Res.* 2012; 42:879–86.
24. Kim HY, Park JW, Joo J, Kim H, Woo SM, Lee WJ, Kim CM. Worse outcome of sorafenib therapy associated with ascites and Child-Pugh score in advanced hepatocellular carcinoma. *J Gastroenterol Hepatol.* 2013; 28:1756–61.
25. Iavarone M, Cabibbo G, Biolato M, Della Corte C, Maida M, Barbara M, Basso M, Vavassori S, Craxi A, Grieco A, Cammà C, Colombo M. Predictors of survival in patients with advanced hepatocellular carcinoma who permanently discontinued sorafenib. *Hepatology.* 2015; 62:784–91.
26. Di Costanzo GG, de Stefano G, Tortora R, Farella N, Addario L, Lampasi F, Lanza AG, Cordone G, Imperato M, Caporaso N. Sorafenib off-target effects predict outcomes in patients treated for hepatocellular carcinoma. *Future Oncol.* 2015; 11:943–51.
27. Personeni N, Bozzarelli S, Pressiani T, Rimassa L, Tronconi MC, Scalfani F, Carnaghi C, Pedicini V, Giordano L, Santoro A. Usefulness of alpha-fetoprotein response in patients treated with sorafenib for advanced hepatocellular carcinoma. *J Hepatol.* 2012; 57:101–07.
28. Vincenzi B, Santini D, Russo A, Addeo R, Giuliani F, Montella L, Rizzo S, Venditti O, Frezza AM, Caraglia M, Colucci G, Del Prete S, Tonini G. Early skin toxicity as a predictive factor for tumor control in hepatocellular carcinoma patients treated with sorafenib. *Oncologist.* 2010; 15:85–92.
29. Bettinger D, Schultheiss M, Knüppel E, Thimme R, Blum HE, Spangenberg HC. Diarrhea predicts a positive response to sorafenib in patients with advanced hepatocellular carcinoma. *Hepatology.* 2012; 56:789–90.
30. Song T, Zhang W, Wu Q, Kong D, Ma W. A single center experience of sorafenib in advanced hepatocellular carcinoma patients: evaluation of prognostic factors. *Eur J Gastroenterol Hepatol.* 2011; 23:1233–38.
31. Shin SY, Lee YJ. Correlation of skin toxicity and hypertension with clinical benefit in advanced hepatocellular carcinoma patients treated with sorafenib. *Int J Clin Pharmacol Ther.* 2013; 51:837–46.
32. Cho JY, Paik YH, Lim HY, Kim YG, Lim HK, Min YW, Gwak GY, Choi MS, Lee JH, Koh KC, Paik SW, Yoo BC. Clinical parameters predictive of outcomes in sorafenib-treated patients with advanced hepatocellular carcinoma. *Liver Int.* 2013; 33:950–57.
33. Bajaj JS, Heuman DM, Hylemon PB, Sanyal AJ, White MB, Monteith P, Noble NA, Unser AB, Daita K, Fisher AR, Sikaroodi M, Gillevet PM. Altered profile of human gut microbiome is associated with cirrhosis and its complications. *J Hepatol.* 2014; 60:940–47.
34. Chassaing B, Etienne-Mesmin L, Gewirtz AT. Microbiota-liver axis in hepatic disease. *Hepatology.* 2014; 59:328–39.
35. American Association for the Study of Liver Diseases, European Association for the Study of the Liver. Hepatic encephalopathy in chronic liver disease: 2014 practice guideline by the European Association for the Study of the Liver and the American Association for the Study of Liver Diseases. *J Hepatol.* 2014; 61:642–59.
36. Bruix J, Sherman M, and American Association for the Study of Liver Diseases. Management of hepatocellular carcinoma: an update. *Hepatology.* 2011; 53:1020–22.
37. Reig M, Rimola J, Torres F, Darnell A, Rodriguez-Lope C, Forner A, Llach N, Ríos J, Ayuso C, Bruix J. Postprogression survival of patients with advanced hepatocellular carcinoma: rationale for second-line trial design. *Hepatology.* 2013; 58:2023–31.
38. Choi GH, Han S, Shim JH, Ryu MH, Ryoo BY, Kang YK, Kim KM, Lim YS, Lee HC. Prognostic Scoring Models for Patients Undergoing Sorafenib Treatment for Advanced Stage Hepatocellular Carcinoma in Real-Life Practice. *Am J Clin Oncol.* 2017; 40:167–74.
39. Kudo M, Ueshima K, Arizumi T. Real-life clinical practice with sorafenib in advanced hepatocellular carcinoma: a single-center experience. *Dig Dis.* 2012; 30:609–16.
40. Pinter M, Sieghart W, Huckle F, Graziadei I, Vogel W, Maieron A, Königsberg R, Weissmann A, Kornek G, Matejka J, Stauber R, Buder R, Grünberger B, et al. Prognostic factors in patients with advanced hepatocellular carcinoma treated with sorafenib. *Aliment Pharmacol Ther.* 2011; 34:949–59.
41. Villanueva A, Llovet JM. Targeted therapies for hepatocellular carcinoma. *Gastroenterology.* 2011; 140:1410–26.
42. Lencioni R, Llovet JM. Modified RECIST (mRECIST) assessment for hepatocellular carcinoma. *Semin Liver Dis.* 2010; 30:52–60.



# Nivolumab in patients with advanced hepatocellular carcinoma (CheckMate 040): an open-label, non-comparative, phase 1/2 dose escalation and expansion trial

Anthony B El-Khoueiry,\*Bruno Sangro,\*Thomas Yau, Todd S Crocenzi, Masatoshi Kudo, Chiun Hsu, Tae-You Kim, Su-Pin Choo, Jörg Trojan, Theodore H Welling 3rd, Tim Meyer, Yoon-Koo Kang, Winnie Yeo, Akhil Chopra, Jeffrey Anderson, Christine dela Cruz, Lixin Lang, Jaclyn Neely, Hao Tang, Homa B Dastani, Ignacio Melero

## Summary

**Background** For patients with advanced hepatocellular carcinoma, sorafenib is the only approved drug worldwide, and outcomes remain poor. We aimed to assess the safety and efficacy of nivolumab, a programmed cell death protein-1 (PD-1) immune checkpoint inhibitor, in patients with advanced hepatocellular carcinoma with or without chronic viral hepatitis.

**Methods** We did a phase 1/2, open-label, non-comparative, dose escalation and expansion trial (CheckMate 040) of nivolumab in adults ( $\geq 18$  years) with histologically confirmed advanced hepatocellular carcinoma with or without hepatitis C or B (HCV or HBV) infection. Previous sorafenib treatment was allowed. A dose-escalation phase was conducted at seven hospitals or academic centres in four countries or territories (USA, Spain, Hong Kong, and Singapore) and a dose-expansion phase was conducted at an additional 39 sites in 11 countries (Canada, UK, Germany, Italy, Japan, South Korea, Taiwan). At screening, eligible patients had Child-Pugh scores of 7 or less (Child-Pugh A or B7) for the dose-escalation phase and 6 or less (Child-Pugh A) for the dose-expansion phase, and an Eastern Cooperative Oncology Group performance status of 1 or less. Patients with HBV infection had to be receiving effective antiviral therapy (viral load  $<100$  IU/mL); antiviral therapy was not required for patients with HCV infection. We excluded patients previously treated with an agent targeting T-cell costimulation or checkpoint pathways. Patients received intravenous nivolumab 0·1–10 mg/kg every 2 weeks in the dose-escalation phase (3+3 design). Nivolumab 3 mg/kg was given every 2 weeks in the dose-expansion phase to patients in four cohorts: sorafenib untreated or intolerant without viral hepatitis, sorafenib progressor without viral hepatitis, HCV infected, and HBV infected. Primary endpoints were safety and tolerability for the escalation phase and objective response rate (Response Evaluation Criteria In Solid Tumors version 1.1) for the expansion phase. This study is registered with ClinicalTrials.gov, number NCT01658878.

**Findings** Between Nov 26, 2012, and Aug 8, 2016, 262 eligible patients were treated (48 patients in the dose-escalation phase and 214 in the dose-expansion phase). 202 (77%) of 262 patients have completed treatment and follow-up is ongoing. During dose escalation, nivolumab showed a manageable safety profile, including acceptable tolerability. In this phase, 46 (96%) of 48 patients discontinued treatment, 42 (88%) due to disease progression. Incidence of treatment-related adverse events did not seem to be associated with dose and no maximum tolerated dose was reached. 12 (25%) of 48 patients had grade 3/4 treatment-related adverse events. Three (6%) patients had treatment-related serious adverse events (pemphigoid, adrenal insufficiency, liver disorder). 30 (63%) of 48 patients in the dose-escalation phase died (not determined to be related to nivolumab therapy). Nivolumab 3 mg/kg was chosen for dose expansion. The objective response rate was 20% (95% CI 15–26) in patients treated with nivolumab 3 mg/kg in the dose-expansion phase and 15% (95% CI 6–28) in the dose-escalation phase.

**Interpretation** Nivolumab had a manageable safety profile and no new signals were observed in patients with advanced hepatocellular carcinoma. Durable objective responses show the potential of nivolumab for treatment of advanced hepatocellular carcinoma.

**Funding** Bristol-Myers Squibb.

## Introduction

Worldwide, liver cancer accounts for more than 850 000 new cancer cases annually, and approximately 90% of these are hepatocellular carcinoma.<sup>1,2</sup> Chronic infection with hepatitis C virus (HCV) or hepatitis B virus (HBV) is the leading cause of hepatocellular carcinoma.<sup>3</sup> Hepatocellular carcinoma is often diagnosed at advanced stages of disease for which highly effective therapies are

insufficient. At present, sorafenib, a small-molecule multikinase inhibitor, is the only evidence-based systemic treatment option for patients with advanced hepatocellular carcinoma.<sup>2,4,5</sup> In previously untreated patients with advanced disease, the median overall survival was 10·7 months in those treated with sorafenib and 7·9 months in those who received placebo (hazard ratio [HR] 0·69, 95% CI 0·55–0·87;  $p < 0·001$ ).<sup>6</sup> In selected

Lancet 2017; 389: 2492–502

Published Online

April 20, 2017

[http://dx.doi.org/10.1016/S0140-6736\(17\)31046-2](http://dx.doi.org/10.1016/S0140-6736(17)31046-2)

S0140-6736(17)31046-2

See [Comment](#) page 2448

\*Joint first authors

USC Norris Comprehensive Cancer Center, Los Angeles, CA, USA (A B El-Khoueiry MD); Clínica Universidad de Navarra and CIBERED, Pamplona, Spain (B Sangro MD); University of Hong Kong, Hong Kong Special Administrative Region, China (T Yau MD); Providence Cancer Center, Portland, OR, USA (T S Crocenzi MD); Kindai University Faculty of Medicine, Osaka, Japan (M Kudo MD); National Taiwan University Hospital, Taipei, Taiwan (C Hsu MD); Seoul National University Hospital, Seoul, South Korea (T-Y Kim MD); National Cancer Center, Singapore (S-P Choo MBBS); Goethe University Hospital and Cancer Center, Frankfurt, Germany (J Trojan MD); University of Michigan School of Medicine, Ann Arbor, MI, USA (T H Welling MD); Royal Free Hospital, London, UK (T Meyer MD); Asan Medical Center, University of Ulsan, Seoul, South Korea (Y-K Kang MD); Chinese University of Hong Kong, Hong Kong Special Administrative Region, China (W Yeo MD); Johns Hopkins Singapore International Medical Centre, Singapore (A Chopra MD); Bristol-Myers Squibb, Princeton, NJ, USA (J Anderson MD, C dela Cruz MD, L Lang PhD, J Neely PhD, H Tang PhD, H B Dastani PhD); Biomedical Research Network in Oncology (CIBERONC), Pamplona, Spain (I Melero); and Center for Applied Medical Research (CIMA), Pamplona, Spain (I Melero)

## Research in context

### Evidence before this study

Patients with advanced hepatocellular carcinoma who have tumours that are not amenable to surgical resection or local treatment have few effective treatment options. Although treatment with multikinase inhibitors provides some overall survival benefit—for example, sorafenib in previously untreated patients and regorafenib in sorafenib progressors—an unmet need remains in many patients. Chronic inflammatory conditions in the liver, such as cirrhosis and viral hepatitis, result in some degree of immunosuppression within the hepatocellular carcinoma tumour microenvironment, making immune checkpoints attractive therapeutic targets. We searched PubMed from Sept 1, 2010, to Sept 1, 2016, for articles using search terms “advanced HCC” and “immunotherapy OR immune checkpoint AND HCC”. Non-English articles, review articles, and meta-analysis references were excluded. We identified one relevant phase 1 clinical trial from 2013 evaluating the cytotoxic T-lymphocyte antigen (CTLA-4) checkpoint inhibitor tremelimumab in a small cohort of patients with advanced hepatocellular carcinoma who were infected with hepatitis C virus (HCV), which reported a manageable safety profile as well as preliminary evidence of antitumour and antiviral activity. Several preclinical studies have provided evidence in support of immunotherapeutic approaches for hepatocellular carcinoma, including the immunogenicity of transformed hepatocytes and immunosuppressive tumour microenvironments containing infiltrating lymphocytes. However, evidence showing the usefulness of immune checkpoint inhibitors in the treatment of patients with advanced hepatocellular carcinoma has been very limited. As early as 2010, reports have shown that programmed cell death protein-1 (PD-1) inhibitors can be potent immuno-oncology agents in patients with metastatic melanoma, providing rationale for immune checkpoint therapies in multiple other malignancies. When the CheckMate 040 trial

began in 2012, several trials of nivolumab in metastatic tumour settings were ongoing. Whether liver-related toxicities from immune checkpoint inhibitors would be affected by concomitant HCV or hepatitis B virus (HBV) infection in patients with hepatocellular carcinoma was not known.

### Added value of this study

To our knowledge, this is the first report of a PD-1 checkpoint inhibitor in patients with advanced hepatocellular carcinoma. The CheckMate 040 trial is a prospective, non-comparative, phase 1/2 dose study of nivolumab that assessed safety and clinical benefit across multiple hepatocellular carcinoma aetiologies, including patients with HCV or HBV infection. The efficacy of nivolumab monotherapy was evaluated as a first-line treatment in patients who had not previously received sorafenib or were intolerant and as a second-line treatment in those with previous disease progression on sorafenib.

### Implications of all the available evidence

Since the CheckMate 040 trial began, nivolumab has been approved in the USA and European Union for the treatment of melanoma, refractory non-small cell lung cancer, advanced renal cell carcinoma, and Hodgkin lymphoma; and squamous cell carcinoma of the head and neck and urothelial carcinoma (only in the USA). Studies have shown that nivolumab monotherapy provides improved overall survival or clinical benefit in these approved indications. In this study in patients with advanced hepatocellular carcinoma, nivolumab showed encouraging objective response rates and overall survival. The safety profile of nivolumab was manageable and no new safety signals were observed. These findings support further investigation of nivolumab as a treatment option for patients with advanced hepatocellular carcinoma; a phase 3 randomised study of nivolumab monotherapy compared with sorafenib is underway.

Correspondence to:  
Dr Anthony B El-Khoueiry,  
USC Norris Comprehensive  
Cancer Center, Los Angeles,  
CA 90033, USA  
[elkhoei@med.usc.edu](mailto:elkhoei@med.usc.edu)

patients who tolerated sorafenib but progressed while on therapy, another multikinase inhibitor, regorafenib, has been reported to provide an overall survival benefit compared with placebo (10·6 months vs 7·8 months; HR 0·62, 95% CI 0·50–0·78;  $p<0\cdot001$ ).<sup>7</sup>

Immunotherapies that inhibit the immune checkpoint interaction between programmed cell death protein-1 (PD-1) and programmed death-ligand 1 (PD-L1) have shown substantial survival benefit in some patients with metastatic carcinomas of multiple tissue origins.<sup>8–11</sup> The presence of tumour-infiltrating lymphocytes expressing PD-1 in hepatocellular carcinoma lesions and their correlation with outcome suggest that immunotherapeutic approaches might be useful in this setting.<sup>12–15</sup>

Nivolumab is a fully human immunoglobulin G4 monoclonal antibody that disrupts PD-1 immune checkpoint signalling and thereby restores the antitumour activity of otherwise suppressed effector

T cells. CheckMate 040 is an ongoing, global, phase 1/2 study of nivolumab in patients with advanced hepatocellular carcinoma with or without chronic viral hepatitis who were previously treated or untreated with sorafenib. In this first report of a PD-1 checkpoint inhibitor for the treatment of advanced hepatocellular carcinoma, we detail nivolumab safety and efficacy results from the dose-escalation and dose-expansion phases of CheckMate 040.

## Methods

### Study design and participants

We did a multicentre, non-comparative, open-label, phase 1/2 study in patients with advanced hepatocellular carcinoma with or without chronic viral hepatitis (HCV or HBV) to evaluate the safety and efficacy of nivolumab as a monotherapy (CheckMate 040). The dose-escalation phase was conducted at seven hospitals or academic centres in four countries or territories (USA, Spain,



Hong Kong, and Singapore) and the dose-expansion phase was conducted at 39 sites in 11 countries (Canada, UK, Germany, Italy, Japan, South Korea, Taiwan, and the countries or territories involved in dose escalation).

Eligible patients were at least 18 years old with histologically confirmed advanced hepatocellular carcinoma (not amenable to curative surgery or local treatment); use of archival tissue samples was allowed. Fresh tumour biopsy was required at baseline if no other record of histological diagnosis was available. Patients in the dose-escalation phase and patients in the HCV-infected and HBV-infected cohorts of the expansion phase included those whose disease progressed while receiving at least one previous line of systemic therapy, including sorafenib, or who were intolerant of or refused sorafenib treatment. Patients were also required to have Child-Pugh scores of 7 or less (Child-Pugh A or B7) for the dose-escalation phase and 6 or less (Child-Pugh A) for the dose-expansion phase at screening, and an Eastern Cooperative Oncology Group (ECOG) performance status of 1 or less. Patients with HBV infection were required to be receiving effective antiviral therapy and have a viral load less than 100 IU/mL at screening; antiviral therapy was not required for patients with HCV infection. Patients who had previously been treated with an agent targeting T-cell costimulation or checkpoint pathways (including those targeting PD-1, PD-L1 or PD-L2, CD137, or cytotoxic T-lymphocyte antigen [CTLA-4]) were excluded. Additional eligibility criteria are in the appendix. All patients provided written informed consent, and the study protocol and amendments were approved by each site's institutional review board or independent ethics committee.

See Online for appendix

Procedures

Patients received intravenous nivolumab every 2 weeks. In the dose-escalation phase, patients were enrolled into three cohorts on the basis of hepatocellular carcinoma aetiology (without viral hepatitis, HCV-infected, and HBV-infected). Across these cohorts, sequential patient groups (of up to six patients per dose level for doses

0.1–3.0 mg/kg and up to 13 patients for 10 mg/kg) received the following doses of nivolumab: 0.1 mg/kg (patients with HBV infection only), 0.3 mg/kg, 1.0 mg/kg, 3.0 mg/kg, or 10 mg/kg (patients without viral hepatitis [ie, uninfected] only) in a 3+3 design with the intention of determining the maximum-tolerated dose. Dose-limiting toxicities were determined on the basis of the incidence and intensity of adverse events occurring up to 2 weeks after the third nivolumab dose. Patients were treated until a confirmed complete response was achieved (dose-escalation phase only) or until disease progression or unacceptable toxicity occurred.

Safety assessments were done continuously during treatment and up to 100 days after the last dose or until all treatment-related adverse events were resolved to baseline or deemed irreversible by the investigator; adverse events were assessed using the National Cancer Institute Common Terminology Criteria for Adverse Events (NCI CTCAE; version 4.03). Patients were followed up for survival every 3 months.

We analysed investigator-assessed tumour response using the Response Evaluation Criteria In Solid Tumors (RECIST; version 1.1) for key study endpoints.<sup>16</sup> Exploratory endpoints included tumour assessments by modified RECIST (mRECIST; assessed by blinded independent central review). RECIST version 1.1 was used for assessment of the primary endpoint because it is well established and provides a more conservative estimation of response than mRECIST. Assessment by RECIST version 1.1 also allows for comparisons of response data with pivotal studies in patients with hepatocellular carcinoma (eg, sorafenib/SHARP trial).<sup>6</sup> mRECIST has not been prospectively validated and has not been evaluated for immuno-oncology therapies. Tumour biopsies collected at baseline were retrospectively used for analysis of PD-L1 expression by immunohistochemistry. Details on tumour assessments and measurement of tumour PD-L1 expression are in the appendix. In patients infected with HCV or HBV, HCV RNA and HBV surface antigen (HBsAg), respectively, were measured from patient sera at baseline and on treatment. Serum anti-HBs levels were also measured.

We assessed patient-reported health status in the dose-expansion phase using the three-level version of the European Quality of Life-5 Dimensions utility index (EQ-5D-3L) and visual analogue scale (EQ-5D-VAS).<sup>17</sup> Patients completed the EQ-5D-3L at baseline and every 6 weeks through week 25 while on treatment. The analysis population included those who had a baseline EQ-5D-3L assessment and at least one post-baseline assessment. Additional details on the methodology for assessing patient-reported outcomes are in the appendix.

Outcomes

The primary endpoint of the dose-escalation phase was safety and tolerability, based on incidence of adverse events, serious adverse events, adverse events leading to

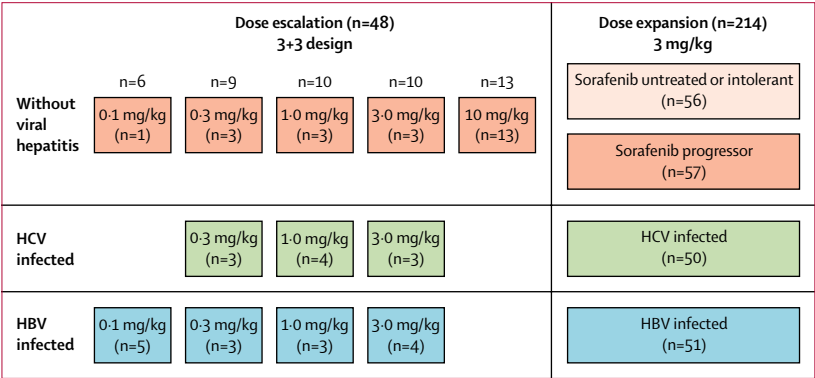


Figure 1: Trial design  
HCV=hepatitis C virus. HBV=hepatitis B virus.



discontinuation, and deaths. The primary endpoint of the dose-expansion phase was objective response rate. Key secondary endpoints included objective response rate (dose-escalation phase only), complete response rate, disease control rate, duration of response, time to response, time to progression, progression-free survival, overall survival, and response stratified by PD-L1 expression. Additionally, patient-reported quality of life measures and tumour response evaluation using mRECIST were exploratory endpoints. Secondary and exploratory endpoints not reported here are provided in the appendix.

### Statistical analysis

We used descriptive statistics to characterise safety analyses for all treated patients and to characterise patient-reported quality of life outcomes in patients treated in the dose-expansion phase. We estimated 95% CIs using the Clopper-Pearson method for objective response rate and the conventional Wald method for patient-reported outcomes. We used Kaplan-Meier methodology to determine medians and 95% CIs for

duration of response and overall survival. We determined sample sizes for each dose in the dose-escalation phase (3–13 patients) on the basis of observed toxicities, not statistical considerations. For the dose-expansion phase, we chose sample sizes of approximately 50 treated patients per cohort to improve estimations of efficacy. With a minimum of 50 patients, the lower bound of the 95% CI for a hypothetical response rate of 20% would be 10%.

This study is registered with ClinicalTrials.gov, number NCT01658878.

### Role of the funding source

The study was designed by the authors in collaboration with the funder (Bristol-Myers Squibb). The authors and funder were responsible for data collection, and the sponsor was responsible for data analysis. The authors and funder were involved in data interpretation, development of the report, and the decision to submit. The corresponding author had full access to all of the data and the final responsibility to submit for publication.

	Escalation phase				Expansion phase				
	Uninfected (n=23)	HCV infected (n=10)	HBV infected (n=15)	All patients (n=48)	Uninfected untreated/intolerant (n=56)	Uninfected progressor (n=57)	HCV infected (n=50)	HBV infected (n=51)	All patients (n=214)
Median age (years)	61 (54–72)	67 (60–74)	62 (46–66)	62 (55–69)	66 (59–71)	65 (60–71)	65 (61–73)	55 (42–66)	64 (56–70)
≥65 years	8 (35%)	6 (60%)	6 (40%)	20 (42%)	33 (59%)	29 (51%)	25 (50%)	13 (25%)	100 (47%)
Sex									
Female	6 (26%)	4 (40%)	2 (13%)	12 (25%)	8 (14%)	15 (26%)	8 (16%)	12 (24%)	43 (20%)
Male	17 (74%)	6 (60%)	13 (87%)	36 (75%)	48 (86%)	42 (74%)	42 (84%)	39 (76%)	171 (80%)
Race									
White	19 (83%)	8 (80%)	1 (7%)	28 (58%)	38 (68%)	34 (60%)	29 (58%)	4 (8%)	105 (49%)
Asian	2 (9%)	2 (20%)	14 (93%)	18 (38%)	16 (29%)	22 (39%)	18 (36%)	45 (88%)	101 (47%)
Black	2 (9%)	0	0	2 (4%)	1 (2%)	1 (2%)	2 (4%)	2 (4%)	6 (3%)
Other	0	0	0	0	1 (2%)	0	1 (2%)	0	2 (1%)
ECOG performance status 1*	9 (39%)	4 (40%)	6 (40%)	19 (40%)	16 (29%)	22 (39%)	15 (30%)	24 (47%)	77 (36%)
Extrahepatic metastases	16 (70%)	6 (60%)	12 (80%)	34 (71%)	36 (64%)	41 (72%)	25 (50%)	42 (82%)	144 (67%)
Vascular invasion	8 (35%)	5 (50%)	6 (40%)	19 (40%)	13 (23%)	18 (32%)	17 (34%)	15 (29%)	63 (29%)
Child-Pugh score									
5	19 (83%)	8 (80%)	14 (93%)	41 (85%)	43 (77%)	37 (65%)	27 (54%)	42 (82%)	149 (70%)
6	4 (17%)	2 (20%)	1 (7%)	7 (15%)	12 (21%)	20 (35%)	20 (40%)	9 (18%)	61 (29%)
7–9	0	0	0	0	1 (2%)	0	3 (6%)	0	4 (2%)
α-fetoprotein ≥400 µg/L†	6 (26%)	3 (30%)	6 (40%)	15 (31%)	15 (27%)	22 (39%)	17 (34%)	25 (49%)	79 (37%)
Previous treatment									
Surgical resection	15 (65%)	8 (80%)	13 (87%)	36 (75%)	34 (61%)	36 (63%)	18 (36%)	40 (78%)	128 (60%)
Radiotherapy‡	6 (26%)	2 (20%)	2 (13%)	10 (21%)	9 (16%)	17 (30%)	4 (8%)	11 (22%)	41 (19%)
Local treatment for HCC§	8 (35%)	6 (60%)	10 (67%)	24 (50%)	24 (43%)	28 (49%)	25 (50%)	40 (78%)	117 (55%)
Systemic therapy	19 (83%)	6 (60%)	15 (100%)	40 (83%)	23 (41%)	57 (100%)	32 (64%)	47 (92%)	159 (74%)
Sorafenib¶	17 (74%)	5 (50%)	15 (100%)	37 (77%)	15 (27%)	57 (100%)	30 (60%)	43 (84%)	145 (68%)

Data are median (IQR) or n (%). HCV=hepatitis C virus. HBV=hepatitis B virus. HCC=hepatocellular carcinoma. ECOG=Eastern Cooperative Oncology Group. \*All patients had a baseline ECOG performance status of 0 or 1. †Baseline α-fetoprotein levels were not available for ten patients; dose escalation (n=1), dose expansion (n=9). ‡Internal or external, and could include radioembolisation. §Includes transcatheter arterial chemoembolisation and transcatheter embolisation. ¶Reasons for previous treatment failure with sorafenib therapy included disease progression (165 [63%] of 262) and sorafenib intolerance (13 [5%] of 262); four (2%) of 262 patients experienced sorafenib treatment failure due to other reasons.

**Table 1: Patient demographics, baseline characteristics, and previous treatment**

## Results

The cutoff date for this analysis was Aug 8, 2016. Between Nov 26, 2012, and Aug 8, 2016, 262 patients with advanced hepatocellular carcinoma with or without HCV or HBV infection were treated: 48 patients in the dose-escalation phase and 214 in the dose-expansion phase (figure 1). Intravenous nivolumab monotherapy doses were 0·1–10 mg/kg every 2 weeks in the dose-escalation phase,

and cohorts included 23 patients without viral hepatitis, ten patients with HCV infection, and 15 patients with HBV infection. Across these three cohorts, six patients were assigned to nivolumab 0·1 mg/kg, nine patients to 0·3 mg/kg, ten patients to 1 mg/kg, ten patients to 3 mg/kg, and 13 patients to 10 mg/kg, every 2 weeks. Only patients in the cohort without viral hepatitis were assigned to the maximum dose of 10 mg/kg.

	Escalation phase				Expansion phase				
	Uninfected (n=23)	HCV infected (n=10)	HBV infected (n=15)	All patients (n=48)	Uninfected untreated/intolerant (n=56)	Uninfected progressor (n=57)	HCV infected (n=50)	HBV infected (n=51)	All patients (n=214)
Continuing treatment	1 (4%)	1 (10%)	0	2 (4%)	20 (36%)	10 (18%)	14 (28%)	14 (27%)	58 (27%)
Discontinued treatment	22 (96%)	9 (90%)	15 (100%)	46 (96%)	36 (64%)	47 (82%)	36 (72%)	37 (73%)	156 (73%)
Disease progression	18 (78%)	9 (90%)	15 (100%)	42 (88%)	29 (52%)	42 (74%)	24 (48%)	37 (73%)	132 (62%)
Study drug toxicity	1 (4%)	0	0	1 (2%)	4 (7%)	0	4 (8%)	0	8 (4%)
Unrelated adverse event	1 (4%)	0	0	1 (2%)	0	4 (7%)	4 (8%)	0	8 (4%)
Patient decision*	0	0	0	0	2 (4%)	1 (2%)	3 (6%)	0	6 (3%)
Complete response	2 (9%)	0	0	2 (4%)	0	0	0	0	0
Other/not reported	0	0	0	0	1 (2%)	0	1 (2%)	0	2 (1%)

Data are n (%). HCV=hepatitis C virus. HBV=hepatitis B virus. \*Includes patients who withdrew consent.

**Table 2: Patient disposition at data cutoff (Aug 8, 2016)**

	0·1 mg/kg (n=6)		0·3 mg/kg (n=9)		1 mg/kg (n=10)		3 mg/kg (n=10)		10 mg/kg (n=13)		All patients (n=48)	
	Any grade	Grade 3/4	Any grade	Grade 3/4	Any grade	Grade 3/4	Any grade	Grade 3/4	Any grade	Grade 3/4	Any grade	Grade 3/4
Treatment-related serious AEs	1 (17%)*	1 (17%)*	1 (11%)†	1 (11%)†	0	0	0	0	1 (8%)‡	0	3 (6%)	2 (4%)
AEs leading to discontinuation	0	0	1 (11%)§	1 (11%)§	0	0	1 (10%)¶	1 (10%)¶	1 (8%)	1 (8%)	3 (6%)	3 (6%)
Treatment-related deaths	0	0	0	0	0	0	0	0	0	0	0	0
Patients with a treatment-related AE	4 (67%)	2 (33%)	8 (89%)	3 (33%)	8 (80%)	5 (50%)	9 (90%)	2 (20%)	11 (85%)	0	40 (83%)	12 (25%)
Treatment-related AEs**												
Rash	1 (17%)	0	2 (22%)	0	2 (20%)	0	2 (20%)	0	4 (31%)	0	11 (23%)	0
Pruritus	2 (33%)	0	3 (33%)	0	0	0	1 (10%)	0	3 (23%)	0	9 (19%)	0
Diarrhoea	0	0	3 (33%)	0	0	0	1 (10%)	0	1 (8%)	0	5 (10%)	0
Decreased appetite	1 (17%)	0	2 (22%)	0	1 (10%)	0	0	0	1 (8%)	0	5 (10%)	0
Fatigue	1 (17%)	1 (17%)	2 (22%)	0	1 (10%)	0	0	0	0	0	4 (8%)	1 (2%)
Asthenia	0	0	1 (11%)	0	0	0	1 (10%)	0	1 (8%)	0	3 (6%)	0
Weight decreased	0	0	1 (11%)	0	0	0	0	0	2 (15%)	0	3 (6%)	0
Nausea	0	0	1 (11%)	0	0	0	1 (10%)	0	1 (8%)	0	3 (6%)	0
Dry mouth	0	0	1 (11%)	0	1 (10%)	0	0	0	1 (8%)	0	3 (6%)	0
Laboratory treatment-related AEs**												
AST increase	0	0	2 (22%)	2 (22%)	3 (30%)	2 (20%)	1 (10%)	1 (10%)	4 (31%)	0	10 (21%)	5 (10%)
ALT increase	0	0	2 (22%)	2 (22%)	1 (10%)	0	2 (20%)	1 (10%)	2 (15%)	0	7 (15%)	3 (6%)
Lipase increase	1 (17%)	1 (17%)	1 (11%)	0	4 (40%)	4 (40%)	2 (20%)	1 (10%)	2 (15%)	0	10 (21%)	6 (13%)
Amylase increase	1 (17%)	0	0	0	4 (40%)	1 (10%)	2 (20%)	1 (10%)	2 (15%)	0	9 (19%)	2 (4%)
Anaemia	0	0	1 (11%)	0	1 (10%)	1 (10%)	0	0	2 (15%)	0	4 (8%)	1 (2%)
Hypoalbuminaemia	0	0	1 (11%)	0	1 (10%)	0	0	0	1 (8%)	0	3 (6%)	0
Hyponatraemia	0	0	0	0	2 (20%)	0	0	0	1 (8%)	0	3 (6%)	0

Data are n (%). AE=adverse event. AST=aspartate aminotransferase. ALT=alanine aminotransferase. \*Pemphigoid (n=1). †Adrenal insufficiency (n=1). ‡Liver disorder (n=1). §Malignant neoplasm progression (n=1). ¶Grade 3 ALT increase (n=1), grade 2 AST increase. ||Grade 3 blood bilirubin increase (n=1). \*\*Treatment-related AEs reported in ≥5% of all patients, any grade.

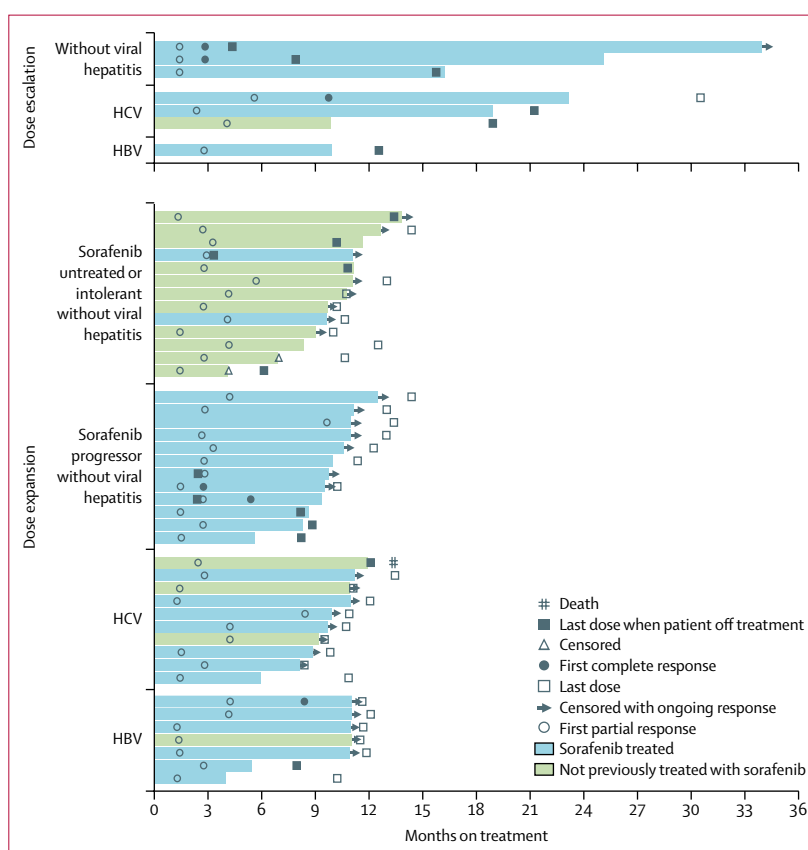
**Table 3: Safety and tolerability of nivolumab in the dose-escalation phase**

Patient demographics, baseline disease characteristics, and previous treatments are presented in table 1. In the dose-escalation phase, the overall median age was 62 years (IQR 55–69; table 1). Patients were heavily pretreated and 37 (77%) of 48 patients had previously been treated with sorafenib. Extrahepatic metastases were present in 34 (71%) patients and vascular invasion was present in 19 (40%) patients; all patients were reported as Child-Pugh class A with Child-Pugh scores of 5 or 6 at baseline.

In the dose-escalation phase, 46 (96%) of 48 patients discontinued treatment; 42 (88%) discontinued due to disease progression (table 2). Two patients (4%; both without viral hepatitis) discontinued after achieving a complete response (per study protocol) and entered the follow-up period. Other reasons for discontinuation included study drug-related toxicity in one patient and adverse events unrelated to treatment in another patient. After discontinuation of nivolumab, 23 (48%) patients were treated with a subsequent therapy (appendix). At the time of data cutoff, two of the 48 patients in the dose-escalation phase were continuing treatment with nivolumab.

One dose-limiting toxicity (grade 2 hepatic impairment) was reported in a patient in the cohort without viral hepatitis who received 10 mg/kg, which resolved within 7 days. A maximum tolerated dose was not reached. Grade 3/4 treatment-related adverse events occurred in 12 (25%) of 48 patients (table 3). Treatment-related adverse events that occurred in more than 10% of patients were rash in 11 (23%) patients, aspartate aminotransferase (AST) increase in ten (21%) patients, alanine aminotransferase (ALT) increase in seven (15%) patients, lipase increase in ten (21%) patients, amylase increase in nine (19%) patients, and pruritus in nine (19%) patients. Treatment-related serious adverse events were reported in three (6%) patients (pneumonia [n=1], adrenal insufficiency [n=1], liver disorder [n=1]). Grade 3/4 select adverse events, those with a potential inflammatory mechanism requiring more frequent monitoring, were adrenal insufficiency (n=1), diarrhoea (n=1), hepatitis (n=2), infusion hypersensitivity (n=1), and acute kidney injury (n=1; appendix). One patient without viral hepatitis who received nivolumab 3 mg/kg discontinued due to treatment-related ALT and AST increases without concomitant changes in liver function. 30 (63%) of 48 patients in the dose-escalation phase died, and no deaths were determined to be related to nivolumab therapy.

The overall objective response rate was 15% (95% CI 6–28; appendix) in the dose-escalation phase, including three complete responses and four partial responses. Responses occurred early in treatment; of the seven patients who achieved an objective response, five responded within 3 months of treatment initiation (figure 2). The disease control rate was 58% (95% CI 43–72) and the median time to progression was 3.4 months (95% CI 1.6–6.9). The median duration of response was 17 months (95% CI 6–24) and the 6-month and 9-month



**Figure 2: Time to response and duration of response**

Duration of response (months) to nivolumab for the 49 patients who achieved a complete or partial response in the dose-escalation or dose-expansion phases. HCV=hepatitis C virus. HBV=hepatitis B virus.

overall survival rates were both 66% (95% CI 51–78). Median overall survival for patients in the dose-escalation phase was 15.0 months (95% CI 9.6–20.2).

On the basis of the results from the dose-escalation phase and from studies of nivolumab in other tumour types,<sup>18</sup> a dose of 3 mg/kg was selected for the dose-expansion phase. 214 patients with advanced hepatocellular carcinoma were treated in the dose-expansion phase in four cohorts: 56 patients were not infected with HCV or HBV and had not been treated with sorafenib previously or were intolerant, 57 had disease progression on sorafenib, 50 patients were infected with HCV, and 51 were infected with HBV (figure 1). Patients enrolled in the dose-expansion phase had comparable demographics and baseline disease characteristics to those in the dose-escalation phase (table 1). 145 (68%) of 214 patients had previously been treated with sorafenib.

As of Aug 8, 2016, 58 (27%) of 214 patients enrolled in the dose-expansion phase were continuing treatment. Disease progression was the most common reason for discontinuation, occurring in 132 (62%) of 214 patients. Eight patients (4%) discontinued after experiencing study drug toxicity (table 2).

	Uninfected untreated/ intolerant (n=56)	Uninfected progressor (n=57)	HCV infected (n=50)	HBV infected (n=51)	All patients (n=214)
Objective response*	13 (23%; 13 to 36)	12 (21%; 11 to 34)	10 (20%; 10 to 34)	7 (14%; 6 to 26)	42 (20%; 15 to 26)
Complete response	0	2 (4%)	0	1 (2%)	3 (1%)
Partial response	13 (23%)	10 (18%)	10 (20%)	6 (12%)	39 (18%)
Stable disease	29 (52%)	23 (40%)	23 (46%)	21 (41%)	96 (45%)
Progressive disease	13 (23%)	18 (32%)	14 (28%)	23 (45%)	68 (32%)
Not evaluable	1 (2%)	4 (7%)	3 (6%)	0	8 (4%)
Duration of response*					
KM median	8.4 (8.3 to NE)	NR	9.9 (4.5 to 9.9)	NR	9.9 (8.3 to NE)
Ongoing, n/N (%)	8/13 (62%)	7/12 (58%)	8/10 (80%)	5/7 (71%)	28/42 (67%)
Disease control*	42 (75%; 62 to 86)	35 (61%; 48 to 74)	33 (66%; 51 to 79)	28 (55%; 40 to 69)	138 (64%; 58 to 71)
Disease control with stable disease for ≥6 months	22 (39%; 27 to 53)	22 (39%; 26 to 52)	17 (34; 21 to 49)	18 (35%; 22 to 50)	79 (37%; 30 to 44)
Overall survival					
6 months	89% (77 to 95)	75% (62 to 85)	85% (72 to 93)	84% (71 to 92)	83% (78 to 88)
9 months	82% (68 to 90)	63% (49 to 74)	81% (66 to 90)	70% (55 to 81)	74% (67 to 79)
KM median	NR	13.2 (8.6 to NE)	NR	NR	NR
Progression-free survival*					
KM median	5.4 (3.9 to 8.5)	4.0 (2.6 to 6.7)	4.0 (2.6 to 5.7)	4.0 (1.3 to 4.1)	4.0 (2.9 to 5.4)

Unless otherwise indicated, data are n (%; 95% CI); n (%); months (95% CI); or % (95% CI). HCV=hepatitis C virus. HBV=hepatitis B virus. KM=Kaplan-Meier estimate. NR=not reached. NE=not estimable. RECIST=Response Evaluation Criteria In Solid Tumors. \*Determined by investigator assessment using RECIST version 1.1.

**Table 4: Nivolumab efficacy in the dose-expansion phase**

An objective response was observed in 42 patients (20%; 95% CI 15–26) who received nivolumab 3 mg/kg every 2 weeks in the dose-expansion phase (table 4). Objective responses included three complete responses and 39 partial responses. Stable disease was observed in 96 (45%) patients, and thus disease control was observed in 138 patients (64%). Among the 202 patients who were evaluable and had at least one post-baseline target lesion assessment, substantial reductions in tumour burden were observed in all cohorts (figure 3). Best reductions from baseline in tumour burden are shown in figure 4. Most of the objective responses occurred before 3 months (29 of 42; 69%), similar to the time-to-response profile observed in the dose-escalation phase (figure 2). 28 (67%) of the 42 patients with a response had ongoing responses at the time of data cutoff. The median duration of response was 9.9 months (95% CI 8.3 to not estimable [NE]). Most disease stabilisations lasted at least 6 months, as reported in 79 of 138 patients (57%) with disease control. In the dose-expansion phase, the median time to progression was 4.1 months (95% CI 3.7–5.5). The 6-month overall survival rate was 83% (95% CI 78–88) and the 9-month overall survival rate was 74% (95% CI 67–79) with nivolumab 3 mg/kg in patients in the dose-expansion phase (table 4). The 6-month progression-free survival rate was 37% (95% CI 30–43) and the 9-month progression-free survival rate was 28% (95% CI 22–35).

Objective responses occurred in 13 (23%) of 56 patients without viral hepatitis who had not previously been treated with sorafenib or were intolerant and 12 (21%) of

57 sorafenib progressors without viral hepatitis (table 4); 15 responses were ongoing. The three complete responses in the dose-expansion phase occurred in two patients without viral hepatitis who had progression on sorafenib therapy and one patient with HBV infection (who had previously been treated with sorafenib). Disease control was seen in 42 (75%) of 56 patients without viral hepatitis who had not previously been treated with sorafenib or were intolerant and 35 (61%) of 57 patients in the sorafenib progressor cohort without viral hepatitis. 6-month overall survival in patients without viral hepatitis who had not previously been treated with sorafenib or were intolerant was 89% (95% CI 77 to 95; 48 at risk) and 75% (95% CI 62 to 85; 43 at risk) in the sorafenib progressor cohort without viral hepatitis (table 4). Median overall survival in the sorafenib progressor without viral hepatitis cohort was 13.2 months (95% CI 8.6 to NE); medians were not reached in the other dose-expansion cohorts.

Objective response rates were ten (20%) of 50 patients infected with HCV and seven (14%) of 51 patients infected with HBV (table 4); 13 responses were ongoing. Disease control was achieved in 33 (66%) patients infected with HCV and 28 (55%) patients infected with HBV. 6-month overall survival was 85% (95% CI 72–93) in the cohort with HCV infection (38 at risk) and 84% (95% CI 71–92) in the cohort with HBV infection (43 at risk). Nivolumab exhibited limited antiviral activity. The kinetics of HCV RNA levels over time were assessed in patients infected with HCV with advanced hepatocellular carcinoma, and no patient achieved a sustained virological response for more than

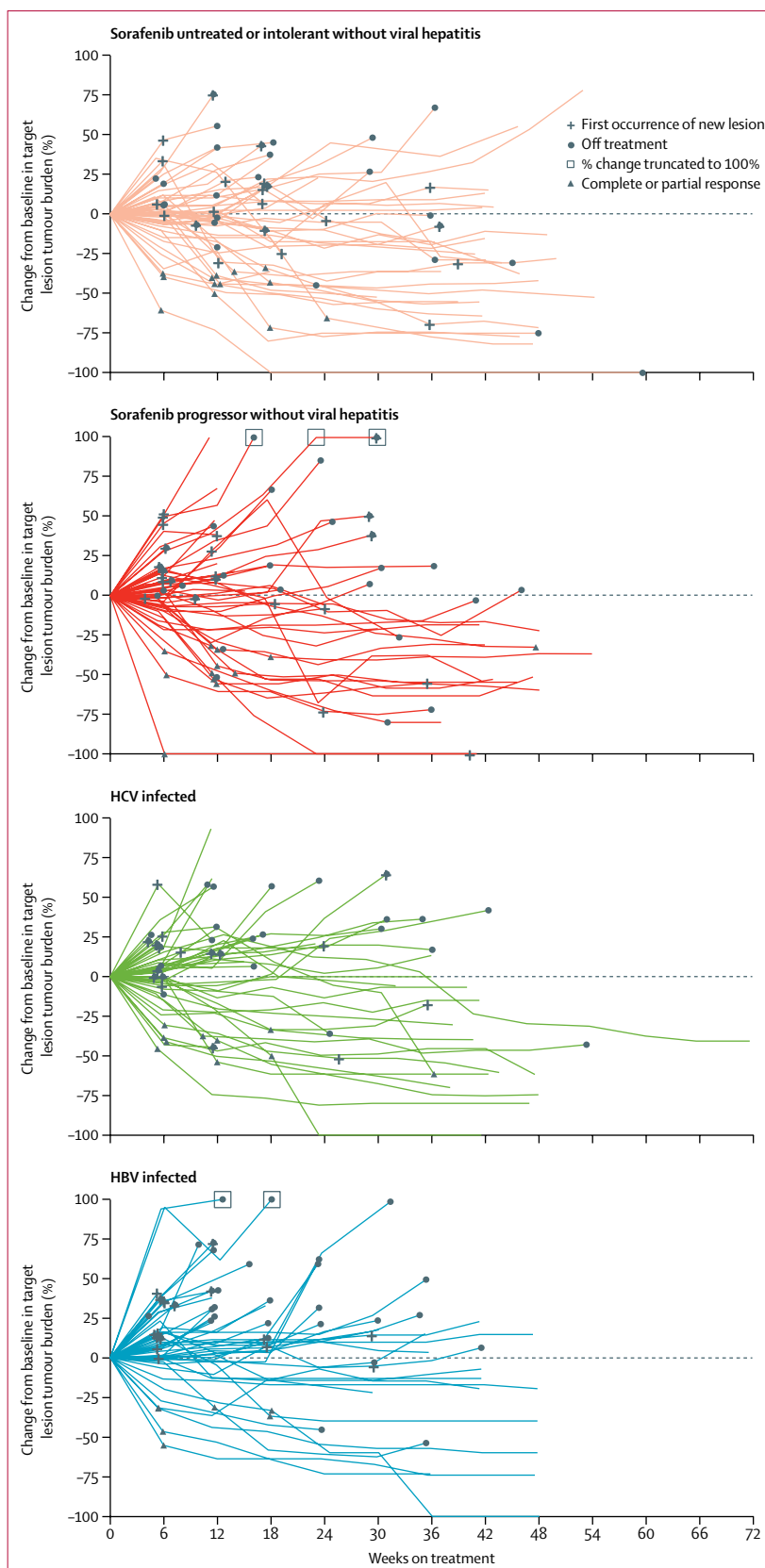
24 weeks. Some patients infected with HCV had transient reductions in HCV RNA. No patients had reactivation of HBV, and no instances of anti-HBs seroconversion were noted among patients infected with HBV.

In the dose-expansion phase, the objective response rate was analysed using mRECIST by blinded independent central review in the 145 patients who had previously been treated with sorafenib (irrespective of hepatocellular carcinoma aetiology); under these criteria the objective response rate was 27 (19%) of 145 patients, including five patients with a complete response (appendix).

The overall safety profile of nivolumab in patients in the dose-expansion phase was comparable to that observed in the dose-escalation phase. Grade 3/4 treatment-related adverse events were seen in 40 (19%) patients and grade 3/4 treatment-related serious adverse events were seen in nine (4%) patients (appendix). Symptomatic treatment-related adverse events were comparable in patients with and without HCV or HBV infection. Adverse events led to discontinuation in 24 patients, and there were no treatment-related deaths.

As a secondary endpoint, PD-L1 expression levels were retrospectively assessed as a potential biomarker for nivolumab therapy in the 174 (81%) of 214 patients with available data in the dose-expansion phase. Membrane expression of PD-L1 on at least 1% of tumour cells was observed in 34 (20%) of 174 patients at baseline; 140 (80%) patients had PD-L1 expression on less than 1% of tumour cells (table 5). Objective responses were observed in nine (26%) of 34 patients with PD-L1 expression on at least 1% of tumour cells (95% CI 13–44) and in 26 (19%) of 140 patients with PD-L1 on less than 1% of tumour cells (95% CI 13–26).

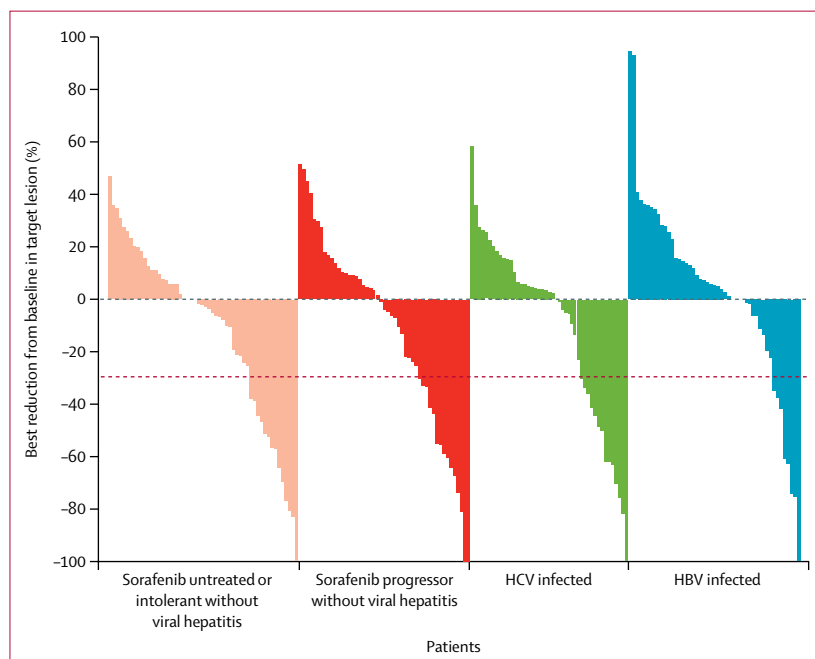
Among patients in the dose-expansion phase who were on treatment at the data cutoff, the EQ-5D-3L completion rate exceeded 90% at each timepoint through week 25. EQ-5D-3L index scores were stable while on treatment with no significant changes from baseline (mean 0·856, 95% CI 0·827 to 0·884) to week 25 (0·829, 0·786 to 0·872); mean change from baseline was –0·015 (–0·051 to 0·021). EQ-5D-VAS scores were also stable, with no significant changes from baseline (mean 73·0, 95% CI 69·0 to 77·1) to week 25 (75·4, 70·0 to 80·9); mean change from baseline was 3·2 (–1·2 to 7·5). Comparable results were observed in patients who had previously been treated with sorafenib. For this patient subpopulation, EQ-5D-3L scores were not appreciably changed from baseline (mean 0·853, 95% CI 0·816 to 0·889) through week 25 (0·825, 0·773 to 0·877); mean change from baseline was –0·014 (–0·058 to 0·030). Similarly, EQ-5D-VAS scores were stable from baseline (mean 73·9, 95% CI 69·2–78·6) through week 25 (75·8, 69·3–82·4); mean change from baseline was 3·1 (–1·3 to 7·6).



**Figure 3: Percentage change in tumour burden**

Percentage change in tumour lesion size from baseline over time in the dose-expansion phase (n=202). HCV=hepatitis C virus. HBV=hepatitis B virus.





**Figure 4: Best percentage change in tumour burden**

Best percentage change in tumour lesion size from baseline over time in the dose-expansion phase (n=202). Red dash indicates a 30% reduction. HCV=hepatitis C virus. HBV=hepatitis B virus.

	Escalation phase (n=44)*	Expansion phase (n=174)*
PD-L1 $\geq 1\%$ †	11 (25%)	34 (20%)
Objective response	3/11 (27%; 6–61)	9/34 (26%; 13–44)
Complete response	1 (9%)	1 (3%)
Partial response	2 (18%)	8 (24%)
Stable disease	0	16 (47%)
Progressive disease	7 (64%)	9 (26%)
Not determined	1 (9%)	0
PD-L1 $< 1\%$ †	33 (75%)	140 (80%)
Objective response	4/33 (12%; 3–28)	26/140 (19%; 13–26)
Complete response	2 (6%)	2 (1%)
Partial response	2 (6%)	24 (17%)
Stable disease	19 (58%)	62 (44%)
Progressive disease	8 (24%)	46 (33%)
Not determined	2 (6%)	6 (4%)

Data are n (%); n/N (%; 95% CI). PD-L1=programmed death-ligand 1.  
 \*Four patients in the dose-escalation phase and 40 patients in the dose-expansion phase did not have tumour PD-L1 expression data available.  
 †PD-L1 membrane expression on tumour cells.

**Table 5: PD-L1 expression on tumour cells and response**

## Discussion

Previous studies<sup>6,7,19</sup> in advanced hepatocellular carcinoma of first-line sorafenib have shown response rates of 2–3% and second-line regorafenib has shown a response rate of 7%. In this phase 1/2 study, treatment with nivolumab resulted in substantial tumour reductions and objective

response rates of 15–20% irrespective of line of therapy in patients with advanced hepatocellular carcinoma. Notably, the disease control rate was 58% in the dose-escalation phase and 64% in the dose-expansion phase, which could have positively affected overall survival. Baseline tumour cell PD-L1 status did not have an apparent effect on response rates. Median duration of response in both phases of the study (as high as 17 months in the dose-escalation phase) suggests that in the treatment of patients with advanced hepatocellular carcinoma, nivolumab might offer durable responses when other existing therapies have not.<sup>6,19</sup> Median overall survival relative to sorafenib was encouraging in a population enriched in patients with metastatic disease and with previous treatment with sorafenib.<sup>20,21</sup>

In the dose-escalation phase, the safety profile of nivolumab in patients with hepatocellular carcinoma was consistent with that observed in other tumour types.<sup>9,10,22–25</sup> To our knowledge, all previous studies of PD-1 inhibitors have excluded patients with chronic viral hepatitis. Hepatic safety events in virally infected patients with hepatocellular carcinoma treated with a CTLA-4 checkpoint inhibitor have been reported.<sup>26</sup> Therefore, we evaluated viral aetiologies in separate cohorts in this study to identify any unique safety signals. We noted no new nivolumab safety signals. Safety findings from the dose-escalation phase were consistent with those in a larger group of patients from the dose-expansion phase.

The comparable objective response results in patients who had not previously been treated with sorafenib or were intolerant and in patients with disease progression on sorafenib suggest that nivolumab efficacy is not affected by previous sorafenib treatment status. In addition to potentially supporting nivolumab as a viable second-line therapy for patients with disease progression on multikinase inhibitors (as shown with a median overall survival of more than 13 months in patients without viral hepatitis with previous progression on sorafenib), the objective response rate of 23% and 9-month overall survival of 82% in untreated patients supports the investigation of nivolumab as a first-line therapy for patients with advanced hepatocellular carcinoma. This study was not powered for statistical comparisons between patients who were infected with HCV or HBV, or who did not have viral hepatitis; however, responses were observed irrespective of hepatocellular carcinoma aetiology. Treatment with nivolumab was associated with stable patient-reported outcomes, including indicators of health status and quality of life, irrespective of previous treatment with sorafenib.

A limitation of this study is the lack of randomised control arms. A subsequent randomised cohort-expansion phase of CheckMate 040 is evaluating nivolumab compared with sorafenib in the first-line setting. Although objective responses occurred in this study regardless of PD-L1 expression on tumour cells (using 1% of tumour cells expressing PD-L1 as a cutoff), future studies will need to evaluate the expression of PD-1 and

PD-L1 on tumour-infiltrating lymphocytes as potentially valuable biomarkers. Inhibition of PD-L1 signalling by non-tumour cells could contribute to the efficacy of nivolumab in patients who have low (<1%) levels of PD-L1 expression on tumour cells. Although PD-L1 is not yet established as a consistently reliable biomarker across tumour types or lines of therapy, it is also possible that in a larger patient population, patients who have a higher proportion of tumour cells expressing PD-L1 might achieve greater benefit. An in-depth characterisation of tumour-infiltrating T-cell and macrophage subsets, including their expression of PD-1 and PD-L1, could be important for future biomarker assessments in patients with advanced hepatocellular carcinoma. Additionally, for more meaningful median overall survival results in the dose-expansion patient cohorts, longer follow-up will be needed.

Results from subsequent comparative, randomised phases of CheckMate 040 will further inform the therapeutic potential of nivolumab in patients with advanced hepatocellular carcinoma who have few existing treatment options. Nivolumab might provide favourable efficacy with a good safety profile in the context of the available targeted therapies. A phase 3 randomised study of nivolumab monotherapy compared with sorafenib in the first-line setting is ongoing.

#### Contributors

ABE-K, BS, TSC, THW, JA, CdC, and IM conceived and designed the study. ABE-K, BS, TY, TSC, MK, CH, T-YK, S-PC, JT, THW, TM, Y-KK, WY, AC, and IM recruited patients and collected the data. JA, CdC, LL, JN, HT, and HBD analysed the data. All authors interpreted the data and were involved in development, review, and approval of the manuscript.

#### Declaration of interests

ABE-K has received research support from Astex, received personal fees from Merrimack, and served as an adviser for Bristol-Myers Squibb, AstraZeneca, Bayer, Genentech, and Novartis. BS has received speaking and consulting fees from Bristol-Myers Squibb and Bayer and consulting fees from AstraZeneca, Transgene, and Adaptimmune. TY has received speaking fees and research support from Bristol-Myers Squibb and has served as an adviser to Bristol-Myers Squibb. TSC has received research support from Bristol-Myers Squibb. S-PC has received speaking fees from Bristol-Myers Squibb. JT has received speaking and consulting fees from Bristol-Myers Squibb and Bayer. TM has served as a consultant for Bristol-Myers Squibb, Bayer, Ipsen, and Eisai. Y-KK has received consulting fees from Bristol-Myers Squibb, Ono Pharmaceutical Co, Bayer, Blueprint, AstraZeneca, Pfizer, Dicerna, and Mirna. WY has received research support from Bristol-Myers Squibb and has served as an adviser to Bristol-Myers Squibb. ACh has received research support and personal fees from Bristol-Myers Squibb, Bayer, Astellas, MSD, and Boehringer Ingelheim, and has received personal fees from Janssen Oncology, Bayer, Lilly, AstraZeneca, Roche, and Mundipharma. JA, JN, and HBD are employees and stockholders of Bristol-Myers Squibb. CdC, LL, and HT are employees of Bristol-Myers Squibb. IM has received research support and personal fees from Bristol-Myers Squibb. MK, CH, T-YK, and THW declare no competing interests.

#### Acknowledgments

This study was supported by Bristol-Myers Squibb (Princeton, NJ, USA) and by Ono Pharmaceutical Co (Osaka, Japan). We thank the patients and their families, and investigators and research staff at all study sites. The PD-L1 immunohistochemistry 28-8 pharmDx assay was developed by Dako North America (Carpinteria, CA, USA). Lisa Dauffenbach of Mosaic Laboratories (Lake Forest, CA, USA) and Cyrus Hedvat from

Bristol-Myers Squibb contributed to analyses of PD-L1 immunohistochemical staining. TM is supported by the NIHR Biomedical Research Centre at University College London Hospitals. We acknowledge Jon Wigginton (MacroGenics Inc, Rockville, MD, USA) for early development of the CheckMate 040 protocol and Ashok Gupta (MedImmune) for serving as an early medical lead for CheckMate 040. Editorial assistance was provided by Jeff Bergen of Chrysalis Medical Communications (Hamilton, NJ, USA) and was funded by Bristol-Myers Squibb.

#### References

- 1 Torre LA, Bray F, Siegel RL, et al. Global cancer statistics, 2012. *CA Cancer J Clin* 2015; **65**: 87–108.
- 2 Llovet JM, Zucman-Rossi J, Pikarsky E, et al. Hepatocellular carcinoma. *Nat Rev Dis Primers* 2016; **2**: 16018.
- 3 McGlynn KA, Petrick JL, London WT. Global epidemiology of hepatocellular carcinoma: an emphasis on demographic and regional variability. *Clin Liver Dis* 2015; **19**: 223–38.
- 4 European Association for the Study of the Liver, European Organisation for Research and Treatment of Cancer. EASL-EORTC clinical practice guidelines: management of hepatocellular carcinoma. *J Hepatol* 2012; **56**: 908–43.
- 5 National Comprehensive Cancer Network. Clinical Practice Guidelines in Oncology. Hepatobiliary Cancers. Version 1.2017. 2017. [https://www.nccn.org/professionals/physician\\_gls/f\\_guidelines.asp](https://www.nccn.org/professionals/physician_gls/f_guidelines.asp) (accessed April 3, 2017).
- 6 Llovet JM, Ricci S, Mazzaferro V, et al. Sorafenib in advanced hepatocellular carcinoma. *N Engl J Med* 2008; **359**: 378–90.
- 7 Bruix J, Qin S, Merle P, et al. Regorafenib for patients with hepatocellular carcinoma who progressed on sorafenib treatment (RESORCE): a randomised, double-blind, placebo-controlled, phase 3 trial. *Lancet* 2017; **389**: 56–66.
- 8 Whiteside TL, Demaria S, Rodriguez-Ruiz ME, et al. Emerging opportunities and challenges in cancer immunotherapy. *Clin Cancer Res* 2016; **22**: 1845–55.
- 9 Weber JS, D'Angelo SP, Minor D, et al. Nivolumab versus chemotherapy in patients with advanced melanoma who progressed after anti-CTLA-4 treatment (CheckMate 037): a randomised, controlled, open-label, phase 3 trial. *Lancet Oncol* 2015; **16**: 375–84.
- 10 Motzer RJ, Escudier B, McDermott DF, et al. Nivolumab versus everolimus in advanced renal-cell carcinoma. *N Engl J Med* 2015; **373**: 1803–13.
- 11 Topalian SL, Drake CG, Pardoll DM. Immune checkpoint blockade: a common denominator approach to cancer therapy. *Cancer Cell* 2015; **27**: 450–61.
- 12 Prieto J, Melero I, Sangro B. Immunological landscape and immunotherapy of hepatocellular carcinoma. *Nat Rev Gastroenterol Hepatol* 2015; **12**: 681–700.
- 13 Shi F, Shi M, Zeng Z, et al. PD-1 and PD-L1 upregulation promotes CD8<sup>+</sup> T-cell apoptosis and postoperative recurrence in hepatocellular carcinoma patients. *Int J Cancer* 2011; **128**: 887–96.
- 14 Flecken T, Schmidt N, Hild S, et al. Immunodominance and functional alterations of tumor-associated antigen-specific CD8<sup>+</sup> T-cell responses in hepatocellular carcinoma. *Hepatology* 2014; **59**: 1415–26.
- 15 Breous E, Thimme R. Potential of immunotherapy for hepatocellular carcinoma. *J Hepatol* 2011; **54**: 830–34.
- 16 Eisenhauer EA, Therasse P, Bogaerts J, et al. New response evaluation criteria in solid tumours: revised RECIST guideline (version 1.1). *Eur J Cancer* 2009; **45**: 228–47.
- 17 EuroQol Group. EuroQol: a new facility for the measurement of health-related quality of life. *Health Policy* 1990; **16**: 199–208.
- 18 Topalian SL, Hodi FS, Brahmer JR, et al. Safety, activity, and immune correlates of anti-PD-1 antibody in cancer. *N Engl J Med* 2012; **366**: 2443–54.
- 19 Cheng AL, Kang YK, Chen Z, et al. Efficacy and safety of sorafenib in patients in the Asia-Pacific region with advanced hepatocellular carcinoma: a phase 3 randomised, double-blind, placebo-controlled trial. *Lancet Oncol* 2009; **10**: 25–34.
- 20 Bruix J, Raoul JL, Sherman M, et al. Efficacy and safety of sorafenib in patients with advanced hepatocellular carcinoma: subanalyses of a phase III trial. *J Hepatol* 2012; **57**: 821–29.

For the phase 3 trial see  
ClinicalTrials.gov number  
NCT02576509

- 21 Cheng AL, Guan Z, Chen Z, et al. Efficacy and safety of sorafenib in patients with advanced hepatocellular carcinoma according to baseline status: subset analyses of the phase III sorafenib Asia-Pacific trial. *Eur J Cancer* 2012; **48**: 1452–65.
- 22 Borghaei H, Paz-Ares L, Horn L, et al. Nivolumab versus docetaxel in advanced nonsquamous non-small-cell lung cancer. *N Engl J Med* 2015; **373**: 1627–39.
- 23 Brahmer J, Reckamp KL, Baas P, et al. Nivolumab versus docetaxel in advanced squamous-cell non-small-cell lung cancer. *N Engl J Med* 2015; **373**: 123–35.
- 24 Ansell SM, Lesokhin AM, Borrello I, et al. PD-1 blockade with nivolumab in relapsed or refractory Hodgkin's lymphoma. *N Engl J Med* 2015; **372**: 311–19.
- 25 Ferris RL, Blumenschein G, Jr, Fayette J, et al. Nivolumab for recurrent squamous-cell carcinoma of the head and neck. *N Engl J Med* 2016; **385**: 1856–67.
- 26 Sangro B, Gomez-Martin C, de la Mata M, et al. A clinical trial of CTLA-4 blockade with tremelimumab in patients with hepatocellular carcinoma and chronic hepatitis C. *J Hepatol* 2013; **59**: 81–88.

# Clinical significance of Akt2 in advanced pancreatic cancer treated with erlotinib

ERI BANNO<sup>1</sup>, YOSUKE TOGASHI<sup>1,2</sup>, MARCO A. DE VELASCO<sup>1</sup>, TAKURO MIZUKAMI<sup>1</sup>, YU NAKAMURA<sup>1</sup>, MASATO TERASHIMA<sup>1</sup>, KAZUKO SAKAI<sup>1</sup>, YOSHIHIKO FUJITA<sup>1</sup>, KEN KAMATA<sup>3</sup>, MASAYUKI KITANO<sup>3,4</sup>, MASATOSHI KUDO<sup>3</sup> and KAZUTO NISHIO<sup>1</sup>

<sup>1</sup>Department of Genome Biology, Kindai University Faculty of Medicine, Osaka-Sayama, Osaka 589-8511;

<sup>2</sup>Division of Cancer Immunology, EPOC, National Cancer Center, Kashiwa, Chiba 277-8577;

<sup>3</sup>Department of Gastroenterology and Hepatology, Kindai University Faculty of Medicine, Osaka-Sayama, Osaka 589-8511; <sup>4</sup>Second Department of Internal Medicine, Wakayama Medical University, Wakayama, Wakayama 641-8509, Japan

Received December 6, 2016; Accepted March 29, 2017

DOI: 10.3892/ijo.2017.3961

**Abstract.** Akt2 is an isoform of Akt, and an association between Akt2 and resistance to epidermal growth factor receptor (EGFR) tyrosine kinase inhibitors (TKIs) has been suggested in pancreatic cancer (PC) *in vitro*. In this study, we investigated the association between Akt2 expression as evaluated using immunohistochemistry and the outcome of patients with advanced PC who had received treatment with erlotinib (an EGFR-TKI). Although the difference was not significant, patients with high levels of Akt2 expression tended to have a poorer response and a shorter progression-free survival period after treatment with erlotinib plus gemcitabine than those with low expression levels ( $P=0.16$  and  $0.19$ , respectively). *In vitro*, an *Akt2*-amplified PC cell line and *Akt2*-overexpressed cell lines exhibited resistance to anti-EGFR therapies, including erlotinib, but combined treatment with BYL719 (a PI3K inhibitor) cancelled this resistance. Our findings suggest that Akt2 might be associated with the resistance to anti-EGFR

therapies, especially the use of erlotinib against PC, and that this resistance can be overcome by combined treatment with a PI3K inhibitor. Akt2 expression could become a predictive biomarker for erlotinib resistance in PC.

## Introduction

Pancreatic cancer (PC) remains a deadly disease. Gemcitabine has been considered as the standard therapy for patients with unresectable or metastatic disease for over a decade (1,2). Recently, overall survival (OS) has been significantly prolonged using combination therapies, such as gemcitabine plus erlotinib, a combination of oxaliplatin, irinotecan, fluorouracil and leucovorin (FOLIFRINOX), a combination of nab-paclitaxel and gemcitabine, or a combination of nanoliposomal irinotecan, fluorouracil and leucovorin (NAPOLI-1) (3-6). However, despite such recent progress, the OS rate of PC patients is still <5% (1,2). Erlotinib, an epidermal growth factor receptor (EGFR) tyrosine kinase inhibitor (TKI), was the first drug approved for the treatment of PC after showing a survival benefit when combined with gemcitabine over traditional gemcitabine alone (3). Although PC has been well characterized at the genetic level, the molecular mechanisms linking genetic changes to the aggressive nature of this disease remain unclear (7). Multiple genetic alterations, such as K-ras mutation or the loss of *p53* and *SMAD4*, are thought to influence the progression of PC (8). Nevertheless, to date, the inhibition of EGFR by erlotinib is the only targeted approach to demonstrate a survival benefit.

The PI3K/Akt/mTOR pathway, which is located downstream of the EGFR pathway and regulates cell survival and apoptosis, is frequently upregulated or altered in many cancers, and components of the PI3K/Akt/mTOR pathway can also be targeted in the treatment of many cancers (9). Among them, the inhibition of mTOR with rapalogs has initially shown a clinical efficacy in some solid tumors (10). More recently, many agents in clinical development have been designed to inhibit other components of this pathway, including Akt, PI3K and PTEN.

**Correspondence to:** Dr Kazuto Nishio, Department of Genome Biology, Kindai University Faculty of Medicine, 377-2 Ohno-higashi, Osaka-Sayama, Osaka 589-8511, Japan  
E-mail: knishio@med.kindai.ac.jp

**Abbreviations:** CRC, colorectal cancer; CT, computed tomography; EGFP, enhanced green fluorescent protein; EGFR, epidermal growth factor receptor; EUS-FNA, endoscopic ultrasonography-guided fine needle aspiration; FBS, fetal bovine serum; HNSCC, head and neck squamous cell carcinoma; LAd, lung adenocarcinoma; LSq, lung squamous cell carcinoma; NSCLC, non-small cell lung cancer; OS, overall survival; PC, pancreatic cancer; PFS, progression-free survival; TCGA, the Cancer Genome Atlas; TKI, tyrosine kinase inhibitor; SD, standard deviations

**Key words:** pancreatic cancer, Akt2, anti-EGFR therapy, erlotinib, PI3K inhibitor

Akt, the major downstream component of the PI3K/Akt/mTOR pathway, is a serine/threonine kinase that plays a critical role in regulating diverse cellular function including cell growth, proliferation, survival, glucose metabolism, genome stability, transcription and protein synthesis, and neurovascularization (9). The Akt family has three isoforms: Akt1, Akt2 and Akt3. These isoforms are structurally homologous but exhibit distinct features. Akt1 and Akt2 are ubiquitously expressed, whereas Akt3 is found predominantly in the brain, heart and kidneys (11). The Akt isoforms are known to carry specific genetic alterations in different tumor types. *Akt1* amplification has been detected in gastric adenocarcinoma, and the selective activation of *Akt3* in combination with a loss of PTEN has been found in sporadic melanoma (12). In contrast, amplification or high levels of expression of *Akt2* are frequently found in human pancreatic, lung, colorectal, ovarian, and breast cancers (12-19), and high *Akt2* expression levels are positively correlated with the aggressiveness of cancer or poor survival rates in colorectal, ovarian, and breast cancers (16-19). In PC, the activation of the PI3K/Akt/mTOR pathway is a biological indicator of aggressiveness (20), and a recent report has shown that EGFR-TKI resistance in PC is associated with the upregulation of the PI3K/Akt/mTOR pathway *in vitro* (21). Thus, high *Akt2* expression levels have been hypothesized to induce resistance to the EGFR-TKI, erlotinib, in patients with PC. In this study, we investigated the association between the *Akt2* expression level and the outcome of patients with advanced PC who had received erlotinib treatment as well as the contribution of *Akt2* to resistance to anti-EGFR therapies *in vitro*.

## Materials and methods

**Patients and clinical specimens.** Twenty-six patients with advanced PC that received Tarceva® (erlotinib) treatment in combination with gemcitabine at Kindai University Hospital between 2010 and 2014 were included. Among them, 22 patients who had been diagnosed based on the results of endoscopic ultrasonography-guided fine needle aspiration (EUS-FNA) participated in this study. Progression-free survival (PFS) was defined as the time from the initiation of erlotinib treatment until the first observation of disease progression or death from any cause, while OS was defined as the time from the initiation of erlotinib treatment until death from any cause. The stage of disease was classified according to the clinical TNM staging system. Tumor response was evaluated using computed tomography (CT) according to the Response Evaluation Criteria in Solid Tumors. This study was performed retrospectively and was approved by the ethics committee of the Kindai University Faculty of Medicine.

**Immunohistochemistry.** The immunohistochemical method used in this study has been previously described (22). Briefly, 4- $\mu$ m tissue sections from formalin-fixed, paraffin-embedded blocks were sectioned and placed onto charged slides. The slides were then deparaffinized and hydrated; endogenous peroxidase activity was blocked using 3% H<sub>2</sub>O<sub>2</sub> in methanol and normal goat serum. The slides were incubated in a rabbit polyclonal antibody specific for Akt2 (1:200; Proteintech Chicago, IL, USA) overnight at 4°C. Immunohistochemical staining was performed using the rabbit Vectastain Elite

ABC kit (Vector Laboratories, Burlingame, CA, USA), and the slides were developed in diaminobenzidine (DAB kit, Thermo Fisher Scientific, Waltham, MA, USA) according to the manufacturer's protocols, then counterstained with hematoxylin. The staining assessment was performed using ImageJ software (<http://imagej.nih.gov/ij/>).

**Cell culture and reagents.** The HCC827, PC-9, Ma-1, and H358 cell lines [human non-small cell lung cancer (NSCLC) cell lines] and the BxPC-3 and PANC-1 cell lines (human PC cell lines) were maintained in RPMI-1640 medium (Sigma-Aldrich, St. Louis, MO, USA) with 10% fetal bovine serum (FBS; Sigma-Aldrich). The CCK81 cell line [a human colorectal cancer (CRC) cell line] and the gpIRES-293 cell line were maintained in DMEM medium (Nissui Pharmaceutical, Tokyo, Japan) with 10% FBS. All the cells were maintained in a 5% CO<sub>2</sub>-humidified atmosphere at 37°C. Erlotinib and BYL719 were purchased from Selleck Chemicals (Houston, TX, USA).

**Copy number assay.** The *Akt2* copy number was determined using a commercially available and predesigned TaqMan Copy Number assay (Applied Biosystems, Foster City, CA, USA), as described previously (23). Genomic DNA was extracted from each of the cell lines using the QIAamp DNA Mini kit (Qiagen, Hilden, Germany), according to the manufacturer's instructions. The primer ID used for *Akt2* was Hs04028824\_cn. The *TERT* locus was used for the internal reference copy number. Human genomic DNA (Takara, Shiga, Japan) was used as a normal control. A PCR analysis was performed using the ABI PRISM 7900HT Sequence Detection system (Applied Biosystems), and the results were analyzed using CopyCaller software version 2.0 (Applied Biosystems). The experiment was performed in triplicate.

**Real-time reverse-transcription PCR (RT-PCR).** A total of 1  $\mu$ g of RNA was isolated from the cells using Isogen reagent (Nippon Gene, Tokyo, Japan) and then converted to cDNA using the Gene Amp RNA-PCR kit (Applied Biosystems). Real-time PCR was performed using SYBR Premix Ex Taq and Thermal Cycler Dice (Takara) under the following conditions: 95°C for 5 min, followed by 50 cycles of 95°C for 10 sec and 60°C for 30 sec, as described previously (23). *GAPDH* was used to normalize the expression levels in the subsequent quantitative analyses. The experiment was performed in triplicate. The primers used for this study were as follows: *Akt2* F, CCGCCTGTGCTTTGTGATGG; R, TTTCCAGCTTGATGTCGCGG. *GAPDH* F, GCACCGTCAAGGCTGAGAAC; and R, ATGGTGGTGAAGACGCCAGT.

**In vitro growth inhibition assay.** The growth-inhibitory effects of the drugs were examined using a 3-(4, 5-di-methylthiazol-2-yl)-2,5-diphenyltetrazolium bromide assay (MTT; Sigma-Aldrich), as described previously (23). The experiment was performed in triplicate.

**Plasmid construction, viral production, and stable transfectants.** The methods used in this section have been previously described (24). Complementary DNA (cDNA) encoding human full length *Akt2* was prepared by PCR using Prime



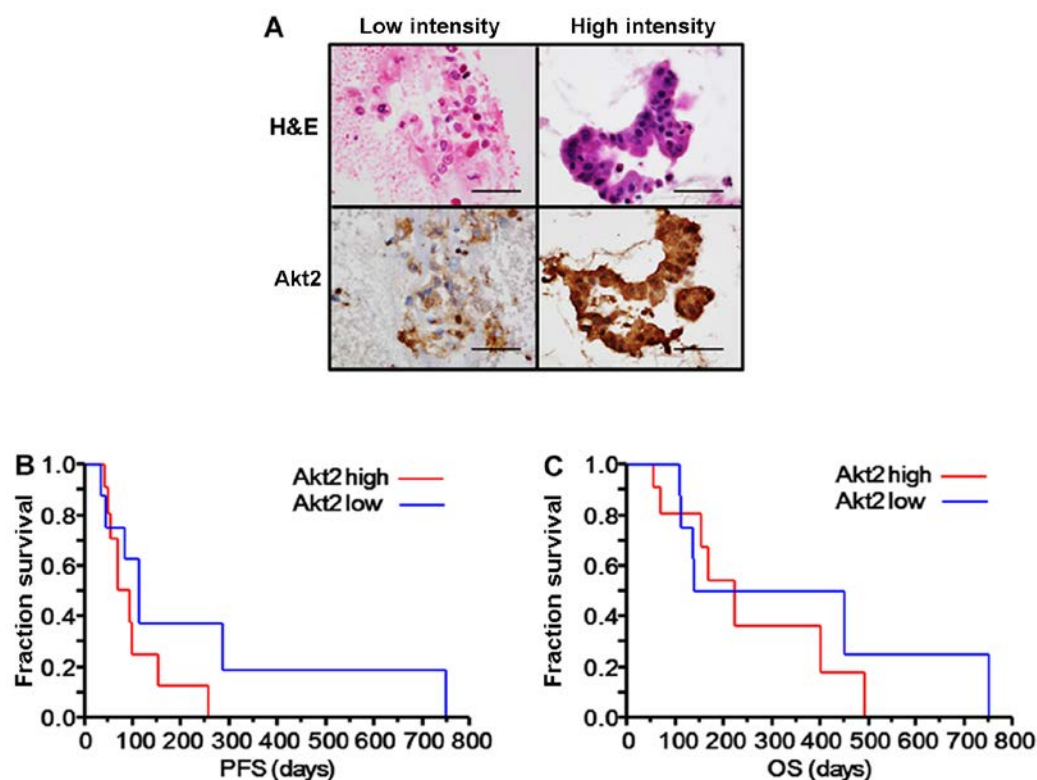


Figure 1. Akt2 expression and outcome of patients with advanced pancreatic cancer (PC) treated with erlotinib. (A) Hematoxylin and eosin (H&E) staining and immunohistochemical (IHC) staining for Akt2 in patients with advanced PC. Deparaffinized sections from endoscopic biopsied tumors were analyzed using H&E and IHC staining. The staining intensity was determined by the relative mean grey value (mean grey value/maximum grey value) using ImageJ software, and the patients were divided into two groups: a low intensity group (relative mean grey value <70%) and a high intensity group (relative mean grey value  $\geq$ 70%). Scale bar, 50  $\mu$ m. (B) Kaplan-Meier curve of progression-free survival (PFS). Patients with a high Akt2 intensity tended to have a shorter PFS than those with a low intensity (median PFS; 92 vs. 113 days,  $P=0.19$ ). (C) Kaplan-Meier curve of overall survival (OS). Patients with a high Akt2 intensity tended to have a shorter OS than those with a low intensity (median OS; 224 vs. 295 days,  $P=0.59$ ).

STAR HS DNA polymerase (Takara) and the following primers: forward, 5'-GGGAATTCGCCGCGCATGAATGAGG TGTCTGTCATCAAAG-3'; reverse, 5'-CCCTCGAGGCCCA GTCACCTCGCGGATGCTGGC-3'. The full length *Akt2* was subcloned into a pCR-Blunt II-TOPO cloning vector (Invitrogen, Carlsbad, CA, USA) as *EcoRI-XhoI* fragments. *Akt2* in the TOPO cloning vector was cut out and transferred to a pQCLIN retroviral vector (Clontech Laboratories, Inc., Palo Alto, CA, USA) together with the enhanced green fluorescent protein (EGFP) following the internal ribosome entry site sequence (IRES) to monitor the expression of the inserts indirectly. The nucleotide sequence of the construct was verified by DNA sequence analysis. A pVSV-G vector (Clontech) for the constitution of the envelope and the pQCLIN-IG constructs were cotransfected into gpIRES-293 cells using FuGENE6 transfection reagent (Roche Diagnostics, Basel, Switzerland). After 48 h of transfection, the culture medium was collected and viral particles were concentrated by centrifugation at 15,000  $\times$  g for 3 h at 4°C. The viral pellet was suspended in fresh DMEM medium. The titer of the viral vector was calculated using the EGFP-positive cells that were infected by the serial dilution of virus-containing media, and the multiplicity of infection was determined. The vectors and the stable viral transfectant BxPC-3, Ma-1, and CCK81 cell lines were designated as pQCLIN-EGFP, pQCLIN-Akt2, BxPC-3/EGFP, BxPC-3/Akt2, Ma-1/EGFP, Ma-1/Akt2, CCK81/EGFP, and CCK81/Akt2, respectively.

**Western blot analysis.** The western blot analysis was performed as described previously (24). Subconfluent cells were washed with cold phosphate-buffered saline (PBS) and lysed using lysis A buffer containing 1% Triton X-100, 20 mM Tris-HCl (pH 7.0), 5 mM EDTA, 50 mM sodium chloride, 50 mM pyrophosphate, 50 mM sodium fluoride, 1 mM sodium orthovanadate, and a protease inhibitor mix, Complete™ (Roche Diagnostics). Whole-cell lysates were separated using SDS-PAGE and were blotted onto a polyvinylidene fluoride membrane. The membrane was blocked for 1 h with 5% skim milk in a TBS buffer (pH 8.0) with 0.1% Tween-20. The membrane was then washed 3 times with TBS and incubated overnight with the primary antibody at 4°C. After washing 3 times with TBS, the membrane was incubated with a horseradish peroxidase-conjugated secondary antibody for 1 h at room temperature. The membrane was then washed, followed by visualization using an ECL detection system and LAS-4000 (GE Healthcare, Buckinghamshire, UK). Rabbit antibodies specific for EGFR, phospho-EGFR, Akt, phospho-Akt, caspase-3, cleaved caspase-3, and  $\beta$ -actin were obtained from Cell Signaling (Beverly, MA, USA). To evaluate the influence of the drugs on phosphorylation and an apoptosis-related molecule, the cells were stimulated for 1-3 and 24 h, respectively.

**Database analysis.** To analyze the prevalence of *Akt2* amplification and high expression levels, the cBioPortal for Cancer

Genomics database (<http://www.cbiportal.org/public-portal/>) was searched (25,26). Within the database, The Cancer Genome Atlas (TCGA) datasets (<http://cancergenome.nih.gov/>) of several cancers are analyzed.

**Statistical analysis.** Continuous variables were analyzed using Student's t-test, and the results were expressed as the average and standard deviations (SD). The univariate relationship between each independent variable was examined using the Fisher's exact test. The statistical analyses were two-tailed and were performed using Microsoft Excel (Microsoft, Redmond, WA, USA) and JMP Pro 11 (SAS Institute, Cary, NC, USA).  $P < 0.05$  was considered statistically significant.

## Results

**Akt2 expression and patient characteristics.** A total of 22 patients with advanced PC and a good performance status (0-1) who had been diagnosed based on the results of EUS-FNA were enrolled in this study. The patients with PC ranged in age from 17 to 70 years, with a median age of 61 years, and the male: female ratio was 12:10. To evaluate the relationship between Akt2 expression and prognosis, an immunohistochemical analysis was performed using biopsy specimens from these patients (Fig. 1A). Three of the 22 specimens could not be evaluated properly using immunohistochemistry for Akt2 because of the poor conditions of the samples and were excluded from additional analyses. The staining intensity was determined as the relative mean grey value (mean grey value/maximum grey value) using ImageJ software, and the patients were divided into two groups: a low intensity group (relative mean grey value  $< 70\%$ ,  $n=8$ ) and a high intensity group (relative mean grey value  $\geq 70\%$ ,  $n=11$ ). No significant differences in the patient characteristics were observed between the two groups, but patients with a high Akt2 intensity tended to have a poorer response to erlotinib plus gemcitabine (0/11 vs. 2/8,  $P=0.16$ ) (Table I). Though the difference was not significant, patients with a high Akt2 intensity also tended to have a shorter PFS (median PFS: 92 vs. 113 days,  $P=0.19$ ) (Fig. 1B) and OS after the initiation of erlotinib plus gemcitabine (median OS: 224 days vs. 295 days,  $P=0.59$ ) (Fig. 1C). These results suggest that Akt2 might be associated with erlotinib resistance in advanced PC.

**Akt2 copy number, Akt2 gene expression, and Akt2 protein expression in diverse cancer cell lines.** To investigate the relationship with Akt2 expression and the response to anti-EGFR therapies, we evaluated the Akt2 gene copy numbers, Akt2 gene expression, and Akt2 protein expression in several cancer cell lines for which anti-EGFR therapies are commonly used. Seven diverse cancer cell lines (four NSCLC cell lines, one CRC cell line, and two PC lines) were used because the PANC-1 cell line has been reported to exhibit Akt2 amplification and the other cell lines are sensitive to anti-EGFR therapies. The Akt2 gene copy number, Akt2 gene expression, and Akt2 protein expression for these cell lines were estimated using a copy number assay, real-time RT-PCR, and western blotting, respectively. The PANC-1 cell line had high copy numbers of the Akt2 gene (40 copies) and the Akt2 gene expression level was also markedly elevated, whereas

Table I. Patient characteristics and associations with Akt2 expression.

Patients characteristics	Akt2 intensity		P-value <sup>b</sup>
	Low (n=8)	High (n=11)	
Age, years			
<60	4	5	1.0
$\geq 60$	4	6	
Gender			
Male	4	7	0.66
Female	4	4	
T stage			
T1-3	5	5	0.65
T4	3	6	
N stage			
N0	3	7	0.37
N1-3	5	4	
M stage			
M0	3	2	0.60
M1	5	9	
Treatment line of erlotinib plus gemcitabine			
First line	4	5	1.0
Second line or later	4	6	
Response to erlotinib plus gemcitabine			
PR	2	0	0.16
SD or PD	6	11	
Median PFS (days) <sup>a</sup>	113	92	0.19
Median OS (days) <sup>a</sup>	295	224	0.59

PR, partial response; SD, stable disease; PD, progressive disease; PFS, progression-free survival; OS, overall survival. <sup>a</sup>PFS and OS were defined as the time from the initiation of erlotinib treatment until disease progression or death from any cause and the time from the initiation of erlotinib treatment until death from any cause, respectively. <sup>b</sup>PFS and OS were analyzed using the log-rank test, and the others were analyzed using the Fisher's exact test.

the other cell lines had neither a high Akt2 copy number nor a high expression level (Fig. 2A and B). Western blot analysis also revealed that Akt2 protein was highly expressed in the PANC-1 cell line (Fig. 2C).

**Combined effect of erlotinib and a PI3K inhibitor in an Akt2-amplified and highly expressed PANC-1 cell line.** To investigate the influence of Akt2 on the resistance to anti-EGFR therapies, the effect of erlotinib against the PANC-1 cell line (an Akt2-amplified and highly expressed cell line) was tested using an MTT assay. As is shown in Fig. 3A, the PANC-1 cell

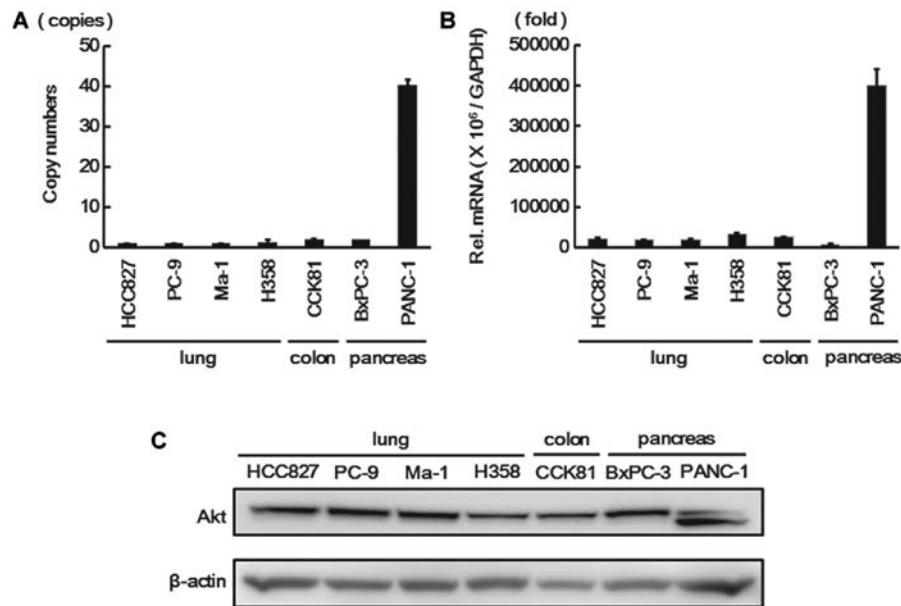


Figure 2. *Akt2* copy number, *Akt2* expression, and *Akt2* protein expression in diverse cancer cell lines. (A) *Akt2* copy number. The copy number for *Akt2* was determined using a TaqMan Copy Number assay. A copy number gain for *Akt2* was observed only in the PANC-1 cell line (40 copies). Columns, mean of independent triplicate experiments; error bars, SD. (B) *Akt2* expression. The *Akt2* expression level was estimated using real-time RT-PCR. *GAPDH* was used to normalize the expression levels. The *Akt2* expression level in the PANC-1 cell line was particularly high compared with those in the other cell lines. Columns, mean of independent triplicate experiments; error bars, SD. (C) *Akt2* protein expression. Western blotting was performed to confirm *Akt* expression. *Akt2* protein was highly expressed in the PANC-1 cell line, compared with the other cell lines.  $\beta$ -actin was used as an internal control.

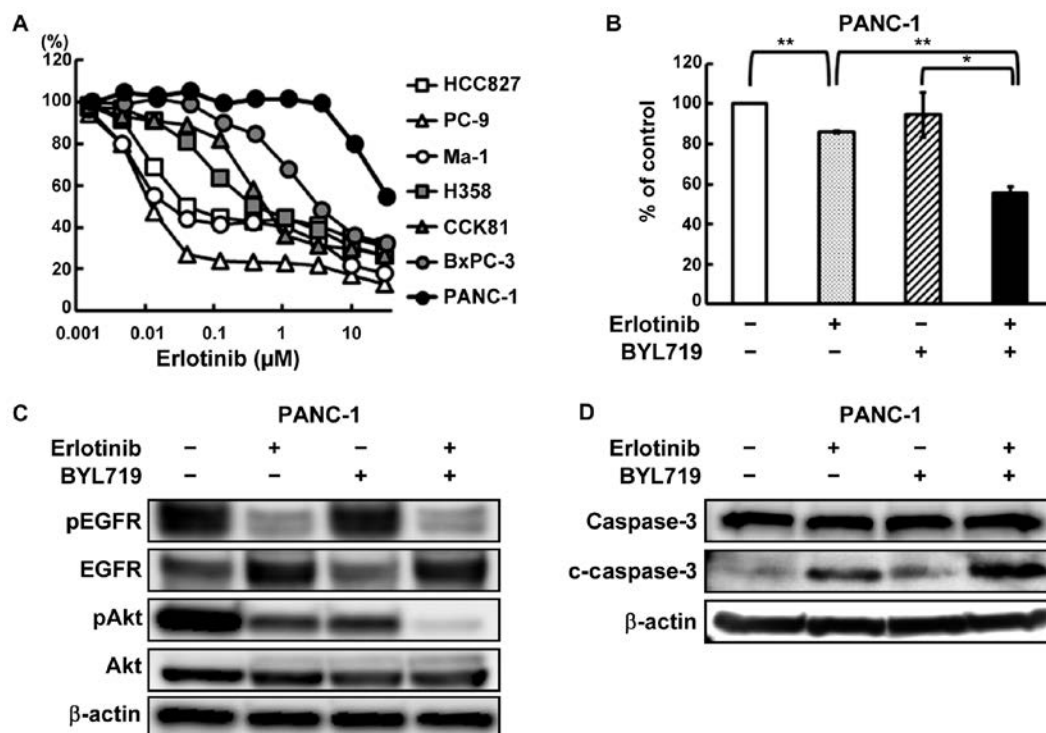


Figure 3. Combined effect of erlotinib and BYL719 in an *Akt2*-amplified and highly expressed PANC-1 cell line. (A) Growth inhibitory effects of erlotinib in diverse cancer cell lines. The cells were exposed to each concentration of erlotinib for 72 h, and the growth inhibitory effects were evaluated using an MTT assay. The HCC827, PC-9, and Ma-1 cell lines (non-small cell lung cancer cell lines harboring *EGFR* mutations) were hypersensitive to erlotinib. The PANC-1 cell line was particularly resistant to erlotinib. Lines, mean of independent triplicate experiments. (B) Growth inhibitory effects of erlotinib and/or BYL719 in the PANC-1 cell line. The cells were treated with 10  $\mu$ M of erlotinib and/or 2  $\mu$ M of BYL719 for 72 h, and the growth inhibitory effects were evaluated using an MTT assay. The combined treatment of erlotinib and BYL719 inhibited the cellular growth more intensively, compared with erlotinib monotherapy. Columns, mean of independent triplicate experiments; error bars, SD; \* $P$ <0.05; \*\* $P$ <0.01. (C) Phosphorylation of EGFR and Akt in the PANC-1 cell line. The cells were treated with 10  $\mu$ M of erlotinib and/or 2  $\mu$ M of BYL719, and the samples were collected 1 h after drug stimulation. The phosphorylation of Akt persisted in the erlotinib monotherapy, while the combined treatment with BYL719 decreased the phosphorylation of Akt.  $\beta$ -actin was used as an internal control. pEGFR, phospho-EGFR; pAkt, phospho-Akt. (D) Expression of an apoptosis-related molecule in the PANC-1 cell line. Twenty-four hours after the cells were exposed to the drugs (erlotinib, 10  $\mu$ M; BYL719, 2  $\mu$ M), the samples were collected. Although erlotinib or BYL719 monotherapy did not increase the expression of cleaved caspase-3, the combined treatment increased the expression.  $\beta$ -actin was used as an internal control. c-caspase-3, cleaved caspase-3.

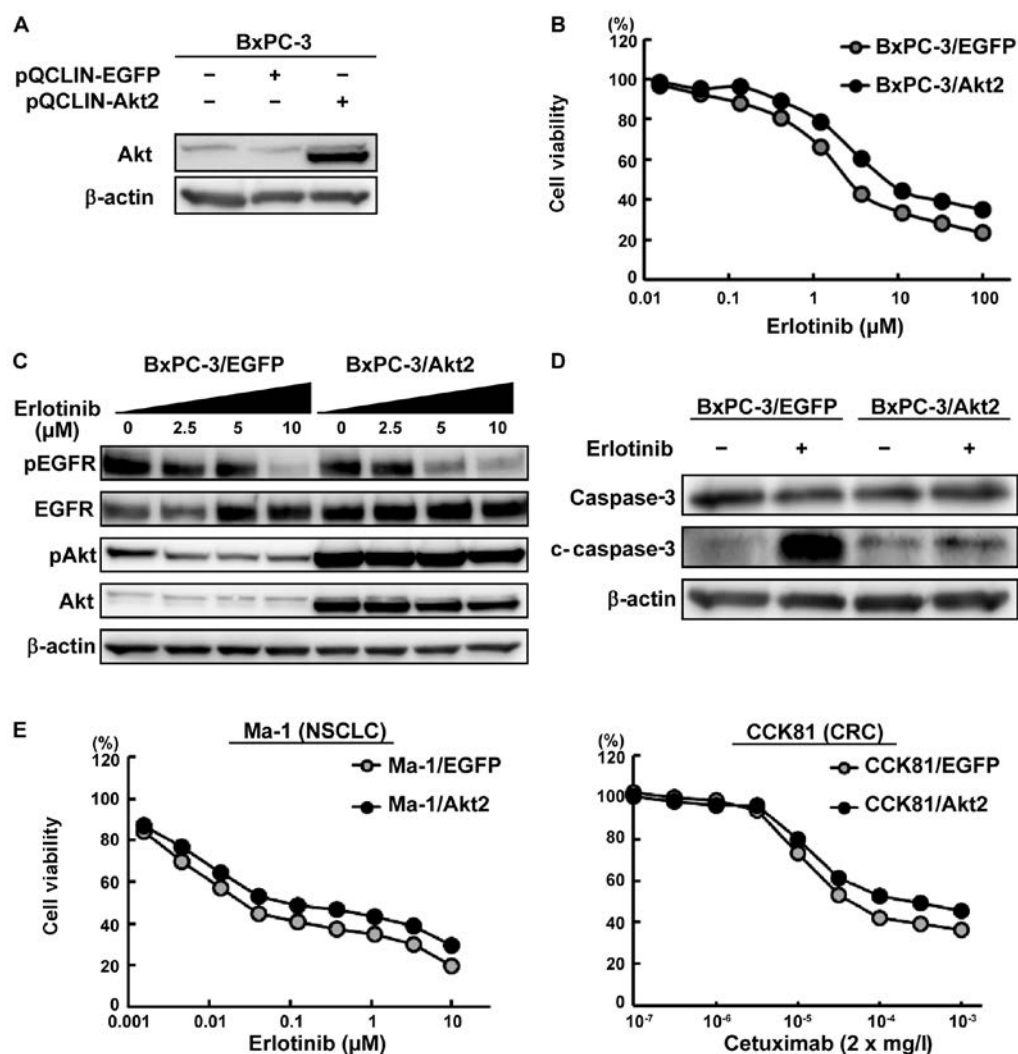


Figure 4. Influence of *Akt2*-overexpression on the efficacy of anti-EGFR therapies against PC, colorectal cancer (CRC) or non-small cell lung cancer (NSCLC) cell lines. (A) *Akt2* protein expression in the BxPC-3 cell lines. To investigate the influence of *Akt2*, an *Akt2*-overexpressed cell line was retrovirally created. An *EGFP*-overexpressed cell line was used as an internal control. The BxPC-3/*Akt2* cell line exhibited the overexpression of *Akt2* protein.  $\beta$ -actin was used as an internal control. (B) Growth inhibitory effects of erlotinib in the BxPC-3 cell lines. The cells were exposed to each concentration of erlotinib for 72 h, and the growth inhibitory effects were evaluated using an MTT assay. The sensitivity to erlotinib was weakened in the BxPC-3/*Akt2* cell line, compared with the control. Lines, mean of independent triplicate experiments. (C) Phosphorylation of EGFR and Akt in the Bx-PC3 cell lines. Three hours after the cells were treated with the indicated concentration of drugs, the samples were collected. Erlotinib inhibited the phosphorylation of EGFR and Akt in a dose-dependent manner in the BxPC-3/*EGFP* cell line. In contrast, the phosphorylation of Akt strongly persisted in the BxPC-3/*Akt2* cell line regardless of the inhibition of the phosphorylation of EGFR.  $\beta$ -actin was used as an internal control. pEGFR, phospho-EGFR; pAkt, phospho-Akt. (D) Expression of an apoptosis-related molecule in the BxPC-3 cell lines. Twenty-four hours after the cells were treated with the drug (erlotinib, 2.5  $\mu$ M), the samples were collected. Erlotinib increased the expression of cleaved caspase-3 to a greater extent in the BxPC-3/*EGFP* cell line but did not increase the expression in the BxPC-3/*Akt2* cell line.  $\beta$ -actin was used as an internal control. c-caspase-3, cleaved caspase-3. (E) Growth inhibitory effects in NSCLC and CRC cell lines. The Ma-1/*Akt2* cell line (human NSCLC cell line) and CCK81/*Akt2* cell line (human CRC cell line) were resistant to erlotinib and cetuximab, respectively. The cells were exposed to each concentration of erlotinib/cetuximab for 72 h, and the growth inhibitory effects were evaluated using an MTT assay. Lines, mean of independent triplicate experiments.

line was particularly resistant to erlotinib, compared with the other cell lines that did not exhibit either amplification or a high *Akt2* expression level. Next, the combined effect of erlotinib and BYL719, a PI3K inhibitor, was examined in the PANC-1 cell line. The combined treatment of erlotinib and BYL719 inhibited the cellular growth more intensively than erlotinib monotherapy (Fig. 3B). This combined effect in the PANC-1 cell line has already been reported (21), but we also confirmed the efficacy of combination therapy in this study. Whereas the phosphorylation of Akt persisted after erlotinib monotherapy, the combined treatment decreased the phosphorylation of Akt (Fig. 3C). In contrast to erlotinib or BYL719 monotherapy,

the combined treatment of erlotinib and BYL719 increased the expression level of an apoptosis-related molecule, cleaved caspase-3 (Fig. 3D).

#### *Akt2* overexpression led to resistance to anti-EGFR therapies.

To evaluate the contribution of *Akt2* to the EGFR-TKI response, a stably *Akt2*-overexpressed PC cell line was created. The BxPC-3 cell line was mainly used because this PC cell line is intermediately sensitive to erlotinib with no *Akt2* amplification or high expression (Figs. 2 and 3A). The stably *EGFP*-expressed cell line was used as a control. *Akt2*-overexpression was confirmed using a western blot analysis (Fig. 4A). Then, we



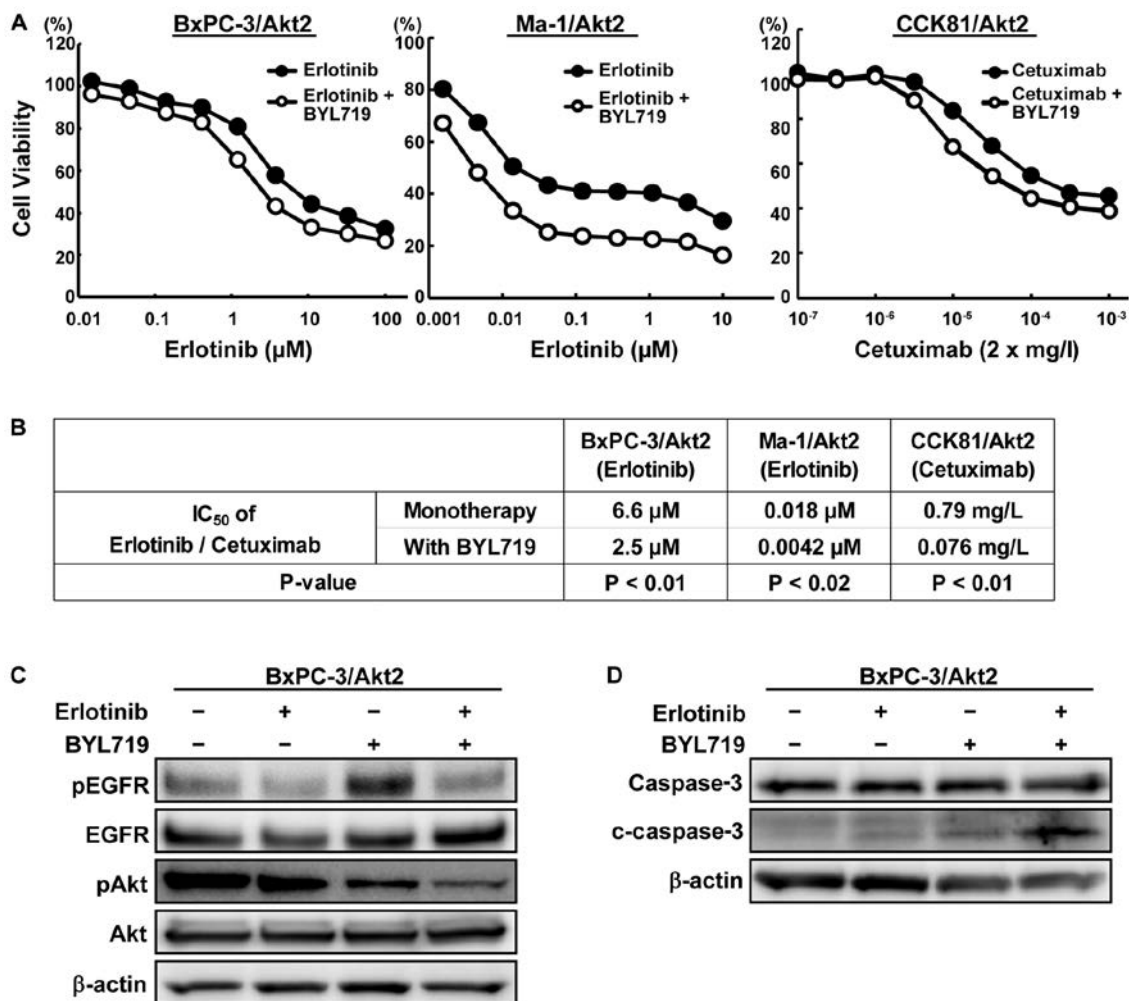


Figure 5. Combined effect of anti-EGFR therapy and BYL719 in the Akt2-overexpressed cell lines. (A) Growth inhibitory effects of the combined treatment of erlotinib/cetuximab and BYL719 in the Akt2-overexpressed cell lines. Cells were exposed to each concentration of erlotinib/cetuximab with or without BYL719 (BxPC-3, 4 μM; CCK81 and Ma-1, 2 μM) for 72 h, and the growth inhibitory effects were evaluated using an MTT assay. The combined treatment with erlotinib/cetuximab and BYL719 strongly inhibited the cellular growth compared with erlotinib/cetuximab monotherapy. Lines, mean of independent triplicate experiments. (B) IC<sub>50</sub> values of erlotinib/cetuximab with or without BYL719 in the Akt2-overexpressed cell lines. The IC<sub>50</sub> values of erlotinib/cetuximab were significantly lower in the combination therapy than in the monotherapy. (C) Phosphorylation of EGFR and Akt in the BxPC-3/Akt2 cell line. Three hours after the cells were exposed to the drugs (erlotinib, 5 μM; BYL719, 4 μM), the samples were collected. The phosphorylation of Akt was inhibited to a greater degree by the combined treatment than the erlotinib monotherapy. β-actin was used as an internal control. pEGFR, phospho-EGFR; pAkt, phospho-Akt. (D) Expression of an apoptosis-related molecule in the BxPC-3/Akt2 cell line. Twenty-four hours after the cells were exposed to the drugs (erlotinib, 5 μM; BYL719, 4 μM), the samples were collected. In contrast to erlotinib or BYL719 monotherapy, the combined treatment increased the expression of cleaved caspase-3 to a greater extent. β-actin was used as an internal control. c-caspase-3, cleaved caspase-3.

performed a growth inhibition assay using this cell line and found that the BxPC-3/Akt2 cell line was resistant to erlotinib (Fig. 4B). In contrast, Akt2-overexpression was not associated with gemcitabine resistance. In western blot analyses, erlotinib inhibited the phosphorylation of EGFR and Akt in a dose-dependent manner in the control cells. In contrast, the phosphorylation of Akt strongly persisted in the BxPC-3/Akt2 cell line, although erlotinib inhibited the phosphorylation of EGFR (Fig. 4C). The erlotinib-induced elevation in the expression level of cleaved caspase-3 in the BxPC-3/Akt2 cell line was lower than that in the control cells (Fig. 4D). Furthermore, similar experiments were also performed in other cell lines (Ma-1 and CCK81), demonstrating the resistance to anti-EGFR therapies in Akt2-overexpressed cell lines (Fig. 4E). These results indicate that Akt2 might be related to resistance to anti-EGFR therapies.

*Combined effect of anti-EGFR therapies and a PI3K inhibitor in the Akt2-overexpressed cell lines.* To investigate the effect of a PI3K inhibitor on the drug resistance induced by Akt2 overexpression, we performed growth inhibition assays using erlotinib/cetuximab and BYL719 in the Akt2-overexpressed lines. The combined treatment with erlotinib/cetuximab and BYL719 considerably inhibited the cellular growth, compared with the monotherapy (Fig. 5A). The IC<sub>50</sub> values of erlotinib/cetuximab were significantly lower in the combination therapy than in the monotherapy (Fig. 5B). In the BxPC-3/Akt2 cell line, the phosphorylation of Akt was also markedly inhibited by the combined treatment with BYL719 compared with erlotinib alone (Fig. 5C). Compared with monotherapy, the combined treatment with BYL719 increased the expression of cleaved caspase-3 to a greater extent (Fig. 5D). These results indicate that Akt2 can be associated with resistance to



Table II. High RNA expression and gene amplification of *Akt2* in TCGA database.

Cancer type	Amplification		RNA expression	
	No. of samples	No. of samples with amplification (%)	No. of samples	No. of samples with a high expression level (%)
PC	145	11 (8)	178	25 (14)
LAd	230	3 (1.3)	230	21 (9.1)
LSq	178	8 (4.5)	178	24 (13.5)
CRC	212	3 (1.4)	244	17 (7)
HNSCC	279	4 (1.4)	279	27 (9.7)

PC, pancreatic cancer; LAd, lung adenocarcinoma; LSq, lung squamous cell carcinoma; CRC, colorectal adenocarcinoma; HNSCC, head and neck squamous cell carcinoma. Gene amplification and RNA expression were evaluated by genome sequencing and RNA sequencing, respectively. High RNA expressed samples were defined as those with a Z-score >2.0.

anti-EGFR therapies via the PI3K-Akt pathway and that such resistance can be overcome by a PI3K inhibitor.

*Akt2* amplification and high *Akt2* expression levels in several cancers from TCGA datasets. Next, we analyzed the TCGA database to investigate the frequencies of *Akt2* amplification and high expression levels in several cancers. Data for PC, lung adenocarcinoma, lung squamous cell carcinoma, CRC, and head-and-neck squamous cell carcinoma (HNSCC) were analyzed since EGFR-TKIs or anti-EGFR monoclonal antibodies are clinically used for the treatment of these cancers. A high *Akt2* expression level was defined as a Z-score >2.0 using RNA sequencing. Samples with a high *Akt2* expression level were found at a relative high frequency of 7-14%. In contrast, the frequency of *Akt2* amplification was not so high, except for PC (8%), and *Akt2* amplification was correlated with the *Akt2* expression level. Among all the cancers that were examined, the frequencies of both *Akt2* amplification and a high expression level were the highest for PC (Table II).

## Discussion

In this study, we revealed the possible association between high *Akt2* expression levels and erlotinib resistance in clinical specimens of advanced PC. In addition, *in vitro* experiments also demonstrated this association and the efficacy of combined treatment with a PI3K inhibitor for overcoming resistance. Although a previous *in vitro* study demonstrated an association between *Akt2* and erlotinib resistance (21), to the best of our knowledge, this is the first study to show this association in clinical specimens of advanced PC.

EGFR is a cell membrane growth factor receptor characterized by tyrosine kinase activity that plays a crucial role in the control of key cellular transduction pathways (27). At present, targeting EGFR is one of the most effective anticancer strategies available, and anti-EGFR therapies are now widely used for the treatment of PC, NSCLC, CRC, and HNSCC (27). For advanced PC, erlotinib is the first drug for which a superiority of combination therapy with gemcitabine in terms of OS and PFS, has been documented in a large randomized trial, but the achievable improvement has remained limited (3).

This unsatisfactory outcome has encouraged a number of studies which have attempted to identify molecular markers capable of predicting the efficacy of erlotinib in patients with PC (1,27). *EGFR* mutation or amplification has been a potential predictor of the response to EGFR-TKI treatment or patient prognosis in several cancers (27), and EGFR-TKIs are known to be effective against NSCLC harboring *EGFR* mutations (28). Several studies, however, have demonstrated that neither *EGFR* amplification nor *EGFR* mutation is a predictive biomarker for the response to erlotinib in PC (29,30). *KRAS* mutations, which act downstream of the EGFR pathway, have been characterized as a predictive biomarker for resistance to anti-EGFR antibodies in CRC (31). In PC, however, *K-ras* mutations, which occur in 90% of PC, have not been recognized as a predictive biomarker for resistance to erlotinib in combination with gemcitabine (29). These previous studies highlight the need to explore alternative explanations for responses to erlotinib and to identify markers that can predict the efficacy of erlotinib in patients with PC. Recently, alterations of the PI3K-Akt pathway, which is active downstream of the EGFR pathway, have been implicated as potential mechanisms of resistance to anti-EGFR therapies in CRC and lung adenocarcinoma (32-35). Amplification and high expression levels of *Akt2* are also reportedly associated with resistance to erlotinib in PC *in vitro* (21). The present study showed a tendency toward a poorer response and a shorter PFS and OS for erlotinib plus gemcitabine in patients with advanced PC harboring high *Akt2* expression. Furthermore, *in vitro* experiments showed that *Akt2* is associated with the resistance to anti-EGFR therapies, and a TCGA dataset showed that the frequencies of both *Akt2* amplification and high expression levels are relatively high in PC. These findings suggest that *Akt2* expression could be a predictive biomarker for resistance to erlotinib in PC. In addition, in our *in vitro* experiments, the combined treatment of erlotinib and a PI3K inhibitor was able to overcome this resistance, indicating that this combined treatment might be a promising strategy for the treatment of patients who are resistant to anti-EGFR therapies because of high *Akt2* expression levels.

A previous report showed that a high *Akt2* expression detected using immunohistochemistry was observed in 40%

of cases, consistent with the results of the present study, but a correlation with the survival of patients with PC was not seen (14). In the previous study, all the patients had received curative surgical resections and did not receive erlotinib treatment (14). In contrast, we focused on patients with advanced PC treated with erlotinib plus gemcitabine and showed a tendency toward a poorer outcome among patients with high Akt2 expression levels. The PI3K/Akt/mTOR pathway regulates cell survival and apoptosis (9), and *Akt2* expression is reportedly associated with prognosis and aggressiveness in other cancers (16-19). In addition, Akt2, which is active downstream of the EGFR pathway, seems to be associated with erlotinib resistance. Therefore, the tendency toward a poorer outcome among patients with advanced PC with high Akt2 expression levels who had been treated with erlotinib plus gemcitabine, as observed in the present study, seems reasonable.

The present study had some limitations. First, the study was relatively small and was performed retrospectively, and we could not show a significant correlation between Akt2 expression and the response to erlotinib. Only a few patients with advanced PC are eligible for surgical resection (1), and cytological examinations such as EUS or CT-guided FNA, which is an invasive method, are not routinely performed when cancer is almost certainly diagnosed using dynamic CT imaging (36). Consequently, predictive biomarkers in advanced PC are difficult to investigate and studies like ours are very rare. At our institute, however, EUS-FNA is commonly conducted (37). Therefore, the present study might be valuable from the aspect of its use of rare biopsy specimens despite the small number of available samples. In addition, the present study, showing Akt2 expression as a biomarker candidate, encourages the use of aggressive biopsies in patients with advanced PC. Recently, evaluation of gene amplification has become feasible using a liquid biopsy, which detects cell-free circulating tumor DNA in the blood (38,39). Liquid biopsies are less invasive than EUS-FNA and might be useful for the detection of biomarkers such as gene amplification.

As a second limitation, we could not evaluate Akt2 gene amplification and expression because of the poor sample conditions. Due to the small amount of biopsied tissue obtained using EUS-FNA, we could not extract a sufficient amount of DNA/RNA for such analyses. Instead, we analyzed the TCGA database to investigate the frequencies of *Akt2* amplification and high expression levels. The frequencies of *Akt2* amplification and high expression in PC are not as high as those of other gene alterations, such as those of the *K-ras* mutation. Recently, however, molecular targeted therapy for low-frequency alterations has been developed. For example, the frequencies of *ALK* rearrangements and uncommon *EGFR* mutations in NSCLC are as low as 5 and 10%, respectively (40,41). Patients with *ALK* rearrangements are well known to respond dramatically to crizotinib (40), and in a recent post hoc analysis and our *in vitro* studies, afatinib was reported to be effective for patients harboring uncommon *EGFR* mutations, including exon 18 mutations, the *S768I* mutation, and the *L861Q* mutation (42-44). Thus, the low frequencies of gene alterations should not be overlooked, and effective biomarkers for the detection and treatment of PC are eagerly anticipated, but not yet defined. Therefore, Akt2 expression in PC might be valuable in treatment with erlotinib. To eliminate these limitations and to

confirm our findings, further analyses including multi-center studies are desirable.

In conclusion, we found an association between high Akt2 expression levels and resistance to erlotinib in both clinical specimens of advanced PC and several cell lines. A high Akt2 expression level might be a predictive biomarker for resistance to anti-EGFR therapies, especially erlotinib, in patients with PC. Our present study was, however, very small and was performed retrospectively. Therefore, further large-scale studies are needed to confirm these findings.

## Acknowledgements

We thank Mr. Shinji Kurashimo, Mr. Yoshihiro Mine, Ms. Eiko Honda, Ms. Tomoko Kitayama, and Ms. Ayaka Kurumatani for their technical assistance, and we thank Dr Yoshimi Hosono for the pathological review. This study was supported in part by Grant-in-Aid for Research Activity start-up (15H06754).

## References

1. Ryan DP, Hong TS and Bardeesy N: Pancreatic adenocarcinoma. *N Engl J Med* 371: 1039-1049, 2014.
2. Vincent A, Herman J, Schulick R, Hruban RH and Goggins M: Pancreatic cancer. *Lancet* 378: 607-620, 2011.
3. Moore MJ, Goldstein D, Hamm J, Figer A, Hecht JR, Gallinger S, Au HJ, Murawa P, Walde D, Wolff RA, *et al*; National Cancer Institute of Canada Clinical Trials Group: Erlotinib plus gemcitabine compared with gemcitabine alone in patients with advanced pancreatic cancer: A phase III trial of the National Cancer Institute of Canada Clinical Trials Group. *J Clin Oncol* 25: 1960-1966, 2007.
4. Conroy T, Desseigne F, Ychou M, Bouché O, Guimbaud R, Bécauarn Y, Adenis A, Raoul JL, Gourgou-Bourgade S, de la Fouchardière C, *et al*; Groupe Tumeurs Digestives de Unicancer; PRODIGE Intergroup: FOLFIRINOX versus gemcitabine for metastatic pancreatic cancer. *N Engl J Med* 364: 1817-1825, 2011.
5. Von Hoff DD, Ervin T, Arena FP, Chiorean EG, Infante J, Moore M, Seay T, Tjuland SA, Ma WW, Saleh MN, *et al*: Increased survival in pancreatic cancer with nab-paclitaxel plus gemcitabine. *N Engl J Med* 369: 1691-1703, 2013.
6. Wang-Gillam A, Li CP, Bodoky G, Dean A, Shan YS, Jameson G, Macarulla T, Lee KH, Cunningham D, Blanc JF, *et al*; NAPOLI-1 Study Group: Nanoliposomal irinotecan with fluorouracil and folinic acid in metastatic pancreatic cancer after previous gemcitabine-based therapy (NAPOLI-1): A global, randomised, open-label, phase 3 trial. *Lancet* 387: 545-557, 2016.
7. Kozak G, Blanco FF and Brody JR: Novel targets in pancreatic cancer research. *Semin Oncol* 42: 177-187, 2015.
8. Macgregor-Das AM and Iacobuzio-Donahue CA: Molecular pathways in pancreatic carcinogenesis. *J Surg Oncol* 107: 8-14, 2013.
9. Thorpe LM, Yuzugullu H and Zhao JJ: PI3K in cancer: Divergent roles of isoforms, modes of activation and therapeutic targeting. *Nat Rev Cancer* 15: 7-24, 2015.
10. Ocana A, Vera-Badillo F, Al-Mubarak M, Templeton AJ, Corrales-Sanchez V, Diez-Gonzalez L, Cuenca-Lopez MD, Seruga B, Pandiella A and Amir E: Activation of the PI3K/mTOR/AKT pathway and survival in solid tumors: Systematic review and meta-analysis. *PLoS One* 9: e95219, 2014.
11. Nitulescu GM, Margina D, Juzenas P, Peng Q, Olaru OT, Saloustros E, Fenga C, Spandidos DA, Libra M and Tsatsakis AM: Akt inhibitors in cancer treatment: The long journey from drug discovery to clinical use (Review). *Int J Oncol* 48: 869-885, 2016.
12. Martini M, De Santis MC, Braccini L, Gulluni F and Hirsch E: PI3K/AKT signaling pathway and cancer: An updated review. *Ann Med* 46: 372-383, 2014.
13. Ruggeri BA, Huang L, Wood M, Cheng JQ and Testa JR: Amplification and overexpression of the AKT2 oncogene in a subset of human pancreatic ductal adenocarcinomas. *Mol Carcinog* 21: 81-86, 1998.

14. Yamamoto S, Tomita Y, Hoshida Y, Morooka T, Nagano H, Dono K, Umeshita K, Sakon M, Ishikawa O, Ohigashi H, *et al*: Prognostic significance of activated Akt expression in pancreatic ductal adenocarcinoma. *Clin Cancer Res* 10: 2846-2850, 2004.
15. Dobashi Y, Kimura M, Matsubara H, Endo S, Inazawa J and Ooi A: Molecular alterations in AKT and its protein activation in human lung carcinomas. *Hum Pathol* 43: 2229-2240, 2012.
16. Rychahou PG, Kang J, Gulhati P, Doan HQ, Chen LA, Xiao SY, Chung DH and Evers BM: Akt2 overexpression plays a critical role in the establishment of colorectal cancer metastasis. *Proc Natl Acad Sci USA* 105: 20315-20320, 2008.
17. Nakayama K, Nakayama N, Kurman RJ, Cope L, Pohl G, Samuels Y, Velculescu VE, Wang TL and Shih IeM: Sequence mutations and amplification of PIK3CA and AKT2 genes in purified ovarian serous neoplasms. *Cancer Biol Ther* 5: 779-785, 2006.
18. Bacus SS, Altomare DA, Lyass L, Chin DM, Farrell MP, Gurova K, Gudkov A and Testa JR: AKT2 is frequently upregulated in HER-2/neu-positive breast cancers and may contribute to tumor aggressiveness by enhancing cell survival. *Oncogene* 21: 3532-3540, 2002.
19. Bellacosa A, de Feo D, Godwin AK, Bell DW, Cheng JQ, Altomare DA, Wan M, Dubeau L, Scambia G, Masciullo V, *et al*: Molecular alterations of the AKT2 oncogene in ovarian and breast carcinomas. *Int J Cancer* 64: 280-285, 1995.
20. Edling CE, Selvaggi F, Buus R, Maffucci T, Di Sebastiano P, Friess H, Innocenti P, Kocher HM and Falasca M: Key role of phosphoinositide 3-kinase class IB in pancreatic cancer. *Clin Cancer Res* 16: 4928-4937, 2010.
21. Wong MH, Xue A, Julovi SM, Pavlakis N, Samra JS, Hugh TJ, Gill AJ, Peters L, Baxter RC and Smith RC: Cotargeting of epidermal growth factor receptor and PI3K overcomes PI3K-Akt oncogenic dependence in pancreatic ductal adenocarcinoma. *Clin Cancer Res* 20: 4047-4058, 2014.
22. De Velasco MA, Tanaka M, Yamamoto Y, Hatanaka Y, Koike H, Nishio K, Yoshikawa K and Uemura H: Androgen deprivation induces phenotypic plasticity and promotes resistance to molecular targeted therapy in a PTEN-deficient mouse model of prostate cancer. *Carcinogenesis* 35: 2142-2153, 2014.
23. Arao T, Ueshima K, Matsumoto K, Nagai T, Kimura H, Hagiwara S, Sakurai T, Haji S, Kanazawa A, Hidaka H, *et al*: FGF3/FGF4 amplification and multiple lung metastases in responders to sorafenib in hepatocellular carcinoma. *Hepatology* 57: 1407-1415, 2013.
24. Togashi Y, Kogita A, Sakamoto H, Hayashi H, Terashima M, de Velasco MA, Sakai K, Fujita Y, Tomida S, Kitano M, *et al*: Activin signal promotes cancer progression and is involved in cachexia in a subset of pancreatic cancer. *Cancer Lett* 356 (2 Pt B): 819-827, 2015.
25. Cerami E, Gao J, Dogrusoz U, Gross BE, Sumer SO, Aksoy BA, Jacobsen A, Byrne CJ, Heuer ML, Larsson E, *et al*: The cBio cancer genomics portal: An open platform for exploring multi-dimensional cancer genomics data. *Cancer Discov* 2: 401-404, 2012.
26. Gao J, Aksoy BA, Dogrusoz U, Dresdner G, Gross B, Sumer SO, Sun Y, Jacobsen A, Sinha R, Larsson E, *et al*: Integrative analysis of complex cancer genomics and clinical profiles using the cBioPortal. *Sci Signal* 6: pii, 2013.
27. Ciardiello F and Tortora G: EGFR antagonists in cancer treatment. *N Engl J Med* 358: 1160-1174, 2008.
28. Mitsudomi T and Yatabe Y: Mutations of the epidermal growth factor receptor gene and related genes as determinants of epidermal growth factor receptor tyrosine kinase inhibitors sensitivity in lung cancer. *Cancer Sci* 98: 1817-1824, 2007.
29. da Cunha Santos G, Dhani N, Tu D, Chin K, Ludkovski O, Kamel-Reid S, Squire J, Parulekar W, Moore MJ and Tsao MS: Molecular predictors of outcome in a phase 3 study of gemcitabine and erlotinib therapy in patients with advanced pancreatic cancer: National Cancer Institute of Canada Clinical Trials Group Study PA.3. *Cancer* 116: 5599-5607, 2010.
30. Tzeng CW, Frolov A, Frolova N, Jhala NC, Howard JH, Buchsbaum DJ, Vickers SM, Heslin MJ and Arnoletti JP: Epidermal growth factor receptor (EGFR) is highly conserved in pancreatic cancer. *Surgery* 141: 464-469, 2007.
31. Karapetis CS, Khambata-Ford S, Jonker DJ, O'Callaghan CJ, Tu D, Tebbutt NC, Simes RJ, Chalchal H, Shapiro JD, Robitaille S, *et al*: K-ras mutations and benefit from cetuximab in advanced colorectal cancer. *N Engl J Med* 359: 1757-1765, 2008.
32. Sartore-Bianchi A, Martini M, Molinari F, Veronese S, Nichelatti M, Artale S, Di Nicolantonio F, Saletti P, De Dosso S, Mazzucchelli L, *et al*: PIK3CA mutations in colorectal cancer are associated with clinical resistance to EGFR-targeted monoclonal antibodies. *Cancer Res* 69: 1851-1857, 2009.
33. De Roock W, Claes B, Bernasconi D, De Schutter J, Biesmans B, Fountzilas G, Kalogeras KT, Kotoula V, Papamichael D, Laurent-Puig P, *et al*: Effects of KRAS, BRAF, NRAS, and PIK3CA mutations on the efficacy of cetuximab plus chemotherapy in chemotherapy-refractory metastatic colorectal cancer: A retrospective consortium analysis. *Lancet Oncol* 11: 753-762, 2010.
34. Sos ML, Koker M, Weir BA, Heynck S, Rabinovsky R, Zander T, Seeger JM, Weiss J, Fischer F, Frommolt P, *et al*: PTEN loss contributes to erlotinib resistance in EGFR-mutant lung cancer by activation of Akt and EGFR. *Cancer Res* 69: 3256-3261, 2009.
35. Jeannot V, Busser B, Brambilla E, Wislez M, Robin B, Cadranet J, Coll JL and Hurbain A: The PI3K/AKT pathway promotes gefitinib resistance in mutant KRAS lung adenocarcinoma by a deacetylase-dependent mechanism. *Int J Cancer* 134: 2560-2571, 2014.
36. Tamm EP, Bhosale PR and Lee JH: Pancreatic ductal adenocarcinoma: Ultrasound, computed tomography, and magnetic resonance imaging features. *Semin Ultrasound CT MR* 28: 330-338, 2007.
37. Kitano M, Kudo M, Yamao K, Takagi T, Sakamoto H, Komaki T, Kamata K, Imai H, Chiba Y, Okada M, *et al*: Characterization of small solid tumors in the pancreas: The value of contrast-enhanced harmonic endoscopic ultrasonography. *Am J Gastroenterol* 107: 303-310, 2012.
38. Diaz LA Jr and Bardelli A: Liquid biopsies: Genotyping circulating tumor DNA. *J Clin Oncol* 32: 579-586, 2014.
39. Heitzer E, Ulz P and Geigl JB: Circulating tumor DNA as a liquid biopsy for cancer. *Clin Chem* 61: 112-123, 2015.
40. Gridelli C, Peters S, Sgambato A, Casaluze F, Adjei AA and Ciardiello F: ALK inhibitors in the treatment of advanced NSCLC. *Cancer Treat Rev* 40: 300-306, 2014.
41. Roengvoraphoj M, Tsongalis GJ, Dragnev KH and Rigas JR: Epidermal growth factor receptor tyrosine kinase inhibitors as initial therapy for non-small cell lung cancer: Focus on epidermal growth factor receptor mutation testing and mutation-positive patients. *Cancer Treat Rev* 39: 839-850, 2013.
42. Yang JC, Sequist LV, Geater SL, Tsai CM, Mok TS, Schuler M, Yamamoto N, Yu CJ, Ou SH, Zhou C, *et al*: Clinical activity of afatinib in patients with advanced non-small-cell lung cancer harbouring uncommon EGFR mutations: A combined post-hoc analysis of LUX-Lung 2, LUX-Lung 3, and LUX-Lung 6. *Lancet Oncol* 16: 830-838, 2015.
43. Kobayashi Y, Togashi Y, Yatabe Y, Mizuuchi H, Jangchul P, Kondo C, Shimoji M, Sato K, Suda K, Tomizawa K, *et al*: EGFR exon 18 mutations in lung cancer: Molecular predictors of augmented sensitivity to afatinib or neratinib as compared with first- or third-generation TKIs. *Clin Cancer Res* 21: 5305-5313, 2015.
44. Banno E, Togashi Y, Nakamura Y, Chiba M, Kobayashi Y, Hayashi H, Terashima M, de Velasco MA, Sakai K, Fujita Y, *et al*: Sensitivities to various epidermal growth factor receptor-tyrosine kinase inhibitors of uncommon epidermal growth factor receptor mutations L861Q and S768I: What is the optimal epidermal growth factor receptor-tyrosine kinase inhibitor? *Cancer Sci* 107: 1134-1140, 2016.



## Images of the Month

### A Case of Type II Enteropathy-Associated T-Cell Lymphoma in a Patient With Ulcerative Colitis

Yoriaki Komeda<sup>1</sup>, Hiroshi Kashida<sup>1</sup>, Toshiharu Sakurai<sup>1</sup>, Masashi Kono<sup>1</sup>, Tomoyuki Nagai<sup>1</sup>, Yutaka Asakuma<sup>1</sup>, Satoru Hagiwara<sup>1</sup>, Shigenaga Matsui<sup>1</sup>, Tomohiro Watanabe<sup>1</sup>, Takaaki Chikugo<sup>2</sup> and Masatoshi Kudo<sup>1</sup>

*Am J Gastroenterol* 2017;112:833; doi:10.1038/ajg.2017.56



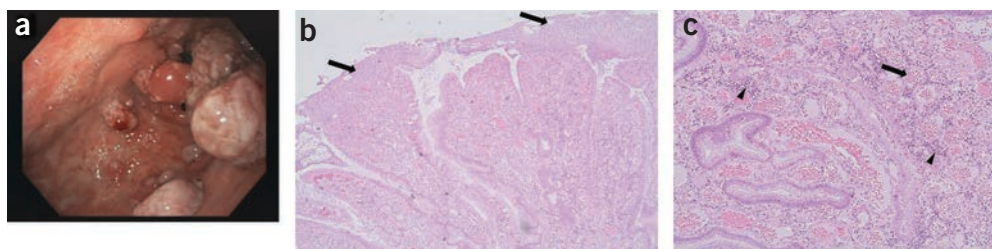
A 65-year-old man presented 7 years after being treated by a local physician for left-sided ulcerative colitis (UC). A colonoscopy suggested that the UC was nearly in remission, but, unexpectedly, a rectal biopsy revealed lymphoma. The patient was referred to our hospital. Colonoscopy revealed edematous and fine granular mucosa with tiny erosions extending from the sigmoid colon to the rectum (**a**). Abdominal computed tomography revealed wall thickening at multiple sites in the jejunum; one site showed mass formation. Enteroscopy showed fine, granular, edematous mucosa extending from the duodenum into the jejunum. There were ulcerated areas, and at one site a mass occupied half the lumen (**b**). Biopsy specimens from the small and large intestines revealed that the epithelium of the crypts and the stromal tissue were infiltrated by abnormal lymphocytes that were positive for CD3, CD7, CD8, and CD56 and negative for CD4, CD20, TIA1, and granzyme B (**c**). The findings led to a diagnosis of enteropathy-associated T-cell lymphoma in immunostaining. After diagnosis, symptoms of intestinal obstruction developed and laparoscopic partial resection of the jejunum was performed. During the fifth course of chemotherapy, the patient developed septicemia and disseminated intravascular coagulopathy, which led to his death 7 months after presentation. (Informed consent was obtained from the patient's family to publish these images.)

<sup>1</sup>Department of Gastroenterology and Hepatology, Kindai University Faculty of Medicine, Osaka-Sayama, Osaka, Japan; <sup>2</sup>Department of Pathology, Kindai University Faculty of Medicine, Osaka-Sayama, Osaka, Japan.

### Recurrent Gastrointestinal Bleeding due to Multiple Pyogenic Granulomas in the Stomach

Matthias C Reichert<sup>1</sup>, Michael Schuster<sup>1</sup>, Yoo-Jin Kim<sup>2</sup> and Frank Lammert<sup>1</sup>

*Am J Gastroenterol* 2017;112:833; doi:10.1038/ajg.2016.599



A 77-year-old woman with compensated liver cirrhosis (Child-Pugh stage A) due to chronic hepatitis C virus infection was referred to our department with recurrent upper gastrointestinal bleeding, requiring blood transfusion (500 ml packed red blood cells). Esophagogastroduodenoscopy revealed red, hyperemic, smooth polyps in the gastric antrum (**a**), which bled on contact with the endoscope. Multiple polyps were resected using snare polypectomy with prophylactic clip applications. Histopathological analysis revealed highly vascularized polypoid lesions, each with erosions, fibrinous exudate, and acute inflammation of the surface (**b**, arrows). The striking outgrowth of congestive capillary vessels (**c**, arrow), accompanied by acute and chronic inflammatory infiltrates (**c**, arrowheads) resembling granulation tissue, led to the diagnosis of pyogenic granuloma. During follow-up (7 months), the patient showed no further episodes of gastrointestinal bleeding, and hemoglobin levels remained stable at 9 g/dl. Pyogenic granulomas are benign vascular tumors that can be resected endoscopically. Multiple pyogenic granulomas in the stomach are very rare. (Informed consent was obtained from the patient to publish these images.)

<sup>1</sup>Department of Medicine II, Saarland University Medical Center, Homburg, Germany; <sup>2</sup>Institute of Pathology, Saarland University Medical Center, Homburg, Germany.

**Original Paper**

# The Overall Survival of Patients with Hepatocellular Carcinoma Correlates with the Newly Defined Time to Progression after Transarterial Chemoembolization

Tadaaki Arizumi Kazuomi Ueshima Mina Iwanishi Tomohiro Minami  
Hirokazu Chishina Masashi Kono Masahiro Takita Norihisa Yada  
Satoru Hagiwara Yasunori Minami Hiroshi Ida Yoriaki Komeda  
Mamoru Takenaka Toshiharu Sakurai Tomohiro Watanabe  
Naoshi Nishida Masatoshi Kudo

Department of Gastroenterology and Hepatology, Kindai University Faculty of Medicine,  
Osaka-Sayama, Japan

**Keywords**

Hepatocellular carcinoma · Kinki criteria · Overall survival · Time to progression after transarterial chemoembolization · Transarterial chemoembolization

**Abstract**

**Aim/Background:** The ultimate aim of any treatment for hepatocellular carcinoma (HCC) is to improve overall survival (OS); however, the clinical significance of time to progression (TTP) after transarterial chemoembolization (TACE) is unclear. This retrospective study examined the association between OS and the newly defined time to TACE progression (TTTP) to assess whether TTTP can be an alternative to OS in HCC patients with Barcelona Clinic Liver Cancer (BCLC) stage B. **Methods:** Between January 2006 and December 2013, 592 patients with HCC (BCLC B1,  $n = 118$ ; BCLC B2,  $n = 170$ ) underwent TACE. TTTP was then redefined as time to progression from the first image taken after TACE. The relationship between TTTP and OS was then examined based on survival time. **Results:** Survival analysis revealed significant differences in the OS of patients with BCLC B1 and those with BCLC B2 (median OS: 42.3 months, 95% confidence interval [CI] 34.4–50.7; and 29.3 months, 95% CI 26.1–37.6, respectively,  $p = 0.0348$ ). The median TTTP values were 9.5 months (95% CI 7.0–10.9) and 5.3 months (95% CI 4.6–6.7), respectively ( $p = 0.0078$ ). There was a moderate positive correlation between OS and TTTP for both B1 ( $R^2 = 0.6563$ ,  $p = 0.0045$ ) and B2 ( $R^2 = 0.6433$ ,  $p = 0.0052$ ) substages. There was also a positive correlation between OS and TTTP for the combined B1 and B2 substages

Masatoshi Kudo, MD, PhD  
Department of Gastroenterology and Hepatology  
Kindai University Faculty of Medicine  
377-2 Ohno-Higashi, Osaka-Sayama 589-8511 (Japan)  
E-Mail m-kudo@med.kindai.ac.jp



( $R^2 = 0.6590$ ,  $p = 0.0024$ ). **Conclusions:** There was a moderate correlation between the TTTP and OS of patients with HCC after TACE therapy, where the patients with short TTTP represented short OS, indicating that TTTP is an alternative parameter for survival analysis of HCC patients with BCLC stage B tumors who undergo TACE.

© 2017 S. Karger AG, Basel

## Introduction

Despite recent diagnostic and therapeutic advances, hepatocellular carcinoma (HCC) is still the third-most lethal malignancy worldwide and is associated with increasing mortality [1]. Nationwide follow-up surveys conducted by the Liver Cancer Study Group of Japan show that the total number of liver cancer deaths began to increase sharply in 1975, peaked in 2004, and declined again thereafter. It is noteworthy that the establishment of a nationwide HCC surveillance program contributed to improved overall survival (OS) rates [2]. With respect to treatment, sorafenib is effective for cases of advanced HCC [3, 4], and various embolic materials and catheters have been developed for transarterial chemoembolization (TACE) [5]. These advances have contributed to improved OS rates in the past decade. In addition to OS, studies examining the efficacy of anticancer agents and other interventions have examined time to progression (TTP), which is generally defined as the time from initiation of treatment intervention to tumor progression per Response Evaluation Criteria in Cancer of the Liver (RECIST), and is evaluated by comparing pretreatment images with follow-up images.

However, insufficient deposition of lipiodol, which is indicative of TACE failure, may mean that patients undergo further rounds of TACE, irrespective of whether tumor progression per RECIST is detected. In other words, whether or not progression is confirmed, TACE may be repeated in patients that show a progressive disease. Because this means that multiple TACE procedures could be performed even after tumor progression is confirmed, TTP (as a surrogate measure of evaluating survival) is not suitable for patients treated with TACE.

The effects of TACE can also be masked by the emergence of a new lesion, which is considered progressive disease according to the modified RECIST [6] and the Response Evaluation Criteria in Cancer of the Liver (RECICL) criteria [7]. Although TACE is recommended for patients with Barcelona Clinic Liver Cancer (BCLC) stage B HCC [8], a majority of patients undergoing TACE actually harbor multiple intrahepatic tumors or a single large hepatic tumor. Under these conditions, it is easily assumed that these HCCs will have a high frequency of intrahepatic metastasis; also, because of the biological characteristics of HCC, new lesions are likely to appear.

The appearance of new lesions immediately after TACE is indicative of “progression” and so the treatment response will be classified as progressive disease according to the RECIST and mRECIST criteria, despite any favorable response noted in the initially treated tumor. Currently, sorafenib is the only treatment strategy available after failure of TACE [9, 10]. However, in clinical practice, “progression” is not determined by development of a new small lesion, and switching from TACE to sorafenib or other therapies does not necessarily happen at this point. In such cases, it is conceivable that a favorable response by the treated tumor would improve survival, irrespective of the development of new lesions.

Although many clinical trials of TACE alone or targeted agents in combination with TACE use OS as a primary endpoint, it takes a long time before its effects are proved [11–13]. Furthermore, the OS benefit is diluted by prolonged post-progression survival [14], because post-trial treatments such as intra-arterial infusion chemotherapy, sorafenib, or other trial agents (including regorafenib, lenvatinib, or immunotherapy) can have a chance of marked antitumor effect, resulting in longer post-progression survival irrespective both in the testing

and control arms. However, TTP can be evaluated over a shorter period of time than OS; therefore, it would be a more desirable endpoint if it actually correlated with OS. To date, no trial except one [15] has used TTP as a primary endpoint because, as mentioned above, it is unsuitable for assessing the effects of TACE therapy [16]. So far, it is generally well known that TTP based on RECIST does not correlate with OS in targeted agent trials probably because treatment in both testing and control arms is often followed by other post-treatment anti-cancer agents or procedures [17–19]. In case of a TACE combination trial, the dilution effect on OS by post-trial anticancer treatment would be much larger since the OS of BCLC stage B HCC patients is longer than the OS of BCLC stage C HCC patients.

The aim of this study was to ascertain whether the newly defined time to TACE progression (TTTP) is a useful parameter for assessing the effects of TACE on HCC. Thus, we analyzed the correlation between OS and TTTP among HCC patients who underwent conventional TACE (cTACE) therapy.

## Materials and Methods

### *Patients*

Between January 2006 and August 2013, 592 patients with HCC underwent cTACE as a first-line treatment at Kindai University Hospital. Of these, 288 who had undergone cTACE during their clinical course and met the inclusion criteria were enrolled in this retrospective study. All patients satisfied the diagnostic criteria for HCC set out in the American Association for the Study of the Liver Disease guidelines. Clinicopathological variables, including demographic parameters, tumor staging (based on the number of focal lesions and the maximum diameter of contrast-enhanced [CE] lesions), Child-Pugh score, and BCLC stage, were collected at the time of referral (i.e., prior to treatment). The inclusion criteria were as follows: (1) a diagnosis of HCC based on histological examination, radiologic findings of early enhancement followed by late washout on CE-CT, or dynamic MRI; (2) performance status of 0; and (3) Child-Pugh class A or B preserved liver function. The exclusion criteria were as follows: (1) concomitant antineoplastic treatment and (2) lack of data before and after cTACE due to missing medical records. Patient characteristics are summarized and presented in Table 1. The patient population comprised 213 men and 75 women. Overall, 180 patients (62.5%) were positive for the antihepatitis C virus antibodies, 27 (9.4%) were positive for the hepatitis B virus surface antigen, and 81 (28.1%) were negative for both. 244 patients (84.8%) were classified as Child-Pugh class A. Epirubicin, miriplatin, and cisplatin were used as the TACE chemoagent in 265, 20, and 3 patients, respectively.

### *Kinki Criteria*

For substaging according to the Kinki criteria, patients were classified according to their Child-Pugh score (5–7 points or 8–9 points) and according to the number and diameter of the tumors using the Milan criteria and the up-to-seven criteria. Substage B1 cases had a Child-Pugh score of 5–7 and met the up-to-seven criteria; substage B2 cases had a Child-Pugh score of 5–7 and exceeded the up-to-seven criteria; substage B3 cases had a Child-Pugh score of 8–9 and any tumor status [20–23].

### *TACE Technique*

The right femoral artery was accessed using an 18-gauge Seldinger needle and a 4-Fr sheath inserted. The celiac artery was catheterized using a 4.2-Fr catheter, through which a 2.2-Fr microcatheter (Shirabe®; Piolax, Yokohama, Japan) was advanced coaxially into the common or proper hepatic artery. Rotational angiography was then performed to evaluate the vessels feeding identified tumors. The tip of the catheter was then placed into the segmental and subsegmental feeding arteries with assistance from selective hepatic angiography and/or tracking navigation imaging. Chemoembolization was then performed using 60–120 mg of miriplatin (Miripla®; Sumitomo Dainippon Pharma, Osaka, Japan), 20–50 mg of epirubicin (Epirubicin®; Nippon Kayaku, Tokyo, Japan), or 50–100 mg of cisplatin (IA-call®; Nippon Kayaku) emulsified in iodized oil (Lipiodol® Ultra-Fluid; Guerbet, Paris, France) containing gelatin sponge particles (Gelpart®; Nippon Kayaku, or Gelfoam®; Upjohn, Kalamazoo, MI, USA). The injection volume of the emulsion (<8 mL) was based on the tumor volume. Neither drug-eluting-bead TACE (DEB-TACE) nor balloon-occluded TACE (B-TACE) were utilized in this study.

**Table 1.** Characteristics of hepatocellular carcinoma patients treated with conventional transarterial chemoembolization therapy

Characteristic	All patients (N = 288)	B1 substage (n = 118)	B2 substage (n = 170)
Age, years	73 (67–77) <sup>a</sup>	74 (69–77.75) <sup>a</sup>	72.5 (66.25–77) <sup>a</sup>
Sex			
Male	213 (74.0)	86 (72.9)	127 (74.7)
Female	75 (26.0)	32 (27.1)	43 (25.3)
Child-Pugh score			
5	160 (55.6)	71 (60.2)	89 (52.4)
6	84 (29.2)	36 (30.5)	48 (28.2)
7	44 (15.3)	11 (9.3)	33 (19.4)
Virus status <sup>b</sup>			
HBV	27 (9.4)	12 (10.2)	15 (8.8)
HCV	180 (62.5)	77 (65.3)	103 (60.6)
Virus negative	81 (28.1)	29 (24.6)	52 (30.6)
Serum ALT, IU/L	37 (25.75–57.25) <sup>a</sup>	38 (22.25–61) <sup>a</sup>	37 (26.25–54.75) <sup>a</sup>
Serum ALP, IU/mL	334.5 (253–454.75) <sup>a</sup>	320.5 (242–448.25) <sup>a</sup>	348 (269–462.5) <sup>a</sup>
Serum platelets, 10 <sup>4</sup> /μL	12.7 (9.1–16.925) <sup>a</sup>	11.7 (8.7–15.5) <sup>a</sup>	13.35 (9.8–18.25) <sup>a</sup>
Serum AFP, ng/mL	25 (7–208)	20 (6.25–84.75) <sup>a</sup>	32 (8–360) <sup>a</sup>
Chemoagents			
Epirubicin	265 (92.0)	111 (94.1)	154 (90.6)
Miriaplatin	20 (6.9)	7 (5.9)	13 (7.6)
Cisplatin	3 (1.0)	0 (0)	3 (1.8)

Values are shown as *n* (%), unless otherwise indicated. ALT, alanine aminotransferase, ALP, alkaline phosphatase, AFP, alpha-fetoprotein, HBV, hepatitis B virus, HCV, hepatitis C virus.

<sup>a</sup> Dispersion variables are shown as median values (25–75%). <sup>b</sup> Cases testing positive for HBV surface antigen were considered cases of HBV-related hepatocellular carcinoma (HCC); those testing positive for HCV antibody were considered cases of HCV-related HCC.

#### Time to TACE Progression

CE-CT or CE-MRI was initially performed at 1 month after TACE therapy to obtain baseline images. These were then compared with images taken every 1–3 months after therapy. To assess the target lesions, the 5 largest tumors were selected from the intrahepatic lesions for the total of maximum diameter of each viable lesion in one dimension measurement. Progression was defined as a  $\geq 20\%$  increase relative to the post-treatment images (baseline images) in the summed diameter of the 5 largest tumors on post-treatment images. The appearance of vascular invasion or extrahepatic spread was also regarded as progression. TTTP was defined as the interval from the day of baseline images after treatment to the time of progression. For example, if a  $\geq 20\%$  increase in the summed diameter was observed on images obtained 1 month after baseline, progression was deemed to have occurred at 1 month after treatment: the TTTP would therefore be 1 month.

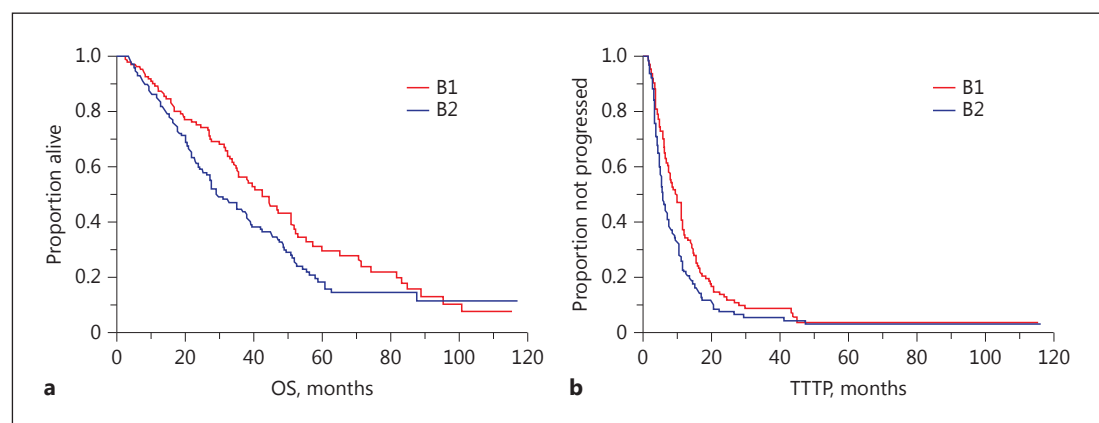
#### Statistical Analysis

The outcome of interest, OS, was calculated from the date of the first cTACE to the date of death or last clinic follow-up. Patients were followed up until October 2016. OS was calculated using 2 methods. First, institutional electronic medical records were checked to confirm each patient's vital status or date of death, if available. Second, all patients who remained alive and patients of unknown vital status were censored at the last known clinical follow-up date. Kaplan-Meier survival curves were plotted, and the significance of differences was assessed using the log-rank test. Categorical variables were compared using the Bonferroni-corrected Mann-Whitney U test. Differences with a two-tailed *p* value of  $< 0.05$  were considered statistically significant. To examine relationships between TTTP and OS of the patients, the Pearson correlation test was applied. Any discrepancies between OS and TTTP were identified from correlation plots. All analyses were performed using the SPSS Medical Pack for Windows, version 10.0 (SPSS, Inc., Chicago, IL, USA).

**Table 2.** Relationship between TTTP and OS in patients with B1 substage hepatocellular carcinoma

TTTP range	Patients (N = 118)	Median OS (95% CI), months	25th–75th percentile of OS
0–5 months	34	27.0 (2.2–84.5)	8.5–40.4
5–10 months	32	24.7 (5.6–100.4)	13.9–39.4
10–15 months	21	30.2 (8.0–108.7)	15.7–50.3
15–20 months	13	47.0 (16.0–113.4)	31.4–55.0
20–25 months	6	46.4 (23.5–71.1)	39.2–55.3
25–30 months	3	54.5 (46.7–88.4)	50.6–71.5
30–35 months	2	34.4 (33.4–35.3)	33.9–34.8
35–40 months	1	37.4 (37.4–37.4)	37.4–37.4
40–45 months	4	62.7 (44.0–88.2)	44.0–83.1
45–50 months	0		
>50 months	2	89.2 (63.2–115.2)	76.2–102.1

TTTP, time to transarterial chemoembolization progression; OS, overall survival; CI, confidence interval.



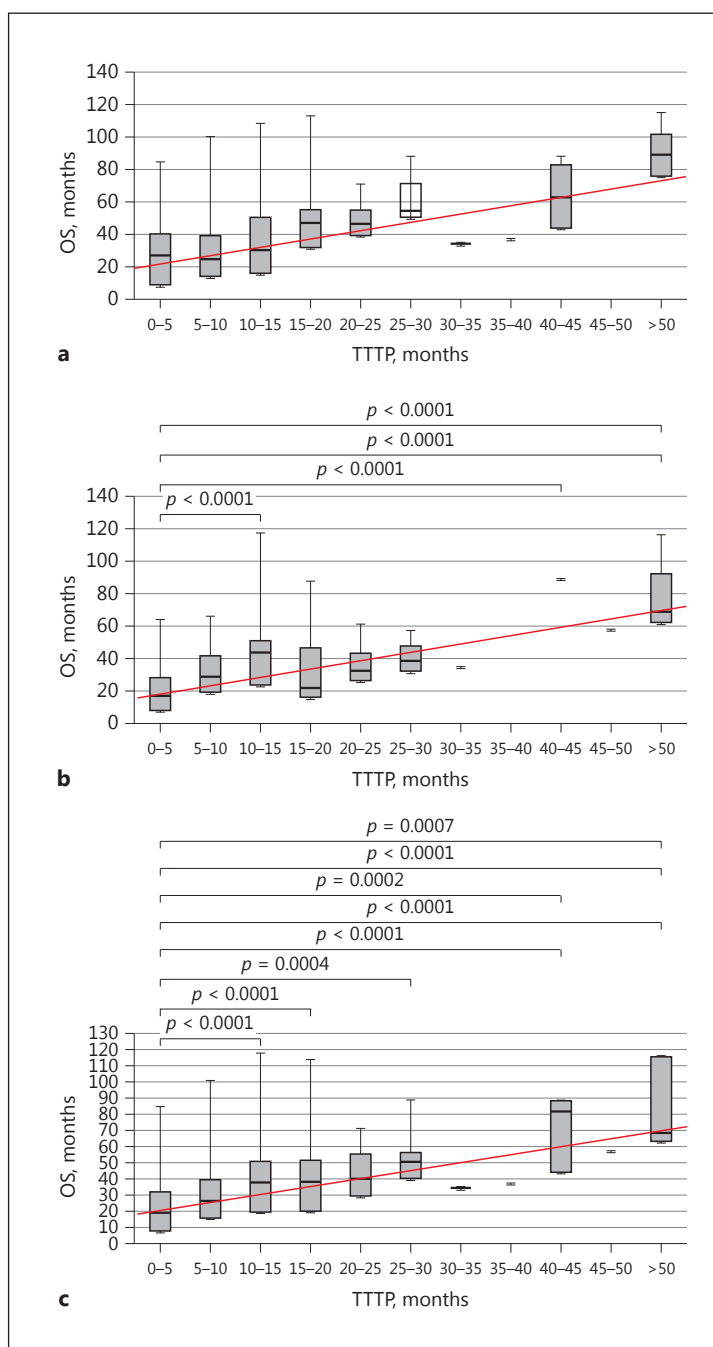
**Fig. 1.** Comparison of overall survival (OS) (**a**) and the newly defined time to transarterial chemoembolization progression (TTTP) (**b**) in patients with B1 and B2 substage hepatocellular carcinoma. **a** Comparison of survival curves reveals median OS values of 42.3 months (95% confidence interval [CI] 34.4–50.7) and 29.3 months (95% CI 26.1–37.6) for the B1 and B2 substage groups, respectively ( $p = 0.0348$ ). **b** Comparison of survival curves reveals median TTTP values of 9.5 months (95% CI 7.0–10.9) and 5.3 months (95% CI 4.6–6.7) for the B1 and B2 substage groups, respectively ( $p = 0.0078$ ).

## Results

### OS and TTTP

The median OS value for BCLC substage B1 and B2 patients combined was 35.3 months (95% confidence interval [CI] 31.4–41.7). When we compared OS and TTTP among the B1 and B2 substage groups using Kaplan-Meier estimates, we found a significant intergroup difference in the median OS values: 42.3 months (95% CI 34.4–50.7) for group B1 and 29.3 months (95% CI 26.1–37.6) for group B2 ( $p = 0.0348$ ) (Fig. 1a). Further comparison revealed a significant difference between the groups in terms of the median TTTP, with values of 9.5 months (95% CI 7.0–10.9) for group B1 and 5.3 months (95% CI 4.6–6.7) for group B2 ( $p = 0.0078$ ) (Fig. 1b).

**Fig. 2.** Correlation plots of overall survival (OS) and time to transarterial chemoembolization progression (TTTP). The correlation between OS (y axis) and TTTP (x axis) for the B1 (a) and B2 (b) substage groups was assessed separately. A combined analysis was also conducted (c). Each *p* value shown in the panels was calculated by Bonferroni-corrected Mann-Whitney U test. Both substages demonstrated a positive moderate correlation, with  $R^2$  values of 0.6563 ( $p = 0.0045$  by Pearson correlation test) (a) and 0.6433 ( $p = 0.0052$ ) (b) for the B1 and B2 substages, respectively. The combined 2 substages (c) also exhibited a positive correlation with each other ( $R^2 = 0.6590$ ,  $p = 0.0024$ ).



#### Association between OS and TTTP

To determine the effect of TTTP on OS, we classified TTTP into subgroups based on duration, with a 5-month range per group.

The median OS values for each TTTP range in the B1 substage group are presented in Table 2. Although there was no significant difference in the median OS among these subgroups, Pearson correlation analysis revealed the positive correlation between TTTP and OS where the patients with short TTTP represented short OS and those with long TTTP showed long OS; the median OS values (25–75th percentile) of the group with a TTTP range of 0–5 months and those of the group with TTP >50 months were 89.2 months (76.2–102.1) and 27.0 months



**Table 3.** Relationship between TTTP and OS in patients with B2 substage hepatocellular carcinoma

TTTP range	Patients (N = 170)	Median OS (95% CI), months	25th–75th percentile of OS
0–5 months	81	16.9 (0.4–63.9)	7.4–27.9
5–10 months	37	28.8 (7.7–65.6)	18.8–41.5
10–15 months	26	43.6 (11.5–116.9)	23.4–50.7
15–20 months	13	21.5 (15.2–87.3)	16.0–46.6
20–25 months	4	32.2 (22.4–60.5)	26.0–43
25–30 months	3	38.3 (25.3–56.8)	31.8–47.5
30–35 months	1	34.7 (34.7–34.7)	34.7–34.7
35–40 months	0		
40–45 months	1	88.8 (88.8–88.8)	88.8–88.8
45–50 months	1	57.5 (57.5–57.5)	57.5–57.5
>50 months	3	68.2 (55.6–115.7)	61.9–92.0

TTTP, time to transarterial chemoembolization progression; OS, overall survival; CI, confidence interval.

**Table 4.** Relationship between TTTP and OS in patients with B1 and B2 substage hepatocellular carcinoma

TTTP range	Patients (N = 288)	Median OS (95% CI), months	25th–75th percentile of OS
0–5 months	115	19.4 (0.4–84.5)	8.1–32.2
5–10 months	69	26.7 (5.6–100.4)	16.3–40.0
10–15 months	47	37.7 (8.0–116.9)	19.9–50.5
15–20 months	26	38.4 (15.2–113.4)	20.5–51.6
20–25 months	10	40.2 (22.4–71.1)	19.6–55.3
25–30 months	6	50.6 (25.3–88.4)	40.4–56.2
30–35 months	3	34.7 (33.4–35.3)	34.1–35.0
35–40 months	1	37.4 (37.4–37.4)	37.4–37.4
40–45 months	5	81.4 (44.0–88.8)	44.1–88.2
45–50 months	1	57.5 (57.5–57.5)	57.5–57.5
>50 months	5	68.2 (55.6–115.7)	63.2–115.1

TTTP, time to transarterial chemoembolization progression; OS, overall survival; CI, confidence interval.

(8.5–40.4), respectively ( $R^2 = 0.6563$ ,  $p = 0.0045$ ) (Fig. 2a; Table 2). For the B2 substage group, the corresponding median OS values are presented in Table 3. A significant difference was observed for the median OS in several comparisons: between the groups with OS of 0–5 and 10–15 months ( $p < 0.0001$ ), 0–5 and 40–45 months ( $p < 0.0001$ ), 0–5 and >50 months ( $p < 0.0001$ ), and 5–10 and >50 months ( $p < 0.0001$ ) subgroups. In addition, there was a significant positive correlation between OS and TTTP in B2 substages by Pearson correlation analysis ( $R^2 = 0.6433$ ,  $p = 0.0052$ ) (Fig. 2b).

The median OS values for each TTTP range when the B1 and B2 substages were combined are presented in Table 4. There was also a significant difference in the median OS between the groups with OS of 0–5 and 10–15 months ( $p < 0.0001$ ), 0–5 and 15–20 months ( $p < 0.0001$ ), 0–5 and 25–30 months ( $p = 0.0004$ ), 0–5 and 40–45 months ( $p < 0.0001$ ), 0–5 and >50 months ( $p < 0.0001$ ), 5–10 and 40–45 months ( $p = 0.0002$ ), 5–10 and >50 months ( $p < 0.0001$ ), and 10–15 and >50 months ( $p = 0.0007$ ) subgroups. A significant positive correlation was observed between OS and TTTP for the combined B1 and B2 substages ( $R^2 = 0.6590$ ;  $p = 0.0024$ ) (Fig. 2c).

## Discussion

Here, we compared OS and TTTP among patients with substage B1 and B2 HCC. The results according to the Kinki criteria showed that those with substage B1 HCC undergoing cTACE had longer OS and TTTP than those with substage B2 undergoing cTACE. Moreover, OS correlated with TTTP: patients with a longer OS also had a longer TTTP.

Despite administering standard-of-care therapy according to established guidelines, in clinical practice we sometimes encounter patients who present with tumor progression shortly after treatment. These tumors may be resistant to further treatment and the patients often have a poor prognosis.

Early intrahepatic metastasis of HCC may be caused by dissemination of tumor cells via the portal vein [24]. Insufficient deposition of lipiodol may allow TACE-resistant tumors to survive; subsequent dissemination of residual HCC cells via the portal vein leads to early recurrence and a poor prognosis [25]. Here, we assumed that the inefficacy of various post-treatments against the highly malignant tumors meant that patients with a short TTTP also had a short OS.

Currently, many clinical trials of TACE use OS as the primary endpoint because it is not clear whether TTP per RECIST truly reflects OS. Here, we observed median OS values of 42.3 months for the B1 substage group and 29.3 months for the B2 substage group. These median survival times are quite long (>2 years); therefore, any clinical trial that uses OS as an endpoint would require a very long follow-up period. However, the median values for TTTP were 9.5 months for the B1 group and 5.3 months for the B2 group; these times are clearly much shorter and correlate with OS. Thus, the data suggest that TTTP is a suitable endpoint of clinical trials because it requires a shorter follow-up period than OS.

Having said that, a few cTACE-naïve patients showed a discrepancy between OS and TTTP (i.e., some showed a long OS and a short TTTP). One possible reason for this is that a second round of cTACE might have been effective, thereby extending OS. For example, several types of anticancer agents can be used alongside with cTACE. Such second-line chemotherapy agents might have improved the treatment effects. In addition, new TACE procedures such as DEB-TACE (which uses drug-eluting beads) and B-TACE (which uses balloon occlusion techniques) were available for the second round. Another possible reason is that post-cTACE treatment might have been effective, thereby contributing to the long OS observed in some cases with a short TTTP. For example, the use of sorafenib to treat patients with TACE-refractory disease and a short TTTP actually prolongs OS [9, 10]. However, in general we found that OS correlated with TTTP in patients with B1 or B2 substage HCC. Taken together, these results suggest that TTTP can predict OS after TACE. Thus, TTTP is a potential surrogate endpoint for OS in future clinical trials testing the effects of TACE, or new agents combined with TACE, on HCC.

## Disclosure Statement

The authors have no conflicts of interest to declare.

## References

- 1 Jemal A, Siegel R, Xu J, Ward E: Cancer statistics, 2010. *CA Cancer J Clin* 2010;60:277–300.
- 2 Kudo M: Surveillance, diagnosis, treatment, and outcome of liver cancer in Japan. *Liver Cancer* 2015;4:39–50.
- 3 Cheng AL, Kang YK, Chen Z, Tsao CJ, Qin S, Kim JS, Luo R, et al: Efficacy and safety of sorafenib in patients in the Asia-Pacific region with advanced hepatocellular carcinoma: a phase III randomised, double-blind, placebo-controlled trial. *Lancet Oncol* 2009;10:25–34.
- 4 Llovet JM, Bruix J: Molecular targeted therapies in hepatocellular carcinoma. *Hepatology* 2008;48:1312–1327.
- 5 Minami Y, Minami T, Chishina H, Arizumi T, Takita M, Kitai S, Yada N, et al: Balloon-occluded transcatheter arterial chemoembolization for hepatocellular carcinoma: a single-center experience. *Oncology* 2015;89(suppl 2):27–32.
- 6 Lencioni R, Llovet JM: Modified RECIST (mRECIST) assessment for hepatocellular carcinoma. *Semin Liver Dis* 2010;30:52–60.
- 7 Kudo M, Ueshima K, Kubo S, Sakamoto M, Tanaka M, Ikai I, Furuse J, et al: Response Evaluation Criteria in Cancer of the Liver (RECICL) (2015 revised version). *Hepatol Res* 2016;46:3–9.
- 8 Bruix J, Reig M, Sherman M: Evidence-based diagnosis, staging, and treatment of patients with hepatocellular carcinoma. *Gastroenterology* 2016;150:835–853.
- 9 Ogasawara S, Chiba T, Ooka Y, Kanogawa N, Motoyama T, Suzuki E, Tawada A, et al: Efficacy of sorafenib in intermediate-stage hepatocellular carcinoma patients refractory to transarterial chemoembolization. *Oncology* 2014;87:330–341.
- 10 Arizumi T, Ueshima K, Minami T, Kono M, Chishina H, Takita M, Kitai S, et al: Effectiveness of sorafenib in patients with transcatheter arterial chemoembolization (TACE) refractory and intermediate-stage hepatocellular carcinoma. *Liver Cancer* 2015;4:253–262.
- 11 Kudo M, Han G, Finn RS, Poon RT, Blanc JF, Yan L, Yang J, et al: Brivanib as adjuvant therapy to transarterial chemoembolization in patients with hepatocellular carcinoma: a randomized phase III trial. *Hepatology* 2014;60:1697–1707.
- 12 Meyer T, Kirkwood A, Roughton M, Beare S, Tsochatzis E, Yu D, Davies N, et al: A randomised phase II/III trial of 3-weekly cisplatin-based sequential transarterial chemoembolisation vs embolisation alone for hepatocellular carcinoma. *Br J Cancer* 2013;108:1252–1259.
- 13 Zhou B, Yan Z, Liu R, Shi P, Qian S, Qu X, Zhu L, et al: Prospective study of transcatheter arterial chemoembolization (TACE) with ginsenoside Rg3 versus TACE alone for the treatment of patients with advanced hepatocellular carcinoma. *Radiology* 2016;280:630–639.
- 14 Terashima T, Yamashita T, Takata N, Nakagawa H, Toyama T, Arai K, Kitamura K, et al: Post-progression survival and progression-free survival in patients with advanced hepatocellular carcinoma treated by sorafenib. *Hepatol Res* 2016;46:650–656.
- 15 Kudo M, Imanaka K, Chida N, Nakachi K, Tak WY, Takayama T, Yoon JH, et al: Phase III study of sorafenib after transarterial chemoembolisation in Japanese and Korean patients with unresectable hepatocellular carcinoma. *Eur J Cancer* 2011;47:2117–2127.
- 16 Llovet JM, Di Bisceglie AM, Bruix J, Kramer BS, Lencioni R, Zhu AX, Sherman M, et al: Design and endpoints of clinical trials in hepatocellular carcinoma. *J Natl Cancer Inst* 2008;100:698–711.
- 17 Cainap C, Qin S, Huang WT, Chung IJ, Pan H, Cheng Y, Kudo M, et al: Linifanib versus Sorafenib in patients with advanced hepatocellular carcinoma: results of a randomized phase III trial. *J Clin Oncol* 2015;33:172–179.
- 18 Zhu AX, Park JO, Ryoo BY, Yen CJ, Poon R, Pastorelli D, Blanc JF, et al: Ramucirumab versus placebo as second-line treatment in patients with advanced hepatocellular carcinoma following first-line therapy with sorafenib (REACH): a randomised, double-blind, multicentre, phase 3 trial. *Lancet Oncol* 2015;16:859–870.
- 19 Llovet JM, Decaens T, Raoul JL, Boucher E, Kudo M, Chang C, Kang YK, et al: Brivanib in patients with advanced hepatocellular carcinoma who were intolerant to sorafenib or for whom sorafenib failed: results from the randomized phase III BRISK-PS study. *J Clin Oncol* 2013;31:3509–3516.
- 20 Kudo M: Heterogeneity and subclassification of Barcelona Clinic Liver Cancer Stage B. *Liver Cancer* 2016;5:91–96.
- 21 Arizumi T, Ueshima K, Iwanishi M, Minami T, Chishina H, Kono M, Takita M, et al: Validation of Kinki Criteria, a modified substaging system, in patients with intermediate stage hepatocellular carcinoma. *Dig Dis* 2016;34:671–678.
- 22 Arizumi T, Ueshima K, Iwanishi M, Minami T, Chishina H, Kono M, Takita M, et al: Validation of a modified substaging system (Kinki Criteria) for patients with intermediate-stage hepatocellular carcinoma. *Oncology* 2015;89(suppl 2):47–52.
- 23 Kudo M, Arizumi T, Ueshima K, Sakurai T, Kitano M, Nishida N: Subclassification of BCLC B stage hepatocellular carcinoma and treatment strategies: proposal of modified Bolondi's Subclassification (Kinki Criteria). *Dig Dis* 2015;33:751–758.
- 24 Sakon M, Umeshita K, Nagano H, Eguchi H, Kishimoto S, Miyamoto A, Ohshima S, et al: Clinical significance of hepatic resection in hepatocellular carcinoma: analysis by disease-free survival curves. *Arch Surg* 2000;135:1456–1459.
- 25 Adachi E, Matsumata T, Nishizaki T, Hashimoto H, Tsuneyoshi M, Sugimachi K: Effects of preoperative transcatheter hepatic arterial chemoembolization for hepatocellular carcinoma. The relationship between postoperative course and tumor necrosis. *Cancer* 1993;72:3593–3598.

## CASE REPORT

# A Case of Waldenstrom Macroglobulinemia with Temporary Appearance of 7S IgM Half Molecule

Mayumi Imoto<sup>1,6</sup>, Koji Yoshida<sup>2</sup>, Yasuhiro Maeda<sup>3</sup>, Ken-Ichi Nakae<sup>1</sup>, Masatoshi Kudo<sup>4</sup>,  
Ikunosuke Sakurabayashi<sup>5</sup>, Toshiyuki Yamada<sup>6</sup>, Toshinori Kamisako<sup>1,7</sup>

<sup>1</sup> Department of Clinical Laboratory, Kindai University Hospital, Ohnohigashi, Osakasayama, Japan

<sup>2</sup> Faculty of Biology-Oriented Science and Technology, Kindai University, Kinokawa, Wakayama, Japan

<sup>3</sup> Department of Hematology, National Hospital Organization Osaka Minami Medical Center, Kidohigashi-machi, Kawachinagano, Japan

<sup>4</sup> Department of Gastroenterology and Hepatology, Kindai University Faculty of Medicine, Ohnohigashi, Osakasayama, Japan

<sup>5</sup> Department of Integrated Medicine, Saitama Memorial Hospital, Minumaku, Saitama, Japan

<sup>6</sup> Department of Clinical Laboratory Medicine, Jichi Medical University, Yakushiji, Shimotsuke, Japan

<sup>7</sup> Department of Clinical Laboratory Medicine, Kindai University Faculty of Medicine, Ohnohigashi, Osakasayama, Japan

## SUMMARY

**Background:** We encountered a rare case of Waldenstrom macroglobulinemia with temporary appearance of 7S IgM half molecule and with monoclonal proteins binding to agarose gel.

**Methods:** The patient's serum and urine were analyzed using sodium dodecyl sulfate-polyacrylamide gel electrophoresis and immunoblotting. The N-terminal amino acid sequences of the IgM with abnormal mass (68 kDa) were determined and compared with those of known immunoglobulin.

**Results:** The 68 kDa IgM consisted of a defective  $\mu$  chain (36 kDa) and an intact  $\kappa$  chain. N-terminal amino acid sequence analysis demonstrated that the defective  $\mu$  chain had the variable region of IgM. The agarose gel-binding ability of the IgM- $\kappa$  M-protein was lost after reduction or alkaline treatment of serum.

**Conclusions:** The 7S half molecule IgM in the present case may miss a large part of the constant region of the  $\mu$  chain.

(Clin. Lab. 2017;63:983-989. DOI: 10.7754/Clin.Lab.2017.170106)

## Correspondence:

Mayumi Imoto  
Department of Clinical Laboratory  
Kindai University Hospital  
377-2 Ohnohigashi  
589-8511 Osakasayama  
Japan  
Phone: +81 72-366-0221  
Fax: +81 72-366-0206  
Email: maimoto@zmail.plala.or.jp

## KEY WORDS

7S IgM half-molecule, N-terminal amino acid sequence, agarose gel binding, Waldenstrom macroglobulinemia

## LIST OF ABBREVIATIONS

LMW - low molecular weight  
SDS-PAGE - sodium dodecyl sulfate-polyacrylamide gel electrophoresis

## INTRODUCTION

The half-molecule (HM) immunoglobulin (Ig) consists of a light chain and a structurally defective heavy chain. In 1969, Hobbs et al. [1] first reported HM IgG in a patient with soft tissue plasmacytoma. Thus far, HM IgG

[1], IgA [2,3], and IgM [4] have been reported; however, the number of cases is small. In 1999, we reported the first case of HM 7S IgM in a patient with Waldenstrom macroglobulinemia [4]. In this initial case, 20 N-terminal amino acid residues of the defective  $\mu$  chain sequence were identical to those of the intact  $\kappa$  chain. Here we report another case of HM 7S IgM, which temporarily appeared in the blood and urine of a patient with Waldenstrom macroglobulinemia. In this patient, the serum IgM- $\kappa$  M-protein showed an agarose gel-binding ability. We report the immunochemical characteristics of these abnormal proteins.

## CASE

The patient was a 60-year-old male referred to our hospital because of hyper- $\gamma$  globulinemia. The laboratory findings were white blood cell count: 6,900/ $\mu$ L (4,000 - 8,000/ $\mu$ L), red blood cell count: 373 x 10<sup>4</sup>/ $\mu$ L (420 - 540 x 10<sup>4</sup>/ $\mu$ L), hematocrit: 35.7% (39 - 51%), hemoglobin concentration: 122 g/L (125 - 175 g/L), and total protein: 101 g/L (65 - 82 g/L). The IgM level was 58.88 g/L (0.7 - 4.7 g/L), showing a marked increase, and the IgG and IgA levels were 6.51 g/L (8.0 - 20 g/L) and 0.49 g/L (0.7 - 4.7 g/L), respectively. The M-protein zone (49.3%, 49.8 g/L) was noted in the fast  $\gamma$  region on serum fractionation and urine Bence Jones protein (BJP) was positive. Rheumatoid factor was 7 IU/mL (< 15 IU/mL). In the bone marrow, lymphocytes were increased up to 12.1% (CD19: 48.4%, CD20: 56.8%) was observed while normal plasma cells accounted for 1.2%. Based on these data, the patient was clinically diagnosed with Waldenstrom macroglobulinemia. On serum immunoelectrophoresis (IEP), IgM- $\kappa$  M-protein was identified (Figure 1). On serum immunofixation electrophoresis (IFE), not only the bands reactive with anti- $\mu$  and anti- $\kappa$  chain antibodies but also the bands reactive with anti- $\gamma$ , anti- $\alpha$ , and anti- $\lambda$  chain antibodies, suggesting that the M-proteins were bound to agarose and remained even after deproteinization (Figure 2). Apart from the M-protein band, faint bands reacting to anti- $\mu$  and  $\kappa$  chain antibodies were observed on the anode side (Figure 2). A band reactive with anti- $\mu$  chain and  $\kappa$ -type BJP was detected in urine on IFE (Figure 3). This finding suggested the existence of low molecular weight (LMW) IgM. The possible LMW IgM disappeared after 3 weeks of chemotherapy with fludarabine phosphate.

## MATERIALS AND METHODS

### Materials

PD-10 (GE Healthcare, Buckinghamshire, UK) was used to replace urine with buffer, and Minicon (Millipore, Billerica, MA, USA) was used to concentrate urine. For immunological reactions, rabbit anti-human Ig, anti-human  $\gamma$  chain, anti-human  $\alpha$  chain, anti-human

$\mu$  chain, anti-human  $\kappa$  chain, and anti-human  $\lambda$  chain antibodies (DAKO, Copenhagen, Denmark) were used. For IEP, a commercial IEP agarose plate (Helena, Beaumont, TX, USA) was used with ionic strength 0.06 veronal buffer (pH 8.6) [5]. Titan Gel IFE (Helena) was used for IFE. For molecular weight markers, a LMW marker kit (GE Healthcare) was used. As secondary antibody, peroxidase-labeled goat anti-rabbit Ig (MBL, Nagoya, Japan) was used. Polyvinylidene difluoride (PVDF) membrane (Millipore) was used for immunoblotting.

### Molecular mass estimation of LMW IgM

The molecular weight of LMW IgM was investigated both with and without dithiothreitol (DTT) using sodium dodecyl sulfate-polyacrylamide gel electrophoresis (SDS-PAGE). DTT was used as the reducing agent. For SDS-PAGE, 7 - 15% and 10 - 15% gradient polyacrylamide gels were prepared following the method reported by Laemmli [6]. Protein was stained with Coomassie Brilliant Blue R-250 (CBB). Immunoblotting was performed using a blotting device (BIO CRAFT, Tokyo, Japan) in which proteins were electrically transferred to PVDF membrane at 200 mA for 45 minutes, and the blot was stained by peroxidase-labeled enzyme immunoassay employing Towbin's method [7].

### Two-dimensional electrophoresis of LMW IgM

Two-dimensional electrophoresis was performed to estimate the components of LMW IgM [4]. Using the patient's urine, the first SDS-PAGE (1st PAGE) was performed without reducing treatment, and the target band was excised from the gel. This gel fragment was reduced with DTT in 37°C for 60 minutes and applied to the second SDS-PAGE (2nd PAGE) to analyze the components of LMW IgM.

### N-terminal amino acid sequence analysis of LMW IgM

The N-terminal amino acid sequences of LMW IgM were analyzed as previously reported [8]. After SDS-PAGE of the target abnormal  $\mu$  and  $\kappa$  chains, the proteins were transferred to a PVDF membrane and stained. The N-terminal amino acid sequences were analyzed using a 477-A Protein Sequencer (ABI, Foster City, CA, USA). The determined N-terminal amino acid sequences were compared with the FASTA version 3 database.

### Reactivity of IgM- $\kappa$ M-protein with agarose gel

Agar gel (1.5%), agarose gel (1.5%), and agar/agarose mixture gel (agar:agarose = 1:1) were used for electrophoresis. After electrophoresis, the gels were deproteinized and desalted, and the protein binding state was observed by protein staining. The patient's serum was serially diluted 2-fold, and the maximum dilution factor showing the reactivity was investigated. To investigate the mechanism of binding to agarose, the patient's serum was subjected to treatment with 30 mM DTT, 4 M



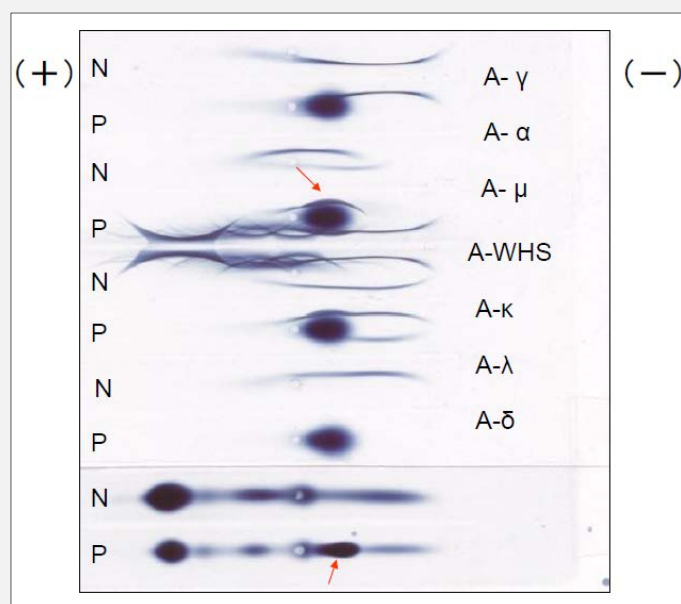


Figure 1. Immunoelectrophoretic pattern of the patient's serum.

IgM-κ M-protein was identified in the β over the fast γ region. A protein band indicated by the arrow was present at a site corresponding to M-protein. N - normal serum, P - patient's serum, A-γ - anti-human γ heavy chain antibodies, A-α - anti-human α heavy chain antibodies, A-μ - anti-human μ heavy chain antibodies, A-WHS - anti-human whole serum antibodies, A-κ - anti-human κ light chain antibodies, A-λ - anti-human λ light chain antibodies, A-δ - anti-human δ heavy chain antibodies.

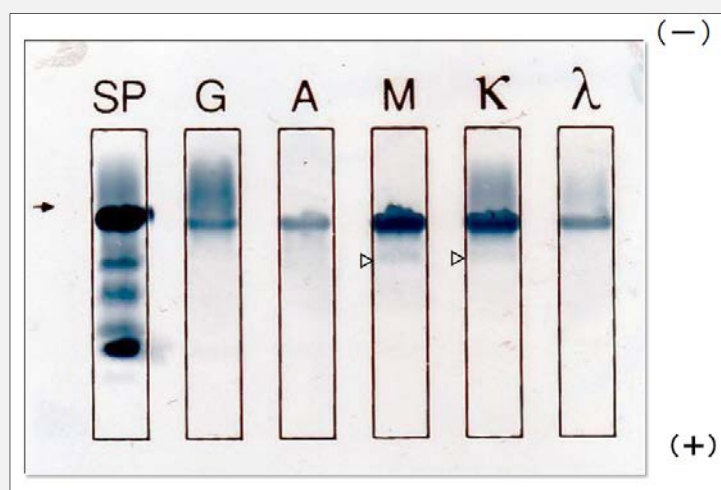
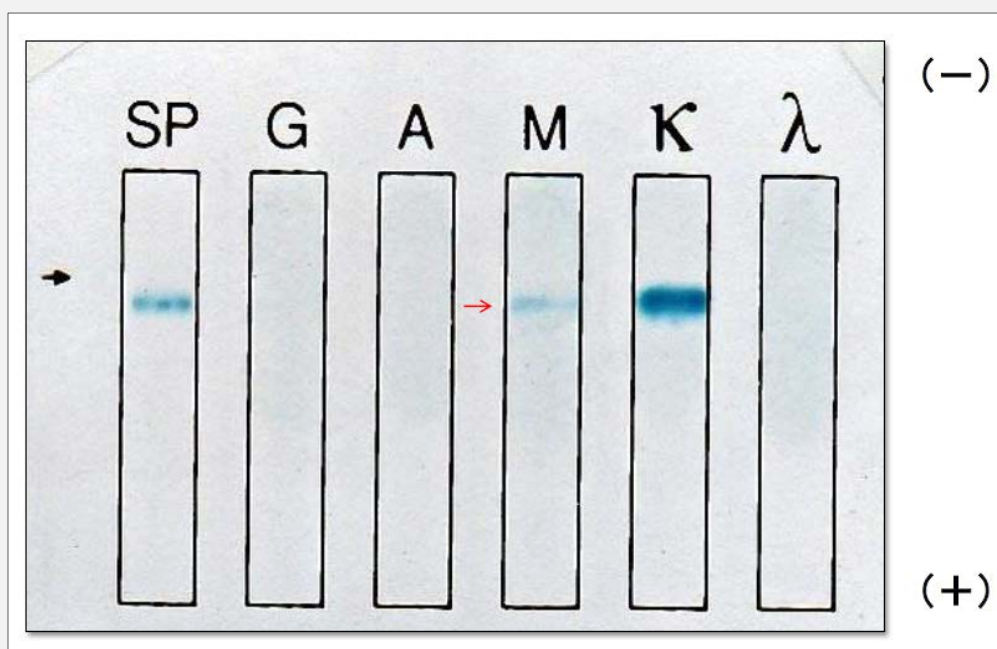


Figure 2. Immunofixation electrophoresis pattern of the patient's serum.

Bands reactive with anti-γ (lane G), α (lane A), and λ (lane λ) chain antibodies were observed in the position corresponding to IgM-κ type M-protein. Furthermore, bands (⤵) reacting to antibody μ and κ were slightly observed on the anode side. The position of the samples applied is indicated by the arrow. SP - stain protein, G - anti-human γ heavy chain antibodies, A - anti-human α heavy chain antibodies M - anti-human μ heavy chain antibodies, κ - anti-human κ light chain antibodies, λ - anti-human λ light chain antibodies.



**Figure 3. Immunofixation pattern of the patient's urine.**

A band detected with anti- $\mu$  heavy chain antibodies in addition to  $\kappa$ -type Bence Jones protein was observed (red arrow). The sample application point is indicated by a black arrow. SP - stain protein, G - anti-human  $\gamma$  heavy chain antibodies, A - anti-human  $\alpha$  heavy chain antibodies, M - anti-human  $\mu$  heavy chain antibodies,  $\kappa$  - anti-human  $\kappa$  light chain antibodies,  $\lambda$  - anti-human  $\lambda$  light chain antibodies.

urea, 1 M acetic acid, 1.7 M KOH, 10% Triton X-100, and 1 M NaCl [9]. The patient's serum and treatment solution were mixed at 3:1 and applied to agarose gel electrophoresis. The gel was deproteinized and stained with CBB.

## RESULTS

### Molecular mass estimation of LMW IgM and confirmation of components by two-dimensional electrophoresis

In serum, the 193 kDa and 68 kDa bands reacted with anti- $\mu$  chain antibodies under non-reducing conditions. In urine, only the 68 kDa band reacted. With anti- $\kappa$  chain antibody, the 193, 68, 43, and 28 kDa (BJP- $\kappa$ ) bands reacted, other than IgG (162 kDa), in serum, and the 68, 43, and 28 kDa bands reacted in urine (Figure 4). After reducing treatment, the 74 (normal size), 49, and 36 kDa bands reacted with anti- $\mu$  chain antibodies in serum, and a 36 kDa band was the main reactive band in urine (Figure 5). The two-dimensional electrophoresis revealed that the 68 kDa IgM was composed of a defective 36 kDa  $\mu$  chain and an intact 28 kDa  $\kappa$  chain (Figure 6).

### N-terminal amino acid sequence analysis

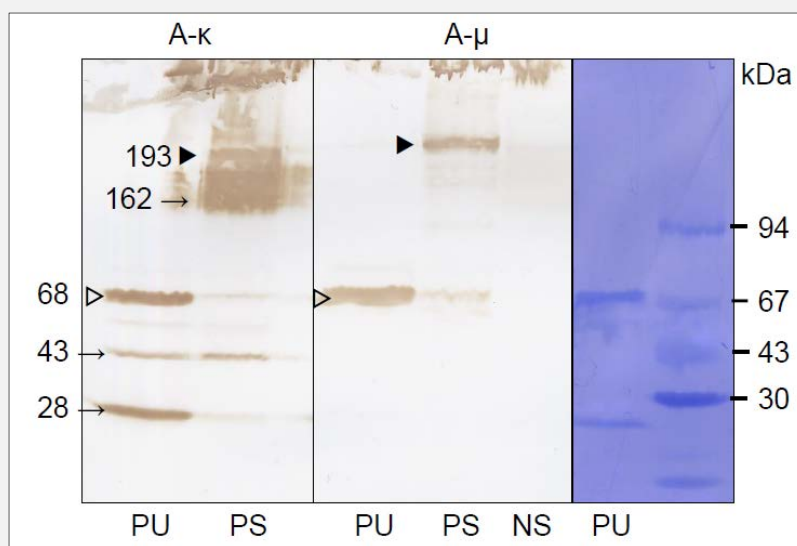
The 36 kDa band had N-terminal sequences sharing 94% identity with those of a known IgM V-L [10] and the  $\kappa$  chain shares 100% identity with that of a known  $\kappa$  chain (FASTA, version3).

### Reactivity with agarose gel

On IEP with three types of gel: 1.5% agar, 1.5% agarose gel, and agar/agarose gel mixture, M-protein was detected in serum even at a dilution of 256 times (IgM: 23 mg/dL). The agarose gel-binding ability was lost after reduction by 30 mM DTT or after alkaline treatment with 1.7 M KOH (Figure7).

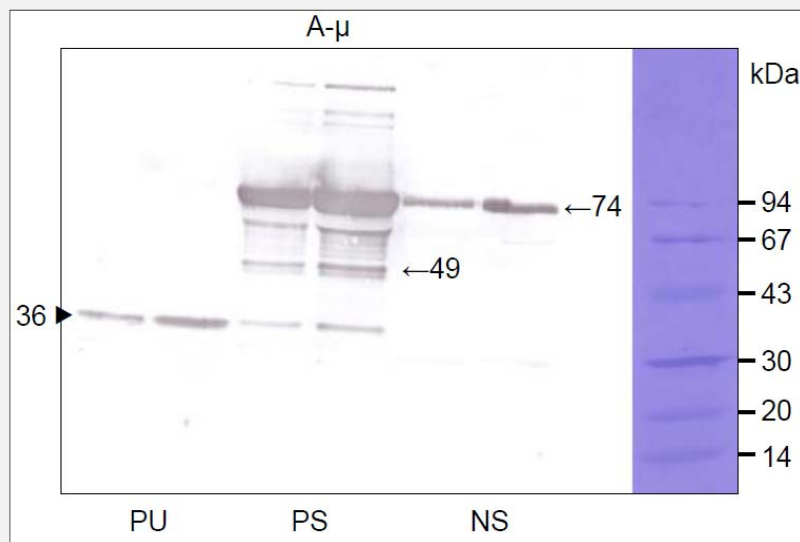
## DISCUSSION

We suspected the appearance of LMW IgM in the patient serum and urine as an anti- $\mu$  chain antibodies-reactive band. Sequential analyses of immunoblot suggested that the LMW IgM was composed of a defective  $\mu$  chain and an intact  $\kappa$  chain. The molecular size and N-terminus structure of the defective  $\mu$  chain suggested the deficit of CH2 to CH4 domains. Finally, the LMW IgM is defined as a half molecule 7S IgM with a defec-



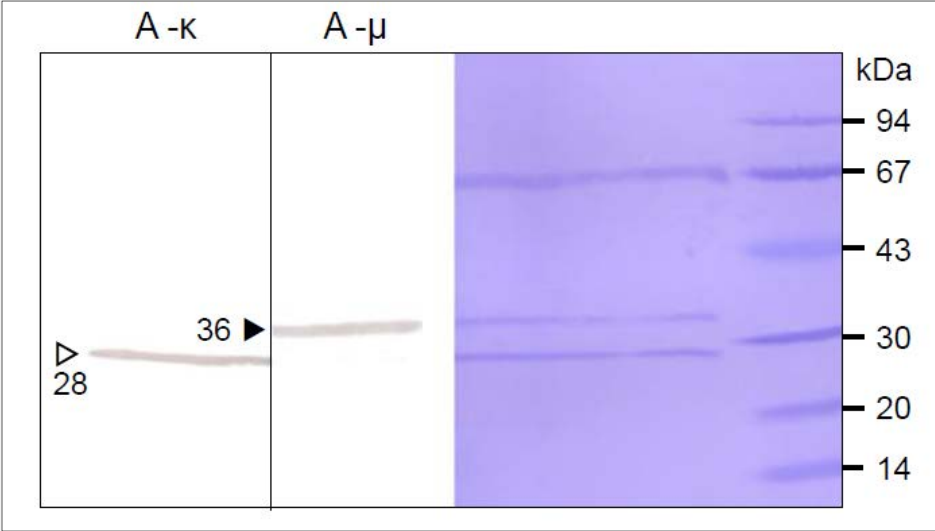
**Figure 4. Immunoblotting of the patient's serum and urine under non-reducing conditions.**

In serum, bands at 193 kDa (▶) and 68 kDa (▷) were detected with anti-μ heavy chain antibodies under non-reducing conditions. In urine and serum, a 68 kDa band (▷) was detected. With anti-κ light chain antibodies, the 193, 68, 43, and 28 kDa bands were detected in addition to IgG (162 kDa) in serum, and the 68, 43, and 28 kDa bands were recognized in urine. The panel on the right represents PU and standard molecular weight marker protein staining. A-μ - anti-human μ heavy chain antibodies, A-κ - anti-human κ light chain antibodies, NS - normal serum, PS - patient's serum, PU - patient's urine.



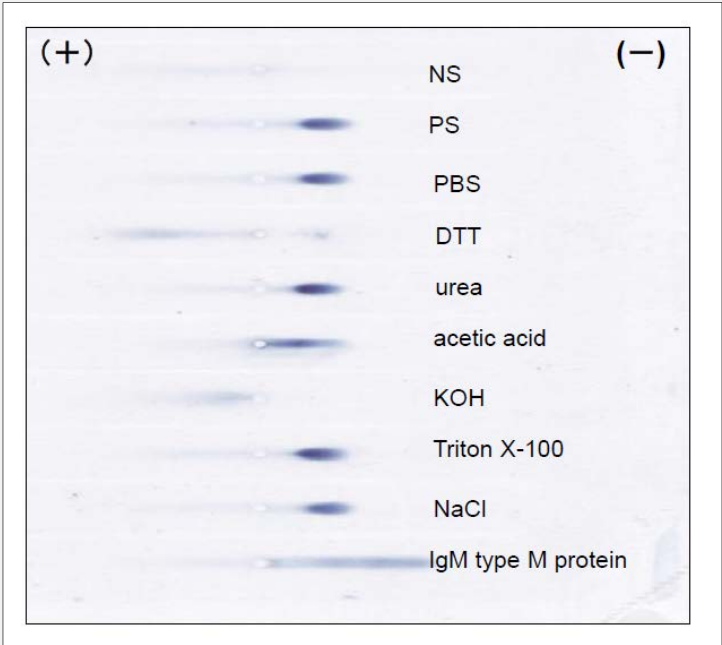
**Figure 5. Immunoblotting of the patient's serum and urine under reducing conditions.**

After reducing treatment, 74 (normal size), 49, and 36 kDa bands were detected with anti-μ heavy chain antibodies in serum, and a 36 kDa band was the main band in urine. The panel on the right represents PU and standard molecular weight marker protein staining. A-μ - anti-human μ heavy chain antibodies, NS - normal serum, PS - patient's serum, PU - patient's urine.



**Figure 6. Immunoblotting of low molecular weight IgM (second PAGE).**

The protein with a molecular weight of 68 kDa before reduction was separated into anti-μ heavy chain reactive 36 kDa (▶) and anti-κ light chain reactive 28 kDa (▷) bands. A-μ - anti-human μ heavy chain antibodies, A-κ - anti-human κ light chain antibodies. The panel on the right represents PU and standard molecular weight marker protein staining.



**Figure 7. Analysis of the agarose-binding ability of the M-protein after chemical treatment.**

The reactivity was lost after reduction by 30 mM DTT or after alkaline treatment with 1.7 M KOH.

tive  $\mu$  chain. Several  $\mu$  chain-related bands other than the 63 kDa band with unusual molecular mass were observed in this patient. Although we did not perform sequence studies on those because of poor recovery of materials, speculations as below may be possible from the experience of the first case [4]. The 43 kDa band, which reacted only with anti- $\kappa$  chain antibodies (Figure 4), is assumed to be the second half-molecule 7S IgM comprised of one  $\kappa$  chain with the normal molecular weight and a  $\mu$  chain with a large defect missing the constant region reactive with the anti- $\mu$  chain antibodies. The 49 kDa band, reactive only with anti- $\mu$  chain antibodies after reduction treatment (Figure 5), is assumed to be a low-molecular-weight  $\mu$  chain starting with the C1 region missing the VH region based on the analytical results of the first case.

The HM 7S IgM in the present case disappeared after chemotherapy. The appearance of it should be discussed. Since we did not analyze the structure of the main IgM- $\kappa$  M-protein, it is unknown whether it was derived from a different clone of the M-protein clone or a newly generated clone. If the former estimate is present, the different clone might produce defective IgM. Based on the findings of the first case, we consider it rather to be an abnormal production of the clone.

It has been recognized that some IgM M-protein binds to agarose or agar gel and disturbs M-protein typing in IEP or IFE from before. Upon experiencing a similar phenomenon, we studied a chemical interaction between IgM M-protein and gels. Agar gels are comprised of agarose as well as agarpectin, and M-protein, reactive with agar gel, has been frequently reported [11] and is considered to be the result of binding to the sulfate group in agarpectin through ionic bonding [11]. For this reason, we investigated whether the binding was influenced by increased salt concentrations (up to 1 M NaCl) in deproteinization. However, no change was observed. We observed that the agarose gel-binding ability of the IgM was lost when treated with 30 mM DTT or 1.7 M KOH. These results indicate that the binding ability is disrupted by cleavage of the S-S bond of the M-protein and that it requires the pentamer form of IgM. In addition, from the IEP image of Figure 1, it seems that IgM molecules bind to agarose in this case.

Finally, the accumulation of rare cases like our case should contribute to better understandings of IgM M-protein production.

#### Acknowledgement:

We are grateful to Dr. Hyogo Sinohara, Emeritus Professor, Kindai University, and Dr. Kozo Tatara, Professor, The Open University of Japan, for instruction in this study.

#### Declaration of Interest:

The authors declare no conflict of interest.

#### References:

1. Hobbs JR, Jacobs A. A half-molecule GK plasmacytoma. *Clin Exp Immunol* 1969;5:199-207 (PMID: 4984125).
2. Spiegelberg HL, Fishkin BG. Human myeloma IgA half-molecules. *J Clin Invest* 1976;58:1259-65 (PMID: 993344).
3. Sakurabayashi I, Kin K, Kawai T. Human IgA1 half-molecules: clinical and immunologic features in a patient with multiple myeloma. *Blood* 1979;53:269-78 (PMID: 367466).
4. Imoto M, Ishikawa K, Yamamoto K, et al. Occurrence of heavy chain of 7S IgM half-molecule whose NH<sub>2</sub>-terminal sequence is identical with that of kappa light chain sequence in patients with Waldenstrom macroglobulinemia. *Clin Chim Acta* 1999;282:77-88 (PMID: 10340436).
5. Grabar P, Williams CA. [Method permitting the combined study of the electrophoretic and the immunochemical properties of protein mixtures; application to blood serum]. *Biochim Biophys Acta* 1953;10:193-4 (PMID: 13041735).
6. Laemmli UK. Cleavage of structural proteins during the assembly of the head of bacteriophage T4. *Nature* 1970;227:680-5. (PMID: 5432063).
7. Towbin H, Staehelin T, Gordon J. Electrophoretic transfer of proteins from polyacrylamide gels to nitrocellulose sheets: procedure and some applications. *Proc Natl Acad Sci USA* 1979;76:4350-4 (PMID: 388439).
8. Yamamoto K, Sinohara H. Isolation and characterization of mouse countertrypsin, a new trypsin inhibitor belonging to the mammalian fetuin family. *J Biol Chem* 1993;268:17750-3 (PMID: 7688730).
9. Imoto M, Sinohara H, Sakurabayashi I, Akiyama T, Furuta I, Sasaki T. A new type of temperature-dependent serum M protein: a case of IgG-lambda type multiple myeloma. *Clin Chm Acta* 2003;334:153-6 (PMID: 12867286).
10. Ayadi H, Mihaesco E, Congy N, et al. H chain V region sequences of three human monoclonal IgM with anti-myelin-associated glycoprotein activity. *J Immunol* 1992;148:2812-6 (PMID: 1374100).
11. Levy DE, Horner AA, Solomon A. Immunoglobulin-Sulfated Polysaccharide Interactions. *J Exp Med* 1981;153:883-96 (PMID: 7252414).





## Case report

# Stent migration during EUS-guided hepaticogastrostomy in a patient with massive ascites: Troubleshooting using additional EUS-guided antegrade stenting



Ken Kamata, Mamoru Takenaka\*, Kosuke Minaga, Shunsuke Omoto, Takeshi Miyata, Kentaro Yamao, Hajime Imai, Masatoshi Kudo

Department of Gastroenterology and Hepatology, Kindai University School of Medicine, Osaka, Japan

## ARTICLE INFO

## Article history:

Received 21 March 2017

Accepted 30 May 2017

## Keywords:

EUS-guided biliary drainage

EUS-guided hepaticogastrostomy

EUS-guided antegrade stenting

## ABSTRACT

EUS-guided hepaticogastrostomy (EUS-HGS) is useful for treating obstructive jaundice. However, stent migration may sometimes occur both during and after the procedure. This report describes a patient with pancreatic cancer and massive ascites who underwent EUS-HGS combined with EUS-guided antegrade stenting (EUS-AS), with additional EUS-AS playing a role in troubleshooting for stent migration during EUS-HGS.

© 2017 Pan-Arab Association of Gastroenterology. Published by Elsevier B.V. All rights reserved.

## Introduction

Although EUS-guided biliary drainage (EUS-BD) is increasingly used as an alternative treatment for patients with biliary obstruction who fail standard endoscopic retrograde cholangiopancreatography, adverse events may sometimes occur [1,2]. For example, a recent systematic analysis of 1192 patients who underwent EUS-BD found that stent migration occurred in 32 (2.68%) cases, with stent migration into the abdominal cavity having high mortality rate [3,4]. This report describes a patient who experienced stent migration during EUS-guided hepaticogastrostomy (EUS-HGS), with additional EUS-guided antegrade stenting (EUS-AS) playing a role in troubleshooting to prevent bile leakage.

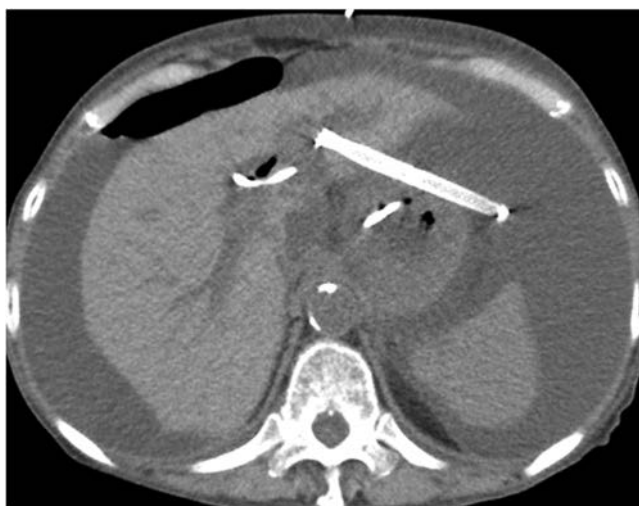
## Case presentation

A 66-year-old woman with advanced pancreatic cancer, duodenal stenosis, and massive ascites presented with obstructive jaundice caused by lower bile duct obstruction. A duodenal metal stent had been deployed for duodenal stenosis. Endoscopic retrograde transpapillary drainage was attempted; however, deep cannulation into the bile duct was unsuccessful because the indwelling

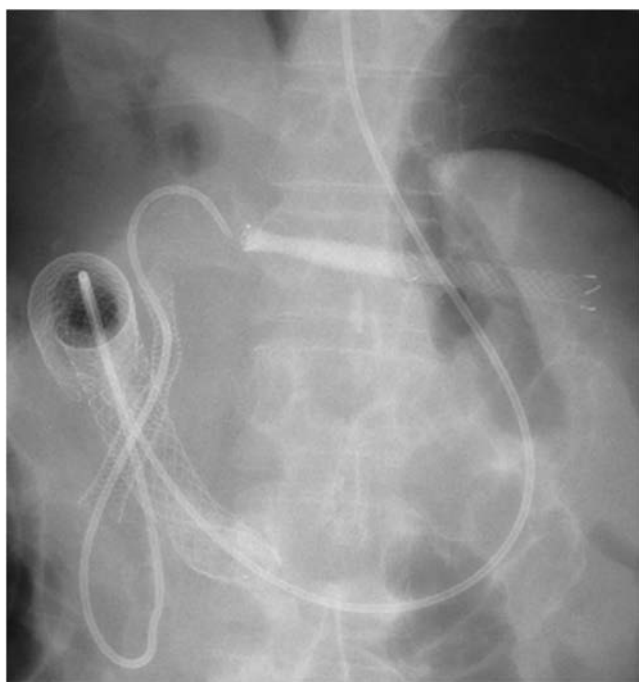
duodenal stent limited the ability to manipulate the scope. Thus, EUS-HGS combined with EUS-AS was performed. The intrahepatic biliary branch duct of segment 3 (B3) was punctured with a 19-gauge needle. Because the EUS image showed massive ascites around the gastric lumen, it was technically challenging to puncture B3. The echoendoscope was pushed adhesively to the gastric lumen with a strong angle position, enabling puncture of B3 without ascites intervening between the liver parenchyma and the gastric lumen. A 0.035-inch guide wire was passed through the needle until it reached the duodenum via the ampulla, 6 and 7-Fr bougie dilators were serially advanced over the guide wire to dilate the puncture site and part of the bile duct stricture. A covered metal stent (CMS) (diameter, 10 mm; length, 6 cm) for the EUS-AS was placed over the ampulla across the lower bile duct obstruction. Subsequently, EUS-HGS was performed. During deployment of the CMS (diameter, 10 mm; length, 8 cm), its luminal side was migrated towards the intraperitoneal cavity. Stent migration was caused by ascites flowing in the space separating the liver and stomach when the echoendoscope was pulled out from the gastric lumen (Fig. 1). The scope was immediately changed to a duodenal scope and a 6-Fr endoscopic nasobiliary drainage tube placed in the intrahepatic bile duct across the CMS that had been placed in the lower bile duct to reduce bile leakage (Fig. 2). After the procedure, the patient's obstructive jaundice improved and her abdominal distention decreased due to the reduction in ascites volume. The patient resumed eating 5 days after surgery with no bile peritonitis. A recent study reported that a stent length  $\geq 3$  cm in the

\* Corresponding author at: Department of Gastroenterology and Hepatology, Kindai University School of Medicine, 377-2 Ohno-higashi, Osaka-sayama 589-8511, Japan.

E-mail address: [mamoxyo45@gmail.com](mailto:mamoxyo45@gmail.com) (M. Takenaka).



**Fig. 1.** CT scan shows that the luminal side of the stent had migrated towards the intraperitoneal cavity.



**Fig. 2.** Fluoroscopic image shows placement of the 6-Fr endoscopic nasobiliary drainage tube in the intrahepatic bile duct.

gastrointestinal lumen can prevent stent migration after deployment in EUS-HGS [5,6]. In this case, metal stents longer than 10 cm may be suitable. Severe ascites may cause inward stent migration, which may require EUS-AS troubleshooting during EUS-HGS

## References

- [1] Itoi T, Sofuni A, Itokawa F, et al. Endoscopic ultrasonography-guided biliary drainage. *J Hepatobiliary Pancreat Sci* 2010;17:611–6.
- [2] Alvarez-Sánchez MV, Jenssen C, Faiss S, et al. Interventional endoscopic ultrasonography: an overview of safety and complications. *Surg Endosc* 2014;28:712–34.
- [3] Wang K, Zhu J, Xing L, Wang Y, Jin Z, Li Z. Assessment of efficacy and safety of EUS-guided biliary drainage: a systematic review. *Gastrointest Endosc* 2016;83:1218–27.
- [4] Martins FP, Rossini LGB, Ferrari AP. Migration of a covered metallic stent following endoscopic ultrasound-guided hepaticogastrostomy. *Endoscopy* 2010;42:E126–7.
- [5] Ogura T, Yamamoto K, Sano T, et al. Stent length is impact factor associated with stent patency in endoscopic ultrasound-guided hepaticogastrostomy. *J Gastroenterol Hepatol* 2015;30:1748–52.
- [6] Nakai Y, Isayama H, Yamamoto N, et al. Safety and effectiveness of a long, partially covered metal stent for endoscopic ultrasound-guided hepaticogastrostomy in patients with malignant biliary obstruction. *Endoscopy* 2016;48:1125–8.



Original Research

# Ramucirumab as second-line treatment in patients with advanced hepatocellular carcinoma following first-line therapy with sorafenib: Patient-focused outcome results from the randomised phase III REACH study



Ian Chau <sup>a,\*</sup>, Markus Peck-Radosavljevic <sup>b</sup>, Christophe Borg <sup>c</sup>, Peter Malfertheiner <sup>d</sup>, Jean Francois Seitz <sup>e</sup>, Joon Oh Park <sup>f</sup>, Baek-Yeol Ryoo <sup>g</sup>, Chia-Jui Yen <sup>h</sup>, Masatoshi Kudo <sup>i</sup>, Ronnie Poon <sup>j</sup>, Davide Pastorelli <sup>k</sup>, Jean-Frederic Blanc <sup>l</sup>, Hyun Cheol Chung <sup>m</sup>, Ari D. Baron <sup>n</sup>, Takuji Okusaka <sup>o</sup>, L. Bowman <sup>p</sup>, Zhanglin Lin Cui <sup>p</sup>, Alicia C. Girvan <sup>p</sup>, Paolo B. Abada <sup>p</sup>, Ling Yang <sup>q</sup>, Andrew X. Zhu <sup>r</sup>

<sup>a</sup> Royal Marsden Hospital, London and Surrey, United Kingdom

<sup>b</sup> Allgemeines Krankenhaus Wien, Vienna and Klinkum Klagenfurt am Wörthersee, Klagenfurt, Austria

<sup>c</sup> Hospital Jean Minjoz, Besançon, France

<sup>d</sup> Universitätsklinikum Magdeburg, Magdeburg, Germany

<sup>e</sup> Hôpital La Timone, Aix-Marseille University, Marseille, France

<sup>f</sup> Samsung Medical Center, Sungkyunkwan University School of Medicine, Seoul, Republic of Korea

<sup>g</sup> Asan Medical Center, Seoul, Republic of Korea

<sup>h</sup> National Cheng Kung University Hospital, Tainan, Taiwan

<sup>i</sup> Kinki University School of Medicine, Osaka-Sayama, Osaka, Japan

<sup>j</sup> The University of Hong Kong, Hong Kong

<sup>k</sup> Istituto Oncologico Veneto IRCCS, Padova, Italy

<sup>l</sup> Hepato-Gastroenterology and Digestive Oncology Unit, Centre Medico-chirurgical Magellan, CHU Bordeaux, France

<sup>m</sup> Yonsei Cancer Center, Yonsei University Health System, Seoul, Republic of Korea

<sup>n</sup> Sutter Health California Pacific Medical Center, San Francisco, CA, USA

<sup>o</sup> National Cancer Center Hospital, Tokyo, Japan

<sup>p</sup> Eli Lilly and Company, Indianapolis, IN, USA

<sup>q</sup> Eli Lilly and Company, Bridgewater, NJ, USA

<sup>r</sup> Massachusetts General Hospital Cancer Center, Harvard Medical School, Boston, MA, USA

Received 15 March 2017; accepted 2 May 2017

Available online 4 June 2017

\* Corresponding author: Department of Medicine, Royal Marsden Hospital, Downs Road, Sutton, Surrey, SM2 5PT, United Kingdom. Fax: +44 208 661 3890.

E-mail address: [ian.chau@rmh.nhs.uk](mailto:ian.chau@rmh.nhs.uk) (I. Chau).

**KEYWORDS**

Ramucirumab;  
Sorafenib;  
Hepatocellular  
carcinoma;  
Patient-focused  
outcomes;  
Quality of life;  
Performance status

**Abstract Purpose:** To report patient-focused outcomes as measured by quality of life (QoL) and performance status (PS) in REACH, a phase III placebo-controlled randomised study, assessing ramucirumab in advanced hepatocellular carcinoma (HCC) patients who received prior sorafenib.

**Methods:** Eligible patients had advanced HCC, Child-Pugh A, PS 0 or 1 and prior sorafenib. Patients received ramucirumab (8 mg/kg) or placebo (1:1) on day 1 of a 2-week cycle. QoL was assessed by FACT Hepatobiliary Symptom Index (FHSI)-8 and EuroQoL (EQ-5D) at baseline; cycles 4, 10, and 16; and end of treatment. PS was assessed at baseline, each cycle, and end of treatment. Deterioration in FHSI-8 was defined as a  $\geq 3$ -point decrease from baseline and PS deterioration was defined as a change of  $\geq 2$ . Both intention-to-treat and pre-specified subgroup of patients with baseline serum alpha-fetoprotein (AFP)  $\geq 400$  ng/mL were assessed.

**Results:** There were 565 patients randomised to ramucirumab and placebo. Compliance with FHSI and EQ-5D was high and similar between groups. In the ITT population, deterioration in FHSI-8, EQ-5D, and PS was similar between ramucirumab and placebo. In patients with baseline AFP  $\geq 400$  ng/mL, ramucirumab significantly reduced deterioration in FHSI-8 at the end of treatment compared with placebo ( $P = 0.0381$ ), and there was a trend towards a delay in the deterioration of symptoms in FHSI-8 (HR 0.690;  $P = 0.054$ ) and PS (HR 0.642;  $P = 0.057$ ) in favour of ramucirumab.

**Conclusions:** We report one of the most comprehensive data sets of QoL and symptom burden in patients undergoing systemic therapy for advanced HCC. Ramucirumab was associated with no worsening of QoL. In patients with baseline AFP  $\geq 400$  ng/mL, the significant survival benefit observed in patients treated with ramucirumab was coupled with a trend in patient-focused outcome benefits.

**Clinical trial registration:** NCT01140347.

© 2017 Elsevier Ltd. All rights reserved.

## 1. Introduction

Hepatocellular carcinoma (HCC) constitutes a significant global disease burden, with an estimated 782,000 new cases and 745,000 deaths in 2012, surpassing gastric cancer as the second most common cause of cancer death in the world [1]. For patients with advanced HCC who are not candidates for locoregional therapy, such as liver resection and transplantation or transarterial (chemo) embolisation, systemic therapy with sorafenib is currently the standard of care. This is based on two randomised controlled trials (RCTs) [2,3] showing overall survival benefits of sorafenib over placebo. However, for both studies, another important end-point, time to symptomatic progression, was not significantly different between the two arms. This end-point was also included as a co-primary outcome with overall survival in the pivotal SHARP study [2].

Cancer-related symptoms and the associated impact on health-related quality of life (QoL) in patients with HCC are complex. Overall effects can be related to the background liver disease and cancer burden, as well as treatment-related adverse reactions. Patients with liver disease including cirrhosis or hepatitis virus infection could have compromised QoL at baseline. Compared with the general population, patients with HCC have worse QoL in physical, psychological, functional well-being and hepatobiliary symptoms [4]. Even compared

with patients who had chronic liver disease, patients with HCC had worse physical well-being and overall QoL [4].

Although QoL data have been reported for systemic therapy, including octreotide and tamoxifen [4], comprehensive QoL data are sparse for more contemporary targeted therapy. Even for sorafenib, apart from time to symptomatic progression, no further detailed QoL data have been published from the two pivotal RCTs. In other recently published RCTs evaluating brivanib [5,6], everolimus [7], erlotinib [8], sunitinib [9], linifanib [10] and regorafenib [11], very limited or no QoL data were reported.

Ramucirumab is a monoclonal antibody targeting against vascular endothelial growth factor (VEGF) receptor 2. REACH was a multinational phase III RCT evaluating ramucirumab plus best supportive care versus placebo plus best supportive care as second-line treatment for patients with advanced HCC who had disease progression during or after sorafenib or were intolerant to sorafenib [12]. In the intention-to-treat (ITT) population, there was no overall survival benefit for ramucirumab over placebo (hazard ratio [HR] 0.87;  $P = 0.14$ ). However, in a protocol pre-defined patient subpopulation with serum alpha-fetoprotein (AFP)  $\geq 400$  ng/mL, there was a statistically and clinically meaningful survival advantage for ramucirumab over placebo (HR 0.67;  $P = 0.006$ ) [12]. Herein, we report

patient-focused outcome measures, including QoL and performance status (PS), from the REACH study.

## 2. Methods

### 2.1. Study design and patients

The REACH study design has been published previously [12]. Patients included in this study were at least 18 years of age with histologically or cytologically confirmed advanced HCC, stage B or C Barcelona Clinic Liver Cancer score, and a Child-Pugh score of less than 7 (Child-Pugh A). At study entry, patients were required to have an Eastern Cooperative Oncology Group PS of 0 or 1, prior sorafenib therapy, documented disease progression during or after discontinuation of sorafenib therapy or had discontinued sorafenib therapy after an adverse drug reaction despite dose reduction.

### 2.2. Procedures

Patients were randomised 1:1 to receive ramucirumab 8 mg/kg or placebo intravenously on day 1 of a 2-week cycle until disease progression, unacceptable toxicity, or withdrawal of consent. All patients received supportive care without active cytotoxic therapy. Clinician-assessed PS was collected at baseline, before every cycle, and at the end of study treatment. Local radiological imaging was performed at baseline, every 6 weeks during the first 6 months of treatment, and every 9 weeks thereafter.

Patient-reported outcomes, including cancer-related symptoms and health-related QoL, were assessed using the FHSI-8 and the EuroQoL (EQ-5D). These assessments were made at baseline, before cycle 4 (approximately 6 weeks following the first infusion of study therapy), and every 12 weeks thereafter (every 6 cycles) until the end of study therapy. An end of treatment visit occurred within 7 d after the decision was made to discontinue all study therapy. The instruments were administered together and in sequential order, with the FHSI-8 presented first followed by presentation of the EQ-5D.

FHSI-8 was a self-administered questionnaire with specific focus on the most frequent and concerning symptoms experienced by patients with hepatobiliary malignancies [13]. This 5-point assessment (scored 0 to 4) for eight symptoms included symptoms more specific to hepatobiliary cancer (jaundice and stomach pain/discomfort) and some that were associated with generalised advanced/metastatic malignancy (weight loss and fatigue). The total score (range 0–32) was calculated as a simple summation of eight symptom items, with a higher score representing fewer symptoms according to scoring guidelines. The minimally important differences (MIDs) in FHSI-8 scores had been previously reported as 2 to 3 points [14].

The EQ-5D version used in REACH is a validated QoL assessment consisting of a descriptive system and visual analogue scale (VAS) [15]. The descriptive system scale is comprised of the following five dimensions: mobility, self-care, usual activities, pain/discomfort and anxiety/depression. Each dimension has three levels of severity. Each EQ-5D health state was converted to a single summary utility score by applying a formula that attaches weights to each of the answers in each dimension. The VAS is a vertical scale wherein end-points are labelled ‘best imaginable health state’ and ‘worst imaginable health state.’ Index-based summary score is typically interpreted along a continuum where 1 represents best possible health and 0 represents dead [16]. The MIDs in EQ-5D have been reported as 0.06 to 0.08 for EQ-5D index and 0.07 for EQ-5D VAS in all cancers, with the lower bounds likely to represent a closer estimate of true MIDs [16].

### 2.3. Statistical considerations

Overall survival was analysed using a log-rank test stratified by randomisation strata. In patients with baseline AFP  $\geq 400$  ng/mL, survival analysis was pre-specified in the protocol. Percentage of compliance with FHSI and EQ-5D was calculated as the number of completed assessments divided by the number of expected assessments (patients still on study).

For cancer-related symptoms and QoL, descriptive analyses were assessed at each cycle, as well as the change from baseline. Time to FHSI-8 deterioration was defined as the time from the randomisation date to the first date with a  $\geq 3$ -point decrease (based on 32-point scale) from baseline. Three or more points difference was chosen based on previously reported MID in HCC [14]. Any missing values were excluded from the analysis. The individual symptom analysis compared time to deterioration of each FHSI-8 item between treatment arms, with the deterioration threshold defined as 0.5 standard deviation of baseline scores of each item [17]. In case of no FHSI-8 deterioration, the subject was censored at the time of the last FHSI recording. Time to PS deterioration between treatment arms was defined as the time from the randomisation date to the first date that a change to PS  $\geq 2$  was observed. Kaplan–Meier method and Cox proportional hazards regression model were used to assess time to deterioration [18,19]. In case of no PS greater than 2, the subject was censored at the time of the last PS recording. Time to FHSI-8 deterioration and PS deterioration was assessed for the ITT population and the subpopulation of patients with baseline AFP  $\geq 400$  ng/mL. Analysis of FHSI-8 association with tumour response was determined by using the FHSI-8 score most proximal to the determination of best tumour response according to Response Evaluation Criteria In Solid Tumors criteria [20]. The relationship between FHSI-8 and best tumour size change was



estimated by using simple linear regression and reporting the slope and statistical significance of the derived linear relationship.

### 3. Results

Between November 2010 and April 2013, 565 patients were enrolled in the REACH study, with 283 randomly assigned to ramucirumab and 282 to placebo. Table 1 shows baseline characteristics for each treatment group for the ITT population and the subpopulation of patients with baseline AFP  $\geq 400$  ng/mL. Baseline characteristics were balanced between the two treatment groups for both populations. Table 2 shows the FHSI-8 and EQ-5D assessment compliance rates. Compliance was high at the pre-specified measurement time points. Due to the rapidly progressive nature of the disease in this setting, fewer patients were expected to complete the QoL assessment at cycles 10 and 16 although the compliance rates remained high. Most patients were able to complete the QoL instruments at their individual end of treatment visit, and thus the number of patients was higher at the end of treatment measurement than at cycle 16.

Table 3 shows the FHSI-8 total scores. In the ITT population, the mean end of treatment FHSI-8 score change from baseline was numerically slightly greater in the placebo group compared with the ramucirumab group ( $P = 0.3722$ ), although the changes in both arms were less than the MID of 2–3 for FHSI-8 scores. In

Table 2

Compliance for FHSI-8 and EQ-5D assessment.

QoL assessment	ITT		AFP $\geq 400$ ng/mL	
	Ramucirumab	Placebo	Ramucirumab	Placebo
FHSI-8				
compliance, <i>n</i> of expected (%)				
Baseline	272 (96.1)	267 (94.7)	118 (99.2)	124 (94.7)
Cycle 4	164 (88.6)	142 (84.5)	64 (92.8)	55 (85.9)
Cycle 10	72 (78.3)	43 (81.1)	22 (84.6)	10 (76.9)
Cycle 16	48 (78.7)	24 (77.4)	18 (90.0)	7 (77.8)
End of treatment	172 (62.1)	201 (72.8)	80 (67.2)	98 (76.6)
EQ-5D				
compliance, <i>n</i> of expected (%)				
Baseline	273 (96.5)	267 (94.7)	118 (99.2)	124 (94.7)
Cycle 4	163 (88.1)	143 (85.1)	64 (92.8)	55 (85.9)
Cycle 10	74 (80.4)	43 (81.1)	22 (84.6)	10 (76.9)
Cycle 16	48 (78.7)	25 (80.6)	18 (90.0)	7 (77.8)
End of treatment	172 (62.1)	200 (72.5)	80 (67.2)	98 (76.6)

Abbreviations: AFP, alpha-fetoprotein; EQ-5D, EuroQoL; FHSI-8, FACT Hepatobiliary Symptom Index; ITT, intention-to-treat; QoL, quality of life.

patients with baseline AFP  $\geq 400$  ng/mL, the magnitude of deterioration of the FHSI-8 score from baseline was more pronounced in the placebo group compared with the ramucirumab group. The mean deterioration of  $-3.73$  in the placebo group was deemed to be higher than the MID of 2–3 for the FHSI-8 score. Ramucirumab significantly reduced deterioration in FHSI-8 at the end of treatment compared with placebo ( $P = 0.0381$ ).

Table 1

Patient baseline demographics and clinical characteristics.

Baseline demographics	ITT		AFP $\geq 400$ ng/mL	
	Ramucirumab ( <i>N</i> = 283)	Placebo ( <i>N</i> = 282)	Ramucirumab ( <i>N</i> = 119)	Placebo ( <i>N</i> = 131)
Age (years), median (range)	64 (28–87)	62 (25–85)	61 (34–84)	60 (25–83)
Gender (male), <i>n</i> (%)	236 (83.4)	242 (85.8)	92 (77.3)	110 (84.0)
Race, <i>n</i> (%)				
White	139 (49.1)	137 (48.6)	50 (42.0)	49 (37.4)
African American	Included in other	Included in other	1 (0.8)	0 (0)
Asian	131 (46.3)	135 (47.9)	66 (55.5)	78 (59.5)
Other	13 (4.6)	10 (3.5)	2 (1.7)	4 (3.1)
ECOG PS, <i>n</i> (%)				
0	159 (56.2)	153 (54.3)	60 (50.4)	63 (48.1)
1	124 (43.8)	129 (45.7)	59 (49.6)	68 (51.9)
Child-Pugh Class A, <i>n</i> (%)	277 (97.9)	276 (97.9)	115 (96.6)	129 (98.5)
Baseline BCLC score, <i>n</i> (%)				
Stage B	33 (11.7)	34 (12.1)	11 (9.2)	9 (6.9)
Stage C	250 (88.3)	248 (87.9)	108 (90.8)	122 (93.1)
Macrovascular invasion present, <i>n</i> (%)	82 (29.0)	79 (28.0)	43 (36.1)	44 (33.6)
Extrahepatic spread present, <i>n</i> (%)	207 (73.1)	200 (70.9)	85 (71.4)	101 (77.1)
Aetiology of liver disease <sup>a</sup> , <i>n</i> (%)				
Hepatitis B	100 (35.3)	101 (35.8)	53 (44.5)	66 (50.4)
Hepatitis C	77 (27.2)	77 (27.3)	35 (29.4)	28 (21.4)
Other <sup>b</sup>	106 (37.5)	104 (36.9)	46 (38.7)	49 (37.4)

Abbreviations: AFP, alpha-fetoprotein; BCLC, Barcelona Conference Liver Cancer; ECOG PS, Eastern Cooperative Oncology Group performance status; ITT, intention-to-treat; N, number of patients in the ITT population.

<sup>a</sup> As reported on the case report form.

<sup>b</sup> Other includes significant alcohol use, steatohepatitis, haemochromatosis, other, and unknown.

Table 3  
FHSI-8 total scores.

FHSI-8 scores	ITT		AFP $\geq 400$ ng/mL	
	Ramucirumab	Placebo	Ramucirumab	Placebo
FHSI-8 total score, mean (SD)				
Baseline	26.17 (4.898)	26.70 (4.647)	25.84 (5.030)	25.92 (4.978)
Cycle 4	25.98 (4.251)	26.28 (5.313)	25.86 (4.196)	25.52 (4.846)
Cycle 10	26.30 (4.731)	27.54 (4.043)	25.82 (4.807)	27.80 (4.686)
Cycle 16	26.50 (4.861)	28.50 (3.050)	25.24 (5.389)	28.29 (3.147)
End of treatment	23.66 (5.964)	24.28 (6.552)	23.80 (5.685)	22.58 (6.560)
End of treatment FHSI-8 score change from baseline, mean (SD)	–2.44 (5.561)	–2.86 (5.618)	–2.21 (5.627)	–3.73 (5.875)
<i>P</i> -value from <i>t</i> -test for end of treatment FHSI-8 score change from baseline	0.3722		0.0381	

Abbreviations: AFP, alpha-fetoprotein; FHSI-8, FACT Hepatobiliary Symptom Index; ITT, intention-to-treat; SD, standard deviation.

An analysis of tumour response and FHSI-8 demonstrated a linear association between FHSI-8 symptom deterioration and change in tumour size in the ITT population (slope = 0.1312;  $P = 0.0023$ ; Fig. 1A). This linear association was also observed in patients with baseline AFP  $\geq 400$  ng/mL (slope = 0.1979;  $P = 0.0057$ ; Fig. 1B). Thus, patients with tumour progression were more likely to experience worse cancer-related symptom burden.

Table 4 shows the EQ-5D summary index and VAS scores. In the ITT population, the mean change for EQ-5D summary index was –0.129 and –0.144 for ramucirumab and placebo, respectively, compared with baseline. In patients with baseline AFP  $\geq 400$  ng/mL, the magnitude of deterioration was more pronounced on the placebo arm, with a mean change of –0.120 and –0.191 for ramucirumab and placebo, respectively.

For both ramucirumab and placebo groups, QoL as measured by the EQ-5D was maintained while patients were active on study treatment (i.e. before disease progression), but the decline in QoL was notable at the end of treatment visits. The decline of the EQ-5D scores at end of treatment suggests a correlation with disease progression, which was the most common reason (79% of patients) to discontinue study treatment.

In the ITT population, there was no significant difference in the time to first deterioration in FHSI-8 total score  $\geq 3$  between ramucirumab and placebo (HR 1.037; 95% CI: 0.802–1.341;  $P = 0.782$ ; Fig. 2A). The median time was 3.2 months for ramucirumab and 3.1 months for placebo. In patients with baseline AFP  $\geq 400$  ng/mL, there was a trend towards more prolonged time to first deterioration in FHSI-8 total score  $\geq 3$  in favour of ramucirumab (HR 0.690; 95% CI: 0.470–1.014;  $P = 0.054$ ; Fig. 2B). The median time was 2.9 months for ramucirumab and 1.6 months for placebo.

In the ITT population, there was no significant difference in the time to first deterioration in PS  $\geq 2$  between ramucirumab and placebo (HR 0.891; 95% CI: 0.651–1.220;  $P = 0.471$ ) (Fig. 3A). Although there were

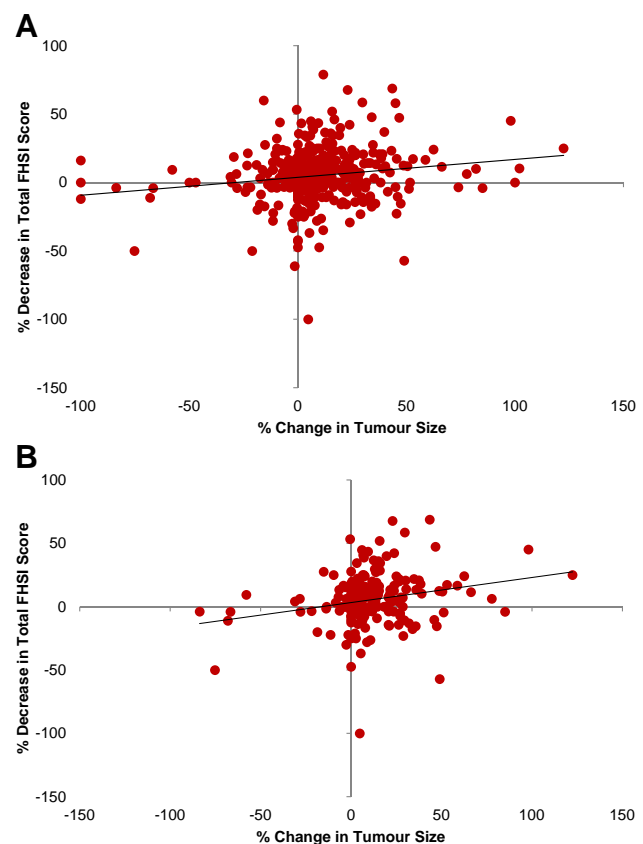


Fig. 1. (A) Percent change from baseline in best tumour measure versus percent change from baseline in FHSI score at best tumour measure in ITT population. (B) Percent change from baseline in best tumour measure versus percent change from baseline in FHSI score at best tumour measure in patients with baseline AFP  $\geq 400$  ng/mL. AFP, alpha-fetoprotein; FHSI, Functional Assessment in Cancer Therapy (FACT) Hepatobiliary Symptom Index; ITT, intention-to-treat.

a large number of censored events, suggesting many patients had documented radiological disease progression and came off study before the documentation of PS deterioration, sensitivity analysis showed missing data had no impact on the results. In patients with baseline

Table 4

EQ-5D summary index and VAS scores.

EQ-5D scores	ITT				AFP $\geq 400$ ng/mL			
	<i>N</i>	<u>Ramucirumab</u>	<i>N</i>	<u>Placebo</u>	<i>N</i>	<u>Ramucirumab</u>	<i>N</i>	<u>Placebo</u>
		Mean (SD)		Mean (SD)		Mean (SD)		Mean (SD)
EQ-5D index score								
Baseline	271	0.783 (0.218)	266	0.827 (0.191)	116	0.778 (0.215)	123	0.807 (0.202)
Cycle 4	168	0.782 (0.225)	146	0.795 (0.245)	68	0.792 (0.207)	54	0.753 (0.271)
Cycle 10	74	0.788 (0.255)	46	0.867 (0.131)	21	0.804 (0.254)	10	0.887 (0.123)
Cycle 16	49	0.806 (0.240)	25	0.871 (0.106)	18	0.810 (0.196)	7	0.896 (0.102)
End of treatment	168	0.672 (0.315)	193	0.705 (0.309)	78	0.688 (0.314)	95	0.635 (0.314)
Change from baseline in EQ-5D index score								
Cycle 4	166	−0.038 (0.189)	145	−0.046 (0.245)	67	−0.031 (0.208)	53	−0.071 (0.277)
Cycle 10	71	−0.054 (0.212)	45	0.003 (0.148)	21	−0.024 (0.206)	10	0.034 (0.191)
Cycle 16	47	−0.062 (0.214)	25	−0.012 (0.085)	18	−0.028 (0.192)	7	−0.009 (0.114)
End of treatment	166	−0.129 (0.290)	190	−0.144 (0.280)	77	−0.120 (0.320)	93	−0.191 (0.297)
EQ-5D VAS score								
Baseline	271	72.0 (18.15)	265	72.6 (17.93)	117	73.2 (17.72)	124	72.1 (18.96)
Cycle 4	167	72.8 (18.02)	148	73.1 (18.70)	68	73.7 (17.23)	56	70.9 (16.96)
Cycle 10	75	73.9 (18.75)	46	78.4 (16.35)	22	74.5 (20.05)	10	84.9 (13.30)
Cycle 16	49	77.4 (18.82)	25	81.1 (12.04)	18	73.8 (24.91)	7	87.4 (9.09)
End of treatment	169	62.4 (20.30)	199	65.7 (20.31)	79	62.7 (20.56)	98	61.9 (19.78)
Change from baseline in EQ-5D VAS score								
Cycle 4	165	−1.2 (16.37)	146	−1.3 (18.39)	67	−2.4 (19.91)	55	−4.0 (18.59)
Cycle 10	72	−2.0 (13.46)	45	3.8 (15.58)	22	−0.8 (17.24)	10	8.0 (11.60)
Cycle 16	47	−0.2 (17.16)	25	3.6 (13.41)	18	−0.2 (23.86)	7	7.6 (10.50)
End of treatment	168	−10.8 (19.18)	196	−9.0 (18.26)	79	−11.8 (21.27)	97	−11.9 (18.42)

Abbreviations: AFP, alpha-fetoprotein; EQ-5D, EuroQoL; ITT, intention-to-treat; SD, standard deviation; VAS, visual analogue scale.

AFP  $\geq 400$  ng/mL, there was once again a trend towards more prolonged time to first deterioration in PS  $\geq 2$  in favour of ramucirumab (HR 0.642; 95% CI: 0.405–1.017;  $P = 0.057$ ; Fig. 3B).

Fig. 4 shows a summary of time to deterioration of individual FHSI-8 symptom items in patients with baseline AFP  $\geq 400$  ng/mL. With each item, there appeared to be a trend towards benefit with ramucirumab, with the most notable being delayed worsening of pain.

#### 4. Discussion

In the ITT analysis of patient-focused outcomes, there were no significant treatment differences in FHSI-8, EQ-5D, time to symptomatic deterioration, and PS deterioration. However, in the pre-specified subpopulation of patients with baseline AFP  $\geq 400$  ng/mL, ramucirumab significantly reduced deterioration in FHSI-8 at the end of treatment compared with placebo ( $P = 0.0381$ ), and there was a trend towards more prolonged time to symptom and PS deterioration in favour of ramucirumab. In addition, increase in tumour size was coupled with deterioration of cancer-related symptoms as measured by FHSI-8 assessment. Demonstrating the biological plausibility of the symptom improvement with tumour size changes enhances the sense of robustness for the strong time to deterioration results seen with the FHSI-8. Therefore, in this subgroup, not only was a significant survival benefit observed with

ramucirumab (HR 0.67;  $P = 0.006$ ), the survival benefit appears to be coupled with benefits in patient-focused outcome (i.e. delay in worsening of disease-related symptoms and PS).

The FACT-Hep, originally developed to assess disease-specific issues in hepatobiliary cancers [21], was a 45-item self-report instrument to measure QoL in this particular group of patients. The eight most commonly endorsed items were retained in this symptom index, comprising pain, weight loss, nausea, jaundice, back pain, stomach pain/discomfort, and two fatigue items (lack of energy and feeling fatigued), to form the FHSI-8. Higher scores reflected better QoL or fewer symptoms. In addition, there were significant correlations between better QoL scores and better patient-assessed PS. Nevertheless, in the original development of FACT-Hep and FHSI, notably only approximately 20% of the patients in the validation set had HCC and a larger proportion (nearly 40%) of patients had metastatic colorectal cancer [13,21].

However, the reliability of FACT-Hep and FHSI-8 were validated in an independent cohort of predominantly HCC patients (85%) [14]. Importantly, this study established the MID estimates to be 2 to 3 points for FHSI. In addition, patients in this study underwent liver-directed locoregional therapy with TACE or 90-Yttrium microspheres and not systemic therapy. Nevertheless, FHSI was used in assessing systemic treatment in both our current REACH study as well as other pivotal RCTs in HCC [2,3].

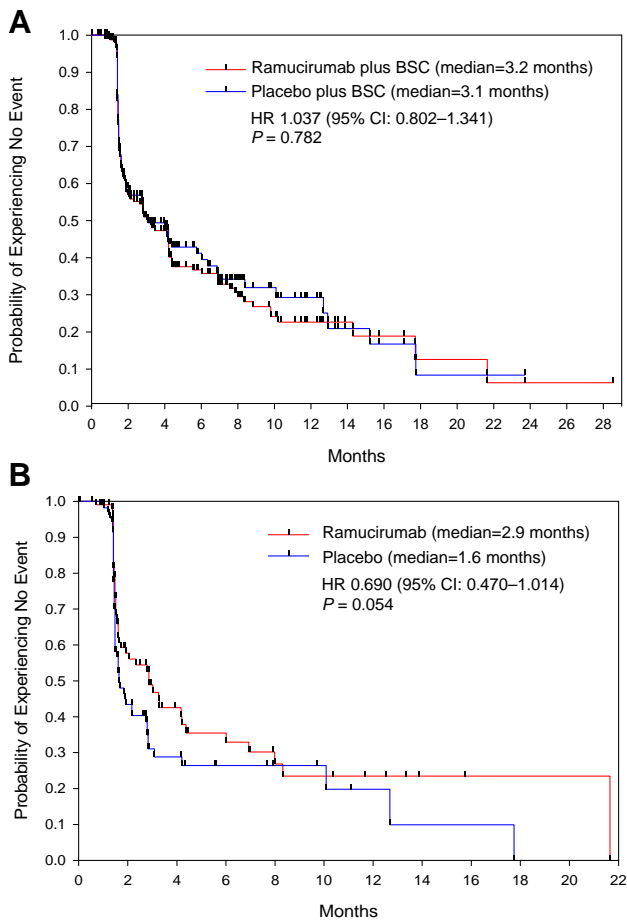


Fig. 2. (A) Time to first deterioration in FHSI-8 total score in ITT population. (B) Time to first deterioration in FHSI-8 total score in patients with baseline AFP  $\geq 400$  ng/mL. AFP, alpha-fetoprotein; BSC, best supportive care; CI, confidence interval; FHSI-8, Functional Assessment in Cancer Therapy (FACT) Hepatobiliary Symptom Index; HR, hazard ratio; ITT, intention-to-treat.

For the EQ-5D assessment, there was evidence in our data that patients experiencing radiological disease progression also noticed deterioration in QoL, which was greater than the MID. Although intuitively one would have expected this in advanced cancers, it is in fact poorly documented in published literature. In a recent systematic review [22], only four studies assessed this: one in colorectal cancer (panitumumab); two in breast cancer (lapatinib); and one in renal cell cancer (pazopanib) across all solid tumours. All reported that being progression-free had a statistically significant positive association with better QoL, with or without decreased disease symptoms. However, there could be publication bias. In the REACH study, there was a significant improvement in progression-free survival for ramucirumab in the ITT population and the subpopulation of patients with baseline AFP  $\geq 400$  ng/mL [12]; the relatively long interval between QoL assessments might have precluded detection of QoL differences

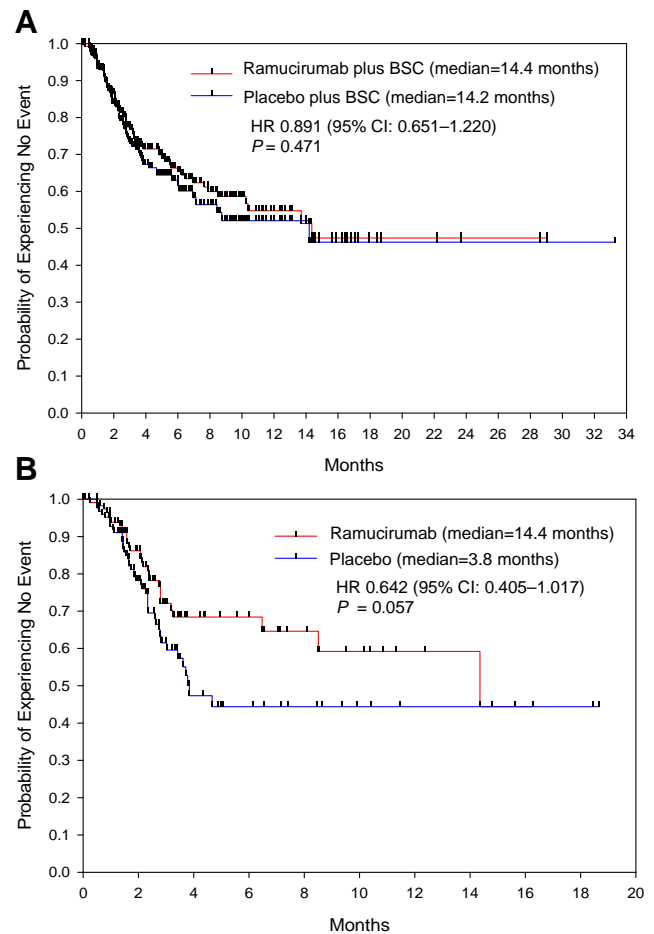


Fig. 3. (A) Time to first deterioration in ECOG PS in ITT population. (B) Time to first deterioration in ECOG PS in patients with baseline AFP  $\geq 400$  ng/mL. AFP, alpha-fetoprotein; BSC, best supportive care; CI, confidence interval; ECOG PS, Eastern Cooperative Oncology Group performance status; HR, hazard ratio; ITT, intention-to-treat.

between the two arms. Clinically important differences could have been missed, especially when only 12 weekly assessments were made in the latter part of patient study participation in a disease setting with a very short progression-free interval. We did not assess time to deterioration of EQ-5D scores since FHSI was more specific to HCC compared with the more generic EQ-5D.

In recent years, many large-scale RCTs have been performed to assess novel systemic agents to improve the outcome of patients with advanced HCC not amenable to locoregional liver-directed therapy. Yet, very sparse QoL data have been reported. In SHARP [2] and Asia-Pacific [3] studies, only time to deterioration of FHSI scores was reported. The studies, however, defined deterioration as  $\geq 4$  points decline in FHSI scores. No other QoL data have been published from these two pivotal studies of sorafenib. Only through observational data has there been a suggested impact of

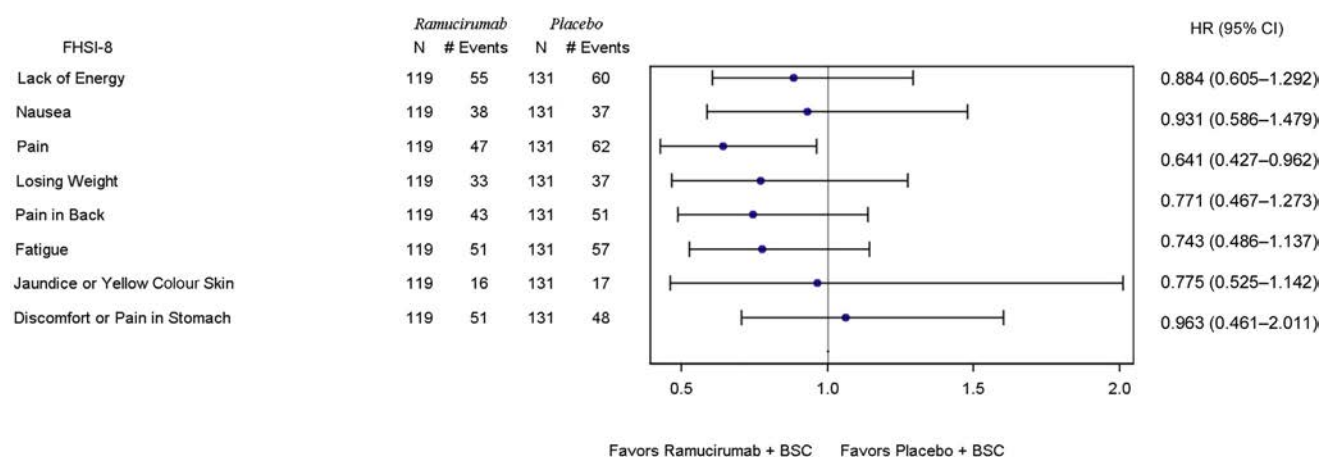


Fig. 4. Summary of time to deterioration of FHSI-8 symptom items in patients with baseline AFP  $\geq 400$  ng/mL. BSC, best supportive care; CI, confidence interval; FHSI-8, Functional Assessment in Cancer Therapy (FACT) Hepatobiliary Symptom Index; HR, hazard ratio; AFP, alpha-fetoprotein.

sorafenib toxicity on QoL in the first week of therapy [23]. Subsequent first-line RCTs only reported physical and role function as measured by EORTC QLQc30 in the BRISK-FL study evaluating brivanib [6]. Three other studies reporting no QoL data yet evaluated erlotinib [8], sunitinib [9] and linifanib [10]. A total of 4857 patients were recruited in these first-line studies. In second-line studies, no QoL data were reported from the BRISK-PS study evaluating brivanib [5], whereas another study evaluating everolimus only reported time to 5% deterioration in global QoL and physical function scales as measured by EORTC QLQc30 [7]. A total of 941 patients were enrolled in these studies. Hence, our current report provides an important and much more comprehensive source of QoL data in patients with advanced HCC undergoing systemic treatment. Another strength of our study was the placebo-controlled study design, which allowed an appreciation of symptom burden from the disease alone (placebo arm) rather than with the addition of toxicities from active treatment. Most recently, the RESORCE study reported a survival benefit in favour of regorafenib in patients who progressed after first-line sorafenib [11]. Patients had to be able to tolerate sorafenib to be eligible. However, there was a statistically significant worsening of QoL for regorafenib compared with placebo despite overall survival benefit and ability to tolerate sorafenib.

There are several limitations in our analysis. Although compliance was high for assessable patients, the absolute number of patients eligible for assessment became very low for cycles 10 and 16 due to the rapidly progressive nature of the disease. As the first treatment assessment was only performed 6 weeks from randomisation, this might not have captured early treatment-related toxicity and its impact on patients' QoL as could be seen with sorafenib [14]. It was unknown how missing data might have impacted results. A high proportion of censored patients in the assessment of time to PS

deterioration might have resulted from patients taken off study due to radiological progression before PS deterioration.

In conclusion, we report one of the most comprehensive data sets of QoL and symptom burden in patients undergoing systemic therapy for advanced HCC. Ramucirumab treatment was associated with maintenance of QoL in this group of patients. In patients with baseline AFP  $\geq 400$  ng/mL, a significant survival benefit was observed with ramucirumab coupled with benefits in patient-focused outcome.

### Funding

This work was supported by Eli Lilly and Company.

### Conflict of interest statement

MP-R has been both an advisor and a speaker for Bayer, Eli Lilly and Company, Bristol-Myers Squibb, and Novartis and has been an advisor and also received grant support from Bayer and ArQule. LB, ZLC, ACG, PBA and LY are all employees and stockholders of Eli Lilly and Company. AXZ received research funding from Eli Lilly and Company.

Ian Chau is a member of Advisory Board of Sanofi Oncology, Eli-Lilly, Bristol Meyers Squibb, MSD, Bayer, Roche, Five Prime Therapeutics and received research funding from Janssen-Cilag, Sanofi Oncology, Merck-Serono, Novartis and received honorarium from Taiho, Pfizer, Amgen, Eli-Lilly, Gilead Science. Joon Oh Park received funding from the Celgene, Astra Zeneca and honorarium from Celgene. Jean-Frédéric Blanc received honorarium from Bayer, Bristol-Myers-Squibb. Hyun Cheol Chung is a member of Advisory Board of Eli-Lilly, Bristol Meyers Squibb, MSD, Celltrion, Quintiles and received funding from Eli-Lilly, GSK, MSD and honorarium from Merck Serono.



Okusaka Takuji is a member of Advisory Board of Eli-Lilly and received funding from Eli-Lilly, Chugai Pharmaceutical, Eisai, Novartis, Shizuoka, Takeda, Yakult, Onco, Taiho, Nippon Boehringer Ingelheim, Kowa, Kyowa Hakko Kirin, Merck Serono, Ono Pharmaceutical, Bayer Yakuhin, Pfizer Japan, Astra-Zeneca, Dainippon Sumitomo Pharma, Nobelpharma, Zeria Pharmaceutical, GSK, Nono Carrier, Baxter and the honorarium from Chugai, Eisai, Novartis, Yakult, Taiho, Nippon, Merck Serono, Ono, Bayer, Dainippon Sumitomo Pharma, Nobelpharma, Zeria, Nono Carrier, Baxter, BMS, Nippon Chemiphar, Daiichi Sankyo, Nippon Kayaku, Astellas. Andrew Zhu received research funding from Eli-Lilly. The employment and stock of Lee Bowman, Zhanglin Cul, Paolo Abada is associated with Eli Lilly and Paolo Abada's pending patent is from Eli Lilly. All other remaining authors declare no conflicts of interests.

## Acknowledgements

The authors thank the patients, their families, the study sites and the study personnel who participated in this clinical trial. Eli Lilly and Company contracted with inVentiv Health Clinical for writing support, provided by Dr. Jarrett Coffindaffer, and editorial support, provided by Ms. Teri Tucker.

IC would like to thank National Health Service funding to the National Institute for Health Research Biomedical Research Centre at the Royal Marsden NHS Foundation Trust and The Institute of Cancer Research.

## References

- [1] Ferlay J, Soerjomataram I, Dikshit R, Eser S, Mathers C, Rebelo M, et al. Cancer incidence and mortality worldwide: sources, methods and major patterns in GLOBOCAN 2012. *Int J Cancer* 2015;136(5):E359–86.
- [2] Llovet JM, Ricci S, Mazzaferro V, Hilgard P, Gane E, Blanc JF, et al. Sorafenib in advanced hepatocellular carcinoma. *N Engl J Med* 2008;359(4):378–90.
- [3] Cheng AL, Kang YK, Chen Z, Tsao CJ, Qin S, Kim JS, et al. Efficacy and safety of sorafenib in patients in the Asia-Pacific region with advanced hepatocellular carcinoma: a phase III randomised, double-blind, placebo-controlled trial. *Lancet Oncol* 2009;10(1):25–34.
- [4] Fan SY, Eiser C, Ho MC. Health-related quality of life in patients with hepatocellular carcinoma: a systematic review. *Clin Gastroenterol Hepatol* 2010;8(7):559–64. e1–10.
- [5] Llovet JM, Decaens T, Raoul JL, Boucher E, Kudo M, Chang C, et al. Brivanib in patients with advanced hepatocellular carcinoma who were intolerant to sorafenib or for whom sorafenib failed: results from the randomized phase III BRISK-PS study. *J Clin Oncol* 2013;31(28):3509–16.
- [6] Johnson PJ, Qin S, Park JW, Poon RT, Raoul JL, Philip PA, et al. Brivanib versus sorafenib as first-line therapy in patients with unresectable, advanced hepatocellular carcinoma: results from the randomized phase III BRISK-FL study. *J Clin Oncol* 2013;31(28):3517–24.
- [7] Zhu AX, Kudo M, Assenat E, Cattan S, Kang YK, Lim HY, et al. Effect of everolimus on survival in advanced hepatocellular carcinoma after failure of sorafenib: the EVOLVE-1 randomized clinical trial. *JAMA* 2014;312(1):57–67.
- [8] Zhu AX, Rosmorduc O, Evans TR, Ross PJ, Santoro A, Carrilho FJ, et al. SEARCH: a phase III, randomized, double-blind, placebo-controlled trial of sorafenib plus erlotinib in patients with advanced hepatocellular carcinoma. *J Clin Oncol* 2015;33(6):559–66.
- [9] Cheng AL, Kang YK, Lin DY, Park JW, Kudo M, Qin S, et al. Sunitinib versus sorafenib in advanced hepatocellular cancer: results of a randomized phase III trial. *J Clin Oncol* 2013;31(32):4067–75.
- [10] Cainap C, Qin S, Huang WT, Chung IJ, Pan H, Cheng Y, et al. Linifanib versus Sorafenib in patients with advanced hepatocellular carcinoma: results of a randomized phase III trial. *J Clin Oncol* 2015;33(2):172–9.
- [11] Bruix J, Qin S, Merle P, Granito A, Huang YH, Bodoky G, et al. Regorafenib for patients with hepatocellular carcinoma who progressed on sorafenib treatment (RESORCE): a randomised, double-blind, placebo-controlled, phase 3 trial. *Lancet* 2017;389(10064):56–66.
- [12] Zhu AX, Park JO, Ryoo BY, Yen CJ, Poon R, Pastorelli D, et al. Ramucirumab versus placebo as second-line treatment in patients with advanced hepatocellular carcinoma following first-line therapy with sorafenib (REACH): a randomised, double-blind, multicentre, phase 3 trial. *Lancet Oncol* 2015;16(7):859–70.
- [13] Yount S, Cella D, Webster K, Heffernan N, Chang C, Odom L, et al. Assessment of patient-reported clinical outcome in pancreatic and other hepatobiliary cancers: the FACT Hepatobiliary Symptom Index. *J Pain Symptom Manage* 2002;24(1):32–44.
- [14] Steel JL, Eton DT, Cella D, Olek MC, Carr BI. Clinically meaningful changes in health-related quality of life in patients diagnosed with hepatobiliary carcinoma. *Ann Oncol* 2006;17(2):304–12.
- [15] EuroQol—a new facility for the measurement of health-related quality of life. *Health Policy* 1990;16(3):199–208.
- [16] Pickard AS, Neary MP, Cella D. Estimation of minimally important differences in EQ-5D utility and VAS scores in cancer. *Health Qual Life Outcomes* 2007;5:70.
- [17] Norman GR, Sloan JA, Wyrwich KW. Interpretation of changes in health-related quality of life: the remarkable universality of half a standard deviation. *Med Care* 2003;41(5):582–92.
- [18] Kaplan EL, Meier P. Non parametric estimation from incomplete observations. *J Am Stat Assoc* 1958;53:457–81.
- [19] Cox DR. Regression models and life tables. *J R Stat Soc A* 1972;29:187–220.
- [20] Eisenhauer EA, Therasse P, Bogaerts J, Schwartz LH, Sargent D, Ford R, et al. New response evaluation criteria in solid tumours: revised RECIST guideline (version 1.1). *Eur J Cancer* 2009;45(2):228–47.
- [21] Heffernan N, Cella D, Webster K, Odom L, Martone M, Passik S, et al. Measuring health-related quality of life in patients with hepatobiliary cancers: the functional assessment of cancer therapy-hepatobiliary questionnaire. *J Clin Oncol* 2002;20(9):2229–39.
- [22] Gutman SI, Piper M, Grant MD, Basch E, Olinisky DM, Aronson N. AHRQ methods for effective health care. In: Progression-free survival: what does it mean for psychological well-being or quality of life? Rockville (MD): Agency for Healthcare Research and Quality (US); 2013.
- [23] Brunocilla PR, Brunello F, Carucci P, Gaia S, Rolle E, Cantamessa A, et al. Sorafenib in hepatocellular carcinoma: prospective study on adverse events, quality of life, and related feasibility under daily conditions. *Med Oncol* 2013;30(1):345.

GUIDELINES

# Asia–Pacific clinical practice guidelines on the management of hepatocellular carcinoma: a 2017 update

Masao Omata<sup>1,2</sup> · Ann-Lii Cheng<sup>3</sup> · Norihiro Kokudo<sup>4</sup> · Masatoshi Kudo<sup>5</sup> · Jeong Min Lee<sup>6</sup> · Jidong Jia<sup>7</sup> · Ryosuke Tateishi<sup>8</sup> · Kwang-Hyub Han<sup>9</sup> · Yoghesh K. Chawla<sup>10</sup> · Shuichiro Shiina<sup>11</sup> · Wasim Jafri<sup>12</sup> · Diana Alcantara Payawal<sup>13</sup> · Takamasa Ohki<sup>14</sup> · Sadahisa Ogasawara<sup>15</sup> · Pei-Jer Chen<sup>16</sup> · Cosmas Rinaldi A. Lesmana<sup>17,18</sup> · Laurentius A. Lesmana<sup>17</sup> · Rino A. Gani<sup>18</sup> · Shuntaro Obi<sup>19</sup> · A. Kadir Dokmeci<sup>20</sup> · Shiv Kumar Sarin<sup>21</sup>

Received: 6 January 2017 / Accepted: 2 May 2017 / Published online: 15 June 2017  
© The Author(s) 2017. This article is an open access publication

**Abstract** There is great geographical variation in the distribution of hepatocellular carcinoma (HCC), with the majority of all cases worldwide found in the Asia–Pacific region, where HCC is one of the leading public health problems. Since the “Toward Revision of the Asian Pacific Association for the Study of the Liver (APASL) HCC Guidelines” meeting held at the 25th annual conference of the APASL in Tokyo, the newest guidelines for the

treatment of HCC published by the APASL has been discussed. This latest guidelines recommend evidence-based management of HCC and are considered suitable for universal use in the Asia–Pacific region, which has a diversity of medical environments.

**Keywords** Hepatocellular carcinoma · Asia–Pacific · APASL · Treatment algorithm

✉ Masao Omata  
aug8808@yahoo.co.jp

<sup>1</sup> Department of Gastroenterology, Yamanashi Prefectural Central Hospital, Kofu-city, Yamanashi, Japan

<sup>2</sup> The University of Tokyo, Tokyo, Japan

<sup>3</sup> Department of Oncology and Internal Medicine, National Taiwan University Hospital, National Taiwan University Cancer Center and Graduate Institute of Oncology, National Taiwan University, Taipei, Taiwan

<sup>4</sup> Hepato-Biliary-Pancreatic Surgery Division and Artificial Organ and Transplantation Division, Department of Surgery, Graduate School of Medicine, The University of Tokyo, Tokyo, Japan

<sup>5</sup> Department of Gastroenterology and Hepatology, Kindai University School of Medicine, Osaka-Sayama, Osaka, Japan

<sup>6</sup> Department of Radiology and Institute of Radiation Medicine, Seoul National University College of Medicine, Seoul, Republic of Korea

<sup>7</sup> Beijing Key Laboratory of Translational Medicine on Cirrhosis, National Clinical Research Center for Digestive Diseases, Liver Research Center, Beijing Friendship Hospital, Capital Medical University, Beijing, China

<sup>8</sup> Department of Gastroenterology, Graduate School of Medicine, The University of Tokyo, Tokyo, Japan

<sup>9</sup> Department of Internal Medicine, Yonsei University College of Medicine, Seoul, Republic of Korea

<sup>10</sup> Department of Hepatology, Postgraduate Institute of Medical Education and Research, Chandigarh, India

<sup>11</sup> Department of Gastroenterology, Juntendo University, Tokyo, Japan

<sup>12</sup> Department of Medicine, Aga Khan University and Hospital, Karachi, Pakistan

<sup>13</sup> Department of Hepatology, Cardinal Santos Medical Center, Manila, Philippines

<sup>14</sup> Department of Gastroenterology, Mitsui Memorial Hospital, Tokyo, Japan

<sup>15</sup> Department of Gastroenterology and Nephrology, Graduate School of Medicine, Chiba University, Chiba, Japan

<sup>16</sup> Department of Internal Medicine, National Taiwan University Hospital, Taipei, Taiwan

<sup>17</sup> Digestive Disease and GI Oncology Center, Medistra Hospital, University of Indonesia, Jakarta, Indonesia

<sup>18</sup> Department of Internal Medicine, Cipto Mangunkusumo Hospital, University of Indonesia, Jakarta, Indonesia

<sup>19</sup> Third Department of Internal Medicine, Teikyo University School of Medicine, Chiba, Japan

## Introduction

Liver cancer is currently the second most common cause of cancer-related death worldwide [1], and hepatocellular carcinoma (HCC) accounts for more than 90% of liver cancers [2]. There has been a marked increase in HCC-related annual death rates during the past two decades, with the majority of all cases of HCC worldwide found in the Asia–Pacific region [3]. Thus, HCC represents a major public health problem in the Asia–Pacific region.

The Asian Pacific Association for the Study of the Liver (APASL) HCC guidelines were published in 2010 [4], being the oldest of the major guidelines. The “Toward Revision of the APASL HCC Guidelines” meeting was held at the 25th annual conference of the APASL in Tokyo on February 23, 2016. The attendees consisted of expert hepatologists, hepatobiliary surgeons, radiologists, and oncologists from the Asia–Pacific region. These members have discussed and debated the contents of the newest guideline. The new guideline is evidence based and is considered to be generally accepted in the Asia–Pacific region, which has a diversity of medical environments. The evidence and recommendations in the guideline have been graded according to the Grading of Recommendations Assessment, Development and Evaluation (GRADE) system (Table 1) [5, 6]. The finalized recommendations for the management of HCC are presented in this review.

## Epidemiology and risk factors

Liver cancer is the sixth most common cancer worldwide, being the fifth most common in males (7.5% of total) and the ninth in females (3.4% of total) [7]. Each year, approximately 78,200 new cases are diagnosed [7]. The prognosis for liver cancer is very poor (overall mortality to incidence rate, 0.95). The most frequent type is HCC, a cancer derived from liver hepatocytes. There are other types of liver cancer, such as intrahepatic cholangiocarcinoma (derived from biliary cells), sarcomas, and so forth, which should also be taken into account. Worldwide, approximately 80% of HCC cases are caused by hepatitis B virus (HBV) and/or hepatitis C virus (HCV) infection, especially in the setting of established cirrhosis or advanced fibrosis. The highest age-adjusted incidence rates (>20/100,000) are recorded in East Asia (North and South Korea, China, and Vietnam) and sub-Saharan

Africa [8]. Approximately 75% of liver cancers occur in Asia, with China accounting for more than 50% of the world’s burden [9]. The incidence of HCC is likely to increase over the next 10–20 years and to peak around 2030.

The global age distribution of HCC varies by region, sex, and etiology. Globally, the rate of males suffering from HCC is higher than that of females, with male-to-female ratio ranging between 2:1 and 4:1, with the difference being much greater in high-risk areas. The sex disparity in rates is not well understood, although most liver cancer risk factors are more prevalent in males than females. Differences in sex steroid hormones, immune responses, and epigenetics could be related to the higher rates among males. These variations of age-specific patterns are likely related to the differences in the dominant hepatitis virus in the population, the age at viral infection, as well as the existence of other risk factors. In addition to sex differences, racial/ethnic disparity within multiethnic populations is also notable. Rates of liver cancer among persons of the same ethnicity also vary by geographic location; For example, liver cancer rates among Chinese populations outside China are lower than the rates reported by Chinese registries.

The single largest risk factor for development of HCC is cirrhosis of any etiology, which is present in 70–90% of those who have primary liver cancer [10]. In Africa and Asia, where HBV is endemic, 60% of HCC is associated with HBV, 20% is related to HCV, and the remaining is distributed among other risk factors. The risk of HCC developing among patients chronically infected with HBV ranges from 10- to 100-fold greater compared with the rates in uninfected people, depending on the markers and populations that are evaluated. In HCV infection, the relative risk (RR) for HCC developing in patients with serologically confirmed HCV infection is estimated to be 17-fold. The effect of high rates of alcohol abuse in Asia (as in the rest of the world) and the recent (10–15 year) obesity and type 2 diabetes mellitus (DM) epidemic in Asia may increase the HCC incidence in the next 25 years. In addition, patients who have multiple risk factors are not uncommon in the Asia–Pacific region [i.e., HBV/HCV, alcohol/HBV or HCV, DM/HBV or HCV, and HCV/human immunodeficiency virus (HIV)].

The incidence of HCC has remained the same over the last 20 years in most Asian–Pacific countries, except Singapore, where the incidence for males and females has fallen over the last 30 years. China and Taiwan have reported increasing incidence of HCC for males and females. This may be due to increasing awareness of reporting and better screening services. The country with the highest incidence rate, however, is Mongolia, with an age-standardized rate per 100,000 persons of 78.1.

<sup>20</sup> Department of Gastroenterology, Ankara University School of Medicine, Ankara, Turkey

<sup>21</sup> Department of Hepatology, Institute of Liver and Biliary Sciences, New Delhi, India

**Table 1** Grading of evidence and recommendations (adapted from the GRADE system [5, 6])

	Notes	Symbol
Grading of evidence		
High quality	Further research is very unlikely to change our confidence in the estimate of effect	A
Moderate quality	Further research is likely to have an important impact on our confidence in the estimate of effect and may change the estimate	B
Low or very low quality	Further research is very likely to have an important impact on our confidence in the estimate of effect and is likely to change the estimate. Any estimate of effect is uncertain	C
Grading of recommendation		
Strong recommendation warranted	Factors influencing the strength of the recommendation included the quality of the evidence, presumed important patient outcomes, and cost	1
Weaker recommendation	Variability in preferences and values, or more uncertainty: more likely a weak recommendation is warranted. Recommendation is made with less certainty; higher cost or resource consumption	2

Even within specific geographic regions, however, there is great variability. In Australia, as in the USA, traditionally very low-incidence regions, there has been a substantial increase (two- to threefold) in HCC incidence over the last 25 years, most probably due to immigration of people from the Asia-Pacific and other regions with high prevalence rates of chronic HBV infection, but also due to the epidemics of chronic HCV infection, possibly obesity, and DM.

## Risk factors for HCC

### HBV

Several meta-analyses have demonstrated that the risk of HCC is 15–20 times greater among HBV-infected individuals compared with the uninfected population [11]. Countries with chronic HBV infection prevalence greater than 2% have increased incidence and mortality rates of HCC [12]. Case-control studies in all regions of Asia have shown that chronic HBV infection is significantly more common among HCC cases than controls with odds ratios (ORs) ranging between 5:1 and 65:1 [13]. Similarly, prospective studies of HBV carriers have consistently demonstrated high RRs for HCC, ranging from 5 to 103 [14].

The lifetime risk of HCC among chronic HBV-infected patients is estimated to be 10–25% [15]. Several factors have been reported to increase the HCC risk among HBV carriers, including demographics (male sex, older age, Asian or African ancestry, family history of HCC), viral [higher levels of HBV replication; HBV genotype; longer duration of infection; coinfection with HCV, HIV, or hepatitis D virus (HDV)]; clinical (cirrhosis), and environmental or lifestyle factors (exposure to aflatoxin, heavy alcohol drinking, or tobacco smoking).

Risks of HCC among HBV-infected patients vary by several factors, the major one being serum HBV-DNA levels. Although there is no discrete cutoff level, having greater than Log<sub>10</sub> 5/mL viral copies confers a 2.5- to threefold greater risk over an 8- to 10-year follow-up period than does having a lower viral load [14]. The cumulative incidence of HCC increases with serum HBV-DNA levels. A recent hospital-based cohort study further validated the HCC risk, showing it started to increase when the HBV-DNA level was higher than 2000 IU/mL [16].

In addition to HBV-DNA levels, the clinical significance of quantitative hepatitis B surface antigen (HBsAg) has become increasingly recognized. Data from the Risk Evaluation of Viral Load Elevation and Associated Liver Disease/Cancer–Hepatitis B Virus (REVEAL–HBV) and the ERADICATE-B study all showed that serum HBsAg  $\geq 1000$  IU/mL and HBV-DNA levels are complementary markers in predicting disease progression to cirrhosis and HCC [17, 18]. Cumulative HCC risk from age 30 to 70 years is estimated to be 87% for those persistently positive for HBsAg and hepatitis B envelope antigen (HBeAg), 12% for those persistently positive for HBsAg only, and 1% for those negative for HBsAg [19]. Therefore, prolonged duration of HBeAg positivity or high HBV-DNA levels may be associated with increased risk of HCC.

In multiple population-based studies, genotype C has been associated with higher risk of HCC than genotypes A, B, and D [20, 21]. In studies controlled for genotype, double mutations in the basal core promoter of the HBV genome were independent predictors of increased risk [22]. Mutations in the precore region of the viral genome also have been associated with risk, although less consistently so [23]. A study in Taiwan reported the importance of perinatal transmission of HBV and maternal virus load as a risk factor for HBV carcinogenesis in a familial clustering of HCC [24]. A family history of liver cancer, particularly



among first-degree relatives, in HBV-infected individuals has been shown to increase the incidence of HCC.

Prevention of chronic HBV infection via vaccination drastically reduces the risk of HCC. In Taiwan, 30 years after the initiation of universal newborn vaccination, HBV carrier rates in persons younger than age 30 have decreased from 10–17% to 0.7–1.7% and rates of HCC have decreased by 80% [25].

Several host and viral factors predictive of HCC risk have been identified, and the Risk Estimation for Hepatocellular Carcinoma in Chronic Hepatitis B (REACH-B) study has developed and validated a predictive score for the risk of development of HCC in 3584 noncirrhotic chronic HBV Taiwanese and a validation cohort with 1050 patients with chronic HBV [26]. The 17-point risk score is composed of five predictors of HCC, including male sex, age, serum alanine aminotransferase (ALT) level, HBeAg status, and serum HBV-DNA level. The risk score can precisely estimate the risk of HCC development at 3, 5, and 10 years of follow-up.

Baseline liver stiffness values could be an independent predictor of HCC in patients with chronic HBV infection, where the 3-year cumulative incidence of HCC was significantly higher in patients with a higher liver stiffness value [27]. A recent Korean study included 1250 chronic HBV patients with baseline liver stiffness values to construct a predictive model for HCC occurrence based on a Cox proportional hazards model [28]. By using multivariate analysis, age, male sex, and liver stiffness values were independent predictors of HCC, whereas HBV-DNA levels >20,000 IU/L showed borderline statistical significance. A predictive model for HCC was developed using these four variables, with a correlation coefficient of 0.905 between predicted and observed risks of HCC occurrence.

It is currently clear that antiviral therapy reduces but does not eliminate the risk of HCC in chronic HBV patients with or without cirrhosis. Emerging data with the currently first-line nucleos(t)ide analogs, entecavir and tenofovir, suggest that the risk of HCC is also reduced under long-term therapies with these agents [29, 30]. The treatment benefit from the reduction of HCC incidence is always greater in patients with high baseline HCC risk, particularly those with cirrhosis. In addition, the reduction of HCC incidence under a high genetic barrier nucleos(t)ide analog is higher in the vast majority of patients who will achieve virological remission compared with those who may maintain detectable viral replication.

## HCV

Prospective studies have shown an increased risk of HCC in HCV-infected cohorts. In Japan, HCV antibody (HCV Ab)-positive cases of HCC accounted for more than 70%

of cases diagnosed over the last 10 years [31]. Recently, its incidence has been decreasing. In Korea, approximately 10–20% of HCC patients are positive for HCV Ab. A meta-analysis of case-control studies showed that individuals positive for HCV Ab had 17 times the risk of HCC compared with the HCV Ab-negative cohort [32]. HCV appears to increase the risk of HCC by not only inducing hepatic inflammation and fibrosis, but also promoting malignant transformation of infected cells. The risk is highest among cases with cirrhosis where HCC develops at rate of 1–4% per year, though rates up to 8% have been reported in Japan [33]. The Hepatitis C Antiviral Long Term Treatment Against Cirrhosis (HALT-C) trial showed that 8% of patients without cirrhosis but with advanced fibrosis developed HCC [34]. Other risk factors that increase the risk of HCC in infected patients include male sex, coinfection with HIV or HBV, HCV genotype 1b, older age, presence of DM and obesity, and high level of chronic alcohol consumption. There is no consistent evidence that HCV viral load or quasispecies are important in determining the risk of progression to HCC.

## HBV/HCV coinfection

Three meta-analyses have confirmed that patients with dual HBV/HCV infection have an increased risk of HCC [11, 35, 36]. Different mechanisms have been hypothesized as being associated with development of HBV- or HCV-related HCC. Both viruses could play an active role at different steps of the carcinogenic process when they are present together in hepatocytes, and may be synergistic in causing HCC.

## Alcohol

A recent meta-analysis of 19 prospective studies estimated a 16% increased risk of liver cancer among consumers of three or more drinks per day and a 22% increased risk among consumers of six or more drinks per day [37]. Higher risks were found even for the lowest dose of alcohol (25 g/day), corresponding to approximately two drinks per day [38]. Chronic alcohol use of more than 80 g per day for longer than 10 years increases the risk for HCC by fivefold [32]. A recent meta-analysis showed a dose-response relationship between alcohol intake and liver cancer with RR of 1.19 [95% confidence interval (CI) 1.12–1.27], 1.40 (95% CI 1.25–1.56), and 1.81 (95% CI 1.50–2.19) for 25, 50, and 100 g of alcohol intake per day, respectively [39]. A study from the University of Michigan confirmed that alcohol consumption had a dose-dependent effect on the risk of HCC; the risk increased after 1500 g-years of alcohol exposure (60 g per day for at least 25 years) [40].



However, there is no safety limit for the effects of alcohol on the liver. In a study from Japan involving 804 HCC cases, the multivariate-adjusted hazard ratios (HRs; 95% CI) for alcohol intakes of 0.1–22.9, 23.0–45.9, 46.0–68.9, 69.0–91.9, and >92.0 g per day compared with occasional drinkers were 0.88 (0.57–1.36), 1.06 (0.70–1.62), 1.07 (0.69–1.66), 1.76 (1.08–2.87), and 1.66 (0.98–2.82), respectively [41]. In females who drank more than 23.0 g per day, a significantly increased risk was noted when compared with social drinkers (HR 3.60; 95% CI 1.22–10.66). A meta-analysis of four studies performed to assess the decline of liver cancer risk over time for former drinkers found that the risk of liver cancer falls after cessation by 6–7% a year, but an estimated time period of 23 years is required after drinking cessation before the risk returns to that of nondrinkers, with a large 95% CI of 14–70 years [42].

Alcohol acts synergistically with preexisting chronic liver disease, such as HCV, HBV, and fatty liver disease, as well as lifestyle choices, such as smoking and obesity, to further increase the risk of HCC in these disease states. In a retrospective cohort study by Berman et al. [43], the patients with cirrhosis due to a combination of HCV and alcohol had a significantly higher risk of HCC than those with cirrhosis due to alcohol alone (HR 11.2; 95% CI 2.3–55.0). Patients with HCV and alcohol exposure had a reduced tumor-free survival compared with those with HCV alone [44]. A multivariate analysis of 553 patients with HCC and 160 control subjects affected with HBV from China by Zhu et al. [45] revealed that heavy alcohol use, smoking, and positive family history of liver cancer are associated with HCC development among patients with HBV infection. A prospective case–control study of 210 subjects from the University of Michigan found that there was a dose-dependent relationship between alcohol and tobacco exposure with risk of HCC and synergistic index of 3.3 [40]. History of smoking and alcohol abuse worsened prognosis independently of each other, especially in viral hepatitis-related and early HCC. Abstinence from either reduced HCC-specific mortality, but only after 10 years of cessation [46]. An analysis of 2260 Taiwanese males from the REVEAL-HBV study cohort showed that the risk of HCC increased synergistically in alcohol users who had extreme obesity compared with those without extreme obesity and with nonusers of alcohol [47]. A study from Italy enrolled 465 HCC patients and compared them with 618 cirrhotic patients without HCC and 490 healthy controls, evaluating the association among DM and alcohol abuse in the HCC group versus both control groups. This study showed that, for alcohol abuse alone, the OR for HCC was 3.7 (95% CI 2.5–5.4) and

49.0 (95% CI 21.5–111.8) in DM with significant alcohol intake [48].

### Nonalcoholic fatty liver disease (NAFLD)

Meta-analyses of DM and HCC have consistently estimated RRs of 2.0–2.5 and have found that the relationship is consistent across various populations and is independent of other risk factors [49–51]. Several studies have reported that obesity is also related to liver cancer [52]. In comparing normal-weight persons with overweight and obese persons, a meta-analysis of 11 cohort studies found significant liver cancer risks among overweight and obese persons [53]. Similarly, a meta-analysis of four studies of metabolic syndrome and HCC estimated a significant RR of 1.81 [54]. Although the RRs of DM, obesity, and metabolic syndrome do not approach those of HCV or HBV, they are far more prevalent conditions than HCV and HBV in developed countries. Given the increasing prevalence of these conditions, the proportion of HCC related to obesity, DM, and metabolic syndrome will likely increase in the future.

The results of recent studies demonstrated that HCC is more prevalent in the setting of obesity and insulin resistance, and may occur in nonalcoholic fatty liver disease (NAFLD) patients without cirrhosis. Indeed, in a recent retrospective cohort study that evaluated trends in HCC etiology among adult recipients of liver transplantation (LT) from 2002 to 2012, the number of patients undergoing LT for HCC secondary to nonalcoholic steatohepatitis (NASH) increased by nearly fourfold, whereas the number of patients with HCC secondary to HCV increased by only twofold [55]. Available data suggest that obesity increases the risk of HCC 1.5- to fourfold. One large meta-analysis included seven cohort studies of 5037 overweight subjects (body mass index 25–30 kg/m<sup>2</sup>) and ten studies of 6042 obese subjects (body mass index >30 kg/m<sup>2</sup>); compared with normal-weight people, HCC risk increased 17% in those who were overweight and 89% in those who were obese [53]. In a study from Japan that looked at the recurrence of HCC after ablation therapy in NASH patients, increased visceral fat was an independent risk factor for recurrence of HCC at 3 years (75.1 versus 43.1% with low visceral fat) [56]. In a similar trend seen in many studies, type 2 DM was associated with a substantially increased risk of HCC. Although it is possible that the increased HCC risk associated with DM seen in these studies may be mediated through the development of NAFLD, the presence of multiple pathogenic mechanisms common to obesity, insulin resistance, and NAFLD suggests that this link may not be mediated through NAFLD per se.

Evidence of the development of HCC in noncirrhotic patients continues to accumulate in case reports or case series. Obesity, insulin resistance, and the proinflammatory milieu of NASH may mediate carcinogenesis directly. In a recent study analyzing 1419 HCC cases that were related to NASH (120 cases), HCV (1013 cases), and alcohol (286 cases), cirrhosis was present in only 58.3% of NASH-related HCC cases [57]. Limited available data suggest that risk factors for the development of NASH without cirrhosis include older age, male sex, and metabolic syndrome [58]. In a study of 87 Japanese NASH patients with HCC, Yasui et al. [59] found that 56% of cases were noncirrhotic, and it was noted that males developed HCC at a less advanced stage of liver fibrosis than females. Hashimoto et al. [58] examined 34 cases of NASH-related HCC and found that there was a prevalence of advanced age, male sex, obesity, and type 2 DM; 12% of the patients had stage 1 or 2 fibrosis, and 88% had advanced fibrosis (stage 3–4). These HCC patients tended to be older, male, and have metabolic syndrome.

### Budd–Chiari syndrome

Twelve studies were conducted in Asian countries between 1958 and 2008 to evaluate the prevalence of HCC in Budd–Chiari syndrome patients; the pooled prevalence of HCC was 17.6% in Budd–Chiari syndrome patients and 26.5% in inferior vena cava obstruction patients [60]. There was no statistically significant difference in sex, age, or site of obstruction between HCC and non-HCC groups. It has not been clarified whether HCC occurred only in cirrhosis patients. The prevalence of HCC in Budd–Chiari syndrome patients is highly variable, ranging from 2.0 to 51.6%, as the diagnostic criteria and the methods are significantly discrepant among studies, which potentially influence the prevalence of HCC, and the length of follow-up was also different [61, 62]. In addition, it is necessary to consider carefully that occurrence of HCC is difficult to identify using dynamic computed tomography (CT) or dynamic magnetic resonance imaging (MRI) because of the changes in venous drainage associated with venous outflow obstruction. Further studies are necessary to evaluate the risk factors for HCC in Budd–Chiari syndrome.

### HCC in other liver diseases

Other notable causes of cirrhosis can increase the risk of the development of HCC. In patients with genetic hemochromatosis, in whom cirrhosis is established, the RR for liver cancer is approximately 20-fold higher. The incidence of liver cancer in individuals with stage 4 primary biliary cholangitis (PBC) is similar to the incidence in patients with HCV and cirrhosis, and this suggests that

PBC confers a high risk for HCC [63]. Patients with autoimmune hepatitis and cirrhosis also have an increased incidence of liver cancer [64]. In addition, HCC has been reported in patients with Wilson disease. However, a recent report indicated that the risk of HCC was low in Wilson disease even in cases of cirrhosis [65].

### Host genetics

HCC develops in only a small percentage of those infected with HCV or HBV. Host genetic makeup may be an important factor that influences progression to HCC. Two meta-analyses identified variants of tumor necrosis factor (TNF) associated with a higher risk of HCC [66, 67]. They showed that TNF $\alpha$ -308 AA and AG variants (versus GG) were associated with a significantly increased risk of HCC. A recent meta-analysis concluded that null genotypes of glutathione *S*-transferase (GST) genes (*GSTM1* or *GSTT1*) were associated with an increased risk of HCC [68].

### Aflatoxin

Aflatoxin B1 is a major hepatocarcinogen [69], which acts in part by causing mutations of codon 249, a mutational hotspot of the p53 tumor suppressor gene. Aflatoxin B1 exposure, however, is more common in areas where HBV is the dominant virus, including sub-Saharan Africa, Southeast Asia, and China. Within these areas, higher levels are found among rural than urban populations [70], among males than females [71], and among persons chronically infected with HBV [72]. Aflatoxin B1 is metabolized by CYP2E1, which is induced by alcohol. Thus, alcohol may have an incremental genotoxic effect on aflatoxin B1. One case–control study suggests that combining aflatoxin B1 load and alcohol intake has a synergistic and a statistically significant effect on RR (RR = 35) [73]. There is a synergistic association between aflatoxin B1 and HBV in increasing the risk of HCC. Compared with persons with neither risk factor, the risk of HCC is reported to be fourfold greater among persons with elevated levels of aflatoxin B1, sevenfold greater among chronic HBV carriers, and 60-fold greater among persons with both factors [74, 75]. Evidence suggests that there is also a synergistic effect between aflatoxin B1 and HCV infection [76].

### Tobacco

In 2004, the International Agency for Research on Cancer (IARC) concluded that there was sufficient evidence that tobacco smoking increased the risk of liver cancer [77]. A recent meta-analysis estimated that there was a 1.5-fold increased risk of HCC among current smokers, a risk

similar to that imposed by obesity [78]. Inconsistent findings in studies of the same populations, and the correlation of smoking with other risk factors, such as HBV, HCV infection, and alcohol consumption, have made the relationship between tobacco and HCC difficult to define.

### Coffee and tea

Recent meta-analyses have examined the association between coffee and tea and the risk of HCC [79, 80]. The coffee meta-analysis found a significant 40% reduced risk of HCC among consumers, and tea was associated with a nonsignificant 23% reduced risk. Compounds in coffee that potentially have chemopreventive effects include diterpenes, chlorogenic acid, and caffeine [81]. Diterpenes are lipids that inhibit enzyme expression and enzymatic activity, induce detoxifying enzymes, and regulate signaling pathways [82]. Chlorogenic acid is a polyphenol that increases the activity of detoxifying enzymes [83]. Caffeine has antioxidant properties and increases the metabolic rate and energy expenditure, which could potentially regulate weight and reduce the risk of developing metabolic syndrome [84]. Similarly, tea contains bioactive compounds, including caffeine and polyphenolic compounds. One specific polyphenol, epigallocatechin-3-gallate, has shown promise as a chemopreventive agent by inhibiting enzymatic activities, cell invasion, angiogenesis, and metastasis [85].

### HCC in children

HCC is rare among adolescents and accounts for less than 1% of all malignant neoplasms among children younger than 20 years [86]. Hence, the risk factors are not well studied. Hepatoblastoma is the most common primary hepatic malignancy (48%); HCC is the second most common primary liver malignancy of childhood (27%), with vascular tumors and sarcomas making up the rest. HCC has an incidence of 0.3–0.45 cases per million per year and represents an increasingly common indication for LT in children [87]. HCC is more common in adolescents (10–14 years), more common in males than in females with a 3:1 preponderance, and tends to present with more advanced disease in children than in adults. HCC incidence increases significantly with age. Overall, only 0.5–1% of cases occur before the age of 20 years. The incidence of HCC in chronic HBV carriers is approximately 100-fold greater than that in the HBV-negative population and is more common in areas with high endemic HBV infection rates [88].

The decrease of HBV because of neonatal vaccination has led to a reduction of cases in childhood, which will, in time, be reflected in the adult population [89]. Although

HCV is a known risk factor for HCC in adults, it is rare in children, and there is only a single case report of this occurrence requiring a transplant [90].

Inherited metabolic disorders, specifically hereditary tyrosinemia,  $\alpha$ -1-antitrypsin deficiency, and glycogen storage disease type 1, are associated with childhood cirrhosis and HCC. Tyrosinemia I (fumarylacetoacetate hydrolase deficiency) is an autosomal recessive inborn error of tyrosine metabolism that leads to liver failure in infancy or chronic liver disease with cirrhosis. Without treatment, there is a high risk of HCC in childhood or early adolescence. HCC is also associated with glycogen storage disease types I and IV [91].

Only approximately 30% of pediatric cases of HCC are associated with cirrhosis or preexisting liver abnormality, in contrast to adult HCC in which cirrhosis is present in 70–90% of cases. Similarly,  $\alpha$ -1-antitrypsin deficiency exhibits a different mechanism for carcinogenesis, where liver injury results from abnormal and chronic regenerative signaling from the sick cells to younger, less sick hepatocytes: chronic regeneration in the presence of tissue injury leading to adenomas and ultimately to carcinomas. It was recently suggested that progressive familial intrahepatic cholestasis type 2 (PFIC 2), associated with a mutation of the *ABCB11* gene resulting in deficiency of bile salt export pump (BSEP; a membrane canalicular bile acid transporter), represents a specific and previously unrecognized risk for HCC in young children [92].

### Epidemiology of HCC in Asia-Pacific countries

#### Japan

In Japan, HCC ranks as the fifth most common cancer, being the fourth most common in males and the sixth in females. Nationwide follow-up surveys by the Liver Cancer Study Group of Japan (LCSGJ) show that the age-standardized incidence rate of HCC and total number of deaths from HCC in Japan in males have shown a gradual declining trend since 2004 [7]. In 2012, a total of 30,690 people died of liver cancer in Japan. Although Japan is one of the Asia-Pacific countries with a high HCC incidence rate, the cause of HCC in Japan differs greatly from other countries in the region. Chronic HCV infection is more common than chronic HBV infection in Japan; chronic HCV infection accounts for 64.7% of HCCs. Chronic HBV infection, on the other hand, accounts for only 15.1% of HCCs [93]. In the near future, the prevalence of HCV-related HCC is expected to decrease because of the falling prevalence of HCV and deaths of older HCV patients from unrelated causes [94].

Japan has created the world's first nationwide HCC surveillance program. Japan introduced a liver cancer screening program as early as the 1980s. In 1999, the Japan Society of Hepatology (JSH) began the Eliminate Liver Cancer Program [95]. In addition, the Basic Act on Hepatitis Measures enacted by the Japanese Ministry of Health, Labour and Welfare in 2009 established a system by which public health centers and clinics could perform blood tests free of charge for the general public to check for infection with HBV or HCV. Other possible reasons for the declining incidence rate may be the great success of post-natal HBV vaccination, screening of donated blood, and efforts to educate the general public about HCV.

### India

In India, information on HCC is inadequate. Based on cancer registries in five Indian urban populations (Mumbai, Bangalore, Chennai, Delhi, and Bhopal) over a period of two decades, liver cancer ranks as the fifth most frequent cancer for both sexes [96]. However, the cancer registries in India probably do not provide accurate estimates of HCC prevalence due to their predominantly urban location and because the sources of information on cancers are from cytology, oncology sites, and municipal registers of death. The available data indicate that the age-adjusted incidence rate of HCC in India for males ranges from 0.7 to 7.5 and for females from 0.2 to 2.2 per 100,000 population per year [97]. The incidence of HCC in patients with cirrhosis in India is 1.6% per year. The male-to-female ratio for HCC in India is 4:1. The age of presentation varies from 40 to 70 years. The age-standardized mortality rate for HCC in India for males is 6.8 per 100,000 population and for females is 5.1 per 100,000 population. In India, HBV and HCV infection and alcohol consumption are the main causes of HCC [98]. Reports from tertiary care centers in India on HCC indicate that 70–97% of patients with HCC had underlying cirrhosis of the liver at the time of diagnosis. Approximately one-quarter of HCC cases diagnosed in India do not have any known predisposing risk factors [99]. The presence of any HBV marker (HBsAg positive or presence of HBV antibodies even in absence of HBsAg) increases the risk of HCC [100]. Moreover, huge regional differences in the prevalence of HBV and HCV infection might exist in India (i.e., the prevalence of HCV infection was the highest in the Punjab area). These differences might translate into large differences in the incidence of HCC between states. Because of the discrepant and isolated reports on genetic risk factors for HCC, the data are currently insufficient to implicate any genetic risk factor for HCC in India. The unpublished data from various tertiary care centers suggest that the incidence of HCC is increasing in India.

### Australia

Liver cancer is relatively uncommon in Australia, where it ranks 15th in males and 20th in females [101]. However, over the last three decades, HCC incidence rates have been rising in Australia, both from cases attributed to HCV and from HBV, the latter related to migration from high-prevalence countries [101]. Data from the New South Wales Cancer Registry indicate that age-standardized primary liver cancer incidence rates have increased from 2.0 and 0.5 per 100,000 population in 1972 in males and females, respectively, to 7.4 and 2.9 per 100,000 population in 2004 [102]. Other known risk factors for the increasing incidence of HCC include HBV/HCV coinfection and cirrhosis due to various other causes. According to an Australian study of HCC incidence as stratified by different chronic liver diseases, the HCC incidence rate of patients with HBV mono-infection was markedly higher than that of those with HCV mono-infection (9.5 versus 6.9 cases per 10,000 population-years) [103]. A recent population-based linkage study showed that Asian-born residents with chronic HBV were 30 times more likely to suffer HCC compared with Australian-born residents [104]. The incidence of HCC with chronic viral hepatitis is associated with increasing age, male sex, and other comorbidities. The highest age-specific risk of developing HCC occurs among people aged 75 years and older, being over 14 times the risk for those aged under 45 years. The risk in male patients is threefold higher than that in females [103].

### China

Liver cancer is the second most common cancer in China. Overall, the estimated incidence rate of HCC is 40.0 in males and 15.3 in females per 100,000 population. HCC is ranked as the second most common cause of cancer mortality in males after lung cancer, while it ranked third in females, after lung and gastric cancer. Approximately 383,203 persons die of liver cancer every year in China, which accounts for 51% of deaths from liver cancer worldwide. The mortality rate of liver cancer is higher in males (37.4/100,000) than in females (14.3/100,000) [105]. In China, some identified risk factors, such as HBV, HCV, aflatoxin B1, alcohol consumption, and tobacco smoking, contribute to the incidence and mortality related to HCC. In particular, HBV infection contributes to large number of liver cancer deaths and cases (63.9%). For HCV, its rate in liver cancer deaths and cases is lower than that of HBV (27.7% overall; 27.3% in males and 28.6% in females), but is still higher than that of aflatoxin exposure (25% of the population), alcohol drinking (15.7%), and tobacco smoking (13.9%) [106].



Despite the high incidence of liver cancer throughout China, a decreasing trend has been observed in some regions because of neonatal vaccination for HBV infection. According to the IARC and Cancer Incidence in Five Continents, the age-adjusted incidence rate of HCC has been in on decline in Shanghai since the 1970s and in Tianjin since the 1980s [107, 108].

### Hong Kong

According to the report from the Hong Kong Cancer Registry 2012, liver cancer ranks as the fourth most common cancer and the third most common cause of cancer death. The incidence and mortality of liver cancer are higher in males (fourth and third, respectively, among all cancers) than in females (tenth and fourth, respectively, among all cancers). In Hong Kong, the incidence of HCC increases with age, and the highest age-specific rate occurs among people aged 75 years and older, accounting for 152.4 per 100,000 population. However, over the past 25 years, the incidence of HCC in different age groups (especially age >40 years) has shown an apparently downward trend, which may be explained partly by the declining rate of HBV infection due to the institution of universal HBV vaccination since 1988. Since 1992, chronic HBV has been the major cause of HCC in Hong Kong, accounting for 80% cases in 1992 and 78% cases in 2006. From 1992 to 2006, the proportion of HCV-related HCC increased from 3 to 6.3% [109].

### Korea

In South Korea, liver cancer is the fourth most common cancer in males and the sixth most common cancer in females. The age-standardized incidence rate is 46.5 per 100,000 population (males, 45/100,000; females, 12/100,000). The incidence increases for age over 40 years, reaching a peak at age of 55 years [110]. However, the incidence of liver cancer among Korean males and females declined from 1999 to 2010. HBV is the most common infectious etiologic factor for liver cancer in Korea (70–80%), followed by HCV. HCC is the third leading cause of cancer mortality in Korea. The successful changes in the rates of liver cancer mortality in Korea were not solely due to Korea's HBV vaccination efforts, but also depended on its 10-year plan for cancer control, implemented by the government in 1996. With the introduction of the National Cancer Screening Program (NCSP) in 1999, males and females aged over 40 years with chronic hepatitis (HBsAg or HCV Ab positive) and liver cirrhosis patients, regardless of HBV or HCV infection, are offered screening for HCC.

### New Zealand

New Zealand cancer census data from 1981 to 2004 indicated that the age-standardized incidence rate of HCC was 30.3 per 100,000 population in Pacific Islander males and 9.8 per 100,000 population in Pacific Islander females, compared with 4.1 per 100,000 population and 2.1 per 100,000 population for their European counterparts. This suggests that the rate of HCC in the Pacific is 7 and 4 times higher than that in Europe for males and females, respectively [111].

### Taiwan

A survey from the Taiwan Cancer Registration System documented that the incidence rate of HCC had increased gradually in 1994 to 2007. The rate in males was higher than that in females. HBV infection is the most important cause of HCC, but this phenomenon is changing [112]. From 1981 to 1985, HBV-related HCC accounted for 88% of cases, whereas from 1995 to 2000, the proportion of HBV-related HCC had decreased to 59%, whereas the proportion of HCV-related HCC had increased to 31%. For HBV-related HCC, the ratio between males and females was 6.4, whereas for HCV-related HCC, it was 1.7 [113].

### Iran

Although the true prevalence of HCC in Iran is unknown, it is considered to be a low-risk area for HCC with an incidence less than five per 100,000 population. In contrast to Western countries, alcohol consumption has a minor role in HCC development in Iran. A study on the risk factors of HCC in southern Iran revealed that only 2.8% of HCC patients had history of excess alcohol intake. The same study showed that the predominant cause of HCC in the studied group was HBV followed by HCV infections with incidence of 52.1 and 8.5%, respectively. Approximately 80% of HCC patients were positive for at least one of the known HBV markers. Thus, HBV infection appears to be the most common cause of HCC in Iran [114].

### Pakistan

Unfortunately, no population-based study was available from which a true prevalence and incidence rate of HCC could be ascertained. Most of the studies were hospital based, consisting of case series with small sample size, or they had a highly selected population. However, a few cancer registries have been established in Pakistan. From the 1970s until the mid-1990s, HBV was the most common etiologic factor for HCC in Pakistan. Afterwards, a shift in HCC etiology was observed with a steady rise in HCV-



related HCC cases. The age-standardized rate for HCC is 7.64 per 100,000 population in males and 2.8 per 100,000 population in females. The male-to-female ratio is 3.6:1. The usual age of presentation is in the fifth and sixth decades [115].

### Vietnam

Liver cancer is the leading cause of cancer-related death in males and the second most common for females in Vietnam [116]. Vietnam is a country with a high prevalence of HBV infection (an estimated 12.3% of males and 8.8% of females are chronically infected with HBV). Thus, HBV was the most common etiologic factor for HCC in Vietnam [117]. A recent study reported that the estimated chronic HBV prevalence increased from 6.4 million cases in 1990 to approximately 8.4 million cases in 2005 and was projected to decrease to 8.0 million by 2025 [118]. However, the estimated HBV-related HCC incidence increased from 9400 in 1990 to 25,000 in 2025. Although universal infant HBV vaccination will reduce the chronic HBV prevalence in Vietnam over the next two decades, the HBV-related HCC burden will continue to rise.

### Mongolia

The estimated incidence rate of HCC in Mongolia is 54.1 per 100,000 world standard population, one of the highest worldwide [119]. Although universal vaccination for HBV has been implemented and sterilization of medical devices is being improved, the prevalence of chronic HBV and HCV infection is still over 10%. HCV-related HCCs are more common than HBV-related cancers. In addition, coinfection with HBV and HCV occurs frequently [117]. Due to the lack of a surveillance system, the majority of cancers are diagnosed in advanced stages.

### Other countries

Liver cancer is one of the most common causes of cancer-related death in other Southeast Asian countries, such as Cambodia, Lao People's Democratic Republic, Myanmar, and Papua New Guinea [116]. Although there is little epidemiologic information from those countries in regard to HCC, it is assumed that the high prevalence rate of HBV infection is related to the occurrence of HCC.

### Summary

Although it is difficult to accurately predict future changes in disease epidemiology, the overall global incidence of HCC is predicted to rise in the next few years until a

plateau is reached by 2020. Subsequent decreases in the rates of HCC have been predicted, resulting at least in part from expected improvements in the control of HBV and HCV infection. However, as the contributions of HBV and HCV diminish, other risk factors, such as DM and obesity, may become increasingly important drivers of future HCC incidence trends.

### Prevention

#### Prevention of HBV-related HCC

##### Recommendations

1. As primary prophylaxis for HCC, universal HBV vaccination in infants should be implemented in all countries, especially in HBV-endemic areas (A1).
2. As secondary prophylaxis for HCC development, effective and potentially long-term antiviral therapy should be started in all patients with chronic hepatitis B infection and active liver disease (B1).

The most common risk factor for HCC is chronic HBV infection, which accounts for more than 50% of all cases globally and 60–80% in some Asian countries such as China, Korea, and Vietnam [120]. Strategies to prevent HBV-related HCC include universal hepatitis B vaccination to reduce new infection as primary prevention, antiviral treatment to prevent disease progression by effectively suppressing HBV replication and regular surveillance to detect HCC in earlier stage as secondary prevention, and combination of curative therapies and adjuvant antiviral treatment to increase survival and prevent recurrence for HCC patients as tertiary prevention [2, 121, 122].

#### Primary prophylaxis of HBV-related HCC: vaccination to decrease the rate of HBV infection

The aim of primary prophylaxis in HBV-related HCC is to prevent new HBV infection in healthy individuals. The universal vaccination programs carried out in countries with endemic HBV have resulted in a significant decline in the prevalence rate of HBsAg and incidence of HCC [10]. As an excellent example, the universal hepatitis B immunization program for newborns started in 1984 in Taiwan has significantly reduced the prevalence rates of HBsAg, acute and chronic hepatitis B, and cirrhosis, decreasing HCC incidence by more than 80% and more than 90% among cohorts vaccinated at birth, over 30 years [123, 124]. Similarly, a national survey showed that the prevalence of HBsAg declined from 9.75% in 1992 to

7.18% in 2006 and among children younger than 5 years old declined from 9.67% in 1992 to 0.96% in 2006 in Mainland China, where universal infant HBV vaccination started in 1992 [125]. More importantly, a recent report of a 30-year follow-up study demonstrates that the HCC incidence rate also decreased by 84% in vaccinated cohort in Qidong area of eastern China [126].

### **Secondary prophylaxis of HBV-related HCC: antiviral treatment to reduce incidence of HCC in chronic HBV infection**

Studies have revealed that a variety of factors are involved in HCC occurrence among chronic hepatitis B patients, including demographic, viral, and environmental factors. A large-scale cohort study (REVEAL-HBV study) carried out in Taiwan demonstrated that the incidence rate of HCC was correlated with serum viral load (1.3 and 14.9% for HBV-DNA < 300 copies/mL and  $\geq 1,000,000$  copies/mL, respectively) during a mean follow-up of 11.4 years [127]. Even patients with moderate HBV-DNA level (60–2000 IU/mL) also had a substantially increased risk of HCC and mortality compared with uninfected individuals [128].

Many studies have shown that antiviral treatment can decrease the incidence of HCC. A landmark randomized control trial (RCT), the Cirrhosis and Lamivudine Monotherapy (CALM) study, showed that, compared with placebo group, lamivudine therapy significantly reduced the risk of HCC in chronic hepatitis B patients with advanced fibrosis and cirrhosis (7.4 versus 3.9%) [129]. Meta-analyses confirmed the beneficial effect of antiviral treatment on reducing HCC risk, no matter whether using lamivudine, adefovir, entecavir, tenofovir or interferon [130, 131]. However, virological response was related to the clinical outcome of patients. The incidence of HCC in patients with sustained viral suppression was significantly lower compared with patients with suboptimal response [132]. A follow-up study showed that entecavir is more effective than lamivudine in prevention of HCC due to higher potency and minimal risk of resistance, with 5-year cumulative incidence of HCC of 7 and 20%, respectively [133]. Furthermore, the preventive efficacy of antiviral therapy can be translated to general population; for example, since launched in 2003, a viral hepatitis therapy program has significantly reduced incidence and mortality of HCC in the general population of Taiwan (HR was 0.86 for HCC incidence and 0.76 for HCC mortality) [134]. Of note is that suppression of viral replication in chronic hepatitis B patients by antiviral treatment could reduce but not eliminate the risk of HCC, especially in patients with cirrhosis [135–137]. Kim et al. reported that the risk of HCC remained after HBsAg seroclearance in chronic

hepatitis B patients, especially in males, those who achieved HBsAg seroclearance at >50 years, and those who had liver cirrhosis [138]. Therefore, regular surveillance is important in patients receiving antiviral therapy, even in patients who lost HBsAg due to tumor detection at early stage.

### **Prevention of HCV-related HCC**

#### *Recommendations*

1. In chronic HCV infection, patients who obtained sustained virologic response (SVR) had considerably reduced risk of HCC. However, older age, low platelet count, and/or presence of cirrhosis despite SVR are associated with higher risk for HCC development and warrant surveillance (A1).

In chronic HCV infection, a meta-analysis of retrospective studies implies that the risk of HCC is reduced among patients with HCV who achieve SVR with antiviral therapy with interferon or interferon plus ribavirin [139–142]. Findings on the effect of SVR on liver-related clinical outcomes are similar to those of retrospective, and often smaller, studies from Japan [143–147], the results of which supported an approximately 70–90% reduction in the risk of liver-related clinical outcomes over a follow-up period of 2–6 years in patients achieving SVR. This was reaffirmed by a recent study on 33,005 HCV-infected individuals who received treatment, whose authors concluded that the risk of HCC after HCV cure, though considerably reduced, remains relatively high at 0.33% per year [148].

According to the HALT-C and EPIC studies, a continued elevated risk of HCC in patients with advanced chronic HCV, even in those who achieved SVR, was evident [139]. The 5-year risk of HCC developing in noncirrhotic patients was 4.8%. It has been suggested that the incidence of HCC in patients with cirrhosis from HCV only increases substantially once the platelet count is less than  $100 \times 10^9/L$ . Furthermore, older age and presence of cirrhosis at the point of SVR are associated with a higher risk of HCC, warranting surveillance [148].

Although these studies have validated that there is a reduced incidence of HCC in treated patients, there are no data that demonstrate that treating or eradicating HCV completely eliminates the risk for HCC. Thus, it seems prudent to continue surveillance of patients with HCV and cirrhosis who have achieved viral clearance on therapy. Surveillance is recommended in SVR patients with any histologic stage of HCV with comorbidities, such as alcohol abuse and DM, all of which are established independent risk factors for HCC disease progression [148–151].

While the most commonly observed clinical benefits in SVR patients were the consequence of the arrest of fibrosis progression, regression of preexisting cirrhosis could be documented [152–157]. However, regressed cirrhosis is not a reason to withhold surveillance. The recent new arrival of direct-acting antiviral (DAA) therapy allowed for the achievement of SVR in over 90% of treated patients, irrespective of liver fibrosis stage [158–160]. However, there is no evidence that successful DAA therapy reduces the incidence of HCC in patients with HCV cirrhosis. Maintaining surveillance for SVR patients with advanced liver fibrosis, independently of the histologic response to therapy, is highly recommended.

### Prevention of metabolic-related HCC

#### Recommendations

1. Nonalcoholic fatty liver disease (NAFLD) and nonalcoholic steatohepatitis (NASH) are associated with a significant risk of HCC development, which is higher in the presence of cirrhosis (A2).
2. A significant proportion of patients may suffer HCC even in the absence of cirrhosis (B2).
3. Metabolic syndrome and its components, especially DM and obesity, are associated with a high risk of HCC in patients with NASH (A2).

The estimated prevalence of NASH in the general population ranges from 2 to 3% [161]. Contrary to earlier studies, recent data revealed that up to 44% of cases of NAFLD can progress to NASH even in the absence of inflammation at baseline [162] and approximately 23% of cases of NASH progress to cirrhosis over the next 10–15 years [163]. In general, up to 30–40% and 10–15% of cases of NASH do have advanced fibrosis and cirrhosis, respectively, at initial diagnosis [163]. Although the overall incidence of HCC depends on the stage of underlying NAFLD and associated comorbid conditions, HCC can develop in the absence of cirrhosis in such cases [164]. The incidence of HCC in patients with NASH cirrhosis has been reported to be 2.3–4.0% per year [165, 166].

Metabolic syndrome and components of metabolic syndrome have been associated with the development of HCC [167]. In a meta-analysis of 38,940 cases of cancers (43 articles), Esposito et al. [168] found an association of metabolic syndrome with HCC ( $RR = 1.43$ ,  $p < 0.0001$ ), and the association was stronger in Asians ( $p = 0.002$ ). Moreover, the estimated risk of HCC was high in overweight ( $RR = 1.48$ ; 95% CI 1.31–1.67) and obese ( $RR = 1.83$ ; 95% CI 1.59–2.11) individuals. Tanaka et al. [169] reported that overweight or obesity increased the risk of liver cancer among Japanese population in the meta-

analysis. Consistent with these findings, a significant association of DM and HCC was estimated ( $RR = 2.31$ ; 95% CI 1.87–2.84) by Wang et al. in a meta-analysis of 17 case-control and 32 cohort studies [170]. Longer duration of DM and treatment with insulin or sulfonylureas was also associated with a higher risk of HCC, while a lower risk of HCC was found with metformin treatment. In another meta-analysis of 25 cohort studies, a higher incidence of HCC was found in 17 studies [summary relative risks (SRRs) = 2.01; 95% CI 1.61–2.51] among diabetics compared with nondiabetic patients. However, due to the presence of significant heterogeneity among studies ( $Q = 136.68$ ,  $p < 0.001$ ,  $I^2 = 87.6\%$ ), a subgroup analysis was performed to control for confounders and DM was associated with a higher HCC-related mortality ( $SRR = 1.56$ ; 95% CI 1.30–1.87) [51].

Because HBV and HCV are predominant risk factors responsible for a high burden of liver diseases in the Asia-Pacific region, Chen et al. [171] evaluated the influence of obesity, DM and HBV/HCV infections on the risk of HCC. This meta-analysis found that the positive association with obesity was independent of DM or infections with HBV/HCV.

In general, the relationship between DM, obesity, metabolic syndrome, and HCC is linked with development of NAFLD, and theoretically all are interlinked with each other. Considering the significant burden of NASH (i.e., 2–3% of the global population) and a global rise in the burden of obesity and DM, it is expected that there will be a further increase in the burden of NASH and HCC in the foreseeable future unless considerable preventive measures are taken [172]. Most of the studies have used the Western criteria for obesity, and one can expect an even higher risk if similar estimates are calculated using the Asian criteria for obesity. Higher HCC-related mortality rates have been reported in DM compared with non-DM patients ( $RR = 2.43$ ; 95% CI 1.66–3.55) [170]. Furthermore, due to limited available treatment options, patients with NASH-related cirrhosis carry a significant risk for HCC development. Moreover, many other aspects must be explored; for instance, the role of impaired glucose metabolism, dyslipidemia, and the effect of concomitant use of alcohol must be evaluated [167]. Hence, it is imperative to implement measures to reduce the burden of factors associated with NAFLD/NASH.

So far, the major key preventive measures here include “healthier diet” and lifestyle modification, which should be explained and promoted to every individual who is at risk of or has suffered from such metabolic derangements. Dietary modifications according to underlying risk factors, such as DM, obesity, dyslipidemia, and hypertension, should be promoted. Regular walking and exercise also

have a major role in the control of metabolic syndrome and NAFLD/NASH. Treatment of concomitant metabolic conditions with statins and metformin may also have beneficial effects on portal hypertension, complications of liver cirrhosis, and HCC prevention [173]. The efficacy of metformin as a preventive agent in a clinically relevant rat model of HCC was evaluated and was associated with a reduction in fibrotic and inflammatory markers and a 44% decrease in HCC incidence when administered in an early phase by suppressing the receptors for advanced glycation end products and inhibiting activation of hepatic progenitor cells [174]. However, these preclinical findings must be confirmed in clinical studies.

Bariatric surgery could be recommended for patients with morbid obesity, which may reduce liver fibrosis but carries a risk of decompensation in patients with advanced liver cirrhosis [173]. Furthermore, periodic screening for HCC in patients with NASH will help to identify HCC cases at early stage. Patients with NASH cirrhosis should be considered for HCC screening according to the American Association for the Study of Liver Diseases (AASLD)/American College of Gastroenterology (ACG) practice guidelines [175]. The other systemic review of NAFLD recommended biannual imaging screening in cirrhosis patients [176]. However, screening recommendations have not yet accounted for the increasing number of patients suffering from HCC even though up to 50% of cases may occur in the absence of cirrhosis [59]. The latest European guidelines suggested that the PNPLA3 rs738409 C > G gene polymorphism has been associated with an increased HCC risk and might provide patient risk stratification for tailored HCC surveillance in NAFLD. However, no recommendation can currently be made on the timing of surveillance or its cost-effectiveness [177].

### Tertiary prevention

#### Recommendations

1. Interferon did not reduce the recurrence-free survival (RFS) rate in HBV-related HCC after curative treatment. However, it is possible it improved overall survival (OS) (A2).
2. Nucleos(t)ide analogs may be effective in reducing the risk of recurrent HBV-related HCC after curative treatment (B2).
3. Interferon-based antiviral treatments after curative therapy in HCV-related HCC may reduce the risk of recurrence and improve survival rates (A2).

### Tertiary prevention for HBV-related HCC

HBV viral load has been shown to have an important role in carcinogenesis in patients with chronic HBV liver disease, and recently, HBV viral load has also been reported to be involved in recurrence after radical treatment of HCC [178]. In a retrospective study of 72 patients and a prospective study of 200 patients with hepatic resection for HBV-related HCC, both conducted by Hung et al. [179, 180], patients with a high serum HBV viral load at the time of tumor resection showed a significantly higher recurrence rate compared with patients with a low viral load. Therefore, antiviral and antiinflammatory therapies after curative treatment may be crucial in preventing HCC recurrence and improving survival.

#### Interferon

A small RCT was performed to evaluate the safety and efficacy of 16 weeks of interferon  $\alpha$ -2b therapy after hepatic resection in a group of patients with predominantly HBV-related HCC [181]. The RR of death after interferon treatment was 0.42 (95% CI 0.17–1.05,  $p = 0.06$ ). Subset analysis showed that adjuvant interferon had no survival benefit for pTNM stage I/II tumors (5-year survival 90% in both groups,  $p = 0.91$ ), but prevented early recurrence and improved the 5-year survival of patients with stage III/IVA tumors from 24 to 68% ( $p = 0.04$ ). After this study, another similar RCT was conducted by Chen et al. [182]. A total of 268 patients were allocated randomly to receive either 53 weeks of adjuvant interferon  $\alpha$ -2b treatment or observation alone. The primary endpoint of this study was RFS. The median RFS in the interferon  $\alpha$ -2b and control arms was 42.2 and 48.6 months, respectively ( $p = 0.83$ ). In this study, adjuvant interferon  $\alpha$ -2b did not reduce the postoperative recurrence of HBV-related HCC. HCC recurrence after ablative treatment modalities is also common. Although patients who received medical ablation usually exhibit compensated hepatic functional status, the frequent recurrence of HCC after successful ablation contributes to short-term survival. A small RCT was conducted to evaluate the effectiveness of interferon therapy in preventing HCC recurrence after successful medical ablation therapy for primary tumors [183]. The cumulative HCC recurrence rate of the patients treated with interferon- $\alpha$  and the control group was 25 and 40% at the end of 1 year, and 47 and 90% at the end of 4 years, respectively ( $p = 0.01$ ). Furthermore, this study also showed that the prevention of HCC recurrence using interferon- $\alpha$  was effective in HBV-related HCC [183].



### Nucleos(t)ide analogs

A retrospective study was conducted to evaluate the efficacy with or without using nucleos(t)ide analogs in patients following curative treatments for HBV-related HCC [184]. Cumulative OS rates of HCC were significantly different between the two groups ( $p < 0.01$ ), and cumulative RFS rates of HCC were also significantly different ( $p < 0.01$ ). Yin et al. [185] also reported that nucleos(t)ide analogs improved not only liver function but recurrence and OS rates. In another study, improvements of liver function and OS rates were reported even if the recurrence rates were not significantly different between groups treated with and without nucleos(t)ide analogs [186, 187]. In addition, a large-scale nationwide cohort study was reported from the Taiwan National Health Insurance Research Database [188]. Among 100,938 newly diagnosed HCC patients, they identified 4569 HBV-related HCC patients who received curative liver resection for HCC. The risk of first tumor recurrence was compared between patients who did not (untreated cohort,  $n = 4051$ ) and did (treated cohort,  $n = 518$ ) take nucleos(t)ide analogs. The treated cohort had a higher prevalence of liver cirrhosis when compared with the untreated cohort (48.6 versus 38.7%,  $p < 0.001$ ), but had a lower risk of HCC recurrence [ $n = 106$  (20.5%) versus  $n = 1765$  (43.6%),  $p < 0.001$ ] and lower overall risk of death [ $n = 55$  (10.6%) versus  $n = 1145$  (28.3%),  $p < 0.001$ ]. After adjusting for competing mortality, the treated cohort had a significantly lower 6-year HCC recurrence rate (45.6%; 95% CI 36.5–54.6% versus untreated, 54.6%; 95% CI 52.5–56.6%,  $p < 0.001$ ). Six-year overall mortality was 29.0% (95% CI 20.0–38.0%) for the treated and 42.4% (95% CI 40.0–44.7%,  $p < 0.001$ ) for the untreated cohort. On modified Cox regression analysis, administration of nucleos(t)ide analogs (HR 0.67; 95% CI 0.55–0.81,  $p < 0.001$ ) was independently associated with a reduced risk of HCC recurrence. One study elucidated the superior choice of nucleos(t)ide analogs [189]. A total of 865 HBV-related HCC patients received antiviral treatment at diagnosis or immediately following surgery (adefovir 10 mg per day in 300 patients, entecavir 0.5 mg per day in 325 patients, and lamivudine 100 mg per day in 240 patients). The 1-, 2-, and 3-year resistance rates were 0.9, 1.8, and 2.5%, respectively, for the entecavir group; 3.0, 8.3, and 12.0%, respectively, for the adefovir group; and 21.7, 31.7, and 39.6%, respectively, for the lamivudine group. The 3-year RFS for the entecavir group also differed significantly compared with the adefovir and lamivudine groups (HR 0.810; 95% CI 0.656–0.999,  $p = 0.049$  and HR 0.737; 95% CI 0.591–0.919,  $p < 0.01$ ). A randomized, placebo-controlled trial by Jang et al. [190] also showed that

preemptive lamivudine therapy in patients receiving transarterial chemoembolization (TACE) significantly reduced the incidence of HBV reactivation ( $p < 0.01$ ), overall hepatitis ( $p = 0.02$ ), and severe hepatitis ( $p = 0.035$ ) due to HBV reactivation after repeated TACE. However, prevention of HCC by preemptive lamivudine therapy was not shown because of advanced stage of HCC in patients receiving TACE in that trial [190]. Further prospective RCTs using a larger number of patients are required to assess its role in tertiary prevention of HCC.

### Tertiary prevention of HCV-related HCC

HCC is characterized by very frequent recurrence even after successful initial treatments, either surgical resection or medical ablation, and the risk of recurrence remains high for many years. Recurrence is particularly frequent with HCV-related HCC, and a substantial proportion of recurrences, especially in the late phase, is thought to represent *de novo*, or multicentric, hepatocarcinogenesis [191–193].

### Interferon

Antiviral therapy, such as interferon, might reduce the overall incidence of recurrence by preventing *de novo* carcinogenesis. Indeed, several small-sized RCTs, performed in Japan or Taiwan, showed that the incidence of recurrence was reduced in HCV-related HCC by interferon therapy subsequent to initial HCC treatment [194, 195]. Other RCTs, also performed in Japan or Taiwan, failed to find a significant delay in the first recurrence with interferon therapy, but the second or third recurrence was significantly reduced especially in sustained responders, and the OS was improved [196–198]. Another RCT in Italy did not detect effects of interferon therapy on early recurrence but did find an effect for late recurrence: after an interval of more than 2 years, the rate seemed to be reduced among interferon responders [199]. These data are compatible with the hypothesis that *de novo* carcinogenesis was prevented by successful antiviral therapy. On the other hand, three reports on long-term observation of recurrence after interferon therapy following HCC treatment showed that the recurrence rate in interferon-treated patients decreased over time, suggesting that the growth of residual microscopic tumors had been delayed by interferon (in fact, the two presumed mechanisms are not necessarily mutually exclusive) [200–202]. Most of these studies used interferon monotherapy and suffered from low sustained response rates because most patients had advanced fibrosis or cirrhosis. Preventive effects of interferon on HCC recurrence have yet to be reevaluated using current, more efficient protocols.



### DAA therapy

DAA therapies are promising pan-genotypic agents used to eradicate HCV. However, there is no evidence that DAA therapy will prevent HCC recurrence. One study by Reig et al. [203] reported that eradication of HCV with DAAs led to an unexpected HCC recurrence in some cases, and others reported DAAs did not lead to an unexpected HCC recurrence [204–206], although there is no evidence that SVR after DAA therapy reduces the incidence of recurrence in HCC patients receiving curative treatments. Furthermore, prospective studies are needed.

### Other tertiary preventions of HCC

Microscopic, intrahepatic residual tumors, including intrahepatic metastases, are a possible cause of HCC recurrence. Theoretically, adjuvant chemotherapy may reduce or delay such recurrences, but few chemotherapeutic agents have been effective against HCC and many of them may be hepatotoxic.

### Chemotherapy

Hasegawa et al. [207] reported RCT using oral administration of uracil-tegafur after curative hepatic resection but found no beneficial effects on recurrence and a possible adverse effect on OS. Bruix et al. [208] assessed the efficacy and safety of sorafenib versus placebo as adjuvant therapy in patients with HCC after surgical resection or local ablation. It was a double-blind, placebo-controlled study of patients with HCC with complete radiologic response after surgical resection ( $n = 900$ ) or local ablation ( $n = 214$ ) at 202 sites (hospitals and research centers) in 28 countries. At final analysis, 464 RFS events had occurred (270 in the placebo group and 194 in the sorafenib group). Median follow-up for RFS was 8.5 months in the sorafenib group and 8.4 months in the placebo group. There was no difference in median RFS between the two groups (33.3 versus 33.7 months, respectively; HR 0.940; 95% CI 0.780–1.134; one-sided  $p = 0.26$ ) [208]. In 1996, Muto et al. [209] reported that administration of polyenoic acid, an acyclic retinoid, reduced the recurrence of HCC in RCT. Updated, long-term data were published subsequently [210], postulating that the eradication of premalignant or latent malignant clones was the mechanism of action. However, in a large-scale RCT, the superiority of acyclic retinoid over placebo could not be validated, 600 mg per day was shown to be the optimal dose, and treatment may possibly reduce the recurrence of HCV-related HCC, particularly after 2 years [211]. The investigators concluded that administration of 600 mg per day of acyclic retinoid to patients with HCV-related HCC

who have completed curative therapy might improve survival for those classified as having Child–Pugh class A disease, for whom liver function was relatively stable in subanalysis [212]. Other adjuvant treatments have not been shown to prolong RFS (Table 2).

## Diagnosis and surveillance

### Imaging modalities

#### Ultrasound (US) and contrast-enhanced ultrasound (CEUS)

#### Recommendations

1. Ultrasonography (US) is a screening test and not a diagnostic test for confirmation (B2).
2. Contrast-enhanced US (CEUS) is useful for characterization of US-detected liver nodules and is as sensitive as dynamic computed tomography (CT) or dynamic magnetic resonance imaging (MRI) in the diagnosis of HCC (B2).

As the prognosis of HCC depends largely on the stage at which the tumor is detected, detection of HCC early in its development is critical to improve the survival of affected patients [218–220]. Although ultrasonography (US) is the most widely used modality for HCC screening and surveillance, the reported sensitivity of surveillance US is in the range of 40–81% with specificity of 80–100% [221–225]. According to a recent meta-analysis study, among B-mode US, contrast-enhanced US (CEUS), contrast-enhanced (CT), and gadolinium-enhanced (MRI), B-mode US has the lowest sensitivity and positive predictive value (59.3, 77.4%) while the other three imaging modalities show similar pooled per-lesion sensitivity and positive predictive value (73.6–84.4%, 83.6–89.3%) [226]. Therefore, US is not advocated as a diagnostic test for confirmation due to overlapped imaging features of benign and malignant cirrhotic nodules on US.

Key alterations during hepatocarcinogenesis include angiogenesis, changes in cellularity, the transporters of hepatocytes, and decrease in the number and function of Kupffer cells [227]. Among them, hemodynamic alteration of the nodules, composed of increased arterial flow and decreased portal flow, is the most important change for the diagnosis of HCC [228–230]. However, B-mode US cannot demonstrate tumor vascularity, and color Doppler imaging and power Doppler imaging have low sensitivity for detecting the microflow in the nodules [231–235]. CEUS using microbubble contrast agents and low mechanical index (MI) contrast-specific imaging techniques has been

**Table 2** Adjuvant treatments preventing hepatocellular carcinoma recurrence

Refs.	Study design	Drug	Patients	Outcomes
Takami et al. [213]	RCT	Meloxicam	Meloxicam ( $n = 111$ ) versus control ( $n = 113$ )	Negative. 3-year RFS 53.9% in meloxicam group versus 57.0% in controls
Habu et al. [214]	RCT	Menaquinone	Menaquinone ( $n = 21$ ) versus control ( $n = 19$ )	Positive. Assessing only recurrence event: 9.5% in menaquinone group versus 47.4% in controls
Mizuta et al. [215]	RCT	Menatetrenone	Menatetrenone ( $n = 32$ ) versus control ( $n = 29$ )	Positive. 24-month recurrence rate 39.0% in menatetrenone group versus 83.2% in controls and also assessing overall survival
Hotta et al. [216]	RCT	Menatetrenone	Menatetrenone ( $n = 21$ ) versus control ( $n = 24$ )	Positive on recurrence event: 33.3% in menatetrenone group versus 50.0% in controls, but negative on cumulative recurrence rate
Yoshida et al. [217]	RCT	Menatetrenone	Menatetrenone ( $n = 367$ ) versus controls ( $n = 181$ )	Second interim analysis indicated that vitamin K2 did not prevent disease occurrence or death, with HR of 1.150 (95% CI 0.843–1.570, $p = 0.811$ )

proved to be useful for characterizing liver tumors [235, 236]. Moreover, as Sonazoid microbubbles are phagocytosed by Kupffer cells, Kupffer imaging can be achieved [237]. CEUS can provide superior sensitivity to detect arterial hypervascularity and better demonstration of rapid wash-out for non-HCC malignancy and very late wash-out of HCC compared with dynamic CT or dynamic MRI [238–240]. In addition, CEUS has several other advantages including relative inexpensiveness, no nephrotoxicity of the contrast agents, and no ionizing radiation. In general, CEUS shares many features with dynamic CT and dynamic MRI, but as they are purely intravascular, in cholangiocarcinoma a discordant enhancement pattern is observed on CEUS [236, 238, 241–243]. The AASLD removed CEUS from their guidelines in part because of the perceived possibility of false-positive HCC diagnosis in patients with intrahepatic cholangiocarcinoma [63, 242], but according to recent studies, wash-out time  $>55$  s identified patients with HCC with the highest level of accuracy (92.7%) while wash-out time  $\leq 55$  s correctly identified the vast majority of non-HCC malignancies (diagnostic accuracy 98.3%) [244, 245]. In terms of diagnostic accuracy of CEUS for small HCC, recent meta-analysis studies demonstrated that pooled per-lesion sensitivity and positive predictive value of CEUS are similarly high (84.4 and 89.3%) compared with CT (73.6 and 85.8%) and MRI (77.5 and 83.6%), with better cost-effectiveness than CT or MRI [226, 246, 247]. A comparison of the diagnostic ability for hepatic nodules between CEUS using Sonazoid and contrast-enhanced CT showed that the sensitivity and accuracy were significantly higher for the former (95.4 and 94.7%) than the latter (85.2 and 82.3%) [248]. In real clinical practice, however, given that

cirrhotic liver has a limited sonic window for whole-liver evaluation and that there is a strong need for CT or MRI for tumor staging, use of CEUS as a first-line diagnostic approach, albeit possible, may not be more cost-effective than CT or MRI. As of now, it is generally accepted that CEUS is a cost-effective second-line imaging modality for rapid diagnosis of HCC once the liver focal lesion is detected on US, although dynamic CT or dynamic MRI is the gold standard for characterization of small nodules at high risk for HCC in cirrhotic liver in Western guidelines [2, 249].

## CT and MRI

### Recommendations

1. Dynamic CT, dynamic MRI, or gadolinium ethoxybenzyl diethylenetriamine pentaacetic acid (Gd-EOB-DTPA)-enhanced MRI is recommended as a first-line diagnostic tool for HCC when a screening test result is abnormal (A1).
2. Hallmark of HCC during dynamic CT scan or dynamic MRI is the presence of arterial enhancement, followed by wash-out of the tumor in the portal venous and/or delayed phases (A1).
3. HCC is diagnosed on the basis of imaging criteria in patients belonging to the high-risk group (chronic hepatitis B, chronic hepatitis C or cirrhosis) (A1).
4. The combined interpretation of dynamic and hepatobiliary phase of Gd-EOB-DTPA-enhanced MRI with diffusion-weighted imaging (DWI) can improve the diagnostic accuracy of MR imaging for the detection of HCC (B2).

Once a screening test result is abnormal or there is clinical suspicion of HCC, imaging plays a very important role for diagnosis and staging of this tumor [218, 250–252]. The radiological stage is used to inform clinical decision-making, optimize treatment strategies, and determine eligibility and priority for LT [252, 253]. As mentioned above, in addition to typical hemodynamic changes of HCC such as increased arterial flow and decreased portal flow, several pathologic changes can occur during development of HCC, including changes in cellularity, the transporters of hepatocytes such as organic anionic transporting polypeptides (OATP), and a decrease in the number and function of Kupffer cells [218, 227, 229, 254–257]. Accumulating data demonstrate that OATP8 expression level decreases during hepatocarcinogenesis prior to reduction in portal venous flow and prior to complete neoarterialization and to elevation of arterial flow, which may allow higher sensitivity for detection of malignant changes [257, 258]. The most reliable diagnostic tests for HCC diagnosis are quadruple-phase, multidetector CT (MDCT) and dynamic MRI including late hepatic arterial, portal venous, and delayed phase imaging at about 3–5 min after contrast administration [259–261]. Dynamic CT and dynamic MRI with extracellular gadolinium agents permit diagnosis and staging of HCC based mainly on assessment of vascularity [218, 251]. Presence of arterial enhancement followed by wash-out has sensitivity and specificity of 90 and >95%, respectively, and positive predictive value approximating 100% among the group having high risk for developing HCC, e.g., those with liver cirrhosis [262–265]. When extracellular agents are used, dynamic CT and dynamic MRI permit diagnosis and staging of HCC based mainly on assessment of vascularity, and the hallmark of HCC on CT or MRI is presence of arterial hyperenhancement (wash-in) followed by wash-out of the tumor in the portal venous and/or delayed phases [224, 266–268]. Sangiovanni et al. [269] also reported that the sensitivity of contrast-enhanced MDCT, and MRI using extracellular contrast medium for 1–2-cm HCCs was 44 and 44%, with 100% specificity. This may be explained by the fact that its diagnostic hallmark is often unseen in small HCCs ( $\leq 2$  cm), resulting from incomplete neoangiogenesis [224]. According to several recent meta-analysis studies on the diagnostic accuracy of US, CT, and MRI [225, 226, 270, 271], the per-lesion sensitivity of MRI for nodular HCC of all sizes is 77–100%, while that of CT is 68–91%, and MRI showed at least equivalent or higher per-lesion sensitivity compared with MDCT and therefore could be the preferred imaging modality for diagnosis of HCCs [269, 272–275]. The per-lesion sensitivity, stratified by size, was 100% for both modalities for nodular HCCs > 2 cm, 44–47% (MRI) and 40–44% (CT) for 1–2 cm HCCs [269, 272, 276], and 29–43% (MRI) and

10–33% (CT) for HCCs < 1 cm [269, 273, 276]. To date, there are insufficient data regarding the specificity of the combined criteria of wash-in and wash-out appearance in subcentimeter cirrhotic nodules for HCC diagnosis on dynamic CT or dynamic MRI.

More recently, cell-specific contrast agents other than nonspecific extracellular gadolinium-based contrast media such as superparamagnetic iron oxide (SPIO) particles or in conjunction with gadolinium-based contrast agents (double contrast) or gadolinium ethoxybenzyl diethylenetriamine pentaacetic acid (Gd-EOB-DTPA) have been shown to be highly sensitive for detection of HCC, particularly for small tumors [218, 270, 277–285]. Several studies demonstrated that hepatobiliary contrast media, gadoxetate disodium (Gd-EOB-DTPA, Primovist, Bayer Healthcare, Berlin, Germany) and gadobenate dimeglumine (Gd-BOPTA, Multihance, Bracco, Milan, Italy), have higher overall sensitivity than dynamic CT or dynamic MRI using nonspecific gadolinium chelates [218, 270, 281–285]. A recent meta-analysis study demonstrated that Gd-EOB-DTPA-enhanced MRI showed significantly higher per-lesion sensitivity than MRI performed with other contrast agents (87 versus 74%) [270]. However, it should be noted that approximately 10–20% of HCCs may appear as iso- to hyperintense nodules on hepatobiliary phase (HBP) images [268, 286]. Despite the great advantage of Gd-EOB-DTPA-enhanced MRI for detection of liver malignancies, one possible pitfall of Gd-EOB-DTPA-enhanced MRI arises from absence of its equilibrium phase, which can show better wash-out of HCC than portal phase of dynamic CT or dynamic MRI. Indeed, hypointensity relative to the liver in the transitional phase (1–5 min) of Gd-EOB-DTPA-enhanced MRI may reflect hyperenhancement of liver parenchyma rather than deenhancement of a mass (“pseudo-wash-out”), thereby lowering the specificity for HCC diagnosis [252, 287]. Therefore, to maintain specificity, only portal venous phase “wash-out” should be used for a noninvasive HCC diagnosis, because malignant lesions other than HCCs, such as intrahepatic cholangiocarcinoma as well as hemangioma, can show hypointensity on the transitional phase and/or HBP [224, 288, 289].

Furthermore, diffusion-weighted imaging (DWI) may improve the diagnostic performance of MRI for small HCCs by demonstrating higher cellularity of HCC [290–292]. However, although hypointensity on the HBP and diffusion restriction could improve the sensitivity for the diagnosis of HCC, these findings are not specific to HCC and can be found in other hepatic tumors [224]. Other ancillary imaging features favor HCC diagnosis, including presence of intralesional fat, mild to modest hyperintensity on T2-weighted images [259, 293, 294], and morphologic findings such as intratumoral hemorrhage, fatty

metamorphosis, and nodule-in-nodule architecture [252, 259]. However, great caution is still required when applying these ancillary imaging features for atypically enhancing cirrhotic nodules in order to retain high specificity, facing clinicians with the dilemma of balancing sensitivity and specificity [224].

Although CT hepatic arteriography (CTHA) and CT during arterial portography (CTAP) images have been used as the gold-standard diagnostic method for estimating the malignancy grade based on hemodynamic alteration, this has fallen out of favor in most practice settings except in some countries due to its invasiveness and high false-positive diagnosis rates [229, 295–297].

Hypovascular nodules associated with liver cirrhosis include low-grade dysplastic nodule (LGDN) or high-grade dysplastic nodules (HGDN), early HCCs, and well-differentiated HCCs [218, 255, 266, 298–302]. As there are significant overlaps in enhancement patterns on dynamic CT or dynamic MRI [295–297, 303, 304], the sensitivity of dynamic CT or dynamic MRI in detection of borderline nodules is quite low [301]. When detectable, most borderline lesions have a low–low–low, iso–low–low, or iso–iso–low enhancement pattern compared with adjacent background liver parenchyma on CT or MRI during the hepatic arterial, portal venous, and delayed phases [218, 301, 305, 306]. However, because expression of OATP8 decreases during hepatocarcinogenesis before complete neoarterialization, early HCCs may be more frequently visible on the HBP images of Gd-EOB-DTPA-enhanced MRI as hypointense nodules [289, 296, 297, 300, 307–313]. HBP hypointensity is a strong predictor of premalignancy or malignancy, and its presence favors HGDN or early HCC over LGDN or cirrhotic nodule [310, 314–316]. Although several imaging features are reported to be associated with interval progression to hypervascular HCCs, including large (>9–10 mm diameter) nodule size on initial imaging, nodule growth speed, hyperintensity on T2-weighted images or DWI, hyperintensity on pre-T1-weighted imaging, and intratumoral fat components [289, 315, 317, 318], it is quite challenging to differentiate early HCC from HGDN based on MRI findings [315]. More recently, when hypovascular nodules are detected by MDCT and MRI, the guidelines published by the JSH recommend use of CEUS using Sonazoid and Gd-EOB-DTPA-enhanced MRI [319]. The guidelines published by the JSH stated that hypovascular nodules that are hypointense in the hepatobiliary phase of Gd-EOB-DTPA-enhanced MRI and hypoechoic in the Kupffer phase of CEUS using Sonazoid can almost always be diagnosed as early HCC even without biopsy. However, it is highly likely that there may be some overlaps between early HCCs and HGDNs on both

Gd-EOB-DTPA-enhanced MRI and CEUS using Sonazoid, so these noninvasive diagnostic criteria for hypovascular nodules need to be confirmed with further studies. As of now, those hypovascular nodules showing hypointensity on HBP of Gd-EOB-DTPA-enhanced MRI and decreased uptake in the Kupffer phase of CEUS using Sonazoid require biopsy and pathologic confirmation, as they possess high malignant or premalignant potential.

## Tumor markers

### Recommendations

1. Alpha-fetoprotein (AFP) is not recommended as a confirmatory test in small HCC (B1).
2. The cut-off value of AFP should be set at 200 ng/mL for surveillance programs when used in combination with US (B2).
3. The cut-off value of AFP can be set at lower value in a population with hepatitis virus suppression or eradication (B2).

Tumor markers for HCC are used in diagnosis and treatment evaluation and during follow-up after treatment. The diagnostic performance of tumor markers is evaluated in terms of sensitivity, specificity, and likelihood ratios for positive and negative results (LR+/LR−) [320]. There is an inverse relationship between sensitivity and specificity according to cut-off values. Setting a lower cut-off value increases sensitivity and decreases specificity, and vice versa. A tumor marker with high LR+ is useful in confirming diagnosis, whereas a tumor marker with high LR− is useful in exclusive diagnosis. Those likelihood ratios also change according to cut-off values. The serum level of a tumor marker usually increases as the total tumor volume increases. This fact indicates that the sensitivity of a tumor marker essentially decreases as the target tumor size gets smaller when the cut-off value is fixed.

Since surveillance with alpha-fetoprotein (AFP) alone is only acceptable in a population-based setting and not recommended for high-risk population for HCC [321], the optimal cut-off value of AFP for surveillance should be determined on the premise that it is examined simultaneously with US. In such a situation, lower cut-off value increases the frequency of recall procedures and subsequent negative results and decreases the efficiency of the program.

Combination of two or more tumor markers may contribute to increased sensitivity without decreasing specificity when the correlation among them is small enough. However, to date the efficacy of adding another tumor marker to a surveillance program with US and AFP has not



been fully assessed, especially in terms of cost-effectiveness.

## AFP

AFP has served as a diagnostic test for HCC since the 1970s, when most patients with HCC were diagnosed at advanced stage and with clinical symptoms [322]. Concentration higher than 500 ng/mL was diagnostic. However, the usefulness of AFP as a diagnostic test in small HCCs is limited. According to a systematic review, the sensitivity, specificity, and LR+ of AFP in HCC smaller than 5 cm in diameter ranged from 0.49 to 0.71, 0.49 to 0.86, and 1.28 to 4.03, respectively, with cut-off value of 20 ng/mL and from 0.04 to 0.31, 0.76 to 1.0, and 1.13 to 54.25, respectively, with cut-off value of 200 ng/mL [323]. In meta-analysis, AFP with cut-off value of 200 ng/mL showed a better combined LR+ than with that of 20 ng/mL (5.85 versus 2.45). The cut-off value of AFP should be set at 200 ng/mL instead of 20 ng/mL when used with US in a surveillance program, considering its efficiency.

It is well known that AFP levels increase in patients with active hepatitis or cirrhosis and without HCC, reflecting necroinflammation and regeneration; this fact is the major cause of its low specificity in high-risk population. On the other hand, AFP levels decrease according to decreased hepatitis activity by nucleos(t)ide analogs in chronic hepatitis B and by interferon-based treatments in chronic hepatitis C. In fact, increased sensitivity of AFP in those populations was reported, setting lower cut-off values [324, 325].

## Des-gamma-carboxyprothrombin (DCP)

Des-gamma-carboxyprothrombin (DCP), also known as prothrombin induced by vitamin K absence-II (PIVKA-II), is an abnormal prothrombin protein that is increased in the serum of HCC patients. Since the report by Liebman et al. [326], DCP has been recognized as not only a highly specific marker for HCC but also a predictor of prognosis of HCC patients [327, 328]. According to a systematic review, the sensitivity, specificity, and LR+ of DCP in HCC smaller than 5 cm in diameter ranged from 0.14 to 0.54, 0.95 to 0.99, and 6.86 to 29.7, respectively, with cut-off value of 40 mAU/mL and from 0.07 to 0.56, 0.72 to 1.0, and 3.56 to 13.0, respectively, with cut-off value of 100 mAU/mL [323]. In meta-analysis, DCP with cut-off value of 40 mAU/mL showed a better combined LR+ than with that of 100 mAU/mL (12.60 versus 4.91). According to a more recent systematic review, DCP showed better diagnostic performance than AFP in diagnosis of early HCC in terms of area under the receiver operating characteristic (ROC) curves (0.84 versus 0.68) [329]. However,

funnel plot analysis suggested the presence of publication bias in DCP studies ( $p = 0.02$ ). In fact, in a large-scale study enrolling 1377 patients with HCC and 355 with chronic hepatitis or cirrhosis, the diagnostic performance of DCP was inferior to that of AFP in terms of area under the ROC curves in small (<5 cm) HCC [330].

## *Lens culinaris* agglutinin-reactive fraction of AFP (AFP-L3)

AFP-L3 is a fucosylated variant of AFP that reacts with *Lens culinaris* agglutinin A and can differentiate an increase in AFP due to HCC from that in patients with benign liver disease [331–333]. According to a systematic review, the sensitivity, specificity, and LR+ of AFP-L3 in HCC smaller than 5 cm in diameter ranged from 0.22 to 0.33, 0.93 to 0.94, and 4.63 to 30.8, respectively, with cut-off value of 10% and from 0.21 to 0.49, 0.94 to 1.0, and 8.06 to 45.1, respectively, with cut-off value of 15% [323]. In meta-analysis, AFP-L3 with cut-off value of 15% showed better combined LR+ than with that of 10% (13.1 versus 4.89). One of the major drawbacks of AFP-L3 was that it could not be measured when the AFP value was less than 10 ng/mL. Recently, a highly sensitive assay system was developed which enables AFP-L3 measurement in the range of AFP less than 10 ng/mL [334].

## Glypican-3 (GPC3)

Glypican-3 (GPC3) is a heparan sulfate proteoglycan anchored to the plasma membrane. It has been reported that GPC3 messenger RNA levels are increased in HCC [335, 336]. Whereas the role of GPC3 in immunohistochemical staining was established [337], the reported diagnostic performance of serum GPC3 was inconsistent, mainly due to heterogeneous and unestablished assay system [338].

## Other tumor markers

Various tumor markers have been proposed including Golgi protein 73 (GP73) [339], osteopontin [340], circulating cell free DNA [341], and microRNAs [342]. However, none of them were introduced into daily practice, mainly due to significant heterogeneity in reports and lack of profitability regarding cost-effectiveness.

## Combination of tumor markers

Simultaneous measurement of tumor markers enables improved sensitivity without deteriorating specificity when they have weak association. The sensitivity, specificity, and LR+ of AFP and DCP in small HCC were reported to be 0.48, 0.99, and 48 with cut-off value of 200 ng/mL for AFP



and 40 mAU/mL for DCP [343]. A more recent systematic review reported that the area under the ROC curve was not improved by the combination of DCP and AFP (0.83) compared with DCP alone (0.84) [329].

## Diagnostic algorithm

### Recommendations

1. Typical HCC can be diagnosed by imaging, regardless of its size, if a typical vascular pattern (i.e., arterial enhancement with portal venous wash-out) is obtained on dynamic CT, dynamic MRI, or CEUS (A1).
2. Nodular lesions that show an atypical imaging pattern (e.g., iso- or hypovascular in the arterial phase or arterial hypervascularity alone without portal venous wash-out) should undergo further examination (A1).
3. Gd-EOB-DTPA-enhanced MRI can detect the earliest initial change of HCC, including HGDN, and early HCC (B1).

This section of the guidelines is markedly revised from the APASL 2010 guidelines [4]. Various studies have verified the usefulness of Gd-EOB-DTPA-enhanced MRI for diagnosis of HCC [268, 286, 296, 297, 300, 311–313, 317, 318, 344–363], although this method is not yet included in the AALSD or European Association for Study of the Liver (EASL) guidelines [2, 63, 364, 365]. Only the updated APASL diagnostic algorithm includes Gd-EOB-DTPA-enhanced MRI as a first-line diagnostic tool for HCC, similar to the JSH-LCSGJ guideline [366].

Many institutions use US to screen for HCC, followed by dynamic CT or dynamic MRI for subsequent examinations. When a lesion is intensely enhanced in the arterial phase and shows hypoenhancement in the equilibrium phase by dynamic CT or transitional phase by Gd-EOB-DTPA-enhanced MRI, a diagnosis of HCC is unproblematic; however, benign hypervascular lesions (such as high-flow-type hemangioma), cholangiocarcinoma or combined HCC must be ruled out. When the hepatobiliary phase of Gd-EOB-DTPA-enhanced MRI or the Kupffer phase of CEUS using Sonazoid confirms a defect in these hypervascular nodules, the lesion is diagnosed as HCC.

When a lesion shows low attenuation in the equilibrium phase of dynamic CT, even though it is not intensely enhanced during the early arterial phase, it is possible that a more sensitive tool may diagnose it as hypervascular HCC; thus, either Gd-EOB-DTPA-enhanced MRI or CEUS is necessary. Gd-EOB-DTPA-enhanced MRI is useful for differentiating HCC (even early HCC) from a dysplastic nodule (DN) [299, 309, 367, 368].

Among the nodular lesions associated with liver cirrhosis, LGDN and HGDN (both of which are considered to

be precancerous lesions), early HCC, and nodule-in-nodule liver cancer are regarded as nonhypervascular [299, 309, 367, 368]. The most sensitive modalities that can objectively depict the early carcinogenic process are (1) Gd-EOB-DTPA-enhanced MRI, followed by (2) CTAP/CTHA [369, 370], and (3) CEUS [237, 362, 371]. Portal blood flow may be maintained in some cases of DN and early HCC, but is reduced in other nodules, although arterial blood flow in cases of DN and early HCC will not have increased yet.

The hepatobiliary phase of Gd-EOB-DTPA-enhanced MRI can detect the earliest initial changes suggestive of HCC. The second earliest initial carcinogenic changes are detected by CTAP and the third earliest by CTHA or CEUS (an increase in intranodular arterial blood flow). However, because CTHA and CTAP are invasive tests, they are only performed in a few countries. Indeed, they are not common in the majority of countries in the Asia-Pacific region. Since Gd-EOB-DTPA-enhanced MRI can identify initial carcinogenic changes earlier than CTHA and CTAP [258, 357, 372], the latter have been almost completely replaced by Gd-EOB-DTPA-enhanced MRI. Hypervascular lesions depicted as nodule-in-nodule or as entire hypervascular nodules can be interpreted as advanced cancer, even though they are very small (<2 cm).

Dynamic CT and Gd-EOB-DTPA-enhanced MRI show high sensitivity for arterial blood flow, but cannot detect arterial vascularity in some nodules (detection depends on acquisition timing, tumor location, and liver function), even though lesions appear hypervascular on CEUS. Nodules showing intense enhancement on dynamic CT and Gd-EOB-DTPA-enhanced MRI are assumed to exhibit high intensity on T2-weighted images and DWIs of MRI.

It is recommended that institutions specializing in liver cancer use Gd-EOB-DTPA-enhanced MRI rather than dynamic CT, even when no tumor is detected on US. Institutions that cannot perform Gd-EOB-DTPA-enhanced MRI as the first-line modality may use dynamic CT as a first screening/diagnostic step, even when no nodule is evident on US; however, it is absolutely essential that Gd-EOB-DTPA-enhanced MRI or CEUS be performed when dynamic CT does not identify hallmarks of HCC (i.e., arterial enhancement with venous wash-out) in the detected nodule.

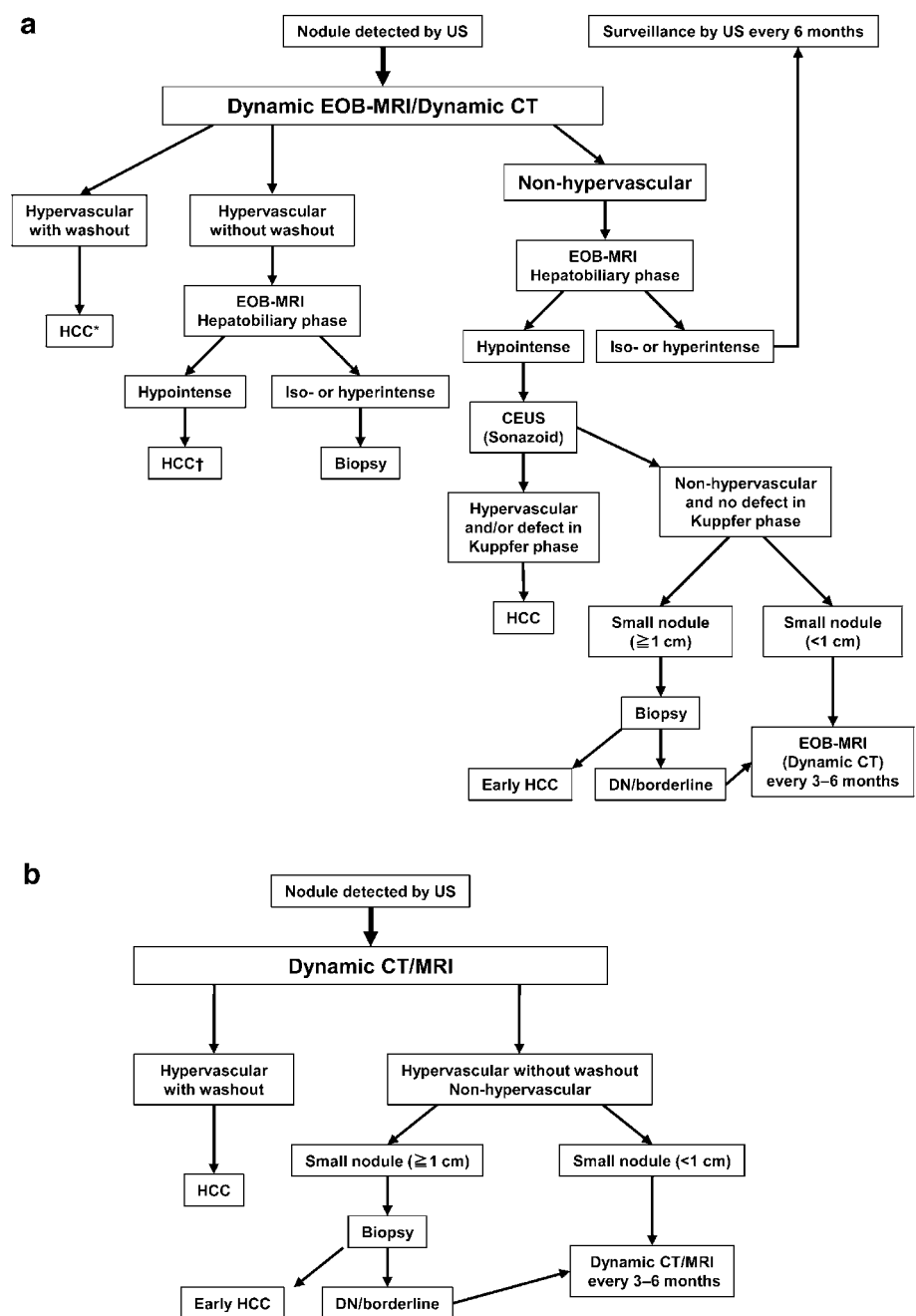
If Gd-EOB-DTPA-enhanced MRI (or dynamic CT) identifies a hypervascular nodule with venous wash-out, a definitive diagnosis of HCC can be made. If Gd-EOB-DTPA-enhanced MRI (or dynamic CT) shows a hypervascular nodule without venous wash-out, a diagnosis of HCC can be made if the nodule shows hypointensity in the hepatobiliary phase of Gd-EOB-DTPA-enhanced MRI. Also, in this case, another modality or MRI sequence should be used to rule out high-flow-type hemangioma,

because the latter can exhibit characteristics similar to HCC. If the hepatobiliary phase of Gd-EOB-DTPA-enhanced MRI identifies the nodule as isointense or hyperintense, biopsy is necessary to confirm the diagnosis (Fig. 1a).

Isointense or hyperintense nonhypervascular nodules in the hepatobiliary phase of Gd-EOB-DTPA-enhanced MRI can enter the routine surveillance protocol. However, nonhypervascular hypointense nodules have high potential for malignant transformation [296, 297, 311–313, 317, 318, 345, 346, 351, 355, 356, 373–379], therefore CEUS study

using Sonazoid is highly recommended. HCC can be correctly diagnosed by CEUS if hypervascularity and/or a defect in the Kupffer phase is observed. Even when a nodule is hypovascular on CEUS with an evident defect in the Kupffer phase, a finding of hypointensity in the hepatobiliary phase of Gd-EOB-DTPA-enhanced MRI is highly suggestive of malignancy [300]. Accordingly, biopsy is recommended for nodules 1.0 cm or larger to make a differential diagnosis between early HCC and a DN. If a nodule is diagnosed as a DN or a borderline lesion, intensive follow-up (every 3–6 months) with Gd-EOB-

**Fig. 1** Diagnostic algorithm for hepatocellular carcinoma using multiple modalities (a) and only dynamic CT/MRI (b) (APASL 2016). \*Cavernous hemangioma sometimes shows hypointensity on the equilibrium (transitional) phase of dynamic Gd-EOB-DTPA MRI (pseudo-wash-out). It should be excluded by further MRI sequences and/or other imaging modalities. †Cavernous hemangioma usually shows hypointensity on the hepatobiliary phase of Gd-EOB-DTPA MRI. It should be excluded by other MRI sequences and/or other imaging modalities



DTPA-enhanced MRI (or dynamic CT) is recommended. Intensive follow-up is also recommended for nodules smaller than 1.0 cm (Fig. 1a). In field practice, multiple imaging modalities are not available at all institutions. Thus, a diagnostic algorithm based on using only dynamic CT (or MRI) is shown in Fig. 1b.

## Surveillance

### Recommendations

1. Surveillance for HCC should be undertaken in high-risk groups of patients and is recommended (B2). The high-risk groups of patients for whom a surveillance strategy is recommended are described in Table 3.
2. Measurement of AFP alone is not recommended for routine surveillance of HCC (A1).
3. The combination of US and serum AFP measurement performed biannually should be used as a surveillance strategy for HCC (B2).

Surveillance is continuous monitoring for disease occurrence and includes application of a diagnostic test in subjects who are predisposed to develop a given disease. The primary motive of a surveillance strategy is to achieve a reduction in disease-related mortality through prompt diagnosis (stage migration), which could, in turn, increase the cost-effectiveness and applicability of certain curative therapies. To consider an intervention effective, it must result in an increase in longevity of approximately 90 days,

and if this goal can be attained at a cost of less than approximately US \$50,000 per year of life gained, it can be deemed cost-effective [380].

### Which modality is to be used for surveillance?

Tests that are widely available include tumor markers, such as AFP, and various imaging techniques, including US, CT, and MRI of the abdomen.

#### US

US is widely used for surveillance of HCC; its widespread popularity is due to its potential advantages of being noninvasive, an absence of risks associated with the procedure, and good acceptance by patients at a relatively moderate cost. A meta-analysis that included 19 studies showed US to be less effective in detecting early-stage HCC (demonstrating sensitivity of only 63%). However, it could detect the vast majority of HCCs before the disease would present clinically (depicting pooled sensitivity of approximately 94%) [223]. In a study by Sato et al. [381] including 1431 patients with chronic HCV, US-based surveillance performed by trained operators resulted in early detection of HCC with average tumor size of  $1.6 \pm 0.6$  cm and only 1.4% of cases exceeded tumor size of 30 mm. Thus, it was suggested that US-based surveillance performed biannually was adequate for early detection of HCC at size smaller than 3 cm [381]. The performance of US in an HCC surveillance strategy strongly depends on the quality of the equipment and the expertise of the performing operator. Thus, special training is warranted for ultrasonographers.

#### CT

Existing evidence does not support routine use of CT scan as part of the surveillance strategy for HCC. Patients with a  $\geq 1$  cm nodule in the liver are recommended to undergo a contrast-enhanced CT scan of the abdomen as a confirmatory test for the diagnosis of HCC, including unenhanced, arterial, venous, and delayed phase imaging. A randomized trial in 2013 examined 163 patients who had compensated cirrhosis. These patients were tested with either annual CT plus biannual AFP measurements or biannual US plus serum AFP measurements. The combination of biannual US and AFP was marginally more sensitive at detecting HCC compared with annual CT (sensitivity and specificity of 71.4 and 97.5%, respectively, versus 66.7 and 94.4%, respectively). This approach was deemed more cost-effective as well [222].

**Table 3** Groups where HCC surveillance is recommended

	HCC risk (per year)
Cirrhotic hepatitis patients	
HBV	3–5%
HCV	2–7%
NASH	2–4%
Genetic hemochromatosis	Unknown, but probably >1.5%
Primary biliary cirrhosis	2–3%
Alpha 1 antitrypsin (A1AT) deficiency	Unknown, but probably >1.5%
Autoimmune hepatitis	
Other etiologies	Unknown
Chronic HBV carriers	
Noncirrhotic (HBsAg positive)	
Asian females >50 years	0.3–0.6%
Asian males >40 years	0.4–0.6%
Africans aged >20 years	NA
History of HCC in the family	NA

## MRI

Similar to the recommendations made for CT scanning of the abdomen, no existing evidence is available to recommend use of abdominal MRI as part of a routine surveillance strategy for detecting HCC. For patients with a  $\geq 1$  cm nodule in the liver, dynamic imaging, such as contrast-enhanced MRI of the abdomen, is often needed as a confirmatory test.

## AFP and other serum markers

Measurement of serum AFP levels is a commonly used strategy for surveillance of HCC because it is widely available, inexpensive, and easy to perform. However, AFP has suboptimal performance as a serological test for surveillance of HCC because it depicts fluctuating levels in patients with cirrhosis with a flare of HCV or HBV infection, in exacerbations of the underlying liver disease, or with the occurrence of HCC [382]. Abnormal serum AFP levels can be detected in only a meager proportion of early-stage HCC tumors (10–20%), which has been correlated now with a particular subtype of HCC depicting an aggressive behavior (S2 class, EpCAM positive) [383]. AFP level of 10.7 ng/ml showed the best combination of specificity (78.1%) and sensitivity (77.2%), a cutoff that approaches the routine limits of normalcy [384].

Other serum markers, such as (DCP),  $\alpha$ -fucosidase, AFP-L3%, and GPC3, are used predominantly in the diagnostic rather than surveillance setting. The presence of elevated AFP-L3% is correlated with an HCC tumor with shorter doubling time, and raised serum DCP levels might be indicative of microinvasion [327, 385]. The HALT-C trial studied the AFP and DCP levels of 39 patients with HCC at diagnosis and 1 year before diagnosis. Neither test alone, nor the combination of the two, was adequate for HCC surveillance because the sensitivity of these two markers was very low when they were used either alone or in combination for the strategy to be considered efficacious and cost-effective in detecting HCC at an early stage [386]. Thus, at present, other than AFP, none of these markers can be recommended routinely as part of a surveillance strategy in patients at risk for HCC [327, 387].

## Combination of imaging and serum markers

Conflicting results have been obtained in studies regarding combination of imaging modalities with serum biomarkers for surveillance of HCC.

The pooled data of a meta-analysis that included 19 studies revealed the combination of US and serum AFP measurement versus US alone to be less specific, no better at detecting subclinical and early-stage HCC, and also not

cost-effective. Although the combination of US and serum AFP resulted in marginally increased sensitivity of 69% compared with 63% for US, this result was not statistically significant [209].

In contrast, a recent study demonstrated that serum AFP at cut-off of 20 ng/ml had specificity and sensitivity of 93.3 and 52.9%, respectively, whereas US had specificity and sensitivity of 74.2 and 92.0%, respectively. A combination of US and AFP demonstrated specificity and sensitivity of 68.3 and 99.2%, respectively. It was shown that, when using a cutoff level at 20 ng/ml and AFP level increase of  $\geq 2$  times from its nadir in the past 12 months, the combination of AFP and US depicted improved specificity of 71.5% and sensitivity of 99.2% [388].

The benefit of surveillance was demonstrated in a subset of patients with chronic HBV by Zhang et al. [389], in which biannual US and serum AFP measurement decreased mortality from HCC by 37%. Compliance with scheduled tests was depicted to be approximately 58.2%.

Several reports indicated the cost-effectiveness of HCC surveillance, and that US combined with AFP has been shown to increase quality-adjusted life years in patients who suffered from HCC, especially those who underwent resection or transplantation [390, 391]. The cost-effectiveness of HCC surveillance depends on the potential of receiving curative therapy in high-risk patients. Thus, if patients are ineligible for treatments due to severe liver disease or other comorbidities, HCC surveillance is not necessary.

## Surveillance interval

The surveillance interval should depend on the median tumor doubling time, which in HCC is demonstrated to be 80–117 days. Thus, a 6-month surveillance interval seems to be a reasonable choice. A meta-analysis has demonstrated that the pooled sensitivity of a US-based 6-month surveillance strategy drops to 50 from 70% for an annual program [223]. A study by Anderson et al. [392] demonstrated that semiannual US surveillance for HCC in cirrhotic patients improves clinical outcomes at a reasonable cost.

In a RCT that enrolled patients with compensated cirrhosis, no significant difference was documented in the rate of HCC detection by using an US-based surveillance strategy every 3 or 6 months [393]. Thus, in the light of current evidence, biannual US with AFP-based surveillance seems appropriate and is currently recommended.

## Who should be screened and who should not be screened?

The economic scenario in each country dictates the threshold at which a surveillance program can be

considered cost-effective. Patients who have liver cirrhosis and those who have chronic HBV infection (even in the absence of cirrhosis) constitute the high-risk group (Table 3) [394].

#### *Cirrhotic patients*

Studies depicting cost-effectiveness suggest that an incidence of HCC of  $\geq 1.5\%$  per year would require implementing a surveillance strategy in patients with cirrhosis [395], which would be irrespective of the etiology involved [396, 397]. The presence of late-stage decompensated cirrhosis (Child–Pugh class C) prohibits use of potentially curative therapies, thus implementing surveillance strategies may not be a cost-effective approach in this subset of patients [398]. Cost-effectiveness of HCC surveillance depends on the potential of receiving curative therapy in high-risk patients. Thus, if patients are ineligible for treatments due to severe liver disease or other comorbidities, HCC surveillance is not necessary. An exception to this is patients who are on a wait list for liver transplantation, who should undergo screening for HCC regardless of their liver functional status, because detecting tumors that exceed the conventional criteria may help formulate priority policies for liver transplantation. A recent Danish nationwide cohort study of patients suffering from alcohol-related cirrhosis of the liver demonstrated that the 5-year cumulative risk of HCC was only 1.0% [399]. Thus, it was suggested that a surveillance strategy in this subset of patients might not prove to be cost-effective. However, further studies are needed to verify these findings.

#### *Noncirrhotic patients*

Patients with chronic HBV infection are also prone to HCC development in the noncirrhotic stage. The cut-off for the annual incidence of HCC is still ill defined in this subset of patients, although opinions from expert groups suggest that surveillance strategies are needed if the incidence of HCC is at least 0.2% per year [63]. The incidence of HCC developing in adult African or Asian active chronic HBV carriers or those having a history of HCC in the family exceeds this value, and Asian patients having high HBV-DNA levels ( $>10,000$  copies/mL) in serum are linked to a yearly risk of more than 0.2%/year [127].

A recent study by Lok et al. [400] showed that HCC can occur in noncirrhotic patients with chronic HCV who suffer advanced fibrosis (METAVIR F3). Because the transition to cirrhosis from advanced fibrosis cannot be determined accurately, patients with chronic HCV with bridging fibrosis can be considered for surveillance; however, further data are needed before making this recommendation. Noninvasive methods to ascertain liver fibrosis, such as transient elastography (TE), appear to be novel tools to stratify patients at different HCC risks [401]. On the other hand, HCV-infected patients without cirrhosis remain at risk for HCC even after achieving SVR. Fibrotic stage (F2 or 3), old age, gamma-glutamyl transferase ( $\gamma$ GT) levels, and DM carry high risk of HCC occurrence in noncirrhotic patients, and these patients should be followed carefully for HCC after SVR [402, 403].

Patients with NAFLD who do not have underlying cirrhosis might also benefit from surveillance strategies, because emerging evidence suggests an increased risk of HCC development in this subset of patients [404]; however, more data on this aspect are needed before this strategy is recommended routinely [63]. Groups for whom HCC surveillance is uncertain are shown in Table 4.

#### *Treated chronic viral hepatitis*

Patients who achieve sustained HBV-DNA suppression or HBeAg seroconversion in chronic HBV and SVR in chronic HCV have increased; however, those treatments do not eliminate the risk of HCC completely [405, 406]. Thus, surveillance can be offered to treated patients with chronic HCV who have advanced fibrosis or cirrhosis even after achieving SVR and also to patients with chronic HBV who remain at risk of HCC due to various baseline factors.

## **Treatments**

### **Liver resection (LR) and liver transplantation (LT)**

#### *Recommendations*

1. Liver resection (LR) is a first-line curative treatment for HCC among Child–Pugh class A patients when resectability is confirmed in terms of tumor burden and

**Table 4** Groups in which HCC surveillance is uncertain

Patient group	HCC risk (per year)
Chronic hepatitis C-induced advanced fibrosis	$<1.5\%$
Chronic hepatitis B carriers younger than 50 years (females) or 40 years (males)	$<0.2\%$
NAFLD, noncirrhotic stage	$<1.5\%$



liver functional reserve by multidisciplinary evaluation (B2).

2. Liver transplantation (LT) provides the best curative treatment for all HCC patients from an oncologic point of view, and is recommended as a first-line treatment for HCC among Child–Pugh class B and C patients, if the liver graft is available (A1).
3. For cirrhotic Child–Pugh class A patients with HCC, resectability should be discussed in a multidisciplinary team, and LT may be a second-line treatment in a salvage fashion (B2).

The optimal surgical strategy for HCC has been controversial so far, as indicated by the great difference in the indication for liver resection (LR) and LT for HCC among major algorithms worldwide [407]. When considering LR for HCC, the extent of radical resection to remove the tumor, as well as the functional reserve of the diseased liver and the volume of the future liver remnant, must be taken into account. LT is now an established surgical treatment for HCC patients. In contrast to LR, there is no restriction for the indication of LT, at least in terms of liver function, and LT, which could potentially cure both the diseased liver and HCC, is superior to any other conventional therapeutic options from an oncologic point of view. It is now a matter of debate how best to select those to be offered LR or LT among HCC patients [408]. This section summarizes the current opinions regarding LR and LT for HCC.

## LR

Recent advances in surgical technique and postoperative management have made LR safe even for those with cirrhosis; however, there is still no consensus regarding the tumor burden and the liver functional reserve suitable for surgical removal with adequate survival. Indeed, in the current most popular guidelines, surgery is restricted to those patients in the very early or early stages of disease [Barcelona-Clinic Liver Cancer (BCLC) score 0–A] [2, 409]. However, LR in the real world is completely different from the BCLC recommendations, as demonstrated in the recent multicenter study reporting that 50% of patients with intermediate or advanced HCC are treated routinely with surgery in tertiary referral centers worldwide [410]. Thus, it seems difficult to set clear indication of LR for HCC at present, and LR should at least be considered in a multidisciplinary setting as a potentially curative therapy for not only patients with BCLC stage 0–A, but also patients with BCLC stages B and C. At present, however, the AASLD and EASL guidelines [2, 63], following the BCLC recommendations, set narrower indication for LR. LR is only recommended for those with single nodule and Child–Pugh class A without evidence of portal hypertension.

In contrast, LR is indicated for more progressed HCC in terms of tumor burden and for more diseased patients in terms of liver function in the treatment algorithms of Asian countries [411]. Firstly, in terms of tumor burden: The Japanese treatment algorithm recommends LR for those with single HCC (any size, regardless of macrovascular invasion) and those with multiple nodules within 3 in number (any size) [366, 412, 413]. The Hong Kong treatment algorithm recommends LR for those with early tumor ( $\leq 5$  cm,  $\leq 3$  tumor nodules, no intrahepatic venous invasion) and intermediate tumor ([1]  $\leq 5$  cm, either  $>3$  tumor nodules or with intrahepatic venous invasion, or [2]  $>5$  cm, 3 tumor nodules, and no intrahepatic venous invasion) [414]. The Korean treatment algorithm adopts wider indication of resection for HCC in which LR is allowed for those with curatively treatable disease (no limit regarding tumor burden) [415]. Secondly, in terms of liver functional reserve: The Japanese treatment algorithm recommends LR for those with Liver Damage A and B [412]. The Hong Kong treatment algorithm recommends LR for those with Child–Pugh class A and B early tumor and those with Child–Pugh class A intermediate tumor [414].

## LT

LT is the only treatment that offers the real chance of a cure for both HCC and the underlying liver cirrhosis; the shortage of liver grafts and the possibility of tumor recurrence, however, are strong limiting factors. To minimize HCC recurrence, the Milan criteria are now accepted as the gold-standard patient selection criteria in terms of tumor burden: solitary HCC less than 5 cm in diameter or within 3 nodules less than 3 cm in diameter, and without radiological evidence of vascular invasion or distant metastasis [416]. The most widely accepted criteria for the expansion of Milan are the University of California, San Francisco (UCSF) criteria: solitary tumor  $\leq 65$  mm in diameter, or 2–3 tumors, each with diameter  $\leq 45$  mm and total tumor diameter  $\leq 80$  mm, and without radiological evidence of vascular invasion or distant metastasis [417]. While it is widely accepted that the Milan criteria are too strict in terms of posttransplant recurrence rate and could definitely be expanded to some extent without impairing patient outcome, one must always be aware that any kind of expansion in tumor size or number includes the potential to worsen the posttransplant survival in patients with HCC [418]. The “metroticket paradigm” well describes this principle: the longer the distance beyond the conventional indication criteria with more aggressive tumor burden, the higher the price in terms of postoperative impairment in survival. Excessive expansion of inclusion criteria will result in a significant increase in organ demand, with a consequent increase in waiting time and a deterioration of

OS among patients with HCC as a whole in the corresponding region [419]. Moreover, the allocation system should take into account how much the extension of criteria for HCC patients will negatively influence the wait list of patients without HCC. According to studies based on the US transplant registry using Markov models, patients beyond the Milan criteria would need to achieve 5-year survival of above 60% to prevent a substantial decrease in the life-years available to the entire population of candidates for LT [420].

The Milan criteria are also standard indication criteria for LT for HCC patients in Asian countries. However, in Asia where living-donor liver transplantation (LDLT) is the mainstay for LT, things are somewhat different from region to region [421]. Unlike deceased-donor LT, LDLT is not limited by the restrictions imposed by the nationwide allocation system, and the indication for LDLT in patients with HCC often depends on institutional or case-by-case considerations, balancing the burden on the donor, the operative risk, and the OS benefit for the recipient. Caution should be paid to the possible increased recurrence rate in LDLT when compared with deceased-donor LT [422], while reports of this issue seem conflicting [423]. In Japan, each center has developed institutional expansion criteria, while National Insurance covers only those within the Milan criteria. In Taiwan and Hong Kong, the UCSF criteria [417] are adopted. In Mainland China, Hangzhou or Chengdu criteria are used with satisfactory outcome [424]. In Korea, the UCSF or Milan criteria are basically used, but LDLT can be offered for any HCC without distant metastasis under National Insurance coverage. In conclusion, the Milan criteria are still the gold-standard criteria of LT for HCC patients worldwide, and seem best to be included in the treatment algorithm for HCC to set the tumor burden limitation.

The indication of LT for HCC in terms of liver functional reserve is based on the model for end-stage liver disease (MELD) score with additional points in Western countries [418]. Consequently, LT can be offered for those with Child–Pugh class A as shown in the BCLC algorithm, if they satisfy the Milan criteria [425]. In contrast, in Asian countries, where liver grafts are extremely scarce, LT is recommended for those with decompensated liver cirrhosis (Child–Pugh class B and C) in patients with HCC as well as in those with other diseases.

## LR versus LT

LT is definitely superior to LR or other locoregional treatments from the oncologic viewpoint, since it enables the widest possible resection margins and completely removes the diseased liver at risk of developing HCC. Considering that 5-year survival after LR for HCC among

those with Child–Pugh class B is around 60% at a maximum [426, 427], LT should be recommended for such patients, if the graft is available. On the contrary, there is ongoing controversy regarding the indication of LR and LT for HCC among those with Child–Pugh class A liver dysfunction [428–431]. As mentioned above, LT is recommended as a primary treatment for HCC among those with Child–Pugh class A with evidence of portal hypertension in Western countries; however, given the shortage of liver grafts, the selection of patients who can achieve a comparable outcome by LR is a matter of debate [429, 432, 433]. Chapman et al. [434] reported significantly worse patient survival and RFS of LR compared with LT among noncirrhotic patients with HCC within the Milan criteria. Similarly, Adam et al. [435] reported worse outcomes of LR against LT among those with solitary HCC with diameter less than 5 cm. The significantly impaired RFS of LR was observed even for those with solitary HCC less than 3 cm in diameter. On the contrary, Vitale et al. [436] found that LR achieved better patient survival regardless of tumor stage provided that the patient's MELD score was less than 10. According to the meta-analysis performed by Proneth et al. [437], resectable HCC should primarily be resected as a good alternative to LT when both LR and LT seem feasible, although the data collected for the meta-analysis were of low quality of evidence. Some European authors reported that salvage LT following LR may have poorer outcomes than upfront LT [438, 439], although those are retrospective single-center observational studies. LR versus LT for those initially admissible for both treatments should be investigated by well-designed prospective study. In addition, one should always be aware that intention-to-treat analysis, not just survival from operation, should be considered when comparing LT and LR.

In contrast, in Asian countries where locoregional treatments are the mainstay strategy for HCC, LT is not recommended for Child–Pugh class A patients [411], and LR achieved 5-year survival rate of around 60% among Child–Pugh class A recipients even with portal hypertension [440], and when restricted to Child–Pugh class A patients within the Milan criteria, the 5-year survival rate reaches above 70% [441, 442]. Given the absolute scarcity of liver grafts and excellent locoregional treatment strategies in Asian countries, Child–Pugh class A, noncirrhotic patients with HCC should firstly undergo LR rather than LT if both are feasible, and the resectability of HCC should be evaluated in a multidisciplinary fashion for Child–Pugh class A, cirrhotic patients. Several methods for estimation of liver functional reserve, such as indocyanine green retention rate at 15 min (ICG-15), 99mTc-galactosyl human serum albumin (GSA) scintigraphy, 13C-methacetin breath test (LiMAx), MELD score, serum albumin-

bilirubin (ALBI) grade, aspartate transaminase-to-platelet ratio index (APRI), and FibroScan may be helpful for further stratification among Child–Pugh class A patients to elucidate better candidates for LR (or LT).

## Decisions on resectability of HCC

### The perspective of surgeons

While discussing the resectability of HCC, both technical and oncological aspects should be taken into consideration, as for the case of colorectal liver metastases. Satisfactory long-term prognosis is required to justify surgical resection, even if a tumor is technically and safely resectable. However, it is quite difficult to define “satisfactory prognosis,” because various points need to be considered, including social, ethical, economic, and emotional issues. Thus, in this section, we focus on the technical aspects related to the resectability of HCC.

In general, the surgical indications for HCC are decided not only according to the conditions of the tumor, but also according to the liver function, because HCC is frequently associated with liver dysfunction or cirrhosis caused by viral hepatitis, steatohepatitis, alcohol abuse, etc. Extensive resection of noncancerous liver parenchyma, which is a risk factor for fatal postoperative liver failure, should be avoided as much as possible. To prevent postoperative liver failure, accurate preoperative estimation of both the liver functional reserve and liver volume to be resected is essential.

There are several methods available to estimate the liver functional reserve, such as determination of the Child–Pugh score, the MELD score, determination of the hepatic venous pressure gradient, 99mTc-galactosyl serum albumin liver scintigraphy, and measurement of the ICG R15. Although, in Western countries, determination of the Child–Pugh score is the standard method, it provides too rough an estimate to allow accurate quantitative evaluation of the liver functional reserve or accurate prediction of the surgical risk in patients with liver dysfunction. On the other hand, in Asian countries, the ICG R15 value is regarded as an important parameter to estimate the liver function and tolerable resection volume. Especially in Japan, the so-called Makuuchi’s criteria [443], which include ICG R15, have been widely applied to determine the surgical indications and surgical procedures for HCC. Several authors have reported achieving zero or very low mortality with use of these criteria [444, 445]. Despite the ICG test being associated with some minor, but practical problems, such as the slight invasiveness associated with the injection of ICG and the long time needed for the test, we recommend that the ICG test also be performed in Asia-Pacific

countries other than Japan, because the safety of the surgery is coming to be regarded as the first priority in this region.

The MELD score, which is calculated from laboratory values for creatinine, bilirubin, and international normalized ratio for prothrombin time, is well known as a good predictor to guide care in patients with end-stage liver disease awaiting transplantation. However, it is not useful to decide indication of resection, because it assesses only the degree of synthetic dysfunction but not the severity of portal hypertension. The hepatic venous pressure gradient is also a well-known factor adopted in treatment algorithms advocated by the BCLC group. However, it is not used in clinical practice, because of the difficulty of direct measurement.

To increase the safety of surgical resection, it is also important to accurately estimate the liver volume to be resected and the liver volume to be preserved. Recently, a three-dimensional (3-D) virtual hepatectomy simulation software has been developed, which enables estimation of the anatomic relationships between the tumors and vessels in the liver. Preoperative volumetric estimation becomes easier and more accurate with the use of this software [446]. By applying the results of the preoperative volume estimation to Makuuchi’s criteria, the surgical indications in HCC patients with underlying liver cirrhosis can be determined more precisely, increasing the safety of liver surgery. Because this evaluation method requires the aforementioned expensive software and digital data obtained by MDCT, it may be difficult or impossible to apply at all institutions. However, manual volumetric estimation, which was the method employed before the introduction of the 3-D simulation software, is a useful substitute and should be considered in difficult situations. If the liver volume that can be preserved is too small compared with the estimated liver function, portal vein embolization is a good choice to avoid the risk of liver failure. This method, which was originally developed for treatment of hilar bile duct carcinoma [447], can be applied to obtain sufficient remnant liver volume before major hepatectomy for HCC. If preoperative evaluations suggest that the future liver remnant would be insufficient, portal vein embolization is a useful method to ensure the safety of major hepatectomy by increasing the volume of the contralateral “remnant” lobe.

The accumulated experience and tremendous efforts of preceding surgeons have remarkably increased the safety and expanded the indications of liver surgery in patients with HCC. If liver function can be preserved, the range of “technically resectable” HCC will also expand. However, whether HCC tumors are technically/practically resectable or not should be decided considering the clinical practice recommendations at each institution. In addition to the skill level and experience of the surgeons, a

multidisciplinary approach is also important to cope with various kinds of complication. Institution-related conditions are expected to become more and more significant in the future.

In conclusion, the resectability of HCC has to be determined with first priority accorded to the safety of resection. Appropriate and accurate preoperative evaluations by expert surgeons and institutions are indispensable.

### The perspective of hepatologists

Hepatic resection is a quite complicated surgical procedure among various operative methods. When considering hepatic resection for HCC, surgeons have to evaluate tumor location and liver functional reserve and decide an appropriate extent of resection and specific resection technique such as limited resection and systematic resection. Although there are several algorithms to guide secure hepatic resection, the detailed operative plan can only be formed by well-experienced hepatobiliary surgeons in marginally resectable cases. Therefore, the role of hepatologists is limited to monitoring surgeons' skill based on outcomes such as in-hospital mortality. It is well known that in-hospital mortality is strongly affected by the number of hepatic resections performed annually in a hospital [448]. In other words, the resectability of HCC in terms of safety differs markedly among surgeons, hospitals, and countries. Basically, hepatic resection should be performed by surgeons specialized in hepatobiliary surgery rather than general gastroenterological surgeons. If hepatologists judge their surgeons not to be prepared for difficult hepatic surgery, they have to recommend referral to other hospitals with well-experienced hepatobiliary surgeons or, in some "ablatable" cases, to another department with expertise in local ablative therapy.

### Local ablation

#### Recommendations

1. Percutaneous ablation therapies should be performed on patients with HCC, generally for Child–Pugh class A or B patients with three or fewer tumors, each 3 cm or less in diameter (B1).
2. Ethanol injection is a treatment of choice only in cases in which radiofrequency ablation (RFA) cannot be performed safely because of either enterobiliary reflux, adhesion between the tumor and the gastrointestinal tract, or other reasons (B1).
3. RFA is recommended as an image-guided percutaneous ablation technique (A1).
4. RFA is an acceptable alternative to resection for HCC 3 cm or smaller in Child–Pugh class A or B patients (B1).

5. RFA is a first-line treatment in HCC 2 cm or smaller in Child–Pugh class A or B cirrhosis (B1).

Image-guided percutaneous ablation therapies include ethanol injection [449–451], microwave ablation (MWA) [452], radiofrequency ablation (RFA) [453–455], and others. They are potentially curative, minimally invasive, and easily repeatable for recurrence. They are mainly performed on patients with small HCC, generally in Child–Pugh class A or B patients with three or fewer tumors each 3 cm or less in diameter.

Percutaneous ethanol injection was first reported in the early 1980s [449–451], and was long the standard in ablation. Survival of patients treated with ethanol injection has been reported to be 38–60% at 5 years [456–459]. Local tumor progression after percutaneous ethanol injection has been reported to occur in 6–31% depending on the tumor size [456, 458, 460, 461]. Percutaneous ethanol injection has been considered a safe procedure, with mortality and morbidity of 0–3.2% and 0–0.4%, respectively [458–460, 462]. Nowadays, ethanol injection is a treatment of choice only in cases in which RFA cannot be performed safely because of either enterobiliary reflux, adhesion between the tumor and the gastrointestinal tract, or other reasons.

Percutaneous MWA, in which cancer tissue is ablated by dielectric heat produced by microwave energy emitted from the inserted bipolar-type electrode, was introduced into clinical practice in the 1990s [452]. The first-generation MWA has been replaced by RFA in Japan [463], because of small volume of ablation. New-generation MWA systems incorporating antenna cooling and high-power generation have received considerable attention [464]. New-generation MWA may create a more predictable ablation zone, and a larger ablation volume in a shorter procedure time. However, its cumulative reported experience is limited. Further studies are needed, especially from the viewpoint of long-term survival.

In RFA, radiofrequency energy emitted from the exposed portion of the electrode is converted into heat, which causes necrosis of the tumor. RFA has recently been the most widely used ablation technique for HCC. Its survival has been reported to be 39.9–68.5% at 5 years and local tumor progression to be 2.4–27.0% [465–470]. Mortality and morbidity of RFA have been reported to be 0.9–7.9% and 0–1.5%, respectively [465–469]. Compared with RFA alone, combination of RFA with TACE may increase the volume of necrosis [471, 472], and might improve overall survival [473, 474]. Likewise, hepatic arterial balloon occlusion during RFA might extend the area of ablation and decrease tumor recurrence from the same subsegment as the ablated tumor [475].

Irreversible electroporation (IRE) is a nonthermal tumor ablation technique that uses electric pulses to induce cell



death, while preserving the structural integrity of bile ducts and vessels. IRE seems to be useful for tumors near a major Glisson's sheath [476].

There have been five RCTs comparing RFA with ethanol injection. Four of them demonstrated superiority of RFA over ethanol injection, in terms of treatment response, recurrence, and OS [455, 477–479], while the other trial showed that OS was not significantly different between RFA and ethanol injection [480]. Ethanol injection, however, does not require special instruments and is cheaper. Ethanol injection might be a treatment of choice in very small HCC.

An RCT comparing RFA with first-generation MWA demonstrated that the number of treatment sessions was fewer in RFA, although complete therapeutic effect, major complications, and local tumor progression were not statistically different between the two therapies [481].

It is not easy to compare outcomes between RFA and surgical resection; the indications are different between the two treatments. Furthermore, indications for each treatment are different from institution to institution. Thus, a case adjudged to be treatable by RFA or surgical resection at an institution may not be given the same treatment at another. There have been four RCTs comparing RFA with surgical resection. Three of them showed that OS was similar between RFA and surgical resection. A trial on patients with a solitary HCC 5 cm or smaller showed that OS and disease-free survival (DFS) were not statistically different between RFA and resection, but complications were more frequent and severe after surgery [482]. Another trial on patients with nodular diameters of less than 4 cm and up to 2 nodules showed that there were no statistically significant differences between RFA and surgical resection in terms of OS and RFS [483]. In another trial on patients with HCC 3 cm or smaller in diameter, there was no significant difference in DFS or OS between RFA and hepatectomy, although the incidence of postoperative complications and hospital stay were significantly greater in hepatectomy [484]. The remaining study on patients within the Milan criteria showed that OS and RFS were significantly lower in RFA than in surgical resection [485].

Concerning OS, some nonrandomized comparative studies reported that RFA had similar survival to resection [486–497], while others found that resection was associated with higher survival [426, 498–502]. Even in studies which reported that surgical resection was superior to RFA, there was no significant difference in OS between RFA and surgical resection in patients with HCC 2 cm or smaller in diameter [426] or 3 cm or smaller in diameter [499–501]. In one study, RFA had better long-term survival than surgical resection after propensity score analysis [503]. RFA was associated with fewer major complications [494, 500] and shorter hospital stay [494]. RFA may be more cost-

effective than surgical resection [504]. Most studies reported that RFS was higher in surgical resection than in RFA, although OS was not significantly different between RFA and surgical resection in them. This is probably because surgical resection removes a much larger volume of liver parenchyma, which may result in removal of some occult metastases and reduction of new carcinogenesis but may be prone to liver decompensation. In addition, most recurrence can be treated curatively by iterative RFA [469] but not by repeated surgical resection. Although further RCTs are warranted to compare ablation with surgical resection [505], data available at present suggest that OS is not significantly different between RFA and surgical resection. Various innovations, such as CEUS [506] and multimodality fusion imaging [507], would improve outcomes in ablation.

Ablation is less invasive and less expensive. Because patients with HCC have been markedly aging, minimally invasive therapies such as ablation would play a more important role. Because many Asian countries are still developing, from the viewpoint of medical economics, highly cost-effective therapies such as ablation should have priority. Ablation techniques, especially RFA, may be an alternative to surgery in selected cases.

## Transarterial chemoembolization (TACE)

### Recommendations

1. Transarterial chemoembolization (TACE) is recommended as a first-line treatment of HCC for patients with unresectable, large/multifocal HCCs who do not have vascular invasion or extrahepatic spread (A1).
2. Selective TACE can be performed in patients with small tumors in whom ablation is difficult to perform because of tumor location or medical comorbidities (B1).
3. Selective or superselective TACE should be attempted in order to preserve nontumorous liver parenchyma, maximize treatment effect, and minimize complications (A1).
4. TACE using drug-eluting beads has similar therapeutic efficacy with less systemic adverse events compared with conventional TACE (B2).
5. Other treatment strategies might be considered for patients with HCC who are not suitable for or do not response to repeated TACE (B2).
6. Transarterial radioembolization (TARE) with yttrium-90-loaded resin/glass beads may be used as an alternative locoregional treatment for unresectable HCC (B2).



Although the normal liver receives a dual blood supply from the hepatic artery and the portal vein, HCC is supplied almost exclusively by the hepatic artery [508]. TACE exploits the preferential hepatic arterial supply of HCC for targeted delivery of chemotherapeutic agents, usually mixed with lipiodol, followed by embolization or reduction in arterial flow using various types of particles (e.g., gel-foam particles), while sparing the surrounding liver parenchyma [509]. TACE is currently considered as the mainstay of therapy for unresectable, large/multifocal HCCs without vascular invasion or extrahepatic spread [510]. TACE provided a significant survival benefit in selected HCC patients with preserved liver function and adequate performance status [511–514]. Therefore, the guidelines published by the EASL and AASLD recommend TACE as a first-line, noncurative therapy for non-surgical patients with large/multifocal HCC who do not have vascular invasion or extrahepatic spread [2, 63]. In addition, according to the guidelines published by the JSH [515], hepatectomy or TACE is recommended if there are 2 or 3 tumors of less than 3 cm, and TACE or hepatic arterial infusion chemotherapy is recommended if there are 4 or more tumors. In addition, TACE can be performed in patients at early stage in whom RFA is difficult to perform because of tumor location or medical comorbidities [516]. TACE is also the first-line therapy for downstaging tumors that exceed the criteria for LT.

As TACE usually does not induce significant liver dysfunction even in cirrhotic patients and treatment-related mortality is less than 5% [516, 517], the benefits of TACE procedure should not be offset by treatment-induced liver failure. TACE is associated with transient postembolization syndrome, but incidence of severe events has been reported to be less than 5%, including hepatic insufficiency, liver abscess, acute cholecystitis or gastrointestinal bleeding [517, 518]. Important predisposing factors are major portal vein obstruction, compromised hepatic functional reserve, biliary obstruction, previous biliary surgery, excessive amount of iodized oil, and nonselective embolization [519]. Therefore, selective or superselective TACE should be attempted to maximize tumor necrosis and to minimize procedure-related complications by preserving nontumorous liver parenchyma [520, 521].

However, there is no standardized protocol for TACE in terms of treatment schedule or type and dosage of anticancer agent. In addition, predictions of its therapeutic efficacy are limited by the use of nonstandardized embolic material. TACE performed with drug-eluting beads (DEB-TACE) loaded with doxorubicin has been shown to modify the pharmacokinetics of the injected chemotherapy, allowing longer intratumoral exposure and less systemic exposure of the drug, reducing toxicity [522, 523]. In prospective clinical trials, liver toxicity and

systemic adverse effects occur less frequently after DEB-TACE than conventional TACE. Although there is no significant benefit of DEB-TACE over conventional TACE with respect to objective response, selected patient groups such as those with Child–Pugh class B, ECOG performance status 1, bilobar disease, and recurrent disease showed a significant increase in objective response in DEB-TACE group [524]. Furthermore, DEB-TACE was associated with improved tolerability, with a significant reduction in serious liver toxicity and side-effects [524]. Despite these promising results, use of DEB-TACE in Asia has been relatively low compared with Western countries [2, 415, 525]. So far, in Asia, there has been no robust evidence favoring use of DEB-TACE in terms of efficacy and cost-effectiveness. Therefore, further research is required to address this issue.

Although TACE is considered the standard of care for nonsurgical HCCs that are also ineligible for percutaneous ablation, those with so-called bulky tumor burden (tumor size >5 cm) and Child–Pugh class B showed the worst survival outcomes (median OS of about 9 months) [526]. Furthermore, several scoring systems [i.e., SNACOR [527], hepatoma-embolisation prognostic (HAP) score [528], modified HAP score [529], Selection for TrAnsarterial chemoembolisation TrEatment (STATE) score [530], and the Chiba HCC in intermediate-stage prognostic (CHIP) score [531]] have been developed, identifying a subgroup with unfavorable outcomes. Among them, STATE score based upon tumor burden (up-to-7 criteria), albumin level, and C-reactive protein level was suggested as an objective point score to guide the decision regarding the first treatment, showing that lower STATE score was associated with worse outcome [530]. In a similar context, the Assessment for Retreatment with TACE (ART) score, an objective point score to guide the decision regarding retreatment with TACE, was developed based upon an increase of aspartate aminotransferase by >25%, Child–Pugh score increase, and absence of radiological response [532]. Higher ART score was associated with major adverse events after the second TACE ( $P = 0.011$ ) [532]. Based upon these findings, sequential use of the STATE and ART scores was suggested to identify the most suitable and unsuitable patients for multiple TACE sessions [530]. So, for such a population with relatively unfavorable outcomes primarily owing to tumor burden and/or liver function, other treatment options based upon multidisciplinary approaches, including a switch of treatment modality from TACE to sorafenib or hepatic arterial infusion chemotherapy, might also be considered. Vice versa, even for large/multinodular HCC, active curative treatments including LT (e.g., within up-to-7 criteria), or so-called downstaging strategies might be tried in selected cases [533–535].

According to conventional size-based response evaluation criteria, i.e., World Health Organization (WHO) criteria [536], the reported rate of objective response ranges between 16 and 60% [513, 517]. The Response Evaluation Criteria in Solid Tumors (RECIST) [537] generally ignore tumor necrosis, and thus may underestimate treatment response [538]. In contrast, two enhancement criteria, the EASL criteria [539] and the modified RECIST (mRECIST) [540], have demonstrated superior efficacy for assessing treatment response and predicting survival outcome compared with the WHO criteria or RECIST [541–543]. The objective response rate using enhancement criteria ranges between 58 and 86%, and 20–41% achieve complete response [538, 541–543]. In addition, the biological response based upon changes in tumor markers after treatment might be used as an ancillary method for assessment of overall response [544, 545].

Another issue related to TACE is the concept of “failure” or “refractoriness” to TACE. So far, several studies have tried to address this [366, 525, 546–548]. The JSH has provided a definition of TACE failure/refractoriness as two or more consecutive ineffective responses seen within the treated tumors, two or more consecutive progressions in the liver (including an increase in the tumor number), continuous elevation of tumor markers right after TACE, appearance of vascular invasion, and appearance of extrahepatic spread [366]. Similarly, according to Raoul et al. [546], a switch of treatment modality from TACE to others including sorafenib might be considered for those who have progression after two sessions of TACE. However, there is still no consensus regarding the definition of TACE failure or refractoriness. Moreover, there is no proven therapy for the purpose of rescue, although sorafenib rescue might improve survival in patients who experience TACE failure, compared with those who continue TACE [549, 550]. Other treatment modalities including internal or external radiotherapy and new molecular targeted agents have been studied as potential rescue therapies for patients with TACE failure.

Many attempts have been made to improve the treatment outcomes of TACE. Combination of sorafenib and TACE might be an eligible option [551]. However, a RCT comparing the efficacy in HCC treated with sorafenib or placebo plus DEB-TACE showed that combination therapy did not improve outcome [552].

Transarterial radioembolization (TARE) involves injection of implantable radioactive microspheres into tumor-feeding arteries in order to expose the tumor to highly concentrated radiation while protecting the normal parenchyma. TARE using yttrium-90 is an evolving and promising regional therapy, which can complement or replace TACE [2, 415, 553]. In a European phase II study of patients with intermediate or advanced HCC, TARE

resulted in 40.4% objective tumor response rate with median survival of 15 months [554]. In another large retrospective cohort study conducted in the USA, the median survival of TARE-treated patients with portal vein invasion was significantly shorter than those without invasion (10 versus 15.3 months) [555, 556]. In a recent prospective multicenter Korean study, the 3-month tumor response rate was 57.5% and the 3-year OS rate was 75% [557]. Although there is not enough evidence confirming clinical benefit of TARE compared with conventional TACE, TARE might be recommended to patients who are not good candidates for TACE due to bulky tumor and/or portal vein invasion, based on published data.

## Radiation therapy

### Recommendations

1. Although stereotactic body radiotherapy (SBRT) and proton beam (also carbon ion beam) are reasonable options for patients who have failed other local therapies, radiotherapy (RT) has not been shown to improve outcomes for patients with HCC. However, RT may be considered for symptomatic bony metastases (C2).

Although HCC is considered to be a radiosensitive tumor, it also is located in a radiosensitive organ. Due to the development of three-dimensional conformal radiation therapy (3D-CRT), radiotherapy (RT) can be performed more safely for patients with HCC without severe toxicity. Technological developments for targeting HCC precisely with RT [intensity-modulated RT (IMRT) and image-guided approaches, including stereotactic body radiotherapy (SBRT)] can improve the benefit and reduce the risk. However, they do not alter the high recurrence rates in other nontreated areas of the liver. There are no large-scale RCTs demonstrating an effect of any form of RT on survival and no consensus regarding the optimal use of this therapy. Thus, RT is not recommended in the AASLD and EASL guidelines for treating HCC [2, 63]. Even though strong evidence is lacking, RT may be one of the promising treatment options for HCC.

### Indications

The lack of strong evidence to support RT for patients with HCC is reflected in the various recommendations of expert groups in different countries. The AASLD and EASL guidelines do not address use of external-beam RT for treatment of HCC [2, 63]. Consensus-based guidelines from the National Comprehensive Cancer Network (NCCN) list external-beam RT (conformal or stereotactic)

as an alternative option to ablation or arterially directed therapies for patients with unresectable HCC who have contraindications for liver transplantation. An expert consensus group of the Americas Hepato-Pancreato-Biliary Association (AHPBA) concluded that RT can provide local control for some unresectable HCC lesions, that better RT planning and delivery (for example, hypofractionation, stereotactic treatment, proton beam, and carbon ion beam therapy) have the advantage of increasing the radiation dose to unresectable HCC without causing severe toxicity, and that strategies combining RT with other therapies merit continued evaluation [558]. SBRT and proton beam (also carbon ion beam) are reasonable options for patients who have not responded to other local modalities and have no extrahepatic disease, limited tumor burden, and relatively good liver function. Where available, proton beam and carbon ion beam irradiation is a reasonable approach for patients with large HCC with or without tumor thrombus of vessels.

### Contraindications

The radiation dose must be relatively low to minimize the radiation effect on normal liver included in the treatment field. Use of RT should be limited to patients with sufficient liver function (Child–Pugh score 7 or less) and liver volume outside the radiation field. Patients with Child–Pugh score of 8 or more have elevated risk of radiation-induced hepatic toxicity or liver failure [559]. A relative contraindication to RT is previous hepatic radiation to the same segment of the liver. While retreatment may be possible in select cases, these patients should be evaluated in a tertiary care center by experts on hepatic RT [560, 561].

### Efficacy

#### 3D-CRT

With the development of 3D-CRT techniques, RT can be performed more safely to the HCC with less liver toxicity. Most available data are from retrospective or single-center studies [562, 563]. A phase II trial in France reported sustained local tumor control in 78% of patients with early-stage HCC (one nodule and  $\leq 5$  cm, or two nodules and  $\leq 3$  cm) who were treated with 3D-CRT [564]. One of the problems with RT is the high intrahepatic recurrence rate outside of the high-dose irradiation area, which may be caused in part by difficulties with accurately targeting HCC during conventional RT treatment planning [565].

#### SBRT

SBRT (sometimes called stereotactic radiosurgery) is a technique in which a limited number of high-dose RT with hypofractionation (typically 3–6) are delivered to a small, definite target using multiple, nonparallel radiation beams. The beams converge on the target lesion, minimizing radiation exposure to other normal tissue or organs. This targeting makes it possible to treat a lesion in either a single or limited number of dose fractions. Experience with SBRT for HCC is increasing [566–569]. In the largest series, 93 patients (Child–Pugh A: 69 patients; Child–Pugh B: 24 patients) with small HCCs (median 2 cm; range 1–6 cm) who were not eligible for surgical resection or RFA were treated with SBRT [566]. The in-field complete response rate was 16%, but the in-field progression-free survival at 3 years was 92%.

#### Charged-particle radiation therapy

There is a growing body of evidence, primarily from Japan, supporting use of proton beam and carbon ion beam irradiation, particularly for patients with large tumors or portal vein thrombus [570–573]. In one study, 162 patients with 192 HCCs were treated with proton beam irradiation [570]. Most tumors had diameter of 3–5 cm. The majority of the patients had past history of receiving other nonsurgical treatments. The 5-year local control and 5-year survival rates were 87 and 24%, respectively.

### Complications

Minimizing radiation-induced complications depends on careful patient selection and radiation treatment planning. The most common acute side-effects include transient fatigue, nausea, vomiting, and right upper quadrant pain. Possible long-term side-effects include worsening hepatic function with ascites, edema, hepatomegaly, thrombocytopenia, and elevated liver function tests. Rarely, cases of radiation-induced biliary stenosis, portal vein thrombosis, or death from radiation-induced liver failure have been reported [574].

### Response assessment

Dynamic CT or dynamic MRI is usually performed at 4 weeks, 2–3 months later, and then at 3-month intervals for at least 1 year. If there has been no recurrence of disease after a year, imaging will be performed every 4–6 months.

## Systemic therapy

### Recommendations

1. Sorafenib is recommended for the first-line treatment of advanced-stage patients (macrovascular invasion or extrahepatic metastasis) who are not suitable for locoregional therapy and who have Child–Pugh class A liver function (A1).
2. Sorafenib may be used with caution in patients with Child–Pugh class B liver function (B2).

### Sorafenib

Sorafenib, a multikinase inhibitor of Raf, vascular endothelial growth factor receptor (VEGFR), platelet-derived growth factor receptor (PDGFR), c-kit, Flt-3, and RET [575], has been approved for the treatment of advanced HCC in patients with Child–Pugh class A liver function worldwide. The approval is generally based on the results of two phase III, double-blind, placebo-controlled trials [576, 577]. The first trial (SHARP trial) was conducted primarily in Europe and the USA (HCV: 28.1%, alcoholic liver disease: 26.4%) with the primary end point of OS. The second trial was conducted primarily in the Asia–Pacific population (HBV: 73%) with an almost identical design to the SHARP trial. Sorafenib resulted in a similar survival benefit in these two different patient populations. The hazard ratios of OS and time to radiological progression were 0.69 and 0.58 in the SHARP trial and 0.68 and 0.57 in the Asia–Pacific trial. Exploratory subgroup analyses of the two trials indicated that sorafenib treatment prolonged survival regardless of patient age, performance status, and tumor burden (vascular invasion or extrahepatic spread). However, sorafenib rarely induced radiological responses (SHARP trial: 2%, Asia–Pacific trial: 3.3%). Sorafenib at dosage of 400 mg twice daily is generally well tolerated. The most common drug-related adverse events included diarrhea, fatigue, hand–foot skin reaction, and rash/desquamation, most of which were grade 1 or 2. The most common causes of treatment interruption or dose reduction were hand–foot skin reaction, rash, and diarrhea.

The efficacy of sorafenib in patients with Child–Pugh class B liver function has never been prospectively studied by RCTs. Several noninterventional studies investigated the efficacy and safety of sorafenib in HCC patients with Child–Pugh class A versus class B liver function. HCC patients with Child–Pugh class B liver function, compared with those with Child–Pugh class A liver function, had shorter duration of sorafenib use (Child–Pugh class B: 8.4 weeks; Child–Pugh class A: 13.6 weeks) [578] and

shorter median OS (Child–Pugh class B: 3.8–4.5 months; Child–Pugh class A: 10–13 months) [579–581] but similar rates of adverse events. Patients with Child–Pugh score 7, compared with patients with Child–Pugh score 8 or 9, had higher median OS time, but the difference did not reach statistical significance [580–583]. Taken together, patients with Child–Pugh class B liver function did not suffer excessive risk with sorafenib use, but they were more likely to develop hepatic decompensation [584], which limited continuation of sorafenib and thus survival. Therefore, sorafenib may be used with caution in patients with Child–Pugh score 7 and is generally not suggested for patients with Child–Pugh score >7 or decompensated cirrhosis.

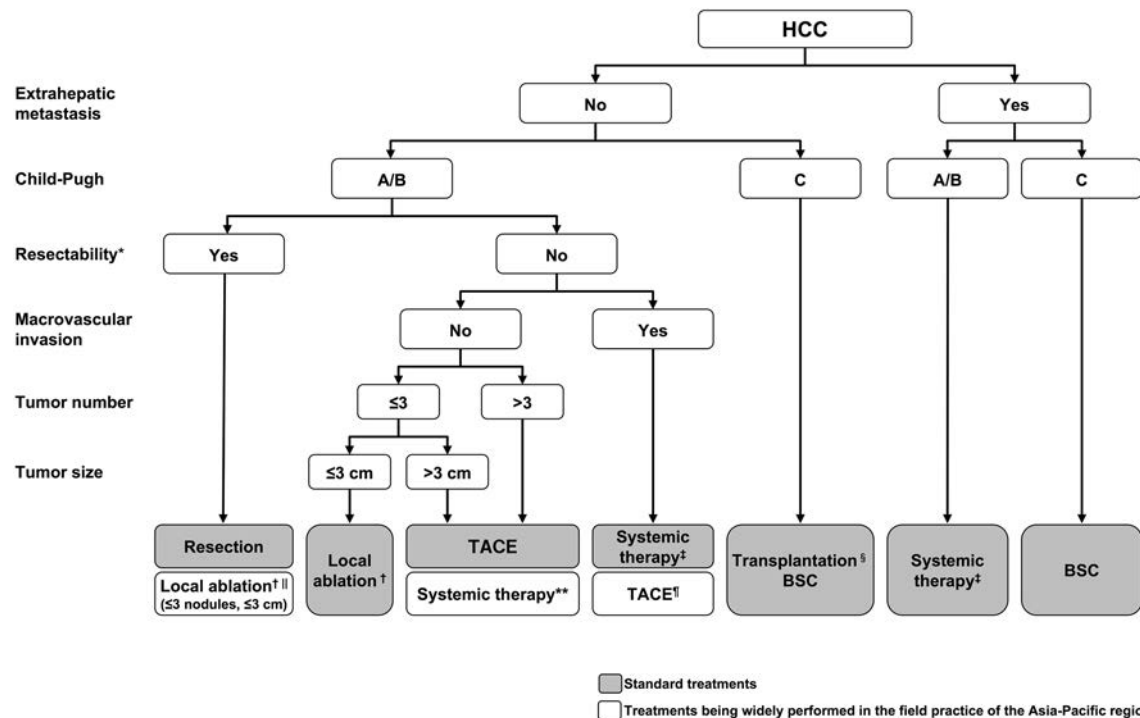
### Regorafenib

Regorafenib, a novel multikinase inhibitor, has more potent inhibitory activities against multiple angiogenic pathways (VEGFR, PDGFR, TIE2, and FGFR) and oncogenic pathways (RET, KIT, c-RAF/RAF-1, and BRAF) than sorafenib [585]. Regorafenib, administered at 160 mg once daily for 3 weeks in each 4-week cycle, has been investigated for its efficacy and safety as a second-line treatment in a phase III double-blind RCT (RESORCE trial) [586]. Regorafenib, compared with placebo, significantly reduced the risks of death (HR 0.62; 95% CI 0.50–0.78;  $p < 0.001$ ) and progression or death (HR 0.46; 95% CI 0.37–0.56;  $p < 0.001$ ) in 573 HCC patients (regorafenib: 379 patients; placebo: 194 patients) with Child–Pugh class A liver function who had progression on sorafenib. The median OS and progression-free survival (regorafenib versus placebo) were 10.6 versus 7.8 months and 3.1 versus 1.5 months, respectively. The overall response rate (regorafenib versus placebo) was 10.6 versus 4.1%, respectively ( $p = 0.005$ ). Rates of grade  $\geq 3$  adverse events were 79.7% with regorafenib and 58.5% with placebo. The most common grade  $\geq 3$  adverse events included hypertension, hand–foot skin reaction, fatigue, and diarrhea.

### Treatment algorithm

The latest treatment algorithm is evidence based and attempts to be comprehensible and suitable for universal use in the Asia–Pacific region, which has a diversity of medical environments (Fig. 2). The order of columns corresponds to the decision-making process of treatment in field practice. Standard treatments with high evidence levels and treatments being widely performed in field practice in the Asia–Pacific region are demonstrated. The results of ongoing trials, which will be announced in the near future, or further planning of prospective studies will present possibilities for changing standard treatments. It is greatly hoped that promising results will be delivered from





**Fig. 2** Treatment algorithm for hepatocellular carcinoma (APASL 2016). \*Decisions regarding resectability should be discussed in a multidisciplinary team. †RFA is recommended as the first choice for the local ablation. ‡Currently, sorafenib and regorafenib are drugs that have shown clinical benefits in phase III studies. See text for use of systemic therapy. §Liver transplantation is recommended when indicated. ||Local ablation is an alternative treatment in

the Asia-Pacific region. Although there are various treatments being performed in limited institutions or countries, those treatments which do not have sufficient supporting evidence are not indicated in terms of universal use in this region.

RFA for resectable patients ( $\leq 3$  cm,  $\leq 3$  nodules) and TACE for patients with macrovascular invasion (no extrahepatic metastasis) are often performed in field practice in the Asia-Pacific region. The JSH consensus-based guidelines and the Hong Kong Liver Cancer staging system are similar protocols recommended based on these points [414, 548]. Despite insufficient evidence for standard treatments at the moment, RFA for resectable patients ( $\leq 3$  cm,  $\leq 3$  nodules) and TACE for patients with macrovascular invasion (no extrahepatic metastasis) are categorized as treatments being widely performed in field practice in the Asia-Pacific region.

Recently, the concept of conversion from TACE to sorafenib before the appearance of macrovascular invasion or extrahepatic metastasis has been advocated by clinicians from both Europe and Japan [366, 546, 548]. This point of controversy in clinical practice has been discussed since the approval of sorafenib for treatment of HCC. Although only a few retrospective studies have reported the

resectable patients ( $\leq 3$  cm and  $\leq 3$  nodules). Choice of treatments should be discussed in a multidisciplinary team. ¶TACE is an alternative treatment in patients with macrovascular invasion (no extrahepatic metastasis). Choice of treatments should be discussed in a multidisciplinary team. \*\*Treatment conversion from TACE to systemic therapy is recommended for patients in whom TACE is expected to be ineffective

effectiveness of this concept [549, 550, 587], conversion from TACE to systemic therapy appears to be a reasonable treatment strategy. In fact, in field practice, sorafenib has been administered to a considerable number of patients without either macrovascular invasion or extrahepatic metastasis [588]. Thus, this treatment algorithm recommends treatment conversion from TACE to systemic therapy for patients in whom TACE is ineffective.

The other unique point of this algorithm is the indication for hepatic resection. It does not include strictly defined conditions for hepatic resection. According to the Japanese guidelines, resection is recommended in several treatment arms, thereby making these recommendations complicated and confusing [366, 547]. On the other hand, indications for resection are limited, such as a single lesion and normal hepatic portal vein pressure, according to the BCLC staging system [409]. These selection criteria appear to be too strict and unsuitable for use in the Asia-Pacific region. It may be difficult to define criterion for resectability that are generally applicable in countries with varying medical environments. In this treatment algorithm, indications for resection are not strictly defined in order to allow surgeons and hepatologists to collaborate in deciding on therapeutic strategies. Thus, this algorithm recommends that decisions



**Table 5** Ongoing clinical trials of immune checkpoint inhibitors for advanced hepatocellular carcinoma

Drug	Phase	Design	Study number
<i>First-line</i>			
Nivolumab versus sorafenib	III	Randomized, open label	NCT02576509
Nivolumab plus ipilimumab (anti-CTLA-4) versus nivolumab versus sorafenib	II	Randomized, open label	NCT01658878
<i>Second-line</i>			
Nivolumab	Ib	Open label	NCT01658878
Pembrolizumab (anti-PD-1)	II	Open label	NCT02702414
Pembrolizumab versus placebo	III	Randomized, double blind, placebo controlled	NCT02702401
Nivolumab plus galunisertib (GSK- $\beta$ inhibitor)	II	Open label	NCT02423343
Durvalumab (anti-PD-L1) plus tremelimumab versus durvalumab versus tremelimumab	II	Randomized, open label	NCT02519348
Durvalumab plus ramucirumab (anti-VEGFR)	I	Open label	NCT02572687
PDR001 (anti-PD-1) plus capmatinib (cMet inhibitor) versus PDR001	Ib/II	Open label	NCT02795429

regarding resectability are discussed by a multidisciplinary team, including surgeons and hepatologists. It is also important for surgeons and hepatologists to provide feedback on treatment outcomes to one another.

## Clinical trials for new compounds on the horizon

### Molecular targeted agents

In addition to sorafenib and regorafenib, a variety of molecular targeted agents have been thoroughly investigated, including sunitinib [589], brivanib [590, 591], linafanib [592], ramucirumab (angiogenesis inhibitors) [593], erlotinib (EGFR inhibitor) [594], and everolimus (mTOR inhibitor) [595]. However, none have shown survival benefits in either first-line or second-line setting in phase III RCTs. The results of large randomized phase III trials for lenvatinib (first-line) and cabozantinib (second-line) will soon be available. All of these trials were conducted in biomarker-unselected HCC patients. Recently, tivantinib was found effective in MET-high subgroup of patients [596], and MET-high-enriched randomized phase III studies were initiated. The latest early-phase trials for selective c-Met inhibitors, tepotinib [597], capmatinib [598], as well as selective FGFR4 inhibitor FGF401 are being conducted in biomarker-enriched HCC patients.

### Immunotherapy

Immuno-oncology is an emerging area of drug development. Major breakthroughs have been achieved in agents targeting immune checkpoint proteins, such as cytotoxic T lymphocyte antigen-4 (CTLA-4) and programmed cell death-1 (PD-1), in patients with various types of cancer

[599–603]. These immune checkpoint inhibitors restore and sustain activation of either primed or effector T cells to exert T cell-mediated cancer cell killing. Tremelimumab, an anti-CTLA-4 antibody, resulted in an objective response rate of 17.6%, a disease control rate of 76.4%, and time to progression of 6.48 months in 21 HCV-related HCC patients who had failed at least one line of systemic therapy [604]. Nivolumab, an anti-PD-1 antibody, is currently being investigated as a second-line therapy in a phase I/II trial. The preliminary data from its dose expansion cohort showed an objective response of 20% and a 9-month OS rate of 74% in 214 HCC patients [605]. The objective responses were observed in all etiology groups. Adverse events were generally tolerable and manageable in these two trials. Moreover, a significant proportion of patients with chronic HBV or HCV infection had reduction of viral load with study treatment. These promising results indicate an important step toward a new paradigm of systemic therapy for advanced HCC. More clinical trials using immune checkpoint inhibitors alone or in combination with immunotherapy or molecular targeted therapy are ongoing (Table 5).

**Acknowledgements** We appreciate Kiyoshi Hasegawa (The University of Tokyo), Nobuhisa Akamatsu (The University of Tokyo), Amna Subhan (Aga Khan University and Hospital), Tomoko Saito (Chiba University), Masanori Inoue (Chiba University), Toru Wakamatsu (Chiba University), Masayuki Yokoyama (Chiba University), and Tomoyuki Ishigami (Chiba University) for assistance that greatly improved the guidelines.

### Compliance with ethical standards

**Conflict of interest** Masao Omata received fees for being a speaker, consultant, and advisory board member from Bayer, Boehringer Ingelheim, Bristol-Myers Squibb, Otsuka, Astellas, Gilead Sciences, Chugai, Mitsubishi Tanabe, Kyorin, Merck Sharp and Dohme,

Dainippon Sumitomo, Vertex Pharmaceuticals, Takeda, Merck Serono, and Zeria. Ann-Lii Cheng received consultant fees from Novartis, Merck Serono, Eisai, Merck Sharp and Dohme, ONXEO, Bayer, Bristol-Myers Squibb, and Ono Pharmaceutical. Norihiro Kokudo received research grants from Dainippon Sumitomo, Astellas, and Taiho. Masatoshi Kudo received lecture fees from Bayer, Eisai, Merck Sharp and Dohme, and Ajinomoto, research grants from Chugai, Otsuka, Takeda, Dainippon Sumitomo, Daiichi Sankyo, Merck Sharp and Dohme, Eisai, Bayer, and AbbVie, and consulting or advisory fees from Kowa, Merck Sharp and Dohme, Bristol-Myers Squibb, Bayer, Chugai, and Taiho. Jidong Jia received consultation and speaker fees from Bristol-Myers Squibb, Gilead, Merck Sharp and Dohme, Novartis, and Roche. Sadahisa Ogasawara received a consulting or advisory fee from Bayer and Eisai and honoraria from Bayer and Eisai. Jeong Min Lee, Ryosuke Tateishi, Kwang-Hyub Han, Yoghesh K. Chawla, Shuichi Shiina, Wasim Jafri, Diana Alcantara Payawal, Takamasa Ohki, Pei-Jer Chen, Cosmas Rinaldi A. Lesmana, Laurentius A. Lesmana, Rino A. Gani, Shuntaro Obi, A. Kadir Dokmeci, and Shiv Kumar Sarin declare that they have no conflict of interest.

**Open Access** This article is distributed under the terms of the Creative Commons Attribution 4.0 International License (<http://creativecommons.org/licenses/by/4.0/>), which permits unrestricted use, distribution, and reproduction in any medium, provided you give appropriate credit to the original author(s) and the source, provide a link to the Creative Commons license, and indicate if changes were made.

## References

- World Health Organization. Cancer. <http://www.who.int/mediacentre/factsheets/fs297/en/>. Accessed 16 April 2017
- European Association For The Study of the Liver; European Organisation For Research And Treatment Of Cancer. EASL-EORTC clinical practice guidelines: management of hepatocellular carcinoma. *J Hepatol* 2012;56:908–943
- Lozano R, Naghavi M, Foreman K, Lim S, Shibuya K, Aboyans V, et al. Global and regional mortality from 235 causes of death for 20 age groups in 1990 and 2010: a systematic analysis for the Global Burden of Disease Study 2010. *Lancet* 2012;380:2095–2128
- Omata M, Lesmana LA, Tateishi R, Chen PJ, Lin SM, Yoshida H, et al. Asian Pacific Association for the Study of the Liver consensus recommendations on hepatocellular carcinoma. *Hepatol Int* 2010;4:439–474
- Guyatt GH, Oxman AD, Vist GE, Kunz R, Falck-Ytter Y, Alonso-Coello P, et al. GRADE: an emerging consensus on rating quality of evidence and strength of recommendations. *BMJ* 2008;336:924–926
- Schünemann HJ, Oxman AD, Brozek J, Glasziou P, Jaeschke R, Vist GE, et al. Grading quality of evidence and strength of recommendations for diagnostic tests and strategies. *BMJ* 2008;336:1106–1110
- International Agency for Research on Cancer. GLOBOCAN 2012: Estimated cancer incidence, mortality and prevalence worldwide in 2012. <http://globocan.iarc.fr/Default.aspx/>. Accessed 16 April 2017
- Yang JD, Roberts LR. Hepatocellular carcinoma: a global view. *Nat Rev Gastroenterol Hepatol* 2010;7:448–458
- Lai CL, Ratziu V, Yuen MF, Poynard T. Viral hepatitis B. *Lancet* 2003;362:2089–2094
- El-Serag HB. Epidemiology of viral hepatitis and hepatocellular carcinoma. *Gastroenterology* 2012;142:1264–1273
- Shi J, Zhu L, Liu S, Xie WF. A meta-analysis of case-control studies on the combined effect of hepatitis B and C virus infections in causing hepatocellular carcinoma in China. *Br J Cancer* 2005;92:607–612
- McGlynn KA, London WT. The global epidemiology of hepatocellular carcinoma: present and future. *Clin Liver Dis* 2011;15:223–243
- Doe JE, Paddle GM. The evaluation of carcinogenic risk to humans: occupational exposures in the spraying and application of insecticides. *Regul Toxicol Pharmacol* 1994;19:297–308
- Chen CJ, Iloeje UH, Yang HI. Long-term outcomes in hepatitis B: the REVEAL-HBV study. *Clin Liver Dis* 2007;11:797–816
- World Health Organization. Hepatitis B. <http://www.who.int/mediacentre/factsheets/fs204/en/>. Accessed 16 April 2017
- Tseng TC, Liu CJ, Chen CL, Wang CC, Su TH, Kuo SF, et al. Serum hepatitis B virus-DNA levels correlate with long-term adverse outcomes in spontaneous hepatitis B e antigen seroconverters. *J Infect Dis* 2012;205:54–63
- Tseng TC, Liu CJ, Yang HC, Su TH, Wang CC, Chen CL, et al. High levels of hepatitis B surface antigen increase risk of hepatocellular carcinoma in patients with low HBV load. *Gastroenterology* 2012;142:1140–1149
- Tseng TC, Liu CJ, Yang HC, Su TH, Wang CC, Chen CL, et al. Serum hepatitis B surface antigen levels help predict disease progression in patients with low hepatitis B virus loads. *Hepatology* 2013;57:441–450
- Liaw YF. HBeAg seroconversion as an important end point in the treatment of chronic hepatitis B. *Hepatol Int* 2009;3:425–433
- Liu CJ, Kao JH. Global perspective on the natural history of chronic hepatitis B: role of hepatitis B virus genotypes A to. *J Semin Liver Dis* 2013;33:97–102
- Kao JH, Chen PJ, Lai MY, Chen DS. Hepatitis B genotypes correlate with clinical outcomes in patients with chronic hepatitis B. *Gastroenterology* 2000;118:554–559
- Yang HI, Yeh SH, Chen PJ, Iloeje UH, Jen CL, Su J, et al. Associations between hepatitis B virus genotype and mutants and the risk of hepatocellular carcinoma. *J Natl Cancer Inst* 2008;100:1134–1143
- Kao JH, Chen PJ, Chen DS. Recent advances in the research of hepatitis B virus-related hepatocellular carcinoma: epidemiologic and molecular biological aspects. *Adv Cancer Res* 2010;108:21–72
- Chen CH, Chen YY, Chen GH, Yang SS, Tang HS, Lin HH, et al. Hepatitis B virus transmission and hepatocarcinogenesis: a 9 year retrospective cohort of 13676 relatives with hepatocellular carcinoma. *J Hepatol* 2004;40:653–659
- Chang MH, You SL, Chen CJ, Liu CJ, Lee CM, Lin SM, et al. Decreased incidence of hepatocellular carcinoma in hepatitis B vaccinees: a 20-year follow-up study. *J Natl Cancer Inst* 2009;101:1348–1355
- Yang HI, Yuen MF, Chan HL, Han KH, Chen PJ, Kim DY, et al. Risk estimation for hepatocellular carcinoma in chronic hepatitis B (REACHB): development and validation of a predictive score. *Lancet Oncol* 2011;12:568–574
- Jung KS, Kim SU, Ahn SH, Park YN, Kim Do Y, Park JY, et al. Risk assessment of hepatitis B virus-related hepatocellular carcinoma development using liver stiffness measurement (FibroScan). *Hepatology* 2011;53:885–894
- Kim DY, Song KJ, Kim SU, Yoo EJ, Park JY, Ahn SH, et al. Transient elastography-based risk estimation of hepatitis B virus-related occurrence of hepatocellular carcinoma: development and validation of a predictive model. *Oncol Targets Ther* 2013;6:1463–1469
- Kim WR, Loomba R, Berg T, Aguilar Schall RE, Yee LJ, Dinh PV, et al. Impact of long-term tenofovir disoproxil fumarate on

- incidence of hepatocellular carcinoma in patients with chronic hepatitis B. *Cancer* 2015;121:3631–3638
30. Wong GL, Chan HL, Mak CW, Lee SK, Ip ZM, Lam AT, et al. Entecavir treatment reduces hepatic events and deaths in chronic hepatitis B patients with liver cirrhosis. *Hepatology* 2013;58:1537–1547
  31. Fasani P, Sangiovanni A, De Fazio C, Borzio M, Bruno S, Ronchi G, et al. High prevalence of multinodular hepatocellular carcinoma in patients with cirrhosis attributable to multiple risk factors. *Hepatology* 1999;29:1704–1707
  32. Donato F, Tagger A, Gelatti U, Parrinello G, Boffetta P, Albertini A, et al. Alcohol and hepatocellular carcinoma: the effect of lifetime intake and hepatitis virus infections in men and women. *Am J Epidemiol* 2002;155:323–331
  33. Fattovich G, Giustina G, Degos F, Tremolada F, Diodati G, Almasio P, et al. Morbidity and mortality in compensated cirrhosis type C: a retrospective follow-up study of 384 patients. *Gastroenterology* 1997;112:463–472
  34. Lok AS, Everhart JE, Wright EC, Di Bisceglie AM, Kim HY, Sterling RK, et al. Maintenance peginterferon therapy and other factors associated with hepatocellular carcinoma in patients with advanced hepatitis C. *Gastroenterology* 2011;140:840–849
  35. Donato F, Boffetta P, Puoti M. A meta-analysis of epidemiological studies on the combined effect of hepatitis B and C virus infections in causing hepatocellular carcinoma. *Int J Cancer* 1998;75:347–354
  36. Cho LY, Yang JJ, Ko KP, Park B, Shin A, Lim MK, et al. Coinfection of hepatitis B and C viruses and risk of hepatocellular carcinoma: systematic review and meta-analysis. *Int J Cancer* 2011;128:176–184
  37. Turati F, Galeone C, Rota M, Pelucchi C, Negri E, Bagnardi V, et al. Alcohol and liver cancer: a systematic review and meta-analysis of prospective studies. *Ann Oncol* 2014;25:1526–1535
  38. Bagnardi V, Blangiardo M, La Vecchia C, Corrao G. A meta-analysis of alcohol drinking and cancer risk. *Br J Cancer* 2001;85:1700–1705
  39. Corrao G, Bagnardi V, Zambon A, La Vecchia C. A meta-analysis of alcohol consumption and the risk of 15 diseases. *Prev Med* 2004;38:613–619
  40. Marrero JA, Fontana RJ, Fu S, Conjeevaram HS, Su GL, Lok AS. Alcohol, tobacco and obesity are synergistic risk factors for hepatocellular carcinoma. *J Hepatol* 2005;42:218–224
  41. Shimazu T, Sasazuki S, Wakai K, Tamakoshi A, Tsuji I, Sugawara Y, et al. Alcohol drinking and primary liver cancer: a pooled analysis of four Japanese cohort studies. *Int J Cancer* 2012;130:2645–2653
  42. Heckley GA, Jarl J, Asamoah BO, G-Gerdtham U. How the risk of liver cancer changes after alcohol cessation: a review and meta-analysis of the current literature. *BMC Cancer* 2011;11:446
  43. Berman K, Tandra S, Vuppalanchi R, Ghabril M, Sandrasegaran K, Nguyen J, et al. Hepatic and extrahepatic cancer in cirrhosis: a longitudinal cohort study. *Am J Gastroenterol* 2011;106:899–906
  44. Shimauchi Y, Tanaka M, Koga K, Itano S, Ishii K, Kumashiro R, et al. Clinical characteristics of patients in their 40 s with HCV antibody-positive hepatocellular carcinoma. *Alcohol Clin Exp Res* 2000;24:64S–67S
  45. Zhu GT, Lou GQ, Shi JP. To investigate the relationship of alcohol intake and hepatocellular carcinoma among patients with hepatitis B virus infection. *Zhonghua Shi Yan He Lin Chuang Bing Du Xue Za Zhi* 2011;25:328–330 (in Chinese)
  46. Shih WL, Chang HC, Liaw YF, Lin SM, Lee SD, Chen PJ, et al. Influences of tobacco and alcohol use on hepatocellular carcinoma survival. *Int J Cancer* 2012;131:2612–2621
  47. Loomba R, Yang HI, Su J, Brenner D, Ilse U, Chen CJ. Obesity and alcohol synergize to increase the risk of incident hepatocellular carcinoma in men. *Clin Gastroenterol Hepatol* 2010;8:891–898
  48. Balbi M, Donadon V, Ghersesti M, Grazioli S, Valentina GD, Gardenal R, et al. Alcohol and HCV chronic infection are risk cofactors of type 2 diabetes mellitus for hepatocellular carcinoma in Italy. *Int J Environ Res Public Health* 2010;7:1366–1378
  49. Chen J, Han Y, Xu C, Xiao T, Wang B. Effect of type 2 diabetes mellitus on the risk for hepatocellular carcinoma in chronic liver diseases: a meta-analysis of cohort studies. *Eur J Cancer Prev* 2015;24:89–99
  50. El-Serag HB, Richardson PA, Everhart JE. The role of diabetes in hepatocellular carcinoma: a case-control study among United States veterans. *Am J Gastroenterol* 2001;96:2462–2467
  51. Wang C, Wang X, Gong G, Ben Q, Qiu W, Chen Y, et al. Increased risk of hepatocellular carcinoma in patients with diabetes mellitus: a systematic review and meta-analysis of cohort studies. *Int J Cancer* 2012;130:1639–1648
  52. Saunders D, Seidel D, Allison M, Lyratzopoulos G. Systematic review: the association between obesity and hepatocellular carcinoma—epidemiological evidence. *Aliment Pharmacol Ther* 2010;31:1051–1063
  53. Larsson SC, Wolk A. Overweight, obesity and risk of liver cancer: a meta-analysis of cohort studies. *Br J Cancer* 2007;97:1005–1008
  54. Jinjuvadia R, Patel S, Liangpunsakul S. The association between metabolic syndrome and hepatocellular carcinoma: systematic review and meta-analysis. *J Clin Gastroenterol* 2014;48:172–177
  55. Wong RJ, Cheung R, Ahmed A. Nonalcoholic steatohepatitis is the most rapidly growing indication for liver transplantation in patients with hepatocellular carcinoma in the U.S. *Hepatology* 2014;59:2188–195
  56. Ohki T, Tateishi R, Shiina S, Goto E, Sato T, Nakagawa H, et al. Visceral fat accumulation is an independent risk factor for hepatocellular carcinoma recurrence after curative treatment in patients with suspected NASH. *Gut* 2009;58:839–844
  57. Mittal S, Sada YH, El-Serag HB, Kanwal F, Duan Z, Temple S, et al. Temporal trends of non-alcoholic fatty liver disease-related hepatocellular carcinoma in the veteran affairs population. *Clin Gastroenterol Hepatol* 2015;13:594–601
  58. Hashimoto E, Yatsuji S, Tobari M, Taniai M, Torii N, Tokushige K, et al. Hepatocellular carcinoma in patients with nonalcoholic steatohepatitis. *J Gastroenterol* 2009;44(Suppl 19):89–95
  59. Yasui K, Hashimoto E, Komorizono Y, Koike K, Arai S, Imai Y, et al. Characteristics of patients with nonalcoholic steatohepatitis who develop hepatocellular carcinoma. *Clin Gastroenterol Hepatol* 2011;9:428–433
  60. Ren W, Qi X, Yang Z, Han G, Fan D. Prevalence and risk factors of hepatocellular carcinoma in Budd-Chiari syndrome: a systematic review. *Eur J Gastroenterol Hepatol* 2013;25:830–841
  61. Shrestha SM, Okuda K, Uchida T, Maharjan KG, Shrestha S, Joshi BL, et al. Endemicity and clinical picture of liver disease due to obstruction of the hepatic portion of the inferior vena cava in Nepal. *J Gastroenterol Hepatol* 1996;11:170–179
  62. Simson IW. The causes and consequences of chronic hepatic venous outflow obstruction. *S Afr Med J* 1987;72:11–14
  63. Bruix J, Sherman M, American Association for the Study of Liver Diseases. Management of hepatocellular carcinoma: an update. *Hepatology* 2011;53:1020–1022
  64. Ferenci P, Fried M, Labrecque D, Bruix J, Sherman M, Omata M, et al. World Gastroenterology Organisation guideline.

- Hepatocellular carcinoma (HCC): a global perspective. *J Gastrointest Liver Dis* 2010;19:311–317
65. van Meer S, de Man RA, van den Berg AP, Houwen RH, Linn FH, van Oijen MG, et al. No increased risk of hepatocellular carcinoma in cirrhosis due to Wilson disease during long-term follow-up. *J Gastroenterol Hepatol* 2015;30:535–539
  66. Guo YM, Wei WY, Shen XZ. Tumour necrosis factor 308 polymorphisms and hepatocellular carcinoma risk: a meta-analysis. *Hepatogastroenterology* 2010;57:926–931
  67. Qin H, Liu B, Shi T, Liu Y, Sun Y, Ma Y. Tumour necrosis factor- $\alpha$  polymorphisms and hepatocellular carcinoma: a meta-analysis. *J Int Med Res* 2010;38:760–768
  68. White DL, Li D, Nurgalieva Z, El-Serag HB. Genetic variants of glutathione S-transferase as possible risk factors for hepatocellular carcinoma: a HuGE systematic review and meta-analysis. *Am J Epidemiol* 2008;167:377–389
  69. Overall evaluations of carcinogenicity: an updating of IARC Monographs volumes 1 to 42. IARC. Overall evaluations of carcinogenicity: an updating of IARC monographs volumes 1 to 42. IARC Monogr Eval Carcinog Risks Hum Suppl 1987;7:1–440
  70. Wild CP, Hall AJ. Primary prevention of hepatocellular carcinoma in developing countries. *Mutat Res* 2000;462:381–393
  71. Plymoth A, Viviani S, Hainaut P. Control of hepatocellular carcinoma through hepatitis B vaccination in areas of high endemicity: perspectives for global liver cancer prevention. *Cancer Lett* 2009;286:15–21
  72. Sun CA, Wu DM, Wang LY, Chen CJ, You SL, Santella RM. Determinants of formation of aflatoxin-albumin adducts: a seven-township study in Taiwan. *Br J Cancer* 2002;87:966–970
  73. Bulatao-Jayme J, Almero EM, Castro MC, Jardeleza MT, Salamat LA. A case-control dietary study of primary liver cancer risk from aflatoxin exposure. *Int J Epidemiol* 1982;11:112–119
  74. Qian GS, Ross RK, Yu MC, Yuan JM, Gao YT, Henderson BE, et al. A follow-up study of urinary markers of aflatoxin exposure and liver cancer risk in Shanghai, People's Republic of China. *Cancer Epidemiol Biomarkers Prev* 1994;3:3–10
  75. Ross RK, Yuan JM, Yu MC, Wogan GN, Qian GS, Tu JT, et al. Urinary aflatoxin biomarkers and risk of hepatocellular carcinoma. *Lancet* 1992;339:943–946
  76. Kuang SY, Lekawanvijit S, Maneekarn N, Thongsawat S, Brodovicz K, Nelson K, et al. Hepatitis B 1762T/1764A mutations, hepatitis C infection, and codon 249 p53 mutations in hepatocellular carcinomas from Thailand. *Cancer Epidemiol Biomarkers Prev* 2005;14:380–384
  77. U.S. Department of Health and Human Service. SURGEN GENERAL. GOV. The Health Consequences of smoking–50 years of progress: a report of the surgeon general, 2014. <http://www.surgeongeneral.gov/library/reports/50-years-of-progress/>. Accessed 16 April 2017
  78. Lee YC, Cohet C, Yang YC, Stayner L, Hashibe M, Straif K. Meta-analysis of epidemiologic studies on cigarette smoking and liver cancer. *Int J Epidemiol* 2009;38:1497–1511
  79. Bravi F, Bosetti C, Tavani A, Gallus S, La Vecchia C. Coffee reduces risk for hepatocellular carcinoma: an updated meta-analysis. *Clin Gastroenterol Hepatol* 2013;11:1413–1421
  80. Fon Sing M, Yang WS, Gao S, Gao J, Xiang YB. Epidemiological studies of the association between tea drinking and primary liver cancer: a meta-analysis. *Eur J Cancer Prev* 2011;20:157–165
  81. Cavin C, Holzhäuser D, Scharf G, Constable A, Huber WW, Schilter B. Cafestol and kahweol, two coffee specific diterpenes with anticarcinogenic activity. *Food Chem Toxicol* 2002;40:1155–1163
  82. Muriel P, Arauz J. Coffee and liver diseases. *Fitoterapia* 2010;81:297–305
  83. Boettler U, Sommerfeld K, Volz N, Pahlke G, Teller N, Somoza V, et al. Coffee constituents as modulators of Nrf2 nuclear translocation and ARE (EpRE)-dependent gene expression. *J Nutr Biochem* 2011;22:426–440
  84. Ludwig IA, Clifford MN, Lean ME, Ashihara H, Crozier A. Coffee: biochemistry and potential impact on health. *Food Funct* 2014;5:1695–1717
  85. Yang CS, Wang X, Lu G, Picinich SC. Cancer prevention by tea: animal studies, molecular mechanisms and human relevance. *Nat Rev Cancer* 2009;9:429–439
  86. Moore SW, Davidson A, Hadley GP, Kruger M, Poole J, Stones D, et al. Malignant liver tumors in South African children: a national audit. *World J Surg* 2008;32:1389–1395
  87. Mann JR, Kasthuri N, Raafat F, Pincott JR, Parkes SE, Muir KR, et al. Malignant hepatic tumours in children: incidence, clinical features and aetiology. *Paediatr Perinat Epidemiol* 1990;4:276–289
  88. Hall AJ, Winter PD, Wright R. Mortality of hepatitis B positive blood donors in England and Wales. *Lancet* 1985;1:91–93
  89. Chang MH. Hepatitis B virus and cancer prevention. *Recent Results Cancer Res* 2011;188:75–84
  90. Malik S, Dekio F, Wen JW. Liver transplantation in a child with multifocal hepatocellular carcinoma hepatitis C and management of post-transplant viral recurrence using boceprevir. *Pediatr Transplant* 2014;18:E64–E68
  91. Manzia TM, Angelico R, Toti L, Cillis A, Ciano P, Orlando G, et al. Glycogen storage disease type Ia and VI associated with hepatocellular carcinoma: two case reports. *Transplant Proc* 2011;43:1181–1183
  92. Zen Y, Vara R, Portmann B, Hadzic N. Childhood hepatocellular carcinoma: a clinicopathological study of 12 cases with special reference to EpCAM. *Histopathology* 2014;64:671–682
  93. Kudo M, Namki I, Ichida T, Ku Y, Kokudo N, Sakamoto M, et al. 19th Zenkoku genpatsusei kangan tsuiseki chosa hokoku (2006–2007). *Kanzo* 2016; 57:45–73 (**Japanese**)
  94. POLARIS Observatory. Hepatitis C. <http://polarisobservatory.org/polaris/hepC.htm>. Accessed 16 April 2017
  95. Kudo M. Japan's successful model of nationwide hepatocellular carcinoma surveillance highlighting the urgent need for global surveillance. *Liver Cancer* 2012;1:141–143
  96. Acharya SK. Epidemiology of hepatocellular carcinoma in India. *J Clin Exp Hepatol* 2014;4:S27–S33
  97. International Agency for Research on Cancer. Cancer incidence in five continents. <http://Ci5.iarc.fr/>. Accessed 16 April 2017
  98. Paul SB, Chalamasetty SB, Vishnubhatla S, Madan K, Gamanagatti SR, Batra Y, et al. Clinical profile, etiology and therapeutic outcome in 324 hepatocellular cancer in India. *Oncology* 2009;77:162–171
  99. Sarin SK, Thakur V, Gupta RC, Saigal S, Malhotra V, Thyagarajan SP, et al. Profile of hepatocellular carcinoma in India: an insight into the possible etiologic associations. *J Gastroenterol Hepatol* 2001;16:666–673
  100. Kumar M, Kumar R, Hissar SS, Saraswat MK, Sharma BC, Sakhuja P, et al. Risk factors analysis for hepatocellular carcinoma in patients with and without cirrhosis: a case-control study of 213 hepatocellular carcinoma patients from India. *J Gastroenterol Hepatol* 2007;22:1104–1111
  101. Law MG, Roberts SK, Dore GJ, Kaldor JM. Primary hepatocellular carcinoma in Australia, 1978–1997: increasing incidence and mortality. *Med J Aust* 2000;173:403–405
  102. Tracey E, Chen S, Baker D, Bishop J, Jelfs P. Cancer in New South Wales: Incidence and Mortality 2004. Cancer Institute, NSW, 2006



103. Walter SR, Thein HH, Gidding HF, Amin J, Law MG, George J, et al. Risk factors for hepatocellular carcinoma in a cohort infected with hepatitis B or C. *J Gastroenterol Hepatol* 2011;26:1757–1764
104. Amin J, O'Connell D, Bartlett M, Tracey E, Kaldor J, Law M, et al. Liver cancer and hepatitis B and C in New South Wales, 1990–2002: a linkage study. *Aust N Z J Public Health* 2007;31:475–482
105. Tanaka M, Katayama F, Kato H, Tanaka H, Wang J, Qiao YL, et al. Hepatitis B and C virus infection and hepatocellular carcinoma in China: a review of epidemiology and control measures. *J Epidemiol* 2011;21:401–416
106. Fan JH, Wang JB, Jiang Y, Xiang W, Liang H, Wei WQ, et al. Attributable causes of liver cancer mortality and incidence in China. *Asian Pac J Cancer Prev* 2013;14:7251–7256
107. Zhou X, Tang Z, Yu Y. Changing prognosis of primary liver cancer: some aspects to improve long-term survival. *Zhonghua Zhong Liu Za Zhi* 1996;18:211–213 (**Article in Chinese**)
108. Lin J. A study on aetiological factors of primary hepato-carcinoma in Tianjin China. *Zhonghua Liu Xing Bing Xue Za Zhi* 1991;12:346–349
109. Yuen MF, Cheng CC, Laufer JJ, Lam SK, Ooi CG, Lai CL. Early detection of hepatocellular carcinoma increases the chance of treatment: Hong Kong experience. *Hepatology* 2000;31:330–335
110. Park JW. Hepatocellular carcinoma in Korea: introduction and overview. *Korean J Gastroenterol* 2005;45:217–226 (**Article in Korean**)
111. Meredith I, Sarfati D, Ikeda T, Blakely T. Cancer in Pacific people in New Zealand. *Cancer Causes Control* 2012;23:1173–1184
112. Lu SN, Su WW, Yang SS, Chang TT, Cheng KS, Wu JC, et al. Secular trends and geographic variations of hepatitis B virus and hepatitis C virus-associated hepatocellular carcinoma in Taiwan. *Int J Cancer* 2006;119:1946–1952
113. Chang MH, Chen CJ, Lai MS, Hsu HM, Wu TC, Kong MS, et al. Universal hepatitis B vaccination in Taiwan and the incidence of hepatocellular carcinoma in children: Taiwan Childhood Hepatoma Study Group. *N Engl J Med* 1997;336:1855–1859
114. Zidan A, Scheuerlein H, Schüle S, Settmacher U, Rauchfuss F. Epidemiological pattern of hepatitis B and hepatitis C as etiological agents for hepatocellular carcinoma in Iran and worldwide. *Hepat Mon* 2012;12:e6894
115. Hafeez Bhatti AB, Dar FS, Waheed A, Shafique K, Sultan F, Shah NH. Hepatocellular Carcinoma in Pakistan: national Trends and Global Perspective. *Gastroenterol Res Pract* 2016;2016:5942306
116. WHO. Cancer country profiles 2014. <http://www.who.int/cancer/country-profiles/en/>. Accessed 16 April 2017
117. Raza SA, Clifford GM, Franceschi S. Worldwide variation in the relative importance of hepatitis B and hepatitis C viruses in hepatocellular carcinoma: a systematic review. *Br J Cancer* 2007;96:1127–1134
118. Nguyen VT, Law MG, Dore GJ. An enormous hepatitis B virus-related liver disease burden projected in Vietnam by 2025. *Liver Int* 2008;28:525–531
119. Baatarkhuu O, Kim DY, Bat-Ireedui P, Han KH. Current situation of hepatocellular carcinoma in Mongolia. *Oncology* 2011;81(Suppl 1):148–151
120. de Martel C, Maucourt-Boulch D, Plummer M, Franceschi S. World-wide relative contribution of hepatitis B and C viruses in hepatocellular carcinoma. *Hepatology* 2015;62:1190–1200
121. Asia-Pacific Working Party on Prevention of Hepatocellular Carcinoma. Prevention of hepatocellular carcinoma in the Asia-Pacific region: consensus statements. *J Gastroenterol Hepatol* 2010;25:657–663
122. Wong VWS, Chan HLY. Prevention of hepatocellular carcinoma: a concise review of contemporary issues. *Ann Hepatol* 2012;11:284–293
123. Ni YH, Chang MH, Wu JF, Hsu HY, Chen HL, Chen DS. Minimization of hepatitis B infection by a 25-year universal vaccination program. *J Hepatol* 2012;57:730–735
124. Chiang CJ, Yang YW, You SL, Lai MS, Chen CJ. Thirty-year outcomes of the national hepatitis B immunization program in Taiwan. *JAMA* 2013;310:974–976
125. Liang X, Bi S, Yang W, Wang L, Cui G, Cui F, et al. Epidemiological serosurvey of hepatitis B in China-declining HBV prevalence due to hepatitis B vaccination. *Vaccine* 2009;27:6550–6557
126. Qu C, Chen T, Fan C, Zhan Q, Wang Y, Lu J, et al. Efficacy of neonatal HBV vaccination on liver cancer and other liver diseases over 30-year follow-up of the Qidong hepatitis B intervention study: a cluster randomized controlled trial. *PLoS Med* 2014;11:e1001774
127. Chen CJ, Yang HI, Su J, Jen CL, You SL, Lu SN, et al. Risk of hepatocellular carcinoma across a biological gradient of serum hepatitis B virus DNA level. *JAMA* 2006;295:65–73
128. Chen JD, Yang HI, Iloeje UH, You SL, Lu SN, Wang LY, et al. Carriers of inactive hepatitis B virus are still at risk for hepatocellular carcinoma and liver-related death. *Gastroenterology* 2010;138:1747–1754
129. Liaw YF, Sung JJ, Chow WC, Farrell G, Lee CZ, Yuen H, et al. Lamivudine for patients with chronic hepatitis B and advanced liver disease. *N Engl J Med* 2004;351:1521–1531
130. Papatheodoridis GV, Lampertico P, Manolakopoulos S, Lok A. Incidence of hepatocellular carcinoma in chronic hepatitis B patients receiving nucleos(t)ide therapy: a systematic review. *J Hepatol* 2010;53:348–356
131. Singal AK, Salameh H, Kuo YF, Fontana RJ. Meta-analysis: the impact of oral anti-viral agents on the incidence of hepatocellular carcinoma in chronic hepatitis B. *Aliment Pharmacol Ther* 2013;38:98–106
132. Eun JR, Lee HJ, Kim TN, Lee KS. Risk assessment for the development of hepatocellular carcinoma: according to on-treatment viral response during long-term lamivudine therapy in hepatitis B virus-related liver disease. *J Hepatol* 2010;53:118–125
133. Hosaka T, Suzuki F, Kobayashi M, Seko Y, Kawamura Y, Sezaki H, et al. Long-term entecavir treatment reduces hepatocellular carcinoma incidence in patients with hepatitis B virus infection. *Hepatology* 2013;58:98–107
134. Chiang CJ, Yang YW, Chen JD, You SL, Yang HI, Lee MH, et al. Significant reduction in end-stage liver diseases burden through the national viral hepatitis therapy program in Taiwan. *Hepatology* 2015;61:1154–1162
135. Cho JY, Paik YH, Sohn W, Cho HC, Gwak GY, Choi MS, et al. Patients with chronic hepatitis B treated with oral antiviral therapy retain a higher risk for HCC compared with patients with inactive stage disease. *Gut* 2014;63:1943–1950
136. Aghemo A, Lampertico P, Colombo M. Assessing long-term treatment efficacy in chronic hepatitis B and C: between evidence and common sense. *J Hepatol* 2012;57:1326–1335
137. Kong Y, You H, Jia J. Oral antiviral therapy reduces the risk of hepatocellular carcinoma in persons with chronic hepatitis B infection: combining evidence and common sense. *Hepatol Int* 2016;10:239–241
138. Kim GA, Lee HC, Kim MJ, Ha Y, Park EJ, An J, et al. Incidence of hepatocellular carcinoma after HBsAg seroclearance in chronic hepatitis B patients: a need for surveillance. *J Hepatol* 2015;62:1092–1099



139. Morgan TR, Ghany MG, Kim HY, Snow KK, Shiffman ML, De Santo JL, et al. Outcome of sustained virological responders with histologically advanced chronic hepatitis C. *Hepatology* 2010;52:833–844
140. Cammà C, Giunta M, Andreone P, Craxi A. Interferon and prevention of hepatocellular carcinoma in viral cirrhosis: an evidence-based approach. *J Hepatol* 2001;34:593–602
141. Akamatsu M, Yoshida H, Shiina S, Teratani T, Obi S, Tateishi R, et al. Sustained viral response prolonged survival of patients with C-viral hepatocellular carcinoma. *Liver Int* 2006;26:536–542
142. Yu ML, Lin SM, Chuang WL, Dai CY, Wang JH, Lu SN, et al. A sustained virological response to interferon or interferon/ribavirin reduces hepatocellular carcinoma and improves survival in chronic hepatitis C: a nationwide, multicentre study in Taiwan. *Antivir Ther* 2006;11:985–994
143. Ikeda K, Saitoh S, Arase Y, Chayama K, Suzuki Y, Kobayashi M, et al. Effect of interferon therapy on hepatocellular carcinogenesis in patients with chronic hepatitis type C: a long-term observation study of 1,643 patients using statistical bias correction with proportional hazard analysis. *Hepatology* 1999;29:1124–1130
144. Kasahara A, Hayashi N, Mochizuki K, Takayanagi M, Yoshioka K, Kakumu S, et al. Risk factors for hepatocellular carcinoma and its incidence after interferon treatment in patients with chronic hepatitis C. Osaka Liver Disease Study Group. *Hepatology* 1998;27:1394–1402
145. Makiyama A, Itoh Y, Kasahara A, Imai Y, Kawata S, Yoshioka K, et al. Characteristics of patients with chronic hepatitis C who develop hepatocellular carcinoma after a sustained response to interferon therapy. *Cancer* 2004;101:1616–1622
146. Shiratori Y, Ito Y, Yokosuka O, Imazeki F, Nakata R, Tanaka N, et al. Antiviral therapy for cirrhotic hepatitis C: association with reduced hepatocellular carcinoma development and improved survival. *Ann Intern Med* 2005;142:105–114
147. Yoshida H, Tateishi R, Arakawa Y, Sata M, Fujiyama S, Nishiguchi S, et al. Benefit of interferon therapy in hepatocellular carcinoma prevention for individual patients with chronic hepatitis C. *Gut* 2004;53:425–430
148. El-Serag HB, Kanwal F, Richardson P, Kramer J. Risk of hepatocellular carcinoma after sustained virological response in Veterans with hepatitis C virus infection. *Hepatology* 2016;64:130–137
149. Chang KC, Hung CH, Lu SN, Wang JH, Lee CM, Chen CH, et al. A novel predictive score for hepatocellular carcinoma development in patients with chronic hepatitis C after sustained response to pegylated interferon and ribavirin combination therapy. *J Antimicrob Chemother* 2012;67:2766–2772
150. van der Meer AJ, Feld JJ, Hofer H, Almasio PL, Calvaruso V, Fernández-Rodríguez CM, et al. Risk of cirrhosis-related complications in patients with advanced fibrosis following hepatitis C virus eradication. *J Hepatol* 2016; (Epub ahead of print)
151. Arase Y, Kobayashi M, Suzuki F, Suzuki Y, Kawamura Y, Akuta N, et al. Effect of type 2 diabetes on the risk for malignancies includes hepatocellular carcinoma in chronic hepatitis C. *Hepatology* 2013;57:964–973
152. Shiratori Y, Imazeki F, Moriyama M, Yano M, Arakawa Y, Yokosuka O, et al. Histologic improvement of fibrosis in patients with hepatitis C who have sustained response to interferon therapy. *Ann Intern Med* 2000;132:517–524
153. Poynard T, McHutchison J, Manns M, Trepo C, Lindsay K, Goodman Z, et al. Impact of pegylated interferon alfa-2b and ribavirin on liver fibrosis in patients with chronic hepatitis C. *Gastroenterology* 2002;122:1303–1313
154. Arif A, Levine RA, Sanderson SO, Bank L, Velu RP, Shah A, et al. Regression of fibrosis in chronic hepatitis C after therapy with interferon and ribavirin. *Dig Dis Sci* 2003;48:1425–1430
155. Pol S, Carnot F, Nalpas B, Lagneau JL, Fontaine H, Serpaggi J, et al. Reversibility of hepatitis C virus-related cirrhosis. *Hum Pathol* 2004;35:107–112
156. Everson GT, Balart L, Lee SS, Reindollar RW, Shiffman ML, Minuk GY, et al. Histological benefits of virological response to peginterferon alfa-2a monotherapy in patients with hepatitis C and advanced fibrosis or compensated cirrhosis. *Aliment Pharmacol Ther* 2008;27:542–551
157. George SL, Bacon BR, Brunt EM, Mihindukulasuriya KL, Hoffmann J, Di Bisceglie AM. Clinical, virologic, histologic, and biochemical outcomes after successful HCV therapy: a 5-year follow-up of 150 patients. *Hepatology* 2009;49:729–738
158. Bourlière M, Bronowicki JP, de Ledinghen V, Hézode C, Zoulim F, Mathurin P, et al. Ledipasvir-sofosbuvir with or without ribavirin to treat patients with HCV genotype 1 infection and cirrhosis non-responsive to previous protease-inhibitor therapy: a randomised, double-blind, phase 2 trial (SIRIUS). *Lancet Infect Dis* 2015;15:397–404
159. Charlton M, Everson GT, Flamm SL, Kumar P, Landis C, Brown RS Jr, et al. Ledipasvir and Sofosbuvir Plus Ribavirin for Treatment of HCV Infection in Patients With Advanced Liver Disease. *Gastroenterology* 2015;149:649–659
160. Leroy V, Angus P, Bronowicki JP, Dore GJ, Hezode C, Pianko S, et al. Daclatasvir, sofosbuvir, and ribavirin for hepatitis C virus genotype 3 and advanced liver disease: a randomized phase III study (ALLY-3 +). *Hepatology* 2016;63:1430–1441
161. Bellentani SSF, Marino M, Bedogni G. Epidemiology of non-alcoholic fatty liver disease. *Dig Dis* 2010;28:155–161
162. McPherson S, Hardy T, Henderson E, Burt AD, Day CP, Anstee QM. Evidence of NAFLD progression from steatosis to fibrosis-steatohepatitis using paired biopsies: implications for prognosis and clinical management. *J Hepatol* 2015;62:1148–1155
163. Matteoni CAYZ, Gramlich T, Boparai N, Liu YC, McCullough AJ. Nonalcoholic fatty liver disease: a spectrum of clinical and pathological severity. *Gastroenterology* 1999;116:1413–1419
164. Guzman GBE, Petrovic LM, Chejfec G, Layden TJ, Cotler SJ. Does nonalcoholic fatty liver disease predispose patients to hepatocellular carcinoma in the absence of cirrhosis? *Arch Pathol Lab Med* 2008;132:1761–1766
165. Yatsuji S, Hashimoto E, Tobari M, Taniai M, Tokushige K, Shiratori K. Clinical features and outcomes of cirrhosis due to non-alcoholic steatohepatitis compared with cirrhosis caused by chronic hepatitis C. *J Gastroenterol Hepatol* 2009;24:248–254
166. Ascha MS, Hanounieh IA, Lopez R, Tamimi TA, Feldstein AF, Zein NN. The incidence and risk factors of hepatocellular carcinoma in patients with nonalcoholic steatohepatitis. *Hepatology* 2010;51:1972–1978
167. Scalera A, Tarantino G. Could metabolic syndrome lead to hepatocarcinoma via non-alcoholic fatty liver disease? *World J Gastroenterol* 2014;20:9217–9228
168. Esposito K, Chiodini P, Colao A, Lenzi A, Giugliano D. Metabolic syndrome and risk of cancer: a systematic review and meta-analysis. *Diabetes Care* 2012;35:2402–2411
169. Tanaka K, Tsuji I, Tamakoshi A, Matsuo K, Ito H, Wakai K, et al. Obesity and liver cancer risk: an evaluation based on a systematic review of epidemiologic evidence among the Japanese population. *Jpn J Clin Oncol* 2012;42:212–221
170. Wang P, Kang D, Cao W, Wang Y, Liu Z. Diabetes mellitus and risk of hepatocellular carcinoma: a systematic review and meta-analysis. *Diabetes Metab Res Rev* 2012;28:109–122
171. Chen Y, Wang X, Wang J, Yan Z, Luo J. Excess body weight and the risk of primary liver cancer: an updated meta-analysis of prospective studies. *Eur J Cancer* 2012;48:2137–2145
172. Bacon BR, Farahvash MJ, Janney CG, Neuschwander-Tetri BA. Nonalcoholic steatohepatitis: an expanded clinical entity. *Gastroenterology* 1994;107:1103–1109

173. Traussnigg S, Kienbacher C, Halilbasic E, Rechling C, Kazemi-Shirazi L, Hofer H, et al. Challenges and Management of Liver Cirrhosis: practical Issues in the Therapy of Patients with Cirrhosis due to NAFLD and NASH. *Dig Dis* 2015;33:598–607
174. DePeralta DK, Wei L, Ghoshal S, Schmidt B, Lauwers GY, Lanuti M, et al. Metformin prevents hepatocellular carcinoma development by suppressing hepatic progenitor cell activation in a rat model of cirrhosis. *Cancer* 2016;122:1216–1227
175. Chalasani N, Younossi Z, Lavine JE, Diehl AM, Brunt EM, Cusi K, et al. The diagnosis and management of non-alcoholic fatty liver disease: practice Guideline by the American Association for the Study of Liver Diseases, American College of Gastroenterology, and the American Gastroenterological Association. *Hepatology* 2012;55:2005–2023
176. Rinella ME. Nonalcoholic fatty liver disease: a systematic review. *JAMA* 2015;313:2263–2273
177. European Association for the Study of the Liver; (EASL); European Association for the Study of Diabetes (EASD); European Association for the Study of Obesity (EASO). EASL–EASD–EASO Clinical Practice Guidelines for the management of non-alcoholic fatty liver disease. *J Hepatol* 2016;64:1388–1402
178. Wu JC, Huang YH, Chau GY, Su CW, Lai CR, Lee PC, et al. Risk factors for early and late recurrence in hepatitis B-related hepatocellular carcinoma. *J Hepatol* 2009;51:890–897
179. Hung IF, Poon RT, Lai CL, Fung J, Fan ST, Yuen MF. Recurrence of hepatitis B-related hepatocellular carcinoma is associated with high viral load at the time of resection. *Am J Gastroenterol* 2008;103:1663–1673
180. Hung IF, Wong DK, Poon RT, Fong DY, Chui AH, Seto WK, et al. Risk factors and post-resection independent predictive score for the recurrence of hepatitis B-related hepatocellular carcinoma. *PLoS One* 2016;11:e0148493
181. Lo CM, Liu CL, Chan SC, Lam CM, Poon RT, Ng IO, et al. A randomized, controlled trial of postoperative adjuvant interferon therapy after resection of hepatocellular carcinoma. *Ann Surg* 2007;245:831–842
182. Chen LT, Chen MF, Li LA, Lee PH, Jeng LB, Lin DY, et al. Long-term results of a randomized, observation-controlled, phase III trial of adjuvant interferon Alfa-2b in hepatocellular carcinoma after curative resection. *Ann Surg* 2012;255:8–17
183. Lin SM, Lin CJ, Hsu CW, Tai DI, Sheen IS, Lin DY, et al. Prospective randomized controlled study of interferon-alpha in preventing hepatocellular carcinoma recurrence after medical ablation therapy for primary tumors. *Cancer* 2004;100:376–382
184. Nishikawa H, Nishijima N, Arimoto A, Inuzuka T, Kita R, Kimura T, et al. Effect of nucleoside analog use in patients with hepatitis B virus-related hepatocellular carcinoma. *Hepatol Res* 2014;44:608–620
185. Yin J, Li N, Han Y, Xue J, Deng Y, Shi J, et al. Effect of antiviral treatment with nucleotide/nucleoside analogs on post-operative prognosis of hepatitis B virus-related hepatocellular carcinoma: a two-stage longitudinal clinical study. *J Clin Oncol* 2013;31:3647–3655
186. Kuzuya T, Katano Y, Kumada T, Toyoda H, Nakano I, Hirooka Y, et al. Efficacy of antiviral therapy with lamivudine after initial treatment for hepatitis B virus-related hepatocellular carcinoma. *J Gastroenterol Hepatol* 2007;22:1929–1935
187. Piao CY, Fujioka S, Iwasaki Y, Fujio K, Kaneyoshi T, Araki Y, et al. Lamivudine treatment in patients with HBV-related hepatocellular carcinoma—using an untreated, matched control cohort. *Acta Med Okayama* 2005;59:217–224
188. Wu CY, Chen YJ, Ho HJ, Hsu YC, Kuo KN, Wu MS, et al. Association between nucleoside analogues and risk of hepatitis B virus-related hepatocellular carcinoma recurrence following liver resection. *JAMA* 2012;308:1906–1914
189. Huang G, Yang Y, Shen F, Pan ZY, Fu SY, Lau WY, et al. Early viral suppression predicts good postoperative survivals in patients with hepatocellular carcinoma with a high baseline HBV-DNA load. *Ann Surg Oncol* 2013;20:1482–1490
190. Jang JW, Choi JY, Bae SH, Yoon SK, Chang UI, Kim CW, et al. A randomized controlled study of preemptive lamivudine in patients receiving transarterial chemo-lipiodolization. *Hepatology* 2006;43:233–240
191. Kumada T, Nakano S, Takeda I, Sugiyama K, Osada T, Kiriya S, et al. Patterns of recurrence after initial treatment in patients with small hepatocellular carcinoma. *Hepatology* 1997;25:87–92
192. Poon RT, Fan ST, Ng IO, Lo CM, Liu CL, Wong J. Different risk factors and prognosis for early and late intrahepatic recurrence after resection of hepatocellular carcinoma. *Cancer* 2000;89:500–507
193. Sakon M, Umeshita K, Nagano H, Eguchi H, Kishimoto S, Miyamoto A, et al. Clinical significance of hepatic resection in hepatocellular carcinoma: analysis by disease-free survival curves. *Arch Surg* 2000;135:1456–1459
194. Ikeda K, Arase Y, Saitoh S, Kobayashi M, Suzuki Y, Suzuki F, et al. Interferon beta prevents recurrence of hepatocellular carcinoma after complete resection or ablation of the primary tumor: a prospective randomized study of hepatitis C virus-related liver cancer. *Hepatology* 2000;32:228–232
195. Kubo S, Nishiguchi S, Hirohashi K, Tanaka H, Shuto T, Yamazaki O, et al. Effects of long-term postoperative interferon-alpha therapy on intrahepatic recurrence after resection of hepatitis C virus-related hepatocellular carcinoma. A randomized, controlled trial. *Ann Intern Med* 2001;134:963–967
196. Shiratori Y, Shiina S, Teratani T, Imamura M, Obi S, Sato S, et al. Interferon therapy after tumor ablation improves prognosis in patients with hepatocellular carcinoma associated with hepatitis C virus. *Ann Intern Med* 2003;138:299–306
197. Hung CH, Lee CM, Wang JH, Tung HD, Chen CH, Lu SN. Antiviral therapy after non-surgical tumor ablation in patients with hepatocellular carcinoma associated with hepatitis C virus. *J Gastroenterol Hepatol* 2005;20:1553–1559
198. Ishikawa T, Higuchi K, Kubota T, Seki K, Honma T, Yoshida T, et al. Combination PEG-IFN a-2b/ribavirin therapy following treatment of hepatitis C virus-associated hepatocellular carcinoma is capable of improving hepatic functional reserve and survival. *Hepatogastroenterology* 2012;59:529–532
199. Mazzaferro V, Romito R, Schiavo M, Mariani L, Camerini T, Bhoori S, et al. Prevention of hepatocellular carcinoma recurrence with alpha-interferon after liver resection in HCV cirrhosis. *Hepatology* 2006;44:1543–1554
200. Sakaguchi Y, Kudo M, Fukunaga T, Minami Y, Chung H, Kawasaki T. Low-dose, long-term, intermittent interferon-alpha-2b therapy after radical treatment by radiofrequency ablation delays clinical recurrence in patients with hepatitis C virus-related hepatocellular carcinoma. *Intervirology* 2005;48:64–70
201. Nishiguchi S, Tamori A, Kubo S. Effect of long-term postoperative interferon therapy on intrahepatic recurrence and survival rate after resection of hepatitis C virus-related hepatocellular carcinoma. *Intervirology* 2005;48:71–75
202. Kanogawa N, Ogasawara S, Chiba T, Saito T, Motoyama T, Suzuki E, et al. Sustained virologic response achieved after curative treatment of hepatitis C virus-related hepatocellular carcinoma as an independent prognostic factor. *J Gastroenterol Hepatol* 2015;30:1197–1204
203. Reig M, Marino Z, Perello C, Inarrairaegui M, Ribeiro A, Lens S, et al. Unexpected early tumor recurrence in patients with hepatitis C virus -related hepatocellular carcinoma undergoing interferon-free therapy: a note of caution. *J Hepatol* 2016;65:719–726

204. The ANRS Collaborative Study Group on Hepatocellular Carcinoma (ANRS CO22 HEPATHER, CO12 CirVir and CO23 CUPILT cohorts). Lack of evidence of an effect of direct-acting antivirals on the recurrence of hepatocellular carcinoma: Data from three ANRS cohorts. *J Hepatol* 2016;65:734–740
205. Conti F, Buonfiglioli F, Scuteri A, Crespi C, Bolondi L, Caraceni P, et al. Early occurrence and recurrence of hepatocellular carcinoma in HCV-related cirrhosis treated with direct-acting antivirals. *J Hepatol* 2016;65:727–733
206. Minami T, Tateishi R, Nakagomi R, Fujiwara N, Sato M, Enooku K, et al. The impact of direct-acting antivirals on early tumor recurrence after radiofrequency ablation in hepatitis C-related hepatocellular carcinoma. *J Hepatol* 2016;65:1272–1273
207. Hasegawa K, Takayama T, Ijichi M, Matsuyama Y, Imamura H, Sano K, et al. Uracil-tegafur as an adjuvant for hepatocellular carcinoma: a randomized trial. *Hepatology* 2006;44:891–895
208. Bruix J, Takayama T, Mazzaferro V, Chau GY, Yang J, Kudo M, et al. Adjuvant sorafenib for hepatocellular carcinoma after resection or ablation (STORM): a phase 3, randomised, double-blind, placebo-controlled trial. *Lancet Oncol* 2015;16:1344–1354
209. Muto Y, Moriwaki H, Ninomiya M, Adachi S, Saito A, Takasaki KT, et al. Prevention of second primary tumors by an acyclic retinoid, polyprenic acid, in patients with hepatocellular carcinoma. Hepatoma Prevention Study Group. *N Engl J Med* 1996;334:1561–1567
210. Takai K, Okuno M, Yasuda I, Matsushima-Nishiwaki R, Uematsu T, Tsurumi H, et al. Prevention of second primary tumors by an acyclic retinoid in patients with hepatocellular carcinoma. Updated analysis of the long-term follow-up data. *Intervirology* 2005;48:39–45
211. Okita K, Izumi N, Matsui O, Tanaka K, Kaneko S, Moriwaki H, et al. Peretinoin after curative therapy of hepatitis C-related hepatocellular carcinoma: a randomized double-blind placebo-controlled study. *J Gastroenterol* 2015;50:191–202
212. Okita K, Izumi N, Ikeda K, Osaki Y, Numata K, Ikeda M, et al. Survey of survival among patients with hepatitis C virus-related hepatocellular carcinoma treated with peretinoin, an acyclic retinoid, after the completion of a randomized, placebo-controlled trial. *J Gastroenterol* 2015;50:667–674
213. Takami Y, Eguchi S, Tateishi M, Ryu T, Mikagi K, Wada Y, et al. A randomised controlled trial of meloxicam, a Cox-2 inhibitor, to prevent hepatocellular carcinoma recurrence after initial curative treatment. *Hepatol Int* 2016;10:799–806
214. Habu D, Shiomi S, Tamori A, Takeda T, Tanaka T, Kubo S, et al. Role of vitamin K2 in the development of hepatocellular carcinoma in women with viral cirrhosis of the liver. *JAMA* 2004;292:358–361
215. Mizuta T, Ozaki I, Eguchi Y, Yasutake T, Kawazoe S, Fujimoto K, et al. The effect of menatetrenone, a vitamin K2 analog, on disease recurrence and survival in patients with hepatocellular carcinoma after curative treatment: a pilot study. *Cancer* 2006;106:867–872
216. Hotta N, Ayada M, Sato K, Ishikawa T, Okumura A, Matsumoto E, et al. Effect of vitamin K2 on the recurrence in patients with hepatocellular carcinoma. *Hepatogastroenterology* 2007;54:2073–2077
217. Yoshida H, Shiratori Y, Kudo M, Shiina S, Mizuta T, Kojiro M, et al. Effect of vitamin K2 on the recurrence of hepatocellular carcinoma. *Hepatology* 2011;54:532–540
218. Choi JY, Lee JM, Sirlin CB. CT and MR imaging diagnosis and staging of hepatocellular carcinoma: part I. Development, growth, and spread: key pathologic and imaging aspects. *Radiology* 2014;272:635–654
219. Singal AG, Pillai A, Tiro J. Early detection, curative treatment, and survival rates for hepatocellular carcinoma surveillance in patients with cirrhosis: a meta-analysis. *PLoS Med* 2014;11:e1001624
220. Khalili K, Menezes R, Kim TK, Kochak Yazdi L, Jang HJ, Sharma S, et al. The effectiveness of ultrasound surveillance for hepatocellular carcinoma in a canadian centre and determinants of its success. *Can J Gastroenterol Hepatol* 2015;29:267–273
221. Bolondi L, Sofia S, Siringo S, Gaiani S, Casali A, Zironi G, et al. Surveillance programme of cirrhotic patients for early diagnosis and treatment of hepatocellular carcinoma: a cost effectiveness analysis. *Gut* 2001;48:251–259
222. Pocha C, Dieperink E, McMaken K, Knott A, Thuras P, Ho S. Surveillance for hepatocellular cancer with ultrasonography vs. Computed tomography—a randomised study. *Aliment Pharmacol Ther* 2013;38:303–312
223. Singal A, Volk ML, Waljee A, Salgia R, Higgins P, Rogers MA, et al. Meta-analysis: surveillance with ultrasound for early-stage hepatocellular carcinoma in patients with cirrhosis. *Aliment Pharmacol Ther* 2009;30:37–47
224. Yoon JH, Park JW, Lee JM. Noninvasive diagnosis of hepatocellular carcinoma: Elaboration on korean liver cancer study group-national cancer center korea practice guidelines compared with other guidelines and remaining issues. *Korean J Radiol* 2016;17:7–24
225. Colli A, Fraquelli M, Casazza G, Massironi S, Colucci A, Conte D, et al. Accuracy of ultrasonography, spiral ct, magnetic resonance, and alpha-fetoprotein in diagnosing hepatocellular carcinoma: a systematic review. *Am J Gastroenterol* 2006;101:513–523
226. Hanna RF, Miloushev VZ, Tang A, Finklestone LA, Brejt SZ, Sandhu RS, et al. Comparative 13-year meta-analysis of the sensitivity and positive predictive value of ultrasound, CT, and MRI for detecting hepatocellular carcinoma. *Abdom Radiol (NY)*. 2016;41:71–90
227. Lee JM, Yoon JH, Kim KW. Diagnosis of hepatocellular carcinoma: newer radiological tools. *Semin Oncol* 2012;39:399–409
228. Coleman WB. Mechanisms of human hepatocarcinogenesis. *Curr Mol Med* 2003;3:573–588
229. Ueda K, Matsui O, Kawamori Y, Nakanuma Y, Kadoya M, Yoshikawa J, et al. Hypervascular hepatocellular carcinoma: evaluation of hemodynamics with dynamic CT during hepatic arteriography. *Radiology* 1998;206:161–166
230. Lee JM, Choi BI. Hepatocellular nodules in liver cirrhosis: mR evaluation. *Abdom Imaging* 2011;36:282–289
231. Tanaka S, Kitamura T, Fujita M, Nakanishi K, Okuda S. Color doppler flow imaging of liver tumors. *AJR Am J Roentgenol* 1990;154:509–514
232. Tanaka S, Kitamura T, Fujita M, Kasugai H, Inoue A, Ishiguro S. Small hepatocellular carcinoma: differentiation from adenomatous hyperplastic nodule with color doppler flow imaging. *Radiology* 1992;182:161–165
233. Koito K, Namieno T, Morita K. Differential diagnosis of small hepatocellular carcinoma and adenomatous hyperplasia with power doppler sonography. *AJR Am J Roentgenol* 1998;170:157–161
234. Hatanaka K, Kudo M, Minami Y, Ueda T, Tatsumi C, Kitai S, et al. Differential diagnosis of hepatic tumors: value of contrast-enhanced harmonic sonography using the newly developed contrast agent, sonazoid. *Intervirology* 2008;51(Suppl 1):61–69
235. D'Onofrio M, Crosara S, De Robertis R, Canestrini S, Mucelli RP. Contrast-enhanced ultrasound of focal liver lesions. *AJR Am J Roentgenol* 2015;205:W56–W66
236. Kim TK, Jang HJ. Contrast-enhanced ultrasound in the diagnosis of nodules in liver cirrhosis. *World J Gastroenterol* 2014;20:3590–3596

237. Kudo M. Defect reperfusion imaging with sonazoid®: a breakthrough in hepatocellular carcinoma. *Liver Cancer* 2016;5:1–7
238. Wilson SR, Kim TK, Jang HJ, Burns PN. Enhancement patterns of focal liver masses: discordance between contrast-enhanced sonography and contrast-enhanced CT and MRI. *AJR Am J Roentgenol* 2007;189:W7–W12
239. Jang HJ, Kim TK, Burns PN, Wilson SR. CEUS: an essential component in a multimodality approach to small nodules in patients at high-risk for hepatocellular carcinoma. *Eur J Radiol* 2015;84:1623–1635
240. Jang HJ, Kim TK, Burns PN, Wilson SR. Enhancement patterns of hepatocellular carcinoma at contrast-enhanced US: comparison with histologic differentiation. *Radiology* 2007;224:898–906
241. Wilson SR, Burns PN. Microbubble-enhanced us in body imaging: what role? *Radiology* 2010;257:24–39
242. Vilana R, Forner A, Bianchi L, Garcia-Criado A, Rimola J, de Lope CR, et al. Intrahepatic peripheral cholangiocarcinoma in cirrhosis patients may display a vascular pattern similar to hepatocellular carcinoma on contrast-enhanced ultrasound. *Hepatology* 2010;51:2020–2029
243. Galassi M, Iavarone M, Rossi S, Bota S, Vavassori S, Rosa L, et al. Patterns of appearance and risk of misdiagnosis of intrahepatic cholangiocarcinoma in cirrhosis at contrast enhanced ultrasound. *Liver Int* 2013;33:771–779
244. de Sio I, Iadevaia MD, Vitale LM, Niosi M, Del Prete A, de Sio C, et al. Optimized contrast-enhanced ultrasonography for characterization of focal liver lesions in cirrhosis: a single-center retrospective study. *Unit Eur Gastroenterol J* 2014;2:279–287
245. Wildner D, Bernatik T, Greis C, Seitz K, Neurath MF, Strobel D. CEUS in hepatocellular carcinoma and intrahepatic cholangiocellular carcinoma in 320 patients - early or late washout matters: a subanalysis of the DEGUM multicenter trial. *Ultraschall Med* 2015;36:132–139
246. Niu Y, Huang T, Lian F, Li F. Contrast-enhanced ultrasonography for the diagnosis of small hepatocellular carcinoma: a meta-analysis and meta-regression analysis. *Tumour Biol* 2013;34:3667–3674
247. Westwood M, Joore M, Grutters J, Redekop K, Armstrong N, Lee K, et al. Contrast-enhanced ultrasound using SonoVue® (sulphur hexafluoride microbubbles) compared with contrast-enhanced computed tomography and contrast-enhanced magnetic resonance imaging for the characterisation of focal liver lesions and detection of liver metastases: a systematic review and cost-effectiveness analysis. *Health Technol Assess* 2013;17:1–243
248. Hatanaka K, Kudo M, Minami Y, Maekawa K. Sonazoid-enhanced ultrasonography for diagnosis of hepatic malignancies: comparison with contrast-enhanced CT. *Oncology* 2008;75(Suppl 1):42–47
249. Cantisani V, David E, Meloni FM, Dietrich CF, Badea R, Messineo D, et al. Recall strategies for patients found to have a nodule in cirrhosis: is there still a role for CEUS? *Med Ultrason* 2015;17:515–520
250. Neri E, Bali MA, Ba-Ssalamah A, Boraschi P, Brancatelli G, Alves FC, et al. ESGAR consensus statement on liver MR imaging and clinical use of liver-specific contrast agents. *Eur Radiol* 2016;26:921–931
251. Lee JM, Trevisani F, Vilgrain V, Wald C. Imaging diagnosis and staging of hepatocellular carcinoma. *Liver Transpl* 2011;17(Suppl 2):S34–43
252. Choi JY, Lee JM, Sirlin CB. CT and MR imaging diagnosis and staging of hepatocellular carcinoma: part II. Extracellular agents, hepatobiliary agents, and ancillary imaging features. *Radiology* 2014;273:30–50
253. Pomfret EA, Washburn K, Wald C, Nalesnik MA, Douglas D, Russo M, et al. Report of a national conference on liver allocation in patients with hepatocellular carcinoma in the United States. *Liver Transpl* 2010;16:262–278
254. Kitao A, Zen Y, Matsui O, Gabata T, Nakanuma Y. Hepatocarcinogenesis: multistep changes of drainage vessels at ct during arterial portography and hepatic arteriography–radiologic-pathologic correlation. *Radiology* 2009;252:605–614
255. Matsui O. Imaging of multistep human hepatocarcinogenesis by CT during intra-arterial contrast injection. *Intervirology* 2004;47:271–276
256. Vavricka SR, Jung D, Fried M, Grutzner U, Meier PJ, Kullak-Ublick GA. The human organic anion transporting polypeptide 8 (SLCO1B3) gene is transcriptionally repressed by hepatocyte nuclear factor 3beta in hepatocellular carcinoma. *J Hepatol* 2004;40:212–218
257. Kitao A, Matsui O, Yoneda N, Kozaka K, Shinmura R, Koda W, et al. The uptake transporter OATP8 expression decreases during multistep hepatocarcinogenesis: correlation with gadoxetic acid enhanced MR imaging. *Eur Radiol* 2011;21:2056–2066
258. Kogita S, Imai Y, Okada M, Kim T, Onishi H, Takamura M, et al. Gd-EOB-DTPA-enhanced magnetic resonance images of hepatocellular carcinoma: correlation with histological grading and portal blood flow. *Eur Radiol* 2010;20:2405–2413
259. American College of Radiology. Liver imaging reporting and data system <http://www.Acr.Org/quality-safety/resources/lirads/>. Accessed 16 April 2017
260. Kim MJ, Choi JY, Lim JS, Kim JY, Kim JH, Oh YT, et al. Optimal scan window for detection of hypervascular hepatocellular carcinomas during MDCT examination. *AJR Am J Roentgenol* 2006;187:198–206
261. Goshima S, Kanematsu M, Kondo H, Yokoyama R, Miyoshi T, Nishibori H, et al. MDCT of the liver and hypervascular hepatocellular carcinomas: optimizing scan delays for bolus-tracking techniques of hepatic arterial and portal venous phases. *AJR Am J Roentgenol* 2006;187:W25–W32
262. Hatfield MK, Beres RA, Sane SS, Zaleski GX. Percutaneous imaging-guided solid organ core needle biopsy: coaxial versus noncoaxial method. *AJR Am J Roentgenol* 2008;190:413–417
263. Forner A, Vilana R, Ayuso C, Bianchi L, Sole M, Ayuso JR, et al. Diagnosis of hepatic nodules 20 mm or smaller in cirrhosis: prospective validation of the noninvasive diagnostic criteria for hepatocellular carcinoma. *Hepatology* 2008;47:97–104
264. Kim TK, Lee KH, Jang HJ, Haider MA, Jacks LM, Menezes RJ, et al. Analysis of gadobenate dimeglumine-enhanced mr findings for characterizing small (1–2-cm) hepatic nodules in patients at high risk for hepatocellular carcinoma. *Radiology* 2011;259:730–738
265. Rimola J, Forner A, Tremosini S, Reig M, Vilana R, Bianchi L, et al. Non-invasive diagnosis of hepatocellular carcinoma ≤2 cm in cirrhosis. Diagnostic accuracy assessing fat, capsule and signal intensity at dynamic MRI. *J Hepatol* 2012;56:1317–1323
266. Marrero JA, Hussain HK, Nghiem HV, Umar R, Fontana RJ, Lok AS. Improving the prediction of hepatocellular carcinoma in cirrhotic patients with an arterially-enhancing liver mass. *Liver Transpl* 2005;11:281–289
267. Lee JH, Lee JM, Kim SJ, Baek JH, Yun SH, Kim KW, et al. Enhancement patterns of hepatocellular carcinomas on multiphasicmultidetector row CT: comparison with pathological differentiation. *Br J Radiol* 2012;85:e573–e583
268. Choi JW, Lee JM, Kim SJ, Yoon JH, Baek JH, Han JK, et al. Hepatocellular carcinoma: imaging patterns on gadoxetic acid-enhanced MR Images and their value as an imaging biomarker. *Radiology* 2013;267:776–786



269. Sangiovanni A, Manini MA, Iavarone M, Romeo R, Forzenigo LV, Fraquelli M, et al. The diagnostic and economic impact of contrast imaging techniques in the diagnosis of small hepatocellular carcinoma in cirrhosis. *Gut* 2010;59:638–644
270. Lee YJ, Lee JM, Lee JS, Lee HY, Park BH, Kim YH, et al. Hepatocellular carcinoma: diagnostic performance of multidetector CT and MR imaging—a systematic review and meta-analysis. *Radiology* 2015;275:97–109
271. Ye F, Liu J, Ouyang H. Gadolinium ethoxybenzyl diethylenetriamine pentaacetic acid (Gd-EOB-DTPA)-enhanced magnetic resonance imaging and multidetector-row computed tomography for the diagnosis of hepatocellular carcinoma: a systematic review and meta-analysis. *Medicine (Baltimore)*. 2015;94:e1157
272. Burrell M, Llovet JM, Ayuso C, Iglesias C, Sala M, Miquel R, et al. MRI angiography is superior to helical CT for detection of HCC prior to liver transplantation: an explant correlation. *Hepatology* 2003;38:1034–1042
273. Kim YK, Kim CS, Chung GH, Han YM, Lee SY, Chon SB, et al. Comparison of gadobenate dimeglumine-enhanced dynamic MRI and 16-MDCT for the detection of hepatocellular carcinoma. *AJR Am J Roentgenol* 2006;186:149–157
274. Krinsky GA, Lee VS, Theise ND, Weinreb JC, Rofsky NM, Diflo T, et al. Hepatocellular carcinoma and dysplastic nodules in patients with cirrhosis: prospective diagnosis with MR imaging and explantation correlation. *Radiology* 2001;219:445–454
275. Lim JH, Kim CK, Lee WJ, Park CK, Koh KC, Paik SW, et al. Detection of hepatocellular carcinomas and dysplastic nodules in cirrhotic livers: accuracy of helical CT in transplant patients. *AJR Am J Roentgenol* 2000;175:693–698
276. Rode A, Bancel B, Douek P, Chevallier M, Vilgrain V, Picaud G, et al. Small nodule detection in cirrhotic livers: evaluation with US, spiral CT, and MRI and correlation with pathologic examination of explanted liver. *J Comput Assist Tomogr* 2001;25:327–336
277. Kim YK, Kwak HS, Kim CS, Chung GH, Han YM, Lee JM. Hepatocellular carcinoma in patients with chronic liver disease: comparison of SPIO-enhanced MR imaging and 16-detector row CT. *Radiology* 2006;238:531–541
278. Ward J, Guthrie JA, Scott DJ, Atchley J, Wilson D, Davies MH, et al. Hepatocellular carcinoma in the cirrhotic liver: double-contrast MR imaging for diagnosis. *Radiology* 2000;216:154–162
279. Yoo HJ, Lee JM, Lee MW, Kim SJ, Lee JY, Han JK, et al. Hepatocellular carcinoma in cirrhotic liver: double-contrast-enhanced, high-resolution 3.0T-MR imaging with pathologic correlation. *I. Invest Radiol* 2008;43:538–546
280. Hanna RF, Kased N, Kwan SW, Gamst AC, Santosa AC, Hasanein T, et al. Double-contrast MRI for accurate staging of hepatocellular carcinoma in patients with cirrhosis. *AJR Am J Roentgenol* 2008;190:47–57
281. Hanna RF, Aguirre DA, Kased N, Emery SC, Peterson MR, Sirlin CB. Cirrhosis-associated hepatocellular nodules: correlation of histopathologic and MR imaging features. *Radiographics* 2008;28:747–769
282. Park G, Kim YK, Kim CS, Yu HC, Hwang SB. Diagnostic efficacy of gadoxetic acid-enhanced MRI in the detection of hepatocellular carcinomas: comparison with gadopentetate dimeglumine. *Br J Radiol* 2010;83:1010–1016
283. Hamm B, Staks T, Mühler A, Bollow M, Taupitz M, Frenzel T, et al. Phase I clinical evaluation of Gd-EOB-DTPA as a hepatobiliary MR contrast agent: safety, pharmacokinetics, and MR imaging. *Radiology* 1995;195:785–792
284. Filippone A, Blakeborough A, Breuer J, Grazioli L, Gschwend S, Hammerstingl R, et al. Enhancement of liver parenchyma after injection of hepatocyte-specific MRI contrast media: a comparison of gadoxetic acid and gadobenate dimeglumine. *J Magn Reson Imaging* 2010;31:356–364
285. Lee DH, Lee JM, Baek JH, Shin C-I, Han JK, Choi BI. Diagnostic performance of gadoxetic acid-enhanced liver MR imaging in the detection of HCCs and allocation of transplant recipients on the basis of the Milan criteria and UNOS guidelines: correlation with histopathologic findings. *Radiology* 2015;274:149–160
286. Kitao A, Matsui O, Yoneda N, Kozaka K, Kobayashi S, Koda W, et al. Hypervascular hepatocellular carcinoma: correlation between biologic features and signal intensity on gadoxetic acid-enhanced MR images. *Radiology* 2012;265:780–789
287. Joo I, Lee JM, Lee DH, Jeon JH, Han JK, Choi BI. Noninvasive diagnosis of hepatocellular carcinoma on gadoxetic acid-enhanced MRI: can hypointensity on the hepatobiliary phase be used as an alternative to washout? *Eur Radiol* 2015;25:2859–2868
288. Hope TA, Fowler KJ, Sirlin CB, Costa EA, Yee J, Yeh BM, et al. Hepatobiliary agents and their role in LI-RADS. *Abdom Imaging* 2015;40:613–625
289. Joo I, Lee JM. Recent advances in the imaging diagnosis of hepatocellular carcinoma: value of gadoxetic acid-enhanced MRI. *Liver Cancer* 2016;5:67–87
290. Park MJ, Kim YK, Lee MW, Lee WJ, Kim Y-S, Kim SH, et al. Small hepatocellular carcinomas: improved sensitivity by combining gadoxetic acid-enhanced and diffusion-weighted MR imaging patterns. *Radiology* 2012;264:761–770
291. Xu PJ, Yan FH, Wang JH, Lin J, Ji Y. Added value of breath-hold diffusion-weighted MRI in detection of small hepatocellular carcinoma lesions compared with dynamic contrast-enhanced MRI alone using receiver operating characteristic curve analysis. *J Magn Reson Imaging* 2009;29:341–349
292. Li X, Li C, Wang R, Ren J, Yang J, Zhang Y. Combined application of gadoxetic acid disodium-enhanced magnetic resonance imaging (MRI) and diffusion-weighted imaging (DWI) in the diagnosis of chronic liver disease-induced hepatocellular carcinoma: a meta-analysis. *PLoS One* 2015;10:e0144247
293. Kadoya M, Matsui O, Takashima T, Nonomura A. Hepatocellular carcinoma: correlation of MR imaging and histopathologic findings. *Radiology* 1992;183:819–825
294. Matsui O, Kadoya M, Kameyama T, Yoshikawa J, Arai K, Gabata T, et al. Adenomatous hyperplastic nodules in the cirrhotic liver: differentiation from hepatocellular carcinoma with MR imaging. *Radiology* 1989;173:123–126
295. Ferrell LD, Crawford JM, Dhillon AP, Scheuer PJ, Nakanuma Y. Proposal for standardized criteria for the diagnosis of benign, borderline, and malignant hepatocellular lesions arising in chronic advanced liver disease. *Am J Surg Pathol* 1993;17:1113–1123
296. Kobayashi S, Matsui O, Gabata T, Koda W, Minami T, Ryu Y, et al. Intranodular signal intensity analysis of hypovascular high-risk borderline lesions of HCC that illustrate multi-step hepatocarcinogenesis within the nodule on Gd-EOB-DTPA-enhanced MRI. *Eur J Radiol* 2012;81:3839–3845
297. Kobayashi S, Matsui O, Gabata T, Koda W, Minami T, Ryu Y, et al. Relationship between signal intensity on hepatobiliary phase of gadolinium ethoxybenzyl diethylenetriaminepentaacetic acid (Gd-EOB-DTPA)-enhanced MR imaging and prognosis of borderline lesions of hepatocellular carcinoma. *Eur J Radiol* 2012;81:3002–3009
298. Sakamoto M. Pathology of early hepatocellular carcinoma. *Hepatol Res* 2007;37(Suppl 2):S135–S138
299. Sakamoto M, Hirohashi S, Shimozato Y. Early stages of multistep hepatocarcinogenesis: adenomatous hyperplasia and early hepatocellular carcinoma. *Hum Pathol* 1991;22:172–178
300. Ichikawa T, Sano K, Morisaka H. Diagnosis of pathologically early HCC with EOB-MRI: experiences and current consensus. *Liver Cancer* 2014;3:97–107



301. Choi BI, Lee JM, Kim TK, Burgio MD, Vilgrain V. Diagnosing borderline hepatic nodules in hepatocarcinogenesis: imaging performance. *AJR Am J Roentgenol* 2015;205:10–21
302. Park YN, Kim MJ. Hepatocarcinogenesis: imaging-pathologic correlation. *Abdom Imaging* 2011;36:232–243
303. Kudo M. Imaging diagnosis of hepatocellular carcinoma and premalignant/borderline lesions. *Semin Liver Dis* 1999;19:297–309
304. Shinmura R, Matsui O, Kadoya M, Kobayashi S, Terayama N, Sanada J, et al. Detection of hypervascular malignant foci in borderline lesions of hepatocellular carcinoma: comparison of dynamic multi-detector row ct, dynamic mr imaging and superparamagnetic iron oxide-enhanced mr imaging. *Eur Radiol* 2008;18:1918–1924
305. Lee J, Lee WJ, Lim HK, Lim JH, Choi N, Park MH, et al. Early hepatocellular carcinoma: Three-phase helical ct features of 16 patients. *Korean J Radiol* 2008;9:325–332
306. Ito K. Hepatocellular carcinoma: conventional MRI findings including gadolinium-enhanced dynamic imaging. *Eur J Radiol* 2006;58:186–199
307. Bartolozzi C, Battaglia V, Bargellini I, Bozzi E, Campani D, Pollina LE, et al. Contrast-enhanced magnetic resonance imaging of 102 nodules in cirrhosis: correlation with histological findings on explanted livers. *Abdom Imaging* 2013;38:290–296
308. Sano K, Ichikawa T, Motosugi U, Sou H, Muhi AM, Matsuda M, et al. Imaging study of early hepatocellular carcinoma: usefulness of gadoxetic acid-enhanced mr imaging. *Radiology* 2011;261:834–844
309. Kudo M. Early hepatocellular carcinoma: definition and diagnosis. *Liver Cancer* 2013;2:69–72
310. Kanefuji T, Takano T, Suda T, Akazawa K, Yokoo T, Kamimura H, et al. Factors predicting aggressiveness of non-hypervascular hepatic nodules detected on hepatobiliary phase of gadolinium ethoxybenzyl diethylene-triamine-pentaacetic-acid magnetic resonance imaging. *World J Gastroenterol* 2015;21:4583–4591
311. Ichikawa S, Ichikawa T, Motosugi U, Sano K, Morisaka H, Enomoto N, et al. Presence of a hypovascular hepatic nodule showing hypointensity on hepatocyte-phase image is a risk factor for hypervascular hepatocellular carcinoma. *J Magn Reson Imaging* 2014;39:293–297
312. Kobayashi S, Matsui O, Gabata T, Koda W, Minami T, Ryu Y, et al. Gadolinium ethoxybenzyl diethylenetriamine pentaacetic acid-enhanced magnetic resonance imaging findings of borderline lesions at high risk for progression to hypervascular classic hepatocellular carcinoma. *J Comput Assist Tomogr* 2011;35:181–186
313. Iannicelli E, Di Pietropaolo M, Marignani M, Briani C, Federici GF, Delle Fave G, et al. Gadoxetic acid-enhanced mri for hepatocellular carcinoma and hypointense nodule observed in the hepatobiliary phase. *Radiol Med* 2014;119:367–376
314. Golfieri R, Grazioli L, Orlando E, Dormi A, Lucidi V, Corcioni B, et al. Which is the best MRI marker of malignancy for atypical cirrhotic nodules: hypointensity in hepatobiliary phase alone or combined with other features? Classification after Gd-EOB-DTPA administration. *J Magn Reson Imaging* 2012;36:648–657
315. Yoon JH, Lee JM, Yang HK, Lee KB, Jang J-J, Han JK, et al. Non-hypervascular hypointense nodules  $\geq 1$  cm on the hepatobiliary phase of gadoxetic acid-enhanced magnetic resonance imaging in cirrhotic livers. *Dig Dis* 2014;32:678–689
316. Yamamoto A, Ito K, Tamada T, Higaki A, Kanki A, Sato T, et al. Newly developed hypervascular hepatocellular carcinoma during follow-up periods in patients with chronic liver disease: observation in serial gadoxetic acid-enhanced MRI. *AJR Am J Roentgenol* 2013;200:1254–1260
317. Kim YK, Lee WJ, Park MJ, Kim SH, Rhim H, Choi D. Hypovascular hypointense nodules on hepatobiliary phase gadoxetic acid-enhanced MR images in patients with cirrhosis: potential of DW imaging in predicting progression to hypervascular HCC. *Radiology* 2012;265:104–114
318. Hyodo T, Murakami T, Imai Y, Okada M, Hori M, Kagawa Y, et al. Hypovascular nodules in patients with chronic liver disease: risk factors for development of hypervascular hepatocellular carcinoma. *Radiology* 2013;266:480–490
319. Kudo M, Matsui O, Izumi N, Iijima H, Kadoya M, Imai Y; Liver Cancer Study Group of Japan. Surveillance and diagnostic algorithm for hepatocellular carcinoma proposed by the liver cancer study group of Japan: 2014 update. *Oncology* 2014;87 Suppl 1:7–21
320. Irwig L, Tosteson AN, Gatsonis C, Lau J, Colditz G, Chalmers TC, Mosteller F. Guidelines for meta-analyses evaluating diagnostic tests. *Ann Intern Med* 1994;120:667–676
321. McMahon BJ, Bulkow L, Harpster A, Snowball M, Lanier A, Sacco F, Dunaway E, et al. Screening for hepatocellular carcinoma in Alaska natives infected with chronic hepatitis B: a 16-year population-based study. *Hepatology* 2000;32:842–846
322. Kew MC. Alpha-fetoprotein. In: Read AE, editor. *Modern trends in gastroenterology*. London: Butterworths; 1975. Vol. 5, p. 91
323. Tateishi R, Yoshida H, Matsuyama Y, Mine N, Kondo Y, Omata M. Diagnostic accuracy of tumor markers for hepatocellular carcinoma: a systematic review. *Hepatol Int* 2008;2:17–30
324. Wong GL, Chan HL, Tse YK, Chan HY, Tse CH, Lo AO, Wong VW. On-treatment alpha-fetoprotein is a specific tumor marker for hepatocellular carcinoma in patients with chronic hepatitis B receiving entecavir. *Hepatology* 2014;59:986–995
325. Minami T, Tateishi R, Kondo M, Nakagomi R, Fujiwara N, Sato M, et al. Serum alpha-fetoprotein has high specificity for the early detection of hepatocellular carcinoma after hepatitis C virus eradication in patients. *Medicine (Baltimore)*. 2015;94:e901
326. Liebman HA, Furie BC, Tong MJ, Blanchard RA, Lo KJ, Lee SD, et al. Des-gamma-carboxy (abnormal) prothrombin as a serum marker of primary hepatocellular carcinoma. *N Engl J Med* 1984;310:1427–1431
327. Koike Y, Shiratori Y, Sato S, Obi S, Teratani T, Imamura M, et al. Des-gamma-carboxy prothrombin as a useful predisposing factor for the development of portal venous invasion in patients with hepatocellular carcinoma: a prospective analysis of 227 patients. *Cancer* 2001;91:561–569
328. Imamura H, Matsuyama Y, Miyagawa Y, Ishida K, Shimada R, Miyagawa S, et al. Prognostic significance of anatomical resection and des-gamma-carboxy prothrombin in patients with hepatocellular carcinoma. *Br J Surg* 1999;89:1032–1038
329. Li C, Zhang Z, Zhang P, Liu J. Diagnostic accuracy of des-gamma-carboxy prothrombin versus alpha-fetoprotein for hepatocellular carcinoma: a systematic review. *Hepatol Res* 2014;44:E11–E25
330. Nakamura S, Nouse K, Sakaguchi K, Ito YM, Ohashi Y, Kobayashi Y, et al. Sensitivity and specificity of des-gamma-carboxy prothrombin for diagnosis of patients with hepatocellular carcinomas varies according to tumor size. *Am J Gastroenterol* 2006;101:2038–2043
331. Sato Y, Nakata K, Kato Y, Shima M, Ishii N, Koji T, et al. Early recognition of hepatocellular carcinoma based on altered profiles of alpha-fetoprotein. *N Engl J Med* 1993;328:1802–1806
332. Taketa K, Endo Y, Sekiya C, Tanikawa K, Koji T, Taga H, et al. A collaborative study for the evaluation of lectin-reactive alpha-fetoproteins in early detection of hepatocellular carcinoma. *Cancer Res* 1993;53:5419–5423
333. Aoyagi Y, Isemura M, Yosizawa Z, Suzuki Y, Sekine C, Ono T, et al. Fucosylation of serum alpha-fetoprotein in patients with

- primary hepatocellular carcinoma. *Biochim Biophys Acta* 1985;830:217–223
334. Kagebayashi C, Yamaguchi I, Akinaga A, Kitano H, Yokoyama K, Satomura M, et al. Automated immunoassay system for AFP-L3% using on-chip electrokinetic reaction and separation by affinity electrophoresis. *Anal Biochem* 2009;388:306–311
  335. Hsu HC, Cheng W, Lai PL. Cloning and expression of a developmentally regulated transcript MXR7 in hepatocellular carcinoma: biological significance and temporospatial distribution. *Cancer Res* 1997;57:5179–5184
  336. Zhu ZW, Friess H, Wang L, Abou-Shady M, Zimmermann A, Lander AD, Korc M, et al. Enhanced glypican-3 expression differentiates the majority of hepatocellular carcinomas from benign hepatic disorders. *Gut* 2001;48:558–564
  337. International Consensus Group for Hepatocellular Neoplasia. The International Consensus. Group for Hepatocellular Neoplasia. Pathologic diagnosis of early hepatocellular carcinoma: a report of the international consensus group for hepatocellular neoplasia. *Hepatology* 2009;49:658–664
  338. Jia X, Liu J, Gao Y, Huang Y, Du Z. Diagnosis accuracy of serum glypican-3 in patients with hepatocellular carcinoma: a systematic review with meta-analysis. *Arch Med Res* 2014;45:580–588
  339. Dai M, Chen X, Liu X, Peng Z, Meng J, Dai S. Diagnostic value of the combination of golgi protein 73 and alpha-fetoprotein in hepatocellular carcinoma: a meta-analysis. *PLoS One* 2015;10:e0140067
  340. Wan HG, Xu H, Gu YM, Wang H, Xu W, Zu MH. Comparison osteopontin vs AFP for the diagnosis of HCC: a meta-analysis. *Clin Res Hepatol Clin Res Hepatol Gastroenterol* 2014;38:706–714
  341. Liao W, Mao Y, Ge P, Yang H, Xu H, Lu X, Sang X, et al. Value of quantitative and qualitative analyses of circulating cell-free DNA as diagnostic tools for hepatocellular carcinoma: a meta-analysis. *Med (Baltimore)*. 2015;94:e722
  342. Lin XJ, Chong Y, Guo ZW, Xie C, Yang XJ, Zhang Q, Li SP, et al. A serum microRNA classifier for early detection of hepatocellular carcinoma: a multicentre, retrospective, longitudinal biomarker identification study with a nested case-control study. *Lancet Oncol* 2015;16:804–815
  343. Sassa T, Kumada T, Nakano S, Uematsu T. Clinical utility of simultaneous measurement of serum high-sensitivity des-gamma-carboxy prothrombin and Lens culinaris agglutinin A-reactive alpha-fetoprotein in patients with small hepatocellular carcinoma. *Eur J Gastroenterol Hepatol* 1999;11:1387–1392
  344. Junqiang L, Yinzhong W, Li Z, Shunlin G, Xiaohui W, Yanan Z, et al. Gadoteric acid disodium (Gd-EOBDTPA)-enhanced magnetic resonance imaging for the detection of hepatocellular carcinoma: a meta-analysis. *J Magn Reson Imaging* 2014;39:1079–1087
  345. Matsuda M, Tsuda T, Yoshioka S, Murata S, Tanaka H, Hirooka M, et al. Incidence for progression of hypervascular HCC in hypovascular hepatic nodules showing hyperintensity on gadoteric acid-enhanced hepatobiliary phase in patients with chronic liver diseases. *Jpn J Radiol* 2014;32:405–413
  346. Jang KM, Kim SH, Kim YK, Choi D. Imaging features of subcentimeter hypointense nodules on gadoteric acid-enhanced hepatobiliary phase MR imaging that progress to hypervascular hepatocellular carcinoma in patients with chronic liver disease. *Acta Radiol* 2015;56:526–535
  347. Matsuda M, Ichikawa T, Amemiya H, Maki A, Watanabe M, Kawaida H, et al. Preoperative gadoteric Acid-enhanced MRI and simultaneous treatment of early hepatocellular carcinoma prolonged recurrence-free survival of progressed hepatocellular carcinoma patients after hepatic resection. *HPB Surg* 2014;2014:641685
  348. Yamashita T, Kitao A, Matsui O, Hayashi T, Nio K, Kondo M, et al. Gd-EOB-DTPA-enhanced magnetic resonance imaging and alpha-fetoprotein predict prognosis of early-stage hepatocellular carcinoma. *Hepatology* 2014;60:1674–1685
  349. Park VY, Choi JY, Chung YE, Kim H, Park MS, Lim JS, et al. Dynamic enhancement pattern of HCC smaller than 3 cm in diameter on gadoteric acid-enhanced MRI: comparison with multiphasic MDCT. *Liver Int* 2014;34:1593–1602
  350. Yu MH, Kim JH, Yoon JH, Kim HC, Chung JW, Han JK, et al. Small ( $\leq 1$ -cm) hepatocellular carcinoma: diagnostic performance and imaging features at gadoteric acid-enhanced MR imaging. *Radiology* 2014;271:748–760
  351. Komatsu N, Motosugi U, Maekawa S, Shindo K, Sakamoto M, Sato M, et al. Hepatocellular carcinoma risk assessment using gadoteric acid-enhanced hepatocyte phase magnetic resonance imaging. *Hepatol Res* 2014;44:1339–1346
  352. Kim KA, Kim MJ, Choi JY, Park MS, Lim JS, Chung YE, et al. Detection of recurrent hepatocellular carcinoma on post-operative surveillance: comparison of MDCT and gadoteric acid-enhanced MRI. *Abdom Imaging* 2014;39:291–299
  353. Phongkitkarun S, Limsamutpetch K, Tannaphai P, Jatchavala J. Added value of hepatobiliary phase gadoteric acid-enhanced MRI for diagnosing hepatocellular carcinoma in high-risk patients. *World J Gastroenterol* 2013;19:8357–8365
  354. Zhao XT, Li WX, Chai WM, Chen KM. Detection of small hepatocellular carcinoma using gadoteric acid-enhanced MRI: is the addition of diffusion-weighted MRI at 3.0T beneficial? *J Dig Dis* 2014;15:137–145
  355. Inoue T, Hyodo T, Murakami T, Takayama Y, Nishie A, Higaki A, et al. Hypovascular hepatic nodules showing hypointense on the hepatobiliary-phase image of Gd-EOB-DTPA-enhanced MRI to develop a hypervascular hepatocellular carcinoma: a nationwide retrospective study on their natural course and risk factors. *Dig Dis* 2013;31:472–479
  356. Toyoda H, Kumada T, Tada T, Niinomi T, Ito T, Sone Y, et al. Non-hypervascular hypointense nodules detected by Gd-EOB-DTPA-enhanced MRI are a risk factor for recurrence of HCC after hepatectomy. *J Hepatol* 2013;58:1174–1180
  357. Ooka Y, Kanai F, Okabe S, Ueda T, Shimofusa R, Ogasawara S, et al. Gadoteric acid-enhanced MRI compared with CT during angiography in the diagnosis of hepatocellular carcinoma. *Magn Reson Imaging* 2013;31:748–754
  358. An C, Park MS, Kim D, Kim YE, Chung WS, Rhee H, et al. Added value of subtraction imaging in detecting arterial enhancement in small ( $< 3$  cm) hepatic nodules on dynamic contrast-enhanced MRI in patients at high risk of hepatocellular carcinoma. *Eur Radiol* 2013;23:924–930
  359. Lee JM, Yoon JH, Joo I, Woo HS. Recent advances in CT and MR imaging for evaluation of hepatocellular carcinoma. *Liver Cancer* 2012;1:22–40
  360. Inoue T, Kudo M, Komuta M, Hayaishi S, Ueda T, Takita M, et al. Assessment of Gd-EOB-DTPA-enhanced MRI for HCC and dysplastic nodules and comparison of detection sensitivity versus MDCT. *J Gastroenterol* 2012;47:1036–1047
  361. Eso Y, Marusawa H, Osaki Y. Education and imaging. Hepatobiliary and pancreatic: detection of early hepatocellular carcinoma by enhanced magnetic resonance imaging. *J Gastroenterol Hepatol* 2012;27:416
  362. Alaboudy A, Inoue T, Hatanaka K, Chung H, Hyodo T, Kumano S, et al. Usefulness of combination of imaging modalities in the diagnosis of hepatocellular carcinoma using Sonazoid®-enhanced ultrasound, gadolinium diethylene-triamine-pentaacetic acid-enhanced magnetic resonance imaging, and contrast-

- enhanced computed tomography. *Oncology* 2011;81(Suppl 1):66–72
363. Golfieri R, Renzulli M, Lucidi V, Corcioni B, Trevisani F, Bolondi L. Contribution of the hepatobiliary phase of Gd-EOB-DTPA-enhanced MRI to Dynamic MRI in the detection of hypovascular small ( $\leq 2$  cm) HCC in cirrhosis. *Eur Radiol* 2011;21:1233–1242
  364. Rieke J, Seidensticker M, Mohnike K. Noninvasive diagnosis of hepatocellular carcinoma in cirrhotic liver: current guidelines and future prospects for radiological imaging. *Liver Cancer* 2012;1:51–58
  365. Bota S, Piscaglia F, Marinelli S, Pecorelli A, Terzi E, Bolondi L. Comparison of international guidelines for noninvasive diagnosis of hepatocellular carcinoma. *Liver Cancer* 2012;1:190–200
  366. Kudo M, Matsui O, Izumi N, Iijima H, Kadoya M, Imai Y, et al. JSH consensus-based clinical practice guidelines for the management of hepatocellular carcinoma: 2014 update by the Liver Cancer Study Group of Japan. *Liver Cancer* 2014;3:458–468
  367. Sakamoto M, Hirohashi S. Natural history and prognosis of adenomatous hyperplasia and early hepatocellular carcinoma: multi-institutional analysis of 53 nodules followed up for more than 6 months and 141 patients with single early hepatocellular carcinoma treated by surgical resection or percutaneous ethanol injection. *Jpn J Clin Oncol* 1998;28:604–608
  368. Kojiro M. Pathology of hepatocellular carcinoma. In: Okuda K, Tabor E, editors. *Liver Cancer*. New York: Churchill Livingstone; 1997
  369. Tajima T, Honda H, Taguchi K, Asayama Y, Kuroiwa T, Yoshimitsu K, et al. Sequential hemodynamic change in hepatocellular carcinoma and dysplastic nodules: cT angiography and pathologic correlation. *AJR Am J Roentgenol* 2002;178:885–897
  370. Hayashi M, Matsui O, Ueda K, Kawamori Y, Gabata T, Kadoya M. Progression to hypervascular hepatocellular carcinoma: correlation with intranodular blood supply evaluated with CT during intraarterial injection of contrast material. *Radiology* 2002;225:143–149
  371. Kudo M, Hatanaka K, Maekawa K. Newly developed novel ultrasound technique, defect reperfusion ultrasound imaging, using sonazoid in the management of hepatocellular carcinoma. *Oncology* 2010;78(Suppl 1):40–45
  372. Tada T, Kumada T, Toyoda H, Ito T, Sone Y, Okuda S, et al. Diagnostic accuracy for macroscopic classification of nodular hepatocellular carcinoma: comparison of gadolinium ethoxybenzyl diethylenetriamine pentaacetic acid-enhanced magnetic resonance imaging and angiography-assisted computed tomography. *J Gastroenterol* 2015;50:85–94
  373. Joishi D, Ueno A, Tanimoto A, Okuda S, Masugi Y, Emoto K, et al. Natural course of hypovascular nodules detected on gadoxetic acid-enhanced MR imaging: presence of fat is a risk factor for hypervascularization. *Magn Reson Med Sci* 2013;12:281–287
  374. Motosugi U. Hypovascular hypointense nodules on hepatocyte phase gadoxetic acid-enhanced MR images: too early or too progressed to determine hypervascularity. *Radiology* 2013;267:317–318
  375. Takechi M, Tsuda T, Yoshioka S, Murata S, Tanaka H, Hirooka M, et al. Risk of hypervascularization in small hypovascular hepatic nodules showing hypointense in the hepatobiliary phase of gadoxetic acid-enhanced MRI in patients with chronic liver disease. *Jpn J Radiol* 2012;30:743–751
  376. Takayama Y, Nishie A, Nakayama T, Asayama Y, Ishigami K, Kakihara D, et al. Hypovascular hepatic nodule showing hypointensity in the hepatobiliary phase of gadoxetic acid-enhanced MRI in patients with chronic liver disease: prediction of malignant transformation. *Eur J Radiol* 2012;81:3072–3078
  377. Akai H, Matsuda I, Kiryu S, Tajima T, Takao H, Watanabe Y, et al. Fate of hypointense lesions on Gd-EOB-DTPA-enhanced magnetic resonance imaging. *Eur J Radiol* 2012;81:2973–2977
  378. Motosugi U, Ichikawa T, Sano K, Sou H, Onohara K, Muhi A, et al. Outcome of hypovascular hepatic nodules revealing no gadoxetic acid uptake in patients with chronic liver disease. *J Magn Reson Imaging* 2011;34:88–94
  379. Kumada T, Toyoda H, Tada T, Sone Y, Fujimori M, Ogawa S, et al. Evolution of hypointense hepatocellular nodules observed only in the hepatobiliary phase of gadoxetate disodium-enhanced MRI. *AJR Am J Roentgenol* 2011;197:58–63
  380. Laupacis A, Feeny D, Detsky AS, Tugwell PX. How attractive does a new technology have to be to warrant adoption and utilization? Tentative guidelines for using clinical and economic evaluations. *CMAJ* 1992;146:473–481
  381. Sato T, Tateishi R, Yoshida H, Ohki T, Masuzaki R, Imamura J, et al. Ultrasound surveillance for early detection of hepatocellular carcinoma among patients with chronic hepatitis C. *Hepatol Int* 2009;3:544–550
  382. Di Bisceglie AM, Sterling RK, Chung RT, Everhart JE, Dienstag JL, Bonkovsky HL, et al. Serum alpha-fetoprotein levels in patients with advanced hepatitis C: results from the HALT-C Trial. *J Hepatol* 2005;43:434–441
  383. Hoshida Y, Nijman SM, Kobayashi M, Chan JA, Brunet JP, Chiang DY, et al. Integrative transcriptome analysis reveals common molecular subclasses of human hepatocellular carcinoma. *Cancer Res* 2009;69:7385–7392
  384. Paul SB, Gulati MS, Sreenivas V, Madan K, Gupta AK, Mukhopadhyay S, et al. Evaluating patients with cirrhosis for hepatocellular carcinoma: value of clinical symptomatology, imaging and alpha-fetoprotein. *Oncology* 2007;72(Suppl 1):117–123
  385. Kumada T, Nakano S, Takeda I, Kiriya S, Sone Y, Hayashi K, et al. Clinical utility of Lens culinaris agglutinin-reactive alpha-fetoprotein in small hepatocellular carcinoma: special reference to imaging diagnosis. *J Hepatol* 1999;30:125–130
  386. Lok AS, Sterling RK, Everhart JE, Wright EC, Hoefs JC, Di Bisceglie AM, et al. Des-gamma-carboxy prothrombin and alpha-fetoprotein as biomarkers for the early detection of hepatocellular carcinoma. *Gastroenterology* 2010;138:493–502
  387. Sterling RK, Jeffers L, Gordon F, Sherman M, Venook AP, Reddy KR, et al. Clinical utility of AFP-L3% measurement in North American patients with HCV-related cirrhosis. *Am J Gastroenterol* 2007;102:2196–2205
  388. Chang TS, Wu YC, Tung SY, Wei KL, Hsieh YY, Huang HC, et al. Alpha-fetoprotein measurement benefits hepatocellular carcinoma surveillance in patients with cirrhosis. *Am J Gastroenterol* 2015;110:836–844
  389. Zhang BH, Yang BH, Zhang ZY. Randomized controlled trial of screening for hepatocellular carcinoma. *J Cancer Res Clin Oncol* 2004;130:417–422
  390. Lin OS, Keefe EB, Sanders GD, Owens DK. Cost-effectiveness of screening for hepatocellular carcinoma in patients with cirrhosis due to chronic hepatitis C. *Aliment Pharmacol Ther* 2004;19:1159–1172
  391. Patel D, Terrault NA, Yao FY, Bass NM, Ladabaum U. Cost-effectiveness of hepatocellular carcinoma surveillance in patients with hepatitis C virus-related cirrhosis. *Clin Gastroenterol Hepatol* 2005;3:75–84
  392. Andersson KL, Salomon JA, Goldie SJ, Chung RT. Cost effectiveness of alternative surveillance strategies for hepatocellular carcinoma in patients with cirrhosis. *Clin Gastroenterol Hepatol* 2008;6:1418–1424

393. Trinchet JC, Chaffaut C, Bourcier V, Degos F, Henrion J, Fontaine H, et al. Ultrasonographic surveillance of hepatocellular carcinoma in cirrhosis: a randomized trial comparing 3- and 6-month periodicities. *Hepatology* 2011;54:1987–1997
394. El-Serag HB, Davila JA. Surveillance for hepatocellular carcinoma: in whom and how? *Therap Adv Gastroenterol* 2011;4:5–10
395. Sarasin FP, Giostra E, Hadengue A. Cost-effectiveness of screening for detection of small hepatocellular carcinoma in western patients with Child-Pugh class A cirrhosis. *Am J Med* 1996;101:422–434
396. Fattovich G, Stroffolini T, Zagni I, Donato F. Hepatocellular carcinoma in cirrhosis: incidence and risk factors. *Gastroenterology* 2004;127:S35–S50
397. Sangiovanni A, Prati GM, Fasani P, Ronchi G, Romeo R, Manini M, et al. The natural history of compensated cirrhosis due to hepatitis C virus: a 17-year cohort study of 214 patients. *Hepatology* 2006;43:1303–1310
398. Trevisani F, Santi V, Gramenzi A, Di Nolfo MA, Del Poggio P, Benvegna L, et al. Surveillance for early diagnosis of hepatocellular carcinoma: is it effective in intermediate/advanced cirrhosis? *Am J Gastroenterol* 2007;102:2448–2457
399. Jepsen P, Ott P, Andersen PK, Sørensen HT, Vilstrup H. Risk for hepatocellular carcinoma in patients with alcoholic cirrhosis: a Danish nationwide cohort study. *Ann Intern Med* 2012;156:841–847, W295
400. Lok AS, Seeff LB, Morgan TR, di Bisceglie AM, Sterling RK, Curto TM, et al. Incidence of hepatocellular carcinoma and associated risk factors in hepatitis C-related advanced liver disease. *Gastroenterology* 2009;136:138–148
401. Martinez SM, Crespo G, Navasa M, Forns X. Noninvasive assessment of liver fibrosis. *Hepatology* 2011;53:325–335
402. Huang CF, Yeh ML, Tsai PC, Hsieh MH, Yang HL, Hsieh MY, et al. Baseline gamma-glutamyl transferase levels strongly correlate with hepatocellular carcinoma development in non-cirrhotic patients with successful hepatitis C virus eradication. *J Hepatol* 2014;61:67–74
403. Huang CF, Yeh ML, Huang CY, Tsai PC, Ko YM, Chen KY, et al. Pretreatment glucose status determines HCC development in HCV patients with mild liver disease after curative antiviral therapy. *Med (Baltimore)*. 2016;95:e4157
404. Leung C, Yeoh SW, Patrick D, Ket S, Marion K, Gow P, et al. Characteristics of hepatocellular carcinoma in cirrhotic and non-cirrhotic non-alcoholic fatty liver disease. *World J Gastroenterol* 2015;21:1189–1196
405. Bruno S, Stroffolini T, Colombo M, Bollani S, Benvegna L, Mazzella G, et al. Sustained virological response to interferon-alpha is associated with improved outcome in HCV-related cirrhosis: a retrospective study. *Hepatology* 2007;45:579–587
406. Sung JJ, Tsoi KK, Wong VW, Li KC, Chan HL. Meta-analysis: Treatment of hepatitis B infection reduces risk of hepatocellular carcinoma. *Aliment Pharmacol Ther* 2008;28:1067–1077
407. Song P, Tobe RG, Inagaki Y, Kokudo N, Hasegawa K, Sugawara Y, et al. The management of hepatocellular carcinoma around the world: a comparison of guidelines from 2001 to 2011. *Liver Int* 2012;32:1053–1063
408. Bruix J, Gores GJ, Mazzaferro V. Hepatocellular carcinoma: clinical frontiers and perspectives. *Gut* 2014;63:844–855
409. Bruix J, Reig M, Sherman M. Evidence-Based Diagnosis, Staging, and Treatment of Patients With Hepatocellular Carcinoma. *Gastroenterology* 2016;150:835–853
410. Torzilli G, Belghiti J, Kokudo N, Takayama T, Capussotti L, Nuzzo G, et al. A snapshot of the effective indications and results of surgery for hepatocellular carcinoma in tertiary referral centers: is it adherent to the EASL/AASLD recommendations?: an observational study of the HCC East-West study group. *Ann Surg* 2013;257:929–937
411. Han KH, Kudo M, Ye SL, Choi JY, Poon RT, Seong J, et al. Asian consensus workshop report: expert consensus guideline for the management of intermediate and advanced hepatocellular carcinoma in Asia. *Oncology* 2011;81(Suppl 1):158–164
412. Kokudo N, Hasegawa K, Akahane M, Igaki H, Izumi N, Ichida T, et al. Evidence-based clinical practice guidelines for hepatocellular carcinoma: the Japan Society of Hepatology 2013 update (3rd JSH-HCC Guidelines). *Hepatol Res* 2015;45
413. Kudo M, Kitano M, Sakurai T, Nishida N. General rules for the clinical and pathological study of primary liver cancer, nationwide follow-up survey and clinical practice guidelines: the Outstanding Achievements of the Liver Cancer Study Group of Japan. *Dig Dis* 2015;33:765–770
414. Yau T, Tang VY, Yao TJ, Fan ST, Lo CM, Poon RT. Development of Hong Kong Liver Cancer staging system with treatment stratification for patients with hepatocellular carcinoma. *Gastroenterology* 2014;146:1691–1700
415. Korean Liver Cancer Study Group (KLCSG); National Cancer Center, Korea (NCC). KLCSG-NCC Korea practice guideline for the management of hepatocellular carcinoma. *Gut Liver* 2014;9:267–317
416. Mazzaferro V, Regalia E, Doci R, Andreola S, Pulvirenti A, Bozzetti F, et al. Liver transplantation for the treatment of small hepatocellular carcinomas in patients with cirrhosis. *N Engl J Med* 1996;334:693–699
417. Yao FY, Ferrell L, Bass NM, Watson JJ, Bacchetti P, Venook A, et al. Liver transplantation for hepatocellular carcinoma: expansion of the tumor size limits does not adversely impact survival. *Hepatology* 2001;33:1394–1403
418. Toso C, Mazzaferro V, Bruix J, Freeman R, Mentha G, Majno P. Toward a better liver graft allocation that accounts for candidates with and without hepatocellular carcinoma. *Am J Transplant* 2014;14:2221–2227
419. Clavien PA, Lesurtel M, Bossuyt PM, Gores GJ, Langer B, Perrier A. Recommendations for liver transplantation for hepatocellular carcinoma: an international consensus conference report. *Lancet Oncol* 2012;13:e11–e22
420. Volk ML, Vijan S, Marrero JA. A novel model measuring the harm of transplanting hepatocellular carcinoma exceeding Milan criteria. *Am J Transplant* 2008;8:839–846
421. Akamatsu N, Sugawara Y, Kokudo N. Living donor liver transplantation for patients with hepatocellular carcinoma. *Liver Cancer* 2014;3:108–118
422. Fisher RA, Kulik LM, Freise CE, Lok AS, Shearon TH, Brown RS Jr, et al. Hepatocellular carcinoma recurrence and death following living and deceased donor liver transplantation. *Am J Transpl* 2007;7:1601–1608
423. Liang W, Wu L, Ling X, Schroder PM, Ju W, Wang D, et al. Living donor liver transplantation versus deceased donor liver transplantation for hepatocellular carcinoma: a meta-analysis. *Liver Transpl* 2012;18:1226–1236
424. Xu X, Lu D, Ling Q, Wei X, Wu J, Zhou L, et al. Liver transplantation for hepatocellular carcinoma beyond the Milan criteria. *Gut* 2016;65:1035–1041
425. Vitale A, Morales RR, Zanusi G, Farinati F, Burra P, Angeli P, et al. Barcelona Clinic Liver Cancer staging and transplant survival benefit for patients with hepatocellular carcinoma: a multicentre, cohort study. *Lancet Oncol* 2011;12:654–662
426. Hasegawa K, Kokudo N, Makuuchi M, Izumi N, Ichida T, Kudo M, et al. Comparison of resection and ablation for hepatocellular carcinoma: a cohort study based on a Japanese nationwide survey. *J Hepatol* 2013;58:724–729
427. Giulianti F, Ardito F, Pinna AD, Sarno G, Giulini SM, Ercolani G, et al. Liver resection for hepatocellular carcinoma  $\leq 3$  cm:



- results of an Italian multicenter study on 588 patients. *J Am Coll Surg* 2012;215:244–254
428. Cucchetti A, Djulbegovic B, Tsalatsanis A, Vitale A, Hozo I, Piscaglia F, et al. When to perform hepatic resection for intermediate-stage hepatocellular carcinoma. *Hepatology* 2015;61:905–914
  429. Facciuto ME, Rochon C, Pandey M, Rodriguez-Davalos M, Samaniego S, Wolf DC, et al. Surgical dilemma: liver resection or liver transplantation for hepatocellular carcinoma and cirrhosis. Intention-to-treat analysis in patients within and outwith Milan criteria. *HPB (Oxford)* 2009;11:398–404
  430. Santambrogio R, Kluger MD, Costa M, Belli A, Barabino M, Laurent A, et al. Hepatic resection for hepatocellular carcinoma in patients with Child-Pugh's A cirrhosis: is clinical evidence of portal hypertension a contraindication? *HPB (Oxford)*. 2013;15:78–84
  431. Silva MF, Sapisochin G, Strasser SI, Hewa-Geeganage S, Chen J, Wigg AJ, et al. Liver resection and transplantation offer similar 5-year survival for Child-Pugh-Turcotte A HCC-patients with a single nodule up to 5 cm: a multicenter, exploratory analysis. *Eur J Surg Oncol* 2013;39:386–395
  432. Chua TC, Saxena A, Chu F, Morris DL. Hepatic resection for transplantable hepatocellular carcinoma for patients within Milan and UCSF criteria. *Am J Clin Oncol* 2012;35:141–145
  433. Muscari F, Foppa B, Carrere N, Kamar N, Peron JM, Suc B. Resection of a transplantable single-nodule hepatocellular carcinoma in Child-Pugh class A cirrhosis: factors affecting survival and recurrence. *World J Surg* 2011;35:1055–1062
  434. Chapman WC, Klintmalm G, Hemming A, Vachharajani N, Majella Doyle MB, DeMatteo R, et al. Surgical treatment of hepatocellular carcinoma in North America: can hepatic resection still be justified? *J Am Coll Surg* 2015;220:628–637
  435. Adam R, Bhangui P, Vibert E, Azoulay D, Pelletier G, Duclos-Vallee JC, et al. Resection or transplantation for early hepatocellular carcinoma in a cirrhotic liver: does size define the best oncological strategy? *Ann Surg* 2012;256:883–891
  436. Vitale A, Huo TL, Cucchetti A, Lee YH, Volk M, Frigo AC, et al. Survival benefit of liver transplantation versus resection for hepatocellular carcinoma: impact of MELD score. *Ann Surg Oncol* 2015;22:1901–1907
  437. Proneth A, Zeman F, Schlitt HJ, Schnitzbauer AA. Is resection or transplantation the ideal treatment in patients with hepatocellular carcinoma in cirrhosis if both are possible? A systematic review and metaanalysis. *Ann Surg Oncol* 2014;21:3096–3107
  438. Belghiti J, Cortes A, Abdalla EK, Régimbeau JM, Prakash K, Durand F, et al. Resection prior to liver transplantation for hepatocellular carcinoma. *Ann Surg* 2003;238:885–892
  439. Bhangui P, Allard MA, Vibert E, Cherqui D, Pelletier G, Cunha AS, et al. salvage versus primary liver transplantation for early hepatocellular carcinoma: do both strategies yield similar outcomes? *Ann Surg* 2016;264:155–163
  440. Ishizawa T, Hasegawa K, Aoki T, Takahashi M, Inoue Y, Sano K, et al. Neither multiple tumors nor portal hypertension are surgical contraindications for hepatocellular carcinoma. *Gastroenterology* 2008;134:1908–1916
  441. Shindoh J, Makuuchi M, Matsuyama Y, Mise Y, Arita J, Sakamoto Y, et al. Complete removal of the tumor-bearing portal territory decreases local tumor recurrence and improves disease-specific survival of patients with hepatocellular carcinoma. *J Hepatol* 2016;64:594–600
  442. Lim KC, Chow PK, Allen JC, Siddiqui FJ, Chan ES, Tan SB. Systematic review of outcomes of liver resection for early hepatocellular carcinoma within the Milan criteria. *Br J Surg* 2012;99:1622–1629
  443. Makuuchi M, Kosuge T, Takayama T, Yamazaki S, Kakazu T, Miyagawa S, et al. Surgery for small liver cancers. *Semin Surg Oncol* 1993;9:298–304
  444. Torzilli G, Makuuchi M, Inoue K, Takayama T, Sakamoto Y, Sugawara Y, et al. No-mortality liver resection for hepatocellular carcinoma in cirrhotic and noncirrhotic patients: is there a way? A prospective analysis of our approach. *Arch Surg* 1999;134:984–992
  445. Lau H, Man K, Fan ST, Yu WC, Lo CM, Wong J. Evaluation of preoperative hepatic function in patients with hepatocellular carcinoma undergoing hepatectomy. *Br J Surg* 1997;84:1255–1259
  446. Kamiyama T, Nakagawa T, Nakanishi K, Kamachi H, Onodera Y, Matsushita M, et al. Preoperative evaluation of hepatic vasculature by three-dimensional computed tomography in patients undergoing hepatectomy. *World J Surg* 2006;30:400–409
  447. Makuuchi M, Thai BL, Takayasu K, Takayama T, Kosuge T, Gunvén P, et al. Preoperative portal embolization to increase safety of major hepatectomy for hilar bile duct carcinoma: a preliminary report. *Surgery* 1990;107:521–527
  448. Sato M, Tateishi R, Yasunaga H, Horiguchi H, Yoshida H, Matsuda S, et al. Mortality and morbidity of hepatectomy, radiofrequency ablation, and embolization for hepatocellular carcinoma: a national survey of 54,145 patients. *J Gastroenterol* 2012;47:1125–1133
  449. Sugiura N, Takara K, Ohto M, Okuda K, Hirooka N. Ultrasound image-guided percutaneous intratumor ethanol injection for small hepatocellular carcinoma. *Acta Hepatol Jpn* 1983; 24:920 (Japanese)
  450. Livraghi T, Festi D, Monti F, Salmi A, Vettori C. US-guided percutaneous alcohol injection of small hepatic and abdominal tumors. *Radiology* 1986;161:309–312
  451. Shiina S, Yasuda H, Muto H, Tagawa K, Unuma T, Ibukuro K, et al. Percutaneous ethanol injection in the treatment of liver neoplasms. *AJR Am J Roentgenol* 1987;149:949–952
  452. Seki T, Wakabayashi M, Nakagawa T, Itho T, Shiro T, Kunieda K, et al. Ultrasonically guided percutaneous microwave coagulation therapy for small hepatocellular carcinoma. *Cancer* 1994;74:817–825
  453. Rossi S, Di Stasi M, Buscarini E, Cavanna L, Quaretti P, Squassante E, et al. Percutaneous radiofrequency interstitial thermal ablation in the treatment of small hepatocellular carcinoma. *Cancer J Sci Am* 1995;1:73–81
  454. Livraghi T, Goldberg SN, Lazzaroni S, Meloni F, Solbiati L, Gazelle GS. Small hepatocellular carcinoma: treatment with radio-frequency ablation versus ethanol injection. *Radiology* 1999;210:655–661
  455. Shiina S, Teratani T, Obi S, Sato S, Tateishi R, Fujishima T, et al. A randomized controlled trial of radiofrequency ablation with ethanol injection for small hepatocellular carcinoma. *Gastroenterology* 2005;129:122–130
  456. Ebara M, Okabe S, Kita K, Sugiura N, Fukuda H, Yoshikawa M, et al. Percutaneous ethanol injection for small hepatocellular carcinoma: therapeutic efficacy based on 20-year observation. *J Hepatol* 2005;43:458–464
  457. Shiina S, Tagawa K, Niwa Y, Unuma T, Komatsu Y, Yoshiura K, et al. Percutaneous ethanol injection therapy for hepatocellular carcinoma: results in 146 patients. *AJR Am J Roentgenol* 1993;160:1023–1028
  458. Sung YM, Choi D, Lim HK, Lee WJ, Kim SH, Kim MJ, et al. Long-term results of percutaneous ethanol injection for the treatment of hepatocellular carcinoma in Korea. *Korean J Radiol* 2006;7:187–192
  459. Shiina S, Tateishi R, Imamura M, Teratani T, Koike Y, Sato S, et al. Percutaneous ethanol injection for hepatocellular



- carcinoma: 20-year outcome and prognostic factors. *Liver Int* 2012;32:1434–1442
460. Livraghi T, Giorgio A, Marin G, Salmi A, de Sio I, Bolondi L, et al. Hepatocellular carcinoma and cirrhosis in 746 patients: long-term results of percutaneous ethanol injection. *Radiology* 1995;197:101–108
  461. Ishii H, Okada S, Nose H, Okusaka T, Yoshimori M, Takayama T, et al. Local recurrence of hepatocellular carcinoma after percutaneous ethanol injection. *Cancer* 1996;77:1792–1796
  462. Di Stasi M, Buscarini L, Livraghi T, Giorgio A, Salmi A, De Sio I, et al. Percutaneous ethanol injection in the treatment of hepatocellular carcinoma. A multicenter survey of evaluation practices and complication rates. *Scand J Gastroenterol* 1997;32:1168–1173
  463. Shiina S, Teratani T, Obi S, Hamamura K, Koike Y, Omata M. Nonsurgical treatment of hepatocellular carcinoma: from percutaneous ethanol injection therapy and percutaneous microwave coagulation therapy to radiofrequency ablation. *Oncology* 2002;62(Suppl 1):64–68
  464. Lubner MG, Brace CL, Hinshaw JL, Lee FT Jr. Microwave tumor ablation: mechanism of action, clinical results, and devices. *J Vasc Interv Radiol* 2010;21:S192–S203
  465. Lencioni R, Cioni D, Crocetti L, Franchini C, Pina CD, Lera J, et al. Early-stage hepatocellular carcinoma in patients with cirrhosis: long-term results of percutaneous image-guided radiofrequency ablation. *Radiology* 2005;234:961–967
  466. Tateishi R, Shiina S, Teratani T, Obi S, Sato S, Koike Y, et al. Percutaneous radiofrequency ablation for hepatocellular carcinoma. An analysis of 1000 cases. *Cancer* 2005;103:1201–1209
  467. Livraghi T, Meloni F, Di Stasi M, Rolle E, Solbiati L, Tinelli C, et al. Sustained complete response and complications rates after radiofrequency ablation of very early hepatocellular carcinoma in cirrhosis: is resection still the treatment of choice? *Hepatol* 2008;47:82–89
  468. Yan K, Chen MH, Yang W, Wang YB, Gao W, Hao CY, et al. Radiofrequency ablation of hepatocellular carcinoma: long-term outcome and prognostic factors. *Eur J Radiol* 2008;67:336–347
  469. Shiina S, Tateishi R, Arano T, Uchino K, Enooku K, Nakagawa H, et al. Radiofrequency ablation for hepatocellular carcinoma: 10-year outcome and prognostic factors. *Am J Gastroenterol* 2012;107:569–577
  470. Kim YS, Lim HK, Rhim H, Lee MW, Choi D, Lee WJ, et al. Ten-year outcomes of percutaneous radiofrequency ablation as first-line therapy of early hepatocellular carcinoma: analysis of prognostic factors. *J Hepatol* 2013;58:89–97
  471. Kitamoto M, Imagawa M, Yamada H, Watanabe C, Sumioka M, Satoh O, et al. Radiofrequency ablation in the treatment of small hepatocellular carcinomas: comparison of the radiofrequency effect with and without chemoembolization. *AJR Am J Roentgenol* 2003;181:997–1003
  472. Morimoto M, Numata K, Kondou M, Nozaki A, Morita S, Tanaka K. Midterm outcomes in patients with intermediate-sized hepatocellular carcinoma: a randomized controlled trial for determining the efficacy of radiofrequency ablation combined with transcatheter arterial chemoembolization. *Cancer* 2010;116:5452–5460
  473. Song MJ, Bae SH, Lee JS, Lee SW, Lee SW, do Song S, You CR, et al. Combination transarterial chemoembolization and radiofrequency ablation therapy for early hepatocellular carcinoma. *Korean J Intern Med* 2016;31:242–252
  474. Xie H, Wang H, An W, Ma W, Qi R, Yang B, et al. The efficacy of radiofrequency ablation combined with transcatheter arterial chemoembolization for primary hepatocellular carcinoma in a cohort of 487 patients. *PLoS One* 2014;9:e89081
  475. Kobayashi M, Ikeda K, Kawamura Y, Hosaka T, Sezaki H, Yatsuji H, et al. Randomized controlled trial for the efficacy of hepatic arterial occlusion during radiofrequency ablation for small hepatocellular carcinoma—direct ablative effects and a long-term outcome. *Liver Int* 2007;27:353–359
  476. Scheffer HJ, Nielsen K, de Jong MC, van Tilborg AA, Vieveen JM, Bouwman AR, et al. Irreversible electroporation for non-thermal tumor ablation in the clinical setting: a systematic review of safety and efficacy. *J Vasc Interv Radiol* 2014;25:997–1011
  477. Lencioni RA, Allgaier HP, Cioni D, Olschewski M, Deibert P, Crocetti L, et al. Small hepatocellular carcinoma in cirrhosis: randomized comparison of radio-frequency thermal ablation versus percutaneous ethanol injection. *Radiology* 2003;228:235–240
  478. Lin SM, Lin CJ, Lin CC, Hsu CW, Chen YC. Radiofrequency ablation improves prognosis compared with ethanol injection for hepatocellular carcinoma < or = 4 cm. *Gastroenterology* 2004;127:1714–1723
  479. Lin SM, Lin CJ, Lin CC, Hsu CW, Chen YC. Randomised controlled trial comparing percutaneous radiofrequency thermal ablation, percutaneous ethanol injection, and percutaneous acetic acid injection to treat hepatocellular carcinoma of 3 cm or less. *Gut* 2005;54:1151–1156
  480. Brunello F, Veltri A, Carucci P, Pagano E, Ciccone G, Moretto P, et al. Radiofrequency ablation versus ethanol injection for early hepatocellular carcinoma: a randomized controlled trial. *Scand J Gastroenterol* 2008;43:727–735
  481. Shibata T, Iimuro Y, Yamamoto Y, Maetani Y, Ametani F, Itoh K, et al. Small hepatocellular carcinoma: comparison of radiofrequency ablation and percutaneous microwave coagulation therapy. *Radiology* 2002;223:331–337
  482. Chen MS, Li JQ, Zheng Y, Guo RP, Liang HH, Zhang YQ, et al. A prospective randomized trial comparing percutaneous local ablative therapy and partial hepatectomy for small hepatocellular carcinoma. *Ann Surg* 2006;243:321–328
  483. Feng K, Yan J, Li X, Xia F, Ma K, Wang S, et al. A randomized controlled trial of radiofrequency ablation and surgical resection in the treatment of small hepatocellular carcinoma. *J Hepatol* 2012;57:794–802
  484. Fang Y, Chen W, Liang X, Li D, Lou H, Chen R, et al. Comparison of long-term effectiveness and complications of radiofrequency ablation with hepatectomy for small hepatocellular carcinoma. *J Gastroenterol Hepatol* 2014;29:193–200
  485. Huang J, Yan L, Cheng Z, Wu H, Du L, Wang J, et al. A randomized trial comparing radiofrequency ablation and surgical resection for HCC conforming to the Milan criteria. *Ann Surg* 2010;252:903–912
  486. Hong SN, Lee SY, Choi MS, Lee JH, Koh KC, Paik SW, et al. Comparing the outcomes of radiofrequency ablation and surgery in patients with a single small hepatocellular carcinoma and well-preserved hepatic function. *J Clin Gastroenterol* 2005;39:247–252
  487. Yamagiwa K, Shiraki K, Yamakado K, Mizuno S, Hori T, Yagi S, et al. Survival rates according to the Cancer of the Liver Italian Program scores of 345 hepatocellular carcinoma patients after multimodality treatments during a 10-year period in a retrospective study. *J Gastroenterol Hepatol* 2008;23:482–490
  488. Yamakado K, Nakatsuka A, Takaki H, Yokoi H, Usui M, Sakurai H, et al. Early-stage hepatocellular carcinoma: radiofrequency ablation combined with chemoembolization versus hepatectomy. *Radiology* 2008;247:260–266
  489. Kim GA, Shim JH, Kim MJ, Kim SY, Won HJ, Shin YM, et al. Radiofrequency ablation as an alternative to hepatic resection for single small hepatocellular carcinomas. *Br J Surg* 2016;103:126–135
  490. Jiang L, Yan L, Wen T, Li B, Zeng Y, Yang J, et al. Comparison of outcomes of hepatic resection and radiofrequency ablation for

- hepatocellular carcinoma patients with multifocal tumors meeting the barcelona-clinic liver cancer stage A classification. *J Am Coll Surg* 2015;221:951–961
491. Kang TW, Kim JM, Rhim H, Lee MW, Kim YS, Lim HK, et al. Small hepatocellular carcinoma: radiofrequency ablation versus nonanatomic resection-propensity score analyses of long-term outcomes. *Radiology* 2015;275:908–919
  492. Yang HJ, Lee JH, Lee DH, Yu SJ, Kim YJ, Yoon JH, et al. Small single-nodule hepatocellular carcinoma: comparison of transarterial chemoembolization, radiofrequency ablation, and hepatic resection by using inverse probability weighting. *Radiology* 2014;271:909–918
  493. Cucchetti A, Piscaglia F, Cescon M, Serra C, Colecchia A, Maroni L, et al. An explorative data-analysis to support the choice between hepatic resection and radiofrequency ablation in the treatment of hepatocellular carcinoma. *Dig Liver Dis* 2014;46:257–263
  494. Zhou Z, Lei J, Li B, Yan L, Wang W, Wei Y, Cheng K. Liver resection and radiofrequency ablation of very early hepatocellular carcinoma cases (single nodule <2 cm): a single-center study. *Eur J Gastroenterol Hepatol* 2014;26:339–344
  495. Tohme S, Geller DA, Cardinal JS, Chen HW, Packiam V, Reddy S, et al. Radiofrequency ablation compared to resection in early-stage hepatocellular carcinoma. *HPB (Oxford)*. 2013;15:210–217
  496. Takayama T, Makuuchi M, Hasegawa K. Single HCC smaller than 2 cm: surgery or ablation? Surgeon's perspective. *J Hepatob Pancreat Sci* 2010;17:422–424
  497. Hung HH, Chiou YY, Hsia CY, Su CW, Chou YH, Chiang JH, et al. Survival rates are comparable after radiofrequency ablation or surgery in patients with small hepatocellular carcinomas. *Clin Gastroenterol Hepatol* 2011;9:79–86
  498. Vivarelli M, Guglielmi A, Ruzzenente A, Cucchetti A, Bellusci R, Cordiano C, et al. Surgical resection versus percutaneous radiofrequency ablation in the treatment of hepatocellular carcinoma on cirrhotic liver. *Ann Surg* 2004;240:102–107
  499. Guglielmi A, Ruzzenente A, Valdegamberi A, Pachera S, Campagnaro T, D'Onofrio M, et al. Radiofrequency ablation versus surgical resection for the treatment of hepatocellular carcinoma in cirrhosis. *J Gastrointest Surg* 2008;12:192–198
  500. Gory I, Fink M, Bell S, Gow P, Nicoll A, Knight V, et al. Radiofrequency ablation versus resection for the treatment of early stage hepatocellular carcinoma: a multicenter Australian study. *Scand J Gastroenterol* 2015;50:567–576
  501. Huang J, Hernandez-Alejandro R, Croome KP, Yan L, Wu H, Chen Z, et al. Radiofrequency ablation versus surgical resection for hepatocellular carcinoma in Childs A cirrhotics-a retrospective study of 1,061 cases. *J Gastrointest Surg* 2011;15:311–320
  502. Yun WK, Choi MS, Choi D, Rhim HC, Joh JW, Kim KH, et al. Superior long-term outcomes after surgery in child-pugh class A patients with single small hepatocellular carcinoma compared to radiofrequency ablation. *Hepatol Int* 2011;5:722–729
  503. Lee YH, Hsu CY, Chu CW, Liu PH, Hsia CY, Huang YH, et al. Radiofrequency ablation is better than surgical resection in patients with hepatocellular carcinoma within the Milan criteria and preserved liver function: a retrospective study using propensity score analyses. *J Clin Gastroenterol* 2015;49:242–249
  504. Cucchetti A, Piscaglia F, Cescon M, Colecchia A, Ercolani G, Bolondi L, et al. Cost-effectiveness of hepatic resection versus percutaneous radiofrequency ablation for early hepatocellular carcinoma. *J Hepatol* 2013;59:300–307
  505. Hasegawa K, Kokudo N, Shiina S, Tateishi R, Makuuchi M. Surgery versus radiofrequency ablation for small hepatocellular carcinoma: start of a randomized controlled trial (SURF trial). *Hepatol Res* 2010;40:851–852
  506. Claudon M, Dietrich CF, Choi BI, Cosgrove DO, Kudo M, Nolsøe CP, et al. Guidelines and good clinical practice recommendations for Contrast Enhanced Ultrasound (CEUS) in the liver—update 2012: a WFUMB-EFSUMB initiative in cooperation with representatives of AFSUMB, AIUM, ASUM, FLAUS and ICUS. *Ultrasound Med Biol* 2013;39:187–210
  507. Krücker J, Xu S, Venkatesan A, Locklin JK, Amalou H, Glossop N, et al. Clinical utility of real-time fusion guidance for biopsy and ablation. *J Vasc Interv Radiol* 2011;22:515–524
  508. Nakashima T, Kojiro M. Pathologic characteristics of hepatocellular carcinoma. *Semin Liver Dis* 1986;6:259–266
  509. Yamada R, Sato M, Kawabata M, Nakatsuka H, Nakamura K, Takashima S. Hepatic artery embolization in 120 patients with unresectable hepatoma. *Radiology* 1983;148:397–401
  510. Liapi E, Geschwind JF. Transcatheter and ablative therapeutic approaches for solid malignancies. *J Clin Oncol* 2007;25:978–986
  511. Lo CM, Ngan H, Tso WK, Liu CL, Lam CM, Poon RT, et al. Randomized controlled trial of transarterial lipiodol chemoembolization for unresectable hepatocellular carcinoma. *Hepatology* 2002;35:1164–1171
  512. Llovet JM, Real MI, Montana X, Planas R, Coll S, Aponte J, et al. Arterial embolisation or chemoembolisation versus symptomatic treatment in patients with unresectable hepatocellular carcinoma: a randomised controlled trial. *Lancet* 2002;359:1734–1739
  513. Llovet JM, Bruix J. Systematic review of randomized trials for unresectable hepatocellular carcinoma: chemoembolization improves survival. *Hepatology* 2003;37:429–442
  514. Llovet JM, Bruix J. Novel advancements in the management of hepatocellular carcinoma in 2008. *J Hepatol* 2008;48(Suppl 1):S20–S37
  515. Kudo M, Okanoue T. Management of hepatocellular carcinoma in Japan: consensus-based clinical practice manual proposed by the Japan Society of Hepatology. *Oncology* 2007;72(Suppl 1):2–15
  516. El-Serag HB, Marrero JA, Rudolph L, Reddy KR. Diagnosis and treatment of hepatocellular carcinoma. *Gastroenterology* 2008;134:1752–1763
  517. Caturelli E, Siena DA, Fusilli S, Villani MR, Schiavone G, Nardella M, et al. Transcatheter arterial chemoembolization for hepatocellular carcinoma in patients with cirrhosis: evaluation of damage to nontumorous liver tissue-long-term prospective study. *Radiology* 2000;215:123–128
  518. Chan AO, Yuen MF, Hui CK, Tso WK, Lai CL. A prospective study regarding the complications of transcatheter intraarterial lipiodol chemoembolization in patients with hepatocellular carcinoma. *Cancer* 2002;94:1747–1752
  519. Chung JW, Park JH, Han JK, Choi BI, Han MC, Lee HS, et al. Hepatic tumors: predisposing factors for complications of transcatheter oily chemoembolization. *Radiology* 1996;198:33–40
  520. Iwamoto S, Sanefuji H, Okuda K. Angiographic subsegmentectomy for the treatment of patients with small hepatocellular carcinoma. *Cancer* 2003;97:1051–1056
  521. Matsui O, Kadoya M, Yoshikawa J, Gabata T, Arai K, Demachi H, et al. Small hepatocellular carcinoma: treatment with subsegmental transcatheter arterial embolization. *Radiology* 1993;188:79–83
  522. Varela M, Real MI, Burrel M, Forner A, Sala M, Brunet M, et al. Chemoembolization of hepatocellular carcinoma with drug eluting beads: efficacy and doxorubicin pharmacokinetics. *J Hepatol* 2007;46:474–481
  523. Meza-Junco J, Montano-Loza AJ, Liu DM, Sawyer MB, Bain VG, Ma M, et al. Locoregional radiological treatment for hepatocellular carcinoma; Which, when and how? *Cancer Treat Rev* 2012;38:54–62

524. Lammer J, Malagari K, Vogl T, Pilleul F, Denys A, Watkinson A, et al. Prospective randomized study of doxorubicin-eluting-bead embolization in the treatment of hepatocellular carcinoma: results of the PRECISION V study. *Cardiovasc Intervent Radiol* 2010;33:41–52
525. Cheng AL, Amarapurkar D, Chao Y, Chen PJ, Geschwind JF, Goh KL, et al. Re-evaluating transarterial chemoembolization for the treatment of hepatocellular carcinoma: consensus recommendations and review by an International Expert Panel. *Liver Int* 2014;34:174–183
526. Lee S, Kim BK, Song K, Park JY, Ahn SH, Kim SU, et al. Subclassification of Barcelona Clinic Liver Cancer B and C hepatocellular carcinoma: a cohort study of the multicenter registry database. *J Gastroenterol Hepatol* 2016;31:842–847
527. Kim BK, Shim JH, Kim SU, Park JY, do Kim Y, Ahn SH, et al. Risk prediction for patients with hepatocellular carcinoma undergoing chemoembolization: development of a prediction model. *Liver Int* 2016;36:92–99
528. Kadalayil L, Benini R, Pallan L, O’Beirne J, Marelli L, Yu D, et al. A simple prognostic scoring system for patients receiving transarterial embolization for hepatocellular cancer. *Ann Oncol* 2013;24:2565–2570
529. Park Y, Kim SU, Kim BK, Park JY, do Kim Y, Ahn SH, et al. Addition of tumor multiplicity improves the prognostic performance of the hepatoma arterial-embolization prognostic score. *Liver Int* 2016;36:100–107
530. Huckle F, Pinter M, Graziadei I, Bota S, Vogel W, Muller C, et al. How to STATE suitability and START transarterial chemoembolization in patients with intermediate stage hepatocellular carcinoma. *J Hepatol* 2014;61:1287–1296
531. Ogasawara S, Chiba T, Ooka Y, Kanogawa N, Motoyama T, Suzuki E, et al. A prognostic score for patients with intermediate-stage hepatocellular carcinoma treated with transarterial chemoembolization. *PLoS One* 2015;10:e0125244
532. Sieghart W, Huckle F, Pinter M, Graziadei I, Vogel W, Muller C, et al. The ART of decision making: retreatment with transarterial chemoembolization in patients with hepatocellular carcinoma. *Hepatology* 2013;57:2261–2273
533. Mazzaferro V, Llovet JM, Miceli R, Bhoori S, Schiavo M, Mariani L, et al. Predicting survival after liver transplantation in patients with hepatocellular carcinoma beyond the Milan criteria: a retrospective, exploratory analysis. *Lancet Oncol* 2009;10:35–43
534. Bolondi L, Burroughs A, Dufour JF, Galle PR, Mazzaferro V, Piscaglia F, et al. Heterogeneity of patients with intermediate (BCLC B) Hepatocellular Carcinoma: proposal for a subclassification to facilitate treatment decisions. *Semin Liver Dis* 2012;32:348–359
535. Parikh ND, Waljee AK, Singal AG. Downstaging hepatocellular carcinoma: a systematic review and pooled analysis. *Liver Transpl* 2015;21:1142–1152
536. Miller AB, Hoogstraten B, Staquet M, Winkler A. Reporting results of cancer treatment. *Cancer* 1981;47:207–214
537. Therasse P, Arbuck SG, Eisenhauer EA, Wanders J, Kaplan RS, Rubinstein L, et al. New guidelines to evaluate the response to treatment in solid tumors. European Organization for Research and Treatment of Cancer, National Cancer Institute of the United States, National Cancer Institute of Canada. *J Natl Cancer Inst* 2000;92:205–216
538. Kim BK, Kim KA, Park JY, Ahn SH, Chon CY, Han KH, et al. Prospective comparison of prognostic values of modified Response Evaluation Criteria in Solid Tumours with European Association for the Study of the Liver criteria in hepatocellular carcinoma following chemoembolisation. *Eur J Cancer* 2013;49:826–834
539. Bruix J, Sherman M, Llovet JM, Beaugrand M, Lencioni R, Burroughs AK, et al. Clinical management of hepatocellular carcinoma. Conclusions of the Barcelona-2000 EASL conference. European Association for the Study of the Liver. *J Hepatol* 2001;35:421–430
540. Lencioni R, Llovet JM. Modified RECIST (mRECIST) assessment for hepatocellular carcinoma. *Semin Liver Dis* 2010;30:52–60
541. Jung ES, Kim JH, Yoon EL, Lee HJ, Lee SJ, Suh SJ, et al. Comparison of the methods for tumor response assessment in patients with hepatocellular carcinoma undergoing transarterial chemoembolization. *J Hepatol* 2013;58:1181–1187
542. Shim JH, Lee HC, Kim SO, Shin YM, Kim KM, Lim YS, et al. Which response criteria best help predict survival of patients with hepatocellular carcinoma following chemoembolization? A validation study of old and new models. *Radiology* 2012;262:708–718
543. Gillmore R, Stuart S, Kirkwood A, Hameeduddin A, Woodward N, Burroughs AK, et al. EASL and mRECIST responses are independent prognostic factors for survival in hepatocellular cancer patients treated with transarterial embolization. *J Hepatol* 2011;55:1309–1316
544. Arai T, Kobayashi A, Ohya A, Takahashi M, Yokoyama T, Shimizu A, et al. Assessment of treatment outcomes based on tumor marker trends in patients with recurrent hepatocellular carcinoma undergoing trans-catheter arterial chemo-embolization. *Int J Clin Oncol* 2014;19:871–879
545. Lee YK, Kim SU, Kim do Y, Ahn SH, Lee KH, Lee do Y, et al. Prognostic value of alpha-fetoprotein and des-gamma-carboxy prothrombin responses in patients with hepatocellular carcinoma treated with transarterial chemoembolization. *BMC Cancer* 2013;13:5
546. Raoul JL, Sangro B, Forner A, Mazzaferro V, Piscaglia F, Bolondi L, et al. Evolving strategies for the management of intermediate-stage hepatocellular carcinoma: available evidence and expert opinion on the use of transarterial chemoembolization. *Cancer Treat Rev* 2011;37:212–220
547. Kim HY, Park JW, Joo J, Jung SJ, An S, Woo SM, et al. Severity and timing of progression predict refractoriness to transarterial chemoembolization in hepatocellular carcinoma. *J Gastroenterol Hepatol* 2012;27:1051–1056
548. Kudo M, Izumi N, Kokudo N, Matsui O, Sakamoto M, Nakashima O, et al. Management of hepatocellular carcinoma in Japan: Consensus-Based Clinical Practice Guidelines proposed by the Japan Society of Hepatology (JSH) 2010 updated version. *Dig Dis* 2011;29:339–364
549. Ogasawara S, Chiba T, Ooka Y, Kanogawa N, Motoyama T, Suzuki E, et al. Efficacy of sorafenib in intermediate-stage hepatocellular carcinoma patients refractory to transarterial chemoembolization. *Oncology* 2014;87:330–341
550. Arizumi T, Ueshima K, Minami T, Kono M, Chishina H, Takita M, et al. Effectiveness of sorafenib in patients with transcatheter arterial chemoembolization (TACE) refractory and intermediate-stage hepatocellular carcinoma. *Liver Cancer* 2015;4:253–262
551. Park JW, Amarapurkar D, Chao Y, Chen PJ, Geschwind JF, Goh KL, et al. Consensus recommendations and review by an International Expert Panel on Interventions in Hepatocellular Carcinoma (EPOIHCC). *Liver Int* 2013;33(3):327–337
552. Lencioni R, Llovet JM, Han G, Tak WY, Yang J, Guglielmi A, et al. Sorafenib or placebo plus TACE with doxorubicin-eluting beads for intermediate stage HCC: the SPACE trial. *J Hepatol* 2016;64:1090–1098
553. Poon RT, Cheung TT, Kwok PC, Lee AS, Li TW, Loke KL, et al. Hong Kong consensus recommendations on the management of hepatocellular carcinoma. *Liver Cancer* 2015;4:51–69

554. Mazzaferro V, Sposito C, Bhoori S, Romito R, Chiesa C, Morosi C, et al. Yttrium-90 radioembolization for intermediate-advanced hepatocellular carcinoma: a phase 2 study. *Hepatology* 2013;57:1826–1837
555. Salem R, Lewandowski RJ, Mulcahy MF, Riaz A, Ryu RK, Ibrahim S, et al. Radioembolization for hepatocellular carcinoma using Yttrium-90 microspheres: a comprehensive report of long-term outcomes. *Gastroenterology* 2010;138:52–64
556. Sangro B, Carpanese L, Cianni R, Golfieri R, Gasparini D, Ezziddin S, et al. Survival after yttrium-90 resin microsphere radioembolization of hepatocellular carcinoma across Barcelona clinic liver cancer stages: a European evaluation. *Hepatology* 2011;54:868–878
557. Kim do Y, Park BJ, Kim YH, Han KH, Cho SB, Cho KR, et al. Radioembolization with Yttrium-90 resin microspheres in hepatocellular carcinoma: a multicenter prospective study. *Am J Clin Oncol* 2015;38:495–501
558. Schwarz RE, Abou-Alfa GK, Geschwind JF, Krishnan S, Salem R, Venook AP, et al. Nonoperative therapies for combined modality treatment of hepatocellular cancer: expert consensus statement. *HPB (Oxford)*. 2010;12:313–320
559. Culleton S, Jiang H, Haddad CR, Kim J, Brierley J, Brade A, et al. Outcomes following definitive stereotactic body radiotherapy for patients with Child-Pugh B or C hepatocellular carcinoma. *Radiother Oncol* 2014;111:412–417
560. Lanciano R, Lamond J, Yang J, Feng J, Arrigo S, Good M, et al. Stereotactic body radiation therapy for patients with heavily pretreated liver metastases and liver tumors. *Front Oncol* 2012;2:23
561. Seol SW, Yu JI, Park HC, Lim DH, Oh D, Noh JM, et al. Treatment outcome of hepatic re-irradiation in patients with hepatocellular carcinoma. *Radiat Oncol J* 2015;33:276–283
562. Liang SX, Zhu XD, Lu HJ, Pan CY, Li FX, Huang QF, et al. Hypofractionated three-dimensional conformal radiation therapy for primary liver carcinoma. *Cancer* 2005;103:2181–2188
563. Oh D, Lim DH, Park HC, Paik SW, Koh KC, Lee JH, et al. Early three-dimensional conformal radiotherapy for patients with unresectable hepatocellular carcinoma after incomplete transcatheter arterial chemoembolization: a prospective evaluation of efficacy and toxicity. *Am J Clin Oncol* 2010;33:370–375
564. Mornex F, Girard N, Beziat C, Kubas A, Khodri M, Trepo C, et al. Feasibility and efficacy of high-dose three-dimensional conformal radiotherapy in cirrhotic patients with small-size hepatocellular carcinoma non-eligible for curative therapies—mature results of the French Phase II RTF-1 trial. *Int J Radiat Oncol Biol Phys* 2006;66:1152–1158
565. Voroney JP, Brock KK, Eccles C, Haider M, Dawson LA. Prospective comparison of computed tomography and magnetic resonance imaging for liver cancer delineation using deformable image registration. *Int J Radiat Oncol Biol Phys* 2006;66:780–791
566. Choi BO, Jang HS, Kang KM, Lee SW, Kang YN, Chai GY, et al. Fractionated stereotactic radiotherapy in patients with primary hepatocellular carcinoma. *Jpn J Clin Oncol* 2006;36:154–158
567. Yoon SM, Lim YS, Park MJ, Kim SY, Cho B, Shim JH, et al. Stereotactic body radiation therapy as an alternative treatment for small hepatocellular carcinoma. *PLoS One* 2013;8:e79854
568. Takeda A, Sanuki N, Eriguchi T, Kobayashi T, Iwabuchi S, Matsunaga K, et al. Stereotactic ablative body radiotherapy for previously untreated solitary hepatocellular carcinoma. *J Gastroenterol Hepatol* 2014;29:372–379
569. Takeda A, Sanuki N, Tsurugai Y, Iwabuchi S, Matsunaga K, Ebinuma H, et al. Phase 2 study of stereotactic body radiotherapy and optional transarterial chemoembolization for solitary hepatocellular carcinoma not amenable to resection and radiofrequency ablation. *Cancer* 2016;122:2041–2049
570. Chiba T, Tokuyue K, Matsuzaki Y, Sugahara S, Chuganji Y, Kagei K, et al. Proton beam therapy for hepatocellular carcinoma: a retrospective review of 162 patients. *Clin Cancer Res* 2005;11:3799–3805
571. Sugahara S, Oshiro Y, Nakayama H, Fukuda K, Mizumoto M, Abei M, et al. Proton beam therapy for large hepatocellular carcinoma. *Int J Radiat Oncol Biol Phys* 2010;76:460–466
572. Hata M, Tokuyue K, Sugahara S, Kagei K, Igaki H, Hashimoto T, et al. Proton beam therapy for hepatocellular carcinoma with portal vein tumor thrombus. *Cancer* 2005;104:794–801
573. Abe T, Saitoh J, Kobayashi D, Shibuya K, Koyama Y, Shimada H, et al. Dosimetric comparison of carbon ion radiotherapy and stereotactic body radiotherapy with photon beams for the treatment of hepatocellular carcinoma. *Radiat Oncol* 2015;10:187
574. Hawkins MA, Dawson LA. Radiation therapy for hepatocellular carcinoma: from palliation to cure. *Cancer* 2006;106:1653–1663
575. Wilhelm S, Carter C, Lynch M, Lowinger T, Dumas J, Smith RA, et al. Discovery and development of sorafenib: a multikinase inhibitor for treating cancer. *Nat Rev Drug Discov* 2006;5:835–844
576. Llovet JM, Ricci S, Mazzaferro V, Hilgard P, Gane E, Blanc JF, et al. Sorafenib in advanced hepatocellular carcinoma. *N Engl J Med* 2008;359:378–390
577. Cheng AL, Kang YK, Chen Z, Tsao CJ, Qin S, Kim JS, et al. Efficacy and safety of sorafenib in patients in the Asia-Pacific region with advanced hepatocellular carcinoma: a phase III randomised, double-blind, placebo-controlled trial. *Lancet Oncol* 2009;10:25–34
578. Lencioni R, Kudo M, Ye SL, Bronowicki JP, Chen XP, Dagher L, et al. GIDEON (Global Investigation of therapeutic decisions in hepatocellular carcinoma and Of its treatment with sorafenib): second interim analysis. *Int J Clin Pract* 2014;68:609–617
579. Hollebecque A, Cattani S, Romano O, Sergent G, Mourad A, Louvet A, et al. Safety and efficacy of sorafenib in hepatocellular carcinoma: the impact of the Child-Pugh score. *Aliment Pharmacol Ther* 2011;34:1193–1201
580. Pressiani T, Boni C, Rimassa L, Labianca R, Fagioli S, Salvagni S, et al. Sorafenib in patients with Child-Pugh class A and B advanced hepatocellular carcinoma: a prospective feasibility analysis. *Ann Oncol* 2013;24:406–411
581. Ogasawara S, Chiba T, Ooka Y, Kanogawa N, Saito T, Motoyama T, et al. Sorafenib treatment in Child-Pugh A and B patients with advanced hepatocellular carcinoma: safety, efficacy and prognostic factors. *Invest New Drugs* 2015;33:729–739
582. Kim JE, Ryoo BY, Ryu MH, Chang HM, Suh DJ, Lee HC, et al. Sorafenib for hepatocellular carcinoma according to Child-Pugh class of liver function. *Cancer Chemother Pharmacol* 2011;68:1285–1290
583. Kim HY, Park JW, Joo J, Kim H, Woo SM, Lee WJ, et al. Worse outcome of sorafenib therapy associated with ascites and Child-Pugh score in advanced hepatocellular carcinoma. *J Gastroenterol Hepatol* 2013;28:1756–1761
584. D'Amico G, Garcia-Tsao G, Pagliaro L. Natural history and prognostic indicators of survival in cirrhosis: a systematic review of 118 studies. *J Hepatol* 2006;14:217–231
585. Wilhelm SM, Dumas J, Adnane L, Lynch M, Carter CA, Schutz G, et al. Regorafenib (BAY 73-4506): a new oral multikinase inhibitor of angiogenic, stromal and oncogenic receptor tyrosine kinases with potent preclinical antitumor activity. *Int J Cancer* 2011;129:245–255
586. Bruix J, Qin S, Merle P, Granito A, Huang YH, Bodoky G, et al. Regorafenib for patients with hepatocellular carcinoma who progressed on sorafenib treatment (RESORCE): a randomised,



- double-blind, placebo-controlled, phase 3 trial. *Lancet* 2017;389:56–66
587. Ogasawara S, Chiba T, Ooka Y, Suzuki E, Inoue M, Wakamatsu T, et al. Analysis of sorafenib outcome: focusing on the clinical course in patients with hepatocellular carcinoma. *PLoS One* 2016;11:e0161303
  588. Kudo M, Lencioni R, Marrero JA, Venook AP, Bronowicki JP, Chen XP, et al. Regional differences in sorafenib-treated patients with hepatocellular carcinoma: GIDEON observational study. *Liver Int* 2016;36:1196–1205
  589. Cheng AL, Kang YK, Lin DY, Park JW, Kudo M, Qin S, et al. Sunitinib versus sorafenib in advanced hepatocellular cancer: results of a randomized phase III trial. *J Clin Oncol* 2013;31:4067–4075
  590. Johnson PJ, Qin S, Park JW, Poon RT, Raoul JL, Philip PA, et al. Brivanib versus sorafenib as first-line therapy in patients with unresectable, advanced hepatocellular carcinoma: results from the randomized phase III BRISK-FL study. *J Clin Oncol* 2013;31:3517–3524
  591. Llovet JM, Decaens T, Raoul JL, Boucher E, Kudo M, Chang C, et al. Brivanib in patients with advanced hepatocellular carcinoma who were intolerant to sorafenib or for whom sorafenib failed: results from the randomized phase III BRISK-PS study. *J Clin Oncol* 2013;31:3509–3516
  592. Cainap C, Qin S, Huang WT, Chung IJ, Pan H, Cheng Y, et al. Linifanib versus Sorafenib in patients with advanced hepatocellular carcinoma: results of a randomized phase III trial. *J Clin Oncol* 2015;33:172–179
  593. Zhu AX, Park JO, Ryoo BY, Yen CJ, Poon R, Pastorelli D, et al. Ramucirumab versus placebo as second-line treatment in patients with advanced hepatocellular carcinoma following first-line therapy with sorafenib (REACH): a randomised, double-blind, multicentre, phase 3 trial. *Lancet Oncol* 2015;16:859–870
  594. Zhu AX, Rosmorduc O, Evans TR, Ross PJ, Santoro A, Carrilho FJ, et al. SEARCH: a phase III, randomized, double-blind, placebo-controlled trial of sorafenib plus erlotinib in patients with advanced hepatocellular carcinoma. *J Clin Oncol* 2015;33:559–566
  595. Zhu AX, Kudo M, Assenat E, Cattani S, Kang YK, Lim HY, et al. Effect of everolimus on survival in advanced hepatocellular carcinoma after failure of sorafenib: the EVOLVE-1 randomized clinical trial. *JAMA* 2014;312:57–67
  596. Santoro A, Rimassa L, Borbath I, Daniele B, Salvagni S, Van Laethem JL, et al. Tivantinib for second line treatment of advanced hepatocellular carcinoma: a randomized, placebo-controlled phase 2 study. *Lancet Oncol* 2013;14:55–63
  597. Qin S, Lim HY, Ryoo BY, Li C, Chen W, Cheng AL. Tolerability and activity of tepotinib in Asian patients with advanced hepatocellular carcinoma (HCC). *J Clin Oncol* 2016;34 (suppl; abstr 4072), 2016
  598. Tanwandee T, Sukeepaisarnjaroen W, Chan SL, Choo SP, Han G, Sriuranpong V, et al. A phase (Ph) II study of the efficacy and safety of the cMET inhibitor capmatinib (INC280) in patients (pts) with advanced hepatocellular carcinoma (HCC). *J Clin Oncol* 2016;34 (suppl; abstr 4074), 2016
  599. Hodi FS, O'Day SJ, McDermott DF, Weber RW, Sosman JA, Haanen JB, et al. Improved survival with ipilimumab in patients with metastatic melanoma. *N Engl J Med* 2010;363:711–723
  600. Topalian SL, Hodi FS, Brahmer JR, Gettinger SN, Smith DC, McDermott DF, et al. Safety, activity, and immune correlates of anti-PD-1 antibody in cancer. *N Engl J Med* 2012;366:2443–2454
  601. Brahmer J, Reckamp KL, Baas P, Crino L, Eberhardt WE, Poddubskaya E, et al. Nivolumab versus docetaxel in advanced squamous-cell non-small-cell lung cancer. *N Engl J Med* 2015;373:123–135
  602. Robert C, Schachter J, Long GV, Arance A, Grob JJ, Mortier L, et al. Pembrolizumab versus ipilimumab in advanced melanoma. *N Engl J Med* 2015;372:2521–2532
  603. Garon EB, Rizvi NA, Hui R, Leighl N, Balmanoukian AS, Eder JP, et al. Pembrolizumab for the treatment of non-small-cell lung cancer. *N Engl J Med* 2015;372:2018–2028
  604. Sangro B, Gomez-Martin C, de la Mata M, Inarrairaegui M, Garralda E, Barrera P, et al. A clinical trial of CTLA-4 blockade with tremelimumab in patients with hepatocellular carcinoma and chronic hepatitis C. *J Hepatol* 2013;59:81–88
  605. El-Khoueiry AB, Sangro B, Yau T, Crocenzi TS, Kudo M, Hsu C, et al. Nivolumab in patients with advanced hepatocellular carcinoma (CheckMate 040): an open-label, non-comparative, phase 1/2 dose escalation and expansion trial. *Lancet* 2017 (Epub ahead of print)



# Liver Resection for Hepatocellular Carcinoma Associated With Hepatic Vein Invasion: A Japanese Nationwide Survey

Takashi Kokudo,<sup>1,2</sup> Kiyoshi Hasegawa,<sup>1</sup> Yutaka Matsuyama,<sup>3</sup> Tadatoshiki Takayama,<sup>4</sup> Namiki Izumi,<sup>5</sup> Masumi Kadoya,<sup>6</sup> Masatoshi Kudo,<sup>7</sup> Shoji Kubo,<sup>8</sup> Michiie Sakamoto,<sup>9</sup> Osamu Nakashima,<sup>10</sup> Takashi Kumada,<sup>11</sup> and Norihiro Kokudo<sup>1</sup>; for the Liver Cancer Study Group of Japan

Because of the rarity of hepatic vein tumor thrombus (HVTT) compared with portal vein tumor thrombus (PVTT) in patients with hepatocellular carcinoma, little is known about this disease entity. The aim of this study was to evaluate the prognosis of each treatment modality for HVTT through an analysis of data collected in a Japanese nationwide survey. We analyzed data for 1,021 Child-Pugh A hepatocellular carcinoma patients with HVTT without inferior vena cava invasion registered between 2000 and 2007. Of these patients, 540 who underwent liver resection (LR) and 481 who received other treatments were compared. Propensity scores were calculated, and we successfully matched 223 patients (49.0% of the LR group). The median survival time in the LR group was 2.89 years longer than that in the non-LR group (4.47 versus 1.58 years,  $P < 0.001$ ) and 1.61 years longer than that in the non-LR group (3.42 versus 1.81 years,  $P = 0.023$ ) in a propensity score-matched cohort. After curative resection, median survival times were similar between patients with HVTT in the peripheral hepatic vein and those with HVTT in the major hepatic vein (4.85 versus 4.67 years,  $P = 0.974$ ). In the LR group, the postoperative 90-day mortality rate was 3.4% (16 patients). In patients without PVTT, the median survival time was significantly better than that in patients with PVTT (5.67 versus 1.88 years,  $P < 0.001$ ). **Conclusion:** LR is associated with a good prognosis in hepatocellular carcinoma patients with HVTT, especially in patients without PVTT. (HEPATOLOGY 2017;66:510-517).

According to the American Association for the Study of Liver Diseases/Barcelona Clinic for Liver Cancer staging system and treatment guidelines, hepatocellular carcinoma (HCC) associated with macroscopic vascular invasion is regarded as an advanced stage of disease with almost zero hope for a cure.<sup>(1)</sup> The only proposed treatment option for this group of patients is palliative sorafenib chemotherapy.<sup>(2)</sup> However, the reported median survival time

(MST) of patients with macroscopic vascular invasion treated with sorafenib is as short as 8.1 months.<sup>(3)</sup> Recently, we reported that the survival benefit of liver resection (LR) in HCC patients with portal vein tumor thrombus (PVTT) is significant, resulting in an MST of 2.87 years with a 5-year survival rate of 39.1% in a Japanese nationwide survey.<sup>(4)</sup> Therefore, surgical intervention might also play some role in the treatment of patients with hepatic vein tumor thrombus (HVTT).

*Abbreviations:* CI, confidence interval; HCC, hepatocellular carcinoma; HR, hazard ratio; HVTT, hepatic vein tumor thrombus; IVCTT, inferior vena cava tumor thrombus; LR, liver resection; mHVTT, major HVTT; MST, median survival time; pHVTT, peripheral HVTT; PVTT, portal vein tumor thrombus; TACE, transcatheter arterial chemoembolization.

Received February 3, 2017; accepted April 18, 2017.

Additional Supporting Information may be found at [onlinelibrary.wiley.com/doi/10.1002/hep.29225/supinfo](http://onlinelibrary.wiley.com/doi/10.1002/hep.29225/supinfo).

Supported by a grant-in-aid for a nationwide follow-up survey of primary liver cancer.

Copyright © 2017 by the American Association for the Study of Liver Diseases.

View this article online at [wileyonlinelibrary.com](http://wileyonlinelibrary.com).

DOI 10.1002/hep.29225

*Potential conflict of interest:* Dr. Izumi is on the speakers' bureau for Gilead, Bayer, and Otsuka. Dr. Kokudo received grants from Bayer and Daiippon Sumitomo.

Because of its rarity, compared with PVTT, little is known about HVTT. As a result of recent advances in surgical techniques and perioperative management, aggressive surgical resection for HCC with HVTT has been proposed by several tertiary centers.<sup>(5-8)</sup> Recently, a member of our group reported the largest single-center case series of patients with HVTT who had undergone LR, resulting in an MST of longer than 4 years.<sup>(5)</sup> However, the number of patients enrolled in such studies is generally too small to lead to a definite conclusion.

The aim of this study was to evaluate the survival benefit of LR for HCC patients with hepatic vein invasion through analysis of a large-scale prospective cohort study based on the latest data available from a Japanese nationwide survey.

## Patients and Methods

### PATIENTS

Since 1965, the Liver Cancer Study Group of Japan has been performing nationwide surveys of patients with primary liver cancer. Patients are registered and followed up as reported.<sup>(9)</sup> The collection and registration of data for patients with HCC were performed with the approval of each institution participating in the nationwide survey. The number of registered institutions was 645, accounting for approximately one third of all HCC patients treated in Japan. To analyze the recent results, we set the study period from 2000 to 2007 (latest data available). The presence of HVTT and PVTT was determined based on the radiological

findings. HVTT was categorized as tumor thrombosis in a peripheral hepatic vein (pHVTT, Vv1), in a major hepatic vein (mHVTT, Vv2), or in the inferior vena cava (IVCTT, Vv3); and PVTT was categorized into main trunk/contralateral branch (Vp4), first-order branch (Vp3), second-order branch (Vp2), and third-order branch (Vp1), according to the Japanese staging system.<sup>(10)</sup> Postoperative mortality was defined as any death other than tumor progression within 90 days of surgery.

### STATISTICAL ANALYSIS

Statistical analyses were performed using JMP software, version 12.2.0 (SAS Institute Inc., Cary, NC). Categorical variables were analyzed using the chi-squared test. Continuous variables were analyzed using the Wilcoxon rank-sum test. Overall survival curves were determined using the Kaplan-Meier method and compared using the log-rank test. Propensity scores were created using logistic regression modeling of the probability of a patient undergoing LR based on age, sex, viral infection (hepatitis B and/or C virus), positive serum alpha-fetoprotein ( $\geq 15$  ng/mL), serum albumin (grams per deciliter),  $\log_{10}$ (total bilirubin) (milligrams per deciliter), prothrombin time (percentage), platelet count ( $10^4$  per microliter), gastroesophageal varices, multiple tumors (three or more), tumor size (centimeters), extent of HVTT, and presence of PVTT (Vp2-3). Because the  $\log_{10}$ (total bilirubin) tended to show a normal distribution for the entire cohort compared to serum total bilirubin level, this parameter was used instead (Supporting Fig. S1). A 1:1 match without

### ARTICLE INFORMATION:

From the <sup>1</sup>Hepato-Biliary-Pancreatic Surgery Division, Department of Surgery, Graduate School of Medicine, University of Tokyo, Tokyo, Japan; <sup>2</sup>Division of Gastroenterological Surgery, Saitama Cancer Center, Saitama, Japan; <sup>3</sup>Department of Biostatistics, School of Public Health, University of Tokyo, Tokyo, Japan; <sup>4</sup>Department of Digestive Surgery, Nihon University School of Medicine, Tokyo, Japan; <sup>5</sup>Department of Gastroenterology, Musashino Red Cross Hospital, Tokyo, Japan; <sup>6</sup>Department of Radiology, Shinshu University School of Medicine, Matsumoto, Japan; <sup>7</sup>Department of Gastroenterology and Hepatology, Kinki University School of Medicine, Osaka, Japan; <sup>8</sup>Department of Hepato-Biliary-Pancreatic Surgery, Osaka City University Graduate School of Medicine, Osaka, Japan; <sup>9</sup>Department of Pathology, Keio University School of Medicine, Tokyo, Japan; <sup>10</sup>Department of Clinical Laboratory Medicine, Kurume University Hospital, Kurume, Japan; <sup>11</sup>Department of Gastroenterology, Ogaki Municipal Hospital, Ogaki, Japan.

### ADDRESS CORRESPONDENCE AND REPRINT REQUESTS TO:

Norihiro Kokudo, M.D.  
Hepato-Biliary-Pancreatic Surgery Division  
Department of Surgery  
Graduate School of Medicine  
University of Tokyo

7-3-1 Hongo, Bunkyo-ku  
Tokyo, Japan  
E-mail: KOKUDO-2SU@h.u-tokyo.ac.jp  
Tel: +81338155411

TABLE 1. Baseline Characteristics of 1,266 Patients With Hepatic Vein Invasion According to Treatment Type

Patient Characteristics	LR Group (n = 651)*	Non-LR Group (n = 615)*	P
Age (years)	64.0 (11.0)	68.3 (10.6)	<0.001
Sex (male/female)	542/109 (83.3/16.7)	489/126 (79.5/20.5)	0.087
Hepatitis B virus infection	166 (25.8)	97 (15.8)	<0.001
Hepatitis C virus infection	269 (41.8)	340 (55.6)	<0.001
Serum albumin (g/dL)	3.92 (0.45)	3.74 (0.49)	<0.001
Serum total bilirubin (mg/dL)	0.82 (0.51)	0.98 (0.74)	<0.001
Prothrombin time (%)	88.7 (17.1)	85.9 (15.9)	0.001
Platelet count ( $10^4/\mu\text{L}$ )	19.0 (8.69)	16.5 (8.68)	<0.001
Gastroesophageal varices	52 (8.4)	156 (25.6)	<0.001
Alpha-fetoprotein ( $\geq 15$ ng/mL)	434 (67.2)	459 (75.0)	0.002
Multiple tumors ( $\geq 3$ )	126 (19.7)	283 (46.6)	<0.001
Tumor size (cm)	8.78 (5.13)	7.77 (5.00)	<0.001
Extent of PVTT			<0.001
Vp1	191 (29.3)	128 (20.8)	
Vp2	137 (21.0)	157 (25.5)	
Vp3	92 (14.1)	173 (28.1)	
Extent of HVTT			0.035
pHVTT	332 (51.0)	274 (44.6)	
mHVTT	208 (32.0)	207 (33.7)	
IVCTT	111 (17.1)	134 (21.8)	

Data are the mean (standard deviation) or number (percentage) unless otherwise indicated.

\*Missing data were not included for baseline characteristics.

replacement was performed using logit (propensity score) through the nearest available matching, setting the caliper at 0.05. A multivariate analysis was performed using a Cox proportional hazards model and the backward elimination procedure.  $P < 0.10$  was set as the cutoff value for the elimination. The following nine variables were examined as potential risk factors: age  $>70$  years, gastroesophageal varices, platelet count  $<100,000/\mu\text{L}$ , positive serum alpha-fetoprotein ( $\geq 15$  ng/mL), number of tumors  $\geq 3$ , tumor size (centimeters), presence of PVTT (Vp2-3), mHVTT, and LR. Liver cirrhosis and poor cancer cell differentiation were also examined in patients who underwent LR. All statistical analyses were two-tailed.  $P < 0.05$  was considered to indicate statistical significance.

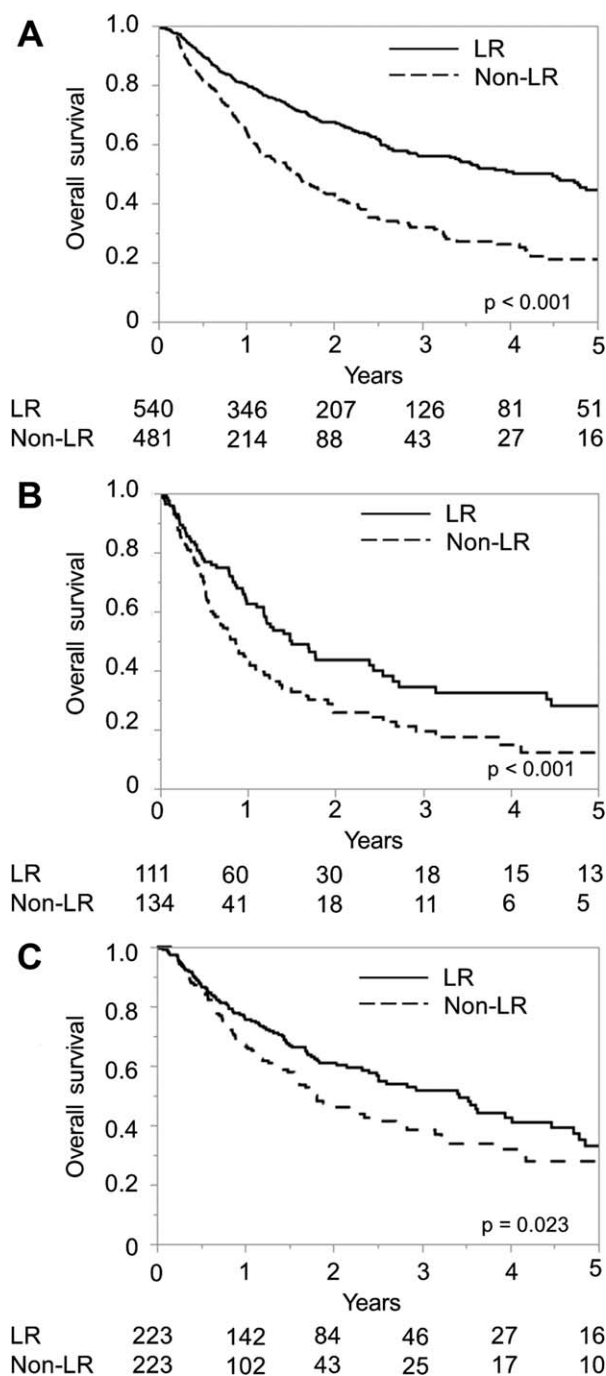
## Results

A total of 77,268 patients with HCC were registered between 2000 and 2007. Among these patients, 11,432 with missing data regarding HVTT and 62,904 without HVTT were excluded from the present analysis. Among the remaining 2,932 patients with HVTT, 740 Child-Pugh B patients, 368 Child-Pugh C patients, and 54 patients with missing data regarding their Child-Pugh classification and/or main treatment were excluded. Among the 1,770 Child-

Pugh A patients with HVTT, 264 Vp4 patients, 235 patients with distant metastasis, and 5 patients with missing data regarding their survival time were excluded. Finally, a total of 1,266 Child-Pugh A patients with HVTT were included in the present analysis. The extent of HVTT was as follows: pHVTT, 606 patients (47.9%); mHVTT, 415 patients (32.8%); and IVCTT, 245 patients (19.4%).

The median follow-up period was 2.08 years (95% confidence interval [CI] 1.90-2.26). The MST after diagnosis according to the extent of HVTT was as follows: pHVTT, 3.15 years (95% CI 2.50-3.84); mHVTT, 2.03 years (95% CI 1.68-2.49); and IVCTT, 1.16 years (95% CI 0.92-1.46). Hepatitis C virus infection, defined as a positive status for hepatitis C virus antibody, was seen in 609 patients (48.5%). Hepatitis B virus infection, defined as a positive hepatitis B surface antigen status, was present in 263 patients (20.9%).

Of the 1,266 patients with HVTT, 651 underwent LR (LR group) and 615 received other treatments (non-LR group). In the non-LR group, 335 patients (54.5%) received transcatheter arterial chemoembolization (TACE), 143 patients (23.3%) received systemic or hepatic arterial infusion chemotherapy, 50 patients (8.1%) received ablation therapy, 69 (11.2%) patients received best supportive care, and 18 patients (2.9%) underwent other treatments. Because sorafenib was only available after 2009 in Japan, none of the



**FIG. 1.** Kaplan-Meier estimates for survival according to treatment type for (A) 1,021 patients with HVTT, (B) 245 patients with IVCTT, and (C) 446 patients with HVTT who were matched according to propensity score. Numbers below the x axis indicate the number of patients at risk.

patients received sorafenib as an initial treatment. Table 1 shows the characteristics of the patients according to the treatment procedure: the non-LR

group tended to have a poorer liver function status and a more advanced stage of disease compared with the LR group.

In the pHVTT/mHVTT patients, the MST after diagnosis for the LR group was 2.89 years longer than that for the non-LR group (4.47 years [95% CI 3.40–5.15] versus 1.58 years [95% CI 1.30–1.83];  $P < 0.001$ ) (Fig. 1A). The survival rates at 1, 3, and 5 years after diagnosis were 80.0%, 56.6%, and 44.2% for the LR group and 63.7%, 32.6%, and 20.3% for the non-LR group, respectively. In the non-LR group, the MST after diagnosis according to treatments was as follows: TACE, 1.61 years (95% CI 1.29–2.01); systemic or hepatic arterial infusion chemotherapy, 0.87 years (95% CI 0.74–1.13); and best supportive care, 0.52 years (95% CI 0.24–0.95). A multivariate analysis performed to determine the risk factors for overall survival also identified non-LR treatment (hazard ratio [HR] = 1.61, 95% CI 1.30–2.01;  $P < 0.001$ ) as one of the most significant risk factors (Supporting Table S1). The reason for death is shown in Supporting Table S2. The frequency of non-cancer-related deaths was comparable in the two groups (10.6% versus 11.9%,  $P = 0.512$ ), and the median cancer-specific survival time for the LR group was 3.91 years longer than that for the non-LR group (6.12 years, 95% CI 4.78–not available, versus 2.21 years, 95% CI 1.81–2.85;  $P < 0.001$ ) (Supporting Fig. S2).

On the other hand, in IVCTT patients, the MST after diagnosis for the LR group was 0.64 years longer than that for the non-LR group (1.48 years, 95% CI 1.16–2.52, versus 0.84 years, 95% CI 0.61–1.07;  $P < 0.001$ ) (Fig. 1B). The survival rates at 1 and 3 years after diagnosis were 63.2% and 33.1% for the LR group and 42.3% and 20.1% for the non-LR group, respectively. In the non-LR group, the MST after diagnosis according to treatments was as follows: TACE, 0.84 years (95% CI 0.58–1.17); systemic or hepatic arterial infusion chemotherapy, 1.28 years (95% CI 0.51–2.41); and best supportive care, 0.49 years (95% CI 0.18–0.93).

To confirm the survival benefit of LR in Child-Pugh A patients with pHVTT/mHVTT, the propensity scores were calculated for 455 patients in the LR group and 380 patients in the non-LR group. We successfully matched 223 patients in the LR group (49.0% of the LR group) and 223 patients in the non-LR group (58.7% of the non-LR group) based on their propensity scores. In the non-LR group, 126 patients (56.5%) received TACE, 38 patients (17.0%) received systemic or hepatic arterial infusion chemotherapy, 37



**TABLE 2. Baseline Characteristics of 446 Patients With HVTT Matched by Propensity Score According to Treatment Type**

Patient Characteristics	LR Group (n = 223)	Non-LR Group (n = 223)	P
Age (years)	66.3 (10.4)	67.5 (11.0)	0.139
Sex (male/female)	187/36 (83.9/16.1)	183/40 (82.1/17.9)	0.614
Viral infection	150 (67.3)	152 (68.2)	0.840
Serum albumin (g/dL)	3.82 (0.44)	3.86 (0.44)	0.543
Serum total bilirubin (mg/dL)	0.84 (0.31)	0.90 (0.59)	0.749
Prothrombin time (%)	87.3 (18.2)	87.8 (15.9)	0.883
Platelet count ( $10^4/\mu\text{L}$ )	16.9 (7.31)	17.5 (9.18)	0.983
Gastroesophageal varices	30 (13.5)	26 (11.7)	0.567
Alpha-fetoprotein ( $\geq 15$ ng/mL)	152 (68.2)	150 (67.3)	0.840
Tumor size (cm)	8.07 (4.36)	7.93 (5.78)	0.184
Multiple tumors ( $\geq 3$ )	74 (33.2)	70 (31.4)	0.685
pHVT/mHVT	129/94 (57.9/42.2)	126/97 (56.5/43.5)	0.774
PVTT (Vp2-3)	90 (40.4)	90 (40.4)	1.000

Data are the mean (standard deviation) or number (percentage) unless otherwise indicated.

patients (16.6%) received ablation therapy, 15 (6.7%) patients received best supportive care, and 7 patients (3.1%) underwent other treatments. Table 2 shows that the main characteristics of these patients did not differ between the two groups. The MST after diagnosis in the LR group was 1.61 years longer than that in the non-LR group (3.42 years, 95% CI 2.40-4.47, versus 1.81 years, 95% CI 1.48-2.48;  $P = 0.023$ ) (Fig. 1C). Furthermore, the survival rates at 1, 3, and 5 years after diagnosis were 75.6%, 51.8%, and 33.1% for the LR group and 67.1%, 37.0%, and 27.9% for the non-LR group, respectively.

The operative procedures and outcomes of the patients in the LR group who underwent curative resection according to the extent of HVTT are shown in Table 3. Major hepatectomy was the most frequent procedure for all types of HVTT. The MST after surgery according to the extent of HVTT was as follows: pHVT, 4.85 years (95% CI 3.38-not available); mHVT, 4.67 years (95% CI 3.32-5.88); and IVCT, 1.37 years (95% CI 1.07-4.21). The survival curves were similar between patients with pHVT and

those with mHVT (Fig. 2A). The recurrence-free survival after surgery according to the extent of HVTT was as follows: pHVT, 2.36 years (95% CI 1.38-3.17); mHVT, 0.88 years (95% CI 0.75-1.32); and IVCT, 0.82 years (95% CI 0.42-1.10). The most frequent site of recurrence was intrahepatic for patients with pHVT and mHVT, whereas distant metastasis was the most frequent site for patients with IVCT. The postoperative 90-day mortality rate was 4.2% (23 patients) for the entire population and was higher for patients with IVCT (pHVT, 4.3%; mHVT, 1.8%; IVCT, 9.9%). A multivariate analysis performed to determine the risk factors for overall survival after LR in patients with pHVT/mHVT identified the presence of PVTT (Vp2-3) (HR = 1.91, 95% CI 1.34-2.70;  $P < 0.001$ ), number of tumors  $\geq 3$  (HR = 1.88, 95% CI 1.28-2.71;  $P = 0.002$ ), gastroesophageal varices (HR = 1.85, 95% CI 1.13-2.90;  $P = 0.016$ ), and poor cancer cell differentiation (HR = 1.57, 95% CI 1.02-2.35;  $P = 0.040$ ) as significant risk factors (Table 4). In patients without PVTT (Vp2-3), the MST was significantly better than

**TABLE 3. Operative Procedures and Outcomes for Patients Who Underwent Curative Resection**

	pHVT (n = 305)*	mHVT (n = 170)*	IVCT (n = 71)*
Major hepatectomy <sup>†</sup>	175 (59.9)	124 (76.5)	51 (75.0)
Median survival time (years)	4.85 (95% CI 3.38-n.a.)	4.67 (95% CI 3.32-5.88)	1.37 (95% CI 1.07-4.21)
Recurrence-free survival (years)	2.36 (95% CI 1.38-3.17)	0.88 (95% CI 0.75-1.32)	0.82 (95% CI 0.42-1.10)
Site of the first recurrence			
Intrahepatic	92 (32.7)	60 (38.0)	17 (23.9)
Distant metastasis	14 (5.0)	18 (11.4)	9 (12.7)
Both	17 (6.0)	16 (10.1)	15 (21.1)
Median hospital stay (days)	21 (IQR 15-36)	23 (IQR 16-46)	26 (IQR 18-55)
90-Day mortality	13 (4.3)	3 (1.8)	7 (9.9)

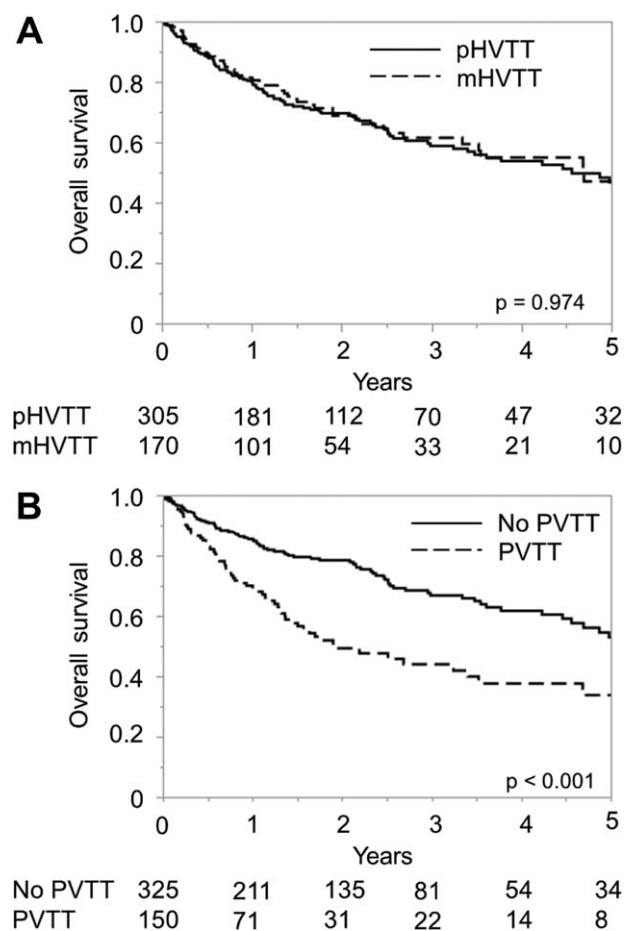
Data are the mean (standard deviation) or number (percentage) unless otherwise indicated.

\*Missing data were not included for baseline characteristics.

<sup>†</sup>More than three Couinaud's segments.

Abbreviation: n.a., not available.





**FIG. 2.** Kaplan-Meier estimates for survival after curative resection for patients with HVT. (A) pHVTT and mHVTT. (B) Presence or absence of PVTT (Vp2-3). Numbers below the x axis indicate the number of patients at risk.

that in patients with PVTT (5.67 years, 95% CI, 4.54–not available, versus 1.88 years, 95% CI 1.35–3.50;  $P < 0.001$ ) (Fig. 2B).

## Discussion

The current study revealed that LR has a significant survival benefit with an acceptable postoperative mortality rate for patients with HVT, even in the propensity score-matched patient groups. Coexisting PVTT was a significant risk factor for survival after LR, and patients without PVTT had an MST of more than 5 years. These results indicate that HVT is different from PVTT and should not be considered as an advanced stage for palliative treatment.

A worldwide consensus on the management of HCC associated with macroscopic vascular invasion does not

yet exist. Surgical resection has been performed successfully in patients with PVTT in Eastern countries,<sup>(7,11)</sup> and several reports arising from Western countries also discuss this approach.<sup>(8,12)</sup> On the other hand, little is known about HVT. This lack of knowledge is probably because HVT is relatively rare, compared with PVTT, in patients with HCC.<sup>(13)</sup> Indeed, in this nationwide survey, hepatic vein invasion was observed in only 4.5% of the entire population. As a result, most studies have reported the results for HVT together with those for PVTT, and studies focusing on HVT alone have been rare.<sup>(3,7,14)</sup> Thus, the poor prognosis of macroscopic vascular invasion may be highly affected by the population with PVTT, and the results concerning patients with HVT might not have been correctly evaluated. Considering that the MST after LR was more than 4 years in patients with HVTs and more than 5 years in patients without PVTT, HVT *per se* is different from PVTT. As a prospective trial other than a nationwide survey would be difficult to conduct because of the rarity of this disease, the present study provides the highest level of evidence available regarding this issue.

Surgical treatment for HVTs is technically demanding, and a major hepatectomy is often required. The 90-day mortality rate was higher in patients with HVT than in those without (3.4% versus 1.2%,  $P < 0.001$ ). However, there was no difference between the two groups in patients who underwent major hepatectomy (3.3% versus 2.0%,  $P = 0.147$ ). These results are comparable with those of other reports.<sup>(15,16)</sup> In addition, although complication data were not available, the postoperative hospital stay was also comparable to that reported in a previous Japanese nationwide survey.<sup>(15)</sup> Thus, the present findings justify the consideration of surgical treatment for HCC patients with HVT.

Sorafenib has been established as a new standard treatment option for advanced HCC.<sup>(1,2)</sup> The effectiveness of sorafenib for HCC patients with macroscopic vascular invasion has also been reported.<sup>(3)</sup> Since sorafenib became available in Japan in 2009, hardly any patients received it during the presently reported study period. Therefore, the prognosis of the

**TABLE 4. Multivariate Analysis to Identify Prognostic Factors Associated With Survival After Liver Resection Among Patients With HVT**

Risk Factors	<i>P</i>	HR (95% CI)
Number of tumors $\geq 3$	0.002	1.88 (1.28–2.71)
PVTT (Vp 2–3)	$<0.001$	1.91 (1.34–2.70)
Gastroesophageal varices	0.016	1.85 (1.13–2.90)
Poor cancer cell differentiation	0.040	1.57 (1.02–2.35)

non-LR group might be slightly better now, thanks to the introduction of sorafenib. However, sorafenib is essentially a palliative treatment; and the expected survival time is normally no longer than 1 year in patients with macroscopic vascular invasion, and the average prolongation of survival is 3.2 months.<sup>(3)</sup> Considering that the MST was more than 4 years and the average prolongation of survival was 2.89 years in the LR group, the survival benefit of LR in patients with HVTT is likely to exist even in the present era of sorafenib treatment.

Available evidence regarding the most suitable treatment strategies for IVCTT is extremely limited because of the rarity of the disease. Indeed, in our nationwide surveillance, the frequency of IVCTT was as small as 1.4%. Surgical resection for IVCTT patients has been reported to result in an MST similar to that in the present report.<sup>(5,13)</sup> However, considering that complete resection is difficult in IVCTT patients and the MSTs were similar between the LR group and the chemotherapy group (1.48 versus 1.28 years), the surgical indications for IVCTT patients require further investigation and comparison with sorafenib treatment. Furthermore, neoadjuvant and/or adjuvant treatment including sorafenib and/or radiotherapy together with LR might be a promising strategy for IVCTT patients.<sup>(17,18)</sup>

In a comparison between the IVCTT and mHVTT groups, while the recurrence-free survival was similar, the MST was significantly poorer in the IVCTT group. This finding can be explained by differences in the sites of recurrence (Table 3). In the mHVTT group, the most frequent type of recurrence was intrahepatic limited recurrence (63.8%), while distant metastasis and/or intrahepatic recurrence were the most common sites in the IVCTT group (58.5%). As long as the recurrence is confined to the liver, at least one of several effective treatment options can be selected, including repeated LR, radiofrequency ablation, and TACE. Therefore, HVTT by itself is not a systemic disease, and control of intrahepatic recurrence should be undertaken in these cases as in cases of HCC without vascular invasion. Furthermore, aggressive surgical treatment might be justifiable for HVTT to avoid progression to IVCTT, which can be considered a systemic disease in which distant metastasis is likely to occur frequently. These results were similar to those of our recent single-center report.<sup>(5)</sup>

Concerning other treatment modalities for HVTT, the MSTs were similar in HVTT patient groups treated with TACE (1.61 versus 1.38 years), chemotherapy

(0.87 versus 0.88 years), and best supportive care (0.52 versus 0.36 years) compared with those in PVTT patient groups.<sup>(4)</sup> On the other hand, the MST was significantly better in patients with HVTT than in those with PVTT after LR (4.47 versus 2.87 years), indicating that the survival benefit of LR is more significant among patients with HVTT than among those with PVTT. Recently, yttrium-90 radioembolization and other new radiation procedures have produced favorable outcomes in patients with macroscopic vascular invasion.<sup>(19–22)</sup> However, such studies are not specified for patients with HVTTs, and future study is essential.

One of the limitations of our study was that although we tried to eliminate the selection bias of the LR group through propensity score-based matching, the possibility of other biases that were not considered in the present study certainly exists. To the best of our knowledge, this is the largest case series to be reported for HVTT. Considering that the MST was more than 4 years after LR, LR should be considered for patients with HVTT before resorting to palliative treatment, including sorafenib. Another limitation is that, although this article demonstrated a survival benefit of LR in HCC patients with HVTT using data from a nationwide survey, the study was limited to patients in Japan, and the etiology of HCC in Japan is mainly viral infection, especially infection with the hepatitis C virus. Thus, these results should be validated using an international database.

Another limitation is the low frequency of HVTT in the entire HCC population. Particularly, patients who are considered to show the most benefit from surgical resection, i.e., those without IVCTT or PVTT, are estimated to be a small proportion. However, due to its rarity, evidence concerning this disease entity is scarce, and a prospective trial is theoretically difficult. Although the number is small, the present report would certainly contribute to prolonging the survival in some patients who suffer from HCC with HVTT.

In conclusion, LR is associated with a good prognosis, with an MST of more than 4 years in HCC patients with HVTT. As long as the hepatic vein invasion is limited to the major hepatic veins, LR should be the treatment of first choice, especially in patients with good liver function.

## REFERENCES

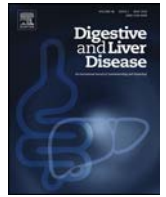
- 1) Forner A, Llovet JM, Bruix J. Hepatocellular carcinoma. *Lancet* 2012;379:1245–1255.

- 2) Llovet JM, Ricci S, Mazzaferro V, Hilgard P, Gane E, Blanc JF, et al. Sorafenib in advanced hepatocellular carcinoma. *N Engl J Med* 2008;359:378-390.
- 3) Bruix J, Raoul JL, Sherman M, Mazzaferro V, Bolondi L, Craxi A, et al. Efficacy and safety of sorafenib in patients with advanced hepatocellular carcinoma: subanalyses of a phase III trial. *J Hepatol* 2012;57:821-829.
- 4) Kokudo T, Hasegawa K, Matsuyama Y, Takayama T, Izumi N, Kadoya M, et al. Survival benefit of liver resection for hepatocellular carcinoma associated with portal vein invasion. *J Hepatol* 2016;65:938-943.
- 5) Kokudo T, Hasegawa K, Yamamoto S, Shindoh J, Takemura N, Aoki T, et al. Surgical treatment of hepatocellular carcinoma associated with hepatic vein tumor thrombosis. *J Hepatol* 2014; 61:583-588.
- 6) **Zhang YF, Wei W**, Guo ZX, Wang JH, Shi M, Guo RP. Hepatic resection versus transcatheter arterial chemoembolization for the treatment of hepatocellular carcinoma with hepatic vein tumor thrombus. *Jpn J Clin Oncol* 2015;45:837-843.
- 7) **Shaohua L, Qiaoxuan W**, Peng S, Qing L, Zhongyuan Y, Ming S, et al. Surgical strategy for hepatocellular carcinoma patients with portal/hepatic vein tumor thrombosis. *PLoS One* 2015;10:e0130021.
- 8) Pesi B, Ferrero A, Grazi GL, Cescon M, Russolillo N, Leo F, et al. Liver resection with thrombectomy as a treatment of hepatocellular carcinoma with major vascular invasion: results from a retrospective multicentric study. *Am J Surg* 2015;210:35-44.
- 9) Hasegawa K, Kokudo N, Makuuchi M, Izumi N, Ichida T, Kudo M, et al. Comparison of resection and ablation for hepatocellular carcinoma: a cohort study based on a Japanese nationwide survey. *J Hepatol* 2013;58:724-729.
- 10) Kudo M, Izumi N, Kokudo N, Matsui O, Sakamoto M, Nakashima O, et al. Management of hepatocellular carcinoma in Japan: Consensus-Based Clinical Practice Guidelines proposed by the Japan Society of Hepatology (JSH) 2010 updated version. *Dig Dis* 2011;29:339-364.
- 11) **Minagawa M, Makuuchi M**. Treatment of hepatocellular carcinoma accompanied by portal vein tumor thrombus. *World J Gastroenterol* 2006;12:7561-7567.
- 12) Roayaie S, Jibara G, Taouli B, Schwartz M. Resection of hepatocellular carcinoma with macroscopic vascular invasion. *Ann Surg Oncol* 2013;20:3754-3760.
- 13) Wang Y, Yuan L, Ge RL, Sun Y, Wei G. Survival benefit of surgical treatment for hepatocellular carcinoma with inferior vena cava/right atrium tumor thrombus: results of a retrospective cohort study. *Ann Surg Oncol* 2013;20:914-922.
- 14) Pawlik TM, Poon RT, Abdalla EK, Ikai I, Nagorney DM, Belghiti J, et al. Hepatectomy for hepatocellular carcinoma with major portal or hepatic vein invasion: results of a multicenter study. *Surgery* 2005;137:403-410.
- 15) Kenjo A, Miyata H, Gotoh M, Kitagawa Y, Shimada M, Baba H, et al. Risk stratification of 7,732 hepatectomy cases in 2011 from the National Clinical Database for Japan. *J Am Coll Surg* 2014;218:412-422.
- 16) Li GZ, Speicher PJ, Lidsky ME, Darrabie MD, Scarborough JE, White RR, et al. Hepatic resection for hepatocellular carcinoma: do contemporary morbidity and mortality rates demand a transition to ablation as first-line treatment? *J Am Coll Surg* 2014;218:827-834.
- 17) Kermiche-Rahali S, Di Fiore A, Drioux F, Di Fiore F, François A, Scotté M. Complete pathological regression of hepatocellular carcinoma with portal vein thrombosis treated with sorafenib. *World J Surg Oncol* 2013;11:171.
- 18) Takano M, Kokudo T, Miyazaki Y, Kageyama Y, Takahashi A, Amikura K, et al. Complete response with sorafenib and transcatheter arterial chemoembolization in unresectable hepatocellular carcinoma. *World J Gastroenterol* 2016;22:9445-9450.
- 19) **Edeline J, Crouzet L**, Campillo-Gimenez B, Rolland Y, Pracht M, Guillygomarc'h A, et al. Selective internal radiation therapy compared with sorafenib for hepatocellular carcinoma with portal vein thrombosis. *Eur J Nucl Med Mol Imaging* 2016;43:635-643.
- 20) **Garin E, Rolland Y**, Edeline J, Icard N, Lenoir L, Laffont S, et al. Personalized dosimetry with intensification using <sup>90</sup>Y-loaded glass microsphere radioembolization induces prolonged overall survival in hepatocellular carcinoma patients with portal vein thrombosis. *J Nucl Med* 2015;56:339-346.
- 21) Memon K, Kulik L, Lewandowski RJ, Mulcahy MF, Benson AB, Ganger D, et al. Radioembolization for hepatocellular carcinoma with portal vein thrombosis: impact of liver function on systemic treatment options at disease progression. *J Hepatol* 2013;58:73-80.
- 22) **Xi M, Zhang L**, Zhao L, Li QQ, Guo SP, Feng ZZ, et al. Effectiveness of stereotactic body radiotherapy for hepatocellular carcinoma with portal vein and/or inferior vena cava tumor thrombosis. *PLoS One* 2013;8:e63864.

Author names in bold designate shared co-first authorship.

## Supporting Information

Additional Supporting Information may be found at [onlinelibrary.wiley.com/doi/10.1002/hep.29225/supinfo](http://onlinelibrary.wiley.com/doi/10.1002/hep.29225/supinfo).



## Image of the Month

## Portal vein stenting for portal vein stenosis caused by bile duct cancer

Ken Kamata<sup>a</sup>, Mamoru Takenaka<sup>a,\*</sup>, Masakatsu Tsurusaki<sup>b</sup>, Masatoshi Kudo<sup>a</sup><sup>a</sup> Department of Gastroenterology and Hepatology, Kindai University Faculty of Medicine, Japan<sup>b</sup> Department of Radiology, Kindai University Faculty of Medicine, Japan

Portal vein stenting has been used in the treatment of malignant portal venous obstruction [1]. The patient was a 74-year-old man who underwent left hepatic trisegmentectomy and biliary reconstruction for hilar cholangiocarcinoma. Lung metastasis occurred 3 months after surgery and chemotherapy was initiated. Four months later, the patient experienced hepatic encephalopathy with elevated serum ammonia concentration (126  $\mu\text{g/dL}$ ). Abdominal CT confirmed portal vein stenosis due to lymph node recurrence around the hilar bile duct (Fig. 1). As conservative treatment was ineffective, he underwent portal vein stenting. Segment 5 of the portal vein was punctured with a 21-gauge needle under guidance of ultrasonography and fluoroscopy. Portal portography distal to the point of portal stenosis confirmed collateral circulation via the esophageal veins. Two stents, one of diameter 8 mm and length 4 cm and the other of diameter 8 mm and length 3 cm (S.M.A.R.T. CONTROL stents) were inserted into the site of portal vein stenosis. Portal portography after stent deployment showed the disappearance of hepatofugal collateral circulation (Fig. 2). His

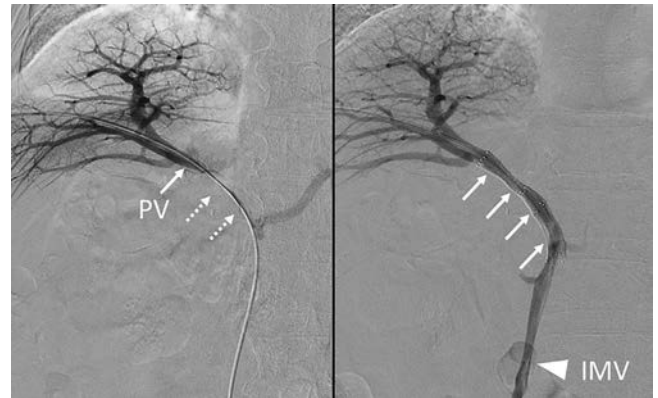


Fig. 2.

serum ammonia concentration decreased to 35  $\mu\text{g/dL}$  3 days after the procedure, and recurrence of hepatic encephalopathy was not observed.

## Disclosure

All authors disclosed no financial relationships relevant to this publication.

## References

- [1] Yamakado K, Nakatsuka A, Tanaka N, et al. Malignant portal venous obstruction treated by stent placement: significant factors affecting patency. *Journal of Vascular and Interventional Radiology* 2001;12:1407–15.

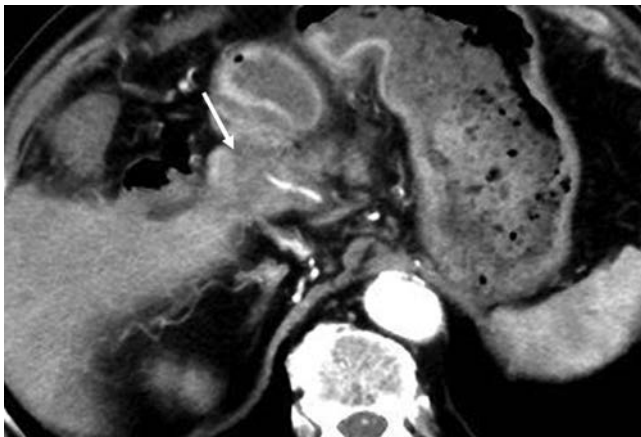


Fig. 1.

\* Corresponding author at: Department of Gastroenterology and Hepatology, Kindai University Faculty of Medicine, 377-2 Ohno-Higashi, Osaka-Sayama, 589-8511, Japan. Fax: +81 72 367 2880.

E-mail address: [mamoxyo45@gmail.com](mailto:mamoxyo45@gmail.com) (M. Takenaka).



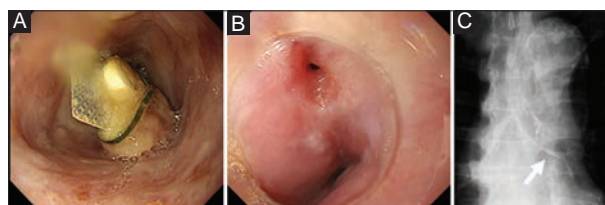
## Endoscopic treatment of tracheoesophageal fistula using the over-the-scope-clip system

Shigenaga Matsui, Hiroshi Kashida, Yutaka Asakuma, Masatoshi Kudo

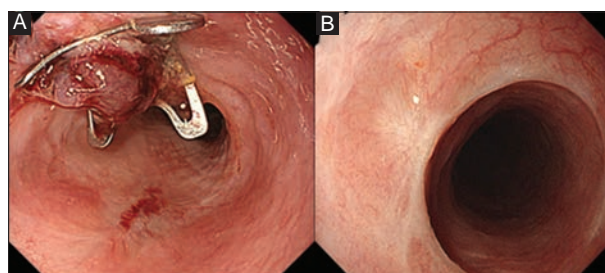
Kindai University Faculty of Medicine, Japan

An 84-year-old man with dysphagia was referred to our hospital for examination. The patient's medical history included endoscopic submucosal dissection for superficial esophageal cancer 2 years previously. Gastrointestinal endoscopy revealed an esophageal foreign body, a press-through pack (PTP) (Fig. 1A). The PTP was successfully removed endoscopically. After extraction of the PTP, the patient presented with continuous fever and a cough. Gastrointestinal endoscopy and fluoroscopy revealed a tracheoesophageal fistula in the esophagus (Fig. 1B,C). The tracheoesophageal fistula was endoscopically closed with the Over-The-Scope Clip (OTSC) system (Fig. 2A). The patient's symptoms were immediately improved. Gastrointestinal endoscopy after 2 months revealed a scar with complete fistula closure (Fig. 2B).

The management of tracheoesophageal fistulas is associated with high morbidity and mortality and remains an interdisciplinary challenge. For patients with benign tracheoesophageal fistulas, treatment is always initially supportive, followed by definitive surgical correction [1]. The OTSC system is a new technique that is becoming established as a reliable method for the endoscopic closure of fistulas, bleeds, perforations and other gastrointestinal lesions [2]. The major benefits of the OTSC are its speed and ease of



**Figure 1** (A) Gastrointestinal endoscopy revealed an esophageal foreign body, a press-through pack. (B) Esophageal orifice of the tracheoesophageal fistula. (C) Fluoroscopy revealed a tracheoesophageal fistula (arrow)



**Figure 2** (A) The fistula was closed endoscopically using the over-the-scope clip system. (B) Scar of complete fistula closure

deployment, and the persistent sealing of tracheoesophageal fistulas.

Department of Gastroenterology and Hepatology, Kindai University Faculty of Medicine, Japan

Conflict of Interest: None

Correspondence to: Shigenaga Matsui, MD, PhD, Department of Gastroenterology and Hepatology, Kindai University Faculty of Medicine, Osaka, Japan, Tel.: +81 723 66 0221, Fax: +81 723 67 2880, e-mail: ma2i@med.kindai.ac.jp

Received 30 May 2017; accepted 1 June 2017  
published online 26 July 2017

DOI: <https://doi.org/10.20524/aog.2017.0181>

### References

1. Reed ME, Mathisen DJ. Tracheoesophageal fistula. *Chest Surg Clin N Am* 2003;**13**:271-289.
2. Richter-Schrag HJ, Glatz T, Walker C, Fischer A, Thimme R. First-line endoscopic treatment with over-the-scope clips significantly improves the primary failure and rebleeding rates in high-risk gastrointestinal bleeding: A single-center experience with 100 cases. *World J Gastroenterol* 2016;**22**:9162-9171.



# SCIENTIFIC REPORTS

OPEN

## Contribution of C1485T mutation in the HBx gene to human and murine hepatocarcinogenesis

Satoru Hagiwara<sup>1</sup>, Naoshi Nishida<sup>1</sup>, Ah-Mee Park<sup>2</sup>, Yoriaki Komeda<sup>1</sup>, Toshiharu Sakurai<sup>1</sup>, Tomohiro Watanabe<sup>1</sup> & Masatoshi Kudo<sup>1</sup>

Received: 2 May 2017

Accepted: 11 August 2017

Published online: 05 September 2017

Although Hepatitis B virus (HBV) X gene mutations are frequently detected in HBV-related human hepatocellular carcinoma (HCC) patients, causative HBx mutations in the development of HCC have not yet been determined. We herein identified C1485T and C1653T mutations in the HBx gene as independent risk of HCC for HBV through the analysis using serum from chronic hepatitis B patients. We generated transgenic mice expressing wild-type (WT-HBxTg) and mutant (C1485T-HBxTg) HBx to assess the carcinogenic potential of mutated HBx. C1485T-HBxTg mice were more susceptible to diethylnitrosamine-induced hepatocarcinogenesis than WT-HBxTg mice and control non-Tg mice. The promotion of hepatocarcinogenesis in C1485T-HBxTg mice was accompanied by the activation of  $\beta$ -catenin and Jun N-terminal kinase (JNK) signaling pathways as well as the production of reactive oxygen species, whereas the activation of nuclear factor-kappa B in the livers of C1485T-HBxTg mice was attenuated. These results demonstrate that the HBx C1485T mutation contributes to human and murine hepatocarcinogenesis.

Hepatocellular carcinoma (HCC) is the third leading cause of cancer death worldwide and chronic hepatitis B virus (HBV) infection is one of the most important etiologies for the development of HCC<sup>1,2</sup>. Thus, HBV-related hepatocarcinogenesis is a global health issue. However, the molecular mechanisms responsible for the development of HBV-related HCC have not yet been elucidated in detail.

HBV exerts its oncogenic effects through the integration of its small double-stranded DNA into the host genome of hepatocytes. It is now generally accepted that HBV integration into the host genome plays a critical role in the development of HBV-related HCC<sup>3–5</sup>. Among all portions of HBV genes, the oncogenic role of the HBV-X (HBx) gene in the occurrence of HBV-related hepatocarcinogenesis has been the focus of previous studies because most patients with HBV-related HCC are positive for the expression of HBx at the protein level<sup>6</sup>. The HBx gene encodes a protein of 154 amino acid residues that is composed of an N-terminal negative regulatory/antiapoptotic domain and C-terminal transactivation/proapoptotic domain<sup>7</sup>. Although the exact mechanisms by which the integration of HBx into the host genome causes HCC currently remain unclear, one possible explanation may be the functions of intact HBx as a transcription regulator<sup>8</sup>. It is now generally accepted that the HBx protein positively and negatively regulates the expression of genes associated with apoptosis, inflammation, and oncogenesis and thereby induces hepatocarcinogenesis<sup>9,10</sup>. Mutations in the HBx gene have also been implicated in HBV-related hepatocarcinogenesis in addition to the role of intact HBx as a transcription regulator. Several studies have demonstrated that HCC-associated HBx mutants more strongly promote oncogenesis than intact HBx<sup>11</sup>. For example, HBx mutants with a C-terminal truncation promote or inhibit cell proliferation in a manner that depends on deletion sites<sup>12</sup>. However, the molecular mechanisms by which the functions of HBx are altered in the presence of HBx mutations and cause the promotion of HBV-related hepatocarcinogenesis have not yet been elucidated in detail. This is also the case for HBx C1653T and C1485T mutations associated with the occurrence of HCC in patients with HBV genotype C in Japan<sup>9,10</sup>. Therefore, alterations in HBx functions in the presence of HCC-associated mutations need to be examined in more detail in order to clarify the pathogenesis of HBV-related hepatocarcinogenesis.

The present study aimed to examine the characteristics of HBx mutations that increase the risk of the emergence of HCC in chronic hepatitis B (CHB) patients with genotype C and to elucidate the roles of these HBx

<sup>1</sup>Department of Gastroenterology and Hepatology, Kindai University Faculty of Medicine, Osaka-Sayama, Japan.

<sup>2</sup>Department of Microbiology, Kindai University Faculty of Medicine, Osaka-Sayama, Japan. Correspondence and requests for materials should be addressed to N.N. (email: [naoshi@med.kindai.ac.jp](mailto:naoshi@med.kindai.ac.jp))

Variables	non-HCC (n = 40)	HCC (n = 40)	p-value
Age (years), median (range)	49.5 (20–77)	53.5 (34–82)	N.S.
Sex (male), n (%)	35 (88%)	35 (88%)	N.S.
HBV-DNA >5 (PCR, log copies/mL), n (%)	23 (58%)	23 (58%)	N.S.
Positive for HBeAg, n (%)	18 (45%)	16 (40%)	0.82
ALT (IU), median (range)	39 (9–246)	44.5 (16–322)	0.69
Pre-core mutation, n (%)	12 (30%)	16 (40%)	0.48
Core promoter mutation, n (%)	23 (58%)	34 (85%)	0.013*
Cirrhosis, n (%)	6 (15%)	23 (58%)	<0.001*
HBx;C1653T mutation	5 (12.5)	15 (37.5)	0.019*
HBx;C1485T mutation	2 (5)	11 (27.5)	0.007*
HBx;C1470A mutation	5 (12.5)	8 (20)	0.55
HBx;C1479A mutation	3 (7.5)	6 (15)	0.48
HBx;C1575G mutation	2 (5)	4 (10)	0.68

**Table 1.** Characteristics and incidences of various HBx gene mutations in patients with or without HCC. HCC, hepatocellular carcinoma; HBeAg, hepatitis B e antigen; PCR, polymerase chain reaction; ALT, alanine aminotransferase; pre-core mutation, a guanine-to-adenine substitution at nucleotide 1896 in the pre-core region; core promoter mutation, an adenine-to-thymine substitution at nucleotide 1762 and guanine-to-adenine substitution at nucleotide 1764 in the core promoter region; N.S., not significant. \*Significant difference;  $p < 0.05$ .

Variables	Odds ratio	95% CI	p-value
Core promoter mutation	3.13	0.88–11.18	0.079
Cirrhosis	11.67	3.37–40.42	<0.001
C1653T mutation	4.70	1.16–18.97	0.030
C1485T mutation	7.75	1.26–47.88	0.027

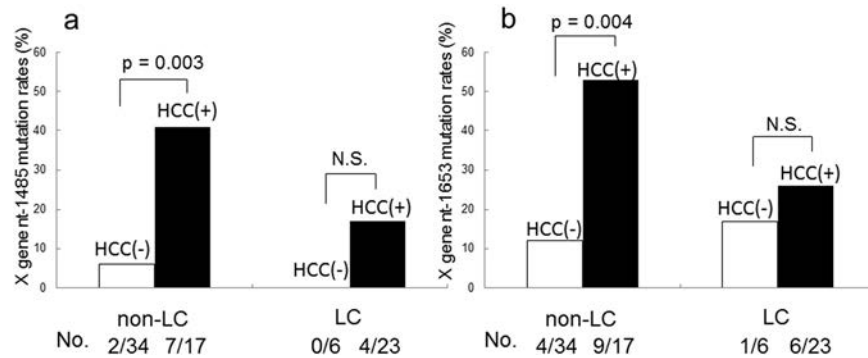
**Table 2.** Results of a multivariate analysis using a logistic regression model for assessing risk factors for carcinogenesis. CI, confidence interval; core promoter mutation, an adenine-to-thymine substitution at nucleotide 1762 and guanine-to-adenine substitution at nucleotide 1764 in the core promoter region. \*Significant difference;  $p < 0.05$ .

mutations in the emergence of HCC from damaged livers. We herein demonstrated that HBx C1653T and C1485T mutations are associated with the development of HBV-related hepatocarcinogenesis and also that the latter mutation induces malignant transformation in hepatocytes upon over-expression.

## Results

**Patient characteristics and mutational profile of the HBx gene.** In order to examine the causative HBx mutations that lead to the development of HBV-related HCC, we initially attempted to identify the sites of mutations in HBx in CHB patients with or without HCC. For this purpose, CHB patients with or without HCC were retrospectively analyzed in this study. Clinicopathological factors were compared between patients with or without HCC after matching for age, sex, and HBV DNA levels. As shown in Table 1, no significant differences were observed in the positive ratio of HBeAg or serum alanine aminotransferase (ALT) levels between patients with or without HCC. As expected, the ratio of liver cirrhosis (LC) and presence of core promoter mutation were significantly higher in patients with HCC than in those without HCC.

Since the regions of HBx, the precore, and core promoter in HBV are important for pathogenesis, we sequenced these regions using a specific primer set and examined mutations in these regions. We found that the presence of a double core promoter mutation (A1762T and G1764A) correlated with the development of HCC, as reported previously<sup>13</sup> (data not shown). We then attempted to identify HBx mutations associated with HBV-related hepatocarcinogenesis and found five different HBx mutations (C1653T, C1485T, C1470A, C1479A, and C1575G) in CHB patients. In the non-HCC group, 6 patients had a single mutation, 4 had 2 mutations, and 1 had 3 mutations in the HBx gene. In the HCC group, 20 patients had a single mutation, 7 had 2 mutations, 2 had 3 mutations, and 1 had 4 mutations in the HBx gene. Among these five HBx mutations, C1485T and C1653T mutations were more frequently detected in HCC than in non-HCC cases (Table 1). The factors identified as significant by a univariate analysis, as listed above, were subjected to a multivariate analysis using a logistic regression model. The presence of the C1485T or C1653T mutation in HBx in combination with LC was identified as an independent factor for the development of HCC (Table 2). Following the identification of the susceptible viral mutations (the C1485T HBx or C1653T HBx mutation) and host factor (the presence of LC) for HBV-related hepatocarcinogenesis in the multivariate analysis, we compared the frequencies of HBx mutations between HCC and non-HCC cases in the context of background liver conditions, i.e. the presence of LC. We compared the



**Figure 1.** Frequencies of C1485T and C1653T mutation in non-LC and LC cases. Frequencies of C1485T (a) and C1653T (b) mutations in non-LC and LC cases. White columns represent non-HCC and black gray columns represent HCC patients sample. The numbers in the bottom line mean positive patients number/total patients number.

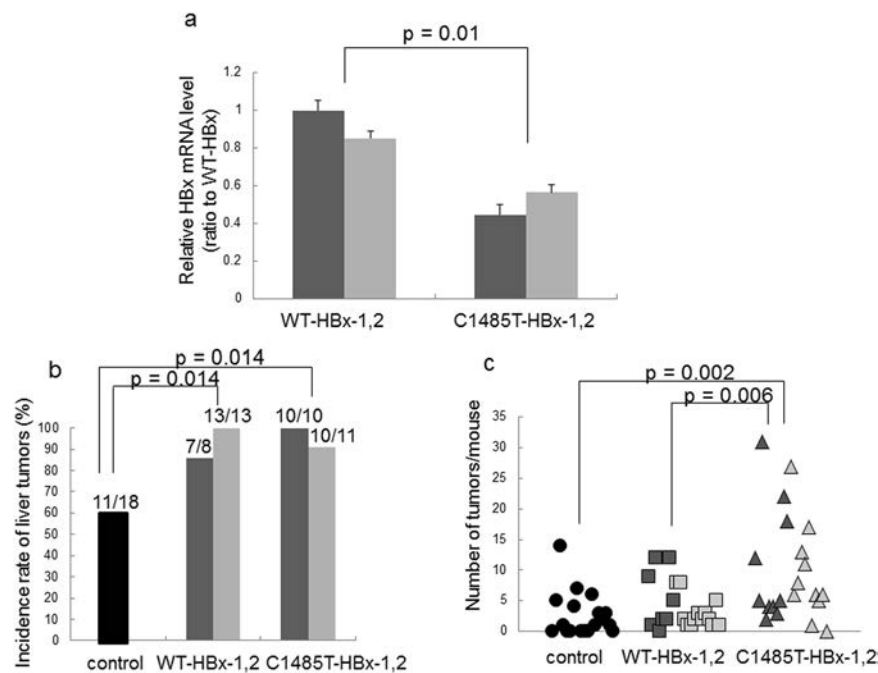
frequencies of C1485T and C1653T mutations in LC and non-LC cases. The analysis of patients with non-LC revealed that C1485T and C1653T mutations were more frequent in HCC than in non-HCC cases ( $p = 0.003$  and  $p = 0.004$  for the C1485T and C1653T mutations, respectively; Fig. 1a,b). In addition, there is a trend showing that these mutations were also more frequent even in HCC cases with LC, although a significant difference was not observed in this cohort. Collectively, these results suggest that C1485T and C1653T mutations in HBx contribute more significantly to HBV-related hepatocarcinogenesis in patients without LC than in those with LC where direct role of HBx should be less critical.

**Incidence of HCC in wild-type (WT) and mutant HBx transgenic (Tg) mice.** Since the presence of the C1485T mutation showed a higher odds ratio for the development of HCC than the C1653T mutation (Table 2), we focused on the role of C1485T mutation on carcinogenesis and then attempted to directly confirm the oncogenic potential of C1485T-HBx in an *in vivo* experimental model. We created Tg mice overexpressing the HBx C1485T mutation (referred to as C1485T-HBxTg) and WT-HBx (WT-HBxTg). We established two Tg lines overexpressing WT-HBxTg and two Tg lines overexpressing C1485T-HBx. As shown in Fig. 2a, we detected the enhanced expression of HBx mRNA in each Tg mouse, but not in control non-Tg mice.

Previous studies showed that the integrated sites of HBV into host genome play important roles in the development of HCC<sup>4,5</sup>. We initially tried to determine the integration sites of HBx gene into host genomes. No specific gene loci were identified as integration sites of transgenes in any of WT-HBxTg and C1485T-HBxTg mice (Supplementary Table 1), suggesting that the integration event should result in structural alterations of known cancer-related genes that could enhance oncogenic pathways. Subsequently, we tried to evaluate the development of liver tumor in WT-HBxTg and C1485T-HBxTg mice. For this purpose, these two Tg mice and control non-Tg WT-C57BL/6 mice were subjected to an injection of diethylnitrosamine (DEN) in order to accelerate hepatocarcinogenesis. As shown in Fig. 2b, the number of male mice that developed liver tumor was significantly higher in the C1485T-HBxTg mouse lines than in control non-Tg mice eight months after the injection of DEN ( $p = 0.014$ ; Fig. 2b). Similarly, each male WT-HBxTg mouse line showed a significantly higher incidence of tumors than control non-Tg mice ( $p = 0.014$ ; Fig. 2b). Although no significant difference was observed in the incidence of liver tumors in male mice among the two C1485T-HBxTg mouse lines and two WT-HBxTg mouse lines, there was a significant difference in the number of liver tumors per body between these two lines; the tumor emergence was significantly higher in C1485T-HBxTg mice than in WT-HBxTg mice ( $p = 0.060$ ) as well as control non-Tg mice ( $p = 0.002$ ; Fig. 2c) for male mice. Although the same experiment was performed with female mice, the incidence of liver tumors was low (data not shown). Such low incidence of tumor emergence in female mice may be attributed to the characteristics of DEN-induced hepatocarcinogenesis utilized in this study<sup>14</sup>. Therefore, we used male mice for further analyses.

It might be possible that difference in sensitivity to DEN-induced hepatocarcinogenesis between WT-HBxTg mice and C1485T-HBxTg mice may be caused by different expression levels of HBx between these two lines. Therefore, we performed a quantitative PCR analysis, and found that the HBx mRNA level was not higher, or rather lower, in mice overexpressing C1485T-HBx, which was more susceptible for hepatocarcinogenesis, than in those carrying WT-HBx overexpression (Fig. 2a). Thus, the higher incidence of tumor emergence in C1485T-HBxTg mice could be caused by C1485T mutation rather than the expression levels of HBx. Collectively, these results strongly suggest that hepatocytes overexpressing C1485T-HBx show higher sensitivity to DEN-induced carcinogenesis than those overexpressing intact HBx.

**Increased cell proliferation in livers of C1485T-HBxTg mice.** In order to confirm the effects of WT- and C1485T-HBx on hepatocyte proliferation, we compared the degree of DNA synthesis in livers after the DEN injection using BrdU staining. As shown in Fig. 3, the greater incorporation of BrdU was observed in the nuclei of hepatocytes in mice overexpressing C1485T-HBx than in those overexpressing WT-HBx and those not expressing HBx (Fig. 3a,b). Moreover, a cell-cycle analysis using cyclin D1 staining also revealed higher numbers of cyclin D1-positive hepatocytes in mice overexpressing C1485T-HBx than in those overexpressing WT-HBx (Fig. 3c,d).



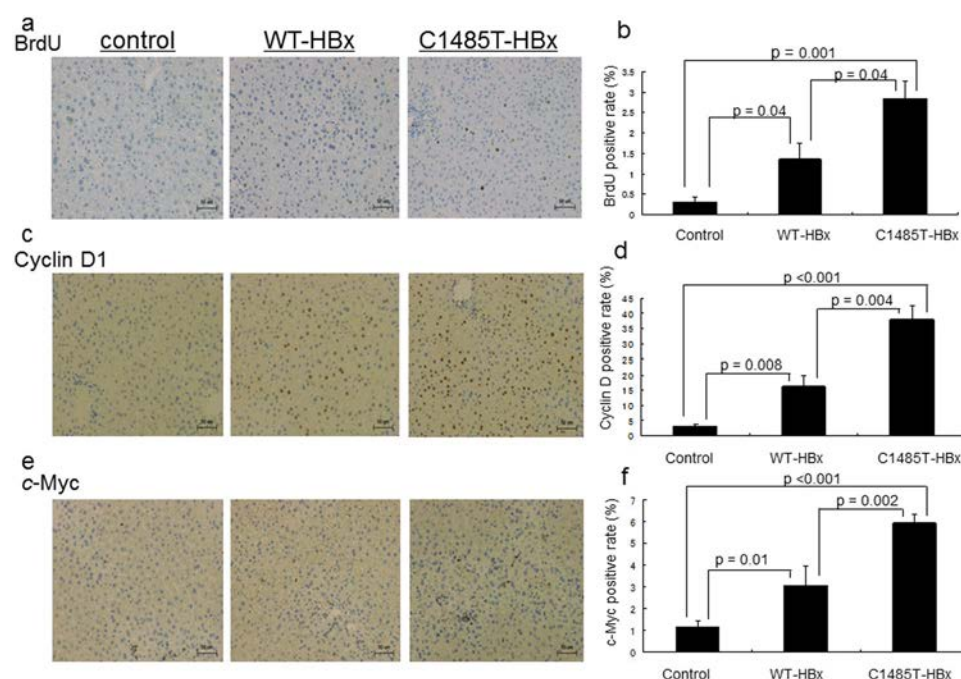
**Figure 2.** Sensitivity to diethylnitrosamine-induced hepatocarcinogenesis in HBx-transgenic mice. (a) HBx mRNA levels in HBx (WT)-transgenic Tg and HBx (C1485T)-Tg mice. Liver were obtained from 6 weeks old male HBx-WT Tg mice and HBx-C1485T-Tg mice. HBx mRNA levels of the liver were determined. The mRNA levels were normalized by  $\beta$ -actin and shown as ratio to one HBx (WT) Tg mice line 1. Data show mean  $\pm$  standard error ( $n = 4$ ). Dark gray and light gray columns represent the different lines of the original mice (dark gray Tg line 1, light gray Tg line 2). (b) Comparison of the incidence of liver tumors in control non-Tg mice and HBx transgenic mice. Male control non-Tg mice, male HBx-WT Tg mice, and male HBx-C1485T-Tg mice were treated with intraperitoneal injection of diethylnitrosamine (DEN, 25 mg/kg) and then the incidence of liver tumors was determined 8 months after the injection ( $n = 8-13$ ). Dark and light gray columns represent the different lines of the original Tg mice (dark gray Tg line 1, light gray Tg line 2). (c) The number of tumors in each male mouse is represented as a circle in control non-Tg mice, as a square in HBx (WT) mice and as a triangle in HBx (C1485T) mice in the graph. Dark and light gray symbols represent the different lines of the original Tg mouse.

Consistent with the results of BrdU and cyclin D1 staining, the expression of the oncogenic protein, c-myc, was significantly enhanced in the hepatocytes of mice overexpressing C1485T-HBx than in those overexpressing WT-HBx and those not expressing HBx (Fig. 3e,f).

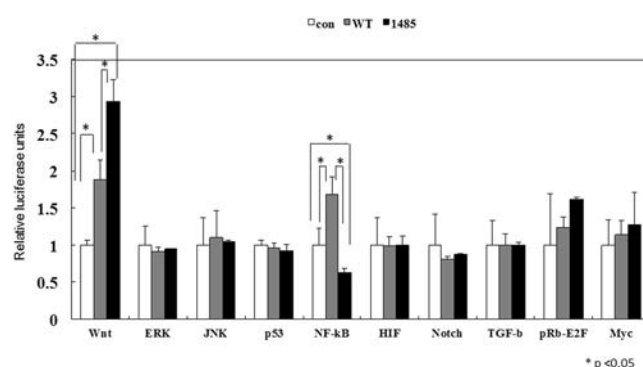
#### Effects of mutant HBx expression on the activation of cancer-related signaling pathways.

Following confirmation of the effects of C1485T-HBx on hepatocyte proliferation, as assessed by BrdU and cyclin D1 staining, we attempted to identify the signaling pathways responsible for enhanced hepatocyte proliferation. We analyzed the transcriptional activity of WT- and C1485T-HBx genes using the Signal Finder Reporter Array, as previously reported<sup>15</sup> (Fig. 4). Expression vectors containing WT- or C1485T-HBx were transfected into HepG2 cells in order to compare their effects on the activation of several oncogenic pathways (Wnt, extracellular signal-regulated kinase (ERK), Jun N-terminal kinase (JNK), p53, nuclear factor-kappa B (NF- $\kappa$ B), hypoxia induced factor (HIF), Notch, transforming growth factor- $\beta$  (TGF- $\beta$ ), retinoblastoma protein (pRb)-E2F, and Myc. Transfection with WT- and C1485T-HBx enhanced the transcriptional activity of the Wnt signaling cascade more than the control empty vector. This increase in transcriptional activity was significantly greater in HepG2 cells overexpressing C1485T-HBx than in those overexpressing WT-HBx ( $p = 0.007$ ; Fig. 4). In contrast, HepG2 cells overexpressing C1485T-HBx showed weaker NF- $\kappa$ B transcriptional activity than those overexpressing control and WT-HBx ( $p = 0.028$  vs. control;  $p < 0.001$  vs. wild type-HBx; Fig. 4), whereas the transfection of WT-HBx into HepG2 cells enhanced NF- $\kappa$ B transcriptional activity than that of the control ( $p = 0.012$ ; Fig. 4). The transfection of the WT- or C1485T-HBx gene into HepG2 cells did not alter reporter gene activity regulated by the ERK, JNK, p53, HIF, Notch, TGF- $\beta$ , pRb-E2F, or Myc signaling pathways, probably because these signaling pathways are constitutively activated in HepG2 cells, as previously described<sup>16</sup>.

**Suppression of NF- $\kappa$ B in livers of C1485T-HBxTg mice.** The results of the Signal Finder reporter assay suggested that the presence of C1485T-HBx in hepatocytes inhibited the activation of NF- $\kappa$ B. This result prompted us to investigate the effects of C1485T-HBx on the NF- $\kappa$ B pathway *in vivo*. The phosphorylation and degradation of inhibitor of NF- $\kappa$ B (I $\kappa$ B)- $\alpha$  is an indispensable step for the translocation of NF- $\kappa$ B subunits into the nucleus, followed by the transcription of target genes<sup>17</sup>. We initially analyzed the level of I $\kappa$ B - $\alpha$  phosphorylation (p-I $\kappa$ B - $\alpha$ ) in the livers of male control non-Tg and Tg mice carrying WT-HBx and C1485T-HBx four hours



**Figure 3.** Enhanced proliferation and cell cycle progression in HBx C1485T-transgenic mice. Male control non-Tg mice, male HBx-WT Tg mice (Tg line 1), and male HBx-C1485T-Tg mice (Tg line 1) were treated with intraperitoneal injection of diethylnitrosamine (DEN, 100 mg/kg). Four hours prior sacrifice BrdU was injected intraperitoneally, and mice were sacrificed at 48 hours after DEN injection. Liver sections were prepared and immunohistochemical staining for BrdU (a,b), cyclin D1 (c,d), and c-myc (e,f) was performed. Representative results from at least three independent experiments ( $n = 4$ ) are shown in panels a, c, and e. Cells positive for each nuclear staining were counted by Image J software and the percentage to total nuclear numbers were shown in graph (b,d,f). Results were shown as mean  $\pm$  standard error.

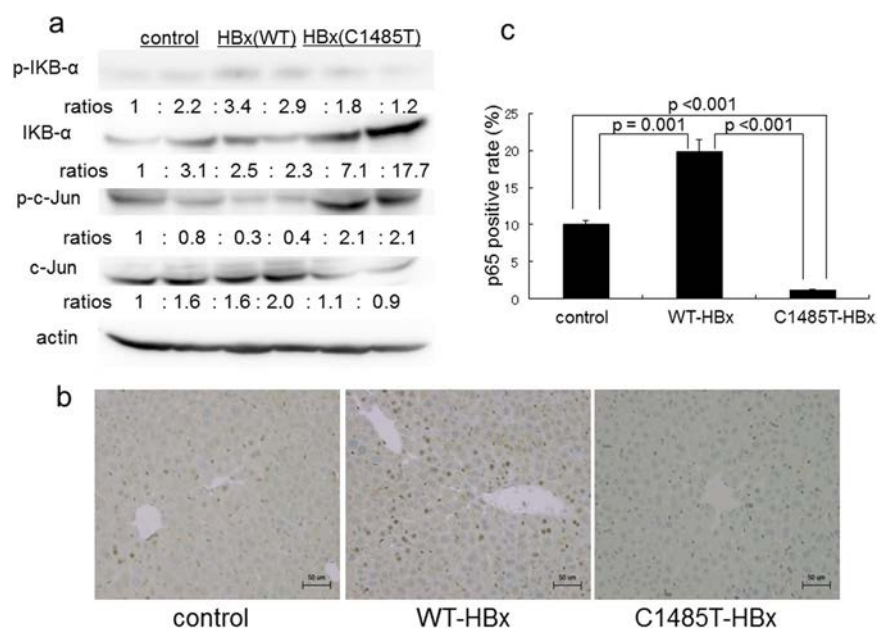


**Figure 4.** Effect of mutant HBx expression on the activation of cancer-related signaling pathways. Transcription factor activities in HepG2 cells overexpressing HBx were measured by using the Signal Finder luciferase reporter system. HepG2 cells were transfected with expression vector of wild type HBx (dark gray), C1485T HBx (black), or an empty vector (white). 2 days after transfection, cell lysate were used for this assay. The results are presented as relative luciferase activity mean  $\pm$  standard error ( $n = 3$ ).

after the administration of DEN. As shown in Fig. 5a, the expression of p-I $\kappa$ B- $\alpha$  in the liver was significantly reduced in C1485T-HBxTg mice than in control non-Tg and WT-HBxTg mice. In contrast, the expression of I $\kappa$ B- $\alpha$  in the liver was markedly reduced in WT-HBxTg mice than in C1485T-HBxTg mice. Consistent with the results obtained from immunoblotting, the nuclear expression of p65, a major component of NF- $\kappa$ B subunits, in hepatocytes was attenuated in C1485-HBxTg mice than in WT-HBxTg and control non-Tg mice (Fig. 5b,c). Thus, the results of immunoblotting and tissue staining strongly suggest the suppression of NF- $\kappa$ B activation in the livers of C1485T-HBxTg mice.

We then investigated the activation of JNK signaling pathways because previous studies reported that the up-regulation of the JNK pathway is associated with the down-regulation of NF- $\kappa$ B signaling pathways<sup>18</sup>. The expression of phosphorylated c-Jun in the liver was stronger in C1485T-HBxTg than in WT-HBxTg mice as





**Figure 5.** Attenuation of NF- $\kappa$ B activation in the liver of C1485T-HBx transgenic mice. Male control non-Tg mice, male HBx-WT Tg mice (Tg line 1), and male HBx-C1485T-Tg mice (Tg line 1) were treated with intraperitoneal injection of diethylnitrosamine (DEN, 100 mg/kg) and liver tissues were obtained 4 hours later. **(a)** Immunoblot analysis for total and phosphorylated I $\kappa$ B- $\alpha$  and c-jun, with actin as a loading control; each number represents the ratio to the control samples on the lane 1. Lane 1, 2; control non-Tg mice, lane 3, 4; HBx wild type transgenic mice, lane 5, 6; HBx C1485T transgenic mice. **(b,c)** Immunohistochemical staining of NF- $\kappa$ B subunit, p65, in the liver. Mice ( $n = 4$ , each group) were treated with intraperitoneal injection of DEN as described in **(a)** and liver tissues were obtained 48 hours after DEN injection. Cells positive for nuclear p65 staining were counted by Image J software and the percentage to total nuclear number were shown as mean  $\pm$  standard error.

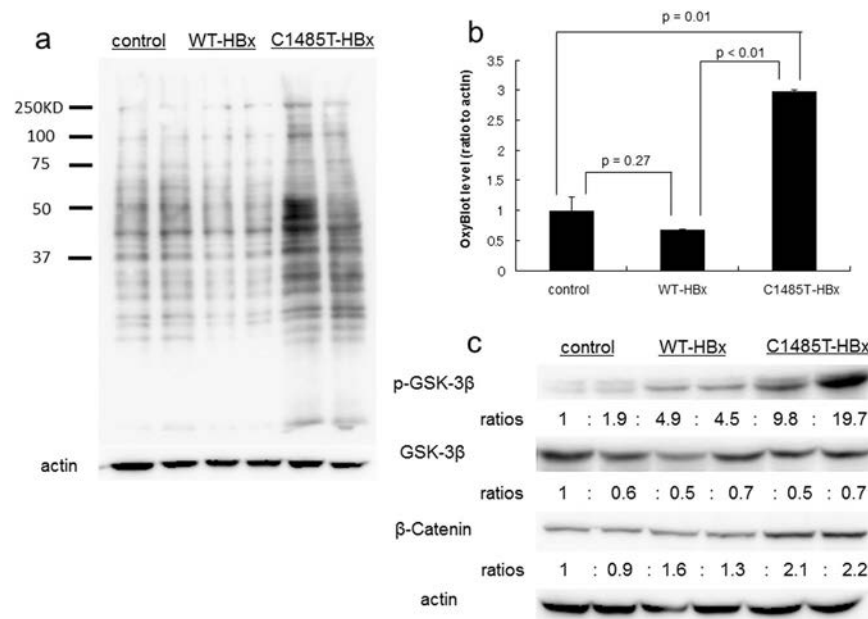
assessed by immunoblotting (Fig. 5a). Thus, it is conceivable that the presence of C1485T-HBx interferes with NF- $\kappa$ B signaling, the effects of which were accompanied by the activation of c-Jun with the potent ability to accelerate cell proliferation, as reported previously<sup>18</sup>.

The production of reactive oxygen species (ROS) in response to the activation of JNK-c-Jun pathways has been implicated in murine hepatocarcinogenesis<sup>19</sup>. Consistent with this finding, oxidized protein levels were significantly higher in C1485T-HBxTg mice than in WT-HBxTg mice, as assessed by OxyBlot<sup>20</sup> (Fig. 6a,b). Collectively, these results suggest that the promotion of hepatocarcinogenesis induced by the overexpression of HBx-C1485T is accompanied by the enhanced activation of JNK signaling pathways and subsequent production of ROS.

**Activation of Wnt/ $\beta$ -catenin signaling pathways in livers of C1485T-HBxTg mice.** We examined the activation status of Wnt signaling pathways because the reporter gene assay showed an increase in activation of the Wnt signaling pathway in WT- and C1485T-HBx-overexpressing cells, particularly in those overexpressing HBx-C1485T. The expression of phosphorylated glycogen synthase kinase-3 $\beta$  (p-GSK3 $\beta$ ) and  $\beta$ -catenin, key signaling molecules in the Wnt pathway<sup>21</sup>, was examined by immunoblotting. p-GSK3 $\beta$  expression levels in the liver were higher in C1485T-HBx mice than in control non-Tg and WT-HBxTg mice. Consistent with the results obtained for p-GSK3 $\beta$ ,  $\beta$ -catenin levels in the liver were higher in C1485T-HBxTg mice than in WT-HBxTg mice (Fig. 6c). Thus, the promotion of DEN-induced hepatocarcinogenesis observed in C1485T-HBxTg mice was characterized by the enhanced activation of the Wnt signaling pathway combined with attenuated activation of NF- $\kappa$ B signaling pathways.

## Discussion

In the present study, we demonstrated that the C1485T HBx mutation is involved in hepatocarcinogenesis in human and mice. This result is supported by the findings of human studies and experimental models of hepatocarcinogenesis. In human studies utilizing age, sex, and HBV-DNA-matched serum samples obtained from CHB patients, we found that the incidence of HCC was higher in patients bearing C1485T or C1653T HBx mutations than in those bearing wild type HBx. Consistent with the findings of human studies, experimental models of DEN-induced hepatocarcinogenesis revealed that C1485T-HBxTg mice were more susceptible to the development of HCC than WT-HBxTg and non-Tg mice. To the best of our knowledge, this is the first study to conduct an *in vivo* phenotypic analysis on C1485T-HBxTg mice. Collectively, the findings obtained from human and mouse studies support our conclusion that the C1485T mutation in the HBx gene is a susceptible factor for the development of HBV-related hepatocarcinogenesis.



**Figure 6.** Enhancement of GSK3 $\beta$  and Wnt activation in the liver of C1485T-HBx transgenic mice. Male control non-Tg mice, male HBx-WT Tg mice (Tg line 1), and male HBx-C1485T-Tg mice (Tg line 1) were treated with intraperitoneal injection of diethylnitrosamine (DEN, 100 mg/kg) and liver tissues were obtained 4 hours later. (a) Protein oxidation of liver lysate from acute DEN-treated mice was determined by oxyblot analysis kit. Lane 1, 2; control non-Tg mice, lane 3, 4; HBx wild type transgenic mice, lane 5, 6; HBx C1485T transgenic mice. (b) The signal intensity of each lane from oxyblot result (a) was determined by Image J software. The bar graph presented mean  $\pm$  standard error (n = 3). (c) Immunoblot analysis for total and phosphorylated GSK- $\beta$  and  $\beta$ -catenin with actin as a loading control; each number represents the ratio to the control samples on the lane 1. Lane 1, 2; control non-Tg mice, lane 3, 4; HBx wild type transgenic mice, lane 5, 6; HBx C1485T transgenic mice.

A large number of studies have confirmed the oncogenic roles played by the HBx protein in hepatocarcinogenesis<sup>22</sup>. Since several mutations have been detected in HBx not only in HCC tissues, but also background liver tissue, mutations in HBx have been implicated in the pathogenesis of HBV-related HCC. However, the effects of HBx mutations on the development of HCC currently remain unclear. In the present study, we analyzed the serum of 80 case-matched HBV genotype C-positive patients with or without HCC in order to identify and clarify HBx mutations associated with HBV-related hepatocarcinogenesis. We found that HBV carrying the C1485T mutation in the HBx gene is involved in the pathogenesis of HBV-related HCC. These results are consistent with previous findings by Muroyama *et al.* showing that the C1485T mutation in the HBx gene was associated the development of HBV genotype C-related HCC<sup>10</sup>. Thus, our results together with these findings suggest that the C1485T mutation in HBx might increase the risk of HCC associated with HBV genotype C. Furthermore, the occurrence of the C1485T mutation was markedly higher in HCC patients without LC than in those with LC in our cohort. Therefore, the C1485T mutation in HBx appears to be involved in the development of HCC even in the cases without LC and thereby acts as a potent oncogenic accelerator independent from liver fibrosis.

On the other hand, a previous study showed that HBV sequences derived from tumor and non-tumor tissues were different<sup>23</sup>, indicating that HBx mutations in the serum do not always reflect those in the HCC tissue. In this regards, our preliminary studies show that C1485T mutation was successfully detected in the HCC tissue in 3 of 5 patients bearing such mutation in the serum (data not shown). Previous study also showed that the HBx codon-38 change in human HCC, which is attributed to the presence of C1485T, was detected in corresponding non-tumor tissues, and was consistent with those in serum<sup>10</sup>. These data suggest that detection of the HBxC1485T mutation in the serum, in combination with the analysis of HCC tissue, could be an informative molecular marker to predict the clinical outcome of CHB patients.

The relationship between the C1485T mutation and emergence of HCC has not been confirmed in HBV genotype A infection<sup>24,25</sup>. Thus, the C1485T mutation in HBx is involved in the pathogenesis of HCC in the presence of HBV genotype C, but not genotype A. In this regard, the infection by HBV genotype C is known to be more strongly associated with severe hepatitis than genotype A of HBV<sup>26</sup>. Since the accumulation of hepatocyte DNA damage is parallel to the severity of hepatitis<sup>27–29</sup>, HBV genotype C infection is regarded as a strong inducer of hepatocyte DNA damage. Thus, the accumulation of DNA damage due to persistent infection with HBV genotype C may act synergistically with the C1485T HBx mutation to promote hepatocarcinogenesis. This is consistent with our phenotypic analysis of C1485T-HBxTg mice in that the spontaneous development of HCC has not been observed in these mice without the administration of DEN (data not shown). Therefore, DEN-induced DNA damage may be a prerequisite for the increased susceptibility of C1485T-HBxTg mice to HCC.

Although several studies have suggested a relationship between mutations in HBx and the development of HCC, specific role of these mutations in hepatocarcinogenesis is still unclear. The relationship observed between HBx mutations and the development of HCC may be an epiphenomenon associated with alternations in the liver microenvironment due to persistent inflammation. Therefore, we established Tg mice carrying C1485T-HBx for the first time and performed a phenotypic analysis. The results obtained from male Tg mice revealed a higher incidence of HCC in C1485T-HBxTg mice than in WT-HBxTg mice following a challenge with DEN. Furthermore, an immunohistochemical analysis revealed that the incorporation of BrdU and expression of cyclin D1 in hepatocytes were stronger in C1485T-HBxTg mice than in WT-HBxTg mice. Thus, the higher incidence of hepatocarcinogenesis in C1485T-HBx Tg mice is linked to the abnormal regulation of the cell cycle and enhanced cell proliferation. Since HBx is a multifunctional protein that not only activates transcriptional transactivation, but also mediates cell growth via proliferation and apoptosis<sup>30</sup>, our results suggest that the C1485T mutation induces hepatocarcinogenesis through enhanced cell proliferation and cell cycle progression. On the other hand, the incidence of liver tumors was low in female mice compared to male mice. Naugler *et al.* showed that DEN-induced hepatocarcinogenesis requires interleukin-6 (IL-6) production by Kupffer cells and that such IL-6 production is negatively regulated by estrogen<sup>14</sup>. Thus, cell proliferation induced by IL-6 could be involved in DEN-induced hepatocarcinogenesis in male mice.

Regarding the mechanisms responsible for enhanced tumorigenesis in C1485T-HBxTg mice, we characterized cancer-related signaling pathways in the presence of C1485T-HBx genes. Reporter gene assays that the transactivation of Wnt signaling pathways was markedly enhanced in HepG2 cells overexpressing C1485T-HBx than in those expressing WT-HBx. Consistently, immunoblotting revealed that the expression of p-GSK3 $\beta$  and  $\beta$ -catenin in the liver was significantly stronger in C1485T-HBxTg mice than in WT-HBxTg mice. Since the activation of the Wnt signaling pathway induces the expression of downstream oncogenic proteins, such as c-myc and cyclin D1, which are overexpressed in the liver of C1485T-HBxTg mice<sup>31</sup>, these results strongly suggest that C1485T-HBx enhances cell cycle progression through the activation of Wnt signaling pathways. Given the fact that WT-HBx also induces HBV-related carcinogenesis through the activation of the Wnt/ $\beta$ -catenin signaling pathways<sup>32</sup>, our results indicate that the presence of the C1485T HBx mutation further enhances hepatocarcinogenesis by augmenting Wnt/ $\beta$ -catenin signaling pathways.

The suppression of NF- $\kappa$ B activation was significantly greater in HepG2 cells overexpressing C1485T-HBx than in those overexpressing WT-HBx. Consistent with this result, the activation of NF- $\kappa$ B was markedly suppressed in the livers of C1485T-HBxTg mice, as assessed by the expression of phospho-I $\kappa$ B  $\alpha$  and degradation of I $\kappa$ B  $\alpha$ . Furthermore, the nuclear translocation of p65, a major NF- $\kappa$ B subunit, in hepatocytes was more strongly inhibited in C1485T-HBxTg mice than in WT-HBxTg mice. Thus, the emergence of HCC caused by C1485T-HBx is also attributed to the suppression of NF- $\kappa$ B. Such suppression of NF- $\kappa$ B in the presence of C1485T- mutation is in contrast to previous findings showing that HBx induces malignant transformation through the inhibition of hepatocyte apoptosis and promotion of angiogenesis in an NF- $\kappa$ B-dependent manner<sup>33, 34</sup>. This discrepancy in the status of NF- $\kappa$ B activation may be partially explained by the types of cells that show the activation of NF- $\kappa$ B. Maeda *et al.* demonstrated that hepatocyte-specific IKK $\beta$ -deficient mice exhibited a marked increase in hepatocarcinogenesis caused by DEN<sup>35</sup>. In addition, the enhancement in hepatocarcinogenesis observed in this hepatocyte-specific NF- $\kappa$ B -deficient mice was accompanied by an increase in the accumulation of ROS<sup>35</sup>. Consistent with the findings reported by Maeda *et al.*, enhancements in DEN-induced hepatocarcinogenesis in C1485T-HBxTg mice were characterized by significant increase of ROS with the suppression of NF- $\kappa$ B activation in the liver, which are involved in hepatocarcinogenesis in C1485T-HBxTg mice treated with DEN.

The increase of phosphorylated c-Jun is another characteristic associated with the development of HCC in the presence of C1485T-HBx in mice model. It should be noted, however, that no difference was detected in JNK activation in HepG2 cells overexpressing WT-HBx gene and C1485T-HBx gene in the reporter gene assay (Fig. 4). The discrepancy of JNK activation between *in vitro* and *in vivo* experiments can be partially explained by the fact that JNK pathway is constitutively activated in HepG2 cells, which makes difficult to detect a significant difference in cell line study<sup>16</sup>.

Regarding the mechanisms responsible for the activation of c-Jun in mice model, we speculate that the accumulation of ROS induced by the suppression of NF- $\kappa$ B plays a role in the activation of JNK signaling pathways. The accumulation of ROS has been reported to induce the oxidative inhibition of mitogen-activated protein kinase (MAPK) phosphatases, which are enzymes responsible for terminating the activation of JNK, and then cause the persistent activation of JNK signaling<sup>36</sup>. Since JNK signaling pathways are regarded as an important contributor to hepatocyte proliferation and HCC development<sup>37–39</sup>, the activation of these pathways may be involved in enhanced hepatocarcinogenesis observed in C1485T-HBxTg mice. In addition, activation of JNK is reportedly contributed to the expansion and proliferation of stem-progenitor cells<sup>40</sup>; the C1485T-HBxTg mice showed an increase of CD133<sup>+</sup> stem-progenitor cells compared to WT-HBxTg mice after treated with DEN (data not shown). Based on these findings, the accumulation of ROS followed by the activation of JNK may also be contributed to C1485T-HBx -dependent hepatocarcinogenesis.

In conclusion, we identified a novel mutation in the HBx gene that accelerates hepatocarcinogenesis. In human studies, we found that the C1485T HBx mutation was more frequent in the sera of patients with HCC than in those without HCC. In experimental models of hepatocarcinogenesis, C1485T-HBxTg mice were more susceptible to the development of HCC than WT-HBxTg mice. The development of HCC in the presence of the C1485T-HBx mutation is associated with the enhanced activation of the Wnt and JNK signaling pathways, decreased activation of NF- $\kappa$ B signaling pathways, and accumulation of ROS. We consider the results of the present study to be of significance in terms of basic research and clinical perspectives. From a basic research standpoint, C1485T-HBxTg mice are a useful tool for the study of the molecular mechanisms underlying HBx-related hepatocarcinogenesis. Our results suggest, from a clinical viewpoint, that a screening of C1485T-HBx mutation in serum might represent a promising approach for predicting the emergence of HCC for CHB, particularly in patients carrying HBV genotype C.

## Methods

**Patient characteristics.** In order to analyze the mutational profile of HBV, we selected 80 out of 185 consecutive hepatitis B surface antigen-positive patients who visited Kindai University Hospital between January 1998 and December 2005. Among these patients, 40 harbored HCC, while 40 had never had this condition. Age, sex, and HBV DNA levels were matched between HCC-positive and -negative groups. Refer to the Supplementary Materials and Methods for more details.

The study protocol conformed to the ethical guidelines of the 1975 Declaration of Helsinki and was approved by the Institutional Review Board of Kindai University Faculty of Medicine. Written informed consent was obtained from all patients recruited in the study. All animals received humane care and the study protocol complied with the institution's guidelines.

**HBV-DNA status of patients.** Samples from all patients were examined for the following serological markers: the hepatitis B surface antigen, hepatitis B e antigen, anti-HBe antibody, HBV DNA level, and HBV genotype.  $\alpha$ -Fetoprotein, the lens culinaris A-reactive fraction of  $\alpha$ -fetoprotein, and des- $\gamma$ -carboxy prothrombin were also examined. Regarding the genotype of HBV, all patients had genotype C infection. Further details on the methods used to assess these parameters are described in the Supplementary Materials and Methods. Patient characteristics according to the presence or absence of HCC are listed in Table 1.

### Reporter assays on HB-transfected HepG2 cells for the detection of altered cellular signaling.

We conducted reporter assays to clarify differences in transcriptional activities between WT and mutant HBx. The HBx gene was amplified from the serum DNA of CHB patients. The primers for WT-HBx were: 5'-ttCTCGAGATGGCTGCTCGGGTGTGC-3' (HBx forward) and 5'-ttGATATCTCAGACGGAGGTGAAAAAG-3' (HBx reverse), and amplified products were cloned into the pEBMulti-Hyg expression vector (Wako Pure Chemical). Regarding the C1485T mutation in HBx, we used the same primer set as that used for the construction of HBx-mutant Tg mice (see below). Transfection of the plasmid (control, WT-HBx, C1485T-HBx, empty vector) into HepG2 cells was performed using Fuge-6 (Roche) following the manufacturer's instructions. The expression of the HBx protein was confirmed by immunocytochemistry using an anti-HBx antibody (BioVendor, Modrice, Czech Republic). These cells were used in subsequent reporter assays.

The reporter assay for the cancer pathway was performed using the Cignal Finder Cancer 10-Pathway Reporter Array (SA Biosciences, Fredrick, MD) according to the manufacturer's instructions. HepG2 cells transfected with the pEBMulti expression vector containing WT- or C1485T-HBx were seeded onto a 96-well plate. Forty-eight hours after transfection, cell lysates were added to Luciferase Assay Reagent II, and firefly luciferase activity was measured. An empty construct was used as a negative control for the normalization of transcriptional activity.

**DEN-initiated tumorigenesis in transgenic mice.** Transgenic mice expressing WT- and C1485T-HBx were generated using C57/BL6 mice (Charles River Laboratories Japan, Yokohama, Japan). Details on the construction are provided in the Supplementary Materials and Methods. The animal experiments were approved by the institutional Animal Care and Use Committee of Kindai University and performed in accordance with the institutional guidelines.

Two-week-old Tg and non-Tg mice were intraperitoneally injected with DEN at 25 mg/kg body weight (Sigma-Aldrich, St Louis, MO). Eight months after the injection, mice were euthanized with an overdose of pentobarbital (200 mg/kg) and cut open for photography and tissue harvesting. Livers were excised, weighed, and examined for macroscopic lesions. According to standard methods, livers were fixed in 10% neutral buffered formalin (Wako Pure Chemical, Osaka, Japan), dehydrated, embedded in paraffin, sectioned serially at 5  $\mu$ m, and stained with hematoxylin and eosin. Tumorous and non-tumorous liver tissues were stored immediately at  $-80^{\circ}\text{C}$ . Identification of integration sites of transgene in the C57/BL6 mice was described in Supplementary Materials and Methods.

**Western blots and analysis of protein oxidation in hepatocytes.** DEN (100 mg/kg body weight) was intraperitoneally injected into 4-week-old Tg and non-Tg mice 4 hours before sacrifice. The liver tissue of Tg mice was homogenized with CellLytic-MT Mammalian Tissue Lysis/Extraction reagent (Sigma-Aldrich, St. Louis, MO) containing a protease inhibitor (Complete; Roche Diagnostics, Mannheim, Germany) and phosphatase inhibitor cocktail (Nacalai Tesque, Kyoto, Japan). Tissue lysates were electrophoresed on a reducing sodium dodecyl sulfate (SDS)-polyacrylamide gel and electroblotted onto a polyvinylidene difluoride (PVDF) membrane. The membrane was blocked with 5% skimmed milk and incubated with anti-phospho-ser32-I $\kappa$ B- $\alpha$ , anti-c-Jun, anti-phospho-ser73-c-Jun, anti-signal transducer and activator of transcription (STAT) 3, anti-phospho-ser727-STAT3, anti-GSK3 $\beta$ , anti-phospho-ser9-GSK3 $\beta$ , anti- $\beta$ -Catenin (Cell Signaling Technology, Inc. Danvers, MA), and anti- $\beta$ -actin (Sigma-Aldrich, St. Louis, MO) antibodies. Protein levels were detected using horseradish-peroxidase-linked secondary antibodies and the ECL-plus System (GE Healthcare, Buckinghamshire, UK). In order to evaluate signal intensity, Western blot image data were quantified using ImageJ software (NIH, Bethesda, MD).

Protein oxidation was assessed using the OxyBlot Protein Oxidation Detection Kit (Millipore Bioscience Research Reagents, Temecula, CA). Twenty micrograms of protein was reacted with dinitrophenylhydrazine for 15 min, followed by neutralization with a solution containing glycerol and 2-mercaptoethanol, resolved using 10% SDS-polyacrylamide gel electrophoresis, and transferred to a PVDF membrane using a semidry transfer system (BioRad). Membranes were then blocked with phosphate buffer saline Tween (0.05% Tween-20) containing 0.1% bovine serum albumin at room temperature for 1 hour, and incubated with a rabbit anti-2,4-dinitrophenol antibody (1:150) overnight at  $4^{\circ}\text{C}$ . The secondary antibody incubation was performed using a horseradish peroxidase-conjugated anti-rabbit IgG (1:300) at room temperature for 1 hour. Immunoreactivity was visualized by enhanced chemiluminescence using ECL plus reagents (GE Healthcare, Piscataway, NJ).



**Immunohistochemistry.** DEN (100 mg/kg body weight) was intraperitoneally injected into 4-week-old Tg and non-Tg mice. Four or 48 hours after the injection, mice were sacrificed and subjected to immunohistochemical analyses. In *in vivo* bromodeoxyuridine (BrdU) labeling, BrdU (50 mg/kg, Wako) was injected 4 hours prior to sacrifice. The liver was isolated, fixed in 20% formalin for 18 h, and stained using the BrdU *In-Situ* Detection kit (BD Pharmingen, San Diego, CA). Immunohistochemistry was performed with a Histofine SAB-PO Kit (Nichirei Biosciences, Tokyo, Japan). Anti-cyclin D1 (Cell Signaling; Beverly, MA), anti-c-myc (Santa Cruz Biotechnology, Santa Cruz, CA), and anti-NF- $\kappa$ B p65 (Cell Signaling) antibodies were used as primary antibodies.

**Statistical analysis.** In order to compare differences between patients with or without HCC, categorical and continuous variables were analyzed using Fisher's exact test and the Mann-Whitney U test, respectively. Factors with a significant difference detected in univariate analyses were subjected to multivariate analyses using a logistic regression analysis model. A *p* of <0.05 was considered to be significant. All analyses were performed with SPSS software (version 11.5; SPSS Inc., Chicago, IL).

## References

- Mittal, S. & El-Serag, H. B. Epidemiology of hepatocellular carcinoma: consider the population. *J Clin Gastroenterol.* **47**(Suppl), S2–6 (2013).
- El-Serag, H. B. Epidemiology of viral hepatitis and hepatocellular carcinoma. *Gastroenterology.* **142**, 1264–1273 (2012).
- Hai, H., Tamori, A. & Kawada, N. Role of hepatitis B virus DNA integration in human hepatocarcinogenesis. *World J Gastroenterol.* **20**, 6236–6243 (2014).
- Sung, W. K. *et al.* Genome-wide survey of recurrent HBV integration in hepatocellular carcinoma. *Nat Genet.* **44**, 765–9 (2012).
- Fujimoto, A. *et al.* Whole-genome mutational landscape and characterization of noncoding and structural mutations in liver cancer. *Nat Genet.* **48**, 500–9 (2016).
- Xu, C., Zhou, W., Wang, Y. & Qiao, L. Hepatitis B virus-induced hepatocellular carcinoma. *Cancer Lett.* **345**, 216–222 (2014).
- Lavanchy, D. Hepatitis B virus epidemiology, disease burden, treatment, and current and emerging prevention and control measures. *J Viral Hepat.* **11**, 97–107 (2004).
- Ng, S. A. & Lee, C. Hepatitis B virus X gene and hepatocarcinogenesis. *J Gastroenterol.* **46**, 974–990 (2011).
- Tanaka, Y. *et al.* Specific mutations in enhancer II/core promoter of hepatitis B virus subgenotypes C1/C2 increase the risk of hepatocellular carcinoma. *J Hepatol.* **45**, 646–653 (2006).
- Muroyama, R. *et al.* Nucleotide change of codon 38 in the X gene of hepatitis B virus genotype C is associated with an increased risk of hepatocellular carcinoma. *J Hepatol.* **45**, 805–812 (2006).
- Chen, W. N., Oon, C. J., Leong, A. L., Koh, S. & Teng, S. W. Expression of integrated hepatitis B virus X variants in human hepatocellular carcinomas and its significance. *Biochem Biophys Res Commun.* **276**, 885–892 (2000).
- Idrissi, M. E. *et al.* HBx triggers either cellular senescence or cell proliferation depending on cellular phenotype. *J Viral Hepat.* **23**, 130–138 (2016).
- Yang, Z. *et al.* Naturally occurring basal core promoter A1762T/G1764A dual mutations increase the risk of HBV-related hepatocellular carcinoma: a meta-analysis. *Oncotarget.* **7**, 12525–12536 (2016).
- Naugler, W. E. *et al.* Gender disparity in liver cancer due to sex differences in MyD88-dependent IL-6 production. *Science.* **317**, 121–4 (2007).
- Park, S. G. I, Chung, C., Kang, H., Kim, J. Y. & Jung, G. Up-regulation of cyclin D1 by HBx is mediated by NF-kappaB2/BCL3 complex through kappaB site of cyclin D1 promoter. *J Biol Chem.* **281**, 31770–31777 (2006).
- Yang, X. & Chan, C. *et al.* Repression of PKR mediates palmitate-induced apoptosis in HepG2 cells through regulation of Bcl-2. *Cell Res.* **19**, 469–86 (2009).
- Verstrepen, L. *et al.* TLR-4, IL-1R and TNF-R signaling to NF-kappaB: variations on a common theme. *Cell Mol Life Sci.* **65**, 2964–2978 (2008).
- Oeckinghaus, A., Hayden, M. S. & Ghosh, S. Crosstalk in NF- $\kappa$ B signaling pathways. *Nat Immunol.* **12**, 695–708 (2011).
- Sakurai, T. *et al.* Hepatocyte necrosis induced by oxidative stress and IL-1 alpha release mediate carcinogen-induced compensatory proliferation and liver tumorigenesis. *Cancer Cell* **14**, 156–165 (2008).
- Kurien, B. T. & Scofield, R. H. Other Notable Methods of Membrane Protein Detection: A Brief Review. *Methods Mol Biol.* **1314**, 357–370 (2015).
- Anastas, J. N. & Moon, R. T. WNT signalling pathways as therapeutic targets in cancer. *Nat Rev Cancer.* **13**, 11–26 (2013).
- Liu, S., Koh, S. S. & Lee, C. G. Hepatitis B Virus X Protein and Hepatocarcinogenesis. *Int J Mol Sci.* **17**(6), pii: E940 (2016).
- Zhang, A. Y. *et al.* Hepatitis B virus full-length genomic mutations and quasispecies in hepatocellular carcinoma. *J Gastroenterol Hepatol.* **31**, 1638–45 (2016).
- Erhardt, A. *et al.* Mutations of the core promoter and response to interferon treatment in chronic replicative hepatitis B. *Hepatology.* **31**, 716–725 (2000).
- Sugauchi, F. *et al.* Epidemiologic and virologic characteristics of hepatitis B virus genotype B having the recombination with genotype C. *Gastroenterology.* **124**, 925–932 (2003).
- Croagh, C. M., Desmond, P. V. & Bell, S. J. Genotypes and viral variants in chronic hepatitis B: A review of epidemiology and clinical relevance. *World J Hepatol.* **7**, 289–303 (2015).
- Yu, S. J. & Kim, Y. J. Hepatitis B viral load affects prognosis of hepatocellular carcinoma. *World J Gastroenterol.* **20**, 12039–12044 (2014).
- Nishida, N. *et al.* Unique features associated with hepatic oxidative DNA damage and DNA methylation in non-alcoholic fatty liver disease. *J Gastroenterol Hepatol.* **31**, 1646–53 (2016).
- Nishida, N. *et al.* Reactive oxygen species induce epigenetic instability through the formation of 8-hydroxydeoxyguanosine in human hepatocarcinogenesis. *Dig Dis.* **31**, 459–66 (2013).
- Bouchard, M. J. & Schneider, R. J. The enigmatic X gene of hepatitis B virus. *J Virol.* **78**, 12725–12734 (2004).
- Logan, C. Y. & Nusse, R. The Wnt signaling pathway in development and disease. *Annu Rev Cell Dev Bio.* **20**, 781–810 (2004).
- Cha, M. Y., Kim, C. M., Park, Y. M. & Ryu, W. S. Hepatitis B virus X protein is essential for the activation of Wnt/beta-catenin signaling in hepatoma cells. *Hepatology* **39**, 1683–1693 (2004).
- Pan, J., Duan, L. X., Sun, B. S. & Feitelson, M. A. Hepatitis B virus X protein protects against anti-Fas-mediated apoptosis in human liver cells by inducing NF-kappa B. *J Gen Virol.* **82**, 171–182 (2001).
- Liu, L. P. *et al.* The role of NF-kappaB in Hepatitis b virus X protein-mediated upregulation of VEGF and MMPs. *Cancer Invest.* **28**, 443–451 (2010).
- Maeda, S., Kamata, H., Luo, J. L., Leffert, H. & Karin, M. IKKbeta couples hepatocyte death to cytokine-driven compensatory proliferation that promotes chemical hepatocarcinogenesis. *Cell.* **121**, 977–990 (2005).
- Kamata, H. *et al.* Reactive oxygen species promote TNFalpha-induced death and sustained JNK activation by inhibiting MAP kinase phosphatases. *Cell.* **120**, 649–661 (2005).



37. Eferl, R. *et al.* Liver tumor development. c-Jun antagonizes the proapoptotic activity of p53. *Cell* **112**, 181–192 (2003).
38. Sakurai, T. *et al.* p38 $\alpha$  inhibits liver fibrogenesis and consequent hepatocarcinogenesis by curtailing accumulation of reactive oxygen species. *Cancer Res.* **73**, 215–224 (2013).
39. Sakurai, T., Maeda, S., Chang, L. & Karin, M. Loss of hepatic NF-kappa B activity enhances chemical hepatocarcinogenesis through sustained c-Jun N-terminal kinase 1 activation. *Proc Natl Acad Sci USA* **103**, 10544–51 (2006).
40. Hagiwara, S. *et al.* Activation of JNK and high expression level of CD133 predict a poor response to sorafenib in hepatocellular carcinoma. *Br J Cancer* **106**, 1997–2003 (2012).

## Acknowledgements

This work was supported by a Health Labor Sciences Research Grant from the Ministry of Health Labour and Welfare of Japan (H22-Clinical Oncology-General-015) and a grant from the Smoking Research Foundation (N.N. and T.W.).

## Author Contributions

Study concept and design (S.H., T.S., and N.N.); analysis and interpretation of data (S.H., T.S., A.-M.P., Y.K., N.N., T.W., and M.K.); statistical analysis (S.H.); provision of samples (S.H., T.S., and A.-M.P.); drafting the manuscript (S.H., T.W., and N.N.); obtaining funding (M.K.).

## Additional Information

**Supplementary information** accompanies this paper at doi:[10.1038/s41598-017-10570-0](https://doi.org/10.1038/s41598-017-10570-0)

**Competing Interests:** The authors declare that they have no competing interests.

**Publisher's note:** Springer Nature remains neutral with regard to jurisdictional claims in published maps and institutional affiliations.



**Open Access** This article is licensed under a Creative Commons Attribution 4.0 International License, which permits use, sharing, adaptation, distribution and reproduction in any medium or format, as long as you give appropriate credit to the original author(s) and the source, provide a link to the Creative Commons license, and indicate if changes were made. The images or other third party material in this article are included in the article's Creative Commons license, unless indicated otherwise in a credit line to the material. If material is not included in the article's Creative Commons license and your intended use is not permitted by statutory regulation or exceeds the permitted use, you will need to obtain permission directly from the copyright holder. To view a copy of this license, visit <http://creativecommons.org/licenses/by/4.0/>.

© The Author(s) 2017

# New Era of the Management of Liver Diseases and Liver Cancer: State-of-the-Art Progress in 2017

Masatoshi Kudo

Department of Gastroenterology and Hepatology, Kindai University Faculty of Medicine, Osaka-Sayama, Japan

Kitahata et al. [1] reported the abdominal ultrasound (US) findings of hepatic malignant lymphoma in 25 patients. They found that the US imaging features of hepatic malignant lymphoma differ, depending on the tumor diameter.

Tsutsui et al. [2] reported clinicopathological study of autoimmune hepatitis (AIH) cases that were difficult to differentiate from drug-induced liver injury (DILI). According to them, acute-onset AIH histopathologically presents with features of acute hepatitis and lacks a specific diagnostic method; finally, AIH is often difficult to differentiate from DILI. Therefore, they attempted to investigate the final clinical diagnosis of these cases, and compare the clinical, biochemical, and histological characteristics of AIH vs. DILI. They concluded that the Digestive Disease Week Japan 2004 scale was useful in differentiating AIH from DILI when the Digestive Disease Week Japan 2004 scale score was  $\geq 5$ . The histologic features of AIH were characterized by cobblestone hepatocellular change, interface hepatitis, and plasma cell infiltration of the portal region.

Yada et al. [3] presented the diagnosis of fibrosis and activity by a combined use of strain and shear wave imaging in patients with liver disease. According to them, the combined use of strain and shear wave imaging (combinational elastography) for cases without jaundice and congestion might be useful in evaluating fibrosis and inflammation. They concluded that the results obtained from their

research might impact the development of future diagnostic equipments and the direction of practical guidelines.

Kobayashi et al. [4] presented the ability of cytokeratin-18 fragments and FIB-4 index to diagnose the overall and mild fibrosis nonalcoholic steatohepatitis (NASH) in Japanese nonalcoholic fatty liver disease patients. They concluded that among several laboratory markers, FIB-4 index and CK-18F demonstrated the ability to diagnose NASH and also the form of the disease with mild fibrosis.

Imoto et al. [5] stated that 2 single nucleotide polymorphisms, upstream of the interferon- $\lambda$  (IFNL) 3 gene, are associated with spontaneous clearance of the hepatitis C virus (HCV) in symptomatic patients with acute hepatitis C. Although these 2 single nucleotide polymorphisms, rs8099917, and rs12979860, have established their significance in HCV clearance, the detailed mechanisms of their roles remain unknown. Therefore, they attempted to clarify the factors affecting IFNL3 production and assess the roles of IFNL3 in the mechanisms of the innate immune response to spontaneously clear HCV in patients with acute hepatitis C. They found that primary HCV infection triggers the production of IFNL3. As a first line of defense in the innate immune system against invading HCV, increased IFNL3 levels play an important role.

Seo et al. [6] compared the effect of Sofosbuvir plus Ribavirin (RBV) treatment with pegylated interferon plus RBV treatment in patients with chronic hepatitis C (CHC) gen-

otype 2. They found that the treatment with Sofosbuvir plus RBV results in not only higher sustained virological response (SVR), but also improves the liver function and the degree of fibrosis as assessed with the use of pathophysiological biomarkers, such as hyaluronic acid, bone morphogenetic protein 7 and connective tissue growth factor.

Umehara et al. [7] studied 415 CHC patients who were treated with interferon-based therapy and investigated the risk factor of hepatocarcinogenesis. They concluded that the serum albumin level was the strongest risk factor for carcinogenesis after SVR achievement in this retrospective study. In addition, this factor was also associated with hepatocellular carcinoma (HCC) development in patients with slight liver fibrosis. Furthermore, the serum albumin level was more sensitive than the progression of liver fibrosis in the prediction of HCC development, and careful follow-up for the detection of HCC may be necessary in such high-risk patients.

Kono et al. [8] found that direct-acting antivirals (DAAs) dramatically improve the sustained pre-treatment characteristics related to sustained liver damage after SVR of chronic CHC patients since continuous liver damage after SVR may be a risk of HCC. Also, the high FIB-4 index, low albumin level, and fatty liver before DAA treatment were associated with a risk of sustained liver damage with AFP and ALT elevation after SVR, suggesting that patients with these factors should be carefully monitored for emergence of HCC.

Ida et al. [9] attempted to clarify whether DAAs can efficiently prevent the occurrence of HCC after SVR, as observed in the interferon-based therapy. They analyzed the clinical features of patients in whom HCC developed after achievement of SVR with DAAs for chronic HCV infection. They concluded that HCC can develop even after SVR by DAAs, especially when patients have a past history of HCC. In this high-risk group, surveillance for HCC detection after achievement of SVR is required. They also stated that even if HCC developed after SVR, curative anticancer therapy was applicable in most cases.

Iwamoto et al. [10] observed that the cumulative incidence of new intrahepatic recurrence was significantly higher in patients with non-hypervascular hypointense hepatic nodules than those without non-hypervascular hypointense hepatic nodules ( $p < 0.0001$ ). Multivariate analysis revealed that the presence of non-hypervascular hypointense hepatic nodules were independent risk factors for new intrahepatic recurrence. These results were consistent with 3 previous reports [11–13].

Arizumi et al. [14] described that tumor characteristics classified as Barcelona Clinic Liver Cancer (BCLC) stage B

HCC are heterogeneous, thus, subclassification such as Kinki criteria is necessary. However, tumors in stage B also include various size and number of HCCs even with Kinki criteria, which should lead to heterogeneity for the overall survival (OS). Therefore, they attempted to clarify how size and number of tumors affect the OS and time to progression in patients with Kinki criteria stage B2 tumors and treated with transarterial chemoembolization (TACE). They found that while significant differences in the OS are observed between BCLC subclasses B1 and B2, no such differences were observed within BCLC sub-substage B2. However, there were statistical differences in time to progression between BCLC sub-substage B2b and B2c/B2a sub-substage patients. Based on these results, B2b substage HCC patients may be good candidates for systemic therapy rather than TACE to improve the survival by preserving the liver function. In addition, they state that since BCLC substage B2 patients with multiple tumors are less responsive to cTACE than BCLC substage B1 patients, further clinical trials are needed to confirm this hypothesis.

Arizumi et al. [15] presented time to transcatheter arterial chemoembolization refractoriness in patients with HCC in Kinki criteria stages B1 and B2. They found that TACE refractoriness occurred earlier in substage B2 HCC than in substage B1 HCC. Thus, the number of TACE sessions performed before the onset of TACE refractoriness was smaller in substage B2 HCC. Moreover, liver function impairment was detected earlier in substage B2 HCC than in substage B1 HCC. In substage B2 HCC, the early onset of TACE refractoriness is assumed to be responsible for the shorter survival than that in substage B1 HCC. They concluded that TACE monotherapy may be limited in efficacy for substage B2 HCC, and inventive therapeutic strategies, such as combination therapies, may be necessary to improve the effects of TACE. Furthermore, when the onset of TACE refractoriness is confirmed, TACE may need to be switched to other therapies, such as hepatic arterial infusion chemotherapy or systemic therapy such as sorafenib, sorafenib-regorafenib sequential therapy, as soon as possible.

Ishikawa et al. [16] described that balloon-occluded transcatheter arterial chemoembolization (B-TACE) using miriplatin is a new strategy for HCC. Therefore, they attempted to evaluate the hemodynamic changes with/without balloon occlusion of the hepatic artery and correlation of cone-beam CT (CB-CT) pixels and CT value after B-TACE for HCC. They found that CB-CT pixel values with balloon occlusion were significantly higher than those without balloon occlusion. However, CB-CT pixel values after balloon occlusion decreased in some cases. In

addition, in the increased group, postoperative CT value was clearly higher, and local recurrence suppressed. By performing CB-CT before and after balloon occlusion, it may be possible to predict the effect of B-TACE using mriplatin. Whereas lower CB-CT pixel values after balloon occlusion groups may be ineffective, there is a need to consider other strategies. Finally, they concluded that following balloon occlusion, intratumoral arterial flow may change, presumably due to a collateral pathway. B-TACE for HCC lesions showing decreased pixel values after balloon occlusion CB-CT may have a poor short-term therapeutic effect compared to those with increased pixel values.

Hiraoka et al. [17] evaluated the relationship of hepatic function with repeated TACE and prognosis after sorafenib treatment in various patient cohorts. They found that the ALBI score gradually worsens with continued TACE, though the ratio of worsening hepatic function is not low even after a few procedures. In addition, downgrading from ALBI-1 during the introduction of sorafenib might be a factor related to poor prognosis. They concluded that for considering the development of new molecular targeted agents [18–21] and other therapeutic modalities including hepatic arterial infusion chemotherapy [22, 23], consideration of therapeutic options that prolong the prognosis of patients with advanced and unresectable HCC are needed. Also, it is important to maintain the liver function by avoiding ineffective TACE that provide poor response with declined liver function at the time of TACE refractoriness, when TACE may be a harmful option, and promptly switch to the systemic therapy such as sorafenib followed by regorafenib.

Ueshima et al. [24] reported a single-institute experience of Sorafenib-regorafenib sequential therapy in advanced HCC. They reported that the median progression-free survival by this sequential treatment was 9.2 months (95% CI 2.3–16.1), the objective response rate was 9.1%, and the disease control rate was 72.7%. They concluded that Sorafenib and regorafenib sequential therapy represents a safe and effective treatment option for patients with advanced HCC.

Nishida et al. [25] described the role of immune checkpoint blockade in the treatment for human HCC. They described that several immune checkpoints are involved in the suppression of an antitumor immune response. Antibodies against these checkpoints such as anti-programmed cell death-1 (PD-1), anti-PD-ligand 1 (PD-L1), and anti-cytotoxic T-lymphocyte-associated antigen 4 (CTLA-4) are now clinically available for the treatment of human

cancers [26]. Currently, clinical trials of anti-PD-1 antibody (nivolumab, pembrolizumab) and anti-PD-L1 antibody (durvalumab), both individually and in combination with anti-CTLA-4 antibody (ipilimumab, durvalumab), are ongoing. At the end of phase I/II trials of nivolumab (CheckMate 040), an objective response rate was observed in 20% of the 214 HCC patients who received 3 mg/kg of nivolumab every 2 weeks (expansion cohort), and a disease control rate was observed in 64% of the patients [27]. Based on the promising results from the present phase III clinical trial of molecular targeting agents [28], new strategies for the treatment of advanced HCC can be designed for the better control of tumor growth. However, mutational heterogeneity of HCC cells eventually leads to the development of resistance to these chemotherapeutic agents [29–31]. Recent studies have shown that the inhibition of immune checkpoints has a great potential to be effective against advanced HCCs that have become drug resistant. However, considering the immunosuppressive tumor microenvironment and the mutation burden of HCC, which could be related to the antigenicity of the tumor, immunotherapy using immune checkpoint inhibitors could have its limitations. The limited tumor responses seen during the clinical trials of immune checkpoint monotherapy have prompted investigations into combination therapies using immune checkpoint inhibitors with molecular targeted agents, such as Lenvatinib.

Recent progress of diagnostic modalities and biomarkers make it easy to diagnose HCC in its early stage, enabling the application of curative treatments, such as resection [32–34], ablation [35–40], and transplantation [41–43]. In intermediate stage HCC, it is important to sub-classify the BCLC-B stage, and systemic therapy may be more suitable [44, 45] for patients with TACE refractoriness or systemic therapy may even be the 1st line therapy for those who may easily develop TACE failure [46]. In advanced HCC, intra-arterial infusion chemotherapy [32, 40] and targeted therapy including sorafenib and 2nd line agent, regorafenib are used. Lenvatinib is also a promising agent since its non-inferiority to sorafenib was shown recently. Current ongoing clinical trials of immune checkpoint inhibitors, PD-1/PD-L1 antibody including monotherapy, combination therapy with CTLA-4, combination therapy with targeted agents, and combination therapy with locoregional therapy are very promising [19].

Finally, I strongly believe that this special issue “New Era of the Management of Liver Diseases: State-of-the-Art Progress in 2017” will be beneficial and invaluable for all readers who have specialized in liver diseases, especially liver cancer.



## References

- Kitahata S, Hiraoka A, Kudo M, Murakami T, Ochi M, Izumoto H, Ueki H, Kaneto M, Aibiki T, Okudaira T, Yamago H, Miyamoto Y, Iwasaki R, Tomida H, Mori K, Kishida M, Miyata H, Tsubouchi E, Hirooka M, Koizumi Y, Ninomiya T, Hiasa Y, Michitaka K: Abdominal ultrasound findings of tumor-forming hepatic malignant lymphoma. *Digest Dis* 2017, in press.
- Tsutsui A, Harada K, Tsuneyama K, Senoh T, Nagano T, Takaguchi K, Ando M, Nakamura S, Mizobuchi K, Kudo M: Clinicopathological study of autoimmune hepatitis cases that were difficult to differentiate from drug-induced liver injury. *Digest Dis* 2017, in press.
- Yada N, Tamaki N, Koizumi Y, Hirooka M, Nakashima O, Hiasa Y, Izumi N, Kudo M: Diagnosis of fibrosis and activity by a combined use of strain and shear wave imaging in patients with liver disease. *Digest Dis* 2017, in press.
- Kobayashi N, Kumada T, Toyoda H, Tada T, Ito T, Kage M, Okanoue T, Kudo M: Ability of cytokeratin-18 fragments and FIB-4 index to diagnose overall and mild fibrosis nonalcoholic steatohepatitis in Japanese nonalcoholic fatty liver disease patients. *Digest Dis* 2017, in press.
- Imoto S, Kim S, Amano K, Iio E, Yoon S, Hirohata S, Yano Y, Ishikawa T, Katsushima S, Komeda T, Fukunaga T, Chung H, Kokuryu H, Horie Y, Hatae T, Fujinami A, Kim S, Kudo M, Tanaka Y: Serum IFN- $\gamma$  levels correlate with serum HCV RNA levels in symptomatic patients with acute hepatitis C. *Digest Dis* 2017, in press.
- Seo K, Kim S, Kim S, Ohtani A, Kobayashi M, Kato A, Morimoto E, Saijo Y, Kim K, Imoto S, Kim C, Yano Y, Kudo M, Hayashi Y: Comparison of Sofosbuvir plus Ribavirin treatment with pegylated interferon plus Ribavirin treatment for chronic hepatitis C genotype 2. *Digest Dis* 2017, in press.
- Umehara Y, Hagiwara S, Nishida N, Sakurai T, Ida H, Minami Y, Takita M, Minami T, Chishina H, Ueshima K, Komeda Y, Arizumi T, Watanabe T, Kudo M: Hepatocarcinogenesis is associated with serum albumin levels after sustained virological responses with interferon based therapy in patients with hepatitis C. *Dig Dis* 2017, in press.
- Kono M, Nishida N, Hagiwara S, Minami T, Chishina H, Arizumi T, Minaga K, Kamata K, Komeda Y, Sakurai T, Takenaka M, Takita M, Yada N, Ida H, Minami Y, Ueshima K, Watanabe T, Kudo M: Unique characteristics associated with sustained liver damage in chronic hepatitis C patients treated with direct acting antivirals. *Digest Dis* 2017, in press.
- Ida H, Hagiwara S, Kono M, Minami T, Chishina H, Arizumi T, Takita M, Yada N, Minami Y, Ueshima K, Nishida N, Kudo M: Hepatocellular carcinoma after achievement of sustained viral response with daclatasvir and asunaprevir in patients with chronic hepatitis C virus infection. *Digest Dis* 2017, in press.
- Iwamoto T, Imai Y, Igura T, Kogita S, Sawai Y, Fukuda K, Yamaguchi Y, Matsumoto Y, Nakahara M, Morimoto O, Ohashi H, Fujita N, Kudo M, Takehara T: Non-hypervascular hypointense hepatic nodules during the hepatobiliary phase of Gd-EOB-DTPA-enhanced MRI as a risk factor of intrahepatic distant recurrence after radiofrequency ablation of hepatocellular carcinoma. *Digest Dis* 2017, in press.
- Toyoda H, Kumada T, Tada T, Niinomi T, Ito T, Sone Y, Kaneoka Y, Maeda A: Non-hypervascular hypointense nodules detected by Gd-EOB-DTPA-enhanced MRI are a risk factor for recurrence of HCC after hepatectomy. *J Hepatol* 2013;58:1174–1180.
- Lee DH, Lee JM, Lee JY, Kim SH, Kim JH, Yoon JH, Kim YJ, Lee JH, Yu SJ, Han JK, Choi BI: Non-hypervascular hepatobiliary phase hypointense nodules on gadoxetic acid-enhanced MRI: risk of HCC recurrence after radiofrequency ablation. *J Hepatol* 2015;62:1122–1130.
- Toyoda H, Kumada T, Tada T, Sone Y, Maeda A, Kaneoka Y: Non-hypervascular hypointense nodules on Gd-EOB-DTPA-enhanced MRI as a predictor of outcomes for early-stage HCC. *Hepatol Int* 2015;9:84–92.
- Arizumi T, Minami T, Chishina H, Kono M, Takita M, Yada N, Hagiwara S, Minami Y, Ida H, Ueshima K, Kamata K, Minaga K, Komeda Y, Takenaka M, Sakurai T, Watanabe T, Nishida N, Kudo M: Impact of tumor factors on survival in patients with hepatocellular carcinoma classified based on kinki criteria stage B2. *Digest Dis* 2017, in press.
- Arizumi T, Minami T, Chishina H, Kono M, Takita M, Yada N, Hagiwara S, Minami Y, Ida H, Ueshima K, Kamata K, Minaga K, Komeda Y, Takenaka M, Sakurai T, Watanabe T, Nishida N, Kudo M: Time to transcatheter arterial chemoembolization refractoriness in patients with hepatocellular carcinoma in Kinki criteria stages B1 and B2. *Digest Dis* 2017, in press.
- Ishikawa T, Imai M, Owaki T, Sato H, Nozawa Y, Sano T, Iwanaga A, Seki K, Honma T, Yoshida T, Kudo M: Hemodynamic changes on cone-beam computed tomography during balloon-occluded transcatheter arterial chemoembolization using miriplatin for hepatocellular carcinoma: a Preliminary Study. *Digest Dis* 2017, in press.
- Hiraoka A, Kumada T, Kudo M, Hirooka M, Koizumi Y, Hiasa Y, Tajiri K, Toyoda H, Tada T, Ochi H, Joko K, Shimada N, Deguchi A, Ishikawa T, Imai M, Tsuji K, Michitaka K: Hepatic function during repeated TACE procedures and prognosis after introducing sorafenib in patients with unresectable HCC – multicenter analysis. *Digest Dis* 2017, in press.
- Kudo M: Molecular targeted therapy for hepatocellular carcinoma: where are we now? *Liver Cancer* 2015;4:I–VII.
- Kudo M: Immune checkpoint blockade in hepatocellular carcinoma. *Liver Cancer* 2015;4:201–207.
- Kudo M: Regorafenib as second-line systemic therapy may change the treatment strategy and management paradigm for hepatocellular carcinoma. *Liver Cancer* 2016;5:235–244.
- Zhang B, Finn RS: Personalized Clinical Trials in hepatocellular carcinoma based on biomarker selection. *Liver Cancer* 2016;5:221–232.
- Obi S, Sato S, Kawai T: Current status of hepatic arterial infusion chemotherapy. *Liver Cancer* 2015;4:188–199.
- Lin CC, Hung CF, Chen WT, Lin SM: Hepatic arterial infusion chemotherapy for advanced hepatocellular carcinoma with portal vein thrombosis: impact of early response to 4 weeks of treatment. *Liver Cancer* 2015;4:228–240.
- Ueshima K, Nishida N, Kudo M: Sorafenib-regorafenib sequential therapy in advanced hepatocellular carcinoma: a single-institute experience. *Digest Dis* 2017, in press.
- Nishida N, Kudo M: Role of immune checkpoint blockade in the treatment for human hepatocellular carcinoma. *Digest Dis* 2017, in press.
- Kudo M: Immune checkpoint inhibition in hepatocellular carcinoma: basics and Ongoing Clinical Trials. *Oncology* 2017;92(suppl 1):50–62.
- El-Khoueiry AB, Sangro B, Yau T, Crocenzi TS, Kudo M, Hsu C, Kim TY, Choo SP, Trojan J, Welling THR, Meyer T, Kang YK, Yeo W, Chopra A, Anderson J, Dela Cruz C, Lang L, Neely J, Tang H, Dastani HB, Melero I: Nivolumab in patients with advanced hepatocellular carcinoma (CheckMate 040): an open-label, non-comparative, phase 1/2 dose escalation and expansion trial. *Lancet* 2017;389:2492–2502.
- Kudo M: A New Era of Systemic Therapy for hepatocellular carcinoma with regorafenib and lenvatinib. *Liver Cancer* 2017;6:177–184.
- Nishida N, Kudo M: Recent advancements in comprehensive genetic analyses for human hepatocellular carcinoma. *Oncology* 2013;84(suppl 1):93–97.
- Nishida N, Chishina H, Arizumi T, Takita M, Kitai S, Yada N, Hagiwara S, Inoue T, Minami Y, Ueshima K, Sakurai T, Kudo M: Identification of epigenetically inactivated genes in human hepatocellular carcinoma by integrative analyses of methylation profiling and pharmacological unmasking. *Dig Dis* 2014;32:740–746.
- Nishida N, Kitano M, Sakurai T, Kudo M: Molecular mechanism and prediction of sorafenib chemoresistance in human hepatocellular carcinoma. *Dig Dis* 2015;33:771–779.



- 32 Kudo M, Izumi N, Sakamoto M, Matsuyama Y, Ichida T, Nakashima O, Matsui O, Ku Y, Kokudo N, Makuuchi M: Survival analysis over 28 years of 173,378 patients with hepatocellular carcinoma in Japan. *Liver Cancer* 2016;5:190–197.
- 33 Ho MC, Hasegawa K, Chen XP, Nagano H, Lee YJ, Chau GY, Zhou J, Wang CC, Choi YR, Poon RT, Kokudo N: Surgery for intermediate and advanced hepatocellular carcinoma: a consensus report from the 5th Asia-Pacific primary liver cancer expert meeting (APPLE 2014). *Liver Cancer* 2016;5:245–256.
- 34 Kudo M: Surveillance, diagnosis, treatment, and outcome of liver cancer in Japan. *Liver Cancer* 2015;4:39–50.
- 35 Teng W, Liu KW, Lin CC, Jeng WJ, Chen WT, Sheen IS, Lin CY, Lin SM: Insufficient ablative margin determined by early computed tomography may predict the recurrence of hepatocellular carcinoma after radiofrequency ablation. *Liver Cancer* 2015;4:26–38.
- 36 Kudo M: Locoregional therapy for hepatocellular carcinoma. *Liver Cancer* 2015;4:163–164.
- 37 Kang TW, Rhim H: Recent advances in tumor ablation for hepatocellular carcinoma. *Liver Cancer* 2015;4:176–187.
- 38 Lencioni R, de Baere T, Martin RC, Nutting CW, Narayanan G: Image-guided ablation of malignant liver tumors: recommendations for clinical validation of novel thermal and non-thermal technologies – A Western perspective. *Liver Cancer* 2015;4:208–214.
- 39 Lin CC, Cheng YT, Chen MW, Lin SM: The effectiveness of multiple electrode radiofrequency ablation in patients with hepatocellular carcinoma with lesions more than 3 cm in size and barcelona clinic liver cancer stage A to B2. *Liver Cancer* 2016;5:8–20.
- 40 Kitai S, Kudo M, Nishida N, Izumi N, Sakamoto M, Matsuyama Y, Ichida T, Nakashima O, Matsui O, Ku Y, Kokudo N, Makuuchi M; Liver Cancer Study Group of Japan: Survival benefit of locoregional treatment for hepatocellular carcinoma with advanced liver cirrhosis. *Liver Cancer* 2016;5:175–189.
- 41 Poon RT, Cheung TT, Kwok PC, Lee AS, Li TW, Loke KL, Chan SL, Cheung MT, Lai TW, Cheung CC, Cheung FY, Loo CK, But YK, Hsu SJ, Yu SC, Yau T: Hong Kong consensus recommendations on the management of hepatocellular carcinoma. *Liver Cancer* 2015;4:51–69.
- 42 Clinical practice guidelines for hepatocellular carcinoma differ between Japan, United States, and Europe. *Liver Cancer* 2015;4:85–95.
- 43 Chow PK, Choo SP, Ng DC, Lo RH, Wang ML, Toh HC, Tai DW, Goh BK, Wong JS, Tay KH, Goh AS, Yan SX, Loke KS, Thang SP, Gogna A, Too CW, Irani FG, Leong S, Lim KH, Thng CH: National cancer centre Singapore consensus guidelines for hepatocellular carcinoma. *Liver Cancer* 2016;5:97–106.
- 44 Geschwind JF, Gholam PM, Goldenberg A, Mantry P, Martin RC, Piperdi B, Zigmont E, Imperial J, Babajanyan S, Foreman PK, Cohn A: Use of transarterial chemoembolization (TACE) and sorafenib in patients with unresectable hepatocellular carcinoma: US regional analysis of the GIDEON registry. *Liver Cancer* 2016;5:37–46.
- 45 Tsurusaki M, Murakami T: Surgical and locoregional therapy of HCC: TACE. *Liver Cancer* 2015;4:165–175.
- 46 Arizumi T, Ueshima K, Minami T, Kono M, Chishina H, Takita M, Kitai S, Inoue T, Yada N, Hagiwara S, Minami Y, Sakurai T, Nishida N, Kudo M: Effectiveness of Sorafenib in patients with transcatheter arterial chemoembolization (TACE) refractory and intermediate-stage hepatocellular carcinoma. *Liver Cancer* 2015;4:253–262.

# Abdominal Ultrasound Findings of Tumor-Forming Hepatic Malignant Lymphoma

Shogo Kitahata<sup>a</sup> Atsushi Hiraoka<sup>a</sup> Masatoshi Kudo<sup>b</sup> Taisei Murakami<sup>a</sup>  
Marie Ochi<sup>a</sup> Hirofumi Izumoto<sup>a</sup> Hidetaro Ueki<sup>a</sup> Miho Kaneto<sup>a</sup>  
Toshihiko Aibiki<sup>a</sup> Tomonari Okudaira<sup>a</sup> Hiroka Yamago<sup>a</sup> Yuji Miyamoto<sup>a</sup>  
Ryuichiro Iwasaki<sup>a</sup> Hideomi Tomida<sup>a</sup> Kenichiro Mori<sup>a</sup> Masato Kishida<sup>a</sup>  
Hideki Miyata<sup>a</sup> Eiji Tsubouchi<sup>a</sup> Masashi Hirooka<sup>c</sup> Yohei Koizumi<sup>c</sup>  
Tomoyuki Ninomiya<sup>a</sup> Yoichi Hiasa<sup>b</sup> Kojiro Michitaka<sup>a</sup>

<sup>a</sup>Gastroenterology Center, Ehime Prefectural Central Hospital, Matsuyama, <sup>b</sup>Kindai University School of Medicine, Department of Gastroenterology and Hepatology, Osaka, and <sup>c</sup>Department of Gastroenterology and Metabology, Ehime University Graduate School of Medicine, Toon, Japan

## Keywords

Hepatic malignant lymphoma · Ultrasonography · Contrast-enhanced ultrasonography · Perflubutane

## Abstract

**Aim/Background:** Evaluations of abdominal ultrasonography (US) findings of primary and secondary tumor-forming hepatic malignant lymphoma (HML) have not been adequately reported. In this study, we elucidated US and contrast-enhanced US (CEUS) findings in patients with HML. **Materials/Methods:** From January 2006 to March 2017, 25 patients with HML were enrolled (primary 7, secondary 18), each of whom was diagnosed pathologically. They were divided into 2 groups based on tumor diameter (cutoff, 30 mm). US imaging findings were retrospectively analyzed. **Results:** All tumors in patients with a small HML (<30 mm in diameter, small group,  $n = 14$ ) were revealed as homo-

geneous hypo-echoic type (100%), with penetrating sign observed in only 1 patient. Tumors in 11 patients in the small group, examined with CEUS, showed homogeneous enhancement in the early vascular phase (91%) and a washout pattern in the portal phase (100%), and they were revealed as defective in the post-vascular phase (100%). In the large group ( $\geq 30$  mm;  $n = 11$ ), tumors were revealed as a heterogeneous hypo-echoic lesion in 10 (91%) and penetrating sign was observed in 8 (73%). Dilatation of the distal intrahepatic bile duct by the tumor was observed in 4 patients in the large group. In 7 large group patients examined with CEUS, imaging findings in the early vascular phase varied, with 5 (71%) showing a washout pattern in the portal phase and 5 (71%) revealed as defective in the post-vascular phase. **Conclusion:** We found that US imaging features of HML differ depending on the tumor diameter.

© 2017 S. Karger AG, Basel

A malignant lymphoma (ML) is known to be derived from lymphatic tissue. Evaluations of abdominal ultrasonography (US) findings of primary and secondary tumor-forming hepatic ML (HML) tumors have not been adequately reported. It is generally considered that an HML is revealed as a homogeneous hypo-echoic lesion [1–3] that often includes a portal or hepatic vein inside of the tumor without invasion (penetrating sign) [4, 5] in conventional US findings. However, a small number of patients with HML shows that there is a lack of deterministic findings in US and contrast-enhanced US (CEUS) examinations. As a result, differential diagnosis from other types of malignant hepatic tumors, such as hepatocellular carcinoma (HCC) [6, 7] and cholangiocellular carcinoma (CCC) [8], is difficult in some cases using US. In the present study, we elucidated US and CEUS findings obtained in patients with HML.

## Materials and Methods

We enrolled 25 patients diagnosed with HML based on pathological findings, obtained from examinations performed at our hospitals from January 2006 to March 2017. The definition of primary HML proposed by Ohsawa et al. [9] was used in this study. All underwent US examinations, while CEUS was performed in 18 (72%) with HI VISION Preirus (probe: EUP-C715, 3.0 MHz, MI 0.2; Hitachi, Tokyo, Japan) or Logic E9 (probe: C1-6-D, 3.4 MHz, MI 0.25, GE Healthcare Medical Systems, Milwaukee, WI, USA, Perflubutane (Sonazoid®; Daiichi Sankyo Co. Ltd., Tokyo, Japan) (0.5 mL/kg of body weight) was injected as the contrast agent for each CEUS examination. The arterial phase of CEUS imaging was identified at 10–60 s after, and the post-vascular phase at 10 min after the injection. The portal phase of CEUS imaging was identified at 1–2 min after perflubutane injection. Findings of US and CEUS were evaluated in a retrospective manner. When the antibody for hepatitis C virus (HCV)/HCV-RNA or hepatitis B surface antigen was detected, the patients were determined to have a chronic HCV or hepatitis B virus (HBV) infection.

Fischer's exact test was used for comparisons with the EZR package [10] using the R program. The study protocol was approved by the Institutional Ethics Committee of Ehime Prefectural Central Hospital (No. 28–52).

## Results

The clinical characteristics of the present cohort are shown in Table 1 (median age 70 years, interquartile range 58–81 years; 15 males, 10 females; 7 primary, 18 secondary; 6 HCV, 5 HBV, 14 no liver disease; diffuse large B-cell lymphoma [DLBCL],  $n = 13$ , DLBCL + mucosa-associated lymphoid tissue,  $n = 2$ , mucosa-associated lymphoid

tissue [11],  $n = 2$ , Hodgkin's lymphoma,  $n = 2$ , B-cell lymphoma [details unknown],  $n = 2$ , DLBCL + methotrexate-associated lymphoproliferative disorders [MTX-LPD],  $n = 1$ , T-cell lymphoma + MTX-LPD,  $n = 1$ , adult T-cell lymphoma,  $n = 1$ , MTX-LPD [12],  $n = 1$ ). The median tumor size was 26 mm (interquartile range 17–50 mm). Although all lesions were revealed as hypo-echoic with conventional US, the internal echo was revealed as heterogeneous in 10 and homogeneous in 15. The border of the tumor was unclear in 11. Inside the tumor, penetrating sign was detected in 9 patients. Dilatation of the distal intrahepatic bile duct by the tumor was observed in 4.

When the cohort was divided into 2 groups according to tumor diameter ( $<30$  mm, small group,  $n = 14$ ;  $\geq 30$  mm, large group,  $n = 11$ ), the tumors of 10 patients in the large group were revealed as a heterogeneous hypo-echoic tumor, 9 had an unclear boundary, and 8 had penetrating sign. Dilatation of the distal intrahepatic bile duct by the tumor was observed in only 4 of the large group cases. On the contrary, all in the small group were revealed as homogeneous hypo-echoic tumors, while 12 had a clear boundary and only 1 had penetrating sign.

Eighteen patients were examined with CEUS. In the arterial phase, 13 showed a homogeneous enhancement, 2 a basket pattern, and 2 an avascular area, while 1 had a spoke-wheel pattern in the early vascular phase. In addition, 16 showed a washout pattern in the portal phase and 2 were revealed as iso-vascular. All were shown as a defect in the post-vascular phase. The 18 patients who were examined with CEUS were divided into 2 groups based on tumor diameter ( $<30$  mm, small group,  $n = 11$ ;  $\geq 30$  mm, large group,  $n = 7$ ). Among those patients in the large group in whom CEUS was performed, 3 showed homogeneous enhancement, 2 had avascular area, 1 showed a basket pattern, 1 had a spoke-wheel pattern in the early vascular phase, and 5 showed a washout pattern in the portal phase, while all were revealed as a defect in the post-vascular phase. Among the 11 patients in the small group, 10 showed homogeneous enhancements and 1 a basket pattern in the early vascular phase, while all had a washout pattern in the portal phase and were revealed as a defect in the post-vascular phase.

The clinical characteristics of patients with primary ( $n = 7$ ) and secondary ( $n = 18$ ) HML are shown in Table 2. In the primary HML group ( $n = 7$ ), 5 had a heterogeneous hypo-echoic tumor with an unclear boundary and 5 had a large-sized tumor ( $\geq 30$  mm). All were examined with CEUS. Images obtained in the early vascular phase showed various features, including 5 tumors with a washout pattern in the portal phase, which were revealed as a defect in the post-vascular phase. Among those in the secondary

**Table 1.** Clinical characteristics of tumor-forming hepatic malignant lymphoma divided by size

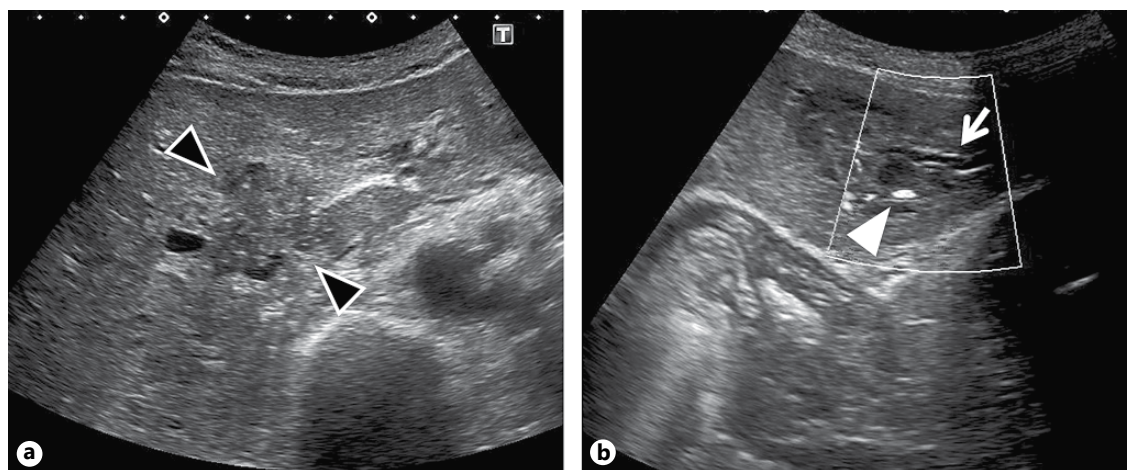
Case Number	Age, years/ sex	Primary/ secondary	HBV/ HCV	Conventional abdominal ultrasonography				CEUS			Pathological diagnosis
				tumor size, mm	internal echo	boundary	penetrating sign	dilatation of intrahepatic bile duct by tumor	early vascular phase	portal phase	
1	64/M	Primary	-/-	100	Hetero/hypo	Unclear	+	+	Hypervascular basket pattern chaotic vessels	Iso-vascular Defect	DLBCL
2	71/F	Primary	-/-	58	Hetero/hypo	Unclear	-	-	Iso-vascular with avascular area	Washout Defect	DLBCL + MTX-LPD
3	61/M	Primary	+/-	54	Hetero/hypo	Unclear	+	-	Hypervascular homogeneous enhancement	Washout Defect	MALT
4	67/M	Secondary	+/-	54	Hetero/hypo	Unclear	+	+	NE		B-cell lymphoma (details unknown)
5	84/F	Secondary	-/+	52	Hetero/hypo	Unclear	+	-	NE		DLBCL
6	40/M	Secondary	-/-	50	Hetero/hypo	Clear	+	-	NE		DLBCL
7	36/M	Primary	-/-	33	Hetero/hypo	Unclear	-	-	Iso-vascular with avascular area	Iso-vascular Defect	B-cell lymphoma (details unknown)
8	53/M	Secondary	-/+	33	Homo/hypo	Clear	-	-	Hypervascular homogeneous enhancement	Washout Defect	DLBCL
9	90/M	Secondary	-/-	32	Hetero/hypo	Unclear	+	+	Hypervascular spoke-wheel pattern	Washout Defect	DLBCL
10	89/F	Secondary	-/-	32	Hetero/hypo	Unclear	+	+	NE		DLBCL
11	83/M	Primary	-/+	30	Hetero/hypo	Unclear	+	-	Hypervascular homogeneous- enhancement	Washout Defect	DLBCL + MALT
12	86/M	Secondary	-/+	27	Homo/hypo	Clear	-	-	Hypervascular homogeneous- enhancement	Washout Defect	DLBCL
13	54/F	Secondary	-/-	26	Homo/hypo	Clear	-	-	NE		T-cell lymphoma + MTX-LPD

**Table 1.** (continued)

Case Number	Age, years/ sex	Primary/ secondary	HBV/ HCV	Conventional abdominal ultrasonography				CEUS			Pathological diagnosis	
				tumor size, mm	internal echo	boundary	penetrating sign	dilatation of intrahepatic bile duct by tumor	early vascular phase	portal phase		post-vascular phase
14	78/F	Secondary	-/-	26	Homo/hypo	Unclear	+	-	Hypervascular homogeneous enhancement	Washout	Defect	MTX-LPD
15	58/M	Primary	-/-	22	Homo/hypo	Clear	-	-	Hypervascular homogeneous enhancement	Washout	Defect	MALT
16	43/M	Secondary	-/-	20	Homo/hypo	Unclear	-	-	NE			DLBCL
17	80/F	Secondary	-/+	19	Homo/hypo	Clear	-	-	Hypervascular homogeneous enhancement	Washout	Defect	Hodgkin's lymphoma
18	70/F	Secondary	+/-	17	Homo/hypo	Clear	-	-	Iso-vascular homogeneous enhancement	Washout	Defect	DLBCL
19	81/F	Secondary	-/+	17	Homo/hypo	Clear	-	-	Hypervascular homogeneous enhancement	Washout	Defect	DLBCL
20	87/M	Secondary	-/-	15	Homo/hypo	Clear	-	-	Iso-vascular homogeneous enhancement	Washout	Defect	DLBCL
21	73/F	Secondary	+/-	15	Homo/hypo	Clear	-	-	Iso-vascular homogeneous enhancement	Washout	Defect	DLBCL
22	69/F	Primary	-/-	11	Homo/hypo	Clear	-	-	Hypervascular basket pattern	Washout	Defect	DLBCL + MALT
23	55/M	Secondary	-/-	10	Homo/hypo	Clear	-	-	Iso-vascular homogeneous enhancement	Washout	Defect	Adult T-cell lymphoma
24	64/M	Secondary	+/-	10	Homo/hypo	Clear	-	-	Iso-vascular homogeneous enhancement	Washout	Defect	DLBCL
25	74/M	Secondary	-/-	7	Homo/hypo	Clear	-	-	NE			Hodgkin's lymphoma
CEUS, contrast-enhanced ultrasonography; hetero, heterogeneous; homo, homogeneous; hypo, hypo-echoic; NE, not examined; DLBCL, diffuse large B-cell lymphoma; MTX-LPD, methotrexate-associated lymphoproliferative disorders; MALT, mucosa-associated lymphoid tissue.												

CEUS, contrast-enhanced ultrasonography; hetero, heterogeneous; homo, homogeneous; hypo, hypo-echoic; NE, not examined; DLBCL, diffuse large B-cell lymphoma; MTX-LPD, methotrexate-associated lymphoproliferative disorders; MALT, mucosa-associated lymphoid tissue.





**Fig. 1.** Case 1: an 89-year-old Japanese female with diffuse large B-cell lymphoma. A heterogeneous hypo-echoic nodule with an unclear boundary (black arrowhead) was detected in the second segment of the liver (32 mm in diameter) by conventional abdominal ultrasonography (US; **a**). Penetrating sign (hepatic vein: white ar-

rowhead) was detected inside of the tumor and dilatation of the intrahepatic bile duct (arrow) by the tumor was observed (**b**). Pathologically, the tumor was diagnosed as secondary hepatic malignant lymphoma (diffuse large B-cell lymphoma).

HML group ( $n = 18$ ), 13 had a homogeneous hypo-echoic tumor and 12 showed a clear boundary. In addition, a small-sized tumor ( $<30$  mm) was found in 12 of these cases. CEUS was performed in 11 of the patients in the secondary HML group. Of those, 10 showed to be enhanced homogeneously in the early vascular phase, while all showed a washout pattern in the portal phase and were revealed as a defect in the post-vascular phase. In both primary and secondary tumor-forming HMLs, there were similar tendencies found in findings obtained with US and CEUS. Although the percentage of large-sized tumors was greater in the primary cases, the difference was not significant (5 of 7 (71.4%) vs. 6 of 18 (33.3%);  $p = 0.177$ ).

#### Representative Cases

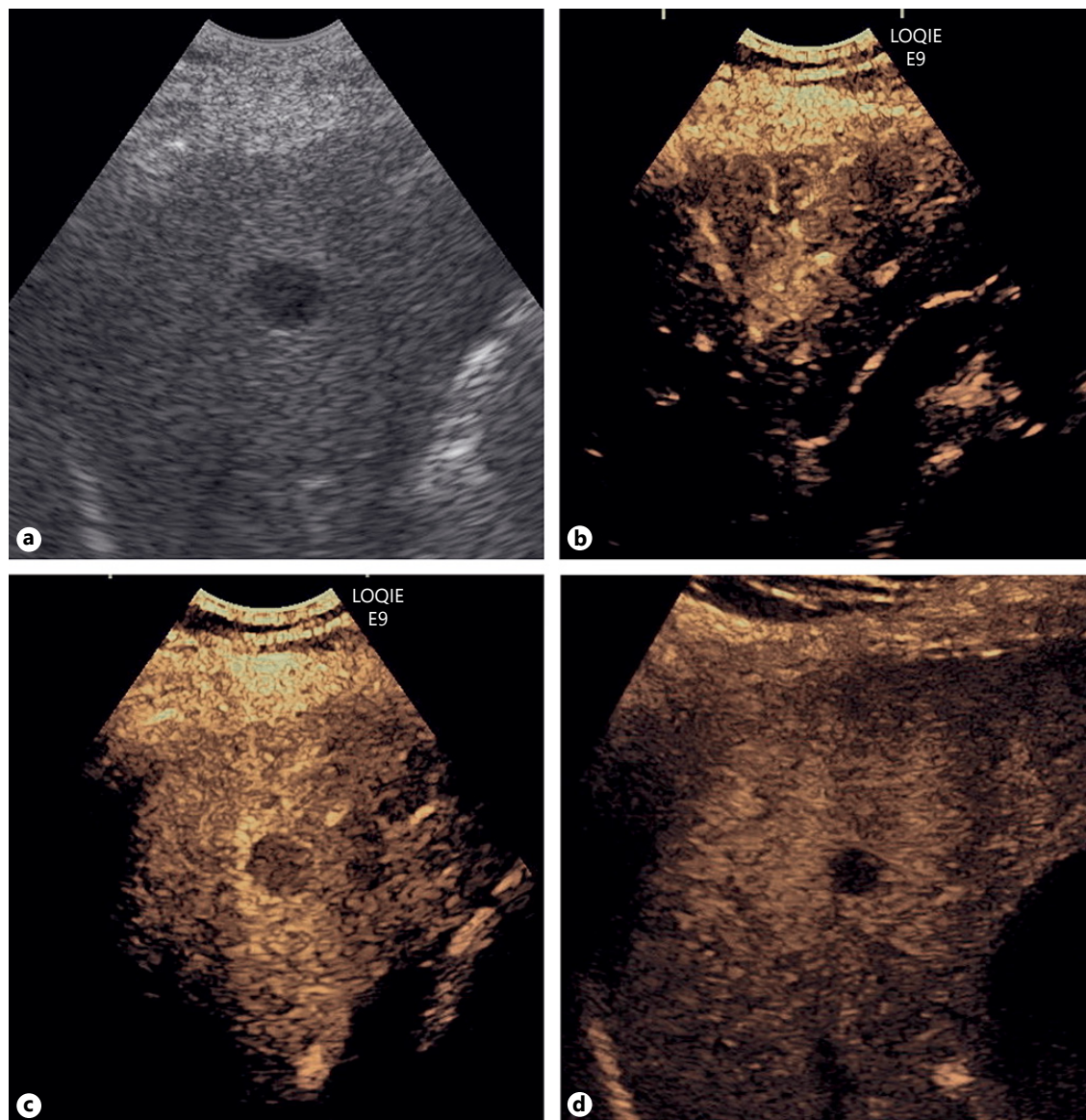
**Case 1.** An 89-year-old Japanese female was referred to Ehime Prefectural Central Hospital with elevated liver enzymes. A hepatic tumor (32 mm in diameter) was detected in the second segment of the liver and revealed as a heterogeneous hypo-echoic nodule with an unclear boundary (Fig. 1). Intraperitoneal lymphadenopathy and pancreatic mass were shown in full-body CT scan. Penetrating sign was detected inside of the tumor and dilatation of the intrahepatic bile duct by tumor was also observed. Pathologically, the tumor was diagnosed as secondary hepatic DLBCL, including microscopic findings showing diffuse proliferation of medium-to-large atypical lymphocytes with hematoxylin and eosin (H&E) staining, and positive findings for the anti-CD-20 antibody following immune staining.

**Table 2.** Conventional ultrasonography findings of primary and secondary tumor-forming hepatic malignant lymphoma

	<30 mm		≥30 mm	
	homo/ hypo	hetero/ hypo	homo/ hypo	hetero/ hypo
Primary HML ( $n = 7$ )	2	0	0	5
Secondary HML ( $n = 18$ )	12	0	1	5

HML, hepatic malignant lymphoma; hetero, heterogeneous; homo, homogeneous; hypo, hypo-echoic.

**Case 2.** A 73-year-old Japanese female was referred to Ehime Prefectural Central Hospital due to lymphadenopathy. A hepatic tumor (15 mm in diameter) was detected in the fifth segment of the liver by conventional US (Fig. 2), and lymphadenopathy was shown in full-body CT scan. The tumor was revealed as a homogeneous hypo-echoic nodule with a clear boundary in conventional US images. With CEUS, homogeneous enhancement in the early vascular phase and a washout pattern in the portal phase were observed, respectively. The tumor was revealed as a defect in the post-vascular phase. The tumor was diagnosed as secondary hepatic DLBCL, with microscopic findings including diffuse proliferation of medium-to-large atypical lymphocytes with H&E staining, and positive findings for the anti-CD-20 antibody in immune staining.



**Fig. 2.** Case 2: a 73-year-old Japanese female with diffuse large B-cell lymphoma. A hepatic tumor (15 mm in diameter) was revealed as a homogeneous hypo-echoic nodule with a clear boundary in the fifth segment of the liver by conventional B-mode of abdominal ultrasonography (US; **a**). In contrast-enhanced US with per-

flubutane (CEUS), homogeneous enhancement in the early vascular phase (**b**) and a washout pattern in the portal phase (**c**) were observed, respectively. In the post-vascular phase of CEUS, the tumor was revealed as a defect (**d**).

## Discussion

ML is known as a malignant tumor that is derived from lymphatic tissue, while it has been noted that HML comprise approximately 8% of focal hepatic lesions [13]. A primary HML has been reported to be a very rare malignancy, representing 0.41–1% of extra-nodal lymphomas [14–16]. On the contrary, it is well known that ML shows frequent invasion, as it has been reported in approximate-

ly 50–60% of autopsy cases with that tumor [16, 17]. Secondary HML has been reported to often progress from ML and the diffuse invasive type is most frequent [18].

It is considered that US findings of both primary and secondary tumor-forming HML have not been adequately evaluated. Although a needle biopsy procedure for ML has a high rate for accurate diagnosis (85%) [19], differential diagnosis including other malignant hepatic tumors (e.g., HCC, CCC) can be difficult in some cases of

HML using US findings [20] and even with other modalities [21, 22]. Lack of deterministic findings for US and CEUS has been thought to be the reason why only a small number of patients have been reported with an HML.

In general, an HML is revealed as a homogeneous hypo-echoic lesion [1–3], and often includes the portal vein or hepatic vein inside of the tumor without invasion (penetrating sign) in conventional US findings [4, 5]. Based on the present results, image findings of HML might differ depending on the tumor diameter. In our study, small tumors (<30 mm in diameter) were revealed as homogeneous hypo-echoic lesions, the same as previously reported, whereas penetrating sign [5] was not detected in nearly all cases. On the contrary, in large tumors (≥30 mm in diameter) penetrating sign was detected, though 91% (10/11) were revealed as a heterogeneous hypo-echoic lesion. In addition, dilatation of the distal intrahepatic bile duct by tumor was observed in 4 cases, making it difficult to distinguish it from CCC.

Trenker et al. [23] reported that HML had no specific tendencies in CEUS findings for the early vascular and post-vascular phases. In the present cohort, image findings in the early vascular phase of CEUS for the large group varied, while those for the small group nearly always showed an enhanced homogeneity and a washout pattern in the portal phase, and defect in the post-vascular phase. Our results also suggest that CEUS findings can differ according to tumor size. In US and CEUS imaging, similar tendencies were observed in both types of tumor-forming HML according to tumor size (<30 or ≥30 mm; Table 2).

Past reports have suggested that development of an HML might be associated with chronic HBV or HCV in-

fection [24, 25], as they have been described as possible trigger factors for immune activation, potentially leading to benign or malignant lymphoproliferative disorders. HBV or HCV infection was detected in 44% of the present cohort. When a hepatic tumor is revealed as typical HCC in CEUS findings but as a homogeneous hypo-echoic lesion in patients with chronic HBV or HCV infection, HML should be kept in mind for differential diagnosis. As confirmed by the present results, diagnosis of HML is often difficult with only US and CEUS imaging, and remains an important issue, indicating the importance of the role of a pathological examination for obtaining a definitive diagnosis. Of course, when a typical small-sized (<30 mm) HCC is shown to be clear homogenous hypo-echoic with a clear boundary in conventional US, biopsy and general examinations for screening of the lymph nodes including imaging should be considered [26, 27].

To the best of our knowledge, no previous reports have noted differences in image findings of HML obtained with US and CEUS. It is important to keep in mind that US findings vary according to tumor size in cases of primary and secondary HML. A limitation of the present study is the small number of patients. Thus, our findings are too limited for definitive conclusions. Therefore, accumulation of cases and studies with a greater number of patients is needed.

## Disclosure Statement

There are no financial disclosures, grants from any organs, conflicts of interest, and/or acknowledgements for the authors to declare.

## References

- 1 Elsayes KM, Menias CO, Willatt JM, Pandya A, Wiggins M, Platt J: Primary hepatic lymphoma: imaging findings. *J Med Imaging Radiat Oncol* 2009;53:373–379.
- 2 Low G, Leen E: Diagnosis of periportal hepatic lymphoma with contrast-enhanced ultrasonography. *J Ultrasound Med* 2006;25:1059–1062.
- 3 Asaoka T, Tono T, Kaneko A, Kin Y, Iwazawa T, Ohnishi T, Nakano Y, Yano H, Okamoto S, Monden T: A resected case of primary hepatic malignant lymphoma. *Jpn J Gastroenterol Surg* 2006;39:203–208.
- 4 Lu Q, Zhang H, Wang WP, Jin YJ, Ji ZB: Primary non-Hodgkin's lymphoma of the liver: sonographic and CT findings. *Hepatobiliary Pancreat Dis Int* 2015;14:75–81.
- 5 Apicella PL, Mirowitz SA, Weinreb JC: Extension of vessels through hepatic neoplasms: MR and CT findings. *Radiology* 1994;191:135–136.
- 6 Kudo M: Breakthrough imaging in hepatocellular carcinoma. *Liver Cancer* 2016;5:47–54.
- 7 Kudo M: Defect reperfusion imaging with sonazoid®: a breakthrough in hepatocellular carcinoma. *Liver Cancer* 2016;5:1–7.
- 8 Salvatore V, Gianstefani A, Negrini G, Allegritti G, Galassi M, Piscaglia F: Imaging diagnosis of hepatocellular carcinoma: recent advances of contrast-enhanced ultrasonography with sonoVue®. *Liver Cancer* 2016;5:55–66.
- 9 Ohsawa M, Aozasa K, Horiuchi K, Kataoka M, Hida J, Shimada H, Oka K, Wakata Y: Malignant lymphoma of the liver. Report of five cases and review of the literature. *Dig Dis Sci* 1992;37:1105–1109.
- 10 Kanda Y: Investigation of the freely available easy-to-use software “EZ” for medical statistics. *Bone Marrow Transplant* 2013;48:452–458.
- 11 Doi H, Ichikawa S, Hiraoka A, Ichiryu M, Nakahara H, Ochi H, Tanabe A, Kodama A, Hasebe A, Miyamoto Y, Ninomiya T, Horiike N, Takamura K, Kawasaki H, Kameoka C, Kan M, Doi S, Soga Y, Tamura H, Maeda T, Asaki A, Seno S, Iguchi H, Hasegawa T: Primitive neuroectodermal tumor of the pancreas. *Intern Med* 2009;48:329–333.
- 12 Miyagawa K, Shibata M, Noguchi H, Hayashi T, Oe S, Hiura M, Abe S, Harada M: Methotrexate-related primary hepatic lymphoma in a patient with rheumatoid arthritis. *Intern Med* 2015;54:401–405.



- 13 Sans M, Andreu V, Bordas JM, Llach J, López-Guillermo A, Cervantes F, Bruguera M, Mondelo F, Montserrat E, Terés J, Rodés J: Usefulness of laparoscopy with liver biopsy in the assessment of liver involvement at diagnosis of Hodgkin's and non-Hodgkin's lymphomas. *Gastrointest Endosc* 1998;47:391–395.
- 14 Zentar A, Tarchouli M, Elkaoui H, Belhamidi MS, Ratbi MB, Bouchentouf SM, Ali AA, Bounaim A, Sair K: Primary hepatic lymphoma. *J Gastrointest Cancer* 2014;45:380–382.
- 15 Noronha V, Shafi NQ, Obando JA, Kummur S: Primary non-Hodgkin's lymphoma of the liver. *Crit Rev Oncol Hematol* 2005;53:199–207.
- 16 Freeman C, Berg JW, Cutler SJ: Occurrence and prognosis of extranodal lymphomas. *Cancer* 1972;29:252–260.
- 17 Levitan R, Diamond HD, Craver LF: The liver in Hodgkin's disease. *Gut* 1961;2:60–71.
- 18 Fukuya T, Honda H, Murata S, Yasumori K, Hayashi T, Ishibashi H, Matsumata T, Masuda K: MRI of primary lymphoma of the liver. *J Comput Assist Tomogr* 1993;17:596–598.
- 19 Quinn SF, Sheley RC, Nelson HA, Demlow TA, Wienstein RE, Dunkley BL: The role of percutaneous needle biopsies in the original diagnosis of lymphoma: a prospective evaluation. *J Vasc Interv Radiol* 1995;6:947–952.
- 20 Liu GJ, Wang W, Lu MD, Xie XY, Xu HX, Xu ZF, Chen LD, Wang Z, Liang JY, Huang Y, Li W, Liu JY: Contrast-enhanced ultrasound for the characterization of hepatocellular carcinoma and intrahepatic cholangiocarcinoma. *Liver Cancer* 2015;4:241–252.
- 21 Chen BB, Murakami T, Shih TT, Sakamoto M, Matsui O, Choi BI, Kim MJ, Lee JM, Yang RJ, Zeng MS, Chen RC, Liang JD: Novel imaging diagnosis for hepatocellular carcinoma: consensus from the 5th Asia-Pacific primary liver cancer expert meeting (APPLE 2014). *Liver Cancer* 2015;4:215–227.
- 22 Joo I, Lee JM: Recent advances in the imaging diagnosis of hepatocellular carcinoma: value of gadoteric acid-enhanced MRI. *Liver Cancer* 2016;5:67–87.
- 23 Trenker C, Kunsch S, Michl P, Wissniowski TT, Goerg K, Goerg C: Contrast-enhanced ultrasound (CEUS) in hepatic lymphoma: retrospective evaluation in 38 cases. *Ultraschall Med* 2014;35:142–148.
- 24 Ferri C, La Civita L, Monti M, Longombardo G, Greco F, Pasero G, Zignego AL: Can type C hepatitis infection be complicated by malignant lymphoma? *Lancet* 1995;346:1426–1427.
- 25 Schöllkopf C, Smedby KE, Hjalgrim H, Rostgaard K, Panum I, Vinner L, Chang ET, Glimelius B, Porwit A, Sundström C, Hansen M, Adami HO, Melbye M: Hepatitis C infection and risk of malignant lymphoma. *Int J Cancer* 2008;122:1885–1890.
- 26 Kudo M: Clinical practice guidelines for hepatocellular carcinoma differ between Japan, United States, and Europe. *Liver Cancer* 2015;4:85–95.
- 27 Chow PK, Choo SP, Ng DC, Lo RH, Wang ML, Toh HC, Tai DW, Goh BK, Wong JS, Tay KH, Goh AS, Yan SX, Loke KS, Thang SP, Gogna A, Too CW, Irani FG, Leong S, Lim KH, Thng CH: National cancer centre Singapore consensus guidelines for hepatocellular carcinoma. *Liver Cancer* 2016;5:97–106.

# Clinicopathological Study of Autoimmune Hepatitis Cases That Were Difficult to Differentiate from Drug-Induced Liver Injury

Akemi Tsutsui<sup>a</sup> Kenichi Harada<sup>c</sup> Koichi Tsuneyama<sup>d</sup> Tomonori Senoh<sup>a</sup>  
Takuya Nagano<sup>a</sup> Koichi Takaguchi<sup>a</sup> Midori Ando<sup>b</sup> Satoko Nakamura<sup>b</sup>  
Koichi Mizobuchi<sup>b</sup> Masatoshi Kudo<sup>e</sup>

<sup>a</sup>Department of Hepatology, and <sup>b</sup>Department of Pathology, Kagawa Prefectural Central Hospital, Kagawa,

<sup>c</sup>Department of Human Pathology, Kanazawa University Graduate School of Medical Sciences, Kanazawa,

<sup>d</sup>Department of Pathology and Laboratory Medicine, Tokushima University Graduate School, Tokushima, and

<sup>e</sup>Department of Gastroenterology and Hepatology, Kindai University Faculty of Medicine, Osaka-Sayama, Japan

## Keywords

Autoimmune hepatitis · Cobblestone hepatocellular change · Digestive Disease Week Japan 2004 scale · Drug-induced liver injury · Emperipolesis · Histologic features

## Abstract

**Aim:** Acute-onset autoimmune hepatitis (AIH) histopathologically presents with features of acute hepatitis and lacks a specific diagnostic method. Also, AIH is often difficult to differentiate from drug-induced liver injury (DILI). We aimed to investigate the final clinical diagnosis of these cases, and compare the clinical, biochemical, and histological characteristics of AIH vs. DILI. **Methods:** We examined the Digestive Disease Week Japan 2004 (DDW-J) scale scores, AIH scores, clinical data, and pathological findings in 20 patients in whom it was difficult to differentiate autoimmune liver disease from DILI. **Results:** In cases with a DDW-J scale score of  $\geq 5$ , there was a good correlation between the final diagnosis and DDW-J scale assessments, but in cases with a DDW-J scale score of  $\leq 4$  they did not correlate well. The scores for pathological findings, such as cobblestone hepatocellular

change ( $p = 0.015$ ), interface hepatitis ( $p = 0.012$ ), and prominent plasma cells in portal areas ( $p = 0.011$ ), were higher in the AIH group than in the DILI group. **Conclusion:** This study showed that DDW-J scale was useful for differentiating AIH from DILI in cases with a DDW-J scale score of  $\geq 5$ . The histologic features of AIH were characterized by cobblestone hepatocellular change, interface hepatitis, and plasma cell infiltration of the portal region.

© 2017 S. Karger AG, Basel

## Introduction

Acute-onset autoimmune hepatitis (AIH) histopathologically presents with features of acute hepatitis and lacks a specific diagnostic method. Also, AIH is often difficult to differentiate from drug-induced liver injury (DILI). These conditions are mediated by immunological reactions, and thus show considerable resemblance in clinical and histopathologic features [1–6].

Early immunosuppressive therapy typically contains disease activity in patients with idiopathic AIH and can



**Table 1.** Patient characteristics

Age, years	52±12.2 (30–72)
Gender, male/female	4/16
Alanine aminotransferase, IU/L	911.9±586 (152–2,061)
Aspartate transaminase, IU/L	702±594 (120–2,168)
Total bilirubin, mg/dL	5.5±5.9 (0.4–20.8)
Alkaline phosphatase, IU/L	546±269 (303–1,306)
γ-Glutamyltranspeptidase, IU/L	251±183 (18–790)
Immunoglobulin G, mg/dL	1,814±637 (917–3,200)
Antinuclear antibodies (positive/negative)	13/7
Anti-mitochondrial antibody M2 (positive/negative)	3/17

lead to disease remission [7, 8]. Similarly, prompt identification and discontinuation of offending drugs halts ongoing liver injury in cases with DILI [5]. Failure to properly treat AIH and DILI could result in clinically devastating acute or chronic outcomes [5, 6]. Chronic AIH could also lead to hepatocarcinogenesis in the future [9–11].

Two major mechanisms are mainly proposed in the development of DILI. First, the dose-dependent (intrinsic) hepatotoxicity caused by the use of drugs, such as acetaminophen and aspirin. The other is idiosyncratic (unpredictable) hepatotoxicity that can be caused by most of the drugs. This mechanism is classified into 2 groups: immunologic and metabolic [12, 13]. Drugs that cause immunity-related DILI can trigger immune response against hepatic proteins, which can lead to a clinical course similar to AIH [3]. Many drugs have been reported to cause this condition, called drug-induced AIH [2, 14, 15]. However, it is difficult to distinguish between classic AIH and drug-induced AIH, as serological and histological findings of these conditions are quite similar [1–6, 16, 17].

The histologic classification of DILI has been reported recently along with detailed descriptions of histologic features and corresponding differential diagnosis for each injury pattern [18]. Characteristic histologic features of AIH have also been well documented in the literature [19, 20]. However, there is no individual histologic feature that is absolutely indicative of either DILI or AIH; thus, the evaluation of liver biopsy in determining AIH vs. DILI may be a significant challenge.

Recently, clinical scales or scores have been developed to facilitate the diagnosis of DILI. In Japan, the Digestive Disease Week Japan 2004 (DDW-J) scale, which is highly sensitive and specific, was developed by modifying the Council for International Organizations of Medical Sci-

ences/the Roussel Uclaf Causality Assessment Method (CIOMS/RUCAM) scale [21–24]. However, there were also discrepancies. In the manual of DDW-J scale, it is described that differential diagnoses of idiopathic AIH and DILI are difficult.

In this study, we examined DDW-J scale scores, AIH scores, clinical data, and pathological findings in 20 patients in whom it was difficult to differentiate autoimmune liver disease from DILI. We aimed to investigate the final clinical diagnosis of these cases, and compare the clinical, biochemical, and histological characteristics of AIH vs. DILI. Furthermore, we wanted to investigate the method of differential diagnosis of AIH vs. DILI.

## Methods

### Subjects

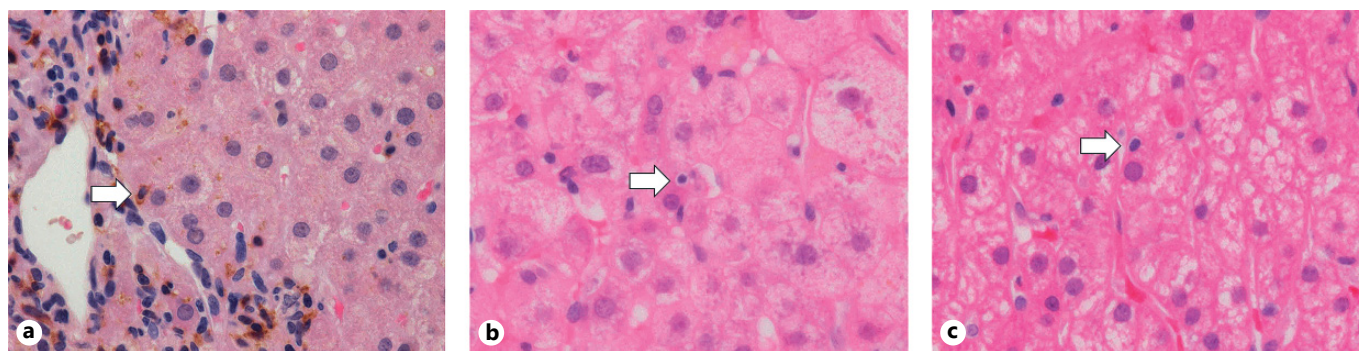
The study comprised 20 patients in whom it was difficult to differentiate AIH from DILI, who underwent liver biopsy, did not have a previous history of liver injury, and were followed up for more than one year, in Kagawa Prefectural Central Hospital from April 2010 to December 2015 (Table 1). Clinical and laboratory data were obtained from medical records in the hospital. The diagnosis of DILI was based on the DDW-J scale and clinical course [21–24]. The diagnosis of AIH was based on a scoring system proposed by the International Autoimmune Hepatitis Group and clinical course [25]. The pathological findings and clinical data were also compared between patients finally diagnosed with AIH and those with DILI.

### The DDW-J Scale

DDW-J scale was developed by modifying the CIOMS/RUCAM scale [21–23]. In particular, the factor of co-medication was excluded, and the factors of drug lymphocyte stimulation test and eosinophilia were included according to Japan's clinical environment. Each case was assessed according to DDW-J scale, a Japanese clinical diagnostic criteria for DILI [24]. First, the cases were scored for 8 indicated items: time to onset, course, risk factors, other causes, previous information on hepatotoxicity, eosinophilia, drug-lymphocyte stimulation test, and response to re-administration. Based on the total scores, individual cases were classified into 3 grades with respect to the diagnosis of DILI: 5 or more, probable; 3–4, possible; 2 or less, unlikely. Then, the cases were classified into hepatocellular, cholestatic, and mixed hepatocellular and cholestatic type according to the serum levels of alanine aminotransferase (ALT) and alkaline phosphatase (ALP). Hepatocellular type was defined as  $ALT > 2 \times$  upper limit of the normal range (ULN) and  $ALP \leq ULN$ , or  $R \geq 5$ , where the  $R$  value was calculated as  $(ALT/ULN)/(ALP/ULN)$ . Cholestatic type was defined as  $ALT \leq ULN$  and  $ALP > 2 \times ULN$ , or  $R \leq 2$ . The mixed type was defined as  $ALT > 2 \times ULN$ ,  $ALP > ULN$ , and  $R > 2$  and  $< 5$ .

### The Final Clinical Diagnosis

A final diagnosis of DILI was based on the following criteria: diseases other than autoimmune liver disease were excluded, DDW-J scale score was  $\geq 3$ , liver injury improved regardless of the



**Fig. 1.** High-power images of emperipolesis. **a** Detection of emperipolesis by immunostaining; the liver tissue collected by needle biopsy was immunostained for CD8 followed by H&E. The white arrow denotes a CD8 positive lymphocyte among the hepatocytes.

**b** Case of autoimmune hepatitis, **(c)** case of drug-induced liver injury. Emperipolesis based on entry of lymphocytes into hepatocytes, was characterized by a halo around the nucleus of lymphocytes. (Needle biopsy, H&E).

**Table 2.** Histologic features evaluated in this study

Histologic features	Evaluation	Score
CZN (Centrozonal necrosis)	Yes/no	1/0
Perivenular necroinflammatory activity	Yes/no	1/0
Lobular necrosis/inflammation (not including CNZ)	Severe/moderate/mild/none	3/2/1/0
Cobblestone hepatocellular change	Severe/moderate/mild/none	3/2/1/0
Hepatocyte rosettes	Yes/no	1/0
Pigmented macrophages	Yes/no	1/0
Prominent plasma cells in intra-acinar areas	Yes/no	1/0
Perivenular fibrosis	Severe/moderate/mild/none	3/2/1/0
Portal inflammation	Severe/moderate/mild/none	3/2/1/0
Interface hepatitis	Severe/moderate/mild/none	3/2/1/0
Prominent plasma cells in portal areas	Severe/moderate/mild/none	3/2/1/0
Bile duct injury	Yes/no	1/0
Portal fibrosis	F4/F3/F2/F1/F0	4/3/2/1/0
Cholestasis	Yes/no	1/0
Mitosis	Yes/no	1/0
Emperipolesis	Yes/no	1/0

presence or absence of treatment, and the liver injury did not relapse during the follow-up period. A final diagnosis of AIH was based on the following criteria: when the pre-treatment AIH score was  $\geq 10$  (definitive/suspected diagnosis), post-treatment AIH score was 12–17 (suspected), and the liver injury relapsed during the follow-up period. Furthermore, a diagnosis of AIH was made, regardless of the presence or absence of liver injury relapse, when the pre-treatment AIH score was  $\geq 10$  (definitive/suspected) and the post-treatment AIH score was  $\geq 18$  (definitive).

#### Liver Biopsy and Histological Examination

Liver biopsy specimens obtained from these patients were fixed in 10% formalin and embedded in paraffin, and were processed routinely for histological diagnosis. The emperipolesis, based on entry of lymphocytes into hepatocytes, was characterized by a halo around the nucleus of lymphocytes in hematoxylin and eosin (H&E)-stained liver sections. Miao et al. [26] reported that the lymphocytes in hepatocytes were predominantly as CD8 T-cells.

Therefore, emperipolesis was evaluated on H&E-stained and double (immunostaining CD8+ H&E) stained slides (Fig. 1a). The 20 biopsy slides were evaluated concomitantly by 3 experienced pathologists (K.T., S.N., and K.M.) blinded to the clinical information using a standardized histologic scoring sheet. Scoring was done by consensus. The features listed in Table 2 were scored and recorded in the standardized scoring sheets. The scores for pathological findings were also compared between patients finally diagnosed with AIH and those with DILI.

#### Statistical Analysis

Data are reported as means ( $\pm$ SDs) for continuous variables or proportion of patients with a condition. Between-group differences were assessed using the Mann-Whitney U test for consistent variables. For all statistical analyses, we used the Excel statistical software package (Bell Curve for Excel; Social Survey Research Information Co., Ltd., Tokyo, Japan). A value of  $p < 0.05$  was considered statistically significant.

**Table 3.****a** Final diagnosis according to AIH score

Final diagnosis	AIH score (pre-treatment)		
	≥16 points definitive diagnosis	10–15 points suspected diagnosis	≤9 points
AIH	2	6	0
DILI	0	2	6
PBC (hepatitis type)	0	0	2
Unclassifiable	0	2	0
Total	2	10	8

Final diagnosis	AIH score (post-treatment)		
	≥18 points definitive diagnosis	12–17 points suspected diagnosis	≤11 points
AIH	5	3	0
DILI	0	1	7
PBC (hepatitis type)	0	1	1
Unclassifiable	0	1	1
Total	5	6	9

**b** Final diagnosis according to DDW-J scale score

Final diagnosis	DDW-J scale score		
	≥5 points probable	3–4 points possible	≤2 points unlikely
AIH	0	4	4
DILI	6	2	0
PBC (hepatitis type)	0	1	1
Unclassifiable	0	2	0
Total	6	9	5

## Results

### *The Final Clinical Diagnosis*

A final diagnosis was AIH in 8 patients, DILI in 8, primary biliary cholangitis (hepatitis type) in 2, and unclassifiable in 2. All 5 cases with an AIH score (post-treatment) of ≥18 were finally diagnosed with AIH (Table 3a). All 6 cases with a DDW-J scale score of ≥5 were finally diagnosed with DILI. In cases with a DDW-J scale score of ≥5, there was a good correlation between the final diagnosis and DDW-J scale assessments, but in cases with a DDW-J scale score of ≤4 they did not correlate well (Table 3b).

### *Comparison of Clinical Features between AIH and DILI Cases*

The clinical data were compared between patients finally diagnosed with AIH ( $n = 8$ ) and those with DILI

( $n = 8$ ). Clinical characteristics of patients with AIH and DILI are summarized in Table 4. The mean age and female gender of the AIH vs. DILI population were  $49.6 \pm 15.4$  vs.  $50.9 \pm 10.5$  years ( $p = 0.834$ ) and 75% vs. 88% female ( $p = 0.587$ ). Immunoglobulin G level was higher in the AIH cases ( $2,064 \pm 530$  mg/dL) than in the DILI cases ( $1,455 \pm 484$  mg/dL;  $p = 0.018$ ). The AIH cases were characterized by positive ANA status ( $p = 0.053$ ) and lower albumin level ( $p = 0.082$ ).

### *Comparison of Histologic Features between AIH and DILI Cases*

The scores for pathological findings were compared between patients finally diagnosed with AIH ( $n = 8$ ) and those with DILI ( $n = 8$ ). The data for the comparison between AIH and DILI are summarized in Table 5. The scores for pathological findings, such as cobblestone he-

**Table 4.** Comparison of clinical features between AIH and DILI cases

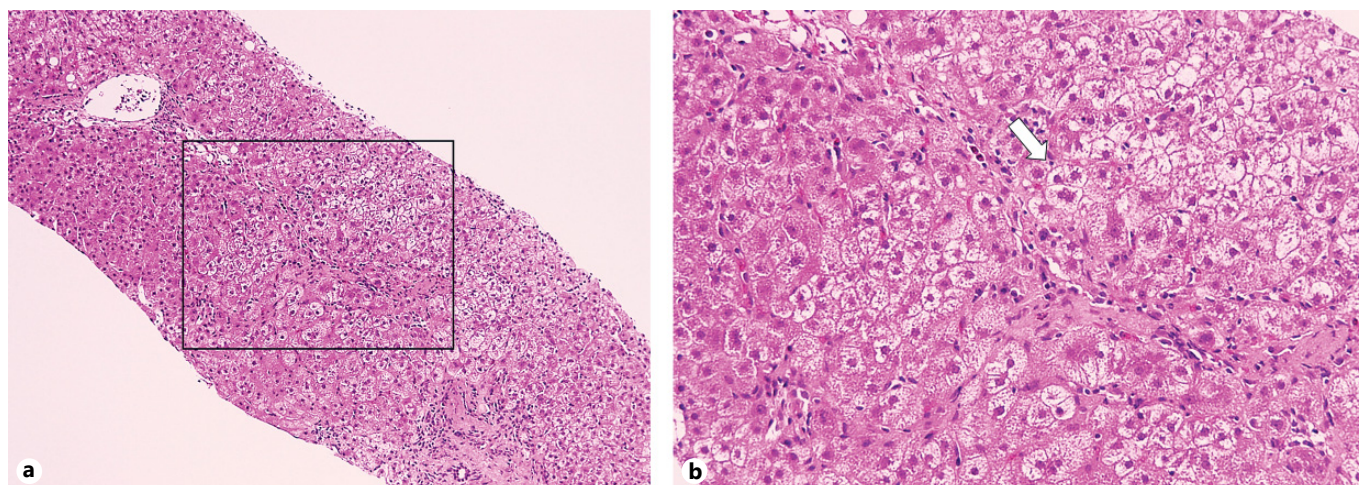
	AIH group (n = 8)	DILI group (n = 8)	p value
Age, years	49.6±15.4 (30–72)	50.9±10.5 (36–67)	0.834
Gender, male/female	2/6	1/7	0.587
Alanine aminotransferase, IU/L	1,015.6 (152–2,061)	920.1 (273–1,732)	0.793
Aspartate transaminase, IU/L	778.1 (120–2,168)	519.5 (100–976)	0.372
Total bilirubin, mg/dL	5.0 (1.6–10.9)	4.85 (0.8–20.8)	0.207
Alkaline phosphatase, IU/L	488.9 (200–692)	549.8 (303–1,049)	0.637
γ-Glutamyltranspeptidase, IU/L	201.1 (58–342)	224.6 (92–453)	0.875
Antinuclear antibodies (positive/negative)	7/1	3/5	0.053
Immunoglobulin G, mg/dL	2,064 (1,341–2,669)	1,454.8 (917–2,437)	0.018*
Immunoglobulin M, mg/dL	167.1 (69–342)	142.1 (71–290)	0.713
WBC, μ/L	5,962 (4,300–8,300)	5,538 (3,000–10,200)	0.494
Peripheral eosinophil, %	2.8 (0–9.9)	2.9 (1.3–10.4)	0.833
Platelet, ×10,000 μ/L	20.2 (13–28.4)	22.2 (13.1–30.9)	0.599
Prothrombin time, %	80.6 (66–97)	88.4 (33–124)	0.172
Albumin, g/dL	3.7 (3.1–4.7)	4.3 (3.4–5)	0.082

\*  $p < 0.05$  Mann-Whitney test.

**Table 5.** Comparison of histologic features between AIH and DILI cases

Histologic features	Evaluation	Cases, n	Score (mean)	p value
CZN (Centrozonal necrosis)	Yes/no	AIH 4/4	0.50	0.27
		DILI 4/4	0.50	
Perivenular necroinflammatory activity	Yes/no	AIH 5/3	0.63	0.50
		DILI 3/5	0.38	
Lobular necrosis/inflammation (not including CNZ)	Severe/moderate/mild/none	AIH 3/0/5/0	1.75	0.14
		DILI 0/1/6/1	1.00	
Cobblestone hepatocellular change	Severe/moderate/mild/none	AIH 0/4/4/0	1.50	0.015*
		DILI 0/0/6/2	0.75	
Hepatocyte rosettes	Yes/no	AIH 3/5	0.38	0.14
		DILI 0/8	0.00	
Pigmented macrophages	Yes/no	AIH 4/4	0.63	0.52
		DILI 6/2	0.75	
Plasma cell infiltration in the liver parenchyma	Yes/no	AIH 3/5	0.38	0.055
		DILI 0/8	0.00	
Perivenular fibrosis	Severe/moderate/mild/none	AIH 0/1/5/2	0.88	0.078
		DILI 0/0/2/6	0.25	
Portal inflammation	Severe/moderate/mild/none	AIH 1/4/3/0	1.75	0.059
		DILI 0/2/3/3	0.88	
Interface hepatitis	Severe/moderate/mild/none	AIH 1/4/3/0	1.75	0.012*
		DILI 0/0/5/3	0.63	
Prominent plasma cells in portal areas	Severe/moderate/mild/none	AIH 0/5/3/0	1.63	0.011*
		DILI 0/0/5/3	0.63	
Bile duct injury	Yes/no	AIH 3/5	0.38	0.52
		DILI 2/6	0.25	
Portal fibrosis	F4/F3/F2/F1/F0	AIH 0/1/2/6/0	1.38	0.34
		DILI 1/0/1/3/3	1.13	
Cholestasis	Yes/no	AIH 0/7	0.00	0.20
		DILI 2/6	0.25	
Mitosis	Yes/no	AIH 0/7	0.00	0.21
		DILI 2/6	0.25	
Emperipolesis	Yes/no	AIH 8/0	1.0	0.20
		DILI 6/2	0.75	





**Fig. 2.** Cobblestone hepatocellular changes. **a** Low-power image, **(b)** high-power image. Cobblestone hepatocellular changes comprised cluster of small and monomorphic hepatocytes with typi-

cally clear hydropic cytoplasm, reflecting increased regenerative activity. Rosette-like formations (white arrow) are seen in cobblestone hepatocellular changes. (Needle biopsy, H&E).

patocellular change ( $p = 0.015$ ; Fig. 2), interface hepatitis ( $p = 0.012$ ), and prominent plasma cells in portal areas ( $p = 0.011$ ), were higher in the AIH group than in the DILI group. Hepatocyte rosettes were noted in 3 cases of the AIH group, but in none of the DILI group. Centrozonal necrosis was found in 4 cases (4/8 cases, 50%) each in the AIH and DILI group (Fig. 3). Emperipolesis was found in all cases (8/8 cases, 100%) of the AIH group, and in 6 cases (6/8 cases, 75%) of the DILI group (Fig. 1b, c).

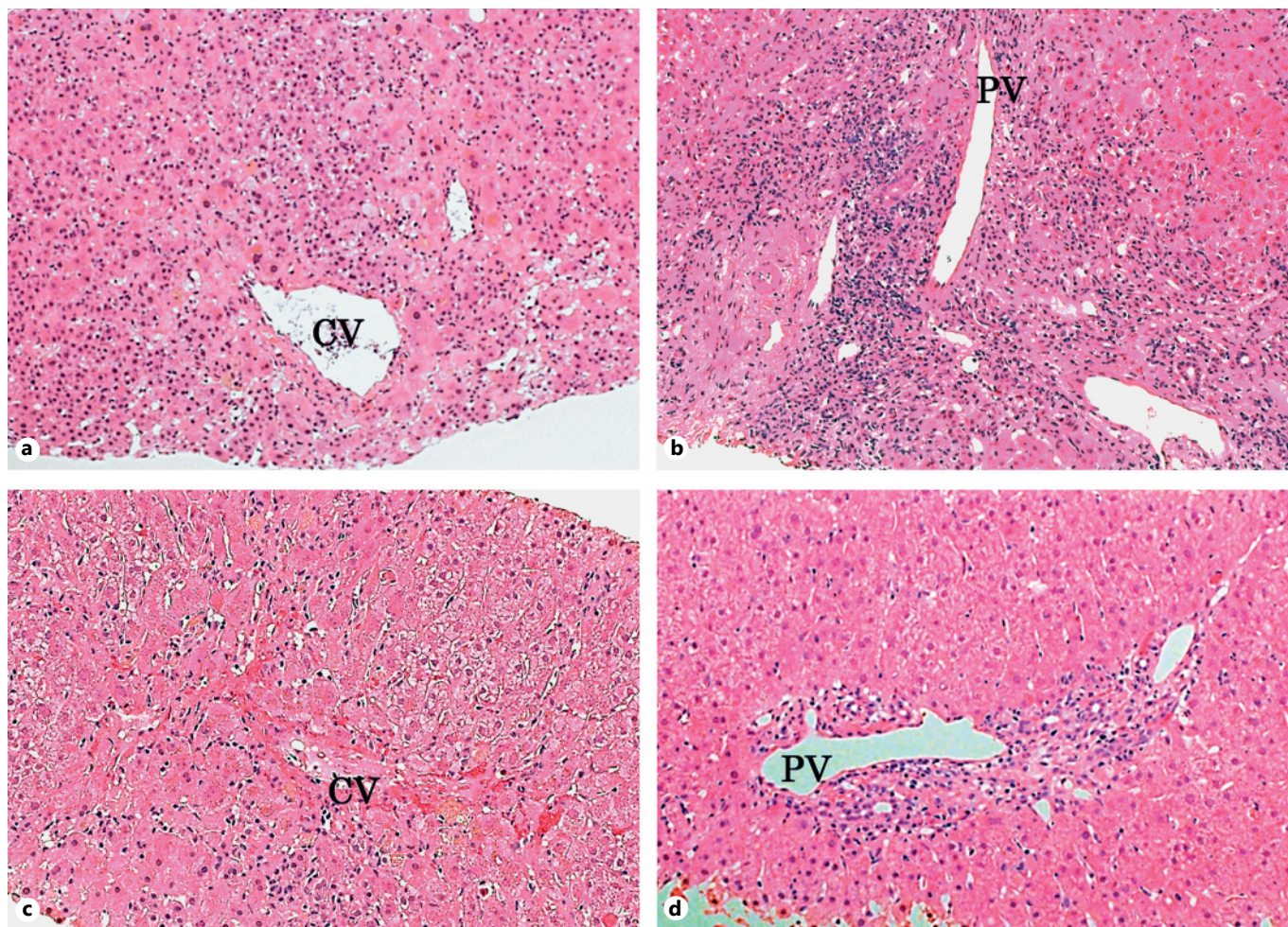
## Discussion

We examined the DDW-J scale scores, AIH scores, clinical data, and pathological findings in 20 patients in whom it was difficult to differentiate autoimmune liver disease from DILI. As a result, the final diagnosis was AIH in 8 patients, DILI in 8. Then, we compared the clinical, biochemical, and histological characteristics of AIH vs. DILI. The data obtained in this study were summarized as follows. (i) In cases with a DDW-J scale score of  $\geq 5$ , there was a good correlation between the final diagnosis and DDW-J scale assessments, but in cases with a DDW-J scale score of  $\leq 4$  they did not correlate well. (ii) The scores for pathological findings, such as cobblestone hepatocellular change ( $p = 0.015$ ), interface hepatitis ( $p = 0.012$ ), and prominent plasma cells in portal areas ( $p = 0.011$ ), were higher in the AIH group than in the DILI group.

The DDW-J scale, which is highly sensitive and specific, was developed by modifying the CIOMS/RUCAM scale [21–23]. It was proposed as an objective tool for the diagnosis of DILI, and has been widely used in Japan [24]. Based on the total scores, individual cases were classified into 3 grades with respect to a diagnosis of DILI: probable, possible, unlikely (Table 2). It was found in this study that all 6 cases with a DDW-J scale score of  $\geq 5$  (probable DILI) were finally diagnosed with DILI, suggesting a good correlation between the final clinical diagnosis and DDW-J scale assessment. However, in cases with a DDW-J scale score of  $\leq 4$ , the final diagnosis and DDW-J scale assessments did not correlate well. We reported a similar result in another study before [27]. Therefore, the DDW-J scale scores appear to be useful for differentiating AIH from DILI. Thus, gathering accurate information for DDW-J scale scores is one of the essentials of accurate diagnosis of DILI, and liver biopsy was useful for differentiating AIH from DILI in cases with a DDW-J scale score of  $\leq 4$ .

In our study, the scores for pathological findings, such as cobblestone hepatocellular change, interface hepatitis, and plasma cell infiltration of the portal region, were higher in the AIH group than in the DILI group, and rosette formation was noted in 3 cases of the AIH group, but in none of the DILI group. It has been reported that interface hepatitis, plasmacytic infiltration, and hepatocyte rosetting are characteristic features of AIH [20]. Liver cell plates are thickened by regeneration, and rosette-like formations are commonly seen in AIH. Fukuda et al. [28] reported that regenerating hepatocytes show a cobble-





**Fig. 3.** Medium-power images of centrozonal necrosis (CZN). **a, b** Case of autoimmune hepatitis. Centrilobular injury with prominent hepatocellular necrosis occurs in conjunction with periportal activity and interface hepatitis. **c, d** Case of drug-in-

duced liver injury. Well-demarcated centrilobular confluent necrosis is common, and the portal inflammatory reaction may be poorly developed or even absent. (Needle biopsy, H&E) CV, central vein; PV, portal vein.

stone appearance. It seems conceivable that cobblestone hepatocellular change which have not been previously described, may lead to characteristic feature of AIH, especially early in the course of AIH. Further investigations with more accumulated cases are required.

Emperipolesis has been widely described in patients with AIH, but its significance and the diagnostic value have not been quantitated. Emperipolesis, based on entry of lymphocytes into hepatocytes, was characterized by a halo around the nucleus of lymphocytes in H&E-stained liver sections. However, it is very difficult to detect it because a halo around the nucleus of hepatocytes in H&E is often seen. Miao et al. [26] reported that CD8 T cells were the major cell type of lymphocytes infiltrating hepatocytes in AIH. Therefore, we evaluated emperipolesis on

an H&E-stained and double (immunostaining CD8+ H&E) stained slides. In our study, emperipolesis was noted in all cases (8/8, 100%) of the AIH group, and in 6 cases (6/8, 75%) of the DILI group. Miao et al. [26] described that emperipolesis is associated with more severe necroinflammatory and fibrotic changes. We consider that emperipolesis is a characteristic feature of AIH; however, it may be seen in not only AIH but also in other liver diseases with severe necroinflammatory changes.

In our study, centrozonal necrosis was found in 4 cases (50%) each in the AIH and DILI groups. The centrilobular pattern of injury has been postulated that it may represent an early stage of otherwise classic AIH [29, 30]. Centrilobular injury with prominent hepatocellular necrosis and mononuclear inflammation occurs in up to

17% of AIH cases, either as an isolated finding (rarely) or in conjunction with periportal activity and interface hepatitis [29–32]. This centrilobular necroinflammatory injury pattern is not specific for AIH, but may also be seen in adverse drug reactions. As histologic features associated with drug-induced hepatitis, well-demarcated centrilobular confluent necrosis is common, and the portal inflammatory reaction may be poorly developed or even absent [33]. According to Suzuki et al. [1], no single feature was indicative of AIH or DILI, but rather the combination of distinct findings. We considered that the evaluation of portal inflammatory reaction appears to be useful for differentiating AIH from DILI when centrilobular necroinflammatory injury pattern was found.

Our study has limitations. First, our sample size was rather small. Second, there is a possibility that some of the observed histologic features may have been influenced by a set of drugs incriminated in the included DILI cases

and/or clinical presentation of AIH (acute vs. chronic presentation). Lastly, our preliminary modeling efforts were only based on statistical results of this small sample without cross-validation.

In conclusion, this study showed that DDW-J scale was useful for differentiating AIH from DILI in cases with a DDW-J scale score of  $\geq 5$ . The histologic features of AIH were characterized by cobblestone hepatocellular change, interface hepatitis, and plasma cell infiltration of the portal region.

However, there were also cases in whom it was difficult to differentiate AIH from DILI. Further investigation is needed to incorporate the knowledge into current clinicopathologic diagnosis.

## Disclosure Statement

There are no conflicts of interest to declare.

## References

- Suzuki A, Brunt EM, Kleiner DE, Miquel R, Smyrk TC, Andrade RJ, Lucena MI, Castiella A, Lindor K, Bjornsson E: The use of liver biopsy evaluation in discrimination of idiopathic autoimmune hepatitis versus drug-induced liver injury. *Hepatology* 2011;54:931–939.
- Bjornsson E, Talwalkar J, Treeprasertsuk S, Kamath PS, Takahashi N, Sanderson S, Neuhäuser M, Lindor K: Drug-induced autoimmune hepatitis: clinical characteristics and prognosis. *Hepatology* 2010;51:2040–2048.
- Liu ZX, Kaplowitz N: Immune-mediated drug-induced liver disease. *Clin Liver Dis* 2002;6:755–774.
- Utrecht J: Immunoallergic drug-induced liver injury in humans. *Semin Liver Dis* 2009;29:383–392.
- Abboud G, Kaplowitz N: Drug-induced liver injury. *Drug Saf* 2007;30:277–294.
- Kirk AP, Jain S, Pocock S, Thomas HC, Sherlock S: Late results of the Royal Free Hospital prospective controlled trial of prednisolone therapy in hepatitis B surface antigen negative chronic active hepatitis. *Gut* 1980;21:78–83.
- Milkiewicz P, Hubscher SG, Skiba G, Hathaway M, Elias E: Recurrence of autoimmune hepatitis after liver transplantation. *Transplantation* 1999;68:253–256.
- Soloway RD, Summerskill WH, Baggenstoss AH, Geall MG, Gitnick GL, Elveback IR, Schoenfield LJ: Clinical, biochemical, and histological remission of severe chronic active liver disease: a controlled study of treatments and early prognosis. *Gastroenterology* 1972;63:820–833.
- Kwak HW, Park JW, Koh YH, Lee JH, Yu A, Nam BH: Clinical characteristics of patients with cryptogenic hepatocellular carcinoma in a hepatitis B virus-endemic area. *Liver Cancer* 2016;5:21–36.
- Borgas DL, Gao JS, Tong M, de la Monte SM: Potential role of phosphorylation as a regulator of aspartyl-(asparaginyl)-beta-hydroxylase: relevance to infiltrative spread of human hepatocellular carcinoma. *Liver Cancer* 2015;4:139–153.
- Ho DW, Lo RC, Chan LK, Ng IO: Molecular pathogenesis of hepatocellular carcinoma. *Liver Cancer* 2016;5:290–302.
- Watkins PB, Seeff LB: Drug-induced liver injury: summary of a single topic clinical research conference. *Hepatology* 2006;43:618–631.
- Leise MD, Poterucha JJ, Talwalkar JA: Drug-induced liver injury. *Mayo Clin Proc* 2014;89:95–106.
- Germano V, Picchianti Diamanti A, Baccano G, Natale E, Onetti Muda A, Priori R, Valesini G: Autoimmune hepatitis associated with infliximab in a patient with psoriatic arthritis. *Ann Rheum Dis* 2005;64:1519–1520.
- Pelli N, Setti M: Atorvastatin as a trigger of autoimmune hepatitis. *J Hepatol* 2004;40:716.
- Manns MP, Czaja AJ, Gorham JD, Krawitt EL, Mieli-Vergani G, Vergani D, Vierling JM: Diagnosis and management of autoimmune hepatitis. *Hepatology* 2010;51:2193–2213.
- Kuzu UB, Oztas E, Turhan N, Saygili F, Suna N, Yildiz H, Kaplan M, Akpınar MY, Akdoğan M, Kacar S, Kilic ZM, Koksas AS, Odemis B, Kayacetin E: Clinical and histological features of idiosyncratic liver injury: dilemma in diagnosis of autoimmune hepatitis. *Hepatol Res* 2016;46:277–291.
- Kleiner DE: The pathology of drug-induced liver injury. *Semin Liver Dis* 2009;29:364–372.
- Dienes HP, Erberich H, Dries V, Schirmacher P, Lohse A: Autoimmune hepatitis and overlap syndromes. *Clin Liver Dis* 2002;6:349–362, vi.
- Czaja AJ: Autoimmune hepatitis; in McSweeney R (ed). *Pathology of the Liver*. Churchill Livingstone, 2007.
- Tajiri K, Shimizu Y: Practical guidelines for diagnosis and early management of drug-induced liver injury. *World J Gastroenterol* 2008;14:6774–6785.
- Hanatani T, Sai K, Tohkin M, Segawa K, Kimura M, Hori K, Kawakami J, Saito Y: A detection algorithm for drug-induced liver injury in medical information databases using the Japanese diagnostic scale and its comparison with the Council for International Organizations of Medical Sciences/the Roussel Uclaf Causality Assessment Method scale. *Pharmacoepidemiol Drug Saf* 2014;23:984–988.
- Watanabe M, Shibuya A, Miura Y, Adachi S, Okuwaki Y, Ono K, Hidaka H, Nakazawa T, Soma K, Saigenji K: Validity study of DDW-J2004 scoring scale for drug-induced liver injury. *Kanzo* 2007;48:219–226.
- Takikawa H, Onji M, Takamori Y, Murata Y, Taniguchi H, Ito T, Watanabe M, Ayada M, Maeda N, Nomoto M, Murata H, Ohmori S, Hisamochi A, Sumida T: Proposal of diagnostic criteria for drug-induced liver injury revised by the DDW-J 2004 Workshop. *Kanzo* 2005;46:85–90.



- 25 Alvarez F, Berg PA, Bianchi FB, Bianchi L, Burroughs AK, Cancado EL, Chapman RW, Cooksley WG, Czaja AJ, Desmet VJ, Donaldson PT, Eddleston AL, Fainboim L, Heathcote J, Homberg JC, Hoofnagle JH, Kakumu S, Krawitt EL, Mackay IR, MacSween RN, Maddrey WC, Manns MP, McFarlane IG, Meyer zum Büschenfelde KH, Zeniya M, et al: International Autoimmune Hepatitis Group Report: review of criteria for diagnosis of autoimmune hepatitis. *J Hepatol* 1999;31:929–938.
- 26 Miao Q, Bian Z, Tang R, Zhang H, Wang Q, Huang S, Xiao X, Shen L, Qiu D, Krawitt EL, Gershwin ME, Ma X: Emperipolesis mediated by CD8 T cells is a characteristic histopathologic feature of autoimmune hepatitis. *Clin Rev Allergy Immunol* 2015;48:226–235.
- 27 Tsutsui A, Nakanuma Y, Takaguchi K, Nakamura S, Shibata H, Baba N, Senoh T, Nagano T, Ikeda H: Comparison of liver biopsy findings with the digestive disease week Japan 2004 scale for diagnosis of drug-Induced liver injury. *Mediators Inflamm* 2015;2015: 913793.
- 28 Fukuda Y, Miyazawa Y, Imoto M, Koyama Y, Nakano I, Nagura H, Kato K: In situ distribution of enolase isozymes in chronic liver disease. *Am J Gastroenterol* 1989;84:601–605.
- 29 Hofer H, Oesterreicher C, Wrba F, Ferenci P, Penner E: Centrilobular necrosis in autoimmune hepatitis: a histological feature associated with acute clinical presentation. *J Clin Pathol* 2006;59:246–249.
- 30 Zen Y, Notsumata K, Tanaka N, Nakanuma Y: Hepatic centrilobular zonal necrosis with positive antinuclear antibody: a unique subtype or early disease of autoimmune hepatitis? *Hum Pathol* 2007;38:1669–1675.
- 31 Misdraji J, Thiim M, Graeme-Cook FM: Autoimmune hepatitis with centrilobular necrosis. *Am J Surg Pathol* 2004;28:471–478.
- 32 Pratt DS, Fawaz KA, Rabson A, Dellelis R, Kaplan MM: A novel histological lesion in glucocorticoid-responsive chronic hepatitis. *Gastroenterology* 1997;113:664–668.
- 33 Jay H: Scheuer's Liver Biopsy Interpretation. 8th edition, Saunders: Elsevier, 2010.

# Diagnosis of Fibrosis and Activity by a Combined Use of Strain and Shear Wave Imaging in Patients with Liver Disease

Norihisa Yada<sup>a</sup> Nobuhura Tamaki<sup>b</sup> Yohei Koizumi<sup>c</sup> Masashi Hirooka<sup>b</sup>  
Osamu Nakashima<sup>d</sup> Yoichi Hiasa<sup>b</sup> Namiki Izumi<sup>c</sup> Masatoshi Kudo<sup>a</sup>

<sup>a</sup>Department of Gastroenterology and Hepatology, Kindai University Faculty of Medicine, Osaka-Sayama,

<sup>b</sup>Department of Gastroenterology and Hepatology, Musashino Red Cross Hospital, Tokyo, <sup>c</sup>Department of Gastroenterology and Metabolism, Ehime University Graduate School of Medicine, Toon, and <sup>d</sup>Department of Clinical Laboratory Medicine, Kurume University Hospital, Kurume, Japan

## Keywords

Combined use of strain and shear wave imaging ·  
Combined use of elastography · Combinational  
elastography · Shear wave imaging · Strain imaging

## Abstract

**Objective:** Performing shear wave imaging is simple, but can be difficult when inflammation, jaundice, and congestion are present. Therefore, the correct diagnosis of liver fibrosis using shear wave imaging alone might be difficult in mild-to-moderate fibrosis cases. Strain imaging can diagnose liver fibrosis without the influence of inflammation. Therefore, the combined use of strain and shear wave imaging (combinational elastography) for cases without jaundice and congestion might be useful for evaluating fibrosis and inflammation. **Methods:** We enrolled consecutive patients with liver disease, without jaundice or liver congestion. Strain and shear wave imaging, blood tests, and liver biopsy were performed on the same day. The liver fibrosis index (LF index) was calculated by strain imaging; real-time tissue elastography, and the shear wave velocity ( $V_s$ ) was calculated by shear wave imaging. Fibrosis index (F index) and activity index (A index) were calculated as a multiple regression equation for

determining hepatic fibrosis and inflammation using histopathological diagnosis as the gold standard. The diagnostic ability of F index for fibrosis and A index for inflammation were compared using LF index and  $V_s$ . **Results:** The total number of enrolled cases was 388. The area under the receiver operating characteristic (AUROC) was 0.87, 0.80, 0.83, and 0.80, at diagnosis of fibrosis stage with an F index of F1 or higher, F2 or higher, F3 or higher, and F4, respectively. The AUROC was 0.94, 0.74, and 0.76 at diagnosis of activity grade with an A index of A1 or higher, A2 or higher, and A3, respectively. The diagnostic ability of F index for liver fibrosis and A index for inflammation was higher than for other conventional diagnostic values. **Conclusions:** The combined use of strain and shear wave imaging (combinational elastography) might increase the positive diagnosis of liver fibrosis and inflammation.

© 2017 S. Karger AG, Basel

## Introduction

In the ultrasonic elastography, the shear wave imaging method calculates the tissue elastic modulus by measuring the propagation speed of the shear wave.

Shear wave imaging is simple to perform, but can be difficult when inflammation, jaundice, and congestion are present. Therefore, it is difficult to diagnose liver fibrosis using shear wave imaging alone in mild-to-moderate fibrosis cases. Strain imaging is a device for the color mapping of tissue relative distortion and can diagnose liver fibrosis in the presence of inflammation, but it is highly dependent on measurement techniques and requires operator training. The Europe and United States guidelines for hepatitis recommended the combined use of shear wave imaging and serum tests. Strain imaging excludes the influence of inflammation, and allows a more accurate diagnosis of fibrosis. Therefore, the combined use of strain and shear wave imaging (combinational elastography) for cases without jaundice and congestion might be useful to evaluate fibrosis and inflammation. Using pathological diagnosis as the gold standard, we developed an algorithm to calculate the degree of fibrosis and inflammation, and examined its diagnostic usefulness.

## Patients and Methods

### Patients

This study analyzed data from UMIN000022089. This was a multi-center prospective study performed at Kindai University Hospital (Osaka-Sayama, Japan), Musashino Red Cross Hospital (Tokyo, Japan), and Ehime University Hospital (Toon, Japan). We enrolled consecutive patients with liver disease initially tested by liver biopsy without jaundice or liver congestion between April 2016 and September 2017. Strain and shear wave imaging, blood tests, and liver biopsy were performed on the same day. The Fibrosis index (F index) and Activity index (A index) were calculated as a multiple regression equation to determine hepatic fibrosis and inflammation using histopathological diagnosis as the gold standard. Their utility was evaluated using K-fold cross validation. The study protocol conformed to the Declaration of Helsinki and was approved by the ethics committee at the Kindai University Faculty of Medicine. Each patient provided informed consent to participate in the study.

### Clinical and Laboratory Assessments

Blood samples were taken after overnight fasting and on the same day as the liver biopsy. Laboratory tests, including aspartate aminotransferase, alanine aminotransferase, total bilirubin, and platelet count were assessed using automated methods.

### Real-Time Tissue Elastography

Real-time tissue elastography (RTE) was performed after overnight fasting with ultrasound (HI VISION Ascendus; Hitachi, Tokyo, Japan) and EUP-C251 convex type probe (5–1 MHz, 50 mm radius scan width, 75° field of view scan angle; Hitachi, Tokyo, Japan), as previously reported [1, 2]. Because the RTE

displays the relative amount of distortion, the analysis area was set as the whole RTE area. Another analyst blinded to patient characteristics, calculated the liver F index (LF index). Three sets of 5 heart beat images were measured and 3 consecutive frames were selected where the RTE image was most stable. One frame taking the median among the LF index obtained from each of the 3 frames was set as the optimum frame. Eleven image features and the LF index acquired by strain histogram measurements from one optimum frame were calculated as follows: mean relative strain value (MEAN), standard deviation of relative strain value (SD), percentage of low strain area (percentage of blue color area – %AREA), complexity of low strain area (calculated as perimeter 2/area – COMP), skewness (SKEW), kurtosis (KURT), entropy (ENT), textural complexity, inverse difference moment (IDM), angular second moment (ASM), contrast (CON), and correlation (COR).

### Shear Wave Measurement

Shear wave measurement (SWM) is a shear wave imaging method. SWM was performed after overnight fasting with ultrasound (HI VISION Ascendus) and EUP-C251 convex-type probe. Using the reliability index, the percentage of the net amount of effective shear wave velocity ( $V_sN$ ), it was determined whether SWM was appropriate for measurements [3]. Measurements where  $V_sN$  was 50% or greater were performed 5 times, and the median value of shear wave  $V_s$  was calculated.

### Pathological Analysis

Liver biopsy was performed with an 18-gauge cutting biopsy. Pathological tissues were paraffin fixed, and stained with hematoxylin & eosin and Masson-Trichrome. A blind reading was performed by a specialized liver pathologist. For pathological diagnosis, fibrosis stage (F stage) and activity grade (A grade) were calculated according to the New Inuyama classification [4]. Only samples with a sufficient amount of tissue collected for pathological diagnosis were analyzed. All cases were analyzed. In addition, those judged as liver cirrhosis by imaging diagnosis and those with platelet counts of 100,000 or less were established as criteria for clinical liver cirrhosis.

### F Index and A Index

Using the pathological diagnostic values F stage and A grade as teacher data, multiple regression equations were calculated using 11 feature quantities and SWM. Using  $k$ -fold cross validation, verification statistics were performed, where  $k = 6$ , and models that gave the best verification statistics were determined. The diagnostic ability of F index for fibrosis and A index for inflammation were compared with LFI and  $V_s$ .

### Statistical Analysis

Descriptive statistics are shown as mean  $\pm$  SD, median, or percentage, as appropriate. Correlations were analyzed using Spearman's rank correlation coefficient. The ranking correlation was analyzed using the Jonckheere-Terpstra trend test. Diagnostic abilities were compared using the area under the receiver operating characteristic (AUROC).  $p < 0.05$  was considered significant. Analysis was performed using SPSS Statistics 20 (IBM, Armonk, NY, USA), JMP 8.0 (SAS Institute Inc.), and R Version 3.3.3 (The R Foundation).



## Results

### Demographics and Baseline Features

The total number of enrolled cases was 388: 205 cases were at Musashino Red Cross Hospital, 106 cases were at Ehime University Hospital, and 77 cases were at Kindai University Hospital.

### Serological Markers

The data of the analysis subject were aspartate aminotransferase  $74.4 \pm 8.7$  IU, alanine aminotransferase  $88.6 \pm 12.7$  IU, serum bilirubin  $0.98 \pm 0.065$  mg/dL, and platelet count  $170,000 \pm 4,000/\mu\text{L}$ . Cases with severe jaundice were not included.

### Background Liver Disease

The subjects analyzed included chronic hepatitis C, nonalcoholic fatty liver disease, chronic hepatitis B, primary biliary cholangitis, and autoimmune hepatitis at 51.8, 11.1, 5.9, 5.9, and 5.4%, respectively. Alcoholic liver injury and drug-induced liver disease were also observed. Patients with congestive liver were not included (Table 1).

### Pathological Analysis

The number of cases by pathological F1 stage was 182 in F1, accounting for about 47% of cases, and A1 accounted for 241 cases and 62%, respectively. Thirteen cases were clinical cases of cirrhosis. There were only 9 cases in the A3 grade. As the F stage increased, the A grade significantly tended to increase ( $r = 0.58$ ,  $p < 0.01$ ; Table 2).

### Calculate F Index and A Index

The F index was calculated as follows:

$$\text{F index} = -12.259 - 0.0199 \times \text{MEAN} - 0.0069 \times \text{SD} + 0.0068 \times \% \text{AREA} - 0.0214 \times \text{COMP} - 0.0772 \times \text{SKEW} + 0.0862 \times \text{KURT} + 1.6659 \times \text{ENT} - 1.3422 \times \text{IDM} + 42.1004 \times \text{ASM} + 0.0011 \times \text{CON} + 8.2076 \times \text{COR} + 1.3869 \times V_s$$

The A index was calculated as follows:

$$\text{A index} = -7.408 - 0.0370 \times \text{MEAN} - 0.0019 \times \text{SD} - 0.0218 \times \% \text{AREA} - 0.0059 \times \text{COMP} + 0.1884 \times \text{SKEW} - 0.2159 \times \text{KURT} - 0.3597 \times \text{ENT} - 5.1614 \times \text{IDM} + 2.6551 \times \text{ASM} + 0.0006 \times \text{CON} + 15.1157 \times \text{COR} + 0.5748 \times V_s$$

### Comparison between Each Evaluation Value and Pathological Diagnosis

The LF index,  $V_s$ , and F index showed a significant upward trend with F stage ( $p < 0.001$ ; Jonckheere-Terpstra trend test,  $r = 0.305$ ,  $0.571$ , and  $0.609$ ; Spearman's rank correlation coefficient). The  $V_s$  and A index also showed

**Table 1.** Background liver disease

Liver disease	n (%)
HCV	201 (51.8)
NAFLD	432 (11.1)
HBV	23 (5.9)
PBC	23 (5.9)
AIH	21 (5.4)
ALD	17 (4.4)
DILI	7 (1.8)
Others	65 (16.8)

This table shows liver disease of patients. Patients with congestive liver were not included. Hepatitis C (HCV) was most.

HCV, hepatitis C; NAFLD, nonalcoholic street hepatitis; HBV, hepatitis B; PBC, primary biliary cholangitis; AIH, autoimmune hepatitis; ALD, alcoholic liver disease; DILI, drug-induced liver disease.

**Table 2.** Number of patients with pathological tissue diagnosis

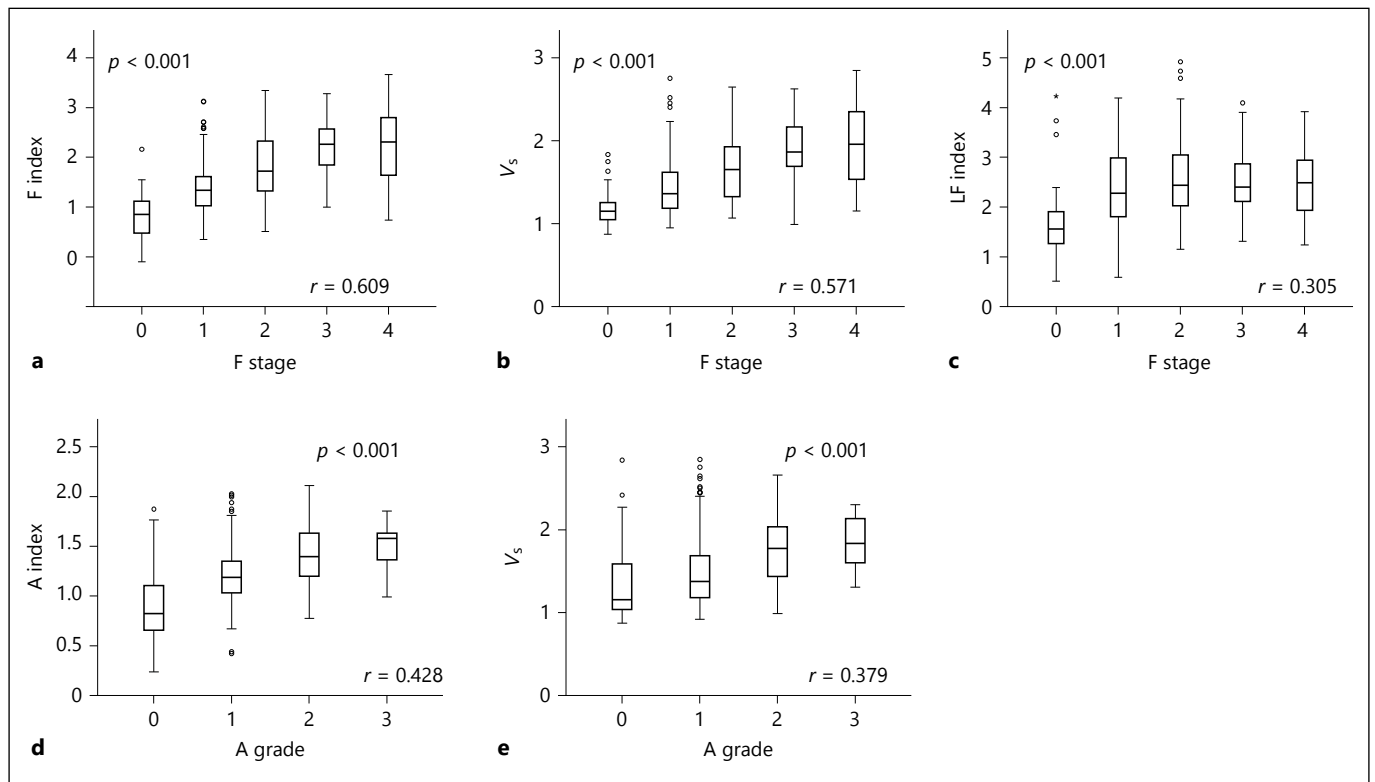
	A0	A1	A2	A3	NE	Total
F0	26	28	1	3	0	55
F1	4	158	19	1	0	182
F2	0	35	38	2	0	75
F3	0	10	20	4	0	34
F4	0	10	17	2	13 (Clinical cirrhosis)	32
Total	30	241	95	9	13	388

Thirteen cases were clinical cases of cirrhosis. As the F stage increased, the A grade significantly tended to increase ( $r = 0.58$ ,  $p < 0.01$ ). NE, not evaluated.

a significant upward trend with A grade ( $p < 0.001$ ,  $r = 0.379$ , and  $0.428$ ). However, the LF index did not significantly correlate with inflammation ( $r = 0.291$ ; Fig. 1).

### Comparison of Diagnostic Ability of Each Evaluation Value

The F stage diagnostic ability of the F index, LF index, and  $V_s$  was compared using the AUROC. For the diagnosis of F1 or higher, the AUROC at F index, LF index, and  $V_s$  were 0.87, 0.83, and 0.81, respectively. Similarly, for the diagnosis of F2 or higher, they were 0.80, 0.79, and 0.62, respectively. For the diagnosis of F3 or higher, the AUROC at F index, LF index, and  $V_s$  were 0.83, 0.81, and 0.59, respectively and for the F4 diagnosis, they were 0.80, 0.79, and 0.59, respectively. The diagnostic ability of F index was the best for each fibrosis stage. The A grade diagnos-



**Fig. 1.** Comparison between each evaluation value and pathological diagnosis. Open circles were outliers. The LF index,  $V_s$ , and F index showed a significant upward trend with F stage ( $p < 0.001$ ; Jonckheere-Terpstra trend test,  $r = 0.305$ ,  $0.571$ , and  $0.609$ ; Spearman's rank correlation coefficient).  $V_s$  and A index also showed a

significant upward trend with A grade ( $p < 0.001$ ,  $r = 0.379$ , and  $0.428$ ). However, the LF index did not significantly correlate with inflammation ( $r = 0.291$ ). **a** F index by F stage, **b**  $V_s$  by F stage, **c** LF index by F stage, **d** A index by A grade, **e**  $V_s$  by A grade.

tic ability of A index, and  $V_s$  was compared by AUROC. For the diagnosis of A1 or higher, the AUROC at A index, and  $V_s$  were 0.94 and 0.85, respectively. Similarly, for the diagnosis of A2 or higher, they were 0.74 and 0.75, respectively. For the diagnosis of A3 or higher, they were 0.76 and 0.75, respectively. In activity diagnosis, the diagnostic ability of A index is not inferior to  $V_s$  (Table 3).

## Discussion

The determination of liver fibrosis severity is very important since fibrosis is one of the important risk factor of hepatocarcinogenesis. Once liver cancer is detected by imaging [5–7] or biomarkers [8, 9], several treatment interventions are applied such as resection [10, 11], ablation [5, 12, 13], transarterial chemoembolization [14, 15], hepatic arterial infusion chemotherapy [16, 17] or systemic therapy [18–21]. A number of studies have investigated shear wave imaging as a noninvasive diagnostic method

for liver fibrosis [22–25]. However, shear wave imaging is affected by hepatic fibrosis and inflammation, jaundice, and congestion [26–28]. This is why the diagnosis of mild-to-moderate hepatic fibrosis is difficult by shear wave imaging alone, despite elastography being a useful noninvasive diagnostic method for hepatic fibrosis described in the hepatitis clinical practice guidelines of the World Federation for Ultrasound in Medicine and Biology (WFUMB), The European Association of the Study of the Liver, and the American Association for the Study of Liver Diseases [29–31].

Strain imaging such as RTE is not affected by inflammation, jaundice, or congestion [1, 2, 32, 33]. In this study, we analyzed only cases without jaundice and congestion to evaluate fibrosis and inflammation. The combined use of strain and shear wave imaging was used to diagnose hepatic fibrosis and inflammation. It was confirmed that the diagnostic ability of F index for liver fibrosis diagnosis and A index for inflammation were higher than other conventional diagnostic values.

**Table 3.** Comparison of diagnostic ability of each evaluation value

Diagnosis level	Evaluation value	Cutoff value	Sensitivity	Specificity	Accuracy	AUROC
F $\geq$ 1	F index	1.162	0.761	0.759	0.760	0.871
	V <sub>s</sub>	1.258	0.770	0.778	0.771	0.826
	LF index	1.901	0.746	0.745	0.746	0.809
F $\geq$ 2	F index	1.524	0.740	0.739	0.740	0.804
	V <sub>s</sub>	1.507	0.735	0.735	0.735	0.794
	LF index	2.282	0.587	0.585	0.585	0.621
F $\geq$ 3	F index	1.748	0.750	0.750	0.750	0.826
	V <sub>s</sub>	1.633	0.724	0.725	0.725	0.809
	LF index	2.322	0.553	0.555	0.554	0.594
F=4	F index	1.770	0.690	0.699	0.698	0.799
	V <sub>s</sub>	1.617	0.667	0.662	0.662	0.778
	LF index	2.361	0.571	0.573	0.573	0.584
A $\geq$ 1	A index	0.982	0.868	0.867	0.868	0.936
	V <sub>s</sub>	1.220	0.769	0.767	0.769	0.852
A $\geq$ 2	A index	1.270	0.689	0.690	0.690	0.741
	V <sub>s</sub>	1.540	0.702	0.701	0.702	0.750
A=3	A index	1.366	0.667	0.704	0.704	0.763
	V <sub>s</sub>	1.643	0.667	0.667	0.667	0.753

The diagnostic ability of F index was the best for each fibrosis stage. In Activity diagnosis, the diagnostic ability of A index is not inferior to V<sub>s</sub>.

However, the number of cases in this study was small. Liver tissues for pathological diagnoses were only obtained by biopsy; therefore, the influence of sampling error could not be eliminated. There was also a bias because there were few cases with high levels of inflammation.

Although various diseases were included in this study, it will be essential to investigate whether there are any common factors between all these diseases in the future. Furthermore, it will be necessary to investigate whether this method can be applied to all cases because the disease is diverse. However, the combined use of strain and shear wave imaging might increase the diagnostic capabilities. These results might impact the development policy of future diagnostic equipment, and the direction of practical guidelines.

## Conclusions

The combined use of strain and shear wave imaging (combinational elastography) might increase the ability to diagnose liver fibrosis and inflammation.

## Acknowledgments

This research was supported by the Research Program on Hepatitis of the Japan Agency for Medical Research and Development.

## Disclosure Statement

The authors declare that they have no conflicts of interest.

## References

- 1 Yada N, Kudo M, Morikawa H, Fujimoto K, Kato M, Kawada N: Assessment of liver fibrosis with real-time tissue elastography in chronic viral hepatitis. *Oncology* 2013; 84(suppl 1):13–20.
- 2 Yada N, Kudo M, Kawada N, Sato S, Osaki Y, Ishikawa A, Miyoshi H, Sakamoto M, Kage M, Nakashima O, Tonomura A: Noninvasive diagnosis of liver fibrosis: utility of data mining of both ultrasound elastography and serological findings to construct a decision tree. *Oncology* 2014;87(suppl 1):63–72.
- 3 Yada N, Sakurai T, Minami T, Arizumi T, Takita M, Hagiwara S, Ueshima K, Ida H, Nishida N, Kudo M: A newly developed shear wave elastography modality: with a Unique Reliability Index. *Oncology* 2015;89(suppl 2): 53–59.
- 4 Ichida F, Tsuji T, Omata M, Ichida T, Inoue K, Kamimura T, Yamada G, Hino K, Yokosuka O, Suzuki H: New Inuyama classification; new criteria for histological assessment of chronic hepatitis. *Int Hepatol Commun* 1996;6:112–119.
- 5 Kudo M: Surveillance, diagnosis, treatment, and outcome of liver cancer in Japan. *Liver Cancer* 2015;4:39–50.

- 6 Hsu C, Chen BB, Chen CH, Ho MC, Cheng JC, Kokudo N, Murakami T, Yeo W, Seong J, Jia JD, Han KH, Cheng AL: Consensus development from the 5th Asia-Pacific primary liver cancer expert meeting (APPLE 2014). *Liver Cancer* 2015;4:96–105.
- 7 Ichikawa S, Ichikawa T, Motosugi U, Sano K, Morisaka H, Enomoto N, Matsuda M, Fujii H: Was hypervascular hepatocellular carcinoma visible on previous gadoxetic acid-enhanced magnetic resonance images? *Liver Cancer* 2015;4:154–162.
- 8 Toyoda H, Kumada T, Tada T, Sone Y, Kaneoka Y, Maeda A: Tumor markers for hepatocellular carcinoma: simple and significant predictors of outcome in patients with HCC. *Liver Cancer* 2015;4:126–136.
- 9 Kudo M: Risk of hepatocellular carcinoma in patients with hepatitis C virus who achieved sustained virological response. *Liver Cancer* 2016;5:155–161.
- 10 Kudo M, Izumi N, Sakamoto M, Matsuyama Y, Ichida T, Nakashima O, Matsui O, Ku Y, Kokudo N, Makuuchi M: Survival analysis over 28 years of 173,378 patients with hepatocellular carcinoma in Japan. *Liver Cancer* 2016;5:190–197.
- 11 Ho MC, Hasegawa K, Chen XP, Nagano H, Lee YJ, Chau GY, Zhou J, Wang CC, Choi YR, Poon RT, Kokudo N: Surgery for intermediate and advanced hepatocellular carcinoma: a consensus report from the 5th Asia-Pacific primary liver cancer expert meeting (APPLE 2014). *Liver Cancer* 2016;5:245–256.
- 12 Kudo M: Locoregional therapy for hepatocellular carcinoma. *Liver Cancer* 2015;4:163–164.
- 13 Kang TW, Rhim H: Recent advances in tumor ablation for hepatocellular carcinoma. *Liver Cancer* 2015;4:176–187.
- 14 Tsurusaki M, Murakami T: Surgical and locoregional therapy of HCC: TACE. *Liver Cancer* 2015;4:165–175.
- 15 Kitai S, Kudo M, Nishida N, Izumi N, Sakamoto M, Matsuyama Y, Ichida T, Nakashima O, Matsui O, Ku Y, Kokudo N, Makuuchi M; Liver Cancer Study Group of Japan: Survival benefit of locoregional treatment for hepatocellular carcinoma with advanced liver cirrhosis. *Liver Cancer* 2016;5:175–189.
- 16 Obi S, Sato S, Kawai T: Current status of hepatic arterial infusion chemotherapy. *Liver Cancer* 2015;4:188–199.
- 17 Lin CC, Hung CF, Chen WT, Lin SM: Hepatic arterial infusion chemotherapy for advanced hepatocellular carcinoma with portal vein thrombosis: impact of early response to 4 weeks of treatment. *Liver Cancer* 2015;4:228–240.
- 18 Kudo M: Molecular targeted therapy for hepatocellular carcinoma: where are we now? *Liver Cancer* 2015;4:I–VII.
- 19 Kudo M: Regorafenib as second-line systemic therapy may change the treatment strategy and management paradigm for hepatocellular carcinoma. *Liver Cancer* 2016;5:235–244.
- 20 Zhang B, Finn RS: Personalized clinical trials in hepatocellular carcinoma based on biomarker selection. *Liver Cancer* 2016;5:221–232.
- 21 Kudo M: Immune checkpoint blockade in hepatocellular carcinoma. *Liver Cancer* 2015;4:201–207.
- 22 Friedrich-Rust M, Wunder K, Kriener S, Sotoudeh F, Richter S, Bojunga J, Herrmann E, Poyndar T, Dietrich CF, Vermehren J, Zeuzem S, Sarrazin C: Liver fibrosis in viral hepatitis: noninvasive assessment with acoustic radiation force impulse imaging versus transient elastography. *Radiology* 2009;252:595–604.
- 23 Colletta C, Smirne C, Fabris C, Toniutto P, Rapetti R, Minisini R, Pirisi M: Value of two noninvasive methods to detect progression of fibrosis among HCV carriers with normal aminotransferases. *Hepatology* 2005;42:838–845.
- 24 Ziol M, Handra-Luca A, Kettaneh A, Christidis C, Mal F, Kazemi F, de Ledinghen V, Marcellin P, Dhumeaux D, Trinchet JC, Beaugrand M: Noninvasive assessment of liver fibrosis by measurement of stiffness in patients with chronic hepatitis C. *Hepatology* 2005;41:48–54.
- 25 Shaheen AA, Wan AF, Myers RP: FibroTest and FibroScan for the prediction of hepatitis C-related fibrosis: a systematic review of diagnostic test accuracy. *Am J Gastroenterol* 2007;102:2589–2600.
- 26 Arena U, Vizzutti F, Corti G, Ambu S, Stasi C, Bresci S, Moscarella S, Boddi V, Petrarca A, Laffi G, Marra F, Pinzani M: Acute viral hepatitis increases liver stiffness values measured by transient elastography. *Hepatology* 2008;47:380–384.
- 27 Millonig G, Reimann FM, Friedrich S, Fonouni H, Mehrabi A, Buchler MW, Seitz HK, Mueller S: Extrahepatic cholestasis increases liver stiffness (FibroScan) irrespective of fibrosis. *Hepatology* 2008;48:1718–1723.
- 28 Colli A, Pozzoni P, Berzuini A, Gerosa A, Canovi C, Molteni EE, Barbarini M, Bonino F, Prati D: Decompensated chronic heart failure: increased liver stiffness measured by means of transient elastography. *Radiology* 2010;257:872–878.
- 29 Ferraioli G, Filice C, Castera L, Choi BI, Sporea I, Wilson SR, Cosgrove D, Dietrich CF, Amy D, Bamber JC, Barr R, Chou YH, Ding H, Farrokh A, Friedrich-Rust M, Hall TJ, Nakashima K, Nightingale KR, Palmeri ML, Schafer F, Shiina T, Suzuki S, Kudo M: WFUMB guidelines and recommendations for clinical use of ultrasound elastography: part 3: liver. *Ultrasound Med Biol* 2015;41:1161–1179.
- 30 European Association for the Study of the Liver. Electronic address: easloffice@easloffice.eu: EASL Recommendations on Treatment of Hepatitis C 2016. *J Hepatol* 2017;66:153–194.
- 31 AASLD/IDSA HCV Guidance Panel: Hepatitis C guidance: AASLD-IDSA recommendations for testing, managing, and treating adults infected with hepatitis C virus. *Hepatology* 2015;62:932–954.
- 32 Fujimoto K, Kato M, Kudo M, Yada N, Shiina T, Ueshima K, Yamada Y, Ishida T, Azuma M, Yamasaki M, Yamamoto K, Hayashi N, Takehara T: Novel image analysis method using ultrasound elastography for non-invasive evaluation of hepatic fibrosis in patients with chronic hepatitis C. *Oncology* 2013;84 (suppl 1):3–12.
- 33 Yada N, Sakurai T, Minami T, Arizumi T, Takita M, Hagiwara S, Ida H, Ueshima K, Nishida N, Kudo M: Influence of liver inflammation on liver stiffness measurement in patients with autoimmune hepatitis evaluation by combinational elastography. *Oncology* 2017;92(suppl 1):10–15.



# Ability of Cytokeratin-18 Fragments and FIB-4 Index to Diagnose Overall and Mild Fibrosis Nonalcoholic Steatohepatitis in Japanese Nonalcoholic Fatty Liver Disease Patients

Natsuko Kobayashi<sup>a</sup> Takashi Kumada<sup>a</sup> Hidenori Toyoda<sup>a</sup> Toshifumi Tada<sup>a</sup>  
Takanori Ito<sup>a</sup> Masayoshi Kage<sup>b</sup> Takeshi Okanoue<sup>c</sup> Masatoshi Kudo<sup>d</sup>

<sup>a</sup>Department of Gastroenterology and Hepatology, Ogaki Municipal Hospital, Ogaki, <sup>b</sup>Department of Diagnostic Pathology, Kurume University Hospital, Kurume, <sup>c</sup>Saiseikai Suita Hospital, Suita, and <sup>d</sup>Department of Gastroenterology and Hepatology, Kindai University Faculty of Medicine, Sayama, Japan

## Keywords

Cytokeratin-18 fragments · FIB-4 index · Nonalcoholic fatty liver · Nonalcoholic steatohepatitis · Mild fibrosis

## Abstract

**Background:** Several laboratory markers used in lieu of liver biopsy are reportedly useful in the diagnosis of nonalcoholic steatohepatitis (NASH). In the present study, we investigated the diagnostic impact of various non-invasive markers for predicting NASH. **Methods:** A total of 229 nonalcoholic fatty liver disease (NAFLD) patients who underwent liver biopsy were enrolled for the study. The diagnostic ability of various markers to diagnose NASH from NAFLD was investigated. **Results:** A total of 140 patients were histologically diagnosed with NASH. Of these, 104 had degree 0–2 fibrosis (F0–2), and 36 had degree 3–4 fibrosis (F3–4). Multiple logistic regression analysis identified hyaluronic acid (HA) (OR 1.014; 95% CI 1.002–1.026;  $p = 0.024$ ), FIB-4 index (OR 2.097; 95% CI 1.177–3.735;  $p = 0.012$ ), and cytokeratin-18 fragments (CK-18F) (OR 1.002; 95% CI 1.001–1.002;  $p < 0.001$ ) as factors independently associated with the diagnosis of NASH. The areas under the receiver operating characteristic curves (AUROCs) of HA, FIB-4 index, and CK-18F for the diagnosis of NASH were 0.77, 0.76, and 0.72, respectively. In ad-

dition, FIB-4 index (OR 1.907; 95% CI 1.063–3.419;  $p = 0.03$ ) and CK-18F (OR 1.002; 95% CI 1.001–1.002;  $p < 0.001$ ) could differentiate between NASH and NAFL, even when NASH patients with advanced fibrosis (F3–4) were excluded. AUROCs of FIB-4 index and CK-18F for the diagnosis of NASH with mild fibrosis (F0–2) from NAFLD were 0.70 and 0.70, respectively. **Conclusions:** FIB-4 index and CK-18F have good diagnostic abilities not only for NASH overall, but also for NASH with mild fibrosis.

© 2017 S. Karger AG, Basel

## Introduction

Nonalcoholic fatty liver disease (NAFLD) is one of the most common liver diseases in both Western and Asian countries [1, 2]. In Japan, approximately 14% of screened patients reportedly have NAFLD [3]. In addition, with the rising numbers of patients with obesity and diabetes mellitus, the incidence of NAFLD is steadily increasing.

NAFLD is histologically further classified into nonalcoholic fatty liver (NAFL) and nonalcoholic steatohepatitis (NASH) [4]. NAFL is defined as the presence of hepatic steatosis with no evidence of hepatocellular injury in the form of ballooning of hepatocytes. NASH is

defined as the presence of hepatic steatosis and inflammation, with hepatocyte ballooning, and with or without fibrosis. NASH, but not NAFL, has a high risk of liver-related disease, such as hepatic encephalopathy, rupture of esophageal and gastric varices, and hepatocellular carcinoma [5, 6]. Once hepatocellular carcinoma is detected by imaging [7–9] or tumor markers [10, 11], several treatment interventions are applied, such as resection [12], ablation [13–15], transarterial therapy [16–19] or systemic therapy [20–22]. Therefore, it is important to differentiate NASH from more benign forms of NAFL.

Liver biopsy is the gold standard for the definitive diagnosis of NASH, but it is associated with problems such as high cost, bleeding risk, and sampling error [23]. Therefore, it is considered important to identify and validate non-invasive markers for predicting NASH without liver biopsy.

Several blood markers and various clinical prediction models, such as adiponectin, cytokeratin-18 (CK-18), and NAFLD fibrosis score (NFS), have been reported useful for differentiating NASH from NAFL [24–26]. However, there are few clinical reports comparing many such markers at the same time in a single group of patients.

In this study, we clarified the ability of various markers to diagnose and distinguish between NASH and NAFL in patients with NAFLD. In addition, we investigated the ability of these markers in diagnosing NASH with mild fibrosis (F0–2) from NAFLD.

## Methods

### *Study Population*

Between 1999 and 2013, 241 consecutive patients with NAFLD underwent liver biopsy for the diagnosis of NASH at Ogaki Municipal Hospital. Twelve of these patients were excluded for the following reasons: (i) other causes of chronic liver disease (e.g., primary biliary cholangitis, autoimmune hepatitis),  $n = 7$ ; (ii) suspected drug-induced NASH,  $n = 1$ ; and (iii) insufficient evaluation of NASH/NAFL classification on pathological findings,  $n = 4$ . Finally, we enrolled 229 NAFLD patients based on histopathological findings.

### *Definitions of Hypertension, Diabetes Mellitus, and Dyslipidemia*

Hypertension was defined as systolic blood pressure  $\geq 135$  mm Hg or diastolic blood pressure  $\geq 85$  mm Hg after 5 min of rest, or use of any antihypertensive medication. Diabetes mellitus was diagnosed based on the criteria of the American Diabetes Association [27], as follows: (1) casual plasma glucose  $\geq 200$  mg/dL, (2) fasting plasma glucose  $\geq 126$  mg/dL, (3) 2-h post-glucose load  $\geq 200$  mg/dL (oral glucose tolerance test), or (4) use of any antihyperglycemic medication. Dyslipidemia was

defined as low-density lipoprotein cholesterol (LDL-C)  $\geq 140$  mg/dL, high-density lipoprotein cholesterol (HDL-C)  $< 40$  mg/dL, triglycerides  $\geq 150$  mg/dL, or treatment with lipid-lowering medication.

### *Definitions of NAFLD*

NAFLD was diagnosed according to the latest guidelines established by the American Association for the Study of Liver Diseases [28] as follows: (1) fatty change of the liver is observed by imaging or histologically; (2) no marked alcohol drinking habit is present (ethanol intake of  $< 210$  g/week for men and  $< 140$  g/week for women); (3) no presence of other factors inducing fatty change of the liver; and (4) no chronic liver disease with clear etiology, such as viruses (hepatitis C virus, hepatitis B virus), primary biliary cholangitis, and autoimmune hepatitis.

### *Histopathological Examination of the Liver and Definitions of NASH/NAFL*

Percutaneous liver biopsy was performed with a 17-gauge needle under ultrasonographic guidance. The liver biopsy specimens were immediately fixed in 10% formalin and embedded in paraffin. The specimens were evaluated by 2 experienced physicians, a hepatologist (T.O.) and a pathologist (K.M), who specialize in NAFLD. Both were blinded to all clinical data. Patients were histologically classified as having NASH or NAFL based on the classification of Matteoni et al. [29], as follows: type 1, fatty liver alone; type 2, fat accumulation and lobular inflammation; type 3, fat accumulation and ballooning degeneration; type 4, fat accumulation, ballooning degeneration, and either Mallory-Denk body or fibrosis. Types 1 and 2 were classified as NAFL, and types 3 and 4 were classified as NASH. Furthermore, NASH with mild fibrosis was defined by stage 0–2 fibrosis (F0–2), and NASH with severe fibrosis was defined by stage 3–4 fibrosis (F3–4) on the basis of the 5-grade scale proposed by Brunt et al. [30], as follows: stage 0, normal connective tissue; stage 1, pericellular or perivenular fibrosis in zone 3 (pericentral vein area); stage 2, zone 3 perisinusoidal/pericellular fibrosis with focal or extensive periportal fibrosis; stage 3, bridging or septal fibrosis; and stage 4, cirrhosis.

### *Routine Laboratory Examination*

Blood samples were obtained at the time of liver biopsy in a fasting state as well as during regular examinations, and blood counts and blood biochemistry tests were conducted using standard methods. All remaining sera were immediately frozen and kept at  $-80^{\circ}\text{C}$  until use.

### *Measurement of NASH-Related Biomarkers*

Serum concentrations of NASH-related biomarkers that have demonstrated the ability to discriminate NASH from NAFLD were determined by immunoassays. Hyaluronic acid (HA) was measured using the latex agglutination method (Wako Pure Chemical Industries, Osaka, Japan). Total CK-18 and cytokeratin-18 fragments (CK-18F) were measured using an M65 ELISA Kit and M30 Apoptosense (PEVIVA AB, Bromma, Sweden), respectively. Type IV collagen 7 s was measured using the latex agglutination method (Sekisui, Tokyo, Japan). Adiponectin was measured using a Human Adiponectin ELISA kit (Circulex, Naganano, Japan). Human tissue inhibitor of metalloproteinase-1 (hTIMP-1) was measured with an hTIMP kit (Daiichi Fine Chemical,

**Table 1.** Patient characteristics

	NAFL ( <i>n</i> = 89)	NASH ( <i>n</i> = 140)	<i>p</i> value
Age, years	46 (34–58)	56 (45–64)	<0.001
Gender, male/female, <i>n</i> (%)	58 (34.8)/ 31 (65.2)	64 (45.7)/ 76 (54.3)	0.004
BMI, kg/m <sup>2</sup>	25.9 (23.6–28.4)	27.1 (25.0–29.7)	0.023
Presence of diabetes mellitus, <i>n</i> (%)	39 (43.8)	65 (46.4)	0.786
Presence of dyslipidemia, <i>n</i> (%)	56 (62.9)	72 (51.4)	0.102
Presence of hypertension, <i>n</i> (%)	34 (38.2)	63 (45.0)	0.339
Matteoni classification, <i>n</i> (%)	1: 37 (41.6) 2: 52 (58.4)	3: 12 (8.6) 4: 128 (91.4)	
Brunt classification staging		10 (7.1)/ 62 (44.3)/ 32 (22.9)/ 30 (21.4)/ 6 (4.3)	
Continuous variables are expressed as medians (interquartile range). Categorical variables are expressed as numbers (percentages).			
BMI, body mass index; NAFL, nonalcoholic fatty liver; NASH, nonalcoholic steatohepatitis.			

Toyama, Japan) and matrix metalloproteinase 2 was measured using the matrix metalloproteinase 2 Activity Assay System (GE Healthcare, USA).

#### Calculation of Complex Markers Related to NASH Diagnosis and Liver Fibrosis

Complex markers were calculated using the following formulae:

i. FIB-4 index = aspartate aminotransferase (AST) (IU/L) × age (years)/platelet count (10<sup>9</sup>/L) × alanine aminotransferase (ALT) (IU/L)<sup>1/2</sup> [31].

ii. AST to platelet ratio index (APRI) = (AST [IU/L]/upper limit of normal AST [IU/L]) × 100/platelet count (10<sup>9</sup>/L) [32].

iii. AST/ALT ratio (AAR) = AST (IU/L)/ALT (IU/L)

iv. NFS =  $-1.675 + 0.037 \times \text{age (years)} + 0.094 \times \text{body mass index (kg/m}^2) + 1.13 \times \text{impaired fasting glucose}^*/\text{diabetes (yes = 1; no = 0)} + 0.99 \times \text{AST/ALT ratio} - 0.013 \times \text{platelet count (10}^9\text{/L)} - 0.66 \times \text{albumin (g/dL)}$ . \*Impaired fasting glucose, fasting blood glucose  $\geq 110$  mg/dL [26].

v. Forn's index =  $7.811 - 3.131 \times \ln(\text{platelet count [10}^9\text{/L)}) + 0.781 \times \ln(\text{gamma-glutamyl transpeptidase, } \gamma\text{-GTP [IU/L)}) + 3.467 \times \ln(\text{age}) - 0.014 \times \text{cholesterol (mg/dL)}$  [33].

#### Statistical Analysis

Statistical analyses were performed with EZR (Saitama medical Center, Jichi Medical University, Saitama, Japan), which is a graphical user interface for R (The R Foundation for Statistical Computing, Vienna, Austria) [34]. Continuous variables were expressed as medians (interquartile range). Categorical variables were expressed as numbers (percentages). Continuous variables were compared using the Mann-Whitney U test, and categorical variables were compared using the chi-square test. Multiple logistic regression was used to estimate the ability to discriminate between NASH and NAFL with the following parameters: HA,

type IV collagen 7s, total CK-18, CK-18F, branched chain amino acid/tyrosine molar ratio (BTR), AAR, APRI, FIB-4 index, Forn's index, and NFS. The same parameters were also used to estimate the ability of discriminating NASH with mild fibrosis and NAFLD.

The diagnostic performance of the scoring systems was assessed using receiver operating characteristic (ROC) curve analysis. The most commonly used index of accuracy is the area under the ROC curve (AUROC), with values close to 1.0 indicating high diagnostic accuracy. Sensitivity and specificity were calculated using maximum (sensitivity + specificity - 1) as the cutoff level in the ROC curve analysis [35]. Statistical significance was defined as  $p < 0.05$ .

The study protocol was in compliance with the Helsinki Declaration and was approved by the institutional review board of Ogaki Municipal Hospital. All patients provided written informed consent for using their clinical data and the analyses of biopsy specimens and serum samples.

## Result

### Patient Characteristics

Table 1 shows the patient characteristics. A total of 229 patients who underwent liver biopsy were investigated. Histological diagnosis was NAFL in 89 patients and NASH in 140. Among NASH patients, 104 had stage 0–2 fibrosis (F0–2), and 36 had stage 3–4 fibrosis (F3–4). The median age of NAFL patients was 46 years (34–58 years), and there was a predominance of males (65.2%). The median age of NASH patients was 56 years (45–64 years),

**Table 2.** Differentiation of NASH from NAFL in univariate analysis

	NAFL ( <i>n</i> = 89)	NASH ( <i>n</i> = 140)	<i>p</i> value
Platelet count, ×10 <sup>4</sup> /μL	24.0 (21.3–29.7)	23.5 (19.3–28.5)	0.140
Hemoglobin, g/dL	14.9 (13.7–16.1)	14.2 (13.4–15.1)	0.003
AST, IU/L	36.0 (24.1–53.0)	60.0 (42.8–91.5)	<0.001
ALT, IU/L	70.0 (33.0–110.0)	85.0 (54.8–135.8)	0.012
γ-GTP, IU/L	60.0 (33.5–97.0)	64.0 (42.0–94.0)	0.186
Total bilirubin, mg/dL	0.60 (0.40–0.80)	0.70 (0.50–0.90)	0.076
Albumin, g/dL	4.5 (4.3–4.7)	4.4 (4.3–4.6)	0.145
Cholinesterase, IU/L	417.5 (356.3–491.3)	375.0 (325.0–446.0)	0.003
Glucose, mg/dL	107.1 (93.1–131.8)	108.7 (96.0–132.0)	0.354
Hemoglobin A1c, %	5.2 (4.8–6.2)	5.6 (5.0–6.1)	0.258
Total cholesterol, mg/dL	203.3 (179.1–227.5)	197.8 (176.4–225.4)	0.325
Triglycerides, mg/dL	152.6 (109.4–204.3)	140.0 (108.4–190.4)	0.455
LDL-C, mg/dL	109.5 (59.0–137.5)	94.5 (48.0–123.4)	0.035
HDL-C, mg/dL	47.7 (40.0–79.5)	54.7 (43.5–100.0)	0.081
Phospholipid, mg/dL	213.0 (188.0–237.0)	214.5 (194.9–232.9)	0.636
Insulin, μU/mL	11.8 (7.3–19.2)	12.6 (7.9–22.6)	0.405
Ferritin, ng/mL	138.0 (82.5–237.3)	195.5 (101.7–349.2)	0.006
Adiponectin, μg/mL	4.9 (3.9–6.9)	5.9 (4.3–7.8)	0.055
HA, ng/mL	23.7 (13.1–38.1)	59.6 (27.8–69.1)	<0.001
Type IV collagen 7s, ng/mL	3.4 (3.0–3.9)	4.1 (3.5–5.3)	<0.001
Total CK-18, U/L	604.8 (401.6–961.0)	1,145.6 (628.4–1,742.6)	<0.001
CK-18F, U/L	275.6 (188.1–442.4)	591.1 (323.7–1,114.7)	<0.001
hTIMP-1, ng/mL	213.6 (155.3–266.7)	214.3 (164.0–286.2)	0.681
hMMP-2, ng/mL	335.5 (202.0–383.9)	340.1 (184.5–432.2)	0.477
Zn, μg/dL	79 (71.0–91.0)	80 (71.5–88.0)	0.936
BTR	7.0 (6.3–8.0)	6.47 (5.5–7.4)	<0.001
AAR	0.55 (0.45–0.73)	0.72 (0.54–0.95)	<0.001
APRI	0.35 (0.26–0.58)	0.68 (0.43–1.17)	<0.001
FIB-4 index	0.78 (0.55–1.20)	1.61 (0.91–2.63)	<0.001
Forn's index	4.08 (2.68–5.01)	5.17 (3.75–6.21)	<0.001
NFS	–2.83 (–4.0 to –1.65)	–2.04 (–3.28 to –0.54)	<0.001

Continuous variables are expressed as medians (interquartile range).

NASH, nonalcoholic steatohepatitis; NAFL, nonalcoholic fatty liver; AST, aspartate aminotransferase; ALT, alanine aminotransferase; γ-GTP, gamma-glutamyl transpeptidase; LDL-C, low-density lipoprotein cholesterol; HDL-C, high-density lipoprotein cholesterol; CK-18, cytokeratin-18; CK18-F, cytokeratin-18 fragment; hTIMP-1, human tissue inhibitor of metalloproteinase-1; hMMP-2, human matrix metalloproteinase 2; BTR, branched chain amino acid/tyrosine molar ratio; AAR, aspartate aminotransferase/alanine aminotransferase ratio; APRI, aspartate aminotransferase/platelet ratio index; NFS, NAFLD fibrosis score.

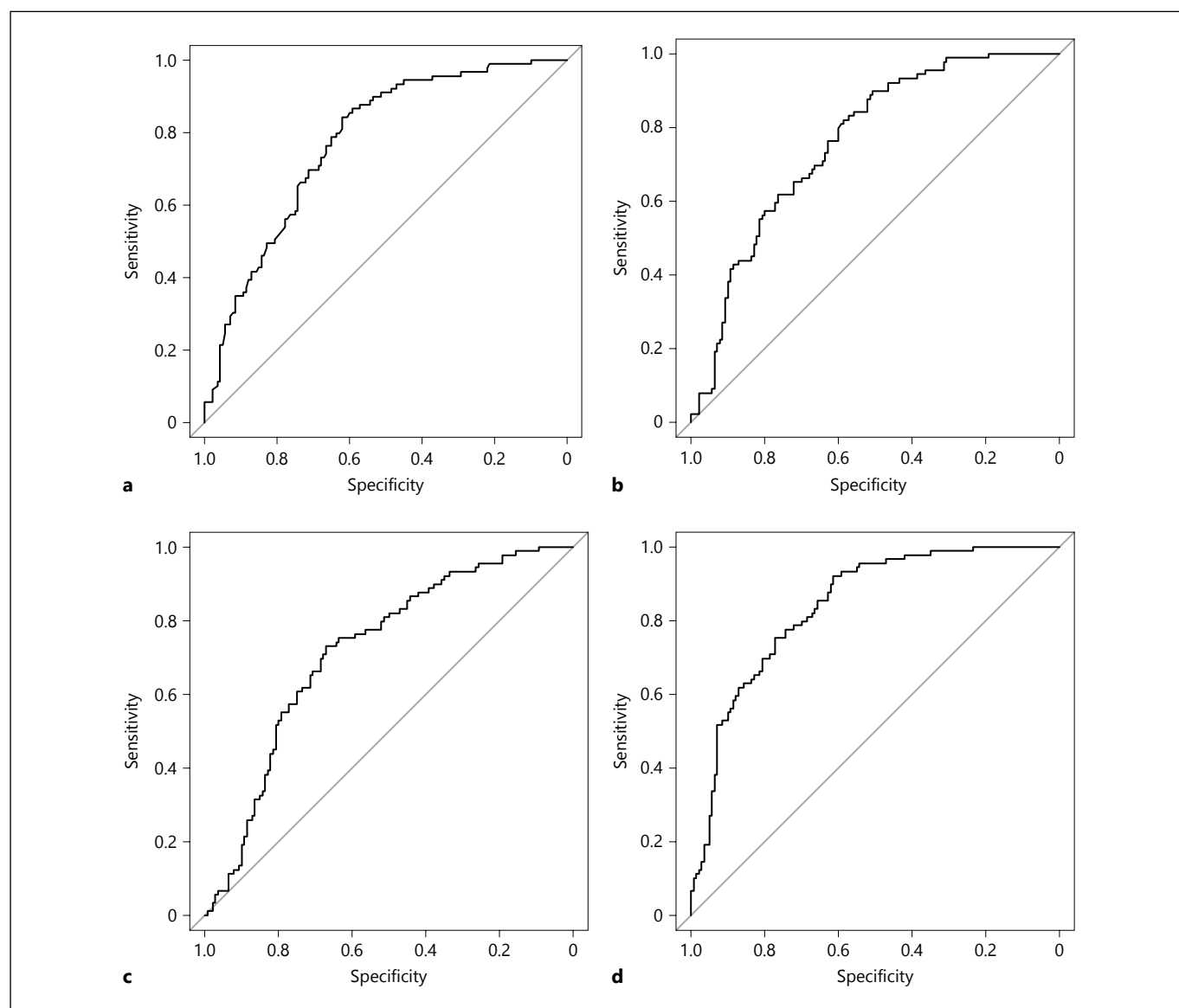
and there was a predominance of females (54.3%). There were significant differences between the NAFL and NASH groups in terms of age, gender, and body mass index.

#### *Differentiation of NASH from NAFL*

As shown in Table 2, the following factors were significantly different between NAFL and NASH patients in the univariate analysis: hemoglobin, AST, ALT, cholinesterase, LDL-C, ferritin, HA, type IV collagen 7s, total CK-18, CK-18F, BTR, AAR, APRI, FIB-4 index, Forn's index,

and NFS. Multiple logistic regression analysis identified HA (OR 1.014; 95% CI 1.002–1.026; *p* = 0.024), FIB-4 index (OR 2.097; 95% CI 1.177–3.735; *p* = 0.012), and CK-18F (OR 1.002; 95% CI 1.001–1.002; *p* < 0.001) as factors independently associated with the diagnosis of NASH. The AUROCs of HA, FIB-4 index, and CK-18F for the diagnosis of NASH were 0.77 (95% CI 0.71–0.83), 0.76 (95% CI 0.69–0.82), and 0.72 (95% CI 0.65–0.78), respectively (Fig. 1a–c). The cutoff value, sensitivity, and specificity of each parameter are presented in Table 3. Figure 1d shows the ROC curve using the combination of HA,





**Fig. 1.** ROC curves of HA, FIB-4 index, and CK-18F for diagnosing NASH. The AUROCs of HA (**a**), FIB-4 index (**b**), and CK-18F (**c**) for diagnosing NASH were 0.77 (95% CI 0.71–0.83), 0.76 (95% CI 0.69–0.82), and 0.72 (95% CI 0.65–0.78), respectively. The AUROC of the combination of HA, FIB-4 index, and CK-18F for the diag-

nosis of NASH was 0.84 (95% CI 0.78–0.88; **d**). ROC, receiver operating characteristic; HA, hyaluronic acid; CK-18F, cytokeratin-18 fragment; NASH, nonalcoholic steatohepatitis; AUROC, area under the receiver operating characteristic curve.

FIB-4 index, and CK-18F. The AUROC of this combination for the diagnosis of NASH was 0.84 (95% CI 0.78–0.88).

#### *Differentiation of NASH with Mild Fibrosis from NAFL*

We then investigated the ability of these markers to diagnose NASH with mild fibrosis from NAFLD. As

shown in Table 4, the following factors differed significantly between patients with NAFL and NASH with mild fibrosis in the univariate analysis: hemoglobin, AST, ALT, total bilirubin, HDL-C, ferritin, HA, type IV collagen 7s, total CK-18, CK-18F, BTR, AAR, APRI, FIB-4 index, and Forn's index. Multiple logistic regression analysis identified FIB-4 index (OR 1.907; 95% CI 1.063–3.419;  $p = 0.030$ ) and CK-18F (OR 1.002; 95% CI 1.001–1.002;

**Table 3.** Diagnostic performance of HA, FIB-4 index, and CK-18F for the diagnosis of definitive NASH

Parameter	Cutoff value	Sensitivity, %	Specificity, %	AUROC (95% CI)
HA, ng/mL	45.1	62	84	0.77 (0.71–0.83)
FIB-4 index	1.56	51	89	0.76 (0.69–0.82)
CK-18F, U/L	408	67	73	0.72 (0.65–0.78)

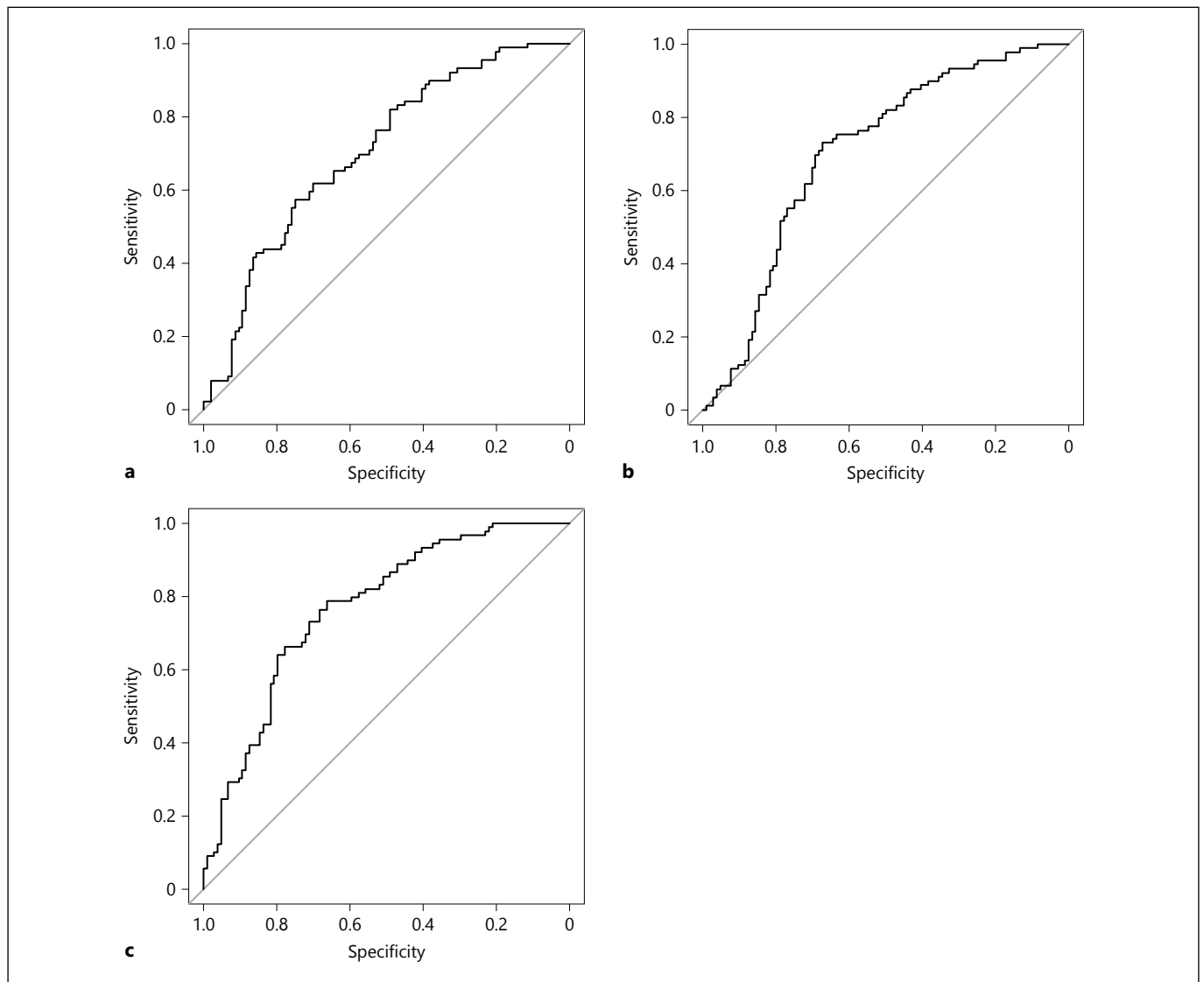
HA, hyaluronic acid; CK18-F, cytokeratin-18 fragment; NASH, nonalcoholic steatohepatitis; AUROC, area under the receiver operating characteristic curve.

**Table 4.** Differentiation of NASH with mild fibrosis from NAFL in univariate analysis

	NAFL ( <i>n</i> = 89)	NASH (F0–2) ( <i>n</i> = 104)	<i>p</i> value
Platelet count, ×10 <sup>4</sup> /μL	24.0 (21.3–29.7)	24.3 (20.9–28.7)	0.909
Hemoglobin, g/dL	14.9 (13.7–16.1)	14.4 (13.5–15.1)	0.041
AST, IU/L	36.0 (24.0–53.0)	55.0 (41.8–81.3)	<0.001
ALT, IU/L	70.0 (33.6–110)	90.5 (56.8–158.5)	0.005
γ-GTP, IU/L	60.0 (33.5–97.0)	62.0 (39.0–90.0)	0.653
Total bilirubin, mg/dL	0.60 (0.40–0.80)	0.70 (0.50–0.90)	0.047
Albumin, g/dL	4.5 (4.3–4.7)	4.5 (4.3–4.7)	0.744
Cholinesterase, IU/L	417.5 (356.3–491.3)	391.0 (337.0–449.0)	0.084
Glucose, mg/dL	107.1 (93.1–131.8)	105.0 (94.8–122.3)	0.749
Hemoglobin A1c, %	5.2 (4.8–6.2)	5.4 (5.0–6.1)	0.447
Total cholesterol, mg/dL	203.3 (179.1–227.5)	205.7 (185.9–227.0)	0.816
Triglycerides, mg/dL	152.6 (109.4–204.2)	148.0 (106.7–191.4)	0.455
LDL-C, mg/dL	109.5 (59.0–137.5)	94.8 (48.3–132.8)	0.108
HDL-C, mg/dL	47.7 (40.0–79.5)	55.3 (44.1–102.3)	0.047
Phospholipid, mg/dL	213.0 (188.0–237.0)	215.7 (195.0–233.7)	0.542
Insulin, μU/mL	11.8 (7.3–19.2)	10.9 (7.7–20.2)	0.726
Ferritin, ng/mL	138.0 (82.5–237.7)	193.2 (93.5–345.7)	0.043
Adiponectin, μg/mL	4.9 (3.9–6.9)	5.5 (4.0–7.4)	0.541
HA, ng/mL	23.7 (13.1–38.1)	45.5 (23.9–74.1)	<0.001
Type IV collagen 7s, ng/mL	3.4 (3.0–3.9)	4.0 (3.4–4.5)	<0.001
Total CK-18, U/L	604.8 (401.6–960.9)	1,145.6 (553.7–1,724.0)	<0.001
CK-18F, U/L	275.6 (188.1–442.4)	589.7 (311.0–1,086.6)	<0.001
hTIMP-1, ng/mL	213.6 (155.3–266.7)	202.2 (151.1–280.8)	0.681
hMMP-2, ng/mL	335.5 (202.0–383.9)	296.3 (178.4–405.6)	0.49
Zn, μg/dL	79 (71.0–91.0)	82 (73.0–89.0)	0.499
BTR	7.0 (6.3–8.0)	6.7 (5.6–7.6)	0.029
AAR	0.55 (0.45–0.73)	0.65 (0.52–0.84)	0.006
APRI	0.35 (0.26–0.58)	0.58 (0.36–1.01)	<0.001
FIB-4 index	0.78 (0.55–1.20)	1.25 (0.84–1.98)	<0.001
FOR's index	4.08 (2.68–5.01)	4.66 (3.54–5.57)	0.017
NFS	–2.83 (–4.01 to –1.65)	–2.38 (–3.48 to –1.45)	0.065

Continuous variables are expressed as medians (interquartile range).

NASH, nonalcoholic steatohepatitis; NAFL, nonalcoholic fatty liver; AST, aspartate aminotransferase; ALT, alanine aminotransferase; γ-GTP, gamma-glutamyl transpeptidase; LDL-C, low-density lipoprotein cholesterol; HDL-C, high-density lipoprotein cholesterol; CK-18, cytokeratin-18; CK18-F, cytokeratin-18 fragment; hTIMP-1, human tissue inhibitor of metalloproteinase-1; hMMP-2, human matrix metalloproteinase 2; BTR, branched chain amino acid/tyrosine molar ratio; AAR, aspartate aminotransferase/alanine aminotransferase ratio; APRI, aspartate aminotransferase/platelet ratio index; NFS, NAFLD fibrosis score.



**Fig. 2.** ROC curves of FIB-4 index and CK-18F for diagnosing NASH with mild fibrosis. The AUROCs of FIB-4 index (**a**) and CK-18F (**b**) for diagnosing NASH with mild fibrosis were 0.70 (95% CI 0.63–0.77) and 0.70 (95% CI 0.63–0.77), respectively. The AUROC of the combination of FIB-4 index and CK-18F for the

diagnosis of NASH with mild fibrosis was 0.77 (95% CI 0.70–0.83) (**c**). ROC, receiver operating characteristic; CK-18F, cytokeratin-18 fragment; NASH, nonalcoholic steatohepatitis; AUROC, area under the receiver operating characteristic curve.

$p < 0.001$ ) as factors independently associated with the diagnosis of NASH with mild fibrosis. The AUROCs of FIB-4 index and CK-18F for the diagnosis of NASH with mild fibrosis from NAFLD were 0.70 (95% CI 0.63–0.77) and 0.70 (95% CI 0.63–0.77), respectively (Fig. 2a, b). The cutoff value, sensitivity, and specificity of each factor are presented in Table 5. Figure 2c shows the ROC curve using the combination of FIB-4 index and CK-18F. The AUROC of this combination for the diagnosis of NASH with mild fibrosis was 0.77 (95% CI 0.70–0.83).

## Discussion

In the present study, we demonstrated that HA, FIB-4 index, and CK-18F had good diagnostic ability for NASH. Based on ROC analysis, the respective diagnostic abilities of HA, FIB-4 index, and CK-18F were 0.77, 0.76, and 0.72. These 3 parameters were independently selected as being diagnostic of NASH by multiple logistic regression analysis using numerous covariates. The AUROC of the combination of these 3 parameters for diagnosing NASH was

**Table 5.** Diagnostic performance of FIB-4 index and CK-18F for the diagnosis of definitive NASH with mild fibrosis

Parameter	Cutoff value	Sensitivity, %	Specificity, %	AUROC (95% CI)
FIB-4 index	0.854	57	75	0.70 (0.63–0.77)
CK-18F, U/L	407.8	67	73	0.70 (0.63–0.77)

CK18-F, cytokeratin-18 fragment; NASH, nonalcoholic steatohepatitis; AUROC, area under the receiver operating characteristic curve.

over 0.8. In addition, FIB-4 index and CK-18F had good ability to diagnose NASH with mild fibrosis in the entire NAFLD patient population. The AUROC of the combination of these 2 parameters for the diagnosis of NASH with mild fibrosis was approximately 0.8.

The usefulness of several non-invasive markers for diagnosing NASH, such as serum biomarkers, scoring systems, and imaging methods, has been shown in previous reports [36]. However, it is currently unclear which among the various markers are most useful for diagnosing NASH in clinical practice. Hence, in this study we tried to comprehensively compare these non-invasive, NASH-related markers at the same time in a single group of patients. We investigated many parameters, such as platelet count, hemoglobin, AST, ALT,  $\gamma$ -GTP, total bilirubin, albumin, cholinesterase, glucose, hemoglobin A1c, total cholesterol, triglycerides, LDL-C, HDL-C, phospholipid, insulin, ferritin, BTR, and Zn in routine laboratory examination. In addition, we also evaluated adiponectin, HA, type IV collagen 7s, total CK-18, CK-18F, hTIMP-1, and MMP-2 as NASH-related biomarkers, and AAR, APRI, FIB-4 index, Forn's index, and NFS as complex markers. Several studies have shown that the NASH-related biomarkers and complex markers listed above are capable of diagnosing NASH [24–26, 33, 37–43]. However, in this study there were no significant differences in platelet count,  $\gamma$ -GTP, total bilirubin, albumin, glucose, hemoglobin A1c, total cholesterol, triglyceride, HDL-C, phospholipid, insulin, adiponectin, hTIMP-1, MMP-2, or Zn in the univariate analysis.

Our results identified CK-18F and FIB-4 index as useful markers for diagnosing not only NASH overall, but also NASH with mild fibrosis. Hepatocyte apoptosis is considered to be one of the etiologies of NASH [44]. CK-18F is regarded as a marker of apoptosis, and is produced by CK-18 being broken down by caspase3 during the apoptotic process [45]. Several studies have demonstrated the utility of CK-18F as a diagnostic marker for NASH

[45]. In a recent meta-analysis [46] of 838 patients in 10 studies, the AUROC for CK-18F in the identification of NASH was 0.845, with 77% sensitivity and 71% specificity. Disadvantages of using CK-18F are that they are not routinely measured in daily practice in Japan and there is no established cutoff value for identifying steatohepatitis. In a recent 2014 study of 424 patients, Cusi et al. [47]. reported that CK-18 had limitations in identifying NASH. However, our study demonstrated that CK-18F was useful in distinguishing NAFL from NASH.

FIB-4 index, a non-invasive complex marker, is used to assess hepatic fibrosis that is calculated based on age and 3 standard biochemical values (platelet count, ALT, and AST). A recent meta-analysis evaluating the use of FIB-4 index described a pooled sensitivity of 84% and specificity of 69% for diagnosing NAFLD-related advanced fibrosis [43]. However, there have been no previous reports on the usefulness of clinical parameters including FIB-4 index for the diagnosis of NASH with mild fibrosis. In general, patients with NASH have a poorer prognosis than the general population. Death secondary to NASH results from cardiovascular events, malignancy, and liver diseases, in that order [48]. For these reasons, NASH is a disease requiring routine follow-up and comprehensive medical intervention. Various treatments for NASH have been developed, but as of now only weight loss [49], vitamin E [50], and pioglitazone [51] are considered as established therapies. Identification and treatment of NASH, particularly at an early stage, may lead to a decrease in its mortality rate.

This study has several limitations, including a retrospective single-center design, small patient population, and patient selection bias. In addition, we did not evaluate the patatin-like phospholipase domain-containing 3 gene that has been implicated in NASH differentiation [52]. Further prospective studies with larger numbers of NAFLD patients are warranted, including those investigating the role of the patatin-like phospholipase domain-containing 3 gene.



Several laboratory markers are useful in diagnosing NASH in patients with NAFLD. In this study, FIB-4 index and CK-18F demonstrated the ability to diagnose NASH, and also the form of the disease with mild fibrosis. Further validation studies using FIB-4 index and CK-18F are needed in the future. In addition, it is necessary to consider whether these markers are related to the prognosis NASH patients.

## References

- Angulo P: Nonalcoholic fatty liver disease. *N Engl J Med* 2002;346:1221–1231.
- Torres DM, Harrison SA: Diagnosis and therapy of nonalcoholic steatohepatitis. *Gastroenterology* 2008;134:1682–1698.
- Suzuki A, Angulo P, Lymp J, St Sauver J, Muto A, Okada T, Lindor K: Chronological development of elevated aminotransferases in a nonalcoholic population. *Hepatology* 2005;41:64–71.
- Chalasani N, Younossi Z, Lavine JE, Diehl AM, Brunt EM, Cusi K, Charlton M, Sanyal AJ: The diagnosis and management of non-alcoholic fatty liver disease: practice guideline by the American gastroenterological association, American association for the study of liver diseases, and american college of gastroenterology. *Gastroenterology* 2012;142:1592–1609.
- Adams LA, Lymp JF, St Sauver J, Sanderson SO, Lindor KD, Feldstein A, Angulo P: The natural history of nonalcoholic fatty liver disease: a population-based cohort study. *Gastroenterology* 2005;129:113–121.
- Hashimoto E, Yatsuji S, Kaneda H, Yoshioka Y, Taniai M, Tokushige K, Shiratori K: The characteristics and natural history of Japanese patients with nonalcoholic fatty liver disease. *Hepatol Res* 2005;33:72–76.
- Ichikawa S, Ichikawa T, Motosugi U, Sano K, Morisaka H, Enomoto N, Matsuda M, Fujii H: Was hypervascular hepatocellular carcinoma visible on previous gadoteric acid-enhanced magnetic resonance images? *Liver Cancer* 2015;4:154–162.
- Joo I, Lee JM: Recent advances in the imaging diagnosis of hepatocellular carcinoma: value of gadoteric acid-enhanced MRI. *Liver Cancer* 2016;5:67–87.
- Kudo M: Surveillance, diagnosis, treatment, and outcome of liver cancer in Japan. *Liver Cancer* 2015;4:39–50.
- Toyoda H, Kumada T, Tada T, Sone Y, Kaneoka Y, Maeda A: Tumor markers for hepatocellular carcinoma: simple and significant predictors of outcome in patients with HCC. *Liver Cancer* 2015;4:126–136.
- Kudo M: Risk of hepatocellular carcinoma in patients with hepatitis c virus who achieved sustained virological response. *Liver Cancer* 2016;5:155–161.
- Ho MC, Hasegawa K, Chen XP, Nagano H, Lee YJ, Chau GY, Zhou J, Wang CC, Choi YR, Poon RT, Kokudo N: Surgery for intermediate and advanced hepatocellular carcinoma: a consensus report from the 5th Asia-Pacific primary liver cancer expert meeting (apple 2014). *Liver Cancer* 2016;5:245–256.
- Kudo M: Locoregional therapy for hepatocellular carcinoma. *Liver Cancer* 2015;4:163–164.
- Kang TW, Rhim H: Recent advances in tumor ablation for hepatocellular carcinoma. *Liver Cancer* 2015;4:176–187.
- Lencioni R, de Baere T, Martin RC, Nutting CW, Narayanan G: Image-guided ablation of malignant liver tumors: recommendations for clinical validation of novel thermal and non-thermal technologies – a western perspective. *Liver Cancer* 2015;4:208–214.
- Tsurusaki M, Murakami T: Surgical and locoregional therapy of HCC: TACE. *Liver Cancer* 2015;4:165–175.
- Geschild JF, Gholam PM, Goldenberg A, Mantry P, Martin RC, Piperdi B, Zigmont E, Imperial J, Babajanyan S, Foreman PK, Cohn A: Use of transarterial chemoembolization (TACE) and sorafenib in patients with unresectable hepatocellular carcinoma: us regional analysis of the gideon registry. *Liver Cancer* 2016;5:37–46.
- Obi S, Sato S, Kawai T: Current status of hepatic arterial infusion chemotherapy. *Liver Cancer* 2015;4:188–199.
- Lin CC, Hung CF, Chen WT, Lin SM: Hepatic arterial infusion chemotherapy for advanced hepatocellular carcinoma with portal vein thrombosis: impact of early response to 4 weeks of treatment. *Liver Cancer* 2015;4:228–240.
- Kudo M: Molecular targeted therapy for hepatocellular carcinoma: where are we now? *Liver Cancer* 2015;4:I–VII.
- Kudo M: Regorafenib as second-line systemic therapy may change the treatment strategy and management paradigm for hepatocellular carcinoma. *Liver Cancer* 2016;5:235–244.
- Zhang B, Finn RS: Personalized clinical trials in hepatocellular carcinoma based on biomarker selection. *Liver Cancer* 2016;5:221–232.
- Bravo AA, Sheth SG, Chopra S: Liver biopsy. *N Engl J Med* 2001;344:495–500.
- Machado MV, Coutinho J, Carepa F, Costa A, Proença H, Cortez-Pinto H: How adiponectin, leptin, and ghrelin orchestrate together and correlate with the severity of nonalcoholic fatty liver disease. *Eur J Gastroenterol Hepatol* 2012;24:1166–1172.
- Feldstein AE, Wieckowska A, Lopez AR, Liu YC, Zein NN, McCullough AJ: Cytokeratin-18 fragment levels as noninvasive biomarkers for nonalcoholic steatohepatitis: a multicenter validation study. *Hepatology* 2009;50:1072–1078.
- Angulo P, Hui JM, Marchesini G, Bugianesi E, George J, Farrell GC, Enders F, Saksena S, Burt AD, Bida JP, Lindor K, Sanderson SO, Lenzi M, Adams LA, Kench J, Thorneau TM, Day CP: The NAFLD fibrosis score: a noninvasive system that identifies liver fibrosis in patients with NAFLD. *Hepatology* 2007;45:846–854.
- Diagnosis and classification of diabetes mellitus. *Diabetes Care* 2010;33(suppl 1):S62–S69.
- Chalasani N, Younossi Z, Lavine JE, Diehl AM, Brunt EM, Cusi K, Charlton M, Sanyal AJ: The diagnosis and management of non-alcoholic fatty liver disease: practice guideline by the American association for the study of liver diseases, American college of gastroenterology, and the American gastroenterological association. *Hepatology* 2012;55:2005–2023.
- Matteoni CA, Younossi ZM, Gramlich T, Boparai N, Liu YC, McCullough AJ: Nonalcoholic fatty liver disease: a spectrum of clinical and pathological severity. *Gastroenterology* 1999;116:1413–1419.
- Brunt EM, Janney CG, Di Bisceglie AM, Neuschwander-Tetri BA, Bacon BR: Nonalcoholic steatohepatitis: a proposal for grading and staging the histological lesions. *Am J Gastroenterol* 1999;94:2467–2474.
- Sterling RK, Lissen E, Clumeck N, Sola R, Correa MC, Montaner J, Sulkowski M, Torriani FJ, Dieterich DT, Thomas DL, Messinger D, Nelson M: Development of a simple noninvasive index to predict significant fibrosis in patients with HIV/HCV coinfection. *Hepatology* 2006;43:1317–1325.

## Disclosure Statement

The authors declare no conflicts of interests.

## Financial Support

There is no grant or other financial support for this study.

- 32 Wai CT, Greenson JK, Fontana RJ, Kalbfleisch JD, Marrero JA, Conjeevaram HS, Lok AS: A simple noninvasive index can predict both significant fibrosis and cirrhosis in patients with chronic hepatitis C. *Hepatology* 2003;38:518–526.
- 33 Forns X, Ampurdanès S, Llovet JM, Aponte J, Quintó L, Martínez-Bauer E, Bruguera M, Sánchez-Tapias JM, Rodés J: Identification of chronic hepatitis c patients without hepatic fibrosis by a simple predictive model. *Hepatology* 2002;36:986–992.
- 34 Kanda Y: Investigation of the freely available easy-to-use software “EZ” for medical statistics. *Bone Marrow Transplant* 2013;48:452–458.
- 35 Youden WJ: Index for rating diagnostic tests. *Cancer* 1950;3:32–35.
- 36 Arulanandan A, Loomba R: Non-invasive testing for NASH and NASH with advanced fibrosis: are we there yet? *Curr Hepatol Rep* 2015;14:109–118.
- 37 Manousou P, Kalambokis G, Grillo F, Watkins J, Xirouchakis E, Pleguezuelo M, Leandro G, Arvaniti V, Germani G, Patch D, Calvaruso V, Mikhailidis DP, Dhillon AP, Burroughs AK: Serum ferritin is a discriminant marker for both fibrosis and inflammation in histologically proven non-alcoholic fatty liver disease patients. *Liver Int* 2011;31:730–739.
- 38 Sakugawa H, Nakayoshi T, Kobashigawa K, Yamashiro T, Maeshiro T, Miyagi S, Shiroma J, Toyama A, Nakayoshi T, Kinjo F, Saito A: Clinical usefulness of biochemical markers of liver fibrosis in patients with nonalcoholic fatty liver disease. *World J Gastroenterol* 2005;11:255–259.
- 39 Abdelaziz R, Elbasel M, Esmat S, Essam K, Abdelaaty S: Tissue inhibitors of metalloproteinase-1 and 2 and obesity related non-alcoholic fatty liver disease: is there a relationship. *Digestion* 2015;92:130–137.
- 40 Toyoda H, Kumada T, Kiriya S, Tanikawa M, Hisanaga Y, Kanamori A, Tada T, Murakami Y: Higher hepatic gene expression and serum levels of matrix metalloproteinase-2 are associated with steatohepatitis in non-alcoholic fatty liver diseases. *Biomarkers* 2013;18:82–87.
- 41 Giannini E, Botta F, Fasoli A, Ceppa P, Risso D, Lantieri PB, Celle G, Testa R: Progressive liver functional impairment is associated with an increase in AST/ALT ratio. *Dig Dis Sci* 1999;44:1249–1253.
- 42 Kruger FC, Daniels CR, Kidd M, Swart G, Brundyn K, van Rensburg C, Kotze M: APRI: a simple bedside marker for advanced fibrosis that can avoid liver biopsy in patients with NAFLD/NASH. *S Afr Med J* 2011;101:477–480.
- 43 Sun W, Cui H, Li N, Wei Y, Lai S, Yang Y, Yin X, Chen DF: Comparison of fib-4 index, nafld fibrosis score and bard score for prediction of advanced fibrosis in adult patients with non-alcoholic fatty liver disease: a meta-analysis study. *Hepatol Res* 2016;46:862–870.
- 44 Feldstein AE, Canbay A, Angulo P, Taniai M, Burgart LJ, Lindor KD, Gores GJ: Hepatocyte apoptosis and fas expression are prominent features of human nonalcoholic steatohepatitis. *Gastroenterology* 2003;125:437–443.
- 45 Leers MP, Kölgén W, Björklund V, Bergman T, Tribbick G, Persson B, Björklund P, Ramaekers FC, Björklund B, Nap M, Jörnvall H, Schutte B: Immunocytochemical detection and mapping of a cytokeratin 18 neo-epitope exposed during early apoptosis. *J Pathol* 1999;187:567–572.
- 46 Chen J, Zhu Y, Zheng Q, Jiang J: Serum cytokeratin-18 in the diagnosis of non-alcoholic steatohepatitis: a meta-analysis. *Hepatol Res* 2014;44:854–862.
- 47 Cusi K, Chang Z, Harrison S, Lomonaco R, Bril F, Orsak B, Ortiz-Lopez C, Hecht J, Feldstein AE, Webb A, Loudon C, Goros M, Tio F: Limited value of plasma cytokeratin-18 as a biomarker for NASH and fibrosis in patients with non-alcoholic fatty liver disease. *J Hepatol* 2014;60:167–174.
- 48 Rafiq N, Bai C, Fang Y, Srishord M, McCullough A, Gramlich T, Younossi ZM: Long-term follow-up of patients with nonalcoholic fatty liver. *Clin Gastroenterol Hepatol* 2009;7:234–238.
- 49 Promrat K, Kleiner DE, Niemeier HM, Jackvony E, Kearns M, Wands JR, Fava JL, Wing RR: Randomized controlled trial testing the effects of weight loss on nonalcoholic steatohepatitis. *Hepatology* 2010;51:121–129.
- 50 Sanyal AJ, Chalasani N, Kowdley KV, McCullough A, Diehl AM, Bass NM, Neuschwander-Tetri BA, Lavine JE, Tonascia J, Unalp A, Van Natta M, Clark J, Brunt EM, Kleiner DE, Hoofnagle JH, Robuck PR: Pioglitazone, vitamin e, or placebo for nonalcoholic steatohepatitis. *N Engl J Med* 2010;362:1675–1685.
- 51 Ratzliff V, Giral P, Jacqueminet S, Charlotte F, Hartemann-Heurtier A, Serfaty L, Podevin P, Lacorte JM, Bernhardt C, Bruckert E, Grimaldi A, Poynard T: Rosiglitazone for nonalcoholic steatohepatitis: one-year results of the randomized placebo-controlled fatty liver improvement with rosiglitazone therapy (flirt) trial. *Gastroenterology* 2008;135:100–110.
- 52 Romeo S, Kozlitina J, Xing C, Pertsemlidis A, Cox D, Pennacchio LA, Boerwinkle E, Cohen JC, Hobbs HH: Genetic variation in pnp1a3 confers susceptibility to nonalcoholic fatty liver disease. *Nat Genet* 2008;40:1461–1465.

# Serum IFN- $\lambda$ 3 Levels Correlate with Serum Hepatitis C Virus RNA Levels in Symptomatic Patients with Acute Hepatitis C

Susumu Imoto<sup>a</sup> Soo Ryang Kim<sup>a</sup> Keisuke Amano<sup>f</sup> Etsuko Iio<sup>n</sup>  
Seitetsu Yoon<sup>g</sup> Shigeya Hirohata<sup>g</sup> Yoshihiko Yano<sup>b</sup> Toru Ishikawa<sup>h</sup>  
Shinji Katsushima<sup>j</sup> Toshiki Komeda<sup>j</sup> Toyokazu Fukunaga<sup>k</sup> Hobyung Chung<sup>c</sup>  
Hiroyuki Kokuryu<sup>i</sup> Yutaka Horie<sup>l</sup> Takashi Hatae<sup>d</sup> Aya Fujinami<sup>e</sup> Soo Ki Kim<sup>a</sup>  
Masatoshi Kudo<sup>m</sup> Yasuhito Tanaka<sup>o</sup>

<sup>a</sup>Department of Gastroenterology, Kobe Asahi Hospital, <sup>b</sup>Department of Gastroenterology, Kobe University Graduate School of Medicine, <sup>c</sup>Department of Gastroenterology, Kobe City Hospital Organization, Kobe City Medical Center, and <sup>d</sup>Educational Center for Clinical Pharmacy, and <sup>e</sup>Medical Biochemistry, Kobe Pharmaceutical University, Kobe, <sup>f</sup>Department of Gastroenterology, Kurume University Medical School, Kurume, <sup>g</sup>Department of Gastroenterology, Hyogo Prefectural Kakogawa Medical Center, Kakogawa, <sup>h</sup>Department of Gastroenterology and Hepatology, Saiseikai Niigata Daini Hospital, Niigata, <sup>i</sup>Hepato-Gastroenterological Section, Kyoto-Katsura Hospital, and <sup>j</sup>Department of Gastroenterology, National Hospital Organization Kyoto Medical Center, Kyoto, <sup>k</sup>Department of Gastroenterology and Hepatology, Kitano Hospital, Osaka, <sup>l</sup>Department of Gastroenterology, Saiseikai Gotsu Hospital, Gotsu, <sup>m</sup>Department of Gastroenterology and Hepatology, Kinki University, School of Medicine, Osaka-Sayama, and <sup>n</sup>Gastroenterology and Metabolism, Nagoya City University, Graduate School of Medical Sciences, and <sup>o</sup>Department of Virology and Liver Unit, Nagoya City University Graduate School of Medical Sciences, Nagoya, Japan

## Keywords

Symptomatic acute hepatitis C · Hepatitis C virus · Interferon- $\lambda$ 3 · Single nucleotide polymorphism rs8099917 · Spontaneous hepatitis C virus clearance · Interferon- $\alpha$  · Interferon- $\beta$

## Abstract

**Background:** Recent genome-wide association studies demonstrated that 2 single nucleotide polymorphisms (SNPs), upstream of the interferon- $\lambda$  (IFNL) 3 gene, are associated with the spontaneous clearance of hepatitis C virus (HCV) in symptomatic patients with acute hepatitis C (AHC).

Although these 2 SNPs, rs8099917 and rs12979860, have established their significant roles in the innate immunity response to spontaneously clear HCV in patients with AHC, the detailed mechanisms of their roles remain largely unknown.

**Aim:** This study is aimed at clarifying the factors affecting IFNL3 production and assessing the roles of IFNL3 in AHC.

**Materials and Methods:** A total of 21 AHC patients who visited the hospital within 10 days after symptom onset were assessed. As controls, 23 healthy volunteers (HVs) were examined. Serum IFNL3 levels were quantified using an in-house, IFNL3-specific chemiluminescence enzyme immunoassay (CLEIA) kit. Serum IFNL1, IFN- $\alpha$ , IFN- $\beta$ , and IFN- $\gamma$  induced protein-10 (IP-10) levels were assayed using

commercial enzyme-linked immunosorbent assay (ELISA) kits. **Results:** At baseline, serum IFNL3 levels were higher in AHC patients than in HVs ( $p < 0.0001$ ). The higher levels in AHC patients did not differ between patients with the rs8099917 TT genotype and those with the non-TT (TG/GG) genotype ( $p = 0.546$ ). Serial measurement of serum IFNL3 levels did not predict the outcome of conventional AHC. However, serum IFNL3 levels at baseline correlated positively with the HCV RNA levels ( $p = 0.005$ ). Following HCV eradication, serum IFNL3 levels reduced to within the range obtained for HVs. Baseline serum IFNL1 levels did not differ significantly between AHC patients and HVs ( $p = 0.284$ ). Serum levels of IFNL1 and IFNL3 at baseline also showed no correlative power ( $p = 0.288$ ). Serum IFN- $\alpha$  and IFN- $\beta$  were detected together with remarkably high serum IFNL3 levels in only one patient who progressed to acute liver failure (ALF). **Conclusion:** These findings indicate that serum IFNL3 levels at baseline are higher in AHC patients regardless of the rs8099917 polymorphism, and primary HCV infection triggers the production of IFNL3. As a first line of defense in the innate immune system against invading HCV, increased IFNL3 levels play an important role, but serum IFNL3 levels are not the principal determinant of the clinical course of conventional AHC.

© 2017 S. Karger AG, Basel

## Introduction

Chronic hepatitis C virus (HCV) infection is a major global health burden. In Japan, approximately 2 million people are chronically infected with HCV [1], however, new occurrences of primary HCV infection are now rare and there are various estimated routes of HCV transmission. HCV infection is one of the major risks of hepatocarcinogenesis. When hepatocellular carcinoma is detected by imaging [2–5] or tumor markers [6, 7], several treatment interventions are applied, such as resection [8, 9], ablation [2, 10], transarterial chemoembolization [11, 12], hepatic arterial infusion chemotherapy [13, 14] or systemic therapy [15–17].

Following HCV infection, spontaneous viral clearance occurs in 25% of individuals [18]. Acute HCV infection is usually asymptomatic, with only a minority of patients presenting with symptoms. Clinical evidence indicates that patients with icteric acute hepatitis C (AHC) have a particularly high chance of clearing the virus spontaneously [19, 20].

Recently, several large genome-wide association studies demonstrated that 2 single nucleotide polymorphisms

(SNPs), upstream of the interferon- $\lambda$  (IFNL) 3 gene, are associated with spontaneous clearance of HCV in AHC [21, 22]. However, these 2 SNPs (rs8099917 and rs12979860) are located some distance from the IFNL3 gene itself [23], therefore, it has remained unclear whether patients with acute HCV infection and the favorable genotype produce larger amounts of IFNL3 (formerly known as IL28B) compared with those having the unfavorable genotype.

For a long time, commercial enzyme-linked immunosorbent assay (ELISA) kits could not distinguish IFNL2 and IFNL3 in the serum due to their considerable amino acid sequence homology [24, 25]. To assess the influence of the 2 SNPs on IFNL3 production, we measured serum IFNL3 levels in patients with primary HCV infection using a newly developed, IFNL3-specific, in-house chemiluminescence enzyme immunoassay (CLEIA) kit [26].

Based on the enhanced data obtained, we studied the factors affecting serum IFNL3 levels and assessed the roles of this cytokine in patients with acute HCV infection.

## Patients and Methods

### Study Subjects

This study enrolled 21 Japanese patients with clinical AHC who visited the hospital within 10 days after symptom onset. According to the criteria proposed by Grebely et al. [22], AHC was defined as serum alanine aminotransferase (ALT) levels over 400 U/L, and HCV RNA positivity with anti-HCV antibody negativity or anti-HCV antibody positivity at a low cutoff index ( $<10$ ), on the day of the initial visit. All patients were negative for hepatitis B virus and human immunodeficiency virus and had no other liver diseases from infective, toxic, or autoimmune causes.

Patients with HCV clearance were identified by 6 successive undetectable serum HCV RNA tests, 4 weeks apart ( $n = 3$ ). Progression from AHC to chronic hepatitis C (CHC) was defined as detectable serum HCV RNA for up to 6 months after the initial visit ( $n = 8$ ). The remaining patients were administered IFN-based therapies within 3 months after the first visit ( $n = 10$ ). Serum samples were collected from the patients at the first medical examination and, as a rule, every 4 weeks thereafter, and stored at  $-80^{\circ}\text{C}$  until testing.

As controls, serum samples were obtained from 23 healthy Japanese adult subjects without HCV, hepatitis B virus or human immunodeficiency virus infection [27].

### Study Design

This was a multicenter, prospective cohort study of serum IFNL3 levels in patients with recent primary HCV infection. The study protocol conformed to the ethical guidelines of the 1975 Declaration of Helsinki and was approved by the institutional Ethics Committee of the Kobe Asahi Hospital (no.12–1) and by the Ethics Committee of each institute. Written informed consent was obtained from all patients.



### SNP Genotyping

The SNP rs8099917 was determined by TaqMan polymerase chain reaction (PCR) using the ABI TaqMan allelic discrimination kit (7900HT Fast Real-Time PCR System; Applied Biosystems, Carlsbad, CA, USA). The SNPs, rs12979860 and rs368234815, were genotyped using the previously described assay [28].

### Measurement of Serum IFNL1, IFNL3, IFN- $\alpha$ , IFN- $\beta$ , and IP-10 Levels

IFNL1 levels were determined with the human IFNL1 ELISA Ready-Set Go (NatuTec, Frankfurt, Germany). This assay was validated in the range between 8.0 and 100 pg/mL. IFNL3 levels were evaluated by the newly developed CLEIA system [26]. This system enables quantification of IFNL3, specifically with no cross-detection of IFNL2 in the range from 0.1 to 1,000 pg/mL [27]. The human IFN- $\alpha$  All Subtype ELISA (detection range 1.95–125 pg/mL) and human IFN- $\beta$  ELISA kits (detection range 1.2–150 pg/mL) were purchased from PBL (Piscataway, NJ, USA). For the measurement of IP-10 levels, an ELISA kit (BD OptEIA Set Human IP-10, detection range 7.8–500 pg/mL; Becton Dickinson Biosciences, San Diego, CA, USA) was used.

### Determination of HCV Genotypes and Viral Load

HCV genotypes were determined by PCR according to the previously described method [29]. Serum HCV RNA levels were measured using the Roche COBAS TaqMan HCV Autoassay V2.0, with a detection limit of 15 IU/mL (Roche Diagnostics KK, Tokyo, Japan).

### Statistical Analyses

Differences between 2 groups were assessed by the Mann-Whitney U test. Continuous variables were compared using the Wilcoxon signed-rank test. Correlations of serum IFNL3 levels with serum total bilirubin (T-Bil), ALT, HCV RNA, IFNL1, and IP-10 levels were evaluated by Spearman's rank correlation coefficient. A *p* value below 0.05 was considered significant. All the analyses were performed using Ekuseru-Tokei 2015 (Social Survey Research Information Co., Ltd.).

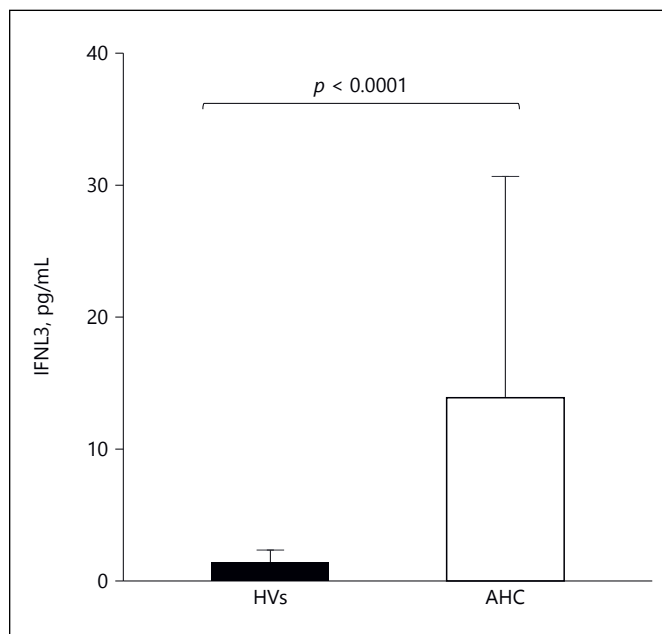
## Results

### Patient Baseline Characteristics

The characteristics of the AHC patients are shown in Table 1. The mean age was 56.0  $\pm$  21.6 years. The HCV genotype distribution was as follows: GT 1b, *n* = 15; GT 2a, *n* = 5; GT 2b, *n* = 1. Various routes of HCV infection were estimated. Perfect linkage disequilibrium existed among the 3 SNPs: rs8099917, rs12979860, and rs368234815.

### Serum IFNL3 Levels were Higher in Patients with AHC than in Healthy Volunteers

We compared serum IFNL3 levels between the AHC and healthy volunteer (HV) groups (mean  $\pm$  SD: 1.4  $\pm$  0.9 pg/mL). IFNL3 levels in the AHC group were significantly higher than those in the HV group (Fig. 1). The only



**Fig. 1.** Serum IFNL3 levels in AHC patients (*n* = 21) were compared with those in HVs (*n* = 23) by the Mann-Whitney U test. All samples were collected from patients at their initial visit.

**Table 1.** Patient baseline characteristics

Factor	Values
Number	21 (9 male, 12 female)
Age, years	56.0 $\pm$ 21.6
Estimated routes of HCV transmission (iatrogenic/sexual contact/tattoo/unknown)	6/3/3/9
HCV genotype (1b/2a/2b)	15/5/1
SNP rs8099917 (TT:non-TT)	18:3
SNP rs12979860 (CC:non-CC)	18:3
SNP rs368234815 (TT/TT:non-TT/TT)	18:3
T-Bil, mg/dL	5.8 $\pm$ 5.1
ALT, U/L	1,325.0 $\pm$ 814.7
IFNL1, pg/mL	134.5 $\pm$ 250.4
IFNL3, pg/mL	13.9 $\pm$ 16.7
IP-10, pg/mL	3,337.2 $\pm$ 1,724.3
HCV RNA, KIU/mL	5,165.8 $\pm$ 8,181.1

Data are presented as mean  $\pm$  SD.

case of ALF [30] without hepatic coma had the highest serum IFNL3 level (77.1 pg/mL) at baseline among those in the AHC group. This patient also had a high HCV RNA level (7.4 log IU/mL) at baseline. Later, this patient's serum IFNL3 level further increased to its peak value (291.5

**Table 2.** Serial measurement of serum clinical and immunologic parameters in a patient with AHC who progressed to ALF and cleared HCV after completing corticosteroid therapy

Case A (F, 53 years)							
Day	IFNL1	IFNL3	IFN- $\alpha/\beta$	T-Bil	ALT	HCV RNA	PT-INR
Initial visit	291.0	77.1	*/4.3	3.2	3,132	7.4	1.32
Day 4**	572.0	291.5	15.2/15.1	5.8	2,552	8.1	1.44
Day 8	174.0	34.0	*/*	8.8	997	8.0	1.58
Day 10	473.0	267.7	*/*	11.0	849	8.4	1.33
Day 14	210.0	97.5	*/*	15.7	852	8.1	0.98
Day 17	243.0	153.6	*/*	16.4	802	8.3	0.87
Day 25	151.0	75.5	*/*	22.4	358	7.8	0.85
Day 60	7.5	3.1	*/*	2.5	71	4.1	n.d.
Day 74	19.3	2.3	*/*	1.4	64	1.7	n.d.
Day 88	27.5	15.0	3.8/6.3	0.9	16	3.7	n.d.
Day 106	77.0	2.0	*/*	0.6	34	*	n.d.

\*\* Measurement of various parameters at day 4 was performed immediately before steroid pulse therapy.

Intravenous and oral corticosteroid administrations were performed from day 4 to day 25, including steroid pulse therapy (methylprednisolone 1,000 mg/day from day 4 to day 6) and steroid mini-pulse therapy (methylprednisolone 500 mg/day from day 7 to day 8).

This patient had the rs8099917 TT genotype.

F, female; PT-INR, prothrombin time-international normalized ratio; \*, not detected; n.d., not done; IFNL1, IFNL3, IFN- $\alpha$ , and IFN- $\beta$ , pg/mL; HCV RNA, log IU/mL.

pg/mL) accompanied by an increase in the serum HCV RNA level (8.1 log IU/mL), immediately before corticosteroid therapy (Table 2).

Additionally, we compared serum IFNL1 levels between AHC patients and HVs ( $n = 23$ , mean  $\pm$  SD:  $110.3 \pm 255.4$  pg/mL) and detected no significant difference between the 2 groups ( $p = 0.284$ ; Fig. 2).

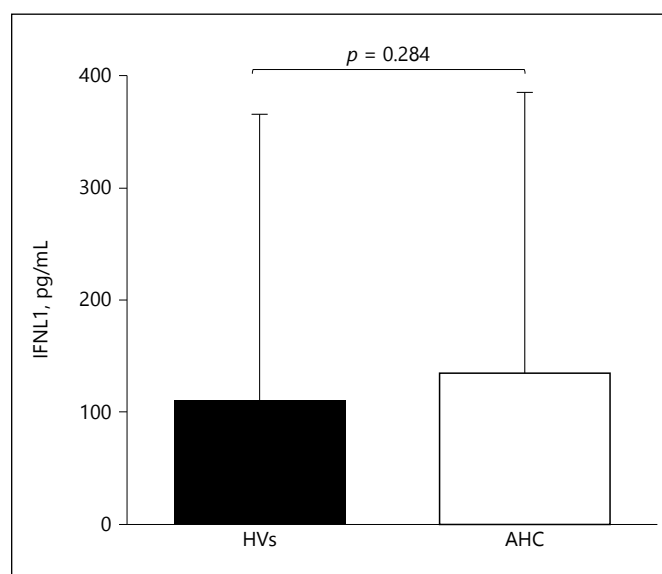
#### *Serum IFNL3 Levels did not Vary with the SNP rs8099917 Genotype, but Correlated with Serum HCV RNA Levels in Patients with AHC*

We compared serum IFNL3 levels between AHC patients with the rs8099917 TT genotype and those with the non-TT genotype. No significant difference was detected between the 2 genotypes (Fig. 3).

Next, we examined whether serum IFNL3 levels correlated with some clinical parameters and immunologic parameters in the AHC group. Serum IFNL3 levels were positively correlated solely with the serum HCV RNA levels ( $p = 0.005$ ). Baseline serum IFNL1 and IFNL3 levels also showed no correlative power (Table 3).

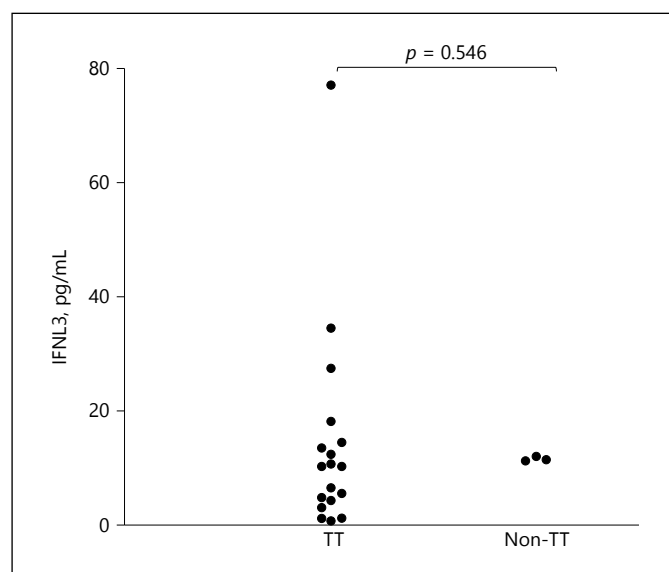
#### *Changes in the Serum IFNL3 Levels Cannot Predict the Clinical Course of Conventional AHC*

In 2 patients who recovered spontaneously from AHC, along with the clearance of HCV, the serum IFNL3 levels



**Fig. 2.** Serum IFNL1 levels in AHC patients ( $n = 21$ ) were compared with those in HVs ( $n = 23$ ) by the Mann-Whitney U test. All samples were collected from patients at their initial visit.

decreased to the range of the HV group, and persisted in this range thereafter. The changes in serum IFNL3 levels, however, were not predictive of spontaneous HCV eradication. Both of these patients had the TT genotype of rs8099917 SNP (Table 4).



**Fig. 3.** Serum IFNL3 levels at baseline in the AHC group were compared between patients with the IFNL3 rs8099917 TT genotype ( $n = 18$ ) and those with the non-TT genotype ( $n = 3$ ) by the Mann-Whitney U test.

**Table 3.** Correlation of serum IFNL3 levels with clinical or immunologic parameters at baseline in patients with AHC ( $n = 21$ )

Factor	CC with IFNL3	<i>p</i> value
T-Bil, mg/dL	0.015	0.949
ALT, U/L	0.211	0.358
IFNL1, pg/mL	0.243	0.288
IP-10, pg/mL	0.116	0.618
HCV RNA, KIU/mL	0.586	0.005

CC, Spearman's rank correlation coefficient.

Among the 8 patients who progressed to CHC, serum IFNL3 levels were compared at baseline and 6 months later. In 2 cases, the serum IFNL3 levels decreased to within the range of the HV group, together with the decline in the serum HCV RNA levels. In 6 cases, the serum IFNL3 levels did not differ greatly between baseline and 6 months after their first medical examination (Fig. 4).

Finally, serum IFNL1 levels also failed to predict the clinical course of conventional AHC (Table 4; Fig. 5).

#### *IFN- $\alpha$ and IFN- $\beta$ Were Detected in Only One Patient Who Progressed to ALF*

We also quantified IFN- $\alpha$  and IFN- $\beta$  in HVs ( $n = 23$ ) and all of the AHC patients ( $n = 21$ ) at the initial examination.

Neither cytokine was detected in the HV group or in 20 of the AHC patients. However, IFN- $\beta$  was detected in one AHC patient who progressed to ALF.

Moreover, we periodically measured IFN- $\alpha$  and IFN- $\beta$  for up to 6 months after the initial visit in the 8 patients who progressed to CHC. In the 2 patients who spontaneously cleared HCV, periodic measurements of the 2 cytokines were performed for up to 6 months after HCV RNA disappearance. We did not detect IFN- $\alpha$  and IFN- $\beta$  in any of these patients.

In the one case who progressed to ALF, IFN- $\alpha$  and IFN- $\beta$  were detected on day 4 after the initial examination. However, 2 cytokines rapidly became undetectable after corticosteroid therapy was initiated. Additionally, serum IFNL3 levels were temporarily decreased soon after the corticosteroid therapy was initiated, however, in accordance with the increase in the HCV RNA levels, it rapidly increased again. After the completion of the corticosteroid therapy, serum IFNL3 levels decreased, but, interestingly, ahead of HCV clearance, transiently increased again together with the reappearance of IFN- $\alpha$  and IFN- $\beta$  (Table 2).

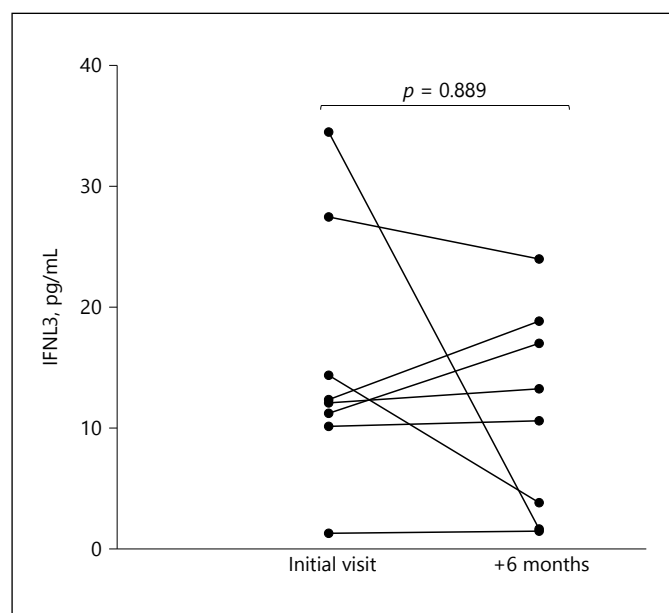
## Discussion

Recent genome-wide association studies identified that 2 SNPs, rs8099917 and rs12979860 (favorable allele TT and CC, respectively), upstream of the IFNL3 gene, are involved in the efficacy of IFN-based treatment in patients with CHC [31–33].

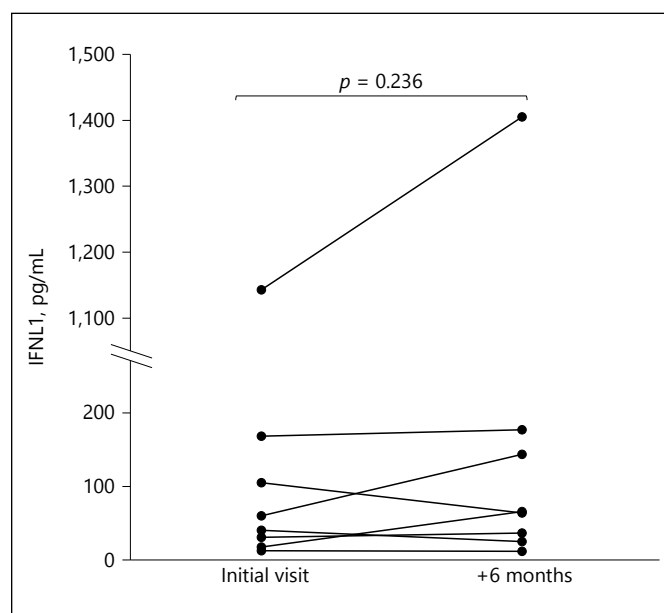
Subsequent studies demonstrated that the same 2 SNPs are strongly associated with the spontaneous clearance of acute HCV infection [21, 22].

However, the mechanistic link between these 2 SNPs and IFNL3 production is unknown. Because IFNL2 and IFNL3 share 97.5% amino acid identity [24, 25], specific detection of each IFNL has been difficult. Finally, Sugiyama et al. [26] constructed a highly IFNL3-specific assay system having little or no cross-reactivity with IFNL2.

Using this CLEIA kit, Aoki et al. [27] quantified the serum IFNL3 levels in patients with CHC for the first time. Although serum IFNL3 levels were higher in CHC patients than in HVs, the levels did not differ between patients with the rs8099917 TT genotype and those with the non-TT genotype, and were unrelated to the response to IFN-based therapy. In CHC patients, serum IFNL3 levels positively correlated with inflammatory and fibrosis markers.



**Fig. 4.** Serial serum IFNL3 levels in patients who progressed from acute to chronic HCV infection ( $n = 8$ ). The value of  $p$  was determined by the Wilcoxon signed-rank test.



**Fig. 5.** Serial serum IFNL1 levels in patients who progressed from acute to chronic HCV infection ( $n = 8$ ). The value of  $p$  was determined by the Wilcoxon signed-rank test.

**Table 4.** Serial measurement of serum clinical and immunologic parameters in patients who resolved spontaneously from acute HCV infection

Day	IFNL1	IFNL3	T-Bil	ALT	HCV RNA
<i>Case B (F, 64 years)</i>					
Initial visit	55.5	3.1	10.4	1,359	5.2
Day 18	125	0.7	1.2	56	1.6
Day 33	145	15.9	0.9	145	5.4
Day 54	143	0.9	0.4	12	2.5
Day 82	100	0.8	0.4	10	*
<i>Case C (M, 61 years)</i>					
Initial visit	5.4	13.5	15.3	1,814	6.9
Day 24	12.6	0.8	13.4	55	2.3
Day 31	7.5	0.8	8.3	64	<1.2
Day 46	*	1.6	3.1	148	2.7
Day 81	0.1	0.8	1.2	18	*

Serum IFN- $\alpha$  and IFN- $\beta$  were not detected in any day in these 2 patients.

These 2 patients had the rs8099917 TT genotype.

M, male; F, female; \*, not detected; HCV RNA, log IU/mL.

In our study, although serum IFNL3 levels at baseline were also higher in AHC patients than in HVs, the levels did not differ between the rs8099917 genotypes. Serial measurement of serum IFNL3 levels did not correlate with the outcome of conventional AHC. In AHC patients,

however, serum IFNL3 levels at baseline correlated positively only with the serum HCV RNA levels. Moreover, in patients who recovered from AHC, in terms of HCV clearance, serum IFNL3 levels decreased to, and persisted within, the range of HVs.



Hepatocytes [34], myeloid dendritic cells type 2 (mDCs2; BDCA3<sup>+</sup>DCs) [35], and plasmacytoid DCs (pDCs) [35] are capable of producing IFNL3 in response to HCV.

Yoshio et al. [35] used the IFNL3-specific CLEIA kit in co-culture experiments with the same number of mDCs2 from healthy Japanese donors with the rs8099917 TT genotype or non-TT genotype and the same amount of cell-cultured HCV, and reported that IFNL3 levels produced from mDCs2 were significantly higher in subjects with the rs8099917 TT genotype than in those with the non-TT genotype.

A more recently identified SNP, rs368234815, is located in exon 1 of the IFNL4 gene, and its favorable allele, TT/TT, is more highly associated with HCV clearance than the 2 previously reported SNPs [28, 36]. IFNL4 protein can be produced by individuals who carry the  $\Delta$ G allele of the rs368234815 variant, but not by individuals who are homozygous for the TT allele because this allele has a frame shift insertion that ablates IFNL4 production. Several explanations for why the loss of IFNL4 confers an improved clinical outcome have been proposed, but the reason remains unclear. In Caucasians and Asians, except for individuals of African ancestry, high linkage disequilibrium has been observed: between rs12979860 and rs368234815 in the former [36], and among rs8099917, rs12979860, and rs368234815 in the latter [37]. Therefore, it is estimated that the existence of the IFNL4 rs368234815 favorable genotype (i.e., the genotype participating in the loss of IFNL4 creation) has a causal role in the clinical course of HCV clearance [38, 39].

Interestingly, Bibert et al. [36], using a real-time PCR system, demonstrated that induction of IFNL3 mRNA relies on the rs368234815 favorable TT/TT genotype, but not the rs12979860 favorable CC genotype, in peripheral blood mononuclear cells obtained from Caucasian patients with CHC and HVs and stimulated with the ds RNA analogue poly (I:C).

The SNP rs8099917 is located 8.9 kb upstream of the promoter region of the IFNL3 gene itself, and hence outside of the IFNL4 gene [23]. Due to its location, it is less likely that this genetic variant has any effect on the transcriptional level of IFNL3 [27]. Incidentally, the SNP rs12979860 is located within intron 1 of the IFNL4 gene [23].

Since it is not possible to set experimental conditions carried out by Yoshio et al. [35] or Bibert et al. [36] in the living body, it is difficult to verify these results.

Although several clinical studies of the SNPs, rs8099917 and rs12979860, have established their antiviral innate immunity-exerting roles in spontaneous HCV clearance

in AHC patients, the detailed mechanisms remain largely unknown, even after measurement of serum IFNL3 levels specifically.

Especially noteworthy are our findings that serum IFNL3 levels statistically correlate exclusively with HCV RNA levels in patients with AHC and decrease to the range of HVs after spontaneous HCV clearance. The IFNLs receptor is expressed by human hepatocytes, the primary cellular targets of HCV [40]. Therefore, our data indicate that primary HCV infection triggers the production of IFNL3.

The major source for the production of serum IFNL3 may be hepatocytes in patients with conventional AHC. In HCV exposure-experiments using primary human hepatocytes [34, 41, 42], HCV robustly stimulated IFNLs production at the protein level, but no induction of IFN- $\alpha$  was observed and no induction or only minimal induction of IFN- $\beta$  was observed. In addition, other IFNL3-producing cells, that is, human mDCs2 [35] and pDCs [35] cultured with HCV released small amounts of IFN- $\alpha$  and IFN- $\beta$  in the human mDCs2 and large amounts of these cytokines in pDCs. Moreover, our clinical investigation revealed that IFN- $\alpha$  and IFN- $\beta$  were not detected in any patients except one who progressed to ALF.

These results suggest that hepatic IFNLs could be a principal driver of IFN-stimulated genes (ISGs) induction in primary HCV infection [42]. Among the IFNL subtypes, IFNL3 has the most potent bioactivity (followed by IFNL1 and IFNL2) [43]. Hence, the role of IFNL3 to induce ISGs as a first line of defense is extremely important in the innate immune response against invading HCV [44]. Accordingly, IFNL3 dampens HCV replication and protects against HCV spreading effectively.

In the one and only patient who progressed to ALF, IFN- $\alpha$  and IFN- $\beta$  were detected together with remarkably high serum IFNL3 levels. Such phenomena are interpreted as double safeguard mechanisms of the host to protect against fatal HCV infection and may serve as important markers to predict progression to ALF. In addition, after corticosteroid therapy, in accordance with the mild increase in HCV RNA level, serum IFNL3 level transiently increased again, and IFN- $\alpha$  and IFN- $\beta$  were also detected preceding successful HCV eradication. We speculated that IFNL3, IFN- $\alpha$ , and IFN- $\beta$  cooperated to strongly inhibit HCV replication because type I and III IFNs differ greatly in their levels of ISG induction with a clearly detectable hierarchy (IFN- $\beta$  > IFN- $\alpha$  > IFNL3 > IFNL1 > IFNL2), and stimulation with either IFN- $\beta$  or IFNLs results in a similar long-lasting ISG induction whereas IFN- $\alpha$  causes transient ISG induction [43].

The dynamics of IFNL1 are similar to those of IFNL3 in supernatants from colon cancer cells cultured with nucleotide analogues (adefovir or tenofovir), but these associations are not found in IFNL1 levels in serum samples from patients undergoing treatment with nucleotide analogues. Serum samples are inappropriate to the measurement of IFNL1 levels for unknown reasons [45]. Therefore, based on these experimental findings and our clinical data indicating that serum IFN1 and IFNL3 levels do not correlate in patients with AHC, we cannot discuss serum IFNL1 levels at this time.

There is only one previously published report regarding serum IFNL1, IFNL2, and IFNL3 levels in AHC patients. Langhans et al. [46] investigated 19 patients with AHC and reported that serum IFNL1 levels were always higher for up to 6 months after the initial visit in patients with spontaneous resolution of acute HCV infection compared with those who progressed to CHC. Although we quantified serum IFNL1 levels using the same kit, our findings differed. The previous study is limited by the measurement of IFNL2 and IFNL3 together, without differentiation. We used the newly developed IFNL3-specific CLEIA kit and found no relationship between serum IFNL3 levels and the clinical course of acute HCV infection.

Our data indicate that endogenous IFNLs alone are insufficient to resolve primary HCV infection. As mentioned in the "Introduction", clinical evidence indicates that AHC patients with jaundice have a higher chance of spontaneous HCV clearance. Therefore, it may be that not only the existence or initiation of another innate immune system in addition to the rs8099917 favorable genotype, but also the activation of the adaptive immune system, is indispensable for successful HCV clearance. The roles of dendritic cells that harmonize the innate and adaptive immune system by stimulating natural killer cells and activating CD4<sup>+</sup> and CD8<sup>+</sup> T cells are also important, although further studies are required to evaluate the functions of dendritic cells in acute HCV infection [47].

Aoki et al. [27] also quantified serum IFNL3 levels in patients with acute hepatitis A ( $n = 34$ ), acute hepatitis B ( $n = 2$ ), and acute hepatitis E ( $n = 9$ ), as well as in CHC patients. All samples were collected from patients whose ALT levels were 2 times higher than the upper limit of the normal range. Only in the acute hepatitis E group were the IFNL3 levels significantly higher than in the HV group ( $p < 0.0001$ ). Hepatitis A virus (HAV) and hepatitis E virus (HEV) are hepatotropic RNA viruses

transmissible by the enterofecal route (HCV is also a hepatotropic RNA virus, but it is a blood-borne virus). Although further studies are needed, Aoki et al. [27] hypothesized that the differences in serum IFNL3 levels were due to distinct mechanisms of recognition of HAV and HEV by the host. In Japan, autochthonous HEV strains of genotypes 3 and 4 are circulating, and the latter, which is especially indigenous to the Hokkaido region, is significantly associated with ALF [48]. It has been reported that serum HEV RNA levels in patients infected with genotype 4 HEV are higher than those infected with genotype 3 HEV [49]. In addition, the high replication activity of genotype 4 HEV was reproduced in a cell culture system using the HE-JF5/15F strain of this genotype recovered from a patient with fulminant hepatitis (i.e., ALF with hepatic coma) [50]. Based on these reports, we speculate that increased levels of serum HEV RNA are produced in patients with ALF in Japan. Gut epithelial cells also have the ability to produce IFNLs in response to enteric viruses [39]. HEV principally replicates in the liver and is shed into the intestinal lumen via the bile duct. Therefore, high serum IFNL3 levels may be released by gut epithelial cells in response to the large amount of HEV in ALF patients mainly infected with genotype 4 HEV. The high mean serum IFNL3 levels in the acute hepatitis E group may be due to the frequent presence of ALF.

## Conclusion

Serum IFNL3 levels at baseline were increased in patients with acute HCV infection regardless of the rs8099917 polymorphism. Serum IFNL3 levels were associated only with the serum HCV RNA levels. The major source for the production of serum IFNL3 may be hepatocytes in patients with conventional AHC. As a first line of defense in the innate immune system against invading HCV, increased levels of serum IFNL3 play an important role, but they are not the principal determinant of the outcome of conventional AHC.

## Special Thanks

Serum IFNL3 levels were measured at the Research Center for Hepatitis and Immunology, National Center for Global Health and Medicine, Ichikawa, Japan, as a kind favor to Professor and Director, Masashi Mizokami, and former Chief, Kazumoto Murata.

## Acknowledgments

The authors thank the members for assistance with various aspects of this study. Members (listed in alphabetical order) include Soji Abe (Saiseikai Niigata Daini Hospital, Niigata, Japan), Kazuo Higuchi (Saiseikai Niigata Daini Hospital, Niigata, Japan), Mika Matsui (Kobe Asahi Hospital, Kobe, Japan), Hiroshi Matsuoka (Saiseikai Gotsu Hospital, Gotsu, Japan), Kentaro Matsuura (Gastroenterology and Metabolism, Nagoya City University, Graduate School of Medical Science, Nagoya, Japan), Takanori Matsuura

(Hyogo Prefectural Kakogawa Medical Center, Kakogawa, Japan), Yasushi Seo (Seo Clinic, Himeji, Japan), Miyuki Taniguchi (Kobe Asahi Hospital, Kobe, Japan), and Sachiyo Yoshio (National Center for Global Health and Medicine, Ichikawa, Japan).

## Disclosure Statement

The authors have no conflict of interest to declare.

## References

- 1 Chung H, Ueda T, Kudo M: Changing trends in hepatitis C infection over the past 50 years in Japan. *Intervirol* 2010;53:39–43.
- 2 Kudo M: Surveillance, diagnosis, treatment, and outcome of liver cancer in Japan. *Liver Cancer* 2015;4:39–50.
- 3 Kudo M: Clinical practice guidelines for hepatocellular carcinoma differ between Japan, United States, and Europe. *Liver Cancer* 2015;4:85–95.
- 4 Kudo M: Breakthrough imaging in hepatocellular carcinoma. *Liver Cancer* 2016;5:47–54.
- 5 Joo I, Lee JM: Recent advances in the imaging diagnosis of hepatocellular carcinoma: value of gadoteric acid-enhanced MRI. *Liver Cancer* 2016;5:67–87.
- 6 Toyoda H, Kumada T, Tada T, Sone Y, Kaneoka Y, Maeda A: Tumor markers for hepatocellular carcinoma: simple and significant predictors of outcome in patients with HCC. *Liver Cancer* 2015;4:126–136.
- 7 Kudo M: Risk of hepatocellular carcinoma in patients with hepatitis C virus who achieved sustained virological response. *Liver Cancer* 2016;5:155–161.
- 8 Kudo M, Izumi N, Sakamoto M, Matsuyama Y, Ichida T, Nakashima O, Matsui O, Ku Y, Kokudo N, Makuuchi M: Survival analysis over 28 years of 173,378 patients with hepatocellular carcinoma in Japan. *Liver Cancer* 2016;5:190–197.
- 9 Ho MC, Hasegawa K, Chen XP, Nagano H, Lee YJ, Chau GY, Zhou J, Wang CC, Choi YR, Poon RT, Kokudo N: Surgery for intermediate and advanced hepatocellular carcinoma: a consensus report from the 5th Asia-Pacific primary liver cancer expert meeting (apple 2014). *Liver Cancer* 2016;5:245–256.
- 10 Kudo M: Locoregional therapy for hepatocellular carcinoma. *Liver Cancer* 2015;4:163–164.
- 11 Tsurusaki M, Murakami T: Surgical and locoregional therapy of HCC: TACE. *Liver Cancer* 2015;4:165–175.
- 12 Arizumi T, Ueshima K, Minami T, Kono M, Chishina H, Takita M, Kitai S, Inoue T, Yada N, Hagiwara S, Minami Y, Sakurai T, Nishida N, Kudo M: Effectiveness of sorafenib in patients with transcatheter arterial chemoembolization (TACE) refractory and intermediate-stage hepatocellular carcinoma. *Liver Cancer* 2015;4:253–262.
- 13 Obi S, Sato S, Kawai T: Current status of hepatic arterial infusion chemotherapy. *Liver Cancer* 2015;4:188–199.
- 14 Lin CC, Hung CF, Chen WT, Lin SM: Hepatic arterial infusion chemotherapy for advanced hepatocellular carcinoma with portal vein thrombosis: impact of early response to 4 weeks of treatment. *Liver Cancer* 2015;4:228–240.
- 15 Kudo M: Molecular targeted therapy for hepatocellular carcinoma: where are we now? *Liver Cancer* 2015;4:I–VII.
- 16 Geschwind JF, Gholam PM, Goldenberg A, Mantry P, Martin RC, Piperdi B, Zigmont E, Imperial J, Babajanyan S, Foreman PK, Cohn A: Use of transarterial chemoembolization (TACE) and sorafenib in patients with unresectable hepatocellular carcinoma: us regional analysis of the gideon registry. *Liver Cancer* 2016;5:37–46.
- 17 Kudo M: Immune checkpoint blockade in hepatocellular carcinoma. *Liver Cancer* 2015;4:201–207.
- 18 Micallef JM, Kaldor JM, Dore GJ: Spontaneous viral clearance following acute hepatitis C infection: a systematic review of longitudinal studies. *J Viral Hepat* 2006;13:34–41.
- 19 Gerlach JT, Diepolder HM, Zachoval R, Gruener NH, Jung MC, Ulsenheimer A, Schraut WW, Schirren CA, Waechter M, Backmund M, Pape GR: Acute hepatitis C: high rate of both spontaneous and treatment-induced viral clearance. *Gastroenterology* 2003;125:80–88.
- 20 Santantonio T, Wiegand J, Gerlach JT: Acute hepatitis C: current status and remaining challenges. *J Hepatol* 2008;49:625–633.
- 21 Thomas DL, Thio CL, Martin MP, Qi Y, Ge D, O'Huigin C, Kidd J, Kidd K, Khakoo SI, Alexander G, Goedert JJ, Kirk GD, Donfield SM, Rosen HR, Tobler LH, Busch MP, McHutchison JG, Goldstein DB, Carrington M: Genetic variation in IL28B and spontaneous clearance of hepatitis C virus. *Nature* 2009;461:798–801.
- 22 Grebely J, Petoumenos K, Hellard M, Matthews GV, Suppiah V, Applegate T, Yeung B, Marks P, Rawlinson W, Lloyd AR, Booth D, Kaldor JM, George J, Dore GJ: Potential role for interleukin-28B genotype in treatment decision-making in recent hepatitis C virus infection. *Hepatology* 2010;52:1216–1224.
- 23 O'Brien TR, Prokunina-Olsson L, Donnelly RP: IFN- $\lambda$ 4: The paradoxical new member of the interferon lambda family. *J Interferon Cytokine Res* 2014;34:829–838.
- 24 Sheppard P, Kindsvogel W, Xu W, Henderson K, Schlutsmeyer S, Whitmore TE, Kuestner R, Garrigues U, Birks C, Roraback J, Ostlander C, Dong D, Shin J, Presnell S, Fox B, Haldeman B, Cooper E, Taft D, Gilbert T, Grant FJ, Tackett M, Krivan W, McKnight G, Clegg C, Foster D, Klucher KM: IL-28, IL-29 and their class II cytokine receptor IL-28R. *Nat Immunol* 2003;4:63–68.
- 25 Kotenko SV, Gallagher G, Baurin VV, Lewis-Antes A, Shen M, Shah NK, Langer JA, Sheikh F, Dickensheets H, Donnelly RP: IFN-lambda mediates antiviral protection through a distinct class II cytokine receptor complex. *Nat Immunol* 2003;4:69–77.
- 26 Sugiyama M, Kimura T, Naito S, Mukaide M, Shinauchi T, Ueno M, Ito K, Murata K, Mizokami M: Development of specific and quantitative real-time detection PCR and immunoassays for  $\lambda$ 3-interferon. *Hepatol Res* 2012;42:1089–1099.
- 27 Aoki Y, Sugiyama M, Murata K, Yoshio S, Kurosaki M, Hashimoto S, Yatsushashi H, Nomura H, Kang JH, Takeda T, Naito S, Kimura T, Yamagiwa Y, Korenaga M, Imamura M, Masaki N, Izumi N, Kage M, Mizokami M, Kanto T: Association of serum IFN- $\lambda$ 3 with inflammatory and fibrosis markers in patients with chronic hepatitis C virus infection. *J Gastroenterol* 2015;50:894–902.
- 28 Prokunina-Olsson L, Muchmore B, Tang W, Pfeiffer RM, Park H, Dickensheets H, Hergott D, Porter-Gill P, Mumy A, Kohaar I, Chen S, Brand N, Tarway M, Liu L, Sheikh F, Astemborski J, Bonkovsky HL, Edlin BR, Howell CD, Morgan TR, Thomas DL, Rehmann B, Donnelly RP, O'Brien TR: A variant upstream of IFNL3 (IL28B) creating a new interferon gene IFNL4 is associated with impaired clearance of hepatitis C virus. *Nat Genet* 2013;45:164–171.

- 29 Tanaka Y, Hanada K, Mizokami M, Yeo AE, Shih JW, Gojobori T, Alter HJ: A comparison of the molecular clock of hepatitis C virus in the united states and Japan predicts that hepatocellular carcinoma incidence in the united states will increase over the next two decades. *Proc Natl Acad Sci U S A* 2002;99:15584–15589.
- 30 Mochida S, Takikawa Y, Nakayama N, Oketani M, Naiki T, Yamagishi Y, Ichida T, Tsubouchi H: Diagnostic criteria of acute liver failure: a report by the intractable hepato-biliary diseases study group of Japan. *Hepatol Res* 2011;41:805–812.
- 31 Tanaka Y, Nishida N, Sugiyama M, Kurosaki M, Matsuura K, Sakamoto N, Nakagawa M, Korenaga M, Hino K, Hige S, Ito Y, Mita E, Tanaka E, Mochida S, Murawaki Y, Honda M, Sakai A, Hiasa Y, Nishiguchi S, Koike A, Sakaida I, Imamura M, Ito K, Yano K, Masaki N, Sugauchi F, Izumi N, Tokunaga K, Mizokami M: Genome-wide association of IL28B with response to pegylated interferon-alpha and ribavirin therapy for chronic hepatitis C. *Nat Genet* 2009;41:1105–1109.
- 32 Suppiah V, Moldovan M, Ahlenstiel G, Berg T, Weltman M, Abate ML, Bassendine M, Spengler U, Dore GJ, Powell E, Riordan S, Sheridan D, Smedile A, Fragomeli V, Müller T, Bahlo M, Stewart GJ, Booth DR, George J: IL28B is associated with response to chronic hepatitis C interferon-alpha and ribavirin therapy. *Nat Genet* 2009;41:1100–1104.
- 33 Ge D, Fellay J, Thompson AJ, Simon JS, Shianna KV, Urban TJ, Heinzen EL, Qiu P, Bertelsen AH, Muir AJ, Sulkowski M, McHutchison JG, Goldstein DB: Genetic variation in IL28B predicts hepatitis C treatment-induced viral clearance. *Nature* 2009;461:399–401.
- 34 Thomas E, Gonzalez VD, Li Q, Modi AA, Chen W, Noureddin M, Rotman Y, Liang TJ: HCV infection induces a unique hepatic innate immune response associated with robust production of type III interferons. *Gastroenterology* 2012;142:978–988.
- 35 Yoshio S, Kanto T, Kuroda S, Matsubara T, Higashitani K, Kakita N, Ishida H, Hiramatsu N, Nagano H, Sugiyama M, Murata K, Fukuhara T, Matsuura Y, Hayashi N, Mizokami M, Takehara T: Human blood dendritic cell antigen 3 (BDCA3)(+) dendritic cells are a potent producer of interferon- $\lambda$  in response to hepatitis C virus. *Hepatology* 2013;57:1705–1715.
- 36 Bibert S, Roger T, Calandra T, Bochud M, Cerny A, Semmo N, Duong FH, Gerlach T, Malinverni R, Moradpour D, Negro F, Müllhaupt B, Bochud PY: IL28B expression depends on a novel TT/-G polymorphism which improves HCV clearance prediction. *J Exp Med* 2013;210:1109–1116.
- 37 Ochi H, Miki D, Hayes CN, Abe H, Hayashida Y, Kubo M, Chayama K: IFNL4/IL-28B haplotype structure and its impact on susceptibility to hepatitis C virus and treatment response in the Japanese population. *J Gen Virol* 2014;95:1297–1306.
- 38 Nagaoki Y, Imamura M, Kawakami Y, Kan H, Fujino H, Fukuhara T, Kobayashi T, Ono A, Nakahara T, Naeshiro N, Urabe A, Yokoyama S, Miyaki D, Murakami E, Kawaoka T, Tsuge M, Hiramatsu A, Aikata H, Takahashi S, Hayes CN, Ochi H, Chayama K: Interferon lambda 4 polymorphism affects on outcome of telaprevir, pegylated interferon and ribavirin combination therapy for chronic hepatitis C. *Hepatol Res* 2014;44:E447–E454.
- 39 Lazear HM, Nice TJ, Diamond MS: Interferon- $\lambda$ : immune functions at barrier surfaces and beyond. *Immunity* 2015;43:15–28.
- 40 Kotenko SV: IFN- $\lambda$ s. *Curr Opin Immunol* 2011;23:583–590.
- 41 Marukian S, Andrus L, Sheahan TP, Jones CT, Charles ED, Ploss A, Rice CM, Dustin LB: Hepatitis C virus induces interferon- $\lambda$  and interferon-stimulated genes in primary liver cultures. *Hepatology* 2011;54:1913–1923.
- 42 Park H, Serti E, Eke O, Muchmore B, Prokuni-Olsson L, Capone S, Folgori A, Rehmann B: IL-29 is the dominant type III interferon produced by hepatocytes during acute hepatitis C virus infection. *Hepatology* 2012;56:2060–2070.
- 43 Bolen CR, Ding S, Robek MD, Kleinstein SH: Dynamic expression profiling of type I and type III interferon-stimulated hepatocytes reveals a stable hierarchy of gene expression. *Hepatology* 2014;59:1262–1272.
- 44 Wieland S, Makowska Z, Campana B, Calabrese D, Dill MT, Chung J, Chisari FV, Heim MH: Simultaneous detection of hepatitis C virus and interferon stimulated gene expression in infected human liver. *Hepatology* 2014;59:2121–2130.
- 45 Murata K, Asano M, Matsumoto A, Sugiyama M, Nishida N, Tanaka E, Inoue T, Sakamoto M, Enomoto N, Shirasaki T, Honda M, Kaneko S, Gatanaga H, Oka S, Kawamura YI, Dohi T, Shuno Y, Yano H, Mizokami M: Induction of IFN- $\lambda$ 3 as an additional effect of nucleotide, not nucleoside, analogues: a new potential target for HBV infection. *Gut* 2016, pii: gutjnl-2016-312653.
- 46 Langhans B, Kupfer B, Braunschweiger I, Arndt S, Schulte W, Nischalke HD, Nattermann J, Oldenburg J, Sauerbruch T, Spengler U: Interferon-lambda serum levels in hepatitis C. *J Hepatol* 2011;54:859–865.
- 47 Yoshio S, Kanto T: Host-virus interactions in hepatitis B and hepatitis C infection. *J Gastroenterol* 2016;51:409–420.
- 48 Abe T, Aikawa T, Akahane Y, Arai M, Asahina Y, Atarashi Y, Chayama K, Harada H, Hashimoto N, Hori A, Ichida T, Ikeda H, Ishikawa A, Ito T, Kang J, Karino Y, Kato H, Kato M, Kawakami M, Kitajima N, Kitamura T, Masaki N, Matsubayashi K, Matsuda H, Matsui A, Michitaka K, Mihara H, Miyaji K, Miyakawa H, Mizuo H, Mochida S, Moriyama M, Nishiguchi S, Okada K, Saito H, Sakugawa H, Shibata M, Suzuki K, Takahashi K, Yamada G, Yamamoto K, Yamanaka T, Yamato H, Yano K, Mishihiro S: Demographic, epidemiological, and virological characteristics of hepatitis E virus infections in Japan based on 254 human cases collected nationwide. *Kanzo* 2006;47:384–391 (In Japanese).
- 49 Takahashi M, Okamoto H: Features of hepatitis E virus infection in humans and animals in Japan. *Hepatol Res* 2014;44:43–58.
- 50 Tanaka T, Takahashi M, Takahashi H, Ichiyama K, Hoshino Y, Nagashima S, Mizuo H, Okamoto H: Development and characterization of a genotype 4 hepatitis E virus cell culture system using a HE-JF5/15F strain recovered from a fulminant hepatitis patient. *J Clin Microbiol* 2009;47:1906–1910.



# Comparison of Sofosbuvir Plus Ribavirin Treatment with Pegylated Interferon Plus Ribavirin Treatment for Chronic Hepatitis C Genotype 2

Kayo Seo<sup>a</sup> Soo Ki Kim<sup>c</sup> Soo Ryang Kim<sup>c</sup> Aya Ohtani<sup>d</sup> Mana Kobayashi<sup>d</sup>  
Airi Kato<sup>d</sup> Eri Morimoto<sup>d</sup> Yuka Saijo<sup>d</sup> Ke Ih Kim<sup>d</sup> Susumu Imoto<sup>c</sup>  
Chi Wan Kim<sup>c</sup> Yoshihiko Yano<sup>b</sup> Masatoshi Kudo<sup>e</sup> Yoshitake Hayashi<sup>a</sup>

<sup>a</sup>Division of Molecular Medicine and Medical Genetics, Department of Pathology, and <sup>b</sup>Center for Infectious Diseases, Kobe University Graduate School of Medicine, <sup>c</sup>Department of Gastroenterology, and <sup>d</sup>Department of Pharmacy, Kobe Asahi Hospital, Kobe, and <sup>e</sup>Department of Gastroenterology and Hepatology, Kinki University Faculty of Medicine, Osaka-Sayama, Japan

## Keywords

Chronic hepatitis C genotype 2 · Sofosbuvir plus ribavirin · Liver function · Fibrosis marker · Hepatocellular carcinoma marker

## Abstract

**Background:** Sofosbuvir plus ribavirin (RBV) therapy showed higher sustained virological response at 12 weeks after treatment (SVR12) than pegylated interferon (peg-IFN) plus RBV; however, liver function, fibrosis, and hepatocellular carcinoma markers have not been assessed so far. **Summary:** Patients ( $n = 21$ ) receiving Sofosbuvir plus RBV and those ( $n = 24$ ) receiving peg-IFN plus RBV were enrolled in this study. Changes in alanine aminotransferase (ALT) and  $\alpha$ -fetoprotein (AFP) levels, platelet (PLT) counts, FIB-4, and aspartate aminotransferase-to-platelet ratio index (APRI) in both groups were assessed in patients achieving SVR12. Also, fibrosis regression was assessed using pathophysiological biomarkers, such as hyaluronic acid, bone morphogenetic protein 7 (BMP-7), and connective tissue growth factor (CTGF) in the Sofosbuvir plus RBV group. In both groups, while the reduction in ALT levels was significant that of AFP was not. Compared with the baseline, although serum PLT count at the

end of treatment (EOT) was significantly higher in the Sofosbuvir plus RBV group, it was significantly lower in the peg-IFN plus RBV group. Although a significant decline in fibrosis markers such as FIB-4 and APRI was observed between the baseline and at EOT in the Sofosbuvir plus RBV group, no significant change of these markers was observed in the peg-IFN plus RBV group. Moreover, BMP-7 and CTGF were significantly lower at EOT than the baseline in the Sofosbuvir plus RBV group. **Key Message:** The treatment with Sofosbuvir plus RBV results in not only a higher SVR, but also improves the liver function and the degree of fibrosis.

© 2017 S. Karger AG, Basel

## Introduction

When hepatocellular carcinoma (HCC) [1, 2] is diagnosed by imaging or tumor markers, treatment interventions are applied, such as resection [3–5], ablation [6–8], transplantation [9], transarterial chemoembolization, transarterial infusion chemotherapy [10, 11] or systemic therapies [12–14]. Hepatitis C virus (HCV) infection is a common cause of chronic hepatitis and hepatocarcinogenesis worldwide [15, 16].



In recent years, treatment of HCV has changed drastically with the development and administration of direct-acting antivirals (DAA) in clinical practice.

DAA therapy with Sofosbuvir (Gilead Sciences), the oral nucleotide analog inhibitor of HCV-specific non-structural protein (NS)5B polymerase, plus ribavirin (RBV) for patients infected with HCV genotype 2 has demonstrated a higher rate of sustained virological response at 12 weeks after treatment (SVR12) and greater safety than treatment with pegylated interferon (peg-IFN) and RBV [17–22].

The prevention of HCC and regression of liver fibrosis have been the main topic of study and discussion in the community of liver experts for decades. The eradication of HCV by treatment with IFN has been shown to prevent HCC [23–27]. Moreover, sustained responders have shown fibrosis stabilization or fibrosis regression by treatment with IFN [28–30].

Nonetheless, prevention of HCC and regression of fibrosis with Sofosbuvir plus RBV treatment for patients with chronic hepatitis C (CHC) genotype 2 remains to be clarified.

After IFN treatment, alanine aminotransferase (ALT) and  $\alpha$ -fetoprotein (AFP) levels [31] are significantly associated with hepatocarcinogenesis; thus, measuring their levels is useful in predicting the future HCC risk [32].

Liver biopsy is the gold standard for assessing liver fibrosis, but serial liver biopsies are challenging due to their invasiveness and high rate of complications. Numerous fibrosis markers have been classified into 2 categories [33]. One used in assessing liver fibrosis is a common chemical test mostly for estimating the degree of fibrosis. FIB-4 and the aspartate aminotransferase-to-platelet ratio index (APRI) in this category have been demonstrated to be accurate in staging chronic liver diseases before antiviral treatment and in the prediction of hepatic fibrosis in HCV patients [34–36]. Fibrosis biomarkers classified in another category, such as hyaluronic acid, bone morphogenetic protein 7 (BMP-7), and connective tissue growth factor (CTGF), are used to assess liver fibrosis pathophysiologically, and have been reported to increase in patients with chronic liver disease, liver damage, and cirrhosis. The elevation in these serum levels may express progression of liver fibrogenesis [37–41]. To date, no study has been made on the use of pathophysiological fibrosis biomarkers for assessing liver fibrosis regression following DAA therapy.

The aim of the present study was to evaluate the impact of Sofosbuvir plus RBV treatment, as compared with that of peg-IFN plus RBV treatment, on changes in liver function, fibrosis markers, and HCC marker with the use of

**Table 1.** Patient baseline characteristics

	Sofosbuvir plus RBV (n = 21)	Peg-IFN plus RBV (n = 24)	p value
Age, years	59.76±13.33	49.08±13.04	0.020
Gender, men/women	12/9	16/8	0.511
AST, IU/L	45.35±26.69	47.71±50.72	0.839
ALT, IU/L	47.56±26.78	67.25±91.62	0.949
AFP, ng/mL	7.00±5.91	8.58±20.4	0.232
PLT, $\times 10^4/\text{mm}^3$	16.84±4.70	20.16±6.64	0.118
FIB-4	3.04±2.71	1.76±1.35	0.044
APRI	0.93±0.89	0.77±0.93	0.122
HCV RNA, logIU/mL	6.29±0.75	6.24±0.79	0.794

Data are shown as means  $\pm$  SD.

ALT, FIB-4 and APRI, AFP, respectively. Additionally, fibrosis regression was assessed using pathophysiological biomarkers, such as hyaluronic acid, BMP-7, CTGF, in the Sofosbuvir plus RBV group.

## Patients and Methods

All patients were seen at Kobe Asahi Hospital and diagnosed with CHC genotype 2 infection.

Twenty-one patients (12 men and 9 women, mean  $59.8 \pm 13.3$  years of age, Table 1) were administered Sofosbuvir 400 mg/day per os and RBV twice daily per os (600 mg/day for body weight (BW)  $\leq 60$  kg, 800 mg/day for BW  $> 60 \sim \leq 80$  kg or 1,000 mg/day for BW  $> 80$  kg) for 12 weeks. Patients with Child-Pugh A liver cirrhosis and those with previous treatment with IFN were included in the present study.

Twenty-four patients (16 men and 8 women, mean  $49.1 \pm 13.0$  years of age, Table 1) were administered peg-IFN  $\alpha$ -2b (1.5  $\mu\text{g}/\text{kg}$  BW) subcutaneously once a week and RBV twice daily per os (600 mg/day for BW  $\leq 60$  kg, 800 mg/day for BW  $> 60 \sim \leq 80$  kg or 1,000 mg/day for BW  $> 80$  kg) for 24 weeks, from 2008 to 2014. The patients received  $> 80\%$  of the scheduled dosage; those with liver cirrhosis were excluded from the study.

Included in the study were patients demonstrating hemoglobin levels of  $\geq 11$  g/dL (women) or  $\geq 12$  g/dL (men), platelet (PLT) count  $\geq 9 \times 10^4/\text{mm}^3$ , HCV RNA  $\geq 4.0$  log IU/mL, neutrophil count  $\geq 1,500/\text{mm}^3$ , and thyroid stimulating hormone levels within normal limits. Those demonstrating human immunodeficiency virus or hepatitis B coinfection, creatinine clearance  $< 50$  mL/min, liver disease other than CHC, evidence of advanced liver disease such as liver cirrhosis (Child-Pugh B and C) under Sofosbuvir plus RBV treatment, preexisting psychiatric conditions, or a history of severe psychiatric disorder were excluded.

## Laboratory Tests and Calculated Scores

HCV RNA levels and genotypes were examined through the COBAS TaqMan HCV test, with a lower limit of quantification of 1.2 log IU/mL.

Serum BMP-7 levels were assayed using a solid-phase, enzyme-linked immunosorbent assay kit Quantikine ELISA kit (Quantikine® ELISA, R&D Systems, Inc., MN, USA, Cat. No, DBP700) based on the sandwich principle, according to the manufacturer's instructions. Serum CTGF levels were assayed using a solid-phase enzyme-linked immunosorbent assay kit (OmniKine® ELISA, LifeSpan BioScience, Inc., USA, Cat. No, OK-0109) based on the sandwich principle, according to the manufacturer's instructions.

APRI and FIB-4 scores were calculated as surrogate markers of liver fibrosis as follows:

APRI = (aspartate aminotransferase (AST) [IU/L]/upper limit of normal)/PLT count (expressed as platelets  $\times 10^9/L$ )  $\times 100$ .

FIB-4 score = age (years)  $\times$  AST [IU/L]/(PLT count ( $\times 10^9/L$ )  $\times \sqrt{ALT [IU/L]}$ )

The APRI score was calculated using Wai's formula [42], and the FIB-4 score was calculated using Sterling's formula [43].

#### Efficacy Assessment

Rapid virological response (RVR), end-of-treatment response (ETR), and SVR12 were defined as undetectable serum HCV RNA at 4 weeks, at the end of treatment (EOT), and 12 weeks after the EOT, respectively. The primary endpoint in this study was at 12 weeks after the EOT. The baseline serum levels of ALT, AFP, PLT count, FIB-4, and APRI were compared with those at EOT and at 12 weeks after the EOT in patients of both groups who achieved SVR12. The baseline levels of hyaluronic acid, BMP-7, and CTGF were compared with those at EOT in patients of the Sofosbuvir plus RBV group.

#### Statistical Analysis

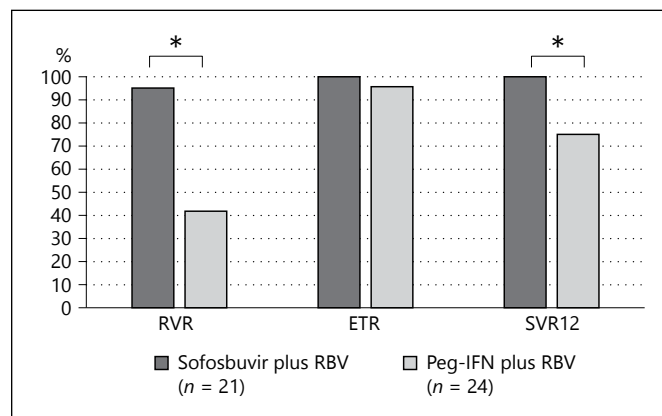
The Mann-Whitney U test and the  $\chi^2$  test were used to compare the baseline data of the Sofosbuvir plus RBV group with those of the peg-IFN plus RBV group. Fisher's exact test was used to compare the rate of SVR12 in the Sofosbuvir plus RBV group with that in the peg-IFN plus RBV group. The Wilcoxon signed-rank test was used to compare the baseline data, comprising the serum levels of ALT, AFP, the PLT count, the FIB-4, and APRI scores with those at EOT and at SVR12, and to compare the baseline data of hyaluronic acid, BMP-7, and CTGF with those at EOT. Variables with a  $p$  value  $< 0.05$  were considered statistically significant. All statistical analyses were carried out using Excel Statistics 2011 by SSRI.

## Results

#### Treatment Efficacy

In the Sofosbuvir plus RBV group, all patients achieved ETR and SVR12; only one patient did not achieve RVR (Fig. 1). On the contrary, RVR, ETR, and SVR12 were achieved in 41.7% (10/24), 95.8% (23/24), and 75.0% (18/24) of the peg-IFN plus RBV group (Fig. 1).

A significant difference in RVR and SVR12 was observed between the Sofosbuvir plus RBV and peg-IFN plus RBV groups (RVR:  $p < 0.001$ , SVR12:  $p = 0.023$ , Fig. 1).



**Fig. 1.** Virological response to treatment with Sofosbuvir plus RBV and peg-IFN plus RBV. All patients treated with Sofosbuvir plus RBV achieved ETR (100%) and SVR12 (100%); only one patient did not achieve RVR (95.2%). RVR, ETR, and SVR12, respectively, were achieved in 41.7% (10/24), 95.8% (23/24), and 75.0% (18/24) of patients in the peg-IFN plus RBV group. A significant difference was observed in RVR and SVR12 between the 2 groups (RVR:  $p < 0.001$ ; SVR12:  $p = 0.023$ ). RBV, ribavirin; peg-IFN, pegylated interferon; RVR, rapid virological response; ETR, end-of-treatment response; SVR12, sustained virological response at 12 weeks after treatment. \*  $p < 0.05$ .

#### Assessment of Liver Function

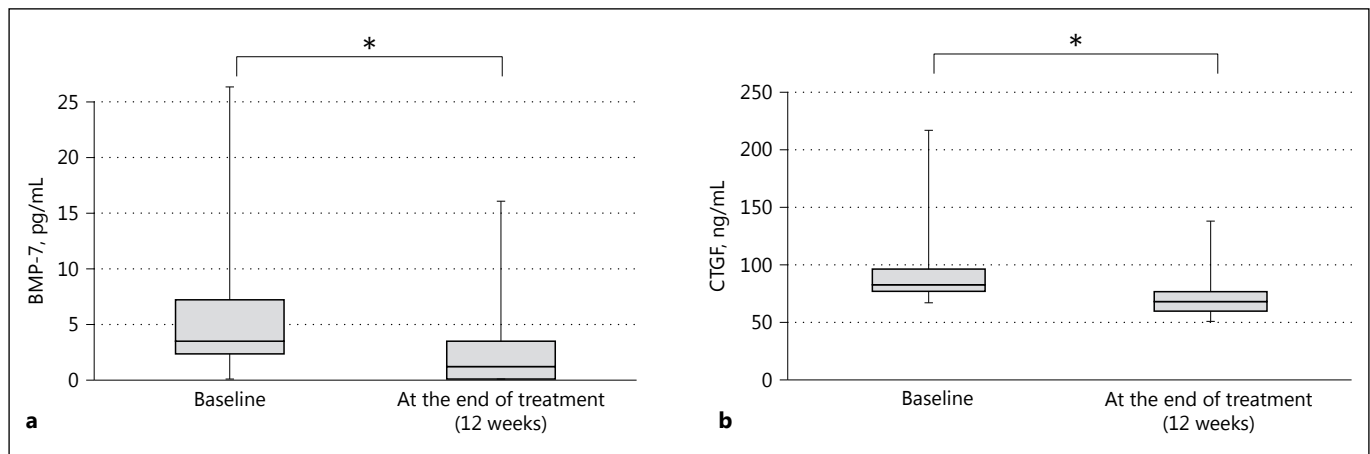
In the Sofosbuvir plus RBV group, the serum ALT level at EOT (20.67 IU/L;  $p = 0.001$ ) and at SVR12 (20.00 IU/L;  $p < 0.001$ ) was significantly lower than the baseline (47.56 IU/L, Table 2). Similarly, in the peg-IFN plus RBV group, a significant reduction in the serum ALT level was observed (baseline: 45.36 IU/L, EOT: 20.29 IU/L;  $p = 0.002$ ; SVR12: 13.21 IU/L;  $p = 0.001$ , Table 2).

#### Assessment of AFP as HCC Tumor Marker

No significant reduction in serum AFP value was observed in either the Sofosbuvir plus RBV group (baseline: 7.00 ng/mL, EOT: 6.00 ng/mL;  $p = 0.094$ ; SVR12: 4.81 ng/mL;  $p = 0.074$ , Table 2) or the peg-IFN plus RBV group (baseline: 4.55 ng/mL, EOT: 3.36 ng/mL;  $p = 0.075$ ; SVR12: 3.21 ng/mL;  $p = 0.124$ , Table 2).

#### Assessment of Liver Fibrosis

In the Sofosbuvir plus RBV group, the serum PLT count was significantly higher at EOT ( $19.14 \times 10^4/mm^3$ ;  $p = 0.026$ ) than the baseline ( $16.84 \times 10^4/mm^3$ ). In the peg-IFN plus RBV group, on the contrary, it was significantly lower ( $15.95 \times 10^4/mm^3$ ;  $p = 0.003$ ) than the baseline ( $20.74 \times 10^4/mm^3$ ). No significant difference was observed between baseline and SVR12 values in either the Sofosbuvir plus RBV group ( $18.03 \times 10^4/mm^3$ ;  $p = 0.199$ )



**Fig. 2.** Comparison of serum BMP-7 and CTGF levels between the baseline and at the end of therapy in the Sofosbuvir plus RBV group. **a** The serum BMP-7 level at the end of treatment (2.49 pg/mL) was lower than the baseline (5.62 pg/mL;  $p = 0.012$ ). **b** The

serum CTGF level at the end of treatment (72.59 ng/mL) was lower than the baseline (98.51 ng/mL;  $p < 0.001$ ). BMP-7, bone morphogenetic protein 7; CTGF, connective tissue growth factor; RBV, ribavirin. \*  $p < 0.05$ .

**Table 2.** Comparison of baseline, end of therapy, and SVR12 data in the Sofosbuvir plus RBV group ( $n = 21$ ) and peg-IFN plus RBV ( $n = 18$ ) group

	Treatment group	Baseline	At the end of treatment (12 weeks or 24 weeks)	$p$ value	Achieved SVR12	$p$ value
ALT, IU/L	Sofosbuvir/RBV	47.56±26.78	20.67±12.64	0.001	20.00±14.60	<0.001
	Peg-IFN/RBV	45.36±40.23	20.29±24.29	0.002	13.21±5.09	0.001
AFP, ng/mL	Sofosbuvir/RBV	7.00±5.91	6.00±3.65	0.094	4.81±2.81	0.074
	Peg-IFN/RBV	4.55±3.64	3.36±2.23	0.075	3.21±1.98	0.124
PLT, $\times 10^4/\text{mm}^3$	Sofosbuvir/RBV	16.84±4.70	19.14±6.16	0.026	18.03±5.65	0.199
	Peg-IFN/RBV	20.74±6.04	15.95±5.70	0.003	20.06±5.81	0.594
FIB-4	Sofosbuvir/RBV	3.04±2.71	2.17±1.44	0.006	2.39±1.72	0.002
	Peg-IFN/RBV	1.51±1.34	2.07±1.57	0.141	1.52±0.85	0.470
APRI	Sofosbuvir/RBV	0.93±0.89	0.41±0.28	<0.001	0.45±0.30	0.001
	Peg-IFN/RBV	0.57±0.60	0.52±0.64	0.438	0.29±0.14	0.041

Data are shown as means  $\pm$  SD.

or the peg-IFN plus RBV group ( $20.06 \times 10^4/\text{mm}^3$ ;  $p = 0.594$ ) (Table 2).

In the Sofosbuvir plus RBV group, a significant decline was observed in FIB-4 and APRI scores: baseline (FIB-4: 3.04, APRI: 0.93), at EOT (FIB-4: 2.17;  $p = 0.006$ , APRI: 0.41;  $p < 0.001$ ), at SVR12 (FIB-4: 2.39;  $p = 0.002$ , APRI: 0.45;  $p = 0.001$ , Table 2). In the peg-IFN plus RBV group, a significant reduction was observed between the baseline APRI score (0.57) and at SVR12 (0.29;  $p = 0.041$ , Table 2). In the Sofosbuvir plus RBV group, serum hyaluronic acid at EOT (223.75 ng/mL) was lower than the baseline (323.40 ng/mL), with no significant difference ( $p = 0.60$ , data not shown). Also, the serum BMP-7 level

at EOT (2.49 pg/mL) was lower than the baseline (5.62 pg/mL;  $p = 0.012$ , Fig. 2a), and a significant decline was observed in the baseline serum CTGF level (98.51 ng/mL) and at EOT (72.59 ng/mL;  $p < 0.001$ , Fig. 2b).

## Discussion

In phase 3 clinical trials, Sofosbuvir plus RBV treatment for patients infected with HCV genotype 2 showed SVR12 in 97% of treatment-naïve patients, in 93% of patients ineligible to receive interferon, and in 86–90% of previously treated patients [20–23]. In the present study,

all patients treated with Sofosbuvir plus RBV achieved SVR12, at a significantly higher rate than that in patients treated with peg-IFN plus RBV. The liver function also improved because of HCV elimination.

Although prevention of HCC after the eradication of HCV has a direct effect on the prognosis of patients infected with HCV, HCC sometimes develops even after such eradication. ALT and AFP are factors significantly associated with the development of HCC, and a decrease in their values is associated with a reduction in HCC risk [32]. The cutoff values of ALT and AFP for the prediction of HCC risk have been determined at 40 IU/L and 6.0 ng/mL, respectively [32]. A decrease in these values after IFN treatment might reduce HCC risk even in patients without HCV eradication [32]. In the present study, although ALT levels at SVR12 were significantly lower than the baseline, no significant decline in AFP value was observed in either group. Nonetheless, the baseline serum level of AFP >6.0 ng/mL decreased to less than 6.0 ng/mL in the Sofosbuvir plus RBV group, suggesting that treatment with Sofosbuvir plus RBV may prevent occurrence of HCC, as does the treatment with peg-IFN plus RBV.

Preventing the development of liver cirrhosis and ameliorating liver fibrosis is the main objective of treating CHC. Although liver biopsy is the gold standard for assessing the regression of liver fibrosis after DAA treatment, serial liver biopsies, for monitoring dynamic changes in liver fibrosis after the achievement of SVR, pose difficulty because of the invasiveness of the procedure and the higher rate of complications. Therefore, such assessment is gradually being replaced by non-invasive methods currently used in clinical practice [44]. In the present study, after treatment, the regression of liver fibrosis was assessed in both groups with the use of fibrosis markers such as PLT, FIB-4, and APRI, that have been demonstrated to be accurate predictors of hepatic fibrosis in HCV patients [34–36]. Several studies have demonstrated a significant decline in liver fibrosis, as determined by FIB-4 and APRI scores in treatment with Sofosbuvir-based regimens [45, 46]. In the present study also, a significant reduction in FIB-4 and APRI scores was observed in the Sofosbuvir plus RBV group; moreover, in evaluating the stages of fibrosis, the PLT count was higher at EOT than the baseline. In the peg-IFN plus RBV group, however, the PLT count at EOT was lower than the baseline, presumably due to side effects; also, compared with the baseline, no significant difference was observed in the FIB-4 score at EOT and at SVR12, the reason being partly due to the exclusion of patients with liver cirrhosis. The baseline FIB-4 score was significantly lower in this group than in the Sofosbuvir plus RBV group.

Additionally, fibrosis regression was assessed using pathophysiological biomarkers, after treatment with Sofosbuvir plus RBV. These biomarkers are pathophysiologically derived from extracellular matrix turnover and/or from changes in fibrogenic cell types, in particular hepatic stellate cells and myofibroblasts [47]; among these, hyaluronic acid is considered the best biomarker [37]. In the present study, the decline in hyaluronic acid was observed in the Sofosbuvir plus RBV group, but without significant change. Transforming growth factor beta (TGF- $\beta$ ) is a non-invasive biomarker of fibrogenesis [48]; however, it is functionally and immunologically difficult to detect it in blood due to its binding to latent TGF- $\beta$ -binding proteins [49, 50], alpha 2-macroglobulin [51], and other ligands. Thus, the measurement of serum TGF- $\beta$  levels is difficult. In the present study, we investigated the correlation of BMP-7 and CTGF with TGF- $\beta$  [47, 52]. BMP-7, a member of the TGF- $\beta$  superfamily, plays a key role in liver organogenesis and development [53, 54]; it has anti-apoptotic, anti-inflammatory, and proliferation-stimulating effects [55, 56], its serum level has been higher in patients with chronic liver disease than in healthy controls [38, 39], and its levels in patients with fibrosis of grades 1, 2, 3, and 4 have been higher than in controls [38]. On the contrary, CTGF is a biomarker of fibrogenesis which reflects TGF- $\beta$  activity [47] and is recognized as an important mediator in fibrogenic pathways as deduced from emerging results of liver fibrosis. It is used to assess the severity of fibrotic remodeling processes [55]. Its level in serum is reported to be already high in fibrosis stage F1 and suitable for determining hepatic fibrosis, and it is most powerful in patients with chronic HCV infection [41]. In the present study, including patients with compensated cirrhosis, treated with Sofosbuvir plus RBV demonstrated a significant decline in levels of serum BMP-7 and CTGF. We assume that these results, indicating decline of TGF- $\beta$ , show clinical improvement in hepatic fibrosis in the Sofosbuvir plus RBV group. Although BMP-7 is suppressed by CTGF [57], both serum BMP-7 and CTGF levels declined after treatment, in our study. It is suspected that the decline in CTGF and TGF- $\beta$  directly induces the decrease in BMP-7. This is the first study that assesses the improvement of hepatic fibrosis, in CHC genotype 2 patients treated with DAA, with the use of pathophysiological biomarkers, such as BMP-7 and CTGF. Improvement of hepatic fibrosis in patients with liver cirrhosis could not be assessed because of the small number of patients. Therefore, a large-scale and longer follow-up study is needed to verify our conclusions.



In conclusion, the treatment with Sofosbuvir plus RBV resulted in not only higher SVR, but also improved liver function, and it ameliorated the degree of fibrosis.

## Ethics Statement

Informed written consent was obtained from each patient, and the study protocol conformed to the ethical guidelines approved by the Ethics Committee of Kobe Asahi Hospital.

## Disclosure Statement

The authors have no conflict of interest to disclose.

## Acknowledgement

We are indebted to Ms. Mika Matsui for her assistance in the preparation of the manuscript.

## References

- Arizumi T, Ueshima K, Minami T, Kono M, Chishina H, Takita M, Kitai S, Inoue T, Yada N, Hagiwara S, Minami Y, Sakurai T, Nishida N, Kudo M: Effectiveness of Sorafenib in patients with transcatheter arterial chemoembolization (TACE) refractory and intermediate-stage hepatocellular carcinoma. *Liver Cancer* 2015;4:253–262.
- Tsurusaki M, Murakami T: Surgical and locoregional therapy of HCC: TACE. *Liver Cancer* 2015;4:165–175.
- Kudo M, Izumi N, Sakamoto M, Matsuyama Y, Ichida T, Nakashima O, Matsui O, Ku Y, Kokudo N, Makuuchi M: Survival analysis over 28 years of 173,378 patients with hepatocellular carcinoma in Japan. *Liver Cancer* 2016;5:190–197.
- Ho MC, Hasegawa K, Chen XP, Nagano H, Lee YJ, Chau GY, Zhou J, Wang CC, Choi YR, Poon RT, Kokudo N: Surgery for intermediate and advanced hepatocellular carcinoma: a consensus report from the 5th Asia-Pacific primary liver cancer expert meeting (APPLE 2014). *Liver Cancer* 2016;5:245–256.
- Kudo M: Surveillance, diagnosis, treatment, and outcome of liver cancer in Japan. *Liver Cancer* 2015;4:39–50.
- Kudo M: Locoregional therapy for hepatocellular carcinoma. *Liver Cancer* 2015;4:163–164.
- Teng W, Liu KW, Lin CC, Jeng WJ, Chen WT, Sheen IS, Lin CY, Lin SM: Insufficient ablative margin determined by early computed tomography may predict the recurrence of hepatocellular carcinoma after radiofrequency ablation. *Liver Cancer* 2015;4:26–38.
- Kang TW, Rhim H: Recent advances in tumor ablation for hepatocellular carcinoma. *Liver Cancer* 2015;4:176–187.
- Clinical practice guidelines for hepatocellular carcinoma differ between Japan, United States, and Europe. *Liver Cancer* 2015;4:85–95.
- Obi S, Sato S, Kawai T: Current status of hepatic arterial infusion chemotherapy. *Liver Cancer* 2015;4:188–199.
- Lin CC, Hung CF, Chen WT, Lin SM: Hepatic arterial infusion chemotherapy for advanced hepatocellular carcinoma with portal vein thrombosis: impact of early response to 4 weeks of treatment. *Liver Cancer* 2015;4:228–240.
- Kudo M: Immune checkpoint blockade in hepatocellular carcinoma. *Liver Cancer* 2015;4:201–207.
- Kudo M: Molecular targeted therapy for hepatocellular carcinoma: where are we now? *Liver Cancer* 2015;4:I–VII.
- Zhang B, Finn RS: Personalized clinical trials in hepatocellular carcinoma based on biomarker selection. *Liver Cancer* 2016;5:221–232.
- Kiyosawa K, Sodeyama T, Tanaka E, Gibo Y, Yoshizawa K, Nakano Y, Furuta S, Akahane Y, Nishioka K, Purcell RH, et al: Interrelationship of blood transfusion, non-A, non-B hepatitis and hepatocellular carcinoma: analysis by detection of antibody to hepatitis C virus. *Hepatology* 1990;12(4 pt 1):671–675.
- Niederer C, Lange S, Heintges T, Erhardt A, Buschkamp M, Hurter D, Nawrocki M, Kruska L, Hensel F, Petry W, Haussinger D: Prognosis of chronic hepatitis C: results of a large, prospective cohort study. *Hepatology* 1998;28:1687–1695.
- Omata M, Nishiguchi S, Ueno Y, Mochizuki H, Izumi N, Ikeda F, Toyoda H, Yokosuka O, Nirei K, Genda T, Umemura T, Takehara T, Sakamoto N, Nishigaki Y, Nakane K, Toda N, Ide T, Yanase M, Hino K, Gao B, Garrison KL, Dvory-Sobol H, Ishizaki A, Omote M, Brainard D, Knox S, Symonds WT, McHutchison JG, Yatsuhashi H, Mizokami M: Sofosbuvir plus ribavirin in Japanese patients with chronic genotype 2 HCV infection: an open-label, phase 3 trial. *J Viral Hepat* 2014;21:762–768.
- Lawitz E, Mangia A, Wyles D, Rodriguez-Torres M, Hassanein T, Gordon SC, Schultz M, Davis MN, Kayali Z, Reddy KR, Jacobson IM, Kowdley KV, Nyberg L, Subramanian GM, Hyland RH, Arterburn S, Jiang D, McNally J, Brainard D, Symonds WT, McHutchison JG, Sheikh AM, Younossi Z, Gane EJ: Sofosbuvir for previously untreated chronic hepatitis C infection. *N Engl J Med* 2013;368:1878–1887.
- Jacobson IM, Gordon SC, Kowdley KV, Yoshida EM, Rodriguez-Torres M, Sulkowski MS, Shiffman ML, Lawitz E, Everson G, Bennett M, Schiff E, Al-Assi MT, Subramanian GM, An D, Lin M, McNally J, Brainard D, Symonds WT, McHutchison JG, Patel K, Feld J, Pianko S, Nelson DR: Sofosbuvir for hepatitis C genotype 2 or 3 in patients without treatment options. *N Engl J Med* 2013;368:1867–1877.
- Zeuzem S, Dusheiko GM, Salupere R, Mangia A, Flisiak R, Hyland RH, Illeperuma A, Svarovskaia E, Brainard DM, Symonds WT, Subramanian GM, McHutchison JG, Weiland O, Reesink HW, Ferenci P, Hezode C, Esteban R: Sofosbuvir and ribavirin in HCV genotypes 2 and 3. *N Engl J Med* 2014;370:1993–2001.
- Morio K, Imamura M, Kawakami Y, Nakahara T, Nagaoki Y, Kawaoka T, Tsuge M, Hiramatsu A, Aikata H, Hayes CN, Makokha GN, Ochi H, Amano H, Arataki K, Moriya T, Ito H, Tsuji K, Kohno H, Waki K, Tamura T, Nakamura T, Chayama K: ITPA polymorphism effects on decrease of hemoglobin during sofosbuvir and ribavirin combination treatment for chronic hepatitis C. *J Gastroenterol* 2017;52:746–753.
- Sugimoto K, Kim SK, Kim SR, Kobayashi M, Kato A, Morimoto E, Imoto S, Kim CW, Tanaka Y, Kudo M, Yano Y, Hayashi Y: Efficacy and safety of sofosbuvir plus ribavirin treatment for patients with chronic hepatitis C genotype 2. *Dig Dis* 2016;34:627–631.
- Asahina Y, Tsuchiya K, Tamaki N, Hirayama I, Tanaka T, Sato M, Yasui Y, Hosokawa T, Ueda K, Kuzuya T, Nakanishi H, Itakura J, Takahashi Y, Kurosaki M, Enomoto N, Izumi N: Effect of aging on risk for hepatocellular carcinoma in chronic hepatitis C virus infection. *Hepatology* 2010;52:518–527.
- Imai Y, Kawata S, Tamura S, Yabuuchi I, Noda S, Inada M, Maeda Y, Shirai Y, Fukuzaki T, Kaji I, Ishikawa H, Matsuda Y, Nishikawa M, Seki K, Matsuzawa Y: Relation of interferon therapy and hepatocellular carcinoma in patients with chronic hepatitis C. *Osaka Hepatocellular Carcinoma Prevention Study Group. Ann Intern Med* 1998;129:94–99.
- Ikeda K, Saitoh S, Arase Y, Chayama K, Suzuki Y, Kobayashi M, Tsubota A, Nakamura I, Murashima N, Kumada H, Kawanishi M: Effect of interferon therapy on hepatocellular carcinogenesis in patients with chronic hepatitis type C: A long-term observation study of 1,643 patients using statistical bias correction with proportional hazard analysis. *Hepatology* 1999;29:1124–1130.



- 26 Yoshida H, Shiratori Y, Moriyama M, Arakawa Y, Ide T, Sata M, Inoue O, Yano M, Tanaka M, Fujiyama S, Nishiguchi S, Kuroki T, Imazeki F, Yokosuka O, Kinoyama S, Yamada G, Omata M: Interferon therapy reduces the risk for hepatocellular carcinoma: national surveillance program of cirrhotic and noncirrhotic patients with chronic hepatitis C in Japan. IHIT Study Group. Inhibition of Hepatocarcinogenesis by Interferon Therapy. *Ann Intern Med* 1999;131:174–181.
- 27 Kudo M: Risk of hepatocellular carcinoma in patients with hepatitis C virus who achieved sustained virological response. *Liver Cancer* 2016;5:155–161.
- 28 Bruno S, Stroffolini T, Colombo M, Bollani S, Benvenuto L, Mazzella G, Ascione A, Santantonio T, Piccinino F, Andreone P, Mangia A, Gaeta GB, Persico M, Fagioli S, Almasio PL: Sustained virological response to interferon-alpha is associated with improved outcome in HCV-related cirrhosis: a retrospective study. *Hepatology* 2007;45:579–587.
- 29 Kim JH, Kim MN, Han KH, Kim SU: Clinical application of transient elastography in patients with chronic viral hepatitis receiving antiviral treatment. *Liver Int* 2015;35:1103–1115.
- 30 Cordero-Ruiz P, Carmona-Soria I, Rodriguez-Tellez M, Caunedo-Alvarez A, Quezada-Pacheco RH, Flores-Cucho A, Romero-Gomez M, Vilches-Arenas A: Long-term follow-up of patients with chronic hepatitis C treated with  $\alpha$ -interferon and ribavirin antiviral therapy: clinical and fibrosis impact of treatment response. *Eur J Gastroenterol Hepatol* 2017;29:792–799.
- 31 Toyoda H, Kumada T, Tada T, Sone Y, Kaneoka Y, Maeda A: Tumor markers for hepatocellular carcinoma: simple and significant predictors of outcome in patients with HCC. *Liver Cancer* 2015;4:126–136.
- 32 Asahina Y, Tsuchiya K, Nishimura T, Murooka M, Suzuki Y, Tamaki N, Yasui Y, Hosokawa T, Ueda K, Nakanishi H, Itakura J, Takahashi Y, Kurosaki M, Enomoto N, Nakagawa M, Kakinuma S, Watanabe M, Izumi N:  $\alpha$ -fetoprotein levels after interferon therapy and risk of hepatocarcinogenesis in chronic hepatitis C. *Hepatology* 2013;58:1253–1262.
- 33 Gressner OA, Gao C: Monitoring fibrogenic progression in the liver. *Clin Chim Acta* 2014;433:111–122.
- 34 Rosenberg WM, Voelker M, Thiel R, Becka M, Burt A, Schuppan D, Hubscher S, Roskams T, Pinzani M, Arthur MJ: Serum markers detect the presence of liver fibrosis: a cohort study. *Gastroenterology* 2004;127:1704–1713.
- 35 Yosry A, Fouad R, Alem SA, Elsharkawy A, El-Sayed M, Asem N, Hassan E, Ismail A, Esmat G: FibroScan, APRI, FIB4, and GUCI: Role in prediction of fibrosis and response to therapy in Egyptian patients with HCV infection. *Arab J Gastroenterol* 2016;17:78–83.
- 36 Bonnard P, Elsharkawy A, Zalata K, Delarocque-Astagneau E, Biard L, Le Foulher L, Hassan AB, Abdel-Hamid M, El-Daly M, Gamal ME, El Kassas M, Bedossa P, Carrat F, Fontanet A, Esmat G: Comparison of liver biopsy and noninvasive techniques for liver fibrosis assessment in patients infected with HCV-genotype 4 in Egypt. *J Viral Hepat* 2015;22:245–253.
- 37 Lydatakis H, Hager IP, Kostadelou E, Mpourmpoulas S, Pappas S, Diamantis I: Non-invasive markers to predict the liver fibrosis in non-alcoholic fatty liver disease. *Liver Int* 2006;26:864–871.
- 38 Tacke F, Gabel E, Bataille F, Schwabe RF, Hellerbrand C, Klebl F, Straub RH, Luedde T, Manns MP, Trautwein C, Brenner DA, Scholmerich J, Schnabl B: Bone morphogenetic protein 7 is elevated in patients with chronic liver disease and exerts fibrogenic effects on human hepatic stellate cells. *Dig Dis Sci* 2007;52:3404–3415.
- 39 Cao H, Shu X, Chen LB, Zhang K, Xu QH, Li G: [The relationship of expression of BMP-7 in the liver and hepatic inflammation and fibrosis in patients with chronic HBV infection]. *Zhonghua Shi Yan He Lin Chuang Bing Du Xue Za Zhi* 2010;24:101–103.
- 40 Aktug Demir N, Kolgelier S, Inkaya AC, Sumner S, Demir LS, Pehlivan FS, Arslan M, Arpacı A: Are bone morphogenetic protein-7 (BMP-7) serum levels correlated with development of hepatic fibrosis? *J Infect Dev Ctries* 2014;8:605–610.
- 41 Kovalenko E, Tacke F, Gressner OA, Zimmermann HW, Lahme B, Janetzko A, Wiederholt T, Berg T, Muller T, Trautwein C, Gressner AM, Weiskirchen R: Validation of connective tissue growth factor (CTGF/CCN2) and its gene polymorphisms as non-invasive biomarkers for the assessment of liver fibrosis. *J Viral Hepat* 2009;16:612–620.
- 42 Wai CT, Greenon JK, Fontana RJ, Kalbfleisch JD, Marrero JA, Conjeevaram HS, Lok AS: A simple noninvasive index can predict both significant fibrosis and cirrhosis in patients with chronic hepatitis C. *Hepatology* 2003;38:518–526.
- 43 Sterling RK, Lissen E, Clumeck N, Sola R, Correa MC, Montaner J, Sulkowski M, Torriani FJ, Dieterich DT, Thomas DL, Messinger D, Nelson M: Development of a simple noninvasive index to predict significant fibrosis in patients with HIV/HCV coinfection. *Hepatology* 2006;43:1317–1325.
- 44 Lackner C, Struber G, Liegl B, Leibl S, Ofner P, Bankuti C, Bauer B, Stauber RE: Comparison and validation of simple noninvasive tests for prediction of fibrosis in chronic hepatitis C. *Hepatology* 2005;41:1376–1382.
- 45 Elsharkawy A, Abdel Alem S, Fouad R, El Raziky M, El Akel W, Abdo M, Tantawi O, AbdAllah M, Bourliere M, Esmat G: Changes in Liver stiffness measurements and Fibrosis scores following Sofosbuvir based treatment regimens without Interferon. *J Gastroenterol Hepatol* 2017, Epub ahead of print.
- 46 Bachofner JA, Valli PV, Kroger A, Bergamin I, Kunzler P, Baserga A, Braun D, Seifert B, Moncssek A, Fehr J, Semela D, Magenta L, Mullhaupt B, Terziroli Beretta-Piccoli B, Mertens JC: Direct antiviral agent treatment of chronic hepatitis C results in rapid regression of transient elastography and fibrosis markers fibrosis-4 score and aspartate aminotransferase-platelet ratio index. *Liver Int* 2017;37:369–376.
- 47 Gressner AM, Yagmur E, Lahme B, Gressner O, Stanzel S: Connective tissue growth factor in serum as a new candidate test for assessment of hepatic fibrosis. *Clin Chem* 2006;52:1815–1817.
- 48 Roth S, Michel K, Gressner AM: (Latent) transforming growth factor beta in liver parenchymal cells, its injury-dependent release, and paracrine effects on rat hepatic stellate cells. *Hepatology* 1998;27:1003–1012.
- 49 Breitkopf K, Lahme B, Tag CG, Gressner AM: Expression and matrix deposition of latent transforming growth factor beta binding proteins in normal and fibrotic rat liver and transdifferentiating hepatic stellate cells in culture. *Hepatology* 2001;33:387–396.
- 50 Hyytiäinen M, Penttinen C, Keski-Oja J: Latent TGF- $\beta$  binding proteins: extracellular matrix association and roles in TGF- $\beta$  activation. *Crit Rev Clin Lab Sci* 2004;41:233–264.
- 51 Crookston KP, Webb DJ, Lamarre J, Gonias SL: Binding of platelet-derived growth factor-BB and transforming growth factor- $\beta$  1 to  $\alpha$ 2-macroglobulin in vitro and in vivo: comparison of receptor-recognized and non-recognized  $\alpha$ 2-macroglobulin conformations. *Biochem J* 1993;293 (pt 2):443–450.
- 52 Wang S, Hirschberg R: Bone morphogenetic protein-7 signals opposing transforming growth factor  $\beta$  in mesangial cells. *J Biol Chem* 2004;279:23200–23206.
- 53 Weiskirchen R, Meurer SK: Bone morphogenetic protein-7 in focus: a member of the transforming growth factor- $\beta$  superfamily is implicated in the maintenance of liver health. *Hepatology* 2007;45:1324–1325.
- 54 Ozkaynak E, Rueger DC, Drier EA, Corbett C, Ridge RJ, Sampath TK, Oppermann H: OP-1 cDNA encodes an osteogenic protein in the TGF- $\beta$  family. *EMBO J* 1990;9:2085–2093.
- 55 Gressner OA, Gressner AM: Connective tissue growth factor: a fibrogenic master switch in fibrotic liver diseases. *Liver Int* 2008;28:1065–1079.
- 56 Sugimoto H, Yang C, LeBleu VS, Soubasakos MA, Giraldo M, Zeisberg M, Kalluri R: BMP-7 functions as a novel hormone to facilitate liver regeneration. *FASEB J* 2007;21:256–264.
- 57 Abreu JG, Ketpura NI, Reversade B, De Robertis EM: Connective-tissue growth factor (CTGF) modulates cell signalling by BMP and TGF- $\beta$ . *Nat Cell Biol* 2002;4:599–604.

# Hepatocarcinogenesis Is Associated with Serum Albumin Levels after Sustained Virological Responses with Interferon-Based Therapy in Patients with Hepatitis C

Yasuko Umehara Satoru Hagiwara Naoshi Nishida Toshiharu Sakurai  
Hiroshi Ida Yasunori Minami Masahiro Takita Tomohiro Minami  
Hirokazu Chishina Kazuomi Ueshima Yoriaki Komeda Tadaaki Arizumi  
Tomohiro Watanabe Masatoshi Kudo

Department of Gastroenterology and Hepatology, Kindai University Faculty of Medicine, Osaka-Sayama, Japan

## Keywords

Interferon · Carcinogenesis · Sustained virological responses · Serum albumin level

## Abstract

**Objective:** It is a generally accepted fact that eradication of hepatitis virus C inhibits the subsequent development of hepatocellular carcinoma (HCC). On the contrary, a significant population of patients developed HCC despite sustained virological responses (SVRs) to interferon (IFN) therapy. **Methods:** A total of 415 patients with chronic hepatitis C, who were treated at our hospital between 2004 and 2014, were enrolled for this study. We examined the risk factors for HCC development after IFN therapy. **Results:** After analyzing various clinical parameters, it was concluded that a serum albumin (ALB) level <4.0 g/dL and the presence or absence of SVR achievement were risk factors for the development of HCC. When analyzing pre- and posttreatment factors, only a serum ALB level <4.0 g/dL was considered a significant risk fac-

tor. The presence or absence of liver fibrosis progression was not identified as a risk factor. **Conclusions:** In patients with a serum ALB level <4.0 g/dL before IFN therapy, hepatic carcinogenesis after SVR achievement need to be considered. Furthermore, the serum ALB level may be more useful than the degree of fibrosis for the prediction of HCC after SVR in chronic hepatitis C.

© 2017 S. Karger AG, Basel

## Introduction

In Japan, the number of hepatitis virus C (HCV)-infected patients is estimated to be approximately 1.5 million. Persistent liver infection with HCV causes chronic hepatitis, liver cirrhosis, and hepatocellular carcinoma (HCC) [1, 2]. In Japan, the annual number of patients who die of HCC is approximately 30,000, with 70% of HCC originating from chronic hepatitis with HCV infection [1, 2]. Thus, eradication

of HCV is quite important for the promotion of health [3].

HCV-related HCC develops in a stepwise manner through the stages of chronic hepatitis and liver cirrhosis. HCV-related HCC is a typical example of inflammation-related cancer, and therefore eradication of HCV at an early stage of chronic hepatitis is considered to be very effective for the prevention of subsequent hepatocarcinogenesis [4]. In fact, several studies reported that the subsequent incidence of HCC decreased in patients in whom HCV was successfully eliminated by interferon (IFN) therapy [5–7]. However, these studies also indicated that the inhibitory effects on carcinogenesis were limited despite the achievement of sustained virological responses (SVRs) to IFN in elderly patients, those with advanced liver cirrhosis, or those with a high serum  $\alpha$ -fetoprotein (AFP) level after treatment [5–9]. Thus, a significant population of patients with HCV-related liver diseases develops HCC despite the achievement and maintenance of SVR. Careful follow-up for the early detection of HCC is mandatory for such high-risk patients even after achievement of SVR [1, 10]. In this retrospective study, we attempted to identify clinical parameters strongly associated with the emergence of HCC in patients with SVRs to IFN.

## Methods

### Subjects

Patients with chronic hepatitis C who were treated at our hospital between 2004 and 2014 were enrolled in this study. Patients with autoimmune hepatitis, primary biliary cirrhosis, co-infection with hepatitis B virus, or an alcohol intake of  $\geq 50$  g/day were excluded. Furthermore, we excluded patients with an IFN administration period of less than 24 weeks, those with an observation period of less than 1 year after the completion of IFN therapy, those with HCC development during IFN therapy, and those with a history of HCC. Finally, we analyzed 415 patients treated with regimens involving IFN. The study protocol was approved by the Ethics Committee of Kindai University Faculty of Medicine, and this study was performed in accordance with the Helsinki Declaration.

### Methods

For HCC diagnosis, contrast-enhanced CT or Gd-EOB-DTPA-enhanced MRI monitoring was performed. For patients in whom a contrast medium could not be used due to allergy or kidney dysfunction, contrast-enhanced ultrasonography was performed.

### Definition of Responses to IFN Therapy

IFN was administered for 24–72 weeks. Patients who remained negative for serum HCV-RNA, 24 weeks after the completion of IFN therapy, were regarded as the state of SVRs. Patients who re-

**Table 1.** Background of registered patients

Factors	Value
Patients, <i>n</i>	415
Age, years, mean (SD)	58.0 (11.7)
Males/females, <i>n</i>	191/224
BMI, kg/m <sup>2</sup> , mean (SD)	23.1 (4.3)
Liver histology	
Activity, A0-1/2-3	94/172
Fibrosis, F0-2, 3-4	199/67
WBC count, $\mu$ L, mean (SD)	5,511 (4,428)
Hb, g/dL, mean (SD)	14.8 (10.2)
Platelet counts, $\times 10^4/\mu$ L, mean (SD)	17.8 (6.5)
Total bilirubin, mg/dL, mean (SD)	0.71 (0.3)
Albumin, g/dL, mean (SD)	4.30 (2.0)
$\gamma$ -GTP, IU/L, mean (SD)	53.3 (56.4)
Total cholesterol, mg/dL, mean (SD)	177.8 (55.3)
Fasting blood sugar, mg/dL, mean (SD)	102.7 (27.0)
DM medication, present/absent	29/386
ALT, IU/L, mean (SD)	71.7 (73.6)
AFP, ng/mL, mean (SD)	11.3 (37.5)
HCV serotype, 1/2/unknown	280/102/33
IFN regimen, combination therapy with	
DAAs, present/absent	45/370
Previous IFN therapy, present/absent	129/286
Combination therapy with UDCA, present/absent	132/283

BMI, body mass index; DM, diabetes mellitus; IFN, interferon; UDCA, ursodeoxycholic acid; WBC, white blood cells; GTP, glutamyl transpeptidase; ALT, alanine aminotransferase; AFP,  $\alpha$ -fetoprotein; HCV, hepatitis C virus; IFN, interferon; DAA, direct-acting antiviral.

maintained positive for HCV-RNA, 24 weeks after the completion of IFN therapy, were regarded as the state of non-SVRs. HCV-RNA was determined using qualitative Amplicor or TaqMan HCV assay (Roche Molecular Diagnostics, Tokyo, Japan).

### Statistical Analysis

Risk factors for HCC were analyzed using Cox's regression model. To determine the cumulative incidence curve, the Kaplan-Meier method was used. Significance was tested using the log-rank test. A *p* value of less than 0.05 was regarded as significant.

## Results

### Patient Background

A total of 415 patients with a mean age of 58 years were enrolled in this retrospective study. They consisted of 191 males and 224 females. Two hundred and sixty-six patients received liver biopsy, and the stage of fibrosis was evaluated as 0–2 in 199 patients and 3–4 in 67. The mean serum albumin (ALB), alanine amino-

**Table 2.** Examination of risk factors for carcinogenesis using pretreatment factors and antiviral effects

Factors	Category	Univariate analysis		Multivariate analysis	
		hazard ratio (95% CI)	<i>p</i> value	hazard ratio (95% CI)	<i>p</i> value
Age, years	0: <60	1	0.065	1	0.411
	1: >60	2.113 (0.956–4.073)		1.494 (0.574–3.885)	
Gender	0: male	1	0.765		
	1: female	0.765 (0.364–1.607)			
BMI, kg/m <sup>2</sup>	0: <25	1	0.441		
	1: >25	1.385 (0.605–3.168)			
Fibrosis stage, F0–2, 3–4	0: F0–2	1	0.001	1	0.105
	1: F3–4	4.357 (1.833–10.356)		2.222 (0.846–5.835)	
Platelet counts, ×10 <sup>4</sup> /μL	0: <15	1	0.056	1	0.831
	1: >15	0.485 (0.231–1.019)		1.108 (0.431–2.852)	
Albumin, g/dL	0: <4	1	<0.001	1	0.021
	1: >4	0.132 (0.060–0.292)		0.306 (0.112–0.840)	
γ-GTP, IU/L	0: <65	1	0.283		
	1: >65	1.569 (0.690–3.566)			
Total cholesterol, mg/dL	0: <221	1	0.211		
	1: >221	0.279 (0.380–2.058)			
DM medication	0: absent	1	0.409		
	1: present	1.057 (0.560–5.492)			
ALT, IU/L	0: <30	1	0.035	1	0.267
	1: >30	4.696 (1.114–19.785)		3.231 (0.407–25.635)	
AFP, ng/mL	0: <6	1	<0.001	1	0.056
	1: >6	5.642 (2.532–12.575)		2.678 (0.974–7.366)	
IFN regimen, combination therapy with DAAs	0: absent	1	0.617		
	1: present	0.597 (0.079–4.506)			
SVR	0: non SVR	1	<0.001	1	0.048
	1: SVR	0.202 (0.096–0.425)		0.383 (0.148–0.991)	

BMI, body mass index; DM, diabetes mellitus; IFN, interferon; SVR, sustained virological response; ALT, alanine aminotransferase; AFP, α-fetoprotein; DAA, direct-acting antiviral; GTP, glutamyl transpeptidase.

transferase (ALT), and AFP levels were 4.3 g/dL, 71.7 IU/L, and 11.3 ng/mL, respectively. The subjects included 29 patients treated for diabetes mellitus (DM; Table 1).

#### *Identification of Risk Factors for Hepatocarcinogenesis Using Pretreatment Factors and Antiviral Effects*

The age, sex, body mass index, stage of fibrosis, platelet count (PLT), ALB, γ-glutamyltransferase, total cholesterol, DM treatment, ALT, AFP, presence or absence of direct-acting antiviral (DAA) therapy, and presence or absence of SVR achievement were investigated to evaluate the possible association for the development of HCC. On univariate analysis using Cox's regression model, the stage of fibrosis, ALB, ALT, AFP, and presence or absence of SVR achievement were extracted as significant factors. These factors identified by univariate analysis are shown to be risk factors for the development

of HCC in patients bearing HCV infection in previous reports [5–7]. In addition to these 5 factors, age and PLT ( $p < 0.1$ ) were also examined using multivariate analysis. Interestingly, multivariate analysis revealed that among 7 factors, only ALB levels and status of SVR were defined as risk factors for HCC development (Table 2). Thus, these initial analyses suggest that serum levels of ALB and status of SVR are associated with the development of HCC.

#### *Examination of Risk Factors for Carcinogenesis Using Pre-/Posttreatment Factors and Antiviral Effects*

We next tried to analyze the involvement of post-treatment factors in the development of HCC. To this end, age, sex, body mass index, stage of fibrosis, PLT, ALB, γ-glutamyltransferase, total cholesterol, DM treatment, baseline or posttreatment ALT, baseline or posttreatment AFP, presence or absence of DAA ther-

**Table 3.** Examination of risk factors for carcinogenesis using pre-/posttreatment factors and antiviral effects

Factors	Category	Univariate analysis		Multivariate analysis	
		hazard ratio (95% CI)	p value	hazard ratio (95% CI)	p value
Age, years	0: <60	1	0.065	1	0.342
	1: >60	2.113 (0.956–4.073)		1.597 (0.608–4.191)	
Gender	0: male	1	0.765		
	1: female	0.765 (0.364–1.607)			
BMI, kg/m <sup>2</sup>	0: <25	1	0.441		
	1: >25	1.385 (0.605–3.168)			
Fibrosis stage, F0–2, 3–4	0: F0–2	1	0.001	1	0.099
	1: F3–4	4.357 (1.833–10.356)		2.279 (0.856–6.066)	
Platelet counts, ×10 <sup>4</sup> /μL	0: <15	1	0.056	1	0.473
	1: >15	0.485 (0.231–1.019)		1.470 (0.513–4.217)	
Albumin, g/dL	0: <4	1	<0.001	1	0.021
	1: >4	0.132 (0.060–0.292)		0.295 (0.104–0.834)	
γ-GTP, IU/L	0: <65	1	0.283		
	1: >65	1.569 (0.690–3.566)			
Total cholesterol, mg/dL	0: <221	1	0.211		
	1: >221	0.279 (0.380–2.058)			
DM medication	0: absent	1	0.409		
	1: present	1.057 (0.560–5.492)			
Pre-ALT, IU/L	0: <30	1	0.035	1	0.382
	1: >30	4.696 (1.114–19.785)		2.583 (0.308–21.649)	
Post-ALT, IU/L	0: <30	1	<0.001	1	0.329
	1: >30	4.629 (2.200–9.740)		2.205 (0.451–10.791)	
Pre-AFP, ng/mL	0: <6	1	<0.001	1	0.056
	1: >6	5.642 (2.532–12.575)		2.678 (0.974–7.366)	
Post-AFP, ng/mL	0: <6	1	<0.001	1	0.152
	1: >6	6.927 (3.238–14.819)		2.216 (0.747–6.577)	
IFN regimen, combination therapy with DAAs	0: absent	1	0.617		
	1: present	0.597 (0.079–4.506)			
SVR	0: non SVR	1	<0.001	1	0.943
	1: SVR	0.202 (0.096–0.425)		0.940 (0.174–5.097)	

BMI, body mass index; DM, diabetes mellitus; IFN, interferon; SVR, sustained virological response; ALT, alanine aminotransferase; AFP, α-fetoprotein; DAA, direct-acting antiviral.

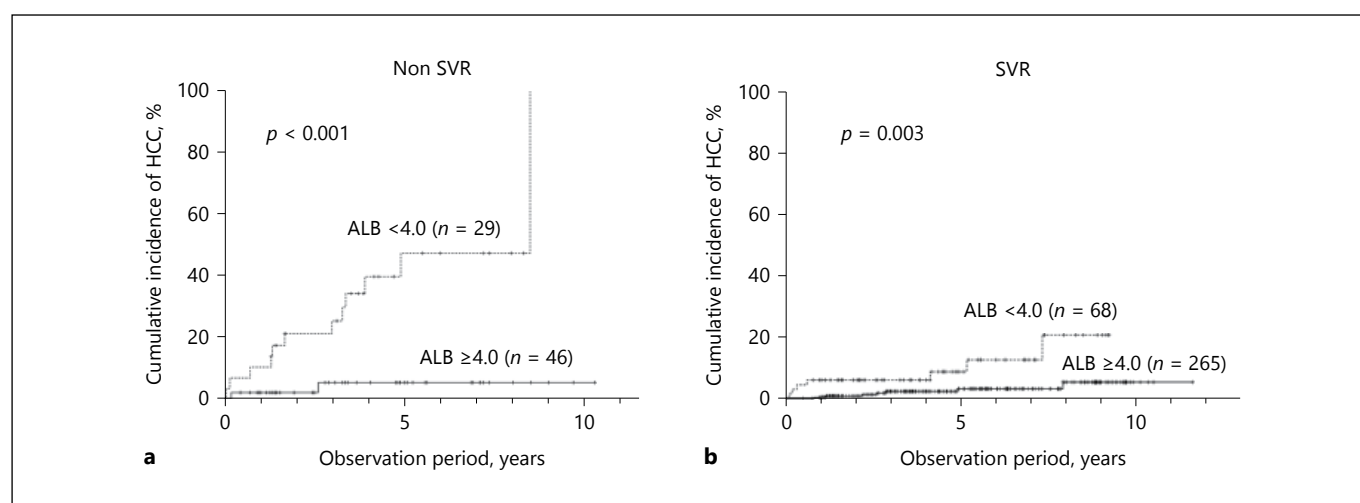
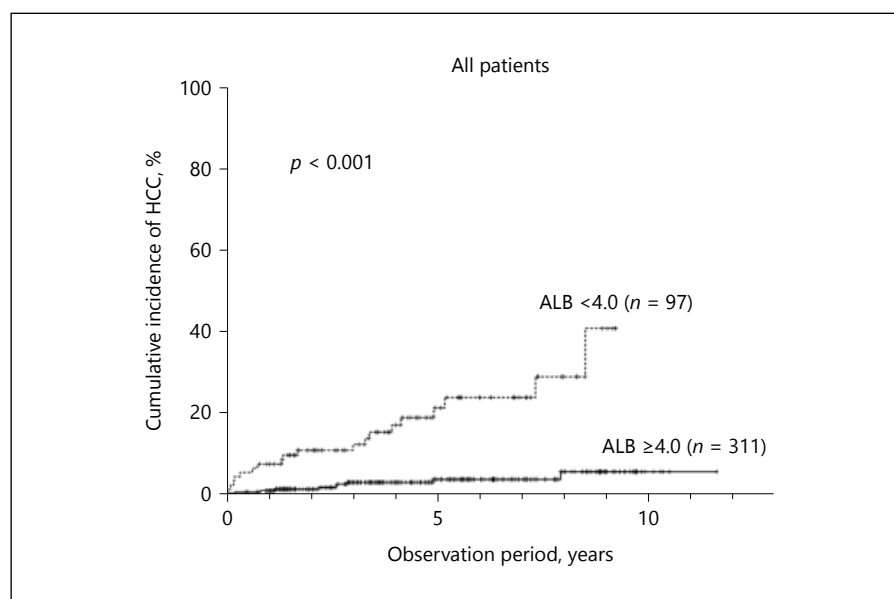
apy, and presence or absence of SVR achievement were subjected to univariate analysis. Serum samples were obtained at 24 weeks after the completion of IFN therapy. On univariate analysis using Cox's regression model, the post-ALT and post-AFP levels were identified as significant factors in addition to the stage of fibrosis, ALB, ALT, AFP, and presence or absence of SVR achievement. In addition to these factors, age and PLT ( $p < 0.1$ ) were again evaluated using multivariate analysis. In this second multivariate analysis, the ALB level was again identified as a risk factor for carcinogenesis (Table 3). Thus, baseline-pretreatment ALB level is the best useful biomarker for the prediction of HCC development in our retrospective analyses.

#### *Changes in the Cumulative Incidence of HCC with Respect to the Serum ALB Level (Analysis with Respect to the Presence or Absence of SVR Achievement)*

Having identified the serum ALB level as the most useful marker for HCC development, we tried to identify a sub-population of patients exhibiting higher risks. First, subjects with a serum ALB level <4.0 g/dL were compared with those with >4.0 g/dL. The cumulative incidence of HCC was significantly higher in the former group than in the latter group (Fig. 1;  $p < 0.001$ ). Thus, the serum ALB level is a sensitive marker for the prediction of HCC development. Subsequently, subjects were subdivided into 4 groups based on serum ALB level and status of SVR achievement. In both SVR-achieved and non-SVR-achieved groups with a serum ALB level <4.0



**Fig. 1.** Comparison of the cumulative incidence of HCC with respect to the serum ALB level. When comparing patients with a serum ALB level <4.0 g/dL with those with a serum ALB level ≥4.0 g/dL, the cumulative incidence of HCC was significantly higher in the former ( $p < 0.001$ ).

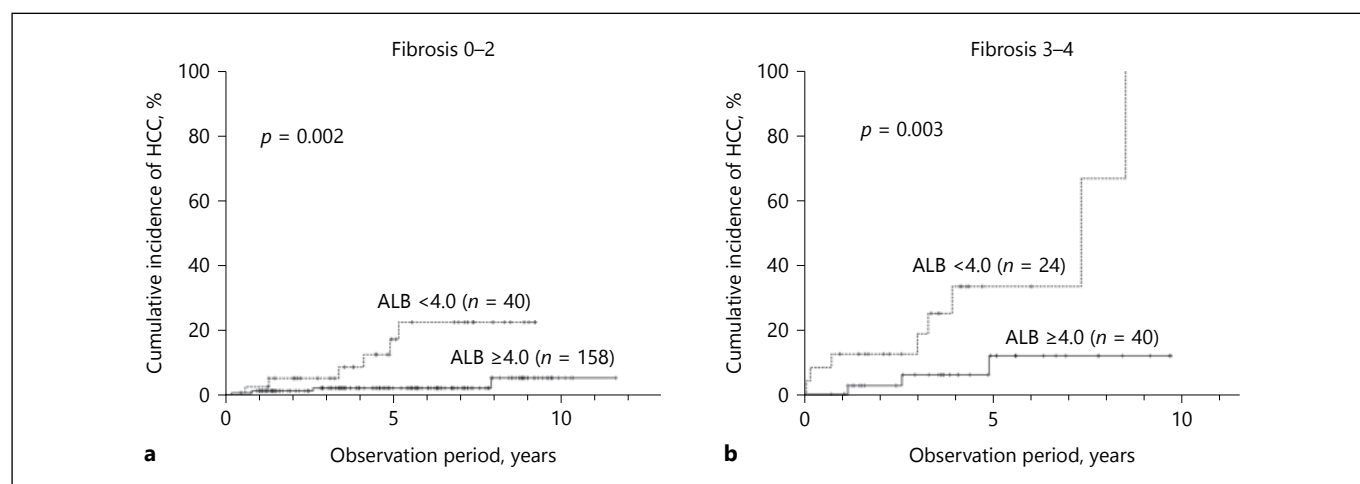


**Fig. 2.** Comparison of the cumulative incidence of HCC with respect to the serum ALB level and presence or absence of SVR achievement. Among the non-SVR-achieved patients, those with a serum ALB level <4.0 g/dL were compared with those with a serum ALB level ≥4.0 g/dL. In the former, the cumulative incidence

of HCC was significantly higher (**a**;  $p < 0.001$ ). Among the SVR-achieved patients, those with a serum ALB level <4.0 g/dL were compared with those with a serum ALB level ≥4.0 g/dL. In the former, the cumulative incidence of HCC was significantly higher (**b**;  $p = 0.003$ ).

g/dL, the cumulative incidences of HCC were significantly higher (Fig. 2a, analysis involving non-SVR-achieved patients:  $p < 0.001$ ; Fig. 2b, analysis involving SVR-achieved patients:  $p = 0.003$ ). These data suggest that the serum ALB level is the most sensitive marker for the prediction of HCC development regardless of SVR achievement.

The degree of fibrosis is strongly associated with the development of HCC [29]. We, therefore, tried to evaluate the relationship between serum ALB level and the degree of fibrosis in this study. Subjects were subdivided into 4 groups based on serum ALB level and degree of fibrosis. Among the fibrosis 0–2 patients, those with a serum ALB level <4.0 g/dL were compared with those with



**Fig. 3.** Comparison of the cumulative incidence of HCC with respect to the serum ALB level and presence or absence of liver fibrosis progression. Among the fibrosis 0–2 patients, those with a serum ALB level <4.0 g/dL were compared with those with a serum ALB level ≥4.0 g/dL. In the former, the cumulative incidence of

HCC was significantly higher (**a**;  $p = 0.002$ ). Among the fibrosis 3–4 patients, those with a serum ALB level <4.0 g/dL were compared with those with a serum ALB level ≥4.0 g/dL. In the former, the cumulative incidence of HCC was significantly higher (**b**;  $p = 0.003$ ).

a serum ALB level ≥4.0 g/dL. The cumulative incidence of HCC was significantly higher in the former group than in the latter group (Fig. 3a;  $p = 0.002$ ). Among the fibrosis 3–4 patients, those with a serum ALB level <4.0 g/dL were compared with those with a serum ALB level ≥4.0 g/dL. The cumulative incidence of HCC was significantly higher in the former group than in the latter group (Fig. 3b,  $p = 0.003$ ). Taken together, these data suggest that the serum ALB level is the most useful marker for the development of HCC irrespective of liver fibrosis stage or SVR achievement.

## Discussion

It has been well-established that IFN treatment against chronic hepatitis for the eradication of HCV prevents the development of HCC. For example, Nishiguchi et al. [11] conducted a prospective study involving patients with liver cirrhosis C, and reported that the risk of HCC was significantly reduced when IFN administration led to an SVR or persistent ALT normalization. In line with the results of this prospective study, Ikeda et al. [12] retrospectively examined the cumulative incidence of HCC with respect to the IFN treatment response in patients with chronic hepatitis C and found that the incidence of HCC was much lower in patients with SVR than in those without IFN treatment or without SVR after the initial

IFN therapy. In addition to these studies, many studies reported that the induction of SVR by IFN therapy prevents subsequent hepatocarcinogenesis [13–16]. Therefore, it can be concluded that the achievement of SVR by IFN therapy is the most effective strategy for the prevention of HCC in patients with HCV-related liver diseases.

On the contrary, the development of HCC occurs in a significant population of HCV-infected patients even after successful induction of SVR. Once HCC occurs, several treatment options including resection [17], ablation [18–20], hepatic arterial chemoembolization [21], transarterial infusion chemotherapy [22, 23], and systemic therapy [24–26] are applied. Previous studies attempted to identify risk factors for such hepatocarcinogenesis. The male gender, an advanced age, alcohol consumption, fatty liver, and DM are considered to increase the risk of HCC after successful induction of SVR [5–7, 27, 28]. As for serum biomarkers for the prediction of HCC after SVR induction, a couple of studies indicated that no significant reduction in the AFP level after IFN therapy was a risk factor for carcinogenesis [5–7]. Furthermore, liver fibrosis is considered to be the most important risk factor for carcinogenesis after SVR achievement, as shown by Morgan et al. [29] who reported that SVR achievement decreased the hazard ratio of hepatocarcinogenesis in patients with advanced stages of liver fibrosis. In this study, we tried to clarify the risk factors for HCC development in patients after SVR in a retrospective manner.

In this study, the serum ALB level and presence or absence of SVR achievement were identified as significant risk factors for carcinogenesis when analyzing pretreatment factors and antiviral effects. In addition to these factors, the ALT and AFP levels after IFN therapy, which were previously reported as risk factors for carcinogenesis [5, 6], were analyzed. Only the serum ALB level prior to the treatment was identified as a significant factor. Regarding the importance of ALB as a predictor for HCC development, Asahina et al. [6] reported that a reduction in the serum ALB level after IFN therapy was a risk factor for carcinogenesis after IFN therapy, independent of age, sex, liver fibrosis, fatty liver, posttreatment ALT and AFP levels. Importantly, a reduction in the serum ALB level after IFN therapy was identified as a risk factor, which is independent of SVR achievement. The importance of the reduction in serum ALB level was confirmed by multivariate analysis since this parameter was more useful for the prediction of HCC development than the posttreatment AFP level. Consistent with the results of Asahina et al. [6], our retrospective univariate and multivariate analyses revealed that the serum ALB before treatment is the most sensitive marker for the prediction of HCC development in patients with successful induction of SVR. Although the posttreatment AFP level and severity of liver fibrosis were also identified as significant risk factors for hepatocarcinogenesis by univariate analysis in study, these parameters were not identified by multivariate analysis. Furthermore, we confirmed that the serum ALB level prior to the treatment exhibits significant correlation to subsequent HCC development, irrespective of SVR status or liver fibrosis stages. Collectively, our retrospective analysis supports the idea that the serum ALB level is more important than the liver fibrosis stages, post-AFP levels, and SVR status for the prediction of HCC development.

The reasons for no significant correlation between HCC development and liver fibrosis remains unknown at present. When analyzing Kaplan-Meier curves, the incidence of HCC after SVR achievement was found to be significantly higher in patients with a serum ALB level <4.0 than in those with a serum ALB level >4.0, and was independent of the severity of liver fibrosis. It should be noted, however, that the incidence of HCC is highest in patients with advanced stages of liver fibrosis (3–4) and serum ALB level <4.0, which suggests the involvement of the severity of liver fibrosis in the development of HCC. This finding together with the fact that the synthetic capacity of ALB reduces with the progression of liver fibrosis, the progression of liver fibrosis and a reduction in the

serum ALB level may act together to promote hepatocarcinogenesis. Therefore, it is difficult to disregard the involvement of liver fibrosis in the development of HCC after induction of SVR.

Interestingly, the incidence of HCC is significantly higher in patients with serum ALB level <4.0 than in those with serum ALB level >4.0 in the early stages of liver fibrosis group. This finding suggests that SVR-mediated inhibitory effects on carcinogenesis are limited in patients exhibiting impaired hepatic synthetic capacity in spite of early stages of liver fibrosis. Thus, careful follow-up for the detection of HCC is necessary in such patients even if the liver fibrosis is not so severe. Another interpretation of this finding comes from the fact that the ALB level reflects the systemic nutritional status regardless of the progression of liver fibrosis. Thus, hepatocarcinogenesis may not be inhibited in malnutrition patients with a reduction in the ALB level.

Branched chain amino acids (BCAAs) improve amino acid imbalance in patients with chronic liver disease. Although several modes of actions, including reduction of angiogenesis and promotion of insulin-dependent hepatocyte proliferation, have been proposed for BCAA's beneficial effects in chronic liver diseases, one of the most important action of BCAA is the promotion of ALB synthesis by oxidative-stress-reducing and oxidized-albumin-lowering actions [30, 31]. In addition, it has been recently reported that oral administration of BCAAs leads to the inhibition of hepatocarcinogenesis through the synthesis of ALB and the reduction in the oxidative stress level [32]. In this study, we identified serum ALB level <4.0 as the strongest risk factor for HCC development in patients with HCV-related liver diseases. This finding suggests that oral supplementation of BCAAs is beneficial for patients exhibiting serum ALB level <4.0 for the prevention of hepatocarcinogenesis.

In conclusion, the serum ALB level was identified as the strongest risk factor for carcinogenesis after SVR achievement in this retrospective study. Importantly, this factor was also associated with HCC development in patients with slight liver fibrosis. The serum ALB level was more sensitive than the progression of liver fibrosis for the prediction of HCC development, and careful follow-up for the detection of HCC may be necessary in such high-risk patients.

#### Disclosure Statement

There are no conflicts of interest to declare.

## References

- 1 Kudo M: Surveillance, diagnosis, treatment, and outcome of liver cancer in Japan. *Liver Cancer* 2015;4:39–50.
- 2 Kudo M, Izumi N, Sakamoto M, Matsuyama Y, Ichida T, Nakashima O, Matsui O, Ku Y, Kokudo N, Makuuchi M: Survival analysis over 28 years of 173,378 patients with hepatocellular carcinoma in Japan. *Liver Cancer* 2016;5:190–197.
- 3 Kudo M: Clinical practice guidelines for hepatocellular carcinoma differ between Japan, United States, and Europe. *Liver Cancer* 2015; 4:85–95.
- 4 Poon RT, Cheung TT, Kwok PC, Lee AS, Li TW, Loke KL, Chan SL, Cheung MT, Lai TW, Cheung CC, Cheung FY, Loo CK, But YK, Hsu SJ, Yu SC, Yau T: Hong Kong consensus recommendations on the management of hepatocellular carcinoma. *Liver Cancer* 2015;4: 51–69.
- 5 Osaki Y, Ueda Y, Marusawa H, Nakajima J, Kimura T, Kita R, Nishikawa H, Saito S, Henmi S, Sakamoto A, Eso Y, Chiba T: Decrease in alpha-fetoprotein levels predicts reduced incidence of hepatocellular carcinoma in patients with hepatitis C virus infection receiving interferon therapy: a single center study. *J Gastroenterol* 2012;47:444–451.
- 6 Asahina Y, Tsuchiya K, Nishimura T, Murooka M, Suzuki Y, Tamaki N, Yasui Y, Hosokawa T, Ueda K, Nakanishi H, Itakura J, Takahashi Y, Kurosaki M, Enomoto N, Nakagawa M, Kakinuma S, Watanabe M, Izumi N:  $\alpha$ -fetoprotein levels after interferon therapy and risk of hepatocarcinogenesis in chronic hepatitis C. *Hepatology* 2013;58:1253–1262.
- 7 Oze T, Hiramatsu N, Yakushijin T, Miyazaki M, Yamada A, Oshita M, Hagiwara H, Mita E, Ito T, Fukui H, Inui Y, Hijioka T, Inada M, Katayama K, Tamura S, Yoshihara H, Inoue A, Imai Y, Hayashi E, Kato M, Miyagi T, Yoshida Y, Tatsumi T, Kasahara A, Hamasaki T, Hayashi N, Takehara T: Post-treatment levels of  $\alpha$ -fetoprotein predict incidence of hepatocellular carcinoma after interferon therapy. *Clin Gastroenterol Hepatol* 2014;12:1186–1195.
- 8 Toyoda H, Kumada T, Tada T, Sone Y, Kaneoka Y, Maeda A: Tumor Markers for hepatocellular carcinoma: simple and significant of outcome in patients with HCC. *Liver Cancer* 2015;4:126–136.
- 9 Kudo M: Risk of hepatocellular carcinoma in patients with hepatitis C virus who achieved sustained virological response. *Liver Cancer* 2016;5:155–161.
- 10 Joo I, Lee JM: Recent advances in the imaging diagnosis of hepatocellular carcinoma: value of gadoteric acid-enhanced MRI. *Liver Cancer* 2016;5:67–87.
- 11 Nishiguchi S, Kuroki T, Nakatani S, Morimoto H, Takeda T, Nakajima S, Shiomi S, Seki S, Kobayashi K, Otani S: Randomised trial of effects of interferon-alpha on incidence of hepatocellular carcinoma in chronic active hepatitis C with cirrhosis. *Lancet* 1995;346:1051–1055.
- 12 Ikeda K, Saitoh S, Arase Y, Chayama K, Suzuki Y, Kobayashi M, Tsubota A, Nakamura I, Murashima N, Kumada H, Kawanishi M: Effect of interferon therapy on hepatocellular carcinogenesis in patients with chronic hepatitis type C: a long-term observation study of 1,643 patients using statistical bias correction with proportional hazard analysis. *Hepatology* 1999;29:1124–1130.
- 13 Yoshida H, Shiratori Y, Moriyama M, Arakawa Y, Ide T, Sata M, Inoue O, Yano M, Tanaka M, Fujiyama S, Nishiguchi S, Kuroki T, Imazeki F, Yokosuka O, Kinoyama S, Yamada G, Omata M: Interferon therapy reduces the risk for hepatocellular carcinoma: national surveillance program of cirrhotic and noncirrhotic patients with chronic hepatitis C in Japan. *IHIT Study Group. Inhibition of hepatocarcinogenesis by interferon therapy. Ann Intern Med* 1999;131:174–181.
- 14 Imai Y, Kawata S, Tamura S, Yabuuchi I, Noda S, Inada M, Maeda Y, Shirai Y, Fukuzaki T, Kaji I, Ishikawa H, Matsuda Y, Nishikawa M, Seki K, Matsuzawa Y: Relation of interferon therapy and hepatocellular carcinoma in patients with chronic hepatitis C. *Osaka Hepatocellular Carcinoma Prevention Study Group. Ann Intern Med* 1998;129:94–99.
- 15 Kasahara A, Hayashi N, Mochizuki K, Takayanagi M, Yoshioka K, Kakumu S, Iijima A, Urushihara A, Kiyosawa K, Okuda M, Hino K, Okita K: Risk factors for hepatocellular carcinoma and its incidence after interferon treatment in patients with chronic hepatitis C. *Osaka Liver Disease Study Group. Hepatology* 1998;27:1394–1402.
- 16 Okanoue T, Itoh Y, Minami M, Sakamoto S, Yasui K, Sakamoto M, Nishioji K, Murakami Y, Kashima K: Interferon therapy lowers the rate of progression to hepatocellular carcinoma in chronic hepatitis C but not significantly in an advanced stage: a retrospective study in 1148 patients. *Viral Hepatitis Therapy Study Group. J Hepatol* 1999;30:653–659.
- 17 Ho MC, Hasegawa K, Chen XP, Nagano H, Lee YJ, Chau GY, Zhou J, Wang CC, Choi YR, Poon RT, Kokudo N: Surgery for intermediate and advanced hepatocellular carcinoma: a consensus report from the 5th Asia-Pacific primary liver cancer expert meeting (APPLE 2014). *Liver Cancer* 2016;5:245–256.
- 18 Kudo M: Locoregional therapy for hepatocellular carcinoma. *Liver Cancer* 2015;4:163–164.
- 19 Kang TW, Rhim H: Recent advances in tumor ablation for hepatocellular carcinoma. *Liver Cancer* 2015;4:176–187.
- 20 Lencioni R, de Baere T, Martin RC, Nutting CW, Narayanan G: Image-guided ablation of malignant liver tumors: recommendations for clinical validation of novel thermal and non-thermal technologies – a western perspective. *Liver Cancer* 2015;4:208–214.
- 21 Tsurusaki M, Murakami T: Surgical and locoregional therapy of HCC: TACE. *Liver Cancer* 2015;4:165–175.
- 22 Obi S, Sato S, Kawai T: Current status of hepatic arterial infusion chemotherapy. *Liver Cancer* 2015;4:188–199.
- 23 Lin CC, Hung CF, Chen WT, Lin SM: Hepatic arterial infusion chemotherapy for advanced hepatocellular carcinoma with portal vein thrombosis: impact of early response to 4 weeks of treatment. *Liver Cancer* 2015;4: 228–240.
- 24 Kudo M: Molecular targeted therapy for hepatocellular carcinoma: where are we now? *Liver Cancer* 2015;4:I–VII.
- 25 Kudo M: Regorafenib as second-line systemic therapy may change the treatment strategy and management paradigm for hepatocellular carcinoma. *Liver Cancer* 2016;5:235–244.
- 26 Geschwind JF, Gholam PM, Goldenberg A, Mantry P, Martin RC, Piperdi B, Zigmont E, Imperial J, Babajanyan S, Foreman PK, Cohn A: Use of transarterial chemoembolization (TACE) and sorafenib in patients with unresectable hepatocellular carcinoma: US regional analysis of the GIDEON registry. *Liver Cancer* 2016;5:37–46.
- 27 Hung CH, Lee CM, Wang JH, Hu TH, Chen CH, Lin CY, Lu SN: Impact of diabetes mellitus on incidence of hepatocellular carcinoma in chronic hepatitis C patients treated with interferon-based antiviral therapy. *Int J Cancer* 2011;128:2344–2352.
- 28 Arase Y, Kobayashi M, Suzuki F, Suzuki Y, Kawamura Y, Akuta N, Kobayashi M, Sezaki H, Saito S, Hosaka T, Ikeda K, Kumada H, Kobayashi T: Effect of type 2 diabetes on risk for malignancies includes hepatocellular carcinoma in chronic hepatitis C. *Hepatology* 2013;57:964–973.
- 29 Morgan RL, Baack B, Smith BD, Yartel A, Pitasi M, Falck-Ytter Y: Eradication of hepatitis C virus infection and the development of hepatocellular carcinoma: a meta-analysis of observational studies. *Ann Intern Med* 2013; 158:329–337.
- 30 Ohno T, Tanaka Y, Sugauchi F, Orito E, Hasegawa I, Nukaya H, Kato A, Matunaga S, Endo M, Tanaka Y, Sakakibara K, Mizokami M: Suppressing effect of oral administration of branched-chain amino acid granules on oxidative stress and inflammation in HCV-positive patients with liver cirrhosis. *Hepatol Res* 2008;38:683–688.
- 31 Fukushima H, Miwa Y, Shiraki M, Gomi I, Toda K, Kuriyama S, Nakamura H, Wakahara T, Era S, Moriaki H: Oral branched-chain amino acid supplementation improves the oxidized/reduced albumin ratio in patients with liver cirrhosis. *Hepatol Res* 2007;37:765–770.
- 32 Setoyama H, Tanaka M, Nagumo K, Naoe H, Watanabe T, Yoshimaru Y, Tateyama M, Sasaki M, Watanabe H, Otogiri M, Maruyama T, Sasaki Y: Oral branched-chain amino acid granules improve structure and function of human serum albumin in cirrhotic patients. *J Gastroenterol* 2017;52:754–765.



# Unique Characteristics Associated with Sustained Liver Damage in Chronic Hepatitis C Patients Treated with Direct Acting Antivirals

Masashi Kono Naoshi Nishida Satoru Hagiwara Tomohiro Minami  
Hirokazu Chishina Tadaaki Arizumi Kosuke Minaga Ken Kamata  
Yoriaki Komeda Toshiharu Sakurai Mamoru Takenaka Masahiro Takita  
Norihisa Yada Hiroshi Ida Yasunori Minami Kazuomi Ueshima  
Tomohiro Watanabe Masatoshi Kudo

Department of Gastroenterology and Hepatology, Kindai University Faculty of Medicine, Osaka-Sayama, Japan

## Keywords

Chronic hepatitis C · Direct acting antivirals · Liver damage · Hepatocellular carcinoma

## Abstract

**Background and Aims:** Direct-acting antivirals (DAAs) dramatically improve the sustained virological response (SVR) of chronic hepatitis C (CHC) patients. However, continuous liver damage after SVR may be a risk of hepatocellular carcinoma (HCC). We clarified pretreatment characteristics related to sustained liver damage after SVR. **Methods:** A total of 286 CHC patients were treated with an interferon-free DAA regimen. Among them, 250 patients achieved SVR for 12 weeks after the end of treatment (SVR12); these individuals were classified based on  $\alpha$ -fetoprotein (AFP) and alanine transaminase (ALT) levels posttreatment. Baseline characteristics significantly associated with AFP >5 ng/mL and ALT level  $\geq 20$  IU/L after SVR were clarified using multivariate analyses. **Results:** Among the pretreatment factors examined, serum AFP values and the presence of fatty liver (FL) were significantly associated with abnormal AFP ( $p < 0.0001$ )

and ALT levels 12 weeks after SVR12 (SVR24;  $p = 0.0109$ ). For 126 patients who showed an increase in baseline AFP level, FL, fibrosis-4 (FIB-4) index, and albumin levels before treatment were related to abnormal AFP at SVR24 ( $p = 0.0005$ , 0.0232, and 0.0400 for FL, FIB-4 index, and albumin, respectively). Similarly, for 150 patients with abnormal baseline ALT levels, FL was associated with an ALT level  $\geq 30$  IU/L after SVR ( $p = 0.0430$ ). **Conclusions:** High FIB-4 index, low albumin level, and FL before DAA treatment were associated with a risk of sustained liver damage with AFP and ALT elevation after SVR; patients with these factors should be carefully monitored for emergence of HCC.

© 2017 S. Karger AG, Basel

## Introduction

At least 150 million people are infected with hepatitis C virus (HCV) worldwide [1]. The critical goal in the management of chronic hepatitis C (CHC) is to achieve a sustained virological response (SVR) that represents contentious HCV elimination. So far, a significant num-

ber of reports have shown that achievement of SVR has a strong impact on the improvement of liver damage and emergence of hepatocellular carcinoma (HCC), which leads to the reduction of liver disease-related mortality [2–4]. However, 2.3 and 5.5% of CHC patients who achieved SVR through interferon (IFN)-based treatment reportedly developed HCC during the average observation periods of 5 and 10 years, respectively [5]. When HCC is detected by imaging [6–10] or biomarkers [11, 12], treatments are performed by means of resection [13, 14], ablation [15–18], transarterial chemoembolization [13, 19–21], intrahepatic arterial infusion chemotherapy [22, 23] or systemic therapy [20, 24–26].

In contrast, it is conceivable that contentious liver damage and regeneration, which are manifested by increases in serum alanine transaminase (ALT) and  $\alpha$ -fetoprotein (AFP) levels, are critical conditions for the development of HCC [27, 28]. Indeed, previous studies have suggested that the elevation of AFP and ALT levels in CHC patients treated with IFN could be a risk for the emergence of HCC [5, 29–31].

In comparison with an IFN-based regimen, IFN-free direct-acting antiviral (DAA) treatments show less adverse effects and a higher SVR rate with shorter treatment periods. Therefore, such treatments can be widely applied to patients carrying HCV, including the elderly, those with advanced liver fibrosis, and those who fail to obtain SVR with IFN-based regimen [32]. However, a subset of patients do not show an improvement of serum AFP and ALT levels regardless of SVR, suggesting that damage to and the regeneration of hepatocytes still lingers on even after the elimination of HCV. As high AFP and ALT levels after SVR could be a surrogate marker for sustained liver damage and HCC emergence [5, 30], characterization of such patients is important for the management of patients with HCV after viral elimination.

In the present study, we focused on this issue and clarified specific pretreatment characteristics related to abnormal AFP and ALT levels after SVR in patients who were treated with an IFN-free DAA regimen.

## Materials and Methods

### Patients

Between September 2014 and April 2016, 286 CHC patients were treated with an IFN-free DAA regimen at Kindai University hospital. DAA treatment includes daclatasvir (DCV) + asunaprevir (ASV), sofosbuvir (SOF)/ledipasvir (LDV), ombitasvir (OBV) + paritaprevir (PTV)/rilonavir (r) or SOF + ritonavir

(RIB). For the treatment of patients with HCV genotype 1, one of the following regimens was applied: DCV + ASV for 24 weeks, SOF/LDV for 12 weeks, or OBV + PTV/r for 12 weeks. In the DCV + ASV regimen, DCV was administered once a day at a dose of 60 mg, and ASV was administered twice a day at a dose of 100 mg. In the SOF/LDV regimen, SOF was administered once a day at a dose of 400 mg, and LDV was administered once a day at a dose of 90 mg. In the OBV + PTV/r regimen, OBV was administered once a day at a dose of 25 mg, PTV was administered once a day at a dose of 150 mg and r was administered once a day at a dose of 100 mg. For the treatment of patients with HCV genotype 2, SOF + RIB was administered for 12 weeks; specifically, SOF was administered once a day at a dose of 400 mg, and RIB was administered at a total dose of 1,000–1,200 mg/day based on body weight, in accordance with the standard treatment protocol for Japanese patients.

An undetectable HCV-RNA at 12 and 24 weeks after the end of treatment (EOT) was defined as SVR12 and SVR24, respectively. Patients testing positive for HCV-RNA 12 weeks after the EOT were defined as non-SVR. Among 286 patients who underwent DAA treatment, 7 patients developed HCC within one year after DAA initiation and were eliminated from the analysis because of the concern that microscopic HCC might already have emerged prior to DAA treatment. In addition, 29 patients were excluded because SVR12 was not achieved. Finally, 250 patients who showed SVR12 after IFN-free DAA treatment were enrolled in this study. Patient age, sex, previous history of HCC, presence of diabetes mellitus (DM), hyperlipidemia (HL), and hypertension (HT) were evaluated. The presence of fatty liver (FL) was also assessed using ultrasonography. Table 1 shows the baseline characteristics of the 250 patients enrolled in this study. The patient population includes 119 men and 131 women (median age, 69 years; range 26–90 years). Sixty of the patients had a past history of HCC development, while 54 also suffered from DM, 34 were HL, 128 had a history of HT, and 77 had a history of FL. Additionally, 67 patients had undergone previous anti-HCV treatments. Among the 250 patients who achieved SVR12, 100 patients were treated with DCV + ASV, 86 patients were treated with SOF + LDV, 17 patients were treated with OBV + PTV/r, and 47 patients were treated with SOF + RIB, respectively. Before DAA treatment, the median HCV-RNA level was 5.9 log/mL (range 2.2–7.6 log/mL) and the median fibrosis-4 (FIB-4) index was 5.1 (range 0.39–31). Other notable baseline values are as follows: serum AST level (median, 52.1 IU/L, range 11–292 IU/L); ALT level (median, 51 IU/L, range 6–506 IU/L); ALB level (median, 3.9 g/dL range 2.3–5.1 g/dL); platelet (PLT) count (median,  $14.2 \times 10^4/\mu\text{L}$ , range  $2.5\text{--}40.6 \times 10^4/\mu\text{L}$ ); AFP level (median, 16.5 ng/mL, range 1–701 ng/mL); and estimated glomerular filtration rate (median, 70.7, range 3–118; (Table 1).

### Follow-up

The follow-up period was started from the initiation of the DAA treatment until 24 weeks after the EOT; HCV-RNA, AST, ALT, ALB, PLT, AFP levels were evaluated at SVR12 and SVR24. The HCV-RNA level was determined using the qualitative AmpliCor or TaqMan HCV assay (Roche Molecular Diagnostics, Tokyo, Japan).

This study was conducted according to the ethical guidelines of the Declaration of Helsinki amended in 2002. Informed consent

was obtained from each patient; the study was approved by the ethics commission of Kindai University Hospital (approval number: 28–251).

#### Statistical Analysis

For univariate analyses, age, FIB-4 index, AST, ALT, ALB, AFP, ferritin levels, PLT counts, and estimated glomerular filtration rate were analyzed as continuous variables. Patient sex; treatment history of HCV; past history of HCC; and presence of DM, HL, HT, and FL were treated as categorical variables. For the comparison of categorical variables, the Pearson's chi-square test was applied. For the comparison of continuous variables, the Student's *t* test and the one-way factorial analysis of variance were applied.

Subsequently, baseline factors with significant differences on univariate analysis were analyzed using multiple logistic regression analysis. For logistic regression analysis, continuous variables found to be significant in univariate analyses were categorized as follows:  $\geq 3.25$  and  $\leq 3.24$  for FIB-4 index;  $\leq 3.7$ ,  $3.8$ – $4.1$ , and  $\geq 4.2$  g/dl for ALB level;  $< 70$ ,  $70$ – $74$ , and  $\geq 75$  years for age; and  $< 30$ ,  $30$ – $59$ , and  $\geq 60$  IU/L for AST level. If FIB-4 index was selected as an item for multivariate analysis, age, AST and ALT levels, and PLT count were excluded from analysis because these were known to be confounding factors for FIB-4 index. All *p* values were 2-sided, and a *p* value of  $< 0.05$  was considered to be significant. Statistical analyses were performed using the Statistical Package for the Social Sciences software, version 11.5J (SPSS; Chicago, IL, USA).

## Results

### Baseline Characteristics of the Patients Associated with Sustained Abnormal AFP and ALT Levels after SVR

A subset of the patients evaluated presented with abnormal levels of serum AFP and ALP, even after the achievement of SVR12. We tried to elucidate the clinical backgrounds of these individuals, related to the sustained increase of AFP and ALT levels after SVR, by analyzing 250 patients who achieved SVR12. For this analysis, we classified patients based on their AFP levels 24 weeks after EOT (at SVR24); the total 250 patients were stratified into a group of 181 patients with AFP levels  $\leq 5$  ng/mL, a group of 30 patients with AFP levels =  $6$ – $9$  ng/mL, and a group of 13 patients with AFP levels  $\geq 10$  ng/mL (26 were missing). The pretreatment factors significantly related to AFP level at SVR24 included a history of HCC emergence, FIB-4 index, and AST, ALB, and AFP levels, and PLT counts on univariate analysis; a history of HCC, higher FIB-4 index, higher pretreatment AST level, lower pretreatment ALB level and PLT count, and higher AFP level were associated with an increase in AFP level at SVR24 ( $p = 0.0443$  for the history of HCC,  $p < 0.0001$  for FIB-4 index,  $p = 0.0005$  for pretreatment AST level,  $p < 0.0001$  for pretreatment ALB level,  $p < 0.0001$  for pre-

**Table 1.** Baseline clinical characteristics of patients

Clinical factors	Baseline characteristics <sup>1</sup>
Gender, male/female	119/131
Age, year, median (range)	69 (26–90)
HCV-RNA, log IU/L, median (range)	5.9 (2.2–7.6)
FIB-4 index, median (range)	5.1 (0.39–31)
AST level, IU/L, median (range)	52.1 (11–292)
ALT level, IU/L, median (range)	51 (6–506)
Albumin level, g/dL, median (range)	3.9 (2.3–5.1)
Platelet counts, $\times 10^3/\mu\text{L}$ , median (range)	14.2 (2.5–40.6)
AFP level, ng/mL, median (range)	16.5 (1–701)
eGFR, mL/min/1.73 m <sup>2</sup> , median (range)	70.7 (3–118)
Previous antiviral treatment (with/without)	67/183
Past history of HCC (with/without)	60/190
Diabetes mellitus (with/without)	54/196
Hyperlipidemia (with/without)	34/216
Hypertension (with/without)	128/122
Fatty liver (with/without)	77/173

<sup>1</sup> Number of patients or median value (range) were shown.

Two hundred and fifty patients were analyzed; 100 patients were treated with DCV + ASV, 86 cases treated with SOF/LDV, 17 cases treated with OBV + PTV/r, and 47 cases treated with SOF + RIB, respectively.

DCV, daclatasvir; ASV, asunaprevir; SOF, sofosbuvir; LDV, ledipasvir; OBV, ombitasvir; PTV/r, paritaprevir; RIB, ritonavir; HCC, hepatocellular carcinoma; HCV, hepatitis C virus; AST, aspartate transaminase; ALT, alanine aminotransferase; AFP, alpha-fetoprotein; eGFR, estimated glomerular filtration rate.

treatment PLT count, and  $p < 0.0001$  for pretreatment AFP level; Table 2). Based on the results of multivariable logistic regression analysis, pretreatment AFP level was identified as an independent factor that was associated with AFP levels at SVR24 ( $p < 0.0001$ ; Table 2).

Similarly, we classified patients based on the ALT levels at SVR24; 175 patients showed an ALT level  $< 20$  IU/L, 39 patients had an ALT level of  $20$ – $29$  IU/L, and 23 patients had an ALT level  $\geq 30$  IU/L (13 were missing). The pretreatment factors significantly related to the ALT level at SVR24 were age, presence of FL, FIB-4 index, pretreatment AST level, pretreatment ALT level, and pretreatment PLT counts ( $p = 0.0025$  for age,  $p = 0.0113$  for FL,  $p = 0.0269$  for FIB-4 index,  $p < 0.0001$  for pretreatment AST level,  $p < 0.0001$  for pretreatment ALT level, and  $p = 0.0495$  for pretreatment PLT counts; Table 3). According to multivariable logistic regression analysis, the presence of FL was identified as an independent factor that was significantly associated with an increase in ALT level at SVR24 ( $p = 0.0109$ ; Table 3).

**Table 2.** Association between pretreatment factors and AFP value after SVR

Pretreatment factors	Patients classified based on AFP value at the time of SVR24 <sup>1</sup>			<i>p</i> value	
	<5 ng/mL ( <i>n</i> = 181)	6–9 ng/mL ( <i>n</i> = 30)	>0 ng/mL ( <i>n</i> = 13)	univariate <sup>3</sup>	multivariate <sup>4</sup>
Age, years	69.9 (68.2–71.6)	66.6 (62.4–70.8)	68.3 (61.9–74.6)	0.3263	
Gender, male/female	83/98	15/15	8/5	0.5230	
Treatment history of HCV (with/without)	47/134	9/21	6/7	0.2777	
Past history of HCC (with/without)	37/144	10/20	6/7	0.0443	0.4341
Past history of diabetes (with/without)	39/142	6/24	2/11	0.8616	
Lipid metabolism (with/without)	23/158	7/23	0/13	0.0983	
Hypertension (with/without)	89/92	18/12	6/7	0.5197	
Fatty liver (with/without)	50/131	11/19	6/7	0.2540	
FIB-4 index <sup>2</sup>	4.28 (3.69–4.86)	7.55 (6.11–8.99)	11.7 (9.52–13.89)	<0.0001	0.2273
AST, IU/L	47.0 (42.2–51.9)	69.1 (57.1–81.1)	70.3 (52.0–88.5)	0.0005	
ALT, IU/L	45.7 (38.8–52.7)	60.7 (43.6–77.7)	52.9 (27.0–78.8)	0.2630	
Albumin, g/dL	4.06 (4.00–4.13)	3.68 (3.52–3.84)	3.55 (3.30–3.80)	<0.0001	0.0832
Platelet counts, ×10 <sup>4</sup> /μL	15.1 (14.2–16.0)	10.9 (8.6–13.1)	7.2 (3.8–10.6)	<0.0001	
AFP, ng/mL	7.44 (–0.07–14.9)	32.1 (13.8–50.4)	121.5 (93.7–149.3)	<0.0001	<0.0001
Ferritin, ng/mL	131.9 (70.1–193.8)	208.7 (79.5–337.9)	77.36 (–169.8–325.1)	0.4903	
eGFR, mL/min/1.73 m <sup>2</sup>	68.7 (65.5–72.0)	75.0 (67.0–83.0)	74.3 (62.1–86.4)	0.2731	

AST, aspartate transaminase; ALT, alanine aminotransferase; AFP, alpha-fetoprotein; eGFR, estimated glomerular filtration rate.

<sup>1</sup> Mean value and 95% CI were shown for contentious variables, and the number of patients in each category was shown for categorical variables.

<sup>2</sup> FIB-4 index = age (year) × AST (IU/L)/PLT (10<sup>9</sup>/L) × ALT (IU/L)<sup>1/2</sup>.

<sup>3</sup> For comparison of contentious variables between multiple groups, one-way factorial analysis of variance was performed. For comparison of categorical variables, the Pearson's chi-squared test was applied.

<sup>4</sup> *p* values by multiple logistic regression analysis.

**Table 3.** Association between pretreatment factors and ALT value after SVR

Pretreatment factors	Patients classified based on ALT value at the time of SVR24 <sup>1</sup>			<i>p</i> values	
	<20 IU/L ( <i>n</i> = 175)	20–29 IU/L ( <i>n</i> = 39)	>30 μ/L ( <i>n</i> = 23)	univariate <sup>3</sup>	multivariate <sup>4</sup>
Age, years	70.4 (68.7–72.1)	67.5 (63.9–71.1)	61.9 (57.2–66.6)	0.0025	
Gender, male/female	76/99	22/17	15/8	0.0708	
Treatment history of HCV (with/without)	48/127	13/26	6/17	0.7378	
Past history of HCC (with/without)	42/133	10/29	4/19	0.7420	
Past history of diabetes (with/without)	37/138	7/32	8/15	0.2668	
Lipid metabolism (with/without)	21/154	7/32	4/19	0.5230	
Hypertension (with/without)	92/83	20/19	11/12	0.9092	
Fatty liver (with/without)	46/129	11/28	13/10	0.0113	0.0109
FIB-4 index <sup>2</sup>	4.69 (4.04–5.35)	6.27 (4.88–7.65)	6.71 (4.91–8.51)	0.0269	0.5048
AST, IU/L	46.1 (41.0–51.2)	57.4 (46.5–68.2)	88.5 (74.4–102.6)	<0.0001	
ALT, IU/L	42.3 (35.1–49.6)	52.2 (36.8–67.6)	97.2 (77.2–117.3)	<0.0001	
Albumin, g/dL	3.98 (3.91–4.05)	3.95 (3.79–4.11)	3.89 (3.69–4.09)	0.7108	
Platelet counts, ×10 <sup>4</sup> /μL	14.7 (13.8–15.7)	12.1 (10.1–14.1)	13.2 (10.6–15.8)	0.0495	
AFP, ng/mL	13.5 (5.1–21.9)	26.2 (8.3–44.1)	27.3 (4.3–50.3)	0.2921	
Ferritin, ng/mL	115.5 (57.8–173.1)	141.1 (5.2–276.9)	270.5 (126.4–414.5)	0.1447	
eGFR, mL/min/1.73 m <sup>2</sup>	68.6 (65.3–71.8)	72.0 (65.1–78.8)	79.7 (70.8–88.7)	0.06	

AST, aspartate transaminase; ALT, alanine aminotransferase; AFP, alpha-fetoprotein; eGFR, estimated glomerular filtration rate.

<sup>1</sup> Mean value and 95% CI were shown for contentious variables, and the number of patients in each category was shown for categorical variables.

<sup>2</sup> FIB-4 index = age (year) × AST (IU/L)/PLT (10<sup>9</sup>/L) × ALT (IU/L)<sup>1/2</sup>.

<sup>3</sup> For comparison of contentious variables between multiple groups, one-way factorial analysis of variance was performed. For comparison of categorical variables, the Pearson's chi-squared test was applied.

<sup>4</sup> *p* values by multiple logistic regression analysis.



**Table 4.** Association between pretreatment factors and AFP value after SVR among patients with baseline AFP >5 ng/mL

Pretreatment factors	Patients classified based on AFP value at the time of SVR24 <sup>1</sup>		<i>p</i> value univariate analysis <sup>3</sup>
	<5 mg/mL ( <i>n</i> = 55)	>5 mg/mL ( <i>n</i> = 43)	
Age, years	71.0 (68.2–73.9)	66.4 (63.2–69.7)	0.0357
Gender, male/female	32/23	23/20	0.6422
Treatment history of HCV (with/without)	18/37	14/29	0.9859
Past history of HCC (with/without)	21/34	17/26	0.8915
Past history of diabetes (with/without)	13/42	8/35	0.5469
Lipid metabolism (with/without)	5/50	7/36	0.2814
Hypertension (with/without)	28/27	24/19	0.6292
Fatty liver (with/without)	7/48	16/27	0.0045
FIB-4 index <sup>2</sup>	5.87 (4.47–7.27)	8.29 (6.71–9.88)	0.0247
AST, IU/L	67.3 (57.9–76.6)	67.8 (57.2–78.4)	0.9450
ALT, IU/L	67.1 (55.4–78.8)	56.8 (43.6–70.0)	0.2513
Albumin, g/dL	3.93 (3.80–4.05)	3.68 (3.54–3.82)	0.0123
Platelet counts, ×10 <sup>4</sup> /μL	12.9 (11.4–14.3)	10.1 (8.5–11.8)	0.0155
Ferritin, ng/mL	162.0 (32.8–291.3)	170.6 (33.0–308.2)	0.9270
eGFR, mL/min/1.73 m <sup>2</sup>	67.0 (60.7–73.3)	76.4 (69.3–83.5)	0.0537

AST, aspartate transaminase; ALT, alanine aminotransferase; AFP, alpha-fetoprotein; eGFR, estimated glomerular filtration rate.

<sup>1</sup> Mean value and 95% CI were shown for contentious variables, and the number of patients in each category was shown for categorical variables.

<sup>2</sup> FIB-4 index = age (year) × AST (IU/L)/PLT (10<sup>9</sup>/L) × ALT (IU/L)<sup>1/2</sup>.

<sup>3</sup> For comparison of contentious variables between 2 groups, the Student *t* test was performed. For comparison of categorical variables, the Pearson's chi-squared test was applied.

#### *Baseline Characteristics that Affect the Posttreatment AFP Level in Patients with Abnormal AFP Levels before Treatment*

Next, we focused on patients with AFP levels >5 ng/mL before treatment to identify baseline characteristics that related to a sustained increase of serum AFP levels after the DAA treatment. In 250 patients who achieved SVR12, 126 showed a pretreatment AFP level >5 ng/mL; we classified these patients into 2 groups based on their AFP values at SVR24: specifically, 55 patients with an AFP level >5 ng/mL and 55 patients with an AFP level ≤5 ng/mL (28 were missing) were considered. In the univariate analysis, age, presence of FL, high FIB-4 index, low ALB level, and low PLT counts were significantly associated with the posttreatment AFP level >5 ng/mL at SVR24 (*p* = 0.0357 for age, *p* = 0.0045 for FL, *p* = 0.0247 for FIB-4 index, *p* = 0.0123 for ALB level, and *p* = 0.0155 for PLT count; Table 4). In the multivariate analysis, presence of FL, high FIB-4 index, and low pretreatment ALB level were independently associated with a posttreatment AFP level >5 ng/mL at SVR24 (OR and 95% CI were 6.64 and 2.22–22.86, *p* = 0.0005 for the presence of FL; 4.46 and 1.21–19.76, *p* = 0.0232 for FIB-4 index ≥3.25; and 3.96 and 1.35–

12.80, *p* = 0.0115 for pretreatment ALB ≤3.7 vs. 3.8–4.1. Age and PLT count were excluded from analysis because these were confounding factors for FIB-4 index; Fig. 1).

#### *Baseline Characteristics Associated with Posttreatment ALT Level at SVR24 in Patients with Abnormal ALT Levels before Treatment*

Among 250 patients who achieved SVR12, 150 patients showed a pretreatment ALT level ≥30 IU/L; we classified these patients into 2 groups based on the ALT value at SVR24, with 51 patients having an ALT level ≥20 IU/L and 92 patients having an ALT level <20 IU/L (7 were missing). In the univariate analysis, age, presence of FL, and high pretreatment AST level were significantly associated with a posttreatment ALT level ≥20 IU/L at SVR24 (*p* = 0.0191 for age, *p* = 0.0447 for presence of FL, and *p* = 0.0211 for pretreatment AST level; Table 5). In the multivariate analysis, the presence of FL and high AST level were identified to be independently associated with a posttreatment ALT level ≥20 IU/L at SVR24 (OR and 95% CI were 2.2 and 1.02–4.78, *p* = 0.0430 for FL; and 2.22 and 1.04–4.88, *p* = 0.0368 for pretreatment AST level ≥60 vs. 30–59, respectively; Fig. 2).

**Table 5.** Association between pretreatment factors and ALT value after SVR among patients with baseline ALT  $\geq 30$  IU/ml

Pretreatment factors	Patients classified based on ALT value at the time of SVR24 <sup>1</sup>		<i>p</i> value
	<20 IU/L ( <i>n</i> = 92)	>20 IU/L ( <i>n</i> = 51)	univariate analysis <sup>3</sup>
Age, years	68.8 (66.2–71.3)	63.7 (60.3–67.1)	0.0191
Gender, male/female	46/46	33/18	0.0902
Treatment history of HCV (with/without)	30/62	16/35	0.8795
Past history of HCC (with/without)	25/67	13/38	0.8272
Past history of diabetes (with/without)	21/71	12/39	0.9238
Lipid metabolism (with/without)	9/83	9/42	0.1744
Hypertension (with/without)	47/45	26/25	0.9903
Fatty liver (with/without)	23/69	21/30	0.0447
FIB-4 index <sup>2</sup>	5.47 (4.41–6.54)	6.95 (5.52–8.39)	0.1051
AST, IU/L	61.1 (53.0–69.2)	77.2 (66.3–88.1)	0.0211
ALT, IU/L	62.7 (50.8–74.7)	79.1 (63.1–95.2)	0.1070
Albumin, g/dL	3.95 (3.85–4.06)	3.88 (3.74–4.02)	0.4011
Platelet counts, $\times 10^4/\mu\text{L}$	13.8 (12.6–15.1)	11.9 (10.2–13.7)	0.0810
AFP, ng/mL	22.2 (7.5–36.9)	31.8 (11.9–51.7)	0.4451
Ferritin, ng/mL	137.8 (46.4–229.3)	225.2 (46.4–229.3)	0.2713
eGFR, mL/min/1.73 m <sup>2</sup>	72.2 (67.8–76.7)	76.9 (70.9–82.9)	0.2191

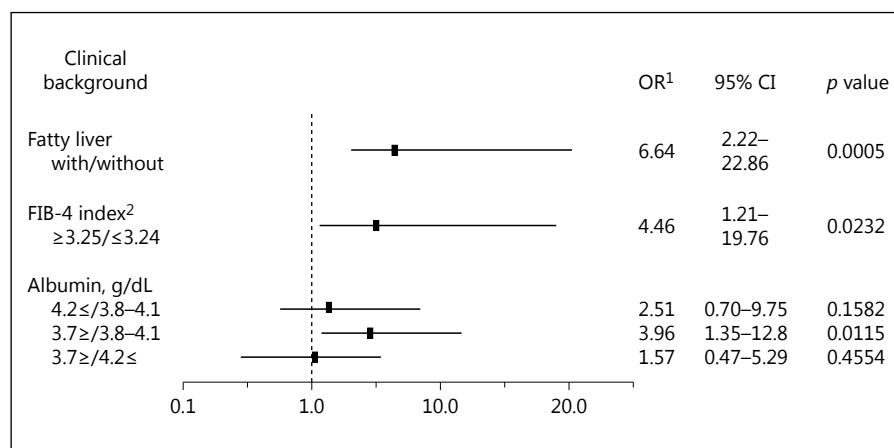
AST, aspartate transaminase; ALT, alanine aminotransferase; AFP, alpha-fetoprotein; eGFR, estimated glomerular filtration rate.

<sup>1</sup> Mean value and 95% CI were shown for contentious variables, and the number of patients in each category was shown for categorical variables.

<sup>2</sup> FIB-4 index = age (year)  $\times$  AST (IU/L)/PLT ( $10^9/\text{L}$ )  $\times$  ALT (IU/L)<sup>1/2</sup>.

<sup>3</sup> For comparison of contentious variables between 2 groups, the Student *t* test was performed. For comparison of categorical variables, the Pearson's chi-squared test was applied.

**Fig. 1.** OR of baseline characteristics for relative risk of sustained increase of AFP after SVR among patients with baseline AFP  $> 5$  ng/mL. ORs and their 95% CI are shown as dots and horizontal bars. For multivariate Cox regression analysis, we categorized contentious variables as follows;  $\geq 3.25$  and  $\leq 3.24$  for FIB-4 index,  $\leq 3.7$ , 3.8–4.1, and  $\geq 4.2$  g/dL for pretreatment ALB, respectively. *p* values by multiple logistic regression analysis are shown. Age and PLT count were excluded from multivariate analysis because these are confounding factor with FIB-4. <sup>1</sup> OR = odds ratio. <sup>2</sup> FIB-4 index = age (year)  $\times$  AST (IU/L)/PLT ( $10^9/\text{L}$ )  $\times$  ALT (IU/L)<sup>1/2</sup>.



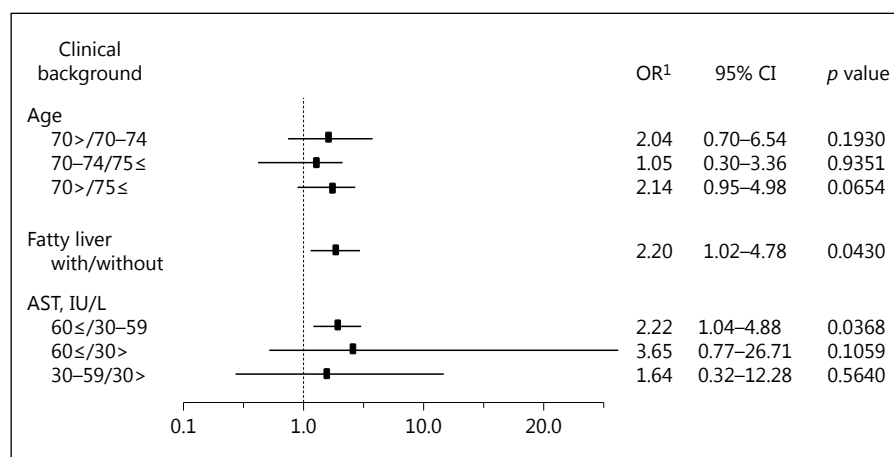
## Discussion

Recent advancement of antiviral treatment using an IFN-free DAA regimen has allowed patients to achieve SVR even in refractory cases, such as in the elderly, in those with advanced liver fibrosis, and in those who were

non-responders to previous IFN-based treatment. However, a subset of patients continued to demonstrate sustained abnormal ALT and AFP levels even after the achievement of SVR. It is conceivable that an increase in ALT and AFP levels should reflect contentious damage and the regeneration of hepatocytes, which should be a

**Fig. 2.** OR of baseline characteristics for relative risk of sustained increase of ALT after SVR among patients with baseline ALT  $\geq 30$  IU/L. ORs and their 95% CI are shown as dots and horizontal bars. For multivariate Cox regression analysis, we categorized age and pretreatment AST as follows;  $<70$ ,  $70-74$ , and  $\geq 75$  years old for age,  $<30$ ,  $30-59$ , and  $\geq 60$  IU/L for pretreatment AST, respectively. *p* values by multiple logistic regression analysis are shown.

<sup>1</sup> OR, odds ratio.



risk for HCC emergence. In this study, we successfully clarified the unique baseline characteristics related to high AFP and ALT values after SVR in CHC patients treated with DAAs.

With respect to the CHC patients who achieved SVR12 in this study, the pretreatment factors significantly related to an increase in AFP levels after SVR were high FIB-4 index, high AST levels, low ALB levels, low PLT counts, and high AFP levels; as such, all of these patients should reflect a progression of liver fibrosis. In multivariate analysis, pretreatment AFP level was the only factor that affected AFP levels after SVR (Table 2). Similarly, the presence of FL, high FIB-4 index, high AST level, high ALT level, and low PLT count were revealed as significant pretreatment factors for the presence of abnormal ALT values after SVR by univariate analysis; the presence of FL was the only independent factor that contributed to the sustained increase in serum ALT levels after the achievement of SVR (Table 3).

Subsequently, we specifically focused on patients with abnormal baseline AFP ( $\geq 5$  ng/mL) and ALT ( $\geq 30$  IU/L) levels to determine the factors that showed a negative impact on the improvement of AFP and ALT levels after treatment. Univariate analysis revealed that older age, the presence of FL, high FIB-4 index, low ALB levels, and low PLT counts were the refractory factors for the decrease in AFP level after SVR. Among them, FL, high FIB-4 index, and low ALB levels were revealed as independent factors for sustained AFP increase in multivariate analysis. In addition, FL was also the only factor independently related to sustained abnormal ALT levels after the achievement of SVR.

As previously reported, AFP levels were significantly different between patients with mild (F0-F2) and ad-

vanced (F3-F4) liver fibrosis, where the average AFP value in patients with F0-F2 was 10 ng/mL and in those with F3-F4, was 23 ng/mL [33]. However, generally, AFP levels decrease through antiviral therapy, and patients with AFP levels  $<6$  ng/mL often show a low incidence of HCC emergence regardless of HCV elimination [5]. Conversely, among SVR patients after pegylated-IFN and RBV treatment, a high AFP value  $\geq 5$  ng/mL is reportedly associated with a high incidence of HCC emergence [34].

In contrast, it has also been reported that the cumulative incidence of HCC was significantly higher even in SVR patients with an ALT level  $\geq 40$  IU/L and an AFP level  $\geq 10$  ng/mL [5]. High ALT and AFP values reflect present damage and the regeneration of hepatocytes; it is possible that hepatocytes carrying DNA damage should act as a seed for transformation and their subsequent regeneration led to the emergence of HCC. In addition, FL reportedly induces oxidative DNA damage in cancer-related genes, which can also be a risk for HCC [35]. Recent reports have also indicated that CHC patients with metabolic features, such as DM, HL, and obesity after IFN therapy shows a higher incidence of HCC emergence than those without metabolic features and that these findings were with respect to both SVR and non-SVR patients [36]. As IFN-free DAA treatment is widely applicable in patients under high risk of HCC, patients with FL, high FIB-4 index, and low ALB level should be carefully monitored for HCC emergence even after the achievement of SVR.

In this study, we found that patients with progressive liver fibrosis and FL could be refractory to the improvement of AFP and ALT levels after elimination of HCV. However, the current study has several limitations. First, because of the limited period of observation after SVR, we

could not evaluate the relationship between AFP and ALT levels after SVR and the emergence of HCC. Second, our single-center analysis may carry a selection bias for patient inclusion. For example, the number of patients included in this study with metabolic features, such as DM, HL, and HT, which might also be a risk for HCC in CHC patients after SVR, was limited. To generalize our findings, these results should be confirmed by further studies using a larger patient cohort.

In conclusion, it is difficult to improve abnormal AFP and ALT levels in patients with advanced liver fibrosis with a high FIB-4 index, low ALB level, and FL even after the elimination of HCV. These baseline factors could

predict contentious damage and regeneration of hepatocytes, and thus, be a risk for HCC after achievement of SVR. Therefore, it is necessary to pay attention to the emergence of HCC after DAA treatment in such patients.

## Disclosure Statement

This work was supported in part by a grant-in-aid for scientific research (KAKENHI: 16K09382) from the Japanese Society for the Promotion of Science (N.N.), a grant from the Smoking Research Foundation (N.N.), the Japan Health Foundation (N.N.). The authors declare that they have no conflict of interest.

## References

- Shire NJ, Sherman KE: Epidemiology of hepatitis C virus: a battle on new frontiers. *Gastroenterol Clin North Am* 2015;44:699–716.
- Singal AG, Volk ML, Jensen D, Di Bisceglie AM, Schoenfeld PS: A sustained viral response is associated with reduced liver-related morbidity and mortality in patients with hepatitis C virus. *Clin Gastroenterol Hepatol* 2010;8:280–288, 288.e281.
- Bruno S, Stroffolini T, Colombo M, Bollani S, Benvegna L, Mazzella G, Ascione A, Santantonio T, Piccinino F, Andreone P, Mangia A, Gaeta GB, Persico M, Fagioli S, Almasio PL: Sustained virological response to interferon-alpha is associated with improved outcome in HCV-related cirrhosis: a retrospective study. *Hepatology* 2007;45:579–587.
- George SL, Bacon BR, Brunt EM, Mihindukulasuriya KL, Hoffmann J, Di Bisceglie AM: Clinical, virologic, histologic, and biochemical outcomes after successful HCV therapy: a 5-year follow-up of 150 patients. *Hepatology* 2009;49:729–738.
- Asahina Y, Tsuchiya K, Nishimura T, Murooka M, Suzuki Y, Tamaki N, Yasui Y, Hosokawa T, Ueda K, Nakanishi H, Itakura J, Takahashi Y, Kurosaki M, Enomoto N, Nakagawa M, Kakinuma S, Watanabe M, Izumi N:  $\alpha$ -fetoprotein levels after interferon therapy and risk of hepatocarcinogenesis in chronic hepatitis C. *Hepatology* 2013;58:1253–1262.
- Kudo M: Surveillance, diagnosis, treatment, and outcome of liver cancer in Japan. *Liver Cancer* 2015;4:39–50.
- Clinical practice guidelines for hepatocellular carcinoma differ between Japan, United States, and Europe. *Liver Cancer* 2015;4:85–95.
- Ichikawa S, Ichikawa T, Motosugi U, Sano K, Morisaka H, Enomoto N, Matsuda M, Fujii H: Was hypervascular hepatocellular carcinoma visible on previous gadoxetic acid-enhanced magnetic resonance images? *Liver Cancer* 2015;4:154–162.
- Joo I, Lee JM: Recent advances in the imaging diagnosis of hepatocellular carcinoma: value of gadoxetic acid-enhanced MRI. *Liver Cancer* 2016;5:67–87.
- Kudo M: Breakthrough imaging in hepatocellular carcinoma. *Liver Cancer* 2016;5:47–54.
- Toyoda H, Kumada T, Tada T, Sone Y, Kaneoka Y, Maeda A: Tumor markers for hepatocellular carcinoma: simple and significant predictors of outcome in patients with HCC. *Liver Cancer* 2015;4:126–136.
- Kudo M: Risk of hepatocellular carcinoma in patients with hepatitis C virus who achieved sustained virological response. *Liver Cancer* 2016;5:155–161.
- Kudo M, Izumi N, Sakamoto M, Matsuyama Y, Ichida T, Nakashima O, Matsui O, Ku Y, Kokudo N, Makuuchi M: Survival analysis over 28 years of 173,378 patients with hepatocellular carcinoma in Japan. *Liver Cancer* 2016;5:190–197.
- Ho MC, Hasegawa K, Chen XP, Nagano H, Lee YJ, Chau GY, Zhou J, Wang CC, Choi YR, Poon RT, Kokudo N: Surgery for intermediate and advanced hepatocellular carcinoma: a consensus report from the 5th Asia-Pacific primary liver cancer expert meeting (APPLE 2014). *Liver Cancer* 2016;5:245–256.
- Kudo M: Locoregional therapy for hepatocellular carcinoma. *Liver Cancer* 2015;4:163–164.
- Kang TW, Rhim H: Recent advances in tumor ablation for hepatocellular carcinoma. *Liver Cancer* 2015;4:176–187.
- Teng W, Liu KW, Lin CC, Jeng WJ, Chen WT, Sheen IS, Lin CY, Lin SM: Insufficient ablative margin determined by early computed tomography may predict the recurrence of hepatocellular carcinoma after radiofrequency ablation. *Liver Cancer* 2015;4:26–38.
- Lin CC, Cheng YT, Chen MW, Lin SM: The effectiveness of multiple electrode radiofrequency ablation in patients with hepatocellular carcinoma with lesions more than 3 cm in size and barcelona clinic liver cancer stage A to B2. *Liver Cancer* 2016;5:8–20.
- Tsurusaki M, Murakami T: Surgical and locoregional therapy of HCC: TACE. *Liver Cancer* 2015;4:165–175.
- Arizumi T, Ueshima K, Minami T, Kono M, Chishina H, Takita M, Kitai S, Inoue T, Yada N, Hagiwara S, Minami Y, Sakurai T, Nishida N, Kudo M: Effectiveness of Sorafenib in patients with transcatheter arterial chemoembolization (TACE) refractory and intermediate-stage hepatocellular carcinoma. *Liver Cancer* 2015;4:253–262.
- Geschwind JF, Gholam PM, Goldenberg A, Mantry P, Martin RC, Piperdi B, Zigmont E, Imperial J, Babajanyan S, Foreman PK, Cohn A: Use of transarterial chemoembolization (TACE) and sorafenib in patients with unresectable hepatocellular carcinoma: US regional analysis of the GIDEON registry. *Liver Cancer* 2016;5:37–46.
- Obi S, Sato S, Kawai T: Current status of hepatic arterial infusion chemotherapy. *Liver Cancer* 2015;4:188–199.
- Lin CC, Hung CF, Chen WT, Lin SM: Hepatic arterial infusion chemotherapy for advanced hepatocellular carcinoma with portal vein thrombosis: impact of early response to 4 weeks of treatment. *Liver Cancer* 2015;4:228–240.
- Kudo M: Molecular targeted therapy for hepatocellular carcinoma: where are we now? *Liver Cancer* 2015;4:I–VII.
- Zhang B, Finn RS: Personalized clinical trials in hepatocellular carcinoma based on biomarker selection. *Liver Cancer* 2016;5:221–232.
- Kudo M: Immune checkpoint blockade in hepatocellular carcinoma. *Liver Cancer* 2015;4:201–207.



- 27 Tateyama M, Yatsushashi H, Taura N, Motoyoshi Y, Nagaoka S, Yanagi K, Abiru S, Yano K, Komori A, Migita K, Nakamura M, Naga-hama H, Sasaki Y, Miyakawa Y, Ishibashi H: Alpha-fetoprotein above normal levels as a risk factor for the development of hepatocel-lular carcinoma in patients infected with hep-atitis C virus. *J Gastroenterol* 2011;46:92–100.
- 28 Tarao K, Rino Y, Ohkawa S, Tamai S, Miyaka-wa K, Takakura H, Endo O, Yoshitsugu M, Watanabe N, Matsuzaki S: Close association between high serum alanine aminotransfer-ase levels and multicentric hepatocarcinogen-esis in patients with hepatitis C virus-associ-ated cirrhosis. *Cancer* 2002;94:1787–1795.
- 29 Okanoue T, Itoh Y, Minami M, Sakamoto S, Yasui K, Sakamoto M, Nishioji K, Murakami Y, Kashima K: Interferon therapy lowers the rate of progression to hepatocellular carcino-ma in chronic hepatitis C but not significant-ly in an advanced stage: a retrospective study in 1148 patients. *Viral Hepatitis Therapy Study Group. J Hepatol* 1999;30:653–659.
- 30 Iwasaki Y, Takaguchi K, Ikeda H, Makino Y, Araki Y, Ando M, Kobashi H, Kobatake T, Tanaka R, Tomita M, Senoh T, Kawaguchi M, Shimoe T, Manabe K, Kita K, Shimamura J, Sakaguchi K, Shiratori Y: Risk factors for he-patocellular carcinoma in Hepatitis C patients with sustained virologic response to interfer-on therapy. *Liver Int* 2004;24:603–610.
- 31 Tanaka H, Tsukuma H, Kasahara A, Hayashi N, Yoshihara H, Masuzawa M, Kanda T, Kashiwagi T, Inoue A, Kato M, Oshima A, Kinoshita Y, Kamada T: Effect of interferon therapy on the incidence of hepatocellular carcinoma and mortality of patients with chronic hepatitis C: a retrospective cohort study of 738 patients. *Int J Cancer* 2000;87: 741–749.
- 32 EASL recommendations on treatment of hep-atitis C 2015. *J Hepatol* 2015;63:199–236.
- 33 Okamura Y, Ashida R, Yamamoto Y, Ito T, Sugiura T, Uesaka K: FIB-4 index is a predic-tor of background liver fibrosis and long-term outcomes after curative resection of hepato-cellular carcinoma. *Ann Surg Oncol* 2016;23: 467–474.
- 34 Oze T, Hiramatsu N, Yakushijin T, Miyazaki M, Yamada A, Oshita M, Hagiwara H, Mita E, Ito T, Fukui H, Inui Y, Hijioka T, Inada M, Katayama K, Tamura S, Yoshihara H, Inoue A, Imai Y, Hayashi E, Kato M, Miyagi T, Yo-shida Y, Tatsumi T, Kasahara A, Hamasaki T, Hayashi N, Takehara T: Post-treatment levels of  $\alpha$ -fetoprotein predict incidence of hepato-cellular carcinoma after interferon therapy. *Clin Gastroenterol Hepatol* 2014;12:1186–1195.
- 35 Nishida N, Yada N, Hagiwara S, Sakurai T, Kitano M, Kudo M: Unique features associ-ated with hepatic oxidative DNA damage and DNA methylation in non-alcoholic fatty liver disease. *J Gastroenterol Hepatol* 2016;31: 1646–1653.
- 36 Nahon P, Bourcier V, Layese R, Audureau E, Cagnot C, Marcellin P, Guyader D, Fontaine H, Larrey D, De Ledinghen V, Ouzan D, Zou-lim F, Roulot D, Tran A, Bronowicki JP, Zar-ski JP, Leroy V, Riachi G, Cales P, Peron JM, Alric L, Bourliere M, Mathurin P, Dharancy S, Blanc JF, Abergel A, Serfaty L, Mallat A, Grange JD, Attali P, Bacq Y, Wartelle C, Dao T, Benhamou Y, Pilette C, Silvain C, Christidis C, Capron D, Bernard-Chabert B, Zucman D, Di Martino V, Thibaut V, Salmon D, Ziolo M, Sutton A, Pol S, Roudot-Thoraval F: Erad-ication of hepatitis C virus infection in pa-tients with cirrhosis reduces risk of liver and non-liver complications. *Gastroenterology* 2017;152:142–156.e142.

# Hepatocellular Carcinoma after Achievement of Sustained Viral Response with Daclatasvir and Asunaprevir in Patients with Chronic Hepatitis C Virus Infection

Hiroshi Ida Satoru Hagiwara Masashi Kono Tomohiro Minami  
Hirokazu Chishina Tadaaki Arizumi Masahiro Takita Norihisa Yada  
Yasunori Minami Kazuomi Ueshima Naoshi Nishida Masatoshi Kudo

Department of Gastroenterology and Hepatology, Faculty of Medicine, Kindai University, Osaka-Sayama, Japan

## Keywords

Direct-acting antivirals · Hepatitis C virus · Hepatocellular carcinoma · Sustained viral response

## Abstract

**Background:** Interferon-based antiviral therapies against hepatitis C virus (HCV) infection have been shown to reduce the incidence of hepatocellular carcinoma (HCC) in patients with sustained viral response (SVR). Recently, direct-acting antivirals (DAAs) have been proven to be much more effective in achieving SVR than interferon-based therapies. However, whether DAAs can efficiently prevent the occurrence of HCC after SVR remains controversial. To clarify this issue, we analyzed the clinical features of patients in whom HCC developed after achievement of SVR with DAAs for chronic HCV infection. **Summary:** Among patients who achieved SVR with daclatasvir and asunaprevir ( $n = 100$ ), HCC developed in 17 patients (HCC group;  $n = 17$ ) and did not develop in 83 patients (non-HCC group;  $n = 83$ ) during a mean observation period of 15 months. A multivariate Cox proportional hazards analysis identified past history of HCC and male sex as significant risk factors for the emergence of HCC after DAAs. Sixteen cases with HCC after DAAs were in the very early or early stage (16/17, 94.1%), and one case was in the

advanced stage (1/17, 5.9%) with portal venous tumor thrombus. Radiofrequency ablation and/or transarterial chemoembolization were performed in most cases as curative therapy (16/17, 94.1%). **Key Messages:** SVR by DAAs did not completely prevent the occurrence of HCC. However, even if HCC did develop after SVR, curative anticancer therapy was applicable in most cases.

© 2017 S. Karger AG, Basel

## Introduction

Hepatocellular carcinoma (HCC) is the third most common cause of death worldwide [1]. Hepatitis C virus (HCV) infection and hepatitis B virus infection are the major causes of HCC [2]. HCV is common in southeast Asia, Japan, South America, and South Africa [3]. HCV infection causes chronic hepatitis for a long period, resulting in the development of liver cirrhosis [4]. HCC arises from liver cirrhosis and chronic hepatitis with high incidence [5]. Therefore, antiviral therapy and surveil-

The view expressed in this article is the authors' view and is not an official position of the institution or funder.

lance for HCC are important [6, 7]. Once HCC is detected by imaging [8–11] or biomarkers [12, 13], several treatments are applied, such as resection [14], ablation [15–19], transarterial chemoembolization (TACE) [20–22], hepatic arterial infusion chemotherapy [23, 24] or systemic therapy [25–27].

Interferon has been used for chronic HCV infection (CHC) since 1990s. Initially, the rate of sustained viral response (SVR) was about 10% [28]. After ribavirin and pegylated-interferon became available, the rate of SVR reached 40–50% [29]. These interferon-based antiviral therapies have been shown to reduce the incidence of HCC in patients with SVR [30]. However, interferon is not applicable to all patients with HCV because of its possible side effects and underlying diseases in the patients [31].

Recently direct-acting antivirals (DAAs) have been proven to be much more effective in achieving SVR than interferon-based therapies in patients with CHC. Daclatasvir (DCV) and asunaprevir (ASV) were the first approved DAAs in Japan. DCV and ASV are inhibitors of non-structural protein 5A and NS3/4A of HCV, respectively. A phase III clinical trial of DCV and ASV in patients with HCV genotype 1b revealed SVR rates of 84.0% in non-cirrhotic patients and 90.9% in cirrhotic patients [32]. Currently, more effective DAAs, including the NS5B inhibitor sofosbuvir, are available, which can achieve SVR rates of more than 95% [33]. However, whether SVR achieved by these DAAs can efficiently prevent the occurrence of HCC after SVR remains controversial. To clarify this issue, we retrospectively analyzed the clinical features of CHC patients who developed HCC after achievement of SVR with DCV and ASV.

## Methods

In this study, DAAs (DCV 60 mg p.o. + ASV 100 mg p.o. b.i.d. for 24 weeks) were administered to 120 patients with CHC and serotype 1. The treatment was initiated between September 2014 and July 2015. SVR was assessed by real-time RT-PCR after 12 weeks of DAA treatment. Twenty patients with failure to achieve SVR and/or suspected HCC at initiation of DAA treatment were excluded. Finally, 100 patients were eligible for this study. Routine surveillance including tumor markers and ultrasound sonography was performed to detect suspected HCC after the DAA treatment. The final diagnosis of HCC was confirmed by contrast ultrasound sonography, contrast-enhanced CT (CE-CT), or contrast-enhanced MRI (CE-MRI). The observation period was from September 2014 to January 2017. The baseline clinical parameters before DAA treatment (age, sex, whole blood cell count, alanine aminotransferase, albumin, alpha-fetoprotein [AFP], past history of HCC) were collected from the individual patient

**Table 1.** Baseline characteristics of the patients with SVR by DAAs

	SVR ( <i>n</i> = 100)
Age, years, median (range)	72.5 (26–87)
Male/female	46/54
Serotype 1, <i>n</i> (%)	100 (100)
ALT, IU/L, median (range)	37 (7–309)
ALB, g/dL, median (range)	3.95 (2.6–5.1)
PLT, ×10,000/mm <sup>3</sup> , median (range)	11.7 (2.5–32.2)
Fib-4 index, median (range)	4.85 (0.40–31.5)
AFP, ng/mL, median (range)	5 (1–701)
Past history of HCC, <i>n</i> (%)	26 (26)
BCLC stage 0/A/B	13/12/1
Number of treatment 1/≥2	11/15
Latest Tx before DAA	
resection/RFA/TACE	4/21/1

BCLC, Barcelona clinical liver cancer; latest Tx, latest treatment for HCC before DAA treatment; RFA, radiofrequency ablation; TACE, transarterial chemoembolization.

records in our hospital. When HCC developed after the end of DAA treatment (EOT), the HCC stages and subsequent therapies were analyzed.

Statistical analyses for comparisons between the 2 groups described later were performed by the Mann-Whitney U test, chi-square test, Wilcoxon signed-rank test, Cochran-Armitage test, and univariate Cox proportional hazards regression analysis using Bell Curve for Excel version 2.0. This study was approved by the Ethical Committee of our institute.

## Results

The baseline characteristics at initiation of DAA therapy are shown in Table 1. The median age was 72.5 years, female sex was more dominant than male sex, serotype was 1 in all cases, median fibrosis-4 (Fib-4) index was 4.85, and 26 patients had a past history of HCC (26/100, 26%). Among the total patients (*n* = 100), 17 patients developed HCC (HCC group, 17/100, 17%) and 83 patients did not develop HCC (non-HCC group, 87/100, 87%) during the observation period (Table 2). The clinical parameters at initiation of DAA treatment were compared between the 2 groups.

In the HCC group, male sex was more dominant, AFP was higher, Fib-4 index was higher, and past history of HCC was more common compared with the non-HCC group (Table 2). AFP at initiation of DAA treatment was compared with that at EOT. In the non-HCC group, AFP was significantly decreased after DAA therapy compared

**Table 2.** Baseline characteristics of the patients with SVR by DAAs in the HCC and non-HCC groups

	HCC group ( <i>n</i> = 17)	Non-HCC group ( <i>n</i> = 83)	<i>p</i> value
Age, years, median (range)	72 (57–83)	73 (26–87)	0.71
Age >65 years, <i>n</i> (%)	14 (82.4)	66 (61.4)	0.79
Age >75 years, <i>n</i> (%)	7 (41.2)	37 (44.6)	0.80
Male, <i>n</i> (%)	13 (76.4)	33 (39.8)	0.006
ALT, IU/L	45 (8–181)	37 (7–309)	0.28
ALB, IU/L	3.9 (2.6–4.5)	4.0 (2.6–5.1)	0.30
PLT, ×10,000/mm <sup>3</sup>	8.5 (2.5–18.1)	11.9 (2.5–32.2)	0.07
AFP, ng/mL	9.0 (2.0–35.1)	4 (1–701)	0.009
Fib-4 index	5.68 (1.78–31.5)	4.67 (0.40–22.4)	0.008
Fib-4 ≥3.25, <i>n</i> (%)	14 (82.3)	60 (72.2)	0.39
Past history of HCC, <i>n</i> (%)	12 (70.6)	14 (16.9)	<0.001

Mann-Whitney U test/chi-square test.

**Table 3.** Comparison of AFP levels at the initiation and end of DAA treatment

	HCC group ( <i>n</i> = 17)	Non-HCC group ( <i>n</i> = 83)
AFP pre, ng/mL, median (range)	9 (2–351)	4 (1–701)
AFP EOT, ng/mL, median (range)	5 (2–96)	3 (1–136)
<i>p</i> value	0.35	<0.001

Wilcoxon signed-rank test.

AFP, alpha-fetoprotein; AFP pre, AFP levels before DAA treatment; AFP EOT, AFP levels at end of DAA treatment.

**Table 4.** AFP-positive rates at the initiation and end of DAA treatment (cutoff value: 10 ng/mL)

	HCC group ( <i>n</i> = 17)	Non-HCC group ( <i>n</i> = 83)	<i>p</i> value
AFP pre >10, ng/mL, <i>n</i> (%)	8 (47.1)	24 (28.9)	0.14
AFP EOT >10, ng/mL, <i>n</i> (%)	4 (23.5)	60 (8.5)	<0.001

Chi-square test.

AFP, alpha-fetoprotein; AFP pre, AFP levels before DAA treatment; AFP EOT, AFP levels at end of DAA treatment.

with the HCC group (Table 3). In the HCC group, the AFP-positive rate at EOT was significantly higher than that in the non-HCC group, when the cutoff value for AFP was 10 ng/mL (Table 4).

Next, we analyzed the detailed past history of HCC before DAA treatment. The number of treatments for previous HCC in the HCC group was significantly higher than that in the non-HCC group (Table 5). Barcelona clinical liver cancer stage and latest type of therapy for

previous HCC did not differ significantly between the 2 groups. Univariate Cox proportional hazards analyses identified the past history of HCC and male sex as significant risk factors for the emergence of HCC after DAA treatment (Table 6). A multivariate analysis confirmed that past history of HCC and male sex were significant risk factors for HCC development after DAA therapy (Table 7). The cumulative incidence of HCC after SVR was significantly higher in patients with past history of



**Table 5.** Past history of HCC before DAA treatment

	HCC ( <i>n</i> = 17)	Non-HCC ( <i>n</i> = 83)	<i>p</i> value
Past history of HCC, <i>n</i> (%)	12 (70.6)	14 (16.9)	<0.001
Number of treatment for previous HCC 0/1/≥2	5/4/8	69/7/7	<0.001
Latest BCLC stage 0/A/B	5/6/1	8/6/0	0.34
Latest Tx before DAA resection/RFA/TACE	2/9/1	2/12/0	0.76
Time from latest HCC to DAAs, days	125 (29–1,618)	636 (47–3,017)	0.16

Cochran-Armitage test/Mann-Whitney U test.

BCLC, Barcelona clinical liver cancer; latest Tx, latest treatment for HCC before DAA treatment; RFA, radio-frequency ablation; TACE, transarterial chemoembolization.

**Table 6.** Univariate Cox proportional hazards regression analyses

	Hazard ratio	95% CI	<i>p</i> value
Male vs. female	4.61	1.50–14.2	0.008
Age >65 years	1.2	0.36–4.33	0.73
Age >75 years	1.0	0.38–2.62	0.99
Fib-4 index >3.25	1.55	0.45–5.42	0.49
PLT pre <100,000/mm <sup>3</sup>	0.92	0.83–1.01	0.08
PLT EOT <100,000/mm <sup>3</sup>	1.57	0.60–4.06	0.36
Fib-4 index >3.25	1.55	0.45–5.42	0.49
AFP pre >10 ng/mL	1.67	0.64–4.33	0.08
AFP EOT >10 ng/mL	2.99	0.96–9.29	0.06
Past history of HCC + vs. –	8.54	3.00–24.29	<0.001

pre, values before DAA treatment; EOT, values at end of DAA treatment.

**Table 7.** Multivariate Cox proportional hazards regression analysis

	Hazard ratio	95% CI	<i>p</i> value
Male vs. female	3.42	1.10–10.67	0.008
Past history of HCC+ vs. –	7.07	2.46–20.33	<0.001

HCC than in patients without past history of HCC (*p* < 0.001; Fig. 1).

Among the 17 patients in the HCC group, 12 patients had a past history of HCC and were thus recurrences of HCC. The remaining 5 patients had no past history of HCC (Table 8), and were thus first occurrences of HCC. We compared the stages and therapies of HCC after DAA treatment between these 2 groups with recurrence of HCC (*n* = 12) and first occurrence of HCC (*n* = 5; Table 8). In both groups, all cases were in the very early and early stage, except for one case in the recurrence group. Radiofrequency ablation was applicable in most cases, resulting in complete remission.

Early occurrences of HCC within 12 weeks after EOT were observed in 5 patients (Table 9). All of these patients had a past history of HCC. In the 5 cases, the duration between latest HCC and initiation of DAA treatment was variable, ranging from 75 to 1,818 days. In case 1, RFA was performed 11 months before DAA therapy, and local recurrence of HCC was observed at EOT. Subsequently RFA was performed, resulting in complete remission (Fig. 2). In case 2, curative resection of HCC was performed 5 years before DAA therapy; nevertheless, recurrence of HCC was observed soon after DAA initiation. In case 3, TACE was carried out 5 months before DAA initiation. Although CE-CT showed complete remission of

**Table 8.** Stages and therapy of HCC after DAA treatment

	Recurrence of HCC ( <i>n</i> = 12)	First occurrence of HCC ( <i>n</i> = 5)
BCLC stage (0/A/B/C)	5/6/0/1	3/2/0/0
Treatment of HCC RFA/TACE/HAIC	11/1*/1	5/0/0
Successful complete remission, <i>n</i> (%)	11 (92)	5 (100)

\* RFA with TACE.

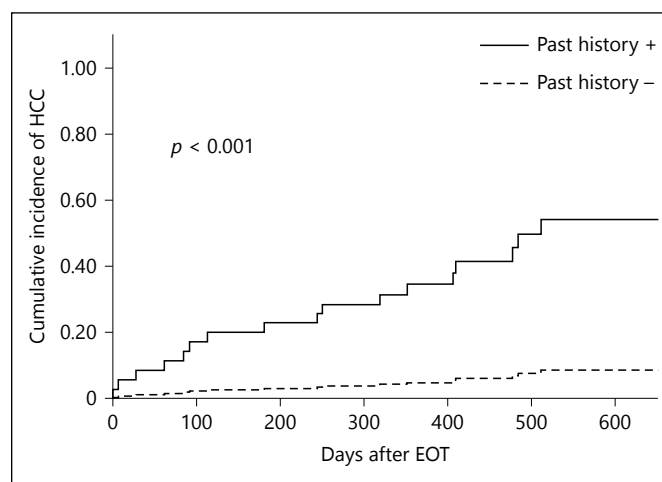
BCLC, barcelona clinical liver cancer; HAIC, hepatic arterial injection chemotherapy; RFA, radiofrequency ablation; TACE, transarterial chemoembolization.

**Table 9.** Early recurrences of HCC after EOT (within 3 months)

	Age	Gender	Latest HCC BCLC	Latest Tx for previous HCC	Latest HCC to DAA, days	DCV + ASV, weeks	EOT to HCC, days	HCC BCLC	Tx for HCC
Case 1	82	M	0	RFA	327	24	0	A	RFA
Case 2	77	M	0	Resection	1,618	24	7	A	RFA
Case 3	83	M	A	TACE	153	24	28	C*	HAIC
Case 4	72	F	0	RFA	653	24	62	0	RFA
Case 5	83	M	0	RFA	75	8	84	A	RFA

BCLC, barcelona clinical liver cancer; Tx for HCC, treatment for recurrent HCC; C\*, HCC with PVTT; HAIC, hepatic arterial injection chemotherapy.

**Fig. 1.** Cumulative incidence of hepatocellular carcinoma (HCC) emergence according to the past history of HCC, before direct-acting antiviral (DAA) treatment. Data were evaluated by using the Kaplan-Meier method ( $p < 0.001$ ). EOT, end of DAA treatment.

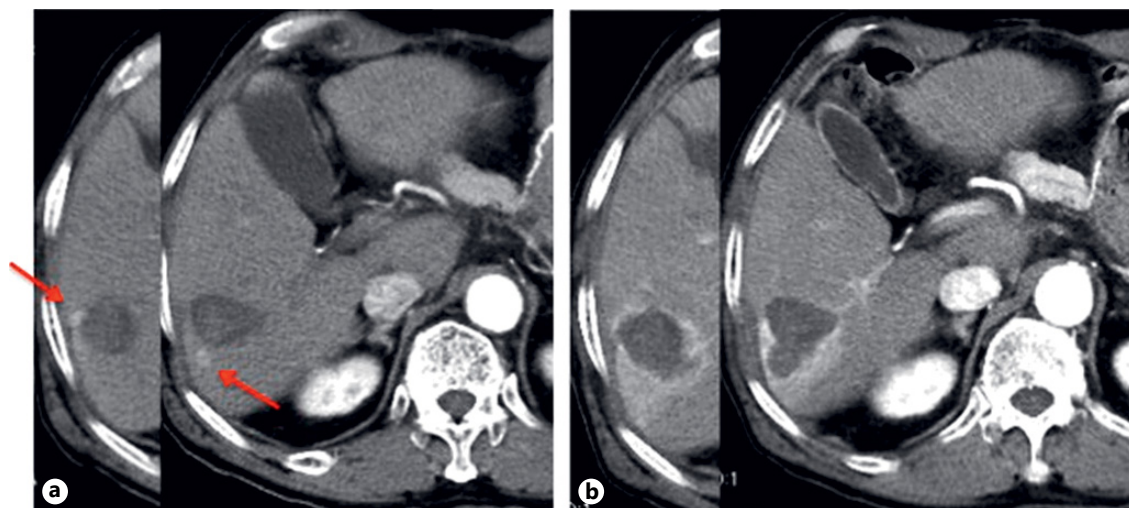


HCC before DAA therapy, portal venous tumor thrombus developed soon after EOT (Fig. 3).

Finally, we analyzed patients without a past history of HCC before DAA therapy ( $n = 74$ ). We did not detect any significant risk factors for the occurrence of HCC ( $n = 5$ ), possibly because of the small sample number (data not shown).

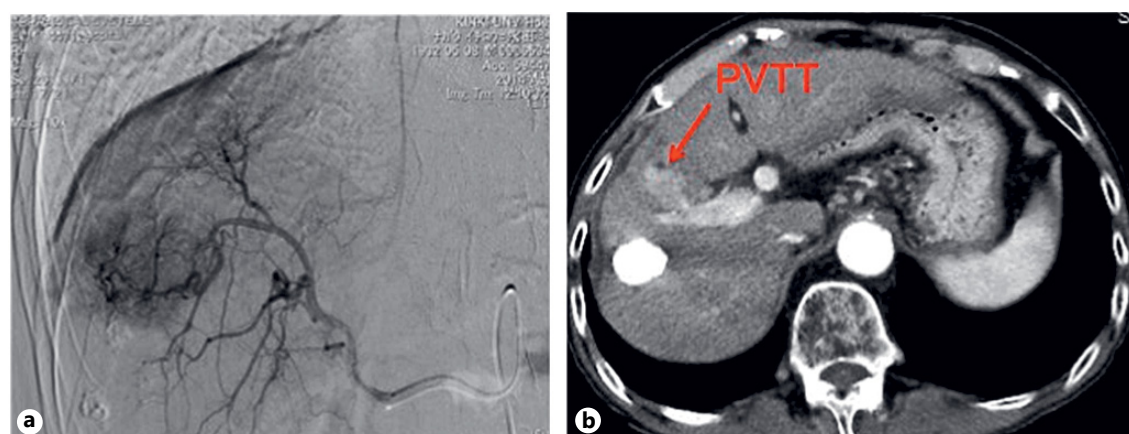
## Discussion

Chronic HCV infection is considered to be one of the major risk factors for the development of HCC [2]. Chronic inflammation induced by HCV may lead to the accumulation of genetic mutations and epigenetic alterations in hepatocytes, resulting in hepatic carcinogenesis



**Fig. 2.** Recurrent hepatocellular carcinoma (HCC) at end of direct-acting antiviral (DAA) treatment in an 82-year-old male (case 1). **a, b** Arterial phase of contrast-enhanced CT shows local recurrent

HCCs (arrows) near the previously ablated area. Alpha-fetoprotein was 4 ng/mL. **c, d** Radiofrequency ablation was performed for HCC, resulting in complete remission.



**Fig. 3.** Recurrent hepatocellular carcinoma (HCC) with portal venous tumor thrombus (PVTT) after direct-acting antiviral (DAA) treatment in an 83-year-old-male (case 3). **a** Conventional trans-arterial chemoembolization using epirubicin and Lipiodol with Gelpart was performed for HCC. DAA treatment was started at 153 days after confirmation of complete remission by contrast-

enhanced CT. Alpha-fetoprotein (AFP) was 9 ng/mL at initiation of DAA treatment. **b** HCC developed with PVTT (arrow) at 4 weeks after end of DAA treatment. AFP was 7 ng/mL at the time of HCC development. Hepatic intra-arterial chemotherapy with cisplatin was performed for HCC.

[34]. Interferon-based therapies have been available as antiviral therapies for a long time [35]. SVR by interferon can reduce the risk of HCC development [30], possibly via termination of additional accumulation of genetic alterations. The effect of interferon has been further enhanced by its combination with protease inhibitors, such as telaprevir or simeprevir [36, 37]. However, the indications for interferon are limited and careful management

is required because of its adverse effects, such as thrombocytopenia and autoimmune diseases [38].

As the first generation of interferon-free antiviral treatments, DCV and ASV were approved in 2014 [32, 39]. The rate of SVR with DCV and ASV is more than 90%, unless the target HCV is drug-resistant [40]. We are now in the age when almost 100% SVR can be achieved by DAAs, including sofosbuvir for CHC [33]. Our con-

cern was whether SVR by DAAs can efficiently inhibit hepatic carcinogenesis.

In the present study, SVR by DCV and ASV did not completely inhibit the emergence of HCC. HCC developed in 17 patients (17/100, 17%). In some cases, such as case 1, HCC appeared in proximity to a previously ablated area and was considered to be a local recurrence. In other cases, recurrent HCC was considered to be de novo cancer, although it was sometimes difficult to distinguish local recurrence from de novo cancer. It was also possible that minor intrahepatic metastasis already existed before DAA treatment. Past history of HCC is considered to be one of the most significant risk factors for HCC recurrence. Indeed, our univariate and multivariate Cox proportional hazards analyses identified past history of HCC and male sex as significant risk factors for the emergence of HCC after DAA treatment.

Early occurrences of HCC within 12 weeks after EOT were observed in 5 patients in the present study. It may be noteworthy that all 5 patients had a past history of HCC. In case 3, portal venous tumor thrombus developed soon after the initiation of DAA treatment. Unfortunately, curative therapy was not applicable for recurrent HCC. It is possible that CE-CT was not sufficient to determine complete remission of HCC after TACE because of the accumulation of Lipiodol. In this regard, assessment of the therapeutic effect of TACE should have been performed by CE MRI, instead of CE-CT. However, it is also possible that rapid suppression of the anticancer immune system by rapid clearance of HCV by the DAA therapy resulted in rapid growth of HCC [41].

There are several reports consistent with our observations of unexpected early recurrence of HCC after SVR by DAAs. Reig et al. [42] reported that 16 of 58 patients (16/58, 27.6%) with past history of HCC developed recurrence of HCC after DAA treatment during a median follow-up of 5.7 months. They concluded that HCC recurrence could occur with an unexpected high rate even after DAA therapy. Conti et al. [43] reported that occurrence and recurrence of HCC were not reduced in CHC despite DAA treatment. While both of these reports clearly suggest that DAAs cannot completely prevent HCC even after SVR, they did not include comparisons with a control group, such as interferon-treated patients. The present study also lacks a control group.

There are several previous reports involving comparisons of effects between DAAs and interferon on hepatic carcinogenesis. Among CHC patients with no past history of HCC, Kobayashi et al. [44] assessed HCC development in patients with SVR after DAA or interferon-based

regimens. To fairly compare the risk of HCC between the 2 groups, they performed a propensity score-matching analysis. They found no significant difference in the rates of HCC development between the 2 groups, and thus concluded that SVR by DAAs reduces the incidence of HCC in CHC patients to the same extent as SVR by interferon. Another report showed that the risks of early HCC occurrence and recurrence after SVR were similar between interferon-based and interferon-free therapies [45]. These reports clearly show that SVR by DAAs does not increase the risk of HCC.

Based on the above reports, the main factor that can account for the high rate of HCC occurrence in our study may be the high rate of past history of HCC (26/100, 26%). In the HCC group, the median Fib-4 index was 5.68 and most cases (14/17, 82%) had advanced fibrosis. Fibrosis is considered to result from long-term chronic inflammation, during which genetic and epigenetic alterations can accumulate in hepatocytes [34]. Actually, HCC developed in 5 patients among those with no past history of HCC (5/74, 6.8%). Preexisting hepatic fibrosis before DAA treatment may be a cause of HCC development in these cases. There is some consistency with a previous report indicating that Fib-4 index exceeding 3.25 was one of the risk factors for HCC development after SVR by DAAs [44].

AFP is not only a tumor marker of HCC, but also a marker of regeneration of hepatocytes [46]. Regeneration of hepatocytes is active in the liver of CHC patients, wherein AFP may exhibit high values. Either interferon or DAAs can terminate active regeneration of hepatocytes, meaning that AFP can become normalized after SVR. Asahina et al. [47] reported that higher post-interferon treatment AFP level was identified as an independent factor significantly associated with HCC development. In agreement with their observation for interferon, a decrease in AFP after DAA treatment was observed in the non-HCC group, while the decrease in AFP was not significant in the HCC group. An insignificant decrease in AFP after EOT would indicate residual HCC or hepatitis, such as non-alcoholic steatohepatitis. Careful attention should be paid to the detection of HCC after DAA treatment, especially when AFP is not decreased at EOT.

There are certain limitations to this study. First, it was a retrospective and non-controlled study. Second, only DCV and ASV were administered to the patients in this study. Currently, several sets of DAAs are available, and analyses of HCC after treatment with other kinds of DAAs are in progress. As the background of CHC pa-



tients treated with interferon is quite different from that of patients treated with DAAs, comparisons with interferon are being performed using propensity score-matching analyses.

In conclusion, HCC can develop even after SVR by DAAs, especially when patients have a past history of HCC. In this high-risk group, surveillance for HCC detection after achievement of SVR is required.

## Acknowledgments

The authors thank Alison Sherwin, PhD, from Edanz Group ([www.edanzediting.com/ac](http://www.edanzediting.com/ac)) for editing a draft of this manuscript.

## Disclosure Statement

The authors declare no conflicts of interest.

## References

- Parkin DM, Bray F, Ferlay J, Pisani P: Global cancer statistics, 2002. *CA Cancer J Clin* 2005; 55:74–108.
- Donato F, Tagger A, Chiesa R, Ribero ML, Tomasoni V, Fasola M, Gelatti U, Portera G, Boffetta P, Nardi G: Hepatitis B and C virus infection, alcohol drinking, and hepatocellular carcinoma: a case-control study in Italy. *Brescia HCC Study. Hepatology* 1997;26: 579–584.
- Kim SR, Kudo M, Hino O, Han KH, Chung YH, Lee HS; Organizing Committee of Japan-Korea Liver S: Epidemiology of hepatocellular carcinoma in Japan and Korea. A review. *Oncology* 2008;75(suppl 1):13–16.
- Ahmad W, Ijaz B, Javed FT, Gull S, Kausar H, Sarwar MT, Asad S, Shahid I, Sumrin A, Khaliq S, Jahan S, Pervaiz A, Hassan S: A comparison of four fibrosis indexes in chronic HCV: development of new fibrosis-cirrhosis index (FCI). *BMC Gastroenterol* 2011;11: 44.
- Chen SL, Morgan TR: The natural history of hepatitis C virus (HCV) infection. *Int J Med Sci* 2006;3:47–52.
- Kudo M: Surveillance, diagnosis, treatment, and outcome of liver cancer in Japan. *Liver Cancer* 2015;4:39–50.
- Kudo M: Clinical practice guidelines for hepatocellular carcinoma differ between Japan, United States, and Europe. *Liver Cancer* 2015; 4:85–95.
- Hsu C, Chen BB, Chen CH, Ho MC, Cheng JC, Kokudo N, Murakami T, Yeo W, Seong J, Jia JD, Han KH, Cheng AL: Consensus development from the 5th Asia-Pacific primary liver cancer expert meeting (APPLE 2014). *Liver Cancer* 2015;4:96–105.
- Ichikawa S, Ichikawa T, Motosugi U, Sano K, Morisaka H, Enomoto N, Matsuda M, Fujii H: Was hypervascular hepatocellular carcinoma visible on previous gadoxetic acid-enhanced magnetic resonance images? *Liver Cancer* 2015;4:154–162.
- Chen BB, Murakami T, Shih TT, Sakamoto M, Matsui O, Choi BI, Kim MJ, Lee JM, Yang RJ, Zeng MS, Chen RC, Liang JD: Novel imaging diagnosis for hepatocellular carcinoma: consensus from the 5th Asia-Pacific primary liver cancer expert meeting (APPLE 2014). *Liver Cancer* 2015;4:215–227.
- Kudo M: Breakthrough imaging in hepatocellular carcinoma. *Liver Cancer* 2016;5:47–54.
- Toyoda H, Kumada T, Tada T, Sone Y, Kaneoka Y, Maeda A: Tumor markers for hepatocellular carcinoma: simple and significant predictors of outcome in patients with HCC. *Liver Cancer* 2015;4:126–136.
- Kudo M: Risk of hepatocellular carcinoma in patients with hepatitis C virus who achieved sustained virological response. *Liver Cancer* 2016;5:155–161.
- Ho MC, Hasegawa K, Chen XP, Nagano H, Lee YJ, Chau GY, Zhou J, Wang CC, Choi YR, Poon RT, Kokudo N: Surgery for intermediate and advanced hepatocellular carcinoma: a consensus report from the 5th Asia-Pacific primary liver Cancer expert meeting (APPLE 2014). *Liver Cancer* 2016;5:245–256.
- Kudo M: Locoregional therapy for hepatocellular carcinoma. *Liver Cancer* 2015;4:163–164.
- Teng W, Liu KW, Lin CC, Jeng WJ, Chen WT, Sheen IS, Lin CY, Lin SM: Insufficient ablative margin determined by early computed tomography may predict the recurrence of hepatocellular carcinoma after radiofrequency ablation. *Liver Cancer* 2015;4:26–38.
- Kang TW, Rhim H: Recent advances in tumor ablation for hepatocellular carcinoma. *Liver Cancer* 2015;4:176–187.
- Lencioni R, de Baere T, Martin RC, Nutting CW, Narayanan G: Image-guided ablation of malignant liver tumors: recommendations for clinical validation of novel thermal and non-thermal technologies – a western perspective. *Liver Cancer* 2015;4:208–214.
- Lin CC, Cheng YT, Chen MW, Lin SM: The effectiveness of multiple electrode radiofrequency ablation in patients with hepatocellular carcinoma with lesions more than 3 cm in size and barcelona clinic liver cancer stage A to B2. *Liver Cancer* 2016;5:8–20.
- Tsurusaki M, Murakami T: Surgical and locoregional therapy of HCC: TACE. *Liver Cancer* 2015;4:165–175.
- Kitai S, Kudo M, Nishida N, Izumi N, Sakamoto M, Matsuyama Y, Ichida T, Nakashima O, Matsui O, Ku Y, Kokudo N, Makuuchi M; Liver Cancer Study Group of Japan: Survival benefit of locoregional treatment for hepatocellular carcinoma with advanced liver cirrhosis. *Liver Cancer* 2016;5:175–189.
- Kudo M, Izumi N, Sakamoto M, Matsuyama Y, Ichida T, Nakashima O, Matsui O, Ku Y, Kokudo N, Makuuchi M: Survival analysis over 28 years of 173,378 patients with hepatocellular carcinoma in Japan. *Liver Cancer* 2016;5:190–197.
- Obi S, Sato S, Kawai T: Current status of hepatic arterial infusion chemotherapy. *Liver Cancer* 2015;4:188–199.
- Lin CC, Hung CF, Chen WT, Lin SM: Hepatic arterial infusion chemotherapy for advanced hepatocellular carcinoma with portal vein thrombosis: impact of early response to 4 weeks of treatment. *Liver Cancer* 2015;4: 228–240.
- Kudo M: Molecular targeted therapy for hepatocellular carcinoma: where are we now? *Liver Cancer* 2015;4:I–VII.
- Kudo M: Regorafenib as second-line systemic therapy may change the treatment strategy and management paradigm for hepatocellular carcinoma. *Liver Cancer* 2016;5:235–244.
- Kudo M: Immune checkpoint blockade in hepatocellular carcinoma. *Liver Cancer* 2015;4: 201–207.
- Douglas DD, Rakela J, Lin HJ, Hollinger FB, Taswell HF, Czaja AJ, Gross JB, Anderson ML, Parent K, Fleming CR, et al: Randomized controlled trial of recombinant alpha-2a-interferon for chronic hepatitis C. Comparison of alanine aminotransferase normalization versus loss of HCV RNA and anti-HCV IgM. *Dig Dis Sci* 1993;38:601–607.
- Sjogren MH, Sjogren R Jr, Lyons MF, Ryan M, Santoro J, Smith C, Reddy KR, Bonkovsky H, Huntley B, Faris-Young S: Antiviral response of HCV genotype 1 to consensus interferon and ribavirin versus pegylated interferon and ribavirin. *Dig Dis Sci* 2007;52: 1540–1547.
- van der Meer AJ, Veldt BJ, Feld JJ, Wedemeyer H, Dufour JF, Lammert F, Duarte-Rojo A, Heathcote EJ, Manns MP, Kuske L, Zeuzem S, Hofmann WP, de Knecht RJ, Hansen BE, Janssen HL: Association between sustained virological response and all-cause mortality among patients with chronic hepatitis C and advanced hepatic fibrosis. *JAMA* 2012;308: 2584–2593.

- 31 Mulhall BP, Younossi Z: Impact of adherence on the outcome of antiviral therapy for chronic hepatitis C. *J Clin Gastroenterol* 2005; 39:S23–S27.
- 32 Kumada H, Suzuki Y, Ikeda K, Toyota J, Karino Y, Chayama K, Kawakami Y, Ido A, Yamamoto K, Takaguchi K, Izumi N, Koike K, Takehara T, Kawada N, Sata M, Miyagoshi H, Eley T, McPhee F, Damokosh A, Ishikawa H, Hughes E: Daclatasvir plus asunaprevir for chronic HCV genotype 1b infection. *Hepatology* 2014;59:2083–2091.
- 33 Mizokami M, Yokosuka O, Takehara T, Sakamoto N, Korenaga M, Mochizuki H, Nakane K, Enomoto H, Ikeda F, Yanase M, Toyoda H, Genda T, Umemura T, Yatsushashi H, Ide T, Toda N, Nirei K, Ueno Y, Nishigaki Y, Betular J, Gao B, Ishizaki A, Omote M, Mo H, Garri-son K, Pang PS, Knox SJ, Symonds WT, McHutchison JG, Izumi N, Omata M: Ledipasvir and sofosbuvir fixed-dose combination with and without ribavirin for 12 weeks in treatment-naïve and previously treated Japanese patients with genotype 1 hepatitis C: an open-label, randomised, phase 3 trial. *Lancet Infect Dis* 2015;15:645–653.
- 34 Nishida N, Goel A: Genetic and epigenetic signatures in human hepatocellular carcinoma: a systematic review. *Curr Genomics* 2011; 12:130–137.
- 35 Ciesek S, Manns MP: Hepatitis in 2010: the dawn of a new era in HCV therapy. *Nat Rev Gastroenterol Hepatol* 2011;8:69–71.
- 36 Furusyo N, Ogawa E, Nakamuta M, Kajiwarra E, Nomura H, Dohmen K, Takahashi K, Satoh T, Azuma K, Kawano A, Tanabe Y, Kotoh K, Shimoda S, Hayashi J; Kyushu University Liver Disease Study (KULDS) Group: Telaprevir can be successfully and safely used to treat older patients with genotype 1b chronic hepatitis C. *J Hepatol* 2013;59:205–212.
- 37 Izumi N, Hayashi N, Kumada H, Okanoue T, Tsubouchi H, Yatsushashi H, Kato M, Ki R, Komada Y, Seto C, Goto S: Once-daily simeprevir with peginterferon and ribavirin for treatment-experienced HCV genotype 1-infected patients in Japan: the CONCERTO-2 and CONCERTO-3 studies. *J Gastroenterol* 2014; 49:941–953.
- 38 Slim J, Afridi MS: Managing adverse effects of interferon-alfa and ribavirin in combination therapy for HCV. *Infect Dis Clin North Am* 2012;26:917–929.
- 39 Chayama K, Takahashi S, Toyota J, Karino Y, Ikeda K, Ishikawa H, Watanabe H, McPhee F, Hughes E, Kumada H: Dual therapy with the nonstructural protein 5A inhibitor, daclatasvir, and the nonstructural protein 3 protease inhibitor, asunaprevir, in hepatitis C virus genotype 1b-infected null responders. *Hepatology* 2012;55:742–748.
- 40 McPhee F, Suzuki Y, Toyota J, Karino Y, Chayama K, Kawakami Y, Yu ML, Ahn SH, Ishikawa H, Bhore R, Zhou N, Hernandez D, Mendez P, Kumada H: High sustained virologic response to daclatasvir plus asunaprevir in elderly and cirrhotic patients with hepatitis C virus genotype 1b without baseline NS5A polymorphisms. *Adv Ther* 2015;32:637–649.
- 41 Serti E, Chepa-Lotrea X, Kim YJ, Keane M, Fryzek N, Liang TJ, Ghany M, Rehermann B: Successful interferon-free therapy of chronic hepatitis C virus infection normalizes natural killer cell function. *Gastroenterology* 2015; 149:190–200.e2.
- 42 Reig M, Marino Z, Perello C, Inarrairaegui M, Ribeiro A, Lens S, Diaz A, Vilana R, Darnell A, Varela M, Sangro B, Calleja JL, Fornis X, Bruix J: Unexpected high rate of early tumor recurrence in patients with HCV-related HCC undergoing interferon-free therapy. *J Hepatol* 2016;65:719–726.
- 43 Conti F, Buonfiglioli F, Scuteri A, Crespi C, Bolondi L, Caraceni P, Foschi FG, Lenzi M, Mazzella G, Verucchi G, Andreone P, Bril-lanti S: Early occurrence and recurrence of he-patocellular carcinoma in HCV-related cir-rhosis treated with direct-acting antivirals. *J Hepatol* 2016;65:727–733.
- 44 Kobayashi M, Suzuki F, Fujiyama S, Kawamu-ra Y, Sezaki H, Hosaka N, Suzuki Y, Saitoh S, Arase Y, Ikeda K, Kumada H: Sus-tained virologic response by direct antiviral agents reduces the incidence of hepatocellular carcinoma in patients with HCV infection. *J Med Virol* 2017;89:476–483.
- 45 Nagata H, Nakagawa M, Asahina Y, Sato A, Asano Y, Tsunoda T, Miyoshi M, Kaneko S, Otani S, Kawai-Kitahata F, Murakawa M, Nit-ta S, Itsui Y, Azuma S, Kakinuma S, Nouchi T, Sakai H, Tomita M, Watanabe M, Ochanomizu Liver Conference Study G: Effect of in-terferon-based and -free therapy on early oc-currence and recurrence of hepatocellular carcinoma in chronic hepatitis C. *J Hepatol* 2017, pii: S0168-8278(17)32070-6.
- 46 Chen MF, Liaw YF, Chen MF: Alpha fetopro-tein and hepatic regeneration. *Gastroenterol-ogy* 1979;76:660.
- 47 Asahina Y, Tsuchiya K, Nishimura T, Mura-oka M, Suzuki Y, Tamaki N, Yasui Y, Hosoka-wa T, Ueda K, Nakanishi H, Itakura J, Taka-hashii Y, Kurosaki M, Enomoto N, Nakagawa M, Kakinuma S, Watanabe M, Izumi N:  $\alpha$ -fetoprotein levels after interferon therapy and risk of hepatocarcinogenesis in chronic hepatitis C. *Hepatology* 2013;58:1253–1262.

# Non-Hypervascular Hypointense Hepatic Nodules during the Hepatobiliary Phase of Gadolinium-Ethoxybenzyl-Diethylenetriamine Pentaacetic Acid-Enhanced MRI as a Risk Factor of Intrahepatic Distant Recurrence after Radiofrequency Ablation of Hepatocellular Carcinoma

Takayuki Iwamoto<sup>a</sup> Yasuharu Imai<sup>a</sup> Takumi Igura<sup>a</sup> Sachiyo Kogita<sup>a</sup>  
Yoshiyuki Sawai<sup>a</sup> Kazuto Fukuda<sup>a</sup> Yoshitaka Yamaguchi<sup>a</sup> Yasushi Matsumoto<sup>a</sup>  
Masanori Nakahara<sup>a</sup> Osakuni Morimoto<sup>b</sup> Hiroshi Ohashi<sup>c</sup> Norihiko Fujita<sup>d</sup>  
Masatoshi Kudo<sup>e</sup> Tetsuo Takehara<sup>f</sup>

<sup>a</sup>Department of Gastroenterology, <sup>b</sup>Department of Gastroenterological Surgery, <sup>c</sup>Department of Pathology, and <sup>d</sup>Department of Radiology, Ikeda Municipal Hospital, Ikeda, <sup>e</sup>Department of Gastroenterology and Hepatology, Kindai University Faculty of Medicine, Osaka-Sayama, and <sup>f</sup>Department of Gastroenterology and Hepatology, Osaka University Graduate School of Medicine, Suita, Japan

## Keywords

Hepatocellular carcinoma · Non-hypervascular hypointense hepatic nodules · Radiofrequency ablation · Gadolinium-ethoxybenzyl-diethylenetriamine pentaacetic acid-enhanced MRI · Recurrence

## Abstract

**Background:** Non-hypervascular hypointense hepatic nodules during the hepatobiliary phase of gadolinium-ethoxybenzyl-diethylenetriamine pentaacetic acid (Gd-EOB-DTPA)-enhanced MRI have been reported to be associated with intrahepatic distant recurrence (IDR) after hepatectomy or radiofrequency ablation (RFA) for hepatocellular carcinoma (HCC). IDR is categorized into hypervascular transformation

of non-hypervascular hypointense hepatic nodules and new intrahepatic recurrence. The aim of this study was to evaluate the relationship between non-hypervascular hypointense hepatic nodules on Gd-EOB-DTPA-enhanced MRI and IDR after RFA, focusing on new intrahepatic recurrence. **Methods:** Ninety-one consecutive patients with 115 HCCs undergoing pretreatment Gd-EOB-DTPA-enhanced MRI and RFA for treatment of HCC were enrolled. **Results:** Of the 91 patients who underwent RFA for HCC, 24 had non-hypervascular hypointense hepatic nodules on pretreatment Gd-EOB-DTPA-enhanced MRI. Recurrences were observed in 15 and 19 patients with and without non-hypervascular hypointense hepatic nodules, respectively. Of the 15 recurrences in patients with non-hypervascular hypointense hepatic nodules, 10 patients had new intrahepatic recurrences.

The cumulative incidence of new intrahepatic recurrence was significantly higher in patients with non-hypervascular hypointense hepatic nodules than in those without non-hypervascular hypointense hepatic nodules ( $p < 0.0001$ ). Multivariate analysis revealed that the presence of non-hypervascular hypointense hepatic nodules and Child-Pugh score were independent risk factors for new intrahepatic recurrence. **Conclusions:** Non-hypervascular hypointense hepatic nodules during the hepatobiliary phase of Gd-EOB-DTPA-enhanced MRI were a useful predictive factor for IDR, particularly for new intrahepatic recurrence, after RFA.

© 2017 S. Karger AG, Basel

## Introduction

Hepatocellular carcinoma (HCC) is one of the most common cancers worldwide [1–3]. In the United States, HCC incidence rates are increasing. This increase is probably caused by an increase in the number of patients with chronic hepatitis C virus (HCV) infection due to injection drug abuse, or an increase in the number of patients with obesity and diabetes mellitus [4, 5]. In Japan, HCC is still ranked as the most common cause of death from malignant neoplasms, though HCC rates are decreasing due to a reduction in patients with HCV infection [1, 6]. The advent of direct-acting antivirals has provided high sustained viral response rates in patients with HCV infection. However, the achievement of a sustained viral response does not eliminate the risk of HCC completely, particularly in patients with liver cirrhosis complications [7]. The detection of HCC in the early stage is important for prognosis and for selecting appropriate therapeutic methods.

The diagnostic performance of various imaging modalities for HCC, such as ultrasound [8–10], multidetector-row CT (MDCT) [11, 12], angiography-assisted CT [13], and MRI [14] has improved notably, and small HCC less than 2 cm in diameter can be detected. The diagnostic performance of CT during hepatic arteriography and CT during arteriography for small hypervascular HCC have been reported to be the most sensitive [15–17]. However, because CT during hepatic arteriography and CT during arteriography are invasive, dynamic CT and MRI are recommended for regular screening of HCC in Japan [18]. Because gadolinium-ethoxybenzyl-diethylenetriamine pentaacetic acid (Gd-EOB-DTPA) is selectively taken up by hepatocytes and excreted into bile ducts, information about hepatocyte function can be obtained [19]. The diagnostic performance was improved

with Gd-EOB-DTPA enhanced MRI when the hepatobiliary phase was added to dynamic studies for evaluation [20–25]. The detection of non-hypervascular hypointense hepatic nodules was increased by Gd-EOB-DTPA enhanced MRI. Recently, non-hypervascular hypointense hepatic nodules during the hepatobiliary phase in HCC patients have been reported to be a significant risk factor for the recurrence after HCC treatment [26–28]. In these reports, intrahepatic recurrence includes hypervascular transformation of non-hypervascular hypointense hepatic nodules during the hepatobiliary phase of pretreatment Gd-EOB-DTPA-enhanced MRI [25]. In patients with non-hypervascular hypointense hepatic nodules, there are a few reports about the evaluation of intrahepatic distant recurrence (IDR) rates except hypervascular transformation of non-hypervascular hypointense hepatic nodules during the hepatobiliary phase of pretreatment Gd-EOB-DTPA-enhanced MRI.

The purpose of the present study was to evaluate the relationship between non-hypervascular hypointense hepatic nodules on Gd-EOB-DTPA-enhanced MRI and IDR after radiofrequency ablation (RFA) [29], focusing on new intrahepatic recurrence.

## Methods

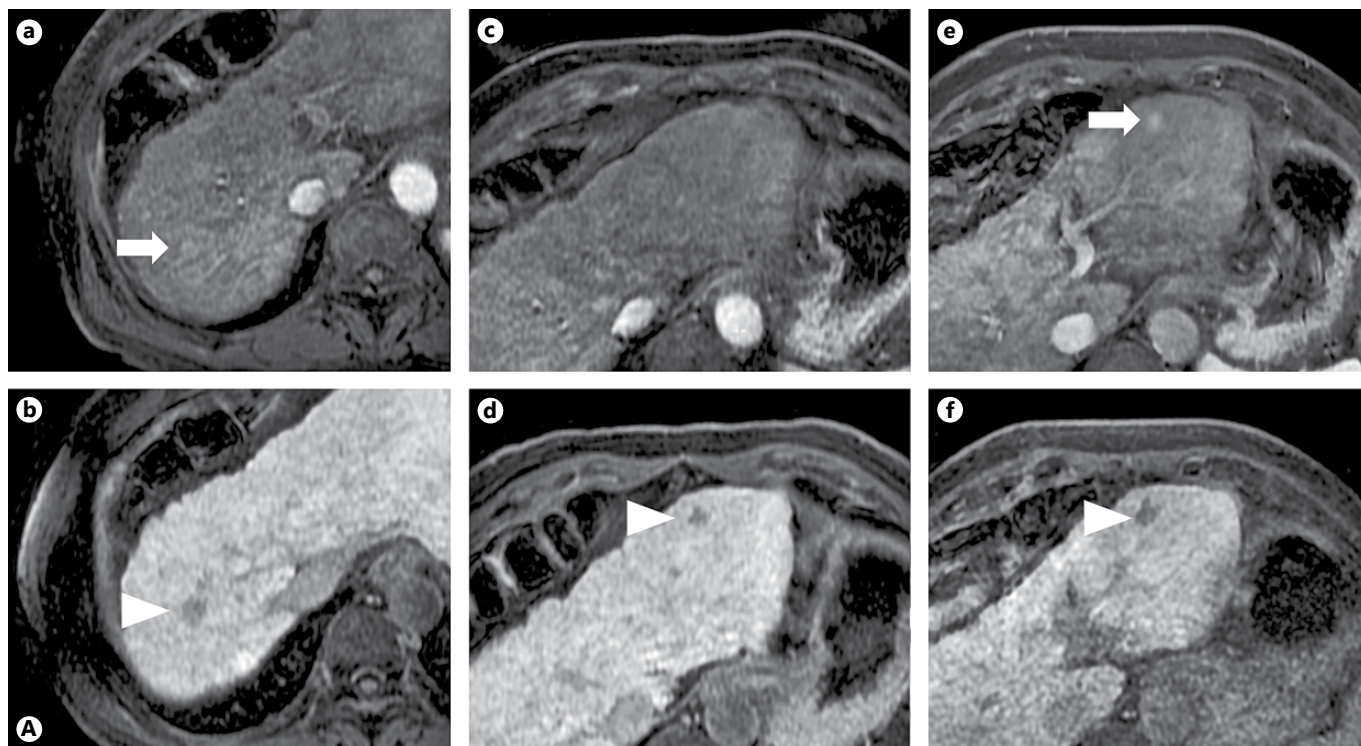
### Patients

This retrospective study was approved by Institutional Review Board of Ikeda Municipal Hospital, and the requirement for informed consent was waived. This study was conducted in compliance with the Declaration of Helsinki. At our institution between March 2008 and January 2015, 91 consecutive patients with 115 HCC underwent RFA. The inclusion criteria of this study were as follows: (1) patients who had HCC diagnosed based on the typical vascular pattern of HCC defined by the American Association for the Study of Liver Disease [30]; (2) patients who underwent Gd-EOB-DTPA-enhanced MRI within 2 months of RFA between March 2008 and January 2015; and (3) patients who did not undergo pretreatment including hepatectomy, RFA, or percutaneous ethanol injection. We enrolled patients who underwent transcatheter arterial chemoembolization (TACE) prior to RFA when the treatments were sequentially performed.

### Diagnosis of HCC Recurrence

The diagnosis of HCC recurrence was made using the typical vascular pattern of HCC defined by the American Association for the Study of Liver Disease. The typical vascular pattern is defined as hypervascularity in the arterial phase, and washout in portal venous and equilibrium phase. In Gd-EOB-DTPA-enhanced MRI, the diagnosis of HCC was also made when the lesion showed arterial hypervascularity and hypointensity in the hepatobiliary phase or arterial hypervascularity, portal venous phase washout, and hypointensity in hepatobiliary phase. However, some of the non-hypervascular nodules that emerged during the follow-up period





**Fig. 1.** A 66-year-old woman with hepatitis C of a hypervascular transformation of non-hypervascular hypointense hepatic nodules during the hepatobiliary phase of gadolinium-ethoxybenzyl-diethylenetriamine pentaacetic acid (Gd-EOB-DTPA)-enhanced MRI. **a** In the arterial phase, Gd-EOB-DTPA-enhanced MRI shows a slightly hypervascular nodule in segment 8 (arrow), **(b)** with hypointensity during the hepatobiliary phase of Gd-EOB-DTPA-enhanced MRI (arrow head). **c** Gd-EOB-DTPA-enhanced

MRI does not show a hypervascular focal lesion, **(d)** whereas the hepatobiliary phase of Gd-EOB-DTPA-enhanced MRI shows a hypointense nodule in segment 3 (arrow head). **e** After 7 months of RFA for HCC in segment 8, a non-hypervascular hypointense nodule in segment 3 became a hypervascular nodule (arrow), **(f)** with growing hypointense nodules during the hepatobiliary phase image of Gd-EOB-DTPA-enhanced MRI (arrow head).

were diagnosed by liver biopsy. Histological diagnosis of HCC was made according to the histological criteria of the International Consensus Group for Hepatocellular Carcinoma by one pathologist with more than 10 years of experience.

Recurrence was categorized into local tumor progression (LTP), IDR, and extra-hepatic metastases (EM). LTP was defined as the development of a new hypervascular tumor adjacent to the ablation zone. IDR was defined as a new nodular HCC, which developed at a location away from the ablation zone. Moreover, the type of IDR in this study was categorized as follows: (1) recurrence of hypervascular transformation of non-hypervascular hypointense hepatic nodules (Fig. 1A) and (2) new intrahepatic recurrence (Fig. 1B). Patients with LTP and EM recurrence after RFA were excluded for further analyses.

#### *Assessment of Non-Hypervascular Hypointense Hepatic Nodules*

Non-hypervascular hypointense hepatic nodules were defined as follows; (1) low intensity signal nodules during the hepatobiliary phase of Gd-EOB-DTPA-enhanced MRI and (2) nodule diameter greater than 3.5 mm. Hypervascular nodules on dynamic CT or Gd-EOB-DTPA-enhanced MRI and high intensity signal nodules

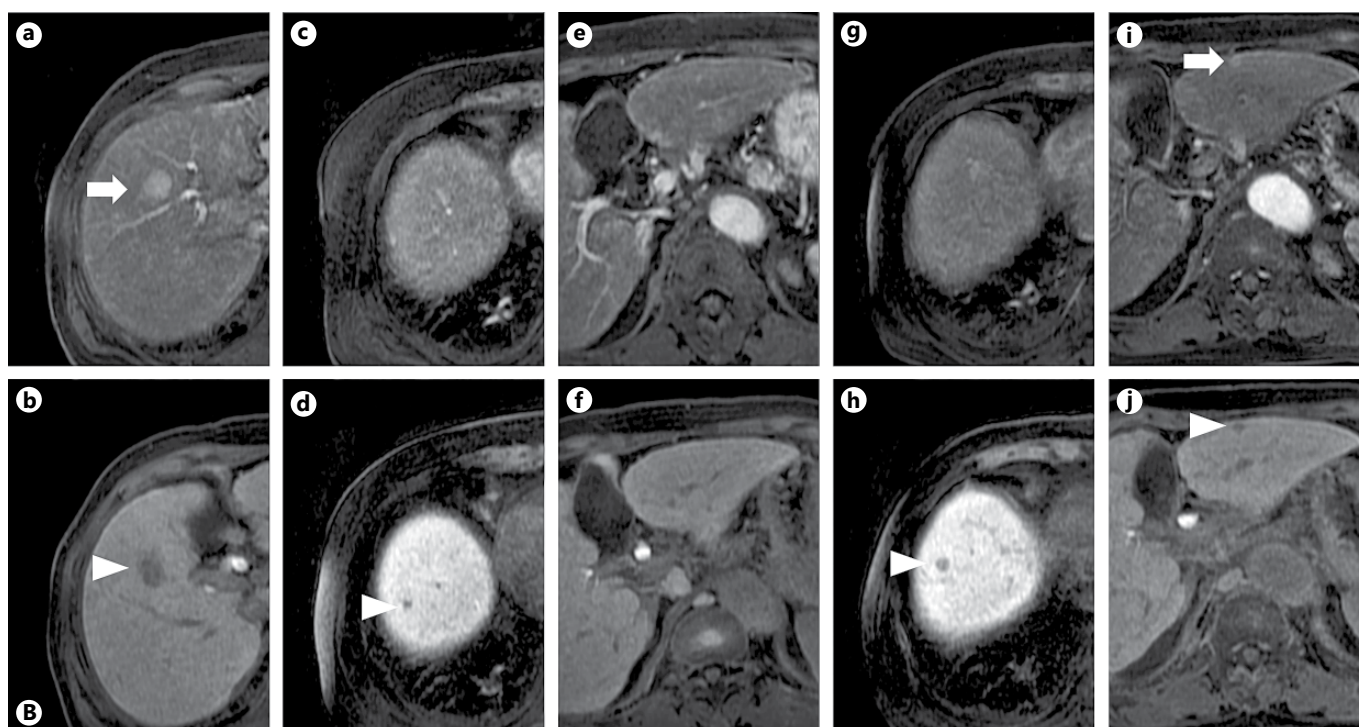
on heavily T2-weighted images on Gd-EOB-DTPA-enhanced MRI were excluded.

#### *Treatment and Follow-Up*

One of the three hepatologists with more than 10 years of experience performed RFA percutaneously under real-time ultrasound guidance using a 17-gauge single electrode with a 2- or 3-cm exposed tip (Cool-tip; RF Ablation System, Covidien, Boulder, Colombia, CO). We used artificial pleural effusion or ascites when it was difficult to detect the guideline of the electrode for RFA because nodules were located on the liver surface, in the hepatic dome, or adjacent to the gastrointestinal tract or gallbladder. One to two sessions of RFA were performed to achieve complete necrosis of the tumor.

After RFA, dynamic CT and Gd-EOB-DTPA-MRI were performed no later than 7 days and 1 month to evaluate for complications and treatment efficacy. Treatment efficacy was evaluated by side-by-side comparison between pretreatment CT/MRI and post-treatment CT/MRI with the consensus between an abdominal radiologist and the RFA operator, both with more than 10 years of experience. If a viable tumor was observed on posttreatment imaging modalities, additional treatment was performed. Dynamic CT





**Fig. 1.** **B** A 78-year-old woman with hepatitis C recurrence of a new intrahepatic lesion. **a** In the arterial phase, Gd-EOB-DTPA-enhanced MRI shows a hypervascular nodule of segment 5 (arrow), **(b)** with hypointensity during the hepatobiliary phase of Gd-EOB-DTPA-enhanced MRI (arrow head). **c** Gd-EOB-DTPA-enhanced MRI does not show a hypervascular focal lesion in segment 8, **(d)** whereas the hepatobiliary phase image shows a hypointense nodule (arrow head). **e, f** In segment 3, Gd-EOB-DTPA-enhanced

MRI does not show any focal lesion in the arterial or hepatobiliary phase. **g, h** After 1 year 6 months of RFA of HCC in segment S5, the non-hypervascular hypointense hepatic nodule during the hepatobiliary phase of Gd-EOB-DTPA-enhanced MRI in segment 8 increased slightly in size (arrow). **i** A new hypervascular nodule emerged in segment 3 (arrow), **(j)** with hypointensity during the hepatobiliary phase of Gd-EOB-DTPA-enhanced MRI (arrow head).

or Gd-EOB-DTPA-MRI was performed every 3 months after complete treatment until January 2015. The blood test and monitoring of tumor markers were also performed every 3 months.

#### Dynamic MDCT and MR Examinations

Dynamic MDCT was performed by 64-channel MDCT scanners (Discovery CT 750HD; GE Healthcare, Milwaukee, WI, USA). The slice thickness was 5 mm. All patients were given 600 mg of iodine per kilogram of body weight with 300 or 370 mg/mL of nonionic contrast medium and a maximum dose of 150 mL per patient. The warmed contrast medium was administered intravenously with a mechanical power injector at 2.5–5 mL/s with a fixed injection duration of 30 s through a 20-gauge catheter inserted into an arm vein. Dynamic triple-phase CT was performed immediately before contrast medium administration and during the hepatic arterial-dominant, portal venous-dominant, and equilibrium phases 30–45, 65–80, and 180–205 s, respectively, after initiating the contrast material injection [31, 32].

Gd-EOB-DTPA-enhanced MRI was performed using a 1.5 T MR scanner (Signa EXCITE HD version 12; GE Healthcare) [32, 33]. Unenhanced, arterial, portal, late, and hepatobiliary phase images were obtained just before and 25, 70, 180 s, and 20 min, respectively, after bolus injection of 25  $\mu$ mol/kg body weight (0.1

mL/kg) Gd-EOB-DTPA (Primovist; Bayer-Schering Pharma, Osaka Japan) at a rate of 2.0 mL/s, using T1-weighted 3-dimensional gradient-echo sequences in a single breath hold (18–20 s). Liver acquisition with volume acceleration with fat saturation was used as a sequence, and the MR parameters were TR, 4.5 ms; TE, 2.2 ms; flip angle, 12°; SENSE factor, 2; slice thickness, 5 mm; slice interval, 2.5 mm; matrix, 192  $\times$  320; and field of view, 360 mm.

#### Statistical Analysis

Recurrence curves were estimated using the Kaplan-Meier method. The univariate and multivariate Cox proportional hazards models were used for the analysis of risk factors related to recurrence, independently [34]. Various factors were analyzed as follows: age, sex, etiology (e.g., HBV and HCV), Child-Pugh score, albumin, total bilirubin, prothrombin, platelet count, tumor size, number of tumors, alpha-fetoprotein, protein induced by vitamin K absence or antagonist-2, presence of diabetes mellitus, history of TACE, fibrosis-4 index. Factors showing statistical significance in the univariate analysis were subsequently analyzed using the multivariate Cox proportional hazard regression model with stepwise selection.

All statistical analyses were performed with EZR (Saitama Medical Center, Jichi Medical University, Saitama, Japan), which

is a graphical user interface for R (The R Foundation for Statistical Computing, Vienna, Austria). More precisely, it is a modified version of R commander designed to add statistical functions frequently used in biostatistics [35]. All *p* values were derived from 2-tailed tests, with *p* < 0.05 considered statistically significant.

## Results

### *Patient Characteristics and Evaluation of Non-Hypervascular Hypointense Hepatic Nodules*

The characteristics of the 91 patients studied are presented in Table 1. There were 50 men and 41 women with a mean age of 72.9 years. The mean tumor size was 16.0 ± 6.5 mm (mean ± SD; range 5–39 mm). Fifty-seven (62.6%) of the 91 patients received TACE before RFA.

Of the 91 patients with a median follow-up of 39.5 ± 21.9 months (mean ± SD; range 2–87) after RFA, non-hypervascular hypointense hepatic nodules were observed in 24 (26.4%) patients on pretreatment Gd-EOB-DTPA-enhanced MRI. We categorized patients into 2 groups, with and without non-hypervascular hypointense hepatic nodules.

### *Cumulative Incidence of Recurrence*

HCC recurrence was observed in 34 patients after RFA. Overall cumulative incidence of recurrence at 1, 3, and 5 years were 13.5, 41.4, and 47.2%, respectively.

HCC recurrence was observed in 15 (62.5%) patients with non-hypervascular hypointense hepatic nodules, and 19 (28.4%) patients without non-hypervascular hypointense hepatic nodules. Of the 15 recurrences in patients with non-hypervascular hypointense hepatic nodules, 10 were new intrahepatic recurrences. The cumulative incidence of IDR of HCC was significantly higher in patients with non-hypervascular hypointense hepatic nodules than in patients without non-hypervascular hypointense hepatic nodules (*p* < 0.0001, Fig. 2A; cumulative recurrence rates at 1, 3, and 5 years; 33.3, 69.9, and 69.9% in patients with non-hypervascular hypointense hepatic nodules; 6.1, 30.6, and 37.8% in patients without non-hypervascular hypointense hepatic nodules, respectively). In univariate analysis, tumor number, Child-Pugh score, and the presence of non-hypervascular hypointense nodules were extracted as factors for recurrence with a *p* value of less than 0.20. Multivariate analysis revealed that independent risk factors for recurrence were Child-Pugh score and the presence of non-hypervascular hypointense nodules (Table 2).

**Table 1.** Baseline characteristics of 91 patients

Age, years, mean ± SD (range)	72.9±8.7 (49–89)
Gender, male/female	50/41
Etiology (HBV-related/HCV-related/ alcoholic/other)	9/59/7/16
Child-Pugh classification (A/B)	79/12
Albumin, g/dL, mean ± SD	3.69±0.43
Total bilirubin, mg/dL, mean ± SD	0.99±0.53
Prothrombin, %	82.1±10.5
Platelet count, ×10 <sup>4</sup> /mL	10.9±4.14
Tumor size, mm, mean ± SD (range)	16.0±6.5 (5.0–39.0)
Number of tumors (single/multiple)	70/21
AFP, ng/dL, mean ± SD (range)	31.6±68.7 (1.53–491.0)
PIVKA II, mAU/mL, mean ± SD (range)	145.9±623.6 (10.0–5,240.0)
Diabetes mellitus (absent/present)	60 (65.9)/31 (34.1)
TACE (absent/present)	57 (62.6)/34 (37.4)
Fib-4 index	6.54±3.77 (1.24–21.2)

HBV, hepatitis B virus; HCV, hepatitis C virus; AFP, alpha-fetoprotein; PIVKA II, protein induced by vitamin K absence or antagonists II; TACE, transcatheter arterial chemoembolization; Fib-4, fibrosis-4 index.

New intrahepatic recurrence was observed in 29 patients, of which 3 were diagnosed with HCC recurrence histologically. Twenty-nine recurrences of a new intrahepatic lesion were observed in 10 and 19 patients with and without non-hypervascular hypointense hepatic nodules, respectively. The cumulative incidence of new intrahepatic recurrence was also significantly higher in patients with non-hypervascular hypointense hepatic nodules than in patients without non-hypervascular hypointense hepatic nodules (*p* = 0.02, Fig. 2B; cumulative recurrence rates at 1, 3, and 5 years; 25.9, 50.9, and 50.9% in patients with non-hypervascular hypointense hepatic nodules; 6.1, 30.6, and 37.8% in patients without non-hypervascular hypointense hepatic nodules, respectively). In univariate analysis, tumor number, Child-Pugh score, and the presence of non-hypervascular hypointense hepatic nodules were extracted as factors for recurrence with a *p* value of less than 0.20. Multivariate analysis revealed that independent risk factors for new intrahepatic recurrence were Child-Pugh score and the presence of non-hypervascular hypointense hepatic nodules (Table 3).

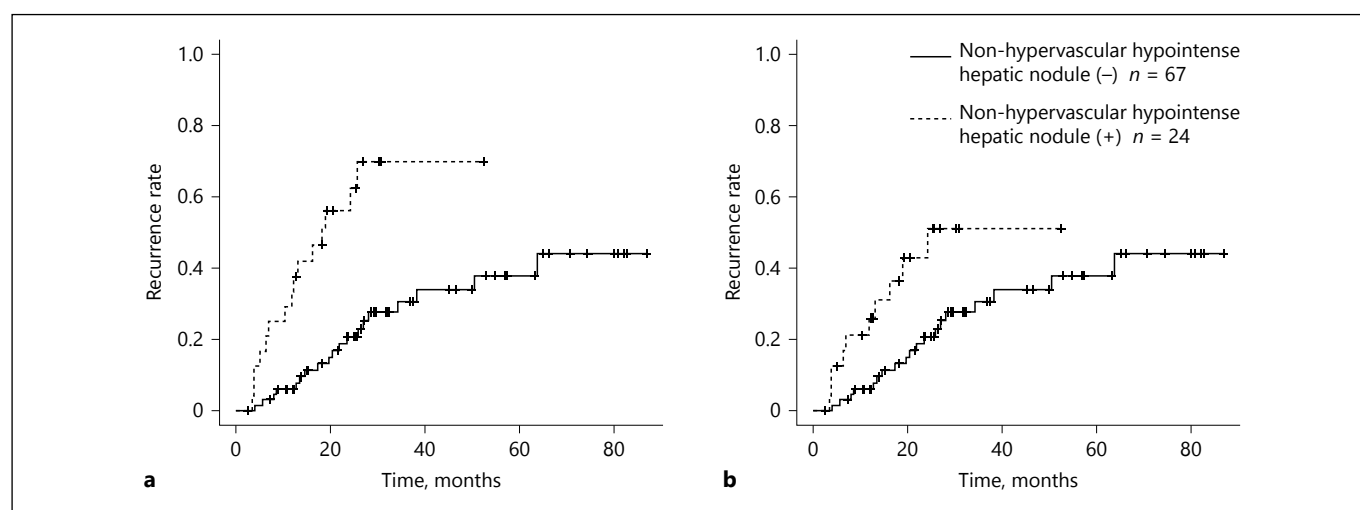
## Discussion

Various factors related to recurrence after RFA for HCC have been reported, such as tumor diameter, tumor number, serum alpha-fetoprotein levels, serum protein induced by vitamin K absence or antagonist-2 levels, an-

**Table 2.** Univariate and multivariate analyses of factors associated with intrahepatic distant recurrence after radiofrequency ablation

Factor	Univariate analysis		Multivariate analysis	
	risk ratio (95% CI)	<i>p</i> value	risk ratio (95% CI)	<i>p</i> value
Age, years	0.99 (0.96–1.04)	0.81		
Gender, male	1.30 (0.65–2.60)	0.46		
Etiology (HCV or others)	0.93 (0.46–1.89)	0.85		
Child-Pugh score (B)	2.45 (1.06–5.65)	0.04	2.87 (1.23–6.69)	0.01
Platelet count, $\times 10^4/\text{mL}$	0.99 (0.91–1.08)	0.83		
Tumor size	1.02 (0.97–1.07)	0.43		
Number of tumors (multiple)	1.84 (0.87–3.85)	0.11		
AFP	1.00 (0.99–1.01)	0.21		
PIVKA II	1.00 (0.99–1.00)	0.91		
Diabetes mellitus (present)	1.28 (0.65–2.55)	0.47		
TACE (present)	1.17 (0.59–2.32)	0.65		
Fib-4 index	1.03 (0.94–1.12)	0.53		
Non-hypervascular hypointense hepatic nodule (present)	4.03 (1.99–8.18)	<0.01	4.37 (2.13–8.86)	<0.01

HCV, hepatitis C virus; AFP, alpha-fetoprotein; PIVKA II, protein induced by vitamin K absence or antagonists II; TACE, transcatheter arterial chemoembolization; Fib-4, fibrosis-4 index.



**Fig. 2.** Cumulative incidence of intrahepatic distant recurrence of HCC after RFA in patients with and without non-hypervascular hypointense hepatic nodules during the hepatobiliary phase image of Gd-EOB-DTPA-enhanced MRI. **a** Comparison of cumulative incidence of total intrahepatic distant HCC recurrence after RFA in patients with and without non-hypervascular hypointense hepatic nodules during the hepatobiliary phase of Gd-EOB-DTPA-enhanced MRI. The cumulative incidence of recurrence was significantly higher in patients with non-hypervascular hypointense

hepatic nodules than in those without non-hypervascular hypointense hepatic nodules ( $p < 0.0001$ ). **b** Comparison of cumulative incidence of new intrahepatic recurrence after RFA in patients with and without non-hypervascular hypointense hepatic nodules. The cumulative incidence of new intrahepatic recurrence was significantly higher in patients with non-hypervascular hypointense hepatic nodules than in those without non-hypervascular hypointense hepatic nodules ( $p = 0.02$ ).

ti-HCV, Child-Pugh score, and platelet count [36–40]. However, due to the variety of recurrence forms such as LTP, IDR, and EM, the evaluation for risk factors related to HCC recurrence after treatment is complicated. Previous studies have reported that most recurrences after

RFA were not LTP but distant recurrence [36, 41]. The frequency of IDR in this study was similar to that of previous studies [36, 37, 41]. Toyoda et al. [26, 28] reported that the presence of non-hypervascular hypointense hepatic nodules detected during the hepatobiliary phase of

**Table 3.** Univariate and multivariate analyses of factors associated with new intrahepatic recurrence after radiofrequency ablation

Factor	Univariate analysis		Multivariate analysis	
	risk ratio (95% CI)	<i>p</i> value	risk ratio (95% CI)	<i>p</i> value
Age, years	0.99 (0.95–1.03)	0.63		
Gender, male	1.53 (0.71–3.30)	0.28		
Etiology (HCV or others)	0.84 (0.39–1.77)	0.64		
Child-Pugh score (B)	3.02 (1.28–7.12)	0.01	3.36 (1.41–7.99)	<0.01
Platelet count, $\times 10^4/\text{mL}$	0.99 (0.91–1.09)	0.91		
Tumor size	1.02 (0.97–1.07)	0.52		
Number of tumors (multiple)	2.00 (0.91–4.42)	0.09		
AFP	1.00 (0.99–1.01)	0.74		
PIVKA II	1.00 (0.99–1.00)	0.95		
Diabetes mellitus (present)	1.30 (0.62–2.72)	0.49		
TACE (present)	1.35 (0.65–2.81)	0.42		
Fib-4 index	1.03 (0.94–1.13)	0.48		
Non-hypervascular hypointense hepatic nodule (present)	2.71 (1.22–6.00)	0.02	2.97 (1.41–6.67)	<0.01

HCV, hepatitis C virus; AFP, alpha-fetoprotein; PIVKA II, protein induced by vitamin K absence or antagonists II; TACE, transcatheter arterial chemoembolization; Fib-4, fibrosis-4 index.

Gd-EOB-DTPA-enhanced MRI is a risk factor for HCC recurrence after treatment, especially multicentric recurrence. In addition, they found that the majority of multicentric recurrence involved the hypervascular transformation of non-hypervascular hypointense hepatic nodules preoperatively with Gd-EOB-DTPA-enhanced MRI. However, a higher recurrence rate was observed in patients with non-hypervascular hypointense hepatic nodules even when the nodules themselves did not progress to HCC in their recent study [28]. In their study, they reported that the presence of non-hypervascular hypointense hepatic nodules detected during the hepatobiliary phase of Gd-EOB-DTPA-enhanced MRI is a risk factor for HCC recurrence after treatment. Lee et al. [27] classified the HCC recurrence after RFA into 3 groups (LTP, IDR, and EM), and they found a significantly higher cumulative incidence of IDR in patients with non-hypervascular hypointense hepatic nodules after RFA for early stage HCCs.

Our study confirmed that HCC recurrence after RFA was significantly higher in patients with non-hypervascular hypointense hepatic nodules than in those without non-hypervascular hypointense hepatic nodules, which was consistent with previous reports [26, 27]. The independent risk factors for HCC recurrence after RFA were Child-Pugh score and the presence of non-hypervascular hypointense hepatic nodules. In addition, we categorized IDR into 2 forms of recurrence, hypervascular transformation of non-hypervascular hy-

pointense hepatic nodules and new intrahepatic recurrence. We revealed that the rate of new intrahepatic recurrence was also significantly higher in patients with non-hypervascular hypointense hepatic nodules than in those without non-hypervascular hypointense hepatic nodules. Furthermore, multivariate analysis revealed that independent risk factors for new hepatic recurrence were also Child-Pugh score and the presence of non-hypervascular hypointense hepatic nodules. The results of our study are in good accordance with the very recent report by Inoue et al. [42]. These results suggest that patients with non-hypervascular hypointense nodules during the hepatobiliary phase of Gd-EOB-DTPA-enhanced MRI need intensive follow-up after RFA because non-hypervascular hypointense hepatic nodules not only have a potential of hypervascular transformation but also are a risk factor for the new intrahepatic recurrence.

There are some limitations to this study. First, this study was conducted retrospectively and the number of patients was not large. A larger prospective study is needed to confirm our findings. Second, we did not evaluate the outcomes of patients with non-hypervascular hypointense hepatic nodules. It is important to investigate survival rates in patients with non-hypervascular hypointense hepatic nodules compared with those without non-hypervascular hypointense hepatic nodules. Finally, we could not exclude the possibility that recurrences included the intrahepatic metastasis of the treated HCC.



In conclusion, non-hypervascular hypointense hepatic nodules during the hepatobiliary phase of Gd-EOB-DTPA-enhanced MRI were a useful predictive factor for the recurrence of IDR, particularly for new intrahepatic recurrence.

## Disclosure Statement

The authors declare that no financial or other conflict of interest exists in association with the content of the article.

## References

- Torre LA, Bray F, Siegel RL, Ferlay J, Lortet-Tieulent J, Jemal A: Global cancer statistics, 2012. *CA Cancer J Clin* 2015;65:87–108.
- Jemal A, Bray F, Center MM, Ferlay J, Ward E, Forman D: Global cancer statistics. *CA Cancer J Clin* 2011;61:69–90.
- Ferlay J, Soerjomataram I, Dikshit R, Eser S, Mathers C, Rebelo M, Parkin DM, Forman D, Bray F: Cancer incidence and mortality worldwide: sources, methods and major patterns in GLOBOCAN 2012. *Int J Cancer* 2015;136:E359–E386.
- Mittal S, El-Serag HB: Epidemiology of hepatocellular carcinoma: consider the population. *J Clin Gastroenterol* 2013;47(suppl):S2–S6.
- Altekruse SF, McGlynn KA, Reichman ME: Hepatocellular carcinoma incidence, mortality, and survival trends in the United States from 1975 to 2005. *J Clin Oncol* 2009;27:1485–1491.
- Umemura T, Ichijo T, Yoshizawa K, Tanaka E, Kiyosawa K: Epidemiology of hepatocellular carcinoma in Japan. *J Gastroenterol* 2009;44(suppl 19):102–107.
- Wirth TC, Manns MP: The impact of the revolution in hepatitis C treatment on hepatocellular carcinoma. *Ann Oncol* 2016;27:1467–1474.
- Kudo M: Breakthrough imaging in hepatocellular carcinoma. *Liver Cancer* 2016;5:47–54.
- Chen BB, Murakami T, Shih TT, Sakamoto M, Matsui O, Choi BI, Kim MJ, Lee JM, Yang RJ, Zeng MS, Chen RC, Liang JD: Novel imaging diagnosis for hepatocellular carcinoma: consensus from the 5th Asia-Pacific primary liver cancer expert meeting (APPLE 2014). *Liver Cancer* 2015;4:215–227.
- Salvatore V, Gianstefani A, Negrini G, Allegretti G, Galassi M, Piscaglia F: Imaging diagnosis of hepatocellular carcinoma: recent advances of contrast-enhanced ultrasonography with SonoVue®. *Liver Cancer* 2016;5:55–66.
- Kudo M: Surveillance, diagnosis, treatment, and outcome of liver cancer in Japan. *Liver Cancer* 2015;4:39–50.
- Hsu C, Chen BB, Chen CH, Ho MC, Cheng JC, Kokudo N, Murakami T, Yeo W, Seong J, Jia JD, Han KH, Cheng AL: Consensus development from the 5th Asia-Pacific primary liver cancer expert meeting (APPLE 2014). *Liver Cancer* 2015;4:96–105.
- Clinical practice guidelines for hepatocellular carcinoma differ between Japan, United States, and Europe. *Liver Cancer* 2015;4:85–95.
- Joo I, Lee JM: Recent advances in the imaging diagnosis of hepatocellular carcinoma: value of gadoteric acid-enhanced MRI. *Liver Cancer* 2016;5:67–87.
- Matsui O, Takashima T, Kadoya M, Ida M, Suzuki M, Kitagawa K, Kamimura R, Inoue K, Konishi H, Itoh H: Dynamic computed tomography during arterial portography: the most sensitive examination for small hepatocellular carcinomas. *J Comput Assist Tomogr* 1985;9:19–24.
- Hayashi M, Matsui O, Ueda K, Kawamori Y, Kadoya M, Yoshikawa J, Gabata T, Takashima T, Nonomura A, Nakanuma Y: Correlation between the blood supply and grade of malignancy of hepatocellular nodules associated with liver cirrhosis: evaluation by CT during intraarterial injection of contrast medium. *AJR Am J Roentgenol* 1999;172:969–976.
- Ueda K, Matsui O, Kawamori Y, Nakanuma Y, Kadoya M, Yoshikawa J, Gabata T, Nonomura A, Takashima T: Hypervascular hepatocellular carcinoma: evaluation of hemodynamics with dynamic CT during hepatic arteriography. *Radiology* 1998;206:161–166.
- Kokudo N, Hasegawa K, Akahane M, Igaki H, Izumi N, Ichida T, Uemoto S, Kaneko S, Kawasaki S, Ku Y, Kudo M, Kubo S, Takayama T, Tateishi R, Fukuda T, Matsui O, Matsuyama Y, Murakami T, Arii S, Okazaki M, Makuuchi M: Evidence-based clinical practice guidelines for hepatocellular carcinoma: the Japan Society of hepatology 2013 update (3rd JSH-HCC Guidelines). *Hepatol Res* 2015;45.
- Schuhmann-Giampieri G, Schmitt-Willich H, Press WR, Negishi C, Weinmann HJ, Speck U: Preclinical evaluation of Gd-EOB-DTPA as a contrast agent in MR imaging of the hepatobiliary system. *Radiology* 1992;183:59–64.
- Vogl TJ, Kummel S, Hammerstingl R, Schellenbeck M, Schumacher G, Balzer T, Schwarz W, Muller PK, Bechstein WO, Mack MG, Sollner O, Felix R: Liver tumors: comparison of MR imaging with Gd-EOB-DTPA and Gd-DTPA. *Radiology* 1996;200:59–67.
- Huppertz A, Balzer T, Blakeborough A, Breuer J, Giovagnoni A, Heinz-Peer G, Laniado M, Manfredi RM, Mathieu DG, Mueller D, Reimer P, Robinson PJ, Strotzer M, Taupitz M, Vogl TJ: Improved detection of focal liver lesions at MR imaging: multicenter comparison of gadoteric acid-enhanced MR images with intraoperative findings. *Radiology* 2004;230:266–275.
- Bluemke DA, Sahani D, Amendola M, Balzer T, Breuer J, Brown JJ, Casalino DD, Davis PL, Francis IR, Krinsky G, Lee FT Jr, Lu D, Paulson EK, Schwartz LH, Siegelman ES, Small WC, Weber TM, Welber A, Shamsi K: Efficacy and safety of MR imaging with liver-specific contrast agent: U.S. multicenter phase III study. *Radiology* 2005;237:89–98.
- Saito K, Kotake F, Ito N, Ozuki T, Mikami R, Abe K, Shimazaki Y: Gd-EOB-DTPA enhanced MRI for hepatocellular carcinoma: quantitative evaluation of tumor enhancement in hepatobiliary phase. *Magn Reson Med* 2005;4:1–9.
- Huppertz A, Haraida S, Kraus A, Zech CJ, Scheidler J, Breuer J, Helmberger TK, Reiser MF: Enhancement of focal liver lesions at gadoteric acid-enhanced MR imaging: correlation with histopathologic findings and spiral CT—initial observations. *Radiology* 2005;234:468–478.
- Ichikawa S, Ichikawa T, Motosugi U, Sano K, Morisaka H, Enomoto N, Matsuda M, Fujii H: Was hypervascular hepatocellular carcinoma visible on previous gadoteric acid-enhanced magnetic resonance images? *Liver Cancer* 2015;4:154–162.
- Toyoda H, Kumada T, Tada T, Niinomi T, Ito T, Sone Y, Kaneoka Y, Maeda A: Non-hypervascular hypointense nodules detected by Gd-EOB-DTPA-enhanced MRI are a risk factor for recurrence of HCC after hepatectomy. *J Hepatol* 2013;58:1174–1180.
- Lee DH, Lee JM, Lee JY, Kim SH, Kim JH, Yoon JH, Kim YJ, Lee JH, Yu SJ, Han JK, Choi BI: Non-hypervascular hepatobiliary phase hypointense nodules on gadoteric acid-enhanced MRI: risk of HCC recurrence after radiofrequency ablation. *J Hepatol* 2015;62:1122–1130.
- Toyoda H, Kumada T, Tada T, Sone Y, Maeda A, Kaneoka Y: Non-hypervascular hypointense nodules on Gd-EOB-DTPA-enhanced MRI as a predictor of outcomes for early-stage HCC. *Hepatol Int* 2015;9:84–92.
- Kudo M: Locoregional therapy for hepatocellular carcinoma. *Liver Cancer* 2015;4:163–164.
- Bruix J, Sherman M: Management of hepatocellular carcinoma: an update. *Hepatology* 2011;53:1020–1022.

- 31 Onishi H, Kim T, Imai Y, Hori M, Nagano H, Nakaya Y, Tsuboyama T, Nakamoto A, Tatsumi M, Kumano S, Okada M, Takamura M, Wakasa K, Tomiyama N, Murakami T: Hypervascular hepatocellular carcinomas: detection with gadoxetate disodium-enhanced MR imaging and multiphasic multidetector CT. *Eur Radiol* 2012;22:845–854.
- 32 Makino Y, Imai Y, Igura T, Kogita S, Sawai Y, Fukuda K, Iwamoto T, Okabe J, Takamura M, Fujita N, Hori M, Takehara T, Kudo M, Murakami T: Feasibility of extracted-overlay fusion imaging for intraoperative treatment evaluation of radiofrequency ablation for hepatocellular carcinoma. *Liver Cancer* 2016;5: 269–279.
- 33 Kogita S, Imai Y, Okada M, Kim T, Onishi H, Takamura M, Fukuda K, Igura T, Sawai Y, Morimoto O, Hori M, Nagano H, Wakasa K, Hayashi N, Murakami T: Gd-EOB-DTPA-enhanced magnetic resonance images of hepatocellular carcinoma: correlation with histological grading and portal blood flow. *Eur Radiol* 2010;20:2405–2413.
- 34 Cox D: Regression models and life-tables. *J R Stat Soc* 1972;187–220.
- 35 Kanda Y: Investigation of the freely available easy-to-use software “EZ” for medical statistics. *Bone Marrow Transplant* 2013;48:452–458.
- 36 Shiina S, Tateishi R, Arano T, Uchino K, Enooku K, Nakagawa H, Asaoka Y, Sato T, Masuzaki R, Kondo Y, Goto T, Yoshida H, Omata M, Koike K: Radiofrequency ablation for hepatocellular carcinoma: 10-year outcome and prognostic factors. *Am J Gastroenterol* 2012;107:569–577.
- 37 Choi D, Lim HK, Rhim H, Kim YS, Lee WJ, Paik SW, Koh KC, Lee JH, Choi MS, Yoo BC: Percutaneous radiofrequency ablation for early-stage hepatocellular carcinoma as a first-line treatment: long-term results and prognostic factors in a large single-institution series. *Eur Radiol* 2007;17:684–692.
- 38 N’Kontchou G, Mahamoudi A, Aout M, Ganne-Carrie N, Grando V, Coderc E, Vicaute E, Trinchet JC, Sellier N, Beaugrand M, Seror O: Radiofrequency ablation of hepatocellular carcinoma: long-term results and prognostic factors in 235 Western patients with cirrhosis. *Hepatology* 2009;50:1475–1483.
- 39 Lee DH, Lee JM, Lee JY, Kim SH, Han JK, Choi BI: Radiofrequency ablation for intrahepatic recurrent hepatocellular carcinoma: long-term results and prognostic factors in 168 patients with cirrhosis. *Cardiovasc Intervent Radiol* 2014;37:705–715.
- 40 Tateishi R, Shiina S, Akahane M, Sato J, Kondo Y, Masuzaki R, Nakagawa H, Asaoka Y, Goto T, Otomo K, Omata M, Yoshida H, Koike K: Frequency, risk factors and survival associated with an intrasubsegmental recurrence after radiofrequency ablation for hepatocellular carcinoma. *PLoS One* 2013; 8:e59040.
- 41 Lencioni R, Cioni D, Crocetti L, Franchini C, Pina CD, Lera J, Bartolozzi C: Early-stage hepatocellular carcinoma in patients with cirrhosis: long-term results of percutaneous image-guided radiofrequency ablation. *Radiology* 2005;234:961–967.
- 42 Inoue M, Ogasawara S, Chiba T, Ooka Y, Wakamatsu T, Kobayashi K, Suzuki E, Tawada A, Yokosuka O: Presence of non-hypervascular hypointense nodules on Gadolinium-ethoxybenzyl-diethylenetriamine pentaacetic acid-enhanced magnetic resonance imaging in patients with hepatocellular carcinoma. *J Gastroenterol Hepatol* 2017;32:908–915.

# Impact of Tumor Factors on Survival in Patients with Hepatocellular Carcinoma Classified Based on Kinki Criteria Stage B2

Tadaaki Arizumi Tomohiro Minami Hirokazu Chishina Masashi Kono  
Masahiro Takita Norihisa Yada Satoru Hagiwara Yasunori Minami  
Hiroshi Ida Kazuomi Ueshima Ken Kamata Kosuke Minaga Yoriaki Komeda  
Mamoru Takenaka Toshiharu Sakurai Tomohiro Watanabe Naoshi Nishida  
Masatoshi Kudo

Department of Gastroenterology and Hepatology, Kindai University Faculty of Medicine, Osaka-Sayama, Japan

## Keywords

Barcelona clinic liver cancer stage B · Hepatocellular carcinoma · Kinki criteria · Overall survival · Transarterial chemoembolization

## Abstract

**Background:** Tumors classified based on the Barcelona Clinic Liver Cancer (BCLC) stage B hepatocellular carcinoma (HCC) are heterogeneous in nature. Previously, the Kinki criterion was proposed for a more precise subclassification of tumors in BCLC-stage B. However, tumors in sub-stage B2 include various size and number of HCCs even with the Kinki criteria, which could lead to heterogeneity for overall survival (OS). In this study, we assessed how the size and number of tumors affect the OS and time to progression (TTP) in patients with Kinki criteria stage B2 tumors and treated with transarterial chemoembolization (TACE). **Methods:** Of 906 HCC patients treated with TACE at Kindai University Hospital, 236 patients with HCC considered as Kinki criteria stage B2 were examined. They were classified into the following 4 groups according to the maximum tumor diameter and number of tumors: B2a group, tumor size  $\leq 6$  cm and total number of tumors  $\leq 6$ ; B2b group, size  $\leq 6$  cm and number  $> 6$ ; B2c group, size  $> 6$  cm and number  $\leq 6$ ; and B2d group, size

$> 6$  cm and number  $> 6$ . The OS and TTP of patients in each group were compared. **Results:** There were 131 patients (55.5%) in the B2a group, 58 (24.6%) in the B2b group, 41 (17.4%) in the B2c group, and 6 (0.03%) in the B2d group. Comparison of the survivals revealed that the median OS was 2.8 years (95% CI 2.0–3.5) in the B2a group, 2.8 years (95% CI 2.0–3.3) in the B2b group, 1.9 years (95% CI 0.8–4.0) in the B2c group, and 2.3 years (95% CI 1.2–ND [no data]) in the B2d group, respectively ( $p = 0.896$ ). The median TTP in B2a, B2b, B2c, and B2d sub-substage HCC were 13.2, 12.1, 13.8, and 11.5 months, respectively ( $p = 0.047$ ). The median TTP in B2a + B2c sub-substage patients was longer than that in B2b + B2d sub-substage HCC patients (14.0 months and 10.4 months;  $p = 0.002$ ). **Conclusion:** No significant differences were observed in the OS among HCC patients subclassified based on the maximum tumor diameter and tumor number in Kinki criteria stage B2. Consequently, Kinki criteria stage B2 HCC is a homogeneous subgroup in terms of OS prediction. However, shorter TTP in B2b+B2c sub-substage HCC patients than that in B2a + B2c sub-substage HCC patients suggests that different treatment strategy, such as systemic therapy with targeted agents instead of TACE, may be suitable to preserve the liver function.

© 2017 S. Karger AG, Basel

## Introduction

Hepatocellular carcinoma (HCC) is the fifth most common cancer in the world, and the third leading cause of cancer-related death worldwide [1]. The total number of deaths from liver cancer in Japan has decreased since its peak in 2004. According to recent analysis from 2012, 30,690 people died from liver cancer in Japan [2, 3]. As in other malignancies, evidence-based and accurate staging and treatment decisions determine the outcome of HCC patients [4, 5]. The Barcelona Clinic Liver Cancer (BCLC) staging system is the most widely used and accepted staging system for HCC, and has been endorsed by the European Association for the Study of Liver and the American Association for the Study of Liver Diseases. The BCLC staging system classifies HCC patients into 5 stages (0, A, B, C, and D), and allocates treatment strategy accordingly [6–10].

In the BCLC staging system, the intermediate stage (B) is defined as asymptomatic, multinodular tumors without an invasive pattern (multinodular tumor, Child-Pugh class A-B, and performance status 0), and transarterial chemoembolization (TACE) is recommended as a first-line treatment. TACE is reportedly not effective in patients with tumors  $\geq 7$  cm in diameter and  $\geq 4$  tumors since TACE is less effective for large and multiple tumors and impairs hepatic function [9]. Superselective TACE with lipiodol reportedly offers satisfactory levels of local control with a lower risk of complications [3, 11–14].

We previously proposed the Kinki criteria for subclassification of BCLC stage-B HCC and demonstrated their efficacy [15–17]. As in previous studies, survival was prolonged in HCC patients meeting the up-to-7 criteria; they were classified as having BCLC stage B but had smaller or fewer tumors. Therefore, criteria based on the up-to-7 criteria were also proposed [18]. According to the proposed Kinki criteria, B2-stage HCC that does not meet the up-to-7 criteria includes large and multiple liver tumors. In case of liver cancer involving a single or few tumors, survival can be prolonged by curative treatment even in larger liver cancers [19, 20]. On the contrary, a complete cure for multiple liver tumors is considered difficult, and treatment strategies in the Japanese guidelines do not include curative treatment for such cancers [10, 21, 22]. Because the tumor characteristics of large and multiple liver cancers may differ, it is questionable whether these 2 types of tumors can be dealt with identically. Therefore, in this study, we assessed whether the tumor diameter and number affected the survival in Kinki criteria stage B2 HCC patients.

## Materials and Methods

### Patients

Between January 2003 and August 2013, 906 patients with HCC were treated with conventional TACE (cTACE) as a first-time treatment at Kinki University Hospital. Of these patients, 753 who met the inclusion criteria were selected for the retrospective study. All patients satisfied the diagnostic criteria for HCC as per the American Association for the Study of Liver Diseases guidelines. Clinicopathological variables including demographic data, full blood count, albumin levels, alpha-fetoprotein levels, alanine aminotransferase levels, alkaline phosphatase levels, tumor stage (including number of focal lesions and maximum tumor diameter), Child-Pugh class, and BCLC prognostic score were collected at the time of referral to our unit, prior to treatment. The inclusion criteria for this study were: (1) diagnosis of HCC based on histological examination or radiologic findings showing early enhancement followed by late washout on contrast-enhanced CT or dynamic magnetic resonance imaging; (2) performance status of 0; and (3) Child-Pugh class A or B liver cirrhosis. The exclusion criteria were: (1) concomitant antineoplastic treatment and (2) patients whose details were unknown because medical records before and after cTACE were missing. The study was approved by the research Ethics Committee at our institution. We posted research content on a website; we also gave the patients the right to refuse participation in the study.

### Modified Bolondi Classification (Kinki criteria)

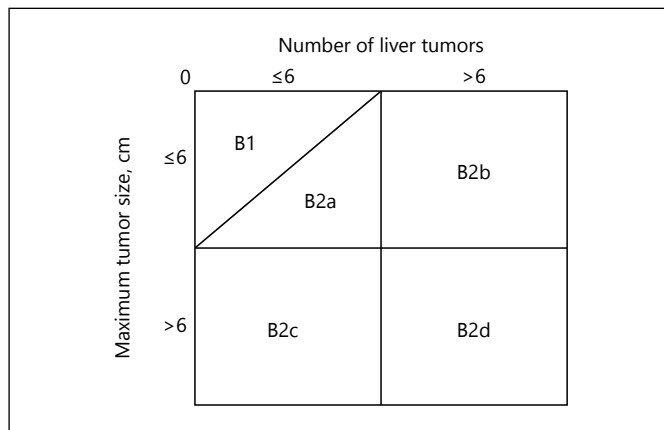
To determine a substage based on Kinki criteria, the patients' Child-Pugh scores and status according to Milan and up-to-7 criteria (based on the number and diameter of tumors) were determined. Patients with a Child-Pugh score of 5–7 and meeting the up-to-7 criteria were classified as subclass B1, those with a Child-Pugh score of 5–7 and exceeding the up-to-7 criteria were classified as subclass B2, and those with a Child-Pugh score of 8–9 and any up-to-7 criteria status were classified as subclass B3 [15].

Subclass B2 was further subdivided into the following 4 subclasses according to the maximum tumor diameter and tumor number: subclass B2a,  $\leq 6$ -cm diameter and  $\leq 6$  tumors; subclass B2b,  $\leq 6$ -cm diameter and  $> 6$  tumors; subclass B2c,  $> 6$ -cm diameter and  $\leq 6$  tumors; and subclass B2d,  $> 6$ -cm diameter and  $> 6$  tumors. Survival was compared and analyzed among these subclasses (Fig. 1). The diameter of viable lesions, as determined from images taken before TACE, was used as the baseline value. The time to progression (TTP) was defined as the duration for the tumor diameter to increase by  $\geq 20\%$  in one direction since the day TACE was administered, according to the modified Response Evaluation Criteria in Solid Tumors [23]. Moreover, because subclass B2 represents multiple liver tumors, cases where new lesions appeared without an increase in tumor diameter were not regarded as progression.

### Statistical Analysis

Univariate survival analysis was performed using the Kaplan-Meier method. The overall survival (OS) analysis ended at the time of death or the last follow-up visit. Survivals between the groups were compared using the log-rank test. For multiple comparisons, the Bonferroni correction was applied. A  $p$  value  $< 0.05$  was considered statistically significant. All analyses were performed using the SPSS Medical Pack for Windows, version 10.0 (SPSS, Inc., Chicago, IL, USA).





**Fig. 1.** Subclassification of Kinki criteria stage B2 hepatocellular carcinoma. Kinki criteria stage B2 was categorized into the following 4 subclasses according to the maximum tumor diameter and tumor number: subclass B2a,  $\leq 6$ -cm diameter and  $\leq 6$  tumors; subclass B2b,  $\leq 6$ -cm diameter and  $> 6$  tumors; subclass B2c,  $> 6$ -cm diameter and  $\leq 6$  tumors; and subclass B2d,  $> 6$ -cm diameter and  $> 6$  tumors.

## Results

### Baseline Characteristics

Among the 753 patients who received cTACE sessions during their clinical course, 261 (34.7%), 425 (56.4%), and 67 (8.9%) patients had BCLC stage A, BCLC stage B, and BCLC stage C tumors, respectively. Of the 425 BCLC stage B patients, 158 (37.2%), 236 (55.5%), and 31 (7.3%) were subclass B1, subclass B2, and subclass B3 according to the Kinki criteria, respectively. Of the 236 subclass-B2 patients, 131 (55.5%), 58 (24.6%), 41 (17.4%), and 6 (0.03%) were subclass B2a, B2b, B2c, and B2d, respectively.

### Overall Survival

In BCLC subclass B2 patients, the median OS was 2.5 years (95% CI 2.2–3.1). When the OS among patients treated with cTACE and belonging to the subclass B2a, B2b, B2c, and B2d groups were compared, the median OS times were 2.6 years (95% CI 2.0–3.5), 2.8 years (95% CI 2.0–3.3), 1.9 years (95% CI 0.8–4.0), and 2.3 years (95% CI 1.2–ND [no data]), respectively ( $p = 0.896$ ; Fig. 2a).

When the  $\leq 6$ -cm diameter (B2a and B2b groups;  $n = 189$ ) and  $> 6$ -cm diameter (B2c and B2d groups;  $n = 47$ ) groups were compared, the median OS times were 2.6 years (95% CI 2.2–3.1) and 1.9 years (95% CI 1.3–3.7), respectively. There was no significant difference between the 2 groups ( $p = 0.585$ ; Fig. 2b). Likewise, for the  $\leq 6$ -tu-

mor (B2a and B2c groups;  $n = 64$ ) and  $> 6$ -tumor groups (B2b and B2d groups;  $n = 172$ ), the median OS times were 2.8 years (95% CI 2.0–3.2) and 2.5 years (95% CI 2.0–3.5), respectively. There was no significant difference between the 2 groups ( $p = 0.759$ ; Fig. 2c).

### TTP after cTACE Therapy

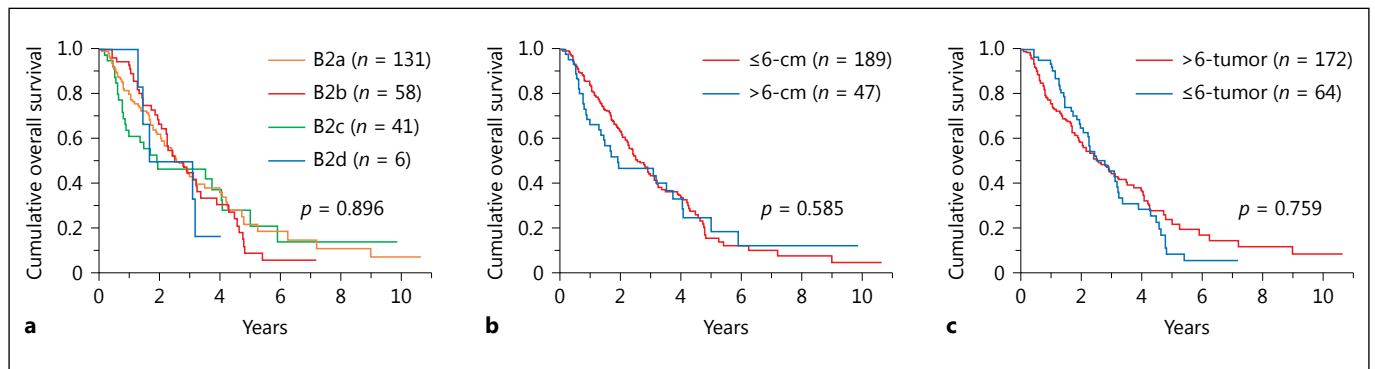
In the BCLC subclass B2 patients, the median TTP was 13 months (95% CI 11.1–16.3). For the B2a, B2b, B2c, and B2d groups, the median TTP was 13.2 months (95% CI 11.1–17.6), 12.1 months (95% CI 6.9–16.1), 13.8 months (95% CI 6.8–37), and 11.5 months (95% CI 1.6–29.3), respectively ( $p = 0.047$ ; Fig. 3a).

The median TTP was 13 months (95% CI 10.9–16.6) in the  $\leq 6$ -cm diameter group (B2a and B2b groups) and 12.3 months (95% CI 7.3–29.3) in the  $> 6$ -cm diameter group (B2c and B2d groups), with no significant difference between the 2 groups ( $p = 0.196$ ; Fig. 3b). Conversely, the median TTP was 14.0 months (95% CI 11.5–17.6) in the  $\leq 6$ -tumor group (B2a and B2c groups) and 10.4 months (95% CI 6.9–15.2) in the  $> 6$ -tumor group (B2b and B2d groups), with a significant difference between the 2 groups ( $p = 0.002$ ; Fig. 3c).

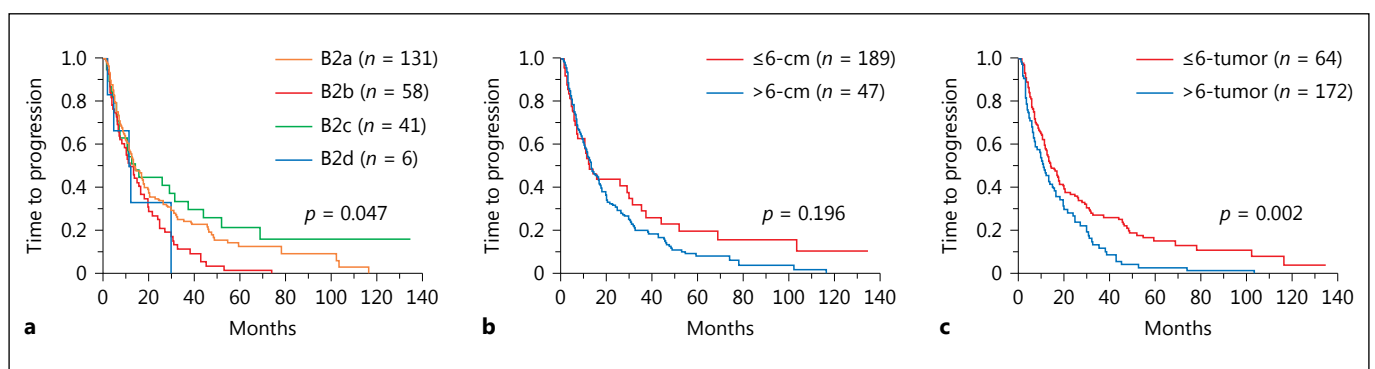
## Discussion

In this study, we subdivided Kinki criteria subclass B2 HCC according to maximum tumor diameter and tumor number, and compared the OS among the new subclasses. However, no significant differences were observed among these subgroups. Moreover, no significant differences in survival were observed when patients were grouped according to the maximum tumor diameter or tumor number alone. There may be confounding factors for the possible reason of no OS difference among sub-subclassification of BCLC B2 stage.

cTACE prolongs the survival in BCLC stage B patients who meet the up-to-7 criteria (B1 sub-stage), that is, in HCC patients with a few small nodules, compared to those who do not [16]. On the contrary, cTACE is not only ineffective but may also diminish the hepatic functional reserve in patients not meeting the up-to-7 criteria (B2 substage). Because cTACE has little effect on prolonging survival, other treatment strategies such as hepatic arterial infusion chemotherapy (HAIC) or sorafenib are potentially the first-line treatments of choice [24–26]. Indeed, BCLC subclass B2 patients do not respond well to cTACE; it is less effective in these patients than in subclass B1 patients. Therefore, BCLC substage B2 patients appear



**Fig. 2.** Overall survival (OS) according to Kinki criteria stage B2 (**a**;  $p = 0.896$ ), maximum tumor size (**b**;  $p = 0.585$ ), and number of liver tumors (**c**;  $p = 0.759$ ).



**Fig. 3.** Time to progression (TTP) according to Kinki criteria stage B2 (**a**;  $p = 0.047$ ), maximum tumor size (**b**;  $p = 0.196$ ), and number of liver tumors (**c**;  $p = 0.002$ ).

to be an appropriate target group for combination therapy with cTACE [27, 28] or other strategies including systemic therapy with sorafenib, regorafenib or lenvatinib [29–31].

A possible reason for the lack of differences in survival between large and multiple liver cancers at BCLC stage B2 is that patients with large liver cancer may have microsatellite lesions even if they have 1–3 liver tumors. As satellite lesions may become more detectable with increased tumor diameter [32–34], prognosis in patients with microsatellite lesions is poor [2, 35]. Thus, it is also plausible that patients with large, but few liver tumors, who were treated with cTACE, may have had microsatellite lesions. These may have caused recurrent tumors after treatment, and consequently, there was no difference in survival between large and multiple HCCs. When large HCCs exceed a certain size, despite a low tumor number, it may need to be treated in the same manner as multiple HCCs.

On the contrary, TTP was significantly different for groups classified by tumor number. A high tumor number is known to be associated with intrahepatic cancer spread and lower survival rates [36, 37], and may have contributed to the significant difference in TTP in our study. Despite the difference in TTP, no significant difference was observed in the OS. Previous studies conducted on BCLC stage B patients revealed that the OS in substage B1 patients was better than that in substage B2 patients. One possible explanation is that in our institute the majority of BCLC B2 substage HCC, especially multiple tumors more than 6 tended to receive HAIC or switch to systemic therapy with sorafenib after TACE refractory. Therefore, the OS was similar between B2b and B2c/B2a even though TTP in B2b sub-substage HCC patients was significantly shorter than that in B2c/B2a sub-substage HCC patients. Switching from ineffective TACE to sorafenib or HAIC might have contributed to the improved OS in B2b sub-substage HCC patients,

similar to the OS of B2a sub-substage HCC patients. B2b sub-substage HCC is a subgroup that is easily predictive of TACE refractoriness; therefore, their TTP is normally worse than in B2a sub-substage HCC patients. A superselective TACE, which is a curative treatment, may be repeated before the disease progresses in some patients, and thus, a complete cure may be achievable. A number of such patients may have been included in our study. Since TTP is the duration between pretreatment imaging and posttreatment imaging showing progression, in patients undergoing TACE, TTP may need to be assessed by a method uniquely adapted to the characteristics of TACE.

Although the number of patients analyzed in this study was adequate, the retrospective design of the study might have led to bias in patient selection. To address these limitations and independently validate the results of this study, we are currently designing a prospective multicenter study that investigates a larger patient cohort.

## Conclusion

Although BCLC subclass B2 HCC, which includes multiple and large liver tumors, was subclassified and analyzed in terms of the maximum tumor diameter and tumor number, no significant differences in the OS were

observed, probably because of the selection bias due to retrospective study design. While significant differences in the OS are observed between BCLC subclasses B1 and B2, no such differences were observed within BCLC sub-substage B2. However, statistical differences in TTP between BCLC sub-substage B2b and B2c/B2a sub-substage patients were observed. Based on these results, we can conclude that B2b substage HCC patients may be good candidates for systemic therapy rather than TACE to improve the survival by preserving the liver function. Since BCLC substage B2 patients with multiple tumors are less responsive to cTACE than BCLC substage B1 patients, further clinical trials are needed to confirm this hypothesis.

## Ethics Statement

Research was ethically conducted in accordance with the World Medical Association Declaration of Helsinki. The research content was posted on a website, and the study protocol was approved by the appropriate institutional Ethics Committees.

## Disclosure Statement

The authors declare that they have no financial conflict of interest.

## References

- 1 Llovet JM, Burroughs A, Bruix J: Hepatocellular carcinoma. *Lancet* 2003;362:1907–1917.
- 2 Kudo M: Surveillance, diagnosis, treatment, and outcome of liver cancer in Japan. *Liver Cancer* 2015;4:39–50.
- 3 Kudo M, Izumi N, Sakamoto M, Matsuyama Y, Ichida T, Nakashima O, Matsui O, Ku Y, Kokudo N, Makuuchi M: Survival analysis over 28 years of 173,378 patients with hepatocellular carcinoma in Japan. *Liver Cancer* 2016;5:190–197.
- 4 Ho MC, Hasegawa K, Chen XP, Nagano H, Lee YJ, Chau GY, Zhou J, Wang CC, Choi YR, Poon RT, Kokudo N: Surgery for intermediate and advanced hepatocellular carcinoma: a consensus report from the 5th Asia-Pacific primary liver cancer expert meeting (apple 2014). *Liver Cancer* 2016;5:245–256.
- 5 Chow PK, Choo SP, Ng DC, Lo RH, Wang ML, Toh HC, Tai DW, Goh BK, Wong JS, Tay KH, Goh AS, Yan SX, Loke KS, Thang SP, Gogna A, Too CW, Irani FG, Leong S, Lim KH, Thng CH: National cancer centre singapore consensus guidelines for hepatocellular carcinoma. *Liver Cancer* 2016;5:97–106.
- 6 EASL-EORTC clinical practice guidelines: Management of hepatocellular carcinoma. *J Hepatol* 2012;56:908–943.
- 7 Diaz-Gonzalez A, Reig M, Bruix J: Treatment of hepatocellular carcinoma. *Dig Dis* 2016;34:597–602.
- 8 Bruix J, Reig M, Sherman M: Evidence-based diagnosis, staging, and treatment of patients with hepatocellular carcinoma. *Gastroenterology* 2016;150:835–853.
- 9 Yamakado K, Miyayama S, Hirota S, Mizunuma K, Nakamura K, Inaba Y, Maeda H, Matsuo K, Nishida N, Aramaki T, Anai H, Koura S, Oikawa S, Watanabe K, Yasumoto T, Furuichi K, Yamaguchi M: Subgrouping of intermediate-stage (BCLC stage B) hepatocellular carcinoma based on tumor number and size and child-pugh grade correlated with prognosis after transarterial chemoembolization. *Jpn J Radiol* 2014;32:260–265.
- 10 Clinical practice guidelines for hepatocellular carcinoma differ between Japan, United States, and Europe. *Liver Cancer* 2015;4:85–95.
- 11 Tsurusaki M, Murakami T: Surgical and locoregional therapy of HCC: TACE. *Liver Cancer* 2015;4:165–175.
- 12 Yamakado K, Miyayama S, Hirota S, Mizunuma K, Nakamura K, Inaba Y, Maeda A, Matsuo K, Nishida N, Aramaki T, Anai H, Koura S, Oikawa S, Watanabe K, Yasumoto T, Furuichi K, Yamaguchi M: Hepatic arterial embolization for unresectable hepatocellular carcinomas: do technical factors affect prognosis? *Jpn J Radiol* 2012;30:560–566.
- 13 Kudo M: Locoregional therapy for hepatocellular carcinoma. *Liver Cancer* 2015;4:163–164.
- 14 Kitai S, Kudo M, Nishida N, Izumi N, Sakamoto M, Matsuyama Y, Ichida T, Nakashima O, Matsui O, Ku Y, Kokudo N, Makuuchi M; Liver Cancer Study Group of Japan: Survival benefit of locoregional treatment for hepatocellular carcinoma with advanced liver cirrhosis. *Liver Cancer* 2016;5:175–189.
- 15 Kudo M, Arizumi T, Ueshima K, Sakurai T, Kitano M, Nishida N: Subclassification of bcl b stage hepatocellular carcinoma and treatment strategies: proposal of modified bolondi's subclassification (kinki criteria). *Dig Dis* 2015;33:751–758.

- 16 Arizumi T, Ueshima K, Iwanishi M, Minami T, Chishina H, Kono M, Takita M, Kitai S, Inoue T, Yada N, Hagiwara S, Ida H, Minami Y, Sakurai T, Kitano M, Nishida N, Kudo M: Validation of a modified substaging system (kinki criteria) for patients with intermediate-stage hepatocellular carcinoma. *Oncology* 2015;89(suppl 2):47–52.
- 17 Kudo M: Heterogeneity and subclassification of barcelona clinic liver cancer stage B. *Liver Cancer* 2016;5:91–96.
- 18 Hiraoka A, Kumada T, Nouse K, Tsuji K, Ito-bayashi E, Hirooka M, Kariyama K, Ishikawa T, Tada T, Toyoda H, Kawasaki H, Hiasa Y, Michitaka K: Proposed new sub-grouping for intermediate-stage hepatocellular carcinoma using albumin-bilirubin grade. *Oncology* 2016;91:153–161.
- 19 Lin CC, Cheng YT, Chen MW, Lin SM: The effectiveness of multiple electrode radiofrequency ablation in patients with hepatocellular carcinoma with lesions more than 3 cm in size and barcelona clinic liver cancer stage A to B2. *Liver Cancer* 2016;5:8–20.
- 20 Poon RT, Cheung TT, Kwok PC, Lee AS, Li TW, Loke KL, Chan SL, Cheung MT, Lai TW, Cheung CC, Cheung FY, Loo CK, But YK, Hsu SJ, Yu SC, Yau T: Hong kong consensus recommendations on the management of hepatocellular carcinoma. *Liver Cancer* 2015;4:51–69.
- 21 Kudo M, Matsui O, Izumi N, Iijima H, Kadoya M, Imai Y, Okusaka T, Miyayama S, Tsuchiya K, Ueshima K, Hiraoka A, Ikeda M, Ogasawara S, Yamashita T, Minami T, Yamakado K: JSH consensus-based clinical practice guidelines for the management of hepatocellular carcinoma: 2014 update by the liver cancer study group of Japan. *Liver Cancer* 2014;3:458–468.
- 22 Kudo M, Kitano M, Sakurai T, Nishida N: General rules for the clinical and pathological study of primary liver cancer, nationwide follow-up survey and clinical practice guidelines: the outstanding achievements of the liver cancer study group of Japan. *Dig Dis* 2015;33:765–770.
- 23 Lencioni R, Llovet JM: Modified recist (mRECIST) assessment for hepatocellular carcinoma. *Semin Liver Dis* 2010;30:52–60.
- 24 Ueshima K, Kudo M, Tanaka M, Kumada T, Chung H, Hagiwara S, Inoue T, Yada N, Kitai S: Phase I/II study of sorafenib in combination with hepatic arterial infusion chemotherapy using low-dose cisplatin and 5-fluorouracil. *Liver Cancer* 2015;4:263–273.
- 25 Lin CC, Hung CF, Chen WT, Lin SM: Hepatic arterial infusion chemotherapy for advanced hepatocellular carcinoma with portal vein thrombosis: Impact of early response to 4 weeks of treatment. *Liver Cancer* 2015;4:228–240.
- 26 Obi S, Sato S, Kawai T: Current status of hepatic arterial infusion chemotherapy. *Liver Cancer* 2015;4:188–199.
- 27 Arizumi T, Ueshima K, Minami T, Kono M, Chishina H, Takita M, Kitai S, Inoue T, Yada N, Hagiwara S, Minami Y, Sakurai T, Nishida N, Kudo M: Effectiveness of sorafenib in patients with transcatheter arterial chemoembolization (TACE) refractory and intermediate-stage hepatocellular carcinoma. *Liver Cancer* 2015;4:253–262.
- 28 Geschwind JF, Gholam PM, Goldenberg A, Mantry P, Martin RC, Piperdi B, Zigmont E, Imperial J, Babajanyan S, Foreman PK, Cohn A: Use of transarterial chemoembolization (TACE) and sorafenib in patients with unresectable hepatocellular carcinoma: us regional analysis of the gideon registry. *Liver Cancer* 2016;5:37–46.
- 29 Kudo M: Molecular targeted therapy for hepatocellular carcinoma: Where are we now? *Liver Cancer* 2015;4:I–VII.
- 30 Kudo M: Regorafenib as second-line systemic therapy may change the treatment strategy and management paradigm for hepatocellular carcinoma. *Liver Cancer* 2016;5:235–244.
- 31 Kudo M: Immune checkpoint blockade in hepatocellular carcinoma. *Liver Cancer* 2015;4:201–207.
- 32 Wu TH, Yu MC, Chen TC, Lee CF, Chan KM, Wu TJ, Chou HS, Lee WC, Chen MF: Encapsulation is a significant prognostic factor for better outcome in large hepatocellular carcinoma. *J Surg Oncol* 2012;105:85–90.
- 33 Truant S, Boleslawski E, Duhamel A, Bouras AF, Louvet A, Febvay C, Leteurtre E, Huet G, Zerbib P, Dharancy S, Hebbat M, Pruvot FR: Tumor size of hepatocellular carcinoma in noncirrhotic liver: a controversial predictive factor for outcome after resection. *Eur J Surg Oncol* 2012;38:1189–1196.
- 34 Lim C, Mise Y, Sakamoto Y, Yamamoto S, Shindoh J, Ishizawa T, Aoki T, Hasegawa K, Sugawara Y, Makuuchi M, Kokudo N: Above 5 cm, size does not matter anymore in patients with hepatocellular carcinoma. *World J Surg* 2014;38:2910–2918.
- 35 Hung IF, Wong DK, Poon RT, Fong DY, Chui AH, Seto WK, Fung JY, Chan AC, Yuen JC, Tiu R, Choi O, Lai CL, Yuen MF: Risk factors and post-resection independent predictive score for the recurrence of hepatitis b-related hepatocellular carcinoma. *PLoS One* 2016;11:e0148493.
- 36 Heng-jun G, Yao-jun Z, Min-shan C, Meixian C, Jun-ting H, Li X, Lau WY: Rationality and effectiveness of transarterial chemoembolization as an initial treatment for BCLC B stage HBV-related hepatocellular carcinoma. *Liver Int* 2014;34:612–620.
- 37 Ogasawara S, Chiba T, Ooka Y, Kanogawa N, Motoyama T, Suzuki E, Tawada A, Azemoto R, Shinozaki M, Yoshikawa M, Yokosuka O: A prognostic score for patients with intermediate-stage hepatocellular carcinoma treated with transarterial chemoembolization. *PLoS One* 2015;10:e0125244.



# Time to Transcatheter Arterial Chemoembolization Refractoriness in Patients with Hepatocellular Carcinoma in Kinki Criteria Stages B1 and B2

Tadaaki Arizumi Tomohiro Minami Hirokazu Chishina Masashi Kono  
Masahiro Takita Norihisa Yada Satoru Hagiwara Yasunori Minami  
Hiroshi Ida Kazuomi Ueshima Ken Kamata Kosuke Minaga  
Yoriaki Komeda Mamoru Takenaka Toshiharu Sakurai  
Tomohiro Watanabe Naoshi Nishida Masatoshi Kudo

Department of Gastroenterology and Hepatology, Faculty of Medicine, Kindai University,  
Osaka Sayama, Japan

## Keywords

Hepatocellular carcinoma · Kinki criteria · Transarterial chemoembolization · Time to untreatable progression · TACE refractoriness · Barcelona clinic liver cancer stage B

## Abstract

**Background:** Transarterial chemoembolization (TACE) is recommended for patients with hepatocellular carcinoma (HCC) in Barcelona Clinic Liver Cancer (BCLC) stage B. However, because of the heterogeneity of HCC in BCLC stage B; various subclassification systems have been proposed to predict the prognosis of patients. Previously, we proposed the Kinki criteria for precise classification of HCC cases in BCLC stage B. In this study, we compared the time to TACE refractoriness in HCC patients with Kinki criteria substages B1 and B2-HCC. **Summary:** Between January 2006 and December 2013, 592 HCC patients (substage B1,  $n = 118$ ; substage B2,  $n = 170$ ) underwent TACE. Time to progression under TACE treatment was defined as the time to untreatable progression (TTUP). TTUP and changes in liver function were analyzed in patients with substages B1 and B2-HCC. The median TTUP was 25.7 months (95% CI 19.3–37.3) and 16.4

months (95% CI 13.1–20.2) in patients with substage B1-HCC and substage B2-HCC, respectively ( $p = 0.0050$ ). In patients with substage B2-HCC, median Child-Pugh scores after the first TACE session was significantly different from those after third and fifth TACE sessions (first-third,  $p = 0.0020$ ; first-fifth,  $p = 0.0008$ ). **Key Message:** TACE refractoriness occurred earlier in patients with substage B2-HCC than those with substage B1-HCC; deterioration of liver function with repeated TACE was more obvious in HCC cases with stage-B1 tumor. Shorter TTUP and impaired liver function due to repeated TACE could be responsible for the shorter survival in patients with substage B2-HCC.

© 2017 S. Karger AG, Basel

## Introduction

Hepatocellular carcinoma (HCC) is the third leading cause of cancer-related deaths worldwide [1–4]. HCC may develop at multiple sites on the liver and can give rise to numerous tumors with the potential to metastasize. Transarterial chemoembolization (TACE) is the standard treatment for HCC patients in the intermediate stage [5–

10], without inducing severe liver damage. However, multiple sessions of TACE lead to the refractoriness of treatment and deterioration of liver function, called as TACE failure/refractoriness [11–14].

We proposed the Kinki criteria wherein Barcelona Clinic Liver Cancer (BCLC) stage B classified HCCs into 3 substages using the Child-Pugh classification (5–7 points or 8–9 points) combined with the “beyond Milan” criteria and the “within” and “out of” the “up-to-7” criteria [15–18]. Based on the Kinki criteria, substage B1-HCC, which falls within the up-to-7 criteria, patients have a relatively small number of tumors or tumors with a small diameter. Substage B1-HCC patients are also candidates for resection [10, 19, 20] and ablation [21–23], in addition to TACE. By contrast, substage B2-HCC, which falls out of the up-to-7 criteria, patients carry multiple or large size of tumors; the overall survival and time to TACE progression were generally shorter in patients with substage B2-HCC than those carrying substage B1-HCC. Moreover, for substage B1-HCC, complete response could be achieved by performing superselective TACE without affecting the liver function. By contrast, complete response to TACE is hard to achieve for cases in substage B2-HCC. Based on the characteristics of tumors, multiple session of TACE is generally required for cases in substage B2, which may in turn result in a deterioration of liver function. In addition, superselective TACE is difficult to perform for substage B2-HCC cases because metastatic tumors are observed in the entire liver. Consequently, anticancer agents are administered, which could affect the non-cancerous liver and may result in a damage of liver function.

In Japan, the criteria for TACE refractoriness proposed by the Japan Society of Hepatology (JSH) are generally applied to determine the indication of TACE [14]. Because substage B2-HCC progressed more than substage B1-HCC, the former is more refract to TACE, which results in a shorter time to untreatable progression (TTUP). In this study, we compared the TTUP and alteration of liver function between the patients with substage B1 and B2-HCC.

## Material and Methods

### Patients

Between January 2006 and August 2013, 592 patients with HCC underwent conventional TACE (cTACE) as a first-line treatment at Kindai University Hospital. Of these patients, 288 who had undergone cTACE during their clinical course and met the inclusion criteria were selected for this retrospective study. All patients

satisfied the diagnostic criteria for HCC according to the American Association for the Study of Liver Diseases guidelines. Data on clinicopathological variables, including demographic data, full blood count, albumin levels, alpha-fetoprotein levels, alanine aminotransferase levels, alkaline phosphatase levels, tumor stage (including the number of focal lesions and maximum tumor diameter), Child-Pugh class, and BCLC prognostic score were obtained at the time of referral to our unit prior to treatment. The inclusion criteria for this study were: (1) diagnosis of HCC based on histological examination or radiologic findings showing early enhancement followed by late washout on contrast-enhanced CT or dynamic MRI; (2) performance status of 0; and (3) Child-Pugh class A or B liver cirrhosis. The exclusion criteria were: (1) concomitant antineoplastic treatment and (2) patients whose details were unknown because medical records before and after cTACE were missing. Patient characteristics are summarized and presented in Table 1. The patient population comprised 213 men and 75 women. Overall, 180 patients (62.5%) were positive for the anti-hepatitis C virus antibodies, 27 (9.4%) were positive for the hepatitis B virus surface antigen, and 81 (28.1%) were negative for both. A total of 244 patients (84.8%) were classified as Child-Pugh class A. Epirubicin, miriplatin, and cisplatin were used as the TACE chemoagent in 265, 20, and 3 patients, respectively.

### Modified Bolondi Classification (Kinki Criteria)

To determine a substage based on the Kinki criteria, the patients' Child-Pugh scores and status according to the Milan and up-to-7 criteria (based on the number and diameter of the tumors) were determined. Patients with a Child-Pugh score of 5–7 and meeting the up-to-7 criteria were classified as substage B1, those with a Child-Pugh score of 5–7 and exceeding the up-to-7 criteria were classified as substage B2, and those with a Child-Pugh score of 8–9 and any up-to-7 criteria status were classified as substage B3 [16, 24].

### TACE Technique

The right femoral artery was accessed with an 18-gauge Seldinger needle, and a 4-Fr sheath was subsequently inserted. The celiac artery was selectively catheterized using a 4.2-Fr catheter. A 2.2-Fr microcatheter (Shirabe®; Piolax, Yokohama, Japan) was advanced coaxially through the catheter into the common or proper hepatic artery. Rotational angiography was performed to evaluate the feeding vessels of identified HCCs. The tip of the catheter was selectively placed into feeding segmental and subsegmental arteries using the findings of selective hepatic angiography and/or tracking navigation imaging. Chemoembolization was performed using 60–120 mg of miriplatin (Miripla®; Sumitomo Dainippon Pharma, Osaka, Japan), 20–50 mg of epirubicin (Epirubicin®; Nippon Kayaku, Tokyo, Japan), or 50–100 mg of cisplatin (IACall®; Nippon Kayaku) emulsified with iodized oil (Lipiodol® Ultra-Fluid; Guerbet, Paris, France) and gelatin sponge particles (Gelpart®; Nippon Kayaku or Gelfoam®; Upjohn, Kalamazoo, MI, USA). The injection volume of the emulsion was determined based on the tumor volumes (<8 mL). Drug-eluting-bead TACE or balloon-occluded TACE was not utilized in this study.

### Definition of TACE Refractoriness

A CT scan was performed within 3 months of the TACE procedure to evaluate the radiological response of the tumor(s) to the treatment. Follow-up CT or MRI was performed every 3–4 months.

**Table 1.** Characteristics of hepatocellular carcinoma patients treated with cTACE

Characteristic	All (n = 288)	B1 stage (n = 118)	B2 stage (n = 170)
Age			
Median (25–75%)	73 (67–77)*	74 (69–77.75)*	72.5 (66.25–77)*
Gender			
Male	213 (74.0)	86 (72.9)	127 (74.7)
Female	75 (26.0)	32 (27.1)	43 (25.3)
Child-Pugh score			
5	160 (55.6)	71 (60.2)	89 (52.4)
6	84 (29.2)	36 (30.5)	48 (28.2)
7	44 (15.3)	11 (9.3)	33 (19.4)
Virus status <sup>†</sup>			
HBV	27 (9.4)	12 (10.2)	15 (8.8)
HCV	180 (62.5)	77 (65.3)	103 (60.6)
Virus negative	81 (28.1)	29 (24.6)	52 (30.6)
Serum ALT, IU/L			
Median (25–75%)	37 (25.75–57.25)*	38 (22.25–61)*	37 (26.25–54.75)*
Serum ALP level, IU/mL			
Median (25–75%)	334.5 (253–454.75)*	320.5 (242–448.25)*	348 (269–462.5)*
Serum platelets, 10 <sup>4</sup> /μL			
Median (25–75%)	12.7 (9.1–16.925)*	11.7 (8.7–15.5)*	13.35 (9.8–18.25)*
Serum AFP, ng/mL			
Median (25–75%)	25 (7–208)*	20 (6.25–84.75)*	32 (8–360)*

ALT, alanine aminotransferase; ALP, alkaline phosphatase; AFP, alpha-fetoprotein; HBV, hepatitis B virus; HCV, hepatitis C virus.

\* Dispersion variables are shown as median values (25–75%).

<sup>†</sup> Cases testing positive for HBV surface antigen (HBsAg) were regarded as cases of HBV-related HCC, and cases testing positive for hepatitis C antibody (HCV Ab) were regarded as cases of HCV-related HCC.

The definition of TACE refractoriness was based on the JSH Consensus Guidelines [14]. The radiological response to TACE was evaluated using the initial CT or MRI within 3 months after TACE treatment. According to the definition of TACE refractoriness by the JSH, the onset of TACE refractoriness was determined when examination immediately after TACE showed 2 increases in the number or diameter of intrahepatic lesions, appearance of extrahepatic spread, or appearance of vascular invasion. Because TACE is, in principle, contraindicated for patients with Child-Pugh class C HCC, TACE refractoriness was also defined as Child-Pugh class C HCC in this study. TTUP was defined as the time from the first TACE session to confirmation of TACE refractoriness. TTUP was assessed in patients with substage B1 and those with substage B2 HCC.

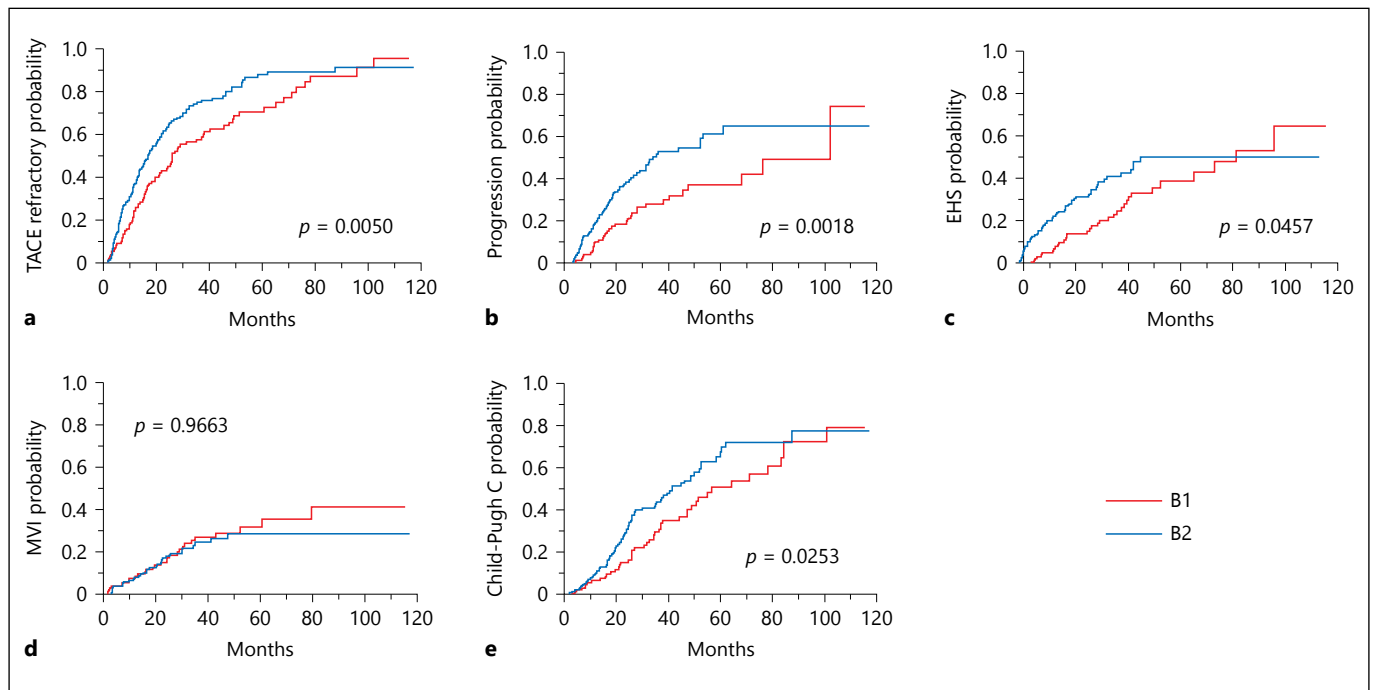
#### Statistical Analysis

Survival curves were estimated using the Kaplan-Meier method, with death as the primary endpoint for the analysis of overall survival. Patients who failed to meet the endpoint were censored at the time of the last follow-up visit. Survival rates were compared between the groups using the log-rank test, and categorical variables were compared using the chi-square test. Comparisons of categorical variables between the groups were conducted using the Mann-Whitney U test. The level of significance was set at  $p < 0.05$ . All analyses were performed using the SPSS Medical Pack for Windows, version 10.0 (SPSS, Inc., Chicago, IL, USA).

## Results

### Time to Untreatable Progression

The median TTUP was 25.7 months (95% CI, 19.3–37.3) in patients with substage B1 HCC and 16.4 months (95% CI 13.1–20.2) in patients with substage B2 HCC, showing a statistically significant difference ( $p = 0.0050$ ; Fig. 1a). In patients with an increased number or diameter of intrahepatic lesions, the median TTUP was 101.8 months (95% CI 47.2–not evaluated [NE]) in those with substage B1 HCC and 33.6 months (95% CI 25.3–53.0) in those with substage B2 HCC, showing a statistically significant difference ( $p = 0.0018$ ; Fig. 1b). In patients with visible extrahepatic spread, the median TTUP was 80.7 months (95% CI 51.9–NE) in those with substage B1 HCC and 48.6 months (95% CI 35.7–NE) in those with substage B2 HCC, showing a statistically significant difference ( $p = 0.0457$ ; Fig. 1c). In patients with visible vascular invasion, TTUP did not reach a median in patients with either substage B1 or B2 HCC, and no statistically significant difference was observed ( $p = 0.9663$ ; Fig. 1d).



**Fig. 1.** Time to untreatable progression. **a** The median time to untreatable progression (TTUP) was 25.7 months (95% CI, 19.3–37.3) in patients with substage B1 hepatocellular carcinoma (HCC) and 16.4 months (95% CI 13.1–20.2) in patients with substage B2 HCC ( $p = 0.0050$ ). **b** In patients with increased number or diameter of intrahepatic lesions, the median TTUP was 101.8 months (95% CI 47.2–not evaluated [NE]) in those with substage B1 HCC and 33.6 months (95% CI 25.3–53.0) in those with substage B2 HCC ( $p = 0.0018$ ). **c** In patients with visible extrahepatic spread,

the median TTUP was 80.7 months (95% CI 51.9–NE) in patients with substage B1 HCC and 48.6 months (95% CI 35.7–NE) in patients with substage B2 HCC ( $p = 0.0457$ ). **d** In patients with visible vascular invasion, TTUP did not reach a median in patients with either substage B1 or B2 HCC ( $p = 0.9663$ ). **e** In patients with Child-Pugh class C HCC, the median TTUP was 56.4 months (95% CI 46.8–82.8) in patients with substage B1 HCC and 41.0 months (95% CI 29.5–51.7) in patients with substage B2 HCC ( $p = 0.0253$ ).

In patients with Child-Pugh class C HCC, the median TTUP was 56.4 months (95% CI 46.8–82.8) in patients with substage B1 HCC and 41.0 months (95% CI 29.5–51.7) in patients with substage B2 HCC, showing a statistically significant difference ( $p = 0.0253$ ; Fig. 1e).

#### *The Number of TACE Sessions before Untreatable Progression*

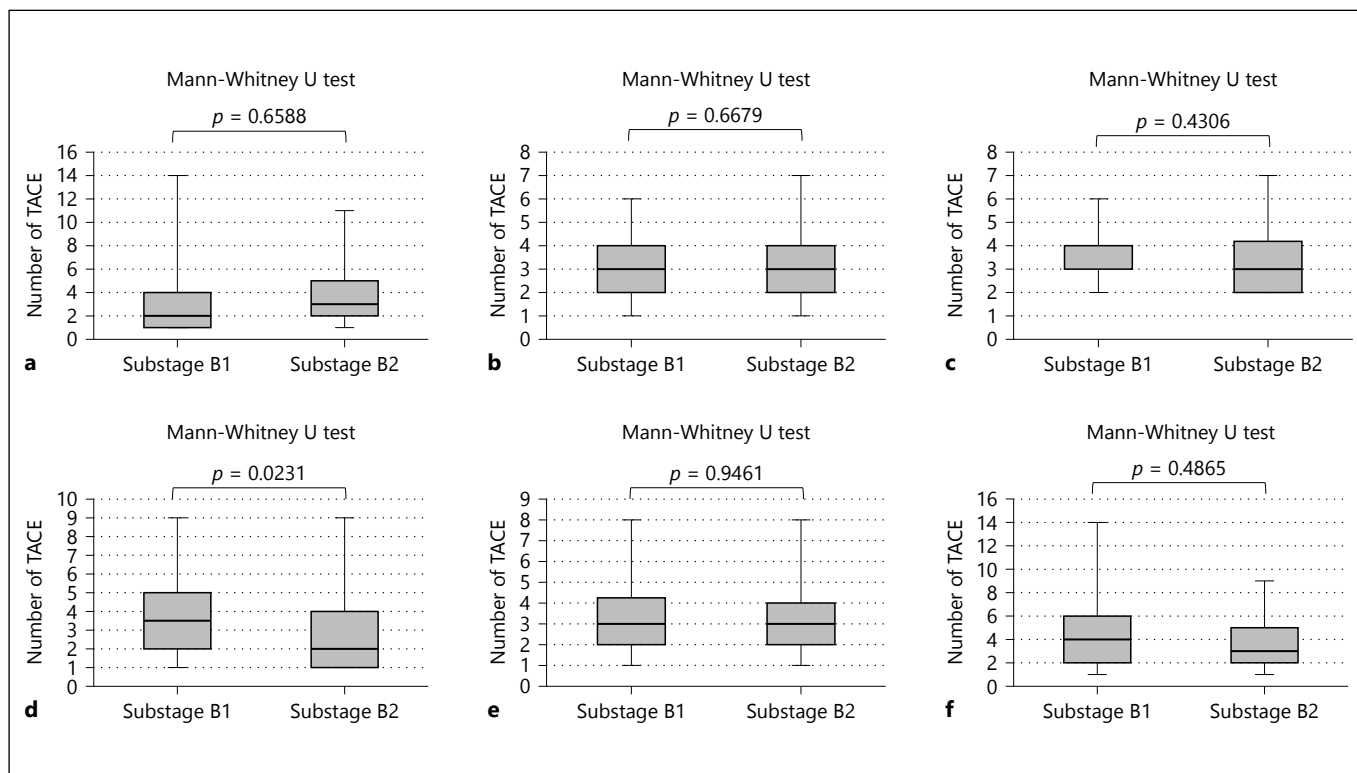
The median total number of TACE sessions (25–75th percentile) was 2 (1–4) in patients with substage B1 HCC and 3 (2–5) in patients with substage B2 HCC ( $p = 0.4306$ ; Fig. 2a). The median number of TACE sessions performed before TTUP was 3 (2–4) in patients with substage B1 HCC and 2 (2–4) in patients with substage B2 HCC, showing no statistically significant difference ( $p = 0.6679$ ; Fig. 2b). The median number of TACE sessions before the number or diameter of intrahepatic lesions increased was 4 (3–4.75) in patients with substage B1 HCC and 3 (2–4.75) in patients with substage B2 HCC, show-

ing no statistically significant difference ( $p = 0.6588$ ; Fig. 2c). The median number of TACE sessions before visible extrahepatic spread was 3.5 (2–5) in patients with substage B1 HCC and 2 (2–4) in patients with substage B2 HCC, showing a statistically significant difference ( $p = 0.0231$ ; Fig. 2d). The median number of TACE sessions before visible vascular invasion was 3 (2–5) in patients with substage B1 HCC and 3 (2–4) in patients with substage B2 HCC, showing no statistically significant difference ( $p = 0.9461$ ; Fig. 2e). In patients with Child-Pugh class C HCC, the median number of TACE sessions was 4 (2–6) in patients with substage B1 HCC and 3 (2–5) in patients with substage B2 HCC, showing no statistically significant difference ( $p = 0.4865$ ; Fig. 2f).

#### *Changes in Liver Function*

In patients with substage B1 HCC, after the first TACE session, the Child-Pugh scores were 5 points in 71 patients (60.2%), 6 points in 36 patients (30.5%), and 7





**Fig. 2.** Number of TACE. **a** The total number of transarterial chemoembolization (TACE) sessions ( $p = 0.6588$  by Mann-Whitney U test). **b** The number of TACE sessions performed before the time to untreatable progression (TTUP;  $p = 0.6679$ ). **c** The number of TACE sessions performed before the number or diameter of intrahepatic lesions increased ( $p = 0.4306$ ). **d** The number of TACE ses-

sions performed before visible extrahepatic spread ( $p = 0.0231$ ). **e** The number of TACE sessions performed before visible vascular invasion ( $p = 0.9461$ ). **f** The number of TACE sessions performed before the development of Child-Pugh class C hepatocellular carcinoma ( $p = 0.4865$ ).

points in 11 patients (9.3%), and the median score was 5 points (5–6). After the third TACE session, the Child-Pugh scores were 5 points in 34 patients (57.6%), 6 points in 13 patients (22.0%), 7 points in 8 patients (13.6%), 8 points in 3 patients (5.0%), and 9 points in 1 patient (1.7%), and the median score was 5 points (5–6). After the fifth TACE session, the Child-Pugh scores were 5 points in 15 patients (55.6%), 6 points in 7 patients (25.9%), 7 points in 4 patients (14.8%), and 8 points in 1 patient (3.7%), and the median score was 5 points (5–6; Fig. 3). No statistically significant differences in changes in liver function were observed between any sessions (first-third,  $p = 0.0825$ ; first-fifth,  $p = 0.2475$ ; third-fifth,  $p = 0.8406$ ; Fig. 4a).

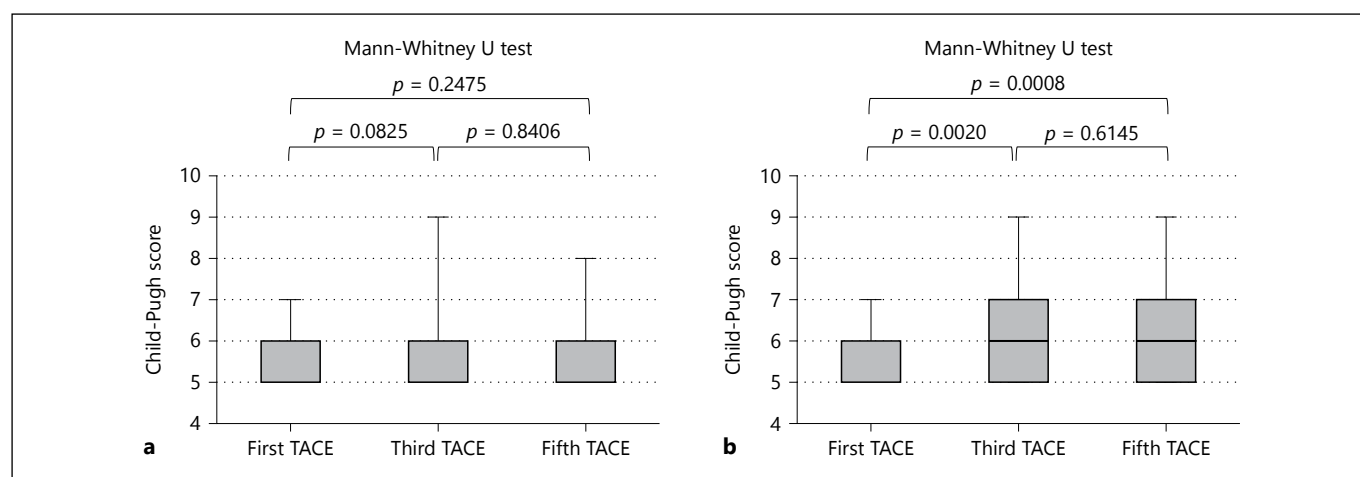
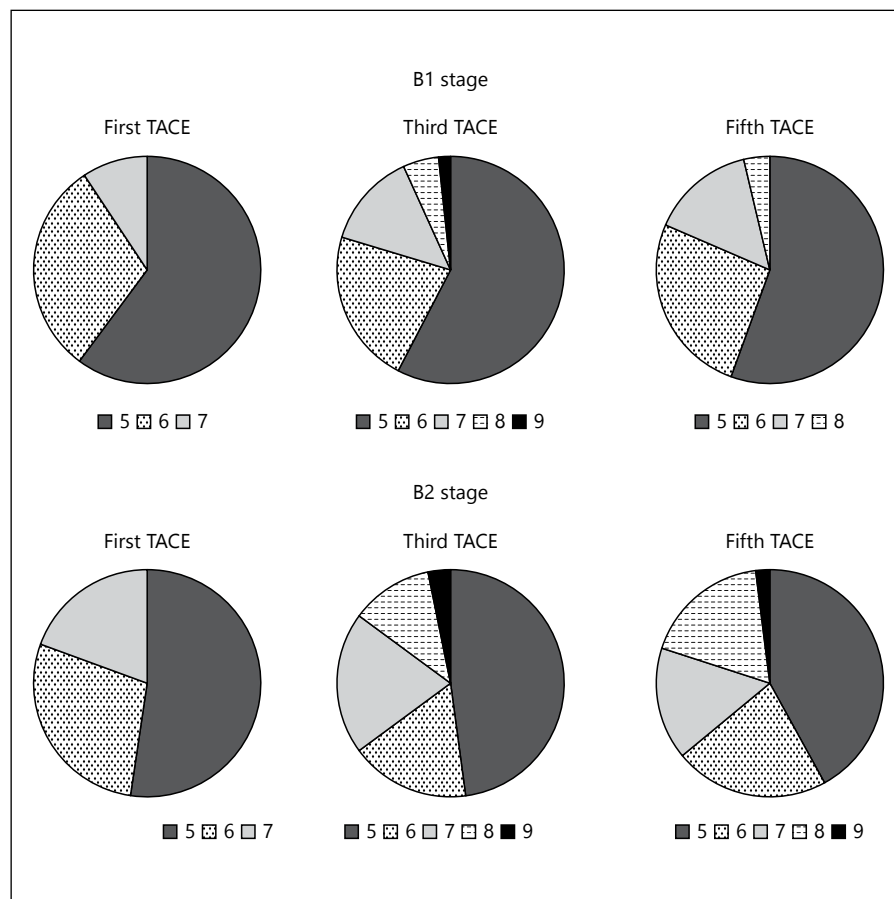
In patients with substage B2 HCC, after the first TACE session, the Child-Pugh scores were 5 points in 89 patients (52.4%), 6 points in 48 patients (28.2%), and 7 points in 33 patients (19.4%), and the median score was 5 points (5–6). After the third TACE session, the Child-

Pugh scores were 5 points in 45 patients (47.9%), 6 points in 16 patients (17.0%), 7 points in 19 patients (20.2%), 8 points in 11 patients (11.7%), and 9 points in 3 patients (3.2%), and the median score was 6 points (5–7). After the fifth TACE session, the Child-Pugh scores were 5 points in 21 patients (42%), 6 points in 11 patients (22%), 7 points in 8 patients (16%), 8 points in 9 patients (18%), and 9 points in 1 patient (2%), and the median score was 6 points (5–7; Fig. 3). The liver function after both the third and fifth TACE sessions significantly differed from that after the first TACE session (first-third,  $p = 0.0020$ ; first-fifth,  $p = 0.0008$ ; third-fifth,  $p = 0.6145$ ; Fig. 4b).

## Discussion

TACE refractoriness occurred earlier in substage B2 HCC than in substage B1 HCC. Thus, the number of TACE sessions performed before the onset of TACE re-

**Fig. 3.** Child-Pugh scores after transarterial chemoembolization (TACE). In patients with substage B1 hepatocellular carcinoma (HCC), the Child-Pugh scores after the first TACE session were 5 points in 71 patients (60.2%), 6 points in 36 patients (30.5%), and 7 points in 11 patients (9.3%). The Child-Pugh scores after the third TACE session were 5 points in 34 patients (57.6%), 6 points in 13 patients (22.0%), 7 points in 8 patients (13.6%), 8 points in 3 patients (5.0%), and 9 points in 1 patient (1.7%). The Child-Pugh scores after the fifth TACE session were 5 points in 15 patients (55.6%), 6 points in 7 patients (25.9%), 7 points in 4 patients (14.8%), and 8 points in 1 patient (3.7%). In patients with substage B2 HCC, the Child-Pugh scores after the first TACE session were 5 points in 89 patients (52.4%), 6 points in 48 patients (28.2%), and 7 points in 33 patients (19.4%). The Child-Pugh scores after the third TACE session were 5 points in 45 patients (47.9%), 6 points in 16 patients (17.0%), 7 points in 19 patients (20.2%), 8 points in 11 patients (11.7%), and 9 points in 3 patients (3.2%). The Child-Pugh scores after the fifth TACE session were 5 points in 21 patients (42%), 6 points in 11 patients (22%), 7 points in 8 patients (16%), 8 points in 9 patients (18%), and 9 points in 1 patient (2%).



**Fig. 4.** Comparison of Child-Pugh scores after transarterial chemoembolization (TACE). **a** In patients with substage B1 hepatocellular carcinoma (HCC), the median Child-Pugh scores (25–75th percentile) were all 5 points (5–6) after the first, third, and fifth TACE sessions. No statistically significant differences in changes in liver function were observed between any sessions (first-third,  $p = 0.0825$ ; first-fifth,  $p = 0.2475$ ; third-fifth,  $p =$

0.8406). **b** In patients with substage B2 HCC, the median Child-Pugh scores (25–75th percentile) were 5 points (5–6) after the first TACE session, 6 points (5–7) after the third TACE session, and 6 points (5–7) after the fifth TACE session. Liver function after both the third and fifth TACE sessions significantly differed from that after the first TACE session (first-third,  $p = 0.0020$ ; first-fifth,  $p = 0.0008$ ; third-fifth,  $p = 0.6145$ ).

fractoriness was smaller in substage B2 HCC. Moreover, liver function impairment was detected earlier in substage B2 HCC than in substage B1 HCC. In substage B2 HCC, the early onset of TACE refractoriness is assumed to be responsible for the shorter survival than that in substage B1 HCC.

This study showed no significant difference in the time to vascular invasion between substages B1 and B2 HCC. However, significant differences in other variables were observed. As substage B2 HCC is a more advanced tumor stage than substage B1 HCC, treatment with TACE once is insufficient for the former. Moreover, intrahepatic and extrahepatic metastases are assumed to occur in early stages, and the number of TACE sessions performed before extrahepatic metastasis was smaller for substage B2 HCC than for substage B1 HCC, which could be attributed to the difficulty in controlling intrahepatic lesions with TACE. Although only TACE is currently recommended for the treatment of BCLC stage B HCC, the survival is short for multiple or huge hepatomas, even for those based on the subclassification of criteria other than the Kinki criteria [25–28]. Treatment with TACE alone may be limited in efficacy for patients with substage B2 HCC including multiple or huge HCCs.

TACE with molecular-targeted agents is expected to more strongly prevent tumor recurrence or regrowth because of the inhibitory effect of the agents on enhanced angiogenesis [29–32]. Moreover, prolongation of the period in which tumor progression can be controlled by TACE could be expected. In addition, reduced frequency of performing TACE is also assumed to contribute to the prevention of liver function deterioration. Although global studies on combination treatment of TACE and molecular-targeted agents were conducted, no favorable results have been obtained to date [33–35]. Furthermore, currently, clinical studies on immune checkpoint inhibitors are conducted in patients with HCC [36]. Immune checkpoint inhibitors might also be effective in preventing HCC progression after TACE, in addition to molecular-targeted agents. Thus, clinical studies on combination treatment of TACE and immune checkpoint inhibitors may also be warranted to identify methods for improving the therapeutic effects of TACE, especially in patients with substage B2 HCC.

In patients with substage B1 HCC, no substantial changes in liver function were observed even after repeated administration of TACE. By contrast, in patients with substage B2 HCC, the liver function after the third and fifth TACE sessions deteriorated compared with that after the first TACE session. As the liver function is

impaired by TACE, it is recommended to perform TACE as selectively as possible [11, 37, 38]. However, it is difficult to perform TACE selectively, especially for multiple HCCs, and TACE could also affect the normal liver and, consequently, impair the liver function. Thus, in case of multiple hepatomas at substage B2, treatment with hepatic arterial infusion chemotherapy [39, 40] may be preferable because it can preserve the liver function and is effective for multiple HCCs. Moreover, because of early onset of TACE refractoriness and impaired liver function in substage B2 HCC, administration of molecular-targeted agents, such as sorafenib, is worth considering.

This study has some limitations. Although the number of patients analyzed in this study was adequate, the retrospective design of the study might have led to bias in patient selection. To address these limitations and independently validate the results of this study, we are currently designing a relevant prospective, multicenter study in a larger patient cohort.

## Conclusion

TACE refractoriness occurred earlier in patients with substage B2 HCC than in patients with substage B1 HCC. TACE for patients with substage B2 HCC resulted in the administration of drugs to a wider area of the liver; consequently, the liver function deteriorated after TACE in patients with substage B2 HCC. Moreover, TACE monotherapy may be limited in efficacy for substage B2 HCC, and inventive therapeutic strategies, such as in combination with other therapies, may be necessary to improve the effects of TACE. Furthermore, when the onset of TACE refractoriness is confirmed, TACE may need to be switched to other therapies, such as hepatic arterial infusion chemotherapy or sorafenib, as soon as possible.

## Ethics Statement

Research was ethically conducted in accordance with the World Medical Association Declaration of Helsinki. We posted the research content on a website, and the study protocol was approved by the appropriate institutional Ethics Committees.

## Disclosure Statement

The authors declare no conflicts of interest.

## References

- Parkin DM, Bray F, Ferlay J, Pisani P: Estimating the world cancer burden: globocan 2000. *Int J Cancer* 2001;94:153–156.
- Kim Y, Han KH: Epidemiology and surveillance of hepatocellular carcinoma. *Liver Cancer* 2012;1:2–14.
- El-Serag HB: Hepatocellular carcinoma. *N Engl J Med* 2011;365:1118–1127.
- Altekruse SF, McGlynn KA, Reichman ME: Hepatocellular carcinoma incidence, mortality, and survival trends in the United States from 1975 to 2005. *J Clin Oncol* 2009;27:1485–1491.
- Bruix J, Reig M, Sherman M: Evidence-based diagnosis, staging, and treatment of patients with hepatocellular carcinoma. *Gastroenterology* 2016;150:835–853.
- Tsurusaki M, Murakami T: Surgical and locoregional therapy of HCC: TACE. *Liver Cancer* 2015;4:165–175.
- Chow PK, Choo SP, Ng DC, Lo RH, Wang ML, Toh HC, Tai DW, Goh BK, Wong JS, Tay KH, Goh AS, Yan SX, Loke KS, Thang SP, Gogna A, Too CW, Irani FG, Leong S, Lim KH, Thng CH: National cancer centre Singapore consensus guidelines for hepatocellular carcinoma. *Liver Cancer* 2016;5:97–106.
- Kudo M: Locoregional therapy for hepatocellular carcinoma. *Liver Cancer* 2015;4:163–164.
- Kitai S, Kudo M, Nishida N, Izumi N, Sakamoto M, Matsuyama Y, Ichida T, Nakashima O, Matsui O, Ku Y, Kokudo N, Makuuchi M; Liver Cancer Study Group of Japan: Survival benefit of locoregional treatment for hepatocellular carcinoma with advanced liver cirrhosis. *Liver Cancer* 2016;5:175–189.
- Kudo M, Izumi N, Sakamoto M, Matsuyama Y, Ichida T, Nakashima O, Matsui O, Ku Y, Kokudo N, Makuuchi M: Survival analysis over 28 years of 173,378 patients with hepatocellular carcinoma in Japan. *Liver Cancer* 2016;5:190–197.
- Arizumi T, Ueshima K, Minami T, Kono M, Chishina H, Takita M, Kitai S, Inoue T, Yada N, Hagiwara S, Minami Y, Sakurai T, Nishida N, Kudo M: Effectiveness of Sorafenib in patients with transcatheter arterial chemoembolization (TACE) refractory and intermediate-stage hepatocellular carcinoma. *Liver Cancer* 2015;4:253–262.
- Arizumi T, Ueshima K, Chishina H, Kono M, Takita M, Kitai S, Inoue T, Yada N, Hagiwara S, Minami Y, Sakurai T, Nishida N, Kudo M: Validation of the criteria of transcatheter arterial chemoembolization failure or refractoriness in patients with advanced hepatocellular carcinoma proposed by the LCSGJ. *Oncology* 2014;87(suppl 1):32–36.
- Raoul JL, Gilabert M, Piana G: How to define transarterial chemoembolization failure or refractoriness: a European perspective. *Liver Cancer* 2014;3:119–124.
- Kudo M, Matsui O, Izumi N, Kadoya M, Okusaka T, Miyayama S, Yamakado K, Tsuchiya K, Ueshima K, Hiraoka A, Ikeda M, Ogasawara S, Yamashita T, Minami T: Transarterial chemoembolization failure/refractoriness: JSH-LCSGJ criteria 2014 update. *Oncology* 2014;87(suppl 1):22–31.
- Kudo M: Heterogeneity and subclassification of barcelona clinic liver cancer stage B. *Liver Cancer* 2016;5:91–96.
- Kudo M, Arizumi T, Ueshima K, Sakurai T, Kitano M, Nishida N: Subclassification of BCLC B stage hepatocellular carcinoma and treatment strategies: proposal of modified bolondi's subclassification (Kinki criteria). *Dig Dis* 2015;33:751–758.
- Arizumi T, Ueshima K, Iwanishi M, Minami T, Chishina H, Kono M, Takita M, Kitai S, Inoue T, Yada N, Hagiwara S, Minami Y, Ida H, Sakurai T, Kitano M, Nishida N, Kudo M: Validation of Kinki criteria, a modified sub-staging system, in patients with intermediate stage hepatocellular carcinoma. *Dig Dis* 2016;34:671–678.
- Arizumi T, Ueshima K, Iwanishi M, Minami T, Chishina H, Kono M, Takita M, Kitai S, Inoue T, Yada N, Hagiwara S, Ida H, Minami Y, Sakurai T, Kitano M, Nishida N, Kudo M: Validation of a modified substaging system (Kinki criteria) for patients with intermediate-stage hepatocellular carcinoma. *Oncology* 2015;89(suppl 2):47–52.
- Kudo M: Surveillance, diagnosis, treatment, and outcome of liver cancer in Japan. *Liver Cancer* 2015;4:39–50.
- Clinical practice guidelines for hepatocellular carcinoma differ between Japan, United States, and Europe. *Liver Cancer* 2015;4:85–95.
- Teng W, Liu KW, Lin CC, Jeng WJ, Chen WT, Sheen IS, Lin CY, Lin SM: Insufficient ablative margin determined by early computed tomography may predict the recurrence of hepatocellular carcinoma after radiofrequency ablation. *Liver Cancer* 2015;4:26–38.
- Kang TW, Rhim H: Recent advances in tumor ablation for hepatocellular carcinoma. *Liver Cancer* 2015;4:176–187.
- Lencioni R, de Baere T, Martin RC, Nutting CW, Narayanan G: Image-guided ablation of malignant liver tumors: recommendations for clinical validation of novel thermal and non-thermal technologies – A Western perspective. *Liver Cancer* 2015;4:208–214.
- Kudo M: Recent trends in the management of hepatocellular carcinoma with special emphasis on treatment with regorafenib and immune checkpoint inhibitors. *Dig Dis* 2016;34:714–730.
- Ramaswami R, Pinato DJ, Kubota K, Ishizuka M, Arizumi T, Kudo M, Jang JW, Kim YW, Pirisi M, Allara E, Sharma R: Prognostic subclassification of intermediate-stage hepatocellular carcinoma: a multicenter cohort study with propensity score analysis. *Med Oncol* 2016;33:114.
- Yamakado K, Miyayama S, Hirota S, Mizunuma K, Nakamura K, Inaba Y, Yamamoto S, Matsuo K, Nishida N, Aramaki T, Anai H, Kora S, Oikawa S, Watanabe K, Yasumoto T, Furuichi K, Yamaguchi M: Prognosis of patients with intermediate-stage hepatocellular carcinomas based on the Child-Pugh score: subclassifying the intermediate stage (Barcelona Clinic Liver Cancer stage B). *Jpn J Radiol* 2014;32:644–649.
- Hiraoka A, Kumada T, Nouse K, Tsuji K, Ito-bayashi E, Hirooka M, Kariyama K, Ishikawa T, Tada T, Toyoda H, Kawasaki H, Hiasa Y, Michitaka K: Proposed new sub-grouping for intermediate-stage hepatocellular carcinoma using albumin-bilirubin grade. *Oncology* 2016;91:153–161.
- Bolondi L, Burroughs A, Dufour JF, Galle PR, Mazzaferro V, Piscaglia F, Raoul JL, Sangro B: Heterogeneity of patients with intermediate (BCLC B) hepatocellular carcinoma: proposal for a subclassification to facilitate treatment decisions. *Semin Liver Dis* 2012;32:348–359.
- Geschwind JF, Gholam PM, Goldenberg A, Mantry P, Martin RC, Piperdi B, Zigmont E, Imperial J, Babajanyan S, Foreman PK, Cohn A: Use of transarterial chemoembolization (TACE) and sorafenib in patients with unresectable hepatocellular carcinoma: US regional analysis of the GIDEON registry. *Liver Cancer* 2016;5:37–46.
- Zhang B, Finn RS: Personalized clinical trials in hepatocellular carcinoma based on biomarker selection. *Liver Cancer* 2016;5:221–232.
- Kudo M: Regorafenib as second-line systemic therapy may change the treatment strategy and management paradigm for hepatocellular carcinoma. *Liver Cancer* 2016;5:235–244.
- Kudo M: Molecular targeted therapy for hepatocellular carcinoma: where are we now? *Liver Cancer* 2015;4:I–VII.
- Kudo M, Imanaka K, Chida N, Nakachi K, Tak WY, Takayama T, Yoon JH, Hori T, Kumada H, Hayashi N, Kaneko S, Tsubouchi H, Suh DJ, Furuse J, Okusaka T, Tanaka K, Matsui O, Wada M, Yamaguchi I, Ohya T, Meinhardt G, Okita K: Phase III study of sorafenib after transarterial chemoembolisation in Japanese and Korean patients with unresectable hepatocellular carcinoma. *Eur J Cancer* 2011;47:2117–2127.
- Kudo M, Han G, Finn RS, Poon RT, Blanc JF, Yan L, Yang J, Lu L, Tak WY, Yu X, Lee JH, Lin SM, Wu C, Tanwandee T, Shao G, Walters IB, Dela Cruz C, Poultar V, Wang JH: Brivanib as adjuvant therapy to transarterial chemoembolization in patients with hepatocellular carcinoma: a randomized phase III trial. *Hepatology* 2014;60:1697–1707.



- 35 Lencioni R, Llovet JM, Han G, Tak WY, Yang J, Guglielmi A, Paik SW, Reig M, Kim Y, Chau GY, Luca A, del Arbol LR, Leberre MA, Niu W, Nicholson K, Meinhardt G, Bruix J: Sorafenib or placebo plus TACE with doxorubicin-eluting beads for intermediate stage HCC: the SPACE trial. *J Hepatol* 2016;64: 1090–1098.
- 36 Kudo M: Immune checkpoint blockade in hepatocellular carcinoma. *Liver Cancer* 2015;4: 201–207.
- 37 Yamakado K, Miyayama S, Hirota S, Mizunuma K, Nakamura K, Inaba Y, Maeda A, Matsuo K, Nishida N, Aramaki T, Anai H, Koura S, Oikawa S, Watanabe K, Yasumoto T, Furuichi K, Yamaguchi M: Hepatic arterial embolization for unresectable hepatocellular carcinomas: do technical factors affect prognosis? *Jpn J Radiol* 2012;30:560–566.
- 38 Ogasawara S, Chiba T, Ooka Y, Kanogawa N, Motoyama T, Suzuki E, Tawada A, Kanai F, Yoshikawa M, Yokosuka O: Efficacy of sorafenib in intermediate-stage hepatocellular carcinoma patients refractory to transarterial chemoembolization. *Oncology* 2014;87:330–341.
- 39 Obi S, Sato S, Kawai T: Current status of hepatic arterial infusion chemotherapy. *Liver Cancer* 2015;4:188–199.
- 40 Lin CC, Hung CF, Chen WT, Lin SM: Hepatic arterial infusion chemotherapy for advanced hepatocellular carcinoma with portal vein thrombosis: impact of early response to 4 weeks of treatment. *Liver Cancer* 2015;4:228–240.

# Hemodynamic Changes on Cone-Beam Computed Tomography during Balloon-Occluded Transcatheter Arterial Chemoembolization Using Miriplatin for Hepatocellular Carcinoma: A Preliminary Study

Toru Ishikawa<sup>a</sup> Michitaka Imai<sup>a</sup> Takashi Owaki<sup>a</sup> Hiroki Sato<sup>a</sup>  
Yujiro Nozawa<sup>a</sup> Tomoe Sano<sup>a</sup> Akito Iwanaga<sup>a</sup> Keiichi Seki<sup>a</sup> Terasu Honma<sup>a</sup>  
Toshiaki Yoshida<sup>a</sup> Masatoshi Kudo<sup>b</sup>

<sup>a</sup>Department of Gastroenterology and Hepatology, Saiseikai Niigata Daini Hospital, Niigata, and <sup>b</sup>Department of Gastroenterology and Hepatology, Kindai University Faculty of Medicine, Osaka-Sayama, Japan

## Keywords

Miriplatin · Cone-beam CT · Balloon-occluded transcatheter arterial chemoembolization · Pixel · CT value

## Abstract

**Background/Aim:** Balloon-occluded transcatheter arterial chemoembolization (B-TACE) using miriplatin (MPT) is anticipated as a new strategy for hepatocellular carcinoma (HCC). This study was aimed at evaluating the hemodynamic changes with/without balloon occlusion of the hepatic artery, correlation of cone-beam CT (CBCT) pixels, and CT value after B-TACE for HCC. **Methods:** A total of 52 patients with HCC, who underwent B-TACE using MPT in addition to the balloon-occluded CBCT hepatic arteriography, were studied. **Results:** After balloon occlusion, CBCT pixel values increased in 37 lesions, whereas it decreased in 15 lesions. Intratumoral CT values after B-TACE were lower with decreased CBCT pixel values than with increased CBCT pixel values. **Conclusion:** Hemodynamic changes on CBCT during balloon occlusion can be used to predict the efficacy of B-TACE using MPT.

© 2017 S. Karger AG, Basel

## Introduction

Cone-beam CT (CBCT) using a flat panel detector (FPD) is an imaging methodology of CT, which is different from conventional CT [1].

CBCT has various artifacts that are not available in conventional CT. Currently, CBCT technology has improved with artifact reduction, and is already well-established in the diagnosis of hepatocellular carcinoma (HCC) [2].

Miriplatin (MPT, Miripla; Sumitomo Dainippon Pharma Co., Ltd., Osaka, Japan) is a specifically designed drug for transarterial chemoembolization (TACE) of HCCs [3]. Balloon-occluded TACE (B-TACE) is a modification of the treatment strategy that is anticipated to improve drug concentration in the tumor [4].

The degree of lipiodol accumulation in a tumor post-TACE correlates with the risk of local recurrence. We have previously reported that the Hounsfield unit value of a tumor obtained from conventional CT immediately after B-TACE with MPT is predictive of the recurrence risk [5].

However, to the best of our knowledge, only a few reports have investigated the correlation of hemodynamics between balloon occlusion CBCT and conventional CT values immediately after B-TACE. The present study is aimed at evaluating the hemodynamic changes with/without balloon occlusion of the hepatic artery and correlation of CT value after B-TACE for HCC.

## Methods

### *Patients and Methods*

#### *Study Cohort*

A total of 52 patients (52 nodules) with HCC who underwent B-TACE using MPT (Miripla; Sumitomo Dainippon Pharma Co., Ltd., Osaka, Japan) at Saiseikai Niigata Daini Hospital between December 2015 and May 2017 were included in this study.

All patients received a comprehensive evaluation by dynamic contrast CT prior to treatment. The study exclusion criteria were: (1) tumor size  $\geq 5$  cm; (2) intentionally incomplete TACE because of tumor infiltration; (3)  $\geq 4$ -month interval between TACE and initial CT during follow-up observation; (4) no CT done during follow-up observation; and (5) nodules with locoregional therapy such as percutaneous ethanol injection, microwave coagulation therapy, laser ablation, and radiofrequency ablation as additional treatment, (6) extrahepatic metastasis of HCC, and (7) other malignancies.

#### *TACE Protocol and CBCT Imaging*

In all cases, vascular access was achieved using the Seldinger technique. Briefly, the femoral artery was punctured, and a 5-Fr introducer was inserted followed by a 5-Fr catheter. A microballoon catheter (Attendant, Terumo, Tokyo, Japan or Logos, Piolax, Kanagawa, Japan) was then advanced into the selective or super-selective branches of the tumor's feeding arteries through a 5-Fr catheter. The microballoon catheter was introduced over a 0.014-inch guide wire (Chikai; Asahi Intec, Aichi, Japan). The tip of the microballoon catheter was positioned in the tumor's feeding artery. CBCT using an Allura Clarity FD20 (Philips, Best, The Netherlands) hepatic arteriography (CB-CTHA) was performed before and after the inflation of the balloon. Six hundred projection images with X-ray parameters of tube voltage 117–123 kV, pulse width 5–10 ms, and tube current 50–325 mA were obtained by 5.2-s acquisitions with 240°C-arm rotation around the patient. The FPD was used for image acquisition, which has a focal spot-detector distance of 120 cm with a 19-inch field of view. The acquisition images by FPD were automatically transferred to an Xtravision workstation (Philips) and reconstructed with artifact reduction. CB-CTHA with/without balloon occlusion was performed for areas containing HCC nodule.

The first CB-CTHA scan started 7–10 s after the initiation of a transcatheter hepatic arterial injection of 5–15 mL of nonionic contrast material (iopamidol, iopamiron® 150 iodine, 150 mg I/mL; Bayer HealthCare, Osaka, Japan) at a speed of 0.5–1.0 mL/s using the automated power injector, and the second scan started 30 s after the first scan ended.

The appropriate injection rate for CB-CTHA was determined by the maximum injection rate (which was basically dependent on the vessel caliber) that would not cause a backward flow of contrast

material on the hepatic arteriography. The injection rate was the same before and after the inflation of the balloon. The balloon was inflated to a diameter 5–10% larger than that of the occluded artery. Subsequently, MPT was prepared by mixing 60 or 120 mg (1 or 2 vials) of MPT hydrate in 3 or 6 mL of lipiodol. The maximum dose of MPT was limited to 120 mg.

MPT infusion was performed after balloon occlusion. MPT infusion was continued under balloon occlusion until HCC was filled with MPT or portal venous branches were beginning to be filled with MPT. Fluoroscopy and digital subtraction angiography during B-TACE procedures observed whether any limitation of MPT inflow into non-tumorous liver parenchyma and dense accumulation in HCC nodule were present, and whether or not anastomotic vessels with collateral artery were present. Then the balloon was deflated.

Conventional CT was performed immediately after the B-TACE. All conventional CT images were obtained using a multi-detector-row helical CT scanner (Aquilion PRIM; Toshiba Medical Systems, Tokyo, Japan). The parameters for scanning were as follows: collimation, 1 mm; reconstruction, 3 mm; pitch, 15; amperage, 300 mA s; kilo voltage, 120 kVp. The images were transferred to the PACS as DICOM data.

Using the EV Insite net software, regions of interest were placed on both CBCT and conventional CT DICOM images, adjusted to 1-mm slice thickness, at the same position. The automatically generated average pixels were recorded.

#### *Ethics Statement*

The study was approved by the Ethics Committee of Saiseikai Niigata Daini Hospital and was conducted in accordance with the principles of the Declaration of Helsinki. The study protocol was approved, and written informed consent was obtained from all participating patients.

#### *Statistical Analysis*

Variable data are expressed as mean  $\pm$  SD. Categorical variables were compared using  $\chi^2$  test or Fisher's exact test, where appropriate. Continuous variables were compared using the independent sample Student's *t* test or one-way repeated analysis of variance. Values of  $p < 0.05$  were considered to indicate statistically significant differences. Statistical processing was performed using Stat-View version 5.0 software (SAS Institute, Cary, NC, USA).

## Results

The study included 52 patients (40 males and 12 females; mean age  $72.32 \pm 7.78$  years), with a total of 52 nodules that were treated with B-TACE using MPT. The average diameter of the nodules on conventional CT was  $27.69 \pm 6.82$  mm (Table 1). The nodules were located at segment S1 ( $n = 2$ ), S2 ( $n = 3$ ), S3 ( $n = 3$ ), S4 ( $n = 7$ ), S5 ( $n = 6$ ), S6 ( $n = 7$ ), S7 ( $n = 5$ ), and S8 ( $n = 19$ ).

CBCT pixel values with balloon occlusion were significantly higher than those without balloon occlusion ( $p = 0.002$ ; Fig. 1). CBCT pixel values increased after balloon occlusion in 37 of the 52 tumors, whereas it decreased after balloon occlusion in 15 tumors. The clinical

**Table 1.** Baseline characteristics of the study population

Demographic variables	Mean ± SD	Range
Age, years	72.32±7.78	50–89
Gender, male:female	40:12	
Etiology (HBV/HCV/NonHBVNonHCV)	9/26/17	
Size, mm	27.69±6.82	10–40
Location (S1/2/3/4/5/6/7/8)	2/3/3/7/6/7/5/19	
Cone-beam CT (pixel)	185.01±98.17	64.0–626.4
Balloon cone-beam CT (pixel)	237.72±179.91	94.6–1,198.1
Post-CT value (HU)	340.36±215.74	122.1–109.2

HBV, hepatitis B virus; HCV, hepatitis C virus; HU, Hounsfield unit.

**Table 2.** Clinical features according to pixel changes after balloon occluded cone-beam CT angiography

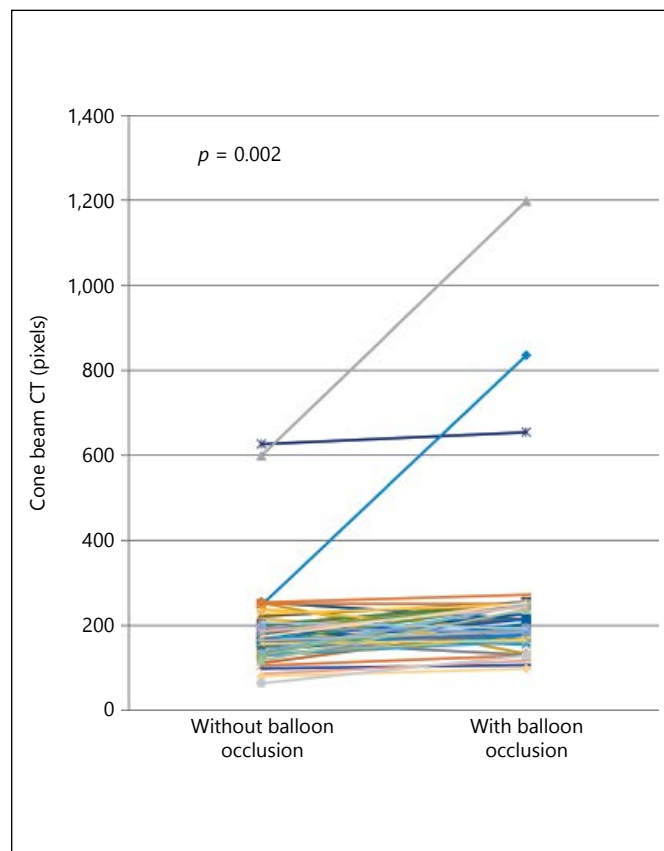
Demographic variables	Decreased	Increased	<i>p</i> value
Age, years	71.40±9.65	72.70±7.01	0.589
Gender, male:female	13:2	27:10	0.288
Etiology (HBV/HCV/ nonHBV vs. nonHCV)	1/6/8	8/20/9	0.126
Size, mm	26.00±5.73	28.37±7.17	0.259
Location (S1/2/3/4/5/6/7/8)	0/2/0/2/1/3/1/6	2/1/3/5/5/4/4/13	0.746
Cone-beam CT (pixel)	175.34±55.53	188.92±111.35	0.656
Balloon cone-beam CT (pixel)	162.93±42.15	268.92±204.67	0.048
Post-CT value (HU)	208.26±62.66	393.91±232.78	0.003

HBV, hepatitis B virus; HCV, hepatitis C virus; HU, Hounsfield unit.

features of the nodules with increased or decreased pixel values are given in Table 2. There was no significant difference at baseline between groups with increased and decreased pixel values; however, the CT value after B-TACE in the increased pixel group was significantly higher than that in the decreased pixel group ( $p = 0.003$ ).

## Discussion

TACE was established for the treatment of HCC when surgical resection [6] or other locoregional treatments [7–13] is not indicated. High concentrations of the drug-delivery vehicle lipiodol in the tumor at the time of treatment are associated with lower risks of local tumor recurrence [14]. MPT (cis-[[((1R, 2R)-1, 2-cyclohexanediamine-N,N0)bis(-myristato)]-platinum(II) monohydrate; Sumitomo Dainippon Pharma Co., Ltd., Osaka, Japan) is a novel lipophilic cisplatin derivative that can be suspended in lipiodol [3, 15, 16].

**Fig. 1.** Changes in cone-beam CT pixels with and without balloon occlusion of the hepatic artery.

Theoretically, MPT is a good agent in terms of its higher solubility, stability in lipiodol, and gradual release within the tumor.

However, a recent study reported that the local recurrence rate was significantly higher for MPT than for epirubicin with mitomycin C in lipiodol-based superselective TACE for HCC [17].

This inferior local control with MPT can be attributed to its higher viscosity. Various methods of administration with MPT are currently being studied to increase its therapeutic efficacy. Irie et al. [4] revealed that dense accumulation in the HCC nodule could be achieved by B-TACE with doxorubicin and mitomycin C.

We previously reported that B-TACE with MPT achieved relatively good local control of HCC (local recurrence rate, 11.1% at 6 months and 26.2% at 12 months) [5]. The mechanism of improved local control can be explained by the presence of anastomotic vessels, viscosity of lipiodol emulsion, and difference in size between the peripheral vessels in normal parenchyma and the vessels



feeding into the HCC. Moreover, we concluded that the plain CT value immediately after B-TACE with MPT is a predictive factor for local recurrence [5].

However, some lesions were not responsive to B-TACE. Currently, CBCT technology has improved with artifact reduction and is already well-established in the diagnosis of HCC [2]. Furthermore, it is possible that CBCT can be successfully used to predict HCC tumor outcome post-TACE [18].

This study was aimed at evaluating the hemodynamic changes with/without balloon occlusion of the hepatic artery and correlation of CT values after B-TACE for HCC.

We speculated that CBCT with/without balloon occlusion can provide useful information for the analysis of hemodynamic changes.

In this study, CB-CT pixel values with balloon occlusion were significantly higher than those without balloon occlusion. However, CB-CT pixel values after balloon occlusion decreased in some cases.

In the increased group, postoperative CT value was clearly higher, and local recurrence may be suppressed. By performing CB-CT before and after bal-

loon occlusion, it may be possible to predict the effect of B-TACE using MPT. Whereas lower CB-CT pixel values after balloon occlusion groups may be considered to be ineffective, there is a need to consider other strategies.

In conclusion, following balloon occlusion, intratumoral arterial flow can change, presumably due to a collateral pathway. B-TACE for HCC lesions showing decreased pixel values after balloon occlusion CBCT may have a poor short-term therapeutic effect compared to those with increased pixel values.

## Disclosure Statement

The authors declare that no conflict of interest exists.

## Financial Disclosure

The authors declare that they do not have a current financial arrangement or affiliation with any organization that may have a direct interest in their work.

## References

- Wallace MJ, Kuo MD, Glaiberman C, Binkert CA, Orth RC, Soulez G: Three-dimensional C-arm cone-beam CT: applications in the interventional suite. *J Vasc Interv Radiol* 2009; 20:S523–537.
- Higashihara H, Osuga K, Onishi H, Nakamoto A, Tsuboyama T, Maeda N, Hori M, Kim T, Tomiyama N: Diagnostic accuracy of C-arm CT during selective transcatheter angiography for hepatocellular carcinoma: comparison with intravenous contrast-enhanced, biphasic, dynamic MDCT. *Eur Radiol* 2012;22:872–879.
- Okusaka T, Okada S, Nakanishi T, Fujiyama S, Kubo Y: Phase II trial of intra-arterial chemotherapy using a novel lipophilic platinum derivative (SM-11355) in patients with hepatocellular carcinoma. *Invest New Drugs* 2004;22:169–176.
- Irie T, Kuramochi M, Takahashi N: Dense accumulation of lipiodol emulsion in hepatocellular carcinoma nodule during selective balloon-occluded transarterial chemoembolization: measurement of balloon-occluded arterial stump pressure. *Cardiovasc Interv Radiol* 2013;36:706–713.
- Ishikawa T, Abe S, Inoue R, Sugano T, Watanabe Y, Iwanaga A, Seki K, Honma T, Nemoto T, Takeda K, Yoshida T: Predictive factor of local recurrence after balloon-occluded TACE with miriplatin (MPT) in hepatocellular carcinoma. *PLoS One* 2014;9:e103009.
- Ho MC, Hasegawa K, Chen XP, Nagano H, Lee YJ, Chau GY, Zhou J, Wang CC, Choi YR, Poon RT, Kokudo N: Surgery for intermediate and advanced hepatocellular carcinoma: a consensus report from the 5th Asia-Pacific primary liver cancer expert meeting (apple 2014). *Liver Cancer* 2016;5:245–256.
- Tsurusaki M, Murakami T: Surgical and locoregional therapy of HCC: TACE. *Liver Cancer* 2015;4:165–175.
- Kudo M: Locoregional therapy for hepatocellular carcinoma. *Liver Cancer* 2015;4:163–164.
- Kudo M, Izumi N, Sakamoto M, Matsuyama Y, Ichida T, Nakashima O, Matsui O, Ku Y, Kokudo N, Makuuchi M: Survival analysis over 28 years of 173,378 patients with hepatocellular carcinoma in Japan. *Liver Cancer* 2016;5:190–197.
- Kudo M: Surveillance, diagnosis, treatment, and outcome of liver cancer in Japan. *Liver Cancer* 2015;4:39–50.
- Obi S, Sato S, Kawai T: Current status of hepatic arterial infusion chemotherapy. *Liver Cancer* 2015;4:188–199.
- Yamada R, Sato M, Kawabata M, Nakatsuka H, Nakamura K, Takashima S: Hepatic artery embolization in 120 patients with unresectable hepatoma. *Radiology* 1983;148:397–401.
- Matsui O, Kadoya M, Yoshikawa J, Gabata T, Arai K, Demachi H, Miyayama S, Takashima T, Unoura M, Kogayashi K: Small hepatocellular carcinoma: treatment with subsegmental transcatheter arterial embolization. *Radiology* 1993;188:79–83.
- Fujita T, Ito K, Tanabe M, Yamatogi S, Sasai H, Matsunaga N: Iodized oil accumulation in hypervascular hepatocellular carcinoma after transcatheter arterial chemoembolization: comparison of imaging findings with CT during hepatic arteriography. *J Vasc Interv Radiol* 2008;19:333–341.
- Hanada M, Baba A, Tsutsumishita Y, Noguchi T, Yamaoka T: Intra-hepatic arterial administration with miriplatin suspended in an oily lymphographic agent inhibits the growth of human hepatoma cells orthotopically implanted in nude rats. *Cancer Sci* 2009;100:189–194.
- Hanada M, Baba A, Tsutsumishita Y, Noguchi T, Yamaoka T, Chiba N, Nishikaku F: Intra-hepatic arterial administration with miriplatin suspended in an oily lymphographic agent inhibits the growth of tumors implanted in rat livers by inducing platinum-DNA adducts to form and massive apoptosis. *Cancer Chemother Pharmacol* 2009;64:473–483.
- Miyayama S, Yamashiro M, Shibata Y, Hashimoto M, Yoshida M, Tsuji K, Toshima F, Matsui O: Comparison of local control effects of superselective transcatheter arterial chemoembolization using epirubicin plus mitomycin C and miriplatin for hepatocellular carcinoma. *Jpn J Radiol* 2012;30:263–270.
- Ishikawa T, Abe S, Hoshii A, Yamada Y, Iiduka A, Nemoto T, Takeda K, Yoshida T: Cone-beam computed tomography correlates with conventional helical computed tomography in evaluation of lipiodol accumulation in HCC after chemoembolization. *PLoS One* 2016;11:e0145546.

# Hepatic Function during Repeated TACE Procedures and Prognosis after Introducing Sorafenib in Patients with Unresectable Hepatocellular Carcinoma: Multicenter Analysis

Atsushi Hiraoka<sup>a</sup> Takashi Kumada<sup>c</sup> Masatoshi Kudo<sup>d</sup> Masashi Hirooka<sup>e</sup>  
Yohei Koizumi<sup>e</sup> Yoichi Hiasa<sup>e</sup> Kazuto Tajiri<sup>f</sup> Hidenori Toyoda<sup>c</sup>  
Toshifumi Tada<sup>c</sup> Hironori Ochi<sup>b</sup> Koji Joko<sup>b</sup> Noritomo Shimada<sup>g</sup>  
Akihiro Deguchi<sup>h</sup> Toru Ishikawa<sup>i</sup> Michitaka Imai<sup>i</sup> Kunihiko Tsuji<sup>j</sup>  
Kojiro Michitaka<sup>a</sup> on behalf of the Real-life Practice Experts for HCC (RELPEC)  
Study Group and HCC 48 Group (hepatocellular carcinoma experts from  
48 clinics)

<sup>a</sup>Ehime Prefectural Central Hospital, Gastroenterology Center, and <sup>b</sup>Matsuyama Red-Cross Hospital, Hepato-Biliary Center, Matsuyama, <sup>c</sup>Ogaki Municipal Hospital, Department of Gastroenterology and Hepatology, Gifu, <sup>d</sup>Kindai University Faculty of Medicine, Department of Gastroenterology and Hepatology, Osaka, <sup>e</sup>Ehime University Graduate School of Medicine, Department of Gastroenterology and Metabolism, Toon, <sup>f</sup>Toyama University Hospital, Department of Gastroenterology, Toyama, <sup>g</sup>Ootakanomori Hospital, Department of Gastroenterology, Chiba, <sup>h</sup>Kagawa-Rosai Hospital, Department of Gastroenterology, Marugame, <sup>i</sup>Saiseikai Niigata Daini Hospital, Department of Gastroenterology, Niigata, and <sup>j</sup>Teine Keijinkai Hospital, Center of Gastroenterology, Sapporo, Japan

## Keywords

Hepatocellular carcinoma · Barcelona clinic liver cancer-B · Transarterial catheter chemoembolization · Hepatic function · Child-Pugh · Albumin-bilirubin-grade

## Abstract

**Background/Aim:** We evaluated the relationship of hepatic function with repeated transarterial catheter chemoembolization (TACE) and prognosis after sorafenib treatment in various patient cohorts. **Methods:** Study 1 comprised of 212 Barcelona clinic liver cancer stage-B (BCLC-B) HCC patients classified as Child-Pugh A (CP-A) and who had received repeated TACE treatments (r-TACE) (naïve:recurrence = 66:

146). Study 2 comprised of 435 patients with unresectable HCC classified as CP-A in who sorafenib was introduced (naïve:recurrence = 37:398; CP score 5:6 = 282:153; macrovessel invasion [MVI]+: extrahepatic metastasis [EHM]+ both negative = 124:226:143). Changes in hepatic function along with CP and albumin-bilirubin (ALBI) score/grade during r-TACE in Study 1, and prognosis after introducing sorafenib in Study 2 were evaluated. **Results:** Hepatic function worsened to CP-B in 9–14% with each TACE procedure, while 18–21% had a change of classification from ALBI-1 to ALBI-2. When the prognosis of patients with the best CP score of 5 was analyzed, those with ALBI-1 ( $n = 154$ ) had a better outcome than those with ALBI-2 ( $n = 128$ ) (MST 17.5 vs. 9.9 months;  $p = 0.01$ ), while ALBI-1 ( $n = 43$ ) patients also showed

a better outcome than ALBI-2 ( $n = 34$ ) patients with a CP score of 5 without MVI/EHM (MST: 17.5 vs. 10.0 months;  $p = 0.029$ ). The Akaike's Information criterion for ALBI-grade (MST: grade 1 vs. 2 = 16.9 vs. 10.4 months;  $p = 0.001$ ) was also better than that for CP (MST: score 5 vs. 6 = 14.4 vs. 10.5 months;  $p = 0.003$ ) (3195.6 vs. 3197.5) in all 435 patients.

**Conclusion:** The rate of patients with downgraded hepatic function during r-TACE, especially with regard to ALBI-grade, was not low. ALBI-grade was shown to be a better hepatic function assessment tool than CP in patients receiving sorafenib treatment. Strict judgment of TACE-refractory status in patients with unresectable HCC is needed to improve prognosis before downgrading the hepatic function.

© 2017 S. Karger AG, Basel

## Introduction

For treating unresectable hepatocellular carcinoma (HCC) patients, especially those with Barcelona clinic liver cancer (BCLC)-stage B (BCLC-B), transarterial catheter chemoembolization (TACE) has been recommended [1] and used as an effective option for prolonging prognosis worldwide [2–8]. Recently, sorafenib [9, 10], a molecular targeting drug, has also been found to be effective for the treatment of unresectable HCC in patients with good hepatic function (Child-Pugh A, CP-A) [11, 12].

To prolong the prognosis of patients with unresectable HCC, the notion of TACE-refractory status, which has been proposed in both western countries [13, 14] and Japan [15, 16] following the development of sorafenib, has become important. It is well known that hepatic function and tumor status have a strong influence on the prognosis of HCC patients [17–20]. When sorafenib is administered to patients with unresectable HCC, it is generally understood that better hepatic function will relate to good prognosis. However, many with unresectable HCC have a history of repeated TACE treatments prior to the introduction of sorafenib, and few reports have evaluated how repeated TACE procedures influence such patients with good hepatic function. Recently, albumin-bilirubin (ALBI)-score/grade has been proposed as a new hepatic function assessment method [21], while the usefulness of ALBI-grade for the assessment of prognosis in HCC in comparison with Child-Pugh has also been examined [19, 22–26].

To elucidate the relationship between repeated TACE and changes in hepatic function with each procedure, and evaluate the importance of hepatic function for improving prognosis after the introduction of sorafenib in unresectable HCC patients with good hepatic function (CP-

A), especially in those without macro-vessel invasion (MVI)/extrahepatic metastasis (EHM), we evaluated changes in hepatic function in patients with repeated TACE, and compared the assessment of hepatic function between Child-Pugh and ALBI-grade at the time of sorafenib introduction in relation to prognosis.

## Materials and Methods

We analyzed 2 different cohorts. In Study 1, changes in hepatic function (Child-Pugh score, ALBI-score/grade) during repeated TACE procedures for the treatment of BCLC-B HCC patients classified as CP-A were evaluated. Study 2 was performed to elucidate the relationship between hepatic function and prognosis after the introduction of sorafenib by comparing between Child-Pugh score/class and ALBI-grade.

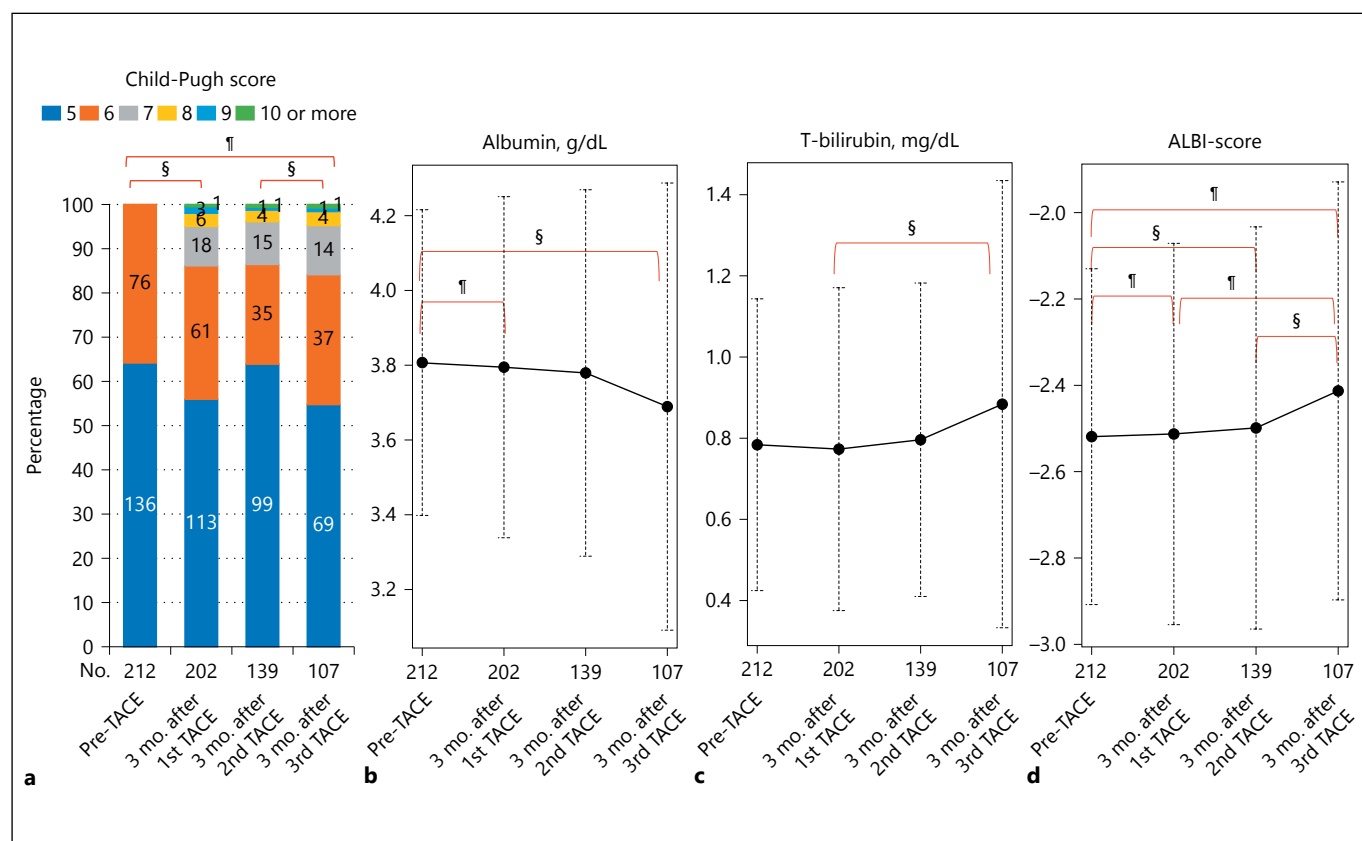
For Study 1, which focused on elucidating changes in hepatic function during repeated TACE procedures, we enrolled 212 BCLC-B HCC patients with good hepatic reserve function (CP-A) who underwent repeated TACE at Ehime Prefectural Central Hospital from January 2000 to December 2016. In Study 2, we analyzed 435 BCLC-B patients with CP-A in whom sorafenib was introduced at our 9 institutions from May 2009 to December 2016 to evaluate prognosis from the viewpoint of hepatic function.

In the 212 patients in Study 1, hepatic function was examined prior to beginning TACE, then 3 months after the initial, 3 months after the second, and 3 months after the third TACE procedure. As for the 435 patients in Study 2, we compared the Child-Pugh score with ALBI-grade for predicting prognosis following the introduction of sorafenib to examine a suitable assessment method for hepatic function at the beginning of sorafenib treatment.

Dynamic computed tomography or magnetic resonance imaging was performed 3 months after each TACE procedure. When recurrence was diagnosed, TACE was performed again and the process repeated, when possible. For TACE, a microcatheter was inserted into the artery feeding the tumor in the most selective manner possible, then a segmental or subsegmental procedure was performed. Epirubicin hydrochloride (Farmorubicin<sup>®</sup>, Pfizer Japan Inc., Tokyo, Japan) prior to January 2010, or miriplatin hydrate (MIRIPLA<sup>®</sup>, Sumitomo Dainippon Pharma Co., Ltd., Osaka, Japan) from January 2010, was injected together with lipiodol in all cases, after which a gelatin sponge cut into small fragments (Gelfoam<sup>®</sup>, Upjohn, Kalamazoo, MI, USA) prior to August 2006, or small gelatin sponge fragments (Gelpart<sup>®</sup>, Nippon Kayaku Co., Ltd., Tokyo, Japan) from September 2006 were used for embolization. The goal of embolization was to eliminate tumor staining without complete obstruction of the hepatic artery.

For assessment of tumors, the BCLC-B subclassification system previously proposed by Kudo [27] was used. Hepatic function was assessed using both Child-Pugh score/classification and ALBI-score/grade. In patients positive for the anti-hepatitis C virus (HCV), HCC was considered to be due to HCV, while it was considered to be caused by hepatitis B virus in patients positive for hepatitis B surface antigen. Patients negative for both anti-HCV and hepatitis B surface antigen were identified as non-viral (nonBnonC) HCC.

All protocols in Study 1 and Study 2 were approved by our Institutional Ethics Committee (IRB No. 28–57).



**Fig. 1.** Changes in (a) Child-Pugh score, (b) serum albumin, (c) total-bilirubin, (d) and ALBI-score during clinical course of BCLC-B HCC patients with Child-Pugh A who underwent repeated TACE procedures. ¶  $p < 0.01$ , §  $p < 0.05$ ; Holm's method.

### Statistical Analysis

Statistical analysis was performed using Welch's  $t$  test, Student's  $t$  test, Mann-Whitney U test, repeated measures of analysis of variance, or Friedman analysis, as appropriate. Prognosis was analyzed using a log-rank test with the Kaplan-Meier method. When multiple comparisons were performed, Holm's method was used. Discriminatory abilities of the scoring models were assessed using Akaike's Information criterion (AIC). All statistical analyses were performed using Easy R (EZR) version 1.29 (Saitama Medical Center, Jichi Medical University, Saitama, Japan), a graphical user interface for the R Statistical Computing Environment (R Foundation, Vienna, Austria). All  $p$  values were derived from 2-tailed tests, with  $p < 0.05$  accepted as statistically significant.

## Results

### Study 1

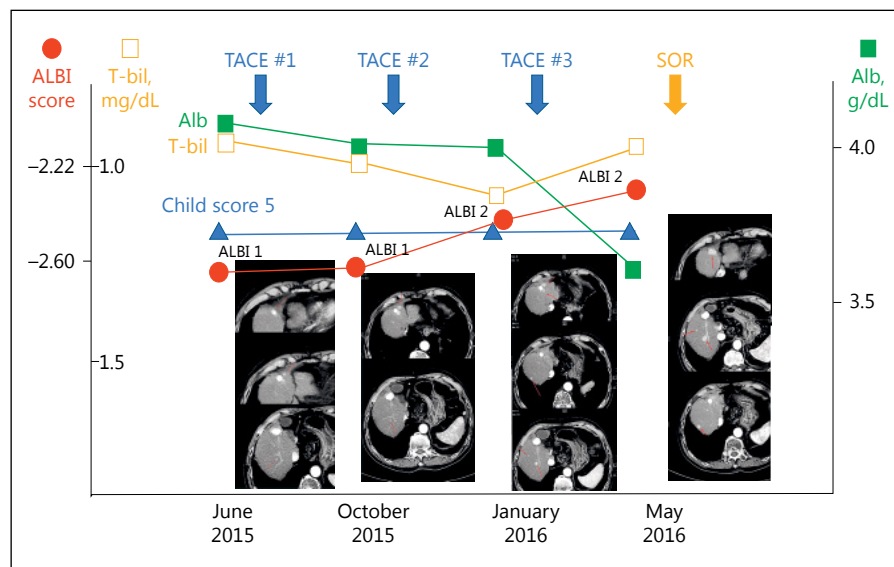
Changes in Child-Pugh score for the 212 patients classified as CP-A (baseline, pre-TACE) are shown in Figure 1a. The number of patients classified as BCLC-B1 was 73

and as BCLC-B2 was 139. There were 136 patients with a Child-Pugh score of 5 and 76 with a Child-Pugh score of 6 (Table 1). At 3 months after the first, second, and third TACE procedure, the Child-Pugh score of patients classified as CP-A increased to 7 or more in 13.8, 13.5, and 15.9%, respectively. In addition, serum levels of albumin and total-bilirubin were slightly worse (Fig. 1b, c), while ALBI-score significantly worsened in association with repeated TACE procedures (Fig. 1d). The ratios of deviation from CP-A at 3 months after each TACE procedure were 13.8, 8.6, and 12.1%, respectively, while those of patients who had deviated from ALBI-1 were 21.4, 19.2, and 18.4%, respectively.

The clinical course of a representative case, a 76-year-old Japanese male, is shown in Figure 2. Following 2 treatments with radiofrequency ablation against HCC, TACE was repeatedly performed for HCC recurrence (BCLC-B1). Although no changes in Child-Pugh score were observed during the clinical course, ALBI-score/grade worsened.



**Fig. 2.** Representative cases. A 76-year-old Japanese male with Child-Pugh A liver cirrhosis due to HCV. After radiofrequency ablation (RFA) twice for hepatocellular carcinoma (HCC), transarterial catheter chemoembolization (TACE) was repeatedly performed for HCC recurrence (BCLC-B1: maximum 1 cm in diameter, 5 nodules). Although no changes in Child-Pugh score were observed during the clinical course, ALBI-score/grade worsened. Alb, albumin; T-bil, total-bilirubin; SOR, sorafenib treatment.



**Table 1.** Clinical characteristics of 212 patients treated with repeated transarterial chemoembolization at Ehime Prefectural Central Hospital

Age, years (IQR)	72* (64–77)
Gender, male/female	163/49
Etiology, HCV/HBV/HDV and HCV/others	162/6/2/42
AST, IU/L	53* (35–78)
ALT, IU/L	44* (26–66)
Platelets, 10 <sup>4</sup> /μL	11.3* (7.9–15.9)
Total-bilirubin, mg/dL	0.7* (0.6–1.0)
Albumin, g/dL	3.8* (3.5–4.1)
Prothrombin time, %	85.0* (77.6–95.9)
Child-Pugh score, 5/6	136/76
ALBI-grade, 1/2	88/124
Naïve/recurrence	65/147
BCLC-B subclassification, B1/B2	73/139

\* Mean value. Values in parenthesis are interquartile range.

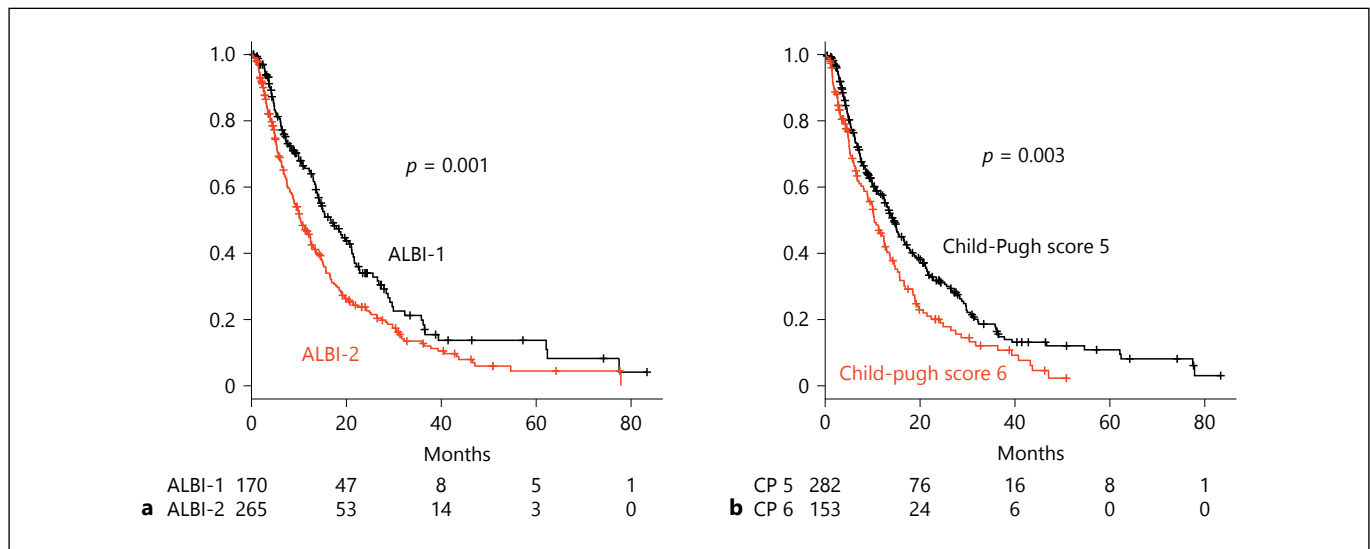
HCV, hepatitis C virus; HBV, hepatitis B virus; nonBnonC, negative for both HBV and HCV; ALBI-grade, albumin-bilirubin grade; AST, aspartate aminotransferase; ALT, alanine aminotransferase; BCLC, Barcelona clinic liver cancer stage.

## Study 2

In this study, 435 HCC patients with CP-A were treated using sorafenib, of which 170 were ALBI-1 and 265 were ALBI-2. Patients with a Child-Pugh score of 5 comprised of 154 patients classified as ALBI-1 and 128 as ALBI-2. On the contrary, 89.5% of patients rated as Child-Pugh 6 were ALBI-2. Adverse events (AEs) at all grades were observed in 236 (54.2%) patients (total: 288 events; hand-foot syndrome [HFS]: 85, diarrhea: 37, appetite

loss: 29, erythema multiforme/rash: 26, general fatigue: 25, others: 86), with 93 grade 3 or 4 AEs observed in 84 (19.3%) (appetite loss: 15, HFS: 13, liver function abnormality: 10, general fatigue 10, diarrhea: 9, gastrointestinal bleeding: 9, others: 27). There were no significant differences regarding sorafenib medication period, total amount of sorafenib, and therapeutic response at 2–3 months after starting sorafenib between ALBI-1 and ALBI-2 patients (Table 2). Both ALBI-grade and Child-Pugh score showed good stratification of prognosis (MST: ALBI-1 vs. ALBI-2, 16.9 vs. 10.4 months,  $p = 0.001$ ; Child-Pugh score 5 vs. 6, 14.4 vs. 10.5 months;  $p = 0.003$ ). However, the AIC for ALBI-grade was smaller as compared to that for Child-Pugh score (3,195.6 vs. 3,197.5; Fig. 3).

Of the 435 patients with CP-A, we analyzed 282 with Child-Pugh 5 according to ALBI-grade and found that those classified as ALBI-1 showed better prognosis than those classified as ALBI-2 after the introduction of sorafenib (MST: 17.5 vs. 9.9 months;  $p = 0.010$ ; Fig. 4a). On the contrary, there was no significant difference in BCLC classification between these groups (data not shown,  $p = 0.843$ ). When the same analysis was performed in 77 of the 282 patients with Child-Pugh 5 after exclusion of MVI/EHM patients, the prognosis of those with ALBI-1 ( $n = 43$ ) was better than that of those with ALBI-2 ( $n = 34$ ) after introducing sorafenib (MST: 17.5 vs. 10.0 months;  $p = 0.039$ ; Fig. 4b). All grades of AE were observed in 43 (55.6%) of these patients (total events: 46 events; HFS: 16, diarrhea: 6, appetite loss: 5, general fatigue: 4, others: 15), while 20 AEs (grades 3 or 4) were observed in 18 patients (23.4%; HFS: 5, diarrhea: 4, appetite loss: 3, others: 8). There was no sig-



**Fig. 3.** Overall survival after introducing sorafenib in all Child-Pugh A patients ( $n = 435$ ). **a** The median survival time (MST) for ALBI-1 ( $n = 170$ ) as compared to ALBI-2 ( $n = 265$ ) patients (16.9 vs. 10.4 months;  $p = 0.001$ , AIC: 3,195.6). **b** The MST for patients

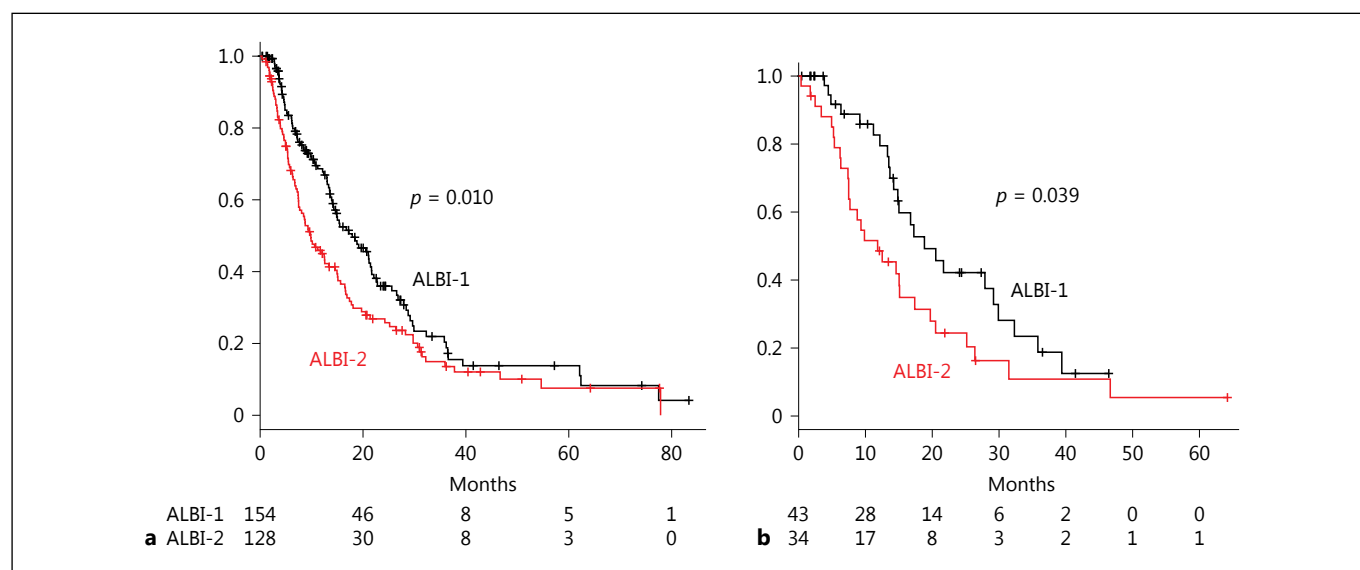
with a Child-Pugh (CP) score of 5 ( $n = 282$ ) as compared to those with a score of 6 ( $n = 153$ ) (14.4 vs. 10.5 months;  $p = 0.003$ , AIC: 3,197.5).

**Table 2.** Characteristics of Child-Pugh A patients classified as ALBI-1 and -2 treated with sorafenib ( $n = 435$ )

	ALBI-1 ( $n = 170$ )	ALBI-2 ( $n = 265$ )	<i>p</i> value
Age, years	69.0±10.6*	68.6±9.3*	0.726
Gender, male/female	147/23	224/41	0.578
Etiology (HCV/HBV/HCV and HCV/others)	75/39/1/55	128/60/1/76	0.249
AST, IU/L	44.8±30.4*	62.1±37.7*	<0.001
ALT, IU/L	36.7±36.2*	44.8±31.4*	0.025
Platelets, 10 <sup>4</sup> /μL	17.1±13.2*	14.4±7.2*	0.016
Total-bilirubin, mg/dL	0.65±0.26*	0.88±0.38*	<0.001
Albumin, g/dL	4.2±0.3*	3.5±0.3*	<0.001
Prothrombin time, %	93.3±15.4*	86.5±10.9*	<0.001
Child-Pugh score, 5/6	154/16	128/137	<0.001
BCLC classification, A/B/C	7/55/108	17/86/162	0.517
Naïve/recurrence	19/151	18/247	0.110
Positive for MVI, %	43 (25.3)	82 (30.9)	0.205
Positive for EHM, %	95 (55.9)	135 (50.9)	0.315
Therapeutic response at first follow-up with imaging modality 2–3 months after introducing sorafenib (CR/PR/SD/PD/ND)	2/13/49/74/32	2/26/73/125/39	0.511
Second-line treatment after sorafenib (performed/not performed/with sorafenib)	57/91/22	65/160/40	0.012
Average period of sorafenib treatments, months	7.6±9.7*	7.6±10.7*	0.939
Total amount of sorafenib, mg	110,034.6±146,217.7*	122,006.1±372,562.0*	0.710
Reasons for stopping sorafenib treatment (in treatment/PD/AE/unknown)	22/80/47/21	13/138/74/40	0.106

\* Mean value ± SD.

ALBI-grade, albumin-bilirubin grade; HCV, hepatitis C virus; HBV, hepatitis B virus; nonBnonC, negative for both HBV and HCV; AST, aspartate aminotransferase; ALT, alanine aminotransferase; BCLC, Barcelona clinic liver cancer stage; MVI, major vessel invasion; EHM, extrahepatic metastasis; CR, complete response; PR, partial response; SD, stable disease; PD, progressive disease; ND, no data; AE, adverse event.



**Fig. 4.** Overall survival of patients with a Child-Pugh score of 5 after introducing sorafenib. **a** Among all patients with a Child-Pugh (CP) score of 5 ( $n = 282$ ), the median survival time (MST) for those classified as ALBI-1 ( $n = 154$ ) was better than that of those classified as ALBI-2 ( $n = 128$ ) (17.5 vs. 9.9 months;  $p = 0.010$ ).

**b** Analysis of 77 patients with CP 5 and BCLC-B. After exclusion of cases with major vessel invasion and/or extrahepatic metastasis, the MST of these patients classified as ALBI-1 ( $n = 43$ ) was better than that of those classified as ALBI-2 ( $n = 34$ ) (17.5 vs. 10.0 months;  $p = 0.039$ ).

nificant difference with regard to the BCLC-B subclassification (Kindai criteria) [27] between these groups ( $p = 0.752$ ; Table 3). The number of past TACE performed in patients with ALBI-1 was  $3.0 \pm 2.7$ , while that in patients with ALBI-2 was  $3.9 \pm 3.0$  ( $p = 0.156$ ). The period of sorafenib medication, total amount of sorafenib, and therapeutic response at 2–3 months after starting sorafenib were not significantly different between patients classified as ALBI-1 and those classified as ALBI-2 (Table 3). However, the frequency of treatments after discontinuing sorafenib was greater in ALBI-1 patients, after exclusion of 9 cases that continued sorafenib ( $p = 0.007$ ).

## Discussion

TACE has been reported to be effective as a palliative treatment for HCC patients classified as BCLC-B [2–4]. Recently, following the development of sorafenib therapy, the concept of TACE-refractory status has been proposed in both western countries and Japan [15, 16]. Ogasawara et al. [28] and Arizumi et al. [29] both reported that the overall survival period of patients whose treatment was switched to sorafenib due to TACE-refractory status was better than those who continued undergoing TACE after becoming TACE-refractory.

Many patients with unresectable HCC have a history of repeated TACE treatments prior to beginning sorafenib. When MVI or EHM is observed, clinicians will often switch from TACE to the next therapy without hesitation. However, such a switch in TACE-refractory patients is not always attempted in those without MVI or EHM, and classified as CP-A. In fact, 23.4% of Japanese clinicians continue TACE even with TACE-refractory patients [15]. Thus, we considered some possible explanations regarding these findings. First, even though results of imaging findings were matched to the Japanese definition of TACE-refractory, clinicians judged the therapeutic response as SD. It is also possible that some clinicians want to re-try TACE by changing chemo-agents, embolization particles, or catheter devices, such as beads [30, 31] or a balloon catheter [32, 33]. Even after excluding patients who no longer continued with TACE because of worsening hepatic function or progression of HCC, the present findings showed that repeated TACE procedures made hepatic function worse at a fixed frequency, while the deviation rate for worsened grade according to an increased number of TACE procedures was larger when patients were assessed using ALBI-grade rather than Child-Pugh classification. Our results suggest that tenacious continued TACE procedures might reduce not only hepatic function, but also prognosis after switching to the next therapeutic modality.

**Table 3.** Characteristics of Child-Pugh 5 patients classified as ALBI-1 and -2 without macrovessel invasion or extrahepatic metastasis treated with sorafenib (*n* = 77)

	ALBI-1 ( <i>n</i> = 43)	ALBI-2 ( <i>n</i> = 34)	<i>p</i> value
Age, years	71.4±10.0	70.3±7.5	0.573
Gender, male/female	37/6	31/3	0.600
Etiology (HCV/HBV/HCV and HCV/others)	21/8/0/14	16/6/0/12	0.839
AST, IU/L	40.9±24.1*	62.4±31.2*	0.004
ALT, IU/L	33.0±25.3*	54.0±25.5*	0.002
Platelets, 10 <sup>4</sup> /μL	16.2±6.6*	14.5±6.5*	0.301
Total-bilirubin, mg/dL	0.62±0.22*	0.79±0.30*	0.006
Albumin, g/dL	4.1±0.3*	3.7±0.2*	<0.001
Prothrombin time, %	95.9±12.8*	88.6±8.8*	0.010
BCLC-B subclassification (B1/B2)	8/35	6/28	0.752
Number of TACE procedures for BCLC-B stage HCC before sorafenib treatment	3.0±2.7*	3.9±3.0*	0.156
Naïve/recurrence	1/42	1/33	0.823
Therapeutic response at first follow-up with imaging modality 2–3 months after introducing sorafenib (CR/PR/SD/PD/ND)	1/5/16/11/10	0/2/9/18/5	0.538
Second-line treatment after sorafenib (performed/not performed/with sorafenib) <sup>§</sup>	21/13/9	9/25/0	0.287
Average period of sorafenib treatments, months	8.9±10.5*	7.2±9.4*	0.425
Total amount of sorafenib, mg	127,055.2±126,631.1*	84,533.1±118,115.2*	0.166
Reasons for stopping sorafenib treatment (in treatment/PD/AE/unknown)	9/18/11/5	0/16/12/6	0.039

\* Mean value ± SD.

<sup>§</sup> After exclusion of 9 cases that continued sorafenib, the frequency of treatments after discontinuing sorafenib was greater in ALBI-1 patients (*p* = 0.007).

ALBI-grade, albumin-bilirubin grade; HCV, hepatitis C virus; HBV, hepatitis B virus; nonBnonC, negative for both HBV and HCV; AST, aspartate aminotransferase; ALT, alanine aminotransferase; BCLC, barcelona clinic liver cancer stage; CR, complete response; PR, partial response; SD, stable disease; PD, progressive disease; ND, no data; AE, adverse event.

Even among patients with the best Child-Pugh score of 5, those classified as ALBI-1 had a better overall survival as compared to those classified as ALBI-2, with the same results observed after exclusion of patients with MVI/EHM (MST: 17.5 vs. 10.0 months, *p* = 0.039). Our findings suggest that the introduction of sorafenib to TACE-refractory patients with the best ALBI-grade 1 may be more effective in prolonging prognosis. We considered the major reason for this finding was that treatment after sorafenib failure was more easily performed in patients classified as ALBI-1 as compared to ALBI-2 because of their good reserve hepatic function. A recent report by Piinato noted that the ability to predict post-sorafenib overall survival was easier when based on ALBI-grade than on Child-Pugh classification [34]. Moreover, this study found that the median post-sorafenib overall survival in ALBI-1, -2, and -3 patients eligible for second-line therapy was 17.5, 7.5, and 1.9 months, respectively (*p* < 0.001). Thus, maintaining a

good ALBI-grade (1) when introducing sorafenib is thought to be important to improve the prognosis of unresectable HCC patients. If ALBI-grade is 2 at diagnosis of BCLC-B and unresectable HCC, then TACE-refractory status should be assessed more strictly for avoiding a worsening hepatic function more with continuing TACE, so as to not lose the chance of switching to a molecular target drug. High levels of tumor markers [35] (positive for 2 of the following factors: alpha-fetoprotein >100 ng/mL, fucosylated alpha-fetoprotein >10%, des-gamma carboxyprothrombin >100 mAU/mL) after 2 TACE procedures was reported to be poor as a prognostic marker in HCC patients with BCLC-B [36], thus it is important to focus on malignant potential and maintain hepatic function other than response in such patients.

The present results suggest that ALBI-score gradually worsens with continued TACE, though the ratio of worsening hepatic function is not low even after a few



procedures. In addition, downgrading from ALBI-1 at the introduction of sorafenib might be a factor related to poor prognosis. Nevertheless, the present study has some limitations, including its retrospective nature and the small number of patients, making it difficult to form definitive conclusions. Hence, additional examinations with larger numbers of patients will be needed.

For considering development of new molecular target drugs [11, 37–39] and other therapeutic modalities including hepatic arterial infusion chemotherapy [40, 41] in the future, analyses of therapeutic options that prolong the

prognosis of patients with advanced and unresectable HCC are needed. It is also important to keep maintenance of hepatic function in mind by avoiding TACE that may have less effect or be harmful, and promptly switch the therapeutic modality in TACE-refractory patients, when possible.

## Disclosure Statement

There are no financial disclosures, grants from any organs, conflicts of interest, and/or acknowledgements for the authors to declare.

## References

- Bruix J, Han KH, Gores G, Llovet JM, Mazzaferro V: Liver cancer: approaching a personalized care. *J Hepatol* 2015;62:S144–S156.
- Cammà C, Schepis F, Orlando A, Albanese M, Shahied L, Trevisani F, Andreone P, Craxi A, Cottone M: Transarterial chemoembolization for unresectable hepatocellular carcinoma: meta-analysis of randomized controlled trials. *Radiology* 2002;224:47–54.
- Lo CM, Ngan H, Tso WK, Liu CL, Lam CM, Poon RT, Fan ST, Wong J: Randomized controlled trial of transarterial lipiodol chemoembolization for unresectable hepatocellular carcinoma. *Hepatology* 2002;35:1164–1171.
- Takayasu K, Arii S, Ikai I, Omata M, Okita K, Ichida T, Matsuyama Y, Nakanuma Y, Kojiro M, Makuuchi M, Yamaoka Y: Prospective cohort study of transarterial chemoembolization for unresectable hepatocellular carcinoma in 8510 patients. *Gastroenterology* 2006;131:461–469.
- Kudo M: Surveillance, diagnosis, treatment, and outcome of liver cancer in Japan. *Liver Cancer* 2015;4:39–50.
- Clinical practice guidelines for hepatocellular carcinoma differ between Japan, United States, and Europe. *Liver Cancer* 2015;4:85–95.
- Kudo M: Locoregional therapy for hepatocellular carcinoma. *Liver Cancer* 2015;4:163–164.
- Tsurusaki M, Murakami T: Surgical and locoregional therapy of HCC: TACE. *Liver Cancer* 2015;4:165–175.
- Llovet JM, Ricci S, Mazzaferro V, Hilgard P, Gane E, Blanc JF, de Oliveira AC, Santoro A, Raoul JL, Forner A, Schwartz M, Porta C, Zeuzem S, Bolondi L, Greten TF, Galle PR, Seitz JF, Borbath I, Haussinger D, Giannaris T, Shan M, Moscovici M, Voliotis D, Bruix J: Sorafenib in advanced hepatocellular carcinoma. *N Engl J Med* 2008;359:378–390.
- Tanaka K, Shimada M, Kudo M: Characteristics of long-term survivors following sorafenib treatment for advanced hepatocellular carcinoma: report of a workshop at the 50th Annual Meeting of the Liver Cancer Study Group of Japan. *Oncology* 2014;87(suppl 1):104–109.
- Kudo M: Molecular Targeted Therapy for Hepatocellular Carcinoma: where Are We Now? *Liver Cancer* 2015;4:I–VII.
- Nakanishi H, Kurosaki M, Tsuchiya K, Yasui Y, Higuchi M, Yoshida T, Komiya Y, Takaura K, Hayashi T, Kuwabara K, Nakakuki N, Takada H, Ueda M, Tamaki N, Suzuki S, Itakura J, Takahashi Y, Izumi N: Novel pre-treatment scoring incorporating C-reactive protein to predict overall survival in advanced hepatocellular carcinoma with sorafenib treatment. *Liver Cancer* 2016;5:257–268.
- Dufour JF, Bargellini I, De Maria N, De Simone P, Goulis I, Marinho RT: Intermediate hepatocellular carcinoma: current treatments and future perspectives. *Ann Oncol* 2013;24(suppl 2):ii24–ii29.
- Hucke F, Sieghart W, Pinter M, Graziadei I, Vogel W, Muller C, Heinzl H, Waneck F, Trauner M, Peck-Radosavljevic M: The ART strategy: sequential assessment of the ART score predicts outcome of patients with hepatocellular carcinoma re-treated with TACE. *J Hepatol* 2014;60:118–126.
- Kudo M, Matsui O, Izumi N, Kadoya M, Okusaka T, Miyayama S, Yamakado K, Tsuchiya K, Ueshima K, Hiraoka A, Ikeda M, Ogasawara S, Yamashita T, Minami T: Transarterial chemoembolization failure/refractoriness: JSH-LCSGJ criteria 2014 update. *Oncology* 2014;87(suppl 1):22–31.
- Kudo M, Matsui O, Izumi N, Iijima H, Kadoya M, Imai Y, Okusaka T, Miyayama S, Tsuchiya K, Ueshima K, Hiraoka A, Ikeda M, Ogasawara S, Yamashita T, Minami T, Yamakado K: JSH consensus-based clinical practice guidelines for the management of hepatocellular carcinoma: 2014 update by the Liver Cancer Study Group of Japan. *Liver Cancer* 2014;3:458–468.
- Kudo M, Chung H, Osaki Y: Prognostic staging system for hepatocellular carcinoma (CLIP score): its value and limitations, and proposal for a new staging system, the Japan Integrated Staging Score (JIS score). *J Gastroenterol* 2003;38:207–215.
- Kudo M, Chung H, Haji S, Osaki Y, Oka H, Seki T, Kasugai H, Sasaki Y, Matsunaga T: Validation of a new prognostic staging system for hepatocellular carcinoma: the JIS score compared with the CLIP score. *Hepatology* 2004;40:1396–1405.
- Hiraoka A, Kumada T, Kudo M, Hirooka M, Tsuji K, Itobayashi E, Kariyama K, Ishikawa T, Tajiri K, Ochi H, Tada T, H. T, Nouse K, Joko K, Kawasaki H, Hiasa Y, Michitaka K: Real-Life Practice Experts for HCC (RELPEC) Study Group and HCC 48 Group (hepatocellular carcinoma experts from 48 clinics): Albumin-bilirubin (ALBI) grade as part of the evidence-based clinical practice guideline for HCC of the Japan Society of hepatology: a comparison with the liver damage and child-pugh classifications. *Liver cancer* 2017;6:204–215.
- Kudo M, Izumi N, Sakamoto M, Matsuyama Y, Ichida T, Nakashima O, Matsui O, Ku Y, Kokudo N, Makuuchi M: Survival analysis over 28 years of 173,378 patients with hepatocellular carcinoma in Japan. *Liver Cancer* 2016;5:190–197.
- Johnson PJ, Berhane S, Kagebayashi C, Sato-mura S, Teng M, Reeves HL, O'Beirne J, Fox R, Skowronska A, Palmer D, Yeo W, Mo F, Lai P, Iñarrairaegui M, Chan SL, Sangro B, Miksad R, Tada T, Kumada T, Toyoda H: Assessment of liver function in patients with hepatocellular carcinoma: a new evidence-based approach-the ALBI grade. *J Clin Oncol* 2015;33:550–558.
- Hiraoka A, Kumada T, Michitaka K, Toyoda H, Tada T, Ueki H, Kaneto M, Aibiki T, Okudaira T, Kawakami T, Kawamura T, Yamago H, Suga Y, Miyamoto Y, Tomida H, Azemoto N, Mori K, Miyata H, Ninomiya T, Kawasaki H: Usefulness of albumin-bilirubin grade for evaluation of prognosis of 2584 Japanese patients with hepatocellular carcinoma. *J Gastroenterol Hepatol* 2016;31:1031–1036.

- 23 Chen RC, Cai YJ, Wu JM, Wang XD, Song M, Wang YQ, Zheng MH, Chen YP, Lin Z, Shi KQ: Usefulness of albumin-bilirubin grade for evaluation of long-term prognosis for hepatitis B-related cirrhosis. *Journal of viral hepatitis* 2017;24:238–245.
- 24 Chan AW, Chong CC, Mo FK, Wong J, Yeo W, Johnson PJ, Yu S, Lai PB, Chan AT, To KF, Chan SL: Incorporating albumin-bilirubin grade into the cancer of the liver Italian program system for hepatocellular carcinoma. *J Gastroenterol Hepatol* 2017;32:221–228.
- 25 Wang YY, Zhong JH, Su ZY, Huang JF, Lu SD, Xiang BD, Ma L, Qi LN, Ou BN, Li LQ: Albumin-bilirubin versus Child-Pugh score as a predictor of outcome after liver resection for hepatocellular carcinoma. *Br J Surg* 2016; 103:725–734.
- 26 Kudo M: Albumin-Bilirubin grade and hepatocellular carcinoma treatment algorithm. *Liver cancer* 2017;6:185–188.
- 27 Kudo M, Arizumi T, Ueshima K, Sakurai T, Kitano M, Nishida N: Subclassification of BCLC B stage hepatocellular carcinoma and treatment strategies: proposal of modified bolondi's subclassification (Kinki Criteria). *Dig Dis* 2015;33:751–758.
- 28 Ogasawara S, Chiba T, Ooka Y, Kanogawa N, Motoyama T, Suzuki E, Tawada A, Kanai F, Yoshikawa M, Yokosuka O: Efficacy of sorafenib in intermediate-stage hepatocellular carcinoma patients refractory to transarterial chemoembolization. *Oncology* 2014;87: 330–341.
- 29 Arizumi T, Ueshima K, Minami T, Kono M, Chishina H, Takita M, Kitai S, Inoue T, Yada N, Hagiwara S, Minami Y, Sakurai T, Nishida N, Kudo M: Effectiveness of sorafenib in patients with transcatheter arterial chemoembolization (TACE) refractory and intermediate-stage hepatocellular carcinoma. *Liver Cancer* 2015;4:253–262.
- 30 Aliberti C, Benea G, Tilli M, Fiorentini G: Chemoembolization (TACE) of unresectable intrahepatic cholangiocarcinoma with slow-release doxorubicin-eluting beads: preliminary results. *Cardiovasc Intervent Radiol* 2008;31:883–888.
- 31 Skowasch M, Schneider J, Otto G, Weinmann A, Woerns MA, Dueber C, Pitton MB: Mid-term follow-up after DC-BEAD-TACE of hepatocellular carcinoma (HCC). *Eur J Radiol* 2012;81:3857–3861.
- 32 Ishikawa T, Abe S, Inoue R, Sugano T, Watanabe Y, Iwanaga A, Seki K, Honma T, Nemoto T, Takeda K, Yoshida T: Predictive factor of local recurrence after balloon-occluded TACE with miriplatin (MPT) in hepatocellular carcinoma. *PLoS One* 2014; 9:e103009.
- 33 Minami Y, Minami T, Chishina H, Arizumi T, Takita M, Kitai S, Yada N, Hagiwara S, Tsurusaki M, Yagyu Y, Ueshima K, Nishida N, Murakami T, Kudo M: Balloon-occluded transcatheter arterial chemoembolization for hepatocellular carcinoma: a single-center experience. *Oncology* 2015;89(suppl 2):27–32.
- 34 Pinato DJ, Yen C, Bettinger D, Ramaswami R, Arizumi T, Ward C, Pirisi M, Burlone ME, Thimme R, Kudo M, Sharma R: The albumin-bilirubin grade improves hepatic reserve estimation post-sorafenib failure: implications for drug development. *Aliment Pharmacol Ther* 2017;45:714–722.
- 35 Toyoda H, Kumada T, Tada T, Sone Y, Kaneoka Y, Maeda A: Tumor markers for hepatocellular carcinoma: simple and significant predictors of outcome in patients with HCC. *Liver Cancer* 2015;4:126–136.
- 36 Hiraoka A, Ishimaru Y, Kawasaki H, Aibiki T, Okudaira T, Toshimori A, Kawamura T, Yamago H, Nakahara H, Suga Y, Azemoto N, Miyata H, Miyamoto Y, Ninomiya T, Hirooka M, Abe M, Matsuura B, Hiasa Y, Michitaka K: Tumor markers AFP, AFP-L3, and DCP in hepatocellular carcinoma refractory to transcatheter arterial chemoembolization. *Oncology* 2015;89:167–174.
- 37 Kudo M: Immune checkpoint blockade in hepatocellular carcinoma. *Liver Cancer* 2015;4: 201–207.
- 38 Kudo M: Regorafenib as second-line systemic therapy may change the treatment strategy and management paradigm for hepatocellular carcinoma. *Liver Cancer* 2016;5:235–244.
- 39 Zhang B, Finn RS: Personalized clinical trials in hepatocellular carcinoma based on biomarker selection. *Liver Cancer* 2016;5:221–232.
- 40 Obi S, Sato S, Kawai T: Current status of hepatic arterial infusion chemotherapy. *Liver Cancer* 2015;4:188–199.
- 41 Lin CC, Hung CF, Chen WT, Lin SM: Hepatic arterial infusion chemotherapy for advanced hepatocellular carcinoma with portal vein thrombosis: impact of early response to 4 weeks of treatment. *Liver Cancer* 2015;4: 228–240.

# Sorafenib-Regorafenib Sequential Therapy in Advanced Hepatocellular Carcinoma: A Single-Institute Experience

Kazuomi Ueshima Naoshi Nishida Masatoshi Kudo

Department of Gastroenterology and Hepatology, Kindai University Faculty of Medicine, Osaka-Sayama, Japan

## Keywords

Hepatocellular carcinoma · Sorafenib-regorafenib sequential therapy · Second-line treatment · Sorafenib · Regorafenib

## Abstract

**Objectives:** Previously, no therapeutic agent has been known to improve the overall survival compared with placebo in patients with hepatocellular carcinoma (HCC), who have progressed after sorafenib. In this patient population, regorafenib was first demonstrated to confer a survival benefit in the RESORCE trial, and subsequently it was approved as a second-line treatment for patients with advanced HCC. An open-label expanded access program (EAP) of regorafenib was implemented for compassionate use. We investigated the efficacy and safety of regorafenib based on our experience of the RESORCE trial and the EAP. **Methods:** Data from 5 patients from the RESORCE trial and 6 from the EAP were analyzed retrospectively. All patients had tolerated prior sorafenib and were progressing during sorafenib treatment. **Results:** The median progression-free survival was 9.2 months (95% CI 2.3–16.1). One patient achieved a partial response and 7 achieved stable disease. The objective re-

sponse rate was 9.1%, and the disease control rate was 72.7%. No treatment-associated mortalities were observed. Grade 3 hypophosphatemia was observed in 2 patients, grade 2 anorexia was observed in 5 patients, and grade 3 neutropenia was observed in 2 patients. Grade 2 and grade 3 thrombocytopenia were observed in 2 and 3 patients, respectively. All treatment-related adverse events were improved by reduction or interruption of regorafenib. Five patients showed decreased serum albumin levels. **Conclusion:** Sorafenib and regorafenib sequential therapy presents a safe and effective treatment option for patients with advanced HCC.

© 2017 S. Karger AG, Basel

## Introduction

Sorafenib is the standard treatment for patients with advanced-stage (Barcelona Clinic Liver Cancer [BCLC] stage C) hepatocellular carcinoma (HCC) with vascular invasion and/or extrahepatic spread, and also for patients with intermediate-stage disease (BCLC stage B) who do not respond to transcatheter arterial chemoembolization (TACE) [1–5].

Following the approval of sorafenib, several other molecular targeted agents have been investigated for first-line use as an alternative to sorafenib or as a second-line treatment for patients with progressive disease or those intolerant to sorafenib. However, in trials of these agents, primary endpoints were not met [6–12]. Thus, sorafenib remains the only systemic therapeutic agent available for the treatment of advanced HCC.

In May 2016, the results of a regorafenib phase III study (RESORCE) were first reported, and were subsequently published in 2017 [13], and represent a promising treatment option for patients progressing on sorafenib [14]. Subsequently, an open-label expanded access program (EAP) of regorafenib treatment in patients with HCC who have progressed after sorafenib was conducted for compassionate use in patients in Japan from March 2017 to June 2017.

In this study, we investigated the efficacy and safety of regorafenib based on our experience of the RESORCE study and the EAP.

## Materials and Methods

We participated in the RESORCE study, a phase III global trial to investigate the efficacy and safety of regorafenib compared with placebo in HCC patients progressing on sorafenib [13]. Thirteen patients were registered to the RESORCE trial, 5 of who were allocated to the regorafenib arm. From March 2017 to May 2017, 6 patients were registered to the EAP at our hospital. In total, data from 11 patients registered to these 2 trials were investigated in this study.

The inclusion and exclusion criteria were almost identical between the RESORCE study and the EAP. Eligible patients had unresectable HCC, confirmed by pathological or radiographic findings, and were BCLC stage B or C. Patients must have tolerated sorafenib ( $\geq 400$  mg daily for at least 20 of 28 days before continuation) and were required to have Child-Pugh A liver function. Patients were excluded if they had discontinued sorafenib for intolerable toxicity.

Patients received 160 mg regorafenib orally once daily for 3 weeks in each 4-week cycle, with best supportive care. Treatment interruption and dose reductions (to 120 mg and then to 80 mg) were permitted according to toxicity.

Progression-free survival (time from the initial administration to radiological or clinical disease progression or death), time to progression (time from the initial administration to radiological or clinical disease progression), objective response rate (complete or partial response), and disease control rate (complete response, partial response, or stable disease maintained for  $\geq 6$  weeks) were assessed by investigators, according to the modified Response Evaluation Criteria in Solid Tumors [15]. Adverse events were graded according to the National Cancer Institute Common Terminology Criteria for Adverse Events (NCI-CTCAE) version 4.03.

These trials were approved by the institutional review board of our hospital and complied with Good Clinical Practice guidelines.

**Table 1.** Patient background

Age, years, median (range)	64.6 (40–77)
Gender	
Male	8
Female	3
Etiology	
HBV	3
HCV	4
NBNC	3
AL	1
Child-Pugh score	
Score 5	5
Score 6	6
ECOG Performance status	
0	10
1	1
TNM stage according to LCSGJ	
Stage III	1
Stage IVA	2
Stage IVB	8
BCLC stage	
BCLC B	1
BCLC C	10
UICC	
Stage II	1
Stage IIIB	2
Stage IVB	8
Major vessel invasion	
Yes	4
No	7
Extrahepatic metastasis	
Yes	8
No	3

LCSGJ, Liver Cancer Study Group of Japan; BCLC, Barcelona Clinic Liver Cancer; UICC, Union for International Cancer Control.

## Results

### Baseline Characteristics

The median age of patients was 64.6 years (range 40–77). Eight were male and 3 were female. HCC derived from HBV, HCV, nonHBV, and alcohol was 3, 4, 3, and 1, respectively. Five patients had a Child-Pugh score of 5 and 6 had a Child-Pugh score of 6, with good performance status. Most patients had major vessel invasion and/or extrahepatic spread and were classified as BCLC stage C (Table 1).

### Treatment

The reason for the discontinuation of sorafenib was progressive disease. The last dose of sorafenib was 800 mg daily in 6 patients and 400 mg in 5 patients. The me-

dian duration of prior sorafenib treatment was 5.9 months. The starting dose of regorafenib was 160 mg daily. At the data cutoff date (30 June 2017), 4 patients remained on treatment. In the remaining 7 patients, the reasons for treatment discontinuation were disease progression ( $n = 5$ , 45.5%) and withdrawal of consent ( $n = 2$ , 18.2%). The median duration of regorafenib treatment was 6.8 months in the RESORCE trial and 2.6 months in the EAP.

### Efficacy

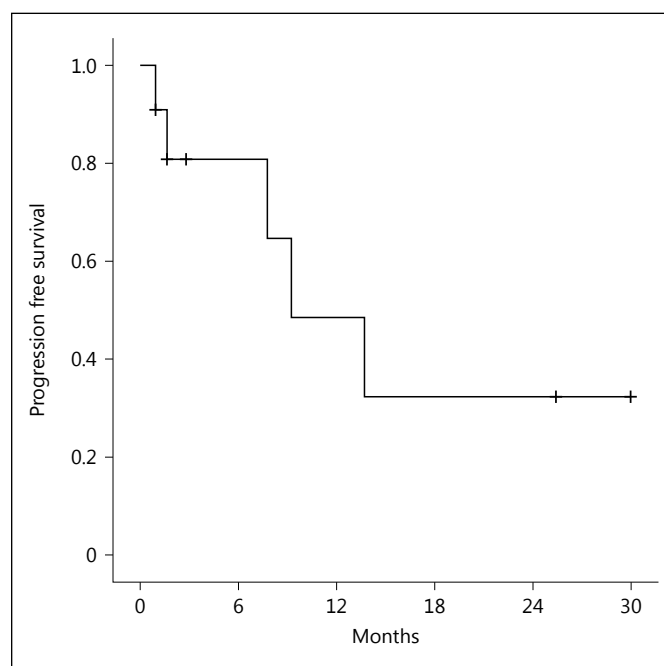
The median progression-free survival was 9.2 months (95% CI 2.3–16.1; Fig. 1). One patient achieved a partial response (Fig. 2a, b) and 7 patients achieved stable disease. The objective response rate was 9.1% and the disease control rate was 72.7% (Table 2).

### Safety

All patients were assessed for toxicity. No treatment-associated mortalities were observed. The drug-related adverse events are summarized in Table 2. No G4 events were observed. Grade 3 hypophosphatemia without symptoms was observed in 2 patients, grade 2 anorexia was observed in 5 patients, and grade 3 neutropenia was observed in 2 patients. Grade 2 and grade 3 thrombocytopenia were observed in 2 and 3 patients, respectively. All treatment-related adverse events were improved by the reduction or interruption of regorafenib treatment. Toxicities of regorafenib tended to be similar to those of sorafenib (Table 3). Five patients showed decreased serum albumin levels,  $<3.0$  mg/dL. The changes in serum albumin levels are shown in Figure 3.

### Discussion

Regorafenib is a small molecule that inhibits angiogenic kinases (VEGFR1/3, platelet-derived growth factor receptor-beta, and fibroblast growth factor receptor 1) and the mutant oncogenic kinases KIT, RET, and B-RAF [16]. A multicenter, open-label, phase II safety study revealed that regorafenib had acceptable tolerance and showed evidence of antitumor activity in patients with intermediate or advanced HCC who had progressed to sorafenib [17]. Subsequently, the randomized, placebo-controlled, phase III RESORCE trial was conducted and demonstrated a statistically significant advantage in the overall survival from 7.8 months with placebo to 10.6 months with regorafenib in patients progressing on sorafenib [13]. Regorafenib has been approved for clinical



**Fig. 1.** Progression-free survival. Kaplan-Meier estimate of progression-free survival from start of treatment to data cutoff date of 30 June 2017. The median progression-free survival was 9.2 months (95% CI 2.3–16.1).

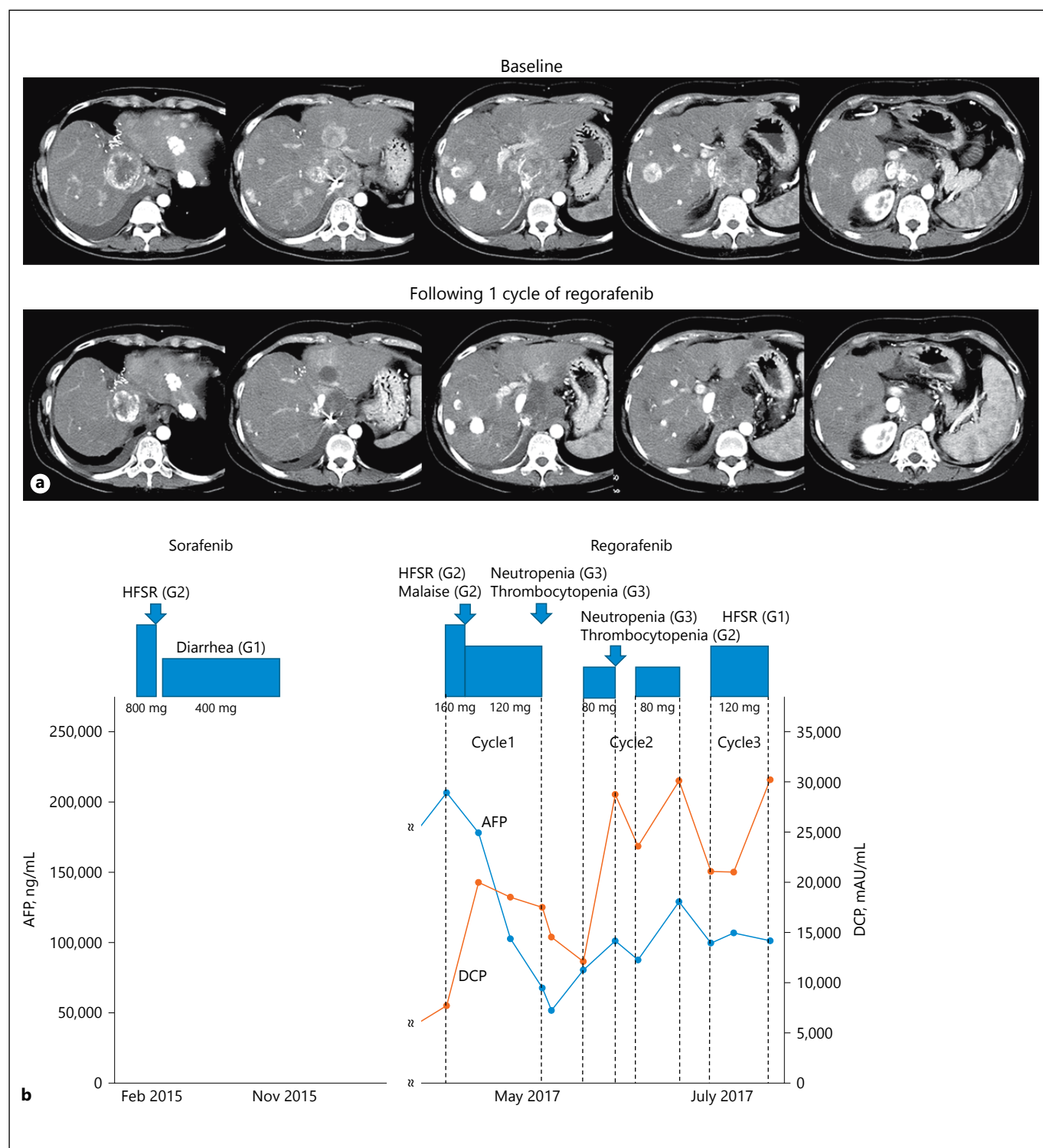
cal use since June 2017 as a second-line treatment for patients with advanced HCC and progression on sorafenib.

In our hospital, 11 HCC patients were treated with regorafenib. Despite the failure of sorafenib treatment, a partial response was observed in one patient, and 7 patients achieved stable disease with relatively high tolerance. All patients had disease progression on sorafenib and had received long-term sorafenib treatment.

Des-gamma-carboxyprothrombin [18] level was increased following administration of regorafenib, but decreased immediately after the reduction or interruption of regorafenib in the patient who showed a partial response (Fig. 2b). This paradoxical change in des-gamma-carboxyprothrombin caused by ischemic changes in hepatocytes is frequently observed with sorafenib treatment [19].

The toxicities associated with regorafenib, such as hand-foot skin reaction, hypertension, or diarrhea, are similar to those of sorafenib because of structural similarities between the 2 agents. From our experience, sorafenib toxicities tended to reappear with successive regorafenib treatment. If treatment-related adverse events were observed in prior sorafenib treatment, careful





**Fig. 2. a** CT scan images of EAP case with partial response. **a, b** CT scan images of an EAP case (**a**) of a 40-year-old female with HCC in multiple locations in the liver. The right pleural effusion was the result of prior TACE without ascites. After one cycle of regorafenib, some tumors disappeared, and almost all showed hypovascular changes and shrinkage. The clinical course of this case is

shown in **b**. Alpha-fetoprotein (AFP) was decreased after the administration of regorafenib. Des-gamma-carboxyprothrombin (DCP) was increased after the administration of regorafenib, but reduction or interruption of regorafenib caused DCP level to decrease. This phenomenon is frequently associated with sorafenib treatment. **b** Clinical course of EAP case with partial response.

**Table 2.** Response rate and disease control rate

Response	<i>n</i>	%
Complete response	0	0
Partial response	1	9.1
Stable disease	7	63.6
Progressive disease	2	18.2
Not evaluable	1	9.1
ORR		9.1
DCR		72.7

ORR, objective response rate; DCR, disease control rate.

**Table 3.** Drug-related adverse event

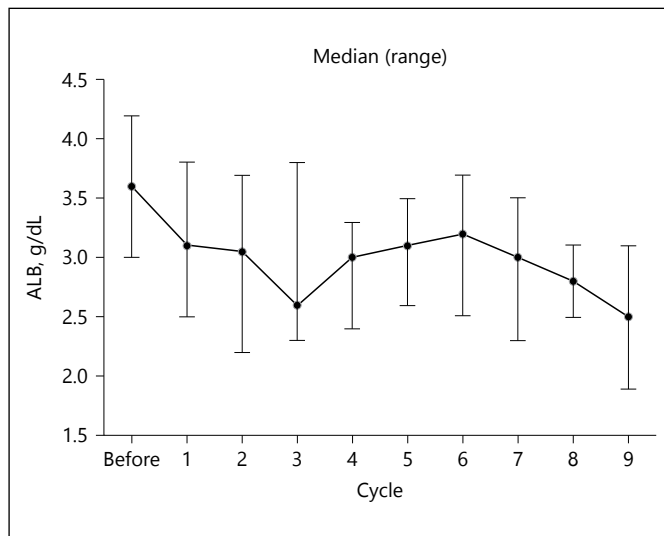
Case	Sorafenib (as a prior treatment)		Regorafenib	
	adverse events	grade	adverse events	grade
Case 1	Alopecia	G1	Hypoalbuminemia	G2
			Hypophosphatemia	G3
			Weight loss	G2
			Anorexia	G2
Case 2	HFSR	G2	HFSR	G3
Case 3	Hypertension	G1	Hypertension	G3
			Proteinuria	G2
Case 4	HFSR	G2	Malaise	G2
			Anorexia	G2
Case 5	Lipase increased	G3	Lipase increased	G3
			Proteinuria	G3
Case 6	Proteinuria	G2	Hypertension	G3
	Hypertension	G2	Hypothyroidism	G2
	Hypothyroidism	G2	Anorexia	G2
	Diarrhea	G2	Anemia	G2
	Dysgeusia	G2	Hypophosphatemia	G3
	Alopecia	G1	Thrombocytopenia	G2
Case 7	HFSR	G2	Diarrhea	G2
	Diarrhea	G1	Anorexia	G2
	Alopecia	G1		
Case 8	Pruritus	G1	Malaise	G2
	HFSR	Unknown	Anorexia	G1
Case 9	Thrombocytopenia	G3	Thrombocytopenia	G2
	Neutropenia	G3	Neutropenia	G3
	Hypertension	G2		
	HFSR	G2		
Case 10	HFSR	G2	HFSR	G1
	Diarrhea	G1	Malaise	G2
			Thrombocytopenia	G3
			Neutropenia	G3
Case 11	No data		Nothing	
	HFSR	G2	HFSR	G3

HFSR, hand-foot skin reaction.

management during successive regorafenib treatment is required, with a focus on the adverse events observed during sorafenib treatment.

The emergence of regorafenib in the clinical field has impacted HCC treatment options. Kudo [20] performed

a simple comparison of the overall survival between TACE alone (from the placebo arm of the brivanib-TACE trial, which has the most conclusive overall survival data on TACE alone) and sorafenib-regorafenib sequential therapy (the regorafenib arm of the RESORCE trial). The



**Fig. 3.** Change in serum albumin levels.

overall survival for TACE alone in patients with intermediate-stage disease and patients with advanced-stage disease receiving sorafenib-regorafenib sequential therapy were almost identical, at 26.0 and 26.1 months, respectively. To maximize the therapeutic potential of regorafenib when locoregional therapy, especially TACE, is refractory [21, 22], patients should immediately receive sorafenib-regorafenib sequential therapy while the liver function is preserved.

## References

- Llovet JM, Ricci S, Mazzaferro V, Hilgard P, Gane E, Blanc JF, de Oliveira AC, Santoro A, Raoul JL, Forner A, Schwartz M, Porta C, Zeuzem S, Bolondi L, Greten TF, Galle PR, Seitz JF, Borbath I, Haussinger D, Giannaris T, Shan M, Moscovici M, Voliotis D, Bruix J: Sorafenib in advanced hepatocellular carcinoma. *N Engl J Med* 2008;359:378–390.
- Cheng AL, Kang YK, Chen Z, Tsao CJ, Qin S, Kim JS, Luo R, Feng J, Ye S, Yang TS, Xu J, Sun Y, Liang H, Liu J, Wang J, Tak WY, Pan H, Burock K, Zou J, Voliotis D, Guan Z: Efficacy and safety of sorafenib in patients in the Asia-Pacific region with advanced hepatocellular carcinoma: a phase III randomised, double-blind, placebo-controlled trial. *Lancet Oncol* 2009;10:25–34.
- Kudo M, Izumi N, Sakamoto M, Matsuyama Y, Ichida T, Nakashima O, Matsui O, Ku Y, Kokudo N, Makuuchi M: Survival analysis over 28 years of 173,378 patients with hepatocellular carcinoma in Japan. *Liver Cancer* 2016;5:190–197.
- Kudo M: Locoregional therapy for hepatocellular carcinoma. *Liver Cancer* 2015;4:163–164.
- Clinical practice guidelines for hepatocellular carcinoma differ between Japan, United States, and Europe. *Liver Cancer* 2015;4:85–95.
- Cheng AL, Kang YK, Lin DY, Park JW, Kudo M, Qin S, Chung HC, Song X, Xu J, Poggi G, Omata M, Pitman Lowenthal S, Lanzalone S, Yang L, Lechuga MJ, Raymond E: Sunitinib versus sorafenib in advanced hepatocellular cancer: Results of a randomized phase III trial. *J Clin Oncol* 2013;31:4067–4075.
- Cainap C, Qin S, Huang WT, Chung JJ, Pan H, Cheng Y, Kudo M, Kang YK, Chen PJ, Toh HC, Gorbunova V, Eskens FA, Qian J, McKee MD, Ricker JL, Carlson DM, El-Nowiem S: Linifanib versus sorafenib in patients with advanced hepatocellular carcinoma: results of a randomized phase III trial. *J Clin Oncol* 2015;33:172–179.
- Johnson PJ, Qin S, Park JW, Poon RT, Raoul JL, Philip PA, Hsu CH, Hu TH, Heo J, Xu J, Lu L, Chao Y, Boucher E, Han KH, Paik SW, Robles-Avina J, Kudo M, Yan L, Sobhon-slidsuk A, Komov D, Decaens T, Tak WY, Jeng LB, Liu D, Ezzeddine R, Walters I, Cheng AL: Brivanib versus sorafenib as first-line therapy in patients with unresectable, advanced hepatocellular carcinoma: Results from the randomized phase III BRISK-FL study. *J Clin Oncol* 2013;31:3517–3524.
- Llovet JM, Decaens T, Raoul JL, Boucher E, Kudo M, Chang C, Kang YK, Assenat E, Lim HY, Boige V, Mathurin P, Fartoux L, Lin DY, Bruix J, Poon RT, Sherman M, Blanc JF, Finn RS, Tak WY, Chao Y, Ezzeddine R, Liu D, Walters I, Park JW: Brivanib in patients with advanced hepatocellular carcinoma who were intolerant to sorafenib or for whom sorafenib failed: results from the randomized phase III BRISK-PS study. *J Clin Oncol* 2013;31:3509–3516.

Limitations of the present study were that it was a single institute study with a small sample size, and the duration of observation in the EAP was relatively short.

In conclusion, sorafenib and regorafenib sequential therapy is an effective treatment option for patients with advanced HCC. Patients who are suitable for regorafenib treatment should be carefully selected to ensure a successful treatment outcome.

## Acknowledgments

We thank Clare Cox, PhD, from Edanz Group ([www.edanz-editing.com/ac](http://www.edanz-editing.com/ac)) for editing a draft of this manuscript.

## Ethics Statement

No approval was required for this retrospective study.

## Disclosure Statement

The authors declare no conflicts of interest.

## Author Contributions

K.U. analyzed the data and wrote the paper. N.N. and M.K. contributed to this study for patient inclusion.

- 10 Zhu AX, Kudo M, Assenat E, Cattani S, Kang YK, Lim HY, Poon RT, Blanc JF, Vogel A, Chen CL, Dorval E, Peck-Radosavljevic M, Santoro A, Daniele B, Furuse J, Jappe A, Perraud K, Anak O, Sellami DB, Chen LT: Effect of everolimus on survival in advanced hepatocellular carcinoma after failure of sorafenib: the EVOLVE-1 randomized clinical trial. *JAMA* 2014;312:57–67.
- 11 Zhu AX, Park JO, Ryoo BY, Yen CJ, Poon R, Pastorelli D, Blanc JF, Chung HC, Baron AD, Pfiffer TE, Okusaka T, Kubackova K, Trojan J, Sastre J, Chau I, Chang SC, Abada PB, Yang L, Schwartz JD, Kudo M: Ramucirumab versus placebo as second-line treatment in patients with advanced hepatocellular carcinoma following first-line therapy with sorafenib (REACH): a randomised, double-blind, multicentre, phase 3 trial. *Lancet Oncol* 2015;16: 859–870.
- 12 Kudo M: Molecular targeted therapy for hepatocellular carcinoma: where are we now? *Liver Cancer* 2015;4:I–VII.
- 13 Bruix J, Qin S, Merle P, Granito A, Huang YH, Bodoky G, Pracht M, Yokosuka O, Rosmorduc O, Breder V, Gerolami R, Masi G, Ross PJ, Song T, Bronowicki JP, Ollivier-Hourmand I, Kudo M, Cheng AL, Llovet JM, Finn RS, LeBerre MA, Baumhauer A, Meinhart G, Han G; RESORCE Investigators: Regorafenib for patients with hepatocellular carcinoma who progressed on sorafenib treatment (RESORCE): a randomised, double-blind, placebo-controlled, phase 3 trial. *Lancet* 2017;389:56–66.
- 14 Kudo M: Regorafenib as second-line systemic therapy may change the treatment strategy and management paradigm for hepatocellular carcinoma. *Liver Cancer* 2016;5: 235–244.
- 15 Lencioni R, Llovet JM: Modified recist (mRECIST) assessment for hepatocellular carcinoma. *Semin Liver Dis* 2010;30:52–60.
- 16 Wilhelm SM, Dumas J, Adnane L, Lynch M, Carter CA, Schutz G, Thierauch KH, Zopf D: Regorafenib (bay 73–4506): a new oral multi-kinase inhibitor of angiogenic, stromal and oncogenic receptor tyrosine kinases with potent preclinical antitumor activity. *Int J Cancer* 2011;129:245–255.
- 17 Bruix J, Tak WY, Gasbarrini A, Santoro A, Colombo M, Lim HY, Mazzaferro V, Wiest R, Reig M, Wagner A, Bolondi L: Regorafenib as second-line therapy for intermediate or advanced hepatocellular carcinoma: multicentre, open-label, phase II safety study. *Eur J Cancer* 2013;49:3412–3419.
- 18 Toyoda H, Kumada T, Tada T, Sone Y, Kaneoka Y, Maeda A: Tumor markers for hepatocellular carcinoma: Simple and significant predictors of outcome in patients with HCC. *Liver Cancer* 2015;4:126–136.
- 19 Ueshima K, Kudo M, Takita M, Nagai T, Tatsumi C, Ueda T, Kitai S, Ishikawa E, Yada N, Inoue T, Hagiwara S, Minami Y, Chung H, Sakurai T: Des-γ-carboxyprothrombin may be a promising biomarker to determine the therapeutic efficacy of sorafenib for hepatocellular carcinoma. *Dig Dis* 2011;29:321–325.
- 20 Kudo M: A new era of systemic therapy for hepatocellular carcinoma with regorafenib and lenvatinib. *Liver Cancer* 2017;6:177–184.
- 21 Kudo M: Surveillance, diagnosis, treatment, and outcome of liver cancer in Japan. *Liver Cancer* 2015;4:39–50.
- 22 Arizumi T, Ueshima K, Minami T, Kono M, Chishina H, Takita M, Kitai S, Inoue T, Yada N, Hagiwara S, Minami Y, Sakurai T, Nishida N, Kudo M: Effectiveness of sorafenib in patients with transcatheter arterial chemoembolization (TACE) refractory and intermediate-stage hepatocellular carcinoma. *Liver Cancer* 2015;4:253–262.

# Role of Immune Checkpoint Blockade in the Treatment for Human Hepatocellular Carcinoma

Naoshi Nishida Masatoshi Kudo

Department of Gastroenterology and Hepatology, Kindai University Faculty of Medicine, Osaka-Sayama, Japan

## Keywords

Hepatocellular carcinoma · Treatment · Immune checkpoint inhibitors · Molecular targeting agent

## Abstract

With the development of molecular targeting therapy, several treatment options for advanced hepatocellular carcinoma (HCC) have become available in cases where curative and other palliative treatments, such as radiofrequency ablation, surgical resection, and transarterial chemoembolization, are not applicable. However, with the detection of a variety of mutations in cancer-related genes in a single tumor, molecular heterogeneity is commonly observed in HCC. Therefore, mutations in the major cellular signaling pathways underlie the development of resistance to molecular targeting agents. On the contrary, immune checkpoint inhibitors have proven effective in patients who are refractory to conventional treatments and molecular targeting therapy. Several clinical trials are currently investigating the efficacy of immune checkpoint inhibitors both individually and in combination with other types of anticancer agents. In this review, we focus on the potential of immune checkpoint blockade in the treatment of human HCC.

© 2017 S. Karger AG, Basel

## Introduction

Hepatocellular carcinoma (HCC) is still one of the leading causes of cancer-related mortalities worldwide, accounting for more than 780,000 deaths per year [1]. Recurrences after curative treatments, such as resection and ablation [2, 3], are one of the characteristics of this tumor, which results in a rapid progression of the tumor to a more advanced stage. So far, the administration of sorafenib has been the only treatment for advanced stage HCC resistant to curative and other palliative treatments, such as radiofrequency ablation (RFA) [4, 5], hepatic resection [6], and transcatheter arterial chemoembolization (TACE) [7, 8]. Based on clinical trials of molecular targeting agents, regorafenib, a drug currently indicated for metastatic colon cancer and unresectable gastrointestinal stromal tumors, is also known to be effective in sorafenib-resistant HCC patients [9, 10]. Another multi-kinase inhibitor, lenvatinib that targets vascular endothelial growth factor receptor 1–3, fibroblast growth factor receptor 1–4, rearranged during transfection, KIT proto-oncogene receptor tyrosine kinase (KIT), and platelet-derived growth factor receptor [11], has shown success in phase III frontline HCC trials [12, 13]. However, tumors acquire drug resistance through acquisition of somatic



mutations [14, 15]. The heterogeneous mutational profiles of HCCs that account for their genetic diversity are well described [16, 17]. The emergence of mutations disrupting targeted signaling pathways results in the development of resistance to the corresponding molecular targeting agents [14]. However, immunotherapy, using immune checkpoint inhibitors, is a promising approach for HCC patients non-responsive to other treatments including molecular targeting therapies [18–22]. Since immunotherapy targets the immune cells to restore an antitumor immune reaction, the response should not be disrupted by the presence of specific driver mutations [23]. Furthermore, once an antitumor response has been achieved, long-term effects could be expected. Here, we summarize the application of immune checkpoint inhibitors, and describe enhancement of the effect of immune modulation in the treatment of advanced HCC.

### **Treatment of HCC with Immune Checkpoint Inhibitors**

Several immune checkpoints are involved in the suppression of an antitumor immune response [24]. Antibodies against these checkpoints such as anti-programmed cell death-1 (PD-1), anti-PD-ligand 1 (PD-L1), and anti-cytotoxic T-lymphocyte-associated antigen 4 (CTLA-4) are now clinically available for treatment of human cancers. CTLA-4 is constitutively expressed in regulatory T cells (Treg) and activated T cells. It binds to its ligands CD80 and CD86 on antigen-presenting cells and interrupts T cell activation by competing with the costimulatory molecule CD28. CTLA-4 would rather be involved in the initial phase of an immune response, mainly in the regional lymph nodes by regulating the activation of CD4<sup>+</sup> T cells. However, for the regulation of T cell responses in peripheral tissues, the binding of PD-1 to PD-L1 is believed to be critical. PD-1 is present in several types of immune cells, such as CD4<sup>+</sup>, CD8<sup>+</sup> T cells, Treg, B cells, monocytes, and dendritic cells [24]. There are 2 types of PD-1 ligands, PD-L1 and PD-L2; the former is expressed in hematopoietic, endothelial, and some kinds of parenchymal cells, whereas the latter is detected specifically in hematopoietic cells. Cancer cells, including HCC, express PD-L1; therefore, blocking the engagement of PD-1 with PD-L1 should directly restore the attack of tumor cells by cytotoxic T cells [23]. A phase II trial of tremelimumab, a CTLA-4 inhibitor in patients with hepatitis C virus-related HCCs, showed a partial response rate (PR) of 17.6%, disease control rate (DCR) of 76.4%,

and time to progression periods (TTP) of 6.48 months (95% CI 3.95–9.14) [25]. Patients without reductions in the serum levels of IFN- $\gamma$  during the treatment showed greater tumor reduction than those with reductions in IFN- $\gamma$  [25].

Currently, clinical trials of anti-PD-1 antibody (nivolumab, pembrolizumab) and anti-PD-L1 antibody (durvalumab) both individually and in combination with anti-CTLA-4 antibody (ipilimumab, durvalumab) are ongoing [18]. At the end of phase I/II trials of nivolumab (CheckMate 040), an objective response rate (OR) was observed in 20% of the 214 HCC patients who received 3 mg/kg of nivolumab every 2 weeks (expansion cohort), and a DCR was observed in 64% of the patients [26]. In sorafenib-treated patients, 19% showed an OR including 5 cases with complete response, suggesting that immune checkpoint blockade could be effective even in the cases refractory to molecular targeting agents [26]. An evaluation of the association between PD-L1 expression and response to the anti-PD-L1 antibody revealed no significant difference in the OR between the PD-L1-positive (26%) and PD-L1-negative (19%) HCC patients. An analysis of the association in 44 patients of the dose-escalation cohort showed a 27% and 12% OR in patients with PD-L1-positive and PD-L1-negative tumors, respectively [26]. Based on the data from the dose-escalation and expansion cohorts, there is probably a trend between PD-L1 expression and tumor response; PD-L1-positive tumors show a better response than the PD-L1-negative tumors, although not significant. Since the anti-PD-1 antibody can interact both with tumor tissues and lymphoid tissues, it would be effective in some PD-L1-negative HCCs as well. Conversely, since several immunosuppressive molecules, including the immune checkpoint molecules, help establish an immunosuppressive tumor microenvironment, the expression of PD-L1 on HCC cells is not necessarily a marker of good anti-PD-1 antibody response. Therefore, a combination of PD-L1 expression and other biomarkers could be potentially useful predictors of the anti-tumor effects of immune checkpoint inhibitors.

### **Combination of Immune Checkpoint Inhibitors with Other Treatments for HCC**

Based on the data from the CheckMate 040 study, especially in sorafenib-resistant HCC patients, monotherapy with anti-PD-1 antibody is expected to produce results comparable to those from phase III clinical trials of sorafenib and regorafenib [7, 9, 26]. Table 1 compares the

**Table 1.** Comparison of the clinical trials of molecular targeting agents and anti-PD-1 antibody in advanced hepatocellular carcinoma

Drug	Classification	Clinical trial	Subjects	Number of patients	OR, %	DCR, %	TTP (95% CI)	OS (95% CI)	Ref.
Sorafenib	Mutikinase inhibitor	SHARP (Phase III)	HCC patients who had not received previous systemic treatment	299	2	43	5.5 (4.1–6.9)	10.7 (9.4–13.3)	2
Regorafenib	Mutikinase inhibitor	RESCORE (Phase III)	HCC patients who tolerated and progressed on sorafenib	379	11	65	3.2 (2.9–4.2)	10.6 (9.1–12.1)	3
Nivolumab	Anti-PD-1 antibody	CheckMate 040 (Phase I/II)	HCC patients who progressed while receiving at least one previous line of systemic therapy, including sorafenib, or who were intolerant of or refused sorafenib treatment	214	20	64	9.9 (8.3–N.E.)*	N.R.	16

TTP and OS are shown as median (month). OR, objective response; DCR, disease control rate; TTP, time to progression (duration of response); OS, overall survival; N.E, not estimated; N.R., not reached. Ref., reference number cited in the text.

\* Duration of response.

OR, DCR, and median TTP from the clinical trials of (a) sorafenib in advanced HCC patients without any previous systemic treatment (Phase III: SHARP trial), (b) regorafenib in patients with HCC progression, who were previously on sorafenib treatment (Phase III: RESCORE trial), and (c) nivolumab in advanced HCC patients who were either sorafenib untreated or intolerant and progressor. Currently, phase III trials comparing the efficacies of nivolumab with sorafenib are ongoing.

Several other novel trials combining immune checkpoint inhibitors with other treatments are also underway. It was reported that a phase II study of tremelimumab as a single agent to treat HCC revealed a PR of 17.6%, a median TTP of 6.48 months, and a median overall survival of 8.2 months [25]. On the contrary, Duffy et al. have reported the effect of tremelimumab, an anti-CTLA-4 antibody, in combination with RFA or TACE in advanced HCC patients; 26.3% of patients showed a PR, a median TTP of 7.4 months, and an overall survival of 12.3 months [27]. Interestingly, tremelimumab in combination with ablation induced the accumulation of intratumoral CD8<sup>+</sup> T cells. Depending on the treated region, ablation induced a decrease in tumor volume as well, leading to the

release of tumor-associated antigens from HCC cells and activated CD8<sup>+</sup> T cells, which in turn could have enhanced the antitumor effect of tremelimumab to tumors at a distance [27]. The effectiveness of tremelimumab at lower doses, in combination with RFA or TACE, indicates that immune checkpoint inhibitors are more effective in combination with other conventional treatments, rather than as a single agent.

A combination of anti-PD-L1 and radiation has been shown to be more effective in suppressing tumor growth and improving survival in a murine HCC model, compared to these treatments given individually [28]. Radiation by activating interferon (IFN)- $\gamma$ /transducers and activator of transcription (STAT3) signaling induced the expression of PD-L1 and infiltration of CD8<sup>+</sup> T cell in HCCs resulting in the antitumor effect of anti-PD-L1.

In the HCC microenvironment, immunosuppressive cytokines, chemokines, and stromal cells could counter the effects of immune checkpoint inhibitors [29]. For example, a high IL-6 expression in cancer-associated fibroblasts reportedly can lead to both the recruitment of immunosuppressive myeloid-derived cells and the induction of immune checkpoints molecules, which in turn could

result in the establishment of an immunosuppressive microenvironment [30]. Therefore the combination of agents that inhibit IL-6 and immune checkpoints could also have the potential to overcome anti-PD-L1 resistance.

Chen et al. [31] also reported an improvement in the tumor response to anti-PD-1 therapy by intervening with the hypoxic and immunosuppressive microenvironments using agents, such as inhibitors of stromal cell-derived 1 $\alpha$  (C-X-C receptor type 4: CXCR4). They showed that sorafenib-induced hypoxia promotes the expression of PD-L1 as well as the induction of immunosuppressive Treg and M2-type macrophages, with CXCR4 mediating the recruitment of these cells. Inhibition of CXCR4 suppressed the tumor growth, reduced metastasis, and improved survival in combination with anti-PD-1 after sorafenib treatment [31].

## Conclusion

Based on the promising results from the present phase III clinical trial of molecular targeting agents, new strategies for treatment of advanced HCC can be designed for the better control of tumor growth [13]. However, mutational heterogeneity of HCC cells eventually leads to the development of resistance to these chemotherapeutic agents [14, 32, 33]. Recent studies have shown that the inhibition of immune checkpoints has a great potential to

be effective against advanced HCCs that have become drug resistant. However, considering the immunosuppressive tumor microenvironment and the mutation burden of HCC, which could be related to the antigenicity of the tumor, immunotherapy using immune checkpoint inhibitors could have its limitations. The limited tumor responses seen during the clinical trials of immune checkpoint monotherapy have prompted investigations into combination therapies using immune modulators with chemotherapeutic agents.

## Acknowledgements

This work was supported in part by Grant-in-Aid for Scientific Research (KAKENHI: 16K09382) from the Japanese Society for the Promotion of Science (N. Nishida) and a grant from the Smoking Research Foundation (N. Nishida).

## Disclosure Statement

The authors have no conflicts of interest to disclose.

## Author Contributions

Naoshi Nishida drafted the manuscript and wrote the final version. Masatoshi Kudo approved the final version of the manuscript.

## References

- 1 Kudo M: Surveillance, diagnosis, treatment, and outcome of liver cancer in Japan. *Liver Cancer* 2015;4:39–50.
- 2 Kudo M, Izumi N, Sakamoto M, Matsuyama Y, Ichida T, Nakashima O, Matsui O, Ku Y, Kokudo N, Makuuchi M: Survival analysis over 28 years of 173,378 patients with hepatocellular carcinoma in Japan. *Liver Cancer* 2016;5:190–197.
- 3 Harlan LC, Parsons HM, Wiggins CL, Stevens JL, Patt YZ: Treatment of hepatocellular carcinoma in the community: disparities in standard therapy. *Liver Cancer* 2015;4:70–83.
- 4 Kudo M: Locoregional therapy for hepatocellular carcinoma. *Liver Cancer* 2015;4:163–164.
- 5 Kang TW, Rhim H: Recent advances in tumor ablation for hepatocellular carcinoma. *Liver Cancer* 2015;4:176–187.
- 6 Ho MC, Hasegawa K, Chen XP, Nagano H, Lee YJ, Chau GY, Zhou J, Wang CC, Choi YR, Poon RT, Kokudo N: Surgery for Intermediate and Advanced Hepatocellular Carcinoma: A consensus report from the 5th asia-pacific primary liver cancer expert meeting (APPLE 2014). *Liver Cancer* 2016;5:245–256.
- 7 Llovet JM, Ricci S, Mazzaferro V, Hilgard P, Gane E, Blanc JF, de Oliveira AC, Santoro A, Raoul JL, Forner A, Schwartz M, Porta C, Zeuzem S, Bolondi L, Greten TF, Galle PR, Seitz JF, Borbath I, Häussinger D, Giannaris T, Shan M, Moscovici M, Voliotis D, Bruix J, SHARP Investigators Study Group: Sorafenib in advanced hepatocellular carcinoma. *NEngl J Med* 2008;359:378–390.
- 8 Tsurusaki M, Murakami T: Surgical and Locoregional Therapy of HCC: TACE. *Liver Cancer* 2015;4:165–175.
- 9 Bruix J, Qin S, Merle P, Granito A, Huang YH, Bodoky G, Pracht M, Yokosuka O, Rosmorduc O, Breder V, Gerolami R, Masi G, Ross PJ, Song T, Bronowicki JP, Ollivier-Hourmand I, Kudo M, Cheng AL, Llovet JM, Finn RS, LeBerre MA, Baumhauer A, Meinhardt G, Han G; RESORCE Investigators.: Regorafenib for patients with hepatocellular carcinoma who progressed on sorafenib treatment (RESORCE): a randomised, double-blind, placebo-controlled, phase 3 trial. *Lancet* 2017;389:56–66.
- 10 Kudo M: Regorafenib as second-line systemic therapy may change the treatment strategy and management paradigm for hepatocellular carcinoma. *Liver Cancer* 2016;5:235–244.
- 11 Ikeda K, Kudo M, Kawazoe S, Osaki Y, Ikeda M, Okusaka T, Tamai T, Suzuki T, Hisai T, Hayato S, Okita K, Kumada H: Phase 2 study of lenvatinib in patients with advanced hepatocellular carcinoma. *J Gastroenterol* 2017;52:512–519.
- 12 Cheng AL, Finn RS, Qin S, Han KH, Ikeda K, Piscaglia F, Baron AD, Park JW, Han G, Jasssem J, Blanc JF, Vogel A, Komov, Je Evans TR, López-López C, Dutcus CE, Ren M, Kraljevic S, Tamai T, Kudo M: Phase III trial of lenvatinib (LEN) vs sorafenib (SOR) in first-line treatment of patients (PTS) with unresectable hepatocellular carcinoma (uHCC). *J Clin Oncol* 2017;35(suppl):abstr 4001.
- 13 Kudo M: A new era of systemic therapy for hepatocellular carcinoma with regorafenib and lenvatinib. *Liver cancer* 2017;6:177–184.

- 14 Nishida N, Kitano M, Sakurai T, Kudo M: Molecular mechanism and prediction of sorafenib chemoresistance in human hepatocellular carcinoma. *Dig Dis* 2015;33:771–779.
- 15 Nishida N, Arizumi T, Hagiwara S, Ida H, Sakurai T, Kudo M: MicroRNAs for the prediction of early response to sorafenib treatment in human hepatocellular carcinoma. *Liver cancer* 2017;6:113–125.
- 16 Nishida N, Kudo M, Nishimura T, Arizumi T, Takita M, Kitai S, Yada N, Hagiwara S, Inoue T, Minami Y, Ueshima K, Sakurai T, Yokomichi N, Nagasaka T, Goel A: Unique association between global DNA hypomethylation and chromosomal alterations in human hepatocellular carcinoma. *PloS one* 2013;8:e72312.
- 17 Nishida N, Kudo M: Alteration of epigenetic profile in human hepatocellular carcinoma and Its clinical implications. *Liver Cancer* 2014;3:417–427.
- 18 Kudo M: Immune checkpoint inhibition in hepatocellular carcinoma: basics and ongoing clinical trials. *Oncology* 2017;92(suppl 1):50–62.
- 19 Kudo M: Molecular targeted agents for hepatocellular carcinoma: current status and future perspectives. *Liver Cancer* 2017;6:101–112.
- 20 Kudo M: Molecular targeted therapy for hepatocellular carcinoma: where are we now? *Liver Cancer* 2015;4:I–vii.
- 21 Kudo M: Immune checkpoint blockade in hepatocellular carcinoma. *Liver Cancer* 2015;4: 201–207.
- 22 Zhang B, Finn RS: Personalized clinical trials in hepatocellular carcinoma based on biomarker selection. *Liver Cancer* 2016;5:221–232.
- 23 Zhou G, Sprengers D, Boor PPC, Doukas M, Schutz H, Mancham S, Pedroza-Gonzalez A, Polak WG, de Jonge J, Gaspersz M, Dong H, Thielemans K, Pan Q, JNM IJ, Bruno MJ, Kwekkeboom J: Antibodies against immune checkpoint molecules restore functions of tumor-infiltrating T cells in hepatocellular carcinomas. *Gastroenterology* 2017, pii: S0016-5085(17)35802-X.
- 24 Prieto J, Melero I, Sangro B: Immunological landscape and immunotherapy of hepatocellular carcinoma. *Nat Rev Gastroenterol Hepatol* 2015;12:681–700.
- 25 Sangro B, Gomez-Martin C, de la Mata M, Inarrairaegui M, Garralda E, Barrera P, Riezu-Boj JI, Larrea E, Alfaro C, Sarobe P, Lasarte JJ, Perez-Gracia JL, Melero I, Prieto J: A clinical trial of CTLA-4 blockade with tremelimumab in patients with hepatocellular carcinoma and chronic hepatitis C. *J Hepatol* 2013;59:81–88.
- 26 El-Khoueiry AB, Sangro B, Yau T, Crocenzi TS, Kudo M, Hsu C, Kim TY, Choo SP, Trojan J, Welling THR, Meyer T, Kang YK, Yeo W, Chopra A, Anderson J, Dela Cruz C, Lang L, Neely J, Tang H, Dastani HB, Melero I: Nivolumab in patients with advanced hepatocellular carcinoma (CheckMate 040): an open-label, non-comparative, phase 1/2 dose escalation and expansion trial. *Lancet* 2017; 389:2492–2502.
- 27 Duffy AG, Ulahannan SV, Makorova-Rusher O, Rahma O, Wedemeyer H, Pratt D, Davis JL, Hughes MS, Heller T, ElGindi M, Uppala A, Korangy F, Kleiner DE, Figg WD, Venzon D, Steinberg SM, Venkatesan AM, Krishnasamy V, Abi-Jaoudeh N, Levy E, Wood BJ, Greten TF: Tremelimumab in combination with ablation in patients with advanced hepatocellular carcinoma. *J Hepatol* 2017;66:545–551.
- 28 Kim KJ, Kim JH, Lee SJ, Lee EJ, Shin EC, Seong J: Radiation improves antitumor effect of immune checkpoint inhibitor in murine hepatocellular carcinoma model. *Oncotarget* 2017;8:41242–41255.
- 29 Nishida N, Kudo M: Immunological micro-environment of hepatocellular carcinoma and Its clinical implication. *Oncology* 2017; 92(suppl 1):40–49.
- 30 Liu H, Shen J, Lu K: IL-6 and PD-L1 blockade combination inhibits hepatocellular carcinoma cancer development in mouse model. *Biochem Biophys Res Commun* 2017;486:239–244.
- 31 Chen Y, Ramjiawan RR, Reiberger T, Ng MR, Hato T, Huang Y, Ochiai H, Kitahara S, Unan EC, Reddy TP, Fan C, Huang P, Bardeesy N, Zhu AX, Jain RK, Duda DG: CXCR4 inhibition in tumor microenvironment facilitates anti-programmed death receptor-1 immunotherapy in sorafenib-treated hepatocellular carcinoma in mice. *Hepatology* 2015;61: 1591–1602.
- 32 Nishida N, Kudo M: Recent advancements in comprehensive genetic analyses for human hepatocellular carcinoma. *Oncology* 2013; 84(suppl 1):93–97.
- 33 Nishida N, Chishina H, Arizumi T, Takita M, Kitai S, Yada N, Hagiwara S, Inoue T, Minami Y, Ueshima K, Sakurai T, Kudo M: Identification of epigenetically inactivated genes in human hepatocellular carcinoma by integrative analyses of methylation profiling and pharmacological unmasking. *Dig Dis* 2014;32: 740–746.

**Editorial**

# Lenvatinib in Advanced Hepatocellular Carcinoma

Masatoshi Kudo

Department of Gastroenterology and Hepatology, Kindai University Faculty of Medicine,  
Osaka-Sayama, Japan

Prof. M. Kudo

Editor *Liver Cancer***Introduction**

Sorafenib has been the standard therapy for patients with unresectable hepatocellular carcinoma (HCC) since 2007, when it was shown to prolong survival, as verified in the SHARP trial [1] and a study conducted in the Asia-Pacific region [2].

Since then, other molecular-targeted agents superior to sorafenib in efficacy or safety in the first-line treatment of HCC were developed and tested in clinical trials (Table 1) [3]. However, a superiority trial of sunitinib [4] and noninferiority followed by superiority studies of brivanib or linifanib versus sorafenib [5, 6] were reported as negative; a superiority trial of sorafenib plus erlotinib versus sorafenib was also unsuccessful [7]. Furthermore, both the SARAH (sorafenib versus radioembolization in advanced HCC) and the SIRveNIB (study to compare selective internal radiation therapy versus sorafenib in locally advanced HCC) trials failed, as reported at the 2017 annual meetings of the European Association for the Study of the Liver and the American Society of Clinical Oncology (ASCO) [8, 9]. These negative trials indirectly indicate the difficulty in achieving the predefined primary overall survival (OS) endpoint in HCC patients and the better-than-expected superiority of sorafenib in prolonging survival.

Against this background, the success of the phase III noninferiority trial of lenvatinib versus sorafenib with OS as the endpoint, as presented at the 2017 ASCO annual meeting, is an unprecedented and groundbreaking achievement in the past 10 years, promising an alternative molecular-targeted therapy option for HCC patients [10].

Masatoshi Kudo, MD, PhD  
Department of Gastroenterology and Hepatology  
Kindai University Faculty of Medicine  
377-2 Ohno-Higashi, Osaka-Sayama 589-8511 (Japan)  
E-Mail m-kudo@med.kindai.ac.jp



**Table 1.** Phase III clinical trials of the agents targeting for hepatocellular carcinoma

Early stage (adjuvant)	Peretinoin vs. placebo (NIK-333)	Phase II/III	Negative
	Sorafenib vs. placebo (STORM)	Phase III	Negative
	Peretinoin vs. placebo (NIK-333)	Phase III	Ongoing
Intermediate stage (combination with TACE)	Sorafenib (Post TACE)	Phase III	Negative
	Brivanib (BRISK-TA)	Phase III	Terminated
	TSU-68 (ORIENTAL)	Phase III	Terminated
	Sorafenib (TACE 2)	Phase III	Negative
Advanced stage (first line)	Sunitinib vs. sorafenib (SUN1170)	Phase III	Negative
	Linifanib vs. sorafenib (LiGHT)	Phase III	Negative
	Brivanib vs. sorafenib (BRISK-FL)	Phase III	Negative
	SOR + erlotinib vs. sorafenib (SEARCH)	Phase III	Negative
	SOR + doxorubicin vs. sorafenib (CALGB808028)	Phase III	Negative
	Sorafenib ± HAIC (SILIUS)	Phase III	Negative
	Lenvatinib vs. sorafenib (REFLECT)	Phase III	Positive
	Nivolumab vs. sorafenib (CheckMate-459)	Phase III	Ongoing
	SIRT vs. sorafenib (SARAH)	Phase III	Negative
	SIRT vs. sorafenib (SIRveNIB)	Phase III	Negative
Advanced stage (second line)	Brivanib vs. placebo (BRISK-PS)	Phase III	Negative
	Everolimus vs. placebo (EVOLVE-1)	Phase III	Negative
	Ramcirumab vs. Placebo (REACH)	Phase III	Negative
	S-1 vs. placebo (S-CUBE)	Phase III	Negative
	Tivantinib vs. placebo (METIV-HCC)	Phase III	Negative
	Regorafenib vs. placebo (RESOUCÉ)	Phase III	Positive
	Ramcirumab vs. placebo (REACH-2)	Phase III	Ongoing

HAIC, hepatic arterial infusion chemotherapy.

## History of the Development of Lenvatinib

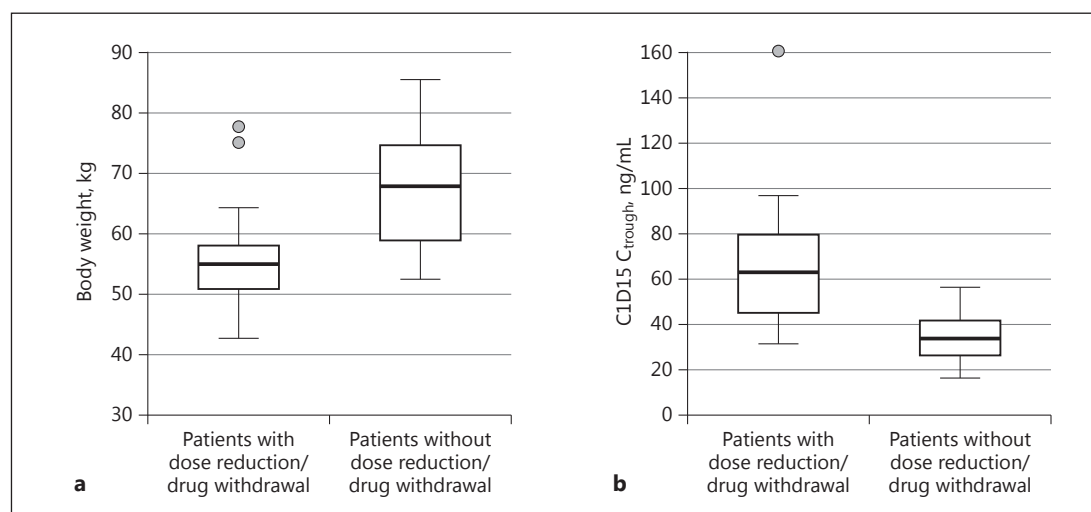
Lenvatinib, which was discovered in an exploratory study for an angiogenesis inhibitor, mainly inhibits vascular endothelial growth factor (VEGF) receptors (VEGFR1, VEGFR2, and VEGFR3), fibroblast growth factor (FGF) receptors (FGFR1, FGFR2, FGFR3, and FGFR4), KIT, and RET [11]. Lenvatinib is an extremely effective inhibitor of tumor angiogenesis that simultaneously interferes with these tumor angiogenesis-related molecules and suppresses growth signals mediated by VEGFRs and FGFRs [12].

A daily dose of 24 mg was initially determined based on the results of a phase I trial for the treatment of solid tumors and other subsequent studies in other types of cancer; however, the dose was reduced to 12 mg after another phase I trial addressing the effect of lenvatinib metabolism on liver function in HCC patients [13].

The phase II study, conducted in Japan and South Korea, confirmed the high antitumor activity of lenvatinib with manageable adverse events in HCC patients [14].

## Relationship between Safety and Body Weight in the HCC Phase II Trial

In the phase II study, a uniform daily dose of 12 mg irrespective of body weight and surface area led to dose reduction in a large proportion of patients: dose adjustment in 34 of 46 patients (74%) because of treatment-related adverse events and withdrawal in 10 patients (22%) because of toxicity. Close examination of patient characteristics indicated that body weight and serum lenvatinib levels were likely to be associated with dose reduction or early



**Fig. 1.** **a** Boxplot of body weight for patients with and without adverse events that led to dose reduction or dose withdrawal within 30 days of lenvatinib treatment initiation. **b** Boxplot of lenvatinib C<sub>trough</sub> level 15 days after lenvatinib treatment initiation for patients with and without adverse events that led to dose reduction or withdrawal within 30 days. C1D15, cycle 1 day 15; C<sub>trough</sub>, minimum concentration of lenvatinib. Cited from Ikeda et al. [14].

withdrawal. More precisely, patients who had dose reduction or early therapy withdrawal within 30 days of lenvatinib treatment were significantly lighter (median weight, 54.1 vs. 67.6 kg) and had a significantly higher minimum plasma concentration of lenvatinib (trough concentration [C1D15C<sub>trough</sub>], 62.4 vs. 33.9 ng/mL; Fig. 1).

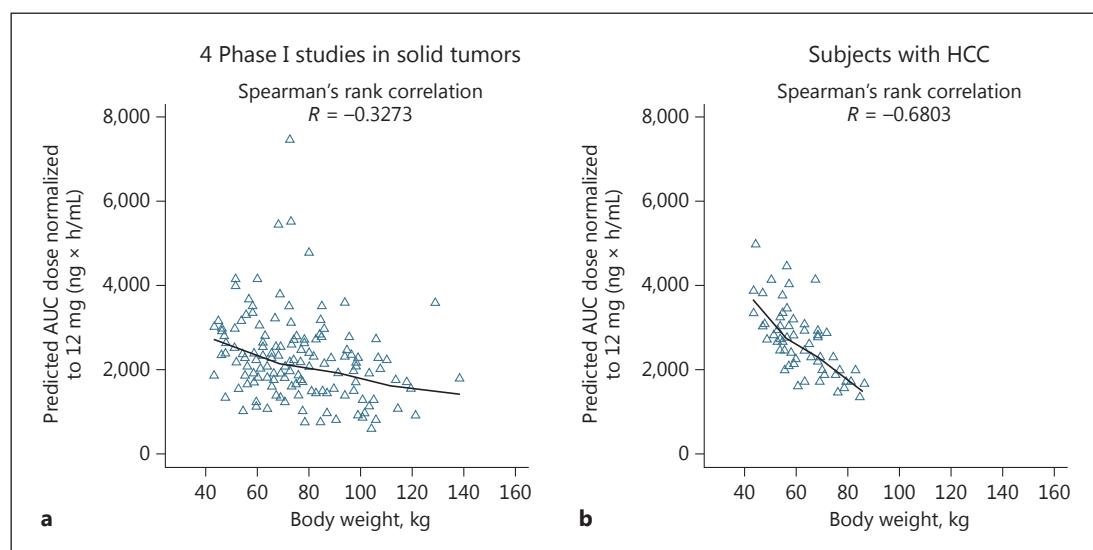
### Pharmacokinetics of Lenvatinib and Rationale for Weight-Based Dosing in HCC Patients

#### *Relationship between Body Weight and Plasma Level of Lenvatinib in HCC Patients*

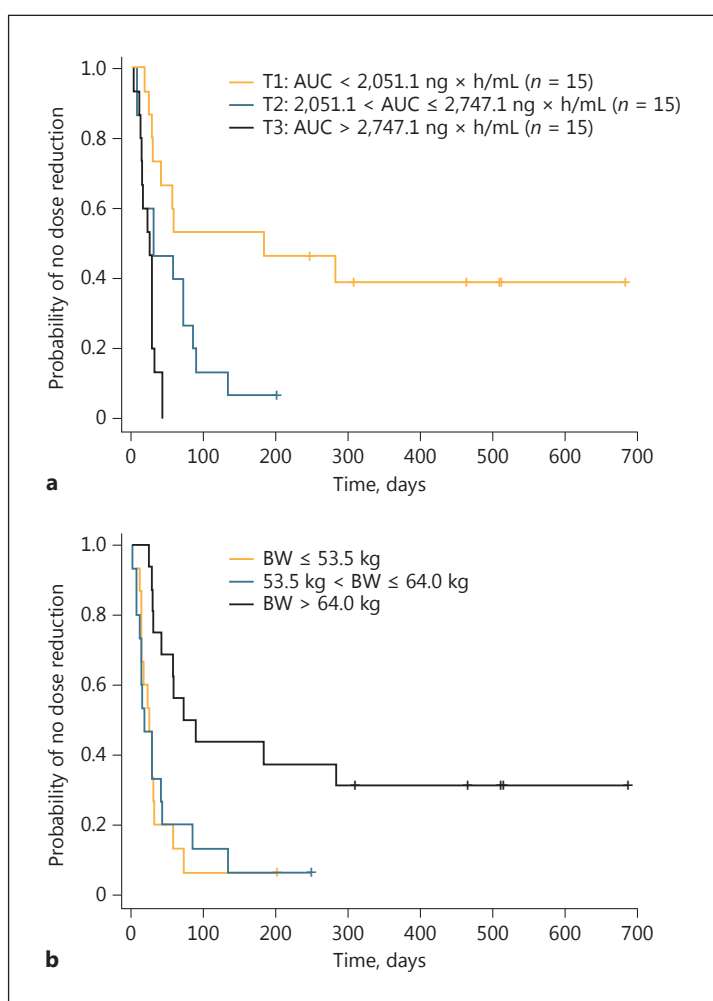
Following the phase I and II studies, population pharmacokinetics was analyzed in 65 HCC patients enrolled in these trials and in 155 patients with solid cancer and 232 healthy individuals enrolled in other clinical studies [15]. A relationship between body weight and plasma lenvatinib level (represented by the area under the blood concentration-time curve [AUC]) was detected, indicating that exposure to lenvatinib increased as body weight decreased (Fig. 2). This trend was more prominent in HCC patients than in patients with other types of solid cancer, suggesting that this relationship particularly impacts HCC patients.

#### *Relationship between the Pharmacokinetics of Lenvatinib and Dose Reduction or Withdrawal in HCC Patients*

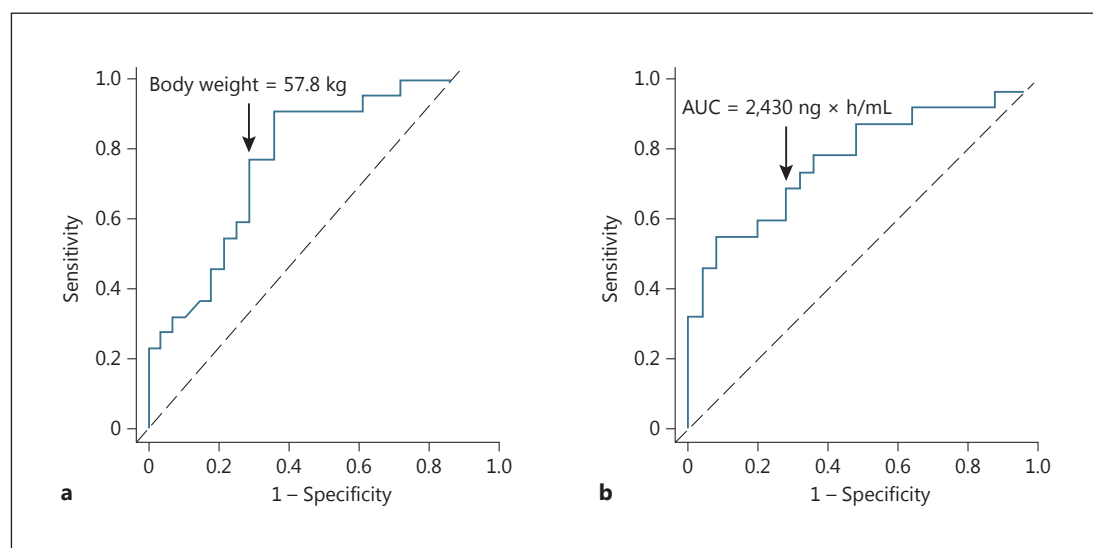
Forty-five patients enrolled in trials for HCC treatment were grouped into a low AUC group (<2,050 ng × h/mL), intermediate AUC group (>2,050 ng × h/mL, ≤2,750 ng × h/mL), and high AUC group (>2,750 ng × h/mL) to examine the relationship between AUC and time to dose reduction or withdrawal of lenvatinib. Kaplan-Meier plots clearly showed that time to dose reduction or withdrawal decreased as AUC increased (Fig. 3a). Body weight was also related to time to dose reduction or withdrawal; time to dose reduction or withdrawal decreased as body weight decreased, demonstrating that dose reduction or withdrawal is required earlier in lighter patients than in heavier patients (Fig. 3b).



**Fig. 2.** Relationship between model-predicted lenvatinib exposure and body weight. AUC, area under the plasma concentration-time curve at steady state; HCC, hepatocellular carcinoma. Cited from Tamai et al. [15].



**Fig. 3.** Kaplan-Meier plots of time to first TEAE leading to lenvatinib withdrawal or dose reduction stratified by tertiles of lenvatinib AUC (a) or body weight (b). AUC, area under the plasma concentration-time curve at steady state; TEAE, treatment-emergent adverse event; BW, body weight. Cited from Tamai et al. [15].



**Fig. 4.** ROC curve for the occurrence of TEAEs leading to dose reduction or discontinuation during cycle 1. **a** Body weight. **b** Lenvatinib AUC. AUC, area under plasma concentration-time curve at steady state; ROC, receiver operating characteristics; TEAE, treatment-emergent adverse event. Cited from Tamai et al. [15].

#### *Optimal Body Weight and AUC Cutoff Value for Lenvatinib Adjustment in HCC Treatment*

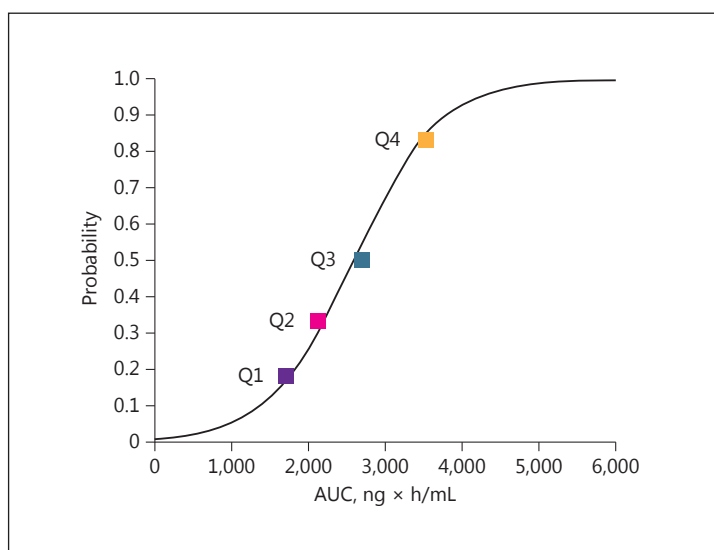
Strong correlations between lenvatinib withdrawal, blood concentration (AUC), and body weight indicated that dose adjustment by body weight and AUC may improve the safety of lenvatinib in the treatment of patients with HCC. Sensitivity and specificity values for predicting early occurrence (within 30 days after the start of therapy) of dose reduction and withdrawal using each body weight cutoff value were calculated to draw receiver operating characteristic (ROC) curves (Fig. 4a). The optimal body weight cutoff value (the point at which the distance between the top-left corner of the graph and the ROC is smallest) that most effectively distinguished the high-risk group for early withdrawal or dose reduction of lenvatinib was 57.8 kg, with a sensitivity of 0.77 and a specificity of 0.67 (false-positive rate, 0.33). Similarly, the best AUC cutoff value was 2,430 ng × h/mL with a sensitivity of 0.71 and a specificity of 0.71 (false-positive rate, 0.29) (Fig. 4b).

#### *Significance of Maintaining the AUC within a Certain Range and Dose Adjustment in HCC Treatment with Lenvatinib*

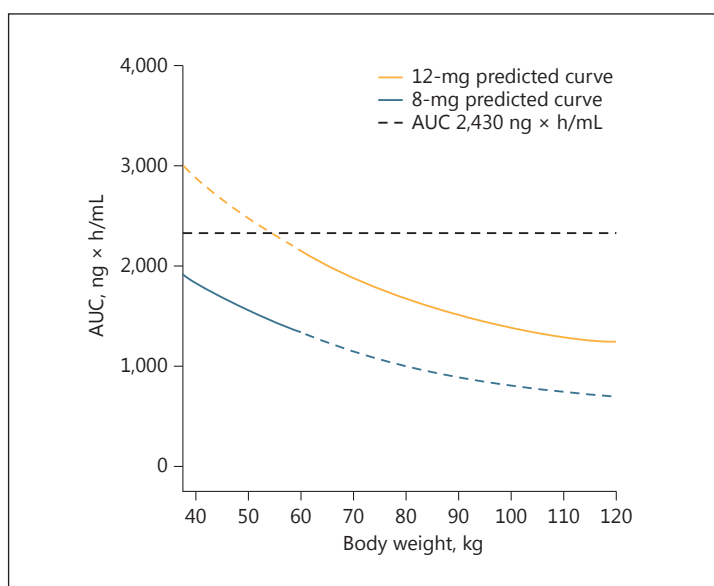
The AUC was better for predicting early withdrawal or dose reduction of lenvatinib than other factors such as sex, body weight, age, liver function, platelet count, Eastern Cooperative Oncology Group performance status, Child-Pugh class, hepatitis viral status, portal vein tumor thrombus, prior chemotherapy, prior antihypertensive therapy, and prior surgery. An AUC probability curve (Fig. 5) can predict early withdrawal or dose reduction of lenvatinib. Consequently, the AUC needs to be maintained below a certain level to reduce the occurrence of early withdrawal or dose reduction; for example, lenvatinib dose adjustment to maintain the AUC value below the optimal cutoff (2,430 ng × h/mL) may be recommended.

Based on the findings that the optimal body weight cutoff for a similar prediction was 57.8 kg, the predicted AUC values for weight-based dosing (daily dose of 12 or 8 mg in patients with a body weight ≥60 or <60 kg, respectively) were calculated and plotted against body weight (Fig. 6). The predicted AUC values were in the range of 1,540–2,050 ng × h/mL in patients with a body weight <60 kg, and 1,410–2,310 ng × h/mL in those with a body weight

**Fig. 5.** Plot of the model-predicted probability of the occurrence of TEAEs leading to dose reduction or discontinuation during cycle 1 versus lenvatinib AUC. Filled squares represent the observed probability of responders for each AUC group, plotted at the median AUC of each group. Q1 group 25th percentile; Q2 group >25th percentile and 50th percentile; Q3 group >50th percentile and 75th percentile; Q4 group >75th percentile. AUC, area under plasma concentration-time curve at steady state; TEAE, treatment-emergent adverse event. Cited from Tamai et al. [15].



**Fig. 6.** Simulated body weight versus lenvatinib AUC for the 12- and 8-mg dose groups. AUC indicates area under the plasma concentration-time curve at steady state, indicating that this weight-based dosing is adequate. Cited from Tamai et al. [15].



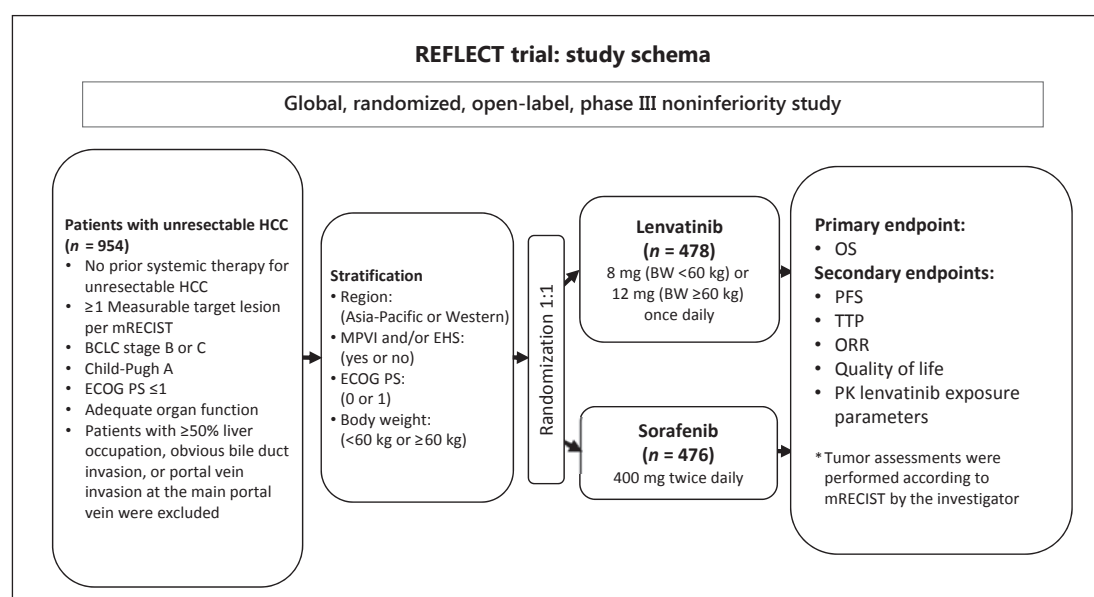
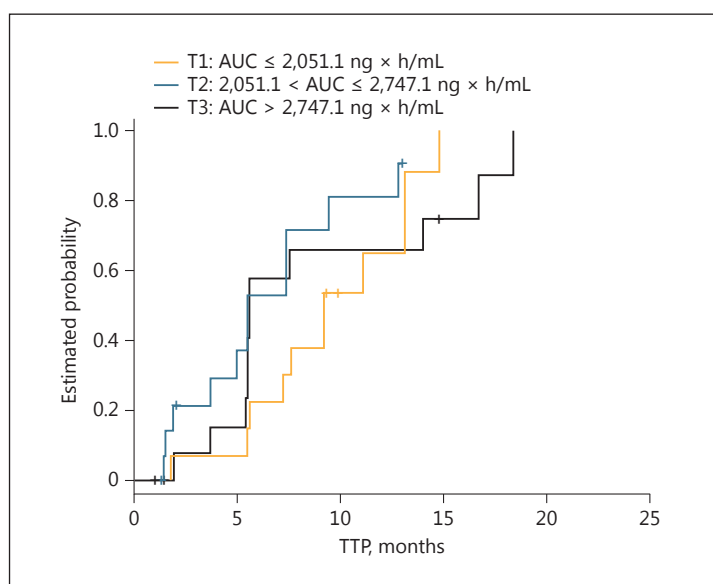
$\geq 60$  kg. These AUC ranges were quite similar and lower than  $2,430 \text{ ng} \times \text{h/mL}$  in both body weight categories, indicating that this weight-based dose adjustment may efficiently reduce early withdrawal and dose reduction of lenvatinib.

#### *Relationship between the AUC and Efficacy in HCC Treatment with Lenvatinib*

Because the lenvatinib dose adjustment to reduce the AUC could impair efficacy, patients enrolled in the phase II trial testing an initial daily dose of 12 mg were grouped into a low AUC group ( $<2,050 \text{ ng} \times \text{h/mL}$ ), an intermediate AUC group ( $>2,050 \text{ ng} \times \text{h/mL}$ ,  $\leq 2,750 \text{ ng} \times \text{h/mL}$ ), and a high AUC group ( $>2,750 \text{ ng} \times \text{h/mL}$ ) to examine a relationship between AUC and efficacy. There was no trend in time-to-progression (TTP) among the three groups (Fig. 7), suggesting that a certain level of efficacy can be maintained even when the AUC is small.



**Fig. 7.** Kaplan-Meier estimates of TTP, stratified by tertiles of lenvatinib AUC. TTP is similar among the 3 groups. AUC, area under the plasma concentration-time curve at steady state; TTP, time to progression. Cited from Tamai et al. [15]



**Fig. 8.** Study diagram of the REFLECT trial. This is a global, randomized, open-label, phase III noninferiority study.

### Results of the Phase III REFLECT Trial

The results of the REFLECT trial, a phase III study of lenvatinib, were presented at the ASCO annual meeting on June 4, 2017.

Patients with unresectable HCC who had not received systemic chemotherapy were randomized in a 1:1 ratio. Treatment was continued until disease progression or onset of an unacceptable adverse event. The primary endpoint was noninferiority in OS with a predefined noninferiority margin of 1.08. Secondary endpoints were progression-free survival (PFS), TTP, objective response rate (ORR), and safety (Fig. 8).

**Table 2.** Results of the REFLECT trial

	Lenvatinib (95% CI) (n = 478)	Sorafenib (95% CI) (n = 476)	Hazard ratio (95% CI)
Median OS, months	13.6 (12.1–14.9)	12.3 (10.4–13.9)	0.92 (0.79–1.06)
Median PFS, months*	7.4 (6.9–8.8)	3.7 (3.6–4.6)	0.66 (0.57–0.77)
Median TTP, months*	8.9 (7.4–9.2)	3.7 (3.6–5.4)	0.63 (0.53–0.73)
ORR, n (%)	115 (24)	44 (9)	–

OS, overall survival; PFS, progression-free survival; TTP, time to progression; ORR, overall response rate.  
\*  $p < 0.0001$ .

**Table 3.** Possible reasons for the success of REFLECT trial

- Good trial design
  - Weight-based dosing (12 vs. 8 mg)
  - Noninferiority trial design
- Potent anticancer activity over sorafenib
- Acceptable toxicity
- Longer treatment duration due to better tolerability, especially less hand-foot-skin reaction (5.7 vs. 3.7 months)

**Table 4.** Possible reasons for not achieving superiority

- AFP imbalance favoring sorafenib arm
- Hepatitis C-related HCC imbalance favoring for sorafenib arm
- By excluding patients with main portal vein tumor thrombus and tumor burden  $\geq 50\%$ , patients were relatively good prognostic population in both arms, leading to long postprogression survival (PPS) who likely received post trial treatments
- OS benefit was diluted by long PPS

Among 954 patients enrolled, 478 and 476 were assigned to the lenvatinib group and the sorafenib group, respectively. Noninferiority in the primary OS endpoint was statistically confirmed (13.6 vs. 12.3 months; hazard ratio, 0.92 [95% CI, 0.79–1.06]). Increases in PFS, TTP, and ORR in the lenvatinib group were statistically significant (Table 2). Common adverse events of lenvatinib were hypertension, diarrhea, decreased appetite, weight loss, and fatigue, which was in good agreement with a previous study [4].

Because this study did not consider the  $\alpha$ -fetoprotein (AFP) level as a stratification factor, the lenvatinib group included more patients with a high AFP level ( $\geq 200$  ng/mL) than the sorafenib group. After adjustment of the AFP imbalance, lenvatinib proved nominally superior to sorafenib in OS based on the post hoc analysis.

Taken together, the findings of the REFLECT trial showed that lenvatinib was statistically noninferior to sorafenib in OS and yielded statistically and clinically significant improvements in PFS, TTP, and ORR, indicating that lenvatinib is a highly promising first-line therapy for patients with unresectable HCC.

### Insights into the Success of the REFLECT Trial

Several key factors might have contributed to this clinically meaningful success, the first in the past 10 years, in confirming the noninferiority of an alternative therapy to sorafenib. The REFLECT trial was the first anti-HCC trial that used a noninferiority trial design with body

**Table 5.** Stratification factors in first-line phase III clinical trials in hepatocellular carcinoma

Study arm vs. placebo arm	SUN1170 (sunitinib)	BRISK-FL (brivanib)	LiGHT (linifanib)	SEARCH (+erlotinib)	CheckMate-459 (nivolumab)	REFLECT (lenivatinib)
Stratification factor	Region Vascular invasion and/or extrahepatic spread Prior TACE	ECOG-PS score Extrahepatic spread and/or vascular invasion Study site	Region ECOG-PS score Vascular invasion and/or extrahepatic spread Hepatitis B virus infection	Region ECOG-PS score Vascular invasion and/or extrahepatic spread Smoking status	Etiology Region Vascular invasion and/or extrahepatic spread	Region ECOG-PS score Vascular invasion and/or extrahepatic spread Body weight

**Table 6.** Recommendations for the design of phase II and phase III trials for patients with HCC (cited and modified from [24])

Aim	Factor	Considerations and recommendations
To select the target population	BCLC stage	Include patients according to the specific BCLC stage (A–C)
	Child-Pugh classification	Include patients in Child-Pugh A to minimize deaths unrelated to HCC
	Biomarker-based enrichment	Include subpopulations with specific activations of the signaling pathway or oncogenic drivers
To choose the appropriate primary endpoints	Overall survival	In phase III studies assessing primary treatments
	Time to recurrence	In phase II/III studies assessing adjuvant treatments
	Time to progression or overall response rate	In phase II studies assessing primary treatments
	Surrogate endpoints	Time to recurrence, time to progression and overall response have to be assessed according to the modified RECIST criteria
	Composite endpoints	Progression-free survival is a vulnerable endpoint in HCC
To decide the adequate control treatment group	Adjuvant therapy after resection or local ablation	Placebo for control treatment group
	Intermediate-stage disease test group	Transcatheter arterial chemoembolization for the control treatment group
	First-line treatment for advanced-stage disease test group	Sorafenib plus supportive care for the control treatment group
	Second-line treatment for advanced-stage disease test group	Placebo plus supportive care for the control treatment group
To stratify factors before randomization	Adjuvant	High risk (size >3 cm, MVI and satellites) and geographical region
	Intermediate stage	Child-Pugh class, AFP and geographical region
	First-line advanced stage	ECOG scale, MVI, EHS and geographical region
	Second-line advanced stage	ECOG scale, MVI, EHS, geographical region, AFP of >400 ng/mL and type of progression

AFP,  $\alpha$ -fetoprotein; BCLC, Barcelona Clinic Liver Cancer; ECOG, Eastern Cooperative Oncology Group; EHS, extrahepatic spread; HCC, hepatocellular carcinoma; MVI, macrovascular invasion; RECIST, response evaluation criteria in solid tumors.

weight-based daily doses (12 or 8 mg). The GIDEON study used different doses of sorafenib according to the patients, with an initial dose of 800 mg in 45.5% of the Japanese subpopulation; however, there was no clear evidence of the efficacy of lower sorafenib dosing [16]. In the REFLECT trial, efficacy was maintained and toxicity remained within acceptable limits in all body weight categories. In particular, there were few cases of hand-foot syndrome and patients were able to sustain therapy for longer periods (5.7 months in the lenvatinib arm vs. 3.7 months in the sorafenib arm) (Table 3). The antitumor activity was high, with a favorable ORR of 24%.

The AFP level and macrovascular invasion were not used as independent stratification factors, resulting in an imbalance unfavorable to the lenvatinib group, with a higher number of sorafenib-responsive hepatitis C patients [17] in the sorafenib group. This may be one of

the reasons why the superiority of lenvatinib in OS was not verified. In addition, the exclusion of patients with a tumor thrombus invading the main portal trunk (Vp4) and those with tumors occupying more than 50% of the liver might have resulted in the selective recruitment of patients who were highly likely to receive post-trial treatment and consequently to have a good prognosis [18–22] in both treatment arms. If so, post-trial treatment may have contributed to prolonging post-progression survival in both the lenvatinib and sorafenib arms, making that the OS benefit of lenvatinib may have been diluted since the hazard ratio of OS becomes high when post-progression survival is long [23, 24] (Table 4). Stratification by AFP level was not common when the REFLECT trial was started, and indeed, none of the relevant past and ongoing clinical studies of first-line therapies include AFP among stratification factors (Table 5). Furthermore, according to a report by Llovet et al. [25], the AFP level is not a recommended factor for stratification in first-line trials (Table 6). Analysis of covariance, which was performed to address the AFP imbalance, showed significant improvement in OS with lenvatinib compared to sorafenib (nominal  $p = 0.0342$ ).

## Conclusions

Lenvatinib is the first anti-HCC agent for which noninferiority to sorafenib was statistically confirmed since the approval of sorafenib for the treatment of HCC approximately 10 years ago. The application for an additional indication for HCC has already been submitted in June 2017 in Japan, before anywhere else in the world. Therefore, therapeutic options in addition to sorafenib will become available in the near future for the treatment of unresectable HCC. Therapeutic combinations involving a tyrosine kinase inhibitor, such as lenvatinib, with an immune checkpoint inhibitor have potential as future treatment strategies [26].

## References

- 1 Llovet JM, Ricci S, Mazzaferro V, Hilgard P, Gane E, Blanc JF, de Oliveira AC, et al: Sorafenib in advanced hepatocellular carcinoma. *N Engl J Med* 2008;359:378–390.
- 2 Cheng AL, Kang YK, Chen Z, Tsao CJ, Qin S, Kim JS, Luo R, et al: Efficacy and safety of sorafenib in patients in the Asia-Pacific region with advanced hepatocellular carcinoma: a phase III randomised, double-blind, placebo-controlled trial. *Lancet Oncol* 2009;10:25–34.
- 3 Kudo M: Molecular targeted agents for hepatocellular carcinoma: current status and future perspectives. *Liver Cancer* 2017;6:101–112.
- 4 Cheng AL, Kang YK, Lin DY, Park JW, Kudo M, Qin S, Chung HC, et al: Sunitinib versus sorafenib in advanced hepatocellular cancer: results of a randomized phase III trial. *J Clin Oncol* 2013;31:4067–4075.
- 5 Johnson PJ, Qin S, Park JW, Poon RT, Raoul JL, Philip PA, Hsu CH, et al: Brivanib versus sorafenib as first-line therapy in patients with unresectable, advanced hepatocellular carcinoma: results from the randomized phase III BRISK-FL study. *J Clin Oncol* 2013;31:3517–3524.
- 6 Cainap C, Qin S, Huang WT, Chung IJ, Pan H, Cheng Y, Kudo M, et al: Linifanib versus sorafenib in patients with advanced hepatocellular carcinoma: results of a randomized phase III trial. *J Clin Oncol* 2015;33:172–179.
- 7 Zhu AX, Rosmorduc O, Evans TR, Ross PJ, Santoro A, Carrilho FJ, Bruix J, et al: SEARCH: a phase III, randomized, double-blind, placebo-controlled trial of sorafenib plus erlotinib in patients with advanced hepatocellular carcinoma. *J Clin Oncol* 2015;33:559–566.
- 8 Vilgrain V, Bouattour M, Sibert A, Lebtahi R, Ronot M, Pageaux G-P, Guio B, Barraud H, Silvain C, G  rolami R, Oberti F, Raoul JL, Costentin C, Samuel D, Dinut A, Pereira H, Chatellier G, Castera L: SARAH trial (Sorafenib vs. Radioembolization in Advanced Hepatocellular Carcinoma). *J Hepatol* 2017;66:S63–S94.
- 9 Chow PK, et al: Phase III multi-centre open-label randomized controlled trial of selective internal radiation therapy (SIRT) versus sorafenib in locally advanced hepatocellular carcinoma: the SIRveNIB study. *J Clin Oncol* 2017;35(suppl;abstr 4002).
- 10 Cheng A, Finn R, Qin S, et al: Phase III trial of lenvatinib (LEN) vs sorafenib (SOR) in first-line treatment of patients (pts) with unresectable hepatocellular carcinoma (uHCC). *J Clin Oncol* 2017;35(suppl;abstr 4001).
- 11 Tohyama O, Matsui J, Kodama K, Hata-Sugi N, Kimura T, Okamoto K, Minoshima Y, et al: Antitumor activity of lenvatinib (e7080): an angiogenesis inhibitor that targets multiple receptor tyrosine kinases in preclinical human thyroid cancer models. *J Thyroid Res* 2014;2014:638747.

- 12 Yamamoto Y, Matsui J, Matsushima T, Obaishi H, Miyazaki K, Nakamura K, Tohyama O, et al: Lenvatinib, an angiogenesis inhibitor targeting VEGFR/FGFR, shows broad antitumor activity in human tumor xenograft models associated with microvessel density and pericyte coverage. *Vasc Cell* 2014;6:18.
- 13 Ikeda M, Okusaka T, Mitsunaga S, Ueno H, Tamai T, Suzuki T, Hayato S, et al: Safety and pharmacokinetics of lenvatinib in patients with advanced hepatocellular carcinoma. *Clin Cancer Res* 2016;22:1385–1394.
- 14 Ikeda K, Kudo M, Kawazoe S, Osaki Y, Ikeda M, Okusaka T, Tamai T, et al: Phase 2 study of lenvatinib in patients with advanced hepatocellular carcinoma. *J Gastroenterol* 2017;52:512–519.
- 15 Tamai T, Hayato S, Hojo S, Suzuki T, Okusaka T, Ikeda K, Kumada H: Dose finding of lenvatinib in subjects with advanced hepatocellular carcinoma based on population pharmacokinetic and exposure-response analyses. *J Clin Pharmacol* 2017, Epub ahead of print.
- 16 Kudo M, Lencioni R, Marrero JA, Venook AP, Bronowicki JP, Chen XP, Dagher L, et al: Regional differences in sorafenib-treated patients with hepatocellular carcinoma: GIDEON observational study. *Liver Int* 2016;36:1196–1205.
- 17 Jackson R, Psarelli EE, Berhane S, Khan H, Johnson P: Impact of viral status on survival in patients receiving sorafenib for advanced hepatocellular cancer: a meta-analysis of randomized phase III trials. *J Clin Oncol* 2017;35:622–628.
- 18 Nagahama H, Okada S, Okusaka T, Ishii H, Ikeda M, Nakasuka H, Yoshimori M: Predictive factors for tumor response to systemic chemotherapy in patients with hepatocellular carcinoma. *Jpn J Clin Oncol* 1997;27:321–324.
- 19 Chung GE, Lee JH, Kim HY, Hwang SY, Kim JS, Chung JW, Yoon JH, et al: Transarterial chemoembolization can be safely performed in patients with hepatocellular carcinoma invading the main portal vein and may improve the overall survival. *Radiology* 2011;258:627–634.
- 20 Kudo M: Molecular targeted therapy for hepatocellular carcinoma: where are we now? *Liver Cancer* 2015;4:I–vii.
- 21 Kudo M: Why does every hepatocellular carcinoma clinical trial using molecular targeted agents fail? *Liver Cancer* 2012;1:59–60.
- 22 Llovet JM, Hernandez-Gea V: Hepatocellular carcinoma: reasons for phase III failure and novel perspectives on trial design. *Clin Cancer Res* 2014;20:2072–2079.
- 23 Broglio KR, Berry DA: Detecting an overall survival benefit that is derived from progression-free survival. *J Natl Cancer Inst* 2009;101:1642–1649.
- 24 Terashima T, Yamashita T, Takata N, Nakagawa H, Toyama T, Arai K, Kitamura K, et al: Post-progression survival and progression-free survival in patients with advanced hepatocellular carcinoma treated by sorafenib. *Hepatol Res* 2016;46:650–656.
- 25 Llovet JM, Zucman-Rossi J, Pikarsky E, Sangro B, Schwartz M, Sherman M, Gores G: Hepatocellular carcinoma. *Nat Rev Dis Primers* 2016;2:16018.
- 26 El-Khoueiry AB, Sangro B, Yau T, Crocenzi TS, Kudo M, Hsu C, Kim TY, et al: Nivolumab in patients with advanced hepatocellular carcinoma (CheckMate 040): an open-label, non-comparative, phase 1/2 dose escalation and expansion trial. *Lancet* 2017;389:2492–2502.



Original Paper

# Validation and Potential of Albumin-Bilirubin Grade and Prognostication in a Nationwide Survey of 46,681 Hepatocellular Carcinoma Patients in Japan: The Need for a More Detailed Evaluation of Hepatic Function

Atsushi Hiraoka<sup>a</sup> Kojiro Michitaka<sup>a</sup> Takashi Kumada<sup>b</sup> Namiki Izumi<sup>c</sup>  
Masumi Kadoya<sup>d</sup> Norihiro Kokudo<sup>e</sup> Shoji Kubo<sup>f</sup> Yutaka Matsuyama<sup>g</sup>  
Osamu Nakashima<sup>h</sup> Michiie Sakamoto<sup>i</sup> Tadatoshii Takayama<sup>j</sup>  
Takashi Kokudo<sup>k</sup> Kosuke Kashiwabara<sup>l</sup> Masatoshi Kudo<sup>m</sup>  
The Liver Cancer Study Group of Japan

<sup>a</sup>Gastroenterology Center, Ehime Prefectural Central Hospital, Matsuyama, <sup>b</sup>Department of Gastroenterology, Ogaki Municipal Hospital, Ogaki, <sup>c</sup>Department of Gastroenterology, Musashino Red Cross Hospital, Tokyo, <sup>d</sup>Department of Radiology, Shinshu University School of Medicine, Matsumoto, <sup>e</sup>National Center for Global Health and Medicine, Tokyo, <sup>f</sup>Department of Hepato-Biliary-Pancreatic Surgery, Osaka City University Graduate School of Medicine, Osaka, <sup>g</sup>Department of Biostatistics, School of Public Health, University of Tokyo, Tokyo, <sup>h</sup>Department of Clinical Laboratory Medicine, Kurume University Hospital, Kurume, <sup>i</sup>Department of Pathology, Keio University School of Medicine, <sup>j</sup>Department of Digestive Surgery, Nihon University School of Medicine, and <sup>k</sup>Hepato-Biliary-Pancreatic Surgery Division, Department of Surgery, Graduate School of Medicine, and <sup>l</sup>Department of Biostatistics, School of Public Health, Graduate School of Medicine, University of Tokyo, Tokyo, and <sup>m</sup>Department of Gastroenterology and Hepatology, Kindai University School of Medicine, Osaka, Japan

## Keywords

Hepatocellular carcinoma · Albumin-bilirubin grade · TNM stage · Japan Integrated Staging · Prognosis · Modified albumin-bilirubin grade

## Abstract

**Background/Aim:** Recently, albumin-bilirubin (ALBI) scoring/grading, consisting of only albumin and total bilirubin, has been proposed. We examined the efficacy of this grading system for determining hepatic function in patients with hepatocellular carcinoma (HCC). **Methods/Materials:** The prognoses of 46,681 HCC patients based on results obtained from a nationwide survey conducted in Japan from 2001 to 2007 were evaluated using (1) Japan

Atsushi Hiraoka, MD, PhD  
Gastroenterology Center, Ehime Prefectural Central Hospital  
83 Kasuga-cho  
Matsuyama, Ehime 790-0024 (Japan)  
E-Mail hirage@m.ehime-u.ac.jp

Integrated Staging (JIS), consisting of Child-Pugh classification and TNM staging (TNM), (2) modified JIS (m-JIS), consisting of liver damage grading and TNM, and (3) ALBI-TNM (ALBI-T), consisting of ALBI grading and TNM, and the results were compared. A subanalysis was also performed to define a cutoff value for ALBI scores for a more detailed stratification of hepatic function. **Results:** ALBI-T, JIS, and m-JIS each showed good capacity for the stratification of prognoses. Although the Akaike information criterion for ALBI-T was nearly equal to that for JIS and m-JIS, the Kaplan-Meier curves and median survival times obtained with ALBI-T were always superior to the corresponding scores. When the indocyanine green retention test (<30%) was used as an additional cutoff value for ALBI score (–2.270, area under the curve 0.828) to divide ALBI grade into 4 levels (modified ALBI [mALBI] grade), mALBI grade was able to stratify the prognosis of patients at any TNM stage in order of grade. Modified ALBI-T (mALBI-T), using mALBI grading and TNM, produced a more detailed stratification for prognosis. **Conclusion:** The predictive value for prognosis of ALBI-T was found to be equal to that of JIS and m-JIS. In addition, mALBI grading and mALBI-T, as proposed in the present study, might provide a more detailed assessment of the hepatic function and prognosis of HCC patients.

© 2017 S. Karger AG, Basel

## Introduction

The Child-Pugh classification [1] is used worldwide as a standard assessment tool for hepatic function in hepatocellular carcinoma (HCC) patients, while it is also a part of the Evidence-Based Clinical Practice Guidelines for HCC of the Japan Society of Hepatology (JSH) as well as liver damage grading [2, 3]. Recently, a new assessment tool for hepatic function, albumin-bilirubin (ALBI) grading, which consists of only albumin and total bilirubin, has been proposed [4]. As compared to other assessment methods, ALBI grade, simply based on 2 common serological factors and determined by serial ALBI scoring, is thought to be advantageous, because the score can also be arbitrarily divided into more detailed grades when necessary.

As a total staging system for HCC, the Japan Integrated staging (JIS) system has also been proposed [5], which consists of the Child-Pugh classification and TNM staging of the Liver Cancer Study Group of Japan (LCSGJ) [6, 7]; JIS has been shown to have a better ability to predict prognosis than the Cancer of the Liver Italian Program (CLIP) scoring system [8, 9]. On the other hand, the usefulness of modified JIS (m-JIS) for grading liver damage as compared to JIS has been proposed for patients who undergo an indocyanine green retention test (ICG-r15) [10]. However, some issues regarding the analysis of hepatic function with the ICG-r15 have been reported, including problems related to the requirement of injection, the risk of anaphylactic shock, and difficulties with obtaining accurate results for patients with marked constitutional jaundice or a portosystemic shunt [11]. As a result, data for the ICG-r15 obtained from a retrospective cohort are often lacking. Recently, ALBI-TNM scoring (ALBI-T), which is composed of JIS used with ALBI grading, was reported to have good prognostic value in 2,584 Japanese HCC patients treated at 2 different institutions [12].

To evaluate whether ALBI grading can be used for hepatic functional assessment instead of Child-Pugh classification and liver damage grading, and to establish a more useful method for the assessment of hepatic function, we compared ALBI grading, Child-Pugh classification, and liver damage grading in the present study. In addition, we examined ALBI scoring/grading for its ability to provide a more detailed evaluation of hepatic function and predict prognosis in Japanese HCC patients using data from a nationwide survey.

## Subjects and Methods

### Patients

From January 2001 to December 2007, details regarding 64,928 treatment-naïve patients with HCC in Japan were recorded using a nationwide survey system. Of these patients, we analyzed 46,681 in the present study, after exclusion of cases lacking serological (albumin, total bilirubin, and prothrombin time) or clinical data (information about ascites or hepatic coma) for Child-Pugh classification or LCSGJ TNM staging. In patients positive for anti-hepatitis C virus (HCV) or hepatitis B surface antigen, HCC was considered to be due to HCV or hepatitis B virus (HBV), respectively. Those negative for both anti-HCV and hepatitis B surface antigen were judged as having nonviral (nonBnonC) HCC.

### Assessment Methods for Hepatic Function and Prognosis

Child-Pugh classification, liver damage grading, and ALBI grading were used for assessment of hepatic function. ALBI score and ALBI grade were defined as follows:  $(\log_{10} \text{bilirubin } [\mu\text{mol/L}] \times 0.66) + (\text{albumin } [\text{g/L}] \times -0.085)$  (grade 1, 2, and 3 =  $\leq -2.60$ ,  $> -2.60$  to  $-1.39$ , and  $> -1.39$ , respectively) [4]. The prognoses of the 46,681 patients with HCC (total group) were assessed using ALBI-T and JIS, while those of the 31,011 patients after excluding those without ICG-r15 results (ICG group) were evaluated using ALBI-T, JIS, and m-JIS. In addition, we compared the potential for predicting prognosis of each score (ALBI-T, JIS, and m-JIS) in HCC patients within the Milan criteria (single lesion  $\leq 5$  cm, or 2 or 3 lesions each 3 cm in size) [13] who were treated with curative therapy (surgical resection, ablative treatment) in both groups. Percutaneous ethanol injection [14, 15] and mainly radiofrequency ablation [16–18] were performed as ablative therapy methods.

As an additional analytic technique, we evaluated the cutoff value for ALBI score by dividing ALBI grade 2 into subgrades (2a and 2b) obtained with the ICG-r15 to produce a modified ALBI grade (mALBI grade) divided into 4 subgrades, because ALBI score is serial and ALBI grade 2 is thought to have a wide range. To evaluate mALBI grading for its ability to assess hepatic function, the prognostic predictive value of modified ALBI-T (mALBI-T), calculated using mALBI grade and LCSGJ TNM stage (mALBI grade 1, 2a, 2b, and 3 = score 0, 1, 2, and 3, respectively; LCSGJ TNM stage I, II, III, and IV = score 0, 1, 2, and 3, respectively), was examined in both groups.

### Statistical Analysis

Prognosis was analyzed using a log-rank test with the Kaplan-Meier method. The discriminatory abilities of the scoring models were assessed using the Akaike information criterion (AIC) [19]. Pearson test, receiver operating characteristic, and area under the curve (AUC) values were calculated for comparisons between ALBI score and the ICG-r15. For multiple comparisons, Holm's method was used. All statistical analyses were performed using Easy R (EZR) version 1.29 (Saitama Medical Center, Jichi Medical University, Saitama, Japan) [20], a graphical user interface for the R statistical Computing Environment (R Foundation, Vienna, Austria). All *p* values were derived from two-tailed tests, with *p* < 0.05 accepted as statistically significant.

## Results

The clinical features of the patients in the total group (*n* = 46,681) are shown in Table 1. The median age was 68 years (interquartile range: 61–74); 33,316 were male and 13,365 were female (HCV, HBV, HBV and HCV, nonBnonC, and unknown: *n* = 30,478, 6,124, 821, 8,743, and 515, respectively; Child-Pugh class A, B, and C: *n* = 34,829, 10,111, and 1,741, respectively; LCSGJ TNM stage I, II, III, and IV: *n* = 7,783, 21,018, 12,843, and 5,037, respectively [IVa and IVb: *n* = 2,927 and 2,110, respectively]; ALBI grade 1, 2, and 3: *n* = 15,968, 27,771, and 2,942, respectively). Surgical resection was performed on 14,551 patients as the initial treatment, while it was ablative therapy for 13,359, transcatheter arterial chemoembolization [21] for 13,995, and other treatments or none for 4,776. The number of patients within the Milan criteria was 25,814 (55.3%).

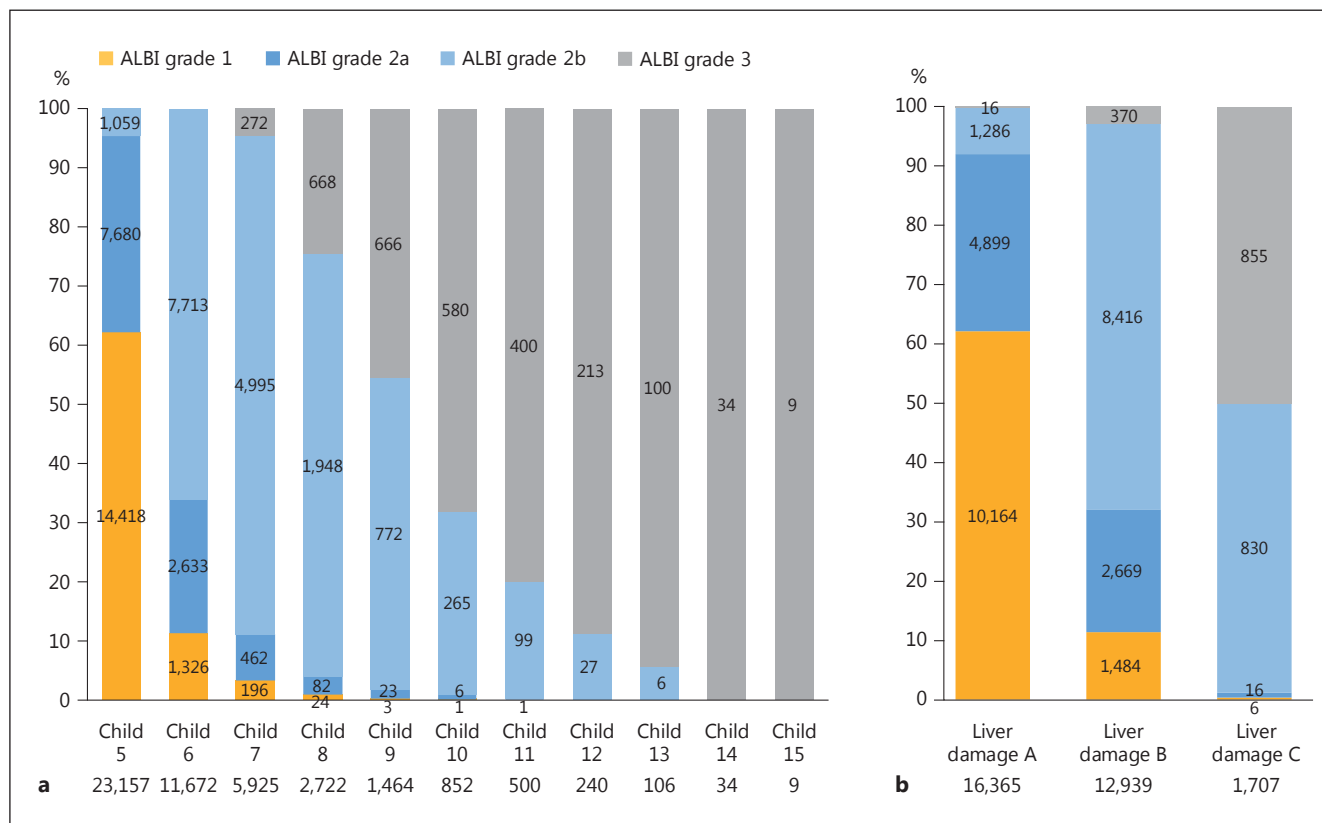
The distribution of ALBI grades for each Child-Pugh score is shown in Figure 1a. The patients classified as Child-Pugh class A consisted of 15,744 with ALBI grade 1 and 19,085

**Table 1.** Clinical features of the patients ( $n = 46,681$ ; total group)

Median age (IQR), years	68 (61–74)
Gender	
Male	33,316
Female	13,365
Etiology	
HCV	30,478
HBV	6,124
HBV and HCV	821
nonBnonC	8,743
Unknown	515
Child-Pugh class	
A	34,829
B	10,111
C	1,741
ALBI grade	
1	15,968
2	27,771
3	2,942
Liver damage grade	
A	16,365
B	12,939
C	1,707
No data	15,670
Median albumin (IQR), g/dL	3.7 (3.3–4.0)
Median total bilirubin (IQR), mg/dL	9 (0.6–1.2)
Median prothrombin time (IQR), %	82 (71–93)
Median platelet count (IQR), $\times 10^4/\mu\text{L}$	11.6 (8.0–16.4)
Median ICG-r15 rate (IQR) <sup>1</sup> , %	19 (12–29)
Median tumor size (IQR), cm	3 (2.0–5.0)
Tumor number	
Single	26,106
Multiple	20,402
No data	173
Vascular invasion of tumor present, $n$ (%)	6,368 (13.6)
Extrahepatic metastasis present, $n$ (%)	2,110 (4.5)
LCSGJ TNM stage	
I	7,783
II	21,018
III	12,843
IVa	2,927
IVb	2,110
Treatment	
Resection	14,551
Ablative therapies	13,359
TACE	13,995
Others	2,341
None	2,435

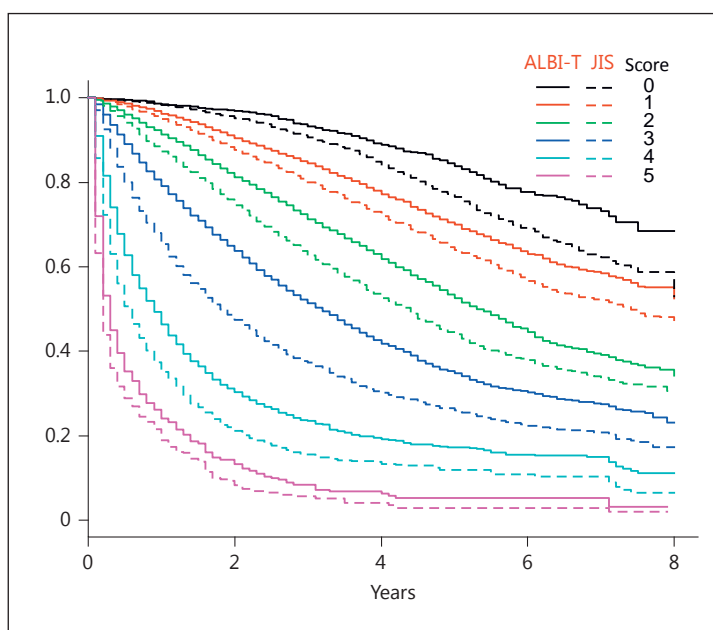
IQR, interquartile range; HCV, hepatitis C virus; HBV, hepatitis B virus; nonBnonC, negative for both HBV and HCV; ALBI, albumin-bilirubin; ICG-r15, indocyanine green retention test; LCSGJ, Liver Cancer Study Group of Japan; TACE, transcatheter arterial chemoembolization.

<sup>1</sup>  $n = 31,011$  (ICG group).



**Fig. 1. a** Distribution of albumin-bilirubin (ALBI) grade for each Child-Pugh score in the total group. **b** Distribution of ALBI grades for each liver damage grade in the ICG group.

**Fig. 2.** Kaplan-Meier curves for albumin-bilirubin (ALBI) grades and TNM staging scores of the Liver Cancer Study Group of Japan (ALBI-T) (solid lines) and Japan Integrated Staging (JIS) scores (broken lines) in the total group. The scores for ALBI-T were always superior to the corresponding JIS scores.





**Table 2.** Comparison of MST between ALBI-T, JIS, and mALBI-T among Japanese hepatocellular carcinoma patients ( $n = 46,681$ ; total group) and those within the Milan criteria treated curatively ( $n = 18,886$ )

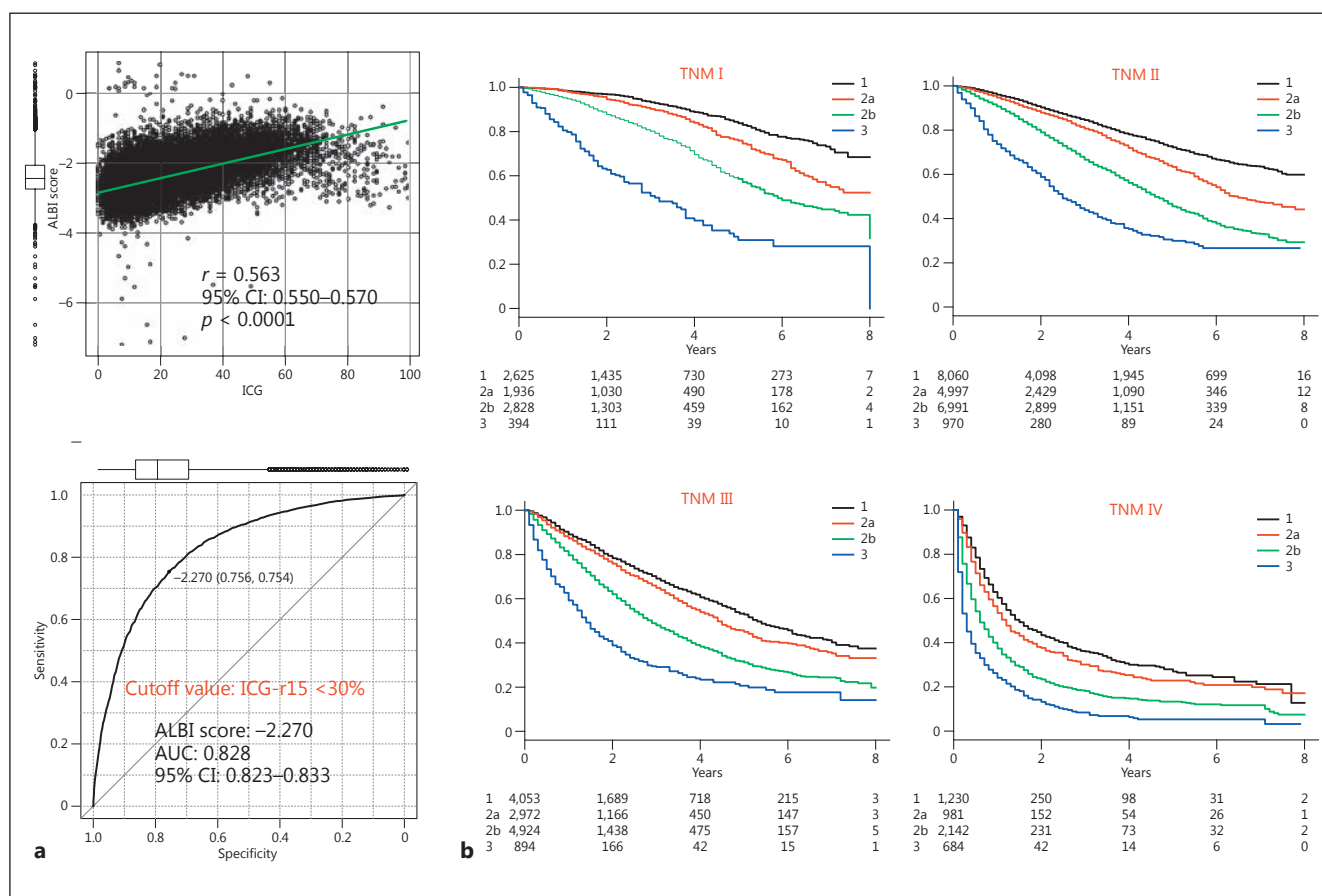
Score	ALBI-T			JIS			mALBI-T		
	MST, years	95% CI, years	<i>n</i>	MST, years	95% CI, years	<i>n</i>	MST, years	95% CI, years	<i>n</i>
<i>All patients (n = 46,681)</i>									
0	NA	NA-NA	2,625	NA	8.0-NA	5,908	NA	NA-NA	2,625
1	NA	8.0-NA	12,824	7.4	7.1-8.0	18,242	NA	NA-NA	10,289
2	5.4	5.2-5.6	16,435	4.4	4.2-4.5	13,531	6.0	5.8-5.6	12,354
3	3.2	3.0-3.3	10,096	1.8	11.7-2.0	6,430	4.2	4.0-4.4	11,334
4	0.9	0.9-1.0	4,017	0.6	0.5-0.06	2,036	2.5	2.4-2.6	6,543
5	0.3	0.2-0.3	684	0.2	0.2-0.2	534	0.8	0.7-0.9	2,852
6	-	-	-	-	-	-	0.3	0.2-0.3	684
AIC	256,952.4			256,356.7			256,955.5		
<i>Patients within the Milan criteria treated curatively (n = 18,886)</i>									
0	NA	NA-NA	2,178	NA	NA-NA	4,818	NA	NA-NA	2,178
1	NA	8-NA	8,465	NA	7.8-NA	10,637	NA	NA-NA	6,568
2	6.1	5.8-6.5	6,958	5.3	4.9-5.8	2,959	7.1	6.5-NA	5,568
3	4.7	4.4-5.6	1,223	3.8	3.3-4.5	453	5.2	5.0-5.7	3,707
4	3.3	2.2-NA	62	NA	1.2-NA	19	4.2	3.7-4.6	803
5	-	-	-	-	-	-	3.3	2.2-NA	62
AIC	57,365.5			57,416.3			57,133.3		

ALBI-T, albumin-bilirubin grading and TNM staging; JIS, Japan Integrated Staging; mALBI-T, modified ALBI-T; MST, median survival time; NA, not available; AIC, Akaike information criterion.

with ALBI grade 2, while those classified as Child-Pugh class B were composed of 223 with ALBI grade 1, 8,282 with ALBI grade 2, and 1,606 with ALBI grade 3; the patients classified as Child-Pugh class C contained 1 with ALBI grade 1, 404 with ALBI grade 2, and 1,336 with ALBI grade 3. Even among the Child-Pugh class B patients, the rate of ALBI grade 3 was not small.

The Kaplan-Meier curves for JIS and ALBI-T of the total group ( $n = 46,681$ ) are shown in Figure 2. The AIC value for ALBI-T for the total group was 256,952.4, while that for JIS was 256,356.7, and the Kaplan-Meier curves and median survival time (MST) for each ALBI-T score were superior to those for JIS (Fig. 2; Table 2).

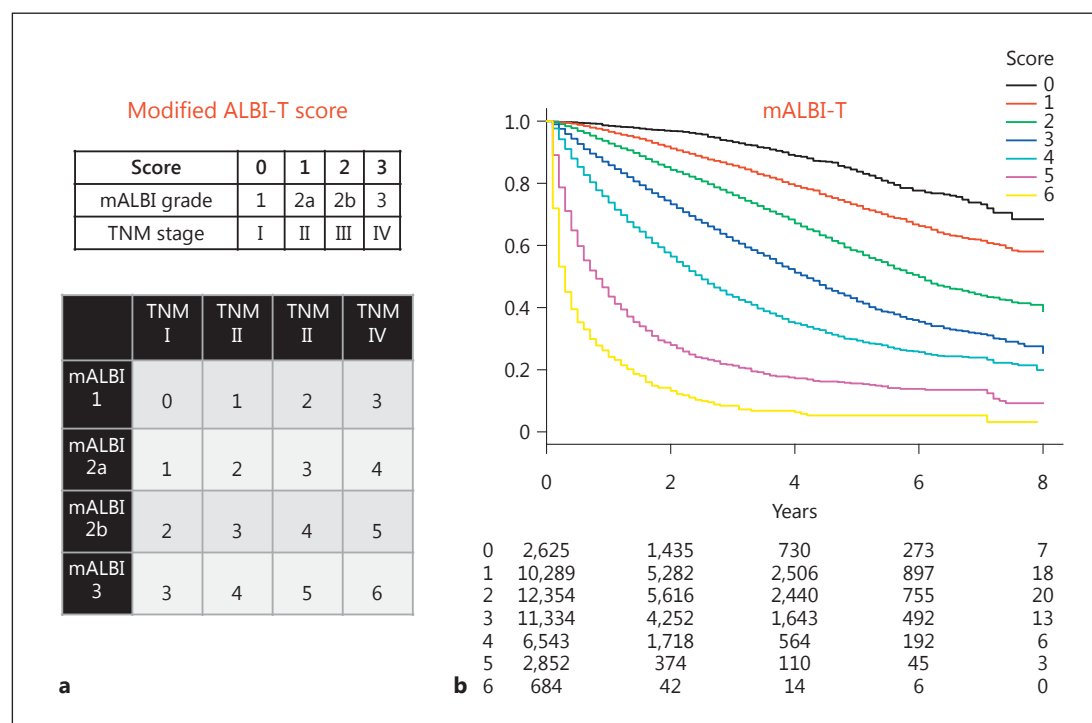
The subanalysis of 31,011 of the patients in the total group with data for the ICG-r15 (ICG group) showed that the ICG-r15 had a good correlation with ALBI score ( $r = 0.563$ ; 95% CI: 0.550–0.570;  $p < 0.0001$ ). Among the 31,011 patients with results for the ICG-r15, surgical resection was performed on 13,487, while it was ablative therapy for 7,669, transcatheter arterial chemoembolization for 7,761, and other treatments or non for 2,094. The number of patients within the Milan criteria was 17,188 (55.4%). The cutoff value for ALBI score for the ICG-r15 ( $<30\%$ ), an indicator for performance of a subsegmentectomy in the Makuuchi criteria [22, 23], was  $-2.270$  (AUC 0.828; 95% CI: 0.823–0.833) (Fig. 3a). The distribution of ALBI grades among the grades for liver damage is shown in Figure 1b. ALBI grade 3 was mainly included in liver damage grade C, while the frequency of ALBI grade 3 was very low among the patients with liver damage grade B. When ALBI grade 2 was divided into 2 subgroups (ALBI grades 2a and 2b) according to the cutoff value for the ICG-r15 ( $<30\%$ ) (ALBI score:  $-2.270$ ), thus conducting a division into 4 ALBI grades (mALBI grade), the ratio of the better subgroup (ALBI grade 2a: score  $\leq -2.270$ ) became lower when the Child-Pugh



**Fig. 3. a** A good relationship ( $r = 0.563$ ; 95% CI: 0.550–0.570;  $p < 0.0001$ ) was observed between indocyanine green retention test (ICG-r15) and albumin-bilirubin (ALBI) score results. The cutoff value for ALBI score for the ICG-r15 (<30%) was -2.270 (AUC 0.828; 95% CI: 0.823–0.833). **b** For each Liver Cancer Study Group of Japan (LCSGJ) TNM stage, good stratification for prognosis of patients with each modified ALBI (mALBI) grade was shown. There were significant differences between each mALBI grade for each LCSGJ TNM stage, as shown by multiple comparisons with Holm's method ( $p < 0.01$ ).

score became larger (Fig. 1a). In each TNM stage, a good ability to stratify prognosis according to the newly established subgroups for ALBI grade (mALBI grades 1, 2a, 2b, and 3) was observed, and there was a statistically significant difference between each mALBI grade in all stages for prognosis ( $p < 0.01$ , Holm's method) (Fig. 3b). When an analysis was performed with mALBI grade in the same manner as with ALBI-T and JIS, patient prognosis could be stratified with the additional grades provided by mALBI-T (Fig. 4). In addition to a greater number of scores for stratification, use of mALBI-T also resulted in a better MST for each score as compared to the corresponding scores for ALBI-T and JIS in the total group (Table 2).

For the 31,011 patients in the ICG group, the AIC value for ALBI-T was similar to that for JIS and m-JIS (157,696.4, 157,591.4, and 157,630.9, respectively), while that for mALBI-T was 157,668.7. mALBI-T showed a better MST for each score as compared to the corresponding scores for ALBI-T, JIS, and m-JIS in the ICG group (Table 3). In the ICG group, those for ALBI-T, JIS, m-JIS, and mALBI-T for the HCC patients within the Milan criteria ( $n = 17,188$ ) were 60,213.2, 60,258.3, 60,279.7, and 59,971.2, respectively (data not shown), while those for the patients treated curatively ( $n = 21,156$ ) were 83,595.4, 83,637.2, 83,611.8, and 83,500.6, respectively (data not shown), and those for the patients within the Milan criteria and treated



**Fig. 4. a** Scores for each factor (modified albumin-bilirubin [mALBI] grades 1, 2a, 2b, and 3 = scores 0, 1, 2, and 3; Liver Cancer Study Group of Japan TNM stages I, II, III, and IV = scores 0, 1, 2, and 3), mALBI grade, and TNM stage. Those were summed to calculate the mALBI-T score (scores 0–6). **b** Kaplan-Meier curves for mALBI-T showing good stratification for prognosis, as shown by each mALBI-T score in the total group ( $n = 46,681$ ).

curatively ( $n = 13,404$ ) were 41,054.6, 41,107.9, 41,094.1, and 40,887.7, respectively (Table 3). For the 18,886 patients within the Milan criteria treated curatively in the total group, those for ALBI-T, JIS, and mALBI-T were 57,365.5, 57,416.3, and 57,133.3, respectively (Table 2).

## Discussion

For treatment of HCC patients, use of a total staging system which integrates both liver function stage and tumor burden stage has become important for accurate prediction of prognosis, as it provides good information for decision-making regarding therapy. Various staging systems have been reported, such as those investigated in the Okuda [24], CLIP [8], Tokyo [25], BALAD [26], and BALAD2 [27, 28] studies. Kudo proposed JIS as a useful prognostic staging system, and showed its consistency with Child-Pugh classification and the TNM staging of the LCSGJ [5, 9]. However, there are some issues, including the fact that the Child-Pugh classification has subjective (ascites, hepatic coma) and confounding factors (albumin, ascites) and was not constructed in a statistical manner. Moreover, albumin, total bilirubin, and prothrombin time are treated as semiquantitative factors in that classification. On the other hand, ALBI-T, which consists of ALBI grading and TNM staging, has been proposed as a new total staging system for HCC [12], and validation studies have already been reported [29, 30].

In the present cohort, ALBI-T showed an almost similar AIC to that of JIS for the total group, as well as for those within the Milan criteria and treated curatively. However, the MST

**Table 3.** Comparison of MST between ALBI-T, JIS, m-JIS, and mALBI-T ( $n = 31,011$ ; ICG group) and those within the Milan criteria treated curatively ( $n = 13,404$ ) among hepatocellular carcinoma patients in whom the ICG-r15 was examined

Score	ALBI-T			JIS			m-JIS			mALBI-T		
	MST, years	95% CI, years	<i>n</i>	MST, years	95% CI, years	<i>n</i>	MST, years	95% CI, years	<i>n</i>	MST, years	95% CI, years	<i>n</i>
<i>Patients in whom the ICG-r15 was examined (n = 31,011)</i>												
0	NA	NA-NA	1,615	NA	NA-NA	3,584	NA	NA-NA	2,208	NA	NA-NA	1,615
1	NA	NA-NA	8,962	8.0	7.4-NA	13,206	7.8	7.3-NA	14,387	NA	NA-NA	7,532
2	5.6	5.4-5.8	11,520	4.5	4.4-4.7	9,412	4.8	4.6-5.0	7,152	6.2	6.0-6.5	8,685
3	3.5	3.3-3.6	6,677	2.0	1.9-2.2	3,842	3.2	3.0-3.4	5,302	4.4	4.2-4.5	7,574
4	1.1	1.0-1.2	2,042	0.7	0.6-0.8	872	1.1	1.0-1.2	1,734	2.7	2.5-2.9	4,073
5	0.5	0.4-0.7	195	0.4	0.2-0.7	95	0.4	0.3-0.5	228	1.0	0.9-1.1	1,337
6	-	-	-	-	-	-	-	-	-	0.5	0.4-0.7	195
AIC	157,696.4			157,591.4			157,630.9			157,668.7		
<i>Patients within the Milan criteria treated curatively in whom the ICG-r15 was examined (n = 13,404)</i>												
0	NA	NA-NA	1,390	NA	NA-NA	3,034	NA	NA-NA	1,916	NA	NA-NA	1,390
1	NA	NA-NA	6,041	NA	NA-NA	8,041	NA	NA-NA	9,025	NA	NA-NA	4,946
2	6.2	5.9-6.8	5,118	5.2	4.9-5.8	2,049	5.5	4.9-5.8	1,868	7.3	6.7-NA	3,931
3	4.7	4.4-5.2	819	3.5	2.8-4.2	274	4.6	4.2-5.2	541	5.2	4.9-5.6	2,591
4	2.6	1.9-4.0	36	2.5	1.2-NA	6	2.5	1.9-4.5	54	4.2	3.5-4.6	510
5	-	-	-	-	-	-	-	-	-	2.6	1.9-4.0	36
AIC	41,054.6			41,107.9			41,094.1			40,887.7		

ICG-r15, indocyanine green retention test; ALBI-T, albumin-bilirubin grading and TNM staging; JIS, Japan Integrated Staging; m-JIS, modified JIS; mALBI-T, modified ALBI-T; MST, median survival time; NA, not available; AIC, Akaike information criterion.

for each ALBI-T score was superior to that for the corresponding JIS score. Although ALBI grade is calculated with only those 2 factors, ALBI-T compared favorably with not only JIS but also m-JIS in the ICG group. In addition, several patients in the present cohort were excluded due to a lack of data for Child-Pugh class (e.g., ascites, hepatic coma) or liver damage grade (ICG-r15). Thus, the simply calculated ALBI grade is thought to be useful for retrospective analysis as well as for predicting prognosis, especially for patients scheduled to undergo curative treatment such as resection or ablative therapy.

In Japan, HCC is often diagnosed at an earlier stage than in Western countries. Kudo et al. [31] recently reported that the number of cases of small-sized HCC has increased because recognition of the importance of surveillance for high-risk patients with chronic liver diseases has varied widely in Japan. Nevertheless, the prognosis for Japanese patients with HCC has improved [31]. Minagawa et al. [6] reported that LCSCJ TNM staging was more appropriate for early-stage HCC cases, while JIS has been proposed as a better total staging system than CLIP scoring [5, 9, 32]. On the other hand, the recent trend for HCC etiology in Japan has rapidly changed [33, 34]. The main etiology of HCC in Japanese patients has been reported to be HCV infection [33, 35]. Development of direct-acting antiviral drug therapy for HCV [36, 37] has led to an extremely high rate of HCV elimination, allowing for maintenance of hepatic function without progression of hepatic fibrosis after sustained virologic response (SVR). However, treatment of HCC after SVR with direct-acting antiviral drug therapy remains controversial, because the incidence of HCC after SVR in a group of interferon-free patients was reported to be >2-fold higher than that in an interferon-based therapy group (7.29 vs. 3.09% and 6.23 vs. 3.01%) [38]. In addition, the number of nonBnonC HCC cases has been increasing [33, 34] in association with the aging of society.

Based on these dynamic changes, it is expected that the frequency of HCC among Japanese patients with better hepatic function will increase. In addition, because of the progress in techniques used for imaging, and therapeutic assistant modalities for the diagnosis and treatment of HCC (virtual ultrasonography [39], artificial effusion [40], contrast-enhanced ultrasonography [41, 42], and Gd-EOB-DTPA-enhanced MRI [43, 44]), the frequencies of resection and ablative therapies including radiofrequency ablation will increase; thus, a more suitable hepatic function assessment tool for the recent trend in Japanese HCC is needed. In addition to the usefulness of ALBI-T for Japanese patients, that of modified CLIP scoring [45], modified BCLC (Barcelona Clinic Liver Cancer) staging [46], and BCLC-B substaging using ALBI grading instead of the Child-Pugh classification/scoring system [47] has recently been reported. Thus, the simply calculated ALBI grade can play an important role in the assessment of hepatic function not only in the recent trend of Japanese HCC but also worldwide.

A previous report noted that liver damage grading is now recognized to be superior as a hepatic functional assessment tool, and that the prognosis prediction value of m-JIS is better than that of JIS [10]. Although the prognostic stratification ability (MST of each score) of m-JIS is thought to be superior to that of JIS, the AIC value was similar to that of JIS and ALBI-T. Liver damage grading is used for the assessment of hepatic function in the Evidence-Based Clinical Practice Guidelines for HCC of the JSH [2, 3], though data for the ICG-r15 are frequently lacking because ICG injection is required. In fact, the ICG-r15 was examined in only 66.4% of the patients of the total group. ALBI-T may have a noninferior predictive value, not only as compared to that of JIS but also to that of m-JIS even in patients who undergo ICG testing, while ALBI-T might show a better MST value than JIS and m-JIS. Moreover, the advantages of the ALBI grade are that it is calculated using only 2 common factors (albumin and total bilirubin) and determined based on serial ALBI scores as compared with other methods. In our previous study, there was a good correlation between ICG-r15 rate and ALBI score ( $r = 0.616$ ;  $p < 0.001$ ), and the cutoff value for ALBI score for the ICG-r15 ( $<30\%$ ) was  $-2.222$  (AUC 0.843; sensitivity 0.823; specificity 0.708; 95% CI: 0.827–0.859) [48]. In the present analysis, a similar correlation between ALBI score and ICG-r15 rate was noted, as well as for the cutoff value for ALBI score ( $-2.270$ ; AUC 0.828) for the ICG-r15 ( $<30\%$ ), which is a cutoff indicator for subsegmental cases in the Makuuchi criteria [22, 23]. Because subsegmentectomy has been thought to be the minimal anatomical surgical resection for HCC, we used the ICG-r15 ( $<30\%$ ) for the cutoff indicator of subgrading for ALBI grade 2. Thus, we consider that a division into 4 ALBI grades can be conducted by making 2 subgrades for ALBI grade 2 (2a and 2b) based on the cutoff value (ALBI score  $-2.270$ ) (mALBI grade). For each TNM stage, a good prognostic stratification ability according to mALBI grade was observed. As a result, mALBI-T showed a more detailed stratification among all of our HCC patients, as well as the best value for the AIC among the 4 tested scoring systems for early-stage HCC (Milan criteria) among patients treated curatively. mALBI and mALBI-T might provide more important information for decision-making regarding therapy.

In conclusion, we evaluated the prognostic significance of ALBI grading/ALBI-T for patients with HCC in Japan using data from a nationwide follow-up survey, and confirmed that they were applicable as well as the Child-Pugh classification/JIS and liver damage grading/m-JIS. Moreover, ALBI scoring might have potential for a division into additional grades for a more detailed assessment of hepatic function and prognosis, such as the present proposed mALBI grading and mALBI-T. Prospective examinations are needed for confirmation.

### Acknowledgement

The authors express their gratefulness to Dr. Natsumi Yamashita, Shikoku Cancer Center, for the excellent advice.



## Disclosure Statement

The authors have no conflicts of interest to declare in regard to this study.

## References

- 1 Pugh RN, Murray-Lyon IM, Dawson JL, Pietroni MC, Williams R: Transection of the oesophagus for bleeding oesophageal varices. *Br J Surg* 1973;60:646–649.
- 2 Makuuchi M, Kokudo N, Arii S, Futagawa S, Kaneko S, Kawasaki S, Matsuyama Y, et al: Development of evidence-based clinical guidelines for the diagnosis and treatment of hepatocellular carcinoma in Japan. *Hepatol Res* 2008;38:37–51.
- 3 Japan Society of Hepatology: Clinical Practice Guidelines for Hepatocellular Carcinoma 2013. [http://www.jsh.or.jp/English/guidelines\\_en/Guidelines\\_for\\_hepatocellular\\_carcinoma\\_2013](http://www.jsh.or.jp/English/guidelines_en/Guidelines_for_hepatocellular_carcinoma_2013).
- 4 Johnson PJ, Berhane S, Kagebayashi C, Satomura S, Teng M, Reeves HL, O’Beirne J, et al: Assessment of liver function in patients with hepatocellular carcinoma: a new evidence-based approach – the ALBI grade. *J Clin Oncol* 2015;33:550–558.
- 5 Kudo M, Chung H, Osaki Y: Prognostic staging system for hepatocellular carcinoma (CLIP score): its value and limitations, and a proposal for a new staging system, the Japan Integrated Staging Score (JIS score). *J Gastroenterol* 2003;38:207–215.
- 6 Minagawa M, Ikai I, Matsuyama Y, Yamaoka Y, Makuuchi M: Staging of hepatocellular carcinoma: assessment of the Japanese TNM and AJCC/UICC TNM systems in a cohort of 13,772 patients in Japan. *Ann Surg* 2007;245:909–922.
- 7 Liver Cancer Study Group of Japan: The General Rules for the Clinical and Pathological Study of Primary Liver Cancer, ed 6. Tokyo, Kanehara, 2015.
- 8 Prospective validation of the CLIP score: a new prognostic system for patients with cirrhosis and hepatocellular carcinoma. The Cancer of the Liver Italian Program (CLIP) Investigators. *Hepatology* 2000;31:840–845.
- 9 Kudo M, Chung H, Haji S, Osaki Y, Oka H, Seki T, Kasugai H, et al: Validation of a new prognostic staging system for hepatocellular carcinoma: the JIS score compared with the CLIP score. *Hepatology* 2004;40:1396–1405.
- 10 Nanashima A, Sumida Y, Abo T, Shindou H, Fukuoka H, Takeshita H, Hidaka S, et al: Modified Japan Integrated Staging is currently the best available staging system for hepatocellular carcinoma patients who have undergone hepatectomy. *J Gastroenterol* 2006;41:250–256.
- 11 Kudo M: Albumin-bilirubin grade and hepatocellular carcinoma treatment algorithm. *Liver Cancer* 2017;6:185–188.
- 12 Hiraoka A, Kumada T, Michitaka K, Toyoda H, Tada T, Ueki H, Kaneto M, et al: Usefulness of albumin-bilirubin grade for evaluation of prognosis of 2,584 Japanese patients with hepatocellular carcinoma. *J Gastroenterol Hepatol* 2016;31:1031–1036.
- 13 Mazzaferro V, Regalia E, Doci R, Andreola S, Pulvirenti A, Bozzetti F, Montalto F, et al: Liver transplantation for the treatment of small hepatocellular carcinomas in patients with cirrhosis. *N Engl J Med* 1996;334:693–699.
- 14 Shiina S, Niwa Y, Shiratori Y, Terano A, Omata M: Percutaneous ethanol injection therapy for hepatocellular carcinoma [sic!] (review). *Int J Oncol* 1993;2:669–675.
- 15 Shiina S, Teratani T, Obi S, Hamamura K, Koike Y, Omata M: Percutaneous ethanol injection therapy for liver tumors. *Eur J Ultrasound* 2001;13:95–106.
- 16 Tateishi R, Shiina S, Teratani T, Obi S, Sato S, Koike Y, Fujishima T, et al: Percutaneous radiofrequency ablation for hepatocellular carcinoma. An analysis of 1,000 cases. *Cancer* 2005;103:1201–1209.
- 17 Hiraoka A, Michitaka K, Horiike N, Hidaka S, Uehara T, Ichikawa S, Hasebe A, et al: Radiofrequency ablation therapy for hepatocellular carcinoma in elderly patients. *J Gastroenterol Hepatol* 2010;25:403–407.
- 18 Shiina S, Tateishi R, Arano T, Uchino K, Enooku K, Nakagawa H, Asaoka Y, et al: Radiofrequency ablation for hepatocellular carcinoma: 10-year outcome and prognostic factors. *Am J Gastroenterol* 2012;107:569–577; quiz 578.
- 19 Akaike H: Information theory and an extension of the maximum likelihood principle; in Petrov BN, Csaki F (eds): *Proceedings of the 2nd International Symposium on Information Theory*. Budapest, Akademiai Kiado, 1973, pp 267–281.
- 20 Kanda Y: Investigation of the freely available easy-to-use software “EZ” for medical statistics. *Bone Marrow Transplant* 2013;48:452–458.
- 21 Takayasu K, Arii S, Ikai I, Omata M, Okita K, Ichida T, Matsuyama Y, et al: Prospective cohort study of transarterial chemoembolization for unresectable hepatocellular carcinoma in 8,510 patients. *Gastroenterology* 2006;131:461–469.
- 22 Miyagawa S, Makuuchi M, Kawasaki S, Kakazu T: Criteria for safe hepatic resection. *Am J Surg* 1995;169:589–594.
- 23 Seyama Y, Kokudo N: Assessment of liver function for safe hepatic resection. *Hepatol Res* 2009;39:107–116.
- 24 Okuda K, Ohtsuki T, Obata H, Tomimatsu M, Okazaki N, Hasegawa H, Nakajima Y, et al: Natural history of hepatocellular carcinoma and prognosis in relation to treatment. Study of 850 patients. *Cancer* 1985;56:918–928.

- 25 Tateishi R, Yoshida H, Shiina S, Imamura H, Hasegawa K, Teratani T, Obi S, et al: Proposal of a new prognostic model for hepatocellular carcinoma: an analysis of 403 patients. *Gut* 2005;54:419–425.
- 26 Toyoda H, Kumada T, Osaki Y, Oka H, Urano F, Kudo M, Matsunaga T: Staging hepatocellular carcinoma by a novel scoring system (BALAD score) based on serum markers. *Clin Gastroenterol Hepatol* 2006;4:1528–1536.
- 27 Berhane S, Toyoda H, Tada T, Kumada T, Kagebayashi C, Satomura S, Schweitzer N, et al: Role of the GALAD and BALAD-2 serologic models in diagnosis of hepatocellular carcinoma and prediction of survival in patients. *Clin Gastroenterol Hepatol* 2016;14:875–886.e6.
- 28 Toyoda H, Tada T, Johnson PJ, Izumi N, Kadoya M, Kaneko S, Kokudo N, et al: Validation of serological models for staging and prognostication of HCC in patients from a Japanese nationwide survey. *J Gastroenterol* 2017, Epub ahead of print.
- 29 Chan AW, Chong CC, Mo FK, Wong J, Yeo W, Johnson PJ, Yu S, et al: Applicability of albumin-bilirubin-based Japan Integrated Staging score in hepatitis B-associated hepatocellular carcinoma. *J Gastroenterol Hepatol* 2016;31:1766–1772.
- 30 Harimoto N, Yoshizumi T, Sakata K, Nagatsu A, Motomura T, Itoh S, Harada N, et al: Prognostic significance of combined albumin-bilirubin and tumor-node-metastasis staging system in patients who underwent hepatic resection for hepatocellular carcinoma. *Hepatol Res* 2017, Epub ahead of print.
- 31 Kudo M, Izumi N, Sakamoto M, Matsuyama Y, Ichida T, Nakashima O, Matsui O, et al: Survival analysis over 28 years of 173,378 patients with hepatocellular carcinoma in Japan. *Liver Cancer* 2016;5:190–197.
- 32 Kudo M: Real practice of hepatocellular carcinoma in Japan: conclusions of the Japan Society of Hepatology 2009 Kobe Congress. *Oncology* 2010;78(suppl 1):180–188.
- 33 Tateishi R, Okanoue T, Fujiwara N, Okita K, Kiyosawa K, Omata M, Kumada H, et al: Clinical characteristics, treatment, and prognosis of non-B, non-C hepatocellular carcinoma: a large retrospective multicenter cohort study. *J Gastroenterol* 2015;50:350–360.
- 34 Hiraoka A, Ochi M, Matsuda R, Aibiki T, Okudaira T, Kawamura T, Yamago H, et al: Ultrasonography screening for hepatocellular carcinoma in Japanese patients with diabetes mellitus. *J Diabetes* 2016;8:640–646.
- 35 Ikai I, Arii S, Okazaki M, Okita K, Omata M, Kojiro M, Takayasu K, et al: Report of the 17th Nationwide Follow-Up Survey of Primary Liver Cancer in Japan. *Hepatol Res* 2007;37:676–691.
- 36 Su F, Beste LA, Green PK, Berry K, Ioannou GN: Direct-acting antivirals are effective for chronic hepatitis C treatment in elderly patients: a real-world study of 17,487 patients. *Eur J Gastroenterol Hepatol* 2017;29:686–693.
- 37 Toyoda H, Kumada T, Tada T, Shimada N, Takaguchi K, Senoh T, Tsuji K, et al: Efficacy and tolerability of an IFN-free regimen with DCV/ASV for elderly patients infected with HCV genotype 1B. *J Hepatol* 2017;66:521–527.
- 38 Toyoda H, Tada T, Takaguchi K, Senoh T, Shimada N, Hiraoka A, Michitaka K, et al: Differences in background characteristics of patients with chronic hepatitis C who achieved sustained virologic response with interferon-free versus interferon-based therapy and the risk of developing hepatocellular carcinoma after eradication of hepatitis C virus in Japan. *J Viral Hepat* 2017;24:472–476.
- 39 Hirooka M, Iuchi H, Kumagi T, Shigematsu S, Hiraoka A, Uehara T, Kurose K, et al: Virtual sonographic radiofrequency ablation of hepatocellular carcinoma visualized on CT but not on conventional sonography. *AJR Am J Roentgenol* 2006;186:S255–S260.
- 40 Uehara T, Hirooka M, Ishida K, Hiraoka A, Kumagi T, Kisaka Y, Hiasa Y, et al: Percutaneous ultrasound-guided radiofrequency ablation of hepatocellular carcinoma with artificially induced pleural effusion and ascites. *J Gastroenterol* 2007;42:306–311.
- 41 Hiraoka A, Ichiryu M, Tazuya N, Ochi H, Tanabe A, Nakahara H, Hidaka S, et al: Clinical translation in the treatment of hepatocellular carcinoma following the introduction of contrast-enhanced ultrasonography with Sonazoid. *Oncol Lett* 2010;1:57–61.
- 42 Hiraoka A, Hiasa Y, Onji M, Michitaka K: New contrast enhanced ultrasonography agent: impact of Sonazoid on radiofrequency ablation. *J Gastroenterol Hepatol* 2011;26:616–618.
- 43 Di Martino M, Marin D, Guerrisi A, Baski M, Galati F, Rossi M, Brozzetti S, et al: Intraindividual comparison of gadoxetate disodium-enhanced MR imaging and 64-section multidetector CT in the detection of hepatocellular carcinoma in patients with cirrhosis. *Radiology* 2010;256:806–816.
- 44 Sano K, Ichikawa T, Motosugi U, Sou H, Muhi AM, Matsuda M, Nakano M, et al: Imaging study of early hepatocellular carcinoma: usefulness of gadoxetic acid-enhanced MR imaging. *Radiology* 2011;261:834–844.
- 45 Chan AW, Chong CC, Mo FK, Wong J, Yeo W, Johnson PJ, Yu S, et al: Incorporating albumin-bilirubin grade into the Cancer of the Liver Italian Program system for hepatocellular carcinoma. *J Gastroenterol Hepatol* 2017;32:221–228.
- 46 Chan AW, Kumada T, Toyoda H, Tada T, Chong CC, Mo FK, Yeo W, et al: Integration of albumin-bilirubin (ALBI) score into Barcelona Clinic Liver Cancer (BCLC) system for hepatocellular carcinoma. *J Gastroenterol Hepatol* 2016;31:1300–1306.
- 47 Hiraoka A, Kumada T, Nouse K, Tsuji K, Itobayashi E, Hirooka M, Kariyama K, et al: Proposed new sub-grouping for intermediate-stage hepatocellular carcinoma using albumin-bilirubin grade. *Oncology* 2016;91:153–161.
- 48 Hiraoka A, Kumada T, Kudo M, Hirooka M, Tsuji K, Itobayashi E, Kariyama K, et al: Albumin-bilirubin (ALBI) grade as part of the evidence-based clinical practice guideline for HCC of the Japan Society of Hepatology: a comparison with the liver damage and Child-Pugh classifications. *Liver Cancer* 2017;6:204–215.

## Reply

# ALBI Score as a Novel Tool in Staging and Treatment Planning for Hepatocellular Carcinoma: Advantage of ALBI Grade for Universal Assessment of Hepatic Function

Atsushi Hiraoka<sup>a</sup> Kojiro Michitaka<sup>a</sup> Takashi Kumada<sup>b</sup> Masashi Kudo<sup>c</sup>

<sup>a</sup>Gastroenterology Center, Ehime Prefectural Central Hospital, Matsuyama, <sup>b</sup>Department of Gastroenterology, Ogaki Municipal Hospital, Ogaki, and <sup>c</sup>Department of Gastroenterology and Hepatology, Kindai University Faculty of Medicine, Osaka, Japan

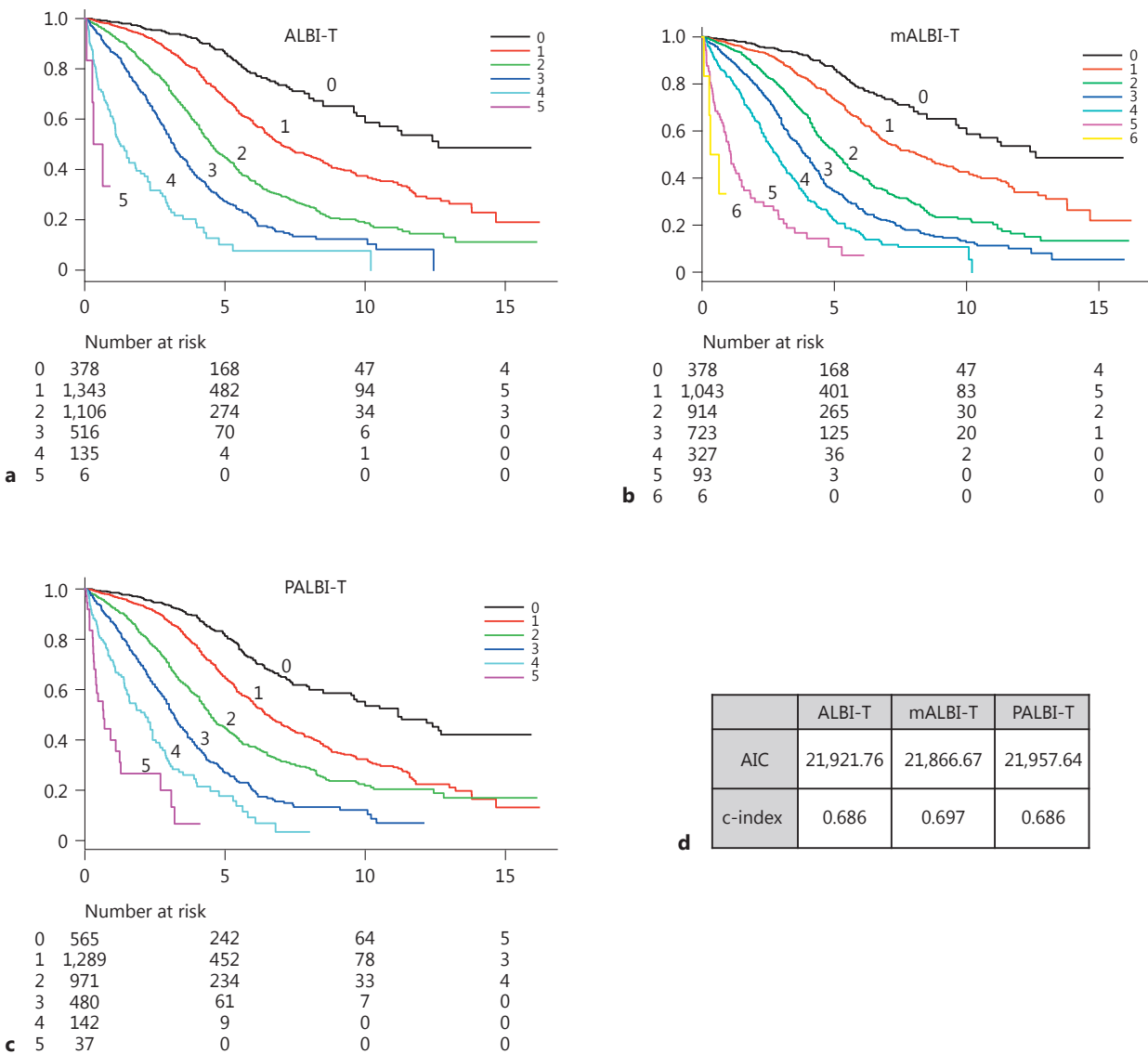
Thank you for your interest in our article titled “Albumin-bilirubin (ALBI) grade as part of the evidence-based clinical practice guideline for HCC of the Japan Society of Hepatology: a comparison with the liver damage and Child-Pugh classification” [1].

Huo et al. have sent an important message in their Letter to the Editor. Incorporation of models based on albumin-bilirubin (ALBI)/platelet-albumin-bilirubin (PALBI) grading, calculated using platelet count, serum albumin, and serum total bilirubin, into current HCC staging systems should be considered in order to refine their prognostic accuracy. There is no doubt that a new detailed assessment tool for hepatic function is needed in order to increase predictive accuracy for prognosis. We agree with their proposal.

Liu et al. [2] reported that the accuracy of PALBI grade was superior to that of ALBI. It is well known that the prognosis of a patient with HCC depends both on hepatic functional reserve and tumor factors. Thus, in order to address the issues raised by Huo et al., we used modified Japan integrated staging (JIS) scoring, which is calculated based on Child-Pugh classification and tumor node metastasis stage (TNM) of the Liver Cancer Study Group of Japan, 6th edition, as well as ALBI-TNM (ALBI-T) [3] and PALBI-TNM (PALBI-T) to validate the comparison with ALBI and PALBI, after excluding 1 patient whose platelet count was unknown ( $n = 3,494$ ). Kaplan-Meier curves for ALBI-T and PALBI-T are presented in Figure 1, and they show similar stratification abilities for prognosis. The c-index was the same value as shown in ALBI-T and PALBI-T scoring, while Akaike's information criterion (AIC) for ALBI-T was slightly better than that for PALBI-T (Table 1). When AIC and c-index were assessed for each etiology, PALBI-T was better in HCC patients with the hepatitis C virus (HCV), while ALBI-T was better in those with hepatitis B virus (HBV), as well as those both without HBV and HCV. Thus, the prognostic predictive values may vary slightly for each etiology. HCV and HBV was detected in 64.6 and 14.5%, respectively, of the patients in our cohort, whereas HBV was the most common etiology in the report by Liu et al. [2].

Of note, it cannot be denied that ALBI grade calculated with only 2 factors, albumin and bilirubin, was not inferior to PALBI and presents a simpler tool for assessment of hepatic function. In fact, a good correlation between ALBI and PALBI scores was observed ( $r = 0.820$ , 95% CI: 0.809–0.831,  $p < 0.0001$ ). Moreover, there

Atsushi Hiraoka, MD, PhD  
Gastroenterology Center  
Ehime Prefectural Central Hospital  
83 Kasuga-cho, Matsuyama, Ehime 790-0024 (Japan)  
E-Mail hirage@m.ehime-u.ac.jp



**Fig. 1.** Overall survival with each assessment tool in combination with tumor node metastasis classification (ALBI-T/mALBI-T/PALBI-T). Overall survival (OS) stratified by ALBI-T (**a**), mALBI-T (**b**), and PALBI-T (**c**) scores. With each, the stratification ability for prognosis was good. Akaike's information criterion (AIC) and c-index were better with mALBI-T compared to the others for assessment of prognosis of the entire patient cohort (**d**).

is an additional advantage with ALBI grade. A modified version has been proposed with 4 grades (1, 2a, 2b, and 3) (modified ALBI [mALBI] grade) for more detailed assessment based on the cut-off value (ALBI score =  $-2.270$ ) for ICG-R15 ( $<30\%$ ) [4]. In the results of additional analyses, AIC and c-index of mALBI/mALBI-T were better than the others (Fig. 1; Table 1).

To improve the accuracy of the prognostic predictive value of HCC staging systems, further validation studies and investigations with international collaboration as well as larger patient cohorts are required. As noted by Huo et al., we agree that incorporation of ALBI/mALBI/PALBI-based models into current HCC staging systems is recommended in order to refine the prognostic accuracy of each system.

**Table 1.** AIC and c-index with ALBI/mALBI/PALBI grades and ALBI-T/mALBI-T/PALBI-T scores

	ALBI	mALBI	PALBI
TNM stage I			
AIC	3,641.5	3,606.6	3,663.7
c-index	0.638	0.680	0.635
TNM stage II			
AIC	9,342.6	9,330.2	9,375.8
c-index	0.613	0.630	0.613
TNM stage III			
AIC	4,606.31	4,604.3	4,609.1
c-index	0.577	0.592	0.585
TNM stage IV			
AIC	774.9	772.2	775.8
c-index	0.597	0.633	0.621
Total			
AIC	22,222.2	22,176.0	22,240.6
c-index	0.609	0.630	0.619
	ALBI-T	mALBI-T	PALBI-T
HCV			
AIC	13,992.7	13,949.1	13,974.7
c-index	0.673	0.686	0.679
HBV			
AIC	1,886.4	1,883.8	1,917.4
c-index	0.750	0.758	0.726
NBNC			
AIC	3,341.4	3,334.6	3,359.5
c-index	0.682	0.689	0.679

AIC, Akaike's information criterion; ALBI, albumin-bilirubin; mALBI, modified ALBI; PALBI, platelet-albumin-bilirubin; TNM, tumor node metastasis classification of the Liver Cancer Study Group of Japan, 6th edition; ALBI-T, ALBI-TNM score; mALBI-T, mALBI-TNM score; PALBI-T, PALBI-TNM score; HCV, hepatitis C virus; HBV, hepatitis B virus; NBNC, negative for both HBV and HCV.

## Disclosure Statement

None of the authors has financial conflicts of interest to disclose concerning this study.

## References

- 1 Hiraoka A, Kumada T, Kudo M, et al: Albumin-bilirubin (ALBI) grade as part of the evidence-based clinical practice guideline for HCC of the Japan Society of Hepatology: a comparison with the liver damage and Child-Pugh classifications. *Liver Cancer* 2017;6:204–215.
- 2 Liu PH, Hsu CY, Hsia CY, et al: ALBI and PALBI grade predict survival for HCC across treatment modalities and BCLC stages in the MELD era. *J Gastroenterol Hepatol* 2017;32:879–886.
- 3 Hiraoka A, Kumada T, Michitaka K, et al: Usefulness of albumin-bilirubin grade for evaluation of prognosis of 2,584 Japanese patients with hepatocellular carcinoma. *J Gastroenterol Hepatol* 2016;31:1031–1036.
- 4 Hiraoka A, Michitaka K, Kumada T, et al: Validation and potential of albumin-bilirubin grade and prognostication in nationwide survey of 46,681 HCC patients in Japan – need for more detailed evaluation of hepatic function. *Liver Cancer* 2017;6:325–336.



# Gankyrin induces STAT3 activation in tumor microenvironment and sorafenib resistance in hepatocellular carcinoma

Toshiharu Sakurai  Norihisa Yada, Satoru Hagiwara, Tadaaki Arizumi, Kosuke Minaga, Ken Kamata, Mamoru Takenaka, Yasunori Minami, Tomohiro Watanabe, Naoshi Nishida and Masatoshi Kudo

Department of Gastroenterology and Hepatology, Faculty of Medicine, Kindai University, Osaka, Japan

## Key words

Bmi1, ERK, hepatocellular carcinoma, interleukin-6, vascular endothelial growth factor

## Correspondence

Toshiharu Sakurai. Department of Gastroenterology and Hepatology, Faculty of Medicine, Kindai University, 377-2 Ohno-Higashi, Osaka-Sayama, Osaka, Japan.  
Tel: +81-75-751-4302; Fax: +81-75-751-4303;  
E-mail: sakurai@med.kindai.ac.jp

## Funding Information

Japan Society for the Promotion of Science, (Grant/Award Number: '17K09396', '26460979').

Received March 22, 2017; Revised July 24, 2017; Accepted July 30, 2017

Cancer Sci 108 (2017) 1996–2003

doi: 10.1111/cas.13341

Most hepatocellular carcinomas (HCC) develop as a result of chronic liver inflammation. We have shown that the oncoprotein gankyrin is critical for inflammation-induced tumorigenesis in the colon. Although the *in vitro* function of gankyrin is well known, its role *in vivo* remains to be elucidated. We investigated the effect of gankyrin in the tumor microenvironment of mice with liver parenchymal cell-specific gankyrin ablation (*Alb-Cre;gankyrin<sup>fl/fl</sup>*) and gankyrin deletion both in liver parenchymal and non-parenchymal cells (*Mx1-Cre;gankyrin<sup>fl/fl</sup>*). Gankyrin upregulates vascular endothelial growth factor expression in tumor cells. Gankyrin binds to Src homology 2 domain-containing protein tyrosine phosphatase-1 (SHP-1), mainly expressed in liver non-parenchymal cells, resulting in phosphorylation and activation of signal transducer and activator of transcription 3 (STAT3). Gankyrin deficiency in non-parenchymal cells, but not in parenchymal cells, reduced STAT3 activity, interleukin (IL)-6 production, and cancer stem cell marker (Bmi1 and epithelial cell adhesion molecule [EpCAM]) expression, leading to attenuated tumorigenic potential. Chronic inflammation enhances gankyrin expression in the human liver. Gankyrin expression in the tumor microenvironment is negatively correlated with progression-free survival in patients undergoing sorafenib treatment for HCC. Thus, gankyrin appears to play a critical oncogenic function in tumor microenvironment and may be a potential target for developing therapeutic and preventive strategies against HCC.

Hepatocellular carcinoma (HCC), the most common form of liver cancer, is the third leading cause of cancer deaths worldwide and is usually associated with a very poor prognosis.<sup>(1)</sup> Given the increase in non-alcoholic steatohepatitis and imminent disappearance of chronic viral hepatitis, hepatosteatosis is a major risk factor for HCC.<sup>(2)</sup> Although a causal relationship between chronic damage, inflammation and carcinogenesis has been widely recognized, the exact molecular mechanism of hepatocarcinogenesis remains to be elucidated.

Hepatic progenitor cells are bipotential cells residing in normal liver and are thought to be implicated in hepatocarcinogenesis.<sup>(3)</sup> A stem cell marker Bmi1 is involved in the regulation of cell proliferation, stem cell maintenance, tumorigenesis and tumor progression.<sup>(4,5)</sup> Bmi1 is overexpressed and acts as an oncogene in several human malignancies, including HCC.<sup>(6,7)</sup> The expression of another “stemness”-related marker epithelial cell adhesion molecule (EpCAM) in HCC is associated with an aggressive biological behavior and poor clinical outcome.<sup>(8)</sup> In chronic inflammation, inflammatory signaling is important for the dedifferentiation and expansion of tumor-initiating cells.<sup>(9–14)</sup>

Gankyrin (also named p28<sup>GANK</sup> or PSMD10) is commonly overexpressed in human cancers.<sup>(15,16)</sup> In our previous study,

we used a conditional gankyrin “floxed” (*gankyrin<sup>fl/fl</sup>*) strain to generate *Villin-Cre;gankyrin<sup>fl/fl</sup>* and *Mx1-Cre;gankyrin<sup>fl/fl</sup>* mice lacking gankyrin in intestinal epithelial cells and inflammatory cells to assess the role of gankyrin in the development of colorectal cancer.<sup>(12)</sup> We found that gankyrin promoted the development of inflammation-induced colorectal cancer. We now describe that gankyrin enhances signal transducer and activator of transcription 3 (STAT3) activation, interleukin (IL)-6 production and subsequent hepatocarcinogenesis in mice exposed to the carcinogen diethylnitrosamine (DEN). Gankyrin upregulates the expression of stem cell markers in tumors. In addition, gankyrin expression in human non-parenchymal cells is inversely correlated with progression free survival (PFS) in HCC patients treated with sorafenib, suggesting that gankyrin expression may be considered as a new biomarker to predict the likelihood of response to sorafenib.

## Methods

**Animals, tumor induction and analysis.** *Gankyrin<sup>fl/fl</sup>* mice were crossed with *Alb-Cre* and *Mx1-Cre* mice (Jackson Laboratory, Bar Harbor, Maine, USA) to generate *Alb-Cre;gankyrin<sup>fl/fl</sup>* and *Mx1-Cre;gankyrin<sup>fl/fl</sup>* mice, respectively.<sup>(12)</sup> Induction of *Mx1-*

*Cre* was achieved with three intraperitoneal injections of 300 µg poly(I:C) (Sigma-Aldrich, St. Louis, MO, USA) every other day to 4–8-week-old mice. All mice were maintained in the C57BL/6 background in filter-topped cages at Kindai University. Male mice (2-week old) were injected intraperitoneally with 25 mg/kg DEN (Sigma). After 8 months on normal chow, mice were killed and analyzed for the presence of HCC. To examine the effect of gankyrin in non-parenchymal cells, we performed bone marrow transplantation (BMT) experiments. Because only 30% of Kupffer cells are reconstituted by donor-derived bone marrow cells 6 months after BMT,<sup>(17)</sup> we gave mice an intravenous injection of liposomal clodronate (200 µL intravenously) before irradiation to deplete Kupffer cells and accelerate macrophage turnover.<sup>(18)</sup> We then flushed the tibias and femurs of donor mice to obtain bone marrow. We injected  $1 \times 10^7$  bone marrow cells into the tail veins of lethally irradiated (11 Gy) recipient mice. Six weeks after BMT, mice were injected intraperitoneally with DEN (100 mg/kg). Four hours after DEN injection, mice were killed and their livers were removed.

All animal procedures were performed according to protocols approved by the Medical Ethics Committee of Kindai University Faculty of Medicine and Institutional Animal Care and in accordance with the recommendations for proper care and use of laboratory animals.

**Biochemical, immunochemical analyses and cell culture.** Real-time quantitative PCR (qPCR), immunoblotting and immunohistochemistry were performed as previously described.<sup>(12,19,20)</sup> The following antibodies were purchased: anti-actin and anti-PSMD10 (gankyrin) from Sigma (St. Louis, MO, USA); anti-Ki67, anti-STAT3, anti-phospho-STAT3, anti-extracellular signal-regulated kinases (ERK), anti-phospho-ERK, anti-p38 and anti-phospho-p38 from Cell Signaling (Danvers, MA, USA); and anti-Src homology 2 domain-containing protein tyrosine phosphatase-1 (SHP-1) from R&D Systems (Minneapolis, MN, USA). Anti-gankyrin antibody was described previously.<sup>(16)</sup> Immunohistochemistry was performed using ImmPRESS reagents (Vector Laboratory, Burlingame, CA, USA) according to the manufacturer's recommendations. Immunofluorescent TUNEL staining was performed to measure apoptosis in paraffin-embedded sections using the *In Situ* Apoptosis Detection Kit, as described by the manufacturer (Takara, Tokyo, Japan) and previous reports.<sup>(12,21)</sup> Nuclei were stained with 4',6-diamidino-2-phenylindole. Duolink fluorescence method was employed to study the interaction between gankyrin and SHP-1, as per the manufacturer's recommendations (Sigma Aldrich). The interaction of gankyrin with SHP-1 was assessed under a confocal laser microscope using antibodies against human gankyrin and SHP-1.

THP-1 cells and Mono Mac 6 cells, an immortalized line of human monocyte, were maintained in RPMI-1640 medium (Gibco, Carlsbad, CA, USA) supplemented with 10% FBS, containing penicillin (100 U/mL) and streptomycin (100 mg/mL) and transfection of gankyrin siRNA (Santa Cruz, Dallas, TX, USA) was carried out using X-treme GENE siRNA Transfection Reagent (Roche, Basel, Switzerland).

**Immunohistochemical analyses of gankyrin expression.** To evaluate gankyrin expression in the tumor microenvironment, we assessed the expression in tumor-infiltrating cells and non-tumor cells at the invasive front of the HCC samples by immunohistochemistry. The evaluation of gankyrin was performed at high magnification ( $\times 100$ ) on the tumor material obtained before receiving sorafenib treatment. The staining status was obtained by calculating the intensity  $\times$  extensity score

(gankyrin expression score) as described previously.<sup>(22)</sup> Intensity of the staining was scored as 0 (negative), 1 (weak) or 2 (strong). Extensity of the staining was scored as 0 (1%–5% of non-tumor cells), 1 (6%–30%), 2 (3%–70%) or 3 (71%–100%). To calculate the intensity  $\times$  extensity score (gankyrin expression score) of non-tumor cells of the HCC samples, five fields were selected at the invasive front as well as within tumors and the average of five fields (magnification  $100 \times$ ) was used to determine the score. Scoring was performed in a blinded fashion by two investigators (T. S. and N. Y.). Samples were considered high expression for gankyrin if the intensity  $\times$  extensity score (gankyrin expression score) was more than a median value. The gankyrin expression score was evaluated in tumor cells as well.

**Patients and specimens.** From May 2009 to June 2010, 38 patients with refractory HCC uncontrolled with standard therapeutic modalities received sorafenib (Nexavar; Bayer HealthCare Pharmaceuticals-Onyx Pharmaceuticals, Leverkusen, Germany) at Kindai University. All pathological specimens of HCC were collected using needle biopsy before sorafenib treatment. Demographic profiles of patients were previously described.<sup>(21)</sup> In addition, liver specimens were collected with needle biopsy in 13 patients who were clinically suspected of non-alcoholic steatohepatitis. The study protocol conformed to the ethical guidelines of the 1975 Declaration of Helsinki and was approved by the institutional review boards. Written informed consent was obtained from all patients for subsequent use of their resected tissues.

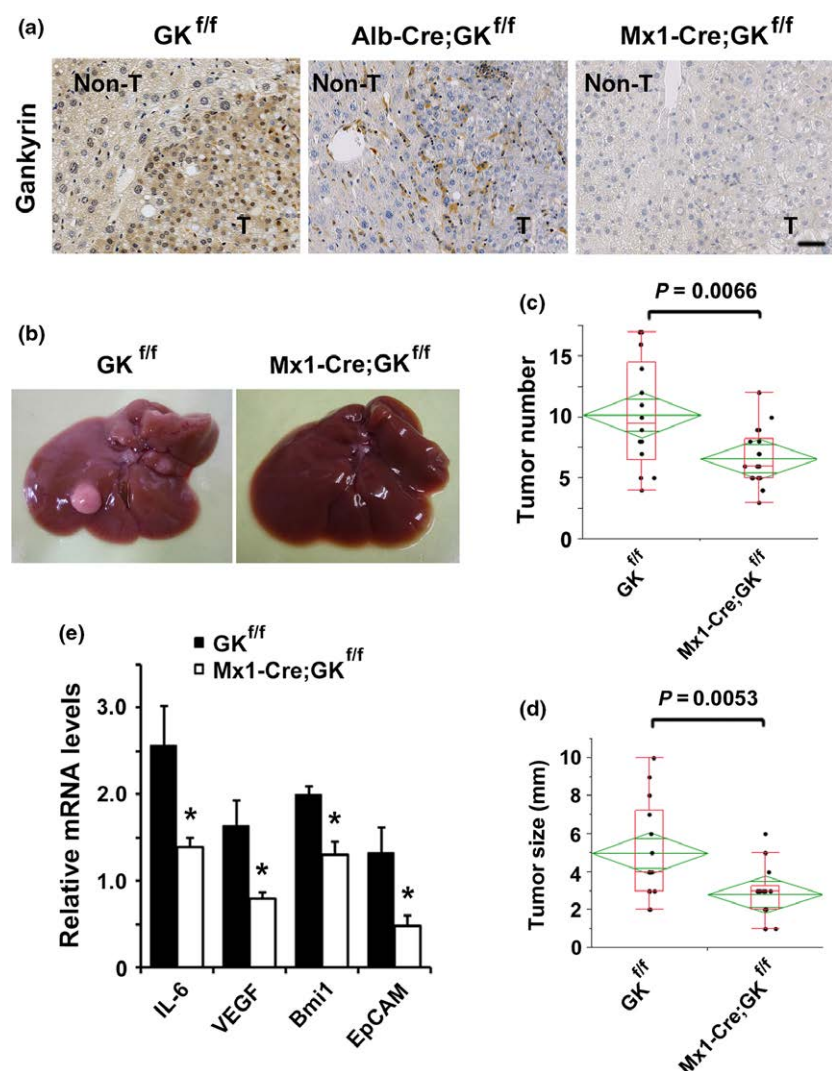
The eligibility criteria for sorafenib therapy were previously described.<sup>(16)</sup> Sorafenib was administered orally at a daily dose of 800 mg divided into two equal doses. Treatment interruptions and up to two dose reductions (first to 400 mg once daily, followed by 400 mg every 2 days) were permitted for drug-related adverse effects (National Cancer Institute-Common Terminology Criteria [NCI-CTC, version 3]). Treatment was continued until the occurrence of radiologic progression, as defined by the Response Evaluation Criteria in Solid Tumors (RECIST, Version 1.1).

**Statistical analysis.** Data are presented as means  $\pm$  SEM. Statistical differences between groups were analyzed using the Fisher's exact test or Student's *t*-test. A value of  $P < 0.05$  was considered statistically significant.

## Results

**Gankyrin deficiency attenuated hepatocarcinogenesis.** We previously generated *Mx1-Cre;gankyrin<sup>fl/fl</sup>* mice by crossing *gankyrin<sup>fl/fl</sup>* mice with *Mx1-Cre* mice. *Mx1-Cre;gankyrin<sup>fl/fl</sup>* mice exhibited gankyrin deletion both in parenchymal cells and non-parenchymal cells of the liver (Fig. 1a and Fig. S1).<sup>(12)</sup> Histomorphology and serum levels of ALT revealed no apparent liver dysfunction in *Mx1-Cre;gankyrin<sup>fl/fl</sup>* mice. The strain failed to exhibit spontaneous liver tumors up to 1 year of age. However, DEN injection on postnatal day 14<sup>(23)</sup> induced well-differentiated HCC in all *gankyrin<sup>fl/fl</sup>* and *Mx1-Cre;gankyrin<sup>fl/fl</sup>* mice (Fig. S2a). *Mx1-Cre;gankyrin<sup>fl/fl</sup>* mice showed gankyrin deletion both in tumor cells and non-parenchymal cells (Fig. 1a). In comparison to *gankyrin<sup>fl/fl</sup>* controls, *Mx1-Cre;gankyrin<sup>fl/fl</sup>* mice exhibited reduced HCC multiplicity and size (Fig. 1b–d). HCC isolated from *Mx1-Cre;gankyrin<sup>fl/fl</sup>* mice exhibited reduced expression of IL-6 and vascular endothelial growth factor (VEGF) (Fig. 1e).

Kupffer cell is a major source of IL-6 production in the liver.<sup>(24)</sup> Therefore, we purified Kupffer cells from *Mx1-Cre;*



**Fig. 1.** Attenuated hepatocarcinogenesis in *Mx1-Cre;gankyrin<sup>f/f</sup>* mice. (a) Control (*GK<sup>f/f</sup>*), *Alb-Cre;gankyrin<sup>f/f</sup>* (*Alb-Cre;GK<sup>f/f</sup>*) and *Mx1-Cre;gankyrin<sup>f/f</sup>* (*Mx1-Cre;GK<sup>f/f</sup>*) mice were challenged with diethylnitrosamine (DEN) and killed after 8 months. Liver sections were examined with immunohistochemistry using gankyrin-specific antibody. Distinction between tumor and non-tumorous liver tissue was made by H&E staining. Non-T, non-tumorous liver tissues; T, tumors. Scale bar, 50  $\mu$ m. (b) Typical examples of macroscopic tumorigenesis in the hepatocellular carcinomas (HCC) model. Livers of control (*GK<sup>f/f</sup>*) and *Mx1-Cre;gankyrin<sup>f/f</sup>* (*Mx1-Cre;GK<sup>f/f</sup>*) mice 8 months after DEN injection are shown. (c) Tumor number and (d) maximal tumor sizes (diameters) in control (*GK<sup>f/f</sup>*, *n* = 14) and *Mx1-Cre;gankyrin<sup>f/f</sup>* (*Mx1-Cre;GK<sup>f/f</sup>*, *n* = 18) mice. (e) RNA was extracted from tumors of *Mx1-Cre;gankyrin<sup>f/f</sup>* (*Mx1-Cre;GK<sup>f/f</sup>*) and *gankyrin<sup>f/f</sup>* (*GK<sup>f/f</sup>*) mice. Relative amounts of mRNA were determined by real-time quantitative PCR (qPCR) and normalized to the amount of actin mRNA. The amount of each mRNA in the untreated liver was given an arbitrary value of 1.0. Data are means  $\pm$  SEM (*n* = 5).

*GK<sup>f/f</sup>* mice and examined whether gankyrin in Kupffer cells affect IL-6 production. We found that gankyrin deletion reduced IL-6 expression in Kupffer cells (Fig. S2b). Immunohistochemistry showed that expression of VEGF was reduced in tumor cells of *Mx1-Cre;GK<sup>f/f</sup>* mice compared with control mice (Fig. S2c). Gankyrin deficiency would downregulate the expression of IL-6 in Kupffer cells and that of VEGF in tumor cells. Thus, the deletion of gankyrin both in parenchymal and non-parenchymal cells inhibited hepatocarcinogenesis.

We evaluated the role of gankyrin in HCC development in the liver parenchymal cells. *Alb-Cre;gankyrin<sup>f/f</sup>* mice were generated by crossing *gankyrin<sup>f/f</sup>* mice with *Alb-Cre* mice. *Alb-Cre;gankyrin<sup>f/f</sup>* mice were negative for gankyrin only in liver parenchymal cells (Fig. 1a and Fig. S1b).<sup>(12)</sup> *Alb-Cre;gankyrin<sup>f/f</sup>* progeny obtained in the expected Mendelian ratio was healthy and failed to show any apparent liver dysfunction. The strain showed no spontaneous liver tumors up to 1 year of age. All *gankyrin<sup>f/f</sup>* and *Alb-Cre;gankyrin<sup>f/f</sup>* mice challenged with DEN developed well-differentiated HCC (Fig. S2a). Gankyrin deficiency in liver parenchymal cells reduced HCC size but not HCC number (Fig. 2a–c). Furthermore, the deletion of gankyrin in tumor cells reduced the expression of VEGF but not IL-6 (Fig. 2d).

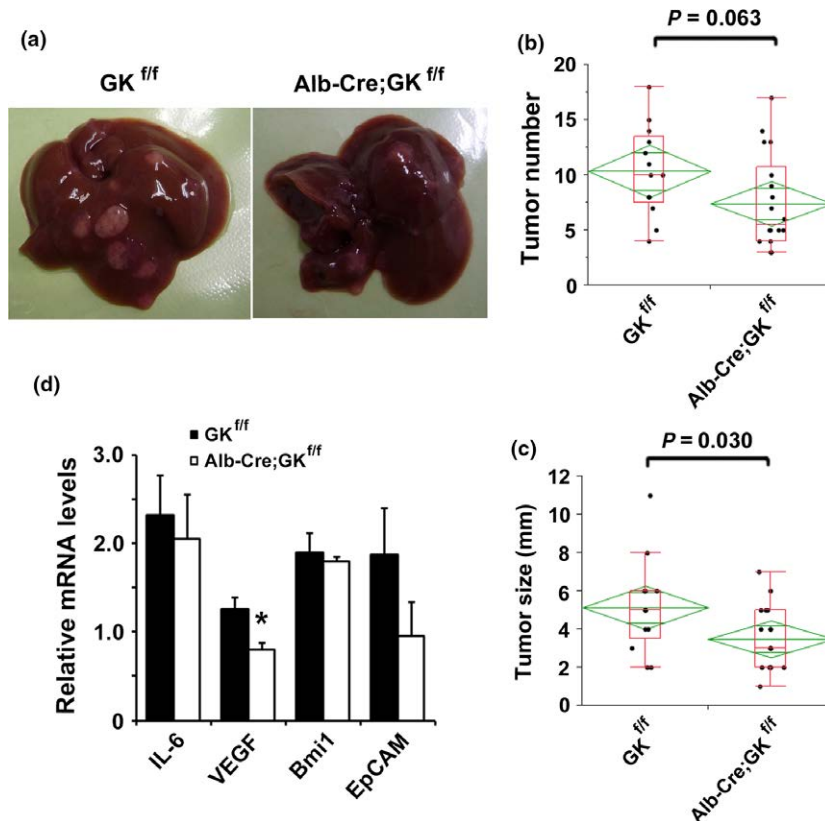
Several studies report that gankyrin promotes proliferation of cancer cells through the inhibition of apoptosis and cell

cycle progression *in vitro*.<sup>(15,25,26)</sup> We assessed the effect of gankyrin on cell death and proliferation *in vivo*. Gankyrin deletion exhibited no significant reduction in apoptosis and proliferation of tumors, as assessed by TUNEL assay and immunohistochemistry using anti-Ki67 antibody, respectively (Fig. S3a,b). Gankyrin deletion affected neither the protein levels of p53 and RB1 nor the mRNA levels of their target genes (Fig. 3a and Fig. S3c).

Next, we examined the differentiation status of HCC obtained from *gankyrin<sup>f/f</sup>*, *Mx1-Cre;gankyrin<sup>f/f</sup>* and *Alb-Cre;gankyrin<sup>f/f</sup>* mice. Analysis of H&E-stained HCC sections did not show any difference in the differentiation status among these strains (Fig. S2a). Epithelial to mesenchymal transition (EMT) is a multistep biological process whereby epithelial cells change in plasticity by transient de-differentiation into a mesenchymal phenotype. Gankyrin overexpression was reported to exhibit EMT phenotype, including loss of the epithelial marker E-cadherin and gain of the mesenchymal marker vimentin in cell lines.<sup>(27)</sup> However, gankyrin deficiency did not show significant difference in expression of EMT-related genes (Fig. S4a,b).

**Gankyrin deficiency inactivated signal transducer and activator of transcription 3/interleukin-6 signaling pathway in the cancer microenvironment.** Studies have shown that STAT3 plays a critical role in HCC development.<sup>(24,28)</sup> We examined the





**Fig. 2.** Attenuated hepatocarcinogenesis in *Alb-Cre;gankyrin<sup>fl/fl</sup>* mice. (a) Typical examples of macroscopic tumorigenesis in the hepatocellular carcinomas (HCC) model. Livers of control (*GK<sup>fl/fl</sup>*) and *Alb-Cre;gankyrin<sup>fl/fl</sup>* (*Alb-Cre;GK<sup>fl/fl</sup>*) mice 8 months after diethylnitrosamine (DEN) injection are shown. (b) Tumor number and (c) maximal tumor sizes (diameters) in control (*GK<sup>fl/fl</sup>*, *n* = 13) and *Alb-Cre;gankyrin<sup>fl/fl</sup>* (*Alb-Cre;GK<sup>fl/fl</sup>*, *n* = 18) mice. (d) RNA was extracted from tumors of *Alb-Cre;gankyrin<sup>fl/fl</sup>* (*Alb-Cre;GK<sup>fl/fl</sup>*) and *gankyrin<sup>fl/fl</sup>* (*GK<sup>fl/fl</sup>*) mice. Relative amounts of mRNA were determined by real-time quantitative PCR (qPCR) and normalized to the amount of actin mRNA. The amount of each mRNA in the untreated liver was given an arbitrary value of 1.0. Data are means ± SEM (*n* = 5).

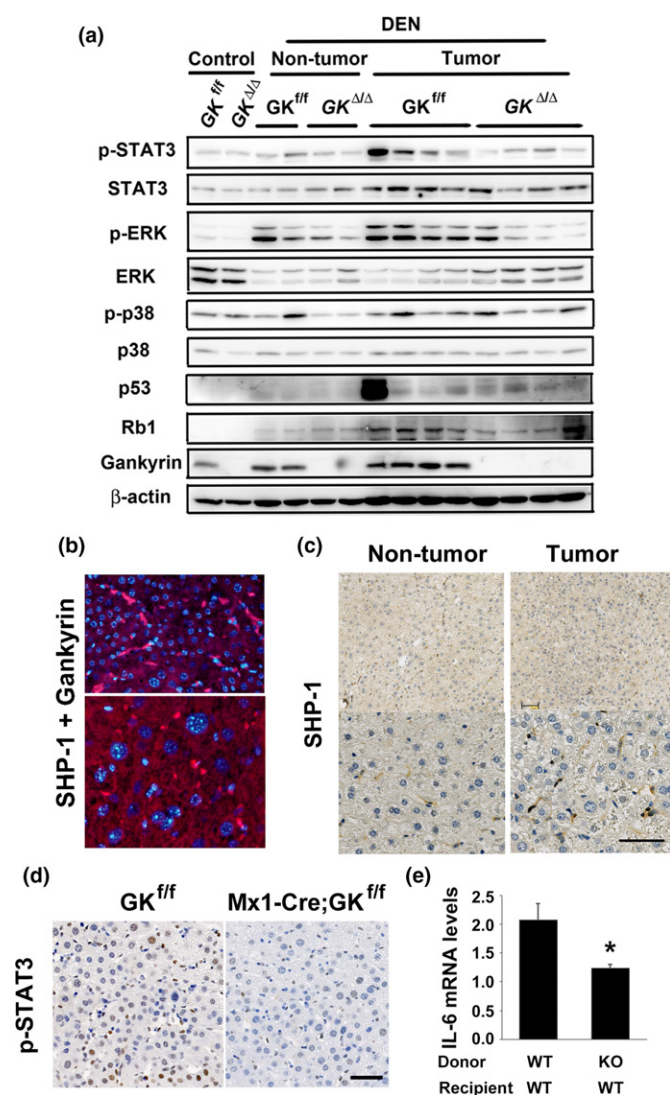
consequences of gankyrin deletion on several signaling pathways in liver parenchymal and non-parenchymal cells. Gankyrin deletion significantly reduced the expression of phosphorylated STAT3 in tumors, and slightly reduced the expression in non-tumor liver tissues (Fig. 3a). Gankyrin-induced pro-inflammatory response enhances the activation of ERK in colorectal tumors.<sup>(12)</sup> This is in line with our result, wherein gankyrin deletion in non-parenchymal cells reduced ERK activity in HCC (Fig. 3a). Previous studies have described a critical role of c-Jun and c-Jun N-terminal kinases (JNK) in the development of HCC.<sup>(20,21,29)</sup> We observed no effect of gankyrin deficiency on JNK activity (Fig. S5a).

SHP-1, a well-known inhibitor of activation-promoting signaling cascades, negatively regulates signaling by STAT3 dephosphorylation.<sup>(12,30)</sup> The Duolink Assay showed the interaction between gankyrin and SHP-1 as red punctate dots in liver tumors (Fig. 3b and Fig. S6), suggestive of STAT3 activation following gankyrin/SHP-1 interaction in non-parenchymal cells where SHP-1 was predominantly expressed (Fig. 3c). HCC isolated from *Mxl-Cre;gankyrin<sup>fl/fl</sup>* mice exhibited reduced expression of IL-6, a downstream molecule of STAT3. To confirm the effect of gankyrin in non-parenchymal cells, we performed bone marrow transplantation (BMT) experiments. Six weeks after BMT, mice were injected intraperitoneally with DEN (100 mg/kg). Four hours after DEN injection, mice were killed and their livers were removed. *GK<sup>fl/fl</sup>* mice rescued with gankyrin-deficient bone marrow exhibited a reduced expression of phosphorylated STAT3 and IL-6 compared with those rescued with wild-type bone marrow (Fig. 3e and Fig. S7). In addition, no difference in IL-6 expression and STAT3 activity was found between *Alb-Cre;gankyrin<sup>fl/fl</sup>* mice and *gankyrin<sup>fl/fl</sup>* controls (Fig. 2d and Fig. S5b). Given that IL-6 produced by non-parenchymal cells activates the transcription factor STAT3

in the liver,<sup>(24)</sup> the decrease in IL-6 production in gankyrin-deficient inflammatory cells may lead to reduced STAT3 activity in tumor cells through a paracrine mechanism. Indeed, immunohistochemistry results showed that the STAT3 activity in tumor cells as well as non-parenchymal cells of *Mxl-Cre;gankyrin<sup>fl/fl</sup>* mice was reduced as compared to that in *gankyrin<sup>fl/fl</sup>* controls (Fig. 3d). These data indicate that gankyrin in non-parenchymal cells plays a crucial role in the regulation of STAT3/IL-6 signaling, which is critical for DEN-induced hepatocarcinogenesis.<sup>(24)</sup>

*Signal transducer and activator of transcription 3* is essential for the expansion of liver cancer stem cell.<sup>(11,12,28)</sup> Inflammatory cytokines such as IL-6 are important for the dedifferentiation and generation of tumor-initiating cells.<sup>(9–14)</sup> HCC isolated from *Mxl-Cre;gankyrin<sup>fl/fl</sup>* mice, but not *Alb-Cre;gankyrin<sup>fl/fl</sup>* mice, exhibited decrease in the expression of stem cell markers Bmi1 and EpCAM as compared to those from controls (Fig. 1e and 2d). Immunohistochemistry showed that expression of Bmi1 was reduced in tumor cells of *Mxl-Cre;GK<sup>fl/fl</sup>* mice compared with control mice (Fig. S8). Taken together, gankyrin in non-parenchymal cells may control STAT3 signaling and stem cell expansion within the tumor microenvironment.

Gankyrin accelerates proteasomal degradation of RB.<sup>(15)</sup> Recently, we reported that gankyrin knockdown reduced STAT3 activities in a myeloid cell line.<sup>(15)</sup> To investigate whether the gankyrin-mediated STAT3 activation depends on degradation of SHP-1 protein, we examined the protein expression level of SHP-1 in the myeloid cell line. Gankyrin knockdown did not affect the protein level of SHP-1 (Fig. S9a), suggesting that gankyrin activates STAT3 by inhibiting the phosphatase activity of SHP-1, but not by accelerating the degradation of SHP-1. Gankyrin knockdown decreased the



**Fig. 3.** Gankyrin deficiency inactivated STAT3/IL-6 signaling pathway in the cancer microenvironment. Control (GK<sup>fl/fl</sup>) and *Mx1-Cre;gankyrin*<sup>fl/fl</sup> (GK<sup>Δ/Δ</sup>) mice were challenged with diethylnitrosamine (DEN) and killed after 8 months. (a) Homogenates of non-treated livers (control), non-tumor colon tissues (non-tumor) and tumors (tumor) were gel-separated and immunoblotted with the indicated antibodies. (b) The interaction of gankyrin with SHP-1 was assessed by Duolink Assay in DEN-treated *gankyrin*<sup>fl/fl</sup> liver. Non-tumor and tumor liver tissues are shown in the upper and lower panels, respectively. (c) Representative images of immunohistochemical detection of SHP-1 in livers (non-tumor) and tumors (tumor) of *gankyrin*<sup>fl/fl</sup> mice challenged with DEN. Scale bar, 50 μm. (d) Representative images of immunohistochemical detection of phosphorylated STAT3 in tumors. Scale bar, 50 μm. (e) Six weeks after BMT, mice were injected intraperitoneally with DEN (100 mg/kg). Four hours after DEN injection, mice were killed and their livers were removed. Relative amounts of IL-6 mRNA were determined by real-time quantitative PCR (qPCR) and normalized to the amount of actin mRNA. The amount of each mRNA in the untreated liver was given an arbitrary value of 1.0. Data are means ± SEM (*n* = 3).

mRNA level of SHP-1 in THP-1 cells (Fig. S9b). Given that gankyrin knockdown did not affect the protein level of SHP-1, gankyrin might be involved in degradation of SHP-1, but it is not the mechanism by which gankyrin activates STAT3. In myeloid cell lines, Mono Mac 6 cells and THP-1 cells, gankyrin knockdown decreased the phosphorylation of STAT3

and the expression of downstream target genes Pim1 and Mcl-1 (Fig. S9b,c).<sup>(12)</sup>

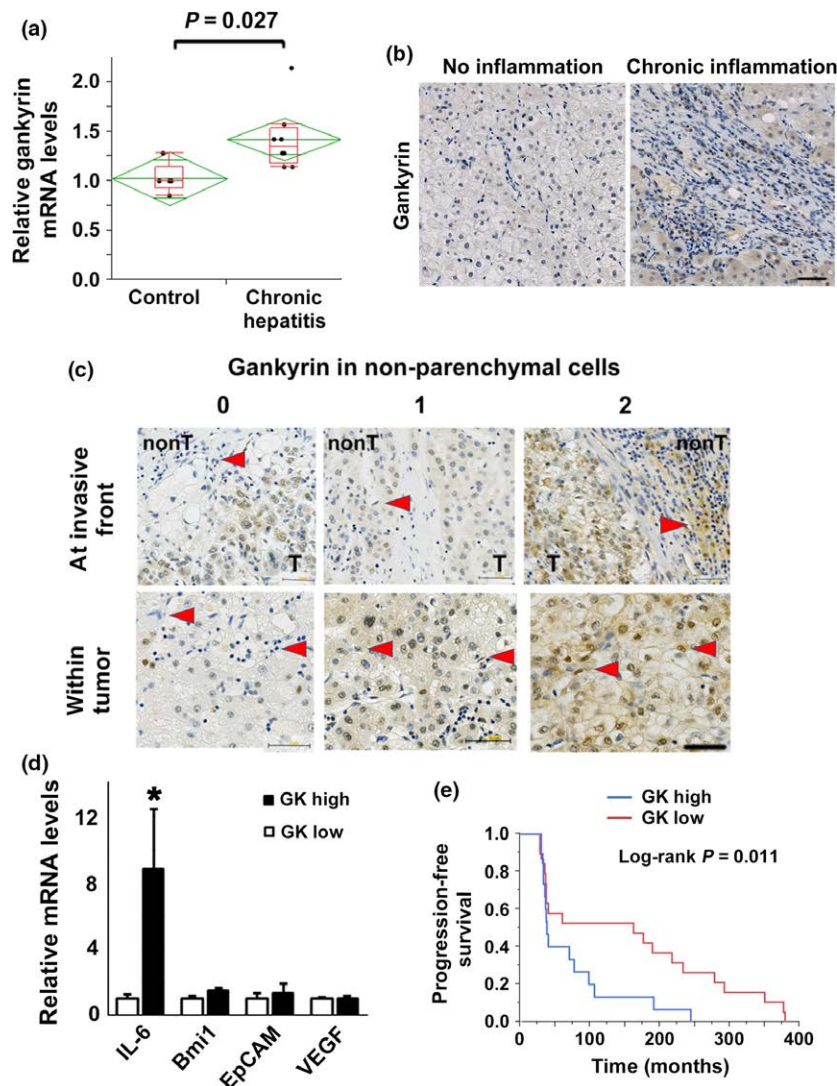
**Gankyrin expression was upregulated in chronic hepatitis.** In our previous study, we showed that longstanding intestinal inflammation increases the expression of gankyrin in the colonic mucosa of patients with inflammatory bowel disease.<sup>(12)</sup> We assessed the association between gankyrin and chronic hepatitis by collecting liver biopsy specimens from patients clinically suspected to have non-alcoholic steatohepatitis. Patient characteristics are shown in Table S1. Patients with chronic hepatitis exhibited an increase in the expression of gankyrin as compared with those without inflammation (Fig. 4a). Thus, gankyrin expression was associated with the disease activity of chronic hepatitis. Immunohistochemical studies has shown that gankyrin expression was enhanced in inflammatory cells as well as hepatocytes (Fig. 4b), indicative of the increased gankyrin expression in non-parenchymal cells and hepatocytes during chronic inflammation.

**Association between gankyrin expression and progression-free survival in patients treated with sorafenib.** Sorafenib is the only anticancer drug with proven prognostic efficacy in HCC. Identification of surrogate biomarkers that predict the biological and clinical efficacy may help us predict the therapeutic response of patients.<sup>(31)</sup> Cancer stem cells have been reported to play a pivotal role in drug resistance of various cancer types. Given the critical role of gankyrin in the regulation of STAT3 signaling and stem cell marker expression, we investigated the association between the therapeutic response to sorafenib and gankyrin expression using human HCC specimens collected prior to treatment. HCC specimens collected before sorafenib treatment were stained with anti-gankyrin antibody (Fig. 4c). Based on immunohistochemistry, patients were divided into high-gankyrin expression and low-gankyrin expression groups. In line with the data in DEN-induced hepatocarcinogenesis model, increased gankyrin expression in non-parenchymal cells, but not in parenchymal cells, is significantly associated with enhanced IL-6 expression (Fig. 4d and Fig. S10a). As regards VEGF, we previously reported that gankyrin expression is significantly associated with VEGF expression in human HCC.<sup>(32)</sup> Our data using *Alb-Cre;gankyrin*<sup>fl/fl</sup> mice indicates a significant relationship between gankyrin and VEGF in tumor cells (Fig. 5). We examined the impact of gankyrin expression in non-parenchymal cells on the therapeutic response of patients treated with sorafenib. A log-rank test using the Kaplan–Meier method showed that the low-gankyrin expression group exhibited significant prolongation of PFS (*P* = 0.011, Fig. 4e), but not overall survival (OS; Fig. S11), as compared to the high-expression group. By contrast, gankyrin expression in tumor cells affected neither PFS nor OS in patients treated with sorafenib (Fig. S10b,c). We have assessed the relationship between gankyrin expression in non-parenchymal cells or parenchymal cells and several clinical parameters, including differentiation and stage of HCC (Table S2 and S3). No significant difference was observed in any parameters other than PFS between gankyrin low and high expression groups.

## Discussion

Studies have shown that gankyrin is upregulated in many HCC cell lines, wherein it promoted the proliferation of cancer cells through the inhibition of apoptosis and cell cycle progression.<sup>(15,25,26)</sup> However, the role of gankyrin in the development of HCC *in vivo* was unclear. Here, we investigated the role of gankyrin in controlling the tumor microenvironment. In our



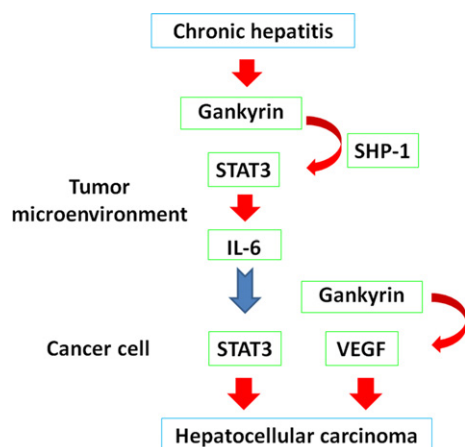


**Fig. 4.** Association between gankyrin expression and poor prognosis in patients treated with sorafenib. (a) Liver specimens were collected using needle biopsy in 13 patients clinically suspected of non-alcoholic steatohepatitis. The expression of gankyrin mRNA in livers without inflammation or fibrosis (control,  $n = 5$ ) and those with inflammation and fibrosis (chronic hepatitis,  $n = 8$ ) was determined by real-time quantitative PCR (qPCR). (b) Representative images of immunohistochemical detection of gankyrin in livers of patients with and without chronic inflammation. Scale bar, 50  $\mu\text{m}$ . (c) Liver specimens of hepatocellular carcinomas (HCC) were taken before sorafenib treatment. Representative images of HCC with intensity of the staining scored as 0 (negative), 1 (weak) or 2 (strong) are shown. Five fields were selected at the invasive front and within tumors. Immunohistochemical detection of gankyrin in non-parenchymal cells of HCC (arrows) are shown. Scale bar, 50  $\mu\text{m}$ . (d) Liver specimens were collected using needle biopsy before sorafenib treatment. The mRNA expression levels of indicated genes in HCC was determined by quantitative real-time qPCR and compared between patients grouped according to the level of gankyrin expression in hepatic non-parenchymal cells as assessed by immunohistochemistry. (e) Association between gankyrin expression and progression-free survival (PFS) in patients with HCC. The Kaplan–Meier method was used to determine the PFS and log-rank test was used to compare PFS between patients grouped according to the level of gankyrin expression in hepatic non-parenchymal cells.

recent study, we revealed that gankyrin upregulates IL-17 and TNF- $\alpha$  expression in lamina propria cells of the colon and accelerates the development of colitis-associated cancer.<sup>(12)</sup> In the present study, we found that gankyrin activates STAT3 through SHP-1 inhibition and IL-6 upregulation in the tumor microenvironment, leading to enhanced hepatocarcinogenesis. Thus, STAT3/IL-6 signaling may mediate the gankyrin-induced cross-talk between tumor cells and non-parenchymal cells.

Gankyrin has been suggested as a regulator for liver tumor-initiating cells.<sup>(12,16,33)</sup> STAT3 activation in inflammatory cells regulates the expansion of cancer stem cells through augmented inflammatory response in the liver.<sup>(11,28)</sup> Thus, it is

generally accepted that cytokine-mediated inflammatory signaling pathways are important for dedifferentiation and generation of tumor-initiating cells.<sup>(9–14)</sup> However, the precise mechanism involved in the activation of cancer-initiating cells in response to pro-inflammatory cytokines has been poorly understood. In this study, we provide the evidence that gankyrin expression in non-parenchymal cells increases levels of cancer stem cell markers (Bmi1 and EpCAM), thereby promoting the expansion of cancer-initiating cells in tumor microenvironment. We show that the molecular interaction between gankyrin and SHP-1 leads to the activation of STAT3 and secretion of pro-inflammatory cytokine IL-6, which may explain the mechanism of gankyrin-induced inflammatory responses by non-parenchymal



**Fig. 5.** The role of gankyrin in the tumor microenvironment and hepatocarcinogenesis. Chronic inflammation enhances gankyrin expression in the human liver. Gankyrin binding to SHP-1 leads to enhanced IL-6 production in the tumor microenvironment. The augmented inflammatory response will activate STAT3, and gankyrin upregulates the expression of vascular endothelial growth factor (VEGF) in tumor cells, which eventually promote the development of hepatocellular carcinoma.

cells. Thus, understanding of the function of gankyrin in non-parenchymal cells has elucidated a part of the molecular mechanism involved in HCC development.

In this study, we used two types of conditional gankyrin-deficient mice: *Alb-Cre;gankyrin<sup>ff</sup>* and *Mx1-Cre;gankyrin<sup>ff</sup>* mice. Gankyrin deletion was confirmed in cancer cells in *Alb-Cre;gankyrin<sup>ff</sup>* mice and non-parenchymal as well as cancer cells in *Mx1-Cre;gankyrin<sup>ff</sup>* mice. DEN-induced HCC development was attenuated in *Alb-Cre;gankyrin<sup>ff</sup>* mice and to a greater extent in *Mx1-Cre;gankyrin<sup>ff</sup>* mice as compared with that in control *gankyrin<sup>ff</sup>* mice. These studies with two types of conditional gankyrin-deficient mice strongly suggest the important role played by gankyrin-expressing non-parenchymal and cancer cells in HCC development. This was supported by our observation that gankyrin expression was enhanced both in non-parenchymal cells and hepatocytes of the liver tissue from patients with chronic hepatitis. In addition, DEN treatment significantly reduced the expression of the proangiogenic factor VEGF in HCC tissues of both *Alb-Cre;gankyrin<sup>ff</sup>* and *Mx1-Cre;gankyrin<sup>ff</sup>* mice. Thus, gankyrin may enhance tumor development through its effect in the tumor cell as well as the tumor microenvironment.

The therapeutic options for advanced-stage HCC are limited, as HCC displays a poor response to systemic treatments such as conventional chemotherapy and radiotherapy. So far,

sorafenib is the only anticancer drug with proven prognostic efficacy in HCC. Identification of surrogate biomarkers that predict the biological and clinical efficacy may help to tailor treatment to every individual patient.<sup>(31)</sup> Sorafenib targets the abnormal activation of ERK often observed in human HCC.<sup>(34)</sup> However, the predictive value of ERK signaling, including VEGF, for the efficacy of sorafenib in HCC remains uncertain.<sup>(35,36)</sup> The activation of other signaling pathways such as JNK and STAT3 may bypass the sorafenib-induced blockade of ERK signaling, resulting in sorafenib resistance.<sup>(21,37)</sup> Thus, JNK and STAT3 signaling pathways are potential predictive biomarkers. To date, no robust predictive biomarker has been developed. In this study, we found a strong correlation between elevated gankyrin expression in the tumor microenvironment and unfavorable PFS in patients treated with sorafenib. Evaluation of gankyrin expression in HCC may be useful to differentiate between responders and non-responders before starting sorafenib treatment and may help to select patients who are likely to benefit from the treatment. STAT3 modulation by gankyrin will contribute to sorafenib resistance, and gankyrin may represent a candidate biomarker to predict the likelihood of response to sorafenib in future HCC patients.

Targeting gankyrin might be a promising strategy for cancer prevention and treatment. Small molecular drugs that inhibit gankyrin have gained increasing interest as therapeutics for liver cancer.<sup>(38)</sup> Given that gankyrin deletion has no effect on liver injury in several hepatitis models (data not shown), gankyrin inhibitors may work without severe adverse side effects. Further work should be performed to obtain more information about the clinical implication of gankyrin and for the development of new therapeutic strategies.

Taken together, gankyrin, upregulated in chronic inflammation, induces STAT3 activation and IL-6 production by binding to SHP-1 in non-parenchymal cells. Such pro-inflammatory cytokine responses may upregulate the expression of stem cell markers in the tumor microenvironment and eventually promote the development of HCC (Fig. 5). Thus, suppression and measurement of gankyrin expression is a promising approach for advanced treatment and personalized management of HCC patients.

## Acknowledgments

This study was supported by JSPS KAKENHI (26460979 and 17K09396) and a Health Labour Sciences Research Grant.

## Disclosure Statement

The authors have no conflict of interest to declare.

## References

- 1 Thorgeirsson SS, Grisham JW. Molecular pathogenesis of human hepatocellular carcinoma. *Nat Genet* 2002; **31**: 339–46.
- 2 Bellentani S. The epidemiology of non-alcoholic fatty liver disease. *Liver Int* 2017; **37**(Suppl 1): 81–4.
- 3 Lo RC, Ng IO. Hepatic progenitor cells: their role and functional significance in the new classification of primary liver cancers. *Liver Cancer* 2013; **2**: 84–92.
- 4 Gargiulo G, Cesaroni M, Serresi M *et al*. In vivo RNAi screen for BMI1 targets identifies TGF-beta/BMP-ER stress pathways as key regulators of neural- and malignant glioma-stem cell homeostasis. *Cancer Cell* 2013; **23**: 660–76.

- 5 Wang MC, Jiao M, Wu T *et al*. Polycomb complex protein BMI-1 promotes invasion and metastasis of pancreatic cancer stem cells by activating PI3K/AKT signaling, an ex vivo, in vitro, and in vivo study. *Oncotarget* 2016; **7**: 9586–99.
- 6 Effendi K, Mori T, Komuta M *et al*. Bmi-1 gene is upregulated in early-stage hepatocellular carcinoma and correlates with ATP-binding cassette transporter B1 expression. *Cancer Sci* 2010; **101**: 666–72.
- 7 Yanai H, Atsumi N, Tanaka T *et al*. Intestinal cancer stem cells marked by Bmi1 or Lgr5 expression contribute to tumor propagation via clonal expansion. *Sci Rep* 2017; **7**: 41838.
- 8 Kim H, Park YN. Hepatocellular carcinomas expressing 'stemness'-related markers: clinicopathological characteristics. *Dig Dis* 2014; **32**: 778–85.

- 9 Adachi T, Sakurai T, Kashida H *et al.* Involvement of heat shock protein  $\alpha$ 4/apg-2 in refractory inflammatory bowel disease. *Inflamm Bowel Dis* 2015; **21**: 31–9.
- 10 Sakurai T, Kashida H, Watanabe T *et al.* Stress response protein cirp links inflammation and tumorigenesis in colitis-associated cancer. *Cancer Res* 2014; **74**: 6119–28.
- 11 Sakurai T, Yada N, Watanabe T *et al.* Cold-inducible RNA-binding protein promotes the development of liver cancer. *Cancer Sci* 2015; **106**: 352–8.
- 12 Sakurai T, Higashitsuji H, Kashida H *et al.* The oncoprotein gankyrin promotes the development of colitis-associated cancer through activation of STAT3. *Oncotarget* 2017; **8**: 24762–76.
- 13 Sakurai T, Kashida H, Komeda Y *et al.* Stress response protein RBM3 promotes the development of colitis-associated cancer. *Inflamm Bowel Dis* 2017; **23**: 66–74.
- 14 Schwitalla S, Fingerle AA, Cammareri P *et al.* Intestinal tumorigenesis initiated by dedifferentiation and acquisition of stem-cell-like properties. *Cell* 2013; **152**: 25–38.
- 15 Higashitsuji H, Itoh K, Nagao T *et al.* Reduced stability of retinoblastoma protein by gankyrin, an oncogenic ankyrin-repeat protein overexpressed in hepatomas. *Nat Med* 2000; **6**: 96–9.
- 16 Mine H, Sakurai T, Kashida H *et al.* Association of gankyrin and stemness factor expression in human colorectal cancer. *Dig Dis Sci* 2013; **58**: 2337–44.
- 17 Kennedy DW, Abkowitz JL. Kinetics of central nervous system microglial and macrophage engraftment: analysis using a transgenic bone marrow transplantation model. *Blood* 1997; **90**: 986–93.
- 18 Van Rooijen N, Sanders A. Liposome mediated depletion of macrophages: mechanism of action, preparation of liposomes and applications. *J Immunol Methods* 1994; **174**: 83–93.
- 19 Sakurai T, Kashida H, Hagiwara S *et al.* Heat shock protein A4 controls cell migration and gastric ulcer healing. *Dig Dis Sci* 2015; **60**: 850–7.
- 20 Sakurai T, Maeda S, Chang L, Karin M. Loss of hepatic NF-kappa B activity enhances chemical hepatocarcinogenesis through sustained c-Jun N-terminal kinase 1 activation. *Proc Natl Acad Sci USA* 2006; **103**: 10544–51.
- 21 Hagiwara S, Kudo M, Nagai T *et al.* Activation of JNK and high expression level of CD133 predict a poor response to sorafenib in hepatocellular carcinoma. *Br J Cancer* 2012; **106**: 1997–2003.
- 22 Remmele W, Stegner HE. Recommendation for uniform definition of an immunoreactive score (IRS) for immunohistochemical estrogen receptor detection (ER-ICA) in breast cancer tissue. *Pathologie* 1987; **8**: 138–40.
- 23 Sakurai T, He G, Matsuzawa A *et al.* Hepatocyte necrosis induced by oxidative stress and IL-1 alpha release mediate carcinogen-induced compensatory proliferation and liver tumorigenesis. *Cancer Cell* 2008; **14**: 156–65.
- 24 Naugler WE, Sakurai T, Kim S *et al.* Gender disparity in liver cancer due to sex differences in MyD88-dependent IL-6 production. *Science* 2007; **317**: 121–4.
- 25 Dawson S, Apcher S, Mee M *et al.* Gankyrin is an ankyrin-repeat oncoprotein that interacts with CDK4 kinase and the S6 ATPase of the 26 S proteasome. *J Biol Chem* 2002; **277**: 10893–902.
- 26 Higashitsuji H, Higashitsuji H, Itoh K *et al.* The oncoprotein gankyrin binds to MDM2/HDM2, enhancing ubiquitylation and degradation of p53. *Cancer Cell* 2005; **8**: 75–87.
- 27 Fu J, Chen Y, Cao J *et al.* p28GANK overexpression accelerates hepatocellular carcinoma invasiveness and metastasis via phosphoinositide 3-kinase/AKT/hypoxia-inducible factor-1alpha pathways. *Hepatology* 2011; **53**: 181–92.
- 28 He G, Yu GY, Temkin V *et al.* Hepatocyte IKKbeta/NF-kappaB inhibits tumor promotion and progression by preventing oxidative stress-driven STAT3 activation. *Cancer Cell* 2010; **17**: 286–97.
- 29 Hagiwara S, Kudo M, Chung H *et al.* Activation of c-Jun N-terminal kinase in non-cancerous liver tissue predicts a high risk of recurrence after hepatic resection for hepatocellular carcinoma. *Hepatol Res* 2012; **42**: 394–400.
- 30 Inoue T, Suzuki Y, Mizuno K, Nakata K, Yoshimaru T, Ra C. SHP-1 exhibits a pro-apoptotic function in antigen-stimulated mast cells: positive regulation of mitochondrial death pathways and negative regulation of survival signaling pathways. *Mol Immunol* 2009; **47**: 222–32.
- 31 Kudo M. Biomarkers and personalized sorafenib therapy. *Liver Cancer* 2014; **3**: 399–404.
- 32 Liu Y, Higashitsuji H, Higashitsuji H *et al.* Overexpression of gankyrin in mouse hepatocytes induces hemangioma by suppressing factor inhibiting hypoxia-inducible factor-1 (FIH-1) and activating hypoxia-inducible factor-1. *Biochem Biophys Res Commun* 2013; **432**: 22–7.
- 33 Qian YW, Chen Y, Yang W *et al.* p28(GANK) prevents degradation of Oct4 and promotes expansion of tumor-initiating cells in hepatocarcinogenesis. *Gastroenterology* 2012; **142**: 1547–58. e14.
- 34 Llovet JM, Ricci S, Mazzaferro V *et al.* Sorafenib in advanced hepatocellular carcinoma. *N Engl J Med* 2008; **359**: 378–90.
- 35 Newell P, Toffanin S, Villanueva A *et al.* Ras pathway activation in hepatocellular carcinoma and anti-tumoral effect of combined sorafenib and rapamycin in vivo. *J Hepatol* 2009; **51**: 725–33.
- 36 Abou-Alfa GK, Schwartz L, Ricci S *et al.* Phase II study of sorafenib in patients with advanced hepatocellular carcinoma. *J Clin Oncol* 2006; **24**: 4293–300.
- 37 Su JC, Tseng PH, Wu SH *et al.* SC-2001 overcomes STAT3-mediated sorafenib resistance through RFX-1/SHP-1 activation in hepatocellular carcinoma. *Neoplasia* 2014; **16**: 595–605.
- 38 Song X, Wang J, Zheng T *et al.* LBH589 Inhibits proliferation and metastasis of hepatocellular carcinoma via inhibition of gankyrin/STAT3/Akt pathway. *Mol Cancer* 2013; **12**: 114.

## Supporting Information

Additional Supporting Information may be found online in the supporting information tab for this article:

- Fig. S1.** Gankyrin expression in the liver.
- Fig. S2.** Diethylnitrosamine (DEN)-induced hepatocellular carcinomas (HCC).
- Fig. S3.** Apoptosis and cell proliferation.
- Fig. S4.** Epithelial to mesenchymal transition (EMT) and gankyrin.
- Fig. S5.** Effects of gankyrin on signaling pathways.
- Fig. S6.** Duolink assay in *Mx1-Cre;GK* mice.
- Fig. S7.** Bone marrow transplantation.
- Fig. S8.** Bmi1 expression in gankyrin-deficient mice.
- Fig. S9.** Effects of gankyrin on SHP-1.
- Fig. S10.** Effects of gankyrin expression in tumor cells.
- Fig. S11.** Effects of gankyrin expression in non-parenchymal cells.
- Table S1.** Characteristics of controls and patients with chronic hepatitis.
- Table S2.** Patient characteristics and gankyrin expression in non-parenchymal cells.
- Table S3.** Patient characteristics and gankyrin expression in tumor cells.

## DISCLOSURE

*All authors disclosed no financial relationships relevant to this publication.*

**Iyad Khamaysi, MD**, Invasive Endoscopy Unit, **Alain Suissa, MD**, Department of Gastroenterology and hepatology, Rambam Health Care Campus, Rappaport Faculty of Medicine, Technion-Israel Institute of Technology, Haifa, Israel

<http://dx.doi.org/10.1016/j.gie.2017.05.047>

## Commentary

Hemobilia, defined as the passage of blood through the biliary tree, can have several causes, including surgical injury to the ducts or adjacent vessels, liver biopsy, bleeding from tumors in the biliary tree, or, as in this case, apparent arteriovenous malformations (AVMs)/telangiectasias in the biliary tree. This patient had Osler-Weber-Rendu syndrome and was at high risk for multiple bleeding events. Interestingly, the bleeding in this case stopped spontaneously, and no therapy was required. Hepatic AVMs were noted, but it is possible that there could have been intraductal AVMs as well. It would have been interesting if the authors had also performed cholangioscopy to look for a target lesion that could have potentially been ablated by argon plasma coagulation or radiofrequency ablation or other methods in an attempt to reduce the risk of a future similar episode.

**Douglas G. Adler, MD, FASGE**  
GIE Associate Editor  
University of Utah School of Medicine  
Salt Lake City, Utah

**Massimo Raimondo, MD**  
Associate Editor for Focal Points

## Utility of contrast-enhanced harmonic EUS for evaluating the effects of steroid therapy in a case of immunoglobulin G4-negative focal autoimmune pancreatitis



A 75-year-old woman was asymptomatic, but contrast-enhanced abdominal CT for hyperamylasemia (1302 U/L) revealed a hypovascular lesion in the pancreatic body and a slightly dilated pancreatic duct on the tail side of the lesion. Her serum immunoglobulin G4 level was 62.9 mg/dL. On positron emission tomography (PET)-CT, the maximum standardized uptake value at the mass lesion was 3.22. Conventional EUS revealed a 25-mm hypoechoic lesion in the pancreatic body. Contrast-enhanced harmonic EUS was then performed with contrast agent (0.015 mL/kg; Sonazoid; Daiichi-Sankyo, Tokyo, Japan). The tumor appeared as an iso-enhancement and homogeneous enhancement with an avascular area. Pathologic findings obtained by EUS-guided FNA with a 22-gauge needle showed prominent infiltration by lymphocytes and plasmacytes, along with fibrosis and storiform fibrosis. We performed minipulse methylprednisolone therapy (2 courses of 500 mg/day, each lasting 3 days/week) to enable a therapeutic

diagnosis. Abdominal CT and PET-CT performed 1 week after treatment showed that both the mass lesion in the pancreatic body and the hot uptake area had disappeared (**A, B**). Conventional EUS showed that the pancreatic mass was reduced in size after treatment. On contrast harmonic EUS, the avascular area disappeared (**C-F, arrowheads**).

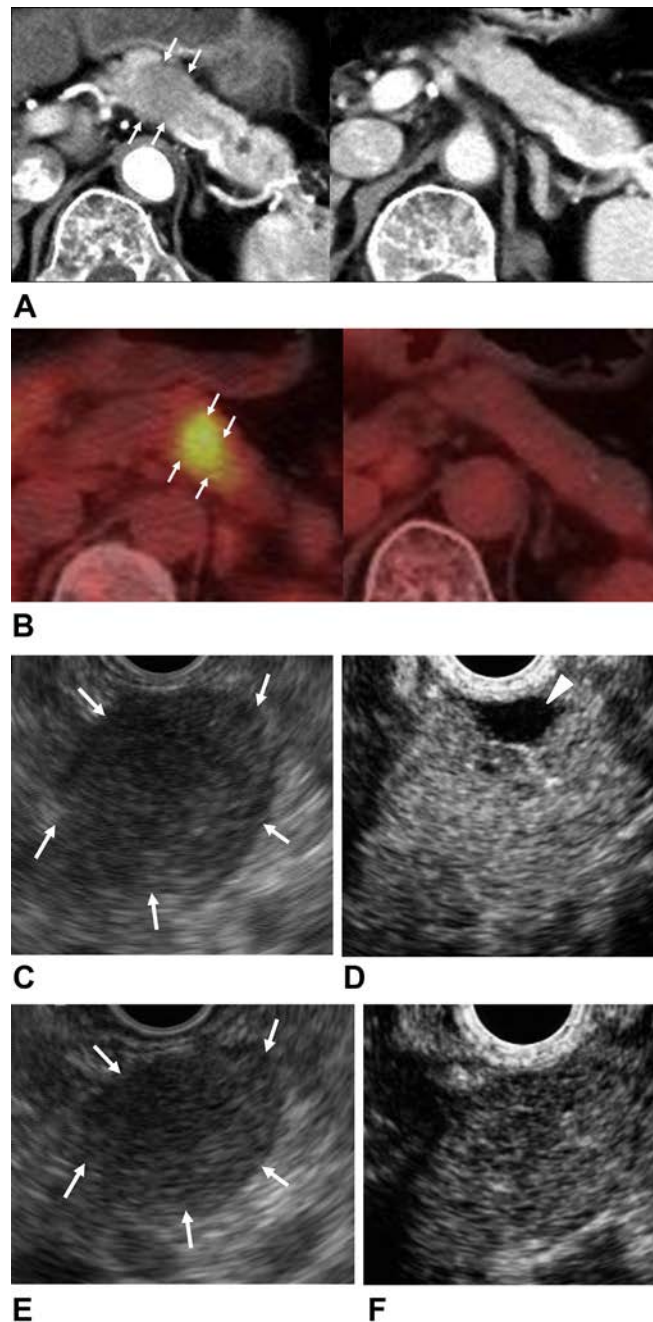
## DISCLOSURE

*All authors disclosed no financial relationships relevant to this publication.*

**Ken Kamata, MD, PhD, Mamoru Takenaka, MD, PhD, Kosuke Minaga, MD, Masatoshi Kudo, MD, PhD**, Department of Gastroenterology and Hepatology, Kindai University School of Medicine, Osaka-Sayama, Japan

<http://dx.doi.org/10.1016/j.gie.2017.06.017>





### Commentary

Autoimmune pancreatitis is a highly heterogeneous disease, developing in young and old patients with highly varied presentations, from diffuse edema of the pancreas to pseudotumors and biliary obstruction. Further muddying the waters, some variants of autoimmune pancreatitis are negative for serum immunoglobulin G subclass 4, making diagnosis more difficult. This patient presented with a pseudotumor caused by autoimmune pancreatitis and had a good response to steroid therapy (the most common first-line agent). This case also illustrates the value of contrast-enhanced EUS. Contrast agents of this kind are very rarely used in the United States because they are not approved by the U.S. Food and Drug Administration, but they are commonly used in Europe and Asia. Contrast agents in EUS can help evaluate solid and cystic tumors, pancreatitis and pancreatic necrosis, and vascular involvement of

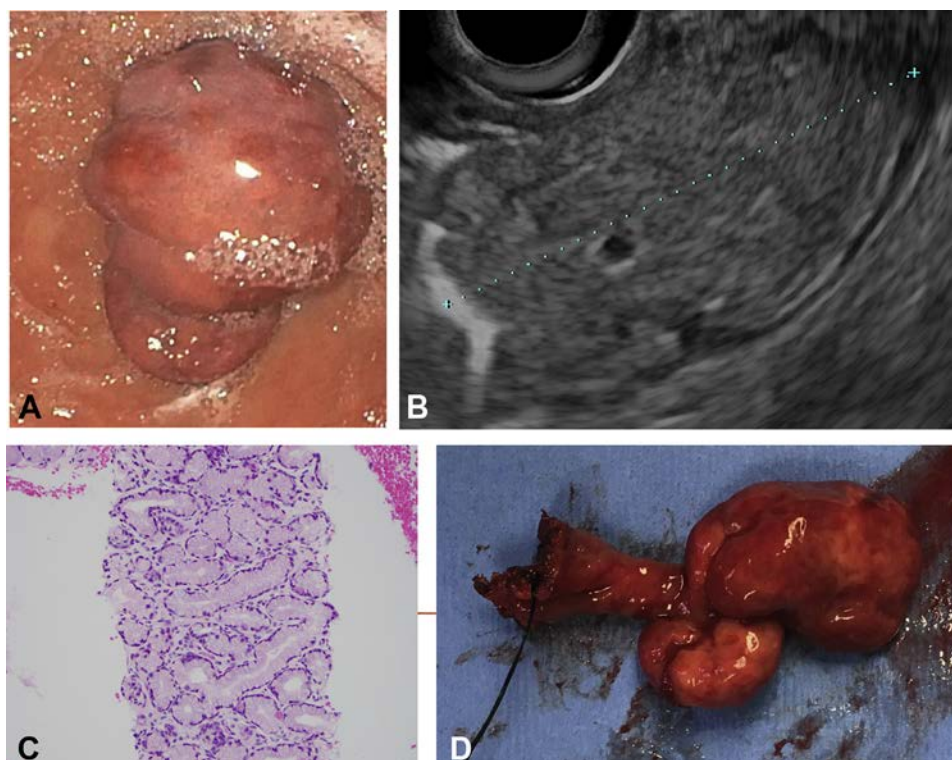


tumors. In this case, contrast-enhanced EUS revealed different findings before and after steroid treatment for this patient, showing how much this technique can allow endosonographers to see beyond what is visible with conventional EUS.

**Douglas G. Adler, MD FASGE**  
**GIE Associate Editor**  
**University of Utah School of Medicine**  
**Salt Lake City, Utah**

**Massimo Raimondo, MD**  
**Associate Editor for Focal Points**

## EUS core biopsy leading to duodenal brunneroma diagnosis



A 56-year-old man presented with vague symptoms of fullness and early satiety. Ultimately, upper endoscopy revealed a large duodenal polyp at least 4 cm long with occasional retrograde protrusion through the pylorus into the stomach (**A**). Biopsy specimens from upper endoscopy demonstrated duodenal mucosa with gastric foveolar metaplasia. The patient underwent EUS to better characterize the lesion, which confirmed a 3.9-cm lesion that appeared to originate from within the deep mucosa, with no involvement of the muscularis propria (**B**). FNA

was nondiagnostic. Fine-needle core biopsy with a fork-tipped needle revealed fragments of benign Brunner glands (**C**). Given the patient's symptoms and the size of the lesion, the patient was referred for surgical resection. In the operating room, gastroenterologists performed upper endoscopy to snare the polyp and tent the lesion for localization. Surgeons were then able to mark the base of the lesion with suture and perform a limited duodenal resection (**D**). Final pathologic examination confirmed a Brunner's gland hamartoma, or brunneroma.

## Validation of serological models for staging and prognostication of HCC in patients from a Japanese nationwide survey

Hienori Toyoda<sup>1</sup> · Toshifumi Tada<sup>1</sup> · Philip J. Johnson<sup>2</sup> · Namiki Izumi<sup>3</sup> ·  
Masumi Kadoya<sup>4</sup> · Shuichi Kaneko<sup>5</sup> · Norihiro Kokudo<sup>6</sup> · Yonson Ku<sup>7</sup> ·  
Shoji Kubo<sup>8</sup> · Takashi Kumada<sup>1</sup> · Yutaka Matsuyama<sup>9</sup> · Osamu Nakashima<sup>10</sup> ·  
Michiie Sakamoto<sup>11</sup> · Tadatoshiki Takayama<sup>12</sup> · Masatoshi Kudo<sup>13</sup> · The Liver Cancer  
Study Group of Japan

Received: 4 January 2017 / Accepted: 7 February 2017 / Published online: 21 February 2017  
© Japanese Society of Gastroenterology 2017

### Abstract

**Background** Two serology-based scoring models for prognostication of patients with hepatocellular carcinoma (HCC), the BALAD and BALAD-2 models, were applied to a Japanese cohort of a nationwide follow-up survey of HCC. The ability of these models to predict the progression of HCC and the deterioration of liver function and to assess prognosis was evaluated.

**Methods** BALAD and BALAD-2 scores were calculated in 24,029 patients from a cohort of Japanese nationwide survey based on the serum levels of five markers (bilirubin, albumin, *lens culinaris* agglutinin-reactive alpha-fetoprotein, alpha-fetoprotein, and des-gamma-carboxy prothrombin) measured at the time of HCC diagnosis. The

associations of these scores with the progression of HCC and liver function and with survival rates were analyzed.

**Results** There were good correlations between BALAD and BALAD-2 scores and the progression of HCC and Child–Pugh class. Both scores accurately categorized patients into risk groups with different survival rates. BALAD-2 showed superior discrimination of patient survival compared with the original BALAD.

**Conclusions** Serology-based scoring models for prognostication, especially the BALAD-2 model, were useful for staging and prognostication of survival in a cohort of Japanese patients with HCC from a nationwide survey.

**Keywords** Hepatocellular carcinoma · Staging · Serological markers · Tumor progression · Liver function · Prognosis

**Electronic supplementary material** The online version of this article (doi:10.1007/s00535-017-1321-6) contains supplementary material, which is available to authorized users.

✉ Hienori Toyoda  
hmtoyoda@spice.ocn.ne.jp

<sup>1</sup> Department of Gastroenterology, Ogaki Municipal Hospital, 4-86 Minaminokawa, Ogaki, Gifu 503-8502, Japan

<sup>2</sup> Institute of Translational Medicine, University of Liverpool, Liverpool, UK

<sup>3</sup> Department of Gastroenterology, Musashino Red Cross Hospital, Tokyo, Japan

<sup>4</sup> Department of Radiology, Shinshu University School of Medicine, Matsumoto, Japan

<sup>5</sup> Department of Gastroenterology, Kanazawa University Hospital, Kanazawa, Japan

<sup>6</sup> Hepato-Biliary-Pancreatic Surgery Division, Artificial Organ and Transplantation Division, Department of Surgery, Graduate School of Medicine, University of Tokyo, Tokyo, Japan

<sup>7</sup> Division of Hepato-Biliary-Pancreatic Surgery, Department of Surgery, Kobe University Graduate School of Medicine, Kobe, Japan

<sup>8</sup> Department of Hepato-Biliary-Pancreatic Surgery, Osaka City University Graduate School of Medicine, Osaka, Japan

<sup>9</sup> Department of Biostatistics, School of Public Health, University of Tokyo, Tokyo, Japan

<sup>10</sup> Department of Clinical Laboratory Medicine, Kurume University Hospital, Kurume, Japan

<sup>11</sup> Department of Pathology, Keio University School of Medicine, Tokyo, Japan

<sup>12</sup> Department of Digestive Surgery, Nihon University School of Medicine, Tokyo, Japan

<sup>13</sup> Department of Gastroenterology and Hepatology, Kinki University School of Medicine, Osaka, Japan

## Introduction

The staging systems of hepatocellular carcinoma (HCC) for assessment of patient outcomes are based on features that influence prognosis, which are broadly classified into two categories, namely, progression of tumors and severity of underlying liver dysfunction. Several staging systems/prognostic scores that combine these factors have been developed [1–6]. The progression of tumors and underlying liver function are usually evaluated by morphology and clinical symptoms in part, which is not objective and can be influenced by methods for evaluations. A recently proposed serology-based staging system for HCC, the BALAD scoring model, for assessing the prognosis of patients with HCC [7], is based solely on the serum levels of five parameters, namely, total bilirubin (T-Bil), albumin (ALB), *lens culinaris* agglutinin A-reactive fraction of alpha-fetoprotein (AFP-L3), alpha-fetoprotein (AFP), and des-gamma-carboxy prothrombin (DCP). The model predicted the outcome of patients with HCC with high discrimination [7]. Recently, an improved serologic staging model, BALAD-2, was developed using a more sophisticated statistical method that treated variables in a continuous manner [8]. Both BALAD and BALAD-2 were reported to have excellent prognostic discrimination in international settings [8, 9], despite large differences across regions in both HCC progression and survival after diagnosis.

In the present study, we applied these two serologic models to 24,029 patients with HCC in Japan, where surveillance of HCC is established and patients are diagnosed with HCC earlier and have longer survival than in Western and other Asian countries. Since 1965, the Liver Cancer Study Group of Japan (LCSGJ) has been conducting biannual nationwide follow-up surveys and prospectively collecting data on patients with HCC in Japan. We conducted this retrospective study based on these prospectively collected data which included variables for BALAD and BALAD-2 scores.

## Patients and methods

### Patients and treatments

A total of 66,554 patients with primary liver cancer were prospectively registered biannually by LCSGJ from more than 750 participating institutions from January 2000 to December 2007 using a registration/questionnaire sheet with more than 180 questions. Data regarding three tumor markers for HCC, specifically AFP, AFP-L3, and DCP, were beginning with the 16th survey. Therefore, the current study used the data from 2000 (16th survey) to 2007 (18th

survey, the latest). The data from 24,029 patients contained all the laboratory variables necessary for calculating the BALAD and BALAD-2 scores, i.e., serum ALB, T-Bil, AFP, AFP-L3, and DCP at diagnosis of HCC, as well as the final prognosis (Supplementary figure S1). HCC was diagnosed on the basis of imaging studies, clinical data, or histopathologic studies at each institution. Treatment types were determined by the treatment algorithm for HCC proposed by Japanese guidelines [10]. The patients were prospectively followed up at each institution. Most patients underwent ultrasonography and measurements of tumor markers every 3 or 4 months, and enhanced computed tomography (CT) or magnetic resonance imaging (MRI) every 6 or 12 months, according to the protocol of the Japanese guidelines [10]. The prognosis of these registered patients was followed until confirmation of death in every survey. Although this study protocol was not submitted to the institutional review board of each institution that participated in the nationwide survey, the data collection and registration of patients with HCC were conducted with the approval of each institution.

BALAD and BALAD-2 scores were assessed in terms of their association with liver dysfunction, based on Child–Pugh class, and the progression of HCC on imaging examinations; progression was assessed based on tumor size, tumor multiplicity, portal vein invasion, and tumor stage. In addition, we used univariate and multivariate analyses to investigate whether BALAD and BALAD-2 scores discriminated the patient survival. Tumor staging was according to TNM criteria of LCSGJ (Supplementary table S1) [11].

### Calculating BALAD and BALAD-2 Scores

BALAD and BALAD-2 scores were calculated based on AFP, AFP-L3, DCP, ALB, and T-Bil levels measured in the serum sample obtained from each patient at the time of HCC diagnosis. The original BALAD score was calculated by simply summing the serum levels of factors indicating both tumor progression (AFP, AFP-L3, and DCP) and liver function (ALB and T-Bil) [7]. The cut-offs for the elevations of AFP, AFP-L3, and DCP were 400 ng/dL, 15%, and 100 mAU/mL, respectively [7]. Liver function was categorized based on serum ALB and T-Bil levels according to the method of Tateishi et al. [12]. ALB level was categorized as above 3.5, 2.8–3.5 g/dL, or below 2.8 g/dL, and scored as 0, 1, or 2, respectively. T-Bil level was categorized as below 1.0, 1.0–2.0 mg/dL, or above 2.0 mg/dL, and scored as 0, 1, or 2, respectively. Liver function was then categorized based on the sum of these 2 scores as A (0 or 1), B (2 or 3), or C (4). The BALAD score is based on the total number of elevated tumor markers and liver function scores.

The BALAD-2 score is calculated using the equation:

$$\begin{aligned} \text{Linear predictor (xb)} = & 0.02 \times (\text{AFP}-2.57) \\ & + 0.012 \times (\text{AFP-L3}-14.19) \\ & + 0.19 \times (\ln(\text{DCP}) - 1.93) \\ & + 0.17 \times ((\text{T-Bil } [\mu\text{mol/L}]^{1/2}) \\ & - 4.50) - 0.09 \times (\text{ALB}[\text{g/L}] \\ & - 35.11), \end{aligned}$$

where T-Bil 1 mg/dL = 17.1  $\mu\text{mol/L}$ , and AFP was capped at 50000 units. Both AFP and DCP are modeled as per 1000 units. Patients are stratified into four prognostic groups according to previously described cut-offs, resulting in four grades: score 1 (low risk,  $\leq -1.74$ ), score 2 ( $-0.91$  to  $> -1.74$ ), score 3 ( $0.24$  to  $> -0.91$ ), and score 4 (high risk,  $> 0.24$ ) [8].

Because the actual values of AFP less than 15 ng/dL and DCP less than 40 mAU/mL were not documented, but described simple as “normal” in the data of nationwide follow-up surveys by LCSGJ, we randomly assigned the number 1–14 ng/dL for AFP and 1–39 mAU/mL for DCP in cases with normal levels of these markers. We assigned 0% for AFP-L3 in cases with undetectable AFP-L3.

### Statistical analyses

Differences in percentages between groups were analyzed using the Chi square test. Differences in means of quantitative values were analyzed using the Mann–Whitney *U* test. Changes in percentages and quantitative values of increases in BALAD and BALAD-2 scores were analyzed with the Cochran–Armitage test and Jonckheere–Terpstra test, respectively. The date of HCC diagnosis was defined as time zero for calculations of survival rates. Survival was defined as the time from diagnosis to death, or last follow-up if death had not occurred. Patients who died were not censored, while surviving patients were censored. The Kaplan–Meier method was used to calculate survival rates, and the log-rank test was used to analyze differences in survival.

The Cox proportional hazard regression model with backward elimination method was used for multivariate analysis. The factors analyzed were age, sex, Child–Pugh class, tumor size, tumor number, portal vein invasion, tumor stage, treatment, and BALAD and BALAD-2 scores. The discriminatory abilities of scoring models were assessed using Akaike Information Criteria (AIC) [13] and Harrell’s *C* statistic [14]. Statistical analysis was performed using JMP statistical software, version 11.0.0 (Macintosh version; SAS Institute, Cary, NC, USA). All *P* values were derived from two-tailed tests, with *P* < 0.05 accepted as statistically significant.

## Results

### Baseline patient characteristics

The median follow-up period after diagnosis was 19.2 months, and the 25th and 75th percentiles were 8.4 and 39.6 months, respectively. Table 1 shows the characteristics of study patients. Males comprised 70.1% of patients, and the mean age was 66.9 years. In the majority of patients, hepatitis C virus (HCV) antibody was positive and was as the cause of chronic liver disease. More than 70% of patients had Child–Pugh [15] class A liver function and HCC was stage I or II in more than 60% of the patients. Serum AFP and DCP levels were below the normal cut-offs (15 ng/mL and 40 mAU/mL) in 33.7 and 42.9% of patients, respectively. Serum AFP-L3 was undetectable in 40.3% of patients.

On calculation of BALAD and BALAD-2 scores, patients were rated as having a BALAD score of 0, 1, 2, 3, 4, and 5 in 9658 (40.2%), 6756 (28.1%), 4135 (17.2%), 2751 (11.4%), 499 (2.1%), and 230 (1.0%) of cases, respectively. BALAD-2 score was 1, 2, 3, and 4 in 7827 (32.6%), 6772 (28.2%), 5510 (22.9%), and 3920 (16.3%) of patients, respectively.

### Association of BALAD and BALAD-2 scores with progression of HCC and liver function

Table 2 shows patient backgrounds, as well as data on liver dysfunction and tumor progression based on BALAD and BALAD-2 scores. Increases in these scores were significantly associated with increased tumor size, as well as higher percentages of patients with worse liver function (Child–Pugh A–C), multiple tumors, portal vein invasion, and increased TNM stage. The associations of BALAD-2 scores with liver dysfunction and tumor progression were more marked and consistent than those of BALAD scores.

### Prognostic significance of BALAD and BALAD-2 scores

Patients’ median survival times and overall 3- and 5-year survival rates are shown in Table 3. Increases in both BALAD and BALAD-2 scores were associated with shortened median survival times and decreased 3- and 5-year survival rates. There were no overlaps in the 95% confidence intervals of median survival times between BALAD-2 scores, whereas there were some overlaps with BALAD. Multivariate analysis showed that BALAD and BALAD-2 scores were associated with patient survival independent of Child–Pugh class, tumor stage, and treatment (Table 4).



**Table 1** Patient characteristics ( $n = 24,029$ )

Age (mean $\pm$ SD, years) (median, IQR)	66.9 $\pm$ 9.6 (68, 61–74)
Sex ratio (male/female)	16,850 (70.1)/7179 (29.9)
HBsAg (positive/negative)	3724 (16.0)/19,618 (84.0)
HCV-Ab (positive/negative)	16,352 (69.5)/7186 (30.5)
Child–Pugh class (A/B/C)	17,533 (74.3)/5230 (22.1)/846 (3.6)
Albumin (mean $\pm$ SD, g/dL)	3.63 $\pm$ 0.56
Total bilirubin (mean $\pm$ SD, mg/dL)	1.13 $\pm$ 1.44
Prothrombin (mean $\pm$ SD, %)	81.2 $\pm$ 16.6
Platelet count (mean $\pm$ SD, $\times 1000/\text{mL}$ )	127 $\pm$ 71
Tumor size (mean $\pm$ SD, cm) (median, IQR)	3.92 $\pm$ 3.70 (2.8, 2.0–4.5)
$\leq 2$ cm/ $> 2$ cm	7966 (34.2)/15,318 (65.8)
Number of tumors (single/multiple)	13,381 (57.0)/10,107 (43.0)
Portal vein invasion (absent/present) <sup>a</sup>	19,876 (88.1)/2680 (11.9)
AFP (median, IQR), $< 15$ ng/mL (%)	175.0 (46.0–974.5), 8086 (33.7)
$< 400$ ng/mL/ $\geq 400$ ng/mL	21,560 (89.7)/2469 (10.3)
AFP-L3 (median, IQR), undetected (%)	21.0 (5.6–49.7), 9682 (40.3)
$< 15\%$ / $\geq 15\%$	20,152 (83.7)/3877 (16.3)
DCP (median, IQR), $< 40$ mAU/mL	283.0 (92.0–1240.0), 10,297 (42.9)
$< 100$ mAU/mL/ $\geq 100$ mAU/mL	19,037 (79.2)/4992 (20.8)
TNM stage (I/II/III/IV)	4791 (22.3)/8943 (41.6)/5684 (26.4)/2081 (9.7)
Treatment (resection/LAT/TACE/others/none)	6859 (28.6)/8600 (35.8)/6221 (25.9)/1378 (5.8)/934 (3.9)

Percentages are given in parentheses

Data were missing in 687 cases for HBsAg, 491 for HCV-Ab, 420 for Child–Pugh class, 706 for prothrombin time, 256 for platelet counts, 745 for tumor size, 541 for tumor number, 1473 for portal vein invasion, 2530 for TNM stage, and 37 for treatment

HBsAg hepatitis B virus surface antigen, HCV-Ab hepatitis C virus antibody, AFP alpha-fetoprotein, AFP-L3 *lens culinaris* agglutinin-reactive AFP, DCP des-gamma-carboxy prothrombin, LAT locoregional ablative therapies including radiofrequency ablation and percutaneous ethanol injection, TACE transarterial chemoembolization

<sup>a</sup> Based on imaging studies

### Discrimination of patient survivals by BALAD and BALAD-2 scores

Figure 1 shows the post-diagnosis survival curves of patients based on BALAD and BALAD-2 scores. Both scores show good discriminatory ability for patient survival rates. In particular, there was no overlap in the 95% confidence intervals of survival curves when categorized by BALAD-2 scores. When survival rates were compared between patients with elevated BALAD scores predominantly due to tumor progression (tumor markers elevation) and those predominantly due to deteriorated liver function (decreases in ALB and T-Bil) among patients with intermediate BALAD score (score 2 and score 3), the survival rates were similar between groups (Supplementary figure S2).

Figure 2 shows the post-diagnosis survival curves by BALAD-2 scores according to the etiology of background liver disease. BALAD-2 scores maintained a good discriminatory ability in all three patient subgroups without overlap of survival curves between scores. When patients were grouped based on the treatment of HCC (Fig. 3), BALAD-2 scores proved equally discriminatory in all

treatment classes without overlap of survival curves. In contrast, BALAD scores showed several overlaps between scores when patients were grouped by etiology or treatment (Supplementary figures S3 and S4). When comparing discriminatory ability of BALAD and BALAD-2 scores with Japan Integrated Staging (JIS) score (Supplementary figure S5), the AICs of BALAD and BALAD-2 models were higher and their Harrell's *C* statistics were lower than those of JIS scoring system (Supplementary table S2). The discriminatory abilities of BALAD and BALAD-2 scores, therefore, were not superior to that of JIS score, but were comparable.

### Discussion

In terms of staging of HCC, the progression of HCC is primarily evaluated by morphology, i.e., the size and number of tumors and the presence of portal vein invasion [11, 16, 17]. Such evaluations are based mainly on imaging studies and postoperative pathologic examinations in patients who have undergone hepatic resection or



**Table 2** Association of BALAD and BALAD-2 scores with hepatitis viral infection, liver function, tumor progression, and treatment in patients with hepatocellular carcinoma ( $n = 24,029$ )

BALAD score	0 ( <i>n</i> = 9568)	1 ( <i>n</i> = 6756)	2 ( <i>n</i> = 4135)	3 ( <i>n</i> = 2751)	4 ( <i>n</i> = 499)	5 ( <i>n</i> = 230)	<i>P</i> value
Age (years)	67.4 ± 8.8	67.5 ± 9.6	66.3 ± 10.2	65.4 ± 10.6	63.9 ± 9.6	62.7 ± 10.2	<0.0001
Sex (male)	6561 (67.9)	4879 (72.2)	2875 (69.5)	1995 (72.5)	363 (72.8)	177 (77.0)	<0.0001
HBsAg positive	1169 (12.5)	1002 (15.2)	781 (19.5)	605 (22.6)	106 (22.0)	61 (27.9)	<0.0001
HCV-Ab positive	7283 (76.9)	4540 (68.6)	2594 (64.2)	1544 (57.2)	278 (57.1)	113 (52.8)	<0.0001
Child–Pugh class-A	7992 (84.3)	5195 (78.4)	2665 (65.6)	1659 (61.2)	22 (4.5)	0	<0.0001
Child–Pugh class-B	1480 (15.6)	1377 (20.8)	1170 (28.8)	818 (30.2)	300 (60.7)	85 (37.6)	<0.0001
Child–Pugh class-C	214 (0.1)	57 (0.8)	229 (5.6)	233 (8.6)	172 (34.8)	141 (62.4)	<0.0001
Platelet count (X1000/ mL)	117 ± 61	131 ± 69	132 ± 78	147 ± 89	125 ± 86	142 ± 94	<0.0001
Tumor size (cm)	2.65 ± 2.62	4.05 ± 3.04	4.81 ± 4.31	6.42 ± 5.02	6.13 ± 5.05	8.34 ± 7.08	<0.0001
Tumor number-solitary	6217 (65.1)	3813 (57.5)	2038 (50.7)	1130 (43.1)	128 (27.7)	55 (26.6)	<0.0001
Tumor number-multiple	3328 (34.9)	2822 (42.5)	1979 (49.3)	1492 (56.9)	334 (72.3)	152 (73.4)	<0.0001
Portal vein invasion − <sup>a</sup>	8957 (98.1)	5795 (91.3)	3143 (81.1)	1649 (64.8)	254 (56.0)	78 (37.9)	<0.0001
Portal vein invasion + <sup>a</sup>	171 (1.9)	552 (8.7)	732 (18.9)	897 (35.2)	200 (44.0)	128 (62.1)	<0.0001
TNM stage-1	3120 (35.5)	1048 (17.3)	459 (12.5)	135 (5.6)	23 (5.8)	6 (3.4)	<0.0001
TNM stage-2	3935 (44.8)	2765 (45.6)	1429 (38.9)	714 (29.7)	76 (19.0)	24 (13.5)	<0.0001
TNM stage-3	1603 (18.3)	1838 (30.3)	1223 (33.2)	841 (35.0)	137 (34.3)	42 (23.6)	<0.0001
TNM stage-4	119 (1.4)	413 (6.8)	567 (15.4)	713 (29.7)	163 (40.9)	106 (59.5)	<0.0001
Treatment-resection	2422 (25.1)	2273 (33.7)	1283 (31.1)	826 (30.1)	45 (9.0)	10 (4.3)	0.9873
Treatment-LAT	5190 (53.9)	2054 (30.4)	923 (22.4)	356 (12.9)	63 (12.6)	14 (6.1)	<0.0001
Treatment-TACE	1792 (18.6)	1974 (29.3)	1342 (32.5)	901 (32.8)	167 (33.5)	45 (19.6)	<0.0001
Treatment-others	118 (1.2)	285 (4.2)	377 (9.1)	424 (15.4)	109 (21.8)	65 (28.3)	<0.0001
Treatment-none	117 (1.2)	162 (2.4)	203 (4.9)	241 (8.8)	115 (23.1)	96 (41.7)	<0.0001
BALAD-2 score	1 ( <i>n</i> = 7827)	2 ( <i>n</i> = 6772)	3 ( <i>n</i> = 5510)	4 ( <i>n</i> = 3920)	<i>P</i> value		
Age (years)	67.5 ± 9.3	67.6 ± 9.4	66.8 ± 9.7	64.6 ± 9.9	<0.0001		
Sex (male)	5560 (71.0)	4699 (69.4)	3828 (69.5)	2763 (70.5)	0.3006		
HBsAg positive	1170 (15.4)	983 (14.9)	842 (15.7)	729 (19.2)	<0.0001		
HCV-Ab positive	5453 (71.2)	4744 (71.2)	3749 (69.4)	2406 (62.9)	<0.0001		
Child–Pugh class-A	7542 (96.7)	5691 (85.7)	3491 (64.6)	899 (23.3)	<0.0001		
Child–Pugh class-B	257 (3.3)	943 (14.2)	1863 (34.5)	2167 (56.2)	<0.0001		
Child–Pugh class-C	2 (0.0)	5 (0.1)	48 (0.9)	791 (20.5)	<0.0001		
Platelet count	139 ± 63	126 ± 66	120 ± 76	117 ± 86	<0.0001		
Tumor size	3.00 ± 2.88	3.70 ± 3.48	4.54 ± 4.13	5.53 ± 5.10	<0.0001		
Tumor number-solitary	5232 (67.7)	3909 (58.7)	2737 (51.0)	1503 (40.3)	<0.0001		
Tumor number-multiple	2499 (32.3)	2747 (41.3)	2632 (49.0)	2229 (59.7)	<0.0001		
Portal vein invasion − <sup>a</sup>	7209 (97.1)	5843 (92.0)	4357 (84.5)	2467 (68.0)	<0.0001		
Portal vein invasion + <sup>a</sup>	217 (2.9)	505 (8.0)	797 (15.5)	1161 (32.0)	<0.0001		
TNM stage-1	2209 (30.9)	1324 (21.6)	817 (16.7)	441 (13.2)	<0.0001		
TNM stage-2	3403 (47.6)	2727 (44.6)	1861 (38.0)	952 (28.5)	<0.0001		
TNM stage-3	1383 (19.4)	1704 (27.9)	1559 (31.9)	1038 (31.1)	<0.0001		
TNM stage-4	153 (2.1)	360 (5.9)	657 (13.4)	911 (27.2)	<0.0001		
Treatment-resection	2776 (35.5)	2217 (32.8)	1348 (24.5)	518 (13.2)	<0.0001		

**Table 2** continued

BALAD-2 score	1 (n = 7827)	2 (n = 6772)	3 (n = 5510)	4 (n = 3920)	P value
Treatment-LAT	3530 (45.2)	2509 (37.1)	1701 (30.9)	860 (22.0)	<0.0001
Treatment-TACE	1302 (16.7)	1716 (25.4)	1831 (33.3)	1372 (35.0)	<0.0001
Treatment-others	117 (1.5)	211 (3.1)	428 (7.8)	622 (15.9)	<0.0001
Treatment-none	88 (1.1)	107 (1.6)	194 (3.5)	934 (13.9)	<0.0001

Percentages are given in parentheses

Data were missing in 687 cases for HBsAg, 491 for HCV-Ab, 420 for Child–Pugh class, 706 for prothrombin time, 256 for platelet counts, 745 for tumor size, 541 for tumor number, 1473 for portal vein invasion, 2530 for TNM stage, and 37 for treatment

HBsAg hepatitis B virus surface antigen, HCV-Ab hepatitis C virus antibody, LAT locoregional ablative therapies including radiofrequency ablation and percutaneous ethanol injection, TACE transarterial chemoembolization

<sup>a</sup> Based on imaging studies

**Table 3** Median survival times and 3- and 5-years survival rates for BALAD and BALAD-2 scores in patients with hepatocellular carcinoma (n = 24,029)

	N	Median survival (years)	95% CI	3-year survival (%)	95% CI	5-year survival (%)	95% CI
BALAD score							
0	9658	7.7	7.3–9.4	85.2	84.3–86.1	68.0	66.3–69.5
1	6576	5.4	5.1–5.8	70.0	68.5–71.4	52.4	50.4–54.4
2	4135	3.7	3.3–4.0	55.2	53.1–57.1	41.7	39.3–44.1
3	2751	2.0	1.8–2.2	41.0	38.6–43.4	29.4	26.6–32.1
4	499	0.8	0.8–0.9	24.4	19.4–29.7	15.9	11.0–21.5
5	230	0.3	0.2–0.4	10.8	6.2–16.9	7.0	3.1–13.0
BALAD-2 score							
1	7827	9.7	8.3–	86.9	85.9–87.8	72.5	70.8–74.1
2	6772	5.8	5.5–6.2	74.8	73.4–76.2	55.8	53.8–57.8
3	5510	3.8	3.6–4.0	57.1	55.4–58.9	40.4	38.2–42.6
4	3920	1.8	1.7–1.9	37.7	35.7–39.5	25.4	23.2–27.7

CI confidence interval

transplantation. However, estimating tumor progression using imaging studies has several shortcomings. The detectability of liver tumors, which influences the determination of tumor multiplicity, depends on the resolution of the imaging modality (ultrasonography, CT, or MRI) and their quality, as well as the skill of the sonographer in case of ultrasonography. Recent advancements in imaging technology, such as multidetector-row CT [18, 19], and MRI [20], have improved the detection of hepatic nodules, resulting in upstaging of HCC progression. In addition, discrepancies between imaging findings and pathologic results are often found in patients who undergo hepatic resection. With imaging studies, it is often difficult to detect microvascular invasion of HCC or minute satellite nodules, both of which are found in pathologic analysis after resection and result in upstaging of HCC progression.

Liver dysfunction in patients with HCC is usually estimated based on the Child–Pugh classification [15]. This classification takes into account the presence and controllability of ascites and hepatic encephalopathy, in addition to

prothrombin time and levels of serum ALB and T-Bil. However, the presence and controllability of ascites and hepatic encephalopathy are largely subjective. Therefore, HCC staging that is based on the morphological evaluation of tumor progression and on liver dysfunction as determined by Child–Pugh classification cannot be fully objective, and therefore cannot be standardized across regions.

The results of the present study, based on the data of a nationwide follow-up survey showed that prognostic scoring based solely on serology were well associated with the progression of HCC and liver dysfunction, and had excellent discriminatory ability for survival in Japanese patients with HCC. Interestingly, the survival rates were similar between patients with the elevation of BALAD score due to tumor progression and those due to liver deterioration, suggesting homogenous survivals in patients with identical scores. The scores of the BALAD and BALAD-2 models were associated with the survival of patients with HCC independent of Child–Pugh class and the morphological features of HCC (Table 4). Previous

**Table 4** Multivariate analysis with backward elimination method for factors associated with survival after diagnosis in patients with hepatocellular carcinoma ( $n = 24,029$ )

Factor	Multivariate analysis	
	<i>P</i> value	Relative risk (95% CI)
Age		
Per 1.0	<0.0001	1.011 (1.008–1.014)
Sex		
Female		
Male	<0.0001	1.128 (1.062–1.198)
Child–Pugh class		
A		1
B	<0.0001	1.631 (1.534–1.736)
C	<0.0001	1.779 (1.565–2.022)
Tumor size		
Per 1.0	<0.0001	1.019 (1.014–1.024)
Portal vein invasion <sup>a</sup>		
Absent		1
Present	<0.0001	1.320 (1.193–1.460)
TNM stage		
1		1
2	<0.0001	1.279 (1.172–1.397)
3	<0.0001	1.757 (1.601–1.929)
4	<0.0001	2.890 (2.528–3.304)
Treatment		
None		1
Resection	<0.0001	0.278 (0.245–0.315)
LAT	<0.0001	0.362 (0.319–0.410)
TACE	<0.0001	0.520 (0.462–0.585)
Others	<0.0001	0.730 (0.641–0.832)
BALAD score		
0		1
1	<0.0001	1.443 (1.339–1.556)
2	<0.0001	1.892 (1.743–2.053)
3	<0.0001	2.579 (2.358–2.821)
4	0.0005	2.634 (2.247–3.087)
5	0.0005	3.846 (3.104–4.766)

Factor	Multivariate analysis	
	<i>P</i> value	Relative risk (95% CI)
Age		
Per 1.0	<0.0001	1.011 (1.008–1.014)
Sex		
Female		
Male	<0.0001	1.129 (1.063–1.199)
Child–Pugh class		
A		1
B	<0.0001	1.293 (1.207–1.386)
C	<0.0001	1.598 (1.406–1.816)

**Table 4** continued

Factor	Multivariate analysis	
	<i>P</i> value	Relative risk (95% CI)
Tumor size		
Per 1.0	<0.0001	1.021 (1.016–1.026)
Number of tumors		
Single		
Multiple	0.0065	1.117 (1.032–1.211)
Portal vein invasion <sup>a</sup>		
Absent		1
Present	<0.0001	1.263 (1.137–1.404)
TNM stage		
1		1
2	<0.0001	1.384 (1.263–1.516)
3	<0.0001	2.073 (1.839–2.336)
4	<0.0001	3.607 (3.044–4.274)
Treatment		
None		1
Resection	<0.0001	0.301 (0.265–0.342)
LAT	<0.0001	0.356 (0.314–0.404)
TACE	<0.0001	0.525 (0.467–0.591)
Others	<0.0001	0.770 (0.676–0.878)
BALAD-2 score		
1		1
2	<0.0001	1.505 (1.387–1.632)
3	<0.0001	2.128 (1.957–2.314)
4	<0.0001	2.816 (2.545–3.116)

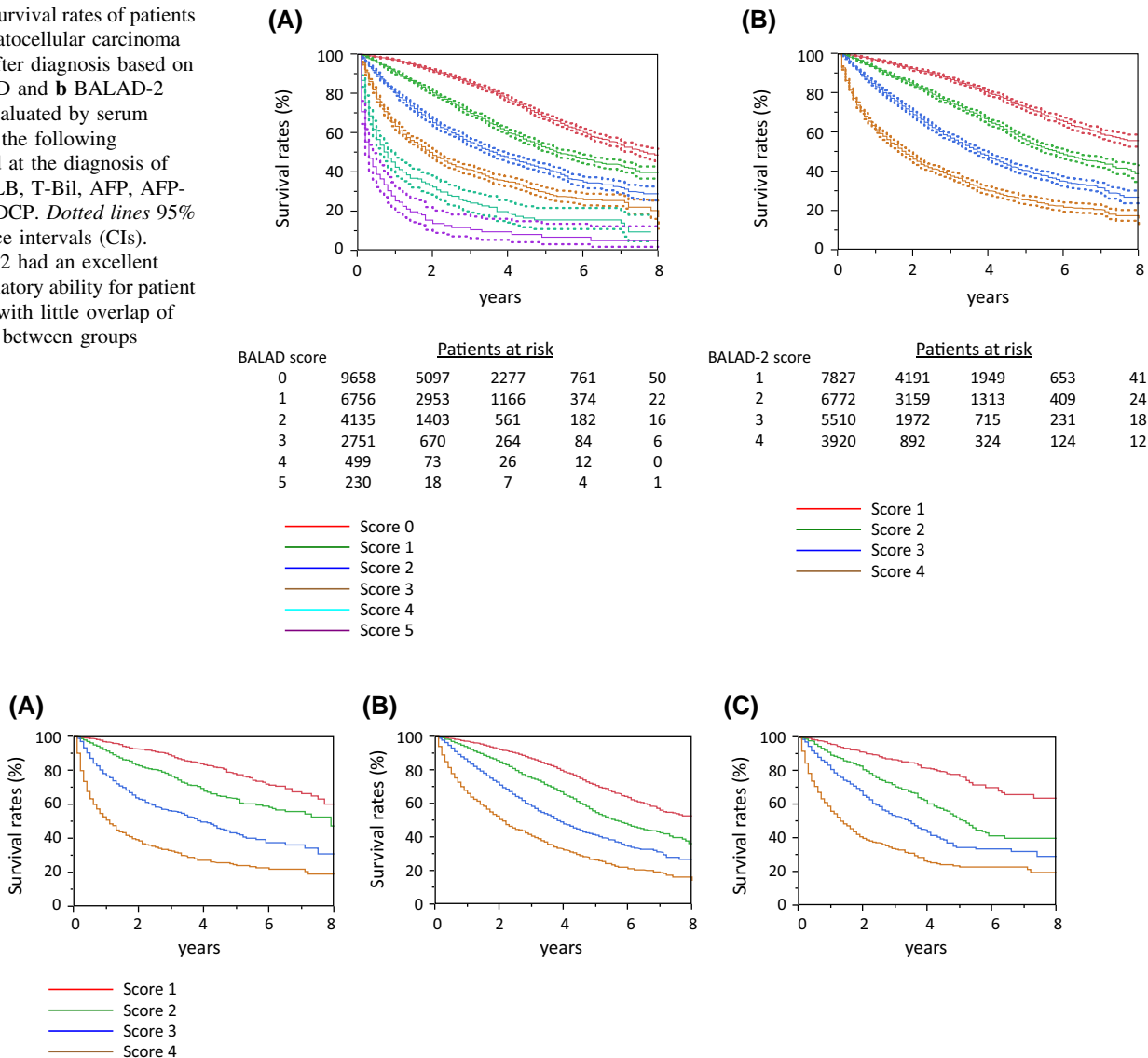
CI confidence interval, LAT locoregional ablative therapies including radiofrequency ablation and percutaneous ethanol injection, TACE transarterial chemoembolization

<sup>a</sup> Based on imaging studies

findings on the usefulness of the BALAD and BALAD-2 models for the prognostication of patients with HCC [7–9] were replicated in this large HCC cohort in Japan, where the survival of patients is long in comparison to Western and other Asian countries. Japanese patients are diagnosed at a much earlier stage, because individuals of the Japanese population who are at risk of HCC (those with chronic liver disease) are more rigorously screened than in Western and other Asian countries, and hence are much more likely to receive potentially curative therapy [21].

The three markers that are incorporated in the BALAD and BALAD-2 scores have the advantage of being commercially available, with regulatory approval in Japan, the USA, and Europe. All three markers are well documented to have prognostic significance when used individually [22–24] and in combination [25]. In addition, previous studies revealed the prognostic significance of serum ALB and T-Bil levels as liver function measures in patients with HCC

**Fig. 1** Survival rates of patients with hepatocellular carcinoma (HCC) after diagnosis based on **a** BALAD and **b** BALAD-2 scores evaluated by serum levels of the following measured at the diagnosis of HCC: ALB, T-Bil, AFP, AFP-L3, and DCP. *Dotted lines* 95% confidence intervals (CIs). BALAD-2 had an excellent discriminatory ability for patient survival with little overlap of 95% CIs between groups



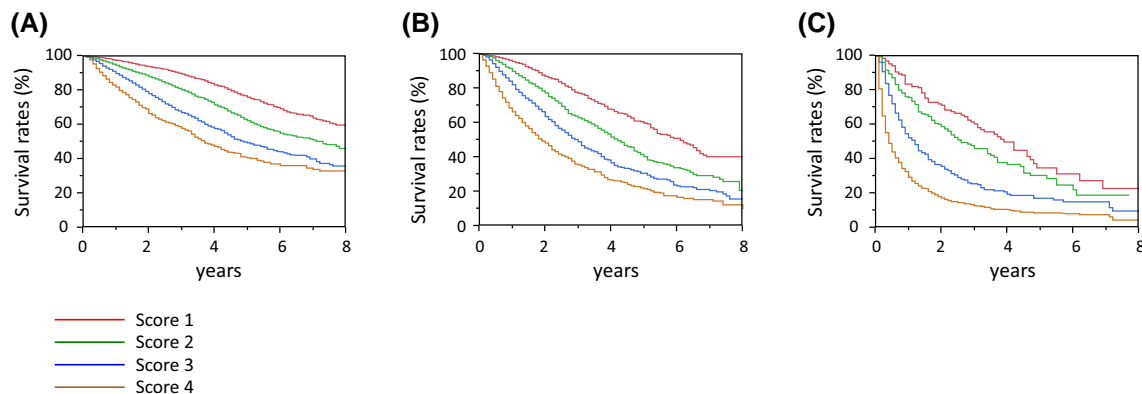
**Fig. 2** Survival rates of patients with hepatocellular carcinoma (HCC) after diagnosis by BALAD-2 scores evaluated by serum levels of the following measured at the diagnosis of HCC: ALB,

T-Bil, AFP, AFP-L3, and DCP. **a** Patients with hepatitis B virus (HBV) infection; **b** patients with hepatitis C virus (HCV) infection; **c** patients without hepatitis virus infection (non-HBV/HCV)

[12, 26]. The combination of these serological indicators of tumor progression and liver function accurately reflected the state of patients with HCC at diagnosis and categorized the risk of death thereafter, at least in Japan where the main etiology of HCC is HCV, many cases are diagnosed in the early stage, and the majority of patients have Child–Pugh class A liver function. In addition, these serological models, especially BALAD-2 model, maintained discriminatory ability in patient subgroups with hepatitis B virus (HBV) or non-HBV/HCV, or in those with intermediate or advanced stages, in addition to HCV-related HCC or early-stage HCC. When compared with JIS scoring systems, these scores did not have superior discriminatory ability. However, the advantage of BALAD or BALAD-2 scores is that the

scorings are objective only based on serum markers, and we believe that it can be of use if they do not show markedly inferior discriminatory ability to JIS, which was shown in this study, or other staging systems of HCC as prognostic models.

When comparing the original BALAD and BALAD-2 models, the latter had a marginally better discrimination. The overlap between risk groups was less evident for BALAD-2 (Table 4; Fig. 2). The superior discrimination of BALAD-2 model was enhanced when patients were grouped by disease stages. Also, regarding the association between BALAD and BALAD-2 scores and tumor progression and liver function, increases in BALAD-2 scores showed more consistent association with the



**Fig. 3** Survival rates of patients with hepatocellular carcinoma (HCC) who undergone **a** curative, **b** intermediate, and **c** palliative or no treatment after diagnosis by BALAD-2 scores evaluated by

serum levels of the following measured at the diagnosis of HCC: ALB, T-Bil, AFP, AFP-L3, and DCP

progression of HCC and the deterioration of liver function (Table 3).

However, the serology-based scoring models have several limitations. First, scoring for prognostication on the basis of serum markers is not applicable to diagnosis, although another serology-based model for the diagnosis of HCC has been reported [9, 27]. Although the selected treatments had close associations with the scores, especially of BALAD-2, these staging models cannot be used for treatment planning. In addition, these models are not applicable in patients who are taking drugs such as warfarin or vitamin K that can influence the levels of tumor markers, and it should be noted that the use of such drugs could not be verified in this study cohort. Finally, these models are used for a “scoring for prognostication” in patients with HCC and not a pure “staging” of HCC such as TNM tumor staging. Therefore, they cannot be discussed in the same line of the staging of other cancers, which oncologists or hepatologists should take into consideration.

There are several limitations of this study. The study patients were a part of all patients in nationwide survey (36.1%) in whom five laboratory variables necessary for calculating the BALAD and BALAD-2 scores were available, although the distributions of HCC stage and Child–Pugh class, as well as tumor size, number, and portal vein invasion, were same between 24,029 study patients and 42,525 patients excluded from the study due to the lack of laboratory variables (data not shown). In addition, actual levels of AFP and DCP were not available in patients with AFP below 15 ng/dL and patients with DCP below 40 mAU/mL and values within these reference ranges were randomly assigned for the calculation of BALAD-2 scores in these cases. Finally, the prognoses of patients who underwent transplantation based on these scores are not known, because few patients with HCC are treated with transplantation in Japan.

In conclusion, we evaluated the prognostic significance of the serology-based BALAD and BALAD-2 scoring models in Japanese patients with HCC in a cohort of a nationwide follow-up survey, and confirmed that these models are applicable for these patients.

#### Compliance with ethical standards

**Conflict of interest** The authors declare that they have no conflict of interest.

#### References

- Okuda K, Ohtsuki T, Obata H, et al. Natural history of hepatocellular carcinoma and prognosis in relation to treatment. Study of 850 patients. *Cancer*. 1985;56:918–28.
- The Cancer of the Liver Italian Program (CLIP) Investigators. A new prognostic system for hepatocellular carcinoma: a retrospective study of 435 patients. *Hepatology*. 1998;28:751–5.
- Chevret S, Trinchet J-C, Mathieu D, et al. A new prognostic classification for predicting survival in patients with hepatocellular carcinoma. *J Hepatol*. 1999;31:133–41.
- Llovet JM, Bru C, Bruix J. Prognosis of hepatocellular carcinoma: the BCLC staging classification. *Semin Liver Dis*. 1999;19:329–38.
- Leung TW, Tang AM, Zee B, et al. Construction of the Chinese University Prognostic Index for hepatocellular carcinoma and comparison with the TNM staging system, the Okuda staging system, and the Cancer of the Liver Italian Program staging system: a study based on 926 patients. *Cancer*. 2002;94:1760–9.
- Kudo M, Chung H, Haji S, et al. Validation of a new prognostic staging system for hepatocellular carcinoma: the JIS score compared with the CLIP score. *Hepatology*. 2004;40:1396–405.
- Toyoda H, Kumada T, Osaki Y, et al. Staging hepatocellular carcinoma by a novel scoring system (BALAD score) based on serum markers. *Clin Gastroenterol Hepatol*. 2006;4:1528–36.
- Fox R, Berhane S, Teng M, et al. Biomarker-based prognosis in hepatocellular carcinoma: validation and extension of the BALAD model. *Br J Cancer*. 2014;110:2090–8.
- Berhane S, Toyoda H, Tada T, et al. Role of the GALAD and BALAD-2 serologic models in diagnosis of hepatocellular carcinoma and prediction of survival in patients. *Clin Gastroenterol Hepatol*. 2016;14:875–86.

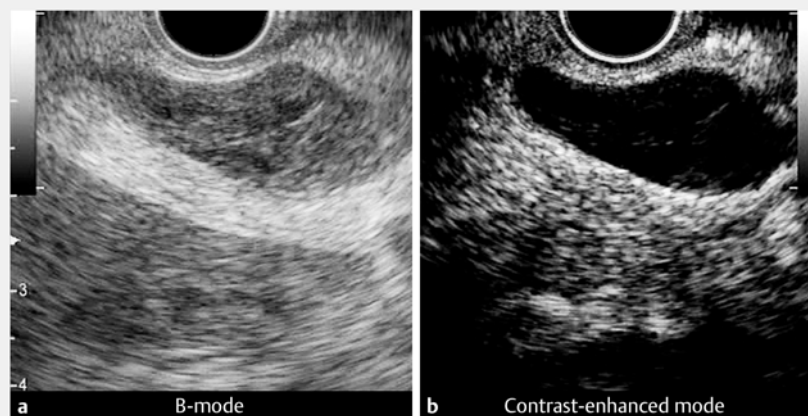


10. Makuuchi M, Kokudo N, Arai S, et al. Development of evidence-based clinical guidelines for the diagnosis and treatment of hepatocellular carcinoma in Japan. *Hepatol Res.* 2008;38:37–51.
11. The Liver Cancer Study Group of Japan. The general rules for the clinical and pathological study of primary liver cancer (English Ed.). 5th ed. Tokyo: Kaneraha & Co. Ltd; 2009.
12. Tateishi R, Yoshida H, Shiina S, et al. Proposal of a new prognostic model for hepatocellular carcinoma: an analysis of 403 patients. *Gut.* 2005;54:419–25.
13. Akaike H. Information theory as an extension of the maximum likelihood principle. In: Petrov BN, editor. Second international symposium on information theory. 1973.
14. Taktak AFG, Eleuteri A, Lake SP, et al. (2007) Evaluation of prognostic models: discrimination and calibration performance. In: Proceedings of the 3rd International Conference on Computational Intelligence in Medicine and Healthcare
15. Pugh RNH, Murray-Lyon IM, Dawson JL, et al. Transection of the oesophagus for bleeding oesophageal varices. *Br J Surg.* 1973;60:646–9.
16. International Union Against Cancer (UICC). Liver. In: Sobin LH, Wittekind CH, editors. TNM classification of malignant tumours. 6th ed. New York: Wiley; 2002. p. 81–3.
17. Vauthey JN, Lauwers GY, Esnaola NF, et al. Simplified staging for hepatocellular carcinoma. *J Clin Oncol.* 2002;127:603–8.
18. Kawata S, Murakami T, Kim T, et al. Multidetector CT: diagnostic impact of slice thickness on detection of hypervascular hepatocellular carcinoma. *Am J Roentgenol.* 2002;179:61–6.
19. Ichikawa T, Erturk SM, Araki T. Multiphasic contrast-enhanced multidetector-row CT of liver: contrast-enhancement theory and practical scan protocol with a combination of fixed injection duration and patients' body-weight-tailored dose of contrast material. *Eur J Radiol.* 2006;58:165–76.
20. Kim HD, Lim YS, Han S, et al. Evaluation of early-stage hepatocellular carcinoma by magnetic resonance imaging with gadoxetic acid detects additional lesions and increases overall survival. *Gastroenterology.* 2015;148:1371–82.
21. Toyoda H, Kumada T, Kiriya S, et al. Impact of surveillance on survival of patients with initial hepatocellular carcinoma: a study from Japan. *Clin Gastroenterol Hepatol.* 2006;4:1170–6.
22. Toyoda H, Kumada T, Osaki Y, et al. Role of tumor markers in assessment of tumor progression and prediction of outcomes in patients with hepatocellular carcinoma. *Hepatol Res.* 2007;37:S166–71.
23. Nagaoka S, Yatsushashi H, Hamada H, et al. The des- $\gamma$ -carboxy prothrombin index is a new prognostic indicator for hepatocellular carcinoma. *Cancer.* 2003;98:2671–7.
24. Nouse K, Kobayashi Y, Nakamura S, et al. Prognostic importance of fucosylated alpha-fetoprotein in hepatocellular carcinoma patients with low alpha-fetoprotein. *J Gastroenterol Hepatol.* 2011;26:1195–200.
25. Toyoda H, Kumada T, Kiriya S, et al. Prognostic significance of simultaneous measurement of three tumor markers in patients with hepatocellular carcinoma. *Clin Gastroenterol Hepatol.* 2006;4:111–7.
26. Johnson PJ, Berhane S, Kagebayashi C, et al. Assessment of liver function in patients with hepatocellular carcinoma: a new evidence-based approach-the ALBI grade. *J Clin Oncol.* 2015;33:550–8.
27. Johnson PJ, Pirrie SJ, Cox TF, et al. The detection of hepatocellular carcinoma using a prospectively developed and validated model based on serological biomarkers. *Cancer Epidemiol Biomark Prev.* 2014;23:144–53.

## Endoscopic ultrasound-guided choledochoduodenostomy with novel use of contrast-enhanced harmonic imaging



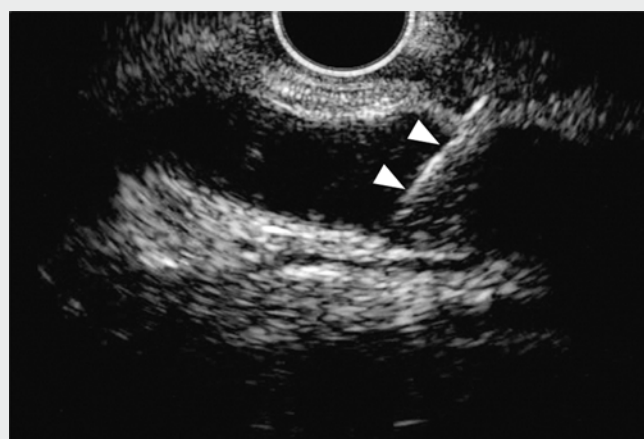
► **Fig. 1** Abdominal computed tomography (CT) scan showing bile duct dilatation and high-density components in the common bile duct, suggesting hemobilia (arrowheads).



► **Fig. 2** Endoscopic ultrasound (EUS) images showing: **a** in B-mode, heterogeneous echogenicity in the common bile duct, but poor visualization; **b** with contrast-enhanced harmonic EUS, the common bile duct as an avascular structure with a clear margin and no pooling of contrast agent in the common bile duct.

Since it was first described in 2001 [1], endoscopic ultrasound-guided choledochoduodenostomy (EUS-CDS) has been increasingly used as an alternative for biliary decompression after failed endoscopic retrograde cholangiopancreatography (ERCP). EUS-CDS has an overall technical success rate of more than 90% [2,3], but puncturing the common bile duct (CBD) can be challenging in patients with hemobilia because it presents as a heterogeneous echogenicity. Here, we present a patient for whom EUS-CDS was successfully performed under contrast-enhanced harmonic EUS (CH-EUS) guidance.

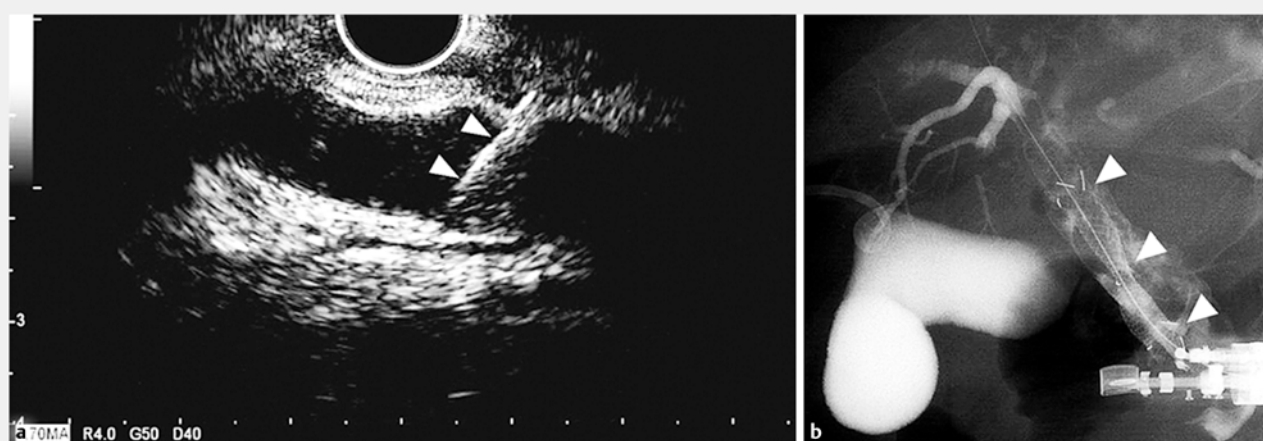
A female patient in her eighties with advanced duodenal cancer was referred to our hospital for treatment of recurrent obstructive jaundice. She had previously undergone duodenal metal stent placement and an external gallbladder drainage catheter had been placed for biliary obstruction due to direct cancer invasion of the ampulla. An abdominal computed tomography (CT) scan revealed bile duct dilatation and high-density components in the CBD, suggesting hemobilia (► **Fig.**



► **Video 1** A sonographic contrast agent (Sonazoid) was injected to determine whether there was active bleeding and to delineate the common bile duct (CBD) from the surrounding tissues during endoscopic ultrasound-guided choledochoduodenostomy. After intravenous infusion of Sonazoid, the CBD was clearly identified, allowing choledochoduodenostomy to be safely performed.

**1).** As her CT scan showed a dilated CBD, we elected to perform EUS-CDS. B-mode EUS revealed heterogeneous echogenicity in the CBD, but the visualization was poor. To determine whether

there was active bleeding and to delineate the CBD from the surrounding tissues, we performed CH-EUS. Immediately after intravenous infusion of 0.015 mL/kg of a sonographic contrast agent (Sonazoid;



► **Fig. 3** Cholechooduodenostomy guided by real-time contrast-enhanced harmonic endoscopic ultrasound showing: **a** the dilated common bile duct being punctured with a 19-gauge aspiration needle (arrowheads); **b** successful deployment of a covered metal stent between the common bile duct and the duodenum (arrowheads) after dilation of the fistula.

Daiichi-Sankyo, Tokyo, Japan), we identified the dilated CBD as an avascular structure, with a clear margin (► **Fig. 2**; ► **Video 1**). There was no pooling of contrast agent in the CBD, so it was punctured with a 19-gauge aspiration needle (► **Fig. 3 a**). After dilating the fistula, we successfully deployed a self-expandable covered metal stent (Niti-S Biliary Covered Stent; 8×60 mm; Taewoong Medical, Seoul, South Korea; ► **Fig. 3 b**). Following this procedure, the patient's condition improved within a few days. To the best of our knowledge, this is the first report of CDS being guided by CH-EUS. CH-EUS may be useful for patients with hemobilia in helping to clearly visualize the CBD.

Endoscopy\_UCTN\_Code\_TTT\_1AS\_2AD

### Competing interests

None

### The Authors

**Kosuke Minaga, Mamoru Takenaka, Ken Kamata, Takeshi Miyata, Kentaro Yamao, Hajime Imai, Masatoshi Kudo**

Department of Gastroenterology and Hepatology, Kindai University Faculty of Medicine, Osaka-Sayama, Japan

### Corresponding author

**Mamoru Takenaka, MD, PhD**

Department of Gastroenterology and Hepatology, Kindai University Faculty of Medicine, 377-2 Ohno-Higashi, Osaka-Sayama, 589-8511, Japan  
Fax: +81-72-3672880  
mamoxyo45@gmail.com

### References

- [1] Giovannini M, Moutardier V, Pesenti C et al. Endoscopic ultrasound-guided bilioduodenal anastomosis: a new technique for biliary drainage. *Endoscopy* 2001; 33: 898–900
- [2] Wang K, Zhu J, Xing L et al. Assessment of efficacy and safety of EUS-guided biliary drainage: a systematic review. *Gastrointest Endosc* 2016; 83: 1218–1227
- [3] Khan MA, Akbar A, Baron TH et al. Endoscopic ultrasound-guided biliary drainage: a systematic review and meta-analysis. *Dig Dis Sci* 2016; 61: 684–703

### Bibliography

DOI <https://doi.org/10.1055/s-0043-117939>

Published online: 13.9.2017

Endoscopy 2017; 49: E281–E282

© Georg Thieme Verlag KG

Stuttgart · New York

ISSN 0013-726X

### ENDOSCOPY E-VIDEOS

<https://eref.thieme.de/e-videos>




*Endoscopy E-Videos* is a free access online section, reporting on interesting cases and new techniques in gastroenterological endoscopy. All papers include a high quality video and all contributions are freely accessible online.

This section has its own submission website at  
<https://mc.manuscriptcentral.com/e-videos>



## BRIEF REPORT

# A case of small invasive gastric cancer arising from *Helicobacter pylori*-negative gastric mucosa: Fundic gland-type adenocarcinoma

Yoriaki Komeda,\*  Tomohiro Watanabe,\* Shigenaga Matsui,\* Hiroshi Kashida,\* Toshiharu Sakurai,\* Masashi Kono,\* Kosuke Minaga,\* Tomoyuki Nagai,\* Satoru Hagiwara,\* Eisuke Enoki<sup>†</sup> and Masatoshi Kudo\*

Departments of \*Gastroenterology and Hepatology and <sup>†</sup>Pathology, Kindai University Faculty of Medicine, Osaka-Sayama, Osaka, Japan

## Key words

chief cell, fundic gland, gastric adenocarcinoma, pepsinogen-I.

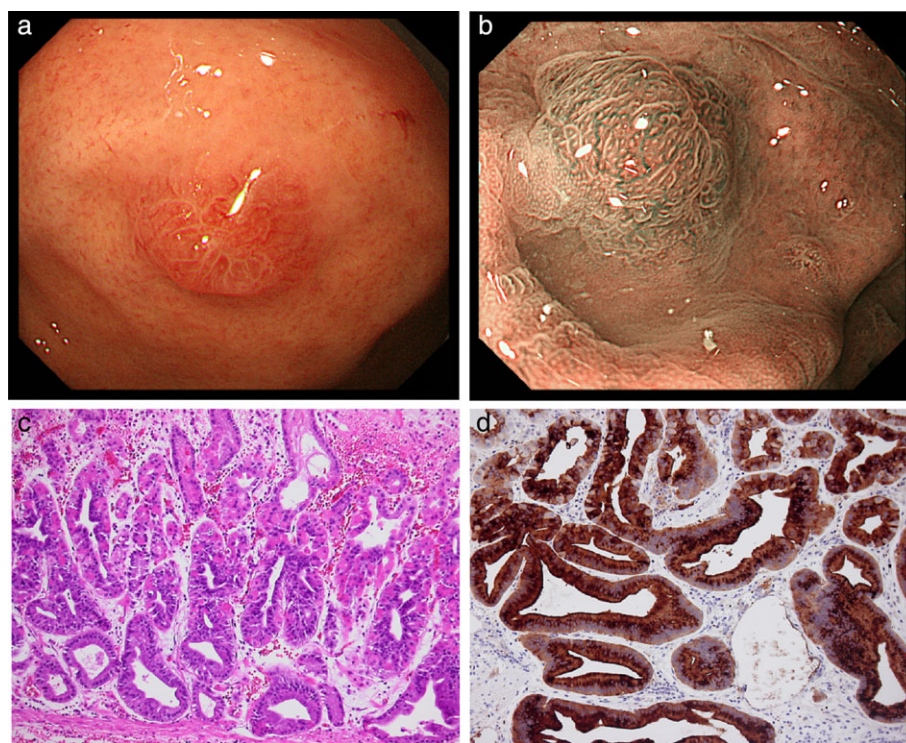
## Correspondence

Yoriaki Komeda Department of Pathology, Kindai University Faculty of Medicine, 377-2 Ohno-Higashi, Osaka-Sayama, Osaka, 589-8511, Japan.  
Email: y-komme@mvb.biglobe.ne.jp

**Declaration of conflict of interest:** The authors declare no conflicts of interest.

A 50-year-old man underwent esophagogastroduodenoscopy for further investigation of mild anemia. Serum antibody titer against *Helicobacter pylori* (*H. pylori*) was below the detection limit.

Esophagogastroduodenoscopy revealed a small reddish elevated lesion, measuring 5 mm in diameter, in the fundus of the stomach without any atrophic change (Fig. 1). Irregular microvascular



**Figure 1** Esophagogastroduodenoscopy revealed a small reddish submucosal tumor like on *H. pylori*-negative gastric mucosa at the fundus in the stomach (Fig. 1a). Magnified narrow band imaging showed irregular microvascular patterns with dilated vessels on tumor surface (Fig. 1b). Hematoxylin and eosin stains revealed a well-differentiated tubular adenocarcinoma with gland architectures that are similar to the fundic glands (Fig. 1c). Immunohistochemical studies revealed that most of tumor cells were positive for pepsinogen-I (Fig. 1d).

patterns with dilated vessels were detected in the tumor surface by magnified narrow band imaging whereas the demarcation line was absent (Fig. 1). The tumor was visualized as a high echoic mass localized to the mucosal layer through endoscopic ultrasonography. Since these findings suggest a gastric tumor originating from the mucosal layer rather than the epithelium, precutting endoscopic mucosal resection (snaring combined with circumferential incision) was performed. Pathological examination of the resected specimen revealed a well-differentiated tubular adenocarcinoma with gland architectures similar to the fundic glands. The tumor was mainly localized in the mucosal layer with invasion into the submucosal layer and most of the tumor surface was covered with nonatypical foveolar epithelium. Immunohistochemical studies revealed that most of the tumor cells were positive for pepsinogen-I and MUC6, but not for H<sup>+</sup>/K<sup>+</sup>-ATPase (Fig. 1), which are aligned with findings that are characteristic of gastric adenocarcinoma of the fundic gland (chief cell-predominant type).<sup>1,2</sup> The differential diagnosis was fundic gland, fundic gland polyps with dysplasia, neuroendocrine tumor (carcinoid), hamartomatous inverted polyps, and low-grade differential adenocarcinoma of the gastric foveolar type.

Gastric adenocarcinoma of the fundic gland type is a rare disease entity, which exhibits a submucosal tumor-like or superficial flat-type elevated lesion on *H. pylori*-negative gastric mucosa in the endoscopic examinations. We need to bear in mind the possibility of gastric adenocarcinoma of the fundic gland type upon encountering such elevated lesions originating from *H. pylori*-negative gastric mucosa.

## Acknowledgments

None.

## References

- 1 Ueyama H, Yao T, Nakashima Y *et al.* Gastric adenocarcinoma of fundic gland type (chief cell predominant type): proposal for a new entity of gastric adenocarcinoma. *Am. J. Surg. Pathol.* 2010; **34**: 609–19.
- 2 Ueyama H, Matsumoto K, Nagahara A, Hayashi T, Yao T, Watanabe S. Gastric adenocarcinoma of the fundic gland type (chief cell predominant type). *Endoscopy.* 2014; **46**: 153–7.





# Rescue EUS-guided intrahepatic biliary drainage for malignant hilar biliary stricture after failed transpapillary re-intervention

Kosuke Minaga<sup>1</sup> · Mamoru Takenaka<sup>1</sup> · Masayuki Kitano<sup>2</sup> · Yasutaka Chiba<sup>3</sup> ·  
Hajime Imai<sup>1</sup> · Kentaro Yamao<sup>1</sup> · Ken Kamata<sup>1</sup> · Takeshi Miyata<sup>1</sup> ·  
Shunsuke Omoto<sup>1</sup> · Toshiharu Sakurai<sup>1</sup> · Tomohiro Watanabe<sup>1</sup> · Naoshi Nishida<sup>1</sup> ·  
Masatoshi Kudo<sup>1</sup>

Received: 31 December 2016 / Accepted: 28 March 2017 / Published online: 19 April 2017  
© Springer Science+Business Media New York 2017

## Abstract

**Background** Treatment of unresectable malignant hilar biliary stricture (UMHBS) is challenging, especially after failure of repeated transpapillary endoscopic stenting. Endoscopic ultrasonography-guided intrahepatic biliary drainage (EUS-IBD) is a recent technique for intrahepatic biliary decompression, but indications for its use for complex hilar strictures have not been well studied. The aim of this study was to assess the feasibility and safety of EUS-IBD for UMHBS after failed transpapillary re-intervention.

**Methods** Retrospective analysis of all consecutive patients with UMHBS of Bismuth II grade or higher who, between December 2008 and May 2016, underwent EUS-IBD after failed repeated transpapillary interventions. The technical success, clinical success, and complication rates were evaluated. Factors associated with clinical ineffectiveness of EUS-IBD were explored.

**Results** A total of 30 patients (19 women, median age 66 years [range 52–87]) underwent EUS-IBD for UMHBS during the study period. Hilar biliary stricture morphology was classified as Bismuth II, III, or IV in 5, 13, and 12 patients, respectively. The median number of preceding endoscopic interventions was 4 (range 2–14). EUS-IBD

was required because the following procedures failed: duodenal scope insertion ( $n = 4$ ), accessing the papilla after duodenal stent insertion ( $n = 5$ ), or achieving desired intrahepatic biliary drainage ( $n = 21$ ). Technical success with EUS-IBD was achieved in 29 of 30 patients (96.7%) and clinical success was attained in 22 of these 29 (75.9%). Mild peritonitis occurred in three of 30 (10%) and was managed conservatively. Stent dysfunction occurred in 23.3% (7/30). There was no procedure-related mortality. On multivariable analysis, Bismuth IV stricture predicted clinical ineffectiveness (odds ratio = 12.7, 95% CI 1.18–135.4,  $P = 0.035$ ).

**Conclusions** EUS-IBD may be a feasible and effective rescue alternative with few major complications after failed transpapillary endoscopic re-intervention in patients with UMHBS, particularly for Bismuth II or III strictures.

**Keywords** Hilar malignant biliary stricture · Endoscopic ultrasonography · EUS-guided biliary drainage · Interventional EUS

Progression of unresectable malignant hilar biliary stricture (UMHBS) leads to persistent obstructive jaundice and cholangitis. The stricture may be caused by malignancies of the bile duct or pancreas, by metastases to the liver, or by lymph nodes around the hilar bile duct. Biliary drainage aims at alleviating symptoms and ameliorating the patient's quality of life. However, effective drainage of biliary stricture at the hepatic hilum is difficult to achieve due to the anatomical complexity of the bile ducts [1]. When appropriate endoscopic expertise is available, stent placement under endoscopic retrograde cholangiopancreatography (ERCP) guidance is generally accepted as first-line palliative therapy for UMHBS [1–7]. Unfortunately,

✉ Mamoru Takenaka  
mamoxyo45@gmail.com

<sup>1</sup> Department of Gastroenterology and Hepatology, Faculty of Medicine, Kindai University, 377-2 Ohno-Higashi, Osaka-Sayama 589-8511, Japan

<sup>2</sup> Second Department of Internal Medicine, School of Medicine, Wakayama Medical University, Wakayama, Japan

<sup>3</sup> Clinical Research Center, Kindai University Hospital, Osaka-Sayama, Japan

subsequent stent dysfunction has been reported in 31–59% of cases, with causes ranging from biliary sludge and food impaction to tumor ingrowth or overgrowth [8–17]. Recent progress in chemotherapy has prolonged patient survival from cancers that cause malignant biliary strictures. Therefore, these patients may require several repeat interventions to manage stent dysfunction. There are several approaches to this. Repeat ERCP is the preferred treatment, allowing mechanical cleaning with a balloon or insertion of a new stent [7, 18]. However, this is sometimes difficult. The reported technical success for such repeat procedures ranges widely from 44 to 96% [8–17]. If repeat ERCP fails, percutaneous transhepatic biliary drainage is an alternative. This is a well-established procedure, but it does have complications. In addition, the external drainage is uncomfortable for the patient [19–22].

Recently, endoscopic ultrasonography-guided biliary drainage (EUS-BD) has been increasingly applied as an alternative for failed transpapillary biliary drainage in patients with malignant biliary obstruction [23–27]. EUS-BD is performed by two different approaches, namely, EUS-guided extrahepatic and EUS-guided intrahepatic biliary drainage (EUS-IBD) [28]. Since EUS-IBD primarily drains the left intrahepatic biliary duct, this technique has not generally been used for complex hilar biliary strictures. To date, few data are available on the indications of EUS-IBD in patients with UMHBS [29–31]. The aim of the current study was to evaluate the technical feasibility and clinical efficacy of EUS-IBD for UMHBS after repeated ERCP-guided transpapillary interventions have failed.

## Materials and methods

This study was a single-center retrospective analysis using a prospectively accumulated database. We reviewed our database to identify all patients who had undergone initial ERCP for malignant hilar biliary stricture between December 2008 and May 2016 in our institution. The protocol to carry out this retrospective study was approved by the Institutional Review Board of Kindai University Faculty of Medicine. EUS-IBD was performed when transpapillary ERCP-guided stenting became ineffective. Relevant data were retrieved from the patients' medical records. All patients had provided written informed consent before undergoing endoscopic procedures.

UMHBS was diagnosed by imaging studies such as computed tomography (CT), magnetic resonance imaging (MRI), ERCP, or EUS. Hilar biliary stricture morphology was assessed according to the Bismuth classification (type I, tumor involves the common hepatic duct distal to the biliary confluence; type II, tumor involves the biliary confluence; type III, tumor involves the biliary confluence

plus the right or left hepatic duct; and type IV, multifocal or tumor involves the confluence and both the right and left hepatic ducts) [32].

EUS-IBD was performed in patients meeting the following criteria: (1) presence of hilar biliary stricture of Bismuth II or higher caused by inoperable malignancy; (2) presence of preceding stent placement under ERCP guidance; (3) presence of cholangitis and/or jaundice after repeated endoscopic transpapillary stenting attempts; and (4) presence of dilated intrahepatic bile duct detected by CT and/or MRI and/or EUS. Contraindications included Eastern Cooperative Oncology Group performance status of 3 or 4, bleeding tendency (prothrombin time international normalized ratio >1.5, <50,000 platelets), or the use of antiplatelet agents.

## Preparation for endoscopy

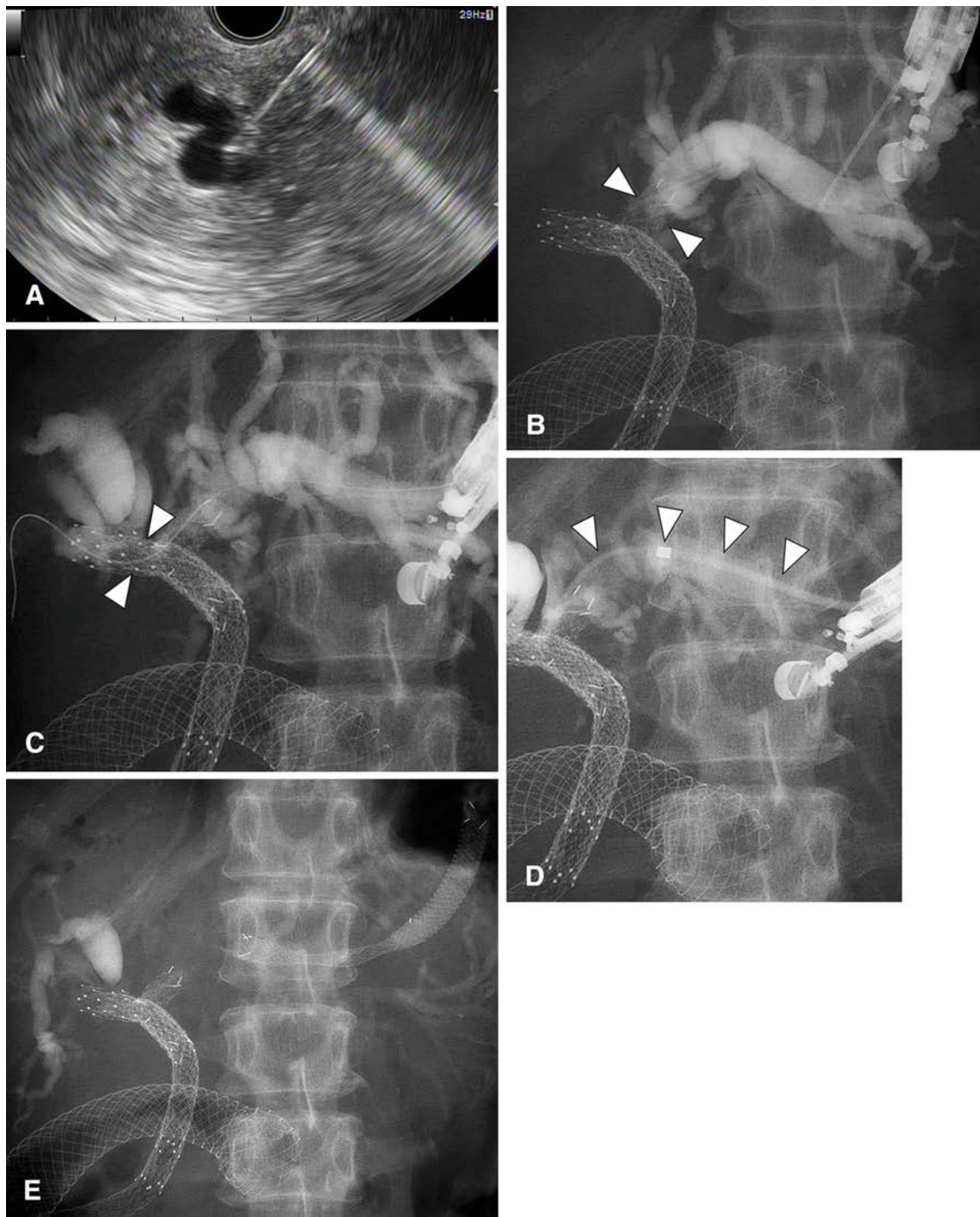
Patients were placed in the prone position with moderate sedation using intravenous midazolam and/or propofol. The level of sedation was titrated to optimize tolerance to the procedure without compromising respiration by using a bispectral index-measuring monitor. Patients were continuously monitored during the procedure with an automated noninvasive blood pressure device, electrocardiography, and pulse oximetry.

## Endoscopic procedure for EUS-IBD

EUS-IBD was performed using an oblique viewing linear array echoendoscope (GF-UCT260; Olympus Medical Systems, Tokyo, Japan). Endosonographic images were observed using an ALOKA ProSound SSD  $\alpha$ -10 (Hitachi Aloka Medical, Tokyo, Japan).

In the present study, the puncture site of the bile duct was selected according to the location of the biliary dilatation. When the left bile duct was predominantly dilated or both left and right bile ducts were dilated on imaging, the left intrahepatic bile duct (LIBD) was punctured from the stomach as this approach has been commonly selected and is well studied for EUS-IBD [25–28]. On the other hand, when the right bile duct was predominantly dilated, the right intrahepatic bile duct was regarded as the puncture target.

After the echoendoscope was introduced into the stomach, the left hepatic lobe and the LIBD were visualized. After visualization of the dilated LIBD from within the stomach, the echoendoscope was manipulated until an appropriate puncture route, free from intervening vessels, was identified. When selecting the LIBD for puncture, the dilated biliary branch duct of B3 was generally chosen as the ideal target. It was punctured with a 19-gauge needle (SonoTip ProControl; Medi-Globe, Rosenheim, Germany) under endosonographic guidance (Fig. 1A, B). Upon



**Fig. 1** Endoscopic ultrasonography-guided intrahepatic biliary drainage (EUS-IBD) after failed transpapillary re-intervention. A case of a 55-year-old female with obstructive jaundice due to gallbladder carcinoma is illustrated. Bilateral multiple biliary metal stentings under ERCP guidance and duodenal stenting had already been performed before EUS-IBD. Abdominal CT revealed dilatation of both left and right intrahepatic bile ducts. **A** The dilated left intrahepatic bile duct of B3 was punctured with a 19-gauge needle under EUS guidance. **B** After puncturing the left intrahepatic bile duct of B3, a small amount of contrast medium was injected, and cholangiography revealed left biliary metal stent occlusion due to

tumor ingrowth (*arrow heads*). **C** A 0.025-inch guidewire was inserted into the biliary system through the needle and advanced from the left intrahepatic bile duct to the right intrahepatic bile duct through the previously placed metal stents. Cholangiography revealed the right biliary metal stent was also occluded due to tumor ingrowth (*arrow heads*). **D** The fistula tract was serially dilated using a tapered biliary bougie dilation catheters (*arrows*). **E** A covered self-expandable metal stent (8 mm in diameter and 10 cm in length) was deployed between the left intrahepatic bile duct and the stomach. After this procedure, the obstructive jaundice completely resolved in a few days, even though EUS-IBD was only performed unilaterally

removal of the stylet, bile was aspirated, followed by contrast injection under fluoroscopic guidance. Thereafter, a sufficient length of 0.025-inch angle-tip guidewire (Revowave; Piolax, Kanagawa, Japan, VisiGlide; Olympus Medical Systems) or a 0.035-inch hydrophilic guidewire (Radifocus; Terumo Co. Ltd., Tokyo, Japan) in difficult cases was inserted into the biliary system through the needle and advanced in an antegrade fashion to the main LIBD (Fig. 1C), and then to the common bile duct, if possible. The fistula tract was serially dilated using either 6-Fr or 7-Fr tapered biliary dilation catheters (Soehendra Biliary Dilation Catheter; Cook, Bloomington, IN, USA) (Fig. 1D) or a 4-mm balloon dilator (REN; Kaneka Medix, Osaka, Japan, MaxPass; Olympus Medical Systems) over the guidewire. Finally, a covered self-expandable metal stent (8 mm in diameter, 8 or 10 cm in length) or a plastic stent (7 Fr in diameter, 10 or 12 cm in length, double pigtail type) was deployed between the LIBD and the stomach (Fig. 1E). When it appeared to be difficult to puncture B3 because of insufficient dilatation or intervening vessels, the biliary branch duct of B2 was punctured instead. In cases with right intrahepatic bile duct dilatation, the procedure was performed by puncturing from the duodenal bulb rather than the stomach. A covered or plastic stent was deployed between the duct and the duodenal bulb in the same way as described for the LIBD. Use of carbon dioxide for endoscopic insufflation was applied during EUS-IBD.

### Outcome definitions and measurements

Outcomes assessed were technical and clinical success rates, complication rate, stent patency, and patients' length of survival. Technical success was defined as successful stent placement between the intrahepatic bile duct and the gastrointestinal lumen, as confirmed by a combination of endoscopy and fluoroscopy. Clinical success was defined as a decrease in serum bilirubin levels to normal levels or by 50% or more within two weeks of stent placement. The incidence of the following complications was calculated: peritonitis, bile leakage, bleeding, stent migration, and stent dysfunction. Stent-related complications were classified as early if within 30 days of stent placement or late if after that point, according to the criteria of Cotton et al. [33]. The stent patency period was defined as the interval between stent placement by EUS-IBD and stent dysfunction or the patient's death. Stent dysfunction was defined as the recurrence of symptoms of biliary obstruction, including obstructive jaundice or cholangitis, with biochemical evidence of cholangitis (leukocytosis, fever, increasing serum bilirubin level) and biliary dilatation on imaging studies. Length of survival was defined as the interval

between stent placement by EUS-IBD and the patient's death.

All patients were followed until study termination (September 30, 2016) or death. When patients could not be directly followed for specific reasons such as moving to another area, their family members or personal physicians were contacted by telephone.

### Statistical analysis

The data were summarized by numbers and percentages for categorical variables or as median values and range for continuous variables. Stent patency and patient survival were evaluated using the Kaplan–Meier method. If stent dysfunction was not evident before death, the patency period was considered equal to the length of survival. Both stent dysfunction and a patient's death were treated as combined endpoints. Univariable and subsequent multivariable logistic regression analyses were performed to explore factors associated with clinical ineffectiveness of EUS-IBD. Odds ratios (ORs) and 95% confidence intervals (CIs) were calculated. The explanatory variables tested in univariable analysis were age, gender, performance status, serum bilirubin level before EUS-IBD, biliary stricture morphology (Bismuth classification), type of stent (plastic vs. metal stent), type of preceding endoscopic stent placement (unilateral vs. bilateral), and number of previously placed metal stents. Variables with a *P* value of <0.1 in this analysis were included in the multivariable logistic regression analysis. Statistical significance was set at a *P* value of <0.05. All statistical analyses were performed using SAS version 9.4 software (SAS Institute Inc., Cary, NC, USA).

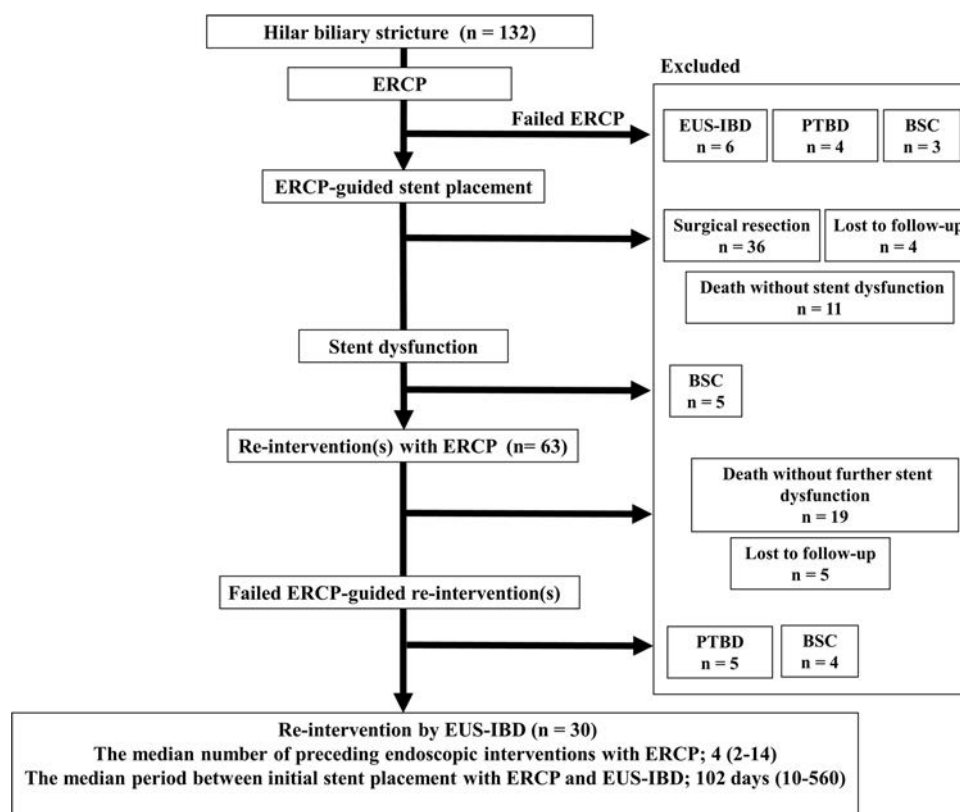
## Results

### Baseline patient characteristics

Between December 2008 and May 2016, 132 consecutive patients underwent ERCP for Bismuth II or higher hilar biliary stricture caused by malignancies. Of these patients, 30 (19 females and 11 males; median age, 66 years [range, 52–87]) underwent EUS-IBD after re-intervention under ERCP guidance became technically unsuccessful or clinically ineffective. The selection of patients is depicted in Fig. 2. Table 1 shows the patient demographics and characteristics, including type of cancer and Bismuth classification. All of the patients had died by the end of the study. Malignancy was histologically confirmed by EUS-guided fine needle aspiration (*n* = 7), surgery for the primary lesion (*n* = 4), bile cytology (*n* = 13), liver biopsy (*n* = 4), or biopsy of duodenal invasion (*n* = 2). The



**Fig. 2** Flow chart demonstrating the selection of patients for the study of endoscopic ultrasonography-guided intrahepatic biliary drainage. *EUS-IBD* endoscopic ultrasonography-guided intrahepatic biliary drainage, *PTBD*, percutaneous transhepatic biliary drainage, *BSC* best supportive care



immediate indications for EUS-IBD were after an ERCP procedure in which there was failure of duodenal scope insertion ( $n = 4$ ), inability to access the papilla after duodenal stent insertion ( $n = 5$ ), or inadequate intrahepatic biliary drainage ( $n = 21$ ) (Table 2). The preceding biliary metal stents had been placed bilaterally in 10 patients and unilaterally in 20 (14 on the right and 6 on the left). The median number of previously placed metal stents was 2 (range 1–4). After the first transpapillary stent placement required replacement, the second procedure failed in four of 30 patients, while the remaining 26 underwent multiple repeated transpapillary re-interventions under ERCP guidance. The median number of such procedures prior to EUS-IBD was 4 (ranging from 2 to 14) and the median period between initial ERCP-guided stent placement and EUS-IBD was 102 days (range 10–560 days).

### Technical and clinical success

EUS-IBD stent placement was technically successful in all but one case (Table 3). According to imaging performed before EUS-IBD, dilatation of the intrahepatic bile duct was observed on both sides in 33.3% (10/30), predominantly on the left in 60% (18/30), and predominantly on the right in 6.7% (2/30). The LIBD was punctured via the stomach in 28 cases (B3 in 23 and B2 in 5) and the right posterior intrahepatic duct via the duodenal bulb in 2. In

the technically failed case, the guidewire slipped out of the biliary system after B3 was punctured. In that case, percutaneous drainage was successfully performed instead. In the 29 patients with technical success, the median procedural time was 39.5 min (ranging from 21 to 68 min). Plastic and metal stents were deployed in 9 and 20 patients, respectively. Clinical success was attained in 22 of 29 (75.9%) or 73.3% of the entire sample of 30. The clinical success rate for Bismuth IV strictures, however, was only 50% (6/12). Among the 22 patients with clinical success, 9 (40.9%) were able to resume chemotherapy after EUS-IBD. The median interval from EUS-IBD until restarting chemotherapy was 25.5 days (ranging from 9 to 48 days).

### Complications, stent patency, and patient survival

Early procedure-related complications not requiring biliary intervention occurred in three patients (10%), all of whom had mild peritonitis managed conservatively with antibiotics (Table 3). Late complications of cholangitis and/or recurrent jaundice due to stent dysfunction occurred in seven patients (23.3%). This was managed endoscopically in three cases by insertion of a plastic stent through the previously deployed metal stent and in 2 with percutaneous drainage. The remaining two patients were in very poor condition and elected supportive care only. Among patients with clinical success, there was no procedure-related or



**Table 1** Clinical characteristics of 30 patients with unresectable malignant hilar biliary stricture who underwent EUS-guided intrahepatic biliary drainage

<i>Clinical characteristics</i>	
Age (years) (median [range])	66 (52–87)
Gender, male/female	11 (36.7)/19 (63.3)
Cause of biliary stricture	
Cholangiocarcinoma	12 (40)
Gallbladder carcinoma	6 (20)
Pancreatic carcinoma	5 (16.7)
Hepatocellular carcinoma	1 (3.3)
Liver metastasis	5 (16.7)
Lymph node metastasis	1 (3.3)
Bismuth classification	
Type II	5 (16.7)
Type III	13 (43.3)
Type IV	12 (40)
Total bilirubin (median [range]) (mg/dL)	7.3 (1.4–23.4)
Serum alkaline phosphatase (median [range]) (mg/dL)	1636.5 (407–4477)
Type of preceding endoscopic stent placement	
Unilateral/bilateral	20/10
Number of previously placed metal stents [median (range)]	2 (1–4)
Number of preceding endoscopic interventions under ERCP guidance [median (range)]	4 (2–14)

*EUS* endoscopic ultrasonography, *ERCP* endoscopic retrograde cholangiopancreatography

30-day mortality. All patients had died by September 30, 2016, the end of the study period. The median period of stent patency in the 22 patients with clinically effective EUS-IBD was 62.5 days (ranging from 31 to 210 days) (Table 3; Fig. 3). The median period of patency for the initial ERCP-placed stent in these same patients had been 91 days (ranging from 14 to 246 days). The median survival for these 22 patients after initial ERCP-guided stent placement was 206 days (ranging from 42 to 610 days). Following clinically successful EUS-IBD, median survival was 64 days (ranging from 31 to 314 days).

### Predictive factors for clinical failure

Excluding the patient with technical failure, factors predicting clinical failure were compared between the seven

**Table 2** Reasons for ERCP re-intervention failure that necessitated EUS-guided intrahepatic biliary drainage

Failure of duodenal scope insertion (%)	4 (13.3)
Failure to access the papilla after duodenal stent insertion (%)	5 (16.7)
Failure to achieve adequate intrahepatic biliary drainage (%)	21 (70)

*EUS* endoscopic ultrasonography, *ERCP* endoscopic retrograde cholangiopancreatography

**Table 3** Outcomes of patients who underwent EUS-IBD for unresectable malignant hilar biliary stricture

<i>Outcome of EUS-IBD</i>	
Technical success (%)	29 (96.7)
Puncture site of the intrahepatic bile duct	
Left B3/B2 (%)	23 (76.7)/5 (16.7)
Right posterior (%)	2 (6.7)
Procedural time (median [range])	39.5 (21–68)
Clinical success (%)	22 (75.9)
Complications (%)	10 (33.3)
Early complications	
Bile peritonitis	3 (10)
Late complications	
Stent dysfunction	7 (23.3)
Bridge to chemotherapy (%)	9 (30)
Stent patency period (days) (median [range])	62.5 (31–210)
Patient survival period (days) (median [range])	64 (31–314)

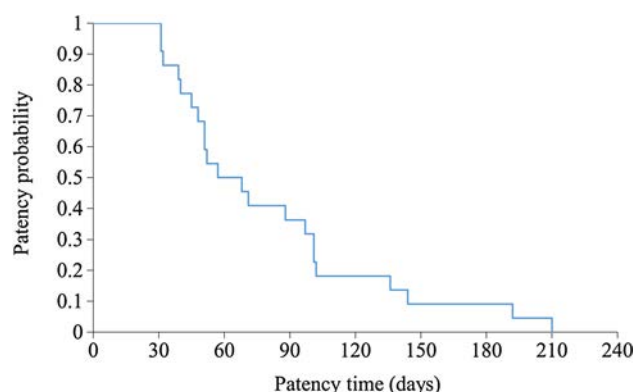
*EUS-IBD* endoscopic ultrasonography-guided intrahepatic biliary drainage

patients who had clinical failure and the 22 with clinical success. Univariable analysis showed that Bismuth classification (Bismuth IV vs. Bismuth II or III, OR 15.9; 95% CI 1.58–162.1;  $P = 0.019$ ) and the type of stent (plastic vs. metal, OR 4.53; 95% CI 0.75–27.39;  $P = 0.099$ ) were considered candidate factors associated with clinical failure of EUS-IBD (Table 4). Thus, these two variables were included in multivariable logistic regression analysis, which revealed that a Bismuth IV stricture was significantly associated with clinical ineffectiveness of EUS-IBD (OR 12.7; 95% CI 1.18–135.4;  $P = 0.035$ ) (Table 5).

### Discussion

In the present study, we retrospectively assessed the technical feasibility and clinical efficacy of EUS-IBD in patients with UMHBS after initially successful ERCP-guided transpapillary stenting ultimately failed. The EUS-IBD was technically successful in all but 1 patient and was clinically successful in three quarters of the patients, a substantial proportion of whom were able to resume chemotherapy.

EUS-IBD is usually applied for primary biliary drainage when ERCP has not succeeded at all. Recently, Ogura et al.



**Fig. 3** Kaplan–Meier graph showing stent patency in patients after clinically effective endoscopic ultrasonography-guided intrahepatic biliary drainage

[31] first described using EUS-BD as a rescue for high-grade hilar stricture after initially successful ERCP stenting eventually failed. They performed EUS-IBD in 10 of 26 patients who failed a first repeated attempt at ERCP stenting, reporting technical success in all 10 and functional success in 9. The fact that a second ERCP stenting procedure failed in 10 of 26 (38.5%) patients with stent dysfunction in their study contrasts with the present study, in which a repeat ERCP stent procedure failed in only four of 30 patients (13.3%), comparable with the previous reports [8–17]. The remaining 86.7% of patients in the present study had a number of successful, repeat ERCP procedures to manage stent dysfunction before EUS-IBD was ultimately required. Inoue et al. [34] retrospectively assessed placement of revisionary metal stent by ERCP following occlusion of bilateral metal stents in 52 patients with malignant hilar biliary obstruction. The median time to recurrent obstruction of the revisionary stents was 68 days. Although their method was quite different from ours, the median stent patency was comparable.

Although EUS-IBD was technically successful in 29 of 30 patients, 7 did not have accompanying clinical success. Further analysis indicated that Bismuth IV biliary stricture

was an independent risk factor for clinical failure. In fact, only 6 of 12 (50%) patients with Bismuth IV strictures had clinical success. A likely explanation for this is the complicated anatomy of Bismuth IV strictures involving both right and left ducts as well as the hilum. EUS-IBD provides only unilateral drainage. This technique, thus, may not be optimal for Bismuth IV strictures.

In a recent systematic analysis of 1192 patients who underwent EUS-BD, complications occurred in 23.3% of patients [35], higher than the complication rate for ERCP reported by Wang et al. [36]. In the present study, bile peritonitis occurred in 10% of the patients and was classified as mild according to the criteria of Cotton et al. [33]. There were no moderate or severe procedure-related complications. If metal stent dysfunction occurs after EUS-IBD, a repeat of the procedure was difficult, as we deployed a stent longer than 8 cm. A previous study showed that a stent  $\geq 3$  cm long placed by EUS-IBD within the gastrointestinal lumen may be suitable to prevent stent migration and achieve long-term stent patency [37]. However, such a placement can sometimes make re-intervention difficult. In the present study, only three of seven patients could be managed endoscopically after stent dysfunction. The development of a new dedicated device for EUS-BD is required and will facilitate re-intervention if needed.

The optimal drainage strategy for treating UMHS has not yet been established and controversies remain, especially regarding the use of unilateral versus bilateral stents [7]. Vienne et al. [38] analyzed the outcomes of drainage after endoscopic stenting and found that effectiveness was significantly associated with a liver volume drainage of  $>50\%$ . This was also associated with longer survival [38]. Drainage of more than half the liver volume often requires placement of multiple stents. Miura et al. [39] analyzed preoperative biliary drainage for malignant hilar biliary stricture, finding that more than one stent was initially placed in only 31 of 122 patients (25.4%), but eventually 69 (56.6%) required multiple stents. They concluded that

**Table 4** Univariable analysis of factors associated with clinical ineffectiveness after EUS-IBD in 29 patients with technically successful procedures

Independent variables	OR	95% CI	P value
Age, years	0.94	0.85–1.05	0.288
Gender, male/female	1.61	0.28–9.20	0.594
Performance status 1 or 2 versus 0	2.25	0.22–22.79	0.492
Serum bilirubin before EUS-IBD $>10$ mg/dL	2.33	0.41–13.17	0.337
Bismuth IV versus Bismuth II or III	15.9	1.58–162.12	0.019
Type of stent, plastic versus metal stent	4.53	0.75–27.39	0.099
Type of preceding stent placement unilateral versus bilateral	3.43	0.35–33.83	0.291
Number of previously placed metal stents	0.70	0.21–2.30	0.557

EUS endoscopic ultrasonography-guided intrahepatic biliary drainage, OR odds ratio, CI confidence interval

**Table 5** Multivariable analysis of factors associated with clinical ineffectiveness after EUS-guided intrahepatic biliary drainage in 29 patients with technically successful procedures

Independent variables	OR	95% CI	P value
Bismuth IV versus Bismuth II or III	12.7	1.18–135.4	0.035
Type of stent, plastic versus metal stent	2.48	0.39–19.23	0.386

EUS endoscopic ultrasonography, OR odds ratio, CI confidence interval

patients with Bismuth II or higher strictures were likely to require multiple stents prior to surgery. These studies suggest that effective drainage of a hilar biliary stricture can frequently be achieved with bilateral or multiple stents. The present study showed the technical and clinical efficacy of EUS-IBD for UMHS for additional unilateral drainage of the liver volume after earlier transpapillary procedures had failed. It would be ideal if dedicated EUS-IBD devices could be developed to achieve safe and effective bilateral drainage of the liver, for example, simultaneously deploying a transpapillary stent in the right intrahepatic bile duct and using EUS-IBD for the LIBD. This might provide more extensive drainage of the liver volume and perhaps longer stent patency and patient survival.

This study has three inherent limitations. First, it was a retrospective study performed in a single institution with a relatively small number of patients. A multicenter study with a larger numbers of patients is needed to further evaluate the efficacy of EUS-IBD for failed repeat endoscopic interventions in patients with UMHS. Second, the study was not comparative. Further prospective randomized controlled studies to compare EUS-IBD with alternative methods such as percutaneous drainage are needed. Third, 68.2% of our patients died of their underlying advanced malignancy without any stent dysfunction. Therefore, stent patency could not be determined precisely. Patency can only be measured in patients with a longer survival.

In conclusion, EUS-IBD appears to be a feasible, safe, and effective rescue method in patients with UMHS, especially those with Bismuth II or III strictures, when repeated ERCP-guided transpapillary interventions become ineffective. Further prospective randomized studies with a larger cohort of patients with UMHS will be required to demonstrate the efficacy and safety of this emerging technique.

**Acknowledgements** This study was supported by grants from the Japan Society for Promotion of Science.

#### Compliance with ethical standards

**Disclosures** Dr. Kosuke Minaga, Dr. Mamoru Takenaka, Dr. Masayuki Kitano, Dr. Yasutaka Chiba, Dr. Hajime Imai, Dr. Kentaro

Yamao, Dr. Ken Kamata, Dr. Takeshi Miyata, Dr. Shunsuke Omoto, Dr. Toshiharu Sakurai, Dr. Tomohiro Watanabe, Dr. Naoshi Nishida, and Dr. Masatoshi Kudo have no conflicts of interest or financial ties to disclose.

#### References



1. De Palma GD, Pezzullo A, Rega M, Persico M, Patrone F, Mastantuono L, Persico G (2003) Unilateral placement of metallic stents for malignant hilar obstruction: a prospective study. *Gastrointest Endosc* 58:50–53
2. Wagner HJ, Knyrim K, Vakil N, Klose KJ (1993) Plastic endoprotheses versus metal stents in the palliative treatment of malignant hilar biliary obstruction. A prospective and randomized trial. *Endoscopy* 25:213–218
3. Dumas R, Demuth N, Buckley M, Peten EP, Manos T, Demarquay JF, Hastier P, Caroli-Bosc FX, Rampal P, Delmont JP (2000) Endoscopic bilateral metal stent placement for malignant hilar stenoses: identification of optimal technique. *Gastrointest Endosc* 51:334–338
4. Cheng JL, Bruno MJ, Bergman JJ, Rauws EA, Tytgat GN, Huijbregtse K (2002) Endoscopic palliation of patients with biliary obstruction caused by nonresectable hilar cholangiocarcinoma: efficacy of self-expandable metallic Wallstents. *Gastrointest Endosc* 56:33–39
5. Chen JH, Sun CK, Liao CS, Chua CS (2006) Self-expandable metallic stents for malignant biliary obstruction: efficacy on proximal and distal tumors. *World J Gastroenterol* 12:119–122
6. Mukai T, Yasuda I, Nakashima M, Doi S, Iwashita T, Iwata K, Kato T, Tomita E, Moriwaki H (2013) Metallic stents are more efficacious than plastic stents in unresectable malignant hilar biliary strictures: a randomized controlled trial. *J Hepatobiliary Pancreat Sci* 20:214–222
7. Kato H, Tsutsumi K, Kawamoto H, Okada H (2015) Current status of endoscopic biliary drainage for unresectable malignant hilar biliary strictures. *World J Gastrointest Endosc* 7:1032–1038
8. Liberato MJ, Canena JM (2012) Endoscopic stenting for hilar cholangiocarcinoma: efficacy of unilateral and bilateral placement of plastic and metal stents in a retrospective review of 480 patients. *BMC Gastroenterol* 12:103
9. Kogure H, Isayama H, Nakai Y, Tsujino T, Ito Y, Yamamoto K, Mizuno S, Yagioka H, Kawakubo K, Sasaki T, Hirano K, Sasahira N, Tada M, Omata M, Koike K (2011) Newly designed large cell Niti-S stent for malignant hilar biliary obstruction: a pilot study. *Surg Endosc* 25:463–467
10. Chahal P, Baron TH (2010) Expandable metal stents for endoscopic bilateral stent-within-stent placement for malignant hilar biliary obstruction. *Gastrointest Endosc* 71:195–199
11. Kim JY, Kang DH, Kim HW, Choi CW, Kim ID, Hwang JH, Kim DU, Eum JS, Bae YM (2009) Usefulness of slimmer and open-cell-design stents for endoscopic bilateral stenting and endoscopic revision in patients with hilar cholangiocarcinoma (with video). *Gastrointest Endosc* 70:1109–1115

12. Lee TH, Moon JH, Kim JH, Park DH, Lee SS, Choi HJ, Cho YD, Park SH, Kim SJ (2013) Primary and revision efficacy of cross-wired metallic stents for endoscopic bilateral stent-in-stent placement in malignant hilar biliary strictures. *Endoscopy* 45:106–113
13. Naitoh I, Hayashi K, Nakazawa T, Okumura F, Miyabe K, Shimizu S, Yoshida M, Yamashita H, Ohara H, Joh T (2012) Side-by-side versus stent-in-stent deployment in bilateral endoscopic metal stenting for malignant hilar biliary obstruction. *Dig Dis Sci* 57:3279–3285
14. Lee TH, Park DH, Lee SS, Choi HJ, Lee JK, Kim TH, Kim JH, Jeong S, Park SH, Moon JH (2013) Technical feasibility and revision efficacy of the sequential deployment of endoscopic bilateral side-by-side metal stents for malignant hilar biliary strictures: a multicenter prospective study. *Dig Dis Sci* 58:547–555
15. Law R, Baron TH (2013) Bilateral metal stents for hilar biliary obstruction using a 6Fr delivery system: outcomes following bilateral and side-by-side stent deployment. *Dig Dis Sci* 58:2667–2672
16. Ishiwatari H, Hayashi T, Ono M, Sato T, Kato J (2013) Newly designed plastic stent for endoscopic placement above the sphincter of Oddi in patients with malignant hilar biliary obstruction. *Dig Endosc* 25(Suppl 2):94–99
17. Kaneko T, Sugimori K, Shimizu Y, Miwa H, Kameta E, Koh R, Numata K, Tanaka K, Maeda S (2014) Efficacy of plastic stent placement inside bile ducts for the treatment of unresectable malignant hilar obstruction (with videos). *J Hepatobiliary Pancreat Sci* 21:349–355
18. Ridditiid W, Rerknimitr R (2012) Management of an occluded biliary metallic stent. *World J Gastrointest Endosc* 4:157–161
19. Jiao D, Huang K, Zhu M, Wu G, Ren J, Wang Y, Han X (2016). Placement of a newly designed Y-configured bilateral self-expanding metallic stent for hilar biliary obstruction: a pilot study. *Dig Dis Sci* doi: [10.1007/s10620-016-4284-1](https://doi.org/10.1007/s10620-016-4284-1) [Epub ahead of print]
20. Yee AC, Ho CS (1987) Complications of percutaneous biliary drainage: benign versus malignant diseases. *AJR Am J Roentgenol* 148:1207–1209
21. Oh HC, Lee SK, Lee TY, Kwon S, Lee SS, Seo DW, Kim MH (2007) Analysis of percutaneous transhepatic cholangioscopy-related complications and the risk factors for those complications. *Endoscopy* 39:731–736
22. Garcarek J, Kurcz J, Guziński M, Janczak D, Sasiadek M (2012) Ten years single center experience in percutaneous transhepatic decompression of biliary tree in patients with malignant obstructive jaundice. *Adv Clin Exp Med* 21:621–632
23. Giovannini M, Moutardier V, Pesenti C, Bories E, Lelong B, Delpero JR (2001) Endoscopic ultrasound-guided bilioduodenal anastomosis: a new technique for biliary drainage. *Endoscopy* 33:898–900
24. Burmester E, Niehaus J, Leineweber T, Huetteroth T (2003) EUS-cholangio-drainage of the bile duct: report of 4 cases. *Gastrointest Endosc* 57:246–251
25. Itoi T, Sofuni A, Itokawa F, Tsuchiya T, Kurihara T, Ishii K, Tsuji S, Ikeuchi N, Umeda J, Moriyasu F, Tsuchida A (2010) Endoscopic ultrasonography-guided biliary drainage. *J Hepatobiliary Pancreat Sci* 17:611–616
26. Artifon EL, Marson FP, Gaidhane M, Kahaleh M, Otoch JP (2015) Hepaticogastrostomy or choledochoduodenostomy for distal malignant biliary obstruction after failed ERCP: Is there any difference? *Gastrointest Endosc* 81:950–959
27. Poincloux L, Rouquette O, Buc E, Privat J, Pezet D, Dapigny M, Bommelaer G, Abergel A (2015) Endoscopic ultrasound-guided biliary drainage after failed ERCP: cumulative experience of 101 procedures at a single center. *Endoscopy* 47:794–801
28. Park DH (2015) Endoscopic ultrasound-guided biliary drainage of hilar biliary obstruction. *J Hepatobiliary Pancreat Sci* 22:664–668
29. Ogura T, Masuda D, Imoto A, Umegaki E, Higuchi K (2014) EUS-guided hepaticogastrostomy for hepatic hilar obstruction. *Endoscopy* 46(Suppl 1):E32–E33
30. Prachayakul V, Aswakul P (2015) Endoscopic ultrasound-guided biliary drainage: bilateral systems drainage via left duct approach. *World J Gastroenterol* 21:10045–10048
31. Ogura T, Onda S, Takagi W, Sano T, Okuda A, Masuda D, Yamamoto K, Miyano A, Kitano M, Takeuchi T, Fukunishi S, Higuchi K (2016). Clinical utility of endoscopic ultrasound-guided biliary drainage as a rescue of re-intervention procedure for high-grade hilar stricture. *J Gastroenterol Hepatol* doi: [10.1111/jgh.13437](https://doi.org/10.1111/jgh.13437). [Epub ahead of print]
32. Bismuth H, Castaing D, Traynor O (1988) Resection or palliation: priority of surgery in the treatment of hilar cancer. *World J Surg* 12:39–47
33. Cotton PB, Eisen GM, Aabakken L, Baron TH, Hutter MM, Jacobson BC, Mergener K, Nemcek A Jr, Petersen BT, Petrini JL, Pike IM, Rabeneck L, Romagnuolo J, Vargo JJ (2010) A lexicon for endoscopic adverse events: report of an ASGE workshop. *Gastrointest Endosc* 71:446–454
34. Inoue T, Naitoh I, Okumura F, Ozeki T, Anbe K, Iwasaki H, Nishie H, Mizushima T, Sano H, Nakazawa T, Yoneda M, Joh T (2016) Reintervention for stent occlusion after bilateral self-expanding metallic stent placement for malignant hilar biliary obstruction. *Dig Endosc* 28:731–737
35. Wang K, Zhu J, Xing L, Wang Y, Jin Z, Li Z (2016) Assessment of efficacy and safety of EUS-guided biliary drainage: a systematic review. *Gastrointest Endosc* 83:1218–1227
36. Wang P, Li ZS, Liu F, Ren X, Lu NH, Fan ZN, Huang Q, Zhang X, He LP, Sun WS, Zhao Q, Shi RH, Tian ZB, Li YQ, Li W, Zhi FC (2009) Risk factors for ERCP-related complications: a prospective multicenter study. *Am J Gastroenterol* 104:31–40
37. Ogura T, Yamamoto K, Sano T, Onda S, Imoto A, Masuda D, Takagi W, Fukunishi S, Higuchi K (2015) Stent length is impact factor associated with stent patency in endoscopic ultrasound-guided hepaticogastrostomy. *J Gastroenterol Hepatol* 30:1748–1752
38. Vienne A, Hobeika E, Gouya H, Lapidus N, Fritsch J, Choury AD, Chrysostalis A, Gaudric M, Pelletier G, Buffet C, Chausade S, Prat F (2010) Prediction of drainage effectiveness during endoscopic stenting of malignant hilar strictures: the role of liver volume assessment. *Gastrointest Endosc* 72:728–735
39. Miura S, Kanno A, Masamune A, Hamada S, Takikawa T, Nakano E, Yoshida N, Hongo S, Kikuta K, Kume K, Hirota M, Yoshida H, Katayose Y, Uuno M, Shimosegawa T (2015) Bismuth classification is associated with the requirement for multiple biliary drainage in preoperative patients with malignant perihilar biliary stricture. *Surg Endosc* 29:1862–1870



## GASTROENTEROLOGY

# Contrast-enhanced harmonic endoscopic ultrasonography for differential diagnosis of submucosal tumors of the upper gastrointestinal tract

Ken Kamata,\* Mamoru Takenaka,\*  Masayuki Kitano,\* Shunsuke Omoto,\* Takeshi Miyata,\* Kosuke Minaga,\* Kentaro Yamao,\* Hajime Imai,\* Toshiharu Sakurai,\* Tomohiro Watanabe,\* Naoshi Nishida,\* Takaaki Chikugo,<sup>†</sup> Yasutaka Chiba,<sup>‡</sup> Haruhiko Imamoto,<sup>§</sup> Takushi Yasuda,<sup>§</sup> Andrea Lisotti,<sup>¶</sup>  Pietro Fusaroli,<sup>¶</sup> and Masatoshi Kudo\*

**Q4** Departments of \*Gastroenterology and Hepatology, <sup>†</sup>Pathology, <sup>§</sup>Surgery, Kindai University Faculty of Medicine, and <sup>‡</sup>Clinical Research Center, Kindai University Hospital, Osaka-sayama, Japan; and <sup>¶</sup>Gastroenterology Unit, Hospital of Imola, University of Bologna, Bologna, Italy

## Key words

endoscopic ultrasound, gastroenterology, stomach.

Accepted for publication 19 February 2017.

## Correspondence

Dr Mamoru Takenaka, Department of Gastroenterology and Hepatology, Kindai University Faculty of Medicine, 377-2 Ohnohigashi, Osaka-sayama 589-8511, Japan. Email: mamoxyo45@gmail.com

**Declaration of conflict of interest:** There are no potential competing interests concerning this study.

**Author contribution:** Ken Kamata was responsible for writing the manuscript, study conception and design, and performing EUS. Mamoru Takenaka did the writing of the manuscript, drafting conception, and design. Masayuki Kitano was responsible for writing the manuscript, drafting conception and design, and performing EUS. Masatoshi Kudo contributed in writing the manuscript, drafting conception and design, and reading EUS. Shunsuke Omoto, Takeshi Miyata, Kosuke Minaga, and Kentaro Yamao performed data collection. Hajime Imai was responsible for data collection and reading EUS. Toshiharu Sakurai, Tomohiro Watanabe, and Naoshi Nishida contributed to the writing and revision of the manuscript. Takaaki Chikugo did the pathological evaluation. Yasutaka Chiba performed statistical analysis. Haruhiko Imamoto and Takushi Yasuda performed the surgical resection. Andrea Lisotti and Pietro Fusaroli did the writing of the manuscript, drafting conception, and design.

**Financial support:** The present study was supported by grants from the Japan Society for the Promotion of Science.

**Guarantor of the article:** Mamoru Takenaka

## Abstract

**Background and Aim:** The study aims to evaluate contrast-enhanced harmonic endoscopic ultrasonography (CH-EUS) for the differential diagnosis of submucosal tumors (SMT) of the upper gastrointestinal tract.

**Methods:** Between June 2008 and May 2015, 157 consecutive patients with submucosal lesions of the upper gastrointestinal tract were evaluated by CH-EUS. This was a single-center retrospective analysis of prospectively collected data in a registry. The data from 73 patients who later underwent surgical resection were analyzed in this study. Surgical specimens served as the final diagnoses. The two CH-EUS variables of blood flow (hyper-enhancement vs hypo-enhancement) and homogeneity of enhancement pattern were evaluated.

**Results:** The final diagnoses were 58 gastrointestinal stromal tumors (GISTs) and 15 benign SMTs (two lipomas, five leiomyomas, five schwannomas, two glomus tumors, and one ectopic pancreas). On CH-EUS, 49 of 58 (84.5%) GISTs presented with hyper-enhancement, whereas 4 of 15 (26.7%) benign SMTs showed hyper-enhancement; 21 of 58 (36.2%) GISTs showed inhomogeneous contrast enhancement, while only 2 of 15 (13.3%) benign SMTs demonstrated inhomogeneous contrast enhancement. If hyper-enhancement was considered to indicate GISTs, the sensitivity, specificity, and accuracy were 84.5%, 73.3%, and 82.2%, respectively. If inhomogeneous enhancement was considered to indicate GISTs, the sensitivity, specificity, and accuracy were 36.2%, 86.7%, and 46.6%, respectively. In lesions of less than 2 cm, hyper-enhancement was a more sensitive indicator of GISTs than inhomogeneous enhancement.

**Conclusions:** Hyper-enhancement and inhomogeneous enhancement were found to be a characteristic of GISTs. CH-EUS was useful for discrimination of benign SMTs from GISTs.



Q5

## Introduction

Endoscopic ultrasound (EUS) is a diagnostic method with high sensitivity for the detection of submucosal tumors (SMTs); however, it is usually difficult to achieve a differential diagnosis between benign and malignant SMTs with conventional EUS.<sup>1,2</sup> EUS fine-needle aspiration (EUS-FNA) allows provision of a tissue specimen from an SMT, which then permits histological and immunohistochemical characterization, although the technique may lack sufficient sensitivity because of insufficient tissue sampling.<sup>3–6</sup> Power Doppler EUS is useful for the assessment of intratumoral vessels in malignant gastrointestinal stromal tumor (GIST).<sup>7</sup> However, it has several limitations, such as blooming of large vessels, motion artifacts, and less sensitivity to the slow flow within intratumoral vessels.

Recently, contrast-enhanced harmonic endoscopic ultrasonography (CH-EUS) was developed specifically for contrast-enhanced harmonic imaging. CH-EUS enables the observation of microcirculation and parenchymal perfusion in tumors, without the presence of Doppler-related artifacts. Sakamoto *et al.* reported on the utility of CH-EUS for predicting the malignancy risk of GISTs.<sup>8</sup> With regard to the differential diagnosis of SMTs of the upper gastrointestinal tract, the diagnostic yield and accuracy of CH-EUS remains largely unknown, although a recent systematic review reported that use of ultrasound contrast agents in EUS appeared useful for differential diagnosis and risk stratification of SMTs.<sup>9</sup> The aim of this study was to evaluate the accuracy of CH-EUS for the differential diagnosis of malignant (GISTs) and benign SMTs.

## Methods

**Study design.** This was a single-center retrospective analysis of prospectively collected data in a registry. The final diagnoses were retrospectively made according to histological specimens obtained from surgical resection or the results of EUS-FNA and clinical course.

**Patients.** A total of 157 consecutive patients with SMTs of the upper gastrointestinal tract underwent fundamental B-mode EUS (FB-EUS) followed by CH-EUS at the Kindai University School of Medicine between June 2008 and May 2015.

Seventy-three patients who underwent surgical resection because of features suggestive of malignancy (i.e., a size of 5 cm or more, enlargement in size during follow-up, heterogeneous enhancement on computed tomography, presence of symptoms, or diagnosis as GIST by EUS-FNA) were analyzed in this study. Patients were not chosen for surgical resection based on CH-EUS findings. This study was performed with the approval of the ethics committee of the Kinki University School of Medicine.

**FB-EUS and CH-EUS.** The echoendoscope used was developed specifically for CH-EUS (GF-UCT260, Olympus Medical Systems Co. Ltd., Tokyo, Japan), and EUS images were analyzed using an ALOKA ProSound SSD  $\alpha$ -10 system (ALOKA Co. Ltd., Tokyo, Japan). After evaluation of the lesions using FB-EUS, the imaging mode was changed to the extended pure harmonic detection mode, which synthesized the filtered second-harmonic components with signals obtained from the phase shift for contrast-

enhanced harmonic imaging. The transmitting frequency and mechanical index were 4.7 MHz and 0.3, respectively. Sonazoid (Daiichi-Sankyo, Tokyo, Japan), which consists of perfluorobutane microbubbles surrounded by a lipid membrane, was used as an ultrasound contrast agent for CH-EUS. Immediately before performing CH-EUS, the contrast agent was reconstituted with 2 mL of sterile water for injection, and a dose of 15  $\mu$ L/kg bodyweight was prepared in a 2-mL syringe. A bolus injection of the ultrasound contrast agent was administered at a speed of 1 mL/s into the antecubital vein. This was followed by a 10-mL saline solution flush to ensure that the entire contrast agent was administered into the circulation.<sup>10</sup>

The CH-EUS lesion examinations lasted for 60 s from injection of the contrast agent, and video sequences of 60 s were stored. Following the methods of previous reports,<sup>8,11</sup> the enhancement patterns were evaluated in terms of homogeneity and the amount of blood flow in the blood-pool phase of the perfusion image (40–60 s after the infusion of Sonazoid). The lesions were divided into different size classes (< 2, 2–5, and > 5 cm), and the enhancement patterns were assessed according to these size classes. The enhancement patterns on CH-EUS were classified as either homogeneous or inhomogeneous enhancement, according to a previous report.<sup>8</sup> Within-lesion blood flow on CH-EUS was quantified according to three patterns: hypo-enhancement, iso-enhancement, or hyper-enhancement; this was performed by comparisons with the surrounding normal tissue, based on the methods in a previous report.<sup>11</sup>

The quantity of blood flow (hypo-enhancement-, iso-enhancement, or hyper-enhancement) and the enhancement pattern (homogeneous enhancement or inhomogeneous enhancement) were independently reviewed by two reviewers (M Kudo and H Imai), who have each performed over 1000 CH-EUS procedures. For the reviews analyzed in this study, which were performed on stored data, the readers were blinded to the final diagnoses. When the independent conclusions of the two reviewers were discordant, third expert reviewer (M Kitano) evaluated the saved images.

**EUS-FNA.** EUS-FNA was performed using 19-gauge, 22-gauge, or 25-gauge needle. A maximum of five passes were made to obtain sufficient material. When sufficient material was obtained, immunohistochemical and hematoxylin–eosin staining were performed.

**Definition.** The reference standard was the pathological finding obtained after surgical resection. GISTs were defined as subepithelial tumors composed of spindle cells that stained positive for c-kit and CD34.

**Statistical analysis.** The categorical variables from the two groups (GIST and benign SMT groups) were compared using a chi-squared test. A chi-squared test was also used for evaluating the results of the dimensional stratification (different lesion size, < 2, 2–5, and > 5 cm). A *P* value of < 0.05 was considered to indicate statistical significance. For testing of interobserver agreement in the CH-EUS findings,  $\kappa$  coefficients of > 0.8, > 0.6, and > 0.4 were considered to indicate excellent, good, and

moderate agreement, respectively. All statistical analyses were performed using SAS software version 9.1 (SAS Institute, Cary, NC, USA).

## Results

The demographic characteristics and the final pathological diagnosis of the 73 patients who underwent surgical resection are shown in Table 1. The final diagnoses were 58 GISTs and 15 benign SMTs, which included lipoma ( $n = 2$ ), leiomyoma ( $n = 5$ ), schwannoma ( $n = 5$ ), ectopic pancreas ( $n = 1$ ), and glomus tumor ( $n = 2$ ). GISTs were located in the gastric fornix ( $n = 12$ ), gastric body ( $n = 31$ ), gastric antrum ( $n = 10$ ), and duodenum ( $n = 5$ ), respectively.

Among the 84 patients who did not undergo surgical resection, 79 underwent EUS-FNA. In five patients, EUS-FNA was not performed because the lesion size was too small. Out of the 79 patients who underwent EUS-FNA, 51 patients were diagnosed with benign SMT and in 28 patients, the results of EUS-FNA were inadequate. The 28 patients who were not diagnosed with GIST by EUS-FNA and the five patients who did not undergo EUS-FNA were followed up for 1 year, but their tumors did not show any differences in size at the end of this period. Eighty-four patients who

did not undergo surgical resection were not analyzed because only follow-up diagnosis cannot completely rule out the existence of GISTs, and the inclusion of non-resected cases in the analysis could have led to large bias.

Table 2 lists the CH-EUS findings of the lesions divided according to lesion size ( $< 2$ , 2–5, and  $> 5$  cm). A total of 49 GISTs demonstrated hyper-enhancement (Fig. 1) and nine demonstrated hypo-enhancement, whereas four benign SMTs demonstrated hyper-enhancement and 11 demonstrated hypo-enhancement (Fig. 2) ( $P < 0.001$  for a quantitative difference in contrast enhancement between GISTs and benign SMTs). No cases showed iso-enhancement. Analysis of enhancement patterns revealed that 37 GISTs showed homogeneous enhancement and 21 showed inhomogeneous enhancement (Fig. 3), whereas 13 benign SMTs showed homogeneous enhancement and two showed inhomogeneous enhancement ( $P = 0.165$  for a difference in enhancement patterns between GISTs and benign SMTs). As a result, hyper-enhancement and inhomogeneous enhancement were considered to be highly specific findings for GISTs. If hyper-enhancement was considered to indicate GISTs, the sensitivity, specificity, and accuracy were 84.5%, 78.9%, and 88.3%, respectively (Table 3). If inhomogeneous enhancement was considered to indicate GISTs, the sensitivity, specificity, and accuracy were 36.2%, 86.7%, and 46.6%, respectively (Table 4). In lesions of less than 2 cm, hyper-enhancement was a more sensitive finding for the indication of GISTs than inhomogeneous enhancement (85.0% vs 10.0%; Tables 3, 4). Table 5 lists the results of the combination of both CH-EUS variables (homogeneous/inhomogeneous enhancement and hyper-enhancement/hypo-enhancement) in both lesion groups. Only three GIST cases showed both homogeneous enhancement and hypo-enhancement.

Testing of interobserver agreement between the two readers in the determination of the quantity of blood flow (hyper-enhancement or hypo-enhancement) and enhancement pattern (homogeneous and inhomogeneous enhancement) revealed a high level of reproducibility ( $\kappa$  coefficient 0.723,  $P < 0.01$  and  $\kappa$  coefficient 0.746,  $P < 0.01$ , respectively).

Fine-needle aspirations were performed in all 73 patients who underwent surgical treatment. The percentage of samples judged adequate for histological evaluation was 94.5% for GIST and 53.3% for benign SMT. If SMT lesions showing hyper-enhancement on CH-EUS and/or indicating as GIST by EUS-FNA were defined as GIST, the sensitivity of combining CH-EUS with EUS-FNA results for diagnosing GIST was 100%.

**Table 1** Patient characteristics and final diagnosis

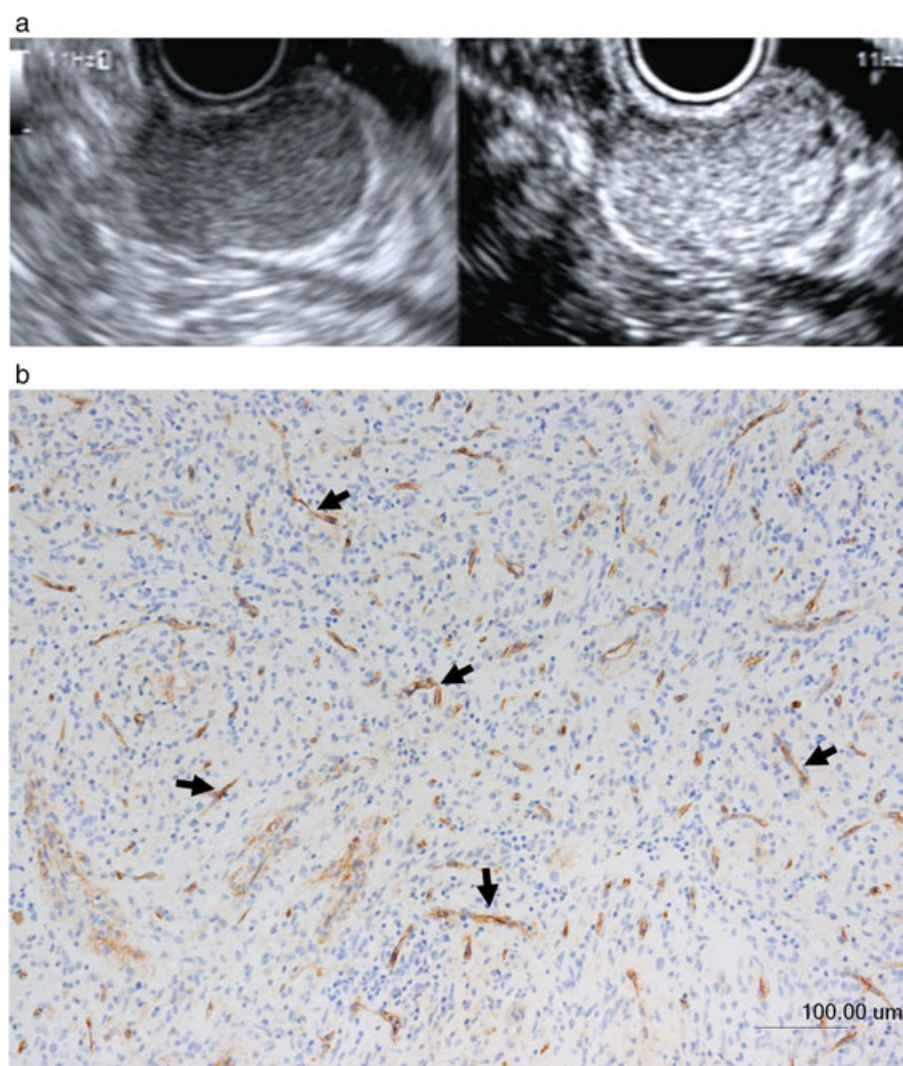
Sex (male/female)	35/38
Mean age, years (range)	62 (24–90)
Median size of the lesion, mm (range)	28 (10–90)
Location (n)	
Esophagus	4
Gastric- Fornix	15
Gastric- Body	36
Gastric- Antrum	13
Duodenum	5
Histology (n)	
GIST	58
Benign SMT	15
Ectopic pancreas	1
Glomus tumor	2
Lipoma	2
Leiomyoma	5
Schwannoma	5

GIST, gastrointestinal stromal tumor; SMT, submucosal tumor.

**Table 2** CH-EUS findings of the lesions divided into different size groups ( $< 2$ ,  $\geq 2$ ,  $< 5$ , and  $> 5$  cm)

		GIST	Benign SMT	P value
Total	Hypo/Hyper	16% ( $n = 9$ )/84% ( $n = 49$ )	73% ( $n = 11$ )/27% ( $n = 4$ )	$< 0.001$
( $n = 73$ )	Homo/Inhomo	64% ( $n = 37$ )/36% ( $n = 21$ )	87% ( $n = 13$ )/13% ( $n = 2$ )	0.165
$< 2$ cm	Hypo/Hyper	15% ( $n = 3$ )/85% ( $n = 17$ )	—	—
( $n = 20$ )	Homo/Inhomo	90% ( $n = 18$ )/10% ( $n = 2$ )	—	—
2–5 cm	Hypo/Hyper	18% ( $n = 6$ )/82% ( $n = 27$ )	77% ( $n = 10$ )/23% ( $n = 3$ )	$< 0.001$
( $n = 46$ )	Homo/Inhomo	58% ( $n = 19$ )/42% ( $n = 14$ )	92% ( $n = 12$ )/8% ( $n = 1$ )	0.056
$> 5$ cm	Hypo/Hyper	0% ( $n = 0$ )/100% ( $n = 5$ )	50% ( $n = 1$ )/50% ( $n = 1$ )	0.608
( $n = 7$ )	Homo/Inhomo	0% ( $n = 0$ )/100% ( $n = 5$ )	50% ( $n = 1$ )/50% ( $n = 1$ )	0.608

CH-EUS, contrast-enhanced harmonic endoscopic ultrasonography; GIST, gastrointestinal stromal tumor; Hypo/Hyper, hypo-enhanced/hyper-enhanced; Homo/Inhomo, homogeneous/inhomogeneous contrast enhancement pattern; SMT, submucosal tumor.



**Figure 1** (a) Contrast-enhanced harmonic endoscopic ultrasonography image of a gastrointestinal stromal tumor demonstrating hyper-enhancement and a homogeneous enhancement pattern. The gastrointestinal stromal tumor is 17 mm in size. The left side is a B-mode endoscopic ultrasound image and the right side, a contrast-enhanced harmonic endoscopic ultrasonography image. (b) Histopathological image of CD 34 stain obtained by surgical resection. Vessels in the tumor are densely depicted (arrows). [Color figure can be viewed at [wileyonlinelibrary.com](http://wileyonlinelibrary.com)]

## Discussion

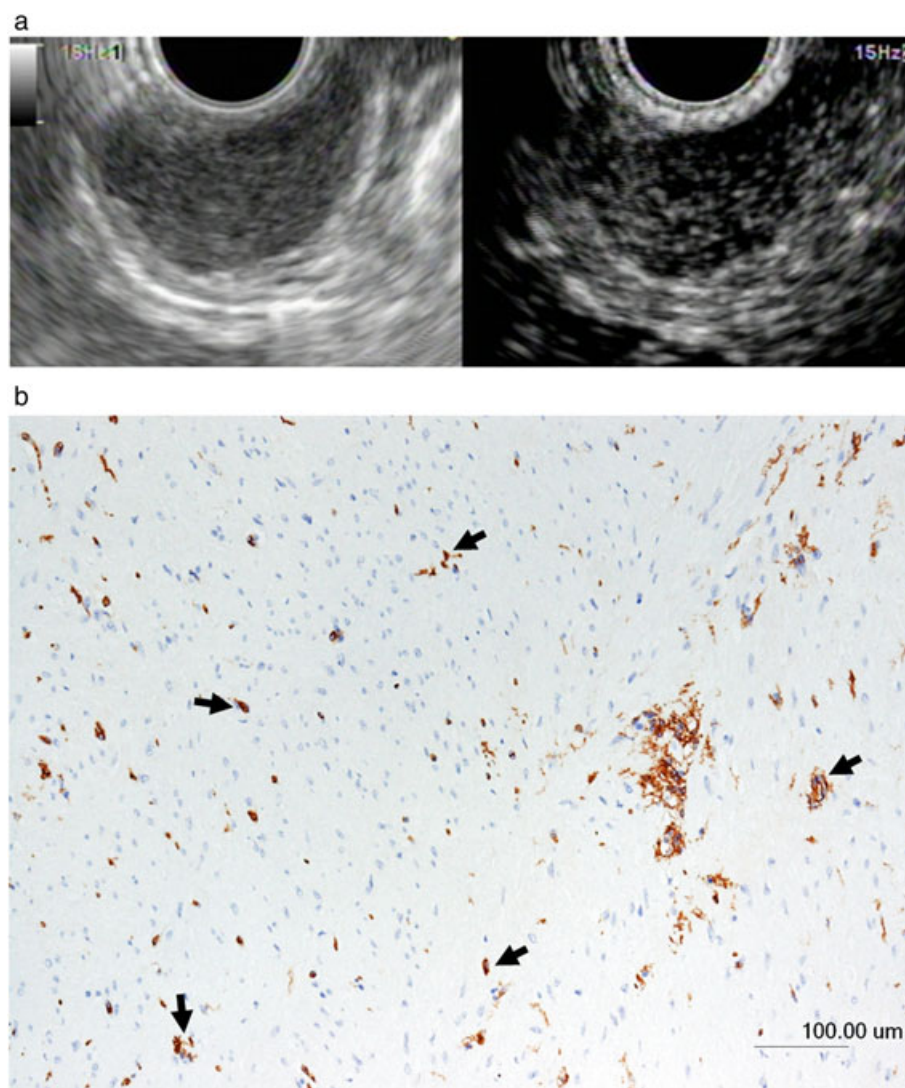
In this study, we assessed CH-EUS for differential diagnosis of SMTs of the upper gastrointestinal tract; these SMTs had a firm diagnosis following surgical resection. Firstly, CH-EUS perfusion images were used to classify the lesions in terms of the amount of blood flow, as hypo-enhancement or hyper-enhancement, and in terms of the pattern of enhancement, as homogeneous or inhomogeneous enhancement. Hyper-enhancement was shown in almost all cases of GIST, with a tendency for homogeneous enhancement to be exhibited in small GIST lesions and inhomogeneous enhancement in larger GIST lesions. By contrast, most benign SMTs showed both hypo-enhancement and a homogeneous enhancement pattern.

Kannengiesser *et al.* reported CH-EUS findings on eight GISTs and nine benign SMTs, with all eight GISTs presenting with hyper-enhancement, findings that were similar to those presented

in this study.<sup>11</sup> We are not aware of any reports describing homogeneous enhancement in SMTs on CH-EUS, although Sakamoto *et al.* reported on the utility of CH-EUS for determination of the degree of malignancy of GISTs.<sup>8</sup> SMTs are frequently found in Japan, as cancer-screening tests are routinely performed.<sup>12</sup> Therefore, in this study, we evaluated a larger number of patients than in previous reports and included an analysis of contrast enhancement pattern and quantity according to different lesion size categories. We demonstrated that an inhomogeneous enhancement pattern had a high specificity for diagnosis of small lesions, although the sensitivity was poor, and that hyper-enhancement was a better predictive finding for lesions of less than 2 cm, as it was for lesions of all sizes.

The diagnostic yield of EUS-FNA for SMTs is insufficient, with reported values ranging from 43.3% to 77.8%.<sup>3,4</sup> However, the diagnostic yield of EUS-FNA for GISTs was 81.6%, which was higher than that for SMTs other than GISTs (62.7%). The Japanese



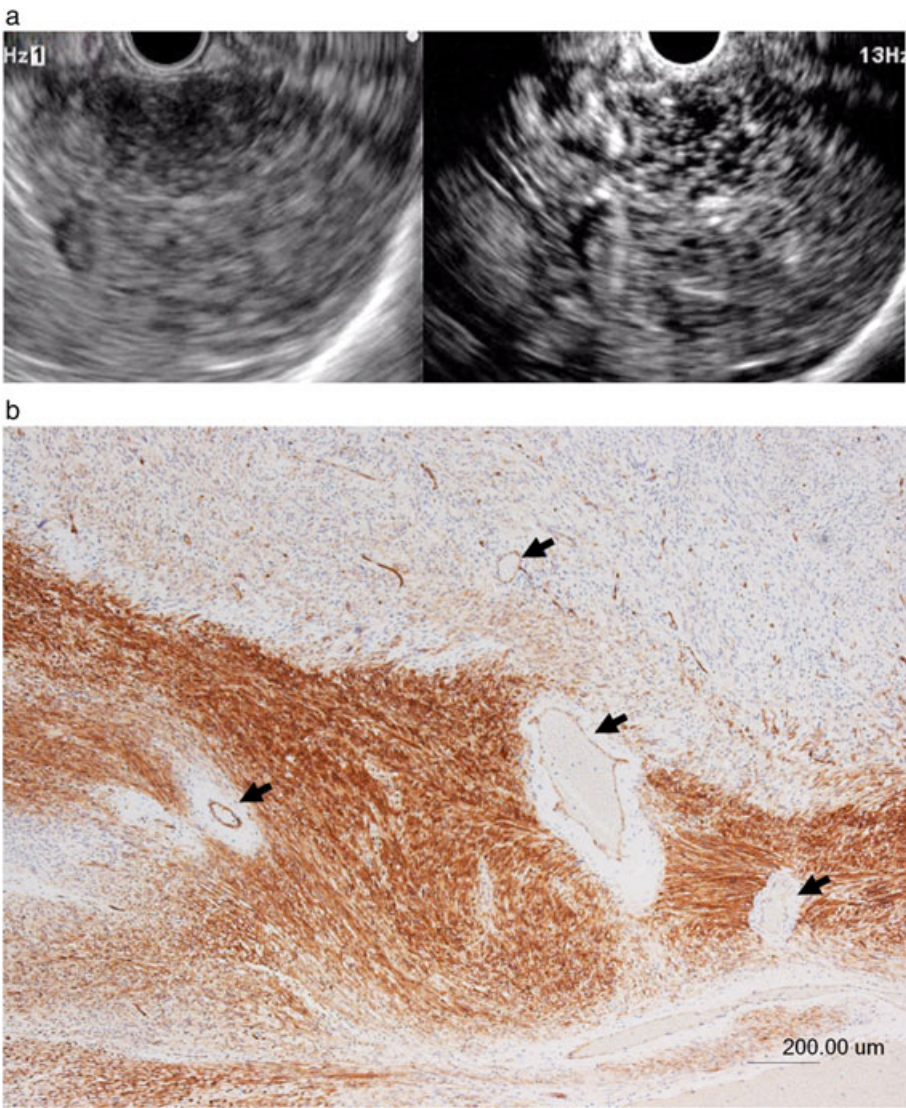


**Figure 2** (a) Contrast-enhanced harmonic endoscopic ultrasonography image of a leiomyoma demonstrating hypo-enhancement and a homogeneous enhancement pattern. The size of the leiomyoma is 30 mm. The left side is a B-mode endoscopic ultrasound image and the right side, a contrast-enhanced harmonic endoscopic ultrasonography image. (b) Histopathological image of CD 34 stain obtained by surgical resection. Vessels in the tumor are sparsely depicted (arrows). [Color figure can be viewed at [wileyonlinelibrary.com](http://wileyonlinelibrary.com)]

guidelines for GISTs state that EUS-FNA has considerable diagnostic yield for lesions of  $\geq 2$  and  $< 5$  cm, whereas lesions of less than 2 cm, without malignant findings and symptoms, should be followed up.<sup>13</sup> The National Comprehensive Cancer Network guidelines also recommended follow-up for SMTs of less than 2 cm.<sup>14</sup> However, the risk of GIST metastasis cannot be accurately predicted without assessment of surgical findings. In our study, hyper-enhancement showed good sensitivity for GISTs, even if the size of the lesion was less than 2 cm. Moreover, CH-EUS may be a useful method for targeted EUS-FNA, as it can help in the selection of suspicious GISTs of less than 2 cm.

This study has several limitations. The study was retrospective, although the data used for analysis were derived from prospectively collected databases. Verification bias cannot be excluded as the CH-EUS results may have influenced decisions on performing EUS-FNA for lesions of less than 2 cm and may

therefore have influenced decisions on the requirement for surgical resection. There were only seven cases with lesions of more than 5 cm. All 20 cases of less than 2 cm were GISTs; therefore, the specificity of CH-EUS was not calculated within this size group. The amount of blood flow and homogeneity of contrast enhancement on CH-EUS were analyzed in a subjective manner. There is a potential for bias resulting from the fact that the readers who assessed the CH-EUS images may have known that there was a high suspicion of GISTs in all cases included in this study, as all of the cases had undergone surgical resection. Lastly, benign SMTs may show various enhancement patterns, which can lead to difficulties in differentiating benign SMTs from GIST in some cases. For example, an ectopic pancreas can show inhomogeneous enhancement as a specific histology. Moreover, as a lipoma usually shows hyperechoic tissue before contrast enhancement, it may not be easy to evaluate the enhancement pattern. To avoid



**Figure 3** (a) Contrast-enhanced harmonic endoscopic ultrasonography image of a gastrointestinal stromal tumor demonstrating hyper-enhancement and an inhomogeneous enhancement pattern. The gastrointestinal stromal tumor is 50 mm in size. The left side is a B-mode endoscopic ultrasound image and the right side, a contrast-enhanced harmonic endoscopic ultrasonography. (b) Histopathological image of CD 34 stain obtained by surgical resection. Many large vessels are depicted in the tumor (arrows). [Color figure can be viewed at [wileyonlinelibrary.com](#)]

**Table 3** Diagnostic accuracy of CH-EUS for discrimination of benign SMTs from GISTs with hyper-enhancement considered to indicate GISTs

	Sensitivity % (95% CI)	Specificity % (95% CI)	PPV % (95% CI)	NPV % (95% CI)	Overall accuracy % (95% CI)
Total	84.5 (49/58)	73.3 (11/15)	92.5 (49/53)	55.0 (11/20)	82.2 (60/73)
(n = 73)	(78.9–88.3)	(51.9–88.0)	(86.4–96.6)	(38.9–66.0)	(73.4–88.2)
< 2 cm	85.0 (17/20)	—	100 (17/17)	0 (0/3)	85.0 (17/20)
(n = 20)	(85.0–85.0)	—	(100–100)	(0)	(85.0–85.0)
2–5 cm	81.8 (27/33)	76.9 (10/13)	90.0 (27/30)	62.5 (10/16)	80.4 (37/46)
(n = 46)	(73.1–87.3)	(54.8–90.7)	(80.4–96.0)	(44.5–73.7)	(67.9–88.2)
5 cm <	100 (5/5)	50.0 (1/2)	83.3 (5/6)	100 (1/1)	85.7 (6/7)
(n = 7)	(84.6–100)	(11.5–50.0)	(70.5–83.3)	(22.9–100)	(63.7–85.7)

CH-EUS, contrast-enhanced harmonic endoscopic ultrasonography; CI, confidence interval; GIST, gastrointestinal stromal tumor; NPV, negative predictive value; PPV, positive predictive value; SMT, submucosal tumor.



**Table 4** Diagnostic accuracy of CH-EUS for discrimination of benign SMTs from GISTs with inhomogeneous-enhancement considered to indicate GISTs

	Sensitivity % (95% CI)	Specificity % (95% CI)	PPV % (95% CI)	NPV % (95% CI)	Overall accuracy % (95% CI)
Total (n = 73)	36.2 (21/58) (30.7–38.7)	86.7 (13/15) (65.3–96.2)	91.3 (21/23) (77.4–97.5)	26.0 (13/50) (19.6–28.9)	46.6 (34/73) (37.8–50.5)
< 2 cm (n = 20)	10.0 (2/20) (10.0–10.0)	— —	100 (2/2) (100–100)	0 (0/18) (0)	10.0 (2/20) (10.0–10.0)
2–5 cm (n = 46)	42.4 (14/33) (34.1–44.9)	92.3 (12/13) (71.2–98.6)	93.3 (14/15) (75.0–98.8)	38.7 (12/31) (29.9–41.4)	56.5 (26/46) (44.6–60.1)
> 5 cm (n = 7)	100 (5/5) (84.6–100)	50 (1/2) (11.5–50)	83.3 (5/6) (70.5–83.3)	100 (1/1) (22.9–100)	85.7 (6/7) (63.7–85.7)

CH-EUS, contrast-enhanced harmonic endoscopic ultrasonography; CI, confidence interval; GIST, gastrointestinal stromal tumor; NPV, negative predictive value; PPV, positive predictive value; SMT, submucosal tumor.

**Table 5** CH-EUS variables (homogenous/inhomogenous and hyper-enhancement/hypo-enhancement) according to lesion type

	Hyper (n = 49)	Hypo (n = 9)
GISTs (n = 58)		
Homogenous (n = 37)	34	3
Inhomogenous (n = 21)	15	6
Benign (n = 15)		
Homogenous (n = 13)	Hyper (n = 4) 3	Hypo (n = 11) 10
Inhomogenous (n = 2)	1	1

CH-EUS, contrast-enhanced harmonic endoscopic ultrasonography; GISTs, gastrointestinal stromal tumors.

this, if benign SMTs, with the exception of leiomyomas, had been excluded, only five cases of benign SMT would have been included in this study. Therefore, we analyzed all types of benign SMTs in this study.

In conclusion, GISTs were characterized by hyper-enhancement and an inhomogeneous enhancement pattern. In lesions of less than 2 cm, hyper-enhancement was a more sensitive finding for indication of GISTs than inhomogeneous enhancement. CH-EUS was useful for discriminating between benign SMTs and GISTs.

## Acknowledgment

The present study was supported by grants from the Japan Society for the Promotion of Science.

## References

- Hwang JH, Saunders MD, Rulyak SJ *et al.* A prospective study comparing endoscopy and EUS in the evaluation of GI subepithelial masses. *Gastrointest. Endosc.* 2005; **62**: 202–8.
- Rosch T, Kapfer B, Will U *et al.* Accuracy of endoscopic ultrasonography in upper gastrointestinal submucosal lesions: a prospective multicenter study. *Scand. J. Gastroenterol.* 2002; **37**: 856–62.
- Mekky MA, Yamao K, Sawaki A *et al.* Diagnostic utility of EUS-guided FNA in patients with gastric submucosal tumors. *Gastrointest. Endosc.* 2010; **71**: 913–19.
- Na HK, Lee JH, Park YS *et al.* Yields and utility of endoscopic ultrasonography-guided 19-gauge trucut biopsy versus 22-gauge fine needle aspiration for diagnosing gastric subepithelial tumors. *Clin Endosc.* 2015; **48**: 152–7.
- Scarpa M, Bertin M, Ruffolo C *et al.* A systematic review on the clinical diagnosis of gastrointestinal stromal tumors. *J. Surg. Oncol.* 2008; **98**: 384–92.
- Philipper M, Hollerbach S, Gabbert HE *et al.* Prospective comparison of endoscopic ultrasound-guided fine-needle aspiration and surgical histology in upper gastrointestinal submucosal tumors. *Endoscopy* 2010; **42**: 300–5.
- Saftoiu A, Vilmann P, Hassan H *et al.* Utility of colour Doppler endoscopic ultrasound evaluation and guided therapy of submucosal tumours of the upper gastrointestinal tract. *Ultraschall Med.* 2005; **26**: 487–95.
- Sakamoto H, Kitano M, Matsui S *et al.* Estimation of malignant potential of GI stromal tumors by contrast-enhanced harmonic EUS (with videos). *Gastrointest. Endosc.* 2011; **73**: 227–37.
- Fusaroli P, Napoleon B, Gincul R *et al.* The clinical impact of ultrasound contrast agents in EUS: a systematic review according to the levels of evidence. *Gastrointest. Endosc.* 2016; **84**: 587–96.
- Kamata K, Kitano M, Omoto S *et al.* Contrast-enhanced harmonic endoscopic ultrasonography for differential diagnosis of pancreatic cysts. *Endoscopy* 2016; **48**: 35–41.
- Kannengiesser K, Mahlke R, Petersen F *et al.* Contrast-enhanced harmonic endoscopic ultrasound is able to discriminate benign submucosal lesions from gastrointestinal stromal tumors. *Scand. J. Gastroenterol.* 2012; **47**: 1515–20.
- Cho JW, Korean ESD Study Group. Current guidelines in the management of upper gastrointestinal subepithelial tumors. *Clin Endosc* 2016; **49**: 235–40.
- Nishida T, Hirota S, Yanagisawa A *et al.* Clinical practice guidelines for gastrointestinal stromal tumor (GIST) in Japan: English version. *Int. J. Clin. Oncol.* 2008; **13**: 416–30.
- Von Mehren M, Randall RL, Benjamin RS *et al.* Gastrointestinal stromal tumors, version 2.2014. *J. Natl. Compr. Cancer Netw.* 2014; **12**: 853–62.

## Review

Nucleotide-binding oligomerization domain 1  
and gastrointestinal disordersBy Tomohiro WATANABE,<sup>\*1,\*2,†</sup> Naoki ASANO,<sup>\*3</sup> Masatoshi KUDO<sup>\*1</sup> and Warren STROBER<sup>\*2</sup>

(Communicated by Shizuo AKIRA, M.J.A.)

**Abstract:** Nucleotide-binding oligomerization domain 1 (NOD1) is an intracellular sensor that detects small peptides derived from the cell wall component of intestinal microflora. NOD1 is expressed in both non-hematopoietic cells such as epithelial cells and hematopoietic cells such as antigen-presenting cells. Detection of its ligand by NOD1 leads to innate immune responses through activation of nuclear factor kappa B and type I interferon as well as induction of autophagy. Innate immune responses through NOD1 activation play an indispensable role both in host defense against microbial infection and in the development of gastrointestinal disorders. Of particular importance, NOD1-mediated innate immune responses are associated with mucosal host defenses against *Helicobacter pylori* (*H. pylori*) infection of the stomach and with the development of pancreatitis. In this review, we discuss the molecular mechanisms by which NOD1 activation leads to the development of *H. pylori*-related gastric diseases and pancreatitis.

**Keywords:** NOD1, *Helicobacter pylori*, pancreatitis

## Introduction

Over the past several decades, our understanding of innate immune system responses has been markedly increased through the intensive study of Toll-like receptors (TLRs).<sup>1)</sup> The TLR system consists of a family of recognition units that respond to microbe-associated molecular patterns (MAMPs) derived from microbes and that are expressed on the cell-surface or endosomes of innate immune cells such as epithelial cells and antigen-presenting

cells (APCs). Activation of TLRs generally leads to pro-inflammatory cytokine responses and enhanced antigen (Ag)-specific adaptive immune responses, both of which are necessary for host defense against microbial infections.<sup>1)</sup> However, in some circumstances such activation can be inappropriate or excessive and in these instances has been implicated in the immuno-pathogenesis of auto-immune diseases.<sup>2)</sup>

More recent studies of innate immune responses have led to the discovery that the TLR-dependent

<sup>\*1</sup> Department of Gastroenterology and Hepatology, Kindai University Faculty of Medicine, Osaka-Sayama, Osaka, Japan.

<sup>\*2</sup> Mucosal Immunity Section, Laboratory of Host Defenses, National Institute of Allergy and Infectious Diseases, National Institutes of Health, Bethesda, MD, U.S.A.

<sup>\*3</sup> Division of Gastroenterology and Hepatology, Tohoku University Graduate School of Medicine, Sendai, Miyagi, Japan.

<sup>†</sup> Correspondence should be addressed: T. Watanabe, Department of Gastroenterology and Hepatology, Kindai University Faculty of Medicine, 377-2 Ohnohigashi Osaka-Sayama, Osaka 589-8511, Japan (e-mail: tomohiro@med.kindai.ac.jp).

Abbreviations: Ag: antigen; AMP: anti-microbial peptide; APC: Antigen presenting cell; ATF6: activating transcription factor 6; CagA: cytotoxin-associated gene A; CARD: caspase activation and recruitment domain; CCKR: cholecystokinin receptor; CCL2: C-C motif chemokine ligand 2; CCR2: C-C chemokine receptor type 2; Cdx2: caudal-type homeobox protein 2; cIAP: cellular inhibitor of apoptosis protein; CXCL: C-X-C motif

chemokine ligand; DAMP: damage-associated molecular pattern; iE-DAP:  $\gamma$ -D-glutamyl meso-diaminopimelic acid; ER: endoplasmic reticulum; GI: gastrointestinal; *H. pylori*: *Helicobacter pylori*; IKK $\epsilon$ : I $\kappa$ B kinase  $\epsilon$ ; IRE1: Inositol-requiring enzyme 1; IRF: interferon regulatory factor; ISGF3: IFN-stimulated gene factor 3; LPS: lipopolysaccharide; LRR: leucine rich repeat; LUBAC: linear ubiquitin chain assembly complex; Lysine: K; MAMP: microbe-associated molecular pattern; MAPK: mitogen activated protein kinase; NOD: nucleotide-binding oligomerization domain; NF- $\kappa$ B: nuclear factor- $\kappa$ B; NLR: NOD-like receptor; OMV: outer membrane vesicle; PERK: protein kinase RNA-like endoplasmic reticulum kinase; PGN: peptidoglycan; PKC: protein kinase C; SLC15: solute carrier family 15; Stat: signal transduction and activator of transcription; TAK1: TGF- $\beta$ -activated kinase 1; TBK1: TANK-binding kinase 1; Th1: T helper type 1; TLR: Toll-like receptor; TRAF: TNF receptor associated factor; T4SS: type IV secretion system; UPR: unfolded protein response; XIAP: X-linked inhibitor of apoptosis.

model of host recognition and response to MAMPs described above are not limited to TLRs. This became apparent from the identification of another family of innate immune receptors called nucleotide-binding oligomerization domain (NOD)-like receptors (NLRs) that also recognize and respond to MAMPs<sup>3)-6)</sup> but differ from TLRs in their structure and in their cytosolic location. In addition, the MAMPs sensed by TLRs and NLRs are markedly different, as is the downstream signaling pathways induced by the MAMPs.<sup>1),3)-6)</sup> These differences make it clear that NLRs constitute an innate immune mechanism that is parallel to but independent of the TLRs mechanism.

NOD1 is a prototypical NLR that detects small peptides (notably  $\gamma$ -D-glutamyl meso-diaminopimelic acid (iE-DAP) and related peptides) derived from peptidoglycan (PGN), a major component of the bacterial cell wall.<sup>7)</sup> Given the fact that PGN containing iE-DAP is present in the cell wall of the Gram-negative bacteria constituting the major class of organisms comprising the gut microflora, NOD1 responses are potentially involved in both homeostatic and host-defense responses to commensal and pathogenic organisms in the gastrointestinal (GI) tract. In fact, there is extensive evidence that NOD1 responses to commensal organisms are not only important during the development of the mucosal immune system early in life,<sup>8)</sup> but also important later on in responses to infection caused by important pathogens such as *Helicobacter pylori* (*H. pylori*).<sup>9)-11)</sup> In addition, there is evidence that NOD1 responses are key factors in the development of pancreatitis as reflected in the experimental pancreatitis caused by cholecystokinin hyperstimulation.<sup>12)-14)</sup> In this review, we focus on these somewhat disparate NOD1-mediated responses with the aim of clarifying how molecular events initiated by NOD1 activation can contribute to both host defense and inflammatory responses.

#### Structure of NOD1 and uptake of NOD1 ligands

NOD1 is structurally similar to other NLR proteins in that it is composed of an N-terminal caspase activation and recruitment domain (CARD), a central NOD and a C-terminal leucine-rich repeat domain (LRR).<sup>3)-6)</sup> As in the case of TLRs containing LRR domains, NOD1 detects its ligand through its C-terminal LRR and ligand binding to this domain leads to oligomerization of NOD1 accompanied by binding and activation of receptor interacting protein

2 (RIP2), the obligate initiator of NOD1 downstream signaling pathways.

Given the fact that NOD1 is expressed in the cytoplasm rather than in the membrane of cells, bacterial PGN needs to gain entry into cells before it can activate NOD1. Obviously, this problem does not apply to ligand associated with invasive bacteria that exhibit various mechanisms of cell entry. However, there exist other pathways of ligand entry that can be potentially used by non-invasive bacteria as well as invasive bacteria. One such pathway involves cellular uptake of bacteria by endocytosis followed by degradation of bacterial components (including PGN) in phago-lysosomes and transport of the peptides derived from degradation across the endosomal membrane by a peptide transporter protein, solute carrier family 15 (SLC15A3 and/or SLC15A4) members.<sup>15),16)</sup> This has been shown by the fact that SLC15A4-deficient mice showed a significant decrease in the NOD1 ligand-induced secretion of cytokine as compared with SLC15A4-intact mice<sup>15)</sup> and SLC15A3-deficient cells have been shown to exhibit reduced production of cytokines upon stimulation with NOD2 ligand.<sup>16)</sup> Interestingly, NOD2 binds to SLC15A and the complex formed includes RIP2, indicating that the transporter protein serves as a "platform" for NOD protein activation at the endosomal interface. Another pathway of NOD1 ligand delivery into the cytoplasm involves outer membrane vesicles (OMVs), *i.e.*, bilayered spherical structures that can be shed from all Gram-negative bacteria.<sup>17)</sup> Such OMVs contain PGN and are taken up by cells via autophagy into autophagosomes. NOD1 ligand is presented to NOD1 by early endosomes, perhaps by a mechanism involving SLC15 transporter proteins as discussed above; this mechanism whatever its nature, also facilitates NOD1 binding to RIP2. Yet a third pathway of NOD1 ligand delivery occurs via direct delivery of ligand by a Type IV bacterial secretion system.<sup>9)</sup> This has been described in relation to delivery of PGN into gastric epithelial cells by *H. pylori* bearing the *cag* pathogenicity island, the latter encoding the genes for the secretion system. However, it applies to any bacterium that expresses a Type IV secretion system.

These findings regarding the delivery systems of NOD1 ligands and PGN strongly suggest that NOD1 can recognize not only invasive bacteria but also extracellular bacteria. As such they suggest that activation of NOD1 is a common event in cells exposed to Gram-negative bacteria.

### NOD1-expressing cells

NOD1 is expressed in a broad range of both hematopoietic cells and non-hematopoietic cells and thus has the potential to fulfill a variety of immunologic functions. Among hematopoietic cells its role in the innate responses of APCs such as macrophages and dendritic cells is most prominent and indeed these cells constitutively express cytoplasmic NOD1 that mediate cytokine responses to NOD1 ligands as already indicated above.<sup>3)–6)</sup> However, while independent NOD1 ligand stimulation elicits rather low level cytokine responses as compared to those elicited by TLR ligands they have a marked ability to enhance concomitant TLR responses.<sup>18),19)</sup> This is most likely due to the fact that NOD1 signaling (as well as NOD2 signaling) engages a down-stream activation pathway that is somewhat independent of and additive to the pathway ordinarily utilized by TLR signaling, such as RIP2 signaling.<sup>3)–6)</sup> Whatever its underlying mechanism, the synergism between NOD1 and TLR signaling has been shown to be necessary for the initiation of substantial adaptive T helper type 1 (Th1), Th2, and Th17 responses.<sup>20),21)</sup> In effect, this means that innate immune sensing of PGN by NOD1 acts cooperatively with sensing of MAMPs by TLRs to promote the development of the robust innate and adaptive responses necessary for eradication of invasive bacteria. A good example of this is the role of NOD1 in a model of *Salmonella typhimurium* infection wherein it has been shown that NOD1 expressed by intestinal lamina propria dendritic cells is indispensable to the elimination of the *Salmonella*.<sup>22)</sup>

Another role of cytosolic NOD1 in microbial infection also related to the fact that its signaling pathway is somewhat independent of that utilized by TLR ligands has been uncovered by Kim *et al.*<sup>23),24)</sup> It has been shown that repeated exposure of APCs to the same or other TLR ligands results in reduced pro-inflammatory cytokine responses and defense against bacteria, probably due to an as yet poorly defined tolerance mechanism.<sup>25)</sup> However, such reduction is more severe in the absence of NOD1 (and NOD2), indicating that responses mediated by the latter ameliorate the tolerance effect.<sup>23),24)</sup> This can be explained by the supposition that mechanisms of TLR and NOD tolerization are different and that NOD responses are preserved in the face of TLR tolerization.

NOD1 (and NOD2) are also expressed by B and T cells but ligands for these innate factors elicit

responses only when the cells are also stimulated via their respective Ag receptors.<sup>26),27)</sup> However, the co-stimulatory responses to NOD1 and NOD2 ligand stimulation in these cells are quite modest and are observed with respect to NOD1 only in the case of tonsil-derived B cells.

Neutrophils are yet another hematopoietic cell that expresses functional NOD1 and indeed it has been shown that bone marrow neutrophils are pre-activated by NOD1 (but not by NOD2) recognition of bacterial PGN translocated from the gut into the bone marrow.<sup>28),29)</sup> In addition, such NOD1-mediated neutrophil pre-activation and its associated increased phagocytic capacity enhances killing of *Streptococcus pneumoniae* and *Staphylococcus aureus* organisms and thus participates in host defense against infection with these bacteria.

As indicated above, NOD1 is also expressed in non-hematopoietic cells and indeed NOD1 responses in such cells may contribute to homeostasis or host defense against pathogens in a manner independent of concomitant NOD1 responses in APCs. This is usually inferred from *in vitro* studies of cell lines or *in vivo* studies of *in situ* cells that are shown to produce NOD1-dependent, epithelial cell-specific anti-microbial peptides (AMPs). NOD1 responses in gut epithelial cells have been the main focus of study in this context corresponding to the fact that such cells are in constant contact with the gut microflora that express NOD1 ligands.<sup>3)–6)</sup> With respect to gut epithelial cell responses affecting homeostasis, it has been shown that NOD1-deficient mice (as well as NOD2-deficient mice) exhibit increased para-cellular permeability as well as decreased RegIII- $\gamma$  production and, as a possible consequence, exhibit increased susceptibility to dextran sulfate-induced colitis.<sup>30)</sup> In addition, qPCR-based assessment of mRNA expression in the ileum or cecum of NOD1-deficient mice revealed that such mice produced lower levels of NOD2, Muc2,  $\alpha$ - and  $\beta$ -defensins as well as keratinocyte-derived chemokine as compared to NOD1-intact littermates; however, this was not associated with changes in the gut microbiome.<sup>31)</sup> These studies relate to those of NOD2-deficient mice in which it was shown that NOD2 deficiency leads to increased gut permeability, increased microflora-dependent induction of suppressor cells and decreased experimental colitis; thus, NOD2 deficiency (and by extension, NOD1 deficiency) has significant down-stream effects on gut homeostasis.<sup>32)</sup>

Epithelial cell-intrinsic NOD1 responses also contribute to host defense against gut pathogens.

Thus, *H. pylori*, an organism that does not invade the lamina propria, elicits a NOD1-dependent type I IFN and chemokine responses in epithelial cell lines.<sup>9),10)</sup> That this type of response affects host defense was shown by the fact that the gastric cancer cell line with reduced NOD1 expression secrete a reduced amount of AMPs and exhibited a reduced capacity to kill *H. pylori* organisms;<sup>33)</sup> in addition, mice with NOD1 deficiency exhibit increased susceptibility to *H. pylori* infection due to impaired type I IFN and Th1 responses.<sup>34)</sup> Such NOD1-mediated host defense is not limited to *H. pylori* since it has been shown that exposure of cells to enteroinvasive *Escherichia coli* elicits a NOD1-dependent host defense response suggesting that NOD1 signaling in epithelial cells has a very broad capacity to induce host defense factors.<sup>35)</sup> Finally, it should be mentioned that NOD1-deficient mice are more susceptible to *Clostridium difficile* infection which in this case was attributed to decreased neutrophil recruitment occurring as a result of decreased epithelial cell C-X-C motif chemokine ligand 1 (CXCL1) production.<sup>36)</sup>

NOD1 signaling relating to host defense is by no means limited to epithelial cells in the GI tract. This is shown in studies of *Chlamidia trachomatis* infection wherein it has been shown that host defense against infection of the female genital tract by this organism is accompanied by NOD1-mediated induction of IL-1 $\beta$  by trophoblast cells.<sup>37)</sup> In addition, *Chlamydia pneumoniae* infection elicits NOD1 activation followed by IL-8 production in endothelial cells that in this case links NOD1 activation with the development of vascular lesions and coronary heart disease caused by this organism.<sup>38)</sup> Finally, it should be noted that parenchymal cells such as hepatocytes<sup>39)</sup> and pancreatic acinar cells express functional NOD1;<sup>12)–14)</sup> in the latter case, sensing of commensal organism-derived PGN by NOD1 mediates acute and chronic pancreatitis as discussed in greater detail below.<sup>12)–14)</sup>

The NOD1 responses of various types of cells reviewed above is to a great extent regulated by their level of NOD1 expression. As might be expected such expression is up-regulated in an inflammatory milieu such as that accompanied by the generation of type I IFN and IFN- $\gamma$ .<sup>40),41)</sup> The involvement of type I IFN in NOD1 expression has been inferred from studies of *Listeria monocytogenes* infection in which it was observed that increased macrophage NOD1 expression normally induced by this infection is virtually absent in type I IFN receptor-deficient mice.<sup>40)</sup> On the other hand, baseline expression of NOD1 by

epithelial cells is up-regulated by IFN- $\gamma$ , but not TNF- $\alpha$ , and this is mediated by the binding of IFN- $\gamma$ -induced interferon regulatory factor 1 (IRF1) to the NOD1 promoter.<sup>41)</sup>

As mentioned above, NOD1 activation plays a protective role in a wide variety of major bacterial infections such as *Salmonella typhimurium*, *Streptococcus pneumoniae*, *Staphylococcus aureus*, enteroinvasive *Escherichia coli*, *Clostridium difficile*, *Chlamidia trachomatis*, and *Chlamydia pneumoniae*.<sup>22),28),29),36)–38)</sup> In addition, it is involved in the pathogenesis of several important viral infections including cytomegalovirus<sup>42)</sup> and Hepatitis C virus.<sup>43)</sup> Thus, it is clear that NOD1 activation is involved in various kinds of human infectious diseases.

### Signaling pathways of NOD1 (Figure 1)

**NOD1-mediated activation of nuclear factor-kappa B (NF- $\kappa$ B) and mitogen-activated protein kinases (MAPKs).** NOD1 activation resulting from LRR sensing of NOD1 ligand is initiated by a NOD1 conformational change that allows a homotypic interaction between NOD1 CARD domains and NOD1 auto-oligomerization; this, in turn, is followed by recruitment of RIP2, its initial down-stream signaling molecule.<sup>3)–6)</sup> Such RIP2 recruitment is an obligate step in NOD1 (as well as NOD2) signaling since cells from mice deficient in RIP2 are unable to mediate NOD1 (or NOD2) activation of pro-inflammatory cytokine responses.<sup>44),45)</sup> Whether RIP2 signaling is dedicated solely to NODs responses is an important question since RIP2 signaling not dependent on NODs activation may be necessary for an optimal cytokine response in the case of inflammation accompanied by both NODs and TLR stimulation. The answer to this question is somewhat controversial; thus, while earlier reports indicated that TLR responses also were mediated by RIP2<sup>46)–48)</sup> more recent reports indicate that TLR responses are undiminished in the absence of RIP2.<sup>44),45),49)</sup> Despite these recent findings, RIP2 activation appears to be necessary for cytokine responses not stimulated by NOD1 and NOD2 since IFN- $\gamma$  responses in the absence of RIP2 are greatly diminished in Th1 cells stimulated with IL-12 or IL-12 and IL-18,<sup>46)</sup> i.e., a cytokine response clearly not driven by NOD1 and NOD2.

Following its activation by NOD1, RIP2 in a ubiquitinated form (see below) complexes with TAK1-binding protein 2 (TAB2) and TAB3 and then recruits TGF- $\beta$ -activated kinase 1 (TAK1) to form an activator of the I $\kappa$ B kinase (IKK) complex;



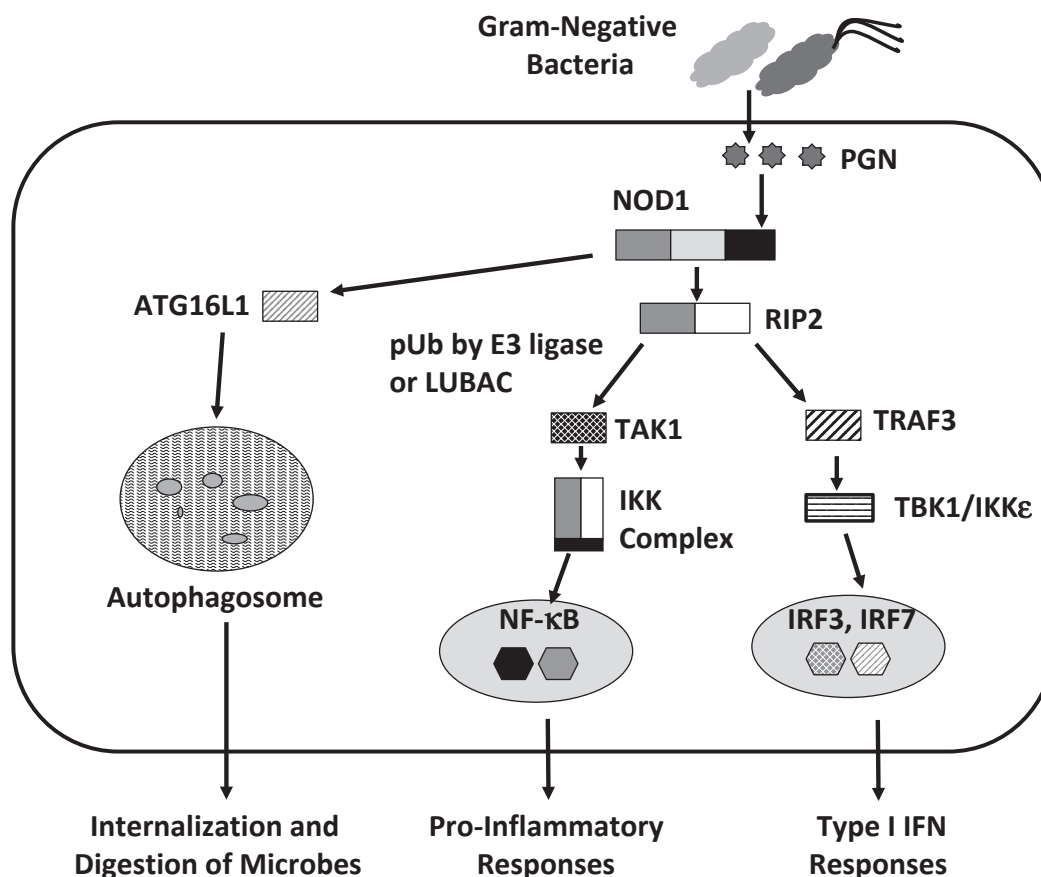


Fig. 1. Signaling pathways of NOD1. Nucleotide-binding oligomerization domain 1 (NOD1) detects peptidoglycan (PGN) derived from Gram-negative bacteria. Sensing of PGN by intracellular NOD1 leads to activation of receptor interacting protein 2 (RIP2). RIP2 subjected to poly-ubiquitination (pUb) by E3 ligases or linear ubiquitin chain assembly complex (LUBAC) interacts with TGF- $\beta$ -activated kinase 1 (TAK1) and I $\kappa$ B kinase (IKK) complex to induce nuclear translocation of nuclear factor- $\kappa$ B (NF- $\kappa$ B) subunits. On the other hand the interaction between RIP2 and TNF receptor associated factor 3 (TRAF3) induces type I IFN responses through nuclear translocation of interferon regulatory factor 3 (IRF3) and IRF7. NOD1 also interacts with ATG16L1 to induce autophagy.

this, in turn, leads to the phosphorylation/degradation of I $\kappa$ B $\alpha$  and nuclear translocation of nuclear factor- $\kappa$ B (NF- $\kappa$ B) subunits that promote transcription of NF- $\kappa$ B target genes through binding to multiple promoter sites.<sup>3)–6)</sup> In addition to NF- $\kappa$ B, mitogen-activated protein kinases (MAPKs) including extracellular signal-regulated kinase, c-JUN N-terminal kinase, and p38 are activated by RIP2.<sup>3)–6)</sup>

The binding of RIP2 to NOD1 is followed by various forms of RIP2 post-translational modification via ubiquitination. Such modification suggests that RIP2 may have various functions (depending on modification) following activation by NOD1 or that activation by NOD1 is controlled by subsequent check-points that prevents down-stream pro-inflammatory responses following inappropriate NOD1 activation.

RIP2 ubiquitination is regulated by a number of E3 ligases including various cellular inhibitor of apoptosis proteins (cIAPs) and TNF-receptor associated factors (TRAFs).<sup>50)–52)</sup> E3 ligases are considered to be involved in Lysine 63 (K63)-linked poly-ubiquitination, acquisition of RIP2 kinase function and autophosphorylation at Tyr 474.<sup>50)–53)</sup> More recently, X-linked inhibitor of apoptosis (XIAP) has also been shown to be an ubiquitinase of RIP2.<sup>54)–56)</sup> This IAP contrasts with the cIAPs mentioned above because it induces linear ubiquitin chain assembly (rather than K63 assembly) via recruitment of a linear ubiquitin chain assembly complex (LUBAC) composed of HOIL1L, HOIP, and SHARPIN.<sup>54)–56)</sup> Both cIAPs-induced polyubiquitination and its accompany auto-phosphorylation and XIAP-induced polyubiquitination have been shown to be associated

with RIP2 down-stream NF- $\kappa$ B activation, although the necessity for cIAPs-induced ubiquitination has been questioned by the fact that cIAP inhibitors do not abrogate RIP2 signaling function (see further discussion below).<sup>57)</sup> Interestingly, mutations in the *XIAP* gene results in an immunodeficiency state known as X-linked lymphoproliferative syndrome type 2.<sup>54),55)</sup> This immunodeficiency may result, at least in part, from the fact that mutations in *XIAP* may cause defective binding to RIP2 or ubiquitination of RIP2 and thus in defective NOD1/2-RIP2 innate responses.<sup>54),55)</sup>

Pellino 3 and ITCH are two additional E3 ligases contributing to RIP2 polyubiquitination. Pellino 3 is a member of a ligase family known to polyubiquitinate IRAKs and thus to augment TLR signaling.<sup>57)</sup> It induces K63 polyubiquitination of RIP2 at sites other than that targeted by cIAPs and does not act via recruitment of LUBAC.<sup>57)</sup> Pellino 3-deficient mice exhibit reduced NOD function and thus its polyubiquitination of RIP2 is thought to be necessary for NOD-mediated innate responses; in this regard, initial Pellino 3-mediated poly-ubiquitination may be necessary for subsequent *XIAP* polyubiquitination and the two E3 ligases may act in tandem to mediate RIP2 activation.<sup>57)</sup> ITCH, in contrast, causes ubiquitination of RIP2 that induces reduced RIP2 activation and thus ITCH deficiency is associated with mucosal inflammation possibly due to inappropriate RIP2-mediated pro-inflammatory function.<sup>58)</sup>

The positive effect of polyubiquitinating E3-ligases on RIP2 activation is counterbalanced by the negative effect of deubiquitinating enzymes that remove poly ubiquitin chains from target molecules. Thus, deubiquitinating enzymes such as A20 and CYLD are negative regulators of NOD-signaling pathways and pro-inflammatory cytokine responses are markedly increased in A20-deficient or CYLD-deficient APCs upon stimulation with NOD ligand.<sup>59)–61)</sup> However, these deubiquitinating factors are not the only negative regulators of NODs; the latter include TRAF4 that binds directly to NOD2.<sup>62),63)</sup> Such negative regulators could conceivably be necessary to prevent excessive NOD inflammatory responses.

**NOD1-mediated activation of type I IFN.** Whereas activation of the NF- $\kappa$ B and MAPK pathways are the major down-stream outcomes of NOD1 signaling, the latter also results in induction of type I IFN production, another important component of the inflammatory response.<sup>10),42),64)</sup> This was initially

discovered by Watanabe *et al.*, who found that gastric and colon cancer cell lines produced a large amount of chemokines upon stimulation with NOD1 ligand and that these included chemokines with the C-X-C motif (CXCL9, CXCL10, and CXCL11) that are dependent on type I IFN responses.<sup>10)</sup> They then found that, as expected, gastric and colonic epithelial cells stimulated with NOD1 ligand induced robust production of IFN- $\beta$  and neutralization of the type I IFN signaling pathway by blockade of the IFN $\alpha/\beta$  receptor resulted in a marked reduction of CXCL10 expression.<sup>10)</sup>

Type I IFN activates transcription of genes related to anti-microbial host defenses by acting through its receptor to induce nuclear translocation of a heterotrimeric complex, called IFN-stimulated gene factor 3 (ISGF3), the latter composed of signal transduction and activator of transcription 1 (Stat1), Stat2, and IRF9.<sup>65)</sup> Thus, in further studies relating NOD1 induction of type I IFN-induced responses to chemokine production Watanabe *et al.* showed that inactivation of ISGF3 via gene-silencing of Stat1 or Stat2 resulted in reduced NOD1 induction of CXCL10. Then, in studies focused on the origin of NOD1-induced CXCL10 production, Watanabe *et al.* conducted studies of bone marrow chimeric mice in which they showed that elevated serum levels of IFN- $\beta$  and CXCL10 seen in NOD1-intact mice treated with NOD1 ligand were markedly decreased in X-irradiated NOD1-deficient mice transplanted with NOD1-intact bone marrow cells, but not in X-irradiated NOD1-intact mice transplanted with NOD1-deficient bone marrow cells.<sup>10)</sup> These results thus suggested that IFN- $\beta$  production followed by IFN- $\beta$ -dependent chemokine responses is an innate immune response induced by NOD1 activation in non-hematopoietic cells, most likely GI epithelial cells. Given the fact that CXCL10 attracts CXCR3-expressing Th1 cells,<sup>66)–68)</sup> it is probable that activation of NOD1 signaling pathways in such epithelial cells is responsible for the generation of IFN- $\beta$  and Th1 responses.

As for the molecular mechanisms leading to IFN- $\beta$  production via NOD1 activation, detailed over-expression and knock-down studies revealed that NOD1 binding to its ligand leads to activation of RIP2 followed by the physical interaction between RIP2 and various TRAFs, such as TRAF2, TRAF5, and TRAF6 that then play a role in RIP2-mediated NF- $\kappa$ B activation.<sup>51),69)</sup> In addition, activated RIP2 interacts with TRAF3 to initiate a signaling pathway that results in induction of type I IFNs.<sup>10)</sup> This

pathway involves activation of TANK-binding kinase 1 (TBK1) and I $\kappa$ B kinase  $\varepsilon$  (IKK $\varepsilon$ ) followed by nuclear translocation of IRF7, a transcription factor acting directly as a transcription factor for type I IFN promoter and indirectly through its induction of type I IFN and the latter's induction of ISGF3.<sup>70),71)</sup> Thus, the RIP2-TRAF3-TBK1-IKK $\varepsilon$ -IRF7 axis plays a key role in the induction of type I IFN responses via NOD1.<sup>10)</sup> The interaction between RIP2 and TRAF3 appears to be a unique feature of NOD1 activation. It is reminiscent of the interaction between MyD88 and TRAF3, which plays an indispensable role in the generation of TLRs-induced type I IFN responses.<sup>72)</sup>

Importantly, sensing of Gram-negative bacteria residing the GI tracts by intracellular NOD1 mediates mucosal host defense against gastric infection of *H. pylori* and development of pancreatitis through induction of type I IFN responses (see below). Moreover, recent studies by Fan *et al.* highlights the importance of NOD1-RIP2-mediated type I IFN responses in anti-viral host defense responses to cytomegalovirus infection of the GI tract.<sup>42)</sup>

**The role of NOD1 in autophagy and in the endoplasmic reticulum stress response.** NOD1 has a surprisingly important role in cellular homeostasis, one involving autophagy and the other, the unfolded protein response. Long-lived proteins and cytoplasmic organelles are degraded or are processed for recycling by a cellular mechanism known as autophagy.<sup>73)</sup> During autophagy double-membrane vacuoles are formed that entrap targeted proteins and subject the latter to proteolytic digestion when the vacuoles are fused with lysosomes. Autophagy also provides machinery for the handling of bacteria that gain cellular entry, but the mechanism that links detection of such bacteria to autophagy is poorly understood. Insight into one such possible mechanism has been reported by Travassos *et al.* who found that invasive bacteria induce autophagic responses via binding of bacterial NOD1 ligand to cellular NOD1 at the bacterial entry site, which then triggers autophagy by NOD1 binding to ATG16L1, an autophagy-inducing protein.<sup>73),74)</sup> Such NOD1-induced autophagy in epithelial cells was shown to control infection with invasive bacteria such as *Shigella flexneri*, but similar NOD1 interactions are presumably involved in the cellular entry of other bacteria as well.

The NOD1-mediated induction of autophagy described above is independent of NOD1 signaling involving RIP2.<sup>74)</sup> However, Irving *et al.* provided

evidence that endosomal co-localization of NOD1 and RIP2 following bacterial OMV uptake leads to autophagy and inflammatory responses in gastric epithelial cells.<sup>17)</sup> Recently, data bearing on whether such RIP2-mediated autophagy depends on ATG16L1 was reported by Sorbara *et al.*<sup>75)</sup> These authors found that epithelial cells subjected to ATG16L1-knockdown exhibit increased chemokine responses upon stimulation with NOD1 ligand. In addition, they found that such increased responses were dependent on RIP2 signaling since they were not seen in RIP2-deficient cells.<sup>75)</sup> Conversely, epithelial cells over-expressing ATG16L1 exhibit markedly decreased K63-linked poly-ubiquitination of RIP2 upon activation of NOD1. These data thus suggest that interaction of NOD1 with ATG16L1 causes inhibition of RIP2 poly-ubiquitination and thus inhibition of NOD1-RIP2 pro-inflammatory signaling. Importantly, such negative regulation of NOD1-RIP2 signaling by ATG16L1 was independent of autophagic responses, implying that the NOD1 induction of autophagy via activation of RIP2 reported by Irving involves an autophagy-inducing mechanism independent of ATG16L1.

The accumulation of unfolded or misfolded proteins caused by endogenous cellular factors or microbial infection can trigger endoplasmic reticulum (ER) stress, a possible pro-inflammatory mechanism underlying Crohn's disease or type 2 diabetes. ER stress induces inflammation by initiating the unfolded protein response (UPR), a process that is marked by the activation of three ER transmembrane receptors: protein kinase RNA-like endoplasmic reticulum kinase (PERK), activating transcription factor 6 (ATF6) and inositol-requiring enzyme 1 (IRE1 $\alpha$ ).<sup>76)</sup> One of these ER receptors, IRE1 $\alpha$ , accounts for the pro-inflammatory potential of the UPR by recruiting TRAF2 to the ER membrane and thus the activation of NF- $\kappa$ B and the production of IL-6.<sup>76)</sup> Unexpectedly, recent studies show that IRE1 $\alpha$ /TRAF2 interaction leading to the induction of NF- $\kappa$ B requires recruitment of NOD1-RIP2 or NOD2-RIP2 and ligand-independent activation of the latter innate immune factors.<sup>77)</sup> Thus, atypical activation of NOD1 (and NOD2) plays important roles in the ER stress-induced inflammatory responses.

#### NOD1 and *Helicobacter pylori* infection

**Activation of NOD1 by *H. pylori*.** Persistent gastric infection of *H. pylori* causes a wide variety of human upper GI tract disorders including chronic gastritis, peptic ulcers, mucosa-associated lymphoid

tissue lymphoma, and gastric cancer.<sup>78)</sup> *H. pylori* organisms are classified into two strains of differing pathogenicity conferred by the expression of cytotoxin-associated gene A (CagA), a virulence protein encoded by the *cagA* gene. The *cagA* gene is one of the 28–30 genes comprising the *cag* pathogenicity island that together provide the proteins necessary for the expression of a syringe needle-like structure known as the type IV secretion system (T4SS) that allows efficient *H. pylori* injection of toxins and bacterial cell wall components into gastric epithelial cells.<sup>78),79)</sup>

Viala *et al.* provided the first evidence that intracellular NOD1 in gastric epithelial cells detects NOD1 ligand derived from *H. pylori* PGN and that such detection has host defense implications.<sup>9)</sup> These authors showed first that such detection was CagA-dependent since *H. pylori* expressing a functional T4SS but not a non-functional T4SS, activated NOD1 as assessed by reporter gene assays. They then showed that NOD1-deficient mice exhibit increased bacterial burdens of T4SS-bearing *H. pylori* organisms as compared with NOD1-intact mice upon acute infection with these organisms.<sup>9)</sup>

Whereas CagA injection of PGN into cells may be the primary mechanism of intra-cellular entry of NOD1 ligand as suggested by Viala *et al.*, NOD1 ligand may also gain entry into the cell in a T4SS-independent fashion via *H. pylori*-derived OMVs. As indicated above, the latter are cell membrane structures released from cells and containing cell contents (such as *H. pylori* PGN) that can be transported across the cell membrane by lipid rafts.<sup>80)</sup> This mechanism of PGN-NOD1 ligand entry has also been shown to have host defense implications in that it results in NOD1-dependent NF- $\kappa$ B activation and pro-inflammatory chemokine responses.<sup>80)</sup> Recently, Irving *et al.* elucidated the molecular mechanism accounting for NOD1-mediated detection of *H. pylori*-derived NOD1 ligand via OMV-transmembrane transport.<sup>17)</sup> They reported that upon entry into the cell, OMVs derived from *H. pylori* induces autophagosome formation in a NOD1 and RIP2-dependent manner and that OMV and their contained PGN then co-localize with both NOD1 and RIP2 in early endosomes.<sup>17)</sup> Thus, these results suggest that *H. pylori*-derived OMVs are internalized and digested into PGN fragments by formation of autophagosomes and that sensing of PGN by NOD1 is achieved in the early endosomes.

**NOD1-mediated mucosal host defense against *H. pylori* (Figure 2 and Table 1).** Host defense elicited by persistent gastric infection of

*H. pylori* is mediated, at least in part, by a strong Th1 immune response since it has been shown that such responses are necessary to obtain reductions in the gastric bacterial load<sup>81),82)</sup> and to correlate with vaccine-induced reductions of *H. pylori* colonization.<sup>83)</sup> Whether these adaptive host defense responses are accompanied or enhanced by innate TLRs-induced immune responses, is uncertain since the stimulatory activity of TLR4 by lipopolysaccharide (LPS) isolated from *H. pylori* is much weaker than that from *Escherichia coli* or *Salmonella typhimurium* and *H. pylori* flagellin has little ability to stimulate TLR5 responses.<sup>84),85)</sup>

On the other hand, studies by Viala *et al.* mentioned above have provided evidence that innate responses, in this case mediated by NOD1, do have a major role in host defense against *H. pylori*. This consists of the fact that NOD1-deficient mice are both susceptible to gastric infection with *H. pylori* and, in addition, exhibit increased gastric bacterial burden upon such infection.<sup>9),10)</sup> One question arising from this observation is if and how activation of an innate NOD1 response might generate an adaptive Th1 response against *H. pylori*. In studies addressing this question and already discussed above in the section of NOD1 signaling pathways, Watanabe *et al.* showed that stimulation of gastric epithelial cells by NOD1 ligand induces a robust production of IFN- $\beta$  and that such type I IFN production leads to a marked production of Th1 chemokines such as CXCL9, CXCL10, and CXCL11.<sup>10)</sup> This suggested that NOD1 activation in gastric epithelial cells triggers adaptive Th1 responses against *H. pylori* via its capacity to induce type I IFN production. *In vivo* support of this conclusion came from studies showing that acute gastric infection of *H. pylori* up-regulates expression of IFN- $\gamma$ , IFN- $\beta$ , and CXCL10 in the gastric mucosa of NOD1-intact mice and that mice that are deficient in NOD1 or type I IFN receptor expression exhibit increased bacterial burden following oral challenge with *H. pylori* as compared with NOD1-intact or type I IFN receptor-intact mice.<sup>10)</sup>

The role of epithelial cells in NOD1 induction of Th1 responses during *H. pylori* infection discussed above is highlighted by the fact that CXCL10 produced by such cells attracts CXCR3-expressing Th1 cells<sup>66)–68)</sup> and that expression of CXCL10 is in fact observed in the stomach of patients with *H. pylori* infection.<sup>86)</sup> Furthermore, since the major Th1 cytokine, IFN- $\gamma$ , up-regulates NOD1 expression,<sup>10),41)</sup> adaptive Th1 cells producing IFN- $\gamma$  may

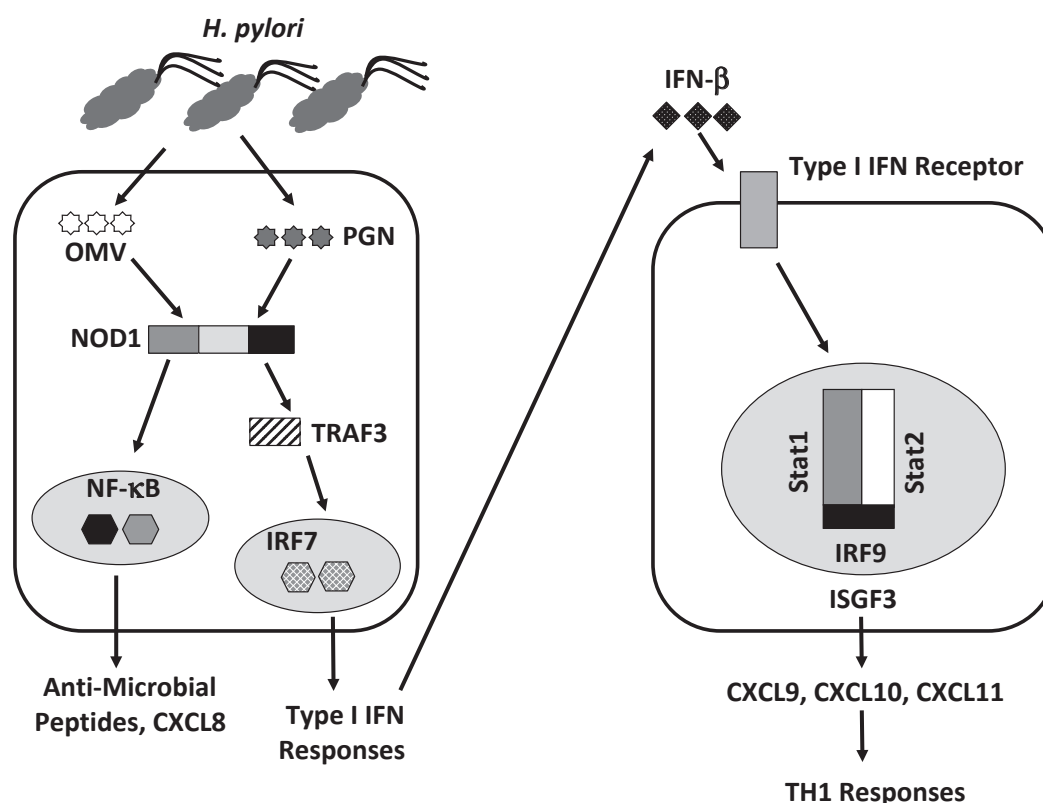


Fig. 2. Involvement of NOD1 in mucosal host defense against *Helicobacter pylori* infection. Nucleotide-binding oligomerization domain 1 (NOD1) expressed in gastric epithelial cells detects peptidoglycan (PGN) or outer membrane vesicles (OMVs) derived from *Helicobacter pylori* (*H. pylori*). Sensing of PGN or OMV by NOD1 causes nuclear translocation of nuclear factor- $\kappa$ B (NF- $\kappa$ B) subunits to induce production of C-X-C motif chemokine ligand 8 (CXCL8) and anti-microbial peptides. Sensing of PGN by NOD1 causes nuclear translocation of interferon regulatory factor 7 (IRF7) through activation of TNF receptor associated factor 3 (TRAF3) to induce production of IFN- $\beta$ . Production of IFN- $\beta$  causes activation of interferon stimulated gene factor 3 (ISGF3), a heterotrimer composed of signal transduction and activator of transcription 1 (Stat1), Stat2, and IRF9 to induce production of T helper type 1 (Th1) chemokines such as CXCL9, CXCL10, and CXCL11.

Table 1. NOD1 activation and gastrointestinal disorders

	NOD1-triggering factors	NOD1-expressing cells	Responses induced by NOD1 activation	Outcome
<i>H. pylori</i> -associated gastritis	Type IV secretion system, OMV transport	Gastric epithelial cells	AMP $\uparrow$ CXCL8 $\uparrow$ CXCL10 $\uparrow$ Type I IFN $\uparrow$	Protection against infection
<i>H. pylori</i> -associated gastric cancer	Type IV secretion system, OMV transport	Gastric epithelial cells	CDX2 $\downarrow$	Cancer development inhibition
Acute pancreatitis	Bacterial translocation	Pancreatic acinar cells	CCL2 $\uparrow$ Type I IFN $\uparrow$	Induction of acute pancreatitis
Chronic pancreatitis	Bacterial translocation	Pancreatic acinar cells	Type I IFN $\uparrow$ CCL2 $\uparrow$ IL-33 $\uparrow$	Induction of chronic pancreatitis



activate innate immune responses through their effect on epithelial expression of NOD1, correlating with the fact that significantly increased expression of NOD1, IFN- $\gamma$ , and CXCL10 has been seen in human gastric biopsies displaying severe *H. pylori*-related gastritis as compared with those displaying mild gastritis.<sup>87)</sup> Taken together, these findings suggest the existence of a positive feedback loop between NOD1 responses of epithelial cells and Th1 responses of lymphoid cells.

As mentioned above, the RIP2-TRAF3-TBK1-IKK $\epsilon$ -IRF7 axis leading to signaling via the type I IFN receptor and activation of ISGF3 plays a major role in NOD1 induction of type I IFN responses in gastric epithelial cells.<sup>10)</sup> Thus, NOD1 activation of CXCL9, CXCL10, and CXCL11 transcription via type I IFN requires nuclear translocation of ISGF3, a complex composed of Stat1, Stat2, and IRF9.<sup>10)</sup> On this basis Watanabe *et al.* examined the activation status of ISGF3 components in the gastric mucosa of mice challenged with *H. pylori* and found that Stat1 and Stat2 activation was enhanced in the gastric mucosa of NOD1-intact mice whereas no such activation was observed in NOD1-deficient mice.<sup>10)</sup> Furthermore, NOD1-intact mice treated with Stat1-specific siRNA exhibited increased bacterial burden of *H. pylori* in the stomach with diminished production of CXCL10 and IFN- $\gamma$ .<sup>10)</sup> Thus, it was evident that NOD1 induction of type I IFN in epithelial cells does require activation of ISGF3.

Interestingly, although NF- $\kappa$ B activation is a major outcome of NOD1-mediated signaling, NOD1-mediated mucosal host defense against acute infection with *H. pylori* does not depend on NF- $\kappa$ B activation. This became apparent from the fact that treatment of *H. pylori*-challenged mice with NF- $\kappa$ B decoy oligonucleotides did not reduce the gastric expression of Th1 chemokines as compared with mice treated with control scrambled oligonucleotides, although treatment with NF- $\kappa$ B decoy oligonucleotides did lead to a marked reduction in the expression of NF- $\kappa$ B-related genes such as TNF and CXCL2.<sup>10)</sup> Thus, NOD1 mediates mucosal host defense against *H. pylori* through the type I IFN-ISGF3 pathway rather than the NF- $\kappa$ B pathway. In line with this conclusion, Hirata *et al.* showed that activation of NF- $\kappa$ B induced by infection with *H. pylori* does not depend upon NOD1.<sup>88)</sup>

Detection of *H. pylori*-derived PGN by NOD1 in gastric epithelial cells induces other anti-microbial responses in addition to those involving type I IFN described above. Thus, *H. pylori* infection of gastric

epithelial cells causes IL-8 production via NOD1-dependent MAPK activation and thereby leads to the migration of neutrophils into the gastric mucosa.<sup>89)</sup> In addition, NOD1 causes epithelial cell release of AMPs capable of direct killing of *H. pylori* organisms.<sup>33)</sup> It is therefore obvious that NOD1 utilizes various pathways to protect the hosts from gastric infection with *H. pylori*.

**NOD1 activation and gastric cancer (Figure 3 and Table 1).** Chronic infection of the gastric mucosa with *H. pylori* is the strongest known risk factor for the development of gastric carcinogenesis.<sup>78)</sup> This is most likely related to the fact that chronic immune stimulation of the mucosal immune system creates a local milieu that supports malignant

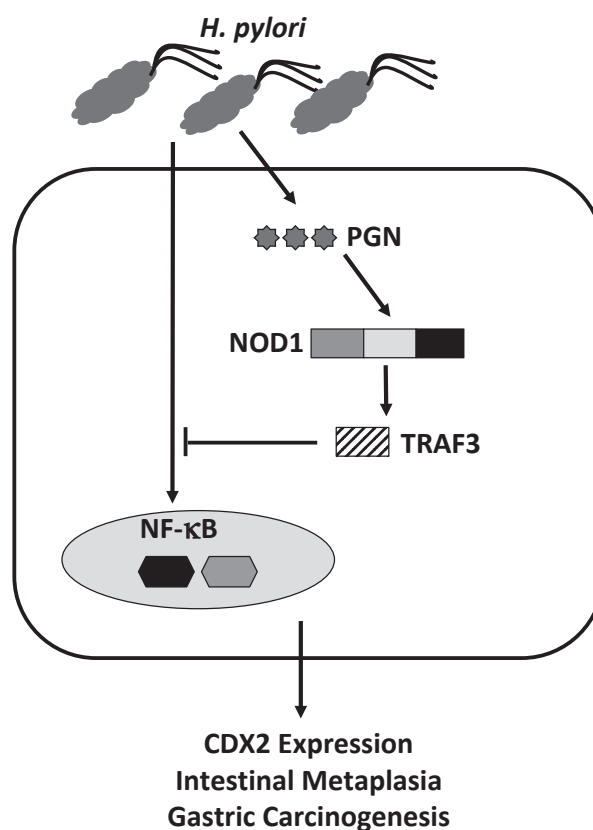


Fig. 3. Involvement of NOD1 in gastric carcinogenesis associated with *Helicobacter pylori* infection. Nucleotide-binding oligomerization domain 1 (NOD1) expressed in gastric epithelial cells detects peptidoglycan (PGN) derived from *Helicobacter pylori* (*H. pylori*). Exposure to *H. pylori* in gastric epithelial cells causes nuclear translocation of nuclear factor- $\kappa$ B (NF- $\kappa$ B) subunits to induce expression of caudal-type homeobox protein 2 (CDX2), a critical factor for intestinal metaplasia and gastric carcinogenesis. This induction of CDX2 expression is negatively regulated by activation of NOD1-TNF receptor associated factor 3 (TRAF3) pathways.

transformation of epithelial cells such as the induction of cytokines that induce transformation of cells with up-regulated oncogenes; however, it is also possible that immune responses can protect against malignant transformation. As described above, NOD1 is a major innate immune sensor of *H. pylori* infection and is therefore likely to be involved in the development of *H. pylori*-associated gastric cancer, either as positive or negative factor. Indeed, Suarez *et al.* performed expression analysis of NOD1 in the human gastric cancer mucosa and non-cancer mucosa<sup>90)</sup> and found that epithelial staining intensity of NOD1 was much lower in gastric cancer mucosa as compared with non-cancer mucosa, suggesting that that in this case, an innate immune response is serving to protect against the development of gastric cancer.<sup>90)</sup>

Caudal-type homeobox protein 2 (Cdx2) is a gastric epithelial cell-derived trans-differentiation factor that plays a pivotal but as yet poorly understood role in the development of “intestinal type” gastric adenocarcinoma; as such its expression serves as a harbinger of eventual development of gastric malignancy.<sup>91)</sup> Thus, as expected, expression of Cdx2 was significantly higher in human gastric cancer mucosa than in non-cancerous mucosa. Asano *et al.*, explored the possibility that NOD1 was affecting malignant transformation via an effect on Cdx2 expression and conducted extensive studies elucidating the molecular mechanisms governing the relation of NOD1 signaling and Cdx2 expression.<sup>11)</sup> They found that Cdx2 expression in epithelial cell lines is induced by infection with *H. pylori* and that such expression is dependent on NF- $\kappa$ B activation. Unexpectedly, they also found that activation of NOD1 negatively regulates *H. pylori*-induced Cdx2 expression since siRNA-mediated knockdown of NOD1 markedly enhanced Cdx2 expression upon exposure to *H. pylori*. In line with previous findings discussed above showing that NOD1/RIP2-mediated TRAF3 activation triggers type I IFN responses rather than NF- $\kappa$ B-related responses,<sup>10)</sup> Cdx2 expression induced by exposure to *H. pylori* was markedly reduced in gastric cancer cells overexpressing TRAF3. They thus concluded that the unique ability of NOD1-activated RIP2 to interact with TRAF3 leads to down-regulation of NF- $\kappa$ B support of Cdx2 expression.

In related studies, Asano *et al.* provide *in vivo* data that support the *in vitro* findings described above.<sup>11)</sup> First, they found that the frequency of goblet cells, highly indicative of pre-cancerous intestinal metaplasia, was more evident in the gastric

mucosa of NOD1-deficient mice 12 months after infection with *H. pylori* than in NOD1-intact mice. Moreover, gastric tissues of NOD1-deficient mice with prolonged *H. pylori* infection exhibited higher levels of Cdx2 expression and lower levels of TRAF3 expression than those of NOD1-intact mice. Moreover, nuclear translocation of NF- $\kappa$ B subunit p65 was enhanced in the gastric tissues of NOD1-deficient mice with prolonged *H. pylori* infection as compared with those of NOD1-intact mice. These *in vivo* studies thus again suggest that NOD1 activation of TRAF3 and the latter's inhibition of NF- $\kappa$ B activation suppress gastric carcinogenesis induced by prolonged *H. pylori* infection. It should be noted that this conclusion meshes quite well with the role of NOD1 as a host defense factor in protection against *H. pylori* infection since in both cases NOD1 is operating via a TRAF3-mediated signaling pathway that favors type I IFN responses rather than NF- $\kappa$ B responses.

#### NOD1 and pancreatitis

**Trypsinogen activation and pancreatitis.** Pancreatitis is one of the major inflammatory disorders of the GI tract and as such has been subjected to considerable research probing its pathogenesis.<sup>92),93)</sup> Nevertheless, it remains poorly understood, particularly with respect to the possible contribution of causative immunologic factors. Recently, it has been discovered that NOD1 plays a major pathogenic role in pancreatitis and will be the focus of this analysis of pancreatitis pathogenesis.<sup>14)</sup>

It is useful to discuss the acute and chronic forms of pancreatitis separately because, while these types of pancreatitis share underlying features, they also have specific manifestations. Acute pancreatitis is defined as sudden inflammation of the exocrine pancreas occurring in a previously normal pancreas and that may undergo resolution without causing permanent pancreatic damage. Chronic pancreatitis is a persistent inflammation of the pancreas usually punctuated by acute exacerbations and occurring in a pancreas that bears the marks of previous episodes of inflammation.<sup>14),94),95)</sup>

An underlying feature of both acute and chronic pancreatitis is dysfunction in the management of potentially corrosive digestive enzymes that are secreted by the pancreas into the intestine and are necessary for normal digestion. In the normal state these enzymes are synthesized in pancreatic acinar cells as inactive pro-enzymes (such as trypsinogen) and are maintained in this state until activated by

enterokinase upon entry into the gut lumen.<sup>96),97)</sup> It is widely believed that pancreatitis is initiated by genetic or environmental factors (the latter including excessive alcohol intake or intake of high fat foods) that cause inappropriate intra-pancreatic activation of pancreatic digestive enzymes, especially trypsinogen, and this is followed by auto-digestion of pancreatic tissue and inflammation.<sup>96),97)</sup>

Strong support of this “trypsin-centered” theory of pancreatitis pathogenesis comes from studies of hereditary pancreatitis in humans.<sup>98)</sup> In these studies it was found that various pancreatitis-associated mutations of PRSS1 gene (the gene encoding the main form of trypsinogen, cationic trypsinogen) lead to a form of trypsinogen that is subject to inappropriate activation or to resistance to intra-cellular degradation after inadvertently activation.<sup>98)</sup> In addition, various mutations of the pancreatitis-associated gene, serine protease inhibitor, Kazal type I (SPINK1) gene (the gene encoding an inhibitor of activated trypsin) impairs negative regulation of trypsinogen activation occurring in acinar cells.<sup>98)</sup> Thus, these genetic studies as well as studies of experimental pancreatitis in mice<sup>14),98)</sup> bolster the concept that inappropriate trypsinogen activation followed by auto-digestion initiates and sustains inflammatory responses of the pancreas.

The trypsin-centered theory of pancreatitis has recently been challenged by an extensive analysis of T7 trypsinogen-depleted mice, *i.e.*, mice that do not synthesize the murine form of trypsin thought to be equivalent to human inflammation-inducing cationic trypsin mentioned above.<sup>99)–101)</sup> Mice deficient in T7 trypsinogen exhibit a marked reduction in activation of trypsinogen but nevertheless exhibit comparable levels of acute and chronic experimental pancreatitis induced by repeated injections of cerulein, a cholecystokinin receptor (CCKR) agonist as observed in wild type mice.<sup>99),100)</sup> These results thus suggested that experimental pancreatitis can occur independently of trypsinogen activation and that pathogenesis of pancreatitis cannot be explained by the trypsin-centered theory alone. It should be noted, however, that these studies do not rule out the possibility that *in vivo*, potentially inflammatory trypsinogen may not consist of T7 trypsinogen alone and that T7 trypsinogen depletion leaves intact other isoforms of trypsinogen that could still be mediating pancreatitis. On this basis, the most reasonable interpretation of studies on the role of trypsinogen activation as an initiator and sustainer of pancreatitis is that such activation is necessary but not sufficient as a cause

of pancreatitis and that other presumably immune-related causes must be operative as well.

**NOD1 activation and acute pancreatitis (Figure 4 and Table 1).** Although in most patients acute pancreatitis is a self-limited inflammation in some patients a severe form of acute pancreatitis occurs that be associated with systemic manifestations of infection.<sup>95)</sup> Ultimately it was found that this clinical outcome was the result of bacterial colonization of the inflamed pancreas followed by infection of necrotic pancreatic tissue.<sup>95)</sup> Thus, such cases provided initial clinical evidence that pancreatitis is associated with disruption of the intestinal barrier followed by entry of intestinal microflora into the circulation and colonization of the pancreas.<sup>12),102)–107)</sup> This was more definitively examined in studies of experimental pancreatitis wherein it was formally shown that mice with pancreatitis have increased bowel permeability and that particles with the size of bacteria have been translocated into the pancreas.<sup>102)–107)</sup> Studies in humans of the types of organisms that enter the circulation by Li *et al.* using 16S rRNA based technology revealed that a broad range of bacteria are detected in the circulation of about 70% of patients; these bacteria were similar to commensal organisms in the GI tract and the latter were presumed to be their origin; however, in some cases the organisms were pathogens, perhaps accounting for the more severe cases of pancreatitis mentioned above.<sup>108)</sup> Of interest, bowel sterilization with a broad range of antibiotics effectively prevented the development of experimental pancreatitis; this finding suggested that translocated organisms play a significant role in pancreatitis pathogenesis.<sup>12),105)–107)</sup>

In initial studies designed to clarify the immune responses against intestinal microflora that might be playing a role in acute pancreatitis Watanabe and his colleagues subjected mice deficient in various innate immune receptors to experimental pancreatitis induced by repeated administration of relatively high doses of cerulein (50 µg/kg), the latter an agent that causes pancreatitis via excessive stimulation of the CCKR.<sup>12)</sup> They found that TLR2 and TLR9 deficient mice exhibited levels of pancreatitis equivalent to that in wild type mice and that TLR4-deficient mice, (that cannot respond to LPS) exhibited somewhat less pancreatitis than wild type mice. However, quite surprisingly, mice deficient in NOD1 were completely resistant to the development of cerulein-induced pancreatitis, indicating that innate recognition of NOD1 ligand derived from gut bacteria plays a major role in the development of pancreatitis. A central

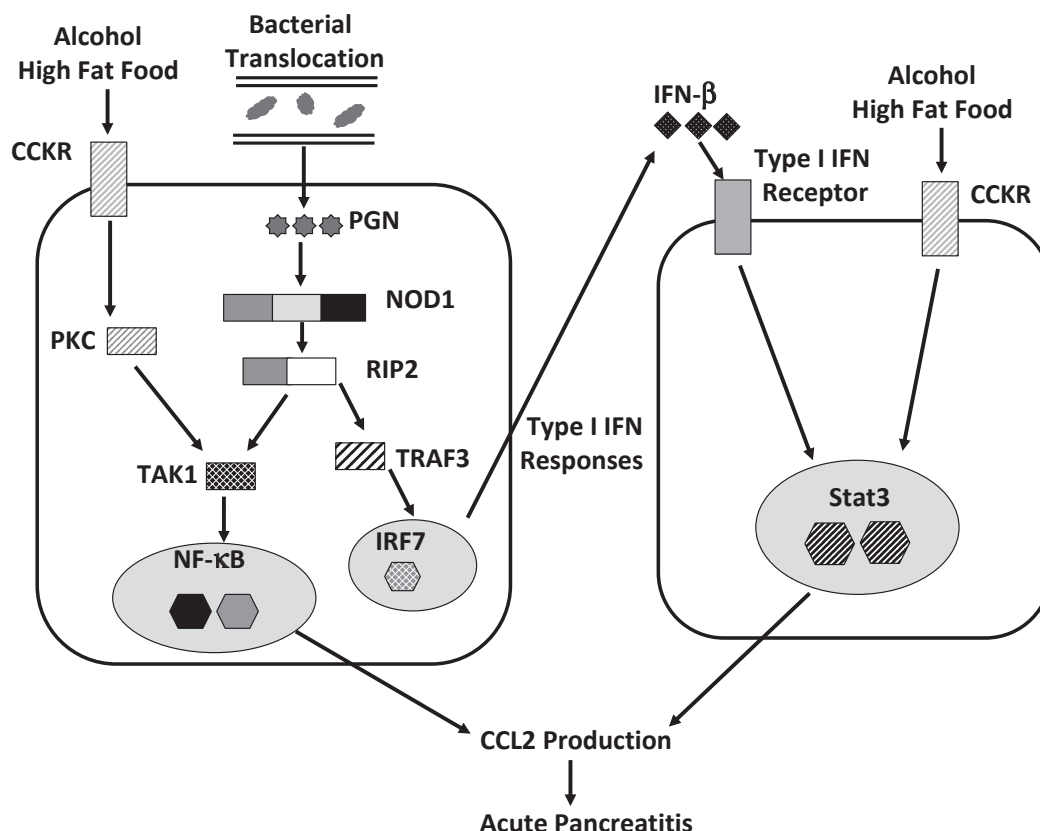


Fig. 4. Involvement of NOD1 in acute pancreatitis. Excessive drinking of alcohol and intake of high fat foods cause cholecystikinin receptor (CCKR) signaling pathways to induce intra-acinar activation of trypsinogen. Nucleotide-binding oligomerization domain 1 (NOD1) expressed in pancreatic acinar cells detects peptidoglycan (PGN) derived from intestinal microflora translocated into the pancreas. CCKR-mediated signaling pathway causes nuclear translocation of nuclear factor-κB (NF-κB) subunits through the interaction between protein kinase C (PKC) and TGF-β-activated kinase 1 (TAK1). NOD1-mediated signaling pathway causes nuclear translocation of NF-κB subunits through the interaction between receptor interacting protein 2 (RIP2) and TAK1. Synergistic activation of NF-κB is achieved by simultaneous activation of CCKR and NOD1. Sensing of PGN by NOD1 causes nuclear translocation of interferon regulatory factor 7 (IRF7) through activation of TNF receptor associated factor 3 (TRAF3) to induce production of IFN-β. Production of IFN-β induced by NOD1 activation acts together with CCKR activation to induce optimal activation of signal transduction and activator of transcription 3 (Stat3). Simultaneous activation of NOD1 and CCKR leads to a robust production of C-C motif chemokine ligand 2 (CCL2) by pancreatic acinar cells through activation of NF-κB and Stat3, which mediates migration of inflammatory myeloid cells into the pancreas.

question raised by this observation as well as the relation of pancreatitis to bacterial translocation discussed above, is why gut bacteria enter the circulation during acute pancreatitis. The most likely answer to this question is that pancreatic inflammation initially arising from trypsin activation sets in motion the intra-pancreatic activation of innate immune receptors that recognize damage-associated molecular patterns (DAMPs) released from dying pancreatic cells and then stimulate the production of a set of cytokines that change gut permeability and mediate bacterial translocation.<sup>109)–111)</sup>

To further define the role of NOD1 in the development of acute pancreatitis, Watanabe *et al.*,

established a new model of acute pancreatitis induced by simultaneous and repeated administration of low doses of cerulein (20 µg/kg) and FK156, an activator of NOD1 that mimics the effect of gut bacteria that have breached the mucosal barrier. The value of this method of inducing pancreatitis resided in the fact that whereas administration of low doses of cerulein alone or NOD1 ligand alone did not induce pancreatitis, the simultaneous administration of these agents does induce pancreatitis; thus this model enables one to analyze the separate molecular mechanisms of inflammation induced by each of the agents causing pancreatitis.<sup>12)</sup>

In initial studies utilizing this model, Watanabe *et al.* conducted bone marrow transplantation studies to determine the type of cells expressing NOD1 in the development of pancreatitis.<sup>12)</sup> They found that one could successfully induce acute pancreatitis in X-irradiated NOD1-intact mice transplanted with NOD1-deficient hematopoietic cells, but not in X-irradiated NOD1-deficient mice transplanted with NOD1-intact hematopoietic cells.<sup>12)</sup> These results strongly suggest NOD1 must be expressed in non-hematopoietic cells, most likely pancreatic acinar cells, to support pancreatitis development.

In related studies they determined the chemokines responsible for development of pancreatitis in this new model of pancreatitis. Here they found that simultaneous activation of NOD1 and cerulein stimulation of the CCKR led to robust production of C-C motif chemokine ligand 2 (CCL2) by pancreatic acinar cells and that mice deficient in C-C chemokine receptor type 2 (CCR2) did not develop pancreatitis.<sup>12)</sup> Thus, CCL2 produced by pancreatic acinar cells emerged as the key pathogenic chemokine in the development of acute pancreatitis induced by simultaneous activation of NOD1 and CCKR.

Finally, Watanabe *et al.* took advantage of the low dose cerulein-NOD1 ligand model of experimental acute pancreatitis described above to analyze the separate and synergistic acinar cell signaling induced by simultaneous NOD1 ligand and low dose cerulein stimulation characterizing the induction of pancreatitis. First, they found that both CCKR stimulation by cerulein and NOD1 signaling by NOD1 ligand was necessary for the activation of NF- $\kappa$ B, the single most important factor in the downstream pathway of pancreatic inflammation. Thus, whereas stimulation of CCKR by low dose cerulein induces protein kinase C (PKC) and TAK1 activation as in previous studies,<sup>112)</sup> the level of such activation by low dose cerulein alone is not sufficient to induce activation of NF- $\kappa$ B; likewise, NOD1 activation of RIP2 also is not sufficient to induce activation of NF- $\kappa$ B. In contrast, simultaneous activation of these pathways by NOD1 ligand and low dose cerulein administered together led to a level of TAK1 activation that was now sufficient to induce activation of NF- $\kappa$ B. This finding is seemingly at odds with the observation alluded to above that high dose cerulein administration is able to induce pancreatitis in the apparent absence of NOD1 ligand. However, this latter observation is more apparent than real, since high dose cerulein is able to induce a sufficient level of inflammation in the pancreas (via trypsin activation?) to cause

translocation of gut bacteria into the circulation and thus stimulation of acinar cells by bacterial NOD1; thus even high dose cerulein requires NOD1 activation, as confirmed by the observation already discussed that high dose cerulein does not induce pancreatitis in the sterilized mouse.

A second set of insights derived from the low dose cerulein-NOD1 ligand pancreatitis model was that synergistic stimulation by NOD1 ligand and cerulein is also necessary for the optimal generation of Stat3, a signaling component necessary for the up-regulation of CCL2 expression, the critically important chemokine necessary for the pancreatic influx of inflammatory macrophages. As noted in previous studies, stimulation of CCKR by cerulein results in the induction of Stat3 activation.<sup>113)</sup> However, such induction is greatly enhanced by type I IFN induced by NOD1 signaling and thus simultaneous activation of NOD1 and CCKR induces synergistic and optimal, activation of Stat3 in pancreatic acinar cells. In addition, in line with the fact that the expression of CCL2 requires transactivation of NF- $\kappa$ B and Stat3,<sup>114)</sup> synergistic activation of NF- $\kappa$ B and Stat3 induced by simultaneous injections with low doses of cerulein and NOD1 ligand is responsible for a robust production of CCL2 by pancreatic acinar cells.

Taken together, the model of experimental acute pancreatitis induced by low dose cerulein and NOD1 ligand provides a rich trove of new insights into the immuno-pathogenesis of pancreatitis that is likely to apply to human pancreatitis. Perhaps the most important of these is the increased recognition that bacteria entering the circulation as a result of DAMPs release in the pancreas and then stimulation of acinar cells via NOD1 are an essential feature of acute pancreatitis pathogenesis.

**NOD1 activation and chronic pancreatitis (Figure 5 and Table 1).** The model of acute pancreatitis described above to investigate the immunologic factors in the pathogenesis of pancreatitis was subsequently used as template by Watanabe *et al.*, as a way to develop a model of chronic pancreatitis. In this chronic model, mice were again administered repeated doses of NOD1 ligand and low doses of cerulein, but in this case this regimen was maintained for a longer period of time. The chronic pancreatitis that ensued was characterized by a massive infiltration of immune cells and the appearance of a characteristic feature of chronic pancreatitis, intense fibrosis and reduction in functional pancreatic parenchymal mass.<sup>13)</sup> As in the acute pancreatitis model, NOD1 expressed in pancreatic



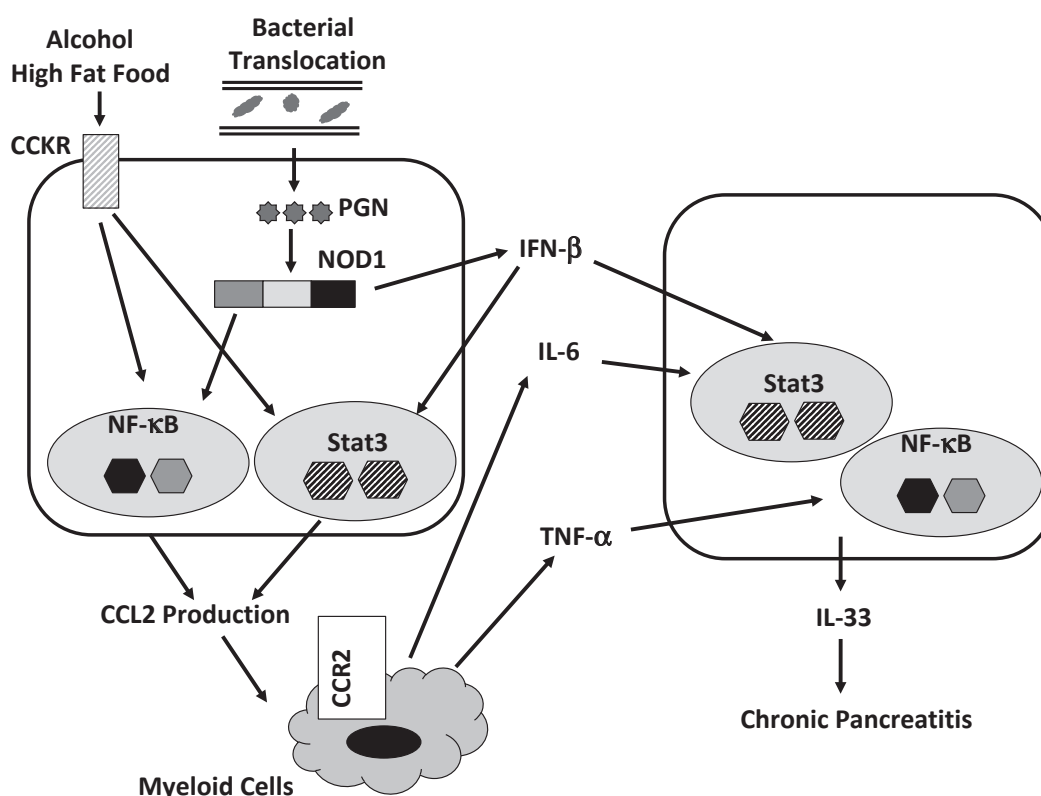


Fig. 5. Involvement of NOD1 in chronic pancreatitis. Simultaneous activation of nucleotide-binding oligomerization domain 1 (NOD1) and cholecystikinin receptor (CCKR) leads to a robust production of C-C motif chemokine ligand 2 (CCL2) through activation of nuclear factor- $\kappa$ B (NF- $\kappa$ B) and signal transduction and activator of transcription 3 (Stat3), which mediates migration of C-C chemokine receptor type 2 (CCR2)-expressing inflammatory myeloid cells into the pancreas. CCR2-expressing inflammatory myeloid cells produce pro-inflammatory cytokines such as TNF- $\alpha$  and IL-6. TNF- $\alpha$  and IFN- $\beta$  produced by myeloid cells and pancreatic acinar cells, respectively, lead to a robust production of IL-33. IL-33 mediates chronic fibro-inflammatory responses of the pancreas.

acinar cells played an indispensable role in the chronic pancreatitis model as shown in studies of chimeric mice: X-irradiated NOD1-intact mice transplanted with NOD1-deficient hematopoietic cells were susceptible to chronic pancreatitis whereas X-irradiated NOD1-deficient mice transplanted with NOD1-intact hematopoietic cells were resistant to chronic pancreatitis. In addition, type I IFN responses were, as in the acute model, again shown to be essential for the development of pancreatitis as shown by the fact that type I IFN receptor-deficient mice were resistant to the development of chronic pancreatitis. The role of type I IFN in the induction of chronic pancreatitis is related to its capacity to elicit Stat3 activation and CCL2 expression necessary for the influx of the inflammatory macrophages that mediate the pancreatic inflammation (as briefly alluded to above in the discussion of acute pancreatitis). In addition, studies of the chronic model disclosed that type I IFN plays a key role in the

macrophage TNF- $\alpha$  production, the cytokine most responsible for acinar cell death. Thus, in these studies it was shown that pancreatic acinar cells derived from the inflamed pancreas and co-cultured with CD11b<sup>+</sup> macrophages release increased amounts of IL-33.<sup>13),14)</sup> Moreover, it was shown that such IL-33 secretion was inhibited by type I IFN receptor Ab or anti-TNF- $\alpha$  Ab, agents that block macrophage TNF- $\alpha$  production and acinar cell IL-33 production, respectively.<sup>13),14)</sup>

In further studies of the chronic pancreatitis model, pancreatic lysates obtained from inflamed pancreas were analyzed to characterize the cytokine and chemokine responses accompanying the chronic pancreatic inflammation. As expected, these studies disclosed that a number of prototypical pro-inflammatory factors are produced in the chronic pancreatic tissue including TNF- $\alpha$ , IL-6, IFN- $\gamma$ , and IFN- $\beta$  among the cytokines and CCL2, CXCL9 and CXCL10 among the chemokines. In addition, the

chronic pancreatitis was accompanied by secretion of several pro-fibrogenic cytokines such as IL-33, IL-13, and TGF- $\beta$ 1.<sup>115)–117)</sup> Thus, chronic and simultaneous activation of NOD1 and CCKR enhances production of cytokines and chemokines that mediate both pro-inflammatory and pro-fibrogenic responses.<sup>13),14)</sup>

Given the importance of pancreatic fibrosis in shaping the character of chronic pancreatitis, the chronic model was also used to define the mechanisms of fibrosis development in chronic pancreatitis. Perhaps the most important finding here was the fact that neutralization of IL-33 signaling by blockade of the IL-33 receptor with anti-ST2 Ab inhibited both inflammatory and fibrogenic responses due to accompanying reduction in the IL33-induced expression of TNF- $\alpha$ , CCL2, IL-13, and TGF- $\beta$ 1. As noted above, IL-33 production by acinar cells is increased upon co-culture with pancreatic myeloid cells (macrophages) that are being stimulated by type I IFN, strongly suggesting that such myeloid cells produce TNF- $\alpha$  that induces IL-33 production by acinar cells.<sup>118)</sup> Thus, the fibrosis of chronic pancreatitis has its origin in the inflammatory effect of macrophages on acinar cells. Finally, it is important to emphasize that IL-33 induction of fibrosis is directly correlated with its induction of IL-13, a cytokine that plays a critical role in tissue fibrogenesis generally<sup>115),116)</sup> as well as in the chronic pancreatitis model studied. The latter was established by studies showing that neutralization of IL-13 (by administration of anti-IL-13 Ab) protected mice from the development of fibrosis and that such neutralization was accompanied by reduced pancreatic expression of TGF- $\beta$ 1, a major effector of fibrosis but not CCL2 and IFN- $\beta$ , major pro-inflammatory factors.<sup>13)</sup> Interestingly, the IL-13 induced by IL-33 was produced by CD4<sup>+</sup> T cells inasmuch as T cell-deficient mice are resistant to the development of chronic pancreatitis.<sup>13)</sup>

### Concluding remarks

This review of NOD1 function discloses that this NLR-type innate intra-cellular sensor of PGN peptides mediates a wide array of immunologic functions affecting host defense including activation of the NF- $\kappa$ B and MAPK responses as well as induction of the type I IFN response. As such, NOD1 plays a surprisingly important role in several inflammatory diseases of the GI tract including *H. pylori* infection of the gastric mucosa and in both acute and chronic pancreatitis. Thus, in *H. pylori* infection NOD1 is essential in the induction of protective type I IFN responses and activation of the ISGF3 signaling

pathway. In addition, NOD1 inhibits gastric carcinogenesis through negative regulation of Cdx2 expression. Finally, in pancreatitis responses to translocated bacteria by NOD1 expressed by acinar cells are responsible both for the influx of inflammatory macrophages and for the acinar cell-destructive effect of TNF- $\alpha$  leading to the expression of IL-33 and pancreatic fibrosis. These newly defined roles of NOD1 in GI inflammation call attention to the possibility that manipulation of NOD1 function can be the focus of new forms of therapy.

### Acknowledgements

This work was supported by Grants-in-Aid for Scientific Research (25293172, 15K15370) from the Japan Society for the Promotion of Science, the Kato Memorial Trust for Nambyo Research, the Naito Foundation, Yakult Bioscience Foundation, SENSHIN Medical Research Foundation, Smoking Research Foundation and Japan Agency for Medical Research and Development (AMED) Grants for Research on Intractable Diseases.

### References

- 1) Akira, S. and Takeda, K. (2004) Toll-like receptor signalling. *Nat. Rev. Immunol.* **4**, 499–511.
- 2) Pisetsky, D.S. (2008) The role of innate immunity in the induction of autoimmunity. *Autoimmun. Rev.* **8**, 69–72.
- 3) Strober, W., Murray, P.J., Kitani, A. and Watanabe, T. (2006) Signalling pathways and molecular interactions of NOD1 and NOD2. *Nat. Rev. Immunol.* **6**, 9–20.
- 4) Franchi, L., Warner, N., Viani, K. and Nunez, G. (2009) Function of Nod-like receptors in microbial recognition and host defense. *Immunol. Rev.* **227**, 106–128.
- 5) Philpott, D.J., Sorbara, M.T., Robertson, S.J., Croitoru, K. and Girardin, S.E. (2014) NOD proteins: regulators of inflammation in health and disease. *Nat. Rev. Immunol.* **14**, 9–23.
- 6) Caruso, R., Warner, N., Inohara, N. and Nunez, G. (2014) NOD1 and NOD2: signaling, host defense, and inflammatory disease. *Immunity* **41**, 898–908.
- 7) Chamaillard, M., Hashimoto, M., Horie, Y., Masumoto, J., Qiu, S., Saab, L., Ogura, Y., Kawasaki, A., Fukase, K., Kusumoto, S., Valvano, M.A., Foster, S.J., Mak, T.W., Nunez, G. and Inohara, N. (2003) An essential role for NOD1 in host recognition of bacterial peptidoglycan containing diaminopimelic acid. *Nat. Immunol.* **4**, 702–707.
- 8) Bouskra, D., Brezillon, C., Berard, M., Werts, C., Varona, R., Boneca, I.G. and Eberl, G. (2008) Lymphoid tissue genesis induced by commensals through NOD1 regulates intestinal homeostasis. *Nature* **456**, 507–510.

- 9) Viala, J., Chaput, C., Boneca, I.G., Cardona, A., Girardin, S.E., Moran, A.P., Athman, R., Memet, S., Huerre, M.R., Coyle, A.J., DiStefano, P.S., Sansonetti, P.J., Labigne, A., Bertin, J., Philpott, D.J. and Ferrero, R.L. (2004) Nod1 responds to peptidoglycan delivered by the *Helicobacter pylori* cag pathogenicity island. *Nat. Immunol.* **5**, 1166–1174.
- 10) Watanabe, T., Asano, N., Fichtner-Feigl, S., Gorelick, P.L., Tsuji, Y., Matsumoto, Y., Chiba, T., Fuss, I.J., Kitani, A. and Strober, W. (2010) NOD1 contributes to mouse host defense against *Helicobacter pylori* via induction of type I IFN and activation of the ISGF3 signaling pathway. *J. Clin. Invest.* **120**, 1645–1662.
- 11) Asano, N., Imatani, A., Watanabe, T., Fushiya, J., Kondo, Y., Jin, X., Ara, N., Uno, K., Iijima, K., Koike, T., Strober, W. and Shimosegawa, T. (2016) Cdx2 expression and intestinal metaplasia induced by *H. pylori* infection of gastric cells is regulated by NOD1-mediated innate immune responses. *Cancer Res.* **76**, 1135–1145.
- 12) Tsuji, Y., Watanabe, T., Kudo, M., Arai, H., Strober, W. and Chiba, T. (2012) Sensing of commensal organisms by the intracellular sensor NOD1 mediates experimental pancreatitis. *Immunity* **37**, 326–338.
- 13) Watanabe, T., Sadakane, Y., Yagama, N., Sakurai, T., Ezoe, H., Kudo, M., Chiba, T. and Strober, W. (2016) Nucleotide-binding oligomerization domain 1 acts in concert with the cholecystokinin receptor agonist, cerulein, to induce IL-33-dependent chronic pancreatitis. *Mucosal Immunol.* **9**, 1234–1249.
- 14) Watanabe, T., Kudo, M. and Strober, W. (2017) Immunopathogenesis of pancreatitis. *Mucosal Immunol.* **10**, 283–298.
- 15) Sasawatari, S., Okamura, T., Kasumi, E., Tanaka-Furuyama, K., Yanobu-Takanashi, R., Shirasawa, S., Kato, N. and Toyama-Sorimachi, N. (2011) The solute carrier family 15A4 regulates TLR9 and NOD1 functions in the innate immune system and promotes colitis in mice. *Gastroenterology* **140**, 1513–1525.
- 16) Nakamura, N., Lill, J.R., Phung, Q., Jiang, Z., Bakalarski, C., de Maziere, A., Klumperman, J., Schlatter, M., Delamarre, L. and Mellman, I. (2014) Endosomes are specialized platforms for bacterial sensing and NOD2 signalling. *Nature* **509**, 240–244.
- 17) Irving, A.T., Mimuro, H., Kufer, T.A., Lo, C., Wheeler, R., Turner, L.J., Thomas, B.J., Malosse, C., Gantier, M.P., Casillas, L.N., Votta, B.J., Bertin, J., Boneca, I.G., Sasakawa, C., Philpott, D.J., Ferrero, R.L. and Kaparakis-Liaskos, M. (2014) The immune receptor NOD1 and kinase RIP2 interact with bacterial peptidoglycan on early endosomes to promote autophagy and inflammatory signaling. *Cell Host Microbe* **15**, 623–635.
- 18) Fritz, J.H., Girardin, S.E., Fitting, C., Werts, C., Mengin-Lecreux, D., Caroff, M., Cavaillon, J.M., Philpott, D.J. and Adib-Conquy, M. (2005) Synergistic stimulation of human monocytes and dendritic cells by toll-like receptor 4 and NOD1- and NOD2-activating agonists. *Eur. J. Immunol.* **35**, 2459–2470.
- 19) Tada, H., Aiba, S., Shibata, K., Ohteki, T. and Takada, H. (2005) Synergistic effect of Nod1 and Nod2 agonists with toll-like receptor agonists on human dendritic cells to generate interleukin-12 and T helper type 1 cells. *Infect. Immun.* **73**, 7967–7976.
- 20) Fritz, J.H., Le Bourhis, L., Sellge, G., Magalhaes, J.G., Fsihi, H., Kufer, T.A., Collins, C., Viala, J., Ferrero, R.L., Girardin, S.E. and Philpott, D.J. (2007) Nod1-mediated innate immune recognition of peptidoglycan contributes to the onset of adaptive immunity. *Immunity* **26**, 445–459.
- 21) Magalhaes, J.G., Rubino, S.J., Travassos, L.H., Le Bourhis, L., Duan, W., Sellge, G., Geddes, K., Reardon, C., Lechmann, M., Carneiro, L.A., Selvanantham, T., Fritz, J.H., Taylor, B.C., Artis, D., Mak, T.W., Comeau, M.R., Croft, M., Girardin, S.E. and Philpott, D.J. (2011) Nucleotide oligomerization domain-containing proteins instruct T cell helper type 2 immunity through stromal activation. *Proc. Natl. Acad. Sci. U.S.A.* **108**, 14896–14901.
- 22) Le Bourhis, L., Magalhaes, J.G., Selvanantham, T., Travassos, L.H., Geddes, K., Fritz, J.H., Viala, J., Tedin, K., Girardin, S.E. and Philpott, D.J. (2009) Role of Nod1 in mucosal dendritic cells during *Salmonella* pathogenicity island 1-independent *Salmonella enterica* serovar Typhimurium infection. *Infect. Immun.* **77**, 4480–4486.
- 23) Kim, Y.G., Park, J.H., Reimer, T., Baker, D.P., Kawai, T., Kumar, H., Akira, S., Wobus, C. and Nunez, G. (2011) Viral infection augments Nod1/2 signaling to potentiate lethality associated with secondary bacterial infections. *Cell Host Microbe* **9**, 496–507.
- 24) Kim, Y.G., Park, J.H., Shaw, M.H., Franchi, L., Inohara, N. and Nunez, G. (2008) The cytosolic sensors Nod1 and Nod2 are critical for bacterial recognition and host defense after exposure to toll-like receptor ligands. *Immunity* **28**, 246–257.
- 25) Liew, F.Y., Xu, D., Brint, E.K. and O'Neill, L.A. (2005) Negative regulation of toll-like receptor-mediated immune responses. *Nat. Rev. Immunol.* **5**, 446–458.
- 26) Petterson, T., Jendholm, J., Mansson, A., Bjartell, A., Riesbeck, K. and Cardell, L.O. (2011) Effects of NOD-like receptors in human B lymphocytes and crosstalk between NOD1/NOD2 and toll-like receptors. *J. Leukoc. Biol.* **89**, 177–187.
- 27) Petterson, T., Mansson, A., Riesbeck, K. and Cardell, L.O. (2011) Nucleotide-binding and oligomerization domain-like receptors and retinoic acid inducible gene-like receptors in human tonsillar T lymphocytes. *Immunology* **133**, 84–93.
- 28) Clarke, T.B., Davis, K.M., Lysenko, E.S., Zhou, A.Y., Yu, Y. and Weiser, J.N. (2010) Recognition of peptidoglycan from the microbiota by Nod1

- enhances systemic innate immunity. *Nat. Med.* **16**, 228–231.
- 29) Hergott, C.B., Roche, A.M., Tamashiro, E., Clarke, T.B., Bailey, A.G., Laughlin, A., Bushman, F.D. and Weiser, J.N. (2016) Peptidoglycan from the gut microbiota governs the lifespan of circulating phagocytes at homeostasis. *Blood* **127**, 2460–2471.
  - 30) Natividad, J.M., Petit, V., Huang, X., de Palma, G., Jury, J., Sanz, Y., Philpott, D., Garcia Rodenas, C.L., McCoy, K.D. and Verdu, E.F. (2012) Commensal and probiotic bacteria influence intestinal barrier function and susceptibility to colitis in *Nod1*<sup>−/−</sup>; *Nod2*<sup>−/−</sup> mice. *Inflamm. Bowel Dis.* **18**, 1434–1446.
  - 31) Robertson, S.J., Zhou, J.Y., Geddes, K., Rubino, S.J., Cho, J.H., Girardin, S.E. and Philpott, D.J. (2013) *Nod1* and *Nod2* signaling does not alter the composition of intestinal bacterial communities at homeostasis. *Gut Microbes* **4**, 222–231.
  - 32) Amendola, A., Butera, A., Sanchez, M., Strober, W. and Boirivant, M. (2014) *Nod2* deficiency is associated with an increased mucosal immunoregulatory response to commensal microorganisms. *Mucosal Immunol.* **7**, 391–404.
  - 33) Grubman, A., Kaparakis, M., Viala, J., Allison, C., Badea, L., Karrar, A., Boneca, I.G., Le Bourhis, L., Reeve, S., Smith, I.A., Hartland, E.L., Philpott, D.J. and Ferrero, R.L. (2010) The innate immune molecule, *NOD1*, regulates direct killing of *Helicobacter pylori* by antimicrobial peptides. *Cell. Microbiol.* **12**, 626–639.
  - 34) Watanabe, T., Asano, N., Kitani, A., Fuss, I.J., Chiba, T. and Strober, W. (2011) Activation of type I IFN signaling by *NOD1* mediates mucosal host defense against *Helicobacter pylori* infection. *Gut Microbes* **2**, 61–65.
  - 35) Kim, J.G., Lee, S.J. and Kagnoff, M.F. (2004) *Nod1* is an essential signal transducer in intestinal epithelial cells infected with bacteria that avoid recognition by toll-like receptors. *Infect. Immun.* **72**, 1487–1495.
  - 36) Hasegawa, M., Yamazaki, T., Kamada, N., Tawaratsumida, K., Kim, Y.G., Nunez, G. and Inohara, N. (2011) Nucleotide-binding oligomerization domain 1 mediates recognition of *Clostridium difficile* and induces neutrophil recruitment and protection against the pathogen. *J. Immunol.* **186**, 4872–4880.
  - 37) Kavathas, P.B., Boeras, C.M., Mulla, M.J. and Abrahams, V.M. (2013) *Nod1*, but not the ASC inflammasome, contributes to induction of IL-1 $\beta$  secretion in human trophoblasts after sensing of *Chlamydia trachomatis*. *Mucosal Immunol.* **6**, 235–243.
  - 38) Opitz, B., Forster, S., Hocke, A.C., Maass, M., Schmeck, B., Hippenstiel, S., Suttorp, N. and Krull, M. (2005) *Nod1*-mediated endothelial cell activation by *Chlamydia pneumoniae*. *Circ. Res.* **96**, 319–326.
  - 39) Scott, M.J., Chen, C., Sun, Q. and Billiar, T.R. (2010) Hepatocytes express functional *NOD1* and *NOD2* receptors: a role for *NOD1* in hepatocyte CC and CXC chemokine production. *J. Hepatol.* **53**, 693–701.
  - 40) Stockinger, S., Reutterer, B., Schaljo, B., Schellack, C., Brunner, S., Materna, T., Yamamoto, M., Akira, S., Taniguchi, T., Murray, P.J., Muller, M. and Decker, T. (2004) IFN regulatory factor 3-dependent induction of type I IFNs by intracellular bacteria is mediated by a TLR- and *Nod2*-independent mechanism. *J. Immunol.* **173**, 7416–7425.
  - 41) Hisamatsu, T., Suzuki, M. and Podolsky, D.K. (2003) Interferon- $\gamma$  augments *CARD4/NOD1* gene and protein expression through interferon regulatory factor-1 in intestinal epithelial cells. *J. Biol. Chem.* **278**, 32962–32968.
  - 42) Fan, Y.H., Roy, S., Mukhopadhyay, R., Kapoor, A., Duggal, P., Wojcik, G.L., Pass, R.F. and Arav-Boger, R. (2016) Role of nucleotide-binding oligomerization domain 1 (*NOD1*) and its variants in human cytomegalovirus control in vitro and in vivo. *Proc. Natl. Acad. Sci. U.S.A.* **113**, E7818–E7827.
  - 43) Vegna, S., Gregoire, D., Moreau, M., Lassus, P., Durantel, D., Assenat, E., Hibner, U. and Simonin, Y. (2016) *NOD1* participates in the innate immune response triggered by Hepatitis C virus polymerase. *J. Virol.* **90**, 6022–6035.
  - 44) Park, J.H., Kim, Y.G., McDonald, C., Kanneganti, T.D., Hasegawa, M., Body-Malapel, M., Inohara, N. and Nunez, G. (2007) *RICK/RIP2* mediates innate immune responses induced through *Nod1* and *Nod2* but not TLRs. *J. Immunol.* **178**, 2380–2386.
  - 45) Park, J.H., Kim, Y.G., Shaw, M., Kanneganti, T.D., Fujimoto, Y., Fukase, K., Inohara, N. and Nunez, G. (2007) *Nod1/RICK* and TLR signaling regulate chemokine and antimicrobial innate immune responses in mesothelial cells. *J. Immunol.* **179**, 514–521.
  - 46) Kobayashi, K., Inohara, N., Hernandez, L.D., Galan, J.E., Nunez, G., Janeway, C.A., Medzhitov, R. and Flavell, R.A. (2002) *RICK/Rip2/CARDIAK* mediates signalling for receptors of the innate and adaptive immune systems. *Nature* **416**, 194–199.
  - 47) Chin, A.I., Dempsey, P.W., Bruhn, K., Miller, J.F., Xu, Y. and Cheng, G. (2002) Involvement of receptor-interacting protein 2 in innate and adaptive immune responses. *Nature* **416**, 190–194.
  - 48) Lu, C., Wang, A., Dorsch, M., Tian, J., Nagashima, K., Coyle, A.J., Jaffee, B., Ocain, T.D. and Xu, Y. (2005) Participation of *Rip2* in lipopolysaccharide signaling is independent of its kinase activity. *J. Biol. Chem.* **280**, 16278–16283.
  - 49) Hall, H.T., Wilhelm, M.T., Saibil, S.D., Mak, T.W., Flavell, R.A. and Ohashi, P.S. (2008) *RIP2* contributes to *Nod* signaling but is not essential for T cell proliferation, T helper differentiation or TLR responses. *Eur. J. Immunol.* **38**, 64–72.
  - 50) Bertrand, M.J., Doiron, K., Labbe, K., Korneluk, R.G., Barker, P.A. and Saleh, M. (2009) Cellular inhibitors of apoptosis *cIAP1* and *cIAP2* are

- required for innate immunity signaling by the pattern recognition receptors NOD1 and NOD2. *Immunity* **30**, 789–801.
- 51) Yang, Y., Yin, C., Pandey, A., Abbott, D., Sasseti, C. and Kelliher, M.A. (2007) NOD2 pathway activation by MDP or *Mycobacterium tuberculosis* infection involves the stable polyubiquitination of Rip2. *J. Biol. Chem.* **282**, 36223–36229.
  - 52) Watanabe, T., Asano, N., Meng, G., Yamashita, K., Arai, Y., Sakurai, T., Kudo, M., Fuss, I.J., Kitani, A., Shimosegawa, T., Chiba, T. and Strober, W. (2014) NOD2 downregulates colonic inflammation by IRF4-mediated inhibition of K63-linked polyubiquitination of RICK and TRAF6. *Mucosal Immunol.* **7**, 1312–1325.
  - 53) Tigno-Aranjuez, J.T., Asara, J.M. and Abbott, D.W. (2010) Inhibition of RIP2's tyrosine kinase activity limits NOD2-driven cytokine responses. *Genes Dev.* **24**, 2666–2677.
  - 54) Damgaard, R.B., Fiil, B.K., Speckmann, C., Yabal, M., zur Stadt, U., Bekker-Jensen, S., Jost, P.J., Ehl, S., Mailand, N. and Gyrd-Hansen, M. (2013) Disease-causing mutations in the XIAP BIR2 domain impair NOD2-dependent immune signalling. *EMBO Mol. Med.* **5**, 1278–1295.
  - 55) Damgaard, R.B., Nachbur, U., Yabal, M., Wong, W.W., Fiil, B.K., Kastirr, M., Rieser, E., Rickard, J.A., Bankovacki, A., Peschel, C., Ruland, J., Bekker-Jensen, S., Mailand, N., Kaufmann, T., Strasser, A., Walczak, H., Silke, J., Jost, P.J. and Gyrd-Hansen, M. (2012) The ubiquitin ligase XIAP recruits LUBAC for NOD2 signaling in inflammation and innate immunity. *Mol. Cell* **46**, 746–758.
  - 56) Tokunaga, F., Sakata, S., Saeki, Y., Satomi, Y., Kirisako, T., Kamei, K., Nakagawa, T., Kato, M., Murata, S., Yamaoka, S., Yamamoto, M., Akira, S., Takao, T., Tanaka, K. and Iwai, K. (2009) Involvement of linear polyubiquitylation of NEMO in NF-kappaB activation. *Nat. Cell Biol.* **11**, 123–132.
  - 57) Yang, S., Wang, B., Humphries, F., Jackson, R., Healy, M.E., Bergin, R., Aviello, G., Hall, B., McNamara, D., Darby, T., Quinlan, A., Shanahan, F., Melgar, S., Fallon, P.G. and Moynagh, P.N. (2013) Pellino3 ubiquitinates RIP2 and mediates Nod2-induced signaling and protective effects in colitis. *Nat. Immunol.* **14**, 927–936.
  - 58) Tao, M., Scacheri, P.C., Marinis, J.M., Harhaj, E.W., Matesic, L.E. and Abbott, D.W. (2009) ITCH K63-ubiquitinates the NOD2 binding protein, RIP2, to influence inflammatory signaling pathways. *Curr. Biol.* **19**, 1255–1263.
  - 59) Hrdinka, M., Fiil, B.K., Zucca, M., Leske, D., Bagola, K., Yabal, M., Elliott, P.R., Damgaard, R.B., Komander, D., Jost, P.J. and Gyrd-Hansen, M. (2016) CYLD limits Lys63- and Met1-linked ubiquitin at receptor complexes to regulate innate immune signaling. *Cell Reports* **14**, 2846–2858.
  - 60) Draber, P., Kupka, S., Reichert, M., Draberova, H., Lafont, E., de Miguel, D., Spilgies, L., Surinova, S., Taraborrelli, L., Hartwig, T., Rieser, E., Martino, L., Rittinger, K. and Walczak, H. (2015) LUBAC-recruited CYLD and A20 regulate gene activation and cell death by exerting opposing effects on linear ubiquitin in signaling complexes. *Cell Reports* **13**, 2258–2272.
  - 61) Hitotsumatsu, O., Ahmad, R.C., Tavares, R., Wang, M., Philpott, D., Turer, E.E., Lee, B.L., Shiffin, N., Advincula, R., Malynn, B.A., Werts, C. and Ma, A. (2008) The ubiquitin-editing enzyme A20 restricts nucleotide-binding oligomerization domain containing 2-triggered signals. *Immunity* **28**, 381–390.
  - 62) Marinis, J.M., Homer, C.R., McDonald, C. and Abbott, D.W. (2011) A novel motif in the Crohn's disease susceptibility protein, NOD2, allows TRAF4 to down-regulate innate immune responses. *J. Biol. Chem.* **286**, 1938–1950.
  - 63) Marinis, J.M., Hutti, J.E., Homer, C.R., Cobb, B.A., Cantley, L.C., McDonald, C. and Abbott, D.W. (2012) IkappaB kinase alpha phosphorylation of TRAF4 downregulates innate immune signaling. *Mol. Cell. Biol.* **32**, 2479–2489.
  - 64) Correa, R.G., Khan, P.M., Askari, N., Zhai, D., Gerlic, M., Brown, B., Magnuson, G., Spreafico, R., Albani, S., Sergienko, E., Diaz, P.W., Roth, G.P. and Reed, J.C. (2011) Discovery and characterization of 2-aminobenzimidazole derivatives as selective NOD1 inhibitors. *Chem. Biol.* **18**, 825–832.
  - 65) Honda, K., Yanai, H., Takaoka, A. and Taniguchi, T. (2005) Regulation of the type I IFN induction: a current view. *Int. Immunol.* **17**, 1367–1378.
  - 66) Christensen, J.E., de Lemos, C., Moos, T., Christensen, J.P. and Thomsen, A.R. (2006) CXCL10 is the key ligand for CXCR3 on CD8+ effector T cells involved in immune surveillance of the lymphocytic choriomeningitis virus-infected central nervous system. *J. Immunol.* **176**, 4235–4243.
  - 67) Hsieh, M.F., Lai, S.L., Chen, J.P., Sung, J.M., Lin, Y.L., Wu-Hsieh, B.A., Gerard, C., Luster, A. and Liao, F. (2006) Both CXCR3 and CXCL10/IFN-inducible protein 10 are required for resistance to primary infection by dengue virus. *J. Immunol.* **177**, 1855–1863.
  - 68) Romagnani, P., Maggi, E., Mazzinghi, B., Cosmi, L., Lasagni, L., Liotta, F., Lazzeri, E., Angeli, R., Rotondi, M., Fili, L., Parronchi, P., Serio, M., Maggi, E., Romagnani, S. and Annunziato, F. (2005) CXCR3-mediated opposite effects of CXCL10 and CXCL4 on TH1 or TH2 cytokine production. *J. Allergy Clin. Immunol.* **116**, 1372–1379.
  - 69) Hasegawa, M., Fujimoto, Y., Lucas, P.C., Nakano, H., Fukase, K., Nunez, G. and Inohara, N. (2008) A critical role of RICK/RIP2 polyubiquitination in Nod-induced NF-kappaB activation. *EMBO J.* **27**, 373–383.
  - 70) Honda, K., Yanai, H., Negishi, H., Asagiri, M., Sato, M., Mizutani, T., Shimada, N., Ohba, Y., Takaoka, A., Yoshida, N. and Taniguchi, T. (2005) IRF-7 is the master regulator of type-I



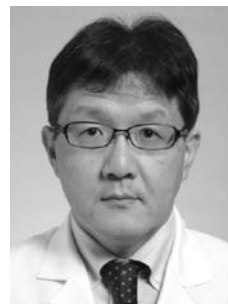
- interferon-dependent immune responses. *Nature* **434**, 772–777.
- 71) Honda, K., Ohba, Y., Yanai, H., Negishi, H., Mizutani, T., Takaoka, A., Taya, C. and Taniguchi, T. (2005) Spatiotemporal regulation of MyD88-IRF-7 signalling for robust type-I interferon induction. *Nature* **434**, 1035–1040.
  - 72) Hacker, H., Redecke, V., Blagoev, B., Kratchmarova, I., Hsu, L.C., Wang, G.G., Kamps, M.P., Raz, E., Wagner, H., Hacker, G., Mann, M. and Karin, M. (2006) Specificity in Toll-like receptor signalling through distinct effector functions of TRAF3 and TRAF6. *Nature* **439**, 204–207.
  - 73) Mizushima, N., Levine, B., Cuervo, A.M. and Klionsky, D.J. (2008) Autophagy fights disease through cellular self-digestion. *Nature* **451**, 1069–1075.
  - 74) Travassos, L.H., Carneiro, L.A., Ramjeet, M., Hussey, S., Kim, Y.G., Magalhaes, J.G., Yuan, L., Soares, F., Chea, E., Le Bourhis, L., Boneca, I.G., Allaoui, A., Jones, N.L., Nunez, G., Girardin, S.E. and Philpott, D.J. (2010) Nod1 and Nod2 direct autophagy by recruiting ATG16L1 to the plasma membrane at the site of bacterial entry. *Nat. Immunol.* **11**, 55–62.
  - 75) Sorbara, M.T., Ellison, L.K., Ramjeet, M., Travassos, L.H., Jones, N.L., Girardin, S.E. and Philpott, D.J. (2013) The protein ATG16L1 suppresses inflammatory cytokines induced by the intracellular sensors Nod1 and Nod2 in an autophagy-independent manner. *Immunity* **39**, 858–873.
  - 76) Celli, J. and Tsolis, R.M. (2015) Bacteria, the endoplasmic reticulum and the unfolded protein response: friends or foes? *Nat. Rev. Microbiol.* **13**, 71–82.
  - 77) Keestra-Gounder, A.M., Byndloss, M.X., Seyffert, N., Young, B.M., Chavez-Arroyo, A., Tsai, A.Y., Cevallos, S.A., Winter, M.G., Pham, O.H., Tiffany, C.R., de Jong, M.F., Kerrinnes, T., Ravindran, R., Luciw, P.A., McSorley, S.J., Baumber, A.J. and Tsolis, R.M. (2016) NOD1 and NOD2 signalling links ER stress with inflammation. *Nature* **532**, 394–397.
  - 78) Hatakeyama, M. (2014) *Helicobacter pylori* CagA and gastric cancer: a paradigm for hit-and-run carcinogenesis. *Cell Host Microbe* **15**, 306–316.
  - 79) Fischer, W. (2011) Assembly and molecular mode of action of the *Helicobacter pylori* Cag type IV secretion apparatus. *FEBS J.* **278**, 1203–1212.
  - 80) Kaparakis, M., Turnbull, L., Carneiro, L., Firth, S., Coleman, H.A., Parkington, H.C., Le Bourhis, L., Karrar, A., Viala, J., Mak, J., Hutton, M.L., Davies, J.K., Crack, P.J., Hertzog, P.J., Philpott, D.J., Girardin, S.E., Whitchurch, C.B. and Ferrero, R.L. (2010) Bacterial membrane vesicles deliver peptidoglycan to NOD1 in epithelial cells. *Cell Microbiol.* **12**, 372–385.
  - 81) D'Elia, M.M., Manghetti, M., De Carli, M., Costa, F., Baldari, C.T., Burroni, D., Telford, J.L., Romagnani, S. and Del Prete, G. (1997) T helper 1 effector cells specific for *Helicobacter pylori* in the gastric antrum of patients with peptic ulcer disease. *J. Immunol.* **158**, 962–967.
  - 82) Itoh, T., Wakatsuki, Y., Yoshida, M., Usui, T., Matsunaga, Y., Kaneko, S., Chiba, T. and Kita, T. (1999) The vast majority of gastric T cells are polarized to produce T helper 1 type cytokines upon antigenic stimulation despite the absence of *Helicobacter pylori* infection. *J. Gastroenterol.* **34**, 560–570.
  - 83) Garhart, C.A., Heinzel, F.P., Czinn, S.J. and Nedrud, J.G. (2003) Vaccine-induced reduction of *Helicobacter pylori* colonization in mice is interleukin-12 dependent but gamma interferon and inducible nitric oxide synthase independent. *Infect. Immun.* **71**, 910–921.
  - 84) Ferrero, R.L. (2005) Innate immune recognition of the extracellular mucosal pathogen, *Helicobacter pylori*. *Mol. Immunol.* **42**, 879–885.
  - 85) Andersen-Nissen, E., Smith, K.D., Strobe, K.L., Barrett, S.L., Cookson, B.T., Logan, S.M. and Aderem, A. (2005) Evasion of Toll-like receptor 5 by flagellated bacteria. *Proc. Natl. Acad. Sci. U.S.A.* **102**, 9247–9252.
  - 86) Eck, M., Schmausser, B., Scheller, K., Toksoy, A., Kraus, M., Menzel, T., Muller-Hermelink, H.K. and Gillitzer, R. (2000) CXC chemokines Gro(alpha)/IL-8 and IP-10/MIG in *Helicobacter pylori* gastritis. *Clin. Exp. Immunol.* **122**, 192–199.
  - 87) Allison, C.C., Ferrand, J., McLeod, L., Hassan, M., Kaparakis-Liaskos, M., Grubman, A., Bhathal, P.S., Dev, A., Sievert, W., Jenkins, B.J. and Ferrero, R.L. (2013) Nucleotide oligomerization domain 1 enhances IFN-gamma signaling in gastric epithelial cells during *Helicobacter pylori* infection and exacerbates disease severity. *J. Immunol.* **190**, 3706–3715.
  - 88) Hirata, Y., Ohmae, T., Shibata, W., Maeda, S., Ogura, K., Yoshida, H., Kawabe, T. and Omata, M. (2006) MyD88 and TNF receptor-associated factor 6 are critical signal transducers in *Helicobacter pylori*-infected human epithelial cells. *J. Immunol.* **176**, 3796–3803.
  - 89) Allison, C.C., Kufer, T.A., Kremmer, E., Kaparakis, M. and Ferrero, R.L. (2009) *Helicobacter pylori* induces MAPK phosphorylation and AP-1 activation via a NOD1-dependent mechanism. *J. Immunol.* **183**, 8099–8109.
  - 90) Suarez, G., Romero-Gallo, J., Piazuelo, M.B., Wang, G., Maier, R.J., Forsberg, L.S., Azadi, P., Gomez, M.A., Correa, P. and Peek, R.M. Jr. (2015) Modification of *Helicobacter pylori* peptidoglycan enhances NOD1 activation and promotes cancer of the stomach. *Cancer Res.* **75**, 1749–1759.
  - 91) Camilo, V., Barros, R., Sousa, S., Magalhaes, A.M., Lopes, T., Mario Santos, A., Pereira, T., Figueiredo, C., David, L. and Almeida, R. (2012) *Helicobacter pylori* and the BMP pathway regulate CDX2 and SOX2 expression in gastric cells. *Carcinogenesis* **33**, 1985–1992.

- 92) Cosen-Binker, L.I. and Gaisano, H.Y. (2007) Recent insights into the cellular mechanisms of acute pancreatitis. *Can. J. Gastroenterol.* **21**, 19–24.
- 93) Lankisch, P.G., Apte, M. and Banks, P.A. (2015) Acute pancreatitis. *Lancet* **386**, 85–96.
- 94) Braganza, J.M., Lee, S.H., McCloy, R.F. and McMahon, M.J. (2011) Chronic pancreatitis. *Lancet* **377**, 1184–1197.
- 95) Frossard, J.L., Steer, M.L. and Pastor, C.M. (2008) Acute pancreatitis. *Lancet* **371**, 143–152.
- 96) Logsdon, C.D. and Ji, B. (2013) The role of protein synthesis and digestive enzymes in acinar cell injury. *Nat. Rev. Gastroenterol. Hepatol.* **10**, 362–370.
- 97) Saluja, A.K., Lerch, M.M., Phillips, P.A. and Dudeja, V. (2007) Why does pancreatic overstimulation cause pancreatitis? *Annu. Rev. Physiol.* **69**, 249–269.
- 98) Whitcomb, D.C. (2010) Genetic aspects of pancreatitis. *Annu. Rev. Med.* **61**, 413–424.
- 99) Dawra, R., Sah, R.P., Dudeja, V., Rishi, L., Talukdar, R., Garg, P. and Saluja, A.K. (2011) Intra-acinar trypsinogen activation mediates early stages of pancreatic injury but not inflammation in mice with acute pancreatitis. *Gastroenterology* **141**, 2210–2217 e2.
- 100) Sah, R.P., Dudeja, V., Dawra, R.K. and Saluja, A.K. (2013) Cerulein-induced chronic pancreatitis does not require intra-acinar activation of trypsinogen in mice. *Gastroenterology* **144**, 1076–1085 e2.
- 101) Ji, B. and Logsdon, C.D. (2011) Digesting new information about the role of trypsin in pancreatitis. *Gastroenterology* **141**, 1972–1975.
- 102) Medich, D.S., Lee, T.K., Melhem, M.F., Rowe, M.I., Schraut, W.H. and Lee, K.K. (1993) Pathogenesis of pancreatic sepsis. *Am. J. Surg.* **165**, 46–50; discussion 51–2.
- 103) Gianotti, L., Munda, R., Alexander, J.W., Tchervenkov, J.I. and Babcock, G.F. (1993) Bacterial translocation: a potential source for infection in acute pancreatitis. *Pancreas* **8**, 551–558.
- 104) Runkel, N.S., Moody, F.G., Smith, G.S., Rodriguez, L.F., LaRocco, M.T. and Miller, T.A. (1991) The role of the gut in the development of sepsis in acute pancreatitis. *J. Surg. Res.* **51**, 18–23.
- 105) Mithofer, K., Fernandez-del Castillo, C., Ferraro, M.J., Lewandrowski, K., Rattner, D.W. and Warshaw, A.L. (1996) Antibiotic treatment improves survival in experimental acute necrotizing pancreatitis. *Gastroenterology* **110**, 232–240.
- 106) Fritz, S., Hartwig, W., Lehmann, R., Will-Schweiger, K., Kommerell, M., Hackert, T., Schneider, L., Buchler, M.W. and Werner, J. (2008) Prophylactic antibiotic treatment is superior to therapy on-demand in experimental necrotising pancreatitis. *Crit. Care* **12**, R141.
- 107) Foitzik, T., Fernandez-del Castillo, C., Ferraro, M.J., Mithofer, K., Rattner, D.W. and Warshaw, A.L. (1995) Pathogenesis and prevention of early pancreatic infection in experimental acute necrotizing pancreatitis. *Ann. Surg.* **222**, 179–185.
- 108) Li, Q., Wang, C., Tang, C., He, Q., Li, N. and Li, J. (2013) Bacteremia in patients with acute pancreatitis as revealed by 16S ribosomal RNA gene-based techniques\*. *Crit. Care Med.* **41**, 1938–1950.
- 109) Yasuda, T., Ueda, T., Shinzeki, M., Sawa, H., Nakajima, T., Takeyama, Y. and Kuroda, Y. (2007) Increase of high-mobility group box chromosomal protein 1 in blood and injured organs in experimental severe acute pancreatitis. *Pancreas* **34**, 487–488.
- 110) Yasuda, T., Ueda, T., Takeyama, Y., Shinzeki, M., Sawa, H., Nakajima, T., Ajiki, T., Fujino, Y., Suzuki, Y. and Kuroda, Y. (2006) Significant increase of serum high-mobility group box chromosomal protein 1 levels in patients with severe acute pancreatitis. *Pancreas* **33**, 359–363.
- 111) Kono, H. and Rock, K.L. (2008) How dying cells alert the immune system to danger. *Nat. Rev. Immunol.* **8**, 279–289.
- 112) Satoh, A., Gukovskaya, A.S., Nieto, J.M., Cheng, J.H., Gukovsky, I., Reeve, J.R. Jr., Shimosegawa, T. and Pandol, S.J. (2004) PKC-delta and -epsilon regulate NF-kappaB activation induced by cholecystokinin and TNF-alpha in pancreatic acinar cells. *Am. J. Physiol. Gastrointest. Liver Physiol.* **287**, G582–G591.
- 113) Yu, J.H., Kim, K.H. and Kim, H. (2006) Suppression of IL-1beta expression by the Jak 2 inhibitor AG490 in cerulein-stimulated pancreatic acinar cells. *Biochem. Pharmacol.* **72**, 1555–1562.
- 114) Deshmene, S.L., Kremlev, S., Amini, S. and Sawaya, B.E. (2009) Monocyte chemoattractant protein-1 (MCP-1): an overview. *J. Interferon Cytokine Res.* **29**, 313–326.
- 115) Fichtner-Feigl, S., Strober, W., Geissler, E.K. and Schlitt, H.J. (2008) Cytokines mediating the induction of chronic colitis and colitis-associated fibrosis. *Mucosal Immunol.* **1** (Suppl 1), S24–S27.
- 116) McHedlidze, T., Waldner, M., Zopf, S., Walker, J., Rankin, A.L., Schuchmann, M., Voehringer, D., McKenzie, A.N., Neurath, M.F., Pflanz, S. and Wirtz, S. (2013) Interleukin-33-dependent innate lymphoid cells mediate hepatic fibrosis. *Immunity* **39**, 357–371.
- 117) Cayrol, C. and Girard, J.P. (2014) IL-33: an alarmin cytokine with crucial roles in innate immunity, inflammation and allergy. *Curr. Opin. Immunol.* **31C**, 31–37.
- 118) Mancuso, G., Midiri, A., Biondo, C., Beninati, C., Zummo, S., Galbo, R., Tomasello, F., Gambuzza, M., Macri, G., Ruggeri, A., Leanderson, T. and Teti, G. (2007) Type I IFN signaling is crucial for host resistance against different species of pathogenic bacteria. *J. Immunol.* **178**, 3126–3133.

(Received May 13, 2017; accepted May 31, 2017)

## Profile

Tomohiro Watanabe graduated from Kyoto University School of Medicine in 1993. He trained in Internal Medicine and Gastroenterology at Kobe City General Hospital. He started research on liver immunology at Department of Gastroenterology and Hepatology, Kyoto University Graduate School of Medicine (Prof. Tsutomu Chiba) and obtained a Ph.D. in 2002. He worked as a postdoctoral fellow at Mucosal Immunity Section, Laboratory of Host Defenses, National Institutes of Health (Dr. Warren Strober) and studied the immuno-pathogenesis of inflammatory bowel diseases and *Helicobacter pylori*-associated gastritis between 2003 and 2006. He then moved back to Department of Gastroenterology and Hepatology, Kyoto University Graduate School of Medicine (Prof. Tsutomu Chiba) as an assistant professor and then was assigned as an associate professor in 2011. In 2016, He became an associate professor at Department of Gastroenterology and Hepatology, Kindai University Faculty of Medicine (Prof. Masatoshi Kudo). He has been studying the immuno-pathogenesis of gastrointestinal disorders including inflammatory bowel diseases, *Helicobacter pylori*-associated gastritis, pancreatitis, and IgG4-related diseases.



# New Paradigm in Gastrointestinal Cancer Treatment

Masatoshi Kudo

Department of Gastroenterology and Hepatology, Kindai University Faculty of Medicine, Osaka-Sayama, Japan

The first Kindai International Symposium on Gastrointestinal Cancer (KISGIC) was held on July 8, 2017 in Osaka, Japan. The main theme of this symposium was: “New paradigm in gastrointestinal cancer treatment.” This symposium focused on recent progress on upper gastrointestinal cancer, lower intestinal cancer, pancreaticobiliary cancer, and liver cancer.

Endoscopic submucosal dissection (ESD) has been widely used in the resection of superficial esophageal cancers. Since its use has been extended to cases involving large esophageal tumors occupying nearly the whole lumen or the whole circumference of the lumen, the occurrence of esophageal stricture has increased. Although endoscopic injection of triamcinolone (TA) is widely used for the prevention of postoperative stricture, a significant number of patients still develop stricture after TA injection therapy. Okamoto et al. [1] performed a retrospective review of the data from 57 patients treated with near- or whole-circumferential ESD and with TA injection. They found that an extensive circumferential mucosal defect (covering more than 75% of the circumference) was associated with a high risk of developing postoperative esophageal stricture, even after preventive injection of TA. Authors concluded that endoscopic TA injection is not sufficient for the prevention of esophageal stricture in patients bearing a mucosal defect covering more than seven-eighths of the circumference after ESD. In such cases, alternative strategies, including the application of

polyglycolic acid sheets with fibrin glue with or without TA injection, may be useful to avoid postoperative stricture.

Gastric cancer is the third leading cause of cancer-related deaths worldwide. Geographically, gastric cancer is very common in East Asia, where the prevalence rate of *Helicobacter pylori* infection is high. Chronic gastric infection due to *H. pylori* initially causes chronic active gastritis, which can then lead to the development of peptic ulcers, atrophic gastritis, and gastric cancer. A protective effect against gastric cancer has been reported to persist for more than 10 years after *H. pylori* eradication. Therefore, *H. pylori* can be considered one of the most important causes of gastric cancer. *H. pylori*-associated gastric cancer is one of the best examples of inflammation-related cancer. Therefore, it is clear that eradication of *H. pylori* reduces the risk for gastric cancer even in the presence of severe gastric atrophy and intestinal metaplasia. Thus, *H. pylori* eradication is the most effective strategy for the prevention of gastric cancer. Adachi et al. [2] attempted to determine whether metronidazole (MNZ)-based triple therapy is superior to clarithromycin (CAM)-based triple therapy as a first-line eradication treatment for *H. pylori*. They found that MNZ-based triple therapy containing esomeprazole and amoxicillin (AMPC) is superior to clarithromycin (CAM)-based triple therapy containing esomeprazole and AMPC as a first-line eradication treatment against *H. pylori*.

Colorectal cancer is one of the most common fatal malignancies worldwide. Inflammatory bowel disease (IBD), comprising ulcerative colitis and Crohn's disease, is thought to result from aberrant activation of the intestinal immune system and is a major risk factor for colorectal cancer, so-called colitis-associated cancer. Cancer stem cells, the microenvironment, and the immune system interact with each other through cytokines. In the context of chronic inflammation, immune responses would affect proliferation of stem cells and increase the expression of stem cell markers. The expression of stress response proteins and gankyrin that functionally link chronic inflammation and tumorigenesis in IBD is significantly correlated with that of a stem cell marker Bmi1. In mice, Bmi1 is required for intestinal tumorigenesis. Yamada et al. [3] found a significant association between Bmi1 expression and chronic inflammation in IBD patients. Their study represents the first report of the expression of Bmi1 in inflammation-associated colorectal cancer that is associated with refractory clinical course. Therefore, Bmi1 might be involved in the mechanistic connection between chronic inflammation and tumorigenesis in IBD.

Sakurai et al. [4] reported prophylactic suturing closure of mucosal defects after endoscopic resection of colorectal tumors in patients at a high risk of bleeding after ESD, who receive anti-thrombotics or anti-platelet agents.

Computer-aided diagnosis (CAD) is becoming a next-generation tool for the diagnosis of human disease. The CAD of colon polyps has been reported previously. Previous studies have reported the usefulness of CAD for colon polyps. The higher rate of correct diagnoses using a CAD system suggests the potential for this diagnostic tool to improve the quality of colonoscopic examinations. In addition to conventional CAD, a convolutional neural network (CNN) system utilizing artificial intelligence has been developing rapidly over the past 5 years. Komeda et al. [5] attempted to generate a unique CNN-CAD system with an amoxicillin (AMPC) function that studied endoscopic images extracted from movies obtained with colonoscopes used in routine examinations. They found that the accuracy of the 10-fold cross-validation is 0.751, where the accuracy is the ratio of the number of correct answers over the number of all the answers produced by the CNN and the decisions by the CNN were correct in 7 of 10 cases. Therefore, they concluded that a CNN-CAD system using routine colonoscopy might be useful for the rapid diagnosis of colorectal polyp classification.

Colonoscopic removal of adenomatous polyps or early cancer prevents death from colorectal cancer. ESD, which enables endoscopists to perform en bloc resection of flat or depressed colorectal tumors larger than 20 mm, has recently been introduced and become a standard procedure in Japan. Although postoperative bleeding (POB) is a major complication associated with ESD, risk factors for POB have not been fully identified. Okamoto et al. [6] found that anti-thrombotic therapy and rectal tumor location were strongly associated with POB in colorectal ESD. The incidence of POB was higher in patients who received heparin bridge therapy as a replacement of anti-thrombotic therapy than that in patients who did not receive heparin bridge therapy.

Colorectal cancer is one of the most common cancers, and 8–29% of patients with colorectal cancer have obstruction-related symptoms. Because obstructive colorectal cancer can be fatal, emergent management is needed. It was reported that the morbidity and mortality rates associated with emergent surgery were high. In the last few decades, there have been many reports about the usefulness of self-expanding metal stents (SEMS) for obstructive colorectal cancer. SEMS are used as a bridge to surgery (BTS) and for palliative therapy. A systematic review revealed that SEMS placement as a BTS has a lower stoma formation rate and complication rate than emergent surgery. However, concerns have been raised regarding the possibility for exacerbation of the oncological prognosis. A few RCTs and a cohort study have shown a significantly higher local disease recurrence rate with SEMS use than emergent surgery. The cancer recurrence rate has been shown to be higher in the subgroup of patients with stent-related perforations; thus, it is suggested that a lower perforation rate may improve the prognosis. Small diameter stents mitigate the mechanical impact of the stents on the tumor and the colonic wall, and can reduce the perforation rate. Ogawa et al. [7] found that the 18-mm diameter stents were effective similar to 22-mm diameter stents. Because 18-mm diameter stents are easy to handle and produce less mechanical stress, they have the potential to decrease the perforation rate and mitigate the stent's impact on the tumors. 18-mm diameter stents can be useful and safe, especially as a BTS.

Narrow band imaging (NBI), which visualizes vessel and surface patterns in detail, is generally considered to provide useful diagnostic information about gastrointestinal lesions identified via endoscopy. Several studies have indicated that NBI observations of colorectal polyps are very useful, accurate predictors of histology. The Japan NBI Expert Team (JNET) proposed a new NBI clas-



sification system for colorectal tumors in June 2014. In this classification system, types 1, 2A, 2B, and 3 correspond to hyperplastic polyps including sessile serrated polyps, low-grade dysplasia, high-grade dysplasia, shallow submucosal invasive carcinomas, and deep submucosal invasive carcinomas, respectively. To validate this system, Komeda et al. [8] performed a retrospective image evaluation study in which 199 colorectal tumors previously assessed by NBI magnifying endoscopy were classified by three blinded experienced colonoscopists using the JNET system. They concluded that JNET classification is useful for the diagnosis of hyperplastic polyps/sessile serrated polyps, low-grade dysplasia, and deep submucosal invasive, but not shallow submucosal invasive lesions. For low-confidence cases, magnified chromoendoscopy is recommended to ensure correct diagnoses.

The number of reports on the utility of contrast-enhanced harmonic endoscopic ultrasonography (CH-EUS) in the differential diagnosis of pancreatic masses has been increasing. CH-EUS depicted the hypoenhancement of pancreatic carcinomas with high sensitivity (89–96%) and specificity (64–94%). Nonetheless, the visual evaluation of CH-EUS scans may be influenced by the endosonographers' subjective impressions. Recent studies have described the quantitative perfusion analysis of pancreatic diseases using a time-intensity curve (TIC), which graphs the changes in signal intensity over time within a region of interest after infusion of an ultrasound contrast agent. Omoto et al. [9] attempted to clarify if quantitative perfusion analysis with CH-EUS characterizes pancreatic tumors and to find the most accurate hemodynamic parameter of TIC for differentiating pancreatic carcinoma from other pancreatic tumors. They found that pancreatic carcinomas exhibited markedly different TIC patterns from the other tumor types, with intensity at 60 s ( $I_{60}$ ) being the most accurate diagnostic parameter. Quantitative perfusion analysis is useful for differentiating pancreatic carcinomas from other pancreatic tumors.

Intraductal papillary mucinous neoplasms (IPMNs) are a well-characterized group of intraductal mucin-producing cystic neoplasms of the pancreas with malignant potential. In the 2012 international consensus guidelines, high-risk IPMN included 2 clinical categories with “high-risk stigmata” and “worrisome features,” and different therapeutic strategies were recommended for both groups. It is recommended that patients with “high-risk stigmata” should be treated by surgical resection. Patients who have “worrisome features” and additional high-risk signs should also undergo resection, while patients with

“worrisome features” alone should receive careful follow-up. The “high-risk stigmata” of IPMNs that can be detected by EUS are an enhancing solid component inside the cyst and dilatation of the main pancreatic duct ( $>10$  mm). Additional high-risk signs among the “worrisome features” are a definite mural nodule and suspected main duct involvement. Thus, the current guidelines focus on the morphological features of IPMN as revealed by EUS. On the other hand, although not described in previous reports, clinical experience suggests that evidence of chronic pancreatitis (CP) is frequently identified in the background pancreatic parenchyma of IPMN patients by EUS (EUS-CP findings). CP is a well-known risk factor for pancreatic malignancy, including pancreatic ductal adenocarcinoma (PDAC). However, the relationship remains unclear between malignant transformation of IPMN and pathological changes of the pancreatic parenchyma, such as atrophy, inflammation, and fibrosis. Moreover, changes of the background parenchyma are not considered to be a high-risk sign for malignant IPMN in the current guideline. Takenaka et al. [10] hypothesized that EUS-CP findings might be associated with malignant IPMN. To examine this hypothesis, they utilized a database of 69 consecutive patients with IPMNs who underwent preoperative EUS and surgical resection. They found that the detection of EUS-CP findings in the pancreatic parenchyma of IPMN patients was associated with invasive IPMC. They also stated that when EUS examination of IPMN is performed, the background parenchyma should be evaluated in addition to the morphological features of the tumor itself.

The gold standard procedure for biliary drainage (BD) is transpapillary drainage during endoscopic retrograde cholangiopancreatography (ERCP). However, ERCP may not be possible in patients with an inaccessible biliary orifice, such as patients with a surgically altered anatomy or duodenal involvement of the tumor. Alternative drainage options in these patients include surgical biliary bypass or percutaneous transhepatic BD; however, these procedures are associated with some adverse events. EUS-guided BD (EUS-BD) techniques such as EUS-guided choledochoduodenostomy (CDS), hepaticogastrostomy (HGS), antegrade stenting (AGS), and rendezvous stenting have recently been shown to be useful for BD after unsuccessful ERCP. Among these procedures, CDS and rendezvous stenting require the echoendoscope to reach the duodenum. Therefore, HGS or AGS is indicated in patients with an inaccessible duodenum. However, HGS is associated with a higher risk of adverse events compared with the other methods. When stent dysfunc-

tion occurs, re-intervention is more difficult after AGS alone than after HGS or CDS. Imai et al. [11] attempted to evaluate the technical success, functional success, adverse events, re-intervention rate, and stent patency before (HGS alone) and after (HGS with AGS) combining both methods and to compare these outcomes between the two groups. They found that although the technical success rate of HGS with AGS was lower than that of HGS, HGS with AGS was superior to HGS in terms of adverse events rate and stent patency in patients receiving chemotherapy. In other words, EUS-HGS both with and without AGS has equivalent short-term safety and efficacy when performed by experts. However, HGS plus AGS is preferred in patients undergoing chemotherapy because it allows for longer stent patency.

Risk factors for PDAC include diabetes mellitus, chronic pancreatitis, obesity, a family history of pancreatic cancer, and a history of smoking or alcohol consumption. Kamata et al. [12] attempted to evaluate the association between risk factors for PDAC and malignant IPMN. They found that there was no significant association between the risk factors for PDAC and malignant IPMN. The presence of several risk factors, especially a positive smoking history in addition to the presence of the mural nodules, is an indication for surgical resection in patients with IPMN.

EUS-guided fine-needle aspiration (EUS-FNA) has been widely used for the diagnosis of both inflammatory and tumor lesions located in and adjacent to the gastrointestinal tract. EUS-FNA has been considered to be a safe technique with few complications, as shown in recent review articles in which EUS-FNA-related morbidity and mortality rates were reported to be <1%. It should be noted, however, that needle tract seeding, although uncommon, can occur after diagnostic EUS-FNA and that this complication affects the prognosis of patients. Although an accurate value for the frequency of needle tract seeding caused by EUS-FNA has not been reported, the number of case reports on needle tract seeding have been rapidly increasing, especially in Japan. Minaga et al. [13] attempted to re-evaluate the safety of EUS-FNA because this complication may have a significant influence on patients' prognoses. They concluded that considering this serious complication, EUS-FNA should be performed only when the results obtained by this procedure are useful for therapeutic decision making. In addition, needle tract seeding following EUS-FNA might be avoided by setting the needle tract line within the surgical resection margins, if technically possible. Carefully planned endoscopic and imaging surveillance of the puncture sites

could lead to the early detection of needle tract seeding, which may improve the prognosis.

Primary sclerosing cholangitis (PSC) is a chronic cholestatic liver disorder characterized by multiple fibrotic strictures of the intra- and extrahepatic biliary tree. Previous studies have shown that >40% of deaths in patients with PSC are related to cholangiocarcinoma, gallbladder carcinoma, or colorectal carcinoma. Cholangiocarcinoma is the most relevant of these, with a lifetime risk in PSC patients of around 7–14% and a prognosis including a 5-year survival of <10%. Primary hepatic adenosquamous carcinoma (ASC) is defined as a rare subtype of cholangiocarcinoma, accounting for 2–3% of cholangiocarcinomas. ASC contains both adenocarcinoma and squamous cell carcinoma components, tends to present more aggressive clinicopathologic features, and has a poorer prognosis than other cholangiocarcinomas. Yamao et al. [14] first reported the first case of hepatic ASC in a patient with PSC. They concluded that patients with PSC should be recognized as being at risk of hepatic ASC, in addition to general cholangiocarcinoma, hepatocellular carcinoma (HCC), and metastatic liver tumor.

Pancreatic cancer has a poor prognosis, and early diagnosis is important for improved outcomes. Small pancreatic cancers have a better prognosis, although detection and diagnosis of noninvasive or small invasive lesions are often challenging. Pancreatic intraepithelial neoplasia (PanIN) is considered a precursor for invasive pancreatic cancer. PanIN is defined as a microscopic papillary or flat and noninvasive epithelial neoplasm arising from the pancreatic ductal epithelium. PanIN is divided into two subtypes: low-grade PanIN (previously reported as PanIN-1 and -2) and high-grade PanIN (previously reported as PanIN-3) involving a carcinoma in situ. As high-grade PanIN does not involve a mass-forming lesion, its diagnosis is challenging by imaging. Detection of high-grade PanIN involves the presence of an abnormal main pancreatic duct (MPD) form, including localized MPD stenosis with distal MPD dilation, focal ductal branch dilation, and cyst formation. Exacerbation of these findings with tumor progression is also a sign of high-grade PanIN. However, the natural history and time to progression of high-grade PanIN remain unclear. Yamao et al. [15] reported two cases of high-grade PanIN without morphological changes in the MPD over relatively long periods. They concluded that when findings of localized MPD stenosis and distal MPD dilation are detected, a definite diagnosis of high-grade PanINs should be considered by pancreatic juice cytology. Even if a definite diagnosis cannot be obtained, strict follow-up ob-

ervation study should be performed. Re-examination should also be considered, particularly in cases with some risk factors for pancreatic cancer, even if there is no change in the MPD form.

EUS-guided pancreatic drainage has been described as a new drainage technique after an unsuccessful transpapillary approach for pancreatic duct strictures. Kamata et al. [16] reported a case who could not continue chemotherapy and was forced to stop chemotherapy due to repeated pancreatitis. Findings indicated that the pancreatic duct stone caused repeat pancreatitis, resulting in the discontinuation of chemotherapy. Although transpapillary pancreatic duct drainage was considerable, pancreatic duct drainage over the tumor and the pancreatic duct stricture was limited. The presence of the tumor in the head of the pancreas made stone removal more difficult. EUS-guided pancreatic drainage was successful in this patient; therefore, this technique may constitute salvage therapy when the transpapillary approach is difficult.

The early-stage pancreatic cancer (e-PC; stage I/II) detection rate is quite low at approximately 25%. Sakamoto et al. [17] conducted a study to evaluate the feasibility of a social program (the Kishiwada project) wherein their hospital, which specializes in PC and primary care medical offices (PMOs), used clinical findings to detect e-PC. They concluded that this social program with collaborations between medical centers that specialize in PC and PMOs used clinical findings, suggesting that not only general internal medicine offices (GIMs) but also other PMOs and indirect findings by US may play an important role in improving the e-PC detection rate.

Repeated pancreatic juice cytology via endoscopic naso-pancreatic drainage (ENPD) is found to have high diagnostic yield and might be useful for the diagnosis of e-PC. EUS-FNA is also helpful for confirming the diagnosis of early pancreatic carcinoma, but its role is limited with respect to carcinoma in situ as no tumor has formed at this stage. Miyata et al. [18] reported that a case of repeated pancreatic juice cytology via ENPD was effective in the diagnosis of pancreatic carcinoma in situ. They speculated that a weak low echoic area around the MPD stricture on EUS might be related to the inflammatory changes accompanying carcinoma in situ of the pancreas.

HCC is the second leading cause of cancer mortality in the world. Sorafenib is an agent that has improved the time-to-progression (TTP) and overall survival (OS) in advanced stages of HCC with vascular invasion and/or extrahepatic spread [19]. Sorafenib is recommended by the consensus-based treatment algorithm for HCC pro-

posed by the Japan Society of Hepatology [20–22]. According to this algorithm, sorafenib is indicated in patients diagnosed with Child-Pugh stage A HCC with extrahepatic spread or vascular invasion. Sorafenib is also recommended in patients with Child-Pugh stage A HCC where transcatheter arterial chemoembolization (TACE) [23–26] and hepatic arterial infusion chemotherapy [26–28] are not indicated. Ogawa et al. [29] attempted to determine the relationship between treatment outcomes and hand-foot syndrome, and post-progression treatment after sorafenib therapy. They found that in sorafenib therapy, the patients with hand-foot syndrome and those who received postprogression treatment showed good OS. They also noted that the best results were observed when therapy was initiated at Child-Pugh grade A-5, which indicates that it is preferable to start sorafenib at the time when liver function is still well preserved. Starting sorafenib at a reduced dose in Japanese patients is also thought to lead to a better OS.

HCC is the fifth most common malignant tumor and the third cause of cancer death in the world. Advances of hepatic resection [27] and radiofrequency ablation [28, 30, 31] as curative treatments have improved the prognosis of HCC. However, it is well known that there is frequent recurrence after curative treatments for HCC. TACE has been performed as a palliative treatment against unresectable HCC in the patients with/without a past history of treatments, especially in BCLC-B (intermediate) stage HCC [32], and has been reported to be effective for improving prognosis of the patients with HCC. Recently, new criteria for predicting poor prognosis of HCC, time to TACE progression (TTTP), have been proposed [33]. TTTP showed a moderate correlation to OS after progression in the patients with BCLC-B HCC treated with TACE. Izumoto et al. [34] performed the validation study of the relationship between TTTP and OS after TACE. They concluded that TTTP showed a good correlation with OS. In the patients with the short TTTP, especially less than 5 months, it might be difficult to improve prognosis with repeated TACE procedure. In such cases, re-consideration of therapeutic strategy, switching treatment from TACE to tyrosine kinase inhibitors, might be needed [20, 35]. In addition, TTTP may be a good surrogate endpoint of OS in the TACE combination trial with molecular targeted agents or immune checkpoint inhibitors or both [26, 36].

Kudo and Arizumi [37] reviewed molecular targeted therapy in combination with TACE of negative trials such as post-TACE, BRISK-TA, SPACE, ORIENTAL, and TACE-2 trials. They state that TACE is the first-line treat-



ment for intermediate-stage HCC; however, repeated TACE sessions tend to impair liver function, resulting in shorter prognosis. Reducing the frequency of TACE, which is generally repeated upon tumor progression, is a challenging issue in the treatment of patients with intermediate-stage HCC. To address this issue, previous trials combined molecular targeted agents with TACE; however, the safety and efficacy of this combination could not be demonstrated, and none of the combination therapies is currently recommended. In such cases, post-trial treatment likely affects OS, making it difficult to evaluate treatment outcomes using OS. Instead of OS, TTP/progression-free survival is used as a primary endpoint in some trials; however, whether TTP/progression-free survival based on RECIST is an appropriate endpoint in clinical trials of TACE combination therapies remains unclear. In general, TTP corresponds to the period between randomization or the day of study initiation and disease progression. In their previous study, they proposed a novel endpoint, "time to TACE progression (TTTP)," as a progression-free period specific to patients treated with TACE and defined as the time from the initial TACE effect evaluation to progression [33]. They also verified that TTTP is correlated with OS, suggesting that TTTP could be a surrogate endpoint for OS and a better primary endpoint than OS for use in clinical studies of TACE in combination with molecular targeted agents or immunotherapy. They concluded that many clinical trials investigated the efficacy of TACE combined with molecular targeted agents; however, none of them demonstrated an OS benefit of the combination strategy or even improved TTP/progression-free survival. Nevertheless, these studies showed the antitumor effect of the molecular targeted agents as adjuvant therapy. It is important to consider the reasons for the negative outcomes of these trials and to carefully plan future clinical trials of combination therapy with TACE.

Kudo reviewed the 2017 update of systemic therapy for HCC. The author pointed out that tumor reduction effect and toxicity of current standard of care (sorafenib) remain unsatisfactory. The development of novel molecular targeted agents, as alternatives to sorafenib, has been attempted up to now, although there are many difficulties unique to HCC to overcome. Nevertheless, the efficacy of 3 molecular targeted agents in succession has recently been proven. Two are the second-line agents, regorafenib and cabozantinib, which developed on sorafenib therapy. Another one is the first-line agent, lenvatinib, which was proven to be noninferior to sorafenib. Another group of agents that are attracting considerable interest are im-

mune checkpoint inhibitors, such as anti-programmed cell death 1 (PD-1), programmed cell death-ligand 1 (PD-L1), or cytotoxic T-lymphocyte-associated antigen 4 (CTLA-4) antibodies that kill cancer cells via a unique mechanism. The expected therapeutic effects of some of these agents are now being investigated in phase III studies. The most recent topics is the combination therapy of PD-1/PD-L1 with other immune checkpoint inhibitor, CTLA-4, or with tyrosine kinase inhibitor, or locoregional therapies, such as resection, ablation or TACE. He concluded that increased options for treatment using a molecular targeted agent and immune checkpoint inhibitors will benefit more HCC patients, but adequate selection of the treatment is important and should be actively explored.

Kudo reviewed the most updated topic, immuno-oncology in HCC. Clinical trials are currently ongoing to evaluate the utility of antibodies against PD-1, PD-L1, and CTLA-4 as monotherapy or combination therapy in patients with HCC. Results of combination treatment with the anti-PD-L1 antibody durvalumab and the anti-CTLA-4 antibody tremelimumab in HCC were presented at the 2017 annual meeting of ASCO. Response rates were 25% in all 40 patients and 40% in the 20 uninfected patients, both of which are encouraging. TACE and radiofrequency ablation can activate tumor immunogenicity by releasing tumor-associated antigen and by inducing the migration of cytotoxic T lymphocytes to small intrahepatic metastatic nodules. Subsequent administration of anti-PD-1 antibody could control these small intrahepatic metastatic nodules. In a nonclinical study, the combination of pembrolizumab and lenvatinib inhibited the cancer immunosuppressive environments induced by tumor-associated macrophages and Tregs. This, in turn, decreased the levels of TGF- $\beta$  and IL-10, the expression of PD-1, and the inhibition of Tim-3, triggering anticancer immunity mediated by immunostimulatory cytokines such as IL-12. Studies such as these may provide insight into the appropriate molecular targeted agents to be used with immune checkpoint inhibitors.

Nishida and Kudo [38] described activation of oncogenic signaling and tumor immunosuppressive microenvironment in HCC. They stated that vascular endothelial growth factor (VEGF) induces myeloid-derived suppressor cell accumulation, inhibit maturation of dendritic cells, and induce Treg cells. VEGF also exerts immunosuppressive function through the expression of immune checkpoint molecules on CD8+ T cells, such as PD-1, T cell immunoglobulin and mucin domain 3 (TIM-3) and CTLA-4. Immunoregulatory enzyme, indoleamine 2,3-

dioxygenase, is overexpressed in HCC cell lines and human HCC tissues, which is an independent prognostic factor for HCC patients. Indoleamine 2,3-dioxygenase is upregulated by proinflammatory cytokines, such as interferon- $\gamma$ , and inhibits T cell activation and promotes expansion of Treg cells. Similarly, lactic acid, which is generated through glycolysis in tumor cells, stimulates the expression of VEGF and M2-like polarization of tumor-associated macrophages. Activation of NF- $\kappa$ B could also increase the expression of immunosuppressive cytokines, such as IL-2, IL-6, and IL-8 in cancer cells. They concluded that from this point of view, it is conceivable

that combination with inhibitors of oncogenic signaling improve the antitumor effect of anti-PD-1 and PD-L1 antibody.

Finally, I strongly believe this supplementary issue of *Oncology* focusing on “New paradigm in gastrointestinal cancer treatment” will be an invaluable one for all the readers of *Oncology*.

## Disclosure Statement

The author has no conflicts of interest to declare.

## References

- Okamoto K, Matsui S, Watanabe T, Asakuma Y, Komeda Y, Okamoto A, Ishikawa R, et al: Clinical analysis of esophageal stricture in patients treated with intralesional triamcinolone injection after endoscopic submucosal dissection for superficial esophageal cancer. *Oncology* 2017;93(suppl 1):9–14.
- Adachi T, Matsui S, Watanabe T, Okamoto K, Okamoto A, Kono M, Yamada M, et al: Comparative study of clarithromycin- versus metronidazole-based triple therapy as first-line eradication for *Helicobacter pylori*. *Oncology* 2017;93(suppl 1):15–19.
- Yamada M, Sakurai T, Komeda Y, Nagai T, Kamata K, Minaga K, Yamao K, et al: Clinical significance of Bmi1 expression in inflammatory bowel disease. *Oncology* 2017;93(suppl 1):20–26.
- Sakurai T, Adachi T, Kono M, Arizumi T, Kamata K, Minaga K, Yamao K, et al: Prophylactic suturing closure is recommended after endoscopic treatment of colorectal tumors in patients with antiplatelet/anticoagulant therapy. *Oncology* 2017;93(suppl 1):27–29.
- Komeda Y, Handa H, Watanabe T, Nomura T, Kitahashi M, Sakurai T, Okamoto A, et al: Computer-aided diagnosis based on convolutional neural network system for colorectal polyp classification: preliminary experience. *Oncology* 2017;93(suppl 1):30–34.
- Okamoto K, Watanabe T, Komeda Y, Kono T, Takashima K, Okamoto A, Kono M, et al: Risk factors for postoperative bleeding in endoscopic submucosal dissection of colorectal tumors. *Oncology* 2017;93(suppl 1):35–42.
- Ogawa S, Ishii T, Minaga K, Nakatani Y, Hatamaru K, Akamatsu T, Seta T, et al: The feasibility of 18-mm diameter colonic stents for obstructive colorectal cancers. *Oncology* 2017;93(suppl 1):43–48.
- Komeda Y, Kashida H, Sakurai T, Asakuma Y, Tribonias G, Nagai T, Kono M, et al: Magnifying narrow band imaging (NBI) for the diagnosis of localized colorectal lesions using the Japan NBI Expert Team (JNET) classification. *Oncology* 2017;93(suppl 1):49–54.
- Omoto S, Takenaka M, Kitano M, Miyata T, Kamata K, Minaga K, Arizumi T, et al: Characterization of pancreatic tumors with quantitative perfusion analysis in contrast-enhanced harmonic Endoscopic Ultrasonography. *Oncology* 2017;93(suppl 1):55–60.
- Takenaka M, Masuda A, Shiomi H, Yagi Y, Zen Y, Sakai A, Kobayashi T, et al: Chronic pancreatitis finding by endoscopic ultrasonography in the pancreatic parenchyma of IPMNs is associated with invasive IPMC. *Oncology* 2017;93(suppl 1):61–68.
- Imai H, Takenaka M, Omoto S, Kamata K, Miyata T, Minaga K, Yamao K, et al: Utility of endoscopic ultrasound-guided hepaticogastrostomy with antegrade stenting for malignant biliary obstruction after failed endoscopic retrograde cholangiopancreatography. *Oncology* 2017;93(suppl 1):69–75.
- Kamata K, Takenaka M, Nakai A, Omoto S, Miyata T, Minaga K, Matsuda T, et al: Association between the risk factors for pancreatic ductal adenocarcinoma and those for malignant intraductal papillary mucinous neoplasm. *Oncology* 2017;93(suppl 1):102–106.
- Minaga K, Takenaka M, Katanuma A, Kitano M, Yamashita Y, Kamata K, Yamao K, et al: Needle tract seeding: an overlooked rare complication of endoscopic ultrasound-guided fine-needle aspiration. *Oncology* 2017;93(suppl 1):107–112.
- Yamao K, Takenaka M, Imai H, Nakai A, Omoto S, Kamata K, Minaga K, et al: Primary hepatic adenosquamous carcinoma associated with primary sclerosing cholangitis. *Oncology* 2017;93(suppl 1):76–80.
- Yamao K, Takenaka M, Nakai A, Omoto S, Kamata K, Minaga K, Miyata T, et al: Detection of high-grade pancreatic intraepithelial neoplasia without morphological changes of the main pancreatic duct over a long period: importance for close follow-up for confirmation. *Oncology* 2017;93(suppl 1):81–86.
- Kamata K, Takenaka M, Minaga K, Sakurai T, Watanabe T, Nishida N, Kudo M: EUS-guided pancreatic duct drainage for repeat pancreatitis in a patient with pancreatic cancer. *Oncology* 2017;93(suppl 1):87–88.
- Sakamoto H, Harada S, Nishioka N, Maeda K, Kurihara T, Sakamoto T, Higuchi K, et al: A social program for the early detection of pancreatic cancer, the Kishiwada project: a multi-center study. *Oncology* 2017;93(suppl 1):89–97.
- Miyata T, Takenaka M, Omoto S, Kamata K, Minaga K, Yamao K, Imai H, et al: A case of pancreatic carcinoma in situ diagnosed by repeated pancreatic juice cytology. *Oncology* 2017;93(suppl 1):98–101.
- Kudo M: Molecular targeted therapy for hepatocellular carcinoma: where are we now? *Liver Cancer* 2015;4:I–VII.
- Kudo M: Clinical practice guidelines for hepatocellular carcinoma differ between Japan, United States, and Europe. *Liver Cancer* 2015;4:85–95.
- Kudo M, Matsui O, Izumi N, Iijima H, Kadota M, Imai Y, Okusaka T, et al: JSH consensus-based clinical practice guidelines for the management of hepatocellular carcinoma: 2014 update by the Liver Cancer Study Group of Japan. *Liver Cancer* 2014;3:458–468.
- Kokudo N, Hasegawa K, Akahane M, Igaki H, Izumi N, Ichida T, Uemoto S, et al: Evidence-based clinical practice guidelines for hepatocellular carcinoma: the Japan Society of Hepatology 2013 update (3rd JSH-HCC guidelines). *Hepatol Res* 2015;45.
- Kudo M: Locoregional therapy for hepatocellular carcinoma. *Liver Cancer* 2015;4:163–164.
- Kudo M: Surveillance, diagnosis, treatment, and outcome of liver cancer in Japan. *Liver Cancer* 2015;4:39–50.
- Tsurusaki M, Murakami T: Surgical and locoregional therapy of HCC: TACE. *Liver Cancer* 2015;4:165–175.



- 26 Arizumi T, Ueshima K, Minami T, Kono M, Chishina H, Takita M, Kitai S, et al: Effectiveness of sorafenib in patients with transcatheter arterial chemoembolization (TACE) refractory and intermediate-stage hepatocellular carcinoma. *Liver Cancer* 2015;4:253–262.
- 27 Kudo M, Izumi N, Sakamoto M, Matsuyama Y, Ichida T, Nakashima O, Matsui O, et al: Survival analysis over 28 years of 173,378 patients with hepatocellular carcinoma in Japan. *Liver Cancer* 2016;5:190–197.
- 28 Kang TW, Rhim H: Recent advances in tumor ablation for hepatocellular carcinoma. *Liver Cancer* 2015;4:176–187.
- 29 Ogawa C, Morita M, Omura A, Noda T, Kudo A, Matsunaka T, Tamaki H, et al: Hand-foot syndrome and post-progression treatment are the good predictors of better survival in advanced hepatocellular carcinoma treated with sorafenib: a multicenter study. *Oncology* 2017;93(suppl 1):113–119.
- 30 Teng W, Liu KW, Lin CC, Jeng WJ, Chen WT, Sheen IS, Lin CY, et al: Insufficient ablative margin determined by early computed tomography may predict the recurrence of hepatocellular carcinoma after radiofrequency ablation. *Liver Cancer* 2015;4:26–38.
- 31 Lencioni R, de Baere T, Martin RC, Nutting CW, Narayanan G: Image-guided ablation of malignant liver tumors: recommendations for clinical validation of novel thermal and non-thermal technologies – a Western perspective. *Liver Cancer* 2015;4:208–214.
- 32 Kudo M: Heterogeneity and subclassification of barcelona clinic liver cancer stage B. *Liver Cancer* 2016;5:91–96.
- 33 Arizumi T, Ueshima K, Iwanishi M, Minami T, Chishina H, Kono M, Takita M, et al: The overall survival of patients with hepatocellular carcinoma correlates with the newly defined time to progression after transarterial chemoembolization. *Liver Cancer* 2017;6:227–235.
- 34 Izumoto H, Hiraoka A, Ishimaru Y, Murakami T, Kitahata S, Ueki H, Aibiki T, et al: Validation of newly proposed time to TACE progression (TTTP) in intermediate stage hepatocellular carcinoma cases. *Oncology* 2017;93(suppl 1):120–126.
- 35 Kudo M: Regorafenib as second-line systemic therapy may change the treatment strategy and management paradigm for hepatocellular carcinoma. *Liver Cancer* 2016;5:235–244.
- 36 Kudo M: Immune checkpoint blockade in hepatocellular carcinoma. *Liver Cancer* 2015;4:201–207.
- 37 Kudo M, Arizumi T: Molecular targeted therapy in combination with transarterial chemoembolization: lessons from negative trials (Post-TACE, BRISK-TA, SPACE, ORIENTAL and TACE-2). *Oncology* 2017;93(suppl 1):127–134.
- 38 Nishida N, Kudo M: Oncogenic signal and tumor microenvironment in hepatocellular carcinoma. *Oncology* 2017;93(suppl 1):160–164.

# Clinical Analysis of Esophageal Stricture in Patients Treated with Intralesional Triamcinolone Injection after Endoscopic Submucosal Dissection for Superficial Esophageal Cancer

Kazuki Okamoto<sup>a</sup> Shigenaga Matsui<sup>a</sup> Tomohiro Watanabe<sup>a</sup>  
Yutaka Asakuma<sup>a</sup> Yoriaki Komeda<sup>a</sup> Ayana Okamoto<sup>a</sup> Ishikawa Rei<sup>a</sup>  
Masashi Kono<sup>a</sup> Mitsunari Yamada<sup>a</sup> Tomoyuki Nagai<sup>a</sup> Tadaaki Arizumi<sup>a</sup>  
Kosuke Minaga<sup>a</sup> Ken Kamata<sup>a</sup> Kentaro Yamao<sup>a</sup> Mamoru Takenaka<sup>a</sup>  
Toshiharu Sakurai<sup>a</sup> Naoshi Nishida<sup>a</sup> Hiroshi Kashida<sup>a</sup> Takaaki Chikugo<sup>b</sup>  
Masatoshi Kudo<sup>a</sup>

Departments of <sup>a</sup>Gastroenterology and Hepatology and <sup>b</sup>Pathology, Kindai University Faculty of Medicine, Osaka-Sayama, Japan

## Keywords

Esophageal stricture · Endoscopic submucosal dissection · Triamcinolone

## Abstract

**Introduction:** Endoscopic submucosal dissection (ESD) has been widely used in the resection of superficial esophageal cancers. Since its use has been extended to cases involving large esophageal tumors occupying nearly the whole or the whole circumference of the lumen, the occurrence of esophageal stricture has increased. Although endoscopic injection of triamcinolone (TA) is widely used for the prevention of postoperative stricture, a significant number of patients still develop stricture after TA injection therapy. **Methods:** We performed a retrospective study to identify the clinical parameters that predispose post-ESD patients to esophageal stricture after TA injection therapy. **Results:** A total of 207 patients who were diagnosed with superficial esophageal

cancer and subsequently underwent ESD were enrolled in this study. Among these patients, 53 patients and 57 lesions bearing mucosal defects covering greater than two-thirds of the esophageal circumference after ESD were treated with TA injection therapy. The rate of esophageal stricture was found to be highest in cases involving mucosal defects that covered more than seven-eighths of the circumference. **Conclusion:** Endoscopic TA injection is not sufficient for preventing esophageal stricture in patients bearing mucosal defects covering more than seven-eighths of the esophageal circumference after ESD.

© 2017 S. Karger AG, Basel

## Introduction

Endoscopic submucosal dissection (ESD) has now become a standard treatment modality for superficial esophageal cancer [1–3]. ESD has enabled endoscopists

to achieve en bloc resection of large superficial esophageal cancers. Indeed, local recurrence rates are much lower in ESD than in conventional endoscopic mucosal resection (EMR) due to the effectiveness of the en bloc resection [1–3]. Thus, ESD is considered the most useful procedure for resection of superficial esophageal cancer.

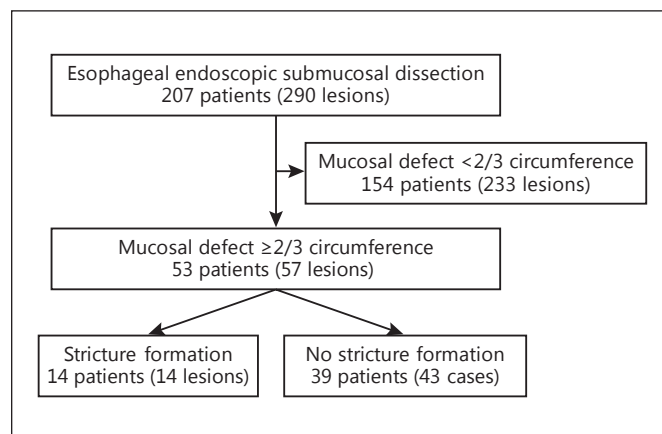
As the indications for ESD for esophageal cancer extend to include larger tumors that occupy near or whole circumference, the complication rate associated with the procedure is rising. Esophageal stricture is the most frequent complication associated with ESD [4]. Ono et al. [5] reported that most patients who underwent near- or whole-circumferential ESD developed postoperative esophageal stricture. Severe esophageal stricture can impair quality of life due to the resultant inability to ingest food, and usually requires multiple sessions of endoscopic balloon dilations (EBDs). Hence, there have been many attempts to reduce the incidence of esophageal stricture. Endoscopic intralesional injection of triamcinolone (TA) is widely used for the prevention of esophageal stricture after ESD. Although endoscopic TA injection can cause delayed perforation upon injection into the muscle layer [6, 7], several clinical studies report the safety and efficacy of its use [8, 9]. It should be noted, however, that a significant proportion (10–20%) of patients still develop postoperative esophageal stricture even after treatment with endoscopic TA injection [8, 9]. Therefore, it is important to identify the subgroup of patients at high risk of developing ESD-related esophageal stricture after TA injection.

In this study, we performed a retrospective review of the data from 57 patients treated with near- or whole-circumferential ESD and with TA injection. We report that an extensive circumferential mucosal defect (covering more than 75% of the circumference) was associated with a high risk of developing postoperative esophageal stricture, even after preventive injection of TA.

## Materials and Methods

### Patients

This was a retrospective study in which we analyzed the clinicopathological factors associated with esophageal stricture after near- or whole-circumferential ESD and endoscopic injection of TA. Between January 2011 and October 2016, a total of 207 patients who were diagnosed with superficial esophageal cancer and subsequently underwent ESD at Kindai University Hospital, Osaka, Japan, were enrolled in this study. Among those 207 patients, ESD was performed in 53 patients for a total of 57 cancerous lesions resulting in mucosal defects covering more than two-thirds of the circumference. Endoscopic injection of TA was performed



**Fig. 1.** Flow diagram showing the patients enrolled in the study. A total of 207 patients who were diagnosed as having superficial esophageal cancer and underwent ESD at Kindai University Hospital were enrolled in this study. Among these 207 patients and 290 lesions, 53 patients bearing 57 lesions underwent ESD with the extent of more than two-thirds of circumferential mucosal defect and then treated with endoscopic injection of TA for the prevention of esophageal stricture. Among 53 patients and 57 lesions, 14 patients exhibited esophageal stricture that required EBD. The 57 lesions were divided into non-esophageal stricture group ( $n = 43$ ) and esophageal stricture group ( $n = 14$ ).

for the 57 lesions. Ethical permission for this study was obtained from the Review Board at Kindai University, Faculty of Medicine. Patients with a history of chemotherapy or radiotherapy for esophageal cancer were excluded from the study.

Clinical parameters were obtained from the medical records of each patient, including age, sex, location of lesion (cervical, upper, middle, lower), longitudinal diameter of the lesion, endoscopic appearance of the lesion (IIa, IIb, IIc), depth of invasion (EP, LPM, MM, SM1, SM2) [5], ESD procedure time, extent of circumferential mucosal defect after ESD (more than 2/3, more than 3/4), and total dose of TA injection. Esophageal stricture was considered present when the patient complained of dysphagia or when a standard endoscope (GIF-Q260J; Olympus Optical, Tokyo, Japan) could not pass through the post-ESD scar.

### Endoscopic Submucosal Dissection

ESD was performed with the patients under conscious sedation by periodic intravenous administration of propofol and pethidine hydrochloride. We used a single-channel upper GI endoscope (GIF-Q260J; Olympus Optical, Tokyo, Japan) with transparent hood and irrigation pump. Carbon dioxide insufflation was used during the procedure. Sodium hyaluronic acid was injected into the submucosal layer to make a submucosal cushion. A flush-knife BT or BTS (DK2620J Fujifilm Medical, Tokyo, Japan) was used to dissect the lesion. The settings of the electrosurgical generator (VIO300 D Erbe Elektromedizin GmbH, Tübingen, Germany) were: soft coagulation (effect 80 W) for marking, endocut I (effect 3, time 2, interval 3) for mucosal incision, swift coagulation (effect 40 W) for submucosal dissection, and soft coagulation (effect

**Table 1.** Clinical parameters associated with esophageal structure

Clinical parameters	Esophageal stricture 14 cases (14 lesions)	Non-esophageal stricture 39 cases (43 lesions)	<i>p</i> value
Age, years	72.3±9.5	68.3±8.6	0.13 <sup>b</sup>
Male/female	12/2 (85.7, 14.3)	38/5 (88.4, 11.6)	0.55 <sup>a</sup>
Location of lesion			
Cervical	1 (7.1)	0	1.00 <sup>a</sup>
Upper	2 (14.3)	1 (2.3)	0.15 <sup>a</sup>
Middle	9 (64.3)	22 (51.2)	0.54 <sup>a</sup>
Lower	2 (14.3)	20 (46.5)	0.06 <sup>a</sup>
Longitudinal diameter of lesion	55.7±14.0	51.4±19.3	0.45 <sup>b</sup>
Endoscopic appearance			
0-IIa	1 (7.1)	1 (2.3)	0.43 <sup>a</sup>
0-IIb	7 (50)	33 (76.7)	0.09 <sup>a</sup>
0-IIc	6 (42.9)	9 (20.9)	0.16 <sup>a</sup>
Depth of invasion			
EP	4 (28.6)	13 (30.2)	1.00 <sup>a</sup>
LPM	6 (42.9)	20 (46.5)	1.00 <sup>a</sup>
MM	3 (21.4)	5 (11.6)	0.39 <sup>a</sup>
SM1	1 (7.1)	0	1.00 <sup>a</sup>
SM2	0	1 (2.3)	1.00 <sup>a</sup>
ESD procedure time	140.1±58.8	99.2±40.5	0.005 <sup>b</sup>
Circumferential extent (CE)			
3/4 ≤ CE ≤1	11 (78.6)	27 (62.8)	0.34 <sup>a</sup>
7/8 ≤ CE ≤1	10 (71.4)	10 (23.3)	0.003 <sup>a</sup>
Total doses of TA, mg	68±24	44.8±23.2	0.06 <sup>b</sup>

Figures in parentheses indicate percentages. ESD, endoscopic submucosal dissection; TA, triamcinolone.  
<sup>a</sup> Fisher's exact test. <sup>b</sup> *t* test.

40 W) for bleeding points. Hemostatic forceps were used for preventive occlusions of the vessels. At the end of the procedure, additional coagulation was carefully performed to prevent delayed bleeding.

#### Endoscopic TA Injection

TA was diluted with 0.9% NaCl to a final concentration of 10 mg/mL. Then, 0.1- to 0.2-mL aliquots were injected at the base of the artificial ulcer using a 25-gauge, 4-mm needle (TOP Corporation). Effective administration of the steroid into the submucosal layer required dissection at the middle level of the submucosal layer to create enough space for the injection. A potential problem with the injection method is the risk of delayed perforation, which may occur if the steroid is injected into the true muscular layer. Therefore, TA must be injected into the submucosal layer.

#### Endoscopic Balloon Dilatation

EBD was performed every 1–4 weeks after ESD. The dilatation was performed in the outpatient department using CRE™ Wire-Guided Esophageal/Pyloric balloon Dilatation Catheters (Boston Scientific, Marlborough, MA, USA). Dilatation therapy was considered successful when the patients reported improvement in dysphagia.

#### Statistical Analysis

Student's *t* test or Fisher's exact test was used in the univariate analysis. A *p* value less than 0.05 was considered significant. Clinical factors considered significant in the univariate analysis were subjected to multivariate analysis and a *p* value less than 0.05 was considered significant.

## Results

#### Flow Diagrams of the Patients

Esophageal stricture is the most frequent complication in ESD. Endoscopic TA injection is one of the most effective treatments for prevention of ESD-associated esophageal stricture [8, 9]. However, a significant proportion of patients still develop esophageal stricture requiring EBD even after endoscopic TA injection. In this retrospective study, we aimed to identify the risk factors for esophageal stricture in patients who underwent near- or whole-circumferential ESD and were treated with TA injection.

As shown in Figure 1, a total of 207 patients who were diagnosed with superficial esophageal cancer and underwent ESD at Kindai University Hospital were enrolled in this study. Among these 207 patients and 290 lesions, 53 patients bearing 57 lesions, underwent ESD which had resulted in a mucosal defect of greater than two-thirds of the esophageal circumference. These patients were then treated with endoscopic injection of TA for the prevention of esophageal stricture. We performed clinicopathological analysis in these 57 lesions.

#### *Risk Factors for Postoperative Esophageal Stricture in Patients Treated with TA Injection*

Among the 53 patients and 57 lesions described above, 14 patients exhibited esophageal stricture requiring EBD. These 57 lesions were divided into 2 groups: the non-esophageal stricture group ( $n = 43$ ) and the esophageal stricture group ( $n = 14$ ). Characteristics of the clinicopathological findings of these lesions are summarized in Table 1. No significant difference was seen in age, sex, tumor location, or depth of tumor invasion for both groups. In contrast, the rate of esophageal stricture was much higher in the cases with a mucosal defect covering more than seven-eighths of the circumference. Total dose of TA injection was higher in the non-esophageal stricture group than in the group with esophageal stricture. We performed multivariate analysis to confirm the results obtained using univariate analysis. As shown in Table 2, a circumferential mucosal defect of more than seven-eighths was identified as an independent risk factor for postoperative esophageal stricture. Conversely, ESD procedure time did not show a significant correlation. Collectively, univariate and multivariate analyses revealed that a mucosal defect covering seven-eighths or more of the circumference was strongly associated with postoperative esophageal stricture in patients treated with TA injection. These data suggest that endoscopic TA injection cannot prevent esophageal stricture in lesions bearing mucosal defects which cover more than seven-eighths of the circumference after ESD.

#### *Case Presentation*

##### *Case 1*

An 84-year-old man was admitted to Kindai University Hospital for ESD of a superficial esophageal cancer. Lugol's iodine staining revealed a lesion that was almost whole circumferential within the esophageal lumen (Fig. 2a). The patient was treated with ESD, which resulted in a whole-circumferential mucosal defect (Fig. 2b). The patient received endoscopic injection of TA for a to-

**Table 2.** Risk factors for postoperative esophageal stricture in patients treated with TA injection

	Odds ratio	95% CI	<i>p</i> value
Procedure time	1.01	1.0–1.03	1.01
More than seven-eighths of circumferential mucosal defect	5.83	1.41–24.12	0.01

tal of 80 mg for the prevention of esophageal stricture. Severe esophageal stricture developed 18 days after the procedure (Fig. 2c).

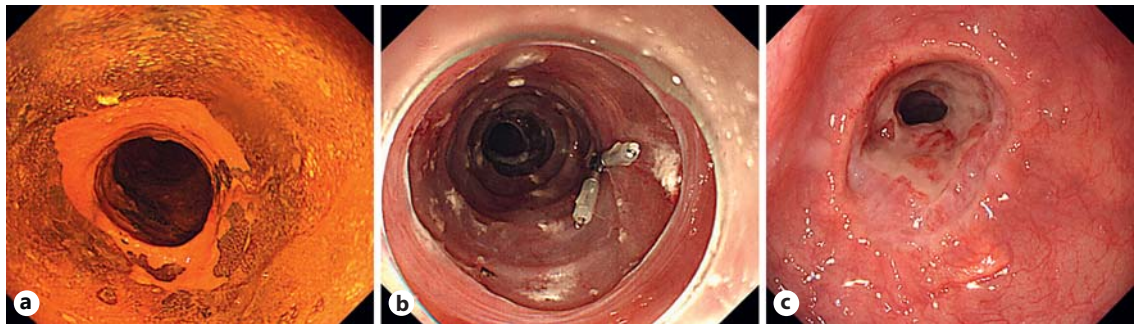
##### *Case 2*

A 54-year-old man was admitted to Kindai University Hospital for ESD of a superficial esophageal cancer. Lugol's iodine staining revealed a lesion occupying approximately two-thirds of the circumference of the esophageal lumen (Fig. 3a). The patient was treated with ESD, which resulted in a mucosal defect covering two-thirds of the lumen circumference (Fig. 3b). The patient received endoscopic injection of TA for a total of 40 mg for the prevention of esophageal stricture. Twenty-eight days after ESD, esophageal stricture had not developed (Fig. 3c).

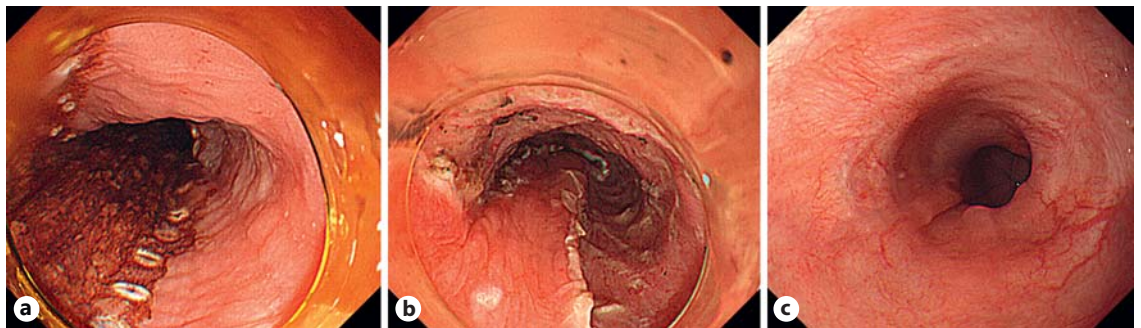
#### **Discussion**

Esophageal submucosal dissection has been established as a minimally invasive and effective modality for the treatment of superficial esophageal cancer [1–3]. This technique has enabled surgeons to perform en bloc resection of superficial esophageal cancers and to make accurate histological diagnoses, especially in terms of depth of invasion. Thus, judgement regarding successful complete resection is much easier in ESD than in conventional EMR. In fact, local recurrence rates of tumors after ESD are lower than those after EMR due to effective en bloc resections [1–3]. The indications for ESD have been extended to large superficial esophageal cancers that occupy almost the whole circumference of the esophageal lumen. Esophageal stricture is the most frequent complication associated with near- or whole-circumferential ESD for such large superficial esophageal cancers. Since esophageal stricture sometimes worsens quality of life, various preventive methods have been





**Fig. 2.** Representative case with esophageal stricture after ESD and TA injection. **a** Lugol's iodine staining revealed a lesion which was almost whole-circumferential within the esophageal lumen. **b** ESD resulted in a whole-circumferential mucosal defect. **c** Severe esophageal stricture developed 18 days after the ESD, despite endoscopic TA injection.



**Fig. 3.** Representative case without esophageal stricture after ESD and TA injection. **a** Lugol's iodine staining revealed a lesion occupying two-thirds of the circumference of esophageal lumen. **b** ESD resulted in a mucosal defect covering two-thirds of the circumference. **c** Esophageal stricture had not developed 28 days after the ESD and endoscopic TA injection.

proposed [4, 7, 10]. Endoscopic injection of TA is widely used in the prevention of esophageal stricture associated with ESD [8, 9]. However, a significant population of patients develop esophageal stricture even after the preventive injection. Therefore, it is important to identify the clinical parameters that predispose ESD treated patients to postoperative esophageal stricture. In this study, we retrospectively analyzed 57 esophageal cancer lesions that occupied greater than two-thirds of the esophageal lumen and that received preventive endoscopic injection of TA. We found that the rate of esophageal stricture was highest in cases when the resulting mucosal defect covered greater than seven-eighths of the esophageal circumference after ESD. Thus, our data suggest that endoscopic TA injection is not sufficient for the prevention of esophageal stricture in cases with mucosal defects covering greater than seven-eighths of the esophageal circumference after ESD.

Since endoscopic TA injection is not sufficiently effective in the prevention of esophageal stricture after near- or whole-circumferential ESD, other preventative strategies need to be considered. Oral prednisolone (30 mg/day) may offer a useful preventive option [11]. However, there are reports linking prednisolone with the development of infectious diseases [12]. Sakaguchi et al. [13] reported the usefulness of polyglycolic acid (PGA) sheets with fibrin glue in the prevention of esophageal stricture after ESD. In line with this, another report showed that the percentage of postoperative stricture after application of PGA sheets was 7.7% in patients with a mucosal defect covering greater than seven-twelfths of the esophageal circumference [14]. Furthermore, Kataoka et al. [15] reported a case in which esophageal stricture was successfully prevented by endoscopic TA injection followed by the application of PGA sheets after a whole-circumferential resection. Therefore, it is important to consider alter-

native strategies including the application of PGA sheets in cases bearing mucosal defects covering greater than seven-eighths of the circumference.

One concern arising from this study is how to optimize TA dosage to most effectively prevent esophageal stricture. TA is injected into the submucosal layer; however, occasionally leakage may occur [10]. Thus, endoscopists often encounter situations in which adequate intralesional distribution of TA is difficult to achieve. In this study, the total dose of TA injected was higher in the patients with esophageal stricture than in those without stricture. However, it remains unknown whether effective doses of TA were actually injected into the submucosal layer in each case. Tracing modalities to confirm adequate distribution of TA would be required to estimate and establish optimal dosage of TA necessary for the prevention of postoperative esophageal stricture.

## Conclusion

We have identified a risk factor for esophageal stricture in patients treated with endoscopic injection of TA. Endoscopic TA injection is not sufficient for the prevention of esophageal stricture in patients bearing a mucosal defect covering more than seven-eighths of the circumference after ESD. In such cases, alternative strategies, including the application of PGA sheets with or without TA injection need to be considered to avoid postoperative stricture.

## Disclosure Statement

The authors have no conflicts of interest to declare.

## References

- Oyama T, Tomori A, Hotta K, Morita S, Kominato K, Tanaka M, Miyata Y: Endoscopic submucosal dissection of early esophageal cancer. *Clin Gastroenterol Hepatol* 2005;3: S67–S70.
- Ono S, Fujishiro M, Niimi K, Goto O, Kodashima S, Yamamichi N, Omata M: Long-term outcomes of endoscopic submucosal dissection for superficial esophageal squamous cell neoplasms. *Gastrointest Endosc* 2009;70:860–866.
- Ono S, Fujishiro M, Koike K: Endoscopic submucosal dissection for superficial esophageal neoplasms. *World J Gastrointest Endosc* 2012;4:162–166.
- Jain D, Singhal S: Esophageal stricture prevention after endoscopic submucosal dissection. *Clin Endosc* 2016;49:241–256.
- Ono S, Fujishiro M, Niimi K, Goto O, Kodashima S, Yamamichi N, Omata M: Predictors of postoperative stricture after esophageal endoscopic submucosal dissection for superficial squamous cell neoplasms. *Endoscopy* 2009;41:661–665.
- Oyama T: Prevention of stricture after large esophageal endoscopic submucosal dissections. *Endoscopy* 2015;47:289–290.
- Yu JP, Liu YJ, Tao YL, Ruan RW, Cui Z, Zhu SW, Shi W: Prevention of esophageal stricture after endoscopic submucosal dissection: a systematic review. *World J Surg* 2015;39: 2955–2964.
- Hashimoto S, Kobayashi M, Takeuchi M, Sato Y, Narisawa R, Aoyagi Y: The efficacy of endoscopic triamcinolone injection for the prevention of esophageal stricture after endoscopic submucosal dissection. *Gastrointest Endosc* 2011;74:1389–1393.
- Takahashi H, Arimura Y, Okahara S, Kodaira J, Hokari K, Tsukagoshi H, Shinomura Y, Hosokawa M: A randomized controlled trial of endoscopic steroid injection for prophylaxis of esophageal stenoses after extensive endoscopic submucosal dissection. *BMC Gastroenterol* 2015;15:1.
- Uno K, Iijima K, Koike T, Shimosegawa T: Useful strategies to prevent severe stricture after endoscopic submucosal dissection for superficial esophageal neoplasm. *World J Gastroenterol* 2015;21:7120–7133.
- Yamaguchi N, Isomoto H, Nakayama T, Hayashi T, Nishiyama H, Ohnita K, Takeshima F, Shikuwa S, Kohno S, Nakao K: Usefulness of oral prednisolone in the treatment of esophageal stricture after endoscopic submucosal dissection for superficial esophageal squamous cell carcinoma. *Gastrointest Endosc* 2011;73:1115–1121.
- Ishida T, Morita Y, Hoshi N, Yoshizaki T, Ohara Y, Kawara F, Tanaka S, Yamamoto Y, Matsuo H, Iwata K, Toyonaga T, Azuma T: Disseminated nocardiosis during systemic steroid therapy for the prevention of esophageal stricture after endoscopic submucosal dissection. *Dig Endosc* 2015;27:388–391.
- Sakaguchi Y, Tsuji Y, Ono S, Saito I, Kataoka Y, Takahashi Y, Nakayama C, Shichijo S, Matsuda R, Minatsuki C, Asada-Hirayama I, Niimi K, Kodashima S, Yamamichi N, Fujishiro M, Koike K: Polyglycolic acid sheets with fibrin glue can prevent esophageal stricture after endoscopic submucosal dissection. *Endoscopy* 2015;47:336–340.
- Iizuka T, Kikuchi D, Yamada A, Hoteya S, Kajiyama Y, Kaise M: Polyglycolic acid sheet application to prevent esophageal stricture after endoscopic submucosal dissection for esophageal squamous cell carcinoma. *Endoscopy* 2015;47:341–344.
- Kataoka M, Anzai S, Shirasaki T, Ikemiyagi H, Fujii T, Mabuchi K, Suzuki S, Yoshida M, Kawai T, Kitajima M: Efficacy of short period, low dose oral prednisolone for the prevention of stricture after circumferential endoscopic submucosal dissection (ESD) for esophageal cancer. *Endosc Int Open* 2015;3:E113–E117.

## Comparative Study of Clarithromycin- versus Metronidazole-Based Triple Therapy as First-Line Eradication for *Helicobacter pylori*

Teppei Adachi Shigenaga Matsui Tomohiro Watanabe Kazuki Okamoto  
Ayana Okamoto Masashi Kono Mitsunari Yamada Tomoyuki Nagai  
Yoriaki Komeda Kosuke Minaga Ken Kamata Kentaro Yamao  
Mamoru Takenaka Yutaka Asakuma Toshiharu Sakurai Naoshi Nishida  
Hiroshi Kashida Masatoshi Kudo

Department of Gastroenterology and Hepatology, Kindai University Faculty of Medicine, Osaka-Sayama, Japan

### Keywords

*Helicobacter pylori* · Clarithromycin · Metronidazole

### Abstract

**Introduction:** Clarithromycin (CAM)-based triple therapy comprising proton pump inhibitors and amoxicillin is administered as first-line eradication treatment against *Helicobacter pylori* infection. However, the eradication rate achieved with CAM-based triple therapy has decreased to <80% owing to the emergence of CAM-resistant strains. This prospective randomized study aimed to compare the efficacy of CAM-based and metronidazole (MNZ)-based triple therapy in terms of *H. pylori* eradication. **Methods:** *H. pylori*-positive patients were treated with CAM-based triple therapy comprising esomeprazole and amoxicillin (EAC group) or with MNZ-based triple therapy comprising esomeprazole and amoxicillin (EAM group). **Results:** *H. pylori* eradication rates achieved in the intention-to-treat (ITT) and per protocol (PP) analyses were 70.6 and 72.7%, respectively, in the EAC group. Eradication rates obtained via ITT and PP analyses were 91.7 and 94.3%, respectively, in the EAM group. In the EAC group, eradication rates were significantly lower in

patients harboring CAM-resistant strains than in those harboring CAM-sensitive strains. In contrast, eradication rates were comparable between patients harboring CAM-resistant strains and those harboring CAM-sensitive strains in the EAM group. **Conclusion:** MNZ-based triple therapy consisting of esomeprazole and amoxicillin is superior to CAM-based triple therapy containing esomeprazole and amoxicillin as first-line eradication treatment against *H. pylori*.

© 2017 S. Karger AG, Basel

### Introduction

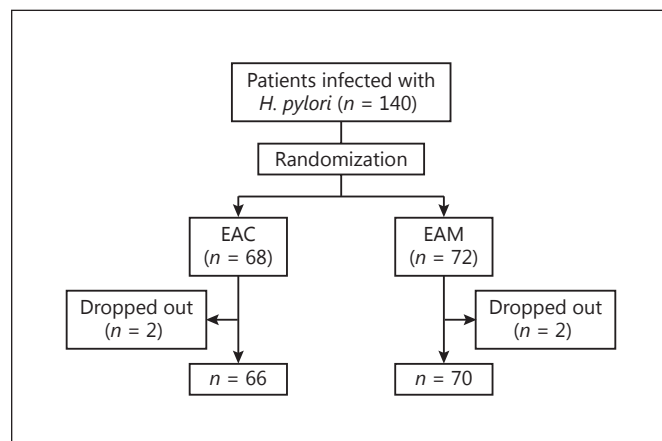
Gastric cancer is the third leading cause of cancer-related deaths worldwide [1]. Geographically, gastric cancer is very common in East Asia, where the prevalence rate of *Helicobacter pylori* infection is high [2]. *H. pylori* is a gram-negative bacterium that colonizes human gastric mucosa and then causes a wide variety of gastric disorders [3]. Chronic gastric infection due to *H. pylori* initially causes chronic active gastritis, which can then lead to the development of peptic ulcers, atrophic gastritis, gastric cancer, and mucosa-associated lymphoid tissue



lymphoma [3]. *H. pylori* infection is now a widely accepted primary cause of gastric cancer [4]. This claim is adequately supported by a large body of epidemiological and clinical evidence. First, around 90% of patients with gastric cancer demonstrate *H. pylori* seropositivity [4, 5]. Second, a prospective and long-term study showed that gastric cancer has been observed more frequently in Japanese patients with *H. pylori* infection than in those without an infection [6]. Third, eradication of *H. pylori* substantially reduced the incidence of gastric cancer in high-risk patients who underwent endoscopic resection [7]. Fourth and finally, a protective effect against gastric cancer has been reported to persist for more than 10 years after *H. pylori* eradication [8]. Therefore, *H. pylori* can be considered one of the most important causes of gastric cancer [9].

*H. pylori*-associated gastric cancer is one of the best examples of inflammation-related cancer [10, 11]. Genetic and epigenetic alterations accumulate within gastric epithelial cells infected with *H. pylori* in response to the progression of chronic inflammation [10, 11]. In fact, advanced stages of *H. pylori*-associated chronic gastritis bearing severe gastric atrophy and intestinal metaplasia are considered precancerous conditions, because gastric cancer tends to originate from gastric mucosa demonstrating these signs [6]. However, it should be noted that eradication of *H. pylori* reduces the risk for gastric cancer even in the presence of severe gastric atrophy and intestinal metaplasia [7]. Thus, *H. pylori* eradication is the most effective strategy for prevention of gastric cancer.

Proton pump inhibitor (PPI)-containing triple therapy with amoxicillin (AMPC) and clarithromycin (CAM) is widely used as a first-line eradication therapy for *H. pylori* in Japan [12]. Patients who demonstrate first-line eradication treatment failure are usually treated with PPI-containing triple therapy comprising AMPC and metronidazole (MNZ) [13, 14]. Although a multicenter study conducted in 2001 reported that the eradication rate using first-line therapy was around 90%, the rate decreased to 70–80% in 2014 [13, 15]. A possible explanation for the decreased eradication rate is the prevalence of CAM-resistant *H. pylori* in Japan [16, 17]. Okamura et al. [16] reported that the rate of CAM resistance is above 30 and 50% in old and young patients, respectively. Therefore, we hypothesized that MNZ-based triple therapy containing PPI and AMPC is superior to CAM-based triple therapy as a first-line eradication option. The aim of this study was to compare the efficacy of MNZ-based triple therapy and CAM-based triple therapy as *H. pylori* eradication treatments.



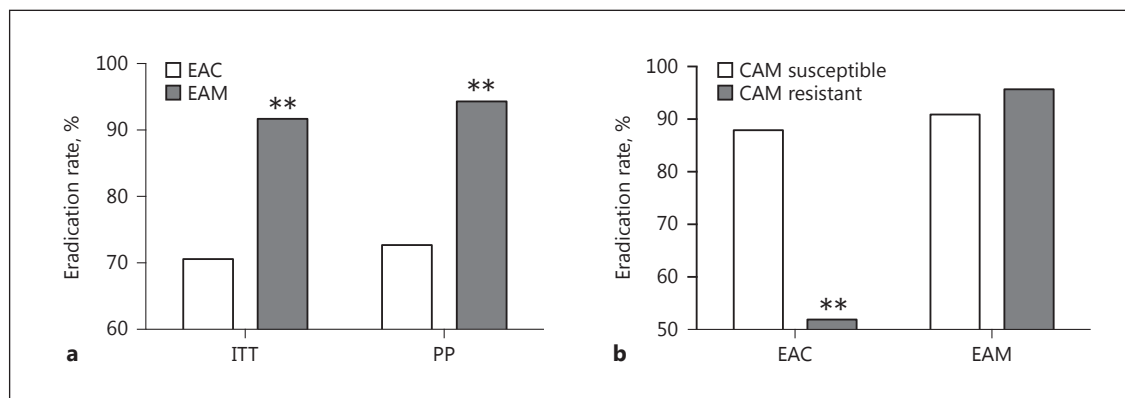
**Fig. 1.** Flow diagram of patient enrollment in this study. EAC, clarithromycin-based triple therapy comprising esomeprazole and amoxicillin; EAM, metronidazole-based triple therapy comprising esomeprazole and amoxicillin.

## Patients

This prospective randomized controlled study was designed to determine whether MNZ-based triple therapy was superior to CAM-based triple therapy as a first-line eradication treatment for *H. pylori*. Patients who underwent esophagogastroduodenoscopy for further examination and follow-up of upper gastrointestinal symptoms and *H. pylori*-associated diseases including peptic ulcers and chronic gastritis at Kindai University Hospital from June 2013 to August 2015 were enrolled. Patients who underwent esophagogastroduodenoscopy for follow-up of postendoscopic submucosal dissection for early gastric cancer were also enrolled. Exclusion criteria were as follows: age <19 years; history of *H. pylori* eradication therapy; allergy to PPI, AMPC, CAM, or MNZ; severe liver dysfunction; severe kidney dysfunction; severe heart disease; pregnancy; alcohol abuse; drug addiction. Written informed consent was obtained from each patient before administering the treatment, and the study protocol was approved by the Kindai University Ethics Committee. In addition, this trial is registered with the University Hospital Medical Information Network (000011203).

## Study Design

A total of 140 patients who met the inclusion criteria and agreed to receive *H. pylori* eradication therapy were enrolled in this study. Assessment of *H. pylori* infection was performed via rapid urease tests, culture methods, serum *H. pylori* antibody tests, and stool *H. pylori* antigen tests. Patients were regarded as *H. pylori*-positive when at least one of these tests yielded positive results. Either CAM-based triple therapy containing esomeprazole and AMPC (EAC) or MNZ-based triple therapy containing esomeprazole and AMPC (EAM) was administered as first-line eradication therapy against *H. pylori*. Patients were randomly divided into two groups: EAC group and EAM group. Patients in the EAC group were administered esomeprazole 20 mg, CAM 400 mg, and AMPC 750 mg twice a day for 7 days, and those in the



**Fig. 2.** *H. pylori* eradication rates. Patients were treated with clarithromycin (CAM)-based triple therapy comprising esomeprazole and amoxicillin (EAC) or metronidazole-based triple therapy comprising esomeprazole and amoxicillin (EAM). Eradication rates were calculated via intention-to-treat (ITT) and per protocol (PP) analyses (a). Eradication rates in the EAC and EAM groups were calculated in patients harboring CAM-susceptible and CAM-resistant strains (b). \*\*  $p < 0.01$ , as compared with EAM group (a) or with CAM-susceptible group (b).

EAM group were administered esomeprazole 20 mg, MNZ 500 mg, and AMPC 750 mg twice a day for 7 days. Eradication of *H. pylori* was confirmed via a urea breath test at 4 weeks after treatment completion. Susceptibility to CAM and MNZ was tested using gastric biopsy specimens obtained during endoscopy as previously described [18, 19].

#### Statistical Analysis

Intention-to-treat (ITT) and per protocol (PP) analyses were used to evaluate the eradication rate.  $\chi^2$  analysis was used for the statistical analysis, and a  $p$  value  $< 0.05$  indicated statistical significance.

## Results

### Patients

A total of 140 patients were enrolled in this study, and 136 patients completed the first-line eradication therapy. As shown in Figure 1, 68 and 72 patients were treated with EAC and EAM protocols, respectively. Two patients in each group dropped out owing to loss to follow-up or poor treatment compliance. None of the patients who completed the first-line eradication therapy showed serious adverse effects that required discontinuation of eradication therapy. As shown in Table 1, no significant differences were observed in terms of baseline characteristics such as age, sex, and diseases between the EAC and EAM groups. In addition, the rate of CAM-resistant *H. pylori* isolated from gastric mucosa samples was comparable between the EAC and EAM groups.

**Table 1.** Clinical characteristics of the patients

	EAC ( <i>n</i> = 68)	EAM ( <i>n</i> = 72)	<i>p</i>
Mean age $\pm$ SD, years	65.1 $\pm$ 10.0	62.7 $\pm$ 11.1	0.71
Sex (male/female)	32/36	36/36	0.93
Diseases			
Gastritis	45	44	0.78
Gastric ulcer	6	9	0.59
Duodenal ulcer	4	5	0.81
Follow-up of post-endoscopic therapy for early gastric cancer	13	14	0.96
Clarithromycin resistance (%)	27/60 (45)	23/67 (34.3)	0.5

EAC, clarithromycin-based triple therapy comprising esomeprazole and amoxicillin; EAM, metronidazole-based triple therapy comprising esomeprazole and amoxicillin.

### Eradication Efficacy

Eradication of *H. pylori* was confirmed via a urea breath test at 4 weeks after the completion of the first-line therapy. As shown in Figure 2a and Table 2, *H. pylori* eradication rates per the ITT and PP analyses were 70.6% (48/68) and 72.7% (48/66), respectively, in the EAC group. Eradication rates obtained in the ITT and PP analyses were 91.7% (66/72) and 94.3% (66/70), respectively, in the EAM group. Thus, the eradication rates in the EAM group were significantly higher than those observed in the EAC group.

We then addressed the effects of CAM resistance on the eradication rates. As shown in Figure 2b and Table 2, the eradication rates were 87.9% (29/33) and 51.9%



**Table 2.** *H. pylori* eradication rates

	EAC (n = 68)	EAM (n = 72)	<i>p</i> ( $\chi^2$ test)
Eradication rate (ITT)	48/68 (72.7)	66/72 (94.3)	0.00135
Eradication rate (PP)	48/66 (70.6)	66/70 (91.7)	0.000644
Clarithromycin susceptible	29/33 (87.9)	40/44 (90.9)	
Clarithromycin resistant	14/27 (51.9)	22/23 (95.7)	
<i>p</i>	0.00345	0.653	

Data are presented as number/total number (%). EAC, clarithromycin-based triple therapy comprising esomeprazole and amoxicillin; EAM, metronidazole-based triple therapy comprising esomeprazole and amoxicillin; ITT, intention to treat; PP, per protocol.

(14/27) in EAC-treated patients harboring CAM-susceptible and CAM-resistant *H. pylori* strains, respectively. In contrast, the eradication rates were 90.9% (40/44) and 95.7% (22/23) in EAM-treated patients bearing CAM-susceptible and CAM-resistant *H. pylori* strains, respectively. Thus, lower eradication rates in the EAC group were associated with a lower rate of eradication in patients harboring CAM-resistant *H. pylori* strains.

## Discussion

CAM-based triple therapy containing PPI and AMPC is frequently used as first-line eradication therapy against *H. pylori* infection in Japan [13, 15]. Although the eradication rate achieved using this first-line regimen was reported to be around 90% in 2001, the rate decreased to less than 80% by 2014 [13, 15]. The progressive increase in the incidence of CAM-resistant *H. pylori* strains is considered to be responsible for the decline in the eradication rate [16, 17]. In this prospective randomized study, we compared the efficacy of EAM with that of EAC. We found that the eradication rate achieved with EAM was much higher than that achieved using EAC in the ITT and PP analyses. This finding was independent of the CAM susceptibility of the strain in the EAM group. On the other hand, the eradication rate achieved using EAC was much lower in patients harboring CAM-resistant strains than in those harboring CAM-susceptible strains. We found that the eradication rates achieved via EAC and EAM were comparable in patients harboring CAM-sensitive *H. pylori* strains (87.9 vs. 90.9%). In contrast, the eradication rate achieved via EAM was much higher than that achieved via EAC against CAM-susceptible *H. pylori*

strains (51.9 vs. 95.7%). The percentage of CAM resistance was 39.3%, whereas that of MNZ resistance was 3.67%. In addition, no major adverse effects requiring discontinuation of eradication treatment were seen in both the EAC and EAM groups. Taken together, our results suggest that MNZ-based triple therapy containing PPI and AMPC is superior to CAM-based triple therapy as a first-line *H. pylori* eradication treatment owing to the high prevalence of CAM resistance and relatively lower prevalence of MNZ resistance. In line with our results, Nishizawa et al. [13] also claimed that MNZ-based therapy was superior to CAM-based therapy.

Vonoprazan (VPZ), a novel potassium-competitive acid blocker, has been recently used as first-line eradication of *H. pylori* [20–22]. Murakami et al. [21] report that the eradication rate achieved with first-line VPZ-based triple therapy containing CAM and AMPC was 92.6% and that achieved with second-line VPZ-based triple therapy containing MNZ and AMPC was 98.0%, even in the presence of CAM-resistant strains. Although the molecular mechanisms accounting for the high VPZ-mediated eradication rates remain unknown, one possible explanation may be enhanced antimicrobial activity of CAM and AMPC in the presence of VPZ [21]. VPZ, which demonstrates a potent ability to inhibit gastric acid production, is considered to create an environment where antimicrobials exert their optimal activity. Thus, CAM-based triple therapy containing VPZ and AMPC could be an effective first-line treatment. It should be noted, however, that the eradication rates achieved with CAM-based triple therapy containing VPZ and AMPC have been reported to be relatively low (86.3, 87.9%) in two studies [20, 22]. Further clinical studies addressing the efficacy of CAM-based triple therapy containing VPZ and AMPC are required to determine the efficacy of this regimen, especially in the setting of CAM-resistant strains.

*H. pylori* eradication is the most effective approach for the prevention of gastric cancer. Eradication of this organism prevents metachronous development of gastric cancer in patients who have undergone endoscopic treatment for early gastric cancer and demonstrate severe gastric atrophy and/or intestinal metaplasia [7]. Thus, eradication of *H. pylori* is also effective for the prevention of gastric carcinogenesis even at advanced stages of chronic gastritis with precancerous mucosal abnormalities such as severe gastric atrophy and/or intestinal metaplasia. Currently, several eradication regimens against *H. pylori* are available. Imprudent selection of eradication regimens might cause the emergence and expansion of antibiotic-resistant strains without the prevention of gastric

cancer. Future studies directly comparing the efficacy and safety of *H. pylori* eradication regimens are necessary to establish an appropriate regimen as a first-line treatment.

In conclusion, MNZ-based triple therapy containing esomeprazole and AMPC is superior to CAM-based triple therapy containing esomeprazole and AMPC as first-line eradication treatment against *H. pylori*.

## References

- 1 Ferlay J, Soerjomataram I, Dikshit R, Eser S, Mathers C, Rebelo M, Parkin DM, Forman D, Bray F: Cancer incidence and mortality worldwide: sources, methods and major patterns in GLOBOCAN 2012. *Int J Cancer* 2015; 136:E359–E386.
- 2 Mentis A, Lehours P, Megraud F: Epidemiology and diagnosis of *Helicobacter pylori* infection. *Helicobacter* 2015;20(suppl 1):1–7.
- 3 Malfertheiner P, Megraud F, O'Morain CA, Gisbert JP, Kuipers EJ, Axon AT, Bazzoli F, Gasbarrini A, Atherton J, Graham DY, Hunt R, Moayyedi P, Rokkas T, Rugge M, Selgrad M, Suerbaum S, Sugano K, El-Omar EM, European Helicobacter and Microbiota Study Group and Consensus panel: Management of *Helicobacter pylori* infection – the Maastricht V/Florence Consensus report. *Gut* 2017;66: 6–30.
- 4 Moss SF: The clinical evidence linking *Helicobacter pylori* to gastric cancer. *Cell Mol Gastroenterol Hepatol* 2017;3:183–191.
- 5 Plummer M, Franceschi S, Vignat J, Forman D, de Martel C: Global burden of gastric cancer attributable to *Helicobacter pylori*. *Int J Cancer* 2015;136:487–490.
- 6 Uemura N, Okamoto S, Yamamoto S, Matsumura N, Yamaguchi S, Yamakido M, Taniguchi K, Sasaki N, Schlemper RJ: *Helicobacter pylori* infection and the development of gastric cancer. *N Engl J Med* 2001;345: 784–789.
- 7 Fukase K, Kato M, Kikuchi S, Inoue K, Uemura N, Okamoto S, Terao S, Amagai K, Hayashi S, Asaka M, Japan Gast Study Group: Effect of eradication of *Helicobacter pylori* on incidence of metachronous gastric carcinoma after endoscopic resection of early gastric cancer: an open-label, randomised controlled trial. *Lancet* 2008;372:392–397.
- 8 Take S, Mizuno M, Ishiki K, Hamada F, Yoshida T, Yokota K, Okada H, Yamamoto K: Seventeen-year effects of eradicating *Helicobacter pylori* on the prevention of gastric cancer in patients with peptic ulcer; a prospective cohort study. *J Gastroenterol* 2015;50:638–644.
- 9 Venerito M, Vasapolli R, Rokkas T, Malfertheiner P: *Helicobacter pylori* and gastrointestinal malignancies. *Helicobacter* 2015; 20(suppl 1):36–39.
- 10 Chiba T, Marusawa H, Ushijima T: Inflammation-associated cancer development in digestive organs: mechanisms and roles for genetic and epigenetic modulation. *Gastroenterology* 2012;143:550–563.
- 11 Shimizu T, Marusawa H, Watanabe N, Chiba T: Molecular pathogenesis of *Helicobacter pylori*-related gastric cancer. *Gastroenterol Clin North Am* 2015;44:625–638.
- 12 Nishida T, Tsujii M, Tanimura H, Tsutsui S, Tsuji S, Takeda A, Inoue A, Fukui H, Yoshio T, Kishida O, Ogawa H, Oshita M, Kobayashi I, Zushi S, Ichiba M, Uenoyama N, Yasunaga Y, Ishihara R, Yura M, Komori M, Egawa S, Iijima H, Takehara T: Comparative study of esomeprazole and lansoprazole in triple therapy for eradication of *Helicobacter pylori* in Japan. *World J Gastroenterol* 2014;20:4362–4369.
- 13 Nishizawa T, Maekawa T, Watanabe N, Harada N, Hosoda Y, Yoshinaga M, Yoshio T, Ohta H, Inoue S, Toyokawa T, Yamashita H, Saito H, Kuwai T, Katayama S, Masuda E, Miyabayashi H, Kimura T, Nishizawa Y, Takahashi M, Suzuki H: Clarithromycin versus metronidazole as first-line *Helicobacter pylori* eradication: a multicenter, prospective, randomized controlled study in Japan. *J Clin Gastroenterol* 2015;49:468–471.
- 14 O'Connor A, Gisbert JP, O'Morain C, Ladas S: Treatment of *Helicobacter pylori* infection 2015. *Helicobacter* 2015;20(suppl 1):54–61.
- 15 Asaka M, Sugiyama T, Kato M, Satoh K, Kuwayama H, Fukuda Y, Fujioka T, Takemoto T, Kimura K, Shimoyama T, Shimizu K, Kobayashi S: A multicenter, double-blind study on triple therapy with lansoprazole, amoxicillin and clarithromycin for eradication of *Helicobacter pylori* in Japanese peptic ulcer patients. *Helicobacter* 2001;6:254–261.
- 16 Okamura T, Suga T, Nagaya T, Arakura N, Matsumoto T, Nakayama Y, Tanaka E: Antimicrobial resistance and characteristics of eradication therapy of *Helicobacter pylori* in Japan: a multi-generational comparison. *Helicobacter* 2014;19:214–220.
- 17 Hu Y, Zhang M, Lu B, Dai J: *Helicobacter pylori* and antibiotic resistance, a continuing and intractable problem. *Helicobacter* 2016; 21:349–363.
- 18 Glupczynski Y, Megraud F, Lopez-Brea M, Andersen LP: European multicentre survey of in vitro antimicrobial resistance in *Helicobacter pylori*. *Eur J Clin Microbiol Infect Dis* 2001;20:820–823.
- 19 Kobayashi I, Muraoka H, Saika T, Nishida M, Fujioka T, Nasu M: Micro-broth dilution method with air-dried microplate for determining MICs of clarithromycin and amoxicillin for *Helicobacter pylori* isolates. *J Med Microbiol* 2004;53:403–406.
- 20 Tsujimae M, Yamashita H, Hashimura H, Kano C, Shimoyama K, Kanamori A, Matsumoto K, Koizumi A, Momose K, Eguchi T, Fukuchi T, Fujita M, Okada A: A comparative study of a new class of gastric acid suppressant agent named vonoprazan versus esomeprazole for the eradication of *Helicobacter pylori*. *Digestion* 2016;94:240–246.
- 21 Murakami K, Sakurai Y, Shiino M, Funao N, Nishimura A, Asaka M: Vonoprazan, a novel potassium-competitive acid blocker, as a component of first-line and second-line triple therapy for *Helicobacter pylori* eradication: a phase III, randomised, double-blind study. *Gut* 2016;65:1439–1446.
- 22 Sakurai K, Suda H, Ido Y, Takeichi T, Okuda A, Hasuda K, Hattori M: Comparative study: vonoprazan and proton pump inhibitors in *Helicobacter pylori* eradication therapy. *World J Gastroenterol* 2017;23:668–675.

## Disclosure Statement

The authors have no conflicts of interest to declare.

# Clinical Significance of Bmi1 Expression in Inflammatory Bowel Disease

Mitsunari Yamada Toshiharu Sakurai Yoriaki Komeda Tomoyuki Nagai  
Ken Kamata Kosuke Minaga Kentaro Yamao Mamoru Takenaka  
Satoru Hagiwara Shigenaga Matsui Tomohiro Watanabe Naoshi Nishida  
Hiroshi Kashida Masatoshi Kudo

Department of Gastroenterology and Hepatology, Kindai University Faculty of Medicine, Osaka-Sayama, Japan

## Keywords

Colitis-associated cancer · Tumor necrosis factor ·  
Infliximab · Stress response · Gankyrin

## Abstract

**Background:** Although the stem cell marker Bmi1 is over-expressed in many malignancies, its role in inflammation-associated cancer is unclear. Colitis-associated cancer (CAC) is caused by chronic intestinal inflammation and often results from refractory inflammatory bowel disease (IBD).

**Methods:** To assess the involvement of Bmi1 in the development of CAC, we analyzed the gene expression of colon tissues collected from 111 patients with IBD and CAC. **Results:** In the colonic mucosa of patients with ulcerative colitis, the expression of Bmi1 correlated significantly with the expression of inflammatory cytokines such as IL-6, IL-17, IL-23, and tumor necrosis factor  $\alpha$  (TNF- $\alpha$ ). In the colonic mucosa of patients with Crohn's disease, the expression of Bmi1 correlated significantly with the expression of TNF- $\alpha$  and IL-23. The expression of Bmi1 was enhanced in the colonic mucosae of refractory IBD, suggesting that Bmi1 expression might be related to increased cancer risk. In addition, patients with high

Bmi1 expression showed significantly lower response rates upon subsequent anti-TNF- $\alpha$  therapy as compared to patients with low Bmi1 expression. In human CAC specimens, the expression of Bmi1 was upregulated in nontumor tissues as well as tumors. **Conclusions:** Bmi1 expression is related to a refractory clinical course of IBD and upregulated in refractory IBD and CAC. Measurement of Bmi1 expression is a promising approach for the advanced treatment and personalized management of IBD patients.

© 2017 S. Karger AG, Basel

## Introduction

Colorectal cancer is one of the most common fatal malignancies worldwide [1, 2]. Inflammatory bowel disease (IBD), comprising ulcerative colitis (UC) and Crohn's disease (CD), is thought to result from aberrant activation of the intestinal immune system [3] and is a major risk factor for colorectal cancer, so-called colitis-associated cancer (CAC) [4]. Indeed, patients with refractory IBD are at higher risk of colorectal cancer than individuals in the general population [5]. Longstanding inflammation

induces stress response proteins such as cold-inducible RNA-binding protein (CIRP), heat shock protein A4 (HSPA4), and RNA-binding motif protein 3 (RBM3), which regulate apoptosis of inflammatory or epithelial cells and expansion of stem cells, leading to the development of CAC [6–8]. In addition, HSPA4 expression could predict poor therapeutic response to steroids in IBD patients. Recently, we reported that the oncoprotein gankyrin activates STAT3 in inflammatory cells and promotes the development of CAC. In UC patients, refractory inflammation is associated with increased gankyrin expression in the colonic mucosa, which increases the risk for CAC [9]. These data suggest that long-term inflammation would result in refractory clinical course and eventually the development of cancer in IBD.

Cancer stem cells, the microenvironment, and the immune system interact with each other through cytokines. In the context of chronic inflammation, immune responses would affect proliferation of stem cells and increase the expression of stem cell markers [10]. The expression of stress response proteins and gankyrin that functionally link between chronic inflammation and tumorigenesis in IBD is significantly correlated with that of the stem cell marker Bmi1 [6–9]. The polycomb group protein Bmi1 is frequently overexpressed in human sporadic colorectal cancer, and the degree of upregulation correlates with disease progression and is predictive of poor patient survival [11]. In mice, Bmi1 is required for intestinal tumorigenesis [12]. Here, we show a significant association between Bmi1 expression and chronic inflammation in IBD patients. This study represents the first report of the expression of Bmi1 in inflammation-associated colorectal cancer that is associated with refractory clinical course. Bmi1 might be involved in the mechanistic connection between chronic inflammation and tumorigenesis in IBD.

## Materials and Methods

### Human Samples

Between April 2011 and March 2013, 111 intestinal samples were obtained from IBD patients and were analyzed for the expression of several genes. CAC specimens were obtained from 10 patients who had undergone colorectal resection.

Thirty colonic mucosal samples were obtained from IBD patients before the initiation of anti-tumor necrosis factor  $\alpha$  (anti-TNF- $\alpha$ ) therapy, and the response to anti-TNF- $\alpha$  therapy was evaluated prospectively. Clinical response was assessed 8 weeks after the treatment. In UC patients, a responder was defined as a person experiencing a decrease of 3 points or more in the full Mayo score or a decrease of 2 points or more in the Mayo clinical score with a

decrease of 1 point or more in the rectal bleeding subscore. In CD, clinical response was defined as a  $\geq 100$ -point decrease from the baseline CDAI score, or as a CDAI score  $< 150$  for patients with a baseline score  $\leq 248$ . The measurement of serum infliximab concentration was performed by KAC Co., Ltd. (Saitama, Japan).

The clinical study protocol conformed to the ethical guidelines of the 1975 Declaration of Helsinki and was approved by the relevant institutional review boards.

### Biochemical and Immunochemical Analyses

Real-time qPCR and immunohistochemistry were previously described [13–16]. The following antibodies were used: anti-Bmi1, anti-CD3, anti-CD20, and anti-CD68 (Dako, Santa Clara, CA, USA). Immunohistochemistry was performed using ImmPRESS<sup>TM</sup> reagents (Vector Laboratory, Burlingame, CA, USA) according to the manufacturer's recommendations. Nuclei were stained with 4',6-diamidino-2-phenylindole (DAPI).

### Statistical Analysis

Differences were analyzed using the Student *t* test. The relationship between the expression of several genes was analyzed by the Spearman rank correlation test. *p* values  $< 0.05$  were considered significant.

## Results

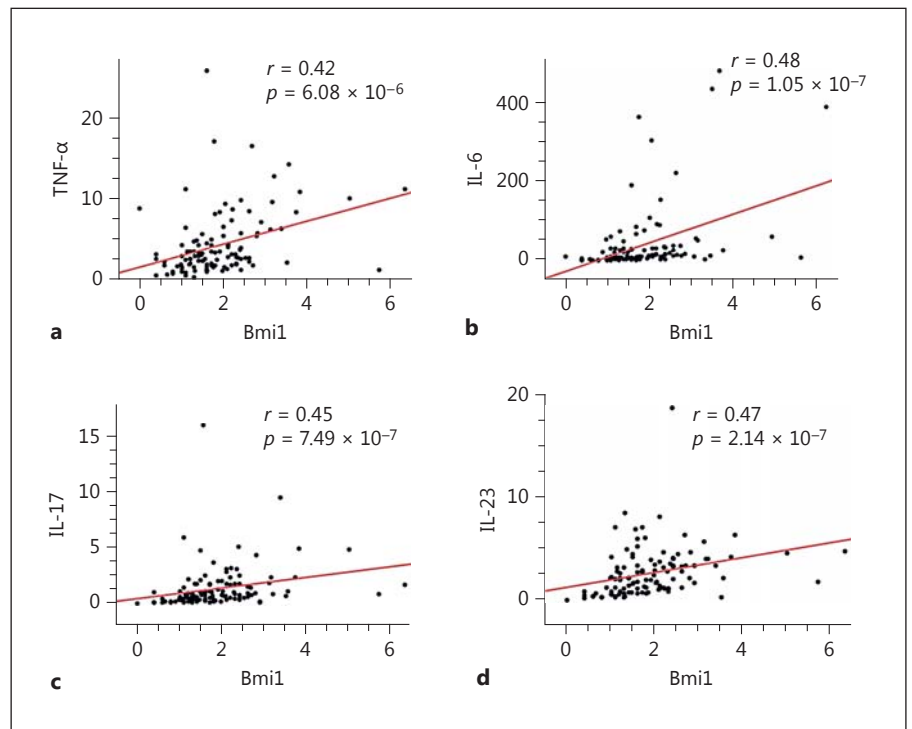
### Association between Bmi1 and Cytokines in the Colonic Mucosa of Patients with IBD

In the colonic mucosa of IBD patients, longstanding intestinal inflammation increases the expression of stress response proteins including CIRP, RBM3, and HSPA4, whose expression correlates significantly with Bmi1 expression [6–8]. Therefore, we explored whether an association exists between Bmi1 expression and cytokine production in IBD patients. Bmi1 expression correlated weakly but significantly with TNF- $\alpha$  and IL-6 expression, with a linear coefficient of 0.42 and 0.48, respectively in the colonic mucosa of UC patients (Fig. 1a, b). IL-23p19 is a specific subunit of IL-23 that acts as a positive regulator of T-helper IL-17-producing cell (Th17) and other IL-17-producing cells [17]. The IL-23/IL-17 pathway has been identified to play a critical role in IBD. A significant correlation was found between *Bmi1* and *IL-17A* or *IL-23p19* mRNA expression in UC patients (Fig. 1c, d).

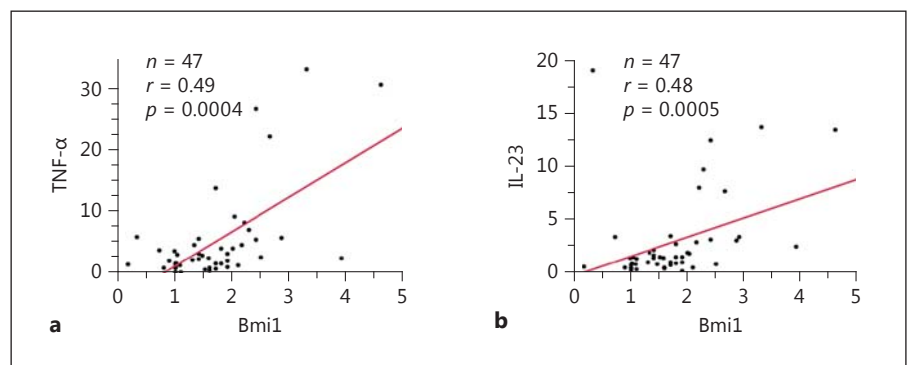
Currently, the biologics with regulatory approval for the management of CD include TNF antagonists and ustekinumab, a monoclonal antibody blocking the biological activity of IL-12 and IL-23 [18, 19]. Bmi1 expression correlated significantly with TNF- $\alpha$  and IL-23 expression, with a linear coefficient of 0.49 and 0.48, respectively in the colonic mucosa of CD patients (Fig. 2a, b).



**Fig. 1.** Association between Bmi1 and inflammatory cytokines in ulcerative colitis. The colonic mucosae were obtained from patients with ulcerative colitis, and gene expression was determined by quantitative real-time qPCR. Scatter plots of relative mRNA levels of Bmi1 and tumor necrosis factor  $\alpha$  (TNF- $\alpha$ ) (a), IL-6 (b), IL-17 (c), and IL-23 (d) are shown.



**Fig. 2.** Association between Bmi1 and inflammatory cytokines in Crohn's disease. The colonic mucosae were obtained from patients with Crohn's disease, and gene expression was determined by quantitative real-time qPCR. Scatter plots of relative mRNA levels of Bmi1 and tumor necrosis factor  $\alpha$  (TNF- $\alpha$ ) (a) and IL-23 (b) are shown.



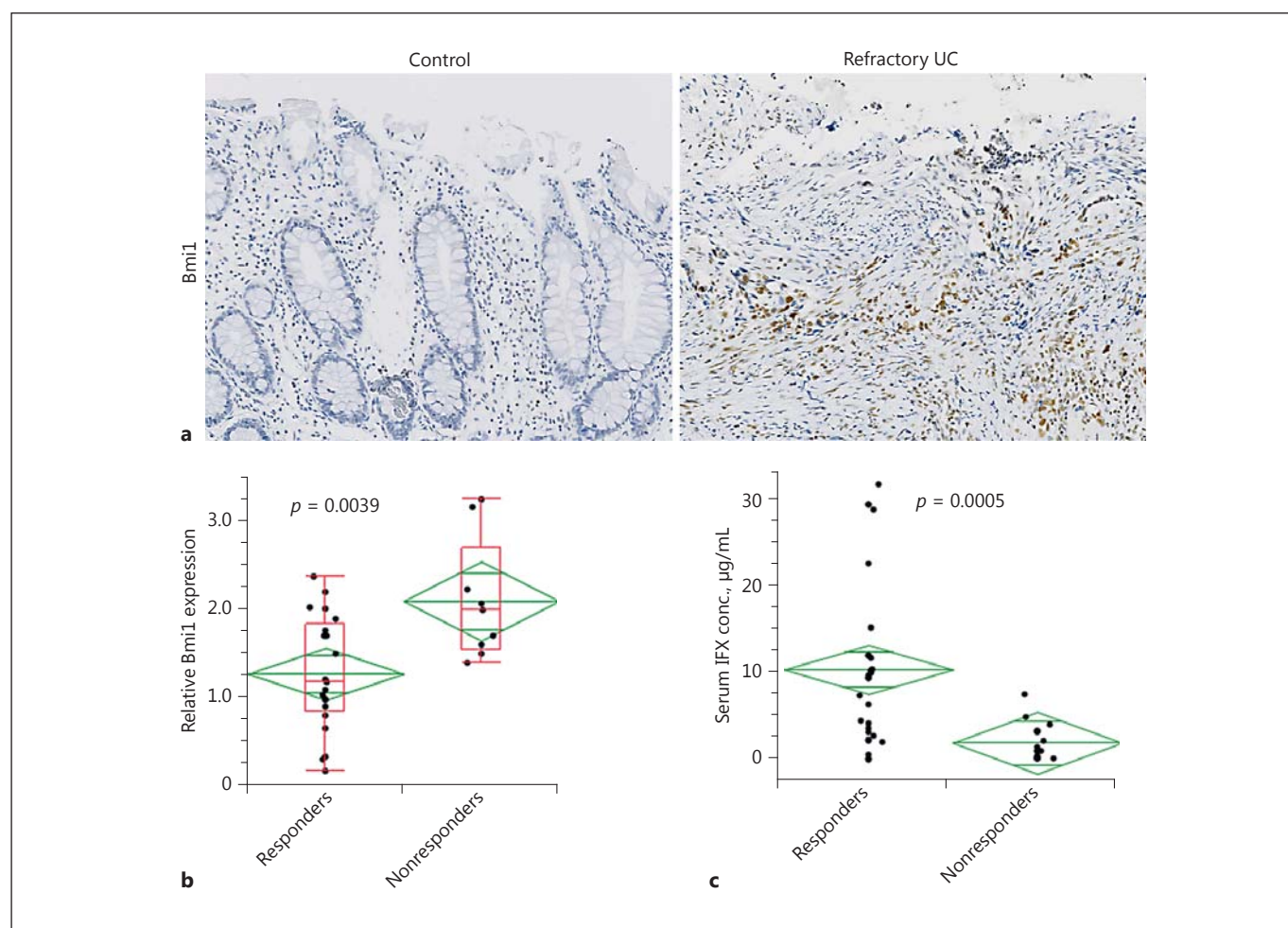
#### *Increased Bmi1 Expression Seen in Refractory IBD Predicts Poor Response to Anti-TNF- $\alpha$ Therapy*

Bmi1 expression levels were increased in patients with refractory IBD associated with long-term inflammation compared with those in controls or IBD patients in remission [7]. Immunohistochemistry was performed to identify the cells expressing Bmi1 in the human intestine. Nonparenchymal cells as well as epithelial cells were found to express Bmi1 protein (Fig. 3a). In chronically inflamed mucosa, Bmi1 expression was enhanced in nonparenchymal cells (Fig. 3a).

We next explored whether an association exists between Bmi1 expression and clinical response to anti-

TNF- $\alpha$  therapy. Thirty colonic mucosal samples were obtained from IBD patients before the initiation of anti-TNF- $\alpha$  therapy, and the response to anti-TNF- $\alpha$  therapy was evaluated prospectively. Among the 30 IBD patients treated with anti-TNF- $\alpha$  therapy and evaluated prospectively, 9 turned out to be resistant to anti-TNF- $\alpha$  therapy. We then determined the correlation of the expression level of Bmi1 to the clinical outcome of anti-TNF- $\alpha$  therapy. The expression level of Bmi1 in the colonic mucosa was  $2.10 \pm 0.23$  in patients without subsequent clinical response to anti-TNF- $\alpha$  therapy, whereas we detected expression levels of  $1.28 \pm 0.14$  in patients with clinical response. Patients with high expression of





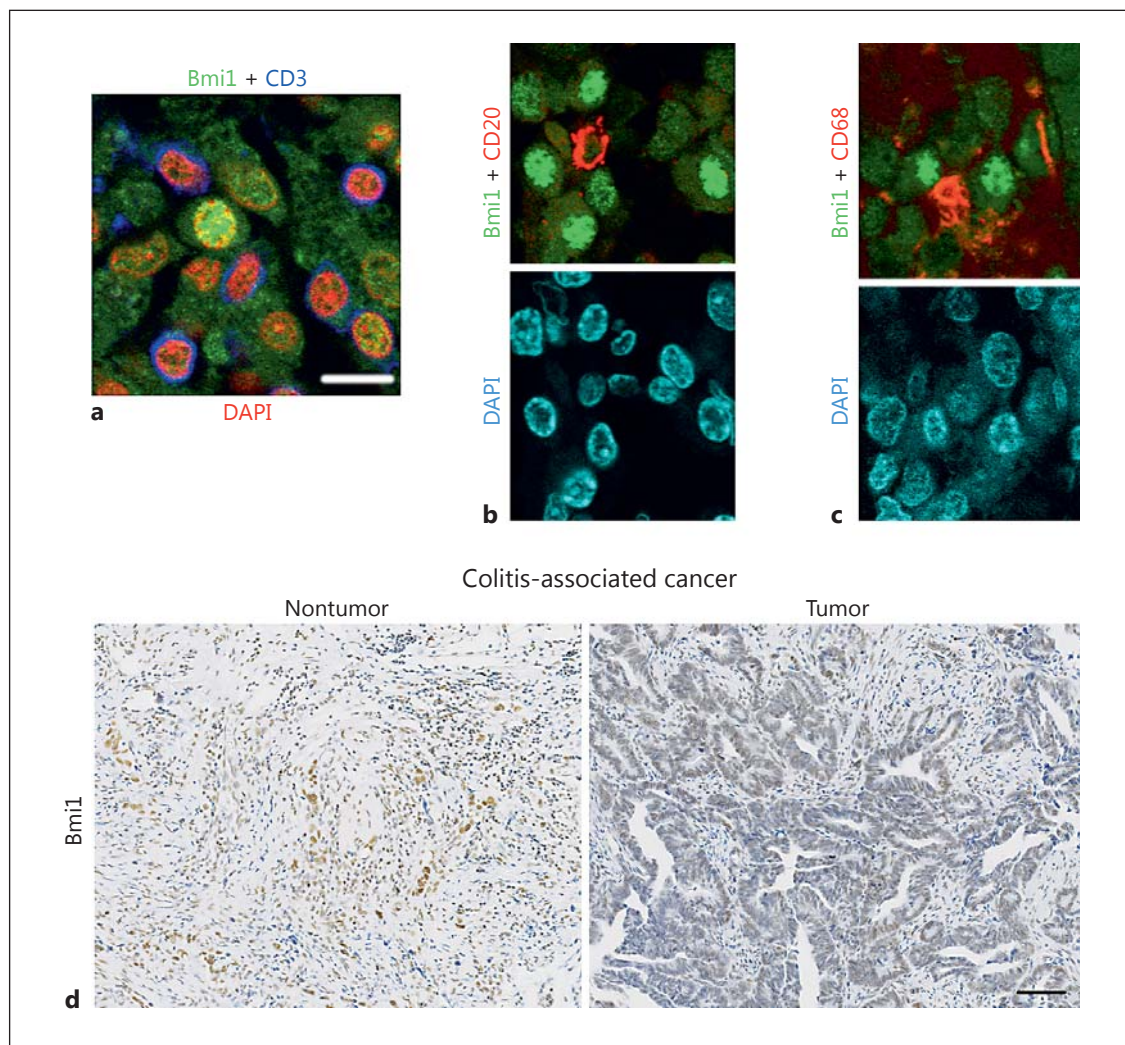
**Fig. 3.** Increased Bmi1 expression seen in refractory inflammatory bowel disease (IBD) predicts poor response to anti-tumor necrosis factor  $\alpha$  (anti-TNF- $\alpha$ ) therapy. **a** Representative images of immunohistochemical findings in human colonic mucosa of patients without IBD and those with refractory IBD using anti-Bmi1 antibody. **b** Relative levels of Bmi1 in colonic tissues of IBD patients

before the initiation of anti-TNF- $\alpha$  therapy, as determined by real-time qPCR (responders,  $n = 21$ ; nonresponders,  $n = 9$ ). The expression level in colonic mucosa of controls was set as 1. **c** The infliximab trough level was determined in patients with IBD. Each dot represents an individual point of infliximab (IFX) trough level measurements. UC, ulcerative colitis.

Bmi1 showed significantly lower response rates upon anti-TNF- $\alpha$  therapy as compared to those with low Bmi1 expression (Fig. 3b). There was no significant difference in age, disease duration, serum C-reactive protein, hemoglobin, or endoscopic findings evaluated using Mayo score between anti-TNF- $\alpha$  therapy responders and nonresponders (Table 1). During anti-TNF- $\alpha$  therapy, the trough levels of anti-TNF- $\alpha$  agents were significantly higher in responders than in nonresponders (Fig. 3c).

#### *Bmi1 Expression Is Enhanced in Human CAC*

Immunohistochemistry showed that Bmi1 was expressed in the mesenchyme of refractory IBD patients (Fig. 3a). As expected, the Bmi1-positive cell population was distinct from CD3-, CD20-, or CD68-expressing differentiated cells (Fig. 4a-c). The expression of Bmi1 was enhanced in the colonic mucosae of refractory IBD [7], suggesting that Bmi1 expression might be related to increased risk for CAC. Consistently, Bmi1 expression was increased in 9 of 10 CACs we examined. Both cancer cells and lamina propria cells expressed Bmi1 protein in human CAC (Fig. 4d).



**Fig. 4.** Bmi1 expression is enhanced in colitis-associated cancer. **a–c** Representative images of immunohistochemical detection of Bmi1 and CD3 (**a**), CD20 (**b**), or CD68 (**c**) in colonic tissues from refractory inflammatory bowel disease patients. **d** Representative images of immunohistochemical findings in human colonic mucosa of patients with colitis-associated cancer using anti-Bmi1 antibody. Scale bar, 100  $\mu$ m. DAPI, 4',6-diamidino-2-phenylindole.

## Discussion

Inflammation is a common and important factor in the pathogenesis of cancer [20]. It has become apparent that the interaction between transformed cells and their close surrounding, including innate immune cells, fibroblasts, and endothelial cells, can be instrumental in the development of many tumors, especially in the context of chronic inflammation [21, 22]. However, the underlying molecular processes involved in this interaction remain to be elucidated. In humans, Bmi1 expression was sig-

nificantly correlated with the expression of inflammatory cytokines, including IL-17 and IL-23. IL-23/IL-17 signaling enhances the immunosuppressive activity of regulatory T cells and reduces CD8<sup>+</sup> cells in tumor, leading to enhanced tumor initiation and promotion [23, 24]. A recent study suggested that colorectal cancer tissue-derived Foxp3+IL-17<sup>+</sup> cells have the capacity to induce cancer-initiating cells in vitro [25]. Chronic inflammation contributes to the expansion of stem cells, leading to the development of cancer [10]. Bmi1 might act as a link between chronic inflammation and tumorigenesis in IBD.

**Table 1.** Clinical characteristics of patients undergoing anti-TNF- $\alpha$  therapy

	Responders (n = 21)	Nonresponders (n = 9)	p value
Age, years	42 $\pm$ 18	42 $\pm$ 19	0.98
Sex (M/F)	13/8	6/2	
Disease duration, years	4.4 $\pm$ 4.2	7.9 $\pm$ 8.3	0.16
Extent of disease			0.72
UC			
Pancolitis	6	4	
Left colitis	6	2	
CD			
Ileitis	6	1	
Ileocolitis	2	2	
Colitis	1	0	
CRP, mg/dL	1.7 $\pm$ 1.5	2.7 $\pm$ 3.8	0.27
Albumin, g/dL	3.5 $\pm$ 0.76	3.2 $\pm$ 0.75	0.34
CMV infection (+/-)	0/21	1/8	0.30
Mayo endoscopic score	2.7 $\pm$ 0.43	2.8 $\pm$ 0.44	0.96

Results are expressed as means  $\pm$  SD, unless otherwise indicated. The presence of cytomegalovirus (CMV) in the colonic mucosa was assessed by PCR. UC, ulcerative colitis; CD, Crohn's disease; CRP, C-reactive protein.

IBD is associated with an increased risk of developing colorectal cancer [5]. Most cases are believed to arise from dysplasia, and surveillance colonoscopy is therefore recommended to detect dysplasia. Early detection of CAC/dysplasia is typically achieved by colonoscopic surveillance with multiple biopsies or alternatively by chromoendoscopy with targeted biopsies of all suspect areas [26]. However, such surveillance programs have a number of limitations such as low yield, high cost, invasiveness, incomplete

patient enrollment, sampling variations, and poor agreement in histopathological interpretation [27]. If a patient's specific risk for developing colorectal cancer is determined more precisely, surveillance strategies could be appropriately personalized and surveillance programs would make considerable progress. No molecular markers are routinely used to stratify IBD patients into groups at low or high risk of developing CAC/dysplasia [28]. We have shown significantly increased Bmi1 expression in mucosal specimens from patients with refractory IBD that is reported to be associated with increased cancer risk [4, 7]. High levels of Bmi1 expression represented a lower response rate upon subsequent anti-TNF- $\alpha$  therapy. Thus, Bmi1 expression reflects the presence of refractory inflammation and is therefore a potential marker for predicting the risk of CAC development. Indeed, Bmi1 expression was increased in human CAC tissues. Analyzing the Bmi1 level in colonoscopy specimens may be utilized to predict the risk of cancer and the prognosis of IBD patients.

Taken together, Bmi1 expression is involved in the refractory clinical course of IBD and upregulated in refractory IBD and CAC. These findings may allow us to further understand the pathogenesis of CAC and also guide personalized and stratified therapeutics.

## Acknowledgments

This study was supported by the Japan Society of Gastroenterology and JSPS KAKENHI (17K09396).

## Disclosure Statement

The authors have no conflicts of interest to declare.

## References

- 1 Jemal A, Siegel R, Ward E, Hao Y, Xu J, Thun MJ: Cancer statistics, 2009. *CA Cancer J Clin* 2009;59:225–249.
- 2 González N, Prieto I, Del Puerto-Nevado L, Portal-Núñez S, Ardura JA, Corton M, Fernández-Fernández B, Aguilera O, Gomez-Guerrero C, Mas S, Moreno JA, Ruiz-Ortega M, Sanz AB, Sanchez-Niño MD, Rojo F, Vivanco F, Esbrit P, Ayuso C, Alvarez-Llamas G, Egido J, García-Foncillas J, Ortiz A; Diabetes-CancerConnect Consortium: 2017 update on the relationship between diabetes and colorectal cancer: epidemiology, potential molecular mechanisms and therapeutic implications. *Oncotarget* 2017;8:18456–18485.
- 3 Chen ML, Sundrud MS: Cytokine networks and T-cell subsets in inflammatory bowel diseases. *Inflamm Bowel Dis* 2016;22:1157–1167.
- 4 Itzkowitz SH, Yio X: Inflammation and cancer IV. Colorectal cancer in inflammatory bowel disease: the role of inflammation. *Am J Physiol Gastrointest Liver Physiol* 2004;287:G7–G17.
- 5 Ullman TA, Itzkowitz SH: Intestinal inflammation and cancer. *Gastroenterology* 2011;140:1807–1816.
- 6 Sakurai T, Kashida H, Watanabe T, Hagiwara S, Mizushima T, Iijima H, et al: Stress response protein Cirp links inflammation and tumorigenesis in colitis-associated cancer. *Cancer Res* 2014;74:6119–6128.
- 7 Adachi T, Sakurai T, Kashida H, Mine H, Hagiwara S, Matsui S, et al: Involvement of heat shock protein A4/Apg-2 in refractory inflammatory bowel disease. *Inflamm Bowel Dis* 2015;21:31–39.
- 8 Sakurai T, Kashida H, Komeda Y, Nagai T, Hagiwara S, Watanabe T, Kitano M, Nishida N, Fujita J, Kudo M: Stress response protein RBM3 promotes the development of colitis-associated cancer. *Inflamm Bowel Dis* 2017;23:66–74.



- 9 Sakurai T, Higashitsuji H, Kashida H, Watanabe T, Komeda Y, Nagai T, Hagiwara S, Kitano M, Nishida N, Abe T, Kiyonari H, Itoh K, Fujita J, Kudo M: The oncoprotein gankyrin promotes the development of colitis-associated cancer through activation of STAT3. *Oncotarget* 2017;8:24762–24776.
- 10 Shigdar S, Li Y, Bhattacharya S, O'Connor M, Pu C, Lin J, et al: Inflammation and cancer stem cells. *Cancer Lett* 2014;345:271–278.
- 11 Clevers H: The cancer stem cell: premises, promises and challenges. *Nat Med* 2011;17:313–319.
- 12 Sangiorgi E, Capecchi MR: Bmi1 is expressed in vivo in intestinal stem cells. *Nat Genet* 2008;40:915–920.
- 13 Sakurai T, Kashida H, Hagiwara S, Nishida N, Watanabe T, Fujita J, Kudo M: Heat shock protein A4 controls cell migration and gastric ulcer healing. *Dig Dis Sci* 2015;60:850–857.
- 14 Sakurai T, Yada N, Watanabe T, Arizumi T, Hagiwara S, Ueshima K, Nishida N, Fujita J, Kudo M: Cold-inducible RNA-binding protein promotes the development of liver cancer. *Cancer Sci* 2015;106:352–358.
- 15 Sakurai T, Kudo M, Umemura A, He G, Elsharkawy AM, Seki E, et al: p38 $\alpha$  inhibits liver fibrogenesis and consequent hepatocarcinogenesis by curtailing accumulation of reactive oxygen species. *Cancer Res* 2013;73:215–224.
- 16 Mine H, Sakurai T, Kashida H, Matsui S, Nishida N, Nagai T, Hagiwara S, Watanabe T, Kudo M: Association of gankyrin and stemness factor expression in human colorectal cancer. *Dig Dis Sci* 2013;58:2337–2344.
- 17 McKenzie BS, Kastelein RA, Cua DJ: Understanding the IL-23-IL-17 immune pathway. *Trends Immunol* 2006;27:17–23.
- 18 Ma C, Fedorak RN, Kaplan GG, Dieleman LA, Devlin SM, Stern N, Kroeker KI, Seow CH, Leung Y, Novak KL, Halloran BP, Huang VW, Wong K, Blustein PK, Ghosh S, Panaccione R: Long-term maintenance of clinical, endoscopic, and radiographic response to ustekinumab in moderate-to-severe Crohn's disease: real-world experience from a multicenter cohort study. *Inflamm Bowel Dis* 2017;23:833–839.
- 19 Mantzaris GJ: Anti-TNFs: originators and biosimilars. *Dig Dis* 2016;34:132–139.
- 20 Schottenfeld D, Beebe-Dimmer J: Chronic inflammation: a common and important factor in the pathogenesis of neoplasia. *CA Cancer J Clin* 2006;56:69–83.
- 21 Balkwill F, Mantovani A: Inflammation and cancer: back to Virchow? *Lancet* 2001;357:539–545.
- 22 Coussens LM, Werb Z: Inflammation and cancer. *Nature* 2002;420:860–867.
- 23 Kortylewski M, Xin H, Kujawski M, Lee H, Liu Y, Harris T, et al: Regulation of the IL-23 and IL-12 balance by Stat3 signaling in the tumor microenvironment. *Cancer Cell* 2009;15:114–123.
- 24 Wu D, Wu P, Huang Q, Liu Y, Ye J, Huang J: Interleukin-17: a promoter in colorectal cancer progression. *Clin Dev Immunol* 2013;2013:436307.
- 25 Yang S, Wang B, Guan C, Wu B, Cai C, Wang M, et al: Foxp3+IL-17+ T cells promote development of cancer-initiating cells in colorectal cancer. *J Leukoc Biol* 2011;89:85–91.
- 26 Rogler G: Inflammatory bowel disease cancer risk, detection and surveillance. *Dig Dis* 2012;30(suppl 2):48–54.
- 27 Gupta RB, Harpaz N, Itzkowitz S, Hossain S, Matula S, Kornbluth A, et al: Histologic inflammation is a risk factor for progression to colorectal neoplasia in ulcerative colitis: a cohort study. *Gastroenterology* 2007;133:1099–1105.
- 28 Farraye FA, Odze RD, Eaden J, Itzkowitz SH: AGA technical review on the diagnosis and management of colorectal neoplasia in inflammatory bowel disease. *Gastroenterology* 2010;138:746–774.

# Prophylactic Suturing Closure Is Recommended after Endoscopic Treatment of Colorectal Tumors in Patients with Antiplatelet/Anticoagulant Therapy

Toshiharu Sakurai Teppei Adachi Masashi Kono Tadaaki Arizumi  
Ken Kamata Kosuke Minaga Kentaro Yamao Yoriaki Komeda  
Mamoru Takenaka Satoru Hagiwara Tomohiro Watanabe Naoshi Nishida  
Hiroshi Kashida Masatoshi Kudo

Department of Gastroenterology and Hepatology, Kindai University, Osaka-Sayama, Japan

## Keywords

Endoscopic submucosal dissection · Laterally spreading tumor · Clip

## Abstract

The prophylactic closure of mucosal defects after endoscopic resection is known to prevent postoperative bleeding in colorectal lesions. However, closure of large mucosal defects is difficult with conventional clips only, and several closure techniques have been previously described; use of an Endoloop, 8-ring loop, or loop clip and a small incision around the mucosal defect. Given that the prophylactic closure requires much cost and time, the application should be limited to high-risk cases. Medication of antithrombotics or antiplatelet agents would be one of the reasonable indications for prophylactic closure of mucosal defects after endoscopic resection of colorectal tumors.

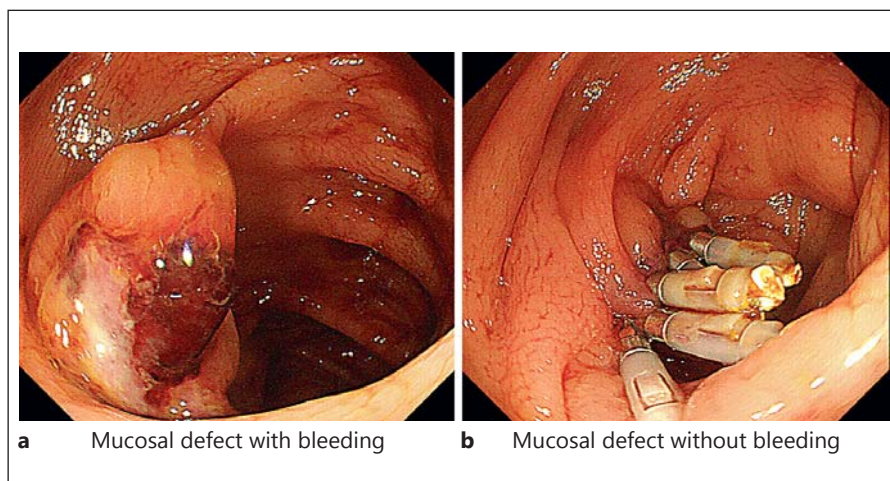
© 2017 S. Karger AG, Basel

A 70-year-old man was admitted to our hospital with a diagnosis of 2 large flat colorectal tumors. He had undergone rectal resection for rectal cancer 3 years before and the postsurgery surveillance colonoscopy showed 2 colorectal laterally spreading tumors, each measuring 20 and 30 mm in diameter, at the transverse and the descending colon, respectively. A stent had been implanted due to abdominal aortic aneurysm 3 years before. Thereafter, he had been taking aspirin (81 mg/day). He had no known allergies, and he drank alcohol occasionally and did not smoke tobacco.

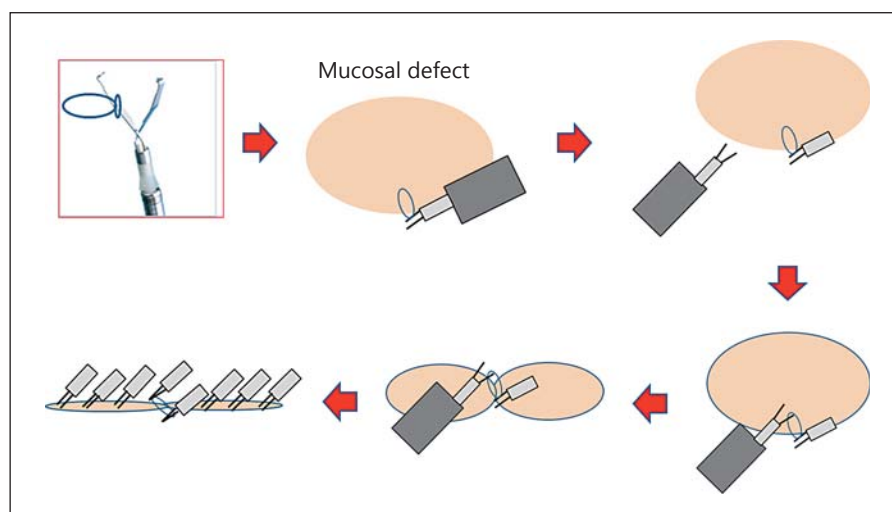
Endoscopic submucosal dissection (ESD) was performed for the 2 colorectal lesions at the same time. Antiplatelet therapy was continued due to high risk of thrombosis after the withdrawal. A larger post-ESD mucosal defect was sutured using endoclips, but not for a smaller one. The next day after ESD, he complained of rectal bleeding. Endoscopy confirmed the source of bleeding was the smaller post-ESD mucosal defect without prophylactic closure (Fig. 1a), but not the larger mucosal wound with prophylactic closure (Fig. 1b). Histopatho-



**Fig. 1.** **a** Endoscopic image of delayed bleeding from the mucosal defect after endoscopic submucosal dissection (ESD), which had not been sutured after the procedure. **b** Endoscopic image of the ESD site of the larger lesion that had been sutured using clips. At this site, no bleeding was found after ESD.



**Fig. 2.** Endoscopic closure of a large mucosal defect using a clip with a ring-shaped nylon loop.



logical examination showed that the larger one was an intramucosal well-differentiated adenocarcinoma without lymphovascular involvement and the smaller one was a sessile serrated adenoma/polyp. Neither recurrence nor complications were found 4 years after endoscopic resection.

A large mucosal defect is made after colorectal ESD, which can be associated with complications such as perforation and bleeding. The prophylactic closure of mucosal defects after endoscopic resection is known to prevent postoperative bleeding and transmural burn syndrome in colorectal lesions [1]. In a retrospective study, prophylactic clip closure after endoscopic resection of sessile colorectal polyps or flat colorectal lesions 2 cm or larger was reported to be effective for preventing delayed bleed-

ing [2]. The currently available clips can be delivered through the endoscope (through-the-scope clips: TT-SCs): Quick Clip (Olympus Japan Inc., Natick, MA, United States), Resolution Clip (Boston Scientific Inc., Natick, MA, USA), and Instinct Clip (Cook Medical Inc., Bloomington, IN, USA). Over-the-scope clips (OTSC system; Ovesco Endoscopy AG, Tübingen, Germany) are also available. Closure of large mucosal defects is difficult with conventional clips only, and several closure techniques have been previously described; use of an Endoloop, 8-ring loop, or loop clip and a small incision around the mucosal defect [3]. The procedure used in our case is described as follows (Fig. 2): a ring-shaped nylon loop (2–3 mm in diameter) was attached to a conventional clip, and the 1st clip with a small loop was placed at an edge of

the mucosal defect. We put one blade of the 2nd clip through the small loop attached to the 1st clip and then placed the 2nd clip at the opposite side of the 1st clip beyond the mucosal defect. It is important that the 1st and the 2nd clips are placed at the points across the maximal diameter, which moves the edges of the mucosal defect closer to each other and makes the subsequent clipping procedure easier. Clips were placed in zipper fashion to completely close the resection site. Given that the prophylactic closure requires much cost and time, the application should be limited to high-risk cases. The present case suggests that medication of antithrombotics or antiplatelet agents would be one of the reasonable indications for prophylactic closure of mucosal defects after endoscopic resection of colorectal tumors.

## Disclosure Statement

The authors have no conflicts of interest to declare.

## References

- 1 Zhang QS, Han B, Xu JH, Gao P, Shen YC: Clip closure of defect after endoscopic resection in patients with larger colorectal tumors decreased the adverse events. *Gastrointest Endosc* 2015;82:904–909.
- 2 Liaquat H, Rohn E, Rex DK: Prophylactic clip closure reduced the risk of delayed postpolypectomy hemorrhage: experience in 277 clipped large sessile or flat colorectal lesions and 247 control lesions. *Gastrointest Endosc* 2013;77:401–407.
- 3 Fujihara S, Mori H, Kobara H, Nishiyama N, Matsunaga T, Ayaki M, Yachida T, Masaki T: Management of a large mucosal defect after duodenal endoscopic resection. *World J Gastroenterol* 2016;22:6595–6609.

# Computer-Aided Diagnosis Based on Convolutional Neural Network System for Colorectal Polyp Classification: Preliminary Experience

Yoriaki Komeda<sup>a</sup> Hisashi Handa<sup>b</sup> Tomohiro Watanabe<sup>a</sup> Takanobu Nomura<sup>c</sup>  
Misaki Kitahashi<sup>c</sup> Toshiharu Sakurai<sup>a</sup> Ayana Okamoto<sup>a</sup> Tomohiro Minami<sup>a</sup>  
Masashi Kono<sup>a</sup> Tadaaki Arizumi<sup>a</sup> Mamoru Takenaka<sup>a</sup> Satoru Hagiwara<sup>a</sup>  
Shigenaga Matsui<sup>a</sup> Naoshi Nishida<sup>a</sup> Hiroshi Kashida<sup>a</sup> Masatoshi Kudo<sup>a</sup>

<sup>a</sup>Department of Gastroenterology and Hepatology, Kindai University Faculty of Medicine, and

<sup>b</sup>Faculty of Science and Engineering and <sup>c</sup>Graduate School of Science and Engineering Research, Kindai University, Osaka-Sayama, Japan

## Keywords

Computer-aided diagnosis · Convolutional neural network · Artificial intelligence · Colon polyp classification · Deep learning

## Abstract

**Background and Aim:** Computer-aided diagnosis (CAD) is becoming a next-generation tool for the diagnosis of human disease. CAD for colon polyps has been suggested as a particularly useful tool for trainee colonoscopists, as the use of a CAD system avoids the complications associated with endoscopic resections. In addition to conventional CAD, a convolutional neural network (CNN) system utilizing artificial intelligence (AI) has been developing rapidly over the past 5 years. We attempted to generate a unique CNN-CAD system with an AI function that studied endoscopic images extracted from movies obtained with colonoscopes used in routine examinations. Here, we report our preliminary results of this novel CNN-CAD system for the diagnosis of colon polyps. **Methods:** A total of 1,200 images from cases of

colonoscopy performed between January 2010 and December 2016 at Kindai University Hospital were used. These images were extracted from the video of actual endoscopic examinations. Additional video images from 10 cases of unlearned processes were retrospectively assessed in a pilot study. They were simply diagnosed as either an adenomatous or nonadenomatous polyp. **Results:** The number of images used by AI to learn to distinguish adenomatous from nonadenomatous was 1,200:600. These images were extracted from the videos of actual endoscopic examinations. The size of each image was adjusted to 256 × 256 pixels. A 10-fold cross-validation was carried out. The accuracy of the 10-fold cross-validation is 0.751, where the accuracy is the ratio of the number of correct answers over the number of all the answers produced by the CNN. The decisions by the CNN were correct in 7 of 10 cases. **Conclusion:** A CNN-CAD system using routine colonoscopy might be useful for the rapid diagnosis of colorectal polyp classification. Further prospective studies in an in vivo setting are required to confirm the effectiveness of a CNN-CAD system in routine colonoscopy.

© 2017 S. Karger AG, Basel

## Introduction

It is now generally accepted that most colorectal cancers originate from adenomas [1–3]. This notion, called the “adenoma-carcinoma sequence,” has been supported by clinical observational studies in which early detection and removal of adenomas efficiently prevented the development of colon cancers [1–3]. The majority of small colorectal polyps are hyperplastic polyps with little or no ability to differentiate into colorectal cancer [4]. Therefore, accurate and objective diagnosis of small colorectal polyps reduces unnecessary biopsies and endoscopic resections, which helps avoid the complications associated with endoscopic procedures. However, it is sometimes difficult even for well-experienced endoscopists to discriminate between hyperplastic polyps and adenomas by conventional white-light observation, image-enhanced endoscopy, and chromoendoscopy [5]. Establishment of an accurate and objective diagnostic tool for the classification of colon polyps would be very useful for both experienced endoscopists and apprentices.

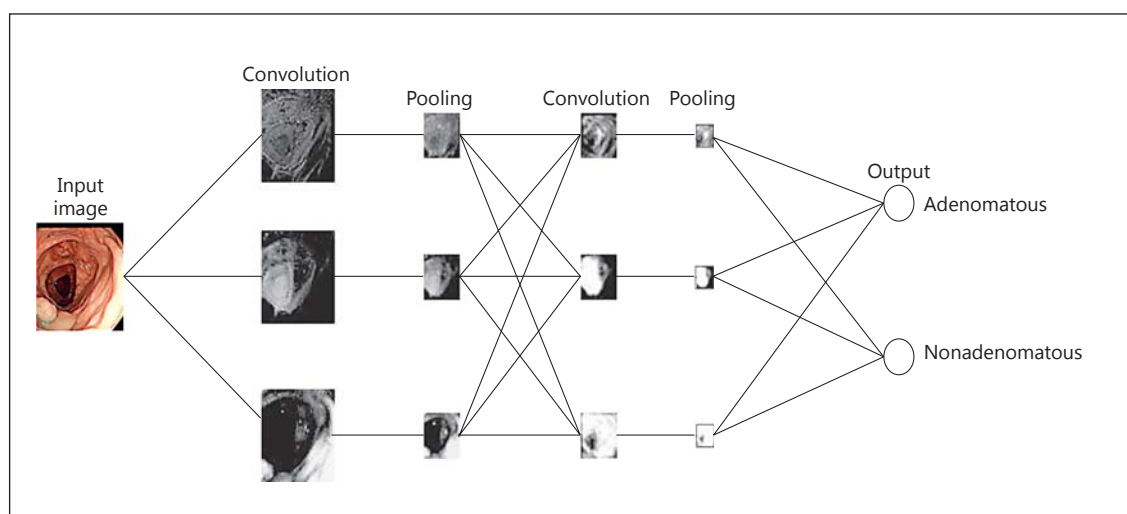
Computer-aided diagnosis (CAD) is becoming a next-generation tool for the diagnosis of human disease [6]. The CAD of colon polyps has been reported on previously [7–16]. Previous studies have reported the usefulness of CAD for colon polyps. CAD for colon polyps has been suggested as a particularly useful tool for trainee colonoscopists, as the use of a CAD system helps avoid the complications associated with endoscopic resections

[9–11]. Moreover, the higher rate of correct diagnoses using a CAD system also suggests the potential for this diagnostic tool to improve the quality of colonoscopic examinations.

In addition to conventional CAD, a convolutional neural network (CNN) system utilizing artificial intelligence (AI) has been developing rapidly over the past 5 years. This system is widely used to recognize human faces on Facebook and in the Google images tool [17]. We hypothesized that a CNN system based on CAD utilizing AI might achieve a higher diagnostic accuracy than conventional CAD without CNN or AI for colorectal polyps. Hence, we attempted to generate a unique CNN-CAD system with an AI function that studied endoscopic images extracted from movies obtained with colonoscopes used in routine examinations. Here, we report our preliminary results of this novel CNN-CAD system for the diagnosis of colon polyps.






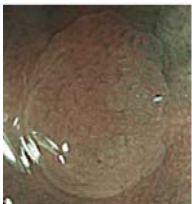
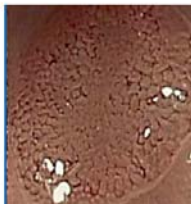



## Methods

A total of 1,200 images from cases of colonoscopy performed between January 2010 and December 2016 at Kindai University Hospital were used. These images were extracted from the video of actual endoscopic examinations. Additional video images from 10 cases of unlearned processes were retrospectively assessed in a pilot study. They were simply diagnosed as either an adenomatous or nonadenomatous polyp. This was a collaborative study between the Department of Gastroenterology and Hepatology, Faculty of Medicine, and the Faculty of Science and Engineering at Kindai University. This study was approved by



**Fig. 1.** Functional architecture of a convolutional neural network.



				
$P_A = 1.0$ $P_N = 0.0$ Incorrect	$P_A = 0.004$ $P_N = 0.996$ Incorrect	$P_A = 0.117$ $P_N = 0.883$ Correct	$P_A = 1.0$ $P_N = 0.0$ Correct	$P_A = 0.0$ $P_N = 1.0$ Correct
				
$P_A = 1.0$ $P_N = 0.0$ Incorrect	$P_A = 1.0$ $P_N = 0.0$ Correct	$P_A = 0.0$ $P_N = 1.0$ Correct	$P_A = 1.0$ $P_N = 0.0$ Correct	$P_A = 1.0$ $P_N = 0.0$ Correct

**Fig. 2.** Experimental results for unlearned data:  $P_A$  and  $P_N$  stand for the probabilities of adenomatous and non-adenomatous, respectively. These probabilities are the output generated by the convolutional neural network.

the Ethics Committee of the Kindai University Faculty of Medicine. The procedures followed were in accordance with the guidelines of the World Medical Association's Declaration of Helsinki.

CNN is a type of artificial neural network that imitates the function of the receptive fields in the human brain. A CNN is one of the major algorithms in deep learning and is a state-of-the-art method in image and speech recognition.

The functional architecture of a CNN is illustrated in Figure 1: the CNN perceives an image as an input, and the output is a class label corresponding to the input image. For instance, the class labels in this study consist of "adenomatous" and "nonadenomatous." As depicted in Figure 1, there are several kinds of layers in the CNN. Each neuron in a layer is connected to the corresponding neurons in the previous layer.

An input image is presented to the first layer, i.e., the left side of Figure 1. The number of neurons in the first layer is equal to the number of pixels in the input image (in a gray-scaled image) or 3 times the number of pixels (in a color image). There are 2 kinds of information processing which are applied iteratively: convolution and pooling.

The convolution process works as a filter that extracts features from images or data in the previous layer. Note that Figure 1 is just a simplified explanation of a CNN. There are a large number of filters in the convolution that are applied simultaneously. The parameter of the filters, which defines the feature to be extracted, is adjusted by learning algorithms. The size of the filters is smaller than that of the layer, so that the filter is repeatedly applied within a stratum.

The pooling process selects the strongest activated value for a feature in a local area that is extracted in the convolution. Through pooling, even if the image is shifted slightly, the classification results are not affected and the size of the layer is reduced by a quarter, as delineated in Figure 1.

For the final layer, all the neurons in one layer are connected to all the neurons in the previous layer. For each connection, a parameter is associated that is also adjusted by learning. The number of neurons in the final layer is equivalent to the number of class labels to be recognized. By using the softmax function, the output of the CNN can be represented as a probability.

## Results

The number of images used by AI to learn to distinguish adenomatous from nonadenomatous was 1,200:600. These images were extracted from the videos of actual endoscopic examinations. The size of each image was adjusted to  $256 \times 256$  pixels. A 10-fold cross-validation was carried out. The accuracy of the 10-fold cross-validation is 0.751, where the accuracy is the ratio of the number of correct answers over the number of all the answers produced by the CNN. The images used for AI learning include images using conventional white-light and narrow-band imaging (NBI) and chromoendoscopy.

Ten additional images of unlearned endoscopic movies were applied as a test, as shown in Figure 2. These images were not used in the training of the CNN.

The output of the CNN was presented as probabilities:  $P_A$  = adenomatous and  $P_N$  = nonadenomatous. The output with the higher probability was regarded as a decision by the CNN. The final evaluation of our CNN was to compare the results of pathological examinations. The decisions by the CNN were correct in 7 of 10 cases.

## Discussion

Removal of colon adenomas has been established as the most efficient strategy for the prevention of colorectal cancers [1–3]. It should be noted, however, that small colorectal polyps include both adenomatous polyps and nonadenomatous polyps, the latter of which have little or no possibility to differentiate into colorectal cancers [4]. Thus, discrimination of adenomatous polyps from nonadenomatous polyps by endoscopic resection is very important to avoid unnecessary removal of colorectal tumors. Although an accurate diagnosis of adenomatous and nonadenomatous polyps by endoscopic findings is absolutely necessary to avoid unnecessary resection of colon polyps, an accurate endoscopic diagnosis of small colorectal polyps is sometimes difficult even for well-trained colonoscopists. Thus, an accurate and reliable diagnostic system is required to discriminate between adenomatous and nonadenomatous polyps in endoscopic findings.

The use of CAD technology has the potential to become a novel diagnostic tool for colorectal tumors. Automatic diagnosis by computer in the CAD system may increase the diagnostic accuracy and reduce the number of unnecessary biopsies and endoscopic resections. As a result, this diagnostic system has the potential to avoid the complications related to unnecessary endoscopic procedures. Initial studies report the usefulness of CAD for colorectal polyps using still images obtained from magnifying NBI observations [12, 13]. As opposed to CAD using still images, 2 Japanese groups have developed CAD with real-time endoscopy [14, 15]. These real-time CAD systems are operated during the actual endoscopic observation. Moreover, Japanese researchers have successfully developed an automated CAD using endocytoscopy based on automated extraction of ultra-magnified nuclear features followed by machine-learning analysis from the same group [9–11]. Thus, a wide variety of CAD systems are available at present. Importantly,

the diagnostic accuracy of these novel methods is higher than that achieved by endoscopic diagnosis by less-experienced endoscopists [9–11].

In this study, we tried to establish a novel CAD system based on CNN and AI. A CNN system is one of the major algorithms in deep learning for AI [17]. Deep learning is a more sophisticated machine-learning method used for computer vision. CNN has the advantage of being able to learn from large data and has led to high accuracy and rapid processing time. Although a CNN-CAD system has been employed for colorectal polyps by using still images of chromoendoscopy in 1 report [17], no studies have used images extracted from movies of real-time routine colonoscopy. Thus, to our knowledge, this is the first report on the utility of CNN based on CAD using real-time endoscopy images. This pilot study demonstrates that our newly developed CNN-CAD system with endoscopic movies might be useful as a fully computer-automated instant diagnostic tool for distinguishing neoplastic changes in colorectal lesions. The diagnostic accuracy for distinguishing nonadenomatous from adenomatous polyps was 70%. The diagnostic accuracy for our CNN-CAD system is not satisfactory at present as compared to previous reports [7–16]. In this regard, we assume that deep learning with 600 or 1,200 images might not be sufficient and, therefore, attribute the relatively low performance to the low number of images.

Alternatively, learning with NBI or pit pattern photographs, rather than conventional white-light photographs, might lead to higher rates of accurate diagnoses, since the former photographs provide clearer features than the latter photographs. In any case, a large number of test cases are absolutely necessary to evaluate the usefulness of our CNN-CAD system. Nonetheless, our CNN-CAD system would still be an attractive choice, since the decision-making process with regard to the removal of colorectal polyps might be simplified by application of this system, especially for less-experienced colonoscopists. Although our CNN-CAD system with colonoscopy videos was applied to discriminate between adenomatous and nonadenomatous polyps in this initial trial, it might be possible to perform differential diagnoses for adenoma, early cancer, and advanced cancer in the future. If our CNN-CAD system can perform an objective evaluation of colorectal tumors, it seems likely that medical malpractice resulting from misdiagnosis could be reduced.

## Conclusion

A CNN-CAD system using routine colonoscopy might be useful for the rapid diagnosis of colorectal polyp classification. Further prospective studies in an in vivo setting are required to confirm the effectiveness of a CNN-CAD system in routine colonoscopy.

## Disclosure Statement

The authors have no conflicts of interest to declare.

## References

- 1 Winawer SJ, Zauber AG, Ho MN, O'Brien MJ, Gottlieb LS, Sternberg SS, Waye JD, Schapiro M, Bond JH, Panish JF, et al: Prevention of colorectal cancer by colonoscopic polypectomy. The National Polyp Study Workgroup. *N Engl J Med* 1993;329:1977–1981.
- 2 Løberg M, Kalager M, Holme Ø, Hoff G, Adami HO, Bretthauer M: Long-term colorectal-cancer mortality after adenoma removal. *N Engl J Med* 2014;371:799–807.
- 3 Zauber AG, Winawer SJ, O'Brien MJ, Lansdorp-Vogelaar I, van Ballegooijen M, Hankey BF, Shi W, Bond JH, Schapiro M, Panish JF, Stewart ET, Waye JD: Colonoscopic polypectomy and long-term prevention of colorectal-cancer deaths. *N Engl J Med* 2012;366:687–696.
- 4 Butterly LF, Chase MP, Pohl H, Fiarman GS: Prevalence of clinically important histology in small adenomas. *Clin Gastroenterol Hepatol* 2006;4:343–348.
- 5 Pohl J, Nguyen-Tat M, Pech O, May A, Rabenstein T, Ell C: Computed virtual chromoendoscopy for classification of small colorectal lesions: a prospective comparative study. *Am J Gastroenterol* 2008;103:562–569.
- 6 Philpotts LE: Can computer-aided detection be detrimental to mammographic interpretation? *Radiology* 2009;253:17–22.
- 7 Fernández-Esparrach G, Bernal J, López-Cerón M, Córdova H, Sánchez-Montes C, Rodríguez de Miguel C, Sánchez FJ: Exploring the clinical potential of an automatic colonic polyp detection method based on the creation of energy maps. *Endoscopy* 2016;48:837–842.
- 8 Takemura Y, Yoshida S, Tanaka S, Onji K, Oka S, Tamaki T, Kaneda K, Yoshihara M, Chayama K: Quantitative analysis and development of a computer-aided system for identification of regular pit patterns of colorectal lesions. *Gastrointest Endosc* 2010;72:1047–1051.
- 9 Mori Y, Kudo SE, Wakamura K, Misawa M, Ogawa Y, Kutsukawa M, Kudo T, Hayashi T, Miyachi H, Ishida F, Inoue H: Novel computer-aided diagnostic system for colorectal lesions by using endocytoscopy (with videos). *Gastrointest Endosc* 2015;81:621–629.
- 10 Mori Y, Kudo SE, Chiu PW, Singh R, Misawa M, Wakamura K, Kudo T, Hayashi T, Katagiri A, Miyachi H, Ishida F, Maeda Y, Inoue H, Nimura Y, Oda M, Mori K: Impact of an automated system for endocytoscopic diagnosis of small colorectal lesions: an international web-based study. *Endoscopy* 2016;48:1110–1118.
- 11 Misawa M, Kudo SE, Mori Y, Nakamura H, Kataoka S, Maeda Y, Kudo T, Hayashi T, Wakamura K, Miyachi H, Katagiri A, Baba T, Ishida F, Inoue H, Nimura Y, Mori K: Characterization of colorectal lesions using a computer-aided diagnostic system for narrow-band imaging endocytoscopy. *Gastroenterology* 2016;150:1531–1532.e3.
- 12 Tischendorf JJ, Gross S, Winograd R, Hecker H, Auer R, Behrens A, Trautwein C, Aach T, Stehle T: Computer-aided classification of colorectal polyps based on vascular patterns: a pilot study. *Endoscopy* 2010;42:203–207.
- 13 Gross S, Trautwein C, Behrens A, Winograd R, Palm S, Lutz HH, Schirin-Sokhan R, Hecker H, Aach T, Tischendorf JJ: Computer-based classification of small colorectal polyps by using narrow-band imaging with optical magnification. *Gastrointest Endosc* 2011;74:1354–1359.
- 14 Takemura Y, Yoshida S, Tanaka S, Kawase R, Onji K, Oka S, Tamaki T, Raytchev B, Kaneda K, Yoshihara M, Chayama K: Computer-aided system for predicting the histology of colorectal tumors by using narrow-band imaging magnifying colonoscopy (with video). *Gastrointest Endosc* 2012;75:179–185.
- 15 Kominami Y, Yoshida S, Tanaka S, Sanomura Y, Hirakawa T, Raytchev B, Tamaki T, Koide T, Kaneda K, Chayama K: Computer-aided diagnosis of colorectal polyp histology by using a real-time image recognition system and narrow-band imaging magnifying colonoscopy. *Gastrointest Endosc* 2016;83:643–649.
- 16 Ribeiro E, Uhl A, Wimmer G, Häfner M: Exploring deep learning and transfer learning for colonic polyp classification. *Comput Math Methods Med* 2016;2016:6584725.
- 17 LeCun Y, Bengio Y, Hinton G: Deep learning. *Nature* 2015;521:436–444.

# Risk Factors for Postoperative Bleeding in Endoscopic Submucosal Dissection of Colorectal Tumors

Kazuki Okamoto<sup>a</sup> Tomohiro Watanabe<sup>a</sup> Yoriaki Komeda<sup>a</sup> Tatsuya Kono<sup>a</sup>  
Kouta Takashima<sup>a</sup> Ayana Okamoto<sup>a</sup> Masashi Kono<sup>a</sup> Mitsunari Yamada<sup>a</sup>  
Tadaaki Arizumi<sup>a</sup> Ken Kamata<sup>a</sup> Kosuke Minaga<sup>a</sup> Kentaro Yamao<sup>a</sup>  
Tomoyuki Nagai<sup>a</sup> Yutaka Asakuma<sup>a</sup> Mamoru Takenaka<sup>a</sup> Toshiharu Sakurai<sup>a</sup>  
Shigenaga Matsui<sup>a</sup> Naoshi Nishida<sup>a</sup> Takaaki Chikugo<sup>b</sup> Hiroshi Kashida<sup>a</sup>  
Masatoshi Kudo<sup>a</sup>

Departments of <sup>a</sup>Gastroenterology and Hepatology and <sup>b</sup>Pathology, Kindai University Faculty of Medicine, Osaka-Sayama, Japan

## Keywords

Colorectal tumors · Endoscopic submucosal dissection · Postoperative bleeding

## Abstract

**Background:** Colonoscopic removal of adenomatous polyps or early cancer prevents death from colorectal cancer. Endoscopic submucosal dissection (ESD), which enables endoscopists to perform en bloc resection of flat or depressed colorectal tumors >20 mm, has recently been introduced and become a standard procedure in Japan. Although postoperative bleeding (POB) is a major complication associated with ESD, risk factors for POB have not been fully identified. **Methods:** A total of 451 patients (509 lesions) who underwent colorectal ESD were retrospectively analyzed to identify clinical parameters associated with POB. **Results:** POB occurred in 14 patients, and 7 of them had received antithrombotic therapy before ESD. Uni- and multivariate analyses revealed that

antithrombotic therapy and rectal tumor location were strongly associated with POB following colorectal ESD. The incidence of POB was higher in patients on heparin bridge therapy (HBT) for the replacement of antithrombotic therapy than in patients with no HBT. Four of 7 patients (57.1%) on antithrombotic therapy experienced POB from the rectal lesions. **Conclusion:** Antithrombotic therapy and rectal lesions result in a higher POB incidence after colorectal ESD.

© 2017 S. Karger AG, Basel

## Introduction

It is now generally accepted that the colonoscopic removal of adenomatous polyps or early cancer prevents death from colorectal cancer [1]. Pedunculated colorectal polyps and flat or depressed colorectal tumors are good indications for endoscopic polypectomy (EP) and endoscopic mucosal resection (EMR), respectively [2, 3]. Al-



though EMR is widely used for endoscopic removal of flat or depressed colorectal tumors, en bloc resection of lesions >20 mm is difficult using EMR [4–6]. A fragmented resection technique called endoscopic piecemeal mucosal resection is often employed in such cases [4–6], but a high incidence of local recurrence has been reported in colorectal tumors treated with this resection technique [4–6]. Endoscopic submucosal dissection (ESD), which allows en bloc resection of flat or depressed colorectal tumors >20 mm, has recently been introduced and become a standard procedure in Japan [4–6]. In fact, many studies addressing the efficacy of ESD show that the rates of en bloc and curative resection are higher in patients treated with ESD than in those treated with EMR [7–11]. In contrast, the local recurrence rate was lower in patients treated with ESD than in those treated with EMR [7–11]. Thus, colorectal ESD has enabled the resection of large flat or depressed colorectal tumors as well as a wide variety of adenomas and early colorectal cancers.

As in case of EP and EMR [12, 13], postoperative bleeding (POB) and perforation are both major complications associated with ESD [14]. The percentages of POB following colorectal ESD [7, 11, 14] are highly variable, ranging from 0.5 to 9.6%. Although the POB rate was lower following colorectal ESD than colorectal EMR in a meta-analysis [2], life-threatening bleeding requiring blood transfusion may occur in patients treated with ESD. Therefore, risk factors for POB following colorectal ESD need to be identified.

Antithrombotic therapy with anticoagulants or antiplatelet agents is widely used for the prevention of ischemic cardiovascular events [15–17]. Although antithrombotic therapy is effective for the prevention of ischemic cardiovascular events, the recent use of anticoagulants or antiplatelet agents is considered a major risk factor for POB following EP and EMR [18–20]. According to the recent guidelines of the Japan Gastroenterological Endoscopic Society (JGES), anticoagulants or antiplatelet agents should not be discontinued before endoscopic procedures with low risk of bleeding since the withdrawal of these drugs may cause new-onset cardiovascular events [21]. On the contrary, anticoagulants or antiplatelet agents must be discontinued in patients bearing a low risk of thromboembolism following withdrawal or replaced by heparin bridge therapy (HBT) in patients at high risk of thromboembolism following withdrawal before endoscopic procedures with a high risk of bleeding, such as EMR and ESD [21]. Recent retrospective studies addressing the safety and efficacy of HBT in colorectal EMR and EP revealed that HBT increases rather than de-

creases the risk of POB [22–24]. It should be noted, however, that clinical studies addressing the safety and efficacy of HBT in colorectal ESD are not available. Here, we performed a retrospective analysis to identify the risk factors for POB in patients who underwent colorectal ESD with or without antithrombotic therapy.

## Patients and Methods

### Patients

This study was a retrospective analysis addressing the safety and efficacy of colorectal ESD. A total of 451 patients (509 lesions) who underwent colorectal ESD at the Kindai University Hospital between April 2010 and February 2017 were enrolled in this study. The Review Board of the Kindai University Faculty of Medicine approved the study design and procedures.

Clinical parameters were obtained from each patient's medical records. They included age, sex, anticoagulant use, antiplatelet agent use, platelet count, prothrombin time (PT), activated partial thromboplastin time (APTT), serum creatinine level, colorectal tumor size, endoscopic tumor appearance (0–IIa, 0–IIa + IIc, 0–IIc, 0–IIc + IIa, 0–Is, 0–Is + IIc, laterally spreading tumor granular [LST-G] homogenous type, LST-G nodular mixed type, LST-nongranular [LST-NG] flat elevated type, and LST-NG pseudodepressed type), tumor histology, and tumor location. Tumor location was classified into cecum, ascending colon, transverse colon, descending colon, sigmoid colon, and rectum.

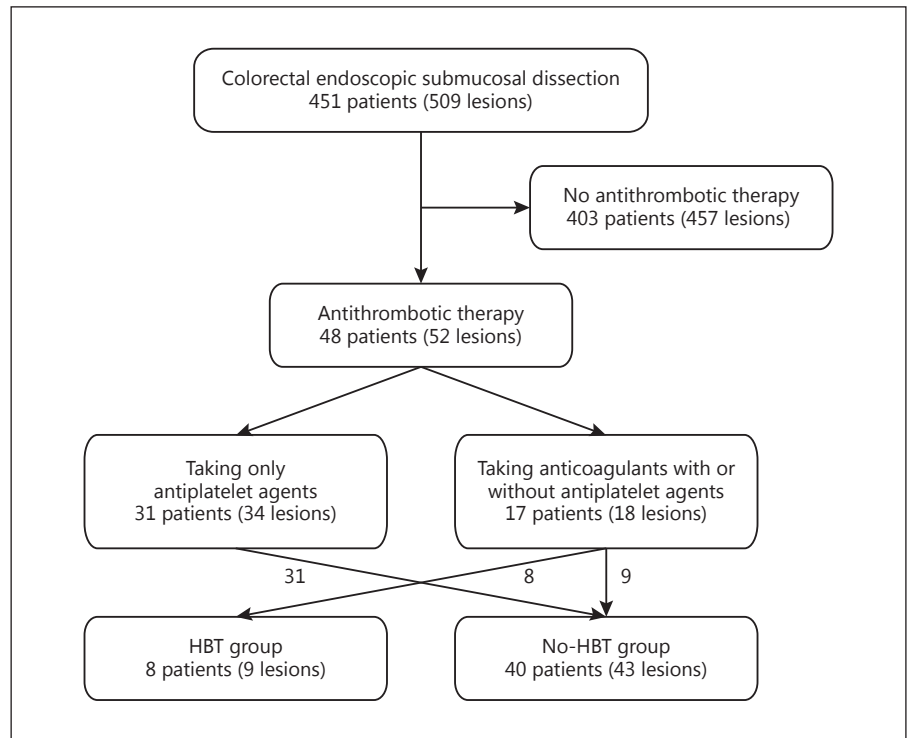
### Management of Anticoagulants and Antiplatelet Agents

Warfarin, dabigatran, rivaroxaban, and edoxaban were used as anticoagulants in this study, while aspirin, ticlopidine, beraprost, cilostazol, eicosapentaenoic acid ethyl ester, and clopidogrel were used as antiplatelet agents. The discontinuation of anticoagulants and/or antiplatelet agents or replacement by HBT was determined by each primary doctor after consultation with cardiologists or neurosurgeons. The discontinuation periods of the above drugs were determined based on the JGES guidelines [21]. HBT was performed using unfractionated heparin sodium, and the dose of heparin was adjusted by monitoring APTT (1.5- to 2.0-fold above the upper limit). HBT was started 3–5 days before ESD and stopped 6 h before ESD. Anticoagulants and antiplatelet agents were resumed 1 or 2 days after ESD.

### ESD Procedure

Colorectal ESD was performed under the condition of conscious sedation with midazolam or diazepam. We used a PCF-290Z colonoscope (Olympus) with a transparent hood and irrigation pump. Carbon dioxide insufflation was used during the procedure. Sodium hyaluronic acid and adrenaline were injected into the submucosal layer to create a submucosal cushion. A flush knife BTS (DK-2620J; Fujifilm) or a DualKnife J (KD-655Q; Olympus) was used to dissect the lesion. The setting of the VIO® 300 D (Electrosurgical Generator) were Endocut I (effect 2, time 3, interval 3) for mucosal incisions, swift coagulation (effect 3/40 W) for submucosal dissections, and soft coagulation (effect 6/80 W) for bleeding points; for preventive occlusions of vessels, hemostatic forceps were used. At the end of the procedure, additional coagulation was carefully performed to prevent delayed bleeding.





**Fig. 1.** Flow diagram of the patients treated with colorectal endoscopic submucosal dissection. HBT, heparin bridge therapy.

#### Postoperative Bleeding

Emergent colonoscopy was performed in cases of melena. POB was defined as active bleeding or an adherent clot on the resection site that required endoscopic treatment.

#### Statistical Analysis

The Student *t* test or Fisher exact test was used in univariate analyses. Values of  $p < 0.05$  were considered significant. Clinical factors that were significant in univariate analysis were subjected to multivariate analysis.

## Results

#### Flow Diagrams of Patient Selection and Treatment Allocation

Four hundred and fifty-one patients (509 lesions) who underwent colorectal ESD were enrolled in this study. A total of 48 patients (52 lesions) received antithrombotic therapy before ESD. Of them, 17 (18 lesions) were treated with anticoagulants with or without antiplatelet agents, and 31 (34 lesions) were treated with antiplatelet agents alone. Six patients were treated with both anticoagulants and antiplatelet agents. The 48 patients (52 lesions) who received antithrombotic therapy before ESD were categorized into the HBT group (8 patients) and no-HBT group

(40 patients). Patients in the no-HBT group had discontinuation of anticoagulants or antiplatelet agents (17 patients), continuation of anticoagulants or antiplatelet agents before ESD (14 patients), and continuation of 1 anticoagulant or antiplatelet agent in the case of  $>2$  drugs before ESD (9 patients). A flow diagram of the patient selection and treatment allocation is shown in Figure 1.

#### Risk Factors for POB following Colorectal ESD

Although POB is a common complication of colorectal ESD, its risk factors have not been identified. Previous studies showed that multiple factors such as size, pedunculated form, and proximal location increase the rate of POB following EP [19, 25, 26]. In addition, antithrombotic therapy, hypertension, chronic renal disease, cardiovascular disease, and advanced age were identified as patient-associated risk factors for delayed bleeding [18–20]. Based on these previous reports, we performed a univariate analysis of the clinical parameters in this retrospective study. As shown in Table 1, POB was seen in 14 patients (14 lesions) among the total 451 patients (509 lesions). Endoscopic hemostasis was required for all 14 patients, and 6 needed blood transfusion. One patient required surgery. No significant correlation was seen between bleeding and tumor-related factors such as size and

**Table 1.** Clinical parameters associated with postoperative bleeding (POB)

Clinical parameters	POB 14 cases (14 lesions)	No POB 437 cases (495 lesions)	<i>p</i> value
Age, years	65.6±12.1	68.3±9.2	0.389 <sup>b</sup>
Males/females	9/5 (64.2/35.8)	236/201 (54.0/46.0)	0.589 <sup>a</sup>
Antithrombotic therapy	7 (50)	45 (8.9)	<0.001 <sup>a</sup>
Anticoagulant agents	3 (21.4)	14 (3.2)	0.009 <sup>a</sup>
Antiplatelet agents	4 (28.6)	39 (7.9)	0.024 <sup>a</sup>
Platelets, $\mu$ L	23.6±9.7	22.3±6.1	0.213 <sup>b</sup>
Prothrombin time, INR	1.06±0.13	1.04±0.47	0.923 <sup>b</sup>
APTT, s	32.1±8.8	28.2±6.9	0.189 <sup>b</sup>
Creatinine, mg/dL	0.95±0.57	0.84±0.84	0.637 <sup>b</sup>
Tumor size, mm	32.2±13.6	30.6±14.1	0.784 <sup>b</sup>
Endoscopic appearance			
0-IIa	0 (0)	1 (0)	1.000 <sup>a</sup>
0-IIa + IIc	0 (0)	8 (1.6)	1.000 <sup>a</sup>
0-IIc	0 (0)	1 (0)	1.000 <sup>a</sup>
0-IIc + IIa	0 (0)	2 (0)	1.000 <sup>a</sup>
0-Is	1 (7.1)	41 (8.3)	1.000 <sup>a</sup>
0-Is + IIc	0 (0)	1 (0)	1.000 <sup>a</sup>
LST-G (homogenous)	0 (0)	83 (17.0)	1.000 <sup>a</sup>
LST-G (nodular mixed)	7 (50)	109 (22.0)	0.022 <sup>a</sup>
LST-NG (flat elevated)	5 (35.7)	156 (31.5)	0.774 <sup>a</sup>
LST-NG (pseudodepressed)	1 (7.1)	93 (18.8)	0.484 <sup>a</sup>
Histology (invasive neoplasm)	0 (0)	8 (1.6)	1.000 <sup>a</sup>
Location			
Cecum	0 (0)	88 (17.8)	1.000 <sup>a</sup>
Ascending colon	2 (14.3)	111 (22.4)	0.745 <sup>a</sup>
Transverse colon	3 (21.4)	132 (26.7)	1.000 <sup>a</sup>
Descending colon	0 (0)	13 (2.6)	1.000 <sup>a</sup>
Sigmoid colon	1 (7.1)	61 (12.3)	1.000 <sup>a</sup>
Rectum	8 (57.1)	90 (18.1)	0.002 <sup>a</sup>

Numbers of cases (%) are shown unless indicated otherwise. APTT, activated partial thromboplastin time; LST, laterally spreading tumor; G, granular; NG, nongranular. <sup>a</sup> Fisher exact test. <sup>b</sup> *t* test.

**Table 2.** Risk factors for postoperative bleeding

	Odds ratio	95% CI	<i>p</i> value
Antithrombotic therapy	4.95	1.48–16.59	0.009
LST-G (mix)	2.12	0.64–7.07	0.22
Rectal tumor	10.81	3.43–34.00	<0.001

LST-G (mix), laterally spreading tumor-granular (nodular mixed).

histology except for the endoscopic appearance of the LST-G mixed nodular type. Interestingly, we found that 8 of 14 patients with POB received ESD for rectal tumors. Thus, the incidence of POB was high in rectal lesions at 8.1% (8/98). Regarding patient-related factors, no signifi-

cant correlation was seen between bleeding and patient-related factors such as age, sex, platelet count, PT, APTT, or serum creatinine level. In contrast, the percentage of POB was much higher in patients with antithrombotic therapy than in those without antithrombotic therapy. Thus, our univariate analysis identified antithrombotic therapy (use of anticoagulants and/or antiplatelet agents) and rectal tumors as risk factors for POB following colorectal ESD.

We then performed multivariate analysis to confirm the results obtained by the univariate analysis. As shown in Table 2, antithrombotic therapy and rectal tumors were identified as independent risk factors for ESD-related POB, whereas the LST-G mixed nodular type did not show a significant correlation. Collectively, these uni- and multivariate analyses revealed that antithrombotic

**Table 3.** Characteristics of patients with or without heparin bridge therapy (HBT)

Clinical parameters	HBT 8 cases (9 lesions)	No HBT 40 cases (43 lesions)	<i>p</i> value
Age, years	72.1±6.3	72.1±7.8	0.980 <sup>b</sup>
Males/females	6/2 (75/25)	28/12 (70/30)	1.000 <sup>a</sup>
Anticoagulant agents	8 (100)	9 (22.5)	0.001 <sup>a</sup>
Antiplatelet agents	1 (12.5)	39 (97.5)	<0.001 <sup>a</sup>
Both	1 (12.5)	8 (20)	1.000 <sup>a</sup>
Tumor size, mm	37.1±11.8	29.7±12.1	0.173 <sup>b</sup>
Histology (invasive neoplasm)	0	0	–
Endoscopic appearance			
0-IIa	0 (0)	4 (9.3)	1.000 <sup>a</sup>
0-IIa + IIc	0 (0)	0 (0)	1.000 <sup>a</sup>
0-IIc	0 (0)	0 (0)	1.000 <sup>a</sup>
0-Is	1 (11.1)	4 (9.3)	1.000 <sup>a</sup>
0-Is + IIc	0 (0)	0 (0)	1.000 <sup>a</sup>
LST-G (homogenous)	2 (22.2)	4 (9.3)	0.275 <sup>a</sup>
LST-G (nodular mixed)	2 (22.2)	10 (23.3)	1.000 <sup>a</sup>
LST-NG (flat elevated)	3 (33.3)	11 (25.6)	0.688 <sup>a</sup>
LST-NG (pseudodepressed)	1 (11.1)	10 (23.3)	0.664 <sup>a</sup>
Location			
Cecum	0 (0)	8 (18.6)	1.000 <sup>a</sup>
Ascending colon	2 (22.2)	8 (18.6)	1.000 <sup>a</sup>
Transverse colon	3 (33.3)	13 (30.2)	1.000 <sup>a</sup>
Descending colon	1 (11.1)	3 (7)	1.000 <sup>a</sup>
Sigmoid colon	0 (0)	2 (4.7)	1.000 <sup>a</sup>
Rectum	3 (33.3)	9 (20.9)	0.415 <sup>a</sup>
Postoperative bleeding	2 (22.2)	5 (11.6)	0.59 <sup>a</sup>

Numbers of cases (%) are shown unless indicated otherwise. LST, laterally spreading tumor; G, granular; NG, nongranular. <sup>a</sup> Fisher exact test. <sup>b</sup> *t* test.

therapy and rectal tumor location are strongly associated with POB caused by ESD.

#### *HBT in and POB following Colorectal ESD*

Having identified the use of anticoagulants and/or antiplatelet agents as a patient-associated risk factor for POB following colorectal ESD, we tried to evaluate the safety and efficacy of HBT. Eight patients received HBT in this study. Seventeen patients discontinued the antithrombotic therapy, 14 patients continued anticoagulants or antiplatelet agents before ESD, and 9 patients continued only 1 anticoagulant or antiplatelet agent in the case of combined therapy. Characteristics of the patients in the HBT group (8 cases) and no-HBT group (40 cases) are summarized in Table 3. The percentages of POB in the no-HBT and HBT group were 11.6% (5/43) and 22.2% (2/9), respectively. Thus, no significant difference in POB was seen between the HBT and no-HBT groups, although the former exhibited a higher rate of POB than the latter.

As shown above, 7 of 52 cases who received antithrombotic therapy exhibited POB. Detailed clinical information on the 7 cases with POB is summarized in Table 4. Two patients who discontinued warfarin and then received HBT experienced POB (Table 4). One patient who was treated with aspirin in combination with cilostazol and then continued therapy with aspirin alone upon ESD experienced POB. Other cases with POB included 1 patient who discontinued aspirin, 1 who continued aspirin, 1 who continued ticlopidine and aspirin, and 1 who discontinued edoxaban. Thus, a wide variety of anticoagulants and antiplatelet agents caused POB.

#### **Discussion**

ESD is widely used to resect flat or depressed colorectal tumors >20 mm [4–6]. The advantages of ESD in colorectal tumor therapy include the higher rate of successful en bloc resection and the lower rate of local recur-

**Table 4.** Clinical characteristics of 7 cases with antithrombotic therapy and postoperative bleeding

Case No.	Age, years	Sex	Tumor characteristics		Anti-coagulants	Antiplatelet agents	HBT	Blood transfusion
			site	size, mm				
1	67	M	A	30	–	aspirin	–	–
2	71	F	R	43	–	ticlopidine	–	yes
3	72	M	R	25	–	aspirin	–	yes
4	70	M	T	20	–	aspirin <sup>1</sup>	–	–
5	68	M	R	32	warfarin	–	yes	–
6	51	M	R	40	edoxaban <sup>1</sup>	–	–	yes
7	83	M	T	45	warfarin	–	yes	–

A, ascending colon; T, transverse colon; R, rectum; HBT, heparin bridge therapy.

<sup>1</sup> Discontinued before endoscopic submucosal dissection.

rence compared with conventional EMR [7–11]. Thus, colorectal ESD has enabled the resection of large flat or depressed colorectal tumors as well as a wide variety of adenomas and early colorectal cancers. POB is a major complication of ESD. Although the rates of POB are comparable among ESD, EMR, and EP, life-threatening bleeding may occur after colorectal ESD. Therefore, the identification of risk factors for POB is important. In this study, we analyzed 451 patients who underwent colorectal ESD at the Kindai University Hospital and found in uni- and multivariate analyses that rectal tumor location and antithrombotic therapy are independent risk factors for bleeding. Thus, rectal tumor location and antithrombotic therapy are likely to increase the risk of POB following colorectal ESD.

Interestingly, the percentage of POB following colorectal ESD was much higher in patients with rectal tumors than that in patients with tumors in the cecum, ascending colon, transverse colon, descending colon, or sigmoid colon. Among 14 POB cases, 8 had bleeding from rectal lesions. These data are in sharp contrast to those of previous reports showing that location in the right hemicolon is an independent risk factor for delayed postpolypectomy bleeding [25, 27]. Thus, rectal location increases the rate of POB following ESD, while right hemicolon location increases the rate of bleeding following EP. The reason for this difference is unknown. Given the fact there are many veins and arteries in the submucosa of the rectum [28], POB may be caused by injury to the submucosal vessels of the rectum during ESD.

As for patient-related factors, we identified antithrombotic therapy as an independent risk factor for POB fol-

lowing colorectal ESD. Consistent with this finding, the use of anticoagulants or antiplatelet agents is considered to promote POB in patients treated with EP or EMR [18–20]. Thus, the use of anticoagulants or antiplatelet agents increases the risk of POB following EMR, EP, and ESD. We performed a detailed analysis of 7 patients with POB treated with anticoagulants and/or antiplatelet agents before ESD. Unfortunately, we could not identify specific antithrombotic drugs that promote POB following colorectal ESD. Intriguingly, 4 (57.1%) of the 7 patients who received antithrombotic therapy had bleeding from rectal lesions. These data altogether suggest that antithrombotic therapy and rectal location are independent risk factors for POB following colorectal ESD and that colonoscopists must be aware of possible bleeding in patients presenting with these risk factors.

According to the JSGE guidelines, HBT is recommended before endoscopic procedures with a high risk of bleeding, such as EMR and ESD in patients at high risk of thromboembolism upon anticoagulant withdrawal [21]. Based on this guideline, HBT is considered a treatment option for patients who are undergoing colorectal EMR or ESD in the presence of antithrombotic therapy. However, recent retrospective studies addressing the safety and efficacy of HBT in colorectal EMR and EP revealed that HBT increases rather than decreases the risk of POB [22–24]. Consistent with the studies cited above, the rate of POB following colorectal ESD tended to be higher in our HBT group than in our no-HBT group, although the difference was not statistically significant. The reasons for the lack of a significant difference in the rate of POB between the HBT and the no-HBT group are currently un-



known. Strict APTT adjustment, overload effects of discontinued anticoagulants, or time of resuming anticoagulants or antiplatelet agents may affect the rate of POB. It should also be noted that the number of patients in this study, especially in the HBT group, is too small to draw a definite conclusion regarding the relationship between colorectal ESD-related POB and HBT. Therefore, prospective multicenter studies are required to confirm the safety and efficacy of HBT in colorectal ESD.

In conclusion, we identified antithrombotic therapy and rectal location as independent risk factors for POB following colorectal ESD. Future studies are required to confirm our findings and decrease the rate of POB following colorectal ESD.

## Disclosure Statement

The authors have no conflicts of interest to declare.

## References

- 1 Zauber AG, Winawer SJ, O'Brien MJ, Lansdorp-Vogelaar I, van Ballegooijen M, Hankey BF, Shi W, Bond JH, Schapiro M, Panish JF, Stewart ET, Waye JD: Colonoscopic polypectomy and long-term prevention of colorectal-cancer deaths. *N Engl J Med* 2012;366:687–696.
- 2 Fujiya M, Tanaka K, Dokoshi T, Tominaga M, Ueno N, Inaba Y, Ito T, Moriichi K, Kohgo Y: Efficacy and adverse events of EMR and endoscopic submucosal dissection for the treatment of colon neoplasms: a meta-analysis of studies comparing EMR and endoscopic submucosal dissection. *Gastrointest Endosc* 2015;81:583–595.
- 3 Tanaka S, Kashida H, Saito Y, Yahagi N, Yamano H, Saito S, Hisabe T, Yao T, Watanabe M, Yoshida M, Kudo SE, Tsuruta O, Sugihara K, Watanabe T, Saitoh Y, Igarashi M, Toyonaga T, Ajioka Y, Ichinose M, Matsui T, Sugita A, Sugano K, Fujimoto K, Tajiri H: JGES guidelines for colorectal endoscopic submucosal dissection/endoscopic mucosal resection. *Dig Endosc* 2015;27:417–434.
- 4 Sauer M, Hildenbrand R, Oyama T, Sido B, Yahagi N, Dumoulin FL: Endoscopic submucosal dissection for flat or sessile colorectal neoplasia >20 mm: a European single-center series of 182 cases. *Endosc Int Open* 2016;4:E895–E900.
- 5 Knabe M, Pohl J, Gerges C, Ell C, Neuhaus H, Schumacher B: Standardized long-term follow-up after endoscopic resection of large, nonpedunculated colorectal lesions: a prospective two-center study. *Am J Gastroenterol* 2014;109:183–189.
- 6 Belderbos TD, Leenders M, Moons LM, Siersema PD: Local recurrence after endoscopic mucosal resection of nonpedunculated colorectal lesions: systematic review and meta-analysis. *Endoscopy* 2014;46:388–402.
- 7 Saito Y, Fukuzawa M, Matsuda T, Fukunaga S, Sakamoto T, Uraoka T, Nakajima T, Ikehara H, Fu KI, Itoi T, Fujii T: Clinical outcome of endoscopic submucosal dissection versus endoscopic mucosal resection of large colorectal tumors as determined by curative resection. *Surg Endosc* 2010;24:343–352.
- 8 Tajika M, Niwa Y, Bhatia V, Kondo S, Tanaka T, Mizuno N, Hara K, Hijioka S, Imaoka H, Ogura T, Haba S, Yamao K: Comparison of endoscopic submucosal dissection and endoscopic mucosal resection for large colorectal tumors. *Eur J Gastroenterol Hepatol* 2011;23:1042–1049.
- 9 Lee EJ, Lee JB, Lee SH, Kim DS, Lee DH, Lee DS, Youk EG: Endoscopic submucosal dissection for colorectal tumors – 1,000 colorectal ESD cases: one specialized institute's experiences. *Surg Endosc* 2013;27:31–39.
- 10 Kobayashi N, Yoshitake N, Hirahara Y, Konishi J, Saito Y, Matsuda T, Ishikawa T, Sekiguchi R, Fujimori T: Matched case-control study comparing endoscopic submucosal dissection and endoscopic mucosal resection for colorectal tumors. *J Gastroenterol Hepatol* 2012;27:728–733.
- 11 Terasaki M, Tanaka S, Oka S, Nakadoi K, Takata S, Kanao H, Yoshida S, Chayama K: Clinical outcomes of endoscopic submucosal dissection and endoscopic mucosal resection for laterally spreading tumors larger than 20 mm. *J Gastroenterol Hepatol* 2012;27:734–740.
- 12 Oka S, Tanaka S, Kanao H, Ishikawa H, Watanabe T, Igarashi M, Saito Y, Ikematsu H, Kobayashi K, Inoue Y, Yahagi N, Tsuda S, Simizu S, Iishi H, Yamano H, Kudo SE, Tsuruta O, Tamura S, Saito Y, Cho E, Fujii T, Sano Y, Nakamura H, Sugihara K, Muto T: Current status in the occurrence of postoperative bleeding, perforation and residual/local recurrence during colonoscopic treatment in Japan. *Dig Endosc* 2010;22:376–380.
- 13 Thirumurthi S, Raju GS: Management of polypectomy complications. *Gastrointest Endosc Clin N Am* 2015;25:335–357.
- 14 Ma MX, Bourke MJ: Complications of endoscopic polypectomy, endoscopic mucosal resection and endoscopic submucosal dissection in the colon. *Best Pract Res Clin Gastroenterol* 2016;30:749–767.
- 15 Sung JJ, Lau JY, Ching JY, Wu JC, Lee YT, Chiu PW, Leung VK, Wong VW, Chan FK: Continuation of low-dose aspirin therapy in peptic ulcer bleeding: a randomized trial. *Ann Intern Med* 2010;152:1–9.
- 16 Witt DM, Delate T, Garcia DA, Clark NP, Hylek EM, Ageno W, Dentali F, Crowther MA: Risk of thromboembolism, recurrent hemorrhage, and death after warfarin therapy interruption for gastrointestinal tract bleeding. *Arch Intern Med* 2012;172:1484–1491.
- 17 Broderick JP, Bonomo JB, Kissela BM, Khoury JC, Moomaw CJ, Alwell K, Woo D, Flaherty ML, Khatri P, Adeoye O, Ferioli S, Kleindorfer DO: Withdrawal of antithrombotic agents and its impact on ischemic stroke occurrence. *Stroke* 2011;42:2509–2514.
- 18 Shibuya T, Nomura O, Kodani T, Murakami T, Fukushima H, Tajima Y, Matsumoto K, Ritsuno H, Ueyama H, Inami Y, Ishikawa D, Matsumoto K, Sakamoto N, Osada T, Nagahara A, Ogihara T, Watanabe S: Continuation of antithrombotic therapy may be associated with a high incidence of colonic post-polypectomy bleeding. *Dig Endosc* 2017;29:314–321.
- 19 Kim HS, Kim TI, Kim WH, Kim YH, Kim HJ, Yang SK, Myung SJ, Byeon JS, Lee MS, Chung IK, Jung SA, Jeon YT, Choi JH, Choi KY, Choi H, Han DS, Song JS: Risk factors for immediate postpolypectomy bleeding of the colon: a multicenter study. *Am J Gastroenterol* 2006;101:1333–1341.
- 20 Hui AJ, Wong RM, Ching JY, Hung LC, Chung SC, Sung JJ: Risk of colonoscopic polypectomy bleeding with anticoagulants and antiplatelet agents: analysis of 1,657 cases. *Gastrointest Endosc* 2004;59:44–48.
- 21 Fujimoto K, Fujishiro M, Kato M, Higuchi K, Iwakiri R, Sakamoto C, Uchiyama S, Kashiwagi A, Ogawa H, Murakami K, Mine T, Yoshino J, Kinoshita Y, Ichinose M, Matsui T; Japan Gastroenterological Endoscopy Society: Guidelines for gastroenterological endoscopy in patients undergoing antithrombotic treatment. *Dig Endosc* 2014;26:1–14.
- 22 Ishigami H, Arai M, Matsumura T, Maruoka D, Minemura S, Okimoto K, Kasamatsu S, Saito K, Nakagawa T, Katsumoto T, Yokosuka O: Heparin-bridging therapy is associated with a high risk of post-polypectomy bleeding regardless of polyp size. *Dig Endosc* 2017;29:65–72.

- 23 Kubo T, Yamashita K, Onodera K, Iida T, Arimura Y, Nojima M, Nakase H: Heparin bridge therapy and post-polypectomy bleeding. *World J Gastroenterol* 2016;22:10009–10014.
- 24 Inoue T, Nishida T, Maekawa A, Tsujii Y, Akasaka T, Kato M, Hayashi Y, Yamamoto S, Kondo J, Yamada T, Shinzaki S, Iijima H, Tsujii M, Takehara T: Clinical features of post-polypectomy bleeding associated with heparin bridge therapy. *Dig Endosc* 2014;26: 243–249.
- 25 Kim JH, Lee HJ, Ahn JW, Cheung DY, Kim JI, Park SH, Kim JK: Risk factors for delayed post-polypectomy hemorrhage: a case-control study. *J Gastroenterol Hepatol* 2013;28: 645–649.
- 26 Watabe H, Yamaji Y, Okamoto M, Kondo S, Ohta M, Ikenoue T, Kato J, Togo G, Matsu-mura M, Yoshida H, Kawabe T, Omata M: Risk assessment for delayed hemorrhagic complication of colonic polypectomy: polyp-related factors and patient-related factors. *Gastrointest Endosc* 2006;64:73–78.
- 27 Buddingh KT, Herngreen T, Haringsma J, van der Zwet WC, Vleggaar FP, Breumelhof R, Ter Borg F: Location in the right hemi-colon is an independent risk factor for delayed post-polypectomy hemorrhage: a multi-center case-control study. *Am J Gastroenterol* 2011;106:1119–1124.
- 28 Lee JH, Lee KH, Chung WS, Hur J, Won JY, Lee DY: Transcatheter embolization of the middle sacral artery: collateral feeder in recurrent rectal bleeding. *AJR Am J Roentgenol* 2004;182:1055–1105.

# The Feasibility of 18-mm-Diameter Colonic Stents for Obstructive Colorectal Cancers

Satoshi Ogawa<sup>a,b</sup> Tatsuya Ishii<sup>b</sup> Kosuke Minaga<sup>b,c</sup> Yasuki Nakatani<sup>b</sup>  
Keiichi Hatamaru<sup>b</sup> Takuji Akamatsu<sup>b</sup> Takeshi Seta<sup>b</sup> Shunji Urai<sup>b</sup>  
Yoshito Uenoyama<sup>b</sup> Yukitaka Yamashita<sup>b</sup> Masatoshi Kudo<sup>c</sup>

<sup>a</sup>Department of Gastroenterology and Hepatology, Kyoto University Graduate School of Medicine, Kyoto,

<sup>b</sup>Department of Gastroenterology and Hepatology, Japanese Red Cross Society Wakayama Medical Center, Wakayama, and <sup>c</sup>Department of Gastroenterology and Hepatology, Kindai University Faculty of Medicine, Osaka-Sayama, Japan

## Keywords

Colonic neoplasms · Self-expanding metal stents · Stent diameter · Bridge to surgery · Perforation

## Abstract

**Objectives:** This study aimed to evaluate the characteristics and the feasibility of 18-mm-diameter stents for obstructive colorectal cancer, comparing the clinical courses with 22-mm-diameter stents. **Methods:** We retrospectively compared 33 consecutive cases treated with 18-mm-diameter stents (bridge to surgery [BTS] in 25, palliative therapy [PAL] in 8) with 27 consecutive cases treated with 22-mm-diameter stents (BTS in 21, PAL in 6) for obstructive colorectal cancer between May 2013 and November 2015 in our institution. **Results:** There were no significant differences between the 18-mm and 22-mm groups in technical success rates (97 and 96%, respectively) and clinical success rates (100 and 100%, respectively). As a BTS, the rates of complications and stoma formation were not significantly different between groups. For PAL, although the rates of complications and stent patency were similar, stent occlusion occurred in 1 pa-

tient (12.5%) in the 18-mm group. **Conclusions:** The 18-mm-diameter stents were similarly effective when compared with 22-mm-diameter stents. Because 18-mm-diameter stents are easy to handle and produce less mechanical stress, they have the potential to decrease the perforation rate and mitigate the stent's impact on the tumors. 18-mm-diameter stents can be useful and safe, especially as a BTS.

© 2017 S. Karger AG, Basel

## Introduction

Colorectal cancer is one of the most common cancers, and 8–29% of patients with colorectal cancer have obstruction-related symptoms [1, 2]. Because obstructive colorectal cancer can be fatal, emergent management is needed. It was reported that the morbidity and mortality rates associated with emergent surgery were high [1, 3, 4]. In the last few decades, there have been many reports about the usefulness of self-expanding metal stents (SEMS) for obstructive colorectal cancer. SEMS are used as a bridge to surgery (BTS) and for palliative therapy

(PAL). A systematic review revealed SEMS placement as a BTS has a lower stoma formation rate and complication rate than emergent surgery [5]. A meta-analysis showed that SEMS placement for PAL is associated with a shorter time to chemotherapy and lower 30-day mortality [6].

Recently, concerns have been raised regarding the possibility for exacerbation of the oncological prognosis. A few randomized controlled trials and a cohort study have shown a significantly higher local disease recurrence rate with SEMS use than emergent surgery [7–10]. According to the European Society of Gastrointestinal Endoscopy (ESGE) guidelines, SEMS placement as a BTS is not recommended as a standard treatment for potentially curable patients with obstructive colorectal cancer [11]. However, one meta-analysis suggests that SEMS as a BTS have no adverse effects in terms of patients' oncological outcomes [12]. The cancer recurrence rate has been shown to be higher in the subgroup of patients with stent-related perforations [9]; thus, it is suggested that a lower perforation rate may improve the prognosis. Small-diameter stents mitigate the mechanical impact of the stents on the tumor and the colonic wall, and can reduce the perforation rate.

To date, few reports examine stent diameter, and the optimal stent diameter has not been determined. In our hospital, we have inserted the Niti-S enteral colonic uncovered stent D-type (Taewoong Medical Inc., Gimpo, Korea) in cases with obstructive colorectal cancer since May 2013. We used 22-mm-diameter stents until May 2014 but now use 18-mm-diameter stents. Then, our study aimed to evaluate the characteristics and the feasibility of 18-mm-diameter stents, comparing them with 22-mm-diameter stents.

## Methods

### Patients

We retrospectively reviewed the endoscopy database and clinical records on all patients who underwent Niti-S enteral colonic uncovered stent placement for obstructive colorectal cancer at the Japanese Red Cross Society Wakayama Medical Center between May 2013 and November 2015. Bowel obstructions were diagnosed through clinical symptoms, CT, and endoscopy.

We analyzed consecutive cases utilizing 18-mm-diameter Niti-S stents from June 2014 to November 2015 and compared them with consecutive cases utilizing 22-mm-diameter stents from May 2013 to May 2014.

Patients who had been followed up at our institution for at least 4 weeks were eligible to be enrolled in this study. Relevant data were retrieved from the medical records of our institution. This study was approved by the Institutional Review Board of our institution. We excluded patients who underwent chemotherapy with the stents inserted, considering the possibility that chemotherapy affects stent patency rate. We followed patients' clinical courses until December 2015.

**Table 1.** Patient characteristics

	18 mm (33 cases)	22 mm (27 cases)	<i>p</i>
Median age (range), years	77 (49–91)	78 (31–97)	0.22
Sex (male/female)	17/16	13/14	0.98
Performance status (0–1/2–4)	27/6	24/3	0.45
Stage (II/IIIa/IIIb/IV)	11/8/3/11	7/7/5/8	0.75
Tumor location (right/left)	12/21	11/16	0.73
Median length of stenosis ± SD, cm	2.8 ± 1.2	3.3 ± 1.4	0.07
Complete/incomplete obstruction	32/1	25/2	0.58
Length of stent (6 cm/8 cm)	31/1	25/2	0.59
Purpose (BTS/PAL)	25/8	21/6	0.85

BTS, bridge to surgery; PAL, palliative therapy.

### Endoscopic Procedure

Before colonic stent placement, all patients underwent abdominal CT scans to evaluate the clinical stage of the tumor and to assess the location and length of the obstruction. Generally, patients underwent enemas for preparation and were maintained under conscious sedation with 0.05 mg/kg intravenous midazolam. Patients were continuously monitored during the procedure with an automated noninvasive blood pressure device, electrocardiogram tracing, and pulse oximetry.

We used Niti-S enteral colonic uncovered D-type stents (Taewoong Medical Inc., Gimpo, South Korea), 18 or 22 mm in diameter and 60 or 80 mm in length.

All procedures were performed under endoscopic and fluoroscopic guidance. We used conventional endoscopes (CF-H260, CF-HQ290, Olympus Medical Systems, Tokyo, Japan) in cases utilizing 22-mm-diameter stents. We also used slim-diameter endoscopes (PCF-Q260AI or GIF-Q260J, Olympus) in cases utilizing 18-mm-diameter stents. We used a guidewire (0.025-inch Visi-Glide, Olympus, or 0.035-inch Jagwire, Boston Scientific Corporation, Natick, MA, USA) and an ERCP catheter (ERCP catheter filiform, MTW Endoscopie W. Haag KG, Wesel, Germany, or Swing Tip Cannula, Olympus) to pass the stricture and select the oral intestinal tract. Thereafter, contrast medium was injected to confirm the position and the length of the stricture. We did not attempt dilation of strictures due to risk of perforation. Stent length was selected to cover the entire stricture adequately.

Abdominal radiographs were obtained 1 day after stent placement to evaluate the degree of stent expansion. To prevent stool impaction, a low residual diet with laxatives, such as magnesium formulations, was recommended.

### Study Design

Patients were divided into two groups according to stent diameters. We retrospectively compared the two groups for patient characteristics, technical success rate, clinical success rate, procedure time, and the time until resumption of diet.

Patients receiving stents as a BTS were followed perioperatively and assessed for complications related to stents, the time interval to operation, laparoscopic resection rate, stoma formation rate, and perioperative complications.

**Table 2.** Results of the procedures

	18 mm (33 cases)	22 mm (27 cases)	<i>p</i>
Median procedure time (range), min	20 (8–65)	25 (11–60)	0.08
Technical success rate, %	97 (32/33)	96 (26/27)	0.86
Clinical success rate, %	100 (32/32)	100 (26/26)	1.00
Mean CROSS before procedure $\pm$ SD	1.2 $\pm$ 1.2	1.3 $\pm$ 1.4	0.70
Mean CROSS after procedure $\pm$ SD	4.0 $\pm$ 0.1	4.0 $\pm$ 0.2	0.44
Mean period of restarting meal $\pm$ SD	1.4 $\pm$ 0.6	2.1 $\pm$ 1.8	0.19
CROSS, ColoRectal Obstruction Scoring System.			

Patients with stents inserted for PAL were followed until their last clinical follow-up, telephone interview, death, or the study endpoint and assessed for complications related to stents, the period of stent patency, and the patency rate during the follow-up period. Stent patency was determined as patients without stent occlusion and still alive.

#### Statistical Analysis

Student *t* test was used for continuous data comparison. Fisher exact probability test and  $\chi^2$  test were used for comparison of categorical data. A *p* value of <0.05 was considered to be significant. All statistical analyses were performed using JMP 12.2 (SAS Institute Inc., Cary, NC, USA).

#### Definitions

We defined the patients receiving stents prior to elective surgery as the BTS group and the patients receiving stents for relief of symptoms as the PAL group.

Technical success was defined as successful stent placement in an appropriate site without complications. Clinical success was defined as effective decompression of the colon with resolution of obstructive symptoms within 72 h of stent placement [5]. The clinical success rate was calculated as the percentage of clinically successful cases relative to the technically successful cases. In cases where the patients underwent multiple stenting procedures, analysis was applied to the initial procedure.

The degree of obstruction was divided into two groups, complete and incomplete. Incomplete obstruction was defined as a narrow stool caliber or the ability to pass only small amounts of liquid stool or gas, and complete obstruction was defined as a lack of an endoscopically visible lumen or the inability to pass stool or gas [13, 14].

Performance status was recorded to determine the clinical condition according to the Eastern Cooperative Oncology Group performance status.

To evaluate the level of oral intake, we used the ColoRectal Obstruction Scoring System (CROSS), which assigns a point score based on the patient's oral intake level: CROSS 0, requiring continuous decompression; CROSS 1, no oral intake; CROSS 2, liquid or enteral nutrient intake; CROSS 3, soft solids, low residue, and full diet with symptoms of stricture; and CROSS 4, soft solids, low residue, and full diet without symptoms of stricture [15, 16].

## Results

### Patient Characteristics

Insertion of 18-mm-diameter stents was attempted in 33 cases (BTS in 25, PAL in 8), and insertion of 22-mm-diameter stents in 27 cases (BTS in 21, PAL in 6). Baseline patient characteristics are summarized in Table 1. Demographic features of both groups were not significantly different.

### Clinical Outcomes and Complications of SEMS Placement

Median procedure time was not significantly different between groups. Technical success rates of the 18- and 22-mm groups were 97% (32/33) and 96% (26/27), respectively. We were unable to pass the guidewire in a patient with ileocecal cancer in the 18-mm group, requiring urgent surgery. Additionally, a perforation related to stent insertion occurred in 1 patient with sigmoid colon cancer in the 22-mm group, and emergent surgery was performed. The perforation occurred at the anal side of the tumor and was caused by the delivery system. The clinical success rates were 100% (32/32) and 100% (26/26), respectively. Procedure time and the time to resumption of an oral diet are shown in Table 2.

The results of patients who underwent stent placement as a BTS are shown in Table 3. Abscess formation around the tumor occurred in 2 cases (one in the 18-mm group and the other in the 22-mm group). Both cases were treated with antibiotics and elective surgery was performed. The median time to surgery was significantly longer in the 18-mm group. The laparoscopic resection rate was high in both groups, and all indications for open surgery were related to tumor infiltration into the surrounding organs. There were no cases of inadequate colonic decompression. Perioperative complications occurred in



**Table 3.** Complications and clinical courses of the bridge-to-surgery cases

	18 mm (25 cases)	22 mm (21 cases)	<i>p</i>
Complication	1/25	2/21	
Perforation	0	1	
Migration	0	0	
Bleeding	0	0	
Occlusion	0	0	
Abscess	1	1	
Median time interval to operation (range), days	26 (18–41)	22 (10–30)	0.003 <sup>a</sup>
Laparoscopic resection rate, %	84 (21/25)	81 (17/21)	0.79
Stoma formation rate, %	0 (0/25)	4.8 (1/21)	0.46

<sup>a</sup> Statistically significant.

only 1 case. In this case, minor leakage occurred and was treated conservatively.

The results of the patients who underwent stent placement for PAL are shown in Table 4. Stent occlusion occurred in 1 patient in the 18-mm group at 73 days postoperatively due to tumor ingrowth and was treated with re-insertion of an additional 18-mm-diameter stent. Bleeding occurred in 1 case in the 22-mm group at 132 days postoperatively and was treated with surgical resection. Among patients in the 18-mm group, 87.5% maintained stent patency until death or the end of follow-up.

## Discussion

This is a single-center retrospective study comprising 60 patients with obstructive colorectal cancer who underwent SEMS placement as a BTS or for PAL. The technical and clinical success rates in our hospital were in line with a previous systematic review with medians of 96.2% (66–100%) and 92% (42–100%), respectively [5]. As the result of this study, 18-mm-diameter stents were feasible, compared with 22-mm-diameter stents.

### *Characteristics of 18-mm-Diameter Stents*

Advantages of the 18-mm-diameter stents include the decrease in mechanical stress and high versatility. Small-diameter stents exert less stress against the tumor and colonic wall. The small outer diameter of the 18-mm stent delivery system (9 Fr) allows easy insertion through the working channel (>3.0 mm) of the endoscope and allows for use of various endoscopes (PCF-Q260AI or GIF-

**Table 4.** Complications and clinical courses of the palliative-therapy cases

	18 mm (8 cases)	22 mm (6 cases)	<i>p</i>
Complication	1/8	1/6	
Perforation	0	0	
Migration	0	0	
Bleeding	0	1	
Occlusion	1	0	
Median period of stent patency (range), days	107.5 (26–194)	182 (13–481)	0.27
Stent patency rate, %	87.5 (7/8)	100 (6/6)	0.37

Q260J, Olympus). In contrast, when inserting 22-mm stents, we have to use conventional endoscopes (CF-H260 or CF-HQ290, Olympus) because the outer diameter of the delivery system is 10 Fr.

Disadvantages of the 18-mm-diameter stent include the risks of occlusion, migration, and inadequate decompression.

### *To Decrease Perforation Rate*

Stent-related perforation may result from 4 causes: (1) guidewire or catheter malpositioning, (2) dilation of the stricture before or after stent placement, (3) stent-induced perforation (tumor and non-tumor local perforation), and (4) proximal colonic distension because of inadequate colonic decompression or excessive air insufflation [17]. A meta-analysis revealed that the overall perforation rate with SEMS is 7.4% [18], but the prevalence of stent-related complications is likely to be underestimated because of subclinical perforations [9].

When using 18-mm-diameter stents, we can use slim scopes, which are flexible and easy to handle. It then becomes easier to maintain a good view of the tumor, especially in the bent positions such as in the sigmoid colon. It is also easier to determine the oral side and pass the guidewire and the catheter safely and precisely. Although there was no significant difference in procedure times, the procedure time of the 18-mm group was shorter than that of the 22-mm group. The reason is possibly that the procedures become easier with a greater choice of scopes.

Next, the strong stent radial force, which is the radially directed expanding force that maintains the luminal patency at the stricture once the stent is deployed, can cause perforation, and the large-diameter stent is associated with late perforations [19]. One meta-analysis reported that procedure-induced perforations accounted

for 19.4% of early perforations and that the remaining early perforation could be caused by failure of the colonic wall to adapt to the expanding forces of the stent [18]. In other words, perforation occurs due to the stent itself; thus, small stents may be advantageous as they create less disruption of the preexisting structure.

Finally, although there was concern regarding the potential for inadequate colonic decompression in the 18-mm group, 18-mm stents improved the CROSS score to the same degree as 22-mm stents in this study.

Therefore, 18-mm stents have the potential to decrease the perforation rate.

#### *BTS*

Although smaller-diameter stents may theoretically increase the migration and occlusion rates, there were no complications noted in the 18-mm group. Lee et al. [20] used the 18-mm-diameter Niti-S uncovered stent in 20 cases as a BTS. They reported no occlusions; migration occurred in 3 cases (15%) before surgery, although elective surgery was performed without additional treatment in all cases [20]. The reason why migration did not occur in our study may be that almost all our cases were complete obstructions. We recognize that it is undesirable to insert stents for incomplete obstruction prophylactically.

As 18-mm stents obtained enough decompression, laparoscopic resections were performed safely, and no cases required stoma formation because of inadequate decompression in either group. In our institution, the interval from SEMS insertion to surgery is longer than in a previous report [21]. The anastomotic leakage rate is higher when the interval is 1–9 days than 10 days or longer [22], although longer intervals may increase the stent-related complication rate. A certain period may allow for better recovery and optimal nutrition [15], and this optimal interval should be established in future studies. Though the interval of the 18-mm group was significantly longer, it is because the waiting time of the surgery has become longer in our hospital nowadays.

We conclude that 18-mm stents as a BTS can decrease the perforation rate without exacerbation of the oncological disease process, because they provide easy handling and lower mechanical stress. Therefore, the 18-mm-diameter stent is feasible and can be useful as a BTS. Larger and longer examinations are needed in the future to evaluate the impact on prognosis.

#### *PAL*

There were no complications, except for 1 case of occlusion in the 18-mm group. According to a previous report,

complications of SEMS placement for PAL happen more often in small-diameter stents [23]. In contrast, a prospective study showed complications and long-term patency were not significantly different in varying stent diameters [24]. Our median patency periods are in line with those of previous reports (90–204 days) [23, 24]. Although there were no significant differences in the patency periods between the 18-mm- and 22-mm-diameter groups in our study, the number of cases is small and follow-up period is short. Then, larger and longer studies are necessary.

#### *Optimal Diameter of SEMS*

Our obstruction and migration rate of the 18-mm group were totally 4.8 and 0%, which is in line with a previous report [25]. In addition, 18-mm stents could get adequate decompression. Actually, no perforations occurred with the Niti-S uncovered 18-mm-diameter stents in our study (33 cases) and Lee et al.'s study (39 cases) [20]. Therefore, we see that 18-mm-diameter stents can be optimal, especially as a BTS.

#### *Limitation*

Our study has several limitations. First, these study outcomes were examined in a single institution retrospectively, and the number of subjects was small. Second, it is necessary to consider the possibility that there is improvement of the operator's technique because the periods of the 18-mm group and 22-mm group are different. A prospective large study is expected to exclude these biases. More than anything, it is necessary to examine the long-term oncological prognosis in 18-mm-diameter stent cases.

#### **Conclusion**

As a BTS, 18-mm-diameter stents are feasible because the effectiveness is not inferior to that of 22-mm-diameter stents in clinical practice. Furthermore, 18-mm-diameter stents may be safer to place, because they are easy to handle and their mechanical stress is small. Moreover, they have the potential to decrease perforation rates and improve long-term prognoses.

For PAL, there was no significant difference in the stent patency period between the stent types. Therefore, 18-mm-diameter stents are feasible. However, the number of cases is small, and follow-up periods were very short. Further study is necessary to confirm the feasibility of 18-mm-diameter stents.

## Acknowledgement

Ishii et al. [26] have already previously reported the data regarding BTS cases in this article in Japanese. Some data are based on Ishii et al.'s data. We added additional cases and investigated further. In addition, because this article was to be written in English, we authored the manuscript.

## Disclosure Statement

The authors have no conflicts of interest to declare.

## Author Contributions

S.O., T.I., K.M., and Y.Y. designed the study. S.O. wrote the initial draft of the manuscript. T.I. and K.M. contributed to analysis and interpretation of data, and assisted in the preparation of the manuscript. Y.N., K.H., T.A., T.S., S.U., Y.U., Y.Y., and M.K. contributed to data collection and interpretation, and critically reviewed the manuscript. The final version of the manuscript was approved by all authors.

## References

- 1 Deans GT, Krukowski ZH, Irwin ST: Malignant obstruction of the left colon. *Br J Surg* 1994;81:1270–1276.
- 2 Willett C, Tepper JE, Cohen A, Orlow E, Welch C: Obstructive and perforative colonic carcinoma: patterns of failure. *J Clin Oncol* 1985;3:379–384.
- 3 Barillari P, Aurello P, De Angelis R, Valabrega S, Ramacciato G, D'Angelo F, Fegiz G: Management and survival of patients affected with obstructive colorectal cancer. *Int Surg* 1992;77:251–255.
- 4 Pearce NW, Scott SD, Karran SJ: Timing and method of reversal of Hartmann's procedure. *Br J Surg* 1992;79:839–841.
- 5 Watt AM, Faragher IG, Griffin TT, Rieger NA, Maddern GJ: Self-expanding metallic stents for relieving malignant colorectal obstruction: a systematic review. *Ann Surg* 2007;246:24–30.
- 6 Zhao XD, Cai BB, Cao RS, Shi RH: Palliative treatment for incurable malignant colorectal obstructions: a meta-analysis. *World J Gastroenterol* 2013;19:5565–5574.
- 7 Alcantara M, Serra-Aracil X, Falco J, Mora L, Bombardo J, Navarro S: Prospective, controlled, randomized study of intraoperative colonic lavage versus stent placement in obstructive left-sided colonic cancer. *World J Surg* 2011;35:1904–1910.
- 8 Gorissen KJ, Tuynman JB, Fryer E, Wang L, Uberoi R, Jones OM, Cunningham C, Lindsey I: Local recurrence after stenting for obstructing left-sided colonic cancer. *Br J Surg* 2013;100:1805–1809.
- 9 Sloothaak DA, van den Berg MW, Dijkgraaf MG, Fockens P, Tanis PJ, van Hooft JE, Bemelman WA: Oncological outcome of malignant colonic obstruction in the Dutch Stent-In 2 trial. *Br J Surg* 2014;101:1751–1757.
- 10 Tung KL, Cheung HY, Ng LW, Chung CC, Li MK: Endo-laparoscopic approach versus conventional open surgery in the treatment of obstructing left-sided colon cancer: long-term follow-up of a randomized trial. *Asian J Endosc Surg* 2013;6:78–81.
- 11 van Hooft JE, van Halsema EE, Vanbiervliet G, Beets-Tan RG, DeWitt JM, Donnellan F, Dumonceau JM, Glynne-Jones RG, Hassan C, Jimenez-Perez J, Meisner S, Muthusamy VR, Parker MC, Regimbeau JM, Sabbagh C, Sagar J, Tanis PJ, Vandervoort J, Webster GJ, Manes G, Barthet MA, Repici A: Self-expandable metal stents for obstructing colonic and extracolonic cancer: European Society of Gastrointestinal Endoscopy (ESGE) Clinical Guideline. *Endoscopy* 2014;46:990–1053.
- 12 Matsuda A, Miyashita M, Matsumoto S, Matsutani T, Sakurazawa N, Takahashi G, Kishi T, Uchida E: Comparison of long-term outcomes of colonic stent as "bridge to surgery" and emergency surgery for malignant large-bowel obstruction: a meta-analysis. *Ann Surg Oncol* 2015;22:497–504.
- 13 Baron TH, Dean PA, Yates MR 3rd, Canon C, Koehler RE: Expandable metal stents for the treatment of colonic obstruction: techniques and outcomes. *Gastrointest Endosc* 1998;47:277–286.
- 14 Repici A, Adler DG, Gibbs CM, Malesci A, Preatoni P, Baron TH: Stenting of the proximal colon in patients with malignant large bowel obstruction: techniques and outcomes. *Gastrointest Endosc* 2007;66:940–944.
- 15 Saito S, Yoshida S, Isayama H, Matsuzawa T, Kuwai T, Maetani I, Shimada M, Yamada T, Tomita M, Koizumi K, Hirata N, Kanazawa H, Enomoto T, Sekido H, Saida Y: A prospective multicenter study on self-expandable metallic stents as a bridge to surgery for malignant colorectal obstruction in Japan: efficacy and safety in 312 patients. *Surg Endosc* 2016;30:3976–3986.
- 16 Colonic Stent Safe Procedure Research Group. [http://colon-stent.com/001\\_main-page\\_en.html](http://colon-stent.com/001_main-page_en.html).
- 17 Baron TH, Wong Kee Song LM, Repici A: Role of self-expandable stents for patients with colon cancer (with videos). *Gastrointest Endosc* 2012;75:653–662.
- 18 van Halsema EE, van Hooft JE, Small AJ, Baron TH, Garcia-Cano J, Cheon JH, Lee MS, Kwon SH, Mucci-Hennekinne S, Fockens P, Dijkgraaf MG, Repici A: Perforation in colorectal stenting: a meta-analysis and a search for risk factors. *Gastrointest Endosc* 2014;79:970–982.e7; quiz 983.e2, 983.e5.
- 19 van Hooft JE, Fockens P, Marinelli AW, Bossuyt PM, Bemelman WA: Premature closure of the Dutch Stent-in I study. *Lancet* 2006;368:1573–1574.
- 20 Lee KM, Shin SJ, Hwang JC, Cheong JY, Yoo BM, Lee KJ, Hahm KB, Kim JH, Cho SW: Comparison of uncovered stent with covered stent for treatment of malignant colorectal obstruction. *Gastrointest Endosc* 2007;66:931–936.
- 21 De Ceglie A, Filiberti R, Baron TH, Ceppi M, Conio M: A meta-analysis of endoscopic stenting as bridge to surgery versus emergency surgery for left-sided colorectal cancer obstruction. *Crit Rev Oncol Hematol* 2013;88:387–403.
- 22 Lee GJ, Kim HJ, Baek JH, Lee WS, Kwon KA: Comparison of short-term outcomes after elective surgery following endoscopic stent insertion and emergency surgery for obstructive colorectal cancer. *Int J Surg* 2013;11:442–446.
- 23 Small AJ, Coelho-Prabhu N, Baron TH: Endoscopic placement of self-expandable metal stents for malignant colonic obstruction: long-term outcomes and complication factors. *Gastrointest Endosc* 2010;71:560–572.
- 24 Im JP, Kim SG, Kang HW, Kim JS, Jung HC, Song IS: Clinical outcomes and patency of self-expanding metal stents in patients with malignant colorectal obstruction: a prospective single center study. *Int J Colorectal Dis* 2008;23:789–794.
- 25 Gianotti L, Tamini N, Nespoli L, Rota M, Bolzonaro E, Frego R, Redaelli A, Antolini L, Ardito A, Nespoli A, Dinelli M: A prospective evaluation of short-term and long-term results from colonic stenting for palliation or as a bridge to elective operation versus immediate surgery for large-bowel obstruction. *Surg Endosc* 2013;27:832–842.
- 26 Ishii T, Minaga K, Ogawa S, Taki M, Yabuuchi Y, Matsumoto H, Akamatsu T, Seta T, Uenoyama Y, Yamashita Y: Usefulness of the 18-mm-diameter Niti-S stent in colonic stenting as a bridge to surgery in patients with obstructive colorectal cancer. *Gastroenterol Endosc* 2016;58:121–129.

## Magnifying Narrow Band Imaging (NBI) for the Diagnosis of Localized Colorectal Lesions Using the Japan NBI Expert Team (JNET) Classification

Yoriaki Komeda<sup>a</sup> Hiroshi Kashida<sup>a</sup> Toshiharu Sakurai<sup>a</sup> Yutaka Asakuma<sup>a</sup>  
George Tribonias<sup>a</sup> Tomoyuki Nagai<sup>a</sup> Masashi Kono<sup>a</sup> Kosuke Minaga<sup>a</sup>  
Mamoru Takenaka<sup>a</sup> Tadaaki Arizumi<sup>a</sup> Satoru Hagiwara<sup>a</sup> Shigenaga Matsui<sup>a</sup>  
Tomohiro Watanabe<sup>a</sup> Naoshi Nishida<sup>a</sup> Takaaki Chikugo<sup>b</sup> Yasutaka Chiba<sup>c</sup>  
Masatoshi Kudo<sup>a</sup>

Departments of <sup>a</sup>Gastroenterology and Hepatology and <sup>b</sup>Pathology, Kindai University Faculty of Medicine, and  
<sup>c</sup>Clinical Research Center, Kindai University Hospital, Osaka-Sayama, Japan

### Keywords

Narrow band imaging · Japan NBI Expert Team (JNET) classification · NBI International Colorectal Endoscopic (NICE) classification · Colorectal tumors · Magnifying endoscopy

### Abstract

**Objective:** The Japan NBI Expert Team (JNET) proposed a new narrow band imaging (NBI) classification system for colorectal tumors in June 2014. In this classification system, types 1, 2A, 2B, and 3 correspond to hyperplastic polyps (HPs) including sessile serrated polyps (SSPs), low-grade dysplasia (LGD), high-grade dysplasia (HGD) to shallow submucosal invasive (SM-s) carcinomas, and deep submucosal invasive (SM-d) carcinomas, respectively. **Methods:** To validate this system, we performed a retrospective image evaluation study, in which 199 colorectal tumors previously assessed by NBI magnifying endoscopy were classified by 3 blinded experienced colonoscopists using the JNET system. The results

were compared with the final pathological diagnoses to determine the JNET classification's accuracy. The interobserver agreement was calculated, and the intraobserver agreement was assessed after 6 months. **Results:** The final pathological diagnoses identified 14 HPs/SSPs, 127 LGDs, 22 HGDs, 19 SM-s carcinomas, and 17 SM-d carcinomas. The respective sensitivities, specificities, positive predictive value, negative predictive value, and accuracies were as follows: Type 1, 85.7, 99.5, 92.3, 98.9, and 98.5%; Type 2A, 96.0, 81.9, 90.3, 92.1, and 90.9%; Type 2B, 75.6%, 90.5, 67.3, 93.4, and 87.4%; and Type 3, 29.4%, 100, 100, 93.8, and 94.0%. The interobserver agreement and the intraobserver agreement were moderate ( $\kappa$  value: 0.52) and excellent ( $\kappa$  value: 0.88), respectively. Lesions presenting as Type 2B during NBI comprised a range of colorectal tumors, including HGDs, SM-s, and SM-d. **Conclusions:** The JNET classification was useful for the diagnosis of HPs/SSPs, LGDs, and SM-d, but not SM-s lesions. For low-confidence cases, magnified chromoendoscopy is recommended to ensure correct diagnoses.

© 2017 S. Karger AG, Basel



## Introduction

Narrow band imaging (NBI), which visualizes vessel and surface patterns in detail, is generally considered to provide useful diagnostic information about gastrointestinal lesions identified via endoscopy [1]. Several studies have indicated that NBI observations of colorectal polyps are very useful, accurate predictors of histology [2–6]. Although previous studies [2–6] addressed the utility of NBI observations (i.e., vascular and surface patterns) for the endoscopic diagnosis of colorectal tumors, a universal definitive classification system has not yet been established. The NBI International Colorectal Endoscopic (NICE) classification, published by the Colon Tumor NBI Interest Group (CTNIG), uses the colors, vessels, and surface patterns observed during endoscopy to classify the results of nonmagnifying evaluations [7, 8]. However, colonoscopists often encounter difficulties with cases classified as NICE Type 2, as this category includes a variety of pathologies ranging from low-grade dysplasia (LGD) to shallow submucosal invasive cancer (SM-s) [9, 10]; the former is suitable for endoscopic mucosal resection (EMR), whereas the latter is indicated for endoscopic submucosal dissection (ESD) [11].

The Japan NBI Expert Team (JNET), which comprises 38 members specialized in colonoscopy, attempted to establish a new NBI classification system for colorectal tumor diagnosis that would overcome the limitations of the NICE classification system. This novel NBI magnifying classification system for colorectal tumors, the JNET classification, was proposed in June 2014 [11]. The JNET classification uses magnifying NBI observations with a focus on vessel and surface patterns to diagnose colorectal tumors as Types 1, 2A, 2B, and 3. Type 1 is characterized by an invisible vessel pattern and a surface pattern comprising dark and white spots, similar to the surrounding normal mucosa. Type 2A is defined as vessels of a regular caliber and distribution (meshed/spiral pattern) and a regular (tubular/branched/papillary) surface pattern. Type 2B is defined as vessels with a variable caliber and irregular distribution and an obscure surface pattern. Type 3 is characterized as a vessel pattern comprising areas of loose or interrupted thick vessels and a surface pattern of amorphous areas (Fig. 1). Types 1, 2A, 2B, and 3 correlate with the pathological diagnoses of hyperplastic polyp (HP) and sessile serrated polyp (SSP), LGD, high-grade dysplasia (HGD) and SM-s cancer (T1a; <1,000  $\mu\text{m}$ ), and deep submucosal invasive cancer (SM-d: T1b;  $\geq 1000 \mu\text{m}$ ), respectively [11]. The NICE and JNET classifications differ most significantly in that Type 2 from

the former is subdivided into Types 2A and 2B in the latter, thus allowing the discrimination of LGD and HGD-SM-s lesions. To evaluate the usefulness of the JNET classification, we conducted a retrospective study to evaluate the interobserver and intraobserver agreement among 3 observers and, thus, determine the usefulness of the JNET classification.

## Methods

### Study Design

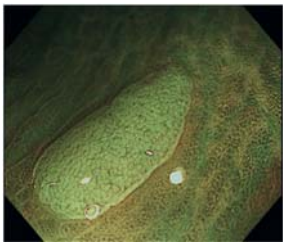
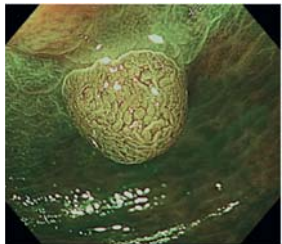
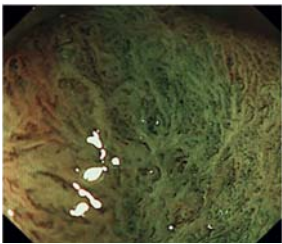

We conducted a retrospective image evaluation study of digital files containing endoscopic images of localized colorectal neoplastic lesions that had been treated with EMR, ESD, or surgical operation from April 2010 to April 2015. Endoscopic images were taken using magnified NBI. The exclusion criteria were advanced colorectal adenocarcinoma, neoplastic lesions associated with inflammatory bowel disease, and polyposis. In addition, colorectal tumors >5 cm were excluded from this study because a precise NBI diagnosis is difficult in such cases. A total of 199 lesions were randomly selected from among 510 colorectal neoplastic lesions subjected to NBI observation at Kindai University Hospital. Per lesion, 1–4 representative NBI magnifying endoscopy images were selected by Y.K. and 3 other observers (H.K., T.S., and Y.A.) who were blinded to the pathological, white light, and chromoendoscopic findings and the clinical information. The 199 lesions were classified according to the JNET system and evaluated by the 3 observers. All evaluated images were obtained via magnifying colonoscopy (device: CF-H260AZI, PCF-260AZI; Olympus Optical Co., Tokyo, Japan).

Initially, the 3 experienced colonoscopists (H.K., T.S., and Y.A.; NBI diagnosis >1,000 cases over >5 years) independently diagnosed the images obtained from the 199 cases. If the individual diagnostic interpretations differed, the 3 reviewers discussed the case until a consensus was obtained. For cases in which a diagnosis of JNET classification was difficult because of inconsistent interpretations between the vessel and surface patterns, the 3 reviewers determined the final JNET diagnosis via consensus after discussion. The consensus NBI diagnosis was then compared with the final pathological diagnosis. Histological diagnoses were reviewed by a pathologist (T.T.) with expertise in the field of colorectal tumors and blinded to the NBI findings. Histopathology was defined according to the World Health Organization classification system [12]. Initially, the interobserver agreement among the 3 observers was calculated. Six months later, the intraobserver agreement was calculated for a single observer (H.K.).

### Statistical Analysis

The sensitivity, specificity, positive predictive value (PPV), negative predictive value (NPV), and accuracy were calculated for each classification category. The interobserver agreement and the intraobserver agreement were calculated using  $\kappa$  coefficients, using the following arbitrary interpretation reported by Landis and Koch [13]: poor, 0–0.20; fair, 0.21–0.40; moderate, 0.41–0.60; substantial, 0.61–0.80; and excellent, 0.81–1.00.



	Type 1	Type 2A	Type 2B	Type 3
Vessel pattern	Invisible <sup>1</sup>	Regular caliber <sup>2</sup> Regular distribution (meshed/spiral pattern)	Variable caliber Irregular distribution	Loose vessel areas Interruption of thick vessels
Surface pattern	Regular dark or white spots Similar to surrounding normal mucosa	Regular (tubular/branched/papillary)	Irregular or obscure	Amorphous area
Most likely histology	Hyperplastic polyp/ Sessile serrated polyp	Low-grade dysplasia	High-grade dysplasia/ Shallow submucosal invasive cancer <sup>3</sup>	Deep submucosal invasive cancer
Endoscopic image				

**Fig. 1.** The Japan Narrow Band Imaging (NBI) Expert Team (JNET) classification. <sup>1</sup> If visible, the caliber in the lesion is similar to that of the surrounding normal mucosa. <sup>2</sup> Microvessels are often distributed in a punctate pattern, and well-ordered reticular or spiral vessels may not be observed in depressed lesions. <sup>3</sup> Deep submucosal invasive cancer may be included. The NBI images corresponding to each JNET type were obtained from patients recruited for this study.

**Table 1.** The relationship between JNET classification and histology

JNET classification	Histology				
	HP/SSP	LGD	HGD	SM-s	SM-d
Type 1 ( <i>n</i> = 13)	12 (92.3)	1 (7.7)			
Type 2A ( <i>n</i> = 135)	2 (1.5)	122 (90.4)	8 (5.9)	2 (1.5)	1 (0.7)
Type 2B ( <i>n</i> = 46)		4 (8.7)	14 (30.4)	17 (37.0)	11 (23.9)
Type 3 ( <i>n</i> = 5)					5 (100)

HP, hyperplastic polyp; SSP, sessile serrated polyp; LGD, low-grade dysplasia; HGD, high-grade dysplasia; SM-s (T1a), shallow submucosal invasive cancer; SM-d (T1b), deep submucosal invasive cancer.

## Results

### JNET Classification

As shown in Figure 1, all 199 colorectal tumors enrolled in this study were classified as JNET Type 1, Type 2A, Type 2B, or Type 3, as has been previously described [11]. Representative NBI pictures from this study that correspond to each JNET type are shown in Figure 1.

### Sensitivity, Specificity, PPV, NPV, and Accuracy of JNET

The pathological analysis of 199 lesions revealed 14 cases of HP/SSP, 127 cases of LGD, 22 cases of HGD, 19 cases of SM-s, and 17 cases of SM-d. Table 1 demonstrates the relationships between JNET categories and histology, whereas Table 2 presents the diagnostic characteristics for each category. The sensitivity, specificity, PPV, NPV, and accuracy for Type 1 were 85.7% (12/14), 99.5% (184/185),

**Table 2.** Performance characteristics (95% CI) of each type in JNET classification

	Sensitivity, %	Specificity, %	PPV, %	NPV, %	Accuracy, %
Type 1	85.7 (57.2–98.2)	99.5 (97.0–100.0)	92.3 (64.0–99.8)	98.9 (64.0–99.8)	98.5 (95.7–99.7)
Type 2A	96.0 (91.0–98.7)	81.9 (71.1–90.0)	90.3 (84.1–94.8)	92.1 (82.7–97.4)	90.9 (86.1–94.6)
Type 2B	75.6 (59.7–87.6)	90.5 (84.8–94.6)	67.3 (52.0–80.5)	93.4 (88.3–96.8)	87.4 (82.0–91.7)
Type 3	29.4 (10.3–56.0)	100 (98.0–100)	100 (47.8–100)	93.8 (89.4–96.8)	94.0 (89.7–96.8)

CI, confidence interval; PPV, positive predictive value; NPV, negative predictive value.

92.3% (12/13), 98.9% (184/186), and 98.5% (196/199), respectively. The corresponding values for Type 2A were 96.0% (122/127), 81.9% (59/72), 90.3% (122/135), 92.1% (59/64), and 90.9% (181/199), respectively; for Type 2B 75.6% (31/41), 90.5% (143/153), 67.3% (143/153), 93.4% (143/153), and 87.4% (174/199), respectively; and for Type 3 29.4% (5/17), 100% (182/182), 100% (5/5), 93.8% (182/194), and 94.0% (187/199), respectively.

#### *Interobserver and Intraobserver Agreement for the JNET Classification*

Moderate interobserver agreement was observed among the 3 observers (vessel/surface pattern  $\kappa$  values = 0.52/0.52). The complete concordance rate for vessel and surface patterns among the 3 observers was 67%. In contrast, the intraobserver agreement was excellent (vessel/surface pattern  $\kappa$  values = 0.87/0.88).

## Discussion

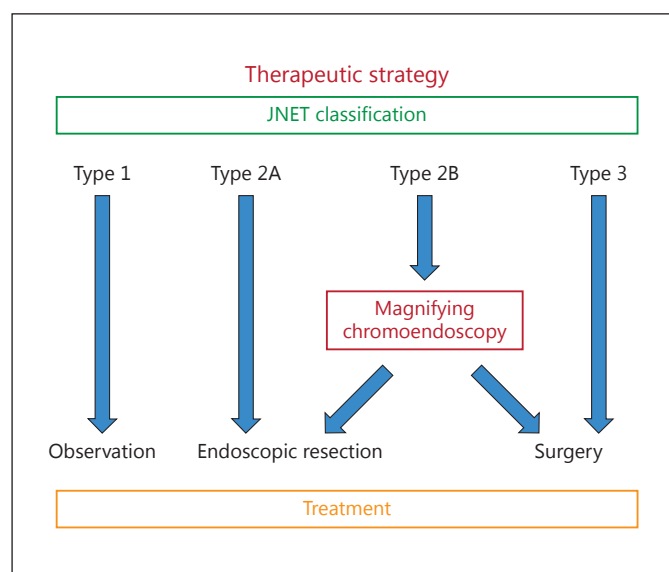
In this study, we obtained preliminary data regarding the clinical utility of the JNET classification system for the diagnosis of colorectal tumors by classifying 199 colorectal lesions through a review of magnifying NBI images and a comparison with pathological findings. The NBI diagnoses of JNET Type 1 and Type 2A correlated strongly with the HP-SSP and LGD types, respectively, suggesting that these lesion types could be diagnosed using the JNET classification alone. In contrast, pathological examination revealed that JNET Type 2B included a wide variety of colorectal tumors ranging from LGD to SM-d lesions. Therefore, a careful consideration of the endoscopic treatment strategy would be required for a diagnosed JNET Type 2B lesion. Similarly, the diagnosis of SM-d lesions according to the JNET classification alone was not satisfactory, as these lesions could be classified as either JNET Type 3 or Type 2B. Conversely, JNET Type 3 cor-

related strongly with SM-d lesions. Taken together, these data suggest that the JNET classification system is a useful tool for the diagnosis of HP-SSP, LGD, and SM-d lesions.

Consistent with a previous report by Sumimoto et al. [14], the sensitivity, specificity, PPV, NPV, and accuracy of the JNET Type 1 classification were satisfactory. These parameters were similarly high for JNET Type 2A, suggesting that HP-SSP and LGD lesions can be accurately diagnosed using the JNET classification alone. The specificity and PPV of the JNET Type 3 classification were both 100%, indicating that JNET Type 3 correlates with the pathological diagnosis of SM-d lesions that require surgical resection. In contrast, the sensitivity, specificity, PPV, NPV, and accuracy were unsatisfactory for Type 2B lesions, as pathological analysis revealed that this category included various types of colorectal tumors while excluding HP/SSP lesions. Therefore, subsequent magnifying chromoendoscopy is strongly recommended for lesions within this category.

Studies have been performed to evaluate the usefulness of the NICE classification for the diagnosis of colorectal tumors since its initial proposal in 2009 [7, 8]. Hattori et al. [9] reported that the risk of failure to detect diminutive and small colorectal invasive cancers using the “resect and discard” strategy might be avoided by using the NICE classification. In another multicenter study, Rees et al. [10] provided evidence that an NBI-assisted optical diagnosis could not currently be recommended for the diagnosis of colorectal polyps in the absence of NBI expertise. These negative findings might be attributable to the inclusion of a wide range of pathologies (from LGD to SM-s [T1a]) within the NICE Type 2 classification.

Therefore, colonoscopists have often encountered difficulties regarding the application of NICE classifications to the endoscopic diagnosis of colorectal tumors, including difficulties regarding the selection of an appropriate endoscopic resection procedure (i.e., choosing between EMR, which is mainly intended for LGD and HGD le-



**Fig. 2.** A therapeutic strategy based on the JNET classification and magnifying chromoendoscopy.

sions, and ESD, which is intended for lesions from HGD to SM-s [T1a]). The JNET classification, which includes NBI magnifying observations, was proposed to resolve these problems. The use of magnifying endoscopy to subdivide the NICE Type 2 category into the JNET Type 2A and Type 2B categories promoted the diagnosis of LGD lesions in both the present study and a previous study [11]. It should be noted, however, that the diagnostic value of the JNET classification is unsatisfactory, especially regarding JNET Type 2A and 2B. Therefore, it is too early to determine the superiority of the JNET classification over the NICE classification until the results of clinical trials that directly address the utilities and accuracies of both classifications are available.

Consistent with the previous study [11], our results support the superiority of the JNET classification over the NICE classification. The utilization of magnifying NBI might partially explain the improved diagnostic accuracy of the JNET classification for LGD lesions. Magnifying endoscopy can optically zoom up to 100 times in real time and reveal detailed pit pattern characteristics, compared with the conventional observations used to differentiate between non-neoplastic polyps and neoplastic colorectal polyps [15, 16].

To our knowledge, this is the first study to demonstrate interobserver and intraobserver colorectal tumor diagnosis agreement regarding the JNET classification.

Although the interobserver agreement was moderate, the intraobserver agreement was excellent. This might be because a significant proportion of JNET Type 2A and Type 2B lesions comprise uncertain or borderline lesions, leading to highly variable diagnoses. The presence of Type 2A–2B borderline lesions might affect not only the interobserver agreement, but also the specificity and sensitivity. Therefore, it was difficult to definitively diagnose a significant proportion of colorectal tumors in this study as Type 2A or Type 2B, which may contribute to the low specificity of Type 2A. The high sensitivities of JNET Type 1 and Type 2A in this study suggest that these types correlate strongly with HP-SSP and LGD, respectively, and can, therefore, be used alone to diagnose these lesions. In contrast, the pathological examination revealed that JNET Type 2B included a wide variety of colorectal tumors, and, therefore, could not specifically indicate HGD or SM-d. Similarly, the diagnosis of SM-d lesions using the JNET classification alone was unsatisfactory, as these lesions exhibit characteristics of both Type 3 and Type 2B. However, JNET Type 3 correlated strongly with SM-d lesions. Taken together, these data suggest that the JNET classification system is a useful tool for the diagnosis of HP/SSP, LGD, and SM-d lesions.

JNET Type 2A and Type 2B had a relatively low specificity and sensitivity, respectively. We attribute this to the fact that JNET Type 2B lesions comprise a variety of colorectal tumors and that a significant proportion of colorectal tumors exhibit Type 2A–2B borderline NBI findings. Therefore, colonoscopists should perform magnifying chromoendoscopy followed by a pit pattern diagnosis for these uncertain 2A–2B borderline lesions. Based on the findings presented in this study, we have devised a flowchart of our strategy, for the selection of endoscopic colorectal tumor treatment, which employs both the JNET classification and chromoendoscopy (Fig. 2).

It should be noted that prospective and multicenter studies that address the usefulness of both the JNET classification and magnifying chromoendoscopy for the diagnosis of colorectal tumors will be required to confirm this concept.

This study has some notable limitations. First, the study was conducted using pre-existing digital image files from medical records. Second, it was conducted at a single center, and JNET classification was performed only by expert colonoscopists. Third, only a few JNET Type 3 cases were included. Finally, this study did not include a comparison with other classification systems, such as the Sano, Hiroshima, Showa, and Jikei classifications [17–20].

In conclusion, the JNET classification is a valid tool for predicting the histology of localized colorectal lesions. A JNET diagnosis of Type 1, 2A, or 3 corresponds to a pathological diagnosis of a HP/SSP, LGD, or SM-d lesion, respectively, without requiring magnifying chromoendoscopy. However, magnifying chromoendoscopy is strongly recommended for the accurate diagnosis of Type 2B and uncertain 2A–2B borderline lesions. Multicenter prospective studies to validate our conclusions should be conducted in the near future.

## Statement of Ethics

Ethical permission for this study was granted by the Review Board of the Kindai University Hospital (approval No. 28-220). The procedures followed were in accordance with the guidelines of the World Medical Association's Declaration of Helsinki (1964, and its later amendments).

## Disclosure Statement

The authors have no conflicts of interest to declare.

## References

- 1 Gono K, Obi T, Yamaguchi M, et al: Appearance of enhanced tissue features in narrow-band endoscopic imaging. *J Biomed Opt* 2004;9:568–577.
- 2 Machida H, Sano Y, Hamamoto Y, et al: Narrow-band imaging in the diagnosis of colorectal mucosal lesions: a pilot study. *Endoscopy* 2004;36:1094–1098.
- 3 Hirata M, Tanaka S, Oka S, et al: Evaluation of microvessels in colorectal tumors by narrow band imaging magnification. *Gastrointest Endosc* 2007;66:945–952.
- 4 Hirata M, Tanaka S, Oka S, et al: Magnifying endoscopy with narrow band imaging for diagnosis of colorectal tumors. *Gastrointest Endosc* 2007;65:988–995.
- 5 East JE, Suzuki N, Bassett P, et al: Narrow band imaging with magnification for the characterization of small and diminutive colonic polyps: pit pattern and vascular pattern intensity. *Endoscopy* 2008;40:811–817.
- 6 Wada Y, Kashida H, Kudo SE, et al: Diagnostic accuracy of pit pattern and vascular pattern analyses in colorectal lesions. *Dig Endosc* 2010;22:192–199.
- 7 Hewett DG, Kaltenbach T, Sano Y, et al: Validation of a simple classification system for endoscopic diagnosis of small colorectal polyps using narrow-band imaging. *Gastroenterology* 2012;143:599–607.
- 8 Hayashi N, Tanaka S, Hewett DG, et al: Endoscopic prediction of deep submucosal invasive carcinoma: validation of the Narrow-Band Imaging International Colorectal Endoscopic (NICE) classification. *Gastrointest Endosc* 2013;78:625–632.
- 9 Hattori S, Iwatate M, Sano W, et al: Narrow-band imaging observation of colorectal lesions using NICE classification to avoid discarding significant lesions. *World J Gastrointest Endosc* 2014;6:600–605.
- 10 Rees CJ, Rajasekhar PT, Wilson A, et al: Narrow band imaging optical diagnosis of small colorectal polyps in routine clinical practice: the Detect Inspect Characterise Resect and Discard 2 (DISCARD 2) study. *Gut* 2016, DOI: 10.1136/gutjnl-2015-310584.
- 11 Sano Y, Tanaka S, Kudo SE, et al: Narrow-band imaging (NBI) magnifying endoscopic classification of colorectal tumors proposed by the Japan NBI Expert Team. *Dig Endosc* 2016;28:526–33.
- 12 Bosman FT, Carneiro F, Hruban RH, et al (eds): WHO Classification of Tumors of the Digestive System, ed 4. Lyon, IARC, 2010.
- 13 Landis R, Koch GG: The measurement of observer agreement for categorical data. *Biometrics* 1977;33:159–174.
- 14 Sumimoto K, Tanaka S, Shigita K, et al: Clinical impact and characteristics of the narrow-band imaging magnifying endoscopic classification of colorectal tumors proposed by the Japan NBI Expert Team. *Gastrointest Endosc* 2016, DOI: 10.1016/j.gie.2016.07.035.
- 15 Fu KI, Sano Y, Kato S, et al: Chromoendoscopy using indigo carmine dye spraying with magnifying observation is the most reliable method for differential diagnosis between non-neoplastic and neoplastic colorectal lesions: a prospective study. *Endoscopy* 2004;36:1089–1093.
- 16 Matsuda T, Fujii T, Saito Y, et al: Efficacy of the invasive/non-invasive pattern by magnifying chromoendoscopy to estimate the depth of invasion of early colorectal neoplasms. *Am J Gastroenterol* 2008;103:2700–2706.
- 17 Sano Y, Ikematsu H, Fu KI, et al: Meshed capillary vessels by use of narrow-band imaging for differential diagnosis of small colorectal polyps. *Gastrointest Endosc* 2009;69:278–283.
- 18 Kanao H, Tanaka S, Oka S, et al: Narrow-band imaging magnification predicts the histology and invasion depth of colorectal tumors. *Gastrointest Endosc* 2009;69:631–636.
- 19 Wada Y, Kudo S, Kashida H, et al: Diagnosis of colorectal lesions with the magnifying narrow-band imaging system. *Gastrointest Endosc* 2009;70:522–531.
- 20 Nikami T, Saito S, Tajiri H, et al: The evaluation of histological atypia and depth of invasion of colorectal lesions using magnified endoscopy with narrow-band imaging. *Gastroenterol Endosc* 2009;51:10–19.

# Characterization of Pancreatic Tumors with Quantitative Perfusion Analysis in Contrast-Enhanced Harmonic Endoscopic Ultrasonography

Shunsuke Omoto<sup>a</sup> Mamoru Takenaka<sup>a</sup> Masayuki Kitano<sup>d</sup> Takeshi Miyata<sup>a</sup>

Ken Kamata<sup>a</sup> Kosuke Minaga<sup>a</sup> Tadaaki Arizumi<sup>a</sup> Kentaro Yamao<sup>a</sup>

Hajime Imai<sup>a</sup> Hiroki Sakamoto<sup>a</sup> Yogesh Harwani<sup>a</sup> Toshiharu Sakurai<sup>a</sup>

Tomohiro Watanabe<sup>a</sup> Naoshi Nishida<sup>a</sup> Yoshifumi Takeyama<sup>b</sup>

Yasutaka Chiba<sup>c</sup> Masatoshi Kudo<sup>a</sup>

Departments of <sup>a</sup>Gastroenterology and Hepatology and <sup>b</sup>Surgery, and <sup>c</sup>Division of Biostatistics, Clinical Research Center, Kindai University Faculty of Medicine, Osaka-Sayama, and <sup>d</sup>Second Department of Internal Medicine, Wakayama Medical University School of Medicine, Wakayama, Japan

## Keywords

Contrast-enhanced harmonic endoscopic ultrasonography · Quantitative perfusion analysis · Pancreatic carcinoma · Time-intensity curve

## Abstract

**Objectives:** This study evaluated whether quantitative perfusion analysis with contrast-enhanced harmonic (CH) endoscopic ultrasonography (EUS) characterizes pancreatic tumors, and compared the hemodynamic parameters used to diagnose pancreatic carcinoma. **Methods:** CH-EUS data from pancreatic tumors of 76 patients were retrospectively analyzed. Time-intensity curves (TIC) were generated to depict changes in signal intensity over time, and 6 parameters were assessed: baseline intensity, peak intensity, time to peak, intensity gain, intensity at 60 s ( $I_{60}$ ), and reduction rate. These parameters were compared between pancreatic carcinomas ( $n = 41$ ), inflammatory pseudotumors ( $n = 14$ ), pancreatic neuroendocrine tumors ( $n = 14$ ), and other tumors ( $n = 7$ ). All

6 TIC parameters and subjective analysis for diagnosing pancreatic carcinoma were compared. **Results:** Values of peak intensity and  $I_{60}$  were significantly lower and time to peak was significantly longer in the groups with pancreatic carcinomas than in the other 3 tumor groups ( $p < 0.05$ ). Reduction rate was significantly higher in pancreatic carcinomas than in pancreatic neuroendocrine tumors ( $p < 0.05$ ). Areas under the receiver-operating characteristic curves for the diagnosis of pancreatic carcinoma using subjective analysis, baseline intensity, peak intensity, intensity gain,  $I_{60}$ , time to peak, and reduction rate, were 0.817, 0.664, 0.810, 0.751, 0.845, 0.777, and 0.725, respectively.  $I_{60}$  was the most accurate parameter for differentiating pancreatic carcinomas from the other groups, giving values of sensitivity/specificity of 92.7/68.6% when optimal cutoffs were chosen. **Conclusions:** In pancreatic carcinomas, TIC patterns were markedly different from the other tumor types, with  $I_{60}$  being the most accurate diagnostic parameter. Quantitative perfusion analysis is useful for differentiating pancreatic carcinomas from other pancreatic tumors.

© 2017 S. Karger AG, Basel



## Introduction

The number of reports on the utility of contrast-enhanced harmonic (CH) endoscopic ultrasonography (EUS) in the differential diagnosis of pancreatic masses has been increasing [1–5]. CH-EUS depicted the hypo-enhancement of pancreatic carcinomas with high sensitivity (89–96%) and specificity (64–94%) [1–5]. Nonetheless, the visual evaluation of CH-EUS scans may be influenced by the endosonographers' subjective impressions [6]. In addition, there was no standardized method to analyze the images after the infusion of an ultrasound contrast agent, particularly regarding how to determine the enhancement pattern of the EUS-depicted pancreatic masses.

Recent studies have described quantitative perfusion analysis of pancreatic diseases using a time-intensity curve (TIC), which depicts the changes in signal intensity over time within a region of interest (ROI) after infusion of an ultrasound contrast agent [7–12]. However, the scanning methods and the parameters evaluated varied between these reports. Therefore, the primary aim of this study was to determine if quantitative perfusion analysis with CH-EUS helps to characterize pancreatic tumors. The secondary aim was to find the most accurate hemodynamic parameter of TIC for differentiating pancreatic carcinoma from other pancreatic tumors.

## Patients and Methods

### *Patients and Study Design*

This retrospective study included patients with a suspect pancreatic mass on the basis of results from computed tomography (CT), magnetic resonance imaging, or transabdominal ultrasonography (US), and who underwent both standard EUS and CH-EUS between February 2011 and February 2012 at the Department of Gastroenterology and Hepatology, Kindai University Faculty of Medicine. Patients were enrolled if the solid component of the mass was >75% of the total volume and if, after EUS examinations, they had undergone surgery or EUS-guided fine-needle aspiration (EUS-FNA) leading to a histological or cytological diagnosis, with a follow-up of at least 12 months. Pancreatic cystic tumors with a content of solid tumor <25% were excluded. The histological or cytological outcome was considered the gold standard diagnosis for the purposes of this study and was used to divide patients into 4 groups: pancreatic carcinomas, pancreatic neuroendocrine tumors, inflammatory pseudotumors, and other tumors.

### *Endoscopic Ultrasonography*

Conventional EUS of the pancreas without a contrast agent was performed first, giving special attention to pancreatic masses. When conventional EUS revealed a solid lesion, images of the ideal scanning plane were displayed to portray the whole area of the

lesion. Thereafter, the imaging mode was changed to the extended pure harmonic detection mode. This mode synthesizes the filtered second harmonic components with signals obtained from the phase shift, which is used for CH imaging. The transmitting frequency and mechanical index were 4.7 MHz and 0.3, respectively. The ultrasound contrast agent Sonazoid (Daiichi-Sankyo, Tokyo, Japan) was used. Immediately before CH-EUS, the contrast agent was reconstituted with 2 mL of sterile water for injection, and a dose of 15  $\mu$ L/kg body weight was prepared in a 1-mL syringe. A bolus injection of the contrast agent was administered. With a frame rate of about 10 images/s, all images and hemodynamic data were acquired using a ProSound Alpha 10 US system (Aloka, Tokyo, Japan). All EUS procedures were performed by 2 endosonographers (M. Kitano and H. Sakamoto). One was responsible for endoscopic manipulation and scanning, and the other for operating the US scanner. Both endosonographers are certified by the Japan Gastroenterological Endoscopy Society and have >10 years of experience with CH-EUS; each has performed >1,000 CH-EUS procedures. Subjective analysis was performed by these endosonographers for diagnosing pancreatic carcinoma. A hypo-enhancement pattern defined pancreatic carcinoma.

### *TIC Analysis*

The acquired images were reviewed using the software "Time Intensity Curve" (ProSound Alpha-10 US system; Aloka, Tokyo, Japan). An ROI was placed over the pancreatic mass to cover an area as large as possible, and a TIC was generated to depict the changes in signal intensity over time within the ROI (Fig. 1). From these data, the software calculated the baseline intensity (dB), and, then, after the injection of contrast medium, the peak intensity (dB), the time to peak (s), the intensity gain (dB), the intensity at 60 s ( $I_{60}$ , dB), and the reduction rate at 60 s (reduction rate [%] =  $[1 - I_{60}/\text{peak intensity}] \times 100$ ) (Fig. 1).

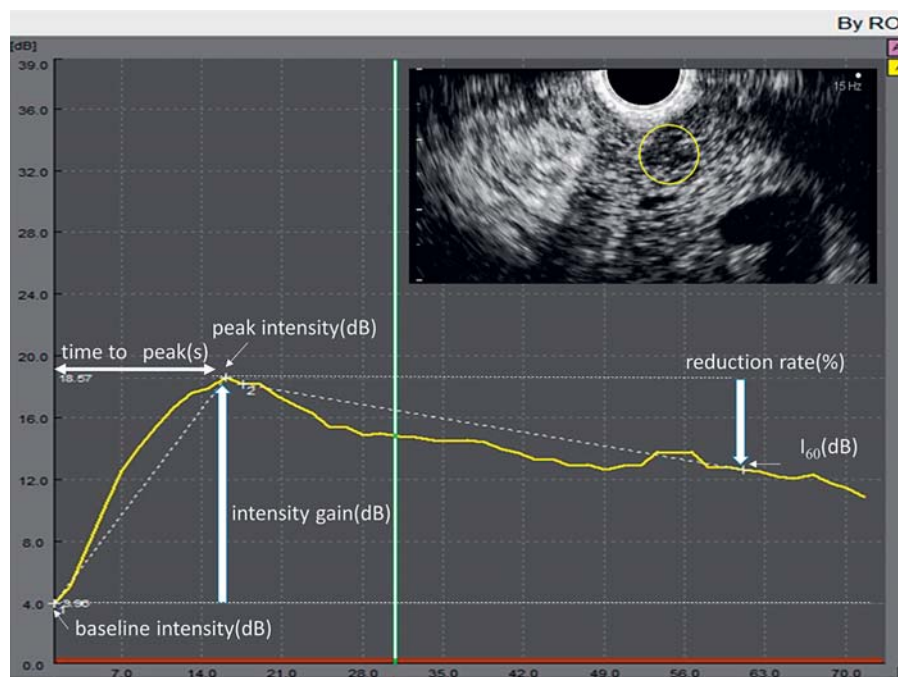
### *Statistical Analysis*

All analyses were performed using the statistical software SAS 9.1.3 (SAS Institute Inc., Cary, NC, USA). The Steel-Dwass test was applied to compare the TIC parameters among the 4 groups. When the  $p$  value was <0.05, the difference was considered statistically significant. For the diagnosis of pancreatic carcinoma, receiver-operating characteristic (ROC) analysis was performed for all TIC parameters to determine the sensitivity, specificity, and odds ratio using the optimal cutoff value.

## Results

During the study period, 76 consecutive patients with suspect pancreatic masses were enrolled. Of the enrolled patients, 44 were men and 32 women; their mean age was  $68.3 \pm 10.2$  years. Table 1 shows the final diagnoses in the 76 patients. There were 41 patients with pancreatic carcinoma, which was diagnosed histologically after surgical resection in 13 cases and EUS-FNA in 28. Six patients with pancreatic neuroendocrine tumor were diagnosed by histological analysis of resected specimens. In the remaining 8 patients, neuroendocrine tumor was diag-

**Fig. 1.** Quantitative perfusion analysis of contrast-enhanced harmonic endoscopic ultrasonography of a pancreatic carcinoma. A region of interest (yellow circle) is placed over the pancreatic mass. Baseline intensity (dB), echo intensity before injection of contrast agent; peak intensity (dB), echo intensity at the peak; time to peak (s), time from injection of contrast medium to peak intensity; intensity gain, echo intensity gain from baseline to peak intensity;  $I_{60}$ , echo intensity 60 s after injection of contrast medium; reduction rate (%), the rate of reduction intensity from the peak to 60 s: reduction rate =  $(1 - I_{60}/\text{peak intensity}) \times 100$ ).



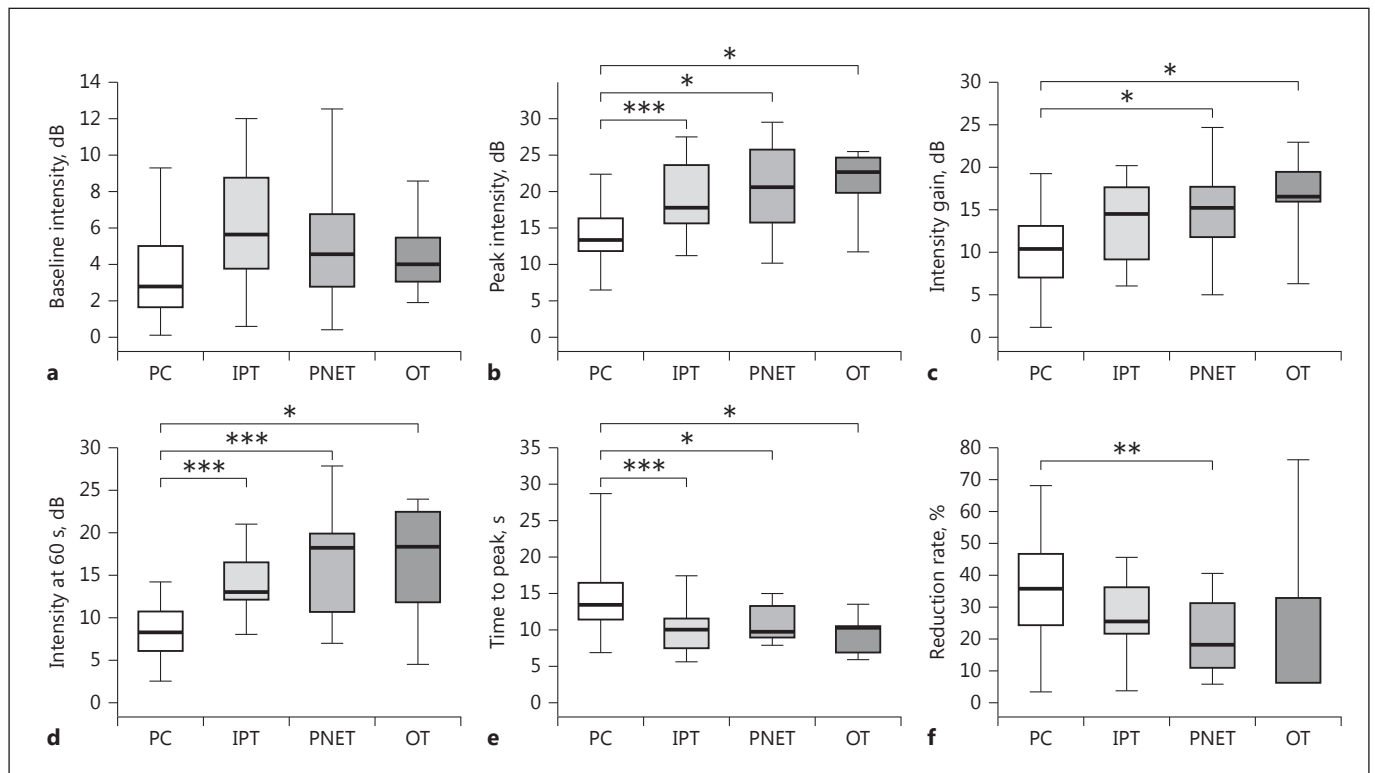
**Table 1.** Patient characteristics

Age (mean $\pm$ SD), years	68.3 $\pm$ 10.2
Gender (males/females)	44/32
Maximum tumor diameter (mean $\pm$ SD), mm	25.9 $\pm$ 16.5
Final diagnosis, total $n$ ( $n$ surgically resected)	
Pancreatic carcinoma	41 (13)
Inflammatory pseudotumor	14 (0)
Pancreatic neuroendocrine tumor	14 (6)
Other tumor	7 (1)
Pancreatic metastasis from RCC	4 (0)
Pancreatic metastasis from BC	2 (0)
Solid pseudopapillary neoplasm	1 (1)
RCC, renal cell carcinoma; BC, breast carcinoma.	

nosed based on EUS-FNA. In all patients with inflammatory pseudotumor, which was diagnosed histologically after EUS-FNA, periodic follow-up with CT and/or EUS revealed a reduction or no change in size. In 10 patients who were suspected of having autoimmune pancreatitis based on the 2011 International Clinical Diagnostic Criteria, tumor reduction was observed after steroid therapy [13]. In the group of 7 patients with other tumors, 4 were pancreatic metastases from renal cell carcinoma, 2 pancreatic metastases from ductal carcinoma of the breast, and 1 was a solid pseudopapillary neoplasm.

There was no significant difference in baseline intensity among the 4 groups (Fig. 2a). After the injection of contrast medium, values of peak intensity and  $I_{60}$  for the pancreatic carcinoma group were significantly lower than those of the other groups ( $p < 0.05$ ) (Fig. 2b, d). Values of intensity gain for the pancreatic carcinoma group were significantly lower than those of the pancreatic neuroendocrine tumor group and the other tumor groups ( $p < 0.05$ ), although there was no significant difference in intensity gain between pancreatic carcinoma and inflammatory pseudotumor groups (Fig. 2c). Instead, time to peak was significantly longer in the pancreatic carcinoma group than in the other groups ( $p < 0.05$ ) (Fig. 2e). Finally, the reduction rate for pancreatic carcinomas was significantly higher than for pancreatic neuroendocrine tumors ( $p < 0.01$ ) (Fig. 2f).

In ROC analysis for the diagnosis of pancreatic carcinomas (Fig. 3), the areas under the curve for subjective analysis, baseline intensity, peak intensity, intensity gain,  $I_{60}$ , time to peak, and reduction rate were 0.817, 0.664, 0.810, 0.751, 0.845, 0.777, and 0.725, respectively. According to the ROC data, the optimal cutoff values for these parameters without subjective analysis were 3.2, 15.1, 13.7, and 12.4 dB, 12.0 s, and 31.4%, respectively. These cutoffs correspond to the values of sensitivity, specificity, and odds ratio (Table 2). In addition, subjective analyses for the diagnosis of pancreatic carcinomas are



**Fig. 2.** Comparison of time-intensity curves (TIC) among 4 types of pancreatic tumors. TIC parameters include baseline intensity (a), peak intensity (b), intensity gain (c), intensity gain at 60 s (d), time to peak (e), and reduction rate (f). PC, pancreatic carcinomas ( $n = 41$ ); IPT, inflammatory pseudotumors ( $n = 14$ ); PNET, pancreatic neuroendocrine tumors ( $n = 14$ ); OT, other tumors ( $n = 7$ ). Values shown are medians (horizontal lines), 25th and 75th percentiles (boxes), and ranges (vertical lines). \*  $p < 0.05$ , \*\*  $p < 0.01$ , \*\*\*  $p < 0.005$  (Steel-Dwass test).

**Table 2.** Receiver-operating characteristic analysis of quantitative perfusion data from contrast-enhanced harmonic endoscopic ultrasonography for the diagnosis of pancreatic carcinoma

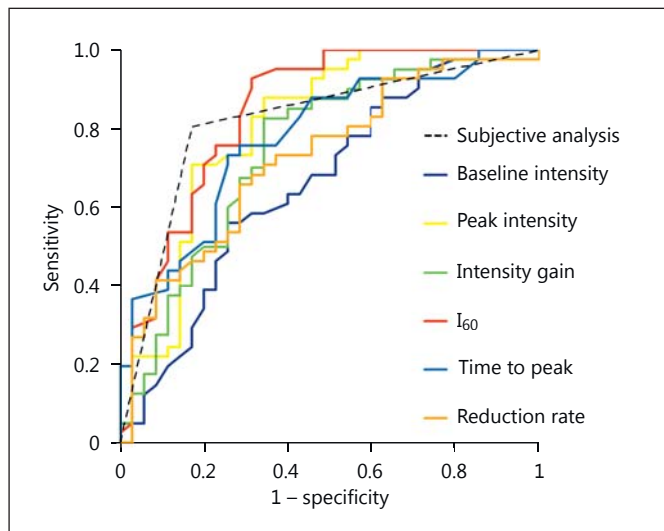
Parameter	AUC	Cutoff	Sensitivity	Specificity	Odds ratio
Subjective analysis	0.817	–	80.4%	82.9%	19.938
Baseline intensity	0.664	3.2 dB	56.1%	74.3%	3.691
Peak intensity	0.810	15.1 dB	70.7%	82.9%	11.681
Intensity gain	0.751	13.7 dB	82.5%	65.7%	9.036
$I_{60}$	0.845	12.4 dB	92.7%	68.6%	27.636
Time to peak	0.777	12.0 s	73.2%	74.3%	7.879
Reduction rate	0.725	31.4%	65.9%	71.4%	4.821

$I_{60}$ , intensity gain at 60 s; AUC, area under the curve.

shown in Table 2. The sensitivity and specificity of subjective analyses were 80.4 and 82.9%. The  $I_{60}$  (cutoff = 12.4 dB) was the most accurate parameter by ROC analysis for the diagnosis of pancreatic carcinomas with 92.7% sensitivity, 68.6% specificity, and an odds ratio of 27.636.

## Discussion

In this study, various TIC parameters were assessed in pancreatic masses and compared in terms of their ability to diagnose pancreatic carcinoma. In pancreatic carci-



**Fig. 3.** Receiver-operating characteristic curves for the diagnostic ability of time-intensity curves of contrast-enhanced harmonic endoscopic ultrasonography for pancreatic carcinoma. The areas under the curve for subjective analysis, baseline intensity, peak intensity, intensity gain, intensity gain at 60 s ( $I_{60}$ ), time to peak, and reduction rate were 0.817, 0.664, 0.810, 0.751, 0.845, 0.777, and 0.725, respectively.

noma patients, TIC patterns markedly differed from the other tumor types. This clinical observation suggests quantitative analysis with CH-EUS is useful in the differential diagnosis of pancreatic masses. There have been some reports on the usefulness of a quantitative analysis of CH-EUS data using TIC in the diagnosis of pancreatic tumors. Seicean et al. [10] compared pancreatic carcinomas and mass-forming chronic pancreatitis in terms of contrast medium uptake and concluded that the uptake ratio (tumor/surrounding tissue) was significantly lower in adenocarcinomas than in pancreatitis, although they analyzed data from 30 patients only. Gheonea et al. [11] assessed various parameters including area under the ROC curve, time to peak, and maximum and median intensity; in their report, the sensitivity and specificity were remarkably high (93.75 and 89.47%), although it was unclear which parameter was used for diagnostic analysis, and the cutoff values for the parameters were not reported. Imazu et al. [8] found that autoimmune pancreatitis ( $n = 8$ ) and pancreatic carcinomas ( $n = 18$ ) had markedly different TIC. Intensity gain of pancreatic mass lesions in patients with autoimmune pancreatitis was significantly higher than in patients with pancreatic carcinomas (accuracy, 100%). Săftoiu et al. [12] reported the usefulness of TIC and an automated computer-aided

diagnostic system based on their TIC data. Matsubara et al. [9] compared the reduction rate from the peak at 1 min between pancreatic carcinomas ( $n = 48$ ), inflammatory pseudotumors ( $n = 27$ ), and pancreatic neuroendocrine tumors ( $n = 16$ ). In their report, the reduction rate was greatest in pancreatic carcinomas followed by mass-forming pancreatitis, autoimmune pancreatitis, and pancreatic neuroendocrine tumors ( $p < 0.05$ ). However, it is difficult to determine the diagnostic accuracy with quantitative analysis because these previous reports enrolled patients with different kinds of diseases and employed different kinds of parameters. Therefore, our study included all solid tumors and assessed various parameters. There are several parameters for diagnosing pancreatic tumors. From these previous reports [7–12], we chose baseline intensity, peak intensity, intensity gain,  $I_{60}$ , time to peak, and reduction rate as parameters for TIC analysis. Peak intensity, intensity gain, and  $I_{60}$  were significantly lower in the pancreatic carcinoma group than in the other groups, while time to peak and reduction rate were higher. These results suggest that pancreatic carcinomas have a slower blood inflow velocity and faster blood outflow velocity, and may reflect the fact that most of these carcinomas have a rich fibrous stroma that usually accounts for the observed hypovascularity [14–16]. However, there are no reports on which TIC parameter represents vessel volume or fibrosis. Further CH-EUS studies on tumors that are all surgically resected are needed to clarify the histological meaning of the 6 TIC parameters used in the present study.

The current study first compared the diagnostic utility of different kinds of TIC parameters using ROC analysis and determined the most reliable TIC parameter. ROC analysis revealed that the best parameter for diagnosing pancreatic carcinomas was  $I_{60}$ . When the cutoff for  $I_{60}$  was set at 12.4 dB, sensitivity and specificity were 92.7 and 68.6%, respectively.  $I_{60}$  had a higher sensitivity than subjective analysis. Eight out of 38 (21%) correctly diagnosed as pancreatic carcinoma by  $I_{60}$  presented an iso-enhancement pattern by subjective analysis. Despite the evaluation by experts, subjective analysis can be difficult to distinguish from iso- or hypo-enhancement patterns. Therefore, the case of iso-enhancement pattern might be a good adaptation of TIC analysis.

Although  $I_{60}$  was lower than subjective analysis in specificity,  $I_{60}$  was higher than subjective analysis in ROC/area under the ROC curve. ROC analysis can change the cutoff in all parameters. When the patient cannot receive EUS-FNA because of anticoagulation therapy or intervening vessel, higher specificity is required.



In the present study, a single ROI was placed over the pancreatic tumor. Some reports used a second, parenchymal ROI in the surrounding tissue and measured the value in the tumor relative to the surrounding tissue [10, 11]. However, when the tumor is large, it is not possible to set 2 ROI (the tumor and the surrounding tissue) on a fixed single image. Moreover, setting 2 ROI may lead to selection bias. Therefore, we chose a single ROI and placed it so as to cover the largest possible tumor area, because the intensity in the tumor is heterogeneous.

Our study has several limitations. A fixed single image without sweep scan technique has to be used in order to obtain TIC. If subjective observation is employed, sweep scanning of the whole lesion with the transducer allows comparison of the tumor and the surrounding tissue in relatively large tumors. It was a retrospective study at a single center, and the sample number was relatively small. Also, some tumors were diagnosed based only on samples obtained by EUS-FNA and follow-up with imaging. A multicenter, prospective study in a larger patient cohort

diagnosed only on surgical resection specimens is needed to clarify the diagnostic utility of quantitative perfusion analysis with CH-EUS.

In conclusion, pancreatic carcinoma exhibited markedly different TIC patterns from inflammatory pseudotumors, pancreatic neuroendocrine tumors, and other pancreatic tumors. Thus, quantitative perfusion analysis is useful to differentiate pancreatic carcinomas from other pancreatic masses.  $I_{60}$  is the most accurate parameter.

## Acknowledgments

This study was supported by grants from the Japan Society for Promotion of Science (No. 22590764 and 25461035).

## Disclosure Statement

The authors have no conflicts of interest to declare.

## References

- 1 Fusaroli P, Spada A, Mancino MG, Caletti G: Contrast harmonic echo-endoscopic ultrasound improves accuracy in diagnosis of solid pancreatic masses. *Clin Gastroenterol Hepatol* 2010;8:629–634.
- 2 Kitano M, Kudo M, Yamao K, et al: Characterization of small solid tumors in the pancreas: the value of contrast-enhanced harmonic endoscopic ultrasonography. *Am J Gastroenterol* 2012;107:303–310.
- 3 Napoleon B, Alvarez-Sanchez MV, Gincul R, et al: Contrast-enhanced harmonic endoscopic ultrasound in solid lesions of the pancreas: results of a pilot study. *Endoscopy* 2010;42:564–570.
- 4 Kitano M, Sakamoto H, Matsui U, et al: A novel perfusion imaging technique of the pancreas: contrast-enhanced harmonic EUS (with video). *Gastrointest Endosc* 2008;67:141–150.
- 5 Gincul R, Palazzo M, Pujol B, et al: Contrast-harmonic endoscopic ultrasound for the diagnosis of pancreatic adenocarcinoma: a prospective multicenter trial. *Endoscopy* 2014;46:373–379.
- 6 Fusaroli P, Kyraios D, Mancino MG, et al: Interobserver agreement in contrast harmonic endoscopic ultrasound. *J Gastroenterol Hepatol* 2012;27:1063–1069.
- 7 Kersting S, Konopke R, Kersting F, et al: Quantitative perfusion analysis of transabdominal contrast-enhanced ultrasonography of pancreatic masses and carcinomas. *Gastroenterology* 2009;137:1903–1911.
- 8 Imazu H, Kanazawa K, Mori N, et al: Novel quantitative perfusion analysis with contrast-enhanced harmonic EUS for differentiation of autoimmune pancreatitis from pancreatic carcinoma. *Scand J Gastroenterol* 2012;47:853–860.
- 9 Matsubara H, Itoh A, Kawashima H, et al: Dynamic quantitative evaluation of contrast-enhanced endoscopic ultrasonography in the diagnosis of pancreatic diseases. *Pancreas* 2011;40:1073–1079.
- 10 Seicean A, Badea R, Stan-Iuga R, Mocan T, Gulei I, Pascu O: Quantitative contrast-enhanced harmonic endoscopic ultrasonography for the discrimination of solid pancreatic masses. *Ultraschall Med* 2010;31:571–576.
- 11 Gheonea D, Streba C, Ciurea T, Săftoiu A: Quantitative low mechanical index contrast-enhanced endoscopic ultrasound for the differential diagnosis of chronic pseudotumoral pancreatitis and pancreatic cancer. *BMC Gastroenterol* 2013;13:2.
- 12 Săftoiu A, Vilman P, Dietrich CF, et al: Quantitative contrast-enhanced harmonic EUS in differential diagnosis of focal pancreatic masses (with videos). *Gastrointest Endosc* 2015;82:59–69.
- 13 Shimosegawa T, Chari ST, Frulloni L, et al: International consensus diagnostic criteria for autoimmune pancreatitis: guidelines of the International Association of Pancreatology. *Pancreas* 2011;40:352–358.
- 14 Numata K, Ozawa Y, Kobayashi N, et al: Contrast-enhanced sonography of pancreatic carcinoma: correlations with pathological findings. *J Gastroenterol* 2005;40:631–640.
- 15 Hata H, Mori H, Matsumoto S, et al: Fibrous stroma and vascularity of pancreatic carcinoma: correlation with enhancement patterns on CT. *Abdom Imaging* 2010;35:172–180.
- 16 Spivak-Kroizman TR, Hostetter G, Posner R, et al: Hypoxia triggers hedgehog-mediated tumor-stromal interactions in pancreatic cancer. *Cancer Res* 2013;73:3235–3247.



# Chronic Pancreatitis Finding by Endoscopic Ultrasonography in the Pancreatic Parenchyma of Intraductal Papillary Mucinous Neoplasms Is Associated with Invasive Intraductal Papillary Mucinous Carcinoma

Mamoru Takenaka<sup>a,e</sup> Atsuhiko Masuda<sup>a</sup> Hideyuki Shiomi<sup>a</sup> Yosuke Yagi<sup>a</sup>  
Yoh Zen<sup>b</sup> Arata Sakai<sup>a</sup> Takashi Kobayashi<sup>a</sup> Yoshifumi Arisaka<sup>a</sup>  
Yoshihiro Okabe<sup>a</sup> Hiromu Kutsumi<sup>a,d</sup> Hirochika Toyama<sup>c</sup> Takumi Fukumoto<sup>c</sup>  
Yonson Ku<sup>c</sup> Masatoshi Kudo<sup>e</sup> Takeshi Azuma<sup>a</sup>

<sup>a</sup>Division of Gastroenterology, Department of Internal Medicine, <sup>b</sup>Division of Diagnostic Pathology, and

<sup>c</sup>Division of Hepato-Biliary-Pancreatic Surgery, Department of Surgery, Kobe University Graduate School of Medicine, <sup>d</sup>Center for Clinical Research and Advanced Medicine Establishment, Shiga University of Medical Science, Kobe, and <sup>e</sup>Department of Gastroenterology and Hepatology, Kindai University Graduate School of Medicine, Osaka-Sayama, Japan

## Keywords

Chronic pancreatitis · Endoscopic ultrasonography · Intraductal papillary mucinous neoplasm · Pancreatic parenchyma

## Abstract

**Background/Objectives:** The recent guideline for intraductal papillary mucinous neoplasms (IPMNs) focuses on morphological features of the lesion as signs of malignant transformation, but ignores the background pancreatic parenchyma, including features of chronic pancreatitis (CP), which is a risk factor for pancreatic malignancies. Endoscopic ultrasonography frequently reveals evidence of CP (EUS-CP findings) in the background pancreatic parenchyma of patients with IPMNs. Therefore, we investigated whether background EUS-CP findings were associated with malignant IPMN.

**Methods:** The clinical data of 69 consecutive patients with IPMNs who underwent preoperative EUS and surgical resection between April 2010 and October 2014 were collected prospectively. The association of EUS-CP findings (total number of EUS-CP findings; 0 vs.  $\geq 1$ ) with invasive IPMN was examined. The association of EUS-CP findings with pathological changes of the background pancreatic parenchyma (atrophy/inflammation/fibrosis) was also examined. **Results:** Among patients with EUS-CP findings, invasive intraductal papillary mucinous carcinoma (IPMC) was significantly more frequent than among patients without EUS-CP findings (42.5% [17/40] vs. 3.4% [1/29],  $p = 0.0002$ ). In addition, patients with EUS-CP findings had higher grades of pancreatic

M. Takenaka, A. Masuda, and H. Shiomi contributed equally to this work.

atrophy and inflammation than patients without EUS-CP findings (atrophy: 72.5% [29/40] vs. 34.5% [10/29],  $p = 0.003$ ; inflammation: 45.0% [18/40] vs. 20.7% [6/29],  $p = 0.04$ ). **Conclusions:** In IPMN patients, detection of EUS-CP findings in the background pancreatic parenchyma was associated with a higher prevalence of invasive IPMC. Accordingly, EUS examination should not only assess the morphological features of the lesion itself, but also EUS-CP findings in the background parenchyma.

© 2017 S. Karger AG, Basel

## Introduction

Intraductal papillary mucinous neoplasms (IPMNs) are a well-characterized group of intraductal mucin-producing cystic neoplasms of the pancreas with malignant potential [1, 2]. In the 2012 international consensus guidelines, high-risk IPMN included two clinical categories with “high-risk stigmata” and “worrisome features,” and different therapeutic strategies were recommended for both groups. It is recommended that patients with “high-risk stigmata” be treated by surgical resection [3–7]. Patients who have “worrisome features” and additional high-risk signs should also undergo resection, while patients with “worrisome features” alone should receive careful follow-up. The “high-risk stigmata” of IPMNs that can be detected by endoscopic ultrasonography (EUS) are an enhancing solid component inside the cyst and dilation of the main pancreatic duct ( $>10$  mm) [3, 8–11]. Additional high-risk signs among the “worrisome features” are a definite mural nodule and suspected main duct involvement [12, 13]. Thus, the current guidelines focus on the morphological features of IPMN as revealed by EUS.

On the other hand, although not described in previous reports, clinical experience suggests that evidence of chronic pancreatitis (CP) is frequently identified in the background pancreatic parenchyma of IPMN patients by EUS (EUS-CP findings). CP is a well-known risk factor for pancreatic malignancy, including pancreatic ductal adenocarcinoma [14–16]. However, the relationship between malignant transformation of IPMNs and pathological changes of the pancreatic parenchyma, such as atrophy, inflammation, and fibrosis, remains unclear. Moreover, changes of the background parenchyma are not considered to be a high-risk sign for malignant IPMN in the current guideline. We hypothesized that EUS-CP findings might be associated with malignant IPMN.

To test this hypothesis, we utilized a database of 69 consecutive patients with IPMNs who underwent preopera-

tive EUS and surgical resection at Kobe University Hospital. We examined the association of EUS-CP findings with the incidence of malignant IPMN and with pathological changes of the background parenchyma in the resected specimens (atrophy, inflammation, and fibrosis).

## Methods

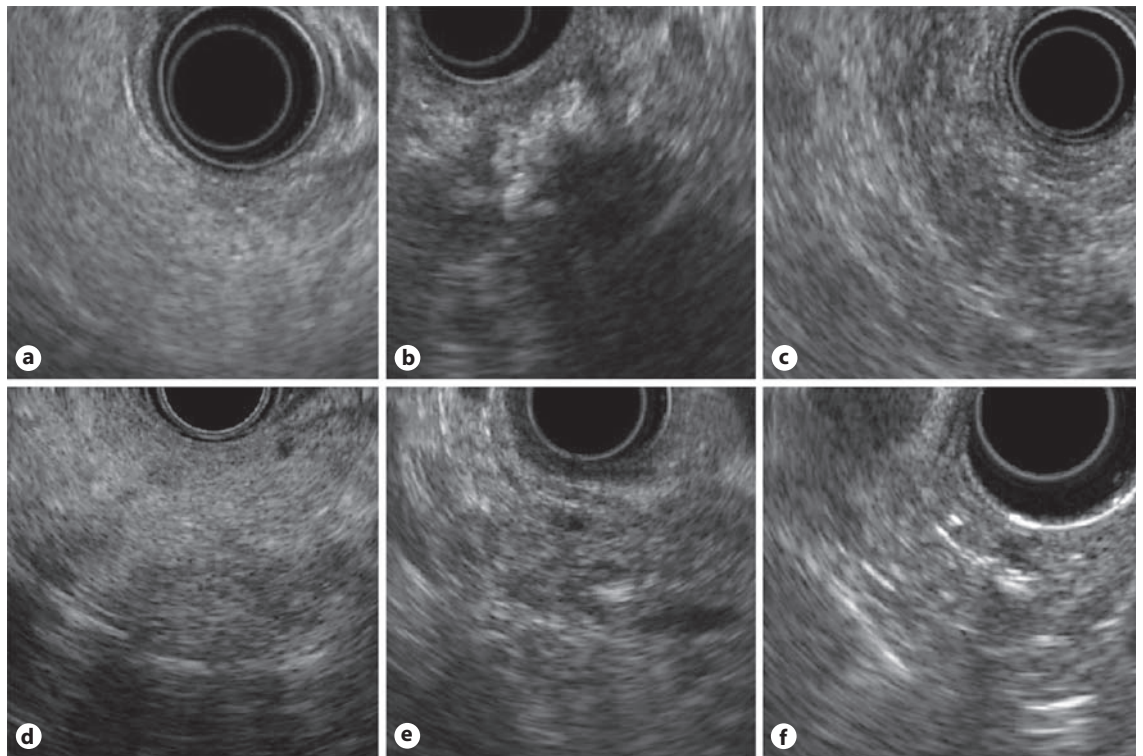
### Study Design

The clinical data of 69 consecutive patients with IPMNs in whom EUS was performed before surgical resection at Kobe University Hospital from April 2010 to October 2014 were collected prospectively. Patients with concomitant pancreatic carcinoma (defined by the presence of two discrete tumors) were excluded. We investigated various clinical and tumor characteristics, including age, sex, abdominal symptoms (presence vs. absence), serum CEA ( $<5$  vs.  $\geq 5$  ng/mL), serum CA19-9 ( $<37$  vs.  $\geq 37$  U/mL), diabetes mellitus (presence vs. absence), habitual drinking (none/sometimes/daily), alcohol consumption ( $<50$  vs.  $\geq 50$  g/day), macroscopic type of IPMN (main duct, mixed, or branch duct type), cyst location (head vs. body/tail), main pancreatic duct diameter ( $<5$ , 5–10,  $>10$  mm), mural nodule in the cyst (presence vs. absence), cyst diameter ( $<30$ , 30–40,  $>40$  mm), and tumor mucin phenotype (intestinal, gastric, pancreatobiliary, or oncocytic). According to the 2012 international consensus guidelines [3], the macroscopic type of IPMN was classified as main duct type (MD-IPMN), mixed type (Mix-IPMN), or branch duct type (BD-IPMN) based on the results of imaging studies, mainly magnetic resonance cholangiopancreatography (MRCP). Tumors were histologically classified into four types (gastric, intestinal, pancreatobiliary, or oncocytic) according to the appearance on hematoxylin and eosin-stained sections and immunohistochemistry with anti-mucin antibodies (MUC1/MUC2/MUC5AC/MUC6). In patients with multiple morphologically distinct IPMNs, each neoplasm was classified depending on the type of the dominant component. Tumors were also classified into low-grade dysplasia, high-grade dysplasia, or invasive intraductal papillary mucinous carcinoma (IPMC). The diameter of the main pancreatic duct and the cyst size were measured by MRCP in most cases. In patients who did not undergo MRCP, measurement was done by an alternative method, such as endoscopic retrograde cholangiopancreatography or computed tomography. The presence of mural nodules was evaluated by EUS and magnetic resonance imaging. Abdominal symptoms were defined as including abdominal or back pain/discomfort, weight loss, appetite loss, and jaundice.

This study was conducted in accordance with the Declaration of Helsinki and its amendments (UMIN-CTR ID: 000021345). The study protocol was approved by the ethics committee of Kobe University School of Medicine (No. 1864). All authors had access to the study data and reviewed and approved the final manuscript.

### Evaluation of the Pancreatic Parenchyma by EUS

Three echo-endoscopes (GF-UCT240, GF-UCT260, or GF-UE260; Olympus, Tokyo, Japan) were used in this study. EUS-CP findings refer to the parenchymal features of CP in the Rosemont classification recently proposed as EUS diagnostic criteria for this condition [17]. These findings included “hyperechoic foci with



**Fig. 1.** Typical EUS-CP findings based on the parenchymal features of CP according to the Rosemont classification. **a** Normal. **b** Hyperechoic foci with shadowing. **c** Lobularity with honeycombing. **d** Lobularity without honeycombing. **e** Hyperechoic foci without shadowing. **f** Stranding. CP, chronic pancreatitis; EUS, endoscopic ultrasonography.

shadowing,” “lobularity with honeycombing,” “lobularity without honeycombing,” “hyperechoic foci without shadowing,” and “stranding” (Fig. 1). “Cysts” is also a parenchymal feature of CP in the Rosemont classification, but it was excluded because IPMN itself affects cyst formation. For the same reason, ductal features of CP in the Rosemont classification were excluded, including “main pancreatic duct calculi,” “irregular main pancreatic duct contour,” “dilated side branches,” “main pancreatic duct dilation,” and “hyperechoic main pancreatic duct margin.”

EUS-CP findings were reviewed prospectively by an endosonographer (M. Takenaka) who was unaware of the other data. All cases were re-examined by a second endosonographer (H. Shiomi), who was also unaware of the other data, and there was a good correlation of EUS-CP findings between the two endosonographers ( $\kappa = 0.80$  for score 0 vs.  $\geq 1$ ,  $p < 0.001$ ). Both endosonographers had experience with more than 1,000 EUS examinations.

#### *Indications for Surgical Resection*

Indications for surgical resection of IPMN at our hospital were decided according to the 2012 International Consensus Guidelines. According to the guidelines, resection is recommended for MD-IPMN. In the case of Mix-IPMN and BD-IPMN, resection is recommended if the patient has “high-risk stigmata.” In patients with “worrisome features” and additional high-risk signs, resection is also recommended.

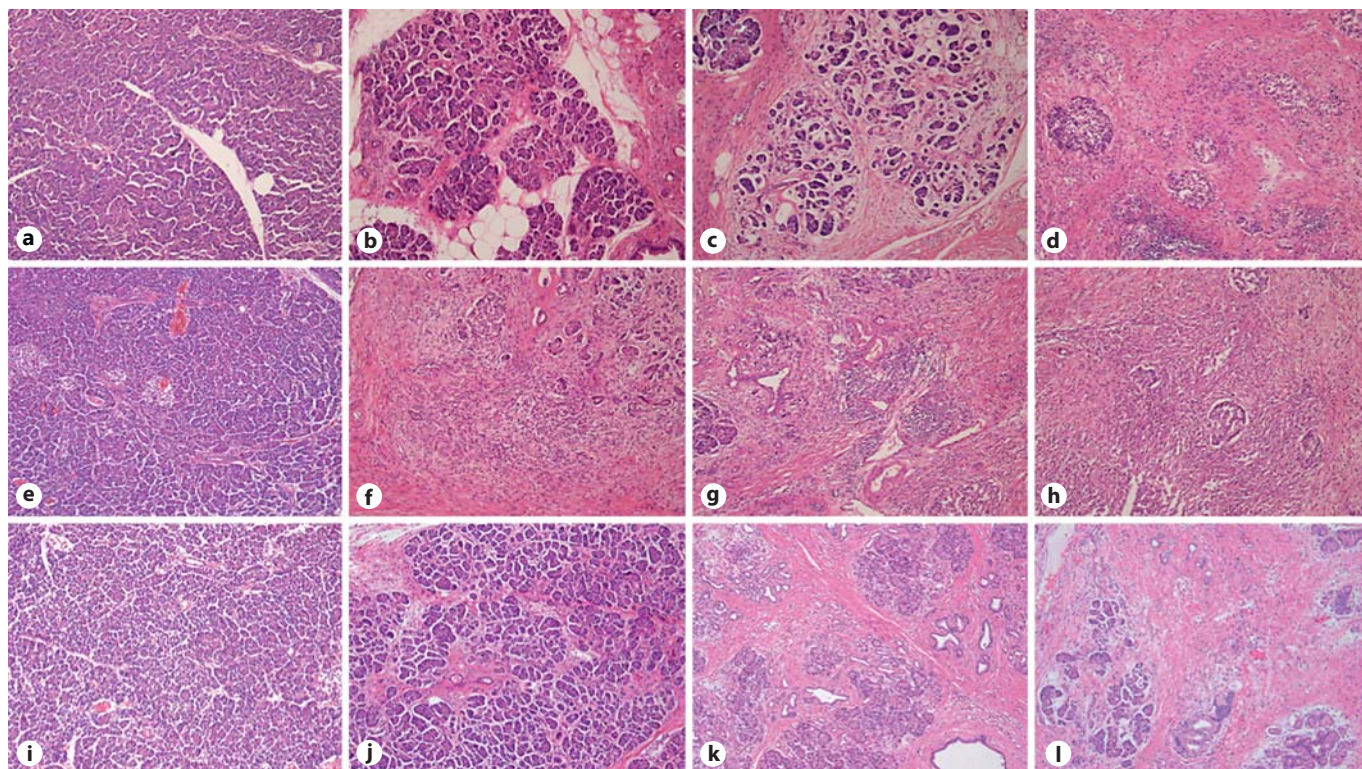
#### *Pathological Evaluation of Pancreatic Parenchymal Atrophy, Inflammation, and Fibrosis*

Hematoxylin and eosin-stained tissue sections from all resected specimens of IPMN were reviewed by a pathologist (Y. Zen), who was blinded to all clinical features. Pancreatic parenchymal atrophy, infiltration of inflammatory cells, and fibrosis were evaluated in the background pancreatic parenchyma. The severity of parenchymal atrophy, inflammation, or fibrosis was graded as 0 (none), 1+ (mild), 2+ (moderate), or 3+ (severe). Representative examples are shown in Figure 2.

#### *Statistical Analysis*

All statistical analyses were conducted using JMP version 11 (SAS Institute, Cary, NC, USA), and all  $p$  values were two-sided. The  $\chi^2$  test (or Fisher exact test, if appropriate) was used to assess associations between categorical variables. To assess the association of the number of EUS-CP findings (0 vs.  $\geq 1$ ) with the incidence of invasive IPMN, we conducted multivariate logistic regression analysis. The binary categorical variable (presence and absence) of the incidence of invasive IPMN was used as an outcome variable. Multivariate binary logistic regression analysis was performed to adjust for potential confounders. The OR was adjusted for age, alcohol consumption, and macroscopic type of IPMN, the  $p$  value of which was  $<0.2$  in univariate analysis. Kappa coefficients were calculated to assess agreement of EUS-CP findings between the two observers. In all analyses,  $p < 0.05$  was considered statistically significant.





**Fig. 2.** Pathological findings of the background pancreas parenchyma in intraductal papillary mucinous neoplasm patients. The figure shows the grading of parenchymal atrophy, inflammation, and fibrosis of the pancreas. **a–d** Parenchymal atrophy of grades 0–3. **a** Grade 0 (no atrophic change). **b** Grade 1 (focal atrophy). **c** Grade 2 (moderate atrophy). **d** Grade 3 (severe atrophy with few

residual acinar cells). **e–h** Inflammation of grades 0–3. **e** Grade 0 (no inflammation). **f** Grade 1 (mild inflammation). **g** Grade 2 (moderate inflammation with lymphoid aggregates). **h** Grade 3 (massive inflammation). **i–l** Fibrosis of grades 0–3. **i** Grade 0 (no fibrosis). **j** Grade 1 (mild fibrosis). **k** Grade 2 (moderate fibrosis). **l** Grade 3 (massive fibrosis).

## Results

### *Association of EUS-CP Findings with Invasive IPMC*

We categorized 69 IPMN patients by clinical features and factors associated with EUS-CP findings. There were 29 patients without EUS-CP findings and 40 patients with at least one EUS-CP finding. The clinical and morphological features of IPMN are summarized with respect to EUS-CP findings in Table 1. Patients with EUS-CP findings were older than those without EUS-CP findings ( $70.2 \pm 1.4$  vs.  $65.0 \pm 1.7$  years,  $p = 0.02$ ). Among the patients with EUS-CP findings, invasive IPMC was significantly more frequent than among those without EUS-CP findings (42.5% [17/40] vs. 3.4% [1/29],  $p = 0.0002$ ) (Table 2). Multivariate analysis showed that detection of EUS-CP findings in the background pancreatic parenchyma was associated with a higher prevalence of invasive IPMC (multivariate OR = 21.9, 95% CI = 3.8–423.1,

$p = 0.0001$ ). Assessment of each EUS-CP finding showed that invasive IPMC was significantly more frequent in the patients with “stranding” than in those without (55% [11/20] vs. 14% [7/49],  $p = 0.002$ ). In addition, invasive IPMC was significantly more frequent in the patients who had “lobularity without honeycombing” than in those without (83% [5/6] vs. 21% [13/63],  $p = 0.004$ ) (Table 3).

### *Association of EUS-CP Findings with Pathological Changes of the Pancreatic Parenchyma*

Table 4 shows the association between the total number of EUS-CP findings and the pathological findings (atrophy/inflammation/fibrosis) in the background pancreatic parenchyma of the IPMN patients. Among patients with EUS-CP findings, higher grades of pancreatic atrophy and inflammation were observed than in those without EUS-CP findings (atrophy: 72.5% [29/40]



**Table 1.** Characteristics of the patients and the IPMNs (number of EUS-CP findings 0 vs. ≥1)

	Number of EUS-CP findings		<i>p</i> value
	0	≥1	
Patients, <i>n</i>	29	40	
Age, years	65.0±1.7	70.2±1.4	0.02
Sex, male/female	17/12	20/20	0.50
Abdominal symptoms	5 (17%)	11 (28%)	0.32
CEA ≥5 ng/mL	8 (28%)	13 (33%)	0.66
CA19-9 ≥37 U/mL	8 (28%)	7 (18%)	0.32
Diabetes mellitus	10 (35%)	13 (33%)	0.86
Habitual drinking (none/sometimes/daily)	14/7/8	22/9/9	0.84
Alcohol consumption ≥50 g/day	1 (3%)	5 (13%)	0.19
<i>Clinical features of IPMN</i>			
Macroscopic type (main duct/mixed/branch duct)	0/16/13	5/24/11	0.08
Location of cyst (head/body-tail)	18/11	24/16	0.86
Diameter of main pancreatic duct (<5/5–10/≥10 mm)	12/10/7	10/14/16	0.26
Mural nodule in cyst	11 (38%)	18 (45%)	0.56
Cyst size (<30/30–40/≥40 mm)	14/8/7	23/3/14	0.08
Mucin phenotype (intestinal/gastric/pancreatobiliary/oncocytic)	8/16/4/1	12/24/4/0	0.64
Invasive IPMC	1 (3%)	17 (43%)	0.0002

Values are presented as *n*, *n* (%), or mean ± SD. *p* < 0.05 was considered statistically significant. CP, chronic pancreatitis; EUS, endoscopic ultrasonography; IPMC, intraductal papillary mucinous carcinoma; IPMN, intraductal papillary mucinous neoplasm.

**Table 2.** Frequency of invasive IPMC in relation to the number of EUS-CP findings

Univariate analysis	Patients, <i>n</i>	Invasive IPMC		<i>p</i> value
		present	absent	
Total	69	18 (26%)	51 (74%)	
EUS-CP findings				
≥1	40	17 (43%)	23 (57%)	0.0002
0	29	1 (3%)	28 (97%)	
Multivariate analysis	Invasive IPMC (outcome variable) <sup>1</sup>			<i>p</i> value
EUS-CP findings (≥1)	21.9 (3.8–423.1)			0.0001

*p* < 0.05 was considered statistically significant. <sup>1</sup> Presented as OR (95% CI). The score presents as follows: 0 (absent), 1+ (present). The OR was adjusted for age, alcohol consumption, macroscopic type of IPMN, of which *p* was <0.2 in Table 1 (univariate analysis). CP, chronic pancreatitis; EUS, endoscopic ultrasonography; IPMC, intraductal papillary mucinous carcinoma.

**Table 3.** Prevalence of invasive IPMC in relation to each EUS-CP finding

	Patients, <i>n</i>	Invasive IPMC		<i>p</i> value
		present	absent	
Total	69	18 (26%)	51 (74%)	
Hyperechoic foci with shadowing				
Present	10	4 (40%)	6 (60%)	0.44
Absent	59	14 (24%)	45 (76%)	
Lobularity with honeycombing				
Present	2	1 (50%)	1 (50%)	0.46
Absent	67	17 (25%)	50 (75%)	
Lobularity without honeycombing				
Present	6	5 (83%)	1 (17%)	0.004
Absent	63	13 (21%)	50 (79%)	
Hyperechoic foci without shadowing				
Present	27	10 (37%)	17 (63%)	0.16
Absent	42	8 (19%)	34 (81%)	
Stranding				
Present	20	11 (55%)	9 (45%)	0.002
Absent	49	7 (14%)	42 (86%)	

*p* < 0.05 was considered statistically significant. CP, chronic pancreatitis; EUS, endoscopic ultrasonography; IPMC, intraductal papillary mucinous carcinoma.

**Table 4.** Association between the number of EUS-CP findings and pathological changes in the background pancreatic parenchyma of IPMN patients

	Patients, <i>n</i>	Atrophy		<i>p</i> value	Inflammation		<i>p</i> value	Fibrosis		<i>p</i> value
		high	low		high	low		high	low	
Total	69	39 (57%)	30 (43%)		24 (57%)	45 (43%)		32 (46%)	37 (54%)	
Total number of EUS-CP findings										
≥1	40	29 (73%)	11 (27%)	0.003	18 (45%)	22 (55%)	0.04	21 (53%)	19 (47%)	0.33
0	29	10 (34%)	19 (66%)		6 (21%)	23 (79%)		11 (38%)	18 (62%)	

Atrophy, inflammation, and fibrosis were divided into two groups based on the grade of pathological findings (high, moderate, or severe; low, none, or mild).  $p < 0.05$  was considered statistically significant. CP, chronic pancreatitis; EUS, endoscopic ultrasonography; IPMN, intraductal papillary mucinous neoplasm.

**Table 5.** Association between each EUS-CP finding and pathological changes in the background pancreatic parenchyma of IPMN patients

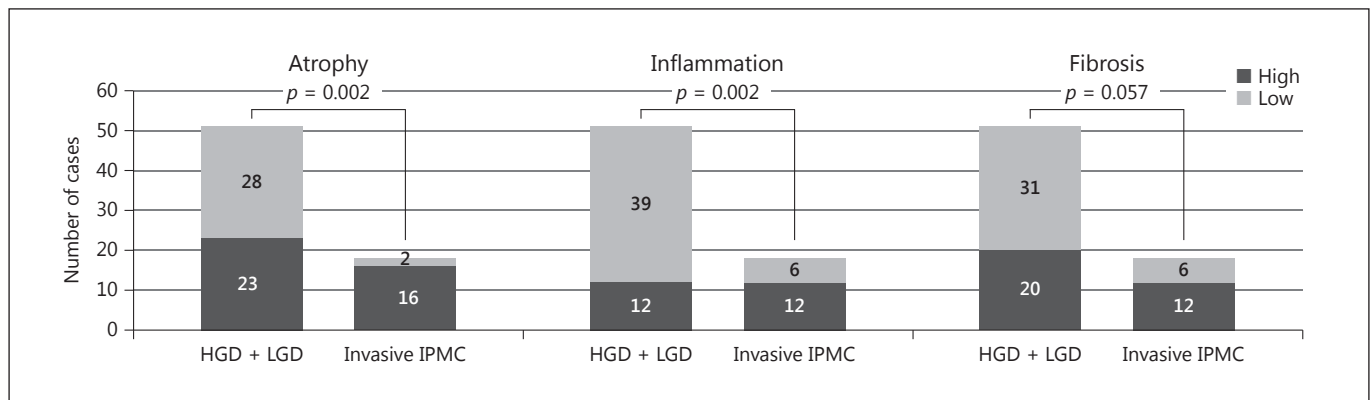
	Patients, <i>n</i>	Atrophy		<i>p</i> value	Inflammation		<i>p</i> value	Fibrosis		<i>p</i> value
		high	low		high	low		high	low	
Total	69	39 (57%)	30 (43%)		24 (57%)	45 (43%)		32 (46%)	37 (54%)	
Hyperechoic foci with shadowing										
Present	10	8 (80%)	2 (20%)	0.17	6 (60%)	4 (40%)	0.09	6 (60%)	4 (40%)	0.50
Absent	59	31 (53%)	28 (47%)		18 (31%)	41 (69%)		26 (44%)	33 (56%)	
Lobularity with honeycombing										
Present	2	2 (100%)	0 (0%)	0.50	0 (0%)	2 (100%)	0.54	2 (100%)	0 (0%)	0.21
Absent	67	37 (55%)	30 (45%)		24 (36%)	43 (64%)		30 (45%)	37 (55%)	
Lobularity without honeycombing										
Present	6	5 (83%)	1 (17%)	0.22	4 (67%)	2 (33%)	0.17	5 (83%)	1 (17%)	0.09
Absent	63	34 (54%)	29 (46%)		20 (32%)	43 (68%)		27 (43%)	36 (57%)	
Hyperechoic foci without shadowing										
Present	27	18 (67%)	9 (33%)	0.22	11 (41%)	16 (59%)	0.45	11 (41%)	16 (50%)	0.47
Absent	42	21 (50%)	21 (50%)		13 (31%)	29 (69%)		21 (50%)	21 (50%)	
Stranding										
Present	20	18 (90%)	2 (10%)	0.0004	11 (55%)	9 (45%)	0.03	15 (75%)	5 (25%)	0.003
Absent	49	21 (59%)	28 (41%)		13 (27%)	36 (73%)		17 (35%)	32 (65%)	

Atrophy, inflammation, and fibrosis were divided into two groups based on the grade of pathological findings (high, moderate to severe; low, none to mild).  $p < 0.05$  was considered statistically significant. CP, chronic pancreatitis; EUS, endoscopic ultrasonography; IPMN, intraductal papillary mucinous neoplasm.

vs. 34.5% [10/29],  $p = 0.003$ ; inflammation: 45.0% [18/40] vs. 20.7% [6/29],  $p = 0.04$ ). Assessment of the pathological correlates with each EUS-CP finding revealed higher grades of pancreatic atrophy, inflammation, and fibrosis in patients with “stranding” than in those without (atrophy: 90% [18/20] vs. 43% [21/49],  $p = 0.0004$ ; inflammation: 56% [11/20] vs. 27% [13/49],  $p = 0.03$ ; fibrosis: 75% [15/20] vs. 35% [17/49],  $p = 0.003$ ) (Table 5).

#### *Association of Pathological Changes in the Pancreatic Parenchyma with Invasive IPMC*

Figure 3 displays the relationship between pathological changes (atrophy, inflammation, and fibrosis) in the background pancreatic parenchyma and invasive IPMC. Higher grades of atrophy and inflammation were significantly associated with the presence of invasive IPMC (atrophy:  $p = 0.002$ ; inflammation:  $p = 0.002$ ). Higher grades of fibrosis were also associated with invasive IPMC, but the relationship was not significant ( $p = 0.057$ ).



**Fig. 3.** Association of pathological changes in the pancreatic parenchyma of intraductal papillary mucinous neoplasm with invasive intraductal papillary mucinous carcinoma (IPMC). The figure displays the relationship between pathological changes (atrophy, inflammation, and fibrosis) in the background pancreatic parenchyma

ma and invasive IPMC.  $p < 0.05$  was considered statistically significant. Atrophy, inflammation, and fibrosis were divided into two groups based on the grade of pathological findings (high, moderate to severe; low, none to mild). HGD, high-grade dysplasia; LGD, low-grade dysplasia.

## Discussion

In this study, we found that the frequency of invasive IPMC was significantly higher in patients with EUS-CP findings than in those without. In other words, IPMN patients with “normal background pancreatic parenchyma” on EUS had a significantly lower rate of malignancy. To the best of our knowledge, this is the first study to examine the association between EUS-CP findings and malignant transformation of IPMNs.

The Rosemont classification has been proposed as EUS criteria for diagnosing CP [17]. The EUS-CP findings used in this study corresponded to the parenchymal features of the Rosemont classification. However, the relationship between EUS findings and pathological findings in patients with CP has not been well characterized, even in the Rosemont classification. One of the reasons for this is that tissue specimens for evaluating the pancreatic parenchyma often cannot be obtained in patients with CP because they rarely undergo surgery. In this study, we were able to examine the relationship between EUS-CP findings and pathological changes of the background pancreatic parenchyma because we used the resected specimens from IPMN patients.

In the Rosemont classification, each EUS finding has a predictive value, and the findings are categorized into major or minor criteria. The major criteria of CP are “hyperechoic foci with shadowing” and “lobularity with honeycombing.” On the other hand, “stranding” and “lobularity without honeycombing” are classified as minor cri-

teria because of poor specificity. In the present study, “stranding” and “lobularity without honeycombing” were frequently observed in the background parenchyma of IPMN patients, which was a discrepancy between our results and the Rosemont classification. This difference might have arisen because the causes of CP were different. The Rosemont classification was mainly based on alcoholic CP. On the other hand, our study did not target alcoholic CP, but instead assessed CP caused by mucin stagnation in IPMN patients. It has been reported that hypersecretion of mucin by IPMNs causes obstruction of the main pancreatic duct, which may induce low-grade pancreatitis [2]. This difference in the pathogenesis of the parenchymal changes might be associated with the difference of major EUS findings.

Alcohol consumption is strongly associated with CP [18–20]. In our study, there were no significant differences in alcohol consumption between the groups with and without EUS-CP findings, but the presence of these findings was associated with pathological changes of the background parenchyma, such as atrophy and inflammation. This indicates that the EUS-CP findings we investigated were not associated with alcohol consumption and that an increase in mucin production with malignant transformation of IPMN might be associated with changes in the background parenchyma.

The present study has some limitations. First, it was difficult to demonstrate the association of each EUS-CP finding with specific pathological features. Even in the Rosemont classification, only “hyperechoic foci with

shadowing” and “cysts” (excluded from this study) have histological correlates such as calcification and pseudocyst, while other factors (including “stranding” and “lobularity with honeycombing”) are not associated with specific histological features. Further studies will be required to clarify the pathological correlates of these findings. Next, this was a retrospective single-center study, and the number of subjects was limited. Thus, larger studies will be necessary to confirm our results.

In conclusion, detection of EUS-CP findings in the pancreatic parenchyma of IPMN patients was associated with invasive IPMC. When EUS examination of IPMN is performed, the background parenchyma should be evaluated in addition to the morphological features of the tumor itself.

## Acknowledgments

We would like to thank the staff of the Center of Clinical Research (Dr. Omori) at Kobe University Hospital for their valuable contributions (advice about statistical analysis). The authors assume full responsibility for the analysis and interpretation of the data in this report.

This work was supported by grants from JSPS KAKENHI (Grants-in-Aid for Scientific Research; grant No. 15624848 to A. Masuda and grant No. 15612795 to H. Kutsumi). This work was also supported by the Research Committee of Intractable Pancreatic Diseases from the Ministry of Health, Labor, and Welfare of Japan (A. Masuda, H. Shiomi, and H. Kutsumi).

## Disclosure Statement

The authors have no conflicts of interest to declare.

## References

- 1 Retter J, Dinter D, Bersch C, Singer MV, Lohr M: Acute recurrent pancreatitis curtaining an intraductal papillary mucinous tumor of the pancreas. *J Gastrointest Liver Dis* 2007;16:445–447.
- 2 Kloppel G: Clinicopathologic view of intraductal papillary-mucinous tumor of the pancreas. *Hepatogastroenterology* 1998;45:1981–1985.
- 3 Tanaka M, Fernandez-del Castillo C, Adsay V, et al: International consensus guidelines 2012 for the management of IPMN and MCN of the pancreas. *Pancreatology* 2012;12:183–197.
- 4 Mimura T, Masuda A, Matsumoto I, et al: Predictors of malignant intraductal papillary mucinous neoplasm of the pancreas. *J Clin Gastroenterol* 2010;44:e224–e229.
- 5 Crippa S, Fernandez-Del Castillo C, Salvia R, et al: Mucin-producing neoplasms of the pancreas: an analysis of distinguishing clinical and epidemiologic characteristics. *Clin Gastroenterol Hepatol* 2010;8:213–219.
- 6 Suzuki Y, Atomi Y, Sugiyama M, et al: Cystic neoplasm of the pancreas: a Japanese multi-institutional study of intraductal papillary mucinous tumor and mucinous cystic tumor. *Pancreas* 2004;28:241–246.
- 7 Rodriguez JR, Salvia R, Crippa S, et al: Branch-duct intraductal papillary mucinous neoplasms: observations in 145 patients who underwent resection. *Gastroenterology* 2007;133:72–79; quiz 309–310.
- 8 Aso T, Ohtsuka T, Matsunaga T, et al: “High-risk stigmata” of the 2012 international consensus guidelines correlate with the malignant grade of branch duct intraductal papillary mucinous neoplasms of the pancreas. *Pancreas* 2014;43:1239–1243.
- 9 Ohno E, Hirooka Y, Itoh A, et al: Intraductal papillary mucinous neoplasms of the pancreas: differentiation of malignant and benign tumors by endoscopic ultrasound findings of mural nodules. *Ann Surg* 2009;249:628–634.
- 10 Buscaglia JM, Shin EJ, Giday SA, et al: Awareness of guidelines and trends in the management of suspected pancreatic cystic neoplasms: survey results among general gastroenterologists and EUS specialists. *Gastrointest Endosc* 2009;69:813–820; quiz 820.e1–e17.
- 11 Ridditid W, DeWitt JM, Schmidt CM, et al: Management of branch-duct intraductal papillary mucinous neoplasms: a large single-center study to assess predictors of malignancy and long-term outcomes. *Gastrointest Endosc* 2016;84:436–445.
- 12 Yamamoto N, Kato H, Tomoda T, et al: Contrast-enhanced harmonic endoscopic ultrasonography with time-intensity curve analysis for intraductal papillary mucinous neoplasms of the pancreas. *Endoscopy* 2016;48:26–34.
- 13 Kitano M, Kamata K, Imai H, et al: Contrast-enhanced harmonic endoscopic ultrasonography for pancreatobiliary diseases. *Dig Endosc* 2015;27(suppl 1):60–67.
- 14 Lowenfels AB, Maisonneuve P, Cavallini G, et al: Pancreatitis and the risk of pancreatic cancer. International Pancreatitis Study Group. *N Engl J Med* 1993;328:1433–1437.
- 15 Talamini G, Falconi M, Bassi C, et al: Incidence of cancer in the course of chronic pancreatitis. *Am J Gastroenterol* 1999;94:1253–1260.
- 16 Malka D, Hammel P, Maire F, et al: Risk of pancreatic adenocarcinoma in chronic pancreatitis. *Gut* 2002;51:849–852.
- 17 Catalano MF, Sahai A, Levy M, et al: EUS-based criteria for the diagnosis of chronic pancreatitis: the Rosemont classification. *Gastrointest Endosc* 2009;69:1251–1261.
- 18 Majumder S, Chari ST: Chronic pancreatitis. *Lancet* 2016;387:1957–1966.
- 19 Kume K, Masamune A, Ariga H, Shimosegawa T: Alcohol consumption and the risk for developing pancreatitis: a case-control study in Japan. *Pancreas* 2015;44:53–58.
- 20 Ye W, Lagergren J, Weiderpass E, Nyren O, Adami HO, Ekblom A: Alcohol abuse and the risk of pancreatic cancer. *Gut* 2002;51:236–239.



# Utility of Endoscopic Ultrasound-Guided Hepaticogastrostomy with Antegrade Stenting for Malignant Biliary Obstruction after Failed Endoscopic Retrograde Cholangiopancreatography

Hajime Imai<sup>a</sup> Mamoru Takenaka<sup>a</sup> Shunsuke Omoto<sup>a</sup> Ken Kamata<sup>a</sup>  
Takeshi Miyata<sup>a</sup> Kosuke Minaga<sup>a</sup> Kentaro Yamao<sup>a</sup> Toshiharu Sakurai<sup>a</sup>  
Naoshi Nishida<sup>a</sup> Tomohiro Watanabe<sup>a</sup> Masayuki Kitano<sup>b</sup> Masatoshi Kudo<sup>a</sup>

<sup>a</sup>Department of Gastroenterology and Hepatology, Kindai University Faculty of Medicine, Osaka-Sayama, and

<sup>b</sup>Second Department of Internal Medicine, Wakayama Medical University, Wakayama, Japan

## Keywords

Endoscopic ultrasound-guided hepaticogastrostomy ·  
Endoscopic ultrasound-guided antegrade stenting ·  
Obstructive jaundice · Endoscopic ultrasound-guided  
biliary drainage

## Abstract

**Background:** Endoscopic ultrasound (EUS)-guided biliary drainage (BD) is a well-recognized alternative BD method after unsuccessful endoscopic transpapillary drainage. EUS-guided hepaticogastrostomy (HGS) with antegrade stenting (AGS) was recently applied to the treatment of malignant obstructive jaundice. **Objective:** To assess the efficacy and safety of HGS combined with AGS for treatment of malignant biliary stricture-induced obstructive jaundice. **Design:** Retrospective cohort study. **Setting:** Single academic tertiary care center. **Patients:** From January 2006 to December 2014, endoscopic retrograde cholangiopancreatography was at-

tempted in patients with obstructive jaundice; it was successful in 641 patients and impossible in 154 patients (post-surgically altered anatomy or duodenal stenosis,  $n = 101$ ; difficult cannulation,  $n = 53$ ). In total, 145 patients underwent EUS-guided BD; HGS and HGS with AGS were attempted in 42 patients (Group A, January 2006–August 2011) and 37 patients (Group B, September 2011–December 2014), respectively. **Interventions:** Under EUS and fluoroscopy guidance, HGS and HGS with AGS were performed via needle puncture, guidewire insertion, puncture-hole dilation, and stent placement. **Main Outcome Measurements:** Groups A and B were compared in terms of technical success, functional success, adverse event rates, re-intervention rates, patient survival time, and time to stent dysfunction or patient death. The two groups were also compared in a subgroup analysis of only 28 patients who underwent chemotherapy. **Results:** The technical success rate was significantly higher in Group A than B (97.6 vs. 83.8%,  $p = 0.03$ ). The functional success rate was comparable between the two groups (90.2 vs. 90.3%),

although the rate of adverse events was significantly higher in Group A than B (26.1 vs. 10.8%,  $p = 0.03$ ). The re-intervention rate tended to be higher in Group A than B (16.7 vs. 8.1%,  $p = 0.25$ ). Groups A and B did not differ significantly in terms of median overall patient survival (75 vs. 61 days,  $p = 0.70$ ) or median time to stent dysfunction or patient death (68 vs. 63 days,  $p = 0.08$ ). Among patients who underwent chemotherapy, there was no difference in overall patient survival time between the two groups (121 vs. 157 days,  $p = 0.08$ ), although time to stent dysfunction or patient death was significantly shorter in Group A than B (71 vs. 95 days,  $p = 0.02$ ).

**Conclusion:** Although the technical success rate of HGS with AGS was lower than that of HGS, HGS with AGS was superior to HGS in terms of adverse event rate and stent patency in patients receiving chemotherapy.

© 2017 S. Karger AG, Basel

## Introduction

The gold standard procedure for biliary drainage (BD) is transpapillary drainage during endoscopic retrograde cholangiopancreatography (ERCP). However, ERCP may not be possible in patients with an inaccessible biliary orifice, such as patients with a surgically altered anatomy or duodenal involvement of the tumor. Alternative drainage options in these patients include surgical biliary bypass or percutaneous transhepatic BD (PTBD); however, these procedures are associated with some adverse events [1, 2]. Endoscopic ultrasound (EUS)-guided BD (EUS-BD) techniques such as EUS-guided choledochoduodenostomy (CDS), hepaticogastrostomy (HGS), antegrade stenting (AGS), and rendezvous stenting (RVS) have recently been shown to be useful for BD after unsuccessful ERCP [3–16]. Among these procedures, CDS and RVS require the echoendoscope to reach the duodenum. Therefore, HGS or AGS is indicated in patients with an inaccessible duodenum. However, HGS is associated with a higher risk of adverse events compared with the other methods [17]. When stent dysfunction occurs, re-intervention is more difficult after AGS alone than after HGS or CDS [18]. Thus, we began adding AGS during HGS in a single session in September 2011. The aim of this study was to evaluate the technical success, functional success, adverse events, re-intervention rate, and stent patency before (HGS alone) and after (HGS with AGS) combining both methods and to compare these outcomes between the two groups. The two groups were also compared only among patients receiving chemotherapy.



**Fig. 1.** Puncturing the intrahepatic bile duct. A 19-G needle was inserted into the bile duct under endoscopic ultrasound guidance.

## Patients and Methods

### Patients

This study involved a retrospective analysis of data that had been prospectively collected from clinical records and imaging studies. In total, 795 patients were admitted to our hospital from January 2006 to December 2014 for treatment of obstructive jaundice caused by an unresectable malignant biliary stricture. In 88 patients, ERCP, CDS, and RVS were impossible because of an inaccessible duodenum caused by a surgically altered anatomy or duodenal involvement of the tumor. PTBD was performed in 9 patients. In the remaining 79 patients, we performed HGS with or without AGS. From January 2006 to August 2011, HGS alone was performed ( $n = 42$ , Group A). Beginning in September 2011, we added AGS during HGS in a single session ( $n = 37$ , Group B). The characteristics of patients of Groups A and B are shown in Table 1. All patients provided written informed consent to undergo HGS or HGS with AGS, and the study was approved by the ethics committee of our institution.

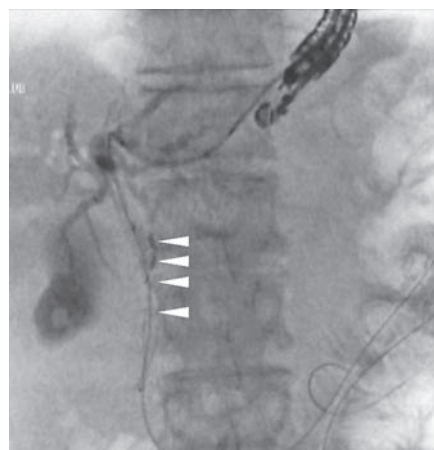
### Techniques

#### HGS

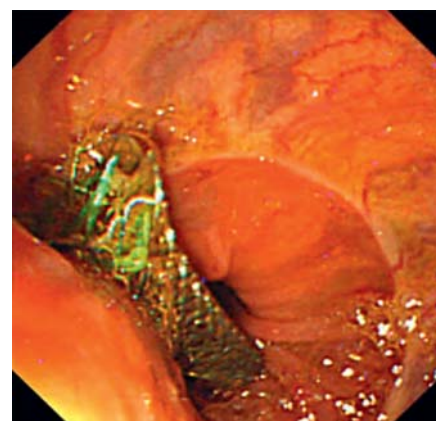
An echoendoscope (GF-UCT240-AL5; Olympus, Tokyo, Japan) was introduced into the stomach and used to visualize the left hepatic bile duct. The scope was manipulated to identify an appropriate puncture route with no interposing vessels. A 19-G needle (SonoTip; Medi-Globe, Aachenmühle, Germany) was inserted into the bile duct under EUS guidance. Bile was aspirated and contrast medium was injected into the bile duct for cholangiography. After confirmation of successful needle puncture by endosonographic and fluoroscopic imaging, a 0.035-inch guidewire (RevoWave; Piolax, Yokohama, Japan) was introduced into the bile duct. The puncture tract was dilated by biliary dilation catheters (6→7→9 Fr). A covered self-expandable metal stent (SEMS) was deployed between the left hepatic bile duct and the stomach.



**Fig. 2.** Insertion of a guide wire. A 0.035-inch guidewire was introduced into the bile duct and manipulated to pass the stricture (arrowheads). The duodenal and/or jejunal lumen was opacified with contrast material to direct the stent placement.



**Fig. 3.** Insertion of the stent at antegrade stenting. An uncovered self-expandable metal stent was deployed across the stricture (arrowheads).



**Fig. 4.** Insertion of the stent at hepaticogastrostomy. A covered self-expandable metal stent was deployed between the left hepatic bile duct and the stomach.

**Table 1.** Characteristics and outcomes of the patients of Groups A and B

	Group A (n = 42)	Group B (n = 37)	p value
Mean age ± SD, years	67.3 ± 13.9	77.0 ± 11.5	0.09
Sex (male/female)	24/18	20/17	0.79
Primary disease, %			
Pancreatic cancer	31.0 (13/42)	24.3 (9/37)	0.51
Bile duct cancer	42.9 (18/42)	29.7 (11/37)	0.23
Lymph node metastasis	26.2 (11/42)	45.9 (17/37)	0.07
Technical success rate, %	97.6	83.8	0.03
Functional success rate, %	90.2	90.3	0.99
Adverse events, %	26.1	10.8	0.03
Re-intervention rate, %	16.7	8.1	0.25
Mean procedure time ± SD, min	73.5 ± 29.4	70.1 ± 30.9	0.67
Median overall survival (range), days	75 (5–354)	61 (16–335)	0.70
Median time to stent dysfunction or patient death (range), days	68 (5–185)	63 (16–335)	0.08

Groups A and B were compared using Fisher exact test, unpaired *t* test, or log-rank test. From January 2006 to August 2011, HGS alone was performed (*n* = 42, Group A). In September 2011, we introduced AGS before deployment of HGS in a single session (*n* = 37, Group B). SD, standard deviation; HGS, EUS-guided hepaticogastrostomy; AGS, EUS-guided antegrade stenting.

#### HGS with AGS

HGS with AGS is a modified HGS technique. An echoendoscope (GF-UCT240-AL5; Olympus, Tokyo, Japan) was introduced into the stomach and used to visualize the left hepatic bile duct. The scope was manipulated to identify an appropriate puncture route with no interposing vessels. A 19-G needle (SonoTip; Medi-Globe, Achenmühle, Germany) was inserted into the bile duct under EUS guidance (Fig. 1). Bile was aspirated and contrast medium was injected into the bile duct for cholangiography. After confirmation of successful needle puncture by endosonographic and

fluoroscopic imaging, a 0.035-inch guidewire (RevoWave, Piolax, Yokohama, Japan) was introduced into the bile duct and manipulated to pass the stricture. The duodenal and/or jejunal lumen was opacified with contrast material to direct the stent placement (Fig. 2). An uncovered SEMS (Zeo Stent; ZEON Medical, Tokyo, Japan) was deployed across the stricture (AGS) (Fig. 3). After AGS, the puncture tract was dilated using biliary dilation catheters (6→7→9 Fr) (Soehendra Biliary Dilation Catheter; Cook Medical, Bloomington, IN, USA). A covered SEMS was deployed between the left hepatic bile duct and the stomach (Fig. 4).

**Table 2.** Characteristics and outcomes of the patients of Groups A and B in chemotherapy

	Group A ( <i>n</i> = 14)	Group B ( <i>n</i> = 14)	<i>p</i> value
Mean age ± SD, years	70.6±6.2	66.1±10.0	0.17
Sex (male/female)	7/7	9/5	0.45
Primary disease, %			
Pancreatic cancer	35.7 (5/14)	7.1 (1/14)	0.07
Bile duct cancer	35.7 (5/14)	35.7 (5/14)	1.0
Lymph node metastasis	28.6 (4/14)	57.1 (8/14)	0.13
Adverse events, %	35.7	14.2	0.19
Re-intervention rate, %	28.6	7.1	0.13
Mean procedure time ± SD, min	59.5±5.4	74.4±6.6	0.09
Median overall survival (range), days	121 (68–354)	157 (52–390)	0.08
Median time to stent dysfunction or patient death (range), days	71 (58–185)	95 (16–335)	0.02

Groups A and B were compared using Fisher exact test, unpaired *t* test, or log-rank test. Between January 2006 and August 2011, HGS alone was performed (*n* = 14, Group A). In September 2011, we introduced AGS before deployment of HGS in a single session (*n* = 14, Group B). SD, standard deviation; HGS, EUS-guided hepaticogastrostomy; AGS, EUS-guided antegrade stenting.

#### Outcome Assessment

The assessed outcomes were the technical and functional success rates, adverse event rate, re-intervention rate, procedure time, overall patient survival time, and time to stent dysfunction or patient death. In Group A, technical success of HGS was defined as successful stent deployment between the left hepatic bile duct and the stomach. In Group B, technical success of HGS with AGS was defined as successful stent deployment at the bile duct stricture (AGS) in addition to successful HGS. Functional success for obstructive jaundice was defined as a decrease in the bilirubin concentration to <40% of the pretreatment value within 2 weeks. The incidence rate of adverse events such as peritonitis, bile leakage, bleeding, stent migration, and stent occlusion was also assessed. Re-intervention was defined as any endoscopic, surgical, or percutaneous procedure that was required to improve symptoms after placement of the stent. The time to stent dysfunction or patient death was defined as the time from stent deployment to biliary re-intervention due to stent dysfunction or the time from stent deployment to patient death. Groups A and B were compared in terms of technical success, clinical success, adverse event outcomes, procedure time, overall patient survival, and time to stent dysfunction or patient death. For the subgroup analysis of only patients who underwent chemotherapy, Groups A and B were compared in terms of overall patient survival and the time to stent dysfunction or patient death.

#### Statistical Analysis

Statistical analysis was performed using SPSS version 11.0 (SPSS Inc., Chicago, IL, USA). Continuous variables were compared between the two groups using Student *t* test. The rates of success, adverse events, and re-intervention were compared between the two groups using Fisher exact test. The Kaplan-Meier method was used to measure overall patient survival and the time to stent dysfunction or patient death. The log-rank test was used to compare Groups A and B in terms of overall patient survival and the time to stent dysfunction or patient death. A two-tailed *p* value of <0.05 was considered statistically significant.

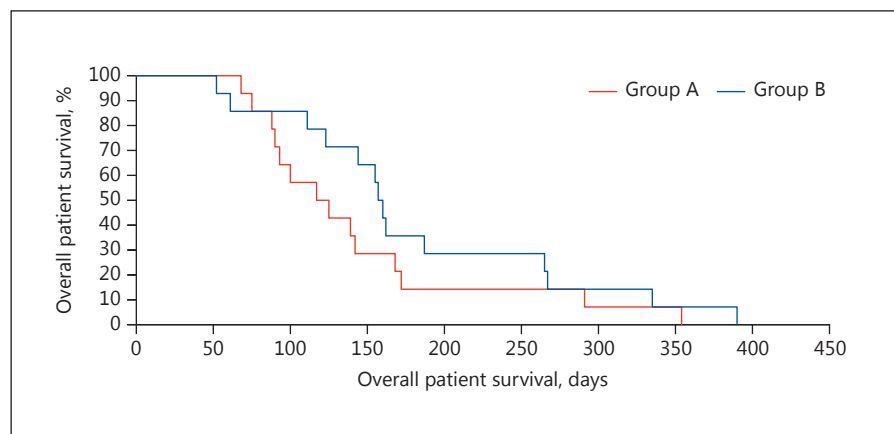
#### Results

The technical success rate was significantly higher in Group A than B (97.6 vs. 83.8%, *p* = 0.03) (Table 1). In Group A, deployment of the covered SEMS between the bile duct and stomach was unsuccessful in only 1 patient. In Group B, AGS failed because a guidewire did not pass the stricture in 6 patients, although the HGS technique was successful in all patients. Functional success was achieved in 37 patients (90.2%) in Group A and 28 patients (90.3%) in Group B. There was no significant difference in the functional success rate between Groups A and B (*p* = 0.99).

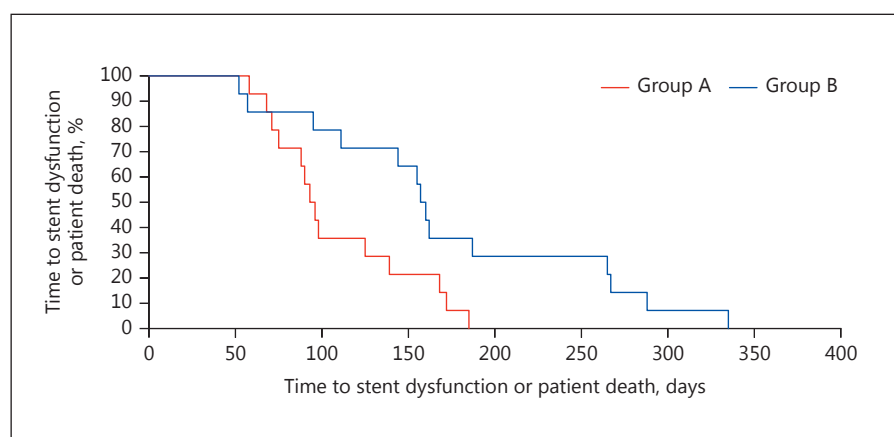
Re-intervention was required in 7 (16.7%) and 3 (8.1%) patients in Groups A and B, respectively (*p* = 0.25). There was no significant difference between Groups A and B in terms of the re-intervention rate, although the rate was higher in Group A. The mean procedure times were 73.4 ± 29.4 and 70.1 ± 30.9 min in Groups A and B, respectively (*p* = 0.67). In Group A, 11 patients (26.2%) had procedural-related adverse events including bile leakage (16.7%, *n* = 7), stent migration (4.8%, *n* = 2), and cholangitis (4.8%, *n* = 2). In Group B, 4 patients (10.8%) had procedural-related adverse events including mild acute pancreatitis (5.4%, *n* = 2), bile leakage (2.7%, *n* = 1), and cholangitis (2.7%, *n* = 1). Two patients with stent migration in Group A required PTBD. All other patients were managed conservatively. There were significant differences in the adverse event rates between Groups A and B (*p* = 0.03). At the time of the retrospective evaluation (June 30, 2015), all patients had died. The median sur-



**Fig. 5.** The Kaplan-Meier curves for the overall patient survival time in Groups A and B among patients who underwent chemotherapy. The median survival times in Groups A and B among patients receiving chemotherapy were 121 and 157 days, respectively ( $p = 0.08$ , log-rank test).



**Fig. 6.** The Kaplan-Meier curves for the median time to stent dysfunction or patient death in Groups A and B among patients who underwent chemotherapy. The median time to stent dysfunction or patient death in Groups A and B among patients receiving chemotherapy were 71 and 95 days, respectively ( $p = 0.02$ , log-rank test).



vival times in Groups A and B were 75 and 61 days, respectively ( $p = 0.70$ ). The median time to stent dysfunction or patient death in Groups A and B were 68 and 63 days, respectively ( $p = 0.08$ ). Groups A and B did not differ significantly in terms of overall patient survival or time to stent dysfunction or patient death. Table 2 shows the detailed characteristics of the patients who underwent chemotherapy. There were no differences in any outcomes between Groups A and B, although the re-intervention rate tended to be higher in Group A than B (28.6 vs. 7.1%,  $p = 0.13$ ). Figures 5 and 6 show the Kaplan-Meier curves for the overall patient survival time and time to stent dysfunction or patient death in Groups A and B among patients who underwent chemotherapy. The median survival times in Groups A and B among patients receiving chemotherapy were 121 and 157 days, respectively ( $p = 0.08$ ). The median time to stent dysfunction or patient death in Groups A and B among patients receiving chemotherapy were 71 and 95 days, respectively ( $p = 0.02$ ).

## Discussion

In 2001, Giovannini et al. [3] published the first report of EUS-guided biliary access from the duodenal bulb followed by plastic stent placement after failed ERCP. Several EUS-BD methods such as CDS, HGS, AGS, and RVS were subsequently reported with respect to the utility of BD methods after unsuccessful ERCP [4–12]. These reports concluded that CDS is indicated in cases of distal biliary obstruction. However, CDS is sometimes difficult to perform because the duodenum is inaccessible due to tumor invasion or after surgical reconstruction. In such cases, HGS or AGS is regarded as the preferred method. Although the choice of transluminal drainage does not appear to affect the adverse event rate, HGS is associated with a higher risk of adverse events [17].

HGS with AGS may have an advantage with respect to adverse events, re-intervention method, and stent patency. HGS with AGS may prevent or reduce adverse events because AGS is carried out without dilation of the HGS

fistula and prevents bile leakage during the dilation of the fistula [18]. Indeed, our results showed that the adverse event rate in Group B (10.8%) is significant lower than that in Group A (26.2%). In particular, the rate of bile leakage in Group B (2.7%) was lower than that in Group A (14.3%). However, mild acute pancreatitis occurred in 2 patients with obstructive jaundice caused by lymph node metastasis of gastric cancer in Group B. A stent deployed not only at the stricture but also at the major papilla may cause acute pancreatitis by compression of the pancreatic duct orifice. Another study using AGS also showed acute pancreatitis after treatment in 8.3% of patients [18]. These results suggest that we must consider the possibility of acute pancreatitis after AGS and avoid stent deployment at the papilla.

If stent occlusion occurs in patients who have undergone AGS alone, re-intervention is very difficult. However, re-intervention can be easily performed through the HGS stent in patients who have undergone HGS with AGS [18]. Indeed, we placed the plastic stent through the HGS stent in 3 patients (Group A,  $n = 1$ ; Group B,  $n = 2$ ) in whom stent occlusion occurred.

Another reason to perform HGS with AGS is that longer stent patency might be obtained than with HGS or AGS only. When one stent becomes occluded, the other stent offers an outlet and avoids obstructive jaundice. One report described stent dysfunction between CDS and HGS [19]. According to that study, stent occlusion resulted in a higher dysfunction rate in HGS than CDS. However, data regarding stent patency in EUS-BD is lacking because of short follow-up periods and survival times. In the present study, Groups A and B did not differ sig-

nificantly in terms of the median time to stent dysfunction or patient death (68 vs. 63 days,  $p = 0.08$ ), but the median time to stent dysfunction or patient death among patients receiving chemotherapy was longer in Group B than A (95 vs. 71 days,  $p = 0.02$ ).

The technical success rate was lower in Group B than A in the current study. The technique of HGS with AGS is similar to that of transgastric RVS. In previous reports about transgastric RVS, the technical success rate ranged from 44 to 100% [20–24]. The most frequent reason for failure of RVS was difficulty in passing the guidewire through the stricture. In our study, 6 cases were attributed to failure to pass a guidewire through the stricture. In these cases, we decided during the procedure to perform HGS.

Our study has two limitations: its retrospective design and performance at a single center. The retrospective nature of the study could have allowed for potential bias in patient selection, limiting the validity of the conclusions. Because the study was conducted at an expert center, the results may not apply universally.

In conclusion, this study shows that EUS-HGS both with and without AGS has equivalent short-term safety and efficacy when performed by experts. However, HGS plus AGS is preferred in patients undergoing chemotherapy because it allows for longer stent patency.

## Disclosure Statement

The authors have no conflicts of interest to declare.

## References

- Smith AC, Dowsett JF, Russell RC, et al: Randomised trial of endoscopic stenting versus surgical bypass in malignant low bile duct obstruction. *Lancet* 1994;344:1655–1660.
- Stoker J, Lameris JS: Complications of percutaneously inserted biliary Wallstents. *J Vasc Interv Radiol* 1993;4:767–772.
- Giovannini M, Moutardier V, Pesenti C, et al: Endoscopic ultrasound-guided bilioduodenal anastomosis: a new technique for biliary drainage. *Endoscopy* 2001;33:898–900.
- Will U, Thieme A, Fuedner F, et al: Treatment of biliary obstruction in selected patients by endoscopic ultrasonography (EUS)-guided transluminal biliary drainage. *Endoscopy* 2007;39:292–295.
- Burmester E, Niehaus J, Leineweber T, et al: EUS-cholangio-drainage of the bile duct: report of 4 cases. *Gastrointest Endosc* 2003;57:246–251.
- Kim YS, Gupta K, Mallery S, et al: Endoscopic ultrasound rendezvous for bile duct access using a transduodenal approach: cumulative experience at a single center. A case series. *Endoscopy* 2010;42:496–502.
- Siddiqui AA, Sreenarasimhaiah J, Lara LF, et al: Endoscopic ultrasound-guided transduodenal placement of a fully covered metal stent for palliative biliary drainage in patients with malignant biliary obstruction. *Surg Endosc* 2011;25:549–555.
- Hara K, Yamao K, Niwa Y, et al: Prospective clinical study of EUS-guided choledochoduodenostomy for malignant lower biliary tract obstruction. *Am J Gastroenterol* 2011;106:1239–1245.
- Komaki T, Kitano M, Sakamoto H, et al: Endoscopic ultrasonography-guided biliary drainage: evaluation of a choledochoduodenostomy technique. *Pancreatol* 2011;11(suppl 2):47–51.
- Dhir V, Bhandari S, Bapat M, et al: Comparison of EUS-guided rendezvous and precut papillotomy techniques for biliary access (with videos). *Gastrointest Endosc* 2012;75:354–359.

- 11 Vila JJ, Perez-Miranda M, Vazquez-Sequeiros E, et al: Initial experience with EUS-guided cholangiopancreatography for biliary and pancreatic duct drainage: a Spanish national survey. *Gastrointest Endosc* 2012;76:1133–1141.
- 12 Nguyen-Tang T, Binmoeller KF, Sanchez-Yague A, et al: Endoscopic ultrasound (EUS)-guided transhepatic antegrade self-expandable metal stent (SEMS) placement across malignant biliary obstruction. *Endoscopy* 2010;42:232–236.
- 13 Artifon EL, Safatle-Ribeiro AV, Ferreira FC, et al: EUS-guided antegrade transhepatic placement of a self-expandable metal stent in hepatico-jejunal anastomosis. *JOP* 2011;12:610–613.
- 14 Weilert F, Binmoeller KF, Marson F, et al: Endoscopic ultrasound-guided antegrade treatment of biliary stones following gastric bypass. *Endoscopy* 2011;43:1105–1108.
- 15 Park DH, Jang JW, Lee SS, et al: EUS-guided transhepatic antegrade balloon dilation for benign bilioenteric anastomotic strictures in a patient with hepaticojejunostomy. *Gastrointest Endosc* 2012;75:692–693.
- 16 Iwashita T, Yasuda I, Doi S, et al: Endoscopic ultrasound-guided antegrade treatments for biliary disorders in patients with surgically altered anatomy. *Dig Dis Sci* 2013;58:2417–2422.
- 17 Dhir V, Artifon EL, Gupta K, et al: Multi-center study on endoscopic ultrasound-guided expandable biliary metal stent placement: choice of access route, direction of stent insertion, and drainage route. *Dig Endosc* 2014;26:430–435.
- 18 Ogura T, Masuda D, Imoto A, et al: EUS-guided hepaticogastrostomy combined with fine-gauge antegrade stenting: a pilot study. *Endoscopy* 2014;46:416–421.
- 19 Hara K, Yamao K, Mizuno N, et al: Endoscopic ultrasonography-guided biliary drainage: who, when, which, and how? *World J Gastroenterol* 2016;22:1297–1303.
- 20 Artifon EL, Marson FP, Gaidhane M, et al: Hepaticogastrostomy or choledochoduodenostomy for distal malignant biliary obstruction after failed ERCP: is there any difference? *Gastrointest Endosc* 2015;81:950–959.
- 21 Iwashita T, Lee JG, Shinoura S, et al: Endoscopic ultrasound-guided rendezvous for biliary access after failed cannulation. *Endoscopy* 2012;44:60–65.
- 22 Maranki J, Hernandez AJ, Arslan B, et al: Interventional endoscopic ultrasound-guided cholangiography: long-term experience of an emerging alternative to percutaneous transhepatic cholangiography. *Endoscopy* 2009;41:532–538.
- 23 Kahaleh M, Hernandez AJ, Tokar J, et al: Interventional EUS-guided cholangiography: evaluation of a technique in evolution. *Gastrointest Endosc* 2006;64:52–59.
- 24 Kawakubo K, Isayama H, Sasahira N, et al: Clinical utility of an endoscopic ultrasound-guided rendezvous technique via various approach routes. *Surg Endosc* 2013;27:3437–3443.

# Primary Hepatic Adenosquamous Carcinoma Associated with Primary Sclerosing Cholangitis

Kentaro Yamao<sup>a</sup> Mamoru Takenaka<sup>a</sup> Hajime Imai<sup>a</sup> Atsushi Nakai<sup>a</sup>  
Shunske Omoto<sup>a</sup> Ken Kamata<sup>a</sup> Kosuke Minaga<sup>a</sup> Takeshi Miyata<sup>a</sup>  
Toshiharu Sakurai<sup>a</sup> Tomohiro Watanabe<sup>a</sup> Naoshi Nishida<sup>a</sup> Ippei Matsumoto<sup>b</sup>  
Yosihumi Takeyama<sup>b</sup> Takaaki Chikugo<sup>c</sup> Masatoshi Kudo<sup>a</sup>

Departments of <sup>a</sup>Gastroenterology and Hepatology, <sup>b</sup>Surgery, and <sup>c</sup>Pathology, Kindai University Faculty of Medicine, Osaka-Sayama, Japan

## Keywords

Adenosquamous carcinoma · Primary sclerosing cholangitis · Liver tumor · Cholangiocarcinoma · Liver abscess · Ulcerative colitis

## Abstract

**Introduction:** Primary sclerosing cholangitis (PSC) is a chronic cholestatic liver disorder characterized by multiple fibrotic strictures of the bile duct. More than 40% of deaths in PSC patients are related to malignant tumors, including cholangiocarcinoma. Primary hepatic adenosquamous carcinoma (ASC) is a rare subtype of cholangiocarcinoma containing adenocarcinoma (AC) and squamous cell carcinoma (SCC) components, with a poorer prognosis than other cholangiocarcinomas. We report the first case of a hepatic ASC in a patient with PSC. **Case Report:** A 28-year-old man was referred for diagnosis and treatment of a liver abscess suspected by contrast-enhanced computed tomography (CE-CT). He had a history of ulcerative colitis and PSC. Abdominal CE-CT revealed a 60-mm-diameter ring-shaped mass with central necrosis in the left lobe. Magnetic resonance imaging demonstrated a poorly circumscribed low-signal-

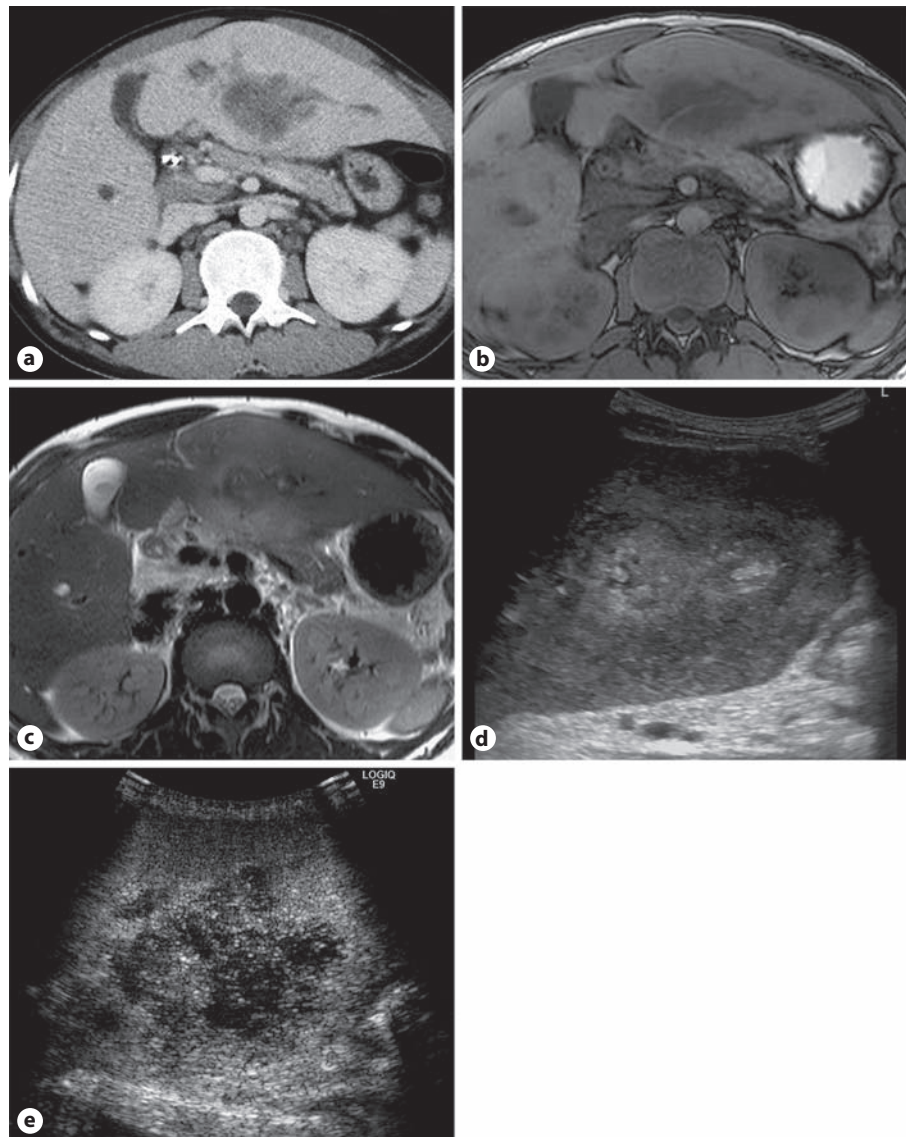
intensity mass in T1-weighted imaging and a high-signal-intensity mass with a scattered low-signal-intensity area in T2-weighted imaging. Abdominal ultrasonography showed a hypoechoic component with a diffuse hyperechoic area in the tumor. Ultrasound-guided biopsy and histological examination showed tumor cells with both squamous and glandular differentiation. Left lobectomy was performed. Microscopic examination revealed 2 components, including moderately differentiated AC and well-differentiated SCC. The final diagnosis was hepatic ASC. **Conclusion:** This is the first reported case of hepatic ASC in a patient with PSC. Patients with PSC should be recognized as being at a risk of not only general cholangiocarcinoma, hepatocellular carcinoma, and metastatic liver tumor, but also ASC.

© 2017 S. Karger AG, Basel

## Introduction

Primary sclerosing cholangitis (PSC) is a chronic cholestatic liver disorder characterized by multiple fibrotic strictures of the intra- and extrahepatic biliary tree. Previous studies have shown that >40% of deaths in patients





**Fig. 1.** **a** Contrast-enhanced abdominal computed tomography. A mass 62 × 45 cm in diameter showing a low-density tumor with an irregularly enhanced rim in the left lobe. **b** Magnetic resonance imaging. T1-weighted image demonstrated a poorly circumscribed low-signal-intensity mass. **c** T2-weighted image demonstrated a high-signal-intensity mass with a scattered low-signal-intensity area in the left lobe. **d** Ultrasonography showed a hypoechoic component with a diffuse hyperechoic area in the tumor. **e** Contrast-enhanced ultrasonography showed an avascular area in the tumor.

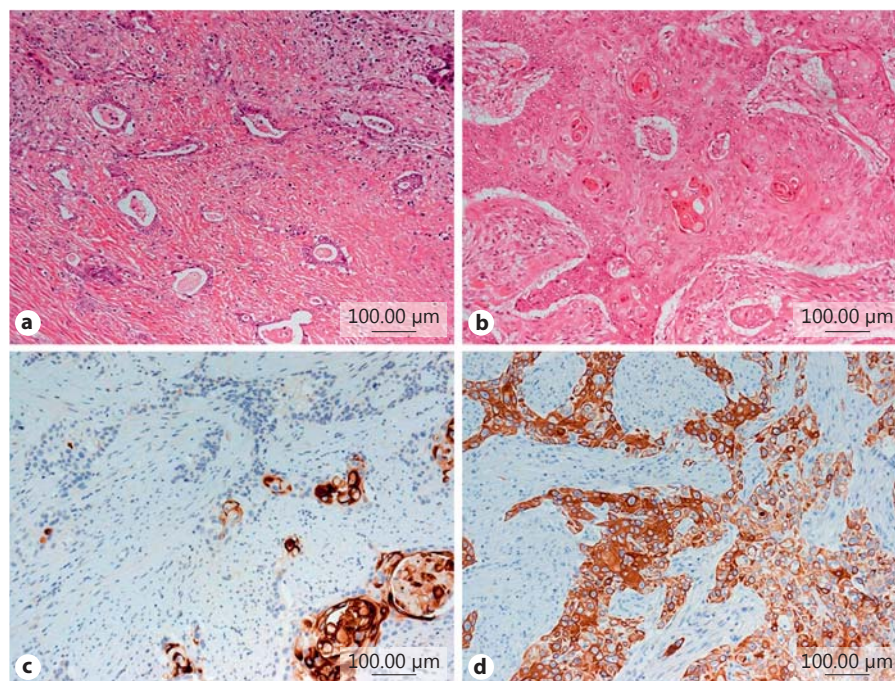
with PSC are related to cholangiocarcinoma, gallbladder carcinoma, or colorectal carcinoma [1, 2]. Cholangiocarcinoma is the most relevant of these, with a lifetime risk in PSC patients of around 7–14% and a prognosis including a 5-year survival of <10% [2].

Primary hepatic adenosquamous carcinoma (ASC) is defined as a rare subtype of cholangiocarcinoma, accounting for 2–3% of cholangiocarcinomas [3–5]. ASC contains both adenocarcinoma (AC) and squamous cell carcinoma (SCC) components, tends to present more aggressive clinicopathologic features, and has a poorer prognosis than other cholangiocarcinomas [6, 7]. Barr and Hancock [8] first reported a case of primary hepatic

ASC in 1975, since when several cases of histologically defined primary hepatic ASC have been reported in the literature [3, 9–12]; however, none have been reported in patients with PSC. We herein report the first case of hepatic ASC in a patient with PSC.

### Case Report

A 28-year-old man was referred for diagnosis and treatment of a liver abscess suspected by abdominal contrast-enhanced computed tomography (CT). The patient's chief complaints were fever and epigastric pain. He was a nonsmoker and had no history of alcohol abuse. He had a 10-year history of ulcerative colitis and a



**Fig. 2.** **a** AC; HE stain. **b** Immunostaining for carcinoembryonic antigen revealed cytoplasm-positive staining for AC. **c** SCC; HE stain. **d** Immunostaining for cytokeratin 5/6 revealed cytoplasm-positive staining for SCC. AC, adenocarcinoma; HE, hematoxylin and eosin; SCC, squamous cell carcinoma.

3-year history of PSC. Endoscopic biliary drainage was performed regularly to exchange the biliary stent in the left bile duct with the stenosis due to PSC.

The results of relevant laboratory studies were total bilirubin 3.4 mg/dL (normal 0.3–1.2 mg/dL), aspartate transaminase 72 IU/L (normal 13–33 IU/L), alanine transaminase 56 IU/L (normal 8–42 IU/L), alkaline phosphatase 1,554 U/L (normal 106–322 U/L), albumin 2.9 g/dL (normal 4.1–5.1 g/dL), C-reactive protein 8.07 mg/dL (normal 0–0.14 mg/dL), white blood cells 16,800/mL (normal 2,800–9,200/mL), prothrombin time international normalized ratio 1.32, indocyanine green retention rate at 15 min 26.0% (normal 0–10%), carcinoembryonic antigen 6.1 ng/mL (normal <5.0 ng/mL), carbohydrate antigen 19–9,290 U/mL (normal <37 U/mL), and SCC antigen 5.1 ng/mL (0–1.5 ng/mL). The patient tested negative for hepatitis B viral surface antigen and hepatitis C viral antibody.

Abdominal contrast-enhanced CT showed an enhanced ring-shaped mass measuring 62 × 45 mm in diameter with central necrosis in the left lobe (Fig. 1a). Magnetic resonance imaging demonstrated a poorly circumscribed low-signal-intensity mass in T1-weighted images (Fig. 1b) and a high-signal-intensity mass with a scattered low-signal intensity area in T2-weighted images (Fig. 1c). Positron emission tomography showed increased <sup>18</sup>F-fluorodeoxyglucose uptake (maximum standardized uptake value: 9.59) in the tumor. These findings, especially the inflammatory reaction, led to suspicion of a liver abscess, but increasing tumor markers indicated a malignant liver tumor.

Abdominal ultrasonography showed a hypoechoic mass with a partial hyperechoic area (Fig. 1d), and contrast-enhanced ultrasonography showed a heterogeneous hypoechoic tumor with a partially avascular area (Fig. 1e). Ultrasonography-guided biopsy was performed, and histological examination revealed tumor cells with both squamous and glandular differentiation. The diagnosis was ASC.

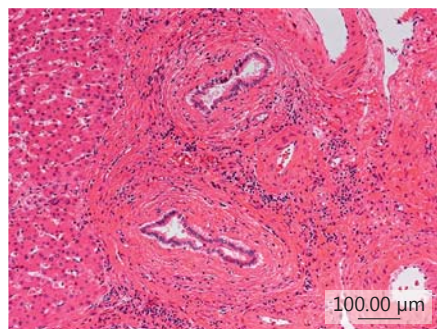
Left lobectomy was performed. The cut surface of the resection specimen showed a yellowish-white solid tumor, measuring 65 × 55 × 45 mm, with partial necrosis. Microscopic examination revealed 2 components, including moderately differentiated AC (Fig. 2a) and well-differentiated SCC (Fig. 2b). The SCC component was predominant over the AC component and occupied >80% of the tumor. There was also a transitional area between the 2 components. Immunohistochemistry revealed carcinoembryonic antigen and cytokeratin 7 expression in most glandular and transitional epithelia (Fig. 2c), but no expression in the stratified squamous epithelia, whereas cytokeratin 5/6 was expressed in most of the SCC (Fig. 2d). A final diagnosis of hepatic ASC was made on the basis of the histological and immunohistochemical findings. Periductal concentric fibrosis of the bile ducts (onion skin-like appearance) suggested the presence of PSC (Fig. 3).

Recurrence was detected in the liver by follow-up examination 1 month postoperatively, and the patient died of ASC recurrence 2 months after surgery.

## Discussion

PSC is a chronic inflammatory liver disease of unknown etiology, primarily targeting cholangiocytes at any portion of the biliary tree. Liver transplantation is currently the only effective treatment. PSC shows a close association with inflammatory bowel disease, mainly ulcerative colitis. As in many chronic inflammatory conditions, PSC may be complicated by cancer development, which accounts for >40% of deaths in patients with PSC





**Fig. 3.** Periductal concentric fibrosis of the bile ducts was present (onion skin-like appearance).

[1, 2, 13]. Cholangiocarcinoma, gallbladder carcinoma, and colorectal carcinoma have been variably associated with PSC, with prevalences of up to 13–14% [14].

ASC is a rare subtype of cholangiocarcinoma with more aggressive clinical and pathological features than other cholangiocarcinomas, and the prognosis of patients with hepatic ASC is extremely poor. Kobayashi et al. [6] reported a mean survival time for patients with hepatic ASC of 8.7 months, and the overall 1-, 2-, and 3-year survival rates after surgery were 38.5, 16.2, and 10.8%, respectively. Uenishi et al. [15] reported a 1-year survival rate for intrahepatic cholangiocarcinoma of 68%, indicating that the prognosis of patients with primary hepatic ASC was poorer than that of patients with the common type of hepatic cholangiocarcinoma.

Chronic inflammation of the biliary tree is thought to be caused by PSC, congenital biliary abnormalities, and hepatolithiasis. The pathogenesis of ASC is still unclear, but it may be caused by continuous irritation of the bile ducts by chronic inflammation or associated with congenital cysts of the biliary tract [16]. Barr and Hancock [8] and Hamaya et al. [17] found no normal epithelium in the tumors they observed, which contained only AC, AC metaplasia, and SCC components, leading them to suggest that ASC may arise from squamous metaplasia of AC cells. In the present case, recurrent acute inflammation due to PSC and/or retrograde cholangitis due to placement of the biliary stent initially led to chronic inflammation, which may then have been responsible for metaplastic changes in the biliary epithelium. The AC component was, therefore, located near the intrahepatic bile duct and was surrounded by the SCC component, with a transitional area between the 2 components.

Liver tumors in patients with PSC include cholangiocarcinoma, hepatocellular carcinoma, metastatic liver tu-

mor, and liver abscess [18, 19]. Imaging of the tumor as a low-density lesion surrounded by a highly enhanced rim on CT may resemble the findings for cholangiocarcinoma, metastatic liver disease, and liver abscess. ASC is a rare subtype of cholangiocarcinoma, and an accurate pre-biopsy diagnosis by radiological imaging was difficult in this case. However, echo-guided ultrasound biopsy was useful for diagnosis, and echo-enhanced tissue sampling enabled biopsy of the optimal part of the tumor, avoiding the necrotic area.

In conclusion, this is the first report describing resection of a hepatic ASC in a patient with PSC. Patients with PSC should be recognized as being at risk of hepatic ASC, in addition to general cholangiocarcinoma, hepatocellular carcinoma, and metastatic liver tumor.

### Statement of Ethics

Written informed consent was obtained from the patient for publication of this case report.

### Disclosure Statement

The authors declare that they have no competing interests.

### Funding Sources

No funding was received.

### Author Contributions

K.Y. drafted the manuscript. A.N., S.O., K.K., K.M., and T.M. worked on clinical data acquisition. H.I. contributed to the treatment of the patient. M.T., I.M., Y.T., and M.K. revised the manuscript critically for important intellectual content. T.C. performed the pathological analysis. All authors read and approved the final manuscript.

### References

- 1 Fevery J, Henckaerts L, Van Oirbeek R, Vermeire S, Rutgeerts P, Nevens F, Van Steenberghe W: Malignancies and mortality in 200 patients with primary sclerosing cholangitis: a long-term single-centre study. *Liver Int* 2012; 32:214–222.
- 2 Bergquist A, Ekblom A, Olsson R, Kornfeldt D, Loof L, Danielsson A, Hultcrantz R, Lindgren S, Prytz H, Sandberg-Gertzén H, Almer S, Granath F, Broome U: Hepatic and extrahepatic malignancies in primary sclerosing cholangitis. *J Hepatol* 2002;36:321–327.

- 3 Nakajima T, Kondo Y: A clinicopathologic study of intrahepatic cholangiocarcinoma containing a component of squamous cell carcinoma. *Cancer* 1990;65:1401–1404.
- 4 Nishioka T, Kubo S, Tanaka S, Wakasa K, Takemura S, Kinoshita M, Hamano G, Kuwae Y, Shibata T, Suehiro S: Outcomes of hepatic resection in intrahepatic cholangiocarcinoma patients with diabetes, hypertension, and dyslipidemia: significance of routine follow-up. *Liver Cancer* 2016;5:107–120.
- 5 Yoh T, Hatano E, Yamanaka K, Nishio T, Seo S, Taura K, Yasuchika K, Okajima H, Kaido T, Uemoto S: Is surgical resection justified for advanced intrahepatic cholangiocarcinoma? *Liver Cancer* 2016;5:280–289.
- 6 Kobayashi M, Okabayashi T, Okamoto K, Namikawa T, Araki K: A clinicopathologic study of primary adenosquamous carcinoma of the liver. *J Clin Gastroenterol* 2005;39:544–548.
- 7 Yeh CN, Jan YY, Chen MF: Adenosquamous carcinoma of the liver: clinicopathologic features in 12 patients and review of the literature. *Int Surg* 2002;87:125–129.
- 8 Barr RJ, Hancock DE: Adenosquamous carcinoma of the liver. *Gastroenterology* 1975;69:1326–1330.
- 9 Hayashi T, Mizuki A, Yamaguchi T, Hasegawa T, Kunihiro T, Tsukada N, Matsuoka K, Orikasa H, Yamazaki K: Primary adenosquamous carcinoma of the liver which produces granulocyte-colony-stimulating factor and parathyroid hormone related protein: association with leukocytosis and hypercalcemia. *Intern Med* 2001;40:631–634.
- 10 Takahashi H, Hayakawa H, Tanaka M, Okamura K, Kosaka A, Mizumoto R, Katsuta K, Yatani R: Primary adenosquamous carcinoma of liver resected by right trisegmentectomy: report of a case and review of the literature. *J Gastroenterol* 1997;32:843–847.
- 11 Yeh CN, Jan YY, Chen MF: Adenosquamous carcinoma of the liver: clinicopathologic study of 10 surgically treated cases. *World J Surg* 2003;27:168–172.
- 12 Yokota H, Matoba M, Tonami H, Hasegawa T, Saito H, Kurose N: Imaging findings in primary adenosquamous carcinoma of the liver: a case report. *Clin Imaging* 2007;31:279–282.
- 13 Bergquist A, Said K, Broome U: Changes over a 20-year period in the clinical presentation of primary sclerosing cholangitis in Sweden. *Scand J Gastroenterol* 2007;42:88–93.
- 14 Bonato G, Cristofori L, Strazzabosco M, Fabris L: Malignancies in primary sclerosing cholangitis – a continuing threat. *Dig Dis* 2015;33(suppl 2):140–148.
- 15 Uenishi T, Hirohashi K, Kubo S, Yamamoto T, Yamazaki O, Kinoshita H: Clinicopathological factors predicting outcome after resection of mass-forming intrahepatic cholangiocarcinoma. *Br J Surg* 2001;88:969–974.
- 16 Ochiai T, Yamamoto J, Kosuge T, Shimada K, Takayama T, Yamasaki S, Ozaki H, Nakanishi Y, Mukai K: Adenosquamous carcinoma with different morphologic and histologic components arising from the intrahepatic bile duct: report of a case. *Hepatogastroenterology* 1996;43:663–666.
- 17 Hamaya K, Nose S, Mimura T, Sasaki K: Solid adenosquamous carcinoma of the liver. A case report and review of the literature. *Acta Pathol Jpn* 1991;41:834–840.
- 18 Kudo M: Surveillance, diagnosis, treatment, and outcome of liver cancer in Japan. *Liver Cancer* 2015;4:39–50.
- 19 Kudo M, Izumi N, Sakamoto M, Matsuyama Y, Ichida T, Nakashima O, Matsui O, Ku Y, Kokudo N, Makuuchi M: Survival analysis over 28 years of 173,378 patients with hepatocellular carcinoma in Japan. *Liver Cancer* 2016;5:190–197.



# Detection of High-Grade Pancreatic Intraepithelial Neoplasia without Morphological Changes of the Main Pancreatic Duct over a Long Period: Importance for Close Follow-Up for Confirmation

Kentaro Yamao<sup>a</sup> Mamoru Takenaka<sup>a</sup> Atsushi Nakai<sup>a</sup> Shunsuke Omoto<sup>a</sup>

Ken Kamata<sup>a</sup> Kosuke Minaga<sup>a</sup> Takeshi Miyata<sup>a</sup> Hajime Imai<sup>a</sup>

Toshiharu Sakurai<sup>a</sup> Tomohiro Watanabe<sup>a</sup> Naoshi Nishida<sup>a</sup> Ippei Matsumoto<sup>b</sup>

Yosihumi Takeyama<sup>b</sup> Takaaki Chikugo<sup>c</sup> Masatoshi Kudo<sup>a</sup>

Departments of <sup>a</sup>Gastroenterology and Hepatology, <sup>b</sup>Surgery, and <sup>c</sup>Pathology, Kindai University Faculty of Medicine, Osaka-Sayama, Japan

## Keywords

Pancreatic cancer · High-grade pancreatic intraepithelial neoplasia · Carcinoma in situ · Localized main pancreatic duct stenosis · Distal main pancreatic duct dilation

## Abstract

Pancreatic intraepithelial neoplasia (PanIN) is a microscopic papillary noninvasive lesion arising from the pancreatic ductal epithelium. However, the natural history and time to progression of high-grade PanIN remain unclear. Herein, we report 2 cases of high-grade PanIN without morphological changes of the main pancreatic duct (MPD) over relatively long periods. In the first case, a 63-year-old man was identified with MPD dilation. Magnetic resonance cholangiopancreatography showed localized stenosis in the pancreatic body with distal MPD dilation. Endoscopic retrograde pancreatography (ERP) was attempted because of possible high-grade PanIN but was unsuccessful. At 15-month follow-up, there was no change in the form of the MPD in various im-

ages. However, ERP was re-performed because of possible high-grade PanIN, and cytology showed adenocarcinoma. Postoperative pathology indicated diffuse lesions corresponding to high-grade PanINs in the MPD stenosis and surrounding branches. Final diagnosis was high-grade PanIN. In the second case, a 77-year-old man was identified with MPD dilation. Magnetic resonance cholangiography showed localized stenosis in the MPD of the pancreatic head with distal MPD dilation. He was diagnosed with MPD stenosis caused by chronic pancreatitis, and further examination was not recommended. At 25 months, the patient was referred to our hospital because of a mild change in MPD dilation. ERP showed localized irregular stenosis in the MPD, and cytology showed suspected adenocarcinoma. Postoperative pathology indicated a localized lesion with high-grade PanIN in the branch duct around the MPD stenosis. Final diagnosis was high-grade PanIN. In conclusion, we report 2 cases of high-grade PanIN without morphological changes of the MPD over relatively long periods. Even if a definite diagnosis is not obtained at initial examination, a strict follow-up observa-

tional study should be performed. Re-examination, including ERP, should also be considered in cases with risk factors of pancreatic cancer, even if there is no change in MPD form.

© 2017 S. Karger AG, Basel

## Introduction

Pancreatic cancer has a poor prognosis, and early diagnosis is important for improved outcomes. Small pancreatic cancers have a better prognosis [1], although detection and diagnosis of noninvasive or small invasive lesions are often challenging. Pancreatic intraepithelial neoplasia (PanIN) is considered a precursor for invasive pancreatic cancer [2]. PanIN is defined as a microscopic papillary or flat and noninvasive epithelial neoplasm arising from the pancreatic ductal epithelium. PanIN is divided into 2 subtypes: low-grade PanIN (previously reported as PanIN-1 and -2) and high-grade PanIN (previously reported as PanIN-3) involving a carcinoma in situ [2, 3]. As high-grade PanIN does not involve a mass-forming lesion, its diagnosis is challenging by imaging. Detection of high-grade PanIN involves the presence of an abnormal main pancreatic duct (MPD) form, including localized MPD stenosis with distal MPD dilation, focal ductal branch dilation, and cyst formation. Exacerbation of these findings with tumor progression is also a sign of high-grade PanIN. However, the natural history and time to progression of high-grade PanIN remain unclear. Herein, we report 2 cases of high-grade PanIN without morphological changes in the MPD over relatively long periods.

## Case Presentation

### Case 1

A 63-year-old man was admitted to our hospital with first ever complaint of back pain in February 2015. He had a medical history of surgery for esophageal cancer without recurrence. He had a smoking history of 40 cigarettes per day for 40 years and an al-

cohol history of 8 cups of whisky per day for 35 years. Abdominal ultrasonography (US) showed dilation of the MPD. Contrast-enhanced computed tomography (CE-CT) and magnetic resonance cholangiopancreatography (MRCP) showed localized stenosis of the MPD in the pancreatic body with distal dilation but no obvious tumor at the site of stenosis (Fig. 1a). Endoscopic US (EUS) showed no mass lesion around the stenosis (Fig. 1b). Endoscopic retrograde pancreatography (ERP) was attempted. However, deep cannulation was unsuccessful, and pathological diagnosis was not performed. Although these findings suggested high-grade PanIN or small pancreatic cancer, the patient was followed up, as there was no definitive diagnosis.

Follow-up examinations were performed for 15 months (3-month intervals) using CT and MRCP. There were no obvious changes in the form of the MPD at follow-up (Fig. 1c). Similar findings were observed by EUS (Fig. 1d). However, ERP was re-performed because of the potential for high-grade PanIN. ERP showed no evidence of abnormalities in the pancreatic head but localized irregular stenosis in the pancreatic body with distal MPD dilation (Fig. 1e). Cytology of pancreatic juice was obtained by aspiration, brushing, and through endoscopic nasopancreatic drainage (ENPD), although only the brush cytology sample showed adenocarcinoma.

The patient underwent a distal pancreatectomy with splenectomy along the line of the right side of the portal vein. Pancreatography of the resected specimen showed irregular stenosis around the margin and dilation of the distal MPD and branches (Fig. 1f). The branches around the MPD stenosis had poor contrast. Microscopically, postoperative pathology indicated diffuse lesions corresponding to high-grade PanINs in the irregular MPD stenosis and surrounding branches (Fig. 1g, h). Immunohistochemical study indicated positive MUC-5AC and -6 staining and negative MUC-1 and -2 staining. Severe fibrosis with numerous inflammatory cells and disappearance of acinar cells were observed around the MPD stenosis. An 8-mm diameter branch-type intraductal papillary mucinous adenoma (IPMA) was observed at the tail of the pancreas but separate from the high-grade PanIN of the MPD. Final diagnosis was high-grade PanIN of the main and branch MPD (Tis N0 M0, stage 0 [UICC-7]) and IPMA. The postoperative course was uneventful, and the patient was discharged and is doing well without recurrence at 10 months following surgery.

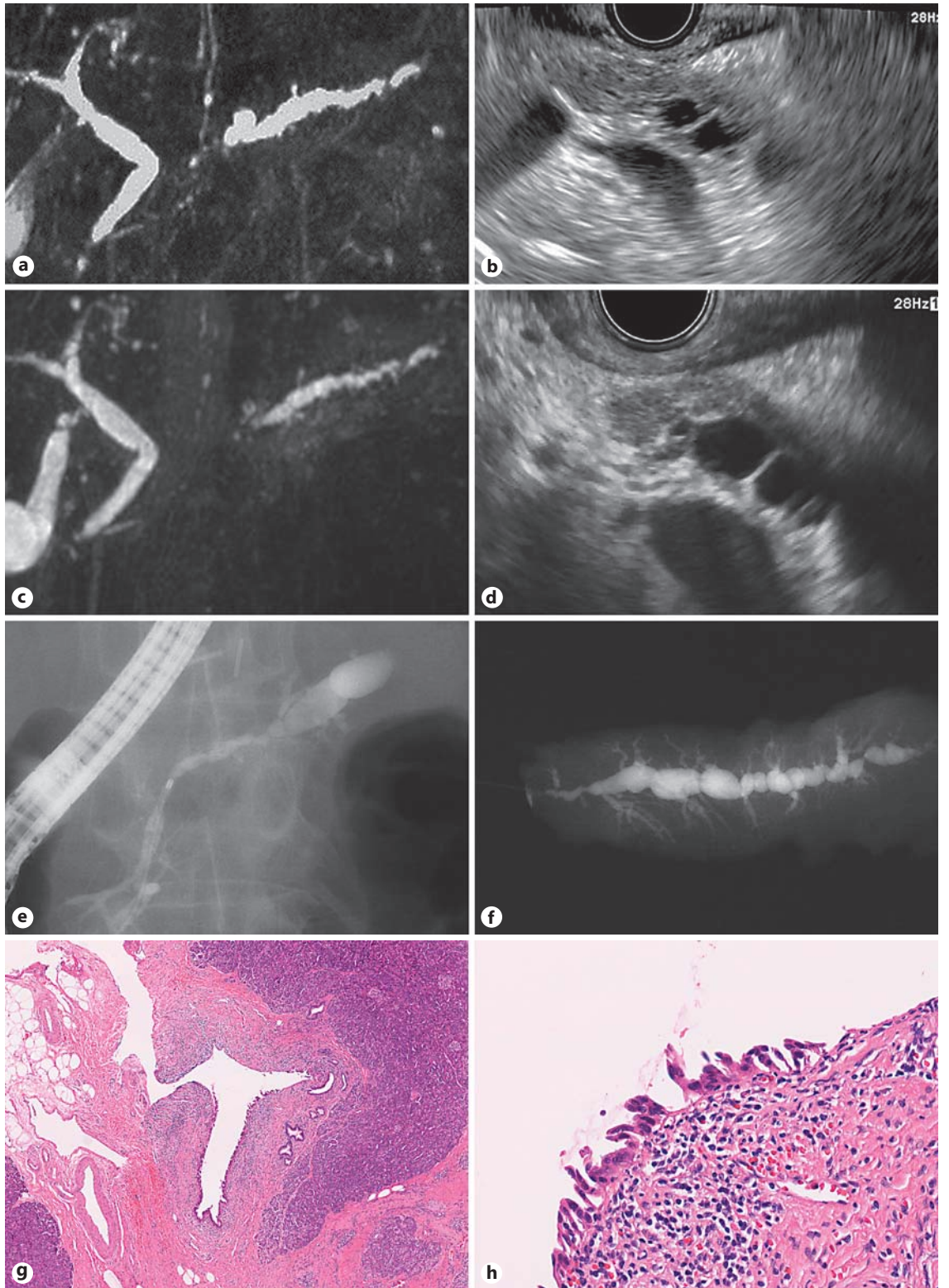
### Case 2

In a 77-year-old man, first ever symptoms of MPD dilation were detected in October 2012, 25 months before referral to our hospital. He had a medical history of cerebral infarction and atrial fibrillation. He had a smoking history of 40 cigarettes per day for 55 years and an alcohol history of 2 bottles of beer per day for 50

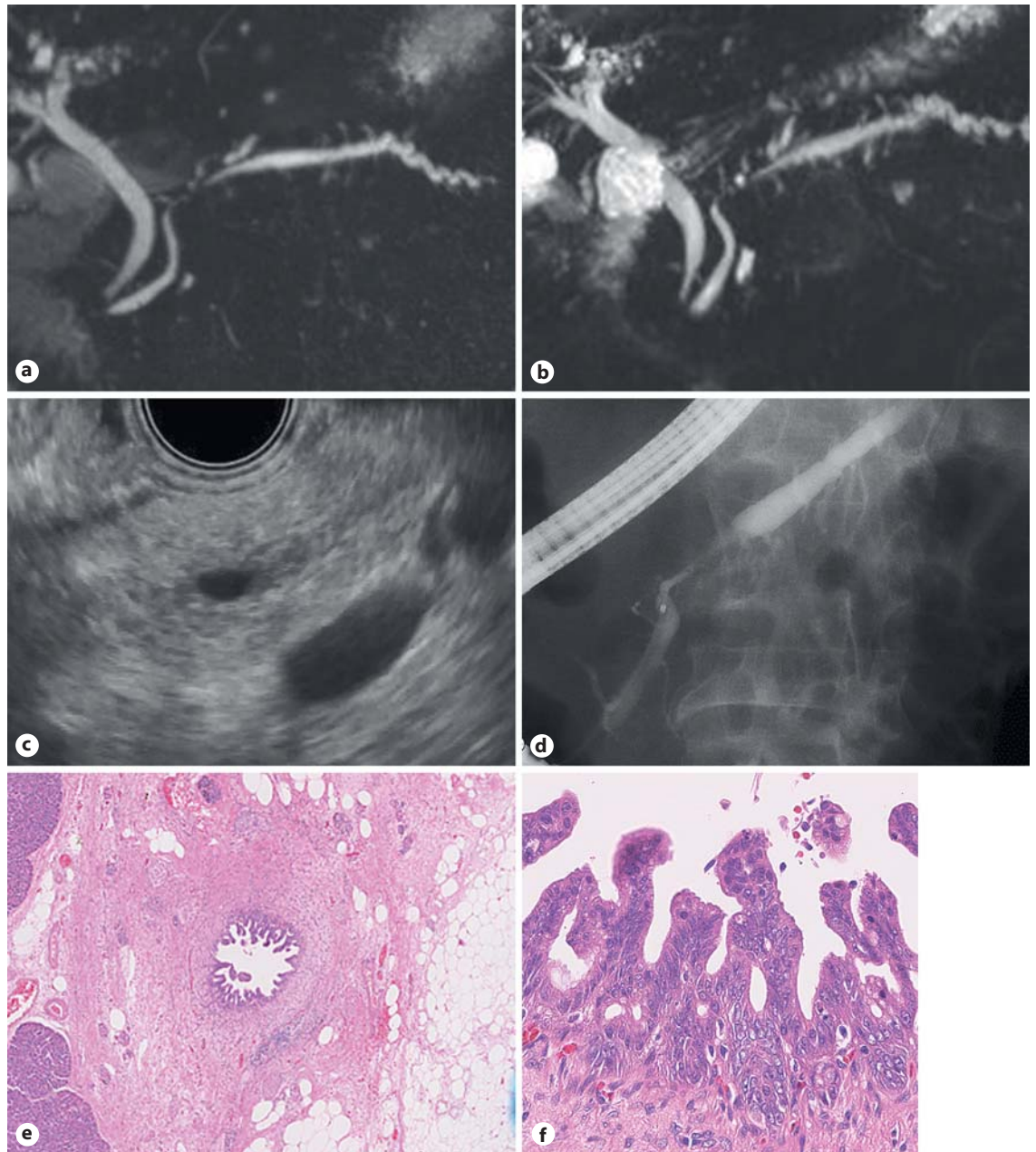
**Fig. 1.** Case 1. **a** Magnetic resonance cholangiopancreatography (MRCP) demonstrated stenosis of the main pancreatic duct (MPD) in the pancreatic head and body and distal MPD dilation. **b** Endoscopic ultrasonography (EUS) revealed no evidence of a mass lesion around the MPD stenosis. **c** MRCP at 15-month follow-up showed no change in MPD stenosis and distal dilation (see **a**). **d** EUS at 15-month follow-up showed no change in MPD form. **e** Endoscopic retrograde pancreatography demonstrated no apparent abnormalities in the pancreatic head of the MPD but local-

ized irregular stenosis in the pancreatic body. **f** Postoperative pancreatography revealed irregular stenosis around the margin and dilation of the distal MPD and branches. The branches around the MPD stenosis had poor contrast. **g, h** Macroscopic pathological findings in the MPD, with evidence of high-grade pancreatic intraepithelial neoplasia. The irregular stenosis of the MPD in the pancreatic body was associated with severe fibrosis and numerous inflammatory cells.

(For figure see next page.)







**Fig. 2.** Case 2. **a** Magnetic resonance cholangiopancreatography (MRCP) revealed MPD stenosis in the pancreatic head and distal MPD dilation. **b** MRCP at 25-month follow-up showed no change of the MPD stenosis and slight worsening of the distal dilation. **c** EUS demonstrating the MPD stenosis without a mass lesion. **d** ERP demonstrating the localized irregular stenosis of the MPD in the pancreatic body. **e, f** Macroscopic pathological findings of the branch pancreatic duct, with evidence of high-grade pancreatic intraepithelial neoplasia.

years. He had received several examinations in October 2012 by a local doctor, with abdominal US showing a 5-mm MPD dilation. CE-CT and MRCP showed localized stenosis of the MPD in the pancreatic head and dilation with distal MPD, although no obvious tumor was observed (Fig. 2a). The diagnosis at that time was MPD stenosis caused by chronic pancreatitis, and the patient was

recommended for observation. Ultrasonography was performed 1 year after, with no change in the form of the MPD. However, the patient was referred to our hospital because of a mild change in the size of the MPD in November 2014 (25 months after his initial visit). CE-CT and MRCP showed stenosis of the MPD in the pancreatic head and distal MPD dilation, although no obvious tumor



at the site of stenosis was observed and the form of the MPD was similar to that 25 months before (Fig. 2b). EUS showed no mass lesion around the MPD stenosis (Fig. 2c). Nevertheless, we performed ERP given the potential for a high-grade PanIN. ERP showed localized irregular stenosis of the MPD in the pancreatic body (Fig. 2d). Aspiration cytology and ENPD repeated cytology were performed, with 1 aspiration cytology sample showing suspected adenocarcinoma. The patient underwent a subtotal stomach-preserving pancreatoduodenectomy.

Microscopically, postoperative pathology indicated a localized lesion with high-grade PanIN in the branch duct around the MPD stenosis (Fig. 2e, f). Immunohistochemical study indicated positive MUC-6 staining and negative MUC-1, -2, and -5AC staining. Severe fibrosis with numerous inflammatory cells and disappearance of acinar cells were observed around the MPD stenosis. A 10-mm diameter branch-type IPMA was observed at the head of the pancreas, separate from the high-grade PanIN of the MPD. The final diagnosis was high-grade PanIN of the branch duct (Tis N0 M0, stage 0 [UICC-7]) and IPMA. The postoperative course was uneventful, and the patient was discharged and is doing well without recurrence at 32 months following surgery.

## Discussion

Patients with pancreatic cancer have an extremely poor prognosis because of the difficulty of early detection and the highly progressive tumor speed. Nevertheless, the 5-year survival rate of patients with high-grade PanIN is 85.8% [1]. Thus, early detection of pancreatic cancer is critical for improved prognosis. PanINs are defined as non-mass-forming lesions found only in the pancreatic ductal epithelium [2]. Detection of high-grade PanIN involves the presence of an abnormal MPD form, including localized MPD stenosis with distal MPD dilation, focal ductal branch dilation, and cyst formation. Exacerbation of these findings with tumor progression is also a sign of high-grade PanIN.

However, there was no evidence of new tumor appearance or exacerbation of the MPD form at long-term follow-up in our 2 cases of high-grade PanIN (case 1, 15 months; case 2, 25 months), indicating no or slight progression during this period. The long follow-up period in case 1 was because there was no definitive diagnosis of pancreatic cancer (ERP was unsuccessful), while case 2 was followed up in a nonspecialized hospital where the initial MPD abnormality was detected. Although there was no definitive diagnosis of PanINs at the initial hospital visits, if present, these findings without morphological changes of the MPD suggest that the progression time of PanINs was very slow.

In a genomic analysis of autopsy patients with pancreatic cancer to evaluate the clonal relationships between primary and metastatic cancers, Yachida et al. [4] report-

ed a progression time between tumor genesis and PanIN (until the progression of the invasive carcinoma) of 11.7 years. These data support our findings of the presence of high-grade PanINs during the 1- to 2-year period from initial findings to surgery in our 2 cases. To our knowledge, there is only 1 reported case of high-grade PanIN in which diagnosis of malignancy was difficult and with a follow-up of more than 1 year. However, in that case, the form of the MPD changed markedly at 2.5 years after initial examination [5]. Therefore, our 2 cases without morphological changes of the MPD are important for clinical practice.

As high-grade PanINs are non-mass-forming lesions and are difficult to visualize, EUS-guided fine-needle aspiration biopsy, which is generally performed to diagnose pancreatic cancer, is not effective. There are previous reports using cytology with pancreatic juice, including repeated cytology of pancreatic juice obtained using an ENPD tube and brush cytology, for diagnosis of high-grade PanINs and small pancreatic cancer. Using repeated cytology with an ENPD tube, Liboshi et al. [6] reported a sensitivity, specificity, and accuracy of detecting high-grade PanIN and small pancreatic cancer of 100, 83.3, and 95%, respectively, while Mikata et al. [7] reported a sensitivity, specificity, and accuracy of detecting pancreatic cancer, including advanced pancreatic cancer, of 80, 100, and 87%, respectively, which was significantly higher than the sensitivity, specificity, and accuracy obtained when using single cytology. Further, 1 study reported diagnosis using brush cytology in a high-grade PanIN patient [5]. Thus, these methods can be used to directly and efficiently collect the specimens of pancreatic duct epithelium lesions, which are otherwise difficult to perform using EUS-guided fine-needle aspiration.

The 2016 revised clinical guidelines for pancreatic cancer using evidence-based medicine published by the Japan Pancreas Society suggest a number of risk factors for pancreatic cancer, including family history of pancreatic cancer, diabetes, obesity, chronic pancreatitis, intraductal papillary mucinous neoplasm, pancreatic cysts, smoking, and heavy drinking [8]. Our 2 cases had intraductal papillary mucinous neoplasm, smoking, and heavy drinking as risk factors. Thus, cases with localized MPD stenosis and distal MPD dilation should be closely monitored for potential high-grade PanIN, even if the form of the MPD does not change at follow-up observation. Further, patients with some risk factors for pancreatic cancer should be more carefully monitored. In such cases, ERP with pancreatic juice cytology should be considered for definitive diagnosis.

In conclusion, we reported 2 cases of high-grade PanIN without morphological changes of the MPD over relatively long periods. When findings of localized MPD stenosis and distal MPD dilation are detected, a definite diagnosis of high-grade PanINs should be considered by pancreatic juice cytology. Even if a definite diagnosis cannot be obtained, strict follow-up observational study should be performed. Re-examination should also be considered, particularly in cases with some risk factors for pancreatic cancer, even if there is no change in the MPD form.

### Statement of Ethics

Written informed consent was obtained from both patients for publication of this case report.

### Disclosure Statement

The authors declare that they have no competing interests.

### Funding Sources

No funding was received.

### Author Contributions

K.Y. drafted the manuscript. A.N., S.O., K.K., K.M., and T.M. performed clinical data acquisition. H.I. contributed to the treatment of the patient. M.T., I.M., Y.T., and M.K. critically revised the manuscript for important intellectual content. T.C. performed the pathological analysis. All authors read and approved the final manuscript.

### References

- 1 Egawa S, Toma H, Ohigashi H, Okusaka T, Nakao A, Hatori T, et al: Japan Pancreatic Cancer Registry; 30th year anniversary: Japan Pancreas Society. *Pancreas* 2012;41:985–992.
- 2 Hruban RH, Adsay NV, Albores-Saavedra J, Compton C, Garrett ES, Goodman SN, et al: Pancreatic intraepithelial neoplasia: a new nomenclature and classification system for pancreatic duct lesions. *Am J Surg Pathol* 2001;25:579–586.
- 3 Basturk O, Hong SM, Wood LD, Adsay NV, Albores-Saavedra J, Biankin AV, et al: A revised classification system and recommendations from the Baltimore Consensus Meeting for Neoplastic Precursor Lesions in the Pancreas. *Am J Surg Pathol* 2015;39:1730–1741.
- 4 Yachida S, Jones S, Bozic I, Antal T, Leary R, Fu B, et al: Distant metastasis occurs late during the genetic evolution of pancreatic cancer. *Nature* 2010;467:1114–1117.
- 5 Seki M, Ninomiya E, Hayashi K, Gotoh H, Koga R, Saiura A, et al: Widespread and multifocal carcinomas in situ (CISs) through almost the entire pancreas: report of a case with preoperative cytological diagnosis. *Langenbecks Arch Surg* 2010;395:589–592.
- 6 Iiboshi T, Hanada K, Fukuda T, Yonehara S, Sasaki T, Chayama K: Value of cytodiagnosis using endoscopic nasopancreatic drainage for early diagnosis of pancreatic cancer: establishing a new method for the early detection of pancreatic carcinoma in situ. *Pancreas* 2012;41:523–529.
- 7 Mikata R, Ishihara T, Tada M, Tawada K, Saito M, Kurosawa J, et al: Clinical usefulness of repeated pancreatic juice cytology via endoscopic naso-pancreatic drainage tube in patients with pancreatic cancer. *J Gastroenterol* 2013;48:866–873.
- 8 Yamaguchi K, Okusaka T, Shimizu K, et al: Clinical practice guidelines for pancreatic cancer 2016 from the Japan Pancreas Society: a synopsis. *Pancreas* 2017;46:595–604.

# EUS-Guided Pancreatic Duct Drainage for Repeat Pancreatitis in a Patient with Pancreatic Cancer

Ken Kamata Mamoru Takenaka Kosuke Minaga Toshiharu Sakurai  
Tomohiro Watanabe Naoshi Nishida Masatoshi Kudo

Department of Gastroenterology and Hepatology, Kindai University School of Medicine, Osaka-Sayama, Japan

## Keywords

Pancreatic cancer · Endoscopic ultrasonography · Pancreatitis

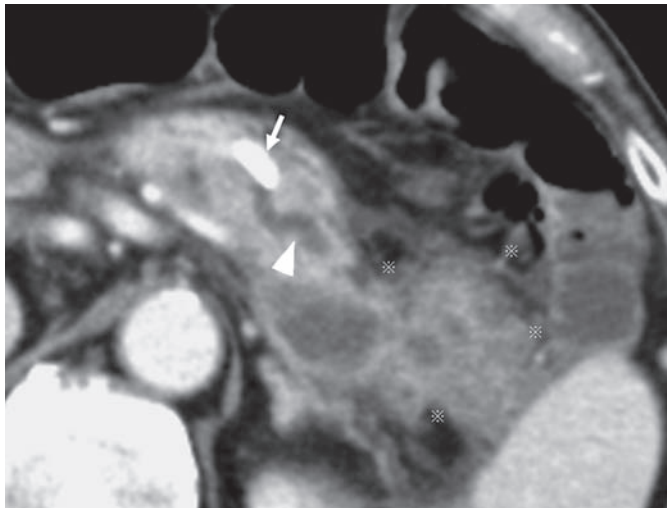
## Abstract

Endoscopic ultrasound-guided pancreatic drainage (EUS-PD) was performed in a patient with unresectable pancreatic cancer who developed pancreatitis. In this case, EUS-PD was useful as salvage therapy for pancreatitis as the transpapillary approach was difficult.

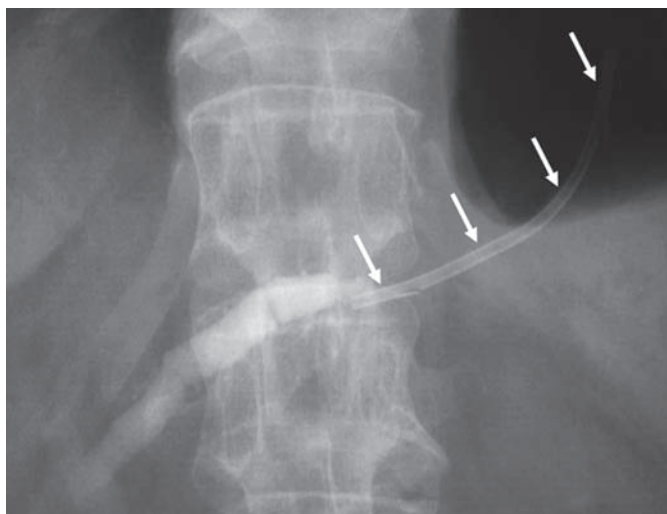
© 2017 S. Karger AG, Basel

Endoscopic ultrasound-guided pancreatic drainage (EUS-PD) has been described as a new drainage technique after unsuccessful transpapillary approach for pancreatic duct strictures [1–3]. Our patient was a 74-year-old man with unresectable pancreatic cancer receiving chemotherapy. Due to repeated pancreatitis, however, he could not continue treatment and was forced to stop chemotherapy. The patient had no history of chronic pancreatitis but abdominal CT showed a pancreatic duct stone in the main pancreatic duct at the pancreatic body. The main pancreatic duct was slightly dilated

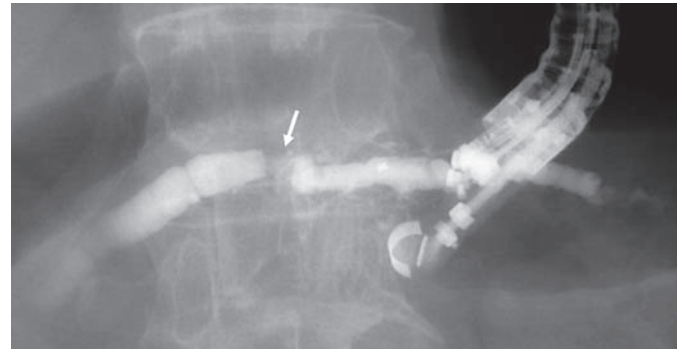
from the tail side of the stone, with localized pancreatitis observed around the pancreatic tail (Fig. 1). The pancreatic cancer was located in the pancreatic head, whereas the pancreatic stone was located in the pancreatic body (Fig. 1). After pancreatitis was resolved, transpapillary pancreatic duct drainage was attempted, but the guide wire could not be deployed over the pancreatic duct stricture caused by the tumor. Then, EUS-PD was performed to prevent pancreatitis induced by a pancreatic duct stricture. The patient was placed under sedation with a bolus infusion of 0.05 ml/kg propofol. The dilated pancreatic duct from the tail side of the stone, as viewed echoendoscopically (GF-UCT260; Olympus) from the stomach position, was punctured with a 19-gauge needle (Sonotip; Medi-Globe), with correct puncturing confirmed with contrast medium (Fig. 2). A 0.025-inch guidewire (Visi-Glide2; Olympus) was inserted toward the pancreatic tail. After dilating the fistulous tract using a diathermic dilator, a 7-Fr plastic stent (7 cm in length; Boston Scientific) was successfully deployed (Fig. 3). There were no complications during the procedure. Seven days later, the patient's serum amylase concentration had decreased to 88 U/L and he started dietary intake. One month after the procedure, he resumed chemotherapy, with no recurrence of pancreatitis to date. Findings in this patient in-



**Fig. 1.** Abdominal CT image of the patient, showing dilation of the main pancreatic duct (arrowhead) from the stone (arrow) to the tail side with localized pancreatitis (※) observed around the pancreatic tail.



**Fig. 3.** Fluoroscopic image showing the deployment of a 7-Fr plastic stent (arrows) at the tail side from the stone between the pancreatic duct in the body of the pancreas and the gastric body.



**Fig. 2.** Fluoroscopic image showing that the defect was a pancreatic stone (arrow) in the pancreatic body.

indicated that the pancreatic duct stone caused repeat pancreatitis, resulting in discontinuation of chemotherapy. Although transpapillary pancreatic duct drainage was considerable, pancreatic duct drainage over the tumor and the pancreatic duct stricture was limited. The presence of the tumor in the head of the pancreas may have made stone removal more difficult. EUS-PD may constitute salvage therapy when the transpapillary approach is difficult.

#### Disclosure Statement

All authors disclosed no financial relationships relevant to this publication.

#### References

- 1 Itoi T, Kasuya K, Sofuni A, et al: Endoscopic ultrasonography-guided pancreatic duct access: techniques and literature review of pancreatography, transmural drainage and rendezvous techniques. *Dig Endosc* 2013;25:241–252.
- 2 Kurihara T, Itoi T, Sofuni A, et al: Endoscopic ultrasonography-guided pancreatic duct drainage after failed endoscopic retrograde cholangiopancreatography in patients with malignant and benign pancreatic duct obstructions. *Dig Endosc* 2013;25(suppl 2):109–116.
- 3 Tyberg A, Sharaiha RZ, Kedia P, et al: EUS-guided pancreatic drainage for pancreatic strictures after failed ERCP: a multicenter international collaborative study. *Gastrointest Endosc* 2017;85:164–169.



# A Social Program for the Early Detection of Pancreatic Cancer: The Kishiwada Katsuragi Project

Hiroki Sakamoto<sup>a</sup> Satoshi Harada<sup>a</sup> Nobu Nishioka<sup>a</sup> Kazuo Maeda<sup>b</sup>  
Takamasa Kurihara<sup>c</sup> Tateki Sakamoto<sup>d</sup> Kazuhide Higuchi<sup>e</sup> Masayuki Kitano<sup>f</sup>  
Yoshifumi Takeyama<sup>g</sup> Masafumi Kogire<sup>h</sup> Masatoshi Kudo<sup>i</sup>

<sup>a</sup>Department of Gastroenterology, Katsuragi Hospital, <sup>b</sup>Internal Medicine, Maeda Clinic, <sup>c</sup>Internal Medicine, Kurihara Clinic, <sup>d</sup>Internal Medicine and Pediatrics, Sakamoto Clinic, and <sup>e</sup>2nd Department of Internal Medicine, Osaka Medical College, Osaka-Sayama, <sup>f</sup>Second Department of Internal Medicine, Wakayama Medical University Hospital, Wakayama, and Departments of Surgery at <sup>g</sup>Kindai University Faculty of Medicine and <sup>h</sup>Kishiwada City Hospital, and <sup>i</sup>Department of Gastroenterology and Hepatology, Kindai University Hospital, Osaka-Sayama, Japan

## Keywords

Pancreatic cancer · Early pancreatic cancer · Intraductal papillary mucinous neoplasm · Endoscopic ultrasound · Kishiwada Katsuragi project

## Abstract

**Objectives:** The early-stage pancreatic cancer (e-PC; stage I/II) detection rate is quite low at approximately 25%. The aim of this study was to evaluate the feasibility of a social program (the Kishiwada Katsuragi project) wherein our hospital, which specializes in PC, and primary care medical offices (PMOs) used clinical findings to detect e-PC. **Methods:** Patients with a score of  $\geq 2$  points on clinical findings were enrolled: symptoms of abdominal pain/back pain (1 point), new-onset diabetes (1 point), high amylase (AMY) and/or pancreatic AMY (P-AMY) (1 point), high carbohydrate antigen 19-9 (1 point), and ultrasonography (US) findings including direct (e.g., a solid pancreatic tumor) and/or indirect findings (e.g., dilatation of a pancreatic diameter of  $\geq 2.5$  mm

and/or cystic lesions) (2 points) were evaluated using the protocol for social programs. **Results:** Between November 2014 and December 2016, 244 patients were enrolled by 41 PMOs as cooperative facilities, and 15 e-PC cases (53.6%) of the 28 PC patients were detected. The mean clinical finding score of the e-PC group ( $3.13 \pm 1.9$ ) was significantly higher than that of the overall non-PC group ( $2.1 \pm 0.4$ ) ( $p < 0.05$ ). “High AMY/P-AMY” and “symptoms” were significantly more frequent in the e-PC group than in the non-PC group ( $p < 0.05$ ). Although the sensitivity of direct findings by US was 40.0%, that of indirect findings was 93.3% in the e-PC group. Nine and 6 of the 15 patients with e-PC were enrolled via general internal medicine offices (GIMs) and other PMOs without GIMs (general surgery,  $n = 3$ ; urology,  $n = 2$ ; otolaryngology,  $n = 1$ ). **Conclusion:** This social program with collaborations between medical centers that specialize in PC and PMOs used clinical findings, suggesting that not only GIMs but also other PMOs and indirect findings by US may play an important role in improving the e-PC detection rate.

© 2017 S. Karger AG, Basel

## Introduction

Pancreatic cancer (PC) is generally associated with a poor prognosis and is difficult to diagnose early enough for surgical resection, the only potentially curative treatment for PC, to be performed. Indeed, only 25% of PC patients have early-stage PC (e-PC) at the time of detection [1, 2].

A screening program is needed to improve the detection rate of e-PC. Previous studies have identified various risk groups and factors (a family history of PC and pancreatitis, smoking, alcohol consumption, diabetes (DM), obesity, and cystic lesions, including intraductal papillary mucinous neoplasm and main pancreatic duct [MPD] dilatation), but few standard programs are available for screening high-risk patients. Evidence-based clinical guidelines for PC were published by the Japan Pancreas Society (JPS) in 2006, with the third edition released in 2013 [3]. The guidelines include a protocol for diagnosing and treating PC. The sections of Clinical questions 1 and 2 suggest several risk factors that may be involved in the development of PC [4–11].

The guidelines include a protocol for a social program to diagnose e-PC by consulting clinical findings (the

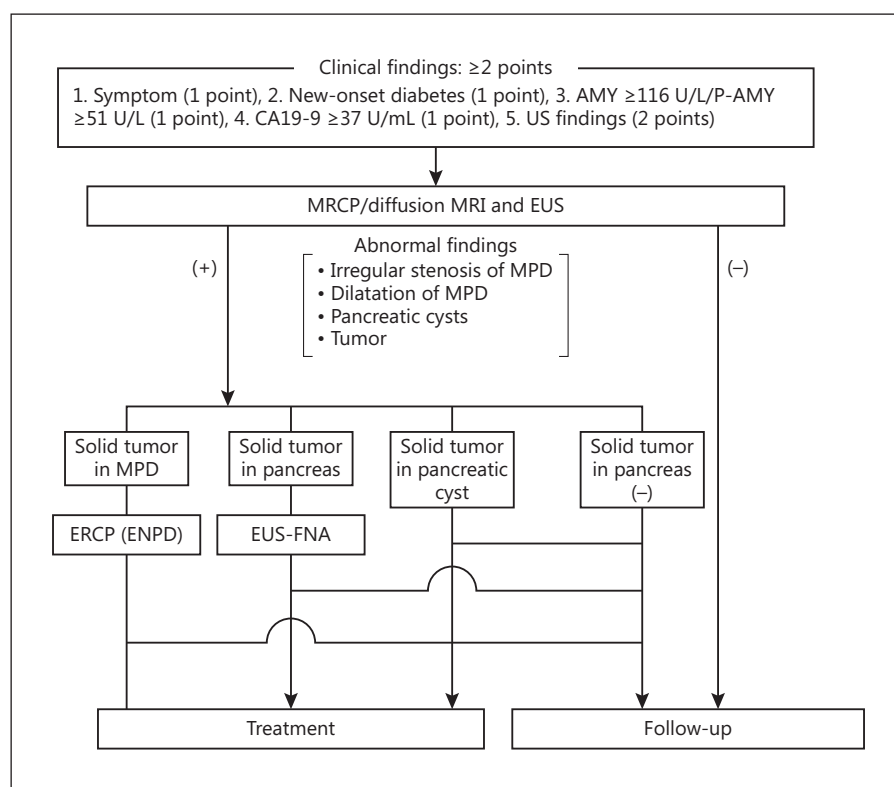
Kishiwada Katsuragi project). The aim of the present study was to evaluate the feasibility of such a social program via collaboration between our medical center, which specializes in PC, and primary-care medical offices (PMOs).

## Patients and Methods

Forty-one PMOs, including 27 general internal medicine offices (GIMs) and 14 other PMOs (otolaryngology,  $n = 4$ ; general surgery,  $n = 3$ ; orthopedic surgery,  $n = 2$ ; gynecology,  $n = 2$ ; urology,  $n = 2$ , and psychiatry,  $n = 1$ ), were enrolled. If a patient presented with  $\geq 2$  points for 5 clinical findings, they were examined in accordance with the protocol for social programs for diagnosing e-PC (Fig. 1). If a patient did not receive ultrasonography (US) and/or did not undergo a carbohydrate antigen 19-9 (CA19-9) examination by the PMO at entry into this study, then they received these evaluations before undergoing magnetic resonance cholangiopancreatography (MRCP) including magnetic resonance imaging (MRI), and endoscopic ultrasound (EUS) at our institution.

Between November 2014 and October 2016, 244 patients in whom PC was suspected based on the clinical findings (at the co-operating facilities) were evaluated. Twenty-eight (11.5%) of these 244 patients were ultimately diagnosed with PC. This study received approval from the ethics committee of Katsuragi Hospital.

**Fig. 1.** The protocol for the social program for diagnosing early-stage pancreatic cancer. ENPD, endoscopic nasopancreatic drainage; ERCP, endoscopic retrograde cholangiopancreatography; EUS, endoscopic ultrasonography; FNA, fine-needle aspiration; MPD, main pancreatic duct; MRCP, magnetic resonance cholangiopancreatography; MRI, magnetic resonance imaging; US, ultrasonography; CA19-9, carbohydrate antigen 19-9; P-AMY, pancreatic amylase.



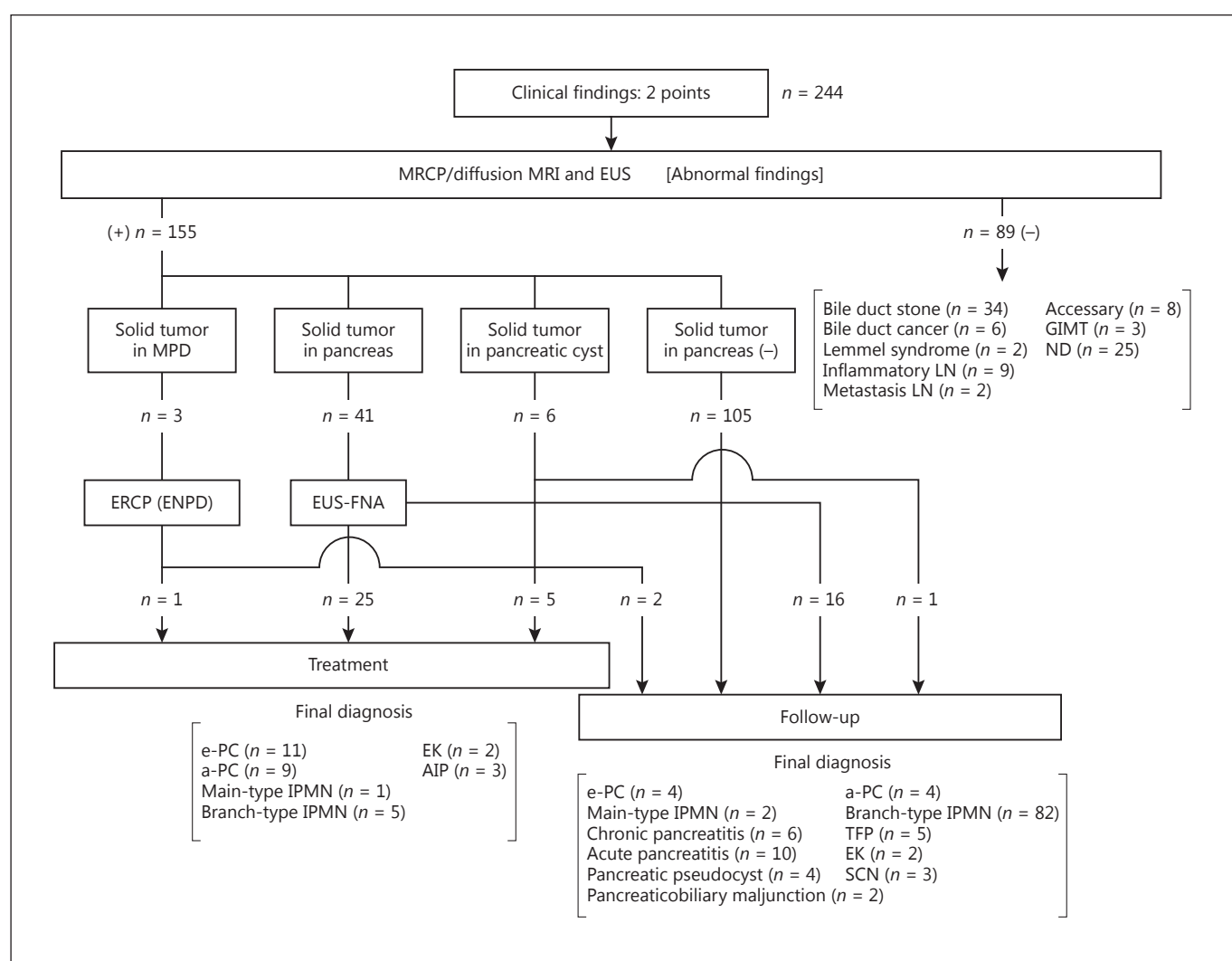
### Clinical Findings

Patients with 2 points for the following clinical findings were diagnosed with suspected PC: (1) symptoms (abdominal pain or fatigue, or back pain) (1 point) [3], (2) new-onset DM (1 point) [12–14], (3) a high amylase (AMY) level ( $\geq 116$  U/L) and/or pancreatic amylase (P-AMY) level ( $\geq 51$  U/L) (1 point) [3], (4) a high CA19-9 level ( $\geq 37$  U/mL) (1 point) [15–17], and (5) US findings (2 points) [18, 19]. The US findings included direct (e.g., a solid pancreatic tumor) and indirect findings (e.g., dilatation of the MPD to a diameter of  $\geq 2.5$  mm or a pancreatic cyst). DM was defined as a fasting blood sugar level of  $\geq 126$  mg/dL, a casual blood glucose level of  $\geq 200$  mg/dL, or HbA1c (NGSP)  $\geq 6.5\%$ .

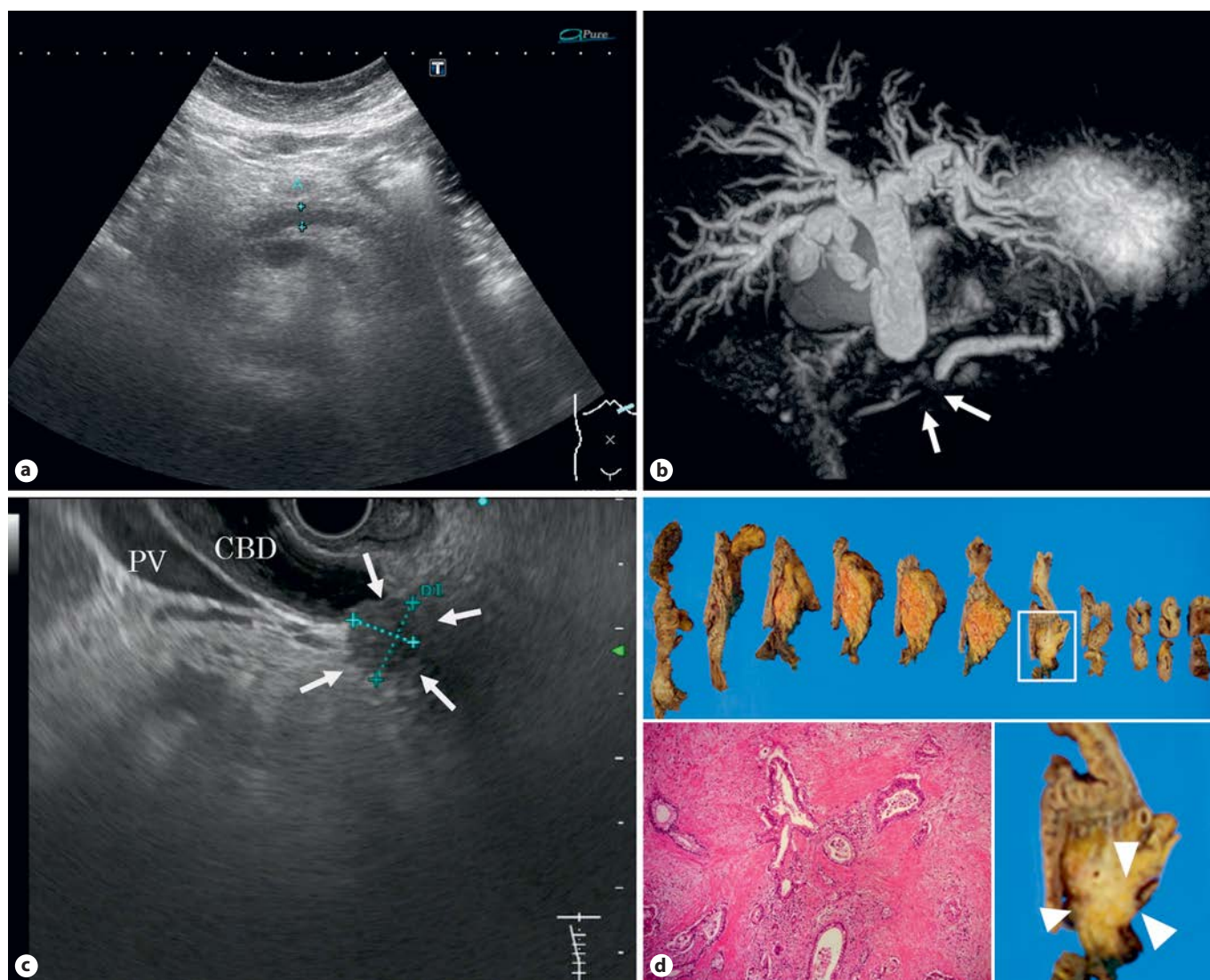
### Protocol for Social Programs for Diagnosing e-PC (Fig. 1)

The JPS guidelines include a protocol for diagnosing and treating PC [3]. The protocol in the present study (the Kishiwada project) referenced the protocol for the diagnosis of PC.

Patients who were enrolled based on their clinical findings underwent diffusion-weighted imaging (DWI) MRI and MRCP, and EUS (GF-UC240P-AL5; Olympus, Tokyo, Japan) was performed. If EUS revealed a solid mass in the pancreas, then EUS-fine needle aspiration (EUS-FNA) was performed [20, 21]. If the findings revealed irregular stenosis in the MPD or dilatation of the MPD, then endoscopic retrograde cholangiopancreatography was performed, and a cytological examination of pancreatic juice samples obtained by multiple endoscopic nasopancreatic drainage (ENPD) samplings was performed (Fig. 1).



**Fig. 2.** Clinical characteristics of patients. a-PC, advanced pancreatic cancer; e-PC, early-stage pancreatic cancer; EK, neuroendocrine; LN, lymph node; AIP, autoimmune pancreatitis; TFP, tumor-forming pancreatitis; GIMT, gastrointestinal mesenchymal tumor; SCN, serous cyst adenoma; IPMN, intraductal papillary mucinous neoplasm; ND, no disease. For all other abbreviations, see Figure 1.



**Fig. 3.** A 66-year-old woman positive at entry for 3 points (“symptoms [abdominal pain]” and “US findings”) of 5 clinical findings from a primary-care medical office. **a** Ultrasonography did not detect a tumor without dilatation of the main pancreatic duct. **b** Magnetic resonance cholangiopancreatography shows stenosis and dilatation of the main pancreatic duct (arrow). **c** Endoscopic ultrasonography shows a low-echoic lesion measuring 18 mm in diameter (arrow) adjacent to the bile duct. The histological diag-

nosis was adenocarcinoma by endoscopic ultrasonography-fine needle aspiration. **d** She received subtotal stomach-preserving pancreatoduodenectomy. The resected specimen showed a white solid tumor, measuring 20 × 18 mm (arrowheads). A pathologic examination of the resected specimen showed invasive ductal carcinoma, moderately differentiated. The final pathological diagnosis was stage IIA pancreatic cancer. PV, portal vein; CBD, common bile duct.

#### DWI-MRI and MRCP Techniques

MRI examinations were carried out with a 2.0-Tesla unit (Vantage Titan, Toshiba, Japan) with a 12-channel body and spine matrix coil combination. DWI was performed as a part of the routine abdomen MRI protocol for the evaluation of hepato-pancreato-biliary ducts in our institution. The protocol included axial fat-sat T1-weighted images, axial T2-weighted images, axial T2-weighted half-Fourier acquisition single-shot turbo spin echo images, coronal 2D MRCP, coronal 3D MRCP, and DWI images.

Apparent diffusion coefficient maps were automatically reconstructed for all DWI.

#### Diagnosis and Classification of PC

The final diagnoses were made according to the histology of the resected tumor. For patients who did not undergo surgical resection, the final diagnoses were made according to the histology or cytology of samples obtained by EUS-FNA or ENPD. In cases where pancreatic malignancy was excluded by EUS-FNA or



ENPD, the final diagnosis was confirmed by following the patient for at least 6 months.

Tumor classification was performed accordance with the Union for International Cancer Control (UICC) guidelines for PC. In this study, e-PC was defined as stage 0-IIB and advanced PC (a-PC) was defined as stage III-IV accordance with the UICC guidelines.

#### Statistical Analyses

The mean total scores of the e-PC, a-PC, and non-PC groups were compared using Wilcoxon's signed-rank test. The  $\chi^2$  test was used to compare the frequencies of each clinical findings category between the e-PC, a-PC, and non-PC groups. Sensitivities for detecting pancreatic findings (direct and indirect) by MRCP were calculated and compared between the e-PC and a-PC groups. A  $p$  value  $<0.05$  was considered to be statistically significant.

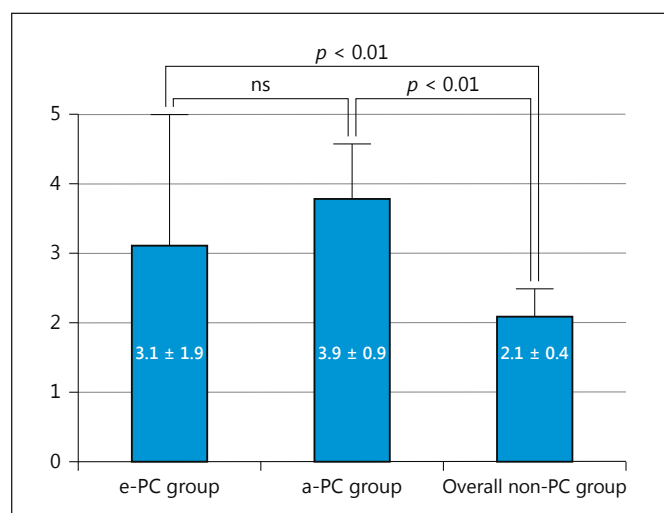
## Results

Among the 244 cases diagnosed with PC based on the clinical findings, pancreatic disease was detected in 155 cases (63.5%), while diseases other than pancreatic disease were detected in 64 (26.2%), and 25 cases (10.3%) were found to have no disease at all (Fig. 2).

Three of these 155 patients received a cytodiagnosis using pancreatic juice obtained by ENPD, as EUS revealed a tumor in the MPD; they were therefore diagnosed with adenocarcinoma by cytology of the ENPD sample. One of these 3 patients underwent distal pancreatectomy, and the other 2 received best supportive care because they were elderly. Forty-one cases in whom EUS revealed a tumor in the pancreas parenchyma underwent EUS-FNA. The final UICC tumor classification of pancreatic adenocarcinoma revealed that 15 of the 28 PC (53.6%) cases were e-PC (stage IA,  $n = 4$ ; IB,  $n = 1$ ; IIA,  $n = 4$ ; IIB,  $n = 6$ ); 11 and 4 patients in the e-PC group received surgery and best supportive care because 4 patients were elderly, respectively (Fig. 3). Thirteen of the 28 PC (46.4%) cases were a-PC (stage III,  $n = 4$ ; IV,  $n = 9$ ); 9 and 4 patients in the a-PC group received chemotherapy and best supportive care, respectively. In 105 cases, EUS revealed a cystic lesion or pancreatic swelling but did not reveal a solid tumor in the pancreas; therefore, these patients are being followed up without EUS-FNA or ENPD (Fig. 2).

#### Comparison of the Mean Total Scores at Entry among the e-PC, a-PC, and Non-PC Groups (Fig. 4)

The average total scores were  $3.1 \pm 1.9$ ,  $3.9 \pm 0.9$ , and  $2.1 \pm 0.4$  in the e-PC, a-PC, and non-PC groups, respectively. The average total score of the e-PC and a-PC group

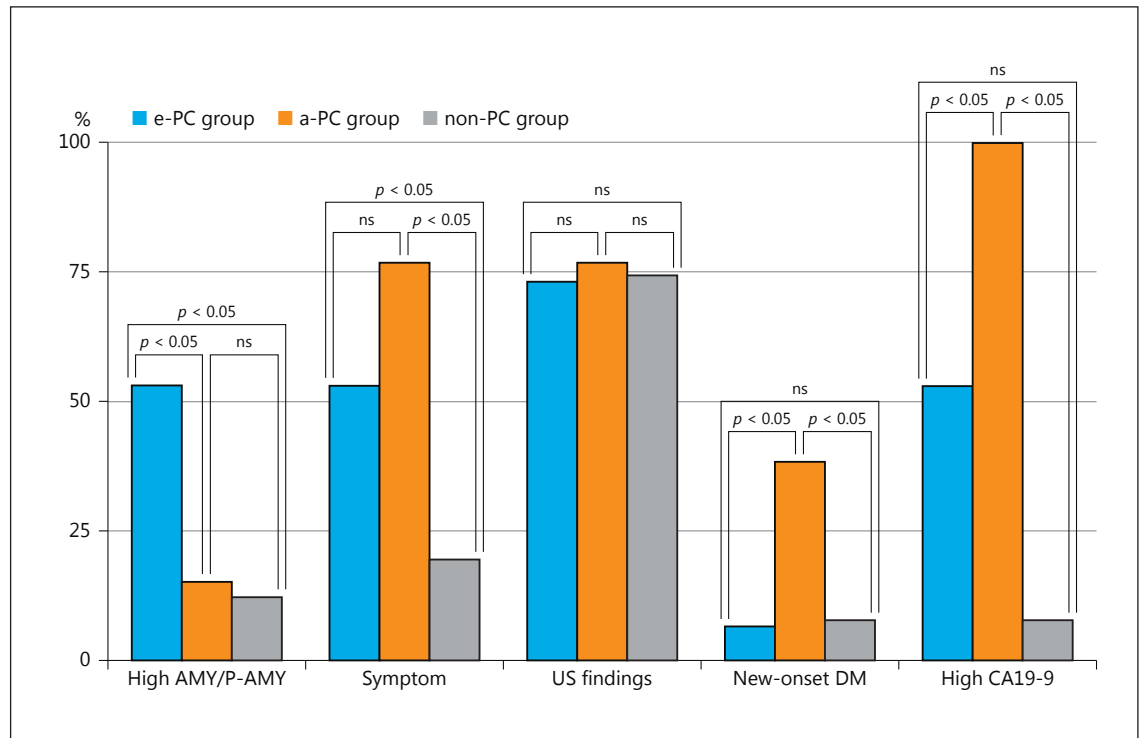


**Fig. 4.** A comparison of the mean total scores at entry among the early-stage pancreatic cancer (e-PC), advanced pancreatic cancer (a-PC), and non-pancreatic cancer (non-PC) groups. ns, not significant.

was significantly higher than that of the non-PC group ( $p < 0.05$ ). There were no significant differences in the average total score between the e-PC and a-PC groups (Fig. 4).

#### Comparison of Each Score Item among the e-PC, a-PC, and Non-PC Groups (Fig. 5)

“High AMY/P-AMY” was found in 8 of 15 (53.3%), 2 of 13 (15.4%), and 36 of 216 (16.7%) patients in the e-PC, a-PC, and non-PC groups, respectively; the frequency in the e-PC group was significantly higher than in the other groups ( $p < 0.05$ ). “Symptoms” was found in 8 of 15 (53.3%), 10 of 13 (77%), and 42 of 216 (19.4%) patients in the e-PC, a-PC, and non-PC groups, respectively; the frequency in the e-PC and a-PC groups was significantly higher than in the non-PC group ( $p < 0.05$ ). “US findings” was found in 11 of 15 (73.3%), 10 of 13 (66%), and 160 of 216 (74.5%) patients in the e-PC, a-PC, and non-PC groups, respectively, which was not significantly different. “New-onset DM” was found in 1 of 15 (6.7%), 5 of 13 (38.5%), and 17 of 216 (7.9%) patients in the e-PC, a-PC, and non-PC groups, respectively; the frequency in the e-PC group was significantly higher than in the other groups ( $p < 0.05$ ). “High CA19-9 levels” was found in 8 of 15 (53.3%), 13 of 13 (100%), and 17 of 216 (7.9%) patients in the e-PC, a-PC, and non-PC groups, respectively; the frequency in the e-PC group was significantly higher than in the non-PC group ( $p < 0.05$ ).



**Fig. 5.** A comparison of each score item among the early-stage pancreatic cancer (e-PC), advanced pancreatic cancer (a-PC), and non-pancreatic cancer (non-PC) groups. P-AMY, pancreatic amylase; US, ultrasonography; DM, diabetes mellitus; CA19-9, carbohydrate antigen 19-9; ns, not significant.

#### Clinical Findings of the PC Patients at Entry

Nine of the 15 (60.0%) patients in the e-PC group, were enrolled via GIMs, while the remaining 6 (40.0%) were enrolled via PMOs (general surgery,  $n = 3$ ; urology,  $n = 2$ ; otolaryngology,  $n = 1$ ). Six patients with abdominal pain in the e-PC group had acute pancreatitis; the abdominal pain coincided with a high AMY level. Abnormal US findings were detected at entry in 11 of the 15 (73.3%) patients in the e-PC group, and the remaining 4 (26.7%) were enrolled via facilities in which US was not conducted. After having being introduced to our hospital, all of these patients underwent US. The total sensitivity of direct detection by US (both US findings at entry and at our institution) was 40.0% (6 of 15) in the e-PC group. The total sensitivity for detecting MPD dilatation by US was 66.7% (10 of 15) in the e-PC group. The sensitivity for detecting a cystic lesion by US was 20.0% (3 of 15) in the e-PC group. The overall sensitivity of indirect US findings (MPD dilatation and/or cystic lesion) by US was 93.3%.

#### Comparison of the Sensitivities of Detecting Pancreatic Findings by MRCP between the e-PC and a-PC Groups (Table 1)

The sensitivities for detecting pancreatic carcinoma by diffusion MRI were 33.3% (5 of 15) and 92.3% (12 of 13) in the e-PC and a-PC groups, respectively, which was significantly different ( $p < 0.05$ ). The sensitivities for detecting MPD dilatation by MRCP were 93.3% (14 of 15) and 84.6% (11 of 13) in the e-PC and a-PC groups, respectively. The sensitivities for detecting MPD cystic lesion by MRCP were 26.7% (4 of 15) and 38.5% (5 of 13) in the e-PC and a-PC groups, respectively. There were no significant differences in the indirect findings for MPD dilatation and MPD cystic lesions between the e-PC and a-PC groups.

#### Discussion

PC is one of most lethal malignant cancers, ranking fifth in mortality related to cancer worldwide. The overall 5-year survival rate of PC has been reported to be

**Table 1.** Total sensitivities for detecting pancreatic findings by diffusion magnetic resonance imaging (MRI) and magnetic resonance cholangiopancreatography (MRCP) between the early-stage pancreatic cancer (e-PC) and advanced pancreatic cancer (a-PC) groups

	Direct finding on diffusion MRI, <i>n</i> (%)	Indirect findings on MRCP, <i>n</i> (%)		
	solid tumor	MPD dilatation	cystic lesion	MPD dilatation and/ or cystic lesions
e-PC group ( <i>n</i> = 15)	5 (33.3)	14 (92.3)	4 (26.7)	8 (100)
a-PC group ( <i>n</i> = 13)	12 (92.3)	11 (84.6)	5 (38.5)	6 (100)
	} <i>p</i> < 0.05		} ns	

MPD, main pancreatic duct; ns, not significant.

around 1–4% [22]. Egawa et al. [23] analyzed 32,619 cumulative records from 1981 to 2007. The survival curve in their report was divided into that for patients who underwent pancreatectomy and that for those who had unresectable disease. There was a significant increase in the survival rate in the patients who underwent resection. Chiang et al. [24] compared the clinicopathological characteristics and prognosis of large PC (tumor size >2 cm) and small PC (tumor size ≤2 cm) patients undergoing resection. Small-PC and large-PC patients had a similar prognosis after resection [23]. A high albumin level (>3.5 g/dL) and early-stage disease (stage I, II) were favorable prognosis factors for small-PC patients. The detection of PC at an early stage and the performance of curative surgery can be expected to improve the long-term patient outcomes.

Hanada et al. [4, 22] reported that a social program for the early diagnosis of PC, with collaborations between Onomichi Hospital, specialists in PC from medical centers, and general practitioners (Onomichi project), was useful for the early detection of PC. Developing an effective screening strategy for PC will require the establishment of a network wherein facilities specializing in PC cooperate with medical offices of various channels. Screening for cases of PC is simple and easy for various doctors, and a sensitive screening method that is safe with low invasiveness eagerly waited.

The pathogenesis of neoplasm remains unclear, but some risk factors have been noted for identifying candidates for screening, such as DM, obesity, cigarette smoking, a family history of PC, chronic pancreatitis, and intraductal papillary mucinous neoplasm. Evidence-based clinical guidelines for PC were published by the Japan Pancreas Society (JPS) in 2013 [3]. The sections of Clinical questions 1 and 2 suggest some risk factors that may

be involved in the development of PC [4–11]. With reference to this information, this social program (Kishidawa Katsuragi project) adopted clinical findings.

We compared each item in the scores among the e-PC, a-PC, and non-PC groups. “US findings” showed no significant difference among the three groups. Three of the five clinical findings (“symptoms,” “new onset DM,” and “high CA19-9”) were more frequent in the a-PC group than in the other groups. In contrast, “high AMY/P-AMY” was significantly more frequent in the e-PC group than in the other groups. Six patients with abdominal pain in the e-PC group had acute pancreatitis; abdominal pain coincided with a high AMY/P-AMY level. Thus, regarding the clinical findings, abdominal pain in patients with a high AMY/P-AMY level was important for the detection of e-PC. Homma et al. [25] reported that, in a study of 10,162 asymptomatic individuals, abnormal CA19-9 levels were only noted in 18 (0.2%) subjects. Although their study used a variety of screening tests, only 4 cases of PC (0.04%) were detected [25]. The measurement of CA19-9 levels alone was therefore ineffective as a screening test for PC, especially in asymptomatic individuals. In our study, when the finding of a high CA19-9 level was combined with at least one other clinical finding, the rate of CA19-9 elevation in the e-PC group at entry was 53.3%. As such, the combined finding of a high CA19-9 level and another clinical finding may be useful for detecting e-PC.

In this study, the total (both US findings at entry and our institution) sensitivity for detecting a direct finding by US was 40.0% in the e-PC group. However, the sensitivities for indirect findings, such as MPD dilatation or cystic lesions, by US were high and were therefore deemed very important for the detection of e-PC. Although the diagnostic ability of US depends on the operator’s experi-

ence and the patient's condition (in terms of obesity and bowel gas content), US remains useful noninvasive, convenient technique, and it is associated with lower costs than multiple detector computed tomography (MDCT), MRCP/diffusion MRI, and EUS, which are necessary primary imaging modalities for diagnosing e-PC.

Although there were no significant differences in the average total score between the e-PC and a-PC groups, the average total scores of the e-PC and a-PC groups were significantly higher than those of the overall non-PC groups at entry. Therefore, our findings suggested that if the average score for clinical findings was  $\geq 3$ , we should strongly doubt pancreatic cancer and perform a more detailed inspection with MRCP/diffusion MRI, EUS and MDCT.

In the Kishiwada Katsuragi project, patients who were enrolled according to clinical findings initially underwent MRCP/diffusion MRI. MDCT involves radiation exposure and carries an unpredictable risk of an allergic response to the iodine contrast medium; however, MRCP/diffusion MRI carries no such risk or exposure requirements. In addition, MRCP is a noninvasive and increasingly common procedure in cases of biliary and pancreatic diseases and is as sensitive as endoscopic retrograde cholangiopancreatography in detecting pancreatic carcinomas [26–28]. Furthermore, diffusion MRI measures the Brownian motion (random thermal diffusion) of molecules in tissues and depicts locoregional characteristics of water diffusion. Thus, diffusion MRI can be used to distinguish neoplastic lesions from the surrounding normal tissues without the need for an imaging contrast agent. Diffusion MRI can be used for the diagnosis of PC. In our study, patients who were enrolled based on their clinical findings initially underwent diffusion MRI/MRCP. In our study, the sensitivities of detecting direct finding by diffusion MRI were 33.3 and 92.3% in the e-PC and a-PC groups, respectively. Although diffusion MRI was useful for detecting a-PC, it was not sufficient to detect e-PC. However, in the e-PC group, the sensitivities for overall indirect findings, including dilatation of the

MPD and/or cysts, was 100%, suggesting that these findings were very important for detecting e-PC.

In the Kishiwada Katsuragi project, we hoped that the clinical findings would allow e-PC to be readily detected by any PMO. Therefore, 41 PMOs (27 GIMs and 14 other PMOs) were enrolled as cooperative facilities, including 27 GIMs and 14 other types of PMO (general surgery, urology, and orthopedics departments) to determine which clinical findings were most closely associated with the detection of PC. Six (6/15) of all patients with e-PC were detected by other PMOs, suggesting that the participation of other PMOs, as well as GIMs, plays an important role in improving the e-PC detection rate. Regarding the clinical findings at entry, the rates of patients with symptoms, high AMY/P-AMY, high CA19-9, and new-onset DM were lower than those with US findings in the e-PC groups; however, these findings were important for the detection of PC because 4 of the 15 (26.7%) patients were from facilities in which US was not conducted.

The present study is associated with several limitations, including the small study population. Further examinations are therefore necessary. The accumulation of a greater number of cases and the modification of the clinical finding score will be necessary to improve the efficiency of PC detection.

In conclusion, social programs with collaborations between medical centers that specialize in PC and PMOs used clinical findings, suggesting that not only GIMs but also other PMOs may be important for the early detection of PC. Findings from US and MRCP/diffusion MRI, especially indirect findings such as dilatation of the MPD and cystic lesions, were useful for the detection of e-PC. Further studies with the accumulation of a greater number of cases are necessary to confirm our findings.

## Disclosure Statement

There are no companies in a relation of conflict of interest requiring disclosure in relation to this paper.

## References

- 1 Egawa S, Toma H, Ohigashi H, Okusaka T, Nakao A, Hatori T, Maguchi H, Yanagisawa A, Tanaka M: Japan Pancreatic Cancer Registry; 30th year anniversary: Japan Pancreas Society. *Pancreas* 2012;41:985–992.
- 2 D'Haese JG, Werner J: Resectability of pancreatic cancer: new criteria. *Radiologe* 2016; 56:318–324.
- 3 Yamaguchi K, Okusaka T, Shimizu K, Furuse J, Ito Y, Hanada K, Shimosegawa T: Committee for revision of clinical guidelines for pancreatic cancer of Japan Pancreas Society. EBM-based clinical guidelines for pancreatic cancer (2013) issued by the Japan Pancreatic Society: a synopsis. *Jpn J Clin Oncol* 2014;44: 883–888.



- 4 Hanada K, Okazaki A, Hirano N, Izumi Y, Teraoka Y, Ikemoto J, Kanemitsu K, Hino F, Fukuda T, Yonehara S: Diagnostic strategies for early pancreatic cancer. *J Gastroenterol* 2015; 50:147–154.
- 5 Okano K, Suzuki Y: Strategies for early detection of resectable pancreatic cancer. *World J Gastroenterol* 2014;20:11230–11240.
- 6 Raimondi S, Lowenfels AB, Morselli-Labate AM, Maisonneuve P, Pezzilli R: Pancreatic cancer in chronic pancreatitis; aetiology, incidence and early detection. *Best Pract Res Clin Gastroenterol* 2010;24:349–358.
- 7 McKay CJ, Glen P, McMillan DC: Chronic inflammation and pancreatic cancer. *Best Pract Res Clin Gastroenterol* 2008;22:65–73.
- 8 Rebours V, Boutron-Ruault MC, Schnee M, Férec C, Maire F, Hammel P, Ruszniewski P, Lévy P: Risk of pancreatic adenocarcinoma in patients with hereditary pancreatitis: a national exhaustive series. *Am J Gastroenterol* 2008;103:111–119.
- 9 Klein AP, Brune KA, Petersen GM, Goggins M, Tersmette AC, Offerhaus GJ, Griffin C, Cameron JL, Yeo CJ, Kern S, Hruban RH: Prospective risk of pancreatic cancer in familial pancreatic cancer kindreds. *Cancer Res* 2004;64:2634–2638.
- 10 Canto MI, Harinck F, Hruban RH, Offerhaus GJ, Poley JW, Kamel I, Nio Y, Schulick RS, Bassi C, Kluijdt I, Levy MJ, Chak A, Fockens P, Goggins M, Bruno M: International Cancer of Pancreas Screening (CAPS) Consortium. International Cancer of the Pancreas Screening (CAPS) consortium summit on the management of patients with increased risk for familial pancreatic cancer. *Gut* 2013;62:339–347.
- 11 Brune KA, Lau B, Palmisano E, Canto M, Goggins MG, Hruban RH, Klein AP: Importance of age of onset in pancreatic cancer kindreds. *J Nat Cancer Inst* 2010;102:119–126.
- 12 Pannala R, Basu A, Petersen GM, Chari ST: New-onset diabetes: a potential clue to the early diagnosis of pancreatic cancer. *Lancet Oncol* 2009;10:88–95.
- 13 Ogawa Y, Tanaka M, Inoue K, Yamaguchi K, Chijiwa K, Mizumoto K, Tsutsu N, Nakamura YA: A prospective pancreatography study of the prevalence of pancreatic carcinoma in patients with diabetes mellitus. *Cancer* 2002;94:2344–2349.
- 14 Mizuno S, Nakai Y, Isayama H, Yanai A, Tahagara N, Miyabayashi K, Yamamoto K, Kawakubo K, Mohri D, Kogure H, Sakaki T, Yamamoto N, Sahahira N, Hirano K, Tsujino T, Ljichi H, Takeishi K, Akanuma M, Taka M, Koike K: Risk factors and early signs of pancreatic cancer in diabetes: screening strategy based on diabetes onset age. *J Gastroenterol* 2013;48:238–246.
- 15 Pleskow DK, Berger HJ, Gyves J, Allen E, McLean A, Podolsky DK: Evaluation of a serologic marker, CA19-9, in the diagnosis of pancreatic cancer. *Ann Intern Med* 1989;110:704–709.
- 16 Marrelli D, Caruso S, Pedrazzani C, Neri A, Fernandes E, Marini M, Pinto E, Roviello F: CA19-9 serum levels in obstructive jaundice: clinical value in benign and malignant conditions. *Am J Surg* 2009;198:333–339.
- 17 Glenn J, Steinberg WM, Kurtzman SH, Steinberg SM, Sindelar WF: Evaluation of the utility of a radioimmunoassay for serum CA19-9 levels in patients before and after treatment of carcinoma of the pancreas. *J Clin Oncol* 1988; 6:462–468.
- 18 Nakaizumi A, Tatsuta M, Uehara H, Iishi H, Yamamura H, Okuda S, Kitamura T: A prospective trial of early detection of pancreatic cancer by ultrasonographic examination combined with measurement of serum elastase 1. *Cancer* 1992;69:936–940.
- 19 Tanaka S, Nakao M, Ioka T, Takakura R, Takano Y, Tsukuma H, Uehara H, Suzuki R, Fukuda J: Slight dilatation of the main pancreatic duct and presence of pancreatic cysts as predictive signs of pancreatic cancer: a prospective study. *Radiology* 2010;254:965–972.
- 20 Sakamoto H, Kitano M, Komaki T, Noda K, Chikugo T, Kudo M: Small cell carcinoma of the pancreas: role of EUS-FNA and subsequent effective chemotherapy using carboplatin and etoposide. *J Gastroenterol* 2009;44: 432–438.
- 21 Sakamoto H, Kitano M, Komaki T, Noda K, Chikugo T, Dote K, Takeyama Y, Das K, Yamao K, Kudo M: Prospective comparative study of the EUS guided 25-gauge FNA needle with the 19-gauge Trucut needle and 22-gauge FNA needle in patients with solid pancreatic masses. *J Gastroenterol Hepatol* 2008;55: 1785–1788.
- 22 Hanada K, Okazaki A, Hirano N, Izumi Y, Minami T, Ikemoto J, Kanemitsu K, Hino F: Effective screening for early diagnosis of pancreatic cancer. *Best Pract Res Clin Gastroenterol* 2015;29:929–939.
- 23 Egawa S, Toma H, Ohigashi H, Okusaka T, Nakao A, Hatori T, Maguchi H, Yanagisawa A, Tanakan M: Japan Pancreatic Cancer Registry; 30th year anniversary: Japan Pancreas Society. *Pancreas* 2012;41:985–992.
- 24 Chiang KC, Yeh CN, Lee WC, Jan YY, Hwang TL: Prognostic analysis of patients with pancreatic head adenocarcinoma less than 2 cm undergoing resection. *World J Gastroenterol* 2009;15:4305–4310.
- 25 Homma T, Tsuchiya R: The study of the mass screening of persons without symptoms and of the screening of outpatients with gastrointestinal complains or icterus for pancreatic cancer in Japan, using CA19-9 and elastase-1 or ultrasonography. *Int J Pancreatol* 1991;9: 119–124.
- 26 Lopez Hänninen E, Amthauer H, Hosten N, Ricke J, Böhmig M, Langrehr J, Hintze R, Neuhaus P, Wiedenmann B, Rosewicz S, Felix R: Prospective evaluation of pancreatic tumors: accuracy of MR imaging with MR cholangiopancreatography and MR angiography. *Radiology* 2002;224:34–41.
- 27 Adamek HE, Albert J, Breer H, Weitz M, Schilling D, Riemann JF: Pancreatic cancer detection with magnetic resonance cholangiopancreatography and endoscopic retrograde cholangiopancreatography: a prospective controlled study. *Lancet* 2000;356:190–193.
- 28 Holzapfel K, Reiser-Erkan C, Fingerle AA, Erkan M, Eiber MJ, Rummeny EJ, Friess H, Kleeff J, Gaa J: Comparison of diffusion-weighted MR imaging and multidetector-row CT in the detection of liver metastases in patients operated for pancreatic cancer. *Abdom Imaging* 2011;36:179–184.

# A Case of Pancreatic Carcinoma in situ Diagnosed by Repeated Pancreatic Juice Cytology

Takeshi Miyata Mamoru Takenaka Shunsuke Omoto Ken Kamata  
Kosuke Minaga Kentaro Yamao Hajime Imai Masatoshi Kudo

Department of Gastroenterology and Hepatology, Kindai University Faculty of Medicine, Osaka-Sayama, Japan

## Keywords

Pancreatic carcinoma in situ · Pancreatic juice cytology

## Abstract

Repeated pancreatic juice cytology via endoscopic nasopancreatic drainage (ENPD) has a high diagnostic yield and might be useful for the diagnosis of early-stage pancreatic cancer. A 67-year-old man presented with a pancreatic cyst occasionally detectable in the body of the pancreas by ultrasonography (US). No obvious pancreatic tumor was detected by US, computed tomography (CT), magnetic resonance cholangiopancreatography, and endoscopic ultrasound (EUS) (although the latter did reveal a weak, low echoic area). Endoscopic retrograde pancreatography showed irregular narrowing of the main pancreatic duct (MPD) at the pancreatic body. Pancreatic juice cytology was also performed, but did not give evidence of a malignancy. Therefore, the patient was followed up. CT and EUS performed after 3 months showed the same findings as did endoscopic retrograde pancreatography; however, the results of repeated pancreatic juice cytology performed via ENPD tube revealed a suspected malignancy on 2 of 6 occasions. Therefore, we performed a central pancreatectomy. Histopathological exami-

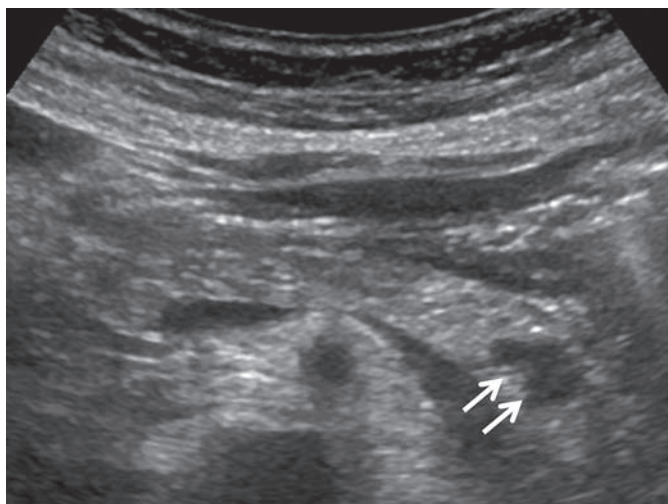
nation of a resected specimen revealed carcinoma in situ in the narrow MPD at the body of the pancreas. In the current case, repeated pancreatic juice cytology via ENPD was effective. A weak low echoic area around the MPD stricture on EUS might be related to the inflammatory change accompanying carcinoma in situ of the pancreas.

© 2017 S. Karger AG, Basel

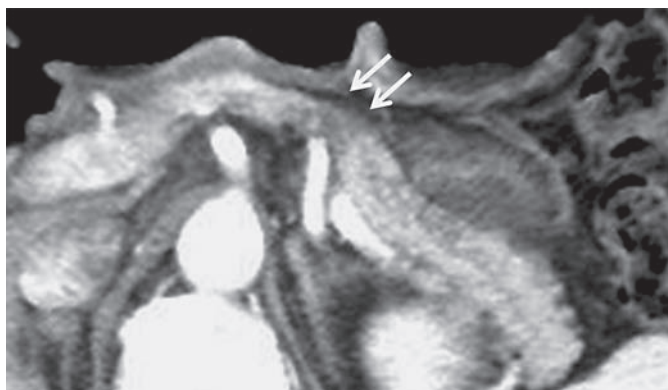
## Introduction

Repeated pancreatic juice cytology via endoscopic nasopancreatic drainage (ENPD) is found to have a high diagnostic yield and might be useful for the diagnosis of early-stage pancreatic cancer [1]. Endoscopic ultrasound (EUS)-guided fine-needle aspiration is also helpful for confirming the diagnosis of early pancreatic carcinoma, but its role is limited with respect to carcinoma in situ as no tumor has formed at this stage [2]. A weak low echoic area around the main pancreatic duct (MPD) stricture on EUS might be related to inflammatory changes accompanying carcinoma in situ of the pancreas.

Here, we report the case of repeated pancreatic juice cytology via ENPD, which was effective.



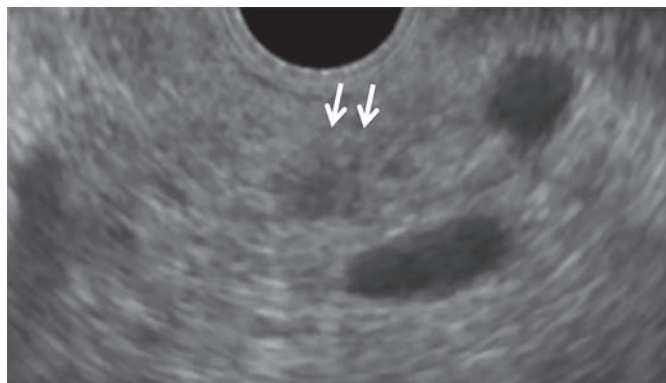
**Fig. 1.** An ultrasonography image showing a pancreatic cyst in the body of the pancreas (arrows).



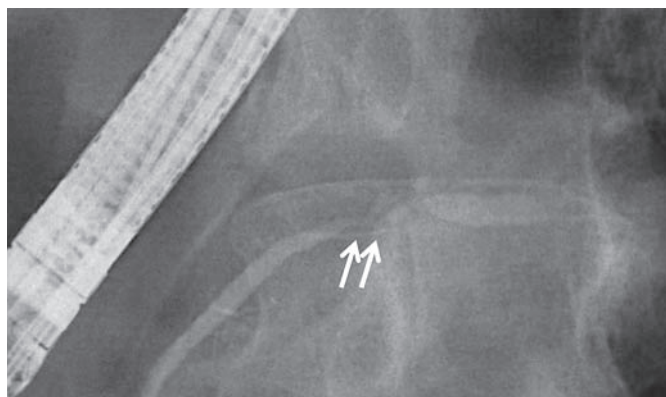
**Fig. 2.** A computed tomography image showing a pancreatic cyst in the body, and dilation of the main pancreatic duct (arrows).



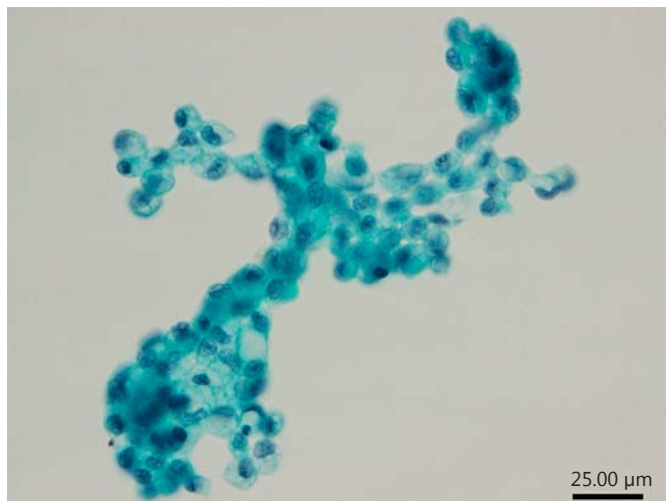
**Fig. 3.** A magnetic resonance cholangiopancreatography image showing irregular narrowing of the main pancreatic duct at the pancreatic body (arrows).



**Fig. 4.** An endoscopic ultrasound image showing a weak low echogenic area around the narrowing of the main pancreatic duct at the pancreatic body (arrows).

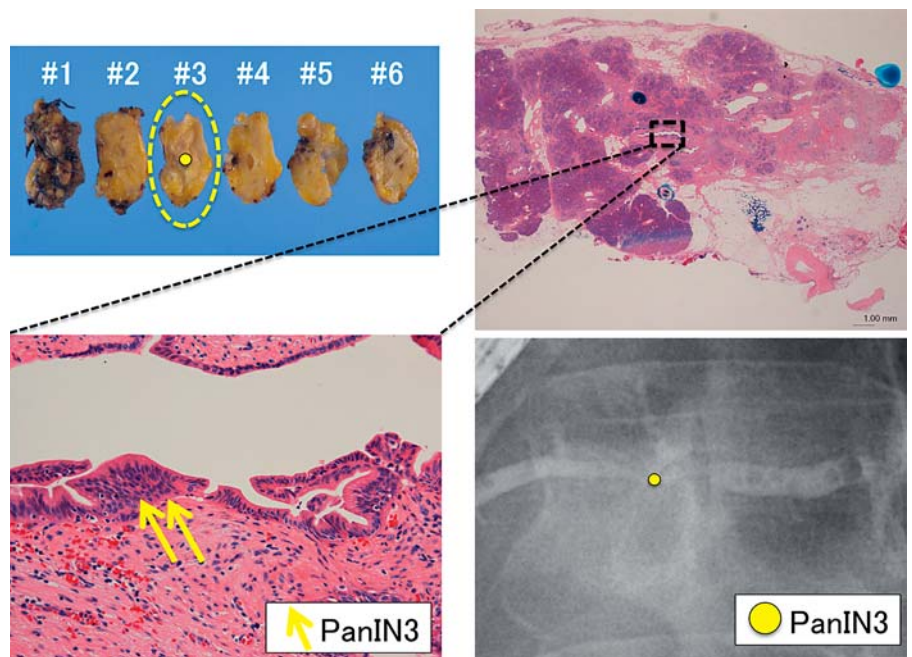


**Fig. 5.** An endoscopic retrograde pancreatography image showing irregular narrowing of the main pancreatic duct at the pancreatic body (arrows).

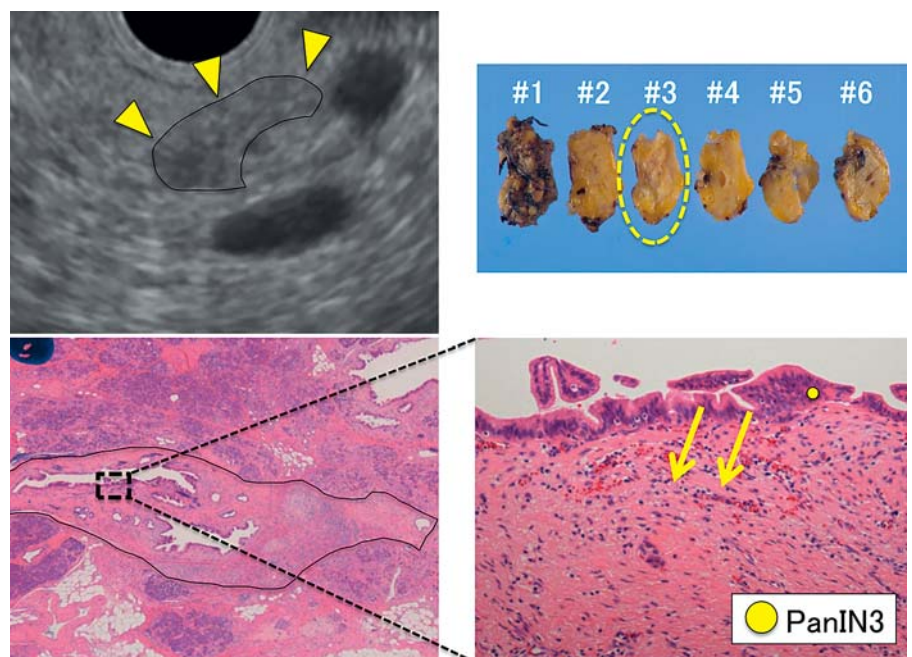


**Fig. 6.** Pancreatic juice cytology obtained by endoscopic nasopancreatic drainage tube revealing suspected malignancy.





**Fig. 7.** Histopathological examination of the resected specimen shows carcinoma in situ at the part of the narrow main pancreatic duct in the body of the pancreas (arrows).



**Fig. 8.** Histopathological examination of the resected specimen shows inflammatory change seen around the carcinoma (arrows) in situ detected by endoscopic ultrasound (arrowheads).

## Case Report

We describe a 67-year-old man with a pancreatic cyst occasionally detectable in the body of the pancreas by ultrasonography (US) (Fig. 1). Tumor markers (CEA, CA19-9, DUPAN2, and Span1) were within normal limits. Computed tomography (CT) also revealed a pancreatic cyst (diameter, 15 mm) in the body of

the pancreas and dilation of the MPD (Fig. 2). Magnetic resonance cholangiopancreatography showed localized irregular narrowing of the MPD at the pancreatic body (Fig. 3), and EUS showed a weak low echoic area around this point (Fig. 4). No obvious pancreatic tumor was detected by US, CT, magnetic resonance cholangiopancreatography, and EUS (although the latter did reveal a weak low echoic area). Endoscopic retrograde pancreatography



showed irregular narrowing of the MPD at the pancreatic body (Fig. 5). Pancreatic juice cytology was also performed, but did not give evidence of a malignancy. Therefore, the patient was followed up. CT and EUS performed 3 months later showed the same findings as did endoscopic retrograde pancreatography; however, the results of repeated pancreatic juice cytology via ENPD tube revealed a suspected malignancy on 2 of 6 occasions (Fig. 6). Taking all imaging findings into consideration, we suspected pancreatic carcinoma in situ at the pancreatic body. Therefore, we performed a central pancreatectomy. Histopathological examination of a resected specimen revealed carcinoma in situ in the narrow MPD at the body of the pancreas (Fig. 7). The resected margin of the pancreas was negative, and no lymph node metastasis was detected. Inflammatory change (inflammatory cell infiltration and fibrosis) were observed around the carcinoma in situ, at the site matched to the low echoic area detected by EUS (Fig. 8). The patient is still alive 3 years following surgery, and no adjuvant chemotherapy was required.

## Discussion

Previous studies showed that ENPD had a high diagnostic yield and might be useful for the diagnosis of early-stage pancreatic cancer [1]. In the current case, repeated

pancreatic juice cytology via ENPD was also effective. EUS-guided fine-needle aspiration is also helpful for confirming the diagnosis of early pancreatic carcinoma, but its role is limited with respect to carcinoma in situ as no tumor has formed at this stage [2]. A weak low echoic area around the MPD stricture on EUS might be related to the inflammatory changes accompanying carcinoma in situ of the pancreas.

## Disclosure Statement

The authors have no conflicts of interest to declare.

## References

- 1 Mikata R, Ishihara T, Yokosuka O, et al: Clinical usefulness of repeated pancreatic juice cytology via endoscopic naso-pancreatic drainage tube in patients with pancreatic cancer. *J Gastroenterol* 2013;48:866–873.
- 2 Hanada K, Okazaki A, Yonehara S, et al: Diagnostic strategies for early pancreatic cancer. *J Gastroenterol* 2015;50:147–154.

# Association between the Risk Factors for Pancreatic Ductal Adenocarcinoma and Those for Malignant Intraductal Papillary Mucinous Neoplasm

Ken Kamata<sup>a</sup> Mamoru Takenaka<sup>a</sup> Atsushi Nakai<sup>a</sup> Shunsuke Omoto<sup>a</sup>  
Takeshi Miyata<sup>a</sup> Kosuke Minaga<sup>a</sup> Tomohiro Matsuda<sup>a</sup> Kentaro Yamao<sup>a</sup>  
Hajime Imai<sup>a</sup> Yasutaka Chiba<sup>d</sup> Toshiharu Sakurai<sup>a</sup> Tomohiro Watanabe<sup>a</sup>  
Naoshi Nishida<sup>a</sup> Takaaki Chikugo<sup>b</sup> Ippei Matsumoto<sup>c</sup> Yoshifumi Takeyama<sup>c</sup>  
Masatoshi Kudo<sup>a</sup>

Departments of <sup>a</sup>Gastroenterology and Hepatology, <sup>b</sup>Pathology, and <sup>c</sup>Surgery, Kindai University Faculty of Medicine, and <sup>d</sup>Clinical Research Center, Kindai University Hospital, Osaka-Sayama, Japan

## Keywords

Intraductal papillary mucinous neoplasm · Pancreatic ductal adenocarcinoma · Smoking history · Risk factors

## Abstract

**Background and Aims:** Risk factors for pancreatic ductal adenocarcinoma (PDAC) include diabetes mellitus, chronic pancreatitis, obesity, a family history of pancreatic cancer, and a history of smoking or alcohol consumption. The aim of this study was to evaluate the association between risk factors for PDAC and malignant intraductal papillary mucinous neoplasm (IPMN). **Methods:** The study included 134 consecutive patients with IPMN who underwent surgical resection at Kindai University Hospital between April 2009 and March 2015. Data on the presence or absence of mural nodules (MNs) and risk factors for PDAC were evaluated.

Multivariable logistic regression analysis was performed with malignant IPMN as the outcome variable and MNs and risk factors for PDAC as explanatory variables. **Results:** The odds ratio of malignant IPMN to MNs was 3.88 (95% confidence interval [CI] 1.53–9.84;  $p = 0.004$ ), whereas that of malignant IPMN to smoking history was 1.66 (95% CI 0.74–3.71;  $p = 0.22$ ). When the presence of MNs was considered as a predictive factor for malignancy, the sensitivity and specificity were 88.5 and 32.1%, respectively, whereas when the presence of both smoking history and MNs was considered, the specificity improved to 73.2%, with a decrease in sensitivity to 42.3%. **Conclusions:** The presence of both a smoking history and MNs was a valuable predictive factor for malignant IPMN with high specificity. A smoking history should be considered before surgical resection in addition to the presence of MNs.

© 2017 S. Karger AG, Basel

## Introduction

Intraductal papillary mucinous neoplasm (IPMN) is diagnosed by several imaging modalities, such as ultrasonography, computed tomography, magnetic resonance cholangiopancreatography, and endoscopic ultrasonography. The 2012 international consensus guidelines for the management of IPMN define the presence of mural nodules (MNs) as high-risk stigmata, and IPMN with MN is an indication for surgical resection [1]. Pathologically, IPMN is classified as low, intermediate, or high-grade dysplasia or as invasive [2]. Invasive IPMN at an advanced stage mimics ordinary pancreatic ductal adenocarcinoma (PDAC). Diabetes mellitus (DM), chronic pancreatitis (CP), obesity, a family history of pancreatic cancer, a smoking history, and alcohol consumption are well-known risk factors for PDAC [3–8]. However, the association of these risk factors with malignant IPMN, including high-grade dysplasia and invasive disease, is poorly understood. In this study, we evaluated a database of 134 consecutive patients with IPMN who underwent surgical resection and assessed the association of risk factors for PDAC with malignant IPMN.

## Patients and Methods

### Study Design

The present study was a single-center retrospective study using prospectively collected data. The final diagnoses were made according to histological specimens obtained during surgical resection. This study was performed with the approval of the ethics committee of Kinki University School of Medicine.

### Patients

A total of 134 consecutive patients with IPMN who underwent surgical resection for IPMN at our hospital between April 2009 and March 2015 were included. Patients who underwent surgical resection for PDAC concomitant with IPMN were excluded from the study. Data were collected prospectively before surgical resection and included the presence or absence of MNs, DM (HbA1c [National Glycohemoglobin Standardization Program]  $\geq 6.5$ ), CP, obesity (body mass index  $>30$ ), family history of pancreatic cancer, smoking history (former and current smoker), and alcohol consumption ( $>37.5$  g/day). For DM, information on disease duration and the presence or absence of rapid progression was also collected. For smoking history, pack-years data were also collected.

### Definitions

IPMN was classified into main duct type, mixed type, or branch duct type based on imaging studies and according to the 2012 international consensus guidelines [1]. The reference standard was the pathological findings after surgical resection. Malignant IPMN was defined as high-grade dysplasia or invasive disease. Benign IPMN was defined as low- and moderate-grade dysplasia and bor-

**Table 1.** Patient characteristics ( $n = 134$ )

Mean age $\pm$ SD, years	69.8 $\pm$ 8.61
Gender, $n$	
Male	69
Female	65
Location of resected IPMN, $n$	
Head	94
Body	30
Tail	10
Type of IPMN, $n$	
Main duct type	19
Mixed type	41
Branch duct type	74
Final diagnosis, $n$	
Malignant IPMN <sup>a</sup>	78
Benign IPMN <sup>b</sup>	56

SD, standard deviation; IPMN, intraductal papillary mucinous neoplasm. <sup>a</sup> High-grade dysplasia and invasive. <sup>b</sup> Low- and intermediate-grade dysplasia.

derline malignancy. MN was defined as a protrusion of the cyst wall into its lumen that was detected by imaging modalities, such as ultrasonography, computed tomography, magnetic resonance cholangiopancreatography, or endoscopic ultrasonography. Former smokers were defined as patients who had stopped smoking  $>1$  year before surgical resection. Current smokers were defined as patients who were smoking at the time of surgery.

### Statistical Analysis

To examine factors affecting malignant IPMN, a multivariable logistic regression analysis was performed in which the outcome variable was malignant IPMN and the explanatory variables were MNs, DM, CP, obesity, family history of pancreatic cancer, smoking history, and alcohol consumption. The sensitivity, specificity, and accuracy for diagnosing malignant IPMN using MNs and/or risk factors for PDAC were calculated. All statistical analyses were performed using JMP software version 13 (SAS Institute, Cary, NC, USA).

## Results

The characteristics of the 134 patients are shown in Table 1. According to the pathological classification, the number of malignant and benign IPMNs was 78 (58%) and 56 (42%), respectively. The presence or absence of MNs and/or the risk factors for PDAC in the 134 patients are shown in Table 2. MNs were preoperatively detected in 107 patients and not detected in 27 patients. Table 3 shows the association between the presence or absence of risk factors and malignant or benign IPMN. All patients with CP had malignant IPMN; CP was excluded from the

**Table 2.** MNs and risk factors for PDAC ( $n = 134$ )

MN in cyst, $n$	
Present	107
Absent	27
DM (HbA1c [NGSP] $\geq 6.5\%$ ), $n$	
Present	36
Disease duration	
Within 3 years	31
More than 3 years	5
Absent	98
CP, $n$	
Present	9
Absent	125
Obesity (BMI $>30$ ), $n$	
Present	9
Absent	125
Smoking history, $n$	
Present	58
Pack-years	
More than 40	32
20–39	25
1–19	1
Absent	76
Alcohol consumption ( $>37.5$ g/day), $n$	
Present	25
Absent	109
Family history of pancreatic cancer, $n$	
Present	7
Absent	127

MN, mural nodule; PDAC, pancreatic ductal adenocarcinoma; DM, diabetes mellitus; NGSP, National Glycohemoglobin Standardization Program; CP, chronic pancreatitis; BMI, body mass index.

multivariable logistic regression analysis for malignant IPMN despite the strong association of CP with malignant IPMN.

Patients with DM within 3 years of disease duration had high rates of malignant IPMN. Regarding smoking history, the number of pack-years was positively related to the rate of malignant IPMN and the presence of MNs.

#### *Multivariable Logistic Regression Analysis Using Malignant IPMN as an Outcome Variable*

The results of the multivariable logistic regression analysis are shown in Table 4. Using a cutoff value of  $p = 0.25$ , the presence of MNs and smoking history were identified as factors positively associated with malignant

**Table 3.** Association between MNs and other risk factors and malignant or benign IPMN

	Benign ( $n = 56$ )	Malignant ( $n = 78$ )
MNs, $n$		
Absent	18	9
Present	38	69
DM, $n$		
Absent	43	55
Present	13	23
Disease duration		
Within 3 years	1	4
More than 3 years	12	19
CP, $n$		
Absent	56	69
Present	0	9
Obesity, $n$		
Absent	52	73
Present	4	5
Smoking, $n$		
Absent	37	39
Present	19	39
Pack-years		
More than 40	10	22
20–39	8	17
1–19	1	0
Alcohol, $n$		
Absent	48	61
Present	8	17
Family history, $n$		
Absent	51	76
Present	5	2

MN, mural nodule; IPMN, intraductal papillary mucinous neoplasm; DM, diabetes mellitus; CP, chronic pancreatitis.

IPMN. Family history was negatively associated with malignant IPMN and was excluded from further analysis.

#### *Sensitivity, Specificity, and Accuracy for Diagnosing Malignant IPMN Using MNs and/or Smoking History*

As an additional analysis, we assessed the accuracy of MNs and/or smoking history for the diagnosis of malignant IPMN considering the results of the multivariable logistic regression analysis. When the presence of MNs was considered an indicator of malignancy, the sensitivity, specificity, positive predictive value (PPV), negative predictive value, and accuracy with 95% confidence inter-



**Table 4.** Multivariable logistic regression analysis of the association between MNs and the risk factors for PDAC and malignant IPMN<sup>a</sup>

	Odds ratio	95% CI	<i>p</i> value
<i>Malignant IPMN (outcome variable)</i>			
MN	3.88	1.53–9.84	0.004
DM	1.41	0.58–3.43	0.45
Obesity	0.52	0.12–2.24	0.38
Smoking history	1.66	0.74–3.71	0.22
Alcohol consumption	1.40	0.48–4.05	0.54
Family history of pancreatic cancer	0.22	0.04–1.34	0.10

MN, mural nodule; PDAC, pancreatic ductal adenocarcinoma; IPMN, intraductal papillary mucinous neoplasm; CI, confidence interval; DM, diabetes mellitus. <sup>a</sup> CP was excluded from this analysis because the initial analysis showed that the value of CP was unstable.

vals were 88.5% (82.7–93.2), 32.1% (24.1–38.8), 64.5% (60.3–68.0), 66.7% (49.9–80.4), and 64.9% (58.2–70.5), respectively. The specificity of the diagnosis using only the presence of MNs was low; therefore, we evaluated the diagnostic ability using both MNs and smoking history. Considering both the presence of MNs and a positive smoking history as indicators of malignancy, the sensitivity, specificity, PPV, negative predictive value, and accuracy with 95% confidence intervals were 42.3% (35.4–48.4), 73.2% (63.6–81.7), 68.8% (57.6–78.6), 47.7% (41.4–53.2), and 55.2% (47.2–62.3), respectively.

## Discussion

The frequency of high-grade dysplasia or invasive main duct type IPMN is approximately 70% [1, 9]. By contrast, the rate of high-grade dysplasia or invasive branch duct type IPMN is lower; therefore, the indications for the surgical resection of IPMNs, especially for branch duct IPMNs, remain controversial [1, 9]. In this study, we evaluated 134 patients with resected IPMNs and found that 58.2% were malignant. MNs are considered as high-risk stigmata, and 107 of the 134 patients (79.9%) underwent surgical resection because of the presence of MNs; however, the PPV of MNs for malignant IPMN was 64.5%, which was not a satisfactory result. The identification of factors with good predictive value for malignant IPMN is necessary.

Several studies investigated the association of environmental, personal, and hereditary risk factors with the oc-

currence or degree of IPMN [10–14]. Capurso et al. [10] compared 390 patients with IPMN with 390 matched controls and found that a history of DM, CP, and a family history of pancreatic cancer were all independent risk factors for IPMN. Carr et al. [11] examined the association between IPMN malignant progression and smoking in 324 resected IPMNs and found no significant difference in the percentage of invasive IPMNs between smokers and nonsmokers (22 vs. 18%,  $p = 0.5$ ). However, among patients with invasive IPMN, smokers were younger than nonsmokers at the time of diagnosis (65 vs. 72 years,  $p = 0.01$ ). This indicated that smoking might promote IPMN malignant progression. Rezaee et al. [12] reported that patients with main duct type IPMNs were more frequently smokers than patients with mixed and branch duct type IPMNs ( $p = 0.03$ ). However, there was no difference between the 2 groups in terms of the risk of high-grade dysplasia or invasive carcinoma.

The present study showed no significant difference in the incidence of malignant IPMNs between smoking and nonsmoking groups. However, the odds ratio of smoking (1.66) in patients with malignant IPMN was higher than that of environmental, personal, and hereditary risk factors. Moreover, considering a positive smoking history in combination with the presence of MNs as indications for surgery, the PPV and specificity for malignant IPMN increased from 64.5 to 68.8% and from 32.1 to 73.2%, respectively, although the accuracy decreased.

This study had several limitations. The study used a retrospective design and included a small number of patients who underwent surgical resection. The results of the analysis should be validated in a prospective larger study. CP was excluded from the multivariable logistic regression analysis of the association between MNs and the risk factors for PDAC and malignant IPMN because the value of CP was unstable, as all patients with CP had malignant IPMNs. However, CP may be associated with malignant IPMN.

In conclusion, there was no significant association between the risk factors for PDAC and malignant IPMN. The presence of several risk factors, especially a positive smoking history in addition to the presence of MNs, is an indication for surgical resection in patients with IPMN.

## Disclosure Statement

There are no potential competing interests concerning this study.

## Author Contributions

Ken Kamata: writing of the manuscript, study conception and design, and performing endoscopic ultrasonography. Mamoru Takenaka: writing of the manuscript, drafting conception and design. Atsushi Nakai: data collection. Shunsuke Omoto: data collection. Takeshi Miyata: data collection. Kosuke Minaga: data collection. Tomohiro Matsuda: data collection. Kentaro Yamao: data

collection. Hajime Imai: data collection. Yasutaka Chiba: statistical analysis. Toshiharu Sakurai, Tomohiro Watanabe, and Naoshi Nishida: contribution to writing and revising the manuscript. Takaaki Chikugo: pathological evaluation. Ippei Matsumoto and Yoshifumi Takeyama: surgical resection. Masatoshi Kudo: writing of the manuscript and drafting conception and design. Guarantor of the manuscript: Mamoru Takenaka.

## References

- 1 Tanaka M, Fernández-del Castillo C, Adsay V, et al: International consensus guidelines 2012 for the management of IPMN and MCN of the pancreas. *Pancreatol* 2012;12:183–197.
- 2 Adsay NV, FukushimaN, Furukawa T, et al: Intraductal neoplasms of the pancreas; in Bosman FT, Hruban RH, Cameiro F, et al (eds): *WHO Classification of Tumors of the Digestive System*. WHO Classification of Tumors, ed 4. Lyon, IARC, 2010, pp 304–313.
- 3 Ben Q, Xu M, Ning X, et al: Diabetes mellitus and risk of pancreatic cancer: a meta-analysis of cohort studies. *Eur J Cancer* 2011;47:1928–1937.
- 4 Ueda J, Tanaka M, Ohtsuka T, et al: Surgery for chronic pancreatitis decreases the risk for pancreatic cancer: a multicenter retrospective analysis. *Surgery* 2013;153:357–364.
- 5 Lin Y, Kikuchi S, Tamakoshi A, et al: Obesity, physical activity and the risk of pancreatic cancer in a large Japanese cohort. *Int J Cancer* 2007;120:2665–2671.
- 6 Jacobs EJ, Chanock SJ, Fuchs CS, et al: Family history of cancer and risk of pancreatic cancer: a pooled analysis from the Pancreatic Cancer Cohort Consortium (PanScan). *Int J Cancer* 2010;127:1421–1428.
- 7 Matsuo K, Ito H, Wakai K, et al: Cigarette smoking and pancreas cancer risk: an evaluation based on a systematic review of epidemiologic evidence in the Japanese population. *Jpn J Clin Oncol* 2011;41:1292–1302.
- 8 Tramacere I, Scottie L, Jenab M, et al: Alcohol drinking and pancreatic cancer risk: a meta-analysis of the dose-risk relation. *Int J Cancer* 2010;126:1474–1486.
- 9 Tanaka M, Chari S, Adsay V, et al: International consensus guidelines for management of intraductal papillary mucinous neoplasms and mucinous cystic neoplasms of the pancreas. *Pancreatol* 2006;6:17–32.
- 10 Capurro G, Boccia S, Salvia R, et al: Risk factors for intraductal papillary mucinous neoplasm (IPMN) of the pancreas: a multicentre case-control study. *Am J Gastroenterol* 2013;108:1003–1009.
- 11 Carr RA, Roch AM, Shaffer K, et al: Smoking and IPMN malignant progression. *Am J Surg* 2017;213:494–497.
- 12 Rezaee N, Khalifian S, Cameron JL, et al: Smoking is not associated with severe dysplasia or invasive carcinoma in resected intraductal papillary mucinous neoplasms. *J Gastrointest Surg* 2015;19:656–665.
- 13 Leal JN, Kingham TP, D'Angelica MI, et al: Intraductal papillary mucinous neoplasms and the risk of diabetes mellitus in patients undergoing resection versus observation. *J Gastrointest Surg* 2015;19:1974–1981.
- 14 Sturm EC, Roch AM, Shaffer KM, et al: Obesity increases malignant risk in patients with branch-duct intraductal papillary mucinous neoplasm. *Surgery* 2013;154:803–809.

# Needle Tract Seeding: An Overlooked Rare Complication of Endoscopic Ultrasound-Guided Fine-Needle Aspiration

Kosuke Minaga<sup>a</sup> Mamoru Takenaka<sup>a</sup> Akio Katanuma<sup>b</sup> Masayuki Kitano<sup>c</sup>  
Yukitaka Yamashita<sup>d</sup> Ken Kamata<sup>a</sup> Kentaro Yamao<sup>a</sup> Tomohiro Watanabe<sup>a</sup>  
Hiroyuki Maguchi<sup>b</sup> Masatoshi Kudo<sup>a</sup>

<sup>a</sup>Department of Gastroenterology and Hepatology, Kindai University Faculty of Medicine, Osaka-Sayama,

<sup>b</sup>Center for Gastroenterology, Teine-Keijinkai Hospital, Sapporo, <sup>c</sup>Second Department of Internal Medicine, Wakayama Medical University School of Medicine, and <sup>d</sup>Department of Gastroenterology and Hepatology, Japanese Red Cross Society Wakayama Medical Center, Wakayama, Japan

## Keywords

Endoscopic ultrasound · Endoscopic ultrasound-guided fine-needle aspiration · Needle tract seeding · Tumor seeding · Seeding

## Abstract

Endoscopic ultrasound-guided fine-needle aspiration (EUS-FNA) has been widely used for diagnosis of both inflammatory and tumor lesions located in and adjacent to the gastrointestinal tract. EUS-FNA has been considered to be a safe technique with few complications, as shown in recent review articles in which EUS-FNA-related morbidity and mortality rates were reported to be <1%. It should be noted, however, that needle tract seeding, although uncommon, can occur after diagnostic EUS-FNA and that this complication affects the prognosis of patients. Although an accurate value for the frequency of needle tract seeding caused by EUS-FNA has not been reported, the numbers of case reports on needle tract seeding have been rapidly increasing, especially in Ja-

pan. These case reports regarding EUS-FNA-related needle tract seeding prompted us to reevaluate the safety of EUS-FNA because this complication may have a significant influence on patients' prognoses. In this review, we summarize the clinical features and outcomes of needle tract seeding after EUS on the basis of the previously reported cases and provide useful information to prevent and reduce this serious complication.

© 2017 S. Karger AG, Basel

## Introduction

Since the first description in 1992 by Vilman et al. [1], the utility and efficacy of endoscopic ultrasound-guided fine-needle aspiration (EUS-FNA) have been well established in the diagnoses of a wide variety of lesions located in and adjacent to the gastrointestinal tract. Although EUS-FNA itself has been considered to be a very safe diagnostic modality with <1% of morbidity and mortality

rates [2], it is not free from complications. The most common complications of EUS-FNA include infections, bleeding, and pancreatitis. Moreover, a number of recent case studies have highlighted the importance of needle tract seeding as a rare but serious complication associated with EUS-FNA. Although an accurate value for the frequency of needle tract seeding following EUS-FNA has not been reported yet, the numbers of case reports regarding needle tract seeding have been increasing, especially those by Japanese endosonographers. Probably, this complication remains underreported. In this review, we summarize the clinical features and outcomes of needle tract seeding obtained from an extensive analysis of previously published reported cases.

## Methods

This review is based on the results of searches performed in the Medline/PubMed and Cochrane Library electronic databases of studies published between June 1996 and June 2017 using the keywords “EUS OR endoscopic ultrasound” AND “seeding.” The initial search identified 80 articles. Of these, 32 articles were considered relevant to this review through the screening of their titles. After careful reading of the abstracts, the complete texts were obtained for potentially relevant articles. Finally, we included a total of 29 references focusing on EUS-FNA-related complications and found 15 case reports regarding needle tract seeding following EUS-FNA.

## Risk of Needle Tract Seeding following EUS-FNA

According to large retrospective surveys, the rate of needle tract seeding caused by percutaneous abdominal FNA is extremely low and ranges from 0.003 to 0.009% [3, 4]. Furthermore, a previous study suggested that needle tract seeding and/or peritoneal dissemination may be disregarded as possible complications following EUS-FNA because the rate of such complications is lower in EUS-FNA than in percutaneous FNA [5]. However, it has been suggested that the frequency of needle tract seeding might have been underestimated in previous studies because disease mortality was calculated without clear recognition of tumor dissemination [6]. More accurate rates of needle tract seeding caused by EUS-FNA have been obtained by later retrospective analyses. In cases of pancreatobiliary tumors, many studies have provided evidence that the EUS-FNA procedure itself did not increase the risk of needle tract seeding, peritoneal dissemination, or decreased survival [7–12]. For example, Ngamruengphong et al. [7] performed a retrospective study to ad-

dress whether preoperative EUS-FNA for pancreatic cancer is associated with an increased risk of stomach or peritoneal recurrence and whether the procedure affects long-term survival. In this retrospective study in 256 patients who underwent surgery with curative intent, preoperative EUS-FNA was performed in 208 patients, and a total of 16 patients had peritoneal recurrence. This group of 16 patients with peritoneal or gastric recurrence was composed of 5 patients in the non-EUS-FNA group and 11 patients in the EUS-FNA group. A multivariate analysis did not find a significant correlation between preoperative EUS-FNA and cancer recurrence in the stomach or peritoneal cavity [7]. Similar results were obtained in 2 other retrospective studies in which EUS-FNA did not increase the risk of tumor dissemination through the needle tract in pancreatic cancer [10, 11]. Regarding mucinous pancreatic cystic lesions, the PIPE study was conducted to assess the frequency of postoperative peritoneal seeding in patients with intraductal papillary mucinous neoplasm. In this study, preoperative EUS-FNA was not associated with an increased frequency of peritoneal seeding in patients who underwent surgery [8].

However, we need to be cautious in the interpretation of the results of these studies for the following reasons. First, the number of patients in these studies might be too small to sufficiently estimate the actual frequency of needle tract seeding, a rare complication of EUS-FNA. Second, the follow-up periods of these studies were rather short to observe the incidence or outcome of needle tract seeding. Taken together, these retrospective studies do not provide clinical evidence that needle tract seeding is a complication associated with EUS and that awareness of this complication is absolutely necessary before EUS-FNA.

In contrast to the retrospective studies shown above, a prospective study by Levy et al. [13] provided valuable information about the causal linkage of EUS-FNA to tumor dissemination. They evaluated the presence of malignant cells within gastrointestinal luminal fluid in patients who received diagnostic EUS-FNA for extraluminal sites, pancreatic cancer in this case. Surprisingly, post-FNA luminal fluid cytology was positive in 3 (11.5%) of 26 patients with pancreatic cancer, which suggested that translocation of malignant cells from pancreatic cancer tissue into the lumen of the gastrointestinal tract was evoked in a significant population of patients after diagnostic EUS-FNA [13]. Unfortunately, it remains unknown whether such translocation of malignant cells into the gastrointestinal lumen results in colonization and dissemination of tumor cells. Thus, the clinical significance of these results needs



**Table 1.** Clinical features and outcomes of 15 published cases of needle tract seeding following EUS-FNA

First author, year [ref.]	Country	Diagnosis, tumor staging	Details of EUS-FNA			Time interval	Details of tumor seeding		Outcomes
			puncture lumen	needle diameter, gauge	passes, <i>n</i>		seeding site	tumor size, mm	
Shah, 2004 [15]	USA	perigastric lymph node metastasis from malignant melanoma	transgastric	22	1	6 months	posterior gastric wall	30	surgery, further follow-up unknown
Paquin, 2005 [16]	Canada	pancreatic adenocarcinoma, T1N0M0	transgastric	22	5	21 months	posterior gastric wall	50	palliative chemotherapy, died 12 months after diagnosis
Doi, 2008 [17]	Japan	mediastinal lymph node metastasis from gastric cancer	transesophageal	19	1	21 months	esophageal wall	8	radiation, the lesion resolved after 2 months
Ahmed, 2011 [18]	USA	pancreatic adenocarcinoma, T2N0M0	transgastric	–	multiple	nearly 4 years	gastric wall	45	died with another malignancy
Chong, 2011 [19]	Australia	pancreatic adenocarcinoma, T2N0M0	transgastric	22	2	26 months	posterior gastric wall	40	unresectable, further follow-up unknown
Katanuma, 2012 [20]	Japan	pancreatic adenocarcinoma, T2N0M0	transgastric	22	4	22 months	posterior gastric wall	–	surgery, further follow-up unknown
Anderson, 2013 [21]	USA	pancreatic adenocarcinoma	–	–	–	–	gastroesophageal junction	10	not reported
Sakurada, 2015 [22]	Japan	pancreatic adenosquamous carcinoma, T2N0M0	transgastric	22	–	19 months	posterior gastric wall	20	surgery (curatively resected), further follow-up unknown
Minaga, 2015 [23]	Japan	pancreatic adenocarcinoma, T3N0M0	transgastric	22	3	8 months	posterior gastric wall	12	surgery, no recurrence after 27 months of follow-up
Tomonari, 2015 [24]	Japan	pancreatic adenocarcinoma, T3N0M0	transgastric	22	2	28 months	gastric wall	32	surgery, further follow-up unknown
Kita, 2016 [25]	Japan	pancreatic adenocarcinoma	transgastric	22	2	7 months	posterior gastric wall	–	not reported
Yamabe, 2016 [26]	Japan	intraductal papillary mucinous carcinoma	transgastric	25	–	3 months	posterior gastric wall	24	palliative chemotherapy, died 26 months after diagnosis
Minaga, 2016 [27]	Japan	pancreatic adenocarcinoma, T1N0M0	transgastric	22	3	24 months	posterior gastric wall	30	surgery, no recurrence after 18 months of follow-up
Iida, 2016 [28]	Japan	pancreatic adenocarcinoma, T3N0M0	transgastric	22	3	6 months	posterior gastric wall	18	surgery, re-recurrence in the upper gastric posterior wall
Goel, 2017 [29]	Australia	metastatic squamous cell carcinoma in the celiac axis of unknown origin	transgastric	19	2	11 months	posterior gastric wall	50	unresectable, further follow-up unknown

EUS-FNA, endoscopic ultrasound-guided fine-needle aspiration.

to be clarified. However, the results of this study indicate that translocation of tumor cells into the gastrointestinal lumen might be involved in the development of tumor dissemination following EUS-FNA [6]. Collectively, previous retrospective and prospective studies have not clearly shown the accurate rate or outcome of needle tract seeding after EUS-FNA. Given that the occurrence of this complication is very low, the numbers of recruited patients in these studies might have been too small to draw definitive conclusions. Further prospective studies with a large number of patients are awaited to fully define the clinical characteristics of needle tract seeding following EUS-FNA. Therefore, at present, our knowledge regarding EUS-FNA-related needle tract seeding is exclusively obtained from case reports. In the following paragraphs, we discuss clinical characteristics of needle tract seeding through detailed analysis of each case report.

### Cases of Needle Tract Seeding in the Literature

The first case of tumor dissemination caused by EUS-FNA was reported by Hirooka et al. [14] in 2003. They reported a case of EUS-FNA-caused peritoneal dissemination of an intraductal papillary mucinous tumor of stage I with T1N0M0. Since this first report of tumor dissemination, needle tract seeding has been reported in 15 cases following EUS-FNA [15–29]. Notably, 9 of 15 cases were reported from Japan. The details of the individual cases are shown in Table 1. Moreover, 12 (80%) of 15 cases of needle tract seeding were caused by diagnostic EUS-FNA of pancreatic cancer and pancreatic cystic tumors. In all 12 cases, the tumors were located in the body or tail of the pancreas. In 13 (86.7%) of 15 cases, EUS-FNA was performed via the gastric body to preferentially diagnose pancreatic body or tail lesions. No reports described the tumor seeding following EUS-FNA for pancreatic head lesions, which can be explained by the fact that the needle tract site may be resected together with a primary tumor in pancreatic head cancer. These data suggest that endosonographers need to bear in mind the possibility of needle tract seeding when performing EUS-FNA for resectable tumors located in the pancreatic body or tail.

Regarding the EUS-FNA procedure, a 22-G FNA needle was used in the majority of cases with EUS-related needle tract seeding. In most cases, vacuum suction from a syringe during the puncture was applied. The median number of needle passes was 2 (range 1–5). Whether the risk of tumor seeding is associated with the needle size or number of passes remains uncertain.

The interval from EUS-FNA to detection of needle tract seeding varies widely, with a median interval of 20 months (range 3–48). For detection of the seeding tumor, gastroscopy and imaging modalities, especially positron emission tomography, have been useful. Abnormal accumulation of fluorine-18-deoxyglucose locally into the seeding sites was detected in 6 cases.

In terms of the seeding site, tumor seeding was located in the gastric wall in 13 (86.7%) cases, in the esophageal wall in 1 case, and in the gastroesophageal junction in 1 case. The median seeding tumor size was 30 mm (range 8–50). Most of the seeding tumors manifested as a submucosal tumor-like mass because the tumor mainly arose from the submucosal muscle layer or serosa but not from the mucosal layer.

Regarding treatment of EUS-related needle tract seeding, surgical resection was performed in 7 cases. In 1 case of needle tract seeding that occurred in the esophageal wall, radiation therapy successfully resolved the lesion. In 2 cases, palliative chemotherapy was selected, and in the remaining 5 cases, the treatment methods were not reported. Among the 7 cases treated with surgical resection for EUS-FNA-related needle tract seeding, no tumor recurrence was observed in the 2 cases treated at our hospital at 27 and 18 months of follow-up, respectively, after surgical resection of the seeded lesions [23, 27]. In the other 5 cases treated with surgical resection, no detailed information about the patients' outcomes and follow-up was obtained. Thus, the long-term prognosis of surgically resected needle tract seeding is not well known. Most recently, Iida et al. [28] reported a re-recurrence case after radical surgical resection for EUS-FNA-related tumor seeding. In this case, distal gastrectomy was performed for needle tract seeding that occurred on the lower posterior wall of the gastric body. At 21 months after distal gastrectomy, re-recurrence was detected on the upper posterior wall of the operated gastric body. The authors suggested that total gastrectomy rather than simple surgical resection should be considered in such cases [28].

Although the optimal treatment strategy for needle tract seeding has not been established, early detection and surgical resection of needle tract seeded lesions may be very effective for achieving long-term survival in some cases. However, further studies are necessary to fully define the clinical characteristics of needle tract seeding cases that can be successfully treated with surgical resection. Moreover, it should also be emphasized that cautious follow-up of the needle puncture sites by performing endoscopy and imaging modalities for early detection of needle tract seeding is of great importance to ensure radical cure.

## Prevention of Needle Tract Seeding

As mentioned earlier, needle tract seeding after EUS-FNA is a serious complication that may worsen patients' prognoses. Consequently, the question arises as to how we can perform EUS-FNA safely without increasing the risk of needle tract seeding. In this regard, a couple of suggestions have been made to reduce the risk of needle tract seeding. Fujii and Levy [6] reported that the risk of needle tract seeding may be reduced by performing EUS-FNA only when the results obtained by this procedure are useful for a patient's management. Technically, it is important to set the needle tract sites within the surgical resection margins in the cases of patients with resectable tumors to avoid needle tract seeding. Most cases of needle tract seeding have occurred after diagnostic EUS against lesions located in the pancreatic body or tail. In such cases, needle tract sites may be set in the gastric body, which may not be resected by surgery. Therefore, the risk-benefit ratio of EUS-FNA should be carefully considered in patients with potentially resectable lesions of the pancreatic body or tail, as Hirooka et al. suggested [14].

Careful follow-up using endoscopy and imaging modalities is necessary in cases in which the needle tract site is outside the surgical resection margins. In such cases, it may be mandatory to detect needle tract seeding before metastases occur to resect curatively.

## Conclusions

Needle tract seeding following EUS-FNA is a rare but serious complication that may impair patients' survival. Therefore, endosonographers should bear in mind the possibility of needle tract seeding before EUS-FNA. Considering this serious complication, EUS-FNA should be performed only when the results obtained by this procedure are useful for therapeutic decision-making. Needle tract seeding following EUS-FNA might be avoided by setting the needle tract line within the surgical resection margins, if technically possible. Carefully planned endoscopic and imaging surveillance of the puncture sites could lead to early detection of needle tract seeding, which may improve the prognosis. Further prospective studies with a larger cohort are required to estimate the risk of needle tract seeding following EUS-FNA.

## Disclosure Statement

The authors have no financial conflicts of interest to declare concerning this article.

## References

- 1 Vilmann P, Jacobsen GK, Henriksen FW, et al: Endoscopic ultrasonography with guided fine needle aspiration biopsy in pancreatic disease. *Gastrointest Endosc* 1992;38:172–173.
- 2 Wang KX, Ben QW, Jin ZD, et al: Assessment of morbidity and mortality associated with EUS-guided FNA: a systematic review. *Gastrointest Endosc* 2011;73:283–290.
- 3 Smith EH: Complications of percutaneous abdominal fine-needle biopsy. *Radiology* 1991;178:253–258.
- 4 Jenssen C, Alvarez-Sánchez MV, Napoléon B, et al: Diagnostic endoscopic ultrasonography: assessment of safety and prevention of complications. *World J Gastroenterol* 2012;18:4659–4676.
- 5 Micames C, Jowell PS, White R, et al: Lower frequency of peritoneal carcinomatosis in patients with pancreatic cancer diagnosed by EUS-guided FNA versus percutaneous FNA. *Gastrointest Endosc* 2003;58:690–695.
- 6 Fujii LL, Levy MJ: Basic techniques in endoscopic ultrasound-guided fine needle aspiration for solid lesions: adverse events and avoiding them. *Endosc Ultrasound* 2014;3:35–45.
- 7 Ngamruengphong S, Xu C, Woodward TA, et al: Risk of gastric or peritoneal recurrence, and long-term outcomes, following pancreatic cancer resection with preoperative endosonographically guided fine needle aspiration. *Endoscopy* 2013;45:619–626.
- 8 Yoon WJ, Daglilar ES, Fernández-del Castillo C, et al: Peritoneal seeding in intraductal papillary mucinous neoplasm of the pancreas patients who underwent endoscopic ultrasound-guided fine-needle aspiration: the PIPE Study. *Endoscopy* 2014;46:382–387.
- 9 El Chafic AH, Dewitt J, Leblanc JK, et al: Impact of preoperative endoscopic ultrasound-guided fine needle aspiration on postoperative recurrence and survival in cholangiocarcinoma patients. *Endoscopy* 2013;45:883–889.
- 10 Ikezawa K, Uehara H, Sakai A, et al: Risk of peritoneal carcinomatosis by endoscopic ultrasound-guided fine needle aspiration for pancreatic cancer. *J Gastroenterol* 2013;48:966–972.
- 11 Tsutsumi H, Hara K, Mizuno N, et al: Clinical impact of preoperative endoscopic ultrasound-guided fine-needle aspiration for pancreatic ductal adenocarcinoma. *Endosc Ultrasound* 2016;5:94–100.
- 12 Ngamruengphong S, Swanson KM, Shah ND, et al: Preoperative endoscopic ultrasound-guided fine needle aspiration does not impair survival of patients with resected pancreatic cancer. *Gut* 2015;64:1105–1110.
- 13 Levy MJ, Gleeson FC, Campion MB, et al: Prospective cytological assessment of gastrointestinal luminal fluid acquired during EUS: a potential source of false-positive FNA and needle tract seeding. *Am J Gastroenterol* 2010;105:1311–1318.

- 14 Hirooka Y, Goto H, Itoh A, et al: Case of intraductal papillary mucinous tumor in which endosonography-guided fine-needle aspiration biopsy caused dissemination. *J Gastroenterol Hepatol* 2003;18:1323–1324.
- 15 Shah JN, Fraker D, Guerry D, et al: Melanoma seeding of an EUS-guided fine needle track. *Gastrointest Endosc* 2004;59:923–924.
- 16 Paquin SC, Gariépy G, Lepanto L, et al: A first report of tumor seeding because of EUS-guided FNA of a pancreatic adenocarcinoma. *Gastrointest Endosc* 2005;61:610–611.
- 17 Doi S, Yasuda I, Iwashita T, et al: Needle tract implantation on the esophageal wall after EUS-guided FNA of metastatic mediastinal lymphadenopathy. *Gastrointest Endosc* 2008;67:988–990.
- 18 Ahmed K, Sussman JJ, Wang J, et al: A case of EUS-guided FNA-related pancreatic cancer metastasis to the stomach. *Gastrointest Endosc* 2011;74:231–233.
- 19 Chong A, Venugopal K, Segarajasingam D, et al: Tumor seeding after EUS-guided FNA of pancreatic tail neoplasia. *Gastrointest Endosc* 2011;74:933–935.
- 20 Katanuma A, Maguchi H, Hashigo S, et al: Tumor seeding after endoscopic ultrasound-guided fine-needle aspiration of cancer in the body of the pancreas. *Endoscopy* 2012;44(suppl 2):E160–E161.
- 21 Anderson B, Singh J, Jafri SF, et al: Tumor seeding following endoscopic ultrasonography-guided fine-needle aspiration of a celiac lymph node. *Dig Endosc* 2013;25:344–345.
- 22 Sakurada A, Hayashi T, Ono M, et al: A case of curatively resected gastric wall implantation of pancreatic cancer caused by endoscopic ultrasound-guided fine-needle aspiration. *Endoscopy* 2015;47(suppl 1):E198–E199.
- 23 Minaga K, Kitano M, Yamashita Y: Surgically resected needle tract seeding following endoscopic ultrasound-guided fine-needle aspiration in pancreatic cancer. *J Hepatobiliary Pancreat Sci* 2015;22:708–709.
- 24 Tomonari A, Katanuma A, Matsumori T, et al: Resected tumor seeding in stomach wall due to endoscopic ultrasonography-guided fine needle aspiration of pancreatic adenocarcinoma. *World J Gastroenterol* 2015;21:8458–8461.
- 25 Kita E, Yamaguchi T, Sudo K: A case of needle tract seeding after EUS-guided FNA in pancreatic cancer, detected by serial positron emission tomography/CT. *Gastrointest Endosc* 2016;84:869–870.
- 26 Yamabe A, Irisawa A, Shibukawa G, et al: Rare condition of needle tract seeding after EUS-guided FNA for intraductal papillary mucinous carcinoma. *Endosc Int Open* 2016;4:E756–E758.
- 27 Minaga K, Kitano M, Enoki E, et al: Needle-tract seeding on the proximal gastric wall after EUS-guided fine-needle aspiration of a pancreatic mass. *Am J Gastroenterol* 2016;111:1515.
- 28 Iida T, Adachi T, Ohe Y, et al: Re-recurrence after distal gastrectomy for recurrence caused by needle tract seeding during endoscopic ultrasound-guided fine-needle aspiration of a pancreatic adenocarcinoma. *Endoscopy* 2016;48(suppl 1):E304–E305.
- 29 Goel A, Hon KCA, Chong A: Needle tract tumor seeding following endoscopic ultrasound-guided fine needle aspiration of metastatic squamous cell carcinoma. *Clin Gastroenterol Hepatol* 2017, DOI 10.1016/j.cgh.2017.04.024.



# Hand-Foot Syndrome and Post-Progression Treatment Are the Good Predictors of Better Survival in Advanced Hepatocellular Carcinoma Treated with Sorafenib: A Multicenter Study

Chikara Ogawa<sup>a,f</sup> Masahiro Morita<sup>a</sup> Akina Omura<sup>a</sup> Teruyo Noda<sup>a</sup>  
Atsushi Kubo<sup>a</sup> Toshihiro Matsunaka<sup>a</sup> Hiroyuki Tamaki<sup>a</sup>  
Mitsushige Shibatoge<sup>a</sup> Akemi Tsutsui<sup>b</sup> Tomonori Senoh<sup>b</sup> Takuya Nagano<sup>b</sup>  
Kouichi Takaguchi<sup>b</sup> Joji Tani<sup>c</sup> Asahiro Morishita<sup>c</sup> Hirohito Yoneyama<sup>c</sup>  
Tsutomu Masaki<sup>c</sup> Akio Moriya<sup>d</sup> Masaharu Ando<sup>d</sup> Akihiro Deguchi<sup>e</sup>  
Yasutaka Kokudo<sup>e</sup> Yasunori Minami<sup>f</sup> Kazuomi Ueshima<sup>f</sup> Toshiharu Sakurai<sup>f</sup>  
Naoshi Nishida<sup>f</sup> Masatoshi Kudo<sup>f</sup>

<sup>a</sup>Department of Gastroenterology and Hepatology, Takamatsu Red Cross Hospital, and <sup>b</sup>Department of Hepatology, Kagawa Prefectural Central Hospital, Takamatsu, <sup>c</sup>Department of Gastroenterology and Neurology, Faculty of Medicine, Kagawa University, Miki, <sup>d</sup>Department of Gastroenterology, Mitoyo General Hospital, Kan-onji, <sup>e</sup>Department of Gastroenterology, Kagawa Rosai Hospital, Marugame, and <sup>f</sup>Department of Gastroenterology and Hepatology, Kindai University Faculty of Medicine, Osaka-Sayama, Japan

## Keywords

Hepatocellular carcinoma · Sorafenib · Hand-foot syndrome

## Abstract

**Objective:** To determine the relationship between treatment outcomes and hand-foot syndrome (HFS), and the relationship between survival rate and post-progression treatment after sorafenib therapy. **Methods:** The study assessed 314 patients with advanced hepatocellular carcinoma (HCC) treated with sorafenib at 5 general hospitals in Kagawa Prefecture, Japan. **Results:** At the start of sorafenib therapy, 23.6% of the patients had HCC of a Child-Pugh class other than A. The initial sorafenib dose was 800 mg in 9.2% of the patients and 400 mg in 64.3%. Time to progression was 129 days (95% CI:

87.3–170.7) and the median overall survival (OS) was 392 days (95% CI: 316.0–468.0). The OS of the patients with Child-Pugh class A HCC was significantly better than that of the patients with Child-Pugh class B HCC ( $p < 0.0001$ ). The survival curves for Child-Pugh class A-5 points and class A-6 points were significantly different, with that for class A-5 points being better ( $p < 0.0001$ ). A significant difference was observed between the patients who exhibited HFS and those who did not, with the former exhibiting a better survival rate ( $p < 0.001$ ). In addition, the survival rate of the patients who received post-progression treatment after sorafenib therapy was significantly better than that of the patients who did not ( $p < 0.001$ ). **Conclusion:** In sorafenib therapy, patients with HFS and those who received post-progression treatment exhibited good OS.

© 2017 S. Karger AG, Basel

## Introduction

Hepatocellular carcinoma (HCC) is the second leading cause of cancer mortality in the world [1]. Sorafenib is an agent that has improved the time to progression and overall survival (OS) in advanced stages of HCC with vascular invasion and/or extrahepatic spread [2]. Sorafenib has been administered in accordance with the consensus-based treatment algorithm for HCC proposed by the Japan Society of Hepatology [3–6]. According to this algorithm, sorafenib is indicated for patients diagnosed with Child-Pugh class A HCC with extrahepatic spread or vascular invasion. Sorafenib is also recommended for patients with Child-Pugh class A HCC where transcatheter arterial chemoembolization (TACE) [7–11] and hepatic arterial infusion chemotherapy [12, 13] are not indicated. In the present study, we examined the efficacy of sorafenib treatment and the clinical outcome in 314 patients at 5 general hospitals in Kagawa Prefecture, Japan.

## Subjects and Methods

### Patients

Between June 2009 and January 2016, 314 patients with advanced HCC were treated with sorafenib at 5 general hospitals in Kagawa Prefecture, Japan. The diagnosis of HCC was made based on histological or radiological findings using contrast-enhanced

computed tomography and/or dynamic magnetic resonance imaging [14, 15]. The responses of all patients were evaluated using the modified Response Evaluation Criteria in Solid Tumors (mRECIST) [16].

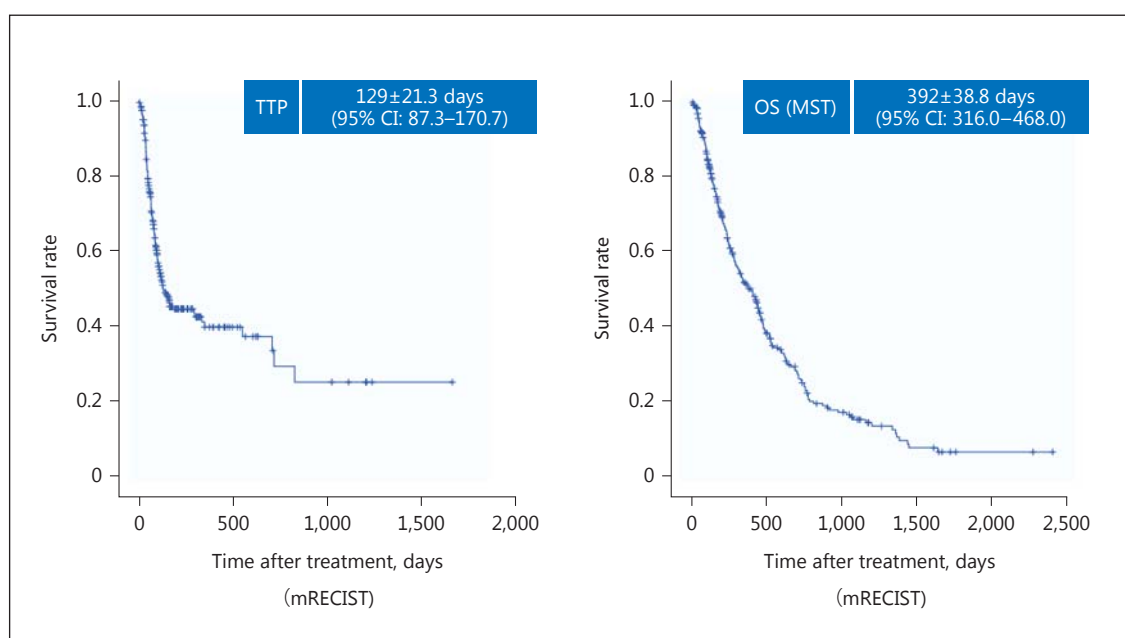
### Statistical Analyses

Univariate analysis was used to identify predictors of survival using the Kaplan-Meier method, and comparisons were performed using the log-rank test. A *p* value of <0.05 was considered statistically significant. All analyses were performed using SPSS version 22.0 for Windows (IBM, Armonk, NY, USA).

## Results

### Baseline Characteristics

The study included 254 men and 60 women. Their mean age was  $72.5 \pm 9.46$  years (range: 38–91), their mean height was  $160.4 \pm 9.12$  cm (range: 125.7–179.0), and their mean weight was  $58.6 \pm 11.9$  kg (range: 27–101.9). There were 43 patients with hepatitis B virus infection, 175 patients with hepatitis C virus infection, and 96 patients with other forms of liver disease. In 57 patients, HCC had been newly diagnosed, whereas in 257 patients it had recurred. There were 295 patients with a history of treatment for HCC and 19 patients with no such history. The mean initial sorafenib dose was  $391.7 \pm 159$  mg/day (range: 200–800).



**Fig. 1.** Kaplan-Meier curves of time to progression (TTP) and overall survival (OS) of patients with sorafenib treatment. MST, median survival time; mRECIST, modified Response Evaluation Criteria in Solid Tumors.

**Table 1.** Patient characteristics by Child-Pugh class

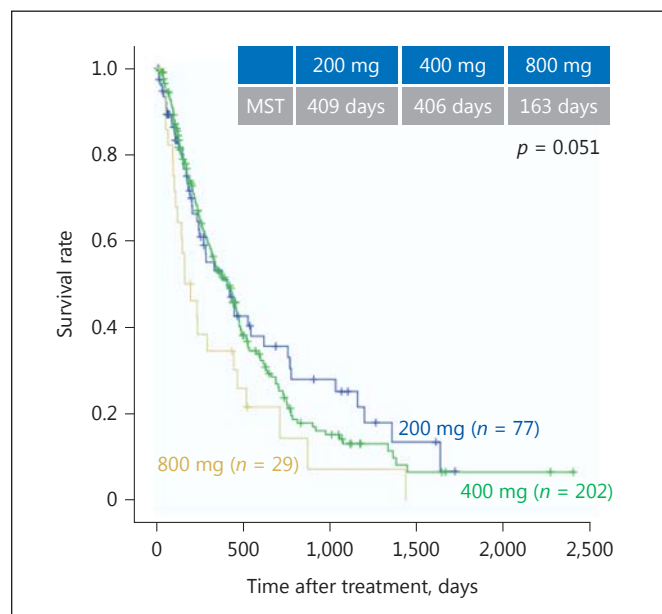
	Child-Pugh class A (n = 181)	Child-Pugh class B (n = 55)	<i>p</i>
Sex (male/female)	196/44	58/16	ns
Age (<70/≥70 years)	82/158	37/37	0.014
Height (<160/≥160 cm)	94/140	29/45	ns
Weight (<60/≥60 kg)	140/94	43/31	ns
Background (HBV/HCV/other)	33/130/77	10/45/19	ns
Initial manifestation/recurrence	39/201	18/56	ns
Tumors (<4/≥5)	114/115	29/45	ns
AFP (<200/≥200 ng/mL)	128/108	34/37	ns
DCP (<400/≥400 mAU/mL)	110/125	24/44	ns
AFP-L3 (<10/≥10%)	39/87	8/25	ns
Stage (III or lower/IVa/IVb)	106/40/94	36/18/20	ns

AFP, α-fetoprotein; DCP, des-gamma-carboxyprothrombin.

The Child-Pugh class and score at the initiation of sorafenib therapy was A-5 points in 129 patients, A-6 points in 111 patients, B-7 points in 48 patients, and B-8 points or higher in 26 patients. Sorafenib therapy was initiated in stage I in 6 patients, stage II in 51 patients, stage III in 85 patients, stage IVa in 58 patients, and stage IVb in 114 patients. The mean observation period in the present study was  $223 \pm 277$  days (range: 2–1,665). The indications for starting sorafenib were distal metastasis in 39.8% of the patients, unresponsiveness to TACE in 39.5%, inability to perform TACE in 8.9%, severe vascular invasion in 10.8%, and other reasons in 1.0%. The lung was the site of distant metastasis in 54 patients, the bone in 39 patients, lymph nodes in 36 patients, the adrenal glands in 14 patients, and the peritoneal cavity in 13 patients (some patients had metastases to multiple sites).

#### OS and Radiological Evaluation

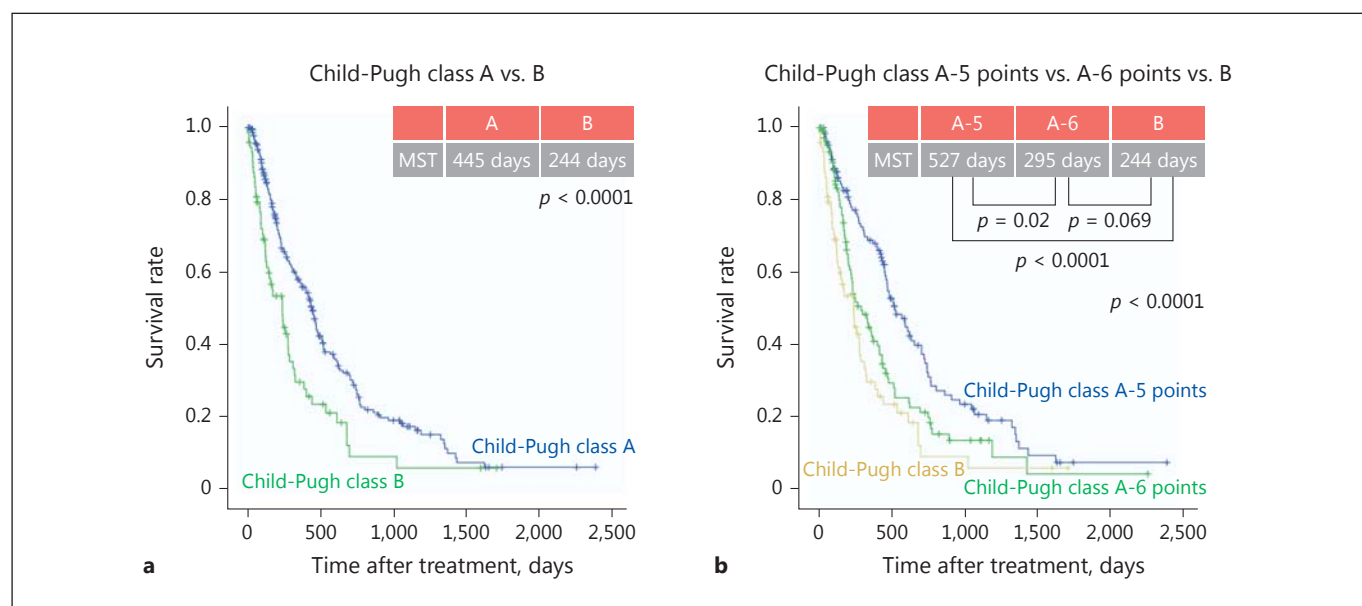
The results of sorafenib therapy were a time to progression of  $129 \pm 21.3$  days (95% CI: 87.3–170.7) and a median OS (median survival time [MST]) of  $392 \pm 38.8$  days (95% CI: 316.0–468.0) (Fig. 1). A complete response, partial response, stable disease, progressive disease, and incomplete evaluation were observed in 10, 25, 113, 147, and 19 patients, respectively. The overall response rate was 11.1%, and the tumor control rate was 47.4%. An initial sorafenib dose of 200 mg was administered to 77 patients, 400 mg to 202 patients (the most common dose), 600 mg to 6 patients, and 800 mg to 29 patients. The mean duration of sorafenib administration was 223.6 days, and the mean durations for the 200-, 400-, 600-, and 800-mg doses were 212.6, 242.2, 155, and 136.8 days, respectively.



**Fig. 2.** Kaplan-Meier curves of overall survival (median survival time [MST]) of the patients in the standard-dose group, the half-dose group, and the quarter-dose group (by initial dose).

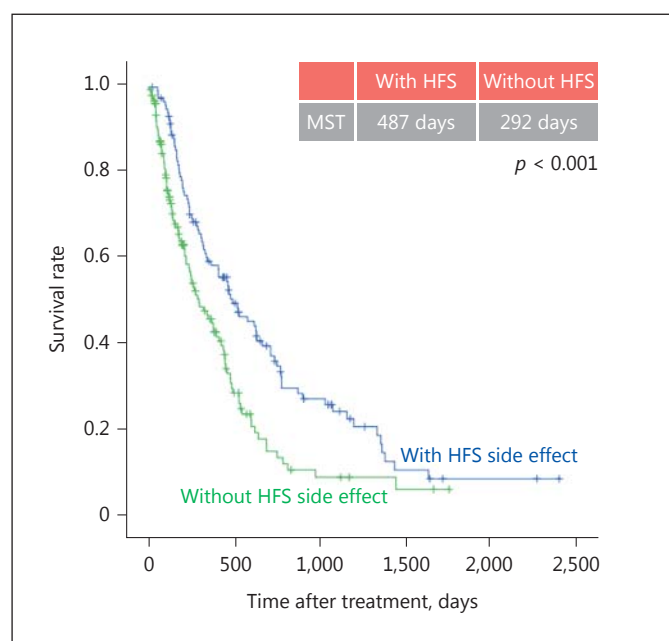
Disparities between institutions regarding the initial sorafenib dose were observed. The survival rate with a 400-mg initial dose was significantly higher than that with an 800-mg initial dose (Fig. 2).

A significant difference in patient characteristics according to Child-Pugh class was only observed for age (<70 years, ≥70 years;  $p = 0.014$ ); no significant differences were observed for the other variables (Table 1). Re-



**Fig. 3.** Survival curves by Child-Pugh class and score at the start of therapy. **a** Kaplan-Meier curves of overall survival (median survival time [MST]) of the patients with Child-Pugh class A and Child-Pugh class B hepatocellular carcinoma (HCC). There was a significant difference between class A and class B. **b** Kaplan-Meier curves of overall survival (MST) of the patients with Child-Pugh

class A-5 points and Child-Pugh class A-6 points. There was a significant difference between class A-5 points and class A-6 points. Child-Pugh class B HCC had worse results than class A HCC, but the results for class A-6 points were close to those for class B (no significant difference between class A-6 points and class B).

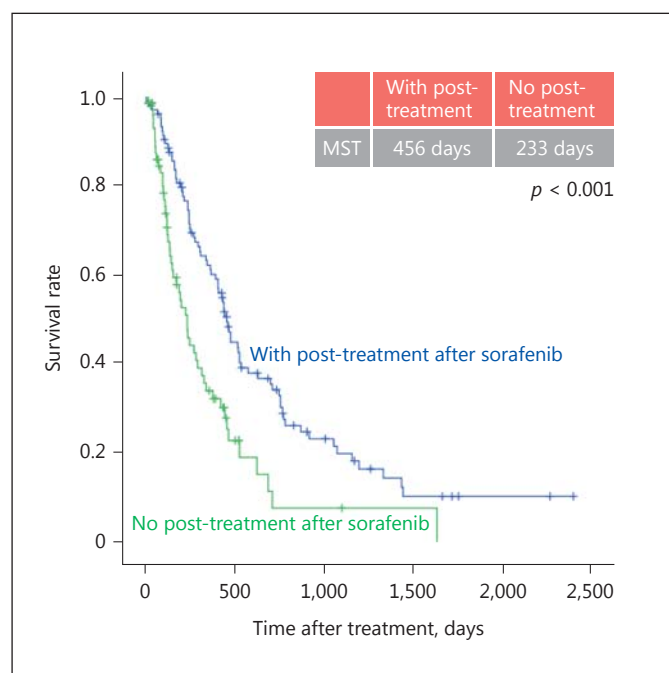


**Fig. 4.** Kaplan-Meier curves of overall survival (median survival time [MST]) of the patients with a hand-foot syndrome (HFS) side effect and those without an HFS side effect. Overall survival was significantly longer among the patients who exhibited HFS as a side effect.

Regarding survival rate, a significant difference was observed between Child-Pugh class A and class B, with the former being better ( $p < 0.0001$ ). Further, OS was significantly different between Child-Pugh class A-5 points and class A-6 points, with class A-5 points being better ( $p = 0.02$ ); however, OS was not significantly different between Child-Pugh class A-6 points and class B ( $p = 0.069$ ). The best OS was observed when treatment was initiated at Child-Pugh class A-5 points (Fig. 3).

Next, we examined the onset of hand-foot syndrome (HFS), which is an adverse effect of sorafenib. During the observation period, HFS was observed in 118 patients (37.6%), with the mean number of days until onset being  $29.6 \pm 33.8$  (range: 1–227). By grade, adverse effects were observed in 43 patients with grade I HCC (14.0%), 42 patients with grade II HCC (13.8%), and 24 patients with grade III HCC (7.9%). The number of days until onset of HFS was less than 1 month from initiation of sorafenib therapy for 65.3% of the patients who exhibited HFS. Regarding differences in OS based on the presence or absence of HFS, the MST of the patients with HFS was 487 days, while that of the patients without HFS was 292 days; this difference was statistically significant ( $p = 0.001$ ) (Fig. 4). The MSTs of the patients who underwent post-





**Fig. 5.** Kaplan-Meier curves of overall survival (median survival time [MST]) of the patients who received post-treatment after sorafenib therapy and those who did not. Overall survival was significantly longer among the patients who received post-treatment after sorafenib therapy.

progression treatment after sorafenib therapy and of those who did not were 456 and 233 days, respectively, with those who underwent post-progression treatment exhibiting a better OS ( $p < 0.001$ ) (Fig. 5).

## Discussion

Sorafenib is a multitargeted tyrosine kinase inhibitor that suppresses tumor proliferation and angiogenesis. This agent carries a mild-to-moderate toxicity profile and exhibits antitumor activity against various solid tumors [17]. It was the first systemic agent that was proven to prolong the survival of patients with advanced HCC in two phase III trials [2, 18], and it is now the standard of care for systemically treated patients [5, 19–22]. The initial sorafenib dose recommended in the Sorafenib Hepatocellular Carcinoma Assessment Randomized Protocol (SHARP) trial and the Asia-Pacific trial was 800 mg/day, but since sorafenib came into clinical use, there have been reports of lower initial doses. A large trial conducted among Japanese people, who have a smaller body surface area than Europeans and Americans, reported little dif-

ference between starting at 400 and 800 mg/day. In the roughly 7 years since sorafenib was approved in Japan, several studies have reported using other initial doses besides 800 mg.

Some have also reported administering sorafenib to patients other than those with Child-Pugh class A disease [23, 24]. In addition, better therapeutic results have been reported in patients who exhibited HFS, compared to those who did not [25, 26]. In the present study, in which we examined the outcomes of sorafenib administration in 314 patients at 5 general hospitals in Kagawa Prefecture, Japan, the results of the present study also showed comparable results.

In the present study, only about 10% of the patients started at an initial dose of 800 mg, but their median OS was 392 days, which is better than the results of the SHARP and Asia-Pacific trials. Regarding liver function at the start of treatment, about one-fourth of the patients had Child-Pugh class B disease. The good OS results achieved even against a background of poor liver function are thought to have been largely because administration had started at an optimal stage for some patients and because of the benefits of post-progression treatment after sorafenib therapy, as the importance of post-progression treatment after sorafenib has already been reported [27].

Moreover, methods of preventing and treating HFS have been established since sorafenib came into clinical use, so the results were likely less affected by dropouts due to HFS compared to when the drug was first approved. Previously, patients who exhibited HFS had better results than those who did not; a similar trend was observed in the present study.

Regarding liver function at the start of therapy, in the GIDEON (Global Investigation of Therapeutic Decisions in Hepatocellular Carcinoma and of Its Treatment with Sorafenib) trial the group of Child-Pugh class A patients had better OS than the group that started at Child-Pugh class B [28]; this was also observed in the present study. In the present study, even among the Child-Pugh class A patients, the group that started at class A-5 points had a significantly better OS than the group that started at class A-6 points; however, the OS of the group that started at class A-6 points was not significantly different from that of the Child-Pugh class B group. This suggests that among Child-Pugh class A patients, starting sorafenib when liver functions are well preserved, such as at class A-5 points, is preferable. The positive results observed in the present study for patients who underwent post-progression treatment such as TACE, hepatic arte-

rial infusion chemotherapy, or ablation [29–32] after sorafenib therapy also indicate that initiating therapy when liver function is well preserved (Child-Pugh class A-5 points) is beneficial.

## Conclusion

The best results were observed when therapy was initiated at Child-Pugh class A-5 points, which indicates that it is preferable to start sorafenib at the time when liver function is still well preserved. Starting sorafenib at a reduced dose in Japanese patients is also thought to lead to

a better OS. Among the patients who exhibited HFS, those who were able to receive post-progression treatment after sorafenib therapy had good OS, which suggests that addressing this side effect is important for preserving the remaining hepatic reserve. The recent success of new systemic therapy agents [33, 34] and immunotherapies [35] will be expected to further improve survival among patients with advanced HCC.

## Disclosure Statement

The authors have no conflicts of interest to declare.

## References

- McGlynn KA, Petrick JL, London WT: Global epidemiology of hepatocellular carcinoma: an emphasis on demographic and regional variability. *Clin Liver Dis* 2015;19:223–238.
- Llovet JM, Ricci S, Mazzaferro V, Hilgard P, Gane E, Blanc JF, et al: Sorafenib in advanced hepatocellular carcinoma. *N Engl J Med* 2008; 359:378–390.
- Kudo M, Izumi N, Kokudo N, Matsui O, Sakamoto M, Nakashima O, et al: Management of hepatocellular carcinoma in Japan: Consensus-Based Clinical Practice Guidelines proposed by the Japan Society of Hepatology (JSH) 2010 updated version. *Dig Dis* 2011;29:339–364.
- Kudo M, Ueshima K: Positioning of a molecular-targeted agent, sorafenib, in the treatment algorithm for hepatocellular carcinoma and implication of many complete remission cases in Japan. *Oncology* 2010;78(suppl 1): 154–166.
- Kudo M: Treatment of advanced hepatocellular carcinoma with emphasis on hepatic arterial infusion chemotherapy and molecular targeted therapy. *Liver Cancer* 2012;1:62–70.
- Kudo M: Clinical practice guidelines for hepatocellular carcinoma differ between Japan, United States, and Europe. *Liver Cancer* 2015; 4:85–95.
- Kudo M: Locoregional therapy for hepatocellular carcinoma. *Liver Cancer* 2015;4:163–164.
- Kudo M: Surveillance, diagnosis, treatment, and outcome of liver cancer in Japan. *Liver Cancer* 2015;4:39–50.
- Tsurusaki M, Murakami T: Surgical and locoregional therapy of HCC: TACE. *Liver Cancer* 2015;4:165–175.
- Arizumi T, Ueshima K, Minami T, Kono M, Chishina H, Takita M, et al: Effectiveness of sorafenib in patients with transcatheter arterial chemoembolization (TACE) refractory and intermediate-stage hepatocellular carcinoma. *Liver Cancer* 2015;4:253–262.
- Geschwind JF, Gholam PM, Goldenberg A, Mantry P, Martin RC, Piperdi B, et al: Use of transarterial chemoembolization (TACE) and sorafenib in patients with unresectable hepatocellular carcinoma: US regional analysis of the GIDEON registry. *Liver Cancer* 2016;5:37–46.
- Obi S, Sato S, Kawai T: Current status of hepatic arterial infusion chemotherapy. *Liver Cancer* 2015;4:188–199.
- Lin CC, Hung CF, Chen WT, Lin SM: Hepatic arterial infusion chemotherapy for advanced hepatocellular carcinoma with portal vein thrombosis: impact of early response to 4 weeks of treatment. *Liver Cancer* 2015;4: 228–240.
- Chen BB, Murakami T, Shih TT, Sakamoto M, Matsui O, Choi BI, et al: Novel imaging diagnosis for hepatocellular carcinoma: consensus from the 5th Asia-Pacific Primary Liver Cancer Expert Meeting (APPLE 2014). *Liver Cancer* 2015;4:215–227.
- Joo I, Lee JM: Recent advances in the imaging diagnosis of hepatocellular carcinoma: value of gadoxetic acid-enhanced MRI. *Liver Cancer* 2016;5:67–87.
- Lencioni R, Llovet JM: Modified RECIST (mRECIST) assessment for hepatocellular carcinoma. *Semin Liver Dis* 2010;30:52–60.
- Strumberg D, Richly H, Hilger RA, Schleucher N, Korfee S, Tewes M, et al: Phase I clinical and pharmacokinetic study of the novel Raf kinase and vascular endothelial growth factor receptor inhibitor BAY 43-9006 in patients with advanced refractory solid tumors. *J Clin Oncol* 2005;23:965–972.
- Cheng AL, Kang YK, Chen Z, Tsao CJ, Qin S, Kim JS, et al: Efficacy and safety of sorafenib in patients in the Asia-Pacific region with advanced hepatocellular carcinoma: a phase III randomised, double-blind, placebo-controlled trial. *Lancet Oncol* 2009;10:25–34.
- Alves RC, Alves D, Guz B, Matos C, Viana M, Harriz M, et al: Advanced hepatocellular carcinoma. Review of targeted molecular drugs. *Ann Hepatol* 2011;10:21–27.
- Peck-Radosavljevic M: Drug therapy for advanced-stage liver cancer. *Liver Cancer* 2014; 3:125–131.
- Keating GM, Santoro A: Sorafenib: a review of its use in advanced hepatocellular carcinoma. *Drugs* 2009;69:223–240.
- Saraswat VA, Pandey G, Shetty S: Treatment algorithms for managing hepatocellular carcinoma. *J Clin Exp Hepatol* 2014;4(suppl 3): S80–S89.
- Nishikawa H, Osaki Y, Endo M, Takeda H, Tsuchiya K, Joko K, et al: Comparison of standard-dose and half-dose sorafenib therapy on clinical outcome in patients with unresectable hepatocellular carcinoma in field practice: a propensity score matching analysis. *Int J Oncol* 2014;45:2295–2302.
- Morimoto M, Numata K, Kondo M, Kobayashi S, Ohkawa S, Hidaka H, et al: Field practice study of half-dose sorafenib treatment on safety and efficacy for hepatocellular carcinoma: a propensity score analysis. *Hepatol Res* 2015;45:279–287.
- Vincenzi B, Santini D, Russo A, Addeo R, Giuliani F, Montella L, et al: Early skin toxicity as a predictive factor for tumor control in hepatocellular carcinoma patients treated with sorafenib. *Oncologist* 2010;15:85–92.

- 26 Otsuka T, Eguchi Y, Kawazoe S, Yanagita K, Ario K, Kitahara K, et al: Skin toxicities and survival in advanced hepatocellular carcinoma patients treated with sorafenib. *Hepatol Res* 2012;42:879–886.
- 27 Arizumi T, Ueshima K, Takeda H, Osaki Y, Takita M, Inoue T, et al: Comparison of systems for assessment of post-therapeutic response to sorafenib for hepatocellular carcinoma. *J Gastroenterol* 2014;49:1578–1587.
- 28 Kudo M, Ikeda M, Takayama T, Numata K, Izumi N, Furuse J, et al: Safety and efficacy of sorafenib in Japanese patients with hepatocellular carcinoma in clinical practice: a subgroup analysis of GIDEON. *J Gastroenterol* 2016;51:1150–1160.
- 29 Kang TW, Rhim H: Recent advances in tumor ablation for hepatocellular carcinoma. *Liver Cancer* 2015;4:176–187.
- 30 Lencioni R, de Baere T, Martin RC, Nutting CW, Narayanan G: Image-guided ablation of malignant liver tumors: recommendations for clinical validation of novel thermal and non-thermal technologies – a Western perspective. *Liver Cancer* 2015;4:208–214.
- 31 Lin CC, Cheng YT, Chen MW, Lin SM: The effectiveness of multiple electrode radiofrequency ablation in patients with hepatocellular carcinoma with lesions more than 3 cm in size and Barcelona Clinic Liver Cancer stage A to B2. *Liver Cancer* 2016;5:8–20.
- 32 Kitai S, Kudo M, Nishida N, Izumi N, Sakamoto M, Matsuyama Y, et al: Survival benefit of locoregional treatment for hepatocellular carcinoma with advanced liver cirrhosis. *Liver Cancer* 2016;5:175–189.
- 33 Kudo M: Molecular targeted therapy for hepatocellular carcinoma: where are we now? *Liver Cancer* 2015;4:I–VII.
- 34 Kudo M: Regorafenib as second-line systemic therapy may change the treatment strategy and management paradigm for hepatocellular carcinoma. *Liver Cancer* 2016;5:235–244.
- 35 Kudo M: Immune checkpoint blockade in hepatocellular carcinoma. *Liver Cancer* 2015;4:201–207.

# Validation of Newly Proposed Time to Transarterial Chemoembolization Progression in Intermediate-Stage Hepatocellular Carcinoma Cases

Hirofumi Izumoto<sup>a</sup> Atsushi Hiraoka<sup>a</sup> Yoshihiro Ishimaru<sup>b</sup> Tadashi Murakami<sup>b</sup>  
Shogo Kitahata<sup>a</sup> Hidetaro Ueki<sup>a</sup> Toshihiko Aibiki<sup>a</sup> Tomonari Okudaira<sup>a</sup>  
Yuji Miyamoto<sup>a</sup> Hiroka Yamago<sup>a</sup> Ryuichiro Iwasaki<sup>a</sup> Hideomi Tomida<sup>a</sup>  
Kenichiro Mori<sup>a</sup> Masato Kishida<sup>a</sup> Eiji Tsubouchi<sup>a</sup> Hideki Miyata<sup>a</sup>  
Tomoyuki Ninomiya<sup>a</sup> Hideki Kawasaki<sup>a</sup> Masashi Hirooka<sup>c</sup> Bunzo Matsuura<sup>c</sup>  
Masanori Abe<sup>c</sup> Yoichi Hiasa<sup>c</sup> Kojiro Michitaka<sup>a</sup> Masatoshi Kudo<sup>d</sup>

<sup>a</sup>Gastroenterology Center and <sup>b</sup>Department of Radiology, Ehime Prefectural Central Hospital, Matsuyama,

<sup>c</sup>Department of Gastroenterology and Metabology, Ehime University Graduate School of Medicine, Toon, and

<sup>d</sup>Department of Gastroenterology and Hepatology, Kindai University School of Medicine, Osaka-Sayama, Japan

## Keywords

Hepatocellular carcinoma · Conventional transarterial chemoembolization · Barcelona Clinic Liver Cancer stage B · Transarterial chemoembolization-refractory status · Time to transarterial chemoembolization progression · Overall survival

## Abstract

**Background/Aim:** Determination of failure of transarterial chemoembolization (TACE) for treatment of Barcelona Clinic Liver Cancer stage B (BCLC-B) hepatocellular carcinoma (HCC) has become important because of the development of tyrosine kinase inhibitor (TKI) treatment. We evaluated the usefulness and efficacy of the newly proposed time to TACE progression (TTTP). **Patients and Methods:** From 2006 to 2016, 192 BCLC-B HCC patients [median age 72 years,

male/female ratio = 149/43, Child-Pugh score 5/6/7 = 106/56/30, albumin-bilirubin (ALBI) grade 1/2 = 64/128, Kin-ki criteria B1/B2 = 64/128] were enrolled. TTTP was defined based on a previous report and first imaging performed 3 months after initial TACE had been used to obtain baseline images. The patients were divided into three groups according to TTTP (<5, 5–10, and ≥10 months; group I, II, and III, respectively). We evaluated the relationship between TTTP and overall survival (OS) as well as the prognostic factors for death. **Results:** The median number of TACE procedures was 4 (interquartile range 3–7). There was a moderate correlation between TTTP and OS ( $r = 0.527$ , 95% CI 0.416–0.622,  $p < 0.001$ ). The median survival for group I ( $n = 78$ ), II ( $n = 49$ ), and III ( $n = 65$ ) was 24.6, 34.7, and 49.5 months, respectively (group I vs. group II,  $p = 0.023$ ; group I vs. group III,  $p < 0.001$ ; group II vs. group III,  $p = 0.037$ ; Holm's method). ALBI grade 2 (HR 1.548, 95% CI 1.004–2.388,  $p = 0.048$ ), al-



pha-fetoprotein (>100 ng/mL) (HR 1.540, 95% CI 1.035–2.291,  $p = 0.033$ ), and TTTP (<5 months) (HR 2.157, 95% CI 1.447–3.215,  $p < 0.001$ ) were significant prognostic factors for death in multivariate Cox hazard analysis. **Conclusion:** In patients with reduced TTTP, especially <5 months, it might be difficult to improve prognosis with a repeated TACE procedures. In such cases, reconsideration of the therapeutic strategy might be needed when possible.

© 2017 S. Karger AG, Basel

## Introduction

Hepatocellular carcinoma (HCC) is the fifth most common type of malignant tumor [1] and the third leading cause of cancer death throughout the world [2], though progress in the methods used for hepatic resection [3–6] and radiofrequency ablation [7–14] as curative treatments has improved the prognosis of affected patients. However, it is well known that recurrence of HCC frequently occurs following curative treatment. Transarterial chemoembolization (TACE) [15–19] has been developed as a palliative treatment for unresectable HCC in patients with or without a past history of treatments, especially for those in Barcelona Clinic Liver Cancer stage B (BCLC-B) (intermediate), and reported to be effective for improving patient prognosis.

Recently, systemic therapies with tyrosine kinase inhibitor (TKI) have been developed as treatments for unresectable HCC [20–26]. With recognition of the therapeutic effectiveness of TKI against HCC, the notion of TACE-refractory status has been proposed as an indication for switching from TACE to TKI [27], and Ogasa-wara et al. [28] and Arizumi et al. [19] reported the clinical importance of switching to sorafenib for intermediate-stage HCC patients to improve their prognosis.

The importance of determining TACE-refractory status and predicting progression in patients who have undergone repeated TACE procedures has increased, and as a new criterion for predicting poor prognosis, time to TACE progression (TTTP) has been proposed recently [29]. It has been shown that TTTP has a moderate correlation with overall survival (OS) after progression in patients with stage BCLC-B HCC who have been treated with TACE.

In the present study, we examined the usefulness of TTTP for predicting the prognosis in HCC patients with BCLC-B and good hepatic function (Child-Pugh score ≤7) who underwent repeated TACE procedures.

## Patients and Methods

### Patients

From 2006 to 2016, 205 patients with Kinki criteria B1 or B2 substage HCC [30] were treated with TACE. After excluding 13 patients because of lack of follow-up imaging data for evaluation of TTTP, 192 were enrolled in this study.

### Diagnosis and Treatment of HCC

HCC was diagnosed based on an increasing course of alpha-fetoprotein (AFP) as well as dynamic CT [31], MRI [32], contrast-enhanced US with perfluorobutane (Sonazoid®; Daiichi Sankyo Co., Ltd., Tokyo, Japan) [33, 34], and/or pathological findings. Tumor node metastasis (TNM) stage was determined using the criteria reported in studies for staging of HCC conducted by the Liver Cancer Study Group of Japan (LCSGJ, 6th edition) [35]. Prior to 2005, all enrolled patients were treated based on the HCC strategy developed by Ehime Prefecture Hospital. For those beyond the Milan criteria [36], surgical resection, if possible, was selected, while TACE was performed when surgical resection could not be performed [8]. Since 2005, all treatments were performed following the Japanese practical guidelines for HCC [37] whenever possible after obtaining written informed consent from each patient.

### Kinki Criteria for Substaging of BCLC-B HCC

Using the reported Kinki criteria [30], patients were classified according to Child-Pugh score (5–7 or 8–9 points) and tumor burden (Milan criteria [36], up-to-seven criteria [38]). Staging for patients with a Child-Pugh score of 5–7 and within the up-to-seven criteria was B1, for those with a Child-Pugh score of 5–7 and beyond the up-to-seven criteria B2, and for those with a Child-Pugh score of 8–9 and any tumor status B3 [39].

### TACE Procedure

All nodules treated with TACE were shown to be hypervascular. Two experienced radiologists (Y.I., T.M.) and a hepatologist (A.H.) performed the TACE procedures, for which a microcatheter was inserted into the artery feeding the tumor in a manner as superselective as possible following conventional hepatic angiography, after which a segmental or subsegmental TACE procedure was performed. Prior to the procedure, antegrade flow in the portal vein and absence of obstruction of the main trunk of the portal vein were confirmed by US, dynamic CT, and portography findings obtained via the superior mesenteric artery. Epirubicin hydrochloride (Farmorubicin®; Pfizer Japan Inc., Tokyo, Japan), before January 2010, or miriplatin hydrate (MIRIPLA®; Sumitomo Dainippon Pharma Co., Ltd., Osaka, Japan), after February 2010, was injected together with Lipiodol in all cases, after which a gelatin sponge cut into small fragments (Gelfoam®; Upjohn, Kalamazoo, MI, USA), before August 2006, or small gelatin sponge fragments (Gelpart®; Nippon Kayaku Co., Ltd., Tokyo, Japan), after September 2006, were used for embolization. The goal of embolization was disappearance of tumor staining without complete obstruction of the hepatic artery. Three months after TACE, dynamic CT and/or EOB-MRI were performed. When intrahepatic recurrence was confirmed, the TACE procedure was repeated.

**Table 1.** Clinical characteristics of 192 patients with BCLC-B hepatocellular carcinoma

Age, years	72 (64–77)
Gender (male/female)	149/43
Etiology (HCV/HBV/HBV+HCV/ alcohol/others)	149/5/1/11/26
Aspartate aminotransferase, IU/L	52 (35–79)
Alanine aminotransferase, IU/L	39 (25–65)
Platelets, $\times 10^4$ cells/ $\mu$ L	10.8 (7.2–15.0)
Total bilirubin, mg/dL	0.8 (0.6–1.0)
Albumin, g/dL	3.8 (3.4–4.0)
Prothrombin time, %	81.5 (73.9–91.0)
Child-Pugh class (5/6/7)	106/56/30
ALBI grade (1/2)	64/128
Alpha-fetoprotein, ng/mL	30.1 (9.1–160.325)
Fucosylated alpha-fetoprotein, %	4.95 (0.5–22.5)
PIVKA-II, mAU/mL	85 (29–594.5)
Maximum tumor size, cm	1.9 (1.2–3.4)
Tumor number (single/multiple)	2/190
TNM stage of LCSGJ (II/III)	104/88
Kinki criteria (B1/B2)	64/128
Naïve/recurrence	52/140
TTTP (<5/5–10/ $\geq 10$ months)	78/49/65

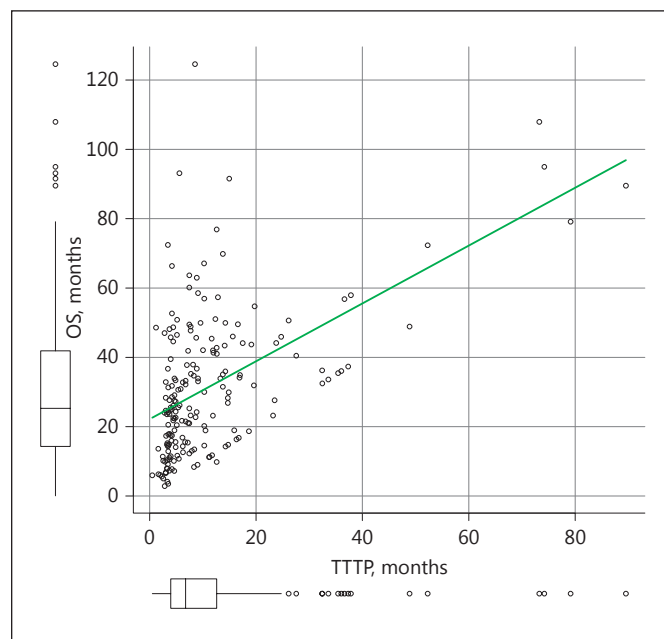
Values are presented as *n* or median (interquartile range). ALBI, albumin-bilirubin; BCLC-B, Barcelona Clinic Liver Cancer stage B; HBV, hepatitis B virus; HCV, hepatitis C virus; LCSGJ, Liver Cancer Study Group of Japan 6th edition; PIVKA-II, protein induced by vitamin K absence or antagonist-II; TNM, tumor node metastasis; TTTP, time to transarterial chemoembolization progression.

#### Time to TACE Progression

TTTP was defined based on findings previously reported [29]. For baseline imaging, the results of dynamic CT or EOB-MRI performed 3 months after the initial TACE were used, then findings from dynamic CT or EOB-MRI obtained 3 months after TACE were utilized for comparison to the baseline images. To assess the target lesions, the five largest tumors shown in the images were selected from intrahepatic lesions for calculating the total maximum diameter (two-dimensional measurement) of each viable lesion. When the total maximum diameter as compared to that seen in the baseline images was  $\geq 1.2$  times larger, progression was determined.

When complete response was noted in the first imaging, the date of confirmed recurrence of HCC was defined as the date of progression, while the appearance of vascular invasion or extrahepatic spreading was also regarded as progression. Patients were divided into three groups based on TTTP (<5 months [group I], 5–10 months [group II], and  $\geq 10$  months [group III]), then OS after progression was evaluated.

Written informed consent was obtained from all patients prior to treatment. The study protocol was in compliance with the Helsinki Declaration and approved by the Institutional Ethics Committee of Ehime Prefectural Central Hospital (No. 29–36).



**Fig. 1.** Correlation between time to transarterial chemoembolization progression (TTTP) and overall survival (OS) after introducing transarterial chemoembolization (TACE). There was a moderate correlation between TTTP and OS after introducing TACE as treatment for Barcelona Clinic Liver Cancer stage B hepatocellular carcinoma patients ( $r = 0.527$ , 95% CI 0.416–0.622,  $p < 0.001$ ).

#### Statistical Analysis

Statistical analyses were performed using the Kaplan-Meier method with log-rank test, and Pearson correlation test, Student *t* test, Welch test, Mann-Whitney test,  $\chi^2$  test, or Fisher exact test, as appropriate. Multiple comparisons were analyzed using Holm's method. Statistical significance was defined as  $p < 0.05$ . Statistical analyses were performed using EZR, a graphical user interface for R, version 1.32 (The R Foundation for Statistical Computing, Vienna, Austria).

#### Results

The clinical background information is shown in Table 1. The median number of TACE procedures was 4 (interquartile range 3–7). There was a modest correlation between TTTP and OS ( $r = 0.527$ , 95% CI 0.416–0.622,  $p < 0.001$ ) (Fig. 1).

The OS rate for each group based on TTTP was analyzed. Stratification ability using survival curves for each of those groups was good, with significant differences between them observed. The median survival time for group I ( $n = 78$ ) was 24.6 months, while that of group II ( $n = 49$ )

**Table 2.** Cox hazard analysis of prognostic factors for death after introduction of transarterial chemoembolization

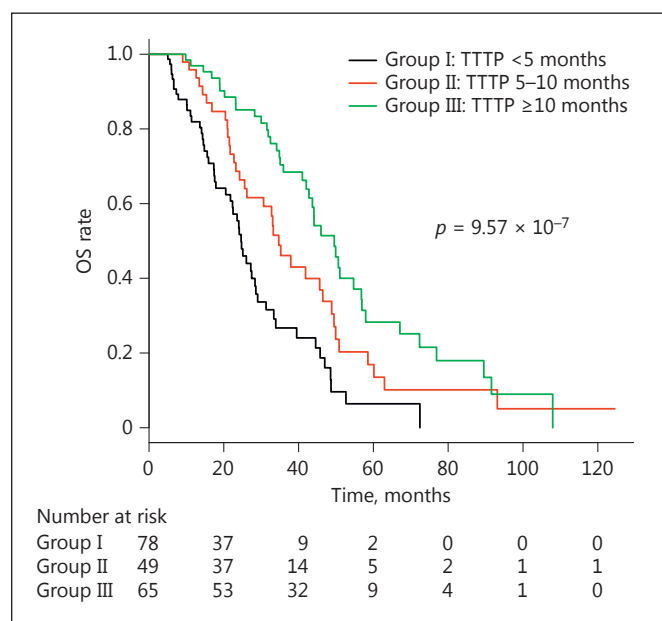
	Univariate			Multivariate		
	HR	95% CI	<i>p</i> value	HR	95% CI	<i>p</i> value
Age (≥65 years)	1.139	0.754–1.72	0.573	–	–	–
Gender (female)	1.425	0.935–2.171	0.100	–	–	–
Positive for hepatitis C virus	1.184	0.758–1.851	0.458	–	–	–
Aspartate aminotransferase (>40 IU/L)	1.636	1.104–2.423	0.014	1.459	0.964–2.207	0.074
Alanine aminotransferase (>40 IU/L)	1.233	0.867–1.753	0.244	–	–	–
Platelets (>10×10 <sup>4</sup> cells/μL)	0.711	0.500–1.023	0.059	–	–	–
Child-Pugh B (7)	1.386	0.864–2.222	0.176	–	–	–
Albumin-bilirubin (grade 2)	1.887	1.265–2.814	0.002	1.548	1.004–2.388	0.048
Alpha-fetoprotein (>100 ng/mL)	1.554	1.506–2.285	0.025	1.540	1.035–2.291	0.033
Fucosylated alpha-fetoprotein (>10%)	1.357	0.938–1.963	0.105	–	–	–
PIVKA-II (>100 mAU/mL)	1.488	1.041–2.127	0.029	1.180	0.789–1.764	0.421
Maximum tumor diameter (>5 cm)	1.347	0.740–2.452	0.330	–	–	–
TNM stage III of LCSGJ	1.498	1.053–2.132	0.025	1.084	0.735–1.600	0.682
Kinki criteria B2	1.308	0.895–1.911	0.165	–	–	–
Recurrence of hepatocellular carcinoma	1.024	0.678–1.546	0.910	–	–	–
TTTP (<5 months)	2.514	1.731–3.650	<0.001	2.157	1.447–3.215	<0.001

LCSGJ, Liver Cancer Study Group of Japan 6th edition; PIVKA-II, protein induced by vitamin K absence or antagonist-II; TNM, tumor node metastasis; TTTP, time to transarterial chemoembolization progression.

was 34.7 months and that of group III (*n* = 65) 49.5 months (group I vs. group II, *p* = 0.023; group I vs. group III, *p* < 0.001; group II vs. group III, *p* = 0.037, respectively; Holm's method) (Fig. 2).

In univariate Cox hazard analysis, aspartate aminotransferase (>40 IU/L), albumin-bilirubin (ALBI) grade 2, AFP (>100 ng/mL), protein induced by vitamin K absence or antagonist-II (PIVKA-II) (>100 mAU/mL), TNM stage III, and TTTP (<5 months) were significant prognostic factors for death after TACE introduction for BCLC-B HCC. Multivariate analysis showed that ALBI grade 2 (HR 1.548, 95% CI 1.004–2.388, *p* = 0.048), AFP (>100 ng/mL) (HR 1.540, 95% CI 1.035–2.291, *p* = 0.033), and TTTP (<5 months) (HR 2.157, 95% CI 1.447–3.215, *p* < 0.001) were significant prognostic factors (Table 2).

In a comparison between Kinki criteria B1 (*n* = 64) and B2 (*n* = 128) cases, Child-Pugh score/classification was not significantly different (*p* = 0.818), while the frequency of TNM stage III was greater in the B2 subgroup (*p* = 0.001) (data not shown). Although the survival curve for the B1 cases was superior to that of the B2 cases, no significant difference was seen (median survival time: B1 vs. B2 = 44.1 vs. 34.1 months, *p* = 0.161). Furthermore, no significant difference was observed between B1 and B2 with regard to TTTP (median TTTP: B1 vs. B2 = 7.2 vs. 6.8, *p* = 0.899).



**Fig. 2.** Overall survival (OS) rates in each group based on time to transarterial chemoembolization progression (TTTP) grouping. Significant differences were observed among the OS rate values for all groups. The median survival time for group I (*n* = 78, TTTP <5 months) was 24.6 months, for group II (*n* = 49, TTTP 5–10 months) 34.7 months, and for group III (*n* = 65, TTTP ≥10 months) 49.5 months (group I vs. group II, *p* = 0.023; group I vs. group III, *p* < 0.001; group II vs. group III, *p* = 0.037, respectively; Holm's method).

## Discussion

TACE-refractory status has been proposed in studies conducted in both Western and Asian countries [27, 40, 41]. Switching to TKI is considered important for improvement of prognosis in patients with BCLC-B HCC who are confirmed to be TACE refractory [19, 28]. The usefulness of sorafenib for advanced HCC was demonstrated in the SHARP [20] and Asia-Pacific [42] trials. Moreover, regorafenib has been proposed for use as a second-line agent in cases receiving sorafenib therapy [21], while the effectiveness of lenvatinib as another first-line TKI agent for unresectable HCC has recently been reported [22, 23]. In the future, determination of TACE-refractory status will increase in importance along with the introduction of therapeutic options for improvement of prognosis in HCC patients because of the increasing number of effective TKI treatments presently under development.

TTTP has been proposed as a new factor for determining progression in patients undergoing repeated TACE treatments. From the viewpoint of therapeutic response to TACE, TTTP showed a moderate correlation to OS after introduction of TACE, and OS was reduced in the patients with shorter TTTP (group I) as compared to the others. These results were similar to those of the previous report that originally proposed TTTP [29].

In addition, maintained hepatic function is important for improving the prognosis of BCLC-B HCC patients, except for therapeutic response to repeated TACE procedures. In our previous study, hepatic function worsened with repeated TACE procedures [43], as determined with the use of the newly proposed ALBI score [44–46]. Some reports have noted the usefulness of ALBI grade for patients undergoing sorafenib treatment and for subclassification of BCLC-B HCC [47–49]. In fact, ALBI grade 2, but not Child-Pugh class B (score 7), was shown to be an independent risk factor for death by Cox hazard analysis findings in the present study. Since TKI therapy is recommended for patients with good hepatic function, it is important to keep in mind that non-effective TACE can also harm hepatic function, thus possibly reducing the opportunity for TKI treatment in the future.

Although the OS of the Kinki criteria B1 subgroup was not superior to that of the B2 subgroup in our study, previous reports with larger cohorts of patients classified as BCLC-B [30] according to the Kinki and Bolondi [49] criteria, used with Child-Pugh score, or the MICAN criteria [48], used with ALBI grade, have found that a

lower subgrade is related to better prognosis. In our results, TTTP did not show significant differences when compared between the Kinki criteria B1 and B2 subgroups ( $p = 0.899$ ). The response to TACE might be similar for each subgrade of BCLC-B. For BCLC-B HCC patients treated with TACE in this multiple TKI era, prolonging postprogression survival is thought to be necessary for improving OS, thus identification of patients who easily develop TACE failure or refractory status has become important [50]. TTTP may be suitable for determining the optimal timing for switching to TKI while avoiding worsened hepatic function.

Our study has some limitations. First, this was a validation study based on retrospective analyses. Furthermore, all analyzed patients were treated at the same institution. Finally, a suitable assessment method for hepatic function with regard to TKI treatment remains to be established. In the future, a prospective study with a larger cohort treated at multiple institutions will be needed.

In conclusion, TTTP may be a good surrogate endpoint for use in a TACE combination trial with TKI or immunotherapy, because TTTP correlates with OS. In patients with reduced TTTP, especially <5 months, it might be difficult to improve prognosis by repeated TACE procedures. In such cases, reconsideration of the therapeutic strategy, including switching treatment from TACE to TKI, may be necessary.

## Disclosure Statement

None of the authors has any financial disclosures, grants from any organs, or conflicts of interest to declare.

## References

- 1 Parkin DM, Bray F, Ferlay J, Pisani P: Estimating the world cancer burden: Globocan 2000. *Int J Cancer* 2001;94:153–156.
- 2 Parkin DM, Bray F, Ferlay J, Pisani P: Global cancer statistics, 2002. *CA Cancer J Clin* 2005; 55:74–108.
- 3 Song TJ, Ip EW, Fong Y: Hepatocellular carcinoma: current surgical management. *Gastroenterology* 2004;127(5 suppl 1):S248–S260.
- 4 Seyama Y, Kokudo N: Assessment of liver function for safe hepatic resection. *Hepatol Res* 2009;39:107–116.
- 5 Kudo M, Izumi N, Sakamoto M, Matsuyama Y, Ichida T, Nakashima O, Matsui O, et al: Survival analysis over 28 years of 173,378 patients with hepatocellular carcinoma in Japan. *Liver Cancer* 2016;5:190–197.



- 6 Ho MC, Hasegawa K, Chen XP, Nagano H, Lee YJ, Chau GY, Zhou J, et al: Surgery for intermediate and advanced hepatocellular carcinoma: a consensus report from the 5th Asia-Pacific Primary Liver Cancer Expert Meeting (APPLE 2014). *Liver Cancer* 2016;5: 245–256.
- 7 Tateishi R, Shiina S, Teratani T, Obi S, Sato S, Koike Y, Fujishima T, et al: Percutaneous radiofrequency ablation for hepatocellular carcinoma. An analysis of 1000 cases. *Cancer* 2005;103:1201–1209.
- 8 Hiraoka A, Horiike N, Yamashita Y, Koizumi Y, Doi K, Yamamoto Y, Hasebe A, et al: Efficacy of radiofrequency ablation therapy compared to surgical resection in 164 patients in Japan with single hepatocellular carcinoma smaller than 3 cm, along with report of complications. *Hepatogastroenterology* 2008;55: 2171–2174.
- 9 Hiraoka A, Michitaka K, Horiike N, Hidaka S, Uehara T, Ichikawa S, Hasebe A, et al: Radiofrequency ablation therapy for hepatocellular carcinoma in elderly patients. *J Gastroenterol Hepatol* 2010;25:403–407.
- 10 Kudo M: Surveillance, diagnosis, treatment, and outcome of liver cancer in Japan. *Liver Cancer* 2015;4:39–50.
- 11 Poon RT, Cheung TT, Kwok PC, Lee AS, Li TW, Loke KL, Chan SL, et al: Hong Kong consensus recommendations on the management of hepatocellular carcinoma. *Liver Cancer* 2015;4:51–69.
- 12 Kudo M: Clinical practice guidelines for hepatocellular carcinoma differ between Japan, United States, and Europe. *Liver Cancer* 2015; 4:85–95.
- 13 Kang TW, Rhim H: Recent advances in tumor ablation for hepatocellular carcinoma. *Liver Cancer* 2015;4:176–187.
- 14 Lencioni R, de Baere T, Martin RC, Nutting CW, Narayanan G: Image-guided ablation of malignant liver tumors: recommendations for clinical validation of novel thermal and non-thermal technologies – a Western perspective. *Liver Cancer* 2015;4:208–214.
- 15 Takayasu K, Arii S, Ikai I, Omata M, Okita K, Ichida T, Matsuyama Y, et al: Prospective cohort study of transarterial chemoembolization for unresectable hepatocellular carcinoma in 8510 patients. *Gastroenterology* 2006; 131:461–469.
- 16 Hiraoka A, Kumagi T, Hirooka M, Uehara T, Kurose K, Iuchi H, Hiasa Y, et al: Prognosis following transcatheter arterial embolization for 121 patients with unresectable hepatocellular carcinoma with or without a history of treatment. *World J Gastroenterol* 2006;12: 2075–2079.
- 17 Kudo M: Locoregional therapy for hepatocellular carcinoma. *Liver Cancer* 2015;4:163–164.
- 18 Tsurusaki M, Murakami T: Surgical and locoregional therapy of HCC: TACE. *Liver Cancer* 2015;4:165–175.
- 19 Arizumi T, Ueshima K, Minami T, Kono M, Chishina H, Takita M, Kitai S, et al: Effectiveness of sorafenib in patients with transcatheter arterial chemoembolization (TACE) refractory and intermediate-stage hepatocellular carcinoma. *Liver Cancer* 2015;4:253–262.
- 20 Llovet JM, Ricci S, Mazzaferro V, Hilgard P, Gane E, Blanc JF, de Oliveira AC, et al: Sorafenib in advanced hepatocellular carcinoma. *N Engl J Med* 2008;359:378–390.
- 21 Bruix J, Qin S, Merle P, Granito A, Huang YH, Bodoky G, Pracht M, et al: Regorafenib for patients with hepatocellular carcinoma who progressed on sorafenib treatment (RESORCE): a randomised, double-blind, placebo-controlled, phase 3 trial. *Lancet* 2017; 389:56–66.
- 22 Ikeda K, Kudo M, Kawazoe S, Osaki Y, Ikeda M, Okusaka T, Tamai T, et al: Phase 2 study of lenvatinib in patients with advanced hepatocellular carcinoma. *J Gastroenterol* 2017; 52:512–519.
- 23 Cheng AL, Finn RS, Qin S, Han KH, Ikeda K, Piscaglia F, Baron AD, et al: Phase III trial of lenvatinib (LEN) vs sorafenib (SOR) in first-line treatment of patients (pts) with unresectable hepatocellular carcinoma (uHCC) (abstract). *J Clin Oncol* 2017;35:4001.
- 24 Kudo M: Molecular targeted therapy for hepatocellular carcinoma: where are we now? *Liver Cancer* 2015;4:i–vii.
- 25 Kudo M: Regorafenib as second-line systemic therapy may change the treatment strategy and management paradigm for hepatocellular carcinoma. *Liver Cancer* 2016;5:235–244.
- 26 Kudo M: Immune checkpoint blockade in hepatocellular carcinoma. *Liver Cancer* 2015;4: 201–207.
- 27 Kudo M, Matsui O, Izumi N, Kadoya M, Okusaka T, Miyayama S, Yamakado K, et al: Transarterial chemoembolization failure/refractoriness: JSH-LCSGJ criteria 2014 update. *Oncology* 2014;87(suppl 1):22–31.
- 28 Ogasawara S, Chiba T, Ooka Y, Kanogawa N, Motoyama T, Suzuki E, Tawada A, et al: Efficacy of sorafenib in intermediate-stage hepatocellular carcinoma patients refractory to transarterial chemoembolization. *Oncology* 2014;87:330–341.
- 29 Arizumi T, Ueshima K, Iwanishi M, Minami T, Chishina H, Kono M, Takita M, et al: The overall survival of patients with hepatocellular carcinoma correlates with the newly defined time to progression after transarterial chemoembolization. *Liver Cancer* 2017;6: 227–235.
- 30 Kudo M, Arizumi T, Ueshima K, Sakurai T, Kitano M, Nishida N: Subclassification of BCLC B stage hepatocellular carcinoma and treatment strategies: proposal of modified Bolondi's subclassification (Kinki criteria). *Dig Dis* 2015;33:751–758.
- 31 Bruix J, Sherman M: Management of hepatocellular carcinoma. *Hepatology* 2005;42: 1208–1236.
- 32 Sano K, Ichikawa T, Motosugi U, Sou H, Muhi AM, Matsuda M, Nakano M, et al: Imaging study of early hepatocellular carcinoma: usefulness of gadoxetic acid-enhanced MR imaging. *Radiology* 2011;261:834–844.
- 33 Hiraoka A, Hiasa Y, Onji M, Michitaka K: New contrast enhanced ultrasonography agent: impact of Sonazoid on radiofrequency ablation. *J Gastroenterol Hepatol* 2011;26: 616–618.
- 34 Kudo M: Breakthrough imaging in hepatocellular carcinoma. *Liver Cancer* 2016;5:47–54.
- 35 The Liver Cancer Study Group of Japan Society of Hepatology: The General Rules for the Clinical and Pathological Study of Primary Liver Cancer, ed 6. Tokyo, Kanehara & Co Ltd, 2015, p 26.
- 36 Mazzaferro V, Regalia E, Doci R, Andreola S, Pulvirenti A, Bozzetti F, Montalto F, et al: Liver transplantation for the treatment of small hepatocellular carcinomas in patients with cirrhosis. *N Engl J Med* 1996;334:693–699.
- 37 The Japan Society of Hepatology: Clinical Practice Guidelines for Hepatocellular Carcinoma 2013. [https://www.jsh.or.jp/English/guidelines\\_en/Guidelines\\_for\\_hepatocellular\\_carcinoma\\_2013](https://www.jsh.or.jp/English/guidelines_en/Guidelines_for_hepatocellular_carcinoma_2013) (accessed August 1, 2017).
- 38 D'Amico F, Schwartz M, Vitale A, Tabrizian P, Roayaie S, Thung S, Guido M, et al: Predicting recurrence after liver transplantation in patients with hepatocellular carcinoma exceeding the up-to-seven criteria. *Liver Transpl* 2009;15:1278–1287.
- 39 Kudo M: Heterogeneity and subclassification of Barcelona Clinic Liver Cancer Stage B. *Liver Cancer* 2016;5:91–96.
- 40 Huckle F, Sieghart W, Pinter M, Graziadei I, Vogel W, Muller C, Heinzl H, et al: The ART-strategy: sequential assessment of the ART score predicts outcome of patients with hepatocellular carcinoma re-treated with TACE. *J Hepatol* 2014;60:118–126.
- 41 Dufour JF, Bargellini I, De Maria N, De Simone P, Goulis I, Marinho RT: Intermediate hepatocellular carcinoma: current treatments and future perspectives. *Ann Oncol* 2013; 24(suppl 2):ii24–ii29.
- 42 Cheng AL, Kang YK, Chen Z, Tsao CJ, Qin S, Kim JS, Luo R, et al: Efficacy and safety of sorafenib in patients in the Asia-Pacific region with advanced hepatocellular carcinoma: a phase III randomised, double-blind, placebo-controlled trial. *Lancet Oncol* 2009; 10:25–34.
- 43 Hiraoka A, Kumada T, Kudo M, Hirooka M, Koizumi Y, Hiasa Y, Tajiri K, et al: Hepatic function during repeated TACE procedures and prognosis after introducing sorafenib in patients with unresectable HCC – multicenter analysis. *Dig Dis* 2017;35:602–610.

- 44 Johnson PJ, Berhane S, Kagebayashi C, Sato-mura S, Teng M, Reeves HL, O'Beirne J, et al: Assessment of liver function in patients with hepatocellular carcinoma: a new evidence-based approach – the ALBI grade. *J Clin Oncol* 2015;33:550–558.
- 45 Hiraoka A, Kumada T, Michitaka K, Toyoda H, Tada T, Ueki H, Kaneto M, et al: Usefulness of albumin-bilirubin grade for evaluation of prognosis of 2584 Japanese patients with hepatocellular carcinoma. *J Gastroenterol Hepatol* 2016;31:1031–1036.
- 46 Hiraoka A, Kumada T, Kudo M, Hirooka M, Tsuji K, Itobayashi E, Kariyama K, et al: Albumin-bilirubin (ALBI) grade as part of the evidence-based clinical practice guideline for HCC of the Japan Society of Hepatology: a comparison with the liver damage and Child-Pugh classifications. *Liver Cancer* 2017;6: 204–215.
- 47 Ogasawara S, Chiba T, Ooka Y, Suzuki E, Kanogawa N, Saito T, Motoyama T, et al: Liver function assessment according to the albumin-bilirubin (ALBI) grade in sorafenib-treated patients with advanced hepatocellular carcinoma. *Invest New Drugs* 2015;33:1257–1262.
- 48 Hiraoka A, Kumada T, Nouse K, Tsuji K, Itobayashi E, Hirooka M, Kariyama K, et al: Proposed new sub-grouping for intermediate-stage hepatocellular carcinoma using albumin-bilirubin grade. *Oncology* 2016;91: 153–161.
- 49 Bolondi L, Burroughs A, Dufour JF, Galle PR, Mazzaferro V, Piscaglia F, Raoul JL, et al: Heterogeneity of patients with intermediate (BCLC B) hepatocellular carcinoma: proposal for a subclassification to facilitate treatment decisions. *Semin Liver Dis* 2012;32:348–359.
- 50 Kudo M: A new era of systemic therapy for hepatocellular carcinoma with regorafenib and lenvatinib. *Liver Cancer* 2017;6:177–184.

# Transarterial Chemoembolization in Combination with a Molecular Targeted Agent: Lessons Learned from Negative Trials (Post-TACE, BRISK-TA, SPACE, ORIENTAL, and TACE-2)

Masatoshi Kudo Tadaaki Arizumi

Department of Gastroenterology and Hepatology, Kindai University Faculty of Medicine, Osaka-Sayama, Japan

## Keywords

Hepatocellular carcinoma · Transarterial chemoembolization · Clinical trial · Molecular targeted agent · Sorafenib · Brivanib · Orantinib

## Abstract

The multikinase inhibitor sorafenib is the first oral molecular targeted agent with proven prognostic benefit in unresectable advanced hepatocellular carcinoma (HCC). However, as with other drugs, sorafenib has its limitations, and various clinical trials have been conducted to develop novel molecular targeted agents for use alone or in combination with existing locoregional therapies. Despite this, clinical trials of molecular targeted agents combined with transarterial chemoembolization (TACE) have not reported major treatment outcomes to date. In this review, we describe previous clinical trials of combination therapy with TACE and a molecular targeted agent in patients with unresectable HCC.

© 2017 S. Karger AG, Basel

## Introduction

The survival benefit of sorafenib in unresectable advanced hepatocellular carcinoma (HCC) was demonstrated in the Sorafenib Hepatocellular Carcinoma As-

essment Randomized Protocol (SHARP) and Asia-Pacific studies [1, 2]. In 2007, sorafenib was approved in the EU and USA, where it became a first-line agent for unresectable advanced HCC. Transarterial chemoembolization (TACE) is the first-line treatment option for intermediate-stage HCC [3–6]; however, repeated TACE sessions tend to impair liver functional reserve. Reducing the frequency of TACE, which is generally repeated upon tumor progression, is a challenging issue in the treatment of patients with intermediate-stage HCC. To address this issue, previous trials combined molecular targeted agents with TACE; however, the safety and efficacy of this combination could not be demonstrated, and none of the combination therapies is currently recommended.

In the SHARP study, subanalysis showed that the hazard ratio (HR) for overall survival (OS) in patients with HCC with no vascular invasion or extrahepatic spread, which are regarded as good indications for TACE, was 0.52 and, thus, extremely good in the sorafenib group. The median survival of these patients was extended approximately 1.5-fold [7], suggesting that the addition of sorafenib as adjuvant therapy to TACE improves prognosis. The combination of TACE with sorafenib does not simply represent the administration of 2 types of treatment; the combination is expected to extend the period during which TACE controls tumor progression because sorafenib strongly suppresses post-TACE tumor recur-

rence and progression by inhibiting hypoxia-induced angiogenesis. In addition, the detrimental effect on liver function may be suppressed by reducing the frequency of TACE. Sorafenib combined with TACE is expected to improve the survival of patients with intermediate-stage HCC, which is the goal of TACE, by extending the time to progression (TTP) to the advanced stage while maintaining liver function [8].

## The Post-TACE Study

### Background

TACE is used as a first-line treatment for unresectable HCC; however, the procedure is hardly curative in clinical practice and needs to be repeated multiple times. Repeated TACE may promote the deterioration of liver function. Based on the apparent role of angiogenesis and the upregulation of vascular endothelial growth factor (VEGF) associated with tumor recurrence after TACE, a study was designed with the objective of delaying the recurrence of HCC and prolonging OS by administering sorafenib after TACE. Sorafenib is an inhibitor of several tyrosine kinases involved in the growth of tumor cells and angiogenesis, such as Raf, VEGF receptor, and platelet-derived growth factor (PDGF) receptor. This placebo-controlled phase III study designated the Post-TACE study was conducted in Japan and Korea [9].

### Methods

Patients with unresectable HCC and Child-Pugh A liver function who had imaging findings of objective treatment response (complete response or partial response) at 1–3 months after TACE were included. These patients were randomly assigned to 2 groups for sorafenib or placebo administration. The primary and secondary endpoints of the study were TTP and OS, respectively.

### Results

A total of 458 patients (387 from Japan and 71 from Korea) were registered to the study between April 2006 and July 2009. These patients were randomized to the sorafenib ( $n = 229$ ) or placebo ( $n = 229$ ) arms. The median TTP, the primary endpoint of the study, was 5.4 and 3.7 months in the sorafenib and placebo groups, respectively (HR 0.87 [95% CI 0.70–1.09];  $p = 0.252$ ) (Table 1). The median OS, the secondary endpoint of the study, was 29.7 months in the sorafenib group, whereas

a median value was not reached in the placebo group (HR 1.06 [95% CI 0.69–1.64];  $p = 0.790$ ). A subanalysis in Japanese patients showed that the median TTP was 3.9 and 3.7 months in the sorafenib and placebo arms, respectively, with a HR of 0.94 and no significant intergroup difference. In Korean patients, however, the HR was 0.38 and TTP was clearly longer in the sorafenib group.

### Possible Reasons for Failure

In this study, the primary endpoint TTP did not differ significantly between the groups. One possible reason for this is the timing of sorafenib administration. TACE promotes the production of VEGF by triggering ischemic conditions. Therefore, for sorafenib to produce the expected effects, it may be necessary to inhibit angiogenesis occurring soon after TACE. However, because the study included only patients who responded to TACE, approximately 60% of the patients in the sorafenib group underwent drug treatment 9 weeks after TACE. This long waiting period might have contributed to the loss of the additive effect of sorafenib.

In addition, the mean daily dose in the sorafenib group was as low as 386 mg because of many cases of dose reduction (73%) and interruption (91%). By contrast, the mean daily dose of sorafenib was 797 mg in the SHARP study, and the occurrence of dose reduction (26%) and interruption (44%) was low. In the Asia-Pacific study, the mean daily dose of sorafenib was 795 mg, with a low occurrence of dose reduction (31%) and interruption (43%), and the study outcomes were markedly different from those of the Post-TACE study. The Post-TACE study was conducted before the results of the SHARP study were revealed to be positive, and Japanese patients did not participate in the SHARP or Asia-Pacific study; therefore, physicians in the Post-TACE study who may have been unfamiliar with the management of the side effects of sorafenib, especially hand-foot skin reaction, used the drug at low doses and short duration, resulting in poor treatment outcomes.

Although no significant intergroup difference was observed between Japan and Korea, significant differences in TTP were observed between Korea and Japan. This could be attributed to the considerably longer treatment duration in Korean patients than in Japanese patients (median 31 vs. 16 weeks), which generated a good HR. Furthermore, patient backgrounds were different between the 2 countries, with a higher proportion of elderly patients and a greater number of lesions in Japanese than in Korean patients.



**Table 1.** Clinical trials of TACE combined with molecular targeted agents

	Post-TACE ( <i>n</i> = 458)		BRISK-TA ( <i>n</i> = 502)		SPACE ( <i>n</i> = 307)		ORIENTAL ( <i>n</i> = 888)		TACE-2 ( <i>n</i> = 313)	
	sorafenib ( <i>n</i> = 229)	placebo ( <i>n</i> = 227)	brivanib ( <i>n</i> = 249)	placebo ( <i>n</i> = 253)	sorafenib ( <i>n</i> = 154)	placebo ( <i>n</i> = 153)	orantinib ( <i>n</i> = 444)	placebo ( <i>n</i> = 444)	sorafenib ( <i>n</i> = 157)	placebo ( <i>n</i> = 156)
Phase	III		III (immature/ terminated)		II		III (terminated due to interim analysis)		III (terminated due to interim analysis)	
mOS, months	29.7	NR	26.4	26.1	NR	NR	31.1	32.3	21.1	19.7
HR (95% CI)	1.06 (0.69–1.64)		0.90 (0.66–1.23)		0.898 (0.606–1.330)		1.090 (0.878–1.352)		0.91 (0.67–1.24)	
<i>p</i> value	0.79		0.528		0.295		0.435		0.57	
mTTP, months	5.4	3.7	8.4	4.9	5.6	5.5	ND	ND	7.9 <sup>a</sup>	7.8 <sup>a</sup>
HR (95% CI)	0.87 (0.70–1.09)		0.61 (0.48–0.77)		0.797 (0.588–1.080)		ND		0.99 (0.77–1.27)	
<i>p</i> value	0.252		<0.0001		0.072		ND		0.94	
Primary endpoint	TTP		OS		TTP		OS		PFS	
Definition of progression	RECICLE		mRECIST		mRECIST		TACE discontinuation criteria		RECIST 1.1	
Median DOT of study drug	17 weeks		24.0 weeks		21.0 weeks		43.6 weeks		17.1 weeks	

TACE, transarterial chemoembolization; mOS, median overall survival; NR, not reached; HR, hazard ratio; mTTP, median time to progression; ND, no data; PFS, progression-free survival; DOT, duration of treatment. <sup>a</sup> Progression-free survival was used in the TACE-2 study.

## The BRISK-TA Study

### Background

Brivanib inhibits the signal transduction pathway of fibroblast growth factor receptor in addition to the VEGF receptor, and its mechanism of action is, therefore, different from that of sorafenib. Based on the action of brivanib, a phase III study was designed to investigate the efficacy and safety of the drug as an adjuvant therapy to TACE in patients with unresectable HCC [10].

### Methods

At 83 institutes in 12 countries, a total of 502 patients were treated with TACE and randomly allocated to receive brivanib (*n* = 249) or placebo (*n* = 253). The period between TACE and drug administration ranged from 48 h to 21 days. TACE was repeated in patients receiving insufficient treatment and in those showing tumor progression or the development of a new lesion. Drug administration was stopped 2 days before the second or later TACE session and was resumed 3–21 days after TACE. The primary endpoint was OS, and secondary endpoints were time to disease progression, which is a composite endpoint, time to extrahepatic spread or vascular invasion (TTES/VI), and the number of TACE sessions. In the study, extrahepatic metastasis/spread, vascular invasion, death, exacerbation to Child-Pugh C, and a reduction in performance status by 2 points were defined as disease progression.

### Results

Between August 2009 and August 2012, 502 patients were allocated to receive brivanib (*n* = 249) or placebo (*n* = 253). The median OS, the primary endpoint of the study, was 26.4 and 26.1 months in the brivanib and placebo arms, respectively (HR 0.90 [95% CI 0.66–1.23]; *p* = 0.5280) (Table 1). Regarding the secondary endpoints, the median time to disease progression was 12.0 and 10.9 months in the brivanib and placebo arms, respectively (HR 0.94 [95% CI 0.72–1.22]; *p* = 0.6209). However, the brivanib group had a longer TTES/VI (HR 0.64 [95% CI 0.45–0.90]; *p* = 0.0096) and fewer TACE sessions (HR 0.72 [95% CI 0.61–0.86]; *p* = 0.0002). The median TTP was 8.4 months in the brivanib group and 4.9 months in the placebo group; the former had a significantly longer TTP (HR 0.61 [95% CI 0.48–0.77]; *p* < 0.0001). The response rate per mRECIST [11] was 48 and 42% in the brivanib and placebo groups (odds ratio 1.28 [95% CI 0.90–1.83]), with 22 and 11% for complete response and 9 and 18% for progressive disease (PD), respectively.

### Possible Reasons for Failure

The survival benefit of brivanib was not demonstrated in a phase III trial comparing OS noninferiority between brivanib and sorafenib as a first-line treatment for unresectable advanced HCC (the BRISK-FL study) and another phase III study that compared brivanib and placebo as a second-line treatment following sorafenib (the BRISK-PS study). Consequently, the BRISK-TA study

was terminated 2 years earlier than originally planned, after enrolling only 502 patients, which was a markedly smaller cohort than the originally planned 870 patients. Although the primary endpoint OS did not differ significantly between the groups, TTES/VI, TTP, and response rate were significantly different, suggesting that brivanib delays tumor progression and metastasis. Because of the early termination of the study, in addition to patients, the number of deaths (needed to calculate the primary endpoint OS) was 164, accounting for 32% of the initially anticipated number of deaths (520). This early termination also makes evaluation of drug efficacy difficult; however, the intergroup differences in TTES/VI and TTP, as well as the reduced number of TACE sessions, suggest that brivanib had a positive anticancer effect. If the study had been continued, it might have met its primary endpoint of prolonging overall survival.

## The SPACE Study

### Background

The SPACE study, which involved the use of drug-eluting beads loaded with doxorubicin (DEBDOX), was conducted at 85 institutes in 13 countries, but not in Japan. This phase II study investigated the safety and efficacy of TACE with doxorubicin-eluting beads (DEB-TACE) combined with sorafenib or placebo in patients with unresectable intermediate-stage (BCLC stage B) HCC. Based on the findings of the Post-TACE study indicating that VEGF production is upregulated in response to TACE-induced ischemia, which suggests that early administration of sorafenib is necessary, in the SPACE study, TACE was performed after the initiation of sorafenib treatment [12].

### Methods

Patients registered at 85 institutes in 13 countries were randomly allocated to receive sorafenib or placebo. Sorafenib or placebo was administered 3–7 days before DEB-TACE. After the first DEB-TACE, the second and latter DEB-TACE procedures were performed at 3, 7, and 13 months and every 6 months thereafter. The primary endpoint was TTP, and the secondary endpoints were OS, TTES/VI, time to untreatable progression (TTUP) by TACE, and safety. The criteria for untreatable progression by TACE were defined as the occurrence of vascular invasion or extrahepatic spread, sustained ascites, Child-Pugh class B, Eastern Cooperative Oncology Group (ECOG) performance status score of  $\geq 2$ , and platelet

count of  $<60,000/\mu\text{L}$ . A 1-tailed test was used to analyze the differences between the groups, with significance set at 15% ( $\alpha = 0.15$ ).

### Results

Of 307 patients, 154 received sorafenib and 153 received placebo. The median TTP, the primary endpoint of the study, was 169 and 166 days in the sorafenib and placebo groups, respectively, thereby achieving the primary endpoint (HR 0.797 [95% CI 0.588–1.08];  $p = 0.072$ ) (Table 1). However, the secondary endpoints of OS and TTES/VI did not reach the median value in both groups (HR 0.898 [95% CI 0.606–1.33];  $p = 0.295$  for OS, and HR 0.621 [95% CI 0.321–1.20];  $p = 0.076$  for TTES/VI). The median TTUP was 95 and 224 days in the sorafenib and placebo groups, respectively (HR 1.586 [95% CI 1.200–2.096];  $p = 0.999$ ). The number of patients with TACE-untreatable progression was 110 and 96 in the sorafenib and placebo groups, respectively. The frequency of DEB-TACE was once in 35.9% of sorafenib patients and 19.2% of placebo patients. Comparison between Asian and non-Asian patients showed that the proportion of Asian patients who underwent DEB-TACE once was 24.1% in the sorafenib group and 22.0% in the placebo group, and among non-Asian patients it was 42.4% in the sorafenib group and 17.8% in the placebo group. TTP in Asian patients was 24 months in the sorafenib group and 16.1 months in the placebo group, and TTP in non-Asian patients was 25.0 months in the sorafenib group and 24.0 months in the placebo group.

### Possible Reasons for Clinically Unmeaningful Results

The SPACE study achieved the primary endpoint of TTP; however, no significant difference was observed in the secondary endpoint of OS. Similarly, TTUP did not show significant differences or was considerably shorter in the sorafenib group, inconsistent with the outcome initially anticipated. In this study, DEB-TACE was performed at 3, 7, and 13 months and every 6 months thereafter using the method-designated scheduled TACE, in which TACE is performed at fixed intervals. Even when intrahepatic lesions responded favorably to TACE, unnecessary repetition of TACE might have impaired liver function or increased the side effects of sorafenib. Unlike scheduled TACE, TACE is performed when needed in Japan using a method designated “on-demand TACE.”

In this study, many patients had fewer TACE sessions, which may have occurred because the criteria for TACE-untreatable progression were not appropriate. Although

vascular invasion and extrahepatic spread are adequate criteria, Child-Pugh B, sustained ascites, and a platelet count of  $<60,000/\mu\text{L}$  may not indicate that patients are untreatable with TACE. The Japan/Korea Post-TACE study suggested that sorafenib might extend TTP if sorafenib is administered for a long period of time; however, in the SPACE study, sorafenib administration was terminated early based on the criteria for TACE-untreatable progression.

In addition, treatment duration of sorafenib was too short, i.e., only 21 weeks. In Asian patients, median treatment duration of sorafenib was 30 weeks, resulting in a favorable HR of 0.720 ( $p = 0.078$ ), whereas in non-Asian patients, median treatment duration of sorafenib was just 17.4 weeks, resulting in a poor HR of 0.865 ( $p = 0.243$ ). This implies that treatment duration is very important in the TACE combination trial similar to the Post-TACE study.

## ORIENTAL Study

### Background

A phase I/II study showed promising efficacy and safety of orantinib, a molecular targeted agent that inhibits VEGF, PDGF, and fibroblast growth factor receptors in patients with advanced HCC [13]. In light of the promising outcomes, a phase II study was conducted to evaluate the efficacy of combination therapy with TACE and orantinib. The results showed improved progression-free survival (PFS), the primary endpoint of the study, suggesting the additive effect of the combination of orantinib and TACE [14]. Accordingly, a phase III (ORIENTAL) study was conducted in Japan, Korea, and Taiwan [15].

### Methods

Between December 2010 and November 2013, 889 patients with unresectable HCC were registered at 75 institutes located in the 3 countries and subsequently allocated to receive orantinib or placebo. The primary endpoint was OS, and the secondary endpoints were time to TACE failure (TTTF), time to treatment failure, and safety.

### Results

Of 889 patients initially registered, 1 withdrew and the remaining patients were allocated to receive orantinib ( $n = 444$ ) or placebo ( $n = 444$ ). Follow-up was initially planned to continue until November 2016; however, the study was terminated after an interim analysis based on

the recommendation of the Data Monitoring Committee, which provides independent assessment of efficacy and safety, because data analysis suggested that the primary endpoint of the study (OS) would not be achieved. The median OS was 31.1 and 32.3 months in the orantinib and placebo groups, respectively (HR 1.090 [95% CI 0.878–1.352];  $p = 0.435$ ) (Table 1). The median OS in patients with BCLC stage B HCC was 31.1 and 26.6 months in the orantinib and placebo groups, respectively (HR 0.837 [95% CI 0.624–1.124];  $p = 0.236$ ). The median TTTF, a secondary endpoint, was 23.9 and 19.8 months in the orantinib and placebo groups, respectively (HR 0.887 [95% CI 0.725–1.086];  $p = 0.245$ ). In addition, the median TTTF in patients with a low level of VEGF-C was 25.5 and 18.4 months in the orantinib and placebo groups, respectively (HR 0.695;  $p = 0.0196$ ).

### Possible Reasons for Failure

OS, the primary endpoint of this study, did not differ significantly between the groups, whereas TTTF was significantly extended in patients with low levels of VEGF-C in the orantinib group. Additionally, orantinib tended to prolong OS in patients with BCLC stage B HCC, which is a recommended indication for TACE. The study was terminated early because of the interim analysis results that orantinib had no survival benefit in combination with TACE. Because patients with unresectable HCC were targeted in this study, patients with BCLC stage B HCC, the conventional indication for TACE, accounted for only 50% of all patients. The remaining subjects were BCLC stage A or C. Intergroup comparison after excluding patients with BCLC stage B HCC revealed that OS was poor in the orantinib group, which might have worsened the OS of the entire orantinib group.

Comparison of OS between patients with and without orantinib dose reduction showed that OS was significantly prolonged in patients with dose reduction, whereas OS was shorter in patients without dose reduction than in the placebo group. Comparison by country showed that the proportion of patients with dose reduction was approximately 50% in Japan, whereas only 30% of patients had dose reduction in Korea and Taiwan. Side effects were the primary reason for dose reduction in approximately 90% of patients, suggesting the importance of controlling drug adverse effects. OS tended to be prolonged in the orantinib group compared to the placebo group in Japan, whereas the opposite tendency was observed in Korea and Taiwan. This suggested that OS was longer in Japan because of the proper dose modification and adequate management of side effects.

## The TACE-2 Study

### Background

Twenty institutes in England participated in this study, which aimed to clarify whether combination therapy with DEB-TACE and sorafenib suppresses tumor progression and extends OS [16].

### Methods

Patients were allocated to receive sorafenib or placebo, and DEB-TACE was performed within 2–5 weeks after administration of sorafenib or placebo. Subsequently, DEB-TACE was repeated when an additional TACE session was necessary based on imaging findings. The primary endpoint was PFS, and the secondary endpoints were OS and TTP.

### Results

A total of 313 patients were registered for the study and randomized to the sorafenib ( $n = 157$ ) or placebo ( $n = 156$ ) arms. The median PFS per RESIST version 1.1, the primary endpoint of the study, was 7.9 months (95% CI 7.4–9.1) and 7.8 months (95% CI 7.0–10.7) in the sorafenib and placebo arms, respectively (HR 0.99 [95% CI 0.77–1.27];  $p = 0.94$ ). The median OS, the secondary endpoint, was 21.1 months (95% CI 14.7–29.3) and 19.7 months (95% CI 16.7–23.2) in the sorafenib and placebo groups, respectively (HR 0.91 [95% CI 0.67–1.24];  $p = 0.57$ ). The authors concluded that these results, taken together with those from the SPACE trial, provide definitive evidence that DEB-TACE combined with sorafenib therapy does not improve outcome compared to DEB-TACE alone.

### Possible Reasons for Failure

In this trial, no significant difference in PFS or OS was observed, showing no beneficial effect of sorafenib. DEB-TACE was repeated at the discretion of the physician, even before confirming the progression. Because progression was defined based on RECIST 1.1, sorafenib treatment was terminated at the point of appearance of new intrahepatic lesions. Therefore, it is possible that DEB-TACE was repeated before sorafenib could produce the anticipated benefit, rendering the study results insignificant. The appearance of new intrahepatic lesions does not always indicate that TACE or sorafenib is not effective and should be switched to another treatment option, because intrahepatic metastatic recurrence through the portal vein frequently occurs in HCC. This is a biological characteristic of HCC even after resection, ablation, or

superselective TACE in cases in which HCC nodules are large ( $>2$  cm) [17]. Therefore, the definition of progression in patients undergoing TACE based on RECIST 1.1 or mRECIST is not adequate.

Even in the absence of significant differences between patients treated with TACE alone and those treated with TACE combined with a molecular targeted agent, studies showed the antitumor effect of molecular targeted therapy in an adjuvant setting. However, the TACE-2 study did not show intergroup differences or an antitumor effect of sorafenib in the adjuvant setting. This was similar to the STORM study, which investigated the efficacy of sorafenib as adjuvant to resection or radiofrequency ablation and found no effect of sorafenib on suppressing recurrence as adjuvant therapy for HCC [18]. These findings suggest that concurrent administration of sorafenib has no effect on the suppression of disease progression based on RECIST and that TACE may be combined with more potent agents, such as immunotherapy or a drug causing a significant response in the tumor, such as lenvatinib [19]. Another possible explanation for the negative results is the trial design, especially the definition of progression. As stated earlier, progression based on RESIST 1.1 or mRECIST may not be adequate in trials of TACE combination therapies [12].

### Proposal of a New Primary Endpoint in TACE Combination Trials

In phase III studies evaluating the effects of cancer treatment, the primary endpoint is OS in principle. However, in previous combination studies with TACE, the median OS ranged from 18 months (shortest) to 32 months (longest) (Table 1), suggesting that the duration of the study needs to be extremely long when evaluating OS as a primary endpoint. In clinical studies that are terminated early because of tumor progression or adverse effects, patients often receive various post-trial treatments, such as hepatic artery infusion chemotherapy [20–22], ablation [23–25], or systemic therapy [26–29]. In such cases, post-trial treatment likely affects OS, making it difficult to evaluate treatment outcomes using OS, especially in studies of TACE in patients with intermediate-stage HCC.

Instead of OS, TTP/PFS is used as a primary endpoint in some trials; however, whether TTP/PFS based on RECIST is an appropriate endpoint in clinical trials of TACE combination therapies remains unclear. In general, TTP corresponds to the period between random-



ization or the day of study initiation and disease progression. However, in patients treated with TACE, the procedure is often repeated before the tumor diameter exceeds the pretreatment diameter. Additionally, patients with indications appropriate for TACE often have multiple lesions and are likely to develop new ones, which leads to the question of whether a new lesion should be considered as PD.

In our previous study, we proposed a novel endpoint, “time to TACE progression (TTTP),” as a progression-free period specific to patients treated with TACE and defined as the time from the initial TACE effect evaluation to progression [30]. TTTP was determined using images taken 1 month after TACE as baseline images and by designating PD as the time at which the sum of the diameters of the 5 largest tumors is larger than the baseline diameter by  $\geq 20\%$  or the time of appearance of extrahepatic spread or vascular invasion. TTTP is better suited for evaluating the effect of TACE in clinical practice. We also verified that TTTP is correlated with OS, suggesting that TTTP could be a surrogate endpoint for OS and a

better primary endpoint than OS for use in clinical studies of TACE in combination with molecular targeted agents.

## Conclusion

Many clinical trials investigated the efficacy of TACE combined with molecular targeted agents; however, none of them demonstrated an OS benefit of the combination strategy or even improved TTP/PFS. Nevertheless, these studies showed the antitumor effect of the molecular targeted agents as adjuvant therapy. It is important to consider the reasons for the negative outcomes of these trials and to carefully plan future clinical trials of combination therapy with TACE.

## Disclosure Statement

The authors have no conflicts of interest to declare.

## References

- Llovet JM, Ricci S, Mazzaferro V, Hilgard P, Gane E, Blanc JF, de Oliveira AC, et al: Sorafenib in advanced hepatocellular carcinoma. *N Engl J Med* 2008;359:378–390.
- Cheng AL, Kang YK, Chen Z, Tsao CJ, Qin S, Kim JS, Luo R, et al: Efficacy and safety of sorafenib in patients in the Asia-Pacific region with advanced hepatocellular carcinoma: a phase III randomised, double-blind, placebo-controlled trial. *Lancet Oncol* 2009;10:25–34.
- Kudo M: Locoregional therapy for hepatocellular carcinoma. *Liver Cancer* 2015;4:163–164.
- Kudo M: Surveillance, diagnosis, treatment, and outcome of liver cancer in Japan. *Liver Cancer* 2015;4:39–50.
- Tsurusaki M, Murakami T: Surgical and locoregional therapy of HCC: TACE. *Liver Cancer* 2015;4:165–175.
- Arizumi T, Ueshima K, Minami T, Kono M, Chishina H, Takita M, Kitai S, et al: Effectiveness of sorafenib in patients with transcatheter arterial chemoembolization (TACE) refractory and intermediate-stage hepatocellular carcinoma. *Liver Cancer* 2015;4:253–262.
- Bruix J, Raoul JL, Sherman M, Mazzaferro V, Bolondi L, Craxi A, Galle PR, et al: Efficacy and safety of sorafenib in patients with advanced hepatocellular carcinoma: subanalyses of a phase III trial. *J Hepatol* 2012;57:821–829.
- Geschwind JF, Gholam PM, Goldenberg A, Mantry P, Martin RC, Piperdi B, Zigmont E, et al: Use of transarterial chemoembolization (TACE) and sorafenib in patients with Unresectable hepatocellular carcinoma: US regional analysis of the GIDEON registry. *Liver Cancer* 2016;5:37–46.
- Kudo M, Imanaka K, Chida N, Nakachi K, Tak WY, Takayama T, Yoon JH, et al: Phase III study of sorafenib after transarterial chemoembolisation in Japanese and Korean patients with unresectable hepatocellular carcinoma. *Eur J Cancer* 2011;47:2117–2127.
- Kudo M, Han G, Finn RS, Poon RT, Blanc JF, Yan L, Yang J, et al: Brivanib as adjuvant therapy to transarterial chemoembolization in patients with hepatocellular carcinoma: a randomized phase III trial. *Hepatology* 2014;60:1697–1707.
- Lencioni R, Llovet JM: Modified RECIST (mRECIST) assessment for hepatocellular carcinoma. *Semin Liver Dis* 2010;30:52–60.
- Lencioni R, Llovet JM, Han G, Tak WY, Yang J, Guglielmi A, Paik SW, et al: Sorafenib or placebo plus TACE with doxorubicin-eluting beads for intermediate stage HCC: the SPACE trial. *J Hepatol* 2016;64:1090–1098.
- Kanai F, Yoshida H, Tateishi R, Sato S, Kawabe T, Obi S, Kondo Y, et al: A phase I/II trial of the oral antiangiogenic agent TSU-68 in patients with advanced hepatocellular carcinoma. *Cancer Chemother Pharmacol* 2011;67:315–324.
- Inaba Y, Kanai F, Aramaki T, Yamamoto T, Tanaka T, Yamakado K, Kaneko S, et al: A randomised phase II study of TSU-68 in patients with hepatocellular carcinoma treated by transarterial chemoembolisation. *Eur J Cancer* 2013;49:2832–2840.
- Kudo M, Cheng A-L, Park J-W, Park JH, Liang P-C, Hidaka H, Izumi N, Heo J, Lee YJ, Sheen I-S, Chiu C-F, Arioka H, Morita S, Arai Y: Orantinib versus placebo combined with transcatheter arterial chemoembolization in patients with unresectable hepatocellular carcinoma (ORIENTAL): a randomised, double-blind, placebo-controlled, multicentre, phase 3 study. *Lancet Gastroenterol Hepatol* 2017, Epub ahead of print.
- Meyer T, Fox R, Ma YT, Ross PJ, James MW, Sturgess R, Stubbs C, et al: Sorafenib in combination with transarterial chemoembolisation in patients with unresectable hepatocellular carcinoma (TACE 2): a randomised placebo-controlled, double-blind, phase 3 trial. *Lancet Gastroenterol Hepatol* 2017;2:565–575.
- Nakashima O, Sugihara S, Kage M, Kojiro M: Pathomorphologic characteristics of small hepatocellular carcinoma: a special reference to small hepatocellular carcinoma with indistinct margins. *Hepatology* 1995;22:101–105.

- 18 Bruix J, Takayama T, Mazzaferro V, Chau GY, Yang J, Kudo M, Cai J, et al: Adjuvant sorafenib for hepatocellular carcinoma after resection or ablation (STORM): a phase 3, randomised, double-blind, placebo-controlled trial. *Lancet Oncol* 2015;16:1344–1354.
- 19 Cheng A, Finn R, Qin S, et al: Phase III trial of lenvatinib (LEN) vs sorafenib (SOR) in first-line treatment of patients (pts) with unresectable hepatocellular carcinoma (uHCC). *J Clin Oncol* 2017;35(suppl):abstr 4001.
- 20 Obi S, Sato S, Kawai T: Current status of hepatic arterial infusion chemotherapy. *Liver Cancer* 2015;4:188–199.
- 21 Lin CC, Hung CF, Chen WT, Lin SM: Hepatic arterial infusion chemotherapy for advanced hepatocellular carcinoma with portal vein thrombosis: impact of early response to 4 weeks of treatment. *Liver Cancer* 2015;4:228–240.
- 22 Ueshima K, Kudo M, Tanaka M, Kumada T, Chung H, Hagiwara S, Inoue T, et al: Phase I/II study of sorafenib in combination with hepatic arterial infusion chemotherapy using low-dose cisplatin and 5-fluorouracil. *Liver Cancer* 2015;4:263–273.
- 23 Teng W, Liu KW, Lin CC, Jeng WJ, Chen WT, Sheen IS, Lin CY, et al: Insufficient ablative margin determined by early computed tomography may predict the recurrence of hepatocellular carcinoma after radiofrequency ablation. *Liver Cancer* 2015;4:26–38.
- 24 Kang TW, Rhim H: Recent advances in tumor ablation for hepatocellular carcinoma. *Liver Cancer* 2015;4:176–187.
- 25 Lencioni R, de Baere T, Martin RC, Nutting CW, Narayanan G: Image-guided ablation of malignant liver tumors: recommendations for clinical validation of novel thermal and non-thermal technologies – a Western perspective. *Liver Cancer* 2015;4:208–214.
- 26 Kudo M: Molecular targeted therapy for hepatocellular carcinoma: where are we now? *Liver Cancer* 2015;4:I–VII.
- 27 Kudo M: Regorafenib as second-line systemic therapy may change the treatment strategy and management paradigm for hepatocellular carcinoma. *Liver Cancer* 2016;5:235–244.
- 28 Zhang B, Finn RS: Personalized clinical trials in hepatocellular carcinoma based on biomarker selection. *Liver Cancer* 2016;5:221–232.
- 29 Kudo M: Immune checkpoint blockade in hepatocellular carcinoma. *Liver Cancer* 2015;4:201–207.
- 30 Arizumi T, Ueshima K, Iwanishi M, Minami T, Chishina H, Kono M, Takita M, et al: The overall survival of patients with hepatocellular carcinoma correlates with the newly defined time to progression after transarterial chemoembolization. *Liver Cancer* 2017;6:227–235.

# Systemic Therapy for Hepatocellular Carcinoma: 2017 Update

Masatoshi Kudo

Department of Gastroenterology and Hepatology, Kindai University Faculty of Medicine, Osaka-Sayama, Japan

## Keywords

Systemic therapy · Hepatic arterial infusion chemotherapy · Molecular targeted therapy · Immune checkpoint inhibitor

## Abstract

Systemic therapy for hepatocellular carcinoma (HCC) changed drastically after the introduction of the molecular targeted agent sorafenib in 2007. Sorafenib provides an additional therapeutic option for patients with extrahepatic spread or vascular invasion, resulting in improved survival even among patients with advanced HCC; however, the toxicity of sorafenib and its unsatisfactory antitumor effects remain unsolved issues. The development of novel molecular targeted agents as alternatives to sorafenib has been limited by difficulties unique to HCC. Recent studies have demonstrated the efficacy of two molecular targeted agents, the second-line agent regorafenib, which is used after sorafenib failure, and the first-line agent lenvatinib, which has been shown to be noninferior to sorafenib. Another category of agents that are attracting considerable interest are immune checkpoint inhibitors such as anti-PD-1/PD-L1 or CTLA-4 antibodies, which kill cancer cells via a unique mechanism. The therapeutic effects of some of these agents are currently under investigation in phase III studies. The most recent topics

of interest are the combination of anti-PD-1/PD-L1 therapies with other immune checkpoint inhibitors, such as anti-CTLA-4 antibodies, or with a tyrosine kinase inhibitor, or with locoregional therapies such as resection, ablation, or trans-arterial chemoembolization.

© 2017 S. Karger AG, Basel

## Introduction

Systemic therapy against hepatocellular carcinoma (HCC) changed drastically following the introduction of the molecular targeted agent sorafenib in 2007. The introduction of sorafenib provided an additional therapeutic option for HCC patients with extrahepatic spread or vascular invasion, and survival improved to some extent even among patients with advanced HCC. Although novel molecular targeted agents have been tested to overcome the poor antitumor effect and toxicity associated with sorafenib, none of them showed satisfactory results for various reasons.

Another category of agents that attracted considerable attention in recent years is that of immune checkpoint inhibitors [1]. These include anti-programmed cell death protein 1 (PD-1)/anti-programmed cell death protein

ligand 1 (PD-L1) or cytotoxic T-lymphocyte-associated antigen 4 (CTLA-4) antibodies, which kill cancer cells via a unique mechanism involving immune responses. Phase III studies of some of these agents are currently ongoing, and expectations are high regarding their therapeutic effects. However, the high cost of these agents has become an important social issue, and there is an increasing need to establish appropriate biomarkers. This article describes the current status, problems, and future perspectives of recent clinical trials of new anti-HCC agents [1–4].

## Molecular Targeted Agents

Sorafenib is an oral kinase inhibitor that exerts antitumor effects through the following mechanisms: (1) tumor growth suppression mediated by targeting serine/threonine kinases that are components of the Raf/MEK/ERK pathway (e.g., C-Raf, wild-type B-Raf, and mutant V600E B-Raf), a common downstream pathway of signals transduced via VEGFR, PDGFR, and EGFR; and (2) angiogenesis suppression by targeting tyrosine kinases (e.g., VEGFR1, VEGFR2, VEGFR3, PDGFR- $\alpha/\beta$ , RET, and Fms-related tyrosine kinase 3 [FLT3]) [5, 6]. Sorafenib became the standard of care for advanced HCC following confirmation of its effect by significantly improving overall survival (OS) over placebo in two large-scale trials, the SHARP trial [7, 8] and the Asia-Pacific trial [4].

### *Current Status of the Development of Molecular Targeted Agents for HCC*

Several clinical trials have investigated the efficacy of novel molecular targeted agents, mainly as adjuvant therapy after curative treatment, in combination with transarterial chemoembolization (TACE), as first-line therapy for advanced HCC, or as second-line therapy. To date, 20 phase III trials of molecular targeted agents for HCC failed to show a benefit in OS or time to tumor progression (TTP)/progression-free survival (PFS) (Table 1). The results of the phase III trials are outlined in the next paragraphs.

### *Prevention of Recurrence after Curative Treatment (Adjuvant Therapy)*

**Sorafenib.** A phase III trial comparing adjuvant sorafenib to placebo after radiofrequency ablation [9–11] or hepatectomy [12–15] (STORM trial) found no difference in the primary endpoint of recurrence-free survival (RFS) [16]. A possible explanation for the failure of sorafenib to suppress secondary HCC occurrence

and metastatic recurrence is the weak involvement of angiogenesis in the development of microcarcinoma, even in cases of multicentric tumors or intrahepatic metastasis.

**Peretinoin.** This agent acts by removing precancerous lesions and thereby suppresses cancer development by inhibiting the phosphorylation of retinoid nuclear receptors to induce differentiation and apoptosis [17, 18]. A placebo-controlled phase II/III study examining adjuvant peretinoin after hepatectomy or radiofrequency ablation showed significant benefits in the primary endpoint of RFS in the 600 mg peretinoin group, but not in the 300 mg peretinoin group, over placebo [19]. The primary comparison showed no significant differences between the overall peretinoin group and the placebo group. A second phase III trial comparing 600 mg peretinoin with placebo in HCV-positive Child-Pugh class A patients is currently underway (NIK-333 trial). Another trial comparing RFS associated with peretinoin to placebo in HBV-positive patients in Japan, South Korea, and Taiwan is also ongoing (K-333 trial).

### *Combination Therapy with TACE*

**Sorafenib.** A phase III post-TACE trial comparing sorafenib and placebo after TACE [9, 14, 20, 21] was conducted in patients who responded to TACE in Japan and South Korea. However, the primary endpoint of prolonged TTP was not achieved, mainly because of the short treatment duration (17 weeks) and the long period (9 weeks) between TACE and the start of sorafenib or placebo. A phase II study comparing sorafenib and placebo in combination therapy with scheduled TACE using doxorubicin-eluting beads (SPACE trial) was successful [22]. The primary endpoint of prolonged TTP was positive, albeit without clinical meaningfulness. There was no significant difference in the secondary outcome of OS. The time to untreatable progression was shorter in the sorafenib group than in the placebo group. In the TACE 2 trial, which was conducted in the UK, the primary endpoint of prolonged PFS was not achieved [23]. This failure could be attributed to the short sorafenib/placebo treatment duration (17.1 weeks) after TACE, as the definition of progression was determined based on RECIST 1.1: one single new lesion in the liver is determined as “progression” per RECIST 1.1, which is not a good definition for a TACE combination trial [24].

**Orantinib.** This oral kinase inhibitor targets VEGFR2, PDGFR, and FGFR to suppress angiogenesis [25]. A phase III trial comparing orantinib and placebo in combination therapy with TACE (ORIENTAL study) was ter-



**Table 1.** Phase III clinical trials for HCC

	Trial setting	Design	Trial name	Presentation	Publication
Early	Adjuvant (prevention of recurrence)	1 Peretinoin vs. placebo*	NIK-333	ASCO 2010	JG 2014
		2 Sorafenib vs. placebo*	STORM	ASCO 2014	Lancet-O 2015
		3 <i>Peretinoin vs. placebo</i>	<i>NIK-333/K-333</i>		
Intermediate	Improvement of TACE	1 TACE +/- sorafenib*	Post-TACE	ASCO-GI 2010	EJC 2011
		2 TACE +/- brivanib*	BRISK-TA	ILCA 2013	Hepatol 2014
		3 TACE +/- orantinib*	ORIENTAL	EASL 2015	Lancet GH 2017
		4 TACE +/- sorafenib	TACE 2	ASCO 2016	Lancet GH 2017
Advanced	First line	1 Sorafenib vs. sunitinib*	SUN1170	ASCO 2011	JCO 2013
		2 Sorafenib vs. brivanib*	BRISK-FL	AASLD 2012	JCO 2013
		3 Sorafenib vs. linifanib*	LiGHT	ASCO-GI 2013	JCO 2015
		4 Sorafenib +/- HAIC*	SILIUS	EASL 2016	
		5 Sorafenib +/- erlotinib*	SEARCH	ESMO 2012	JCO 2013
		6 Sorafenib +/- doxorubicin*	CALGB808028	ASCO 2016	
		7 Sorafenib vs. SIRT*	SARAH	EASL 2017	
		8 Sorafenib vs. SIRT*	SIRveNIB	ASCO 2017	
		<b>9 Sorafenib vs. lenvatinib</b>	<b>REFLECT</b>	<b>ASCO 2017</b>	
		10 <i>Sorafenib vs. nivolumab</i>	<i>CheckMate-459</i>		
	Second line	1 Brivanib vs. placebo*	BRISK-PS	EASL 2012	JCO 2013
		2 Everolimus vs. placebo*	EVOLVE-1	ASCO-GI 2014	JAMA 2014
		3 Ramucirumab vs. placebo*	REACH	ESMO 2014	Lancet-O 2015
		4 S-1 vs. placebo*	S-CUBE	ASCO-GI 2015	Lancet GH 2017
		<b>5 Regorafenib vs. placebo</b>	<b>RESORCE</b>	<b>WCGC 2016</b>	Lancet 2017
		6 Tivantinib vs. placebo*	METIV-HCC	ASCO 2017	
		7 Tivantinib vs. placebo*	JET-HCC	ESMO 2017	
		<b>8 Cabozantinib vs. placebo</b>	<b>CELESTIAL</b>	(Press release)	
		9 <i>Ramucirumab vs. placebo</i>	<i>REACH-2</i>		
		10 <i>Pembrolizumab vs. placebo</i>	<i>KEYNOTE-240</i>		

Bold type: positive trials; italics: ongoing trials. HCC, hepatocellular carcinoma; TACE, transarterial chemoembolization; HAIC, hepatic arterial infusion chemotherapy; SIRT, selective internal radiation therapy. \* RCT halted or negative results.

minated after the interim analysis because the criteria for trial continuation regarding the primary endpoint of OS were not met [26]. The failure of this trial could be attributed to the considerable toxicity of orantinib.

**Brivanib.** This oral kinase inhibitor targets VEGFR and FGFR. A phase III trial comparing brivanib and placebo in combination with TACE (BRISK-TA study) [27] was terminated during the recruitment phase because of the failure of parallel trials of brivanib as first-line or second-line therapy. Although the agent did not show superiority in OS over placebo, significant improvements in PFS and TTP were reported. In addition, the time to vascular invasion and time to extrahepatic spread were significantly longer in the brivanib arm, suggesting a positive antitumor effect of brivanib.

#### First-Line Therapy for Advanced HCC

**Sunitinib.** This oral kinase inhibitor targets VEGFR, PDGFR, KIT, FLT3, and RET [28]. A phase III study comparing sunitinib and sorafenib as first-line therapy (SUN1170) showed that the primary endpoint of OS was significantly worse in patients receiving sunitinib [29]. There were no differences in the secondary endpoints of PFS and TTP between the two treatment groups. These results were attributed to the high dose reduction and interruption rates due to severe hematological toxicities in the sunitinib group.

**Brivanib.** A phase III study comparing brivanib and sorafenib as first-line therapy (BRISK-FL study) did not prove the noninferiority of brivanib to sorafenib in the primary outcome of OS [30].

**Table 2.** SIRT with <sup>90</sup>Y versus sorafenib in patients with locally advanced hepatocellular carcinoma

	SIRT ( <i>n</i> = 237)	Sorafenib ( <i>n</i> = 222)	HR	<i>p</i> value
Primary endpoint (ITT)				
Median OS, months	8.0	9.9	1.15 (0.94–1.41)	0.18
Secondary endpoint				
Median PFS (ITT), months	4.1	3.7	1.03 (0.85–1.25)	0.76
ORR (RECIST 1.1)	19%	11.6%		0.042
Safety (TEAE, ≥grade 3)				
Fatigue	20%	41%		
Diarrhea	3%	30%		
Abdominal pain	6%	14%		
Hand-foot skin reaction	1%	12%		

Vilgrain et al. [39]. SIRT, selective internal radiation therapy; ITT, intention to treat; OS, overall survival; PFS, progression-free survival; ORR, objective response rate; TEAE, treatment-emergent adverse event.

**Table 3.** The SARAH trial: SIRT with <sup>90</sup>Y versus sorafenib in patients with locally advanced hepatocellular carcinoma

	SIRT ( <i>n</i> = 237)	Sorafenib ( <i>n</i> = 222)	HR	<i>p</i> value
Primary endpoint (ITT)				
Median OS, months	8.0	9.9	1.15 (0.94–1.41)	0.18
Forest plot (ITT)				
Macroscopic vascular invasion (yes)			1.19 (0.92–1.54)	
Main portal vein (yes)			1.39 (0.88–2.19)	

Vilgrain et al. [39]. SARAH Clinical Study Results Investor Presentation, April 24, 2017. SIRT, selective internal radiation therapy; ITT, intention to treat; OS, overall survival

**Table 4.** Phase III multicenter open-label randomized controlled trial of SIRT versus sorafenib in locally advanced hepatocellular carcinoma: the SIRveNIB study

	SIRT ( <i>n</i> = 182)	Sorafenib ( <i>n</i> = 178)	HR	<i>p</i> value
Primary endpoint (ITT)				
Median OS, months	8.54	10.58	1.17	0.203
Secondary endpoint				
Median TTP (overall), months	5.88	5.36	0.93	
Median TTP (liver specific), months	6.08	5.39	0.91	
Tumor response rate	16.5%	1.7%		<0.001
Safety				
Severe AEs	27.7%	50.6%		

Chow et al. [40]. SIRT, selective internal radiation therapy; ITT, intention to treat; OS, overall survival; TTP, time to tumor progression; AE, adverse event.

**Linifanib.** This oral kinase inhibitor targets VEGFR and PDGFR. A phase III study comparing linifanib to sorafenib as first-line therapy (LiGHT trial) did not prove the noninferiority of linifanib to sorafenib in the primary endpoint of OS [31].

**Sorafenib plus Erlotinib.** Erlotinib is an oral kinase inhibitor targeting the EGFR tyrosine kinase. A phase III study assessing the addition of erlotinib to first-line sorafenib therapy (SEARCH study) showed that the primary endpoint of OS was comparable between the sorafenib plus placebo group and the sorafenib plus erlotinib group, confirming no additional effect of erlotinib [32].

**Lenvatinib.** This oral kinase inhibitor targets the receptor tyrosine kinases involved in tumor angiogenesis and malignant transformation (e.g., VEGFR1, VEGFR2, VEGFR3, FGFR1, FGFR2, FGFR3, FGFR4, PDGFR- $\alpha/\beta$ , KIT, and RET) [33]. Following favorable outcomes of a phase II single-arm study on patients with advanced HCC (TTP, 7.4 months; OS, 18.7 months) [34], a phase III study comparing lenvatinib and sorafenib (REFLECT trial) demonstrated that lenvatinib was statistically noninferior in OS (primary endpoint) and resulted in statistically significant and clinically meaningful improvements in PFS, TTP, and ORR (secondary endpoints) [35]. Lenvatinib is currently approved for the treatment of thyroid cancer, and an indication expansion (application submitted in June 2017) is expected to be approved by 2018.

**Intra-Arterial Radioembolization with  $^{90}\text{Y}$ .**  $^{90}\text{Y}$  radioembolization is reported to be effective for the treatment of HCC [36–38]. However, the results of two prospective randomized trials, the SARAH (Sorafenib versus Radioembolization in Advanced Hepatocellular Carcinoma) and SIRveNIB (Study to Compare Selective Internal Radiation Therapy versus Sorafenib in Locally Advanced Hepatocellular Carcinoma) trials were negative, as reported at the 2017 annual meetings of the European Association for the Study of the Liver and the American Society of Clinical Oncology (ASCO) [39, 40] (Tables 2–4). In both trials, the ORR was significantly better in the  $^{90}\text{Y}$  groups; however, there was no statistically significant difference in the primary endpoint of OS. In addition, there was no significant difference in survival benefit in patients with vascular invasion. These negative trials indirectly demonstrate the difficulty in achieving the predefined primary endpoint of improving OS among HCC patients in the first-line setting and the better-than-expected superiority of sorafenib in improving survival among such patients.

**Hepatic Arterial Infusion Chemotherapy.** Hepatic arterial infusion chemotherapy (HAIC) has been reported to be useful in patients with advanced HCC, especially with vascular invasion [41–43]. However, the SILIUS trial, which compared HAIC plus sorafenib with sorafenib alone, could not show any additive effect compared to sorafenib alone in patients with advanced HCC.

#### Second-Line Therapy for Advanced HCC

Sorafenib is the standard of care for advanced HCC. Several agents versus placebo were evaluated as second-line therapy in patients who progressed on sorafenib or those who were intolerant to sorafenib.

**Brivanib.** Brivanib was compared with sorafenib in combination therapy with TACE and as a first-line therapy. It was also evaluated as a second-line therapy in a placebo-controlled study (BRISK-PS trial), in which brivanib showed significantly improved TTP and ORR (secondary endpoint) but not OS (primary endpoint) [44]. The failure of this trial was partly attributed to the higher frequency of vascular invasion in the brivanib arm than in the placebo arm, as the stratification factor was set as “vascular invasion and/or extrahepatic spread.” After this negative trial, vascular invasion thereafter tended to be included as an independent stratification factor in the following second-line trials (Table 5).

**Everolimus.** This selective mTOR inhibitor suppresses angiogenesis and tumor growth. A placebo-controlled phase III study (EVOLVE-1) did not show a significant improvement in the primary outcome of OS [45].

**Tivantinib.** This agent selectively inhibits the hepatocyte growth factor receptor c-MET; strong expression of c-MET in liver cancer tissues is associated with poor prognosis. Following a phase II study that showed significant improvements in OS and TTP among patients with c-MET overexpression who received tivantinib [46, 47], a placebo-controlled phase III study was conducted on patients overexpressing c-MET in liver cancer tissues; this was the first biomarker-selected clinical trial for HCC. To reflect ethnic differences in metabolizing enzyme activities, studies with fundamentally the same design were separately carried out globally (METIV-HCC) and in Japan (JET-HCC) (Table 1). The primary endpoint of METIV-HCC was OS and that of JET-HCC was PFS. However, the primary endpoint of OS or PFS was not met in either trial; the results of the former were reported at ASCO 2017 [48]. According to the results presented at ASCO, OS in the placebo arm was too good (OS, 9.1 months). The reason for this negative trial remains unknown. In addition, c-MET expression was not a prog-

**Table 5.** Phase III clinical trials: advanced stage, second line versus placebo

Study arm vs. placebo arm	BRISK-PS (brivanib) [44]	EVOLVE-1 (everolimus) [45]	REACH (ramucirumab) [50]	S-CUBE (S-1) [52]	RESORCE (regorafenib) [54]	METIV-HCC (tivantinib) [48]	KEYNOTE-240 (pembrolizumab) [69]
Intolerance to sorafenib	12–13%	18.5–20%	13–15%	30.6–33.8%	0%	17–21%	–
Stratification factor	Reason for sorafenib discontinuation ECOG PS score Extrahepatic spread and/or vascular invasion	Region <b>Macrovascular invasion</b>	Region Cause of liver disease	Medical institutions Extrahepatic metastasis and/or vascular invasion	Region ECOG PS score <b>Extrahepatic spread</b> <b>Vascular invasion</b> AFP	<b>Extrahepatic spread</b> <b>Vascular invasion</b> AFP	Region <b>Vascular invasion</b> AFP

After the BRISK-PS trial, where AFP and MVI imbalance was observed in the testing arm, AFP and MVI started to be included as independent stratification factors in the recent trials, although they are known to be prognostic factors. ECOG PS, Eastern Cooperative Oncology Group performance status; AFP,  $\alpha$ -fetoprotein; MVI, macroscopic vascular invasion.

**Table 6.** Comparison of phase II–III studies [46–48] on tivantinib: second line, MET-high hepatocellular carcinoma

	Phase II				Phase III			
	tivantinib (n = 22)	placebo (n = 15)	HR	p value	tivantinib (n = 226)	placebo (n = 114)	HR	p value
MET-high, overall	48%		–	–	100%		–	–
Sample before SOR	40%		–	–	33% (197)		–	–
Sample after SOR	82%		–	–	67% (394)		–	–
Median OS (95% CI), months	7.2 (3.9–14.6)	3.8 (2.1–6.8)	0.38 (0.18–0.81)	0.01	8.4 (6.8–10.0)	9.1 (7.3–10.4)	0.97 (0.75–1.25)	0.81
Median PFS (95% CI), months	2.2 (1.4–4.6)	1.4 (1.4–1.4)	0.45 (0.21–0.95)	0.02	2.1 (1.9–3.0)	2.0 (1.9–3.6)	0.96 (0.75–1.22)	0.72

SOR, sorafenib; OS, overall survival; PFS, progression-free survival.

nostic factor in this phase III trial (Table 6). The JET-HCC trial was also reported as a negative study without any detailed disclosure of the results. This was presented at ESMO 2017.

**Ramucirumab.** This humanized IgG<sub>1</sub> monoclonal antibody selectively inhibits VEGFR2 [49]. A placebo-controlled phase III study (REACH) showed no significant improvement in the primary endpoint of OS; however, a stratified analysis showed a significant improvement in OS among patients with  $\alpha$ -fetoprotein (AFP) levels  $\geq 400$  ng/mL [50, 51]. In the Japanese cohort, both the overall cohort and the patients with AFP levels  $\geq 400$  ng/mL showed significantly better survival than the placebo arm [50, 51]. A second placebo-controlled phase III study including only patients with AFP levels  $\geq 400$  ng/mL is currently underway (REACH-2).

**S-1.** A cytotoxic agent of S-1 also failed to show survival benefit in patients who progressed or intolerant to sorafenib. This trial was conducted only in Japan [52].

**Regorafenib.** This oral kinase inhibitor targets multiple protein kinases, including VEGFR1, VEGFR2, VEGFR3,

TIE2, PDGFR- $\alpha/\beta$ , FGFR, KIT, RET, RAF-1, and BRAF [53]. Because regorafenib and sorafenib have remarkably similar toxicity profiles due to a similar molecular structure, a placebo-controlled phase III study (RESORCE) was conducted using different inclusion criteria, namely, HCC nonresponsive but tolerant to sorafenib. The results indicated a significant improvement in the primary endpoint of OS (10.6 months with regorafenib vs. 7.8 months with placebo), as well as in PFS and TTP [54]. Regorafenib thus became the first second-line agent with proven improved efficacy when compared to placebo. Following this positive study, an indication expansion for regorafenib was approved in April 2017 in the USA and in May 2017 in Japan, allowing its use in second-line therapy for HCC. Regorafenib is not suitable for the treatment of patients intolerant to sorafenib, and a second-line treatment for this subgroup of patients remains an unmet need (Fig. 1). The success of this trial is attributed to the following four points: (1) only sorafenib progressors were included in the trial (i.e., intolerant patients were excluded); (2) vascular invasion and extrahepatic spread were



set as independent stratification factors; (3) AFP  $\geq 400$  ng/mL was included as a stratification factor; and (4) tolerability was strictly defined as receiving sorafenib  $\geq 400$  mg daily for at least 20 of the last 28 days of treatment (Table 7). Compared with previous negative phase III second-line trials, the only difference in the patient characteristics in the RESORCE trial was the absence of patients intolerant to sorafenib (Table 8). This superb trial design led to the positive results of the RESORCE study [3].

**Cabozantinib.** Cabozantinib is a dual inhibitor of MET/VEGFR2 in tumors. On October 16, 2017, the results of phase 3 CELESTIAL trial of cabozantinib were released by press to be positive by meeting its primary endpoint of prolonging its overall survival in patients with advanced HCC. The details will be presented in the future congress and journal. In the near future, we will have another second-line agent for HCC.

#### Major Difficulties Associated with Clinical Trials of Molecular Targeted Agents in HCC

Many clinical trials of molecular targeted agents did not meet their primary endpoints of prolonging OS, possibly because of the uniqueness of the treatment strategies and modalities with regard to HCC.

#### Molecular and Biological Heterogeneity of HCC

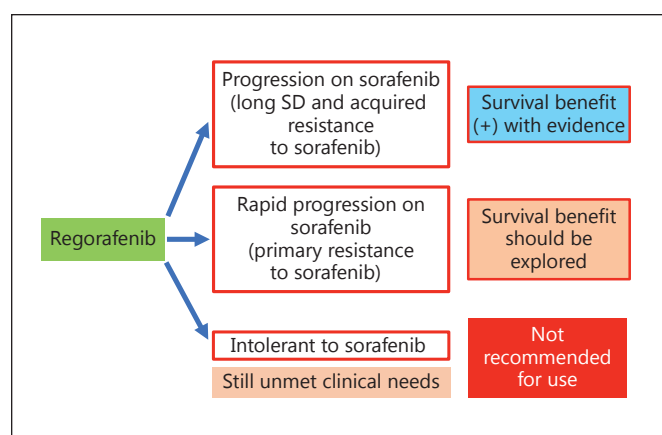
HCCs are very heterogeneous, as is reflected in the tumorigenesis of HCC. The inclusion criteria of clinical trials are mainly based on liver function and tumor stage (e.g., Child-Pugh class A and the presence of extrahepatic spread and/or vascular invasion). However, the recruited patients do not show uniformity in the biological characteristics of the tumors. Therefore, refined patient selection by biomarkers (e.g., genetic abnormalities and expressed proteins) was recently proposed [55]. For example, c-MET overexpression was used as a biomarker in trials of tivantinib [46–48], and RAS was used as a biomarker in a trial of an MEK inhibitor [56]. A trial of an FGFR inhibitor using FGF19 as a biomarker is currently ongoing. However, following the negative outcomes of a phase III study of tivantinib [48] and this phase II study of an MEK inhibitor, development of the two agents was halted. A biomarker selection-based trial design alone may not be sufficient to overcome the difficulties associated with HCC trials; other trial designs may be more important and should be refined.

#### Liver Cancer with Cirrhosis

HCC is frequently associated with liver cirrhosis. Liver cirrhosis poses a considerable problem unique to HCC.

**Table 7.** Reasons for the success of the RESORCE trial (regorafenib)

Good anticancer activity of the agent (compared to placebo)
Acceptable toxicity and tolerability (only patients tolerant to sorafenib)
Superb trial design
Decreasing the imbalance of strong prognostic factors (AFP and vascular invasion were independent stratification factors)
Decreasing post-trial treatment because of the short post-progression survival



**Fig. 1.** Regorafenib use in practice. SD, stable disease.

Because liver function can be impaired in patients with cirrhosis, drugs tend to exert profound toxic effects, sometimes at an irrecoverable level. In such cases, the expected drug effect may not be exerted because dose reductions and interruptions are often inevitable. The balance between the potency and the toxicity of an agent is important for the development of new agents for the treatment of HCC.

#### Importance of the Stratification Factor

The design of a clinical study strongly influences the study outcomes. For example, the stratification factor “vascular invasion and/or extrahepatic spread versus neither of them” has typically been used [29–31]; however, the effect of vascular invasion on prognosis is considerably stronger than the effect of extrahepatic spread. In fact, an imbalance in the presence of vascular invasion favoring placebo may explain the lack of differences in OS between brivanib and placebo as second-line therapy [3, 44]. Different results may be obtained if patients with

**Table 8.** Phase III trials: second line

	RESORCE regorafenib arm [52] (n = 379)	BRISK-PS brivanib arm [44] (n = 263)	EVOLVE-1 everolimus arm [45] (n = 362)	REACH ramucirumab arm [50] (n = 283)
Male	88%	82%	84%	83%
Median age (range), years	64 (19–85)	64 (19–89)	67 (21–86)	64 (28–87)
Asian	41%	48%	38%	46%
ECOG PS 0/1	65/35%	57/39%	59/36%	56/44%
Child-Pugh class A	98%	92%	98%	98%
BCLC stage B/C	14/86%	9/87%	13.5/86.5%	12/88%
MVI	29%	31%	33%	29%
EHS	70%	65%	74%	73%
MVI and/or EHS	80%	–	83%	–
Etiology				
Alcohol	24%	23%	18%	–
HBV	38%	39%	25%	35%
HCV	21%	28%	26%	27%
NASH	7%	–	4%	–
Intolerance to sorafenib	0%	13%	19%	13%

ECOG PS, Eastern Cooperative Oncology Group performance status; BCLC, Barcelona Clinic Liver Cancer; MVI, macroscopic vascular invasion; EHS, extrahepatic spread; NASH, nonalcoholic steatohepatitis.

high AFP values are assigned equally to each group, as observed in the REFLECT trial (lenvatinib), which achieved noninferiority but could not achieve superiority to sorafenib [35].

#### Post-Trial Treatment

In the treatment of HCC, locoregional approaches are generally used, often proactively, even in patients with Child-Pugh class B or C cancer [57–61]. The patients were repeatedly treated locoregionally after the trial, using TACE, ablation, or HAIC, which resulted in improved post-progression survival, and this likely explains the lack of a difference in OS despite a significant difference in PFS. Post-trial treatment is therefore a major factor distinguishing HCC from other solid cancers.

Another issue unique to HCC is that trials of second-line therapies involve patients that have progressed on and those intolerant to sorafenib. Those who have progressed on sorafenib will have a poor prognosis because they have already experienced ineffective sorafenib treatment. However, those who are intolerant to sorafenib will often have considerably better liver function and tumor status because they may have discontinued sorafenib early and therefore can undergo several post-trial treatments, resulting in improved post-progression survival without any difference in OS (Fig. 2) [62].

## Immune Checkpoint Inhibitors

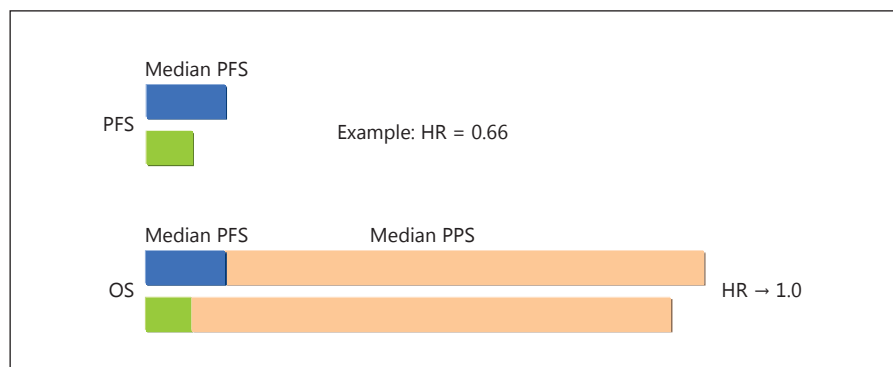
### Immune Checkpoint Inhibitors

PD-1 was discovered by Tasuku Honjo in 1992 in a search for molecules inducing T-cell apoptosis [63]. It was later identified as a receptor that negatively regulates immune responses. After the discovery of the PD-1 ligands PD-L1 and PD-L2 in 2000 [64], blockade of the PD-1/PD-L1 pathway was shown to cancel tumor-induced immune suppression to restore intrinsic immune activities, thereby killing tumors. Treatment strategies based on anti-PD-1/PD-L1 agents that inhibit this pathway were subsequently developed. Blockade of CTLA-4, discovered by James Allison in 1995 [65], was also reported to induce rejection of tumors in mice [66]. Such molecules regulating T-cell activities and their inhibitors are referred to as immune checkpoint molecules and immune checkpoint inhibitors, respectively. In relation to HCC treatment, trials of anti-PD-1 antibodies (nivolumab and pembrolizumab), anti-PD-L1 antibodies (avelumab, durvalumab, and atezolizumab), and anti-CTLA-4 antibodies (ipilimumab and tremelimumab) are currently underway.

#### Nivolumab

Nivolumab (recombinant) is the world's first humanized monoclonal IgG<sub>4</sub> antibody to human PD-1. Promis-

**Fig. 2.** Relationship between progression-free survival (PFS) and overall survival (OS). The HR comes close to 1.0 if post-progression survival (PPS) becomes long due to effective post-trial treatment.



ing outcomes were reported in a phase I/II trial of nivolumab for the treatment of HCC (Checkmate-040), including an ORR of 20% (including 2 cases of complete response) and a disease control rate of 67%; a long-lasting durable response in patients showing an objective response was also characteristic of nivolumab therapy [67]. A trial examining a larger number of cases is currently underway, and the update presented at ASCO 2017 was again promising: OS with nivolumab was 28.6 months among sorafenib-naïve patients and 15 months among sorafenib-experienced patients [68]. A head-to-head phase III trial comparing nivolumab and sorafenib is also ongoing. Following the outcomes of the above-mentioned phase I/II trial [35], the FDA approved nivolumab as second-line treatment for HCC in September 2017 in the USA.

#### Pembrolizumab

Pembrolizumab (recombinant) is another humanized monoclonal IgG<sub>4</sub> antibody to human PD-1. Following a phase II study on HCC, a phase III placebo-controlled study examining second-line pembrolizumab in patients who have progressed on or are intolerant to sorafenib is currently underway [69].

#### Other Immune Checkpoint Inhibitors

All anti-PD-L1 antibodies, avelumab as a monotherapy, atezolizumab in combination with the anti-glypican-3 antibody codrituzumab, and durvalumab in combination with the anti-CTLA-4 antibody tremelimumab, are currently being evaluated in phase I or phase II studies. Inhibitory antibodies against other suppressive immune checkpoint molecules such as TIM3 and Lag3 and agonistic antibodies to OX40 are being investigated in early-stage studies.

#### Combination Therapy Using an Immune Checkpoint Inhibitor with a Molecular Targeted Agent

The results of an open-label phase Ib trial assessing the efficacy and safety of lenvatinib plus pembrolizumab were reported at ESMO 2016. Among 13 cases of solid tumors, a partial response was achieved in 9 cases and stable disease was achieved in 4 cases; this amazing anti-tumor effect had an ORR of 69.2% and a disease control rate of 100% [70]. The efficacy of an immune checkpoint inhibitor in combination with a molecular targeted agent has attracted much interest in recent years. A clinical trial investigating the efficacy of such combination treatment for HCC has already started in Japan and the USA (NCT03006926). The approach is extremely promising because of the additive therapeutic effect of the two agents and the synergistic effect by improving the tumor-induced immunosuppressive microenvironment.

#### Need for Biomarkers

The indications for ipilimumab (anti-CTLA-4 antibody) and nivolumab (anti-PD-1 antibody), which were first approved for use in the treatment of malignant melanoma, are gradually expanding. These agents, which exert favorable therapeutic effects mediated by unique anti-tumor mechanisms, benefit many patients; however, the high cost of treatment is a social problem and a healthcare financial burden. Consequently, there is an increasing need to establish appropriate biomarkers to identify patients who will respond to specific agents or will have adverse events. Given that pembrolizumab is available to patients with PD-L1-positive non-small cell lung cancer, establishing biomarkers will help reduce medical costs. Possible current biomarkers predictive of a response to immune checkpoint inhibitors are PD-L1 expression, tumor-infiltrating lymphocytes, or the mutation burden of each patient.

In May 2017, the FDA approved pembrolizumab for the treatment of any solid tumor confirmed to have high microsatellite instability or deficient mismatch repair [71, 72]. This marks the first approval of a cancer treatment based on specific genetic abnormalities rather than the organ where the tumor originated and points to a future of biomarker-based treatment selection.

## Conclusion

This article outlined most of the current systemic therapies and ongoing clinical trials for HCC. Among the molecular targeted agents, regorafenib was approved for

the treatment of HCC as a second-line agent, and lenvatinib will become clinically available as a first-line agent in 2018. Although increased options for treatment combining molecular targeted agents and immune checkpoint inhibitors will benefit HCC patients, adequate selection of a treatment strategy may become a more important issue.

## Disclosure Statement

The author has no conflicts of interest to declare.

## References

- Kudo M: Immune checkpoint blockade in hepatocellular carcinoma. *Liver Cancer* 2015;4: 201–207.
- Kudo M: Molecular targeted therapy for hepatocellular carcinoma: where are we now? *Liver Cancer* 2015;4:I–VII.
- Kudo M: Regorafenib as second-line systemic therapy may change the treatment strategy and management paradigm for hepatocellular carcinoma. *Liver Cancer* 2016;5:235–244.
- Zhang B, Finn RS: Personalized clinical trials in hepatocellular carcinoma based on biomarker selection. *Liver Cancer* 2016;5:221–232.
- Wilhelm SM, Carter C, Tang L, Wilkie D, McNabola A, Rong H, et al: BAY 43-9006 exhibits broad spectrum oral antitumor activity and targets the RAF/MEK/ERK pathway and receptor tyrosine kinases involved in tumor progression and angiogenesis. *Cancer Res* 2004;64:7099–7109.
- Chang YS, Adnane J, Trail PA, Levy J, Henderson A, Xue D, et al: Sorafenib (BAY 43-9006) inhibits tumor growth and vascularization and induces tumor apoptosis and hypoxia in RCC xenograft models. *Cancer Chemother Pharmacol* 2007;59:561–574.
- Llovet JM, Ricci S, Mazzaferro V, Hilgard P, Gane E, Blanc JF, et al: Sorafenib in advanced hepatocellular carcinoma. *N Engl J Med* 2008; 359:378–390.
- Cheng AL, Kang YK, Chen Z, Tsao CJ, Qin S, Kim JS, et al: Efficacy and safety of sorafenib in patients in the Asia-Pacific region with advanced hepatocellular carcinoma: a phase III randomised, double-blind, placebo-controlled trial. *Lancet Oncol* 2009;10:25–34.
- Kudo M: Locoregional therapy for hepatocellular carcinoma. *Liver Cancer* 2015;4:163–164.
- Kang TW, Rhim H: Recent advances in tumor ablation for hepatocellular carcinoma. *Liver Cancer* 2015;4:176–187.
- Lencioni R, de Baere T, Martin RC, Nutting CW, Narayanan G: Image-guided ablation of malignant liver tumors: recommendations for clinical validation of novel thermal and non-thermal technologies – a Western perspective. *Liver Cancer* 2015;4:208–214.
- Kudo M, Izumi N, Sakamoto M, Matsuyama Y, Ichida T, Nakashima O, et al: Survival analysis over 28 years of 173,378 patients with hepatocellular carcinoma in Japan. *Liver Cancer* 2016;5:190–197.
- Ho MC, Hasegawa K, Chen XP, Nagano H, Lee YJ, Chau GY, et al: Surgery for intermediate and advanced hepatocellular carcinoma: a consensus report from the 5th Asia-Pacific Primary Liver Cancer Expert Meeting (AP-PLE 2014). *Liver Cancer* 2016;5:245–256.
- Kudo M: Surveillance, diagnosis, treatment, and outcome of liver cancer in Japan. *Liver Cancer* 2015;4:39–50.
- Poon RT, Cheung TT, Kwok PC, Lee AS, Li TW, Loke KL, et al: Hong Kong consensus recommendations on the management of hepatocellular carcinoma. *Liver Cancer* 2015;4: 51–69.
- Bruix J, Takayama T, Mazzaferro V, Chau GY, Yang J, Kudo M, et al: Adjuvant sorafenib for hepatocellular carcinoma after resection or ablation (STORM): a phase 3, randomised, double-blind, placebo-controlled trial. *Lancet Oncol* 2015;16:1344–1354.
- Nakamura N, Shidoji Y, Yamada Y, Hatakeyama H, Moriwaki H, Muto Y: Induction of apoptosis by acyclic retinoid in the human hepatoma-derived cell line, HuH-7. *Biochem Biophys Res Commun* 1995;207:382–388.
- Yasuda I, Shiratori Y, Adachi S, Obora A, Takemura M, Okuno M, et al: Acyclic retinoid induces partial differentiation, down-regulates telomerase reverse transcriptase mRNA expression and telomerase activity, and induces apoptosis in human hepatoma-derived cell lines. *J Hepatol* 2002;36:660–671.
- Okita K, Izumi N, Matsui O, Tanaka K, Kaneko S, Moriwaki H, et al: Peretinoin after curative therapy of hepatitis C-related hepatocellular carcinoma: a randomized double-blind placebo-controlled study. *J Gastroenterol* 2015;50:191–202.
- Tsurusaki M, Murakami T: Surgical and locoregional therapy of HCC: TACE. *Liver Cancer* 2015;4:165–175.
- Arizumi T, Ueshima K, Minami T, Kono M, Chishina H, Takita M, et al: Effectiveness of sorafenib in patients with transcatheter arterial chemoembolization (TACE) refractory and intermediate-stage hepatocellular carcinoma. *Liver Cancer* 2015;4:253–262.
- Lencioni R, Llovet JM, Han G, Tak WY, Yang J, Guglielmi A, et al: Sorafenib or placebo plus TACE with doxorubicin-eluting beads for intermediate stage HCC: the SPACE trial. *J Hepatol* 2016;64:1090–1098.
- Meyer T, Fox R, Ma YT, Ross PJ, James MW, Sturgess R, Stubbs C, Stocken DD, Wall L, Watkinson A, Hacking N, Evans TRJ, Collins P, Hubner RA, Cunningham D, Primrose JN, Johnson PJ, Palmer DH: Sorafenib in combination with transarterial chemoembolisation in patients with unresectable hepatocellular carcinoma (TACE 2): a randomised placebo-controlled, double-blind, phase 3 trial. *Lancet Gastroenterol Hepatol* 2017;2:565–575.



- 24 Arizumi T, Ueshima K, Iwanishi M, Minami T, Chishina H, Kono M, et al: The overall survival of patients with hepatocellular carcinoma correlates with the newly defined time to progression after transarterial chemoembolization. *Liver Cancer* 2017;6:227–235.
- 25 Hoekman K: SU6668, a multitargeted angiogenesis inhibitor. *Cancer J* 2001;7(suppl 3): S134–S138.
- 26 Park JW, Cheng AL, Kudo M, Park JH, Liang CP, Hidaka H, et al: A randomized, double-blind, placebo-controlled phase III trial of TSU-68 (orantinib) combined with transcatheter arterial chemoembolization in patients with unresectable hepatocellular carcinoma. *J Hepatol* 2015;62(suppl 1):abstract G06.
- 27 Kudo M, Han G, Finn RS, Poon RT, Blanc JF, Yan L, et al: Brivanib as adjuvant therapy to transarterial chemoembolization in patients with hepatocellular carcinoma: a randomized phase III trial. *Hepatology* 2014;60:1697–1707.
- 28 Mendel DB, Laird AD, Xin X, Louie SG, Christensen JG, Li G, et al: In vivo antitumor activity of SU11248, a novel tyrosine kinase inhibitor targeting vascular endothelial growth factor and platelet-derived growth factor receptors: determination of a pharmacokinetic/pharmacodynamic relationship. *Clin Cancer Res* 2003;9:327–337.
- 29 Cheng AL, Kang YK, Lin DY, Park JW, Kudo M, Qin S, et al: Sunitinib versus sorafenib in advanced hepatocellular cancer: results of a randomized phase III trial. *J Clin Oncol* 2013;31:4067–4075.
- 30 Johnson PJ, Qin S, Park JW, Poon RT, Raoul JL, Philip PA, et al: Brivanib versus sorafenib as first-line therapy in patients with unresectable, advanced hepatocellular carcinoma: results from the randomized phase III BRISK-FL study. *J Clin Oncol* 2013;31:3517–3524.
- 31 Cainap C, Qin S, Huang WT, Chung IJ, Pan H, Cheng Y, et al: Linifanib versus sorafenib in patients with advanced hepatocellular carcinoma: results of a randomized phase III trial. *J Clin Oncol* 2015;33:172–179.
- 32 Zhu AX, Rosmorduc O, Evans TR, Ross PJ, Santoro A, Carrilho FJ, et al: SEARCH: a phase III, randomized, double-blind, placebo-controlled trial of sorafenib plus erlotinib in patients with advanced hepatocellular carcinoma. *J Clin Oncol* 2015;33:559–566.
- 33 Yamamoto Y, Matsui J, Matsushima T, Obashi H, Miyazaki K, Nakamura K, et al: Lenvatinib, an angiogenesis inhibitor targeting VEGFR/FGFR, shows broad antitumor activity in human tumor xenograft models associated with microvessel density and pericyte coverage. *Vasc Cell* 2014;6:18.
- 34 Ikeda K, Kudo M, Kawazoe S, Osaki Y, Ikeda M, Okusaka T, et al: Phase 2 study of lenvatinib in patients with advanced hepatocellular carcinoma. *J Gastroenterol* 2017;52:512–519.
- 35 Kudo M, Finn R, Qin S, Han K-H, Ikeda K, Piscaglia F, Baron A, Park J-W, Han G, Jassem J, Blanc JF, Vogel A, Komov D, Evans TRJ, Lopez C, Dutcus C, Guo M, Saito K, Kraljevic S, Tamai T, Ren M, Cheng A-L: A randomised phase 3 trial of lenvatinib vs. sorafenib in first-line treatment of patients with unresectable hepatocellular carcinoma. *Lancet* 2017, in press.
- 36 Khajornjiraphan N, Thu NA, Chow PK: Yttrium-90 microspheres: a review of its emerging clinical indications. *Liver Cancer* 2015;4: 6–15.
- 37 Edeline J, Gilibert M, Garin E, Boucher E, Raoul JL: Yttrium-90 microsphere radioembolization for hepatocellular carcinoma. *Liver Cancer* 2015;4:16–25.
- 38 Cucchetti A, Cappelli A, Ercolani G, Mosconi C, Cescon M, Golfieri R, et al: Selective internal radiation therapy (SIRT) as conversion therapy for unresectable primary liver malignancies. *Liver Cancer* 2016;5:303–311.
- 39 Vilgrain V, et al: SARA trial: Sorafenib vs Radioembolization in Advanced Hepatocellular Carcinoma. *EASL* 2017, GS012.
- 40 Chow PK, et al: Phase III multi-centre open-label randomized controlled trial of selective internal radiation therapy (SIRT) versus sorafenib in locally advanced hepatocellular carcinoma: the SIRveNIB study. *J Clin Oncol* 2017;35(suppl):abstract 4002.
- 41 Obi S, Sato S, Kawai T: Current status of hepatic arterial infusion chemotherapy. *Liver Cancer* 2015;4:188–199.
- 42 Lin CC, Hung CF, Chen WT, Lin SM: Hepatic arterial infusion chemotherapy for advanced hepatocellular carcinoma with portal vein thrombosis: impact of early response to 4 weeks of treatment. *Liver Cancer* 2015;4: 228–240.
- 43 Ueshima K, Kudo M, Tanaka M, Kumada T, Chung H, Hagiwara S, et al: Phase I/II study of sorafenib in combination with hepatic arterial infusion chemotherapy using low-dose cisplatin and 5-fluorouracil. *Liver Cancer* 2015;4:263–273.
- 44 Llovet JM, Decaens T, Raoul JL, Boucher E, Kudo M, Chang C, et al: Brivanib in patients with advanced hepatocellular carcinoma who were intolerant to sorafenib or for whom sorafenib failed: results from the randomized phase III BRISK-PS study. *J Clin Oncol* 2013;31:3509–3516.
- 45 Zhu AX, Kudo M, Assenat E, Cattani S, Kang YK, Lim HY, et al: Effect of everolimus on survival in advanced hepatocellular carcinoma after failure of sorafenib: the EVOLVE-1 randomized clinical trial. *JAMA* 2014;312:57–67.
- 46 Santoro A, Rimassa L, Borbath I, Daniele B, Salvagni S, Van Laethem JL, et al: Tivantinib for second-line treatment of advanced hepatocellular carcinoma: a randomised, placebo-controlled phase 2 study. *Lancet Oncol* 2013;14:55–63.
- 47 Rimassa L, Abbadessa G, Personeni N, Porta C, Borbath I, Daniele B, et al: Tumor and circulating biomarkers in patients with second-line hepatocellular carcinoma from the randomized phase II study with tivantinib. *Onco-target* 2016;7:72622–72633.
- 48 Rimassa L, Assenat E, Peck-Radosavljevic M, Zagonel V, Pracht M, Rota-Carevoli E, et al: Second-line tivantinib vs placebo in patients with MET-high hepatocellular carcinoma: results of the METIV-HCC phase 3 trial. *ASCO Annual Meeting '17* (abstract 4000). <https://www.arqule.com/wp-content/uploads/Tivantinib-METIV-HCC-Phase-3-trial-ASCO-2017.pdf>.
- 49 Spratlin JL, Cohen RB, Eadens M, Gore L, Camidge DR, Diab S, et al: Phase I pharmacologic and biologic study of ramucirumab (IMC-1121B), a fully human immunoglobulin G<sub>1</sub> monoclonal antibody targeting the vascular endothelial growth factor receptor-2. *J Clin Oncol* 2010;28:780–787.
- 50 Zhu AX, Park JO, Ryoo BY, Yen CJ, Poon R, Pastorelli D, et al: Ramucirumab versus placebo as second-line treatment in patients with advanced hepatocellular carcinoma following first-line therapy with sorafenib (REACH): a randomised, double-blind, multicentre, phase 3 trial. *Lancet Oncol* 2015;16:859–870.
- 51 Kudo M, Hatano E, Ohkawa S, Fujii H, Masumoto A, Furuse J, et al: Ramucirumab as second-line treatment in patients with advanced hepatocellular carcinoma: Japanese subgroup analysis of the REACH trial. *J Gastroenterol* 2017;52:494–503.
- 52 Kudo M, Moriguchi M, Numata K, Hidaka H, Tanaka H, Ikeda M, et al: S-1 versus placebo in patients with sorafenib-refractory advanced hepatocellular carcinoma (S-CUBE): a randomised, double-blind, multicentre, phase 3 trial. *Lancet Gastroenterol Hepatol* 2017;2:407–417.
- 53 Wilhelm SM, Dumas J, Adnane L, Lynch M, Carter CA, Schütz G, et al: Regorafenib (BAY 73-4506): a new oral multikinase inhibitor of angiogenic, stromal and oncogenic receptor tyrosine kinases with potent preclinical antitumor activity. *Int J Cancer* 2011;129:245–255.
- 54 Bruix J, Qin S, Merle P, Granito A, Huang YH, Bodoky G, et al: Regorafenib for patients with hepatocellular carcinoma who progressed on sorafenib treatment (RESORCE): a randomised, double-blind, placebo-controlled, phase 3 trial. *Lancet* 2017;389:56–66.
- 55 Villanueva A: Rethinking future development of molecular therapies in hepatocellular carcinoma: a bottom-up approach. *J Hepatol* 2013;59:392–395.
- 56 Lim HY, Heo J, Choi HJ, Lin CY, Yoon JH, Hsu C, et al: A phase II study of the efficacy and safety of the combination therapy of the MEK inhibitor refametinib (BAY 86-9766) plus sorafenib for Asian patients with unresectable hepatocellular carcinoma. *Clin Cancer Res* 2014;20:5976–5985.
- 57 Kitai S, Kudo M, Nishida N, Izumi N, Sakamoto M, Matsuyama Y, et al: Survival benefit of locoregional treatment for hepatocellular carcinoma with advanced liver cirrhosis. *Liver Cancer* 2016;5:175–189.
- 58 Nishikawa H, Kita R, Kimura T, Ohara Y, Takeda H, Sakamoto A, et al: Clinical efficacy of non-transplant therapies in patients with hepatocellular carcinoma with Child-Pugh C liver cirrhosis. *Anticancer Res* 2014;34:3039–3044.

- 59 Nouse K, Kokudo N, Tanaka M, Kuromatsu R, Nishikawa H, Toyoda H, et al: Treatment of hepatocellular carcinoma with Child-Pugh C cirrhosis. *Oncology* 2014;87(suppl 1):99–103.
- 60 Nouse K, Ito Y, Kuwaki K, Kobayashi Y, Nakamura S, Ohashi Y, et al: Prognostic factors and treatment effects for hepatocellular carcinoma in Child C cirrhosis. *Br J Cancer* 2008; 98:1161–1165.
- 61 Kudo M, Osaki Y, Matsunaga T, Kasugai H, Oka H, Seki T: Hepatocellular carcinoma in Child-Pugh C cirrhosis: prognostic factors and survival benefit of nontransplant treatments. *Dig Dis* 2013;31:490–498.
- 62 Terashima T, Yamashita T, Takata N, Nakagawa H, Toyama T, Arai K, et al: Post-progression survival and progression-free survival in patients with advanced hepatocellular carcinoma treated by sorafenib. *Hepatol Res* 2016;46:650–656.
- 63 Ishida Y, Agata Y, Shibahara K, Honjo T: Induced expression of PD-1, a novel member of the immunoglobulin gene superfamily, upon programmed cell death. *EMBO J* 1992;11: 3887–3895.
- 64 Okazaki T, Honjo T: PD-1 and PD-1 ligands: from discovery to clinical application. *Int Immunol* 2007;19:813–824.
- 65 Krummel MF, Allison JP: CD28 and CTLA-4 have opposing effects on the response of T cells to stimulation. *J Exp Med* 1995;182:459–465.
- 66 Leach DR, Krummel MF, Allison JP: Enhancement of antitumor immunity by CTLA-4 blockade. *Science* 1996;271:1734–1736.
- 67 El-Khoueiry AB, Sangro B, Yau T, Crocenzi TS, Kudo M, Hsu C, et al: Nivolumab in patients with advanced hepatocellular carcinoma (CheckMate 040): an open-label, non-comparative, phase 1/2 dose escalation and expansion trial. *Lancet* 2017;389:2492–2502.
- 68 Crocenzi TS, El-Khoueiry AB, Yau TC, Melero I, Sangro B, Kudo M, et al: Nivolumab (nivo) in sorafenib (sor)-naïve and -experienced pts with advanced hepatocellular carcinoma (HCC): CheckMate040 Study. *J Clin Oncol* 2017;35:abstract 4013.
- 69 Finn RS, Chan SL, Zhu AX, et al: KEYNOTE: Randomized phase III study of pembrolizumab versus best supportive care for second-line advanced hepatocellular carcinoma. *J Clin Oncol* 2017;35(suppl):abstr TPS4143.
- 70 Taylor M, Dutcus CE, Schmidt E, Bagulho T, Li D, Shumaker R, et al: A phase 1b trial of lenvatinib (LEN) plus pembrolizumab (PEM) in patients with selected solid tumors. *Ann Oncol* 2016;27:266–295, abstract 776PD.
- 71 FDA: FDA approves first cancer treatment for any solid tumor with a specific genetic feature. May 23, 2017. <https://www.fda.gov/newsevents/newsroom/pressannouncements/ucm560167.htm>.
- 72 Le DT, Uram JN, Wang H, Bartlett BR, Kemberling H, Eyring AD, et al: PD-1 blockade in tumors with mismatch-repair deficiency. *N Engl J Med* 2015;372:2509–2520.

# Immuno-Oncology in Hepatocellular Carcinoma: 2017 Update

Masatoshi Kudo

Department of Gastroenterology and Hepatology, Kindai University Faculty of Medicine, Osaka-Sayama, Japan

## Keywords

Hepatocellular carcinoma · Nivolumab · Pembrolizumab · Ipilimumab · Tremelimumab

## Abstract

Clinical trials are currently ongoing to evaluate the utility of antibodies against programmed cell death 1 (PD-1), programmed cell death-ligand 1 (PD-L1), and cytotoxic T-lymphocyte-associated antigen 4 (CTLA-4) as monotherapy or combination therapy in patients with hepatocellular carcinoma (HCC). Results of combination treatment with the anti-PD-L1 antibody durvalumab and the anti-CTLA-4 antibody tremelimumab in HCC were presented at the 2017 annual meeting of the ASCO (American Society of Clinical Oncology). Response rates were 25% in all 40 patients and 40% in the 20 uninfected patients, both of which are encouraging. Transcatheter arterial chemoembolization and radiofrequency ablation can activate tumor immunogenicity by releasing tumor-associated antigen and by inducing the migration of cytotoxic T lymphocytes to small intrahepatic metastatic nodules. Subsequent administration of anti-PD-1 antibody could control these small intrahepatic metastatic nodules. In a nonclinical study, the combination of pembrolizumab and lenvatinib inhibited the cancer immunosuppressive environments induced by tumor-associated macrophages and regulatory T cells. This, in turn, decreased the levels of TGF- $\beta$  and IL-10, the expression of PD-1, and the

inhibition of Tim-3, triggering anticancer immunity mediated by immunostimulatory cytokines such as IL-12. Studies such as these may provide insight into the appropriate molecular targeted agents to be used with immune checkpoint inhibitors.

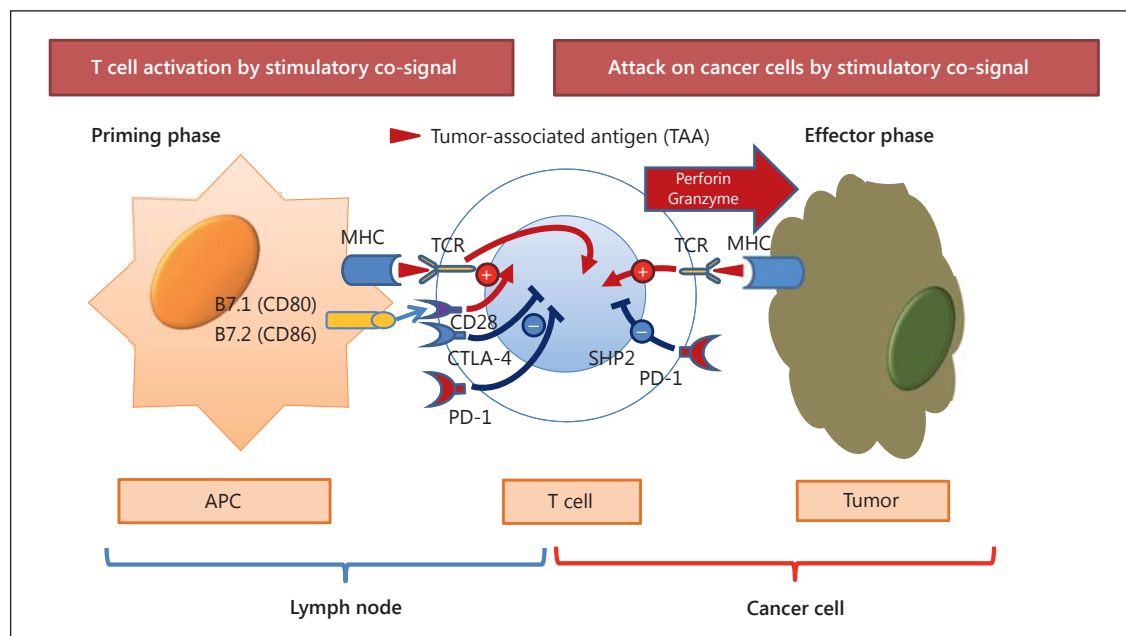
© 2017 S. Karger AG, Basel

## Introduction

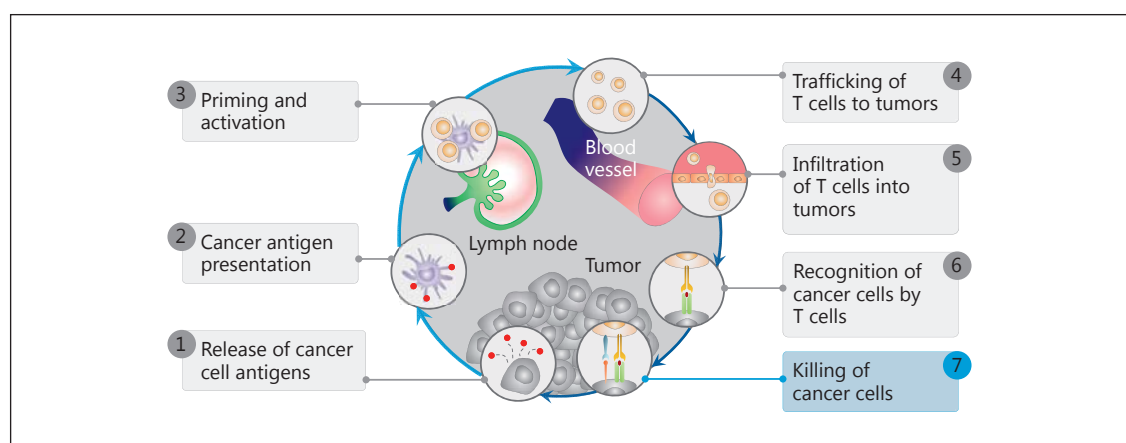
Clinical trials are currently ongoing to evaluate the utility of antibodies against programmed cell death 1 (PD-1), programmed cell death-ligand 1 (PD-L1), and cytotoxic T-lymphocyte-associated antigen 4 (CTLA-4), as monotherapy or combination therapy, in patients with hepatocellular carcinoma (HCC). This article reviews current knowledge of immune checkpoint inhibitors and trends in clinical trials for HCC.

## Theoretical Basis of Enhanced Tumor Immunoreactivity by Immune Checkpoint Inhibitors

During carcinogenesis, the transformation of cancer cells is associated with recognition of tumor-associated antigens (TAAs) by a group of proteins called the major histocompatibility complex (MHC) on the surface of antigen-presenting cells. These cells subsequently migrate to



**Fig. 1.** T cell-mediated cancer immunity including priming phase at the lymph nodes and effector phase at the cancer microenvironment.



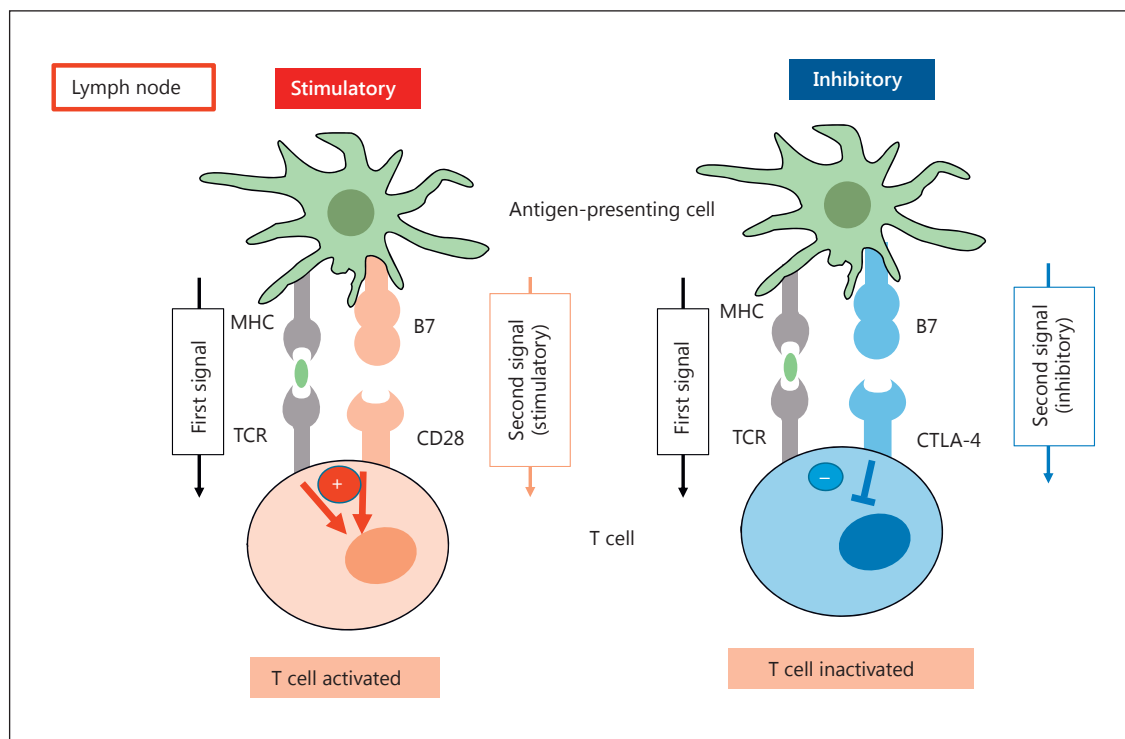
**Fig. 2.** The immune system is capable of eliminating tumor cells through 7 steps. Adapted from Chen and Mellman [1].

lymph nodes, where they present TAAs to T cell receptors (TCR) on the surface of immature T cells (signal 1). Immature T cells cannot be activated by the binding between TAA and TCR (signal 1), but require a co-stimulatory signal (signal 2). This signal is generated when B7 proteins (CD80/B7-1 and CD86/B7-2) on antigen-presenting cells bind to CD28 on immature T cells, inducing the differentiation of these T cells into CD8<sup>+</sup> T cells (priming phase). Subsequently, activated T cells migrate through the blood-

stream to the tumor microenvironment, where they recognize TAAs presented by the MHC on tumor cells and begin to attack the cells by releasing perforin and granzyme (effector phase) (Fig. 1). This process has been called the conventional cancer immunity cycle (Fig. 2) [1].

Although T cells are effective initially, they lose their effect relatively quickly. Previous attempts to enhance anticancer immunity have involved the activation of immune-stimulatory mechanisms by various modalities, in-





**Fig. 3.** There are 2 immune regulatory co-signals: stimulatory and inhibitory co-signals. These are called immune checkpoints. Since affinity of CTLA-4 to B7 is 10 times stronger than that of CD28, second inhibitory co-signal induces T cell in activation.

cluding peptide, dendritic cell, cytokine, and lymphokine-activated killer cell therapy. These attempts, however, seldom produced satisfactory results, largely because the body's innate immune system, which negatively regulates immune responses (immune evasion mechanism), was incompletely understood. In reality, attempts to progressively enhance immune responses reinforce an immune system that negatively regulates immune response in reaction to positive regulation. These theoretical and practical reasons may explain the failure of previous studies that employed immunostimulatory therapy alone.

In humans, immune escape in cancer is mediated largely by two mechanisms: one in the lymph nodes and the other in the tumor microenvironment.

### Cancer Immune Escape and Inhibitors

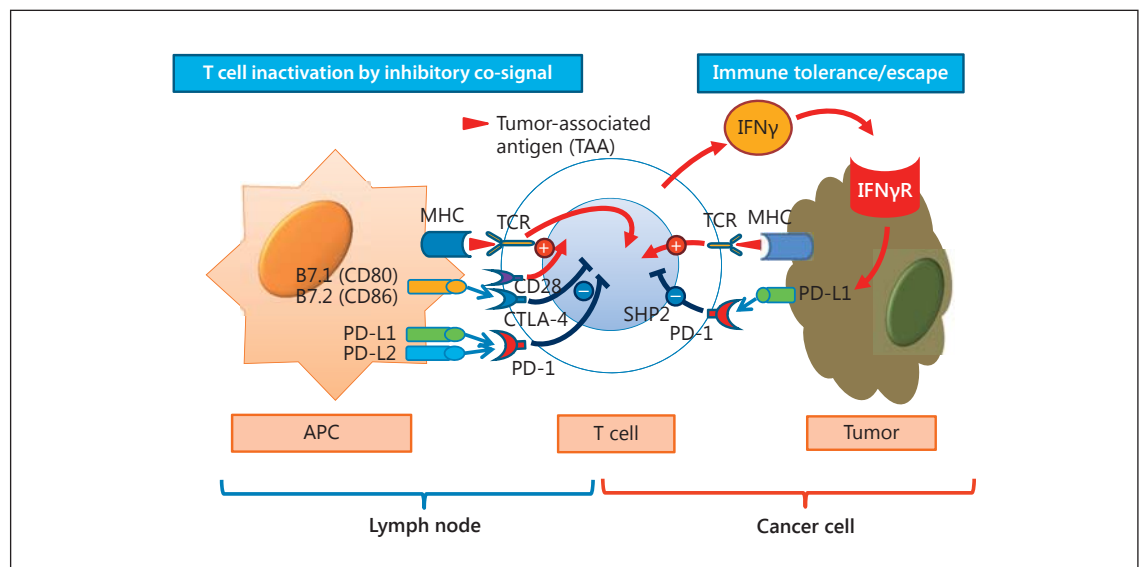
#### *CTLA-4 Pathway and Inhibitors*

The CTLA-4 pathway regulates the proliferation of activated lymphocytes, primarily in the lymph nodes. CTLA-4 is constitutively expressed by regulatory T cells

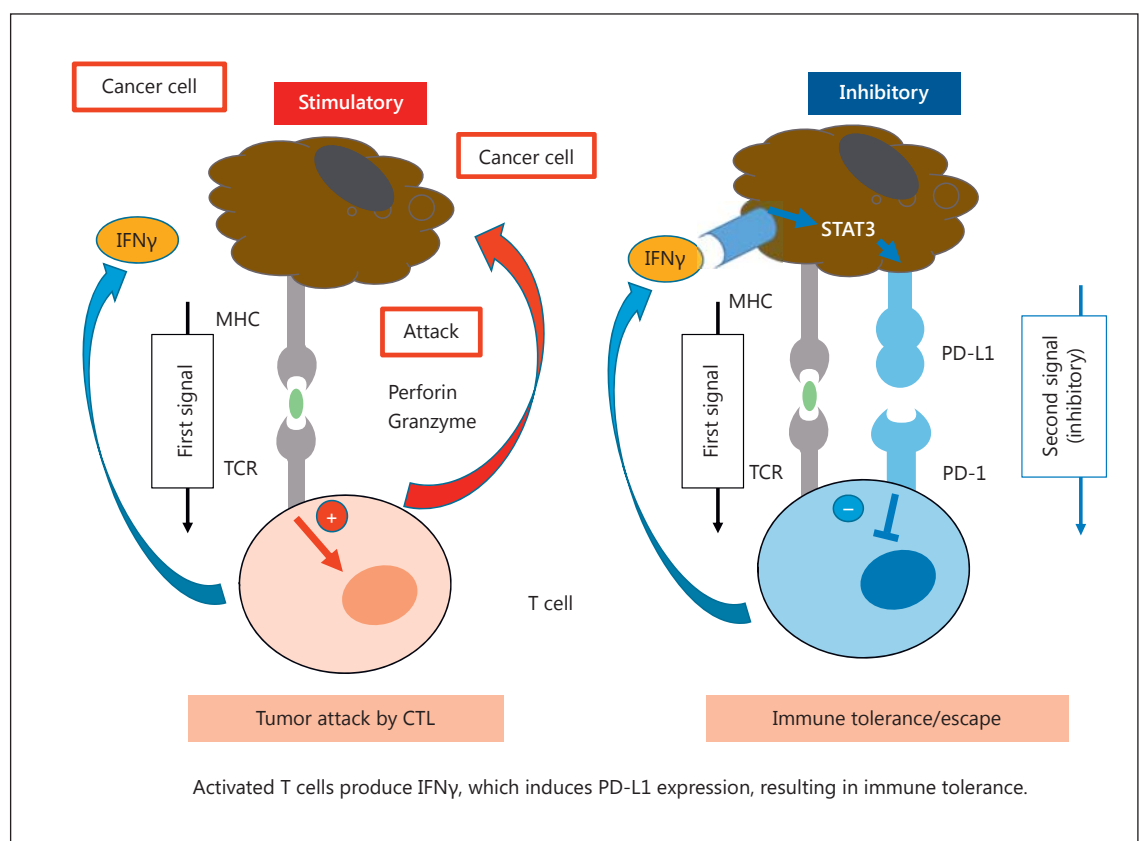
(Tregs), but is also expressed transiently by other types of T cells during the early phase of activation (within 24–48 h). Because CTLA-4 has a  $\geq 10$ -fold greater affinity to B7 than does CD28, the affinity of CTLA-4 to T cells activated via the B7/CD28 pathway (stimulatory signal 2) is  $\geq 10$  times that of CD28. Thus, CTLA-4 binds to B7-1/B7-2 by competing with CD28 and transmits inhibitory signal 2 to the T cell. Under normal physiological conditions, CTLA-4 terminates T cell activity, which is no longer needed to regulate excessive immune response mediated by T cells. However, in cancer, CTLA-4 suppresses the proliferation (activation and production) of T cells that have undergone TAA recognition and differentiation (Fig. 3, 4).

The immunosuppressive mechanism underlying T cell activation in the lymph nodes can be counteracted by antibodies against CTLA-4. The first use of anti-CTLA-4 antibody in cancer treatment was reported in 1996, with this antibody successfully eliminating tumor cells in mice.

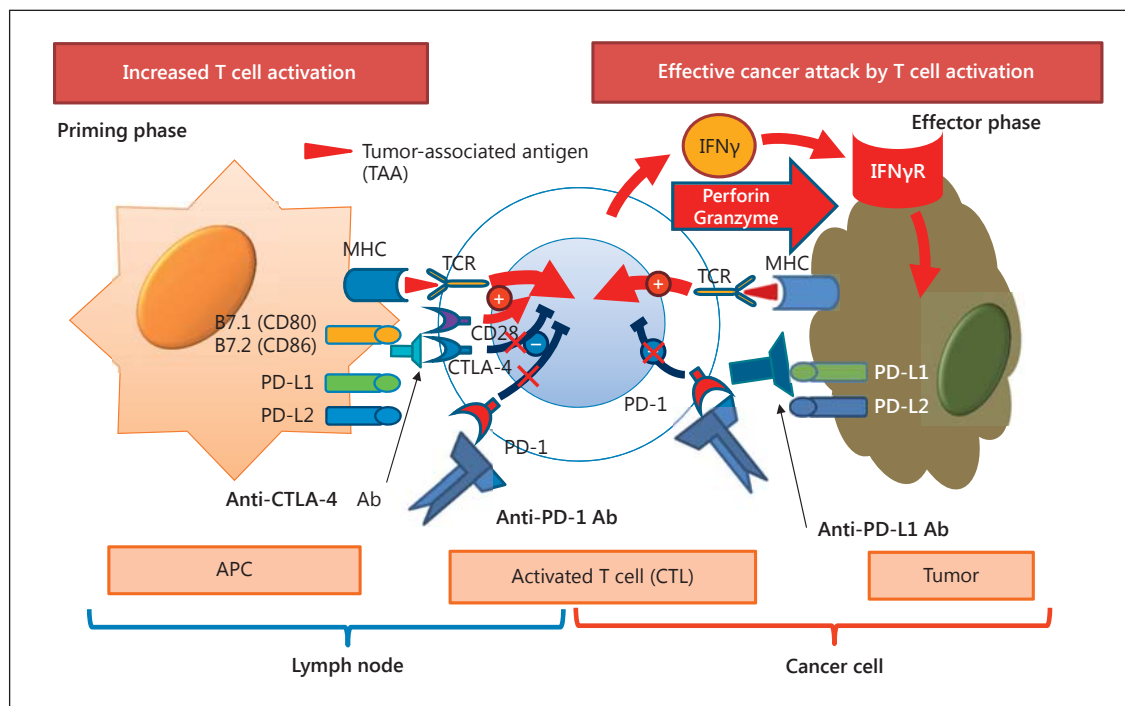
As described above, CTLA-4 is expressed at high levels by Tregs. Accordingly, one of the actions of anti-CTLA-4 antibody may be to downregulate Tregs in the tumor mi-



**Fig. 4.** T cell inactivation and cancer immune escape by CTLA-4, PD-1, and PD-L1. As a result, T cell is failed to be activated at the lymph node.



**Fig. 5.** Immune regulatory co-signaling (immune checkpoints: stimulatory and inhibitory) in cancer microenvironment. At the tumor microenvironment, cytotoxic T cell is inactivated by secondary inhibitory signal through the PD-1/PD-L1 pathway by IFN $\gamma$  produced by transient activation of CTL.



**Fig. 6.** Cancer attack by CTLs activated by the immune checkpoint inhibitors anti-PD-1, anti-PD-L1, and anti-CTLA-4 antibodies. By the administration of anti-CTLA-4, anti-PD-1 and anti-PD-L1 antibodies, T cell activation and effective cancer attack by activated T cell are restored.

croenvironment. Clinical studies are currently underway to aggressively evaluate the efficacy of the anti-CTLA-4 antibodies ipilimumab and tremelimumab.

#### *The PD-1/PD-L1 Pathway and Its Inhibitors*

PD-1, a receptor for co-inhibitory signals, is expressed by T cells and B cells, and in bone marrow, and inhibits antigen-specific activation of T cells by binding to PD-L1/PD-L2. PD-L2 is expressed only by dendritic cells, whereas PD-L1 is expressed by dendritic cells and various tissue types, including blood vessels, heart, lungs, and placenta.

PD-1 is barely detected in normal mice or in peripheral blood of healthy humans, whereas it is expressed in the late phase of T cell activation in response to infection and inflammation. Under these conditions, PD-1 is expressed at particularly high levels by effector T cells circulating in peripheral blood.

In contrast to PD-1, PD-L1 is expressed constitutively in peripheral tissues under normal physiologic conditions. Upon induction of an immune response, almost all immunocompetent cells, including T cells and B cells, start to express PD-L1. In addition, most cancer cells express PD-L1 through a mechanism described below.

By contrast, the expression and function of PD-L2 are limited because it is expressed only by antigen-presenting cells and is involved in the activation of T cells in the lymph nodes. This may explain why the effect of PD-L2 is thought to play a limited role in cancer immunity, whereas anti-PD-1 antibody and anti-PD-L1 antibody are comparably effective.

Upon recognition by surface TCR of tumor antigens presented by the MHC, activated T cells transmit a signal to attack cancer cells by releasing perforin or granzyme and simultaneously delivering cytokines, mainly interferon  $\gamma$ , to cancer cells. In response to this stimulation, cancer cells express PD-L1, which binds to PD-1 as a defense mechanism. This results in the transmission of inhibitory signals to cytotoxic T lymphocytes, thereby reducing their potency (immune evasion or immune tolerance) (Fig. 5).

If anti-PD-1 antibody is administered at this point, it will unlock the negative regulation of the immune response, and enable recovery of the ability to attack cancer cells (Fig. 6). That is, unlike conventional chemotherapy or molecular targeted therapy, antibody therapy improves the potency of attack on cancer cells by restoring

**Table 1.** Immune checkpoint inhibitors in HCC clinical trials

Target cell	Target molecule	Development code	Drug name	Commercial name	Antibody	Company
T lymphocyte	PD-1	BMS-36558 ONO-4538	Nivolumab	Optivo	Fully human IgG4 antibody	ONO/BMS
	PD-1	MK-4375	Pembrolizumab	Keytruda	Humanized IgG4 antibody	Merck
Tumor cell	PD-L1	MPDL3280A	Atezolizumab	Not yet approved	Fully humanized IgG1 antibody	Roche
	PD-L1	MEDI4736	Durvalumab	Not yet approved	Humanized IgG1 antibody	AstraZeneca
	PD-L1	MSB-0010718C	Avelumab	Not yet approved	Humanized IgG1 antibody	Merck-serono
T lymphocyte	CTLA-4	BMS-734016	Ipilimumab	Yervoy	Fully humanized IgG1 antibody	BMS Medarex
	CTLA-4	MEDI1123	Tremelimumab	Not yet approved	Fully humanized IgG2 antibody	AstraZeneca MedImmune

the function of the innate anticancer immune system, a powerful and precise weapon against cancer [2–13]. Anti-PD-L1 antibody has similar effects [14]. In addition, PD-L1 is reported to be a biomarker that can predict the effect of anti-PD-1 antibody [15]. However, some patients with tumors that do not express PD-L1 have also been found to benefit from anti-PD-1 antibody.

#### Development and a Trend of Immune Checkpoint Inhibitors for HCC

Interim results of the phase I/II CheckMate 040 clinical trial of the anti-PD-1 antibody nivolumab in patients with HCC were reported at the 2015 annual meeting of the American Society of Clinical Oncology (ASCO), held in Chicago, IL, USA [16]. Subsequent study outcomes were presented at the ASCO meetings in 2016 and 2017, and the results of the trial were published in *The Lancet* [17]. Based exclusively on these study outcomes, the United States Food and Drug Administration approved nivolumab as second-line treatment agent for HCC in September 22, 2017.

The findings of the dose escalation phase of this phase I/II trial confirmed the safety of nivolumab, at a dose of 3 mg/kg, in HCC patients infected with hepatitis C virus (HCV) or hepatitis B virus (HBV) infection, and at doses up to 10 mg/kg in HCC patients without infection. Moreover, the effectiveness and safety of this agent were evaluated in the 214 patients in the dose escalation and dose

expansion cohorts. Among the 144 (67%) patients with extrahepatic metastases and the 63 (29%) with vascular invasion, 42 (20%) showed a favorable response to nivolumab, including 3 patients who achieved complete response (CR). Also, disease progression was suppressed in 138 of the 214 (64%) patients, and the 9-month survival rate was as high as 74%. These results are considered highly promising, especially because this group of patients had highly advanced HCC.

The waterfall plots show comparable tumor-reducing effects of nivolumab in 3 types of patients, patients without viral hepatitis, whether untreated with or intolerant to sorafenib or progressing on sorafenib, and those infected with HBV or HCV infection, although the effect of nivolumab appeared to be slightly weaker in the HBV group. Some patients began to respond to this drug within 3 months of first administration, with responses being durable for a long period of time. The spider plots also show that this effect was durable not only in patients who achieved CR or partial response, but also in patients with stable disease. However, the drug was ineffective in 30–40% of these patients, with some showing rapid exacerbation of disease, suggesting that this may be the limit of monotherapy.

The 3 patients who achieved CR did so during the early phase of treatment (3–10 months) and currently remain disease-free, including one each for  $\geq 25$  months and  $\geq 33$  months. Similarly, most patients with partial response and stable disease have maintained the disease state, with few developing progressive disease due to the



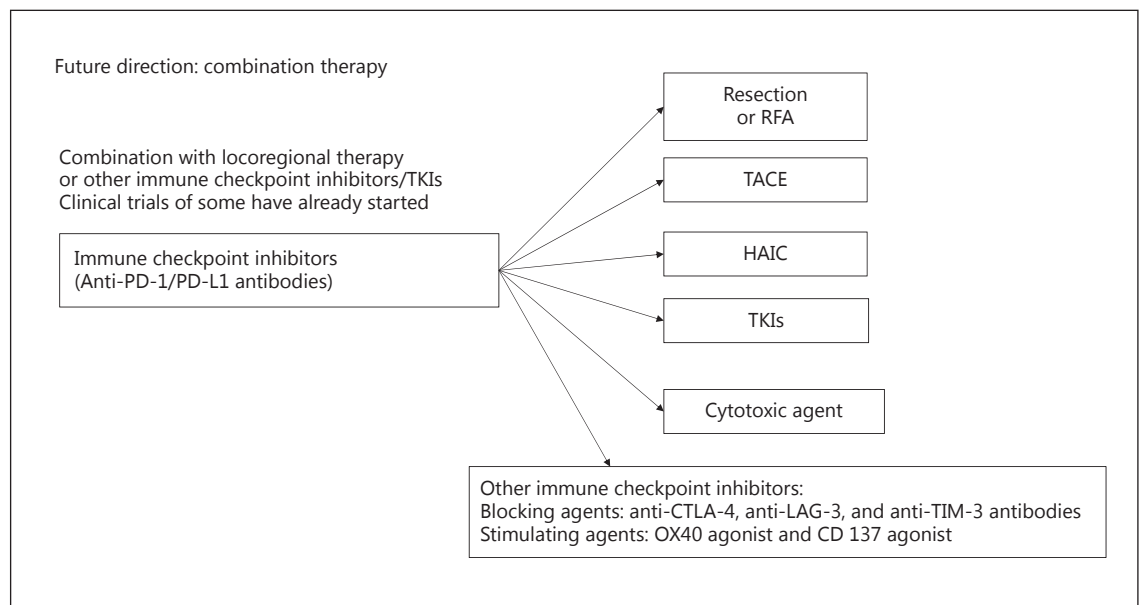
**Table 2.** Immune checkpoint inhibitors: ongoing trials

Drug	Trial name	Clinicaltrials.gov No.	Company	Phase	Subjects, <i>n</i>	Line of therapy	Design	Endpoint	Status
<b>Nivolumab</b> Nivolumab (PD-1 Ab)/ Ipilimumab (CTLA-4 Ab)	CheckMate 040	NCT01658878	BMS/ONO	I/II	42	1 L/2 L	cohort 1: dose escalation	DLT/MTD	completed
	CheckMate 040	NCT01658878	BMS/ONO	I/II	214	1 L/2 L	cohort 2: dose expansion	ORR	completed
	CheckMate 040	NCT01658878	BMS/ONO	I/II	200	1 L	cohort 3: nivolumab vs. sorafenib	ORR	completed
	CheckMate 040	NCT01658878	BMS/ONO	I/II	120	2 L	cohort 4: nivolumab + ipilimumab	safety / tolerability	completed
	CheckMate 040	NCT01658878	BMS/ONO	I/II	–	1 L	cohort 5: nivolumab (Child-Pugh B)	ORR	recruiting
	CheckMate 040	NCT01658878	BMS/ONO	I/II	–	1 L	cohort 6: nivolumab + cabozantinib	ORR	recruiting
	CheckMate 040	NCT01658878	BMS/ONO	I/II	–	1 L	cohort 7: nivolumab + ipilimumab + cabozantinib	ORR	recruiting
	CheckMate 459	NCT02576509	ONO	III	726	1 L	nivolumab vs. sorafenib	OS	completed
<b>Pembrolizumab</b> Pembrolizumab (PD-1 Ab)	KEYNOTE-224	NCT02702414	MSD	II	100	2 L	pembrolizumab (1 arm)	ORR	completed
Pembrolizumab (PD-1 Ab)	KEYNOTE-240	NCT02702401	MSD	III	408	2 L	pembrolizumab vs. placebo	PFS/OS	recruiting
<b>Durvalumab</b> Durvalumab (PD-L1 Ab)/ Tremelimumab (CTLA-4 Ab)	–	NCT02519348	AstraZeneca	II	144	1 L/2 L	durvalumab (arm A) tremelimumab (arm B) durvalumab + tremelimumab (arm C)	safety/ tolerability	recruiting
Durvalumab + Tremelimumab	–	NCT028211754	AstraZeneca	I/II	–	TACE/RFA	1 arm	safety/ tolerability	recruiting
MSBoo11359C (PD-L1 Ab + TGFB Trap)	–	NCT02699515	Merck-serono	I	–	1L	1 arm	safety/ tolerability	recruiting

DLT, dose-limiting toxicity; MTD, maximum tolerated dose; ORR, objective response rate; TTP, time to progression; OS, overall survival; PFS, progression-free survival.

development of drug tolerance. Accordingly, the treatment efficacy of the anti-PD-1 antibody, nivolumab has been sustained (durable response) in patients with HCC, similarly to findings in other types of cancer. This treatment outcome is typical of immune checkpoint inhibitors, and thus, deserves attention. It should also be noted that, despite nivolumab treatment being terminated a few months after the 2 above patients attained CR, both have continued to maintain CR to date. Furthermore, the interim results presented at the 2015 annual meeting of

ASCO included a patient with HCC who initially had innumerable tumors in both lobes, all of which disappeared after 6 weeks of treatment as well as showing a reduction in the  $\alpha$ -fetoprotein level from 21,000 to 283 ng/mL. Another HCC patient initially had a tumor measuring  $\geq 10$  cm in diameter, but this tumor shrunk dramatically to about 2 cm after 48 weeks of treatment. Although liver damage was the most worrisome anticipated grade 3–4 treatment-related side effect, only 9 patients (4%) developed elevated aspartate aminotransferase and only 6 (3%)



**Fig. 7.** Future direction of treatment strategy with immune checkpoint inhibitors is a combination therapy with other check point inhibitor/stimulators, tyrosine kinase inhibitors (TKIs), transarterial chemoembolization (TACE) and resection or ablation. RFA, radiofrequency ablation; HAIC, hepatic arterial infusion chemotherapy.

developed elevated alanine aminotransferase, rates comparable to those observed in patients with other types of cancer. Furthermore, severe liver damage associated with viral hepatitis was not observed.

In summary, (1) the safety profile of monotherapy with the anti-PD-1 antibody, nivolumab was satisfactory in patients with HCC, as in other types of cancer; (2) nivolumab could be used safely in HCC patients infected with HBV or HCV; and (3) nivolumab had a remarkably high response rate as an immunotherapeutic agent with long-lasting efficacy. The durable response of nivolumab was comparable among different cohorts (patients without viral hepatitis and those infected with HBV or HCV) regardless of drug dose or etiology.

Follow-up results presented at the 2017 annual meeting of ASCO showed that the median overall survival was 28.6 months in the sorafenib-naïve group and 15.6 months in the sorafenib-experienced group, both of which are considered astounding [18].

### Other Currently Ongoing Clinical Trials

Table 1 shows immune checkpoint inhibitors that are currently being evaluated in patients with HCC. At present, 5 cohorts are being evaluated in the phase I/II Check-

Mate 040 study: a dose escalation cohort (cohort 1), a dose expansion cohort (cohort 2), a randomized comparative trial with sorafenib (cohort 3), a cohort consisting of patients concurrently treated with nivolumab and the CTLA-4 antibody ipilimumab (cohort 4), and a cohort of patients with Child-Pugh class B liver function (cohort 5) (Table 2).

The results of the phase I/II CheckMate 040 study have led to the design of a phase III clinical trial directly comparing sorafenib and nivolumab, a trial currently underway. Another trial is evaluating the efficacy of the anti-PD-1, pembrolizumab as second-line therapy after sorafenib failure. Early approval of either or both of these anti-PD-1 antibodies nivolumab and pembrolizumab is anxiously awaited.

Compared with anti-PD-1 antibody, the side effects of anti-CTLA-4 antibody tend to be slightly more severe in patients with HCC [19].

### Combination Therapy with Immune Checkpoint Inhibitors

Antibody therapy against PD-L1 and CTLA-4, in addition to PD-1, appears promising as immunotherapy for HCC. Indeed, studies evaluating combination therapy

**Table 3.** Phase I/II combination therapy with durvalumab (PD-L1 Ab) and tremelimumab (CTLA-4 Ab) in HCC

Investigator-assessed response	HBV+ (n = 11)	HCV+ (n = 9)	Uninfected (n = 20)	All (n = 40)
Confirmed ORR (all PR), % (95% CI)	0 (0.0–28.5)	11.1 (0.3–48.2)	30.0 (11.9–54.3)	17.5 (7.3–32.8)
CR + PR (confirmed + unconfirmed), % (95% CI)	9.1 (0.2–41.3)	11.1 (0.3–48.2)	40.0 (19.1–63.9)	25.0 (12.7–41.2)
CR + PR + SD ≥16 weeks (DCR16), % (95% CI)	45.5 (16.7–76.6)	44.4 (13.7–78.8)	70.0 (45.7–88.1)	57.5 (40.9–73.0)

Adapted from Kelley et al. [23]. HCC, hepatocellular carcinoma; ORR, objective response rate; PR, partial response; CR, complete response; SD, stable disease, DCR, disease control rate.

**Table 4.** Combination trials of immune checkpoint inhibitors with TKIs in HCC

Phase	Target	Agent	Company	Trial No.
Ib/II	PD-1 + TGF- $\beta$ receptor I	nivolumab + galunisertib (LY2157299)	Lilly	NCT02423343
I	PD-1 + multikinase	pembrolizumab + lenvatinib	Eisai	NCT03006926
I	PD-1 + multikinase	pembrolizumab + nintedanib	Gustave Roussy	NCT02856425
I	PD-1 + multikinase	PDR001 + sorafenib	Novartis	NCT02988440
I/II	PD-1 + c-Met	PDR001 + capmatinib (INC280)	Novartis	NCT02795429
I	PD-L1 + VEGF	durvalumab + ramucirumab	Astra Zeneca	NCT02572687
I/II	PD-1 + VEGF	nivolumab + cabozantinib	BMS	NCT01658878
I/II	PD-1 + CTLA-4 + VEGF	nivolumab + ipilimumab + cabozantinib	BMS	NCT01658878

TKIs, tyrosine kinase inhibitors; HCC, hepatocellular carcinoma.

with multiple immune checkpoints such as anti-PD-1 antibody plus anti CTLA-4 antibody, are currently underway (Fig. 7). This combination is very effective in patients with malignant melanoma [20, 21], and is being studied in patients with HCC [22]. A rationale for combination therapy with antibodies against PD-1/PD-L1 and CTLA-4 is that inhibition of the PD-1 and PD-L1 pathways cannot stimulate cancer immunity when target lymphocytes (CD8+ T cells) are absent from the tumor microenvironment. However, concurrent use of anti-CTLA-4 antibody ensures inhibition of the B7-CTLA-4 pathway, resulting in CD8+ T cell proliferation in the lymph nodes and their infiltration into tumor tissues, thus strengthening antitumor effects. In addition, anti-CTLA-4 antibody in the tumor microenvironment can inhibit the tumor suppressive effect of Tregs, which express surface CTLA-4. Based on this rationale, several studies are currently investigating the utility of combination therapy with antibodies against CTLA-4, PD-1, and PD-L1 in HCC (Table 2).

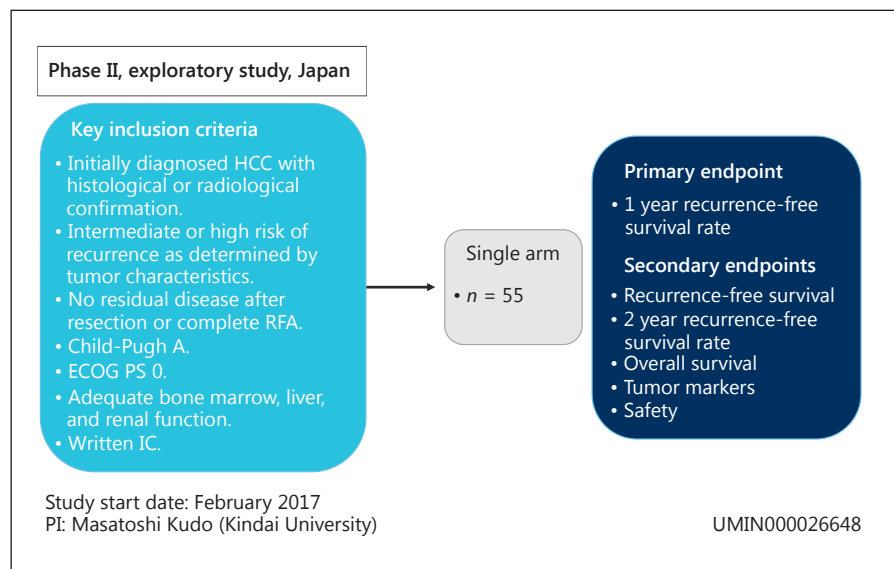
The efficacy of nivolumab and the anti-CTLA-4 antibody ipilimumab has been evaluated in the CheckMate 040 study using various doses and intervals. Another current clinical trial is comparing the effects of combina-

tion therapy with the anti-PD-1 antibody and the anti-CTLA-4 antibody tremelimumab and monotherapy with each antibody in patients with HCC. Treatment outcomes from phase I of this phase I/II trial were presented at the 2017 annual meeting of ASCO, showing objective response rates of 25% in all 40 patients and 40% in the 20 uninfected patients, findings considered quite encouraging (Table 3) [23]. The phase II study is scheduled to end in April 2018.

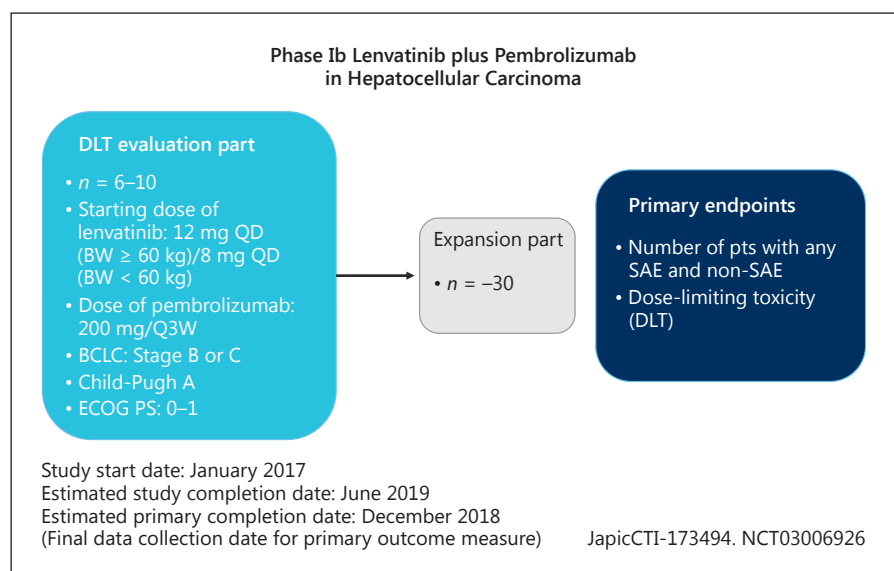
### Immune Checkpoint Inhibitors in Combination with Existing Locoregional Therapy

Other studies are evaluating a different treatment approach for HCC by combining immune checkpoint inhibitors and conventional locoregional therapy. Radiotherapy and locoregional therapies, such as transcatheter arterial chemoembolization (TACE) and radiofrequency ablation (RFA), are thought to activate the immune system and improve the effect of immunotherapy by inducing local inflammation and the release of neoantigens. Accordingly, these locoregional therapies are particularly

**Fig. 8.** Phase II exploratory trial design of adjuvant treatment with anti-PD-1 antibodies in the prevention of recurrence after curative treatment of HCC, which is currently being conducted only in Japan. HCC, hepatocellular carcinoma; IC, informed consent.



**Fig. 9.** Phase Ib lenvatinib plus pembrolizumab in hepatocellular carcinoma, currently being conducted only in Japan. DLT, dose-limiting toxicity; BW, body weight; BCLC, Barcelona Clinic Liver Cancer; pts, patients; SAE, severe adverse effect.



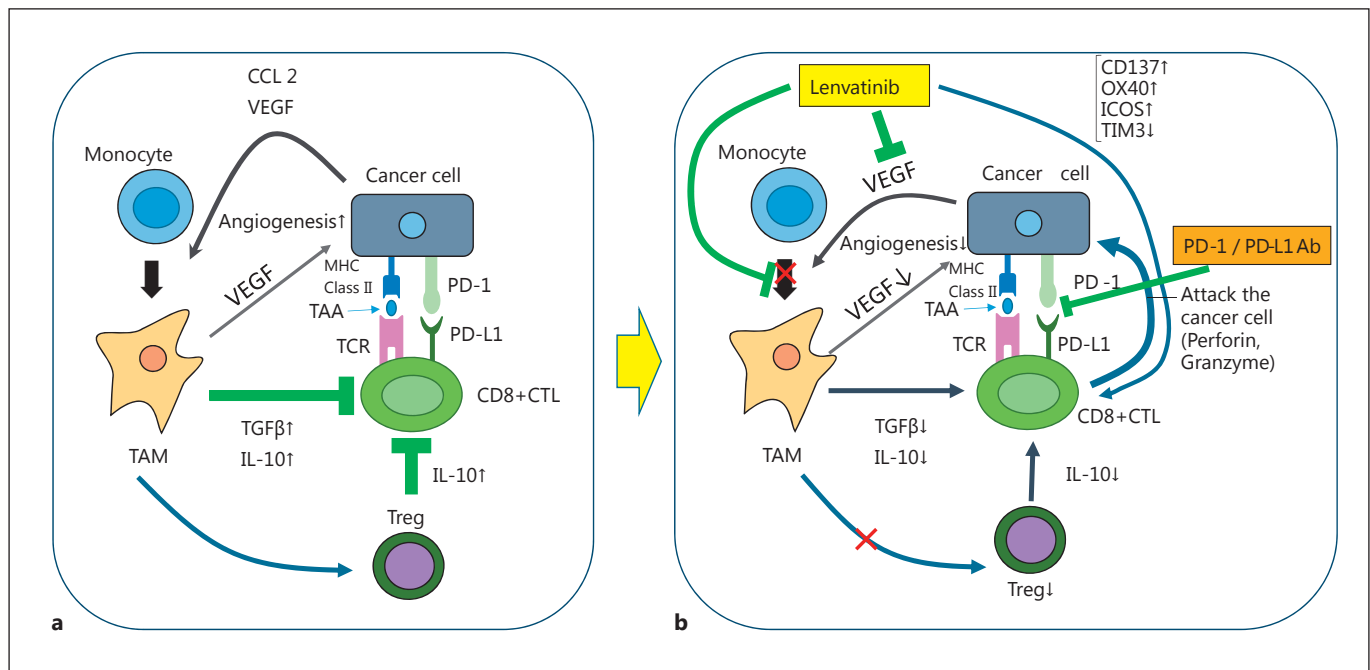
useful for tumors that do not release enough TAA. A recent clinical study reported the treatment efficacy of anti-CTLA-4 antibody combined with locoregional therapy in patients with advanced HCC [24]. In this study (NCT# 01853618), the anti-CTLA-4 antibody tremelimumab was used as adjuvant therapy after performing TACE or RFA on some nodules in patients with advanced HCC. The rate of partial reduction was 26%, and median time to progression and overall survival were 7.4 and 12.3 months, respectively. Moreover, this combination therapy increased the number of CD3+ and CD8+ cells in un-

treated nodules induced by locoregional therapy, a rare phenomenon referred to as the abscopal effect.

These findings suggest that immune checkpoint inhibitors (anti-PD-1, anti-PD-L1, and anti-CTLA-4 antibodies) can be used in combination with TACE or as adjuvant therapy after resection or RFA (Fig. 7).

Tumor recurrence rates are particularly high in patients with HCC, even after curative treatment such as resection or RFA. This is largely attributable to microsatellite lesions that were not detected by preoperative diagnostic imaging. Several clinical trials have evaluated the





**Fig. 10.** Mechanism of synergistic effect by a combination therapy of lenvatinib and PD-1 antibody. **a** Immunosuppressive microenvironment and PD-1/PD-L1 immunosuppression. **b** Lenvatinib and anti-PD-1/PD-L1 antibodies synergistically induce PD-1/PD-L1 blockade and inhibit the immunosuppressive microenvironment.

effects of adjuvant treatment with interferon, retinoids, vitamin K, or sorafenib in patients with these microsatellite lesions, but none has yielded positive outcomes [25–28].

TACE [29–32] and RFA [33–35] induce tumor immunogenicity by releasing TAA and stimulating the migration of cytotoxic T lymphocytes to small intrahepatic metastatic nodules. Thus, subsequent administration of an anti-PD-1 antibody may control these small intrahepatic metastatic nodules [36]. For example, RFA was found to significantly increase the number of tumor antigen-specific T cells in 62% of patients, confirming the release of TAA. This study also showed that recurrence-free survival rates were significantly higher among patients with high levels of tumor antigen-specific T cells than among those with low levels of tumor antigen-specific T cells [37].

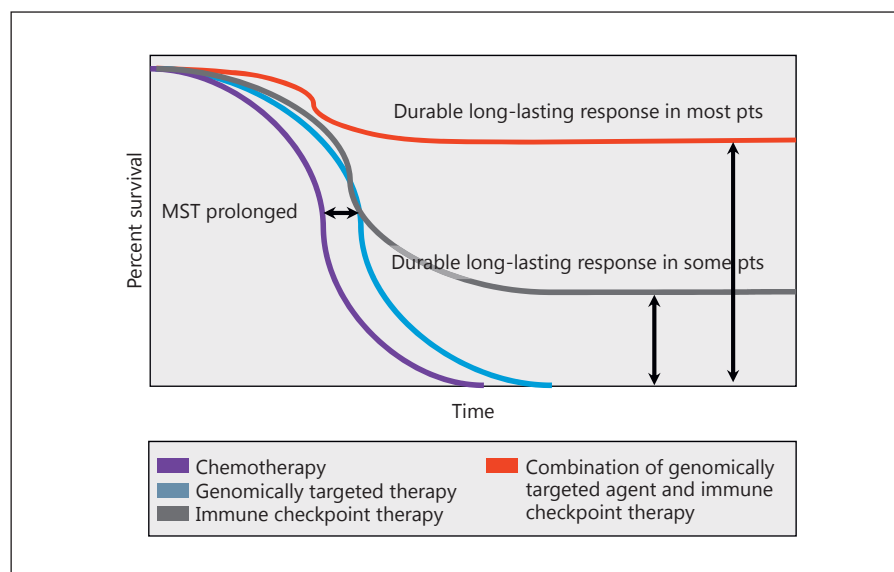
An investigator-initiated clinical trial in Japan is ongoing evaluating the utility of nivolumab as adjuvant therapy after resection [38, 39] or ablation. The combined use of immune checkpoint inhibitors under adjuvant conditions after curative treatment with RFA is expected to serve as an appropriate treatment strategy for preventing recurrence of HCC (Fig. 8).

### Concurrent Use of Immune Checkpoint Inhibitors and Molecularly Targeted Agents

Combination therapy with immune checkpoint inhibitors and molecularly targeted agents [40, 41] has received considerable attention in recent years. Factors that may contribute to the immunosuppressive hepatic environment in patients with liver cancer include hepatic interstitial cells, such as Kupffer cells, dendritic cells, endothelial cells, and hepatic stellate cells, and immunosuppressive cytokines, such as interleukin (IL)-10 and transforming growth factor (TGF)- $\beta$ , as well as the PD-1/PD-L1 pathway. This immunosuppressive environment may be inhibited by combinations of molecularly targeted agents and immune checkpoint inhibitors [42, 43].

Table 4 shows ongoing clinical trials of combination treatments with immune checkpoint inhibitors and molecularly targeted agents. The efficacy of combination therapy with pembrolizumab and lenvatinib in HCC is being tested in Japan (Fig. 9). Previous studies of this combination, presented at ESMO 2016 and ASCO 2017, reported high response rates (50–70%) and long-lasting drug effects (durable response) in patients with solid cancer such as renal and endometrial cancers [44, 45].

**Fig. 11.** Improved overall survival as a result of combination therapy of molecular targeted therapy and immune checkpoint inhibitor will be realistic in the very near future. MST, median survival time; pts, patients. Adapted from Sharma and Allison [46].



Unlike concurrent administration of 2 immune checkpoint inhibitors (PD-1/PD-L1 antibody plus CTLA-4 antibody), combinations with molecularly targeted agents should result in cancer cell suppression by 2 different mechanisms of action. In a preclinical study, pembrolizumab and lenvatinib inhibited cancer immunosuppressive environments induced by tumor-associated macrophages and Tregs, reducing the levels of TGF- $\beta$  and IL-10, the expression of PD-1, and the inhibition of Tim-3, and thereby triggering anticancer immunity mediated by immunostimulatory cytokines such as IL-12 [44] (Fig. 10). These studies may provide insight into the appropriate molecularly targeted agents to be used with immune checkpoint inhibitors.

## Conclusion

Patients who respond favorably to combinations of molecularly targeted agents and immune checkpoint inhibitors may show prolonged survival or achieve a cure [46, 47] (Fig. 11). In addition to prolonging the survival of patients with HCC, combinations of immune checkpoint inhibitors with molecularly targeted agents or locoregional therapy may bring about a true cure, thus causing a paradigm shift in liver cancer therapy. Liver cancer represents a group of highly heterogeneous lesions with variable etiopathogenesis, including viral and non-viral hepatitis. Many patients with liver cancer have impaired liver function and poor physical performance, re-

quiring a variety of treatment options. The invention of immune checkpoint inhibition and the combination strategies centered on checkpoint inhibitors may drastically change the conventional treatment algorithms for HCC.

## Disclosure Statement

The author has no conflicts of interest to declare.

## References

- 1 Chen DS, Mellman I: Oncology meets immunology: the cancer-immunity cycle. *Immunity* 2013;39:1–10.
- 2 Sznol M, Chen L: Antagonist antibodies to PD-1 and B7-H1 (PD-L1) in the treatment of advanced human cancer. *Clin Cancer Res* 2013;19:1021–1034.
- 3 Herbst RS, Soria JC, Kowanetz M, Fine GD, Hamid O, Gordon MS, et al: Predictive correlates of response to the anti-PD-L1 antibody MPDL3280A in cancer patients. *Nature* 2014;515:563–567.
- 4 Shih K, Arkenau HT, Infante JR: Clinical impact of checkpoint inhibitors as novel cancer therapies. *Drugs* 2014;74:1993–2013.
- 5 Philips GK, Atkins M: Therapeutic uses of anti-PD-1 and anti-PD-L1 antibodies. *Int Immunol* 2015;27:39–46.
- 6 Mahoney KM, Freeman GJ, McDermott DF: The next immune-checkpoint inhibitors: PD-1/PD-L1 blockade in melanoma. *Clin Ther* 2015;37:764–782.

- 7 Harshman LC, Drake CG, Wargo JA, Sharma P, Bhardwaj N: Cancer immunotherapy highlights from the 2014 ASCO Meeting. *Cancer Immunol Res* 2014;2:714–719.
- 8 Topalian SL, Drake CG, Pardoll DM: Targeting the PD-1/B7-H1(PD-L1) pathway to activate anti-tumor immunity. *Curr Opin Immunol* 2012;24:207–212.
- 9 Merelli B, Massi D, Cattaneo L, Mandala M: Targeting the PD1/PD-L1 axis in melanoma: biological rationale, clinical challenges and opportunities. *Crit Rev Oncol Hematol* 2014;89:140–165.
- 10 Le DT, Uram JN, Wang H, Bartlett BR, Kemberling H, Eyring AD, et al: PD-1 blockade in tumors with mismatch-repair deficiency. *N Engl J Med* 2015;372:2509–2520.
- 11 Droeser RA, Hirt C, Viehl CT, Frey DM, Nebiker C, Huber X, et al: Clinical impact of programmed cell death ligand 1 expression in colorectal cancer. *Eur J Cancer* 2013;49:2233–2242.
- 12 Ribas A: Tumor immunotherapy directed at PD-1. *N Engl J Med* 2012;366:2517–2519.
- 13 Hamid O, Robert C, Daud A, Hodi FS, Hwu WJ, Kefford R, et al: Safety and tumor responses with lambrolizumab (anti-PD-1) in melanoma. *N Engl J Med* 2013;369:134–144.
- 14 Brahmer JR, Tykodi SS, Chow LQ, Hwu WJ, Topalian SL, Hwu P, et al: Safety and activity of anti-PD-L1 antibody in patients with advanced cancer. *N Engl J Med* 2012;366:2455–2465.
- 15 Gao Q, Wang XY, Qiu SJ, Yamato I, Sho M, Nakajima Y, et al: Overexpression of PD-L1 significantly associates with tumor aggressiveness and postoperative recurrence in human hepatocellular carcinoma. *Clin Cancer Res* 2009;15:971–979.
- 16 El-Khoueiry AB, Melero I, Crocenzi TS, et al: Phase I/II safety and antitumor activity of nivolumab in patients with advanced hepatocellular carcinoma (HCC): CA209-040. *J Clin Oncol* 2015;33(suppl; abstr LBA101). <http://meetinglibrary.asco.org/slides>.
- 17 El-Khoueiry AB, Sangro B, Yau T, Crocenzi TS, Kudo M, Hsu C, et al: Nivolumab in patients with advanced hepatocellular carcinoma (CheckMate 040): an open-label, non-comparative, phase 1/2 dose escalation and expansion trial. *Lancet* 2017;389:2492–2502.
- 18 Todd SC, El-Khoueiry AB, Yau T, Melero I, Sangro B, Kudo M, et al: Nivolumab in sorafenib-naïve and -experienced patients with advanced hepatocellular carcinoma: CheckMate040 Study. *J Clin Oncol* 2017;35(15 suppl):4013.
- 19 Sangro B, Gomez-Martin C, de la Mata M, Inarrairaegui M, Garralda E, Barrera P, et al: A clinical trial of CTLA-4 blockade with tremelimumab in patients with hepatocellular carcinoma and chronic hepatitis C. *J Hepatol* 2013;59:81–88.
- 20 Larkin J, Chiarion-Sileni V, Gonzalez R, Grob JJ, Cowey CL, Lao CD, et al: Combined nivolumab and ipilimumab or monotherapy in untreated melanoma. *N Engl J Med* 2015;373:23–34.
- 21 Postow MA, Chesney J, Pavlick AC, Robert C, Grossmann K, McDermott D, et al: Nivolumab and ipilimumab versus ipilimumab in untreated melanoma. *N Engl J Med* 2015;372:2006–2017.
- 22 Kudo M: Molecular targeted agents for hepatocellular carcinoma: current status and future perspectives. *Liver Cancer* 2017;6:101–112.
- 23 Kelley RK, Abou-Alfa GK, Bendell JC, Kim TY, Borad MJ, Yong WP, et al: Phase I/II study of durvalumab and tremelimumab in patients with unresectable hepatocellular carcinoma(HCC): phase I safety and efficacy analyses. *J Clin Oncol* 2017;35(suppl; abstr 4073).
- 24 Duffy AG, Ulahannan SV, Makorova-Rusher O, Rahma O, Wedemeyer H, Pratt D, et al: Tremelimumab in combination with ablation in patients with advanced hepatocellular carcinoma. *J Hepatol* 2017;66:545–551.
- 25 Yoshida H, Shiratori Y, Kudo M, Shiina S, Mizuta T, Kojiro M, et al: Effect of vitamin K2 on the recurrence of hepatocellular carcinoma. *Hepatology* 2011;54:532–540.
- 26 Bruix J, Takayama T, Mazzaferro V, Chau GY, Yang J, Kudo M, et al: Adjuvant sorafenib for hepatocellular carcinoma after resection or ablation (STORM): a phase 3, randomised, double-blind, placebo-controlled trial. *Lancet Oncol* 2015;16:1344–1354.
- 27 Mazzaferro V, Romito R, Schiavo M, Mariani L, Camerini T, Bhoori S, et al: Prevention of hepatocellular carcinoma recurrence with alpha-interferon after liver resection in HCV cirrhosis. *Hepatology* 2006;44:1543–1554.
- 28 Okita K, Izumi N, Matsui O, Tanaka K, Kaneko S, Moriwaki H, et al: Peritoin after curative therapy of hepatitis C-related hepatocellular carcinoma: a randomized double-blind placebo-controlled study. *J Gastroenterol* 2015;50:191–202.
- 29 Kudo M: Locoregional therapy for hepatocellular carcinoma. *Liver Cancer* 2015;4:163–164.
- 30 Kudo M: Surveillance, diagnosis, treatment, and outcome of liver cancer in Japan. *Liver Cancer* 2015;4:39–50.
- 31 Tsurusaki M, Murakami T: Surgical and locoregional therapy of HCC: TACE. *Liver Cancer* 2015;4:165–175.
- 32 Arizumi T, Ueshima K, Minami T, Kono M, Chishina H, Takita M, et al: Effectiveness of sorafenib in patients with transcatheter arterial chemoembolization (TACE) refractory and intermediate-stage hepatocellular carcinoma. *Liver Cancer* 2015;4:253–262.
- 33 Teng W, Liu KW, Lin CC, Jeng WJ, Chen WT, Sheen IS, et al: Insufficient ablative margin determined by early computed tomography may predict the recurrence of hepatocellular carcinoma after radiofrequency ablation. *Liver Cancer* 2015;4:26–38.
- 34 Kang TW, Rhim H: Recent advances in tumor ablation for hepatocellular carcinoma. *Liver Cancer* 2015;4:176–187.
- 35 Lencioni R, de Baere T, Martin RC, Nutting CW, Narayanan G: Image-guided ablation of malignant liver tumors: recommendations for clinical validation of novel thermal and non-thermal technologies – a Western perspective. *Liver Cancer* 2015;4:208–214.
- 36 Kudo M: Immune checkpoint inhibition in hepatocellular carcinoma: basics and ongoing clinical trials. *Oncology* 2017;92(suppl 1):50–62.
- 37 Mizukoshi E, Yamashita T, Arai K, Sunagozaka H, Ueda T, Arihara F, et al: Enhancement of tumor-associated antigen-specific T cell responses by radiofrequency ablation of hepatocellular carcinoma. *Hepatology* 2013;57:1448–1457.
- 38 Kudo M, Izumi N, Sakamoto M, Matsuyama Y, Ichida T, Nakashima O, et al: Survival analysis over 28 years of 173,378 patients with hepatocellular carcinoma in Japan. *Liver Cancer* 2016;5:190–197.
- 39 Ho MC, Hasegawa K, Chen XP, Nagano H, Lee YJ, Chau GY, et al: Surgery for intermediate and advanced hepatocellular carcinoma: a consensus report from the 5th Asia-Pacific Primary Liver Cancer Expert Meeting (AP-PLE 2014). *Liver Cancer* 2016;5:245–256.
- 40 Kudo M: Molecular targeted therapy for hepatocellular carcinoma: where are we now? *Liver Cancer* 2015;4:I–vii.
- 41 Zhang B, Finn RS: Personalized clinical trials in hepatocellular carcinoma based on biomarker selection. *Liver Cancer* 2016;5:221–232.
- 42 Tiegs G, Lohse AW: Immune tolerance: what is unique about the liver. *J Autoimmun* 2010;34:1–6.
- 43 Kudo M: Immune checkpoint blockade in hepatocellular carcinoma. *Liver Cancer* 2015;4:201–207.
- 44 Kato T, Bao X, Macgrath S, Tabata K, Hori Y, Tachino S, et al: Lenvatinib mesilate (LEN) enhanced antitumor activity of a PD-1 blockade agent by potentiating Th1 immune response. *Ann Oncol* 2016;27(suppl\_6):2PD.
- 45 Makker V, Rasco DW, Dutcus CE: A phase Ib/II trial of lenvatinib (LEN) plus pembrolizumab (Pembro) in patients (Pts) with endometrial carcinoma. *J Clin Oncol* 2017;35(suppl; abstr 5598).
- 46 Sharma P, Allison JP: Immune checkpoint targeting in cancer therapy: toward combination strategies with curative potential. *Cell* 2015;161:205–214.
- 47 Sharma P, Allison JP: The future of immune checkpoint therapy. *Science* 2015;348:56–61.

# Oncogenic Signal and Tumor Microenvironment in Hepatocellular Carcinoma

Naoshi Nishida Masatoshi Kudo

Department of Gastroenterology and Hepatology, Kindai University Faculty of Medicine, Osaka-Sayama, Japan

## Keywords

Hepatocellular carcinoma · Oncogene · Molecular targeting agent · Microenvironment · Immune checkpoint inhibitors

## Abstract

During tumor development, several immunosuppressive molecules are released from cancer cells and contribute to the establishment of immunosuppressive tumor environment. In tumor tissues, cytokines, chemokines, growth factors, and metabolites are present and could counter the effects of immune checkpoint inhibitors. From this point of view, monotherapy of anti-PD-1/PD-L1 antibody might not be enough to exert a sufficient antitumor effect; additional blockade of immunosuppressive molecules in tumor microenvironment could enhance the antitumor effect of anti-PD-1/PD-L1 antibody. Importantly, the production of immunosuppressive molecules in cancer cells is attributed to the activation of cellular signaling through genetic and epigenetic alterations and environmental stimulation, such as inflammation and hypoxia. In this review, we focus on the establishment of immunosuppressive microenvironment of hepatocellular carcinoma in the context of activation of oncogenic signals, and discuss how the immunosuppressive condition could be overcome using tyrosine kinase inhibitors.

© 2017 S. Karger AG, Basel

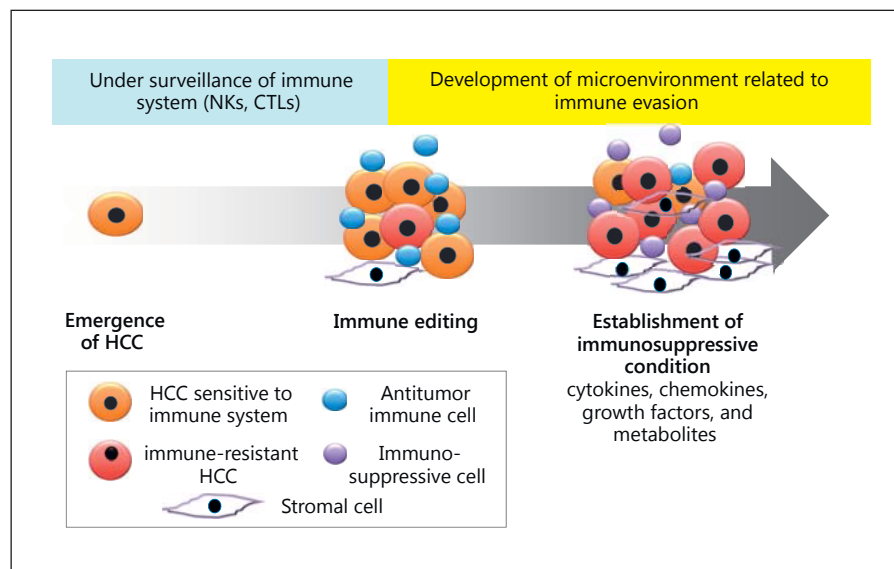
## Introduction

During tumor development, genetic and epigenetic alterations take place that lead to the transformation of hepatocytes [1–5]. These events induce several tumor-associated antigens (TAAs), and a variety of nonsynonymous passenger mutations that could be a source of neoantigen and a target of antitumor immune response.

On the other hand, at the early stage of tumor development, cancer cells are under surveillance of the immune system and could be eliminated by CD8<sup>+</sup> cytotoxic T cells that target TAAs and neoantigens. The extent of TAA-specific CD8<sup>+</sup> T cell responses to hepatocellular carcinoma (HCC) is more prominent in patients with an early stage of tumor compared to those in the late stage, and are correlated with survival of the patients [6]. On the contrary, immunosuppressive environment against cancer cells could develop during the progression of tumor, which is attributed to a selective pressure of the immune system on cancer cells. Consequently, less immunogenic tumor cells could survive and expand, which is a phenomenon called immune editing [7] (Fig. 1). During this process, several cytokines, chemokines, growth factors, and metabolites are released from immune cells as well as cancer cells, and contribute to the establishment of an immunosuppressive condition in tumor [8, 9]. Importantly,



**Fig. 1.** Development of immunosuppressive environment in cancer. At the early stage of tumor, cancer cells are under surveillance of natural killer cells (NKs) and cytotoxic T cells (CTLs). During this process, less immunogenic cancer cells are selected (immune editing). Immunosuppressive cytokines, chemokines, growth factors, and metabolites are released from immune cells and cancer cells, and play a role for the development of immunosuppressive microenvironment in tumor at the advanced stage. HCC, hepatocellular carcinoma.



cellular signals activated through genetic and epigenetic alterations could induce the production of immunosuppressive molecules in HCC tissues [8]. In this review, we focus on the establishment of immunosuppressive microenvironment in the context of activation of oncogenic signaling.

### Activation of Oncogenic Signaling and Immunosuppressive Molecules

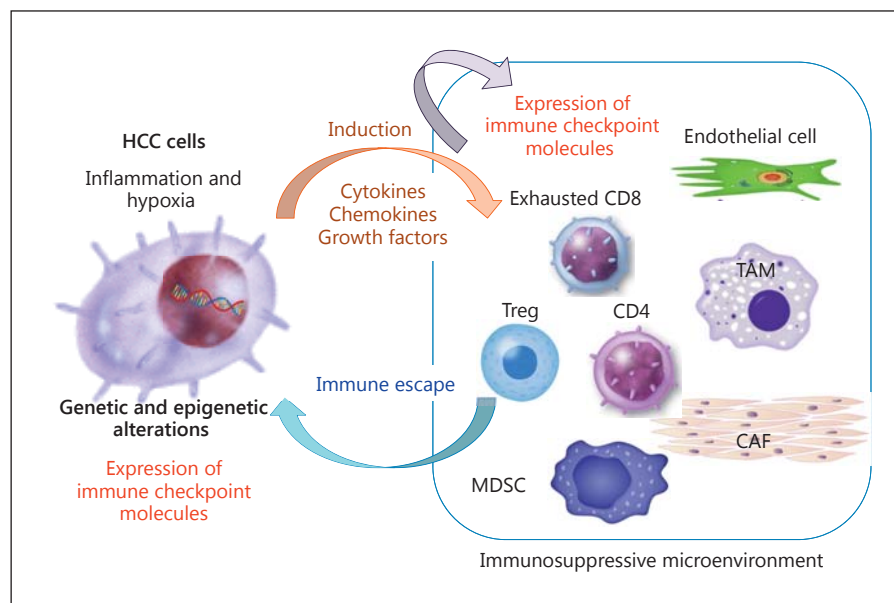
In melanoma cells, it is reported that constitutive activation of mitogen-activated protein kinase (MAPK) by gain-of-function BRAF mutation (BRAF<sup>V600</sup>) induces the increase in interleukin (IL)-6, IL-10, and vascular endothelial growth factor (VEGF), and results in the recruitment of myeloid-derived suppressor cells (MDSCs) and regulatory T (Treg) cells in tumor tissues [10]. It also reduces the expression of major histocompatibility complex class I molecule, and suppresses the CD8<sup>+</sup> T cells and natural killer (NK) cells in tumor microenvironment [11–13]. Reportedly, MAPK inhibition increased the number of antigen-specific CD8<sup>+</sup> T cells in tumor, and more importantly, combination of MAPK/extracellular signal-regulated kinase (MEK) inhibition with anti-programmed death-ligand 1 (PD-L1) antibody induced a synergistic effect for tumor regression compared to monotherapy of MEK inhibitor or anti-PD-L1 antibody [13, 14]. These observations indicate that activation of the oncogenic pathway in cancer cells could play an impor-

tant role for the establishment of immunosuppressive tumor microenvironment.

#### Induction of Growth Factors

So far, overexpression of VEGF and basic fibroblast growth factor are reported in HCC tissues compared to noncancerous livers [15]. VEGF is known to induce MDSC accumulation, inhibit maturation of dendritic cells (DCs), and induce Treg cells [16]. VEGF also exerts immunosuppressive function through the expression of immune checkpoint molecules on CD8<sup>+</sup> T cells, such as PD-1, T-cell immunoglobulin and mucin domain 3 (TIM-3) and cytotoxic T-lymphocyte antigen-4 (CTLA-4) [16]. Expression of VEGF is reportedly controlled by microRNA (miR)-146a as well as hypoxia-inducible factor-1 $\alpha$  (HIF-1 $\alpha$ ), and downregulation of miR-146a through DNA methylation takes place in HCC cells [17]. High expression of transforming growth factor- $\beta$  (TGF- $\beta$ ), which is known as an immune modulator, could also be a predictor of poor prognosis in HCC patients [18]; transcriptional expression of TGF- $\beta$  is induced by the activation of  $\beta$ -catenin, which is one of the commonly mutated genes in HCC [19]. Expression of TGF- $\beta$  leads to the induction of Treg cells, inhibits DCs and NK cell activity [20], and induces expression of TIM-3 on tumor-associated macrophages (TAMs) [21]. Hypoxia in tumor cells also induces HIF-1 $\alpha$  and results in the increase of several immune modulators, such as VEGF, platelet-derived growth factor (PDGF), lactic acid, and adenosine [22].

**Fig. 2.** Role of activation of oncogenic signal in cancer for development of immunosuppressive microenvironment. Oncogenic signal in hepatocellular carcinoma (HCC) cells, which is activated thorough genetic and epigenetic alterations and environmental factors, could induce the components of tumor microenvironment, such as regulatory T (Treg), tumor-associated macrophages (TAM), myeloid-derived suppressor cells (MDSC), and cancer-associated fibroblast (CAF).



#### *Cytokines, Chemokines, and Metabolites*

HCC cells also produce several cytokines, chemokines, and metabolites as immune modulators to the surrounding environment. Amphiregulin, the ligand of endothelial growth factor receptor (EGFR), could be induced in Treg cells as well as tumor cells [23]. Immunoregulatory enzyme, indoleamine 2,3-dioxygenase (IDO), is overexpressed in HCC cell lines and human HCC tissues, which is an independent prognostic factor for HCC patients [24]. IDO is upregulated by proinflammatory cytokines, such as interferon- $\gamma$ , and inhibits T-cell activation and promotes expansion of Treg cells [25, 26]. Similarly, lactic acid, which is generated through glycolysis in tumor cells, stimulates the expression of VEGF and M2-like polarization of TAMs [27]. Activation of NF- $\kappa$ B could also increase the expression of immunosuppressive cytokines, such as IL-2, IL-6, and IL-8 in cancer cells; intratumoral CC chemokine ligand (CCL)-20 prompts the migration of Treg cells through its receptor CCR6 and plays a role for the establishment of immunosuppressive condition in HCC [28].

#### **Conclusion**

The blockade of PD-1-PD-L1 axis is a promising approach for the control of advanced HCC; the phase I/II trials of nivolumab (CheckMate 040) showed an objective response rate of 20% and disease control was observed in

64% of HCC patients [29]. However, several immune modulators are expressed and released from cancer cells through the activation of cellular signaling, which is a consequence of genetic and epigenetic alterations and stimulation of environmental factors such as inflammation and hypoxia (Fig. 2). Therefore, it is conceivable that combination with inhibitors of oncogenic signaling improves the antitumor effect of anti-PD-1 and PD-L1 antibody. For example, IL-6 and PD-L1 blockade combination reportedly inhibits HCC development in mouse model [30]. Inhibition of C-X-C receptor type 4 in tumor microenvironment facilitates anti-PD-L1 immunotherapy of mice HCC [31]. Recently, it was also reported that PD-1 expression promotes tumor growth, where PD-1 binds the downstream effectors of mammalian target of rapamycin (mTOR) and promotes their phosphorylation; the combination of mTOR inhibition with anti-PD-1 antibody results in a synergic tumor regression [32]. Based on these findings, clinical trials of immunomodulation of tumor microenvironment through intervention of oncogenic signaling are ongoing [33–39]. These trials include immune checkpoint inhibition combined with tyrosine kinase inhibitors [40, 41] and other types of immune checkpoint inhibitors such as CTLA-4 antibody as well as immune checkpoint therapy combined with locoregional therapy such as resection [42–44], ablation [45, 46], transarterial chemoembolization [47, 48], and hepatic arterial infusion chemotherapy [49, 50].

## Acknowledgements

This work was supported in part by a Grant-in-Aid for Scientific Research (KAKENHI: 16K09382) from the Japanese Society for the Promotion of Science (N. Nishida) and a grant from the Smoking Research Foundation (N. Nishida).

## Disclosure Statement

The authors have no conflicts of interest to disclose.

## Author Contributions

Naoshi Nishida drafted the manuscript and wrote the final version. Masatoshi Kudo approved the final version of the manuscript.

## References

- 1 Nishida N: Impact of hepatitis virus and aging on DNA methylation in human hepatocarcinogenesis. *Histol Histopathol* 2010;25:647–654.
- 2 Nishida N, Kudo M: Recent advancements in comprehensive genetic analyses for human hepatocellular carcinoma. *Oncology* 2013; 84(suppl 1):93–97.
- 3 Nishida N, Kudo M: Alteration of epigenetic profile in human hepatocellular carcinoma and its clinical implications. *Liver Cancer* 2014;3:417–427.
- 4 Nishida N, Nishimura T, Nakai T, Chishina H, Arizumi T, Takita M, Kitai S, Yada N, Hagiwara S, Inoue T, Minami Y, Ueshima K, Sakurai T, Kudo M: Genome-wide profiling of DNA methylation and tumor progression in human hepatocellular carcinoma. *Dig Dis* 2014;32:658–663.
- 5 Nishida N, Kudo M: Clinical significance of epigenetic alterations in human hepatocellular carcinoma and its association with genetic mutations. *Dig Dis* 2016;34:708–713.
- 6 Flecken T, Schmidt N, Hild S, Gostick E, Drognitz O, Zeiser R, Schemmer P, Bruns H, Eiermann T, Price DA, Blum HE, Neumann-Haefelin C, Thimme R: Immunodominance and functional alterations of tumor-associated antigen-specific CD8+ T-cell responses in hepatocellular carcinoma. *Hepatology* 2014; 59:1415–1426.
- 7 Willmsky G, Schmidt K, Loddenkemper C, Gellermann J, Blankenstein T: Virus-induced hepatocellular carcinomas cause antigen-specific local tolerance. *J Clin Invest* 2013;123: 1032–1043.
- 8 Nishida N, Kudo M: Immunological microenvironment of hepatocellular carcinoma and its clinical implication. *Oncology* 2017; 92(suppl 1):40–49.
- 9 Sia D, Jiao Y, Martinez-Quetglas I, Kuchuk O, Villacorta-Martin C, Castro de Moura M, Putra J, Camprecios G, Bassaganyas L, Akers N, Losic B, Waxman S, Thung SN, Mazzaferro V, Esteller M, Friedman SL, Schwartz M, Villanueva A, Llovet JM: Identification of an immune-specific class of hepatocellular carcinoma, based on molecular features. *Gastroenterology* 2017;153:812–826.
- 10 Sumimoto H, Imabayashi F, Iwata T, Kawakami Y: The BRAF-MAPK signaling pathway is essential for cancer-immune evasion in human melanoma cells. *J Exp Med* 2006;203: 1651–1656.
- 11 Wilmott JS, Long GV, Howle JR, Haydu LE, Sharma RN, Thompson JF, Kefford RF, Hersey P, Scolyer RA: Selective BRAF inhibitors induce marked T-cell infiltration into human metastatic melanoma. *Clin Cancer Res* 2012;18:1386–1394.
- 12 Frederick DT, Piris A, Cogdill AP, Cooper ZA, Lezcano C, Ferrone CR, Mitra D, Boni A, Newton LP, Liu C, Peng W, Sullivan RJ, Lawrence DP, Hodi FS, Overwijk WW, Lizee G, Murphy GF, Hwu P, Flaherty KT, Fisher DE, Wargo JA: BRAF inhibition is associated with enhanced melanoma antigen expression and a more favorable tumor microenvironment in patients with metastatic melanoma. *Clin Cancer Res* 2013;19:1225–1231.
- 13 Mandala M, De Logu F, Merelli B, Nassini R, Massi D: Immunomodulating property of MAPK inhibitors: from translational knowledge to clinical implementation. *Lab Invest* 2017;97:166–175.
- 14 Ebert PJR, Cheung J, Yang Y, McNamara E, Hong R, Moskalenko M, Gould SE, Maecker H, Irving BA, Kim JM, Belvin M, Mellman I: MAP kinase inhibition promotes T cell and anti-tumor activity in combination with PD-L1 checkpoint blockade. *Immunity* 2016;44: 609–621.
- 15 Mise M, Arai S, Higashitani H, Furutani M, Niwano M, Harada T, Ishigami S, Toda Y, Nakayama H, Fukumoto M, Fujita J, Imamura M: Clinical significance of vascular endothelial growth factor and basic fibroblast growth factor gene expression in liver tumor. *Hepatology* 1996;23:455–464.
- 16 Voron T, Colussi O, Marcheteau E, Pernot S, Nizard M, Pointet AL, Latreche S, Bergaya S, Benhamouda N, Tanchot C, Stockmann C, Combe P, Berger A, Zinzindohoue F, Yagita H, Tartour E, Taieb J, Terme M: VEGF-A modulates expression of inhibitory checkpoints on CD8+ T cells in tumors. *J Exp Med* 2015;212:139–148.
- 17 Zhang Z, Zhang Y, Sun XX, Ma X, Chen ZN: microRNA-146a inhibits cancer metastasis by downregulating VEGF through dual pathways in hepatocellular carcinoma. *Mol Cancer* 2015;14:5.
- 18 Peng L, Yuan XQ, Zhang CY, Ye F, Zhou HF, Li WL, Liu ZY, Zhang YQ, Pan X, Li GC: High TGF-beta1 expression predicts poor disease prognosis in hepatocellular carcinoma patients. *Oncotarget* 2017;8:34387–34397.
- 19 Wu J, Lu M, Li Y, Shang YK, Wang SJ, Meng Y, Wang Z, Li ZS, Chen H, Chen ZN, Bian H: Regulation of a TGF-beta1-CD147 self-sustaining network in the differentiation plasticity of hepatocellular carcinoma cells. *Oncogene* 2016;35:5468–5479.
- 20 Sprinzl MF, Reisinger F, Puschnick A, Ringelhan M, Ackermann K, Hartmann D, Schiemann M, Weinmann A, Galle PR, Schuchmann M, Friess H, Otto G, Heikenwalder M, Protzer U: Sorafenib perpetuates cellular anticancer effector functions by modulating the crosstalk between macrophages and natural killer cells. *Hepatology* 2013;57:2358–2368.
- 21 Yan W, Liu X, Ma H, Zhang H, Song X, Gao L, Liang X, Ma C: Tim-3 fosters HCC development by enhancing TGF-beta-mediated alternative activation of macrophages. *Gut* 2015;64:1593–1604.
- 22 Prieto J, Melero I, Sangro B: Immunological landscape and immunotherapy of hepatocellular carcinoma. *Nat Rev Gastroenterol Hepatol* 2015;12:681–700.
- 23 Castillo J, Goni S, Latasa MU, Perugorria MJ, Calvo A, Muntane J, Bioulac-Sage P, Balabaud C, Prieto J, Avila MA, Berasain C: Amphiregulin induces the alternative splicing of p73 into its oncogenic isoform DeltaEx2p73 in human hepatocellular tumors. *Gastroenterology* 2009;137:1805–1815.e1–4.
- 24 Pan K, Wang H, Chen MS, Zhang HK, Weng DS, Zhou J, Huang W, Li JJ, Song HF, Xia JC: Expression and prognosis role of indoleamine 2,3-dioxygenase in hepatocellular carcinoma. *J Cancer Res Clin Oncol* 2008;134:1247–1253.
- 25 Belladonna ML, Orabona C, Grohmann U, Puccetti P: TGF-beta and kynurenines as the key to infectious tolerance. *Trends Mol Med* 2009;15:41–49.

- 26 Mezrich JD, Fechner JH, Zhang X, Johnson BP, Burlingham WJ, Bradfield CA: An interaction between kynurenine and the aryl hydrocarbon receptor can generate regulatory T cells. *J Immunol* 2010;185:3190–3198.
- 27 Colegio OR, Chu NQ, Szabo AL, Chu T, Rherbergen AM, Jairam V, Cyrus N, Brokowski CE, Eisenbarth SC, Phillips GM, Cline GW, Phillips AJ, Medzhitov R: Functional polarization of tumour-associated macrophages by tumour-derived lactic acid. *Nature* 2014;513:559–563.
- 28 Chen KJ, Lin SZ, Zhou L, Xie HY, Zhou WH, Taki-Eldin A, Zheng SS: Selective recruitment of regulatory T cell through CCR6-CCL20 in hepatocellular carcinoma fosters tumor progression and predicts poor prognosis. *PLoS One* 2011;6:e24671.
- 29 El-Khoueiry AB, Sangro B, Yau T, Crocenzi TS, Kudo M, Hsu C, Kim TY, Choo SP, Trojan J, Welling THR, Meyer T, Kang YK, Yeo W, Chopra A, Anderson J, Dela Cruz C, Lang L, Neely J, Tang H, Dastani HB, Melero I: Nivolumab in patients with advanced hepatocellular carcinoma (CheckMate 040): an open-label, non-comparative, phase 1/2 dose escalation and expansion trial. *Lancet* 2017;389:2492–2502.
- 30 Liu H, Shen J, Lu K: IL-6 and PD-L1 blockade combination inhibits hepatocellular carcinoma cancer development in mouse model. *Biochem Biophys Res Commun* 2017;486:239–244.
- 31 Chen Y, Ramjiawan RR, Reiberger T, Ng MR, Hato T, Huang Y, Ochiai H, Kitahara S, Unan EC, Reddy TP, Fan C, Huang P, Bardeesy N, Zhu AX, Jain RK, Duda DG: CXCR4 inhibition in tumor microenvironment facilitates anti-programmed death receptor-1 immunotherapy in sorafenib-treated hepatocellular carcinoma in mice. *Hepatology* 2015;61:1591–1602.
- 32 Li H, Li X, Liu S, Guo L, Zhang B, Zhang J, Ye Q: PD-1 checkpoint blockade in combination with an mTOR inhibitor restrains hepatocellular carcinoma growth induced by hepatoma cell-intrinsic PD-1. *Hepatology* 2017, DOI: 10.1002/hep.29360.
- 33 Kudo M: Immune checkpoint blockade in hepatocellular carcinoma: 2017 update. *Liver Cancer* 2016;6:1–12.
- 34 Kudo M: Recent trends in the management of hepatocellular carcinoma with special emphasis on treatment with regorafenib and immune checkpoint inhibitors. *Dig Dis* 2016;34:714–730.
- 35 Nishida N, Kitano M, Sakurai T, Kudo M: Molecular mechanism and prediction of sorafenib chemoresistance in human hepatocellular carcinoma. *Dig Dis* 2015;33:771–779.
- 36 Smyth MJ, Ngiew SF, Ribas A, Teng MW: Combination cancer immunotherapies tailored to the tumour microenvironment. *Nat Rev Clin Oncol* 2016;13:143–158.
- 37 Kudo M: Immune checkpoint inhibition in hepatocellular carcinoma: basics and ongoing clinical trials. *Oncology* 2017;92(suppl 1):50–62.
- 38 Kudo M: Molecular targeted agents for hepatocellular carcinoma: current status and future perspectives. *Liver Cancer* 2017;6:101–112.
- 39 Kudo M: Immune checkpoint blockade in hepatocellular carcinoma. *Liver Cancer* 2015;4:201–207.
- 40 Kudo M: Regorafenib as second-line systemic therapy may change the treatment strategy and management paradigm for hepatocellular carcinoma. *Liver Cancer* 2016;5:235–244.
- 41 Kudo M: Molecular targeted therapy for hepatocellular carcinoma: where are we now? *Liver Cancer* 2015;4:I–vii.
- 42 Kudo M, Izumi N, Sakamoto M, Matsuyama Y, Ichida T, Nakashima O, Matsui O, Ku Y, Kokudo N, Makuuchi M: Survival analysis over 28 years of 173,378 patients with hepatocellular carcinoma in Japan. *Liver Cancer* 2016;5:190–197.
- 43 Ho MC, Hasegawa K, Chen XP, Nagano H, Lee YJ, Chau GY, Zhou J, Wang CC, Choi YR, Poon RT, Kokudo N: Surgery for intermediate and advanced hepatocellular carcinoma: a consensus report from the 5th Asia-Pacific Primary Liver Cancer Expert Meeting (AP-PLC 2014). *Liver Cancer* 2016;5:245–256.
- 44 Kudo M: Surveillance, diagnosis, treatment, and outcome of liver cancer in Japan. *Liver Cancer* 2015;4:39–50.
- 45 Kang TW: Recent advances in tumor ablation for hepatocellular carcinoma. *Liver Cancer* 2015;4:176–187.
- 46 Lencioni R, de Baere T, Martin RC, Nutting CW, Narayanan G: Image-guided ablation of malignant liver tumors: recommendations for clinical validation of novel thermal and non-thermal technologies – a Western perspective. *Liver Cancer* 2015;4:208–214.
- 47 Kudo M: Locoregional therapy for hepatocellular carcinoma. *Liver Cancer* 2015;4:163–164.
- 48 Tsurusaki M, Murakami T: Surgical and locoregional therapy of HCC: TACE. *Liver Cancer* 2015;4:165–175.
- 49 Obi S, Sato S, Kawai T: Current status of hepatic arterial infusion chemotherapy. *Liver Cancer* 2015;4:188–199.
- 50 Lin CC, Hung CF, Chen WT, Lin SM: Hepatic arterial infusion chemotherapy for advanced hepatocellular carcinoma with portal vein thrombosis: impact of early response to 4 weeks of treatment. *Liver Cancer* 2015;4:228–240.



Original Paper

# Treatment Stage Migration Maximizes Survival Outcomes in Patients with Hepatocellular Carcinoma Treated with Sorafenib: An Observational Study

Clarence Yen<sup>a</sup> Rohini Sharma<sup>a</sup> Lorenza Rimassa<sup>b</sup> Tadaaki Arizumi<sup>c</sup>  
Dominik Bettinger<sup>d, e</sup> Huay Yee Choo<sup>a</sup> Tiziana Pressiani<sup>b</sup>  
Michela E. Burlone<sup>f</sup> Mario Pirisi<sup>f</sup> Laura Giordano<sup>b</sup> Anisa Abdulrahman<sup>a</sup>  
Masatoshi Kudo<sup>c</sup> Robert Thimme<sup>d, e</sup> Joong Won Park<sup>g</sup>  
David James Pinato<sup>a</sup>

<sup>a</sup>Department of Surgery and Cancer, Imperial College London, Hammersmith Hospital, London, UK; <sup>b</sup>Medical Oncology and Haematology Unit, Humanitas Cancer Center, Humanitas Clinical and Research Center, Milan, Italy; <sup>c</sup>Department of Gastroenterology and Hepatology, Kindai University School of Medicine, Osakasayama, Japan; <sup>d</sup>Department of Medicine II, University Medical Center, and <sup>e</sup>Berta Ottenstein Programme, Faculty of Medicine, University of Freiburg, Freiburg, Germany; <sup>f</sup>Department of Translational Medicine, Università degli Studi del Piemonte Orientale “A. Avogadro,” Novara, Italy; <sup>g</sup>Center for Liver Cancer, National Cancer Center Hospital, Goyang, South Korea

## Keywords

Hepatocellular carcinoma · Sorafenib · Treatment stage migration · Prognosis · Treatment-naïve patients

## Abstract

**Background:** Level I evidence supports the use of sorafenib in patients with Barcelona Clinic Liver Cancer (BCLC) stage C hepatocellular carcinoma, where heterogeneity in efficacy exists due to varying clinicopathologic features of the disease. **Aim:** We evaluated whether prior treatment with curative or locoregional therapies influences sorafenib-specific survival. **Methods:** From a prospective data set of 785 consecutive patients from international specialist centres, 264 patients (34%) were treatment naïve (TN) and 521 (66%) were pre-treated (PT), most frequently with transarterial chemoembolization ( $n = 413$ ; 79%). The primary endpoint was overall survival (OS) from sorafenib initiation with prognostic factors tested on uni- and multivariate analyses. **Results:** Median OS for the entire cohort was 9 months; the median sorafenib duration was 2.8 months, with discontinuation being secondary to progression ( $n =$

Dr. David James Pinato, MD, MRes, MRCP (UK), PhD  
NIHR Academic Clinical Lecturer in Medical Oncology  
Imperial College London Hammersmith Campus  
Du Cane Road, London W12 0HS (UK)  
E-Mail david.pinato@imperial.ac.uk

454; 58%) or toxicity ( $n = 149$ ; 19%). PT patients had significantly longer OS than TN patients (10.5 vs. 6.6 months;  $p < 0.001$ ). Compared to TN patients, PT patients had a better Child-Pugh (CP) class (CP A: 57 vs. 47%;  $p < 0.001$ ) and a lower BCLC stage (BCLC A–B, 40 vs. 30%;  $p = 0.007$ ). PT status preserved an independent prognostic role ( $p = 0.002$ ) following adjustment for BCLC stage,  $\alpha$ -fetoprotein, CP class, aetiology, and post-sorafenib treatment status. PT patients were more likely to receive further anticancer treatment after sorafenib (31 vs. 9%;  $p < 0.001$ ). **Conclusion:** Patients receiving sorafenib after having failed curative or locoregional therapies survive longer and are more likely to receive further treatment after sorafenib. This suggests an incremental benefit to OS from sequential exposure to multiple lines of therapy, justifying treatment stage migration in eligible patients.

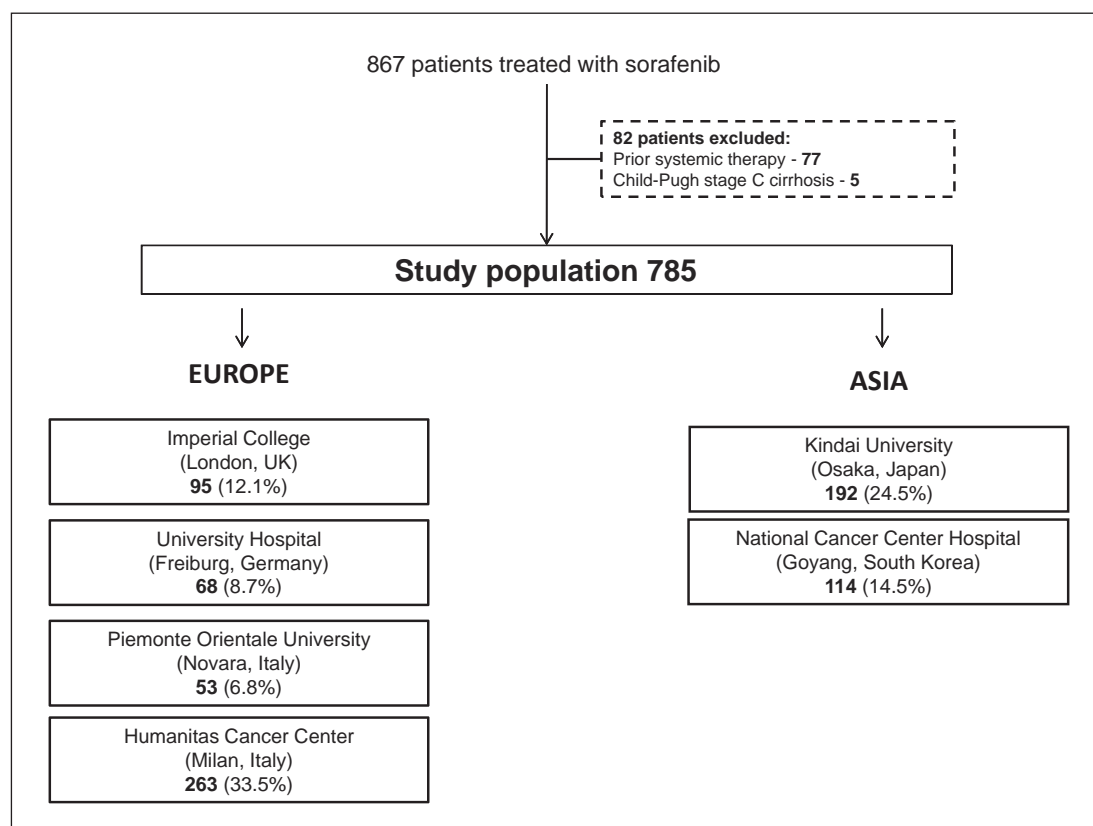
© 2017 S. Karger AG, Basel

## Introduction

Hepatocellular carcinoma (HCC) is the third most common cause of cancer-related death worldwide at a mortality-to-incidence ratio of 0.95 [1, 2] and 5-year survival rates ranging from 5 to 20% [3]. Treatment options for HCC have widened and improved over time to include surgical, locoregional, and systemic therapies [4], and staging algorithms including the Barcelona Clinical Liver Cancer (BCLC) system have facilitated a rational treatment allocation process. Despite increasing efforts addressed at harmonizing management decisions, there is recognized geographical variation in the provision of radical and palliative treatments in HCC where regional preferences and the availability of each treatment modality among the treating multidisciplinary tumour board affect outcomes [5, 6].

The last decade has seen sorafenib emerging as the first systemic agent to produce a survival benefit of approximately 3 months in the treatment of advanced HCC [7, 8]. The magnitude of the survival benefit documented in pre-registration trials is extrapolated from a population of patients with advanced HCC, Child-Pugh (CP) class A, for whom sorafenib represented the first-line option for systemic therapy [9].

In clinical practice, the provision of sorafenib is not solely restricted to treatment-naïve (TN) patients who present with advanced HCC and preserved liver function, but also extends to patients who have progressed after curative or locoregional therapies. The provision of sorafenib as the next most suitable therapy in the context of disease progression or patient ineligibility to further locoregional therapies, a concept also termed “treatment stage migration” [10], is globally the most common indication for the use of sorafenib, as shown in the GIDEON study, where 57% of the patients on sorafenib had previously received local surgical ablative therapy or transarterial chemoembolization (TACE) [11]. Subanalyses of pre-registration trials have initially demonstrated that sorafenib treatment leads to a significant survival advantage over placebo in patients with HCC irrespective of a number of key clinicopathologic features, including disease aetiology, baseline tumour burden, performance status, tumour stage, and prior therapy [12, 13]. However, it is unclear whether TN patients have a life expectancy similar to that of patients who are migrated to sorafenib after failure of radical/locoregional therapies in routine clinical care, where provision of sorafenib does not strictly follow clinical trial eligibility criteria and often extends to subjects with a wider range of liver functional reserve and BCLC stage, variables that are likely to make the expected survival benefit from sorafenib dissimilar to that reported in phase III trial data [14, 15]. Moreover, since the treatment landscape of HCC has recently expanded to include second-line therapies [16, 17], it is important to understand whether treatment sequencing prior to sorafenib might influence the eligibility of patients to receive further systemic treatment lines following sorafenib discontinuation [18].



**Fig. 1.** Study flow chart.

To address these issues, we designed this study aiming to compare and contrast the clinicopathologic features and survival outcomes of patients who received sorafenib for two different clinical indications: (1) as first-line therapy for previously untreated HCC (TN group) or (2) in the context of disease progression or relapse following prior treatment with radical or locoregional therapies (PT group).

## Methods

This observational study was conducted on a prospectively maintained, multicentre data set of 867 consecutive patients receiving sorafenib from 6 tertiary referral centres with HCC multidisciplinary services between 2008 and 2016. From this database, 77 patients who had previously received systemic therapy and 5 CP class C patients were excluded.

The final data set of 785 patients consisted of 449 patients (61.0%) from Europe and 306 (39.0%) from Asia. The European centres included 95 patients (12.1%) from Imperial College London (UK), 68 patients (8.7%) from University Hospital Freiburg (Germany), 53 patients (6.8%) from the Academic Liver Unit in Novara (Italy), and 263 patients (33.5%) from the Humanitas Cancer Center in Milan (Italy). The Asian subgroup included 192 patients (24.5%) from Kindai University, Osakasayama (Japan), and 114 patients (14.5%) from the National Cancer Center Hospital, Goyang (South Korea) (Fig. 1). All patients met the criteria for a histological and/or radiological diagnosis of HCC [10].

Sorafenib was administered after multidisciplinary discussion, either as the first anticancer therapy or in the setting of relapse, failure, or ineligibility to radical or locoregional treatments. The clinical follow-up of the patients during sorafenib treatment included routine blood tests, physical examination, and adverse event assessment before each cycle of sorafenib. Radiologic staging was performed using computerized

Yen et al.: Treatment Stage Migration Maximizes Survival Outcomes in Patients with Hepatocellular Carcinoma Treated with Sorafenib: An Observational Study

**Table 1.** Clinicopathologic features at study baseline

Patient characteristic	Treatment naïve <i>n</i> = 264	Prior treatment <i>n</i> = 521	<i>p</i> value
Median age at sorafenib initiation (range), years	68.6 (59.9–76.2)	69.5 (61.4–76.6)	0.309
Gender			
Male	204 (77.3%)	426 (81.8%)	0.135
Female	60 (22.7%)	95 (18.2%)	
Aetiology			
Hepatitis B virus	58 (22.0%)	125 (24.0%)	<b>0.003</b>
Hepatitis C virus	76 (28.8%)	203 (39.0%)	
Non-viral	130 (49.2%)	193 (37.0%)	
Geography			
Western	197 (74.6%)	282 (54.1%)	<b>&lt;0.001</b>
Eastern	67 (25.4%)	239 (45.9%)	
Extrahepatic spread			
Absent	162 (63.3%)	317 (61.4%)	0.619
Present	94 (36.7%)	199 (38.6%)	
Portal vein invasion			
Absent	170 (64.4%)	397 (76.2%)	<b>&lt;0.001</b>
Present	94 (35.6%)	124 (23.8%)	
α-Fetoprotein			
>400 ng/mL	121 (46.9%)	181 (36.0%)	<b>0.004</b>
<400 ng/mL	137 (53.1%)	322 (64.0%)	
Child-Pugh class			
A	117 (47.2%)	283 (57.3%)	<b>0.009</b>
B	131 (52.8%)	211 (42.7%)	
BCLC stage			
A/B	80 (30.3%)	209 (40.1%)	<b>0.007</b>
C	184 (69.7%)	312 (59.9%)	
Median duration of sorafenib treatment (range), months	2.9 (1.6–6.9)	2.6 (1.4–6.9)	0.755
Previous treatment			
Liver resection	–	148 (28.4%)	–
Liver transplant	–	7 (1.3%)	
RFA	–	168 (32.2%)	
TACE	–	413 (79.3%)	

Bold type denotes significance. BCLC, Barcelona Clinic Liver Cancer; RFA, radiofrequency ablation; TACE, transarterial chemoembolization.

tomography and/or magnetic resonance imaging, as clinically indicated. The patients were re-assessed radiologically for disease response status every 8–12 weeks using the modified RECIST (mRECIST) criteria on contrast-enhanced imaging.

The patients' clinicopathological characteristics, including treatments received prior to and after sorafenib, were collected, and the baseline CP class and BCLC stage were reconstructed [19, 20]. The primary endpoint of this study was overall survival (OS), calculated from the date of sorafenib commencement until death or last follow-up. In addition, we performed a subgroup analysis on post-sorafenib treatment status to explore its confounding effect on survival in the PT and TN groups.

The study was performed following research ethics committee approval from all participating institutions in accordance with the good clinical practice standards published in the Declaration of Helsinki.



### Statistical Analysis

The patients' characteristics were analysed by descriptive statistical methods and are presented as means or medians, as appropriate. Normality was tested with the Shapiro-Wilk test. The Pearson  $\chi^2$  test or Fisher exact test was used for analysis of proportions, as appropriate. Kaplan-Meier curves with log-rank testing were used to perform a univariate survival analysis, with significant factors ( $p < 0.05$ ) being entered into Cox regression models. All statistical analyses were performed using SPSS version 21.0 (IBM Inc., Chicago, IL, USA) and conducted at 95% confidence intervals (95% CI), with a two-tailed level of significance at  $p < 0.05$ .

## Results

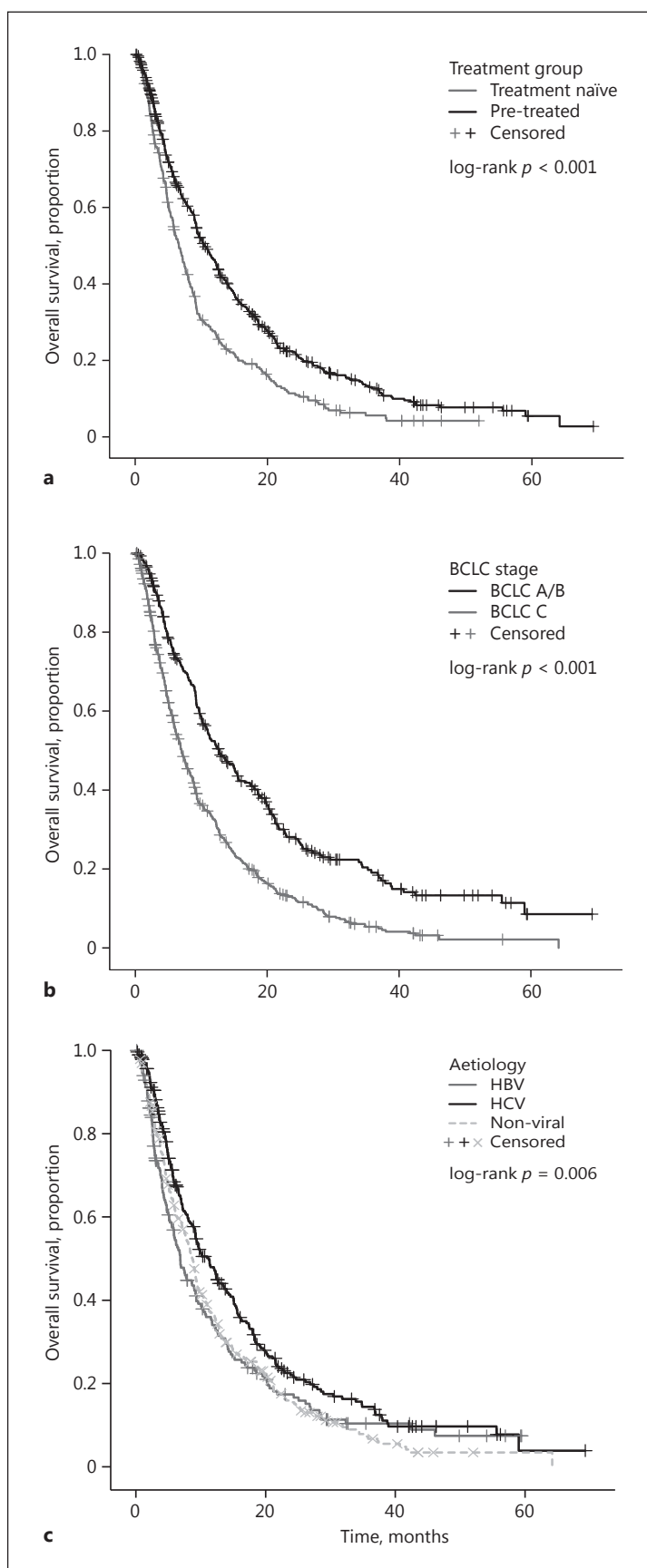
### Patient Characteristics

A total of 785 patients receiving sorafenib for HCC were included: 521 patients (66.4%) had been pre-treated with either potentially curative or locoregional treatment (PT group) and 264 patients (33.6%) were treatment naïve (TN group). The treatment modalities in the PT group included TACE ( $n = 413$ ; 79.3%), radiofrequency ablation (RFA;  $n = 168$ ; 32.2%), and liver resection ( $n = 148$ ; 28.4%). The mean number of prior treatment lines was 2, with 282 patients (54.1%) having received only 1 prior line of treatment.

The differential distribution of the clinical characteristics of the TN and PT patients is presented in Table 1. There were no differences in age at sorafenib initiation, gender distribution, and extrahepatic spread between the TN and PT cohorts at baseline. The treatment duration was similar across the groups: 2.9 months (95% CI: 1.6–6.9) in the TN group and 2.6 months (95% CI: 1.4–6.9) in the PT group ( $p = 0.75$ ). Sorafenib discontinuation primarily followed progression of disease ( $n = 454$ ; 58.1%) and unacceptable toxicity ( $n = 149$ ; 19.0%). Hepatitis C virus (HCV) aetiology was more prevalent in PT than in TN patients ( $n = 203$ , 39.0%, vs.  $n = 76$ , 28.8%;  $p = 0.003$ ). There were more patients treated in Western centres in the TN group ( $n = 197$ ; 74.6%) than in the PT group ( $n = 282$ ; 54.1%) ( $p < 0.001$ ). At baseline, 312 patients (59.9%) in the PT group satisfied BCLC stage C criteria, as compared to 184 patients (69.7%) in the TN group ( $p = 0.007$ ). The PT group had a higher proportion of CP class A patients ( $n = 283$ ; 57.3%) than the TN group ( $n = 117$ ; 47.2%) ( $p = 0.009$ ), as well as lower  $\alpha$ -fetoprotein (AFP) levels, with 181 patients (36.0%) having an AFP level  $>400$  ng/mL in the PT group as compared to 121 patients (46.9%;  $p = 0.004$ ) in the TN group. There were no differences in dose reductions between the two groups ( $n = 99$ , 38.2%, in the TN group and  $n = 170$ , 33.0%, in the PT group;  $p = 0.151$ ).

### Prognostic Relationship between Prior Treatment Status and Sorafenib-Specific Survival in Patients with HCC

Overall, 637 patients (81.1%) had died by the time of analysis, 233 (88.3%) in the TN group and 404 (77.5%) in the PT group. Median OS across the whole study population was 9.0 months (95% CI: 8.2–9.7). The patients in the Eastern centres had a median OS of 8.5 months ( $n = 306$ ; 95% CI: 7.1–9.9 months), while the patients in the Western centres had a non-dissimilar median OS of 9.9 ( $n = 479$ ; 95% CI: 8.2–10.0 months; log-rank  $p = 0.074$ ). On univariate analysis, the patients in the PT cohort had a significantly longer median OS of 10.5 months (95% CI: 9.2–11.8), compared to 6.6 months (95% CI: 5.6–7.6; log-rank  $p < 0.001$ ) in the TN group (Fig. 2a). Other univariate predictors of poorer OS included aetiology of chronic liver disease ( $p = 0.006$ ), AFP  $>400$  ng/mL ( $p < 0.001$ ), portal vein invasion (PVI;  $p < 0.001$ ), extrahepatic spread ( $p < 0.001$ ), CP class ( $p = 0.016$ ), and BCLC stage ( $p < 0.001$ ), as shown in Table 2 and Figure 2. The multivariate analyses revealed prior treatment status to remain an independent predictor of OS (HR 1.32; 95% CI: 1.10–1.57;  $p = 0.002$ ) following adjustment



**Fig. 2.** Kaplan-Meier curves describing the overall survival of patients with hepatocellular carcinoma treated with sorafenib according to prior treatment status (pre-treated or treatment naïve) (**a**), BCLC stage (**b**), and aetiology of the underlying cirrhosis (**c**). BCLC, Barcelona Clinic Liver Cancer; HBV, hepatitis B virus; HCV, hepatitis C virus.

**Table 2.** Univariate and multivariate analyses of survival

	n	Univariate			Multivariate		
		OS, months	95% CI	p value	HR	95% CI	p value
Gender							
Male	630	9.0	8.1–9.8	0.292	–	–	–
Female	155	9.2	7.2–11.2				
Aetiology							
Non-viral	323	8.7	7.8–9.6	<b>0.006</b>	–	–	0.103
Hepatitis B virus	183	6.8	5.4–8.2		1.04	0.83–1.29	
Hepatitis C virus	279	11.3	9.4–13.2		0.84	0.69–1.01	
Geography				0.074	–	–	–
Western	479	9.1	8.2–10.0				
Eastern	306	8.5	7.1–9.9				
α-Fetoprotein							
>400 ng/mL	459	11.8	10.2–13.3	<b>&lt;0.001</b>	–	–	<b>&lt;0.001</b>
<400 ng/mL	302	5.6	4.7–6.6		1.82	1.53–2.16	
Portal vein invasion							
Absent	567	9.9	8.8–11.1	<b>&lt;0.001</b>	–	–	–
Present	218	5.9	4.7–7.0				
Extrahepatic spread							
Absent	479	9.7	8.6–10.8	<b>&lt;0.001</b>	–	–	–
Present	293	7.0	5.7–8.3				
Child-Pugh class							
A	400	9.2	7.9–10.5	<b>0.016</b>	–	–	<b>0.046</b>
B	342	8.6	7.6–9.6		1.19	1.00–1.41	
BCLC stage							
A/B	289	12.7	10.3–15.2	<b>&lt;0.001</b>	–	–	<b>&lt;0.001</b>
C	496	7.0	6.1–7.9		1.65	1.38–1.98	
Treatment group							
Pre-treated	521	10.5	9.2–11.8	<b>&lt;0.001</b>	–	–	<b>0.002</b>
Treatment naïve	264	6.6	5.6–7.6		1.32	1.10–1.57	

Bold type denotes significance. OS, overall survival; BCLC, Barcelona Clinic Liver Cancer.

for aetiology, CP class, BCLC stage, and AFP level (Table 2). When stratified according to BCLC stage, the prior treatment status was able to identify patient subsets with clinically meaningful differences in survival, ranging from 18.6 months for PT BCLC stage A/B patients to 8 months for TN BCLC stage A/B patients who were unfit to receive radical or locoregional therapies (online suppl. Table 1; see [www.karger.com/doi/10.1159/000480441](http://www.karger.com/doi/10.1159/000480441) for all online suppl. material).

We evaluated the relationship between prior treatment status and best type of radiologic response according to the mRECIST criteria. Radiologically proven disease progression was documented in 58 TN patients (63.7%) and 162 PT patients (59.3%), with no difference in response rate between the groups ( $p = 0.22$ ) (Table 3).

In the analysis of treatment after sorafenib discontinuation, we excluded patients on ongoing sorafenib ( $n = 23$ ) or in disease remission ( $n = 7$ ). In the entire study cohort, provision of further anticancer treatment ( $n = 119$ ; 24.2%) was associated with an improved median OS of 18.3 months (95% CI: 13.8–22.9), as compared to 5.8 months (95% CI: 5.0–6.6) among

**Table 3.** Comparison of radiologic responses and the post-sorafenib treatment status between the pre-treated and treatment-naïve patients

	Treatment naïve	Pre-treated	<i>p</i> value
<i>Radiologic response</i>	<i>n</i> = 91	<i>n</i> = 273	
Progressive disease	58 (63.7%)	162 (59.3%)	0.220
Stable disease	28 (30.8%)	75 (27.5%)	
Partial response	5 (5.5%)	32 (11.7%)	
Complete response	0 (0%)	4 (1.5%)	
<i>Treatment after sorafenib discontinuation</i>	<i>n</i> = 157	<i>n</i> = 365	
Best supportive care	136 (90.7%)	237 (69.3%)	<b>&lt;0.001</b>
Further anticancer treatment	14 (9.3%)	105 (30.7%)	

Bold type denotes significance.

the patients who received best supportive care (BSC;  $n = 373$ ; 75.8%;  $p < 0.001$ ), with an HR of 1.8 (95% CI: 1.4–2.2). In the patient cohort receiving further anticancer therapy, 64 patients (53.8%) received further systemic therapy, while 76 (63.9%) of them received locoregional therapy (hepatic arterial infusion chemotherapy or radioembolization), with 21 (17.6%) receiving both locoregional and systemic therapy after sorafenib. Upon sorafenib discontinuation, the patients in the PT group were more likely to receive further anticancer treatment ( $n = 105$ ; 30.7%) than the TN patients ( $n = 14$ ; 9.3%;  $p < 0.001$ ; Table 3).

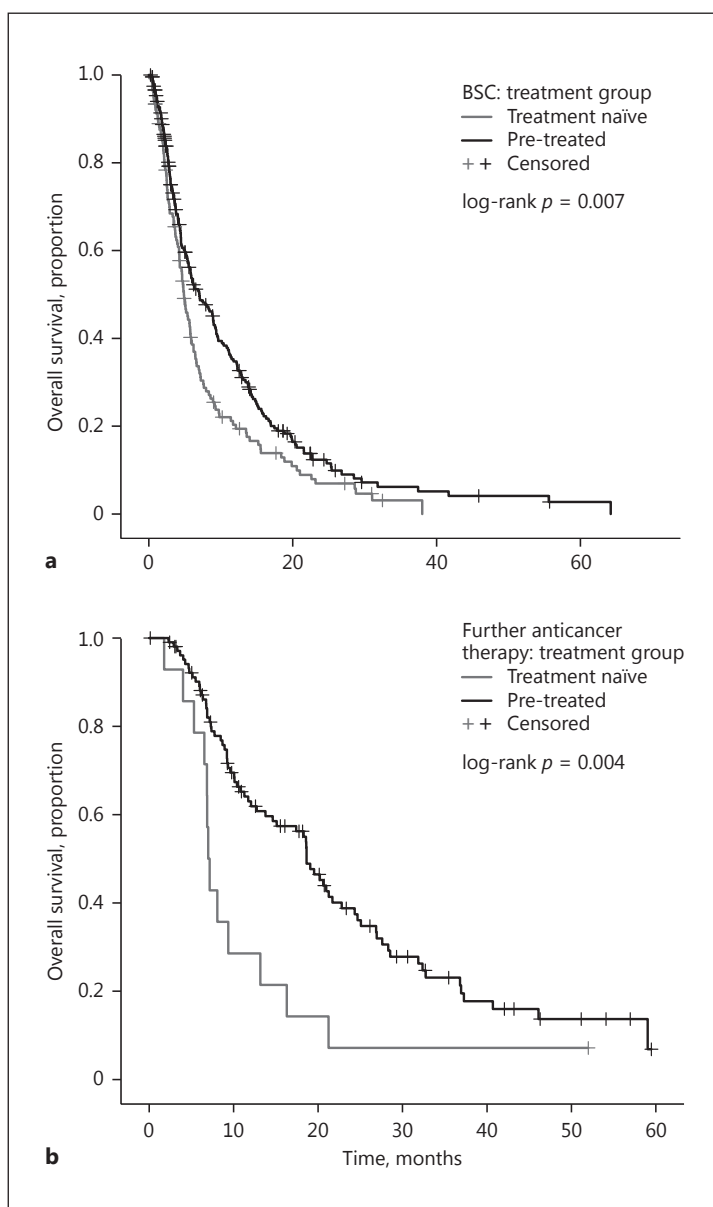
Lastly, we address the potential confounding effect of post-sorafenib therapy status on OS. Among the patients who received BSC after sorafenib discontinuation, the PT group ( $n = 237$ ; 63.5%) had a longer median OS of 7.0 months (95% CI: 5.2–8.9), as compared to the TN group ( $n = 136$ ; 36.5%) with a median OS of 4.9 months (95% CI: 4.2–5.6;  $p = 0.007$ ), with an HR of 1.4 (95% CI: 1.1–1.7) (Fig. 3a). Similarly, among the patients who received further anticancer treatment after sorafenib, the PT group ( $n = 105$ ; 88.2%) had a longer median OS of 18.6 months (95% CI: 16.5–20.8), as compared to 7.0 months (95% CI: 6.5–7.6) in the TN group ( $n = 14$ ; 11.8%;  $p = 0.004$ ; Fig. 3b), with an HR of 2.3 (95% CI: 1.3–4.2). This confirmed that the prognostic stratification imparted by pre-sorafenib treatment status was maintained independently from post-sorafenib treatment.

## Discussion

The multi-targeted tyrosine kinase inhibitor sorafenib has remained the only evidence-based systemic treatment option for patients with HCC for a decade, having been the first compound to demonstrate a significant survival benefit over placebo in two landmark phase III studies [7, 8]. Whilst the positioning of this treatment has initially coincided with the BCLC stage C category of patients (i.e., patients with metastases or PVI, a performance status of 0–2, and preserved liver function), the administration of sorafenib has progressively widened to include patients with earlier-stage disease who have progressed or are deemed ineligible to further radical or locoregional therapies.

These indications, defined within the BCLC guidelines as “treatment stage migration” [10], are based on subgroup analyses of clinical trials showing that sorafenib is more efficacious than placebo in advanced HCC irrespective of prior treatment [12, 13]. In the post-sorafenib era, however, inconclusive evidence exists to demonstrate whether PT and TN patient subpopulations might have a different life expectancy whilst on sorafenib treatment





**Fig. 3.** Kaplan-Meier curves describing the differences in overall survival of patients classified according to prior treatment status following stratification by the type of therapy received after permanent sorafenib cessation: best supportive care (BSC) (**a**) or further active anticancer therapies (**b**).

[21–24]. In addition, expanding level I evidence across the various stages of HCC has importantly shown that the efficacy of sorafenib is strongly dependent on the stage of the disease. The STORM trial has in fact revealed that sorafenib is ineffective in reducing the risk of relapse after resection or RFA in early-stage HCC [25]. Similarly, the SPACE trial and, subsequently, the TACE-2 trial have provided unequivocal evidence that the provision of sorafenib alongside TACE does not improve the survival of patients with intermediate-stage HCC [26–28]. Taken together, the evidence produced to date suggests significant heterogeneity in the clinical activity of sorafenib across stages and indications.

With this in mind, we conducted this study to evaluate whether the survival outcomes of patients receiving sorafenib as first-line anticancer therapy are significantly different from those of patients who are “migrated” to sorafenib after failure of prior radical or locoregional therapies. In our large, consecutive patient series, consisting of a multicentre database from

6 tertiary referral centres across Europe and Asia, we confirmed that sorafenib-specific OS is significantly influenced by the previous anticancer treatment status.

In our study, the patients in the PT group had better liver functional reserve, lower tumour stages, higher AFP levels, and a lower prevalence of PVI, suggesting that the difference in survival observed between the pre-treatment and the treatment-naïve group may be attributed to differences in common clinicopathologic features of the disease [12, 20, 29–33]. However, when we performed multivariate analyses of survival, we found that the 4-month increase in the probability of survival associated with prior treatment was independent of liver functional reserve, stage, aetiology, and AFP levels, which is to suggest that the imbalance of prognostic factors may not entirely explain the difference in survival we observed between the groups.

Our results suggest that patients considered for sorafenib in the context of relapsed/progressive HCC after radical/locoregional therapies are clinically diverse from those who present with de novo metastatic disease – who, in our study, had shorter OS times despite an equal duration of sorafenib treatment and comparable radiologic responses. We cannot discount the possibility that biologic factors intrinsic to the molecular makeup of HCC might be at the basis of the different survival periods observed between the PT and the TN group, more so in light of recent evidence suggesting genomic diversity in the evolution of HCC [34]. It is possible that in the PT group, the HCC might have had a more indolent course that allowed early detection and facilitated the provision of multiple lines of treatment, leading to better patient selection. On the other hand, the diverse distribution of aetiologic factors across groups might be an equally important factor to underpin such biologic heterogeneity. Interestingly, in our study, we found the PT group to comprise more HCV-related cirrhotics, whose survival was significantly superior to those with other aetiologies, echoing evidence from recently published meta-analyses highlighting improved survival among patients with HCV-associated HCC treated with sorafenib [35].

Regardless of the causality, the diversity in prognostic outlook that we document here is a finding of greater consequence with the advent of second-line therapies for HCC. In our study, PT patients were less likely to receive BSC following sorafenib cessation, making this group an optimally suited patient population for further anticancer treatment upon permanent sorafenib cessation.

Our results may also have important implications for optimizing the sequencing of treatments for patients with HCC. Whilst limited by a non-randomized observational study design, our findings suggest that in patients who are initially eligible to radical/locoregional therapies, these should be prioritized over systemic treatment. The use of sorafenib as “salvage” treatment in the context of disease progression or relapse after radical/locoregional therapies does not seem to negatively affect outcome, being conversely associated with an improved survival probability despite the longer time from the original diagnosis of HCC that characterizes the PT group.

We acknowledge a number of limitations to our observations. Firstly, the multicentre observational nature of this study, whilst limiting systematic bias, is influenced by the heterogeneity in the provision of treatments prior to and after sorafenib therapy, with implications for the estimation of survival. Secondly, we could not adjust our analyses for the type or number of TACE procedures, a treatment strategy characterized by wide interinstitutional variability. Despite the acknowledged limitations, our patient data set is fully representative of the population of patients eligible to sorafenib [7, 8, 36]: the median OS of 10.4 months in our PT group is similar to that of the patients treated with TACE in the SHARP trial (median OS: 11.9 months) and with TACE or RFA in the Asian-Pacific trial (median OS: 7.3 and 10.5 months, respectively) [12, 13].

To conclude, in this observational study we have shown that TN patients receiving sorafenib as first-line anticancer therapy have profoundly different survival outcomes from those who received it after prior treatment for HCC. We have highlighted the sources of clinical heterogeneity, including stage and liver functional imbalance, underlying this difference. Indirectly, our study supports the provision of sorafenib in the context of treatment migration following failure of radical or locoregional therapies, and highlights that this patient population is optimally suited for second-line therapies. Whilst we could not control for potential confounders – including a different underlying biology, varying burden of disease within each BCLC stage, and a different and heterogeneity in the criteria for conversion from radical/locoregional to sorafenib – taken together, our study suggests that TN and PT patients should be regarded as different clinical entities, a finding that should be carefully weighted in clinical study design as well as in clinical practice.

### Acknowledgements

D.B. is supported by the Berta Ottenstein Programme, Faculty of Medicine, University of Freiburg. D.J.P. is supported by the National Institute for Health Research (NIHR).

### Disclosure Statement

The authors have no conflicts of interest to disclose.

### Funding Sources

No specific funding was obtained to support the conduction of this study.

### Author Contributions

Study concept and design: D.J.P., C.Y.; acquisition of data: D.J.P. and T.A., D.B., H.Y.C., L.R., M.E.B., T.P., M.P., L.G., A.A., M.K., R.T., J.W.P., and R.S.; analysis and interpretation of data: D.J.P., R.S., L.R., and C.Y.; drafting of the manuscript: C.Y. and D.J.P.; critical revision of the manuscript for important intellectual content: all the authors; statistical analysis: C.Y. and D.J.P.; administrative, technical, or material support: R.S., L.R., J.W.P., R.T., M.K., and M.P.; study supervision: D.J.P.

### References


- 1 Ferlay J, Soerjomataram I, Dikshit R, et al: Cancer incidence and mortality worldwide: sources, methods and major patterns in GLOBOCAN 2012. *Int J Cancer* 2015;136:E359–E386.
- 2 Jemal A, Bray F, Center MM, Ferlay J, Ward E, Forman D: Global cancer statistics. *CA Cancer J Clin* 2011;61:69–90.
- 3 American Cancer Society: Global Cancer Facts and Figures, ed 3. Atlanta, American Cancer Society, 2015.
- 4 Dhir M, Melin AA, Douaiher J, et al: A review and update of treatment options and controversies in the management of hepatocellular carcinoma. *Ann Surg* 2016;263:1112–1125.
- 5 Leoni S, Piscaglia F, Serio I, et al: Adherence to AASLD guidelines for the treatment of hepatocellular carcinoma in clinical practice: experience of the Bologna Liver Oncology Group. *Dig Liver Dis* 2014;46:549–555.
- 6 Park JW, Chen M, Colombo M, et al: Global patterns of hepatocellular carcinoma management from diagnosis to death: the BRIDGE Study. *Liver Int* 2015;35:2155–2166.
- 7 Cheng A-L, Kang Y-K, Chen Z, et al: Efficacy and safety of sorafenib in patients in the Asia-Pacific region with advanced hepatocellular carcinoma: a phase III randomised, double-blind, placebo-controlled trial. *Lancet Oncol* 2009;10:25–34.
- 8 Llovet JJM, Ricci S, Mazzaferro V, et al: Sorafenib in advanced hepatocellular carcinoma. *N Engl J Med* 2008;359:378–390.

- 9 Peck-Radosavljevic M, Greten TF, Lammer J, et al: Consensus on the current use of sorafenib for the treatment of hepatocellular carcinoma. *Eur J Gastroenterol Hepatol* 2010;22:391–398.
- 10 European Association for the Study of the Liver; European Organisation for Research and Treatment of Cancer: EASL-EORTC clinical practice guidelines: management of hepatocellular carcinoma. *J Hepatol* 2012;56:908–943.
- 11 Kudo M, Lencioni R, Marrero JA, et al: Regional differences in sorafenib-treated patients with hepatocellular carcinoma: GIDEON observational study. *Liver Int* 2016;36:1196–1205.
- 12 Cheng AL, Guan Z, Chen Z, et al: Efficacy and safety of sorafenib in patients with advanced hepatocellular carcinoma according to baseline status: subset analyses of the phase III Sorafenib Asia-Pacific trial. *Eur J Cancer* 2012;48:1452–1465.
- 13 Bruix J, Raoul J-L, Sherman M, et al: Efficacy and safety of sorafenib in patients with advanced hepatocellular carcinoma: subanalyses of a phase III trial. *J Hepatol* 2012;57:821–829.
- 14 Pressiani T, Boni C, Rimassa L, et al: Sorafenib in patients with Child-Pugh class A and B advanced hepatocellular carcinoma: a prospective feasibility analysis. *Ann Oncol* 2013;24:406–411.
- 15 Pinter M, Sieghart W, Graziadei I, et al: Sorafenib in unresectable hepatocellular carcinoma from mild to advanced stage liver cirrhosis. *Oncologist* 2009;14:70–76.
- 16 Kudo M: A new era of systemic therapy for hepatocellular carcinoma with regorafenib and lenvatinib. *Liver Cancer* 2017;6:177–184.
- 17 El-Khoueiry AB, Sangro B, Yau T, et al: Nivolumab in patients with advanced hepatocellular carcinoma (CheckMate 040): an open-label, non-comparative, phase 1/2 dose escalation and expansion trial. *Lancet* 2017;389:2492–2502.
- 18 Rimassa L, Pressiani T, Personeni N, Santoro A: Regorafenib for the treatment of unresectable hepatocellular carcinoma. *Expert Rev Anticancer Ther* 2017;17:567–576.
- 19 Johnson PJ, Berhane S, Kagebayashi C, et al: Assessment of liver function in patients with hepatocellular carcinoma: a new evidence-based approach – the ALBI grade. *J Clin Oncol* 2015;33:550–558.
- 20 Llovet JM, Brú C, Bruix J: Prognosis of hepatocellular carcinoma: the BCLC staging classification. *Semin Liver Dis* 1999;19:329–338.
- 21 Baek KK, Kim J-H, Uhm JE, et al: Prognostic factors in patients with advanced hepatocellular carcinoma treated with sorafenib: a retrospective comparison with previously known prognostic models. *Oncology* 2011;80:167–174.
- 22 Devlin P, Cheng S, Vyas R, Parikh ND: Sorafenib associated survival in treatment naïve versus treatment experienced patients with advanced hepatocellular carcinoma. *Gastroenterology* 2016;150:S516.
- 23 Wörns M, Koch S, Niederle IM, et al: The impact of patient and tumour baseline characteristics on the overall survival of patients with advanced hepatocellular carcinoma treated with sorafenib. *Dig Liver Dis* 2013;45:408–413.
- 24 Song T, Zhang W, Wu Q, et al: A single center experience of sorafenib in advanced hepatocellular carcinoma patients. *Eur J Gastroenterol Hepatol* 2011;23:1233–1238.
- 25 Bruix J, Takayama T, Mazzaferro V, et al: Adjuvant sorafenib for hepatocellular carcinoma after resection or ablation (STORM): a phase 3, randomised, double-blind, placebo-controlled trial. *Lancet Oncol* 2015;16:1344–1354.
- 26 Lencioni R, Llovet JM, Han G, et al: Sorafenib or placebo plus TACE with doxorubicin-eluting beads for intermediate stage HCC: the SPACE trial. *J Hepatol* 2016;64:1090–1098.
- 27 Meyer T, Fox R, Ma YT, et al: TACE 2: a randomized placebo-controlled, double-blinded, phase III trial evaluating sorafenib in combination with transarterial chemoembolisation (TACE) in patients with unresectable hepatocellular carcinoma (HCC) – background. *J Clin Oncol* 2016;34(suppl):4018.
- 28 Kudo M, Imanaka K, Chida N, et al: Phase III study of sorafenib after transarterial chemoembolisation in Japanese and Korean patients with unresectable hepatocellular carcinoma. *Eur J Cancer* 2011;47:2117–2127.
- 29 A new prognostic system for hepatocellular carcinoma: a retrospective study of 435 patients: the Cancer of the Liver Italian Program (CLIP) investigators. *Hepatology* 1998;28:751–755.
- 30 Kudo M, Chung H, Osaki Y: Prognostic staging system for hepatocellular carcinoma (CLIP score): its value and limitations, and a proposal for a new staging system, the Japan Integrated Staging Score (JIS score). *J Gastroenterol* 2003;38:207–215.
- 31 Marrero JA, Fontana RJ, Barrat A, et al: Prognosis of hepatocellular carcinoma: comparison of 7 staging systems in an American cohort. *Hepatology* 2005;41:707–716.
- 32 Raoul J-L, Bruix J, Greten TF, et al: Relationship between baseline hepatic status and outcome, and effect of sorafenib on liver function: SHARP trial subanalyses. *J Hepatol* 2012;56:1080–1088.
- 33 Yau T, Chan P, Ng KK, et al: Phase 2 open-label study of single-agent sorafenib in treating advanced hepatocellular carcinoma in a hepatitis B-endemic Asian population. *Cancer* 2009;115:428–436.
- 34 Zhai W, Lim TK-H, Zhang T, et al: The spatial organization of intra-tumour heterogeneity and evolutionary trajectories of metastases in hepatocellular carcinoma. *Nat Commun* 2017;8:4565.
- 35 Jackson R, Psarelli E-E, Berhane S, et al: Impact of viral status on survival in patients receiving sorafenib for advanced hepatocellular cancer: a meta-analysis of randomized phase III trials. *J Clin Oncol* 2017;35:622–628.
- 36 Johnson PJ, Qin S, Park JW, et al: Brivanib versus sorafenib as first-line therapy in patients with unresectable, advanced hepatocellular carcinoma: results from the randomized phase III BRISK-FL study. *J Clin Oncol* 2013;31:3517–3524.



SHORT REPORT

# Imaging and clinicopathological features of nivolumab-related cholangitis in patients with non-small cell lung cancer

Hisato Kawakami<sup>1</sup>  · Junko Tanizaki<sup>1</sup> · Kaoru Tanaka<sup>1</sup> · Koji Haratani<sup>1</sup> · Hidetoshi Hayashi<sup>1</sup> · Masayuki Takeda<sup>1</sup> · Ken Kamata<sup>2</sup> · Mamoru Takenaka<sup>2</sup> · Masatomo Kimura<sup>3</sup> · Takaaki Chikugo<sup>3</sup> · Takao Sato<sup>4</sup> · Masatoshi Kudo<sup>2</sup> · Akihiko Ito<sup>3</sup> · Kazuhiko Nakagawa<sup>1</sup>

Received: 19 February 2017 / Accepted: 3 March 2017 / Published online: 20 March 2017  
© Springer Science+Business Media New York 2017

**Summary** *Background* Nivolumab demonstrates promising efficacy for the treatment of non-small cell lung cancer and other malignancies. The clinical benefit of nivolumab, however, may be hampered by specific immune-related adverse events (irAEs), and little is known regarding nivolumab-related cholangitis. *Methods* A computerized search of our clinical database identified 3 metastatic non-small cell lung cancer patients with nivolumab-related cholangitis. All patients were treated with intravenous nivolumab monotherapy (3.0 mg/kg) every 2 weeks until disease progression or irAEs occurred. Clinical data regarding the duration of nivolumab treatment, symptoms, laboratory abnormalities, pathological findings of liver parenchyma biopsy specimens, and management of nivolumab-related cholangitis were analyzed. *Results* Our analysis revealed that nivolumab-related cholangitis was characterized by (1) localized extrahepatic bile duct dilation without obstruction; (2) diffuse hypertrophy of the extrahepatic bile duct wall; (3) a dominant increase in the biliary tract enzymes alkaline phosphatase and gamma-glutamyl transpeptidase relative to the hepatic enzymes aspartate and alanine aminotransferase; (4) normal or reduced levels of the serum

immunological markers antinuclear antibody, antimitochondrial antibody, smooth muscle antibody, and immunoglobulin G4; (5) the pathological finding of biliary tract cluster of differentiation 8-positive T cell infiltration from liver biopsy; and (6) a moderate to poor response to steroid therapy. *Conclusions* Nivolumab-related cholangitis is associated with distinct imaging and clinicopathological features that distinguish it from acute cholangitis of common etiologies and other immune-related cholangitis. Further studies are warranted to establish the optimal management of patients with this irAE.

**Keywords** Cholangitis · Immune-related adverse event · Nivolumab monotherapy · Programmed death-1

## Introduction

The programmed death-1 (PD-1) receptor is expressed on T cells, whereas programmed death-ligand 1 (PD-L1) is overexpressed on specific types of cancer cells. PD-1 can be activated by binding to PD-L1, which leads to the suppression of T cell (Th1) cytotoxic immune responses. This repression pathway has been demonstrated to play a key role as a tumor immune escape mechanism from host immunity and is upregulated in many tumors and in their surrounding microenvironment. Nivolumab is a fully humanized immunoglobulin G4 (IgG4) monoclonal antibody that blocks the engagement of PD-1 by PD-1 ligands with immune checkpoint inhibitory and antineoplastic activities. Based on the evidence that blockade of the PD-1/PD-L1 pathway with nivolumab leads to remarkable clinical responses in patients with many types of cancer, including melanomas, non-small cell lung cancer (NSCLC), renal cell carcinoma, bladder cancer, and Hodgkin's lymphoma [1–8], the United States Food

✉ Hisato Kawakami  
kawakami\_h@dot.med.kindai.ac.jp

<sup>1</sup> Department of Medical Oncology, Kindai University Faculty of Medicine, 377-2 Ohno-Higashi, Osaka-Sayama, Osaka 589-8511, Japan  
<sup>2</sup> Department of Gastroenterology and Hepatology, Kindai University Faculty of Medicine, 377-2 Ohno-Higashi, Osaka-Sayama, Osaka 589-8511, Japan  
<sup>3</sup> Department of Pathology, Kindai University Faculty of Medicine, 377-2 Ohno-Higashi, Osaka-Sayama, Osaka 589-8511, Japan  
<sup>4</sup> Hospital Pathology, Kindai University Faculty of Medicine, 377-2 Ohno-Higashi, Osaka-Sayama, Osaka 589-8511, Japan

and Drug Administration has approved nivolumab for the treatment of these malignancies.

The clinical benefit of nivolumab, however, may be hampered by specific immune-related adverse events (irAEs) caused by dysregulation of the host immune system [9], whereby unregulated T cells damage the host [10–12]. For nivolumab-treated NSCLC patients, two major irAEs include diarrhea and a rash that affects 8.0–11.0% and 4.0–11.0% of patients, respectively. Hepatitis is also an important irAE that affects 1.0–3.0% of nivolumab-treated patients [8, 13, 14]. However, to date, no information has been available regarding nivolumab-related cholangitis. Herein, we report on a case series of 3 patients with nivolumab-related cholangitis and describe its specific imaging and clinicopathological features.

## Patients and methods

A computerized search of our institution's clinical database identified 3 patients with nivolumab-related cholangitis who had imaging data available at the time irAEs occurred. All patients in our series had unresectable or metastatic NSCLC and were treated with intravenous nivolumab monotherapy (3.0 mg/kg) every 2 weeks until disease progression or irAEs occurred. Clinical data regarding the duration of nivolumab treatment, symptoms, laboratory abnormalities, pathological findings of liver parenchyma (or extrahepatic bile duct) biopsy specimens, and management of nivolumab-related cholangitis were analyzed.

Contrast-enhanced computed tomography (CT) scans of the chest, abdomen, and pelvis were routinely performed immediately prior to (baseline CT) and every 2 months after commencing nivolumab treatment. All patients in the current study underwent abdominal CT and/or additional imaging tests, including endoscopic ultrasonography, endoscopic retrograde cholangiopancreatography, and magnetic resonance cholangiopancreatography, due to abnormal hepatobiliary function test results during or after nivolumab treatment. CT scans performed at the time hepatobiliary function test abnormalities occurred were compared with the baseline and available follow-up CT images to identify serial changes during the clinical course of the treatment.

## Results

### Clinicopathological characteristics

Between December 2015 and October 2016, a total of 91 patients with metastatic or recurrent NSCLC were administered nivolumab at our institution. Our analysis identified 3 patients with nivolumab-related cholangitis, yielding an

incidence rate of 3.3% for this irAE. The patients' baseline characteristics are summarized in Table 1. None of the patients had a history of acute, chronic, or autoimmune cholangitis or pancreatitis prior to commencing nivolumab treatment. Case 3 developed liver metastasis in S8, which was distant from the intrahepatic bile duct. The imaging and clinicopathological features of the 3 patients with nivolumab-related cholangitis in our case series (Cases 1–3) are summarized in Table 2. The clinical manifestations of these cases are comparable to those of obstructive cholangitis, including general fatigue and a mild fever. Biliary enzymes were dominantly increased in all cases, with peak alkaline phosphatase levels of >2000 U/L (reference range, <50 U/L) and peak gamma-glutamyl transpeptidase levels of >800 U/L (reference range, <30 U/L), compared with hepatic enzymes, with peak aspartate aminotransferase levels of 89–142 U/L (reference range, <30 U/L) and peak alanine aminotransferase levels of 70–144 U/L (reference range, <42 U/L) (Fig. 1a–c and Table 2). A moderate increase in total bilirubin levels of ≤3.8 mg/dL was also observed.

In Cases 1 and 3, serological test results for viral hepatitis and antibodies associated with autoimmune hepatitis or cholangitis, including antinuclear antibody, antimitochondrial antibody, and smooth muscle antibody, were negative. In Case 2, the intensity of antinuclear antibody staining was scored as 1+. However, all other serological test results were negative. Serum IgG4 levels were normal in all cases. All patients had an uneventful treatment course until hepatobiliary function test abnormalities occurred. Hepatotoxic medication, herbal drugs, and alcohol were not adopted during nivolumab treatment.

The time course of the hepatobiliary function test abnormalities was identified during nivolumab treatment (9 and 6 courses in Cases 1 and 2, respectively; Fig. 1a–b). In contrast, in Case 3, hepatobiliary function test abnormalities were observed 2 months after the final administration of nivolumab (Fig. 1c). Hepatobiliary function test abnormalities were characterized by a rapid increase and delayed decrease after discontinuation of nivolumab treatment. In Case 3, antibiotic treatment was initially administered on suspicion of infectious cholangitis. In Cases 2 and 3, endoscopic bile duct drainage was performed with plastic stents in place in order to exclude the possibility of cholangitis caused by an obstruction. However, laboratory data indicated little improvement following the procedure. After excluding the possibility of a biliary tract infection, Cases 1 and 2 were treated with steroids (0.5 mg/kg of oral prednisolone, tapered over a 1–2-week period, depending on the patient's condition) and nivolumab was reintroduced due to a rapid, steroid-induced decrease in hepatobiliary enzyme activities. After the second administration of nivolumab with concomitant low doses of prednisolone, however, hepatobiliary function test abnormalities gradually recovered over time (Fig. 1a–b).

**Table 1** Baseline characteristics of the patients ( $N = 3$ ) in our case series

Patient	Sex	Age (y)	Histology	Stage	Site of metastasis	Pre-treatment	Number of cycles <sup>a</sup>	Best response
1	M	64	ADC	Stage IV	Bone	First-line: C + P + V; second-line: N	9	PR
2	F	73	SC	Stage IV	Bone	First-line: NED + S-1; second-line: D; third-line: PEM; fourth-line: N	6	PR
3	F	82	SC	Recurrent	Liver	First-line: C + S-1; second-line: N; third-line: D	12	SD

<sup>a</sup> Number of treatment cycles until hepatobiliary abnormalities occurred

ADC Adenocarcinoma, C Carboplatin, CDDP Cisplatin, D Docetaxel, F Female, M Male, N Nivolumab, NED Nedaplatin, P Paclitaxel, PEM Pemetrexed, PR Partial response, RT Radiotherapy, S-1 tegafur/gimeracil/oteracil, SC Squamous carcinoma, SD Stable disease, V Veliparib, y Years

## Imaging findings

Although clinical manifestations and serological test abnormalities were suggestive of obstructive cholangitis, all of the patients in our case series demonstrated discriminative imaging findings. In all cases, common CT findings included almost typical intrahepatic bile duct dilation, but extensive extrahepatic biliary tract dilation (Fig. 2a–c). In Case 1 and 2, hypertrophy of the gallbladder wall was also observed (Fig. 2a–b). Additionally, all cases exhibited slight subclinical extrahepatic bile duct dilation prior to commencing nivolumab treatment (data not shown). Extrahepatic bile duct dilation progressed during nivolumab treatment and frequently remained after discontinuation of nivolumab treatment, even with steroid or antitumor necrosis factor- $\alpha$  antibody

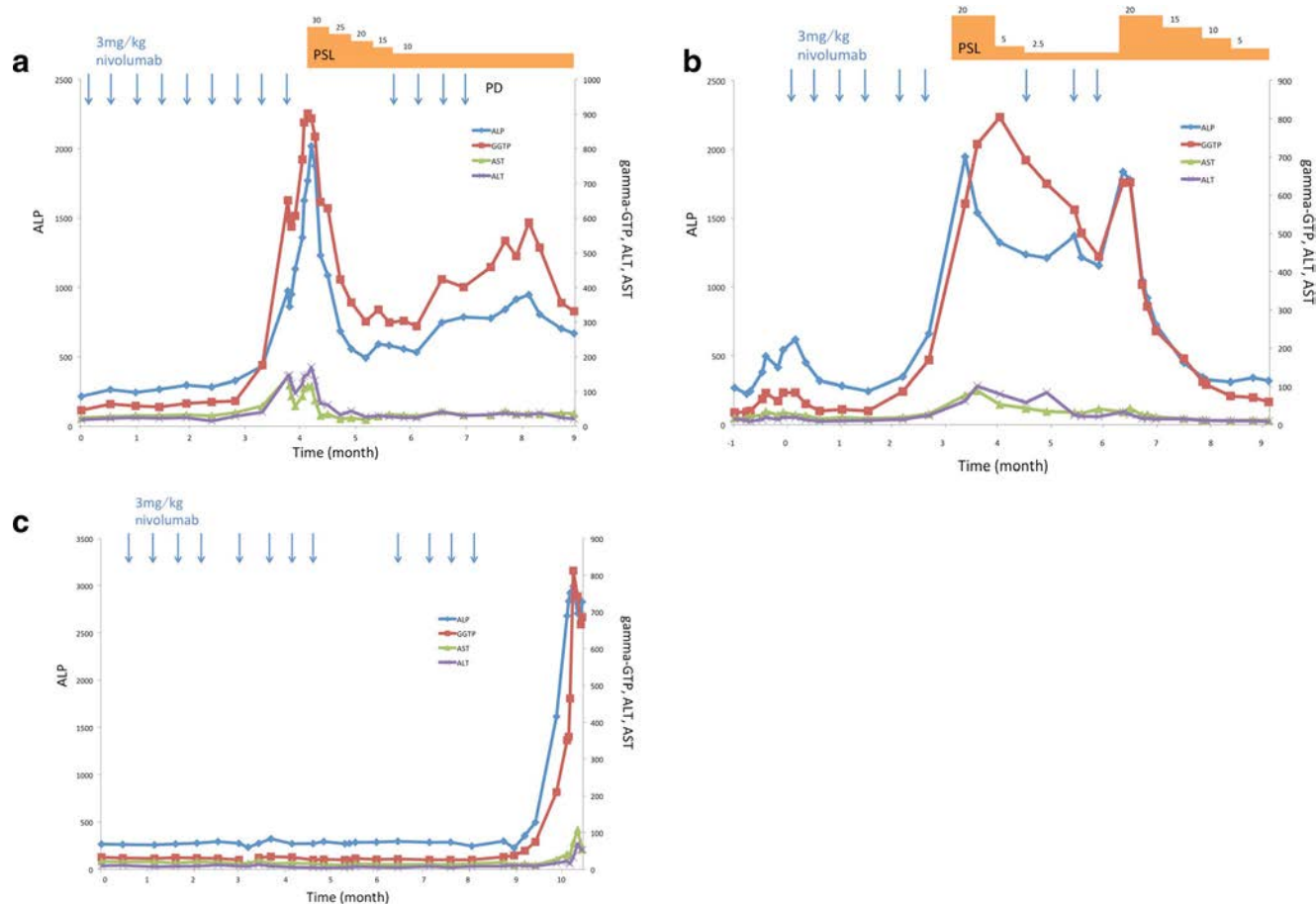
therapy. There was no imaging data to suggest that a lesion (e.g., common bile duct stones or a tumor) was responsible for obstruction of the extrahepatic bile duct. Pancreatic imaging was normal in all cases.

Endoscopic ultrasonography was performed in all cases, demonstrating diffuse hypertrophy of the extrahepatic bile duct (Fig. 3a–c). In Cases 2 and 3, cholangiopancreatography (magnetic resonance cholangiopancreatography in Case 2 and endoscopic retrograde cholangiopancreatography in Cases 2 and 3) demonstrated normal findings in the intrahepatic bile duct and extrahepatic bile duct dilation with distal beaking (Fig. 3d–f). No evidence of an obstruction in the bile duct (e.g., common bile duct stones or a tumor) was detected by either endoscopic ultrasonography or cholangiopancreatography.

**Table 2** Imaging and pathological findings of the patients ( $N = 3$ ) in our case series

Patient	Symptoms	Peak hepatobiliary abnormality and immunological markers	Imaging findings	Pathological findings
1	Fever, abdominal discomfort	ALP: 1769 U/L; $\gamma$ -GTP: 902 U/L; ALT: 144 U/L; AST: 142 U/L; AMA(-); ANA(-); IgG4(-); T-bil: 0.7 mg/dL	CT: Extrahepatic bile duct dilation, hypertrophy of the gallbladder and extrahepatic bile duct; EUS: No obstruction, diffuse hypertrophy of the gallbladder and extrahepatic bile duct, normal intrahepatic bile duct findings.	Liver biopsy: T cell infiltration around the Glisson's capsule (CD8+ T cells were more dominant than CD4+ T cells).
2	Fever, vomiting, abdominal discomfort, diarrhea	ALP: 1947 U/L; $\gamma$ -GTP: 804 U/L; ALT: 101 U/L; AST: 89 U/L; AMA(-); ANA(1+); IgG4(-); T-bil: 3.8 mg/dL	CT: Extrahepatic bile duct dilation; EUS: No obstructive lesions, diffuse hypertrophy of the extrahepatic bile duct, normal intrahepatic bile duct findings; ERCP/MRCP: No obstructive lesions, extrahepatic bile duct dilation.	NA
3	Fever, general fatigue	ALP: 2996 U/L; $\gamma$ -GTP: 813 U/L; ALT: 70 U/L; AST: 108 U/L; AMA(-); ANA(-); IgG4(-); T-bil: 0.8 mg/dL	CT: Extrahepatic bile duct dilation; EUS: No obstruction, diffuse hypertrophy of the extrahepatic bile duct; ERCP: No obstruction, extrahepatic bile duct dilation with distal beaking, normal intrahepatic bile duct findings.	Liver biopsy: T cell infiltration around the Glisson's capsule (CD8+ T cells were more dominant than CD4+ T cells).

ALP Alkaline phosphatase, ALT Alanine aminotransferase, AMA Anti-mitochondrial antibody, ANA Anti-nuclear antibody, AST Aspartate aminotransferase, CD4 Cluster of differentiation 4, CD8 Cluster of differentiation 8, CT Computed tomography, ERCP Endoscopic retrograde cholangiopancreatography, EUS Endoscopic ultrasonography,  $\gamma$ -GTP gamma-glutamyl transpeptidase, IgG4 Immunoglobulin G4, MRCP Magnetic resonance cholangiopancreatography, NA Not available, T-bil Total bilirubin



**Fig. 1** Hepatobiliary function test profile and clinical course. Case 1: A 64-year-old man with a fever, abdominal discomfort, and elevated hepatobiliary function test results during nivolumab treatment. Nivolumab treatment was discontinued 4 cycles after the reintroduction of nivolumab due to disease progression (a). Case 2: A 73-year-old woman with a fever, vomiting, abdominal discomfort, and elevated hepatobiliary function test results during nivolumab treatment. After discontinuing nivolumab treatment due to cholangitis, tumor shrinkage

was maintained for 6 months (b). Case 3: An 82-year-old woman with a fever, general fatigue, and elevated hepatobiliary function test results during nivolumab treatment. The patient developed cholangitis 2 months after the final administration of nivolumab (c). ALP, alkaline phosphatase; ALT, alanine aminotransferase; AST, aspartate aminotransferase; GGTP, gamma-glutamyl transpeptidase; PD, progressive disease; PSL, prednisolone

### Histopathological analysis

Histopathological analysis of liver biopsy specimens was performed for Cases 1 and 3. Although CT scans (or other imaging modalities) revealed minimal changes in the intrahepatic biliary tract, T cell infiltration was observed, especially around the Glisson's capsule (Fig. 4a–b) where cluster of differentiation 8 (CD8)-positive T cells were dominant compared to CD4-positive T cells. Pathological findings (e.g., spotty or bridging necrosis) were not detected, suggesting an acute or subacute response of this irAE.

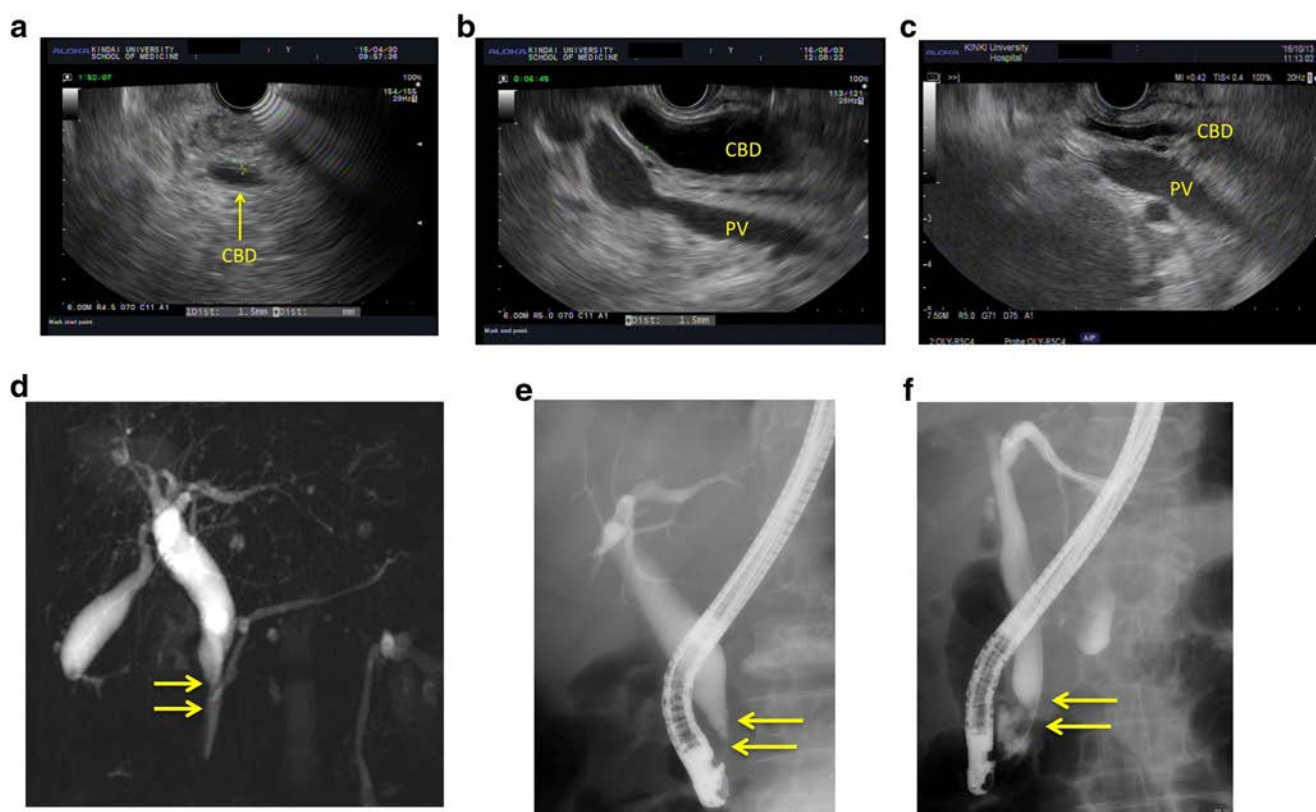
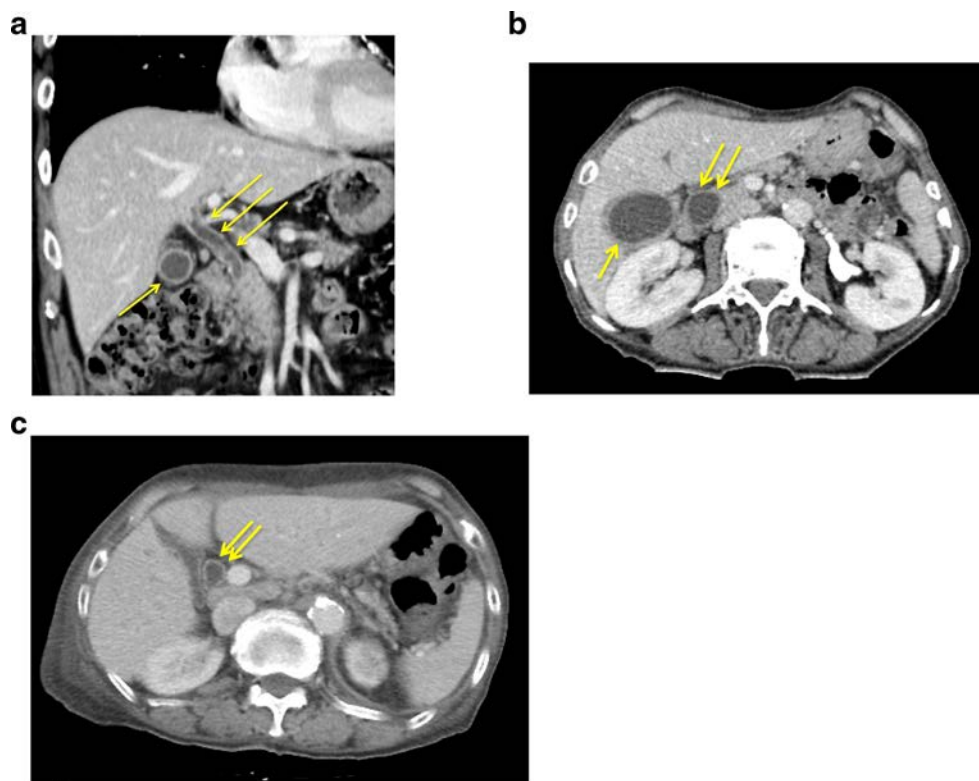
### Discussion

In the present case series, we report on nivolumab-related cholangitis that was detected at a frequency of 3.3% in

nivolumab-treated NSCLC patients. Nivolumab-related cholangitis was characterized by: (1) localized extrahepatic bile duct dilation without obstruction; (2) diffuse hypertrophy of the extrahepatic bile duct wall; (3) a dominant increase in the biliary tract enzymes alkaline phosphatase and gamma-glutamyl transpeptidase relative to the hepatic enzymes aspartate and alanine aminotransferase; (4) normal or reduced levels of the serum immunological markers antinuclear antibody, antimitochondrial antibody, smooth muscle antibody, and immunoglobulin G4; (5) the pathological finding of biliary tract CD8-positive T cell infiltration from liver biopsy; and (6) a moderate to poor response to steroid therapy. Only one case of nivolumab-related cholangitic liver disease has been reported to date [15]. This case was similar to ours, with dominant increases in biliary tract enzymes relative to hepatic enzymes, CD8-positive lymphocyte infiltration on liver biopsy, and a poor response to steroid therapy. Unfortunately,

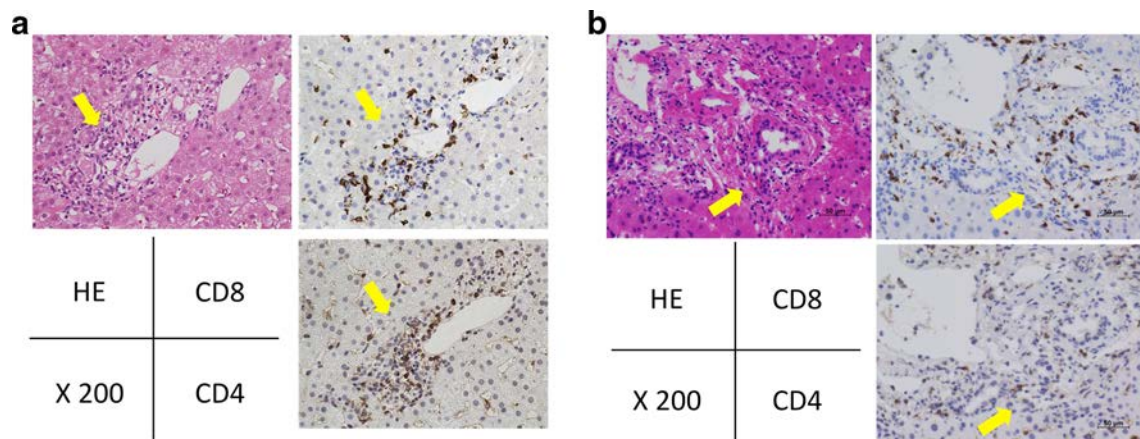


**Fig. 2** Computed tomography (CT) imaging of nivolumab-related cholangitis. Case 1: Coronal contrast-enhanced CT imaging. Extrahepatic bile duct dilation and hypertrophy of the gallbladder wall (arrows) increased from prior CT imaging (data not shown) during nivolumab treatment (**a**). Case 2: Axial contrast-enhanced CT imaging. Extrahepatic bile duct dilation (arrows) increased from prior CT imaging (data not shown) during nivolumab treatment (**b**). Case 3: Axial contrast-enhanced CT imaging. Extrahepatic bile duct dilation (arrows) increased from prior CT imaging (data not shown) even after nivolumab treatment (**c**)



**Fig. 3** Endoscopic ultrasonography demonstrating diffuse hypertrophy of the extrahepatic bile duct in Cases 1 (**a**), 2 (**b**), and 3 (**c**). Case 2: Magnetic resonance cholangiopancreatography demonstrating biliary tract dilation localized to the extrahepatic lesion with distal beaking

(arrows) and no obstruction (**d**). Cases 2 and 3: Endoscopic retrograde cholangiopancreatography demonstrating biliary tract dilation localized to the extrahepatic lesion with distal beaking (arrows) and no obstruction (**e–f**). CBD, common bile duct; PV, portal vein



**Fig. 4** Cases 1 (a) and 3 (b): Hematoxylin and eosin (HE; upper left panel), cluster of differentiation 8 (CD8; upper right panel), and cluster of differentiation 4 (CD4; lower right panel) stained histopathological

specimens demonstrating T cell infiltration (arrows) around the Glisson's capsule (200× magnification)

however, it remains uncertain as to whether this case is fully consistent with our own, given that data are lacking for imaging findings and the status of serum immunological markers. Further accumulation of cases is anticipated to more clearly define the characteristics of this irAE. Moreover, it remains uncertain as to whether this irAE arises exclusively from nivolumab or from other PD-1 and PD-L1 therapies as well. This raises further questions that need to be addressed.

Similar imaging findings are associated with IgG4-related cholangitis, a relatively new disease concept of which patients meet the diagnostic criteria for primary sclerosing cholangitis, but are characterized by different clinicopathological characteristics [16]. Indeed, IgG4-related cholangitis frequently involves the extrahepatic bile ducts, exhibiting generalized, but irregular thickening or a tumefactive lesion [17]. However, IgG4-related cholangitis is frequently associated with other fibrosing conditions, especially autoimmune pancreatitis, and is characterized by elevated serum IgG4 levels, IgG4-positive plasma cell infiltration of the bile ducts, and a favorable response to steroid therapy [16]. Therefore, we reasonably considered our case series of cholangitis patients as a distinct entity of irAE (i.e., nivolumab-related cholangitis). Unlike IgG4-related cholangitis, the patients in our case series did not exhibit a favorable response to steroid therapy, possibly in part, due to insufficient quantities of steroids or “burn out” of nivolumab-related cholangitis. Albeit limited, this suggests that early use of a sufficient quantity of immunosuppressive drugs may be effective in terms of clinical improvement and resolution of imaging, as well as hepatobiliary function test abnormalities, which awaits further evaluation. To establish the optimal management of this newly recognized irAE, more studies are still warranted.

Biliary epithelial cells represent the initial contact points for potential pathogenic microorganisms in the extrahepatic bile duct that ascends from the intestinal tract. These cells express

and secrete chemokines and cytokines, including interferon gamma, tumor necrosis factor-alpha, and interleukin-1, which are important signaling molecules for biliary innate immune defenses given that they can recruit neutrophils, monocytes, or T lymphocytes, and the recruited immune cells can act as a protective response against biliary tract infections [18]. Conversely, given their relatively high expression of human leukocyte antigen class I–II, intercellular adhesion molecule-1, and lymphocyte function-associated antigen-3, biliary epithelial cells are also known to be vulnerable to immune attack [19]. Together, it is possible that in the presence of an appropriate antigen, PD-1 antibody, in association with these adhesion molecules, extensively accelerates the activity of cytotoxic T cells against biliary epithelial cells, resulting in nivolumab-related cholangitis. Indeed, it has been reported that biliary epithelial cell-mediated T cell activation occurs partially via PD-1 ligands in a cell contact-dependent manner in models of primary biliary cirrhosis [20]. In our case series, all patients exhibited mild extrahepatic bile duct dilation immediately prior to commencing nivolumab treatment, suggesting that they had possibly had subclinical or latent cholangitis. Although this may explain why nivolumab-related cholangitis was localized to the extrahepatic bile duct, infiltration of CD8-positive T cells was observed in the intrahepatic bile duct where no obvious imaging abnormalities were detected. Further studies are necessary to understand why this irAE causes dilation and diffuse hypertrophy of the extrahepatic bile duct.

Limitations of this study include potential bias associated with the dosage, duration, and choice of immunosuppressive therapy, which is inevitable in a retrospective analysis, as well as, the small number of patients with a known history of cholangitis after nivolumab treatment. In addition, we could not fully perform the histopathological analyses in all 3 patients due to the retrospective design of our study.

Nivolumab is a novel immunomodulator that demonstrates promising efficacy for the treatment of NSCLC and other malignancies. In addition, alternative anti-PD-1 and anti-PD-L1 antibodies are awaiting approval [21]. Given the incremental use of nivolumab and other drugs of the same class in the treatment of malignant diseases, it is of utmost importance to understand the characteristic imaging findings and clinico-pathological features of nivolumab-related cholangitis that is detected in ~3.0% of nivolumab-treated NSCLC patients. Further study is warranted to establish the optimal management of patients with this irAE.

**Acknowledgements** We wish to thank to our colleagues in the Departments of Medical Oncology, Gastroenterology and Hepatology, and Pathology at Kindai University Faculty of Medicine (Osaka, Japan).

### Compliance with ethical standards

**Conflict of interest** Hisato Kawakami declares that he has no conflict of interest. Junko Tanizaki declares that she has no conflict of interest. Kaoru Tanaka declares that he has no conflict of interest. Koji Haratani declares that he has no conflict of interest. Hidetoshi Hayashi declares that he has no conflict of interest. Masayuki Takeda declares that he has no conflict of interest. Ken Kamata declares that he has no conflict of interest. Mamoru Takenaka declares that he has no conflict of interest. Masatomo Kimura declares that he has no conflict of interest. Takaaki Chikugo declares that he has no conflict of interest. Takao Sato declares that he has no conflict of interest. Masatoshi Kudo declares that he has no conflict of interest. Akihiko Ito declares that he has no conflict of interest. Kazuhiko Nakagawa declares that he has no conflict of interest.

**Funding** None declared.

**Ethical approval** All procedures performed in studies involving human participants were in accordance with the ethical standards of the institutional and/or national research committee and with the 1964 Helsinki declaration and its later amendments or comparable ethical standards.

**Informed consent** Informed consent was obtained from all individual participants included in the study.

### References

- Topalian SL, Hodi FS, Brahmer JR, Gettinger SN, Smith DC, McDermott DF, Powderly JD, Carvajal RD, Sosman JA, Atkins MB, Leming PD, Spigel DR, Antonia SJ, Horn L, Drake CG, Pardoll DM, Chen L, Sharfman WH, Anders RA, Taube JM, McMiller TL, Xu H, Korman AJ, Jure-Kunkel M, Agrawal S, McDonald D, Kollia GD, Gupta A, Wigginton JM, Sznol M (2012) Safety, activity, and immune correlates of anti-PD-1 antibody in cancer. *N Engl J Med* 366:2443–2454. doi:[10.1056/NEJMoa1200690](https://doi.org/10.1056/NEJMoa1200690)
- Brahmer JR, Tykodi SS, Chow LQ, Hwu WJ, Topalian SL, Hwu P, Drake CG, Camacho LH, Kauh J, Odunsi K, Pitot HC, Hamid O, Bhatia S, Martins R, Eaton K, Chen S, Salay TM, Alaparthi S, Grosso JF, Korman AJ, Parker SM, Agrawal S, Goldberg SM, Pardoll DM, Gupta A, Wigginton JM (2012) Safety and activity of anti-PD-L1 antibody in patients with advanced cancer. *N Engl J Med* 366:2455–2465. doi:[10.1056/NEJMoa1200694](https://doi.org/10.1056/NEJMoa1200694)
- Topalian SL, Sznol M, McDermott DF, Kluger HM, Carvajal RD, Sharfman WH, Brahmer JR, Lawrence DP, Atkins MB, Powderly JD, Leming PD, Lipson EJ, Puzanov I, Smith DC, Taube JM, Wigginton JM, Kollia GD, Gupta A, Pardoll DM, Sosman JA, Hodi FS (2014) Survival, durable tumor remission, and long-term safety in patients with advanced melanoma receiving nivolumab. *J Clin Oncol* 32:1020–1030. doi:[10.1200/JCO.2013.53.0105](https://doi.org/10.1200/JCO.2013.53.0105)
- Powles T, Eder JP, Fine GD, Braiteh FS, Loria Y, Cruz C, Bellmunt J, Burris HA, Petrylak DP, Teng SL, Shen X, Boyd Z, Hegde PS, Chen DS, Vogelzang NJ (2014) MPDL3280A (anti-PD-L1) treatment leads to clinical activity in metastatic bladder cancer. *Nature* 515:558–562. doi:[10.1038/nature13904](https://doi.org/10.1038/nature13904)
- Herbst RS, Soria JC, Kowanetz M, Fine GD, Hamid O, Gordon MS, Sosman JA, McDermott DF, Powderly JD, Gettinger SN, Kohrt HE, Horn L, Lawrence DP, Rost S, Leabman M, Xiao Y, Mokatri A, Koeppen H, Hegde PS, Mellman I, Chen DS, Hodi FS (2014) Predictive correlates of response to the anti-PD-L1 antibody MPDL3280A in cancer patients. *Nature* 515:563–567. doi:[10.1038/nature14011](https://doi.org/10.1038/nature14011)
- Hamid O, Robert C, Daud A, Hodi FS, Hwu WJ, Kefford R, Wolchok JD, Hersey P, Joseph RW, Weber JS, Dronca R, Gangadhar TC, Patnaik A, Zarour H, Joshua AM, Gergich K, Ellassa-Schaap J, Algazi A, Mateus C, Boasberg P, Tumeh PC, Chmielowski B, Ebbinghaus SW, Li XN, Kang SP, Ribas A (2013) Safety and tumor responses with lambrolizumab (anti-PD-1) in melanoma. *N Engl J Med* 369:134–144. doi:[10.1056/NEJMoa1305133](https://doi.org/10.1056/NEJMoa1305133)
- Ansell SM, Lesokhin AM, Borrello I, Halwani A, Scott EC, Gutierrez M, Schuster SJ, Millenson MM, Cattray D, Freeman GJ, Rodig SJ, Chapuy B, Ligon AH, Zhu L, Grosso JF, Kim SY, Timmerman JM, Shipp MA, Armand P (2015) PD-1 blockade with nivolumab in relapsed or refractory Hodgkin's lymphoma. *N Engl J Med* 372:311–319. doi:[10.1056/NEJMoa1411087](https://doi.org/10.1056/NEJMoa1411087)
- Rizvi NA, Mazières J, Planchard D, Stinchcombe TE, Dy GK, Antonia SJ, Horn L, Lena H, Minenza E, Mennecier B, Otterson GA, Campos LT, Gandara DR, Levy BP, Nair SG, Zalcman G, Wolf J, Souquet PJ, Baldini E, Cappuzzo F, Chouaid C, Dowlati A, Sanborn R, Lopez-Chavez A, Grohe C, Huber RM, Harbison CT, Baudelet C, Lestini BJ, Ramalingam SS (2015) Activity and safety of nivolumab, an anti-PD-1 immune checkpoint inhibitor, for patients with advanced, refractory squamous non-small-cell lung cancer (CheckMate 063): a phase 2, single-arm trial. *Lancet Oncol* 16:257–265. doi:[10.1016/S1470-2045\(15\)70054-9](https://doi.org/10.1016/S1470-2045(15)70054-9)
- Friedman CF, Proverbs-Singh TA, Postow MA (2016) Treatment of the immune-related adverse effects of immune checkpoint inhibitors: a review. *JAMA Oncol* 2:1346–1353. doi:[10.1001/jamaoncol.2016.1051](https://doi.org/10.1001/jamaoncol.2016.1051)
- Nishimura H, Okazaki T, Tanaka Y, Nakatani K, Hara M, Matsumori A, Sasayama S, Mizoguchi A, Hiai H, Minato N, Honjo T (2001) Autoimmune dilated cardiomyopathy in PD-1 receptor-deficient mice. *Science* 291:319–322
- Chen L (2004) Co-inhibitory molecules of the B7-CD28 family in the control of T-cell immunity. *Nat Rev Immunol* 4:336–347
- Nishimura H, Nose M, Hiai H, Minato N, Honjo T (1999) Development of lupus-like autoimmune diseases by disruption of the PD-1 gene encoding an ITIM motif-carrying immunoreceptor. *Immunity* 11:141–151
- Brahmer J, Reckamp KL, Baas P, Crinò L, Eberhardt WE, Poddubska E, Antonia S, Pluzanski A, Vokes EE, Holgado E, Waterhouse D, Ready N, Gainor J, Arén Frontera O, Havel L, Steins M, Garassino MC, Aerts JG, Domine M, Paz-Ares L, Reck M, Baudelet C, Harbison CT, Lestini B, Spigel DR (2015) Nivolumab versus docetaxel in advanced squamous

- cell non-small-cell lung cancer. *N Engl J Med* 373:123–135. doi:[10.1056/NEJMoa1504627](https://doi.org/10.1056/NEJMoa1504627)
14. Borghaei H, Paz-Ares L, Horn L, Spigel DR, Steins M, Ready NE, Chow LQ, Vokes EE, Felip EE, Holgado E, Barlesi F, Kohlhäufel M, Arrieta O, Burgio MA, Fayette J, Lena H, Poddubskaya E, Gerber DE, Gettinger SN, Rudin CM, Rizvi N, Crinò L, Blumenschein GR Jr, Antonia SJ, Dorange C, Harbison CT, Graf Finckenstein F, Brahmer JR (2015) Nivolumab versus docetaxel in advanced Nonsquamous non-small-cell lung cancer. *N Engl J Med* 373: 1627–1639
  15. Gelsomino F, Vitale G, D’Errico A, Bertuzzi C, Andreone P, Ardizzoni A (2016) Nivolumab-induced cholangitic liver disease: a novel form of serious liver injury. *Ann Oncol*. doi:[10.1093/annonc/mdw649](https://doi.org/10.1093/annonc/mdw649)
  16. Björnsson E, Chari ST, Smyrk TC, Lindor K (2007) Immunoglobulin G4 associated cholangitis: description of an emerging clinical entity based on review of the literature. *Hepatology* 45:1547–1554
  17. Zen Y, Harada K, Sasaki M, Sato Y, Tsuneyama K, Haratake J, Kurumaya H, Katayanagi K, Masuda S, Niwa H, Morimoto H, Miwa A, Uchiyama A, Portmann BC, Nakanuma Y (2004) IgG4-related sclerosing cholangitis with and without hepatic inflammatory pseudotumor, and sclerosing pancreatitis-associated sclerosing cholangitis: do they belong to a spectrum of sclerosing pancreatitis? *Am J Surg Pathol* 28:1193–1203
  18. Wu CT, Davis PA, Luketic VA, Gershwin ME (2004) A review of the physiological and immunological functions of biliary epithelial cells: targets for primary biliary cirrhosis, primary sclerosing cholangitis and drug-induced ductopenias. *Clin Dev Immunol* 11: 205–213
  19. Reynoso-Paz S, Coppel RL, Mackay IR, Bass NM, Ansari AA, Gershwin ME (1999) The immunobiology of bile and biliary epithelium. *Hepatology* 30:351–357
  20. Kamihira T, Shimoda S, Nakamura M, Yokoyama T, Takii Y, Kawano A, Handa M, Ishibashi H, Gershwin ME, Harada M (2005) Biliary epithelial cells regulate autoreactive T cells: implications for biliary-specific diseases. *Hepatology* 41:151–159
  21. Chen L, Han X (2015) Anti-PD-1/PD-L1 therapy of human cancer: past, present, and future. *J Clin Invest* 125:3384–3391



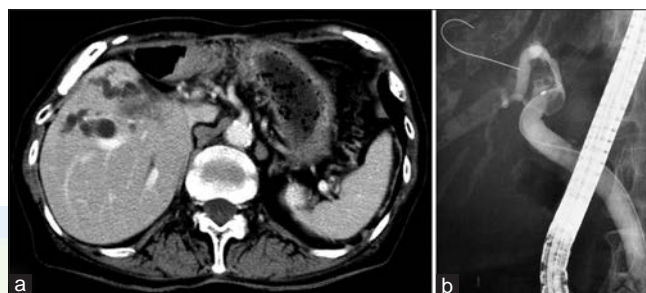
## —Images and Videos—

# Achievement of long-term stent patency in endoscopic ultrasonography-guided right bile duct drainage after left hepatic lobectomy (with video)

Kosuke Minaga, Mamoru Takenaka, Takeshi Miyata, Kentaro Yamao, Ken Kamata, Masayuki Kitano<sup>1</sup>, Masatoshi Kudo

Department of Gastroenterology and Hepatology, Faculty of Medicine, Kindai University, Osaka-Sayama, <sup>1</sup>Second Department of Internal Medicine, School of Medicine, Wakayama Medical University, Wakayama, Japan

A 72-year-old female with advanced rectal cancer presented with obstructive jaundice 6 months after undergoing left hepatic lobectomy for liver metastases. Computed tomography revealed a dilated right intrahepatic bile duct, and a new liver metastasis appeared in her right hepatic lobe [Figure 1a]. Endoscopic retrograde cholangiopancreatography (ERCP) revealed severe stricture at the hepatic hilum; however, insertion of an ERCP catheter into the right anterior intrahepatic duct was unsuccessful [Figure 1b]. Subsequently, endoscopic ultrasonography-guided right hepatic bile duct drainage (EUS-RBD) was attempted. The right anterior intrahepatic duct could be well-visualized with an echoendoscope from the duodenal bulb and was punctured with a 19-gauge aspiration needle [Figure 2a]. A 0.025-inch angle-tip guidewire (VisiGlide 2; Olympus Medical Systems, Tokyo, Japan) was inserted into the biliary system [Figure 2b], and following dilation of the fistula track by a 7-Fr biliary bougie dilator (Soehendra Biliary Dilation Catheter, Cook Medical, Winston-Salem, North Carolina, USA), a covered self-expandable



**Figure 1.** (a) Computed tomography image showing a dilated right intrahepatic bile duct and liver metastasis in the right hepatic lobe. (b) Cholangiography image obtained by endoscopic retrograde cholangiopancreatography showing a severe stricture at the hepatic hilum. Repeated attempts to insert an endoscopic retrograde cholangiopancreatography catheter into the right anterior intrahepatic duct failed

metal stent (10 mm × 100 mm, Niti-S Biliary Covered Stent; Taewoong Medical, Seoul, South Korea) was successfully deployed through the duodenal bulb [Figure 2c and Video 1]. The total procedure time was 42 min. The postoperative period was uneventful, and both jaundice and never mentioned before resolved in

This is an open access article distributed under the terms of the Creative Commons Attribution-NonCommercial-ShareAlike 3.0 License, which allows others to remix, tweak, and build upon the work non-commercially, as long as the author is credited and the new creations are licensed under the identical terms.

**For reprints contact:** [reprints@medknow.com](mailto:reprints@medknow.com)

**How to cite this article:** Minaga K, Takenaka M, Miyata T, Yamao K, Kamata K, Kitano M, *et al.* Achievement of long-term stent patency in endoscopic ultrasonography-guided right bile duct drainage after left hepatic lobectomy (with video). *Endosc Ultrasound* 2017;6:412-3.

Video Available on: [www.eusjournal.com](http://www.eusjournal.com)

Access this article online

Quick Response Code:



Website:

[www.eusjournal.com](http://www.eusjournal.com)

DOI:

10.4103/eus.eus\_9\_17

### Address for correspondence

Dr. Mamoru Takenaka, Department of Gastroenterology and Hepatology, Faculty of Medicine, Kindai University, 377-2 Ohno-Higashi, Osaka-Sayama 589-8511, Japan. E-mail: [mamoxyo45@gmail.com](mailto:mamoxyo45@gmail.com)

**Received:** 2016-10-26; **Accepted:** 2016-11-26



**Figure 2.** (a) The right anterior intrahepatic duct was punctured using a 19-gauge aspiration needle under endosonographic guidance. (b) After the injection of contrast agent, a 0.025-inch guidewire was inserted into the biliary system. (c) A covered metal stent (10 mm wide and 100 mm long) was successfully deployed into the right hepatic bile duct via the duodenal bulb

a week. Chemotherapy was resumed for advanced rectal cancer immediately after discharge. The patient died 767 days after EUS-RBD because of the progression of her underlying disease; however, she remained free of jaundice until death.

EUS-guided biliary drainage is a recently developed alternative technique in patients with biliary obstruction for failed ERCP.<sup>[1,2]</sup> Various techniques have been described; however, limited data are available regarding EUS-RBD<sup>[3-5]</sup> and long-term follow-up data are lacking. This is the first case which attained long-term stent patency in EUS-RBD after left hepatic lobectomy.

The use of the Spyglass System (Boston Scientific, Natick, Massachusetts, USA) to facilitate selective placement of a guidewire in the context of difficult biliary strictures has been reported.<sup>[6]</sup> However, even if a guidewire had been successfully inserted across this stricture, the configuration and site of the stricture would have made placement of a self-expandable metal stent difficult, and a plastic stent would have to be used. Plastic stents tend to occlude within a few months, and the patient would have had to undergo repeat ERCP procedures for palliative drainage. In contrast, EUS-RBD using a self-expandable metal stent allowed long lasting effective drainage.

In conclusion, EUS-RBD could be an effective palliative option for right intrahepatic bile duct drainage, which is expected to maintain the patient's quality of life and achieve long-term stent patency and survival.

### *Declaration of patient consent*

The authors certify that they have obtained all appropriate patient consent forms. In the form the patient has given her consent for her images and other clinical information to be reported in the journal. The patient understand that her name and initial will not be published and due efforts will be made to conceal her identity, but anonymity cannot be guaranteed.

### *Financial support and sponsorship*

Nil.

### *Conflicts of interest*

There are no conflicts of interest.

## REFERENCES

1. Giovannini M, Moutardier V, Pesenti C, *et al.* Endoscopic ultrasound-guided bilioduodenal anastomosis: A new technique for biliary drainage. *Endoscopy* 2001;33:898-900.
2. Poincloux L, Rouquette O, Buc E, *et al.* Endoscopic ultrasound-guided biliary drainage after failed ERCP: Cumulative experience of 101 procedures at a single center. *Endoscopy* 2015;47:794-801.
3. Park SJ, Choi JH, Park DH, *et al.* Expanding indication: EUS-guided hepaticoduodenostomy for isolated right intrahepatic duct obstruction (with video). *Gastrointest Endosc* 2013;78:374-80.
4. Ogura T, Sano T, Onda S, *et al.* Endoscopic ultrasound-guided biliary drainage for right hepatic bile duct obstruction: Novel technical tips. *Endoscopy* 2015;47:72-5.
5. Mukai S, Itoi T, Tsuchiya T, *et al.* EUS-guided right hepatic bile duct drainage in complicated hilar stricture. *Gastrointest Endosc* 2017;85:256-257.
6. Theodoropoulou A, Vardas E, Voudoukis E, *et al.* SpyGlass direct visualization system facilitated management of iatrogenic biliary stricture: A novel approach in difficult cannulation. *Endoscopy* 2012;44:E433-4.